
2018 Annual Meeting of the American Society for Bone and Mineral Research

Palais des congrès de Montréal in Montréal, Québec, Canada September 28 – October 1, 2018

The *Journal of Bone and Mineral Research* (ISSN: 0884-0431 [print]; 1523-4681 [online]) provides a forum for papers of the highest quality pertaining to bone, muscle, and mineral metabolism. Manuscripts are published on the biology and physiology of bone and muscle, relevant systems biology topics (e.g., osteoimmunology), and the pathophysiology and treatment of sarcopenia, and disorders of bone and mineral metabolism. All authored papers and editorial news and comments, opinions, findings, conclusions or recommendations in the *Journal* are those of the author(s) and do not necessarily reflect the views of the *Journal* and its publisher, nor does their publication imply any endorsement.

The JOURNAL OF BONE AND MINERAL RESEARCH (ISSN: 0884-0431), is published monthly on behalf of the American Society for Bone and Mineral Research by Wiley Subscription Services, Inc., a Wiley Company, 111 River St., Hoboken, NJ 07030-5774. Periodical Postage Paid at Hoboken, NJ and additional offices.

Postmaster: Send all address changes to JOURNAL OF BONE AND MINERAL RESEARCH, John Wiley & Sons Inc., C/O The Sheridan Press, PO Box 465, Hanover, PA 17331. **Information for subscribers:** The *Journal of Bone and Mineral Research* is published in 12 issues per year. Institutional subscription prices for 2018 are: Print & Online: US\$1437 (US), US\$1528 (Rest of World), €1097 (Europe), £935 (UK). Prices are exclusive of tax. Asia-Pacific GST, Canadian GST and European VAT will be applied at the appropriate rates. For more information on current tax rates, please go to www.wileyonlinelibrary.com/tax-vat. The price includes online access to the current and all online back files to January 1st 2012, where available. For other pricing options, including access information and terms and conditions, please visit www.wileyonlinelibrary.com/access. **Commercial Reprints:** Beth Ann Rocheleau, Reprints and Eprints Manager, Rockwater, Inc., PO Box 2211, Lexington, SC 29072, USA; Tel: +00 (1)803 359-4578; Fax: +00 (1)803-753-9430; E-mail: asbmr@rockwaterinc.com. For submission instructions, subscription and all other information, visit: www.jbmr.org

The *Journal of Bone and Mineral Research* is the official journal of the American Society for Bone and Mineral Research, 2025 M Street, NW, Suite 800, Washington, DC 20036-3309, USA. **Advertising:** Address advertising inquiries to Joseph Tomaszewski, Advertising Sales Executive, Wiley, 111 River St., Hoboken, NJ 07030, (201) 748-8895 (Tel); jtomaszews@wiley.com (email). Advertisements are subject to editorial approval and must adhere to ASBMR's advertising policy as specified here: <https://onlinelibrary.wiley.com/page/journal/15234681/homepage/Advertise.html>. Publication of the advertisements in JBMR® is not an endorsement of the advertiser's product or service or the claims made for the product in such advertising. **Disclaimer:** No responsibility is assumed, and responsibility is hereby disclaimed, by the American Society for Bone and Mineral Research, the *Journal of Bone and Mineral Research*, and the Publisher for any injury and/or damage to persons or property as a matter of products liability, negligence or otherwise, or from any use or operation of methods, products, instructions or ideas presented in the *Journal*. Independent verification of diagnosis and drug dosages should be made. Discussions, views and recommendations as to medical procedures, choice of drugs and drug dosages are the responsibility of the authors. Advertisers are responsible for compliance with requirements concerning statements of efficacy, approval, licensure, and availability. The *Journal of Bone and Mineral Research* is a **Journal Club™** selection. The Journal is indexed by *Index Medicus*, *Current Contents/Life Science*, *CABS (Current Awareness in Biological Sciences)*, *Excerpta Medica*, *Cambridge Scientific Abstracts*, *Chemical Abstracts*, *Reference Update*, *Science Citation Index*, and Nuclear Medicine Literature Updating and Indexing Service. Copyright © 2018 by the American Society for Bone and Mineral Research. All rights reserved. No part of this publication may be reproduced, stored or transmitted in any form or by any means without the prior permission in writing from the copyright holder. Authorization to photocopy items for internal and personal use is granted by the copyright holder for libraries and other users registered with their local Reproduction Rights Organisation (RRO), e.g. Copyright Clearance Center (CCC), 222 Rosewood Drive, Danvers, MA 01923, USA (www.copyright.com), provided the appropriate fee is paid directly to the RRO. This consent does not extend to other kinds of copying such as copying for general distribution, for advertising or promotional purposes, for creating new collective works or for resale. Special requests should be addressed to: permissions@wiley.com. The *Journal of Bone and Mineral Research* accepts articles for Open Access publication. Please visit <https://authorservices.wiley.com/author-resources/Journal-Authors/licensing-open-access/open-access/onlineopen.html> for further information about OnlineOpen.

GUIDELINES FOR ABSTRACT READERS

The JBMR® Supplement 1 Abstracts serves as a compiled version of the Abstracts. Authors submit their own abstracts and are charged a fee to do so. Each abstract must be sponsored by a current ASBMR member. Authors are responsible for the accuracy of the content that they post. Authors are responsible for ensuring compliance with applicable human subject and animal subject procedures. When an abstract is submitted, one person is identified as the Presenting Author, the person who is expected to present the abstract at the ASBMR Annual Meeting.

The ASBMR depends upon the honesty of the authors and presenters and relies on their assertions that they have had sufficient full access to the data to be and are convinced of its reliability. The ASBMR expects that authors and presenters:

- Will disclose any conflicts of interest, real or perceived.
- Should disclose any relationship that may bias one's presentation or which, if known, could give the perception of bias.
- Will affirm, for any study funded by an organization with a proprietary or financial interest, that they had full access to all the data in the study.
- Are responsible for the content of abstracts, presentations, slides, and reference materials.
- Keep the planning, content and execution of abstracts, speaker presentations, slides, abstracts and reference materials free from corporate influence, bias or control.
- Should give a balanced view of therapeutic options by providing several treatment options, whenever possible, and by always citing the best available evidence.
- Should disclose when any commercial product is not labeled for the use under discussion or that the product is still investigational.

The ASBMR:

- Will note those speakers who have disclosed relationships, including the nature of the relationship and the associated commercial entity.
- Will peer-review the abstracts according to categories, but only to determine which will be selected for oral presentation, for poster presentations or for any awards. Abstracts are not otherwise subject to any quality or content review by ASBMR or JBMR®.
- Expects the audience for the Abstracts to be researchers, physicians and other health and allied health professionals.
- Protects the Abstracts by copyright, and prohibits the reproduction, distribution or transmission of the abstracts without the express written permission of ASBMR.
- Embargoes the Abstracts for public release in written, oral and electronic communications until one hour after the abstract has been presented.

Disclaimer. All authored abstracts, findings, conclusions, recommendations or oral presentations are those of the author(s) and/or speaker(s) and do not reflect the views of the American Society for Bone and Mineral Research or imply any endorsement. No responsibility is assumed, and responsibility is hereby disclaimed, by the American Society for Bone and Mineral Research for any injury and/or damage to persons or property as a matter of products' liability, negligence or otherwise, or from any use or operation of methods, products, instructions or ideas presented in the abstracts or at the ASBMR Annual Meeting. Independent verification of diagnosis and drug dosages should be made. Discussions, views and recommendations regarding medical procedures, choice of drugs and drug dosages are the responsibility of the authors and presenters.

TABLE OF CONTENTS

ASBMR Information	v
Abstract-Based Award Key	??
Abstract Presentation Key	xiii
Abstracts	1
Oral Presentations	1
Late-Breaking Oral Presentations	53
Friday Poster Presentations	61
Saturday Poster Presentations	127
Sunday Poster Presentation	199
Monday Poster Presentations	321
Author Index	441

Orals

LB Orals

Friday Posters

Saturday Posters

Sunday Posters

Monday Posters

JBMR[®] Editorial Board

Editor-in-Chief

Roberto Civitelli

St. Louis, Missouri, USA

Deputy Editors

Lorenz C Hofbauer

Dresden, Germany

Fernando Rivadeneira

Rotterdam, The Netherlands

Jennifer Westendorf

Rochester, Minnesota, USA

Associate Editors

Laura M. Calvi
Rochester, New York, USA

Christa Maes
Leuven, Belgium

Natalie Sims
Melbourne, Australia

Thomas Carpenter
New Haven, Connecticut, USA

Tuan Nguyen
Sydney, Australia

Chan Soo Shin
Seoul, Korea

X. Edward Guo
New York City, New York, USA

Ann Schwartz
San Francisco, California, USA

Marjolein van der Meulen
Ithaca, New York, USA

Benjamin Leder
Boston, Massachusetts, USA

Deborah Veis
St. Louis, Missouri, USA

Editors Emeritus

Juliet E. Compston, Cambridge, United Kingdom

Thomas L Clemens, Baltimore, Maryland, USA

Marc K Drezner, Madison, Wisconsin, USA

John A Eisman, Sydney, Australia

Lawrence G Raisz, Farmington, Connecticut, USA

Editorial Board

Cheryl Ackert-Bicknell, USA

Matthew Allen, USA

Tamara Alliston, USA

Hani Awad, USA

Douglas Bauer, USA

Bob Blank, USA

Steve Boyd, Canada

Miriam Bredella, USA

Marco Brotto, USA

Bjoern Buehring, USA

Andrew Burghardt, USA

David Burr, USA

Bjorn Busse, Germany

Frederic Cailotto, France

Geert Carmeliet, Belgium

Peggy Cawthon, USA

Wenhan Chang, USA

Lin Chen, China

Je-Yong Choi, Korea

Christine Chung, USA

Gregory Clines, USA

Martine Cohen-Solal, France

Celine Colnot, France

Arthur Conigrave, Australia

Sarah Dallas, USA

Douglas Digirolamo, USA

Paola Divieti, USA

Matthew Drake, USA

Colin Dunstan, Australia

Florent Elefteriou, USA

Klaus Engelke, Germany

Roberta Faccio, USA

Joshua Farr, USA

Renny Franceschi, USA

Lora Giangregorio, Canada

Catherine Gordon, USA

Struan Grant, USA

Nuria Guanabens, Spain

Eric Hesse, Germany

Edward Hsiao, USA

Anita Ignatius, Germany

Carlos Isales, USA

David Karasik, USA

Stavroula Kousteni, USA

Christopher Kovacs, Canada

Kenneth Kozloff, USA

Craig Langman, USA

Brendan Lee, USA

Mike Lewiecki, USA

Heather Macdonald, Canada

Michael Mannstadt, USA

Stavros Manolagas, USA

Michael McClung, USA

Craig Munns, Australia

Nicola Napoli, Italy

Keizo Nishikawa, Japan

Barbara Obermayer-Pietsch,
Austria

Eric Orwoll, USA

Merry Oursler, USA

John Pettifor, South Africa

Ling Qin, China

Ling Qin, USA

Frank Rauch, Canada

Martina Rauner, Germany

Lars Rejnmark, Denmark

Brent Richards, Canada

Pamela Robey, USA

Kerrie Sanders, Australia

John Schousboe, USA

Claudia Sedlinsky, Argentina

Pawel Szulc, France

Tingting Tang, China

Elena Tsourdi, Germany

Andre Uitterlinden, The
Netherlands

Andre Van Wijnen, USA

Peter Vestergaard, Denmark

Meiqing Wang, China

Kate Ward, UK

Stuart Warden, USA

Marc Wein, USA

Michael Whyte, USA

Cristiano Zerbini, Brazil

AMERICAN SOCIETY FOR BONE AND MINERAL RESEARCH (ASBMR)

OFFICERS

Michael J. Econs, M.D. President
Bart L. Clarke, M.D., President-Elect
Jane A. Cauley, DrPh, Past-President
Thomas L. Clemens, Ph.D., Secretary-Treasurer
Juliet Compston, M.D., FRCP, Secretary-Treasurer Elect

COUNCILORS

Mary Bouxsein, Ph.D.	Term expires 2018	Anna Spagnoli, M.D.	Term expires 2020
Lorenz Hofbauer, M.D.	Term expires 2019	Johannes Van Leeuwen, Ph.D.	Term expires 2018
Suzanne Jan De Beur, M.D.	Term expires 2018	Kate Ward, Ph.D.	Term expires 2020
Stavroula Kousteni, Ph.D.	Term expires 2019	Peter Ebeling, AO, M.D., FRACP,	Ex-Officio, Term expires 2021
Christopher Kovacs, M.D.	Term expires 2020	Roberto Civitelli, M.D.	Ex-Officio, Term expires 2022
Ernestina Schipani, M.D., Ph.D.	Term expires 2019		

ASBMR STAFF

Lauren Anderson, Senior Program Coordinator	Brittany Jackson, Senior Exhibits and Ancillary Meetings Coordinator
Angela Belusik, Senior Program Manager	Deborah Kroll, Director of Development
Michelle Brereton, Annual Meeting and Planning Logistics Coordinator	Lindsay Kroboth, Marketing Coordinator
Matt Burruss, Senior Conference Manager	David Merli, Senior Exhibit Sales Manager
Amanda Darvill, Senior Marketing Director	Sunny Patel, Accounting Manager
Katie Duffy, Director of Publications	Corie Stretton, Hotel and Housing Service Coordinator
Ann L. Elderkin, P.A., Executive Director	Lauren Strup, Operations Coordinator
Douglas Fesler, Associate Executive Director	Brian Teague, Director of Finance
Brigid Greaney, Registration and Annual Meeting Associate	Lauren Taggart, Operations Manager
Jasmine Guerra, Senior Marketing Coordinator	Jennifer Trotter, Operations Coordinator
John Heiser, Exhibits Sales Coordinator	

ASBMR BUSINESS OFFICE

2025 M Street, NW
Suite 800
Washington, DC 20036-3309
USA
Tel: +1 (202) 367-1161
Fax: +1 (202) 367-2161
E-mail: asbmr@asbmr.org
Internet: <http://www.asbmr.org>

2018 PROGRAM COMMITTEE

President: Michael J. Econs, M.D.
Program Co-Chair: Douglas Bauer, M.D.
Program Co-Chair: Marja Hurley, M.D.
Program Co-Chair: Merry Jo Oursler, Ph.D.

2018 ABSTRACT REVIEWERS

Yousef Abu-Amer, Ph.D.
Cheryl Ackert-Bicknell, Ph.D.
Annette AdaM.S., M.D.
Robert Adler, M.D.
Catherine Anastasopoulou, Ph.D., M.D.
Thomas Levin Andersen, Ph.D.
Paul Anderson, Ph.D.
Laura Bachrach, M.D.
Zvi Bar-shavit, Ph.D.
Sarah Berry, M.D., M.P.H.
Daniel Bikle, Ph.D., M.D.
Dennis Black, Ph.D.
Dana Bliuc, Ph.D., M.D., M.P.H.
Alison Boyce, M.D.
Maria Lorena Brance, Ph.D., M.D.
Sharon Brennan-Olsen, Ph.D.
Giacomina Brunetti, Ph.D.
Angela Bruzzaniti, Ph.D.
Diana Carlone, M.D.
Geert Carmeliet, Ph.D., M.D.
Alesha Castillo, Ph.D.
Peggy Cawthon, Ph.D., M.P.H.
Roland Chapurlat, Ph.D., M.D.
Cyrille Confavreux, Ph.D., M.D.
Carolyn Crandall, M.D., M.S.
Janet Crane, M.D.
Sarah Dallas, Ph.D.
Maria Danila, M.D., M.P.H., M.S.
Jesus Delgado-Calle, Ph.D.
Matthew Drake, Ph.D., M.D.
Amel Dudakovic, Ph.D.
Emma Duncan, FRACP, Ph.D., MBBS
Gustavo Duque, Ph.D., M.D.
Elizabeth Eekhoff, Ph.D., M.D.
Grahame Elder, Ph.D., MBBS
Alessandra Esposito, Ph.D.
Charles Farber, Ph.D.
David Findlay, Ph.D.
Melissa Fiscaletti, M.D., M.S.
Lorraine Fitzpatrick, M.D.
Jackie Fretz, Ph.D.
Robyn Fuchs, Ph.D.
Seiji Fukumoto, Ph.D.
Dana Gaddy, Ph.D.
Erin Gaffney-Stomberg, Ph.D.
Deborah Galson, Ph.D.
Xueqin Gao, Ph.D., M.D., M.S.
Vishnu Garla, M.D.
Luigi Gennari, Ph.D., M.D.
Louis Gerstenfeld, Ph.D.
Ali Ghasem-Zadeh, Ph.D.
Sabrina Gill, M.D., M.P.H.
Anne Gingery, Ph.D.
Natalie Glass, Ph.D.
Francis Glorieux, Ph.D., M.D.
Francesca Gori, Ph.D.
Struan Grant, Ph.D.
Stan Gronthos, Ph.D.
Michael Hadjiargyrou, Ph.D.
Dominique Heymann, Ph.D.
Pamela Hinton, Ph.D.
Lorenz Hofbauer, M.D.
Nicholas Hoyle, Ph.D.
Keith Hruska, M.D.
Keith Hruska, M.D.
Amira Hussein, Ph.D., M.S.
Daisuke Inoue, Ph.D.
Daisuke Inoue, Ph.D., M.D.
Karl Insogna, M.D.
Srividhya Iyer, Ph.D.
Suzanne Jan de Beur, M.D.
Jean Jiang, Ph.D.
Robert Jilka, Ph.D.
Rachelle Johnson, Ph.D.
James Johnston, Ph.D., M.S.
Robert Josse, MBBS
Ivo Kalajzic, M.D., Ph.D.
Fadia Kamal, Ph.D.
David Karasik, Ph.D.
Mustapha Kassem, Ph.D., M.D.
Hiroshi Kawaguchi, M.D.
Deepak Kumar Khajuria, Ph.D.
Alyia Khan, M.D.
Amna Khan, M.D.
Joseph Kindler, Ph.D.
Richard Kremer, Ph.D., M.D.
Nancy Lane, M.D.
Nancy Lane, M.D.
Craig Langman, M.D.
Beata Lanske, Ph.D.
Richard Lee, D.D.S., Ph.D.
Richard Lee, Ph.D., M.D.
Josh Lewis, Ph.D.
X. Sherry Liu, Ph.D.
Jonathan Lowery, Ph.D.
Christa Maes, Ph.D.
Russell Main, Ph.D.
Sarah Manske, Ph.D.
Kim Mansky, Ph.D.
Gabriel Mbalaviele, Ph.D.
Sara McBride-Gagyi, Ph.D.
Mike McClung, M.D.
Megan McGee-Lawrence, Ph.D.
Malachi McKenna, M.P.H.
Malachi McKenna, Ph.D.
Meenal Mehrotra, MBBS
Daniela Merlotti, Ph.D., M.D.
Jane Mitchell, Ph.D.
Sharon Moe, M.D.
Subburaman Mohan, Ph.D.
David Monroe, Ph.D.
Suzanne Morin, M.D., M.S.
Ioanna Mosialou, Ph.D.
Katherine Motyl, Ph.D.
Mark Nanes, M.D.
Dobrawa Napierala, Ph.D.
Tuan Nguyen, Ph.D.
Andreas Niemeier, M.D.
Toru OGASAWARA, Ph.D.
Michael Ominsky, Ph.D.
Orhan K Oz, Ph.D., M.D.
Julie Paik, M.D.
Eleftheros Paschalis, Ph.D.
Jessica Pepe, Ph.D., M.D.
Allison Pettit, Ph.D.
Lilian Plotkin, Ph.D.
Richard Prince, M.D., MBBS
Rhonda Prisby, Ph.D.
Ling Qin, Ph.D.
Alexander Rodriguez, Ph.D.
James Ryaby, Ph.D.
Kenneth Saag, M.D.
Yves Sabbagh, Ph.D.
Fayez Safadi, Ph.D.
Lisa Samelson, Ph.D.
Cheryl Sanchez, M.D.
Erica Scheller, D.D.S., Ph.D.
Tobias Schmidt, Ph.D.
Viral Shah, M.D.
Sue Shapses, Ph.D.
Masako Shimada, Ph.D., M.D.
Dolores Shoback, M.D.
Eileen Shore, Ph.D.
Joe Stains, Ph.D.
Paula Stern, M.D.
Paula Stern, Ph.D.
Elsa Strotmeyer, Ph.D., M.P.H.
Larry Suva, Ph.D.
Hanna Taipaleenmaki, Ph.D.
Josephine Tauer, Ph.D., M.S.
Willi Thompson, Ph.D.
Annegreet Veldhuis-Vlug, Ph.D., M.D.
Annegreet Veldhuis-Vlug, Ph.D., M.D.
Marcella Walker, M.D.
Joseph Wallace, Ph.D.
Xiaofang Wang, D.D.S., Ph.D.
Yongmei Wang, M.D., Ph.D.
Stuart Warden, Ph.D.
Megan Weivoda, Ph.D.
Deborah Wenkert, M.D.
Kenneth White, Ph.D.
Bettina Willie, Ph.D.
Nicole Wright, Ph.D.
Liping Xiao, M.D., Ph.D.
Elaine Yu, Ph.D.
Ayse Zengin, Ph.D.

ASBMR COMMITTEE MEMBERS AND REPRESENTATIVES

ADVOCACY/SCIENCE POLICY COMMITTEE

Deborah Veis, M.D., Ph.D., *Chairperson*
Robert Blank, M.D., Ph.D.
Cyrus Cooper, D.M., FRCP, M.D.
Maureen Devlin, Ph.D.
Patricia Ducey, Ph.D.

Louis Gerstenfeld, Ph.D.
Mark Hamrick, Ph.D.
Roy Morello, Ph.D.
Babatunde Oyajobi, MBBS, Ph.D.
Shivani Sahni, Ph.D.

Deborah Wenkert, M.D.
Stavroula Kousteni, Ph.D.,
Council Liaison
Ann L. Elderkin, P.A., *Staff Liaison*
Douglas Fesler, *Staff Liaison*
Lauren Strup, *Staff Liaison*

DEVELOPMENT COMMITTEE

Shonni Silverberg, M.D., *Co-Chairperson*
Larry Suva, Ph.D., *Co-Chairperson*
Teresita Bellido, Ph.D.
Paola Divieti Pajevic, M.D., Ph.D.

Charles Farber, Ph.D.
Marian Hannan, Ph.D.
Melissa Kacena, Ph.D.
Dolores Shoback, M.D.

Emily Stein, M.D.
Ernestina Schipani, M.D., Ph.D.,
Council Liaison
Deborah Kroll, *Staff Liaison*
Ann L. Elderkin, P.A., *Staff Liaison*

ETHICS ADVISORY COMMITTEE

Elizabeth Shane, M.D., *Chairperson*
Cheryl Ackert-Bicknell, Ph.D.
Richard Bockman, M.D., Ph.D.
Janine Danks, BSc, MSc, Ph.D.
Bess Dawson-Hughes, M.D.

Núria Guañabens, M.D., Ph.D.
Moustapha Kassem, M.D., Ph.D.
Huifang (Linda) Lu, M.D., Ph.D.
Laurie McCauley, D.D.S., Ph.D.
Thomas Weber, M.D.

Johannes van Leeuwen, Ph.D.,
Council Liaison
Ann L. Elderkin, P.A., *Staff Liaison*
Lauren Taggart, *Staff Liaison*

FINANCE COMMITTEE

Thomas Clemens, Ph.D., *Chairperson*
Juliet Compston, M.D., FRCP
Emma Duncan, M.D., Ph.D.
Beatrice Edwards, M.D., FACP

Deborah Galson, Ph.D.
Robert Jilka, Ph.D.
Rene St-Arnaud, Ph.D.
Joseph Stains, Ph.D.

Michael J. Econs, M.D., *Ex Officio*
Anna Spagnoli, M.D., *Council Liaison*
Ann L. Elderkin, P.A., *Staff Liaison*
Brian Teague, *Staff Liaison*

MEMBERSHIP ENGAGEMENT AND EDUCATION COMMITTEE

Nicola Napoli, M.D., *Chairperson*
Susan Bloomfield, Ph.D.
Ching-Lung Cheung, Ph.D.
Claire Edwards, Ph.D.
Amna Khan, MBBS, M.D.
Beata Lecka-Czernik, Ph.D.
Joshua Lewis

Christa Maes, Ph.D.
Morten Frost Nielsen, M.D., Ph.D.
Martina Rauner, Ph.D.
Erica Scheller, D.D.S., Ph.D.
Anne Gingery, Ph.D.
Jonathan Lowery, Ph.D.
Christopher J. Hernandez, Ph.D.

Nicole Wright, Ph.D., MPH
Mary Boussein, Ph.D., *Council Liaison*
Suzanne Jan De Beur, M.D.,
Council Liaison
Douglas Fesler, *Staff Liaison*
Lauren Taggart, *Staff Liaison*
Lauren Strup, *Staff Liaison*
Jennifer Trotter, *Staff Liaison*

DIVERSITY IN BONE AND MINERAL RESEARCH SUBCOMMITTEE

Christopher J. Hernandez, Ph.D.,
Co-Chairperson
Nicole Wright, Ph.D., MPH,
Co-Chairperson
Sunday Akintoye, D.D.S.

Joel Jules, Ph.D.
Kristy Nicks, Ph.D.
Robert Nissenson, Ph.D.
Babatunde Oyajobi, MBBS, Ph.D.
Lilian Plotkin, Ph.D.

Larry Suva, Ph.D.
Sylvia Christakos, Ph.D., *Ex-Officio*
Nicola Napoli, M.D., *MEEC Liaison*
Lauren Taggart, *Staff Liaison*
Jennifer Trotter, *Staff Liaison*

EARLY STAGE INVESTIGATOR SUBCOMMITTEE

Jonathan Lowery, Ph.D., *Co-Chairperson*
Anne Gingery, Ph.D., *Co-Chairperson*
Beth Bragdon, Ph.D.
Joshua Farr, Ph.D.
Tristan Fowler, Ph.D.
Kathleen Hill-Gallant, Ph.D.

Aaron Hudnall, D.O.
Julia Hum, Ph.D.
Aaron James, M.D.
Rachelle Johnson, Ph.D.
Corrine Metzger, MS
Patrick Mulcrone, B.A., B.S.

Hanna Taipaleenmaki, Ph.D.
Megan Weivoda, Ph.D.
Nicola Napoli, M.D., *MEEC Liaison*
Lauren Taggart, *Staff Liaison*
Lauren Strup, *Staff Liaison*

PROFESSIONAL PRACTICE COMMITTEE

Benjamin Leder, M.D., *Chairperson*
Sarah Berry, M.D.
Ghada El-Hajj Fuleihan, M.D., MPH
Nicholas Harvey, MBBC
Valerie Peck, M.D.

Luisa Plantalech, M.D.
Anne Schafer, M.D.
Catherine Van Poznak, M.D.
Peter Vestergaard, M.D., Ph.D.
Elaine Yu, M.D.

Christopher Kovacs, M.D.,
Council Liaison
Douglas Fesler, *Staff Liaison*
Ann L. Elderkin, P.A., *Staff Liaison*
Jennifer Trotter, *Staff Liaison*

PUBLICATIONS COMMITTEE

Michael Mannstadt, M.D., *Chairperson*
Yousef Abu-Amer, Ph.D.
Murat Bastepe, M.D., Ph.D.
Peggy Cawthon, Ph.D., MPH
Dominique Heymann, Ph.D.
Marja Hurley, M.D.

David Karasik, Ph.D.
Meryl S. LeBoff, M.D.
Markus Seibel, M.D., Ph.D.
Roberto Civitelli, M.D., *Ex-Officio*
John Bilezikian, M.D., Ph.D. (hon),
Ex-Officio

Peter Ebeling, AO, M.D., FRACP,
Ex-Officio
Lorenz Hofbauer, M.D., *Council Liaison*
Ann Elderkin, P.A., *Staff Liaison*
Katie Duffy, *Staff Liaison*

WOMEN IN BONE AND MINERAL RESEARCH COMMITTEE

Roberta Faccio, Ph.D., *Chairperson*
Sharon Brennan-Olsen, Ph.D.
Fjola Johannesdottir, Ph.D.
Patricia Juarez Camacho, Ph.D., M.S.
Lamya Karim, Ph.D.

Jenneke Klein-Nulend, Ph.D.
Kim Mansky, Ph.D.
Barbara Obermayer-Pietsch, M.D.
Allison Pettit, Ph.D.
Michaela Reagan, Ph.D.

Archana Sanjay, Ph.D.
Kate Ward, Ph.D., *Council Liaison*
Lauren Taggart, *Staff Liaison*
Lauren Strup, *Staff Liaison*

PRIMER EDITORIAL BOARD - 9th Edition

John Bilezikian, M.D., Ph.D.(hon) *Editor-in-Chief*
Senior Associate Editors
Roger Bouillon, M.D., Ph.D., FRCP
Juliet E. Compston, M.D., FRCP
Thomas Clemens, Ph.D.
Associate Editors
Douglas Bauer, M.D.
Peter Ebeling, AO, M.D., FRACP

Klaus Engelke, Ph.D.
David Goltzman, M.D.
Theresa A. Guise, M.D.
Suzanne M. Jan de Beur, M.D.
Harald Jueppner, M.D.
Karen M. Lyons, Ph.D.
Laurie K. McCauley, D.D.S., Ph.D.
Michael McClung, M.D., FACP
Paul D. Miller, M.D., FACP

Socrates E. Papapoulos, M.D., Ph.D.
G. David Roodman, M.D., Ph.D.
Clifford J. Rosen, M.D.
Ego Seeman, M.D., FRACP
Rajesh V. Thakker, M.D., FRCP
Michael Whyte, M.D.
Mone Zaidi, M.D., Ph.D., FRCP
Murray J. Favus, M.D., *Founding Editor*
Katie Duffy, *Staff Liaison*

ASBMR REPRESENTATIVES TO FASEB

Brendan Boyce, M.D.
Member, Board of Directors

Thomas L. Clemens, Ph.D.
FASEB Finance Committee

Laurie McCauley, D.D.S., Ph.D.
FASEB Editorial Board

Yousef Abu-Amer, Ph.D.
*FASEB Open Access Journal
Editorial Board*

Deborah V. Veis, M.D., Ph.D.
Science Policy Committee (SPC)

Dana Gaddy, Ph.D.
*Animals in Research and Education Issues
Subcommittee, SPC*

Paula Stern, Ph.D.
*Breakthroughs in Bioscience
Subcommittee, SPC, Chair*

Dominique Heymann, Ph.D.
*Breakthroughs in Bioscience
Subcommittee, SPC*

Dolores Shoback, M.D.
*Clinical and Translational Research
Subcommittee, SPC*

Michael Hadjiargyrou, Ph.D.
*Training and Career Resources
Subcommittee, SPC*

Li Xin, Ph.D.
Shared Research Subcommittee, SPC

Louis Gerstenfeld, Ph.D.
*Data Science and Informatics
Subcommittee, SPC*

Roberta Faccio, Ph.D.
Excellence in Science Award Committee

Patricia Ducey, Ph.D.
Research Conferences Advisory Committee

David Karasik, Ph.D.
*Publications and Communications
Committee*

ASBMR REPRESENTATIVES TO OTHER GROUPS

Robert Adler, M.D.
National Bone Health Alliance, Co-Chair

Bart L. Clarke, M.D.
U.S. Bone and Joint Initiative

Stuart L. Silverman, M.D.
*National Osteoporosis Foundation Interspecialty Medical
Council*

Marjorie M. Luckey, M.D.
*National Osteoporosis Foundation Subcommittee on
Implementation of New Guidelines for Practicing Physicians*

Roland Baron, D.D.S., Ph.D.
*International Federation of Musculoskeletal Research Societies,
Co-Chair*

Meghan McGee-Lawrence, Ph.D.
IFMRS Future Global Leaders Committee

Lynda Bonewald, Ph.D.
IFMRS Big Data Working Group, Co-Chair

AWARDS

WILLIAM F. NEUMAN AWARD

Vicki Rosen, Ph.D.

FULLER ALBRIGHT AWARD

Christopher J. Hernandez, Ph.D.

FREDERIC C. BARTTER AWARD

Michael A. Levine, M.D.

LOUIS V. AVIOLI FOUNDERS AWARD

Nicola C. Partridge, Ph.D.

LAWRENCE G. RAISZ AWARD

José Luis Millán, Ph.D.

PAULA STERN ACHIEVEMENT AWARD

Elizabeth Shane, M.D.

SHIRLEY HOHL SERVICE AWARD

Jane A. Cauley, DrPh

STEPHEN M. KRANE AWARD

Marian F. Young, Ph.D.

GIDEON A. RODAN AWARD

Teresita M. Bellido, Ph.D.

ADELE L. BOSKEY AWARD

Marjolein van der Meulen, Ph.D.

PRESIDENT'S RECOGNITION AWARD

Joan A. McGowan, Ph.D.

2018 ASBMR MOST OUTSTANDING BASIC ABSTRACT AWARD

Karin H. Nilsson, M.Sc. Pharm.

2018 ASBMR MOST OUTSTANDING CLINICAL ABSTRACT AWARD

Branko Ristic, M.D., Ph.D.

2018 ASBMR MOST OUTSTANDING TRANSLATIONAL ABSTRACT AWARD

Cyrille B. Confavreux, M.D. Ph.D.

2018 ASBMR PRESIDENT'S AWARD

Fatemeh Mirzamohammadi, M.D.

2018 ASBMR YOUNG INVESTIGATOR AWARD

Named in memory of Robert Heaney and given to the most outstanding abstract in nutrition research.

Emma O. Billington

2018 ASBMR FELIX BRONNER YOUNG INVESTIGATOR AWARD

Yunshu Wu, Ph.D

2018 ASBMR FUND FOR RESEARCH AND EDUCATION YOUNG INVESTIGATOR AWARDS

Amy T. Bunyamin

Jayenth K. Mayur, MBS

2018 ASBMR FUND FOR RESEARCH AND EDUCATION YOUNG INVESTIGATOR AWARDS

In memory of Adele L. Boskey, Ph.D.

For her contributions and trailblazing in the fields of Bone Mineralization and Mechanobiology

Ruban Dhaliwal, M.D., M.P.H.

Frans L. Heyer, M.D.

Leeann D. Louis

2018 ASBMR YOUNG INVESTIGATOR AWARD RECIPIENTS

Supported by donations from AgNovos Healthcare and Amgen, Inc.

Emilie Barruet, Ph.D.	Marie-Therese Haider	Camille M. Parsons
Julian Meyer Berger	Yujiao Han	WanXin Qiao, PhD
Lise Sofie Bislev, M.D.	Jiahui Huang	Biancamaria Ricci, PhD
Niambi S. Brewer	Haemin Kim, Ph.D.	Lina Saad, PhD
ASM Borhan	Sarah Kim, Ph.D.	Jad G. Sfeir, M.D.
Kun Chen, M.D., PhD	Berit A M Larsson, M.D	Albert Shieh, M.D.
Haizi Cheng	Min Joon Lee	Henriette Ejlsmark Svensson, M.D.
Abigail Coffman	Yongjia Li	Wei-Ju Tseng
Diana L. Cousminer, Ph.D.	Stewart A. Low, PhD	Tianlu Wang
Marianne Comeau-Gauthier, M.D.	Sameh Melk	Ren Xu, Ph.D.
Corey M. Dussold	Christophe Merceron, Ph.D.	Sung-Hee Seanna Yoon
Daniel Vladimir Dudenkov, MD	Thomas Merlijn	Randy Yeh, M.D.
Alessandra Esposito, Ph.D.	Jonathan G. Messer, PhD	Ariane Zamarioli, Ph.D.
Pablo Florenzano, M.D.	Kenichi Nagano, D.D.S., Ph.D	Jiajun Zhang, PhD
Erik J. Geiger, M.D.	Laura C. Ortinou, Ph.D	Zoe (Xiaofang) Zhu, D.D.S, Ph.D.
Jessica D. Hathaway-Schrader, Ph.D.	Julien Paccou, M.D., Ph.D.	
Betty Hoac, Ph.D.	Gabriel M. Pagnotti, Ph.D.	

2018 FELLOWS OF THE ASBMR

Yousef Abu-Amer, PhD	Colin Dunstan, PhD	Gordon Klein, MD, MPH.	David Roodman, MD, PhD
John Adams, MD	Richard Eastell, MD	Saija Kontulainen, PhD	Clifford Rosen, MD
Donato Agnusdei, MD	Peter Ebeling, MD	Fernando Lecanda, PhD	Clinton Rubin, PhD
Matthew Allen, PhD	Kristine Ensrud	Beata Lecka-Czernik, PhD	Janet Rubin, M.D.
Andrew Arnold, MD	Solomon Epstein, Mbbch	Michael Lewiecki, MD	Fayez Safadi, M.Phil., PhD
Teresita Bellido, PhD	Jose Luis Ferretti, MD, PhD	Jane Lian, PhD	Elizabeth (Lisa) Samelson, PhD
John Bilezikian, MD	Dana Gaddy, PhD	Robert Marcus, MD	Elliott Schwartz, MD
Robert Blank, MD, PhD	James Gallagher, PhD	Laurie Mccauley, PhD	Elizabeth Shane, MD
Richard Bockman, MD, PhD	Julie Glowacki, PhD	Michael Mcclung, MD	Eileen Shore, Ph.D.
Henry Bone, MD	Susan Greenspan, MD	Paul Miller, MD	Shonni Silverberg, MD
Mary Bouxsein, PhD	Stan Gronthos, PhD	Sharon Moe, MD	Natalie Sims, PhD
Dean Barbara Boyan, PhD	Michael Hadjiargyrou, PhD	Prof Tuan Nguyen, DsC	Emily Stein, MD
Steven Boyd, PhD	Steven Harris, MD	Robert Nissenson, PhD	Rajesh Thakker, M.B., B.Chir.
Jane Cauley, DrPh	Hunter Heath. MD	Eric Orwoll, MD	Andre Van Wijnen, PhD
Lin Chen, MD	Keith Hruska, MD	Nicola Partridge, PhD	Deborah Veis, MD, PhD
Sylvia Christakos, PhD	Marja Hurley, MD	Prof John Pettifor, Mbbch, PhD	Nelson Watts, MD
Roberto Civitelli, MD	Carlos Isales, MD	Carol Pilbeam, PhD, MD	Deborah Wenkert, MD
Bart Clarke, MD	Suzanne Jan de Beur, MD	Richard Prince, MD	Jennifer Westendorf, PhD
Carolyn Crandall, MD, MS	Prof Graeme Jones, M.B.B.S, PhD	Ling Qin, PhD	
Janine Danks, PhD	Sundeep Khosla, MD	Sakamuri Reddy, PhD	
Emma Duncan, PhD	Douglas Kiel, MD, MPH	Jonathan Reeve, D.M DSc	

DISCLOSURE POLICY

The ASBMR is committed to ensuring the balance, independence, objectivity and scientific rigor of all its individually sponsored or industry-supported educational activities. Accordingly, the ASBMR adheres to the requirement set by ACCME that audiences at jointly-sponsored educational programs be informed of a presenter's (speaker, faculty, author, or planner) academic and professional affiliations, and the disclosure of the existence of any significant financial interest or other relationship a presenter or their spouse has with any proprietary entity over the past 12 months producing, marketing, re-selling or distributing health care goods or services, consumed by, or used on patients, with the exemption of non-profit or government organizations and non-health care related companies. When an unlabeled use of a commercial product, or an investigational use not yet approved for any purpose, is discussed during the presentation, it is required that presenters disclose that the product is not labeled for the use under discussion or that the product is still investigational. This policy allows the listener/attendee to be fully knowledgeable in evaluating the information being presented. The On-Site Program book will note those speakers who have disclosed relationships, including the nature of the relationship and the associated commercial entity.

Disclosure should include any affiliation that may bias one's presentation or which, if known, could give the perception of bias. This includes relevant financial affiliations of a spouse or partner. If an affiliation exists that could represent or be perceived to represent a conflict of interest, this must be reported in the abstract submission program by listing the name of the commercial entity and selecting the potential conflict(s) by clicking in the box next to the relationship type. Disclosures will be printed in the program materials. These situations may include, but are not limited to:

DISCLOSURE KEY

13. Grant/Research Support
14. Consultant
15. Speakers' Bureau
16. Major Stock Shareholder
17. Other Financial or Material Support

ABSTRACT PRESENTATION KEY

1001 - 1157	Oral Presentations
1158 - 1177	Late-Breaking Oral Presentations
FRI#	Friday Poster Presentations
SAT#	Saturday Poster Presentations
SUN#	Sunday Poster Presentation
MON#	Monday Poster Presentations
*	Denotes Abstract Presenting Author

1001

The skeletal actions of irisin are mediated through alpha V integrin receptors on osteocytes. Bruce Spiegelman^{*1}, Hyeonwoo Kim¹, Christianne Wrann², Roland Baron³, Mary Bouxsein⁴, Lynda Bonewald⁵, Clifford Rosen⁶. ¹Dana Farber Cancer Center, United States, ²Mass general hospital, United States, ³Harvard dental school, United States, ⁴Beth Israel Deaconess Hospital, United States, ⁵Indiana University, United States, ⁶Maine Medical Center, United States

The effects of physical activity on the skeleton are site and force specific. Irisin, an exercise-induced hormone, is a peptide product cleaved from the muscle membrane protein FNDC5. It rises acutely with activity and enters the circulation. Irisin infusions increase cortical bone mass in mice, although the mechanism is not clear. We hypothesized that irisin would act directly on osteocytes. To test that we studied MLO-Y4 cells, employed short-term irisin injections, and performed OVX in a loss of function mouse model, FNDC5 KO (KO). First, we treated MLO-Y4 cells with irisin in the presence of hydrogen peroxide at amounts sufficient to induce apoptosis. Irisin treatment reduced hydrogen peroxide-induced apoptosis at concentrations of 1-500 ng/ml ($p < 0.01$) well within the physiological concentrations of irisin found in human plasma. Next, we examined SOST expression after irisin treatments. Irisin raised SOST mRNA level in osteocyte cultures in a dose-dependent manner ($p < 0.01$). To examine the regulation by irisin in vivo, we injected recombinant irisin daily into WT mice for 6 days. Irisin injections raised SOST mRNA 4 fold in osteocyte-enriched bones, as well as SOST protein by 50% in serum. To test whether the absence of irisin affected bone turnover, we OVX'd 9 month KO mice and their littermate controls (WT, n=4-5 per genotype). As expected, WT B6 mice lost 35% of their lumbar BV/TV post OVX whereas there was no change in BV/TV for the KO mice ($p < 0.01$ by ANOVA). Osteoclast number, osteoclast surface/ bone surface and eroded surfaces/bone surface all were markedly enhanced in controls but unchanged in KO mice ($p < 0.02$ for genotype by ANOVA). Importantly, WT but not KO mice showed a significant increase in lacuna area and density ($p < 0.01$) after OVX, denoting the absence of osteocytic osteolysis in FNDC5 KO. To assess whether irisin also directly affected osteoclasts, we added irisin (1-10 ng/ml) to WT bone marrow cultures treated with mCSF and RANKL and found a significant dose dependent increase in osteoclast number ($p < 0.001$). Ligand binding studies revealed that irisin interacted with $\alpha V/\beta 5$ integrin, and chemical inhibition of the αV integrins blocked signaling and function by irisin in osteocytes. In sum, irisin acts directly and indirectly on osteocytes by binding to αV integrins. Our results provide new insight into exercise induced changes in the skeleton and potentially offer a new therapeutic approach to treat postmenopausal osteoporosis.

Disclosures: **Bruce Spiegelman, None**

1002

Bone corticalisation requires suppression of glycoprotein 130 signalling in osteocytes, and occurs by region-specific imbalances in bone formation and resorption Emma Walker^{*}, Kim Truong, Narelle Mcgregor, T John Martin, Natalie A Sims. St. Vincent's Institute of Medical Research, Australia

The molecular mechanisms that control bone corticalization (the coalescence of trabeculae to form thick cortical bone during development) are unknown. Recently, it has been shown that this closure of cortical pores requires the intracellular protein SOCS3 in osteocytes. SOCS3 provides negative feedback for STAT3 signaling elicited by a subset of receptors expressed in osteocytes, including leptin receptor (LepR) and glycoprotein 130 (gp130 / Il6st, the receptor for all IL-6 family cytokines). In female mice lacking SOCS3 in osteocytes (Dmp1Cre.Socs3^{f/f}) the phenotype is most extreme, with metaphyseal cortical consolidation being delayed until after 12 weeks of age, when longitudinal bone growth has ceased. This provides a way to identify the specific cytokine receptor that delays corticalization, and a model to study the cellular activities mediating this process. To identify the cellular actions that mediate corticalization, we quantified bone resorbed and formed in female Dmp1Cre.Socs3^{f/f} mice from 12 to 16 weeks of age using co-registered in vivo micro-CT images of the metaphysis. In regions where trabeculae coalesced to form cortical bone, bone formation was significantly and markedly (up to 10-fold) greater than bone resorption. In contrast, in the central region that became trabecular bone, bone resorption dominated (2-fold higher than formation). This indicates that two processes occur during corticalization: (1) bone formation between trabecular struts at the periphery, and (2) resorption of trabeculae in the marrow space. To identify which SOCS3-dependent receptor must be suppressed for cortical bone to form, we sought to rescue the delayed in corticalization by crossing Dmp1Cre.Socs3^{f/f} mice with either Il6st-flox (gp130) mice, or LepR-flox mice. In both females and in males, the cortical defect was fully rescued by gp130 deletion. When quantified at 12 weeks of age, cortical porosity was significantly less in Dmp1Cre.Socs3^{f/f}.Il6st^{f/f} mice compared with Dmp1Cre.Socs3^{f/f} controls (60% less in males, and 77% less in females, $p < 0.001$, n=8-10/group). No such rescue was observed with LepR deletion. In conclusion, the distinct structures of cortical and trabecular bone form by bone formation-mediated closure of cortical pores at the periphery and resorption of trabeculae in the central marrow space. While SOCS3 suppresses signals from multiple receptors expressed in osteocytes, its suppression of gp130 is critical for metaphyseal corticalization.

Disclosures: **Emma Walker, None**

1003

Ablation of Osteopontin in Osteomalacic Hyp Mice Partially Rescues the Deficient Mineralization without Correcting Hypophosphatemia Betty Hoac^{*1}, Tchilalo Boukpe², Daniel J Buss³, Catherine Chaussain², Monzur Murshed¹, Marc D Mckee¹. ¹Faculty of Dentistry, McGill University, Canada, ²School of Dentistry University Paris Descartes Sorbonne Paris Cité, France, ³Department of Anatomy and Cell Biology, McGill University, Canada

Hereditary mutations in the PHEX gene (phosphate-regulating gene with homologies to endopeptidases on the X chromosome) cause the osteomalacic disease X-linked hypophosphatemia (XLH). PHEX is predominately expressed by osteocytes, osteoblasts and odontoblasts, and inactivating mutations in this gene lead to renal phosphate wasting, severe hypomineralization of bones and teeth, hallmark hypomineralized periosteocytic lesions (so-called "halos") that persist despite stable correction of serum phosphate, and the accumulation of mineralization-inhibiting peptides and proteins – including osteopontin (OPN). We have previously identified full-length OPN to be a physiologically relevant substrate for PHEX, and found increased OPN and OPN fragments in protein extracts of human XLH dentin and Hyp (mouse model for XLH) bone, as well as an abundance of OPN localized in the pericellular hypomineralized region around osteocytes. These findings suggest that the accumulation of OPN (and its fragments) may contribute to the mineralization defects observed in XLH/Hyp bone. To investigate the effect of OPN deficiency in Hyp mice, double-null mice for Phex and Opn (Hyp;Opn^{-/-}) were generated, and histomorphometric analysis of resin-embedded, undecalcified bone sections showed significantly reduced osteoid area/bone area of trabecular bone in lumbar vertebrae and decreased average osteocyte lacunar area within the cortical bone of the distal femur, as compared to Hyp bone controls. Furthermore, machine-learning analysis of nano-computed tomography data taken from the mid-diaphysis of the anterior medial tibia confirmed that Hyp;Opn^{-/-} mice had reduced osteocyte lacunar volumes, thus showing partial correction of the characteristic hypomineralized periosteocytic lesions in Hyp mouse bone. Surprisingly, serum biochemistry measurements revealed that the double-null mice had no correction of the hypophosphatemia observed in Hyp mice, indicating that the improved mineralization phenotype observed in Hyp;Opn^{-/-} mice is independent of systemic phosphate-regulating factors. In conclusion, this study shows that OPN accumulation locally in the extracellular matrix of XLH/Hyp bone contributes to its osteomalacia and its hypomineralized periosteocytic lesions, and removal of this mineralization-inhibiting OPN partially rescues the mineralization phenotype without affecting hypophosphatemia.

Disclosures: **Betty Hoac, None**

1004

TGF β regulation of perilacunar/canalicular remodeling is sexually dimorphic Neha S. Dole^{*1}, Cristal S. Yee¹, Claire Acevedo², Courtney M. Mazur¹, Tamara Alliston¹. ¹University of California San Francisco, United States, ²University of Utah, United States

Bone quality, a determinant of fragility, is known to show sex-specific differences. However, the molecular mechanisms responsible for sexually dimorphic bone quality remain unclear, limiting our ability to therapeutically target fragility. Previously, we reported that pharmacologic antagonism of TGF β , a known regulator of bone mass and quality, increases bone mass more robustly in females than in males. Recently, we found that TGF β regulates bone quality through osteocyte-intrinsic stimulation of perilacunar/ canalicular remodeling (PLR) in male mice. Since lactation is a potent PLR agonist and female bone mass is more sensitive to TGF β , we hypothesize that basal and lactation-inducible PLR occurs through a TGF β -dependent mechanism in female bone. We evaluated virgin female and lactating T β R1Ioc^{-/-} mice, where T β R1I is ablated from osteocytes using DMP1-Cre, and their wild type littermates (WT). Micro-CT revealed that seven days of lactation induces bone loss in both genotypes, however bone loss was significantly attenuated in lactating T β R1Ioc^{-/-} mice. Lactation-inducible expression of several PLR genes (MMP13, MMP14, and Cathepsin K (CTSK), TRAP, and ATP6V0D2) was mitigated in T β R1Ioc^{-/-} bones. Further, lactation increased osteocyte lacunar volume in WT but not in T β R1Ioc^{-/-} bones. Thus, osteocyte-intrinsic TGF β is required for maximal induction of PLR during lactation. Analysis of virgin female bone, however, surprisingly revealed sexual dimorphism in the osteocyte-intrinsic role of TGF β . Unlike male mice, virgin T β R1Ioc^{-/-} female mice had no differences in trabecular bone mass compared to WT. Loss of osteocyte intrinsic TGF β signaling caused coordinated repression of key PLR genes in males, however; PLR gene expression was normal in female T β R1Ioc^{-/-} bones. Severe deterioration of osteocyte lacuno-canalicular network (LCN) integrity observed in male T β R1Ioc^{-/-} bones was completely absent in females. Moreover, flexural strength tests demonstrate that, despite normal cortical thickness, male T β R1Ioc^{-/-} bones have decreased ultimate stress and toughness modulus relative to WT. In contrast, these properties are significantly increased in virgin T β R1Ioc^{-/-} females relative to WT controls. Thus, our study shows that, while lactation-inducible PLR is dependent on osteocyte-intrinsic TGF β ; osteocytes possess sexually dimorphic mechanisms to regulate PLR and bone quality during homeostasis.

Disclosures: **Neha S. Dole, None**

1005

Do Drug Holidays Reduce Atypical Femur Fracture Risk?: Results from the Southern California Osteoporosis Cohort Study (SOCS) Annette L. Adams^{*1}, Bonnie H. Li¹, Denison S. Ryan¹, Erik J. Geiger², Richard M. Dell¹, Dennis M. Black². ¹Kaiser Permanente Southern California, United States, ²University of California, San Francisco, United States

Long-term bisphosphonate (BP) use has been associated with increased risk of atypical femur fractures (AFF). BP holidays of 3-5 years have been recommended as a way of balancing the risk of AFF with the intended anti-fracture benefit of the medications, and studies have suggested that women who discontinue BP after 3-5 years of use are not at increased risk for osteoporosis-related fractures. However, whether AFF risk is lowered after discontinuation of BP is uncertain. To address the relationship of time since last BP use and risk of AFF, we conducted a cohort study of women aged ≥ 50 years who were members of Kaiser Permanente Southern California (KPSC) during the period 1/1/2007-9/30/2015. Women were required to have pharmacy benefits and to have been members of KPSC for ≥ 1 year prior to cohort entry. We included in the cohort any woman who had used a BP and had at least one available pre-treatment bone mineral density (BMD) total hip scan. AFFs were identified and verified by physician review of x-ray images for fractures occurring during the study period with ICD-9 diagnosis codes for subtrochanteric or femoral shaft fractures. Women were considered to have discontinued BP if there was a gap >3 months between last BP use and cohort entry anniversaries. We also included information on the following potential confounders of the association between time since discontinuation and AFF: age, race/ethnicity, smoking, height, fracture history, duration of BP use, duration of glucocorticoid use, and pre-treatment total hip T-score. Multivariable time-varying Cox proportional hazards methods were used to estimate hazard ratios (HR) and 95% confidence intervals (CI). The cohort included 152,934 women meeting inclusion criteria with 185 AFF (incidence rate 1.70 per 10,000 person-years). After adjustment for all confounders, there was a 44% reduction in the risk of AFF in the first year after discontinuation compared to women who continued to use BP (HR 0.56, CI 0.38-0.82). In years 1 to 4 after discontinuation, AFF risk was decreased by 80% (HR 0.20, CI 0.10-0.37) and after >4 years, AFF risk was reduced by 78% (HR 0.22, CI 0.08-0.59) compared to current users. These results suggest that among women with BP use of varying duration, discontinuation is associated with substantially decreased risk of AFF. Thus, these results suggest that a drug holiday of 3-5 years would likely markedly reduce AFF risk among long-term BP users.

Disclosures: **Annette L. Adams**, Merck, Grant/Research Support

1006

The Impact of Bisphosphonate Drug Holidays on Fracture Rates Jeffrey Curtis^{*}, Rui Chen, Zixu Li, Tarun Arora, Kenneth Saag, Nicole Wright, Shanette Daigle, Meredith Kilgore, Elizabeth Delzell. University of Alabama at Birmingham, United States

Introduction Discontinuation of bisphosphonates after at least 3-5 years of continuous therapy is becoming increasingly common in the U.S. However, the benefits and risks of stopping bisphosphonates (BPs), and the timing as to when it might be optimal to restart, are unclear. We conducted a population-based cohort study of women on long term BP therapy to evaluate the rate of hip fracture following a drug holiday (temporary or permanent BP discontinuation). Methods Medicare data (2006-2015) were used to identify all women with medical and pharmacy coverage who initiated a BP and were at least 80% adherent for at least 3 years ('baseline'), at which time follow-up began. Patients using other bone therapies (e.g. denosumab, estrogen, teriparatide, calcitonin) were excluded (or censored, if they started after follow-up began). Subgroups defined by exclusive use of specific BPs, and prior fragility fracture, were defined. Crude rates of hip and other types of fractures using validated algorithms were evaluated in relation to continuing BP therapy vs. stopping, and time since stopping. Cox proportional hazards ratios (HRs) evaluated the adjusted risk of stopping for more than 2 years compared to continued use, controlling for potentially confounding factors. Results A total of 160,369 women were eligible for analysis, and 36% underwent a BP drug holiday of >12 months. Overall, during a median (IQR) follow-up of 2.7 (1.5, 4.1) years, there were 4,823 hip fractures. Compared to continued BP use, hip fracture rates were significantly elevated among women undergoing BP drug holidays. Adjusted HRs for the association between drug holiday $>2y$ and hip fracture are shown overall and for key subgroups (Table). Risk was similarly elevated for humerus fractures but not for other fracture types. Conclusions In a large cohort of older U.S. women, a BP drug holiday greater than 2 years was associated with a significantly increased risk for hip fracture but was minimally elevated for other fracture types.

Table: Hip fracture Rate for BP Drug Holiday >2 years

Cohort	Women, n	Number of hip fractures, n	Crude Incidence Rate per 1000 person-years	Adjusted* Hazard Ratio (95% CI)
Any BP	160,369	4,823	14.0	1.22 (1.11 – 1.34)
Alendronate users	81,287	2,245	13.1	1.28 (1.12 – 1.46)
Risedronate users	9,823	269	13.8	1.45 (1.00 – 2.11)
Zoledronate users	13,885	367	18.0	1.31 (0.94 – 1.82)
Prior fragility fracture	6,914	430	37.4	1.38 (1.01 – 1.89)

*Hazard ratio for women with a drug holiday of >2 years compared to persistent users, adjusted for age, region, race, rural or urban, median income, calendar year of study entry, comorbidity (fragility fracture, Charlson comorbidity index), DXA, office visits, office visits with bone specialists, long term care residence, vitamin D deficiency, glucocorticoids, and other factors, assessed...

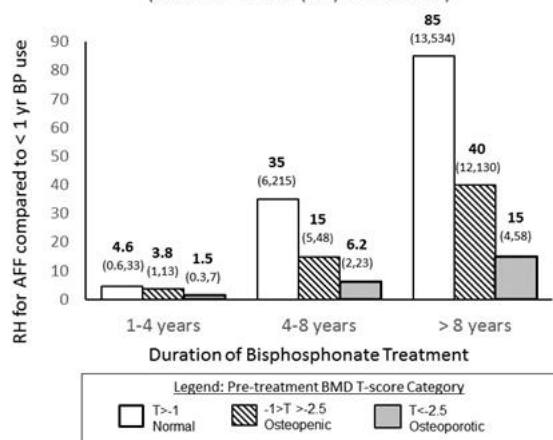
Disclosures: **Jeffrey Curtis**, Amgen, Grant/Research Support, Radius, Consultant, Amgen, Consultant, Radius, Grant/Research Support

1007

Bisphosphonate Use and Risk of AFF Varies by Pre-treatment BMD Level: Results from the Southern California Osteoporosis Cohort Study (SOCS) Dennis M. Black^{*1}, Erik J. Geiger¹, Bonnie H. Li², Denison S. Ryan², Richard M. Dell², Annette L. Adams². ¹University of California, San Francisco, United States, ²Kaiser Permanente Southern California, United States

While most studies have shown bisphosphonate (BP) use and longer duration is associated with increased atypical femur fracture (AFF) risk, the effect might be attenuated if indications for BP treatment, such as BMD, could be controlled. However, no AFF studies have included pre-BP BMD. To test if pre-treatment BMD attenuates the relationship of BP duration to AFF risk, we analyzed data from Kaiser Permanente Southern California (KPSC), an HMO with ~ 4.5 million members. We established a cohort of women >50 yrs with cohort entry from 1/1/2007-9/30/15. We assessed all X-rays with ICD9 coded subtrochanteric or femoral shaft fractures using ASBMR 2014 criteria with verified adjudication by 2 experts. Risk factors including age, Asian race, pretreatment BMD (PT BMD), BP use, fracture hx, height, GC use and smoking hx were available for up to 10 years prior to cohort entry and were updated annually thereafter. PT BMD was defined as total hip BMD before or soon after starting BPs. The relationship of BP duration to AFF risk was assessed before and after inclusion of PT BMD in multivariable (MV) Cox models with time-varying covariates. This analysis included women who had both PT BMD and any BP use (N=152,934). There were 185 AFFs overall. In a MV model (without PT BMD), those with longer BP duration had higher AFF risk. Compared to <1 year BP the relative hazard (RH) for 1-4 yrs of BP use was 3 (CI 1.4,7.3), for 4-8 yrs was 15 (CI 7,33) and >8 yrs was 37 (CI 16,83). PT BMD added to the model did not attenuate the relationship of BP duration to AFF risk. Inclusion of PT BMD also showed those with higher BMD had a 40% AFF risk per SD BMD increase (HR 1.4 (CI 1.2 1.7)). To further study PT BMD and AFF, we performed analyses stratified by PT BMD T-score (T >-1 ; -1 to -2.5; T <-2.5). We consistently observed larger risk increases with BPs for those with higher PT BMD (Figure). For example, in those with normal PT BMD (T >-1) the RH for 4-8 years BP use (vs <1 yr) was 35 compared to 15 in those with osteopenic BMD and compared to 6 in those with osteoporotic BMD (T <-2.5). We conclude that adjustment for PT BMD did not attenuate the relationship of BP use to AFF risk. Surprisingly, our results indicate that women with higher PT BMD have a larger increase in AFF risk with BP use than those with lower BMD. If confirmed in other studies, these results suggest that PT BMD could impact clinical decisions around patient selection for BP initiation and drug holidays.

Increase in AFF Risk with BP Use is Greater For Normal Pre-treatment BMD vs. Osteopenic & Osteoporotic BMD for Each BP Duration (Relative Hazard (RH) and 95% CI)



Disclosures: **Dennis M. Black**, Asahi-Kasei, Consultant, Radius Pharma, Grant/Research Support

1008

Clinical features of 35 patients with 172 spontaneous vertebral fractures after denosumab discontinuation: a single center observational study Elena Gonzalez-Rodriguez*, Berengere Aubry-Rozier, Delphine Stoll, Didier Hans, Olivier Lamy. Lausanne University Hospital, Switzerland

IntroductionIn the absence of bisphosphonate treatment, denosumab discontinuation (DD) induces an increase of B-crosslaps above baseline values for two years, and a complete or partial loss of the BMD gain after one year. This rebound effect is associated with spontaneous clinical vertebral fractures (SCVF) in 1 to 10% of patients. We report the clinical characteristics of 35 patients with SCVF after DD evaluated at our center from July 2015 to March 2018. **Method**We report the cases of 35 patients who received denosumab 60mg every 6 months for 2 to 11 doses. All were on calcium and vitamin D during denosumab treatment and after DD. VF have been documented by MRI. A wide biological assessment, performed at the time of fracture, was strictly normal. A secondary cause of osteoporosis was excluded. Patients did not receive any osteoporosis treatment between DD and the onset of SCVF. **Results**Thirty-four women and one man, 66.3±9.6 years, experienced 172 SCVF (median 5) in the 11.6±2.8 months (median 11; min 7, max 20) following the last denosumab injection. Eight women received a bisphosphonate before denosumab, and nine women received aromatase-inhibitors (AI) with denosumab. Eleven women had prevalent osteoporotic fracture. Twelve women had vertebroplasties with 58 new VF in the following days. The mean B-crosslaps value at the time of SCVF was 1523±588 ng/l. B-crosslaps values increase with the number of denosumab doses (R2=0.28). The number of SCVF was inversely associated with age: 5.4±2.0 vs 2.8±1.3, < vs > 65 years (p<0.001). The delay between DD and the occurrence of SCVF increases with age: 10.4±1.3 vs 12.7±2.6 months, < vs > 65 years (p=0.008). The mean reasons for DD were end of AI or no more osteoporosis (15), omission (7), patient's wish (5), atypical femoral fracture or dental intervention (4). **Conclusion**After denosumab discontinuation, women < 65 years have a higher number of SCVF and in a shorter period than women over 65 years. SCVF are a very severe and frequent clinical complication after DD. A close follow-up for 2 years after DD is necessary. Bisphosphonates may decrease the rebound effect at DD. Studies are urgently needed to better define who and when to treat with denosumab, as well as strategies to avoid SCVF after denosumab discontinuation.

Disclosures: **Elena Gonzalez-Rodriguez**, None

1009

Targeting skeletal endothelium to ameliorate bone loss Ren Xu*¹, Alisha Yallowitz¹, Shawon Debnath¹, Jung-Min Kim², Kazuki Inoue³, Baohong Zhao³, Jae-Hyuck Shim², Laurie Glimcher⁴, Matthew Greenblatt¹. ¹Weill Cornell Medical College, United States, ²University of Massachusetts Medical School, United States, ³Hospital for Special Surgery, United States, ⁴Dana-Farber Cancer Institute and Harvard University Medical School, United States

Recent studies have identified a specialized subset of vascular endothelium in bone termed type H endothelium (CD31^{high}Endomucin^{high}) as an important regulator of bone formation. However, it remains unclear how type H endothelium levels are coupled to anabolic bone formation. Here, we show that the greatly elevated bone formation seen in mice lacking the adaptor protein Schnurri-3 (Shn3^{-/-} mice) is accompanied by an increase in type H endothelium. Osteoblasts control type H endothelium levels, as seen in mice with an

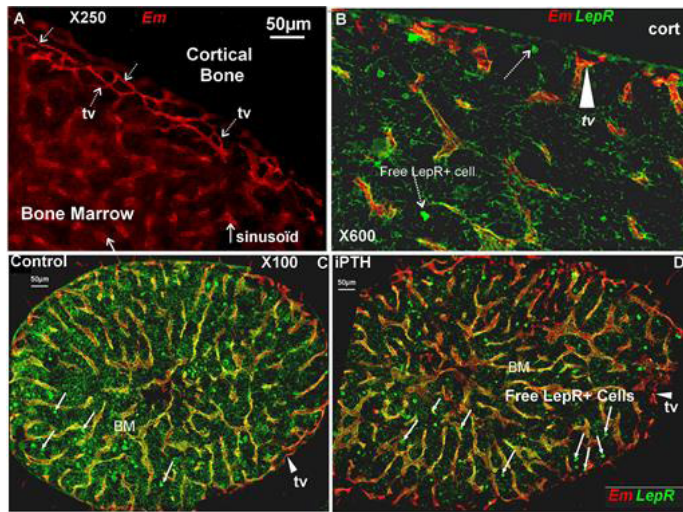
osteoblast-lineage specific Shn3 deletion (Shn3ox mice and Shn3ocn-ert mice). Transcriptomic analysis identified the axon-guidance cue SLIT3 as a proangiogenic factor whose expression in bone is restricted to osteoblasts and is negatively regulated by SHN3. Subsequent analysis of germline and osteoblast specific SLIT3-deficient mice (Slit3ox mice and Slit3dmp1 mice) or mice lacking the SLIT3 receptor ROBO1 demonstrated reduced type H endothelium and low bone mass due to impaired bone formation but intact bone resorption, and SLIT3 is necessary for the high bone mass and increased type H endothelium phenotypes of Shn3^{-/-} mice. This osteo-angio crosstalk pathway is essential for bone healing, as shown by the complete blockade in fracture repair in SLIT3-deficient mice and enhanced fracture repair in Shn3^{-/-} mice. Finally, administration of recombinant SLIT3 both enhanced skeletal fracture healing and counteracted bone loss in a mouse model of postmenopausal osteoporosis. Thus, SLIT3 provides proof-of-principle for a class of vascular-targeted osteo-anabolic therapies to treat bone loss.

Disclosures: **Ren Xu**, None

1010

Intermittent Parathyroid Hormone does not expand type H cell population but impacts transitional vessels by reducing their coverage by Leptin Receptor Positive Pericytes and Upregulating their Expression of Collagen Type 18/Endostatin. Robin Caire*¹, Bernard Roche¹, Tiphanie Picot², Zhiqiao He³, Carmen M Anaci², Mireille Thomas¹, Lydia Campos², Laurence Vico¹, Marie-Hélène Lafage-Proust¹. ¹INSERM 1059, Université de Lyon, France, ²University Hospital Hematology Lab, France, ³BIIGC, Université de Lyon, France

We showed that intermittent administration of Parathyroid Hormone (iPTH), an osteo-anabolic drug, affects bone vessels. Transitional capillaries close to the bone surfaces express both endomucin (Em⁺, Fig1A) and CD31 (type H endothelial cells) and bear pericytes which express Leptin receptor (LepR⁺) and may differentiate into osteoblasts. Increase in Type H cell number is associated with higher bone formation. Thus, our hypothesis was that iPTH impacts transitional vessels by expanding Type H cells. **Methods:** 3 month-old C57/Bl6J female mice were treated with subcut. injections of either PTH 1-84 (100µg/kg/d) or saline (CT) for 7 or 14d (n=6-8/gp). We quantified LepR⁺, CD31⁺, Em⁺ and type H cells by Flow cytometry (FACS) in bone marrow of long bones. Then, we quantified Em and LepR double immunostaining of 40µm-thick tibia transverse cryosections after confocal microscopy acquisition. Next, we analyzed mRNA expression of 87 angiogenesis-related genes in tibiae (PCR Array, Qiagen) of mice treated with PTH 100µg/kg/d, either intermittently or continuously via ALZET minipumps (cPTH) or saline (CT) for 7, 14 and 28d. **Results:** Unexpectedly, FACS data showed that iPTH dramatically decreased the percentage of type H cells by 78 and 90% at d7 and 14, respectively (p<0.001) and of LepR⁺ cells at d14 (-46%, p=0.01 vs CT). Immunostained image quantification showed that the transitional Em⁺ endocortical vessel network was disrupted and intracortical vascular density increased at d14 under iPTH only. In the bone marrow, LepR⁺ cells were essentially perivascular and connected to each other via a dendrite network (Fig1B) which became less dense after 14d of iPTH (-58%, p<0.01 vs CT). Moreover, LepR⁺ vascular coverage was decreased by iPTH in transitional vessels only (-51% p<0.01) while the number of free LepR⁺ cells not attached to vessels increased in the endocortical area only (+49% p<0.01, Fig1CD). Genomic analyses showed that mRNA expression of PEDF, Collagen 18 α1, MMP-2 and TIMP-1 were consistently upregulated by iPTH at 2 or 3 time points, compared to CT and cPTH. Finally, iPTH increased immunostaining of endostatin, a Collagen 18 domain that can potentially become anti-angiogenic after cleavage, in both endocortical (79%, p=0.02) and peri-trabecular transitional microvessels at d14. **Conclusion.** Our results show that iPTH specifically remodels transitional vessels and suggest that iPTH promotes mobilization of LepR⁺ cells from these vessels close to the bone surface.



Disclosures: **Robin Caire**, None

1011

Hypoxia/HIF Signaling Contributes to Bone Homeostasis by Preventing Premature Senescence and Apoptosis of Multipotent Mesenchymal Progenitor Cells

Kassandra Spiller*, Yinshi Ren, Colleen Wu. Duke University, United States

Multipotent mesenchymal progenitors (MMPs) cultured under low oxygen tension exhibit diminished DNA damage, enhanced genomic stability and increased replicative potential. While these findings highlight a role for hypoxia in prolonging MPP lifespan in vitro, the contribution of hypoxic niches in regulating MPP function in vivo has not been fully explored. Notably, the bone microenvironment (BME) displays vascular heterogeneity leading to regional areas of hypoxia. In response to low oxygen, hypoxia inducible factor (HIF) signaling is activated to facilitate oxygen delivery and cellular adaptation to low oxygen. We sought to define the role of hypoxia and HIF signaling in the regulation of MPP function and bone homeostasis. For our studies, we utilized transgenic mice expressing Cre-recombinase under the control of the Leptin Receptor (LepR) promoter (LepR-cre) as LepR marks a population of BM cells enriched for MPPs. Confocal imaging of LepR-cre;tdTomato mice demonstrated that a subset of LepR expressing cells localized to hypoxic perivascular areas and co-stained for HIF transcription factors. Next, to determine the necessity of HIF signaling within LepR cells in regulating bone homeostasis, we crossed mice homozygous for the Hif-2 conditional allele to LepR-cre mice. μ CT and histological analysis of long bones harvested from LepR-cre;Hif-2fl/fl mutant mice revealed a two-fold decrease in trabecular bone volume when compared to littermate controls. Quantification of multinucleated TRAP positive cells demonstrated no differences in osteoclast numbers suggesting diminished trabecular bone volume was not due to aberrant bone remodeling. Interestingly, LepR-cre;Hif-2fl/fl mice had fewer colony forming units – fibroblastic (CFU-F) when compared to littermate controls. To elucidate the potential cellular and molecular mechanism driving phenotypic changes associated with loss of HIF signaling in LepR expressing cells, MPPs were cultured under Hx (1% O₂) and Nx (21% O₂) conditions. Interestingly, hypoxia was associated with decreased β -galactosidase activity, reduced numbers of TUNEL positive cells, and diminished protein expression of p21 and cleaved caspase-3. In addition, hypoxia reduced genotoxic damage as marked by fewer distinct nuclear γ H2AX and 53BP1 foci. Taken together, this data suggests that the hypoxic BME may aid in maintaining bone homeostasis by impairing genotoxic damage to prevent premature senescence and apoptosis of MPPs.

Disclosures: **Kassandra Spiller**, None

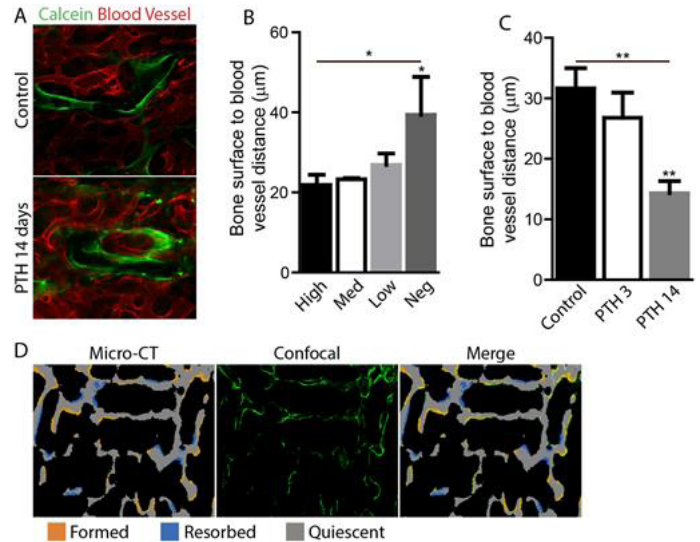
1012

Mineralizing Bone Surfaces Drive Blood Vessel Redistribution Through Asymmetric Angiogenesis

Robert Tower*¹, Chamith Rajapakse¹, Xi Jiang¹, Wei Tong², Nathaniel Dymant¹, Ling Qin¹. ¹University of Pennsylvania, United States, ²Xiehe Hospital, China

Angiogenic-osteogenic coupling is important for establishing and maintaining bone homeostasis. Despite extensive research, it is still not clear whether new bone formation plays a dominant role in recruiting the bone marrow vasculature, or whether vessels move to the bone surface first, bringing mesenchymal progenitors to initiate new bone formation. To address this issue, we first established a 3D confocal imaging approach of tissue-cleared femurs from 12-week-old mice that can accurately measure the distance between bone surfaces and the nearest vessel. We observed a close association between vessels and mineralizing, calcein high bone surfaces (21.9±2.6 vs calcein neg, 39.4±6.5 μ m, p<0.05). Treatment with PTH for 14 days increased vessel association (14.2±1.9 vs control, 31.7±3.3 μ m, p<0.01),

through increased mineralization, but showed no significant change in vessel distance at calcein high surfaces. Next, we performed micro-CT scans on the femur trabecular bone of the same mice at 10 and 12 weeks of age and registered these images to deduct formed and resorbed bone surface within this 2-week period. Furthermore, 12-week micro-CT images were registered with confocal images taken after harvest. Finite element analysis revealed that the top 0.5% strain surfaces at 10 weeks predicts sites of future bone formation with an accuracy of 85.8±1.6%. At 12 weeks, high strain, calcein negative bone surfaces were selected as non-mineralizing sites of future bone formation. These surfaces failed to show any notable vessel recruitment relative to all calcein neg surfaces, demonstrating that blood vessels are recruited to, but do not precede, actively mineralizing bone surfaces. Bone marrow vessels are coated with a basement membrane (BM) for structural stability. Interestingly, immunofluorescent analysis revealed that the vessel surface neighboring calcein high bone displays significantly less staining for collagen type IV (4-fold, p<0.001) and laminin (2-fold, p<0.05), two major components of the BM. This also coincided with increased endomucin staining (a marker for dynamic vessels) (2.5-fold, p<0.01) and a 194% increased angiogenic filipodia density (p<0.01) at the bone-facing surface, compared to the marrow-facing surface. Such differences were not observed in vessels residing in the diaphyseal marrow. Taken together, our results demonstrate that vessel redistributes to mineralizing surfaces via increased asymmetric angiogenesis at the bone-facing vessel surface.



Disclosures: **Robert Tower**, None

1013

The lysosomal protein arylsulfatase B is a key enzyme involved in skeletal turnover

Gretl Hendrickx*¹, Sandra Pohl², Alexandra Angermann¹, Anke Jeschke¹, Timur A Yorgan¹, Tim Rolvien¹, Michael Amling¹, Thomas Braulke², Thorsten Schinke¹. ¹Department of Osteology and Biomechanics, University Medical Center Hamburg-Eppendorf, Germany, ²Department of Biochemistry, Children's Hospital, University Medical Center Hamburg-Eppendorf, Germany

Skeletal pathologies are frequently observed in lysosomal storage disorders, yet the relevance of specific lysosomal enzymes in bone remodeling cell types is poorly defined. Two lysosomal enzymes, i.e. Ctsk (cathepsin K) and Acp5 (also known as tartrate-resistant acid phosphatase), are long known as molecular marker proteins of differentiated osteoclasts. However, whereas the cysteine protease Ctsk is directly involved in the degradation of bone matrix proteins, the molecular function of Acp5 in osteoclasts is still unknown. Here we show that Acp5, in concert with Acp2 (lysosomal acid phosphatase), is required for dephosphorylation of mannose 6-phosphate residues to promote the activity of lysosomal enzymes. Using an unbiased approach, we identified the glycosaminoglycan-degrading enzyme Arsb, mutated in mucopolysaccharidosis type VI (MPS-VI), as an osteoclast marker, whose activity depends on dephosphorylation by Acp2 and Acp5. Similar to Acp2/Acp5^{-/-} mice, Arsb-deficient mice display lysosomal storage accumulation in osteoclasts, impaired osteoclast activity and high trabecular bone mass. Of note, the most severe lysosomal storage was observed in osteocytes from Arsb-deficient mice. Although this pathology did not impair production of Sost and Fgf23, these findings demonstrate that osteocytes participate in bone matrix turnover. Since the influence of enzyme replacement therapy (ERT) on bone remodeling in MPS-VI is still unknown, we additionally treated Arsb-deficient mice by weekly injection of recombinant human ARSB from 12 to 24 weeks of age. We found that the high bone mass phenotype of Arsb-deficient mice and the underlying bone cell deficits were fully corrected by ERT in the trabecular compartment. Taken together, our results do not only demonstrate that the function of Acp5 in osteoclasts is linked to dephosphorylation of lysosomal enzymes, they also provide an important proof-of-principle for the feasibility of ERT to correct bone cell pathologies in lysosomal storage disorders.

Disclosures: **Gretl Hendrickx**, None

1014

Positive effects of intermittent PTH on growing bone and dystrophic muscle in Mdx mouse model of Duchenne Muscular Dystrophy Sung-Hee Seanna Yoon^{*1}, Marc Grynepas², Jane Mitchell¹. ¹University of Toronto, Canada, ²Lunenfeld-Tanenbaum Research Institute, Canada

Duchenne Muscular Dystrophy (DMD) is a progressive muscle disorder caused by genetic mutations on dystrophin encoding gene. With an absence of functional dystrophin, DMD boys show not only muscle wasting and inflammation, but also compromised bone health with high risk of fracture. The use of high dose glucocorticoids (GC) as the gold standard therapy also contributes to bone fragility in DMD boys. Our previous study showed that the prophylactic use of anti-resorptive bisphosphonates increased bone mineral density (BMD) but did not improve bone mechanical properties in the Mdx mouse model of DMD and dramatically decreased bone turnover. Thus, this study examined the effects of daily administered parathyroid hormone (PTH), the only available bone anabolic therapy, on growing bone and dystrophic muscle in the presence of slow-release pellet of prednisone using the Mdx mice. Five-week GC treated Mdx mice showed decreased cortical bone thickness and area ($p < 0.001$), which was significantly improved by PTH treatment ($p < 0.001$). This bone increase by intermittent PTH was through suppression of osteoclasts on endocortical surfaces ($p < 0.001$). GC-induced decreases in toughness and modulus from three-point bending tests were also improved with PTH therapy ($p < 0.05$). While there was no significant effect of muscular dystrophy on cortical bone, Mdx mice showed significantly less volumetric BMD and bone mass of trabecular compartments in lumbar vertebrae. GC or intermittent PTH by themselves did not have significant effect, but the combination of two treatments resulted in significant increase in volumetric BMD ($p < 0.001$) and percent bone volume ($p < 0.01$). Although only trabecular thickness was improved, PTH significantly improved ultimate load and stress, energy to fail, stiffness and modulus compared to control Mdx in vertebral compression test. In the presence of GC, PTH significantly improved all of structural and material properties. Moreover, GC resulted in significantly improved grip strength and endurance in treadmill running, which were maintained and further improved, respectively, in co-treated Mdx mice. All together, our study demonstrated that intermittent PTH significantly improved GC-induced bone loss and maintained or further enhanced dystrophic muscle function that is already improved by GC treatment. These findings could give an insight into the use of teriparatide in DMD boys, and also other forms of GC-induced osteoporotic patients.

Disclosures: *Sung-Hee Seanna Yoon, None*

1015

Deletion of PKA Regulatory Subunit 1A to Increase PKA Activity in Osteoblasts Causes Dramatic Expansion of Trabecular Bone at the Expense of Cortical Bone Carole Le Henaff^{*1}, Florante Ricarte², Joshua Johnson¹, Zhiming He¹, Johanna Warshaw¹, Henry Kronenberg³, Lawrence Kirschner⁴, Nicola Partridge¹. ¹New York University, college of dentistry, United States, ²Molecular Pharmacology Training Program, Sackler Institute of Graduate Biomedical Sciences, New York University School of Medicine, United States, ³Endocrine Unit, Massachusetts General Hospital, Harvard Medical School, United States, ⁴Department of Cancer Biology and Genetics, Internal Medicine, The Ohio State University, Division of Endocrinology, Diabetes, and Metabolism, Department of Internal Medicine, The Ohio State University Wexner Medical Center, United States

Parathyroid hormone (PTH) plays a central role in regulation of calcium metabolism and is the osteoanabolic hormone for treating osteoporosis. We have previously shown that PTH acts through PTHR1 and protein kinase A (PKA) activation to regulate the life cycle of HDAC4 in osteoblastic cells, thus identifying it as a major regulator of Runx2- and Mef2c-dependent transcription in bone. We hypothesized that similar to PTH (1-34) treatment, an increase in PKA activity in osteoblasts will cause an increase in bone accrual. Our study aims to elucidate the effects of increased PKA activity and better understand the actions of PTH (1-34) in bone. Weekly injections of tamoxifen (1mg/10g) were administered to 1 month-old or 5 month-old C57Bl/6 male and female col1CREERT/Prkar1af/fl mice or Prkar1af/fl mice as controls, for 3-4 weeks to delete the PKA regulatory subunit 1A and increase PKA activity. This resulted in a decrease of whole body (-6%), femoral (-24%), and tibial BMD (-22%) in 2 month-old col1CREERT/Prkar1af/fl mice. They were smaller and bones were very brittle with little bone marrow. μ CT showed dramatic excess trabecular bone and absence of cortical bone in vertebrae (Figure 1) and throughout most of the bone marrow cavity in femurs. Surprisingly, no overall BMD changes were observed with 6 month-old mice but they developed tumors in their tails. By μ CT, 6 month-old col1CREERT/Prkar1af/fl mice showed decreases in cortical thickness and cortical BMD and increases in cortical porosity and endocortical perimeter. In trabecular bone, BV/TV, Tb.N and trabecular BMD were increased, while Tb.S decreased. In both age groups, cortical and trabecular bone RNAs showed a substantial increase in bone sialoprotein mRNA levels (3 to 6 fold) with a sharp decrease in osteocalcin (0.2-0.4 fold). Furthermore, genes whose expression is known to be regulated by PTH were significantly changed: SOST expression was decreased to 0.1-0.2 fold, RANKL was upregulated by 2-3 fold and MMP13 was increased by at least 3 fold. These animals mimic mice in which a constitutively-active PTH receptor is expressed under the control of the col1 promoter. Indeed, the overall data show a great increase in trabecular bone mass with breakdown of cortical bone. The bone seems

to be immature and unable to transition to cortical bone. In conclusion, high PKA activity in osteoblasts appears to be involved in increasing immature trabecular bone and resorbing cortical bone.

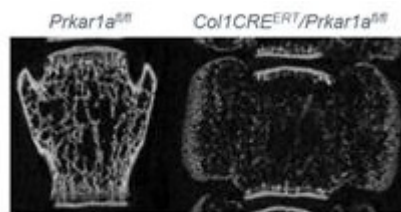


Figure 1 : μ CT images of vertebrae from 2 month-old mice after 3 tamoxifen injections

Disclosures: *Carole Le Henaff, None*

1016

Low bone mass in mice with conditional Wnt1 deletion and a Wnt1 mutation causing early-onset osteoporosis Nele Vollerensen^{*}, Timur Yorgan, Tim Rolvien, Michael Amling, Thorsten Schinck. Department of Osteology and Biomechanics, University Medical Center Hamburg-Eppendorf, Germany

Wnt signaling is long known as a key pathway controlling skeletal remodeling. The more recent identification of WNT1 mutations in individuals with osteogenesis imperfecta type XV or early-onset osteoporosis (EOOP) suggested that Wnt1 is a key ligand stimulating this pathway in osteoblasts. To elucidate the role of Wnt1 in skeletal turnover, we first generated mice with an osteoblast-specific Wnt1 inactivation (Wnt1fl/fl;Runx2-Cre). These mice displayed multiple skeletal fractures, decreased trabecular bone mass and cortical thinning at 24 weeks of age. In contrast, Wnt1 inactivation in osteoclasts did not cause any detectable bone remodeling abnormality in Wnt1fl/fl;Lyz2-Cre mice. We additionally established a mouse model carrying an EOOP-associated recessive Wnt1 mutation (p.Arg-235Trp). Wnt1+/R235W mice displayed decreased trabecular and cortical bone mass at the age of 52 weeks, whereas homozygous Wnt1R235W/R235W mice showed an exacerbated phenotype already evident at 24 weeks of age. To address the clinically relevant question, if Wnt1 mutations interfere with the osteoanabolic influence of intermittent PTH treatment, we finally treated 52 weeks old Wnt1+/R235W mice by daily PTH injection. Using μ CT, dynamic histomorphometry and serum biomarker determination we found no difference between wildtype and Wnt1+/R235W littermates in the response to PTH treatment. Taken together, our results provide further in vivo evidence for a key function of Wnt1 in controlling trabecular and cortical bone remodeling. Moreover, the generation of the Wnt1+/R235W mice will be very informative for understanding the cellular and molecular bases of Wnt1-dependent EOOP. Importantly, the normal response of these mice to intermittent PTH injection strongly suggests that osteoanabolic treatment with teriparatide might be preferable to normalize bone pathologies in individuals with WNT1 mutations.

Disclosures: *Nele Vollerensen, None*

1017

Loss of Hypoxia Inducible Factor-2 Alpha in Mesenchymal Progenitors Increases Bone Mass Accrual and Osteoblastogenesis Christopher Merceron^{*1}, Kavitha Raganathan², Elizabeth Wang¹, Zachary Tata¹, Laura Mangiavini¹, Mohd Parvez Khan¹, Benjamin Levi², Ernestina Schipani¹. ¹Department of Orthopedic Surgery, School of Medicine, University of Michigan, United States, ²Division of Plastic and Reconstructive Surgery, Department of Surgery, University of Michigan, United States

Understanding the mechanisms that control bone mass and osteoblastogenesis is crucial to unveil the pathogenesis of skeletal diseases and identify approaches for their treatment. Osteoblastic cells operate in a hypoxic environment. The transcription factors Hypoxia Inducible Factor-1a (HIF1) and HIF2 are key mediators of the cellular response to hypoxia. Both are expressed in osteoblastic cells. HIF1 is known to be a positive regulator of bone formation and osteoblast differentiation. Conversely, the role of HIF2 in the control of bone mass and osteoblast biology is still poorly understood. To fill this gap of knowledge, we generated mutant mice carrying a loss-of-function mutation of HIF2 in mesenchymal progenitors of the limb bud and their descendants using PRX1-Cre. MicroCT and histomorphometric analyses at 12 weeks of age showed a significant increase in bone mass in mutants. The mineral apposition rate, the bone formation rate and the number of osteoblasts were also augmented. Conversely, in vivo overexpression of HIF2 in the same cells resulted in a delay of the osteogenic front in the calvaria, a thinning of the cortical bone, and an impairment of both bone formation rate and osteoblast number in the trabecular compartment of the long bones. In vitro studies of bone marrow stromal cells expressing a gain-of-function mutation of HIF2 demonstrated that HIF2 is a direct inhibitor of osteoblastogenesis, as shown by analyses of Alkaline Phosphatase (ALP) activity, mineralization and mRNAs encoding osteoblastic markers such as Osterix, ALP, and Osteopontin. Interestingly, the level of Runx2 mRNA was not affected by HIF2, which suggests that HIF2 impairs osteoblastogenesis by acting upstream of Osterix through the modulation of Runx2 activity. Consistent with these

data, we gathered evidence that Sox9, which is emerging as a negative regulator of osteoblastogenesis, is likely to mediate the HIF2-dependent impairment of osteoblast differentiation. Our findings constitute a paradigm shift as activation of the hypoxia signaling pathway has been associated with an increased osteoblast activity through HIF1. They also show that HIF1 and HIF2 have opposing functions in osteoblastic cells. HIF2 can be selectively inhibited by small molecules that are currently in clinical trials in patients with renal carcinoma. Inhibiting HIF2 could thus represent a therapeutic approach for the treatment of the low bone mass observed in chronic diseases, osteoporosis or aging.

Disclosures: **Christophe Merceron**, None

1018

Periosteal skeletal stem cells are a functionally and genetically distinct subset of skeletal stem cells necessary for bone healing Laura Ortinau¹, Hamilton Wang¹, Kevin Lei¹, Yannis Hara¹, Breddan Lee¹, David Scadden², Dongsu Park¹. ¹Baylor College of Medicine, United States, ²Harvard University, United States

The periosteum is critical for bone healing, suggesting skeletal stem cells (SSCs), which are essential for lifelong bone and cartilage regeneration, reside in the periosteum. Therefore, the manipulation of periosteal SSCs (P-SSCs) is a promising therapy for degenerative bone disease and bone defects. Animal models that selectively label a P-SSC subset by myxovirus resistance-1 (Mx1) with either Rosa-DTR or α SMA-GFP expression were used for lineage tracing and fluorescence-activated cell sorting (FACS) analysis. P-SSC migration and bone injury repair was determined using sequential live intravital imaging of the calvaria. Our previous studies revealed that mature osteoblasts turn over rapidly and are replaced by their stem/progenitor cells genetically labeled by the Mx1 promoter *in vivo*. Mx1+ cells are abundantly present (> 50%) in the periosteal (PO) cambial layer (outer bone surface) of calvaria and long bones. To determine the necessity of Mx1+ PO cells in bone healing, we treated the calvaria of Mx1/tomato/DTR mice locally with diphtheria toxin (DT) reducing the number of Mx1+ PO cells by > 90%, while Mx1+ cells in the BM and in the distal periosteum remained unchanged. Sequential imaging of injury repair for 16 days revealed that local DT-mediated deletion of Mx1+ PO cells completely inhibits the recruitment and proliferation of Mx1+ osteogenic cells at the injury site and delays calvaria bone healing. We then determined that Mx1+ PO cells can be further specified by the α SMA mesenchymal marker. Histological and *in vivo* image analysis of Mx1/Tomato/ α SMA-GFP mouse calvaria and tibia revealed that most Mx1+ α SMA+ cells reside in the periosteum and calvarial sutures but are nearly undetectable in the bone marrow (BM). FACS analysis of Mx1/Tomato/ α SMA-GFP mouse periosteum showed that ~80% of Mx1+ α SMA+ PO cells express immunophenotypic SSC markers (CD45-CD31-Ter119-CD140a-CD105+) and highly express known SSC transcripts Grem1, LepR, and Cxcl12. Upon injury to the calvaria, we observed significant migration of Mx1+ α SMA+ P-SSCs out of the coronal suture toward the injury site within 24-48 hours and are present at the injury site 4-7 days post-injury. Further tracking, histology, and *in vivo* imaging 14 days post injury revealed Mx1+ α SMA+ periosteal cells repopulate the outer layer of the callus and supply most of the callus-forming cells and new osteoblasts during fracture healing. In addition, we found that CCR3 and CCR5, receptors for chemokine CCL5, are specifically expressed in Mx1+ α SMA+ P-SSCs. Thus P-SSCs are a functionally and genetically distinct subset of SSCs that are necessary for bone healing

Disclosures: **Laura Ortinau**, None

1019

Cfp1 is Essential for the Initiation of Chondrogenesis and Growth Plate Development Diana Carlone*, Emanuele Pignatti, Lijie Jiang, Manasvi Shah, David Breault. Boston Children's Hospital, United States

Mesenchymal progenitor cells (MPCs) are required for proper specification of the developing limb and perturbations in their capacity to expand and differentiate translate into major skeletal defects. Recent data indicate that epigenetic regulation of gene expression plays an essential role in mediating MPC activity. Precisely how this controls MPCs, including their ability to form bone, remains to be determined. CXXC finger protein 1 (Cfp1) is a critical epigenetic regulatory factor that has been implicated in the control of progenitor cell differentiation, through unknown mechanisms. To address this in bone, we deleted Cfp1 specifically in limb bud mesenchyme using Prx1-Cre. Conditional knockout (cKO) mice died shortly after birth and displayed a complete absence of forelimbs, implying a profound defect in MPC function. Embryonic analysis revealed that cKO forelimbs form but are lost by E14.5. In addition, high-density culture of forelimb mesenchymal cells revealed an intrinsic defect of cKO cells to undergo condensation, indicating that Cfp1 is required for the initiation of chondrogenesis in the developing limb. To decipher the mechanism(s) by which Cfp1 regulates MPCs, we performed whole transcriptome analysis of limb buds (E11.5) from cKO and control mice. This analysis revealed a dramatic reduction in chondrogenic gene markers, including the master transcriptional regulator Sox9, further supporting Cfp1's role in the initial steps of chondrogenesis. In addition, our preliminary data indicate that loss of Cfp1 leads to differential expression of signaling pathways important for chondrogenesis, such as FGF, BMP, Wnt and Shh. In contrast to the forelimb, cKO hindlimbs did develop, but were severely stunted. Moreover, high-density culture of hindlimb mesenchymal cells from cKO mice were able to condense and differentiate, similar to controls, suggesting that Cfp1 also functions in chondrocytes during endochondral ossification. Consistent with this, cKO tibia exhibited abnormal growth plate development with reduced proliferation and

accelerated hypertrophy. In addition, decreased ERK/Mapk signaling and Runx2 expression were observed. Finally, deletion of Cfp1 in chondrocytes using, Col2a1-Cre, resulted in smaller mice with shorter limbs, consistent with a physiological role for Cfp1 in chondrocytes during endochondral ossification. Together, our results show that Cfp1 is an essential modulator of skeletal development, through augmentation of regulatory genes and signaling pathways during the initiation of chondrogenesis and growth plate development. These results highlight the intricate nature of the epigenetic regulatory network in the skeleton.

Disclosures: **Diana Carlone**, None

1020

The Role of GATA4 in Mesenchymal Stem Cell Proliferation and Differentiation Aysha Khalid*, Susan Miranda, Alexandria Slayden, Jerusha Kumpati, Gustavo Miranda. University of Tennessee, United States

GATA4 is a zinc finger transcription factor that has been shown to regulate tissue specific gene expression. Previously, we demonstrated that mice with deletion of Gata4 using Cre-recombinase under the control of the Col1a1 2.3 kb promoter, had significantly reduced trabecular bone properties. However, it is not yet known if GATA4 plays a role in mesenchymal stem cell (MSC) biology or MSC commitment to osteoblasts or adipocytes. Gata4fl/fl mice were crossed with mice expressing Cre-recombinase under the control of the Prx1 promoter, which is expressed in limb bud mesenchyme, to create Gata4 PRX conditional knockout (Gata4 PRX-cKO) mice. The Gata4 PRX-cKO mice showed significantly reduced properties of trabecular bone indicating the importance of early expression of GATA4 in maintaining normal bone mass. Bone marrow stromal cells differentiated for 14 days showed reduced fat accumulation and mineralization, as visualized by Oil Red O and Alizarin Red staining, respectively. Less bone and less fat indirectly suggest a cellular defect in MSCs. qPCR analysis of the cDNA of bone marrow MSCs differentiated for 0-14 days in osteogenic and adipogenic media exhibited the highest level of Gata4 expression in undifferentiated cells. FACS analysis of MSCs from PRX-cKO and wildtype (WT) mice display a significant reduction in the MSC population (Sca1+/CD44+/CD34-/CD45-) in PRX-cKOs. PRX-cKOs also had reduced Giemsa staining in CFU-F assays. The immunocytochemistry of Gata4 PRX-cKO bone marrow MSCs showed fewer nestin positive stem cells as compared to WT bones. Cell proliferation rates were also reduced in Gata4 PRX-cKO primary bone marrow MSCs, as determined by IncuCyte proliferation assays and qPCR analysis of cDNA expression levels of proliferation markers. qPCR analysis of the cDNA of Gata4 PRX-cKO bone marrow MSCs also showed a significant reduction in Wnt ligands and signaling. To determine if Wnts are direct targets of GATA4, ChIP qPCR was performed, and we demonstrate that GATA4 is recruited to enhancers near Wnt3 and Wnt10b. Furthermore, qPCR analysis showed a significant reduction of Gata4 in Wnt10b-knockout mice, indicating a co-regulation between GATA4 and WNT10B. Together, these data suggest that Gata4 PRX-cKO have fewer and slower proliferating MSCs due to a reduction in Wnt signaling, which in turn leads to reduced bone mineral density in Gata4 PRX-cKO bones, as compared to wildtype bones.

Disclosures: **Aysha Khalid**, None

1021

The TGF β Receptor ALK5 is an Essential Regulator of BMP Signaling in the Growth Plate Weiguang Wang*, Hyeleim Chun, Karen Lyons. University of California, Los Angeles, United States

TGF β s and BMPs regulate joint shape, cartilage formation and AC maintenance, but the functions of the TGF β pathway in cartilage *in vivo* are unclear. Cartilage-specific loss of the receptor TGF β RII or the intracellular mediator Smad3 in embryos or young mice leads to osteoarthritis (OA)-like pathologies (1-3). However, no structural alterations were observed when TGF β RII was ablated in articular cartilage (4). Furthermore, TGF β activates Smad2 and Smad3, but the role of Smad2 was unknown. The purpose of this study was to investigate the extent to which TGF β controls cartilage formation and maintenance *in vivo*. We therefore generated mice lacking (a) Smads2 and 3, (b) the TGF β receptor ALK5, and (c) either the BMP receptor ALK1 or both ALK1 and ALK5. Results: Loss of Smad2 in cartilage led to only subtle growth plate abnormalities at birth, but mutants developed OA-like pathologies as they aged. These phenotypes were exacerbated in Smad2/Smad3 cartilage-specific double mutants, demonstrating that both Smad2 and Smad3 transduce TGF β signaling in cartilage. Cartilage-specific loss of ALK5 led to a far more severe, neonatal lethal phenotype. The greater severity of the phenotype demonstrates that the majority of ALK5 action in cartilage occurs independently of Smad2/3 activity. Characterization of the ALK5 phenotype revealed unexpected evidence that BMP signaling was elevated. Because the BMP receptor ALK1 can associate physically with ALK5, we investigated whether ALK1 interacts genetically with ALK5 in cartilage. We found that loss of ALK1 in cartilage did not lead to a discernable phenotype, but the severe chondrodysplasia found in Alk1 mutants was almost completely reversed in Alk1/Alk5 double mutants. This demonstrated a previously unexpected role for ALK1 in the growth plate. Using reporter assays, CRISPR-modified chondrocytes, chemical crosslinking and proximity ligation studies, we found that ALK1 and ALK5 form complexes in cartilage, and that loss of ALK5 leads to formation of new ALK1/ActR1B complexes. These complexes drive high levels of BMP signaling. These studies indicate that contrary to expectation, the primary function of the TGF β receptor ALK5 is not to transduce TGF β signals, but is rather to restrain exuberant BMP signaling by ALK1.1. Serra, R et al. (1997). J Cell Biol. 139, 541-522. Yang, X. et al. (2001). J Cell Biol. 153, 35-463. Shen, J. et al. (2013). Arthritis Rheum. 65, 3107-194. Chen, R. et al. (2015). Am J Pathol. 185, 2875-85



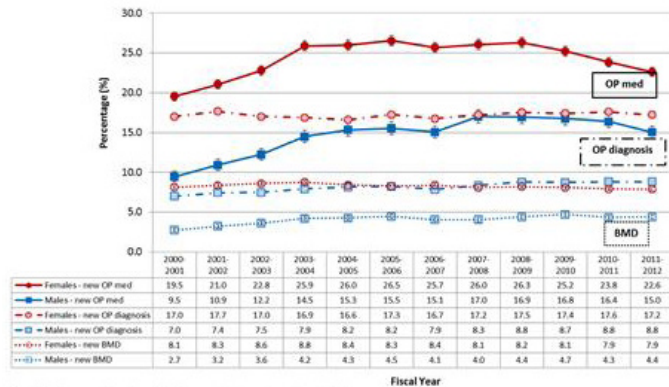
Disclosures: Weiguang Wang, None

1022

Post-Fracture Care gap in Canada from 2000-2001 to 2011-2012: A Nationwide Population-based Analysis Suzanne N Morin^{*1}, Siobhan O'Donnell², Sonia Jean³, Susan Jaglal⁴, Kerry Siminoski⁵, Alexandra Papaioannou⁶, Jacques Brown⁷, Lisa M Lix⁸, William D Leslie⁸. ¹McGill University, Canada, ²Public Health Agency of Canada, Canada, ³Institut national de santé publique du Québec, Canada, ⁴University of Toronto, Canada, ⁵University of Alberta, Canada, ⁶McMaster University, Canada, ⁷Université Laval, Canada, ⁸University of Manitoba, Canada

PURPOSE: A high percentage of Canadians who experience fragility fractures do not receive the osteoporosis (OP) screening or treatments that have been demonstrated to be cost-effective for secondary prevention. We aimed to describe the secular trend in the post-fracture care gap in Canada from 2000-2001 to 2011-2012. **METHODS:** Using linked provincial and territorial health administrative data from the Public Health Agency of Canada's Canadian Chronic Disease Surveillance System (CCDSS), we identified Canadians age 40 years and older who sustained an incident fracture of the hip, humerus, wrist, vertebrae or pelvis during the study period. Outcomes were a new OP diagnosis, bone mineral density (BMD) testing or (in those over 65 years) OP medication prescription (OP med) in the 12 months following the index fracture. **RESULTS:** We identified a total of 900,000 incident fractures among women and 391,700 among men over the study period. Up to 17.7% (95% Confidence Intervals [CI] 17.3-18.1%) of women and 8.8% (8.5-9.2%) of men received a new OP diagnosis, and this improved in men (p for trend <0.001). The percentage of individuals who underwent BMD testing was low, particularly in men (<10%), but increased slightly during the study period (p<0.001). OP med increased up to a maximum of 16.9% (16.1-17.8%) of men and 26.3% (25.7-27.9%) of women by 2008-2009 (p<0.0001). There was a significant downward trend in OP med for women and men during the last 4 years of the study period (p <0.003). (Figure) Age-specific percentages of women and men who received a new OP diagnosis or OP med increased with age, and was highest, in 2011-12, in women 80-84 y (26.4%; 95% CI 25.1-27.9%) and in men ≥ 85 y (19.6%; 95% CI 18.0-21.4%). BMD testing in the year following a fracture was highest in women 55-69 y (12.7%; 95% CI 11.7-13.8% to 13.0%; 95% CI 12.0-14.1%) and men 65-74 y (6.6%; 95% CI 5.6-7.7% to 7.1%; 95% CI 6.0-8.4%), and lowest in the oldest age-groups. **CONCLUSIONS:** As documented in many countries, secondary fracture prevention strategies are infrequently implemented in Canada. Few were given a new diagnosis of OP or underwent BMD testing. Only one in four women and one in six men received a new OP prescription in the year following a major osteoporotic fracture and this proportion decreased significantly in the last 4 years. Ongoing efforts to improve post fracture care through fracture liaison services should be vigorously supported.

Percentage (crude) of Canadians* who received a new OP prescription (med), diagnosis or BMD 12 months after any OP related fracture† by sex, Canada*, 2000-2001 to 2011-2012



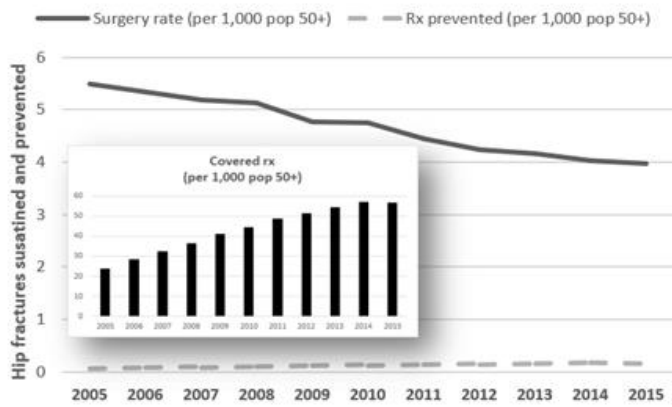
*Aged 65+ for new OP med, and 40+ for new OP diagnosis and new BMD.
 †Any OP related fracture includes hip, forearm, spine, humeral or pelvis.
 *Data do not include YT, NT, NU, AB, NB, NL for new OP med; YT for new OP diagnosis and YT, NT, NU, SK, NS, MB for new BMD.
 Abbreviations: BMD, bone mineral density test; med, medication; OP, osteoporosis.
 Notes: 95% confidence interval shows an estimated range of values which is likely to include the true percentage 19 times out of 20.
 Source: Public Health Agency of Canada using Canadian Chronic Disease Surveillance System data files contributed by provinces and territories.

Disclosures: Suzanne N Morin, Amgen, Grant/Research Support

1023

Hip fractures rates and time trends in use of anti-osteoporosis medications in Denmark for the period 2005 to 2015 Bo Abrahamsen^{*1,2}, Michael K Skjødt¹, Peter Vesteragaard³. ¹Holbæk Hospital, Dept of Medicine, Denmark, ²Univ of Southern Denmark, OPEN, Denmark, ³Aalborg University and University Hospital, Steno Diabetes Center North Jutland, Denmark

Background: Declining use of bisphosphonates (BP) in the United States and Europe may lead to a widening of the treatment gap for osteoporosis and an increase in osteoporotic fracture rates. However, a shift to non-bisphosphonates and to hospital administered i.v. BPs could lead to overestimation of the treatment gap if analyses are based exclusively on BPs and on non-hospital use. We analysed a best-case scenario where all use of BPs, denosumab, raloxifene and PTH analogues - including the oncology area - was contrasted with the trend in hip fracture rates over the same period. **Methods:** Aggregate statistics were obtained from the National Board of Health and the National Medicines Agency on surgically treated hip fracture events and total use in DDD (defined daily doses) of the above medications with number of persons covered assuming a medication possession ratio of 100. The Danish 50+ population was 1.8 mio in 2005 and rose to 2.1 mio in 2015. The number of fractures prevented was estimated by assuming a primary prevention scenario (taken from alendronate FIT, no prior vertebral fracture) with an absolute risk reduction of 0.3 hip fractures per 100 person years. **Results:** A plateau in prevalence of use of osteoporosis medications (bars, fig 1) occurred in 2014. Between 2005 and 2015, hip fracture rates (solid line, fig 1) declined by 30%. Statistically, 363 hip fractures were avoided in 2015 due to osteoporosis medications compared with 133 in 2005 (dotted line, fig 1). However, only 10% of the observed reduction in hip fracture rates is statistically attributable to treatment even in a best-case scenario. **Discussion:** The use of anti-osteoporosis treatment in Denmark reached a plateau in 2014 even in a best-case scenario where all pharmacy and hospital dispensations of osteoporosis drugs is assumed to be for the osteoporosis indication. A limitation to the study is lack of individual adherence data. About 90% of the decline in hip fracture rates appears to be due to factors other than osteoporosis medication; prior studies using APC models have suggested major cohort effects with a transient decrease in rates. The plateau in use of osteoporosis treatment is problematic given the predicted increased age-specific hip fracture rates.



Disclosures: **Bo Abrahamsen**, UCB, Grant/Research Support, Novartis, Grant/Research Support

1024

A Comparison of U.S. and Canadian Osteoporosis Screening and Treatment Strategies: What proportions of postmenopausal women are identified for screening and treatment? Carolyn Crandall^{*1}, Joseph Larson², Joann Manson³, Jane Cauley⁴, Kristine Ensrud⁵, Andrea Lacroix⁶, Jean Wactawski-Wende⁷, Mrirul Datta⁸, Maryam Sattari⁹, John Schousboe¹⁰, William Leslie¹¹. ¹University of California, Los Angeles, United States, ²Fred Hutchinson Cancer Research Center, United States, ³Harvard Medical School, United States, ⁴University of Pittsburgh, United States, ⁵University of Minnesota, United States, ⁶University of California, San Diego, United States, ⁷the State University of New York, United States, ⁸Purdue University, United States, ⁹University of Florida, United States, ¹⁰Park Nicollet Institute, United States, ¹¹University of Manitoba, Canada

Objective. To compare 1) the proportion of postmenopausal women identified for screening under the United States Preventive Services Task Force (USPSTF) and Osteoporosis Canada (CAROC) strategies; and 2) the proportion of women identified for drug treatment under the National Osteoporosis Foundation (NOF) and Canadian Association of Radiologists and Osteoporosis Canada (CAROC) treatment strategies. **Methods.** We used 10-year follow-up data from 111,707 women aged 50-79 years in the WHI Observational Study and Clinical Trials. Fractures were self-reported annually. Bone density information was available for a subset of 8,134 participants. **Results.** For women ≥65 years, 100% were identified for bone mineral density (BMD) screening by the USPSTF and Canadian strategies, 35-74% were identified for treatment under NOF, and 16-37% were identified for treatment under CAROC (range among 5-year age strata) (Table). Among women aged >65 years who experienced major osteoporotic fracture (MOF) during 10-year follow-up, sensitivity for identifying treatment candidates was 50-83% for NOF and 27-52% for CAROC (range among 5-year age strata). Among women 50-64 years-old, 16% of women were identified for BMD screening under the USPSTF strategy; 52% were identified for screening under the Canadian strategy. Among women 50-64 years-old who experienced MOF during follow-up, USPSTF and Canadian strategies identified a small fraction of this group for BMD screening. Specifically, the USPSTF strategy identified 4% of women 50-54 years-old and 36% of women 60-64 years-old for BMD screening at baseline; the Canadian strategy identified 54% of women 50-54 years-old and 61% of women 60-64 years-old for BMD screening at baseline. Among women 50-64 years-old, the NOF strategy identified a larger proportion for drug treatment to prevent fractures (16%) than did the CAROC strategy (3%). Among women aged 50-64 who experienced MOF during follow-up, the NOF strategy had a higher sensitivity for identifying them as treatment candidates at baseline, but sensitivity was low for both strategies (NOF 10-38%; CAROC 1-15%). **Conclusion.** Among women aged 50-64 years, the screening and treatment strategies examined identified only a small proportion of women who subsequently experienced MOF. Among women aged ≥65 years who subsequently experienced MOF, the NOF strategy identified more women for treatment than the CAROC strategy. Osteoporosis screening and treatment strategies warrant reconsideration.

Table. Proportion of Women with Major Osteoporotic Fractures during 10-year Follow-up who are Identified for Bone Mineral Density Testing (under the USPSTF and Canadian Strategies) and Treatment (under the NOF and CAROC strategies)¹

Strategy	Age Group	Total n	Identified for screening, n (%)	MOF Events, n (%)	Sensitivity (95% CI)	Specificity (95% CI)	Positive Predictive Value (95% CI)	Kappa
USPSTF	All Participants	115267	57363 (50%)	14109 (12%)	69.4 (68.6, 70.1)	52.3 (52.0, 52.6)	16.9 (16.6, 17.1)	0.09
	50-54	16420	465 (28%)	1032 (6%)	4.4 (3.1, 5.6)	39.3 (39.0, 39.5)	9.7 (9.0, 10.4)	0.02
	55-59	24523	3273 (13%)	1956 (8%)	19.1 (17.3, 20.8)	87.1 (86.7, 87.6)	11.4 (10.3, 12.5)	0.05
	60-64	27802	7543 (27%)	2731 (10%)	35.6 (34.0, 37.6)	73.6 (73.1, 74.1)	13.0 (12.2, 13.7)	0.05
	65-69	24997	24997 (100%)	3544 (14%)	100.0 (-)	0.0 (-)	14.2 (13.7, 14.6)	-
	70-74	15808	15808 (100%)	3111 (20%)	100.0 (-)	0.0 (-)	19.7 (19.1, 20.3)	-
75-79	5907	5907 (100%)	1732 (29%)	100.0 (-)	0.0 (-)	29.3 (28.2, 30.5)	-	
Canadian	All Participants	115537	62599 (54%)	14105 (12%)	62.9 (62.2, 63.5)	29.9 (29.6, 30.2)	14.1 (13.9, 14.6)	0.04
	50-54	16420	8391 (51%)	1032 (6%)	54.4 (51.3, 57.4)	46.1 (46.3, 46.9)	6.7 (6.2, 7.2)	0.01
	55-59	24523	12373 (50%)	1956 (8%)	63.4 (63.2, 67.6)	50.0 (49.3, 50.6)	8.6 (8.3, 9.3)	0.02
	60-64	27802	15123 (55%)	2731 (10%)	60.6 (59.8, 62.5)	45.0 (45.2, 46.5)	11.0 (10.5, 11.4)	0.02
	65-69	24997	24997 (100%)	3544 (14%)	100.0 (-)	0.0 (-)	14.2 (13.7, 14.6)	-
	70-74	15808	15808 (100%)	3111 (20%)	100.0 (-)	0.0 (-)	19.7 (19.1, 20.3)	-
75-79	5907	5907 (100%)	1732 (29%)	100.0 (-)	0.0 (-)	29.3 (28.2, 30.5)	-	
NOF	All Participants	7226	2184 (30%)	1034 (13%)	50.3 (47.2, 53.3)	75.9 (74.8, 76.9)	23.8 (22.0, 25.6)	0.16
	50-54	1295	93 (7%)	79 (6%)	10.1 (3.3, 16.9)	92.8 (91.3, 94.3)	8.6 (6.8, 14.4)	0.03
	55-59	1690	234 (14%)	138 (8%)	29.0 (21.3, 36.7)	87.3 (85.6, 88.9)	11.1 (12.2, 22.0)	0.12
	60-64	1794	472 (26%)	189 (11%)	37.6 (30.5, 44.5)	78.8 (76.8, 80.6)	11.2 (13.5, 20.9)	0.11
	65-69	1729	624 (36%)	259 (15%)	50.0 (43.8, 56.2)	87.7 (85.3, 90.1)	23.2 (17.9, 24.5)	0.11
	70-74	1100	553 (50%)	250 (23%)	66.8 (63.0, 74.6)	95.2 (91.8, 98.5)	31.1 (27.2, 36.0)	0.17
75-79	388	288 (74%)	122 (31%)	82.8 (76.0, 89.6)	29.7 (24.2, 35.2)	36.1 (29.5, 40.6)	0.09	
CAROC	All Participants	7226	826 (12%)	1034 (13%)	24.1 (22.0, 27.3)	91.1 (91.1, 92.4)	30.9 (27.1, 34.9)	0.18
	50-54	1295	6 (<1%)	79 (6%)	1.3 (0.0, 3.8)	99.6 (99.2, 99.9)	16.7 (0.0, 59.5)	0.01
	55-59	1690	29 (2%)	138 (8%)	4.3 (0.9, 7.8)	98.5 (97.9, 99.1)	20.7 (6.0, 36.4)	0.04
	60-64	1794	119 (7%)	189 (11%)	14.8 (9.7, 19.9)	94.3 (93.2, 95.5)	23.5 (16.3, 31.3)	0.11
	65-69	1729	269 (16%)	259 (15%)	27.0 (21.5, 32.4)	96.4 (94.7, 98.2)	25.1 (20.4, 30.9)	0.13
	70-74	1100	261 (24%)	250 (23%)	35.2 (29.2, 41.2)	79.6 (76.9, 82.4)	33.7 (27.9, 39.5)	0.15
75-79	388	142 (37%)	122 (31%)	61.6 (42.6, 80.6)	70.3 (64.8, 75.8)	44.4 (36.1, 52.6)	0.21	

¹ Major osteoporotic fractures are defined as adjudicated hip fracture or self-report fracture of lower arm/wrist, spine/back, or upper arm/shoulder. USPSTF denotes United States Preventive Services Task Force; CAROC denotes Canadian Association of Radiologists and Osteoporosis Canada; NOF denotes National Osteoporosis Foundation; AUC denotes area under the receiver operating characteristic curve.

Disclosures: **Carolyn Crandall**, None

1025

Screening of high fracture risk in primary care not effective Thomas Merlijn^{*1}, Karin Swart¹, Coen Netelenbos², Petra Elders¹. ¹Department of General Practice and Elderly Care Medicine, VU University Medical Center, Netherlands, ²Department of Internal Medicine, Endocrine Section, VU University Medical Center, Netherlands

Objective: To study whether screening of fracture risk and subsequent treatment of older women in primary care can reduce osteoporotic fractures, in comparison to usual care. **Method:** In the SALT Osteoporosis Study (SOS), a pragmatic randomized trial in women 65-90 years we compared a fracture risk screening program and subsequent treatment with usual care. All women in 224 GP practices in the Netherlands received a questionnaire to assess clinical risk factors for fractures. We randomized 11,331 women with at least one clinical risk factor for fractures (previous fracture, parental hip fracture, low body weight, secondary causes for osteoporosis). Participants in the intervention group underwent bone densitometry and vertebral fracture assessment. Anti-osteoporotic medication was recommended if the 10-year major osteoporotic fracture probability (FRAX) was above an age dependent threshold. The outcomes were time to first osteoporotic fracture and time to first hip fracture, analyzed with Cox proportional Hazard analysis. Self-reported fractures at 18 and 36 months were verified with the GP or hospital. **Results:** The mean follow up was 3,7 years and was complete in 94% of the participants. We identified 573 osteoporotic fractures and 140 hip fractures in the intervention group (n=5734) and 605 osteoporotic fractures and 146 hip fractures in the control group (n=5597). Screening and subsequent treatment had no effect on time to first fracture (HR=0.91, 95%CI=0.81 to 1.02) nor first hip fracture (HR=0.92, 95%CI=0.73 to 1.17). **Conclusion:** Screening and subsequent treatment of older women with increased fracture risk in primary care has no effect or at most limited effect in reduction of osteoporotic fractures. This finding is in line with the main results of two simultaneous trials (SCOOP and ROSE) however a reduction in hip fractures was not reproduced in our trial. Active screening of increased fracture risk in primary care should not be recommended in guidelines.

Disclosures: **Thomas Merlijn**, None

1026

Identification of Prevalent Vertebral Fracture Increases Utilization of Pharmacologic Fracture Prevention Therapy John Schousboe^{*1}, Lisa Lix², Suzanne Morin³, Sheldon Derkach², Mark Bryanton², Masha Alhrbi², William Leslie². ¹Park Nicollet Clinic & HealthPartners Institute, United States, ²University of Manitoba, Canada, ³McGill University, Canada

Purpose: Many guidelines recommend targeted lateral spine imaging for prevalent vertebral fracture assessment (VFA) to aid in fracture risk assessment and identification of those who may benefit from pharmacotherapy. However, whether the findings of VFA impact use of fracture prevention pharmacotherapy is unknown. Our aim was to estimate the association of vertebral fractures documented on VFA with subsequent prescription of pharmacologic fracture prevention therapy (Rx). **Methods:** Since 2010, in Manitoba (Canada) densitometric VFA imaging has been performed at the time of bone densitometry (BMD), in men and women with a central T-score ≤ -1.5 and one of the following: a) age ≥ 70 years; or b) age ≥ 50 years plus historical height loss > 5 cm, measured height loss > 2.5 cm, or chronic systemic glucocorticoid therapy. Among 6652 treatment naive individuals with at least 90 days follow up and VFA imaging (mean [SD] age 76 [7] years, 92% women), 923 (13.9%) had ≥ 1 definite vertebral fractures (positive VFA) using a modified algorithm-based qual-

tative method. Subsequent osteoporosis Rx initiated within the subsequent 12 months was identified using population-based pharmacy data. Logistic regression models were used to estimate the association of positive VFA with Rx prescription, compared to negative VFA. Results: Osteoporosis Rx was initiated by 1527 (23.6%) individuals (39.1% with positive vs 20.7% with negative VFA, p -value<0.001). Positive VFA was associated with subsequent Rx prescription adjusted for FRAX with BMD (OR 2.37 [95% CI 2.04-2.75]), or adjusted for BMD T-score category at any site (OR 2.38 [95% CI 2.03-2.79]). The association of positive VFA with subsequent Rx was highest in those without osteoporosis by BMD criteria, and in those designated (before VFA results are known) to have low to moderate FRAX fracture risk probability (Table). Conclusion: Identification of prevalent vertebral fracture on VFA increases subsequent prescription of fracture prevention medication, particularly for those not already designated to be at high fracture risk or who do not have osteoporotic BMD T-scores. Even amongst those with high fracture risk or osteoporotic BMD T-score, documentation of prevalent vertebral fracture modestly increases prescription of osteoporosis medication. Targeted VFA imaging at the time of BMD can improve identification of those at high risk of fracture for whom fracture prevention therapy is indicated.

Table: Association of Positive vs Negative VFA with Subsequent Rx Prescription, OR (95% CI)

FRAX 10-Year Major Osteoporotic Fracture Risk Category*			WHO BMD T-Score Category ^a	
<10%	10% to 20%	>20%	Osteopenia	Osteoporosis
4.18 (2.84, 6.16)	2.99 (2.43, 3.66)	1.44 (1.14, 1.83)	4.51 (3.48, 5.85)	1.72 (1.43, 2.08)

* p -value<0.001 for interaction between positive VFA and MOF 10-year risk

^a p -value<0.001 for interaction between positive VFA and BMD T-Score Category (based on worst T-score among lumbar spine, total hip, and femoral neck)

Disclosures: John Schousboe, None

1027

The role of apolipoprotein E in fracture healing and osteoblast differentiation

Xiaohua Zong^{*1}, Puvindran Nadesan², James White³, Phillip White³, Gurpreet Baht⁴. ¹Department of Orthopaedic Surgery, Duke Molecular Physiology Institute, Duke University, United States, ²Department of Orthopaedic Surgery, Duke University, United States, ³Department of Medicine, Duke Molecular Physiology Institute, Duke University, United States, ⁴Department of Orthopaedic Surgery, Department of Pathology, Duke Molecular Physiology Institute, Duke University, United States

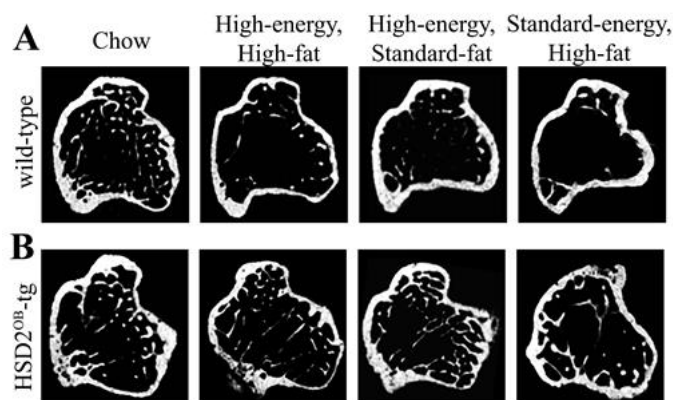
Apolipoprotein E (ApoE) is an extracellular matrix protein involved in the transport of fatty acids. Recent studies link ApoE polymorphisms, found in 20% of the population, to an increased incidence of hip and vertebral fractures and ApoE knockout mice (ApoE^{-/-}) display increased bone mineral density. However, little is known about the function or the mechanism of action of ApoE in bone. Wildtype (WT) and ApoE^{-/-} mice underwent tibial fracture surgery; fracture calluses were assessed for healing at 7-, 14-, and 21-days post injury. μ CT and histological analysis revealed that in ApoE^{-/-} mice fracture calluses contained 50% more bone and deposited tissue was 35% denser than in WT controls. Osteoblast (Ob) differentiation was assessed by measuring colony-forming-units from bone marrow aspirates of unfractured mice. Cultures from ApoE^{-/-} mice contained 40% less progenitor cells; however, Ob differentiation and Ob activity were both doubled in response to loss of ApoE expression. Transcripts for osteogenic markers (Col1, Bsp, Alp) were elevated in Ob cultures from ApoE^{-/-} mice. Conversely, treatment of cultures with exogenous rApoE decreased osteoblast differentiation, mineral formation, and the level of osteogenic transcripts. Due to ApoE's association with lipid metabolism, we investigated the transcript levels of genes involved in fatty acid oxidation and glycolysis. During Ob differentiation in ApoE^{-/-} mice, fatty acid oxidation transcripts were unaltered; however, genes involved in glycolysis were significantly upregulated. Metabolic flux analysis revealed increased glycolytic rate and increased uptake of radio-labeled glucose in ApoE^{-/-} Ob's. Furthermore, transcript and protein levels of glucose transporter 1 (Glut1) were higher in cultured Ob's from ApoE^{-/-} mice. This finding was recapitulated in vivo: immunohistochemistry of fracture calluses from WT and ApoE^{-/-} mice revealed elevated levels of Glut1 expression in ApoE^{-/-} Ob's. Finally, differentiation of ApoE^{-/-} Ob's was more sensitive to glycolytic inhibition than differentiation of WT Ob's and the enhanced fracture healing observed in ApoE^{-/-} mice was ameliorated by high fat diet. These data confirm a negative role for ApoE in bone fracture healing and Ob differentiation. Specifically, loss of ApoE serves to elevate glycolysis within Ob's and subsequently differentiation. This identifies ApoE as a novel target for therapeutic intervention to improve fracture healing or osseous integration of implants.

Disclosures: Xiaohua Zong, None

1028

Osteoblasts Mediate the Adverse Effects of High-fat Diets on Bone and Fat Metabolism Through Glucocorticoid Signalling Sarah Kim*, Holger Henneicke, Sylvia J. Gasparini, Lee Thai, Markus J. Seibel, Hong Zhou. Bone Research Program, ANZAC Research Institute, The University of Sydney, Australia

Overconsumption of energy-dense diets is a major public health challenge due its causal association with obesity, diabetes and poor skeletal health. Most animal studies examining diet-induced obesity and diabetes have focused solely on combined high-energy, high-fat diets. We therefore aimed to define whether the adverse health outcomes are due to the high energy density or high fat content of these diets. Since osteoblasts co-regulate overall energy balance under the control of glucocorticoids, we also examined whether abrogating glucocorticoid signalling in osteoblasts and osteocytes protects mice from diet-induced metabolic and skeletal disturbances. We utilised transgenic (tg) mice in which glucocorticoid signalling has been disrupted in osteoblasts and osteocytes via targeted overexpression of the glucocorticoid-inactivating enzyme, 11 β -hydroxysteroid dehydrogenase type 2 ('HSD2OB-tg' mice). Seven-week-old male tg mice and their wild-type (WT) littermates were fed ad libitum for 18-weeks one of the following diets: High-energy, standard-fat (fat=14% total-energy, 16.3kJ/g); high-energy, high-fat (fat=43% total-energy, 16.3kJ/g); standard-energy, high-fat (fat=43% total-energy, 13.8kJ/g) or standard-chow (fat=14% total-energy, 13.8kJ/g). At endpoint, body composition, serum lipids, glucose handling and bone mass were measured. High-energy feeding, regardless of dietary fat content resulted in significantly increased fat mass in WT mice compared to WT chow-fed mice along with hyperlipidaemia, fasting hyperglycaemia and reduced insulin sensitivity. Both high-energy diets induced significant tibial trabecular and cortical volume loss to a similar extent. WT mice on the standard-energy, high-fat diet remained lean and insulin sensitive but displayed pronounced trabecular and cortical bone loss (Fig.1A). Notably, HSD2OB-tg mice were protected from high-energy diet-induced excessive fat accrual, hyperlipidaemia, insulin resistance, glucose intolerance and bone loss (Fig.1B), despite consuming the same amount as their WT littermates on either high-energy or standard-energy, high-fat diet. We conclude that high energy density rather than high fat content induces metabolic dysfunction in male mice, whereas high dietary fat results in bone loss. Both effects are mediated by glucocorticoid signalling in osteoblasts and osteocytes.



Disclosures: Sarah Kim, None

1029

Bone marrow adipose tissue: white, brown or beige? Hero Robles*¹, Madelyn Lorenz¹, Eric Hilker¹, Kristann Magee¹, Jesse D Procknow¹, Zhaohua Wang¹, Charles A Harris², Clarissa S Craft¹, Erica L Scheller¹. ¹Department of Internal Medicine, Division of Bone and Mineral Diseases, Washington University, United States, ²Department of Internal Medicine, Division of Endocrinology, Metabolism and Lipid Research, Washington University, United States

Adipocytes within the skeleton, collectively known as bone marrow adipose tissue (BMAT), make up approximately 60-70% of bone marrow and 8% of total fat mass in the average adult human. Recent studies have shown that BMAT has the ability to contribute significantly to both peripheral and local metabolism. However, its characterization as a white, brown, or beige adipocyte remains controversial. To clarify this point, we first examined the ultrastructural nature of BMAT using three dimensional electron microscopy (3D-EM). Reconstruction of the bone marrow niche via 3D-EM demonstrated that BMAT has an extensive mitochondrial network interspersed around and between multiple lipid droplets (Fig.1A). We also found that CL316,243 was capable of inducing lipid droplet remodeling in a subset of mouse bone marrow adipocytes in vivo; suggesting that BMAT has a distinctive phenotype which, like beige and brown adipocytes, may undergo adrenergic-induced remodeling and potentially thermogenesis. To address this, we developed two genetic mouse models. In the first, we used UCP1-Cre to drive diphtheria toxin (DTA) expression and cell death after β 3-agonist stimulation (UCP1Cre+/DTA+). This facilitates a quantitative, region-specific analysis of induced UCP1 expression in BMAT and WAT. In the second,

UCP1-Cre mice were crossed with mTmG reporter mice (UCP1Cre+/mTmG+) to allow visualization of UCP1 expressing cells in intact tissues by monitoring GFP expression. As expected, CL316,243 treatment was associated with depletion of inguinal beige adipocytes in adult UCP1Cre+/DTA+ mice and regions of GFP expression in UCP1Cre+/mTmG+ mice. However, despite the extensive mitochondrial network observed with 3D-EM and lipid droplet remodeling after CL316,243, we did not observe loss of BMAT beyond that of control animals in the UCP1Cre+/DTA+ model of induced cell death. Similarly, UCP1-induced conversion of the mTmG transgene did not occur in the BMAT. Our data suggests that BMAT adipocytes are capable of induced lipid droplet remodeling, however, they are not true UCP1-expressing beige or brown adipocytes. This supports a paradigm by which BMAT adipocytes are a unique subpopulation which, based on our EM analyses, is likely specialized to support cells within the skeletal and hematopoietic niche (Fig.1B).

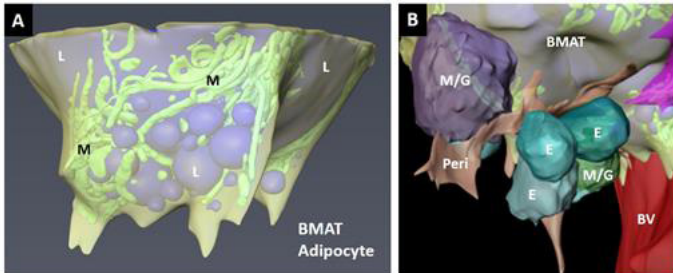


Figure 1. Ultrastructural morphology of the bone marrow adipose tissue (BMAT) niche. (A) BMAT adipocyte from the mouse proximal tibia with small lipid droplets around a large lipid globule (L, blue) which are enmeshed by an extensive mitochondrial network (M, green). Cytoplasm in yellow. **(B)** The BMAT adipocyte adheres to a sinusoidal blood vessel (BV, red) and interfaces directly with cells of the niche including pericytes (peri, tan and pink), myeloid/granulocyte lineage cells (M/G, purple and green) and erythroblasts (E).

Disclosures: **Hero Robles, None**

1030

Lrp4 expression by adipocytes and osteoblasts modulates endocrine actions of sclerostin Soohyun Kim^{*1}, Hao Da¹, Priyanka Kushwaha¹, Zhu Li¹, Thomas Clemens², Ryan Riddle². ¹Johns Hopkins University School of Medicine, United States, ²Johns Hopkins University School of Medicine, Baltimore VA Medical Center, United States

Sclerostin exerts profound local control over bone acquisition and also mediates endocrine communication between fat and bone by regulating Wnt signaling in adipocytes. Consequently, *Sost*^{-/-} mice exhibit a marked decrease in body fat mass as well as the expected increase in bone volume. In the osteoblast, sclerostin's anti-anabolic activity is enhanced by *Lrp4*, which facilitates its interaction with *Lrp5/6*. To determine if *Lrp4* similarly affects sclerostin's endocrine functions, we specifically disrupted *Lrp4* expression in adipocytes and osteoblasts by crossing *Lrp4loxP/loxP* mice with *adipoQ-Cre* (*AdΔLrp4*) or *Ocn-Cre* (*ObΔLrp4*) mice. In vitro, *Lrp4* expression parallels triglyceride deposition in adipocytes and coincides with the ability of sclerostin to enhance fatty acid synthesis. Loss of *Lrp4* function in the adipocyte mirrored the effect of sclerostin-deficiency on whole-body metabolism, as *AdΔLrp4* mice exhibited a reduction in adipocyte hypertrophy and improvements in glucose and lipid homeostasis, including increased glucose and insulin tolerance and reduced serum fatty acids when compared to littermate controls. Intriguingly, loss of *Lrp4* function in the osteoblast, which increases *Sost* expression and the circulating levels of sclerostin, produced the opposite effect. When compared to controls, *ObΔLrp4* mice exhibited significant increases in whole body fat mass and impaired glucose tolerance and insulin sensitivity, despite the development of a high bone mass phenotype. Taken together these data indicate the expression of *Lrp4* by both the adipocyte and osteoblast is required for normal sclerostin endocrine function. Additionally, they suggest that the impact of sclerostin on adipocyte physiology is distinct from its anti-anabolic effect on osteoblast function.

Disclosures: **Soohyun Kim, None**

1031

Maternal Obesity-Mediated Epigenetic Regulation of Osteoblast Differentiation through SATB2 Jin-Ran Chen^{*}, Haijun Zhao, Oxana P. Lazarenko, Kartik Shankar. Arkansas Children's Nutrition Center and the Department of Pediatrics, University of Arkansas for Medical Sciences, United States

Nutritional status during intrauterine and/or early postnatal life has substantial influences on adult offspring health, mostly linked with permanent metabolic changes. However, evidence on the impact of high fat diet (HFD)-induced maternal obesity on regulation of fetal bone development is sparse. Thus, we investigated the effects of maternal obesity in rodents on both fetal skeletal development and epigenetic regulation of osteoblast differentiation in offspring. First, female Sprague-Dawley rats were fed either a low-fat AIN-93G control diet or a high fat diet (HFD) (45% fat calories) for 10 wks starting at 6 wks of age.

After 10 wks of these diets, lean (from control diet) and obese (from HFD) female rats were time-impregnated (n=6 per group) by control diet male rats. At gestational day 18.5 (E18.5), all fetuses were taken and embryonic osteogenic calvarial cells (EOCCs) were isolated. We found epigenetic regulation of polycomb-regulated gene *Ezh2* (Enhancer of zeste homolog 2) in embryonic rat from HFD obese dams. Increased enrichment of repressive histone mark H3K27me3 on the gene body of *SATB2* (ChIP Seq analysis) was associated with aberrant differentiation of EOCCs to mature osteoblasts. Knocking down *Ezh2* in EOCCs and ST2 cells increased *SATB2* expression, on the other hand, *Ezh2* overexpression in EOCCs and ST2 cells decreased *SATB2* expression. These data were consistent with ChIP experimental results showed strong association between H3K27me3, *Ezh2* and *SATB2*. Second, we generated pre-osteoblastic cell specific *Ezh2* conditional knockout mouse model by breeding *Ezh2 flox/flox* and *Osterix-Cre+* mice. In 6-week-old mice, we found significantly increased *SATB2* mRNA and protein expression in bone from *Ezh2flox/flox Osterix-Cre+* conditional knockout mice compared with those from *Ezh2flox/+Cre+*, *Cre+*, *Ezh2flox/flox Cre-*, *Ezh2flox/+Cre-* and wild type mice. These findings indicate maternal HFD-induced obesity-associated decreasing of fetal pre-osteoblastic cell differentiation is under epigenetic control through *SATB2* expression. Supported by USDA-ARS Project #6026-51000-010-05S.

Disclosures: **Jin-Ran Chen, None**

1032

Cellular Senescence in Tendon Aging and Pathology Anne Gingery^{*}, Tamara Tchkonkia, James C Kirkland, Peter C Amadio. Mayo Clinic, United States

Tendons and ligaments are responsible for the integrity and mobility of the musculoskeletal system. Tendon injuries are slow to repair as compared to other musculoskeletal tissues, and the failure to repair tendon damage that occurs with age, overuse, and injury is a significant clinical musculoskeletal challenge. Senescent cells, which are defined as cells growth arrested in response to stress (e.g., telomere shortening, reactive oxygen species, mechanical stress), play an important role in wound healing; however, it has recently been noted that these cells accumulate with age in many tissues and failure to clear these cells contributes to the pathology of age-related diseases. Senescent cells can exhibit a senescence-associated secretory phenotype (SASP) that is thought to mediate disease pathology. Recent work in our tendinopathy model revealed a senescence signature. Further, the incidence of tendinopathy increases with age. Therefore, we tested the hypothesis that senescent cell accumulation contributes to age and injury related tendon pathologies. To test our hypothesis we utilized both mouse models of tendon aging and a rat chronic tendinopathy model (collagenase-induced). Several markers of cellular senescence, including histological marker - senescence associated beta-galactosidase (SABG), gene expression markers p16, p53, as well as SASP factors such as TGF- β , PAI-1, and IGF-1 increased with age. Ablation of p16ink4a positive senescent cells using mice expressing the INK-ATTAC "suicide" transgene or by targeting with senolytics such as dasatinib +quercetin (DQ) reduced markers of senescence, as well as fibrotic markers, in aged (23-24 months) mouse tendons as compared to young tendons (4 months). Furthermore in a chronic Achilles tendinopathy model we found increased expression of SABG, p16, TGF- β , Col3, as well as dysregulation of check point genes indicating that cellular senescence may play a causal role in chronic tendon pathologies. Collectively these data demonstrate that cellular senescence plays a role in tendon aging and in chronic tendinopathy. Furthermore, this work establishes that targeting cellular senescence may provide a novel and much needed therapeutic target for tendon pathologies.

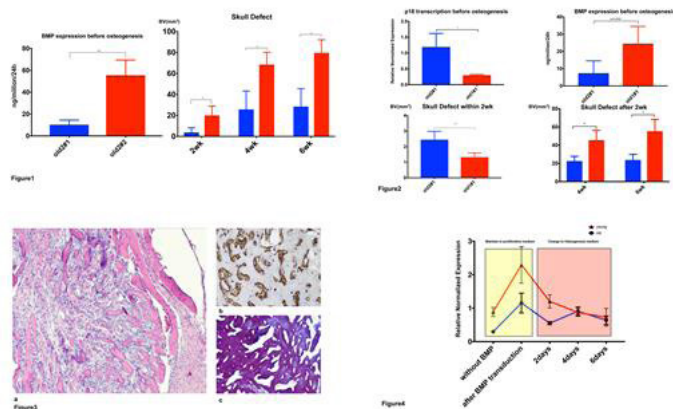
Disclosures: **Anne Gingery, None**

1033

p18 is required and regulated by BMP4 in Muscle-Derived Stem Cell-mediated Osteogenesis and Bone Regeneration during aging Haizi Cheng^{*1,2}, Xueqin Gao¹, Aiping Lu¹, Johnny Huard¹. ¹The University of Texas Health Science Center at Houston, Houston, TX; Steadman Philippon Research Institute, Vail, CO, United States, ²University of Pittsburgh, Pittsburgh, PA, United States

INTRODUCTION: Bone morphogenetic protein 4 (BMP4) induces bone formation by muscle-derived stem cells (MDSCs), and promotes stem cell self-renewal. The cyclin-dependent kinase inhibitors p16INK4A (p16) and p18INK4C (p18) cause early G1-phase cell cycle blockade by targeting cyclin-dependent kinase (CDK) 4/6. It is unclear if p18 correlates directly or inversely with p16 in natural aging. We found that aged MDSC exhibit weakened proliferation and attenuated multi-lineage differentiation potential, but can regenerate bone in a critical-sized skull defect in 6-week-old CD-1 nude mice after transduction with BMP4/green fluorescent protein retrovirus (retro-BMP4/GFP). **METHODS:** Young (3-week-old) and aged (2-year-old) MDSCs, isolated by a modified preplate technique, were transduced with retro-BMP4/GFP. FACS was performed for GFP; BMP4 was quantified by ELISA. MDSCs were then transplanted in a critical-sized calvarial bone defect model using fibrin sealant in CD-1 nude mice. In vivo bone regeneration was measured by microCT bi-weekly for 6 weeks. Gene expression was quantitated by qRT-PCR. Statistical analysis was by unpaired or multiple t-test. **RESULTS:** BMP4-transduced aged MDSCs, when transplanted into the skull defect in CD-1 nude mice, showed significantly improved osteogenesis (Fig. 1); Increased p18 transcription, even with low BMP4 expression, caused aged MDSCs to regenerate more bone in the first 2 weeks; thereafter, more BMP4 induced more bone (Fig. 2). H&E staining demonstrated functional bone formation in the defect area (Fig. 3a). GFP staining confirmed that the newly generated bone was derived from the transplanted BMP4/GFP MDSCs (Fig. 3b). Herovici's staining showed major bone matrix collagen type

I formation in aged MDSCs (Fig. 3c). p18 was temporarily upregulated after BMP4 transduction and before osteogenesis. **DISCUSSION:** BMP4 transduction improved osteogenesis by old MDSCs in vivo. BMP4 transduction in aged MDSCs caused p18 upregulation and p21 and p16 downregulation, conferring characteristics of young MDSCs. p18 and p16 may have compensatory effects, as either can cause cell cycle G1 arrest. BMP4 transduction may result in a transition between p16 and p18. Therefore, regulating the p18:16 ratio using growth factors such as BMP4 could reverse aged stem cells from senescence to quiescence, conditionally increasing the stemness of aging stem cells.



Disclosures: *Haizi Cheng, None*

1034

Male-Female Spatio-Temporal Differences of Age-Related Bone Loss

Julio Carballido-Gamio^{1*}, Elisa A Marques², Sigurdur Sigurdsson³, Kristín Siggeirsdóttir³, Alexandria Jensen^{1,4}, Gunnar Sigurdsson^{3,5,6}, Thor Aspelund^{3,7}, Gudny Eiriksdóttir³, Vilmundur Gudnason^{3,5}, Thomas F Lang⁸, Tamara B Harris². ¹Department of Radiology, School of Medicine, University of Colorado Denver, Denver, CO, United States, ²National Institute on Aging, Intramural Research Program, Laboratory of Epidemiology and Population Sciences, Bethesda, MD, United States, ³Icelandic Heart Association Research Institute, Kópavogur, Iceland, ⁴Department of Biostatistics & Informatics, Colorado School of Public Health, Aurora, CO, United States, ⁵University of Iceland, Reykjavik, Iceland, ⁶Landspítalinn University Hospital, Reykjavik, Iceland, ⁷Centre of Public Health Sciences, University of Iceland, Reykjavik, Iceland, ⁸Department of Radiology and Biomedical Imaging, University of California, San Francisco, CA, United States

Normal aging leads to bone loss, and older women lose bone at a faster rate than men. The spatial distribution of bone loss in the proximal femur is mostly unknown. The objective of this work was to assess the spatio-temporal distribution of the deterioration of bone in older men and women with aging. A better understanding of how age-related loss might affect the fracture-prone regions of the hip could lead to more informed fracture-prevention strategies. A subset of 305 men (74.9±4.8 yr) and 371 age-matched women (74.8±4.7 yr) with no history of fracture were randomly selected from the Age, Gene/Environment Susceptibility-Reykjavik Study (Sigurdsson-2006, Harris-2007). QCT scans of the left proximal femur obtained at baseline and at 5.2±0.4 years follow-up were automatically processed (Carballido-Gamio-2015) to assess local changes in volumetric bone mineral density (vBMD), cortical bone thickness, cortical vBMD, vBMD in a layer adjacent to the endosteal surface, and structure in men and women, as well as sex differences using voxel-based morphometry (VBM) (Ashburner-2000, Carballido-Gamio-2013a), surface-based statistical parametric mapping (SPM) (Friston-1994, Carballido-Gamio-2015), and tensor-based morphometry (TBM) (Davatzikos-1996, Carballido-Gamio-2013b). The statistical assessments of local parametric changes were performed using linear mixed effects models allowing for baseline and time-varying covariates, yielding Student's t-test statistical maps (t-Maps) that were corrected for multiple comparisons (Genovese-2002). The t-Maps in Fig. 1 summarize the results of this study. Except for minor spatial differences, men and women showed similar spatial bone deterioration (Fig. 1A-E). However, compared to older men, older women showed significant larger: 1) losses of trabecular vBMD in the femoral neck and trochanteric region (Fig. 1F); 2) losses of cortical vBMD laterally and at the inferior-anterior cortex (Fig. 1H); 3) losses of endosteal vBMD in the greater trochanter and inferiorly in the femoral neck (Fig. 1J); 4) contractions of the principal compressive group and cortex (Fig. 1G); and 5) expansions of the trabecular compartment in the greater trochanter (Fig. 1G). Using Computational Anatomy and longitudinal QCT scans, we have shown that older women lose more bone than older men with aging, and that they do it in fracture-prone regions according to previous prospective studies (Carballido-Gamio-2013a-b), providing new information on the pathophysiology of osteoporosis.

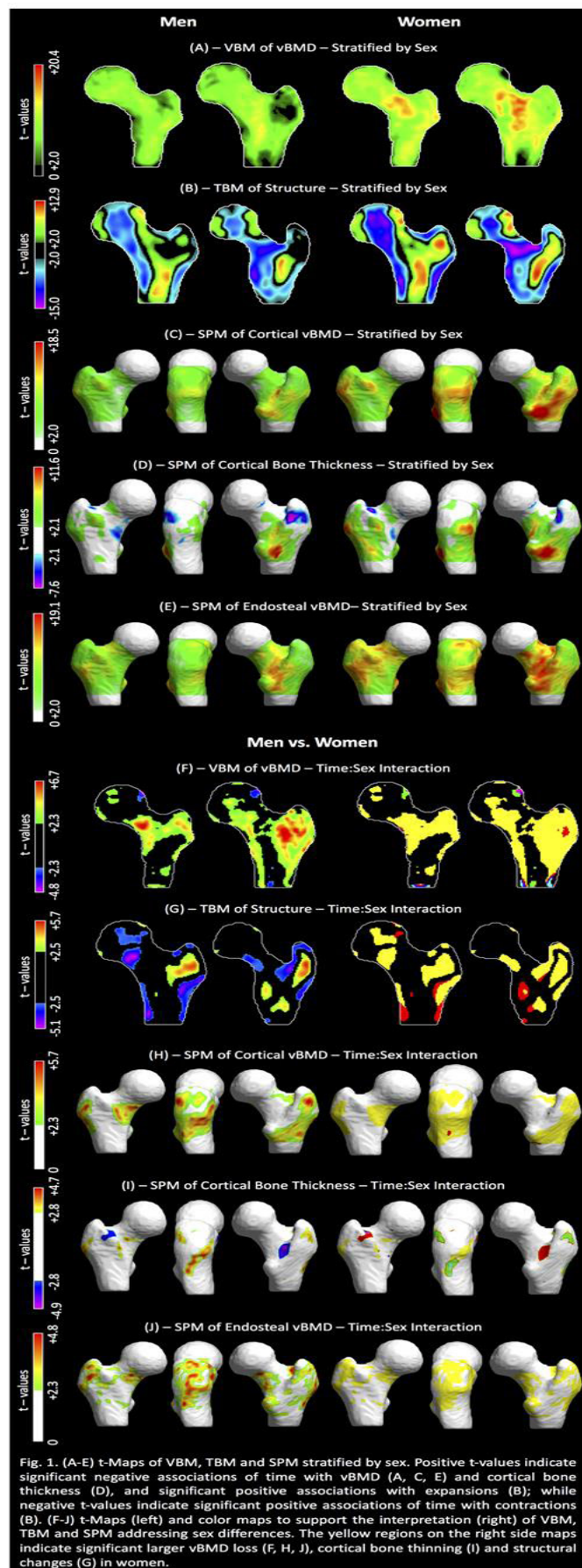


Fig. 1. (A-E) t-Maps of VBM, TBM and SPM stratified by sex. Positive t-values indicate significant negative associations of time with vBMD (A, C, E) and cortical bone thickness (D), and significant positive associations with expansions (B); while negative t-values indicate significant positive associations of time with contractions (B). (F-J) t-Maps (left) and color maps to support the interpretation (right) of VBM, TBM and SPM addressing sex differences. The yellow regions on the right side maps indicate significant larger vBMD loss (F, H, J), cortical bone thinning (I) and structural changes (G) in women.

Disclosures: *Julio Carballido-Gamio, None*

1035

RANKL produced by osteocytes is required for cortical, but not cancellous, bone loss with age Jinhu Xiong*, Keisha Cawley, Ryan Macleod, Maria Almeida, Charles Obrien. University of Arkansas for Medical Sciences, United States

Like humans, mice lose cortical and cancellous bone with advanced age. Previous studies in mice have shown that loss of cortical bone with age is associated with increased osteoclast number at the endocortical surface compared to young adult animals. However, osteoclast number in cancellous bone is reduced in aged mice. These findings suggest that different mechanisms underlie age-associated bone loss in these two skeletal compartments. Osteocytes are an essential source of RANKL for osteoclast formation and recent studies have found that RANKL mRNA is increased in cortical bone of aged mice, suggesting a possible mechanism responsible for the increased endosteal bone resorption. To determine if osteocyte-derived RANKL plays a role in age-associated bone loss, we deleted the RANKL gene using a Dmp1-Cre transgene and compared bones of conditional knockout (CKO) and control (*f/f*) female littermates at 6 and 24 months of age. Serial analysis of bone mineral density (BMD) beginning at 5 months of age showed that control mice maintained stable femoral BMD until 20 months of age, after which it declined. In the spine of control mice, BMD began to decline at 20 months of age. In contrast, BMD in the femur and spine of CKO mice increased until the end of the experiment. MicroCT analysis revealed that femoral cortical thickness in control mice was significantly lower at 24 months compared to 6 months. In contrast, cortical thickness in CKO mice was higher at 24 months than at 6 months. The loss of cortical bone in control mice was due to expansion of the endosteal perimeter with age, which did not occur in CKO mice. Analysis of L4 vertebrae revealed that both genotypes lost cancellous bone volume with age, even though cancellous bone volume was higher in CKO mice compared to controls at both ages. These results demonstrate that RANKL produced by osteocytes is required for the increase in resorption and bone loss that occurs at the endosteal surface in murine long bones. Together with the finding that RANKL mRNA is elevated in cortical bone of aged mice, these results also suggest that the age-associated increase in osteocyte RANKL is a key factor driving cortical bone loss with age. In striking contrast, the loss of cancellous bone with age occurs even in the absence of osteocyte-derived RANKL, demonstrating that different molecular mechanisms underlie the age-associated cellular and structural changes in these two compartments.

Disclosures: **Jinhu Xiong, None**

1036

RANKL+ plasmacytic B and TGFβ+ myeloid cells are attracted to bone marrow during aging by a TRAF3-dependent mechanism to increase bone resorption, decrease bone formation and promote osteoporosis Jinbo Li*, Akram Ayoub, Zhenqiang Yao, Brendan Boyce. University of Rochester Medical Center, United States

Levels of TGFβ1 and RANKL increase in bone marrow (BM) with age and induce lysosomal degradation of TNF receptor-associated factor 3 (TRAF3), a negative regulator of NF-κB signaling, in osteoblast (OB) and osteoclast (OC) precursors, respectively. Mice we generated with TRAF3 conditionally deleted in mesenchymal lineage cells (using Prx-1 Cre) or myeloid cells (using Lys-M Cre) develop accelerated osteoporosis with aging. Low-grade chronic inflammation (LLCI) also induces bone loss during aging; we hypothesize that TGFβ1 and RANKL mediate this loss. We found that BM cells (BMCs) comprise 62±5% of TGFβ1 and 75±7% of RANKL expression in leg bones from 22-m-old mice with significantly higher levels of TGFβ1 (16±3 vs 10±1 ng/ml) and RANKL (644±50 vs 475±19 pg/ml) than in BM from 4-m-old mice. 78% of TGFβ1+ BMCs were CD11b+Ly6GhiLy6C+CCR5+ myeloid cells and 70% of RANKL+ BMCs were B220hiIgM+IgD+CD138+CXCR4+ plasmacytic B cells. The % and absolute # of these cell populations were 2-fold higher in BM from old than young mice. In addition, protein levels of CCL5, a CCR5 ligand, and CXCL12, a CXCR4 ligand, were increased 12- and 16-fold, resp., in BMCs from old than young mice. CCL5 and CXCL12 mRNA levels were 4- and 7-fold higher, resp., in CD45-mesenchymal cells from BM from old mice, but not in CD45+ hematopoietic cells. Of note, mice with TRAF3 conditionally deleted in mesenchymal lineage cells, but not in myeloid cells, had elevated CCL5 and CXCL12 expression, increased BM RANKL+ plasmacytic B and TGFβ1+ myeloid cells, enhanced OC formation and reduced OB differentiation, similar to changes detected in old WT mice. Consistent with these findings, old WT mice treated with the FDA-approved drugs, Plerixafor (P), a CXCR4 antagonist, or Maraviroc (M), a CCR5 antagonist, had significantly reduced absolute #s of plasmacytic B cells (by 59% for P) and myeloid cells (by 49% for P; 57% for M) in BM, and increased vertebral trabecular bone mass (BV/TV: 17±4% for P, 15±4% for M vs 12±2% in Ctrl). Our findings suggest that RANKL+ plasmacytic B cells and TGFβ1+ myeloid cells are attracted to BM in response to increased CXCL12 and CCL5 expressed by mesenchymal cells deficient in TRAF3 either genetically or during aging to promote LLCI-mediated bone loss. Plerixafor and Maraviroc are potential new therapies for osteoporosis that could inhibit bone resorption and enhance bone formation by keeping these RANKL- and TGFβ-expressing cells in blood and away from BM.

Disclosures: **Jinbo Li, None**

1037

Investigating the influence of adult hip shape genetic variants across the life course: findings from a population-based study in adolescents Monika Frysz*^{1,2}, Denis Baird², Jenny Gregory³, Richard Aspden³, Jonathan Tobias⁴, Lavinia Paternoster (Cox)^{1,2}. ¹Population Health Sciences, Bristol Medical School, University of Bristol, United Kingdom, ²MRC Integrative Epidemiology Unit at the University of Bristol, United Kingdom, ³Institute of Medical Science, School of Medicine, Medical Sciences & Nutrition, Aberdeen, United Kingdom, ⁴Musculoskeletal Research Unit, Bristol Medical School, University of Bristol, United Kingdom

Hip shape is a well-recognized risk factor for both hip osteoarthritis (OA) and hip fracture. Recent genome-wide association meta-analysis identified nine loci associated with hip shape in adults (mean age 62, range 48 -74 years), however it is unclear whether the same genetic variants affect hip shape across the life course. In the present study, we investigated the relationship between adult loci and hip shape in adolescents. Hip DXA scans were obtained in offspring from the Avon Longitudinal Study of Parents and Children, at mean ages of 13.8 and 17.8 years. To quantify hip morphology, each image was analysed in Shape software based on a 53-point Statistical Shape Model (SSM). Principal component analysis was used to generate 10 linearly independent modes of variation (hip shape modes (HSMs) using the same model as a previous adult study). Genetic variants which had previously shown genome-wide significant association with specific HSM(s) in adults were tested for association with the same HSM at the two adolescent time points using SNPTTEST (18 tests in total). Complete genotypic and phenotypic data were available from 3550 and 3175 individuals at mean ages of 13.8 and 17.8 years respectively. There was evidence to suggest all genetic variants tested were associated with the relevant HSMs measured in adolescence (Table 1). The directions of effects were consistent with those of adults, although adolescent effect sizes were generally smaller. The strongest evidence was for two variants located near SOX9 (rs2158915 and rs2160442) with consistent effects across both adolescent time points for HSM1 and HSM5, which both capture femoral neck width (FNW). There was also strong evidence of association between rs10743612 (near PTHLH) and HSM1 and between rs6537291 (near HHIP) and HSM2 across both time points. HSM1 scores capture femoral head curvature, whereas both HSM1 and HSM2 capture FNW along with variation in greater and lesser trochanters. The genes implicated by the strongest associations with hip shape in adolescents, namely SOX9, PTHLH and HHIP are known to be involved in endochondral bone formation. In conclusion, variants implicated in endochondral bone formation appear to consistently influence hip shape across the life course, including aspects of hip shape related to risk of hip OA and/or fracture in later life.

Table 1 Genetic associations between genetic variants (previously identified in adult genome-wide meta-analysis) and hip shape in ALSPAC adolescents

HSM	SNP	Locus	Adult meta-analysis N=15,934		Age 14 GWAS N=3,550		Age 18 GWAS N=3,175	
			BETA	P	BETA ¹	P	BETA ²	P
1	rs2158915	SOX9	-0.13	8.47x10 ⁻²⁷	-0.05	9.94x10 ⁻⁸	-0.05	3.25x10 ⁻⁴
1	rs1243579	GSC	0.12	2.85x10 ⁻¹⁴	0.03	0.01	0.02	0.086
1	rs10743612	KLHL42-PTHLH	0.09	2.91x10 ⁻¹²	0.05	1.13x10 ⁻⁵	0.04	0.003
1	rs73197346	RUNX1	-0.11	2.52x10 ⁻¹⁰	-0.05	2.38x10 ⁻⁴	-0.03	0.026
1	rs59341143	NKX3-2	0.098	6.53x10 ⁻¹⁰	0.02	0.102	0.02	0.093
2	rs1966265	FGFR4	0.13	3.73x10 ⁻²⁰	0.05	0.018	0.07	0.003
2	rs6537291	HHIP	-0.07	1.01x10 ⁻⁹	-0.06	0.001	-0.07	0.001
2	rs1885245	ASTN2	0.07	4.95x10 ⁻⁹	0.04	0.019	0.01	0.545
5	rs2160442	SOX9	-0.09	5.18x10 ⁻¹⁴	-0.07	1.36x10 ⁻⁴	-0.10	2.83x10 ⁻⁸

Abbreviations: HSM – Hip shape mode, SNP – Single nucleotide polymorphism, P – P value

¹Results from hip shape GWAS in ALSPAC adolescents (age 14), adjusted for age and gender

²Results from hip shape GWAS in ALSPAC adolescents (age 18), adjusted for age and gender
0.05 a threshold corrected for 18 tests=0.003

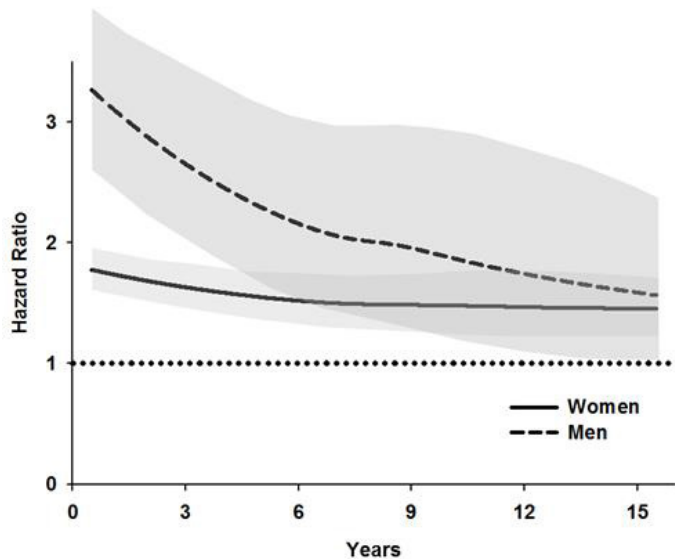
Disclosures: **Monika Frysz, None**

1038

Changes in the Risk of Subsequent Major Osteoporotic Fractures over Time in Men and Women: A Population-Based Observational Study with 25-year Follow Up Suzanne N Morin*¹, Lin Yan², Lisa M Lix², William D Leslie². ¹McGill University, Canada, ²University of Manitoba, Canada

PURPOSE: The risk of subsequent major osteoporotic fractures (MOF: hip, spine, forearm and humerus) following an index fracture is elevated but declines over time. Our aim was to study changes in the risk of subsequent fracture over time, in men and women, to inform the timing of implementation of intensive anti-fracture strategies. **METHODS:** Using the Province of Manitoba (Canada) linked administrative healthcare databases, we performed a matched historical cohort study in 17,721 men and 57,783 women ≥ 50 y who sustained an index MOF during 1989-2006. Rates of subsequent MOF until 2016 were compared with those of age- and sex-matched controls (n=165,965), allowing for at least 10 y and up to 25 y of follow up. Annual crude rates and cumulative incidence for subsequent fractures were estimated, accounting for competing mortality, stratified by sex and age. Hazard ratios (HR) with 95% Confidence Intervals (CI) for subsequent MOF (cases vs. controls) were estimated from Cox proportional hazard models for each of the first 15 y of follow up with a final category for ≥ 15 y, stratified by sex. **RESULTS:** We identified 29,694 index MOF cases (11,028

wrist; 9313 hip; 5799 humerus; 3554 spine). The annual crude rate of subsequent MOF per 1000 person-years among cases was 18.5 (95% CI:17.3-19.8) in men and 29.6 (95% CI: 28.28-30.4) in women. Rate ratios across all follow up years were 2.5 (95% CI 2.3-2.7) in men and 1.6 (95% CI 1.6-1.7) in women compared to controls. The cumulative incidence of subsequent MOF to 25 y was higher in cases vs controls for both sexes and across all age categories except >80 y where this relationship reversed due to competing mortality. HRs for subsequent MOF were higher in men than women, particularly in the first year following the index fracture (HR 3.3, 95% CI 2.6-4.1 in men; HR 1.8, 95% CI 1.7-2.0 in women), and remained very high for men during the first 3 y of follow up. Risk declined over time but remained elevated even ≥ 15 y after the index fracture (HR 1.8, 95% CI 1.4-2.4 in men; 1.5, 95% CI 1.3-1.6 in women). (Figure)CONCLUSIONS: The risk of subsequent MOF was elevated in both sexes over 25 y of follow up with time-dependent attenuation that was most evident in men. The risk of subsequent MOF was higher in men than women, particularly in the first 3 y. These results underscore the importance of timely recognition of fracture events, especially in men, a population in whom secondary prevention is vastly under-implemented.



Disclosures: Suzanne N Morin, None

1039

Advanced glycation endproduct content is increased in cortical bone of the femoral neck in men with type 2 diabetes mellitus Pablo Palomino^{*1}, Heather Hunt¹, Eric Marty², Rehan Saiyed², Matthew Cohn², Joseph Lane², Robert Ritchie³, Bernd Gludovatz², Eve Donnelly¹. ¹Cornell University, United States, ²Hospital for Special Surgery, United States, ³University of California, Berkeley, United States, ⁴UNSW, Australia

Patients with type 2 diabetes mellitus (T2DM) have a greater fracture risk than non-diabetic patients despite having normal to high bone mineral densities. Bone quality in T2DM may be impaired by accelerated accumulation of advanced glycation endproducts (AGEs) due to hyperglycemia. However, the influence of AGEs on bone fragility in vivo is poorly understood. Our objective was to relate bone tissue AGE content, microscale fracture properties, and microscale morphology in cortical bone from patients with and without T2DM. Under IRB approval, femoral neck specimens were retrieved from men undergoing total hip arthroplasty for osteoarthritis. Glycated hemoglobin (HbA1c) was measured pre-operatively. Notched beams (1x1x10mm) were excised from the medial cortex and allocated to two groups based on T2DM diagnosis at time of surgery: type 2 diabetic (T2DM, n=33, age=64.5±8.5y, HbA1c=6.9±0.8%), and non-diabetic (Non-DM, n=32, age=60.3±9.6y, HbA1c=5.5±0.3%). Three-point bending in a variable-pressure SEM was performed on a randomly selected subset of samples (Table 1) to assess initiation toughness and propagation toughness (R-curve slope). After testing, micro-computed tomography (voxel ~3.38µm³) was used to assess crack deflection (tortuosity) and cortical morphometric parameters. Adjacent bone tissue of the full set of samples was homogenized for fluorescence spectrometry to assess total fluorescent AGE content (fAGEs). Statistical analyses were adjusted for patient age. Fluorescent AGE content was 19% higher in T2DM vs. Non-DM bone (p = 0.05) but was not correlated with pre-operative HbA1c. Initiation and propagation toughness, crack tortuosity, and cortical morphometric parameters were similar across groups. Initiation toughness was negatively correlated with fAGEs (R² = 0.13, p = 0.03). When cortical bone fAGEs were compared across patient groups, AGE content was higher in the T2DM group, reflecting increased glycation of the collagen matrix with dysregulated glucose metabolism. In addition, our work demonstrates a common inverse relationship between fAGEs and crack initiation toughness in men with and without T2DM, consistent with prior work that establishes a role for AGEs in bone embrittlement in non-diabetic bone. Because T2DM is associated with an increase in fAGEs, further analyses are required to discern whether these biochemical changes contribute to the greater hip fracture risk with T2DM observed clinically.

Characteristic	T2 Diabetic	Non-diabetic	% Difference vs. non-DM	p
Age				
Full Cohort (T2DM: n = 33, Non-DM: n = 32)	64.5 ± 8.5	60.3 ± 9.6	6.73	0.07
Mechanically Tested (T2DM: n = 19, Non-DM: n = 20)	64.0 ± 8.8	60.9 ± 8.8	4.96	0.52
Micro-CT Scanned (T2DM: n = 14, Non-DM: n = 13)	65.6 ± 9.3	59.8 ± 10.1	9.3	0.23
HbA1c (%)				
Full Cohort	6.9 ± 0.8	5.5 ± 0.3	22.6	<< 0.001
Mechanically Tested	6.7 ± 0.7	5.4 ± 0.3	21.5	<< 0.001
Micro-CT Scanned	6.8 ± 0.8	5.5 ± 0.3	21.1	<< 0.001
BMI (kg/m²)				
Full Cohort	32.1 ± 5.4	30.3 ± 6.4	5.77	0.09
Mechanically Tested	32.1 ± 4.8	29.6 ± 5.3	8.10	0.10
Micro-CT Scanned	32.8 ± 5.0	29.5 ± 4.9	10.6	0.11
Total Fluorescent AGEs (ng quinine/mg collagen)				
Full Cohort (T2DM: n = 32, Non-DM: n = 30)	61.0 ± 23.5	50.3 ± 19.1	19.2	0.05
Mechanically Tested (T2DM: n = 19, Non-DM: n = 19)	56.3 ± 23.8	51.5 ± 16.9	8.91	0.49
Micro-CT Scanned	59.6 ± 25.3	48.3 ± 14.4	20.9	0.17
Porosity (%)				
Micro-CT Scanned	13.1 ± 3.7	12.8 ± 2.8	2.32	0.78
Haversian Canal Diameter (µm)				
Micro-CT Scanned	59.3 ± 11.8	59.4 ± 10.9	0.17	0.98
Haversian Canal Density (#/mm²)				
Micro-CT Scanned	10.2 ± 2.6	10.4 ± 2.7	1.94	0.83

Values shown as mean ± 1 SD. p-values determined by student's t-test or Mann-Whitney U test. p < 0.05 shown in bold.

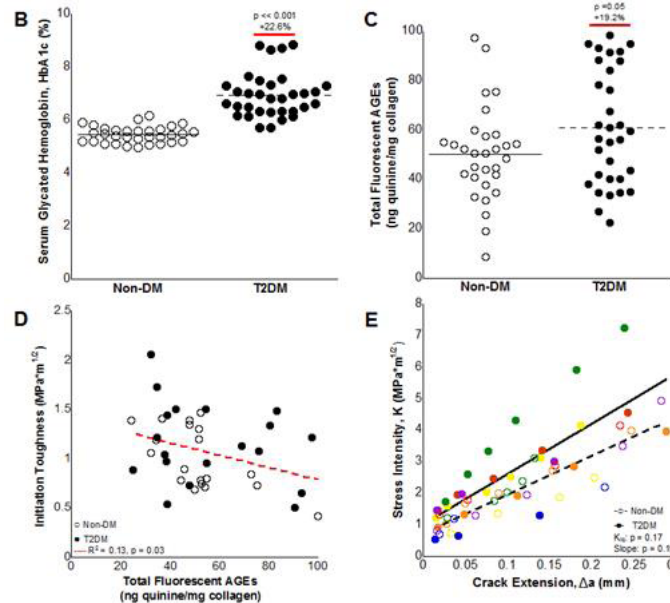


Figure 1: (A) Patient characteristics; (B) Pre-operative glycaemic control was worse in type-2 diabetes mellitus (T2DM) vs. non-diabetic (Non-DM) group; (C) Total fluorescent AGEs were 19% higher in T2DM group for full cohort. (D) Initiation toughness trended toward a negative correlation with total fluorescent AGEs across patient groups in the mechanically tested subset (regression fit: R² = 0.13, p = 0.03). (E) Representative plots of stress intensity vs. crack extension (R-curves) in the non-DM and T2DM groups. Crack initiation and propagation toughness calculated from R-curves were not different between patient groups.

Disclosures: Pablo Palomino, None

1040

Definitions of sarcopenia as predictors of fracture risk independent of FRAx, falls and BMD: A meta-analysis of the Osteoporotic Fractures in Men (MrOS) Study Nicholas Harvey^{*1}, Anders Oden², Eric Orwoll³, Timothy Kwok⁴, Magnus Karlsson⁵, Bjorn Rosengren⁵, Eva Ribom⁶, Peggy Cawthon⁷, Kristine Ensrud⁸, Cyrus Cooper¹, John Kanis⁹, Claes Ohlsson², Dan Mellstrom², Helena Johansson², Eugene McCloskey⁹. ¹MRC Lifecourse Epidemiology Unit, University of Southampton, Southampton SO16 6YD, United Kingdom, ²Centre for Bone and Arthritis Research (CBAR), Sahlgrenska Academy, University of Gothenburg, Gothenburg, Sweden, ³Oregon Health & Science University, Portland, OR, United States, ⁴Department of Medicine & Therapeutics and School of Public Health, The Chinese University of Hong Kong, HK, Hong Kong, ⁵Clinical and Molecular Osteoporosis Research Unit, Department of Clinical Sciences Malmö, Lund University and Department of Orthopedics, Skane University Hospital, Malmö, Sweden, ⁶Department of Surgical Sciences, University of Uppsala, Uppsala, Sweden, ⁷Research Institute, California Pacific Medical Center, San Francisco, CA, United States, ⁸Medicine and Epidemiology & Community Health, University of Minnesota, MN, United States, ⁹Centre for Metabolic Bone Diseases, University of Sheffield, Sheffield, United Kingdom

We have demonstrated that the predictive value for fracture of appendicular lean mass/height² (ALM/ht²) is markedly attenuated by femoral neck BMD (fnBMD). Since the majority of sarcopenia definitions use ALM/ht², and to inform approaches to clinical assessment, our aim was to investigate the predictive value of sarcopenia definitions for incident

fracture, independent of fnBMD , FRAX probability and prior falls. In US, Sweden and Hong Kong MrOS cohorts, we used an extension of Poisson regression to investigate relationships between sarcopenia (y/n) and incident major osteoporotic fracture (MOF: clinical vertebral, hip, wrist, proximal humerus). Sarcopenia definitions tested were those published by Baumgartner, Fielding, Cruz-Jentoft, Morley, Chen, Delmonico, Studenski (1 & 2, using ALM adjusted for BMI). Associations were adjusted for age and time since baseline, and reported as hazard ratio (HR) for first incident MOF. Further analyses adjusted additionally for FRAX MOF probability (available in 7531 men and calculated \pm fnBMD), prior falls (y/n) or fnBMD T-score. Results were synthesized by meta-analysis. Complete data were available for: 5660 men in USA, 2764 in Sweden and 1987 in Hong Kong; (mean ages 73.5, 75.4 and 72.4 years respectively). Mean follow-up time: 8.7 to 10.9 years. Prevalence of sarcopenia ranged from 0.9% (Studenski 2) to 21% (Baumgartner) in US; corresponding figures were 0.4% to 22% in Sweden and 4% to 35% in Hong Kong. Sarcopenia status, by all definitions except those of Studenski, was associated with incident MOF (HR: 1.39 to 1.76), e.g. Cruz-Jentoft (HR: 1.76; 95%CI: 1.38, 2.26); Fielding (HR: 1.60; 95%CI: 1.27, 2.01); Morley (HR: 1.74; 95%CI: 1.29, 2.36). Associations were robust to adjustment for prior falls or FRAX probability (without fnBMD), but were slightly attenuated by adjustment for FRAX (with fnBMD), although remaining statistically significant. Adjustment for fnBMD T-score alone led to marked attenuation to below or borderline statistical significance, e.g. Cruz-Jentoft (HR: 1.34; 95%CI: 1.04, 1.73); Fielding (HR: 1.24; 95%CI: 0.98, 1.56); Morley (HR: 1.24; 95%CI: 0.91, 1.69). Chen (Asian) and Cruz-Jentoft definition behaved similarly. In conclusion, the predictive value for fracture of sarcopenia definitions based on ALM is reduced by inclusion of fnBMD T-score. Given that both ALM and BMD are derived from DXA, these findings suggest that other muscle measures, e.g. from pQCT, might usefully be investigated in characterising sarcopenia status.

Disclosures: *Nicholas Harvey, None*

1041

Muscle mass assessed by D3Cr dilution and incident fractures in older men

Peggy Cawthon^{*1}, Katherine Peters¹, Steven Cummings¹, Eric Orwoll², Andrew Hoffman³, Kristine Ensrud⁴, Jane Cauley⁵, William Evans⁶. ¹California Pacific Medical Center, United States, ²OHSU, United States, ³Stanford, United States, ⁴University of Minnesota, United States, ⁵University of Pittsburgh, United States, ⁶University of California, Berkeley, United States

Muscle mass likely influences fracture risk in several ways: muscle exerts strong forces on bone, and bone must remodel to accommodate these forces; muscle tissue produces myokines which are pro-anabolic on bone; and muscle influences fall risk and thus fracture risk. However, previous studies have been unable to assess the relation between muscle mass and fracture risk given limitations in the widely used approximations of muscle mass. Whole body dual energy x-ray absorptiometry (DXA) measures lean mass (which includes water, muscle, and all other non-bone non-fat tissue), not muscle mass per se. We have previously shown that men with low muscle mass assessed by D3Cr (deuterated creatine) dilution are more likely to have incident injurious falls and worse physical performance. Therefore, in 1388 men (mean age 84.2 yrs) at the Year 14 Visit of the MrOS study, we tested the hypothesis that men with lower D3Cr muscle mass (standardized to body mass) were more likely to fracture than those with higher muscle mass, and that similar associations would not be seen with DXA-based appendicular lean mass/height² (ALM/ht²). Cox proportional hazards models were used to determine the HR for any clinical fracture (N=103), non-vertebral fracture (N=93) or hip fracture (N=21) over 2.4 years of follow-up. Models were adjusted for age and femoral neck BMD, and then further adjusted for 10-year probability of hip fracture from FRAX (with BMD). Fractures were centrally adjudicated. Each SD decrement in D3Cr muscle mass/wgt was associated with a 23-25% increased risk of any clinical or non-vertebral fracture, and a 72% increased risk of hip fracture, after accounting for age, BMD and FRAX (with BMD) ($p < 0.05$). Men in the lowest quartile of D3Cr muscle mass/wgt had an approximate 2-fold increased risk of any clinical or non-spine fracture and an 8-fold increased risk of hip fracture compared to men in the highest quartile, after accounting for age, BMD and FRAX (with BMD). Confidence intervals were wide, especially for hip fracture. Low DXA ALM/ht² was not significantly associated with fracture risk. In conclusion, these results suggest that the D3Cr measure of muscle mass may be a novel risk factor for fracture in older men while DXA ALM/ht² is not useful for fracture prediction. Future studies should investigate the relation between D3Cr muscle mass and fracture in women and younger men.

Table. Multivariate adjusted risk of fracture ([HR(95%CI)] by D₃Cr muscle mass/wgt or ALM/ht² in 1388 older men

	Any clinical fracture (N=103)	Non-spine fracture (N=93)	Hip fracture (N=21)
D₃Cr muscle mass/wgt			
Quartile 1 (lowest)	2.1 (1.1,3.8)	2.3 (1.2,4.3)	8.4 (1.0,68.3)
Quartile 2	1.2 (0.6,2.3)	1.2 (0.6,2.4)	5.3 (0.7,44.2)
Quartile 3	1.5 (0.8,2.8)	1.7 (0.9,3.2)	3.4 (0.4,30.9)
Quartile 4 (highest)	1.0 (referent)	1.0 (referent)	1.0 (referent)
p-trend	0.034	0.027	0.016
Per SD decrement	1.3 (1.01,1.5)	1.3 (1.01,1.6)	1.7 (1.05,2.8)
ALM/ht²			
Quartile 1 (lowest)	0.8 (0.5,1.4)	0.8 (0.5,1.5)	4.9 (0.6,39.2)
Quartile 2	0.7 (0.4,1.2)	0.7 (0.4,1.2)	4.8 (0.6,39.8)
Quartile 3	0.8 (0.4,1.4)	0.9 (0.5,1.6)	5.1 (0.6,43.5)
Quartile 4 (highest)	1.0 (referent)	1.0 (referent)	1.0 (referent)
p-trend	0.345	0.394	0.207
Per SD decrement	0.9 (0.7,1.1)	0.9 (0.7,1.1)	1.3 (0.8, 2.1)

Disclosures: *Peggy Cawthon, None*

1042

Osteoblast-derived NOTUM Reduces Cortical Bone Mass in Mice and the NOTUM Locus is Associated with Bone Mineral Density in Humans

Karin Nilsson^{*1}, Sofia Movérare-Skrtic¹, Petra Henning¹, Thomas Funk-Brentano¹, Maria Nethander¹, Fernando Rivadeneira², Antti Koskela³, Juha Tuukkanen³, Jan Tuckermann⁴, Christine Perret⁵, Ulf Lerner¹, Claes Ohlsson¹. ¹Center for Bone and Arthritis Research at the Sahlgrenska Academy, 41345 Gothenburg, Sweden, ²Department of Internal Medicine, Erasmus University Rotterdam, Rotterdam, The Netherlands, Netherlands, ³Institute of Cancer Research and Translational Medicine, Department of Anatomy and Cell Biology, Faculty of Medicine, University of Oulu, Finland, ⁴Institute of General Zoology and Endocrinology, Universität of Ulm, Germany, ⁵Inserm, Institut Cochin, Paris, France

Osteoporosis is a common skeletal disease, affecting millions of individuals worldwide. There is a medical need to improve the therapy for non-vertebral fractures, mainly caused by reduced cortical bone mass. WNT proteins are crucial regulators of both trabecular and cortical bone mass. It was recently demonstrated that NOTUM is a secreted WNT lipase inactivating WNTs by removing their attached lipid group essential for activation of Frizzled receptors. To determine if NOTUM regulates bone mass, we developed a global Notum^{-/-} mouse model. Although Notum^{-/-} mice were embryonic lethal, adult female Notum^{+/-} displayed specifically increased cortical bone thickness. Notum expression was high in cortical bone and conditional Notum inactivation in mice revealed that osteoblast-lineage cells are the principal source of NOTUM in cortical bone. Importantly, osteoblast-lineage specific Notum inactivation resulted in substantially increased cortical bone thickness and bone strength associated with increased canonical WNT signaling in cortical bone. In contrast, trabecular bone mass was unaffected. Large scale human genetic analyses using the powerful UK Biobank dataset (n = 445921 European subjects) identified two independent genetic variants mapping to the NOTUM locus (17q25.3) that are associated with BMD (P value $< 1 \times 10^{-10}$) as estimated with quantitative ultrasound in the heel. Thus, osteoblast derived NOTUM is an essential regulator of cortical bone thickness and bone strength in mice and genetic variants in the NOTUM locus are associated with BMD variation in humans. Therapies targeting osteoblast-derived NOTUM may prevent non-vertebral fractures.

Disclosures: *Karin Nilsson, None*

1043

Role of Osterix (SP7) in Regulating Osteocyte Biology and Dendrite Formation

Fatemeh Mirzamohammadi^{*1}, Hironori Hojo², Tetsuya Enishi¹, Nicolas Govea¹, Henry M. Kronenberg¹, Marc N. Wein¹. ¹Center for Skeletal Research, Endocrine Unit, Department of Medicine, Massachusetts General Hospital, Harvard Medical School, 50 Blossom Street, Boston, Massachusetts 02114, United States, ²Center for Disease Biology and Integrative Medicine, The University of Tokyo Graduate School of Medicine, 7-3-1 Hongo, Bunkyo-ku, Tokyo 113-8656, Japan

Osteocytes participate in inter-cellular communication through an elaborate network of dendritic projections coursing throughout mineralized bone matrix. Osteocyte projections allow these cells to communicate with each other in order to sense mechanical and hormonal cues that regulate bone homeostasis. SP7, a key transcription factor required for skeletal development, is also required for osteocyte-specific sclerostin (SOST) expression. To study the role of SP7 in osteocytes in more detail, we generated mice lacking SP7 in osteocytes

using DMP1-Cre. Surprisingly, these mice display a dramatic bone phenotype that cannot be explained solely by reduced SOST expression. Specifically, SP7 conditional KO mice display cortical bone porosity due to intracortical bone remodeling. Detailed analysis of osteocyte morphology in these mice revealed a near-complete absence of osteocyte dendrites (Fig.1a,b). We next established an *in vitro* system to study the role of SP7 in osteocyte dendrite formation. When osteoblasts are cultured in 3D collagen gel conditions, they undergo a dramatic cuboidal-to-dendritic morphology change which relies on the presence of SP7 (Fig.1c). Notably, in SP7 knockdown cells, we observe a reduction in the number of large dendrites from each cell, and reduced "spine-like" projections emanating from each dendrite. Therefore, SP7 is required for osteocytes to form dendrites, both *in vivo* and *in vitro*. To determine the molecular mechanisms through which SP7 regulates osteocyte dendrite formation, we performed RNA-seq in OCY454 cells (an osteocyte-specific cell line) after SP7 knockdown or over-expression. To understand the molecular mechanisms through which SP7 controls osteocyte biology, we performed SP7 ChIP-seq to determine its global pattern of chromatin binding in OCY454 cells, and compared its binding pattern in osteocytes versus osteoblasts. These studies revealed a core group of 78 genes whose expression is regulated by SP7 and show nearby SP7 binding sites. Furthermore, amongst SP7-regulated genes, OSTN and PANX3 showed functional effects on osteocyte dendrite formation in our *in vitro* assays using CRISPR/Cas9-mediated knockdown and over-expression approaches. Taken together, these data indicate that SP7 orchestrates the osteoblast-to-osteocyte transition by regulating a group of genes that controls dendrite formation.

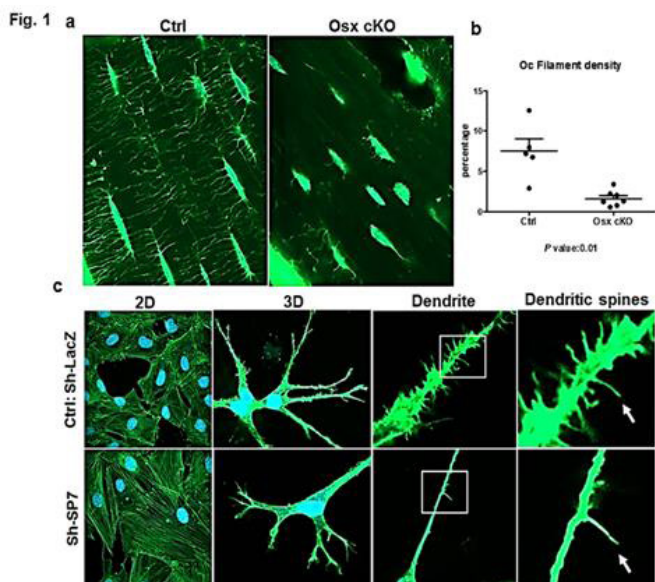


Figure 1. Cortical bone from tibia of 8 week old control and osterix (SP7) conditional knockout mice (a) was stained with phalloidin (green) to mark actin filaments. Control mice show typical dendritic projections, which are absent in osterix mutants. b, quantification of results. c, Control (Ctrl) and osterix (SP7) knockdown (Sh-SP7) MC3T3-E1 osteoblasts were cultured in standard 2D conditions (left), or in 3D collagen gels, then stained with phalloidin (green) and DAPI (blue). Osterix is required for optimal dendrite formation, and for the formation of spine-like projections emanating from each dendrite.

Disclosures: *Fatemeh Mirzamohammadi, None*

1044

Hypermineralization of bones by Col2a1-expressing osteoblasts Yukiko Kuroda*, Koichi Matsuo. Laboratory of Cell and Tissue Biology, Keio University School of Medicine, Japan

Auditory ossicles and specific parts of skeletal bones are highly mineralized; however, cellular mechanisms that enable formation of highly mineralized bone matrix during development are unknown. In this study, we examined developmental ossification processes of highly mineralized bones, such as auditory ossicles and the humerus. Ordinary osteoblasts highly express type I collagen, encoded by Col1a1, and Col1a1-GFP transgenic (Tg) mice also express green fluorescent protein (GFP) at high levels. Unexpectedly, in these Tg mice, osteoblasts in auditory ossicles and in specific regions of the distal humerus express very low GFP levels. Histological analysis of those tissues revealed that a new type of Col1a1low osteoblast, marked by Col1a1 expression lower than that of ordinary osteoblasts, produces highly mineralized bone. These novel cells are genuine osteoblasts, based on their expression of alkaline phosphatase and osteocalcin, their localization along alizarin-labeled new bone, and their terminal differentiation into osteocytes. Curiously, Col1a1low cells were undetectable in auditory ossicles of severely osteopetrotic mice, suggesting that generation of mature Col1a1low osteoblasts marked by robust osteocalcin expression depends on chondroclasts. To define collagen subtypes produced by Col1a1low cells in highly mineralized bones, we compared collagens from auditory ossicles with those from the femoral diaphysis, a skeletal bone exhibiting average bone mineral density. The diaphysis exhibited type I collagen only, while auditory ossicles contained both type I and II collagens as major components of the collagen matrix. Surprisingly, Col1a1low osteoblasts produced type II collagen

at high levels, an activity previously thought unique to chondrocytes. Finally, expression of type I (Col1a1) and type II collagen (Col2a1) transcripts in a mesenchymal stem cell line was induced by exogenous type II collagen, suggesting that the extracellular environment, including the collagen matrix, can stimulate generation of Col2a1-expressing cells. We conclude that Col1a1lowCol2a1high osteoblasts are distinct from previously characterized osteoblasts and form type II collagen-rich, highly mineralized bone matrix. We propose that these Col2a1-expressing cells be called 'hypermineralizing osteoblasts'.

Disclosures: *Yukiko Kuroda, None*

1045

In vivo cell fates of CXCL12+ perisinusoidal bone marrow mesenchymal stromal stem cells Yuki Matsushita*, Noriaki Ono. University of Michigan School of Dentistry, United States

Mesenchymal stem cells (MSCs) are widely believed to stand at the pinnacle of the skeletal cell lineage, playing critical roles in bone formation and regeneration. Although MSCs are retrospectively identified as cells that can self-renew and differentiate into the trilineage, i.e. osteoblasts/cytes, chondrocytes and adipocytes *in vitro* and upon transplantation, their *in vivo* behavior has not been fully elucidated. MSCs are proposed to reside in a perisinusoidal space of bone marrow; reticular stromal cells expressing C-X-C motif chemokine ligand 12 (CXCL12) occupy this position, which are termed as CXCL12-abundant reticular (CAR) cells. Here, we set out to investigate whether CAR cells can behave as MSCs and contribute to bone homeostasis and regeneration. For this purpose, we generated a tamoxifen inducible Cxcl12-creER transgenic line, and analyzed this line with a Rosa26-tdTomato reporter allele, a Cxcl12-GFP allele and a Col1a1(2.3kb)-GFP transgene. Cxcl12-creER specifically marked a subset of CAR cells without marking osteoblasts or chondrocytes upon tamoxifen injection. Virtually all Cxcl12-creER+ cells (96.9%) juxtaposed with endomucin+ sinusoidal endothelial cells. Analysis of colony forming unit-fibroblasts (CFU-Fs) revealed that a small fraction of CFU-Fs (3.7%) were marked by Cxcl12-creER, and that a majority of individual Cxcl12-creER+ colonies could self-renew and differentiate into the trilineage *in vitro*, indicating that Cxcl12-creER can effectively mark perisinusoidal MSCs. Subsequently, we traced the cell fate of Cxcl12-creER+ MSCs *in vivo*. These cells remained mostly dormant in physiological conditions, contributing to trabecular bone osteoblasts, but rarely to cortical bone osteoblasts without producing new reticular cells in growing marrow space. However, these cells were highly reactive, readily proliferating and differentiating into trabecular and cortical osteoblasts after bone marrow ablation and drill-hole injury, respectively. Moreover, these cells also differentiated into chondrocytes beneath the growth plate and converted into marrow adipocytes upon feeding with high-fat diet containing PPARg agonist rosiglitazone. Taken together, our study demonstrated for the first time that a subset of CAR cells can behave as MSCs, revealing unique *in vivo* characteristics of perisinusoidal MSCs that are dormant during steady-state conditions but can become a potent source of differentiated cells during regenerative conditions.

Disclosures: *Yuki Matsushita, None*

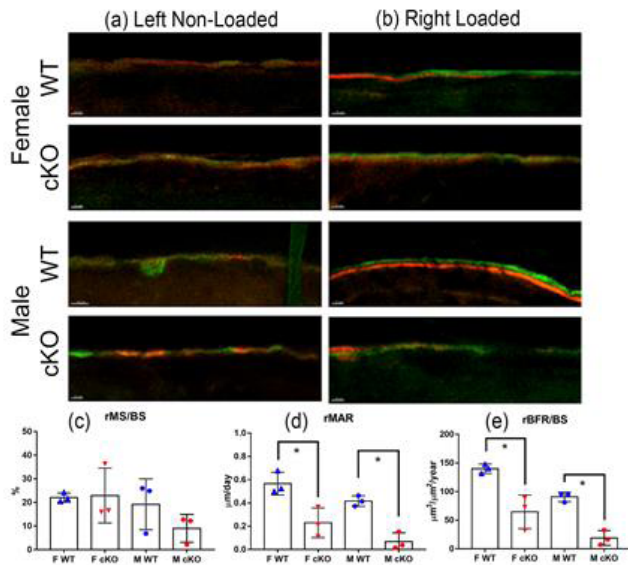
1046

Osteocyte-Specific CXCL12 Expression Is Critical for Load-Induced Bone Formation in Adult Mice Pamela Cabahug-Zuckerman*, Chao Liu, Emily Fang, Alesha Castillo. New York University, United States

Load-bearing exercise is an inexpensive means to counteract osteopenia; however, in older patients, mechanical loading alone may be insufficient to enhance bone mass (1). Identifying key signaling events in load-induced bone accrual could reveal promising therapeutic targets to prevent increased fracture risk in aging (2). Our previous work showed that CXC Motif Chemokine Ligand 12 (CXCL12) expression is enhanced in osteocytes (OCYs) in response to *in vivo* mechanical loading, and that antagonizing its receptor, CXCR4, significantly reduced load-induced bone formation in mice ulnae (3). We hypothesize that osteocyte-specific CXCL12 expression is critical in mechanically-driven bone formation. All procedures were approved by the NYU Institutional Animal Care and Use Committee. We generated male and female mice in which CXCL12 was deleted from OCYs (CXCL12ΔOCY) by crossing CXCL12 floxed mice and 10kb DMP1-Cre transgenic mice (gifts from Drs. Geoffrey Gurtner and Lynda Bonewald, respectively). The 10kb DMP1-Cre has been shown to be robustly expressed in odontoblasts and OCYs, with little to no activity in cells from non-mineralized tissues (4). Growing mice (n=3-8/group) were given fluorochrome labels every two weeks between 4-16 weeks of age. A second group of 16-week-old mice (n=3/group) were subjected to tibial axial cyclic loading (1200μe, 2Hz, 120cycles, 3days/wk for 2 wks) (5). Basal and load-induced periosteal (Ps) and endosteal (Es) mineralizing surface (MS/BS, %), mineral apposition (MAR, μm/day) and bone formation rates (BFR/BS, μm³/μm²/year) were calculated (6) at mid-length. No significant differences were detected in basal bone formation during development. However, relative load-induced Ps rMAR was reduced by 50% in female (p=0.02) and 75% in male (p=0.002) CXCL12ΔOCY mice; and similarly, Ps rBFR/BS was reduced by 50% in female (p=0.01) and 70% in male (p=0.001) CXCL12ΔOCY mice (Figure 1). Es bone formation was not affected by CXCL12 deletion. In summary, OCY-specific CXCL12 expression plays a critical role in load-driven Ps MAR, suggesting that CXCL12 signaling may positively regulate osteogenic differentiation and/or mature osteoblast function. Underlying mechanisms are being explored. Thus, OCY-specific CXCL12 signaling may be a promising target to enhance load-induced bone formation in

the elderly. (1) Gianoudis+ JBMR 2014 (2) Holguin+ JBMR 2016 (3) Leucht+ JOR 2013 (4) Lu+ J Dent Res 2007 (5) Liu+ Bone 2018 (6) Dempster+ JBMR.2013.

Figure 1. Representative images of (a) non-loaded and (b) loaded periosteal bone from Cre- (WT) and Cre+ (cKO) mice. Scale bars = 10 μ m. Relative periosteal (c) MS/BS, (d) MAR and (e) BFR/BS expressed as means \pm SD. * $p < 0.05$.

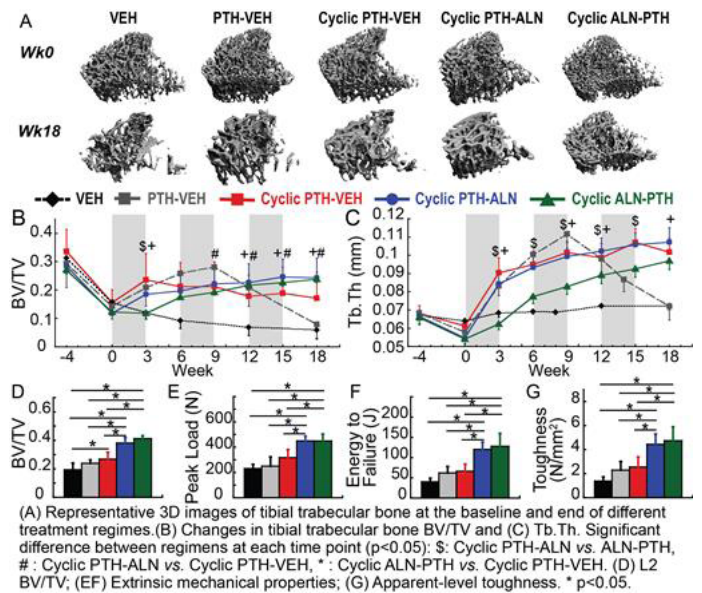


Disclosures: Pamela Cahug-Zuckerman, None

1047

Cyclic and Alternating Parathyroid Hormone (PTH) and Alendronate Treatment Regimens Further Improve Bone Microarchitecture and Strength Beyond Daily and Cyclic PTH Regimens Hongbo Zhao*¹, Wei-Ju Tseng¹, Tien-Jung Lee², Wonsae Lee¹, Yihan Li¹, Chantal De Bakker¹, X. Sherry Liu¹. ¹University of Pennsylvania, United States, ²National Central University, Taiwan

Bone mineral density rapidly decreases upon withdrawal from intermittent PTH treatment despite its potent effect of promoting bone formation. Our previous study showed a continuous anabolic window during the first week of PTH discontinuation in ovariectomized (OVX) rats, which offers a new mechanism in support of a cyclic administration regime with repeated cycles of on and off PTH treatment to maximize the treatment duration. However, osteoclast number increases significantly following the anabolic window. Therefore, we hypothesized that incorporating an anti-resorptive treatment during the off-PTH period of cyclic treatment regimen may further improve the treatment efficacy. 29 4mo-old SD rats underwent OVX surgery and developed osteopenia for 4 wks (51% and 11% reduction in BV/TV and Tb.Th, respectively) before they were assigned to 5 treatment regimens: VEH (n=6, 18-wk saline), PTH-VEH (n=6, 9-wk PTH 40 μ g/kg/day followed by 9-wk saline), Cyclic PTH-VEH (n=7, 3-wk PTH followed by 3-wk saline, 3 cycles), Cyclic PTH-ALN (n=5, 3-wk PTH followed by 3-wk ALN, 3 cycles) and Cyclic ALN-PTH (n=5, 3-wk ALN followed by 3-wk PTH, 3 cycles). In vivo μ CT (Fig A) indicated that bone loss continued in VEH for 18 wks. Meanwhile, 9-wk PTH treatment in the PTH-VEH group led to greater BV/TV and Tb.Th than all the other groups. However, these improvements disappeared after the 9-wk discontinuation from PTH (Fig A-C). On the other hand, Cyclic PTH treatment efficiently maintained the benefit of 3-wk PTH treatment in BV/TV from the 1st cycle of treatment, and increased Tb.Th over the next 2 cycles of treatment. Furthermore, both alternating PTH-ALN and ALN-PTH further improved the benefit of PTH treatment in BV/TV when compared to cyclic PTH-VEH (Fig A-C). Vertebral BV/TV in both cyclic PTH-ALN and ALN-PTH were greater than all other groups (Fig D). Additionally, compression tests of L2 suggested that peak load, energy to failure, and apparent-level toughness were 29%, 45%, and 43% greater in the cyclic PTH-ALN than the cyclic PTH-VEH, and 29%, 48%, and 46% greater in the cyclic ALN-PTH than the cyclic PTH-VEH, respectively (Fig E-G). No difference was found in any of the L2 mechanical properties among VEH, PTH-VEH, and cyclic PTH-VEH (Fig E-G). In summary, cyclic and sequential treatment of PTH and anti-resorptive agent further improve the treatment efficacy of daily and cyclic PTH treatment on bone microarchitecture and bone strength and extend PTH treatment duration.



(A) Representative 3D images of tibial trabecular bone at the baseline and end of different treatment regimens. (B) Changes in tibial trabecular bone BV/TV and (C) Tb.Th. Significant difference between regimens at each time point ($p < 0.05$): \$: Cyclic PTH-ALN vs. ALN-PTH, #: Cyclic PTH-ALN vs. Cyclic PTH-VEH, *: Cyclic ALN-PTH vs. Cyclic PTH-VEH. (D) L2 BV/TV; (E) Extrinsic mechanical properties; (F) Apparent-level toughness. * $p < 0.05$.

Disclosures: Hongbo Zhao, None

1048

Somatic Activating Mutations in MAP2K1 Cause Melorheostosis Heeseog Kang*¹, Smita Jha², Zuoming Deng³, Nadja Fratzl-Zelman⁴, Wayne A. Cabral⁵, Aleksandra Ivovic⁶, Françoise Meylan⁶, Eric P. Hanson⁷, Eileen Lange⁸, James Katz⁹, Paul Roschger⁴, Klaus Klaushofer⁴, Edward W. Cowen¹⁰, Richard M. Siegel¹¹, Timothy Bhattacharyya¹², Joan C. Marini¹. ¹Section on Heritable Disorders of Bone and Extracellular Matrix, NICHD, NIH, United States, ²Clinical and Investigative Orthopedics Surgery Unit, NIAMS, NIH, United States, ³Biodata Mining and Discovery Section, Office of Science and Technology, NIAMS, NIH, United States, ⁴Ludwig Boltzmann Institute of Osteology, Austria, ⁵Molecular Genetics Section, NHGRI, NIH, United States, ⁶Immunoregulation Section, NIAMS, NIH, United States, ⁷Autoimmunity Branch, NIAMS, NIH, United States, ⁸Clinical Research, NIAMS, NIH, United States, ⁹Rheumatology Branch, NIAMS, NIH, United States, ¹⁰Dermatology Branch, NIAMS, NIH, United States, ¹¹Office of Clinical Director, NIAMS, NIH, United States, ¹²Clinical Trials & Outcomes Branch, NIAMS, NIH, United States

Melorheostosis is a rare dysostosis of unknown etiology, with characteristic radiographs of "dripping candle wax". Because of its sporadic occurrence, somatic mutations have been hypothesized as causative, but bone tissue was not previously investigated. We recruited 15 unrelated melorheostosis patients, who underwent paired biopsies of affected and contralateral unaffected bone. Using exome sequencing, we identified somatic mosaic mutations in MAP2K1, encoding the Mitogen-Activated Protein Kinase Kinase 1 (MEK1), in gDNA from affected, but not unaffected bone, of 8 of 15 patients, and confirmed these mutations by ddPCR. Mosaicism for MAP2K1 mutations was also detected in skin overlying bone lesions in some patients, but not in blood samples. Located within the negative regulatory domain of MEK1, these activating mutations (p.Q56P, p.K57E, p.K57N) were previously identified in various malignancies. Immunohistochemical analysis in affected bone displayed a mosaic pattern of activation of ERK1/2, the substrates of MEK1. In addition, flow cytometry of osteoblasts cultured from affected bone demonstrated two cell populations with distinct ph-ERK1/2 levels. Histology of melorheostotic bone was distinctive, with exuberant initial deposition of distinctive parallel layers of primary lamellar bone, followed by intense bone remodeling with increased cellularity. The elevated RANKL/OPG ratio in affected osteoblasts correlates with increased osteoclast number and bone remodeling. In cultured osteoblasts, the MAP2K1 mutations enhanced cell proliferation with increased cyclin D expression. Interestingly, MAP2K1 mutations inhibited BMP2-mediated osteoblast differentiation and mineralization in vitro, underlying the significant elevation of unmineralized osteoid in melorheostotic bone. Melorheostosis, a benign bone overgrowth condition, is caused by somatic mosaicism for MAP2K1 activating mutations previously identified as cancer-associated. Increased MEK1-ERK1/2 signaling enhanced osteoblast growth and bone remodeling, while inhibiting osteoblast differentiation and bone. This is the first demonstration that the MAP2K1 oncogene is important to human bone formation. MEK1 inhibition, already in trials for cancer, may be a treatment for melorheostosis.

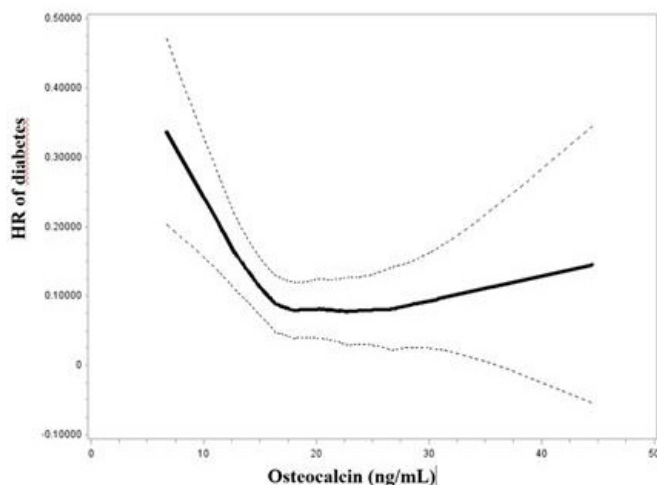
Disclosures: Heeseog Kang, None

1049

Osteocalcin Function On Energy Metabolism Is Conserved In Humans: Results of a 5 Year Prospective Cohort of Diabetes Onset Cyrille Confavreux^{*1}, Pawel Szulc², Matthieu Wargny³, Marie Christine Carlier², Elisabeth Sornay-Rendu², Matthieu Pichelin³, Bertrand Cariou³. ¹INSERM UMR1033 - University of Lyon - Department of Rheumatology, Hospices Civils de Lyon, France, ²INSERM UMR1033 - University of Lyon, France, ³INSERM UMR 1087/CNRS UMR 6291- Department of Endocrinology, University Hospital of Nantes, France

Background. Experimental studies show that bone is an endocrine organ active on energy metabolism through at least one hormone: osteocalcin. In vivo, osteocalcin regulates insulin secretion by pancreatic β -cells and adiponectin secretion by adipocytes. In humans, data are limited to cross-sectional and retrospective studies. The aim of this study is to assess the association between baseline osteocalcin concentration and the prospectively assessed risk of type 2 diabetes mellitus. Methods. The NANTOS project is a 5-year single center prospective cohort study of men and women followed annually for diabetes onset. To be included, these patients had to be prediabetic with an elevated FINRISK, a score risk to predicting diabetes and a fasting blood glucose between 1.1 and 1.26 g/L. At baseline, patients underwent a clinical examination and a morning fast blood withdrawal. Primary endpoint was the onset of diabetes based on abnormal fasting blood glucose >1.26 g/L. Total serum osteocalcin was assessed at baseline using ELECSYS-Roche diagnosis methods. We performed a multivariate survival analysis (Cox model), a Youden analysis and a quartile analysis to analyze the link between osteocalcin and diabetes onset. Results. Among 323 prediabetic individuals with all available data, 40 subjects became diabetic during the follow-up. Median time to diabetes onset was 14.7 months [interquartile range 12.7-26.5 months]. Cox multivariate model has been adjusted for the following parameters: age, BMI, current smoking, alcohol consumption, familial history of diabetes, renal function (creatinin), glycated hemoglobin A1c, HDL-cholesterol and diuretics. Lower total serum osteocalcin was significantly associated with an increased risk of diabetes onset (HR= 1.81 per 1SD decrease [95%CI: 1.14–2.89 ; p<0.05]). Moreover, the lowest quartile (≤ 14.7 ng/mL for men and 16.1ng/mL for females) was also associated with an increased risk of diabetes onset in multivariate analysis (HR= 2.98 vs. three upper quartiles combined, 95%CI: 1.48–6.00; p<0.005). Youden's index found that the osteocalcin concentration of 14.8ng/mL was the most discriminating cut-off in the entire cohort. Individuals who had osteocalcin levels below 14.8 ng/mL had higher risk of incident diabetes mellitus compared with those who had higher osteocalcin levels (HR=3.28, 95%CI: 1.63–6.58, p<0.001). Conclusion. We show for the first time that low osteocalcin concentrations are associated with markedly higher risk of incident type 2 diabetes mellitus in the prospectively assessed prediabetic individuals. These data strengthen the hypothesis that the effect of osteocalcin on energy metabolism, discovered in rodents, may be conserved in humans.

Association between serum total osteocalcin and diabetes risk



Disclosures: Cyrille Confavreux, None

1050

RANK Ligand inhibitors improve muscle function and glucose homeostasis Nicolas Bonnet^{*}, Lucie Bourgoin, Emmanuel Biver, Thierry Chevalley, Melany Hars, Andrea Trombetti, Serge Ferrari. Service of Bone Diseases, Faculty of Medicine (UNIGE), Switzerland

RANKL is a factor of osteoclastogenesis, but is also expressed in muscle, with implications in Duchenne's dystrophy. Data from the FREEDOM trial suggests that RANKL inhibition influence both the risk of falls and the development of diabetes. We investigated

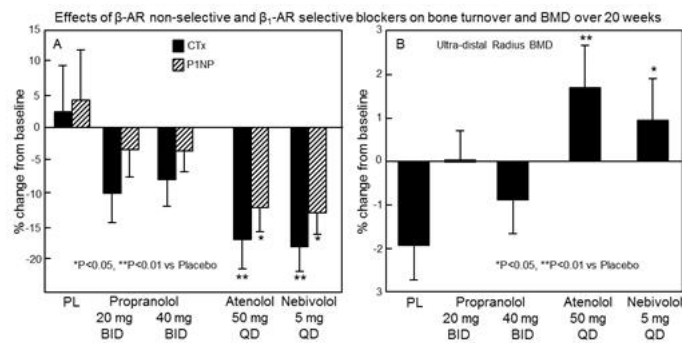
if RANKL inhibitors (OPG or denosumab, Dmab) modify muscle function, and glucose homeostasis in mice overexpressing human RANKL (huRANKL) and in a model of type 2 diabetes (Ppar β -/-). HuRANKL were treated with Dmab (10mg/kg/week) or vehicle (Veh) and Ppar β -/- with Opg-Fc (4mg/kg/week) both for 4 weeks. Muscle function was investigated by running and handgrip test and glucose homeostasis by GTT, ITT and EH clamp. In addition, 18 post-menopausal women treated for osteoporosis with Dmab were evaluated by DXA, HOMA and handgrip (65.0 \pm 1.4years) at baseline and after 3 years. They were matched to 49 controls for age, BMI, BMD and fracture. HuRANKL mice have severe osteoporosis and lower maximal speed and limb force, respectively -41% and -11% vs WT (p<0.05). Although they exhibit a normal body weight, gastrocnemius and soleus mass were lower (-29% and -57% vs WT, p<0.05). ITT AUC was higher, +31% vs WT (p<0.05) and GIR, an index of insulin sensitivity was lower (-24.6%, p<0.05). 2D[14C]-glucose incorporation indicated a lower glucose uptake in soleus (-51.9% vs WT, p<0.05). Dmab increased limb force, gastrocnemius mass (+34.7% and +9.8% vs Veh, p<0.05) and normalized ITT (AUC 464 \pm 25.1 vs 353.9 \pm 8.1 in Dmab, p<0.05). In Ppar β -/-, Opg-Fc increased BV/TV (+107% vs KO Veh, p<0.05) as well as force and muscle volume of the limb (+6.7%, +12%, p<0.05). Moreover, Opg-Fc decreased GTT and ITT AUC (-36.7% and -22.3% vs KO Veh, p<0.05) arguing for a restoration of insulin sensitivity, confirmed by western in muscle. In women, Dmab improved LSBMD, appendicular lean mass and handgrip as compared to controls (0.012 \pm 0.12g/cm², 0.098 \pm 0.27kg, 0.36 \pm 2.3kg, vs -0.046 \pm 0.0712g/cm², -0.22 \pm 0.34kg, and -2.81 \pm 1.64kg, all p<0.05) over 3 years. HOMA was not different between groups. In conclusion, overexpression of huRANKL causes bone loss and impairs muscle function and insulin sensitivity. RANKL inhibitors restored muscle strength and improved insulin sensitivity in both osteoporosis and diabetes mice, while denosumab improved muscle mass and strength in osteoporotic women. Altogether these data point towards a potentially new mechanism linking RANKL to fracture risk, i.e. not only by decreasing bone density, but also muscle strength.

Disclosures: Nicolas Bonnet, None

1051

Sympathetic Outflow Regulates Bone Metabolism in Humans: Evidence from Cellular, Epidemiological, and Direct Interventional Studies Sundeep Khosla^{*1}, Matthew Drake¹, Tammie Volkman¹, Brianne Thicke¹, Sara Achenbach¹, Elizabeth Atkinson¹, Michael Joyner¹, Clifford Rosen², David Monroe¹, Joshua Farr¹. ¹Mayo Clinic, United States, ²Maine Medical Center Research Institute, United States

There is considerable evidence from rodent studies that the sympathetic nervous system (SNS) regulates bone metabolism principally via β 2-adrenergic receptors (β 2-ARs). As results from human studies have been conflicting, we used multiple approaches to evaluate a possible role for SNS regulation of human bone metabolism. RNA sequencing of human bone biopsies and cultured osteoblasts demonstrated absence of β 3-AR, whereas β 1- and β 2-ARs were expressed in both human bone and cultured cells. In a population study, we identified 67 subjects aged > 50 yrs who had used β -blockers for at least 1 yr over the past 5 yrs; 63 were on β 1-selective blockers (atenolol/metoprolol). Relative to non-users (n=185), those on β 1-selective blockers had better HRpQCT-derived bone microarchitecture at both the distal radius and tibia (e.g., 7-9% higher BV/TV and TbN; all p<0.05). We next performed a direct interventional study that also sought to define β -AR selectivity for SNS effects on human bone. 155 postmenopausal women were randomized to one of five treatment groups for 20 wks: (1) Placebo (PL); (2) propranolol, 20 mg BID; (3) propranolol, 40 mg BID; (4) atenolol, 50 mg/d; (5) nebivolol, 5 mg/d. As no clinically available β 2-AR selective antagonists exist, we took advantage of the β 1-AR selectivity gradient of these drugs (propranolol [non-selective] << atenolol [relatively β 1-selective/some β 2-AR antagonism] < nebivolol [highly β 1-AR selective]) to define the β -AR selectivity for SNS effects on bone. Relative to PL, at 20 weeks both atenolol and nebivolol, but neither dose of propranolol, significantly (P < 0.05 by Dunnett's test) reduced serum CTx (by ~20%) and PINP (by ~15%) (Fig. A). Despite the short duration of the intervention, both atenolol and nebivolol significantly increased ultra-distal radius BMD (relative to PL by 3.6% and 2.9%, respectively; Fig. B). Collectively, these studies demonstrate that: (1) β 1- and β 2-ARs, but not β 3-ARs, are expressed in human bone; (2) patients on β 1-selective blockers have better bone microarchitecture; and (3) β 1-selective blockers (atenolol, nebivolol), but not a non-selective β -AR blocker (propranolol), have favorable effects on bone turnover and BMD in postmenopausal women. These 3 independent lines of evidence strongly support a role for the SNS in regulating bone metabolism in humans principally via β 1-ARs and warrant future clinical trials with atenolol or nebivolol for the prevention of bone loss in postmenopausal women.



Disclosures: **Sundeep Khosla**, None

1052

DMP1 overexpression prevents bone alterations, FGF23 elevations and cardiac hypertrophy in mice with chronic kidney disease Corey Dussold^{*1}, Claire Gerber¹, Samantha White¹, Xueyan Wang¹, Connor Francis¹, Lixin Qi¹, Ying Liu², Chaoyuan Li², Jian Q Feng², Myles Wolf³, Valentin David¹, Aline Martin¹. ¹Division of Nephrology and Hypertension, and Center for Translational Metabolism and Health, Northwestern University Feinberg School of Medicine, Chicago, IL, United States, ²Department of Biomedical Sciences, Baylor College of Dentistry, Texas A&M University, Dallas, TX, United States, ³Division of Nephrology, Duke University, Durham, NC, United States

Disordered bone and mineral metabolism is a common complication of chronic kidney disease (CKD), including an exponential increase in production and secretion of the osteocyte-derived hormone fibroblast growth factor 23 (FGF23) during CKD progression. Excess FGF23 is independently associated with increased risk of cardiovascular disease and mortality, perhaps by contributing to development of left ventricular hypertrophy (LVH). Dentin matrix protein 1 (DMP1), an extracellular matrix protein produced by osteocytes, is an established inhibitor of FGF23 production and a promoter of bone mineralization. We hypothesized that overexpression of DMP1 in CKD would improve bone health and prevent FGF23 elevations and consequent adverse cardiovascular outcomes in CKD. We studied the Col4a3KO mouse, an established model of progressive CKD, which typically shows a shortened lifespan (21.4±0.6 weeks). We overexpressed DMP1 (DMP1Tg-3.6Kb Col1a1 promoter) in the bone of WT (DMP1Tg) and Col4a3KO (Col4a3KO/DMP1Tg) animals and we assessed renal function, serum FGF23 and phosphate (Pi) levels, bone and cardiac phenotype in 20 week-old mice, and overall survival. Compared to WT, Col4a3KO mice showed impaired renal function (blood urea nitrogen: 94±18 vs 25±2 mg/dL), reduced cortical bone mineral density (BMD: 1154±14 vs 1194±5 mg/cm³), altered osteocyte morphology and connectivity, an 8-fold increase in serum FGF23 levels, hyperphosphatemia (serum Pi: 9.2±0.6 vs 6.2±0.2 mg/dL), and LVH (LV Mass: 124±7 vs 101±4 mg) (p<0.05 vs WT for each). Overexpression of DMP1 in Col4a3KO/DMP1Tg did not improve renal function but corrected CKD-induced BMD decrease by 40% and fully prevented alterations in osteocyte morphology and connectivity. Col4a3KO/DMP1Tg also showed lower FGF23 levels (631±124 vs 1161±196 pg/mL) resulting in higher serum phosphate levels (11.4±1.0 mg/dL) (p<0.05 vs Col4a3KO for each). As opposed to Col4a3KO, Col4a3KO/DMP1Tg mice did not have LVH (LV Mass: 93±5 mg; NS vs WT). Finally, Col4a3KO/DMP1Tg had improved survival compared to Col4a3KO (24.2±0.9 vs 21.4±0.6 weeks; p<0.05). Overexpression of DMP1 in bone prevented CKD-associated osteocyte alterations and FGF23 elevations, development of LVH and improved survival, despite persistently impaired renal function and worsened hyperphosphatemia. These results support the contribution of FGF23 excess to cardiac injury in CKD and suggest that DMP1 represents a novel therapeutic approach to improve bone and cardiac outcomes in CKD.

Disclosures: **Corey Dussold**, None

1053

Overexpression of PTHrP in Transgenic Mammary Tumors Causes Hypercalcemia and Rapid Fat Wasting but does not Increase Energy Expenditure. Pamela Dann^{*1}, Farzin Takyar¹, Kellen Bean², Rachel Perry¹, Gerald Shulman¹, John Wysolmerski¹. ¹Yale University, United States, ²Yale College, United States

PTHrP has been reported to cause beiging of white adipocyte tissue (WAT) in cancer cachexia by interacting with the PTH1 receptor (PTHR1) to induce a hypermetabolic state associated with fat and muscle wasting. We utilized a tetracycline-regulated bitransgenic, MMTV-rTA;pTet-PTHrP, system to overexpress PTHrP in the MMTV-PyMT model of murine breast cancer (Tet-PTHrP;PyMT mice) in order to ask whether PTHrP might contribute to cachexia in breast cancer. Tet-PTHrP;PyMT mice (10-12 weeks old) with mammary tumors were treated with doxycycline (Dox) to induce PTHrP expression. Within 2-4 days of Dox treatment, the mice developed severe hypercalcemia with elevated levels of circulating

PTHrP in the absence of bone metastases, reproducing the cardinal features of humoral hypercalcemia of malignancy (HHM). HHM in these mice was associated with rapid weight loss; within 4 days of Dox treatment, Tet-PTHrP;PyMT lost 15% of their body mass. There was a dramatic decrease in the weight of all fat pads, and histology and perilipin immunofluorescence demonstrated a decrease in the size of adipocytes characterized by loss of the central lipid droplet but the absence of multi-locular droplets. Immunofluorescence staining demonstrated increased expression of UCP-1 in lipid-depleted adipocytes. None of these changes occurred in control Tet-PTHrP;PyMT mice off Dox. Despite the upregulation of UCP-1 expression, metabolic cage studies were not consistent with a hypermetabolic state. Tet-PTHrP;PyMT mice were studied for two consecutive periods, first off Dox and then on Dox, allowing each mouse to serve as its own control. As expected, when treated with Dox, Tet-PTHrP;PyMT mice lost weight and fat mass as assessed using proton NMR. There were no differences in activity counts but, when placed on Dox, the mice had a decreased VO₂, VCO₂, food and water intake, and energy expenditure. RER was decreased, suggesting an overall increase in fat oxidation. Rates of systemic WAT lipolysis appeared to be elevated as indicated by increased circulating glycerol and non-esterified fatty acids. In order to determine whether these effects of PTHrP were mediated by PTHrP acting on the PTHR1, we also treated mice with an anti-PTHrP blocking antibody. This resulted in normalization of calcium but not PTHrP levels, as well as prevention of weight loss and fat and muscle wasting. Anti-PTHrP treatment also normalized circulating levels of glycerol and fatty acids, consistent with an inhibition of PTHrP-induced WAT lipolysis. Finally, we also treated Tet-PTHrP;PyMT mice with rOPF-Fc to normalize circulating calcium levels. Interestingly, this also prevented weight loss. In summary, overexpression of PTHrP in transgenic breast tumors causes HHM and rapid weight loss. The weight loss is associated with increased WAT lipolysis but decreased overall energy expenditure. Calcium as well as PTHrP levels may contribute to fat wasting.

Disclosures: **Pamela Dann**, None

1054

A novel regulatory network mediated by the miR182-PKR-IFN- β axis plays a key role in osteoclastogenesis and osteoprotection Kazuki Inoue^{*1}, Zhonghao Deng², Yufan Chen³, Gregory Vitone², Eugenia Giannopoulou⁴, Ren Xu⁵, Shiaoqing Gong⁶, David G. Kirsch⁷, Matthew Greenblatt⁸, Anil K. Sood⁸, Liang Zhao³, Baohong Zhao¹. ¹Hospital for Special Surgery, Weill Cornell Medical College, United States, ²Hospital for Special Surgery, United States, ³Nanfeng Hospital, Southern Medical University, China, ⁴New York City College of Technology, City University of New York, United States, ⁵Weill Cornell Medical College, United States, ⁶Department of Molecular Biology, The Rockefeller University, United States, ⁷Duke University Medical Center, United States, ⁸The University of Texas MD Anderson Cancer Center, United States

Bone loss is a severe consequence of diseases such as rheumatoid arthritis (RA) and osteoporosis, in which osteoclasts are a culprit directly responsible for bone destruction. MicroRNAs (miRNAs) are important regulators in various biological and disease settings. miRNA-based therapeutics recently shows significant promise in disease treatment. Such progress however remains underexplored in bone diseases. Here we identify miR-182 as a key positive regulator of osteoclastogenesis, bone homeostasis and pathologic bone resorption using complementary gain and loss-of-function approaches. Myeloid-specific knockout of miR-182 protects mice against excessive osteoclast formation and bone resorption in disease models of ovariectomy-induced osteoporosis and rheumatoid arthritis. An osteoclast precursor (OCP) specific transgenic mouse model of miR-182 showed a complementary phenotype with markedly decreased bone mass and enhanced osteoclastogenesis. Treatment of these disease models with nanoparticles containing miR-182 inhibitors completely suppresses pathologic bone erosion driven by enhanced osteoclastogenesis, highlighting the therapeutic implication of miR-182 inhibition. Mechanistically, we performed genome wide analysis based on two parallel RNA-seq experiments, one with miR-182 deficient OCPs and the other with miR-182 overexpressed OCPs. We found that miR-182 promoted the expression of key osteoclastogenic genes by selectively and significantly suppressing endogenous IFN- β -mediated autocrine inhibitory loop of osteoclastogenesis. We further identified protein kinase double-stranded RNA-dependent (PKR) as a new and essential miR-182 target. Genetic deletion of PKR in OCPs showed increased osteoclast formation and impaired IFN- β -mediated feedback inhibition. The regulatory role of miR-182 is well conserved in human osteoclastogenesis. In RA, the expression levels of miR-182, PKR and IFN- β are significantly altered in monocytes isolated from RA patients, correlated with the osteoclastogenic capacity of the RA OCPs and regulated by TNFi treatment. Collectively, these findings reveal a novel regulatory network in osteoclastogenesis mediated by miR182-PKR-IFN- β axis that plays a key role in bone biology and diseases. The genetic and pharmacological evidence from mouse disease models as well as the correlation between miR-182 and RA disease present miR-182 inhibition as a novel therapeutic strategy to prevent pathologic bone destruction.

Disclosures: **Kazuki Inoue**, None

1055

Transcriptional Co-factor Jab1 is Vital for Mouse Chondrocyte Differentiation

Murali Mamidi*, William Samsa, Ricky Chan, Guang Zhou. Case Western Reserve University, United States

The evolutionarily conserved transcriptional cofactor Jab1 regulates cell proliferation, differentiation, and apoptosis by modulating the activity of various transcription factors. We previously reported that the chondrocyte-specific deletion of Jab1 mutant mice, Col2a1-Cre+; Jab1^{lox/lox}, displayed a lethal chondrodysplasia phenotype at birth. Jab1-deficient chondrocytes displayed increased apoptosis, accelerated chondrocyte hypertrophy, and G2 phase cell cycle arrest. Jab1-deficient chondrocytes also showed enhanced expression of Smad1/5 phosphorylation and increased BMP response, indicating that Jab1 inhibits BMP signalling in chondrocytes to inhibit chondrocyte hypertrophy. To further identify Jab1 downstream targets in chondrocytes, we performed in-depth analysis of Col2a1-Cre+; Jab1^{lox/lox} mouse chondrocytes by various methods in this study. Our immunoprecipitation (IP) results showed that the endogenous Jab1 interacts with endogenous Smad1/5, but not with endogenous Smad2/3 and Smad7. Interestingly, the small molecule inhibitor of type I BMP receptor LDN-193189 can partially block the increased BMP signalling in Jab1 cKO chondrocytes. Indeed, although Jab1 did not directly interact with a key type I BMP receptor Acvr1, the interaction between Smad1/5 and Acvr1 was significantly increased in Jab1-deficient chondrocytes. Thus, Jab1 might negatively regulate BMP signalling during chondrocyte differentiation in part by sequestering Smad1/5 from Acvr1. RNA-Sequencing analysis of Jab1 cKO chondrocytes showed a total of 1993 differentially expressed genes (1060 increased and 933 decreased). Moreover, gene set enrichment analysis (GSEA) showed that Jab1 regulates essential developmental pathways, such as p53, BMP/TGF- β , and apoptosis. Moreover, the reporter assay in Jab1 cKO chondrocytes also demonstrated that Jab1 regulates multiple pathways, including Hedgehog signalling, which is involved in hypertrophic chondrocyte differentiation. Finally, ChIP-qPCR showed that Jab1 might directly regulate key cartilage-specific enhancer elements in Col2a1 and Aggrecan genes. In conclusion, our data showed that Jab1 acts as a transcriptional co-factor to interact with key developmental pathways to control chondrocyte differentiation.

Disclosures: Murali Mamidi, None

1056

Targeting the Hedgehog Signaling Pathway to Ameliorate Metachondromatosis Jiahui Huang*, Douglas Moore, Michael Ehrlich, Wentian Yang. Department of Orthopaedics, Brown University Alpert Medical School and Rhode Island Hospital, United States

Metachondromatosis (MC) is a rare autosomal dominant tumor syndrome featuring the growth of osteochondromas and enchondromas in the long bones and digits. Recently, disease-associated whole-genome sequencing and linkage analysis using high-density SNP arrays uncovered heterozygous early frameshift or nonsense mutations in PTPN11 in >50% of MC cases. PTPN11 encodes the protein-tyrosine phosphatase SHP2, which is required for RAS/ERK pathway activation in most receptor tyrosine kinase, cytokine receptor, and integrin signaling pathways. Germline PTPN11 activating mutations cause Noonan syndrome, whereas PTPN11 mutations that substantially impair SHP2 catalytic activity cause LEOPARD syndrome, both of which include incompletely penetrant skeletal abnormalities. Somatic PTPN11 activating mutations are the most common cause of the childhood myeloproliferative diseases and several solid tumors. It remains unclear how heterozygous loss-of-function PTPN11 mutations cause MC. Using genetically modified animals and biological and biochemical approaches, we report here that Ptpn11 functions as a tumor suppressor in cartilage. Somatic Ptpn11 deletion, likely due to Ptpn11 loss of heterozygosity (LOH) mutations in the Prrx1+ mesenchymal cells, in the Ctsk+ chondroprogenitors, and in the Col2a1+ but not Col10a1+ chondrocytes cause MC (Fig.1). To gain insight into the molecular pathogenesis of MC, differential gene expression array and RNA-seq analysis were carried out using SHP2-sufficient and SHP2-deficient chondrocytes and progenitors, respectively. These assays revealed that multiple genes and pathways that had previously been reported to be critical for chondrocyte proliferation and maturation were affected by Ptpn11 deletion. Ptpn11 deficient chondroid cells had decreased ERK activation and enhanced IHH and PTHrP expression. Treatment of chondroid cells with FGFR or MEK inhibitor also increased Ihh and Pthrp expression. Most importantly, Smoothed inhibition ameliorated the metachondromatosis phenotype in Tg(Ctsk-Cre;Ptpn11^{fl/fl}) mice. Thus, in contrast to its pro-oncogenic role in hematopoietic and epithelial cells, Ptpn11 is a tumor suppressor in cartilage, acting in part via a FGFR/MEK/ERK-dependent pathway in chondroid progenitors to prevent excessive Ihh production and MC formation.

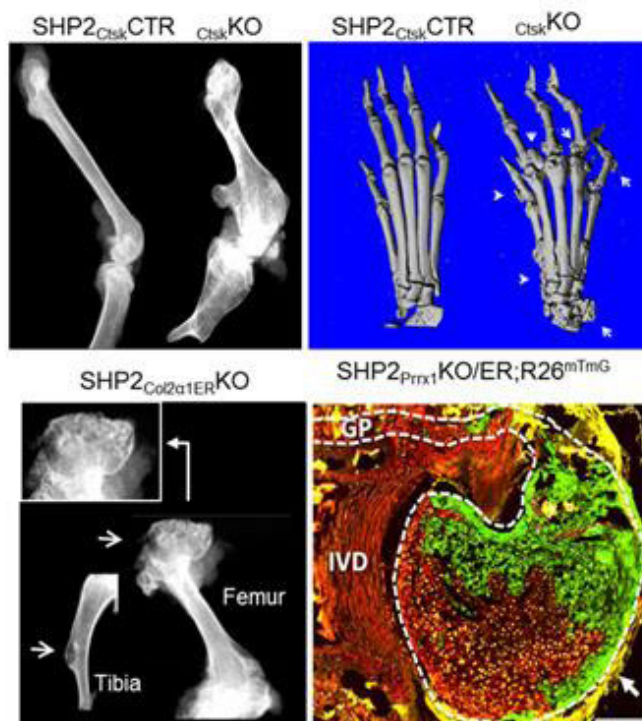


Fig. 1 Mice lacking SHP2 in the Prrx1+, Ctsk+ and Col2a1+ chondroprogenitors develop osteo-chondromas and enchondromas, which recapitulate the features of human metachondromatosis. X-ray (i, iii) and μ CT images (iii) show the growth of osteochondromas and enchondromas on the proximal and distal femur (i, iii) and metatarsal bones (ii). Fluorescent images of vertebrate (iv) showing the growth of osteochondromas comprised of cells derived from SHP2 deficient OCPs.

Disclosures: Jiahui Huang, None

1057

Teasing Apart Endocrine and Inflammatory Control of Cyp27b1 Expression Reveals Vital Relationships of Vitamin D3 Metabolites and Enzyme Levels to Skeletal Health Mark Meyer*¹, Nancy Benkusky¹, Seong Min Lee¹, Melda Onal¹, Martin Kaufmann², Glenville Jones², J. Wesley Pike¹. ¹University of Wisconsin - Madison, United States, ²Queen's University, Canada

The vitamin D endocrine system regulates mineral homeostasis. Terminal activation of vitamin D3 to its hormonal form, 1,25(OH)₂D₃, occurs in the kidney via the cytochrome P450 enzyme CYP27B1. Despite its importance in vitamin D metabolism, the molecular mechanisms underlying the regulation of the gene for this enzyme, Cyp27b1, were unknown. Clinically, fundamental questions of 25(OH)D₃ sufficiency and conversion to 1,25(OH)₂D₃ in health and disease are still hotly debated. To tackle these questions, we identified a set of enhancers defining a kidney-specific control module governed by a renal cell-specific chromatin structure located distal to Cyp27b1 that mediates unique basal and parathyroid hormone (PTH)-, fibroblast growth factor 23 (FGF23)-, and 1,25(OH)₂D₃-mediated regulation of Cyp27b1 expression. Genomic deletion using CRISPR-Cas9 in C57BL/6 mice resulted in a debilitating skeletal phenotype after loss of Cyp27b1 PTH sensitivity (M1-IKO deletion), or a quasi-normal bone mineral phenotype after loss of FGF23 sensitivity (M21-IKO deletion). Furthermore, subsequent new deletions within the M1-IKO enhancer reveal a bimodal expression whereby Cyp27b1 expression is increased by selective removal of a basal suppressor. Refinement of the M21-IKO enhancer deletion narrows the unknown transcription factor mediating FGF23 genomic activity to a few hundred base pairs. A combination of deletions (M1/M21-DKO) resulted in a complete loss of basal as well as endocrine-insensitive renal Cyp27b1 expression. On the other hand, inflammation-induced non-renal cell Cyp27b1 expression, a complication of sarcoidosis and autoimmune diseases, was unaffected by these deletions, thus separating endocrine and inflammatory regulation

of Cyp27b1. We then identified the inflammatory region and subsequently deleted it in vivo leading to the unique loss of inflammation-induced Cyp27b1 activation. Importantly, each of these mouse models represent a unique tissue-specific deletion of 1,25(OH)2D3 production that will allow a detailed exploration of long-standing questions regarding non-renal production, contribution, and action of locally produced 1,25(OH)2D3 as well as assessment of the vital relationships that exist between 25(OH)D3 levels, Cyp27b1/Cyp24a1 expression, and enzymatic conversion of 1,25(OH)2D3 and skeletal health and vitality. We conclude that these models open new avenues for the study of vitamin D metabolism and therapeutic strategies for human health and disease.

Disclosures: Mark Meyer, None

1058

Change in Bone Turnover as a Surrogate for Fracture Outcomes: A Novel Individual-level Analysis of Pooled Anti-resorptive Trials from the FNHI Bone Quality Study

Douglas Bauer^{*1}, Eric Vittinghoff¹, Dennis Black¹, Mary Bouxsein², Li-Yung Lui³, Jane Cauley⁴, Anne De Papp⁵, Andreas Grauer⁶, Sundeep Khosla⁷, Bruce Mitlak⁸, Charles McCulloch¹, Richard Eastell⁹. ¹University of California, San Francisco, United States, ²Harvard Medical School, United States, ³California Pacific Medical Center, United States, ⁴University of Pittsburgh, United States, ⁵Merck & Co., Inc., United States, ⁶Amgen Inc., United States, ⁷Mayo Clinic College of Medicine, United States, ⁸Radius Health, United States, ⁹University of Sheffield, United Kingdom

To determine if treatment-related change in bone turnover markers (BTMs) can be used as a surrogate for fracture risk reduction for drug development, the FNHI Bone Quality Project is compiling individual patient data from as many osteoporosis randomized trials as possible. Thus far, we have compiled individual BTM data on >100,000 individuals from 14 anti-resorptive (AR) osteoporosis treatments trials (5 bisphosphonates and 3 SERMS). One component of the criteria for FDA qualification of a proposed surrogate marker is the Percent of Treatment Explained (PTE). Previous change in BTM analyses from individual trials reported non-vertebral fracture PTEs ranging from 28 to 77%, but analysis methods differed and single studies were too small to give precise estimates. We used our pooled data to estimate PTEs for BTM change, using a novel three-stage procedure. In the first stage, we used a linear mixed model (LMM) to estimate participant-specific total alkaline phosphatase trajectories. In the second, we used additional LMMs to estimate BTM trajectories, using the predicted total alkaline phosphatase values to help impute the BTM for participants with no observed BTM values. In the third, we fit nested models for the effect of treatment on time to vertebral, non-vertebral and hip fracture. PTE was calculated as the percentage change in the coefficient for treatment after adding estimated BTM change, based on the second-stage LMM, to the base model. Confidence intervals were obtained using seemingly unrelated regressions. This pooled analysis includes data from trials that measured at least one of 3 serum BTMs (Bone ALP, PINP and sCTX). Twelve trials (N=48,833) reported 3,532 incident vertebral fractures and 14 trials (N=56,758) reported 5,272 non-vertebral and 702 hip fractures. Pooled PTE estimates ranged from 69-123% for vertebral fracture and from 85-138% for non-vertebral fracture (Table); all were statistically significant. Hip fracture PTEs ranged from 43-139%, but CIs were wide and only the PTE for PINP was statistically significant. In this large pooled analysis of individual data from AR trials, we found that change in BTMs explain a substantial proportion of the vertebral and non-vertebral fracture benefit observed with AR treatments. Despite the challenges of imputing missing BTM values and estimating PTE with precision, our findings are proof of concept for the potential utility of BTMs as surrogate markers in trials of AR treatments.

Table. Percent of Treatment Effect (95% CI) Explained by Change in BTMs in Anti-resorptive Trials with Fracture Outcomes

	Bone ALP	PINP	sCTX
Vertebral (12 trials)	123% (81, 165%) p<0.0005	69% (24, 113%) p=0.003	89% (43, 135%) p<0.0005
Non-vertebral (14 trials)	119% (24, 214%) p=0.014	138% (33, 244%) p=0.01	85% (1, 169%) p=0.048
Hip (14 trials)	55% (-48, 157%) p=0.30	139% (4, 274%) p=0.043	43% (-61, 146%) p=0.42

Disclosures: Douglas Bauer, None

1059

Effect of Denosumab and High-Dose Teriparatide on Peripheral Bone Mineral Density and Microarchitecture

Joy Tsai^{*1}, Amy Yuan¹, Natalie David¹, Hang Lee¹, Mary Bouxsein², Benjamin Leder¹. ¹Massachusetts General Hospital, United States, ²Beth Israel Deaconess Medical Center, United States

Background: In postmenopausal women with osteoporosis, 15 months of combined denosumab (DMAB) and high-dose (HD) teriparatide (TPTD) increases bone mineral den-

sity (BMD) at the spine and hip more and faster than combined DMAB and standard-dose (SD) TPTD. The effects of combined DMAB and HD TPTD on peripheral volumetric BMD and microarchitecture are unknown. Methods: We randomized 69 postmenopausal women ages 52-83yo at high fracture risk to 1 of 2 groups: TPTD 20-mcg (SD) or TPTD 40-mcg QD (HD) given months 0-9 overlapped with DMAB 60-mg SC Q6M given months 3-15. Women were excluded if they ever received IV bisphosphonates (BP) or oral BPs within 6 months. Total, trabecular, & cortical density (Tt.vBMD, Tb.vBMD, Ct.vBMD); trabecular thickness, spacing, & number; and cortical thickness & porosity (Ct.Th, Ct.Po) were measured by high-resolution peripheral QCT of the distal tibia and radius. Results: Tt.vBMD at the tibia increased more in the HD (5.3±5.4%) than the SD group (3.4±1.9%) (p=0.01). Tt.vBMD also increased more in the HD group (2.6±4.4%) than the SD group (1.0±4.5%) at the radius, but this did not meet statistical significance (p=0.06). Ct.vBMD at the tibia increased by 2.2±1.8% in the HD group compared to 1.6 ± 1.5% in the SD group (p=0.13) whereas at the radius Ct.vBMD in the HD group increased by 1.0±2.2% which was significantly greater than the increase in the SD group (0.3±1.5%) (p=0.047). Changes in Tb.vBMD at both the tibia and the radius showed a similar pattern but between group comparisons were not significant. Tb.vBMD at the tibia increased by 1.7±2.0% in the HD group and by 1.2±2.2% in the SD group (p=0.17) whereas at the radius Tb.vBMD increased by 2.2±4.0% in the HD group and by 1.2±4.2% in the SD group (p=0.14). Ct.Po did not increase in either group at the tibia or the radius and there were no between group differences. Conclusions: The TPTD 40-mcg/DMAB combination increases Tt.vBMD at the radius and tibia and Ct.vBMD at the radius more than TPTD 20-mcg/DMAB combination. Moreover, in contrast to the well-described decrease in Ct.vBMD and increase in Ct.Po that is observed with TPTD alone, co-administration of DMAB prevents these deleterious changes even when TPTD is given in double the standard dose. These results show that the HD combination results in more favorable changes in both trabecular and cortical peripheral bone than does the SD combination and may be a useful therapy in patients at high risk of fragility fracture.

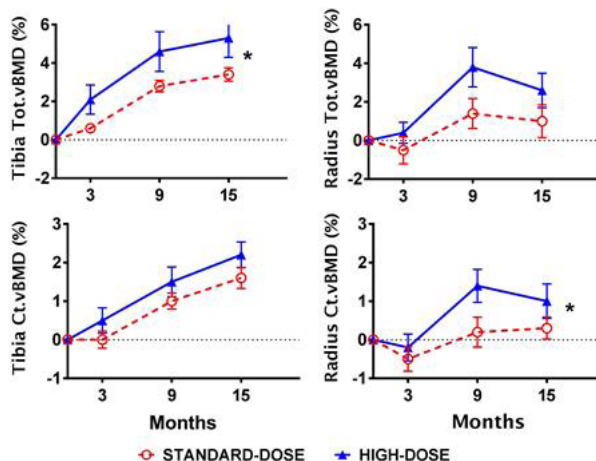


Figure. Mean percent change (SEM) from baseline in Tt.vBMD and Ct.vBMD at 15 months. *p-value <0.05 between groups.

Disclosures: Joy Tsai, None

1060

Effect of Dual-Task Functional Power and Mobility Training on Falls and Physical Function in Older People Living in Retirement Villages: A Cluster Randomised Controlled Trial

Robin Daly^{*1}, Rachel Duckham¹, Jamie Tait¹, Timo Rantalainen², Caryl Nowson¹, Dennis Taaffe³, Keith Hill⁴, Lucy Busija⁵, Kerrie Sanders⁶. ¹Institute for Physical Activity and Nutrition, Deakin University, Australia, ²Gerontology Research Centre, University of Jyväskylä, Australia, ³School of Medical and Health Sciences, Edith Cowan University, Australia, ⁴School of Physiotherapy and Exercise Science, Curtin University, Australia, ⁵Mary MacKillop Institute for Health Research, Australian Catholic University, Australia, ⁶Department of Medicine, University of Melbourne, Australia

Many falls in older people result from an inability to produce a rapid explosive movement when balance is lost often whilst concurrently performing other attention-demanding cognitive or motor tasks. This 12-month cluster RCT examined whether dual task functional high velocity (power) training (DT-FPT) could reduce falls and improve physical function in older adults. Residents (n=300) at risk of falling (mean age 77 y, 73% women) from 22 independent living retirement villages were randomised to DT-FPT involving high velocity strength and mobility training performed simultaneously with cognitive or motor tasks, or a usual care control (CON) group. The intervention consisted of 6 months supervised training (45-60 min, 2/week) at each village followed by a 6 month maintenance program. Falls were monitored monthly by diaries. Secondary outcomes included lower limb muscle strength, power and balance/mobility under single and dual-task (DT) conditions. Data on falls were obtained from 278 (93%) and 250 (83%) participants at 6 and 12 months. Mean exercise adherence for each training phase was 50% and 40%, respectively. Overall 89 falls were

recorded by 65 fallers in the first 6 months. The rate of falls was 30% lower in DT-FPT vs CON [IRR: 0.70 (95% CI 0.42, 1.17)], but this difference was not significant. In contrast, the relative risk (RR) for multiple falls (≥ 2) was significantly lower in DT-FPT [RR 0.30 (95% CI, 0.09, 0.97)]. There were no differences in the risk of falling [RR 0.89 (0.50, 1.60)], injurious falls [RR 1.03 (0.50, 2.13)] or falls requiring medical attention [RR 1.15 (0.33, 3.92)]. During the step-down phase, 76 falls were recorded by 53 fallers (37 had first fall). There were no significant group differences in any falls outcome, with the exception that there were fewer falls requiring medical attention in DT-FPT [RR 0.10 (0.02, 0.54)]. In terms of physical function, DT-FPT significantly improved muscle power (five sit-to-stand, $P < 0.001$), mobility (four square step test, $P < 0.05$) and choice stepping reaction time (CSRT, $P < 0.05$) compared to CON after 6 and 12 months. There were also greater improvements in dual task motor ($P < 0.05$) and cognitive ($P = 0.05$) gait speed and CSRT ($P < 0.05$) in DT-FPT vs CON after 12 months. In conclusion, dual task functional power training reduced the risk of multiple falls and improved muscle power, mobility and dual task performance in the elderly at increased risk of falling residing in retirement villages.

Disclosures: **Robin Daly, None**

1061

Skeletal Benefit/risk of Long-term Denosumab Therapy: A Virtual Twin Analysis of Fractures Prevented To Skeletal Safety Events Observed Serge Ferrari¹, E Michael Lewiecki², Peter W Butler³, David L Kendler⁴, Nicola Napoli⁵, Shuang Huang³, D Barry Crittenden³, Nicola Pannaciuoli³, Ethel Siris⁶, Neil Binkley⁷. ¹Geneva University Hospital, Switzerland, ²New Mexico Clinical Research & Osteoporosis Center, United States, ³Amgen Inc., United States, ⁴University of British Columbia, Canada, ⁵Università Campus Bio-Medico di Roma, Italy, ⁶Columbia University Medical Center, United States, ⁷University of Wisconsin-Madison, United States

Purpose: Osteoporosis (OP) is a chronic disease, yet skeletal safety events—atypical femoral fracture (AFF) and osteonecrosis of the jaw (ONJ)—remain a concern with long-term treatment. Ten years of denosumab (DMAB) therapy in postmenopausal women with OP has demonstrated sustained and low vertebral and nonvertebral fracture rates, with low adverse event rates (Bone Lancet Diabetes Endocrinol 2017). Here, we generated a DMAB skeletal benefit/risk ratio derived from observed data and model-based estimates from the FREEDOM trial and its Extension. Methods: Exposure-adjusted subject incidence per 100,000 subject-years of clinical, major osteoporotic, vertebral, nonvertebral, and hip fractures was calculated for long-term (LT) subjects randomized to DMAB in the 3-year FREEDOM trial and enrolled in the 7-year Extension (follow-up time on DMAB 3 to 10 years). Due to the lack of a long-term placebo group, fracture rates in a hypothetical cohort of 10-year placebo controls (virtual twins [VT]) were estimated: A regression model was generated using data from subjects randomized to PBO during FREEDOM and then enrolled in the Extension; a VT with identical baseline characteristics to each LT subject was derived; and fracture rates were then predicted for the untreated VT group using the regression model. The number of fractures prevented per 100,000 subject-years was calculated as (VT rate – LT rate). AFF and ONJ incidences on DMAB were based on observed cases in the LT group during the Extension; the VT group was assumed to have no AFF or ONJ in the absence of treatment. A skeletal benefit/risk ratio was calculated from fractures prevented per AFF or ONJ observed. Results: This analysis included 2343 subjects. The estimated number of clinical fractures prevented was 1403 per 100,000 subject-years (Table). There was 1 case of AFF and 7 ONJ (mild and moderate), corresponding to rates of 5 (AFF) and 35 (ONJ) per 100,000 subject-years. Hence, there were 281 and 40 clinical fractures prevented per AFF and ONJ observed, respectively. The skeletal benefit/risk ratio for other fracture endpoints is shown below (Table). Conclusions: As long-term placebo-controlled fracture outcome studies in postmenopausal OP are not ethical, the virtual twin model provides a reasonable estimate of untreated fracture rates. Using this model, long-term DMAB therapy has a highly favorable benefit/risk profile when comparing fractures prevented per skeletal adverse event observed.

Table. Ratio of Fractures Prevented per Skeletal Safety Event Observed in Long-term FREEDOM Extension Subjects Using the Virtual Twin Method

	Exposure-adjusted subject incidence per 100,000 subject-years				
	Clinical fractures N = 2343 Exp = 18295	Major osteoporotic fractures ^a N = 2343 Exp = 18772	Vertebral fractures N = 2116 ^b Exp = 18385	Non-vertebral fractures N = 2343 Exp = 18451	Hip fractures N = 2343 Exp = 19742
Long-term	1777	1525	901	1528	149
Twin	3180	2699	1879	2924	297
Ratio ^c	0.56	0.57	0.48	0.53	0.54
Fractures prevented	1403	1174	978	1396	148
Ratio of fractures prevented per AE observed ^d					
AFF (5) ^e	280.6	234.8	195.6	279.2	29.6
ONJ (35) ^f	40.1	33.5	27.9	39.9	4.2

Based on LT denosumab subjects. All results are based on 5000 bootstrap samples.

N = number of LT subjects who had fracture outcome data; Exp = exposure time in subject years indicating the time from FREEDOM baseline to the onset of first event (for subjects who had a fracture event) or end of study or last assessment date, whichever was greater (for subjects who did not have a fracture event)

^aMajor osteoporotic fractures were defined as clinical spine, forearm, hip, or shoulder fracture

^b227 LT subjects had missing vertebral fracture outcome data during FREEDOM and/or its Extension

^c Calculated as (LT rate) / (VT rate)

^d Calculated as (VT rate – LT rate) / AE rate

^e The number in parentheses indicates the AE subject incidence rate per 100,000 subject-years in LT subjects

^f There were 2 mild, 5 moderate, and no severe cases of ONJ in the LT group

AE: Adverse event; AFF: atypical femoral fracture; ONJ: osteonecrosis of the jaw

Disclosures: **Serge Ferrari, AMGEN, UCB, Labatec, Agnovos, Consultant, UCB, MSD, Grant/Research Support**

1062

The Calgary Vitamin D Study: Bone Microarchitecture Effects of Three-Year Supplementation With 400, 4000 or 10000 IU Daily Lauren A Burt^{1*}, Marianne S Rose², Emma O Billington¹, Duncan A Raymond¹, David A Hanley¹, Steven K Boyd¹. ¹McCaig Institute for Bone and Joint Health, Cumming School of Medicine, University of Calgary, Canada, ²Research Facilitation, Alberta Health Services, Canada

Most studies exploring the effect of daily vitamin D supplementation on bone mineral density (BMD) have used dual X-ray absorptiometry (DXA) to evaluate changes, and apart from treatment of vitamin D deficiency, the effect of vitamin D on bone health is unclear. Furthermore, few studies have investigated supplementation of doses at or above the IOM's recommended tolerable upper limit (TUL) of 4000 IU daily. In a 3-year, double-blind RCT, we investigated the effect of daily doses of 400, 4000 and 10000 IU vitamin D on measures of areal BMD (aBMD) using DXA at the hip, and volumetric BMD and estimated strength by high resolution peripheral quantitative computed tomography (HR-pQCT) at the radius and tibia. Participants were healthy men and women 55 to 70 years with DXA T-score above -2.5 and serum 25(OH)D between 30 - 125 nmol/L. Participants consuming <1200 mg/day of calcium received calcium supplementation. At baseline and annual visits participants had standard DXA measurements at the hip. Additionally, the radius and tibia were scanned on a second-generation HR-pQCT (XtremeCT II, SCANCO Medical AG, Switzerland) to measure total volumetric BMD (TtBMD) at baseline, 6, 12, 24 and 36 months. Finite element analysis from HR-pQCT was calculated to estimate failure load. Following an intent-to-treat analysis, we used constrained linear mixed effects models to determine treatment group by time interactions. 311 participants were randomized; 299-303 were included in the primary analysis. Mean (SD) serum 25(OH)D concentrations increased to 76 (18), 115 (23) and 188 (39) nmol/L after 3 months, in 400, 4000 and 10000 IU groups, respectively. Total hip aBMD decreased over study duration, but no difference among treatment groups was detected ($p = 0.868$). In contrast, there were significant group-by-time interactions for TtBMD. Over a period of 3-years, TtBMD decreased at the radius (400 IU: -1.4%, 4000 IU: -2.6% and 10000 IU: -3.6%, $p < 0.001$) and tibia (400 IU: -0.9%, 4000 IU: -1.2% and 10000 IU: -2.1%, $p < 0.001$). We did not observe significant group-by-time interactions for failure load at the radius ($p = 0.259$) or tibia ($p = 0.062$). In this 3-year study of non-osteoporotic individuals with adequate baseline 25(OH)D serum, vitamin D supplementation was associated with no detectable difference in DXA aBMD, but a dose-related decrease in HR-pQCT bone density at the radius and tibia, with the largest decrease occurring in the 10000 IU/day group.

Disclosures: **Lauren A Burt, None**

1063

Physiotherapy Rehabilitation for Osteoporotic Vertebral Fracture - A randomised controlled trial and economic evaluation (PROVE trial): ISRCTN 49117867 Karen Barker^{1*}, Meredith Newman², Nigel Stallard³, Jose Leal¹, Catherine Minns Lowe², Muhammad Javaid¹, Angela Noufaily³, Anish Adhikari¹, David Smith¹, Varsha Gandhi¹, Cyrus Cooper¹, Sarah Lamb¹. ¹University of Oxford, United Kingdom, ²Oxford University Hospitals Foundation Trust, United Kingdom, ³University of Warwick, United Kingdom

Purpose: Vertebral fragility fractures are associated with significant pain and reduction in quality of life. Physical therapy is often recommended for patients and typically includes manual vs. exercise therapy. There is little evidence to support either approach. We investigated the clinical and cost-effectiveness of two different physiotherapy programmes for people with symptomatic osteoporotic vertebral fractures compared with a single session of physiotherapy. Methods: We performed a multicentre, assessor blinded, three-arm randomised trial of 7 sessions of manual therapy vs. exercise therapy delivered over 12 weeks compared to a single one hour session with a specialist physiotherapist in patients with symptomatic vertebral fractures. The co-primary outcomes were quality of life (QUALLEFO 41) and muscle endurance (Timed Loaded Standing (TLS) test) at 12 months. Secondary outcomes were: thoracic kyphosis measured with a Flexicurve ruler, balance evaluated via the Functional Reach (FR) test and physical function by the Short Performance Physical Battery (SPPB), 6 minute walk test and Physical Activity Scale for the Elderly (PACE), a health resource use diary and the EQ-5D-5L at 4 and 12 months. Results: 615 patients were enrolled with 216 patients randomised to the exercise therapy arm, 203 patients to manual therapy arm and 197 to usual care arm. The mean age was 72.1 yrs and 87% were female. At 12 months, there were no significant benefits of either a course of exercise or manual therapy over a single hour session of physiotherapy. For the secondary outcomes, relative to a single session, there is significant improvement from exercise therapy at 4 months in the SPPB, the FR test and the six minute walk test and from manual therapy at four months in TLS and FR. The treatment differences for TLS were significant in those patients under 70 years old, but not older. Neither the manual or exercise physiotherapy interventions were cost-effective relative to a single physiotherapy session using the £20,000 per QALY threshold. Conclusions: In the largest trial assessing physiotherapy in patients with osteoporotic fragility fractures, benefits were seen at 4 months but neither intervention was superior to a single one-hour advice session with a specialist physiotherapist at 12 months. Future research should focus on improving adherence to therapy recommendations.

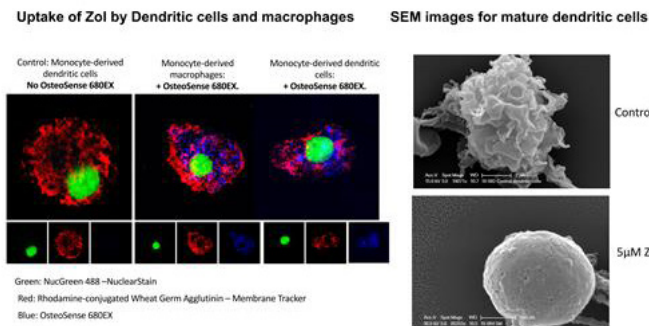
Disclosures: **Karen Barker, None**

1064

Impaired Dendritic Cell Function and Bacterial Load Increase in the Oral Microenvironment as Contributing Factors to the Induction of MRONJ

Ranya Elsayed*¹, Esteban Celis², Hussein Sultan², Christopher Cutler¹, Mahmoud Elashiry¹, Mohamed Meghil¹, Zoya Kurago¹, Mohamed Awad¹, Mohey Eldin El-Shikh³, Mohammed Elsalanty¹, Riham El Sayed³. ¹Department of Oral Biology, Dental College of Georgia, Augusta University, United States, ²Biochemistry and Molecular Biology, Georgia Cancer Center, Medical College of Georgia, Augusta University, United States, ³Queen Mary, University of London, United Kingdom

Previous studies have shown the important role of immune cells during the early stages of bone healing. We propose that anti-resorptive medication-related osteonecrosis of the jaw (MRONJ) may be a consequence of disruption in the local immune response in the bone microenvironment. While bisphosphonates are known to target osteoclasts mainly, immune cells from the same lineage, such as macrophages and dendritic cells (DCs), could also be affected. Our aims were to: 1) test the hypothesis that Zol treatment increases oral bacterial load in vivo and reduces DC uptake of oral bacteria in-vitro. 2) test the hypothesis that Zoledronate (Zol) modulates local immune response by impairing DC differentiation and function. Using immunofluorescence, we confirmed that bisphosphonates are internalized by DCs and macrophages. Phagocytic function and bacterial clearance by murine bone marrow-derived DCs (BMDCs) were impaired by Zol treatment, leading to a significant decrease in the uptake of FITC dextran and inability to phagocytose common periodontal pathogens, such as *P. gingivalis* and *F. nucleatum*, evidenced by flow cytometry. Increased bacterial load was confirmed in oral samples from Zol-treated animals compared to controls. Zol-treated BMDCs demonstrated a significant decrease in the expression of maturation markers MHCI, costimulatory molecules CD86, CD80 and CD83, and inflammatory cytokines IL-6, IL-12, IL-23 interferon gamma (IFN- γ), and increase in the anti-inflammatory cytokine IL-10, as demonstrated by qPCR and flow cytometry. Furthermore, Zol-treated DCs were defective in CCL19-induced migration, consistent with a significant decrease in CCR7 receptor expression. There was also a decrease in the expression of the tetraspanin CD9. Electron microscopy imaging was performed to confirm Zol-induced changes in morphology and cytoskeleton of DCs. Moreover, Zol treatment reduced the capacity of DCs to present OVA peptide to OT-II transgenic mice-derived (OVA specific) T-cells shown by CFSE proliferation assay, with a significant decrease in the production of Th-1 activation cytokines IL-2 and IFN- γ shown by ELISA. In conclusion, Zol treatment causes disruption of DC function, combined with an increase in bacterial load in alveolar bone, both of which could contribute to the pathogenesis of osteonecrosis.



Disclosures: *Ranya Elsayed, None*

1065

Gnas inactivation alters adipose tissue properties during progression to heterotopic ossification

Niambi Brewer*¹, John T Fong², Deyu Zhang², Frederick S Kaplan², Robert J Pignolo³, Eileen M Shore¹. ¹Departments of Orthopaedic Surgery and Genetics, Perelman School of Medicine, University of Pennsylvania, United States, ²Department of Orthopaedic Surgery, Perelman School of Medicine, University of Pennsylvania, United States, ³Division of Geriatric Medicine and Gerontology, Mayo Clinic College of Medicine, United States

Heterotopic ossification (HO) is a common physiological response to severe tissue trauma such as combat blast injuries, high impact trauma, and hip replacements. The investigation of rare genetic disorders provides insight into the aberrant mechanisms that cause HO formation and leads to identification of targets for pharmacological intervention in both genetic and non-genetic forms of HO. HO in the rare genetic disorder, Progressive Osseous Heteroplasia (POH), initiates in subcutaneous soft tissues then progresses into deeper connective tissues. POH is caused by inactivation of GNAS, a gene that encodes the alpha stimulatory subunit of G proteins (G α). Our previous work demonstrated that adipose derived stromal cells (ASCs) from Gnas-KO mice exhibit enhanced osteogenic and impaired adipogenic potential in vitro, supporting that osteogenesis and heterotopic bone in POH occurs at the expense of adipogenesis, however, the pathophysiology of POH remains poorly

understood. To examine the mechanisms and signals that lead to initiation of heterotopic bone caused by GNAS inactivation in osteogenic progenitor cells, we developed an in vivo HO model using Gnas-null mice (Gnas^{fl/fl};Cre-ERT2 or Gnas^{fl/fl};Ai9^{fl/fl};Cre-ERT2) that consistently and reliably induces spontaneous HO. Through microCT, histologic, and immunohistochemistry analyses in cross-sectional and longitudinal studies, this model initiates HO within subcutaneous adipose tissues with progressive expansion over time. Using the same model and methods, we investigated the tissue changes that precede HO formation and identified increased extracellular matrix content, as well as a shift from white to beige adipose tissue, including UCP1 expression and decreased adipocyte size and lipid content. Cell implant studies showed that fluorescent-labeled Gnas-null ASCs form HO when implanted within Gnas-null adipose tissue, as expected. However, wildtype (WT) ASCs also induce HO in a Gnas-null background, although less robustly than mutant ASCs, suggesting that the tissue microenvironment strongly influences cell fate. Further, neither WT nor Gnas-null ASCs implanted into a control background formed HO, supporting that the mutant osteogenic progenitor cells are insufficient to induce HO. These data highlight the importance of the microenvironment within the adipose tissue in supporting ectopic bone formation by Gnas inactivation and provide insights into the pathophysiology of POH and other GNAS-related disorders.

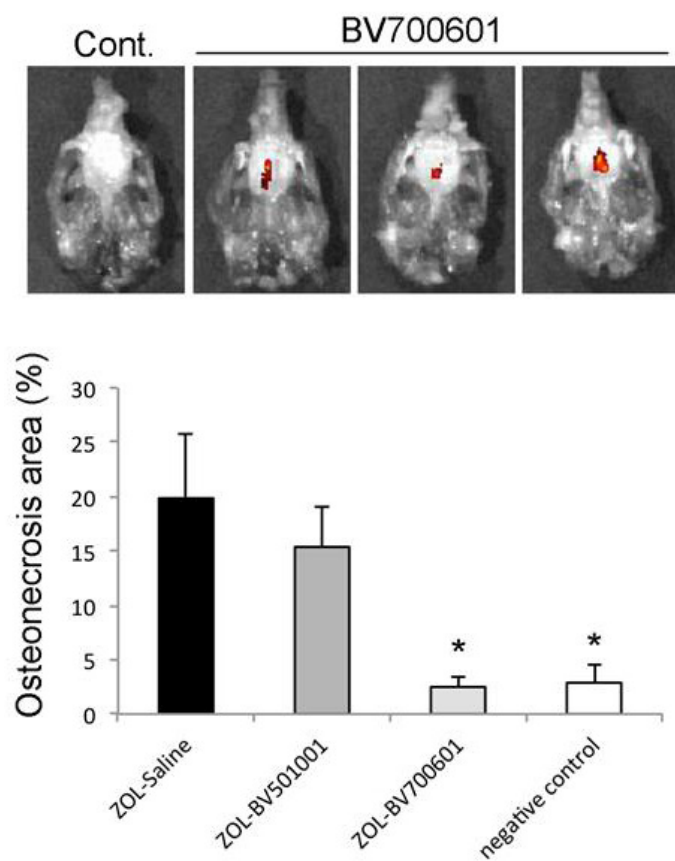
Disclosures: *Niambi Brewer, None*

1066

Prevention of Zoledronate-Induced MRONJ with Indocyanine Green (ICG) Labeled Bisphosphonates

Shuting Sun*¹, Akishige Hokugo², Frank H. (Hal) Ebetino¹, Keivan Sadrerafi¹, Philip Cherian¹, Charles E. McKenna³, Ichiro Nishimura². ¹Biovinc, United States, ²UCLA School of Dentistry, United States, ³Chemistry Department, University of Southern California, United States

Medication-related osteonecrosis of the jaw (MRONJ) is a rare but serious concern, particularly for oral surgery patients who have received a nitrogen-containing bisphosphonate (BP) drug to avoid skeletal complications and bone pain due to multiple myeloma or metastatic bone cancer. We recently introduced the concept of legacy bisphosphonate displacement via local administration with a suitable inactive BP as an approach to prevent or treat BP-associated MRONJ. We have developed an efficient synthesis to provide several novel BP compounds to facilitate efficacy studies. Our synthetic procedures allow for analogs including novel ICG-conjugated BPs which offer a fluorescent imaging moiety that is approved as a human diagnostic. For our therapeutic purpose, we hypothesized that these analogs need to maintain their bone affinity, but not possess pharmacological activity. Potentially useful bone affinity was demonstrated with these new fluorescent BP analogs on incubation with hydroxyapatite although that of BV700601 was higher. Anti-prenylation activity (a marker for inhibition of bone resorption activity) was evaluated in J744.2 macrophages to show that BV501001 (AF647-ZOL) and BV700601 (ICG-C-pRIS) had undetectable activity up to 100 μ M. Efficacy to prevent the development of Zol-induced ONJ was determined in female 8-10 wk old C57B16J mice pretreated with 500 μ g/kg ZOL. Subsequently, mice were subjected to intra-oral injection of vehicle saline, BV501001 (350 μ M) or BV700601 (350 μ M) to the palatal mucosa adjacent to the left maxillary first molar. Ten days later, the maxillary left first molar was extracted. Two weeks after tooth extraction, the maxilla was harvested, subjected to ex vivo fluorescent imaging (IVIS), and the development of osteonecrosis adjacent to the extraction wound was measured in histological cross-sections. The area of necrotic bone over the left palatal bone area in the saline, BV501001, and BV700601 groups was 19.8 \pm 6.0%, 15.4 \pm 3.6%, and 2.5 \pm 0.9% respectively. BV700601 intra-oral injection resulted in the prevention of osteonecrosis development, potentially due to its higher bone affinity than BV501001. Our results provide support for the proposal that local BP displacement prophylaxis, prior to dental surgery, can prevent or mitigate the induction of MRONJ associated with legacy nitrogen containing BP accumulated in the jawbone after routine therapy, while preserving the therapeutic effect of NBPs at other diseased skeletal sites.



Disclosures: **Shuting Sun**, BioVinc, Major Stock Shareholder

1067

The Effect of Androgens on Renal Calcium and Phosphate Handling, Independent of Bone and in Circumstances of Low Dietary Calcium Rougin Khalil^{*1}, Na Ri Kim¹, Ferran Jordi¹, Frank Claessens², Dirk Vanderschueren¹, Brigitte Decallonne¹. ¹KU Leuven, Department of Chronic Diseases, Metabolism & Ageing (CHROMETA), Clinical and Experimental Endocrinology, Leuven, Belgium, ²KU Leuven, Department of Cellular and Molecular Medicine, Molecular Endocrinology, Leuven, Belgium

We have previously shown that orchidectomy (ORX) in adult mice induces hypercalcaemia and upregulation of renal Ca²⁺ and PO₄³⁻ transporters, but also bone loss already after 2 weeks. Pretreatment with a risedronate inhibited bone resorption and hypercalcaemia but confirmed the upregulation of renal Ca²⁺ and PO₄³⁻ transporters, suggesting bone-independent renal effects of androgens. We hypothesize that androgens regulate renal Ca²⁺ and PO₄³⁻ homeostasis, independent of the dietary Ca²⁺ content as well. ORX was performed on 18-week-old male mice (vs SHAM) and pretreated all animals with risedronate. Mice were fed either a normal Ca²⁺ diet (NCD, 1%) or a low Ca²⁺ diet (LCD, 0.02%), while PO₄³⁻ was unchanged (0.6%). At 1 and 2 weeks post-ORX 24 hr urine (metabolic cages) and serum was collected. After sacrifice (2 w post-ORX) kidneys were taken for qPCR of Ca²⁺ and PO₄³⁻ transporters, trabecular bone was analyzed by microCT (L5 vertebra), and femoral bone was analyzed for Ca²⁺ content by ashing. Serum Ca²⁺ and PO₄³⁻, and urinary Ca²⁺ excretion were similar under both diets, but PO₄³⁻ excretion was significantly increased in both the SHAM and ORX groups (239% and 268%, P < 0.0001) under LCD diet. Under LCD, increased serum levels of 1,25-dihydroxyvitamin D and PTH were observed. While risedronate efficiently blocked ORX-induced bone loss under the NCD, microCT analysis revealed that bone resorption was not fully blocked under the LCD, with a decrease in bone volume density of 14% compared to the NCD fed SHAM mice (P < 0.05). Also the femur Ca²⁺ content was significantly reduced in the LCD group (7.2 versus 8.8 mg in the NCD fed SHAM mice, p < 0.0001). Under the NCD an increase of renal Ca²⁺ and PO₄³⁻ transporter expression after ORX was confirmed. In the LCD group a small but significant additional increase of renal Ca²⁺ transporter expression was observed, with a 1.7-fold increase for TRPV5, a 2.1-fold increase for CaBP9K and a 1.5-fold increase for PMCA (vs respectively a 1.6-, 1.5- and 1.3-fold increase for the NCD). Expression of PO₄³⁻ transporters (NaPi-2c, PiT1, PiT2) was similar in both diet groups. In conclusion, low dietary Ca²⁺ results in secondary hyperparathyroidism with ORX-induced bone loss despite treatment with bisphosphonates, and an additional increase in renal Ca²⁺ transporters. These findings underline the

importance of adequate dietary Ca²⁺ intake along with anti-resorptive drugs in circumstances of bone loss post-androgen deprivation.

Disclosures: **Rougin Khalil**, None

1068

PPAR γ in cells of the mesenchymal lineage is dispensable for the age-dependent decline of bone mass and hematopoietic changes in the appendicular skeleton Maria Almeida^{*}, Michela Palmieri, Ha-Neui Kim, Li Han, Xin Zhang, Wen Li, Yonghan He, Robert Weinstein, Daohong Zhou, Stavros Manolagas, Robert Jilka. UAMS, United States

Age-dependent bone loss is associated with an increase in marrow adipocytes. Because both osteoblasts and adipocytes originate from a common mesenchymal progenitor, it has been postulated that this bone loss is due in part to diversion of mesenchymal progenitors to adipocytes at the expense of osteoblasts. Mesenchymal progenitors also give rise to stromal cells, which along with adipocytes, are critical sources of factors that support the hematopoietic stem cell (HSC) niche. With age, HSCs increase but their progeny is skewed toward the myeloid lineage at the expense of lymphoid cells. PPAR γ is a master transcriptional regulator of adipocytes. To investigate the contribution of marrow adipocytes to age-related changes in bone and bone marrow, we generated mice lacking PPAR γ in the mesenchymal lineage of the appendicular skeleton using Prx1-Cre (PPAR Δ Prx1 mice) in the C57BL/6J background. PPAR Δ Prx1 littermates were used as controls. Deletion of PPAR γ was confirmed by qPCR of DNA from cortical bone and RNA from bone marrow-derived stromal cell cultures. Consistently, and in contrast to cells from control mice, rosiglitazone failed to stimulate adipocyte differentiation or to inhibit osteoblast differentiation in ex-vivo bone marrow cultures of 22 month old PPAR Δ Prx1 mice. Cancellous bone volume at the femoral distal metaphysis and cortical thickness at the diaphysis were indistinguishable in PPAR Δ Prx1 and control females and males at 3 and 6 months of age, as determined by micro-CT. Control mice exhibited the expected loss of cortical bone thickness at the diaphysis and the proximal end of the femur, at 22 months of age. The volume of the cancellous bone compartment of the femoral head declined from 60% to 45% between 6 and 22 months of age. However, cortical and cancellous bone mass was indistinguishable between PPAR Δ Prx1 and aged matched controls. Cancellous bone at the distal femur was undetectable in both control and PPAR Δ Prx1 mice. Moreover, the effect of aging on hematopoietic stem cells was unaltered by PPAR γ deletion, as measured by HSC number and circulating B, T, and myeloid cells, using FACS. We conclude that PPAR γ expressed in mesenchymal progenitors and their progeny plays no role in the age-dependent decline of bone mass or the hematopoietic system changes in the appendicular skeleton of mice.

Disclosures: **Maria Almeida**, None

1069

An Antibody against Oxidized Phospholipids Promotes Bone Anabolism by Preventing their Binding to the Scavenger Receptor ScrB1 and thereby their Pro-Apoptotic Effect on Osteoblasts Elena Ambrogini^{*1}, Michela Palmieri¹, Li Han¹, Xuchu Que², Sotirios Tsimikas², Joseph L Witzum², Stavros C Manolagas³, Robert L Jilka³. ¹Center for Osteoporosis and Metabolic Bone Diseases, University of Arkansas for Medical Sciences and the Central Arkansas Veterans Healthcare System, United States, ²Department of Medicine, University of California San Diego, United States, ³Center for Osteoporosis and Metabolic Bone Diseases, Center for Osteoporosis and Metabolic Bone Diseases, University of Arkansas for Medical Sciences and the Central Arkansas Veterans Healthcare System, United States

Oxidized phospholipids (OxPL) are pro-inflammatory products of lipid peroxidation. Scavenger receptors (SRs) and toll-like receptors (TLRs) recognize OxPL and dispose of oxidatively-modified molecules. Natural antibodies (nAbs) of the innate immune system also recognize OxPL and block their deleterious effects. However, persistence and/or excessive amounts of OSEs overwhelm these defense mechanisms and result in several diseases, such as atherosclerosis and osteoporosis. Oxidized phospholipids containing phosphocholine (PC-OxPL) are components of oxidized low density lipoproteins (OxLDLs), and are also present on the surface of apoptotic cells. The nAb IgM E06 recognizes PC-OxPL. It was previously reported that male transgenic mice expressing a single chain (scFv) form of the antigen-binding domain of E06 IgM (E06-scFv) are protected against high fat diet-induced atherosclerosis and bone loss. Remarkably, they also have increased cancellous bone in the distal femur and vertebrae when fed a normal diet. These anabolic effects are associated with increased bone formation. We report here that the same bone phenotype is present also in female E06-scFv mice fed normal diet, and both sexes exhibit an increase in cortical thickness of the diaphyseal femur due to a reduction in medullary area. Together, these findings indicate that lipid peroxidation negatively affects bone under physiologic conditions, in part by restraining bone formation. To elucidate potential mechanisms responsible for this effect, we used qPCR to measure the levels of the SRs and TLRs known to bind PC-OxPL, and found that calvaria osteoblastic cells primarily expressed ScrB1, while CD36, TLR2, 4 and 6 were expressed at 3-30-fold lower levels. Ox-LDL decreased the replication, differentiation and survival of osteoblast progenitors in vitro; and these effects were reversed by purified E06 IgM. Reduction of ScrB1 in calvaria osteoblastic cells using shRNA protected them from OxLDL-induced apoptosis. Furthermore, bone marrow- or calvaria-derived osteoblasts from

ScrB1 knock-out mice were protected from the pro-apoptotic effect of OxLDL, whereas osteoblastic cells from wild type mice were not. Together with published evidence that ScrB1 knock out mice have high bone mass, our results indicate that ScrB1 mediates the deleterious effects of PC-OxPL on osteoblasts and that anti-PC-OxPL antibodies, like E06, may exert their bone anabolic effects in part by preventing OxPL from binding to SR-B1.

Disclosures: **Elena Ambrogini, None**

1070

Change in BMD as a Surrogate for Fracture Risk Reduction in Osteoporosis Trials: Results from Pooled, Individual-level Patient Data from the FNIH Bone Quality Project Dennis Black^{*1}, Eric Vittinghoff¹, Richard Eastell², Douglas Bauer¹, Li-Yung Lui³, Lisa Palermo¹, Charles McCulloch¹, Jane Cauley⁴, Sundeep Khosla⁵, Fernando Marin⁶, Anne De Papp⁷, Andreas Grauer⁸, Mary Bouxsein⁹. ¹University of California, San Francisco, United States, ²University of Sheffield, United Kingdom, ³California Pacific Medical Center, United States, ⁴University of Pittsburgh, United States, ⁵Mayo Clinic, United States, ⁶Eli Lilly and Company, Switzerland, ⁷Merck & Co., Inc., United States, ⁸Amgen, Inc., United States, ⁹Harvard Medical School, United States

To facilitate future drug development in osteoporosis, the FNIH Bone Quality Project aims to identify a surrogate that can be used in place of fracture in future clinical trials. To do so, we compiled and pooled individual patient data from 25 randomized, placebo-controlled osteoporosis trials that enrolled >125,000 subjects. Changes in BMD are an obvious candidate surrogate. One step in the validation of a surrogate biomarker is to estimate the percent of treatment explained (PTE) by the surrogate. Previous analyses of individual trials reported PTEs for BMD change ranging from 4% to ~80%, but analysis methods differed, and single studies were too small to give precise estimates. We used our pooled data to estimate PTE for BMD change, using a two-stage procedure. In the first stage, we used linear mixed models (LMM) to estimate participant-specific BMD trajectories. In the second, we fit nested pooled logistic regression (PLR) models for the effect of treatment on time to vertebral, non-vertebral and hip fractures. PTE was calculated as the percentage change in the coefficient for treatment after adding time-dependent BMD change, based on the first-stage LMM, to the base PLR model. Confidence intervals for PTE were obtained using the method of seemingly unrelated regressions. We analyzed PTE for femoral neck, total hip and lumbar spine BMD for vertebral, hip and non-vertebral fractures including people with at least one BMD measurement. We examined the change in BMD at 24 months, and included all fractures to the end of the trials. The current analyses included 21 trials (including bisphosphonates, SERMs, estrogen, odanacatib, denosumab, PTH1-34, and PTH1-84) with 83,395 subjects with DXA who suffered 4515 vertebral, 6608 non-vertebral and 873 hip fractures. We found that PTE for 24 month change in femoral neck BMD was 65% (95% CI: 53-77%) for vertebral, 74% (95% CI: 43-105%) for non-vertebral and 65% (24-106%) for hip fractures (see Table). The results were similar for total hip, but PTE was lower for lumbar spine BMD. Our results indicate that changes in total hip and femoral neck BMD explain a large proportion of the treatment-related reduction in fracture risk for all 3 fracture types. Importantly, this analysis included therapies with differing mechanisms of action. These data, along with others generated from this project, support the potential value of DXA BMD change as a surrogate for fractures in future trials.

Table. Percent of treatment effect (%; 95% CI) explained by changes in total hip (TH), femoral neck (FN) and lumbar spine (LS) at 24 months for vertebral, hip and non-vertebral fractures.

	Δ TH BMD	Δ FN BMD	Δ LS BMD
Vertebral Fx	66% (55, 77%) p<0.0005	65% (53, 77%) p<0.0005	27% (14, 40%) p<0.0005
Hip Fx	60% (27, 93%) p<0.0005	65% (24, 106%) p=0.002	42% (7, 76%) p=0.019
Non-vertebral Fx	69% (41, 96%) p<0.0005	74% (43, 105%) p<0.0005	56% (25, 87%) p<0.0005

Disclosures: **Dennis Black, Radius Pharmaceutical, Consultant, Asahi-Kasei, Consultant, Roche Diagnostics, Speakers' Bureau**

1071

Probiotic Treatment Using a Mix of Three Lactobacillus Strains Protects Against Lumbar Spine Bone Loss in Healthy Early Postmenopausal Women Claes Ohlsson^{*1}, Dan Curia², Klara Sjögren¹, Per-Anders Jansson³. ¹Centre for Bone and Arthritis Research, Institute of Medicine, the Sahlgrenska Academy at University of Gothenburg, Sweden, ²CTC, Gothia Forum, Sahlgrenska University Hospital, Sweden, ³Department of Molecular and Clinical Medicine, the Sahlgrenska Academy, University of Gothenburg, Sweden

The gut microbiota composition has been associated with several different diseases. Experimental studies using rodents indicate that manipulation of the gut microbiota compo-

sition may alter bone homeostasis and we recently introduced a new term "osteomicrobiology" for the rapidly emerging research field of the role of the gut microbiota in bone health (Trends Endocrinol Metab. 2015 26:69-74). Several recent studies have demonstrated that certain probiotic treatments protect rodents from ovariectomy-induced bone loss but there is no adequately powered clinical study of the effect of probiotic treatment on postmenopausal bone loss in women. The aim of the present study was to determine if a combination of three bacterial strains protects against the rapid lumbar spine bone loss occurring in early postmenopausal women. We performed a multicenter, randomized, placebo-controlled, parallel group, clinical study to evaluate the efficacy on lumbar spine bone mineral density (LS-BMD) and safety of a probiotic treatment consisting of three lactobacillus strains (*L. paracasei* DSM 13434, *L. plantarum* DSM 15312 and DSM 15313; 1x10¹⁰ CFU/capsule once daily for 12 months) in 234 healthy early postmenopausal women (LS-BMD T-score >-2.5; 2-12 years after menopause; mean age 58.6±4.0 (SD) years, mean BMI 24.0±2.7 kg/m²) that were analysed by LS-DXA both at baseline and after 12 months. The primary endpoint was the percentage change from baseline in LS-BMD at 12 months. The LS BMD loss was significant in the placebo group -0.77% (p=0.0006) but not in the probiotic treated group -0.17% (p=0.40). The percentage change in LS-BMD from baseline was small but significantly different in the probiotic group compared with the placebo group (p=0.04; Wilcoxon rank-sum test). The most pronounced protective effect of probiotic treatment was observed for women below the median of 6 years from menopause. For these women, the LS-BMD loss was clearly less pronounced in the probiotic treated group -0.18% (p=0.56) compared with the placebo group -1.21% (P=0.0001). The adverse events were similar between the two groups. In conclusion, probiotic treatment using a mix of three lactobacillus strains protects against lumbar spine bone loss in healthy early postmenopausal women. These findings indicate that the pronounced lumbar spine bone loss occurring during the first years after menopause is reduced by specific probiotic treatment.

Disclosures: **Claes Ohlsson, None**

1072

VK5211, a Novel Selective Androgen Receptor Modulator (SARM), Significantly Improves Lean Body Mass in Hip Fracture Patients: Results of a 12 Week Phase 2 Trial Branko Ristic^{*1}, Vladimir Harhaji², Paul Dan Sirbu³, Moises Irizarry-Roman⁴, Gabor Bucsi⁵, Istvan Szanyi⁵, Neil Binkley⁶, Denise Orwig⁷, Joel Neutel⁸, Ken Homer⁸, Marianne Mancini⁹, Hiroko Masamune⁹, Geoff Barker⁹, Brian Lian⁹. ¹Clinical Center Kragujevac, Clinic for Orthopedics and Traumatology, Serbia, ²Clinical Center of Vojvodina, Clinic for Orthopedic Surgery and Traumatology, Serbia, ³County Hospital for Emergency Sfantul Spiridon Iasi, Clinical Section of Orthopedics and Traumatology, Romania, ⁴Infinite Clinical Research, United States, ⁵PTE ÁK Traumatology and Clinical Surgery, Hungary, ⁶University of Wisconsin School of Medicine and Public Health, United States, ⁷Department of Epidemiology and Public Health, University of Maryland School of Medicine, United States, ⁸Integrum Clinical Research, United States, ⁹Viking Therapeutics, Inc., United States

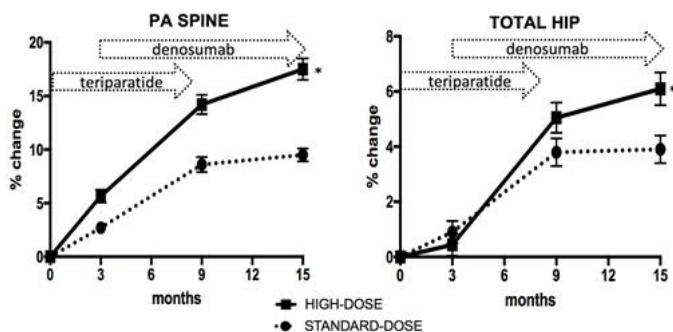
Introduction Hip fractures are a leading cause of disability and morbidity in older people. Post-fracture, an increased catabolic state often leads to loss of muscle, which can impair balance and endurance, potentially increasing the risk of further injury. Anabolic steroids have been shown to improve muscle mass in certain settings. Selective androgen receptor modulators (SARMs) could be similarly effective in older patients who have suffered muscle loss following hip fracture, while potentially avoiding undesired side effects associated with broad-acting anabolic agents. VK5211 is a novel, non-steroidal, orally available SARM that has been shown to improve muscle mass and bone mineral density in animal models. In humans, a prior Phase 1 study demonstrated increases in lean body mass after 21 days of dosing. Purpose A 12 week study was conducted to assess the safety and efficacy of VK5211 in patients who had suffered a hip fracture. Methods A randomized, double-blind, placebo-controlled, multicenter, international Phase 2 trial was conducted to evaluate VK5211 in patients recovering from hip fracture. Patients were randomized to receive daily oral VK5211 doses of 0.5 mg, 1.0 mg, 2.0 mg, or placebo, for 12 weeks. The primary endpoint evaluated change from baseline in lean body mass, less head, in patients receiving VK5211 compared with placebo. Secondary and exploratory endpoints included changes in appendicular lean mass, bone density, and functional performance. Results A total of 108 patients were randomized (83 F, 25 M; mean age 77). Patients receiving VK5211 demonstrated significant increases in lean body mass, less head, after 12 weeks. Placebo-adjusted increases were 4.8% at 0.5 mg, 7.2% at 1.0 mg, and 9.1% at 2.0 mg (p < 0.005 for each). The proportions of patients experiencing at least a 2.0 kg increase were 14% with placebo, 57% at 0.5 mg, 65% at 1.0 mg, and 81% at 2.0 mg (p < 0.01 for each). Patients receiving VK5211 demonstrated improvement in certain measures of functional performance, including the 6-minute walk test and short physical performance battery (these endpoints were not powered for significance). The rates of adverse events were similar in cohorts receiving VK5211 as compared with placebo, and no drug-related SAEs were observed in VK5211-treated patients. Conclusion VK5211 was well-tolerated and produced improvements in lean body mass in hip fracture patients following 12 weeks of dosing. Further evaluation in this setting is warranted.

Disclosures: **Branko Ristic, None**

1073

Rapid and Large BMD Increases in Postmenopausal Women Treated With Combined High-Dose Teriparatide and Denosumab: The DATA-HD Randomized Controlled Trial Benjamin Leder^{*1}, Hang Lee², Natalie David², Richard Eastell³, Tsai Joy². ¹Harvard Medical School, Massachusetts General Hospital, United States, ²Massachusetts General Hospital, United States, ³Mellanby Centre for Bone Research, United Kingdom

In the DATA study, we demonstrated that when given concomitantly, denosumab (DMAB) fully inhibits teriparatide (TPTD)-induced bone resorption while allowing for continued TPTD-induced modeling-based bone formation. These effects on bone turnover, in turn, result in greater gains in hip and spine BMD than can be achieved with either drug alone. We thus hypothesized that combining DMAB with a larger anabolic stimulus, in the form of high-dose TPTD, would further expand the separation between rates of bone formation and resorption and result in even larger and faster increases in bone mass. Methods: 69 postmenopausal osteoporotic women (age 52-83) were randomized to one of two treatments: TPTD 40-mcg (high dose-HD) or TPTD 20-mcg (standard dose-SD) given months 0-9 overlapped with DMAB 60-mg SC given months 3-15 for a total study duration of 15 months. Subjects were excluded for oral BP exposure within 6 months or any exposure to TPTD, DMAB, or IV BPs. Results: At month 15, mean total hip (TH) BMD increased more in the HD ($6.1 \pm 3.4\%$) than the SD group ($3.9 \pm 2.9\%$, $P < 0.001$). Femoral neck (FN) BMD also increased more in the HD than SD group ($6.8 \pm 4.1\%$ vs $4.3 \pm 3.7\%$, $P = 0.04$) as did spine BMD ($17.5 \pm 6.0\%$ vs $9.5 \pm 3.2\%$, $P < 0.001$). Of note, both TH and FN BMD had increased by $>5\%$ and spine BMD by $>14\%$ by month 9 (after only 3 months of TPTD followed by 6 months of combined therapy). Additionally, the relative greater BMD gains in the HD vs the SD group continued to expand during the final 6-months of treatment despite the fact that both groups were receiving identical DMAB monotherapy during this phase. In the initial 3-months of TPTD monotherapy, serum bone formation markers increased significantly more in the HD than SD group (PINP, 402% vs 153%, OC 254% vs 140%), as did bone resorption (CTX, 159% vs 84%). At month 9, OC remained above baseline in the HD but not SD group (+10% vs -27%) and PINP was significantly less suppressed in HD than SD (-32% vs -43%). CTX was also less suppressed in the HD than SD group (-46% vs -69%). Month-15 bone turnover markers (after 6 months of DMAB monotherapy) were similarly suppressed in both groups. Summary: The combination of TPTD 40-mcg and DMAB increases hip and spine BMD faster and more than standard combination therapy or any available single drug. These robust and rapid increases in BMD suggest that by expanding the separation between bone formation and bone resorption, the HD regimen may provide the fastest means of restoring skeletal integrity in osteoporotic patients at the highest risk of fragility fracture. Larger trials are urgently needed to fully evaluate the efficacy and safety of this treatment approach.



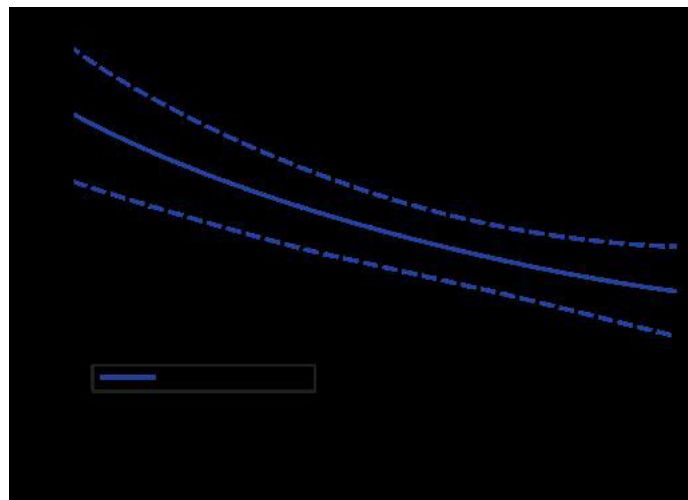
Disclosures: Benjamin Leder, Amgen, Grant/Research Support, Lilly, Grant/Research Support, Amgen, Consultant

1074

T-score as an Indicator of Fracture Risk on Therapy: Evidence From Romosozumab vs Alendronate Treatment in the ARCH Trial Felicia Cosman^{*1}, E. Michael Lewiecki², Peter R. Ebeling³, Eric Hesse⁴, Nicola Napoli⁵, Daria B. Crittenden⁶, Maria Rojeski⁶, Wenjing Yang⁶, Cesar Libanati⁷, Serge Ferrari⁸. ¹Columbia University, United States, ²New Mexico Clinical Research & Osteoporosis Center, United States, ³Monash University, Australia, ⁴University Medical Center Hamburg-Eppendorf, Germany, ⁵Campus Bio-Medico University of Rome, Italy, ⁶Amgen Inc., United States, ⁷UCB Pharma, Belgium, ⁸Geneva University Hospital, Switzerland

BMD is a strong predictor of fracture (fx) risk in untreated patients. Recent evidence suggests that BMD achieved during treatment also reflects fx risk; thus, T-scores are being considered as a target to guide osteoporosis treatment. In ARCH (NCT01631214), romosozumab (Romo), an investigational bone-forming agent with a dual effect of increasing bone formation and decreasing bone resorption, followed by alendronate (ALN) had greater efficacy in fx risk reduction and BMD gains vs ALN alone (Saag NEJM 2017). Of note, a cardiovascular imbalance was observed with Romo in ARCH and a comprehensive assess-

ment of these data is ongoing. Here we explored the relationship between T-scores achieved on-study after 1 year with Romo or ALN and subsequent fx risk. Postmenopausal women with osteoporosis and prior fragility fx were randomized 1:1 to receive Romo 210mg SC QM or ALN 70mg PO QW for 12 months, followed by open-label (OL) ALN 70mg PO QW for ≥ 12 months, with an event-driven primary analysis. We examined change from baseline in BMD and T-scores at 12 months and the relationship between total hip (TH) T-scores at month 12 and subsequent nonvertebral (NVT) fx rates. We also compared fxs in the OL period, including new vertebral (VT) fxs in year 2 (based on month 24 spine radiographs) and clinical, NVT, and hip fxs between arms in the full OL period. ARCH enrolled 4093 patients (2046 Romo, 2047 ALN); mean baseline T-scores were -2.96 at the lumbar spine and -2.80 at the TH. 3465 patients (1739 Romo, 1726 ALN) received ≥ 1 OL ALN dose in the OL period (median 1.9 years follow-up). Mean TH BMD increased by 6.2% for Romo and 2.8% for ALN in the first year, with increases in T-score of 0.31 and 0.15, respectively. At month 12, the achieved TH T-score was associated with the 1-year NVT fx rate observed in the OL period (Figure) and the relationship was independent of the drug received in the first year. During the OL period, when all patients were on ALN, patients who received Romo first had a 75% lower relative risk of new VT fx ($P < 0.001$), and had reductions in clinical (32%, $P = 0.001$), NVT (19%, $P = 0.120$), and hip (40%, $P = 0.041$) fxs vs patients who received ALN first. Higher absolute TH T-scores achieved on therapy at month 12 resulted in subsequent lower fx risk regardless of the treatment received, with ongoing benefits from building a BMD foundation. These data support the concept of a T-score target to improve outcomes in osteoporosis treatment.



Disclosures: Felicia Cosman, Amgen, Eli Lilly, Grant/Research Support, Amgen, Eli Lilly, Speakers' Bureau, Advisory Boards Amgen, Eli Lilly, Merck, and Radius, Other Financial or Material Support, Merck, Radius, Tarsa, Consultant

1075

Breast Cancer Bone Metastases are Attenuated in a Tgif1-deficient Bone Microenvironment Marie-Therese Haider^{*}, Hiroaki Saito, Eric Hesse, Hanna Taipaleenmäki. Molecular Skeletal Biology Laboratory, Department of Trauma, Hand and Reconstructive Surgery, University Medical Center Hamburg-Eppendorf, Hamburg, Germany

Osteoclast activation is a hallmark of breast cancer-induced osteolytic bone disease. However, much less is known about the role of osteoblasts during this process. Our experiments revealed that osteoblast-conditioned medium stimulates breast cancer cell (BCC) migration in vitro ($p < 0.001$), suggesting that osteoblasts may also play a role during early stages of bone metastasis. Furthermore, we identified the homeodomain protein TG-interacting factor-1 (Tgif1) as a strongly up-regulated molecule in osteoblasts upon stimulation by BCCs, indicating a potential role of Tgif1 in the osteoblast-BCC interaction. Indeed, conditioned medium from osteoblasts of mice bearing a germline deletion of Tgif1 (Tgif1^{-/-}) failed to induce BCC migration compared to conditioned medium obtained from wild-type osteoblasts ($p < 0.05$), suggesting that Tgif1 in osteoblasts supports the activation of BCC movement. To better understand this finding, we performed unbiased SILAC and RNA-seq analyses and identified Semaphorin 3E (Sema3E) to be abundantly expressed and secreted by Tgif1^{-/-} osteoblasts. Recombinant Sema3E dose-dependently impaired BCC migration, suggesting that Tgif1 supports BCC migration by suppressing Sema3E expression in osteoblasts. To test the hypothesis that Tgif1 contributes to the initiation of metastatic bone disease in vivo, we employed a syngeneic metastasis model. In support of our hypothesis, bioluminescence imaging revealed a decreased number of bone metastases in Tgif1^{-/-} mice compared to control littermates (36% vs. 56%, respectively) 7 days after intracardiac injection of 4T1-GFP-Luc BCCs. Consistently, the presence of single BCCs or micro-metastases in the tibiae was reduced by 25% in Tgif1^{-/-} mice determined by confocal microscopy. Further histological analyses revealed that BCCs localize in close proximity to Endomucin-positive vascular cells and to osteoblasts. Although Tgif1-deficiency did not affect the number or size of the vessels in the bone marrow, the number and activity of osteoblasts

were reduced compared to control littermates ($p < 0.05$). This suggests that the protective effect on bone metastases might be mediated by the osteoblasts and not by the bone marrow vasculature. In summary, we propose that lack of Tgfr1 in osteoblasts attenuates cancer cell migration and metastases formation, possibly through suppression of *Sema3E*. Thus, our findings establish osteoblasts as important regulators during early stages of bone metastasis.

Disclosures: Marie-Therese Haider, None

1076

TGF-beta inhibition restores the responsiveness to osteoanabolic PTH treatment in the *Crtap*^{-/-} model of recessive Osteogenesis Imperfecta Ingo Grafe*, Jennifer Zieba, Elda Munivez, Yuqing Chen, Ming-Ming Jiang, Brian Dawson, Carrie Jiang, Alexis Castellon, Joseph Slietka, Sandesh Nagamani, Brendan Lee. Department of Molecular and Human Genetics, Baylor College of Medicine, United States

Osteogenesis Imperfecta (OI) is characterized by low bone mass and fractures, and better treatment options are needed. Most cases are caused by dominant type I collagen mutations. Mutations in *CRTAP*, involved in post-translational collagen modifications, cause severe recessive OI. Previously, we have shown that increased TGFβ signaling is a key contributor to the phenotype in OI mouse models, including *Crtap*^{-/-} mice. Intermittent PTH treatment increases BMD in patients with osteoporosis; however, in a randomized clinical trial, we have shown that PTH treatment does not improve aBMD in patients with severe forms of OI. Others have shown TGFβ and PTH signaling interactions, e.g. that TGFβ-inhibition increases PTH signaling and bone mass. Our preliminary *in vitro* studies suggest that BMSCs of *Crtap*^{-/-} mice, cultured in osteogenic conditions, exhibit an increased pSmad2/Smad2 ratio (increased TGFβ signaling), and reduced pCREB/CREB ratio, suggesting impaired PTH signaling. Hence, we hypothesized that inhibition of the increased TGFβ signaling in *Crtap*^{-/-} mice restores the osteoanabolic effects of PTH treatment. To test this hypothesis, we treated 8-week-old *Crtap*^{-/-} and wild-type (WT) mice with PTH (40 μg/kg, 5x/week, s.c.), low-dose of the pan-TGFβ neutralizing antibody 1D11 (Genzyme/Sanofi; 1mg/kg, 3x/week IP), or control treatment (vehicle/control antibody) for 8 weeks. MicroCT of femurs of control treated *Crtap*^{-/-} mice showed reduced BV/TV (36% of WT control) and Cort.Th (88% of WT). In WT mice, PTH treatment increased BV/TV by 29% and Cort.Th by 7%. In contrast, in *Crtap*^{-/-} mice PTH was less effective, only slightly increased BV/TV (by 4% to 40% of WT) and did not improve Cort.Th. Low dose 1D11 treatment in WT mice increased BV/TV (+49%) but Cort.Th was unchanged. In *Crtap*^{-/-} mice 1D11 moderately increased BV/TV (to 57% of WT) and did not increase Cort.Th. Combined 1D11 and PTH treatment increased BV/TV (+66%) and Cort.Th (+5%) in femurs of WT mice. In *Crtap*^{-/-} mice, combined 1D11 and PTH treatment synergistically restored BV/TV and Cort.Th to 96% and 93% of control WT mice, respectively. In summary, we show that inhibition of increased TGFβ signaling restores responsiveness to intermittent PTH treatment in the *Crtap*^{-/-} model of severe recessive OI. Because increased TGFβ signaling also contributes to the skeletal phenotypes in dominant OI, combinatorial anti-TGFβ and PTH treatment might be an attractive new treatment option for patients with OI.

Disclosures: Ingo Grafe, None

1077

Osteocyte Senescence Underlies the Increase in RANKL in Aged Mice via a GATA4 Mediated Mechanism Ha-Neui Kim*, Srividhya Iyer², Jianhui Chang², Li Han¹, Aaron Warren¹, Stavros Manolagas¹, Charles O'Brien¹, Daohong Zhou², Maria Almeida¹. ¹University of Arkansas for Medical Sciences and Central Arkansas Veterans Healthcare System, United States, ²University of Arkansas for Medical Sciences, United States

The accumulation of senescent cells causes age-related diseases and curtails longevity. Old mice exhibit increased number of senescent osteoprogenitors and osteocytes and markers of DNA damage. In addition, the expression of the senescence associated secretory phenotype (SASP) is elevated, as is the expression of RANKL in osteocyte enriched bone shafts. These changes are associated with accumulation of GATA4, a transcription factor that induces the SASP. Elimination of p16 expressing senescent cells in bone decreases osteoclasts and increases bone mass in old mice. However, the cellular and molecular mechanisms mediating these effects remain unknown. Here, we examined whether cellular senescence caused by DNA damage and GATA4 activation could be responsible for the increase in RANKL with old age. We subjected cultured bone marrow-derived stromal cells to 10 Gy of γ -radiation (IR), an established inducer of DNA damage and senescence. After a few passages, the irradiated cells exhibited elevated senescence associated β -galactosidase activity, increased expression of GATA4 and RANKL. Similarly, exposure of *ex-vivo* cultures of osteocyte enriched cortical shafts, from young C57BL/6 mice, to IR caused an increase in γ H2AX, a common marker of DNA damage. IR also increased the levels of GATA4 and RANKL. Overexpression of GATA4, using a retroviral vector, in primary osteoblastic cells or the MLO-Y4 osteocytic cell line increased RANKL and other elements of the SASP including IL-1 α and MMP13. To test whether elimination of senescent cells in old mice altered RANKL levels, we administered the senolytics ABT263 (40 mg/kg body weight), or Bcl-PROTAC (40 mg/kg body weight) for 30 days to 24-month-old female mice. Bone marrow stromal cells from the femurs were cultured in the presence of osteogenic medium for 10 days to collect mRNA. Both the stromal cell cultures and osteocyte-enriched shafts

from mice treated with ABT263 or Bcl-PROTAC had decreased markers of senescence and lower transcript levels of RANKL compared to mice treated with vehicle. Our findings indicate that RANKL is part of the SASP in cells of the osteoblast lineage and that the increase in RANKL with age is caused by DNA damage and GATA4 activation. Together with evidence, presented elsewhere in this meeting, showing that RANKL deletion in osteocytes prevents the loss of cortical bone with aging, this work demonstrates that senescence in osteocytes is a critical mechanism of skeletal aging.

Disclosures: Ha-Neui Kim, None

1078

BLU-782; a highly selective ALK2 inhibitor, designed specifically to target the cause of fibrodysplasia ossificans progressiva Alison Davis*, Brian Hodous², Timothy Labranche¹, Michael Sheets¹, Natasja Brooijmans¹, Joseph Kim¹, Brett Williams¹, Sean Kim¹, Lan Xu³, John Vassiliadis¹, Julia Zhu¹, Ruduan Wang¹, Rachel Stewart⁴, Paul Fleming⁵, Chris Graul⁴, Elliot Greenblatt⁶, Keith Bouchard⁶, Vivek Kadambi¹, Timothy Guzi¹, Jeffrey Hunter⁶, Christoph Lengauer¹, Marion Dorsch¹, Andrew Garner¹. ¹Blueprint Medicines, United States, ²Accent Therapeutics, United States, ³Foghorn Therapeutics, United States, ⁴In vivo, United States, ⁵Akebia Therapeutics, United States, ⁶Alexion Pharmaceuticals, United States

Therapies that precisely target the causative disease driver can lead to profound clinical benefit, while minimizing the potential for off-target toxicities. Fibrodysplasia ossificans progressiva (FOP) is a rare, severely disabling and ultimately life-shortening disease. FOP is characterized by episodic soft tissue edema (flares), and the progressive replacement of skeletal muscle and connective tissue by heterotopic bone. FOP is caused by a gain-of-function mutation in *ACVR1*, which encodes activin-like kinase 2 (ALK2). The most common ALK2 mutation identified in FOP is R206H, which imparts hypersensitivity to BMPs and a neomorphic response to activins. Here we describe the generation and characterization of a highly selective ALK2 inhibitor, designed specifically to target the underlying genetic driver of FOP. To achieve this, we analyzed the Blueprint Medicines proprietary small molecule library, which is annotated against 392 human kinases, for selective ALK2-binding compounds. This analysis identified a novel series of compounds, that exhibited a unique ALK2 selectivity profile. Using structure-guided drug design, we optimized the potency, selectivity and pharmaceutical properties of the initial leads to generate BLU-782. Biochemical genome profiling demonstrated BLU-782 preferentially bound ALK2 with high affinity. In cells, BLU-782 potently inhibited ALK2R206H, while it did not significantly inhibit ALK1, ALK3 or ALK6 activity. The *in vivo* activity of BLU-782 was evaluated using a conditional knock-in ALK2R206H transgenic mouse model, which develops soft tissue edema, inflammation and heterotopic ossification (HO) upon mechanical muscle injury. When dosed prophylactically, BLU-782 inhibited edema and prevented cartilage and bone formation without impacting body weight. Moreover, histological analysis of untreated ALK2R206H mice identified muscle breakdown, endochondral cartilage and heterotopic bone at the injury site. Conversely, in BLU-782-treated ALK2R206H FOP mice, heterotopic bone was absent, while organized muscle repair and regrowth were frequently observed. This establishes that selective ALK2 inhibition in ALK2R206H FOP mice prevents the formation of heterotopic bone and enables skeletal myofiber regeneration to proceed to restore muscle architecture. Collectively, these data demonstrate the selectivity and *in vivo* activity of the investigational agent BLU-782 and support its progression into clinical development.

Disclosures: Alison Davis, Blueprint Medicines, Major Stock Shareholder

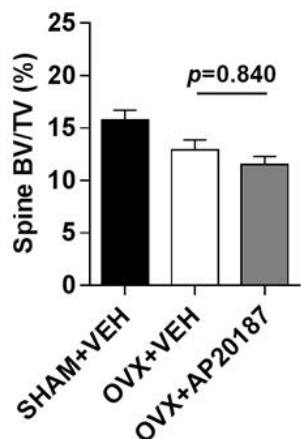
1079

Estrogen Deficiency and Cellular Senescence Represent Independent Mechanisms in the Pathogenesis of Osteoporosis: Evidence from Studies in Mice and Humans Joshua Farr*, David Monroe, Daniel Fraser, Brittany Negley, Brianne Thicke, Jennifer Onken, Robert Pignolo, Tamar Tchkonja, James Kirkland, Sundeep Khosla. Mayo Clinic, United States

Estrogen (E) deficiency is a seminal mechanism in the pathogenesis of osteoporosis. Mounting evidence, however, indicates that cellular senescence, a fundamental aging mechanism that drives multiple age-related diseases, also causes osteoporosis. Recently, we systematically identified an accumulation of senescent cells, characterized by increased p16Ink4a and p21Cip1 levels, in mouse bone with aging. We also found similar results in bone biopsies from older vs younger women, indicating parallel findings in humans. We then demonstrated that senescent cells mediate age-related bone loss using multiple approaches, e.g., treating wild-type (WT) mice with "senolytics" (i.e., drugs that eliminate senescent cells) and reducing senescent cell burden using mice expressing the INK-ATTAC "suicide" transgene via drug (AP20187)-inducible caspase-8 driven by the senescence-associated p16Ink4a promoter. These approaches improved bone mass and strength by suppressing bone resorption and stimulating bone formation. Here, we investigate a possible role for E in the regulation of senescence in bone. In adult (4-month) WT mice, 8 wks post ovariectomy (OVX, n=15) or orchidectomy (ORCH, n=15), we found no changes in p16Ink4a or p21Cip1 mRNA levels in bone vs sex-matched WT mice that underwent sham surgery (SHAM, n=15/sex). We next obtained human bone biopsies from 40 healthy postmenopausal women randomized to either placebo (PL, n=20, 73±6 yrs) or short-term E (STE, n=20, 71±5 yrs) therapy for 3 wks. As compared to PL, STE therapy had no effect on p16Ink4a or p21Cip1 mRNA

levels in human bone. Finally, we randomized 4-month-old female INK-ATTAC mice to SHAM+vehicle (SHAM+VEH, n=11), OVX+VEH (n=10), or OVX+AP20187 (n=17) for 8 wks. As anticipated, OVX+VEH caused bone loss as compared to SHAM+VEH. However, treatment with AP20187, which eliminates senescent cells in INK-ATTAC mice, did not rescue the OVX-induced bone loss (Figure). In addition, there was no evidence of changes in senescence biomarkers, including p16Ink4a, p21Cip1, and EGFP (encoded by the INK-ATTAC transgene), in response to AP20187. Collectively, our data establish that E deficiency and cellular senescence represent independent mechanisms in the pathogenesis of osteoporosis. Moreover, these findings have important implications for testing novel senolytics for skeletal efficacy, as these drugs will need to be evaluated in models of aging, as opposed to the current FDA model of prevention of OVX-induced bone loss.

Effect of AP20187 on OVX-induced bone loss



Disclosures: Joshua Farr, None

1080

Lower CYP27B1 expression impairs osteoblasts activity in adolescent idiopathic scoliosis – a new insight to improve bone quality by vitamin D supplementation Jia Jun Zhang^{*1,2}, Yujia Wang^{1,2}, Carol Cheng^{1,2}, Tsz Ping Lam^{1,2}, Bobby Kin-Wah Ng^{1,2}, Jack Chun-Yiu Cheng^{1,2}, Wayne Yuk-Wai Lee^{1,2}. ¹Department of Orthopaedics and Traumatology, SH Ho Scoliosis Research Laboratory, The Chinese University of Hong Kong, Hong Kong, ²Joint Scoliosis Research Center of the Chinese University of Hong Kong and Nanjing University, The Chinese University of Hong Kong, Hong Kong

Purpose: Altered bone mass and microstructure are associated with curve progression of AIS. Previous studies reported lower serum VitD level and association between polymorphism in VitD receptor (VDR) and low bone mass in AIS. The preliminary finding of our randomized controlled clinical trial (RCT) demonstrated that bone quality improvement by vitamin D (VitD) and calcium supplementation could result in lower chance of curve progression to surgical threshold. Another RCT study showed that AIS subjects with higher serum VitD (>40 nmol/L) showed enhanced response to whole body vibration. These findings suggest that VitD and related metabolic pathway could be candidates underlying low bone mass in AIS. **Method:** This study aimed to study the effect of VitD on the cellular activities of primary osteoblasts and osteocytes derived from AIS patients and control subjects. Primary osteoblasts were isolated from iliac crest trabecular bone biopsies from 10 AIS patients undergoing spinal fusion and 4 age-matched control subjects undergoing respective orthopaedic surgery. Primary osteocytes culture was derived by culturing the osteoblasts in 3D collagen gel. Protein level of CYP27B1 and VDR of osteoblasts were determined by Western blot. The osteoblasts and osteocytes were treated with 1, 25-dihydroxyvitamin D₃ (1,25-VitD) at different concentrations (0, 10, 100 nM) for 7 days with or without vibration (0.3g, 35 Hz, 20 minutes daily). mRNA level of representative osteoblast and osteocyte markers were determined with qPCR. Mann-Whitney test was used for statistical analysis. **Result:** AIS osteoblasts had lower protein level of CYP27B1 but higher VDR when compared with the control. Therefore, AIS osteoblasts were more sensitive to 1,25-VitD treatment. Vibration enhanced the response of AIS osteoblasts and osteocytes to 1,25-VitD treatment as indicated by up-regulation of Runx2, Alp, Spp1, Bglapand Vdr mRNA in primary osteoblasts, and Spp1, Phex, Cx43 and E11 mRNA in primary osteocytes. **Conclusion:** This is the first in vitro evidence showing intrinsically lower ability of CYP27B1 mediated Vit-D activation in AIS osteoblasts, which is speculated to limiting the response of AIS to Vit-D despite higher VDR expression. The additive effect of vibration on 1,25-VitD treatment in AIS is in line with our clinical observation. Taking together, our findings partly support the notion to improve bone quality in AIS subjects with Vit-D supplementation which could be enhanced by WBV.

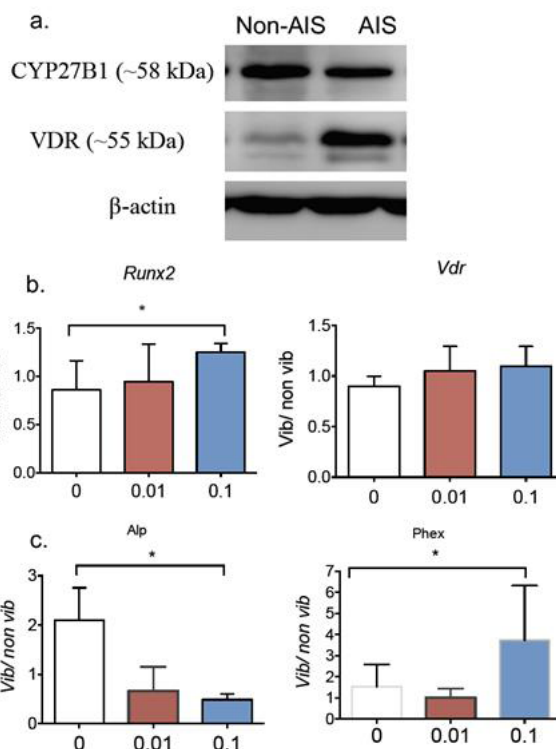


Figure a. Representative image of western blot result of CYP27B1 and VDR
b. mRNA level of representative osteoblast markers in primary osteoblast from AIS and control
c. mRNA level of representative osteocyte markers in primary osteocyte from AIS and control

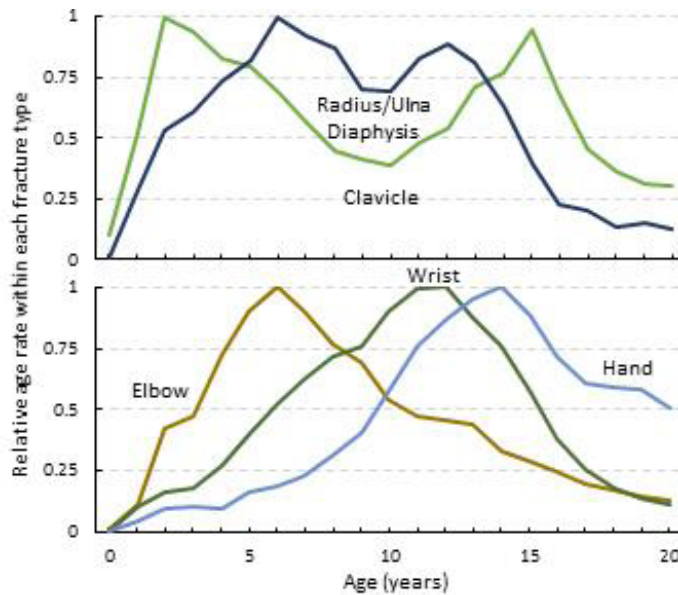
Disclosures: Jia Jun Zhang, None

1081

Age at Peak Fracture Rate Depends on Fracture Type and Trabecular/Cortical Dominance of Fracture Site – Expanding Explanations of Peak Fracture Rate beyond Lag in Mineralization Bjorn Rosengren*, Daniel Jerrhag, Magnus Karlsson. Clinical and Molecular Osteoporosis Research Unit, Departments of Orthopedics and Clinical Sciences, Skane University Hospital and Lund University, Sweden

BACKGROUND Early research on childhood fractures has shown differences in peak fracture rate in boys and girls and between fracture types. Studies have pointed to a major explanatory role of the mineralization lag found during rapid growth, as the two coincide, at least for wrist fractures. This explanation is often used also for other fracture types, however with questionable support in literature. We therefore sought to examine recent age rate patterns of fractures in general, specific fracture types and of fractures located mainly in cortical or mainly in trabecular bone. **METHODS** By use of official in- and out-patient record data for children (≤ 20 years) in Sweden (Skåne region), we ascertained fractures during 3.5 million person-years (py) 1999-2010. To compare age rate patterns between fracture types we normalized the age specific rates within each fracture type to the highest incidence of that specific fracture type. **RESULTS** We found 71,525 fractures during 3.5 million py corresponding to an overall fracture incidence rate of 205 per 10,000 py (boys 254, girls 155). Wrist fractures and hand fractures together accounted for 50% of all fractures. Age rate patterns and age at peak incidence were different between boys and girls, between the 20 examined fracture types and between cortical fractures (examples in top panel of Fig) and trabecular fractures (examples in bottom panel of Fig). Peak fracture age occurred at 13 years for any fracture (boys 14, girls 11) but ranged from 2 to 19 depending on the specific fracture type. The incidence rate ratio (IRR) between boys and girls for any fracture was 1.6 (95% CI 1.6, 1.6). The highest boy to girl IRR was found for fractures of the skull (2.8 [2.6, 3.0]), femur diaphysis (2.6 [2.2, 3.1]) and scapula (2.5 [1.8, 3.7]). The only fracture type more common in girls was of the proximal humerus (0.8 [0.7, 0.9]). **CONCLUSION** Age at peak incidence and age rate patterns are different between boys and girls, between fracture types and between fractures in cortical and trabecular bone. The results challenge the widespread notion that age at peak fracture incidence is determined by the lag in mineralization

during rapid growth and indicate that other factors, such as physical activity patterns and risk taking behavior are important.

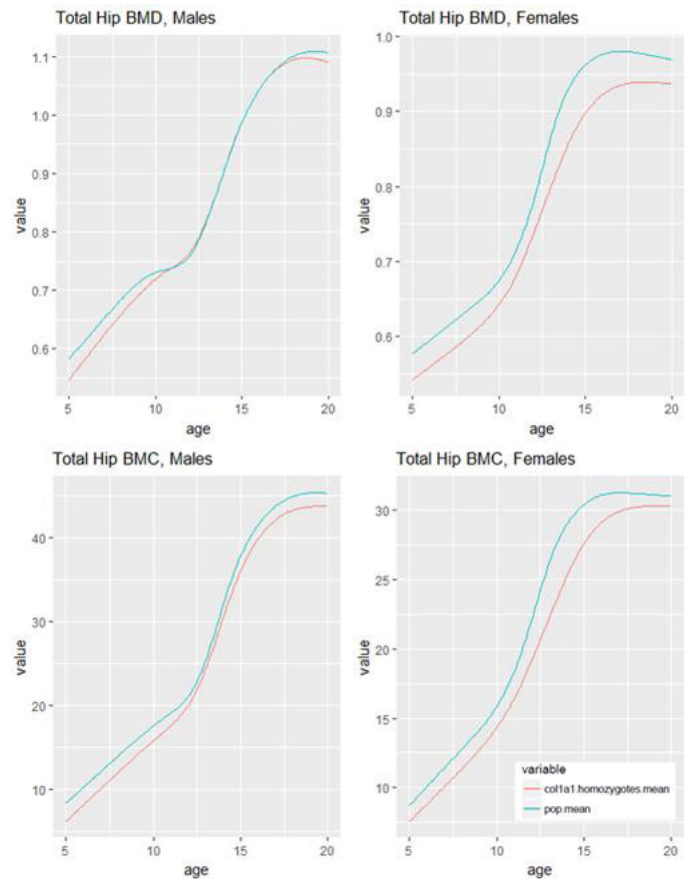


Disclosures: Bjorn Rosengren, None

1082

The COL1A1 Sp1 Variant and Bone Accrual in Childhood Diana Cousminer^{*1}, Shana McCormack¹, Jonathan Mitchell¹, Alessandra Chesi¹, Joan Lappe², Heidi Kalkwarf³, Sharon Oberfield⁴, Vicente Gilsanz⁵, John Shepherd⁶, Andrea Kelly¹, Benjamin Voight⁷, Babette Zemel¹, Struan Grant¹. ¹Children's Hospital of Philadelphia, United States, ²Creighton University, United States, ³Cincinnati Children's Hospital, United States, ⁴Columbia University, United States, ⁵Children's Hospital of Los Angeles, United States, ⁶University of Hawaii, United States, ⁷University of Pennsylvania, United States

Over two decades ago, a low frequency variant (rs1800012) in an Sp1 binding site within the first intron of the type I collagen alpha 1 (COL1A1) gene was reported to be associated with osteoporotic fracture. The influence of this variant is known to vary with age: it only moderately influences adult peak bone mineral density (BMD) but has a relatively pronounced effect in the high bone turnover state of postmenopausal bone loss (Uitterlinden et al, NEJM 1998). Another high bone turnover period is during childhood and adolescence; however, the role of rs1800012 is unclear in this setting. We assessed association between rs1800012 and areal-BMD (aBMD) and bone mineral content (BMC) Z-scores at multiple skeletal sites in the Bone Mineral Density in Childhood study, a mixed-longitudinal, densely phenotyped cohort of healthy children and adolescents (n=1,419). We tested a recessive model using a mixed random effects method accounting for multiple measurements (1-7 annual per subject), adjusting for relevant covariates, in both sex-specific and combined settings. We then tested for pubertal stage interactions in pre-pubertal (Tanner stage (TS) 1), pubertal (TS 2-4), and post-pubertal (TS 5) groups. Finally, SITAR modeling was used in girls and boys separately for each skeletal site; this method reduces complex growth curves into three parameters representing the a-size, b-timing, and c-velocity of bone accrual, and we tested the difference between genotype groups using t tests for each parameter. We found that AA-genotype carriers had significantly lower aBMD and BMC at all skeletal sites prior to puberty, with an effect that was attenuated by TS 5, reflecting significant puberty interactions (e.g. hip neck aBMD $P=2 \times 10^{-6}$). AA carriers began bone accrual later than their peers (later b-timing; e.g. total hip BMC $P=0.005$), and had slower accrual during puberty (slower c-velocity; e.g. total hip BMC $P=0.04$), particularly in girls, and most markedly at the total hip (Fig.1) and femoral neck. Our data suggest that rs1800012 principally affects bone density in a context-specific manner, i.e. during periods of high turnover, both in early and late life, when estrogen levels are low or absent. Investigating the interaction between genetics, maturational phase, and the hormonal milieu can therefore yield important insights into bone gain and loss that may be masked during the relatively quiescent state in adulthood.



Disclosures: Diana Cousminer, None

1083

Reliability of annual changes and monitoring time intervals for bone strength, size, density and micro-architectural development at the distal radius and tibia in children: A 1-year HR-pQCT follow-up Amy Bunyamin^{*1}, Kelsey Björkman², Chantal Kawalilak¹, Seyedmahdi Hosseinitabatabaei³, Adrian Teare¹, James Johnston¹, Saija Kontulainen². ¹Department of Mechanical Engineering, College of Engineering, University of Saskatchewan, Canada, ²College of Kinesiology, University of Saskatchewan, Canada, ³Division of Biomedical Engineering, College of Engineering, University of Saskatchewan, Canada

High-resolution peripheral quantitative computed tomography (HR-pQCT) imaging, together with computational finite element (FE) analysis, offers an attractive method of non-invasively quantifying bone strength development in children. However, evidence of annual change and error in repeated HR-pQCT measures in children are limited, and time intervals required to reliably capture change in pediatric bone strength and micro-architecture have not been defined. Study purposes were to: 1) Quantify annual changes in bone properties at the distal radius and tibia in children; 2) characterize observed mean change in contrast to reported pediatric precision errors (Kawalilak et al. 2017); and 3) estimate monitoring time intervals (MTIs) required to reliably characterize growth and development in bone properties at the distal radius and tibia of children. We analyzed distal radius (7% of ulnar length) and tibia (8% site) bone properties from 38 typically developing children (22 girls; mean baseline age: 10.6 years) obtained from HR-pQCT scanning and FE analysis at baseline and after 1-year. We characterized mean annual changes (via paired t-tests) and contrasted changes in relation to pediatric precision errors. We estimated MTIs based on median annual changes and precision errors. Annual increases (and MTIs) in bone strength (failure load, stiffness, apparent modulus, ultimate stress), total area, cortical thickness and density ranged between 3.2-27.3% (MTIs: 0.5-4.9 years) at the distal radius and 2.5-16.3% (0.5-3.1 years) at the distal tibia. Trabecular area and cortical porosity decreased 2.4% and 22.0% at the distal radius, respectively, and 1.3% and 7.9% at the distal tibia. Observed bone changes exceeded their respective precision errors. MTIs ranged between 0.5-∞ years at the distal radius and 0.4-8.1 years at the distal tibia. Increased bone strength coincided with cortical bone growth, bone consolidation and trabecular coalescence at distal bone ends in children. Estimated MTIs indicated that changes in bone strength and micro-architecture

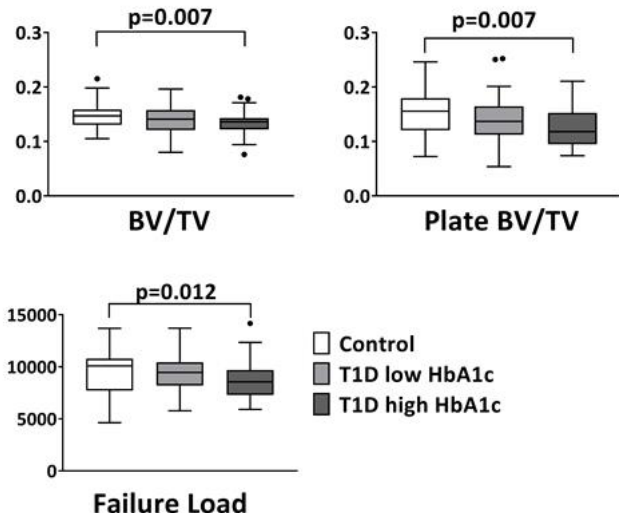
(cortical and trabecular thickness, density, cortical porosity) can be reliably monitored in 1 to 2 year intervals in children.

Disclosures: **Amy Bunyamin, None**

1084

Glycemic Control Influences Trabecular Microarchitecture in Youth with Type 1 Diabetes Deborah Mitchell^{*1}, Signe Caksa², Amy Yuan², Mary Bouxsein², Madhusmita Misra¹. ¹Pediatric Endocrine Unit, Massachusetts General Hospital, United States, ²Endocrine Unit, Massachusetts General Hospital, United States

Fracture risk is elevated in patients with type 1 diabetes (T1D) throughout the lifespan, but the etiology of this risk remains poorly understood. As DXA-based aBMD alone does not explain the increased fracture risk, we hypothesized that bone microarchitecture and trabecular morphology are negatively altered in youth with T1D and that these alterations are influenced by glycemic control as assessed by hemoglobin A1c (HbA1c). We conducted a cross-sectional study of girls ages 10-16 years (62 with T1D and 60 controls). We measured microarchitecture by high-resolution peripheral quantitative computed tomography (HR-pQCT) and trabecular morphology by individual trabecular segmentation (ITS) at the distal radius (7% site) and distal tibia (8% site). We estimated bone strength with micro-finite element analysis. The mean age at diagnosis of T1D was 8.8 ± 3.0 years and the mean duration of disease was 4.8 ± 3.2 years; no subject had microvascular complications. Median HbA1c in the T1D group was 8.5%. The groups were well-matched for age, bone age, pubertal stage, and height. Weight was higher in T1D (Z-score 0.7 ± 0.8 vs. 0.4 ± 0.9 , $p=0.050$), and serum 25OHD was lower (26 ± 8 vs. 33 ± 10 ng/mL, $p<0.001$). We observed no differences in aBMD at the whole body, spine, hip, or radius. At the distal tibia, subjects with T1D had lower bone volume fraction (BV/TV) ($p=0.012$) and trabecular thickness ($p=0.025$), with lower plate BV/TV ($p=0.009$) and axial BV/TV ($p=0.010$) (adjusted for bone age, height, and weight). As shown in Figure 1, after dividing the T1D subjects into those at or below vs. those above the median HbA1c, only those with a high HbA1c ($>8.5\%$) had significantly different microarchitecture and morphology compared to controls, including a 9.5% lower BV/TV and a 19.5% lower plate BV/TV ($p=0.007$ for both comparisons). Micro-finite element analysis revealed a significantly lower failure load in T1D, again limited to those with a high HbA1c (7.1% lower, $p=0.012$). After further adjustment for 25OHD, the association of high HbA1c with trabecular parameters and failure load was attenuated but remained significant. We observed no significant differences in trabecular indices or failure load at the distal radius though numerically these were all lower in the T1D group. In summary, in girls with T1D, hyperglycemia is associated with unfavorable trabecular microarchitecture and morphology early in the course of disease and may contribute to diabetic skeletal fragility.



Disclosures: **Deborah Mitchell, None**

1085

A common SNP in the CYP2R1 promoter decreases transcriptional activity and is associated with low serum 25(OH)D levels and reduced responsiveness to vitamin D supplementation. Jeffrey Roizen^{*1}, Alex Casella², Caela Long¹, Zahra Tara¹, Meizan Lai¹, Hakon Hakonarson¹, Michael Levine¹. ¹The Children's Hospital of Philadelphia, United States, ²University of Maryland, United States

Optimal bone and mineral metabolism, as well as immune and cardiovascular function, depend on normal vitamin D metabolism. Ineffective sunlight exposure and inadequate dietary vitamin D each have well understood roles in the pathophysiology of vitamin D deficiency; however, the extent to which common polymorphisms in genes encoding vitamin D metabolizing enzymes contribute to vitamin D homeostasis remains undefined.

Several genome wide association studies (GWAS) have identified significant associations between serum [25(OH)D] and single nucleotide polymorphisms (SNPs) in or near the locus for CYP2R1, the gene encoding the principal vitamin D 25-hydroxylase enzyme. By targeting DNase hypersensitivity sites we identified rs7949459 as a SNP that is likely in a transcription factor binding site. This SNP is in high linkage disequilibrium with the commonly nearby SNPs identified in GWAS for 25(OH)D (for each of rs10500804, rs10741657, and rs10766192, $D > 0.98$). Using a promoter reporter we found that the minor allele of this SNP causes a greater than 80% decrease in reporter activity. We used CRISPR/Cas9 to generate iPSCs that were homozygote major, homozygote minor and heterozygote at this allele and differentiated these iPSCs into hepatocytes. In iPSCs differentiated to hepatocytes presence of the minor allele significantly decreased CYP2R1 mRNA and 25-hydroxylase activity. Consistent with the idea that this effect was due to changes at rs7949459 rather than off-target effect, the genotype at this allele caused no differences in promoter reporter activity. In a pediatric cohort, presence of a single rs7949459_T allele (the minor allele) was associated as a continuous variable with 25(OH)D ($\beta=0.35$, $SE=0.15$, $p=0.02$). Similarly, the rs7949459_T allele was more common in decreased responders to supplementation (chi-squared analysis $p < 0.03$). Thus, our genetic and cell-based studies provide evidence that this common genetic variation in CYP2R1 has significant effects on CYP2R1 transcription, and provide a functional context for interpreting GWAS that show relationships between circulating 25(OH)D and CYP2R1.

Disclosures: **Jeffrey Roizen, None**

1086

YAP and TAZ deletion in mature osteoblasts reduce bone formation and increase marrow adipocyte accumulation Mengrui Wu^{*1}, Joshua Chou², Dorothy Hu¹, Kenichi Nagano¹, Daniel Brooks³, Mary Bouxsein³, Francesca Gori¹, Roland Baron¹. ¹Harvard School of Dental medicine, United States, ²University of Technology Sydney, Austria, ³Beth Israel Deaconess Medical Center, United States

YAP and TAZ are transcriptional effectors of Hippo signaling, regulating cell fate, tissue development and homeostasis. YAP and TAZ have redundant functions and are often referred as YAP/TAZ, although some distinct functions of YAP or TAZ have been reported. Furthermore, no specific ligands or receptors have been identified that regulate the Hippo cascade. Importantly however the activity of the two key effectors of Hippo signaling, YAP and TAZ, can also be regulated by Wnt signaling. Given that Wnt signaling is one of the most dominant anabolic pathways in bone, interactions between WNT signaling and YAP and/or TAZ may contribute to skeletal homeostasis. To test this hypothesis, we generated mice lacking YAP and/or TAZ in mature osteoblasts. YAP^f/fTAZ^f/fBglap-Cre (DKO), YAP^f/fBglap-Cre (YAP CKO) and TAZ^f/fBglap-Cre (TAZ CKO) mice develop normally and have similar body weight compared to their YAP^f/fTAZ^f/f, YAP^f/f or TAZ^f/f littermates. Double deletion of YAP and TAZ leads to a marked decrease in trabecular number, cortical bone area and cortical thickness as indicated by mCT analysis in 12-week-old mice. Intriguingly, YAP CKO affects only trabecular bone, while TAZ CKO affects mostly cortical bone, revealing for the first time unique functions of these two Hippo effectors in bone. Consistently, histomorphometric analysis shows that DKO female mice display a significant decrease in bone formation rate (BFR/BS = 0.78 ± 0.11 vs. 1.19 ± 0.03 $\mu\text{m}^3/\mu\text{m}^2/\text{year}$, $p=0.02$), while osteoblast and osteoclast numbers remain similar. Active β -catenin levels are largely reduced in DKO long bones and primary osteoblasts, indicating that YAP and TAZ are required for proper canonical Wnt signaling activation. Interestingly, DKO mice also display an increased accumulation of marrow adipocytes and mesenchymal stem cells (MSC) isolated from DKO mice marrow have decreased osteoblast differentiation potency and increased adipocyte differentiation potency, as indicated by alkaline phosphatase and Oil red O staining, respectively. These findings suggest that YAP and TAZ activity is involved in the WNT signaling cascade is a target for anabolic treatment in diseases associated with bone loss and fragility, identifying novel signaling cascades interacting with WNT signaling may help understand how WNT affects bone homeostasis and open novel therapeutic avenues for the treatment of skeletal diseases.

Disclosures: **Mengrui Wu, None**

1087

The Wnt Agonist R-spondin 3: An Unexpected Negative Regulator of Bone Formation Kenichi Nagano^{*2}, Kei Yamana², Hiroaki Saito², Virginia Parkman², Jun Guo¹, Henry Kronenberg¹, Francesca Gori², Roland Baron². ¹Endocrine Unit, Massachusetts General Hospital, United States, ²Division of Bone and Mineral Research, Harvard Medical School and Harvard School of Dental Medicine., United States

Wnt signaling regulates cell proliferation, differentiation and function and its activation exerts a positive action on bone homeostasis. R-spondins (RSpos), cysteine-rich secreted glycoproteins, have been shown to promote canonical Wnt signaling in vitro. Accordingly, RSpos are expected to exert a positive influence on bone formation and mass. Despite the biological and therapeutic importance of Wnt signaling in bone, RSpo molecular mechanisms of action in bone remains elusive. Among the 4 RSpos, RSpo3 is highly expressed in bone and has been found associated with bone density in several GWA studies. We therefore

explored its role and mechanism of action in skeletal homeostasis. While global deletion of RSp3 resulted in embryonic lethality at E10.5, before skeletal development, RSp3^{+/+} mice develop normally and are healthy. Contrary to our expectations, Rsp3 haploinsufficiency led to a significant increase in trabecular (but not cortical) bone mass in both genders and at several time points. Dynamic histomorphometry showed that this gain of bone mass was due to a 4X increase in BFR/BS (23.4±12.7 vs 108±14.3, p<0.01) and osteoblast (OB) number (2.22±0.15 vs 8.52±1.33, p<0.01) whereas osteoclast (OC) number was not altered (0.36±0.05 vs 0.44±0.09, NS). FACS analysis demonstrated a marked increase in the Lin-CD45-CD31-CD51+Sca1+ mesenchymal stem cell (MSC) population in the bone marrow of Rsp3^{+/+} mice (0.36±0.07 vs 0.66±0.09, p<0.05). These MSCs have a higher OB potential, as indicated by CFU-F and CFU-OB assays. Remarkably, absence of RSp3 in E9.5 MEFs, resulted in a significant activation of ERK signaling and an unexpected increase in canonical Wnt signaling that, in turn, leads to accelerated OB differentiation. Inhibition of canonical Wnt signaling by Dkk1, while preventing canonical Wnt signaling activation in wt cells showed significantly less inhibitory potential in RSp3-deleted cells. This finding was confirmed in vivo with RSp3 haploinsufficiency partially preventing the decrease in BFR and BV induced by Dkk1 targeted overexpression in OBs. Thus, our findings reveal a novel and unexpected function of RSp3 as a negative regulator of bone formation and indicate that, despite its co-activating function for canonical Wnt signaling, RSp3 exerts a negative influence on bone homeostasis. This negative effect is, at least in part, exerted via the ERK pathway and the enhancement of Dkk1 inhibitory activity.

Disclosures: **Kenichi Nagano**, None

1088

EZH2 is Regulated by the MiR-23a Cluster to Maintain Bone Mass In Vivo Benjamin Wildman*, Tanner Godfrey, Mohammad Rehan, Yuechuan Chen, Qamarul Hassan. University of Alabama at Birmingham, Institute of Oral Health Research, United States

Differentiation of pre-osteoblasts is critical to controlling in-vivo development and growth of bone. Recent studies highlight the importance of epigenetic regulation in directing osteoblast commitment and function. Here we show that the microRNA-23a cluster (miR-23a, 27a, and 24-2) controls bone mass in-vivo through a previously unknown EZH2 mediated epigenetic mechanism. First, we knocked down the miR-23a cluster in mouse pre-osteoblasts (MC3T3-E1) cells with an anti-microRNA cassette (miRZIP). Next, we created a mouse model that inducibly expresses the miRZIP cassette to knock-down the microRNA cluster (miR-23aCIZIP) in-vivo. Luciferase and Chromatin Immunoprecipitation (ChIP) assays along with RNA sequencing were performed to elucidate the mechanism of miR-23a cluster action in maturing osteoblasts. MiR-23a cluster knockdown increased the intensity of Alkaline Phosphatase staining in MC3T3-E1 cells. Additionally, it upregulated mRNA expression of osteogenic marker genes such as Runx2 and Osteocalcin. Micro-CT analysis of 2 month old femurs showed that trabecular bone volume and trabecular number significantly increased in miR-23aCIZIP mice as compared to controls. Additionally, connective density and trabecular thickness were significantly greater while trabecular space was significantly decreased. Supporting this increased bone mass, Runx2 expression levels were significantly upregulated while the levels of a potent epigenetic repressor Ezh2 were significantly reduced in whole bone RNA sequenced from miR-23aCIZIP mice. Mechanistically, we found that the miR-23a cluster inhibits RUNX2 translation by binding to the 3' UTR of Runx2 mRNA transcripts. Furthermore, ChIP assays revealed RUNX2 binds to the Ezh2 promoter inhibiting transcription in MC3T3-E1 cells. Additional ChIP experiments in miR-23aCIZIP mouse primary calvarial pre-osteoblasts showed that miR-23a cluster knockdown results in decreased binding of the epigenetic repressor EZH2 to osteogenic gene promoters such as Osteocalcin and Runx2, resulting in a more osteogenic transcription program. We developed a novel microRNA cluster knockdown mouse model allowing us to decipher how the miR-23a cluster orchestrates bone mass maintenance in-vivo.

Disclosures: **Benjamin Wildman**, None

1089

Versatile Transcriptional Co-Factor Jab1 is Required for Osteoblast Differentiation and Postnatal Bone Growth William Samsa*, Murali Mamidi, Lindsay Bashur, David Danielpour, Guang Zhou. Case Western Reserve University, United States

Jab1 (Jun activation domain-binding protein 1), also known as Cops5/Csn5, is the fifth subunit of the highly conserved macromolecular complex the COP9 Signalosome. Jab1 plays crucial roles in regulating proliferation, apoptosis, and differentiation. We previously reported that the loss of Jab1 specifically in mouse osteochondral progenitor cells of the limb buds, using a Prx1-cre driver, results in drastically shorter limbs, with highly disorganized epiphyseal growth plates and a severely reduced number hypertrophic chondrocytes. We found increased apoptosis as measured by TUNEL staining and cleaved Caspase 3 IHC in the growth plates of mutant mice. Real-time qPCR analysis of osteoblasts from these mutant mice showed reduced expression of osteoblast differentiation markers. Micromass cultures of E12.5 Jab1-null limb bud cells displayed significantly reduced BMP reporter activity, and decreased expression of Sox9 and its downstream targets. Thus, Jab1 is a master regulator of limb development in mice. To determine the specific role of Jab1 in osteoblast differentiation and postnatal bone growth, we generated a novel mouse model in which Jab1 is deleted specifically in osteoblast precursor cells under the control of the Osterix-cre (Ox-cre) promoter.

These mutant mice appeared normal at birth, but developed progressively worsening dwarfism. Importantly, all of these mutant mice die prior to weaning age. Histological analysis of long bones revealed a disorganized epiphyseal growth plate with a reduced hypertrophic zone in the mutant mice. H&E staining revealed a reduced amount of primary trabeculae, delayed and impaired secondary ossification center formation, and altered bone marrow cellularity that is reminiscent of pancytopenia. Moreover, we show that in ex vivo cultures of primary calvarial osteoblasts, Jab1 is expressed at both the early and late stages of osteoblast differentiation, and that the loss of Jab1 resulted in impaired osteoblast differentiation and reduced mineralization. Furthermore, the loss of Jab1 in primary calvarial osteoblasts resulted in lower phospho-SMAD1/5 expression, indicating reduced BMP signaling activity. Additionally, shRNA knockdown of Jab1 in the preosteoblastic cell line MC3T3 led to a decreased level of Osterix. Thus, Jab1 is necessary for osteoblast differentiation and postnatal bone growth, likely through positively regulating BMP signaling and other master transcriptional factors, such as Osterix.

Disclosures: **William Samsa**, None

1090

Transcription Factor 7 like 2 (TCF7L2) is a Novel Regulator of Osteoblast Functions and Peak Bone Mass in Mice Chandrasekhar Kesavan*¹, Nagraj Puppali², Nikita Bajwa², Subburaman Mohan¹. ¹VA Loma Linda Healthcare System, Loma Linda University, United States, ²VA Loma Linda Healthcare System, United States

It is now well recognized that peak bone mass attained early in life is an important factor affecting the risk of osteoporosis in later years. While the importance of transcription factors such as Runx2 and Osterix in the regulation of osteoblast (OB) development and attainment of peak bone mass is well known, our understanding of transcriptional regulation of OB commitment and differentiation is incomplete. In our effort to identify transcription factors (TFs) that are critical for OB differentiation, we found that expression of TCF7L2, an early acting TF whose mutations have been associated with various clinical diseases, increases several-fold during OB differentiation, in vitro. To elucidate the role of TCF7L2 in OBs, we generated mice with conditional disruption of TCF7L2 in OBs by two generation breeding of TCF7L2 floxed mice and Col1 α 2-Cre mice. All of the pups that were homozygous for the TCF7L2 floxed allele and were Cre positive died either during pregnancy or immediately after birth. Alizarin red staining of skeletons of homozygous TCF7L2 conditional knockout (cKO) pups prior to birth revealed smaller size bones with compromised mineralization. We, therefore, evaluated the skeletal phenotype of heterozygous 4-5 week old cKO mice by micro-CT. Trabecular (Tb) bone volume of the femur was reduced by 30% (P<0.01) in both male and female TCF7L2 heterozygous cKO mice compared to control littermates, mediated by reduced Tb number and thickness and increased Tb separation. In addition, the bone size at the mid-diaphysis of the femur was reduced by 25% (P<0.01). To determine the mechanism for reduced trabecular bone, we evaluated the consequence of knockdown of TCF7L2 expression by treating floxed OBs with adenoviral iCre and found reduced proliferation (25%, P<0.05) as well as differentiation (40%, P<0.05). To identify TCF7L2 target genes, we searched for the presence of putative TCF7L2 regulatory motifs in the promoter region of genes involved in OB differentiation and identified members of the Wnt signaling pathway as direct targets of TCF7L2. We found that expression levels of Wnt1, Wnt16, β -catenin and Axin were reduced by 30-60% (p<0.05) in OBs-derived from heterozygous cKO mice vs. control mice. In conclusion, our findings provide the first evidence that TCF7L2 is a key regulator of OB functions, in vitro and in vivo that acts in part via regulating the expression of Wnt family members.

Disclosures: **Chandrasekhar Kesavan**, None

1091

Osteoblast-intrinsic IRE1a/XBP1s Signaling Regulates Bone Development and Bone Marrow Homeostasis Hongjiao Ouyang*¹, Shankar Revu², Kai Liu², Yuqiao Zhou², Qi Han¹, Faisal Alshalawy¹, Yuji Mishina³, Alejandro Almarza², Donna Stolz², Konstantinos Verdellis², Randal Kaufman⁴. ¹Texas A&M University, United States, ²University of Pittsburgh, United States, ³University of Michigan, United States, ⁴Sanford-Burnham-Prebys Medical Discovery Institute, United States

The inositol-requiring enzyme 1 α (IRE1 α)/X-box binding protein 1 spliced (XBP1s) pathway is an endoplasmic reticulum (ER) stress signaling branch required for the development of secretory organs. IRE1 α is an endoribonuclease that generates Xbp1s from Xbp1 upon ER stress. However, it remains elusive as to how this pathway regulates bone development and homeostasis. Our laboratory generated and characterized mice lacking osteoblast-specific IRE1 α (CKO), and their wild type littermates (WT), by breeding IRE1 α Flox/Flox mice with Osterix-Cre mice. It was found that 2-month-old female IRE1 α CKO mice displayed osteoporosis with decreased osteoblastogenesis, increased bone marrow fat and reduced osteoclastogenesis. On one hand, it was observed that IRE1 α -deficient osteoblasts exhibited exacerbated ER stress and consequently experienced activation of the PRKR-like endoplasmic reticulum kinase (PERK)/eukaryotic translation-initiation factor 2 α subunit (EIF2 α) signal transduction pathway, both in vivo and in vitro, compared with WT counterparts. Consequently, IRE1 α -deficient osteoblasts had a reduced steady-state protein level of β -Catenin, a transcription factor central for canonical Wnt signaling, both in vivo and in

vitro, compared with WT counterparts. Similarly, the bone marrow stromal cells (BMSCs) that were deficient in XBP1, the downstream effector of IRE1 α , also had a reduced β -Catenin protein level in vitro, compared with WT counterparts. LiCl treatment of IRE1 α CKO mice partially but significantly rescued osteoporosis in these mice. These results revealed a novel role of IRE1 α /XBP1s signaling in regulating osteogenesis and bone marrow adipogenesis via modulating Wnt/ β -Catenin signaling. On the other hand, 2-month-old female IRE1 α CKO mice had significant reduction in both the osteoclast number and serum level of RANKL in vivo, compared with WT littermates. Consistently, XBP1-deficient murine BMSCs also had decreased RANKL expression in vitro, compared with WT counterparts. Conversely, XBP1s overexpression in human BMSCs led to an increased RANKL expression and an enhanced capacity of these cells to support osteoclast formation from osteoclast progenitors. Taken together, these data suggest osteoblast-intrinsic ER stress IRE1 α /XBP1s signaling plays essential roles in regulating bone development and bone marrow homeostasis via modulating osteoblast-mediated osteoclastogenesis, osteoblastogenesis as well as bone marrow adipogenesis.

Disclosures: *Hongjiao Ouyang, None*

1092

Osteocyte Notch3 is Responsible for the Osteopenia of Lateral Meningocele Syndrome (LMS) Ernesto Canalis*, Jungeun Yu, Lauren Schilling, Stefano Zanotti. UConn Health, United States

Notch (1 to 4) receptors determine cell fate and function and their expression is cell lineage-dependent. In the osteoblast lineage, Notch3 mRNA is preferentially expressed by osteocytes, and in the myeloid lineage Notch3 is not detected. This suggests that the osteocyte is responsible for the phenotype of skeletal diseases associated with alterations in Notch3 activity. LMS (OMIM 130720), a rare genetic disorder characterized by developmental abnormalities and bone loss, is associated with mutations in exon33 of NOTCH3. The mutations lead to the translation of a truncated protein lacking the PEST domain, and NOTCH3 gain-of-function. We reported a mouse model (Notch3tm1.1Ecan) harboring a Notch3 mutant allele reproducing LMS, where a termination codon was introduced at base pairs 6691-6696 of the Notch3 coding sequence leading to the translation of a truncated 2230 amino acid protein devoid of the PEST domain. Heterozygous Notch3tm1.1Ecan mice develop pronounced osteopenia, but the mechanisms and whether organs outside the skeleton are responsible for the phenotype are unknown. We report that young and mature Notch3tm1.1Ecan mutant mice appear healthy, and histopathology of multiple organs including the brain revealed no abnormalities. This was associated with low levels of Notch3 expression in most organs outside the skeleton. Notch3 target genes were induced in bone extracts from Notch3tm1.1Ecan mice, confirming Notch signal activation. Notch3tm1.1Ecan mice had pronounced cancellous and cortical bone osteopenia. Osteoblast cell replication was enhanced in vitro. This was reflected by an increase in osteoblast and osteocyte number and a modest increase in bone formation in vivo, which was not sufficient to prevent the osteopenic phenotype. Notch3tm1.1Ecan mice had increased osteoclast surface associated with an increase in RANKL expression by the osteocyte. Notch3tm1.1Ecan mutants exhibited enhanced osteoclastogenesis in vitro, possibly related to events operating in vivo. Co-cultures of bone marrow macrophages (BMMs) and osteoblasts from wild type and Notch3tm1.1Ecan mice revealed enhanced osteoclastogenesis in Notch3tm1.1Ecan cells, which was due to osteoblast- and BMM-dependent effects. In conclusion, Notch3 is preferentially expressed by the osteocyte where it increases RANKL to cause the osteopenia of LMS. The function of Notch receptors is cell lineage specific and dependent on their level of expression.

Disclosures: *Ernesto Canalis, None*

1093

Tgfr1-mediated Repression of PAK3 Supports Osteocyte Spreading Simona Bolamperti*¹, Hiroaki Saito¹, Antonio Virgilio Failla², Hanna Taipaleenmäki¹, Eric Hesse¹. ¹Molecular Skeletal Biology Laboratory, Department of Trauma, Hand and Reconstructive Surgery, University Medical Center Hamburg-Eppendorf, Germany, ²Microscopy Imaging Facility, University Medical Center Hamburg-Eppendorf, Germany

Adherence and spreading of osteoblasts on bone surfaces and the formation of an organized lacuno-canalicular network by osteocytes are important for the integrity of the bone tissue. We observed an increased expression of the homeodomain protein TG-interacting factor 1 (Tgfr1) during the spreading of osteoblasts on collagen I-coated surfaces in vitro, suggesting a role of Tgfr1 during this process. In support of this hypothesis, calvarial osteoblasts obtained from mice bearing a germline deletion of Tgfr1 (Tgfr1^{-/-}) and osteocyte-like cells of the OCY454 cell line with a transient knockdown of Tgfr1 were impaired in their capacity to adhere and spread (p<0.05). Furthermore, immunocytochemistry demonstrated that Tgfr1-deficient osteoblasts and osteocytes have a reduced capacity to form focal adhesions and cell protrusions, retaining a more spherical cell shape (p<0.01). Investigation of a panel of factors known to regulate cell spreading revealed an increased expression of the p21-activated kinase 3 (PAK3) in Tgfr1-deficient osteocytes at the mRNA and protein level (p<0.01), suggesting an inhibition of PAK3 expression by Tgfr1. This hypothesis was supported by chromatin immunoprecipitation, which revealed the binding of Tgfr1 to a conserved binding site within the PAK3 promoter. Furthermore, gene reporter assays demonstrated an increased activity of the PAK3 promoter in the absence of Tgfr1 (p<0.01). Mechanistically, inhibition of PAK3 expression in Tgfr1-deficient osteocytes using siRNA restored the capacity of

cells to spread and to form focal adhesions as well as cell protrusions (p<0.001). To confirm these observations in vivo, we analyzed the bones of Tgfr1^{-/-} mice. Tgfr1-deficient osteoblasts appeared to have a less cuboidal appearance compared to cells of control littermates. Furthermore, osteocytes in the trabecular compartment of Tgfr1^{-/-} bones were irregularly shaped and formed a disorganized lacuno-canalicular network (p<0.05). A reminiscent phenotype was found in bones of mice with a targeted deletion of Tgfr1 in mature osteoblasts and osteocytes using the cre-recombinase controlled by the Dmp1-promoter (Dmp1-Cre⁺;Tgfr1 loxP/loxP). This confirms that the altered osteocyte shape is cell-autonomously driven. In summary, our findings demonstrate that Tgfr1-mediated repression of PAK3 is important for osteoblasts and osteocytes to adhere and spread. This mechanism might contribute to the formation of an organized osteocyte network in bone.

Disclosures: *Simona Bolamperti, None*

1094

Osteocytic Kindlin-2 regulates bone mass accrual and maintenance and mediates skeletal response to mechanical loading and PTH anabolism Huiling Cao*¹, Qinnan Yan¹, Dong Wang², Yumei Lai², Simin Lin¹, Yimin Lei¹, Liting Ma¹, Yuxi Guo¹, Yishu Wang¹, Yilin Wang¹, Huanqing Gao¹, Xiaochun Bai³, Chuanju Liu⁴, Jian Q. Feng⁵, Chuanyue Wu¹, Di Chen², Guozhi Xiao¹. ¹Department of Biology and Guangdong Provincial Key Laboratory of Cell Microenvironment and Disease Research, Southern University of Science and Technology, China, ²Department of Orthopedic Surgery, Rush University Medical Center, United States, ³Department of Cell Biology, School of Basic Medical Sciences, Southern Medical University, China, ⁴Department of Orthopedic Surgery, New York University School of Medicine, United States, ⁵Department of Biomedical Sciences, Texas A&M University College of Dentistry, United States

Osteocytes embedded in a mineralized bone matrix regulate bone homeostasis in response to mechanical and other signals by currently unknown mechanisms. This study shows that osteocytes express abundant Kindlin-2, an integrin co-activator, and that deleting Kindlin-2 in osteocytes causes lifelong severe osteopenia in mice. Kindlin-2 loss in osteocytes not only drastically decreases osteoblast number and function, leading to reductions in osteoid production mineralization and bone formation, but also the promotion of osteoclast formation. Mechanistically, Kindlin-2 loss increases sclerostin expression in osteocytes and inhibits β -catenin signaling in osteoblasts and bone formation. Additionally, Kindlin-2 loss in osteocytes promotes the differentiation of mesenchymal stem cells to adipogenic lineage, further reducing osteoblast formation. Furthermore, Kindlin-2 loss increases the activator of nuclear factor-kappaB ligand (Rankl) expression in osteocytes and promotes osteoclast formation and differentiation from bone marrow monocytes. Kindlin-2 loss impairs osteocyte spreading and reduces osteocyte density by increasing cell apoptosis. Importantly, mice lacking Kindlin-2 in osteocytes fail to increase bone mass and mineral density in response to mechanical loading using a tail suspension model. Finally, of clinical significance, Kindlin-2 loss in osteocytes impairs the anabolic actions of intermittent parathyroid hormone in bone in adult ovariectomized mice. These studies uncover a previously unknown function for Kindlin-2 and define novel mechanisms through Kindlin-2 for osteocyte regulation of bone homeostasis.

Disclosures: *Huiling Cao, None*

1095

Specific Gut Bacterium Alters Commensal Microbiota Immunomodulatory Actions Regulating Skeletal Development Jessica Hathaway-Schrader*, Nicole Poulides, Sakamuri Reddy, Caroline Westwater, Chad Novince. Medical University of South Carolina, United States

The commensal gut microbiota critically regulates post-natal skeletal development. We have previously shown the commensal gut microbiota enhances osteoclastogenesis and suppresses osteoblastogenesis, which appears to be mediated by TH17/IL-17 immune response effects in bone marrow and liver. Of interest, segmented filamentous bacteria (SFB) is a genomically distinct commensal gut bacterium that potently directs TH17/IL-17 mediated immunity. Study purpose was to delineate the influence of SFB on commensal gut microbiota immunomodulatory actions regulating post-natal skeletal development. Nine-week-old, female, C57BL/6T^{*} murine-pathogen-free (MPF) mice (*specific-pathogen-free mice colonized by SFB) and #excluded-flora (EF) mice (#specific-pathogen-free mice devoid of SFB) were euthanized, and tissues were collected. Proximal tibia trabecular bone was analyzed by uCT and histomorphometric analyses. Mesenteric lymph node (MLN), liver lymph node (LLN), spleen, and bone marrow cells were isolated for flow cytometric analyses. Ileum, liver, spleen, and bone marrow were assessed for target genes by qRT-PCR and nCounter. IL17 was substantially increased in the ileum of MPF mice, which is in line with SFB induction of TH17/IL-17 immunity. EF vs. MPF mice had decreased body weight and tibia length. Increased proliferative and hypertrophic chondrocyte zone heights in the growth plate of EF mice imply that reduced tibia length is due to altered endochondral bone formation. MPF mice had decreased trabecular bone volume fraction, which was attributed to reduced trabecular number. TRAP+ osteoclast numbers lining trabecular bone were enhanced in MPF vs. EF mice. MPF mice had increased MLN and LLN weight per body weight, upregulated % cytotoxic T-cells in MLNs, and enhanced % helper T-cells in LLNs. Paralleling the increased

osteoclast numbers, the critical osteoclastic transcription factor *Nfatc1* was increased in marrow of MPF mice. Decreased *Col1a1*, but no difference in *Ocn* and *Opn* in the marrow of MPF vs. EF mice, indicate that suppressed early osteoblast activity contributes to the osteopenic trabecular bone phenotype found in MPF mice. *C3*, *C4b*, *C5a* and *Lcn2* were up-regulated in liver and marrow of MPF mice, which provides novel mechanistic insight about commensal gut microbiota osteoimmune response effects. This research notably reveals that specific microbes critically impact commensal gut microbiota immunomodulatory actions regulating post-natal skeletal development.

Disclosures: *Jessica Hathaway-Schrader, None*

1096

Haploid Embryonic Stem Cell-Mediated Targeted Genetic Screening In Vivo Identifies Novel Factors for Bone Development Yujiao Han*, Weiguo Zou. Shanghai Institute of Biochemistry and Cell Biology, China

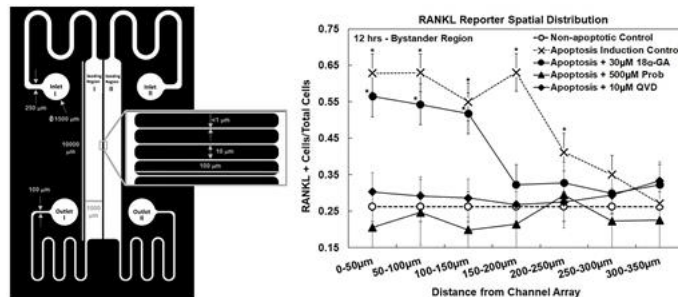
Functional mutagenic screening has been used to identify key factors required for a wide range of developmental processes. However, such screens can only be successfully applied in lower organisms. Here, we develop a knockout (KO)-based screen in mouse using androgenetic haploid embryonic stem cells (haESCs). We screened factors involved in bone development by introducing a sgRNA library containing 216 sgRNAs targeting 72 preselected candidate genes into haESCs, which carried constitutively expressed Cas9 and were injected into oocytes to produce semi-cloned (SC) mice. We produced 426 SC pups and among them, 404 pups carried one sgRNA and covered all 72 genes. The skeletal phenotypes of each SC pups at birth were analyzed by alcian blue and alizarin red staining. Through the screen we identified transcriptional factor *Irx5* as a positive regulator of bone development and the phenotype were validated by the generation of KO mouse lines through zygotic injection. Two lines of *Irx5* KO mouse exhibited obvious decreased bone mass and increased adipogenesis in the bone marrow. Moreover, the deletion of *Irx5* from bone marrow cells prohibited osteoblast differentiation and enhanced adipocyte differentiation ability in vitro. Mechanistically, *IRX5* promotes osteoblastogenesis and inhibits adipogenesis by inhibiting *PPAR γ* expression. We conclude that haESC-mediated SC technology, in combination with a targeted sgRNA library, can be used as a powerful reverse genetic screening strategy in vivo in mouse.

Disclosures: *Yujiao Han, None*

1097

A Novel In Vitro Fluidic Approach to Measuring the Apoptotic Bystander Effect in Osteocyte Networks Sean Mccutcheon*¹, Robert Majeska², David Spray¹, Maribel Vazquez², Mitchell Schaffler². ¹Albert Einstein College of Medicine, United States, ²The City College of New York, United States

Osteocytes are widely regarded as the primary sensors and transducers in bone. In response to apoptosis in nearby cells, osteocytes upregulate RANKL which in turn triggers recruitment and differentiation of osteoclast precursors. How osteocytes sense apoptosis and respond to tissue level stimuli is still under intensive study. The spatial constraints of the lacunar canalicular system (LCS) and the network structure of osteocytes within it are key determinants of sensory and response communication pathways, yet a high throughput in vitro device to study osteocyte behavior in such a confined system has yet to be developed. In this study we utilized a novel multi-scale fluidic device that mimics the architecture and diffusion parameters of the LCS to examine paracrine signaling between dying and surviving osteocytes (the "bystander effect"). The device, (the Macro-micro-nano, or M μ n) consists of two cell seeding regions separated by a 100 μ m-wide channel array. The channel array, which provides conduits similar to canaliculi for osteocyte processes in vivo, is composed of ~900nm-wide channels separated by 10 μ m. When cultured on both sides of the array, MLO-Y4 osteocytes extend processes that form functional gap junction connections within the array channels. To test the bystander effect, apoptosis was induced in osteocytes on one side of the M μ n by heat stress, and RANKL expression was quantified on the non-apoptotic side via a fluorescent RANKL gene reporter system. Apoptosis induction resulted in ~2-fold increase in RANKL-expressing bystander osteocytes after 12h, which diminished with distance from the apoptotic source (Fig); similar to the pattern for osteocyte RANKL expression seen around microdamage sites in vivo. Inhibiting caspase 3 (10 μ M QVD) eliminated this elevation. Activation and spread of RANKL signaling in bystander osteocytes was also prevented by blocking the membrane channel Pannexin 1 (500 μ M Probenecid). However, RANKL signaling in bystander osteocytes was unaffected by inhibiting Connexin 43 (30 μ M 18 α -GA). These data indicate that diffusible paracrine signals and not direct gap junction signaling, are the primary mechanism by which bystander osteocytes respond to nearby apoptosis. Furthermore, the dependency of RANKL activation in bystander osteocytes on the Pannexin 1 channel points to ATP release as a dominant chemical signal in this process.

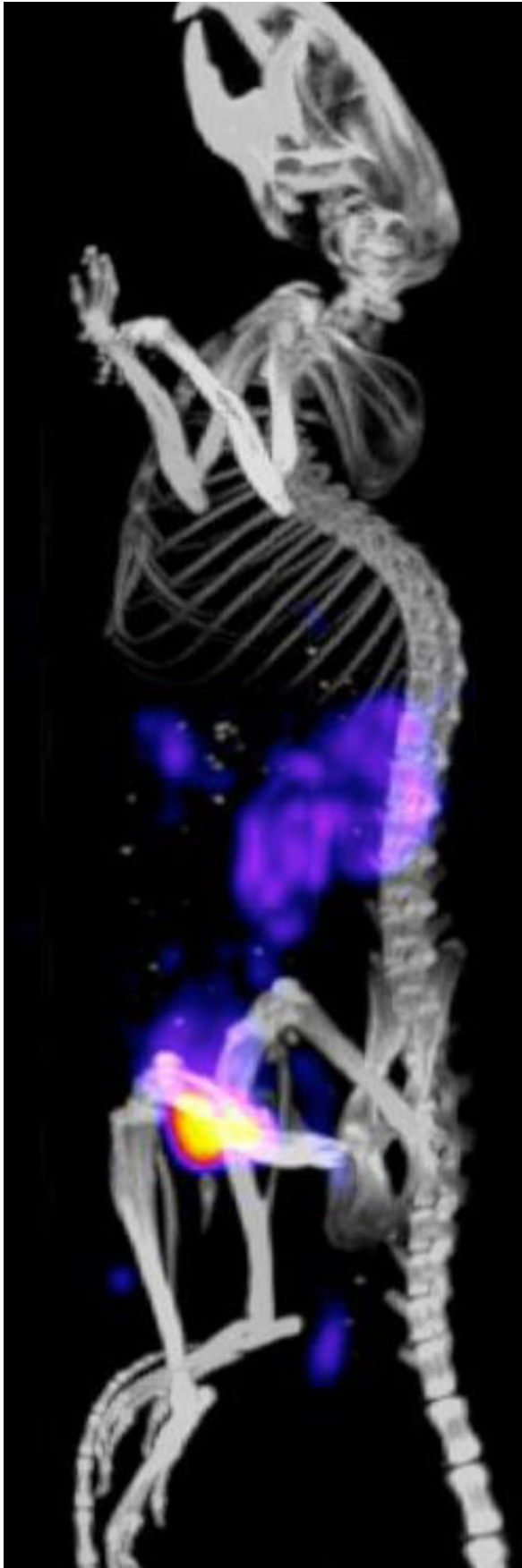


Disclosures: *Sean Mccutcheon, None*

1098

Fracture targeted PTHrP agonists for accelerated bone repair Stewart Low*¹, Jeffery Nielsen², Philip Low². ¹Purdue, United States, ²Purdue University, United States

Background: Over 6 million bone fractures occur in the United States each year, resulting in significant morbidity, mortality, and lost productivity. In general, conventional therapy has focused on mechanically stabilizing fractures with little consideration of a pharmaceutical approach to accelerate fracture repair. Development of locally-applied bone anabolic agents (such as BMP-2) have resulted in accelerated bone growth but have limited approved uses due to the invasiveness of their application (via surgery) and their potential for ectopic bone growth. Likewise, efforts to accelerate fracture repair by systemically-administered anabolic agents have yet to achieve sufficient therapeutic concentrations at the fracture site; We have developed a systemically-administered fracture-targeted therapeutic that demonstrates remarkable specificity to the site of a fracture and significantly accelerates bone repair. With systemic administration, multiple doses of the drug can be administered in a non-invasive manner while targeting allows for therapeutic concentrations of anabolic to accumulate at the fracture site, an objective only previously achieved by local application. Furthermore, by limiting drug accumulation to the fracture site, systemic toxicities are avoided along with any ectopic bone growth associated with local anabolic administration. Methods: Our fracture-targeted bone anabolic agent was prepared by synthesizing a parathyroid hormone-related protein (PTHrP) fragment conjugated to a hydroxyapatite-homing acidic oligopeptide. In vivo experiments were conducted on Swiss Webster mice (10 per group). Femoral fractures were induced with a 3-point bending device and stabilized. Mice were dosed with 30 nmol/kg/d of targeted-PTHrP, non-conjugated (free) PTHrP, or saline. Following a 4-week study, fracture callus densities were measured using microCT. A marked increase in bone density (30%) was observed in the free-PTHrP group over the saline group, whereas a far greater (70%) increase in bone density was observed in the targeted-PTHrP group over the saline group. Further studies confirmed that the greatest difference in ossification occurred early in the fracture healing process (2 weeks), with the fracture callus resolving to cortical bone by 8-weeks. Conclusions By targeting bone anabolic agents to bone fractures, we can deliver sufficient concentrations of anabolic agent to the fracture site to accelerate healing.



Disclosures: *Stewart Low, None*

1099

Mechanical stimulation prevents the decline in anabolic response to prolonged Sclerostin-neutralizing antibodies exposure Maude Gerbaix*, Serge Ferrari. Division of Bone Diseases, Geneva University Hospitals and Faculty of Medicine, Switzerland

Inhibition of sclerostin leads to a massive increase, followed by a drastic down-regulation of bone formation. Whether or not osteoblastic cells remain responsive to anabolic stimuli after the exhaustion of Sclerostin-neutralizing Ab (Scl-Ab) effects on bone formation however remains unclear. We investigated the effects of mechanical stimulation on bone microarchitecture and gene expression in mice continuously exposed to Scl-Ab. Four month-old mice received Scl-Ab (50 mg/kg/w) or Veh for 5 weeks. At week 3, axial compression was applied on the left tibia 3 days per week for 2 weeks. Subgroups of treated and Veh mice were euthanized at 2, 4 and 5 weeks of treatment for analyses of bone microstructure, serum markers and bone gene expression by RT-QPCR. In Scl-Ab animals, P1NP peaked at 2 weeks and decreased at 5 weeks. Scl-Ab increased BV/TV at distal femur and vertebrae (+141%, +157% respectively vs Veh; $p < 0.01$) and femur cortical thickness (Ct.Th) (+22% vs Veh; $p < 0.01$) by 2 weeks; by 4 weeks, Scl-Ab had maximally increased BV/TV at distal femur and vertebrae (+232%, +462% respectively vs Veh; $p < 0.01$) and femur Ct.Th (+30% Veh; $p < 0.01$), with no further gain at 5 weeks. Under continuous Scl-Ab treatment, loading further increased tibia trabecular BV/TV (+14% vs nonloaded tibia; $p < 0.05$) and femur Ct.Th femur (+19% vs nonloaded tibia; $p < 0.05$), as also observed in Veh treated animals. Scl-Ab upregulated *Coll1*, *Bglap*, *Sost* and *Dkk1* genes expression (+74.78%, +135%, +21%, +56% respectively vs Veh; $p < 0.05$) and down-regulated *Posnt* and *NRG1* gene expression (-32%, -24%; respectively vs Veh $p < 0.05$) at week 2, whereas at week 5, gene expression levels did not differ from Veh. Loading further increased *Coll1*, *ALP*, *Wisp1* and *Posnt* genes expression in Scl-Ab as compared to Veh (+17%; +992%; +284%; +31% vs Veh; $p < 0.05$). *NRG1* and *SerpinF1* genes expression were also upregulated by loading under veh and AbScl treatment. In summary, stimulation of osteoblastic gene expression related to bone formation is not sustained with Scl-Ab, as counterregulatory mechanisms such as *Sost* and *Dkk1* are induced, and co-stimulatory pathways, such as periostin, are repressed. Mechanical loading however is able to maintain these bone forming mechanisms despite the continuous inhibition of *Sost*. These observations suggest that lining cells and osteoblast precursors are still responsive and could be further stimulated by mechanisms that are at least partially independent of *Sost* inhibition.

Disclosures: *Maude Gerbaix, None*

1100

An Anti-Angiogenic Agent Induced Osteonecrosis of the Jaw-Like Lesions in Rice Rats (*Oryzomys palustris*) Jonathan Messer*, Jessica Jiron, Abel Abraham, Evelyn Castillo, Josh Yarrow, Don Kimmel, J Ignacio Aguirre. University of Florida, United States

Medication-related osteonecrosis of the jaw (MRONJ) is a potentially serious adverse event seen in patients taking powerful anti-resorptive (pAR), and more recently, antiangiogenic (AA) agents. Multiple recent pre-clinical experiments indicate that combined local factors (e.g., dental infection) and systemic factors (e.g., pARs, etc.) are required to induce MRONJ. However, no pre-clinical experiments have investigated a role for AAs (e.g., anti-VEGF antibody, aVEGF) in MRONJ. We hypothesize that despite lacking anti-resorptive activity, AAs cause MRONJ-like lesions in rice rats with localized periodontitis (PD), which results in progression of oral infection and necrosis of oral soft and hard tissues. Rice rats were randomized at age 4 wks into 3 groups (N=15) that received 1) intravenous (IV) zoledronic acid (ZOL; 80 $\mu\text{g}/\text{kg}$ BW 1X/mo); 2) subcutaneous aVEGF (Genentech rodent cross-species anti-VEGF MAb [B20-4.1.1]; 5mg/kg BW 2X/wk), or 3) IV vehicle (VEH; saline 1X/mo). Bi-weekly oral exams were conducted with binocular loupes (4X) to inspect the oral cavity of rats between ages 4-22 weeks. At each exam, oral lesions were identified and scored using an integral 0-4 severity scoring system, in which 0 was normal and 4 was marked gingival recession with exposed bone (MRONJ-like lesion). At the end of the study, rats were euthanized, and high resolution photographs of jaw quadrants were analyzed. Jaw quadrants were processed for MicroCT analysis and histopathologic assessment. 40% of VEH rats developed spontaneous, localized PD lesions at the interdental region of maxillary molars 2-3 (M2M3) with low-grade severity (1-1.5), as previously described. 55% of ZOL- and 73% of aVEGF-treated rats developed lesions at M2M3 with severity of 1-4. Gross MRONJ-like lesions were detected in 0, 25, and 47% of VEH, ZOL, and aVEGF rats, respectively. MicroCT, histopathologic, and immunohistochemical analyses are ongoing to confirm MRONJ lesions, and determine the extent of morphologic or histologic variation in the affected tissues among the different groups. Our data suggest that AA inhibits healing of focal PD lesions, promoting the development of MRONJ lesions in similar circumstances to those induced by ZOL. This is the first pre-clinical, prospective experiment to establish a potential causal relationship between an AA agent and MRONJ.

Disclosures: *Jonathan Messer, None*

1101

Spinal loading regulates bone remodeling and angiogenesis in a mouse model of postmenopausal osteoporosis Xinle Li^{1*}, Jie Li¹, Daquan Liu¹, Hiroki Yokota², Ping Zhang¹. ¹Department of Anatomy and Histology, School of Basic Medical Sciences, Tianjin Medical University, Tianjin 300070, China, ²Department of Biomedical Engineering, Indiana University-Purdue University Indianapolis, IN 46202, United States

Osteoporosis is characterized by reduced bone mass and deterioration of bone micro-architecture, and an increased risk of fractures. While angiogenesis is essential for repairing of bone disorders such as fracture and osteonecrosis, mechanical loading is reported not only to stimulate bone formation, but also to promote vessel remodeling in osteonecrosis of the femoral head. Spinal loading is one form of loading modalities, in which compressive loads are applied to the lumbar spine. Using ovariectomized (OVX) mice, we examined whether spinal loading prevents bone loss through regulating a Wnt pathway in postmenopausal osteoporosis. Sixty C57BL/6 female mice (~14 weeks) were divided into three groups (n=20): the sham control, OVX, and spinal loading-treated OVX group. Spinal loading (4 N at 10 Hz for 5min/day) was applied for 2 weeks. Bone mineral density (BMD) and bone mineral content (BMC) were measured, and ink perfusion was performed to evaluate angiogenesis. Femora were harvested for bone histomorphometry and Western Blotting, and bone marrow-derived cells were isolated to examine osteoclast development, osteoblast mineralization, and differentiation of endothelial progenitor cells (EPCs). RNA interference for Wnt3a was employed to test whether Wnt3a is involved in bone remodeling and angiogenesis. The results showed that OVX mice presented bone loss with reduction in a vessel volume, and daily application of spinal loading for two weeks significantly increased BMD, BMC, trabecular bone volume, and the number of osteoblasts on bone surface. It also enhanced differentiation and mineralization of osteoblasts. Regarding osteoclasts, the loaded group presented significant reduction in osteoclast activity and suppression of their formation, migration and adhesion. While the levels of RUNX2, alkaline phosphatase, and osteocalcin were increased, those of NFATc1, RANKL, and cathepsin K were decreased by spinal loading. Spinal loading also enhanced a microvascular volume, migration and tube formation of EPCs, and VEGF expression. Transient knockdown of Wnt3a blocked the observed loading effects on osteoclast development, osteoblast mineralization, and differentiation of EPCs. Collectively, this study shows using OVX mice that spinal loading stimulates bone formation and angiogenesis and it suppresses bone resorption via the Wnt pathway. Further understanding of spinal loading can contribute to developing potential therapies for postmenopausal osteoporosis.

Disclosures: *Xinle Li, None*

1102

Low Affinity Bisphosphonate Exerts a Strong Anabolic Effect on Trabecular Bone Abigail Coffman^{1*}, Robert J. Majeska¹, Jelena Basta-Pljakic¹, Mark W. Lundy², Frank H. Ebetino³, Mitchell B. Schaffler¹. ¹City College of New York, United States, ²Indiana University School of Medicine, United States, ³University of Rochester, United States

PURPOSE: Bisphosphonates (BPs) in clinical use to prevent bone loss are characterized by high binding affinity for hydroxyapatite (HA), reflecting bone matrix targeting and high potency of FPPS inhibition. Many BPs with low HA affinity (thus rapid biological clearance) and strong FPPS inhibition have not been developed clinically. Their effects in vivo are not well understood, but BPs with short half-lives and rapid clearance from the body potentially offer certain advantages over long half-lives of current clinical BPs. Here we explored whether one such compound, NE-580251, might have beneficial effects on bone. **METHODS:** Young adult female C57BL/6 mice (15 w.o., JAX, n=5/group, IACUC approved) underwent OVX; they were treated with NE-58025 (NE-025, 200µg/kg daily, sc), Risedronate (RIS, 2.4 µg/kg 3x/wk, sc) or PBS, and sacrificed at 3 mo. NE-025 has much lower HA binding and similar FPPS inhibition than RIS. Sham, baseline and age matched control groups were also studied. Femurs were assessed by µCT (6.7 µm resolution) and trabecular microarchitecture analyzed. Comparisons: ANOVA and post-hoc Tukey test; data shown as mean±SD. **RESULTS:** Tb.V/TV in OVX mice decreased ~70% from baseline. This loss was prevented by RIS, as expected. Surprisingly, Tb.V/TV in NE-025 mice increased >140% vs baseline (p<0.0001), driven by increased Tb.N but with no change in Tb.Th (Fig 1). **DISCUSSION:** The anabolic effect of NE-025 on bone was surprising—particularly its magnitude; its underlying mechanisms are as yet unknown. Most BPs with varying HA binding and FPPS inhibition are anti-apoptotic, at very low doses, and prolonged osteoblast life span might contribute to bone formation. Intriguingly, low concentrations of clinical BPs were also shown to promote osteoblast proliferation in vitro^{5,6}—an effect not seen in vivo. We speculate that the high HA affinity of clinical BPs limit their access to osteoblastic cells in vivo, while osteoclasts may “see” the BPs released from matrix as they initiate resorption. As NE-025 is not retained on bone surfaces nearly as strongly, its presentation to osteoblastic cells is more direct and similar to that seen in vitro. Regardless of mechanism, this remarkable anabolic action of NE-025 on cancellous bone needs to be explored further. **REFERENCES:** 1) Ebetino FH+ Osteoporosis 14:20,1990 2) Fuchs R+ JBMR 23:1689,2008 3) Plotkin LI+ JBC, 280:7317,2005 4) Follet H+ Bone 40:1172,2007 5) Mathov I+ JBMR 16:2050,2001 6) Im GI+ Biomater, 25:4105,2004

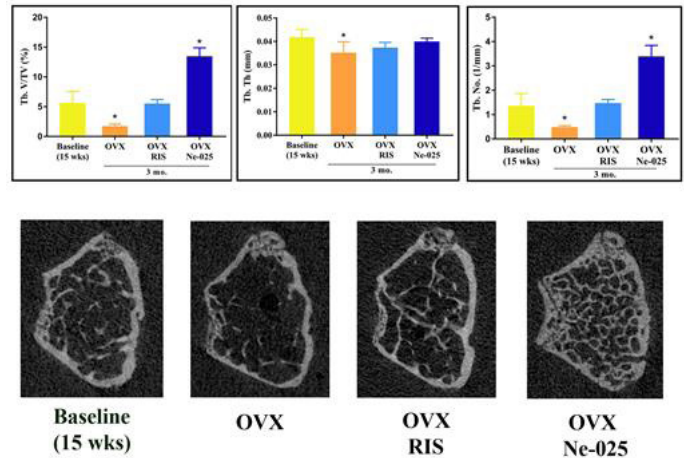


Figure: Trabecular bone architectural changes after 3 months of treatment versus baseline. Lower row images: µCT of femoral metaphyses

Disclosures: *Abigail Coffman, None*

1103

Siglec-15-Targeting Therapy Increases Bone Mass in Rats and Is a Potential Therapeutic Strategy for Juvenile Osteoporosis Dai Sato^{1*}, Masahiko Takahata¹, Masahiro Ota¹, Chie Fukuda², Eisuke Tsuda², Tomohiro Shimizu¹, Hiroki Hamano¹, Sigeto Hiratsuka¹, Akiko Okada², Ryo Fujita¹, Norio Amizuka³, Tomoka Hasegawa³, Nrimasa Iwasaki¹. ¹Department of Orthopaedic Surgery, Faculty of Medicine and Graduate School of Medicine, Hokkaido University, Japan, ²Rare Disease Laboratories, Daiichi Sankyo Co., Ltd., Japan, ³Hokkaido University, Department of Developmental Biology of Hard Tissue, Graduate School of Dental Medicine, Japan

Although osteoporosis is rare in children and adolescents, the number of juvenile patients with secondary osteoporosis increases based on the long-term survival of patients with intractable diseases owing to advances in medical treatments. Therefore, the management of juvenile osteoporosis is gaining importance. However, the treatment of juvenile osteoporosis has not been established due to a lack of data regarding the efficacy and adverse effects of therapeutic agents. The possible adverse effects of the long-term use of antiresorptive therapies on skeletal growth in children is of particular concern. Sialic acid-binding immunoglobulin-like lectin 15 (Siglec-15) is a cell surface receptor that regulates osteoclast development and bone resorption, and its deficiency suppresses bone remodeling in the secondary spongiosa, but not in the primary spongiosa, due to a compensatory mechanism of osteoclastogenesis. This prompted us to develop an anti-Siglec-15 therapy for juvenile osteoporosis. Using growing rats, we investigated the effects of an anti-Siglec-15 neutralizing antibody (Ab) on systemic bone metabolism and skeletal growth, comparing to those of bisphosphonate. Male 6-week-old F344/Jcl rats were randomized into six groups: control (PBS twice per week), anti-Siglec-15 Ab (0.25, 1, or 4 mg/kg every 3 weeks), and alendronate (ALN) (0.028 or 0.14 mg/kg twice per week). Treatment commenced at 6 weeks of age and continued for the next 6 weeks. Changes in bone mass, bone metabolism, bone strength, and skeletal growth during treatment were analyzed. Both anti-Siglec-15 therapy and ALN increased bone mass, bone mineral density and the mechanical strength of both the femora and lumbar spines. Anti-Siglec-15 therapy did not have a significant effect on skeletal growth as evidenced by micro-CT-based measurements of femoral length, high-dose ALN resulted in growth retardation with morphological abnormalities in the metaphysis of femur. ALN therapy decreased the perimeter of osteoclasts relative to the bone perimeter in the primary spongiosa with growth plate dysplasia in histological sections, whereas anti-Siglec-15 Ab therapy did not result in these outcomes. This unique property of the anti-Siglec-15 Ab can probably be attributed to compensatory signaling for Siglec-15 inhibition in the primary spongiosa, but not in the secondary spongiosa. Thus, anti-Siglec-15 therapy could be a safe and effective for juvenile osteoporosis.

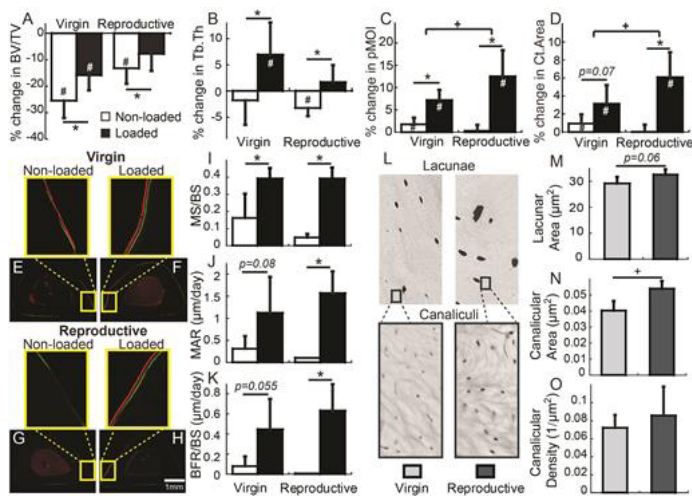
Disclosures: *Dai Sato, Daiichi Sankyo Co., Ltd, Other Financial or Material Support*

1104

Peri-Lacunar/Canalicular (PLC) Remodeling Enhances Mechano-Sensitivity in Rat Maternal Bone when Subjected to Estrogen Deficiency

Yihan Li^{1*}, Chantal De Bakker¹, Wei-Ju Tseng¹, Hongbo Zhao¹, Ashutosh Parajuli², Liyun Wang², X. Sherry Liu¹. ¹University of Pennsylvania, United States, ²University of Delaware, United States

Pregnancy and lactation lead to substantial changes in the skeleton but exert no adverse, or even protective effects on postmenopausal risk of fracture. Our previous study found that rats with multiple reproductive cycles had attenuated ovariectomy (OVX)-induced bone loss compared to virgins. It has been suggested that the osteocyte can actively remodel its peri-lacunar/canalicular (PLC) matrix during lactation. Therefore, we hypothesized that PLC remodeling may enhance bone's mechano-sensitivity by priming the microenvironment of osteocytes, exerting protective effects post-menopause. At age 10mo, Virgin (n=7) and Reproductive (n=6, 2 cycles of pregnancy, lactation, and weaning) rats underwent OVX surgery and, starting at 6wks post-OVX, were subjected to a 2-wk in vivo dynamic loading of the tibia (~1500µe at midshaft). In vivo µCT indicated that virgin and reproductive rats underwent 25% and 13% trabecular bone (Tb) loss in the non-loaded tibia, respectively (Fig A). Loading attenuated OVX Tb loss in virgins and abolished Tb loss in reproductive rats (Fig A). Loading also led to a 7% increase in Tb thickness (Tb.Th) in virgins and abolished OVX-induced reduction in Tb.Th in reproductive rats (Fig B). At the tibial midshaft, loading led to 7% and 13% increased polar moment of inertia (pMOI) in virgin and reproductive rats, respectively (Fig C). Similar results were found in cortical area (Ct.Area, Fig D). Moreover, ANOVA test indicated greater loading responses in pMOI and Ct.Area in reproductive rats than in virgins. Dynamic histomorphometry showed significant increases in periosteal double-labeled bone formation by loading in reproductive rats, while only trends of elevation (p<0.1) were observed in virgins (Fig E-K). Backscattered SEM imaging of tibial cortex indicated a trend toward greater lacunar area (by 11%, p=0.07) and 33% greater canalicular area in reproductive rats than in virgins (Fig L-N), while no difference was found in canaliculi density (Fig O). According to a lacuna-canalliculi system (LCS) fluid flow model [1], the enlarged LCS area in reproductive rats would lead to increased PLC fluid space, resulting in increased fluid shear stress on osteocytes and cell processes. In summary, reproduction and lactation exert long-term functional adaptation in modulating osteocyte LCS environment to enhance bone's mechano-sensitivity to protect the maternal skeleton from future estrogen deficiency. [1] Weinbaum S et al, J Biomech., 1994.



(A-B) Comparisons of % changes in trabecular bone and (C-D) midshaft cortex over the 2-wk loading period between non-loaded and loaded tibia in virgin and reproductive rats. (E-H) Comparisons of representative histology images and (I-K) periosteal bone formation parameters between non-loaded and loaded tibia in virgin and reproductive rats. (L) Comparisons of bSEM images and (M-O) LCS structure between virgin and reproductive rats. p<0.05; # pre- ≠ post-loading; * non-loaded ≠ loaded; + virgin ≠ reproductive.

Disclosures: Yihan Li, None

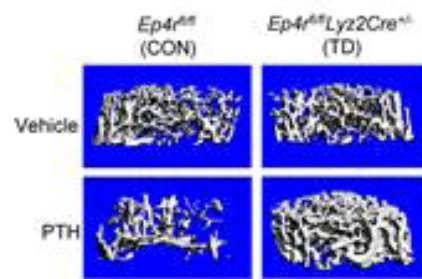
1105

Deletion of Prostaglandin E2 (PGE2) Receptor EP4 in Myeloid Lineage Cells Restores the Anabolic Effects of Continuous PTH in Mice

Shilpa Choudhary*, Joseph Lorenzo, Carol Pilbeam. Musculoskeletal Institute & Department of Medicine, UConn Health, United States

We previously found that the anabolic response to continuously infused PTH in mice is suppressed by the induction of serum amyloid A3 (SAA3). In vitro experiments indicate that SAA3 is produced in myeloid cells in response to RANKL through a mechanism that requires PGE2. We hypothesized that the required PGE2 acts via the EP4 receptor. To test this, we generated Ep4^{fl/fl} (Control, CON) and Ep4^{fl/fl}/iLyz2Cre^{-/-} (targeted deletion in myeloid cells, TD) littermates in a CD-1 background. In bone marrow macrophages (BMMs) from TD mice, cultured with M-CSF +/- RANKL, Ep4r mRNA was reduced >96% compared to CON BMMs. RANKL induced Saa3 mRNA 1600-fold in CON BMMs, which was reduced

by 99% in TD BMMs. RANKL-induced SAA3 protein was undetectable in the culture medium of TD BMMs but easily measured in CON medium. Male (3-mo-old) CON and TD mice (n=6/group) were continuously infused with vehicle or hPTH 1-34 (40 µg/kg/d) for 12 days. Measurements included mRNA from unflushed tibiae after ends removed; serum analyses; and femoral µCT. Data were analyzed by 2-way ANOVA. Vehicle-infused CON and TD mice did not differ in any of the measurements. PTH induced mRNA for cyclooxygenase 2, the major enzyme producing PGE2, equally in CON and TD tibiae (7-fold). In contrast, the induction of Saa3 mRNA (37-fold) by PTH was reduced 91% in TD tibiae. Although PTH infusion caused bone loss in CON mice, decreasing distal femoral trabecular BV/TV 50%, PTH infusion was anabolic in TD mice, increasing BV/TV 64%. PTH increased cortical area and thickness 20-24% and tibial expression of osteogenic genes, Bglap, Igf1 and Wnt10b, only in TD mice. mRNA for Sost, an inhibitor of bone formation, was decreased by PTH only in TD tibiae. PTH elevated serum PINP, a marker of bone formation, >400% in TD mice, compared to 35% in CON mice. In contrast to the striking differences between CON and TD mice in measurements associated with PTH-stimulated bone formation, PTH stimulated factors associated with bone resorption similarly in CON and TD mice. Serum CTX, a marker of bone resorption, was elevated by PTH 5-fold in both CON and TD mice. In addition, PTH increased the Rankl/Opg mRNA ratio similarly in CON and TD tibiae. We conclude that the EP4 receptor in myeloid cells mediates the PGE2 effects required for SAA3 suppression of the bone formation response to continuous PTH. Hence, antagonists of the EP4 receptor may enhance the therapeutic potential of PTH for treating bone diseases.



Disclosures: Shilpa Choudhary, None

1106

The Gut Microbiota Is Required For The Anabolic And Catabolic Effects Of PTH In Bone

Jau-Yi Li*, Mingcan Yu, Abdul Malik Tyagi, Chiara Vaccaro, Jonathan Adams, Rheinallt M. Jones, Roberto Pacifici. School of Medicine, Emory University, United States

There is increasing evidence that the gut microbiome plays a pivotal role in bone health and disease, but the relationship between microbiota and PTH remains unexplored. This study was designed to investigate the role of the gut microbiota in the skeletal effects of PTH. Continuous PTH treatment (cPTH), a model of hyperparathyroidism induces bone catabolism. Conversely, teriparatide treatment, which is modeled by intermittent PTH (iPTH) administration, induces bone anabolism. We investigated if the gut microbiota affects the bone anabolic activity of iPTH by injecting iPTH (80 µg/Kg/day, SC) daily for 4 weeks into 8-week-old germ-free (GF) mice, conventionally raised (Conv.R) mice, and Conv.R mice treated with wide-spectrum antibiotics (Abx). Abx treatment decreased gut bacterial DNA by > 99%. iPTH treatment increased trabecular bone volume (BV/TV), µCT indices of trabecular structure, and bone formation in Conv. R mice, but not in GF mice and Conv. R. mice treated with Abx. Moreover, Abx treatment blocked the capacity of iPTH to induce osteoblast differentiation, to activate Wnt signaling in osteoblastic cells, to increase the number of regulatory T cells (Tregs), and to upregulate the production of Wnt10b by bone marrow CD8+ T cells. Tregs and Wnt10b have been previously reported to mediate the effects of iPTH on Wnt signaling and bone formation. To investigate the role of the gut microbiome in models of hyperparathyroidism, 16-week-old Conv. R. mice and Abx treated Conv. R. mice were infused with cPTH (80µg/kg/day delivered by osmotic pumps) for 2 weeks or fed a low Ca diet (0.01% calcium) for 4 weeks. cPTH and low Ca diet induced trabecular and cortical bone loss and stimulated bone resorption in control mice but not in those treated with Abx. cPTH is known to induce bone loss by upregulating TNF and IL-17 production by T cells and RANKL production by osteocytes. We found that cPTH and low Ca diet stimulated IL-17 and TNF production in Payer's patches and the bone marrow; however, Abx treatment prevented the increase in TNF and IL-17 levels induced by cPTH and low Ca diet. In summary, these findings provide compelling evidence that the microbiota and the gut/bone axis play a critical role in the anabolic and catabolic effects of PTH in bone. The gut microbiota is required for activating both the Tregs/Wnt10b/Wnt signaling pathway that leads to iPTH induced bone anabolism, and the TNF/IL-17/RANKL pathway that causes bone loss in hyperparathyroidism.

Disclosures: Jau-Yi Li, None

1107

Impaired 1,25 dihydroxyvitamin D action underlies the development of enthesopathy in the Hyp mouse model of XLH Eva Liu^{*1}, Janaina Martins², Marie Demay². ¹Brigham and Women's Hospital, MGH, and Harvard Medical School, United States, ²Massachusetts General Hospital and Harvard Medical School, United States

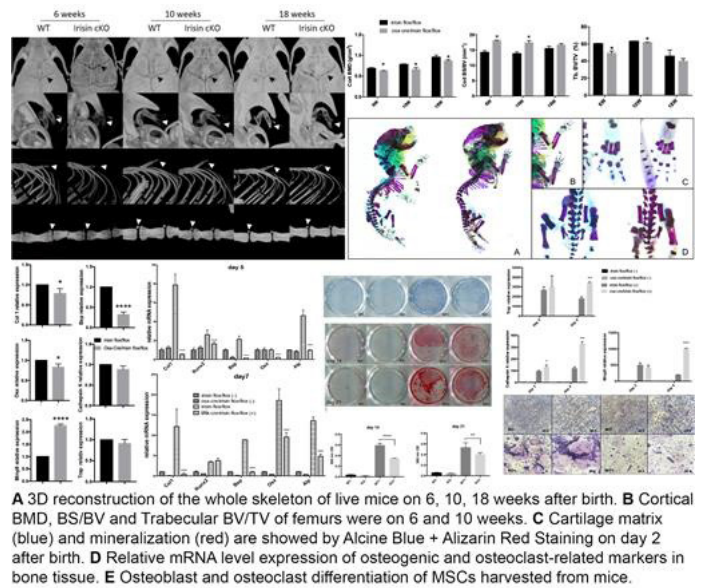
The enthesis is a specialized fibrocartilaginous tissue that forms at the site of attachment of tendon to bone, optimizing the transfer of mechanical stress from muscle to bone. X-linked hypophosphatemia (XLH) is characterized by elevated serum FGF23 levels, leading to decreased production of 1,25 dihydroxyvitamin D (1,25D) and hypophosphatemia. A complication of XLH is enthesopathy, an abnormal mineralization of bone-tendon attachment sites, which leads to pain and impaired mobility. Compared to WT, Achilles tendon entheses in mice with XLH (Hyp) have an expansion of aberrant Safranin O positive (SaO+) hypertrophic enthesopathy cells (HECs). Hyp entheses exhibit increased expression of BMP and IHH target genes, implicating these signaling pathways in the pathogenesis of enthesopathy. Treatment of Hyp mice with either 1,25D or an FGF23 blocking antibody attenuates the enthesopathy phenotype, suggesting that impaired 1,25D action in XLH plays a pathogenic role in the development of enthesopathy. Studies were undertaken to identify a pathogenic role for impaired 1,25D action in the development of enthesopathy. Global ablation of the vitamin D 1-alpha-hydroxylase (Cyp27b1KO) resulted in an enthesopathy phenotype similar to that seen in Hyp mice. The Achilles tendon entheses of Cyp27b1KO and Hyp;Cyp27b1KO mice exhibit an expansion of SaO+ HECs, immunoreactive to BMP induced p-Smad1/5 and the BMP and IHH target genes Sox9, Patched and Runx2. In contrast, entheses from FGF23KO and Hyp;FGF23KO mice which have elevated serum 1,25D levels did not exhibit enthesopathy. Deletion of Cyp27b1 in FGF23KO and Hyp;FGF23KO mice led to an expansion of HECs expressing BMP and IHH targets. Prior studies have demonstrated that BMPs regulate IHH signaling in chondrocytes. Since impaired 1,25D action in mice leads to expression of BMP and IHH target genes in the fibrocartilaginous HECs, studies were performed to address the hypothesis that 1,25D suppresses BMP/IHH signaling, in chondrogenic cells. Primary murine chondrocytes were treated with rhBMP2 with or without 1,25D. 1,25D pretreatment suppressed the induction of BMP and IHH target genes by rhBMP2. These results demonstrate that impaired 1,25D action, rather than direct effects of increased FGF23, underlies the pathogenesis of XLH enthesopathy. They also suggest that optimizing 1,25D treatment will prevent the development of enthesopathy in XLH by suppressing BMP and IHH signaling in entheses.

Disclosures: *Eva Liu, None*

1108

Irisin Deficiency Disturbs Bone Metabolism Zoe (Xiaofang) Zhu^{*1,2}, Jake (Jinkun) Chen^{3,4}, Guofang Shen⁵, Qisheng Tu¹. ¹Tufts University School of Dental Medicine, United States, ²Shanghai Jiaotong Univ., China, ³Division of Oral Biology Tufts University School of Dental Medicine, United States, ⁴Department of Developmental, Molecular and Chemical Biology Sackler School of Graduate Biomedical Sciences Tufts University School of Medicine, United States, ⁵Shanghai Jiaotong Univ., China

Metabolic bone diseases caused by abnormalities of mineralization, such as rickets, osteoporosis, osteopetrosis are among the most common public health issues. Irisin, a recently identified novel hormone-like myokine, is the cleaved and secreted portion of the fibronectin-type III domain-containing 5 (FNDC5). Recent studies reported the involvement of the irisin in many physiological and pathological conditions with bone mineral density changes, such as osteoporotic fractures. In addition, injection of recombinant irisin is shown to have increased bone mass in mice. Those led us to hypothesize that irisin regulates bone metabolism. We first designed and constructed the irisin^{flx/flx} mice. *Ox-Cre/irisin^{flx/flx}* mice, in which irisin was specifically deleted in bone, were created by crossing our *irisin^{flx/flx}* mice with *ostx-cre* mice. The mice were grouped according to the southern blot and standard PCR genotyping results, and phenotypes were analyzed. Gene and protein expression of the irisin were remarkably decreased in bone but no significant difference in other tissue in knockout mice. We found both young and adult irisin knockout mice were smaller and lighter than normal. In vivo analyses using Micro CT showed lower Co. BMD, Co. Thickness and Tb. BV/TV of femurs, and significantly delayed bone development and mineralization of skull, hyoid, ribs, xiphoid and coccyx on 6, 10, 18 weeks after birth in knockout mice. Whole skeleton staining also showed the mineralization delay on P2 in knockout group (as shown on figure). Our assessment indicates increased osteoblast-related genes expression and decreased osteoclast-related genes expression in bone tissues in knockout mice. By harvesting and culturing the MSCs, we identified that the osteoblastogenesis was inhibited and the osteoclastogenesis was increased in MSCs from knockout mice cultured in vitro. For the first time, we established the irisin gene flanked mice: *irisin^{flx/flx}* mice, and *irisin* bone-specific knockout mice model: *Ox-Cre/irisin^{flx/flx}* mice. The *irisin* deficiency mice showed delayed bone formation and mineralization, and increased osteoclastogenesis. Irisin, as a new hormone-like polypeptide, plays an important role in bone metabolism and in the crosstalk between bone and other organs, representing a potential molecule for the prevention and treatment of bone diseases.



A 3D reconstruction of the whole skeleton of live mice on 6, 10, 18 weeks after birth. **B** Cortical BMD, BS/BV and Trabecular BV/TV of femurs were on 6 and 10 weeks. **C** Cartilage matrix (blue) and mineralization (red) are shown by Alcine Blue + Alizarin Red Staining on day 2 after birth. **D** Relative mRNA level expression of osteogenic and osteoclast-related markers in bone tissue. **E** Osteoblast and osteoclast differentiation of MSCs harvested from mice.

Disclosures: *Zoe (Xiaofang) Zhu, None*

1109

Deficits in cortical and trabecular bone microarchitecture increase short-term risk of fracture independently of DXA BMD and FRAX: The Bone Microarchitecture International Consortium (BoMIC) Elizabeth Samelson^{*1}, Serkalem Demissie², Jonathan Adachi³, Shreyasee Amin⁴, Elizabeth Atkinson⁵, Claudie Berger⁶, Emmanuel Biver⁶, Steven Boyd⁷, Lauren Burt⁷, Roland Chapurlat⁸, Thierry Chevalley⁶, Serge Ferrari⁶, David Goltzman⁹, David Hanley⁷, Ching-Ti Liu¹⁰, Marian Hannan¹, Sundeep Khosla⁴, Mattias Lorentzon¹¹, Dan Mellstrom¹², Blandine Merle¹³, Maria Nethander^{14,15}, Claes Ohlsson¹⁵, René Rizzoli⁶, Elisabeth Sornay-Rendu¹³, Daniel Sundh¹¹, Pawel Szulc¹⁶, Bert Van Rietbergen¹⁷, Andy Wong¹⁸, Hanfei Xu², Lajji Yang¹⁹, Mary Boussein²⁰, Douglas Kiel¹. ¹Institute for Aging Research, Hebrew SeniorLife, Harvard Medical School, United States, ²Department of Biostatistics, Boston University School of Public Health, United States, ³Department of Medicine, Michael G. DeGroot School of Medicine, St Joseph's Healthcare - McMaster University, Canada, ⁴Mayo Clinic College of Medicine, United States, ⁵Research Institute of the McGill University Health Centre, Canada, ⁶Division of Bone Diseases, Geneva University Hospitals and Faculty of Medicine, Switzerland, ⁷McCaig Institute for Bone and Joint Health, Canada, ⁸INSERM UMR 1033, Université de Lyon, Hospices Civils de Lyon, Lyon, France, ⁹Departments of Medicine, McGill University and McGill University Health Centre, Canada, ¹⁰Boston University School of Public Health, United States, ¹¹Geriatric Medicine, Centre for Bone and Arthritis Research, Institute of Medicine, University of Gothenburg, Sweden, ¹²Geriatric Medicine, Centre for Bone and Arthritis Research, Institute of Medicine, Sahlgrenska Academy, University of Gothenburg, Sweden, ¹³INSERM UMR 1033, Pavillon F, Hôpital E Herriot, France, ¹⁴Bioinformatics Core Facility, Sahlgrenska Academy, University of Gothenburg, Gothenburg, Sweden, ¹⁵Centre for Bone and Arthritis Research, Institute of Medicine, Sahlgrenska Academy, University of Gothenburg, Gothenburg, Sweden, ¹⁶INSERM UMR1033, University of Lyon, Hôpital Edouard Herriot, France, ¹⁷Department of Biomedical Engineering, Eindhoven University of Technology, Netherlands, ¹⁸Toronto General Hospital, Canada, ¹⁹Institute for Aging Research, Hebrew SeniorLife, United States, ²⁰Dept of Orthopedic Surgery, Harvard Medical School, Center for Advanced Orthopedic Studies, BIDMC, United States

There is a growing need to identify individuals at "imminent" risk of fracture. In particular, since many fractures occur in persons with osteopenia, better approaches for stratifying fracture risk are needed. Thus, we combined data from 7 cohorts to conduct a prospective study of bone microarchitecture, evaluated by HR-pQCT, and 2-year incidence of fracture. Participants included 6,763 individuals (4,768 women, 1,995 men) from the Framingham Osteoporosis Study, Geneva Retirees, Mayo Clinic, CaMos, Qalyor, OFELY, and STRAM-BO cohorts. Participants underwent HR-pQCT scanning (XtremeCT, Scanco Medical AG) at the distal radius and tibia. We estimated hazard ratios (HR) for the association between each bone measure and 2-year fracture incidence, adjusted for age, sex, cohort, height and weight, and then additionally adjusted for femoral neck (FN) areal BMD (aBMD) or FRAX (calculated with FN aBMD) for major osteoporosis fracture. Mean age was 68±9 years (range, 40-96), and 71% were women. Only 8% had FN T-score ≤ -2.5, whereas 55% had

FN T-score between -1.0 and -2.5 and 37% had FN T-score ≥ -1.0 . Two-year cumulative incidence of fracture was 4% (271/6,763). Fractures included 67 (25%) wrist, 34 (13%) spine, 32 (12%) ankle, 28 (10%) rib, 20 (7%) upper arm, 8 (3%) hip and 82 (30%) at the pelvis, lower thigh, and other sites. For each SD decrease in radius cortical indices, fracture risk increased 38% to 73% and remained increased by 29% to 61% after additional adjustment for FN aBMD (Table). Trabecular indices were also significantly associated with 2-year fracture risk, independently of FN aBMD, with adjusted HRs ranging from 1.15 (SD trabecular number) to 1.54 (trabecular volumetric BMD, vBMD). Decreased failure load was associated with nearly a 2-fold (HR=1.97) increased fracture risk, and after adjustment for FN aBMD, HR=1.77. Results for the tibia (not shown) were similar to those for the radius, and findings were similar when models adjusted for FRAX (Table). In this large, community-based population of older adults, cortical and trabecular bone microarchitecture and density predicted short-term risk of fracture, independent of FN aBMD and FRAX. These results indicate that HR-pQCT may be a useful adjunct to traditional assessment of imminent fracture risk in older adults, including those with T-scores above the osteoporosis range.

Bone Measure**	Adjusted for age, sex, cohort, height, and weight		Additional adjustment for DXA FN aBMD		Adjusted for cohort and FRAX for major osteoporotic fracture*	
	HR	95% CI	HR	95% CI	HR	95% CI
Femoral Neck						
aBMD	1.43	1.22-1.69	--	--	--	--
Radius						
Cortical vBMD	1.38	1.17-1.63	1.29	1.08-1.53	1.29	1.10-1.51
Cortical Tissue Mineral Density	1.46	1.16-1.83	1.34	1.04-1.71	1.33	1.07-1.65
Cortical Porosity [†]	0.86	0.70-1.06	0.88	0.72-1.09	0.90	0.74-1.09
Cortical Thickness	1.54	1.30-1.83	1.43	1.20-1.72	1.45	1.23-1.70
Cortical Area	1.73	1.40-2.14	1.61	1.29-2.01	1.53	1.27-1.84
Cortical Area Fraction	1.39	1.19-1.63	1.32	1.12-1.55	1.30	1.12-1.50
Trabecular vBMD	1.64	1.42-1.89	1.54	1.31-1.80	1.53	1.33-1.77
Trabecular Number	1.47	1.29-1.68	1.40	1.21-1.61	1.38	1.21-1.57
SD Trabecular Number**	1.18	1.11-1.26	1.15	1.07-1.24	1.14	1.06-1.23
Trabecular Thickness	1.43	1.23-1.66	1.31	1.12-1.53	1.37	1.19-1.59
Trabecular Spacing [†]	1.24	1.16-1.32	1.20	1.11-1.30	1.18	1.10-1.28
Total Area	0.91	0.72-1.14	0.93	0.73-1.17	1.02	0.86-1.20
Total vBMD	1.63	1.40-1.89	1.52	1.29-1.80	1.49	1.29-1.72
Failure Load	1.97	1.47-2.65	1.77	1.27-2.47	1.55	1.21-1.97

*VAX estimated with femoral neck aBMD
[†]HRs expressed per SD decrease in bone measure, except cortical porosity. SD trabecular number, and trabecular spacing expressed per SD increase.
 **HRs expressed per SD increase in bone measure. vBMD=volumetric bone mineral density.

Disclosures: Elizabeth Samelson, None

1110

Prediction of Incident Hip Fracture: Can we do Better than Femoral Neck aBMD? A Comprehensive Image-Based Assessment in Men and Women Julio Carballido-Gamio^{*1}, Sigurdur Sigurdsson², Kristín Siggeirsdóttir², Alexandria Jensen^{1,3}, Gunnar Sigurdsson^{2,4,5}, Thor Aspelund^{2,6}, Gudny Eiriksdóttir², Vilundur Gudnason^{2,4}, Thomas F Lang⁷, Tamara B Harris⁸. ¹Department of Radiology, School of Medicine, University of Colorado Denver, Denver, CO, United States, ²Icelandic Heart Association Research Institute, Kópavogur, Iceland, ³Department of Biostatistics & Informatics, Colorado School of Public Health, Aurora, CO, United States, ⁴University of Iceland, Reykjavik, Iceland, ⁵Landsþítalinn University Hospital, Reykjavik, Iceland, ⁶Centre of Public Health Sciences, University of Iceland, Reykjavik, Iceland, ⁷Department of Radiology and Biomedical Imaging, University of California, San Francisco, CA, United States, ⁸National Institute on Aging, Intramural Research Program, Laboratory of Epidemiology and Population Sciences, Bethesda, MD, United States

Fragility hip fractures lead to devastating personal and financial effects. DXA aBMD is the clinical standard to assess osteoporosis and hip fracture risk. However, subjects with normal aBMD do fracture, underscoring the necessity of better hip fracture prediction techniques. The objective of this work was to perform a comprehensive image-based assessment of hip fracture prediction using advanced image analyses and machine learning. A subset of 585 men (76.9±5.6 yr) and 796 women (77.0±5.5 yr) from the AGES Reykjavik Study was included in this work, including 100 men and 234 women having incident hip fracture. Using baseline hip QCT scans, 3D parametric maps of vBMD, cortical bone thickness, cortical vBMD and endosteal vBMD, and 2D QCT-derived aBMD maps were generated. Local parametric comparisons were then performed between cases and noncases—stratified by sex—using voxel-based morphometry (VBM) and statistical parametric mapping (SPM) with general linear models allowing for covariates. Statistical multi-parametric modeling (SMPM)—based on principal component analysis (PCA)—was also performed for all the parameters with and without shape. VBM and SPM yielded Student's t-test statistical maps (t-Maps) indicating regions where the parameters were significantly associated with fracture. These regions were subdivided to identify the most significant clusters using fuzzy c-means (FCM). SMPM generated scores for each subject, parameter and PC representing different spatial parametric patterns. Mean parametric values within the FCM clusters and SMPM scores were then used with machine learning elastic net regularization to generate hip fracture prediction models, whose performance was assessed with ROC analyses measuring AUC improvements with respect to mean femoral neck aBMD (FN.aBMD). The full pipeline was performed with stratified 10-fold cross-validation. Fig. 1 summarizes the results of this study with 3 important findings: 1) in men, FN.aBMD was the best predictor; 2) in women, several QCT parameters performed better than FN.aBMD, however, PCA of aBMD maps was the best predictor; and 3) in women with high FN.aBMD, PCA of aBMD maps remained as the best predictor. Our results indicate that FN.aBMD might be a good predictor in men, and that advanced image analyses and machine learning improve aBMD-based pre-

dition in women. Ultimately, QCT enables 3D assessments of both BMD and bone quality that capture diagnostic information that cannot be measured by DXA.

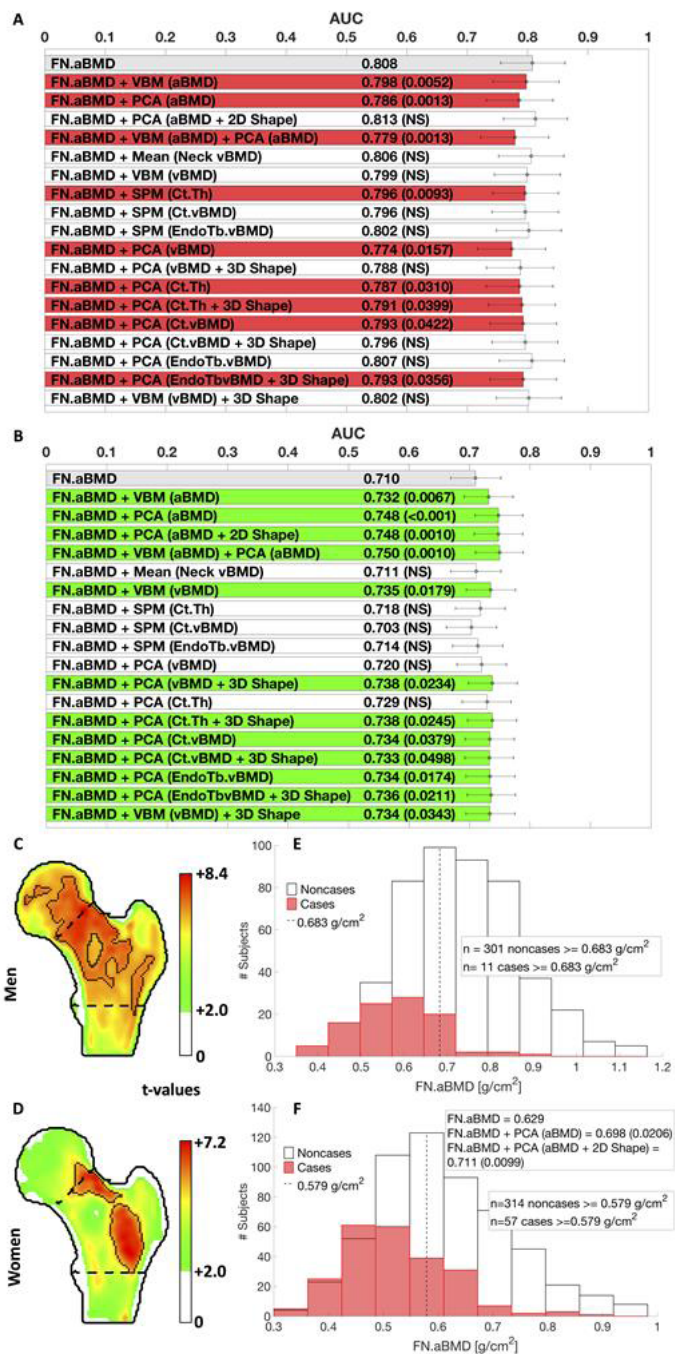


Fig 1. AUCs (p-values) for the prediction models in men (A) and women (B). VBM t-Maps of aBMD comparisons between cases and noncases in men (C) and women (D) with dotted lines enclosing the FCM clusters. Distribution of FN.aBMD values in men (E) and women (F). PCA of aBMD remained as the best predictor in women with high FN.aBMD (F).
 Notes: The femoral head was excluded from the SPM analyses due to the thin cortical bone, and from the 2D VBM and PCA analyses for a more realistic DXA scenario. White pixels in (C) and (D) were not significant after false discovery rate correction for multiple comparisons. Abbreviations: Ct.Th = cortical bone thickness; Ct.vBMD = cortical vBMD; EndoTb.vBMD = vBMD in a layer adjacent to the endosteal surface; NS = nonsignificant.

Disclosures: Julio Carballido-Gamio, None

1111

Deterioration of Bone Microstructure Identifies Women at Imminent Risk of Fragility Fractures Roland Chapurlat^{*1}, Elisabeth Sornay-Rendu¹, Roger Zebaze², Minh Bui², Eric Lespessailles³, Ego Seeman². ¹INSERM UMR 1033, France, ²University of Melbourne, Australia, ³IPROS, France

The burden of fragility fractures in the population arises from women with osteopenia or normal bone mineral density (BMD), not osteoporosis. Microstructural deterioration increases bone fragility out of proportion to the bone loss producing it. Our goal was to determine whether women at imminent risk for fracture, particularly those with osteopenia or normal BMD, are detectable by measuring microstructural deterioration. We measured distal radial microstructure, BMD and the Fracture Risk Assessment (FRAX) score in two prospective studies of postmenopausal women, the OFELY (n = 589) and QUALYOR (n = 1540) studies, in France. Microstructural deterioration of cortical porosity and trabecular density relative to the mean in premenopausal women was measured with high resolution peripheral quantitative tomography and expressed as a Structural Fragility Score (SFS). The thresholds used were a T score of < -2.5 SD for BMD, a FRAX score > 20 and the SFS > 70. Fracture risk associated with BMD, FRAX and the SFS was estimated by odds ratios (OR) using the exact logistic regression method before and after removing the contribution of the other two tools. Among 1996 women (mean age 67 [range 42-96]), during 2 years, 98 had a fracture at a median of 1.06 years; 20.4% had osteoporosis, 79.6% had osteopenia or normal BMD. Neither BMD nor FRAX predicted fracture independent of the Structural Fragility Score. By contrast, the Structural Fragility Score, independent of BMD or FRAX, identified 14 of 20 women with osteoporosis having a fracture (sensitivity 70%, specificity 63.1%, odds ratio, OR 3.95, p=0.01), 29 of 78 women with osteopenia or normal BMD having a fracture (sensitivity 37.2%, specificity 83.6%, OR 3.01, p<0.001) and 19 of 24 women over 70 years of age having major fragility fractures (sensitivity 79.2%, specificity 69.3%, OR 8.52, p<0.001). We conclude that most postmenopausal women at imminent risk for fracture within 2 years remain undetected using BMD or FRAX but are identifiable by measuring microstructural deterioration non-invasively. These women are likely to need prompt treatment that is not triggered using FRAX or BMD.

Disclosures: **Roland Chapurlat**, None

1112

Prevalent Vertebral Fracture Identified on Densitometric Images Predict Incident Fractures in Routine Clinical Practice John Schousboe^{*1}, Lisa Lix², Suzanne Morin³, Sheldon Derkatch², Mark Bryanton², Mashael Alhrbi², William Leslie². ¹Park Nicollet Clinic and HealthPartners Institute, United States, ²University of Manitoba, Canada, ³McGill University, Canada

Purpose: Using vertebral fracture assessment (VFA) on densitometric lateral spine images to identify those with prevalent vertebral fracture is not widely accepted, in part because the predictive validity of VFA in clinical practice has not been established. Our objective was to estimate the associations of prevalent vertebral fractures identified on VFA images obtained during routine practice with incident hip, non-vertebral, major osteoporotic, and clinical vertebral fractures. Methods: Using the Manitoba (Canada) Bone Density database from 2010 onward, VFA images were obtained for 9972 men and women (mean age [SD] 76 [6.9] years) referred for bone densitometry (DXA). Definite prevalent vertebral fractures (positive VFA) were identified in 1575 (15.8%) using a modified algorithm-based qualitative method. Incident fractures were identified using administrative claims data during a mean follow-up of 2.8 [1.7] years. Cox proportional hazards models estimated the associations between positive VFA and incident fractures adjusted for: (1) FRAX (with femoral neck bone mineral density [BMD]) probabilities of major osteoporotic fracture (MOF); (2) FRAX risk factors (age, body mass index, femoral neck BMD, prior fracture, parental hip fracture, glucocorticoid use, alcohol use, smoking, rheumatoid arthritis) as separate covariates; or (3) FRAX risk factors with lumbar spine BMD and osteoporosis drug therapy (Rx). Results: Hazard Ratios (95% CI) for incident fracture in those with positive VFA vs VFA negative for vertebral fracture are shown in the Table. Positive VFA was significantly associated with the incidence of all fracture outcomes. Interaction terms between positive VFA and MOF FRAX with BMD score or BMD T-score category for prediction of fracture at any skeletal site were nonsignificant. Conclusions: Prevalent vertebral fracture identified on densitometric VFA images in routine clinical practice are strongly associated with incident hip, vertebral, and other clinical fractures, adjusted for BMD and other clinical risk factors. These associations do not vary by FRAX with BMD score or BMD T-score level. These associations are similar in strength to those shown in prospective studies using standard radiographs to identify prevalent vertebral fracture, and establish the predictive validity of using VFA at the time of bone densitometry to aid fracture risk assessment in routine clinical practice.

Table: Hazard Ratios (95% CI) for Incident Fracture in Those with Definite vs No Prevalent Vertebral Fracture

Fracture Outcome	Covariates		
	FRAX with BMD MOF Score	FRAX risk factors	FRAX risk factors + LS-BMD + Osteoporosis Rx
Hip Fracture (n=226)	2.20 (1.65, 2.94)	1.95 (1.45, 2.62)	2.13 (1.51, 3.02)
All Non-Vertebral (n=715)	2.10 (1.77, 2.47)	1.99 (1.68, 2.35)	2.08 (1.71, 2.54)
Major Osteoporotic* (n=552)	2.07 (1.71, 2.50)	1.95 (1.61, 2.37)	2.07 (1.65, 2.09)
Clinical Vertebral* (n=93)	2.78 (1.77, 4.35)	2.68 (1.69, 4.23)	3.09 (1.85, 5.16)

*Excludes vertebral fractures during first 12 months of follow-up

Disclosures: **John Schousboe**, None

1113

Screening for Incomplete Atypical Femur Fractures in Bone Density Laboratories Sameh Melk^{*}, Robert Bleakney, Lianne Tile, Rowena Ridout, Heather McDonald-Blumer, Angela Cheung, Moira Kapral, Judite Scher, Alice Demaras. UHN, Canada

Background: Complete atypical femur fractures (AFFs) are a rare complication of anti-resorptive medications used to treat osteoporosis, with reported frequencies of approximately 1 in 1000 patient-years after long-term (6-10 yrs) use. Recent studies suggest that incomplete AFFs (iAFFs) may be more common because approximately 75% of patients with complete AFF have prodromal symptoms prior to their fracture. Imaging with either plain radiographs or densitometer-based techniques may detect an iAFF prior to a complete break. This study examined the frequency of iAFFs at 3 academic bone density laboratories in Toronto. Methods: We screened women either postmenopausal or over age 50 who had been on at least 5 years of oral bisphosphonate therapy or 3 years of intravenous bisphosphonates or denosumab from bone density laboratories at three academic centres in Toronto (Toronto General Hospital, Toronto Western Hospital and Princess Margaret Hospital). All women had to have pain, discomfort or weakness in their upper leg. Subjects underwent a Single Energy (SE)-femur scan using Hologic Discovery or Horizon A densitometers, scanning from above the lesser trochanter to the medial condylar flare, and a plain radiograph of the femur for comparison. Scans were read by an expert with extensive experience in identifying femur characteristics along the AFF spectrum. Results: 1361 women met age and/or postmenopausal criteria and of these, 315 (26%) had leg symptoms, and 255 consented to participate in the study. Of the 545 femurs scans completed, SE-femur identified 2 iAFFs in 2 (0.8%) women, one of whom had a prior AFF on the contralateral side which was not previously recognized as AFF. 13 (5%) women (19 femurs) had an equivocal focal cortical reaction (2 were endosteal). 81 (32%) women (121 femurs) had generalized cortical thickening. Follow-up imaging (SE-femur +/- plain radiograph) 6 months to 2 years later did not yield further iAFFs. SE-femurs detected other abnormalities including vascular calcifications, an intraosseous lipoma, avascular necrosis, enchondromas, tug lesions and gold threads from acupuncture. Conclusions: Incomplete AFFs are rare even in this higher risk group of women on long-term potent anti-resorptive therapy and who have upper leg symptoms. However, they may be more frequent than complete AFFs. Further studies are needed to better define the cost-effectiveness of screening strategies to identify iAFFs in those at risk.

Disclosures: **Sameh Melk**, None

1114

Genomic Prediction of Osteoporosis Using 426,000 Individuals from UK Biobank

Vincenzo Forgetta^{*1}, Julyan Keller-Baruch², Marie Forest¹, Audrey Durand³, Sahir Bhatnagar⁴, John Kemp⁵, John Morris¹, John Kanis^{6,7}, Douglas Kiel⁸, Eugene McCloskey⁹, Helena Johansson^{6,7}, Nicholas Harvey¹⁰, Dave Evans⁵, Joelle Pineau³, William Leslie¹¹, Celia M T Greenwood², J Brent Richards². ¹Centre for Clinical Epidemiology, Lady Davis Institute, Jewish General Hospital, McGill University, Canada, ²Department of Human Genetics, McGill University, Canada, ³School of Computer Science, McGill University, Canada, ⁴Centre for Clinical Epidemiology, Lady Davis Institute, Jewish General Hospital, Canada, ⁵University of Queensland Diamantina Institute, Translational Research Institute, MRC Integrative Epidemiology Unit, University of Bristol, Australia, ⁶Centre for Metabolic Bone Diseases, University of Sheffield, United Kingdom, ⁷Australian Catholic University, United Kingdom, ⁸Institute for Aging Research, Hebrew SeniorLife, Harvard Medical School, Broad Institute of MIT & Harvard, United States, ⁹Mellanby Centre for Bone Research, Centre for Integrated Research in Musculoskeletal Ageing, University of Sheffield, United Kingdom, ¹⁰Medical Research Council Lifecourse Epidemiology Unit, University of Southampton, United Kingdom, ¹¹Department of Medicine (Endocrinology), Department of Radiology (Nuclear Medicine), University of Manitoba, Canada

Background The prediction of clinically relevant traits using genetics has not yet been generally successful, even those which are highly heritable, such as bone density, the measure most often used to diagnose osteoporosis. We tested whether machine learning methods could improve prediction of estimated bone mineral density (eBMD) from genotypes. **Methods** We used the UK Biobank to identify 426,812 individuals with eBMD measures at calcaneal ultrasound and genome-wide genotypes, who were of British descent. Dividing the cohort into separate training (N = 341,450), validation (N = 42,681) and test (N = 42,681) datasets, we first evaluated a prediction model containing only age and sex, two commonly used metrics to identify people for BMD testing. Next, we undertook a genome-wide association study for eBMD in the training set. Using top-ranked SNPs from the GWAS by P-value we trained a machine learning algorithm, least absolute shrinkage and selection operator (LASSO), using six different SNP sets to predict eBMD in the training set. We optimized tuning parameters for these SNP sets in the validation dataset and selected the best performing SNP set for evaluation of prediction in the test dataset. Last, we tested whether genomic pre-screening could identify individuals unlikely to have a diagnosis of osteoporosis by eBMD measurement. **Results** In the test dataset, the variance explained in eBMD by age and sex was 5.8%. The area under the receiver operator curve using age and sex was 71.3% [95% CI: 68.7%-74%] for the diagnosis of osteoporosis. Using the machine learning algorithm and adding genotypic information, the variance explained increased approximately five-fold to 29.7%. The area under the receiver operator curve for the diagnosis of osteoporosis increased to 81.3% (P = 2x10⁻¹⁷, compared to age and sex alone). The maximal combined sensitivity and specificity for the diagnosis of osteoporosis were 75% and 75%, respectively. Including only individuals aged 55-, or 65- and over generated similar prediction performance. **Interpretation** The use of genotypes in a machine learning algorithm resulted in a clinically-relevant improvement in the identification of individuals at risk for eBMD-defined osteoporosis and provides the opportunity to use a genomic pre-screening to focus clinical screening programs.

Disclosures: Vincenzo Forgetta, None

1115

Excess intra-abdominal adipose tissue accumulation increases the risk of fragility fracture: A Mendelian randomization study with Genome-wide association meta-analysis on fracture

Yi-Hsiang Hsu^{*1}, Chia-Yen Chen², Ching-Ti Li³, Douglas Kiel⁴. ¹Harvard Medical School and Broad Institute of MIT and Harvard, United States, ²Analytic and Translational Genetics Unit, Massachusetts General Hospital, United States, ³Dept. Biostatistics, School of Public Health, Boston Univ., United States, ⁴Hebrew SeniorLife and Harvard Medical School, United States

Although high BMI and obesity have been traditionally considered to reduce fracture risk, the association between obesity and the risk of fragility fracture from observational studies is controversial, possibly due to confounding factors and reverse causality. To overcome such challenges, Mendelian randomization (MR) has been proposed to estimate causal relations between an exposure and outcome. MR utilizes genetic risk factors as instrumental variables that are naturally randomized at birth. In addition, the BMI phenotype does not reflect the actual amount of fat tissue that may affect the skeleton. Visceral adipose tissue (VAT) measured by qCT better quantifies metabolically active fat. To determine the causal relation of VAT with the risk of fracture, we selected SNPs associated with VAT from a genome wide association study (GWAS) meta-analysis (10,557 adult Caucasians) as instrumental variables. These SNPs are located in ADAD2, CLSTN2, DCLK2, DNAH10, GJB5, KCNG4, KSR2, LOC642502, LOC92017, MPZ, PCP4L1, PDCD6IP, RREB1, SDHC, TAF1C, TRAM1L1 and WFDC1 GWAS loci. The fracture GWAS meta-analysis was done in 264,973 adult samples from 23 cohort studies (37,857 fracture cases, 227,116 controls). To estimate the per SNP causal relation between VAT and fracture risk, we used the 2-sample MR analytical approach. To increase statistical power, we combined each SNP result into a

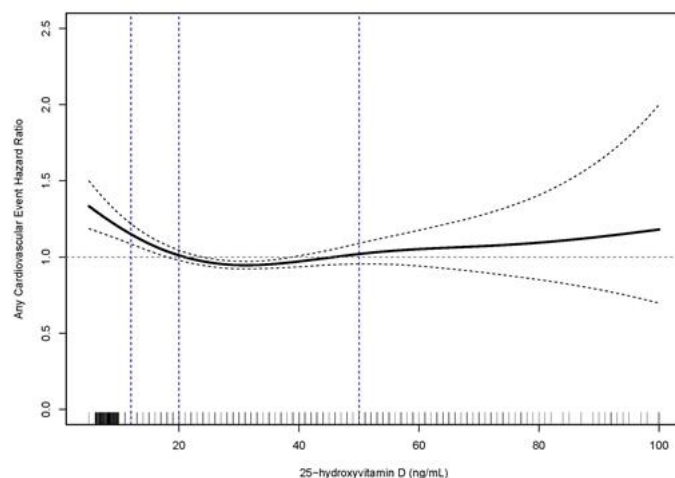
multi-instrument summary-level MR variable. To avoid bias from pleiotropic genetic effects, we applied a newly developed method, the Mendelian Randomization Pleiotropy RESidual Sum and Outlier (MR-PRESSO) test. We found a causal effect of VAT on fracture risk with a 10% increased risk for all fractures per each SD increase in genetically-estimated VAT (OR=1.10, 95%CI=1.04-1.16). We did not detect any pleiotropic biases in our MR analysis. Among tested SNPs, the maximum OR was 1.19 (19% increase risk). We performed MR-analyses on other obesity relevant measurements (Body fat%, waist circumference, hip circumference, waist-hip ratio & overweight). None of them were causally associated with fracture risk. In summary, with robust GWAS studies and genetically-driven MR analyses, we found that VAT, but not other classical obesity indices, causally increase fracture risk. These findings suggest that specific efforts to reduce VAT might lower the risk for fracture. Gender-specific MR-analyses are underway to identify whether the increased fracture risk from VAT is gender-specific.

Disclosures: Yi-Hsiang Hsu, None

1116

Serum 25-Hydroxyvitamin D Values and Risk of Incident Cardiovascular Disease: A Population-Based Retrospective Cohort Study Daniel Dudenkov^{*}, Kristin Mara, Tanya Petterson, Julie Maxson, Tom Thacher. Mayo Clinic, United States

Background: Concentrations of serum 25-hydroxyvitamin D [25(OH)D] below 20 ng/mL and above 50 ng/mL have been associated with chronic adverse events including cardiovascular disease. Our objective was to conduct a comprehensive population-based study in the United States of the relationship of low and high serum 25(OH)D levels with cardiovascular disease. **Methods:** We identified all serum 25(OH)D measurements in adults age 18 years and older residing in Olmsted County, MN between January 1, 2005 and December 31, 2011, using the resources of the Rochester Epidemiology Project. Any new diagnosis of cardiovascular disease (arrhythmia, cardiac arrest, cardiomyopathy, cerebrovascular disease, coronary artery disease, heart failure, myocardial infarction, peripheral vascular disease) was the primary outcome, and time zero was 30 days after first 25(OH)D measurement. Patients were followed until their last clinical visit as an Olmsted County resident, December 31, 2014, or death. Categories of 25(OH)D values were examined using predetermined ranges of interest: <12, 12-19, 20-50 (reference range), and >50 ng/mL. Multivariable Cox proportional hazards models were adjusted for age, BMI, sex, race, smoking history, season of 25(OH)D measurement, hypertension, hyperlipidemia, and Charlson comorbidity index at time of 25(OH)D measurement. **Results:** A total of 11,022 unique persons had a 25(OH)D measurement during the seven year interval, with a mean (±SD) value of 30.0±12.9 ng/mL. Mean age was 54.3±17.2 years, and the majority were female (77.1%) and white (87.6%). There were 4,355 incident diagnoses of cardiovascular disease in this cohort after a median overall follow-up of 4.8 years (IQR 3.4-6.2). Unadjusted cardiovascular disease hazard ratios (HRs) (95% confidence interval) for 25(OH)D values <12, 12-19, and >50 ng/mL, compared to the reference range 20-50 ng/mL, were 1.36 (1.21-1.53), 1.12 (1.03-1.22), and 1.17 (1.02-1.33), respectively. Adjusted hazard ratios for the same 25(OH)D categories were 1.33 (1.17-1.51), 1.22 (1.12-1.33), and 1.15 (1.00-1.31). Figure shows the HRs for cardiovascular outcomes with 25(OH)D values as a continuous variable. **Conclusion:** Values of 25(OH)D <20 ng/mL were associated with the development of a new diagnosis of cardiovascular disease after adjusting for comorbidities. There may also be an association between 25(OH)D >50 ng/mL and cardiovascular disease, although the results are not statistically significant.



Disclosures: Daniel Dudenkov, None

1117

Estradiol and Follicle Stimulating Hormone as Predictors of Onset of Menopause Transition- related Bone Loss in Pre- and Perimenopausal Women

Albert Shieh^{1*}, Gail Greendale¹, Jane Cauley², Carrie Karvonen-Gutierrez³, Carolyn Crandall¹, Arun Karlamangla¹. ¹University of California, Los Angeles, United States, ²University of Pittsburgh, United States, ³University of Michigan, United States

Purpose. The menopause transition (MT) could be an optimal but time-limited window for early interventions to prevent future fractures. In order to intervene before substantial bone loss has occurred, we must be able to determine when a woman is about to begin losing bone. The objective of this study was to examine the ability of single and serial measures of serum estradiol (E2) or follicle stimulating hormone (FSH) to predict the onset of MT-related bone loss. Methods. We used data from 1,113 participants in the Study of Women's Health Across the Nation (SWAN) who had at least 2 measurements of E2 and/or FSH from pre- (regular menstrual bleeding), early peri- (less predictable menstrual bleeding at least once every 90 days), and/or late perimenopause (menstrual bleeding less than once every 90 days), as well as corresponding measurements of bone loss. Onset of MT-related bone loss was defined as a decline in BMD from SWAN baseline to the first follow-up visit after the E2 or FSH measurement that exceeded the site-specific least significant change (3.9% for lumbar spine [LS]; 6.2% for femoral neck [FN]). In our first set of analyses, E2 and FSH (log-transformed, base 2) were each modeled as predictor of MT-related bone loss onset in separate models, using mixed-effects, repeated-measures, modified Poisson regression, adjusted for age, BMI, race/ethnicity, MT stage, and study site. In our second set of analyses, within-woman changes in E2 and FSH from SWAN baseline to a follow-up visit before postmenopause were each modeled as primary predictor in separate models, adjusted for level of E2 or FSH, respectively, plus the above covariates. Results. Single Measures: Each doubling of E2 was associated with 9% and 11% lower risk of bone loss onset at the LS ($p < 0.0001$) and FN ($p = 0.01$). Similarly, each doubling in FSH was associated with a 39% and 27% greater risk of bone loss onset at the LS ($p < 0.0001$) and FN ($p < 0.0001$). Serial Measures: Within-woman change in E2 or FSH did not predict onset of bone loss at either the LS ($p = 0.2$ for E2, 0.8 for FSH) or FN ($p = 0.9$ for E2, 0.5 for FSH) independent of E2 or FSH level. Conclusions. We conclude that that single measures of E2 or FSH early in the MT may aid in prompt identification of women who are about to begin losing bone, and that tracking within-woman change in E2 or FSH does not add independent prediction ability.

Disclosures: **Albert Shieh, None**

1118

The Association between Objectively Measured Physical Activity and Bone Strength and Microarchitecture Among Older Men

Lisa Langsetmo^{1*}, Andrew Burghardt², John Schousboe¹, Peggy Cawthon², Jane Cauley³, Nancy Lane⁴, Kristine Ensrud⁵, Eric Orwoll⁶. ¹University of Minnesota, United States, ²University of California, San Francisco, United States, ³University of Pittsburgh, United States, ⁴University of California, Davis, United States, ⁵University of Minnesota, Minneapolis VA Health Care System, United States, ⁶Oregon Health and Science University, United States

To examine the association between objectively measured physical activity (PA) with bone strength of the distal limbs, we studied 994 older men (mean age 83.9 years, SD 3.9) with 5-day activity assessments and at least 90% wear time (SenseWear Pro3 Armband) at Y7 and Y14 Visit who also had Y14 bone microarchitecture assessments of the distal radius and tibia (Scanco high resolution peripheral quantitative tomography [HR-pQCT]). PA parameters were averaged over the 2 time-points. Armband data along with height, weight, handedness, and smoking status were used to estimate total energy expenditure [TEE], total steps per day, and level of activity: sedentary (<1.5 METs), light (1.5-3 METs), or at least moderate (≥ 3 METs). Peak 30 minute cadence [P30MC] was obtained from data by ordering cadence (counts/minute) by 1 min episodes and then taking mean of the top 30 episodes. Estimated failure load (force required to break) was determined from HR-pQCT data using finite element analysis. Total, cortical, and trabecular volumetric BMD were also computed from HR-pQCT data. We used multiple linear regression models with standardized PA and HR-pQCT variables (yielding effect size) and adjusted for age, race, weight, limb length, education, alcohol use, and smoking history. For partitioned activity time, 1 unit=30 minutes. In the study cohort, the means (SDs) for daily activity were: 2338 (356) kcal [TEE]; 5739 (2696) [step count], 60 (20) counts/minute [P30MC], 67 (28) min [light activity], and 85 (52) min [at least moderate activity]. Higher TEE, step count, and P30MC were each associated with higher failure load of the distal radius (effect size from 0.08 to 0.13) but not with higher volumetric BMD or compartment specific BMD. Higher TEE, step count, and P30MC were each associated with higher failure load of the distal tibia (effect size from 0.19 to 0.21) and also with higher volumetric BMD (effect size from 0.08 to 0.15), higher trabecular BMD (effect size from 0.07 to 0.11), and higher cortical BMD (effect size from 0.09 to 0.13). Time spent in at least moderate activity vs time spent in sedentary behavior was related to bone strength at both sites after adjustment, whereas time spent in light activity was not. These results suggest that at least moderate physical activity averaged over a period of time may have a modest effect on bone strength among older men with slightly stronger effect sizes at a weight-bearing vs. a non-weight-bearing skeletal site.

Table 1: Associations* of Objective Measures of Physical Activity with Failure Load, Total BMD, and Compartmental BMD

Distal Radius	Failure Load	Total BMD	Trabecular BMD	Cortical BMD
Total energy expenditure	0.13 (0.06, 0.20)	0.01 [-0.06, 0.09]	0.05 [-0.03, 0.12]	-0.03 [-0.10, 0.05]
Step Count	0.11 (0.04, 0.18)	0.06 [-0.01, 0.13]	0.05 [-0.02, 0.12]	0.04 [-0.03, 0.11]
Peak 30 min Cadence	0.08 (0.01, 0.15)	0.06 [-0.01, 0.12]	0.05 [-0.02, 0.12]	0.04 [-0.02, 0.11]
Light Activity Time	-0.05 [-0.15, 0.05]	-0.07 [-0.17, 0.03]	-0.03 [-0.13, 0.07]	-0.07 [-0.17, 0.03]
Moderate/Vigorous Activity Time	0.08 (0.03, 0.13)	0.05 (0.00, 0.10)	0.03 [-0.02, 0.09]	0.04 [-0.02, 0.09]
Distal Tibia	Failure Load	Total BMD	Trabecular BMD	Cortical BMD
Total energy expenditure	0.21 (0.14, 0.28)	0.08 (0.01, 0.15)	0.07 (0.00, 0.15)	0.09 (0.02, 0.15)
Step Count	0.20 (0.13, 0.26)	0.15 (0.08, 0.21)	0.10 (0.03, 0.17)	0.13 (0.07, 0.19)
Peak 30 min Cadence	0.19 (0.13, 0.26)	0.15 (0.08, 0.22)	0.11 (0.04, 0.18)	0.13 (0.06, 0.19)
Light Activity Time	-0.03 [-0.13, 0.07]	-0.08 [-0.18, 0.02]	0.00 [-0.10, 0.10]	-0.07 [-0.16, 0.03]
Moderate/Vigorous Activity Time	0.10 (0.05, 0.15)	0.08 (0.03, 0.13)	0.03 [-0.03, 0.08]	0.09 (0.04, 0.14)

*SD increment in outcome variable per 30 minute increment of time variables or per SD increment of other PA variables

Disclosures: **Lisa Langsetmo, None**

1119

Lower Insulin Sensitivity in Patients With High Bone Mass due to a LRP5T253I mutation

Jens-Jacob Lindegaard Lauterlein^{1*}, Anne Pernille Herrmann, Moustapha Kassem, Kurt Højlund, Morten Frost. Department of Endocrinology and Metabolism, Odense University Hospital, Odense, Denmark

The aim of this investigation was to assess the clinical effects of increased Wnt signaling on glucose homeostasis and body composition in individuals with high bone mass (HBM) due to a LRP5T253I mutation. The LDL receptor-related protein 5 (LRP5) is an important co-receptor in the canonical Wnt signaling pathway, and LRP5 is involved in the differentiation of mesenchymal stem cells favoring osteoblastogenesis over adipogenesis as well as substrate utilization, e.g. by favoring β -oxidation of fatty acids in the osteoblast. In vivo, Lrp5 deficient mice display glucose intolerance, impaired pancreatic β -cell function and low bone mass. In humans, loss of function mutations in LRP5 cause severe osteoporosis and impaired glucose metabolism due to reduced β -cell function, whereas LRP5 gain of function mutations causes HBM and has been reported to be associated with reduced insulin resistance (HOMA-IR) and a beneficial fat distribution. We recruited 14 patients with LRP5T253I HBM and 14 healthy age-, sex- and BMI-matched controls. Insulin secretion was assessed using a 1-hour intravenous glucose tolerance test (IVGTT), and insulin sensitivity was measured as insulin-stimulated glucose disposal rates (Rd) using a 3-hour euglycaemic hyperinsulinaemic clamp. Substrate metabolism was evaluated by indirect calorimetry, and body composition was investigated using whole body DXA. One LRP5T253I HBM patient with undiagnosed diabetes (HbA1c: 7.6%, ref. <6.5%) was excluded from further analyses. There was no difference in age (48(5) vs. 47(4) years), BMI (29.4 vs. 29.7 kg/m²) or HbA1c (5.4% in both) between LRP5T253I HBM and controls. Furthermore, we observed no difference in β -cell function between the two groups (IVGTT: normal first and second phase insulin response). Insulin sensitivity was reduced by 25% in LRP5T253I HBM compared to controls (Rd 258(19) vs. 347(26) mg/m²/min, $p < 0.01$), whereas insulin-mediated suppression of hepatic glucose production was intact. Respiratory exchange rate in the insulin-stimulated state was lower in LRP5T253I HBM (0.89 vs. 0.95, $p < 0.05$), consistent with a higher rate of lipid oxidation ($p < 0.05$). There was no difference in the distribution of peripheral and central fat mass between groups. These data indicate that the LRP5T253I mutation impairs glucose metabolism in humans by reducing insulin sensitivity in skeletal muscle. The mutation does not affect hepatic insulin sensitivity, pancreatic β -cell function or fat distribution.

Disclosures: **Jens-Jacob Lindegaard Lauterlein, None**

1120

Genetic and epigenetic defects at the GNAS locus lead to distinct patterns of skeletal growth but similar early-onset obesity

Patrick Hanna^{1*}, Harald Jüppner², Guiomar Perez De Nancars³, Giovanna Mantovani⁴, Alessia Usardi⁵, Susanne Thiele⁶, Agnès Linglart⁷. ¹INSERM U1169 and Paris Sud Paris-Saclay university, Bicêtre Paris Sud hospital, France, ²Endocrine Unit and Pediatric Nephrology Unit, Massachusetts General Hospital and Harvard Medical School, United States, ³Molecular (Epi)Genetics Laboratory BioAraba National Health Institute, OSI Araba University Hospital, Spain, ⁴Fondazione IRCCS 'Ca' Granda Ospedale Maggiore Policlinico Endocrinology and Diabetology Unit, Department of Clinical Sciences and Community Health, University of Milan, Italy, ⁵APHP, Reference Center for rare disorders of the calcium and phosphate metabolism, filière OSCAR and Plateforme d'Expertise Maladies Rares Paris-Sud, Bicêtre Paris Sud hospital, France, ⁶Division of Experimental Pediatric Endocrinology and Diabetes Department of Pediatrics, Center of brain, behavior and metabolism, University of Lübeck, Germany, ⁷APHP, Endocrinology and diabetes for children, Bicêtre Paris Sud hospital, France

Introduction: Pseudohypoparathyroidism type 1A (PHP1A), pseudoPHP (PPHP), and PHP1B are caused by maternal and paternal GNAS mutations, and abnormal methylation at maternal GNAS promoter(s), respectively. Adult PHP1A patients are reportedly obese and short, whereas most PPHP patients are born small. In addition to PTH resistance, PHP1A and PHP1B patients may display early-onset obesity. Objectives: characterize the growth and weight gain patterns in patients with GNAS molecular defects. Methods: Through an

international collaboration, we collected growth and weight data from birth until adulthood for 306 PHP1A/PPHP and 220 PHP1B patients. Results: PHP1A/PPHP patients were smaller at birth than healthy controls, especially PPHP (length z-score PHP1A: -1.1 ± 1.8 ; PPHP: -3.0 ± 1.5). Short stature is observed in 64% and 59% of adult PHP1A and PPHP patients. PHP1B patients displayed early post-natal overgrowth (height z-score at 1 year: 2.2 ± 1.3 and 1.3 ± 1.5 in autosomal dominant and sporadic PHP1B). After birth, both PHP1A and PPHP patients displayed a moderate catch-up growth, but showed a progressive decline in growth velocity and lack of pubertal spurt leading to a final short stature (height z-score: PHP1A: -0.6 ± 1.7 at 3 years, -0.9 ± 1.3 at 10 years, -2.5 ± 1.1 at 18 years; PPHP: -1.5 ± 1.5 at 3 years, -0.2 ± 1.1 at 10 years, -1.9 ± 1.2 at 18 years). PHP1B patients showed a gradual decrease in growth velocity resulting in normal adult height (height z-score: AD-PHP1B: 1.2 ± 0.9 at 3 years, -0.2 ± 1.3 at 10 years, and -0.4 ± 1.1 at 18 years; spor-PHP1B: 1.1 ± 0.9 at 3 years, 0.8 ± 1.3 at 10 years, and -0.4 ± 1.1 at 18 years). Early-onset obesity characterizes GNAS alterations (BMI z-score at 1 year: PHP1A: 3.5 ± 2.3 , AD-PHP1B: 2.5 ± 1.6 and spor-PHP1B: 2.9 ± 1.4) and is associated to significant overweight and obesity in adults (BMI z-score: 1.4 ± 2.6 , 2.1 ± 2.0 , and 1.4 ± 1.9 in PPHP, PHP1A, and PHP1B, respectively). Conclusion: The growth impairment in PHP1A/PPHP may be due to Gsa haploinsufficiency in the growth plates; the paternal XLtas transcript likely contributes to prenatal growth; for all disease variants, a reduced pubertal growth spurt may be due to accelerated growth plate closure. Consequently, early diagnosis and close follow-up is needed in patients with GNAS defects to screen and intervene in case of early-onset obesity and decreased growth velocity.

Disclosures: **Patrick Hanna, None**

1121

Sclerostin Resistance Protects Bone Mass and Improves Insulin Sensitivity in a Mouse Model of Type 1 Diabetes Giulia Leanza^{*1,2}, Francesca Fontana², Rocky Strollo¹, Paolo Pozzilli¹, Nicola Napoli^{1,2}, Roberto Civitelli¹. ¹Campus Bio-Medico University, Italy, ²Washington University in St Louis, United States

Patients with type 1 diabetes (T1D) are at increased risk of fracture, but the mechanisms of such increased bone fragility remain largely unknown. In a preliminary study, we found high circulating levels of the Wnt inhibitor sclerostin (Scl) in T1D patients, suggesting a potential role of Wnt signaling in diabetic bone disease. To test this hypothesis, we introduced the Scl-resistant Lrp5A214V mutation, associated with high bone mass (HBM), in mice carrying the Ins2Akita mutation (Akita), which become spontaneously diabetic at age 4-5 week. Bone mass by DXA was significantly higher in Akita/HBM relative to Akita littermates at 12 weeks (88.2 ± 5.2 vs 67.9 ± 4 mg/cm²; $p < 0.001$; $n = 7-11$), persisting higher for up to 26 weeks (90.2 ± 3.0 vs 70.4 ± 1.7 mg/cm²; $p < 0.001$ $n = 5$) despite overt diabetes. Further analysis by μ CT at age 20 weeks revealed lower trabecular bone volume/total volume (BV/TV) in Akita compared to wild type (WT) mice (0.2 ± 0.02 vs 0.35 ± 0.05 ; $p < 0.05$; $n = 3-5$). Conversely, both trabecular (Tb) and cortical (Ct) parameters were significantly higher in Akita/HBM mutants compared to Akita littermates, including total Ct area (1.6 ± 0.06 vs 1.2 ± 0.07 mm²), Ct bone area (0.9 ± 0.1 vs 0.6 ± 0.05 mm²), and Ct thickness (0.2 ± 0.02 vs 0.1 ± 0.01 mm, $p < 0.001$, $n = 5-7$). Tb BV/TV and Tb thickness were also higher in Akita/HBM mutants relative to Akita littermates (0.4 ± 0.05 vs 0.2 ± 0.02 ; and 0.1 ± 0.02 vs 0.09 ± 0.03 mm, respectively, $p < 0.001$, $n = 3-5$). We found no significant differences in total Ct area between Akita and WT mice, consistent with observations in humans with T1D. As expected, both Akita and Akita/HBM mutants developed diabetes (non-fasting blood glucose > 300 mg/dl), albeit with different onset timing. At 8 weeks, only 40 % of Akita/HBM mice had developed hyperglycemia, compared to 90% of Akita mice ($n = 10$). Only at 12 weeks were most Akita/HBM mice hyperglycemic. Intriguingly at age 6 and 8 weeks, glucose tolerance was significantly better in Akita/HBM relative to Akita mice ($p < 0.05$ for difference in areas under the curve, AUC; $n = 3-6$). Likewise, insulin sensitivity (by intraperitoneal insulin tolerance test) was higher in the Akita/HBM compared to the Akita group ($p < 0.01$ for difference in AUC; $n = 4-8$) at age 7 weeks. In summary, Wnt activation protects bone mass and may retard the onset of metabolic abnormalities in T1D, thus disclosing a potential additional therapeutic advantage to Scl inhibition.

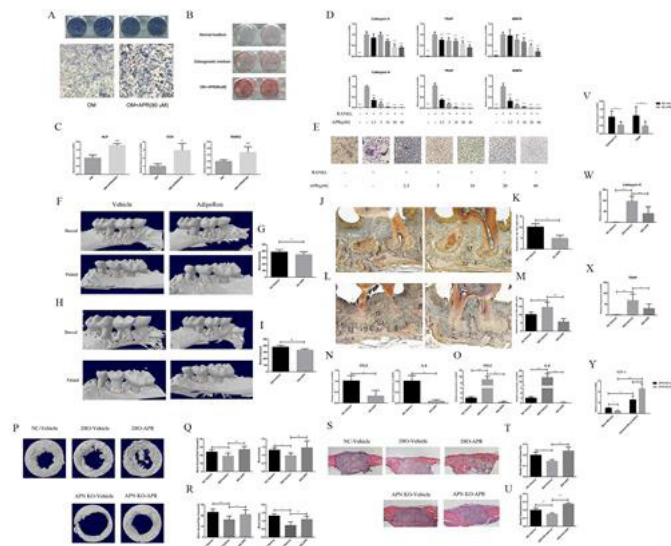
Disclosures: **Giulia Leanza, None**

1122

AdipoRon, an Adiponectin Receptor Agonist, Ameliorates Diabetic Bone Disorders by Inhibiting Osteoclastogenesis and Promoting Bone Formation Xingwen Wu^{*1,2}, Maxwell Tu¹, Wei Qiu¹, Junxiang Lian¹, Youcheng Yu², Jake Chen^{1,3}. ¹Division of Oral Biology, Tufts University School of Dental Medicine, United States, ²Department of dentistry, Zhongshan hospital, Fudan University, China, ³Department of Developmental, Molecular and Chemical Biology Sackler School of Graduate Biomedical Sciences Tufts University School of Medicine, United States

Objectives: Adiponectin (APN), a primary adipokine, has insulin-sensitizing and anti-diabetic properties. Recent literature indicates a strong correlation between low levels of adiponectin and bone disorders. AdipoRon (APR), a recently found orally active small molecules, binds and activates both adiponectin receptors (AdipoR1, R2), with potent effects similar to adiponectin. In this study, we investigated whether APR can ameliorate diabetic bone disorders through inhibiting osteoclastogenesis and promoting bone formation in both in vitro and in vivo models. Materials and Methods: We used experimental periodontitis and

calvarial bone defect mouse models to test our hypothesis. Three types of animals were used including diet-induced obesity (DIO) mice, APN knockout (KO) mice and normal-chow (NC) diet wild type mice as controls. Moreover, RAW 264.7 cells and bone marrow macrophages (BMM) were used to explore if APR can inhibit osteoclastogenesis. Primary calvarial bone osteoblasts were used to test if APR can promote osteogenesis. Results: APR increased the expression level of ALP, RUNX2 and OCN during osteogenic induction of primary calvarial bone osteoblasts (Figs. A-C), while the RANKL-enhanced expressions of Cathepsin K, TRAP and MMP9 were decreased by APR treatment in osteoclastic differentiation of RAW264.7 cells and BMMs (Figs. D, E). APR reduced alveolar bone destruction in experimental periodontitis in NC and DIO mice (Figs. F-O). The expression of CCL2, IL-6 in palatal gingiva and the number of TRAP-stained osteoclasts exhibited significantly increased in DIO-Vehicle group than in NC-vehicle group and the APR treatment decreased the CCL2 and IL-6 production and osteoclast number. APR treatment inhibited osteoclastogenesis of BMMs in both NC and DIO mice (Figs. V-X). APR promoted the healing of calvarial bone defect in DIO and KO mice (Figs. P-U). BV/TV, Tb.N and the percentage of newly formed bone were significantly increased in APR treated group than in vehicle controls. In KO mice, APR treatment increased the chemotactic gradient of SDF-1 between bone marrow and calvarial bone defect site showing a decreased level in bone marrow and an increased level in defect area (Fig. Y). Conclusions: APR could inhibit the inflammatory alveolar bone destruction and promote bone defect healing by inhibiting the osteoclastogenesis, enhancing the mineralization of osteoblasts, and promoting a favorable SDF-1-mediated chemotactic gradient for stem cell migration.



Disclosures: **Xingwen Wu, None**

1123

Selective Deletion of Marrow Adipocytes Leads to Increased Mesenchymal Precursors, a Shift in Lineage Allocation, and Increased Bone Mass with Improved Bone Biomechanics Steven Tommasini^{*1}, Tracy Nelson¹, Chad Faulkner-Filosa¹, Matthew Rodeheffer¹, Clifford Rosen², Dieter Lindskog¹, Mark Horowitz¹. ¹Yale University School of Medicine, United States, ²Maine Medical Center Research Institute, United States

Although marrow adipocytes (MA) were identified more than a century ago, it is only recently that significant progress has been made in understanding the origin, development, and function of these cells that become so prominent in the bone marrow (BM) with age and following injury. We have performed lineage tracing of MA following induction of BM adipogenesis with either rosiglitazone-enriched (rosi) diet or irradiation of double fluorescent mT/mG reporter mice to determine the ontogeny and identity of MA progenitor cells. Following either irradiation or rosi diet in Prx1-Cre:mT/mG mice, all MA were eGFP+ and therefore derived from the Prx1 lineage. Thus, we reasoned that crossing Prx1-Cre mice with mice expressing a Ppar γ /fl allele would ablate MAs. Histologically, the marrow in distal tibia of Cre-negative (control) mice was filled with MA. In contrast, Prx1-Cre:Ppar γ /fl (Cre+) mice had no marrow adipocytes in this space. To determine if MA could be induced in the proximal tibia or femur, mice were sub-lethally irradiated and MAs measured by osmium tetroxide staining. As expected, irradiated control mice had extensive MA appearing below the growth plate, extending through the metaphysis, and into the diaphysis. As in the distal tibia, Cre+ mice had no detectable MA in these bones. To determine how the lack of MA affected bone, long bones were first analyzed by micro-CT. Bones from Cre+ mice had a significant increase in trabecular BV/TV and Tb.Th, and Ct.Th and pMOI. The increased bone mass could be accounted for by the striking increase ($> 50\%$) in CFU-Fs from female and male BM. Biomechanical properties of the femurs were assessed via 4-point bending. Stiffness, maximum load, post-yield deflection, and total work were significantly increased in the Cre+ femurs compared to controls. The uniform tracing of MA by the mesenchymal

progenitor transgene Prx1-Cre bred with mice expressing Ppar γ /fl allowed us to selectively delete MA. Marrow in the distal tibia of these mice was devoid of MA and MA could not be induced in the tibia or femur by x-irradiation, indicating that Prx1 is an early marker of MA ontogeny. The loss of MA resulted in a lineage shift from MA to osteoblasts. Taken together, these data indicate that ablation of MA results in increased bone, which functionally is stronger, suggesting that MA have at least an indirect regulatory effect on bone mass.

Disclosures: **Steven Tommasini**, None

1124

A novel crosstalk between TGF- β /BMP and Wnt families through Smad4 in endochondral ossification Sho Tsukamoto^{*1}, Mai Kuratani¹, Noriko Sekine¹, Misato Okubo¹, Yutaka Nakachi¹, Shinya Tanaka², Eijiro Jimi³, Hiromi Oda², Takenobu Katagiri¹. ¹Division of Pathophysiology, Research Center for Genomic Medicine, Saitama Medical University, Japan, ²Department of Orthopedic Surgery, Saitama Medical University, Japan, ³Faculty of Dental Science, Oral health•Brain health•Total health Research Center, Kyushu University, Japan

Members of the transforming growth factor- β (TGF- β) family, including BMPs, GDFs and Activins, regulate skeletal development in embryos by activating Smad transcription factors. Smad4 is a critical co-activator essential for the Smad-dependent intracellular signaling in target cells. However, the role of the TGF- β family on skeletal growth after birth is still unclear, because Smad4 knockout mice are lethal at early stages in embryos. In the present study, we established Smad4 conditional knockout (Smad4 cKO) mice under the control of tamoxifen by crossing Smad4 floxed mice with CAG-CreERT mice. The established mice were injected tamoxifen at 10-w-old to delete the Smad4 gene in adulthood. On day 23 after the injection, the Smad4 cKO mice showed an increase in bone mass in trabecular bone but not in cortical bone in micro-CT analysis. They also showed an increase in numbers of hypertrophic chondrocytes and osteocalcin-positive bone-forming osteoblasts in growth plates and primary spongiosa, respectively. Bone histomorphometry suggested that the increased bone mass was due to an increase in bone formation rather than a decrease in bone resorption. We found that the osteoblastic cells increased in the Smad4 cKO mice were positive for β -catenin. Quantitative RT-PCR analysis of the Wnt signaling related genes revealed that expression of Wnt7b mRNA was increased in the growth plates of Smad4 cKO mice. The expression of Wnt7b mRNA was decreased in response to BMP-4 stimulation in vitro. Wnt7b was detected in hypertrophic chondrocytes in growth plates in immunohistochemical analysis. Moreover, Wnt7b stimulated mineralization of primary osteoblasts in vitro was greatly enhanced by treatment with Wnt7b. We established double conditional knockout mice of Smad4 and Wnt7b (Smad4;Wnt7b dcKO) crossed with the CAG-CreERT mice. In contrast to the Smad4 single cKO mice, the Smad4;Wnt7b dcKO mice did not show the increase in bone mass after the tamoxifen injection even though they had many hypertrophic chondrocytes. Taken together, our findings suggest that the inhibition of Smad4-dependent signaling pathway in chondrocytes enhances endochondral ossification in vivo by stimulating differentiation to hypertrophic chondrocytes and expression of Wnt7b. This is a novel crosstalk between the TGF- β /BMP and Wnt families through Smad4 in endochondral ossification.

Disclosures: **Sho Tsukamoto**, None

1125

GDF11 Locally Controls Axial Skeletal Patterning and Systemically Improves Bone Formation As Opposed to Myostatin Joonho Suh^{*1}, Je-Hyun Eom¹, Na-Kyung Kim¹, Joo-Cheol Park², Kyung-Mi Woo¹, Jeong-Hwa Baek¹, Hyun-Mo Ryoo¹, Se-Jin Lee³, Yun-Sil Lee¹. ¹Department of Molecular Genetics & Dental Pharmacology, School of Dentistry and Dental Research Institute, Seoul National University, Republic of Korea, ²Department of Oral Histology-Developmental Biology, School of Dentistry and Dental Research Institute, Seoul National University, Republic of Korea, ³Department of Genetics and Genome Sciences, University of Connecticut School of Medicine, United States

Growth and differentiation factor 11 (GDF11) and myostatin (MSTN) are closely related TGF-beta family members that have been reported to have distinct functions. While MSTN is a negative-regulator of muscle mass, the reported functions of GDF11 are more diverse and controversial. Since Gdf11^{-/-} mice display anterior homeotic transformations of vertebrae, it has been suggested that GDF11 expressed from the tail bud forms concentration gradients like a morphogen, and regulates anterior-posterior (A-P) axial skeletal patterning. However, we show here that locally expressed GDF11 determines positional fate of axial skeleton. In detail, we used a Cdx2-Cre transgene to eliminate Gdf11 expression in posterior regions. Cdx2-Cre; Gdf11^{lox/lox} mice exhibited equal vertebral characteristics to Gdf11^{-/-} mice in posterior regions, developing 9 lumbar vertebrae (vs. 6 lumbar vertebrae in wt mice), while displaying normal skeletal phenotype in anterior regions. Interestingly, we also found decreased bone formation in both Gdf11^{-/-} and Cdx2-Cre; Gdf11^{lox/lox} mice. Micro-CT analysis of P0 mice revealed that both bone volume (BV) and bone mineral density (BMD) were significantly diminished in Gdf11^{-/-} mice, and mildly reduced in Cdx2-Cre; Gdf11^{lox/lox} mice compared to wt mice, indicating that GDF11 systemically regulates bone formation. Surprisingly, Mstn^{-/-} P0 mice exhibited enhanced BV and BMD in contrast to Gdf11^{-/-} mice. In addition, micro-CT and DXA analysis showed that temporal deletion of Gdf11 in all tissues of CAG-Cre-ER; Gdf11^{lox/lox} mice, induced by 4-hydroxytamoxifen or tamoxifen injection, reduces bone formation in both E18.5 embryos and young adult mice

aged from 6 to 10 weeks. We also analyzed 10-week old F66 transgenic mice overexpressing Follistatin, a GDF11/MSTN inhibitor, and found that while their muscle mass increased as much as Mstn^{-/-} mice, their BMD significantly decreased compared to that of wt and Mstn^{-/-} mice. Finally, in vitro analysis revealed that osteoblast differentiation was impaired and osteoclastogenesis was enhanced in Gdf11^{-/-} mice, while the opposite was observed in Mstn^{-/-} mice. All of our data strongly suggest that GDF11 locally regulates A-P patterning of axial skeleton, and systemically enhances bone formation as opposed to MSTN. Because GDF11 and MSTN share equal binding molecules, the opposing role of GDF11 in bone formation must be carefully monitored when developing MSTN-targeting drugs to improve bone and muscle mass.

Disclosures: **Joonho Suh**, None

1126

Conditional Disruption of the Osterix (Osx) Gene in Chondrocytes During Early Postnatal Growth Impairs Secondary Ossification in the Mouse Tibial Epiphysis. Weirong Xing^{*1}, Catrina Godwin², Sheila Pourteymoor², Subburaman Mohan¹. ¹VA Loma Linda Healthcare System, Loma Linda University, United States, ²VA Loma Linda Healthcare System, United States

The canonical pathway of endochondral ossification, the process of replacing cartilage with bone, involves apoptosis of hypertrophic chondrocytes followed by vascular invasion to bring in osteoclast and osteoblast precursors to resorb cartilage and produce bone matrix, respectively. However, our recent findings support a new paradigm in which the prepubertal increase in thyroid hormone levels induces IHH and OSX signaling in hypertrophic chondrocytes to transdifferentiate them into osteoblasts and promote secondary ossification at the epiphyses. To test if Osx expressed in chondrocytes contributes to transdifferentiation and secondary ossification, we generated Osx^{lox/lox};Col2-Cre-ERT2 mice and treated them with a single injection of tamoxifen (200 μ g) at postnatal day (P) 3 prior to evaluation of the epiphyseal bone phenotype by microCT, histology, and immunohistochemistry at P21. Vehicle (oil)-treated Osx^{lox/lox};Col2-Cre-ERT2 and tamoxifen-treated Cre-negative Osx^{lox/lox} mice were used as controls. MicroCT analysis of tibial epiphyses revealed that trabecular bone mass was reduced by 23% (P < 0.01) in the Osx conditional knockout (cKO) compared to control mice. Trabecular number and thickness were reduced by 28% and 8%, respectively, while trabecular separation was increased by 24% in the cKO mice (all P < 0.05). Trichrome staining of longitudinal sections of tibial epiphyses showed that bone area and bone area adjusted for total area were decreased by 22% and 18% (both P < 0.01), respectively, in the Osx cKO mice compared to oil-treated vehicle controls. Immunohistochemistry studies revealed that there was abundant expression of OSX in prehypertrophic chondrocytes of control mice which was considerably reduced in the cKO mice. Furthermore, expression of MMP13, COL10, and BSP was reduced in the epiphyses of cKO mice. To determine if Mmp13 and Col10 are direct targets of Osx, we evaluated their expression levels in response to Osx overexpression using lentiviral vectors in ATDC5 chondrocytes. We found that Osx overexpression increased Col10 (2.5-fold P<0.01), Mmp13 (1.5-fold, P<0.05), Alp (9.7-fold, P<0.001) and Bsp (127-fold, P<0.001) expression in ATDC5 chondrocytes. Based on these data, we conclude that Osx expressed in chondrocytes plays an important role in secondary ossification by regulating expression of genes involved in chondrocyte hypertrophy and transdifferentiation.

Disclosures: **Weirong Xing**, None

1127

Mechanical Signals Preserve Bone and Muscle While Suppressing Adiposity in a Murine Model of Complete Estrogen Deprivation Gabriel M. Pagnotti^{*1}, Ryan Pattyn², Laura E. Wright², Sutha K. John², Sreemala Murthy², Trupti Trivedi², Yun She², Clinton T. Rubin³, William R. Thompson², Khalid S. Mohammad², Theresa A. Guise². ¹UIPUI, United States, ²Indiana University, United States, ³Stony Brook University, United States

Adverse musculoskeletal effects, such as bone loss and muscle weakness, are experienced by post-menopausal, breast cancer patients treated with aromatase inhibitors to deplete estrogen production. Bisphosphonates, inhibitors of osteoclastic resorption, reduce bone metastases and cancer-induced fractures, but do not cause disease regression. Mechanical signals generated during exercise are anabolic to bone and muscle; however, many patients are unable to participate in regimented exercise programs due to musculoskeletal symptoms. Low intensity vibrations (LIV), mechanical signals similar to stimuli generated from exercise, previously prevented bone loss in two cancer models without elevating longevity and mitigated fat accrual in ovariectomy models. We hypothesized that LIV could improve musculoskeletal morbidity in mice undergoing complete estrogen deprivation, such as that in postmenopausal breast cancer patients. To generate this model, C57Bl/6 mice ovariectomized at 8w of age and treated with the aromatase inhibitor letrozole daily for 24w were administered either LIV (n=10; 90Hz at 0.4g) or control-LIV treatment (CTL; n=10) for 4w prior to and 24w post-surgery. Whole body DXA scanning performed consecutively every 3w measured lean and fat tissue. LIV significantly increased lean mass (p<0.02) over the 28w-treatment period relative to baseline, while LIV restricted total fat mass by 41% (p<0.001). Forelimb grip strength was 32% greater (p<0.05) in LIV-mice compared to CTL mice at 28w. High-resolution (12 μ m) ex vivo micro-computed tomography was performed on lumbar vertebrae, a mechanosensitive load-bearing site of bone metabolism. BV/TV and

connectivity density of L5 vertebrae were 22% ($p < 0.05$) and 53% ($p < 0.05$) greater, respectively, after 24 of LIV. Dynamic histomorphometry indicated a 70% ($p < 0.05$) greater BFR/BS and 60% greater trend in MS/BS in response to LIV. Mineral apposition rate increased, trending 18% greater in LIV-treated L5 versus those of CTL-mice. Osteoblast numbers were 38% ($p < 0.01$) greater in Von Kossa-stained LIV-treated L5 vertebrae than in CTL sections. TRAP-stained sections indicated a 41% reduction in osteoclast surface ($p < 0.01$) and 37% ($p < 0.05$) fewer numbers of osteoclasts in LIV vertebrae. Together, these data highlight the profound impact of estrogen deprivation on musculoskeletal tissue and support the role of physical activity and mechanical signals in maintaining bone and lean tissue mass while limiting the accrual of fat.

Disclosures: Gabriel M. Pagnotti, None

1128

Alpha-Ketoglutarate Ameliorated the Age-related Osteoporosis via Regulating Histone Methylations of Mesenchymal Stem Cells Yuan Wang*, Liang Xie, Jing Xie, Yuchen Guo, Yuting Liu, Yunshu Wu, Rixin Zheng, Hongke Luo, Xiaofei Zheng, Quan Yuan. State Key Laboratory of Oral Diseases, West China Hospital of Stomatology, Sichuan University, China

Osteoporosis is an age-related progressive bone disorder that seriously threatens the health of aging population. Alpha ketoglutarate (α KG) is an essential intermediate in the tricarboxylic acid (TCA) cycle. Recently, α KG has been reported to possess an anti-aging effect, as the treatment of α KG extended the lifespan and delayed age-related phenotypes in worms. Here we aimed to investigate the effect of α KG on the age-related osteoporosis and senescence-associated (SA) phenotypes of mesenchymal stem cells (MSCs). First, we treated the aged mice with α KG via oral administration (0.25% and 0.75%), and observed a dose dependent increase in bone mass in treated group compared with control group. Moreover, MSCs isolated from α KG-treated mice also exhibited a promoted osteogenic potential. Besides, in vitro supplementation of α KG reduced the expression of SA genes (p16, p21, p53, IL6) in aged MSCs. Similarly, the positive cells of SA- β -gal staining and immunofluorescence (IF) of nuclear senescence-associated markers (laminA/C, γ -H2A.X) were declined by α KG administration. Furthermore, α KG treatment promoted self-renewal, migration, and more importantly, osteogenesis of aged MSCs in vitro. Next, we fed 2m-old adult mice with α KG (0.25%) or distilled water and harvested the bone tissues at 4m/6m-old. MicroCT and histological analyses showed that α KG precluded the progressive bone loss of adult mice upon aging, as evidenced by increased bone mineral density (BMD), trabecular bone volume (BV/TV) and osteoblast number (N.Ob/B.Pm), etc. Additionally, α KG improved the healing of femoral bone defect in an aged rodent model. Since α KG is an indispensable cofactor of the Jumonji C domain-containing (JMJD) family histone demethylases, we hypothesized that the positive effect of α KG on age-related osteoporosis might relate to histone methylations of MSCs. Interestingly, in vitro and in vivo study showed that α KG treatment relieved the overall accumulations of H3K9me3 and H3K27me3 along with aging, but not other histone marks that were reported to be regulators of bone metabolism. In addition, CHIP assay revealed that α KG reduced their enrichment on the promoters of BMP2, BMP4, Nanog and Oct4. In summary, α KG ameliorated the age-related osteoporosis via regulating histone methylations of MSCs, suggesting that α KG might be a potential therapeutic agent for the treatment of osteoporosis.

Disclosures: Yuan Wang, None

1129

Improving Mitochondrial Function via CypD Deletion is Effective in Stimulating Bone Formation Brianna Shares*, Roman Eliseev. University of Rochester, United States

Bone marrow mesenchymal stem cells (BMSCs) are multipotent progenitors that can differentiate into osteoblasts, adipocytes, and chondrocytes. As BMSCs undergo osteogenic differentiation they upregulate use of their mitochondria and oxidative phosphorylation (Ox-Phos). Our data and the literature indicate that active mitochondria are required for osteoblast differentiation. Our lab is investigating if strategies aimed at improving mitochondrial Ox-Phos are effective in stimulating bone formation. One such strategy is inhibition of opening of a non-selective mitochondrial pore called the mitochondrial permeability transition pore (MPTP). MPTP opening is the most common mechanism of mitochondrial dysfunction and is positively regulated by cyclophilin D (CypD). Recently, our lab showed that protecting the mitochondria by genetic removal of CypD protected against age-related bone loss in mice. However, the role of CypD during osteogenic differentiation in physiological and pathological settings has not been fully elucidated. To uncover the role of CypD during osteogenic differentiation, we isolated BMSCs from CypD KO mice and control littermates to perform osteoinduction. Throughout osteogenesis the MPTP closes, which is further desensitized by CypD KO. CypD KO BMSCs show improved mitochondrial function and mineralization during osteogenesis as indicated by metabolic profiling and staining, respectively. In addition, CypD KO BMSCs produced larger ossicles following an ectopic bone formation assay, indicating their increased osteogenic potential. To uncover the role of CypD in a pathological setting, tibial fractures were done on both CypD KO mice and control littermates. At 0, 7, 14, 21, 28, and 35 days post-fracture, blood and bones were collected. Fractured and unfractured tibiae were analyzed via biomechanical testing, histology, IHC and mCT. We observed that CypD KO mice show enhanced fracture healing in regards to bone biomechanical parameters and bone formation when compared to control littermates, which may result from

a truncated cartilage phase and faster ossification phase. This work shows that improving mitochondrial function via CypD genetic deletion is effective in stimulating bone formation, further highlighting the importance of mitochondria for bone formation.

Disclosures: Brianna Shares, None

1130

TRAP as a Novel Regulator of Bone Formation in Osteoblasts at Sites of Bone Remodeling Diana Metz-Estrella*, Tzong-Jen Sheu, J Edward Puzas. University of Rochester, United States

Purpose: Emerging evidence is defining a new role for tartrate-resistant acid phosphatase (TRAP). Literature findings indicate that although TRAP is predominantly produced by osteoclasts, it can be found inside of osteoblasts at sites of bone remodeling. Uptake of residual TRAP through endocytotic mechanisms accounts for this. Moreover, over expression or copious uptake of TRAP in osteoblasts leads to a strong stimulation of bone formation. Can these observations explain the spatial coupling observed during remodeling? That is, is TRAP one of the signals that directs new bone formation to sites of prior resorption and is, in part, responsible for the spatial orientation of osteoblast activity that maintains skeletal microarchitecture? Our recent findings posit a mechanism for how endocytosed TRAP stimulates osteoblastic activity. Methods: In prior work we used a phage-display method to identify osteoblast proteins that demonstrated a high affinity for TRAP. We were able to identify a key intermediate involved in the regulation of cell function. New data indicate that this intermediate plays a dual role in the osteoblast. Using a phosphorylation detection method, sub-cellular fractionation techniques and confocal microscopy we have defined two pathways by which TRAP can stimulate formation. Results: Inside osteoblasts TRAP will enter the cytosol through a process known as endosome escape. In the cytosol TRAP binds to a phosphorylatable protein known as TRIP or TGF β 2-receptor-interacting-protein (with high affinity, $K_d = 10-10M$). TRIP is also known as a component of the protein synthetic initiation factor complex, i.e. eIF3- α . When TRIP is phosphorylated (by the type II TGF β 2 receptor kinase) it acts to initiate translation of proteins used in bone. However, when TRIP is dephosphorylated it can enter the nucleus and act as a co-regulator for the expression of osteoblast-specific genes. Our data indicate that intracellular TRAP is the phosphatase that dephosphorylates TRIP, thereby stimulating the final differentiation of osteoblasts on TRAP-coated resorption surfaces. Conclusion: Site-specific bone formation is required to maintain skeletal microarchitecture. There have been only a few theories presented to explain this phenomenon (i.e. canopy formation and sphingosine kinase). Now, we offer another possibility that can account for how osteoblasts can recognize a resorption lacuna and target formation to precise sites in bone.

Disclosures: Diana Metz-Estrella, None

1131

Osteoclast-derived autotaxin is a characteristic factor controlling bone degradation upon inflammation. Olivier P*¹, Sacha Flammier¹, Fanny Bouguillaut¹, François Duboeuf¹, Gabor Tigyi², Fabienne Coury¹, Irma Machuca-Gayet¹. ¹INSERM U1033, France, ²University of Memphis, United States

Rheumatoid arthritis (RA) patients in sustained clinical remission or low disease activity often continue to accrue bone erosions despite control of inflammation. Osteoclasts are responsible for focal bone erosions and systemic bone loss in RA. Current therapies using anti-resorptive drugs are suboptimal in RA because they could lead to issues by shutting down physiologic remodeling in long term treatment supporting the need for alternative therapies. Autotaxin (ATX) is a secreted lysophospholipase D converting lysophosphatidylcholine into lysophosphatidic acid. ATX is upregulated in the synovial liquid of patients with RA and contributes to synovial inflammation. However, ATX role in bone resorption is totally unknown. We found that ATX was up regulated during the course of osteoclastogenesis and LPS or TNF α applied to mature osteoclasts further enhanced ATX expression. In vitro osteoclast-derived ATX was necessary for bone resorption activity that was blocked by pharmacological ATX inhibitors (PF-8380, BMP22). We generated mice with conditional genetic ablation of ATX in osteoclasts (Δ ATXCtsk mice) that were challenged using LPS injections that induced a 43 % decrease in the trabecular BV/TV (BV/TV) in control mice but had no impact on bone in Δ ATXCtsk mice. The challenge with K/BxN serum transfer that induces severe arthritis revealed that Δ ATXCtsk mice were protected from systemic bone loss, and displayed almost no local bone erosion. Intriguingly, in a non-inflammatory bone loss condition as observed in mice after ovariectomy (OVX), Δ ATXCtsk and control mice revealed similar impact on bone 4 weeks post-OVX with a 30% decrease in BV/TV. As supported by an absence of bone phenotype at steady state on Δ ATXCtsk mice, these results indicate that osteoclast-derived ATX might be dispensable for osteoclast function under non-inflammatory conditions. By using a pharmacological approach on a second inflammatory mouse model exploiting transgenic hTNF mice that develop aggressive arthritis with joint swelling and bone erosions, we found that albeit inefficient on synovitis, BMP22 treatment induced a 28% increase in BV/TV and a 50% decrease in the extent of bone erosion (BS/BV). These results establish that ATX is a new factor produced by osteoclasts that controls inflammation-induced bone loss without interfering with osteoclast function in non-inflammatory conditions. ATX might be a promising therapeutic target for the prevention of bone erosion occurrence in RA.

Disclosures: Olivier P, None

1132

Protease-activated receptor 1 (PAR1) deletion causes enhanced osteoclastogenesis in response to inflammatory signals through a Notch 2-dependent mechanism Judy Kalinowski^{*1}, Sandra Jastrzebski¹, Hicham Drissi², Archana Sanjay¹, Sun-Kyeong Lee¹, Ernesto Canalis¹, Joseph Lorenzo¹. ¹UCConn Health, United States, ²Emory University School of Medicine, United States

We found that protease-activated receptor 1 (PAR1), a G-protein coupled receptor, is transiently expressed in osteoclast (OC) precursor cells during RANKL-induced osteoclastogenesis. Studies of PAR1-deficient (PAR1 KO) and wild-type (WT) mice in homeostasis at 8-weeks-old showed minimal differences in either bone mass or bone cells. However, bone marrow macrophages (BMM) and FACS-purified murine bone marrow OC precursor cells cultured with M-CSF+RANKL produced more OC in PAR1 KO cultures than in WT (22 to 48% more OC in PAR1 KO, $p < 0.01$). To determine if this enhanced osteoclastogenesis with RANKL occurred with other TNF superfamily members, we tested osteoclastogenic responses to the proinflammatory cytokine TNF- α (TNF). Treatment of BMMs with sub-maximal doses of TNF + RANKL produced an enhanced osteoclastogenic response. In vivo we treated WT and PAR1 KO mice with daily injections of TNF over their calvariae for 4 days and examined TRAP+ OC 1 day later. TNF induced a 2.9-fold increase ($p < 0.01$) in OC area in WT mice vs. vehicle controls. Strikingly, TNF increased OC area by 9.5-fold in calvariae of PAR1 KO mice, which was a greater response than in either TNF-treated WT mice or vehicle-treated PAR1 KO mice ($p < 0.01$ for both). Because TNF can activate Notch signaling, we examined if inhibiting Notch2 in PAR1 KO mice abrogated their enhanced OC response to TNF. WT and PAR1 KO mice were treated with TNF over the calvaria and either a control antibody (Ab) or an Ab to the Notch 2 negative regulatory region (N2-NRR Ab), which specifically blocks only Notch 2 signaling. Treatment of PAR1 KO mice with N2-NRR Ab reduced TNF-induced osteoclastogenesis to WT levels ($p < 0.01$) without affecting TNF responses in WT mice. In BMM cultures N2-NRR Ab reduced RANKL-induced OC in PAR1 KO BMMs to levels seen in WT cultures ($p < 0.01$) but did not alter RANKL-induced OC in WT BMMs. PAR1 KO BMMs treated with M-CSF had higher Hes1 mRNA levels (a Notch target gene) by 3.4-fold over WT ($p < 0.01$). RANKL+M-CSF or RANKL+TNF+M-CSF treatment of WT BMMs increased Hes1 mRNA to levels seen in M-CSF-treated PAR1 KO cells but had little additional effect on Hes1 mRNA in PAR1 KO cells. These results demonstrate that both in vivo and in vitro PAR1 deletion causes enhanced osteoclastogenesis in response to inflammatory signals in bone through a Notch 2-dependent mechanism. We speculate that PAR1 activation could be a drug target for the development of treatments for inflammatory bone diseases.

Disclosures: **Judy Kalinowski, None**

1133

Examining the influence of senescent cells on PTH/PTHrP signaling in bone Joseph Gardinier^{*}, Chunbin Zhang, Henry Ford Hospital, United States

Age-related bone loss predisposes both men and women to osteoporosis. The chronic low-grade inflammation produced by the senescent-associated secretory phenotype (SASP) of senescent cells contributes to age-related bone loss. However, the influence of SASP on osteoblast function is poorly understood. Given that parathyroid hormone (PTH)/PTH-related protein signaling plays a key role in regulating osteoblast growth and differentiation, we hypothesize that SASP suppress osteoblast expression of the PTH/PTHrP receptor (PPR). To test this hypothesis, MC3T3 derived osteoblasts were treated with conditioned media (CM) from two models of senescent cells. To model senescence, MC3T3 pre-osteoblast cells were exposed to oxidative stress (350 μ M H₂O₂) or irradiation (10 Gy). The onset of senescence was then verified by the presence of beta galactosidase and expression of several inflammatory cytokines and chemokines such as interleukin-6, interleukin-1 α (IL-1 α), tumor necrosis factor alpha (TNF- α), and chemokine ligand 1. Mature osteoblasts were then treated with CM from each model of senescence for 2 days. Control cells were treated with CM from non-senescent cells. As a result, CM from senescent cells caused a significant reduction in osteoblast PPR expression compared to controls. Antagonists against chemokine receptors 1 and 2 failed to prevent PPR suppression in response to CM. Independently, IL-1 α and TNF- α treatment were able to suppress PPR expression directly, but not IL-6. The impact of SASP on PPR expression was then evaluated in-vivo using C57/Bl6 male mice. Between 2 and 18 months of age, we found an increase in cellular senescence within bone, based on P16ink4a expression, and a decrease in PPR expression that corresponded with a loss in sensitivity to exogenous PTH(1-34) treatment based on c-fos expression. To verify that senescent cells are responsible for the loss in PPR expression, 78-week old mice were treated with a combination of dasatinib and quercetin (DQ). After 1 week of DQ treatment, the presence of senescent markers was significantly reduced, while the expression of PPR was significantly increased. Overall, these data demonstrate that senescent cells suppresses the expression of PPR through their release of cytokines IL-1 α and TNF- α . Targeting the underlying mechanisms that influence PPR expression has the potential to enhance the sensitivity to PTH signaling in bone in an aging population.

Disclosures: **Joseph Gardinier, None**

1134

Argininosuccinate lyase deficiency as a model to study nitric oxide function in Bone Zixue Jin^{*1}, Jordan Kho¹, Brian Dawson¹, Monica Grover², Ming-Ming Jiang¹, Yuqing Chen¹, Brendan Lee¹. ¹Baylor College of Medicine, United States, ²Stanford University, United States

Nitric oxide (NO) is an important signaling molecule that influences a wide range of biological processes, including bone metabolism. Previous studies have shown that NO donors may potentially increase bone mineral density in women with postmenopausal osteoporosis. However, the function of NO in bone metabolism remains controversial in both pharmacological and genetic studies. NO is enzymatically produced by three nitric oxide synthases (nNOS, iNOS and eNOS) from L-arginine. NOS knock out (KO) mice have been used to study NO function; however, analyses have been limited by the potential redundancy of the three NOS isoforms. Argininosuccinate lyase (ASL) is the only mammalian enzyme capable of generating arginine, the sole precursor for NOS-dependent NO synthesis. Moreover, we recently showed that it is also required for channeling extracellular arginine to NOS for NO production. Hence, deletion of ASL leads to a cell- autonomous deficiency of NOS-dependent NO production due to combined loss of endogenous arginine production and extracellular arginine channeling. ASL deficiency is thus a Mendelian model for cell-autonomous, NOS-dependent NO deficiency. To study NO function in bone formation, we generated Asl osteoblastic conditional knockout (cKO) mice by crossing Asl^{flx}/flox mice with osteoblastic-specific Cre transgenic mice. Interestingly, we found that early deletion of Asl from osteoblast precursors using Osterix-Cre transgenic lines (Osx-Asl cKO mice) led to increased bone mass. In contrast, deletion from mature osteoblast using Osteocalcin-Cre transgenic lines (Ocn-Asl cKO mice) led to decreased bone mass. Mechanistically, impaired osteoblast function was observed in both Osx-Asl cKO mice and Ocn-Asl cKO mice, whereas decreased osteoclast number and activity was observed only in Osx-Asl cKO mice. In addition, deletion of Asl in Osx-Asl cKO mice resulted in decreased RANKL/OPG mRNA ratio, thereby reducing bone resorption. Furthermore, we provide evidence that NO generated in early osteoblast lineage inhibits OPG expression, while enhances RANKL expression, at least in part via the cAMP responsive element binding protein (CREB) pathway. Taken together, we established new mouse models to study NO function in bone by conditional deletion of ASL in osteoblastic cells. Our findings reveal that cell-autonomous NO production is important for osteoblast function and stage-dependent osteoblast coupling with osteoclast.

Disclosures: **Zixue Jin, None**

1135

Activin type 1 receptor ALK4 regulates postnatal bone mass Shek Man Chim^{*}, David Maridas, Laura Gamer, Vicki Rosen. Harvard School of Dental Medicine, United States

As effectors of both osteoblast and osteoclast formation and activity, activins have a complex role in the skeleton. Activins signal via complexes containing both type 1 and type 2 receptors; ALK4 is a unique type 1 receptor for activins on skeletal progenitors, while the type 2 receptors utilized by activins, ACVR2A and ACVR2B, also participate in BMP and GDF signaling. As such, modulating ALK4 availability on skeletal target cells is the most direct way to determine the specific effects of activin signaling in the skeleton. Here, we generated mice lacking ALK4 in skeletal progenitor cells (Alk4^{f/f}; Prx1-Cre = Alk4 cKO), and by targeting the type 1 receptor, removed activin signaling from early limb mesoderm without affecting BMP and GDF signaling. We found that newborn Alk4 cKO mice have normal skeletons that could not be distinguished from control littermates in whole mount skeletal preps stained with Alizarin Red and Alcian Blue. Western blot analyses demonstrated that pSmad2 and pSmad1/5/8 levels were unchanged in bone lysates of newborn Alk4 cKO mice. These results suggested that ALK4 is dispensable for formation of limb skeleton. We then performed Micro-CT analyses of Alk4 cKO mice at 2 and 6 months of age and found that removal of ALK4 from skeletal progenitors resulted in significant increases in trabecular bone mass at 2 months (32% compared to littermate controls) and 6 months (67% compared to littermate controls) of age. At each time point, cortical thickness remained unchanged. Bone histomorphometric analysis showed that osteoclast number and bone-eroded area were not changed in Alk4 cKO mice, consistent with a specific effect of activin on bone forming cells. Western blot analyses demonstrated that pSmad2 levels were reduced in bone lysates of Alk4 cKO mice, while pSmad1/5/8 levels were unchanged, providing direct evidence that removal of Alk4 specifically impaired activin signaling without altering BMP signaling. As circulating activin levels increase with age and in patients with inflammatory diseases, physiological states where reduced bone mass is observed, we believe that targeting activin signaling in osteoblasts through ALK4 provides a novel way to control bone mass.

Disclosures: **Shek Man Chim, None**

1136

A Novel Osteolineage-Derived Cancer Associated Fibroblast Population In Primary Tumors Expresses Dkk1 And Enhances Tumor Growth Biancamaria Ricci^{*}, Francesca Fontana, Sahil Mahajan, Roberto Civitelli, Roberta Faccio. Washington University in St Louis, United States

We recently described that mice bearing extra-skeletal tumors have increased levels of the Wnt/ β -catenin inhibitor Dkk1 in circulation and bone marrow fluid. Although Dkk1 is

known to modulate bone remodeling, during tumor progression Dkk1 induces the expansion of myeloid derived suppressor populations to inhibit anti-tumor T cell responses. The goal of this study was to determine the source of Dkk1 and whether Dkk1 acts locally or systemically to exert immune suppressive functions. Dkk1 was highly expressed by osteoblasts (OBs) and osteocytes in mice with extra-skeletal tumors. Although we did not detect expression of Dkk1 in our tumor lines, we found expression in the tumor mass by the cancer-associated fibroblasts (CAFs). Unexpectedly CAFs also expressed two OB-specific markers Osterix (Osx) and Osteocalcin (Ocn), leading to the hypothesis that Dkk1 at tumor site is produced by a novel osteolineage-derived fibroblast population. To test this possibility, we turned to a mouse model carrying the R26R-tdTomato reporter protein (TdTomato) under the control of a TET-off doxycycline *Osx-Cre* (TdTOsx) driven promoter. Doxycycline was administered to moms and pups until weaning to prevent *Osx-Cre* activation in perinatal mesenchymal stem cells and, at 8 weeks of age, mice were orthotopically inoculated with B16 or PyMT cell lines. We found that 3-9% cells in the tumor mass were TdTOsx+. This population expressed several fibroblast markers and Dkk1. Importantly, TdTOsx cells isolated from B16 tumors and co-injected together with B16 cells into WT recipient mice significantly increased tumor growth compared to the tumor line alone. Next, to determine whether *Osx+* cells support tumor progression via production of Dkk1, we generated *Osx-Cre;Dkk1fl/fl* mice and observed a significant reduction in tumor size compared to control mice. Since *Osx-Cre* targets also the OBs, to specifically evaluate the contribution of CAF-derived Dkk1, we generated *Fsp1-Cre;Dkk1fl/fl* mice. Strikingly, tumor growth was also significantly reduced in the *Fsp-Cre;Dkk1fl/fl* mice indicating that fibroblast-derived Dkk1 plays an important role during tumor progression. In summary, we have identified a novel population of CAFs that expresses the osteolineage marker *Osx*, contributes to Dkk1 production and strongly supports tumor growth.

Disclosures: **Biancamaria Ricci**, None

1137

Notch2 is a new marker of breast cancer stem cell and is involved in bone marrow cellular dormancy Mattia Capulli¹, Dayana Hristova², Zoe Valbret¹, Kashmala Carys¹, Ronak Arjan¹, Antonio Maurizi¹, Francesco Masedu¹, Nadia Rucci¹, Anna Teti¹. ¹University of L'Aquila, Italy, ²University of Cambridge, United Kingdom

Tumor dormancy is responsible for breast cancer (BC) relapse after a prolonged disease-free period. Clinical and experimental data indicate bone marrow as a candidate tissue to host BC dormancy. Since dormancy also requires tumor initiation properties to start a secondary disease, we hypothesized that dormancy and initiation represent two sides of the same coin and are regulated by orchestrated signals. We identified a subpopulation of BC cells expressing high levels of Notch2 (Notch2+) that displays the dual properties of dormancy and tumor-initiation, in which Notch2 was the molecular switch mediating these opposing behaviors. In MDA-MB-231 human BC cell line (MDA), Notch2+ cells represented 1-5% of the total population. They did not belong to the classical CD44+/CD24-MDA stem population but were enriched in the HSC stem markers, CD34, c-kit, Tie2 and Cxcr4 (+103,103,102,10fold; $p < 0.01$, respectively), suggesting a unique HSC-mimicry. Notch2+MDA stemness and tumor-initiating ability were confirmed in culture by the generation of more (+2fold; $p=0.00323$) and larger primary mammospheres ($p=0.0001$) and more secondary mammospheres (+15fold; $p=0.0033$) vs Notch2-MDA, despite their lower proliferation in standard 2D-cultures (-54%; $p=0.03$). Similar results were obtained when the HSC stem cell marker Tie2 was used for sorting MDA. When injected intratibially in immunocompromised mice, Notch2+MDA in-bone growth (-70%; $p=0.02$) and dissemination to distant organs (-67%; $p=0.0001$) were lower vs Notch2-MDA, suggesting that the bone microenvironment favors dormancy vs tumor-initiation. In immunocompromised mouse tibias injected with luciferase+MDA that after one month showed no bioluminescence or osteolysis (presumed dormancy), we identified single Notch2+, non-proliferating (Ki67-) MDA located close to the endosteum. In the same mouse model, single treatment with a γ -secretase inhibitor dislodged Notch2+MDA from the endosteum ($p < 0.0001$) and increased distant organ colonization (+3fold of liver metastases; $p=0.0496$) vs vehicle. Conversely, both chronic and acute inflammation proved ineffective in reactivating tumor cells. Key results were confirmed in mouse 4T1 BC cells in vitro and in vivo. Moreover, intratibially injected MDA cells that survived a prolonged chemotherapy treatment (42 days) with doxorubicin (0.1mg/kg) were dormant and Notch2+. In conclusion, our data indicate a key role for Notch2 and HSC-mimicry in BC cell dormancy and tumor-initiating ability.

Disclosures: **Mattia Capulli**, None

1138

Circulating osteoprogenitor cells provide a novel diagnostic biomarker for bone metastasis Hyun Jin Sun¹, Kyung-Hun Lee¹, Kyoung Jin Lee², Serk In Park², Young Joo Park¹, Seock-Ah Lim¹, Sun Wook Cho¹. ¹Seoul National University Hospital, Republic of Korea, ²Korea University College of Medicine, Republic of Korea

The accurate estimation of viable tumors of bone metastases is critical for optimal treatment. However, the current image-based diagnostic modalities have limitations. This study aimed to investigate the potentials of circulating osteoprogenitor cells (cOPs) for diagnosing disease progression and treatment monitoring of bone metastasis. We performed flow cytometric analyses of cOPs in the blood samples from a mouse model of bone metastasis as well

as from breast cancer patients with or without bone metastasis. First, in an *in vivo* bone metastasis models of human breast cancer cells growing in the tibiae of nude mice, flow cytometric analyses of peripheral blood mononuclear cells showed that cOPs (CD15-CD45-Osteocalcin+) were significantly increased as early as 1 week after tumor injection, compared to the non-tumor bearing age-matched control mice, even before the development of detectable bone metastases by BLI as early as 2 weeks. In contrast, histological analyses detected tumor cell colonization in the endosteal niche were observed only at 1 to 2 weeks after tumor injection, and overt metastatic lesions with bone destruction were observed at 4-week. Subsequently, to evaluate the changes of cOPs in response to cancer therapy, zoledronic acid (ZA) was administered immediately after intratibial cancer cell injection. At 1-week after treatment, cOPs were significantly reduced in the ZA-treated group compared with controls in the tumor-bearing bone, while no significant changes in the non-tumor bearing controls were observed. Next, cOPs (CD15-CD34-Osteocalcin+) were analyzed in 98 metastatic breast cancer patients. 61 patients had bone metastasis and 37 had metastasis in other sites than bone. cOPs were significantly higher in bone metastasis than other metastasis group, while serum bone-specific alkaline phosphatase or CTx showed no difference. Due to the heterogeneity of the disease status of bone metastasis, we then divided the patients into two groups, stable ($n=30$) and persistent ($n=31$) groups based on their diagnostic imaging studies performed on 0 and 3 months after blood sampling. cOPs were significantly higher in persistent than stable group with minimal overlaps in the levels of cOPs between groups. Furthermore, 11 patients who had paired sampling before and 3-months after first ZA administration showed that cOPs were significantly decreased after ZA treatment than before. In conclusion, cOPs increased in the micro-metastatic stage of bone metastasis, and changed significantly earlier than detectable lesions in imaging studies. In addition, cOPs increased in actively progressing bone metastasis in our cross-sectional cohort, and decreased in response to a bone-targeting agent, suggesting the potentials of cOPs as diagnostic tools for disease progression and treatment monitoring of bone metastasis.

Disclosures: **Hyun Jin Sun**, None

1139

An IAP Antagonist Inhibits Breast Cancer Metastasis to Bone by Killing Cancer Cells, Inhibiting Osteoclast and Enhancing Osteoblast Differentiation Wei Lei*, Rong Duan, Brendan Boyce, Zhenqiang Yao. University of Rochester Medical Center, United States

Development of breast cancer (BC) bone metastasis (B.Met) depends on cancer-bone cell interactions, in which enhanced osteoclast (OC) formation causes osteolysis, osteoblasts (OB) fail to repair lytic lesions, and factors released from bone or produced locally promote cancer cell growth. We found that SM164, a small molecule compound, which degrades inhibitor of apoptosis proteins (IAPs) to kill cancer cells, also inhibited OC formation and stimulated OB differentiation *in vitro*. We tested its effects on BC B.Met in 5 week-old female athymic nude mice inoculated with MDA-MB-231luciferase cells into their left cardiac ventricles, starting 2d after inoculation. SM164 significantly reduced bioluminescent imaging (BLI) signals in the hind-limbs vs. vehicle ($p < 0.01$) and combined standard chemotherapy (STC): adriamycin, cytoxan and zoledronic acid ($p < 0.01$) after 2, 3 and 4 weeks of treatment. Mice were euthanized on day 29 to evaluate B.Met by histologic analysis. SM164 significantly reduced the number of mice with B.Met (25%; 2/8, $p < 0.05$) compared with vehicle group (100%; 7/7), but STC did not (71%; 5/7). Similarly, mice treated with SM164 had fewer osteolytic lesions in tibiae and femora (9%; 3/32) than those given STC (39%; 11/28; $p < 0.05$) or vehicle (61%; 17/28, $p < 0.05$ vs. vehicle and STC). Both SM164 and STC significantly reduced a bone destruction score evaluated by the presence of tumor in bone marrow, cortical bone, growth plate, secondary ossification center and outside the bone. Importantly, SM164 and STC reduced OC numbers inside metastatic sites, 19+/-8 and 6+/-1.7, respectively, versus 52+/-15/mm² in the vehicle group. SM164 also increased the bone formation rate in vertebrae that had no B.Met (0.84+/-0.19 vs. 0.58+/-0.12 cm²/cm³/d in vehicle, $p < 0.05$). When SM164 was given 2 weeks after cancer inoculation when B.Met was established, it also inhibited cancer cell BLI in the bones 2 weeks later, but this effect did not reach significance histologically. Interestingly, SM164-induced apoptosis of MDA231 cells was dependent on macrophage production of membrane-bound TNF. Finally, SM164 prevented RANKL- and TGFbeta1-induced TRAF3 degradation in macrophages and OB lineage cells, respectively, to inhibit OC and enhance OB differentiation. Our findings suggest that SM164 could act as a novel agent to prevent BC B. Met by simultaneously killing cancer cells, inhibiting OC and enhancing OB differentiation.

Disclosures: **Wei Lei**, None

1140

Bone-targeting Bortezomib significantly increases its efficacy in the treatment of human multiple myeloma *in vitro* and *in vivo* in mice Jianguo Tao*, Venkatesan Srinivasan, Xichao Zhou, Frank Ebetino, Robert Boeckman, Brendan Boyce, Lianping Xing. University of Rochester, United States

Multiple myeloma (MM) is plasma cell malignancy that arises in bone marrow and causes osteolytic lesions throughout the skeleton. It is treated with first-line drugs, such as Bortezomib (Btz), which inhibit proteasomal degradation and kill MM cells. MM is currently incurable in part because adverse effects on non-skeletal tissues, including thrombocytopenia and peripheral neuropathy, limit the amount of drug that can be given, and tumor cells become Btz-resistant. To attempt to circumvent these issues, we have linked Btz to a

bisphosphonate (BP) that binds avidly to bone, but is not anti-resorptive, using novel linkers to generate (BP-Btz) conjugates. We hypothesize that BP-Btz will 1) reduce MM burden and bone destruction and kill Btz-resistant MM cells more effectively than Btz; and 2) have improved efficacy with a slow release rate. We tested the effects of our lead BP-Btz conjugate (BP-Btz1; 3nM) and found that it killed the human MM cell lines, U266, RPMI8226, and JIN3, in vitro with an IC50 similar to Btz. Bone slices that were pre-incubated with BP-Btz1 killed MM cells in vitro, but those pre-incubated with Btz did not. In NSG mice inoculated with JIN3 human MM cells, BP-Btz1 (1x/4d for 3wk) reduced tumor burden and bone destruction as effectively as Btz (1x/2d for 3wk) compared to Veh: CD138+ MM cells (25±14 vs 32±11 vs 48±13%, respectively); lytic lesions: (35±18 vs 40±14 vs 100±10%); and bone volume (42±8 vs 26±21 vs 9±7%). Btz, but not BP-Btz, decreased platelet counts compared to Veh (1038±217 vs 816±192 vs 1132±223). Importantly, a 3-fold higher dose of BP-Btz1 had no systemic side effects in vivo but was able to kill Btz-resistant human MM cells in vitro than needed to kill Btz-sensitive MM cells (9 vs 3nM). To test if varying the release rate of Btz from BP-Btz by altering the linker chemistry affects its efficacy, we synthesized two new BP-Btz conjugates with faster and slower release kinetics vs BP-Btz1. These killed MM cells at a similar IC50 as BP-Btz1 in vitro, but had significantly reduced ability to reduce MM tumor burden in vivo compared to BP-Btz1 and Veh (tumor area: 65±18 (faster) vs 42±25 (slower) vs 23±28 and 79±8%) and bone destruction (spinal paralysis: 20 vs 20 vs 0 and 60%). In summary, BP-Btz1 reduces myeloma cell tumor burden in mice bearing human MM cells and associated bone loss more effectively than Btz with less systemic adverse effects. BP-Btz may represent a novel therapeutic agent to treat patients with MM.

Disclosures: **Jianguo Tao**, None

1141

FGFR and mTOR Signaling Cooperate in Osteosarcoma Pathogenesis and Metastasis Arshiya Bani*¹, Sorrel Bunting¹, Carolina Zanduetta², Susana Martinez-Canarias², Haritz Moreno², Beatriz Moreno², Fernando Lecanda², Agamemnon Grigoriadis¹. ¹King's College London, United Kingdom, ²CIMA Pamplona, Spain

Osteosarcoma (OS) is the most common primary malignancy of the skeleton, occurring primarily in children and adolescents. Metastatic disease is the single most important prognostic factor with a high frequency of patients developing lung metastases. We have recently demonstrated that high FGFR1 signalling in a transgenic model of OS as well as in human OS samples contributes to the pathogenesis and metastasis of OS. Significantly, xenograft OS studies showed that genetic or pharmacological inhibition of FGFR1 decreased lung metastasis. A recent shRNA kinase library screen identified mTOR signaling as a cooperating pathway with FGFR signaling. To validate this finding, we stimulated murine and human OS cell lines with FGF2 and found an increase in pAkt/mTOR signaling and mTOR target genes that was inhibited by the FGFR inhibitor, PD173074. Functional analysis by colony assay showed that FGF2 stimulated colony growth of OS cells, and the mTOR inhibitor, Rapamycin, completely blocked this response. Moreover, shRNA silencing of mTOR prevented FGF2-stimulated cell migration in wound/scratch assays, suggesting functional crosstalk between these pathways. To confirm pathway cooperativity in vivo, we performed xenograft studies. Silencing of mTOR in FGFR1-expressing OS cells reduced tumor formation on a chick chorioallantoic membrane, with reduced mitotic (pHistone-H3) index. Interestingly, using a murine intratibial OS xenograft model, inhibition of FGFR1 and mTOR signaling (AZD4547 and AZD8055, respectively), either alone or in combination, showed a decrease in bioluminescence imaging in the lungs of mice treated with the mTOR inhibitor alone as well as with the combined FGFR/mTOR inhibitors, compared to controls with a marked reduction in both the size and diameter ($p < 0.01$) of spontaneous pulmonary metastatic nodules. No differences were observed in the number of lung nodules and in treated primary tumors. Immunostaining analysis showed a marked decrease in the number of Ki67+ cells in lung metastases of FGFR/mTOR inhibitor-treated mice ($p < 0.01$), whereas no changes in activated caspase-3 were detected. Thus, combinatorial treatment significantly decreased lung metastasis of OS cells. Ongoing analysis of activated FGFR and mTOR pathways in patient-derived tissue microarrays will enable patient stratification that will be useful in the clinical setting to exploit this as a potential anti-metastatic therapy in OS.

Disclosures: **Arshiya Bani**, None

1142

Off-treatment Bone Mineral Density Changes in Postmenopausal Women after 5 Years of Anastrozole Ivana Sestak*¹, Jack Cuzick¹, Glen Blake², Rajesh Patel³, Robert Coleman⁵, Richard Eastell⁴. ¹Centre for Cancer Prevention, Queen Mary University London, United Kingdom, ²Division of Imaging Sciences, King's College London, United Kingdom, ³Imperial College London, United Kingdom, ⁴Academic Unit of Bone Metabolism, Metabolic Bone Centre, Northern General Hospital, United Kingdom, ⁵Academic Unit of Clinical Oncology, Weston Park Hospital, United Kingdom

Background: Anastrozole (A) has been shown to prevent breast cancer in postmenopausal women at increased risk of developing the disease, but has been associated with substantial accelerated bone mineral density (BMD) loss during active treatment. Here, we investigate changes in BMD assessed by dual energy X-ray absorptiometry (DXA) 2 years after treatment cessation in women included in the IBIS-II breast cancer prevention trial.

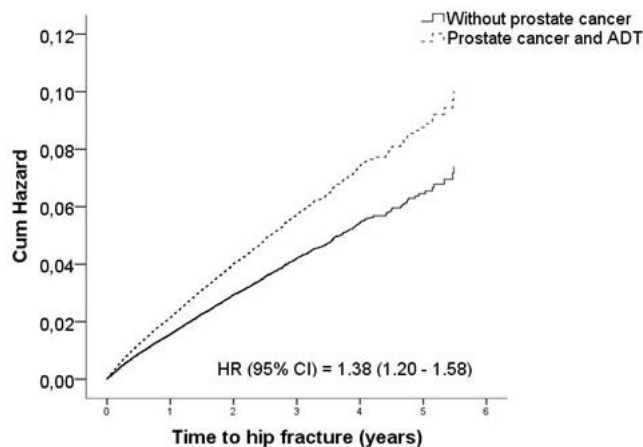
Methods: IBIS II randomly assigned 3864 postmenopausal women to A 1mg/day or placebo (P) for 5 years. 1410 were included in a BMD sub-study and stratified into three strata according to their baseline T-score at spine or femoral neck (stratum I (N=760): T-score > 1.0 and observed; stratum II (N=500): $-1.0 < \text{T-score} < -2.5$ and randomised to weekly risedronate or placebo; stratum III (N=150): $-2.5 < \text{T-score} < -4.0$ or/and two fragility fractures and all on risedronate). The primary objective of this analysis was to investigate whether DXA BMD at the spine and hip changed 2 years after stopping A or P. All results are presented as mean % BMD changes (95% CI) between 5 and 7 years of follow-up. Results: 5 and 7-year BMD data were available for a total of 529 women who did not receive risedronate. In stratum I, cessation of A (N=205) led to an increase in BMD at the spine that was larger than in those on P (N=206) (A=1.29% (95% CI 0.78 to 1.79) vs. P=0.2% (-0.23 to 0.62), $p=0.001$). At the hip, BMD remained unchanged between 5 and 7 years after cessation of A but continued to a decrease in those who had been on P (A=-0.07% (-0.51 to 0.37) vs. P=-1.31% (-1.67 to 0.94), $p < 0.0001$). Similar results were observed for women with osteopenia (stratum II). Those previously on A (N=53) had a significantly larger BMD increase at the spine after treatment cessation compared to those stopping P (N=64) (A=2.81% (1.40 to 4.23) vs. P=0.57% (-0.36 to 1.50); $p=0.007$). Loss of BMD at the hip continued in women who had been on P but increased slightly following cessation of A (A=0.47% (-0.42 to 1.36) vs. P=-1.33% (-2.12 to -0.54); $p=0.003$). Conclusions: These are the first results reporting BMD changes after stopping A in a breast cancer prevention setting. BMD at the lumbar spine improved significantly more in women who were originally randomised to A compared to those who received P. Our results show that the negative effects of A on BMD in the preventive setting are partially reversible.

Disclosures: **Ivana Sestak**, None

1143

Patients with prostate cancer and androgen deprivation therapy have increased risk of fractures – a study from the Fractures and fall injuries in the elderly cohort (FRAILCO) Marit Wallander*¹, Kristian F Axelsson², Dan Lundh³, Mattias Lorentzon⁴. ¹Department of Medicine Huddinge, Karolinska Institute, Sweden, ²Department of Orthopaedic Surgery, Skaraborg Hospital, Sweden, ³School of Health and Education, University of Skovde, Sweden, ⁴Geriatric Medicine, Department of Internal Medicine and Clinical Nutrition, Center for Bone Research at the Sahlgrenska Academy, Sweden

Purpose Androgen-deprivation therapy (ADT) in patients with prostate cancer (PC) is associated to increased risk of fractures compared to PC patients without ADT. Most previous studies are however small or are lacking sufficient data on traditional fracture-related risk factors. In this study, we investigated the relationship between ADT in patients with PC and the risk of incident fractures and non-skeletal fall injuries both compared to those without ADT and compared to patients without PC. Methods We included 179,744 men (79.1 ± 7.9 years (mean ± SD)) from the Swedish registry "Senior alert" (a cohort of elderly individuals) to which national directories were linked in order to study associations regarding fractures, fall injuries, morbidity, mortality and medications. Among these men, we identified 159,662 patients without PC, 6954 with PC and current ADT (prescription of GnRH-agonist within the previous year) and 13,128 patients with PC without ADT. During a total follow-up of approximately 270,300 patient-years we identified 10,916 fractures of which 6525 were major osteoporotic fractures (MOF) including 4860 hip fractures. We performed multivariable Cox regression analyses adjusted for age, weight, height, previous fracture, per oral glucocorticoids, calcium- and vitamin D, alendronate use, rheumatoid arthritis, secondary osteoporosis and estimated alcohol over-consumption, previous falls and Charlson comorbidity index. Results After multivariate adjustment and compared to men without PC, those with PC and ADT had increased risk of any fracture (HR 95% CI: 1.40 (1.28-1.53)), hip fracture (1.38 (1.20-1.58)) and MOF (1.44 (1.28-1.61)) but not of non-skeletal fall injury (1.01 (0.90 - 1.13)). Hazard ratios were similar when comparison was made to patients with PC but without ADT. Patients with PC without ADT did not have increased risk of any fracture (0.97 (0.90-1.05)), hip fracture (0.95 (0.84-1.07)), MOF (1.01 (0.92-1.12)) and had decreased risk of non-skeletal fall injury (0.84 (0.77 - 0.92)). Conclusions Patients with PC and ADT is a fragile patient group with increased risk of fractures compared to patients without PC and compared to those with PC without ADT. We believe that medical treatment in order to prevent fractures should be considered in the routine evaluation of all patients with PC and ADT.

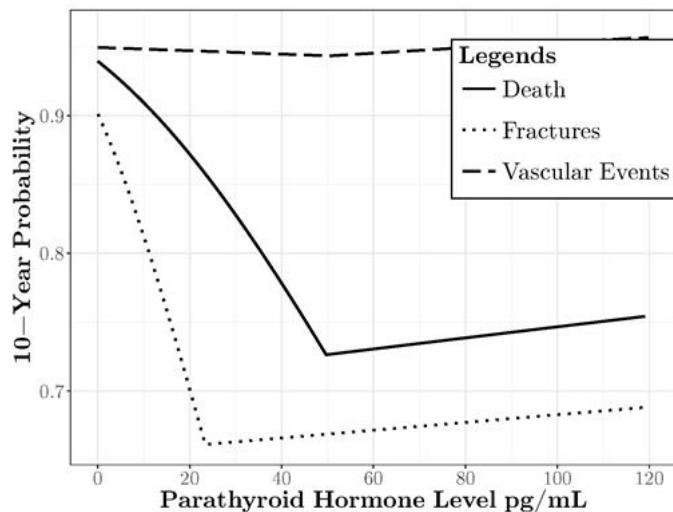


Disclosures: *Marit Wallander, None*

1144

Low Parathyroid Hormone Levels are Associated with Increased Hazards of Fracture and Death in Stage 3 and 4 Chronic Kidney Disease Karen Hansen*¹, Sinong Geng², Zhaobin Kuang², Peggy Peissig³. ¹University of Wisconsin School of Medicine & Public Health, United States, ²University of Wisconsin, United States, ³Marshfield Clinic, United States

Chronic kidney disease (CKD) affects ~20% of older adults. Secondary hyperparathyroidism (sHPT) afflicts over half of stage 3-4 CKD patients. Cross-sectional studies have linked secondary hyperparathyroidism (HPT) to greater risk of fractures, vascular events and death. Thus, the National Kidney Foundation recommends treatment of sHPT in CKD patients. In a recent systematic review, we found no placebo-controlled clinical trials proving that treatment of sHPT reduced fractures, vascular events or death. Three retrospective studies reported that calcitriol and alfacalcidol therapy reduced death. We hypothesized that lower PTH levels at baseline would be associated with lower risk of fractures, vascular events and death in stage 3 and 4 CKD patients. We used Marshfield Clinic electronic health records spanning 1985 to 2013 to assess relationships between baseline PTH levels and subsequent 10-year probabilities of clinical fractures, vascular events and mortality in stage 3 and 4 CKD patients. We studied adults with ≥ 2 PTH measurements at baseline. We used ICD-9 codes to identify subjects' medical conditions, fractures, vascular events and death. In multivariate models, we assessed relationships between serum PTH and the three clinical outcomes, controlling for age, gender and co-morbidities. The 7594 subjects were 68 ± 13 years old and 55% were women. Fractures, vascular events and death occurred in 19%, 60% and 29% of the cohort, respectively. In multivariate models controlling for age, gender, tobacco use, bisphosphonate and hormone therapy, PTH predicted fracture. The PTH value at which the probability of fracture was minimized equaled 23 pg/mL. Below this level, the 10-year probability of fracture dramatically increased (Figure). After controlling for age, gender, tobacco use, vascular disease, diabetes, hypertension, lipids and obesity, PTH was a significant variable in models predicting death. The 10-year probability of death was lowest at a PTH of 50 pg/mL and below this level, the probability of death increased sharply. Vascular event rates were high regardless of PTH values, but rates were lowest at a PTH value of 50 pg/mL. To our knowledge, ours is the first study to suggest that low parathyroid hormone levels are associated with an increased probability of fractures and death in stage 3-4 CKD patients. Findings suggest that over-suppressing PTH with vitamin D analogs might cause harm. Further studies are needed to confirm these findings.



Disclosures: *Karen Hansen, None*

1145

Prevalence and risk of vertebral fractures in primary hyperparathyroidism: A nested case-control study Henriette Ejlsmark-Svensson*^{1,2}, Lise Sofie Bislev^{1,2}, Siv Lajlev², Torben Harsløf², Lars Rolighed³, Tanja Sikjær², Lars Rejnmark^{1,2}. ¹Department of Clinical Medicine, Aarhus University, Denmark, ²Department of Endocrinology and Internal Medicine, Aarhus University Hospital, Denmark, ³Department of Otorhinolaryngology, Head and Neck Surgery, Aarhus University Hospital, Denmark

Introduction Prevalence of vertebral fractures (Vfx) in patients with primary hyperparathyroidism (PHPT) remains uncertain. The presence of Vfx is of importance to choice of treatment. International guidelines recommends parathyroidectomy in patients with PHPT and osteoporosis including the presence of Vfx. We aimed to estimate the prevalence of Vfx, investigate potential risk factors associated with Vfx and whether bone mineral density (BMD) differs between PHPT- and osteoporotic-patients with Vfx. Methods Through the Danish National Patient Register, we identified patients diagnosed with PHPT between 2005-2015. The diagnosis was verified by retrieving biochemistry data. Patients with ionized-calcium levels above and PTH levels in upper third or above upper limit of the reference range were included (averages of two measurements). X-ray reports of the thoracolumbar spine were reviewed by two investigators. Osteoporotic patients with Vfx were identified from our outpatient clinic and matched on age and sex with PHPT patients with Vfx. Results We identified 792 PHPT patients among whom spine X-ray was available from 588 patients. Vfx were present in 122 (21%) patients and were equally frequent among sex (77% females). Fractured patients were older (70 [IQR: 62-77] yrs. vs 63 [55-71] yrs.) and had lower heights (163 [158-169] cm vs 166 [160-172] cm) compared to non-fractured patients (pall <0.02). After stratification by age-groups, the prevalence of Vfx differed significantly between sexes (p<0.01). Ionized-calcium and PTH did not differ between groups. BMD at total hip and forearm were lower in fractured compared to non-fractured patients (pall <0.03) after adjusting for age, sex and BMI. Compared with osteoporotic patients with Vfx (N=108), BMD at the lumbar spine was higher in PHPT patients with Vfx (N=108) (p<0.01). This did not change by excluding patients with lumbar Vfx (p<0.01). Conclusion The severity of PHPT assessed by biochemistry does not seem to be associated with risk of Vfx and the relatively high prevalence of Vfx supports a proactive screening in all patients diagnosed with PHPT. Compared with osteoporosis; Vfx seems to occur at a higher BMD in PHPT.

Disclosures: *Henriette Ejlsmark-Svensson, None*

1146

Fracture Risk Assessment in Women with Breast Cancer Initiating Aromatase Inhibitor Therapy: A Registry-Based Cohort Study William Leslie*¹, Suzanne Morin², Lisa Lix¹, Eugene McCloskey³, Helena Johansson³, Nicholas Harvey⁴, John Kanis³. ¹University of Manitoba, Canada, ²McGill University, Canada, ³Centre for Metabolic Bone Diseases, United Kingdom, ⁴MRC Lifecourse Epidemiology Unit, United Kingdom

PURPOSE: Aromatase inhibitors (AI) for breast cancer induce bone mineral density (BMD) loss and have been reported to increase fracture risk. FRAXR was developed to predict 10-year risk for major osteoporotic fracture (MOF) and hip fracture in the general population. We evaluated the performance of FRAX for fracture prediction in women treated with AI. METHODS: We conducted a BMD registry-based cohort study linked to population-based data for the Province of Manitoba, Canada. We identified women age 40 years or

older initiating AI for breast cancer with at least 12 months AI prescribed (N=1775), with breast cancer but not receiving AI (N=1016), and from the general population (N=34,205) during 2005-2016. FRAX scores were computed with and without BMD. Survival methods (with competing mortality) and Cox proportional hazards models were used to study time to first incident fracture, adjusted for baseline risk, in breast cancer subgroups compared to general population. RESULTS: Mean age at baseline was 65 years for all groups (P=0.607). Cumulative fracture incidence to 10 years showed no significant between-group differences for incident MOF (P=0.198) or any fracture (P=0.157); there was a lower incidence of hip fracture in AI users (P=0.039). FRAX stratified risk for MOF, hip and any fracture equally well in all subgroups (all P-interaction >0.1). At baseline AI users had higher BMI, higher BMD, lower osteoporosis prevalence and fewer prior fractures (P<0.001). When adjusted for FRAX score without BMD and with AI use entered as a secondary cause of osteoporosis (Table, Model 1), AI users were at significantly lower risk for MOF (HR 0.78, 95% CI 0.63-0.97), hip fracture (HR 0.44, 95% CI 0.26-0.73) and any fracture (HR 0.77, 95% CI 0.64-0.92). AI use was no longer significantly associated with fractures when AI use was not entered as secondary osteoporosis (Model 2) or when BMD was included in the FRAX calculation (Model 3). Similar results were seen when analysis was limited to 918 women with at least 5 years of AI use. CONCLUSIONS: Our findings challenge the view that all women with breast cancer initiating AI therapy are at high fracture risk. Fracture probability scores from FRAX stratify fracture risk equally well in women receiving AI therapy as in non-users, but including secondary osteoporosis as a risk factor for AI users overestimated fracture risk.

Table. Hazard ratios (HR) with 95% confidence intervals (CI) for incident fracture according to breast cancer status and aromatase inhibitor (AI) use, adjusted for baseline risk.

	Model 1: Adjusted for FRAX without BMD (+ AI secondary)	Model 2: Adjusted for FRAX without BMD (- AI secondary)	Model 3: Adjusted for FRAX with BMD
Outcome: MOF	HR per SD	HR per SD	HR per SD
General population	1 (REF)	1 (REF)	1 (REF)
Breast cancer, AI user	0.78 (0.63-0.97)	1.02 (0.83-1.27)	1.10 (0.89-1.36)
Breast cancer, non-AI user	0.96 (0.76-1.22)	0.96 (0.76-1.22)	0.97 (0.77-1.23)
Outcome: Hip Fracture	HR per SD	HR per SD	HR per SD
General population	1 (REF)	1 (REF)	1 (REF)
Breast cancer, AI user	0.44 (0.26-0.73)	0.68 (0.41-1.13)	0.78 (0.47-1.30)
Breast cancer, non-AI user	0.75 (0.47-1.19)	0.75 (0.47-1.19)	0.77 (0.48-1.23)
Outcome: Any Fracture	HR per SD	HR per SD	HR per SD
General population	1 (REF)	1 (REF)	1 (REF)
Breast cancer, AI user	0.77 (0.64-0.92)	0.97 (0.81-1.17)	1.03 (0.85-1.24)
Breast cancer, non-AI user	0.95 (0.77-1.16)	0.95 (0.77-1.16)	0.96 (0.78-1.18)

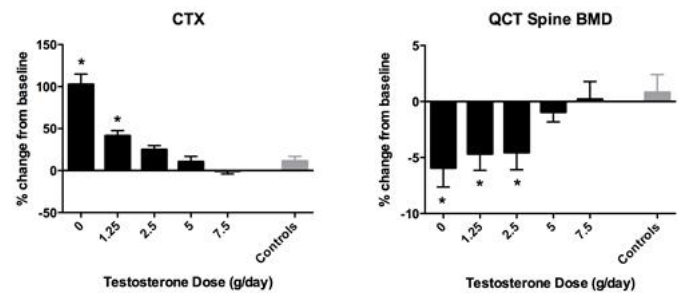
Data from Cox proportional hazards models. Significant results are in boldface. MOF, major osteoporotic fracture. + (with) and - (without) AI use entered as secondary osteoporosis.

Disclosures: **William Leslie, None**

1147

Towards a physiologically-based definition of hypogonadism: Dose-response relationships between testosterone and bone density in older men Elaine Yu*, Benjamin Leder, Hang Lee, Laura Krivicich, Emily Gentile, Sarah Hirsch, Karin Darakananda, David Lin, Joel Finkelstein. Massachusetts General Hospital, United States

Introduction: Testosterone (T) replacement in older men is controversial, partly due to a lack of a physiologically-based definition of late-onset hypogonadism. We previously found that T levels above 200 ng/dL prevented increases in bone resorption and decreases in bone mineral density (BMD) in young men. However, it is not clear whether the same physiologic thresholds apply to older men. Thus, we performed a randomized controlled physiologic study in older men to determine the T thresholds that lead to bone loss. Methods: Healthy men aged 50-75 (n=177) were randomized to 1 of 6 groups. Groups 1-5 received goserelin acetate (Zoladex®, AstraZeneca LP, 3.6 mg q4wk) to induce severe hypogonadism, together with 0 (placebo), 1.25, 2.5, 5, or 7.5 g/day of a T gel (AndroGel®, Abbvie) for 16 weeks. Group 6 (Controls) received placebo Zoladex® and placebo AndroGel®. BMD of lumbar spine was assessed by DXA (L1-L4) and by QCT (L4). Serum C-telopeptide (CTX) was measured at weeks 0 and 16 to assess bone resorption. The mean percent change from baseline of CTX and spine BMD for the Controls was compared with the mean change for each of the other 5 groups using Dunnett's test for multiple comparisons. Results: Mean age at baseline was 65 ± 4 years. Mean baseline T levels were 490 ± 151 ng/dL in the full cohort, and were similar in each of the 6 groups. Mean (± SD) serum T and E levels measured every 4 weeks were 35 ± 34, 206 ± 116, 324 ± 162, 549 ± 290, and 807 ± 381 ng/dL and 3 ± 2, 11 ± 7, 15 ± 7, 28 ± 13, and 36 ± 18 pg/mL in the 0, 1.25, 2.5, 5, and 7.5 g/day T dose groups, respectively, and 533 ± 142 ng/dL and 28 ± 5 pg/mL in the Controls. Serum CTX increased 103 ± 57% in the 0 g/day T group and 41 ± 30% in the 1.25 g/day T group (P<0.01 vs Controls for both), but did not differ significantly from Controls in groups that received 2.5, 5, or 7.5 g/day of T. When assessed by QCT, spine BMD decreased by -6 ± 8%, -5 ± 7%, and -5 ± 8% in groups that received 0, 1.25, or 2.5 g/day of T (P<0.05 vs Controls for each of the 3 groups). There were no differences in DXA spine BMD in any group compared with Controls. Conclusions: The strong dose-response relationships between T dose and CTX and BMD in older men suggest that increased bone resorption and bone loss begin when serum T levels fall below 200-300 ng/dL and serum E2 levels fall below 10-15 pg/mL. These data suggest that the relationship between gonadal steroid levels and bone health is similar in older and younger men.



Disclosures: **Elaine Yu, None**

1148

Mettl3-mediated m6A regulates the fate of bone marrow mesenchymal stem cells and osteoporosis Yunshu Wu*, Liang Xie¹, Mengyuan Wang¹, Yuchen Guo¹, Rui Sheng¹, Jing Li¹, Peng Deng¹, Rixin Zheng¹, Qiuchan Xiong¹, Yizhou Jiang², Ling Ye¹, Xuedong Zhou¹, Shuibin Lin³, Quan Yuan¹. ¹State Key Laboratory of Oral Diseases & National Clinical Research Center for Oral Diseases, West China Hospital of Stomatology, Sichuan University, China, ²Institute for Advanced Study, Shenzhen University, China, ³Center for Translational Medicine, The First Affiliated Hospital, Sun Yat-sen University, China

Aged-related osteoporosis is featured with low bone mass and excessive accumulation of adipocytes. However, explicit mechanisms under which the lineage allocation of bone marrow mesenchymal stem cells (MSCs) favors adipogenic to osteogenic lineage remain unclear. Being the most abundant internal mRNA epigenetic modification, N6-methyladenosine (m6A) exerts great influence in modulating multiple RNA processing events. Recent studies uncovered that m6A modification maintains the proper lineage commitment of functional stem cells and participates in mammalian development and disease control. To study the potential role of m6A methylation and its methyltransferase Mettl3 in MSCs lineage allocation and bone diseases, we first performed immunostaining which showed that Mettl3 is prevalently expressed in murine bone cells and bone marrow. Next, we generated Prx1-Cre driven Mettl3 conditional knockout mice and discovered that decreased m6A level upon loss of Mettl3 in MSCs led to low bone mass and high marrow adiposity in mice, much resembling the pathological features of osteoporosis. In consistent with in vivo phenotypes, cell culturing of primary Mettl3^{fl/fl} and Prx1-Cre;Mettl3^{fl/fl} MSCs revealed that m6A reduction impaired the osteogenic while promoting the adipogenic differentiation potential of mutant MSCs. More interestingly, mice with conditional Mettl3 over-expression in MSCs exhibited less bone loss after ovariectomy, which highlights the therapeutic potential of Mettl3 in preventing estrogen deficiency-induced osteoporosis. Mechanistically, our MeRIP-seq and RNA-seq demonstrated that Mettl3-mediated m6A regulates PTH (parathyroid hormone)/Pth1r (parathyroid hormone receptor-1) signaling axis, one of the most essential pathway in bone homeostasis. Knockout of Mettl3 reduced the translation efficiency of MSCs lineage allocator Pth1r, thus further blocking the downstream pathways, such as cyclic AMP-dependent protein kinase A (PKA) and extracellular signal-regulated kinases (ERK), responsible for the anabolic effect of PTH. In addition, Mettl3 conditional knockout mice displayed an obviously inert response to intermittent PTH injection. They failed to undergo an effective increase in bone remodeling and their excessive accumulation of marrow fat was also hardly alleviated after PTH treatment. Our results demonstrate the pathological outcomes of m6A mis-regulation in MSCs and unveil novel epitranscriptomic mechanism in skeletal health and diseases.

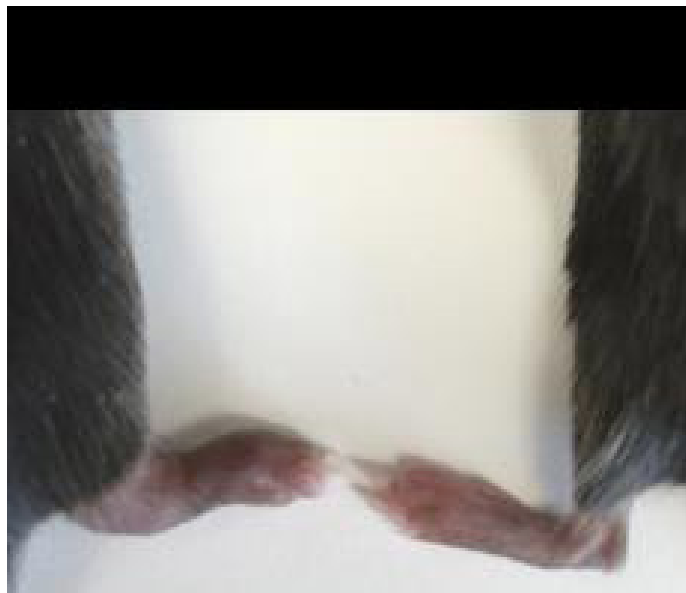
Disclosures: **Yunshu Wu, None**

1149

Fat Regulates Inflammatory Arthritis Yongjia Li¹, Wei Zou¹, Jonathan Brestoff¹, Nidhi Rohatgi¹, Xiaobo Wu², John Atkinson², Charles Harris³, Steven Teitelbaum^{1,4}. ¹Department of Pathology and Immunology, Washington University School of Medicine, St. Louis, United States, ²Division of Rheumatology, Department of Medicine, Washington University School of Medicine, St. Louis, United States, ³Division of Endocrinology, Metabolism and Lipid Research, Department of Medicine, Washington University School of Medicine, St. Louis, United States, ⁴Division of Bone and Mineral Diseases, Department of Medicine, Washington University School of Medicine, St. Louis, United States

Obesity and inflammatory arthritis (IA) are common disorders in western society, yet their relationship is poorly understood. To explore the possible association of fat to IA, we cross-mated diphtheria toxin (DTA) flox/flox mice with those expressing Adiponectin Cre. The resultant mice are fat-free (FF) as they completely lack visible visceral, subcutaneous and brown adipose tissue, confirmed by virtually undetectable circulating adipocyte-specific adipokines. To test whether fat is involved in the pathogenesis of IA, we injected K/BxN

serum into WT and FF mice. K/BxN serum induces severe IA characterized by dramatically enhanced paw and ankle thickness, increased osteoclast number, inflammation and severe bone destruction in WT mice. Surprisingly, FF mice are completely resistant to K/BxN serum-induced inflammatory arthritis. Importantly, transplantation of WT, mature fat into FF mice totally reverses their arthritis resistance suggesting that adipocyte products promote IA. To determine which adipokines are involved in regulating IA, we administered K/BxN serum to adipokine-knock out (KO) mice, including those deleted of adiponectin, leptin, combined adiponectin/leptin (double-KO) or adiponectin. While all other adipokine KO mice develop inflammatory joint disease comparable to WT, adiponectin deficiency totally prevents K/BxN serum induced IA. This observation suggests fat-mediated development of IA requires adipocyte-expressed adiponectin. Consistent with this posture, unlike WT fat, transplantation of adipose tissue derived from adiponectin-deficient mice into FF mice fails to enable K/BxN induced IA. Neutrophils play a key role in inflammatory joint destruction. Using flow cytometry, we established that neutrophils comprise more than 90% of immune cells in synovial fluid of WT mice injected with K/BxN serum, but less than 5% in similarly treated FF and adiponectin-KO mice. These results suggest absence of adiponectin is responsible for the arrested inflammation in the joints of FF and adiponectin-KO mice. Recently it has been reported that alternative pathway of complement activation is critical for IA development as complement component, factor B-deficient mice are resistant to K/BxN induced joint destruction. Since adiponectin (complement factor D) is involved in alternate complement activation, our results suggest that fat is important for IA development by modulating fat-free (FF) alternate complement activation via adiponectin. Our study provides the first direct evidence that fat regulates IA development.



Disclosures: *Yongjia Li, None*

1150

Deletion of Ror2 Promotes Bone Formation by Attenuating IL-6 Signaling

Hiroaki Saito^{*1}, Jonathan Gordon², Josech R. Boyd², Michiru Nishita³, Yasuhiro Minami³, Jane Lian², Gary Stein², Hanna Taipaleenmäki¹, Eric Hesse¹. ¹Molecular Skeletal Biology Laboratory, Department of Trauma, Hand and Reconstructive Surgery, University Medical Center Hamburg-Eppendorf, Germany, ²Department of Biochemistry, College of Medicine, University of Vermont, United States, ³Department of Physiology and Cell Biology Kobe University Graduate School of Medicine, Japan

Canonical Wnt signaling is among the strongest inducers of bone formation while much less is known about non-canonical Wnt signaling in bone mass accrual. Receptor tyrosine kinase-like orphan receptors 1 and 2 (Ror1, Ror2) play an important role in activating non-canonical Wnt signaling. To determine the physiological role of Ror1 and Ror2 in bone formation, we deleted each receptor individually and in combination within the osteoblast lineage using the cre-recombinase under the control of the 2.3 kb fragment of the collagen type 1 promoter (Col1-Cre+). Deletion of Ror1 in 8-week old Col1-Cre+;Ror1fl/fl mice did not show any alteration of the bone phenotype compared to Col1-Cre+;Ror1wt/wt control littermates. However, mice bearing a targeted deletion of Ror2 in osteoblasts (Col1-Cre+;Ror2fl/fl) demonstrated an increase in the number of osteoblasts and in the bone formation rate without changes in bone resorption, thereby augmenting trabecular and cortical bone mass ($p < 0.05$). This phenotype was recapitulated in Ror1/2 double conditional knockout mice (Col1-Cre+;Ror1,2fl/fl), demonstrating that in osteoblasts Ror1 is dispensable while Ror2 inhibits bone formation. In support of these findings, Ror2-deficient mouse embryonic fibroblasts showed an improved osteoblast differentiation. Furthermore, reducing the abundance of Ror2 in Kusa-A1 and Ocy454 osteoblast-like cells using the CRISPR/Cas9 system and in calvarial osteoblasts using the GapmeR technology, increased osteoblast differentiation

and mineralization as well as the expression of the osteoblast-related genes Runx2, alkaline phosphatase and osteocalcin. To elucidate the mechanisms by which Ror2 suppresses bone formation, we performed a genome-wide RNA-seq analysis in Ror2-deficient calvarial osteoblasts. Comprehensive bioinformatics analysis of 699 upregulated and 665 downregulated genes revealed that target genes of the IL-6 and TNF- α pathways (Ccl5, Cxcl1, Cxcl10, Bcl3, Icam1 and Pik3r3) were significantly decreased in Ror2-deficient osteoblasts. Since these cascades are known to impair osteoblast function and bone formation, we hypothesized that lack of Ror2 might attenuate IL-6 signaling. Indeed, phosphorylation of Stat3 and the expression of Socs3 in response to IL-6 treatment were impaired in Ror2-deficient osteoblasts compared to controls. These findings suggest that deletion of Ror2 promotes bone formation and gain in bone mass by attenuating IL-6 signaling in osteoblasts.

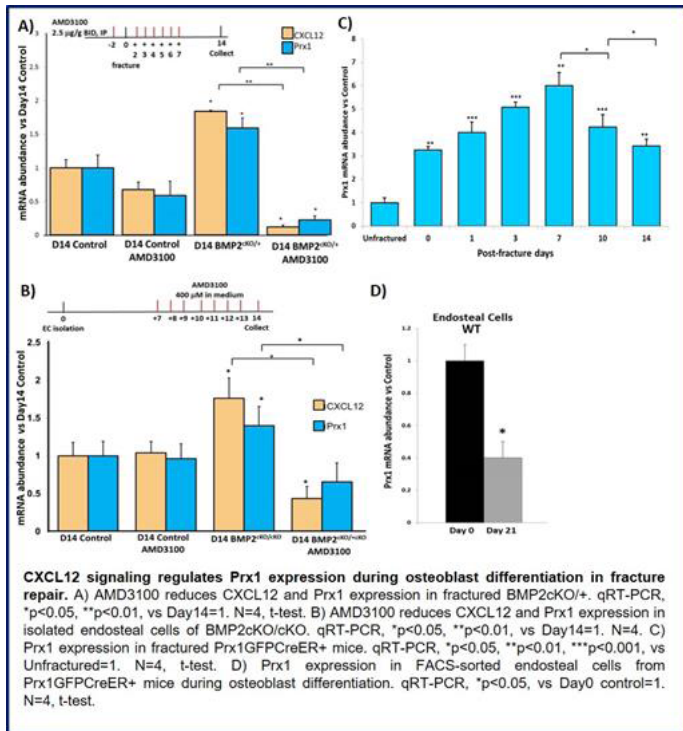
Disclosures: *Hiroaki Saito, None*

1151

BMP2-CXCL12 Axis Regulates Prx1 Expression During Fracture Repair

Alessandra Esposito^{*}, Lai Wang, Tieshi Li, Jie Jiang, Xin Jin, Anna Spagnoli. Rush University Medical Center, United States

Despite the clinical significance of fractures, mechanisms governing the cellular and humoral responses during repair are still not completely known. Studies, including from our laboratory, have reported that Paired Related Homeobox 1 (Prx1) regulates mesenchymal stromal cells differentiation and is postnatally expressed within the periosteum and endosteum. We previously reported that a bone morphogenic protein 2 (BMP2+)-chemokine C-X-C motif-ligand-12 (CXCL12+) endosteal/perivascular cell population is recruited during fracture repair, and that BMP2-dependent osteogenic differentiation requires CXCL12 downregulation. We hypothesize that BMP2-CXCL12 axis regulates Prx1 expression during osteoblast differentiation and such regulation is critical for fracture repair. To support our hypothesis we found that mice haploinsufficient for BMP2 in Prx1 expressing cells (BMP2cKO/+), that have impaired fracture healing, have increased Prx1 mRNA levels and such increase positively correlated with increased levels of CXCL12. Immunofluorescence analysis of calluses from BMP2cKO/+ mice showed an increase of CXCL12+/Prx1+ cells, surrounding endothelial CD31+ cells and co-expressing pericyte markers. Tracing studies using Prx1-GFP-CreER-Rosa26-LacZ mice confirmed that Prx1 expressing cells are pericytes and they lose Prx1 expression with osteo-chondrogenic differentiation. Furthermore, in fractured calluses, Prx1 mRNA expression increased rapidly right after fracture, peaked by day 7, decreased by day 10 and continued to decline by day 14. Impaired fracture healing of BMP2cKO/+ mice was rescued when mice were systemically treated with AMD3100, an inhibitor of CXCL12 signaling, that led to a downregulation of both CXCL12 and Prx1 mRNA expressions (Fig). Isolated endosteal cells from BMP2cKO/cKO mice failed to differentiate into osteoblasts and showed increased Prx1 and CXCL12 mRNA levels; AMD3100 treatment restored osteogenic differentiation and normalized both CXCL12 and Prx1 mRNA expressions (Fig). Interestingly, FACS-sorted GFP+ endosteal cells from Prx1GFPcCreER+ mice cultured under osteogenic conditions differentiated in osteoblasts (Fig) and differentiation was associated with a decrease of Prx1 mRNA expression. Taken together, our in vitro and in vivo studies suggest that Prx1 is a downstream target of CXCL12 signaling during BMP2-induced fracture healing, and a downregulation of Prx1 is required for osteoblast differentiation.



Disclosures: *Alessandra Esposito, None*

1152

Regulation Of 4-aminobutyrate Aminotransferase (Abat) by Dnmt3b Regulates Chondrocyte Metabolism and the Development of OA Jie Shen*, Cuicui Wang, Daofeng Li, Ting Wang, Audrey Mcalinden, Regis O'Keefe. Washington University in St Louis, United States

Recent GWAS studies have implicated a distinct DNA methylation signature in OA patients, suggesting that DNA methyltransferases (Dnmt) have a role in regulating cartilage homeostasis. Our work further established that loss of Dnmt3b in articular chondrocytes (ACs) leads to OA progression, at least in part, due to accelerated TCA cycle and elevated mitochondrial respiration. The goal of this study is to determine the downstream targets of Dnmt3b potentially involved in regulating chondrocyte energy metabolism and in the pathogenesis of OA. RNA-seq and Methyl-seq were performed to investigate the downstream targets of Dnmt3b and integrative analysis revealed an enrichment in genes and pathways that regulate cellular energy metabolism in Dnmt3b LOF ACs. Among these gene targets was Abat. Direct analysis of the Abat promoter confirmed that Dnmt3b LOF resulted in reduced methylation in ACs (50% methylation in Control; and 3% methylation in Dnmt3b LOF). qPCR and western blot further showed that Abat gene and protein expression were induced in Dnmt3b LOF ACs and OA patients. Since Abat catalyzes the metabolism of GABA to succinate, HPLC mass spectrometry validated an increase in succinate (300%) level in Dnmt3b LOF ACs. We further evaluated if Abat was involved in regulation of OXPHOS and AC hypertrophy and found that Abat siRNA resulted in a decrease in OXPHOS as reduced basal OCR (50%), maximal OCR (60%), and ATP production (50%). Abat inhibition in Dnmt3b LOF ACs by Vigabatrin blocked the increase in the expression of Col10a1, Mmp13, and Runx2 observed in the Dnmt3b LOF ACs. In contrast, Abat overexpression led to a marked increase in basal OCR (300%), maximal OCR (500%), and ATP production (500%). Overexpression of Abat stimulated AC hypertrophy as reflected by upregulation of Runx2 (250%) and Mmp13 (600%). The deleterious role of Abat was further confirmed in vivo by intraknee overexpression of Abat via lentiviral virus. Histological analysis revealed that Abat overexpression led to advanced osteoarthritic changes with loss of cartilage and development of osteophytes at 6 weeks post DMM surgery (n=10). More importantly, mice treated with Abat inhibitor, Vigabatrin displayed a protective effect against injury-induced OA progression at 6 and 10 weeks post DMM surgery (n=5). OARSI scoring showed marked lower scores in Vigabatrin treated mice. Taken together, Abat is a target of Dnmt3b and Abat mediated energy metabolism plays a critical role in OA progression.

Disclosures: *Jie Shen, None*

1153

Burosumab Improved Serum Phosphorus, Osteomalacia, Mobility, and Fatigue in the 48-Week, Phase 2 Study in Adults with Tumor-induced Osteomalacia Syndrome Suzanne Jan De Beur¹, Paul D. Miller², Thomas J. Weber³, Munro Peacock⁴, Karl L. Insogna⁵, Rajiv Kumar⁶, Frank Rauch⁷, Diana Luca⁸, Christina Theodore-Oklota⁸, Kathy Lamp⁸, Javier San Martin⁸, Thomas O. Carpenter⁹. ¹Johns Hopkins University School of Medicine, United States, ²Colorado Center for Bone Research, United States, ³Duke University, United States, ⁴Indiana University School of Medicine, United States, ⁵Yale University School of Medicine, United States, ⁶Mayo Clinic College of Medicine, United States, ⁷McGill University, Canada, ⁸Ultragenyx Pharmaceutical Inc., United States

Tumor-induced Osteomalacia (TIO) Syndrome, including Epidermal Nevus Syndrome (ENS), is a rare condition in which tumor-produced fibroblast growth factor 23 (FGF23) leads to decreased renal phosphate reabsorption, impaired 1,25(OH)₂D synthesis, and osteomalacia resulting in pain, weakness, fatigue, decreased mobility, and fractures. Burosumab is a fully human monoclonal antibody against FGF23. In the ongoing open-label Phase 2 CL201T study (NCT02304367), 16 adults with TIO and 1 adult with ENS were treated with burosumab for 48 weeks. All subjects received 0.3-2.0 mg/kg every 4 weeks with the exception of 1 subject that received only 1 dose of 0.3 mg and then 2 doses of 0.15 mg/kg at Weeks 8 and 32. Key endpoints were change in serum phosphorus and histomorphometric indices assessed from paired trans-iliac crest bone biopsies. Fatigue, quality of life, and mobility were also assessed. At baseline, mean age was 53 years, mean serum intact FGF23 was 381 pg/mL, and mean serum phosphorus was 1.6 mg/dL. One subject with TIO discontinued treatment prior to Week 48 to treat tumor progression. Mean (SD) serum phosphorus level averaged across the mid-point of the dose interval through Week 24 was 2.73 mg/dL (0.81). Histomorphometric analysis is reported for 11/13 subjects with paired biopsies that showed osteomalacia at baseline. At Week 48, histomorphometric indices improved as demonstrated by increases in mineralizing surface/bone surface (mean percentage change +227%) and decreases in osteoid thickness (-24%), osteoid volume/bone volume (-24%) and mineralization lag time (-45%). Mean (SD) Global Fatigue Score decreased from 5.7 (2.7) at baseline to 3.8 (2.9) at Week 48 (p=0.0008). The mean (SD) physical component summary score on the Short-Form 36 health assessment increased from 33 (11) at baseline to 39 (11) at Week 48 (p=0.009). Additionally, mean (SD) vitality score increased from 41 (14) to 47 (12) (p=0.0057). The mean (SD) number of sit-to-stand repetitions increased from 6.9 (4.2) at baseline to 8.5 (4.2) at Week 48 (n=13; p=0.0006). All subjects experienced ≥1 adverse event (AE). There were 13 drug-related AEs in 6 subjects, none were serious. There were 11 serious AEs in 5 subjects, none of which were drug-related. In adults with TIO Syndrome, burosumab was associated with increases in serum phosphorus; improvements in osteomalacia, mobility, and quality of life; and reductions in fatigue.

Table 1. Histomorphometric Assessments in UX023-CL201T

Assessment	All Subjects* Mean [Median] (SD)	Normal Range (Recker et al. 1988)
Osteoid V / Bone V, %		
Baseline	19.82 [11.00] (18.47)	0.30 - 3.10
Week 48	13.62 [8.10] (15.09)	
Osteoid Thickness, μM		
Baseline	17.63 [13.60] (11.07)	5.50 - 12.00
Week 48	12.17 [8.20] (9.03)	
Osteoid S / Bone S, %		
Baseline	64.27 [57.00] (28.06)	7.0 - 25.0
Week 48	63.00 [64.00] (24.98)	
Mineralizing S / Bone S, days		
Baseline	2.18 [1.75] (1.70)	0.5 - 8.0
Week 48	6.13 [5.10] (4.83)	
Mineralization Lag Time, days		
Baseline	2138.43 [1567.40] (1865.58)	23.0 - 80.0
Week 48	994.53 [329.00] (2137.32)	

*11 subjects with paired biopsies who also showed osteomalacia at baseline are included in the histomorphometric analyses. S, surface; V, volume

Disclosures: *Suzanne Jan De Beur, Ultragenyx Pharmaceutical Inc., Consultant, Ultragenyx Pharmaceutical Inc., Grant/Research Support, Shire plc, Grant/Research Support, Mereo BioPharma Group Ltd, Grant/Research Support*

1154

Efficacy and Safety of Burosumab, a Fully Human Anti-FGF23 Monoclonal Antibody, for Children 1-4 Years Old with X-linked Hypophosphatemia (XLH) Michael P. Whyte^{*1}, Erik Imel², Gary S. Gottesman¹, Meng Mao³, Alison Skrinar³, Javier San Martin³, Thomas O. Carpenter⁴. ¹Shriners Hospitals for Children, United States, ²Indiana University School of Medicine, United States, ³Ultragenyx Pharmaceutical Inc., United States, ⁴Yale University School of Medicine, United States

In children with X-linked hypophosphatemia (XLH), high circulating levels of fibroblast growth factor 23 (FGF23) cause hypophosphatemia with consequent rickets, skeletal deformities, and growth impairment. We have reported that treatment with burosumab, a fully human monoclonal antibody against FGF23, improved phosphate homeostasis and rickets in 5-12 year-old children with XLH. Study CL205 (NCT02750618) is an open-label, multicenter investigation of the efficacy and safety of burosumab in 13 1-4 year-old children with XLH. Each child received burosumab 0.8 mg/kg SC Q2W, increased to 1.2 mg/kg if hypophosphatemia persisted, for 64 weeks with the option to enroll in an extension study. The primary endpoint was change from baseline in serum phosphorus at Week 40. Other key endpoints included change in rickets severity at Weeks 40 and 64 based on the Thacher Rickets Severity Score (RSS) and the Radiographic Global Impression of Change (RGI-C). All 13 children (mean age 2.9 years; 69% male) completed 64 weeks of burosumab treatment. Though all children had received conventional therapy before enrollment (mean duration 16 months), rickets was apparent at baseline (85% of children had Total RSS \geq 2.0). Rickets, as assessed by RSS, RGI-C, and serum alkaline phosphatase (ALP) activity, significantly improved (Table 1). At Weeks 40 and 64, mean RSS decreased by 59% and 69%, respectively. All children achieved substantial healing (RGI-C Global Score \geq +2.0) by Week 40. Lower limb bowing improved, with 2 and 4 children achieving a lower extremity RGI-C \geq +2.0 at Weeks 40 and 64, respectively. Significant decreases in ALP at Week 40 (-39%) were maintained at Week 64. Consistent with our findings in older children with XLH, serum phosphorus and 1,25(OH)₂D levels increased, with mean values reaching within the normal range. All children experienced \geq 1 adverse event (AE). One child had a serious AE, dental abscess, that was considered unrelated to treatment. All other AEs were mild or moderate, except for a Grade 3 food allergy unrelated to study drug. No child discontinued therapy, showed hyperphosphatemia, or had clinically meaningful increases in circulating calcium or PTH. Consistent with findings in older children with XLH treated with burosumab, Q2W burosumab significantly improved phosphate homeostasis and rickets in 1-4 year-old children with XLH.

Table 1. Burosumab through Week 64 for 1-4 Year-old Children with XLH

Assessment	Q2W (N=13)
Serum Phosphorus, mg/dL, mean (SE)	
Baseline	2.51 \pm 0.08
Week 40	3.47 \pm 0.14 ^a
Week 64	3.40 \pm 0.13 ^a
Serum 1,25(OH)₂D, pg/mL, mean (SE)	
Baseline	45 \pm 5
Week 40	57 \pm 3 ^b
Week 64	56 \pm 3 ^a
Serum ALP, U/L, mean (SE)	
Baseline	549 \pm 54
Week 40	335 \pm 24 ^a
Week 64	334 \pm 22 ^a
RSS Total Score, mean (SE)	
Baseline	2.9 \pm 0.4
Week 40	1.2 \pm 0.1 ^a
Week 64	0.9 \pm 0.1 ^a
RGI-C Global Score, LS mean (SE)	
Week 40	+2.33 \pm 0.07 ^a
Week 64	+2.23 \pm 0.11 ^a
RGI-C Lower Limb Score, LS mean (SE)	
Week 40	+1.26 \pm 0.13 ^a
Week 64	+1.56 \pm 0.12 ^a

^ap<0.0001 and ^bp<0.001 based on LS mean change from baseline. Lower RSS and Higher RGI-C values indicate improvement.

Disclosures: **Michael P. Whyte**, Ultragenyx Pharmaceutical Inc., Consultant, Ultragenyx Pharmaceutical Inc., Grant/Research Support

1155

Incidence of Malignancies in Fibrous Dysplasia: Data from a National Pathology Cohort Marlous Rotman^{*}, Neveen Hamdy, Bas Majoor, Michiel Van De Sande, Judith Bovee, Sander Dijkstra, Olaf Dekkers, Natasha Appelman-Dijkstra. LUMC, Netherlands

Fibrous dysplasia (FD) is reported to be associated with increased risk for breast and thyroid cancer and for the pre-malignant intraductal papillary mucinous neoplasm (IPMN), possibly due to extra-skeletal tissue distribution of GNAS-mutations. Data on further associations of FD with malignant tumors are scarce. Since these associations may have significant clinical implications, we performed a cohort study on tumor occurrence in FD. Pathology reports from patients with confirmed FD were retrieved from the Dutch National pathology registry (PALGA). Incidence rates for malignant tumors were estimated and compared between FD patients and the general Dutch population by calculating standardized morbidity ratios (SMR). In this study, SMRs were calculated for all histologically confirmed FD/GNAS-associated and bone tumors. We also studied the FD associated risk for the three most common malignancies in the Netherlands, e.g. prostate, colorectal and skin cancer; our data on breast cancer have been reported previously. Of the 1146 PALGA FD patients, 177 (M/F; 79/98) also had histological evidence for a malignant tumor. Mean age at FD diagnosis was 47.0 years (1-86yr) and mean age at diagnosis of malignancy was 49.7 years (2-92yr). 207 malignant tumors were documented. Among known GNAS-related and bone tumors, SMR was increased for thyroid cancer (3.71[95%CI 1.13-7.76]) and for osteosarcoma (26.31[95%CI 6.58-59.20]). For the three most prevalent malignancies in The Netherlands, SMRs were increased for prostate cancer (3.08[95%CI 1.82-4.63]) and melanoma (1.99[95%CI 1.05-2.94]), but not for colorectal cancer. Our data confirm that patients with FD have an increased risk for thyroid cancer and osteosarcoma. We also report for the first time an increased risk for a number of other malignancies in FD such as melanoma and prostate cancer, which both have not previously been associated with GNAS-mutations, but no increased risk for pancreatic cancer was found. Our findings raise awareness for the risk of malignancy in FD, although caution should be exerted in the interpretation of these data, as true incidence rates of malignancy might have been underestimated by the inclusion in this study of only patients with histologically-confirmed FD, and the specific role of GNAS mutations in the pathophysiology of FD-related tumors is as yet to be unraveled.

Disclosures: **Marlous Rotman**, None

1156

Abnormal Monocyte Responses in Fibrodysplasia Ossificans Progressiva Emilie Barruet^{*1}, Blanca M Morales¹, Tania Moody¹, Corey J Cain¹, Kelly Wentworth¹, Tea V Chan¹, Amy Ton¹, Tom Hm Ottenhoff², Mariëlle C. Haks², Judith Hellman¹, Mary Nakamura³, Edward C Hsiao¹. ¹UCSF, United States, ²Leiden University Medical Center, Netherlands, ³UCSF/VAMC, United States

Heterotopic ossification (abnormal bone formation in soft tissue) is known to be triggered in inflammatory settings, although the underlying mechanisms are poorly understood. Diseases of heterotopic bone formation such as fibrodysplasia ossificans progressiva (FOP) give valuable insights into human-specific mechanisms of increased bone formation. FOP is associated with mutations in the Activin A type I receptor (ACVR1), a BMP receptor that increases ACVR1 signaling activity and response to both BMP and Activin A ligands. FOP is characterized by progressive and debilitating heterotopic ossification, often occurring in inflammatory flares with pain, erythema, swelling, and localized edema. The forming bone lesions contain multiple cell types, including large numbers of macrophages that may play a key role in modulating osteogenesis. We previously showed that FOP patients have increased serum cytokine levels associated with a chronic inflammatory state. We hypothesized that patients with FOP are in a pro-inflammatory state that increases their sensitivity to inflammatory insults. Using carefully-obtained samples of blood from FOP subjects and relatives, we tested the activation of CD14⁺ primary monocytes with toll-like receptor (TLR) ligands including lipopolysaccharide (LPS), and used immunofluorescence quantification analyses to assay the BMP and NFB pathways. We also analyzed the different subtypes (classical, intermediate and non-classical) of monocytes present in whole blood of FOP patients and found a significant increase in the intermediate monocyte population that is thought to be pro-inflammatory. TLR4 activation by LPS of FOP CD14⁺ primary monocytes increased CCR7 and CXCL10 expression as well as pro-inflammatory cytokine (IL-1RA, IL-3, IL-15, IL-17A), chemokine (MIP-1 α , CCL1), and growth factor (EGF, VEGF) production via prolonged activation of the NFB pathway. Together, these results suggest a pro-inflammatory state at baseline in FOP patients that can be detected in primary monocytes from FOP patients. The insights gained from these studies indicate that modulation of the inflammatory state may be a key strategy for mitigating the devastating progression of FOP. Further study of the inflammatory responses will help identify how disruptions of the normal bone-regulating roles of monocytes and macrophages trigger heterotopic bone formation, and whether these immune targets may be amenable to modulation as part of a comprehensive treatment strategy.

Disclosures: **Emilie Barruet**, None

1157

Albright Hereditary Osteodystrophy (AHO): autosomal dominant shortening of metacarpals and -tarsals caused by a novel splice-site mutation in PTHLH Monica Reyes*¹, Bert Bravenboer², Harald Jüppner¹. ¹Endocrine Unit, Massachusetts General Hospital, United States, ²Department of Endocrinology, Universitair Ziekenhuis Brussel, Belgium

Shortening of metacarpals and/or -tarsals is typically observed in pseudohypoparathyroidism (PHP) type Ia (PHP1A) or pseudo-PHP (PPHP), related disorders that are caused by GNAS mutations involving those exons that encode the α -subunit of the stimulatory G protein (*G α s*). PHP1A patients also develop PTH-resistant hypocalcemia and often resistance to other hormones, while PPHP patients show no hormonal abnormalities. We now investigated a large Caucasian family with shortened metacarpals and -tarsals, as well as reduced adult height. The proband (190/II-1) had normal serum calcium and phosphate levels (2.34 mmol/L and 1.18 mmol/L, respectively), PTH was slightly elevated (75.7 pg/ml) despite a normal 25-OH vitamin D level (39.1 ng/ml); TSH was normal. Nucleotide sequence analysis of GNAS exons 1-13 provided no evidence for a mutation and no epigenetic GNAS changes were detected. Skeletal abnormalities were present also in the proband's sister (190/II-2),

one of this sister's daughters (190/III-1) and two of her three grandchildren (190/IV-1, 190/IV-2), who all had normal calcium, phosphate, PTH, and TSH levels. Whole exome sequencing of the proband's genomic DNA revealed a heterozygous A>G change at nucleotide -3 of PTHLH exon 3 that encodes the last two amino acids of the Pre-Pro sequence and the secreted PTHrP(1-139). The same nucleotide change was also found in the four available family members with similarly shortened metacarpals and -tarsals, but not in two unaffected family members and unrelated spouses. Furthermore, the nucleotide change in PTHLH was not found in public databases thus raising the possibility that it causes the skeletal abnormalities. Complementary DNA derived from immortalized lymphoblastoid cells of the affected male 190/IV-2 and his unaffected sister 190/IV-3 was PCR-amplified using forward primers located in either PTHLH exon 1 or 2, and a reverse primer located in the 3'-non-coding region of exon 3. Nucleotide sequence analysis of both amplicons from 190/IV-2, but not 190/IV-3, revealed a heterozygous insertion of genomic nucleotides -2 and -1 at exon 3, which causes a frame-shift after residue 34 of the PrePro sequence thus encoding 29 novel amino acids that share no homology with PTHrP or any other protein. Our findings extend previous reports indicating that PTHrP haploinsufficiency causes of AHO-like features, which are similar to those observed with GNAS mutations, but do not affect the regulation of mineral ion homeostasis.

Disclosures: Monica Reyes, None

LB-1158

Bone marrow-derived CXCL12 is indispensable for the loss of cortical bone mass caused by estrogen deficiency Filipa Ponte*, Aaron Warren, Ha-Neui Kim, Iyer Srividhya, Li Han, Maria Almeida, Stavros Manolagas. UAMS, United States

The protective effects of estrogens against cortical and cancellous bone loss result from ER α signaling on distinct cell types: mesenchymal cells (targeted by Prx1 or Osx1-Cre) and cells of the myeloid lineage (targeted by LysM-Cre), respectively. However, functional evidence for the ER α gene targets and the molecular changes and mediators of the adverse effects of estrogen deficiency in the two bone compartments is lacking. CXCL12 is a C-X-C motif containing chemo-attractant abundantly expressed in Prx1 cells of the bone marrow and indispensable for B-lymphopoiesis. The mRNA and secreted protein levels of CXCL12 are increased in ER α null bone marrow cells from female ER α fl/Prx1-Cre mice; and so is osteoclastogenesis in co-cultures of ER α null BM stromal or calvaria cells with macrophages. Furthermore, ovariectomy (OVX) increases CXCL12 in the bone marrow plasma in mice and administration of E2 prevents it. To functionally determine whether the increase of CXCL12 with estrogen deficiency contributes to the loss of cortical bone mass and/or the increase in B-cells, we have generated mice with conditional deletion of a CXCL12 allele in mesenchymal progenitors expressing Prx1 (CKO mice). CXCL12-floxed (control) and CKO littermate mice were ovariectomized (OVX) at 4.5 months of age and 6 weeks later sacrificed for analysis. CXCL12 mRNA in bone marrow-derived stromal cell cultures from CKO mice was decreased by more than 90%. Total body weight and cortical thickness (measured by micro-CT) in the mid-shaft of the femur were indistinguishable between estrogen-sufficient control and CKO mice. The number of CD19+ B cells was, however, dramatically decreased in the CKO mice. Loss of estrogens caused the expected decrease in cortical thickness in the control mice. This effect was completely prevented in the CKO mice. OVX increased B cell number in the bone marrow of control mice, but in spite of the low number of B cells in the CKO mice, B cell number increased following OVX. These results demonstrate that mesenchymal/stromal cell-derived CXCL12 is an indispensable mediator of the loss of cortical bone mass, but not the increase in B-cells, caused by estrogen deficiency in mice.

Disclosures: *Filipa Ponte, None*

LB-1159

Marrow adiposity and vascular morphology are regulated by EBF1 in adult bone Seham Alruwaili*, Steven Tommasini², Ben-Hua Sun², Jackie Fretz². ¹Quinnipiac University, United States, ²Yale School of Medicine, United States

EBF1-KO mice have a low bone phenotype. These global knockouts, however, are heavily influenced by the consequences of EBF1-loss from extra-skeletal tissues including kidney development and systemic adiposity changes. Although Osx- and Runx2- driven deletion models of EBF1 have been described with relatively modest phenotypes, we present here that Prx1-driven conditional deletion of EBF1 to the entire mesenchymal lineage results in a prolific increase in marrow adiposity, and aberrations to the cortical vascular network. Young mice, up to 3 months of age had no overt bone phenotype when they were examined by μ CT for bone quality and osmium staining for quantification of marrow adiposity. By contrast, 6 month old animals developed a significant increase in marrow adiposity (increased over 10 fold) without any alteration of the BV/TV, TbN, TbTh, TbSp, cortical radii or thicknesses, nor BS/BV in either the trabecular or cortical region. Upon histological examination, marrow adiposity was greatly increased, and large portions of the marrow space was occupied by dilated sinusoids. Using FACS the CD45-CD34+ endothelial population was increased in Prx1-cre:Ebfl/fl mice. Higher resolution nano-CT revealed that small voids representing osteocyte lacunae were present in both genotypes at equal number and quantity. Larger voids in the bone that trace the vascular network were expanded in the Prx1-cre:Ebfl/fl animals (0.55 + 0.07% vs. 0.95 + 0.40%). Their pathway through the cortex were more distended and torturous in Prx1-cre:Ebfl/fl mice, and large diameter vessels (50-200 μ m) vertically traversing the cortex were uniquely present in the knockouts. FACS separation of various mesenchymal progenitors in 6 month old animals revealed that the abundance of PDGFR α + and PDGFR β + perivascular cell number increased. Markers of other populations, like α SMA were unchanged. This suggests a selective shift in the identity of the MSCs populating Prx1-cre:Ebfl/fl bones. Taken together these data indicate that EBF1 has an integral role in regulating the formation of marrow adipocytes from perivascular progenitors, and functions through these support cells to regulate the bone vascular network of the adult skeleton. It also illustrates a situation where marrow adiposity can increase without a decrease in bone volume. Future research into the mechanism of this phenotype may be useful in enhancing our understanding and treatment of vascular bone diseases.

Disclosures: *Seham Alruwaili, None*

LB-1160

Conditional ablation of Prx1 expressing cells impairs endochondral ossification in postnatal bone repair Lai Wang*, Alessandra Esposito¹, Joseph Temple¹, Tieshi Li¹, Jie Jiang¹, Xin Jin^{1,2}, Anna Spagnoli¹. ¹Department of Pediatrics, Rush University Medical Center, Chicago, United States, ²Department of Orthopaedics, Union Hospital, Tongji Medical College, Huazhong University of Science and Technology, Wuhan, 430022, P.R. China

Fracture healing is a complex process involving endochondral and intramembranous ossification. Cells from the periosteum and endosteum contribute significantly to callus formation through endochondral ossification. Prx1 is postnatally expressed in the periosteum and endosteum, and Prx1CreER transgene-expressing cells are confirmed as osteochondral progenitor cells. In this study, we used Prx1CreER;R26tdTomato to trace the Prx1 expressing progenitor cells, and used Prx1CreER;R26DTA mice to determine the effect of cell ablation of Prx1 expressing cells in fracture healing. Male mutant mice and their littermate controls were subjected to tibia fracture at postnatal age 10-12 weeks. 4-hydroxymoxifen was administered for 6 days started two days before fracture. Mice were euthanized 14 days after fracture. Immunofluorescence analysis showed co-expression of Sox9 and Osx with tdTomato in the callus of Prx1CreER;R26tdTomato mice, confirming that chondrocytes and osteoblasts in the callus are derived from Prx1 progenitor cells. Contrast-enhanced microCT imaging was performed using contrast agent phosphotungstic acid (PTA) to analyze the callus cartilage. MicroCT-PTA imaging analyses revealed that the volume of soft callus was significantly decreased in Prx1CreER;R26DTA mice compared to their control littermates (13.23 \pm 3.48 vs. 8.23 \pm 1.39 mm³, n=3 of each group, p<0.05). Immunofluorescence analyses by confocal microscopy showed that tdTomato fluorescence was decreased in the callus of Prx1CreER;R26DTA;R26tdTomato mice, so did the expression of chondrocyte marker Sox9 and osteoblast marker Osx. In Prx1CreER;R26DTA mice, the decrease in cartilage formation was also detected by Safranin O/Fast Green staining. Interestingly, the fracture callus of Prx1CreER;R26DTA mice showed an increased neovascularization. Quantification with PECAM1+ vessel counting showed a 31.9% of increase in microvessel density in calluses from Prx1CreER;R26DTA mice [1.00 \pm 0.11 for control group (n=5), vs. 1.32 \pm 0.25 for DTA group (n=7), the numbers of PECAM1+ vessels per field were normalized to the control group, p<0.05]. These data indicate that the Prx1-progenitors mediate endochondral ossification. The increased angiogenesis in the callus of Prx1CreER;R26DTA mutant mice may indicate that the failure in bone repair is compensated with increased vascularization.

Disclosures: *Lai Wang, None*

LB-1161

WITHDRAWN

LB-1162

LRP5-deficiency in OsxCreERT2 mice recapitulates intervertebral disc degeneration from aging and mechanical compression Jiannong Dai*, Matthew Silva², Nilsson Holguin¹. ¹IUPUI, United States, ²Washington University in St. Louis, United States

Intervertebral disc (IVD) degeneration putatively activates differentiation of prehypertrophic chondrocyte-like cells. Osterix is a critical transcription factor in mesenchymal stem cell fate, where its loss or loss of WNT signaling diverts differentiation to a chondrocytic lineage, but its role in IVD degeneration and aging is unclear. Using immunofluorescence, osterix was expressed in (pre)osteoblasts of 5 mo and 12 mo vertebra and in the cells of the outer annulus fibrosus (AF) and nucleus pulposus (NP) of healthy 5 mo IVD, but declined with aging (Fig. 1A). IVD degeneration and aging inactivated WNT signaling. Therefore, we suppressed LRP5 (WNT ligand receptor) in 4 mo mice that inducibly targeted osterix-expressing cells (OsxCreERT2) and report WNT signaling (TOPGAL, LRP5 cKO, n=10). Wild-types served as controls (LRP5fl/fl/TOPGAL, WT, n=9). LRP5 cKO and WT were analyzed by histology, qPCR and mechanical testing. In IVDs, depletion of LRP5 in osterix-expressing cells inactivated WNT signaling (Fig. 1B) in the NP by 95% and AF by 45%, reduced osterix expression by 75% (Fig. 1C), degenerated the IVD (Fig. 1D, E) and reduced the compressive and tensile stiffness by 45%. Using RNA-sequencing, LRP5-deficiency in osterix-expressing cells upregulated notochordal cell markers in the IVD. Next, we determined the histological score of young-adult (5 mo) and aged IVD (18 mo) subjected to 1 week of tail compression (model of IVD degeneration, n=5/age). QPCR quantified the expression of genes related to transcription factors (Osterix, RUNX2) and hypertrophic chondrocyte marker MMP13 in 5 mo and 12 mo IVDs subjected to tail compression (n=5-7/age). Adjacent, non-compressed IVD served as controls. Similar to LRP5 cKOs, aging and mechanical compression induced IVD degeneration, but with the most degeneration noted in compressed 18 mo IVD (Fig. 1E). Similarly, aging and compression reduced osterix expression with superposition effects (Fig. 1C). MMP13 expression, and similarly RUNX2, was elevated by compression of IVD, but less so in 12 mo IVD, suggesting a muted expansion of hypertrophic chondrocyte-like cells with aging. Overall, these data show that IVD cells express osterix and inactivation of WNT signaling in these cells can lead to IVD degeneration similar to aging. These data suggest that aging may limit regeneration by depleting the cells necessary to differentiate and/or proliferate prehypertrophic chondrocyte-like cells during IVD degeneration.

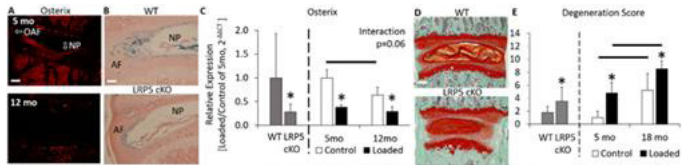


Figure 1. Loss of Osterix-expressing cells via loss of WNT signaling contributes to intervertebral disc degeneration. (A) Fluorescence (Ox/CreERT2-Ai9/td) of Osterix (red, arrows) in the nucleus pulposus (NP) and outer annulus fibrosus (OAF) decreased with aging between 5 and 12 months of age. (B) WNT signaling (blue) in WT (TOPGAL/Lrp5^{fl}) and LRP5 cKO (TOPGAL/Lrp5^{fl}/Ox-CreERT2) mice showing loss with Lrp5-deficiency. (C) Gene expression of Osterix declines with inactivated WNT, aging and compression. (D) Safranin-O images of LRP5 cKO and WT IVD. (E) Greater intervertebral disc degeneration in LRP5 cKO than WT. Aging (5 vs 18 mo), mechanical compression (Control vs Loaded) and in combination induce intervertebral disc degeneration in a respectively increasing order. Scale: (A, D) 100 μ m, (B) 50 μ m. *: vs Control and bar: vs 5 mo, p<0.05

Disclosures: **Jiannong Dai, None**

LB-1163

Childhood Obesity and Fracture Risk: A Region-wide Longitudinal Cohort Study of 466,000 Children and up to 11 Years of Follow-up Daniel Prieto-Alhambra^{*1}, Katherine Butler², Jose Poveda^{3,4}, Daniel Martinez-Laguna^{3,4}, Carlen Reyes^{3,4}, Jennifer Lane¹, Jeroen De Bont^{3,4}, M Kassim Javaid¹, Cyrus Cooper^{1,5}, Jennifer Logue⁶, Talita Duarte-Salles^{3,4}, Dominic Furniss¹. ¹NDORMS, University of Oxford, United Kingdom, ²Stoke Mandeville Hospital, United Kingdom, ³Institut Universitari d'Investigació en Atenció Primària Jordi Gol (IDIAP Jordi Gol), Spain, ⁴CIBERFes, Universitat Autònoma de Barcelona and Instituto de Salud Carlos III, Spain, ⁵MRC Lifecourse Epidemiology Unit, University of Southampton, United Kingdom, ⁶University of Glasgow, United Kingdom

Objectives.As childhood obesity increases, there is growing interest in the impact of Body Mass Index (BMI) upon bone health. This study investigated if there is an association between childhood BMI and fracture risk. **Methods.**A prospective cohort of children with a valid primary care BMI measurement in Catalonia, Spain at age 4 years (± 6 months) between 1/1/2001 and 31/12/2013 were identified in SIDIAP database, and followed up until they turned 15, migrated, died, or until 31/12/2016. Fractures were defined using validated ICD10 codes recorded in primary care. Childhood cumulative incidence (age 4 to 15 years) was calculated by anatomical location and stratified by BMI category (WHO 2007 growth reference). Cox models were used to estimate Hazard Ratios (HR) according to BMI. Results. Of 466,997 children, 9250 (2.0%) had obese range BMIs, 26526 (5.7%) overweight, and 540 (0.1%) underweight range BMIs. We identified 20878 incident fractures. The cumulative incidence of upper limb fracture for children with obese range BMIs was 76.1 per 10,000 (95%CI 58.4-81.1), compared to 62.1 (59.8-63.4) for normal BMI. Lower limb fracture cumulative incidence was 28.7 per 10,000 (18.0-34.1) in those with obese range BMIs and 15.1 (13.9-15.7) in children with normal range BMI. Using BMI as a continuous variable, adjusted hazard ratios (HR; 95%CI) were 1.05 (1.03-1.06) per 1 standard deviation increase for forearm fractures, 1.08 (1.05-1.12) for hand fractures, 1.14 (1.09-1.20) for ankle fractures and 1.15 (1.10-1.19) for foot fractures. Divided by WHO categories, compared to those with normal range BMI, children with obese range BMIs had an adjusted HR (95%CI) of 1.14 (1.0-1.29) for forearm fractures, 1.37 (1.14-1.66) for hand fractures, 1.66 (1.32-2.10) for foot fractures and 1.81 (1.37-2.37) for ankle fractures. Further adjustment for birthweight (available for 310,751 children) did not affect these estimates. **Conclusions.** Childhood obesity is associated with a significantly increased risk of forearm, hand, ankle, and foot fractures. The effect of increased BMI upon fracture risk in adults appears to extend to the paediatric population.

Disclosures: **Daniel Prieto-Alhambra, UCB, Consultant, Amgen, Speakers' Bureau, Servier, Grant/Research Support, Amgen, Grant/Research Support, UCB, Grant/Research Support**

LB-1164

Does Cortical Porosity Predict Incident Fractures in Postmenopausal Women? Camilla Andreassen^{*1}, Åshild Bjørnerem². ¹Department of Clinical Medicine, UiT The Arctic University of Norway, Tromsø, Norway, Department of Orthopaedic Surgery, University Hospital of North Norway, Tromsø, Norway, ²Department of Clinical Medicine, UiT The Arctic University of Norway, Tromsø, Norway, Department of Obstetrics and Gynecology, University Hospital of North Norway, Tromsø, Norway

Measurement of areal bone mineral density (aBMD) using dual-energy x-ray absorptiometry, online Fracture Risk Assessment Tool (FRAX) and the Garvan Fracture Risk Calculator based on clinical risk factors are commonly used approaches for assessment of fracture risk. However, these approaches have limitations and additional bone measurements may enhance the predictive ability of these existing tools. In cross-sectional studies, women with fracture have higher cortical porosity, thinner cortices and smaller cortical cross-sectional area (CSA) than controls. Cortical porosity and thickness are associated with fracture risk independent of aBMD and FRAX, and cortical porosity improved net reclassification of women with fracture compared with FRAX alone. Whether cortical porosity predicts inci-

dent fractures in unclear. We wanted to examine whether cortical porosity of the proximal femur predicts incident fractures (non-vertebral and vertebral) independent of aBMD during 5 years follow-up of postmenopausal women. In this prospective study we pooled 211 postmenopausal women aged 54-94 years at baseline, with prevalent nonvertebral fractures (181 wrist, 26 proximal humerus and 4 hip), and 232 fracture-free controls in a nested case-control study from the Tromsø Study in Norway. We assessed femoral neck (FN) aBMD, and calculated FRAX 10-year probability of major osteoporotic fracture and Garvan 10-year risk for any fragility fracture, and quantified femoral subtrochanteric cortical porosity, thickness, and CSA from CT images using StrAx software. During a mean follow-up of 5.2 years, 80 (18.1%) of 443 women had an incident fracture (28 forearm, 7 proximal humerus, 4 clavicle, 1 rib, 7 hand, 9 hip, 2 patella, 7 ankle, 8 foot, 7 spine). Per standard deviation (SD) higher cortical porosity, thinner cortices, and smaller cortical CSA, hazard ratio (HRs) (95% confidence interval) for fracture were 1.07 (0.86-1.33), 0.97 (0.77-1.21), and 1.15 (0.92-1.44), respectively, all p > 0.10. Cortical porosity of the inner transitional zone predicted incident fractures marginally, HR was 1.23 (0.96-1.56), p = 0.081 adjusted for age, height, weight and prior fracture, and 1.16 (0.91-1.47), p = 0.231 when additionally adjusted for FN aBMD. Per SD higher FN aBMD, FRAX and Garvan estimates, HRs were 1.40 (1.06-1.86), 1.21 (1.01-1.45), and 1.31 (1.11-1.55), respectively, all p < 0.05. Based on this data, FN aBMD, FRAX and Garvan estimates predicted incident fractures in women but cortical porosity did not.

Disclosures: **Camilla Andreassen, None**

LB-1165

Nursing Home Trends in Hip Fracture Rates Follow the Plateau Observed in U.S. Women Sarah Berry^{*1}, Lori Daiello², Andrew Zullo², Kevin McConeghy², Tingting Zhang², Yoojin Lee², Jeffrey Curtis³, Nicole Wright³, Vincent Mor², Douglas Kiel¹. ¹Hebrew SeniorLife, Institute for Aging Research, United States, ²Brown University School of Public Health, United States, ³University of Alabama at Birmingham, School of Public Health, United States

Purpose.A recent U.S. population-based study suggested a decline in the incidence of hip fracture (fx) between 2002-2012 among women in Medicare, followed by a leveling in the rate from 2013-2015. Newly admitted nursing home (NH) residents are particularly vulnerable to hip fx, and it is unclear whether that trend is observed in this high risk group. The purpose of our study was to describe trends in hip fx rates among 2.6 million newly admitted U.S. NH residents from 2007 to 2015, and to examine whether these trends could be explained by differences in resident characteristics. **Methods.** Medicare claims data were linked with the Minimum Data Set (MDS), a federally mandated clinical assessment performed quarterly on NH residents. In each year (2007-2015) we identified newly admitted long-stay (≥ 100 days in the same facility) NH residents. We restricted the sample to residents aged ≥ 65 years enrolled in Medicare Part A. Hip fx was defined using Part A diagnostic codes (ICD-9 & ICD-10). Follow-up time was calculated from the index date until the first hospitalized hip fx event, Medicare disenrollment, death or one year. Incidence rates were calculated as the number of hip fx divided by follow-up time. Poisson regression was used to adjust rates for age, sex, cognition, and transfer dependence. **Results.** The number of newly admitted NH residents decreased from 324,508 in 2007 to 261,550 in 2015. Mean age was similar across the years, but residents were more dependent in transfers over time (50% in 2007 to 64% in 2015). The unadjusted incidence rate of hip fracture decreased from 3.55/100 person-years in 2007 to 3.16/100 person-years in 2013 (Table), with a leveling or modest increase in the rate in 2014-2015. Mortality was relatively constant over time. The adjusted hip fracture rates were lower in magnitude with overlapping confidence intervals, but followed a similar trend as the unadjusted rates with a leveling of the decline in 2013. **Conclusions:** We observed a recent plateau in the incidence rates of hip fx among NH residents, similar to the trend observed in a sample of community-dwelling U.S. women. NH residents have become more functionally dependent, which might be expected to reduce the risk of fx. However, our findings may not be fully explained by differences in mortality, cognition, or transfer dependence. More investigation is required to understand the reason for the leveling in hip fx rates in a high risk NH population.

Year	N	Age Mean(SD)	Female n (%)	Dependent in transfers n (%)	1 year mortality n (%)	1 year hip fx n (%)	Unadjusted IR/100 person yrs (95% CI)	Adjusted IR**/100 person yrs (95% CI)
2007	324,508	84 (8)	223,154 (69)	161,853 (50)	89,940 (28)	5,580 (3.0)	3.55 (3.48, 3.62)	2.70 (2.58, 2.83)
2008	315,270	84 (8)	215,855 (69)	164,034 (52)	84,794 (27)	5,242 (2.9)	3.54 (3.47, 3.61)	2.72 (2.59, 2.85)
2009	299,825	84 (8)	203,100 (68)	163,080 (54)	79,225 (26)	4,681 (2.9)	3.51 (3.44, 3.59)	2.73 (2.60, 2.86)
2010	292,778	83 (8)	197,170 (67)	164,122 (57)	79,567 (27)	4,314 (2.8)	3.38 (3.30, 3.46)	2.67 (2.54, 2.81)
2011	299,964	83 (8)	203,330 (67)	173,764 (58)	79,199 (26)	3,737 (2.7)	3.27 (3.19, 3.34)	2.60 (2.47, 2.73)
2012	282,570	83 (8)	188,389 (67)	169,736 (62)	77,086 (27)	3,383 (2.6)	3.22 (3.14, 3.30)	2.62 (2.49, 2.75)
2013	274,501	83 (8)	181,085 (66)	167,667 (63)	72,288 (26)	3,075 (2.6)	3.16 (3.09, 3.24)	2.60 (2.47, 2.73)
2014	263,427	83 (8)	167,412 (65)	162,993 (64)	72,603 (28)	6,900 (2.6)	3.22 (3.14, 3.31)	2.67 (2.54, 2.81)
2015	261,550	83 (8)	167,412 (65)	161,601 (64)	69,018 (27)	6,789 (2.6)	3.27 (3.18, 3.35)	2.73 (2.60, 2.87)

* Defined as requiring extensive or total assistance with transfers; < 3% missing
** Adjusted for age, sex, cognition, and transfer dependence

Disclosures: **Sarah Berry, Walters Kluwer, Other Financial or Material Support**

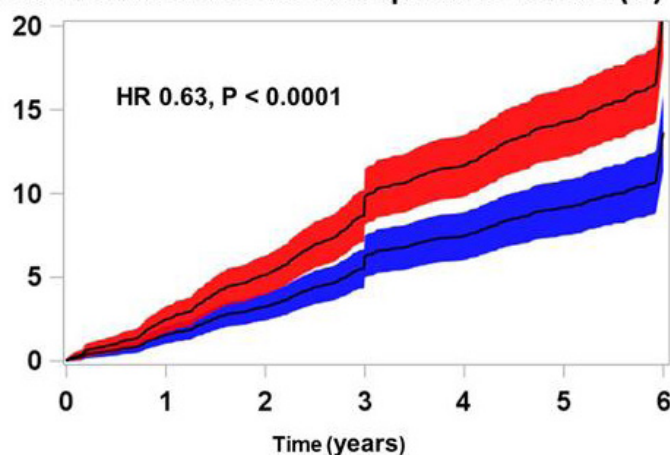
LB-1166

Fracture Prevention in Osteopenic Postmenopausal Women with Zoledronic Acid Every 18 Months, a Randomized Controlled Trial Ian Reid^{*}, Anne Horne, Borislav Mihov, Mark Bolland, Sonja Bastin, Greg Gamble. University of Auckland, New Zealand

Bisphosphonates prevent fractures in patients with osteoporosis but their efficacy in women with osteopenia is unknown. Most fractures in postmenopausal women occur in

osteopenic individuals, so if pharmaceutical intervention is to impact significantly on total fracture numbers, therapies with efficacy in osteopenic postmenopausal women are needed. We report a 6-year, double-blind trial of 2000 osteopenic (i.e. hip T-scores between -1.0 and -2.5) postmenopausal women aged >65 years recruited using electoral rolls. They were randomly assigned to receive 4 infusions of either zoledronic acid 5mg, or normal saline at 18-month intervals. Supplements of vitamin D, but not calcium, were provided. Baseline mean age was 71 (SD 5) years, femoral neck T-score -1.5 (0.5), and median 10-year hip fracture risk 2.3% by FRAX. The primary endpoint of osteoporotic fracture (i.e. osteoporotic non-vertebral fractures or vertebral fractures) occurred in 190 women in the placebo group (227 fractures) and in 122 women in the zoledronic acid group (131 fractures), hazard ratio (HR) 0.63 (95%CI 0.50, 0.79; $P < 0.0001$). The number needed to treat to prevent one woman fracturing was 15. Anti-fracture efficacy was unaffected by baseline BMD, prevalent fracture, calculated fracture risk, age, BMI, or calcium intake. Non-vertebral osteoporotic fractures (HR 0.66, $P = 0.0014$), symptomatic fractures (HR 0.73, $P < 0.0027$), vertebral fractures (odds ratio 0.45, $P = 0.0018$), and height loss ($P < 0.0001$) were also reduced in the zoledronic acid group. There were 41 deaths in the placebo group and 27 in the zoledronic acid group (odds ratio 0.65, 95%CI 0.40, 1.05). Rate ratios for other pre-specified adverse events were: myocardial infarction 0.58 (0.35, 0.94), composite vascular endpoint 0.72 (0.53, 0.98), and cancer 0.68 (0.52, 0.89). Rate ratio for breast cancer was 0.59 (0.35, 0.98). Zoledronic acid prevents fractures in osteopenic women aged >65 years, substantially broadening the target population for pharmaceutical intervention to prevent fractures. The beneficial effects on cancer and vascular disease are consistent with data from some previous studies and suggest that zoledronic acid should be formally trialled for the prevention of these conditions.

Cumulative Incidence Osteoporotic Fracture (%)



Disclosures: **Ian Reid**, Novartis, Other Financial or Material Support

LB-1167

Fracture Risk after Stopping Adjuvant Denosumab in Hormone Receptor Positive Breast Cancer Patients on Aromatase Inhibitor Therapy – an Analysis of 3,425 Postmenopausal Patients in the Phase III ABCSG-18 trial
 Georg Pfeiler¹, Guenther G. Steger², Daniel Egle³, Richard Greil⁴, Florian Fitzal⁵, Viktor Wette⁶, Marija Balic⁷, Ferdinand Haslbauer⁸, Elisabeth Melbinger-Zeintzer⁹, Vesna Bjelic-Radicic¹⁰, Jonas Bergh¹¹, Raimund Jakesz⁵, Christian Marth³, Paul Sevela¹², Brigitte Mlineritsch¹³, Ruth Exner⁵, Christian Fesl¹⁴, Sophie Frantal¹⁴, Christian F Singer¹, Michael Gnant⁵. ¹Medical University of Vienna/ Department of Obstetrics and Gynecology and Comprehensive Cancer Center, Austria, ²Medical University of Vienna/ Department of Internal Medicine I/Oncology, Austria, ³Medical University Innsbruck/ Department of Gynecology, Austria, ⁴Paracelsus Medical University Salzburg/ Department of Internal Medicine III and Salzburg Cancer Research Institute, Austria, ⁵Medical University of Vienna/ Department of Surgery and Comprehensive Cancer Center, Austria, ⁶Breast Center St. Veit/ Glan/ Doctor's Office Wette, Austria, ⁷Medical University Graz/ Department of Oncology, Austria, ⁸Hospital Vöcklabruck/ Department of Internal Medicine, Austria, ⁹Hospital Wolfsberg/ Department of Surgery, Austria, ¹⁰Medical University Graz/ Department of Gynecology, Austria, ¹¹Department of Oncology-Pathology, Karolinska Institutet and Cancer Theme, Karolinska University Hospital, 17176-Stockholm, Sweden, ¹²Karl Landsteiner Institute for Gynecologic Oncology and Senology, Austria, ¹³Paracelsus Medical University Salzburg/ Department of Internal Medicine III, Austria, ¹⁴Austrian Breast & Colorectal Cancer Study Group/ Statistic Department, Austria

Background: Endocrine therapy with aromatase inhibitors (AI) for at least 5 years is standard of care in patients with early hormone receptor (HR+) positive breast cancer. ABCSG-18 has shown (1) a high fracture risk in patients on AI treatment, (2) a significant

reduction of clinical and vertebral fractures by 6-monthly denosumab (HR=0.5, $p < 0.0001$, Lancet 2015). Recent reports indicate an elevated risk of rebound-associated fractures - especially multiple vertebral fractures - after stopping denosumab. Here we present data on fracture risk >6 months after the last dose of denosumab or placebo for patients with HR+ early breast cancer. Methods: In the prospective, double-blind, placebo-controlled phase III ABCSG-18 trial, 3,425 postmenopausal HR+ patients treated with adjuvant AI were enrolled to denosumab 60mg or placebo s.c. q6 months until the prespecified number of 247 first clinical fractures was reached. All patients received at least 2 doses of denosumab (median: 7 doses), the primary trial endpoint was time to first clinical fracture risk. Results: 2,451 patients stopped AI later than 6 months after the last dose of denosumab/placebo. 387 patients ended their AI intake prior to, and 295 patients within 6 months after the last dose of denosumab/placebo. During a median off-treatment follow-up of 36 months, 318 fractures in 199 patients (subject incidence rate 6.2%) have occurred. No difference in overall fracture risk in patients who stopped denosumab compared to patients who stopped placebo could be detected (163 vs 155 fractures in 98 vs 101 patients, time to first fracture: HR 0.92 (0.70, 1.22)). However, when looking specifically at clinical fractures, patients who stopped denosumab had a significantly higher risk of clinical vertebral fractures and multiple clinical vertebral fractures compared to patients who stopped placebo (39 vs 14 fractures in 22 vs 9 patients, HR 2.44 (1.12, 5.32); 28 vs 8 fractures in 11 vs 3 patients, HR 3.52 (0.98, 12.64)). This increased risk of clinical vertebral as well as multiple clinical vertebral fractures in patients who stopped denosumab, only occurred in patients who ended AI treatment prior to or >6 months after the last dose of denosumab/placebo, whereas no difference was seen in patients who ended AI treatment within 6 months of stopping denosumab/placebo. Conclusion: Rebound-associated fractures after termination of adjuvant denosumab therapy may be avoided when stopping bone-compromising AI therapy within 6 months.

Disclosures: **Georg Pfeiler**, Novartis, Grant/Research Support, Pfizer, Grant/Research Support, AstraZeneca, Grant/Research Support, Amgen, Consultant

LB-1168

Burosumab Improved Rickets, Phosphate Metabolism, and Clinical Outcomes Compared to Conventional Therapy in Children with XLH
 Erik Imel¹, Michael P. Whyte², Craig Munns³, Anthony A. Portale⁴, Leanne Ward⁵, Ola Nilsson⁶, Jill H. Simmons⁷, Raja Padidela⁸, Noriyuki Namba⁹, Hae I. Cheong¹⁰, Meng Mao¹¹, Chao-Yin Chen¹¹, Alison Skrinar¹¹, Javier San Martin¹¹, Francis Glorieux¹². ¹Indiana University School of Medicine, United States, ²Shriners Hospitals for Children, United States, ³The Children's Hospital at Westmead, Australia, ⁴University of California, San Francisco, United States, ⁵University of Ottawa, Canada, ⁶Karolinska Institutet, Sweden, ⁷Vanderbilt University School of Medicine, United States, ⁸Royal Manchester Children's Hospital, United Kingdom, ⁹Osaka Hospital, Japan Community, Healthcare Organization; Osaka University Graduate School of Medicine, Japan, ¹⁰Seoul National University Children's Hospital, Republic of Korea, ¹¹Ultragenyx Pharmaceutical Inc., United States, ¹²Shriners Hospital for Children-Canada, McGill University, Canada

In children with X-linked hypophosphatemia (XLH), high circulating levels of fibroblast growth factor 23 (FGF23) cause hypophosphatemia with consequent rickets, skeletal deformities, and growth impairment. Conventional therapy has consisted of multiple daily doses of oral phosphate and active vitamin D (Pi/D). Burosumab is a fully human monoclonal antibody against FGF23 indicated for the treatment of XLH. In the Phase 3 randomized active-control study CL301 (NCT02915705), 61 children with XLH (1-12 years old) were randomized 1:1 to receive open-label subcutaneous burosumab starting at 0.8 mg/kg every 2 weeks (Q2W) or standard XLH doses of Pi/D as prescribed by investigators. Eligibility criteria included a Total Rickets Severity Score (RSS) ≥ 2.0 and prior receipt of Pi/D. The primary endpoint was the radiographic global impression of change (RGI-C) global score for rickets assessed by radiologists blinded to treatment at Week 40 (RGI-C 7-point ordinal scale: worsening of rickets [-3, -2, -1], no change [0], or improvement [+1, +2, +3]). At Week 40, burosumab significantly improved rickets compared with Pi/D. More subjects in the burosumab group had a RGI-C global score $\geq +2.0$ at Week 40, indicating substantial healing, compared with the Pi/D group (21/29, 72% vs 2/32, 6%; odds ratio of 39.1; $p < 0.0001$). Further evidence of rachitic improvement with burosumab included decreased alkaline phosphatase, decreased RSS, and improved lower limb deformity RGI-C compared with Pi/D. Increases in serum phosphorus and TmP/GFR occurred rapidly with burosumab and these values were significantly greater at Week 40 compared with Pi/D. Standing height Z-score increased in both groups, with a least squares mean change (95% CI) of +0.15 (0.05, 0.25) for burosumab and a change of +0.08 (-0.02, 0.19) for Pi/D. The Six Minute Walk Test percent predicted distance increased with burosumab (Baseline to Week 40: 62% to 72%) and was unchanged with Pi/D (76% to 75%). Pre-defined adverse events (AEs) of interest, including hypersensitivity and injection site reaction, were higher in the burosumab group, but were mild to moderate in severity overall, with no discontinuations. There were 4 serious AEs (3 with burosumab, 1 with Pi/D); none were related to treatment and all resolved. In this Phase 3 randomized controlled trial, burosumab Q2W resulted in significantly greater improvement in rickets and serum phosphorus compared with conventional therapy in 1-12 year-old children with XLH.

Assessment	PivD (N = 31)	Burosumab (N = 29)
RGI-C Global Score, LS mean ± SE		
Week 40	+0.77 ± 0.11 ^a	+1.92 ± 0.11 ^a
RSS Total Score, mean ± SE		
Baseline	3.19 ± 0.20	3.17 ± 0.18
Week 40	2.47 ± 0.19	1.13 ± 0.14
LS mean ± SE change from baseline	-0.71 ± 0.14 ^a	-2.04 ± 0.15 ^a
RGI-C Lower Limb Deformity Score, LS mean ± SE		
Week 40	+0.21 ± 0.12 ^a	+0.62 ± 0.16 ^b
Alkaline Phosphatase, mean ± SE		
Baseline	523.44 ± 27.30	510.76 ± 23.19
Week 40	488.69 ± 33.42	380.76 ± 18.47
LS mean ± SE change from baseline	-34.52 ± 18.73 ^a	-131.49 ± 12.52 ^a
Serum Phosphorus, mg/dL, mean ± SE		
Baseline	2.30 ± 0.05	2.42 ± 0.05
Week 40	2.53 ± 0.06	3.30 ± 0.08
LS mean ± SE change from baseline	0.20 ± 0.06 ^a	0.92 ± 0.08 ^a
Standing Height Z Score, mean (SE)		
Baseline	-2.05 ± 0.15	-2.32 ± 0.22
Week 40	-1.97 ± 0.15	-2.12 ± 0.23
6MWT, % predicted norm, mean ± SE		
Baseline	76.20 ± 3.32	62.13 ± 4.81
Week 40	75.28 ± 3.18	71.85 ± 3.08

^aP<0.0001; ^bP<0.05 between treatment groups using the ANCOVA (RGI-C, RSS) and GEE (ALP, phosphorus) model. Decreases in RSS and increases in RGI-C indicate improvement. 6MWT in subjects ≥65yrs-old.

Disclosures: **Erik Imel**, Ultragenyx Pharmaceutical Inc., Other Financial or Material Support, Ultragenyx Pharmaceutical Inc., Grant/Research Support, Ultragenyx Pharmaceutical Inc., Consultant

LB-1169

Continued Improvement in Clinical Outcomes in the Phase 3 Randomized, Double-Blind, Placebo-Controlled Study of Burosumab, an Anti-FGF23 Antibody, in Adults with X-Linked Hypophosphatemia (XLH) Anthony A. Portale¹*, Karl L. Insogna², Karine Briot³, Erik Imel⁴, Peter Kamenický⁵, Thomas Weber⁶, Pisit Pitukcheewanont⁷, Hae I. Cheong⁸, Suzanne Jan De Beur⁹, Yasuo Imanishi¹⁰, Nobuaki Ito¹¹, Robin Lachmann¹², Hiroyuki Tanaka¹³, Farzana Perwad¹⁴, Lin Zhang¹⁵, Christina Theodore-Oklota¹⁵, Matt Mealiffe¹⁵, Javier San Martin¹⁵, Thomas O. Carpenter¹⁶. ¹University of California, San Francisco, United States, ²Yale School of Medicine, United States, ³Centre d'Evaluation des Maladies Osseuses, Hôpital Cochin, France, ⁴Indiana University School of Medicine, United States, ⁵Université Paris-Sud, France, ⁶Duke University Medical Center, United States, ⁷Children's Hospital Los Angeles, University of Southern California Keck School of Medicine, United States, ⁸Seoul National University Children's Hospital, Republic of Korea, ⁹Johns Hopkins University, United States, ¹⁰Osaka City University Graduate School of Medicine, Japan, ¹¹Tokyo University Hospital, Japan, ¹²University College London Hospitals, United Kingdom, ¹³Okayama Saiseikai General Hospital, Japan, ¹⁴University of California, San Francisco, United States, ¹⁵Ultragenyx Pharmaceutical Inc., United States, ¹⁶Yale University School of Medicine, United States

In adults with XLH, excess FGF23 causes hypophosphatemia with consequent fractures/pseudofractures (Fx/PFx), osteomalacia, pain, stiffness, and impaired physical function. In an ongoing, Phase 3, double-blind, multicenter study, we examined the efficacy and safety of burosumab in adults with XLH. Subjects were randomized 1:1 to receive burosumab 1 mg/kg or placebo subcutaneously every 4 weeks. At Week 24, subjects in the placebo group crossed-over to receive burosumab, and all subjects continued treatment for an additional 24 weeks, remaining blinded to prior treatment. The primary endpoint was the proportion of subjects achieving mean serum phosphorus above the lower limit of normal (LLN) at the midpoint of the dosing intervals from Weeks 0-24. A significantly greater percentage of burosumab subjects than placebo subjects attained the primary endpoint (94% vs 8%; p<0.0001). Between Weeks 24-48, 84% (57/68) of burosumab-continuation subjects and 89% (59/66) of crossover subjects were above the LLN at the midpoint of the dosing intervals. At baseline, 65 active Fx/PFx were present in 47% (32/68) of burosumab subjects and 91 Fx/PFx in 58% (38/66) of placebo subjects. At Week 24, 43% (28/65) of Fx/PFx healed with burosumab and 8% (7/91) healed with placebo (odds ratio 16.8, p<0.0001). By Week 48, the burosumab-continuation group showed additional Fx/PFx healing and the crossover group showed healing similar to that of the burosumab-continuation group at Week 24. At Week 24, the burosumab group showed greater reductions than the placebo group in stiffness scores (p=0.011), and non-significant reductions in pain (p=0.092) and physical functioning (p=0.048) scores. At Week 48, both groups showed significant decreases from baseline (or Week 24 for crossover) in stiffness (both p<0.0001), physical functioning (both p<0.001), and pain (both p<0.0001) scores. There was no meaningful difference in subject-reported pain medication use (Week 0→48 opioid: burosumab-continuation 25%→21% of subjects, crossover 20%→18%; non-narcotic: 69%→57%, 65%→52%). Serious AEs were reported in 15 subjects, none were drug-related. There were no meaningful changes in serum calcium, iPTH, nor nephrocalcinosis scores. In adults with XLH, burosumab was associated with

improvements in serum phosphorus, pain, stiffness, and physical functioning, and healing of Fx/PFx. Improvements seen in the burosumab group at Week 24 were replicated in subjects who crossed over from placebo to burosumab.

Assessment	Burosumab Continuation Weeks 0-48 (N = 68)	Crossover Placebo Weeks 0-24 Burosumab Weeks 24-48 (N = 66)
Serum Phosphorus, mg/dL		
Baseline	2.03 ± 0.04	1.92 ± 0.04
Week 22 (Mid-point)	2.91 ± 0.07	2.03 ± 0.04
Week 24 (Trough)	2.53 ± 0.05	2.07 ± 0.04
Week 46 (Mid-point)	2.97 ± 0.07	3.03 ± 0.07
Week 48 (Trough)	2.47 ± 0.06	2.47 ± 0.06
Percentage of Healed Fx/PFx, (% # Fx/PFx / baseline # Fx/PFx)		
Week 24	43 (28 / 65)	8 (7 / 91)
Week 48	63 (41 / 65)	35 (32 / 91)
WOMAC Stiffness Score		
Baseline	64.7 ± 2.5	61.4 ± 2.6
Week 24	53.7 ± 2.5	60.4 ± 2.7
Week 48	45.3 ± 2.7	44.7 ± 2.8
Change at Week 48	-16.0 ± 3.3 ^a	-15.3 ± 3.5 ^a
WOMAC Physical Functioning Score		
Baseline	50.8 ± 2.4	43.9 ± 2.5
Week 24	43.4 ± 2.4	42.7 ± 2.8
Week 48	38.4 ± 2.3	34.7 ± 2.8
Change at Week 48	-7.8 ± 2.1 ^a	-6.4 ± 2.9 ^a
BPI Worst Pain Score		
Baseline	6.8 ± 0.2	6.5 ± 0.2
Week 24	5.8 ± 0.2	6.1 ± 0.3
Week 48	5.6 ± 0.2	4.9 ± 0.3
Change at Week 48	-1.1 ± 0.2 ^a	-1.5 ± 0.2 ^a

Mean or LS mean change from baseline ± SE. ^aP<0.001 vs baseline (or week 24 for placebo) to week 48

Disclosures: **Anthony A. Portale**, Ultragenyx Pharmaceutical Inc., Other Financial or Material Support, Ultragenyx Pharmaceutical Inc., Consultant, Ultragenyx Pharmaceutical Inc., Grant/Research Support

LB-1170

Oral Iron Therapy Normalizes Fibroblast Growth Factor 23 (FGF23) in Patients with Autosomal Dominant Hypophosphatemic Rickets Erik Imel¹*, Ziyue Liu², Melissa Coffman¹, Dena Acton¹, Michael Econs¹. ¹Indiana University School of Medicine, United States, ²Indiana University School of Public Health, United States

Autosomal dominant hypophosphatemic rickets (ADHR) is a rare bone disease caused by mutations impairing cleavage of fibroblast growth factor 23 (FGF23). FGF23 gene expression increases during iron deficiency. In both humans and mice with the ADHR mutation, increased intact FGF23 concentrations and resulting hypophosphatemia occur in the setting of iron deficiency. This clinical trial tested the hypothesis that oral iron administration would normalize FGF23 concentrations in ADHR subjects. Subjects with ADHR were recruited to receive oral iron replacement for 12 months, at a starting dose of 65 mg daily and titrated based on serum iron concentration. Eligibility criteria included: confirmed FGF23 mutation; and either serum iron < 50 mcg/dl; or serum iron 50-100 mcg/dl combined with hypophosphatemia and intact FGF23 >30 pg/ml. Key exclusion criteria were CKD or pregnancy. The primary outcome was decrease in fasting intact FGF23 ≥20% from baseline. All laboratory samples were collected fasting. Six adults (3 male, 3 female) having the R176Q mutation were enrolled. Four subjects completed 12 months and one completed 4 months to date; 1 was lost to followup. At baseline 3/5 subjects had severely symptomatic hypophosphatemia (phosphorus <2.5 mg/dl). Due to symptoms, these 3 subjects also received calcitriol with or without phosphate, concurrent with oral iron: 1 began prior to enrollment, 1 began at the baseline visit, 1 began at month 2. Baseline laboratories included [median (minimum, maximum)]: fasting serum phosphorus 2.1 (<1.0, 2.7 mcg/dl), iron 69 (22, 83 mcg/dl), intact FGF23 171.7 (20.3, 222.6 pg/ml) (See Table). Within 4 months, 4 out of 5 subjects already met the primary outcome, decreasing FGF23 by ≥20% from baseline, and 3 had normalized FGF23 (<70 pg/ml in our laboratory). Overall, median FGF23 concentrations decreased from 171.7 pg/ml at baseline to 47.2 pg/ml at 4 months and 50.1 pg/ml at 12 months. Median ferritin increased from 18.6 mg/ml at baseline to 46.1 ng/ml at month 4 and 143.5 ng/ml at month 12. All 3 subjects with baseline hypophosphatemia normalized serum phosphorus, had markedly improved symptoms, and were able to discontinue calcitriol and phosphate (2 at 4 months, 1 at 9 months). Oral iron treatment normalized serum FGF23 and phosphorus in ADHR subjects. Since iron repletion is necessary to treat iron deficiency, and oral iron treatment was also able to normalize FGF23, oral iron should be the standard therapy for ADHR.

Table	N	FGF23 (pg/ml)	Phosphorus (mg/dl)	Iron (mcg/dl)	Ferritin (ng/ml)	Alkaline phosphatase (U/L)	Creatinine (mg/dl)
Screening	5	52.6 (34.8, 182.7)	2.3 (1.4, 2.9)	53 (10, 81)	-	80.5 (56.0, 135.0)	0.82 (0.53, 1.03)
Baseline	5	171.7 (20.3, 222.6)	2.1 (-1.0, 2.7)	69 (22, 83)	38.6 (7.7, 82.5)	93.0 (82.5, 211.0)	0.70 (0.55, 1.01)
Month 4	5	47.2 (17.3, 77.3)	2.9 (2.1, 3.6)	76 (39, 94)	46.1 (28.8, 92.1)	91.0 (68.0, 195.0)	0.74 (0.52, 0.97)
Month 6	4	25.8 (16.3, 44.8)	3.1 (2.3, 4.2)	95 (44, 133)	86.7 (54.3, 127.0)	89.5 (60.0, 157.0)	0.76 (0.66, 0.86)
Month 12	4	50.1 (19.4, 62.9)	2.9 (2.5, 4.0)	66 (43, 88)	143.5 (49.6, 261.0)	78.0 (60.0, 120.0)	0.75 (0.56, 0.86)

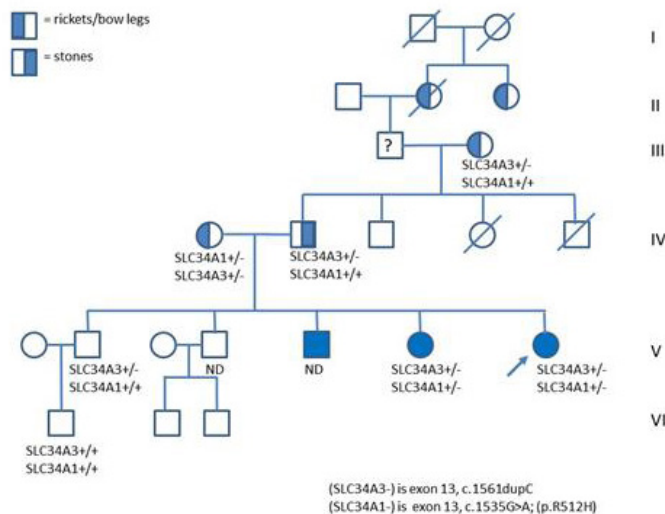
Values are median (minimum, maximum); for Month 6, N=3 for FGF23.

Disclosures: Erik Imel, None

LB-1171

Digenic Inheritance of Heterozygous SLC34A3 and SLC34A1 Mutations in Hereditary Hypophosphatemic Rickets with Hypercalciuria Rebecca Gordon^{*1}, Daniel Doyle², Joshua Zaritsky², Michael Levine¹. ¹The Children's Hospital of Philadelphia, United States, ²Alfred I. duPont Hospital for Children, United States

Hereditary Hypophosphatemic Rickets with Hypercalciuria (HHRH) is an autosomal recessive disorder characterized by renal phosphate wasting due to mutation of SLC34A3 encoding the NPT2c sodium-phosphate cotransporter in the proximal renal tubule. Patients manifest hypophosphatemia with rickets and/or osteomalacia plus low serum levels of FGF23, with consequent elevated 1,25(OH)2D that leads to hypercalciuria and often renal stones. We evaluated a non-consanguineous kindred with apparent dominant transmission of HHRH by next generation sequencing (NGS), and identified digenic heterozygous mutations in both affected sisters: a known missense mutation in SLC34A3 (exon 13, c.1535G>A; p.R512H) and a novel frameshift mutation in SLC34A1 (exon 13, c.1561dupC), which encodes the NPT2a sodium-phosphate cotransporter that is expressed in the proximal renal tubule. Evaluation of all available family members over four generations demonstrated that the mother with bowed legs and short stature also had the same two digenic heterozygous mutations as her two affected daughters; the affected short father and short paternal grandmother carried only the SLC34A3 missense mutation, which was also present in an unaffected short older brother. Another presumed affected older brother, given his bowed legs, refused to participate in these studies. Because both parents carried the identical SLC34A3 mutation it was not possible to determine the parent of origin for this allele in generation V carriers. Therefore, both mutations, on different chromosomes, could have come from the mother. Both affected daughters and the father had clinically significant nephrolithiasis. All available affected family members had low to low-normal serum phosphorus levels with elevated 1,25(OH)2D levels and low serum 25(OH)D levels. Subjects with digenic heterozygous mutations had a more severe phenotype than subjects with only one heterozygous mutation, with variable penetrance. There appeared to be an attenuation of renal phosphate wasting with aging. We conclude that these two affected siblings and their family members demonstrate a novel, digenic basis for pseudo-autosomal dominant inheritance of HHRH. We suggest that NGS of multiple genes involved in phosphate regulation provides a more comprehensive genetic evaluation of patients with hypophosphatemic rickets, and can provide novel insights into the pathogenesis of renal phosphate wasting.



Disclosures: Rebecca Gordon, None

LB-1172

LRP6 Mutation: A New Cause of Autosomal Dominant High Bone Mass Michael P. Whyte^{*1,2}, Gary S. Gottesman¹, Elizabeth L. Lin^{1,2}, William H. Mcalister³, Angela Nenninger¹, Vinieth N. Bijanki¹, Margaret Huskey², Shenghui Duan², Steven Mumm^{1,2}. ¹Center for Metabolic Bone Disease and Molecular Research, Shriners Hospital for Children, United States, ²Division of Bone and Mineral Diseases, Department of Internal Medicine, Washington University School of Medicine at Barnes-Jewish Hospital, United States, ³Mallinckrodt Institute of Radiology, Washington University School of Medicine at St. Louis Children's Hospital, United States

Autosomal dominant gain-of-function mutation of the gene encoding LDL-receptor protein 5 (LRP5) causes high bone mass (HBM). Clinical expressivity ranges from non-syndromic to overt with oropharyngeal exostoses and neurological complications including Chiari I malformation and cranial nerve palsies. LRP5 is a transmembrane receptor with four extracellular YWTD β -propeller domains, which bind WNT, SOST, and DKK1 to regulate osteoblast-mediated bone formation via the canonical WNT pathway. LRP5 activating mutations, which cause HBM by diminishing inhibitory ligand (SOST and DKK1) binding, lie within β -propeller 1. Notably, the LRP6 receptor protein is ~70% homologous to LRP5, and similarly binds LRP5 ligands. Nevertheless, mutations in LRP6 leading to HBM have not been reported. In two HBM American families, we discovered LRP6 mutations that encode alterations within regions homologous to the LRP5 β -propeller 1. In Family 1, two teenage sisters were found by their dentist to have dense mandibles. An 8-year-old boy in Family 2 developed Bell's palsy after suffering trauma to his face and CT imaging revealed increased density of his calvarium and skull base. Subsequent radiographic skeletal surveys of affected individuals from both families showed generalized osteosclerosis and endosteal hyperostosis that mimicked LRP5 HBM. Family 1 (mother and 2 daughters) DXA BMD Z-scores ranged from +5.2 to +9.4 in the spine and +7.8 to +10.1 in the hip, which increased with age. In family 2 (3 generations), Z-scores ranged from +7.3 to +10.3 in the spine and +6.4 to +8.8 in the hip. We found acquired torus palatinus, a variably broad jaw, and an inability to float in our LRP6 HBM families, akin to our LRP5 HBM families. Although serum PINP and CTX were elevated, other studies of bone and mineral metabolism were normal. In family 1, our Ion Torrent HBM platform identified an LRP6 missense mutation c.602C>T, p.A201V confirmed by Sanger sequencing, which is precisely homologous to the previously reported LRP5 HBM mutation c.641C>T, p.A214V. In family 2, Sanger sequencing showed the LRP6 mutation c.553A>C, p.N185H when LRP5 analysis proved negative. This second LRP6 mutation occurs at another homologous LRP5 HBM mutation site but results in a different amino acid change (c.593A>G, p.N198S). Both mutations co-segregated with the HBM phenotype in their respective families. Thus, LRP6 mutations also cause HBM.

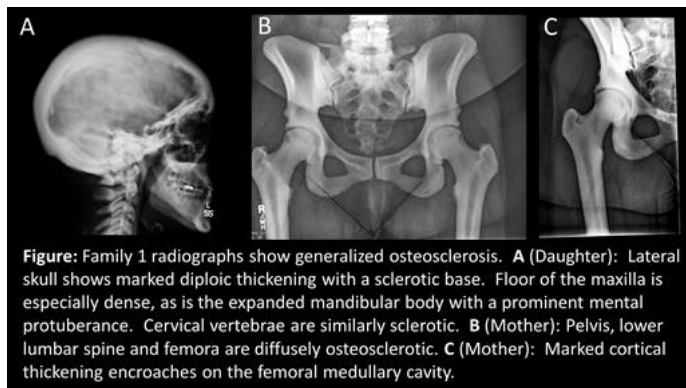


Figure: Family 1 radiographs show generalized osteosclerosis. **A** (Daughter): Lateral skull shows marked diploic thickening with a sclerotic base. Floor of the maxilla is especially dense, as is the expanded mandibular body with a prominent mental protuberance. Cervical vertebrae are similarly sclerotic. **B** (Mother): Pelvis, lower lumbar spine and femora are diffusely osteosclerotic. **C** (Mother): Marked cortical thickening encroaches on the femoral medullary cavity.

Disclosures: Michael P. Whyte, None

LB-1173

Multi-omics approach reveals novel pathogenic indicators of DISH Matthew Veras^{*1}, Neil Tenn¹, Miljan Kuljanin², Gilles Lajoie², James Hammond³, S. Jeffrey Dixon¹, Cheryle Séguin¹. ¹Bone & Joint Institute, The University of Western Ontario, Canada, ²The University of Western Ontario, Canada, ³University of Alberta, Canada

Background: Mice lacking equilibrative transporter 1 (ENT1) develop ectopic spinal calcifications mirroring diffuse idiopathic skeletal hyperostosis (DISH) in humans. Calcifications affecting fibrocartilaginous tissues including the annulus fibrosus (AF) of the intervertebral disc are detected at 2 months-of-age, increase in severity and progress caudally with age. This novel preclinical model allows for unprecedented studies of the molecular mechanisms underlying ectopic calcification at the onset and throughout disease progression; an approach not possible in the clinical population where diagnosis is limited to late stage disease. To decipher the mechanisms driving DISH, we developed an unbiased strategy applying transcriptomic, proteomic, and metabolomic analysis of the ENT1 KO mouse to identify novel pathogenic indicators of DISH. Methods & Results: To identify pathways associated with ectopic calcification, we assessed AF tissue from WT and ENT1^{-/-} mice prior to (2 months-of-age) and following (6 months-of-age) AF calcification. Microarray analysis

revealed massive dysregulation of transcription in the AF of *ENT1*^{-/-} mice compared to WT. Gene ontology analysis showed deregulation of pathways regulating bone mineralization, bone cell development, and biomimetic tissue development; surprisingly, cell cycle processes were the most highly affected pathways. The E2f family of transcription factors and proliferating cell nuclear antigen (PCNA) were implicated in the deregulation of cell cycle progression. Proteomic analysis quantified the expression of over 5000 proteins and identified subsets of dysregulated proteins in *ENT1*^{-/-} tissues. Analysis confirmed transcriptomic data and implicated known modulators of mineralization such as bone sialoprotein and matrix Gla-protein in disease progression. Notably, we confirmed dysregulation of cell-cycle regulators PCNA (7.5-fold increase), CDK1 (5.8-fold increase), and a remarkable 19.7-fold increase in MCM5 expression in *ENT1*^{-/-} vs WT at 6 months-of-age. Significance: This is the first study to associate dysregulation of cell cycle with disorders of ectopic calcification, suggesting a causative link with DISH. This multi-omics analysis using a preclinical model of DISH has provided novel insight into the pathways regulating disease pathogenesis. Combined with ongoing metabolomic analysis, these studies will identify therapeutic targets to prevent or delay the onset of ectopic calcification in DISH patients.

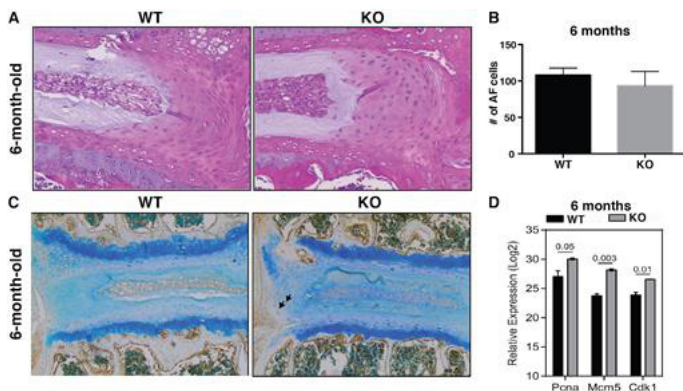


Figure 1. Loss of *ENT1* dysregulates cell cycle-associated proteins in the annulus fibrosus of the intervertebral disc. **A)** 6-month-old WT and *ENT1*^{-/-} mid-coronal T2/T3 intervertebral discs (IVDs) stained with hematoxylin and eosin. *ENT1*^{-/-} sections show disrupted organization of annulus fibrosus (AF) tissue whereby AF cells no longer line concentric collagen lamellae. Furthermore, there appears to be a larger proportion of rounded AF cells. **B)** Counts of AF cells in the right lateral aspect of 6-month-old T2/T3 intervertebral discs. There is no significant difference in the number of AF cells between WT and *ENT1*^{-/-}. **C)** 6-month-old WT and *ENT1*^{-/-} mid-coronal T2/T3 intervertebral disc immunostaining for proliferating cell nuclear antigen (PCNA). There is an absence of PCNA positive cells in the AF of WT intervertebral discs, but numerous PCNA-positive cells in the outer AF of *ENT1*^{-/-} intervertebral discs. **D)** Proteomic analysis of 6-month-old WT and *ENT1*^{-/-} thoracic AF tissue. Proteomics revealed significant upregulation of PCNA, MCM5, and CDK1 protein expression in *ENT1*^{-/-} thoracic AF tissue compared to WT control. Images are representative of n=3 mice per genotype. AF cell counting was performed on n=3 tissue sections per genotype. Proteomics was performed on n=2 mice per genotype (AF tissue from 4 thoracic IVDs per mouse).

Disclosures: **Matthew Veras, None**

LB-1174

Cathepsin K (Ctsk) restrains the periostin (Postn)-mediated increase in cortical size induced by RANKL Nicolas Bonnet¹, Eleni Douni², Serge Ferrari³. ¹University Geneva Hospital (HUG), Switzerland, ²Biomedical Sciences Research Center "Alexander Fleming", ²Department of Biotechnology, Agricultural University of Athens, Greece, ³University Geneva Hospital (HUG), Switzerland

Failure of periosteal apposition to compensate for endosteal resorption may contribute to age-related bone fragility, however this mechanism remains poorly understood. We previously reported that Postn, -expressed by osteocytes and lining cells in response to mechanical forces-, stimulates bone formation, and is eventually degraded by Ctsk. We hypothesized that RANKL would increase mechanically-driven periosteal apposition but these effects be limited by Ctsk-dependent Postn degradation. For this purpose, femur microstructure, periosteal bone formation and cortical strength were evaluated in mice overexpressing huRankL and eventually subjected to limb immobilization (IL) by botox injection, as well as in the progeny of huRANKLTg+ x Ctsk^{-/-} and huRANKLTg+ x Postn^{-/-} mice. huRANKL Tg+ exhibit low BV/TV and CtBV vs WT (1.5±0.2% vs 11±0.9; 0.39±0.02mm³vs 0.52±0.01, p<0.001) but a high CtTV (1.58±0.05mm³ vs 1.17±0.04, p<0.01). Immobilization further decreased BV/TV and CtBV in huRANKLTg+ (-97% & -43% vs the non-IL, p<0.05), and prevented the increase in CtTV (-12% vs non-IL, p<0.05). Accordingly, Postn mRNA levels are increased and Sost decreased in cortical bone of huRANKLTg+ (+73% and -69%, p<0.01), while Postn mRNA and protein decreases and Ctsk mRNA increases in IL (+53% and -34%, p<0.05). In turn genetic deletion of Postn in huRANKL-Tg+ mice prevented the compensatory periosteal growth and aggravated bone fragility. In contrast, in Tg5519-Ctsk^{-/-} mice, Ctsk ablation improved BV/TV but also increased CtTV (+24% vs huRANKLTg+, +67% vs WT, both p<0.05). PsBFR was stimulated vs huRANKLTg+ (+215%), and WT (+1533%), with an increased Postn protein levels. mRNA levels of Runx2, ALP, Col1a and PDGFB were also increased (+100%, +86%, +23%, +191% vs huRANKLTg+, p<0.05). As a consequence, ultimate force was improved in huRANKLTg+-Ctsk^{-/-} (14.7±0.8 vs 9.9±1.3N in huRANKLTg+, p<0.05), reaching cortical strength levels similar to WT. In conclusions, endosteal bone loss induced by high levels of RANKL is accompanied by an increased periosteal bone formation and diameter that is mechanically driven and mediated by Postn. However, the larger bones of huRANKL mice remain weaker than WT because Postn is degraded by Ctsk. In turn, Ctsk inhibition improves periosteal growth and fully restores

bone strength. These findings further delineate the molecular mechanisms that couple bone remodeling / modeling.

Disclosures: **Nicolas Bonnet, None**

LB-1175

Short-Term Intermittent PTH (1-34) Administration, Angiogenesis, and Matrix Metalloproteinase-9 in Femora of Mature and Middle-Aged C57BL/6 Mice Seungyong Lee*, Rhonda Prisby. The University of Texas at Arlington, United States

Intermittent parathyroid hormone administration (iPTH) increases bone volume and matrix metalloproteinase (MMP)-9 secretion. In addition, iPTH alters bone blood vessels by increasing vasodilator capacity, augmenting bone perfusion, and relocating bone marrow blood vessels closer to osteoid seams. Discrepancies exist, however, as to whether iPTH elicits angiogenesis. Since MMP-9 participates in cellular homing and migrating, we theorized that it aids in relocating bone marrow blood vessels. We examined the influence of short-term (i.e., 5- and 10-days) iPTH on angiogenesis, MMP-9 secretion, and the distance between blood vessels and bone in mature (6-8mon; n=30) and middle-aged (10-12mon; n=30) male and female C57BL/6 mice. Mice were divided accordingly: control (CON), 5-days iPTH (5dPTH) and 10-days iPTH (10dPTH). Mice were given a placebo (i.e., PBS; 50 µl/d) or PTH 1-34 (43 µg/kg/d). Right femora were collected and prepared for histology. Frontal sections (5µm) were triple-immunolabeled to identify endothelial cells (i.e., anti-CD31), vascular smooth muscle cells (i.e., anti-αSMA), and MMP-9 (i.e., anti-MMP9). Sections of the distal femoral metaphysis were imaged to determine vascular density, MMP-9 localization, and blood vessel distance to bone. Blood vessels were analyzed according to diameter: 1-29µm, 30-100µm, and 101-200µm. Trabecular bone microarchitecture (i.e., BV/TV [%], Tb.Th [µm], Tb.N [1/mm²], and Tb.Sp [µm]) and bone static (i.e., OS/BS, %, Ob.S/BS, % and Oc.S/BS, %) and dynamic (MAR, mm/day; sLS/BS, %; dLS/BS, %; MS/BS, % and BFR, mm³/mm²/day) properties were examined. Gender-related differences were not observed with this sample size, so female and male data were pooled. The density of 1-29µm and 30-100µm CD31-labeled blood vessels was significantly (p<0.05) higher and tended (p=0.055) to be higher, respectively, in 10dPTH vs. 5dPTH and CON. Further, 30-100µm and 101-200µm αSMA-labeled blood vessels tended (p<0.10) to be higher in 10dPTH vs. 5dPTH. MMP-9 was augmented (p<0.05) in 10dPTH vs. the other groups and MMP-9 was closer (p<0.05) to 1-29µm blood vessels and furthest (p<0.05) from trabecular bone. No differences were observed in distances between blood vessels and bone, bone microarchitecture, and bone static and dynamic properties. In conclusion, bone angiogenesis occurs by 10 days of iPTH (i.e., quicker than changes in trabecular bone), coinciding with augmented MMP-9 secretion closer to the smallest (1-29µm) blood vessels.

Disclosures: **Seungyong Lee, None**

LB-1176

Identification of a Novel Selective Small-Molecule Inhibitor of the BMP Type I Receptor Kinase ACVR1/ALK2 with Disease-Modifying Potential for On-Target Therapy of Fibrodysplasia Ossificans Progressiva (FOP) Ina Kramer¹, Luca Arista², Victoria Head³, Michaela Kneissel¹, Thomas Ullrich², Sabine Guth-Gundel¹. ¹Musculoskeletal Disease Area, Novartis Institutes for BioMedical Research, Switzerland, ²Global Discovery Chemistry, Novartis Institutes for BioMedical Research, Switzerland, ³Translational Medicine, Novartis Institutes for BioMedical Research, Switzerland

Fibrodysplasia ossificans progressiva (FOP) is a devastating ultra-rare disease of painful progressive soft tissue heterotopic ossification (HO) causing ankylosis and immobility of patients with no treatment available to date. It is caused by a recurrent autosomal dominant gain-of-function mutation in the bone morphogenetic protein (BMP) type I receptor ACVR1/ALK2 [(ALK2(R206H))] rendering the receptor hypersensitive to BMP ligands and conferring aberrant responsiveness to Activin A-mediated BMP pathway activation. While clinical trials in FOP are ongoing with therapeutic principles blocking upstream or further downstream events of the mutated ALK2-induced signaling cascade, a direct and selective on-target therapy to normalize the aberrant ALK2 receptor activity is still missing. Here, we describe a novel small-molecule ALK2 kinase inhibitor, SF-86-HL84, which is selective for ALK2 relative to the related BMP type I receptors ALK1, 3 and 6, but also the TGFβ receptor ALK5, in biochemical kinase as well as cellular reporter gene assays. Moreover, SF-86-HL84 demonstrates excellent oral pharmacokinetic and overall drug formulatability properties. We hence tested its therapeutic potential in an inducible mouse model of pediatric FOP (Acvr1tmR206H;R26-CreERT2 mice) in which we induced expression of the mutated Alk2(R206H) allele by tamoxifen dosing starting at about one week of age followed by induction of the disease phenotype by unilateral hind limb skeletal muscle injury at about 10 days of age. Irrespective of whether oral treatment was started in a preventive mode 3 days after injury or a therapeutic setting 2.5 weeks after injury when heterotopic bone was already present, SF-86-HL84 fully suppressed HO following 6 weeks of dosing as assessed by in vivo and ex vivo computed tomography. We also assessed the bone phenotypic consequences of SF-86-HL84 therapy on the growing and aged skeleton by determining structural and functional biomechanical parameters in skeletally growing Acvr1tmR206H;R26-CreERT2 mice as well as intact aged female rats. Neither skeletal long bone growth nor skeletal bone loss during aging were impacted by SF-86-HL84 therapy at doses demonstrating full ther-

apeutic efficacy. Together, our findings reveal that the novel ALK2 inhibitor SF-86-HL84 shows superior in vitro selectivity and compound properties while holding disease-modifying potential for FOP based on its demonstrated in vivo efficacy in a preclinical mouse model of pediatric FOP.

Disclosures: Ina Kramer, Novartis Pharma AG, Other Financial or Material Support

LB-1177

Activin A (ActA) Expression by Fibroadipogenitors (FAPs), But Not Myeloid Cells, Is Necessary for Endochondral Heterotopic Ossification (HO) in Fibrodysplasia Ossificans Progressiva (FOP) Mice Cody M. Elkins*, Chuanmin Cheng, Heather Durai, Nikash Hari, Daniel S. Perrien. Vanderbilt Center for Bone Biology, Division of Clinical Pharmacology, Department of Medicine, Vanderbilt University Medical Center, United States

FOP is a rare, currently untreatable disease, characterized by episodic skeletal muscle inflammation, or 'flares', leading to endochondral heterotopic ossification (EHO), causing pain, joint fusion, loss of mobility, and eventual premature death. The classic causal mutation, ALK2R206H, sensitizes the Type 1 BMP receptor ALK2/ACVR1 to Activin A (ActA)-induced signaling. Expression of ALK2R206H in intramuscular FAPs (CD45-/CD34-/Scal+/PDGFR1 α + cells) is necessary and sufficient to induce EHO in mice. However, the in vivo sources of ActA driving this process are unknown. Pro-inflammatory mac-

rophages (M Φ) express high levels of ActA, play critical roles in innate sterile inflammation and tissue repair, and depletion reduces HO in FOP mice. Thus, we hypothesized that M Φ -derived-ActA is required for injury-induced EHO in FOP. To test this hypothesis, EHO was initiated in FOP mice (R26creERT2;ALK2R206H-FIE α /WT) by tamoxifen-induced expression of ALK2R206H followed by injury of the gastrocnemius with cardiotoxin or crush injury. The area and volume of EHO were measured by plain radiographs and μ CT at 14-21 days after injury. To demonstrate M Φ involvement, CCR2DTR/+ mice, which allow selective killing of M Φ s by treatment with diphtheria toxin (DT), were crossed with FOP mice (CCR2DTR/+;FOP mice). DT treatment depleted >90% of M Φ s and completely prevented the EHO seen in CCR2+/+;FOP mice (p<0.001). Histological examination confirmed that M Φ depletion also blocked muscle repair and led to the formation of small scattered intramembranous dystrophic HO. In contrast, global deletion of ActA prevented EHO in FOP mice without dystrophic ossification, demonstrating that ActA is necessary for EHO in FOP. Next, FAPs from uninjured muscles of FOP mice were injected into injured muscles of ALK2wt/wt recipient mice. Extensive EHO formed in wildtype and Rag2 recipient mice. Surprisingly, myeloid-specific deletion of ActA in Lysmcre/cre;ActAfl/fl recipients did not prevent EHO compared to Lysm+/+;ActAfl/fl recipients, suggesting that M/M Φ expression of ActA is dispensable. In contrast, deletion of ActA in donor FOP FAPs (ActA-/-;FOP) completely prevented EHO without blocking muscle repair or causing dystrophic HO in Rag2 or WT recipients. These data provide the first direct evidence that the autonomous expression of ActA and its autocrine signaling in FAPs is necessary for EHO in FOP mice, while suggesting the critical role of M Φ s in FOP is independent of their ActA expression.

Disclosures: Cody M. Elkins, None

FRI-0001

Acute Kidney Injury in Primary Hyperparathyroidism Cristiana Cipriani^{*1}, Jessica Pepe¹, Federica Biamonte¹, Valeria Fassino¹, Luciano Colangelo¹, Valentina Piazzolla¹, Carolina Clementelli¹, Luciano Niedo², Salvatore Minisola¹. ¹Sapienza University of Rome, Italy, ²UNINT University, Italy

Purpose. The endpoint of the study was to establish the potential role of biomarkers of acute kidney injury in detecting subtle renal damage in patients with primary hyperparathyroidism (PHPT). **Methods.** We studied 69 post-menopausal patients with PHPT and 41 healthy age and sex-matched subjects. Exclusion criteria were: GFR<60 ml/min, chronic inflammatory disease, diabetes, infection, cancer. We measured serum IL-18, calcium (Ca), phosphorus (P), 25(OH)D, PTH, Klotho, plasma intact FGF23, Monocyte Chemoattractant Protein-1 (pMCP-1); urinary Neutrophil Gelatinase-Associated Lipocalin (NGAL), Kidney injury molecule-1 (KIM-1), uMCP-1, creatinine clearance (CrCl), calcium excretion (CaEx) and renal tubular reabsorption of phosphate (TmPO4/GFR). **Results.** Our data showed, as expected, significantly higher mean serum Ca, PTH and CaEx ($p<0.001$) and lower 25(OH)D ($p<0.05$), P and TmPO4/GFR ($p<0.0001$) in PHPT compared to control subjects. Mean FGF23 and Klotho were higher in PHPT (72±48 pg/ml and 811±366 pg/ml, respectively) compared to controls (53±23.5 and 668.6±17; $p<0.02$ and $p<0.05$, respectively). KIM-1/uCr was significantly higher in PHPT (1.4-6±1.3-6) than in controls (9.2-7±7-7; $p<0.05$). Results were confirmed when the analysis was adjusted for CrCl and the presence of hypertension. Significant differences in mean values of NGAL/uCr (1.8-5±1.4-5 and 1-5±8-6, respectively; $p<0.0001$) were observed between PHPT with (n=28) and without kidney stones (n=35). Six PHPT refused kidney ultrasound. Considering together patients and subjects according to the CrCl, difference in Klotho levels were significant between PHPT (956.3±453) and controls (679±219) in those with CrCl > 90 ml/min ($p<0.05$). In the CrCl 60-89 ml/min class, we observed a significant difference in KIM-1/uCr between PHPT (1.3-6±9-7) and controls (8.2-7±3.6-7; $p<0.02$). We found significant positive associations between NGAL/uCr and Ca ($R=0.292$, $p<0.02$) and KIM1/uCr and PTH ($R=0.329$, $p<0.01$). **Conclusions.** There is a subtle kidney injury in patients with PHPT as detected by the use of sensitive biomarkers, particularly KIM-1 and NGAL, well before the deterioration of GFR. Since these molecules are elevated in patients with proximal tubular necrosis, they could reflect an intra-renal damage in PHPT. At present it is unclear if the increased FGF23 levels represent a compensatory mechanism, are expression of PTH-driven effects on bone cells or are related to parathyroid resistance.

Disclosures: Cristiana Cipriani, None

FRI-0002

Changes in Skeletal Microstructure Through Four Years of rhPTH(1-84) Therapy in Hypoparathyroidism Natalie Cusano^{*1}, Mishaela Rubin², John Williams², Sanchita Agarwal², Gaia Tabacco², Yu-Kwang Donovan Tay², Rukshana Majeed², Beatriz Omeragic², John Bilezikian². ¹Lenox Hill Hospital, United States, ²Columbia University Medical Center, United States

Hypoparathyroidism is characterized by low bone turnover, above average areal bone mineral density (BMD), and abnormal structural indices by bone biopsy. We previously reported that patients with hypoparathyroidism on conventional therapy have altered skeletal parameters including elevated cortical BMD using high resolution peripheral quantitative computed tomography (HRpQCT, Scanco Medical) of the distal radius and tibia. No data are available regarding the effects of rhPTH(1-84) on these microstructural indices by HRpQCT. We now report HRpQCT results for 34 hypoparathyroid patients 1, 2, and 4 years after rhPTH(1-84) in comparison to baseline values. The group was comprised of 25 women/9 men; age 47 ± 14 (SD) years; etiology: 20 postsurgical, 14 idiopathic; duration 12 ± 13 years. Prior to therapy with rhPTH(1-84), serum calcium was 8.7 ± 1 mg/dL and PTH 1.4 ± 4 pg/mL. A linear mixed model approach was used, controlling for effects of age, gender, and disease duration. At baseline, areal BMD by DXA was normal/above average: lumbar spine T-score +1.4, femoral neck +0.7, total hip +0.9, 1/3 radius 0.0, ultradistal radius +0.2. Areal BMD demonstrated the following changes at 4 years ($p<0.05$ for all): lumbar spine: +4.7 ± 0.9%, femoral neck +2.1 ± 0.9%, total hip -2.5 ± 0.8%, ultradistal radius -2.8 ± 0.8; no significant change at the 1/3 radius. The HRpQCT results are presented in Table 1. There were declines in volumetric BMD and cortical area, cortical BMD, and cortical thickness at both the radius and tibia but no significant changes in trabecular indices from baseline. Age was a significant negative predictor at the radius in volumetric and cortical BMD and at the tibia in volumetric BMD, cortical area, cortical BMD, and cortical thickness; gender and disease duration had no effect. Using HRpQCT, these data are the first to show changes in cortical parameters in hypoparathyroid patients after therapy with rhPTH(1-84). The data contrast with the BMD data by DXA that seem to mimic the effects of PTH therapy in osteoporosis. Rather, by this high resolution technology, we provide support for the hypothesis that PTH corrects unusually dense cortical bone in this PTH deficient setting by starting the transition towards trabecularization.

Table 1. Changes in Cortical (Ct) HRpQCT indices after 4 years of rhPTH(1-84)

Index	Radius	Tibia
Volumetric BMD	-2.8 ± 0.6	-1.9 ± 0.5
Ct area	-3.8 ± 0.8	-2.9 ± 0.8
Ct BMD	-3.6 ± 0.5	-3.9 ± 0.5
Ct thickness	-3.2 ± 0.9	-2.8 ± 0.8
% change from baseline ± SE		
$p<0.05$ for all		

Disclosures: Natalie Cusano, Shire, Speakers' Bureau, Shire, Grant/Research Support

FRI-0003

Greater Visceral Adipose Tissue is Associated with Impairment of Bone Strength Assessed with HR-pQCT : the OFELY Study Francois Duboeuf^{*}, Elisabeth Sornay-Rendu, Roland Chapurlat. INSERM UMR 1033, Université de Lyon, France

Purpose : The relationship between visceral (VFAT) and subcutaneous (SFAT) fat mass with bone mineral density and microarchitecture is still controversial. Although obesity has been reported not to be protective against fracture, a recent study from the Framingham cohort (1), showed that visceral fat assessed by computed tomography was positively associated with bone quality assessed by HRpQCT. Our aim was to analyze this relationship using the DXA technique to evaluate abdominal fat mass. **Subjects and methods :** 815 women (mean ± SD : age: 60 ± 15 years; BMI: 24 ± 4 kg/m²) from the OFELY study with both whole body DXA (Discovery A, HOLOGIC Inc; Bedford, MA) and HR-pQCT (Xtreme CT, Scanco Medical AG, Switzerland) at the radius and tibia have been included. Abdominal visceral fat (VFAT) and subcutaneous fat (SFAT) areas were assessed using the APEX 4.0.2 software. The bone microarchitectural considered parameters from the HR-pQCT were : Total area (Tt.Ar), cortical area (Ct.Ar), trabecular area (Tb.Ar), Total VBMD (Tt.vBMD), Cortical VBMD (Ct.vBMD), Trabecular vBMD (Tb.vBMD), Cortical thickness (Ct.Th), Cortical porosity (Ct.Po), Trabecular Number (Trab.N), Standard deviation of Trabecular separation (Tb.Sp.SD), Failure Load (FL) and strength (K). We performed multiple linear regression analysis (HR-pQCT parameters as the dependent variable and VFAT or SFAT quartiles as the primary independent variable). All analyzes were adjusted for age and BMI. **Results :** At the radius, Ct.Ar ($p=0.035$), FL ($p=0.006$) and K ($p=0.005$) were significantly lower in the highest quartile of VFAT compared with the other quartiles. At the tibia, Ct.Ar ($p=0.0001$), Tb.Sp.SD ($p=0.001$), FL ($p=0.002$) and K ($p=0.003$) were significantly lower in the highest quartile of VFAT. At the radius Tt.Ar ($p=0.001$) and Tb.Ar (0.006) were significantly lower in the highest quartile of SFAT compared with the other quartiles. At the tibia, Ct.Ar ($p=0.008$) and Tt.Ar ($p=0.016$) were significantly lower in the highest quartile of SFAT. **Conclusion :** We found that highest VFAT and SFAT values are associated with smaller bone size. Highest values of VFAT-but not SFAT are associated with lower bone strength supporting the deleterious effect of VFAT on bone. This could be explained by both a smaller size of the bone and some metabolic effect, such as low-grade inflammation from the VFAT compartment. **1. Visceral Adipose Tissue Is Associated With Bone Microarchitecture...**, J Bone Miner. Res., 25:2:10.

Disclosures: Francois Duboeuf, None

FRI-0004

Effects of parathyroidectomy on the biology of bone tissue in patients with chronic kidney disease and secondary hyperparathyroidism Geovanna O. Pires^{*1,2}, Itamar O. Vieira¹, Fabiana R. Hernandez³, Andre L. Teixeira¹, Ivone B. Oliveira¹, Wagner V. Dominguez¹, Luciene M. Dos Reis¹, Fabio M. Montenegro⁴, Rosa M. Moyses^{1,5}, Aluizio B. Carvalho³, Vanda Jorgetti^{1,2}. ¹Laboratório de Investigação Médica 16, Hospital das Clínicas da Faculdade de Medicina da Universidade de São Paulo, Brazil, ²Hospital Samaritano Américas Serviços Médicos, Brazil, ³Nephrology Division, Federal University of São Paulo, Brazil, ⁴Disciplina de Cabeça e Pescoço, Hospital das Clínicas da Faculdade de Medicina da Universidade de São Paulo, Brazil, ⁵Pos-Graduate Medicine Program, UNINOVE, Brazil

Secondary hyperparathyroidism (SHP) is a complication of chronic kidney disease that compromises skeletal integrity. In patients with SHP undergoing parathyroidectomy (PTx), parathyroid hormone (PTH) levels dramatically fall. The effects of PTx are poorly understood, especially regarding proteins expressed by osteocytes, such as fibroblast growth factor 23 (FGF23), dentin matrix protein 1 (DMP-1), matrix extracellular phosphoglycoprotein (MEPE), sclerostin (Scl), receptor activator of nuclear factor kappa β ligand (RANKL) and osteoprotegerin (OPG), which regulate bone turnover. We aimed to characterize the bone expression of these proteins by immunohistochemistry and correlate them with those of bone histomorphometry before and after PTx. We studied bone biopsies, before and 12 months after PTx, from 23 patients. The attached table reports the results. We observed an improvement in biochemical parameters (Calcium, Phosphorus, Alkaline Phosphatase, and PTH). Also, we observed an improvement in trabecular thickness (Tb.Th), trabecular separation (Tb.Sp), and trabecular number (Tb.N); a decrease in osteoid volume (OV/BV), osteoid thickness (O.Th), osteoid surface (OS/BS), osteoblast surface (Ob.S/BS), eroded surface (ES/BS), osteoclast surface (Oc.S/BS), total osteocytes per bone area (Ost total/B.Ar), total osteocytes per tissue area (Ost total/T.Ar), and fibrosis (Fb.V/TV). But, an impaired mineralization [bone formation rate (BFR/BS), mineralizing surface (MS/BS) and mineralization lag time (Mlt)], after PTx. We found significant increases in Scl and OPG expression and a decrease in the RANKL/OPG ratio after PTx. We detected also correlations in the relative changes before (Δ) and 12 months after PTx between osteocyte proteins and bone histomorphometric parameters: Δ Scl and Δ BV/TV, Δ Tb.N, Δ O.Th and Δ Tb.Sp; Δ RANKL and Δ BV/TV, Δ Tb.N, and Δ Tb.Sp; Δ RANKL/OPG ratio and Δ Ob.S/BS, suggesting the involvement of these proteins in the improvement of bone lesions due to SHP. We conclude that after PTx, significant changes in the bone expression of osteocyte proteins occur and these proteins may potentially regulate bone remodeling.

	Before PTX (N=23)	12 months after PTX (N=23)	p
Clinical data			
Age (years)	41.91 \pm 12.5	-	-
Male (%)	43.4	-	-
Hemodialysis time (months)	96.96 \pm 45.54	-	-
Biochemistry			
Calcium (mg/dl)	10.18 \pm 0.89	9.43 \pm 1.06	0.0214
Phosphorus (mg/dl)	6.83 \pm 2.01	5.33 \pm 1.62	0.0022
Alkaline phosphatase (U/l)	676 (177-2587)	109 (49-233)	<0.0001
PTH-intact (pg/ml)	1960 (597-3587)	58 (1-303)	<0.0001
Histomorphometry			
Tb.Th (μ m)	111.8 \pm 25.27	142.2 \pm 34.8	0.0001
Tb.Sp (μ m)	658.2 (86.39-1299)	585.5 (131-3627)	0.0275
Tb.N (1/mm)	1.34 (0.68-5.39)	1.38 (0.3-4.3)	0.0085
OV/BV (%)	10.57 (1.74-32.4)	4.49 (0.17-17.76)	0.0002
O.Th (μ m)	11.82 \pm 3.06	7.84 \pm 2.17	<0.0001
OS/BS (%)	52.45 \pm 16.41	38.78 \pm 24.96	0.0119
Ob.S/BS (%)	13.43 (4.46-44.1)	1.5 (0-8.9)	<0.0001
ES/BS (%)	15.77 (3.83-25.5)	1.95 (0-14.6)	<0.0001
Oc.S/BS (%)	4.58 (1.2-9.14)	0.34 (0-1.34)	<0.0001
Fb.V/TV (%)	6.76 (0.63-19.05)	0.03 (0-0.94)	<0.0001
BFR/BS (μ m ³ /mm ² /day)	0.17 (0.04-0.43)	0.006 (0.006-0.096)	<0.0001
MS/BS (%)	15.52 (3.93-27.7)	2.92 (0.33-21.9)	<0.0001
Mlt (days)	32.3 (5.6-104.6)	809.9 (7.4-809.9)	<0.0001
Ost total/B.Ar (n/mm ²)	127.8 \pm 45	78.7 \pm 30.6	<0.0001
Ost total/T.Ar (n/mm ²)	27.3 (4.9-75.4)	17.9 (1.6-61.3)	0.0018
Immunohistochemistry			
Scl (%)	3.95 (0.25-37.1)	13.5 (3.03-41.42)	0.0009
OPG (%)	0.74 (0.17-3.03)	2.54 (0.26-16.12)	0.0001
RANKL/OPG (UA)	3.39 (0.37-13.95)	1.50 (0.29-14.35)	0.040

Correlations in relative changes between osteocytes proteins and histomorphometric parameters			
Δ Scl	Δ BV/TV	-0.54	0.007
	Δ O.Th	-0.50	0.0015
	Δ Tb.N	-0.51	0.012
	Δ Tb.Sp	0.51	0.012
Δ RANKL	Δ BV/TV	-0.45	0.046
	Δ Tb.N	-0.55	0.012
Δ RANKL/OPG	Δ Tb.Sp	0.53	0.015
	Δ Ob.S/BS	-0.48	0.033

Values are expressed as the mean and standard deviation or median and extremes. PTx, parathyroidectomy; PTH-intact, parathyroid hormone; BV/TV, bone volume; Tb.Th, trabecular thickness; Tb.Sp, trabecular separation; Tb.N, trabecular number; OV/BV, osteoid volume; O.Th, osteoid thickness; OS/BS, osteoid surface; Ob.S/BS, osteoblastic surface; ES/BS, eroded surface; Oc.S/BS, osteoclastic surface; Fb.V/TV, fibrosis volume; BFR/BS, bone formation rate; MS/BS, mineralizing surface; Mlt, mineralization lag time; Ost total: total number of osteocytes; Ost total/B.Ar: total osteocytes normalized to the trabecular bone area; Ost total/T.Ar: total osteocytes normalized to the tissue area analyzed; Scl, Sclerostin; OPG, osteoprotegerin; RANKL/OPG, receptor activator of nuclear factor kappa β ligand and OPG ratio; UA, Arbitrary unity; r, Spearman correlation coefficient.

Disclosures: Geovanna O. Pires, None

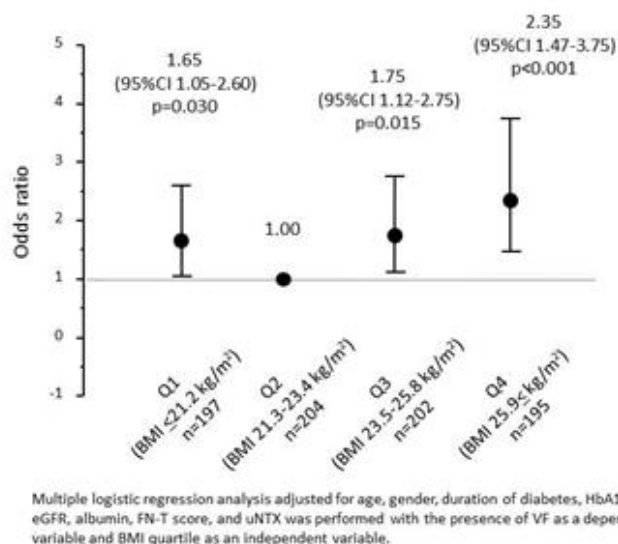
FRI-0005

Overweight and Underweight Are Risk Factors for Vertebral Fractures in Patients with Type 2 Diabetes Mellitus Ipei Kanazawa*, Masakazu Notsu, Ken-Ichiro Tanaka, Toshitsugu Sugimoto. Shimane University Faculty of Medicine, Japan

Purpose: Several studies suggest that obesity may be a risk factor for fracture although the relationship between body mass index (BMI) and fracture risk is unknown in type 2 diabetes (T2DM). We thus aimed to examine the association between BMI and the prevalence of vertebral fracture (VF) in Japanese patients with T2DM. Methods: In this cross-sectional study, 798 subjects (500 men and 298 women) with T2DM were enrolled. Bone mineral density (BMD) of femoral neck (FN) was measured by the dual-energy X-ray absorptiometry. VF was defined by semi-quantitative method using lateral X-ray films of the thoracic and lumbar spine. The association of BMI quartiles (Q1; < 21.2 kg/m², Q2; 21.3 – 23.4 kg/m², Q3; 23.5 – 25.8 kg/m², Q4; 25.9 < kg/m²) with the presence of VF was examined. Results: According to BMI increase, urinary N-terminal cross-linked telopeptide of type-I collagen (uNTX), a bone resorption marker, was significantly decreased, and FN-BMD, FN-T score, and FN-Z score were significantly increased. Subjects in Q2 quartile had less prevalence of VF (29.4%) compared to others in Q1 (43.1%), Q3 (28.6%), and Q4 (41.5%). Multiple logistic regression analyses adjusted for age, gender, duration of diabetes, HbA1c, estimated glomerular filtration rate, and serum albumin showed that Q1, Q3, and Q4 were significantly associated with an increased VF risk compared to Q2 as a reference [Q1; odds ratio (OR) = 1.91, 95% confidence interval (CI) 1.24 – 2.95, p = 0.004, Q3; OR = 1.65, 95%CI 1.07 – 2.55, p = 0.023, and Q4; OR = 2.18, 95%CI 1.39 – 3.41, p < 0.001]. Moreover, these associations remained significant after additional adjustment for femoral neck T score and uNTX (Figure). When the associations were examined separately in men and women, same tendencies were observed as the results of total subjects although some associations became insignificant because the number of the subjects was reduced. Conclusions: This is the first study to show that both overweight and underweight were associated with the BMD-inde-

pendent risk of VF in patients with T2DM. Therefore, body weight modification should be considered to protect diabetes-related bone fragility.

Association between BMI quartile and the risk of VF in patients with T2DM



Disclosures: *Ipppei Kanazawa, None*

FRI-0006

Cinacalcet restores bone quality in CKD-MBD mice by modulating Wnt10b and klothe signaling in bone cells

Jia-Fwu Shyu¹, Tzu-Hui Chu¹, Yi-Jun Lin¹, Lo-Wei Chen², Cheng-Yuan Hsiao¹, Wen-Chih Liu⁴. ¹Department of Biology and Anatomy, National Defense Medical Center, Taiwan, ²Department of Biology and Anatomy, National Defense Medical Center, United Republic of Tanzania, ⁴Graduate Institute of Clinical Medicine, College of Medicine, Taipei Medical University, Taiwan

Chronic kidney disease (CKD) is a global health problem of growing incidence that affects 5 to 15% of the world's population. The mineral and bone disorder (MBD) begins early in CKD consisting of vascular calcification, osteodystrophy, loss of klothe and increased FGF23 secretion. Progress has been made into the causes of CKD-MBD, but they remain largely unknown. Recent studies have suggested that adding a calcimimetic agent, namely cinacalcet, can reduce the risk of fractures in CKD-MBD patients. Further insights into the action of cinacalcet in bone cells might lead to calcium sensing receptor-based drugs that maximize not only the effects of the receptor on the parathyroid glands and kidneys but also on bone. Two-step 5/6 nephrectomy protocol was performed in 8-wk-old male mice. Four weeks later these CKD mice were treated with cinacalcet for 4 more weeks. μ CT images demonstrated obvious deterioration of bone microstructure in CKD mice as compared with the control mice. Moreover, the CKD mice exhibited decreased cortical bone thickness, increased cortical porosity, impaired trabecular bone volume and bone surface density, and decreased trabecular number in comparison with the control mice. Cinacalcet-treated CKD mice revealed significantly increased cortical thickness and significantly reduced cortical porosity compared with saline-treated CKD mice. The roles of Wnt ligands and klothe involved in skeletal physiology and disease is not fully understood yet. We hypothesize that cinacalcet increases bone formation by inducing Wnt10b and klothe expression in bone cells. To test this hypothesis, bone marrow hematopoietic mononuclear cells were isolated from rat femur and tibia. They were induced into osteoclasts by M-CSF and RANKL treatments. In these cells, cinacalcet induced an increase of Wnt10b expression as examined by confocal and Western blot analysis. ELISA analysis also showed increase of Wnt10b expression in supernatant (condition medium) collected from the cinacalcet-treated osteoclasts. Culture of osteoblasts (isolated from neonatal rat calvarias) with the cinacalcet-treated osteoclasts condition medium increased mineralization as indicated by alizarin red staining. In addition, increased klothe expression was found in cinacalcet-treated osteoblasts. Taken together, these results indicate that upregulated Wnt and klothe signaling may be involved in the underlying mechanisms of using cinacalcet to restore bone quality in CKD-MBD mice.

Disclosures: *Jia-Fwu Shyu, None*

FRI-0007

Bone Material Strength Index as Measured by Impact Microindentation in Patients with Primary Hyperparathyroidism and Hypoparathyroidism

Jessica Starr¹, Gaia Tabacco², Rukshana Majeed¹, Beatriz Omeragic¹, Maximo Gomez¹, Leonardo Bandeira³, Mishaela Rubin¹. ¹COLUMBIA UNIVERSITY, United States, ²University Campus Bio-Medico, Italy, ³Instituto FBandeira de Endocrinologia, United States

PTH is a regulator of cortical bone properties. Increased levels in primary hyperparathyroidism (PHPT) lead to cortical bone loss while deficient levels in hypoparathyroidism (HypoPT) increase cortical thickness. Yet the effects of PTH excess and deficiency on cortical bone tissue properties as assessed by in vivo impact microindentation are unknown. We hypothesized that bone material strength index (BMSi) would be decreased in PHPT and increased in HypoPT as compared to euparathyroid controls. Impact microindentation was performed in 50 subjects (PHPT, HypoPT and Control) to assess BMSi at the anterior surface of the mid-tibia diaphysis. Areal bone mineral density (aBMD) (g/cm²) of the lumbar spine (LS), femoral neck (FN), total hip (TH) and distal 1/3 radius (DR) were measured by dual-energy X-ray absorptiometry (DXA) in PHPT and HypoPT. Controls were selected to match either PHPT or HypoPT subjects by age (PHPT [n=13]: 59.3±15 yrs; HypoPT [n=15]: 44.3±12.5 yrs; Controls [n=22]: 49.2±17 yrs) and gender (proportion female: PHPT: 69%; HypoPT: 73%; Controls: 77%). Serum calcium differed between the groups (PHPT: 10.7±1 mg/dl; HypoPT: 8.6±1 mg/dl; Controls: 9.5±1 mg/dl; p<0.001), as did PTH levels (PHPT: 73.6±40 pg/ml; HypoPT: 8.0±4 pg/ml; Controls: 31.4±22 pg/ml; p<0.001). As compared to controls, BMSi was 12% lower in PHPT (Controls: 77.2 ± 8 vs PHPT: 67.8 ± 9; p=0.01) and 11% lower in HypoPT (Controls 77.2 ± 8 vs HypoPT 68.4 ± 10; p=0.02); the differences persisted after adjusting for age and gender. BMSi in PHPT and HypoPT did not differ (p=0.98). DXA T-scores were higher in HypoPT than in PHPT at the FN (HypoPT: -0.13 ± 2 vs PHPT: -1.24 ± 2; p=0.06), TH (HypoPT: 0.03 ± 1 vs PHPT: -0.83 ± 1; p=0.06) and DR (HypoPT: -0.03 ± 1 vs PHPT: -1.38 ± 1; p=0.01), although not at the LS (HypoPT: -0.14 ± 1 vs PHPT: -0.63 ± 2; p=0.45). In conclusion, PHPT and HypoPT subjects have worse cortical bone indentation properties as measured by in vivo impact microindentation of the tibial diaphysis when compared to controls. BMSi is reduced in HypoPT to a similar extent as in PHPT, despite higher aBMD T-scores. These data suggest that measurement of BMSi may reflect a different aspect of skeletal behavior than that assessed by aBMD. The results provide a rationale for future investigations aimed at assessing mechanisms by which abnormal PTH levels impact cortical bone tissue properties and at determining whether BMSi can predict fracture in PHPT and HypoPT patients.

Disclosures: *Jessica Starr, None*

FRI-0008

Parathyroid Gland Localization in Primary Hyperparathyroidism: Evaluation of a Novel Imaging Protocol and Direct Head-to-Head Comparison of Parathyroid 4D-CT and Sestamibi SPECT/CT

Randy Yeh*, Yu-Kwang Donovan Tay, Gaia Tabacco, Laurent Derclé, Jennifer Kuo, Leonardo Bandeira, Catherine Mcmanus, James Lee, John Bilezikian. Columbia University Medical Center, United States

Background Accurate preoperative imaging is critical to the success of minimally invasive parathyroidectomy. At most institutions, technetium 99m (99mTc) sestamibi scintigraphy and ultrasound, often used in combination, are the imaging modalities of choice. A more recent approach, 4-dimensional computed tomography (4D-CT) has demonstrated excellent accuracy in preoperative localization of abnormal parathyroid tissue. In some studies, 4D-CT has appeared to be superior to sestamibi. We evaluated the accuracy of the combined use of 4D-CT and sestamibi SPECT/CT and performed a direct head-to-head comparison of each modality using a one-stop imaging protocol performed on a single SPECT/CT scanner. Methods Four hundred consecutive patients with primary hyperparathyroidism (PHPT) who had parathyroidectomy (PTX) first underwent the combined imaging protocol. The imaging protocol consisted of dual-phase sestamibi SPECT/CT and 4D-CT, with 4D-CT acquired immediately after the delayed phase sestamibi SPECT/CT acquisition and the patient in the same position and SPECT/CT scanner. Using a 4-quadrant analysis, sensitivity, specificity and area under the curve (AUC) for localization were compared for sestamibi SPECT/CT and 4D-CT, alone and in combination. The reference standard for successful PTX was an intraoperative drop in PTH > 50% and pathological confirmation of an adenoma or hyperplasia. Results Combination of 4D-CT/Sestamibi and 4D-CT alone had the highest AUCs of 0.879 [95% CI 0.857 - 0.900] and 0.875 [0.853-0.897] and were not statistically different from each other. Both had a significantly higher AUC than sestamibi alone of 0.784 [0.756-0.811]. 4D-CT had higher sensitivity than sestamibi (79% vs. 58%) and demonstrated sensitivity equal to combined 4D-CT/Sestamibi (80%). While sestamibi showed the highest specificity (99%), both 4D-CT and combined 4D-CT/Sestamibi still demonstrated very high specificity at 96% and 95%, respectively. In a subset analysis, 4D-CT had higher sensitivity than sestamibi in single gland (92% vs. 75%) and multigland disease (58% vs. 31%). Conclusion The combination of 4D-CT/Sestamibi did not improve the accuracy of 4D-CT alone, but was superior to sestamibi alone. 4D-CT provides superior preoperative localization compared to sestamibi in patients with single and multigland disease. 4D-CT should be considered as a first-line modality in the preoperative localization of abnormal parathyroid tissue in primary hyperparathyroidism.

Comparison of Diagnostic Performance of Different Modalities							
Modality	ALL PATIENTS			SINGLE GLAND DISEASE		MULTIGLAND DISEASE	
	AUC (95% CI)	Sensitivity	Specificity	Sensitivity	Specificity	Sensitivity	Specificity
4D-CT	0.875 (0.853-0.897)	79%	96%	92%	97%	58%	88%
Sestamibi SPECT/CT	.784 (0.756-0.811)	58%	99%	75%	99%	31%	96%
4D-CT + Sestamibi SPECT/CT	0.879 (0.857-0.900)	80%	95%	94%	96%	58%	86%

Disclosures: **Randy Yeh, None**

FRI-0053

Slc20a2, encoding the phosphate transporter PiT2, is a novel genetic determinant of bone quality and strength Sarah Beck-Cormier^{*1}, Christopher J. Lelliott², John G. Logan³, David T. Lafont², Victoria D. Leitch³, Natalie C. Butterfield³, Hayley J. Protheroe³, Peter I. Croucher⁴, Paul A. Baldock⁴, Alina Gaultier-Lintia⁵, Gael Nicolas⁶, Nina Bon¹, Sophie Sourice¹, Jérôme Guicheux¹, Laurent Beck¹, Graham R. Williams³, J. H. Duncan Bassett³. ¹Inserm, UMR 1229, RMeS, Regenerative Medicine and Skeleton, Université de Nantes, UFR Odontologie, ONIRIS, Nantes, F-44042, France, ²Mouse Pipelines, Wellcome Trust Sanger Institute, Hinxton, CB10 1SA, United Kingdom, ³Molecular Endocrinology Laboratory, Department of Medicine, Imperial College London, London W12 0NN, United Kingdom, ⁴The Garvan Institute of Medical Research, Sydney, NSW 2010, Australia, ⁵CHU Nantes, Laennec Hospital, Nantes, F-44093, France, ⁶Normandie Univ, UNIROUEN, Inserm U1245 and Rouen University Hospital, Department of Genetics and CNR-MAJ, F 76000, Normandy Center for Genomic and Personalized Medicine, Rouen, France

Fracture susceptibility is currently predicted by assessment of bone mineral density (BMD) but is also determined by bone quality. Bone quality describes the material properties of the skeleton that contribute to strength independently of BMD, and has recently emerged as an important research priority as it cannot currently be integrated into the clinical prediction of fracture risk. Phosphate (Pi) is a major ion component of the bone matrix and its uptake by mineralizing cells is considered a pre-requisite for mineralization. In vertebrates, the type III co-transporters (PiT1/SLC20A1 and PiT2/SLC20A2) are the only sodium-Pi co-transporters known to be expressed in skeletal tissues, and are thought to be essential for Pi delivery during mineralization. To determine the physiological role of PiT2 in tissue mineralization, we performed detailed characterization of the skeletal phenotype of Slc20a2-deficient mice (n=3-6 Slc20a2^{-/-} and wild-type mice per age, per sex) and evaluated the bone phenotype of 21 patients with heterozygous pathogenic variants in SLC20A2 leading to Primary Familial Brain Calcifications (PFBC). We showed that juvenile Slc20a2^{-/-} mice had abnormal endochondral (decreased height of the growth plate, p<0.01) and intramembranous ossification (reduced cranial length (p<0.001), zygomatic width (p<0.01) and mandibular length (p<0.01)), decreased BMD (p<0.001), impaired mineral accrual and short stature. In adult mice, μ CT analysis, quantitative back-scattered electron-scanning electron microscopy (qBSE-SEM) and biomechanical testing revealed small reduced trabecular and cortical volumes (p<0.05 and p<0.001, respectively) and mineralization (p<0.001) but a profound impairment of bone strength (reduced bone stiffness and strength, p<0.001 and p<0.01, respectively). Bone quality was therefore investigated by comparing bone mineral content (BMC) and biomechanical parameters in Slc20a2^{-/-} mice and 320 age and sex-matched wild-type controls. This analysis showed that bone quality was severely impaired in Slc20a2^{-/-} mice. In human, we showed that mean bone density in occipital condyle and thickness of parietal bone spongiosa were decreased in PFBC patients compared to controls, suggesting they may also have impaired skeletal tissues. Altogether, these studies identify Slc20a2 as a physiological regulator of tissue mineralization and highlight a critical role for phosphate transport in the determination of bone quality and strength.

Disclosures: **Sarah Beck-Cormier, None**

FRI-0054

Bone strength and mineralization are regulated independently of bone mass by ephrinB2-dependent autophagic processes in osteocytes Vrahnas Christina^{*1}, Toby Dite¹, Yifang Hu², Huynh Nguyen³, Mark R Forwood³, Keith R Bamberg⁴, Mark J Tobin⁴, Gordon K Smyth², T John Martin¹, Natalie A Sims¹. ¹St. Vincent's Institute of Medical Research, Australia, ²Walter and Eliza Hall Institute of Medical Research, Australia, ³Griffith University, Australia, ⁴Australian Synchrotron, Australia

Bone formation has two phases: a rapid initiation (primary mineralization), followed by slower accrual of mineral (secondary mineralization) that continues until that portion of bone is renewed by remodeling. Initiation of bone mineralization, and late stage osteoblast differentiation, requires expression of EphrinB2 (Efnb2) in the osteoblast lineage, but the function of EphrinB2 in matrix-embedded osteocytes is not known. We previously reported at this meeting that osteocyte-specific EphrinB2 null mice (Dmp1Cre.Efnb2^{f/f}) exhibit an intrinsic defect in material strength. Their brittle bone phenotype was not associated with any change

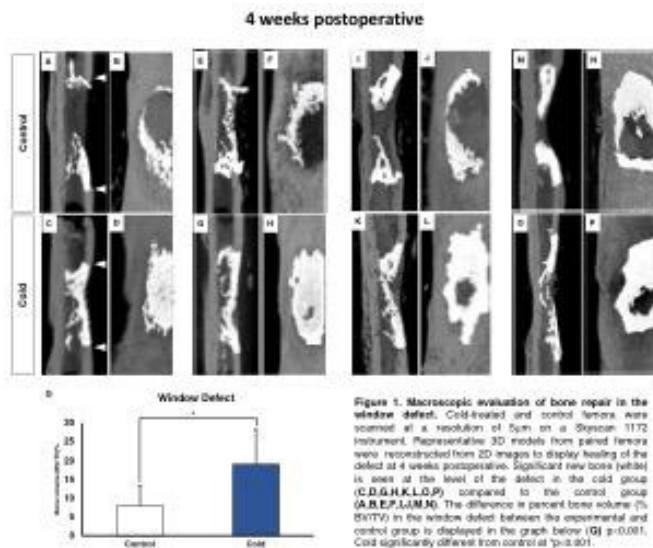
in moment of inertia, osteoblast numbers, nor any defect in the initiation of osteoid mineralization. However, secondary mineralization was significantly accelerated: after initiation of mineralization, mineral:matrix ratio, and carbonate:matrix ratio increased more rapidly in EphrinB2-deficient bones than controls (detected by synchrotron-based Fourier-transform infrared microspectroscopy). This indicated that osteocytic ephrinB2 suppresses mineral accumulation in bone. To identify novel mechanisms by which osteocytes regulate secondary mineralization bone mass, we carried out RNA sequencing of marrow-flushed cortical bone from Dmp1Cre.Efnb2^{f/f} brittle-bone mice and Dmp1Cre control littermates. This revealed 782 significantly up-regulated genes and 1024 down-regulated genes (FDR < 0.05). Genes previously known to regulate mineralization (e.g. Dmp1, Mepe, Sost, Phospho1, Enpp1, Enpp2) were not significantly modified by EphrinB2 deletion, and no regulation of the collagen type I genes (Col1a1 or Col1a2) was detected. By a literature search, we identified that >30% of the top 30 differentially expressed genes are associated with autophagy, a mechanism that mediates intracellular recycling and exocytic secretion. We therefore generated stable ephrinB2-deficient osteocyte cell lines (Ocy454) using shRNA. EphrinB2-deficient osteocytes deposited greater amounts of mineral in vitro than controls. They also showed a significantly greater increase in autophagic flux than control cells (the increase in LC3-II:I ratio in response to chloroquine treatment was increased by 30% compared to controls). This suggests that secondary mineralization of the bone matrix is controlled by autophagic processes in osteocytes, in a manner that is limited by ephrinB2. Such processes may be disrupted in conditions of bone fragility that are independent of bone mass.

Disclosures: **Vrahnas Christina, None**

FRI-0055

Non-invasive Localized Cold Therapy as a New Mode of Bone Repair Enhancement Marianne Comeau-Gauthier^{*}, Daniel Castano, Jose Luis Ramirez-Garcia Luna, Justin Drager, Jake Barralet, Geraldine Merle, Edward Harvey. McGill University, Canada

It has been observed that frequent cold-water exposure results in ectopic bone formation visualized in the outer ear[1,2]. Local cold therapy has been a time-honored treatment for inflammatory and painful musculoskeletal afflictions, but its effect on bone defect healing has never been studied. In vitro studies revealed that although osteoclastogenesis is enhanced upon cold application[3], the effect of hypothermia on osteoblasts is conflicting[4,5]. This project used repeated cold-water exposure as a novel non-invasive adjunct therapy to stimulate bone growth in a bilateral cortical defect model. Bilateral femoral window defects were drilled in 18 adult wild-type male mice. Starting postoperative day 1, one lower extremity was immersed daily in an ice bath for 15 minutes (temperature at bone level=19°C), whereas the other was used as control. Mice were euthanized at postoperative day (POD)-7 (early inflammatory phase) (n=6) and POD-28 (remodeling phase) (n=12). Bone formation was assessed using micro CT and histological analysis for alkaline phosphatase (ALP), tartrate resistant acid phosphatase (TRAP), CD34, and vascular endothelial growth factor (VEGF) to identify osteogenic cells, osteoclasts, endothelial vascular cells and angiogenesis respectively. Lowering the temperature at the defect site during the healing course resulted in a significant increase in bone volume (Fig.1), despite a decrease of the osteoblast activity at 4 weeks. Interestingly, immunohistochemical analysis demonstrated higher expression of VEGF and a greater number of CD34+ stained cells during the inflammatory healing stage (POD-7) accompanied with higher expression of TRAP. Interestingly, at 4 weeks this trend was inverted, and the expression of VEGF and CD34+ was decreased compared to the non-treated group. Our results demonstrate that daily local cold therapy for 4 weeks accelerates/enhances bone healing in a murine model of intramembranous bone repair. Further, our study suggests that this increase in osteogenesis is mediated by the upregulation of the VEGF pathway. Further studies exploring the mechanism of action of local cooling on bone healing, as well as the optimal treatment dose, duration, and frequency are warranted based on the results of this pilot study. If proven effective, local cold therapy can be introduced as a novel, cost effective, and non-invasive treatment modality to enhance bone healing in a clinical setting.



Disclosures: *Marianne Comeau-Gauthier, None*

FRI-0056

A Novel FEM Approach for Evaluating the Fracture Resistance of Human Cortical Bone Demonstrates that Material Heterogeneity Distributes and Attenuates Damage in Cortical Bone from Human Iliac Crest Biopsies
Ahmet Demirtas*¹, Erik Taylor², Eve Donnelly², Ani Ural¹. ¹Villanova University, United States, ²Cornell University, United States

Pathologic or therapeutic compositional changes at the microscale alter fracture resistance at larger length scales. However, the relative importance of these modifications on fracture risk has not been quantified. The aim of this study is to establish a finite element (FE) model capable of simulating the influence of material property alterations on the fracture resistance of human cortical bone biopsies. In particular, we examined the effect of material heterogeneity on the fracture behavior of cortical bone. An FE model was generated of a notched beam excised from an iliac crest biopsy (gender: F, age: 75y) loaded in three-point bending (Fig. 1a) by: (1) micro-computed tomography (μ CT) imaging of the beam at 1.4µm resolution, (2) processing the μ CT image via a MATLAB script to identify the location of cement lines and osteons, and (3) generating the 3D FE model using an image processing software, and a second MATLAB script (Fig. 1b). The model simulated fracture via cohesive extended finite elements (osteons and interstitial bone) and interface elements (cement lines). The influence of material heterogeneity on the fracture behavior of cortical bone was investigated by generating two models with distributions of material properties measured by nanoindentation (1) heterogeneous (HT) (Fig. 1c) and (2) homogeneous (HM), average material properties assigned to all osteons and interstitial bone. The fracture behavior was assessed by comparing the crack and damage volume at the same load. The HT material distribution increased the damage volume but reduced the crack volume compared to the HM material distribution (Fig. 1d,e). A major crack formed following the initial notch in the HM model (Fig. 1f) whereas the fractured elements were distributed in the HT model without the formation of a macrocrack (Fig. 1g). In addition, HT model resulted in greater amounts of low-level damage compared to the small amounts of high-level damage in the HM model (Fig. 1h,i). In conclusion, the current study developed a novel modeling approach that is capable of assessing the influence of material property distribution in human biopsies on their fracture response. The results demonstrated that material heterogeneity promoted energy dissipation and prevented crack growth in the bone. This approach has the potential to provide additional insight into the patient-specific effects of treatments and diseases which can improve fracture risk assessment and therapeutic interventions.

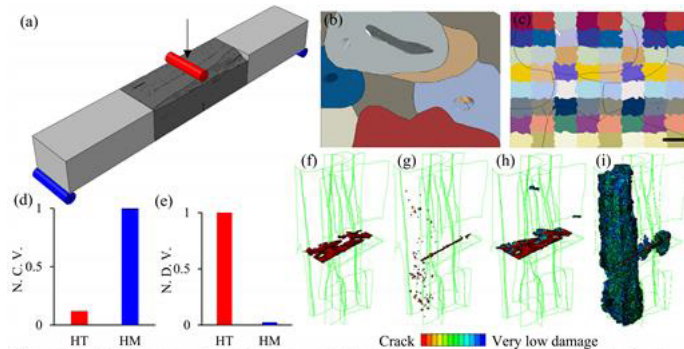


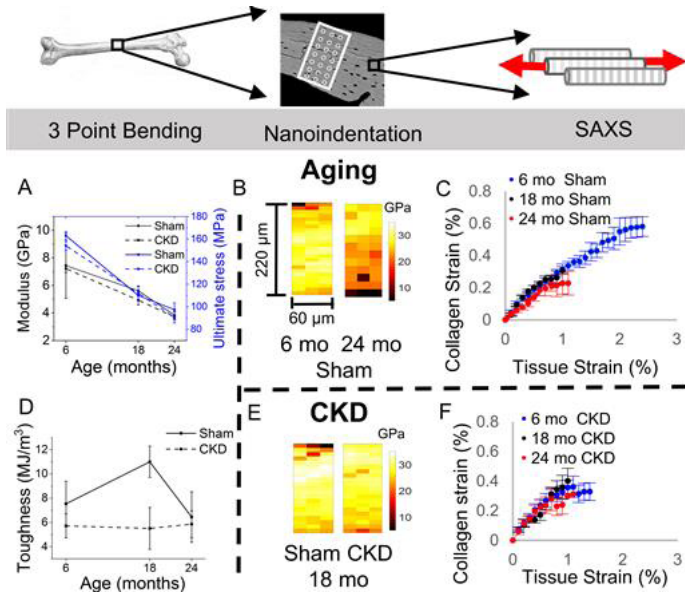
Figure 1: (a) Planar view of three point bending specimen where the dark grey section is the detailed microstructure region. The arrow on red cylinder shows the applied displacement and the blue cylinders show the fixed boundary conditions (span length = 3mm). (b) Cross-sectional view of the detailed model showing the osteons and interstitial bone. (c) Material assignment in HT model based on nanoindentation measurements. Each color represents a different value of material property (Scale bar = 50 µm). (d) Normalized crack volume (NCV) and (e) damage volume (NDV). Crack formation in (f) homogeneous (HM), and (g) heterogeneous (HT) models. Damage formation in (h) HM, and (i) HM models. In (f-i) the cement lines are highlighted with green.

Disclosures: *Ahmet Demirtas, None*

FRI-0057

Aging and Chronic Kidney Disease differently diminish bone mechanics from the nano- to whole-bone scales
Chelsea M Heveran*¹, Charles Schurman², Claire Acevedo³, Eric Schaible⁴, Eric W Livingston⁵, Moshe Levi⁶, Ted Bateman⁵, Tamara Alliston^{2,7}, Karen B King⁸, Virginia L Ferguson¹. ¹Department of Mechanical Engineering, University of Colorado at Boulder, United States, ²Department of Orthopaedic Surgery, University of California San Francisco, United States, ³Department of Mechanical Engineering, University of Utah, United States, ⁴Lawrence Berkeley National Laboratory, United States, ⁵Department of Biomedical Engineering, University of North Carolina, United States, ⁶Department of Biochemistry and Molecular & Cellular Biology, Georgetown University, United States, ⁷UC Berkeley/UCSF Graduate Program in Bioengineering, United States, ⁸Department of Orthopaedics, University of Colorado School of Medicine, United States

Aging and chronic kidney disease (CKD) commonly co-occur and both increase fracture risk. We hypothesized that aging and CKD, which each affect systemic mineral homeostasis and bone turnover, would differently diminish bone strength and toughness. Male C57Bl/6 mice received Sham or 5/6th nephrectomy (to induce CKD) surgeries and were killed after 3 mo at 6 mo (Sham: n = 6; CKD: 7), 18 mo (n = 8; 10), and 24 mo (n = 8; 8). Whole femur mechanics were evaluated via three-point bending (3PB). The femur mid-diaphysis was then dehydrated, embedded, sectioned, and polished. Nanoindentation arrays spanning the cortical thickness assessed reduced modulus (Er). Tissue tensile stress and strain were studied in the ulna-radius complex; collagen nanomechanics were monitored via change in d-spacing from synchrotron Small-Angle X-ray Scattering (SAXS). MicroCT evaluated cortical (midshaft femur) and trabecular (proximal tibia) microarchitecture. For Sham, aging (6 mo to 24 mo) reduced 3PB ultimate stress (-40.2%, $p < 0.05$), modulus (-48.4%, $p < 0.05$), and microscale Er (-9.2%, $p < 0.05$) (Fig 1A-B). Adjusting for age (ANCOVA), higher Er corresponded with lower 3PB ultimate stress ($r^2 = 86%$, $p < 0.05$), with no correlation to 3PB outcomes (Fig 1C). Cortical (\uparrow Ct.Po, \downarrow Ct.Th) and trabecular (\downarrow Tb.N, \downarrow Tb.Th) microarchitecture were lost with aging. Lower Ct.Th contributed to lower ultimate stress (ANCOVA $r^2 = 88%$; $p < 0.05$). CKD at 18 mo vs Sham reduced 3PB toughness (-49.9%, $p < 0.05$), but not ultimate stress or modulus, and microscale variance in Er (-19.8%, $p < 0.05$) (Fig 1D-E). SAXS tissue tensile strain declined with CKD ($p < 0.05$), and collagen fibers assumed greater % total strain ($p < 0.05$) (Fig 1F). Increased % collagen strain reduced 3PB toughness (ANCOVA $r^2 = 27%$; $p < 0.05$). CKD also impacted cortical (\downarrow Ct.Po, \downarrow Ct.Th) and trabecular microarchitecture (\downarrow Tb.N, \downarrow Tb.Th). Lower Tb.Th reduced 3PB modulus and strength (ANCOVA $r^2 = 79-83%$, $p < 0.05$). We show for the first time that aging and CKD differently diminish multiscale bone mechanics. Aging reduced whole bone strength and modulus, which is explained by altered tissue-scale stiffness and microarchitecture but not collagen mechanics. CKD reduced toughness, which is best explained by increased collagen strain burden. Our results demonstrate that aging and CKD may separately contribute to loss of skeletal strength and fracture resistance.



Disclosures: *Chelsea M Heveran, None*

FRI-0058

The Effect of Vitamin D3 Supplementation on Distal Radius Fracture Healing: A Randomized Controlled HR-pQCT Trial F.L. Heyer^{*1}, J.J.A. De Jong¹, P.C. Willems¹, J.J. Arts², S.M.J. Van Kuijk¹, J.A.P. Bons¹, M. Poeze¹, P.P. Geusens¹, B. Van Rietbergen³, J.P. Van Den Bergh¹. ¹Maastricht University Medical Center, Netherlands, ²Eindhoven University of Technology, Netherlands, ³Technical University of Eindhoven, Netherlands

Enhancing fracture healing using systemic therapies is gaining interest. Vitamin D3 is an important factor to consider in bone metabolism, especially in the population at risk for osteoporotic fractures in which there is a substantial prevalence of vitamin D deficiency. Animal studies have shown a positive effect of vitamin D3 supplementation on fracture healing, but evidence from clinical trials is scarce and inconclusive. We performed a randomized controlled trial to assess the effect of vitamin D3 supplementation on distal radius fracture healing using high-resolution peripheral quantitative computed tomography (HR-pQCT) and micro-finite element analysis (μFEA) based outcome parameters. Thirty postmenopausal women with a conservatively treated distal radius fracture were included within two weeks post-fracture and randomized in a control group, a low-dose and a high-dose intervention group receiving 30 000 IU and 75 000 IU vitamin D3 per six weeks equivalent to 700 IU/day and 1 800 IU/day, respectively. After the baseline visit 1-2 weeks post-fracture, follow-up visits were scheduled 3-4, 6-8 and 12 weeks post-fracture. At each visit, HR-pQCT scans of the fractured radius were performed. Cortical and trabecular bone microarchitectural parameters and μFEA derived torsion, compression and bending stiffness were assessed. In addition, venous blood samples were collected to assess serum markers of bone resorption (C-terminal telopeptide of type I collagen; CTX) and bone formation (N-terminal propeptide of type I procollagen; PINP). Serum levels of 25(OH)D3 were <50 nmol/L in 30-40% and <75 nmol/L in 60-90% of included patients. No statistically significant differences were observed between control and low-dose intervention groups in any of the outcome parameters (all p>0.05). High-dose vitamin D3 supplementation resulted in a decreased trabecular number (B -0.22; p<0.01) and lower compression stiffness (B -3.63; p<0.05), together with an increase in the bone resorption marker CTX (B 0.062; p<0.05), after correction for baseline 25(OH)D3-levels. We conclude that vitamin D3 700 IU/day supplementation does not improve distal radius fracture healing and that a dose of 1 800 IU/day may be detrimental to restoring bone stiffness during the first 12 weeks of fracture healing.

Disclosures: *F.L. Heyer, None*

FRI-0059

Differences in Microarchitectural and Nano-mechanical Properties of Bone Between Patients with and without Atypical Femoral Fracture after Prolonged Bisphosphonate Treatment Shijing Qiu^{*1}, Lanny Griffin², George Divine¹, Mahalakshi Honasoge¹, Arti Bhan¹, Shiri Levy¹, Elizabeth Warner¹, Sudhaker Rao¹. ¹Henry Ford Hospital, United States, ²California Polytechnic State University, United States

It is well-known that a small group of patients on long-term bisphosphonate (BP) therapy are predisposed to sustain atypical femoral fracture (AFF). However, the mechanism(s) resulting in AFF remains unclear. The purpose of this study is to determine the association of AFF with bone microarchitecture and remodelling, and its mechanical properties. Iliac bone

biopsies were obtained after double tetracycline labeling from 20 age-matched postmenopausal women with ≥2-year BP treatment, 10 with AFF (aged 67.4 ± 5.36) and 10 without AFF (aged 67.3 ± 6.83). The 5 μm sections were used to measure bone microarchitecture and remodeling status. Nanoindentation was performed on each bone block. As shown in Table, there was very little difference in cortical bone volume (BV/TV), and the nominal difference in cancellous BV/TV between patients with and without AFF was not statistically significant. Interestingly, wall thickness (W.Th) in all bone compartments (cancellous, cortical and endosteal) was significantly decreased in AFF patients. In contrast, erosion surface (ES/BS) and osteoclast surface (Oc.S/BS) in all bone compartments were numerically increased in AFF patients, but only the increase in Oc.S/BS in cortical bone reached statistical significance. Based on numerical data, the insignificant results may have been due to small sample size. Nano-indentation showed that the elastic modulus (E) of cortical bone was significantly increased in AFF patients. In summary, two morphological changes of bone (especially cortical bone) were noted in AFF patients: decreased W.Th and increased osteoclasts and bone resorption areas. Others have reported increased number of osteoclasts after 3 years of alendronate treatment, but approximately 1/3 were giant hyper-nucleated osteoclasts detached from bone surface (NEJM 2009;360:53-62). These osteoclasts have low capacity for bone resorption, producing shallow resorption cavities. Accordingly, accumulation of such abnormal osteoclasts may increase resorption area, but decrease resorption depth. The shallow resorption cavities would reduce W.Th, leading to an expansion of interstitial bone area with higher mineralization degree that may raise elastic modulus. Our previous work indicated that microdamage are much more likely to accumulate in the interstitial areas of cortical bone. Therefore, the increase in fragile interstitial bone is probably a crucial factor for the development of atypical fracture in femoral diaphysis.

Table 1. Comparison of bone histomorphometry and nano-mechanical properties between patients with and without atypical femoral fracture after long-term bisphosphonate treatment

	BV/TV	W.Th	ES/BS	Oc.S/BS	BFR/BS	E	H
Cancellous							
No AFF	19.6 (8.76)	35.4 (4.75)	1.75 (1.94)	0.192 (0.240)	1.75 (2.86)	16.5 (0.160)	2.11 (0.030)
AFF	13.7 (4.73)	29.3 (4.16)*	2.90 (3.39)	0.462 (0.628)	1.24 (2.34)	16.2 (0.170)	2.19 (0.030)
Cortical							
No AFF	95.5 (1.51)	42.2 (3.94)	1.38 (0.719)	0.158 (0.142)	4.23 (3.59)	16.6 (0.150)	2.05 (0.030)
AFF	95.3 (3.04)	36.3 (4.46)*	3.52 (2.17)	0.569 (0.392)*	4.62 (4.44)	17.5 (0.160)*	1.97 (0.027)
Endosteal							
No AFF		37.9 (4.66)	2.00 (0.899)	0.337 (0.271)	3.13 (3.70)		
AFF		32.6 (3.38)*	6.66 (10.7)	1.19 (1.52)	2.35 (4.30)		

* p<0.05

Disclosures: *Shijing Qiu, None*

FRI-0060

Effect of Exercise and Weight on Bone Health in 8-9 Year Old Children Sandra Shefelbine^{*1}, Vineel Kondiboyina¹, Lauren Raine¹, Arthur Kramer¹, Naiman Khan², Charles Hillman¹. ¹Northeastern University, United States, ²University of Illinois at Urbana-Champaign, United States

Obesity has reached epidemic proportions around the world. One in every six children in the United States is obese. It has been observed in various studies that when adjusted for their weight, obese children have lower bone mineral content (BMC) and bone mineral density (BMD), which may explain their high rates of fracture. BMD is an areal estimate and does not take into account the effect bone thickness. Bone mineral apparent density (BMAD=BMC/Area^{1.5}) is a volumetric estimate and has been recommended for assessing bone density in children. The objective of this study was to evaluate the effect of a 9-month physical activity intervention on BMC, bone area, and BMAD of children based on their pretrial weight class (normal weight, NW, and overweight/obese, O/O). Participants included overweight and obese (BMI> 85%, n=148) and healthy weight (n=203) preadolescents (8-9 years old). Their whole body bone mineral density (BMC), area, and bone mineral apparent density were recorded using dual X-ray absorptiometry (DXA). O/O children had a higher total BMC (p<0.001) than normal weight children but when adjusted for their weight BMC was lower in O/O children compared to normal weight children (p<0.001) in both pre-trial and post-trial assessments. Interestingly, pre-trial and post-trial whole body BMAD of O/O children was higher than normal weight children irrespective of adjustment by weight (p<0.001). Nine-months of exercise significantly increased BMC (p<0.001) and area (p=0.006) in both O/O and normal weight, but had no effect on BMAD. BMAD increased more in normal weight children than in O/O children in both the exercise and non-exercise groups (p=0.017). The change in BMAD and BMC due to exercise within weight groups was not significantly different from each other (p=0.53 and p=0.54). Therefore, due to exercise, the increase in the bone mineral content and area for normal weight and O/O children is similar but there is no significant change in the volumetric density. In summary, obesity in 8-9 year olds results in bones with higher BMC, area, and BMAD compared to normal weight bones. Exercise increases BMC and area but not volumetric density (BMAD) in both normal and O/O children. The greater increase in BMC and BMAD over the 9 months in normal weight compared to obese children indicates a slower rate of bone mass accrual, which may have implications for bone health during skeletal growth.

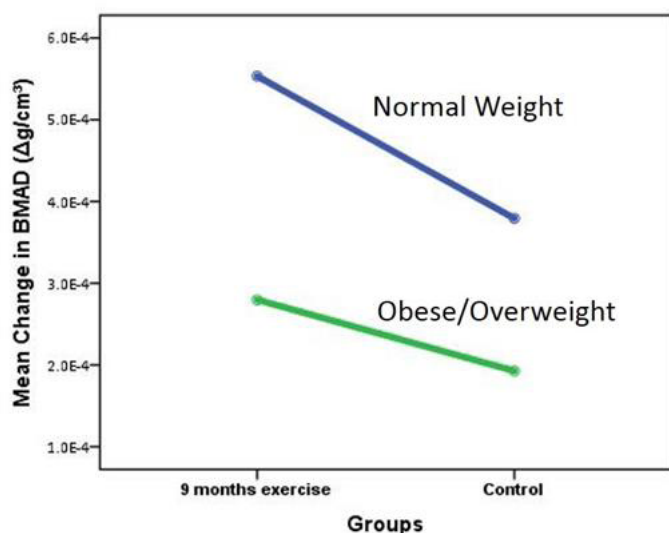


Figure 1: Change in BMAD over a 9 month period by weight class and treatment. Increase in BMAD is greater in normal weight than in O/O in both exercise and control groups. The increase in BMAD in the exercise group is not significantly different from the control group for either O/O or normal weight.

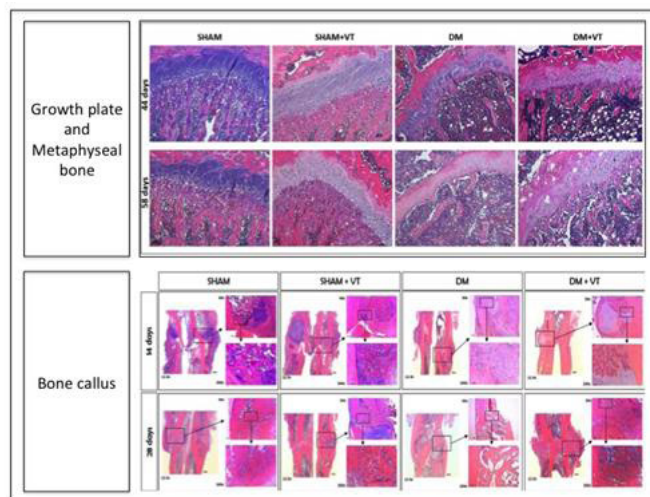
Disclosures: *Sandra Shefelbine, None*

FRI-0061

Uncontrolled hyperglycemia delays bone healing and disrupts the microstructure and gene expression of cartilaginous and bony cells at the growth plate, metaphyseal and subchondral bone in diabetic rats Ariane Zamarioli^{*1}, Beatriz P Trani¹, Maysa S Campos¹, João Paulo B Ximenez², Raquel A Silva³, José B Volpon¹. ¹School of Medicine of Ribeirão Preto, Brazil, ²School of Pharmaceutical Sciences of Ribeirão Preto, Brazil, ³School of Dentistry of Ribeirão Preto, Brazil

The aim of this study was to assess the effects of hyperglycemia on the growth plate, bone quality and fracture healing in diabetic and non-diabetic rats. For this, 112 female Wistar rats (200±10g) were assigned to four groups: (1) SHAM, (2) sham with vibration therapy (SHAM+VT), (3) diabetes mellitus (DM), and (4) DM+VT. Diabetes was induced with a single intravenous injection of streptozotocin. Thirty days after diabetes induction, animals underwent closed bone fracture at the right mid-femur, followed by surgical stabilization of bone fragments. Three days after bone fracture, DM+VT and SHAM+VT rats were subjected to whole-body vibration therapy (50 Hz, 3x/wk, 20 minutes). On days 14 and 28 post-fracture (representing two distinct phases of normal bone healing: soft and hard bone callus formation, respectively), the rats were euthanized, blood was collected for serum bone marker analysis, and both femurs were collected for real time PCR, micro-computed tomography and histological analysis. The left femur was used to assess the quality of growth plate, and both subchondral and metaphyseal bone. The right fractured femur was used to follow bone healing. Diabetes caused detrimental effects on the growth plate, metaphyseal and subchondral bone, as well as a delay in bone healing in hyperglycemic rats, with a decrease of 93% in circulating IGF-1 and an increase in CTX-I level. In intact bone, diabetes caused detrimental changes in growth plate (tridimensional volume, thickness, area of proliferative, hypertrophic and ossification zones and reduction in cells of the ossification and calcified zones), in metaphyseal bone microarchitecture (reduced BV by 90%, BV/TV by 87%, TbN by 85% and Conn.D by 77%) and in subchondral bone (reduction in BV/TV and Tb.Th and, increment in BS/BV and SMI). In bone healing, diabetes caused a delay in cell proliferation, 81% in callus volume and 69% in callus mineralization. The osteoblast differentiation marker RUNX-2 was less expressed in diabetic rats when compared to non-diabetics after 28 days of fracture. Conversely, vibration therapy exerted an osteogenic effect in accelerating bone healing and in increasing bone and cartilage quality, but only in diabetic rats. VT significantly increased the IGF-1 and decreased the RANK-L level. VT was effective at increasing growth plate thickness and at ameliorating metaphyseal microarchitecture (augmented BV by 494%, BV/TV by 386%, TbN by 394% and Conn.D by 233%, Fig 1), but no changes were seen in the subchondral bone. In bone callus, VT accelerated osteogenic and chondrogenic cell proliferation at the fracture callus (Fig 2), thus increasing callus volume by 52%. We concluded that diabetes had detrimental effects on both non-fractured bone quality and fracture healing. Vibration therapy was very effective at counteracting the significant disruption

in bone metabolism, mass and microarchitecture on both non-fractured and fractured femurs of diabetic rats.

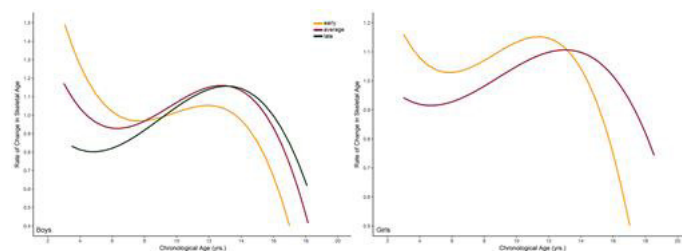


Disclosures: *Ariane Zamarioli, None*

FRI-0110

Identification of a Non-Linear Maturation Trajectory During Adolescence Melanie Boeyer^{*}, Emily Leary, Dana Duren. University of Missouri, United States

Assessments of a child's growth trajectory is of critical importance for clinicians treating skeletal growth and/or developmental disorders (e.g., leg length inequality). Current growth trajectory estimates are based on a child's chronological age and current height, with improvement occurring with the addition of a skeletal age assessment. Unfortunately, the precision of these estimates is rarely narrow, with implications for clinical outcomes. Variability in these estimates may be due, in part, to non-linear developmental patterns (i.e., maturational spurt). To assess the contribution of a maturational spurt to longitudinal growth, we assessed serial left hand-wrist radiographs, using the Fels Method, in 345 healthy boys and girls between 3 and 20 years of age from the Fels Longitudinal Study. The shape of individual developmental trajectories was examined to determine if skeletal age tracked linearly or curvilinearly (4th order fixed effect polynomials) with chronological age. Trajectories that exhibited a curvilinear relationship were further assessed for maturational spurt parameters (e.g., onset, peak, and cessation) using the first and second derivative of the polynomial model. All parameter estimates were determined separately for early, average, and late maturing boys and girls, defined based on the mean relative skeletal age at the parameters of the maturational spurt. Differences in the chronological age and the rate of maturation attained at each parameter were compared among maturity groups using a one-way ANOVA. Most (81%) boys and girls exhibited a curvilinear relationship between chronological age and skeletal age, with the maturational peak occurring most frequently in adolescence. Significant differences ($p < 0.001$) were observed in the chronological age of cessation, with early maturers reaching this milestone 10.8 and 15.2 months earlier than average maturing boys and girls, respectively. Late maturing boys failed to reach cessation prior to 20 years of age. No late maturing girls were identified. Although the parameters of the maturational spurt appear variable, when used in conjunction with other developmental milestones, such as peak height velocity or menarche, finer resolution in growth trajectory estimates will likely be achieved. These results highlight the curvilinear relationship between chronological age and skeletal age and combat the current paradigm that skeletal maturation is a linear process.



Disclosures: *Melanie Boeyer, None*

FRI-0111

Sexual Dimorphism in Cortical and Trabecular Bone Microstructure Appears During Puberty in Chinese Children Ka Yee Cheuk^{*1}, Xiao-Fang Wang², Ji Wang³, Zhendong Zhang³, Fiona Wp Yu¹, Vivian Wy Hung¹, Wayne Yw Lee¹, Ali Ghasem-Zadeh², Roger Zebaze², Tracy Y Zhu¹, X Edward Guo³, Jack Cy Cheng¹, Tsz Ping Lam¹, Ego Seeman². ¹Department of Orthopaedics and Traumatology, The Chinese University of Hong Kong, Hong Kong, ²Departments of Endocrinology and Medicine, Austin Health, University of Melbourne, Australia, ³Bone Bioengineering Laboratory, Department of Biomedical Engineering, Columbia University, United States

Distal forearm fractures during growth are more common in males than females. As metaphyseal cortical bone is formed by coalescence of trabeculae emerging from the periphery of the growth plate, we hypothesized that the later onset of puberty in males produces a longer delay in trabecular bone formation and coalescence resulting in a transient phase of higher cortical porosity, lower matrix mineral density and higher trabecular density than in females. We quantified the non-dominant distal radial microstructure in 433 healthy Chinese boys and girls aged 7 to 17 years using high-resolution peripheral quantitative computed tomography in Hong Kong. Measurements of 110 slices (9.02 mm) were acquired 5 mm proximal to the growth plate of the non-dominant distal radius. Porosity was measured using StrAx1.0; trabecular plate and rod structure were measured using Individual Trabecula Segmentation (ITS). Mechanical properties were estimated using finite element analysis (FEA). Results were after adjusted for age, total bone area, dietary calcium intake and physical activity level. In boys, total bone area was 14.7-18.6% larger throughout puberty, cortical area/total bone area was 5.6% smaller in Tanner stage 2 only, cortical porosity was 8.6-14.9% higher and matrix mineral density was 1.0-2.5% lower in Tanner stage 2 to 5, than in girls. Boys had higher rod BV/TV in Tanner stage 3 and 4, higher plate BV/TV and plate to rod ratio in Tanner stage 5 and 20.4% lower apparent modulus than girls in Tanner stage 2 ($p < 0.05$). A transient phase of higher porosity due to dissociation between bone mineral accrual and linear growth may contribute to higher distal radial bone fragility among Chinese males than females during growth.

Disclosures: **Ka Yee Cheuk**, None

FRI-0112

Elucidating the Mechanism of JAGGED1-mediated Osteoblast Commitment during Maxillary Development Archana Kamalakar^{*}, Melissa Oh, Samir Ballestas, Yvonne Coretha Stephenson, Steven Goudy. Emory University, United States

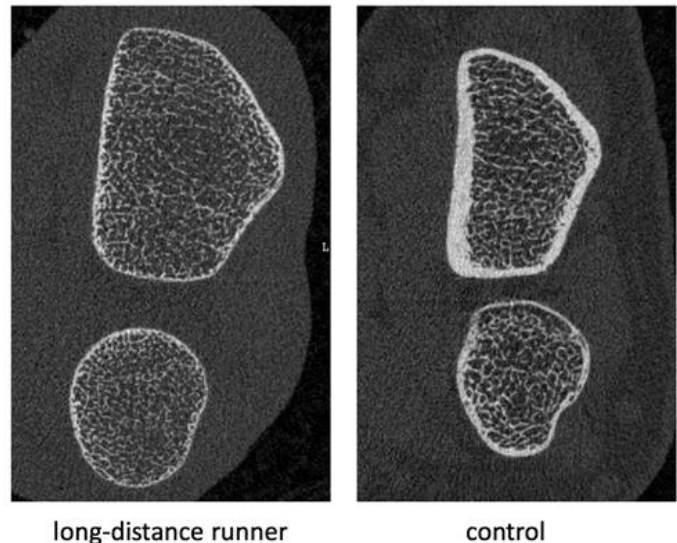
Maxillary bone deficiency (MBD) results from changes in cell signaling mechanisms during maxillary bone development, trauma or surgery. While in adults, bone morphogenetic protein (BMP2) is commonly used to ameliorate MBD, in pediatric cases, it leads to significant pain, erythema and inflammation. Therapies based on stimulation of bone formation without triggering painful inflammation in children with MBD are lacking. JAGGED1 (JAG1), a membrane-bound NOTCH ligand, is required for normal craniofacial development, and Jagged1 mutations in humans are known to cause maxillary bone hypoplasia and Alagille Syndrome, associated with bone demineralization and fractures. We previously demonstrated deficient maxillary osteo- and vasculo- genesis in *Wnt1-cre;Jagged1^{fl/fl}* (Jag1CKO) mice by conditional deletion of *Jagged1* in maxillary mesenchymal stem cells. We hypothesize that a JAG1-NOTCH1 pathway is essential for maxillary development and for differentiation of neural crest cells (osteoblast precursors) during intramembranous ossification. In this study, we investigated the JAG1 signaling pathways in a cranial neural crest cell line, O9-1. We observed significant increase in Notch1 gene expression within 3hrs of JAG1 treatment (5 fold>control) compared to untreated and BMP2-treated cells. As expected, treatment with DAPT, a γ -secretase inhibitor of NOTCH intracellular domain (NICD) cleavage, \pm JAG1, resulted in increased Notch1 gene expression, suggesting a compensatory mechanism in response to lack of NOTCH activity. Furthermore, osteoblast differentiation and maturation markers, Runx2 and OCN, respectively, as well as classic NOTCH1 targets, Hes1 and Hey1, were increased with JAG1 treatment. While Hes1 and Hey1 expression levels were predictably decreased after DAPT treatment, Runx2 and OCN levels were surprisingly constant in the presence of DAPT, indicating that JAG1 effects are independent of NICD cleavage. JAG1 treatment also led to increased JAK2 phosphorylation, which was refractory to DAPT treatment, further implicating the NICD cleavage-independent effects of JAG1. Pharmacologic inhibition of JAK2 phosphorylation upon JAG1 induction reduced Runx2 and OCN gene expression. Collectively, these data suggest that JAK2 is an essential component downstream of a non-canonical JAG1-NOTCH1 pathway through which JAG1 stimulates expression of osteoblast-specific gene targets that contribute to osteoblast differentiation and bone mineralization in maxillary development

Disclosures: **Archana Kamalakar**, None

FRI-0113

Menstrual abnormalities and cortical bone deterioration in young female athletes: an analysis by HR-pQCT Yuriko Kitajima^{*1}, Ko Chiba², Yusaku Isebe², Narihiro Okazaki², Naoko Murakami¹, Michio Kitajima¹, Kiyonori Miura¹, Makoto Osaki², Hideaki Masuzaki¹. ¹Department of Obstetrics and Gynecology, Nagasaki University Graduate School of Biomedical Sciences, Japan, ²Department of Orthopedic Surgery, Nagasaki University Graduate School of Biomedical Sciences, Japan

Purpose Young female athlete such as long-distance runners and rhythmic gymnasts sometimes have menstrual abnormalities, that causes problem with bone metabolism. HR-pQCT is a high resolution quantitative CT which enables us to investigate a patients' bone microstructure non-invasively. The purpose of this study is to investigate bone microstructural changes in young female athletes by HR-pQCT. Method Nineteen female athletes (middle and long-distance runners and rhythmic gymnasts, ages 15-21) and 29 female non-athletes (control, ages 15-23) participated in this study. A questionnaire survey was performed to obtain menstrual history. Distal radius and tibia were scanned by HR-pQCT at the voxel size of 61 μ m (XtremeCT II, Scanco Medical, Switzerland), and cortical and trabecular bone micro-structures were analyzed. Results 84.2% of female athletes had abnormal menstruation. BMI was lower in athletes than in the control group (18.4 and 20.9, respectively, $p < 0.01$). Cortical BMD was lower in athletes than in the control group (880.4 and 920.9 mg/cm³ at the radius, $p < 0.03$; 935.2 and 956.5 mg/cm³ at the tibia, $p < 0.01$). Cortical porosity at the radius was increased in athletes (0.34 and 0.20%, $p = 0.01$). Trabecular BMD, number, and thickness were not significantly different. Conclusion Young female athletes seem to be high risk population of abnormal menstruation and deteriorated cortical bone. Our study suggest that to maintain bone health in young female athletes, monitoring menstrual cycles is important.



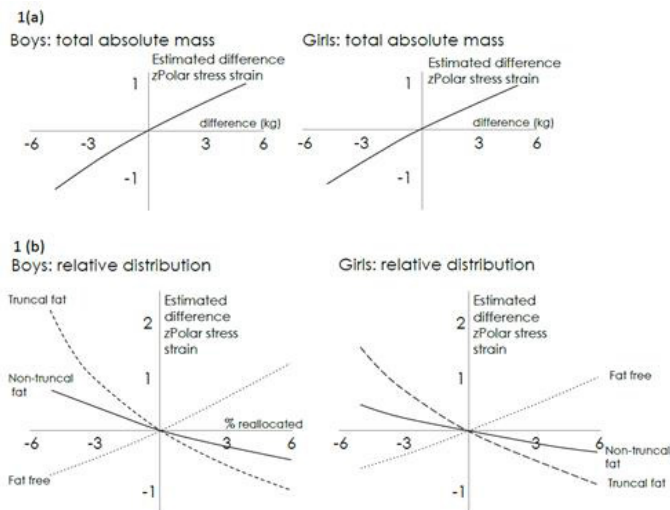
Disclosures: **Yuriko Kitajima**, MARUSAN-AI Co., Ltd., Grant/Research Support

FRI-0114

Body mass is important, but so is its distribution: associations between body composition and bone health measures in 11-12 year old children Peter Simm^{*1}, Dorothea Dumuid², Susan Clifford³, Grace Gell³, Timothy Olds², Melissa Wake³. ¹Dept of Endocrinology, Royal Children's Hospital Melbourne, Australia, ²Alliance for Research in Exercise, Nutrition and Activity, University of South Australia, Australia, ³Murdoch Children's Research Institute, Australia

The drivers of bone mass accrual in childhood remain unclear, with conflicting data about the role of body composition, and the relative impact of the underlying components such as fat mass and fat-free mass. The Child Health Checkpoint is a cross-sectional study of 11-12 year old Australian children, drawn from the national Longitudinal Study of Australian Children (LSAC). 1874 children attended for a single-day session involving multiple health measures, including peripheral quantitative computerised tomography (pQCT) of the non-dominant tibia, and body composition analysis (truncal fat, non-truncal fat, fat free mass) measured by bio-impedance. Compositional multiple linear regression explored the relationship between body composition and bone health measures (trabecular/cortical density and geometry). Novel isocompartmental substitution modelling quantified the differences in bone health associated with the reallocation of mass between body compartments. Models were adjusted for age, height, pubertal stage, socioeconomic status and moderate-vigorous physical activity. 843 subjects (49.3% male) with complete data participated in these analyses. In non-compositional analyses of bone parameters, higher fat-free mass was associated with overall improved skeletal geometry and trabecular density, but lower cortical density.

However, higher truncal and nontruncal fat had the opposite effect. Figure 1(a) shows that polar stress-strain index (SSI) increases linearly with overall mass, consistent with previous studies showing body mass drives improved bone health parameters in young people. Compartmental substitution modelling revealed profoundly opposing effects of different elements of body composition (see figure 1 (b)). For example, a 6% absolute increase in fat-free mass was associated with a 1 SD increase in SSI while a 3% absolute reduction in truncal fat was associated with an approximately 1 SD increase. Effects for non-truncal fat were similar in pattern, but much weaker, to those for truncal fat. These findings emphasize that while heavier children in general have stronger bones, it is higher lean mass combined with lower truncal fat that drives improved outcomes at any given total body mass. The role of non-truncal fat seems less important. If these relationships are confirmed in experimental studies, interventions that maximise fat-free mass and minimise truncal fat could lead to long term, population-wide skeletal health benefits.



Disclosures: Peter Simm, None

FRI-0135

Osteocalcin is necessary and sufficient to mount an acute stress response
Julian Berger*, Lori Khimian, Karsenty Gerard. Columbia University, United States

While trying to identify a common thread between the diverse functions of the hormone we noticed that memory, adaptation to exercise, energy expenditure and male fertility that are all favored by osteocalcin, are survival functions for animals living in hostile conditions such as in the wild. This observation prompted us to ask whether osteocalcin contributes to a quintessential survival function, the acute stress response (ASR). This investigation revealed that osteocalcin exhibits two major features of a stress hormone. First, circulating bioactive osteocalcin levels increase two to four times within 5 to 15 minutes in wild type (WT) mice exposed to any type of stressors. The same is true in rats and humans. The bone's response to stress is specific to osteocalcin, independent of transcriptional events, sympathetic tone or the adrenal glands, but requires the integrity of neurons of the amygdala. Second, analysis of mice lacking Osteocalcin (*Ocn*^{-/-}) or its receptor in peripheral organs (*Gprc6a*^{-/-}) demonstrates that osteocalcin signaling in peripheral organs, is necessary for the full development of the following manifestations of the ASR: increased heart rate, hyperventilation, and enhanced energy expenditure. Anatomical, molecular, genetic, and electrophysiological evidence obtained in WT and *Gprc6a*^{-/-} mice or cells shows that to favor these physiological processes osteocalcin signals in post-ganglionic parasympathetic neurons to inhibit their activity thereby leaving the sympathetic tone unabated. Next to assess the respective contribution of osteocalcin and glucocorticoid signaling in triggering an ASR we analyzed the stress manifestations mentioned above in WT mice that had been adrenalectomized (Adx). Surprisingly, we observed that WT Adx mice have an ASR that is identical in intensity to the one of WT mice. Since corticosterone inhibits Osteocalcin expression, WT Adx mice also display a two- to three-fold increase in circulating osteocalcin. We reasoned that if osteocalcin was sufficient to mount an ASR, the hyperosteocalcinemia of the WT Adx mice might explain why they can mount a full fledge ASR. In support of this hypothesis we observed that *Ocn*^{+/-} Adx mice that yield normal circulating osteocalcin levels, could not mount an ASR. Taken together these results identify osteocalcin as a bona fide stress hormone and reveal that unlike other vertebrates, bony vertebrates use a bone-centric mode of response to an acute stress.

Disclosures: Julian Berger, None

FRI-0136

Mice with reduced visceral and bone marrow adipose tissue have increased bone mass
Louise Grahne*¹, Karin L. Gustafsson¹, Klara Sjögren¹, Petra Henning¹, Vikte Lionikaite¹, Antti Koskela², Juha Tuukkanen², Claes Ohlsson¹, Ingrid Wernstedt Asterholm³, Marie K. Lagerquist¹. ¹Centre for Bone and Arthritis Research, Department of Internal Medicine and Clinical Nutrition, Institute of Medicine, The Sahlgrenska Academy, University of Gothenburg, Sweden, ²Medical Research Center, University of Oulu, Finland, Sweden, ³Unit of Metabolic Physiology, Department of Physiology, Institute of Neuroscience and Physiology, The Sahlgrenska Academy, University of Gothenburg, Sweden

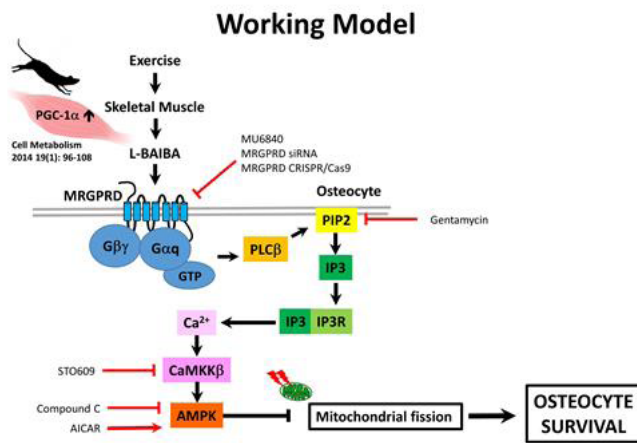
Although obesity is associated with metabolic comorbidities such as diabetes and atherosclerosis, obesity has long been thought to protect against osteoporosis, possibly due to a higher mechanical load. However, these findings are under debate since fat mass – especially visceral fat mass – has been negatively associated with bone mass. Also bone marrow adipose tissue (BMAT) has been negatively associated with bone mass; a suggested mechanism is the competitive differentiation of osteoblasts and marrow adipocytes from bone marrow mesenchymal stromal cells. To further investigate the link between fat and bone mass, we used a mouse model, the RID transgenic mice (Wernstedt Asterholm et al., Cell Metab, 2014), with reduced capacity for adipogenesis in visceral fat. We hypothesized that RID transgenic mice, compared with wild type mice, would develop reduced BMAT in response to high-fat diet (HFD), for 11 weeks, leading to increased bone mass. As expected, RID transgenic mice had reduced HFD-induced weight (-7%, $P < 0.001$) and fat mass (-39%, $P < 0.001$, determined by dual-energy X-ray absorptiometry) gain compared with controls. Furthermore, the bone marrow adiposity, as judged by histological analysis of femur, was decreased in RID transgenic mice and this finding was associated with smaller bone marrow adipocytes than in controls (-20%, $P < 0.05$). In line with our hypothesis, HFD-fed RID transgenic mice displayed an increased bone mass, in long bones and vertebrae, affecting trabecular and cortical parameters. For example, as determined by high-resolution micro-computed tomography, RID transgenic mice had increased percent bone volume (BV/TV) (+11%, $P < 0.05$) and cortical thickness (+10%, $P < 0.01$) in femur and increased trabecular thickness (+6%, $P < 0.01$) in L5 vertebra compared with controls. Furthermore, HFD-fed RID transgenic mice had an increased humeral toughness (+44%, $P < 0.01$), determined by 3-point bending, compared with controls. In conclusion, mice with reduced visceral and bone marrow adipose tissue have increased bone mass.

Disclosures: Louise Grahne, None

FRI-0137

An Osteocyte Protective Metabolite, β -aminoisobutyric Acid, BAIBA Mediates Survival Signals through MRGPRD/Ca²⁺/CaMKK β /AMPK pathway.
Yukiko Kitase*, Lynda Bonewald. Indiana University, United States

Osteoporosis and sarcopenia are age-related diseases that frequently occur together. Evidence is accumulating for molecular crosstalk between muscle and bone that may reciprocally enhance the function of the other tissue in healthy individuals and may reduce degenerative processes with aging. We have previously shown that β -aminoisobutyric acid, BAIBA, a contracting skeletal muscle-derived metabolite, prevents bone loss induced by hindlimb unloading in mice while inhibiting osteocyte apoptosis *in vivo*. *In vitro*, L-BAIBA protects MLO-Y4 osteocyte-like cells from oxidative stress-induced cell death by preventing mitochondrial fission/depolarization (ASBMR2016). We validated that the Mas-related G-protein coupled receptor, type D (MRGPRD) mediates the protective effects of L-BAIBA by both siRNA and CRISPR/Cas9 mediated gene editing. MRGPRD is known to be coupled to the G α_q subunit that induces cytoplasmic calcium ion flux when activated. Since AMPK is critical in maintaining mitochondrial homeostasis and calcium signaling activates AMP-activated protein kinase (AMPK) via the calcium/calmodulin-dependent protein kinase β (CaMKK β), we hypothesized that L-BAIBA activates calcium signaling pathways downstream of MRGPRD leading to activation of AMPK to protect osteocytes from oxidative stress. Pharmacological inhibition of phosphatidylinositol bisphosphate (PIP2) hydrolysis leading to inositol triphosphate (IP3)/Ca²⁺ release using gentamycin blocked the protective effect of L-BAIBA on cell death induced by hydrogen peroxide-mediated oxidative stress in MLO-Y4 cells, as did STO-609, a CaMKK β inhibitor. Treatment with L-BAIBA increased phosphorylation of AMPK indicating an increase in the active form. An AMPK inhibitor, compound C, inhibited L-BAIBA protective effects while the AMPK activator, AICAR, protected MLO-Y4 from oxidative stress-induced cell death. Together these data suggest that the muscle-derived factor, L-BAIBA works to protect osteocytes from cell death induced by oxidative stress through binding to the MRGPRD receptor which leads to stimulation of calcium release followed by CaMKK β -mediated activation of AMPK. This study has revealed a novel pathway for muscle-bone crosstalk by which BAIBA, produced by exercising muscle, has beneficial effects on osteocyte survival.



Disclosures: Yukiko Kitase, None

FRI-0138

Fam210a is a Novel Determinant of Bone and Muscle Ken-Ichiro Tanaka^{*1}, Yingben Xue¹, Loan Nguyen-Yamamoto¹, John A Morris², Ipei Kanazawa³, Toshitsugu Sugimoto³, Simon S Wing⁴, J Brent Richards², David Goltzman¹. ¹Calcium Research Laboratory, Metabolic Disorders and Complications Program, Research Institute of the McGill University Health Centre, Canada, ²Departments of Medicine, Human Genetics, Epidemiology and Biostatistics, McGill University, Jewish General Hospital, Canada, ³Internal Medicine 1, Shimane University Faculty of Medicine, Japan, ⁴Division of Endocrinology, Department of Medicine, McGill University, Canada

Background: Osteoporosis and sarcopenia are common comorbid diseases, however their shared mechanisms are largely unknown. Genome-wide association studies (GWAS) in humans have identified SNPs intronic to FAM210A (family with sequence similarity 210, member a), which are strongly associated with the risk of fracture, but less so with decreased bone mineral density (BMD) [Nat Genet 2012]. Although Fam210a is expressed in a variety of tissues involving muscle, the skeletal function of Fam210a remains unknown. **Methods:** We investigated the effect of FAM210A on bone and muscle using human genetic association data and Fam210a knockout mice. We first examined whether SNPs mapping to FAM210A were associated with bone and muscle traits in adults and children. Next, we examined phenotypes of two-month-old tamoxifen-inducible Fam210a knockout (TFam210a^{-/-}) and tamoxifen-inducible Fam210a muscle-specific knockout (TFam210aMus^{-/-}) mice. The expression and localization of Fam210a were investigated using X-gal staining and immunofluorescence. Their BMD, biomechanical strength, bone micro-architecture using micro-computed tomography (μ CT), bone formation, osteoclast activity, grip strength, and limb lean mass were evaluated. Microarray analysis of muscle cells from TFam210aMus^{-/-} mice was performed. **Results:** We found that genetic variation near FAM210A was associated, through large-scale GWAS studies, with fracture, BMD, and appendicular and whole body lean mass, in humans. In mice Fam210a was localized to muscle mitochondria and cytoplasm, as well as in heart and brain, but not in bone. Grip strength and limb lean mass were reduced in TFam210a^{-/-} mice and TFam210aMus^{-/-} mice. Decreased BMD, bone biomechanical strength and bone formation, and elevated osteoclast activity with micro-architectural deterioration of trabecular and cortical bones, were observed in TFam210a^{-/-} mice. BMD of male TFam210aMus^{-/-} mice was also reduced and osteoclast numbers and surface in TFam210aMus^{-/-} mice were increased. Microarray analysis of muscle cells from TFam210aMus^{-/-} mice identified candidate musculoskeletal modulators involving MMP-12. **Conclusions:** Fam210a has a crucial role in regulating bone structure and function, and may impact osteoporosis through a biological pathway involving muscle as well as through other mechanisms. **Funding Support:** the Canadian Institutes of Health Research (CIHR), MSD Life Science Foundation, Public Interest Incorporated Foundation, The Uehara Memorial Foundation, Mochida Memorial Foundation and by a Richard and Edith Strauss Postdoctoral Fellowship in Medicine from the Research Institute of the McGill University Health Centre

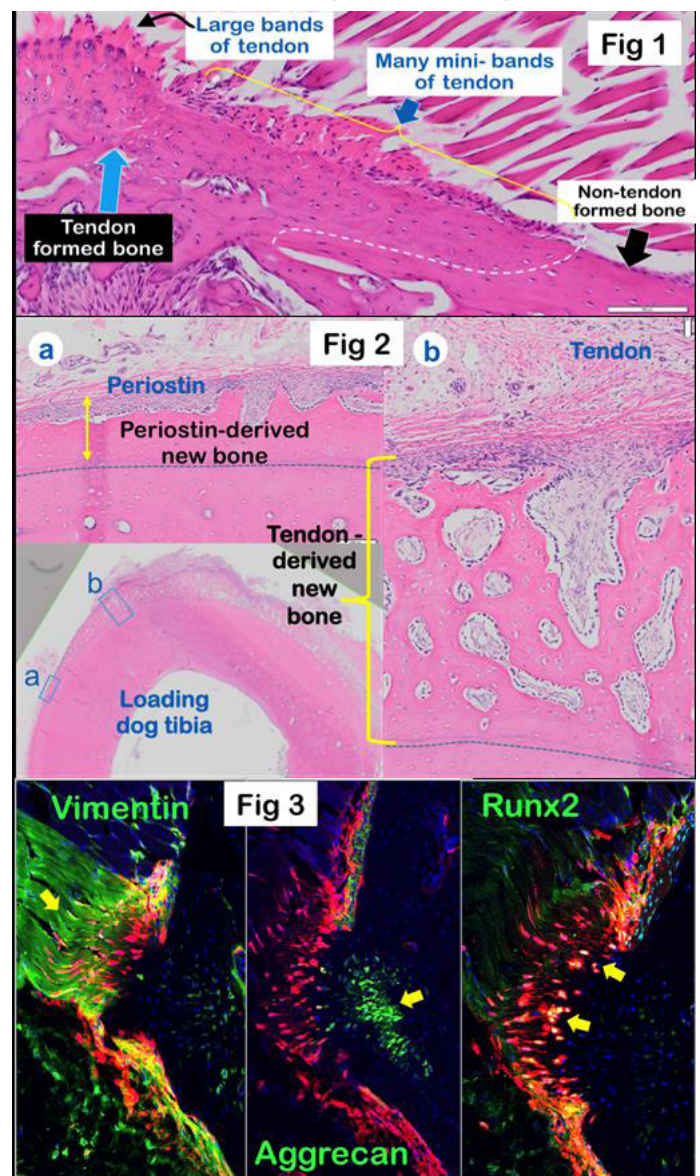
Disclosures: Ken-Ichiro Tanaka, None

FRI-0139

The direct transdifferentiation of tendon cells into bone cells during bone modeling and remodeling Ke Wang^{*1}, Chi Ma¹, Minghao Zheng², Xiaohua Liu¹, Jian Feng¹, Yan Jing¹. ¹Texas A&M University College of Dentistry, United States, ²The University of Western Australia, Australia

For many years, bone is considered to be exclusively formed by its own cells, whereas tendon is thought to assist muscles in body movement. The purpose of this study is to test the direct transdifferentiation of tendon cells into bone. First, we demonstrated that in addition

to long fibrous tendons (commonly observed in literature), there are many mini-tendons that attach muscles to bone, resulting in a huge contact area between tendon and rough/uneven bone compared to smooth and even bone that has no tendon attachment (Fig 1). In these massive junction areas, the histological analyses showed unique features in cell distribution pattern, cell shape, and gene expression profiles (such as high levels of Periostin, Vimentin, Biglycan, DMP1, and Col I) that differ from the non-tendon-attached bone. To address mechanical responses, we applied open-coil springs anchored on miniscrew implants in dog tibia with a force of 0g and 200 g separately. Sixty-day loading resulted in more robust new bone formation in the tendon-bone junction (including more osteons; Fig2a) compared to the periosteum-attached bone(Fig2b). Cell lineage tracing using Gli1-CreERT2-tdTomato mice (induced at 4-weeks old, harvested@5-, 6-, and 7-weeks, separately) displayed strong Gli1+ tendon cells mainly at the tendon-bone junction (including both long and short tendon cells) surrounded by strong aggrecan+ matrices. Initially, there were few red bone cells in the bone underneath. Later, however, more and more red bone cells are observed, which are co-localized with Runx2 and cartilage (aggrecan) and tendon (vimentin) markers (Fig 3), confirming that tendon cells directly transdifferentiate into bone cells. Interestingly, in the 3.2 Col 1-Cre-tdTomato mice (induced and harvested at the same time-frame as the Gli1 tracing line) many more red bone cells are identified in the tendon-bone junction, which are also co-localized with the above cartilage, tendon and bone markers. Furthermore, we used 2.3 Col 1-GFP young adult mice labeled with Alizarin Red for 4 hours to define a relationship between tendon, tendon-derived bone, and mineralization. Non-decalcified frozen confocal imaging revealed that those GFP+ tendon cells form bone cells, and that neither GFP+ tendon cells nor GFP+ osteoblast cells deposit mineral, whereas GFP+ osteocytes do. Thus we propose that the tendon-derived bone cells contribute to bone formation in the tendon-bone attached area, and directly respond to mechanical response.



Disclosures: Ke Wang, None

FRI-0169

Low bone mass and high marrow adiposity in congenic 6T mice are related to shifts in metabolic flexibility within the bone marrow niche. Sheila Bornstein*, Clifford Rosen, Victoria Demambro, Anyonya Guntur, Makoto Fujiwara. Maine Medical Center Research Institute, United States

C3H/HeJ mice have both high bone marrow adipose tissue (MAT) and BMD compared to B6. We made a congenic mouse, B6.C3H.6T (6T), with an inversion on mouse Chr6 from C3H, and backcrossed it into B6Bm (100%BL/6J) ten generations. 6T male and female mice on a high fat diet (HFD) had high BMAT but low trabecular BV/TV and reduced bone formation. We hypothesized that skeletal differences between B6Bm and 6T were related to altered metabolic regulation from genes near or at the inversion site (Chr 6 at ~120MB). To test that hypothesis, we measured body composition in B6Bm and 6T, energy expenditure (EE) on a 13 week regular (LFD) or HFD. We measured whole tibia bone + marrow gene expression (tibial MGE) and cultured bone marrow MSCs from both strains under adipogenic conditions. On a LFD, 16-week old male 6T and B6Bm mice had similar body weights and fat mass, but 6T had greater lean mass, higher RQ, greater daytime EE and were more active. There were no differences in aBMD or trabecular BV/TV between 6T and B6Bm on a LFD. But, on a HFD, 6T gained more weight and fat mass than B6Bm ($p < 0.0001$). Similarly, femoral BV/TV in 6T was 50% lower than B6Bm ($p < 0.03$) and had reduced cortical thickness and enhanced cortical porosity ($p < 0.006$). On a HFD, tibia MGE revealed markedly reduced Sp7, Ocn, Sost, Runx2, and Rankl in 6T vs. B6Bm. 6T BMSCs showed enhanced adipogenic differentiation vs. B6 by Oil Red O staining and was associated with a 1.5 fold increase in Pparg, AdipoQ, and Ccrn4l. Two key regulatory factors for adipogenesis were markedly altered in tibia MGE on a HFD. Aebp1 which promotes adipogenic proliferation and inhibits differentiation, was lower in 6T vs B6Bm ($p < 0.004$). And, Bcl2l13 mRNA, a mitochondria receptor that regulates mitochondrial fission was lower in 6T compared to B6Bm ($p < 0.001$). Consistent with less mitochondria in 6T on a HFD there was lower Pdk4 (pyruvate dehydrogenase kinase 4) than B6Bm, ($p = 0.007$); PDK4 is a mitochondrial enzyme that regulates metabolic flexibility by shifting metabolism from fatty acid to glucose oxidation. In sum, Bcl2l13 and Pparg, two genes located on either side of the Chr 6 inversion exhibited altered regulation and likely play a key role in the skeletal differences between 6T and B6 on a HFD. Metabolic flexibility, i.e. switching from fatty acid to glucose oxidation reflected by gene expression and energy expenditure could lead to impaired bone formation, lower bone mass and greater MAT in the congenic 6T.

Disclosures: *Sheila Bornstein, None*

FRI-0170

Activation of β -catenin signaling in mature osteoblasts versus osteoblast progenitors defines a transcriptional and mutational profile for the transformation of MDS to AML Álvaro Cuesta-Domínguez^{*1}, Ioanna Mosialou¹, Junfei Zhao², Akihide Yoshimi³, Konstantinos Panitsas⁴, Richard A. Friedman⁵, Omar Abdel-Wahab^{3,6}, Raúl Rabadán⁷, Stavroula Kousteni¹. ¹Department of Physiology and Cellular Biophysics, College of Physicians and Surgeons, Columbia University Medical Center, United States, ²Department of Systems Biology, Columbia University Medical Center, United States, ³Human Oncology and Pathogenesis Program, Memorial Sloan Kettering Cancer Center, United States, ⁴Department of Physiology and Cellular Biophysics, College of Physicians and Surgeons, Columbia University, United States, ⁵Biomedical Informatics Shared Resource, Department of Biomedical Informatics, Herbert Irving Comprehensive Cancer Center, College of Physicians and Surgeons, Columbia University Medical Center, United States, ⁶Weill Cornell Medical College and Leukemia Service, Dept. of Medicine, Memorial Sloan Kettering Cancer Center, United States, ⁷Department of Systems Biology and Department of Biomedical Informatics, Columbia University Medical Center, United States

A growing body of evidence indicates that osteoblasts have a pathogenetic role in the development of myelodysplasia (MDS), acute myeloid leukemia (AML) and transformation of MDS to AML. β -catenin activation in osteoblasts induces MDS progressing to AML in mice and is seen in more than 30% of MDS and AML patients. To examine whether the stage of osteoblast differentiation influences disease development or progression, we constitutively activated β -catenin in mature osteoblasts (β cat(ex3)OCN mice) and osteoblast progenitors (β cat(ex3)2.3Col1a1 mice). β cat(ex3)2.3Col1a1 mice develop MDS which rapidly transforms to AML characterized by multi-organ infiltration with myeloid blasts, hematopoietic deregulation and lethality by 6 weeks of age. However, β cat(ex3)OCN mice presented with thrombocytopenia, anemia and lymphocytopenia along with dysplasia in the erythroid and megakaryocyte lineage in the blood and bone marrow, and although they never developed more than 10% of blasts in the marrow they die by 6 weeks of age. These characteristics indicate the development of MDS in β cat(ex3)OCN mice. In agreement with this diagnosis, high throughput, targeted-DNA-sequencing of CD11b+/Gr-1+ myeloid cells from β cat(ex3)OCN mice, identified in-frame deletions in the histone methyltransferases Kmt2d and Setd1e, missense mutations in Cux1 and Braf splice site (previously reported in human MDS) and in the Fanconi anemia complementation group A (FancA) gene associated with defective DNA repair. RNA-seq analysis revealed that genes related to cell cycle (cycD), insulin signaling (InsR, Rtk, Shc) and the oncogene c-myc regulatory cascade (Jund, Cend2, Max, Ddx3x and Id2) were potentially upregulated in LSK cells from β cat(ex3)OCN mice.

Spliceosome regulators Srsf5 and Prpf8 were downregulated in β cat(ex3)OCN LSK versus wild type LSK cells. Interestingly, spliceosomal mutations are the most common genetic alterations in patients with MDS. In addition, expression of the methyltransferases Kmt2a, Kmt2b and Ash1, which induce MLL rearrangement in AML, was increased in LSK cells from leukemic β cat(ex3)2.3Col1a1 mice as compared to LSK cells from MDS β cat(ex3)OCN mice. Notably, spliceosomal deregulation, as seen in LSK cells of β cat(ex3)OCN mice, is highly associated with MLL-rearranged AML, suggesting that increased expression of Kmt2a, Kmt2b and Ash1 may be crucial in the transformative mechanism leading from MDS in β cat(ex3)OCN mice to AML in β cat(ex3)2.3Col1a1 mice.

Disclosures: *Álvaro Cuesta-Domínguez, None*

FRI-0171

Pharmacological Targeting of Osteoblast-Induced MDS and AML Ioanna Mosialou*, Marta Galan-Diez, Andrew Vandenberg, Abdullah Ali, Azra Raza, Stavroula Kousteni. Columbia University, United States

The bone marrow hematopoietic stem cell niche has emerged as a regulator and instigator of hematological myeloid malignancies. Activation of β -catenin signaling in osteoblasts, by deletion of exon3 or by inactivating mutations in APC, induces myelodysplasia (MDS), rapidly progressing to acute myeloid leukemia (AML) in mice. Activated β -catenin signaling is present in osteoblasts of one third of MDS and AML patients and it is the most active pathway in stromal cells of MDS patients suggesting that it may sustain dysplastic hematopoiesis and progression to MDS and AML in humans. Therefore, targeting this pathway may provide a new therapeutic approach for this subgroup of MDS/AML patients. To examine this hypothesis we searched for an FDA-approved compound with the ability to inhibit β -catenin signaling and identified all-trans-retinoic acid (ATRA) as a potential candidate. We show here that treatment of osteoblastic cells with ATRA inhibits the induction of β -catenin target genes by Wnt3a and abrogates nuclear localization of β -catenin, as shown by immunohistochemistry and western blot analysis. These effects are mediated by the retinoic acid receptor α (RAR α) since silencing RAR α , but not RAR β or RAR γ , in osteoblasts abolishes the inhibitory effect of ATRA on Wnt3a-induced β -catenin signaling. Similarly, treatment of leukemic mice expressing constitutively active β -catenin in their osteoblasts with ATRA, inhibited β -catenin signaling as measured by expression of its target genes Axin2 and Lef1 in bone. At the same time, ATRA improved anemia and thrombocytopenia, decreased the percentage of blasts in bone marrow and blood and prolonged overall survival in these leukemic mice as compared to vehicle-treated mice. The response to ATRA treatment of two MDS patients with active β -catenin in their osteoblasts, and not responding to other treatments, was monitored. The hematologic phenotype of the patients improved and disease status stabilized so that patients remain transfusion independent and disease-related symptom-free with a good quality of life thereafter. The improvement in disease status coincided with absence of β -catenin in the nucleus as flow cytometry analysis showed a high percentage of patient osteoblasts expressing activated β -catenin in pre-therapy samples but not in on-therapy samples. These results suggest that ATRA may find a new use in the treatment of the specific portion of MDS/AML patients with activated β -catenin in their osteoblasts.

Disclosures: *Ioanna Mosialou, None*

FRI-0172

Single-cell proteomics reveal bone marrow stromal cell drivers of blood regeneration Nicolas Severe^{*1}, Murat Karabacak², Karin Gustafsson¹, Ninib Baryawno¹, Gabriel Courties¹, Youmna Kfoury¹, Elizabeth Scadden¹, Matthias Nahrendorf¹, Mehmet Toner², David Scadden¹. ¹Massachusetts General Hospital, United States, ²Shriners Hospital for Children, United States

The relationship between bone and blood is ancient in evolutionary terms. All animals since the divergence of fish that have both bones and blood, make blood in their bones. This long history of co-evolution has led to complex interrelationships that are still being defined. The non-hematopoietic compartment, also called stroma, is increasingly recognized as a regulator of hematopoietic stem and progenitor cells (HSPCs) function, but its cellular complexity remains poorly defined. Mass Cytometry (CyTOF) permits quantitation of up to 40 proteins simultaneously at single-cell resolution, thus enabling multi-dimensional analysis of the bone marrow stromal compartment. Using this approach, we identified 28 distinct populations of mouse bone marrow stromal cells. To define the potential hematopoietic relevance of specific clusters of bone marrow stromal cells, we analyzed their cytokine profile enabling us to select 14 candidate clusters. In addition, assessing the response of these groups to systemic challenges of medical relevance, we evaluated cells prior to whole body lethal irradiation and one day later (the time of bone marrow transplantation). We showed that most bone marrow stromal cells were damaged by radiation. Only 3 clusters preserved their cell number despite irradiation and each expressed the extracellular ecto-5'-nucleotidase, CD73. In order to further explore the function of the adenosine-producing enzyme CD73, we used a CD73-knockout mouse model and found that CD73 expressed by stromal cells is a functional driver of HSPCs engraftment and blood regeneration. Furthermore, cytokine profiling analysis one day post-irradiation reveals a unique cluster of CD73+ persisting cells, producing higher level of hematopoietic niche factors, that can be defined by NGFRhigh expression and support hematopoiesis ex-vivo. These data demonstrate that using single-cell multi-dimensional protein analysis with sequential steps of filtering based on cytokine profiling and resistance to radiation enables identification of novel subset of bone

marrow stromal cells capable of regulating HSPCs transplantation and blood regeneration, mediated in part by an interesting adenosine-producing mechanism.

Disclosures: Nicolas Severe, None

FRI-0187

ERR α in primary breast tumours promotes tumour cell dissemination to bone by regulating RANK Geoffrey Vargas^{*1}, Mathilde Bouchet², Casina Kan³, Claire Benetollo⁴, Martine Croset¹, Martine Mazel⁵, Laure Cayrefourcq⁵, Sophie Vacher⁶, Francesco Pantano⁷, Keltouma Driouch⁶, Ivan Bieche⁶, William Jacot⁵, Jane Aubin⁸, Catherine Alix-Panabieres⁵, Philippe Clezardin¹, Edith Bonnelye¹. ¹INSERM-U1033, France, ²ENS-Lyon, France, ³INSERM U1033, Australia, ⁴INSERM U 1028-CNRS UMR 5292-UCBL Lyon 1, France, ⁵Institut Universitaire de Recherche Clinique (IURC)- Montpellier, France, ⁶Institut Curie, France, ⁷University Campus Bio-Medico-Roma, Italy, ⁸University of Toronto, Canada

Bone is the most common metastatic site for breast cancer. Because Estrogen-Related-Receptor alpha (ERR α) has been implicated in cancer cell invasiveness and bone metastasis progression, we determined whether ERR α expression in primary breast tumours could modulate the molecular mechanisms that drive breast cancer cell dissemination to bone. In breast cancer patients, we showed that high ERR α expression level in primary tumours (n=295) was associated with relapse to bone but not to lungs. ERR α expression was also detected in the circulating tumour cells from metastatic breast cancer patients. Using a murine 4T1 breast cancer cell line that spontaneously metastasizes to lung and bone when inoculated orthotopically to animals, we found that ERR α overexpression in 4T1 cells (4T1-ERR α) promoted spontaneous bone micro-metastasis formation whereas lung metastasis formation remained unchanged. RANK was identified as an ERR α regulated gene in 4T1-ERR α primary tumours both as transcriptomic and protein levels. Concomitantly, we showed that RANKL stimulated 4T1-ERR α cells migration as well as the phosphorylation of mTOR in vitro. In line with these data, RANK was up-regulated in human MCF7 breast cancer cells overexpressing ERR α . A positive correlation was also observed between high ERR α /RANK expression levels in primary tumours from patients with breast cancer (n=446) and occurrence of bone metastases (n=248). Furthermore, in order to determine whether inhibition of ERR α abrogates primary tumour outgrowth and tumour cell dissemination to bone, the pharmacological effect of the ERR α inverse agonist C29, which is known to block ERR α transcriptional activity, was studied. We first showed that C29 inhibited RANK mRNA expression in 4T1 and MCF7 breast cancer cells in vitro. Then, 4T1-ERR α cells were inoculated orthotopically and mice were treated with the C29. Reinforcing our data, we found that the pharmacological inhibition of ERR α reduced primary tumour growth, bone micro-metastasis formation in vivo, and decreased RANK expression in situ. In conclusion, our results reveal a novel ERR α /RANK axis through which ERR α in primary breast cancer promotes dissemination of tumour cells to bone. We propose that ERR α may be a useful biomarker to identify breast cancer patients at high risk of relapse in bone.

Disclosures: Geoffrey Vargas, None

FRI-0188

S100A4 Released from Highly Bone-metastatic Breast Cancer Cells Plays a Critical Role in Osteolysis Haemin Kim^{*1}, Sang Il Kim², Hyung Joon Kim³, Brian Y. Ryu², Junho Chung², Zang Hee Lee², Hong-Hee Kim². ¹Hospital for Special Surgery, United States, ²Seoul National University, Republic of Korea, ³Pusan National University, Republic of Korea

Bone metastasis affects more than 80% of patients with breast cancer at advanced stages of the disease and causes severe pain, fracture, hypercalcemia, and nerve compression, leading to increased morbidity and mortality. Communication between cancer cells and skeletal cells in metastatic bone microenvironments is a principal element that drives tumor progression and osteolysis. In this communication, tumor-derived factors play fundamental roles. To identify key molecules associated with breast cancer bone metastasis, we analyzed the gene expression profiles of the bone-metastatic MDA-MB-231 (MDA) and the nonmetastatic MCF7 breast cancer cell lines. Among the genes that were highly differentially expressed, the signal for S100A4 was higher in the MDA than in the MCF7 cell line. Furthermore, a search of NCBI GEO microarray data sets of tumor samples from 65 breast cancer patients (GSE 14020) revealed a significantly higher expression of S100A4 in bone-metastasized tumors than in tumors metastasized to other organs. To further validate in vivo relevance in an animal model of bone metastasis, we established a highly bone-metastatic subline of MDA by utilizing the in vivo selection method previously described. Briefly, MDA cells were injected into the left ventricle of immune-deficient mice and collected from bones after eight weeks. The in vivo selection method was repeated twice to obtain more homogeneous bone metastatic MDA population. This subline (mtMDA) showed a markedly elevated ability to secrete S100A4 protein than its parental partner, which directly stimulated osteoclast formation via the receptor for advanced glycation end products. Recombinant S100A4 stimulated osteoclastogenesis in vitro and bone loss in vivo. Conditioned medium from mtMDA in which S100A4 was knocked down had a reduced ability to stimulate osteoclasts. Furthermore, the S100A4 knockdown cells elicited less bone destruction in mice compared with the control knockdown cells. In addition, administration of an anti-S100A4 monoclonal antibody that we developed attenuated the stimulation of osteoclastogenesis and bone loss

by mtMDA in mice. Taken together, our results suggest that S100A4 released from breast cancer cells is an important player in the osteolysis caused by breast cancer bone metastasis.

Disclosures: Haemin Kim, None

FRI-0189

Granulocyte Colony Stimulating Factor impacts on osteomacs and bone marrow macrophages – implications for prostate cancer osteoblastic lesion formation Susan Millard^{*}, Andy Wu, Simran Kaur, Yaowu He, Lena Batoon, John Hooper, Allison Pettit. Mater Research - UQ, Australia

Macrophages are key participants in the tumor cell-environment interaction and disruption of this is being investigated as a therapeutic strategy. Both resident macrophages and recruited tumor associated macrophages (TAM) contribute to the prostate cancer (PC) bone-bone marrow (BM) environment interactions. However, it is unclear whether the numerous functionally distinct resident macrophage subsets of bone and BM have opposing roles in the evolution of PC metastasis within bone. Granulocyte colony stimulating factor (G-CSF) drives HSC mobilization and reduces endosteal bone formation indirectly via impacts on BM and osteal (osteomacs) macrophages. G-CSF is used clinically to treat neutropenia subsequent to chemotherapy and prophylactic G-CSF was recently shown to also improve response to chemotherapy. Consequently, we characterized G-CSF bone and BM macrophage population impacts in both naive mice and in the context of PC bone metastasis, modelled by growth of RM1(BM) murine PC cells in immune-competent mice. Naive C57Bl/6 mice were treated with bi-daily G-CSF (125ug/kg) or saline for up to 6 days. Histological and flow cytometric assessments were performed at day 4, 6, 8, 10 and 12. In the PC model, G-CSF treatment was initiated 1 day after intratibial injection of RM1(BM) cells and continued until harvest at day 7. Flow cytometry confirmed expansion of F4/80-Ly6G⁺ granulocytes (neutrophils) and collapse of the F4/80+Ly6G⁺ macrophage subset during G-CSF treatment of non-tumor bearing mice. Monocytes (F4/80+Ly6G-CD115hi) were increased by more than 2-fold and Ly6C⁺ macrophages (F4/80+Ly6G-CD115LoLy6C⁺) were increased by 3-fold at the expense of Ly6C⁻ macrophages which decreased by 6-fold. In non-tumor bearing mice G-CSF treatment resulted in loss of F4/80⁺ endosteal osteomacs, which was accompanied by loss of endosteal osteoblasts, suggestive of osteomacs being capture within either the F4/80+Ly6G⁺ or Ly6C⁻ macrophage subsets. Interestingly within G-CSF treated tumor-bearing limbs, F4/80⁺ resident macrophages in adjacent BM were reduced but TAM were minimally affected. Tumor-associated woven bone formation was reduced more than 2-fold in G-CSF treated animals compared to saline-treated controls (p<0.05), but there was no impact on tumor growth. These observations support the PC osteoblastic response occurs through tumor-mediated subversion of normal osteoclast function rather than a de novo pathological mechanism driven by either the tumor or TAM.

Disclosures: Susan Millard, None

FRI-0190

Serum levels of RANKL are increased in primary breast cancer patients in the presence of disseminated tumor cells in the bone marrow. Tilman Rachner^{*1}, Martina Rauner², Andy Göbel², Oliver Hoffmann³, Lorenz Hofbauer², Rainer Kimmig³, Sabine Kasimir-Bauer³, Ann-Kathrin Bittner³. ¹Universitätsklinik Dresden, Germany, ²University Hospital Dresden, Germany, ³University Hospital Essen, Germany

Background: Receptor activator of nuclear factor kappa-B ligand (RANKL) is an essential protein for osteoclast regulation that is associated with benign and malignant bone disease. The activity of RANKL is controlled by its soluble decoy receptor osteoprotegerin (OPG). There is increasing evidence that RANKL may also directly affect breast cancer progression and metastasis to bone. This study was aimed to assess the levels of RANKL and OPG in 509 newly diagnosed breast cancer patients with regard to the presence of disseminated tumor cells (DTCs) in the bone marrow (BM), circulating tumor cells (CTCs) in blood and clinical parameters. Patients and Methods: 509 patients with first diagnosis of breast cancer between Aug 2006 and Dec 2009 were included in our study. Blood and BM sampling was performed before surgery in an adjuvant setting. Blood was collected from each patient and sRANKL and OPG in the serum was measured by ELISA (Biomedica, Vienna, Austria). Two BM aspirates were analyzed for DTCs by immunocytochemistry using the pan-cytokeratin antibody A45-B/B3. In a subgroup of 364 patients, 2 x 5 ml blood was studied for CTCs using the AdnaTest BreastCancer (AdnaGen AG, Hannover, Germany) for the detection of EpCAM, MUC-1, HER-2, and beta-Actin transcripts. Results: Mean serum values for RANKL and OPG were 0.23±0.20 pmol/l and 4.24±1.70 pmol/l, respectively. RANKL levels were significantly lower in women above 60 years of age (0.19 pmol/l vs 0.26 pmol/l; p < 0.0001). This finding was reflected by higher RANKL serum levels and RANKL/OPG ratios in premenopausal patients compared to peri- (p<0.05) and postmenopausal patients (p<0.001), respectively. RANKL/OPG ratios were also higher in patients with lymph node involvement (N1-N3, p=0.03). All other clinical parameters did not influence RANKL or OPG levels. DTCs were detected in 213/509 (42%) patients and CTCs in 81/364 (22%) patients, respectively. However, while RANKL levels were unchanged in patients with detectable CTCs, they significantly increased by 33% (p<0.0001) in patients with DTCs. There was no difference in OPG levels, resulting in an increased RANKL to OPG ratio in patients with DTCs in the bone marrow (0.087 vs. 0.060; p < 0.0001). Conclusion: In conclusion, we show that RANKL serum levels and RANKL/OPG ratios are increased in patients with detectable DTCs in the BM, prior to the establishment of detectable bone metastases. This

finding warrants further investigation as it may provide a rational for novel diagnostic or therapeutic approaches.

Disclosures: Tilman Rachner, None

FRI-0191

Suppression of Breast Cancer Bone metastasis by Osteocytic Connexin Hemichannels, a Potential Therapeutic Target Manuel Riquelme^{*1}, Sumin Gu¹, Zhiqiang An², Jean Jiang¹. ¹Department of Biochemistry and Structural Biology, University of Texas Health Science Center at San Antonio, United States, ²Brown Foundation, Institute of Molecular Medicine, UT Health Houston, United States

Bone is the most preferred site for metastasized breast cancer cells. Osteocytes consist of over 95% of bone cells and play a central role in coordinating the bone formation, remodeling and extracellular environment composition. Mechanical stimulation induces the opening of osteocytic hemichannels formed for connexin43 (Cx43), which mediates the communication between the intracellular and extracellular space. These channels are permeable to molecules like ATP, PGE2, glutamate and others. It has been shown that mechanical loading inhibits intratibial breast cancer growth. Additionally, we have shown that ATP, released by osteocytic hemichannels through the activation of tumor P2X7 receptor, inhibits cancer cell growth and migration. In this study, we determined if Cx43 hemichannels are a potential therapeutic target for treatment of breast cancer bone metastasis and the underlying inhibitory mechanism of ATP. Mechanical loading reduced tumor growth in mice. Interestingly, tumor growth was reduced in osteocyte-specific transgenic mice expressing Cx43R76W, a dominant negative mutation that blocks gap junctions with the enhancement of Cx43 hemichannels. However, mechanical loading increases tumor growth and this increase was inhibited with Cox-2 inhibitor, which blocks prostaglandin synthesis. This data suggest that increased prostaglandin synthesis by mechanical loading associated with exacerbated activity of hemichannels promotes tumor growth. Our lab develops a monoclonal antibody (MC2), which binds to extracellular domain of Cx43 and increases the activity of osteocytic hemichannels in vitro and in vivo. This antibody was immune-reactive in HeLa cells transfected with Cx43, osteocytic MLO-Y4 cells and mouse osteocytes in situ. The weekly injection of MC2 reduced the breast cancer growth in the WT mouse tibia, but not in osteocyte-specific Cx43 knockout mice. As is known, osteocytes Cx43 hemichannels are permeable to ATP. P2X7 specific agonist benzoyl ATP reduced in vitro breast cancer cell migration, increased cytoplasmic free Ca²⁺ and induced formation of tubulin bundles, indicator of cytoskeleton reorganization. The effect of benzoyl ATP required functional CamKII to elicit these phenomena. Our results suggest that Cx43 hemichannels are likely a new target for treating breast cancer, probably through the enhancement of the extracellular ATP levels and the activation of P2X7/CamKII axis to inhibit breast cancer bone growth and metastasis.

Disclosures: Manuel Riquelme, None

FRI-0192

HDAC inhibitors directly stimulate LIFR and induce pro-dormancy effects in breast cancer cells Miranda Sowder^{*1}, Lauren Holtslander¹, Vera Mayhew¹, Samuel Dooyema¹, Rachelle W. Johnson². ¹Vanderbilt University, United States, ²Vanderbilt University Medical Center, United States

Breast cancer cells often metastasize to the bone, where they may remain dormant for years. Our laboratory previously found that loss of leukemia inhibitory factor receptor (LIFR) in breast cancer cells results in poor patient survival and tumor cell exit from dormancy in the bone marrow. Based on our previous finding that the histone deacetylase (HDAC) inhibitor (HDACi) valproic acid (VPA) promotes LIFR expression in breast cancer cells, we hypothesized that HDACi (romidepsin, panobinostat, vorinostat, entinostat) can be used to directly stimulate LIFR through histone acetylation on the LIFR promoter and maintain tumor cell dormancy. HDACi dramatically induced LIFR mRNA (up to 9.5-fold, $p < 0.05-0.0001$) and protein levels by 24 hours in breast cancer cells with low (MCF7, SUM159, D2.0R) and high (MDA-MB-231b, D2A1, 4T1BM2) metastatic potential. MCF7 cells treated with HDACi showed enrichment of acetylated-H3K9 on the LIFR promoter (up to 10.9-fold, $p < 0.05-0.001$), indicating that HDACi directly stimulate LIFR transcription. HDACi also induced other pro-dormancy genes including AMOT and TGFB2 (up to 5.5-fold, $p < 0.05-0.0001$) independent of LIFR, but did not enhance promoter acetylation, suggesting indirect regulation by HDACi. MCF7 cells labeled with CellTrace Violet proliferation dye showed increased dye retention following 8 days of HDACi treatment (4.1-fold, $p = 0.019$), with similar results observed in MDA-MB-231b cells, indicating that HDACi slow tumor cell proliferation. We next investigated LIFR expression in a dataset of primary breast tumors ($n = 20$; Accession: GSE83530) before and after 8 days of VPA treatment. Patients with increased peripheral blood histone acetylation, an indicator of therapeutic efficacy, showed increased LIFR levels in the primary tumor ($p = 0.0513$) compared to patients with unchanged/decreased acetylation levels. To determine whether HDACi promote tumor dormancy in vivo, mice were treated with VPA (~2mg/kg; 3x/wk) following intracardiac inoculation of MCF7 cells, but no significant difference in tumor-induced osteolysis or tumor burden was observed. However, VPA-treated naïve mice exhibited a significant decrease in bone volume (1.3-fold, $p = 0.037$), suggesting that VPA negatively impacts bone remodeling and should be combined with a bone protective agent. Together, our results indicate that

HDACi slow breast cancer cell proliferation and may be therapeutically useful to maintain tumor cells in a chronic dormant state.

Disclosures: Miranda Sowder, None

FRI-0193

Pharmacological Inhibition of Sclerostin Protects From Breast Cancer-induced Osteolytic Disease and Muscle Weakness Eric Hesse^{*}, Saskia Schröder, Diana Zarecneva, Jenny Pamperin, Hiroaki Saito, Hanna Taipaleenmäki. Molecular Skeletal Biology Laboratory, Department of Trauma, Hand and Reconstructive Surgery, University Medical Center Hamburg-Eppendorf, Germany

Patients with breast cancer bone metastases present with osteolytic lesions and often suffer from muscle weakness. Current treatment includes chemotherapy, irradiation and anti-resorptive drugs that restrict bone destruction. Although patients benefit from these therapies, the disease remains irreversible and additional treatments are needed. Recent evidence suggests a role of the Wnt inhibitor sclerostin in cancer-induced bone disease. We therefore hypothesized that targeting sclerostin in metastatic breast cancer may restrict disease progression and restore muscle function. In support of this hypothesis, we determined a significantly higher sclerostin expression in metastatic MDA-MB-231 breast cancer cells (BCCs) compared to non-metastatic MCF-7 BCCs. Osteoblast differentiation and the activity of Wnt signaling in osteoblasts was inhibited by conditioned medium (CM) from MDA-MB-231 BCCs in a dose-dependent manner. Repression of Wnt activity by CM was partially abolished upon antagonizing sclerostin in BCCs using siRNA. Reduction of sclerostin expression in BCCs also restricted cancer cell migration. This indicates that BCC-derived sclerostin impairs bone formation but supports metastatic features. To test whether sclerostin inhibition restores osteoblast function and attenuates metastatic breast cancer, MDA-MB-231 BCCs stably expressing the luciferase gene were delivered by cardiac injection in female SCID mice and metastases were allowed to form prior to treatment with vehicle or anti-sclerostin antibody (Scl-Ab, 100 mg/kg). Weekly bioluminescence imaging revealed a reduced growth of bone metastases in Scl-Ab-treated mice compared to controls. Inhibition of sclerostin did not change the abundance of BCCs at extra-skeletal sites, indicating that BCCs did not relocate to other organs. In addition, sclerostin inhibition prevented breast cancer-induced bone destruction determined by microCT and histological analyses. Interestingly, although Scl-Ab treatment had no effect on muscle function in naïve mice, it protected from cancer-induced reduction of muscle fiber area and loss of muscle function in tumor-bearing mice, and expanded the life span of these animals. In summary, our data demonstrate that pharmacological inhibition of sclerostin reduces bone metastatic burden and reliefs from the suppression of bone formation and muscle weakness with a potential future implication in treating musculoskeletal complications in breast cancer patients.

Disclosures: Eric Hesse, None

FRI-0226

DDRKG1, an essential component of the ufmylation process, regulates osteochondrogenitor fate determination Yangjin Bae^{*}, Adetutu Egunsola, Monika Weisz-Hubshman, Ming-Ming Jiang, Brendan Lee. Baylor College of Medicine, United States

DDRKG1 has been identified as a novel substrate of ufmylation process, a post-translational modification mediated by one of ubiquitin-like proteins. The physiological role of DDRKG1 is varied in multiple tissue types based on others' studies. Moreover, our recent study underscored the critical role of DDRKG1 in cartilage. In brief, we uncovered homozygous mutation of DDRKG1 as a causative mutation of one of rare form of chondrodysplasia, Shohat-type SEMD (spondyloepimetaphyseal dysplasia). We demonstrated that DDRKG1 loss-of-function mutation led to defects in cartilage development in zebrafish. Furthermore, Ddrkg1^{-/-} mutation was embryonic lethal (E11.5) in mice and also resulted in delayed chondrogenic mesenchymal condensation in the limb buds. Mechanistically, we showed that DDRKG1 forms a complex with SOX9 and inhibits ubiquitination-mediated proteasomal degradation of SOX9. Hence, our discovery of DDRKG1 as a causative gene in Shohat-type SEMD provides unprecedented evidence that ufmylation may be required for proper chondrogenesis. Here, to elucidate the cartilage-specific role of DDRKG1, we generated Prx1-Cre; Ddrkg1^{fl/fl} mice, where Ddrkg1 is deleted in limb bud mesenchymal cells. Unlike Ddrkg1^{-/-} mice, Prx1-Cre; Ddrkg1^{fl/fl} mice survive. We observed progressive shortening of the limbs with an abnormal growth plate phenotype in Prx1-Cre; Ddrkg1^{fl/fl} mice compared to Ddrkg1^{fl/fl} mice. The typical columnar structure of chondrocytes in the proliferating zone in Prx1-Cre; Ddrkg1^{fl/fl} mice was mildly disrupted, with shortening of the proliferating zone, while the hypertrophic zone was elongated and also disorganized. Furthermore, we performed RNA-seq analysis from the limb buds of Prx1-Cre; Ddrkg1^{fl/fl} and Ddrkg1^{fl/fl} mice (E13.5). Among the Top Canonical Pathways affected, Role of Osteoblasts, Osteoclasts and Chondrocytes in Rheumatoid Arthritis was significantly regulated (p -value=1.43E-0.3) based on the Ingenuity Pathway Analysis (IPA) of differentially expressed genes (adj. p value < 0.05). Consistent with the IPA result, we found that osteoblast-specific genes such as Alp and Col1a1 were upregulated in the limb buds of Prx1-Cre; Ddrkg1^{fl/fl} by qRT-PCR analysis. These preliminary data suggest that the loss of DDRKG1 in early mesen-

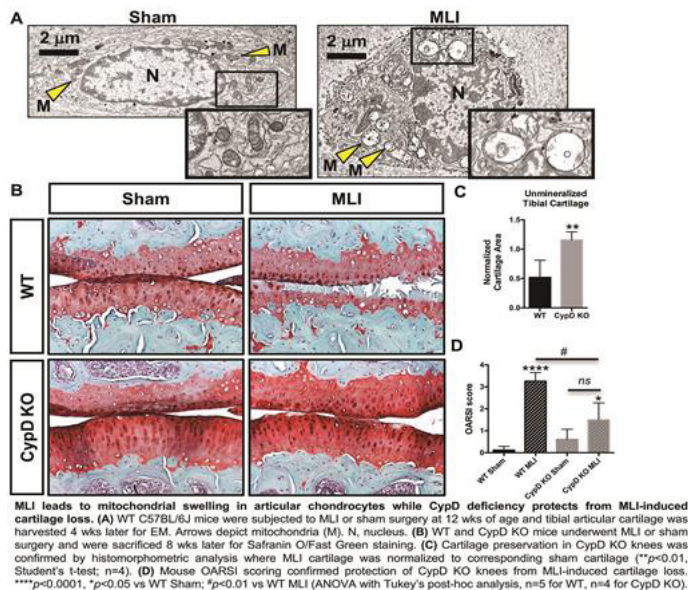
chymal progenitor cells promotes osteoblastic lineage fate determination. The investigation of DDRGK1 role in osteochondroprogenitor fate determination is underway.

Disclosures: **Yangjin Bae**, None

FRI-0227

The role of mitochondrial dysfunction in the development of post-traumatic osteoarthritis Katherine Escalera-Rivera*, Sarah Catheline, Roman Eliseev, Jennifer Jonason. University of Rochester, United States

Osteoarthritis (OA), a debilitating degenerative joint disease characterized by an irreversible loss of articular cartilage, is currently the most common cause of chronic disability in adults. Among the most important risk factors associated with the onset of OA is prior traumatic joint injury. The molecular mechanisms underlying onset and progression of post-traumatic OA (PTOA), however, are still unclear. While mitochondrial dysfunction plays a causative role in a number of degenerative processes following traumatic injury, a relationship between mitochondrial dysfunction and PTOA has not yet been established. Using electron microscopy, we find a greater percentage of swollen mitochondria in joints subjected to meniscal/ligamentous injury (MLI) than in sham joints. Mitochondrial swelling is a consequence of mitochondrial permeability transition pore (MPTP) opening, a process that results in loss of the mitochondrial chemiosmotic membrane gradient. Cyclophilin D (CypD) is currently the only protein genetically proven to be essential for MPTP opening. To test whether inhibition of CypD/MPTP can protect against PTOA, we performed MLI in wild type (WT) C57BL/6J and age-matched CypD knockout (KO) mice and harvested knee joints 8 weeks later for histology. Histomorphometry revealed a ~50% loss of the unmineralized tibial articular cartilage in WT joints while cartilage was maintained in the CypD KO joints. OARSI scoring further revealed that the integrity of the cartilage from the CypD KO joints was significantly better than that of the WT MLI joints. To begin to elucidate the effects of MPTP opening in chondrocytes, we transfected ATDC5 chondrogenic cells with a vector encoding a constitutively active K166Q mutant of CypD (CypDCA). CypDCA expression disrupted mitochondrial membrane integrity leading to release of mtDNA into the cytosol and induction of TLR9 gene expression. Activation of NF- κ B signaling as well as increases in gene expression of pro-inflammatory cytokines, TNF α and IL6, were also observed in the CypDCA cells. Our data, therefore, lead us to propose that chondrocyte mitochondrial dysfunction via MPTP opening and mtDNA-initiated damage-associated molecular pattern (DAMP) signaling causes cartilage catabolism and loss of cell viability following traumatic joint injury. We further suggest that CypD inhibition should be explored as a novel therapeutic strategy for the prevention of PTOA.



Disclosures: **Katherine Escalera-Rivera**, None

FRI-0228

Postnatal inactivation of Dot1L histone methyltransferase in growth plate cartilage impairs longitudinal bone growth Sangita Karki*, Rosa M. Guzzo. UConn Health, United States

Epigenetic regulation by histone modification enzymes is an important component of the regulatory mechanisms controlling skeletal growth and development. Disruptor of telomeric silencing-1 (Dot1L) is the sole histone methyltransferase that catalyzes the methylation of lysine residue 79 in histone 3 (H3K79), an established epigenetic mechanism associated with gene transcription. A recent study showed that Dot1L activity is critical for maintaining joint cartilage homeostasis, however the function of Dot1L in skeletal growth and growth

plate chondrocyte differentiation has not been thoroughly examined. Thus to evaluate the significance of Dot1L function in early postnatal skeletal development, we generated a new inducible, genetic loss of function mouse model using Dot1L^{fl/fl};Aggrecan-CreERT2. Mice were injected with tamoxifen at postnatal day five, and we examined their skeletal phenotype between 3 weeks and 4 months of ages. X-ray imaging showed shortening of the long bones in mice with conditional disruption of Dot1L in growth plate cartilage (Dot1L Δ/Δ mice) by 3 weeks of postnatal development. Alcian blue staining of hindlimbs harvested from Dot1L Δ/Δ mice revealed the presence of lesions and breaks within the cartilage growth plates of the distal femora and proximal tibia, which were not observed in control mice. To explore the molecular basis underlying the growth plate dysplasia in Dot1L Δ/Δ mice, we examined the contribution of Dot1L enzymatic activity on the transcriptional regulation of cartilage genes in vitro. Treatment of mouse primary chondrocytes with a Dot1L specific inhibitor (EPZ 5676, 10 μ M) resulted in global reduction of H3K79 mono- and di-methylation levels by immunoblot analyses. Quantitative PCR analyses further revealed down-regulation of cartilage genes (ie. Sox9, Col2a1) in Dot1L inhibitor-treated chondrocytes as compared to vehicle treated cells. Moreover, inhibition of H3K79 methylation in primary chondrocytes promoted a mature chondrocyte phenotype, as seen by increased type X collagen expression. Together, our data point to a critical role for Dot1L in maintaining growth plate cartilage integrity and in regulating chondrocyte differentiation during postnatal development. Our findings provide an important step toward a deeper understanding of the epigenetic mechanisms that dictate normal skeletal development, and may provide novel insights into the pathophysiology of growth plate dysplasias.

Disclosures: **Sangita Karki**, None

FRI-0229

Ciliary IFT80 Plays a Critical and Necessary Role in Fracture Healing through Regulating IGF β Signaling Pathway Min Liu*, Mohammed Alharbi², Jormay Lim¹, Dana Graves², Shuying Yang¹. ¹Dept. of Anatomy and Cell Biology, School of Dental Medicine, University of Pennsylvania, United States, ²Dept. of Periodontics, School of Dental Medicine, University of Pennsylvania, United States

Rationale: Primary cilia are essential cellular organelles projecting from cell surface to sense and transduce signaling. Intraflagellar transport (IFT) proteins are indispensable for cilia formation and function. However, the precise role and mechanism of IFT protein in regulating bone repair after fracture has not been studied. In this study, we investigated the effect of conditional deletion of IFT80 in chondrocyte on fracture healing in mice. Materials and Methods: IFT80^{fl/fl} mouse model, which has two LoxP sites flanking exon 6 of IFT80, has been generated in our lab. IFT80^{fl/fl} mice were crossed with Col2a1-CreER mice to produce Col2a1; IFT80^{fl/fl} mice. Femur fracture was performed in 12wk old mice from both Col2a1; IFT80^{fl/fl} and IFT80^{fl/fl} mice groups. Tamoxifen was injected at Days 3, 5, and 7 post fractures to delete IFT80 in chondrocytes. Femur samples were collected at day 9, 21 post fractures for analysis. Primary chondrocytes were isolated from IFT80^{fl/fl} mice and infected with adenovirus, which overexpress either Cre or GFP. IF staining was performed to visualize cilia structure and alcian blue staining was used to detect the sulfated proteoglycan deposits. mRNA and protein levels of the markers of chondrogenesis, chondrogenesis and TGF β signaling were measured. Results: Conditional knockout of IFT80 in chondrocytes significantly delayed the fracture healing. Col2a1; IFT80^{fl/fl} mice formed smaller fracture calluses than IFT80^{fl/fl} mice. Radiographic analysis revealed that fracture gap of Col2a1; IFT80^{fl/fl} mice were clearly observed and partially covered mostly by low-density/porous woven bony tissue with significantly lower BV/TV, Tb-N, Tb-Th and greater Tb-Sp. In vitro study showed that IFT80 deletion dramatically reduced cell differentiation, proliferation, and cilia formation. In addition, IFT80 deletion down-regulated TGF- β 1, TGF- β R, and Smad-7 mRNA expression and IF staining revealed a significant reduction of P-Smad2/3 expression in fracture callus. Similarly, primary chondrocytes failed to respond to TGF β stimulation after IFT80 deletion. Finally, we found Foxo1 deletion up-regulated IFT80, Pcm1 and Kd-m3a expression and restored diabetes-reduced cilia formation in chondrocytes. Conclusions: Ciliary IFT80 plays a critical and necessary role in fracture healing through regulating IGF β signaling pathway. IFT proteins and cilia formation might be regulated by Foxo1.

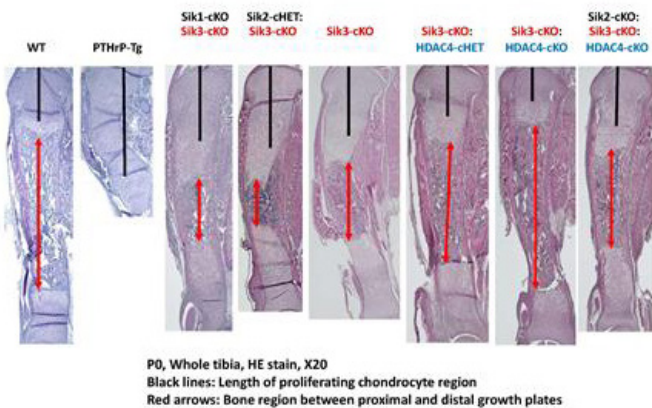
Disclosures: **Min Liu**, None

FRI-0230

PTHrP Targets Salt-induced Kinases to Regulate Chondrocyte Differentiation Shigeki Nishimori*, Marc Wein¹, Kei Sakamoto², Marc Foretz³, Rebecca Berdeaux⁴, Henry Kronenberg¹. ¹Massachusetts General Hospital, United States, ²Nestlé Institute of Health Sciences, Switzerland, ³INSERM, France, ⁴University of Texas, United States

Background: Parathyroid hormone-related protein (PTHrP) inhibits chondrocyte hypertrophy. We have demonstrated in vivo that Histone deacetylase (HDAC) 4 and 5 are mediators of PTHrP signaling in chondrocytes. We have further shown in vivo that PTHrP leads to lower phosphorylation of HDAC4 at the 14-3-3 binding sites and induces subsequent nuclear translocation of HDAC4 (submitted). In the nucleus, HDAC4/5 block Myocyte Enhancer Factor 2 (MEF2) that drives chondrocyte hypertrophy. How PTHrP action leads to lower phosphorylation of HDAC4/5 is not known. Methods: Salt inducible kinase (Sik) 3 influences chondrocyte hypertrophy (Sasagawa, Development, 2012). Sik2 and Sik3 (Sik-

phorylate HDAC4 and HDAC5 at the 14-3-3 binding sites in vitro (Walkinshaw, JBC, 2013). Here, we investigated the roles of SIK family proteins in the PTHrP signaling pathway using mouse genetic models. Surprisingly, the lethal phenotype of the PTHrP-KO mouse is rescued by knocking out the *Sik3* genes. This result is consistent with the model that the PTHrP-KO phenotype requires HDAC4 phosphorylation induced by *Sik3* action. Cyclic AMP signaling leads to protein kinase A-mediated phosphorylation and inactivation of *Sik3* at T467, among other sites. We showed that PTHrP leads to phosphorylation of this site by adding PTH 1-34 (50 nM) to primary rib chondrocytes harvested at birth and using Western blots to assess phosphorylation of *Sik3* T467 by a specific antibody (Patel et al Nature Comm, 2014). The Col2-Cre: *Sik3* conditional KO (*Sik3*-cKO) mouse shows a long proliferating chondrocyte (PC) region, due to delayed chondrocyte hypertrophy. However, it is not as severe as the delay of hypertrophy in the chondrocyte-specific PTHrP transgenic mouse (Weir, PNAS, 1996) that exhibits only round chondrocytes at birth. The more severe phenotype with PTHrP over-expression suggests that other SIK family proteins (*Sik1* or *Sik2*) may control chondrocyte hypertrophy in addition to *Sik3*. By additional deletion of the *Sik1* or *Sik2* gene in the *Sik3*-cKO mouse, we observed longer PC regions and delayed separation of proximal and distal growth plates at birth. These results suggest that *Sik1* and *Sik2* also regulate chondrocyte differentiation, but *Sik2* deletion exhibits more obvious effects. Effects of *Sik1* deletion were more obvious at Embryonic Day 17. *Sik1*-cKO, *Sik2*-cKO, and *Sik1*&*2* double cKO exhibited normal bone phenotypes. By deleting the HDAC4 gene in the *Sik3*-cKO mouse, stepwise shorter PC regions were observed at birth, consistent with the idea that HDAC4 acts downstream of *Sik3* to delay chondrocyte hypertrophy. The longer PC region in the *Sik2*/*Sik3*/HDAC4 triple KO mouse compared to the *Sik3* and HDAC4 double KO mice suggests that *Sik2* can block actions of HDAC5, thereby accelerating hypertrophy. Conclusions: These genetic and in vitro studies suggest that PTHrP acts on growth plate chondrocytes through a *Sik1*, *2*, *3*-HDAC4/5 dependent pathway.



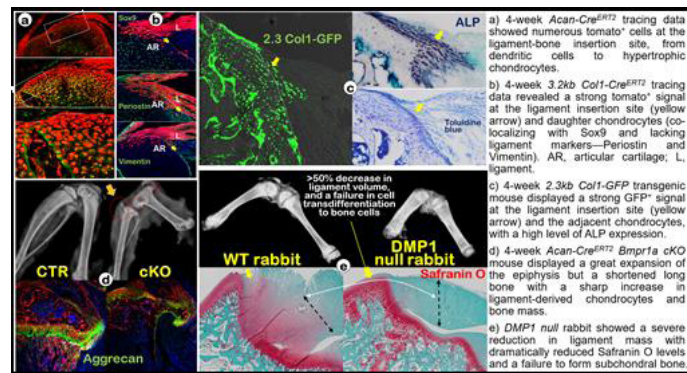
Disclosures: *Shigeki Nishimori, None*

FRI-0231

Direct transdifferentiation of ligament cells into articular chondrocytes that is regulated by Indian hedgehog (IHH) signaling and phosphate levels Jun Wang^{*1}, Chi Ma¹, Hui Li¹, Zhanjun Li², Liangxue Lai², Yan Jing¹, Jian Q. Feng¹. ¹Texas A&M College of Dentistry, United States, ²Jilin Provincial Key Laboratory of Animal Embryo Engineering, Jilin University, China

Articular cartilage is considered to be formed by its own chondrocytes, and currently, the known function of ligaments is to assist muscles in controlling body movement and stabilizing joints. Pathologically, ectopic ossification occurs in ligaments. The aim of this study is to propose a new ligament function: ligaments directly form articular cartilage and subchondral bone during normal development. To test this hypothesis, we first used the Rosa26-tdTomato (tdT) mouse line separately crossed with Gli-CreERT2 and Aggrecan (Acan)-CreERT2 with one-time tamoxifen induction at P5 and harvested at 4-weeks. Both the Gli1 and Acan tracing lines displayed a similar pattern: a) in the distal ligament region there were scattered tdT⁺ ligament cells, but there were numerous tdT⁺ cells at the ligament insertion site; b) many tdT⁺ cells became dendritic cells followed by flat spindle cells, pre-hypertrophic, and then hypertrophic chondrocytes (Fig a). Next, we used the 3.2kb Col1-CreERT2-tdT tracing line with one-time tamoxifen induction for 4-days (P5-P9). A strong tdT⁺ signal was observed in cells at the ligament insertion site and their daughter chondrocytes, which were co-localized with Sox9 and no longer expressed ligament markers (Periostin and Vimentin); b). In a 2.3kb Col1-GFP mouse line, a strong GFP⁺ signal was confirmed in the ligament insertion site and adjacent chondrocytes, in which a high level of alkaline phosphatase was documented (c). To study molecular regulation of direct cell transdifferentiation of ligament into chondrocytes, we deleted *Ihh* in the tdT background using Gli1-CreERT2 and Acan-CreERT2 at P5 and harvested at 4-weeks, separately. These two cKO lines displayed a very similar phenotype, being slightly stronger in the Acan-Cre line: a) a great expansion of the epiphysis but a shortened long bone and b) a sharp increase in the ligament-derived chondrocytes and bone mass, as well as a complete loss of growth plate and metaphysis (d). Finally, in our studies of the newly developed *Dmp1* null rabbit (a hypophosphatemic rickets model), there was a severe reduction in ligament mass and Safranin O levels in ligament at the junction site. These Safranin O⁺ chondrocytes failed to form

mature subchondral bone, leading to expanded knee joint heads (e). Together, our studies support a novel theory: ligament cells directly transdifferentiate into knee chondrocytes and subchondral bone cells, which is regulated by IHH signaling and Pi levels.



Disclosures: *Jun Wang, None*

FRI-0255

Undercarboxylated Osteocalcin Downregulates Pancreatic Lipase Expression in CREB2-Dependent Manner in Pancreatic Acinar Cells Danbi Park^{*1}, Ye-Won Kwon¹, Jeong-Hwa Baek², Kyunghwa Baek¹. ¹Department of Pharmacology, College of Dentistry and Research Institute of Oral Science, Gangneung-Wonju National University, Republic of Korea, ²Department of Molecular Genetics, School of Dentistry and Dental Research Institute, Seoul National University, Republic of Korea

Osteocalcin is an osteoblast-specific secreted protein that has been associated with endocrine roles on multiple aspects of energy metabolism. We explored whether undercarboxylated osteocalcin (ucOC) downregulates pancreatic lipase (PNLIP) expression in pancreatic acinar cells and then identified the downstream signaling pathway. We previously demonstrated that β adrenergic blockade attenuates the body weight/fat mass gain in high fat diet fed mice and such an effect is associated with decrease in PNLIP expression in pancreatic acinar cells. In the present study, we first confirmed that serum ucOC level is inversely correlated with PNLIP expressions, i.e., those mice exhibiting the high level in serum ucOC had the low PNLIP in pancreas. In vitro experiment using primary pancreatic acinar cells and 266-6 cells, ucOC downregulated PNLIP expressions in mRNA and protein level. ucOC increased cellular cAMP level. Rp-cAMPs, KT5720 and H89, cAMP/PKA signaling inhibitors significantly reversed ucOC-induced downregulation of PNLIP expression. ucOC promoted the phosphorylation of cAMP response element-binding protein 2 (CREB2), but not of CREB1. Overexpression of CREB2 significantly suppressed PNLIP expression. The knockdown of CREB2 by siRNA reversed the ucOC-induced downregulation of PNLIP expression. Luciferase reporter assay showed that ucOC suppressed PNLIP promoter transactivation. Overexpression of CREB1 stimulated, but CREB2 suppressed PNLIP promoter activity. Knockdown of G protein-coupled receptor 6A (GPRC6A), a candidate receptor for mediating the response to ucOC in the bone-pancreas endocrine loop, by siRNA reversed the downregulating effect of ucOC on PNLIP expressions. Targeting GPRC6A in 266-6 cells by CRISPR/Cas9 also blocked the suppression effect of ucOC on PNLIP expressions. Taken together, ucOC downregulates pancreatic lipase expression in a cAMP/protein kinase A/CREB2-dependent manner. GPRC6A is a functional osteocalcin sensing receptor that regulate PNLIP expression in pancreatic acinar cells. This work was supported by the National Research Foundation of Korea Grant (NRF-2013R1A1A3008564 and NRF-2017R1A2B1006203).

Disclosures: *Danbi Park, None*

FRI-0256

Ppar γ inhibition in osteoblast / osteocyte (OB/OCY) restores PTH bone anabolism in high fat diet model, importance of glycolysis versus mitochondrial oxidation ratio Lucie Bourgoignie^{*1}, Beatrice Desvergne², Nicolas Bonnet¹. ¹Service of Bone Diseases, Faculty of Medicine (UNIGE), Switzerland, ²Genopode Science & medical University, Switzerland

High fat diet (HFD) is known to induce Ppar γ upregulation as well as disturb glucose metabolism, known to contribute in the inhibition of bone anabolic response to PTH. We hypothesized that specific ablation of Ppar γ in OB/OCY would restore PTH anabolic effects partially by maintaining proper mitochondrial/glycolysis activity. For this purpose, WT females and OB/OCY-specific Ppar γ KO mice (i.e. *Dmp1*-Cre/Lox-Ppar γ -deficient mice) at 16 weeks of age, received either a high fat or chow diet (HF 60% vs CD 10% of fat) for 8 weeks. Half of the mice were treated by intermittent PTH (40 μ g/kg/day) or vehicle (Veh). Bone structure at distal and midshaft femur, bone formation rate (BFR) and osteocalcin were evaluated by microCT, histomorphometry and ELISA. Using the seahorse XF96 system, we measured glycolysis and mitochondrial activity in primary OB from WT and

Ppar γ KO mice. In WT, HFD increased Ppar γ expression in bone (+126% vs CD, $p < 0.001$) and decreased BV/TV (-50.6% vs CD, $p < 0.05$). Anabolic effects of PTH in CD, illustrated by increased BV/TV, cortical thickness (Ct.Th), EcBFR and PsBFR (respectively +92%, +7.9%, +2400% and +290% vs Veh, all $p < 0.05$) were abolished in HFD. In contrast, PTH effects in KO mice under HFD were similar to those obtained in WT under CD. In KO under HFD mice, PTH increased BV/TV, Ct.Th, EcBFR, PsBFR and osteocalcin respectively by +98%, +18%, +580%, +90%, +39% vs Veh, all $p < 0.05$. In Ppar γ KO primary OB, gene expression indicated a reduction in mitochondrial activity (-27% of PDHa1, $p < 0.01$) and an upregulation of Glut1 and Glut4 (+394% and +157%, both $p < 0.001$). Increased in glucose transporter was translated with an increased in glycolysis rate (ECAR, +75% vs WT, $p < 0.01$). Hence, in vitro, osteocalcin response to PTH was magnified in KO vs WT (+97% vs +12.2%, $p < 0.001$). In conclusion, HFD abolishes PTH effects both at the trabecular and cortical structure, suggesting that PTH-based bone fragility treatment in obese and diabetic patients would be less efficient. In contrast, by restoring glycolytic rates, Ppar γ ablation in OB/OCY could maintain the PTH anabolic efficacy. How Ppar γ inhibition in OB/OCY rescue HFD defects remains to be elucidated.

Disclosures: *Lucie Bourgoin, None*

FRI-0257

Allocation of Bone Marrow Stromal Cells into the Adipogenic Lineage is Marked by Enhanced Expression of the Mitophagy Receptor Bcl2l13 Makoto Fujiwara^{*1}, Anyonya Guntur¹, Phuong Le¹, Victoria Demambo¹, Mark Horowitz², Clifford Rosen¹. ¹Maine Medical Center Research Institute, United States, ²Yale University School of Medicine, United States

As with a host of specific transcription factors, metabolic programming may influence the lineage determination of bone marrow stromal cell (BMSC). We previously reported that C3H/HeJ (C3H) mice have higher bone mass yet markedly more marrow adipose tissue than C57BL/6J (B6). We also noted that pre-adipocytes predominantly utilize oxidative phosphorylation (OxPhos) whereas pre-osteoblasts utilize glycolysis. Thus we hypothesized that C3H BMSCs were metabolically programmed to increase bone marrow adipogenesis via enhanced OxPhos. First, we cultured BMSCs from both strains in adipogenic media (AM) and osteogenic media (OM). C3H BMSCs differentiated into more adipocytes at day 9 and osteoblasts at day 14 than B6 BMSCs as measured by Oil Red O and Von Kossa staining respectively. Gene expression patterns in C3H BMSCs also showed greater Pparg, Cebpa, and Adipoq in AM and more Alpl, Runx2, and SP7 in OM. Next we asked whether genetic determinants could be responsible for the cellular phenotypes. C3H mice have an inversion in Chromosome 6 leading to dysregulation in genes at the breakpoint, which include Pparg proximally and Bcl2l13 distally. Bcl2l13 is the mammalian homolog of the yeast ATG32, the mitochondrial receptor protein essential for mitophagy. Gene and protein expression of Bcl2l13 in B6 BMSCs increased 9-fold and 4-fold, respectively at day 9 of adipogenesis, but unchanged in OM. We confirmed a similar pattern in 3T3-L1 cells and in primary cells from the stromal vascular fraction of the inguinal depot. In addition, in BMSCs, a mitochondrial fusion protein Mfn2 was also markedly increased in AM but not changed in OM, and mitochondrial/nuclear DNA ratio (Mt/N DNA) tended to increase in AM. siRNA of Bcl2l13 in 3T3-L1 cells led to more than 80% reduction in protein production, a significant impairment in adipocyte differentiation by Oil Red O staining but not induced apoptosis. Compared to negative control, the Bcl2l13 knock down decreased Mt/N DNA. Interestingly, in silico analysis showed that there are PPARG binding sites in the promoter of Bcl2l13 at full differentiation of 3T3-L1 cells, suggesting that the Pparg-Bcl2l13 interaction leads to enhanced adipogenesis. In sum, we found that the mitophagy receptor Bcl2l13 is essential for adipocyte differentiation, but not osteogenesis, and reflects increased OxPhos. Importantly, mitophagy is essential for adipogenesis and Bcl2l13 reflects how metabolic programming may influence lineage allocation.

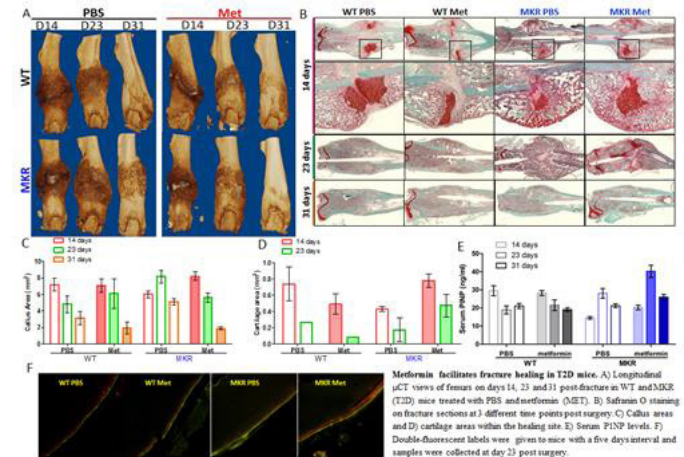
Disclosures: *Makoto Fujiwara, None*

FRI-0258

Metformin Facilitates Fracture Healing in Type-2 Diabetes Mice Yuqi Guo^{*}, Xin Li. NYU College of Dentistry, United States

Diabetes mellitus is a group of chronic diseases characterized by high blood glucose levels. Diabetic patients have a higher risk of sustaining osteoporotic fractures than their non-diabetic counterparts. The fracture healing is usually impaired in diabetics and our understanding of the detrimental effects of hyperglycemia on fracture healing is still inadequate. Effects of diabetes treatments on bone metabolism and fracture are varied. Metformin is the first-line medicine for type-2 diabetes (T2D) and has not been documented with any negative effects on bone. In contrast to most other medicines for T2D, it exhibits a favorable effect on diabetic bone by increasing bone mineral density and decreasing fracture in patients. Here we demonstrated that metformin preserved bone mass and facilitated fracture healing in T2D mice. Closed femoral fracture was induced to the right femur of age-matched normoglycemic and hyperglycemic mice. An intramedullary pin was inserted prior to fracture for stabilization. After fracture, mice were randomly assigned to treatment groups receiving vehicle or metformin daily by intraperitoneal injection. We conducted a temporal histologic analysis to track the healing process by collecting the fractured femora at 14, 23 and 31 days post-fracture. Our results demonstrated that the fracture healing was delayed in T2D mice and metformin rescued the delayed bone healing by facilitating osteogenesis and chondrocytogenesis. The cartilage formation in the endochondral ossification under hy-

perglycemic condition revealed by Safranin O staining was significantly increased at day 14 post-fracture in T2D mice receiving metformin treatment. Serum P1NP levels and double-fluorescent labeling exhibited that metformin stimulated the bone formation at day 23 post-fracture in T2D mice. In vitro culture of human and mouse BMSCs suggested that the impaired osteogenic capacity by hyperglycemia was associated with an impaired mitochondrial respiration. Metformin treatment ameliorated the impairment through stimulating the expression levels of Nrf-1, PGC1 α and Ostrix in pre-osteoblasts. Taken together, our study demonstrated the favorable effects of metformin on bone metabolism in a T2D mouse model and revealed a mechanism by which osteogenesis of BMSCs can be improved.



Disclosures: *Yuqi Guo, None*

FRI-0259

KLF10 regulates skeletal muscle metabolism in mice Malek Kammoun^{*1}, Vladimir Vekler², Jérôme Piquereau², Lydie Nadal-Desbarats³, Philippe Pouletaut¹, Molly Nelson Holte⁴, Malayannan Subramanian⁴, Sabine Bensamoun¹, John Hawse⁴. ¹Université de Technologie de Compiègne, France, ²Univ. Paris-Sud, France, ³Université de Tours, France, ⁴Mayo Clinic, United States

KLF10 is a member of the Krüppel-like family of transcription factors that regulates gene expression in multiple cell and tissue types. Loss of KLF10 expression results in tissue dysfunctions and diseases, many of which present in a sex-specific manner. Deletion of KLF10 in mice leads to an osteopenic bone phenotype only in female mice and polymorphisms in the KLF10 gene are associated with osteoporosis in humans. While KLF10 is well-known for its functions in bone, it is most highly expressed in skeletal muscle. To elucidate the impact of this transcription factor in skeletal muscle, we performed histochemical and electron microscopic analyses of both slow and fast twitch muscles in WT and KLF10 KO mice. The results of these studies revealed a lack of succinate dehydrogenase activity, decreased mitochondrial numbers and changes in mitochondrial shape, enzymatic activity and respiration rates in female, but not male, KLF10 KO mice. We also assessed the activity of specific respiratory chain complexes in situ using saponin-permeabilized skeletal muscle fibers isolated from female WT and KLF10 KO soleus muscle. These studies revealed a significant decrease in respiration rates for complexes I, II and IV in KLF10 KO mice. Metabolite analyses using nuclear magnetic resonance revealed significant differences in multiple metabolites between WT and KLF10 KO muscle further indicating a novel role for KLF10 in muscle metabolism. To understand the molecular mechanisms that underlie these muscle phenotypes, we performed RNA sequencing analyses of WT and KLF10 KO soleus muscle. These studies identified 146 genes whose expression levels were significantly different in KLF10 KO mice, many of which are involved in mitochondrial metabolism and biogenesis. Suppression of KLF10 in C2C12 myocyte precursor cells resulted in decreased mitochondrial numbers and ATP levels. Further, the KLF10 knock-down C2C12 cells also exhibited defects in myocyte differentiation and fusion compared to parental C2C12 cells. In summary, these findings have implicated novel roles for KLF10 in regulating skeletal muscle metabolism and function through altered mitochondrial biogenesis and activity. These phenotypes observed in both KLF10 KO mice and KLF10 knock-down C2C12 cells resemble a number of human diseases associated with mitochondrial myopathies. These models will be useful in identifying novel therapeutic strategies to enhance mitochondrial function and treat such disorders.

Disclosures: *Malek Kammoun, None*

FRI-0260

Fatty acid oxidation is essential for osteoclast development and skeletal homeostasis Priyanka Kushwaha*¹, Conor Beil², Michael J. Wolfgang¹, Ryan C. Riddle¹. ¹Johns Hopkins University School of Medicine, United States, ²Johns Hopkins University, United States

Postnatal skeletal remodeling is an energy demanding process that is linked to nutrient availability and the levels of metabolic hormones. Previously, we demonstrated that mitochondrial long-chain fatty acid oxidation by osteoblasts is required for normal bone accrual and identified a role for the skeleton in whole-body lipid homeostasis. Dietary lipids may also fuel the contralateral arm of the bone remodeling cycle, but the requirement for fatty acid oxidation by osteoclasts has not been studied. To investigate the contribution of fatty acid oxidation to bone resorption, we specifically disrupted expression of carnitine palmitoyltransferase 2, an obligate enzyme in mitochondrial fatty acid β -oxidation in osteoclasts by crossing Cpt2loxP/loxP mice with lysozyme2-Cre transgenic mice (Δ Cpt2). MicroCT revealed that inhibition of long-chain fatty acid oxidation in osteoclasts significantly increased bone volume, secondary to increased trabecular thickness and trabecular number. On the cellular level, TRAP staining revealed dramatic reductions in osteoclast numbers in Δ Cpt2 mice relative to wild-type littermate controls. Similarly, bone marrow cells isolated from Δ Cpt2 mice exhibited a reduced capacity for osteoclast differentiation and pit formation after stimulation with RankL and M-CSF when compared to cells isolated from control mice. These data were further supported by a down-regulation of the expression of osteoclast marker genes, including RANK, Nfatc1, TRAF-6, TNF α and NF- κ B in Cpt2-deficient cultures, despite a compensatory up-regulation of genes involved in glucose utilization. Our data demonstrate that mitochondrial long-chain fatty acid oxidation by the osteoclast is required for normal bone resorption that its inhibition produces an intrinsic defect in osteoclast differentiation.

Disclosures: *Priyanka Kushwaha, None*

FRI-0261

Metabolic characterization of the OCN-Cre;iDTR mouse model supports a relationship between bone health, bone marrow adipose tissue, and overall fitness Heather Fairfield*¹, Samantha Costa¹, Calvin Vary¹, Victoria Demambro¹, Marie Demay², Clifford Rosen¹, Michaela Reagan¹. ¹Maine Medical Center Research Institute, United States, ²Center for Skeletal Research, Massachusetts General Hospital, United States

Background: Many physiological examples demonstrate an inverse correlation between bone marrow adipose tissue (BMAT) volume and bone volume in mice and humans, but few studies have examined this association directly. The question remains whether the skeleton or the adipose it contains drives the correlation, although it has often been postulated that BMAT accumulation causes deterioration of bone. Here we demonstrate for the first time that removing bone cells can induce changes in BMAT and behavior. Methods: We removed osteoblasts and osteocytes from bones using the osteocalcin-cre, inducible diphtheria toxin receptor mouse model (OCN-Cre;iDTR) treated with vehicle (PBS) or diphtheria toxin (DT) every other day for 2 weeks. Long bone cellular and architectural changes were assessed via μ CT, static and dynamic bone histomorphometry, and H&E sections of femora. BMAT was quantified in tibia via OsO4 μ CT and in femur histological sections. Serum was analyzed via mass spectrometry. Changes in body composition were quantified via DEXA PIXMIUS and/or qNMR, and behavioral phenotypes were characterized utilizing metabolic cages. Results: A significant reduction of osteoblasts (Ob.S/BS (%) and N.Ob/B.Pm) upon DT treatment (25-50%, $p < 0.05$) was observed and no bone formation was detected. Many other bone parameters (BV/TV, $p < 0.01$; BMD, $p < 0.001$; and Tb.N, $p < 0.001$) were decreased, while increases in Tb.Sp ($p < 0.001$) and cortical porosity ($p < 0.01$) were observed in DT-treated mice. OsO4 μ CT revealed increased BMAT in DT-treated mice tibia ($p < 0.05$, confirmed by H&E adipocyte counting in the femora) (see Fig 1). Mice had decreased total weight ($p < 0.05$) and lean mass ($p < 0.05$, females; $p = ns$, males). Lipidomic profiling revealed clustering of DT-treated mice based on blood composition of sphingomyelins and glycopeptidolipids; but not triglycerides or diacylglycerols. DT-treated mice also showed less energy expenditure, wheel usage, and food intake (all $p < 0.05$). The majority of these changes, but not BMAT, were normalized after a 3 week recovery. Conclusion: The reciprocal relationship between bone and BMAT we observed mirrors that in osteoporosis, aging and anorexia. We found that removal of bone cells can directly increase BMAT; we will next interrogate the cause and other consequences of this. Our study has important implications in understanding the pathogenesis of elevated BMAT, and the crucial link between skeletal maintenance and overall health in mice and humans.

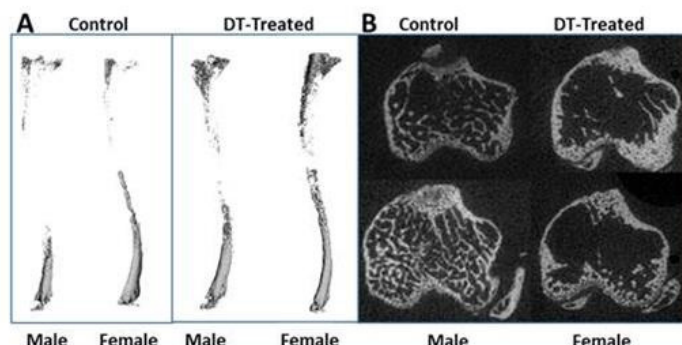


Fig 1. Representative images of A) osmium tetroxide microCT BMAT staining and B) regular microCT of transverse tibial slices from control and DT-treated mice.

Disclosures: *Heather Fairfield, None*

FRI-0262

Complexity in Neuropeptide Y's effects on the skeleton Natalie Ky Wee*¹, Benjamin P Sinder¹, Sanja Novak¹, Xi Wang¹, Brya G Matthews², Boris Zemelman³, Ivo Kalajzic¹. ¹Department of Reconstructive Sciences, University of Connecticut Health Center, United States, ²Department of Molecular Medicine, University of Auckland, New Zealand, ³Center for Learning and Memory, The University of Texas at Austin, United States

Neuropeptide Y (NPY) is involved in multiple processes such as behavior, energy and bone metabolism. Our lab has shown that NPY expression is highly enriched in osteocytes, yet a clear identification of NPY-expressing cells in the skeleton has not been done. Previous studies have relied on global NPY depletion to examine its effects on bone. However, this approach does not distinguish the source of NPY influencing bone. Our aims were to identify which cells within the skeleton express NPY and establish a model that will enable us to differentiate effects of specific NPY deletions. We used a lineage tracing approach (NPYcre x Ai14 TdTomato reporter) to detect NPY expression in bone and have developed the first NPY conditional knockout (NPYcKO) mouse using CRISPR. We crossed our NPYcKO with Hprt-cre to generate a global knockout (NPYKO) and have assessed femurs using microCT, mechanical testing, histomorphometry and flow cytometry. NPY is expressed locally in skeletal sites. In the femur, we observed TdTomato-positive cells in articular chondrocytes, osteocytes and few cells on endosteum and periosteum. Interestingly, NPY expression was heterogeneous within these cell populations. Although NPY is involved in the immune system; we observed no TdTomato positive cells in the bone marrow. We identified a large proportion of osteocytes embedded within calvarial bone were TdTomato positive. To examine NPY's effects, we generated the NPYcKO and confirmed depletion of transcript and protein in our global NPYKO. Male NPYKO mice had a significantly smaller femoral cross-section and impaired bone strength. A reduction in CD51+ osteoprogenitors in the endosteal fraction was observed; whilst dynamic labeling in cancellous bone showed a trend of reduced mineralizing surface in NPYKO. Osteoblast activity (MAR) was increased, consistent with increased BMSC differentiation observed in vitro. Cancellous BFR was unchanged. No skeletal changes were observed in female mice suggesting that there may be sex-specific effects of NPY on bone. Notably, both genders had increased adiposity and thus, metabolic changes were associated with global deletion. This work identified NPY expression in the skeleton and examined the effect of global NPY depletion to bone mass. The differential impact of NPY deletion in cortical and cancellous compartments highlights the complex nature of NPY signaling, which may be from distinct sources that can be dissected with our newly created NPYcKO model.

Disclosures: *Natalie Ky Wee, None*

FRI-0295

Biochemical and phenotypic characterization of mice constitutively expressing epitope-tagged PIT1 transporter in all tissues Clemens Bergwitz*, Sampada Chande, Bryan Ho, Shumayi Syed, Jonathan Fentene. Yale University School of Medicine, United States

Inorganic phosphate (Pi) has an essential role in cell signaling and metabolism and is tightly regulated by parathyroid hormone (PTH), 1,25-dihydroxy vitamin D (1,25-D), and fibroblast growth factor 23 (FGF23) to avoid excess or deficiency. The type III transporters PIT1 and PIT2 have recently emerged as candidates "transceptors" that mediate activation of ERK1/2 by Pi resulting in osteogenic differentiation of smooth vascular and bone cells while pharmacological and genetic inhibition of PIT1 and PIT2 blocks these effects. Because of lack of suitable in vitro models it remains unclear, whether PIT1 or PIT2 regulate PTH, 1,25-D or FGF23. Ablation of Pit1 in mice results in embryonic lethality at E12.5, hypomorphic Pit1 ablation is viable and reduces femur length, but no significant changes of Pi or calcium metabolism were observed. Pit1 transgenic rats on the other hand have reduced trabecular

number on uCT, hyperparathyroidism and hyperphosphatemia, but FGF23 and renal Pi handling were not assessed in these studies. Pit2 null mice have low bone mass, but normal Pi homeostasis at baseline and become hyperphosphatemic when fed a high Pi diet. This goes along with inappropriately low intact FGF23 levels in these mice suggesting that Pit2 is upstream and positively regulating FGF23. To further investigate the regulation of FGF23 and Pi by PIT1, we developed a transgenic mouse expressing epitope-tagged human PIT1 transporter under control of the CMV/chicken beta actin (CAG) promoter and a loxP-stop-loxP (LSL) cassette permitting Cre-mediated activation of transgene expression. Germline excision of the LSL cassette results in expression of the transgene in all mouse tissues (HA-hPit1+/tg). Recombination was confirmed using genomic DNA obtained from tail samples of these mice. Furthermore, expression of HA-hPIT1 was found to be approximately 10-fold above endogenous mouse Pit1 in cultured primary calvaria osteoblasts (PCOB) when assessed by Pit1 immunoblot and qRT-PCR. Also, sodium-dependent 32Pi-uptake was 1.3-fold higher in HA-hPit1+/tg PCOB cultures compared to wildtype (WT) (0.0014± 9.89E-05 vs. 0.0011± 8.52E-05, p=0.037). HA-hPit1+/tg mice showed 1.3-fold higher plasma Pi levels when compared to WT (10.2±0.89, n=11 vs. 7.8±0.62, n=17, p=0.032), while intact FGF23 and urine Pi excretion index (PEI) were normal. These observations are consistent with prior observations in Pit1 transgenic rats and suggest that regulation of Pi homeostasis by type III Pi transporters is more complex than initially expected. Further phenotypic characterization of HA-hPit1+/tg mice and mice with osterix (Osx)-Cre mediated bone-targeted expression of HA-hPit1 is currently underway.

Disclosures: **Clemens Bergwitz, None**

FRI-0296

The role of inorganic pyrophosphate in the pathogenesis of PXE caused by ABCC6 mutations Qiaoli Li*, Jouni Uitto. Thomas Jefferson University, United States

Pseudoxanthoma elasticum (PXE) is a prototype of heritable multisystem ectopic mineralization disorders. It is caused in most cases by loss-of-function mutations in the ABCC6 gene which encodes ABCC6, a putative transmembrane efflux transporter primarily expressed in the liver. Studies in murine models of PXE suggest a unique pathomechanism relating to reduced levels of plasma inorganic pyrophosphate (PPi) as a result of the lack of ABCC6-dependent ATP release in hepatocytes. PPi has been demonstrated, over four decades ago, to be a powerful anti-mineralization factor, which, when present in physiologic concentrations, prevents calcium hydroxyapatite formation in soft connective tissues. The reduced plasma PPi levels raises the possibility to develop pharmacologic approaches for PXE by targeting plasma PPi deficiency. We performed three experiments with attempts to restore plasma PPi levels for treatment of ectopic mineralization in the Abcc6^{-/-} mouse model of PXE. First, the Abcc6^{-/-} mice were administered with stable and non-hydrolyzable PPi analogues, bisphosphonates. The results suggested that selected bisphosphonates, such as etidronate, were able to inhibit ectopic mineralization. Second, the Abcc6^{-/-} mice were crossed with a transgenic mouse overexpressing human ENPP1, an ectonucleotidase that generates PPi through hydrolysis of ATP. The results demonstrated that overexpression of ENPP1 significantly reduced but did not completely prevent ectopic mineralization in the Abcc6^{-/-} mice despite that plasma PPi levels increased to the level of wild type controls. The third experiment focused on inhibition of tissue non-specific alkaline phosphatase (TNAP), the enzyme that degrades PPi. Inhibition of TNAP activity resulted in reduced amount of mineralization in the Abcc6^{-/-} mice despite unchanged plasma PPi levels. The results from three complementary experiments suggest that ABCC6 has other mechanisms, independent of PPi, for prevention of ectopic mineralization under physiologic conditions.

Disclosures: **Qiaoli Li, None**

FRI-0297

BMP2 is Required for Enteseal Bone Formation in Antigen-Induced Arthritis Yukiko Maeda*, Catherine Manning, Ellen Gravalles. University of Massachusetts Medical School, United States

Ankylosing Spondylitis (AS) is a common rheumatic disease with a prevalence of ~0.5% in the general population. AS patients suffer from pain and disability due to inflammation and ossification at enthesial sites, the mechanism of which remains unclear. BMP2 is reported to be upregulated in mesenchymal stem cells derived from AS patients. We studied the role of BMP2 in enthesial bone formation using the antigen-induced arthritis (AIA) model, in which endochondral bone formation occurs at specific enthesial sites about the knee joint. We used limb mesenchymal cell-specific (Prx1-Cre) BMP2 knock out mice (KO) and littermate control mice (WT) to induce AIA in knee joints of 8 and 14 week-old mice. At 8 and 14 weeks of age, both KO and WT mice showed similar inflammation in arthritic knees. Histologic analysis of 8 week-old WT mice revealed endochondral bone formation, angiogenesis and presence of TRAP-positive osteoclasts at entheses by day 15. In contrast, KO mice developed only cartilage but not bone. Furthermore, angiogenesis and osteoclasts were absent at entheses in KO. To examine whether enthesial bone formation was simply delayed in KO mice, we prolonged AIA until day 36; however, enthesial bone formation was again not observed in KO. AIA induced in 14 week-old mice showed enthesial bone formation in WT by day 15. In contrast, KO mice did not develop cartilage or bone at the enthesis. We harvested enthesial cells and bone marrow stromal cells (BMSCs) from 14 week-old WT and KO mice. After 3 weeks in osteoblast differentiation media, enthesial cells and BMSCs from WT mice mineralized, but cells from KO mice did not mineralize.

To explore the molecular mechanism we dissected entheses from 14 week-old WT and KO mice with AIA (day 9) using laser capture microscopy. Gene expression was analyzed using Affymetrix whole transcriptome array. We found that the Wnt antagonist, Sfrp4, was upregulated but Chondroadherin and Cxcl5 were down regulated in KO entheses. Sfrp4 was also upregulated in BMSCs from KO. Signaling Pathway Impact Analysis (SPIA) detected a trend of the Wnt pathway being negatively regulated in KO entheses. These results demonstrate that mesenchymal cell-derived BMP2 regulates enthesial bone formation in the setting of inflammation, possibly through Wnt signaling. Thus may have implications for the pathogenesis of enthesophytes in AS.

Disclosures: **Yukiko Maeda, Abbvie, Grant/Research Support**

FRI-0298

COPB2 Loss of Function Leads to Disrupted Collagen Trafficking and Juvenile Osteoporosis Ronit Marom*, Lindsay C Burrage¹, Mahim Jain², Ingo Grafe¹, Daryl A Scott¹, Jill A Rosenfeld¹, Jason D Heaney¹, Denise Lanza¹, Xiaohui Li¹, Kyu-Sang Joeng¹, Yi-Chien Lee¹, I-Wen Song¹, Joseph M Slepka¹, Dominyka Batkovskytė¹, Zixue Jin¹, Brian C Dawson¹, Shan Chen¹, Yuqing Chen¹, Ming-Ming Jiang¹, Elda M Munivez¹, Vernon R Sutton¹, Cole Kuzawa³, Rossella Venditti⁴, Maryann Weis⁵, Aurélie Clément⁶, Brenna Tresp⁶, Bernardo Blanco-Sánchez⁶, Monte Westerfield⁶, David Eyre⁵, Catherine G Ambrose³, Antonella De Matteis⁴, Brendan Lee¹. ¹Baylor College of Medicine, United States, ²Kennedy Krieger Institute, United States, ³University of Texas Health Science Center at Houston, United States, ⁴TIGEM (Telethon Institute of Genetics and Medicine), Italy, ⁵University of Washington, United States, ⁶University of Oregon, United States

Abnormal collagen trafficking has been implicated in a number of skeletal dysplasias. In a 7-year-old female patient with juvenile osteoporosis, we identified a de novo, heterozygous loss-of-function variant in COPB2, a component of the coatomer complex COPI that is involved with membrane trafficking in the Golgi complex and between the ER and the Golgi complex. The patient presented with recurrent fractures starting at 2 years of age, and low bone mineral density. RNA studies in the patient's lymphoblast cells showed decreased expression of COPB2, consistent with haploinsufficiency. To better understand the molecular consequences of COPB2 haploinsufficiency, we assessed collagen trafficking by immunofluorescence microscopy. In COPB2 siRNA-treated fibroblasts, we observed delayed collagen trafficking with retention of type I collagen in the ER and Golgi, and altered subcellular distribution of Golgi markers. To characterize the effect of COPB2 loss of function on skeletal development, we generated a zebrafish model carrying a frameshift variant (p.Lys10Thrs*12) resulting in an early stop codon in the copb2 gene. copb2-null embryos showed early lethality. Alizarin-red staining of heterozygous larvae at 7 days post-fertilization was reduced, suggesting delayed mineralization. We then generated a mouse model carrying a Copb2 deletion by CRISPR technology. Copb2^{-/-} mice were embryonic lethal. In the heterozygous female mice, uCT analysis showed a 15-20% reduction in spine BV/TV, trabecular number and trabecular thickness. Biomechanical testing of femurs by 3-point bending demonstrated decreased bone strength, with reduced maximal load, stiffness and rigidity in femurs of Copb2^{+/-} female mice, that was associated with decreased cortical thickness and cross-sectional bone area. Interestingly, in spite of the delay in collagen trafficking observed in vitro, collagen post-translational modifications were not altered in bones of Copb2^{+/-} mice. In summary, we identified a loss-of-function variant in COPB2 in a patient with juvenile osteoporosis. Cell studies, zebrafish and mouse models support COPB2 haploinsufficiency as the mechanism of low bone mass in this patient, via disruption of intracellular collagen trafficking. This study underlines the critical role of the COPI complex in bone development and suggests that pathogenic variants in COPB2 should be considered in the genetic differential diagnosis of early-onset osteoporosis.

Members of the Undiagnosed Diseases Network

David R. Adams, Aaron Aday, Mercedes E. Alejandro, Patrick Allard, Euan A. Ashley, Mahshid S. Azamian, Carlos A. Bacing, Eva Baker, Ashok Bajussbramanyam, Hayk Barsbeyan, Gabriel F. Batzi, Alan H. Beag, Babak Behnam, Hugo J. Bellen, Jonathan A. Bernstein, Anna Bican, David P. Bick, Camille L. Birch, Devon Bonner, Braden E. Boone, Bret L. Bostwick, Lauren C. Briere, Ely Brokamp, Donna M. Brown, Matthew Brush, Elizabeth A. Burke, Lindsay C. Burrage, Manish J. Butte, Shan Chen, Gary D. Clark, Terra R. Coakley, Joy D. Cogan, Heather A. Colley, Cynthia M. Cooper, Heidi Cope, William J. Craigie, Precilla D'Souza, Mariska Davids, Jean M. Davidson, Jyoti G. Dayal, Esteban C. Dell'Angelica, Shweta U. Dhar, Katrina M. Dipple, Laurel A. Donnell-Fink, Naghmei Dorrani, Daniel C. Dorset, Emilie D. Douine, David D. Draper, Annika M. Dries, David J. Eckstein, Lisa T. Emrick, Christine M. Eng, Gregory M. Enns, Ascja Eskin, Cecilia Estyves, Tyra Estwick, Laura Fairbrother, Liliana Fernandez, Carlos Ferreira, Paul G. Fisher, Brent L. Fogel, Noah D. Friedman, William A. Gahl, Emily Glatton, Rena A. Godfrey, Alica M. Goldman, David B. Goldstein, Sarah E. Gould, Jean-Philippe F. Gourdine, Catherine A. Groden, Andrea L. Gropman, Melissa Haendel, Rizwan Hamid, Neil A. Hanchard, Lori H. Handley, Matthew R. Herzog, Francis High, Ingrid A. Holm, Jason Hom, Ellen M. Howerton, Yong Huang, Fariha Jamal, Yong-hui Jiang, Jean M. Johnston, Angela L. Jones, Lefkothea Karaviti, David M. Koeller, Isaac S. Kohane, Jennifer N. Kohler, Donna M. Krasnewich, Susan Korrick, Mary Kozura, Elizabeth L. Krieg, Joel B. Krier, Jennifer E. Kyle, Seema R. Lalani, C. Christopher Lau, Jozef Lazar, Kimberly LeBlanc, Brendan H. Lee, Hane Lee, Shawn E. Levy, Richard A. Lewis, Sharyn A. Lincoln, Sandra K. Loo, Joseph Loscalzo, Richard L. Maas, Ellen F. Macnamara, Calum A. MacRae, Valerie V. Maduro, Marta M. Majchenska, May Christine V. Malicdan, Laura A. Mamasova, Teri A. Manolis, Thomas C. Marom, Ronit Marom, Martin G. Martin, Julian A. Martinez-Agosto, Siboli Marwaha, Thomas May, Ailym McCorkie-Rossell, Colleen E. McCormack, Alexa T. McCray, Jason D. Medsker, Thomas O. Metz, Matthew Might, Paolo M. Moretti, Marie Morimoto, John J. Mulvihill, David R. Murdoch, Jennifer L. Murphy, Donna M. Muzny, Michele E. Nehrebecky, Stan F. Nelson, J. Scott Newberry, John H. Newman, Sarah K. Nicholas, Donna Novacic, Jordan S. Orange, James P. Orenco, J. Carl Pallas, Christina GS. Palmer, Jeannette C. Papp, Neil H. Parker, Loren DM. Pena, John A. Phillips III, Jennifer E. Posey, John H. Postlethwaite, Lorraine Potocki, Barbara N. Pusey, Chloe M. Reuter, Amy K. Robertson, Lance H. Rodan, Jill A. Rosenfeld, Jacinda B. Sampson, Susan L. Samson, Kelly Schoch, Molly C. Schroeder, Daryl A. Scott, Prashant Sharma, Vandana Shashi, Edwin K. Silverman, Janet S. Simsheiner, Kevin S. Smith, Rebecca C. Spillmann, Joan M. Stoler, Nicholas Stone, Jennifer A. Sullivan, David A. Swetsch, Queenie K.-G. Tan, Cynthia J. Tiff, Camilo Toro, Alyssa A. Tran, Ting K. Uix, Eric Vlijan, Tigharrie P. Vogel, Daryl M. Waggett, Colleen E. Wahl, Nicole M. Walley, Chris A. Walsh, Melissa Walker, Jium Wan, Michael F. Wandler, Patricia A. Ward, Katrina M. Waters, Bobbie-Jo M. Webb-Robertson, Monte Westerfield, Matthew T. Wheeler, Anastasia L. Wise, Lynne A. Wolfe, Elizabeth A. Worthey, Shinya Yamamoto, John Yang, Yaping Yang, Amanda J. Yoon, Guoyun Yu, Diane B. Zastrow, Chunli Zhao, Allison Zheng

Disclosures: **Ronit Marom, None**

FRI-0299

PIN1 is a new therapeutic target of craniosynostosis Hye-Rim Shin^{*1}, Han-Sol Bae¹, Bong-Su Kim¹, Heein Yoon¹, Young-Dan Cho¹, Woo-Jin Kim¹, Kang Young Choi², Yun-Sil Lee¹, Kyung-Mi Woo¹, Jeong-Hwa Baek¹, Hyun-Mo Ryoo¹. ¹Seoul National University, Republic of Korea, ²Kyungpook National University, Republic of Korea

Gain-of-function mutations in fibroblast growth factor receptors (FGFRs) cause congenital skeletal anomalies including craniosynostosis (CS), which is characterized by the premature closure of craniofacial sutures. Apert syndrome (AS) is one of the severest forms of CS, and the only treatment is surgical expansion of prematurely fused sutures in infants. Previously, we demonstrated that the prolyl isomerase PIN1 plays a critical role in mediating FGFR signaling, and that Pin1^{+/-} mice exhibit delayed closure of cranial sutures. In this study, using both genetic and pharmacologic approaches, we tested whether PIN1 modulation could be used as a therapeutic regimen against AS. In the genetic approach we crossbred Fgfr2S252W^{+/+}, a mouse model of AS, and Pin1^{+/-} mice. Down-regulation of Pin1 gene dosage attenuated premature cranial suture closure and other phenotypes of AS in Fgfr2S252W^{+/+} mutant mice. In the pharmacological approach, we intraperitoneally administered juglone, a PIN1 enzyme inhibitor, to pregnant Fgfr2S252W^{+/+} mutant mice, and found that this treatment successfully interrupted fetal development of AS phenotypes. Primary cultured osteoblasts from Fgfr2S252W^{+/+} mutant mice expressed high levels of FGFR2 downstream target genes, but this phenotype was attenuated by PIN1 inhibition. Post-translational stabilization and activation of RUNX2 in Fgfr2S252W^{+/+} osteoblasts were also attenuated by PIN1 inhibition. Based on these observations, we conclude that PIN1 enzyme activity is important for FGFR2-induced RUNX2 activation and craniofacial suture morphogenesis. Moreover, these findings highlight that juglone or other PIN1 inhibitors represent viable alternatives to surgical intervention for treatment of CS and other hyperostotic diseases.

Disclosures: Hye-Rim Shin, None

FRI-0300

Identifying Genetic Modifiers in Patients with Mild Fibrodysplasia Ossificans Progressiva using Whole Exome Sequencing Kelly Wentworth^{*1}, Tania Moody¹, Kim Taylor¹, Niambi Brewer², Fred Kaplan², Robert Pignolo³, Eileen Shore², Edward Hsiao¹. ¹UCSF, United States, ²UPenn, United States, ³Mayo Clinic, United States

Fibrodysplasia ossificans progressiva (FOP) is an ultra-rare genetic condition characterized by excessive heterotopic bone formation that occurs in response to injury or inflammation. Classic FOP is caused by an autosomal dominant missense mutation in the ACVR1 gene (c.617 G>A; p.R206H), which encodes activin A receptor type 1. This mutation leads to abnormal signaling through the ACVR1 receptor and over-activation of the downstream BMP signaling pathway, resulting in ectopic bone formation in soft tissues and loss of joint function and mobility. FOP is progressive and debilitating disease with no effective medical treatment, and most patients are wheelchair-bound by the third decade of life. There is a wide spectrum of disease severity among FOP patients with the classical R206H mutation, including a very small number who exhibit an unusually mild phenotype, with minimal joint involvement and no significant mobility limitations. We hypothesize that these milder FOP patients may harbor genetic variants that act as modifiers of BMP signaling and confer a protective effect. To test this hypothesis, we performed whole exome sequencing (WES) on a cohort of 23 FOP patients with the ACVR1-R206H mutation. We stratified these patients by disease severity using the CAJIS score (cumulative analogue joint involvement scale), a validated tool for assessing FOP disease burden. Four of the 23 patients had a strikingly mild phenotype defined as a CAJIS score of < 5/30 at age 15 or older. We analyzed the WES data using Ingenuity Variant Analysis software and applied sequential filters to assess for pathogenicity, allele frequency, conservation, and predicted protein function. An additional filter was applied to capture gene variants that are directly involved in BMP signaling, and identified a variant in the BMP receptor BMPRIA in one mildly-affected patient. This variant is not present in the other 19 classically-affected FOP patients. The minor allele frequency of this variant is <1% and is considered rare compared to the general population. It is located in a highly conserved region in the protein kinase domain and is predicted to cause loss-of-function. Since BMPRIA signals through the SMAD 1/5/9 pathway, as does ACVR1, we hypothesize that this variant could potentially attenuate signaling through this pathway, explaining the milder observed phenotype. We are currently testing this hypothesis using human induced pluripotent stem cells derived from FOP patients to determine if this variant alters BMP signaling and to evaluate its potential as a target for pharmacologic treatment. In summary, this study highlights the benefits of using WES combined with a well-defined phenotype analysis to identify rare disease-modifying variants that could be targeted for drug development.

Disclosures: Kelly Wentworth, Clementia Pharmaceuticals, Other Financial or Material Support

FRI-0325

A high resolution Capture-C promoter 'interactome' implicates causal genes at BMD GWAS loci Alessandra Chesi^{*1}, Yadav Wagley², Matthew E. Johnson¹, Sumei Lu¹, Michelle E. Leonard¹, Kenyaita M. Hodge¹, James A. Pippin¹, Elisabetta Manduchi¹, Andrew D. Wells¹, Struan F.A. Grant¹, Kurt D. Hankenson². ¹The Children's Hospital of Philadelphia, United States, ²University of Michigan, United States

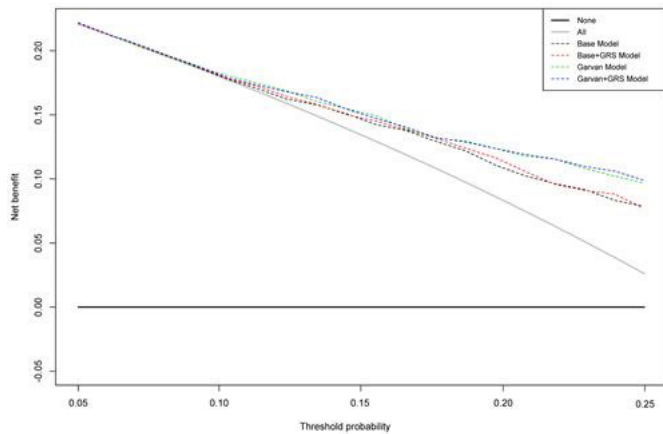
There is clear evidence for a genetic component to osteoporosis pathogenesis. Genome wide association studies (GWAS) have been successful in discovering key genetic variants robustly associated with bone mineral density (BMD), both in children and adults. However, it is known that GWAS only reports genomic signals and not necessarily the precise localization of culprit genes. Given the notable paucity of genomic data available on bone in the public domain, and to improve upon the low resolution of typical Hi-C approaches, we developed a massively parallel, high-resolution Capture-C based method to characterize the genome-wide interactions of all human promoters in osteoblasts. We designed a custom Agilent SureSelect RNA library targeting DpnII restriction fragments overlapping 36,691 promoters of protein-coding, noncoding, antisense, snRNA, miRNA, snoRNA and lincRNA genes. We applied our method of SPATIAL-seq (genome-scale, Promoter-focused Analysis of chromatin Looping) to primary human mesenchymal stem cell (MSC)-derived osteoblasts. We also generated ATAC-seq open chromatin maps from the same MSC-derived osteoblast samples to determine informative proxy SNPs residing in open chromatin for each of 111 BMD GWAS signals at 108 candidate loci. By intersecting our sub-1kb SPATIAL-seq data with our ATAC-seq data, we observed consistent contacts for at least 33 loci. Some 'nearest' genes to the sentinel SNP were supported e.g. SMAD3, SMG6 and SOST1, while at other loci more distant genes were implicated, including EPDR1 at the 'STARD3NL' locus and ING3 at the 'CPED1-WNT16' locus. Remarkably, knockdown of both EPDR1 and ING3 in four primary hMSC donor lines had pronounced inhibitory effects on osteoblastogenesis, including impacting Alizarin red S and histochemical alkaline phosphatase staining. In conclusion, we observed consistent contacts to at least ~30% of BMD GWAS loci using the highest resolution promoter 'interactome' to date in a single, disease-relevant cell type, and revealed two novel genes involved in osteoblastogenesis. Only by identifying the correct genes at BMD loci can GWAS findings be translated to the development of efficacious treatments for osteoporosis.

Disclosures: Alessandra Chesi, None

FRI-0326

Assessing Clinical Utility of Genetic Profiling in Fracture Risk Assessment: A Decision Curve Analysis Thao P. Ho-Le^{*1,2}, Jacqueline R. Center^{1,3}, John A. Eisman^{1,3,4}, Hung T. Nguyen², Tuan V. Nguyen^{1,2,3,4}. ¹Bone Biology Division, Garvan Institute of Medical Research, ²School of Biomedical Engineering, University of Technology, Sydney, Australia, ³St Vincent Clinical School, UNSW Australia, Australia, ⁴School of Medicine, Notre Dame University, Australia

Aims: Genetic profiling has emerged as a useful factor for assessing the distant risk of fracture in asymptomatic individuals. This study was aimed at determining whether adding genetic profiling to clinical risk factors improves clinical decision making for the early identification of individuals at high risk for fracture. **Methods:** The study involved 2188 women and 1324 men aged 60+ years, who have been followed up to 20 years. Bone mineral density (BMD) and clinical risk factors were obtained at baseline. The incidence of fracture and mortality was ascertained during the study period. Sixty-two BMD-associated SNPs were genotyped, and a weighted genetic risk scores (GRS) were constructed for each individual by summing the products of the number of risk alleles and the sex-specific regression coefficients [associated with BMD from GWAS]. We considered 4 Cox's proportional hazard models for predicting 10-year fracture risk: Model I (Base model) included only clinical risk factors (ie age, prior fractures, and fall in previous 12 months); Model II (Garvan model) included clinical risk factors and femoral neck BMD; Model III (Garvan+GRS) included clinical risk factors, femoral neck BMD and GRS; and Model IV (Base+GRS) included clinical risk factors and GRS. **Decision curve analysis** was used to evaluate the clinical net benefit of predictive models: one sums the weighted benefits (true positives) and subtract the weighted harms (false positives), with the weights assigned to true positives and false positives were derived from the threshold probability of fracture. **Results:** In women, for risk threshold above 0.15, the Base+GRS model had a significantly higher net benefit than the Base model (Figure); however, for threshold below 0.15, there was no significant difference in net benefit between the two models. The Garvan model yielded the highest net benefit; adding GRS into the Garvan model did not substantially improve the net benefit. In men with fracture risk greater than 0.15, the Base+GRS model resulted in a better net benefit than the Base model. Interestingly, the Garvan+GRS model did improve the net benefit over and above the Garvan model. **Conclusion:** These results suggest that genetic profiling can provide additional prognostic information to that obtained from clinical risk factors, particularly in women at higher risk of fractures. However, in the presence of BMD in a predictive model, GRS does not further improve net clinical benefit.



Disclosures: *Thao P. Ho-Le, None*

FRI-0327

Bioinformatics Informs GWAS: An Osteoporosis and Epigenetics Study Hui Shen*, Xiao Zhang, Fangtang Yu, Hong-Wen Deng, Melanie Ehrlich. Tulane University, United States

Most genetic variants for osteoporosis identified by genome-wide association studies (GWAS) are mapped to non-coding regions. It is challenging to pinpoint the disease-causal variants and understand their regulatory functions in disease. Here, we employed a novel bioinformatics approach to prioritize osteoporosis-associated genes and potential functional variants by leveraging cell-specific epigenomic and transcriptomic profiles across diverse human cell types. We compiled a list of 275 genes and 11,493 single-nucleotide polymorphisms (SNPs) that were associated with osteoporosis risk in previous GWAS (index SNPs) or that are in high linkage disequilibrium ($r^2 > 0.8$) with the index SNPs. Using comprehensive epigenomic annotations (histone modifications, chromatin segmentation states, DNase I hypersensitivity, and DNA methylation) along with RNA-seq data in osteoblasts and a diverse set of other types of human cells, we identified 16 osteoporosis-associated genes that are preferentially expressed in osteoblasts, and corresponding potential functional SNPs that are mapped to osteoblast-associated enhancer or promoter chromatin. These genes are *CARMN* (host gene for *MIR143* and *MIR145*), *CCDC170*, *GALNT3*, *GPC6*, *HOXA11*, *IGFBP7*, *KLF12*, *PAPPA*, *PDE7B*, *PDGFC*, *PPP6R3*, *PRRX1*, *RERE*, *TBX15*, *TRPS1*, and *TNFRSF11B* (*OPG*). They include some well-known osteoporosis-related genes (e.g., *TNFRSF11B*) and genes that previously received little attention for their potential contribution to osteoporosis risk (e.g., *PDGFC*, *PPP6R3* and *RERE*). Eleven of the genes had enhancer chromatin in the gene body in osteoblasts. Three had enhancer chromatin in intergenic regions. One (*TNFRSF11B*) even had the index SNP embedded in osteoblast-specific enhancer chromatin within the neighboring gene (*COLEC10*) that was silent in osteoblasts and almost all studied cell and tissue types. Some of the index or proxy SNPs also overlapped predicted allelic variation-sensitive binding sites for transcription factors present in osteoblasts. Our study shows how diverse epigenomic and functional annotations can be used to guide the prioritization of novel genes and functional variants in GWAS signals, and highlights a number of promising functional variants that may contribute to osteoporosis risk through influencing osteoblast-specific regulatory elements. Our findings form the basis for future biological studies of the osteoporosis-associated functional variants in model systems.

Disclosures: *Hui Shen, None*

FRI-0343

Regulation of FGF23 and Bone Mass by the Proprotein Convertase Furin Omar Al Rifai*¹, Rachid Essalmani¹, John Creemers², Nabil G. Seidah¹, Mathieu Ferron¹. ¹Institut de recherches cliniques de Montreal, Canada, ²KU Leuven, Belgium

Fibroblast growth factor 23 (FGF23) is a hormone regulating phosphate metabolism, which is secreted by terminally differentiated osteoblasts. Specifically, FGF23 reduces phosphate reabsorption in the proximal tubule of the kidney by decreasing the expression of the sodium/phosphate cotransporters *NaPi2a* and *NaPi2c*. FGF23 proteolytic cleavage by a proprotein convertase (PC) inhibits its activity, since mutations that render FGF23 resistant to cleavage lead in humans to autosomal dominant hypophosphatemic rickets (ADHR), a rare phosphate wasting disorder characterized by increased FGF23 serum level, hypophosphatemia and osteomalacia. Yet, the identity of the PC(s) responsible for FGF23 cleavage in vivo remains undetermined, although it was suggested to be either furin or PC5 based on in vitro evidence. Hence, in the current study we investigate the role of furin and PC5 in the regulation of FGF23 in vivo, and assess their respective requirement for phosphate metabolism and bone mass accrual. OCN-Cre transgenic mice, expressing Cre recombinase under the control

of the human osteocalcin promoter, were crossed with Furin^{fllox}/fllox or Pcsk5^{fllox}/fllox mice to generate mice lacking furin or PC5 specifically in differentiated osteoblasts (i.e., Furin^{nosb}^{-/-} and Pcsk5^{nosb}^{-/-}). Circulating levels of intact FGF23 were significantly increased by more than 25% in Furin^{nosb}^{-/-} mice, but remained unchanged in Pcsk5^{nosb}^{-/-} mice. Despite this raise in active FGF23 there was no change in the expression of *NaPi2a* and *NaPi2c* in the kidney of Furin^{nosb}^{-/-} mice, which maintained normal serum phosphate levels. In addition, bone histology did not reveal sign of osteomalacia in the same animals. These results are consistent with the observation that mice carrying the ADHR mutation (R176Q) in *Fgf23* do not develop hypophosphatemic osteomalacia unless they are fed a low-iron diet [1]. Inactivation of furin in osteoblasts nevertheless resulted in a striking bone phenotype characterized by a 2-fold increase in trabecular bone volume combined with a 15% reduction in cortical thickness and in overall bone mineral density. In three-point bending tests Furin^{nosb}^{-/-} femurs showed reduced bone stiffness. Of note, Pcsk5^{nosb}^{-/-} mice displayed normal bone density. Together these results identify furin as a PC responsible of FGF23 cleavage in vivo, but also suggest that furin in osteoblasts influences bone density through FGF23-independent mechanisms. Ref: (1) Farrow et al. 2011, PNAS, 108: E1146-55.

Disclosures: *Omar Al Rifai, None*

FRI-0344

WITHDRAWN

FRI-0345

Bone-Targeted Pharmacological Inhibition of Notch Signaling Potentiates PTH-induced Bone Gain. Jesus Delgado-Calle*¹, Gerald Wu², Mathew E. Olson¹, Kevin Mcandrews², Jessica H. Nelson¹, Ashley L. Daniel¹, Noriyoshi Kurihara¹, Emily G. Atkinson², Venkat Srinivasan³, Lifeng Xiao³, Frank H. Ebtino³, G. David Roodman¹, Robert K. Boeckman Jr³, Teresita Bellido². ¹Indiana University School of Medicine, Dept. of Medicine, Hematology/Oncology, United States, ²Indiana University School of Medicine, Dept. of Anatomy and Cell Biology, United States, ³University of Rochester, Dept. of Chemistry, United States

Daily injections of PTH (iPTH) cause bone anabolism by increasing osteoblast number and function. However, iPTH also increases bone resorption, which can limit bone gain. Earlier work demonstrated that iPTH activates Notch signaling in osteocytes; and that bone-targeted Notch inhibition using a γ -secretase inhibitor (GSI) conjugated to an alendronate-modified bone-targeting molecule (BT-GSI) decreases Notch signaling in bone, and reduces CTX (-40%) while preserving bone formation, leading to increases in BMD (4-7%) and cancellous bone volume (BV/TV; 30%). Here, we examined if combination of iPTH (anabolic) and BT-GSI (anti-catabolic) increases bone mass to a higher extent than either agent alone. BT-GSI (5mg/kg, 3x/wk) or saline was co-administered with iPTH (100 ng/g/day) or vehicle for 2wks to 4-mo-old mice (n=10/group). iPTH increased *Hes1/5/7* and *Hey1/L* expression in bone, and BT-GSI decreased it to control levels. iPTH increased total (7%) and femoral (13%), and preserved spinal BMD (0%); and BT-GSI potentiated the increase at all bone sites (10, 17, and 7%, respectively). BT-GSI increased by 25% the gain in cancellous BV/TV (L4 and distal femur) and trabecular thickness induced by iPTH, but did not alter iPTH-induced increases in cortical bone area (8%). Co-administration of BT-GSI decreased serum PINP (-30%); however, it preserved the increased bone formation rate (20%) and osteoblast surface (20%) induced by iPTH in cancellous bone. Further, mice receiving iPTH alone or combined with BT-GSI exhibited similar elevated *Alpl*, *Runx2*, *Bglap*, and *Wnt* target genes mRNA levels, and decreased *Sost* in bone. In contrast, co-administration of BT-GSI reduced the increased serum CTX (30%) and osteoclast surface (25%) induced by iPTH to values below those of control mice receiving vehicle. The increased *Rankl/Opg* expression ratio in bone (1.5-fold) induced by iPTH remained unchanged by BT-GSI, and no changes were found in *M-Csf* expression. However, unconjugated GSI reduced *Rankl*-induced osteoclast differentiation in vitro with an EC50 ~0.1 μ M. Importantly, the bone-targeting molecule alone required a dose 10 times higher than GSI to decrease osteoclastogenesis. These results demonstrate that bone-targeted inhibition of the Notch pathway in the frame of anabolic PTH signaling induces a superior bone gain compared to individual treatments and provide the bases for novel therapeutic strategies that reduce bone catabolism while simultaneously preserve bone anabolism.

Disclosures: *Jesus Delgado-Calle, None*

FRI-0346

Overexpression of Sirt1 in Mesenchymal Stem Cells Protects against Glucocorticoid-Induced Osteoporosis by Inhibiting Oxidative Stress and Osteocyte Senescence Qinghe Geng*, Xiaoqing Hu, Jun Wu, Dengshun Miao. Nanjing Medical University, China

Glucocorticoid-induced osteoporosis (GIO) is the most common form of secondary osteoporosis, but molecular mechanisms for their harmful effects on bone are unclear. Although Sirt1 has been suggested as a protective molecule against osteoporosis, it is unknown whether Sirt1 overexpression in mesenchymal stem cells (MSCs) can protect against GIO. To answer this question, 12-week-old male *Prx1-Sirt1*Tg mice with Sirt1 overexpression in

MSCs and WT littermates were injected subcutaneous with either vehicle or dexamethasone (DEX) (1mg/kg/day) for 4 weeks. Bone phenotypes of all models were analyzed at 16 weeks of age. We examined the alterations of expression levels of Sirt1 in bony tissue and found that the mRNA and protein expression levels of Sirt1 were significantly up-regulated in Sirt1Tg mice and were significantly down-regulated in DEX-treated WT mice compared to WT mice, and they were returned to normal levels in DEX-treated Sirt1Tg mice. BMD, cortical and trabecular bone volume and bone mechanical strength, and osteoblastic bone formation parameters including osteoblast number, ALP+ and type I collagen+ areas, MAR, BFR, osteogenic gene expression levels and serum ALP and P1NP levels were all significantly decreased, whereas osteoclastic bone resorption parameters including osteoclast number and surface, RANKL/OPG ratio, serum TRAP-5b and CTX-1 levels were significantly increased in DEX-treated WT mice compared to WT mice, and were normalized in DEX-treated Sirt1Tg mice. To further explore the mechanism underlying the role of Sirt1 overexpression in MSCs in protecting against DEX-induced osteoporosis, we examined the alterations of oxidative stress and cell senescence parameters. Results showed that the ROS levels of bone marrow cells and serum malondialdehyde levels, β -galactosidase and p16 positive osteocytes, protein expression levels of γ H2AX, 8-OHdG, p16, p21 and p53 and inflammatory factors, including TNF α , IL-1 α/β , IL-6 and IL-8 gene expression levels were significantly increased, whereas T-AOC activity and SOD activity, protein expression levels of SOD1/2 and Prdx1/4 were significantly decreased in DEX-treated WT mice compared to WT mice, and were normalized in DEX-treated Sirt1Tg mice. Results of this study demonstrated that overexpression of Sirt1 in MSCs can protect against DEX-induced osteoporosis by inhibiting oxidative stress and osteocyte senescence, thus suggest that Sirt1 in MSCs is a therapeutic target for GIO.

Disclosures: *Qinghe Geng, None*

FRI-0347

Sustained Klotho delivery reduces serum phosphate in a model of diabetic nephropathy Julia Hum^{*1}, Linda O'Bryan², Arun Tatiparthi³, Erica Clinkenbeard⁴, Pu Ni⁴, Martin Cramer², Manoj Bhaskaran², Robert Johnson², Jonathan Wilson², Rosamund Smith², Kenneth White⁴. ¹Marian University, United States, ²Eli Lilly and Company, United States, ³Covance Inc, United States, ⁴Indiana University School of Medicine, United States

Diabetic nephropathy (DN) is a primary cause of end-stage renal disease and is becoming more prevalent due to the global rise of type 2 diabetes. A model of DN, the db/db uninephrectomized (db/db-uni) mouse, is characterized by obesity, as well as compromised renal function. This model also manifests defects in mineral metabolism common in DN including hyperphosphatemia, which leads to severe endocrine disease. The FGF23 co-receptor, α Klotho (α KL), circulates as a soluble, cleaved form ('cKL') and may directly influence phosphate handling. Our study sought to test the effects of cKL on mineral metabolism in db/db-uni mice. Mice were placed into either mild or moderate disease groups based upon the albumin/creatinine ratio (ACR). Body weights of db/db-uni mice were significantly greater across the study compared to lean controls regardless of disease severity. Adeno-associated-cKL (AAV-cKL) administration was associated with increased serum Klotho, intact, bioactive 'iFGF23', and cFGF23 ($p < 0.05$). BUN was improved after cKL administration, and cKL corrected hyperphosphatemia in the high and low ACR db/db-uni group. Interestingly, two weeks after cKL delivery blood glucose levels were significantly reduced in db/db-uni mice with high ACR ($p < 0.05$). Several genes associated with stabilizing active iFGF23 were also increased in the osteoblastic UMR-106 cell line with cKL treatment. It remains to be determined whether increased cKL-FGF23 signaling or increased intact FGF23 acting on the diseased kidney mediates the effects on hyperphosphatemia in DN. In summary, delivery of cKL to a model of DN normalized blood phosphate levels regardless of disease severity.

Disclosures: *Julia Hum, None*

FRI-0348

WITHDRAWN

FRI-0349

1,25-Dihydroxyvitamin D Retards Osteoporosis by Activating Nrf2-Antioxidant Signaling and Inactivating P16 Senescence Signaling Wanxin Qiao^{*1}, Lulu Chen¹, Weiwei Sun¹, David Goltzman², Dengshun Miao¹. ¹Nanjing Medical University, China, ²McGill University, Canada

Vitamin D deficiency has been identified as one of the factors associated with osteoporosis, however, the mechanism of vitamin D deficiency in accelerating the occurrence of osteoporosis is not yet clear. We first employed 1 α (OH)ase heterozygous (1 α (OH)ase^{+/-}) mice as an animal model for 1,25(OH)₂D deficiency. In these mice, serum calcium and phosphorus levels were not reduced significantly, PTH levels were slightly increased, however, serum 1,25(OH)₂D levels were reduced by 30% compared to WT littermates. 1 α (OH)ase^{+/-} mice at 12 months of age displayed severe osteoporotic phenotype, including significantly reduced BMD, trabecular volume, ALP+ osteoblasts, and increased TRAP+ osteoclasts. Mineralization was normal. These mice also displayed an aging phenotype in bone, including significantly increased bone marrow ROS levels, p16+ and β -Gal+ osteocytes. Protein expression levels of nuclear factor erythroid 2-related factor (Nrf2), a mas-

regulator of cellular resistance to oxidants, and its target antioxidant enzyme genes, were down-regulated, and protein expression levels of γ H2AX, a marker for DNA damage, and p16, p19 and p53 were up-regulated. Both the osteoporotic and bone aging phenotypes observed in 1 α (OH)ase^{+/-} mice were rescued by supplementation with exogenous 1,25(OH)₂D3 or with the antioxidant N-acetyl-L-cysteine and by deletion of the p16 gene. Furthermore, we demonstrated that 1,25(OH)₂D3 exerted an antioxidant role by transcriptional regulation of Nrf2 via VDR. Expression levels of Nrf2 gene were upregulated significantly in 1,25(OH)₂D3-treated mouse embryonic fibroblasts (MEFs) from wild-type mice in a dose dependent manner, but not in MEFs from VDR knockout mice. Bioinformatic analysis suggested the presence, in the 5'-flanking region of the Nrf2 promoter, of a VDR response element-like sequence. Chromatin immunoprecipitation demonstrated that the VDR had the ability to physically bind the Nrf2 promoter. Luciferase assays showed that luciferase activity was increased significantly in MEFs transfected with Nrf2-PGL3 plasmid compared with the empty plasmid, and was more pronounced in 1,25(OH)₂D3 treated MEFs transfected with Nrf2-PGL3 plasmid. Nrf2 knock-down significantly down-regulated the expression levels of Nrf2 antioxidant target genes. Taken together, current studies therefore, indicate that 1,25(OH)₂D exerts an anti-osteoporosis role by activation of Nrf2-antioxidant signaling and inactivation of p16 senescence signaling.

Disclosures: *Wanxin Qiao, None*

FRI-0350

Estrogen-stimulated pleiotrophin functions to stimulate osteoblast differentiation and maintain bone mass in IGF binding protein-2 knockout mice Susan D'Costa^{*1}, Gang Xi¹, Victoria Demambro², Clifford Rosen², David Clemmons¹. ¹University of North Carolina at Chapel Hill, United States, ²Maine Medical Center Research Institute, United States

Pleiotrophin (PTN) is an extracellular heparin binding protein that contains a region of sequence that closely resembles IGFBP-2. Both PTN and IGFBP-2 bind to the cell surface receptor RPTP β which leads to activation of AKT. Our previous studies showed that IGFBP-2^{-/-} male mice exhibited reduced trabecular bone mass while female null mice had no reduction but the explanation for this sexual dimorphism was not determined. Since estrogen has been shown to stimulate PTN, we hypothesized that estrogen maintains bone mass in the absence of IGFBP-2 via up-regulation of PTN. Our data showed that although PTN mRNA level was higher in female animals regardless of IGFBP-2 level, PTN mRNA levels in bone were significantly greater in IGFBP-2 knockout compared to wild type females. Analysis of calvarial osteoblasts isolated from IGFBP-2 knockout female mice showed a high level of PTN expression at day 3 and day 6 of differentiation. In addition, the temporal change in expression of PTN in MC-3T3 cells was quite similar to IGFBP-2, increasing from day 0 to day 9 and decreasing after day 12. Knockdown of PTN in MC-3T3 cells using RNAi inhibited osteoblast differentiation which could be rescued by adding back PTN or IGFBP-2. Similar to IGFBP-2, PTN was able to stimulate AKT activation, which is essential for osteoblast differentiation and addition of an anti-fibronectin 3 domain antibody which blocks IGFBP-2 binding to RPTP β , inhibited PTN stimulation of AKT as well as differentiation. The addition of estrogen to MC-3T3 or IGFBP-2 silenced cells stimulated PTN expression and this resulted in enhanced osteoblast differentiation but estrogen had no effect on AKT induction or differentiation when PTN was knocked down. To further support this hypothesis, we also showed that estrogen loss following ovariectomy reduced serum PTN by > 50% while administration of estrogen to WT male mice increased PTN and RPTP β mRNA 1.6 and 2 fold respectively in bone and it induced 1.9 and 2.9 fold increases in IGFBP-2^{-/-} mice. Consistently, our studies in male WT mice showed that estrogen treatment for 16 weeks resulted in a significant increase in aBMD but the response was significantly greater in male IGFBP-2^{-/-} mice. These results demonstrate that estrogen-stimulated PTN functions in a manner similar to IGFBP-2 to stimulate osteoblast differentiation and maintain the bone mass and that in the absence of IGFBP-2, estrogen stimulation of PTN maintains bone mass in female knockout mice.

Disclosures: *Susan D'Costa, None*

FRI-0351

Overexpression of Sirt1 in Mesenchymal Stem Cells Protects against Estrogen Deficiency-Induced Osteoporosis Qian Zhang^{*}, Rong Wang, Jianliang Jin, Dengshun Miao. Nanjing Medical University, China

Previous studies suggest that Sirt1 has a protective role against osteoporosis (OP), however, it is unknown whether overexpression of Sirt1 in mesenchymal stem cells (MSCs) can protect against estrogen deficiency-induced OP. To answer this question, 8-week-old female Prx1-Sirt1 transgenic (Sirt1Tg) mice and WT littermates were surgically ovariectomized (OVX) or sham operated. After 3 months, bone phenotypes of all models were analyzed. BMD, cortical and trabecular bone volume, and osteoblast number, ALP+ and type I collagen+ areas, ALP+ CFU-f forming efficiency and osteogenic gene expression levels were all reduced significantly, whereas TRAP+ osteoclast number and surface, and RANKL/OPG ratio were increased significantly in OVX-WT mice compared to sham-WT mice, however, they were normalized in OVX-Sirt1Tg mice. ROS levels of bone marrow cells, 8-OHdG and β -galactosidase positive osteoblasts and osteocytes, protein expression levels of p16, p21 and p53 were increased significantly, whereas protein expression levels of SOD1/2 and Prdx1/4 were reduced significantly in OVX-WT mice compared to sham-WT mice, however, they were normalized in OVX-Sirt1Tg mice. Furthermore, we demonstrated that estrogen

regulates Sirt1 expression at a transcriptional level mediated via ER α , subsequently, Sirt1 inhibits NF- κ B signaling directly by deacetylating NF- κ B. The mRNA and protein expression levels of Sirt1 in bony tissue were up-regulated significantly in Sirt1Tg mice and were down-regulated significantly in OVX-WT mice compared to sham-WT mice, however, they were returned to normal levels in OVX-Sirt1Tg mice. Bioinformatic analysis suggests the presence of a putative Esr1 response element in the Sirt1 promoter. ChIP demonstrated that the Esr1 had the ability to physically bind the Sirt1 promoter. Luciferase assays showed that luciferase activity was increased significantly in MEFs transfected with Sirt1-PGL3 plasmid compared with the empty plasmid, and was more pronounced in 17 β -estradiol treated MEFs transfected with Sirt1-PGL3 plasmid. Immunoprecipitation demonstrated that Sirt1 could bind to NF- κ B and Sirt1 overexpression in MSCs reduced the acetylation level of NF- κ B and gene expression levels of IL-1 β and IL-8, Mpp3/13. Taken together, current studies therefore, indicate that overexpression of Sirt1 in MSCs can protect against estrogen deficiency-induced OP by inhibition of oxidative stress and osteoblast/osteocyte senescence and inactivation of NF- κ B signaling.

Disclosures: *Qian Zhang, None*

FRI-0392

Gambogic amide, a TrkA agonist, augments skeletal adaptation to mechanical loading through sensory nerve signaling Phuong Hua*, Ryan Tomlinson. Thomas Jefferson University, United States

The periosteal and endosteal surfaces of mature bone are densely innervated by sensory nerves expressing TrkA, the high-affinity receptor for nerve growth factor (NGF). In previous work, we demonstrated that inhibition of TrkA signaling diminished load-induced bone formation. Similarly, administration of exogenous NGF significantly increased load-induced bone formation through activation of Wnt signaling, albeit with the induction of substantial mechanical and thermal hyperalgesia in adult mice. Here, we tested the effect of gambogic amide (GA), a recently identified robust small molecule agonist for TrkA, on hyperalgesia and load-induced bone formation. The right forelimb of adult C57BL/6J mice (n = 7-8 per group) was subjected to non-damaging axial compression (3 N, 100 cycles, 2 Hz rest-inserted) for three consecutive days. GA (0.4 mg/kg) or vehicle (DMSO) was administered one hour prior to the first bout of loading. Behavioral analysis was used to assess pain up to one week after loading. Contrary to our expectations, GA treatment was not associated with diminished use of the loaded forelimb, by forelimb asymmetry testing. In fact, GA-treated mice used the loaded forelimb significantly more than control mice at two time points (1 and 4 days). To further examine GA-induced hyperalgesia, we performed hotplate sensitivity testing at 55 °C. Surprisingly, thermal sensitivity in GA-treated mice was unaffected or significantly decreased following loading. Calcein (10 mg/kg) and alizarin red (30 mg/kg) were administered 3 and 8 days after the initial bout of loading, respectively. Load-induced bone formation was assessed by dynamic histomorphometry using undecalcified sections from the mid-diaphysis of loaded and non-loaded forelimbs. Importantly, GA treatment was associated with a significant increase in relative periosteal bone formation rate (+63%) as compared to vehicle treatment. GA treatment was not associated with alterations in mechanical properties of non-loaded limbs (i.e. femur) as quantified by three-point bending. Furthermore, ulnar sections were stained for static histomorphometric analysis. We observed that GA treatment was associated with an increase in the number of osteoblasts per millimeter of bone surface in loaded limbs (+13%). In total, the results from our study demonstrate that gambogic amide has a beneficial effect on load-induced bone formation without inducing the hyperalgesia observed following exogenous administration of NGF.

Disclosures: *Phuong Hua, None*

FRI-0393

Knockout p16 Protects against Unloading-Induced Intervertebral Disc Degeneration by Inhibiting Oxidative Stress And Cell Senescence Yongxin Ren*, Hui Che. The First Affiliated Hospital of Nanjing Medical University, China

Intervertebral disc degeneration (IVDD) is an integral part of age-related multi-organ aging. The p16 is not only a biomarker, but also an effector for aging, however, the role of p16 in the process of IVDD has not been investigated. In this study, we first examined alterations of p16 expression levels in degenerative human disc specimens and found that p16 expression at both mRNA and protein levels had a positive relationship with the degenerative severe degrees. Then we isolated nucleus pulposus (NP) cells from human discs, in which p16 was overexpression or knockdown, respectively. Our results demonstrated that p16 overexpression inhibited the proliferation of NP cells and induced the senescence of them, in contrast, p16 knockdown played an opposite action on the proliferation and senescence of NP cells. Next, we asked whether p16 knockout could rescue tail suspension-induced IVDD in mice, 3-month-old WT and p16^{-/-} mice were performed with or without tail suspension (TS) for 4 weeks and the phenotypes of lumbar intervertebral discs were analyzed using histopathological, cellular and molecular techniques. MRI evaluation based on Modified Thompson classification revealed that the degree of disc degeneration was increased to double levels of ground WT mice in TS-WT mice and returned to levels of ground WT mice in TS-p16^{-/-} mice. Disc height index, the positive areas of safranin O staining and type II collagen immunostaining in the discs, and the percentage of PCNA+ cells were reduced significantly in TS-WT mice compared with ground WT mice and were largely rescued by p16 deletion. ROS levels, β -galactosidase+ senescence cells and senescence-associated secretory

phenotype (SASP) molecules including the gene expression levels of TNF α , IL-1 α/β and IL-6 and the gene and protein expression levels MMP-3/13, p65-NF- κ B, p19 and p53 were increased significantly, whereas the protein expression levels of Sirt1, SOD1/2, CDK4/6, pRB and E2F1/2 were down-regulated in the discs of TS-WT mice compared with those of ground WT mice, and were all largely rescued by p16 deletion. Our results indicate that p16 deletion can protect against unloading-induced IVDD by stimulating cell proliferation, inhibiting oxidative stress, cell senescence and SASP.

Disclosures: *Yongxin Ren, None*

FRI-0394

FAK expression in osteocytes is dispensable for bone accrual and for the anabolic response of cortical and cancellous bone to mechanical loading in female mice. Amy Y Sato*¹, Troy Li¹, Kevin Mcandrews¹, Alexander G Robling², Teresita Bellido³. ¹Department of Anatomy & Cell Biology, Indiana University School of Medicine, United States, ²Department of Anatomy & Cell Biology, Indiana University School of Medicine, Roudebush Veterans Administration Medical Center, United States, ³Department of Anatomy & Cell Biology, Department of Medicine, Division of Endocrinology, Indiana University School of Medicine, Roudebush Veterans Administration Medical Center, United States

A mechanosome composed of structural and signaling molecules, including the focal adhesion kinase (FAK), transmits mechanical stimuli into pro-survival signaling in osteocytes. Earlier studies showed that FAK activation is required for the anti-apoptotic effects of mechanical stimulation in osteocytes in vitro. However, whether FAK signaling in osteocytes is required for bone accrual or for bone anabolism induced by mechanical loading in vivo remains unknown. We addressed these questions by generating mice lacking FAK in osteocytes (FAKf/f;DMP1-8kbCre: FAK Δ OT) and FAKf/f littermate controls and performed tibial loading in 5-7 mo, female mice. FAK deletion in osteocytes did not alter lean body mass (17 vs 16g), fat mass (8 vs 8g) or total (0.051 vs 0.050g/cm²), spine (0.057 vs 0.057g/cm²) or femur (0.062 vs 0.061g/cm²) BMD, quantified by DXA, or cortical or cancellous bone mass and architecture, quantified by μ CT, for FAK Δ OT vs FAKf/f mice (N=7-16). Body weight and the weight of soleus, gastrocnemius and tibialis anterior muscles were also similar in FAK Δ OT vs FAKf/f mice. The force required to generate equivalent strains in the hindlimbs was 9.6 and 8N for FAK Δ OT and FAKf/f mice, respectively, measured by strain gauges. Tibial loading consisted of a triangle waveform with 0.075sec loading at 4Hz, 0.075sec unloading, and 0.1sec rest, for a total of 5min (1200 cycles), once/d 5x/wk for 2wks. Mechanical loading effects were not detected at the BMD level, regardless of the genotype. However, loaded tibiae from FAKf/f mice showed significant (*p<0.05) gain in the cortical bone fraction (BA/TA: 60 vs *64%) and area (BA: 0.12 vs *0.14mm²), TA (0.20 vs *0.24mm²), and Ct.Th (0.19 vs *0.22mm), without changes in MA (0.08 vs 0.08mm²), in non-loaded vs loaded tibia. Loaded tibia from FAK Δ OT mice showed similar gains compared to control FAKf/f mice in BA/TA (60 vs *66%), BA (0.12 vs *0.15mm²), TA (0.20 vs *0.24mm²), and Ct.Th (0.19 vs *0.22mm), without changes in MA (0.08 vs 0.08mm²), in non-loaded vs loaded, respectively. Loading also led to similar increases in trabecular thickness of proximal tibia cancellous bone in both genotypes, non-loaded vs. loaded (FAKf/f: 0.05 vs *0.06mm; FAK Δ OT: 0.05 vs *0.06mm). Taken together, these findings demonstrate that FAK signaling in osteocytes is not required for bone accrual or for bone anabolism induced by mechanical loading in vivo.

Disclosures: *Amy Y Sato, None*

FRI-0395

IGF1R Deficiency in Periosteal Osteoprogenitors Inhibits Bone Response to Mechanical Loading Tianlu Wang*, Faming Tian, Yongmei Wang, Daniel Bikle. Endocrine Unit, University of California, San Francisco and San Francisco VA Health Care System, United States

Previous studies demonstrated that insulin-like growth factor-1 (IGF1) signaling in mature osteoblasts (OB) and osteocytes is critical for the bone response to mechanical loading. In this study, we investigated the role of IGF1 signaling in periosteal osteoprogenitor cells (POC) using POC specific IGF1 receptor (IGF1R) knockout mice (KO, floxed IGF1R X prx1 promoter driven Cre) and their control littermates (Con, IGF1Rfl/fl no cre). At 12 wks, mice were divided into normal loading (NL), unloading (UL, 14 days tail suspension) and unloading combined with cyclic loading (CycL) group [14 days tail suspension combined with cyclic loading (10N compression, 40cyc/day for 10 days)]. Tamoxifen (Tam) was given 1 dose/day for the first 5 days. In NL group 14 day after tam, μ CT revealed less cortical (Ct.) bone in the KOs compared with the Cons in both genders (male Ct.BV/TV: -11%, Ct.Th: -14%; female Ct.BV/TV: -13%, Ct.Th: -22%, Tb.Th: -8%). Although in both genotypes, UL decreased bone mass compared with NL group, KOs exhibited less cortical bone loss than the Cons (KO male Ct.BV/TV: -6%, female Ct.BV/TV: -3%, Ct.Th: 0%; Con male Ct.BV/TV: -13%, female Ct.BV/TV: -33%, Ct.Th: -25%). Consistently, bone histomorphometry showed reduced cortical and trabecular (Tb) bone formation in KOs in NL in both genders (male Ct.Ec.BFR: -49%, Tb.BFR: -48%; female Ct.Ec.BFR: -48%, Tb.BFR: -53%). Periosteal (Ps) and endocortical (Ec) bone formation rate (BFR) in Cons decreased more dramatically than that in the KOs in response to UL (KO male Ct.Ps.BFR: -79%, female Ct.Ec.BFR: -48%; Con male Ct.Ps.BFR: -88%, female Ct.Ec.BFR: -70%). CycL induced a

greater increase in BFR in Cons than KO (KO male Ct.Ps.BFR:+0.7 fold, KO female Ct.Ec.BFR:+0.4 fold; Con male Ct.Ps.BFR:+2.6 fold, Con female Ct.Ec.BFR:+1.5 fold). In vitro, periosteal cells from each group were cultured in osteogenic medium for 14 days. In NL groups, in both genders, KO cultures formed fewer calcium containing nodules and expressed lower mRNA levels of RUNX2 and osteocalcin (OCN), as determined by QPCR. UL led to less nodule formation in both genotypes, but more dramatic reductions were observed in the KOs compared to the Cons. In response to cycL, more nodules were formed in the Cons than in the KOs, although both genotypes failed to reach significance. Our data indicate that IGF1R in the POC is critical for osteoprogenitor differentiation, bone formation and the skeletal response to mechanical loading, especially in the cortical bone.

Disclosures: **Tianlu Wang**, None

FRI-0396

Mechanical Loading Induces Bone Formation from Pre-Existing Osterix Expressing Cells Heather Zannit*, Matthew Silva. Washington University in St. Louis, United States

Cortical bone formation, which can be stimulated by mechanical loading, occurs when either existing osteoblasts are activated at the bone surface or new osteoblasts are recruited through differentiation or proliferation. The objective of this study was to begin to describe the identity of these bone forming cells. To do this, we utilized tamoxifen inducible *Osx-Cre-ERT2;Ai9/TdTomato* (*iOsx-Ai9*) reporter mice. All experiments used male and female mice aged to 5- and 12-mo subjected to unilateral axial tibial compression. First, the right tibia of *iOsx-Ai9* mice (n=4/age group) were cyclically loaded for 5 days (1200 cycles/day; 7-14 N peak force) and processed for dynamic histomorphometry. We confirmed a significant increase in bone formation in loaded limbs compared to non-loaded controls (p<0.01). Then, to investigate the role of *Osx* lineage cells in this response, *iOsx-Ai9* mice (n=6-15/age group) were pulse labeled with tamoxifen (followed by 3-wk clearance) and the right tibias were cyclically loaded for 5 consecutive days. Mice received BrdU in their drinking water daily, calcein was given 24 hours prior to euthanasia, and tibias were harvested and processed for frozen undecalcified histology. Periosteal compressive surfaces were analyzed in a 2mm region of the mid-diaphysis. Histology revealed both non-loaded and loaded tibias were covered in *Osx*+ cells (>95%) on the periosteum of both 5- and 12-mo animals. Additionally, there was a more than 2-fold increase in the mineralizing surface (calcein+) that is covered with *Osx*+ cells in loaded versus control limbs (p<.001). Furthermore, nearly all (>99%) of mineralizing surfaces were lined with *Osx*+ cells. We also observed both *Osx* and non-*Osx* cells proliferating (BrdU+) at sites of bone formation in 5- and 12-mo mice. These results show that, following mechanical loading, pre-existing cells of the *Osx* lineage cover the vast majority of surfaces where there is active loading-induced bone formation. This indicates that new bone formation shortly after mechanical loading primarily arises from *Osx* lineage cells, not the recruitment of earlier progenitor cells. Our findings of both *Osx*-lineage and non *Osx*-lineage cells proliferating at sites of bone formation validates previous work showing the importance of these cells to loading induced bone formation. To our knowledge, this is the first study to use an inducible reporter mouse to track the origin of bone forming osteoblasts following mechanical stimulation.

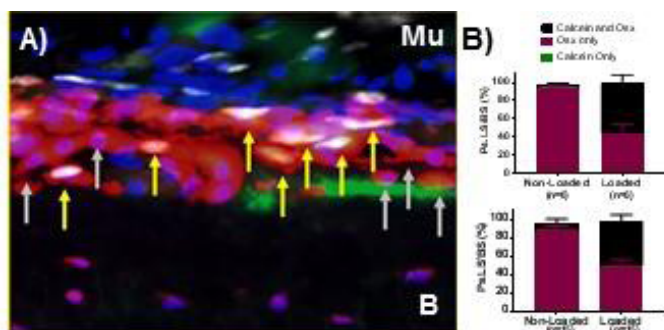


Figure 1. A) Representative image in the ROI of an *iOsx-Ai9* loaded tibia. Mineralizing surface (green) can be seen lined with non-proliferating *Osx* lineage cells (grey arrows) and proliferating *Osx* lineage cells (yellow arrows). B) Percentage of bone surface that is mineralizing with *Osx* lineage or non-lineage cells and just *Osx* lineage cells (Top-5 mo, Bottom-12 mo). Mu-Muscle, B-Bone

Disclosures: **Heather Zannit**, None

FRI-0419

Short-term pharmacologic inhibition of RAGE suppresses bone turnover and muscle atrophy in aging Hannah M. Davis*^{1,2}, Mohammad W. Aref^{1,2}, Alyson L. Essex¹, Sinai Valdez¹, Alexandra Aguilar-Perez^{1,2}, Padmini Deosthale^{1,2}, Fletcher White^{3,4,5}, Jolene Windle⁶, Matthew R. Allen^{1,2,5}, Lilian I. Plotkin^{1,2,5}. ¹Department of Anatomy & Cell Biology, Indiana University School of Medicine, United States, ²Indiana Center for Musculoskeletal Health, United States, ³Department of Anesthesia, Indiana University School of Medicine, United States, ⁴Stark Neuroscience Research Institute, Indiana University School of Medicine, United States, ⁵Roudebush Veterans Administration Medical Center, United States, ⁶Department of Human and Molecular Genetics, Virginia Commonwealth University, Richmond, VA, United States

Young RAGE (receptor for advanced glycation end products) KO mice exhibit increased bone mass and strength due to osteoclast (Oc) defects. Whether pharmacologic RAGE inhibition blocks Oc and prevents bone loss in aging is unknown. We assessed this question using female WT young 5mo and aged 16mo mice treated with Azeliragon (Az), a small molecule RAGE inhibitor being tested as treatment for Alzheimer's Disease and CRISPR/Cas9 global RAGE KO mice. WT mice were injected daily with Az 100µg/d (young), 110µg/d (aged), or vehicle (veh) for 28 days. In 16mo mice, expected age-induced changes in bone geometry and mechanics were observed; and bone formation was suppressed with lower serum P1NP (-39%) and mRNA expression of several osteoblast (Ob) genes. Az treatment did not affect bone geometry or mechanics at either age, but altered bone turnover at the cellular level. In particular, it reduced Oc number/surface on vertebral cancellous and femoral endocortical surfaces at both ages. Consistently, less mature (≥3 nuclei) Oc were obtained in vitro when wildtype bone marrow cells (BMC) were cultured with Az (-30%) or were generated from RAGE KO-derived BMC (-34%). Az also reduced Ob gene expression (OCN, Col1a1, and *Osx*) in bone, serum P1NP levels and vertebral Ob number/surface in both ages. These results suggest pharmacologic and genetic RAGE inhibition decreases Oc and Ob resulting in suppressed bone turnover. In addition, aged veh-treated mice exhibited altered body composition with greater fat mass and less lean mass vs 5mo mice. Consistently, aged veh-treated mice had reduced gastrocnemius (GA), tibialis anterior (TA), and quadriceps (QC) weight (wgt)/body wgt and lower TA mRNA levels of the muscle differentiation marker myoD; whereas muscle atrophy markers atrogen-1 and murf-1 were higher. Az reduced fat mass and increased lean mass; and increased GA (5%) and TA (14%) wgt in 5mo mice and GA (2%), TA (19%), and QC (10%) wgt in 16mo mice. RAGE inhibition also increased the expression of the myogenesis marker myogenin at both ages and restored myoD levels in 16mo mice. Moreover, Az reversed age-induced increased atrogen-1 levels. Overall, these findings reveal that while short-term pharmacologic RAGE inhibition suppresses bone turnover, it does not alter bone architecture or mechanical properties in 5 or 16mo mice. Further, we identified a novel protective effect of RAGE inhibition on skeletal muscle by preventing loss of muscle mass and muscle atrophy in aging.

Disclosures: **Hannah M. Davis**, None

FRI-0420

Anti-Sost/Dkk1 Antibody Therapy Increases Bone Formation in Old Mice, but Does Not Enhance Their Modest Response to Tibial Loading Lisa Lawson*, Michael Brodt, Matthew Silva. Washington University in St. Louis, United States

Bone formation is regulated by the Wnt signaling pathway. Compressive axial loading of the skeleton has been shown to potentially stimulate bone formation and induce expression of osteogenic markers including Sp7 and Col1a1, as well as many Wnt pathway genes. Compared to young-adult mice, however, aged mice exhibit reduced osteogenic responsiveness to skeletal loading. Recent studies suggest that loading-induced activation of the Wnt signaling pathway promotes bone formation in the adult skeleton, and that activation of this pathway may be impaired in the bones of aged mice. Recent work from our lab suggest that these changes may be related to a failure to potentially downregulate *Sost* and *Dkk1* in response to loading. Together, these data suggest that modulating the Wnt signaling pathway by targeting *Sost* and *Dkk1* may be an effective strategy to restore the osteoanabolic effect of loading in aged mice. To investigate this possibility, 22-month old C57BL/6 mice were treated with neutralizing antibodies to *Sost* and *Dkk1* (12.5mg/kg each of anti-*Sost* and anti-*Dkk1*, Amgen) or vehicle, and subjected to daily compressive loading on the right tibia (60 cycles, 2200ue); the left tibia served as a non-loaded control. Bone marrow was removed and tibias were harvested for mRNA isolation. Independent of loading, RT-qPCR showed a marked increase in the expression of Sp7, Runx2, Bglap, and Col1a1 in the non-loaded tibias of antibody-treated mice relative to the non-loaded tibias of vehicle-treated mice. Canonical Wnt pathway target *Axin2* was also elevated in the non-loaded tibias of antibody-treated mice relative to controls. Dynamic histomorphometry showed that independent of loading, antibody treatment was associated with marked increases in measures of bone formation. In the non-loaded tibias of vehicle-treated mice, Ec.MS/BS and Ps.MS/BS were 14.6% and 0.6%, respectively, compared to 95.6% and 25.5%, respectively, in the non-loaded tibias of antibody-treated mice. Ps.MS/BS increased in response to loading in both groups, but antibody treatment did not further increase loading-associated bone formation. In sum, we found anti-*Sost/Dkk1* antibody therapy to be a potent stimulator of bone formation, but that antibody therapy failed to restore a potent osteoanabolic response to tibial loading in aged mice.

Disclosures: **Lisa Lawson**, None

FRI-0421

Association of trajectories of change in bone, lean mass and physical performance with mortality in older men Jian Shen^{*1}, Neeta Parimi², Peggy Cawthon³, Lisa Langsetmo³, Kris Ensrud³, Jane Cauley⁴, Deborah Kado⁵. ¹University of California, San Diego, United States, ²California Pacific Medical Center Research Institute, United States, ³University of Minnesota, United States, ⁴University of Pittsburgh Graduate School of Public Health, United States, ⁵University of California, United States

Musculoskeletal deterioration is an important physiological change observed with aging. Biological cross-talk between bone and muscle may influence the rate of decline, and if so, patterns of concurrent change in musculoskeletal phenotypes may more precisely capture effects of accelerated aging and identify those at high mortality risk. Therefore, we conducted longitudinal analyses of change in bone, muscle and two physical performance parameters with subsequent mortality risk among 3232 men participating in the Osteoporotic Fractures in Men Study (MrOS) (mean age: 79 y). We measured: 1) total hip bone mineral density (BMD); 2) appendicular lean mass (ALM) by DXA; 3) grip strength by hand dynamometry; and 4) gait speed (usual pace over 6 meters, m/s) at up to 4 clinic visits between 2000 and 2009. Using multivariate proportional hazards analyses, all-cause mortality was assessed over an average of 7.1 years following the last clinic visit. We used group-based trajectory models (PROC TRAJ in SAS) to create trajectories based upon identifying patterns of change in each of the 4 parameters. All models were adjusted for age, site, weight loss, fracture history, and self-reported health. For each of the 4 parameters, 3 trajectory groups were identified, each with similar rates of decline. The "high" trajectory group included those with higher values across all visits; the "intermediate" group had values in the middle ranges, and the "low" group had the lowest values over time. Compared to men in the intermediate trajectory group, those in the low trajectory group had an increased mortality risk (HR (95%CI):1.16 (1.02-1.31) for BMD; 1.3 (1.14 -1.48) for ALM; 1.25 (1.1-1.42) for grip strength; and 1.33 (1.12 -1.57) for gait speed. Men in the high trajectory group for gait speed, but not the other 3 high trajectory groups, had lower mortality risk compared to those with an intermediate trajectory. We also found that for each parameter, the single measure at the last visit predicted mortality risk (Table). After adjusting for the last visit measure of each of the 4 parameters, the associations of each of the trajectory groups with mortality risk was no longer significant. These findings suggest that men with elevated mortality risk may follow distinct musculoskeletal trajectories; however, the most proximal musculoskeletal measure of either BMD, ALM, grip strength or gait speed exerts the most influence when estimating mortality risk.

Table. Multivariate adjusted hazard ratios of each musculoskeletal trajectory with all-cause mortality before and after adjusting for the last visit measure

Musculoskeletal trajectory	Full model	Full model + last visit measure
BMD		
Low	1.16 (1.02 to 1.31)	0.95 (0.80 to 1.14)
Intermediate	REF	REF
High	0.97 (0.83 to 1.13)	1.22 (0.98 to 1.52)
ALM		
Low	1.3 (1.14 to 1.48)	1.18 (0.99 to 1.4)
Intermediate	REF	REF
High	1.11 (0.92 to 1.34)	1.24 (0.99 to 1.56)
Grip strength		
Low	1.25 (1.10 to 1.42)	0.93 (0.79 to 1.09)
Intermediate	REF	REF
High	0.89 (0.77 to 1.04)	1.21 (1.01 to 1.45)
Gait speed		
Low	1.33 (1.12 to 1.57)	0.98 (0.80 to 1.19)
Intermediate	REF	REF
High	0.73 (0.64 to 0.83)	0.96 (0.82 to 1.13)
Measure at the last visit (per SD increase)		
BMD	0.90 (0.85 to 0.96)	-
ALM	0.88 (0.81 to 0.96)	-
Grip strength	0.80 (0.75 to 0.85)	-
Gait speed	0.75 (0.70 to 0.80)	-

Full models adjusted for age, clinic site, weight loss from baseline to the last visit, fracture history and self-reported health

Disclosures: **Jian Shen**, None

FRI-0422

Fibroblast growth factor receptor 3 inhibits progression of degeneration in the intervertebral disc in mice Yangli Xie*, Xiaolan Du, Lin Chen, Zuqiang Wang. Department of Rehabilitation Medicine, Center of Bone Metabolism and Repair, State Key Laboratory of Trauma, Burns and Combined Injury, Trauma Laboratory, Daping Hospital, Army Medical University, China

Objective Intervertebral disc (IVD) degeneration is a common degenerative disease, to date the mechanisms during its pathogenesis is largely unknown. Herein we investigated whether FGFR3, a negative regulator of endochondral ossification, is associated with IVD. Methods Immunohistochemistry (IHC) was used to detect the expression of FGFR3 in IVD tissues in mice with different age and from human. Lumbar segmental instability (LSI) model was generated. Deleted FGFR3 in IVD tissue including annulus fibrosus (AF) and endplate (EP) in FGFR3^{flx/flx}; Col2a1-CreERT2 mice by administering tamoxifen. Alterations in IVD structure were evaluated histologically using IVD degeneration scoring system. The expressions of genes associated with IVD homeostasis were analyzed by qRT-PCR and IHC. Results In degenerated IVD from human patients, we found that FGFR3 expression level is decreased in AF and NP, suggesting a possible role for FGFR3 in the IVD homeostasis. The levels of FGFR3 were downregulated in murine IVD tissue during aging process. Gain-of-Function mutation of FGFR3 can play protective role in IVD under LSI condition in mice. Moreover, FGFR3 conditional knockout mice exhibited early onset of IVD degeneration with accelerated IVD matrix degradation, abnormal bone formation in EP and increased bone resorption in vertebra with aging. The elevated Wnt/ β -catenin signaling may be involved in this degeneration process. Conclusions FGFR3 may play a protective role in homeostasis of IVD, and may serve as a potential molecular target for treating disc degenerative diseases.

Disclosures: **Yangli Xie**, None

FRI-0438

Novel Genetic Loci Control L5 Vertebral Trabecular Bone and the Response to Low Calcium Intake in Growing BXD Recombinant Inbred Mice Kritikan Chanpaisaeng^{*1}, Sarah Mace², Perla Reyes-Fernandez¹, James Fleet¹. ¹Department of Nutrition Science, Purdue University, United States, ²Department of Biological Sciences, Purdue University, United States

Epidemiological data show an inverse association between vertebral fractures and trabecular bone (Tb) microarchitecture. This highlights the importance of developing strong Tb microarchitecture to prevent osteoporotic fractures. Because Tb is modulated by genetics (G) and environment (e.g. diet, D), we studied the impact of GxD interactions on Tb at the L5 spine. Mice from 51 BXD recombinant inbred lines were fed either adequate (H, 0.5%) or low (L, 0.25%) Ca diets from 4-12 wks of age. We used micro-computed tomography (μ CT) to measure: bone volume fraction (BV/TV) and Tb tissue mineral density (Tb.TMD), Tb thickness (Tb.Th), separation (Tb.Sp), and number (Tb.N), as well as connectivity density (Conn.D), and structure model index (SMI). The response to dietary Ca restriction (RCR) was calculated for each phenotype in each line. Body size (BS)-corrected residuals were used for statistical analysis. We found that genetics has an independent, strong influence on Tb traits (e.g. BV/TV, narrow sense heritability (h^2)=0.57) but a more modest influence on the RCR (e.g. Tb.N, h^2 =0.28). ANOVA revealed significant main effects for genetics and diet for all traits. Similarly, the RCR was affected by genetics indicating a GxD interaction affecting all Tb traits. BS-corrected line means for each trait and RCR were used for quantitative trait loci (QTL) analysis by composite interval mapping (500 permutations, WinQTL-Cart). We identified 2-5 loci affecting each trait and 1-3 loci affecting the RCR for each trait. Loci controlling Tb.N (chr 2, 12), Tb.Sp (chr 2, 4), Conn.D (chr 1, 12), and SMI (chr 8) were seen in both diet groups providing replication of environmentally robust genetic effects. Loci on chr 2 (Tb.Sp, Tb.N, SMI RCR), chr 12 (Tb.N, Conn.D, Tb.Sp L) and chr 7 (RCR for BV/TV, SMI, Tb.TMD, Tb.Th, Tb.Sp) were found to control multiple phenotypes suggesting the existence of latent traits. Candidate genes underlying selected loci were identified with PROVEAN (protein coding effects) or eQTL analysis in The GeneNetwork (mRNA level effects). On chr 7, we found a non-synonymous coding (Cn) variant and a cis eQTL affecting Lrrk1, a gene that promotes bone resorption. On chr 2, we found a Cn variant of Wisp2, a mesenchymal cell activator of canonical WNT signaling. Within a chr 3 locus, Sec24d has a Cn variant and a cis eQTL that could affect the secretion of extracellular matrix in bone. Our work shows that genetics and diet interact to influence lumbar spine Tb.

Disclosures: **Kritikan Chanpaisaeng**, None

FRI-0439

The large variant of the stimulatory G protein alpha-subunit XLAs regulates bone formation by promoting Wnt signaling Qing He*, Julia Matthias, Lauren Shumate, Murat Bastepe. Massachusetts General Hospital and Harvard Medical School, United States

Mutations of the GNAS complex gene, encoding the alpha-subunit of the stimulatory G protein ($G_{\alpha s}$) and its large variant XLAs, cause multiple diseases that involve bone development, such as Albright's osteodystrophy and progressive osseous heteroplasia. $G_{\alpha s}$ mediates the actions of many hormones or autocrine/paracrine factors primarily by stimulating the cAMP signaling pathway. Although overexpression of XLAs also stimulates cAMP signal-

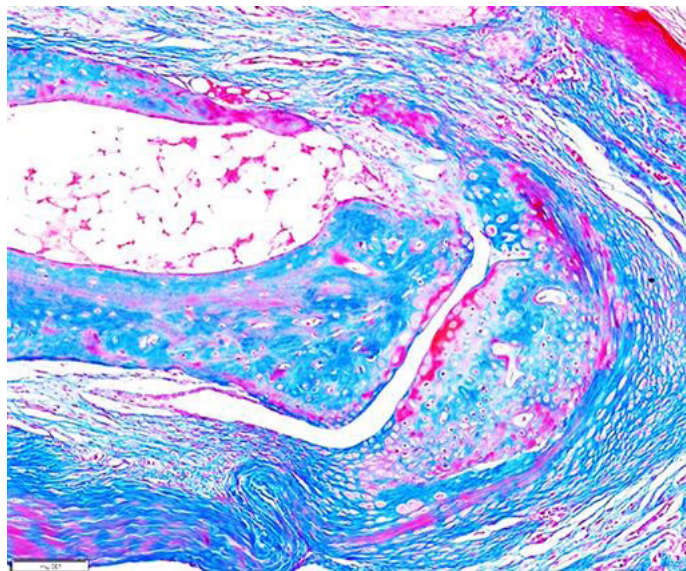
ing, cellular actions of XLAs remain unclear. Moreover, XLAs is expressed in bone cells, but its roles in bone physiology and bone disease are poorly defined. By μ CT and bone histomorphometry analysis, we have demonstrated that XLAs knockout (XLKO) mice have significantly decreased bone mass and thickness at postnatal day 10 because of impaired bone formation. While osteoblast numbers were decreased, osteoclast numbers remained unchanged; surprisingly, osteocyte density was increased in XLKO mice. Consistent with decreased bone formation in XLKO mice, the expression levels of osteogenic markers were dramatically reduced, including alkaline phosphatase, Runx2, osteocalcin, and bone sialoprotein. Calvarial cells isolated from neonatal XLKO mice displayed impaired osteogenic differentiation. Since Wnt signaling has been shown as an important regulator of bone formation and osteogenic differentiation, we examined Wnt signaling and found significantly increased expression of the Wnt inhibitor sclerostin, together with reduced expression of Wnt targets TCF1 and LEF1 in XLKO femurs. Western blot analysis demonstrated decreased skeletal levels of active β -catenin in XLKO mice. Moreover, XLKO calvarial cells showed reduced TOPflash activity at baseline and after Wnt3a stimulation compared to wildtype cells, further confirming repressed Wnt signaling in XLKO samples. Activation of the cAMP signaling pathway can enhance Wnt signaling in bone cells, but RANKL mRNA, a target of cAMP signaling, was increased in XLKO femurs, and CRISPR/Cas9-mediated ablation of XLAs in a mouse osteocyte-like cell line did not diminish cAMP generation, suggesting that the action of XLAs in bone does not occur via cAMP signaling. Taken together, these results imply that XLAs is essential for normal bone formation and osteogenic differentiation, and that its role in bone formation might involve Wnt signaling.

Disclosures: **Qing He**, None

FRI-0440

BMP9 stimulates synovial joint regeneration in mice Ken Muneoka*, Ling Yu, Mingquan Yan, Lindsay Dawson. Texas A&M University, United States

Purpose: A major goal of regeneration science is to develop strategies to stimulate mammalian regeneration. The mouse digit tip is the only part of the limb that displays regenerative ability, amputations at proximal levels result in fibrotic scarring and skeletal truncation. We use the non-regenerating neonatal digit amputation as a test site for factors that can induce regenerative events. Previously we found that BMP2 treatment stimulates bone regeneration by inducing an endochondral ossification center at the amputated digit stump. We now show that subsequent treatment with another BMP family member, BMP9, stimulates the regeneration of a synovial joint. **Methods:** Neonatal digits are amputated mid-way through the sub-terminal phalangeal element (P2) removing the distal half of P2, the terminal phalangeal element (P3) and the intervening P2/P3 joint. After wound closure, a single agarose beads carrying either BMP2 or BMP9 protein is implanted between the wound epidermis and stump. In some experiments, a BMP2 bead implantation is followed by a BMP9 bead implanted 3 or 7 days later. Digits are analyzed using microcomputed tomography (μ CT), histology, immunohistochemistry and in situ hybridization. **Results:** BMP9 treatment induces the regeneration of a skeletal element that articulated with the digit stump in 51% of the digits (n=96). Histological analyses identified an articular cartilage layer lining the regenerated skeletal element and a cavity separating the skeletal element from the stump. The regenerated skeletal element forms as a chondrogenic nodule within 3 days after BMP9 treatment and contains articular chondrocytes identified based on marker gene expression. A cavity lined with cells expressing Prg4 identifies the regenerated cavity as synovial. Studies using mutant mice indicate that BMP9-induced joint regeneration requires the Prg4 gene. Amputation wounds is first treated with BMP2 to induce skeletal regeneration, then treated with BMP9, we show that induced regeneration of bone can be coupled with synovial joint regeneration. **Conclusions:** We have demonstrated for the first time that synovial joint regeneration can be stimulated in a mammalian model of regenerative failure, and have identified BMP9 as a regeneration inducing agent. Combining BMP2 and BMP9 application to induce a complex regenerate establishes a novel strategy for engineering regenerative responses with targeted growth factor treatment.

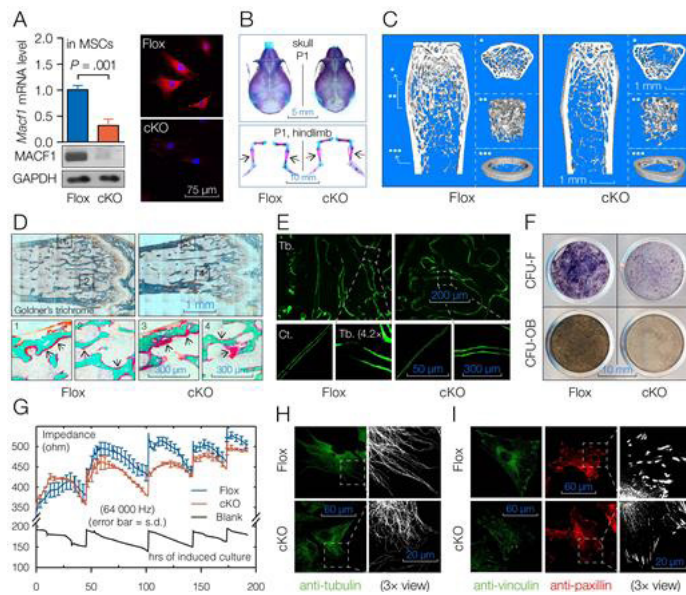


Disclosures: **Ken Muneoka**, None

FRI-0441

Microtubule-Actin Crosslinking Factor 1 Is Essential for Bone Formation in Mice Fan Zhao*¹, Xiaoli Ma¹, Wuxia Qiu², Lifang Hu¹, Airong Qian¹. ¹Northwestern Polytechnical University, China, ²Northwestern Polytechnical, China

The spectraplakins are highly conserved crosslinking proteins that expressed widely in a variety of cell types. In lower animals such as fly, the spectraplakins are encoded by the Short stop (Shot) gene, while in mammals, it is encoded by microtubule-actin crosslinking factor 1 (Macf1). Numerous studies pointed out that MACF1 might serve an important molecular in crosslinking cytoskeletal components during cell migration, adhesion and differentiation. Previous studies also discovered that MACF1 partially colocalizes with the microtubules and microfilaments, has ATPase activity, and controls epidermal migration through regulating focal adhesion and cytoskeleton dynamics. Our previous data demonstrated that MACF1 expression level was lower in osteoporotic bone tissue in mice; In vitro data showed that knockdown of MACF1 in osteoblastic cells inhibited osteoblast differentiation through suppressing the β -catenin/TCF1-Runx2 signaling axis. However, the role of MACF1 in bone metabolism regulation is still poorly understood, no in vivo data are now available to depict its role and mechanism in regulating osteogenic differentiation and bone formation. Being a major factor in cytoskeletal dynamics regulation, increasing evidence have pointed out crucial roles of MACF1 in cellular motabolism. In the present study, we unveiled key roles of MACF1 in osteogenic differentiation and bone formation in vivo. By conditional gene targeting to delete MACF1 in mesenchymal stem cells in mice (panel A), we observed in bones of the MACF1 deficient mice obvious ossification retardation and bone loss (panel B, C and D), which we traced to a decrease of osteoblastic differentiation capability in MSCs (panel E, F and G). Further, we show that MACF1 is essential for the cytoskeleton to regulate osteoblastic differentiation of MSCs (panel H and I). By coupling the results obtained, we have identified key roles of MACF1 in cytoskeleton maintenance in MSCs and bone formation regulation in mice. The data would not only update our knowledge of the spectraplakins in osteoblastic functions, but also offer a new therapeutic target for bone degenerative diseases.



Disclosures: **Fan Zhao, None**

FRI-0442

Epigenetic regulator, Uhrf1, positively controls skeletal muscle differentiation

Yuichiro Sawada^{*1}, Tadahiko Kikugawa¹, Iori Sakakibara², Yusuke Ono³, Yuta Yanagihara⁴, Noritaka Saeki⁴, Hiroyuki Iio¹, Takashi Saika¹, Yuuki Imai⁴. ¹Department of Urology, Ehime University Graduate School of Medicine, Japan, ²Research Center for Advanced Science and Technology, The University of Tokyo, Japan, ³Musculoskeletal Molecular Biology Research Group, Nagasaki University Graduate School of Biomedical Sciences, Japan, ⁴Division of Integrative Pathophysiology, Proteo-Science Center, Ehime University, Japan

Regulation of homeostasis of various cells and tissues requires epigenetic regulation such as DNA methylation and histone modifications, however, the effect of epigenetic regulatory factors on skeletal muscle is still largely unknown. To investigate the relationship between muscle regeneration and epigenetic regulation, we analyzed gene expression levels of various DNA methylation-related factors in mouse skeletal muscle regeneration models induced by cardiotoxin (CTX) injection for TA muscles. As a result, gene expression of Uhrf1 (Ubiquitin-Like PHD And Ring Finger Domain 1), which is responsible for maintenance DNA methylation, was significantly increased at day 4 after muscle injury. To evaluate the function of Uhrf1 in skeletal muscle differentiation and regeneration, Uhrf1 knockout for C2C12 cells, which is a representative myoblastic cell line, were established using CRISPR/Cas9 system and single cell sorting, then, myotube formation and expression of muscle differentiation marker genes were examined. As a result, Uhrf1 knockout C2C12 cells showed remarkably impaired myotube formation, significantly reduced expression of myogenic genes and increased expression of Myh3, an embryonic type myofiber gene. In addition, to investigate the physiological role of Uhrf1, satellite cells, which are stem cells of skeletal muscle, specific Uhrf1 knockout (scKO) mice were generated by crossing Pax7CreERT2 and Uhrf1 floxed mice. Then, the muscle regeneration ability of control and scKO mice were analyzed using CTX model with or without 5-straight-days Tamoxifen injection. Fourteen days after CTX, TA muscles of scKO mice exhibited significantly reduced muscle weight recovery and decreased cross-sectional area of myofibers (n = 3-5) when compared to that of control mice. To examine the potential of satellite cells lacking Uhrf1, single muscle fibers were isolated from EDL muscle of control and scKO mice and cultured for analyses of differentiation and proliferation of satellite cells on the muscle fibers. Immunocytochemistry against Pax7 and MyoD for single muscle fibers revealed that satellite cells on myofibers of scKO mice showed significantly decreased proliferation and impaired differentiation (n = 5 mice, more than 10 fibers/mouse) when compared to that of control mice. These data indicate that Uhrf1 play an important role in proliferation and differentiation of satellite cells, followed by skeletal muscle regeneration and skeletal muscle fiber maturation.

Disclosures: **Yuichiro Sawada, None**

FRI-0464

Targeted epigenetic modulation of bone-specific enhancers regulates mesenchymal cell fate and controls osteoblastic differentiation

Jonathan Gordon^{*1}, Coralee Tye¹, Joseph Boyd¹, Andre Van Wijnen², Janet Stein¹, Gary Stein¹, Jane Lian¹. ¹Department of Biochemistry, Larner College of Medicine, University of Vermont, United States, ²Department of Orthopedic Surgery, Mayo Clinic, United States

Adult bone formation requires a highly regulated program of differentiation from a mesenchymal-derived osteoprogenitor to a mature osteocyte. Epigenetic mechanisms control mesenchymal stromal cell (MSC) commitment to a mature osteoblast through facilitating of binding of transcriptional regulators to promoter regions of genes, however less well understood are inter- and intra-genic regulatory regions that control cell-type-specific gene expression programs. These regulatory elements called cis-regulator modules, are bound by transcription factors (TFs) and specific post-translationally modified histones, and play key roles in the control of tissue morphogenesis. To define novel regulatory regions during osteogenesis, pluripotent CD45-/Ter119-/SCA1+/CD29+/Nestin+/CD146+/aSMA+ MSCs and analogous human MSC populations, were isolated by FACS to obtain a homogenous population of cells that were differentiated to mature osteoblasts. We then used ChIP-seq to develop genome-wide enrichment profiles of intergenic genomic regions of occupied by TFs, cofactors, chromatin regulators, and transcription apparatus occupying osteogenic enhancers in MSCs. Supervised pattern discovery was performed using ChromHMM to segment genomic regions into active, quiescent, TF-bound, transcribed and super-enhancer regions. From this analysis, we identified novel enhancers near genes that are involved in osteogenesis (e.g. SP7, Runx2, Fgfr1). Further novel enhancers for bone formation were predicted in intragenic regions of several osteoblast-related genes. Using a CRISPR-based strategy for targeted epigenetic modification, dCas9 protein fused to the catalytic core of the human acetyltransferase p300 or LSD1/KDM1A was used to alter histone acetylation or histone methylation (respectively) at SP7 enhancer regions. Alterations of histone post-translational modifications at these enhancer regions by targeted dCas9-p300 or dCas9-KDM1A were sufficient to alter expression of SP7 (osterix) and inhibit commitment of progenitors to the osteoblast lineage (dCas9-KDM1) or increase osteoblast-related markers (dCas9-p300). From these studies, we have demonstrated novel regulatory regions, denoted by histone modifications and transcription factor binding sites functioning as enhancers critical for osteogenic differentiation. In addition, we have used a novel epigenetic modification strategy to increase osteoblast-related gene expression. These strategies may be used to modify or enhance osteogenic potential of mesenchymal cells for therapeutic bone regeneration.

Disclosures: **Jonathan Gordon, None**

FRI-0465

Glutamine metabolism is required in skeletal stem cells for appropriate bone regeneration. Yilin Yu*, Anthony Mirando, Leyao Shen, Matthew Hilton, Courtney Karner. Duke University, United States

Skeletal stem cells (SSC) are multipotent progenitor cells postulated to regulate bone mass and regeneration by providing a source of osteoblasts throughout life and in response to injury. With age, the SSC population can be exhausted, resulting in reduced osteoblast formation, decreasing bone mass, and diminished bone regeneration in response to injury. Recent work has focused on defining cell markers of the SSC population, however little is known about the molecular mechanisms regulating the proliferation or maintenance of the SSC population. Glutamine metabolism has emerged as a critical regulator of proliferation and cellular activity in diverse systems. In addition to direct incorporation in polypeptide chains, glutamine is an important oxidative fuel and a precursor of non-essential amino acids, nucleotides, and glutathione. The enzyme glutaminase (GLS) catalyzes the deamination of glutamine to form glutamate, the rate-limiting first step in glutamine metabolism. Here we demonstrate GLS is required in SSC to regulate postnatal bone homeostasis and regeneration. Using GLS activity assays, we discovered GLS activity declines with age in wild type SSC and significantly correlates with depletion of SSC and reduced bone mass observed with aging. Importantly, genetic deletion of a conditional (floxed) GLS allele (Glsf/f) in SSC using LeprCre significantly reduces bone mass in vivo due to decreased osteoblast numbers and bone formation. Moreover, LeprCre;Glsf/f mice had diminished bone regeneration in a non-stabilized tibia fracture model. LeprCre;Glsf/f fracture calluses had reduced cartilage callus formation, diminished bone volume as well as persistent fibrosis at the fracture site. Colony forming unit assays and Brdu incorporation studies demonstrated a significant reduction in proliferation in LeprCre;Glsf/f SSC. Mechanistically, glutamine dependent glutathione and nucleotide biosynthesis are dispensable for SSC proliferation, whereas amino acid transaminase dependent α -ketoglutarate production is critical for SSC proliferation. Collectively, these data highlight the critical role for GLS and glutamine metabolism in SSC to maintain the SSC population and promote postnatal bone mass accrual and bone regeneration in response to fracture. Our data indicate stimulating GLS activity may provide a valuable therapeutic approach to maintain or expand SSC in aged individuals to repair or regenerate bone.

Disclosures: **Yilin Yu, None**

FRI-0466

Zinc Finger Protein 467 Is a Major Determinant of Lineage Allocation and Bone Turnover in Female Mice *Phuong Le*^{*1}, *Weiying Liu*², *Tj Martin*³, *Beate Lanske*⁴, *Roland Baron*², *Clifford Rosen*¹. ¹Maine Medical Center Research Institute, United States, ²Harvard School of Dental Medicine, United States, ³St. Vincent's Institute Medical Research, Australia, ⁴Radius Health, Inc, United States

Zinc finger protein 467 (Zfp467) was originally isolated from mouse endothelial LO cells as an oncostatin M-inducible mRNA. It belongs to the Kruppel-like family of transcription factors and its expression is relatively ubiquitous. Preliminary work implicated Zfp467 as a novel regulator of cell fate by inhibiting osteoblast commitment and stimulating adipocyte differentiation. We (Fan, et al.) reported that Zfp467 is up-regulated 8-fold in RANKL-producing marrow adipocytes from *Prx1cre;PTH1Rfl/fl* mice while Quach, et al. noted that Zfp467 mRNA was suppressed by PTH suggesting that Zfp467 positively influences adipogenesis and is negatively regulated by PTH. In this study, we hypothesized that genetic loss of Zfp467 would lead to an increase in bone mass by shifting marrow cell fate towards osteogenesis. We generated Zfp467^{-/-} mice and performed skeletal and adipose phenotyping. At 16wks of age, Zfp467^{-/-} mice (-/-) were significantly smaller than Zfp467^{+/+} mice (+/+) due to lower fat mass and lean mass ($p < 0.03$). uCT of tibial trabecular (Tb.) bone showed that Tb.BV/TV, Tb.BMD, Tb.N, and Conn.D were significantly higher in -/- vs. +/+ ($p < 0.002$) and lower SMI ($p = 0.005$). Cortical (Ct.) parameters showed smaller Ma.Ar and higher Ct.Ar/Tt.Ar ($p < 0.03$) in -/-. Additionally, Ct.Porosity was significantly lower ($p = .003$) in -/-. Consistent with uCT, histomorphometry showed higher structural parameters of Tb.BV/TV, Tb.N, and Tb.Th ($p < 0.0175$) in -/-. Furthermore, MS/BV, MAR, BFR/BS, and BFR/BV were higher in -/- vs. +/+ ($p < 0.005$). However, Oc.S/BS was also significantly higher in -/- vs. +/+ ($p < 0.05$) indicating an overall increase in bone turnover. Adipocyte ghosts were reduced in the marrow of -/- vs. +/+ mice. Femoral gene expression including *Alpl*, *Sp7*, and *Acp5* were increased ($p < 0.018$) in -/-. In vitro, BMSCs from -/- showed more positive ALP and Von Kossa staining and a decrease in ORO droplets from BMSCs and eMSC. *Adiponectin*, *Cebpa*, *Lepr*, and *Pparg* mRNA were also lower in -/- vs. +/+ ($p < 0.01$). Similarly, *Fabp4* and *Lep* in the inguinal depot were also decreased in -/- vs. +/+ ($p < 0.05$). Taken together, absence of Zfp467 leads to greater bone remodeling with high bone formation and bone mass, together with a decrease in BMAT in female mice. These data support a critical role for Zfp467 in early lineage allocation and provide a novel potential mechanism by which PTH acts in an anabolic manner.

Disclosures: *Phuong Le, None*

FRI-0467

Effects of Notch1 signaling on bone fracture healing *Sanja Novak*^{*1}, *Emilie Roeder*¹, *Brya G Matthews*¹, *Douglas J Adams*², *Ivo Kalajzic*¹. ¹Department of Reconstructive Sciences, University of Connecticut Health Center, United States, ²Department of Orthopaedic Surgery, University of Connecticut Health Center, United States

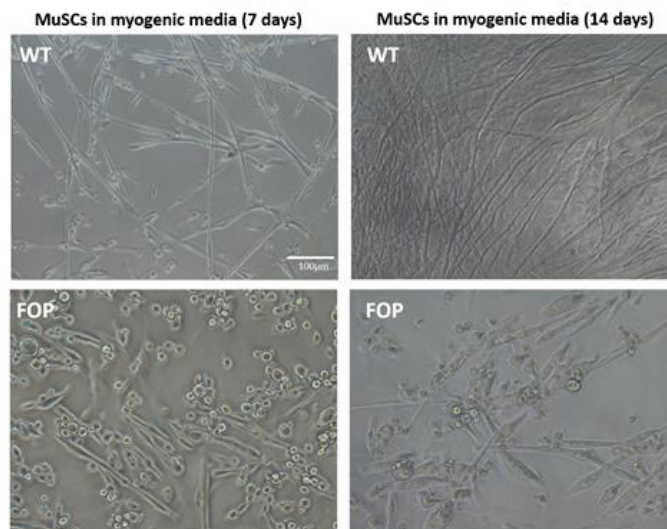
Notch signaling exhibits different effects at different stages of the osteoblast lineage. Notch signaling in progenitor cells increases their proliferation but also inhibits osteogenic differentiation potential. We hypothesize that Notch signaling regulates the expansion, migration and differentiation of mesenchymal progenitor cells and modulates the fracture healing process. Fracture healing was assessed in 8-9-week-old male and female mice. Forced expression of Notch1 intracellular domain (NICD1) was targeted to osteoprogenitor cells using α SMA^{CreERT2} during fracture healing. Stabilized closed transverse femur fractures were generated in experimental mice and littermate controls and Cre activity was induced by injecting tamoxifen on day 0, 2 and 4 post fracture. Increased expression of *Hes1* and *Hey1* in periosteal cell culture (PPC) and callus tissue confirmed NICD1 overexpression. In vitro experiments using PPC overexpressing NICD1 showed increased proliferation and migration compared to controls, but decreased osteogenic differentiation. Histological evaluation of fracture healing in male mice showed that targeted NICD1 overexpression decreased cartilage area 10 days after fracture ($p < 0.05$) and increased mineralized content 14 days after fracture ($p < 0.01$). Fracture calluses with NICD1 overexpression had increased bone mass ($p < 0.05$) with no difference in callus volume compared to controls 3 weeks after fracture. Furthermore, NICD1 overexpression in male animals increased fractured femur strength and stiffness ($p < 0.001$), but also strength and stiffness of intact contralateral femur compared to controls ($p < 0.05$). Overexpression of NICD1 in female mice did not alter callus volume or bone content 3 weeks after fractures, and biomechanical properties of intact contralateral femurs did not differ compared to the controls. Furthermore, using RBPjx floxed mice and crossing them with α SMA^{CreERT2}, we evaluated the effect of Notch signaling deletion on fracture healing. We did not observe changes in callus volume and callus bone mass 3 weeks after fracture. Overexpression of Notch1 signaling in osteoprogenitors following fracture has anabolic effects and leads to increased bone mass and improved biomechanical properties of the fractured femur, while deletion of Notch signaling in α SMA osteoprogenitor cells did not affect the healing process. Further studies are required to understand the discrepancy between in vitro and in vivo effects of NICD overexpression.

Disclosures: *Sanja Novak, None*

FRI-0468

Aberrant muscle tissue repair by mutant ACVR1 FOP muscle stem cells – implications for heterotopic ossification *Alexandra Stanley*^{*1}, *Elisia Tichy*², *Foteini Mourkioti*³, *Eileen M. Shore*⁴. ¹Perelman School of Medicine, University of Pennsylvania, Department of Orthopaedic Surgery, Cell and Developmental Biology Graduate Program, United States, ²Perelman School of Medicine, University of Pennsylvania, Department of Orthopaedic Surgery, United States, ³Perelman School of Medicine, University of Pennsylvania, Departments of Orthopaedic Surgery and Cell and Developmental Biology, United States, ⁴Perelman School of Medicine, University of Pennsylvania, Departments of Orthopaedic Surgery and Genetics, United States

In the rare genetic disease fibrodysplasia ossificans progressiva (FOP), progenitor cells are mis-regulated to differentiate to heterotopic extra-skeletal bone in connective tissues. Mutations in the BMP type I receptor ACVR1/ALK2 cause FOP, with the R206H mutation as the most prevalent. Our lab previously identified that ACVR1R206H increases both BMP ligand-dependent and ligand-independent signaling and promotes increased downstream chondro-/osteogenic gene expression and heterotopic ossification (HO) in FOP patients. HO formation in FOP is often initiated by injury within skeletal muscle. The regenerative potential of skeletal muscle is dependent on the function of muscle stem cells (MuSCs). Quiescent MuSCs are activated within 1-2 days after injury, quickly followed by proliferation, and then differentiation of cells until muscle architecture is restored. We developed an *Acvr1R206H* mouse model that forms HO after cardiotoxin (CTX) injury to skeletal muscle. By 14 days, while muscle of CTX-injured WT animals is fully repaired, muscle tissue from *Acvr1R206H* mice is fibrotic and has not repaired, indicating that muscle healing is impaired by the *Acvr1R206H* mutation. Impaired muscle regeneration is accompanied by a substantial amount of HO within *Acvr1R206H* muscle. BMP signaling has been shown to promote MuSC proliferation and repress their differentiation, leading us to hypothesize that *Acvr1R206H* in MuSCs impairs their ability to regenerate muscle after injury. We examined the effect of the *Acvr1R206H* mutation on MuSC proliferation specifically by isolating MuSCs using fluorescent activated cell sorting. No significant differences between proliferation of MuSCs from WT and FOP injured muscle tissue post-cardiotoxin (CTX) injury were detected, and the number of MuSCs isolated from FOP mice were comparable to that from WT mice. We next investigated the ability of WT and FOP MuSCs to differentiate. We cultured isolated WT and FOP MuSCs in myogenic fusion media and while WT MuSCs differentiate normally to form branching myofibers (high fusion index), FOP MuSCs form underdeveloped fibers that fail to fuse (low fusion index) (Figure One). These data indicate that the *Acvr1R206H* mutation does not alter MuSC proliferation but has a negative impact on their ability to undergo myogenesis. On-going in vivo experiments will further elucidate the role of the MuSCs in response to the *Acvr1R206H* mutation during muscle regeneration in response to tissue injury.



Disclosures: *Alexandra Stanley, None*

FRI-0469

New Insight into SHP2 regulation of Osteogenic Commitment of Mesenchymal Progenitors Lijun Wang^{*1}, Jiahui Huang², Chunlin Zuo², Douglas Moore², Matthew Warman³, Michael Ehrlich¹, Wentian Yang¹. ¹Department of Orthopaedics, Brown University Alpert Medical School and Rhode Island Hospital, United States, ²Brown University Alpert Medical School and Rhode Island Hospital, United States, ³Orthopaedic Research Laboratories and Howard Hughes Medical Institute, Boston Children's Hospital and Harvard Medical School, United States

Chondrocytes and osteoblasts differentiate from mesenchymal stem cells via a common osteochondroprogenitor (OCP). The signaling pathways that control lineage decisions for OCPs are incompletely understood. SHP2 is a ubiquitously expressed protein tyrosine phosphatase and has been identified as an important regulator of the development and homeostasis of multiple tissue and/or organ. The role SHP2 in the skeletal system, however, remains incompletely defined. We conditionally deleted SHP2 in mouse limb and head mesenchyme (using *Prrx1-Cre*), which yielded SHP2-deficient mice with increased cartilage mass and deficient intramembranous and endochondral ossification, suggesting SHP2-deficient OCPs become chondrocytes and not osteoblasts (Fig 1). Consistent with these observations, the expression of the master chondrogenic transcription factor Sox9 and its target genes *Acan*, *Ihh*, *Col2a1*, and *Col10a1* are increased in SHP2-deficient chondroid cells, as revealed by gene expression arrays, qRT-PCR, in situ hybridization, and immunostaining. Mosaic SHP2 deletion at E13.5 in *Prrx1-CreERT2*-expressing OCPs leads to the growth of osteochondromas and enchondromas. Mechanistic *in vivo* and *in vitro* studies demonstrated that SHP2 regulates fate determination of OCPs via the post-translational phosphorylation and SUMOylation of SOX9, at least in part via the PKA signaling pathway. These data indicate that SHP2 is critical for skeletal cell lineage differentiation and thus may be a pharmacologic target for bone and cartilage regeneration.

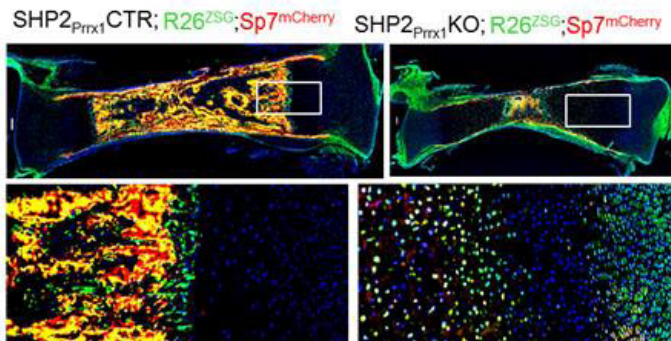


Fig. 1 SHP2 deficiency in the PRRX1+ osteochondroprogenitors (OCPs) impairs osteogenic differentiation. Fluorescent images of P1.5 tibia frozen sections demonstrate that ZsGreen+ OCPs robustly differentiate into OSTERIX+ (red) osteoblasts (green+red=yellow) in *SHP2_{Prrx1}CTR;R26^{ZsG};Sp7^{mCherry}* mice. This process, however, is markedly compromised in *SHP2_{Prrx1}KO;R26^{ZsG};Sp7^{mCherry}* mice. Bottom panels are the enlarged view of the corresponding boxed areas on the top panel.

Disclosures: Lijun Wang, None

FRI-0470

PDGFR β signaling regulates osteogenesis of α SMA labeled periosteal cells. Xi Wang^{*1}, Sanja Novak¹, Danka Grcevic², Brya G Matthews¹, Ivo Kalajzic¹. ¹UCConn Health, United States, ²University of Zagreb, Croatia

The goal of our study is to better understand molecular mechanisms that regulate commitment and differentiation of progenitor cells during bone regeneration. We have shown that alpha smooth muscle actin (α SMA) is a marker for mesenchymal stem cells that contribute to the majority of osteoblasts and chondrocytes in fracture healing. While intact periosteum shows 2.5% α SMA+ cells by flow cytometry, this proportion dramatically increases to 18 \pm 3% on day 4 and 34.8 \pm 5% on day 10 post fracture. Over 60% of the α SMA+ population expresses PDGFR β . We investigated the effect of PDGFR β signaling on α SMA labeled periosteal progenitor cells (PPCs). PPCs were isolated from α SMA-CreERT2/Ai9/Col2.3GFP mice and treated with 4-OH Tamoxifen to induce Cre activity. We treated PPCs with 10ng/ml PDGF-BB and observed a significant increase of EdU+ proliferative cells. PDGF-BB also increased cell migration in a wound healing assay. PDGF-BB also inhibited osteogenic differentiation shown by osteogenic gene expression and GFP expression. To further understand the role of PDGFR β signaling in PPCs, we conditionally deleted PDGFR β using α SMA-CreERT2 crossed with PDGFR β flox/flox mice. *In vitro* deletion of PDGFR β in PPCs resulted in significantly enhanced osteogenic differentiation indicated by ALP and Von Kossa staining. We then performed femur fracture on 12 week old mice and examined the proliferation of periosteal cells upon injury. 4 days after fracture, in the periosteal regions

proximal to fracture site, there was a significant decrease of EdU+ proliferative cells in α SMA PDGFR β del/del mice. 14 days after fracture, there was a trend of more mineralization area/callus area in Cre+ mice (N=8). Overall, PDGFR β is widely expressed in progenitor cells that contribute to fracture healing *in vivo*. Using a conditional deletion mouse model, we have demonstrated that PDGFR β signaling regulates osteogenic differentiation of PPCs. Deleting PDGFR β impaired periosteal cell proliferation, while promoting differentiation. Studies are ongoing to assess the functional outcome of this perturbation on fracture callus composition and biomechanics.

Disclosures: Xi Wang, None

FRI-0501

Drug-induced modulation of gp130 signaling prevents articular cartilage degeneration and promotes repair Ruzanna Shkhyan^{*}, Ben Van Handel, Jacob Bogdanov, Denis Evseenko. University of Southern California, United States

Introduction. Human adult articular cartilage has little capacity for repair, and joint surface injuries often result in osteoarthritis (OA), characterized by loss of matrix, hypertrophy and chondrocyte apoptosis. Inflammation mediated by IL-6 family cytokines has been identified as a critical driver of pro-arthritis changes in mouse and human joints, resulting in a feed-forward process driving expression of matrix degrading enzymes and IL-6 itself. Methods. Medial meniscal tear and focal injury rat models of osteoarthritis. Statistical methods: Student t-test, one-way ANOVA followed by the Newman-Keuls test. All animal experiments were conducted in accordance and under the supervision of the University of Southern California Department of Animal Resources. Results. Human adult articular cartilage has little capacity for repair, and joint surface injuries often result in osteoarthritis (OA), characterized by loss of matrix, hypertrophy and chondrocyte apoptosis. Inflammation mediated by IL-6 family cytokines has been identified as a critical driver of pro-arthritis changes in mouse and human joints, resulting in a feed-forward process driving expression of matrix degrading enzymes and IL-6 itself. Here we show signaling through gp130, the common receptor for IL-6 family cytokines, can have both context- and cytokine-specific effects on articular chondrocytes and that a small molecule gp130 modulator can bias signaling toward anti-inflammatory and anti-degenerative outputs. High throughput screening of 170,000 compounds identified a small molecule gp130 modulator termed Regulator of Cartilage Growth and Differentiation (RCGD 423) that promotes atypical homodimeric signaling in the absence of cytokine ligands, driving transient increases in MYC and pSTAT3 while suppressing oncostatin M- and IL-6-mediated activation of ERK and NF- κ B via direct competition for gp130 occupancy. This small molecule increased proliferation while reducing apoptosis and hypertrophic responses in adult chondrocytes *in vitro*. In a rat partial meniscectomy model, RCGD 423 greatly reduced chondrocyte hypertrophy, loss and degeneration while increasing chondrocyte proliferation beyond that observed in response to the injury. Moreover, RCGD 423 improved cartilage healing in a rat full-thickness osteochondral defect model, increasing proliferation of mesenchymal cells in the defect and also inhibiting breakdown of cartilage matrix in de novo generated cartilage. Conclusion. These results identify a novel strategy for articular cartilage remediation via small molecule-mediated modulation of gp130 signaling.

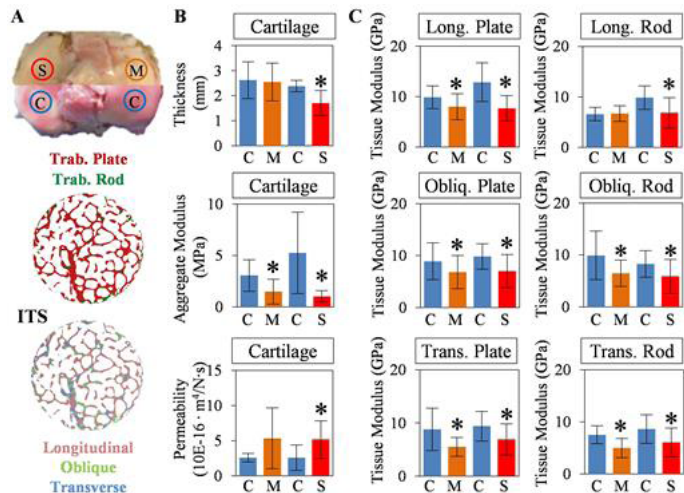
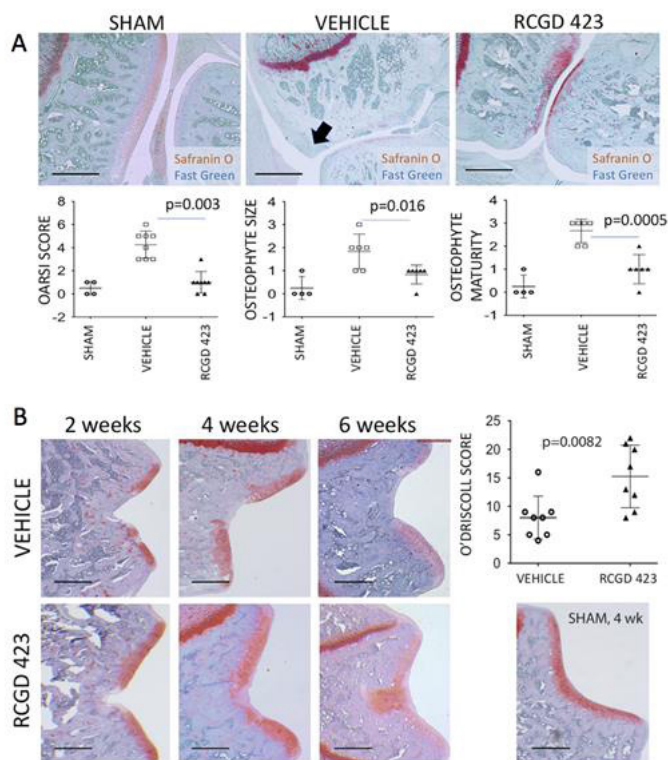


Figure 1. (A) Moderate (M) and severe (S) OA regions and corresponding control (C) regions decomposed by trabecular type and orientation using ITS. (B) Thickness, aggregate modulus and permeability of cartilage and (C) tissue modulus of individual trabeculae measured by microindentation.

Disclosures: *Yizhong Hu, None*

FRI-0503

Reliable change index in the evaluation of joint space loss: a novel method for assessing osteoarthritis progression data from the Osteoarthritis Initiative Camille Parsons¹, Andy Judge², Kirsten Leyland², Hazel Inskip¹, Cyrus Cooper¹. ¹MRC Lifecourse Epidemiology Unit, University of Southampton, United Kingdom, ²University of Bristol, United Kingdom

The reliable change index (RCI) allows for identification of whether observed change between knee joint space width (JSW) measurements is statistically reliable in the presence of measurement error. We aimed to assess the effectiveness of the RCI as a novel approach to estimating osteoarthritis (OA) progression using longitudinal knee JSW measurements, while accounting for the presence of measurement error. Data for these analyses are from the Osteoarthritis Initiative (OAI) public-use data sets. Measurements from 3,469 participants were included. Knee JSW measurements were taken from radiographic images at baseline, and at 12, 24, 36, 48, 72 and 96 months, using a semi-quantitative method. A RCI score was calculated, using the version developed by Christensen and Mendoza, between each OAI study visit for each study participant. The resulting RCI is a continuous score that follows a standard normal distribution, with larger (RCI greater than 1.96) and smaller (RCI less than -1.96) values indicating that the change observed is statistically significant and therefore more than the fluctuations of the measurement. Between consecutive study visits, 53 to 64% of participants had a crude decrease in JSW between study visits. Implementation of the RCI indicated that considerably fewer participants had a statistically reliable decrease in JSW, e.g. 3.1% participants were identified between baseline and 12 month study visits as having meaningful change compared to 53% crude decrease. Similar proportions of statistically reliable decreases were observed between all other OAI study visits. Around 40% of participants had crude increase in JSW between the pairs of study visits under consideration. Use of the RCI dramatically reduced the number of participants that were identified as having an increase, e.g. between 72 and 96 month study visits only 1.4% were identified compared to 39% that were identified using crude differences. As increases in JSW are biologically extremely rare, this shows the impact of measurement error if crude differences are assessed without accounting for measurement error. The RCI provides a useful method to identify change in JSW, removing many of the apparent changes that are likely to be due to measurement error. This method appears to be useful for assessing change in JSW clinical and research settings from radiographs. This method appears to be useful for assessing change in JSW from radiographs in both a clinical and research setting.

Disclosures: *Camille Parsons, None*

Disclosures: *Ruzanna Shkhyan, None*

FRI-0502

Tissue Mechanical Deficiencies Detected in Both Articular Cartilage and Subchondral Trabecular Bone in Osteoarthritic Human Knees Yizhong Hu¹, Eric Y. Yu¹, Ariana Moini¹, Zexi Wang¹, Matthew Scott Heller², Akshay Lakra², Herbert John Cooper², Roshan Pradip Shah², Jeffrey Albert Geller², X. Lucas Lu³, X. Edward Guo¹. ¹Bone Bioengineering Laboratory, Columbia University, United States, ²Department of Orthopaedic Surgery, Columbia University Medical Center, United States, ³Department of Mechanical Engineering, University of Delaware, United States

Cartilage and subchondral bone are key mechanical components in the knee joint and highly vulnerable in osteoarthritis (OA). Histology and specialized MRI sequences reported biochemical deterioration of proteoglycans in OA cartilage. Microstructural analyses of subchondral trabecular bone revealed loss of rod number despite trabecular thickening and bone sclerosis. The biomechanical properties of human OA cartilage and subchondral bone tissue, however, have rarely been examined collectively. In this study, we used microindentation testing to directly quantify tissue mechanical properties in human OA cartilage and subchondral trabecular bone simultaneously. OA (n = 6) and control (n = 4) tibial plateaus were collected from knee replacement patients and cadaver donors. Osteochondral cores were harvested from moderate and severe regions from OA samples and corresponding control regions. From the μ CT scan of each core, cartilage thickness was measured, and subchondral trabecular bone was subjected to Individual Trabecula Segmentation (ITS) for identification of trabecular type and orientation. Each core was subjected to 3 cartilage indentation tests. Aggregate modulus and permeability were calculated based on poroelastic theory. Subchondral bone was then isolated and embedded for microindentation. A total of 212 plates and 156 rods were indented. Bone tissue modulus was calculated from the unloading curve. Cartilage thickness was lower in severe OA regions but remained intact in moderate regions. Cartilage indentation found significantly reduced modulus in all regions. Increased permeability was found only in severe OA regions. Trabecula microindentation revealed consistent and drastic reductions in tissue modulus in OA subchondral bone. On average, a 30% decrease in modulus was found in all regions for longitudinal plates, oblique plates and rods, and transverse plates and rods. The reduced modulus and increased permeability in OA cartilage may be attributable to disintegration of collagen/proteoglycan solid matrix and reduced resistance to fluid flow. Tissue modulus reduction in the subchondral bone despite trabecular thickening indicates increased bone remodeling but compromised mechanical integrity, likely due to poor mineralization. Furthermore, persistent bone changes beneath moderately and severely damaged cartilage may indicate their precedence in OA progression, or different sensitivity of microindentation to cartilage and bone tissue changes.

FRI-0504

Predicting total hip replacement for symptomatic osteoarthritis using radiographs or clinical computed tomography; a prospective case-control study Kenneth Poole*¹, Ilya Burkov¹, Graham Treece¹, Andrew Gee¹, Thomas Turmezei¹, Fjola Johannesdottir¹, Sigurdur Sigurdsson², Tamara Harris⁴, Helgi Jonsson³, Vilundur Gudnason⁵. ¹University of Cambridge, United Kingdom, ²The Icelandic Heart Association, Iceland, ³Public Health Sciences, University of Iceland, Iceland, ⁴Laboratory of Epidemiology and Population Sciences, United States, ⁵Faculty of Medicine, University of Iceland, Iceland

Expert osteoarthritis guidance now advises clinicians not to request imaging when managing patients with hip pain. We evaluated how well a single pelvic radiograph predicted total hip replacement (THR) compared with pain symptoms. From a prospective nested case-control study of 3133 healthy adults, 74 individuals underwent THR for osteoarthritis approximately 3 years after a baseline assessment comprising validated pain questionnaire and hip computed tomography (CT). Each case destined for THR was matched by age and sex to two control individuals. Mean age was 74±5yrs (range 67-89). Baseline variables were performance-tested using receiver-operating-characteristic curve analysis (AUC): hip pain, osteoarthritis grade or minimal joint space width (mJSW) from coronal plane reconstructed radiograph or 3D cortical bone thickness. The location and magnitude of bone thickening associated with THR was highlighted using statistical parametric mapping. Combining hip pain, radiographic osteoarthritis grade and CT gave excellent discrimination of THR (0.90; 0.85,0.95, figure 1). Conversely, hip pain was a poor to marginal predictor (AUC=0.70; 95%CI 0.62,0.78). The AUC for radiographic Kellgren and Lawrence (K&L) osteoarthritis grade alone was 0.87 (0.81,0.92), irrespective of hip pain, with single mJSW being a reasonable discriminator (0.80;0.73,0.87). Osteoarthritis was also associated with a CT-defined crescent of femoral head surface bone thickening (Odds Ratio for THR; 5 per SD thicker; 3:2.7, 0.85 (0.79, 0.91)). In a typical clinical presentation with hip pain, all of the imaging parameters measured ranged from good to excellent in terms of clinical utility. Imaging unequivocally predicted THR for osteoarthritis, whether or not pain had become apparent. Contrary to current guidance, images of patients with hip pain have good to excellent clinical utility for selecting surgically-relevant presentations. If patients with definite hip pain had definite radiological osteoarthritis, 85% went on to THR within 3 years.

Figure 1: Predicting total hip replacement for osteoarthritis within 3 years (+/-2yrs), using baseline hip pain alone versus a adding imaging tests (comparison of area under the ROC curve of the various models)

Model	AUC (95% CI)	Cross-validated AUC*	OR per SD (95% CI)	Hip pain only versus hip pain + imaging (χ ²)	prob > χ ²
hip pain only	0.70 (0.62-0.78)	0.63	2.21 (1.68-2.91)	-	-
Joint Space Width only	0.79 (0.72-0.86)	0.77	0.26 (0.17-0.39)	-	-
[#] hip pain + mJSW	0.80 (0.73-0.87)	0.78	-	5.75	0.0164
OA Score (K&L) only	0.87 (0.81-0.92)	0.85	6.30 (3.96-9.99)	-	-
[#] hip pain + K&L	0.87 (0.82-0.93)	0.85	-	20.35	0.0000
Cortical Thickness only	0.83 (0.77-0.89)	0.81	5.00 (3.24-7.71)	-	-
[#] hip pain + CTh	0.85 (0.79-0.91)	0.83	-	14.30	0.0002
[#] hip pain + K&L + CTh	0.90 (0.85-0.95)	0.88	-	26.80	0.0000

ROC, Receiver operating characteristic; AUC, area under the curve; *Cross Validated; OR, odds ratio per standard deviation (SD); CTh, cortical thickness; mJSW, minimum joint space width; K&L, Kellgren & Lawrence Score; χ²=chi-square test; i vs ii, χ²=9.25, p=0.0024; i vs iii, χ²=2.21, p=0.1375; ii vs iii, χ²=0.48, p=0.4881

Disclosures: **Kenneth Poole, None**

FRI-0505

Beneficial effects of Denosumab on bone loss and bone erosion from results of long-term treatment in the phase 3, DESIRABLE study in patients with rheumatoid arthritis (RA) on background csDMARDs Yoshiya Tanaka*¹, Satoshi Soen², Hisashi Yamanaka³, Toshiyuki Yoneda⁴, Sakae Tanaka⁵, Takaya Nitta⁶, Naoki Okubo⁶, Harry Genant⁷, Désirée Van Der Heijde⁸, Tsutomu Takeuchi⁹. ¹University of Occupational and Environmental Health, Japan, ²Kindai University Nara Hospital, Japan, ³Institute of Rheumatology Tokyo Women's Medical University, Japan, ⁴Osaka University Graduate School of Dentistry, Japan, ⁵The University of Tokyo, Japan, ⁶Daiichi Sankyo Co. Ltd, Japan, ⁷University of California, United States, ⁸Leiden University Medical Center, Netherlands, ⁹Keio University School of Medicine, Japan

Background: The DESIRABLE study demonstrated in RA patients that the first 12 months of treatment with denosumab (DMAb) 60 mg every 6 months (Q6M) or every 3 months (Q3M) significantly inhibited the progression of joint destruction and increased bone mineral density (BMD) compared to placebo. The purpose of this study is to evaluate the safety and efficacy of DMAB 60 mg Q6M or Q3M in RA patients on long-term treatment in the DESIRABLE study. Methods: Upon completion of the 12 months of the double-blind phase (DB) all patients were to receive DMAB 60 mg/Q6M or Q3M and daily supplements of calcium and vitamin D during the following 24 months of the open-label extension phase. Patients were randomized in a 1:1:2:2 ratio to receive one of four treatments (Figure 1). In this analysis, the continuous administration group received 36 months of DMAB treatment,

and the crossover group received 24 months of DMAB treatment (12 month of placebo in DB and 24 months of DMAB treatment). The radiographic evaluation used the van der Heijde modified total Sharp score (mTSS) and BMD of the lumbar spine was measured by dual energy X-ray absorptiometry at 0, 12, 24 and 36 months. Serum CTX-I was also monitored during the study. Results: 667 (placebo/Q6M (P/Q6M), n=113; placebo/Q3M (P/Q3M), n=110; Q6M, n=222; Q3M, n=222) patients received at least one dose of study drug, and 607 (P/Q6M, n=105; P/Q3M, n=103; Q6M, n=199; Q3M, n=200) completed the DB period and entered the long-term extension. In the continuous and the crossover administration groups, sustained inhibition of mTSS and erosion score (mES) progression was observed during long-term treatment phase. No effect on joint space narrowing was observed. In the continuous administration group, increases from the baseline in BMD after 36 months of continued DMAB treatment were 8.9% in Q6M and 9.9% in Q3M group. In the crossover group, BMD changes at 36 month (24 months after the first dose of DMAB) were 6.7% in P/Q6M and 7.6% in P/Q3M group (Figure 2). And similar increases in BMD were observed regardless of glucocorticoid use. In both groups, serum CTX-I was decreased at 1 month after the first dose of DMAB with relatively sustained reductions. Conclusions: A 24 months extension phase of the DESIRABLE study showed that 36 months of DMAB treatment for RA was associated with suppression of mTSS and mES progression, continuous BMD increases, persistent CTX-I reductions and a favorable over all benefit risk profile.

Figure 1: Study design

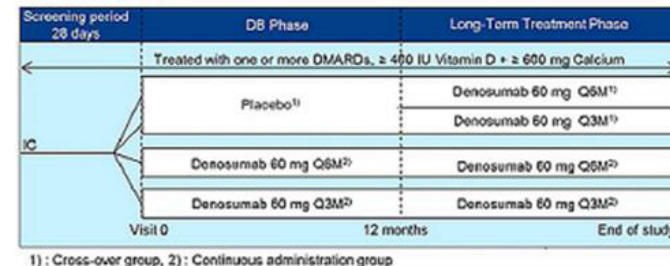
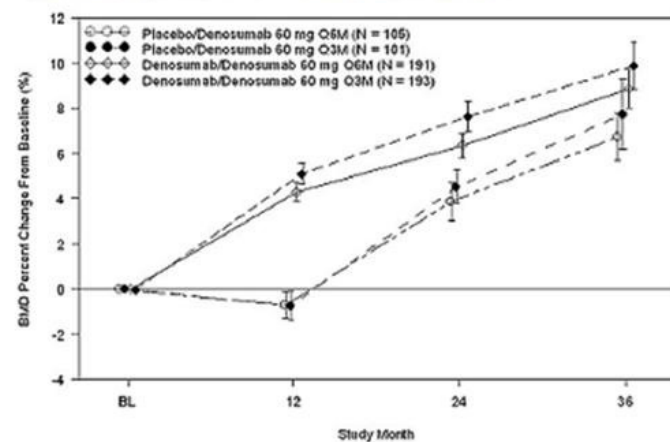


Figure 2: Percentage changes from the baseline in lumbar spine BMD



Disclosures: **Yoshiya Tanaka, Mitsubishi Tanabe, Takeda, Bristol-Myers, Chugai, Astellas, Abbvie, MSD, Daiichi Sankyo, Pfizer, Kyowa Hakkō Kirin, Eisai, Ono, Grant/Research Support, Daiichi-Sankyo, Astellas, Pfizer, Mitsubishi Tanabe, Bristol-Myers, Chugai, YL Biologics, Eli Lilly, Sanofi, Janssen, UCB, Speakers' Bureau**

FRI-0506

WITHDRAWN

FRI-0537

Conditional deletion of Dock7 in the early limb bud results in reduced trabecular bone in both sexes with increased fat mass only in male mice Kathleen A Becker*¹, Daniel J Brooks², Anne Harrington³, Mary L Boussein², Lucy Liaw³, Clifford J Rosen³. ¹Maine Medical Center Research Institute, United States, ²Beth Israel Deaconess Medical Center, Harvard Medical School, United States, ³Maine Medical Center Research Institute, Maine Medical Center, United States

Dock7 is guanine nucleotide exchange factor involved in GTP-loading of small GTPases. While global loss of the Dock7 protein leads to low bone density predominantly in female mice, it is unclear in what cells and tissues Dock7 may function to control bone

metabolism. In order to determine whether Dock7 expression in bone cells is important for development of normal bone density and micro-architecture, Dock7 was conditionally deleted in the early limb bud by breeding a novel model, the floxed exon 3-4 Dock7 allele on the C57BL/6J background, with Prx1-Cre expressing mice. Femurs from 16 wk old female mice expressing the Prx1-Cre (Dock7^{fl/fl};Prx1-Cre) (n=9) were analyzed by micro-computed tomography and compared to female Dock7^{fl/fl} mice (n=8). Female Dock7^{fl/fl};Prx1-Cre mice displayed a reduction in femur length (P=0.002), BV/TV (P=0.035), trabecular (Tb) BMD (P=0.038), and Tb number (P=0.002) with an increase in Tb separation (P=0.0028). Body composition was not altered. The decrease in Tb bone with conditional deletion of Dock7 is similar to what has been previously observed with global loss of the Dock7 protein in Misty mice. Therefore, these data suggest that the Tb bone loss observed in the Dock7^{fl/fl};Prx1-Cre mice was, in part, mediated through loss of Dock7 directly in bone. Unlike Misty mice, cortical thickness (P>0.9999) was unaffected in the Dock7^{fl/fl};Prx1-Cre mice indicating that loss of Dock7 in tissues outside the limb bud may regulate cortical thickness with global loss of Dock7. Similarly, femoral micro-architecture was analyzed in male Dock7^{fl/fl};Prx1-Cre mice (n=9) and compared to Dock7^{fl/fl} mice (n=12). BV/TV (P=0.0003), Tb BMD (P=0.0002), Tb number (P<0.0001), and connectivity density (P<0.0001) were reduced in Dock7^{fl/fl};Prx1-Cre mice with an increase in Tb separation (P<0.0001). No change in femur length was observed. Unlike female mice, the 16 wk old male Dock7^{fl/fl};Prx1-Cre mice had an increase in body mass (P=0.020) and fat mass (P=0.0058) with a reduction in fat free mass (P=0.0036) by DXA. Furthermore, the weight of brown (P=0.0155), inguinal (P=0.0743), and gonadal adipose depots were increased in Dock7^{fl/fl};Prx1-Cre mice compared to Dock7^{fl/fl} mice showing for the first time a sexual dimorphic fat phenotype with deletion of Dock7. Taken together, these data suggest that Dock7 may play a cell autonomous role in controlling bone metabolism warranting further investigation for a role of Dock7 in lineage determination.

Disclosures: *Kathleen A Becker, None*

FRI-0538

The Role of VEGFA from Osteoblast Lineage Cells during Fracture and Cortical Defect Repair Evan Buettmann*, Nicole Migotsky, Susumu Yoneda, Pei Hu, Jennifer McKenzie, Matthew Silva. Washington University in St. Louis, United States

The molecule vascular endothelial growth factor A (VEGFA) has been shown to be indispensable for endochondral and intramembranous ossification following bone injury. However, the dispensability of VEGFA from osteoblast lineage cells at the time of injury in models of endochondral (full fracture) and intramembranous (stress fracture and cortical defect) bone repair remains unknown. Therefore, we sought to determine if inducible genetic deletion of 1) ubiquitous VEGFA and 2) osteoblast lineage VEGFA impairs injury-induced bone formation in mice. First, inducible Cre specificity in our models of fracture and defect repair was verified using an Ai9 (tdTomato) reporter under the Ubiquitin C (UBC), Osterix (Osx) and Dentin Matrix Protein1 (DMP1) CreERT2 driver. Next, these inducible Cre lines were crossed to mice containing floxed VEGFA alleles (VEGFA^{fl/fl}) and either given a femoral fracture, ulnar stress fracture, or tibial defect at 12 weeks of age. Controls were littermate mice without Cre. All mice were given tamoxifen (TAM) continuously starting 2 weeks pre-injury. 1) UBC CreERT2 VEGFA^{fl/fl} (UBC KO) displayed a 96% reduction in VEGFA mRNA from cortical bone that manifested in dramatically reduced bone formation in all injury models. 2) Osx CreERT2 VEGFA^{fl/fl} (Osx KO) and DMP1 CreERT2 VEGFA^{fl/fl} (DMP1 KO) mice both displayed a 35% reduction in VEGFA mRNA from cortical bone. Despite similar deletion efficiencies, only the Osx KO mice displayed a significant reduction in callus bone volume versus controls following full fracture (-27%; p = 0.02; 14 days post-injury) and stress fracture (-58%; p = 0.01; 7 days post-injury). However, neither Osx KO nor DMP1 KO mice demonstrated significant impairments in bone formation following cortical defect (7 days post-injury). Our UBC KO results reaffirm previous pharmacological studies that ubiquitous VEGFA is necessary for injury induced bone formation. The impaired healing in Osx KO but not DMP1 KO animals after fracture suggests that VEGFA from early (osteoprogenitor) but not mature osteoblasts/osteocytes is necessary for maximal periosteal bone formation. On the other hand, the normal healing in the defect model in the Osx and DMP1 KO lines suggests that osteoblast lineage VEGFA is dispensable for intramedullary bone formation. In conclusion, our results show that the requirement for VEGFA varies depending on the injury model and differentiated state of the osteoblast.

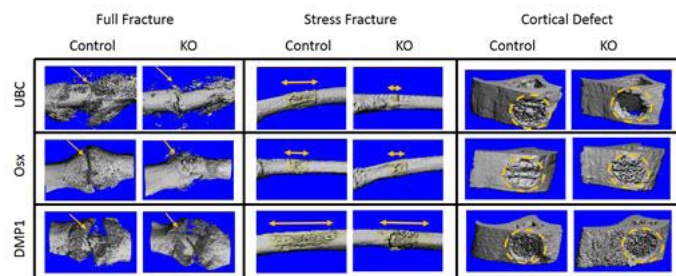


Figure 1. MicroCT reconstructions (10 micron isotropic resolution) of full fracture (day 14), stress fracture (day 7) and tibial defect (day 7) in the littermate control and VEGFA knockout (KO) animals. Ubiquitin C (UBC) CreERT2 VEGFA^{fl/fl} animals (top row) demonstrated greatly diminished bone formation across all injury models (top row). Osterix (Osx) CreERT2 VEGFA^{fl/fl} animals (middle row) demonstrated impaired bone formation following full fracture and stress fracture only. DMP1 (DMP1) CreERT2 VEGFA^{fl/fl} animals (bottom row) demonstrated no differences in healing. Arrows mark the sites of full fracture. Double arrow denotes the stress fracture region in each specimen. Dashed ovals are used to highlight outline of tibial defect.

Disclosures: *Evan Buettmann, None*

FRI-0539

Gene regulatory landscape in primary human mesenchymal stem cell (MSC) during BMP2-induced osteoblast differentiation Alessandra Chesi*¹, Yadav Wagley², Matthew E. Johnson¹, Sumei Lu¹, Michelle E. Leonard¹, Kenya M. Hodge¹, James A. Pippin¹, Elisabetta Manduchi¹, Andrew D. Wells¹, Kurt D. Hankenson², Struan F.A. Grant¹. ¹The Children's Hospital of Philadelphia, United States, ²University of Michigan, United States

Proper bone formation requires the differentiation of osteoblasts from mesenchymal stem cells (MSCs), a process mediated by bone morphogenetic protein (BMP) signaling. To understand the gene regulatory landscape during osteoblast differentiation, we performed ATAC-seq on undifferentiated MSCs and BMP2-differentiated osteoblasts from four human donors to obtain genome-wide maps of open chromatin regions (OCR), where gene regulation is most likely to occur. Of the overall 102,696 OCRs, 56,964 (55%) were common to the two cell types, 36,578 (36%) were osteoblast-specific and only 9,154 (9%) were MSC-specific. Thus, chromatin accessibility increased upon differentiation, and although more than half of the accessible landscape of these two cell types was maintained, more than a third was remodeled de novo to become accessible in the osteoblast lineage. Next, we leveraged a novel chromatin conformation capture technique we developed to investigate the genome-wide 3D contacts of all the promoters in the human genome at high resolution. Our custom Agilent SureSelect RNA library targets DpnII restriction fragments overlapping 36,691 promoters of protein-coding, noncoding, antisense, snRNA, miRNA, snoRNA and lincRNA genes. We applied our SPATIAL-seq (genome-Scale, Promoter-focused Analysis of chromatin Looping) method to both cell types coming from the same donors. In both settings, interacting regions were significantly enriched for open chromatin regions as detected by our ATAC-seq experiments, suggesting a potential regulatory role. They were also enriched for histone marks associated with active chromatin regions in human primary osteoblasts from ENCODE, such as enhancer regions (H3K27ac and H3K4me1), active promoters (H3K4me3), actively transcribed regions (H3K36me3) and transcription factor binding sites (H3K4me2); they also associated with CTCF binding sites and the repressive mark H3K27me3, but not with the repressive mark H3K9me3. We went on to characterize 164,508 chromatin loops specific to the MSC-derived osteoblasts, 136,631 specific to MSCs, and 148,753 loops present in both. Of these, about 10% (15,882, 11,551, and 14,613, respectively) involved open chromatin regions in the corresponding cell type. When intersected with RNAs-seq, these data revealed specific pathways operating in each setting. These unique and high resolution complimentary datasets provide key insights in to the 3D regulatory architecture of human osteoblast differentiation.

Disclosures: *Alessandra Chesi, None*

FRI-0540

Ablation of Gjc1 in the Chondro-Osteogenic Lineage Inhibits Osteoclastogenesis Leading to High Trabecular Bone Mass Francesca Fontana*, Marcus Watkins, Song Dah Woon, Giulia Leanza, Roberto Civitelli. Washington University School of Medicine, United States

The connexins family of gap junction proteins comprises 20 members. Each connexin confers specific permeability and electric conductance to the gap junction they form. Although connexin43 (Cx43) is the most abundant connexin expressed in bone, connexin45 (Cx45) and Cx37 are also present. Missense mutations of the Cx45 gene (Gjc1) in humans have recently been found in families with congenital arrhythmias and skeletal abnormalities. To test the role of Cx45 in bone, we generated Gjc1^{flx/flx}; Tw2-cre mice, where Gjc1 is conditionally inactivated in chondro-osteogenic cells driven by the Dermo1/ Twist2 promoter (cKO). Whereas Cx43 deficiency results in a primarily cortical phenotype, female Gjc1 cKO mice have high trabecular bone mass by μ CT, with >50% higher BV/TV, 75% higher trabecular thickness, and 20% lower trabecular spacing relative to control Gjc1^{flx/flx} mice. Cortical bone mass and geometry are normal. By contrast, male Gjc1 cKO mice

showed no significant abnormalities in trabecular or cortical bone. Using a calcein diffusion assay and FACS analysis to test gap junctional intercellular communication (GJIC), we confirmed that bone marrow stromal cells (BMSC) from Gjc1 cKO mice exhibited higher capacity to transfer calcein from cell to cell. Since these cells abundantly express Cx43, higher GJIC in Cx45 deficient BMSC suggest that Cx45 inhibits Cx43-mediated GJIC, confirming previous data. Furthermore, Gjc1 cKO BMSC were less effective than control BMSC in supporting osteoclastogenesis in co-culture with bone marrow macrophages. This was associated with decreased RANKL expression, without changes in OPG mRNA. Corroborating this finding, histologic analysis revealed 40% decrease in osteoclast number on trabecular surfaces by TRAP-staining of Gjc1 cKO tibiae relative to controls. In vitro, Cx45-deficient BMSC exhibited no obvious osteogenic differentiation defects, consistent with no difference in P1NP levels between Gjc1 cKO and control littermates. Thus, while Cx43's major role is to modulate cortical modeling, Cx45 is a negative regulator of trabecular bone mass, albeit with genetic dysmorphism. Both connexins control osteoclastogenesis by modulating the RANKL/OPG system in osteogenic cells, but in opposite ways and in different bone compartments.

Disclosures: *Francesca Fontana, None*

FRI-0541

A novel role for tissue nonspecific alkaline phosphatase in cranial bone progenitor cells. Hwa Kyung Nam*, Iva Vesela, Nan Hatch. University of Michigan, School of Dentistry, United States

Introduction: Bone growth is dependent upon the presence of self-renewing osteoblast progenitor cell populations. While the contribution of Tissue Nonspecific Alkaline Phosphatase (TNAP) enzyme activity in promoting bone mineralization when expressed in differentiated bone forming cells is well understood, little is known regarding the role of TNAP in bone progenitor cells. Here we investigated the function of TNAP in cranial bone progenitor cells. **Methods:** Synchronized MC3T3E1 cranial osteoblast progenitor cells stably expressing TNAP shRNA and cranial progenitor cells isolated from TNAPko mice were analyzed for cell cyclin and cytokinesis protein expression, FACS based cell cycle progression, cell size, binucleation and FGFR expression when compared to control cells. Erk1,2 phosphorylation was assessed in cranial progenitor cells and tissues of TNAPko mice. **Results:** We find that TNAP is essential for expression of cyclin B1 and D1, as well as for activated forms of the cytokinesis proteins Aurora B and Histone 3. We also find that TNAP functions to promote cranial osteoblast progenitor cell cycle progression, cytokinesis and FGFR2 expression; and that these effects are mediated by erk1,2. **Conclusions:** We propose a model in which TNAP stimulates erk1,2 activity via both phosphate dependent and independent mechanisms, which promotes cell cycle progression, cytokinesis and cell proliferation, and concomitantly feeds back to inhibit FGFR2 expression. Together, our results suggest that the cranial bone abnormalities seen in humans and mice with TNAP deficiency may occur due to diminished erk1,2 activity leading to diminished cranial bone progenitor cell renewal.

Disclosures: *Hwa Kyung Nam, None*

FRI-0542

Global Expression of miR-29 Decoy Decreases Bone Formation and Alters Cortical Bone Morphology in Young Mice Henry Hrdlicka*, Bongjin Shin, Anne Delany, Sun-Kyeong Lee. UConn Health, United States

The miR-29 family of miRNAs positively regulates both osteoblast and osteoclast differentiation. In the osteoblast lineage, miR-29 levels increase as osteoblasts mature and matrix mineralizes; it is thought that miR-29 promotes this process by targeting multiple negative regulators of differentiation. In the osteoclast lineage, miR-29 levels increase in RANKL treated precursors as cells start to fuse; it is thought that miR-29 promotes osteoclastogenesis at least in part by regulating lineage commitment and cell motility. To examine function of miR-29 in normal skeletal physiology in vivo, we created mice globally expressing a miR-29 competitive inhibitor (tough decoy). Specifically, a cassette containing 3 copies of a miR-29 tough decoy within the 3'UTR of the tdTomato reporter was knocked into the Rosa26 locus using CRISPR/Cas9. These mice are viable and fertile. In the current study, we examined the skeletal phenotype of mice carrying one copy of the miR-29 decoy cassette. MicroCT analysis of femurs from 8 week old female mice showed that cortical morphology was significantly altered in miR-29 decoy mice compared with littermate controls. Both endosteal area and perimeter were significantly larger in miR-29 decoy mice (7% increase, $p < 0.01$, $n = 8$), with a trend toward an increase in periosteal area and perimeter ($p = 0.053$ and $p = 0.063$, respectively) in miR-29 decoy mice. Thus, whereas miR-29 decoy mouse bones were larger in diameter, the cortical bone area was not significantly increased. Although trabecular bone volume in the femurs of female miR-29 decoy mice was not altered compared to littermate controls, miR-29 decoy mice had a 60% decrease in bone formation rate ($p = 0.03$, $n = 4$). Unaltered bone volume in the presence of decreased bone formation suggests a decrease in osteoclast number or activity. Investigating the osteoclast potential of bone marrow monocytes from the miR-29 decoy mice in vitro, we found that decoy cells formed 50-70% fewer osteoclasts ($p < 0.01$) compared to controls. miR-29 decoy cells had decreased NFATc1 protein, a transcription factor critical for osteoclastogenesis, and decreased cathepsin K mRNA, indicating decreased osteoclast differentiation and activity. We hypothesize that global inhibition of miR-29 activity decreases bone remodeling,

resulting in relatively mild changes in bone morphology. Whether this decreased remodeling has a significant impact on bone quality will be determined.

Disclosures: *Henry Hrdlicka, None*

FRI-0543

TNAP Deficiency Is the Major Contributor to the Loss of the Mineralization Potential of Trps1 Deficient Osteogenic Cells Sana Khalid*, Byungsoo Chae, Daisy Monier, Mairobys Socorro, Victoria Smethurst, Dobrawa Napierala. Center for Craniofacial Regeneration, Dept. of Oral Biology, McGowan Institute for Regenerative Medicine, University of Pittsburgh School of Dental Medicine, United States

Tissue-Nonspecific Alkaline Phosphatase (TNAP) is critical for mineralization, as evident by hypomineralized skeletal and dental tissues in hypophosphatasia. TNAP is a membrane bound enzyme that generates inorganic phosphate (Pi) by hydrolyzing the mineralization inhibitor pyrophosphate (PPi), and therefore, maintains a Pi/PPi balance conducive for mineralization. Pi is necessary not only for formation of hydroxyapatite, but also acts as a signaling molecule, which regulates osteogenic gene expression. Previous work from our lab demonstrated that 17IIA11 osteogenic cells deficient for the Trps1 transcription factor (Trps1-KD) showed impaired initiation of mineralization in comparison with WT cells. On the molecular level, Trps1-KD cells have significantly decreased expression of several osteogenic genes, including TNAP and, consistently, show reduced TNAP enzymatic activity. We hypothesize that TNAP deficiency in TRPS1-KD cells is the major contributor to the impaired mineralization of these cells. To test our hypothesis, we restored the expression of TNAP in Trps1-KD cells using transposon-mediated genomic integration of a TNAP-expressing construct. We selected 3 clonal cell lines in which TNAP expression was restored to the same level as in WT 17IIA11 cells on the Trps1 deficient background (Trps1-KD;TNAP+ cells) for further analysis. We analyzed the effect of restoring TNAP expression on mineralization, osteogenic gene expression and Pi signaling (as determined by activation of Erk1/2 kinases) employing alizarin red staining, qRT-PCR and Western blot, respectively. Results revealed that restoration of TNAP expression in Trps1 deficient osteogenic cells resulted in increased mineralization. Interestingly, significant upregulation of osteogenic genes Smpd3, Phospho 1, Runx2 and Sp7 (without changing Trps1 expression), and increased Erk1/2 activation in response to elevated exogenous Pi was detected in Trps1-KD;TNAP+ cells in comparison with Trps1-KD. Of note, there was no difference in Pi transporter (Pit1) expression between WT 17IIA11, Trps1-KD and Trps1-KD;TNAP+ cells. On the basis of these results we conclude that impaired mineralization of Trps1 osteogenic cells results mostly from the loss of TNAP expression. Furthermore, our data suggests that TNAP facilitate mineralization not only as a Pi provider but also plays a critical role in expression of osteogenic genes and cellular response to available exogenous Pi.

Disclosures: *Sana Khalid, None*

FRI-0544

Macrophage-secreted Emilin2 Stimulates Chemotaxis and Differentiation in Stromal/Osteoblastic Cells Yukihiko Kohara*, Atsushi Watanabe, Noboru Ogiso, Sunao Takeshita. National Center for Geriatrics and Gerontology, Japan

It was recently reported that in vivo depletion of macrophages resulted in significant reduction in bone formation, suggesting that macrophages have the potential to support bone formation by osteoblasts and contribute to bone metabolism. However, the molecular mechanisms underlying how macrophages stimulate osteogenesis and regulate bone remodeling have not been characterized. In this study, we found that bone marrow macrophage-conditioned medium stimulated chemotaxis in bone marrow stromal ST2 cells. To purify the chemotactic activity from the macrophage-conditioned medium, we performed successive anion-exchange column chromatography by monitoring the chemotactic activity of ST2 cells and identified Emilin2 by LC-MS/MS analysis. Emilin2, a 116 kDa extracellular matrix glycoprotein, is known to regulate cardiac development. Emilin2 mRNA was abundantly expressed in macrophages, but not in the other bone cells. Recombinant Emilin2 protein stimulated chemotaxis in ST2 cells, indicating that macrophages regulate the migration of bone marrow stromal cells through the production of Emilin2. Furthermore, enforced Emilin2 expression in calvaria-derived stromal cells increased calcium deposition, as assessed by Alizarin red staining, and the expression of osteoblast marker genes such as Runx2 and Osteocalcin, as assessed by quantitative RT-PCR. However, increased Emilin2 expression in 3T3-L1 preadipocytes inhibited adipogenesis. These results, taken together, suggest that Emilin2 functions in stromal cells as a mediator of cell fate determination into osteoblasts, while inhibiting the differentiation into adipocytes. Interestingly, the expression of Emilin2 mRNA in macrophages was up-regulated by treatment with IL-4, but not IFN γ and IL-10, which modulate macrophage polarization. IL-4-activated M2a macrophages are known to support tissue repair, including in bone fracture. Therefore, we hypothesize that M2a macrophages regulate bone fracture healing through the production of Emilin2. In fact, Emilin2 expression was transiently up-regulated in repaired tissue after bone injury in 8-week-old male mice. In order to gain insight into the in vivo functions of Emilin2 in bone metabolism, the analysis of Emilin2 knockout mice is now underway.

Disclosures: *Yukihiko Kohara, None*

FRI-0545

Trapidil induces osteogenesis by upregulating the signaling of bone morphogenetic proteins Bongjun Kim*, Hong-Hee Kim, Zang Hee Lee. Department of Cell and Developmental Biology, School of Dentistry, Seoul National University, Republic of Korea

Platelet-derived growth factor receptor (PDGFR) signaling has been shown to inhibit osteogenesis. However, the specific mechanisms by which PDGFR signaling inhibits osteogenic differentiation remain unclear. In the present study, we examined the effect of inhibiting PDGFR with trapidil, a PDGFR antagonist, on osteogenesis *in vitro* and *in vivo*. A rat calvarial defect model was analyzed by micro-computed tomography and histology to determine the pro-osteogenic effect of trapidil *in vivo*. In addition, primary mouse calvarial osteoblast precursors were cultured in osteogenic differentiation medium with trapidil to study the activity and expression of osteogenic markers *in vitro*. We showed that trapidil greatly promoted bone regeneration in a rat calvarial defect model. Further study demonstrated that trapidil induced Smad1/5/9 phosphorylation, MAPK phosphorylation, Runx2 expression, and ALP activity, leading to enhanced osteogenic differentiation *in vitro*. The pro-osteogenic effects of trapidil were inhibited *in vitro* by depletion of ALK3, type I bone morphogenetic protein receptor (BMPR), or treatment with noggin, an antagonist of BMPs. Finally, trapidil showed a synergistic effect with BMP2 on osteogenic differentiation. Trepidil induced BMPR activity through upregulation of BMP signaling, leading to promoted osteogenesis *in vitro* and *in vivo*. Attenuated BMPR activity may be involved in the inhibition of osteogenesis by PDGFR signaling.

Disclosures: **Bongjun Kim**, None

FRI-0546

Regulator of G protein signaling protein 12 is required for osteoblast differentiation through controlling calcium channel/G α i-calcium oscillation-ERK signaling Ziqing Li^{1*}, Tongjun Liu², Alyssa Gilmore², Néstor Más Gómez¹, Claire H Mitchell^{1,3}, Yi-Ping Li⁴, Merry J Oursler⁵, Shuying Yang^{1,2}. ¹Department of Anatomy and Cell Biology, University of Pennsylvania, School of Dental Medicine, United States, ²Department of Oral Biology, School of Dental Medicine, University of Buffalo, State University of New York, United States, ³Department of Physiology, University of Pennsylvania, School of Medicine, United States, ⁴Department of Pathology, University of Alabama in Birmingham, United States, ⁵Department of Medicine, Endocrine Research Unit, Mayo Clinic, United States

Background: Bone homeostasis is intimately relied on the balance between osteoblasts (OBs) and osteoclasts (OCs). Our previous studies revealed that regulator of G protein signaling protein 12 (Rgs12), the largest protein in the Rgs super family, is essential for the terminal differentiation of OCs. However how Rgs12 regulates OB differentiation and function is poorly understood. Methods and materials: OB-targeted Rgs12 conditional knockout (CKO) mice model was generated by crossing Rgs12^{fl/fl} mice with Osterix (Osx)-Cre transgenic mice (Osx; Rgs12^{fl/fl}). Bone architecture changes of 12 weeks old mice were evaluated via micro CT, histology and histomorphometric analyses. For *in vitro* study, OB precursor cells (OPCs) from control mice (Rgs12^{fl/fl}) were transfected with CRE (ad-RGD-Cre) adenovirus, leading a deletion of Rgs12 in OPCs. Molecular events and OB differentiation markers were examined using qPCR, western blot, immunofluorescence and histochemical staining. Calcium (Ca²⁺) oscillation, extracellular Ca²⁺ influx and Ca²⁺ release from endoplasmic reticulum (ER) were detected by live cell imaging. Results: We found that Rgs12 was highly expressed in both OPCs and OBs of Wide Type (WT) mice, and gradually increased during OB differentiation, whereas conditional Rgs12 CKO mice (OSX; Rgs12^{fl/fl}) exhibited a dramatic decrease in cancellous bone mass, evidenced by reduced percentage of trabecular bone volume (BV/TV, 68%), trabecular number (Tb.N, 29%), trabecular thickness (Tb.Th, 81%), bone formation rate (BFR) and increased in trabecular space (Tb.Sp, 340%). Loss of Rgs12 in OPCs *in vitro* significantly inhibited OB differentiation and expression of OB marker genes, resulted in suppression of OB maturation and mineralization. Further, deletion of Rgs12 in OPCs significantly inhibited GTPase activity and impaired Ca²⁺ oscillations via restraints of major Ca²⁺ entry sources (extracellular Ca²⁺ influx and intracellular ER Ca²⁺ release), partially contributed by the blockage of L-type Ca²⁺ channel mediated Ca²⁺ influx. Downstream mediator ERK was also inactive in Rgs12-deficient OPCs, while overexpression of Rgs12 or application of pertussis toxin (PTX) could partially rescue the defective OB differentiation and function via activation of ERK. Conclusion: Our findings reveal that Rgs12 is an important regulator in OB differentiation and function, and highlight Rgs12 as a potential therapeutic target for bone disorders.

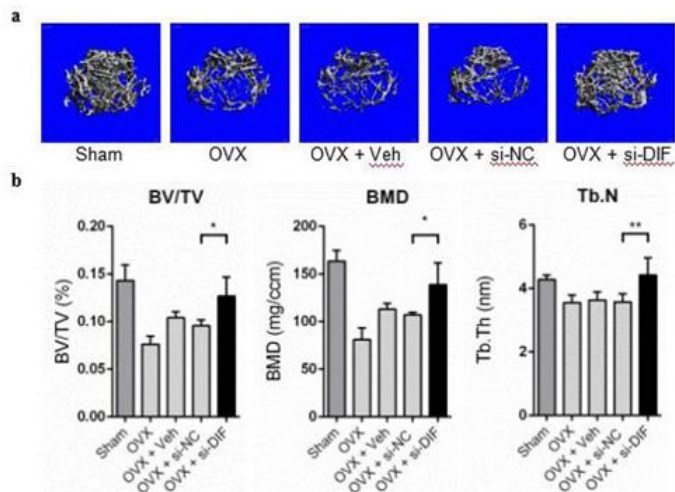
Disclosures: **Ziqing Li**, None

FRI-0547

Lnc-DIF inhibits bone formation via targeting mir-489-3p Zhiping Miao*, Yong Yin, Yan Zhang, Ye Tian, Lifang Hu, Airong Qian. Northwestern Polytechnical University, China

Introduction Long noncoding RNAs (lncRNAs) are a class of transcripts longer than 200 nucleotides. Recently lncRNAs have been focused as important novel regulators for

development, carcinogenesis and osteoporosis. For the purpose of discovering lncRNAs involved in osteogenesis, we initiated characterization of lncRNAs by gene expression profiling analysis. Methods and Results We performed RNA-seq assay on femur tissues from 12 month and 24 month aging C57BL/6 mice. Functional lncRNAs were further screened by correlation analysis to obtain the lncRNAs that were up-regulated by aging and closely related to osteogenesis. We have assessed the expression of lncRNAs in bone-derived mesenchymal stem cells (MSCs) isolated from 12 to 24 month C57BL/6 mice. The expression of Lnc-DIF increased with aging process. Besides, the expression of Lnc-DIF decreased during osteoblastic differentiation processes. We further explored that down-regulation of Lnc-DIF in MC3T3-E1 cell line increased osteogenic gene ALP and RUNX2 expression, ALP activity and calcium nodules. We have found 12 binding sites of mir-489-3p in the sequence of Lnc-DIF through prediction by RNA22. Moreover, luciferase reporter assay proved that Lnc-DIF bond with mir-489-3p. We consistently found that agomir-489-3p increased ALP and RUNX2 expression as well as ALP activity and calcium nodules. For further clarify the mechanism of mir-489-3p, we have predicted its target gene PTPN6 by Gene Coexpression Networks and miranda. Luciferase reporter assay proved that mir-489-3p regulate PTPN6. We have also found the down-regulation of PTPN6 enhanced ALP expression, ALP activity and calcium nodules. To investigate whether the therapeutic inhibition of Lnc-DIF would prevent osteoporosis, we administrated si-Lnc-DIF with osteoblast targeting delivery system in ovariectomy (OVX) C57BL/6 mice model. Micro CT assay have proved that BMD, BV/TV, and Tb.N of OVX mice femurs were all significantly recovered by si-Lnc-DIF treatment. Conclusion In conclusion, we have discovered Lnc-DIF as a novel osteogenic inhibitor. Lnc-DIF inhibits osteoblast differentiation and bone formation through Lnc-DIF - mir-489-3p - PTPN6 pathway. Inhibition of Lnc-DIF recovers bone formation in OVX mice. The finding has revealed a new mechanism of bone formation and provided potential targets for treatment of skeletal disorders.



Disclosures: **Zhiping Miao**, None

FRI-0548

Conditional Deletion of the Glucocorticoid Receptor in Osteoprogenitors Reveals Complex Roles for Glucocorticoid Signaling in Caloric Restriction-Induced Bone Marrow Fat Accumulation Jessica Pierce*, Ke-Hong Ding, Jianrui Xu, Kanglun Yu, Anuj Sharma, Mark Hamrick, William Hill, Xing-Ming Shi, Carlos Isales, Meghan Mcgee-Lawrence. Augusta University, United States

Bone marrow fat storage can be driven by stressors such as aging, inflammation, and increased glucocorticoid (GC) signaling. For example, increased circulation of endogenous GC with age is concurrent with an age-related decline in Hdac3 activity in BMSC-derived osteoblasts, allowing for upregulated GC signaling which may promote marrow fat. GC can induce phenotypic changes by binding and activating the glucocorticoid receptor (GR). Because the metabolic stress of caloric restriction (CR) drives marrow fat accumulation, we sought to test the role of the GR under caloric restriction to further elucidate its role in this model of metabolic stress and determine whether the GR is required for marrow fat storage. Additionally, as sympathetic tone can drive caloric restriction-induced marrow fat storage, we sought to test the role of sympathetic tone as a potential compensatory factor in the response of GR-deficient bone to CR. We hypothesized that blocking sympathetic tone in GR-deficient mice would inhibit the exacerbated marrow adiposity and cortical bone loss induced by CR. GR^{fl/fl} mice were crossed with Osx1-Cre mice to generate GR conditional knockout mice (GR-CKO) and Cre-negative WT controls (6 mo old, n=7 to 8/group) that were subjected to ad libitum (AL), CR (25% reduction), or CR + 0.01% propranolol hydrochloride (administered in drinking water) for 8 weeks. Deletion of the GR within osteoprogenitors protected against osteoblastic lipid accumulation *in vitro* but augmented marrow adiposity *in vivo* (+75% adipocyte density) following caloric restriction. Additionally, DXA analysis (Kubtec Digimus) showed that GR-CKO mice had less femoral cortical bone than GR-WT mice following caloric restriction *in vivo*, while impaired *in vitro* matrix deposition (-81% Alizarin Red fraction) by BMSC-derived osteoblasts isolated from GR-CKO + AL

mice was rescued to GR-WT levels in cells derived from mice subjected to CR. Importantly, GR-CKO mice had decreased femoral cortical bone mass and significantly more marrow fat (+8-fold vs. GR-WT) under ad libitum conditions—with propranolol treatment rescuing bone mineral content but not preventing lipid accumulation induced by CR—indicating a baseline bone phenotype in GR-CKO mice and a potential role for sympathetic tone in rescuing CR-induced bone loss but not marrow adiposity. This work highlights the complex roles of GC signaling in bone health and in the effects of physiological stressors on marrow fat.

Disclosures: **Jessica Pierce**, None

FRI-0549

BAF Chromatin Remodelling Epigenetically Controls Osteogenesis in vivo Tanner Godfrey^{**}, Mohammad Rehan^{*}, Benjamin Wildman, Yuechuan Chen, Quamarul Hassan. University of Alabama at Birmingham, United States

The precise assembly and coordinated function of Brg1 Associated Factors (BAF) complex plays an indispensable role for formation and maintenance of cell-type-specific patterns of accessible DNA, ultimately controlling cellular phenotypic fate. This BAF complex consists of 11 protein subunits encoded by 22 different genes, where different combinations of BAF restrict cell-type specificity. Our lab has identified BAF45a to be a key osteogenic BAF factor required in osteoblasts. Protein-protein interaction studies in vitro established the osteoblast specific BAF composition and in vivo studies show that BAF is a key osteogenic BAF factor required for osteoblastogenesis. We continue to explore the osteoblast specific function of other BAF subunits with the objective to define the osteoblast BAF complex composition and the specific role of different BAF subunits in osteoblasts. The osteoblast-specific BAF complex composition was investigated in differentiating pre-osteoblast cells using anti-BRG1 Immuno-precipitation (IP) mass spectrometry (MS). Osteogenic responsive factors were determined by RT-qPCR following BMP-2 and TGF- β treatment of MC3T3-E1 cells. IP-MS and expression analysis suggest a group of unique and define osteoblast-specific BAF composed of BAF180 (PBRM1), BAF250B and BAF170 interacted with SWI/SNF catalytic subunit BRG1 at day 4 and 14 of differentiation. Treatment with BMP2 resulted in a >2.5 fold increase in Baf45a expression, while TGF- β decreased expression by 50%. BAF45A was found to interact with osteoblast master transcription factor RUNX2 and together regulates osteogenic promoter activity. We developed an osteoblast specific Baf45a knockout model. Osteoblast specific deletion of Baf45a using Osteocalcin-Cre mouse significantly reduced bone volume of the trabecular bone, bone formation rate and bone strength. ChIP experiment was performed to study the epigenetic modification at promoter. Deletion of Baf45a in osteoblasts resulted in drastic decreases in activating histone modification H3K27ac at osteoblast-specific genes. Our data reveal the osteoblastic BAF composition, as well as the osteogenic role of Baf45a. We are in the process of investigating the role of different BAF subunits in the osteoblast development. By understanding these epigenetic mechanisms regulating osteoblasts and bone formation, we hope to uncover potential therapeutic targets to aid the treatment of bone-diseases.

Disclosures: **Tanner Godfrey**^{*}, None

FRI-0550

The N6-methyladenosine demethylase FTO functions in bone to protect osteoblasts from age-related DNA damage Qian Zhang^{*1}, Ryan Riddle¹, Marie-Claude Faugere², Clifford Rosen³, Charles Farber⁴, Thomas Clemens¹. ¹Department of Orthopaedic Surgery, Johns Hopkins University, United States, ²Department of Medicine, University of Kentucky, United States, ³Maine Medical Center, United States, ⁴University of Virginia, United States

The fat mass and obesity-associated gene (FTO) was originally linked to both obesity and bone mineral density in humans by genome wide association studies but its function has remained elusive. FTO encodes a mRNA demethylase that controls mRNA stability via m6Am demethylation of the 5' mRNA cap. To examine the role of FTO in bone, we characterized the phenotype of mice lacking Fto globally (Fto KO) or selectively in osteoblasts (Ftooc-cre^{-/-}). Fto KO mice exhibited reductions in body length and body weight at maturity, and developed age-related reductions in bone volume in both the trabecular and cortical compartments. Ftooc-cre^{-/-} mice developed similar age-related bone deficits with enhanced marrow adiposity but did not exhibit changes in body composition. To explore the mechanism of Fto action in osteoblasts, we examined the impact of Fto loss of function on primary osteoblasts. RNA profiling in osteoblasts following acute disruption of Fto revealed changes in transcripts of genes in the DNA repair pathway including Hsp70, the RNA of which contains a Fto binding motif, and NF- κ B. Fto KO osteoblasts showed increased basal and UV-induced DNA damage as assessed by γ H2AX both in vitro and in vivo. Importantly, inhibition of NF- κ B signaling rescued the phenotype in Fto KO osteoblasts in vitro. These findings suggest that DNA damage in osteoblasts lacking Fto is regulated by Hsp1a-NF κ B signaling. Together, our results indicate that FTO functions intrinsically in the osteoblast to enhance the stability of mRNA products of proteins that function to protect cells from DNA damage.

Disclosures: **Qian Zhang**, None

FRI-0551

Direct reprogramming of mouse fibroblasts into functional osteoblasts by defined factors Hui Zhu^{*1}, Bogdan Conrad², Fan Yang³, Joy Wu¹. ¹Division of Endocrinology, Stanford University School of Medicine, United States, ²Program of Stem Cell Biology and Regenerative Medicine, Stanford University, United States, ³Department of Orthopaedic Surgery, Stanford University School of Medicine, United States

While induced pluripotent stem cells hold promise for skeletal regeneration as a potential source of osteoblasts, the induction of pluripotency followed by directed differentiation into osteoblasts is time-consuming and low yield. In contrast, direct lineage reprogramming without an intervening stem/progenitor cell stage would be a more efficient approach to the generation of osteoblasts. We screened combinations of osteogenic transcription factors and identified a combination of four factors, Runx2, Osx, Dlx5, and ATF4, that rapidly and efficiently reprogram mouse fibroblasts derived from 2.3 kb type I collagen promoter-driven green fluorescent protein (Col2.3GFP) transgenic mice into induced osteoblast cells (iOB). iOB cells exhibit osteoblast morphology, form mineralized nodules, and express both Col2.3GFP and gene markers of osteoblast differentiation. The global transcriptome profiles of iOB cells are similar to primary osteoblasts. Genome-wide DNA methylation analysis demonstrated that within differentially methylated gene loci, the methylation status of iOB cells more closely resembles primary osteoblasts than mouse fibroblasts. We further demonstrate that GFP+ iOBs have transcriptome profiles similar to GFP+ cells harvested from Col2.3GFP mouse bone chips. Functionally, iOBs contribute to bone healing after transplantation into immunodeficient mice in a critical-sized cranial defect model. These findings provide a robust and reliable system to derive osteoblasts for skeletal regeneration.

Disclosures: **Hui Zhu**, None

FRI-0596

Cell Autonomous Sfrp4-Dependent Inhibition of Non-Canonical Wnt Signaling in Osteoclasts Prevents Osteoclastogenesis, Ensuring Normal Cortical Bone Development Kun Chen^{*1}, Pei Ying Ng¹, Dorothy Hu¹, Roland Baron^{1,2}, Francesca Gori¹. ¹Division of Bone and Mineral Research, Harvard Medical School and Harvard School of Dental Medicine, United States, ²Endocrine Unit, Massachusetts General Hospital, United States

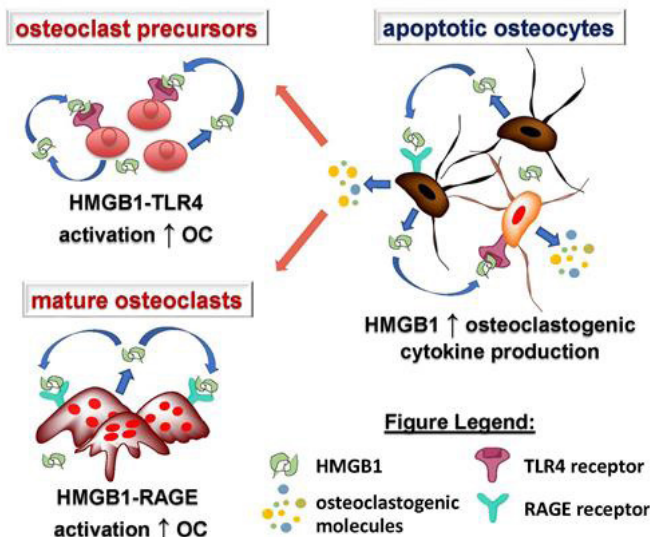
Pyle Disease is a rare skeletal disorder caused by loss of function mutations in the Wnt inhibitor Secreted Frizzled Receptor Protein 4 (Sfrp4). In cortical bone, Sfrp4 is a key regulator of periosteal bone formation and endosteal bone remodeling. The increase in Rankl/Opg ratio and number of endosteal osteoclasts (OCs) in Sfrp4^{-/-} mice, indicate that Sfrp4-mediated signals are involved in osteoblast (OB)-dependent regulation of OC differentiation. We however found that Sfrp4 is also expressed by bone marrow macrophages (BMMs) and its expression increases during Rankl-induced OCgenesis, suggesting that Sfrp4 may be secreted by OCs and regulate OCgenesis in a cell autonomous manner. To test this hypothesis, we explored the mechanisms whereby Sfrp4 and its interference with Wnt signaling regulate OCs. OC differentiation and function were significantly enhanced in Sfrp4^{-/-} BMMs, as indicated by the increase in TRAP+ multinucleated cells, pit assay and OC-specific gene expression. Confirming these findings, Sfrp4-treated wt BMMs were significantly inhibited in their ability to respond to Rankl-induced OC differentiation. Moreover, mix-and-matched co-culture assays demonstrated that Sfrp4 deletion in both OBs or BMMs favors OCgenesis. It is established that while canonical Wnt (cWnt)/Lrp5/6 signaling suppresses OCgenesis, activation of the non-cWnt/Ror2/Jnk cascade is a potent activator of OC differentiation. As expected Sfrp4 deletion resulted in an increase in both cWnt and non-cWnt/Ror2/Jnk signaling in Rankl-induced BMM differentiation. Pharmacological inhibition of cWnt signaling had no effect on the Sfrp4 deficiency-dependent increase in OCgenesis. In contrast, blocking the Ror2/Jnk cascade markedly inhibited OCgenesis. Similarly, while in vitro excision of Lrp5/6 did not alter the effect of Sfrp4 on OCgenesis, in vitro excision of Ror2 significantly impaired it. All together these data reveal a new mechanism whereby combined cell-autonomous effects of Sfrp4 and effects from OB-secreted Sfrp4 regulate OCgenesis. These results are consistent with a paradigm in which the increase in OCs in Sfrp4^{-/-} mice is a consequence of non-cWnt signaling activation overriding the negative effect that activation of cWnt signaling has on OCgenesis. Since deregulated endosteal bone remodeling is a determinant for cortical thickness and porosity, these studies might have implications for the generation of novel therapeutic approaches for the treatment of bone fragility.

Disclosures: **Kun Chen**, None

FRI-0597

Autocrine actions of high mobility group box1 protein (HMGB1) on osteocytes and osteoclasts regulate osteoclastogenesis Hannah M. Davis^{*1,2}, Sinai Valdez¹, Leland J. Gomez¹, Angela Bruzzaniti^{1,2,3}, Lilian I. Plotkin^{1,2,4}. ¹Department of Anatomy & Cell Biology, Indiana University School of Medicine, United States, ²Indiana Center for Musculoskeletal Health, United States, ³Biomedical and Applied Sciences, Indiana University School of Dentistry, United States, ⁴Roudebush Veterans Administration Medical Center, United States

Old age and Cx43 deletion in osteocytes (Ot) increase Ot apoptosis and osteoclastogenesis. Further, prevention of apoptosis in Cx43-deficient MLO-Y4 cells (Cx43def) blocks Oc differentiation induced by Cx43def conditioned media (CM), and blocks the release of the cytokine high mobility group box1 protein (HMGB1) from Cx43def Ot. Inhibition of HMGB1, in turn, lowers RANKL in Cx43def Ot, raising the possibility that HMGB1 mediates osteoclastogenesis induced by apoptotic Ot. We now report that addition of a neutralizing HMGB1 antibody (Ab) to bone marrow cells (BMC) treated with RANKL/MCSF reduces Oc formation. The role of RAGE or TLR4, two HMGB1 receptors, on osteoclastogenesis was tested by adding 1nM HMGB1 plus 100ng/ml RAGE (Azeliragon, Az) or TLR4 (LPS-RS) inhibitors. HMGB1 added during d1-3 increases Oc number, and LPS-RS, but not Az blocks this effect. HMGB1 added during d1-5 or d3-5 did not alter Oc number. Further, while Az or LPS-RS alone during d1-5 did not affect Oc, the combination of both inhibitors decreased Oc number. Moreover, RAGE but not TLR4 inhibition in mature Oc (d3-5) reduced Oc number. This suggests that HMGB1 produced by Oc has autocrine effects on differentiation through TLR4 activation in pre-OCs, followed by RAGE activation. We next tested if RAGE mediates the effects of apoptotic Ot on Oc. Co-culturing Cx43def Ot with WT or RAGE-KO BMC increased Oc number 2 and 4X, respectively vs Cx43+ Ot. Further, Cx43def CM induced 1.6X more Oc than CM from Cx43+ Ot, with or without Az. Similar to Cx43def CM, more Oc were obtained when CM from Ot-enriched long bone cultures of old (21mo) vs young (4mo) mice was added to BMC; an effect that was lost when bones were pre-treated with DEVD, an apoptosis inhibitor. Further, addition of CM from old bones to BMC from WT or RAGE-KO mice increased Oc by 1.3 and 1.7X, respectively, vs young bone CM. Taken together, our findings suggest that apoptotic Ot increase Oc independent of HMGB1/RAGE activation in Oc. Consistent with this, immunodepletion of HMGB1 from Cx43def CM does not prevent Oc formation. However, treatment of Cx43def Ot with HMGB1 Ab followed by HMGB1 immunodepletion, reduced Oc differentiation induced by Cx43def CM, suggesting that autocrine HMGB1 actions stimulate the release of osteoclastogenic signals from Ot. We conclude that HMGB1 exerts dual effects on bone cells, directly promoting Oc differentiation via RAGE and TLR4 activation in Oc and increasing pro-Oc cytokine release from Ot.



Disclosures: *Hannah M. Davis, None*

FRI-0598

EOMES is a novel and essential co-partner of PU.1 and MITF in regulating osteoclast differentiation Blake E. Hildreth Iii^{*1}, Heather A. Carey², Devadoss J. Samuvel¹, Katie A. Thies¹, Jennifer A. Geisler², Thomas J. Rosol³, Ramiro E. Toribio³, Julia F. Charles⁴, Michael C. Ostrowski¹, Sudarshana M. Sharma¹. ¹Medical University of South Carolina Department of Biochemistry and Molecular Biology and Hollings Cancer Center, United States, ²Ohio State University Department of Cancer Biology and Genetics and Comprehensive Cancer Center, United States, ³Ohio State University College of Veterinary Medicine, United States, ⁴Brigham and Women's Hospital and Harvard Medical School Department of Medicine, Division of Rheumatology, Immunology and Allergy, United States

Osteoclasts (OCs) differentiate from myeloid precursors (MPs) and are essential for bone remodeling. Multiple transcription factors (TFs) expressed in MPs and OCs are essential for this process, including PU.1 and MITF. We have shown that PU.1 and MITF physically interact and regulate the transcription of multiple genes essential for OC differentiation and function. However, the full extent of TFs involved, and their hierarchical architecture and interplay, are not well known. Therefore, our goal was to further define the TF network regulating OC differentiation. Functional genomics analysis of OC ChIP-Seq data revealed PU.1/MITF peaks were enriched for the T-box TF EOMES, including many TF loci regulating OC differentiation. ChIP-Seq of EOMES from murine trophoblasts indicated significant overlap with PU.1 at gene loci. Conventional ChIP in MPs and OCs confirmed that EOMES is directly recruited to key PU.1- and MITF-bound TF loci essential for OC differentiation, including Nfatc1 and cFos. Subsequent co-IP demonstrated that EOMES interacts with both PU.1 and MITF. We then evaluated the effects of myeloid-specific deletion of EOMES (EomesΔMP/ΔMP) on OC differentiation and function. EomesΔMP/ΔMP mice had increased bone mass as shown by μCT. Most notably, there was a significant increase in 1) BV/TV and Tb.V/TV in the distal femoral metaphysis; 2) Ct.Th in the distal femoral metaphysis and diaphysis and 3) cumulative BMD. While there was a trend towards an increase in Tb.N (P = 0.065) in EomesΔMP/ΔMP mice, Tb.Sp was significantly reduced. Histomorphometry revealed significantly reduced Oc.N/BS and Oc.S/BS in EomesΔMP/ΔMP mice. EomesΔMP/ΔMP OCs had significantly lower expression of the osteoclastogenic TFs Nfatc1, Fosl2, Prdm1, Jun-B, and Myc, with a significant increase in Ppar-gamma expression. In addition, EomesΔMP/ΔMP OCs had significantly lower expression of the OC marker genes Acp5, Ctsk, Calcr, and Oscar. These findings indicate that 1) MP-specific deletion of EOMES decreases OC differentiation and function and 2) EOMES binds with PU.1 and MITF in both MPs and OCs to TF loci essential for OC differentiation and function. In summary, we have determined that a novel PU.1/MITF binding partner, EOMES, also possess functionality in cells of the OC lineage, of which it is essential for OC differentiation. This is the first evidence of EOMES having a functional role in any cell of the myeloid lineage, and more specifically, OC differentiation.

Disclosures: *Blake E. Hildreth Iii, None*

FRI-0599

RANKL-Sensitive Super-Enhancer Activities Determine Cell Identity During Osteoclastogenesis Min Joon Lee^{*1}, Sungho Park², Keunsoo Kang⁴, Jiyoung Ahn³, Ye-Ji Lee³, Sehwan Mun³, Seyeon Bae³, Kaichi Kaneko³, Kyung-Hyun Park-Min². ¹University of Toronto Faculty of Medicine, Canada, ²Arthritis and Tissue Degeneration Program, David Z. Rosensweig Genomics Research Center, Hospital for Special Surgery, United States, ³Arthritis and Tissue Degeneration Program, Hospital for Special Surgery, United States, ⁴Department of Microbiology, Dankook University, Republic of Korea

Homeostatic osteoclastogenesis from progenitor cells requires precise coordination of cell-type- and site-specific gene expression. Despite substantial advance in the identification of osteoclast master regulators, developing therapeutic interventions for pathologic osteoclasts (e.g. in rheumatoid arthritis, RA) has been challenging due to off-target effects. Targeting tissue-specific and diseases-specific enhancers, a regulatory code located in distal elements, has recently emerged as a new therapeutic potential. Osteoclast-specific transcription is highly organized and is proposed to be driven by enhancers. However, the osteoclast-specific enhancer program is poorly understood and its role in osteoclastogenesis remains unclear. In this study, we profiled enhancers in human osteoclasts by combining bioinformatics and transcriptomics approaches using ChIP-, ATAC-, and RNA-sequencing, and validated the pathophysiological importance of our findings in RA patients. We treated human osteoclast precursors with RANKL for 1 or 3 days, and found that RANKL dynamically regulates super-enhancers, which are large regulatory regions of enhancers previously reported to control cell identity in other cell types. We further identified a new class of RNAs transcribed from super-enhancers (SE-RNAs) in human osteoclasts by integrated analysis of RANKL-regulated transcriptome with osteoclast-specific super-enhancers. These SE-RNAs were associated with the transcription of several key genes important for osteoclastogenesis. Among them, Osteoline, a RANKL-inducible SE-RNA, was found to promote osteoclastogenesis by regulating RANKL-induced NFATc1 gene expression. Knock-down of Osteoline by siRNA suppressed human osteoclastogenesis. Strikingly, we found that Osteoline is only expressed in osteoclasts and not in other cell types. Synovial CD14+ cells isolated from RA patients had significantly elevated Osteoline expression, while those from control CD14+ cells had low, undetectable baseline expression. To the best of our knowledge, our finding

provides the first example of enhancers and super-enhancers in human osteoclasts and highlights the importance of RANKL-induced epigenetic regulation in human osteoclastogenesis. Our results show that RANKL-regulated RNAs transcribed from super-enhancers play an important role in osteoclastogenesis and suggest that manipulating SE-RNAs may offer a novel, cell-specific therapeutic strategy for treating osteoclast-mediated bone diseases.

Disclosures: *Min Joon Lee, None*

FRI-0600

IDH2 is a novel regulator of osteoclast differentiation and function through osteoblastic modulation of ATF-NFATc1-RANKL signaling axis Suk-Hee Lee*, Seung-Hoon Lee, Soon-Young Kim, Eun-Hye Lee, Yeon-Ju Lee, Jung-Eun Kim. Department of Molecular Medicine, CMRI, BK21 Plus KNU Biomedical Convergence Program, School of Medicine, Kyungpook National University, Republic of Korea

Mitochondrial NADP⁺-dependent isocitrate dehydrogenase (IDH2) is an evolutionarily conserved protein that regulates mitochondrial redox balance and energy metabolism via generation of NADPH and α -ketoglutarate, respectively. IDH2 deficiency promotes the mitochondrial dysfunction in multiple cell types and various organs including heart, kidney, and brain. However, the function of IDH2 in bone tissue has not been studied. Here, we investigated the role of IDH2 in bone formation and remodeling using mice with targeted disruption of IDH2. MicroCT demonstrated that the femur of IDH2^{-/-} mice exhibited a 39% (p<0.05) increase in trabecular BV/TV due to a significant increase in Tb.Th and Tb.N and a decrease in Tb.Sp compared to that of wild-type mice. In parallel, a significant reduction of osteoclast number/bone surface was observed in both of vertebrae and long bones from the IDH2-deficient mice, whereas there was no significant change of osteoblast number/bone perimeter between two genotypes. Serological analysis revealed that CTX-1, the marker of osteoclast activity and bone resorption, was reduced in IDH2^{-/-} mice. The RANKL expression level in whole bone marrow from IDH2-deficient mice was decreased in comparison with that of wild-type mice. The RANKL/OPG ratio due to low RANKL was also significantly diminished in the serum of IDH2^{-/-} mice. To investigate the inhibitory effect of IDH2 on the osteoclast differentiation and the associated underlying mechanism of action, bone marrow stromal cells (BMSC) and osteoclast progenitors isolated from IDH2^{-/-} and wild-type mice were used. RANKL gene expression in primary BMSC was significantly decreased at the early stage of IDH2-deficient osteoblast differentiation. Consistent with these findings, the treatment of the serum derived from IDH2-deficient mice remarkably lowered the differentiation capacity of bone marrow-derived osteoclast progenitors. This inactivation of IDH2 was linked to reduced RANKL expression through the ATF4/NFATc1-dependent manner in BMSC, partly via a mitochondrial ATP generation. In the present study, we showed that mice targeted disruption of IDH2 exhibit high bone mass associated with down-regulation of RANKL expression which leads to the inhibition of osteoclast differentiation and bone resorption. Our findings suggest that IDH2 may be a novel positive regulator of osteoclast function and provide a rational of IDH2 as a therapeutic target against bone loss and osteoporosis.

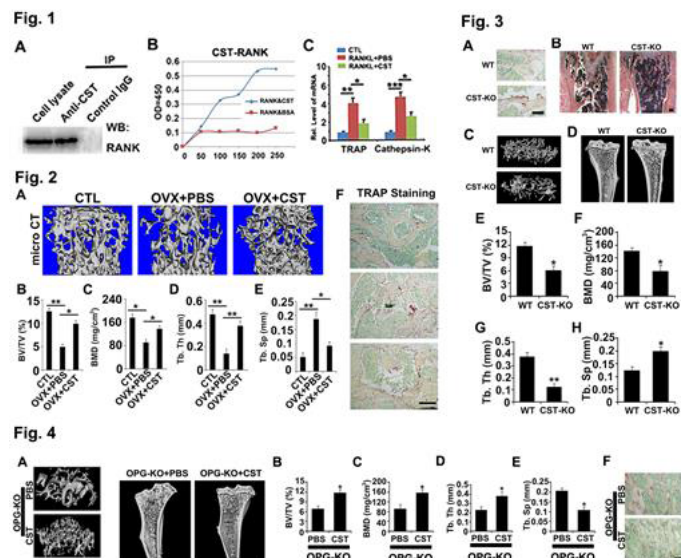
Disclosures: *Suk-Hee Lee, None*

FRI-0601

Cortistatin Directly Binds to RANK and Protects Against Osteoporosis in Mice Weiwei Li^{1*}, Ruize Qu², Xiaomin Chen², Wenhan Wang², John Hayball³, Krasimir Vasilev³, Yunpeng Zhao¹. ¹Shandong University Qilu Hospital, China, ²Shandong University, China, ³University of South Australia, Australia

INTRODUCTION: It is known that RANKL/RANKL signaling pathway plays a critical role in development of osteoporosis[1]. A neuropeptide, cortistatin (CST), is recently reported to be associated with bone metabolism. However, whether CST plays a role in osteoporosis is still unknown.**METHODS:** CST knockout mice (CST^{-/-} of C57BL/6 strain), OPG^{-/-} mice (C57BL/6 strain), micro CT, BMDM, OVX model, CST recombinant protein, co-immunoprecipitation (Co-IP), Solid phase binding assay, Western blot, real time PCR, Histology, immunohistochemistry, unpaired t-tests (Mann-Whitney), paired t-tests, ANOVA.**RESULTS SECTION:** The interaction between CST and RANK was implied by Co-IP (Fig. 1A) and solid phase binding assay (Fig. 1B). BMDM was isolated from WT mice, and RANKL mediated production of osteoclast-associated genes were attenuated by CST (Fig. 1C). Moreover, OVX model was established in WT mice, with or without treatment of 20 μ g CST (twice a week). At 8-week time point, micro CT of vertebra (Fig. 2A) and the parameters, including BV/TV, BMD, Tb.Th and Tb.Sp (Fig. 2B-2E) showed that CST inhibited osteoporosis in OVX model, which was in line with TRAP staining of vertebral body (Fig. 2F). Furthermore, age associated osteoporosis was compared between 10-month old female CST^{-/-} mice and WT mice (N=7 for each group). As a result, loss of CST exaggerated bone loss in tibia, as indicated by TRAP staining (Fig. 3A) and HE staining (Fig. 3B). Micro CT assay (Fig. 3C-3D) as well as its associated statistical analysis of parameters revealed more severe bone loss in CST^{-/-} mice (Fig. 3E-3H). In addition, 2-month old OPG^{-/-} mice were treated with 20 μ g CST (twice a week) for 2 months. As indicated by micro CT image (Fig. 4A), BV/TV, BMD, Tb.Th and Tb.Sp (Fig. 4B-4E), osteoporosis in OPG^{-/-} mice was suppressed by CST treatment. TRAP staining revealed that osteoclast activity in OPG^{-/-} mice was diminished by exogenous CST (Fig. 4F). The values are the mean \pm SD. *p<0.05, **p<0.01 and *** p<0.005 vs. control group.**DISCUSSION:** These results reveal CST as a potential antagonist for osteoporosis through suppressing RANK/RANKL signaling. More

experiments are required to testify the specific mechanisms involved in this process.**SIGNIFICANCE/CLINICAL RELEVANCE:** CST may shed light on treatment of osteoporosis in the future. **REFERENCES:** [1] Luo J, et al, Nature Medicine, 2016



Disclosures: *Weiwei Li, None*

FRI-0602

Hdac3 promotes bone robustness by suppressing osteoclast responsiveness to RANKL and enhancing bone formation Anna Mattson¹, David Molstad¹, Dana Begun¹, Jennifer Westendorf², Merry Jo Oursler¹, Meghan McGeel-Lawrence², Bradley Elizabeth¹. ¹Mayo Clinic, United States, ²Augusta University, United States

Hdac3 is a lysine deacetylase and functions to remove acetyl groups from histones and additional nuclear proteins. HDAC3 levels decline in human bone samples from old as compared to young women; thus, when bone mass decreases with age in humans HDAC3 levels are suppressed. To determine if Hdac3 levels impact osteoclast differentiation and bone resorption, we conditionally deleted Hdac3 in mature osteoclasts by crossing Hdac3^{fl/fl} mice with Ctsk-Cre expressing mice. Hdac3 cKOtsk mice exhibit reduced femoral and tibial bone robustness (bone width relative to length) and increased cortical periosteal osteoclast number and osteoclast size. Trabecular bone volume fraction, bone mineral density, trabecular number and connective density are suppressed with a corresponding increase in trabecular spacing in Hdac3 cKOtsk mice. Hdac3 suppression in mature osteoclasts also reduced healing in a cortical bone defect model. We previously showed that Hdac3 deacetylates the p65 subunit of the NF κ B transcriptional complex to increase DNA binding and transcriptional activity. We hypothesized that elevated NF κ B transcriptional activity of Hdac3 deficient osteoclasts would enhance RANKL signaling. Hdac3 deficient osteoclasts demonstrate increased K310 NF κ B acetylation and NF κ B transcriptional activity. Two downstream transcriptional targets of RANKL-induced activity, NFATc1 and the p65 NF κ B gene locus itself, are likewise elevated in Hdac3 deficient osteoclasts. Hdac3 deficient osteoclasts were hyper-responsive to RANKL and showed elevated osteoclast number and size at all concentrations. Toluidine blue staining of dentin disks cultured with Hdac3 deficient cells was increased by 60%. Osteoclast-specific Hdac3 deficiency decreases cortical and trabecular bone parameters, suggesting that Hdac3 regulates coupling of bone resorption and bone formation. We surveyed a panel of osteoclast-derived coupling factors and found that suppression of Hdac3 diminished S1P production. Osteoclast-derived S1P acts in paracrine to promote bone mineralization. Alizarin red staining of wildtype bone marrow stromal cells cultured with conditioned medium from Hdac3 deficient osteoclasts was markedly reduced. Expression of Alkaline phosphatase, Type Collagen 1a1 and Osteocalcin was also suppressed, but no change in Runx2 expression was observed. Our results demonstrate that Hdac3 controls bone robustness by suppressing osteoclast responsiveness to RANKL and coupling to bone formation.

Disclosures: *Anna Mattson, None*

FRI-0603

Collagen Type VI $\alpha 2$ Chain Deficiency Causes Trabecular Bone Loss by Promoting Osteoclast Differentiation through Enhanced TNF α Signaling Hai Pham^{*}1, Annin Dar¹, Vardit Kram², Li Li¹, Tina Kilts¹, Marian Young¹. ¹Craniofacial and Skeletal Diseases Branch, National Institute of Dental and Craniofacial Research, National Institutes of Health, United States, ²Collagen Type VI $\alpha 2$ Chain Deficiency Causes Trabecular Bone Loss by Promoting Osteoclast Differentiation through Enhanced TNF α Signaling, United States

Collagen type VI monomers are composed of three α -chains ($\alpha 1$, $\alpha 2$, $\alpha 3$) that align in a triple helix that assembles into larger fibrils found in many musculoskeletal tissues. Collagen type VI is widely known for its role in muscular disorders, however its function in bone is still not well understood. Using immunohistochemistry, we examined the expression of collagen type VI during fracture healing, and found that it was enhanced in the callus of healing bone. We further examined all three collagen type VI chains by qPCR and found Col6a2 mRNA highly upregulated at day 14 post-fracture, suggesting it could have a role in bone remodeling. To determine the role of collagen type VI $\alpha 2$ in bone function we analyzed bone mineral density of femora and whole mice's body by DEXA and found it significantly reduced in mice deficient in collagen type VI $\alpha 2$ (Col6a2 KO). Further micro CT analysis of both femora and vertebrae showed significant decreases in bone volume/total volume and trabecular number in Col6a2 KO mice compared to wild-types (WT). To try to understand the cellular basis for the decreased bone mass, we performed double labeling assays by calcein injections, and found no difference in trabecular bone formation between WT and Col6a2 KO mice judged by the mineral appositional rate, bone formation rate, and mineralizing perimeter. This experiment indicated that collagen type VI $\alpha 2$ deficiency does not affect bone formation *in vivo*. When we examined femora sections for the abundance of TRAP positive osteoclasts we discovered that mutant mice exhibited 2.4 times more osteoclasts compared to WT mice, indicating that the primary effect of collagen type VI $\alpha 2$ is on osteoclastogenesis. Since TNF α is well known to promote osteoclastogenesis, we hypothesized that TNF α may be involved in collagen type VI $\alpha 2$ regulation of osteoclastogenesis. To test this, solid phase binding assays were performed and showed specific binding of collagen type VI $\alpha 2$ to TNF α . When we treated bone marrow stromal cells (BMSCs) from WT and Col6a2 KO mice with rmTNF α protein, we found that Col6a2 KO cells expressed higher levels of TNF α mRNA compared to WT cells, suggesting BMSCs from Col6a2 KO mice are highly sensitive to TNF α signaling. Taken together, our data indicate that collagen type VI $\alpha 2$ chain deficiency causes trabecular bone loss by enhancing osteoclast differentiation through enhanced TNF α signaling.

Disclosures: Hai Pham, None

FRI-0604

Dual specificity of the Inpp4b phosphatase in bone remodeling Lina Saad^{*}, Monica Pata, Jean Vacher. IRCM, Canada

Bone remodeling relies on a strict balance between bone formation by the osteoblast and bone resorption by the osteoclast. The differentiation and activation mechanisms of these cells are regulated by multiple signaling cascades including the PI3kinase pathway. Upon external stimulation, phosphatidylinositol kinases and phosphatases are activated and produce short-lived phospholipids second messengers essential in intracellular signaling for cell growth, survival and activation. We isolated and characterized the mouse homologue of the human and rat inositol polyphosphate 4-phosphatase b (Inpp4b) that is highly expressed in osteoclast and to a lower extent in osteoblasts. To gain insight into the role of Inpp4b in bone remodeling, we produced a null allele of Inpp4b. The systemic Inpp4b ablation resulted in an increase in osteoclast number and activity leading to low bone mass and osteoporosis. Inpp4b^{-/-} mice also display an increase in mature osteoblast population resulting in enhancement of bone mineral apposition rate. However, a complete understanding of these regulatory mechanisms was missing. Among several osteoclast signaling cascades responding to RANKL stimulation and upstream of Nfatc1, only the PKC β pathway was modulated in absence of Inpp4b. We show that Inpp4b regulates bone marrow cells differentiation toward mature osteoclasts through the PKC β /GSK-3 β /Nfatc1 pathway and similarly, the PKC β /GSK-3 β -catenin pathway was modulated along Inpp4b^{-/-} osteoblast differentiation. Importantly, pharmacologic inhibition of PKC β in Inpp4b^{-/-} cells results in a significant reduction of NFATc1 gene expression that was associated with a decrease in the level of GSK-3 β inactive phosphorylated form. In addition, co-IP experiments suggest that Inpp4b can interact directly with the phosphorylated forms of PKC β and GSK-3 β . These results provide evidence that the lipid phosphatase Inpp4b is an active protein phosphatase that can modulate PKC β and GSK-3 β protein kinase activities during osteoclast and osteoblast differentiation to control bone remodeling.

Disclosures: Lina Saad, None

FRI-0605

An Unanticipated Role for Sphingosine Kinase-2 in Bone Anabolism Joanne Walker^{*}, Gang-Qing Yao, Meiling Zhu, Ben-Hua Sun, Christine Simpson, Karl Insoigna. Yale University School of Medicine, United States

Release of clastokines may be one mechanism by which osteoclasts modulate bone remodeling. Sphingosine-1-phosphate (S-1-P) is a clastokine with important bone anabolic

functions. Increased S-1-P production by osteoclasts results in increased bone formation *in vivo* (JCI 123:666; Nat. Comm. 5:5215). *In vitro*, S-1-P augments osteoblast differentiation and function. SPHK is the rate-limiting enzyme in S-1-P production and has two isoforms. SPHK1 is a cytoplasmic enzyme that generates S-1-P at the cell membrane for export. SPHK2 is localized to the endoplasmic reticulum, the nucleus, and mitochondria and is thought to generate S-1-P for intracellular actions. To evaluate the roles of SPHK1 and SPHK2 in bone, we examined the skeletal phenotype of mice with selective deletion of SPHK1 in osteoclasts (SPHK1-Oc^{-/-}) mice and mice in which the SPHK2 gene was deleted (SPHK2^{-/-}). Selective deletion of SPHK1 in osteoclasts was accomplished by crossing SPHK1^{fllox}/flox mice with Cathepsin K-Cre⁺ mice and back-crossing these animals to SPHK1^{fllox}/flox mice to yield animals with the genotype SPHK1^{fllox}/flox-CtskCre⁺ /-. BMD by μ CT was quantified at 12-weeks of age in 16 SPHK1-Oc^{-/-} (9F, 7M) and 12 controls (9F, 3M). There were no differences in any of the trabecular or cortical parameters based on genotype or in serum CTx. By contrast SPHK2^{-/-} female mice had a 14% lower spinal BMD ($p < 0.002$) and males a 22% lower BMD at the same site ($p < 0.001$; Fig 1). Trabecular number was reduced in the both male ($p = 0.0004$) and female animals ($p = 0.0002$) and trabecular spacing increased (M: $p = 0.002$; F: $p = 0.0006$). If generation of osteoclast-derived S-1-P is part of the anabolic program in bone entrained by single daily dose PTH, then limiting production of S-1-P should attenuate that anabolic response. SPHK2^{-/-} animals (8 F, 8 M) were treated either with daily (1-34)PTH 80 ng/kg/d or vehicle for 28 days. Wild type controls (8 F, 9 M) were treated in the same manner. At 28 days femoral trabecular BMD increased by 133% in female controls and by 38% in male controls. In SPHK2^{-/-} males, femoral trabecular bone only increased by 7% and in the females by only 54%. In the spine, control females had a 27% increase and the males a 29% increase in BMD while in the SPHK2^{-/-} animals the values were 39% and 17% respectively in the female and male animals. Based on our data we conclude that SPHK2 has an important role in mediating both normal bone remodeling and the anabolic response to PTH.

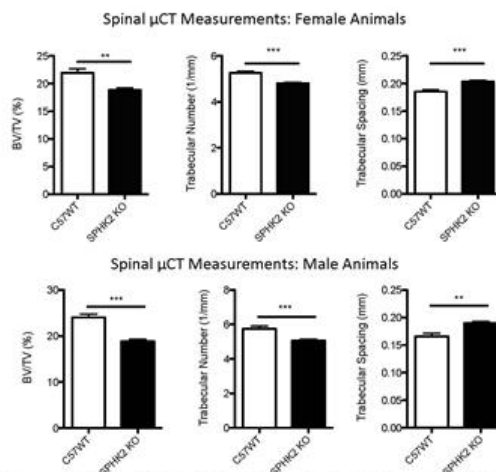


Figure 1. BMD by μ CT was quantified at 12-weeks of age in SPHK2^{-/-} mice. Female and male mice had a low spinal BMD ($p < 0.002$) and ($p < 0.001$), respectively. Trabecular number was reduced in both male ($p = 0.0004$) and female animals ($p = 0.0002$) and trabecular spacing increased (M: $p = 0.002$; F: $p = 0.0006$).

Disclosures: Joanne Walker, None

FRI-0655

Osteocyte Sirt6 has crucial roles in bone and phosphate metabolism Aikebaier Aobulikasimu^{*}1, Zulipiya Aibibula¹, Jinying Piao¹, Shingo Sato², Hiroki Ochi², Kunikazu Tsuji³, Atsushi Okawa¹, Yoshinori Asou¹. ¹Department of Orthopedics Surgery, Tokyo Medical and Dental University, 1-5-45 Yushima Bunkyo-Ku Tokyo Japan, 113-8519, Japan, ²Department of Physiology and Cell Biology, Tokyo Medical and Dental University, 1-5-45 Yushima Bunkyo-Ku Tokyo Japan, 113-8519, Japan, ³Department of Cartilage Regeneration, Tokyo Medical and Dental University, 1-5-45 Yushima Bunkyo-Ku Tokyo Japan, 113-8519, Japan

Aging is a pivotal risk factor for osteoporosis in association with declined activity of vitamin D. FGF23 reduces serum phosphate levels by repressing intestinal phosphate absorption through downregulating 1,25-dihydroxyvitamin D and proximal tubular phosphate resorption. The stress-response and chromatin-silencing factor Sir2, a yeast sirtuin, is a NAD⁺-dependent histone deacetylase. In mammals the sirtuin family contains seven genes encoding sirtuin proteins. Among them, Sirt6 is localized to the nucleus and is involved in transcriptional silencing, genome stability, and longevity. Sirt6 is implicated in the regulation of life span and ageing. We have shown Sirt6 plays roles in the maintenance of the articular cartilage. However, the precise role of Sirt6 in bone metabolism is poorly understood. Here we aimed to examine the role of Sirt6, a mammalian homologue of Sir2, in the osteocyte by analyzing mice lacking Sirt6 in DMP1 expressing cells (DMP1^{Cre}:Sirt6^{f/f} mice;CKO). Mice grew normally and the body weight was not affected by Sirt6 deletion in osteocytes. Five months old male and female CKO have lower trabecular bone volume compared with the control mice both in the femur and the lumbar spine. Serum osteocalcin, a bone formation marker, was decreased in CKO, whereas urine CTX-1, a bone resorption marker, was in-

creased in CKO. Bone histomorphometry analysis indicated MAR and BFR were decreased in CKO. TRAP staining indicated osteoclast number and osteoclast surface were increased in CKO. To elucidate the target of Sirt6 in the osteocyte, qPCR analysis of the cortex bone was employed. As we previously found Sirt6 deficiency enhanced expression of PAI-1, a cell senescence marker, in the chondrocytes, mRNA level of PAI-1 was evaluated with several factors expressed in osteocytes. The results indicated mRNA expression of SOST, FGF23 and PAI-1 was increased in cortical bone of CKO. increased FGF23 levels was associated with reduced phosphate concentration in CKO and also in Sirt6 null mice. Elevated FGF23 in association with reduced phosphate were ameliorated when Sirt6 null mice were crossed with PAI-1 null mice (Sirt6^{-/-}:PAI-1^{-/-} mice). In cultured osteocyte -link MLO-Y4 cells, SOST and PAI-1 were increased by Sirt6 knock down using siRNA. These results indicated Sirt6 regulate bone and phosphate metabolism through, at least in a part, regulation of SOST and FGF23 in osteocytes.

Disclosures: Aikebaier Aobulikasimu, None

FRI-0656

PPAR α is a negative regulator of sclerostin production in osteocytes Amit Chougule*, Lance Stechschulte, Beata Lecka-Czernik. University of Toledo, United States

The nuclear receptor PPAR α is a major regulator of energy production and lipid metabolism, and a pharmacologic target to treat dyslipidemia. Mice deficient in PPAR α are metabolically impaired in response to fasting and high-fat diet, however PPAR α role in maintenance of bone mass has not been studied in details. We have showed that sclerostin protein is under negative control of PPAR α . PPAR α global KO mice (α KO) have larger long bone cavity and thinner cortex, as compared to WT animals. Loss of PPAR α results in decreased bone formation and decreased number of osteoblasts (OB), and increased bone resorption accompanied with increased number of osteoclasts (OC), along with an increase in marrow fat volume (MFV). We analyzed endosteal OB and cortical osteocytes (OT) freshly isolated from femora of WT and α KO mice. OT from α KO have 5-fold increased expression of Sost, while OB have decreased expression of Wnt10b, Wnt16 and CyclinD. Increased Rankl expression in OT correlates with a significant increase in OC, thinner trabeculae and thinner cortex in α KO mice. Consistently, there is 2-fold increase in sclerostin protein levels in α KO femur. Conditioned media (CM) collected from primary cultures of α KO OT have significantly higher sclerostin levels as compared to CM from WT OT. In co-cultures, α KO CM increased expressions of adipogenic markers aP2, CD36 and LPL in recipient WT marrow mesenchymal stem cells (MSC). Depleting sclerostin from α KO CM, decreased adipogenic markers in recipient MSCs, and increased Wnt signaling markers, Wnt10b and Axin2, in MSCs committed to OB lineage. We have identified a PPAR α -specific PPRE sequence (α PPRE) in the Sost promoter located -1.8 kb upstream from the transcription start site. ChIP assay confirmed that PPAR α binds to this α PPRE in basal conditions, and this binding is increased following activation of PPAR α with WY14643 agonist, while it is decreased in the presence of GW6471 antagonist, and is absent when α PPRE is mutated. Increased PPAR α binding correlated with a decreased promoter activity of Sost and its mRNA expression. The effect of OT-specific PPAR α deficiency on bone and energy metabolism is currently tested in 8kb Dmp1CrePPAR α fl/fl mice. In summary, PPAR α acts as a negative regulator of sclerostin expression in OT, which in α KO mice results in decreased bone formation and increased resorption, and increase in MFV. These findings position PPAR α as a pharmacological target controlling sclerostin expression in OT.

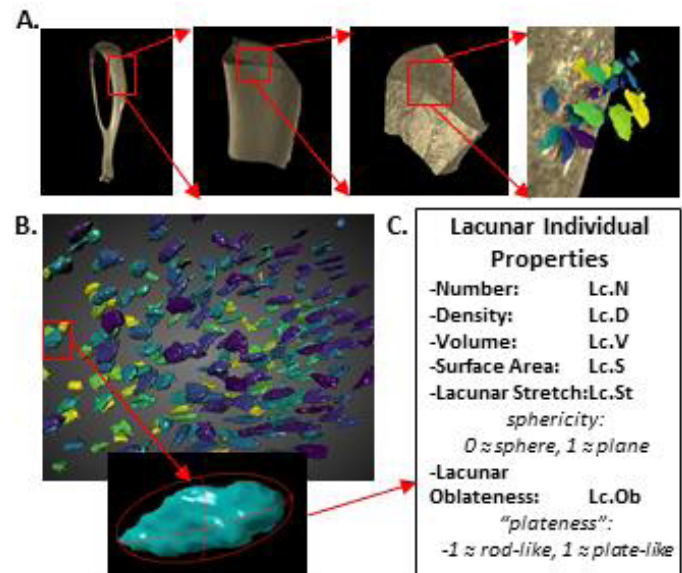
Disclosures: Amit Chougule, None

FRI-0657

Microgravity exposure in growing mice is detrimental to osteocyte lacunar volume and shape Jennifer C. Coulombe^{*1}, Zachary K. Mullen², Ashton M. Weins², Louis S. Stodieck³, Virginia L. Ferguson¹. ¹Department of Mechanical Engineering, University of Colorado, Boulder CO, United States, ²Department of Applied Mathematics, University of Colorado, Boulder CO, United States, ³BioServe Space Technologies, University of Colorado, Boulder, CO, United States

Osteocytes, the primary strain-sensing cell type within bone, perform osteolysis and undergo apoptosis with disuse which may lead to bone fragility in astronauts. Yet the effects of microgravity on osteocyte lacunar morphology and network organization are unknown. This study seeks to evaluate how individual and networks characteristics of osteocyte lacunae are altered by microgravity in regions of tensile and compressive strain in mouse cortical long bone. Female C57Bl/6N, skeletally immature 9 week old mice, n=4/group, were assigned to ground control (GC) and flight (FL; 12.8 days of microgravity, Space Shuttle Endeavour STS-118 mission). GC mice were housed in identical conditions. Tibiae were harvested and matched volumes were scanned with high resolution X-Ray microscopy (XRM; 0.6 μ m voxels, Zeiss, Xradia 520) at 3 mm proximal to the tibiofibular junction. Anterior medial (tensile) and posterior lateral (compressive) regions assessed for influence of in vivo strain. Osteocyte lacunae were evaluated using DragonFly Pro. Osteocyte network characteristics, individual lacunar morphometry, and kriging models of local correlation (i.e., comparing individual measures lacunae to those of their neighbors) were analyzed in R. Two-way ANOVA and Tukey's HSD assessed data for effects of microgravity and strain; significance reported for p < 0.05. Under normal gravity, lacunar volumes were significantly greater in tensile (305.96 \pm 20.1 μ m³) as compared to compressive regions (245.98 \pm 26.17

μ m³). Lacunar stretch₂, Lc.St, and Oblateness₂, Lc.Ob, were also greater in tensile (0.77 \pm 0.01, 0.58 \pm 0.03) than in compressive regions (0.79 \pm 0.01, 0.61 \pm 0.03). Overall, lacunae under compressive strain had -19.6% volume, +3.44% Lc.St and +5.49% Lc.Ob. FL mice showed only -3.1% difference in volume, -0.5% Lc.St, -7.1% Lc.Ob. Kriging demonstrated that lacunar measures were similar to those of neighboring lacunae within each compressive and tensile region. Osteocyte networks remain the same despite exposure to microgravity and strain region. Osteocyte lacunar morphologies undergo shape and volume changes after exposure to microgravity in a strain-dependent manner. These differences in individual lacunae are consistent with those observed in aging³, and may be predictive of diminished osteocyte sensitivity to strain and diminished bone formation⁴. Citations: 1) Patel, TK et al., J. Biomech, 2013 2) Mader, KS et al., Bone, 2013 3) Heveran, CH et al., Bone, 2018 4) Holguin, N et al., J Bone Miner Res, 2016



Disclosures: Jennifer C. Coulombe, None

FRI-0658

Sex divergent role of osteocytic miR21 in the maintenance of osteocyte viability and regulation of bone turnover Hannah M. Davis^{*1,2}, Rafael Pacheco-Costa^{1,2}, Mohammad W. Aref^{1,2}, Alyson L. Essex¹, Emily G. Atkinson^{1,2}, Julian E. Dilley¹, Carmen Herrera¹, Padmini Deosthale^{1,2}, Mircea Ivan³, Matthew R. Allen^{1,2,4}, Teresita M. Bellido^{1,2,4}, Lilian I. Plotkin^{1,2,4}. ¹Department of Anatomy & Cell Biology, Indiana University School of Medicine, United States, ²Indiana Center for Musculoskeletal Health, United States, ³Department of Hematology/Oncology, Indiana University School of Medicine, United States, ⁴Roudebush Veterans Administration Medical Center, United States

The microRNA miR21 regulates bone metabolism by acting directly on osteoblasts (Ob) and osteoclasts (Oc); but its role in osteocytes (Ot) is not completely known. Ot miR21 expression is low in bones from old female mice; and low miR21 levels increase Ot apoptosis. Because Ot apoptosis triggers osteoclastogenesis, we investigated whether Ot miR21 removal increases Oc formation. Surprisingly, high Ot apoptosis in 4-mo female miR21f/f;8kbDMP1-Cre mice with miR21 deletion in Ot (miR21 Δ ot) was accompanied by low bone resorption (and formation) compared to miR21f/f littermates. We now report that Ot miR21 deletion has sex-divergent effects in bone and that the disconnect between Ot apoptosis and Oc number also occurs in 4-mo male miR21 Δ ot (n=12) vs miR21f/f (n=12) mice. However, unlike females, male miR21 Δ ot mice had reduced expression of apoptosis-associated genes (CHOP, Foxo3 and p27) and trends towards lower apoptotic Ot numbers vs miR21f/f mice. Further, Ot miR21 removal had sex-specific effects on femur cortical bone, with lower endocortical turnover in female but higher in male miR21 Δ ot mice (89% more endosteal Oc and 42% higher periosteal BFR). Consistent with these cellular effects, females had no change in bone mass/geometry, whereas miR21 Δ ot males had higher total, spinal and femoral BMD; and increased femoral cortical [10% marrow cavity area, 4% thickness, and 11% MMI] and trabecular [32% BV/TV, 10% thickness, and 20% number] architecture vs miR21f/f mice. To further examine the mechanisms underlying the sex-specific Oc effect of Ot miR21 removal, we generated Oc from wildtype bone marrow cells (BMC) cultured with conditioned media (CM) from Ot-enriched miR21 Δ ot and control bone cultures. Consistent with our in vivo results, addition of CM from miR21 Δ ot females and males led to 0.7-fold less and 3.8-fold more Oc, respectively; independently of whether female or male BMC were used. Further, we found sex-specific changes in Ot-enriched bone lysates with ~60% lower pro-osteoclastogenic cytokines IL6, MCP1, and MCSF mRNA in miR21 Δ ot females, whereas IL1 β and its target DKK1, an Ob inhibitor, were ~80% lower only in miR21 Δ ot males. Collectively, our findings suggest that miR21 exerts a sex-divergent role in Ot, regulating bone mass and architecture through non-cell autonomous effects on Ob and Oc.

Further, we reveal a potential mechanism by which miR21 removal from Ot differentially alters bone turnover by sex-specific regulation of Ot cytokine production.

Disclosures: *Hannah M. Davis, None*

FRI-0659

Osteocyte Density and Viability in Postmenopausal Women after Long-term Bisphosphonate Therapy Shijing Qiu*, George Divine, Mahalakshi Honasoge, Arti Bhan, Shiri Levy, Elizabeth Warner, Sudhaker D Rao. Henry Ford Hospital, United States

Our previous study indicated that short-term (1 year) bisphosphonate (BP) treatment did not affect osteocyte viability in postmenopausal women, but the effect of long-term BP treatment on osteocytes remains unclear. Iliac bone biopsies were obtained from 80 age-matched white postmenopausal women (43 normal volunteers and 37 BP treated patients). The duration of BP exposure was 2 – 17y (median: 7y). Five µm Goldner & trichrome stained sections were used to measure trabecular bone osteocyte density [Ot.Dn (/mm²)], empty lacunar density [EL.Dn (/mm²)], total lacunar density [(TL.Dn (/mm²)), and percent empty lacunae [EL.Dn/TL.Dn (%)]. The difference in each osteocyte-related variable was compared between the 2 groups. As shown in the Table, Ot.Dn was significantly lower in patients with BP treatment than in normal women. In contrast, EL.Dn in BP treated patients was >3 times higher than in the normal women. The extremely increased EL.Dn in BP treated patients resulted in a 4 times higher EL.Dn/TL.Dn ratio. There was also a significant 14% reduction in TL.Dn in the BP treated group. There was no significant correlation between the duration of BP exposure and any osteocyte-related variable. In conclusion, we found that osteocyte viability is dramatically reduced after long-term BP treatment. The significant decrease in total lacunar density and a very high empty lacunar density suggest that part of empty lacunae resulting from osteocyte death are obliterated by mineralized tissue. Combined with our previous work, we postulate that the loss of osteocytes after long-term BP treatment is not due to BP toxicity but rather caused by prolonged and sustained inhibition of bone remodeling. Accumulation of unremodeled old bone characterized by low osteocyte density and hypermineralization will increase bone fragility.

Table 1. Difference in osteocyte-related variables between normal postmenopausal women and BP treated patients

	Normal (n = 43)	BP treated (n =37)	p
Age	64.6 (4.13)	65.7 (4.29)	NS
Ot.Dn	188 (24.2)	119 (31.4)	<0.001
EL.Dn	17.5 (6.52)	58.2 (16.2)	<0.001
TL.Dn	206 (24.1)	177 (30.3)	<0.001
EL.Dn/TL.Dn	8.57 (3.13)	33.3 (10.1)	<0.001

Disclosures: *Shijing Qiu, None*

FRI-0680

Normative Data for Trabecular Bone Score in Men and Women Kara Anderson*, Kara Holloway-Kew, Mark Kotowicz, Natalie Hyde, Julie Pasco. Deakin University, Australia

Purpose Trabecular bone score (TBS) is a novel tool for indirectly assessing trabecular microarchitecture at the lumbar spine, providing information complementary to areal BMD. However, limited reference ranges exist for TBS, particularly in men. The aim of this study was to develop such reference ranges for Australian men and women. Methods This study included 910 men and 780 women (aged 24-98yr) enrolled in the Geelong Osteoporosis Study. TBS was determined by retrospective analysis of lumbar spine DXA scans (Lunar Prodigy) using TBS iNsight software (Version 2.2). Multivariable regression techniques were used to determine best-fit models for TBS incorporating age, height and weight. T-score based classifications were used to assess differences in fracture risk between TBS and BMD using attribute agreement analysis, with partially degraded microarchitecture defined as TBS T-scores of -1.0 to -2.5, and degraded microarchitecture as T-scores below -2.5. Similarly, BMD T-scores of -1.0 to -2.5 indicated osteopenia and T-scores below -2.5 indicated osteoporosis. Results Mean TBS decreases with age in both sexes (Table). Age-related differences in TBS were best modelled with a linear relationship in men (R²=21.5%, p<0.001) and a cubic relationship in women (R²=25.4%, p<0.001). Best models for TBS included linear age and weight in men, and cubic age and linear height in women. The attribute agreement analysis found that 56.2% (95%CI 52.9-59.4) of the men and 55.9% (95%CI 52.2-59.5) of the women had agreements in T-score based classifications of lumbar spine BMD and TBS, meaning that almost half of the men and women were discordant for TBS and BMD categories. Of those considered to have normal lumbar spine BMD, 39.2% of men and 38.5% of women had partially degraded or degraded microarchitecture on the basis of TBS. Conclusion This study provides normative data for TBS in Australian men and women.

Table Mean trabecular bone score in men and women per age decade, given as mean±SD.

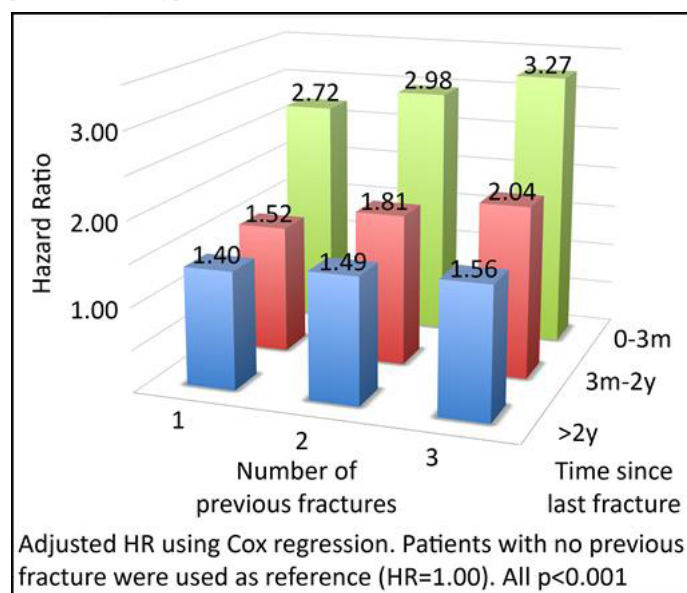
Age (years)	Men (n=910)	Women (n=780)
20-29	1.362±0.113	1.412±0.090
30-39	1.324±0.137	1.397±0.102
40-49	1.289±0.113	1.366±0.124
50-59	1.259±0.127	1.286±0.153
60-69	1.180±0.152	1.243±0.136
70-79	1.149±0.141	1.207±0.136
80+	1.138±0.144	1.180±0.152

Disclosures: *Kara Anderson, None*

FRI-0681

Time since fracture and number of previous fractures are independently associated with risk of new clinical fracture Kristian Axelsson*¹, Dan Lundh², Mattias Lorentzon¹. ¹Department of Geriatrics, Sahlgrenska Academy, Gothenburg University, Sweden, ²School of Bioscience, University of Skovde, Sweden

Background Previous fracture is one of the most important predictors of future fracture. However, previous fracture (yes/no) does not take into account number of fractures and the imminent fracture risk seen during the time period just following a previous fracture. The purpose of this study was to investigate if time since fracture and number of previous fractures are independently associated with risk of new fracture. Methods A total of 429 313 patients (mean age 80.8 (SD 8.2), 58% women, 32% with a previous fracture) were included when visiting a healthcare facility in Sweden during 2008-2014. Patients with previous fracture were divided in three groups depending on number of previous fractures (1, 2, 3 or more) and three groups depending on time since last fracture (0-3 months, 3-24 months, 2 years or more). Each of the nine groups was compared to patients without previous fracture. During a median follow-up time of 1.3 years (IQR 0.6-2.3 years), the risk of any fracture was investigated using a Cox regression model adjusted for several known clinical risk factors (age, sex, weight, height, osteoporosis diagnosis, secondary osteoporosis, rheumatoid arthritis, alcohol related diseases and previous glucocorticoid treatment (≥ 5 mg/day, ≥ 3 months)). To investigate if time since last fracture and number of previous fractures were independently associated with risk of new fracture, a Cox regression model was used. Results Among patients without previous fracture, the number of incident fractures was 18550 (6.4%). Patients with one previous fracture more than 2 years ago had 5527 (9.7%) incident fractures which corresponded to a 1.4 times increased fracture risk (Hazard Ratio (HR) 1.40 (95% CI 1.36-1.44), p<0.001) in an adjusted Cox model compared to patients with no previous fracture, whereas patients with three or more previous fractures and the last fracture within three months had 1111 (22.6%) incident fractures corresponding to a 3.3 times increased fracture risk (HR 3.27 (95% CI 3.06-3.48), p<0.001). Adjusted HR for all the nine groups are presented in Figure 1. Both time since fracture and number of fractures significantly predicted any clinical fracture when used simultaneously in an adjusted Cox model. Conclusions We conclude that time since last fracture and number of fractures are independent predictors of new fracture, indicating that the use of these risk variables could improve fracture risk prediction in existing prediction calculators.



Disclosures: *Kristian Axelsson, None*

FRI-0682

Development of Thresholds for Assessing Radius and Tibia Fragility Fracture Risk Using HR-pQCT – The CaMos Cohort Syed Jafri^{*1}, Lauren Burt², Leigh Gabel², David Hanley³, Steven Boyd². ¹University of Calgary, Canada, ²McCaig Institute for Bone and Joint Health, Department of Radiology, Cumming School of Medicine, University of Calgary, Calgary, Canada, ³McCaig Institute for Bone and Joint Health, Departments of Community Health Sciences and Oncology, Cumming School of Medicine, University of Calgary, Calgary, Canada

Fracture risk assessment tools are important for clinicians to identify patients at risk of fragility fractures. Current densitometry tools do not incorporate bone microarchitecture obtained from 3D imaging devices, which can be leveraged to provide estimates of bone strength using finite element analysis (FEA). Development of thresholds from bone microarchitecture and FEA measures may provide a novel approach to utilizing new high resolution peripheral quantitative computed tomography (HR-pQCT) technology to assess fracture risk. We aimed to develop thresholds that correspond to low bone density (formally known as osteopenia) and osteoporosis using FEA measures based on patient-specific microarchitecture. We then validated our thresholds using fracture data from the Calgary Canadian Multicentre Osteoporosis Study (CaMos). We estimated failure load (N) at the distal radius and tibia by solving FEA models based on HR-pQCT. DXA was assessed to acquire hip aBMD and derive T-scores. Scans were obtained from 866 participants in the Calgary CaMos cohort. A linear regression modeled aBMD-derived T-scores as a function of failure load. Predicted FEA failure load values at -1 and -2.5 T-score cut-offs were used to define thresholds for ranges relevant to low bone density and osteoporosis, respectively. We assessed classification accuracy of our predicted fracture risk thresholds using data from 35 individuals in CaMos who sustained fragility fractures. For women, our model predicted low bone density thresholds at the radius ($\leq 1600\text{N}$) and tibia ($\leq 4800\text{N}$) and osteoporosis thresholds at the radius ($\leq 700\text{N}$) and tibia ($\leq 2800\text{N}$). Predicted thresholds were consistently higher in men, with low bone density thresholds at the radius ($\leq 2000\text{N}$) and tibia ($\leq 5700\text{N}$) and osteoporosis thresholds at the radius ($\leq 800\text{N}$) and tibia ($\leq 3400\text{N}$). Fracture data from our cohort identifies the efficacy of these thresholds to single out individuals at high-risk of fracture (data not shown). These thresholds are the first proposed for interpreting FEA-based failure load estimates from HR-pQCT at the distal radius and tibia. Our future work will validate the use of these thresholds for assessing radius and tibia fragility fracture risk in other cohorts.

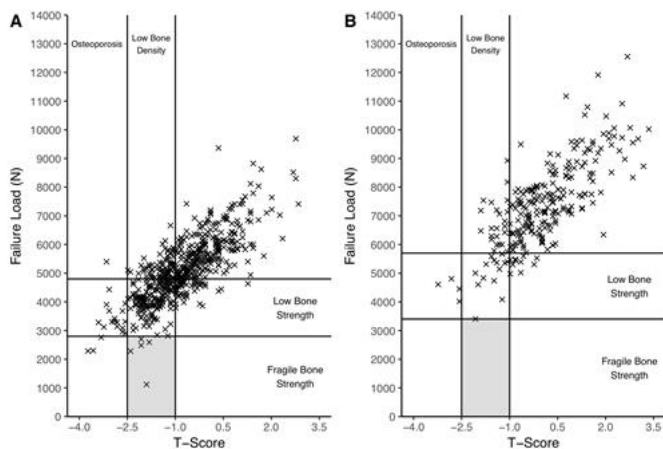


Figure 1. Correlations between measures of hip T-score assessed and tibia failure load for (A) women and (B) men.

Disclosures: Syed Jafri, None

FRI-0683

Automated Identification of Vertebral Compression Fractures Using Artificial Intelligence Convolutional Neural Networks Predicts Incident Non-vertebral and Hip Fracture: The Manitoba BMD Registry Sheldon Derkatch^{*1}, Christopher Kirby², Douglas Kimelman², Mohammad Jafari Jozani¹, J Michael Davidson¹, William Leslie¹. ¹University of Manitoba, Canada, ²St-Boniface Hospital Albrechtsen Research Centre, Canada

Purpose: Detection of vertebral compression fractures aids in future fracture risk assessment and targeting of fracture prevention therapies. Vertebral fracture (VF) recognition can be challenging due to a wide spectrum of appearances and non-fracture deformities. Vertebral fracture assessment (VFA) performed at the time of DXA is often performed by non-radiologists with limited imaging expertise. Aim: To determine if convolutional neural networks (CNNs) can be trained to identify clinically relevant VFs on VFA. Methods: Routine clinical VFA images 2010-2017 from the Manitoba Bone Density Program (GE Lunar Prodigy and iDXA, N=12742) reported by experienced imagers as VF present/absent fol-

lowing the algorithm-based qualitative (ABQ) method were used for CNN training. Criteria for VFA were T-score ≤ -1.5 and (a) age ≥ 70 years; or (b) age ≥ 50 years plus historical height loss >5 cm, measured height loss >2.5 cm, or chronic systemic glucocorticoid therapy. Scans were randomly divided into independent training (60%), validation (10%) and test (30%) sets. The training and validation sets were used to discover effective CNN architectures and training hyperparameters. The best architectures (Inception-ResNetV2 and DenseNet) were then trained on the pooled training and validation sets using the optimized training hyperparameters, and fracture probability predictions were generated using these finalized CNNs as an ensemble. The independent test population (N=3822) was then used to assess CNN concordance with the human "gold standard", and prediction of incident non-vertebral and hip fractures in the subset with linkage to population-based administrative data (N=2813, mean follow up 2.8 years). Results: The CNN ensemble demonstrated AUC 0.94 (95% CI 0.93-0.95) for VF detection in the test data (continuous output, range 0-1); sensitivity 87.4%, specificity 88.4%, accuracy 88.3%, prevalence-adjusted, bias-adjusted kappa 0.77 (dichotomized output, cutoff 0.5). Performance was similarly high for scanner generations, sex, age, body size, and T-score category. "Heatmaps" of regional significance to the CNNs showed strong fracture localization capability. CNN and human detected VF were similarly predictive of any non-vertebral fracture and hip fracture, before and after adjustment for baseline risk (FRAX probability with BMD) (Table). Conclusions: CNNs can identify VFs on VFA images with high accuracy. VFs detected by CNNs in turn predict clinical fracture outcomes.

Table. Hazard ratios (HR) with 95% confidence intervals (CI) for incident fracture in 2813 subjects.

	Model 1: Unadjusted	Model 2: Adjusted for FRAX with BMD
Outcome: Any non-vertebral fracture (N=137) *	HR (95% CI)	HR (95% CI)
Fracture vs No fracture, CNN	2.03 (1.53-2.70)	1.73 (1.29-2.31)
Fracture vs No fracture, Human	2.12 (1.56-2.88)	1.81 (1.33-2.48)
Outcome: Hip Fracture (N=68)	HR (95% CI)	HR (95% CI)
Fracture vs No fracture, CNN	2.76 (1.71-4.46)	1.97 (1.20-3.21)
Fracture vs No fracture, Human	3.08 (1.88-5.07)	2.29 (1.38-3.80)

Data from Cox proportional hazards models. * excludes head/neck, hands/feet, ankle.

Disclosures: Sheldon Derkatch, None

FRI-0684

Clinical Performance of a Beta Version of Trabecular Bone Score (TBS) Including Thickness-based Correction for Soft Tissue Effects: The Manitoba BMD Cohort William D. Leslie^{*1}, Enisa Shevroja², Lisa M. Lix¹, Didier Hans². ¹Department of Medicine (W.D.L.), University of Manitoba, Canada, ²Center of Bone Diseases, DAL-RHU - Lausanne University Hospital, Switzerland

Introduction: Lumbar spine TBS is a texture measurement computed from DXA scans that predicts osteoporotic fractures independently of BMD. The amount of soft tissue in the abdomen impacts the signal to noise ratio and hence has an effect on TBS measurement. To address this, the current software (TBS iNspire®) includes a correction that relies on body mass index (BMI). This correction may be improved by using soft tissue thickness directly estimated by the DXA machine which should be a better indicator of patient morphology. Aim: To test a new TBS calculation based on a correction that relies directly on soft tissue thickness (TBS_{th}) and compare its performance for fracture prediction with the current TBS algorithm (TBSv3). Methods: From a clinical registry of all DXA results for Manitoba, Canada, we identified women and men age >40 years with baseline spine DXA (GE Prodigy) from 1999-2011. Spine TBS were measured using TBSv3 and a beta version (non-calibrated) of the TBS_{th} algorithms by researchers at the University of Lausanne blinded to clinical outcomes. Incident major osteoporotic fractures (MOFs) and hip fractures (HFs) were obtained from population-based health services data. Fracture prediction was estimated from area under the ROC curve (AUC), and comparisons were made (i.e., ΔAUC) using the DeLong method for correlated measures. All analyses were sex-stratified. Results (cf table): 3,827 men (mean age 61.4 years, BMI 26.6 kg/m²) and 34,905 women (mean age 63.3 years, BMI 26.1 kg/m²) met inclusion criteria. TBSv3 exhibited a negative correlation with BMI for both men ($r = -0.04$) and women ($r = -0.02$) while TBS_{th} was now positively correlated ($r = 0.21$ for men, $r = 0.23$ for women), consistent with expectations. Reversals in correlations (from negative to positive) were observed for tissue thickness and abdominal fat percent in both sexes. During a mean follow up of 7.7 years in men, there were 317 incident MOFs and 89 HFs; during 8.9 years in women there were 3,338 incident MOFs and 1,052 HFs. Improvements in fracture prediction were seen with the new TBS algorithm in both men (ΔAUC for MOFs +0.05, $p < 0.001$; HFs +0.03, p NS) and women (ΔAUC for MOFs +0.03, $p < 0.001$; HFs +0.04 $p < 0.001$). Conclusion: The new TBS_{th} algorithm including thickness-based correction for soft tissue effects: (1) is positively associated with BMI (negatively before), and (2) improves fracture prediction in both men and women compared to the current algorithm.

Comparison of clinical performance for current (TBSv3) vs. new TBS (TBS1h)

	Men (n=3827)	Women (n=34,905)
Fracture prediction	AUC (95%CI)	AUC (95%CI)
MOF: L1-L4 TBSv3	0.58[0.54-0.61]	0.63[0.62-0.64]
MOF: L1-L4 TBS1h	0.63[0.59-0.66]*	0.66[0.65-0.67]*
Hip: L1-L4 TBSv3	0.62[0.56-0.68]	0.67[0.65-0.69]
HF: L1-L4 TBS1h	0.65[0.59-0.70]	0.71[0.70-0.73]*

*p<0.001 for TBSv3 vs TBS1h. MOF, Major osteoporotic fracture. HF, hip fracture.

Disclosures: William D. Leslie, None

FRI-0685

Usefulness of the Trabecular Bone Score in dialysis patients Oliver Malle*, Astrid Fahrleitner-Pammer. Medical University of Graz, Dpt. of Internal Medicine, Div. of Endocrinology and Diabetology, Austria

Introduction: The number of patients on dialysis is steadily increasing. Associated comorbidities include cardiovascular diseases and an impaired mineral and bone metabolism leading to a higher fracture possibility, increased morbidity and mortality rate and decreased quality of life. Representing the structural condition of the bone microarchitecture dual-energy X-ray absorptiometry (DXA) is often used in combination with Trabecular Bone Score (TBS) to assess metabolic bone disorders. The aim of this study was to evaluate the clinical relevance of DXA and TBS with regard to fracture prediction in dialysis patients. **Methods:** 82 patients, who underwent dialysis at the university hospital of Graz, were included. All patients were interviewed for prevalent fractures and musculoskeletal pain. Statistical analysis was performed to correlate the results of DXA and TBS with musculoskeletal pain and fracture rate considering the kind and duration of dialysis as well as the number of kidney transplantations. **Results:** 36 out of 82 patients (43.9%) patients suffered from musculoskeletal pain and 32 out of 82 patients (39%) had a positive history of fracture. There was a significant linkage between dialysis duration and fracture rate (p<0.05) as well as musculoskeletal pain (p<0.01). No significant correlation between the DXA- and TBS-parameters and musculoskeletal pain could be established. DXA scores did not correlate with fracture history with the exception of DXA radius measurements. However, a high fracture rate in patients on dialysis significantly correlates with a low TBS (p < 0,001). **Conclusion:** DXA has a limited role in fracture prediction in patients on dialysis. However, the TBS seems to be a better predictor regarding the fracture risk in this patient population.

Osteodensitometry

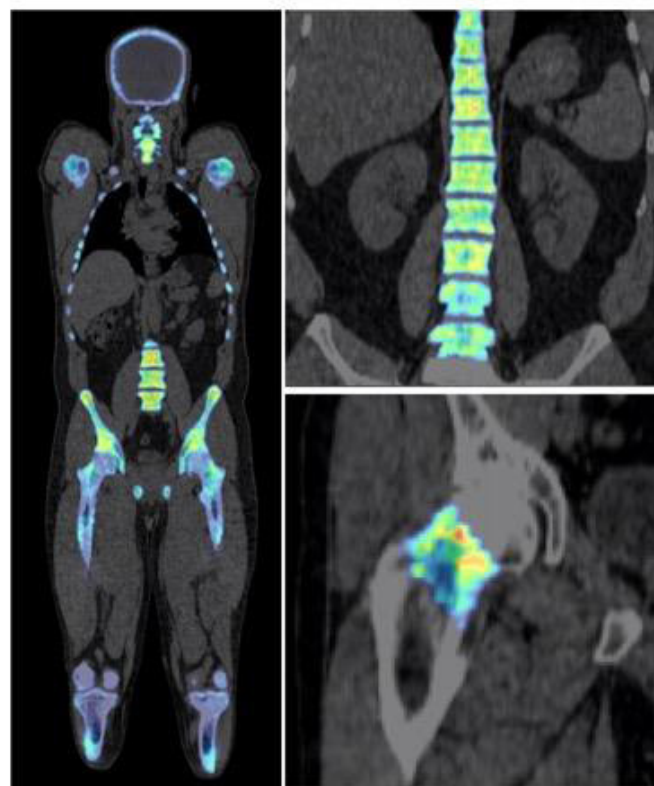
	Patients with history of fracture (n=32)	Patients without history of fracture (n=50)	p-value
L1-L4			
BMD(g/cm ²)	0.877 ± 0.140	0.913 ± 0.176	p=0.69
T-score	-2.0 ± 1.49	-1.86 ± 1.47	p=0.8
Z-score	-1.36 ± 1.22	-1.16 ± 1.16	p=0.47
Femur neck			
BMD(g/cm ²)	0.791 ± 0.127	0.784 ± 0.156	p=0.85
T-score	-1.96 ± 1.12	-2.06 ± 1.14	p=0.67
Z-score	-1.13 ± 0.9	-1.32 ± 1.04	p=0.3
Femur total			
BMD(g/cm ²)	0.801 ± 0.115	0.809 ± 0.147	p=0.85
T-score	-1.85 ± 1.15	-2.03 ± 1.16	p=0.42
Z-score	-1.77 ± 2.47	-1.37 ± 1.12	p=0.71
Radius ultradistal			
BMD(g/cm ²)	0.376 ± 0.096	0.402 ± 0.091	p=0.21
T-score	-3.03 ± 1.81	-2.31 ± 1.74	p=0.08
Z-score	-2.14 ± 2.03	1.61 ± -1.98	p=0.38
Radius 33%			
BMD(g/cm ²)	0.714 ± 0.141	0.781 ± 0.141	p=0.04
T-score	-2.42 ± 1.3	-1.78 ± 1.28	p=0.04
Z-score	-1.74 ± 1.11	-1.13 ± 1.31	p=0.05
Radius total			
BMD(g/cm ²)	0.537 ± 0.105	0.592 ± 0.117	p=0.04
T-score	-2.82 ± 1.5	-2.05 ± 1.54	p=0.04
Z-score	-2.06 ± 1.42	-1.42 ± 1.57	p=0.08
TBS	1.081 ± 0.088	1.174 ± 0.119	p<0.001

Disclosures: Oliver Malle, None

FRI-0686

Assessment of Age Related Changes in Bone Metabolism Using 18F-Sodium Fluoride PET/CT Sylvia Rhodes*, Alexandra Batzdorf, Austin Alexih, Jonathan Guntin, Matthew Peng, Amanda Jankelovits, Justin Kim, Julia Hornyak, Poul Flemming, Abass Alavi, Chamith Rajapakse. University of Pennsylvania, United States

Objectives Integrated Positron Emission Tomography (PET)/Computerized Tomography (CT) imaging with the use of 18F-sodium fluoride (NaF), a hybrid of functional and structural imaging, has the potential for detecting early metabolic changes in bone even in the absence of detectable structural changes [1]. The objective of this study was to investigate the feasibility of using NaF PET/CT as a clinical tool to assess bone metabolism in human subjects. **Methods** 139 healthy subjects (68 females and 71 males with known weight, age range 21-75 years old, BMI 18-43 kg/m²) were administered with the radiotracer NaF, and a PET/CT scan was conducted 90 minutes afterwards. The entire skeleton, vertebra, and femoral neck were segmented from the CT image using an operator-guided semi-automatic algorithm which used Hounsfield threshold 100 for bone. On the fused PET/CT images, standardized uptake values (SUVs) of NaF were calculated at each voxel (Figure 1). SUVs were adjusted for BMI and dosage and then plotted against the age. Drop in SUV for each decade of life was calculated using values at age of 20 years as baseline. **Results** Whole skeleton bone metabolism was negatively correlated with age (females: 3.13% drop in SUV per decade of life, p = 0.004; males: 3.57% drop in SUV per decade of life, p = 0.03). Femoral neck bone metabolism was negatively correlated with age among males (6.88% drop in SUV per decade of life, p = 0.007), but not among females (p = 0.68). Spine bone metabolism was negatively correlated with age among females (5.33% drop in SUV per decade of life, p < 0.001), but not among males (p = 0.30). **Conclusions** NaF PET/CT imaging could provide valuable functional insight regarding bone metabolism in the whole-body skeleton, proximal femur, and spine before conventional structural imaging can detect structural changes that result from substantial physical deterioration. NaF PET/CT based methodology described here has the potential to be an imaging tool that is more sensitive and can lead to earlier detection of metabolic bone diseases. [1] Raynor W, Houshmand S, Gholami S, Emamzadehfard S, Rajapakse CS, Blomberg BA, Werner TJ, Hoiland-Carlsen PF, Baker JF, Alavi A. Evolving Role of Molecular Imaging with (18)F-Sodium Fluoride PET as a Biomarker for Calcium Metabolism. Curr Osteoporos Rep. 2016 Aug;14(4):115-25.



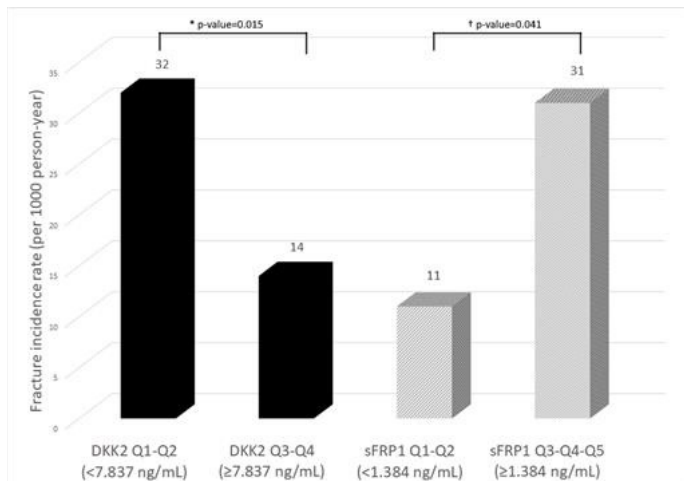
Disclosures: Sylvia Rhodes, None

Friday Posters

FRI-0687

Serum levels of DKK2 and sFRP1 are associated to incident fragility fractures in older women Ana Maria Rodrigues^{*1}, Mónica Eusébio², Ana Catarina Rodrigues³, Joana Caetano-Lopes⁴, Inês Lopes⁵, Jorge M Mendes⁶, Pedro Simões Coelho⁶, João Eurico Fonseca⁵, Jaime Cunha Branco⁷, Helena Canhão¹. ¹EpiDoc Unit – Unidade de Epidemiologia em Doenças Crónicas, CEDOC, Nova Medical School, Lisboa, Portugal, ²Sociedade Portuguesa de Reumatologia, Lisboa, Portugal, ³Faculdade de Medicina da Universidade de Lisboa, Lisboa, Portugal, ⁴Department of Orthopaedic Research, Boston Children's Hospital, Boston, MA, USA; ⁵Department of Genetics, Harvard Medical School, Boston, MA, United States, ⁶Unidade de Investigação em Reumatologia, Instituto de Medicina Molecular, Faculdade de Medicina, Universidade de Lisboa, Centro Académico de Medicina de Lisboa, Portugal, ⁷NOVA IMS, Universidade Nova de Lisboa, Lisboa, Portugal, ⁸Centro de Estudos de Doenças Crónicas (CEDOC) da NOVA Medical School, Universidade Nova de Lisboa (NMS/UNL), Lisboa, Portugal

Background: Secreted Frizzled-related protein-1 (sFRP-1), dickkopf-related protein 2 (DKK2), dickkopf-related protein 1 (DKK1) and sclerostin (SOST) are inhibitors of Wnt signaling and, consequently, inhibitors of osteoblast-mediated bone formation. Our aim is to evaluate the association of serum levels of SOST, DKK1, DKK2 and sFRP-1 with bone mineral density and incident fragility fractures. **Methods:** This longitudinal study analyzed 828 women, aged 65 years old and older, from EpiDoc a population-based cohort. A structured questionnaire was applied during baseline clinical appointment in order to capture prevalent fragility fractures, clinical risk factors for fracture and Osteoporosis diagnosis. Blood was collected to measure serum levels of markers of bone fragility and serum levels of WNT regulators. Vertebral and hip bone mineral density (BMD) were determined by DXA. Two follow-up assessments were performed through a phone call interview and incident fragility fractures were defined by any new self-reported low impact fracture. Multivariate Cox proportional hazards regression models were used to analyze fracture risk, adjusted for clinical risk factors for fracture. **Results:** During a mean follow-up of 2.3±1.0 years, a total of 62 fragility fractures were sustained in 58 women. High serum levels of sFRP-1 were associated with a 1.4-fold increase in fracture risk. Association between sFRP-1 and fracture risk was not independent of BMD. Low serum levels of DKK2 were associated with a 1.6-fold increase of fracture risk in our multivariate model. Association between low levels of DKK2 and fracture risk were independent of BMD. Women in the two lowest quartiles of DKK2 had a fracture rate incidence of 32 per 1000 person-year, while the ones in the highest two quartiles of DKK2 had 14 fragility fractures per 1000 person-year. Serum levels of SOST ($r=0.191$; $p=0.0025$) and DKK1 ($r=-0.1725$; $p=0.011$) were correlated with hip bone mineral density, but not with incident fragility fractures. **Conclusion:** Low serum levels of DKK2 are an independent risk factor for fragility fractures. High serum levels of sFRP-1 are significantly associated with fractures although this association is not independent of BMD. SOST and DKK1 were associated with BMD but not with incident fractures however, the number of new fractures recorded may not allow to detect this association.



Disclosures: Ana Maria Rodrigues, None

FRI-0688

Bone Endosteal But Not Periosteal Changes During Aging At The Distal Radius And Tibia Significantly Differ Between Men And Women As Determined From HRpQCT Images Using A Novel 3D Rigid-Registration Approach Bert Van Rietbergen^{*1}, Emmanuel Biver², Thierry Chevalley², Keita Ito³, Roland Chapurlat⁴, Serge Ferrari². ¹Dept. Biomed. Eng. Eindhoven University of Technology / Dept. Orthopaedics Maastricht University Medical Centre, Netherlands, ²Division of Bone Diseases, University Hospitals and Faculty of Medicine, Switzerland, ³Orthopaedic Biomechanics, Dept. Biomed. Eng. / Dept. Orthopaedics, University Medical Center Utrecht, Netherlands, ⁴SINSERM UMR 1033, Université de Lyon, France

During aging, changes in cortical bone endosteal and periosteal contours have been reported and it was proposed that differences in bone fragility between men and women relate to such changes. However, so far it was not possible to reliably detect these changes in-vivo due to limitations in image resolution and registration. In this study we use High Resolution peripheral Quantitative CT (HRpQCT) scanning in combination with an advanced 3D rigid registration technique to obtain a highly sensitive quantification of periosteal and endosteal changes in-vivo at the distal radius and tibia over time. Goals were first to test the reproducibility of this approach and second to assess differences between men and women in a large cohort. Default periosteal contouring and automatic endosteal autocontouring were applied first to all images. Rigid 3D registration then was used to align follow-up (FU) to baseline (BL) images. To avoid that cortical changes are obscured by the registration, only the cancellous bone compartment was used for registration. Periosteal and endosteal expansion/retraction volumes were determined by overlaying cortical compartments (Fig. 1). The net volume was divided by the BL periosteal or endosteal surface area to calculate an average expansion distance. To test the reproducibility, images from a short-term reproducibility study were used (15 female, 21-47 years, scanned 3 times). To test differences between men and women, images from a subset of the Geneva Retirees Cohort were used (246 female, 60 male, average age 65 years, 3.5 and 7 years FU). Results of the short-term reproducibility study indicated that the least detectable significant change in average periosteal/endosteal expansion was 38/30 microns for the radius and 15/21 microns for the tibia. Results of the cohort study showed significant endosteal expansion at both radius and tibia after 3.5 years that is further increased at 7 years FU (Table 1). The expansion in females was significantly and much higher (1.7 – 4.8 times) than in males. Periosteal changes were much smaller and changes significantly different from zero were found only for the tibia. Differences between male and female were significant ($p<0.01$) for all endosteal measures and for none of the periosteal measures. Although some of the changes found were close to the detection limit, highly significant differences were found between men and women that could explain the development of increased fragility in women

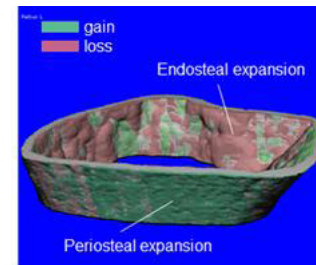


Fig 1: BL-FU overlay image for the cortex

Table 1: Average (SD) expansion in microns

	n	3.5-years FU		7-years FU		
		Periosteal	Endosteal	Periosteal	Endosteal	
Radius Female	148	2.6 (23.1)	37.2 (40.2)**	132	-0.4 (29.9)	71.8 (62.2)**
Male	51	1.7 (27.3)	11.8 (30.9)**	43	-7.0 (28.1)	14.9 (41.8)*
Tibia Female	232	12.3 (21.2)**	36.7 (40.5)**	220	9.6 (37.0)**	69.6 (72.7)**
Male	56	7.9 (23.6)*	21.2 (32.9)**	53	2.5 (35.0)	24.7 (69.2)*

significant different from zero: * $p<0.05$; ** $p<0.01$

Disclosures: Bert Van Rietbergen, Scanco Medical AG, Consultant

FRI-0689

Off-Treatment Bone Mineral Density Changes in Postmenopausal Women after 5 Years of Anastrozole Ivana Sestak^{*}, Jack Cuzick. Centre for Cancer Prevention, Queen Mary University London, United Kingdom

Background: Anastrozole (A) has been shown to prevent breast cancer in postmenopausal women at increased risk of developing the disease, but has been associated with substantial accelerated bone mineral density (BMD) loss during active treatment. Here, we investigate changes in BMD assessed by dual energy X-ray absorptiometry (DXA) 2 years after treatment cessation in women included in the IBIS-II breast cancer prevention trial. **Methods:** IBIS II randomly assigned 3864 postmenopausal women to A 1mg/day or placebo (P) for 5 years. 1410 were included in a BMD sub-study and stratified into three strata ac-

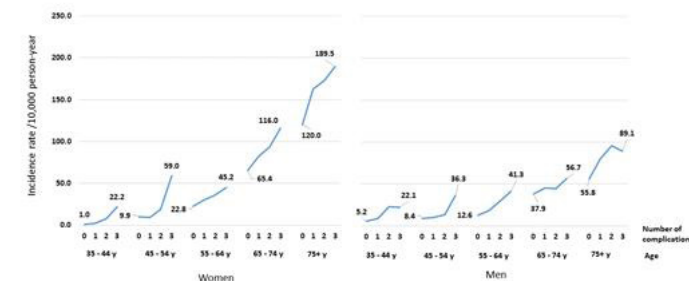
cording to their baseline T-score at spine or femoral neck (stratum I (N=760): T-score>-1.0 and observed; stratum II (N=500): -1.0<T-score>-2.5 and randomised to weekly risedronate or placebo; stratum III (N=150): -2.5<T-score>-4.0 or/and two fragility fractures and all on risedronate). The primary objective of this analysis was to investigate whether DXA BMD at the spine and hip changed 2 years after stopping A or P. All results are presented as mean % BMD changes (95% CI) between 5 and 7 years of follow-up. Results: 5 and 7-year BMD data were available for a total of 529 women who did not receive risedronate. In stratum I, cessation of A (N=205) led to an increase in BMD at the spine that was larger than in those on P (N=206) (A=1.29% (95% CI 0.78 to 1.79) vs. P=0.2% (-0.23 to 0.62), p=0.001). At the hip, BMD remained unchanged between 5 and 7 years after cessation of A but continued to a decrease in those who had been on P (A=-0.07% (-0.51 to 0.37) vs. P=-1.31% (-1.67 to 0.94), p<0.0001). Similar results were observed for women with osteopenia (stratum II). Those previously on A (N=53) had a significantly larger BMD increase at the spine after treatment cessation compared to those stopping P (N=64) (A=2.81% (1.40 to 4.23) vs. P=0.57% (-0.36 to 1.50); p=0.007). Loss of BMD at the hip continued in women who had been on P but increased slightly following cessation of A (A=0.47% (-0.42 to 1.36) vs. P=-1.33% (-2.12 to -0.54); p=0.003). Conclusions: These are the first results reporting BMD changes after stopping A in a breast cancer prevention setting. BMD at the lumbar spine improved significantly more in women who were originally randomised to A compared to those who received P. Our results show that the negative effects of A on BMD in the preventive setting are partially reversible.

Disclosures: *Ivana Sestak, None*

FRI-0738

Microvascular Complications and Risk of Incident Hip Fracture in Type 2 Diabetes: A National Cohort Po-Yin Chang^{*1}, Yi-Ting Wang², Rodrigo J. Valderrábano⁴, Yi-Wen Tsai², Jennifer S. Lee¹. ¹Stanford University School of Medicine, United States, ²National Yang-Ming University Institute of Health and Welfare Policy, Taiwan, ⁴University of Miami Miller School of Medicine, United States

Background: Adults with type 2 diabetes (T2D) have a two-fold hip fracture risk; microvascular complications may further increase the risk. Methods: We followed 90% of all adults with newly diagnosed T2D in Taiwan, from 2001-2005 to 12/31/2013. We compared adults, ages 35 or older, who developed any (n=130,403), two or more (n=46,469), or three (n=9,093) microvascular complications to those who had no complications, matched on age, sex, and T2D duration. The outcome was hospitalized incident hip fractures accompanied by internal fixation or hemiarthroplasty. We reported hazard ratios (HRs) and 95% confidence intervals (CIs) from sex-specific Cox models adjusted for age, T2D duration, comorbidities, T2D medications, and fracture risk factors. Results: During a median 5.7-years of follow-up, 2,999 of 111,747 women and 1,686 of 135,914 men had a hip fracture. Incidence (/10,000 person-years) increased from 41.9 in women with no complications to 91.8 in women with three complications, and in men, from 20.5 to 49.1. Individuals with three complications had an incidence approaching to or greater than those 10 years older with no complications (Fig). Women with one, two, and three complications had a 1.23-fold (CI: 1.14-1.34), 1.79-fold (CI: 1.54-2.08), and 2.59-fold (CI: 1.77-3.98) greater risk of hip fracture, respectively, than those with no complications; for men, the corresponding HRs were 1.33 (CI: 1.19-1.49), 1.92 (CI: 1.58-2.32), and 2.16 (CI: 1.40-3.35). Excluding individuals with cardiovascular diseases did not alter these estimates. Conclusions: Hip fracture risk increased with the number of microvascular complications in T2D adults. Fracture prevention strategies may warrant including T2D adults with multiple microvascular complications.



Disclosures: *Po-Yin Chang, None*

FRI-0739

Cancer Patients who Suffer Fractures are Rarely Assessed or Treated for Osteoporosis: Population-based Data from Manitoba Beatrice Edwards^{*1}, William Leslie², Saeed Al-Azazi², Lin Yan², Lisa Lix², Piotr Czaykowski³, Harminder Singh³. ¹Central Texas Veterans Healthcare System, United States, ²University of Manitoba, Canada, ³University of Manitoba, CancerCare Manitoba, Canada

Background: A care gap has been previously described in the general population whereby individuals with fractures are seldom evaluated or treated for osteoporosis. It is unknown if a similar gap exists for cancer patients. Methods: We linked population-based data (cancer registry, health administrative data, population registry) from Manitoba, Canada to identify cancer cases (first cancer diagnosis excluding non-melanoma skin cancer between 1987 and 2013) with a subsequent major osteoporotic fracture 1997 or later (MOF: hip, clinical spine, forearm, humerus). Performance of a bone mineral density (BMD) test or initiation of osteoporosis therapy over the 12 months post-fracture was analyzed using multivariate logistic regression. Only those who survived for a year after the fracture diagnosis were included. Results: There were 20,656 subjects with a cancer diagnosis who sustained a MOF (females 72.9%, males 27.1%). BMD testing was performed in 11.4% (females 12.8%, males 7.3%), osteoporosis therapy initiated in 22.1% (females 26.1%, males 10.6%), and either BMD or treatment in 28.5% (females 33.0%, males 15.7%). The likelihood of receiving a BMD test or receiving treatment increased from 1997-2000 (15.4%) through 2007-2013 (32.5%). Oncologists were less likely to order BMD or initiate therapy than other clinicians. Logistic regression (Table) showed that BMD testing was more likely to be ordered in cancer patients aged 50-70 years and in those 70 years and older, and in those who sustained fractures between 2007-2013. Osteoporosis therapy was more likely to be initiated in females, in patients who were 50 years of age and older, if fractures occurred in 2001 or later and after vertebral fractures. Finally, either BMD testing and/or osteoporosis therapy initiation was more likely if patients were 50 years of age and older, had a higher socio-economic status, if fractures occurred in 2001 or later, had melanoma, or after vertebral fractures. Conclusions: In cancer patients who sustain a fracture, a care-gap exists whereby the evaluation or treatment for osteoporosis is seldom conducted. This care-gap seems more pronounced in oncologists as compared to other clinicians. We have identified several predictors of testing or initiation of therapy. Care maps need to be developed to reduce variation in care.

Table 1. Likelihood of having a BMD test or osteoporosis treatment initiation

BMD testing	Odds Ratio (95% C.I.)	Treatment initiated	Odds Ratio (95% C.I.)	BMD and/or treatment initiated	Odds Ratio (95% C.I.)
50-70 years of age	6.24 (2.8, 13.4)	Female gender	4.7 (3.6, 6.2)	50-70 years	7.3 (3.8, 14.3)
70 years and older	2.5 (1.1, 5.4)	50-70 years of age	6.2 (2.6, 14.5)	70 years and older	7.7 (3.9, 14.9)
Fracture in 2007-2013	4.7 (3.1, 7.1)	70 years and older	9.9 (4.2, 22.9)	Higher SES	1.4 (1.1, 1.8)
		Fracture in 2000-2006	2.1 (1.7, 2.8)	Fracture in 2001-2006	2.3 (1.8, 2.9)
		Fracture in 2007-2013	2.1 (1.6, 2.7)	Fracture in 2007-2013	7.7 (3.9, 14.9)
		Vertebral fractures	3.9 (3.2, 14.3)	Skin cancer	1.5 (1.1, 2.0)
				Vertebral fractures	2.8 (2.3, 3.6)

SES=socioeconomic status

Disclosures: *Beatrice Edwards, None*

FRI-0740

Risk Factors for Atypical Femur Fractures in a Large, Prospective Cohort Study: A Multivariable Analysis from the Southern California Osteoporosis Cohort Study (SOCS) Erik J. Geiger^{*1}, Dennis M. Black¹, Bonnie H. Li², Denison S. Ryan², Richard M. Dell², Annette L. Adams². ¹University of California, San Francisco, United States, ²Kaiser Permanente Southern California, United States

Atypical femur fractures (AFFs) are rare but serious events. While evidence suggests an increased risk with long-term bisphosphonate (BP) use, examination of other risk factors has been limited. This analysis aimed to assess AFF clinical risk factors together with BP duration in multivariable (MV) analysis in a large, diverse cohort of post-menopausal women. This prospective cohort study included women aged ≥50 years who were members of Kaiser Permanente Southern California (KPSC) during the period 1/1/2007-9/30/2015. Using the 2014 ASBMR criteria, AFFs were adjudicated by expert review (RD) of all X-rays identified from ICD9-coded subtrochanteric or femoral shaft fractures and adjudication verified by a 2nd expert (EG). In addition to age and race, we collected information from KPSC EMRs on the following potential risk factors dating back up to 10 years prior to cohort entry: alcohol use, smoking history, height, fracture history, diabetes, glucocorticoid (GC) use, Charlson score, BP duration and time since BP discontinuation. Time-dependent, MV Cox models were used to estimate hazard ratios (HR) and 95% CIs including all risk factors found significant in unadjusted models. This analysis includes women with any BP use. The overall cohort included 913,367 women with 233 AFFs. In the analysis cohort with any BP use, there were 175,709 women with 206 AFFs. In the MV model, significant risk factors for increased AFF risk included younger age (HR 1.11/5 yr decrease, CI 1.04-1.18) Asian race (HR 3.83, CI 2.79-5.25), shorter height (HR/inch 1.09 CI 1.02-1.15), GC use >1 yr (HR 2.3 CI 1.4-3.6) and history of prior fracture (HR 1.56 CI 1.14-2.14) (see Table). In this fully adjusted model, AFF risk increased with increasing duration of BP use compared to those with <1 year BP use. For 1-4 years of use, the HR was 3.56 (CI 1.53-8.28); for 4-8 years the HR was 19.10 (CI 8.57-42.57); for >8 years the HR was 41.99 (CI 18.47-95.48). Of note, the relationships of Asian race, shorter height and BP duration to AFF risk were attenuated after MV adjustment (Table). Using radiographically-defined AFF and rigorous prospective, multivariable analysis, we identified a number of independent AFF risk factors including Asian race, GC

Friday Posters

use and fracture history. Longer BP duration remained strongly associated with AFF risk, even after full adjustment. These results will be used to develop risk prediction tools to help clinicians individualize BP therapy duration.

Key Risk Factors in MV Model for Increased AFF Risk in 175,709 women >50 years who had used bisphosphonates ^A		
Risk factor	Unadjusted HR (p)	Multivariable Adjusted HR (p)
Younger Age (-5 yrs)	1.02 (0.42)	1.11 (0.003)
Asian race	5.15 (<0.001)	3.83 (<0.001)
GC use > 1 year	2.34 (<0.001)	2.29 (0.0004)
Any fracture hx	1.32 (0.06)	1.56 (0.006)
Shorter Height (-1 inch)	1.16 (<0.001)	1.09 (0.007)
BP duration (vs ≤ 1 year)		
1-4 years	5.6 (<0.001)	3.56 (0.003)
4-8 years	36.4 (<0.001)	19.10 (<0.001)
> 8 years	79.8 (<0.001)	41.99 (<0.001)

^ASmoking and time since BP continuation was also included in model

Disclosures: Erik J. Geiger, None

FRI-0741

Treatment with Statins Is Associated with Higher Volumetric Bone Mineral Density and Lower Cortical Porosity in Older Women Berit Larsson^{*1}, Anna Nilsson¹, Dan Mellstrom¹, Daniel Sundh¹, Mattias Lorentzon². ¹Department of Geriatric Medicine, Institute of Medicine, Sahlgrenska Academy, University of Gothenburg, Sweden, ²Head of Geriatric Medicine, Institute of Medicine, Sahlgrenska Academy, University of Gothenburg, Sweden

Introduction There are conflicting results in the literature whether treatment with statins have an effect on areal bone mineral density and fracture risk. The aim of this study was therefore to investigate if treatment with statins was associated with better bone geometry and microstructure and if these associations were dependent on statin potency. Methods In a large population-based study on older women (75-80 years) a standardized questionnaire was used to assess information regarding diseases, medications and lifestyle. Statin treatment was analyzed as yes/no, and according to statin potency (non-treated vs. simvastatin or atorvastatin/rosuvastatin). Bone geometry and microstructure were measured at the standard site (ultradistal) and at a more proximal section at 14% (distal) of the bone length on radius and tibia using a high-resolution peripheral quantitative computed tomography. Results In the whole cohort of 3028 women (77.8±1.63 [mean±SD]), 803 (26.5%) women were treated with statins. Within this group, 551 (18.2%) took simvastatin, 201 (6.6%) atorvastatin, and 38 (1.3%) took rosuvastatin. Treated women were of similar age (77.9±1.6 vs. 77.8±1.6) and BMI (26.9±4.4 vs. 26.0±4.4) but had higher prevalence of heart disease and other comorbidities than non-treated women. Treatment was associated with a higher total bone mineral density (Tot.vBMD) (3.0%; p<0.001) and with cortical bone parameters, as reflected by a greater cortical area (Ct.Ar) (2.2%; p=0.001), volumetric bone mineral density (Ct.vBMD) (0.6%; p=0.002), and lower cortical porosity (Ct.Po) (-5.2%; p=0.01) at the distal tibia. Similar findings were found for the distal radius with higher Tot.vBMD (4.1%; p<0.001), Ct.Ar (3.2%; p<0.001), Ct.vBMD (0.6%; p<0.001), and lower Ct.Po (-9.7%; p=0.01). Statin use was also associated with greater trabecular bone volume fraction measured in the ultradistal tibia (2.6%; p=0.01) and radius (4.3%; p=0.01). Adjustments for confounders did not substantially alter these associations. Increased statin potency was associated with higher Tot.vBMD, larger Ct.Ar, and lower Ct.Po (Figure 1A-C) at the distal tibia. Conclusion Older women treated with statins had better bone geometry and microstructure at both the tibia and radius, with differences persisting after adjustment for confounders. These associations were dependent on statin potency.

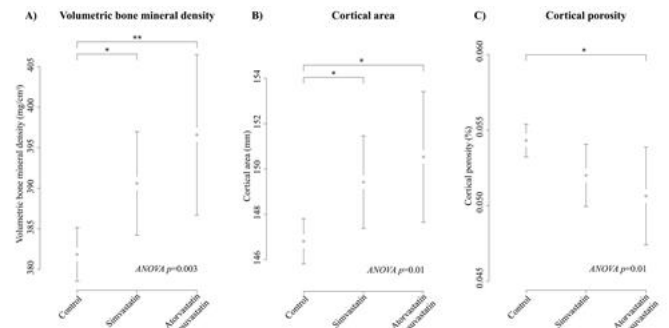


Figure 1 Treatment with statins in categories of potency was associated with increasing volumetric bone mineral density (A) and cortical area (B) as well as decreasing cortical porosity (C). Differences were compared with ANOVA and following post hoc analyses were performed with least significant difference (LSD) and significant levels are presented as *p<0.05, **p<0.01

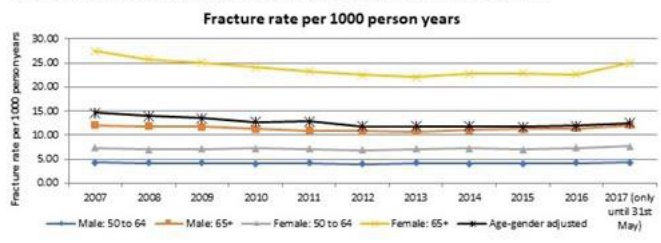
Disclosures: Berit Larsson, None

FRI-0742

Osteoporotic Fracture Trends in a Population of US Managed Care Enrollees: 2007-2017 E. Michael Lewiecki^{*1}, Benjamin Chastek², Kevin Sundquist², Setareh A. Williams³, Deane Leader, Jr.³, Richard J. Weiss³, Yamei Wang³, Lorraine A. Fitzpatrick³, Jeffrey R. Curtis⁴. ¹New Mexico Clinical Research & Osteoporosis Center, United States, ²Optum, United States, ³Radius Health, Inc., United States, ⁴UAB Arthritis Clinical Intervention Program, University of Alabama at Birmingham, United States

Osteoporosis-related fractures (fractures) are a leading cause of morbidity and disability in the US. Epidemiological data on the occurrence of fractures are limited and required to inform healthcare providers, payers, and policymakers on the scope of this disease. The objective of this analysis was to assess the incidence of fractures in a population of managed care enrollees over the past decade. The study included commercial and Medicare Advantage health plan members who had evidence of a qualifying fracture between Jan 2007 and May 2017 (identification period). Fractures were considered qualifying if they were either identified during an inpatient stay or were identified in an outpatient setting based on primary or secondary ICD-9 or ICD-10 accompanied by a repair procedure code. Patients ≥50 years of age with evidence of a qualifying fracture were included. The denominator population comprised of members who were ≥50 years of age during the year of interest. The number of days the member was enrolled in the health plan during the year was calculated and was used to determine the total person-years (py) of enrollment for the denominator. Incidence rate is reported as number of events per 1000 py of enrollment during each year from 2007- May 2017. Rates are presented stratified by age category (50-64 vs ≥65) and gender (male vs. female). Patients were categorized by 5-year age increments and gender, and an overall age-gender adjusted rate was calculated. Of 1,841,263 members with fractures in the identification period, 513,176 met the eligibility criteria. The overall age-gender adjusted rate fell from 14.67/1000 py in 2007 to 11.80/1000 py in 2012, and then did not decrease from 2013- May 2017. Among females ≥65 years old the incidence of fractures declined from 27.49/1000 py in 2007 to 22.08/1000 py in 2013, and then did not decrease from 2014- May 2017. Similarly, among males ≥65 years old incidence decreased from 12.00/1000 py in 2007 to 10.72/1000 py in 2013 and then did not decrease from 2014- May 2017. For males and females ages 50-64 the rates were consistent across years, approximately 4.2 and 7.2 fractures per 1000 py, respectively. The current study findings suggest fracture incidence has remained the same and potentially rising since 2014. The current study results may reflect insufficient osteoporosis diagnosis and treatment and supports the call to action to increase diagnosis and treatment especially in older adults.

Figure. Incidence of Osteoporotic Fractures Per 1000 Person Years: 2007-May 2017



Disclosures: E. Michael Lewiecki, Radius Health, Inc., Consultant, Merck & Co, Consultant, Eli Lilly and Company, Grant/Research Support, Amgen, Consultant, AbbVie, Consultant, Shire, Consultant, Amgen, Grant/Research Support, Merck & Co, Grant/Research Support, Eli Lilly and Company, Consultant, AgNovos Healthcare, Consultant, Alexion Pharmaceuticals, Consultant, TheraNova, Consultant

FRI-0743

An Atlas of Human and Murine Genetic Influences on Osteoporosis John Morris^{*1}, John Kemp², Scott Youlten³, John Logan⁴, Ryan Chai³, Nicholas Vulpesco⁵, Vincenzo Forgetta⁶, Aaron Kleinman⁷, Sindhu Mohanty³, Marcelo Sergio³, Carolina Medina-Gomez⁸, Katerina Trajanoska⁸, Julian Quinn³, Elena Ghirardello⁴, Natalie Butterfield⁴, Katharine Curry⁴, Victoria Leitch⁴, Penny Sparkes⁴, Laetitia Laurent⁶, Anne-Tounisa Adoum⁴, Naila Mannan⁴, Davide Komla-Ebri⁴, Andrea Pollard⁴, Hannah Dewhurst⁴, Stephen Kaptoge⁹, Paul Baldock³, Cyrus Cooper¹⁰, Jonathan Reeve¹¹, Evangelia Ntzani¹², Evangelos Evangelou¹², Claes Ohlsson¹³, David Karasik¹⁴, Fernando Rivadeneira⁸, Cheryl Ackert-Bicknell¹⁵, Douglas Kiel¹⁴, Jonathan Tobias¹⁶, Celia Gregson¹⁶, Nicholas Harvey¹⁰, David Adams¹⁷, Christopher Lelliott¹⁷, David Hinds⁷, Yi-Hsiang Hsu¹⁴, Matthew Maurano⁵, Peter Croucher³, Graham Williams⁴, Duncan Bassett⁴, David Evans², Brent Richards¹. ¹Department of Human Genetics, McGill University, Canada, ²University of Queensland Diamantina Institute, Translational Research Institute, Australia, ³Garvan Institute of Medical Research, Australia, ⁴Molecular Endocrinology Laboratory, Department of Medicine, Imperial College London, United Kingdom, ⁵Institute for Systems Genetics, New York University Langone Medical Center, United States, ⁶Centre for Clinical Epidemiology, Lady Davis Institute, Jewish General Hospital, Canada, ⁷Department of Research, 23andMe, United States, ⁸Department of Internal Medicine, Erasmus Medical Center, Netherlands, ⁹Department of Public Health and Primary Care, University of Cambridge, United Kingdom, ¹⁰MRC Lifecourse Epidemiology Unit, University of Southampton, United Kingdom, ¹¹NIHR Musculoskeletal Biomedical Research Unit, Botnar Research Centre, Nuffield Department of Orthopaedics, Rheumatology and Musculoskeletal Sciences, United Kingdom, ¹²Department of Hygiene and Epidemiology, University of Ioannina Medical School, Greece, ¹³Department of Internal Medicine and Clinical Nutrition, University of Gothenburg, Sweden, ¹⁴Institute for Aging Research, Hebrew SeniorLife, United States, ¹⁵Center for Musculoskeletal Research, Department of Orthopaedics, University of Rochester, United States, ¹⁶Musculoskeletal Research Unit, Department of Translational Health Sciences, University of Bristol, United Kingdom, ¹⁷Wellcome Trust Sanger Institute, Wellcome Genome Campus, United Kingdom

Identifying the genetic determinants of osteoporosis will help to highlight drug targets and understand its biological causes. We therefore performed genome-wide association studies (GWAS) of estimated bone mineral density measured by quantitative heel ultrasound (eBMD, N=426,824) and of bone fracture (Ncases=53,184) in White-British UK Biobank participants. Fracture findings were replicated using 23andMe participants (Ncases=367,900, Ncontrols=363,919). Candidate target genes were identified using functional genomics data and validated with an in-depth mouse screening pipeline. We found 1,106 lead SNPs ($P < 6.6 \times 10^{-9}$) associated with eBMD, mapping to 518 loci (301 novel) and explaining 20% of variance in eBMD. For fracture, we found 14 lead SNPs ($P < 6.6 \times 10^{-9}$), all of which were associated with eBMD. An integrative analysis of human genomic data featuring primary osteoblast and osteocyte Hi-C contact domains, osteoblast open chromatin sites, gene proximity and coding variation enabled us to map genetic associations to a total of 538 target genes. These target genes were enriched for known osteoporosis drug targets and genes involved in bone disorders (OR=58, $P=10^{-75}$). We next undertook skeletal phenotyping of murine knockouts of 126 target genes and found an increased frequency of abnormal skeletal phenotypes ($P < 0.0001$), compared to unselected genes. Multiple lines of evidence converged to suggest a role of DAAM2 in osteoporosis. We therefore generated Daam2 knockout mice for skeletal phenotyping with X-ray microradiography, microtomography and biomechanical testing. We observed large decreases in bone strength in knockout mice (2.14 standard deviations below control strength) likely due to increased cortical porosity and impaired bone quality, despite otherwise normal bone mineral content, bone length, trabecular and cortical parameters. In summary, this atlas of human and murine genetic determinants of osteoporosis has increased the number of associated BMD loci from previous studies 2.5-fold to 518, increasing the variance explained by genetic factors 1.5-fold to 20%. The identified target genes were strongly enriched for genes with known roles in bone biology. Moreover, validation of the DAAM2 target gene in mice led to marked reductions in bone strength and increased cortical bone porosity. This set of identified genes greatly improves our understanding of the genetic determinants of osteoporosis and is expected to identify osteoporosis treatment targets.

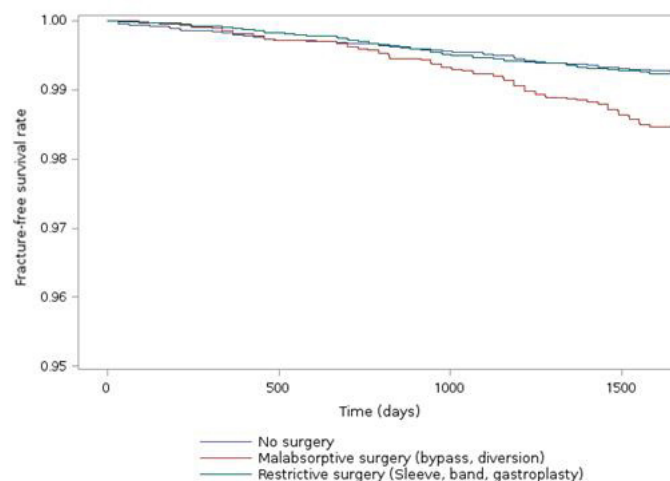
Disclosures: **John Morris, None**

FRI-0744

Risk of fracture after bariatric surgery in France: population based, retrospective cohort study Julien Paccou^{*1}, Niels Martignè¹, Eric Lespessailles², Bernard Cortet¹, Grégoire Ficheur¹. ¹Lille University Hospital, France, ²Université d'Orléans, France

The long-term consequences of bariatric surgery on fracture risk are unclear but are likely to vary by procedure type. Moreover, studies have only been performed in younger

populations than population at risk of osteoporotic fractures. This study aimed to investigate the fracture risk in patients after bariatric surgery versus matched controls. The authors used the National Health Insurance Research Database of France and identified 16,840 patients aged 40 years or older who underwent bariatric surgery with a body mass index (BMI) ≥ 40 kg/m², during January 1, 2011 to June 30, 2012. We paired the cohort of bariatric surgery patients in a one to one ratio with obese people on the following factors: age, sex, Charlson Comorbidity Index; BMI ≥ 50 kg/m². The primary outcome was any diagnosis of major osteoporotic fracture (MOF: hip, humerus, forearm, and vertebral) during the 4.5 years following surgery. Conditional logistic regression was used to investigate the relationships between bariatric surgery and the occurrence of at least one MOF. Similarly, the relationship between bariatric surgery and the risk of forearm fractures and hip fracture was investigated. We also assessed the risk of MOF stratified by surgery type. The mean \pm SD age was 49 ± 7 years, and the groups were predominantly female (78%). The cumulative follow-up was 149,178 person-years. At the end of the study period, there were 174 MOF in the surgical group and 123 MOF in the matched control group. Compared with the control group, the risk of MOF in the surgical group was significantly increased (Odds-Ratio (OR) [95% confidence interval (CI)] = 1.42 [1.13-1.80]). In fracture site-specific analyses, patients with bariatric surgery had an increased risk of forearm fractures (OR=1.73, 95% CI [1.21-2.47]) while it was not the case regarding hip fracture (OR=1.30, 95% CI [0.76-2.24]). For the analysis stratified by surgery type, compared with the control group, the risk of MOF was significantly increased for the malabsorptive bariatric surgery (OR=2.29, 95% CI [1.57-3.36]) whereas no association was found regarding restrictive surgery (OR=1.10, 95% CI [0.71-1.71]) (Figure 1). In patients aged 40 years or older, bariatric surgery was significantly associated with an increased risk of MOF, mainly with malabsorptive procedures. These results provide further evidence that malabsorptive bariatric surgery dramatically increases the risk of fractures.



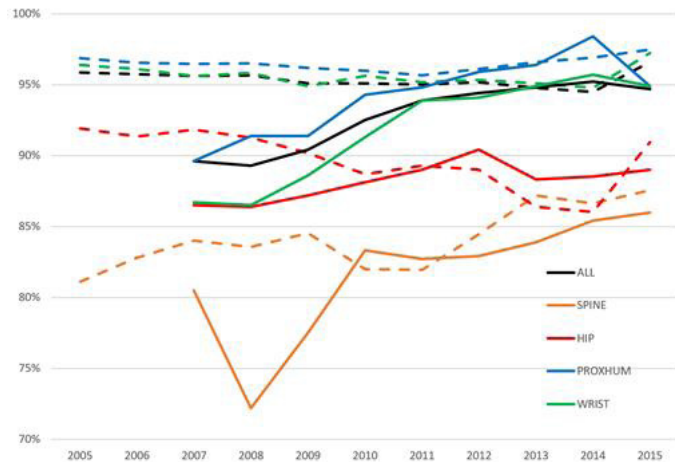
Disclosures: **Julien Paccou, None**

FRI-0745

Secular trends in the initiation of therapy in secondary fracture prevention: widening treatment gaps in Denmark and Spain Daniel Prieto-Alhambra^{*1}, Martin Ernst², Katrine Hass Rubin², Daniel Martinez-Laguna³, M Kassim Javaid¹, Cyrus Cooper⁴, Cesar Libanati⁵, Emese Toth⁵, Bo Abrahamson⁶. ¹Nuffield Department of Orthopaedics, Rheumatology, and Musculoskeletal Sciences (NDORMS), Oxford NIHR Biomedical Research Centre, University of Oxford, United Kingdom, ²OPEN, Institute of Clinical Research, University of Southern Denmark, Denmark, ³GREMPAL Research Group (Idiap Jordi Gol Primary Care Research Institute) and CIBERFes, Universitat Autònoma de Barcelona and Instituto de Salud Carlos III, Spain, ⁴Lifecourse Epidemiology Unit, Southampton University, United Kingdom, ⁵UCB Biopharma Sprl, Belgium, ⁶Holbæk Hospital, Dept of Medicine, Denmark

Purpose: There is a recognised gap in the initiation of anti-osteoporosis therapy for secondary fracture prevention. We used population-based databases in Spain and Denmark to quantify the treatment gap amongst fractured patients in 2005-2015. Methods: Data were extracted from primary care records in Catalonia (SIDAP) and the national hospital database from Denmark, linked to pharmacy dispensation/s from 2005 (2007 for SIDAP) to 2016. Patients with an incident fracture (any but skull/face/digits) in 2005-2015 and aged over 50 years were eligible. Those with prostate, breast, or bone cancer were excluded, as were users of anti-osteoporosis therapy in the year before fracturing. Numbers and % with at least one prescription of anti-osteoporosis treatment in the year following fracture were reported, and treatment gap (those not starting any such therapy) over calendar years depicted. Analyses were stratified by country and fracture site. Results: A total of 131,959 (31,908 wrist, 9,773 hip, 7,664 spine, and 13,230 proximal humerus) and 284,375 (74,911 wrist, 46,171 hip, 8,331 spine, and 29,367 proximal humerus) fracture participants were included from Spain and Denmark respectively. Overall, secondary fracture prevention was more often started

after clinical spine (S 18.3%, DK 15.7%), followed by hip (S 11.5%, DK 10.1%), wrist (S 8.1%, DK 4.4%) and proximal humerus (S 6.9%, DK 3.5%) fractures. Hence treatment coverage was similar for clinical spine and hip, but halved for wrist and proximal humerus in Denmark compared to Spain. Already large treatment gaps increased further in the study period in Spain, from 89.6% for all fractures (80.5% for spine, 89.6% for proximal humerus) in 2007 to 94.7% (86.0% for spine, 94.9% for proximal humerus) in 2015. In Denmark, treatment gaps widened for spine (81.1% in 2005 to 87.6% in 2015), and remained stable for other fractures [Figure 1]. Conclusions: Despite the known imminent fracture risk following a first fracture, unacceptable treatment gaps remain, and have widened in Spain, from 80% to 86% for clinical spine and from 90% to 95% for proximal humerus between 2007 and 2015 respectively. Data from DK suggest a similar trend in treatment gap for clinical spine, but not for other fracture/s. This compares to a 76% treatment gap overall in the 2017 UK Fracture Liaison Service audit. Effective secondary fracture prevention services that can demonstrate closing the treatment gap are urgently required in Europe.



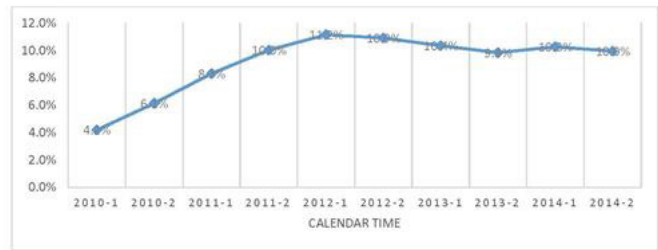
Disclosures: **Daniel Prieto-Alhambra**, UCB, Grant/Research Support, Servier, Grant/Research Support, Pharmo Institute, Grant/Research Support, Amgen, Grant/Research Support

FRI-0746

Temporal Trends and Factors Associated with Bisphosphonate Drug Holidays Jeffrey Curtis*, Rui Chen, Tarun Arora, Shanette Daigle, Robert Matthews, Huifeng Yun, Nicole Wright, Ayesha Jaleel, Elizabeth Delzell, Kenneth Saag. University of Alabama at Birmingham, United States

Background Safety concerns related to osteoporosis (OP) medication use and temporary or permanent cessation of bisphosphonate therapy (e.g. 'drug holidays') have generated appreciable attention in the lay media and medical community. We examined trends and factors associated with BP drug holidays. Methods We assembled a cohort of women ('OP cohort') who had osteoporosis as diagnosed by a physician, fragility fracture, or were treated with any OP therapy using 2009-2015 Medicare data (100% sample). Women with Paget's or malignancy were excluded. Use of any OP therapy was examined in 6 month calendar time intervals during which women had to remain alive with full medical & pharmacy coverage. We identified the subgroup of women ('long term BP user cohort') who had initiated BP therapy and were >=80% adherent with any BP for >=3 years. Women were considered to have taken a BP holiday if they had a gap in BP use > 12 months. We examined patterns of BP drug holidays over time, stratified in 6 month intervals and by cumulative duration of BP drug use. Results From a source population of more than 3 million women with osteoporosis, declining trends in use of all OP therapies were observed. Overall oral BP use fell by more than 50% from 2010 to 2014, although declines plateaued between 2012 and 2014. A total of 160,369 long-term BP users were identified, with mean (SD) age of 78.5 (7.5) years; 71% used alendronate and 51% used alendronate exclusively. Of these, 58,046 (36.2%) women had a BP drug holiday of >12 months. Approximately 10% of long term BP users discontinued each 6 month interval, reaching a peak in 2012 and continuing in a stable fashion thereafter (Figure). The timing of BP drug holidays peaked at a cumulative duration of 5-5.5 years of BP exposure. Numerous factors differed significantly between women taking drug holidays and those who did not including age, fragility fracture, and recent DXA. Conclusion Long term cessation of bisphosphonate therapy after 3-5 years of prior use has become increasingly common in the U.S. The impact on fracture risk and the optimal timing to restart remains of high importance.

Figure: Trends in Bisphosphonate Drug Holidays Over Time



Disclosures: **Jeffrey Curtis**, Radius, Grant/Research Support, Radius, Consultant, Amgen, Grant/Research Support, Amgen, Consultant

FRI-0747

Type 2 Diabetes and HR-pQCT Parameters in Older Men Ann Schwartz*, Neeta Parimi¹, Andrew Burghardt¹, Mary Bouxsein², Elsa Strotmeyer³, Eric Vittinghoff¹, Eric Orwoll⁴, Gina Woods⁵, Dennis Black¹, Nancy Lane⁶, Kristine Ensrud⁷, Nicola Napoli⁸. ¹University of California, San Francisco, United States, ²Harvard Medical School, United States, ³University of Pittsburgh, United States, ⁴Oregon Health and Science University, United States, ⁵University of California, San Diego, United States, ⁶University of California, Davis, United States, ⁷University of Minnesota and Minneapolis VA Health System, United States, ⁸Uniersita Campus Bio-Medico di Roma, Italy

Type 2 diabetes (T2D) may be associated with deficits in bone structure and microarchitecture that contribute to higher fracture risk. Previous studies of high resolution pQCT (HR-pQCT) parameters and T2D have not reported separate results for men. Our study determined associations between T2D and HR-pQCT parameters in older men using data from the Osteoporotic Fractures in Men (MrOS) study, including the diaphyseal tibia as well as the distal tibia and radius. At visit 4, on 1801 MrOS participants at 6 clinical sites, HR-pQCT scans were acquired with SCANCO XtremeCT II scanners at the distal radius (9mm from articular surface), distal tibia (22 mm from articular surface) and diaphyseal tibia (30% of tibia length) and analyzed centrally. Diabetes (DM) was ascertained by self-report of DM diagnosis or use of DM medication. Two men were excluded for lack of data on DM status, and two for possible type 1 DM. Analyses included 1797 men, 288 (16%) with T2D. Linear regression models, adjusted for age, race, BMI and clinic site, were used to compare HR-pQCT parameters by DM status. Mean age was 84 (±4) years in DM and non-DM. Mean weight was greater in DM (83±14 kg) than non-DM (79±12 kg) (p<0.001). Mean height was similar in DM (172±6.7 cm) and non-DM (172±6.9 cm). At all three scan sites, total cross-sectional area was significantly lower in DM than non-DM (Table). Cortical and trabecular area tended to be lower in DM than non-DM as well. Consistent with prior reports, trabecular vBMD and microstructure were either similar between groups, or more favorable in DM compared to non-DM. Total vBMD was similar between groups. However, in contrast to prior reports, there was no difference in cortical porosity between DM and non-DM. At the distal sites, cortical vBMD was similar between groups, but was significantly higher in DM than non-DM at the diaphyseal tibia (1003 vs 995 mg/cm³, p=0.001). Estimated failure load was similar between groups at the distal radius and distal tibia, but was significantly lower in DM than non-DM at the diaphyseal tibia (-2.3%, p=0.010). In summary, in older men T2D was associated with smaller total cross-sectional area at the radius and tibia. Both cortical and trabecular areas appeared to be proportionally smaller as well. At the diaphyseal tibia, smaller total area resulted in lower estimated bone strength despite no deficits in total or cortical vBMD. Smaller bone area may contribute to increased fracture risk in older men with T2D.

Table. Adjusted* Means for Selected HR-pQCT Parameters by Diabetes Status

HR-pQCT measure	DM	No DM	p
Distal Radius			
Estimated failure load (kN)	4.84	4.87	0.755
Total vBMD (mg/cm ³)	277	274	0.510
Total area (mm²)	389	398	0.033
Cortical area (mm ²)	64.8	66.3	0.095
Cortical porosity (%)	1.3	1.4	0.200
Distal Tibia			
Estimated failure load (kN)	13.3	13.5	0.164
Total vBMD (mg/cm ³)	280	279	0.854
Total area (mm²)	874	897	0.010
Cortical area (mm²)	134	139	0.019
Cortical porosity (%)	4.0	4.0	0.981
Diaphyseal Tibia			
Estimated failure load (kN)	19.6	20.1	0.010
Total vBMD (mg/cm ³)	734	730	0.473
Total area (mm²)	430	441	0.004
Cortical area (mm²)	305	313	0.004
Cortical porosity (%)	1.9	1.8	0.585

*Adjusted for age, race, clinic site, BMI

Disclosures: Ann Schwartz, None

FRI-0748

Cluster Analysis of High Resolution Peripheral Quantitative Computed Tomography Parameters Identifies Bone Phenotypes Associated With High Rates of Prevalent Fracture Kate Ward*, Mark Edwards, Leo Westbury, Cyrus Cooper, Elaine Dennison. MRC Lifecourse Epidemiology, University of Southampton, United Kingdom

With increasing use of high-resolution peripheral quantitative computed tomography (HRpQCT) and the extended phenotypic data the technique provides, it is important to assess whether the measurements are associated with fracture risk. The aim of this study was to identify clusters of bone microarchitecture and strength in older men and women from the Hertfordshire Cohort Study and relate them to fracture prevalence and aBMD. We studied 171 women and 188 men, aged 72.1-81.4 years, with HRpQCT (XtremeCT I) images of the distal radius. Standard image analyses were performed for assessment of macrostructure, regional densitometry, cortical (Ct) and trabecular (Tb) microarchitecture, and finite element analysis. K-means partitioning cluster analysis was used to identify four clusters in women and four in men. Prevalent fracture rates and femoral neck aBMD were determined for each cluster. Fifty women and 45 men had fractures. Using microarchitecture and FEA parameters together, in women, there were two phenotypes with fracture risk greater than the reference (lowest fracture prevalence) cluster. Cluster A contained 23 women (10 fracture) with Ct.Ar, Ct.Th, Ct.BMD, Tr.BMD, Tr.Th, stiffness, failure load, and Young's modulus (YM) more than 1SD below the sex-specific cohort mean, and % Tb load (distal) more than 1SD above. The relative risk of fracture [95% confidence interval] was 2.55 [1.28, 5.07], p=0.008 in that cluster. Cluster B (39 women, 14 fracture) had a % Tb load proximal >1SD below the sex-specific cohort mean; relative risk of fracture was 1.93 [0.98, 3.78], p=0.06. Using FEA parameters alone, 3 clusters had significantly greater fracture risk compared to the lowest risk cluster. Two were similar to clusters A and B above, relative risks of fracture were: A 2.40 [1.12, 5.15], p=0.03; B 2.74 [1.46, 5.13], p=0.002; though in B none of the FEA parameters were >1SD below the mean. The third had % Tb load (distal and proximal) >1SD above the sex-specific cohort mean; relative risk of fracture was 2.31 [1.11, 4.78], p=0.02. Fracture rates did not differ significantly by cluster in men, though similar phenotypes to clusters A and B were identified in the analyses. We have demonstrated clusters with cortical and trabecular phenotypes associated with a higher proportion of fractures in women. In men, who had fewer fractures, significant differences in fracture rates were not identified despite similar phenotypes being identified.

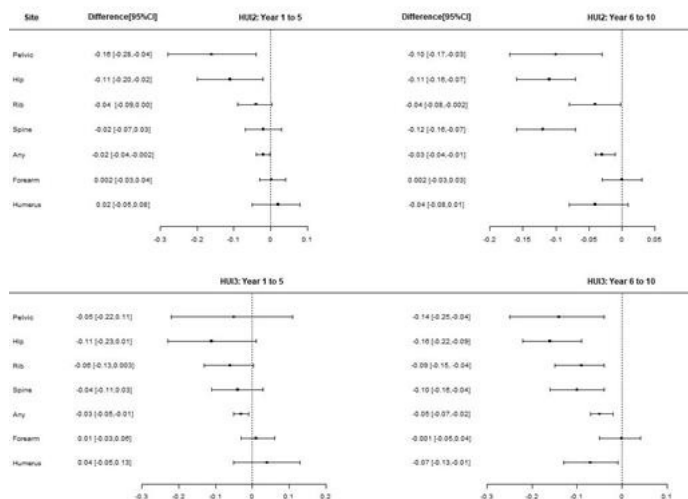
Disclosures: Kate Ward, None

FRI-0804

The Long-term Impact of Incident Low-trauma Fractures on Health-related Quality of Life of Older People: The Canadian Multicentre Osteoporosis Study Asm Borhan*, Alexandra Papaioannou¹, Olga Gajic-Veljanoski², Courtney Kennedy¹, George Ioannidis¹, Claudie Berger³, Wilma Hopman⁴, David Goltzman⁵, Robert Josse⁶, Christopher S Kovacs⁷, David A Hanley⁸, Jerilynn C Prior⁹, Suzanne N Morin⁵, Stephanie M Kaiser¹⁰, Angela M Cheung¹³, Lehana Thabane¹², Jonathan D Adachi¹², The Camos Research Group³. ¹McMaster University & GERAS Centre, Canada, ²GERAS Centre, Canada, ³Camos – McGill University, Canada, ⁴Kingston General Hospital, Canada, ⁵McGill University, Canada, ⁶St. Michael Hospital, Canada, ⁷Memorial University of Newfoundland, Canada, ⁸University of Calgary, Canada, ⁹University of British Columbia, Canada, ¹⁰Dalhousie University, Canada, ¹²McMaster University & St. Joseph's Healthcare Hamilton, Canada, ¹³University of Toronto & University Health Network, Canada

Background Although the short-term impact of incident fractures on health-related quality of life (HRQL) of older people has been confirmed, we lack long-term data. We explored the impact of incident low-trauma fractures on HRQL (measured by Health Utility Index-HUI2/3), among people aged 50 years and older, using 10-year prospective data from the Canadian Multicentre Osteoporosis Study. Both HUI2/3 can capture the general health status and specific domains including mobility, ambulation and pain. Method This study included 2187 men and 5566 women. The HUI2/3 was measured at baseline and year 10, while fragility fractures were ascertained yearly over 10 years and specified by sites (clinical spine, hip, rib, humerus, pelvic, forearm and any). Multivariable regression was used to measure the mean difference, adjusted for baseline HUI score and age, for those with and without fractures. The effect of time periods (years 1 to 5 vs. 6 to 10) and multiple fractures on year 10 HUI score were also examined. Results The median age (men/women: 66/67 years) and baseline HUI scores (0=death, 1=perfect health) for both men (mean±SD: HUI2:0.87±0.13; HUI3: 0.82±0.21) and women (HUI2:0.85±0.15; HUI3:0.80±0.22) were similar. Women and men with incident hip fractures had significant deficits in HRQL: HUI2: -0.11[-0.16, -0.07]; HUI3: -0.15[-0.21, -0.10] and HUI2: -0.19[-0.28, -0.12]; HUI3: -0.15[-0.28, -0.02], respectively. Similarly, clinical spine fractures had substantial deficits on HUI2 among women (-0.07, p<0.001) and men (-0.07, p=0.04). In both sexes, hip fractures had statistically significant negative impact on mobility (men: -0.18, p<0.001; women: -0.16 p<0.001), self-care (men: -0.09, p=0.01; women: -0.18; p<0.001), and ambulation (men: -0.17, p<0.001; women: -0.18; p<0.001). Like hip, clinical spine fractures had substantial deficits on mobility (men: -0.09, p=0.02; women: -0.07; p<0.001), and ambulation (men: -0.10, p=0.02; women: -0.10, p<0.001). Fractures that occurred closer to the follow-up assessment had greater impact on HRQL. However, the impact of hip fractures lasted 5 years or longer (Figure). Multiple hip (-0.15[-0.28, -0.01]) and spine fractures (-0.14[-0.27, -0.004]) significantly impacted the overall HRQL of women only. Humerus and wrist fractures had no long-term impact on HRQL. Conclusion Our analysis suggests that incident low-trauma fractures, in particular hip and clinical spine impact the HRQL of people aged 50+ years for at least 10 years.

Figure: Effect of incident fractures occurred between year 1 to 5 and 6 to 10 on multi-attribute HUI scores at year 10 among women ages 50+ years in the CaMos cohort.



Disclosures: Asm Borhan, None

Friday Posters

FRI-0805

Inappropriate Use of Cost-effectiveness Thresholds as Intervention Thresholds – Potential for Overtreatment of Low Risk Individuals Eugene McCloskey^{*1}, Helena Johansson², Nicholas Harvey³, Juliet Compston⁴, Cyrus Cooper³, John Kanis². ¹Mellanby Centre for Bone Research, University of Sheffield, United Kingdom, ²Centre for Metabolic Bone Diseases, University of Sheffield, United Kingdom, ³MRC Lifecourse Epidemiology Unit, University of Southampton, United Kingdom, ⁴Department of Medicine, Cambridge Biomedical Campus, United Kingdom

Purpose: Cost-effectiveness analysis have traditionally been used to determine appropriate use of relatively expensive treatments. In the UK, the National Institute of Health and Care Excellence (NICE) recently found generic oral bisphosphonates to be cost-effective when prescribed for patients fulfilling screening criteria laid out in NICE CG146 with a 10 year risk of major osteoporotic fracture (MOF) of 1% or more. This 1% threshold has mistakenly been interpreted by some as an intervention threshold; we have compared the impact of this threshold with that advocated by the National Osteoporosis Guideline Group (NOGG). **Methods:** In a simulated age-matched population of 50,633 UK women aged 50-90 years, with risk factor distribution similar to European FRAX derivation cohorts, the NICE and NOGG thresholds were compared including impacts on treatment recommendation and numbers needed to treat (NNT) to prevent a hip fracture. **Results:** All women in the population had a 10-year FRAX MOF probability of ≥1%. As 40,537 fulfilled the NICE CG146 screening criteria, treatment would be recommended in 80.1% of women under the NICE threshold. In contrast, NOGG guidance recommended treatment in 20,465 women (40.8%). At ages 50-54 years, NOGG recommended treatment in 30.8% of women, rising to 63.7% in those aged 85-90 years. In contrast, the NICE threshold treated 61% of 50-54 year olds and 100% of those aged 65 years or older. The median 10-year FRAX hip fracture probability in those identified by NICE for treatment at ages 50-54 years was significantly lower (0.42%) than that in those identified by NOGG (1.07%), suggesting that the NNT would be 2.55 times higher under NICE, assuming the same treatment efficacy in both groups. At 80-85 years, the ratio was 1.32. **Conclusions:** When osteoporosis treatments are very inexpensive, misapplication of cost-effectiveness thresholds as intervention thresholds markedly increases the proportion of postmenopausal women eligible for osteoporosis treatment, an effect that is more marked at younger ages. The higher number needed to treat to prevent a hip fracture, especially at younger ages, is likely to adversely alter the benefit-risk ratio.

Disclosures: Eugene McCloskey, None

FRI-0806

Bending the Curve with Patient Identification and Treatment in Osteoporosis E. Michael Lewiecki^{*1}, Jesse D. Ortendahl², Jacqueline Vanderpuy-Orgle³, Andreas Grauer³, Amanda L. Harmon², Andrea J. Singer⁴. ¹New Mexico Clinical Research & Osteoporosis Center, United States, ²Partnership for Health Analytic Research, LLC, United States, ³Amgen Inc., United States, ⁴Georgetown University Hospital, United States

Purpose: Two million US women and men suffer an osteoporotic fracture every year, often with significant ensuing morbidity, reductions in quality of life, loss of independence, and mortality. Such fractures also contribute to high costs for private payers and Medicare. Given demographic trends, there is an urgent need for better diagnosis and treatment strategies to reduce the clinical and economic burden to the individual and to society. In this study, we aimed to model the expected growth in osteoporotic fractures and simulate the impact of increased case finding and treatment. **Methods:** A microsimulation model was developed to project annual osteoporotic fracture rates and related costs among US women ages 65+ years from 2018-2040. Fracture rates were estimated using FRAX, a commonly used fracture prediction tool, and risk factor prevalence estimates from NHANES, a nationwide survey. Direct and indirect cost inputs were based on published literature and pricing databases. Scenarios, which varied by incorporation of policies aiming to increase diagnosis and treatment, were compared to estimate the potential benefits of encouraging and improving methods of case finding, and incentivizing the appropriate use of treatment. **Results:** Given anticipated population aging and growth, osteoporotic fractures were projected to increase by 68% from 2018 to 2040. The societal costs related to fracture prevention and treatment were expected to rise from \$52 billion in 2018 to over \$87 billion in 2040. Policy-driven increases in diagnosis and treatment of at-risk women could substantially decrease the clinical burden, with increases in treatment preventing up to 6.1 million fractures over the next 22 years. At the same time, efficient methods of case finding leading to higher treatment rates could reduce payer costs by \$21 billion and total societal costs by \$44 billion over the same time period. **Conclusions:** Given a growing population of postmenopausal women in the US population and increasing longevity, there is an expected rise in the economic and clinical burden of osteoporotic fractures. To prevent this rapid growth in fractures, emphasis must be placed on osteoporosis-related interventions. Our analysis found that such measures would simultaneously reduce the clinical burden while reducing costs, a rare combination given the current landscape.

Table 1. Model Projected Clinical and Economic Outcomes

Scenario	Total Fractures (2018-2040)	Fractures Reduced (vs. Base Case)	Total Costs (2018-2040) ^a	Cost Savings (vs. Base Case) ^a
Base Case (11% DXA, 9% Treatment)	61,603,120	-	\$1,674,639.3	-
Increased Case Finding (61% DXA, 31% Treatment)	57,449,128	4,153,993	\$1,635,873.2	\$38,766.0
Increased Treatment (61% DXA, 53% Treatment)	55,457,460	6,145,661	\$1,630,424.9	\$44,214.4

^a Costs reported in millions.

Disclosures: E. Michael Lewiecki, New Mexico Clinical Research & Osteoporosis Center, Other Financial or Material Support, Mereo, Grant/Research Support, Sandoz, Consultant, PFEEx, Grant/Research Support, Ultragenyx, Consultant, Shire, Consultant, Shire, Speakers' Bureau, Amgen, Consultant, Amgen, Grant/Research Support, Radius, Speakers' Bureau, Radius, Consultant, Alexion, Consultant, Alexion, Speakers' Bureau

FRI-0824

The Calgary Vitamin D Study: Safety of Three-Year Supplementation With 400, 4000 or 10000 IU Daily Emma O Billington^{*1}, Lauren A Burt¹, Erin M Davison¹, Marianne S Rose², Sharon Gaudet¹, Michelle Kan¹, Steven K Boyd¹, David A Hanley¹. ¹McCaig Institute for Bone and Joint Health, Cumming School of Medicine, University of Calgary, Canada, ²Research Facilitation, Alberta Health Services, Canada

The Institute of Medicine set the tolerable upper intake level (TUL) for vitamin D at 4000 IU/day. Some suggest the TUL could be 10,000 IU/day. More than 3% of US adults report vitamin D intakes >4000 IU/day, but the safety of this practice is unknown. We conducted a 3-year double-blind RCT to investigate the dose-dependent effects of vitamin D supplementation on bone density and strength; safety was a pre-specified secondary outcome. Healthy adults aged 55-70 with serum 25(OH)D 30-125 nmol/L were randomized to receive 400, 4000 or 10000 IU vitamin D3 daily for 3 years. Calcium supplementation was initiated if dietary calcium intake was <1200mg/day. Fasting blood samples were collected (baseline, 3, 6, 12, 18, 24, 30, 36 months) and serum analyzed for 25(OH)D and calcium. Hypervitaminosis D was defined as 25(OH)D >450 nmol/L; hypercalcaemia as serum calcium >2.55 mmol/L. Hypercalcaemia was defined as 24-hour urine calcium >7.50 mmol or >0.1 mmol/kg body if weight >75kg, measured at baseline, 12, 24, 36 months. Calcium intake was reduced if hypercalcaemia occurred. At visits, adverse events (AEs) and serious adverse events (SAEs), including fractures and falls were reported. Fisher Exact Tests were used to examine relationships between categorical variables. 373 participants (mean [SD]: 62 [4] years, 52% women) were randomized and 343 (92%) completed the study. Drop-outs were similar among groups. Mean (SD) serum 25(OH)D levels at 3 months were 76 (17), 114 (22), 187 (38) nmol/L in the 400, 4000 and 10000 IU groups respectively. No 25(OH)D levels >450 nmol/L were observed at any time point. A total of 2725 AEs occurred in 365 participants, including 66 SAEs in 52 participants (Table 1). The number of participants with AEs (p = 0.999) and SAEs (p = 0.199) were not significantly different between groups. Incidence of hypercalcaemia (range: 2.56-2.64 mmol/L) varied significantly between the 400 IU (0%), 4000 IU (3%) and 10000 IU (9%) groups (p<0.001). Hypercalcaemia occurred in 87 participants; incidence varied significantly between the 400 IU (17%), 4000 IU (22%) and 10000 IU (31%) groups (p = 0.040). In conclusion, vitamin D supplementation for 3 years was not associated with any SAEs or AEs; however, there was a dose-response increase in hypercalcaemia which resolved on repeat testing, and hypercalcaemia which usually resolved with reduction in calcium intake.

Table 1. Incidence of adverse events in a randomized controlled trial comparing vitamin D3 400, 4000 and 10000 IU taken daily for 3 years

	400 IU (n=124)		4000 IU (n=125)		10000 IU (n=124)	
	Total Events, n	Participants Experiencing Event, n (%)	Total Events, n	Participants Experiencing Event, n (%)	Total Events, n	Participants Experiencing Event, n (%)
All Adverse Events	863	121 (98)	968	122 (98)	894	122 (98)
Serious Adverse Events	25	19 (15)	17	12 (10)	24	21 (17)
Adverse Events of Interest						
Hypercalcaemia	0	0 (0)	4	4 (3)	12	11 (9)
Hypercalcaemia						
Any hypercalcaemia	27	21 (17)	40	28 (22)	56	38 (31)
One episode	-	16 (13)	-	20 (16)	-	24 (19)
Two episodes	-	4 (3)	-	4 (3)	-	10 (8)
Three episodes	-	1 (1)	-	4 (3)	-	4 (3)
Falls	5	5 (4)	13	12 (10)	10	8 (6)
Fractures	5	5 (4)	3	3 (2)	8	7 (6)
Nephrolithiasis	0	0 (0)	1	1 (1)	1	1 (1)
Cancer	11	10 (8)	7	7 (6)	13	13 (10)
Infections						
All infections	278	106 (85)	297	100 (80)	287	101 (81)
URTIs	194	89 (72)	204	89 (71)	166	80 (65)
Cardiovascular	38	31 (25)	35	27 (22)	41	30 (24)
Dermatologic	58	36 (29)	62	48 (38)	46	33 (27)

Adverse events and serious adverse events were defined using the standard International Conference on Harmonization Good Clinical Practice (ICH GCP) definition.

Disclosures: Emma O Billington, None

FRI-0825

Natural history of maternal urinary β -C-terminal telopeptide of type I collagen (CTX) in pregnancy, and response to cholecalciferol supplementation: findings from the MAVIDOS trial

Elizabeth Curtis^{*1}, Camille Parsons¹, Kate Maslin¹, Stefania D'Angelo¹, Rebecca Moon¹, Sarah Crozier¹, Fatma Gossiel², Nicholas Bishop³, Stephen Kennedy⁴, Aris Papageorgiou⁴, Robert Fraser⁵, Saurabh Gandhi⁵, Ann Prentice⁶, Hazel Inskip¹, Keith Godfrey¹, Inez Schoenmakers⁶, M Kassim Javaid⁷, Richard Eastell², Cyrus Cooper¹, Nicholas Harvey¹. ¹MRC Lifecourse Epidemiology Unit, University of Southampton, Southampton, United Kingdom, ²Academic Unit of Bone Metabolism, University of Sheffield, Sheffield, United Kingdom, ³Academic Unit of Child Health, Sheffield Children's Hospital, University of Sheffield, Sheffield, United Kingdom, ⁴Nuffield Department of Women's & Reproductive Health, John Radcliffe Hospital, University of Oxford, Oxford, United Kingdom, ⁵Department of Obstetrics and Gynaecology, Sheffield Hospitals NHS Trust, University of Sheffield, Sheffield, United Kingdom, ⁶MRC Human Nutrition Research, Elsie Widdowson Laboratory, Cambridge, United Kingdom, ⁷National Institute for Health Research (NIHR) Oxford Biomedical Research Centre, University of Oxford, United Kingdom

Markers of maternal bone turnover in pregnancy are poorly characterised. In a randomised trial we investigated i) changes in maternal urinary beta-C-terminal telopeptide of type I collagen (CTX) concentrations in pregnancy, and the effect of gestational vitamin D supplementation thereon; and ii) associations between CTX and maternal postnatal bone indices. MAVIDOS is a randomised, double-blind, placebo-controlled trial of 1000 IU/day cholecalciferol vs placebo from 14 weeks gestation to birth. At 14 and 34 weeks gestation, maternal second void urinary CTX was measured using an ELISA (Immunodiagnostic Systems, Boldon, UK) and expressed relative to creatinine (Cr). Maternal bone indices were assessed by DXA (Hologic Discovery) within 2 weeks after delivery. Median CTX concentrations were compared using the Wilcoxon signed-rank test. CTX values were log transformed and standardised to an SD scale. Correlation and linear regression methods were used to explore associations. Beta coefficients represent change in outcome per 1 SD increase in CTX. 636 women (314 placebo, 322 cholecalciferol) were studied. CTX increased overall from 14 to 34 weeks in both groups (median 14 and 34 week CTX: placebo 223.8 and 445.3 μ g/mmol Cr; cholecalciferol 217.5 and 420.0 μ g/mmol Cr; both p=diff 14 to 34 weeks < 0.0001; p=diff for supplementation effect at 34 weeks = 0.06); 14 and 34 week values were correlated in both the placebo (r=0.32) and treatment (r=0.45) groups (both p < 0.0001). In groups combined, 34 week CTX was associated with lower postpartum maternal femoral neck bone area [-0.43cm²/SD (-0.80, -0.07), p=0.02], bone mineral content (BMC) [-0.001g/SD (-0.001, 0.000), p=0.03] and lumbar spine BMC [-0.001g/SD (-0.002, 0.000), p=0.03]. There was no interaction between treatment group and CTX on bone outcomes (p-interaction all > 0.6). Urinary CTX rises from early to late pregnancy, appears to be reduced by gestational cholecalciferol supplementation, and is inversely associated with maternal bone mass post-partum. These findings inform our understanding of bone resorption in pregnancy and the potential relationship with vitamin D metabolism.

Disclosures: Elizabeth Curtis, None

FRI-0826

The association of breastfeeding, maternal smoking, birth weight and maternal diet with bone density and microarchitecture in young adulthood: a 25-year longitudinal study

Yi Yang^{*1}, Feitong Wu¹, Terry Dwyer², Tania Winzenberg¹, Graeme Jones¹. ¹Menzies Institute for Medical Research, University of Tasmania, Australia, ²The George Institute for Global Health, University of Oxford, United Kingdom

Objective: We have previously shown that early life exposures are associated with bone mass assessed by densitometry at age 8 and 16. This study aimed to describe whether these associations persisted to young adulthood and extended to microarchitecture. Method: There were 201 participants followed from birth to age 25. Outcomes measured were bone mineral density (BMD) at the spine, hip and total body (by dual-energy X-ray absorptiometry (DXA)). Trabecular and cortical bone measures were obtained by high resolution peripheral quantitative computerized tomography (HRpQCT) at radius and tibia. Other factors measured were anthropometrics, breastfeeding status, maternal smoking, birth weight and Food Frequency Questionnaire (FFQ) during the third trimester of pregnancy. Result: For participants born prematurely, breastfeeding was associated with improvements in volumetric density (vBMD), porosity in cortical and inner transitional zones, trabecular number (Tb.N) and trabecular bone volume fraction (Tb.BV/TV) at radius or tibia at age 25. Maternal smoking during pregnancy was not associated with participants' porosity and trabecular microarchitecture at age 25. Low birth weight was a positive predictor for spine areal BMD, trabecular vBMD and trabecular separation (Tb.Sp). Maternal meat intake during pregnancy was associated with higher total vBMD and lower porosity at compact cortical, outer and inner transitional zones. Other nutrients (protein, fat, carbohydrate, calcium, magnesium and phosphorus) and food (fish, vegetable, fruit and milk) intake were not associated with any bone measures. For participants born at term, the beneficial effect of breastfeeding was no longer present. Smoking during pregnancy was associated with higher Tb.Sp and inner transitional zone porosity, lower trabecular vBMD, Tb.N and Tb.BV/TV. There was no sig-

nificant association between maternal nutrient and food intake during pregnancy with participants' vBMD and microarchitecture at age 25. Conclusion: There were long-term beneficial associations of breastfeeding, low birth weight, meat intake during pregnancy and vBMD as well as bone microarchitecture in participants born prematurely. Maternal smoking was an early life marker for suboptimal bone trabecular spacing and porosity in those children born at term. This study suggests that early life exposures may have affect bone development until the time of peak bone mass.

Disclosures: Yi Yang, None

FRI-0827

Effect of High-Dose Vitamin D on Bone Microarchitecture assessed via High Resolution Peripheral Quantitative Computed Tomography (HR-pQCT): a Double-Blind RCT

Ursina Meyer^{*1}, Ursula Heilmeyer¹, Robert Theiler², Andreas Egli¹, Heike A. Bischoff-Ferrari². ¹Centre on Aging and Mobility, Department of Geriatrics and Aging Research, University Hospital Zurich and Zurich of University, Switzerland, ²Department of Geriatrics and Aging Research, University Hospital Zurich and Zurich of University, Switzerland

Vitamin D (VitD) is a well-recognized key player in bone and mineral metabolism and VitD supplementation has been widely attributed beneficial effects on musculoskeletal health. However, to date, the optimal supplemental dose remains controversial. In addition, the detailed effect of VitD on bone microarchitecture in humans is still largely unknown as most clinical trials use DXA to assess bone outcomes, a 2D technique that cannot resolve bone microstructure. With the advent of HR-pQCT, a promising, non-invasive imaging tool has emerged which allows for in vivo 3D characterization of human bone microstructure at a spatial resolution of 82 μ m. Therefore, the purpose of this study was to evaluate the effect of two different dosages of daily, 2-year long VitD supplementation (800 IU vs. 2000 IU) on bone microarchitecture using HR-pQCT in elderly seniors. This was a 2-year randomized, double-blind clinical trial. 273 patients aged ≥ 60 y were randomized to receive daily doses of either 2000 IU VitD (HD-group) or the standard-dose of 800 IU VitD (SD-group), and all received 500 mg calcium supplement per day. At baseline and 24 months, aBMD by DXA was measured at the hip and lumbar spine and bone microarchitecture of the distal radius and tibia was imaged by HR-pQCT. Bone structural parameters (0m, 24m, Δ) were computed. General linear models adjusted for age, sex, BMI and baseline bone parameters were employed to compare bone changes over time between treatment groups. At baseline, both groups were similar with respect to mean age, sex, BMI, and serum 25(OH)D levels (Tab 1). After 2 years, higher 25(OH)D levels were observed in the HD-group compared to the SD-group (35.7 \pm 6.8 vs. 28.8 \pm 6.0 ng/ml; p \leq 0.001). While DXA showed similar, small, but not significant increases in mean aBMD over the 2-y follow up for both groups, we noted via HR-pQCT a significant increase in trabecular number in the HD-group (Δ Tb.N 0.056 (SE 0.016) vs. 0.008 (0.016) 1/mm, p = 0.03) at the tibia. No statistical significant differences were found in other structural parameters [trabecular (Tb.Th) or cortical thickness (Ct.Th)], and volumetric BMDs at both sites. We conclude that a high dose VitD supplementation of 2000 IU daily for 2 years might have a slight beneficial effect on bone microarchitecture in seniors by increasing the trabecular number. Further microfinite element analyses are necessary to determine if this translates into improved biomechanical bone properties.

Table 1: Baseline characteristics of n= 196 seniors with HR-pQCT-derived bone microstructure measurements acquired at baseline and after 2 years of Vit D supplementation with either a daily standard dose or high dose Vit D regimen. Values are given as means (standard deviations) unless stated differently. Statistical significance is assumed at a p < 0.05. P-values were calculated using either Student's t-tests or X2 tests, as appropriate.

	Standard Dose Vitamin D: 800 IU	High-Dose Vitamin D: 2000 IU	p-value
N	102	94	
Gender, % female	55%	48%	0.325
Age, yr	70.8 (5.9)	69.8 (6.6)	0.277
BMI, kg/m ²	27.2 (4.1)	27.9 (3.7)	0.228
Serum 25(OH)D level, ng/ml †	18.3 (8)	18.6 (7.9)	0.790
Vitamin D deficient (<20 ng/mL), %	55%	58%	0.932

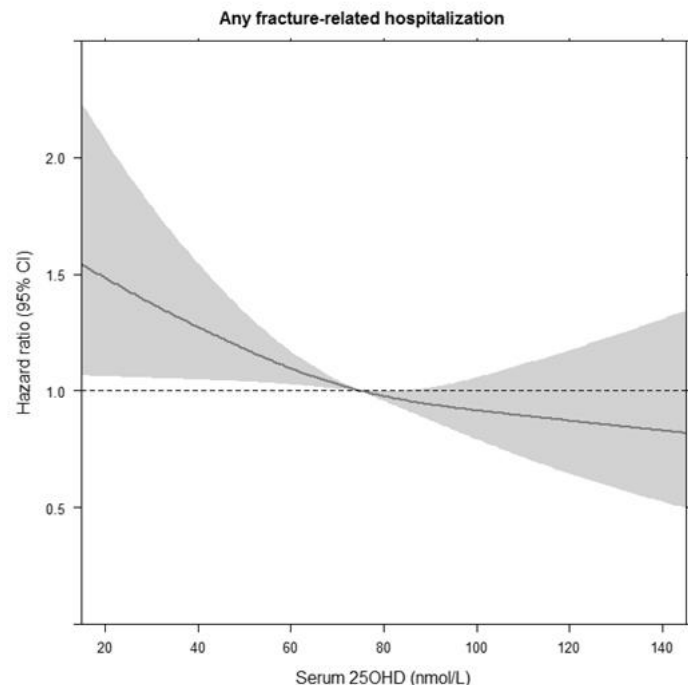
† Serum 25(OH)D level were assessed via the automated Vitamin D assay (Fujirebio).

Disclosures: Ursina Meyer, None

FRI-0828

Vitamin D Status, Bone Quality and Long-Term Risk for Fracture-related Hospitalization in Older Women Kun Zhu^{*1}, Joshua Lewis², Marc Sim², Richard Prince³. ¹Department of Endocrinology and Diabetes, Sir Charles Gairdner Hospital, Australia, ²School of Medical and Health Sciences, Edith Cowan University, Australia, ³Medical School, University of Western Australia, Australia

Aims: We examined the association between plasma 25-hydroxyvitamin D (25OHD) with bone quality and 14.5-year fracture-related hospitalizations in a cohort of older women. **Methods:** The study participants were 1,348 women aged 70-85 years at baseline (1998) from the Perth Longitudinal Study of Aging in Women Study. Assessments include plasma 25OHD concentration using LC-MS/MS at baseline, hip DXA bone mineral density (BMD) at year 1, trabecular bone score (TBS) at year 5, and fracture-related hospitalizations over 14.5 years obtained from the Western Australian Hospital Morbidity Database Collection. **Results:** The mean plasma 25OHD was 66.9 (SD 28.2) nmol/L, and 384 (28.5%), 491 (36.4%) and 473 (35.1%) women had plasma 25OHD <50, 50-75 and ≥75 nmol/L, respectively. Accounting for season of blood sampling, baseline age, BMI and lifestyle factors, women with 25(OH)D ≥75 nmol/L had significantly higher total hip and femoral neck BMD at year 1 (3.3-3.9%) and TBS at year 5 (2.4%) than those with plasma 25OHD <50 nmol/L (all P<0.05). Generalized additive regression models showed that the values for total hip and femoral neck BMD and TBS increased with the increase of plasma 25OHD up to about 100 nmol/L, then levelled off. In the multivariate-adjusted Cox proportional hazards regression analyses, compared with women who had plasma 25OHD <50 nmol/L, those with 25OHD 50-75 and ≥75 nmol/L had significantly lower risk for any fracture (hazard ratio (95% CI): 0.75 (0.58, 0.97) and 0.69 (0.53, 0.90), respectively) and hip fracture-related hospitalization (hazard ratio (95% CI): 0.60 (0.40, 0.91) and 0.61 (0.40, 0.93), respectively). Restricted cubic spline regression models showed that plasma 25OHD below 75 nmol/L was associated with higher risk of any fracture-related hospitalization (Figure) and below 50 nmol/L hip fracture-related hospitalization. **Conclusions:** Our prospective study suggests maintaining serum 25OHD levels of at least 50 nmol/L and ideally up to 75 nmol/L could confer benefit for the long-term prevention of fracture-related hospitalization in community-dwelling older women.



Disclosures: Kun Zhu, None

FRI-0829

High dietary calcium intakes in men, not women, are associated with increased all-cause mortality: the Melbourne Collaborative Cohort Study Alexander Rodriguez^{*1}, David Scott¹, Belal Khan², Allison Hodge³, Dallas English², Graham Giles³, Bo Abrahamson⁴, Peter Ebeling¹. ¹Monash University, Australia, ²University of Melbourne, Australia, ³Cancer Council Victoria, Australia, ⁴University of Southern Denmark, Denmark

Context: The association of dietary calcium with mortality is controversial. A study of older women from the Swedish Mammography Cohort (SMC) suggested higher calcium was associated with a higher mortality risk; while a study of Australian adults from the

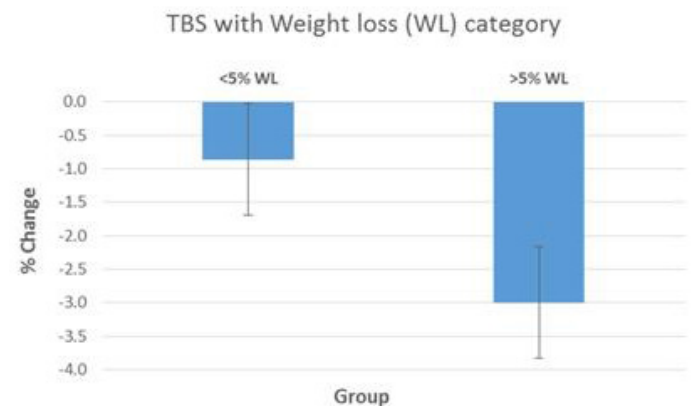
Melbourne Collaborative Cohort Study (MCCS) suggested higher intakes were associated with lower mortality risk. **Objective:** Perform a sex-specific re-analysis of MCCS to evaluate the association of dietary calcium with mortality outcomes and directly compare hazard estimates [95% confidence intervals] in women with those from SMC. **Design:** Prospective, cohort study. **Setting:** Community-dwelling adults. **Patients:** 34,627 individuals (women: 20,834 [60.2%], mean±SD age = 54±8 years) at baseline after excluding those with prevalent CV disease, cancer or incomplete data. **Exposure:** Energy adjusted dietary calcium categorised into levels of consumption (mg/day): <600; 600-999; 1000-1399; ≥1400. **Main outcome:** Mortality from all-causes, any CV disease and myocardial infarction. **Mortality hazards** estimated relative to intakes of 600-999mg/day. **Results:** In women, hazard estimates for calcium intake of ≥1400mg/day did not reach significance for all-cause [HR=0.83; 0.64, 1.08] or CV [HR=1.10; 0.68, 1.78] mortality in adjusted models. In men, intakes of ≥1400mg/day were associated with a 41% increased all-cause mortality risk [HR=1.41; 1.01, 1.97]. There was a trend toward increased CV mortality [HR=1.77; 0.92, 3.13]. In sensitivity analyses excluding those with calcium intakes three standard deviations above the sex-specific mean, for men there was a 54% increased risk of all-cause mortality [HR=1.54; 1.08, 2.19] associated with intakes above 1400mg/day. For women, no hazard estimate reached significance for any outcome. **Conclusion:** Contrary to findings from a similar study conducted in Swedish women, Australian women showed no increase in mortality risk with high calcium intakes. This may reflect differences in calcium handling dynamics, diet or lifestyle factors between the two countries. We identified an increased mortality risk for men.

Disclosures: Alexander Rodriguez, None

FRI-0859

A greater weight loss reduces lumbar spine trabecular bone score in the obese, and this is not influenced by vertebral body structural defects Julia Amariti^{*1}, Stephen Schneider², Karen Hansen³, Yvette Schlüssel¹, Sue Shapses¹. ¹Rutgers University, United States, ²Rutgers Robert Wood Johnson Medical School, United States, ³University of Wisconsin School of Medicine and Public Health, United States

Purpose: Obesity is a risk factor for osteoarthritis and spinal stenosis. Clinicians often recommend weight loss to reduce pain related to osteoarthritis and improve other health outcomes. However, weight loss can result in declines in bone mineral density (BMD), although this is not consistently observed at the lumbar spine (LS). It is hypothesized that this may be due to a higher prevalence of vertebral structural defects, and that LS trabecular bone score (TBS) may be a more sensitive indicator of bone changes due to WL. **Methods:** In this study, we retrospectively examined changes in BMD and trabecular bone scores (TBS) in 88 older overweight/obese women and men (body mass index, BMI, 32.0 ± 4.5 kg/m²; 57 ± 5 years old) who participated in weight loss studies (1-3). We classified weight loss as <5% (mild; n=44) or >5% (moderate; n=44). Because spine osteoarthritis leads to artifacts that spuriously measure the lumbar spine BMD, we assessed dual energy x-ray absorptiometry lumbar spine images for vertebral body exclusion criteria (4). **Results:** Repeated measures ANOVA (group by time) indicated that the trabecular bone score (TBS) was significantly affected by both time (p < 0.001) and degree of weight loss (p = 0.027). Moderate weight loss (-8.4 ± 4.0%) was associated with greater declines in TBS (-3.0 ± 5.5%) than mild weight loss (-2.7 ± 2.2% weight loss, TBS changed by 0.8 ± 4.6%). As expected, BMD decreased (p < 0.05) over time at multiple skeletal sites (ultradistal radius, 33% radius, total body), but this did not differ by weight loss category. By contrast, BMD did not decrease significantly at the lumbar spine, hip or femoral neck. Approximately 40% of subjects had ≥1 vertebrae with focal structural defects prompting vertebral body exclusion. However, when excluding vertebrae with such defects, we still found no association between weight loss and changes in spine BMD. Women experienced a greater decline in TBS than did men, despite similar degrees of weight loss (p < 0.001). **Conclusion:** Weight loss was associated with a decline in TBS, with women experiencing greater declines in TBS than men, despite similar degrees of weight loss. **References:** 1. Sukumar D JBMR 2011; 2. Pop LC Osteopor Int 2017; 3. Pop AJCN 2015; 4. Hansen KE JBMR 2005.



Disclosures: Julia Amariti, None

FRI-0860

Identification of Cellular Senescence and Senescent Secretory Markers as Major Etiologies Underlying Radiotherapy Related Bone Damage

Abhishek Chandra*, Joshua Farr, David Monroe, Rebekah Samsonraj, Haitao Wang, Susan Law, Sundeep Khosla, Robert Pignolo. Mayo Clinic, United States

Radiotherapy reduces cancer burden and improves survivorship, but by-stander effects on healthy tissues such as bone causes insufficiency fractures, and increases risk of morbidity and mortality. Despite extensive efforts, the exact mechanism(s) underlying radiotherapy-induced osteoporosis (RIO) are unclear, and an FDA approved drug to alleviate RIO is still elusive. In our mouse model of RIO, 3-month-old wild-type mice received 16Gy of focal radiation (R) to the metaphyseal region of the right femur, while the contralateral left leg was non-irradiated (NR). We demonstrated in this model that loss in vBMD due to R begins at 2wks and peaks at 4wks. However, since osteoclasts were reduced by 2wks post-R, the exact mechanism behind RIO at 4wks is still incompletely understood. We recently identified cellular senescence and the senescence-associated secretory phenotype (SASP) as causal factors in the pathophysiology of age-related osteoporosis. However, possible roles for cellular senescence and the SASP in RIO have not been defined. Therefore, we performed gene expression profiling of the R bone in comparison to contralateral NR bones from RIO mice and compared markers for senescence and the SASP that were significantly expressed in enriched bone cell populations from old (O) mice as well. Among the senescence-related genes, p15, p16, p21, p27 and their regulator, FoxO1, as well as 12 SASP genes were markedly upregulated in response to R. Strikingly, among the 23 Wnt-pathway genes examined, Wnt-2, -2b, -3, -3a, -5b, -10a, -11, -16, Wif1 and Wisp2 decreased significantly with R; while Axin2, a negative Wnt-regulator had an elevated expression in the R bones. RIO is also associated with bone marrow adiposity (BMA), and we observed increased BMA markers Fabp4, Lpl, ApoE, Plin1, Cebp- α and PPAR- γ in R-bones. In order to identify the bone marrow cells that contributed towards the senescence and SASP observed in R bones, we performed gene expression analysis on magnetic sorted CD14⁺ myeloid cell population 2-weeks post-R. We observed significant increases in Wnt inhibitor, Axin2, the senescence marker, FoxO1 and SASP factors, Ccl2, Ccl4, Ccl5, Ccl6, Ccl7, Cxcl1, Cxcr5 and Mmp12, further confirming that myeloid cells were the major contributors of SASP factors in R bones as compared to NR bones. In conclusion, we have identified that cellular senescence and the SASP are the major etiologies underlying RIO, possibly due to down-regulation of the Wnt-pathway.

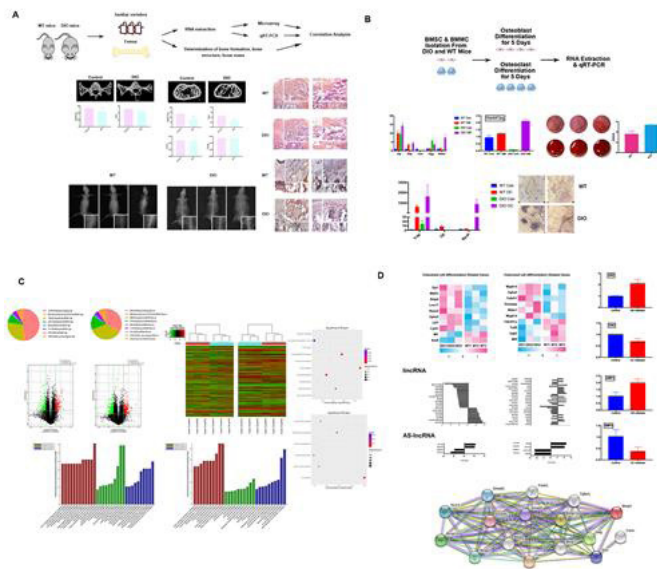
Disclosures: *Abhishek Chandra, None*

FRI-0861

Identification and Characterization of lncRNA-DBD in Diabetic Bone Metabolism

Zhekai Hu*, Qisheng Tu¹, Jake Chen^{1,2}. ¹Division of Oral Biology Tufts University School of Dental Medicine, United States, ²Department of Developmental, Molecular and Chemical Biology Sackler School of Graduate Biomedical Sciences Tufts University School of Medicine, United States

Objective: Mammalian genome contains loci that transcribe long noncoding RNAs (lncRNAs), which can function as essential regulators in diverse cellular processes including stem cell differentiation, cancer development and tissue regeneration via different mechanisms. However, their functions in diabetic bone diseases are largely unknown. In this study, we planned to use a diet induced obesity (DIO) mouse model to identify lncRNAs that attribute to the abnormal skeletal phenotypes under a diabetic condition. Methods: We first generated DIO mouse model and performed histologic staining and computerized tomographic scanning of lumbar vertebra and femur bones from the DIO mice and wide type (WT) mice. In vitro studies included the induction of osteoblast and osteoclast differentiation, quantitative RT-PCR, TRAP and alizarin red S staining. We screened the expression of mRNA and lncRNA in mouse bones through a microarray assay and analyzed the expression profile using bioinformatics. Results: Assessed by the structure model index we found that there was an imbalance between bone formation and bone resorption. Bone microarchitecture was found to be altered, and bone loss increased in lumbar vertebra and femurs of the DIO mice mainly because of impaired remodeling in bone architectures (Fig. A). In vitro experiment findings confirmed the observation (Fig. B). We also screened mRNAs and lncRNAs, and functionally identified a novel candidate lncRNA, termed DBD (Diabetic Bone Disorders), which functioned as an essential regulator in diabetic bone diseases. We further found that DBD highly expressed in osteoblastogenic differentiation and decreased in osteoclastogenic differentiation. In addition, DBD showed a dose-dependent correlation with a neighboring gene Bmp4. Bmp4 plays a pivotal role in osteogenic differentiation and bone formation. Here we showed that Bmp4 regulated the expression of Bmp2, Smad1, Smad2, Shh and Foxh1, potentially through DBD regulation (Fig. C and D). Conclusion: Using RNAs extracted from DIO bone tissues and a microarray assay we have initially identified and characterized a specific lncRNA DBD. DBD level was significantly elevated in diabetic bones. DBD also regulates a neighboring osteogenic gene Bmp4. Currently we are further studying the epigenetic mechanism and molecular signaling of how DBD affects bone metabolism in diabetes. These have great potential to advance our understanding of diabetic related bone disorders.



Disclosures: *Zhekai Hu, None*

FRI-0862

Estrogen depletion alters regulation of mineralization at actively forming osteonal surfaces in a monkey animal model

Eleftherios P. Paschalis*, Sonja Gamsjaeger¹, Stamatia Rokidi¹, Keith Condon², Klaus Klaushofer¹, David Burr². ¹Ludwig Boltzmann Institute of Osteology at the Hanusch Hospital of WGKK and AUA Trauma Centre Meidling, 1st Medical Department, Hanusch Hospital, Heinrich Collin Str. 30, A-1140, Austria, ²Indiana University, School of Medicine, United States

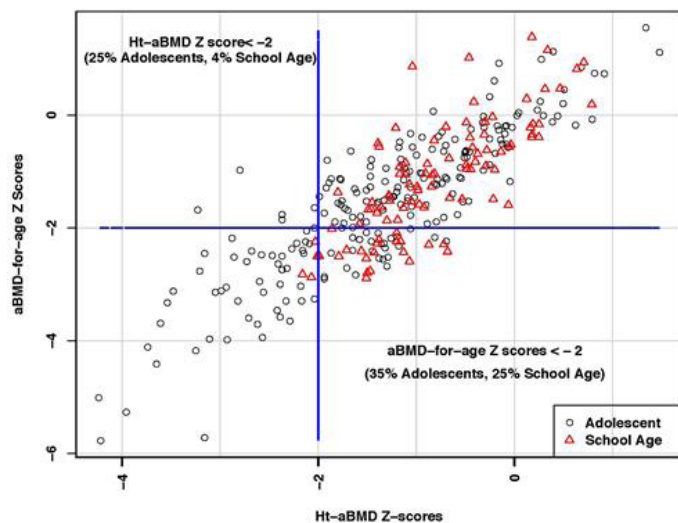
Ovariectomized animal models have been extensively used in osteoporosis research due to the resulting loss of bone mass. The purpose of the present study was to test the hypothesis that estrogen depletion alters mineralization regulation mechanisms in an ovariectomized monkey animal model. We used Raman microspectroscopy to analyze humeri from monkeys that were either SHAM-operated or ovariectomized (N=10 per group). Measurements were made as a function of tissue age based on the presence of multiple fluorescent double labels. Briefly, natural habitat-derived adult female cynomolgus monkeys (*Macaca fascicularis*) were imported from Indonesia, quarantined for 3 months, and screened radiographically to ensure absence of open growth plates and skeletal abnormalities. Double fluorochrome labels were given (calcein, 10 mg/kg, iv) using a 1–12–1 schedule, with sacrifice 7 days after administration. In the present work we focused on osteonal osteoid seams (defined as a surface with evident calcein labels, 1 μ m distance away from the mineralizing front, and for which the Raman spectra showed the presence of organic matrix but not mineral), as well as the youngest mineralized tissue between the second fluorescent label and the mineralizing front, 1 μ m inwards from the front (TA1). The spectroscopically determined parameters of interest were the relative glycosaminoglycan (GAG) and pyridinoline (Pyd) contents in the osteoid, and the mineral content in TA1. In the SHAM animals, there was a significant negative correlation between osteoid GAGs and mineral content (Pearson's $r = -0.83$, $p < 0.0001$), and a positive one between osteoid Pyd and mineral content at TA1 (Pearson's $r = 0.91$, $p < 0.0001$). No significant correlations were evident in the OVX animals (Pearson's $r = -0.26$, and -0.35 , respectively). GAGs are known negative modulators of mineralization. The strong negative correlation between osteoid GAGs and the earliest deposited mineral agrees with previous reports. Pyd is an enzymatic collagen cross-link, involved in collagen fiber formation/stabilization. The highly significant correlation between these two organic matrix attributes in the osteoid and the mineral content of the newly formed bone mineral in the SHAM but not in the OVX animals suggests that in addition to the well-established effects on turnover rates and bone mass, estrogen depletion alters the regulation of mineralization by GAGs and Pyd.

Disclosures: *Eleftherios P. Paschalis, None*

FRI-0877

Low bone mineral density remains highly prevalent in adolescents despite height adjustment: results from the Sickle Cell Clinical Research and Intervention Program (SCCRIP) pediatric cohort Oyebimpe Adesina^{*1}, Guolian Kang², Martha Villavicencio³, Jason Hodges³, Wassim Chemaitilly⁴, Sue Kaste⁵, James Gurney⁶, Babette Zemel⁷, Jane Hankins³. ¹Division of Hematology, University of Washington School of Medicine, United States, ²Department of Biostatistics, St. Jude Children's Research Hospital, United States, ³Department of Hematology, St. Jude Children's Research Hospital, United States, ⁴Department of Pediatric Medicine, Division of Endocrinology, St. Jude Children's Research Hospital, United States, ⁵Department of Radiological Sciences, St. Jude Children's Research Hospital, United States, ⁶School of Public Health, University of Memphis, United States, ⁷Division of Gastroenterology, Hepatology and Nutrition, Children's Hospital of Philadelphia, United States

Purpose Low bone mineral density (BMD) disproportionately affects people with sickle cell disease (SCD), with reported prevalence of 30-50% in children and adolescents. Growth delay is common in SCD, but most BMD studies in pediatric SCD patients fail to account for their short stature. **Methods** We examined low BMD prevalence and clinical correlates in 6 to 18-year-old patients enrolled in the Sickle Cell Clinical Research and Intervention Program (SCCRIP), an ongoing multi-center lifespan SCD cohort study initiated in 2014. SCCRIP participants undergo areal BMD (aBMD) screening from age 6 years, and every 6 years thereafter, using a Hologic dual-energy X-ray absorptiometer (DXA). We stratified subjects into school age children (6-12 years), and adolescents (>12-18 years). Using results of their most recent total body less head DXA scan, we calculated aBMD-for-age and height-adjusted aBMD (Ht-aBMD) Z-scores, based on published values for healthy African American children and adolescents from the Bone Mineral Density in Childhood Study. We defined low BMD as aBMD-for-age Z-score or Ht-aBMD Z-score ≤ -2 ; and, evaluated its associations with demographics and clinical characteristics. Statistical analyses included chi-square, t-test, and multivariate regression analyses. **Results** We examined 308 African American subjects (mean age 12.5 years, 50% female, 73% HbSS/S β thalassemia genotype), and found that 99 (32%, 24 children and 75 adolescents) had low aBMD-for-age, while 58 (19%, 4 children and 54 adolescents) had low Ht-aBMD Z-scores (Figure). In females, low Ht-aBMD Z-scores associated with vitamin D status: 54% deficient, 35% insufficient, and 11% replete (p=0.069). Hip avascular necrosis (AVN) was 5-times more prevalent in males with low versus normal Ht-aBMD Z scores. In multivariate analyses for all patients, low Ht-aBMD Z-scores independently associated with adolescence, chronic pain, and hemoglobin (odds ratios 7.1, 6.9, and 0.8 respectively, p<0.05), not hip AVN (odds ratio 4.5, p=0.11). **Conclusions** Low aBMD is highly prevalent in pediatric SCD. Adjusting for height accounts for the effects of delayed growth on aBMD in children with SCD, yet nearly 20% of subjects (mostly adolescents) still had very low Ht-aBMD Z-scores. Low Ht-aBMD Z-scores associate with older age, chronic pain, and anemia. As the SCCRIP longitudinal cohort matures, future studies will prospectively investigate the association between low Ht-aBMD and markers of SCD severity and morbidity.



Disclosures: Oyebimpe Adesina, None

FRI-0878

Hyponatremia Induced Osteoporosis Julianna Barsony^{*}, Qin Xu, Joseph G. Verbalis. Georgetown University, United States

Growing evidence indicates that chronic hyponatremia represents a significant risk for bone loss, osteoporosis, and fractures in humans. Our prior studies using a rat model of the syndrome of inappropriate antidiuretic hormone secretion (SIADH), demonstrated that hy-

ponatremia causes osteoporosis primarily by increasing osteoclastic bone resorption, thereby liberating stored sodium from bone. Cellular studies have demonstrated increased osteoclast formation and resorptive activity in primary rodent bone marrow macrophages and murine RAW264.7 pre-osteoclastic cells in response to low extracellular fluid (ECF) sodium concentration ([Na⁺]). These studies indicated that osteoclasts can respond to low ECF [Na⁺]. In the present studies, we characterized this response in more detail using gene expression and protein phosphorylation arrays and osteoclast functional assays. We compensated for the osmolality change by adjusting the media osmolality to normal levels with the addition of mannitol. Pathway-specific gene expression array results demonstrated activation of the RANK/PI3K/Akt/mTOR pathway after 24-h exposure to low [Na⁺] (120 mmol/l), compared to normal [Na⁺] (140 mmol/l) media. Phospho-kinase array results supported the findings of the gene expression study. This survival pathway activation generated a burst in osteoclast energy production, as evidenced by ATP measurements in differentiated RAW264.7 cells after culturing in normal and low [Na⁺] for 24 h. Moreover, differentiated osteoclast migration was facilitated through the membrane in a Boyden chamber in low [Na⁺] media compared to migration in normal [Na⁺] media. The potential clinical relevance of osteoclast activation in patients with chronic hyponatremia (131 - 134 mmol/L), having osteoporosis by bone density criteria and prior fractures, was assessed by comparing serum [Na⁺] before and 6 months after starting treatment with denosumab. Administration of denosumab reduced serum [Na⁺] by 2-5 mmol/l (range) compared to baseline in all 4 treatment-naïve patients. No change in serum calcium was found. These combined results therefore support our hypothesis that osteoclast-mediated bone resorption serves to stabilize serum [Na⁺] in hyponatremic patients by releasing sodium from bone stores, and that mTOR inhibitors may be effective in reversing the bone loss in hyponatremic patients without risking aggravation of their hyponatremia.

Disclosures: Julianna Barsony, None

FRI-0879

Bone histomorphometric effects of HIV infection and Antiretroviral therapy Janaina Ramalho^{*1}, Csw Martins¹, Rmr Pereira¹, Thomas Nickolas², Mt Yin², J Galvão³, Margareth Eira⁴, Lm Reis¹, Luzia Furukawa¹, Vanda Jorgetti¹, Rm Moyses^{1,3}. ¹Universidade de São Paulo, Brazil, ²Columbia University, United States, ³UNINOVE, Brazil, ⁴Instituto de Infectologia Emilio ribas, Brazil

Background: Reduction in bone mineral density (BMD) is a known metabolic complication of HIV infection and antiretroviral therapy (ART). We aimed to investigate changes in bone-related proteins and bone histomorphometry in ART-naïve HIV+ men initiating treatment with tenofovir disoproxil fumarate (TDF), lamivudine (3TC) and efavirenz (EFV). **Methods:** In 16 HIV+ men we evaluated bone structure, turnover and mineralization by iliac crest bone biopsy with histomorphometry before and 12 months after ART initiation. BMD was assessed by DXA. RANKL, OPG, SOST, FGF23, IL-6, IL-1 β and TNF α levels in serum and bone were determined using multiplex assays. **Results:** Mean age was 29.8 \pm 5.8 years, mean BMI was 24.4 \pm 2.4, with median HIV RNA level of 28,685 (5,628 - 68,540) copies/mL and mean CD4 of 478 \pm 189 cells. After 12 months, mean CD4 was 739 \pm 232 cells, and all patients had HIV RNA below limit of detection. At baseline, 3 patients (19%) had Z score ≤ -2 at any site. There was a significant reduction in BMD at L1-L4 (0.981 vs. 0.960 g/cm³, p = 0.048), femoral neck (0.887 vs. 0.862 g/cm³, p = 0.001) and total hip (1.029 vs. 1.010 g/cm³, p = 0.04). We observed a trend of increase in 25-OH-vitamin D after 12 months (22.1 \pm 7.4 vs 28.1 \pm 9.2 ng/ml, p 0.06). Reduction in serum RANKL [15.2 (10.0 - 21.9) vs. 10.9 (7.5 - 16.8) pg/ml, p 0.049], TNF α [2.29 (1.78 - 3.37) vs. 1.61 (1.42 - 2.05) pg/ml, p 0.03] and FGF-23 [28.3 (26.2 - 34.9) vs 24.7 (22.1 - 28.3) pg/ml, p 0.04] levels were detected. No significant changes were observed in bone concentration of any protein. Low bone trabecular volume was seen in 25% before and after therapy; whereas the proportion with low bone formation rate and abnormal mineralization lag time increased, albeit not significantly (from 88 to 100%, and from 63 to 75%, respectively). At baseline, increased osteoclastic and eroded surface were seen in 44 and 31%, respectively. ART therapy was associated with an increase in osteoid volume (0.8 (0.3 - 1.4) vs. 2.2 (1.1 - 4.0) %, p 0.02), osteoblastic and osteoclastic surfaces [1.3 (0.5 - 2.3) vs 4.5 (2.5 - 6.8)%, p 0.02, and 0.1 (0.1 - 0.3) vs 0.3 (0.1 - 0.7) %, p 0.04, respectively], and cortical porosity and thickness (3.7 \pm 1.7% vs. 6.3 \pm 3.5%, p 0.049, and 663.5 \pm 163.1mm vs. 886.9 \pm 349.4mm, p 0.04, respectively). **Conclusion:** Abnormalities in bone volume, turnover and mineralization are common in HIV+ men even before ART exposure. These changes did not improve, but worsened after therapy with TDF, 3TC and EFV, which could explain the elevated fracture risk observed in these patients. Our findings emphasize the need for an early detection and management of HIV-related bone disease.

Disclosures: Janaina Ramalho, None

FRI-0880

Low daily dose of glucocorticoids induces trabecular and cortical bones impairment at the femur: a 3D analysis using DXA-based modeling. Arnau Manasanch Berengué^{*1}, Renaud Winzenrieth¹, Ludovic Humbert¹, Edward Leib². ¹Galgo Medical SL, Spain, ²Dept. of Medicine, University of Vermont College of Medicine, United States

INTRODUCTION: The aim of this study was to evaluate the effects of glucocorticoids (GCs) on trabecular and cortical bones at proximal femur using DXA-based 3D modeling. **METHODS:** 402 men and women receiving GCs (≥ 5 mg/day, for ≥ 3 months, predni-

sone equivalent) were included in this study. They were randomly gender-, age- and BMI-matched with 1087 control subjects (1:2 to 1:3). Individuals were included in the control group if they had not received glucocorticoid therapy and if they had a Z-score within -2 to +2 at both spine and femur sites. Clinical data, common clinical risk factors, and dietary habits were available in the medical report of the participants. GCs subjects were stratified depending on their fracture status. Areal BMD (aBMD) was measured at lumbar spine (aBMDLS), total femur (aBMDTot) and femoral neck (aBMDFN). A software algorithm was used to derive QCT-like subject-specific 3D models from the hip DXA scans of the participants and controls and compute the trabecular volumetric BMD (Trabecular vBMD) and the cortical surface BMD (Cortical sBMD). RESULTS: GCs-treated patients had a significantly lower aBMDTot and aBMDFN ($p < 0.05$) when compared with controls while, no difference was observed for aBMDLS ($p = 0.72$). Using 3D modeling, a significantly lower cortical sBMD ($p = 0.02$) at total femur and trabecular vBMD ($p = 0.012$) at neck were observed in GC-treated patients (Figure 1). When stratified based on their fracture status, GCs-treated patients with fracture (all type of osteoporotic fracture) had a significantly lower aBMDTot, cortical sBMD at total femur, trabecular vBMD at both total femur and neck, compared to GCs-treated subjects without fracture (all $p < 0.05$). Cortical sBMD has the strongest association with fracture events in the GCs group, as expressed by an odds ratio per standard deviation decrease of 1.42 [1.08-1.87] and an area under the roc curve of 0.59 [0.54-0.64]. CONCLUSIONS: We observed an impairment of both cortical and trabecular compartments in GCs-treated patients, at total femur for the cortical bone and localized at the neck for the trabecular compartment. Presence of fracture is associated with a low cortical sBMD.

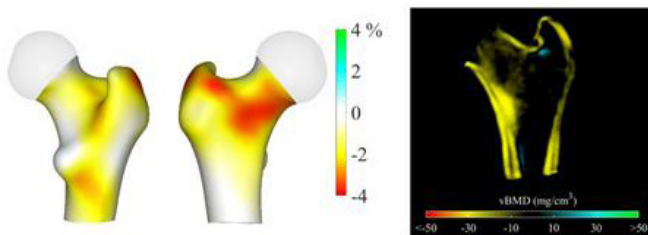


Figure 1: a) 3D distribution of the differences (in %) observed in Cortical sBMD between controls and GCs subjects. Increases are presented in blue-green colour while decreases are presented in yellow-red colours. b) Distribution of the average changes in vBMD observed in both trabecular and cortical bone in the mid coronal between controls and GCs subjects.

Disclosures: **Arnaud Manasanch Berengué**, Galgo Medical, Other Financial or Material Support

FRI-0902

Efficacy of Teriparatide Compared With Risedronate on FRAX®-defined Major Osteoporotic Fractures: A Post-hoc Analysis of the VERO Clinical Trial Jean-Jacques Body^{*1}, Fernando Marin², Piet Geusens³, Cristiano Zerbini⁴, Astrid Fahrleitner-Pammer⁵, Ruediger Moerike⁶, Enrique Casado⁷, Jan Stepan⁸, Salvatore Minisola⁹, Eric Lespessailles¹⁰, Pedro López-Romero², David Kendler¹¹. ¹CHU Brugmann, ULB, Belgium, ²Lilly Research Center Europe, Spain, ³Maastricht University Medical Center, Netherlands, ⁴Centro Paulista de Investigaçao Clínica, Brazil, ⁵Division of Endocrinology, Medical University of Graz, Austria, ⁶Institut Präventive Medizin & Klinische Forschung, Germany, ⁷University Hospital Parc Tauli Sabadell (UAB), Spain, ⁸Institute of Rheumatology and Faculty of Medicine 1, Charles University, Czech Republic, ⁹Sapienza Rome University, Italy, ¹⁰Regional Hospital, University of Orleans, France, ¹¹University of British Columbia, Canada

Background: The VERO trial is an active-controlled fracture endpoint clinical trial that recruited postmenopausal women with low bone mass and prevalent vertebral fractures (VFX). We have previously reported a 52% ($p < .001$) reduction in the relative risk of clinical fractures [a composite of clinical vertebral and non-vertebral fragility fractures] in patients randomized to teriparatide (TPTD) compared to risedronate (RIS). In this original analysis, non-spinal fractures were defined according to the European Guidelines for the Evaluation of Drugs for the Treatment of Osteoporosis. Here we present a post-hoc analysis of the fracture results of the VERO trial restricted to the FRAX®-defined "major" osteoporotic fractures (MOF) (i.e.; clinical vertebral, hip, humerus and forearm), a widely used efficacy endpoint in recent osteoporosis trials. **Patients and Methods:** 1360 postmenopausal women (mean age [SD]: 72.1 [8.7] years) with at least 2 moderate or 1 severe VFX and low bone mass (BMD T-score ≤ -1.5) were randomized (1:1) to SC daily TPTD 20 µg or oral weekly RIS (35 mg) in a double-blind, double-dummy, 2-year trial. Based on the full analysis set (680 patients in each treatment group), we calculated the cumulative incidence of patients and between-treatment comparison based on Kaplan-Meier and stratified log-rank tests, adjusted for antecedent of a recent clinical vertebral fracture in the 12 months before entering the study and recent bisphosphonate use. Patients who were lost to follow-up, died, or completed the study without experiencing a fracture were censored at the last date of contact. Results: 16 patients (2.6%) had ≥ 1 low trauma MOF in the TPTD group compared with 40 patients (6.4%) in the RIS group (hazard ratio 0.40; 95% CI: 0.23-0.68; $p = 0.001$). Table shows the individual fracture location. Absolute MOF risk reduction was 3.8%. Clinical vertebral

fractures were the most frequent fractures: 7 patients in the TPTD group (1.1%) compared to 24 patients (3.9%) in the RIS group (hazard ratio: 0.29; 95% CI: 0.14-0.58; $p = 0.002$). Conclusion: In postmenopausal women with severe osteoporosis, TPTD treatment was more efficacious than RIS, with a 60% lower risk of FRAX-defined major osteoporotic fractures during the 24-month treatment period. **Kendler DL et al. Lancet (2018);391:230-40**

Table: Number of Major Osteoporotic Fractures (FRAX®) by Location (Full Analysis Population)

	Teriparatide (N=680)	Risedronate (N=680)
Clinical vertebral	7	24
Radius	6	10
Hip	2	5
Humerus	4	2

Disclosures: **Jean-Jacques Body**, Eli Lilly and Company, Grant/Research Support, Amgen, Speakers' Bureau

FRI-0903

Association of Alendronate and Risk of Cardiovascular Events in Patients with Hip Fracture Ching-Lung Cheung^{*1}, Chor-Wing Sing¹, Angel Wong¹, Douglas Kiel², Elaine Cheung³, Joanne Lam⁴, Tommy Cheung¹, Esther Chan¹, Annie Kung¹, Ian Wong⁵. ¹The University of Hong Kong, Hong Kong, ²Hebrew SeniorLife, Harvard Medical School, United States, ³United Christian Hospital, Hong Kong, ⁴Queen Mary Hospital, Hong Kong, ⁵UCL School of Pharmacy, United Kingdom

The risk of cardiovascular events (CVE) with alendronate use in real-world hip fracture patients is unknown. This study aimed to investigate the risk of CVE with and without use of alendronate in patients with hip fracture. We conducted a retrospective cohort study using a population-wide database managed by the Hong Kong Hospital Authority. Patients newly diagnosed with hip fracture from 2005 through 2013 were followed until November 6, 2016. Alendronate and other anti-osteoporosis medications use during the study period were examined. We matched treated and non-treated patients based on time-dependent propensity score. The risks of cardiovascular mortality, myocardial infarction, and stroke between treatment groups were evaluated using conditional Cox regression stratified by match pairs. To examine the associations over time, outcomes were assessed at 1-, 3-, 5- and 10-years. Among 34,991 patients with newly diagnosed hip fracture, 4,602 (13.2%) received anti-osteoporosis treatment during follow-up. Physical functioning or survival prospect was not significantly different between treated and non-treated patients. 4,594 treated patients were matched with 13,568 non-treated patients. Results of Cox-regression analysis revealed that alendronate was associated with a significantly lower risk of one-year cardiovascular mortality (HR: 0.33; 95% CI: 0.17-0.65) and incident myocardial infarction (HR: 0.55; 95% CI: 0.34-0.89), whereas marginally significant reduction in risk of stroke was observed at 5- and 10-years (HR at 5-years: 0.82; 95% CI: 0.67-1.1; $p = 0.049$; HR at 10-years: 0.83; 95% CI: 0.69-1.01; $p = 0.065$). The strength of the association declined over time but remained significant. Similar results were observed when all nitrogen-containing bisphosphonates were analyzed together. These findings were robust in multiple sensitivity analyses. Additional studies in other population samples and randomized clinical trials may be warranted to further understand the relationship between use of various anti-osteoporosis medication and risk of CVE in patients with hip fracture.

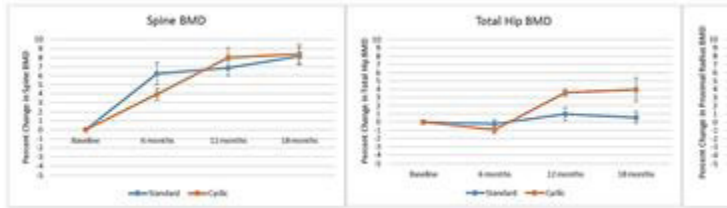
Disclosures: **Ching-Lung Cheung**, None

FRI-0904

Exploring a Teriparatide and Denosumab Sequencing Option: 18 month Interim Results Felicia Cosman^{*1}, David Dempster², Donald McMahon², Jeri Nieves⁴. ¹Columbia University, United States, ²Helen Hayes Hospital, United States, ³Columbia University and Helen Hayes Hospital, United States

In order to maximize the early anabolic effect of teriparatide, and to avoid tachyphylaxis, cyclic therapy might be useful. However, we have previously shown that cyclic teriparatide, in the absence of an intervening antiresorptive agent, does not increase BMD more than standard daily therapy. Since denosumab is a potent antiresorptive agent with a rapid off-effect, it might be the optimal agent to help maximize bone gains with cyclic teriparatide. After baseline evaluation, 70 postmenopausal women with osteoporosis were randomized to a 3-year protocol with: 18 months teriparatide followed by 18 months denosumab (Standard) or 3 separate 12 month cycles of 6 months teriparatide followed by one denosumab dose (Cyclic). Supplements of calcium, if needed, were recommended to achieve total intake >1200 mg/day and vitamin D to maintain serum 25OHD >30 ng/ml. Fasting serum samples for biochemical markers were obtained every 3 months. BMD (DXA) measurements of lumbar spine (LS), total hip (TH), femoral neck (FN), trochanter (TRO) and proximal radius (RAD) were performed every 6 months. Interim results from a pre-planned analysis on women who completed the 18-month protocol ($n = 63$; 30 Standard and 33 Cyclic) are presented here. Baseline descriptive characteristics did not differ between groups (mean age 63.5, LS T-Score -2.7, TH T-Score -1.7, BMI 23.1). BMD increments for LS, TH and RAD are shown in the figure below (mean+SEM). In the LS, BMD increased progressively and similarly in both groups. In the TH, BMD increased in both groups, with a numerically larger

gain at 12 and 18 months in the Cyclic group (p=0.13). Increments in FN BMD were also numerically larger (NS) in the Cyclic Group at 12 and 18 months. There was no precipitous decline in any of the hip sites in the Cyclic group after transition from a single denosumab treatment at 6 months back to teriparatide at 12-18 months. RAD BMD declined progressively over 18 months in Standard, but with Cyclic, RAD BMD increased modestly from 6-18 months. We conclude that over 18 months, the Cyclic regimen resulted in higher BMD than Standard at sites containing more cortical bone, possibly due to minimization of cortical porosity and enhancement of secondary mineralization. Whether this benefit will persist over 36 months is not yet known. Final BMD results from the full 3-year study, including biochemical marker results, will be presented.

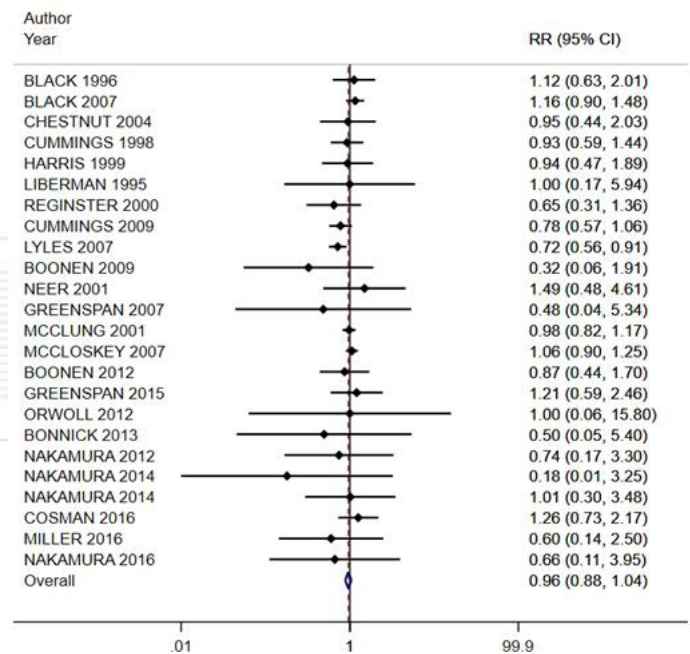


Disclosures: *Felicia Cosman, Amgen, Grant/Research Support, Radius, Speakers' Bureau, Amgen, Speakers' Bureau, Eli Lilly, Speakers' Bureau, Amgen, Consultant, Eli Lilly, Consultant, Radius, Consultant, Eli Lilly, Grant/Research Support*

FRI-0905

Treatments for Osteoporosis Do Not Reduce Overall Mortality Steven R. Cummings*¹, Li-Yung Lui¹, Douglas C. Bauer², Dennis M. Black². ¹San Francisco Coordinating Center, CPMC Research Institute, United States, ²San Francisco Coordinating Center, University of California San Francisco, United States

Background: There has been controversy about whether treatments that reduce the risk of fracture also reduce total mortality. It is a very important issue because, if treatments reduce mortality, then it would be cost-effective for almost all older adults to take a treatment for osteoporosis. Methods: We performed a systematic search for published data from randomized placebo-controlled fracture endpoint trials of treatments for osteoporosis; estrogen therapy and strontium were not included. We included placebo-controlled trials with at least 50 participants in the placebo group and at least one death; trials among those with secondary causes, such as corticosteroid use, were excluded. If there was more than one type of treatment, each treatment arm was compared to the placebo group. The prespecified primary analysis excluded selective estrogen receptor modulators (SERMs) and tibolone that have known hormonal effects that influence conditions besides fractures. A secondary analysis included those agents. As there was no significant heterogeneity (I² = 0% P = 0.73), eligible trials were pooled using a fixed effects model. Results: We identified 32 published trials that included 107,164 participants and 2,803 deaths. Excluding 8 trials of SERMs or tibolone left 24 clinical trials with 63,371 participants and 2,070 deaths. There was no significant effect of treatments on mortality in the primary analysis: risk ratio = 0.96; 95% confidence interval: 0.88 - 1.04 (Figure 1). Similarly, there was no significant effect on mortality when SERMs and tibolone were included (0.99; 0.92 - 1.06). Conclusion: Treatments for osteoporosis do not reduce overall mortality.



Disclosures: *Steven R. Cummings, Amgen, Consultant, Amgen, Grant/Research Support*

FRI-0906

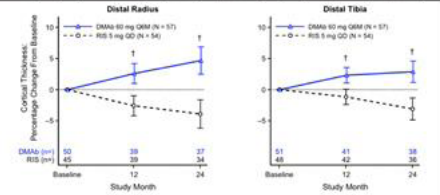
Effect of Denosumab Versus Risedronate on Cortical and Trabecular Bone Microarchitecture by High Resolution Peripheral Quantitative Computed Tomography (HR-pQCT) in Glucocorticoid-treated Individuals Piet Geusens*¹, Stefan Goemaere², Nico Pannaciuoli³, Nancy Lane³, Eric Lespessailles⁵, Osvaldo D. Messina⁶, Roland Chapurlat⁷, Xiang Yin³, Rachel B. Wagman³, Joop Pw Van Den Bergh¹. ¹Maastricht University Medical Center, Netherlands, ²Ghent University Hospital, Belgium, ³Amgen Inc., United States, ⁴University of California, Davis, United States, ⁵University Hospital Orleans, France, ⁶Cosme Argerich Hospital, Argentina, ⁷Hôpital Edouard Herriot, France

Purpose: Glucocorticoid (GC)-induced osteoporosis (GIOP) is the most common secondary cause of osteoporosis, yet many patients with GIOP do not receive osteoporosis therapy. In a study of patients initiating or continuing GC therapy, areal bone mineral density (aBMD) gains were greater with denosumab (DMAB) vs with risedronate (RIS) at the lumbar spine and total hip at 12 and 24 months. This study evaluated the effects of DMAB vs RIS on cortical and trabecular bone microarchitecture by HR-pQCT. Methods: The phase 3, randomized, double-blind, double-dummy, active-controlled study enrolled women and men ≥18 years receiving GC (≥7.5 mg prednisone daily or equivalent) for <3 months (GC-initiating [GC-I]) or ≥3 months (GC-continuing [GC-C]) before screening. All subjects <50 years had a history of osteoporosis-related (OP) fracture. GC-C subjects ≥50 years had lumbar spine, total hip, or femoral neck BMD T-score ≤-2.0; or T-score ≤-1.0 with history of OP fracture. Subjects were randomized 1:1 to subcutaneous DMAb 60 mg every 6 months or oral RIS 5 mg daily for 24 months; all were to receive daily calcium (≥1000 mg) and vitamin D (≥800 IU). In a subset, HR-pQCT (XtremeCT I; Scanco) scans of the distal radius and distal tibia were performed at baseline, Month 12, and Month 24; 110 slices of 82 μm thickness each were acquired, resulting in scan length of ~9 mm. Pixel size of the reconstructed images was 82 μm. Treatment differences (DMAb-RIS) were estimated with an analysis of covariance (ANCOVA) model. Results: 111 subjects (57 DMAb and 54 RIS) enrolled in the substudy. DMAb was associated with significantly greater increases than RIS in cortical thickness, total volumetric BMD (vBMD), and cortical vBMD at the radius and tibia at 12 and 24 months, and in trabecular vBMD at the radius at 12 months and tibia at 24 months (Table). Change in cortical porosity was not different between DMAb and RIS at either timepoint (Table). Results in the GC-I and GC-C subpopulations were overall similar to those in the two subpopulations combined. Conclusion: DMAb was associated with sustained improvements in cortical bone structure, as assessed by HR-pQCT of the radius and tibia, as compared with RIS. It remains to be elucidated whether increased cortical thickness with DMAb is associated with improved bone strength in GIOP. These results provide further support for DMAb as a treatment option for GC-treated patients at increased risk for fracture.

Table. Percentage Change From Baseline and Treatment Difference (DMAb—RIS) at Months 12 and 24 in vBMD and Cortical Microarchitecture at the Distal Radius and Distal Tibia

		Distal Radius		Distal Tibia	
		Month 12	Month 24	Month 12	Month 24
		Total vBMD	DMAb 1.8 (0.7, 2.8)	4.1 (2.6, 5.6)	1.3 (0.4, 2.2)
	RIS	-1.1 (-2.2, -0.1)	-1.7 (-3.3, -0.1)	-0.8 (-1.8, 0.1)	-1.4 (-2.4, -0.4)
	DMAb—RIS	2.9 (1.4, 4.4)*	5.8 (3.6, 7.9)*†	2.2 (0.9, 3.5)*	3.6 (2.2, 5.0)*†
Cortical vBMD	DMAb	0.2 (-0.4, 0.8)	1.2 (0.4, 1.9)	0.5 (-0.1, 1.1)	1.0 (0.4, 1.5)
	RIS	-0.7 (-1.3, -0.1)	-1.4 (-2.2, -0.6)	-0.7 (-1.3, -0.1)	-1.3 (-1.8, -0.7)
	DMAb—RIS	0.9 (0.1, 1.8)*	2.6 (1.5, 3.6)*†	1.2 (0.4, 2.1)*	2.2 (1.4, 3.1)*†
Trabecular vBMD	DMAb	2.3 (0.2, 4.3)	9.4 (1.4, 17.3)	0.8 (-0.3, 1.8)	1.7 (0.7, 2.8)
	RIS	-0.9 (-3.0, 1.1)	-0.7 (-9.0, 7.6)	-0.3 (-1.3, 0.7)	-0.4 (-1.5, 0.6)
	DMAb—RIS	3.2 (0.3, 6.1)*	10.1 (-1.4, 21.6)	1.1 (-0.4, 2.5)	2.1 (0.7, 3.6)*
Cortical porosity	DMAb	2.3 (-2.9, 7.5)	8.5 (1.1, 15.9)	1.3 (-2.5, 5.2)	3.0 (-0.7, 6.6)
	RIS	2.2 (-3.1, 7.6)	10.2 (2.5, 18.0)	2.0 (-1.9, 5.9)	1.7 (-2.1, 5.5)
	DMAb—RIS	0.1 (-7.3, 7.5)	-1.7 (-12.4, 9.0)	-0.7 (-6.1, 4.8)	1.3 (-4.0, 6.6)
Cortical thickness	DMAb	2.6 (1.0, 4.2)	4.7 (2.5, 6.9)	2.3 (1.1, 3.6)	2.9 (1.2, 4.6)
	RIS	-2.6 (-4.2, -1.0)	-3.9 (-6.2, -1.6)	-1.2 (-2.4, 0.1)	-3.1 (-4.9, -1.3)
	DMAb—RIS	5.2 (2.9, 7.4)*	8.6 (5.4, 11.8)*†	3.5 (1.7, 5.2)*†	6.0 (3.5, 8.5)*†

Reported as LS mean (95% CI) and p-value, based on ANCOVA models that included treatment, baseline value, and duration of prior GC use (<12 vs ≥12 months) as covariates
N = no. of subjects enrolled in substudy; n = no. of subjects with observed data
p-value for treatment difference: *p<0.05; †p<0.001



Disclosures: Piet Geusens, Pfizer, Abbott, Lilly, Amgen, MSD, Will, Roche, UCB, BMS, Celgene, Novartis, Grant/Research Support, Amgen, Lilly, Consultant, Pfizer, Abbott, Lilly, Amgen, MSD, Will, Roche, UCB, BMS, Celgene, Novartis, Speakers' Bureau

FRI-0907

Abaloparadite Effect on Bone Mineral Density and Fracture Incidence in Postmenopausal Women with Osteoporosis Aged 80 Years or Older: Results from the ACTIVEExtend Phase 3 Trial Susan Greenspan¹, Fitzpatrick Lorraine², Bruce Mitlak², Yamei Wang², Nicholas C. Harvey³, Chad Deal⁴, Felicia Cosman⁵, Mike McClung⁶. ¹University of Pittsburgh, United States, ²Radius Health, Inc., United States, ³MRC Lifecourse Epidemiology Unit, University of Southampton, United Kingdom, ⁴Cleveland Clinic Foundation, United States, ⁵Columbia University College of Physicians and Surgeons, United States, ⁶Oregon Osteoporosis Center, United States

The risk of fracture increases with increasing age. Thus, it is important to understand efficacy and safety of osteoporosis treatments in elderly patients. In the ACTIVE phase 3 study, 18 months (M) of abaloparadite (ABL) treatment significantly increased bone mineral density (BMD) and reduced the risk of new vertebral, nonvertebral, clinical, and major osteoporotic fractures vs placebo (PBO). Women receiving ABL or PBO in ACTIVE were offered enrollment in the ACTIVEExtend extension study in which both groups received 24M open-label alendronate (ALN) 70 mg weekly for a total of 43M (18M ABL or PBO, 1M for re-consent, and 24M ALN). The objective of this post hoc analysis was to evaluate efficacy and safety of ABL followed by ALN (ABL/ALN) vs PBO/ALN in the subgroup of patients aged ≥80 years in ACTIVEExtend. ACTIVEExtend enrolled postmenopausal women with osteoporosis between the ages of 50 and 85; 558 were from the original ABL group and 581 from the PBO group of the ACTIVE study. Pre-specified endpoints, including BMD, new vertebral, nonvertebral, clinical, and major osteoporotic fractures, were assessed over the 43M period. Nonvertebral fracture endpoints were assessed using the Kaplan-Meier (KM) method, proportional hazard model, and logrank test. A total of 56 ACTIVEExtend patients (29 ABL/ALN; 27 PBO/ALN) were aged ≥80 years at ACTIVE baseline. Mean age was 81.8 years in both groups. Mean percent changes from baseline in total hip, femoral neck, and lumbar spine BMD were all significantly greater with ABL/ALN vs PBO/ALN at all timepoints assessed, except for total hip at M6. At M43, BMD mean percent change from baseline was 5.3% ABL/ALN vs 3.1% PBO/ALN (P=0.024) at the total hip, 4.6% ABL/ALN vs 3.1% PBO/ALN (P=0.044) at the femoral neck, and 17.2% ABL/ALN vs 8.6% PBO/ALN (P<0.0001) at the lumbar spine. Fracture rates were very low in both groups in this small subset of women (new vertebral: 0 ABL/ALN, 1 PBO/ALN; nonvertebral: 1 ABL/ALN, 2 PBO/ALN). Adverse event rates were similar between treatment arms with 78.6% and 81.5% of patients in the ABL/ALN and PBO/ALN groups, respectively reporting ≥1 treatment-emergent adverse event. In conclusion, significant BMD gains were maintained through 43M with ABL/ALN vs PBO/ALN. This post hoc analysis suggests that an ABL/ALN treatment was effective in an elderly subgroup of ACTIVEExtend, with a safety profile similar across treatment arms.

Disclosures: Susan Greenspan, NIH, Grant/Research Support, Lilly, Grant/Research Support, Amgen, Grant/Research Support, PCORI, Grant/Research Support

FRI-0908

Treatment gap following clinical vertebral fracture in the International Cost and Utility Related to Osteoporosis Fractures Study (ICUROS) Mattias Lorentzon¹, Helena Johansson^{2,3}, Nicholas C Harvey⁴, Anders Odén², Kerrie Sanders⁴, Fredrik Borgström⁵, Axel Svedbom⁶, Eugene McCloskey^{2,7}, John Kanis^{2,3}. ¹Geriatric Medicine, Department of Internal Medicine and Clinical Nutrition, Institute of Medicine, Sahlgrenska Academy, University of Gothenburg, Gothenburg and Geriatric Medicine Clinic, Sahlgrenska University Hospital, Mölndal, Sweden, ²Centre for Metabolic Bone Diseases, University of Sheffield, Sheffield, UK, Sweden, ³Institute for Health and Aging, Catholic University of Australia, Melbourne, Australia, United Kingdom, ⁴MRC Lifecourse Epidemiology Unit, University of Southampton, Southampton and NIHR Southampton Biomedical Research Centre, University of Southampton and University Hospital Southampton NHS Foundation Trust, Southampton, United Kingdom, ⁵LIME/MMC, Karolinska Institutet, Stockholm, Sweden, ⁶Mapi, Stockholm, Sweden, ⁷Mellanby Centre for bone research, Department of Oncology and Metabolism, University of Sheffield, Sheffield, United Kingdom

Background Clinical vertebral fractures are among the most severe osteoporotic fractures and lead to increased risk of morbidity and mortality. A prior vertebral fracture increases the risk of a subsequent vertebral fracture by four to five times. The greatest risk reductions with osteoporosis medications have been observed for vertebral fractures. The aim of the present study was to determine the uptake of bone-specific treatment in patients following a clinical vertebral fracture. Methods Adults 50 years or older with a low to moderate energy fracture were included from ten countries in three continents (Europe, S America, Australasia) to the international study on costs and utility for osteoporotic fracture (ICUROS). Patients with clinical vertebral fractures were included within 2 weeks after the fracture, and followed for 18 months. Information about osteoporosis medication (excluding calcium/vitamin D) was collected at 4, 12 and 18 months after the clinical vertebral fracture. Results 750 clinical vertebral fracture cases, 50 years or older, had information on osteoporosis medication. Mean age was 70.3 years and 81% were women. The treatment gap or the proportion of individuals not having fracture preventing treatment, 18 months after the fracture was 67% (95% CI: 63-70). A substantial heterogeneity was observed between countries. For example, in Italy the treatment gap was 99% (95% CI: 97-100, n=116) and in Russia 33% (95% CI: 26-40, n=187). The treatment gap was not significantly different between men and women and did not increase with age. For women, 60-69 years, the treatment gap was 60% (95% CI: 51-67) and for women, 80-89 years, it was 67% (95% CI: 56-78). The corresponding numbers for men were 72% (95% CI: 52-92) and 67% (95% CI: 40-94), respectively. Conclusions Even though a clinical vertebral fracture dramatically increases the risk of subsequent vertebral fracture, and current osteoporosis medications being highly effective in preventing vertebral fractures, most patients do not receive secondary preventive treatment, as demonstrated by the substantial treatment gap in this large international cohort study.

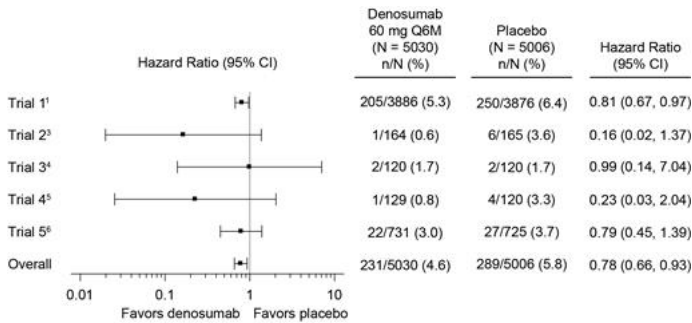
Disclosures: Mattias Lorentzon, None

FRI-0909

A Pooled Analysis of Fall Incidence from Placebo-controlled Trials of Denosumab Eugene McCloskey¹, Richard Eastell¹, Michael McClung², Nico Pannacchiulli³, Christine Wang³, Susan Yue³, Steven R. Cummings⁴. ¹The University of Sheffield, United Kingdom, ²Oregon Osteoporosis Center, United States, ³Amgen Inc., United States, ⁴San Francisco Coordinating Center, United States

Purpose: In the pivotal fracture trial of denosumab in postmenopausal women with osteoporosis (FREEDOM), treatment with denosumab, a RANK ligand (RANKL) inhibitor, resulted in a lower subject incidence of falls not associated with fracture (log rank P-value = 0.02) compared with placebo [1]. In addition to its role in osteoporosis, the RANK/RANKL pathway has also been shown to play a role in muscle strength in a murine model [2]. In an ad hoc exploratory analysis, we pooled data from additional placebo-controlled trials of denosumab to determine the consistency across trials of the reduction in the incidence of falls. Methods: The five placebo-controlled trials that contributed data to the FDA approval of denosumab for the bone loss indication were analyzed. These trials included study populations with low bone mass/osteoporosis and those receiving hormone ablation therapy. Trials in postmenopausal women with osteoporosis (FREEDOM, Trial 1, NCT00089791, [1]) and low bone mass (Trial 2, NCT00091793, [3]), men with osteoporosis (Trial 3, NCT00980174, [4]), women receiving adjuvant aromatase inhibitors for breast cancer (Trial 4, NCT00089661, [5]), and men receiving androgen deprivation therapy for prostate cancer (Trial 5, NCT00089674, [6]) were analyzed. The analysis was stratified by trial and only included data from the placebo-controlled period of each trial. A time-to-event analysis of first fall and exposure-adjusted subject incidence rates of falls (data not shown) were analyzed. Falls were reported as adverse events and not prospectively collected. Results: Kaplan-Meier estimates showed an occurrence of falls in 6.5% of subjects in the placebo groups (N = 5006), compared to 5.2% in denosumab-treated subjects (N = 5030), with an HR (95% CI) of 0.78 (0.66, 0.93), P-value 0.0053. The forest plot of time-to-first occurrence of fall is shown for both the individual studies and overall (Figure), and exposure-adjusted subject incidence rates of falls showed similar results. Heterogeneity in study designs did not permit overall assessment of association with fracture outcomes. Conclusions: Denosumab may reduce the

risk of falls in postmenopausal women with osteoporosis, in addition to the established fracture risk reduction in these patients.



N = Number of subjects who received at least 1 dose of investigational product in Trial 1 (placebo-controlled 36 months), Trial 2 (placebo-controlled first 24 months), Trial 3 (placebo-controlled first 12 months), Trial 4 (placebo-controlled first 24 months), and Trial 5 (placebo-controlled first 36 months).

REFERENCES:

- [1] Cummings S, et al. *N Engl J Med*. 2009;361:756-765.
- [2] Dufresne S, et al. *Receptors Clin Investig*. 2016;3(2):e1323-1-e1323-6.
- [3] Bone HG, et al. *J Clin Endocrinol Metab*. 2008;93(6):2149-2157.
- [4] Langdahl BL, et al. *J Clin Endocrinol Metab*. 2015;100(4):1335-1342.
- [5] Ellis GK, et al. *J Clin Oncol*. 2008;26(30):4875-4882.
- [6] Smith MR, et al. *N Engl J Med*. 2009;361(8):745-755.

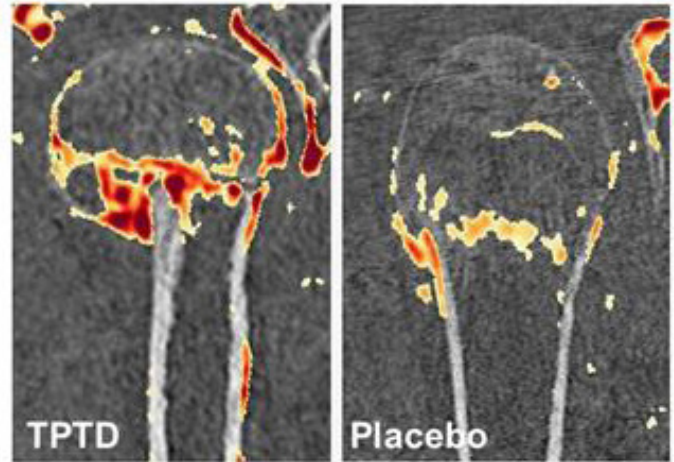
Disclosures: Eugene Mcloskey, Warner Chilcott, Grant/Research Support, Servier, Grant/Research Support, GSK, Consultant, Consilient Healthcare, Consultant, Synexus, Consultant, Amgen, Consultant, Hologic, Grant/Research Support, Tethys, Grant/Research Support, UCB, Consultant, Sanofi-Aventis, Grant/Research Support, Pfizer, Other Financial or Material Support, Roche, Grant/Research Support, Lilly, Grant/Research Support, AstraZeneca, Other Financial or Material Support, Synexus, Grant/Research Support, Internis, Other Financial or Material Support, Amgen, Other Financial or Material Support, Consilient Healthcare, Other Financial or Material Support, Novartis, Grant/Research Support, Pfizer, Grant/Research Support, IOF, Grant/Research Support, MRC, Grant/Research Support, GSK, Grant/Research Support, ActiveSignal, Grant/Research Support, AR UK, Grant/Research Support, Roche, Other Financial or Material Support, Consilient Healthcare, Grant/Research Support, Medtronic, Grant/Research Support, GSK, Other Financial or Material Support, Internis, Grant/Research Support, Amgen, Grant/Research Support, Servier, Other Financial or Material Support, Lilly, Other Financial or Material Support, Merck, Grant/Research Support, UCB, Grant/Research Support, Hologic, Other Financial or Material Support, AstraZeneca, Grant/Research Support, 13 Innovus, Grant/Research Support, ActiveSignal, Consultant, UCB, Grant/Research Support, Unilever, Grant/Research Support

FRI-0910

Teriparatide accelerates proximal humerus fracture consolidation – the TERAFRAP study Christian Muschitz*¹, Judith Haschka¹, Georg Langs², Markus Holzer², Andreas Baierl³, Christoph Pümpel¹, Zora Messner¹, Roland Kocijan¹, Xaver Feichtinger⁴, Rainer Mittermayr⁴, Jakob E. Schanda⁴, Thomas Hausner⁵, Robert Wakolbinger⁶, Jochen Schmidfeld⁶, Christian Fialka⁴, Wolfgang Schima⁷, Heinrich Resch¹. ¹St. Vincent Hospital – Medical Department II – VINFORCE; Academic Teaching Hospital of the Medical University of Vienna, Stumpergasse 13, 1060 Vienna, Austria, ²Medical University of Vienna, Department of Biomedical Imaging and Image-guided Therapy, Computational Imaging Research Lab, Währinger Gürtel 18-20, 1090 Vienna, Austria, ³University of Vienna, Department of Statistics and Operations Research, Oskar-Morgenstern-Platz 1, 1090 Vienna, Austria, ⁴AUVA Trauma Center Meidling, Kundratstrasse 37, 1120 Vienna, Austria, ⁵AUVA Trauma Center Lorenz Böhler, Donaueschingenstraße 13, 1200 Vienna, Austria, ⁶Social Medicine Center East, Department of Traumatology, Langobardenstrasse 122, 1220 Vienna, Austria, ⁷St. Vincent Hospital – Department of Diagnostic and Interventional Radiology; Academic Teaching Hospital of the Medical University of Vienna, Stumpergasse 13, 1060 Vienna, Austria

Purpose: Systemic teriparatide (TPTD) enhances callus formation and mechanical strength after fracture in animal models and in humans. Less data exist on three-dimensional (3D) structural effects at the proximal humerus, a specific non weight-bearing cortical and trabecular bone site with high fracture incidence. **Methods:** This prospective double-blind placebo-controlled study investigated the effects of daily subcutaneous 20 µg TPTD induced changes in 3D bone structure over a 12-weeks treatment period. Untreated postmenopausal women and men with a recent non-surgically treated proximal humerus fracture (≤ 8 days) and without any comorbidity known to affect bone metabolism participated. To quantify localized changes over time, affine and subsequent non-rigid registration of baseline and follow-up high-resolution CT scans (128-row scanner, Somatom Definition AS+, Siemens) were performed. Scans covered proximal and distal humerus, with the arm constrained. At baseline one region of interest at the fracture was annotated for each patient. This region was computationally mapped to the same location in the F/U scan, and average Hounsfield unit values (HU) were extracted in the same region. The **II° objectives** included changes of baseline adjusted values of bone turnover markers (BTM) of formation (PINP) and resorp-

tion (CTX), areal BMD (aBMD: iDXA, DXL) at spine, hip, calcaneus, changes in upper arm mobility (Constant Shoulder Score), pain (VAS) and SF-36 quality of life (QoL) scores. **Results:** Fifty-three of 82 screened patients (42 f, 11 m; mean age 75 years) were randomized either to TPTD or placebo, with 13 patients excluded (surgery, withdrawal). Forty patients finished the trial. In the fracture regions of the TPTD patients superior increases of HU values from baseline to follow up (average delta, +176.1; p<0.001 vs. placebo +125.2; p=0.007) were observed. Simultaneously TPTD induced increases of PINP levels by 59 µg/L, and CTX by 0.31 ng/mL (p<0.005 for both). Areal BMD improved at spine and hip (p<0.05 for both); QoL, VAS and mobility changes were more intense with TPTD compared to placebo (p<0.05 for all). **Conclusion:** After a proximal humerus fracture an early initiation of a daily 12-week administration of TPTD exerts favorable effects at the fracture region through rapid increases of BTM of formation. Additionally these patients benefit from enhanced upper arm mobility, a robust pain reduction and an improvement of their QoL after TPTD.



Disclosures: Christian Muschitz, None

FRI-0911

Localization of Prefracture Lesions in Atypical Femoral Fracture on Straight and Bowed Femurs Young Chang Park*¹, Kyu Hyun Yang². ¹International St. Mary's Hospital, Catholic Kwandong University College of Medicine, Republic of Korea, ²Yonsei University College of Medicine, Republic of Korea

Purpose: The aims of this study were to evaluate the clinical and radiological features of atypical femoral fractures (AFFs) in the straight group and anterolateral femoral bowing group, and to determine which factors were associated with the fracture height of AFFs in the total cohort and each subgroup. **Method:** We separated the 99 patients into two groups according to the presence of anterolateral bowing (straight group vs. bowing group) using anterolateral bowing grading system. Therefore, 43 (43%) patients were classified into the bowing group and the remaining 56 (57%) patients were classified into the straight group. In the bowing group only, the estimated apex height was also measured on a standard anterior-posterior radiograph. The reference line, drawn from the tip of the greater trochanter to the center of the intercondylar notch, was moved parallel in order to touch the most curved (concave) site of the medial femoral cortex. Then, a perpendicular line to the reference line was drawn at the most curved site. The lateral cortex point where this perpendicular line reached was defined as the estimated apex. Clinical and radiological characteristics were compared between the groups. Multivariable linear regression analysis was performed to determine the effect of factors on fracture height. **Results:** In the straight group, 64% of AFFs occurred at the level of the lesser trochanter and subtrochanteric area. The remaining 36% of AFFs were distributed throughout the diaphysis, with decreasing prevalence from the proximal to distal diaphysis. On the other hand, all locations of AFFs in the bowing group were in the diaphyseal area, especially within the range from 40 to 60% of femoral length. The anterolateral bowing grade was not related with the fracture height of AFFs in the bowing group. Patients in the straight group were younger, heavier, and taller, and had a higher bone mineral density, smaller anterior and lateral bowing angles, and more proximal fracture height than those in the bowing group. Multivariable analysis showed that the presence of anterolateral bowing itself was the only factor associated with fracture height in the total cohort (p = 0.001). In the subgroup analysis, weight and lateral bowing angle in the straight group (p = 0.048 and p = 0.036, respectively) and the estimated apex height in the bowing group (p < 0.001) were associated with fracture height. **Conclusion:** The presence of anterolateral bowing and the level of apex of the bowed femur were important factors for the fracture height of AFFs.

Disclosures: Young Chang Park, None

FRI-0962

Beta 2 Adrenergic Receptor Gene Deletion Enhances Periosteal Response to Mechanical Stimulation in Senescent Male Mice Sundar Srinivasan*, Dewayne Threet, Philippe Huber, Brandon Ausk, Leah Worton, Ron Kwon, Steve Bain, Ted Gross, Edith Gardiner. University of Washington, United States

Under physiological load, the sympathetic nervous system (SNS) directly suppresses trabecular bone formation through osteoblastic beta 2 adrenergic receptor (B2AR). Data in a previous report indirectly suggested adult (6 Mo) B2AR-deficient male mice might show an enhanced anabolic response to mechanical stimulation. Here, we tested that hypothesis directly, comparing periosteal mechanical response in B2AR-deficient (*Adrb2*^{-/-}; KO) and *Adrb2*^{+/+} (WT) male mice, in aged (21 Mo) and young adult (5 Mo) animals. Prior to initiation of the study, KO and WT littermates underwent μ Ct scanning at right tibia mid-shaft for structural assessment and strain calculation. Then a 3d/wk, 3wk cantilever bending regimen of right tibia (50 cycles/bout) was applied using an established protocol (1700 μ e normal strain). Mice received calcein labels (d10, d19) for dynamic histomorphometry at periosteum of loaded and contralateral tibia midshafts. Baseline (contralateral) bone formation parameters were higher in tibias from young adult KO mice, with MAR, MS and BFR values +5%, +71%, +81% vs WT, respectively (all $p < 0.05$); however, this difference was not observed in aged bones. On loaded bones of both aged and young adult B2AR KO and WT mice, periosteal MAR, MS and BFR were significantly increased by mechanical stimulation (all $p < 0.02$; loaded vs contralateral). Similarly, in both age groups, bone formation on loaded KO tibias was significantly higher than on loaded WT bones: In aged mice, MS was 80% higher and BFR was 77% higher in KO vs WT; similarly, in young adult, MS and BFR were 96% and 122% higher, respectively, in the KO bones (all $p < 0.05$). *Adrb2* genotype was a significant factor in mid-shaft tibial geometry of young adult but not aged males, with periosteal and cortical areas about 9% smaller in KO mice (both $p < 0.02$ vs WT). This size difference was associated with a higher calculated peak normal strain value for KO tibias vs WT in young adult (1993 ± 87 vs 1698 ± 66 μ e, $p = 0.004$) but not in aged males (1604 ± 35 vs 1553 ± 48 μ e). Thus, B2AR KO enhances mechanical response in aged and young adult male mice, but the response in younger mice is confounded by altered structure and baseline modeling activity. In aged mice, enhancement of MS and BFR by B2AR KO is clear, and unconfounded by structural differences or baseline modeling activity. This genetic study therefore reveals distinct B2AR mediated effects on bone modeling and response to mechanical stimulation.

Disclosures: *Sundar Srinivasan, None*

FRI-0963

Plasminogen is Critical for Bone Fracture Repair by Promoting the Functions of Mesenchymal Progenitors Luqiang Wang*¹, Zhenqiang He², Duan Hao², Richard Mittee³, Yanqing Gong², Ling Qin¹. ¹Department of Orthopaedic Surgery, Perelman School of Medicine, University of Pennsylvania, United States, ²Division of Translational Medicine and Human Genetics, Perelman School of Medicine, University of Pennsylvania, United States, ³Radiation Oncology and Neurosurgery, Perelman School of Medicine, University of Pennsylvania, United States

Plasminogen (Plg) is an inactive proenzyme that can be converted to the active serine protease plasmin for blood clot dissolution and plays a pivotal role in many physiological and pathological processes, such as embryogenesis, wound healing, fibrosis, tumor etc. To understand its function in bone regeneration, we compared the fracture healing process of Plg KO mice with their WT siblings and investigated the action of Plg on mesenchymal progenitors. MicroCT analysis revealed that Plg deficiency in 2-month old female mice causes 39%, 20%, 17%, and 15% decreases in tibial trabecular BV/TV, trabecular number, cortical area, and cortical thickness, respectively, and a 28% increase in trabecular separation ($n = 5$ /group). After a closed, transverse fracture on the tibial midshaft, Plg KO mice displayed drastically delayed fracture healing. In WT mice, callus formation normally peaks at 10 days and fracture site bridges at day 28. However, KO fractures displayed 66% and 57% decreases in callus volume and bone volume, respectively, and unchanged bone volume fraction compared to WT at day 7 post fracture ($n = 6$ mice/group) and similar levels of decreases in callus and bone volumes at day 10 and 14 ($n = 6$ mice/group/time point). KO fractures eventually reached a peak at 28 days but remained non-union at day 42. Histology showed that KO mice have 71% less cartilage formation at the early stage of healing, suggesting that Plg is required for the injury response of periosteal mesenchymal progenitors. In vitro, we found that 20 μ g/ml Plg significantly increases the proliferation of periosteal mesenchymal progenitors by 1.5 fold and inhibits their cell death induced by ischemic condition (anoxia with low glucose). Plg also stimulated progenitor migration by activating MMP9 as shown by zymography analysis. To confirm the actions of Plg on mesenchymal progenitors in vivo, we injected Tomato+ WT mesenchymal progenitors into mice with hindlimb ischemia. Bioluminescence imaging showed that those cells were much less likely to survive and migrate at the injury site in Plg KO mice compared to those in WT mice. Taken together, we demonstrated a critical function of Plg in regulating mesenchymal progenitor proliferation, migration, and survival during the initiation stage of fracture healing. Our study also points out that drugs activating Plg might represent a novel direction for treating fracture non-union.

Disclosures: *Luqiang Wang, None*

FRI-0973

Strain-Specific Response of Inbred Mice to PTH Suggests Significant Genetic Control of the Bone Anabolic Response to Drug Therapy Douglas Adams*¹, Olivia Hart², Renata Rydzik¹, Dana Godfrey², Michael Zuscik², Cheryl Ackert-Bicknell². ¹University of Connecticut, United States, ²University of Rochester, United States

Teriparatide (human PTH:1-34) is an anabolic therapeutic used to treat osteoporosis, demonstrating reduced fracture incidence. However, clinical outcomes demonstrate variable response to PTH, with up to 44% of patients failing to achieve $\geq 3\%$ bone mineral density (BMD) increase after at least 12 months of treatment. Collectively, studies in mice suggest that responses to intermittent PTH vary between strains and anatomical locations, but nearly all studies examined only one strain. Herein we directly compared the response of 3 inbred strains to 4 weeks of intermittent PTH (40 μ g/kg/day) versus saline (control), initiating treatment at 8 weeks of age in male A/J, 129S1/SvImJ (129) and NOD/ShiLJ (NOD) mice ($n = 5$ mice per strain, per treatment). Whole body BMD was measured by DXA (PIXImus II, GE-Lunar). Architecture of femora and L4 vertebrae was measured via microCT imaging. Femora were subjected to 3-point flexure strength tests. Response to PTH was greatest in A/J mice, with significant increases in whole body (10%, $P < 0.001$), femur (20%, $P = 0.001$), and spine (19%, $P = 0.002$) bone mass versus control, with concomitant increases in femoral strength (21%, $P = 0.007$) and stiffness (17%, $P = 0.016$). Nominal gains in whole body BMD occurred in the NOD (4%, $P = 0.062$) and 129 (3%, $P = 0.088$) animals. Modest increases in femoral mass were also observed (NOD = 9%, $P = 0.003$, 129 = 13%, $P = 0.01$). PTH had no effect on bone mass in the spine in either NOD or 129 mice. Femoral strength was increased in the 129 mice (13%, $P = 0.033$), but not in the NOD animals ($P = 0.15$). Reduction of mechanical test data to material properties demonstrated no effects of PTH on matrix material strength and stiffness for any of the three strains examined. This suggests that all gains in bone strength were due to changes in bone size and geometry and likely not due to improvement in material quality. This direct comparison between three commonly used inbred strains strongly reflects the clinical experience with response to PTH treatment ranging from the robust increases in bone seen in the A/J mice to the minimal response observed with the NOD mice. These data confirm that response to PTH is strongly genetically regulated. Identification of genes that control the response to intermittent PTH could provide clinical screening tools to prevent unnecessary Teriparatide treatment, and could elucidate pathways leading to novel or improved anabolic therapies for bone.

Disclosures: *Douglas Adams, None*

FRI-0974

AZP-3404, a Short Peptide Derived from Insulin-like Growth Factor Binding Protein 2 (IGFBP-2), Ameliorates Metabolic Status and Trabecular Bone in Aged-Ovariectomized (OVX) Mice Thomas Delale*¹, Stephane Milano¹, Victoria Demambro², David R Clemmons³, Clifford J Rosen², Thierry Aribat¹. ¹Alize pharma 3, France, ²Maine Medical Center, United States, ³NPT Inc, United States

IGFBP-2 acts on osteoblast differentiation through its heparin-binding domain 1 (HBD-1) and is not dependent on its IGF-binding properties. AZP-3404, a short peptide analog of HBD-1, has been shown to increase trabecular bone formation and improve bone biomechanical properties in young OVX mice. Because bone metabolism, hormonal status and IGF-1/IGFBP system are altered in aging, the aim of this study was to evaluate AZP-3404 treatment on bone and body composition in aged OVX mice. This study was conducted in 13-month aged OVX or sham-operated C57BL/6J female mice. Ten-week treatment with AZP-3404 or vehicle (VHL) was started immediately after surgery ($n = 10$ /group). AZP-3404 was given s.c. twice daily at 1 or 3 mg/kg. During treatment, body composition was monitored by DXA. Post-mortem μ CT was performed to evaluate metaphyseal trabecular and diaphyseal cortical parameters of the femur. At the end of VHL treatment, aged OVX mice gained more body weight and fat mass (g) than the sham-operated animals (+14% and +28% respectively, $p < 0.001$). Femoral trabecular metaphyseal microarchitecture was markedly lower in the sham aged mice compared to young animals. In the aged mice, the farther from the epiphyseal region the scans were performed, the more the effect of OVX on bone was pronounced (VOI1: 0.3-1.05 mm: BV/TV -21%, ns; VOI2: 0.75-1.5 mm: BV/TV -37%, $p < 0.05$). AZP-3404 at 1 mg/kg particularly improved trabecular bone at the VOI where the OVX effect was prominent (BV: +45%, $p < 0.05$; BV/TV: +43%, $p < 0.05$; Tb.Th: +22%, $p < 0.01$; Tb.PF: -24%, $p < 0.01$). In addition, AZP-3404 at 1 mg/kg decreased body weight gain (-6%; $p < 0.01$, vs VHL) and this effect was associated with a decrease in body fat mass (-14%; $p < 0.05$, vs VHL). In conclusion, AZP-3404 significantly improved trabecular microarchitecture at the femoral metaphysis and reduced body weight and fat mass gain in the aged OVX mice. These results support the continued development of AZP-3404 as a novel therapeutic approach for treating trabecular bone loss associated with metabolic disorders in elderly patients.

Disclosures: *Thomas Delale, None*

FRI-0975

AZP-3404, a Short Peptide Derived from Insulin-like Growth Factor Binding Protein 2 (IGFBP-2), Improves Trabecular Bone in Ovariectomized (OVX) Mice Thomas Delale^{*1}, Stephane Milano¹, David R Clemmons², Clifford J Rosen³, Thierry Abrisbat¹. ¹Alizé Pharma 3, France, ²NPT Inc, United States, ³Maine Medical Center, United States

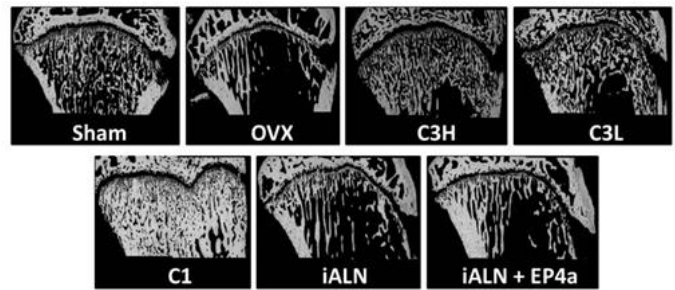
IGFBP-2 is a physiological regulator of osteoblast differentiation, a function that is not dependent on its IGF-binding properties. The heparin-binding domain 1 (HBD-1) of IGFBP-2 replicates this effect and stimulates bone formation in rodents. AZP-3404, a short peptide analog of HBD-1, designed for its osteoblast differentiation activity and improved pharmacokinetics properties is a drug candidate for treatment of bone disorders. This study was conducted to determine the effects of AZP-3404 on bone in ovariectomized (OVX) C57BL/6J female mice. A six-week treatment with AZP-3404 or vehicle (VHL) was initiated 3 weeks after OVX surgery in 8-week animals (n=10/group). OVX effects were confirmed by comparison with a sham-OVX group. AZP-3404 was given s.c. twice a day at 0.3, 1 or 3 mg/kg. rhPTH(1-34) was used as a reference anabolic drug and was injected s.c. at 40 µg/kg daily. During treatment, BMD was monitored by DXA. Post-mortem µCT was performed to evaluate metaphyseal trabecular and diaphyseal cortical long bone parameters. Static and dynamic femoral histomorphometry was also evaluated as well as biomechanical properties of femoral neck. Prior to treatment, OVX animals showed increased body weight (+8%, p<0.001), decreased total (-12%, p<0.001) and vertebral (-23%, p<0.001) BMD compared to sham. Compared to VHL, AZP-3404 increased BMD, especially at the vertebral level (+16.7%, p<0.05) at 3 mg/kg, whereas PTH showed a 4.5% increase. At the distal femoral metaphysis (VOI: 0.3-1.05 mm from epiphysis), AZP-3404 improved trabecular microarchitecture, particularly at 1 mg/kg (BV: +23 %, p<0.01; BV/TV: +18 %, p<0.05; Tb.N: +16 %, p<0.05; Tb. PF: -15%, p<0.01). These effects were more pronounced (e.g.; BV/TV: +37.4 %, p<0.05) at a more proximal VOI (0.75-1.5 mm) and were also observed for tibia (e.g.; BV/TV: +32.0 %, p<0.01). At the same femoral VOIs, PTH showed only 6.5% and 9.7% increases, respectively. PTH also increased femoral cortex thickness by +6.1 % (p<0.01). Static histomorphometry confirmed µCT data. Like PTH, AZP-3404 tended to increase trabecular BFR/TV, while only PTH had an effect on MAR. Importantly, AZP-3404 at 1 mg/kg improved femoral neck strength (maximum load: +11.6%; work-to fracture: +43.3 %; p<0.05). In conclusion, AZP-3404 significantly improved trabecular bone and biomechanical properties in OVX mice supporting its use as a novel therapeutic agent for treating bone disorders associated with trabecular bone loss.

Disclosures: **Thomas Delale, None**

FRI-0976

A Novel Bone Anabolic Conjugated Drug (C3) Can Rebuild Bone in an Ovariectomized (OVX) Rat Model: A Novel Approach for Reversing Osteoporotic Bone Loss Marc Grynpas^{*2}, Zeeshan Sheikh¹, Robert Young³. ¹University of Toronto, Canada, ²Sinai Health System, Canada, ³Simon Fraser University, Canada

Introduction: There is an unmet need to find new anabolic drugs to rebuild bone lost to osteoporosis. By linking a PGE2 receptor analog (EP4a) to a bisphosphonate (ALN) in a conjugated drug (C1), we have shown that bone loss can be recovered. However this conjugated drug does not allow for bone remodeling and results in overproduction of bone that renders bones mechanically weak. In this study we adopted a conjugate bone-targeting approach where a synthetic, stable EP4 agonist is covalently linked to an inactive alendronate (ALN) that still binds to bone and allow physiological bone remodeling (C3). Methods: In this curative experiment, the following 7 groups of rats were treated for 8 weeks via tail vein injection (after losing bone for 12 weeks). 1) Sham, 2) OVX, 3) OVX +C3 low and high (4), 5) OVX+C1, 6) inactive ALN alone and 7) mixture of unconjugated ALN and EP4a (to assess the effect of conjugation) (n=10 for each group). We used microCT to determine bone architecture; static and dynamic histomorphometry to determine bone turnover and biomechanics to measure bone mechanical properties. Results: This experiment demonstrated that C3 treatment significantly increased vertebral bone mineral density and trabecular bone volume versus OVX controls. Biomechanical testing showed that C3 treatment led to significant improvement in the load bearing abilities of the vertebrae compared to OVX controls; C3 stimulated bone formation and increased load bearing in femurs. We have shown in this research study that C3 led to significant anabolic effects on trabecular bone while the effects associated with C1 were beyond physiological levels. Conjugation between the EP4a and ALN components was crucial to the drug's anabolic efficacy as it allowed for the local delivery of EP4a via the bone targeting ability of ALN. Conclusion: The C3 conjugate demonstrated, for the first time, that a combined therapy using an anabolic agent linked to an inactive ALN has significant anabolic effects, yet allow bone remodelling. This would be clinically very useful in the future for treating patients suffering from post-menopausal osteoporosis linked bone loss



Treatment effects of the conjugate drug (C3) in the proximal tibial metaphysis. Representative images scanned using Back Scatter Electron Microscopy (X80 mag)

Disclosures: **Marc Grynpas, None**

FRI-0977

Abaloparatide is as Effective as PTH (1-34) in Improving Bone Formation While PTHrP (1-36) Has Less Effect in Mice. Carole Le Henaff^{*1}, Florante Ricarte², Zhiming He¹, Joshua Johnson¹, Johanna Warshaw¹, Nicola Partridge¹. ¹New York University, college of dentistry, United States, ²Molecular Pharmacology Training Program, Sackler Institute of Graduate Biomedical Sciences, United States

Abaloparatide (ABL), a novel analog of parathyroid hormone-related protein (PTHrP 1-36), has similar bone anabolic effects to teriparatide (PTH 1-34), but lesser bone resorption. As a result, ABL received FDA approval in 2017 and became the second FDA-approved osteoanabolic therapy for the treatment of osteoporosis. This study aims to elucidate the effects of PTH (1-34), PTHrP (1-36), and ABL on bone remodeling, in vivo, in mice. Intermittent daily subcutaneous peptide injections of 80µg/kg/day were administered to 4 month-old C57Bl/6 male mice for 6 weeks (n=10/group). DEXA was performed during the course of the treatment to assess changes in bone mineral density (BMD). Eighteen hours after the final injection, right femurs were harvested for µCT analyses and histomorphometry, sera were assayed for PINP and CTX, and tibiae were separated into cortical, trabecular, and bone marrow fractions for RT-qPCR analyses. Here, we show that ABL resulted in a similar increase in whole body (+5%), femoral (+11.4%), and tibial BMD (+8%) compared with PTH (1-34) and no significant changes were seen with PTHrP (1-36). µCT analyses revealed similar increases in cortical thickness only with ABL (11.9%) and PTH (1-34, 10.7%). Assessment of serum PINP and CTX levels showed that ABL (90ng/ml) was superior to PTH (1-34, 71ng/ml) and PTHrP (1-36, 49.5ng/ml) in stimulating greater levels of PINP, and PTH (1-34, 26.5ng/ml) and ABL (24.5ng/ml) led to increases in CTX (control, 19.3ng/ml). Histomorphometry confirmed an increase in the MAR with PTH (1-34, +39%), ABL (+44%) and the BFR (+70% and +82%, respectively). PTHrP seemed to have no effect on PINP and CTX levels but, surprisingly, had a significant effect on the MAR (+19%) and BFR (+44%). RT-qPCR analyses of trabecular bone showed that PTH (1-34) and ABL led to a similar rise in type-1 collagen, alkaline phosphatase, osteocalcin, and bone sialoprotein mRNA levels. These data show that ABL is equivalent to PTH (1-34) in increasing whole body, femoral, and tibial BMD. Also, PTH (1-34) and ABL exert similar effects on osteoblasts with an increase in osteoblastic gene expression and bone formation rate. Taken together, this study provides greater insight into the effects of PTH (1-34), PTHrP (1-36) and ABL in bone, and confirms that ABL is as effective on osteoanabolic as PTH (1-34).

Disclosures: **Carole Le Henaff, None**

FRI-0978

Vanadyl Acetylacetonate Increases Bone Formation and Inhibits Osteoclast Differentiation in a Diabetes-Related Osteoporotic Rat Model Jayenth Mayur^{*1}, Anthony Lin¹, Maximilian Muñoz¹, Kevin Mesina¹, Atharva Dhole¹, Savannah Roy¹, Daniel Coban¹, Suleiman Sudah², Joseph Benevenia¹, Jessica Cottrell³, David Paglia¹, Sheldon Lin¹. ¹Rutgers New Jersey Medical School, United States, ²Robert Wood Johnson Medical School, United States, ³Seton Hall University, United States

Osteoporosis is typified by deficits in osseous microstructure and cortical weakness. We evaluated Vanadyl Acetylacetonate (VAC), an organic Vanadium salt with an established anabolic role in bone healing, as a potential therapy. This study examined the phenotypic impact of VAC on Type 1 diabetes-related (T1DR) osteoporotic femurs and the cellular mechanism by which VAC controls bone homeostasis. A female T1DR osteoporotic rat model (Verhaeghe et al. 1990) was followed. Right femurs were injected with either 0.1 mL saline solution or 1.5 mg/kg VAC solution. At 4 or 8 weeks post-surgery, rats were sacrificed to evaluate micro-CT (n=6) and torsion testing (n=7) outcomes. At 8 weeks post-surgery, Calcitonin solution (Sims et al. 2014) was injected IP at 7 and 2 days prior to sacrifice to measure bone formation (n=5). To measure osteoclast (OC) differentiation, marrow was extracted 8-weeks post-surgery from contralateral femurs and cultured for 5 days in 3 different media: MCSF (control), MCSF + RANKL, and MCSF + RANKL + 3 mg/mL VAC (n=5; triplicate).

Cells were then fixed using 10% formalin and TRAP stained. At 8 weeks, VAC-treated femora showed a 10% decrease in percent cortical porosity ($p < 0.05$), a 2.4% increase in cortical bone volume/tissue volume (BV/TV) ($p < 0.05$), and a 45% increase in maximum shear stress ($p < 0.005$) (Figure 1A). At 4 weeks, there were no significant changes in cortical bone parameters or mechanical strength. Calcein labeling showed increased mineral apposition (31.4-fold; $p < 0.05$) and bone formation (26.9-fold) rates in VAC-treated femora compared to saline controls (Figure 2). OC quantification in MCSF + RANKL revealed a 91% reduction in OCs ($p < 0.001$) in VAC-treated rats compared to saline controls. In cells extracted from saline controls and cultured in media containing VAC, there was a significant reduction in OCs ($p < 0.001$) compared to cells cultured in the absence of VAC (Figure 1B). This study highlights VAC's effects on bone turnover and osteoclastogenesis in vivo. Calcein labeling suggests that VAC induces bone formation, thus normalizing cortical porosity in T1DR femora. We also found that VAC inhibited OC differentiation in vivo and in vitro, while not impairing supporting cells. An in vitro study (König et al. 2017) similarly showed that human OC differentiation was inhibited by Vanadium ions. In an aging T1DR osteoporotic population, VAC may prove to be an effective clinical adjunct in restoring bone porosity.

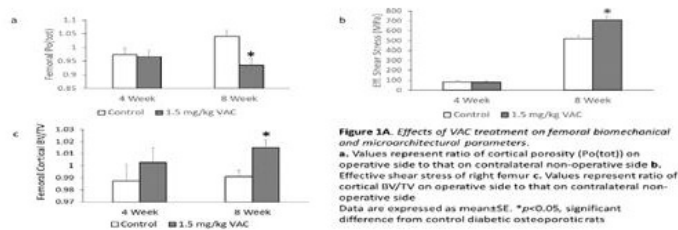


Figure 1A. Effects of VAC treatment on femoral biomechanical and microarchitectural parameters. a. Values represent ratio of cortical porosity (Por(0.05)) on operative side to that on contralateral non-operative side b. Effective shear stress of right femur c. Values represent ratio of cortical BV/TV on operative side to that on contralateral non-operative side. Data are expressed as mean±SE. * $p < 0.05$, significant difference from control diabetic osteoporotic rats

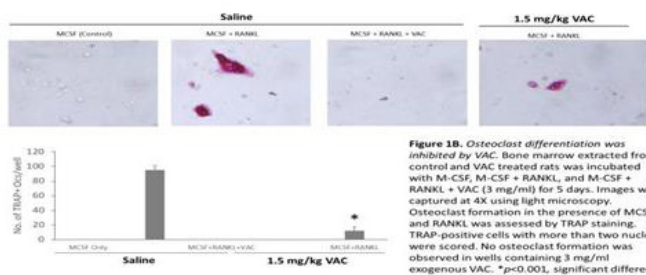


Figure 1B. Osteoclast differentiation was inhibited by VAC. Bone marrow extracted from control and VAC treated rats was incubated with M-CSF, M-CSF + RANKL, and M-CSF + RANKL + VAC (3 mg/ml) for 5 days. Images were captured at 4X using light microscopy. Osteoclast formation in the presence of MCSF and RANKL was assessed by TRAP staining. TRAP-positive cells with more than two nuclei were scored. No osteoclast formation was observed in wells containing 3 mg/ml exogenous VAC. * $p < 0.001$, significant difference from control diabetic osteoporotic rats

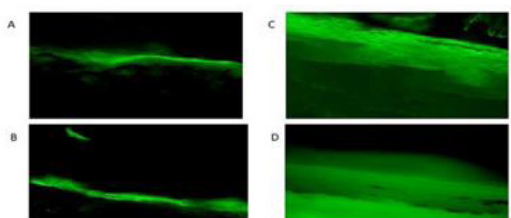


Figure 2. Calcein labeling of femur endosteum at 8 weeks using fluorescent microscopy. Separation between fluorescent endosteal bands signifies new bone growth. A. Control femur image taken at 20X B. VAC treated femur image taken at 20X C. Control femur image taken at 10X D. VAC treated femur image taken at 10X

Disclosures: Jayenth Mayur, None

FRI-0979

Low-intensity Pulsed Ultrasound (LIPUS) Prevents Development of BRONJ-like Pathophysiology in Rat Alveolar Bone Defect Induced by Tooth Removal after Alendronate and Porphyromonas Gingivalis Challenges
 Kouki Hidaka¹, Yuko Mikuni-Takagaki¹, Satoko Wada-Takahashi¹, Makiko Saita², Ryota Kawamata⁴, Takenori Sato¹, Akira Kawata¹, Chihiro Miyamoto¹, Yojiro Maehata¹, Hiroataka Watabe², Nobuyuki Tani-Ishii², Nobuhiro Hamada¹, Shun-Suke Takahashi¹, Shinji Deguchi¹, Ryohei Takeuchi³. ¹Kanagawa Dental University, Graduate School of Dentistry, Department of Oral Science, Japan, ²Kanagawa Dental University, Graduate School of Dentistry, Department of Oral Interdisciplinary Medicine, Japan, ⁴Kanagawa Dental University, Graduate School of Dentistry, Department of Dentomaxillofacial Diagnosis and Treatment, Japan, ⁵Yokosuka City Hospital, Department of Joint Surgery, Japan

Bisphosphonate-related osteonecrosis of the jaw (BRONJ) was first observed in cases of multiple myeloma and metastatic bone cancer treated with nitrogen-containing bisphosphonates (N-BPs) and later in osteoporotic patients undergoing long-term treatment with oral N-BPs. Although the exact cause, induction, and the reason for its site-specific occurrence often after tooth extraction, remain unknown, the disease is often successfully treated with antibiotics. Involvement of human $\gamma\delta$ TCR to phosphoantigens, which can be provided by both certain bacteria and N-BPs, has been suggested (Kalyan S, J Bone Miner Res 2016).

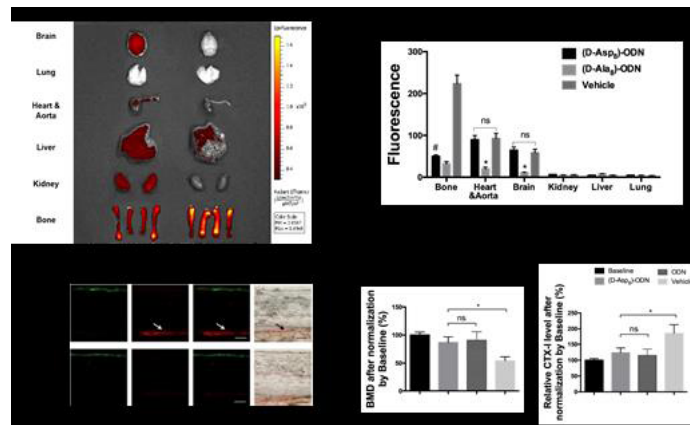
In addition, we found site-specific mechanotransduction in isolated jaw bone osteoblasts which can promote bone remodeling. Namely, mandibular osteoblasts, which thrive under the constant challenge of oral bacteria are unique in expressing molecules such as Bcl-2 and RANKL only when mechanically loaded with LIPUS, and their expression is regulated by $\alpha 5\beta 1$ integrin (Exp Cell Res 2011). Hypothesizing that the sudden loss of occlusal force after tooth extraction may increase the risk of BRONJ, we tested the protective effect of LIPUS as a surrogate occlusal force in a rat BRONJ model prepared in ovariectomized rats by subcutaneously administering 35 $\mu\text{g}/\text{kg}/\text{week}$ alendronate (ALN), a common N-BP, for 5 weeks and then for another 3 weeks with additional periodontopathic *Porphyromonas gingivalis* (Pg) bacteria, by topical application targeting the maxillary first molars. After removing the tooth, LIPUS was applied extrabuccally to the extraction socket 5 times a week for 4 weeks for the experimental ALN+Pg+LIPUS group rats. Consequently, we found delayed healing only in the rats given both ALN and Pg but not in the rats with individual interventions, neither in ALN+Pg+LIPUS group rats. Exposure to daily LIPUS prevented development of deficiencies in ALN+Pg group such as lowered BMD in the alveolar bone, periosteal reaction of new bone formation as well as the eliminated expression of Hsp70, IL-6, Bcl-2 and RANKL mRNAs, all essential to bone regeneration, in the remote leg bone marrow cells. Development of BRONJ-like pathophysiology, at least in this model which is challenged by N-BP and periodontopathic bacteria, was avoidable with LIPUS exposure. In addition to the known effect of LIPUS of inhibiting local inflammation, normalization of the systemic humoral processes of regeneration is likely critical to the maintenance of alveolar bone.

Disclosures: Kouki Hidaka, None

FRI-0980

A Novel Cathepsin K Inhibitor Specifically Approaching Bone Resorption Surface to Suppress Osteoclastic Bone Resorption
 Xiaohao Wu*, Jun Lu, Jin Liu, Lei Dang, Aiping Lu, Ge Zhang. Hong Kong Baptist University, Hong Kong

Recently, the development of Merck's phase III Cathepsin K (CatK) inhibitor Odanacatib (ODN) has been terminated since increased risk for developing stroke was found in ODN-treated patients. Interestingly, our preliminary data revealed that this risk might be due to the non-specific delivery of ODN to non-target tissues. Thus, our study aimed to develop a new inhibitor to selectively approach bone resorption surface to inhibit CatK activity for suppression of osteoclastic bone resorption. The ODN was chemically conjugated with an osteoclast-targeted oligopeptide moiety D-Asp8 to synthesize the (D-Asp8)-ODN conjugate. The selectivity and inhibitory efficiency of (D-Asp8)-ODN conjugate on CatK activity were determined by in vitro enzyme inhibition assay. In vivo distribution of the (D-Asp8)-ODN conjugate was analyzed by biophotonic imaging and histological analysis in an ovariectomized (OVX) mice model of osteoporosis. The CatK activity was measured by enzyme activity assay. In addition, the therapeutic effects of (D-Asp8)-ODN conjugate in OVX mice were measured by ELISA, micro-CT and bone histomorphometry and compared with ODN-treated (positive) as well as vehicle-treated (negative) controls. The (D-Asp8)-ODN conjugate exerted selectively inhibitory effect on CatK activity without off-target effects on other cathepsins (i.e. cathepsin B, S and L), and the inhibitory efficiency was comparable to ODN. Our data further demonstrated that the D-Asp8 could facilitate the conjugated ODN selectively approaching the bone resorption surface and selectively inhibiting the CatK activity in bone tissues without disturbing the CatK activity in non-bone tissues. Furthermore, the (D-Asp8)-ODN conjugate dramatically lowered the serum level of CTX-I (a marker of osteoclastic bone resorption) and attenuated deterioration of bone micro-architecture as compared with vehicle-treated controls in OVX mice during osteoporosis development. More importantly, the in vivo anti-resorptive effect of (D-Asp8)-ODN conjugate was also comparable to that of ODN. Collectively, we demonstrated that the osteoclast-targeted moiety D-Asp8 could facilitate the conjugated ODN selectively approaching bone resorption surface to inhibit the CatK activity for suppression of osteoclastic bone resorption during osteoporosis development in OVX mice. These findings indicate the (D-Asp8)-ODN conjugate as a novel osteoclast-targeted CatK inhibitor candidate for further translational development.



Disclosures: Xiaohao Wu, None

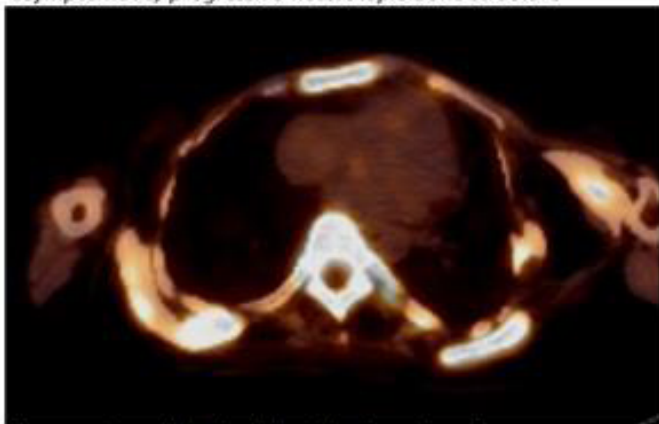
Friday Posters

FRI-1019

[18F]NaF PET/CT can identify a silent “chronic” state of Fibrodysplasia Ossificans Progressiva Esmée Botman^{*1}, Pieter Raijmakers², Maqsood Yaqub², Bernd Teunissen², Coen Netelenbos¹, Lothar Schwarte³, Wouter Lubbers³, Adriaan Lammertsma², Marelise Eekhoff¹. ¹Department of Internal Medicine, section Endocrinology, Netherlands, ²Department of Nuclear Medicine and Radiology, Netherlands, ³Department of anesthesiology, Netherlands

Fibrodysplasia ossificans progressiva (FOP) is a rare, autosomal dominant disorder characterized by heterotopic ossification (HO) in muscles, tendons and ligaments. Flare-ups often precede the formation of HO. Due to progressive contractures without any clinical signs the existence of a chronic, smoldering progressive disease is assumed. Recently, [18F]NaF PET/CT was able to identify ossifying flare-ups, therefore we used the [18F]NaF PET/CT to search for the existence of this assumed but never confirmed “chronic” stage of FOP. Methods: a total of thirteen consecutive [18F]NaF PET/CT-scans from five FOP patients were analyzed. The scans were acquired over 0.5 – 2 years. An in-house tool was used for identifying and analyzing the heterotopic bone structures. Volume of HO and standardized uptake values (SUV) were assessed. Results: Two out of five patients experienced ≥ 1 active clinical flare-ups at the time of the [18F]NaF PET/CT scan. In four out of five patients the serial scans showed progression of HO in the absence of a flare-up or any other clinical signs. This volumetric increase was present for over 10% of the identified HO structures, all were accompanied by increased 18F-sodium fluoride uptake (figure 1). In conclusion, HO may progress throughout the disease and the [18F]NaF PET/CT is a promising modality to identify these asymptomatic, chronically progressive HO lesions. [18F]NaF PET/CT appears to be an adequate imaging technique to detect and follow-up on HO formation both during active an chronic FOP disease. Importantly, future drugs should target both active and chronic HO activities in FOP.

Figure 1. Increased [18F]-Sodium Fluoride uptake in an asymptomatic, progressive heterotopic bone structure



Heterotopic ossification in the right thoracic region. Consecutive [18F]NaF PET/CT-scans obtained within an eight months window showed a volumetric increase of $>5\text{cm}^3$. Increased [18F]-sodium fluoride uptake was found compared to other, non-progressive structures. NB. vertebrae exhibit the highest [18F]-sodium fluoride uptake in the body, due to, among others, mechanical stress

Disclosures: Esmée Botman, None

FRI-1020

Sustained Efficacy and Safety of Burosumab, an Anti-FGF23 Monoclonal Antibody, for 88 Weeks in Children and Early Adolescents with X-Linked Hypophosphatemia (XLH) Thomas O. Carpenter^{*1}, Wolfgang Högl², Erik Imel³, Anthony A. Portale⁴, Annemieke Boot⁵, Agnès Linglart⁶, Raja Padidela⁷, William Van't Hoff⁸, Gary S. Gottesman⁹, Meng Mao¹⁰, Alison Skrinar¹⁰, Javier San Martin¹⁰, Michael P. Whyte⁹. ¹Yale University School of Medicine, United States, ²Birmingham Children's Hospital, United Kingdom, ³Indiana University School of Medicine, United States, ⁴University of California, San Francisco, United States, ⁵University of Groningen, Netherlands, ⁶APHP Hôpital Bicêtre Paris Sud, France, ⁷Royal Manchester Children's Hospital, United Kingdom, ⁸Great Ormond Street Hospital, United Kingdom, ⁹Shriners Hospitals for Children, United States, ¹⁰Ultragenyx Pharmaceutical Inc., United States

In children with X-linked hypophosphatemia (XLH), excess circulating fibroblast growth factor 23 (FGF23) causes hypophosphatemia with consequent rickets, skeletal deformities, and growth impairment. These skeletal abnormalities are associated with pain and impaired physical functioning. We previously reported that treatment with burosumab, a fully human monoclonal antibody against FGF23, improved phosphate homeostasis and rickets severity in children with XLH. Here, we report the long-term data from the Phase 2 Study CL201 (NCT02163577), including data from children who switched from every 4 (Q4W) to every 2 week (Q2W) dosing at Week 64. Fifty-two children with XLH (5-12 years old, Tanner ≤ 2) were randomized 1:1 to receive subcutaneous burosumab Q2W or Q4W for 64 weeks. Doses were titrated up to 2 mg/kg per dose to achieve serum phosphorus levels within 3.5-5.0 mg/dL. All subjects entered the long-term extension at Week 64, in which Q4W-treated subjects changed to the Q2W regimen; treatment continued through Week 88. The significant improvements in Total Rickets Severity Score (RSS) and the Radiographic Global Impression of Change (RGI-C) observed at Week 64 were maintained through Week 88. In the Q4W→Q2W group, 13 (50%) subjects demonstrated substantial healing of rickets (RGI-C $\geq +2$) by Week 64; 3 additional subjects in this group showed substantial healing of rickets by Week 88. Improvements in standing height Z score and distance walked in the 6-Minute Walk Test were sustained through Week 88. Significant increases in serum phosphorus (mg/dL) were maintained through Week 88 (mean [SE]: Q2W 3.36 [0.06]; Q4W→Q2W 3.26 [0.09]). For the 9 subjects who transitioned into adolescence (ranging from ~12 years of age at baseline to 14.6 years of age at Week 88), improvements in serum phosphorus and rickets severity were maintained. One subject had concurrent serious AEs (hospitalization for fever/muscle pain) which resolved within a day. Other AEs were generally mild to moderate in severity; no new serious AEs emerged between Weeks 64-88. No clinically meaningful changes in serum calcium or iPTH occurred. No subject discontinued therapy or developed hyperphosphatemia. Long-term burosumab treatment maintained improvements in clinical outcomes, including rickets severity, growth, and physical ability in children and early adolescents with XLH. Children that changed from the Q4W to Q2W regimen at Week 64 showed continued improvement in rickets severity.

Table 1. Evidence of Long-term Efficacy with Burosumab in CL201

Assessment	Q2W (n=26)	Q4W→Q2W ^a (n=26)
Serum Phosphorus, mg/dL, mean (SE)		
Baseline	2.38 (0.08)	2.28 (0.06)
Week 64	3.35 (0.09)	2.96 (0.07)
Week 88 ^a	3.36 (0.06)	3.26 (0.09)
RSS Total Score, mean (SE)		
Baseline	1.92 (0.23)	1.67 (0.20)
Week 64	0.81 (0.12) ^b	0.94 (0.10) ^b
Week 88 ^a	0.87 (0.14) ^b	0.84 (0.11) ^b
RGI-C Global Score, LS mean (SE)		
Week 64	+1.56 (0.11) ^b	+1.58 (0.11) ^b
Week 88 ^a	+1.67 (0.14) ^b	+1.85 (0.09) ^b
Substantial Healing, (RGI-C $\geq +2.0$), n (%)		
Week 64	15 (58)	13 (50)
Week 88 ^a	15 (58)	16 (62)
Standing Height Z Score, mean (SE)		
Baseline	-1.72 (0.20)	-2.05 (0.19)
Week 64	-1.54 (0.22) ^c	-1.92 (0.16) ^d
Week 88 ^a	-1.47 (0.20) ^b	-1.94 (0.16) ^d
6MWT, percentage predicted norm, mean (SE)		
Baseline	79.32 (2.60)	81.42 (2.96)
Week 64	85.00 (2.03) ^c	84.74 (2.67) ^d
Week 88 ^a	85.55 (1.85) ^d	84.17 (2.70)

^aAt Week 64, Q4W regimen group changed to Q2W regimen through Week 88. ^bP<0.0001 LS mean change from baseline using the GEE model. ^cP<0.001 LS mean change from baseline using the GEE model. ^dP<0.05 LS mean change from baseline using ANCOVA. Decreases in RSS and increases in RGI-C indicate improvement.

Disclosures: Thomas O. Carpenter, Ultragenyx Pharmaceutical Inc., Consultant, Ultragenyx Pharmaceutical Inc., Other Financial or Material Support, Ultragenyx Pharmaceutical Inc., Grant/Research Support

FRI-1021

In a Randomized, Placebo-Controlled Trial Of Teriparatide (TPTD) For Premenopausal Idiopathic Osteoporosis (IOP), Tissue-Level Bone Formation Rate at Baseline and 3 Months Predicts Bone Density Response

Adi Cohen^{*1}, Stephanie Shiau², Nandini Nair¹, John Williams¹, Robert Recker³, Joan Lappe⁴, David Dempster¹, Hua Zhou⁵, Mafo Kamanda-Kosseh¹, Mariana Bucovsky¹, Julie Stubby³, Elizabeth Shane¹. ¹Columbia University Medical Center, United States, ²Mailman School of Public Health, United States, ³Creighton University Medical Center, United States, ⁴Creighton University, United States, ⁵Helen Hayes Hospital, United States

Pre-menopausal women with IOP (PreMenIOP) have marked deficits in bone mass, microstructure and stiffness. On tetracycline-labeled transiliac biopsies, bone formation rate (BFR) varies from very low to elevated. In a pilot study of teriparatide (TPTD) in 21 PreMenIOP, we observed marked increases in BMD, but 20% had no change at any site. We initiated a double-blind, placebo-controlled, single-switchover study of TPTD (20mcg SC QD) in 41 PreMenIOP. Subjects (37±8 yrs) were randomized to ActiveTPTD (n=28) or Placebo (n=13) pens. At 6M, those randomized to Active TPTD continued for 18M; those randomized to Placebo began ActiveTPTD and continued for 24M. Transiliac biopsy was performed at 3M, with tetracycline labelling before initiating and after 2.5M on TPTD or Placebo. Subjects had low lumbar spine (LS) Z scores (-2.2±0.9) and averaged 3±3 fractures. Age, BMI, serum CTX, PINP, LS and radius BMD were similar; total hip (TH) and femoral neck BMD were higher in the Placebo group (p<0.05). During the first 6M, LS BMD increased more in ActiveTPTD than Placebo (5.5±4.2% vs 1.8±4.0%; p=0.01) with no significant differences elsewhere. The ActiveTPTD group had larger 3M increases in cancellous (CAN), endocortical (ENDO) and intracortical BFR (p<0.01-0.001) and larger 3M rises in CTX (+270±420 vs -60±170 pg/mL; p=0.01) and PINP (+61±95 vs -6±9 ng/mL; p=0.02). During the first 12M on active TPTD, BMD increased by 8.2±6.4% at LS, 3.1±4.0% at TH and 2.2±3.8% at FN. As in the pilot study, 20% had no increase in BMD. Baseline BFR predicted 12M change in BMD at LS (CAN: r=0.4, p=0.03; ENDO: r=0.4, p=0.01) and TH (CAN r=0.5, p=0.004). 3M change in ENDO BFR predicted 12M change in BMD at LS and TH (both r=0.5, p=0.02) and in CAN BFR tended to predict TH BMD change (r=0.4; p=0.06). Baseline CTX (not PINP) predicted LS BMD response to TPTD (r=0.4; p=0.03), while 3M changes in CTX and PINP did not. Those randomized to Placebo first (received 12M of TPTD during M6-18) gained less LS BMD on ActiveTPTD than those randomized to ActiveTPTD first (4.1±6.5% vs 10.1±5.4%; p=0.005), but other sites did not differ. Compliance, assessed on returned pens, averaged >90%, did not differ during the 6M RCT or the first 6M or 12M on active TPTD, and did not predict BMD response. In conclusion, these results demonstrate that PreMenIOP have significant increases in lumbar spine BMD after 6 and 12 months of TPTD. They also confirm that a subset of affected women do not respond to TPTD. Both baseline and TPTD-induced 3M increases in tissue-level bone formation rate are significantly associated with BMD response in PreMenIOP.

Disclosures: *Adi Cohen, None*

FRI-1022

Age-related Changes and the Effect of Bisphosphonates on Bone Turnover and Disease Progression in Fibrous Dysplasia of Bone

Pablo Florenzano^{*1,2}, Kristen S Pan^{1,3}, Sydney M Brown¹, Lori C Guthrie¹, Luis Fernandez De Castro¹, Michael T Collins¹, Alison M Boyce¹. ¹Skeletal Diseases and Mineral Homeostasis Section, National Institute of Dental and Craniofacial Research, National Institutes of Health, United States, ²Department of Endocrinology, School of Medicine, Pontificia Universidad Catolica de Chile., United States, ³NIH Medical Research Scholars Program (MRSP), United States

Fibrous dysplasia (FD) is a mosaic disease in which bone is replaced with fibro-osseous tissue, leading to fractures, disability, and pain. FD lesions manifest during the first years of life and expand during childhood, reaching final disease burden by age 15. In vitro data suggests that affected cells apoptose with age, leading to decreased disease activity in adulthood, however no clinical data is available to support this concept. This is relevant for interventional studies with bisphosphonates and other bone-altering medications, which frequently use change in bone turnover markers (BTMs) as surrogate endpoints. The aims of this study are to describe: 1) the natural history of bone turnover in FD, 2) the impact of bisphosphonates on BTMs in FD, and 3) the effect of bisphosphonates on FD lesion expansion and formation during childhood. Methods: Alkaline phosphatase, osteocalcin, NTx, FGF23, RANKL, and skeletal burden score (a validated marker of FD burden) from 179 total subjects were reviewed (mean age at enrollment 19y, range 2-80), including 75 total subjects treated with bisphosphonates. Results: In adults not treated with bisphosphonates, BTMs demonstrated a significant reduction with age: alkaline phosphatase (n=40, p<0.01, r=-0.5), osteocalcin (n=21, p=0.01, r=-0.5), NTx (n=35, p<0.01, r=-0.6), and RANKL (n=18, p<0.05, r=-0.5). FGF23 also demonstrated a significant reduction with age (n=57, p<0.01, r=-0.4). Bisphosphonate treatment (n=30) resulted in an 18% mean reduction in alkaline phosphatase, but in only 17% of subjects did it decline to within the age-specific normal range. Disease progression in children ≤ age 15 was not affected by bisphosphonate treatment [yearly increase in skeletal burden score of 18% for treated subjects (n=15) vs 14% for untreated subjects (n=20), p=ns]. Conclusions: FD is associated with an age-dependent decrease in BTMs in adulthood, with or without bisphosphonate treatment. Bisphosphonates can decrease, but infrequently normalize, BTMs. Bisphosphonate treatment does not prevent

the development or expansion of FD lesions in children. Consideration of the age-related decline in FD-related bone turnover, the lack of effect of bisphosphonates on disease progression, and established side effects in this population, should be made when evaluating use and response of antiresorptive medications in patients with FD.

Disclosures: *Pablo Florenzano, None*

FRI-1023

Trabecular Bone Score in Osteogenesis Imperfecta. Is it useful?

Helena Florez^{*1}, Africa Muxi², Eva Gonzalez³, Ana Monegal¹, Núria Guañabens¹, Pilar Peris¹. ¹Metabolic Bone Diseases Unit, Department of Rheumatology, Hospital Clinic, University of Barcelona, Spain, ²Department of Nuclear Medicine, Hospital Clinic, University of Barcelona, Spain, ³Department of Immunology, Hospital Clinic, University of Barcelona, Spain

The trabecular Bone Score (TBS) is a novel gray-level textural analysis measurement that can be applied to DXA images to estimate trabecular microarchitecture and has been shown to be related to direct measures of bone microarchitecture and fracture risk. Osteogenesis imperfecta (OI) is a congenital bone disease characterised by a low bone mineral density (BMD) and poor bone quality and strength. The usefulness of TBS in OI has been scarcely evaluated. PURPOSE To analyse the clinical usefulness of TBS determination in patients with OI and its relation with anthropometric and clinical features (especially concerning skeletal fractures and BMD results). METHODS Thirty-four patients (23F:11M) with OI with a mean age of 40±15 years (19-70) attending a Metabolic Bone Disease Unit were included. The clinical reports of the patients were reviewed, with especial attention to the clinical features (weight, height and body mass index [BMI]), previous fractures, disease severity, associated mutations and treatments received. Lumbar spine (LS), total hip (TH), and femoral neck (FN) BMD were measured using DXA equipment (Lunar) in all patients. TBS was analysed in LS, and the results were classified in three categories: TBS>1.310 (normal), TBS 1.230-1.310 (partially degraded microarchitecture), TBS<1.230 (degraded microarchitecture). TBS values were compared with a healthy control group of similar age and gender. RESULTS 6/31 patients (19%) had a degraded microarchitecture, 8 (26%) a partially degraded microarchitecture and 17 (55%) normal TBS. All patients with TBS<1.230 were over 40 years old. 97% had a previous history of fractures, most with multiple fractures. Regarding BMD, 61% of the patients had osteoporosis, 36% osteopenia and one had normal values. Most patients had mutations in the COL1A1 or COL1A2 genes (66% and 34%, respectively). No significant differences were observed in BMD or TBS values according to the COL1 gen mutation (COL1A1 vs. COL1A2). A correlation was observed between TBS and age (r=-0.6, p<0.01), LS BMD (r=0.4, p=0.03), TH BMD (r=0.4, p=0.04) and with BMI (r=-0.5, p=0.01). No significant differences were observed on comparing TBS in patients and controls (1.297 vs. 1.399, p=N.S.). CONCLUSION TBS measurement does not seem to be useful for evaluating bone strength in patients with OI. Despite most patients presenting a history of multiple fractures, only 19% showed degraded microarchitecture with TBS. 1 McCloskey EV. J Bone Miner Res. 2016

Disclosures: *Helena Florez, None*

FRI-1024

Achondroplasia Natural History: a Large, Ongoing Multi-Center Cohort Study

Julie Hoover-Fong^{*1}, Michael Bober², Syed Hashmi³, Jacqueline Hecht³, Janet Legare⁴, Mary Ellen Little², John Mcgready¹, Peggy Modaff², Richard Pauli⁴, David Rodriguez-Buritic³, Kerry Schulze¹, Elena Serna³, Cory Smid⁴, Adekemi Alade¹. ¹Johns Hopkins University, United States, ²AI duPont Hospital for Children, United States, ³University of Texas, United States, ⁴University of Wisconsin, United States

Objective: Information lacks about adverse health outcomes related to poor physical function, pain and obstructive/central apnea, and earlier adult and higher infant mortality in achondroplasia. To define the natural history, a large multi-center database with retrospective and prospective functionality was built. Materials/Methods: All available medical records from achondroplasia patients at a skeletal dysplasia center (i.e. Johns Hopkins, AI duPont Hospital, University of Texas, University of Wisconsin) from 1957 to date were gathered. There were 4 primary study domains: 1. Mixed longitudinal anthropometry (i.e. length/ht, wt, head circ); 2. Surgical burden; 3. Sleep disordered breathing; and 4. Radiographic catalogue. Phase 1 was establishment of this well-phenotyped achondroplasia cohort (i.e. Primary Achondroplasia Cohort, PAC). In phase 2, multivariate analysis across study domains will occur. A clinically active sub-cohort from the PAC will participate in prospective studies related to craniofacial structure and obstructive sleep apnea; metabolic health and obesity; neurocognition; and pain/function related to surgery. There is IRB approval. Results: The PAC includes 1,377 subjects (704 M:673 F, mean 15.2±12.1 yr, 75.5% de novo). The Active subcohort includes 471 subjects (250 M:221 F). 5.7% of the PAC were adopted. 39,000+ mixed-longitudinal anthropometric data points were collected to examine length/ht, wt and head circ trajectories. 1,116 subjects had 4,934 surgeries in 5 categories; 151 (10.7%) had no surgery. There were 2,757 ENT procedures (tubes, T&A) in 885 subjects. 138 subjects had 329 brain surgeries (i.e. VP shunt, ventriculostomy) while 250 (18.2%) had a foramen magnum decompression + C1/C2 laminectomy. Spine surgery occurred 430 times in 182 subjects, and 289 had 654 lower extremity procedures (i.e. osteotomy, lengthening). Data from 1556 polysomnograms are available from 666 subjects; 423 (63.3%) have obstructive

sleep apnea. There are 10,354 images from 1,249 subjects. Conclusions: This is the first multi-center natural history study of achondroplasia. We made novel observations about growth velocity and final adult height, surgical burden, and sleep disordered breathing. We are now examining interactions among study domains. This cohort may serve as controls against subjects treated with novel pharmacologic, medical and surgical interventions, and participate in prospective studies.

Disclosures: **Julie Hoover-Fong**, BioMarin, Consultant

FRI-1025

The Effect of Burosumab (KRN23), a Fully Human Anti-FGF23 Monoclonal Antibody, on Osteomalacia in Adults with X-Linked Hypophosphatemia (XLH) Karl L. Insogna^{*1}, Frank Rauch², Peter Kamenický³, Nobuaki Ito⁴, Takuo Kubota⁵, Akie Nakamura⁶, Lin Zhang⁷, Matt Mealiffe⁷, Javier San Martin⁷, Anthony A. Portale⁸. ¹Yale School of Medicine, United States, ²McGill University, Canada, ³Université Paris-Sud, France, ⁴University of Tokyo Hospital, Japan, ⁵Osaka University Hospital, Japan, ⁶Hokkaido University Hospital, Japan, ⁷Ultragenyx Pharmaceutical Inc., United States, ⁸University of California, San Francisco, United States

In adults with XLH, excess FGF23 causes hypophosphatemia, leading to persistent osteomalacia – a defect in bone mineralization due to chronically low serum phosphorus. Osteomalacia is associated with fractures, pseudofractures, delayed fracture healing, and bone pain. Burosumab is a fully human monoclonal antibody against FGF23 under investigation for treatment of XLH. UX023-CL304 is an ongoing, open-label, Phase 3 study investigating the effects of 48 weeks of subcutaneous burosumab, 1.0 mg/kg administered every 4 weeks, on osteomalacia in adults with XLH who have not received oral phosphate and vitamin D therapy within 2 years of enrollment. The primary endpoint is improvement in osteoid volume/bone volume assessed by transiliac bone biopsies obtained at baseline and Week 48. Additional assessments include serum phosphorus, markers of bone turnover, fracture/pseudofracture healing, patient-reported outcomes, and safety. Fourteen subjects enrolled (mean age 40 years, 57% female), 13 completed 48 weeks, and 11 completed paired biopsies. At baseline, subjects demonstrated severe osteomalacia. All osteomalacia-related histomorphometric measures improved significantly at Week 48 (percent change: osteoid volume/bone volume -54%, osteoid thickness -32%, osteoid surface/bone surface -26%, mineralization lag time -52%). Mean serum phosphorus concentration, averaged across the mid-point of the dose cycle between Weeks 0-24, increased by 48%, consistent with previous findings. Markers of bone formation and resorption increased at Week 48 (LS mean increase: P1NP +77%, CTx +36%; both $p < 0.0001$). Of the 4 active pseudofractures detected at baseline, 3 were healed and 1 was missing at Week 48. There were significant reductions in pain (LS mean change -1.86 $p = 0.0054$) and global fatigue (-1.20 $p = 0.0359$) scores. All subjects had ≥ 1 treatment-emergent adverse event (AE). Two subjects experienced serious AEs (migraine; paraesthesia) that were unrelated to treatment and resolved. The safety profile of burosumab was similar to that seen in larger clinical trials, with most AEs mild to moderate in severity. Eleven subjects had 18 procedure-related AEs: 15 for pain and 1 each for itch, headache, and bandage irritation. There were no deaths or incidents of hyperphosphatemia; 1 subject withdrew consent at Week 44. We conclude that treatment with burosumab significantly improves osteomalacia in adults with XLH, which should ameliorate the skeletal complications of this disease.

Table 1. Efficacy Assessments in UX023-CL304

Assessment	All Subjects ^a
Osteoid Volume/Bone Volume, %	
Baseline	26.1 (12.4)
Week 48	11.9 (6.6)
P value ^b	<0.0001
Osteoid Thickness, μm	
Baseline	17.2 (4.1)
Week 48	11.6 (3.1)
P value ^b	<0.0001
Osteoid Surface/Bone Surface, %	
Baseline	91.7 (3.4)
Week 48	67.8 (13.7)
P value ^b	<0.001
Mineralization Lag Time, days^c	
Baseline	1539.8 (1587.1)
Week 48	195.5 (77.7)
P value ^b	<0.05
Serum Phosphorus, mg/dL	
Baseline	2.24 (0.396)
Between Baseline & Week 24, across mid-point of the dose interval	3.31 (0.380)

^an=11 except Baseline OV/BV n=10, Week 48 Mlt n=10, and serum phosphorus n=14. ^bMean percentage change from baseline. ^cUsing imputed results.

Disclosures: **Karl L. Insogna**, Ultragenyx Pharmaceutical Inc., Grant/Research Support, Ultragenyx Pharmaceutical Inc., Other Financial or Material Support, Ultragenyx Pharmaceutical Inc., Consultant

FRI-1026

An overview of the etiology, clinical manifestations, management strategies and complications of hypoparathyroidism from the Canadian National Hypoparathyroidism Registry Rafik El Werfalli^{*1}, Yasser Hakami¹, Manoela Braga¹, Adam Millar², Zubin Punthakee¹, Farhan Tariq¹, J.E.M. Young¹, Aliya Khan¹. ¹McMaster University, Canada, ²University of Toronto, Canada

The Canadian National Hypoparathyroidism Registry (CNHR) was formed in 2014 and enrolment of prevalent and incident cases began following approval by McMaster University Ethics Review Board. Objective(s): • identify the etiology and presenting symptoms of patients with hypoPTH. • evaluate current treatment practice in Canada. • assess differences in presentation based on etiology of the disease. • compare parameters of calcium homeostasis amongst those developing complications of nephrolithiasis or nephrocalcinosis versus those without complications. • assess fracture risk in Canadian patients with hypoPTH. Material and Methods: 118 patients aged >18 years registered in the CNHR were reviewed as per the following inclusion criteria: 1. Chronic HypoPTH (low PTH in the presence of low serum calcium total or ionized below normal reference range for at least 6 months prior to enrolment) 2. HypoPTH (including post-surgery) requiring calcium/calcitriol replacement to maintain normal calcium (total or ionized) calcium level for at least 6 months prior to enrolment 3. Pseudohypoparathyroidism with elevated PTH and low serum calcium (total or ionized) normal vitamin D and hyperphosphatemia were included. We reviewed etiology, clinical presentation, biochemical profile, management strategies, markers of skeletal health including fractures, bone mineral density (BMD), fracture risk and complications including nephrolithiasis/nephrocalcinosis, and basal ganglia calcification. Results: Most patients (72%) had postsurgical hypoparathyroidism, followed by idiopathic/autoimmune disease (25%) and pseudohypoparathyroidism (3%). The mean age of onset was 42.0 years, with mean duration of follow-up of 4 years. All patients were taking calcium supplements (100%); calcitriol was taken by 82.2% and 6 patients were receiving parathyroid hormone. Nephrolithiasis or nephrocalcinosis were present in 24.6% of treated patients despite a mean calcium phosphate product <4.4 mmol²/L². Basal ganglia calcification was present in 8 of the 30 patients reviewed. Hospitalization was required in 40 of the 118 patients for symptoms of hypocalcemia. Conclusion: 1. HypoPTH is associated with a significant disease burden and leads to hospitalization in a large number of patients. 2. Renal complications were present in 24.6% of treated patients despite maintenance of a calcium phosphate product in the desired range (<4.4 mmol²/L²). The ideal calcium phosphate product needs to be reconsidered. 3. Fracture risk was low in the absence of traditional osteoporosis risk factors.

Disclosures: **Rafik El Werfalli**, None

FRI-1027

Bone Remodeling and Bone Mass in Patients with Hypophosphatasemia Laura Lopez-Delgado^{*1}, Leyre Riancho-Zarrabeitia², Maite Garcia-Unzueta¹, Carmen Valero^{1,3}, Jair Tenorio⁴, Marta Garcia-Hoyos¹, Pablo Lapunzina⁴, Jose A. Riancho^{1,3}. ¹Hospital UM Valdecilla, Spain, ²Hospital Sierrallana, Spain, ³Univ Cantabria, IDIVAL, Spain, ⁴Institute of Medical and Molecular Genetics, Spain

Purpose: Hypophosphatasia (HPP) is a rare genetic condition caused by loss-of-function mutations of the gene that encodes the tissue nonspecific alkaline phosphatase (ALPL or TNSALP). It is characterized by low serum levels of ALP. The clinical spectrum of hypophosphatasia (HPP) is broad and variable within families. Adult forms with mild manifestations may be incidentally discovered by the presence of low alkaline phosphatase (ALP) activity in serum. However, it is still unclear whether individuals with persistently low levels of ALP, in the absence of overt manifestations of HPP, present subclinical abnormalities of bone remodeling or bone mass. Methods: The aim of this study was to obtain a better understanding of the skeletal phenotype of adults with low ALP by analyzing bone mineral density (BMD), bone microarchitecture (Trabecular bone score, TBS) and bone turnover markers (P1NP and β -crosslaps). Results: We studied 36 individuals with persistently low serum ALP not related to drug therapy or other secondary cause. In about half of them we identified a heterozygous mutation of the coding region of the ALPL gene. We found that patients with persistently low ALP indeed have a reduced bone turnover. They showed lower levels of P1NP (32.0 \pm 14.4 versus 50.6 \pm 24.0 ng/ml; $p = 0.00089$) and β -crosslaps (0.22 \pm 0.19 versus 0.34 \pm 0.21 ng/ml, $p = 0.008$) than individuals in the control group. However, there were no significant correlations between serum levels of ALP and either P1NP or β -crosslaps among patients with low ALP. Similar levels were found in patients with mutations and those without detected mutations. Despite the decreased bone turnover, there were no significant differences in BMD, bone mineral content or TBS between both patients and controls. Conclusions: These results strongly suggest that patients with persistent hypophosphatasemia have low bone remodelling even though they do not present evident clinical skeletal alterations or decreased BMD. This might render them more susceptible to anti-resorptive-related adverse effects such as the development of atypical femoral fractures.

Disclosures: **Laura Lopez-Delgado**, None

FRI-1028

Clinical Features of Patients with Tumoral Calcinosis: The Mayo Clinic Experience Jad Sfeir*, Kurt Kennel, Matthew Drake. Mayo Clinic, United States

Background: Tumoral calcinosis (TC) is characterized by ectopic tumor-like peri-articular deposits of calcium that can infiltrate muscles and tendons. Epidemiological data is very limited. Primary TC is commonly familial and associated with hyperphosphatemia. Genetic and phenotypic heterogeneity is present, however, and thus patients can have sporadic disease especially when serum phosphate levels are normal. Here we review our experience with this disease. Results: We conducted a retrospective review of patients with radiographic and/or pathologic evidence of calcinosis from January 1985 to December 2016. After excluding secondary causes, such as renal and connective tissue diseases, 33 patients were identified to have primary TC. Patients were primarily Caucasian (78%) women (85%). Approximately half (45.5%) had hyperphosphatemia. Median age at diagnosis for hyperphosphatemic disease was 15.5 years (9.5 – 58.65) versus 66.3 years (55.6 – 75.9) in patients with normophosphatemia. Plain films were required in all patients for the diagnosis of TC. Disease was localized in larger joints sites [hips (27%), shoulders (24%) and elbows (18%)], but smaller joints were almost as common (21% feet and 18% hands). One-third of patients had disease in more than one joint. Surgical excision was performed in two-thirds of patients for symptomatic and/or cosmetic indications. Recurrence occurred in 38%, at a median of 3.5 years after surgery (2 – 8); 75% of those with recurrence had hyperphosphatemia. Only one patient had major complications from surgery including infection, delayed wound healing and prolonged drainage. Sevelamer normalized serum phosphate in 3 out of 4 patients. Etidronate showed no improvement in symptoms or extent of disease. Alendronate and zoledronate were prescribed to 5 patients, but the follow up period was too short to estimate their effect. Conclusion: Although TC was originally thought to primarily affect patients of African descent, our data suggests that Caucasians are at risk too, possibly with a higher prevalence. Hyperphosphatemia was associated with increased TC severity and earlier diagnosis, whereas adults with normophosphatemia have milder disease. Surgery appears to be safe, although the risk of recurrence is substantial. Medical treatment is mostly directed at serum phosphate normalization. Etidronate is largely ineffective but more time is needed to judge the efficacy of newer bisphosphonates.

Disclosures: *Jad Sfeir, None*

FRI-1077

Mechanisms Underlying Increased Osteoclastogenesis in the Mouse Model of Osteogenesis Imperfecta Due to Mutation in Collagen Type I Iris Boraschi*¹, Erène C Niemi², Frank Rauch¹, Mary Nakamura², Svetlana Komarova¹. ¹Shriners Hospital-Canada/ McGill University, Canada, ²University of San Francisco California, United States

Introduction: Osteogenesis imperfecta (OI) is the most common heritable bone fragility disorder, usually caused by dominant mutations in genes coding for collagen type I alpha chains, COL1A1 or COL1A2. Although, osteoclasts do not express or produce collagen, stimulated osteoclastogenesis and bone destruction were reported in OI. Objective: The aim of this study was to examine the osteoclast phenotype in a mouse model of dominant severe OI caused by a Col1a1 mutation, Col1a1Jrt/+ mice. Methods: Bone marrow and spleen osteoclast precursors were extracted, characterized and differentiated into mature osteoclasts by culturing with macrophage colony-stimulating factor and RANKL in vitro. Results: We found that more and larger osteoclasts were formed in vivo from bone marrow and spleen precursors of Col1a1Jrt/+ (OI) mice compared to wild-type littermates (WT). However, expression of the osteoclast markers genes, or signaling by calcium or NFATc1 were not significantly different between WT and OI. Osteoclast precursor frequency was similar in Col1a1Jrt/+ and WT mice, however, OI precursors were more sensitive to RANKL compared to WT. No significant difference was found in the protein expression of RANKL, OPG or RANK between OI and WT bone extracts or in vitro generated osteoblasts or osteoclasts. We have previously established that osteoclast formation is inhibited by collagen type I degradation fragments. The molecular weight of isolated Col1a1Jrt/+ collagen type I was approximately 50 kDa and was easily degradable by cathepsin K. We have previously demonstrated that osteoclast formation is inhibited by collagen type I and, more robustly by its degradation fragments. OI full length collagen type I was more effective in inhibiting osteoclast formation compared to WT, while OI collagen degradation fragments lacked osteoclast-inhibitory activity. Conclusion: We demonstrate that Col1a1 mutation results in an osteoclast phenotype even though osteoclasts themselves do not express this protein. One of the potential mechanisms is rapid degradation of mutated collagen type I resulting in complete lack of fragments with osteoclast inhibitory activity, and thus an absence of a negative feedback for osteoclastogenesis in OI.

Disclosures: *Iris Boraschi, None*

FRI-1078

An antibody against ALK2 extracellular domain reveals a role of dimer formation for signal activation Takenobu Katagiri*¹, Shinnosuke Tsuji², Sho Tsukamoto¹, Mai Kuratani¹, Satoshi Ohte¹, Kiyosumi Takaishi^{2,3}, Yoshihiro Kawaguchi⁴, Jun Hasegawa⁴. ¹Division of Pathophysiology, Research Center for Genomic Medicine, Saitama Medical University, Japan, ²Rare Disease & LCM Laboratories, R&D Division, Daiichi-Sankyo Co., Ltd., Japan, ³Kensuke Nakamura, Modality Research Laboratories, Biologics Division, Daiichi-Sankyo Co., Ltd., Japan, ⁴Modality Research Laboratories, Biologics Division, Daiichi-Sankyo Co., Ltd., Japan

Fibrodysplasia ossificans progressiva (FOP) is a rare autosomal-dominant disorder characterized by heterotopic ossification (HO) in soft tissues. Trauma induces acute progressive ossification in patients with FOP. A recurrent R206H mutation in ALK2, a type I receptor for BMPs, was found in the patients with typical FOP. The mutant ALK2 induces BMP signaling by binding to non-osteogenic ligand, activin A. We have developed rat monoclonal antibodies bind to ALK2 extracellular domain and inhibit signaling in response to ligand stimulation. In the present study, we examined an effect of the ALK2 antibody on HO induced by the mutant receptor and the molecular mechanisms underlying the activity in vitro. We established a novel knock-in mouse line carrying the R206H mutation, in which the mutant ALK2 is induced by Cre-dependent recombination. In mice crossed with CAG-CreERT, trauma-induced HO was observed in tamoxifen-injected mice. Unexpectedly, however, the HO was increased by treatment with the ALK2 antibody. The increase in HO by the antibody was also observed in mice locally injected adenovirus-Cre in skeletal muscle. We carefully examined effects of the antibody on signaling in vitro through mouse and human ALK2 of WT and the R206H forms. We found that the antibody enhanced signaling by mouse R206H, but not human R206H, in the absence of ligands. The F(ab')₂ fragment of the antibody also enhanced mouse R206H, but the Fab fragment did not show such capacity. In addition, the antibody and the F(ab')₂ fragment, but not the F(ab) fragment, induced a dimer formation of ALK2 on the cell surface. By generating chimera and substitution mutations between mouse and human ALK2 sequences, we identified a single residue critical for the responses to the antibody. Substitution of the residue identified in mouse R206H to the human residue caused a suppression of signaling by the antibody. This finding was further supported in human R206H vice versa. Moreover, all of thirteen mutants of human ALK2 found in patients with FOP were suppressed by the antibody in vitro. Taken together, these data suggest that the 2 arms of the antibody form a dimer of ALK2 on the cell surface. The formed dimer of mouse ALK2(R206H) is able to activate signaling in the absence of ligands, although it is inhibited to response to ligands. It was also suggested that the ALK2 antibody inhibits HO in the patients with FOP.

Disclosures: *Takenobu Katagiri, Daiichi-Sankyo Co., Ltd., Grant/Research Support*

FRI-1079

Activation of the pro-fibrotic TGFβ pathway contributes to the multiorgan dysfunctions in the CLCN7-dependent ADO2 Antonio Maurizi*, Mattia Capulli, Anna Curle, Rajvi Patel, Nadia Rucci, Anna Teti. University of L'Aquila, Italy

The chloride channel type 7 (CLCN7) is a ubiquitous gene essential for lysosome function in different cell types. However, missense mutations of CLCN7 are associated only with autosomal dominant osteopetrosis type 2 (ADO2), considered a pure bone disease caused by defective osteoclast function. As a consequence of this classification, ADO2 patients are investigated only for the bone alterations even though the ubiquitous CLCN7 expression suggests that alterations in other organs could also contribute to the patients' morbidities. We tested this hypothesis in a mouse model of ADO2 carrying the heterozygous Clcn7G213R mutation and applied an unbiased large-scale approach. RNA deep sequencing analysis of lungs, muscles and kidney transcriptomes showed an enrichment in the macrophage gene signature and an upregulation of the pro-fibrotic Tgfβ pathway in ADO2 vs WT littermates (p<0.05). In line with these results, histopathological analysis revealed perivascular fibrosis in ADO2 lungs (+1.5fold;p=0.005), muscles (+1.7fold;p=0.04) and kidneys (+3fold;p=0.01), vs WT. Accordingly, upregulation of Col1a1 expression was detected in ADO2 lungs (+6.7fold;p=0.001), muscles (+2.6fold; p=0.001), kidneys (+8fold;p=0.002) and bone marrow (+3.5fold;p<0.01), associated with a higher number of F4/80+ macrophages (+6fold;p<0.01). Macrophages are known to be involved in the onset of fibrosis and are the candidate cells that could induce the observed multiorgan alterations. In line with this hypothesis, ADO2 macrophages revealed higher lysosomal pH (+1.64 pH units;p<0.001), LC3bII accumulation (+1.7fold) and increased p62 expression (+2.7fold), suggesting altered autophagy, which is known to be induced by TGFβ. Real-time RT-PCR confirmed the upregulation of Tgfβ1 and Tgfβ2 in ADO2 lungs and muscles, respectively (+1.5fold;p=0.01 and +2.6fold;p=0.0026), while both Tgfβ1 and Tgfβ2 were upregulated in ADO2 kidneys (+2.4fold; p=0.0008 and +1.4fold;p=0.03). Of note, Tgfβ1 overexpression was also found in the bone marrow (+10fold;p=0.004). Consistently, the TGFβ-activated factors, a-Sma and Grem1, were upregulated in ADO2 lungs (+2.9fold; p<0.0001) and muscles (+11.4fold;p=0.01). Moreover, the activation of the TGFβ pathway was confirmed by increased pSMAD+ cells in the ADO2 lungs (+20 fold;p<0.001). Our work indicates that ADO2 is a systemic disease and that tissue macrophages and activation of the pro-fibrotic TGFβ pathway could mediate ADO2 organ fibrosis.

Disclosures: *Antonio Maurizi, None*

FRI-1080

Autologous Regulatory T Cell Transplantation Enhances Bone Repair in a Mouse Model of Osteogenesis Imperfecta Meenal Mehrotra*, Inhong Kang, Shilpak Chatterjee, Uday Baliga, Shikhar Mehrotra. Medical University of South Carolina, United States

Osteogenesis imperfecta (OI), most common hereditary bone disease, is characterized by reduction in quantity of bone matrix that leads to repeated fractures and bone deformity. Incidence of OI in United States is estimated to be 1/20,000 live births. Long-term treatment to prevent fractures have their own side effects; therefore several strategies are being tested to enhance bone remodeling. It is known that skeletal homeostasis can be dynamically influenced by the immune system. Recent studies have shown that T lymphocytes could be essential in regulating homeostasis, survival and function of not only osteoclasts but osteoblasts as well, thus playing an important role in bone turnover. A previous study demonstrates improved bone formation after delivery of anti-inflammatory regulatory T cells (Treg's) during mesenchymal stem cell based bone regeneration. However, whether T cells, specifically Treg's, play a role in OI, a disease with high turnover and high fracture rates, has never been investigated before. For our studies we used B6C3Fe a/a-Col1a2oim/J (oim) model, which resembles Type III OI, a non-lethal but severe form. Characterization of T lymphocytes demonstrated that splenic T cells from oim mouse exhibited activated phenotype as compared to wild type (WT) T cells, which in turn correlated with higher secretion of effector cytokines, IFN- γ and TNF- α . Furthermore, we also observed that oim mouse exhibited a quantitative decrease in CD4⁺CD25⁺Foxp3⁺ Treg's. Thus, we hypothesized that quantitative restoration of Treg's in OI would inhibit the higher pro-inflammatory cytokine secretion by T cells and lead to better bone formation. Enhanced improvement in trabecular and cortical parameters was observed by Micro-CT when oim mice were transplanted with WT bone marrow (BM) + WT Treg's as compared to those transplanted with WT BM alone. Interestingly, significant improvement in trabecular and cortical parameters was also observed when oim mice were transplanted with Treg's from another oim mouse (auto-transplantation). To determine mechanism of how Treg's mediate healing of bone, we examined their effects on osteoclasts and osteoblasts from oim mice. Conditioned media from WT as well as oim Treg's, not only suppressed osteoclast formation, but also caused a remarkable increase in osteoblast mineralization. Thus, understanding the contribution of Treg's to osteogenesis in OI could help develop autologous immunotherapy based treatment modalities for OI.

Disclosures: Meenal Mehrotra, None

FRI-1081

BMP signaling and BMPR dynamics and interactions are restrained by cell surface heparan sulfate, a mechanism likely altered in Hereditary Multiple Exostoses Christina Mundy*, Evan Yang, Paul Billings, Hajime Takano, Maurizio Pacifici. The Children's Hospital of Philadelphia, United States

Heparan sulfate (HS) is a key component of cell surface and extracellular matrix molecules. The HS chains specifically interact with a variety of signaling proteins, including bone morphogenetic proteins (BMPs), and regulate protein distribution, availability and activity on target cells. A deficiency in HS characterizes the rare pediatric disorder Hereditary Multiple Exostoses. HME is caused by loss-of-function mutations in HS-synthesizing enzymes EXT1 or EXT2 and is characterized by cartilaginous tumors (exostoses/osteochondromas) forming along the growth plate, causing multiple health problems. Previously we showed that genetic or pharmacological interference with HS function rapidly increases canonical BMP signaling, suggesting that HS normally limits BMP signaling. However, the mechanisms of this action remained unclear. Thus, we investigated whether HS regulates cell surface BMP receptor (BMPR) mobility, interactions and signaling. We transfected cell lines with constructs encoding Snap-BMPRII and Snap-BMPRIa fusion proteins. Co-transfected cells rapidly responded to BMP2 treatment with major increases in pSMAD158 levels; interestingly, the same occurred after treatment with HS antagonist Surfen. Such increases were counteracted by Noggin co-treatment, suggesting that they reflected an increase in endogenous BMP at the cell surface. To assess BMPR dynamics, we carried out fluorescence recovery after photobleaching assays and found that receptor mobility decreased after treatment with BMP2 or Surfen, suggesting that the receptors had transitioned to lipid rafts for signaling. To verify such lipid raft re-localization, we separated lipid raft from non-lipid raft cell surface domains by ultracentrifugation and found that treatment with Surfen did in fact shift a significant amount of BMPRII to lipid raft domains compared to untreated cells. Lastly, we performed in situ proximity ligation assays to monitor BMPRIa and BMPRII interactions on live cells and found that treatment with Surfen promoted receptor-receptor oligomerization compared to control cells. In sum, our data indicate that cell surface HS chains restrain BMP signaling by limiting ligand availability and BMPR dynamics and interactions. The HS deficiency in HME could hamper these mechanisms, increasing BMP signaling and inducing osteochondroma formation. Ongoing studies are investigating BMP and BMPR expression and signaling levels in tissues derived from patient osteochondromas.

Disclosures: Christina Mundy, None

FRI-1082

Gene expression profiling of sclerostin antibody-induced therapeutic response in growing Brl/+ mouse model of osteogenesis imperfecta Hsiao Hsin Sung*^{1,2}, Rachel Surowiec³, Rebecca Falzon², Lauren Battle², Chris Stephan², Michelle S. Caird³, Kenneth M. Kozloff³. ¹RIMLS, Department of Rheumatology, Radboudumc, The Netherlands; Department of Oral and Maxillofacial Surgery, University of Michigan. ²Department of Orthopaedic Surgery, University of Michigan, United States, ³Biomedical Engineering, University of Michigan; Department of Orthopaedic Surgery, University of Michigan, United States

Osteogenesis imperfecta (OI) is a genetic disorder caused by mutations in the genes that encode type I collagen. Brl/+ mouse is a model for OI characterized by increased bone fragility and loss in bone mass. Sclerostin antibody (SclAb) is a novel anabolic bone agent that increases bone mass and improves bone fragility in Brl/+ mouse. Unknown is the specific transcriptional response modulated by SclAb in the OI model. The purpose of this study was to assess the differential gene expression induced by SclAb in the trabecular and cortical bone of the Brl/+ OI mouse model after 1 and 5 weeks of treatment. 3 week-old female WT and Brl/+ mice were randomly assigned to SclAb (Amgen) treatment or vehicle injection (PBS), and injected s.c. at 25 mg/kg, 2X/week. Femoral trabecular and cortical samples of Brl/+ and WT mice treated for one and five weeks (Total=8 groups; n=3/group) were carefully dissected, and RNA extractions were processed with the Qiazol and RNeasy micro kit. The RNA integrity number for all samples was above 7.0. RNA-Seq data were analyzed by Funrich, ClustVis, and IpathwaysGuide. qRT-PCR was performed to validate select genes. Statistical analysis was tested with two-tailed unpaired Student's t-test p<0.05 considered as statistically significant. Untreated Brl/+ and WT show high levels of differentially expressed genes (DEGs) at 4 week-old that gradually decrease by 8 week-old (Figure 1A). The length of treatment, type of bone and phenotype determine the SclAb-induced adaptive changes. SclAb-induced cortical response tends to be sustained during the time, unlike the higher-fold change (FC) of differences in the trabecular after 5 week of treatment, possibly due to the catch-up growth (Figure 1B). After 5 weeks of treatment, SclAb seems to restore the gene expression involved in bone remodeling, and collagen organization comparable to a WT level (Figure 1C). In Brl/+ mouse, SclAb induced differential expression of Sost gene (FC>1.5; p<0.05) in both types of bone, and length of treatment (Figure 1 D-E). This is not observed in the trabecular of 1 week-treated WT, suggesting a compensatory mechanism. These data suggest that SclAb regulate differentially the gene expression of cortical and trabecular bone. Understanding the influence of genotype on the therapeutic response is critical for developing patient-specific treatment strategies. In this study, observations of DEGs suggest bone type- and genotype-specific response to therapy between Brl/+ and WT.

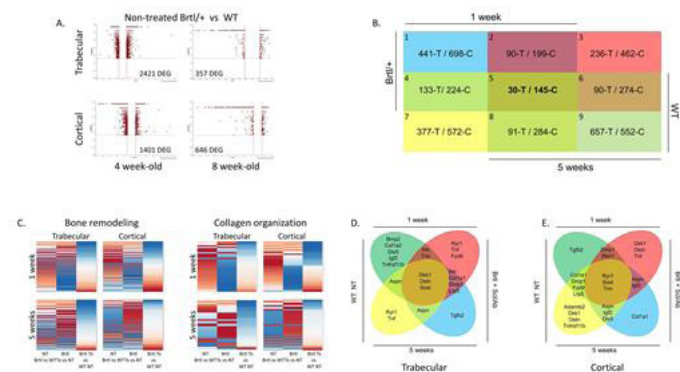


Figure 1. A) Volcano plots showing the global transcriptional changes (>1.5 FC; p<0.05) in trabecular and cortical bone of Brl/+ and WT at 4 and 8 week-old (treated with PBS). The log FC is represented on the x-axis and the y-axis represents the log10 of the p value. B) Venn diagram showing the number of DEGs (>1.5 FC; p<0.05) in all type of genotype, bone type, and treatment duration. Panel 5 shows the overlapping number of genes among the 4 comparisons. Panel 1, 7 shows the early SclAb-induced response in Brl/+ and WT, respectively. Panel 3, 9 shows the late response in Brl/+ and WT, respectively. C) Heatmap, a subset of osteogenic- and collagen-related genes from trabecular and cortical bone of non-treated and treated Brl/+ and WT mice, exhibiting at least 1.5-FC. D-E) Venn diagram showing genes that are differentially expressed (>1.5 FC; p<0.05) in trabecular and cortical bone of Brl/+ treated and WT untreated compared to Brl/+ untreated at 1 and 5 weeks of treatment (SclAb/PBS).

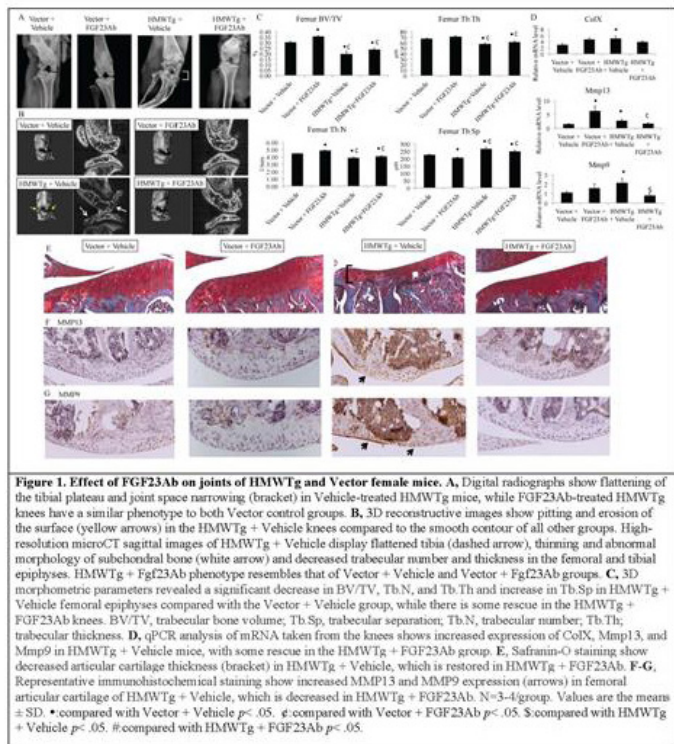
Disclosures: Hsiao Hsin Sung, None

FRI-1083

FGF23 Regulates Wnt/ β -catenin Signaling-mediated Osteoarthritis in Mice Overexpressing High Molecular Weight FGF2 Patience Meo Burt*, Liping Xiao, Marja Hurley. UConn Health, United States

Although humans with X-linked hypophosphatemia (XLH) and the Hyp mouse, a murine homologue of XLH, are known to develop degenerative joint disease, the exact mechanism which drives the osteoarthritic (OA) phenotype remains unclear. Mice that overexpress high molecular weight FGF2 isoforms (HMWTg mice) phenocopy both XLH and Hyp including OA with increased FGF23 production in bone and serum. Since HMWTg cartilage also has increased FGF23 and there is crosstalk between FGF23-Wnt/ β -catenin signaling, the purpose of this study was to determine if OA observed in HMWTg mice is due to FGF23 mediated-canonical Wnt signaling in chondrocytes given that both pathways are implicated in OA pathogenesis. HMWTg OA joints had decreased Dkk1, Sost, and Lrp6 expression

with increased Wnt5a, Wnt7b, Lrp5, Axin2, phospho-GSK3b, Lef1, and nuclear β -catenin as indicated by immunohistochemistry or qPCR analysis. Chondrocytes from HMWTg mice had enhanced alcian blue and alkaline phosphatase staining and increased FGF23, Adamts5, Il-1 β , Wnt7b, Wnt16, and Wisp1 gene expression and phospho-GSK3b protein expression as indicated by Western blot compared to chondrocytes of Vector control and chondrocytes from mice overexpressing the low molecular weight isoform, which were protected from OA. Canonical Wnt-inhibitor treatment rescued some of those parameters in HMWTg chondrocytes, seemingly delaying the initial accelerated chondrogenic differentiation. Neutralizing FGF23Ab treatment was able to partly ameliorate OA abnormalities in subchondral bone and reduce degradative/hypertrophic chondrogenic marker expression in HMWTg joints in vivo (Fig.1). These results demonstrate that osteoarthritis of HMWTg is at least partially due to FGF23 modulated Wnt/ β -catenin signaling in chondrocytes.



Disclosures: *Patience Meo Burt, None*

FRI-1118

Three months of vitamin D3, 2,800 IU/d has an unfavorable effect on muscle strength and physical performance in vitamin D insufficient, hyperparathyroid women – a randomized placebo controlled trial Lise Sofie Bislev*¹, Lene Langagergaard Rødbro¹, Lars Rolighed², Tanja Sikjaer¹, Lars Rejnmark¹. ¹Department of Endocrinology and Internal Medicine, Denmark, ²Department of surgery, Denmark

Introduction: Low vitamin D levels and/or hyperparathyroidism has been associated with reduced muscle strength and postural stability. Methods: In a double-blinded placebo controlled randomized trial, we aimed to investigate effects of vitamin D3 supplementation (2800 IU/d vs. placebo) for three months during wintertime in 81 healthy postmenopausal women with high PTH- and low 25-hydroxy-vitamin D (25(OH)D) (<20 ng/mL). Maximal voluntary isometric muscle strength and maximal force production at upper- and lower extremities was measured with an adjustable dynamometer chair. We assessed physical performance by Time Up to Go test (TUG) and Repeated Chair Stands (RCS). Postural stability was assessed by a stadiometer, body composition by DXA and physical activity by a Physical Activity Scale questionnaire. Results: Median age was 65 (range: 60-76) years. At baseline, p-25(OH)D was 13 \pm 3.7 ng/mL and p-PTH 58 \pm 13.5 ng/mL with no significant differences between groups. Compared with placebo, vitamin D3 supplementation significantly increased levels of 25(OH)D and 1,25(OH)2D by 230% (95% CI: 189% to 272%, *p* < 0.0001) and 58% (190% to 271%, *p* < 0.0001), respectively, and lowered PTH by 17% (-23% to -11%, *p* < 0.0001). Compared with placebo, vitamin D3 had a significant detrimental effect on maximal handgrip strength; -9% (-15% to -3%, *p* < 0.01), knee flexion; -13% (-24% to -2%, *p* = 0.02) and TUG test; 4.4%; (0.1 to 8.6, *p* < 0.05). Total lean body mass and appendicular lean mass index did not change in response to treatment and neither did degree of physical activity. Vitamin D3 supplementation did not affect postural stability or RCS. Changes in 25(OH)D correlated with changes in handgrip (*r* = -0.25, *p* = 0.04), knee flexion (*r* = -0.30, *p* = 0.01) and TUG (*r* = 0.22, *p* = 0.05), whereas changes in PTH did not correlate with any of the stated measurements. Conclusion: Compared with placebo, supplementation with vitamin D3 2800 IU/d had an unfavorable effect on maximal muscle strength and physical

performance. This is the first study to report an unbeneficial effect of a relatively high daily dose of vitamin D3 on muscle strength. Our data warrants against use of too high doses of vitamin D.

Disclosures: *Lise Sofie Bislev, None*

FRI-1119

Analyzing Fall Risk using Smart Phone Application in Subjects with Osteoporosis with and without Falls Krupa Doshi*¹, Seong Moon², Michael Whitaker¹, Thurmon Lockhart². ¹Mayo Clinic, AZ, United States, ²Arizona State University, United States

Background: Fall risk evaluation in osteoporosis is of high priority for research and clinical interventions. Loss of balance and body sway can be important risk factor for falls. We explored use of a wearable smart phone application (SPA) sensor (Lockhart Monitor) capable of measuring postural sway and gait stability in real-time and compared it to traditional force plate sway measurements (AMTI Force Plate). We hypothesized that postural and gait stability measures will differentiate fallers and non-fallers among adults with osteoporosis. Methods: 31 ambulatory adults with osteoporosis (27F, 4M; age (yrs) = 72.4 \pm SD 9.3; 8 fallers) were studied in outpatient endocrinology dept. Postural transition time and static postural stability were measured using force plate and SPA. Dynamic data was collected using the SPA. Subjects were asked to remain standing and follow voice commands from the app. Walking trials were conducted at a self-selected pace over a 10 meter walk-way. Thereafter, a continuous long walking trial was conducted for 120 sec, minimum of 150 gait cycles. Walking aids were allowed. Results: No significant sway differences were observed between fallers and non-fallers' postural stability as measured by sway area, sway path length, and sway velocity using both the force plate and the SPA. However, significant differences were observed between walking patterns of fallers and non-fallers using the SPA (Table 1). Dynamic stability was significantly different (*p* = 0.009) with fallers exhibiting less stable gait as compared to non-fallers. Multiscale entropy in medial-lateral directions during walking was also significantly different (*p* = 0.034) with fallers exhibiting less complexity. Finally, harmonic ratio was significantly different (*p* = 0.009) between fallers and non-fallers. Conclusion: In individuals with osteoporosis, fallers were less stable than non-fallers during walking and exhibited more robot like gait as measured by dynamic gait patterns (dynamic stability, multiscale entropy, and harmonics). Thus, fallers and non-fallers with osteoporosis can be differentiated using dynamic real-time measurements that can be easily captured by a SPA, while traditional postural sway and gait patterns were found to be less sensitive in our study. Thus, dynamic gait assessment promises to be a more sensitive tool to study fall risks and dynamics of walking in adults with osteoporosis as compared to traditional postural sway and gait measurements.

	Dynamic Stability	Multiscale Entropy	Harmonic Ratio
Fallers (n=8)	1.642	10.565	1.921
NonFallers (n=23)	1.48	11.399	1.339
P-value	0.0096	0.0342	0.0094

Disclosures: *Krupa Doshi, None*

FRI-1120

Genetic Basis of Falling Risk Susceptibility Katerina Trajanoska*¹, Felix Day², Carolina Medina-Gomez¹, Andre G. Uitterlinden¹, John Perry², Fernando Rivadeneira¹. ¹Department of Internal Medicine, Erasmus Medical Center, Rotterdam, The Netherlands, Netherlands, ²MRC Epidemiology Unit, University of Cambridge School of Clinical Medicine, Cambridge, United Kingdom

Background: Falls and fall-related injuries are growing healthcare problem in elderly people. Approximately one out of three older adults will experience at least one fall. Multiple factors can increase the risk of falling. We aimed to determine how much of an individual's fall susceptibility can be attributed to genetics. Methods: We conducted the first genome-wide association study (GWAS) to evaluate the genetic variation in fall risk in 89,076 cases and 362,103 controls from the UKBiobank. Individuals were genotyped with the Affymetrix UKBiobank chip. Model included age and sex analysed with BOLT-LMM v.2.3.1. Next, we used LD score regression to: 1). Estimate falling risk heritability 2). Test for genetic correlation with other traits and 3). Identify tissues where expression of genes related to fall-associated variants are enriched. Results: We identified two novel fall loci mapping near PER4 on 7p21.3 (rs2709062, OR=1.03, *p* = 3.4x10⁻⁰⁸) and near TSHZ3 on 19q12 (rs2111530, OR=1.03, *p* = 1.2x10⁻⁰⁸). Falling risk heritability was modest (2.5%). Falls had strong positive genetic correlation with fracture risk (*rg* = 0.35, *se* = 0.05), insomnia (*rg* = 0.42, *se* = 0.05), neuroticism (*rg* = 0.26, *se* = 0.08) and ADHD (*rg* = 0.44, *se* = 0.14); and strong negative genetic correlation with muscle strength (*rg* = -0.24, *se* = 0.04), intelligence (*rg* = -0.12, *se* = 0.04) and social well-being (*rg* = -0.29, *se* = 0.05). Brain and in particular cerebellum tissue showed the highest gene expression enrichment (FDR < 5%) for fall-associated variants. Conclusions: Falling risk constitutes a heritable, heterogeneous and polygenic trait genetically

Friday Posters

correlated with fracture risk and grip strength. The cerebellum tissue enrichment of falls-associated variants corroborates the mediation of postural balance in the etiology of falls.

Disclosures: *Katerina Trajanoska, None*

FRI-1121

Effects of Music-based Multitask Exercise (Jaques-Dalcroze Eurhythmics) versus Multicomponent Exercise on Physical Function, Falls and Brain Plasticity in Older Adults: A Randomized Controlled Trial Mélany Hars^{*1}, Natalia Fernandez², François Herrmann³, René Rizzoli¹, Gabriel Gold³, Patrik Vuilleumier², Andrea Trombetti¹. ¹Division of Bone Diseases, Department of Internal Medicine Specialties, Geneva University Hospitals and Faculty of Medicine, Switzerland, ²Laboratory for Behavioural Neurology and Imaging of Cognition, Campus Biotech, University of Geneva, Switzerland, ³Division of Geriatrics, Department of Internal Medicine, Rehabilitation and Geriatrics, Geneva University Hospitals and Faculty of Medicine, Switzerland

Currently, no robust evidence exists to support one exercise type over another for prevention of physical decline and falls among older adults, primarily because of the lack of comparative trials. The music-based multitask program Jaques-Dalcroze Eurhythmics (JDE) has been shown to increase physical performances and reduce falls [1], but also to improve executive functions, which play a crucial role in falls risk. In the EPHYCOS study, we aimed to i) determine the effectiveness of a JDE exercise intervention compared with a multicomponent (MULTI) exercise intervention—an evidence-based fall prevention program—on physical function and falls, and ii) explore to which extent these interventions are associated with changes in brain structure and brain activity during a cognitive executive task. We conducted a prospective, randomized, single blind comparative effectiveness trial involving 142 community-dwelling older adults (130 women; 74.3 ± 6.5 years) at increased risk of falling. Participants were randomized to i) a JDE exercise program (once weekly, group-based) or ii) a MULTI exercise program (twice weekly, mix of group- and home-based) that included balance, gait, and strength training activities, for 12 months. Physical and falls outcomes were assessed over 12 months. In an exploratory sub-study (n=34), brain structure and function were also assessed through magnetic resonance imaging (MRI). At 12 months, physical performances improved in both groups, but the JDE group improved more than the MULTI group in gait and balance tests (e.g., Timed up & Go and Tinetti tests: p for interaction= 0.013 and 0.030, respectively). The JDE program reduced falls as compared with the MULTI program (adjusted hazard ratio, 0.50 [95%CI, 0.29-0.87]). Exercise-related changes in functional brain MRI showed a decreased activation in the executive network in the JDE group, while an over-recruitment of motor and salience networks was observed in the MULTI group (Figure 1). Finally, an increase of grey matter density across several brain areas was observed in the structural analysis for the JDE group only. In conclusion, JDE exercise results in greater benefits compared with MULTI exercise for a variety of physical outcomes and for falls reduction in older adults. The JDE exercise-related improvements are associated with brain plasticity, including both functional and structural changes in regions related to executive functions. [1] Trombetti et al. Arch Intern Med 2011.

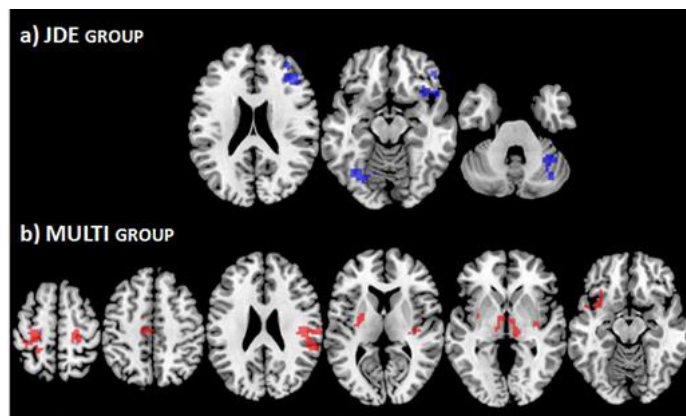


FIGURE 1. ILLUSTRATION OF THE BRAIN AREAS ASSOCIATED WITH CONFLICT RESOLUTION (BASED ON A MODIFIED ERIKSEN FLANKER TASK)
a) In blue, the brain areas reduced after the intervention (i.e. activated at baseline but no more activated at 12-month).
b) In red, the brain areas increased after the training (i.e. not activated at baseline and recruited at 12-month).
 All the clusters presented are significant at the peak-level at $p < 0.001$, uncorrected for multiple comparisons, with a minimum cluster size of 50.

Disclosures: *Mélany Hars, None*

FRI-1122

Effect of Vitamin D3 supplementation on muscle strength in HIV+ postmenopausal women Michael Yin^{*1}, Mariana Bucovsky¹, John Williams¹, Danielle Brunjes¹, Arindam Roychoudhury³, Ivelisse Colon¹, David Ferris², Susan Olender¹, P.Christian Schulz³, Anjali Sharma⁴, Cosmina Zeana², Barry Zingman⁴, Elizabeth Shane¹. ¹Columbia University Medical Center, United States, ²BronxCare Health System, United States, ³Weill Cornell Medical College, United States, ⁴Albert Einstein College of Medicine and Montefiore Medical Center, United States

Background: Both falls and fractures are increased in older HIV+ individuals. Low vitamin D (VitD) levels have been associated with falls, fractures and poor muscle strength in observational studies, and VitD supplementation is associated with increased strength in some treatment studies. We hypothesized that VitD supplementation would improve muscle strength in HIV+ postmenopausal women with low serum VitD (<32 ng/ml). Methods: In a 12-month prospective, randomized, double-blind, placebo-controlled study of 69 HIV+ black and Hispanic postmenopausal women on antiretroviral therapy, we investigated the effects of daily Low (1000 IU; n=31) and Moderate (3000 IU; n=38) VitD doses on muscle mass and strength. The main outcomes were change in lean body mass by DXA and isometric and isokinetic muscle strength in the dominant lower extremity using the Biodex System 4 Pro. Isometric peak torque (force in Kg) was measured in maximum knee extension and flexion held for 6 seconds at 60° and normalized to body weight (Torque/BW, %). Isokinetic measures, from 5 repetitions of knee extension and flexion at 60° per second, included peak torque, work (force x distance, normalized to body weight, Work/BW, %), and average power (work/time, watts). Results: Mean age was 56±5 years, median CD4 count 722 cells/mm³ and 74% had HIV RNA <50 copies/ml. Serum 25-OHD did not differ between groups at baseline, but was higher in the Moderate than Low VitD group at 6 months (33.1±10.3 vs 27.8±8.1 ng/ml, p=0.03) and 12 months (30.2±9.6 vs 24.3±7.6 ng/ml, p=0.007). Baseline lower extremity isometric and isokinetic parameters did not differ between groups. In the Moderate VitD group, there were significant increases in lower extremity isometric torque, and isokinetic torque, work and power at 12 months, with no change in lean mass (Table). In the Low VitD group, the same parameters improved to a lesser extent than the Moderate VitD group, with only 2 parameters reaching significance. There were no statistically significant between-group differences in strength parameters or lean mass. Conclusion: VitD supplementation with 3000 IU daily significantly increased lower extremity muscle torque, work and power in HIV+ postmenopausal women, without a concomitant increase in muscle mass. Future and larger studies will be required to determine the optimal dose of VitD to improve muscle strength and to determine whether supplementation reduces the risk of falls and fractures in HIV+ individuals.

Mean ± SD	Low VitD			Moderate VitD		
	Baseline	12 months	P value	Baseline	12 months	P value
Time						
LE lean mass (kg)	15.3 ± 2.4	14.8 ± 2.8	0.07	15.1 ± 2.9	14.5 ± 2.4	0.04
Isometric						
Torque/BW, extension	125.9 ± 42.8	130.6 ± 38.1	0.16	135.3 ± 47.4	138.9 ± 37.4	0.23
Torque/BW, flexion	59.5 ± 30.0	66.0 ± 19.0	0.03	66.4 ± 27.1	70.7 ± 22.5	0.002
Isokinetic						
Torque/BW, extension	105.4 ± 115.6	117.9 ± 37.0	0.07	33.4 ± 41.6	122.7 ± 36.8	0.001
Torque/BW, flexion	47.7 ± 52.5	56.9 ± 16.5	0.08	15.6 ± 25.9	64.2 ± 21.9	<0.001
Work/BW, extension	94.3 ± 31.3	99.2 ± 30.6	0.38	106.2 ± 36.8	107.2 ± 32.0	0.04
Work/BW, flexion	46.3 ± 18.1	57.0 ± 18.8	0.20	51.1 ± 30.6	62.9 ± 24.2	0.02
Power, extension	44.9 ± 13.9	52.9 ± 20.6	0.01	46.2 ± 14.6	52.5 ± 14.9	<0.001
Power, flexion	19.4 ± 9.0	27.8 ± 11.9	0.16	19.6 ± 12.0	28.0 ± 10.5	0.004

Disclosures: *Michael Yin, None*

SAT-0001

See Friday Plenary Number FRI-0001

SAT-0002

See Friday Plenary Number FRI-0002

SAT-0003

See Friday Plenary Number FRI-0003

SAT-0004

See Friday Plenary Number FRI-0004

SAT-0005

See Friday Plenary Number FRI-0005

SAT-0006

See Friday Plenary Number FRI-0006

SAT-0007

See Friday Plenary Number FRI-0007

SAT-0008

See Friday Plenary Number FRI-0008

SAT-0009**Importance of Recognizing Low Alkaline Phosphatase Levels in a Patient with Decreasing Bone Mineral Density** Nada Alhashemi¹, Christine Derzko².¹University of Toronto, Canada, ²University of Toronto, St Michael's Hospital, Canada

Introduction: Hypophosphatasia is a rare metabolic bone disorder resulting from mutations in the gene encoding tissue nonspecific alkaline phosphatase (TNSALP). The hallmark is a low alkaline phosphatase level. **Case discussion:** A 76 year old woman was referred to the Metabolic Bone Clinic in July 2017 with decreasing bone density despite being on denosumab since 2013. She had longstanding osteoporosis and was on bisphosphonate from 2004 until 2012. She was switched to denosumab in 2013. She gave a history of right 3rd metatarsal - and right 5th digit fractures in the past, while on bisphosphonate. Her medications included denosumab and vitamin D supplements. Examination revealed a body mass index of 20.7 kg/m², increased occiput to wall of > 10 cm, reduced rib to pelvis distance of 1 fingerbreadth. She has scoliosis of the spine with no spine tenderness. Sclera and dentition were unremarkable. Investigations showed a low ALP of 9 U/L. Ca was upper limit of normal at 2.56 mmol/L. Vitamin D was optimal at 100 nmol/L. CBC, Creatinine, TSH were unremarkable. She was noted to have low ALP since June 2016. All documented readings were less than 30 U/L. Dual energy xray absorptiometry from 2017 showed decreasing bone density at the total hip and lumbar spine, from -1.1 to -1.4 and from -1.1 to -2.3 respectively despite being on denosumab. We suspected hypophosphatasia. An elevated urine phosphoethanolamine (PEA) supported the diagnosis, and genetic testing confirmed the mutation. **Discussion:** Hypophosphatasia is a rare inborn error of metabolism resulting from loss of function mutations in the gene encoding TNSALP. TNSALP is expressed in skeleton and teeth. Hypophosphatasia leads to accumulation of TNSALP substrates, including inorganic pyrophosphate (PPi) which is a potent inhibitor of skeletal mineralization. The diagnosis is made by persistently low ALP levels and supported by increased TNSALP substrates including elevated urinary phosphoethanolamine (PEA) and elevated serum pyridoxal 5'-phosphate (PLP). It is important to recognize that persistently low ALP levels may indicate hypophosphatasia. Antiresorptive therapy in such cases may further impair bone mineralization. Treatment involves optimizing vitamin D and calcium. Enzyme replacement therapy with asfotase alfa has been successfully used to treat children and adults.

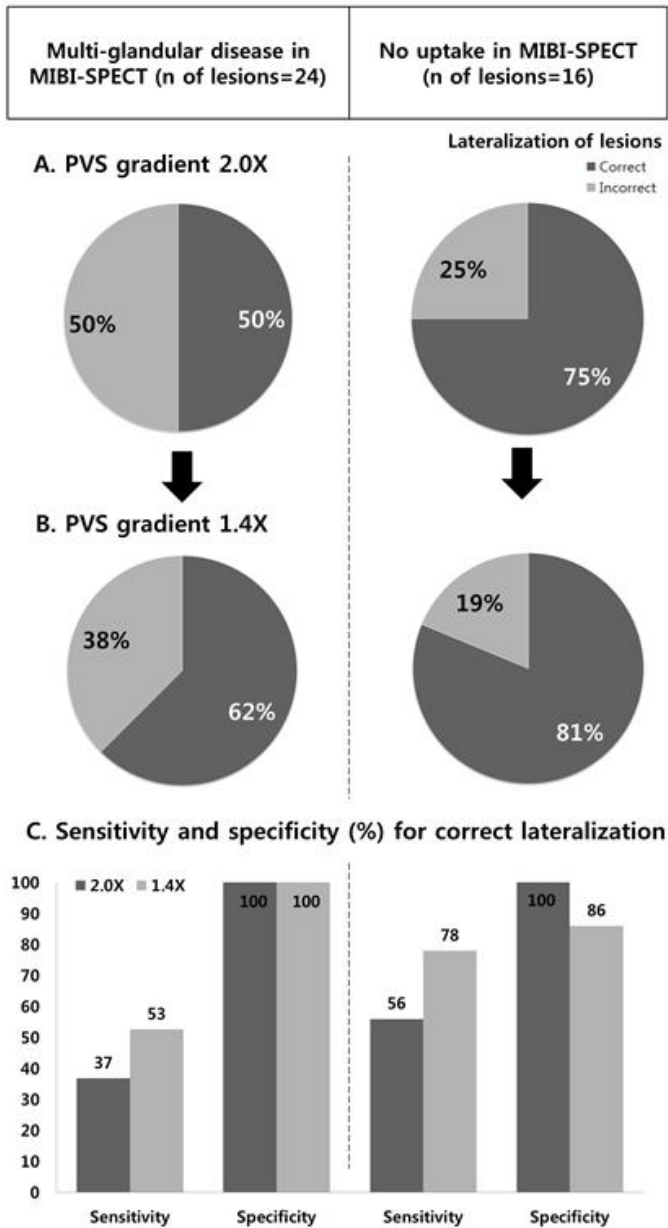
*Disclosures: Nada Alhashemi, None***SAT-0010****Fracture risk in Chronic B-cell Lymphocytic Leukemia: a historic cohort study** Anupam Kotwal*, Jad Sfeir, Matthew Drake. Division of Endocrinology, Diabetes, Metabolism, and Nutrition, United States

Background: Chronic B-cell lymphocytic leukemia (CLL) is a common condition affecting older patients that is usually characterized by a prolonged asymptomatic phase. The effects of CLL on bone health have been limited to advanced disease following chemotherapy. In addition to bone marrow infiltration, increase in circulating levels of cytokines might lead to altered bone metabolism. We aimed to evaluate the rate of fractures and their possible risk factors in patients with CLL. **Methods:** We reviewed all patients with CLL evaluated at Mayo Clinic in Rochester, first diagnosed from 1/1/2000 through 12/31/2010. CLL associated fractures (CAF) were defined as those occurring up to 1 year prior to or any time after CLL diagnosis. Non-parametric tests were used to compare variables in those with or without CAF. **Results:** In this cohort of 107 patients with CLL, median age was 71 years (IQR 62 – 78), 58% (n=62) were males and all patients were Caucasian. No patient was on medication to target CLL. Median follow-up was 8.3 years (IQR 5.1 – 12.7). Thirty four patients (37%) had a CAF, of which 27% were vertebral and 18% proximal femur fractures. Fracture rate was higher in females (44%) as compared to males (23%). Only 3 had >1 fracture. Median time to 1st fracture was 2.5 years after CLL diagnosis (IQR -0.05 to 9.5). We also evaluated for potential risk factors for CAF. Thirty two women (71%) were post-menopausal and they showed a significantly higher rate of CAF compared to pre-menopausal women (46% vs. 25%, respectively; p=0.02). Spontaneous and fall from standing height or less accounted for 87% of CAF. Osteoporosis by BMD criteria was present in 73% of those who sustained a CAF vs. 85% in those who did not (p=0.3), however only 56% of those who fractured had DXA evaluation. Fifteen percent of patients with CAF had a prior fracture history compared to 20% of those without (p=0.5). There was no statistically significant difference in age (p=0.5), BMI (p=0.2), smoking status (p=0.9) and alcohol status (p=0.3) between the two groups. Activity status (only known for 1/4th of the cohort) did not differ between the two groups. There was also no difference between chronic conditions known to impact bone health (such as diabetes mellitus, thyroid disease, renal disease) between the two groups. Mortality was 53% in patients with CAF compared to 49% in those without (p=0.6). Median survival after CLL diagnosis was 5.5 years with no difference between the two groups. Median fracture-to-death time was 1.3 years (IQR 0.4 – 5). **Conclusions:** More than 1/3rd of patients with CLL not receiving targeted therapy had a fracture 1 year prior to or any time after diagnosis, most of which were spontaneous or due to minor trauma. Risk factors included women and post-menopausal status. Impact of CLL on bone metabolism may precede CLL diagnosis, and highlights the need to assess bone health in patients with CLL to reduce fracture risk.

*Disclosures: Anupam Kotwal, None***SAT-0011****Evaluation of an optimal cutpoint of parathyroid venous sampling gradient for localizing elusive cases of primary hyperparathyroidism** Jooyeon Lee¹, Namki Hong¹, Sujin Lee¹, Jong Ju Jeong², Byung Moon Kim³, Dong Joon Kim³, Yumie Rhee¹. ¹Department of Internal Medicine, Severance Hospital, Endocrine Research Institute, Yonsei University College of Medicine, Seoul 120-752, Korea, Republic of Korea, ²Thyroid Cancer Clinic, Yonsei University College of Medicine, Severance Hospital, Seoul, Korea, Republic of Korea, ³Department of Radiology, Yonsei University College of Medicine, Severance Hospital, Seoul, Korea, Republic of Korea

Preoperative localization of abnormal parathyroid tumor before surgery by parathyroid venous sampling (PVS) has been reported to provide useful information in selected recurrent, elusive, or complicated cases of primary hyperparathyroidism (PHPT). Although the 2-fold (2.0X) increase in intact parathyroid hormone (PTH) in PVS has been considered significant, the optimal cutoff for the positive gradient in PVS remains unknown. Among a total of 198 consecutive patients (mean age 58 years, female 75%) with PHPT presented to a tertiary center between 2012 and 2017, 56 subjects who underwent PVS for equivocal or negative results from noninvasive localizations studies or for further confirmation were analyzed. ^{99m}Tc-sestamibi SPECT/CT (MIBI) was performed in all subjects for initial localization study. First, the optimal cutoff for PVS gradient was developed from a dataset of subjects with a single gland disease (n=36) confirmed by MIBI and pathology (development set). Then, the performance of new vs. conventional cutoff (2.0X) for lateralization was compared in subjects with multiple gland uptakes (n=12) or diffuse or no focal uptake (n=8) in MIBI (validation set). In development set, concordant results between radiological/surgical findings and PVS was observed in 25 subjects (right side 13; left side 12), whereas discordant results were found in 11 subjects (opposite direction or no differences in PVS gradient in both sides). Because peak PVS gradient of all subjects in concordant group had a value equal to or higher than 1.4 whereas most of subjects (n=8/11) in the inconsistent group had PVS gradient lower than 1.4, 1.4 fold gradient (1.4X) in PVS was set as a potential alternative threshold. In validation set, applying 1.4X improved correct lateralization of lesions in both multiglandular diseases (50% to 62%) and no focal uptake in MIBI (75% to 81%) compared to 2.0X (Fig.1). Sensitivity for correct lateralization increased from 37% to 53% in multiglandular diseases and 56% to 78% in no uptake in MIBI while the specificity remained high in both conditions (100% in multiglandular diseases and 86% in no uptake in MIBI). In conclusion, PTH gradient cutpoint 1.4X performed better than 2.0X in lateralization of lesions with higher sensitivity for preoperative localization. Our findings suggest that

1.4-fold PTH gradient might provide a more sensitive threshold for localizing parathyroid lesions in selected cases of PHPT, which merits further validation.



SAT-0012

Bone Turnover in Patients With Hypoparathyroidism Treated for 5 Years With Recombinant Human Parathyroid Hormone, rhPTH(1-84), in the Open-Label RACE Study Michael Mannstadt^{*1}, John P. Bilezikian², Henry Bone³, Bart L. Clarke⁴, Douglas Denham⁵, Michael A. Levine⁶, Munro Peacock⁷, Jeffrey Rothman⁸, Dolores M. Shoback⁹, Tamara J. Vokes¹⁰, Mark L. Warren¹¹, Nelson B. Watts¹², Hak-Myung Lee¹³, Nicole Sherry¹³. ¹Massachusetts General Hospital and Harvard Medical School, United States, ²Columbia University, United States, ³Michigan Bone & Mineral Clinic, PC, United States, ⁴Mayo Clinic Division of Endocrinology, Diabetes, Metabolism, and Nutrition, United States, ⁵Clinical Trials of Texas, Inc., United States, ⁶Division of Endocrinology and Diabetes and Center for Bone Health, Children’s Hospital of Philadelphia, United States, ⁷Department of Medicine, Division of Endocrinology, Indiana University School of Medicine, United States, ⁸University Physicians Group – Research Division, United States, ⁹Endocrine Research Unit, SF Department of Veterans Affairs Medical Center, University of California, United States, ¹⁰Section of Endocrinology, University of Chicago Medicine, United States, ¹¹Endocrinology and Metabolism, Physicians East, PA, United States, ¹²Osteoporosis and Bone Health Services, Mercy Health, United States, ¹³Shire Human Genetic Therapies, Inc, United States

Parathyroid hormone (PTH) deficiency in patients with hypoparathyroidism is associated with reduced bone turnover and increased bone mineral density (BMD). In the phase III placebo-controlled REPLACE and dose-blinded RELAY studies, rhPTH(1-84) treatment improved mineral homeostasis and increased bone turnover markers (BTMs) in adults with hypoparathyroidism. In RACE (NCT01297309), an open-label extension of REPLACE and RELAY, treatment with subcutaneous rhPTH(1-84) was initiated at 25 or 50 µg/day. Dose adjustments in 25-µg increments were permitted (up to 100 µg/day) if oral calcium (Ca) and active vitamin D could be reduced and serum Ca maintained at 8.0–9.0 mg/dL. Albumin-corrected serum Ca, 24-h urine Ca, serum phosphate, and serum alkaline phosphatase were measured. Bone turnover was evaluated by serum levels of BTMs; BMD was assessed by dual-energy x-ray absorptiometry. Baseline (BL) was defined as the start of rhPTH(1-84) treatment. Data are presented as mean ± SD. Of 49 patients enrolled (81.6% women; duration of hypoparathyroidism, 15.9±12.49 y), 40 (81.6%) completed 60 months of treatment. Serum Ca was maintained within the target range (BL, 8.4±0.70 mg/dL [n=49]; Month 60 [M60], 8.5±0.78 mg/dL [n=40]). There was a numerical reduction in urinary Ca excretion (BL, 356.7±200.37 mg/24 h [n=48]; M60, 246.3±132.21 mg/24 h [n=40]) and serum phosphate (BL, 4.8±0.58 mg/dL [n=49]; M60, 3.9±0.66 mg/dL [n=40]). Serum alkaline phosphatase levels increased and remained above BL, but within the normal range, over the study (BL, 67.0±18.72 U/L [n=49]; M60, 89.7±29.82 U/L [n=40]). BTMs increased from baseline, peaked at ~1 year following rhPTH(1-84) treatment, and then declined but remained above pretreatment values to M60. BSAP and CTX remained within the normal range and PINP higher than normal over 60 months. BMD was relatively stable, except at the distal one-third radius, where a decline within the normal range was observed at M60 (Table). The most frequently reported adverse events were hypocalcemia (36.7%; n=18); muscle spasms (32.7%; n=16); and nausea, paresthesia, and sinusitis (30.6% each; n=15). Over 5 years, rhPTH(1-84) was associated with an acceptable safety profile, and had sustained pharmacodynamic effects on mineral homeostasis and bone turnover, as shown by maintenance of serum Ca within the target range, decreases in urinary Ca excretion and serum phosphate, increases followed by stabilization in BTMs, and reduced or stable BMD.

Disclosures: Jooyeon Lee, None

BTM	Baseline		Maximum Value		Month 60	
	Mean (SD)	n	Mean (SD)	n	Mean (SD)	n
BSAP, µg/L (Normal 6–30 µg/L)	9.6 (3.32)	48	20.7 (12.18)	45	17.8 (13.82)	37
CTX, ng/L (Normal ≤690 µg/L)	213.0 (172.34)	48	699.1 (469.5)	47	463.7 (388.30)	37
P1NP, µg/L (Normal 20–108 µg/L)	33.7 (19.72)	49	201.5 (160.72)	46	144.1 (153.73)	38
BMD, Z-score	Baseline Mean (SD)	n	Month 60 Mean (SD)	n	Change from Baseline at Month 60 Mean (SD)	n
Lumbar spine	2.13 (1.471)	40	2.13 (1.516)	35	0.10 (0.985)	33
Hip-total	1.57 (1.123)	40	1.54 (1.093)	34	-0.04 (0.583)	32
Hip-femoral neck	1.45 (1.240)	40	1.39 (1.274)	34	-0.02 (0.666)	32
Distal one-third radius	0.94 (0.833)	40	0.50 (1.193)	35	-0.48 (0.962)	33

BMD=bone mineral density; BSAP=bone-specific alkaline phosphatase; BTM=bone turnover marker; CTX=cross-linked c-telopeptide of type 1 collagen; P1NP=aminoterminal propeptide of type 1 collagen

Disclosures: *Michael Mannstadt, Shire, Grant/Research Support, Shire, Consultant*

SAT-0013

Normocalcaemic Hyperparathyroidism: Study Of The Prevalence And Natural History In A United Kingdom Referral Population Marian Schini^{*1}, Richard Jacques¹, Nicola Peel², Jennifer Walsh¹, Richard Eastell¹. ¹University of Sheffield, United Kingdom, ²Sheffield Teaching Hospitals, NHS, United Kingdom

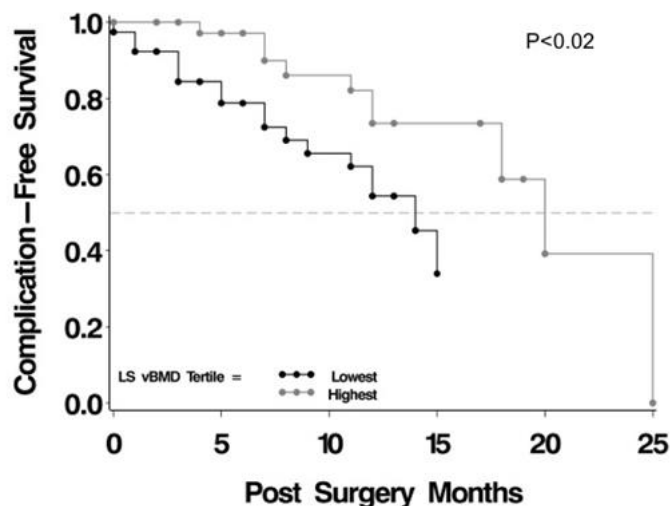
Rationale: Normocalcaemic hyperparathyroidism (NHYP) is characterised by persistently normal calcium levels, elevated PTH values on at least two consecutive measurements, after excluding other causes of secondary hyperparathyroidism. It is usually encountered during the evaluation of secondary osteoporosis. It was recognised by the Third International Workshop on Asymptomatic Primary Hyperparathyroidism (PHPT). The prevalence of the disease in the literature varies significantly due to various definitions used; it is reported to be between 0.1 and 8.9%. The data on the natural history of this disease are sparse and inconclusive. Objectives: to identify the prevalence of NHYP in a UK referral population using the international criteria and study the variability of serum calcium. To compare the variability of serum calcium in NHYP and PHPT. Methodology: We retrospectively evaluated data from 6280 patients referred for a bone mineral density measurement. Using a statistical method (Mahalanobis distance) subjects were identified as 'normal' or 'abnormal' and using the reference intervals for albumin-adjusted calcium and PTH, these patients were divided in different categories. In order to identify NHYP patients, we excluded the ones having either eGFR < 60 ml/min/1.73m² or 25(OH)D < 50nmol/l, or no measurements available. Repeated measurements of calcium were used to calculate the variability. Patients with high PTH and high calcium (PHPT) were also identified and their variability was calculated and compared with the NHYP group. Results: Based on laboratory results on the index day and the evaluation of their medical files, we identified 8 patients (mean age 70y, 86% female) with NHYP (prevalence 0.1%). These patients had laboratory results available for an average of 5 years and the natural history of this disorder was studied. Only 2 patients (0.03%) had consistent normocalcaemia throughout their follow up. The SD for the NHYP group was 0.101 mmol/L (CV 4.0%). Out of the 129 patients identified with high PTH and high calcium, 27 (mean age 73y, 85% female) fulfilled the above-named criteria. Only 48% had persistent hypercalcaemia. The SD of the PHPT patient group was 0.087 mmol/L (CV 3.2%). The comparison of the variances of the two groups showed no statistical difference (p > 0.05). Conclusions: The prevalence of NHYP in our UK referral population is low. NHYP patients often have episodes of hypercalcaemia, so they probably suffer from PHPT. The variability of NHYP and PHPT patients is similar, and this results in about half of patients with PHPT having normal serum calcium at some point.

Disclosures: *Marian Schini, None*

SAT-0014

Low Volumetric Bone Density is a Risk Factor for Complications after Spine Fusion Surgery Yi Liu^{*1}, Alexander Dash¹, Andre Samuel¹, Eric Marty¹, Harold Moore², Brandon Carlson¹, John Carrino¹, Donald McMahon³, Alexander Hughes¹, Han Jo Kim¹, Matthew Cunningham¹, Frank Schwab¹, Richard Bockman¹, Emily Stein¹. ¹Hospital for Special Surgery, United States, ²Weill Cornell Medical College, United States, ³Columbia University, United States

Over 250,000 spine fusion surgeries are performed annually in the US. Complications after fusion result in significant morbidity and healthcare costs. Multiple factors, including osteoporosis, have been suggested to contribute to risk of complication and reoperation. However, most studies have used DXA, which is subject to artifact in patients with spine pathology and may not accurately diagnose osteoporosis in this population. This study investigated volumetric BMD (vBMD) as a risk factor for complication and reoperation after fusion. We hypothesized that patients with low vBMD have higher rates of post-operative complications. Patients enrolled in this retrospective cohort study had initial lumbar spine (LS) fusion at our institution between 1/11 and 12/16, and had pre-operative LS CTs and post-operative imaging available for review. Cox regression analysis was used to relate demographic factors (age, sex, BMI), smoking status, vBMD (T12-L5, using MindWays QCTPro phantomless software), surgical procedure (fusion approach, number of levels, use of bone graft or bone morphogenetic protein), and osteoporosis medications to post-operative outcomes and time to complication. Among 118 patients, mean age was 60±14 years, 59% were women, mean BMI was 28±5 kg/m². Median follow up time was 11 months. Complications occurred in 47 patients, 30% had pseudarthrosis or hardware failure, 26% adjacent degenerative changes, 21% persistent symptoms, and 15% adjacent level fractures. Thirteen patients (11%) required reoperation, 85% within 1 year (median time 4 months). The most common reasons for re-operation were hardware failure (38%), adjacent level fracture (24%) and persistent symptoms (24%). Candidate risk factors for post-operative complication in univariate logistic models (p < 0.2) were tested with Cox time-to-event regression. Only vBMD (T12-L5) was a significant predictor of post-operative complication (p < 0.02, Figure). For each decrease in vBMD of 10 mg/cm³, risk of complication increased by 9%. In summary, we found that low vBMD is a significant risk factor for complications in patients undergoing LS fusion. As CT scans are frequently performed on surgical candidates, this information is readily available and may be helpful to consider in risk stratifying patients prior to surgery. Prospective, controlled studies are needed to confirm our findings and to identify the best strategies for preventing bone loss and lowering risk of complications in this population.



Disclosures: *Yi Liu, None*

SAT-0015

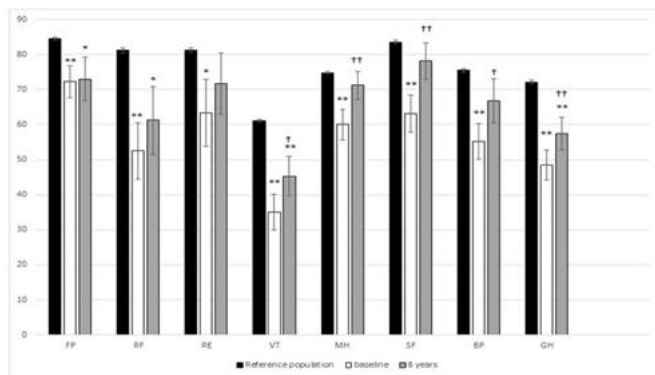
Quality of life in hypoparathyroidism improves with rhPTH(1-84) throughout 8 years of continuous therapy Gaia Tabacco^{*1}, Donovan Tay Yu-Kwang¹, Mishaela Rubin¹, John Williams¹, Beatriz Omeragic¹, Rukshana Majeed¹, Maximo Gomez Almonte¹, Natalie Cusano², John Bilezikian¹. ¹Department of Medicine, Division of Endocrinology, College of Physicians & Surgeons, Columbia University, United States, ²Department of Medicine, Division of Endocrinology, Lenox Hill Hospital, United States

Treatment of hypoparathyroidism with calcium and vitamin D does not improve reduced quality of life (QoL), a characteristic of the disease. rhPTH (1–84) therapy improves QoL metrics for up to 5 years. Information on QoL beyond 5 years has not been available, but is important because there are no limits on duration of rhPTH(1-84) in hypoparathyroidism. Aim of this study is to evaluate the effects of 8 years of continuous rhPTH(1-84) therapy on QoL and to evaluate factors associated with long term benefit. Prospective, open-label

trial. 20 hypoparathyroid subjects were treated with rhPTH(1-84) daily. QoL was evaluated by RAND 36-Item Short Form (SF-36) Health Survey at baseline and through 8 years of therapy. At baseline, all 8 domains of SF-36 were significantly lower than the normal population. rhPTH therapy was associated with a significant improvement in 5 of the 8 domains [vitality, social functioning(SF), mental health(MH), bodily pain(BP) and general health] throughout the study duration. 3 of the 5 domains that were improved at year 8, namely MH, SF and BP, improved to values that were no longer different from normal subjects. Improvement in the mental component summary(MCS) score was sustained through 8 years ($p=0.009$ vs baseline). Improvement in physical component summary (PCS) score, improved through 6 years, and tended to be higher than baseline at years 7 and 8. Lower baseline MCS and PCS scores were associated with a greater likelihood for improvement. A baseline MCS score <238 predicted 90% of the cohort who improved in both MCS and PCS at year 8. A baseline PCS score <245 identified 100% of the cohort who improved at 8 years. There was an inverse relationship between reduction in calcium dosage and improvement in both PCS and MCS. In patients whose both requirement for calcitriol was reduced and duration of disease was shorter improvement in PCS was greater. rhPTH(1-84) improves QoL in hypoparathyroidism. Improvements were more evident in those whose baseline SF-36 levels were lower. Baseline MCS and PCS scores predicted the extent of QoL improvement, but did not explain the entirety of the change. A fall in requirements of calcium and active vitamin D was also associated with an improvement in QoL. The results may be useful for clinicians in deciding which HypoPT patients are likely to benefit from rhPTH(1-84). They also provide a framework for future randomized controlled studies of rhPTH(1-84) on QoL in chronic hypoparathyroidism.

Normative data, baseline and 8y scores for the 8 domains of SF-36 index: physical functioning (PF), role limitations caused by physical health problems (RF), role limitations due to emotional health problems (RE), vitality (VT), mental health (MH) social functioning (SF), bodily pain (BP) and perception of general health (GH).

(* $p<0.05$ vs reference population; ** $p<0.01$ vs reference population; † $p<0.05$ vs baseline; †† $p<0.01$ vs baseline.)



Disclosures: Gaia Tabacco, None

SAT-0016

rhPTH(1-84) in Hypoparathyroidism Is Associated With Stable Renal Function Through 8 Years of Continuous, Uninterrupted Therapy Donovan Tay^{*1}, Gaia Tabacco¹, Natalie Cusano², John Williams¹, Beatriz Omeragic¹, Rukshana Majeed¹, Maximo Gomez Almonte¹, John Bilezikian¹, Mishaela Rubin¹. ¹Columbia University Medical Center, United States, ²Lenox Hill Hospital Department of Medicine, United States

Conventional management of chronic hypoparathyroidism (HypoPT) with calcium and active vitamin D (aVitD) is associated with renal complications such as worsening hypercalciuria, renal stones and renal insufficiency. With rhPTH(1-84) now available as an adjunct therapy in HypoPT, the need for high doses of supplemental calcium and aVitD is markedly reduced. We hypothesized that this reduction in the calcium burden by rhPTH(1-84) would stabilize long-term renal function. This report describes our open-label evaluation of renal function among 24 subjects (mean age: 46±3 years, 75% women; mean duration of disease, 22.9±3 years) treated with rhPTH(1-84) for 8 years of continuous therapy. With rhPTH(1-84), daily supplementation of calcium and aVitD fell progressively. Serum calcium (S.Ca) levels were maintained within the asymptomatic range. 24-hr urine calcium was reduced by 38% from 254±29 mg/d at baseline to 157±37 mg/d at 8 years ($p=0.01$). Of the 11 subjects who were ever on thiazides, the mean dosage fell by 51% from 30±7 to 15±6 mg/day ($p=0.01$); 4 subjects eliminated thiazide use. Renal function was stable throughout the 8-year treatment period. Serum creatinine did not change (0.94±0.04 to 0.95±0.04 mg/dL; $p=NS$). Estimated glomerular filtration rate (eGFR) by MDRD was unchanged (88±4 to 85±4 mL/min/1.73m²; $p=NS$). When stratified according to baseline renal function, those with baseline eGFR <90 mL/min/1.73 m² (n=13) had no change in eGFR (74±5 to 78±4 mL/min/1.73m²; $p=NS$). In those whose eGFR was ≥90 mL/min (n=10), eGFR decreased from 107±6 mL/min to 93±5 mL/min/1.73m²; $p<0.01$, while still remaining in the normal range. Within this stable framework of renal function, S.Ca levels predicted eGFR: for every 1 mg/dL decrease in S.Ca, there was a 5 mL/min/1.73 m² increase in eGFR ($p<0.01$). There were

no associations between eGFR and age, duration of disease, serum phosphate, calcium phosphate product, PTH, or calcium and aVitD dose. One renal stone was reported by 1 patient at year 4. These data suggest that 8 years of continuous rhPTH(1-84) treatment in HypoPT is associated with stable renal function. The results support the idea that reducing the calcium burden by rhPTH(1-84) has salutary effects to maintain renal function, thus potentially addressing a major morbidity in HypoPT. S.Ca may be a surrogate for calcium burden (diet, PTH, Ca and aVitD dose) and a lower S.Ca achieved, may reflect shorter duration in the hypercalcemic range and be renal protective

Disclosures: Donovan Tay, None

SAT-0017

Recognition of persistent low serum alkaline phosphatase in hospitalized adults Justine Vix^{*1}, Thierry Huet², Pascal Roblot³, Françoise Debais¹. ¹Rheumatology department CHU, France, ²Biochemistry department CHU, France, ³Internal medicine department CHU, France

Introduction : Hypophosphatasia (HPP) is a rare genetic disease caused by loss-of-function mutations in the ALPL gene encoding the tissue-non-specific alkaline phosphatase (TNSALP). Mild HPP is usually misdiagnosed in adult age, but should be better recognized in case of low serum alkaline phosphatase (ALP). Methods : Patients were selected from the records of the biochemistry department of Poitiers University Hospital, France. The patients were hospitalized in the departments of rheumatology and internal medicine, between 2007 and 2017. Inclusion criteria were age ≥ 18 years and low serum ALP, with a requirement of 2 low-serum ALP and values ≤ 35 IU/l (normal range : 40-130 IU/l). The aim of this retrospective study was to determine number of patients from whom the persistent low serum ALP value was recognized, and to note if clinical or radiographic findings potentially related to HPP were reported. Results : 37857 hospitalized patients had a serum ALP dosage and 226 of these patients had a least 2 low serum ALP. However, 151 patients had fluctuating low values (mean age 68.9 years ; 56.2 % women) (related to bisphosphonate therapy, severe sepsis, hepatic failure...). Among these 226 patients, 75 patients (51 patients from rheumatology department and 24 from internal medicine department) had persistent low value below 35 IU/l (mean 52.1 years ; 64% women). Mean serum ALP was 29 IU/l (9-35 IU/l) ; the low ALP value was notified in the hospitalization report in 14 patients. A history of fracture was present in 21 patients ; most common recorded fractures were lower limbs in 7 patients (metatarsus, femoral neck...) or vertebral fractures (9 patients). A history of crystalline arthritis or calcific peri-arthritis was noted in 28 patients; radiographic chondrocalcinosis was observed in 10 patients and apatite deposition in 18 patients ; dental abnormalities were reported in 6 patients. Genetic research was conducted in 10 patients and ALPL mutation was found for 6 of them. Conclusion : In these 10 years retrospective study, we found that 0.2% of adult patients hospitalized in rheumatology and internal medicine departments had persistent low serum ALP. An elevated serum ALP value draws more attention than a low value. Physicians are to be aware of the importance of searching for HPP in case of recurrent fractures, musculo-skeletal pain, chondrocalcinosis, dental abnormalities, and to avoid antiresorptive treatments.

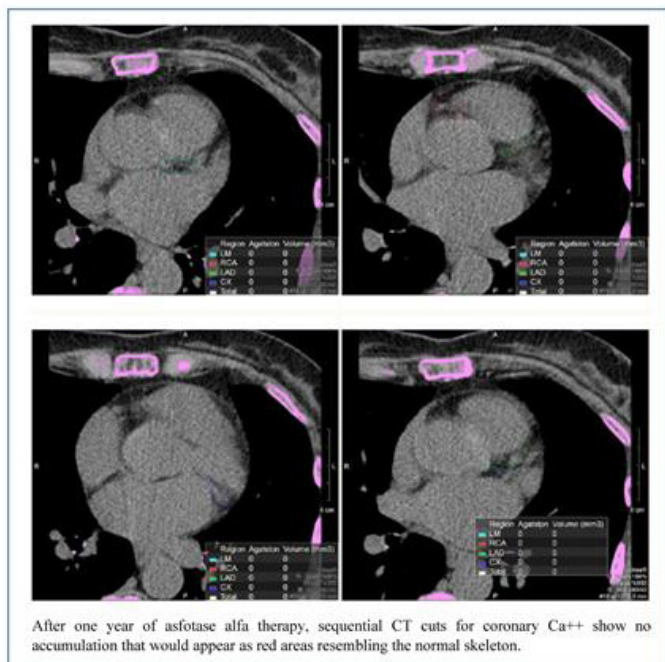
Disclosures: Justine Vix, None

SAT-0018

Coronary Artery Calcification Absence, Assessed by Computed-Tomography, Spanning One Year Of Asfotase Alfa Therapy For A 69-Year-Old Woman With Hypophosphatasia Michael P. Whyte^{*1}, Andy Bierhals². ¹Division of Bone and Mineral Diseases, Department of Internal Medicine, Washington University School of Medicine at Barnes-Jewish Hospital; Center for Metabolic Bone Disease and Molecular Research, Shriners Hospital for Children, United States, ²Mallinckrodt Institute of Radiology, Washington University School of Medicine at Barnes-Jewish Hospital, United States

Hypophosphatasia (HPP) is caused by mutation(s) of the gene that encodes the cell-surface tissue non-specific isoenzyme of alkaline phosphatase (TNSALP). In HPP, extracellular accumulation of the TNSALP substrate inorganic pyrophosphate (ePPI) blocks hydroxyapatite crystal (HA) formation and growth, often causing rickets during infancy or childhood or osteomalacia during adult life. However, seemingly paradoxical ectopic mineralization can occur in HPP, including from hypercalcemia and hyperphosphatemia causing nephrocalcinosis in severe HPP. More mild disturbances in mineral homeostasis in HPP may explain punctate, asymptomatic, corneal calcifications. Also, enthesopathy, osteophytosis, calcific peri-arthritis, and chondrocalcinosis are common in affected adults. In direct contrast, generalized arterial calcification of infancy (GACI) results from mutations in other genes that cause low ePPI levels leading to vascular calcification. In 2015, asfotase alfa (AA), a recombinant HA-targeted TNSALP replacement therapy, was approved for pediatric-onset HPP in the United States. Theoretically, excessive HA-targeted AA could provoke or exacerbate ectopic calcification. However, clinical trials of AA involving all patient ages have been reassuring despite the high on-treatment circulating ALP activity (sometimes, 5000-10,000 U/L). Reassurance has come from skeletal radiographs, retinal ophthalmoscopy, and renal sonography. Nevertheless, coronary artery calcium (C-Ca⁺⁺) has not been studied in HPP, particularly in elderly patients. We investigated, using routinely available computed tomography (CT), a 69-year-old woman with HPP presenting in childhood, who was assessed for C-Ca⁺⁺ before and after one year of standard dose AA therapy. Image acquisition calculated

an Agaston Score and C-Ca⁺⁺ volume using a prospective electrocardiogram (ECG)-gated method. Regions of interest were drawn for each coronary artery, as well as for the coronary artery vascular bed, to calculate the C-Ca⁺⁺ score. No C-Ca⁺⁺ was seen throughout the coronary artery tree at either time point (Figure). Adults with HPP will likely receive AA long-term. Our relatively brief experience with AA treatment for one woman with HPP is reassuring. Baseline and follow-up assessments of additional adult patients will help determine if the ePPI superabundance in HPP is protective against C-Ca⁺⁺, and if AA is safe for adults with various forms of ectopic calcification.



Disclosures: **Michael P. Whyte**, None

SAT-0040

PTH 1-34 Replacement Therapy has Minimal Effect on Quality of Life in Patients with Hypoparathyroidism Rachel I. Gafni^{1*}, Tiffany Hu¹, Lori C. Guthrie¹, Beth A. Brillante¹, Michaele Smith², Robert James³, Michael T. Collins¹. ¹National Institute of Dental and Craniofacial Research, National Institutes of Health, United States, ²Rehabilitation Medicine Department, Clinical Center, National Institutes of Health, United States, ³Rho, Inc, United States

Background: Hypoparathyroidism (hypoPTH) is characterized by hypocalcemia, hyperphosphatemia, and hypercalciuria. Patients with hypoPTH frequently experience neuromuscular irritability, extraskeletal calcifications, decreased bone turnover and poor quality of life (QOL), complaining of fatigue and “brain fog.” Therapy with calcium/calcitriol or parathyroid hormone (PTH) can successfully manage the hypocalcemia, however, the effects of therapy on QOL are unclear. **Methods:** 31 hypoparathyroid subjects (25F, 6M) were treated in an open-label, uncontrolled study with full replacement doses of subcutaneous synthetic PTH 1-34 twice daily for up to 5 years, to maintain a blood calcium of 7.6-9 mg/dL. Subjects completed an SF-36 survey, Fatigue Symptom Inventory (FSI), and 6-minute walk test (6MWT) at baseline, every 6 months on PTH, and at a post-PTH follow-up visit (FU). As duration of therapy varied, analyses were also made using the last treatment time point for all subjects. **Results:** The SF-36 assesses 4 physical components: physical function (PF), physical role limitations (RP), bodily pain (BP), and general health (GH), and 4 mental components: vitality (VT), emotional role limitations (RE), social function (SF) and mental health (MH). Compared to the US population, subjects at baseline had worse scores in RP, GH, VT, and MH (p<0.05). Improvements in mean score were seen only for GH at 6 months and VT at 12 months compared to baseline (p<0.05). At the last treatment time point on PTH, there was an improvement in mean scores for RP, VT, and SF compared to baseline (P<0.05); however, scores at FU were not different from baseline or last treatment on PTH, except for SF, which was had decreased at FU compared to on-PTH (P<0.05). The FSI assesses fatigue severity, frequency, and perceived interference. There were no changes in fatigue frequency at any time point; perceived interference was improved at the 12 and 18-month time points and composite severity was improved only at 60 months (p<0.05). No differences were seen in the 6MWT. **Conclusions:** HypoPTH is associated with decreased QOL compared to the US population. Despite the inherent bias in open-label studies to predict positive effects on QOL, PTH therapy in this study had limited and non-sustained effects on QOL, inconclusive changes in fatigue experience, and no change in the 6MWT.

While PTH 1-34 can adequately manage the hypocalcemia in hypoparathyroidism, its effects on QOL appear to be minimal.

Disclosures: **Rachel I. Gafni**, None

SAT-0053

See Friday Plenary Number FRI-0053

SAT-0054

See Friday Plenary Number FRI-0054

SAT-0055

See Friday Plenary Number FRI-0055

SAT-0056

See Friday Plenary Number FRI-0056

SAT-0057

See Friday Plenary Number FRI-0057

SAT-0058

See Friday Plenary Number FRI-0058

SAT-0059

See Friday Plenary Number FRI-0059

SAT-0060

See Friday Plenary Number FRI-0060

SAT-0061

See Friday Plenary Number FRI-0061

SAT-0062

Second-generation HR-pQCT reveals minor size differences between right and left sides, but no major differences in density or microarchitecture Sanchita Agarwal^{1*}, Bin Zhou², Y Eric Yu², Kyle K Nishiyama¹, Fernando R Rosete¹, Mariana Bucovsky¹, Elizabeth Shane¹, X Edward Guo². ¹Division of Endocrinology, Department of Medicine, Columbia University, United States, ²Bone Bioengineering Laboratory, Department of Biomedical Engineering, Columbia University, United States

Second-generation high-resolution peripheral quantitative computed tomography (HR-pQCT, XCT2, isotropic voxel size 61 μm) permits 3D measurements of bone geometry, density and microstructure in cortical (Ct) and trabecular (Tb) compartments of the distal radius and tibia with high fidelity. Although it is customary to scan the non-dominant limb unless contraindicated (e.g., prior fracture), no study has assessed whether XCT2 measures differ between two sides of the same person. We scanned 68 people (40F, 28M) aged 24 to 80 (mean 40 ± 14), of diverse race (20 Asian, 9 Black, 24 White, 16 Other) and ethnicity (16 Hispanic) with XCT2 at the right (R) and left (L) radius and tibia. Based on the Waterloo handedness and footedness questionnaire, 57 were R dominant, 3 L dominant, 2 ambidextrous and 6 had missing data. As most were R dominant, we compared L versus R sides, without regard to dominance, with a separate analysis by gender. Data were analyzed by paired t-tests and p<0.05 was considered significant. The R radius was larger than the L (Table), with significantly greater Total Area (p=0.015) and Ct Perimeter (0.009) and non-significant trends for larger Tb (p=0.08) and Ct Area (p=0.053). There were no differences in total, Ct or Tb density or in Ct porosity. Tb number was slightly higher on the R (p=0.003). However, as the absolute difference was small (0.04) and below the LSC (0.18), this difference is unlikely to be relevant. Similarly, the R tibia was larger than the L, with significantly greater Total (p=0.01) and Tb Area (p=0.009), non-significant trends for larger Ct Perimeter (p=0.07) and no difference in Ct Area. Total, Ct and Tb density, Ct porosity and Tb number did not differ, though Tb thickness tended to be lower on the R (p=0.07). Analyses based on gender revealed similar trends but size differences were more prominent at the radius in men and the tibia in women (data not shown). In summary, in a group of people that was largely

right-dominant but diverse with respect to age, gender, race and ethnicity, we found that the right radius and tibia were slightly larger than the left, with no difference in total or compartmental densities and minimal differences in Tb microarchitecture. While it is possible that these size differences could affect estimated stiffness, the absence of significant differences in density and microstructure implies that measurements obtained at either site in a given subject will be essentially interchangeable.

Table: Mean \pm SD and absolute difference between measurements at right and left distal radius and tibia

Parameter	RADIUS				TIBIA			
	Left	Right	Difference	p	Left	Right	Difference	p
Tot.Ar (mm ²)	282.8 \pm 64.9	287.9 \pm 68.1	5.109	0.015	715.6 \pm 139.0	723.2 \pm 136.6	7.648	0.010
Tb.Ar (mm ²)	222.9 \pm 58.7	226.9 \pm 61.9	4.050	0.081	580.7 \pm 125.8	589.2 \pm 124.2	8.509	0.009
CT.Ar (mm ²)	63.6 \pm 14.4	64.8 \pm 14.2	1.140	0.053	140.3 \pm 29.3	139.4 \pm 26.6	-0.846	0.408
CT.Pm (mm)	69.9 \pm 8.5	70.5 \pm 8.7	0.663	0.009	102.9 \pm 10.5	103.3 \pm 10.1	0.399	0.073
CT.Th (mm)	1.062 \pm 0.202	1.077 \pm 0.202	0.015	0.214	1.592 \pm 0.288	1.571 \pm 0.256	-0.021	0.146
Tot.vBMD (mgHA/cm ³)	337 \pm 63	338 \pm 68	0.810	0.794	326 \pm 77	318 \pm 61	-8.214	0.131
Tb.vBMD (mgHA/cm ³)	168 \pm 47	169 \pm 47	0.712	0.577	180 \pm 74	173 \pm 47	-7.067	0.280
CT.vBMD (mgHA/cm ³)	924 \pm 55	921 \pm 55	-3.385	0.270	933 \pm 65	933 \pm 62	0.417	0.823
Tb.BV/TV	0.243 \pm 0.068	0.245 \pm 0.069	0.002	0.282	0.258 \pm 0.063	0.256 \pm 0.062	-0.002	0.232
Tb.N (1/mm)	1.429 \pm 0.253	1.464 \pm 0.269	0.035	0.003	1.288 \pm 0.214	1.295 \pm 0.220	0.007	0.430
Tb.Th (mm)	0.235 \pm 0.019	0.234 \pm 0.019	-0.001	0.493	0.258 \pm 0.028	0.256 \pm 0.026	-0.002	0.071
Tb.Sp (mm)	0.670 \pm 0.171	0.657 \pm 0.172	-0.013	0.062	0.760 \pm 0.176	0.753 \pm 0.173	-0.007	0.297
Tb.1/N.SD (mm)	0.259 \pm 0.106	0.251 \pm 0.109	-0.009	0.278	0.348 \pm 0.246	0.315 \pm 0.142	-0.033	0.151
CT.Po (%)	0.603 \pm 0.413	0.647 \pm 0.480	0.044	0.253	2.338 \pm 1.573	2.275 \pm 1.586	-0.062	0.520

Disclosures: *Sanchita Agarwal, None*

SAT-0063

Persistent activation of calcium-sensing receptor increases microcrack and decreases bone strength. Itsuto Endo^{*1,2}, Bingzi Dong³, Yukiyo Ohnishi¹, Yukari Ooguro¹, Kiyoe Kurahashi¹, Masahiro Hiasa⁴, Jumpei Teramachi², Hirofumi Tenshin⁴, Seiji Fukumoto⁶, Masahiro Abe¹, Toshio Matsumoto⁶. ¹Department of Hematology, Endocrinology and Metabolism, Tokushima University Graduate School of Medical Sciences, Japan, ²Department of Chronomedicine, Tokushima University Graduate School of Medical Sciences, Japan, ³Department of Endocrinology and Metabolism, the Affiliated Hospital of Qingdao University, China, ⁴Department of Orthodontics and Dentofacial Orthopedic, Tokushima University, Japan, ⁵Department of Tissue Regulation, Tokushima University, Japan, ⁶Fujii Memorial Institute of Medical Sciences, Tokushima University, Japan

Background: Activating mutations of calcium-sensing receptor (CaSR) cause autosomal dominant hypocalcemia type 1 (ADH1). ADH1 patients exhibited similar to the clinical features of hypoparathyroidism with abnormal calcification of kidney or basal ganglia. However, it is not well known about bone phenotype including bone strength of ADH1 patients. **Methods and Results:** ADH1 model mice (hCaSR A843E knocked-in) mimicked almost all the biochemical features of ADH1 including low bone turnover with decreased PTH secretion, and these phenotype were recovered by subcutaneous injection of PTH(1-34) or oral administration of calcilytic JTT-305. ADH1 mice exhibited smaller body and bone size and lower BMD compared to age-matched WT, and these observations were reversed by PTH(1-34) or JTT-305. Breaking maximum load, stiffness and energy to peak load assessed by 3-point bending test were reduced in ADH1 mice femur regardless of correction by dimension of bone and/or BMD. These corrected bone strength parameters of ADH1 mice were completely recovered by treated with PTH(1-34) or JTT-305. Microcracks assessed by Fuchsin staining were rarely detectable in WT mice, whereas there was a marked increase in both the number and density of microcracks in ADH1 mice femur. PTH(1-34) or JTT-305 reduced microcrack number and density to the similar levels to those in WT mice. Microcrack number and density in ADH1 mice were negatively correlated with the dimension of bone and/or BMD corrected bone strength parameters and were positively correlated with mice ages. The corrected bone strength parameters were negatively correlated with ages of ADH1 mice. **Conclusion:** Accumulation of microcracks due to aging mainly causes decreased bone strength in ADH1 mice. These observations demonstrate that the fracture susceptibility might be increased in aged patients with ADH1.

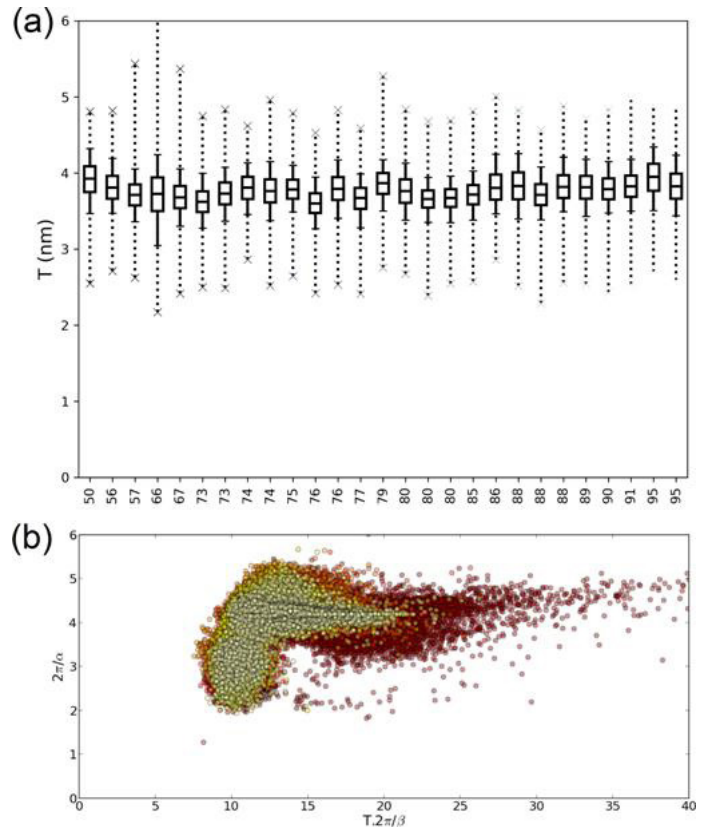
Disclosures: *Itsuto Endo, None*

SAT-0064

Is cortical porosity associated with degraded material quality? Aurelien Gourrier^{*1}, Delphine Farlay², Helene Follet², Georges Boivin². ¹LIPHY CNRS Université Grenoble Alpes, France, ²INSERM UMR 1033 Université de Lyon, France

The mineral nanoscale structure and organization are intrinsic determinants of bone quality. While these material characteristics have been shown to be altered in severe pathological state (e.g. fluorosis, OI), the extent of the fluctuations in healthy individuals is still not fully understood. This study aims to analyze the extent of nanoscale fluctuations that can be expected in a group of healthy individual which main morphological variability is cortical porosity. Transverse sections of 100 μ m in thickness were prepared from the lateral quadrant of the femoral mid-diaphysis of 26 donors aged 50–95 (12 men, 14 women). The samples were analyzed by quantitative scanning small-angle X-ray scattering (qsSAX-SI) using a synchrotron beam of 20 μ m in diameter which allowed resolving histological features. Images of the mineral nanoparticle thickness and organization were thus reconstructed with nanoscale resolution over the full cortical shell (up to 5 \times 11 mm²). The global

mineral nanoparticle thickness distributions reported in fig.1a fall in a range of 3.5 – 4.1 nm (interquartile range), in good agreement with values found in the literature. Significant shifts in average thickness were found between samples, but these remain in a limited range (0.2 – 0.3 nm) as compared to known pathological modifications (e.g. > 1 nm for fluorotic bone). However, a closer examination of the images reveals spatial fluctuations well correlated with histology. In particular, lower thickness values are encountered in the vicinity of the cortical pores/voids. Furthermore, significant perturbations of the mineral organization (higher interparticle distance and shorter correlation length) were also observed (fig.1b) indicating ultrastructural tissue modifications. Our preliminary analysis tends to indicate that cortical bone porosity may be associated with a degraded material quality. While the limited changes in nanoparticle thickness suggests that the global mineralization mechanisms are essentially conserved, the perturbation in their organization indirectly points to alterations of the structure and/or organization of the tissue at the microfibril level. Because microfibrils have been shown to be the main determinants of microelasticity at the lamellar level, these tissue modifications should have an impact on the micro- to macroscopic biomechanical properties. Fig.1: (a) nanoparticle thickness (SAXS) vs age; (b) short range order ($2\pi/\alpha$) vs interparticle distance ($2\pi/\beta$).



Disclosures: *Aurelien Gourrier, None*

SAT-0065

Chondroitin Sulfate and Biglycan Play Pivotal Roles in Bone Toughness via Retaining Bound Water in Bone Matrix Rui Hua^{*1}, Jie Bai², Xiaodu Wang², Jian X. Jiang¹. ¹Department of Biochemistry, UT Health San Antonio, United States, ²Department of Mechanical Engineering, University of Texas at San Antonio, United States

In extracellular bone matrix, proteoglycans (PGs) are one of the structural non-collagenous proteins (NCPs) which reside in the organic interface between hydroxyapatite crystals. Typically, PGs contain long unbranched glycosaminoglycans (GAGs) chains attached to core proteins. Our previous in vitro studies using human cadaveric bone samples showed that PGs might play a pivotal role in sustaining bone toughness via retaining bound water in bone matrix, and chondroitin sulfate (CS) was the major subtype of GAGs which correlated with age-related deterioration of bone toughness. In addition, biglycan, a major subtype of CS-containing PGs, also declined during aging. In this study, we examined the effect of CS and biglycan on the toughness of bone in vivo using WT and biglycan-deficient mouse model. A significant decrease of total GAGs amount was observed in the mineralized compartment of 6-month-old biglycan KO mouse bone matrix. Consistently, a semiquantitative Alcian blue histochemical staining method verified the similar GAG change in biglycan KO mice compared to WT. The tissue-level toughness was investigated using nanoscratch test techniques under both hydrated and dehydrated conditions. The results showed that biglycan deficiency led to a significant reduction of bone toughness for fresh bone specimens. However, after removal of bound water in the bone tissue, the difference between bone tough-

ness of WT and biglycan KO mice was diminished. Moreover, dehydration decreased bone toughness of WT and biglycan KO groups by 22% and 10%, respectively. We have shown that CS and biglycan are important molecules in bone fragility during aging process. Here, we injected CS in 10-month-old WT and biglycan KO mice to test whether supplemental GAGs could improve age-related loss of tissue-level toughness. After intradermal injection of CS (3 mg/kg) for 4 weeks, along with the significant increase of the GAG amount in mineralized matrix of WT group, the bone toughness was greatly improved. Interestingly, the increase of the GAG amount and bone toughness was not observed in biglycan KO mice, possibly caused by the lack of biglycan to retain supplemental CS. In summary, our results demonstrated that CS and biglycan in bone matrix play a pivotal role in retaining bound water in bone matrix, thus imparting the toughness to bone, and supplementation of CS to bone matrix may improve the toughness of bone in mice of 10-month-old.

Disclosures: Rui Hua, None

SAT-0066

Quantitative Computed Tomography (QCT) Analysis of Bone Quality: Consideration of Hierarchical Levels of Variation for Predicting Fracture Risk. Randee Hunter^{*1}, Karen Briley², James Ellis², Amanda Agnew¹. ¹Skeletal Biology Research Laboratory, United States, ²Wright Center of Innovation in Biomedical Imaging, United States

The purpose of this study is to investigate differential skeletal response to systemic and mechanical environments as the source of intra-individual and intra-element variation in bone quality using quantitative computed tomography (QCT). After controlling for patient demographics, a hierarchical consideration of sources of variation could provide clinicians with a mechanism for more discriminant assessments of fracture risk. QCT analysis was performed on ex vivo bilateral radii and tibiae from a cadaveric sample of 76 males (63.7±14.1 yrs) and 34 females (64.4±14.4 yrs). CT scans were acquired using optimized acquisition parameters on a Philips Ingenuity 64-channel system with resulting in-plane resolutions of 0.167mm (radius) and 0.335mm (tibia). Proxies for cortical bone strength, including robustness (Tt.Ar/Le) and area moment of inertia (I), were quantified for sites relative to total length (mm) in the radius (30, 50%) and tibia (38, 50%) using SkyScan CTAn (Bruker) software. Site-specific volumetric bone mineral density (vBMD) was calculated using a QRM cortical phantom. Multiple linear regressions indicate significant relationships for sex, age, and body size (kg) in all segments sites per element for both I and Tt.Ar/Le and (p<0.01). vBMD was not predicted by sex (p>0.05) but was significantly related to age and body size (p<0.01). ANCOVA results indicate significant differences in all variables between segment sites (p<0.01). Pearson correlation coefficients ranging from 0.45 to 0.71 between site-matched variables in both elements indicate a substantial amount of systemic influence. Understanding intra-individual and intra-element variation in cortical bone quality will help advance fracture risk predictions beyond limited areal BMD t-scores. Future work will include dynamic whole bone mechanical testing to determine the biological relevance of these sources of variation.

Disclosures: Randee Hunter, None

SAT-0067

Compressive Bone Strength Index (BSIc) Explains 85% Variance in Experimentally-Derived Distal Radius Failure Load James Johnston^{*1}, Matthew Mcdonald¹, Saija Kontulainen². ¹Department of Mechanical Engineering, University of Saskatchewan, Canada, ²College of Kinesiology, University of Saskatchewan, Canada

Background/Purpose: Peripheral quantitative computed tomography (pQCT) imaging is commonly used to estimate distal radius strength (i.e., failure load) via the compressive bone strength index (BSIc), where $BSIc = (\text{Total area}) \times (\text{Total density})^2$ [1]. This equation is derived from prior research showing that the stress (force/area) required to fracture bone is proportional to density squared [2]. Although commonly reported to estimate distal radius failure load, BSIc has only been validated at the distal tibia (where BSIc explained 85% variance in distal tibia failure load) [1]. It may be possible to advance the BSIc method and apply composite beam theory to account for the relative effects of cortical and trabecular bone in resisting load. The purpose of this study was to assess variance in distal radius failure load predicted by BSIc and a new composite beam index (FCB), along with other bone properties. **Methods:** We evaluated 13 fresh-frozen cadaver forearms, all from female donors (mean age 82.4, SD 8.5 years). We scanned the distal radius using pQCT (0.2mm in-plane pixel size, 2.3mm thickness), and total, cortical and trabecular area and density were analyzed. We calculated BSIc using the equation above. FCB was calculated via $FCB = (\text{Strab}) \times (\text{Etrab}) \times (\text{A-trab}) + (\text{Ecort}) \times (\text{Acort}) \times (\text{Etrab})$, where Strab pertains to density-dependent trabecular bone compressive strength [3] and E pertains to density-dependent elastic moduli of trabecular [4] or cortical [5] bone. Forearms were experimentally tested in axial compression (3mm/s) onto the palm of the hand, and we recorded failure load. We report variance (R²) in experimental failure load predicted by BSIc, FCB and bone properties. **Results:** Variance in failure load appeared to be best predicted by BSIc (R²=85%), total bone mineral content (81%) and FCB (78%). **Conclusions:** BSIc predicted the same, 85% of variance in experimental failure load as previously reported at the distal tibia [1]. This study validates continued use of BSIc when estimating bone strength of the distal radius and for predicting fracture risk. The new FCB strength index explained less variance in failure load than BSIc, likely due to challenges associated with differentiating distal radius cortical from trabecular bone when using pQCT.

References: [1] Kontulainen et al., 2008; [2] Carter and Hayes, 1972; [3] Hvid et al., 1989; [4] Morgan et al., 2003 [5] Snyder & Schneider, 1991

Disclosures: James Johnston, None

SAT-0068

Differences in bone quality between fresh bone and PMMA-embedded bone Hiromi Kimura-Suda^{*1}, Teppei Ito¹, Masahiko Takahata², Tomohiro Shimizu², Fumiya Nakamura¹, Masahiro Ota². ¹Chitose Institute of Science and Technology, Japan, ²Hokkaido University, Japan

Both Fourier transform infrared (FTIR) and Raman imaging are powerful tools for the assessment of bone quality, including parameters such as mineral-to-matrix ratio (mineral/matrix), carbonate-to-phosphate ratio (carbonate/phosphate), crystallinity, and mineral maturity. Conventional FTIR imaging requires the use of a poly(methyl methacrylate) (PMMA) embedding process to prepare thin sections of bone for the assessment of bone quality; however, the PMMA embedding process takes time and causes denaturation of proteins including collagen. Thin sections do not need to be prepared for Raman imaging, which provides information of the bone quality of fresh bone. On the other hand, FTIR imaging provides information on bone quality over a wider area and more quickly than Raman imaging. We have previously developed a quick and easy sectioning method using frozen sectioning instead of PMMA-embedded sectioning to assess the bone quality of fresh calcified bone using FTIR imaging in transmittance mode. We have demonstrated that the mineral/matrix and crystallinity of the thin sections prepared by PMMA embedding were higher than those of sections prepared by frozen sectioning, whereas the carbonate/phosphate of the thin sections prepared by PMMA embedding was lower than that of sections prepared by frozen sectioning. In this study, we clarified the differences in bone quality between fresh bone and PMMA-embedded bone. Femurs were removed from six 12-week-old BALB/cA mice after euthanasia, and thin sections from three mice were prepared by the PMMA embedding procedure, and the thin sections from the other three mice were prepared by the frozen sectioning procedure. In the trabecular bone in the fresh femurs, we found a positive correlation between the mineral/matrix and mineral maturity and a negative correlation between the carbonate/phosphate and mineral/matrix, between the carbonate/phosphate and mineral maturity, and between the carbonate/phosphate and crystallinity; however, no such correlations were observed in the trabecular bone in the femurs embedded in PMMA. Moreover, there was a marked difference in the carbonate/phosphate between the fresh femurs and PMMA-embedded femurs. The carbonate/phosphate of the PMMA-embedded femurs was 30% lower than that of the fresh femurs. We concluded that the carbonate/phosphate may afford a useful parameter for the comparison of bone quality between fresh bone and PMMA-embedded bone.

Disclosures: Hiromi Kimura-Suda, None

SAT-0069

Osseointegrated implants for lower limb amputees: evaluation of bone mineral density Seamus Thomson^{*1}, William Lu¹, Munjed Al Muderis². ¹The University of Sydney, Australia, ²The Osseointegration Group of Australia, Australia

Background and aim(s) The use of dual-energy X-ray absorptiometry (DXA) is a standard clinical procedure for the evaluation of bone mineral density (BMD). Amputee patients are known to have decreased BMD and an increased risk of osteoporosis in the affected proximal femur and hip region. The major cause of these issues in these patients is the absence adequate loading leading to bone resorption in accordance to Wolff's law. In this paper, we present a prospective study reporting changes in BMD among amputees who received osseointegrated implants to determine if the loading through the Osseointegrated implant can overcome the bone resorption issues. **Method** This is a prospective study of 33 patients, consisting of 24 males and 9 females, aged 22-77 (mean = 51.0 ± 2.0) years with one and two-year follow-up. Selection criteria included age over 18 years, unilateral amputees with socket-related problems. All patients received osseointegrated implants press-fitted into the amputated limb. BMD was assessed using DXA in the femoral neck (operative and contralateral) and lumbar spine (L2-L4) regions, and corresponding Z-scores were generated. DXA scans were taken preoperatively as well as one-year and two-years following osseointegration surgery. **Result(s)** Mean BMD and Z-scores of spine, and operative and contralateral sides were generated for all patients. Dependent t-tests were used to test for significant differences (P<0.05) preoperative, one-year, and two-years for mean changes in BMD and Z-scores following surgery. Analysis of the BMD and Z-scores indicated that patients showed improvements at one-year post-surgery. **Conclusion(s)** These results suggest that osseointegrated implants are effective at encouraging bone growth and restoring BMD levels for amputees within a short period of time post-surgery. Osseointegrated implants therefore have the potential to address stress distribution issues associated with socket prostheses and restore the normal bone loading regime in lower limb amputees.

Disclosures: Seamus Thomson, Osseointegration International, Grant/Research Support

SAT-0070

Distal Radius Bone Microarchitecture: what happens between age 25 and old age? Canchen Ma^{*1}, Feng Pan¹, Laura Laslett¹, Kathryn Squibb¹, Roger Zebaze², Tania Winzenberg¹, Graeme Jones¹. ¹Menzies Institute for Medical Research, University of Tasmania, Australia, ²Austin and Repatriation Medical Centre, University of Melbourne, Australia

Purpose: The aim of this study was to describe the differences of bone geometry, volumetric bone mineral density (vBMD) and microarchitecture parameters at the distal radius between older and young adults. Methods: Bone geometry, trabecular and cortical parameters and vBMD at distal radius were collected using high-resolution peripheral computed tomography (HRpQCT) and analysed using StrAx in 201 participants from the prospective Tasmanian Older Adult Cohort study (mean age 72.2 years, range 61.9-89.4 years, female 46.8%) and 196 participants from the T-bone study (mean age 25.5 years, range 24.1-27.6 years, female 38.8%). Unpaired t-tests were used for comparison of means. Results: Older adults had a significantly larger cross-sectional area of the transitional zone (outer 30.96mm² vs. 28.38mm², inner 36.34mm² vs. 32.93mm²) and thicker transitional zone bone area (outer 0.57mm vs. 0.54mm, inner 0.71mm vs. 0.65mm) compared with young adults. In addition, the prevalence of cortical porosity (54% vs. 49%) and porosity of the transitional zone (outer 42% vs. 37%, inner 82% vs. 81%) were significantly higher in older adults than in young adults. vBMD of total bone area (370.73 mg hydroxyapatite (HA)/cm³ vs. 424.57 mg HA/cm³), vBMD of transitional zone (outer 899.29 mg HA/cm³ vs. 959.52 mg HA/cm³, inner 385.47 mg HA/cm³ vs. 408.34 mg HA/cm³), cortical and trabecular vBMD (734.51 mg HA/cm³ vs. 801.04 mg HA/cm³, 114.19 mg HA/cm³ vs. 178.02 mg HA/cm³) were all significantly lower in older adults. There were no significant differences between older and young adults in total, cortical, and trabecular cross-sectional area or cortical and trabecular thickness. Conclusions: Compared to young adults at the time of peak bone mass, older adults have an increase in transitional bone size, decreased vBMD measures and substantially increased prevalence of porosity, with the most significant difference in the compact cortex. Keywords: bone microarchitecture; bone mineral density; high-resolution peripheral quantitative computed tomography

	Older adults (n=201)	Young adults (n=196)	t	p-value
Geometry				
Tl.Ar (mm ²)	286.46(72.36)	275.12(69.06)	1.597	0.111
Ct.Ar (mm ²)	106.93(23.73)	105.25(18.83)	0.780	0.436
Compact cortical Ar (mm ²)	39.63(12.51)	43.95(10.53)	-3.709	<0.001*
Outer TZ Ar (mm ²)	30.96(6.85)	28.38(5.10)	4.249	<0.001*
Inner TZ Ar (mm ²)	36.34(8.96)	32.93(8.07)	3.983	<0.001*
Tb.Ar (mm ²)	179.53(53.73)	169.87(54.46)	1.779	0.076
Ct.Th (mm)	1.96(0.31)	1.97(0.26)	-0.392	0.695
Compact Cortical Thickness (mm)	0.68(0.20)	0.78(0.20)	-5.026	<0.001*
Outer TZ Thickness (mm)	0.57(0.10)	0.54(0.06)	3.640	<0.001*
Inner TZ Thickness (mm)	0.71(0.10)	0.65(0.08)	6.407	<0.001*
vBMD				
Tl.vBMD (mg HA/cm ³)	370.73(80.70)	424.57(69.11)	-7.132	<0.001*
Ct.vBMD (mg HA/cm ³)	734.51(88.98)	801.04(67.53)	-8.377	<0.001*
Compact Cortical vBMD (mg HA/cm ³)	928.57(84.57)	991.24(58.85)	-8.550	<0.001*
Outer TZ vBMD (mg HA/cm ³)	899.29(72.57)	959.52(44.74)	-9.925	<0.001*
Inner TZ vBMD (mg HA/cm ³)	385.47(59.09)	408.34(49.49)	-4.175	<0.001*
Tb.vBMD (mg HA/cm ³)	144.19(59.72)	178.02(51.29)	-6.048	<0.001*
Microarchitecture				
Cortical porosity (%)	54.43(6.96)	49.24(5.41)	8.295	<0.001*
Compact cortical porosity (%)	39.32(6.99)	34.06(4.93)	8.636	<0.001*
Outer TZ porosity (%)	41.72(5.94)	36.71(3.75)	10.010	<0.001*
Inner TZ porosity (%)	81.62(3.98)	80.50(3.47)	3.008	<0.001*
Tb.N (mm ⁻¹)	3.26(0.61)	3.66(0.46)	-7.254	<0.001*
Tb.Th (mm)	0.19(0.01)	0.19(0.01)	0.422	0.673
Tb.CN	0.79(0.25)	0.94(0.24)	-5.869	<0.001*
Tb.Sp (mm)	1.12(0.28)	0.94(0.22)	7.092	<0.001*
Tb.BV/TV (%)	5.14(2.63)	6.19(2.47)	-4.103	<0.001*
Matrix mineral density (%)	67.77(0.90)	67.19(0.83)	6.735	<0.001*

All values are means (standard deviation). Tl.Ar, total cross sectional area; Ct.Ar, total cortical area; TZ: transitional zone; Tb.Ar: trabecular area; Ct.Th: total cortical thickness; Tl.vBMD, total volumetric bone density; Ct.vBMD: volumetric bone density of total cortex; Tb.vBMD: trabecular volumetric bone density; Tb.N, trabecular number; Tb.Th, trabecular thickness; Tb.CN: trabecular connectivity; Tb.Sp: trabecular separation; Tb.BV/TV: trabecular bone volume fraction; HA: hydroxyapatite.
* Statistically significance.

Disclosures: **Canchen Ma, None**

SAT-0071

Osteoarthritis Correlates with High-Speed Exercise and Sesamoid Bone Fracture in Racehorses Heidi Reesink^{*1}, Erin Cresswell², Sean McDonough¹, Scott Palmer¹, Christopher Hernandez¹, Caroline Wollman¹, Bridgette Peal³. ¹Cornell University, United States, ²LifeNet Health, United States, ³North Carolina State University, United States

Fracture of the proximal sesamoid bones (PSBs) is a sudden, unexpected, catastrophic fracture representing the most common fatal musculoskeletal injury in U.S. racehorses. Here, we asked if computed tomography (CT)-measured bone morphologic parameters and macroscopic, micro-CT or histologic evidence of osteoarthritis were correlated with PSB fracture or high-speed exercise. PSBs (n=62) from New York racehorses that sustained a catastrophic fracture (n=8) and controls (n=8) were imaged using high resolution micro-CT.

Each joint was assigned a macroscopic osteoarthritis score by a single board-certified veterinary pathologist, and sagittal PSB histologic sections were scored by 3 blinded observers using the OARSI scale. Logistic and linear regression were performed to identify parameters correlated with fracture and exercise history (measured as total furlongs of exercise). Horses sustaining PSB fracture had greater macroscopic osteoarthritis scores (p=0.005, Fig 1A). PSBs from the intact, contralateral forelimb of horses sustaining fracture had larger osteophytes (p=0.04, Fig 1B) as compared to controls. Fractured bones had increased bone volume fraction (90.39±1.76% vs. 87.20±2.79%, p<0.0001) as compared to controls. Histologic scoring and osteophyte micro-CT revealed strong associations between osteoarthritis and the amount of high-speed exercise (total furlongs, p=0.02 and 0.03, respectively). Catastrophic PSB fracture is associated with increased bone volume fraction, osteophytosis and more advanced macroscopic osteoarthritis in Thoroughbred racehorses. Both macroscopic and histologic osteoarthritis scores were associated with total high-speed furlongs. Monitoring bone volume fraction and osteophytosis in vivo could identify risk factors for catastrophic fracture. Longitudinal imaging studies are required to assess the potential benefit of in vivo CT imaging.

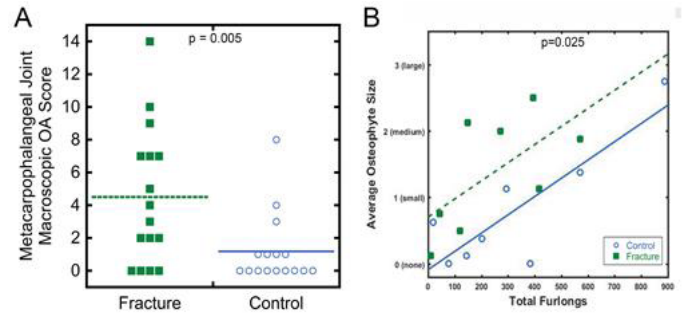


Figure 1. (A) Macroscopic OA scores were higher for horses that experienced fracture vs. controls (p=0.005). (B) Osteophyte size was significantly correlated with fracture (p=0.025) and total distance accrued during high-speed exercise (total furlongs, p=0.001).

Disclosures: **Heidi Reesink, None**

SAT-0110

See Friday Plenary Number FRI-0110

SAT-0111

See Friday Plenary Number FRI-0111

SAT-0112

See Friday Plenary Number FRI-0112

SAT-0113

See Friday Plenary Number FRI-0113

SAT-0114

See Friday Plenary Number FRI-0114

SAT-0115

Elevated RANKL Levels in Pediatric Patients with Metabolic Bone and Neuromuscular Disorders Sara Akhtar Ali^{*}, Leigh Ramos-Platt, Senta Georgia, Pisit Pitukcheewanont. Children's Hospital Los Angeles, United States

Background: Metabolic bone and neuromuscular disorders are not uncommon in pediatrics, many of which lead to pediatric osteoporosis. In addition, the mechanism of bone loss in these conditions has not been established. RANKL (receptor activator of nuclear factor kappaB ligand) and osteoprotegerin (OPG) pathway is responsible for normal bone remodeling, however its role in pediatric metabolic bone and neuromuscular disorders has never been well described. Objective: To quantify RANKL levels in pediatric patients with metabolic bone or neuromuscular disorders compared to controls. Study Design: Subjects, 1-21 years of age, with a diagnosis of either metabolic bone or neuromuscular disorder were enrolled. Free soluble RANKL levels were quantified using a sandwich ELISA (Biomedica Immunoassays BI 20462) and compared to previously published healthy control data using the same assay. Results: One-hundred and twenty-two patients (34 female and 88 male)

from 16 months to 21 years of age were enrolled. Preliminary data showed an overall higher median RANKL level of 0.24 pmol/L (compared to a median level of 0.15 pmol/L in healthy children previously reported) with a mean of 0.28 ± 0.17 pmol/L. Subgroup analysis, when able, was performed using Kruskal-Wallis test showed no statistical significant difference in RANKL levels ($p = 0.33$) among patients with osteogenesis imperfecta ($n = 19$, median = 0.19 pmol/L), rickets ($n = 10$, median = 0.28 pmol/L), hypoparathyroidism ($n = 10$, median = 0.38 pmol/L), pseudohypoparathyroidism ($n = 8$, median = 0.25 pmol/L), steroid-induced osteoporosis ($n = 5$, median = 0.30 pmol/L), and Duchenne Muscular Dystrophy (DMD) ($n = 42$, median = 0.24 pmol/L), though sample size of each diagnosis was small. Mann Whitney U test revealed no significant difference between metabolic bone disorders and neuromuscular disorders ($p = 0.29$); males and females ($p = 0.40$); or history of multiple fractures ($n = 45$, median = 0.22 pmol/L) and no fractures ($n = 77$, median = 0.27 pmol/L, $p = 0.25$). RANKL level was negatively correlated with age (Spearman $r = -.36$, $p < 0.0001$). Conclusions: RANKL levels were elevated in patients with metabolic bone and neuromuscular disorders. RANKL levels were highest in patients with hypoparathyroidism and steroid-induced osteoporosis, as well as DMD. Larger studies should be done to evaluate RANKL for potential targeted therapeutic intervention.

Disclosures: *Sara Akhtar Ali, None*

SAT-0116

SITAR Models of Bone and Body Composition Growth: Prospective Longitudinal Data for U.S. White Girls from Childhood to Adulthood Jodi N Dowthwaite¹, Stephanie A Kliethermes², Tamara A Scerpella². ¹SUNY Upstate Medical University; Binghamton University, United States, ²University of Wisconsin - Madison, United States

Purpose: We aimed to confirm key concepts in pediatric development by evaluating site- and tissue-specific growth patterns, using prospective, longitudinal data from a sample of white girls from Upstate New York. Methods: Data were collected during a study of bone growth in the context of gymnastic exposure; girls were healthy gymnasts or non-gymnasts at enrollment. Height and weight were recorded contemporaneous with annual whole body DXA scans, performed using 1 of 2 Hologic scanners (QDR4500W 1998-2012; Discovery A 2008-2018). A one-time scanner transition affected data for girls measured pre-2008 through post-2010. Cohort and scanner-specific, pediatric regression equations converted QDR data to Discovery-equivalent data before entry into Superimposition by translation and rotation models using "R" (SITAR, Cole et al. 2010). SITAR models use regression B-splines and random effects to produce mean and subject-specific growth curves defined by parameters as follows: size (growth magnitude), tempo (maturation timing) and velocity (growth rate), estimated for numerous outcomes (Table 1). Analysis inclusion criteria were: ≥ 3 annual DXA scans and white, non-Hispanic identification. Affected data were excluded for individuals who developed adverse conditions. Results: SITAR models explained 89% to 98% of variance for all outcomes in 141 girls, representing 3 to 20 annual observations per individual, age range 7.5-30.9 yrs. Mean chronological ages at peak velocity ranged from 12.14 yrs (lean mass) to 13.96 yrs (fat mass), with intermediate ages at peak velocity for all bone outcomes; peak height velocity (PHV) preceded peak velocity for arm bone mineral content (ARMBMC). Conclusion: Our data support the concept that peak lean mass velocity precedes peak BMC velocity at all sites. Furthermore, peak ARMBMC velocity lags ~ 1 yr post-PHV and ~ 0.6 yrs post-peak weight velocity; this lag may contribute to high upper extremity fracture risk during this growth phase, as theorized by pediatric bone researchers. Note that the ARMBMC lag may be moderated in this sample compared to the general population, as many participants were gymnasts exposed to unusual arm loading patterns during growth. Future work will address maturity-specific loading history as a factor in site- and tissue-specific growth curves.

TABLE 1: SITAR Model Results for Growth Curve Properties						
Outcome Variable	df	Size (SE)	Tempo (SE)	Velocity (SE)	Age at Peak Growth Velocity	Variance Explained
Height (cm)	4	137.14 (1.02)	-1.76 (0.11)	1.02 (0.06)	12.33	98.23%
Body Mass (kg)	4	25.88 (1.37)	-3.04 (0.18)	0.75 (0.05)	12.59	93.9%
BMI (kg/m ²)	4	17.17 (0.29)	-2.38 (0.17)	0.99 (0.09)	13.26	89.7%
nbFFM (kg)	4	19.89 (0.699)	-3.34 (0.13)	0.998 (0.04)	12.14	93.98%
Fat Mass (g)	3	8.67 (0.443)	-1.04 (0.17)	1.20 (0.13)	13.96	90.39%
WB BMC (g)	4	1204.79 (14.56)	-1.37 (0.12)	1.06 (0.04)	12.96	97.35%
sumARMBMC (g)	4	132.49 (5.51)	-0.40 (0.15)	0.53 (0.07)	13.28	96.22%
sumLEGBMC (g)	4	437.87 (13.45)	-1.11 (0.13)	0.85 (0.07)	12.93	96.6%
FN BMC (g)	4	2.67 (0.06)	-1.78 (0.18)	0.98 (0.06)	12.53	91.73%
FN BMD (g/cm ²)	4	0.69 (0.01)	-0.995 (0.17)	0.77 (0.08)	13.02	92.94%
L1-L4 BMC (g)	4	20.33 (0.83)	0.16 (0.12)	0.20 (0.05)	13.34	95.59%
L1-L4 BMD (g/cm ²)	4	0.67 (0.01)	-1.82 (0.14)	1.07 (0.04)	12.62	94.13%

Note: N=141 girls for all models; Degrees of Freedom (df) chosen by optimizing BIC
SE= standard error; BMI= body mass index; nbFFM= non-bone fat free mass; WB= whole body;
BMC= bone mineral content; FN= femoral neck; BMD= areal bone mineral density;
L1-L4= Lumbar spine vertebrae 1-4

Disclosures: *Jodi N Dowthwaite, None*

SAT-0117

Low Trabecular Bone Score in Adolescent Female Inpatients with Anorexia Nervosa Yael Levy-Shraga¹, Liana Tripto-Shkolnik², Dana David¹, Iris Vered², Daniel Stein³, Dalit Modan-Moses¹. ¹Pediatric Endocrinology Unit, The Edmond and Lily Safra Children's Hospital, Chaim Sheba Medical Center, Tel-Hashomer, Israel, ²Institute of Endocrinology, Chaim Sheba Medical Center, Tel-Hashomer., Israel, ³Pediatric Psychosomatic Department, The Edmond and Lily Safra Children's Hospital, Chaim Sheba Medical Center, Tel-Hashomer, Israel

Background: Trabecular bone score (TBS) is an emerging technology that provides information regarding bone microarchitecture. A recent study showed that in healthy girls normal TBS (≥ 1.35) was achieved within the first year post-menarche. The aims of our study was to assess TBS in adolescents with anorexia nervosa (AN) and to evaluate correlations with clinical, laboratory and densitometric variables. Methods: A cohort study of 208 adolescent females (mean age 15.6 ± 1.8 yrs) hospitalized because of AN between 2003-2017 was retrospectively assessed. Demographic and clinical data, including age, weight, height, body mass index (BMI), laboratory parameters and bone mineral density (BMD) measurements by dual-energy X-ray absorptiometry (DXA) were retrieved from the medical charts. TBS was assessed by reanalyzing DXA spinal images. Results: Mean TBS was 1.308 ± 0.083 , lower than the values previously described in healthy adolescents ($p < 0.0001$). Compromised microarchitecture was found in 17 participants (8.2%) and partially compromised in 123 (59.1%). TBS was significantly correlated with age, weight standard deviation score (SDS), BMI SDS, BMD measurements of the lumbar spine and total body, luteinizing hormone (LH) and 17 β -estradiol (E2) level, and was negatively correlated with cortisol ($p = 0.017$). Participants with regular menstruation or secondary amenorrhea had higher TBS than participants who were pre-menarche or with primary amenorrhea ($p < 0.001$). A stepwise linear regression analysis identified BMD L1-4 z score and log E2 as independent predictors of TBS. Conclusion: TBS of adolescent females with AN was found to be lower than TBS of healthy adolescents. Prospective longitudinal studies should be undertaken to investigate whether recovery may result in correction of bone microarchitecture.

Disclosures: *Yael Levy-Shraga, None*

SAT-0118

Polyhydramnios: sole risk factor for non-traumatic fractures in 3 infants Geneviève Nadeau^{*}, Marie-Béatrice Saade, Patricia Olivier, Melissa Fisaletti, Marie Laberge-Malot, Philippe Campeau, Nathalie Alos. CHU Sainte-Justine - University of Montreal, Canada

The mechanostat theory postulates that an increased muscle strain and loading will affect bone strength in a corresponding, dose-dependent manner. We now think of multiple mechanostats: their dynamic and set point been different for each bone. The set point adjusts to resist peak forces applied on a bone while allowing it to carry its function efficiently. Ultimately, the overall capacity of a bone to resist strain is not only a function of its mass, but also of its density and unique geometry. These characteristics may be modulated by multiple factors including mechanical usage. Voluntary muscle strain and ground reaction forces seem to have the most predictable impact on bone remodeling. Accordingly, unloading will lead to reduced muscle development (and muscle force) and have a negative effect on the mass, size, and strength of bone with lower fracture thresholds. Low strain has been shown to result in trabecular thinning and endosteal resorption of cortical bone. We present the cases of three patients now aged 2 to 3 years and seen in our Bone Clinic at Sainte-Justine University Hospital between 2013 and 2018. They all presented fractures of lower limbs at an early age (3 to 8 months), and were found to have low bone mineral density upon DXA testing, with Z score of lumbar BMD inferior to -2 SDs. A shared characteristic between patients was that all three pregnancies presented with a polyhydramnios of unknown etiology in the third trimester, as assessed by routine ultrasound. They presented no family history of bone disease, and genetic testing for neuromuscular diseases or bone fragility was negative in all patients. During follow-up, they all showed to be catching up on bone mineral density within the year following the onset of fractures without receiving antiosteoporotic treatments. However, lumbar BMD remained lower than expected (< -1 SD) as based on their anthropometric parameters. Based on the mechanostat theory, we hypothesize that in those patients, polyhydramnios might have played as a significant risk factor for low bone mineral density. A larger amount of liquid in the amniotic cavity could limit the rate and intensity of limb loading, resulting in lower peak force applied on growing bones. No studies have yet investigated a connection between intra-uterine limb strain and bone strength in the perinatal period. This case series could lead the way to researches connecting pre-birth environmental factors to bone strength in infancy.

Disclosures: *Geneviève Nadeau, None*

SAT-0135

See Friday Plenary Number FRI-0135

SAT-0136

See Friday Plenary Number FRI-0136

SAT-0137

See Friday Plenary Number FRI-0137

SAT-0138

See Friday Plenary Number FRI-0138

SAT-0139

See Friday Plenary Number FRI-0139

SAT-0140

Nmp4 regulates bone physiology, obesity, and glucose metabolism Joseph Bidwell*, Ronald Wek, Alexander Robling, Sarah Tersey, Michele Adaway, Carmella Evans-Molina. Indiana University School of Medicine, United States

Recent studies indicate that the skeletal system plays a major role in the maintenance of blood glucose, which in turn can impact the onset of diabetes. The skeleton regulates global energy utilization, in part, by acting as a significant sink for glucose uptake since osteoblasts use glycolysis to fuel bone formation. The bone also acts as an endocrine organ through release of a variety of factors that regulate key aspects of metabolism. *Nmp4* is a ubiquitous transcription factor, and *Nmp4*^{-/-} mice have an unremarkable skeletal phenotype until challenged with any one of several anabolic stimuli (e.g. PTH, *Bmp2*), which elicits enhanced and accelerated bone formation and significantly elevated increases in serum osteocalcin compared to WT mice. *Nmp4*^{-/-} mice harbor more bone marrow osteoprogenitors than WT animals and these cells exhibit enhanced mineralization in culture and a significantly increased capacity for metabolic conversion to glycolysis. Because bone-derived undercarboxylated osteocalcin has been reported to regulate pancreatic β cell function, we hypothesized that *Nmp4*^{-/-} mice may also exhibit changes in glucose metabolism. Interestingly, *Nmp4*^{-/-} mice displayed a significant reduction in pancreatic β cell mass and reduced glucose-stimulated insulin secretion. To test whether *Nmp4* status impacted the β cell adaptive response to obesity, 8 week-old WT and *Nmp4*^{-/-} male mice were randomly placed either on a high fat diet (HFD, adjusted calories diet, 42% from fat) or on a low fat diet (LFD, adjusted calories diet, 12.6% from fat) for 12 weeks. Endpoint parameters included body weight, echo magnetic resonance imaging (echo-MRI), intra-peritoneal glucose tolerance test (IPGTT), insulin tolerance test (ITT), and percent β cell area. As expected the WT mice exhibited a significant HFD-induced weight gain accompanied by a marked increase in percent body fat. The WT mice showed a significant HFD-associated glucose intolerance and insulin insensitivity that was associated with an adaptive increase in the β cell area. Remarkably the HFD-fed *Nmp4*^{-/-} animals were resistant to weight gain and exhibited no significant changes in glucose tolerance, insulin sensitivity, or percent β cell area. We conclude that *Nmp4* mediates a complex regulation of obesity, energy utilization, and bone formation.

Disclosures: *Joseph Bidwell, None***SAT-0141**

Osteocalcin/Oxytocin and NGF/BDNF mRNA levels in bone mediate muscle phenotype dependent response to cold stress challenge in mice Claudia Camerino*, Elena Conte, Maria Rosaria Carratù, Adriano Fonzino, Domenico Tricarico. University of Bari, Italy

Osteocalcin (Ost), Oxytocin (Oxt) and NGF/BDNF exert a protective function on bone, reproduction and cognition under cold stress (CS). Oxt and Ost are also required for muscle regeneration, the latter triggering the increase of IL-6 in myofibers and BDNF in brain. Here, we explored the signaling regulating bone and muscle response to CS. The mRNA levels of *Ngf*, *Ost*, *Oxt* and their receptors (*p75^{ntr}*, *Ntrk1*, *Gprc6a*, *Oxtr*), *Bdnf*, *Ucp1* and *Il-6* in bone, soleus (SOL) and tibialis (TA) muscles from 3 months-old mice exposed to CS were investigated. The expression of different Myosin heavy chain *Mhc2b* (fast-glycolytic), *Mhc1* (slow-oxidative), *Mhc2x* and *Mhc2a* (fast-glycolytic-oxidative) were also investigated. Mice (n= 15) were divided into: controls maintained at room temperature (RT=23°C), exposed to CS at T=4°C for 6h and 5-days (5d). CS exposure for 5d enhanced *Ngf*, but not its receptors, and *Ucp1* genes in bone. *Ucp1* and *Ngf* genes were significantly upregulated by 2 and 1.5 folds respectively in TA after 6h CS. *Ntrk1* was significantly upregulated by 4 and 22 folds respectively in the SOL muscle after 6h and 5d CS, while *p75^{ntr}* was downregulated in both muscles after 6h CS. *Oxt* was upregulated by 5-fold following 5d CS in bone. *Oxtr* and *Il-6* genes were upregulated respectively by 1 and 1.5 folds after 5d CS in SOL. *Ost* increased by 16-fold in bone after 5d, *Gprc6a* was unaffected. *Gprc6a* was upregulated respectively by 3.5 and 2 folds after 6h and 5d CS in TA. *Bdnf* increased by 9.5-fold in bone after 5d CS while it was not affected in muscle. *Mhc2b* was significantly downregulated in SOL respectively by 0.96 and 0.88-folds after 6h and 5d CS vs controls; *Mhc1* only by 0.32-fold after 5d CS in SOL. *Mhc2a* was significantly downregulated by 0.88-fold after 5d CS in TA. *Mhc2x* was not affected following CS. Our study confirms that *Ngf* and *Ucp1* are activated in bone as well as in muscle. *Oxt* and *Ost* are highly expressed in bone and exert phenotype-dependent protective effects towards muscle through up-regulation of their receptors, *Oxtr* in slow-twitch and *Gprc6a* in fast-twitch muscles. CS induced a marked shift of SOL muscle toward the slow-twitch phenotype which is in line with the metabolic need of

the slow-twitch oxidative muscle following thermogenic challenge. CS induced a mild shift of the TA muscle toward the fast-twitch phenotype. IL-6 up-regulation in muscle after CS is consistent with the concept of a coordinated axis between bone and muscle.

Disclosures: *Claudia Camerino, None***SAT-0142**

Bone Defect and Fracture Healing in Dystrophy/utrophin Double Knockout Mice Xueqin Gao*, Xuying Sun¹, Sarah Amra¹, Yan Cui¹, Zhenhan Deng¹, Haizi Cheng¹, Charles Huard¹, Bing Wang², Walter Lowe¹, Johnny Huard¹. ¹University of Texas Health Science Center at Houston, United States, ²University of Pittsburgh, United States

The dystrophin^{-/-} (*mdx*) mouse is a model of Duchenne muscular dystrophy (DMD); however, *mdx* mice have normal lifespan and do not exhibit clinical manifestations seen in DMD patients. The dystrophin^{-/-}/utrophin^{-/-} (Hom) mouse model closely mimics human DMD, with a short life span, and is a more useful DMD model. This study investigated the role of muscle force in bone defect healing, using skull and tibial defects, and tibial fracture, in dystrophic mice. Four-week-old C57BL/10J (B10), *mdx*, dystrophin^{-/-}/utrophin^{+/-} (Het), and Hom mice bred at UTHealth were used. MicroCT analysis showed that a 1-mm skull defect did not heal, whereas a tibial defect of the same size healed fully in 21 days. New bone volume (BV) in the skull defect area was similar among the four groups, although bone density was lower in the Hom group than in the other groups. Tibial defect healing was delayed at day 7 in Hom mice, as evidenced by the lower BV of newly formed bone in the defect area, compared to other groups. Tibial defects were nearly healed by day 21 in all the groups, but newly formed bone density was lower in Hom mice than in the other groups on days 14 and 21. New BV was significantly higher in the tibial defect than in the skull defect in all groups. Herovici's staining showed bone matrix collagen I was less dense in the Hom group than in the other groups. Osteoclasts were decreased in the defect area at day 21 in *mdx*, Het, and Hom mice, compared to the B10 group. MicroCT showed union of tibial fractures in all four groups at 21 days after fracture. Hom mice demonstrated significantly impaired fracture healing compared to B10, *mdx*, and Het mice, as revealed by lower TV, BV, BV/TV and trabecular thickness of callus, and higher mortality after fracture (6/12), whereas no mortalities occurred in the other groups after successful surgery. *mdx* and Het mice did not show impaired fracture healing, as demonstrated by the formation of larger calli (TV), BV, and higher BV/TV, BV density, and trabecular number, and lower trabecular separation, than in the B10 group. H&E staining showed mainly trabecular bone in the fracture site, and lower collagen I density, in Hom mice, compared to other groups. In conclusion, healing of tibial, but not skull, defects were delayed in Hom mice. This was attributed to the lower number of osteoclasts in Hom mice. Tibial fracture healing was also impaired in Hom mice but not in *Mdx* and *Het* mice. Further mechanistic studies are ongoing.

Disclosures: *Xueqin Gao, None***SAT-0143**

Annexin A5 prevents force-mediated bone ridge overgrowth at the enthesis Hisashi Ideno*, Yoshinori Arai², Koichiro Komatsu¹, Kazuhisa Nakashima¹, Satoshi Wada³, Teruhito Yamashita⁴, Ernst Pöschl⁵, Bent Brachvogel⁶, Yoichi Ezura⁷, Akira Nifuji¹. ¹Department of Pharmacology, Tsurumi University School of Dental Medicine, Yokohama, Japan, ²Nihon University, School of Dentistry, Japan, ³Department of Orthodontics, Tsurumi University School of Dental Medicine, Yokohama, Japan, ⁴Division of Hard Tissue Research, Institute for Oral Science, Matsumoto Dental University, Japan, ⁵School of Biological Sciences, University of East Anglia, Norwich Research Park, Norwich, United Kingdom, ⁶Experimental Neonatology, Department of Pediatrics and Adolescent Medicine, Center for Biochemistry, Medical Faculty, University of Cologne, Germany, ⁷Department of Molecular Pharmacology, Medical Research Institute, Tokyo Medical and Dental University, Japan

Tendons are connected to bones by a specialized tissue known as the enthesis. The enthesis transmits muscle contractile forces to the skeleton through the tendons. So far, little is known about the molecular mechanisms of enthesis formation in mature animals. We report here that annexin a5 (*Anxa5*), a member of the annexin family of calcium-dependent phospholipid-binding proteins, plays a critical role in the regulation of bone ridge outgrowth at the entheses. We found that *Anxa5* is highly expressed in the entheses in postnatal and adult mice. In *Anxa5*-deficient (*Anxa5*^{-/-}) mice, the sizes of bone ridge outgrowths at the entheses of tibiae and femur were increased after 7 weeks of age, although there were no obvious differences in the general morphology of long bones. Bone ridge overgrowth at entheses was also observed in muscle attachment sites of the mandibular bone in *Anxa5*^{-/-} mice. This bone overgrowth was not observed at the fibrous enthesis where the fibrocartilage layer does not exist. To examine the effects of mechanical forces, we performed tenotomy in which transmission of contractile forces by the tibial muscle was impaired and hindlimb unloading by tail suspension in mice. In tenotomized mice, bone overgrowth at the entheses in *Anxa5*^{-/-} mice was decreased to a level comparable to that in WT mice at 8 weeks after the operation. Furthermore, the tail-suspended mice showed a decrease in bone overgrowth to similar levels in *Anxa5*^{-/-} and WT mice at 8 weeks after hindlimb unloading, suggesting that bone overgrowth at the enthesis requires mechanical forces. Calcein and Alizarin

Red double labeling revealed more mineralized areas at the enthesis in *Anxa5*^{-/-} mice than WT mice. In *Anxa5*^{-/-} mice, more ALP-expressing cells were observed in the fibrocartilage layer outside of the bone. We further examined effects of *Anxa5* gene knockdown (KD) in primary cultures of chondrocytes and tenocytes in vitro. *Anxa5* KD increased ALP expression in tenocytes and chondrocytes, suggesting that increased ALP activity in the fibrocartilaginous tissue in *Anxa5* KO mice is directly caused by *Anxa5* deletion in tenocytes or fibrocartilage cells. Taken together, these results suggest that *Anxa5* prevents bone overgrowth at the enthesis, whose formation is mediated through mechanical forces brought by muscle loading.

Disclosures: *Hisashi Ideno, None*

SAT-0144

Dysregulation of NF- κ B in Intestinal Epithelial Cells Induces Osteopenia in Mice Ke Ke*, Manoj Arra, Gabriel Mbalaviele, Gaurav Swarnkar, Yousef Abu-Amer. Washington University School of Medicine, United States

Skeletal abnormalities are common co-morbidities of systemic inflammatory syndromes. Patients suffering from Intestinal bowel disease (IBD), including colitis and Crohn's disease, present with skeletal complications. The transcription factor NF- κ B has been implicated in the pathogenesis of numerous inflammatory diseases and elevated NF- κ B activity contributes to these pathologies. However, the mechanism underpinning intestinal inflammation associated bone loss remains vague. Intestinal inflammation generates an inflammatory milieu that leads to dysregulation of mucosal immunity through gut-residing, macrophages, innate lymphoid cells (ILCs) and other cells. ILCs are recently identified mucosal cells considered as the gatekeeper of gut immunity. In our current study we propose that under intestinal inflammation ILCs and other immune cells play a critical role in mediating IBD-induced bone loss. To generate intestinal inflammation we genetically expressed constitutively active IKK2 (IKK2ca) in intestinal epithelial cells (IECs) which represents a sterile non-erosive gut inflammation (IKK2caIEC mice). In addition, we used the well-established dextran sulphate sodium induced IBD (DSS-IBD) model for comparison. Histological staining of intestine sections showed mild intestinal inflammation in IKK2caIEC mice. Both experimental models lost approximately a third of their body weight. Micro-CT analysis showed significant bone loss in both models of IBD. Further Trichrome and TRAP staining in bone sections showed reduced mineralized compartments and increased OC in both models when compared with respective controls. Serum ELISA showed increases expression of inflammatory cytokines like TNF α , IL1 β , IL6, IP10 etc along with increased expression of G-CSF, DKK1 and RANKL which can influence HSC niches and negatively impact osteoblasts. Moreover, ex-vivo cellular analysis in DSS-IBD model showed expansion of whole bone marrow myeloid cell lineage and alteration of intestinal innate lymphoid cell (ILCs) groups. Our finding buttresses the pathogenic role of NF- κ B as the principal player that links gut inflammation with systemic bone loss. Thus, deciphering the cellular and molecular steps contributing to gut-inflammation-induced osteopenia will offer a valuable tool to treat this co-morbidity.

Disclosures: *Ke Ke, None*

SAT-0145

Factors Secreted From MLO-Y4 Osteocyte-Like Cells under Inflammatory Conditions Inhibit C2C12 Myoblast Differentiation Dorit Naot*, Maureen Watson, Ally Choi, David Musson, Jillian Cornish. Department of Medicine, University of Auckland, New Zealand

The presence of healthy muscle adjacent to fracture sites accelerates healing. It has been suggested that muscle supports bone healing through secretion of myokines and by providing a source of stem cells that differentiate into osteoblasts. We developed a co-culture system that allows communication between bone and muscle cells through secreted factors. The aim of the current study was to investigate the effects of factors secreted from osteocyte-like cells on muscle cell differentiation under inflammatory conditions that model early stages of fracture healing. MLO-Y4 osteocyte-like cells were cultured in 6-well plates and C2C12 myoblasts were seeded on inserts (ThinCert™). Inserts were then suspended over the MLO-Y4 cultures and interleukin (IL)-1 β was added at 10ng/mL. Four days later, C2C12 cells were fixed and stained with fluorescently-labeled myosin antibody and DAPI, and fusion index determined. Gene expression was analyzed in RNA from cells collected after 48 hours of co-culture, using real-time PCR with TaqMan® assays. The results present values pooled from three independent biological repeats. The differentiation into myotubes was similar in C2C12 cells cultured alone, treated with IL1 β , or co-cultured with MLO-Y4 cells without IL1 β (fusion index, mean \pm SEM: 27.9 \pm 2.7, 20.41 \pm 2.9 and 30.6 \pm 4.1, respectively). However, in the presence of MLO-Y4 and IL1 β the fusion index was significantly lower; 9.35 \pm 2.7, (P=0.02 in comparison to media alone, one-way ANOVA with Bonferroni's post-hoc). Comparison of gene expression in C2C12 cells treated with IL1 β and cultured alone or in co-culture with MLO-Y4, found lower expression of muscle differentiation markers in co-cultured cells: myogenin (Myog) was 2.4-fold lower and the myosin heavy polypeptides Myh1 and Myh8 were each 8.7-fold lower. In order to determine the specificity of the effect to the cytokine inducing the inflammatory environment, we repeated the experiments replacing IL1 β with TNF α (40ng/mL). We found that the expression of differentiation markers was similarly inhibited; the expression of Myog, Myh1 and Myh8 were 13.7, 9.3 and 10.9-fold lower, respectively, in co-culture. We conclude that under inflammatory conditions, MLO-Y4 cells secrete factors that inhibit the differentiation of C2C12 myoblasts into

myotubes. This inhibition may represent a stage in the process of recruitment of muscle progenitor cells that could potentially differentiate into osteoblasts and contribute to bone repair.

Disclosures: *Dorit Naot, None*

SAT-0146

Region-specific differences in geometric parameters of cortical fibula structure and peroneal muscle forces in football players. Sergio Luscher*¹, Laura Marcela Nociolino^{1,2}, Nicolas Pilot³, Leonardo Pissani³, Gustavo Roberto Cointin¹, Maria Rosa Ulla⁴, Joern Rittweger⁵, Alex Ireland⁶, Jose Luis Ferretti¹, Ricardo Francisco Capozza¹. ¹Center for P-Ca Metabolism Studies (CEMFoC), Natl Univ of Rosario, Argentina, ²Musculoskeletal Biomechanical Studies Unit (UDEBOM), University Institute Gran Rosario (UGR), Argentina, ³Musculoskeletal Biomechanical Studies Unit (UDEBOM), University Institute Gran Rosario (UGR), Argentina, ⁴CEOM- Centro de endocrinología Osteología y Metabolismo de Córdoba, Argentina, ⁵Institute of Aerospace Medicine, German Aerospace Center (DLR); Department of Pediatrics and Adolescent Medicine, University of Cologne, Germany, ⁶School of Healthcare Science, Manchester Metropolitan University, United Kingdom

Structural differences have been described along the cortical human fibula, suggesting distinct, site-specific adaptations to its mechanical environment. The fibula shaft appears insensitive to disuse, whilst the fibula's response to exercise has been little studied. In this study, the cross-sectional moments of inertia concerning lateral and A-P bending (yMI, xMI) and torsion (pMI) and the cross-sectional area and vBMD of cortical bone (CtA, CtD) were pQCT-assessed in 18 serial scans of the fibula taken at every 5% of the 10-90% segment of tibia length, and the maximal strengths of the one-leg jump and the external rotation of the foot were dynamometrically assessed in the dominant (kicking) leg of 19 healthy male footballers (FB) who were trained for 4-8 years and of 15 untrained controls, aged 18-30 years. All MI's were adjusted to CtA to assess the efficiency of distribution of the available cortical tissue to resist each type of deformation. All MI's were consistently larger in FB than in controls throughout the bone (p<0.001), in the order yMI>pMI>xMI. All CtA-adjusted MI's correlated with the strength of the external rotation of the foot (not the one-leg jump) in all subjects, with highest values of both variables for FB, most significantly for the yMI (p<0.001), and with increasing adjustment (r values) toward the middle of the distal region. Correlations between the MI's (y) and CtD (x) ('distribution/quality', d/q curves, indicators of the efficiency of distribution of cortical tissue as a function of its stiffness) calculated for every site scanned were significant for all subjects (p<0.05 to p<0.01) only distally for the yMI and pMI, and nonsignificant for the xMI. Results suggest that FB training would significantly improve fibular resistance to lateral bending, torsion, and A-P bending in that decreasing order, in association with the strength of the lateral peroneal (not soleus/gastrocnemius) muscles only within their anatomic insertion area. The d/q curves suggest that all the above structural improvements (presumably resulting from the controlling work of bone mechanostat) would have been induced beyond the natural influence of cortical tissue stiffness on the easiness of stimulation of the system. This interpretation is in congruence with the observed influence of the strength of muscles which externally rotate or evert the foot on fibula robustness in hominid and predator species for which those movements have high selective connotations.

Disclosures: *Sergio Luscher, None*

SAT-0169

See Friday Plenary Number FRI-0169

SAT-0170

See Friday Plenary Number FRI-0170

SAT-0171

See Friday Plenary Number FRI-0171

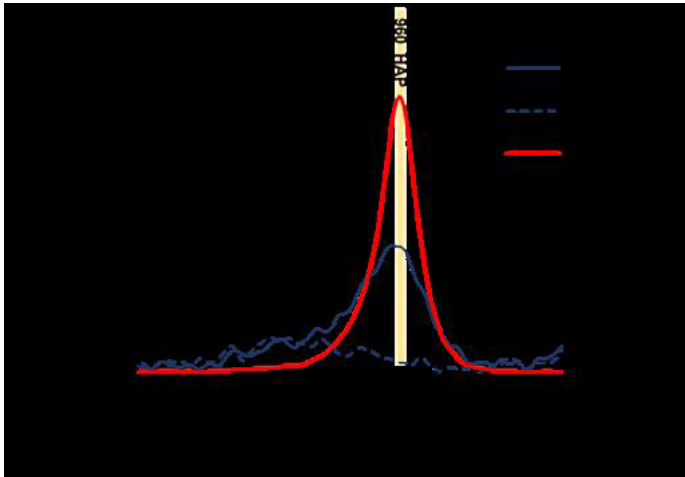
SAT-0172

See Friday Plenary Number FRI-0172

SAT-0173

Osteocalcin and osteopontin mediate osteogenic differentiation of mesenchymal stem/stromal cells by controlling the maturation level of mineral species Marta Carvalho^{*1}, Joaquim Cabral², Cláudia Lobato Da Silva², Deepak Vashishth¹. ¹Center for Biotechnology and Interdisciplinary Studies, Department of Biomedical Engineering, Rensselaer Polytechnic Institute, United States, ²Department of Bioengineering and iBB - Institute of Bioengineering and Biosciences, Instituto Superior Técnico, Universidade de Lisboa, Portugal

Non-collagenous proteins in the bone extracellular matrix, such as osteocalcin (OC) and osteopontin (OPN) are known to control different aspects of mineralization, however their roles in mesenchymal stem/stromal cells (MSC) differentiation are still unknown. The aim of this study was to investigate the roles of OC and OPN in mineral species production during osteogenesis induced by differentiating MSC into osteoblasts. MSC were derived from tibia and femur of bone marrow of 6- to 8- week-old OC^{-/-}OPN^{-/-} mice and Wild-type (WT) control mice. We found that proliferation of OC^{-/-}OPN^{-/-} MSC was affected and their capacity to differentiate into osteoblasts was decreased, although OC^{-/-}OPN^{-/-} MSC were able to differentiate into adipogenic and chondrogenic lineages. After 21 days of osteogenic differentiation, calcium deposition and ALP activity levels of OC^{-/-}OPN^{-/-} MSC demonstrated a significant reduction compared with WT MSC. Using spectroscopic analysis, we found that the maturation of mineral species was affected by the suppression of OC and OPN levels. The mineral species maturation from OC^{-/-}OPN^{-/-} MSC was delayed compared with the control group. After 21 days of osteogenic differentiation, WT MSC presented the peak of hydroxyapatite (HAP) at 960 cm⁻¹, however such a peak was not observed for OC^{-/-}OPN^{-/-} MSC. These results confirm that, at a cellular level, OC and OPN are important regulators of bone mineralization and provide new insights into forming high quality bone, relevant for treatment of fracture healing in older and osteoporotic bone.



Disclosures: *Marta Carvalho, None*

SAT-0174

Osterix-cre expression by itself enhances adipogenic differentiation of stromal cells and affects hematopoiesis Katrin Huck^{*1}, Carla Sens-Albert², Inaam Nakchbandi¹. ¹Max-Planck Institute for Medical Research, Germany, ²University of Heidelberg, Germany

Osterix is a transcription factor in early osteoblast differentiation. It has been used to drive cre recombinase expression and delete floxed genes in cells of the osteoblastic lineage. Its expression in wildtype mice however led to skeletal defects including delayed calvarial calcification and craniofacial deformities. Therefore, the appropriate controls for genetic deletion using osterix cre are not those normally used (homozygous floxed genes in the absence of the promoter (+/+_{fl/fl})). Instead, mice expressing osterix-cre should be used (osx-cre/+_{+/+}). Several published reports deleting various genes using osterix-cre implicated these genes in early adipocyte differentiation and fat metabolism. We evaluated both osteogenic and adipogenic differentiation in vitro of newborn calvarial osteoblasts from mice only carrying osterix-cre and compared these to wildtype littermate controls. Nodule formation was diminished (30% of CT), as was osteocalcin mRNA expression (10% of CT) while the number of preadipocytes was increased (250% of CT). In line with this, PPAR γ mRNA expression was increased (200%), as were other markers of adipocytic differentiation. BMD diminished by 18%, but no differences in dynamic or static bone histomorphometry parameters. Instead there was a 400% increase in the number of adipocytes on bone sections. Osmium tetroxide density was also increased (115% of CT) in the presence of osterix-cre (all results significant at p<0.05 or lower). Because several groups also proposed that bone marrow adipocytes represent part of the hematopoietic stem cell niche we evaluated hematopoiesis in the presence of osterix-cre. While peripheral blood values were normal, both the absolute number and the percentage of hematopoietic stem and progenitor cells were diminished (70% of CT), but administration of doxycycline to silence osterix and hence cre expression

normalized these values. Similarly, the common lymphoid progenitors were diminished, but these recovered after suppression of osterix-cre using doxycycline. In contrast, a decrease in mesenchymal stromal cells did not recover despite doxycycline administration. In summary, the expression of cre-recombinase under the control of osterix should not be used to evaluate mesenchymal stromal cell differentiation to either osteoblasts or to adipocytes. Furthermore, any findings using this promoter in evaluating hematopoiesis might be misleading unless a control containing osterix-cre is included.

Disclosures: *Katrin Huck, None*

SAT-0187

See Friday Plenary Number FRI-0187

SAT-0188

See Friday Plenary Number FRI-0188

SAT-0189

See Friday Plenary Number FRI-0189

SAT-0190

See Friday Plenary Number FRI-0190

SAT-0191

See Friday Plenary Number FRI-0191

SAT-0192

See Friday Plenary Number FRI-0192

SAT-0193

See Friday Plenary Number FRI-0193

SAT-0194

Epigenetic targeting of the myeloma-bone microenvironment in 3D Juraj Adamik^{*1}, Yerneni S Saigopalakrishna², Sree H Pulugulla³, Quanhong Sun¹, Philip E Auron³, Phil G Campbell⁴, Deborah L Galson⁵. ¹Department of Medicine, Hematology/Oncology, UPMC Hillman Cancer Center, University of Pittsburgh, United States, ²Department of Biomedical Engineering, Carnegie Mellon University, United States, ³Department of Biological Sciences, Duquesne University, United States, ⁴Department of Biomedical Engineering, Engineering Research Accelerator, Carnegie Mellon University, United States, ⁵Department of Medicine, Hematology/Oncology, UPMC Hillman Cancer Center, McGowan Institute for Regenerative Medicine, University of Pittsburgh, United States

EZH2, the methyltransferase subunit of Polycomb Repressive Complex 2 (PRC2), catalyzes H3K27me3 histone modifications and epigenetically regulates genes involved in cellular pluripotency and differentiation. EZH2 regulates myeloma (MM) cell survival, and its elevated expression correlates with poor prognosis in MM patients. EZH2 inhibitors including GSK126 showed promising anti-MM effects. We showed that GSK126 rescued MM-induced suppression of BM-MSC osteogenic differentiation, indicating its potential to promote bone healing. We provide evidence that GSK126 blocks MM-induced hyperactivation of osteoclast precursors (OCLp). RNA-seq profiling revealed that inhibition of EZH2 re-activated 115 genes associated with bivalent and/or H3K27me3 promoter signatures including OCL inhibitory factors MafB, Irf8, Bcl6b and Arg1. In contrast, we found that OCLp expansion in MM1.S-conditioned media (MMCM) induced significant gene expression changes, which correlated with TNF and IKK signaling, inflammatory responses and CXC-chemokine receptor pathways. We evaluated the effectiveness of GSK126 in the context of the bone microenvironment in a novel 3-dimensional (3D) model of MM co-cultures (3D-MM). We combined basement membrane extract (BME) hydrogels with devitalized bone slices to mimic the 3D setting of MM with the OCL-resorbing endosteal surface. This enabled us to test GSK126 alone or in combination with bortezomib simultaneously on MM survival and OCLp differentiation and resorption. While GSK126 exhibited potent anti-MM effects and blocked OCL differentiation, mature OCL added to 3D-MM co-cultures increased the IC50MM inhibition dose of both bortezomib and GSK126 by 40% and 50%, respectively. Their synergy on MM cells was further reduced by 70%. 3D-MM co-cultures with total bone marrows of differentially (1-12 months old) aged mice showed selective protection from GSK126, but not bortezomib, on MM viability. Furthermore, the resistance to GSK126 was age-dependent, with the 12-month-old bone marrows causing the greatest

protection of the MM cells. Using confocal microscopy, we found that the resistant MM cells were in close proximity to osteoprogenitor cells, suggesting that this interaction reduces the effectiveness of epigenetic drug targeting against MM. This novel 3D-MM system enables us to rapidly screen drug combinations, and simultaneously evaluate the influence of bone-microenvironmental interactions on MM drug resistance and BM cell responses to the drugs.

Disclosures: *Juraj Adamik, None*

SAT-0195

Metastatic Lesion Types Predict Vertebral Bone Matrix Quality and Strength Stacyann Bailey^{*1}, David Hackney², Marc Stadelmann³, Philippe Zysset³, Ron Alkalay², Deepak Vashishth¹. ¹Rensselaer Polytechnic Institute, United States, ²Beth Israel Deaconess Medical Center, United States, ³University of Bern, Switzerland

Tumor metastasis to the skeleton occurs in more than 80% of all cancer patients[1] and is associated with intractable pain, hypercalcemia, and pathological fractures[2]. Metastatic lesions disrupt normal bone turnover and appear radiologically as osteolytic (bone-destroying), osteoblastic (bone-forming), or mixed with features of both types. Metastatic cells induce oxidative stress within the bone microenvironment and can trigger the formation of molecular cross-links known as advanced glycation end-products (AGEs). AGEs have been shown to be detrimental to bone mechanical properties[3]. However, their role in metastatic bone disease and their contribution to bone fracture remains unclear. This study investigated whether AGE accumulation vary with type of metastatic lesion and whether AGEs in metastatic lesions are predictive of vertebral bone strength. Thoracic and lumbar vertebrae (n=14) were obtained from donors (age 59±7 yrs) with breast, kidney, lung, or prostate cancer. After removal of the endplates and posterior elements, each vertebra was scanned using micro-computed tomography at 24.5µm³ resolution for bone mineral density quantification (µCT100 Scanco, Switzerland). Vertebral bodies were tested in unconfined axial compression until failure and structural properties determined (MTS858 MiniBionix II). The type of lesion in each vertebra i.e. lytic, blastic, or mixed was characterized based on appearance from the µCT dataset. Trabecular bone cores demonstrating these range of lesions were then analyzed for total fluorescent AGEs [4]. Mixed model ANOVA was used to determine the relationship between lesion type and all measured parameters. A significant association with AGEs and lesion type was observed. More specifically, mixed lesions exhibited higher AGEs compared to lytic (p=0.018) and blastic (p=0.015) (Fig 1). A negative correlation between AGEs and BMD was observed for mixed (R² = 0.36, p=0.023) and blastic (R² = 0.44, p=0.0512) lesions. This association remained when the primary cancer was taken into account whereby breast (R² = 0.43, p<0.01) and prostate (R² = 0.58, p<0.01) metastases exhibited higher AGE content with low BMD. Independent of lesion type, AGE was negatively associated with vertebral strength (R² = 0.10, p=0.031). Our results indicate that metastatic bone is heterogeneously modified by AGEs and is lesion dependent. This study provides insight into the role of post-translational modification in bone metastases and may reveal new targets for predicting fracture risk.

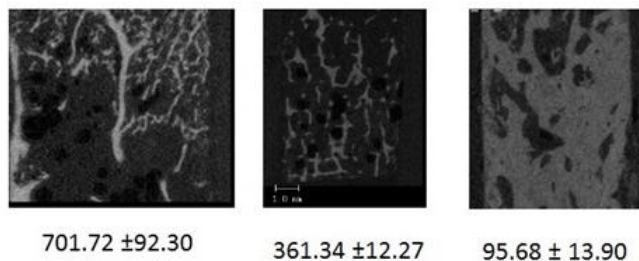


Figure 1: Images from µCT dataset characterizing (from left to right): mixed, lytic, and blastic lesions from trabecular cores of metastatic vertebra analyzed for AGEs (mean and standard deviation displayed below images).

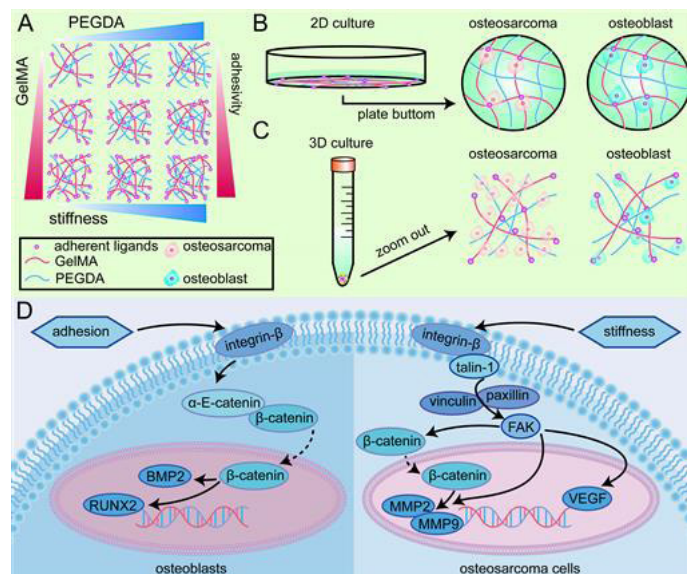
Disclosures: *Stacyann Bailey, None*

SAT-0196

Diacritic impacts of matrix stiffness and adhesion on osteosarcoma cells and osteoblasts Tongmeng Jiang^{*}, Li Zheng, Jinmin Zhao. Guangxi Engineering Center in Biomedical Materials for Tissue and Organ Regeneration & Guangxi Collaborative Innovation Center for Biomedicine, The First Affiliated Hospital of Guangxi Medical University, China

The means of extracellular matrix (ECM) affects osteosarcoma cells and their normal counterparts (osteoblasts) is still unknown. Different natural materials with distinguishable characteristics were used as vehicles for two-dimensional (2D) and three-dimensional (3D) culture. Assays showed that matrix stiffness and adhesion are two main factors influenced on osteosarcoma cells and osteoblasts. We developed hydrogels with different ECM stiffness

and adhesion properties using poly (ethylene glycol) diacrylate (PEGDA) and methacrylated gelatin (GelMA). When cultured in 3D hydrogels, osteosarcoma cells are dependent on the matrix stiffness by regulating the integrin-mediated focal adhesion (FA) pathway, whereas osteoblasts are highly sensitive to the ECM adhesion via the integrin-mediated adherens junction (AJ) pathway. However, when seeded on the 2D hydrogels, osteosarcoma cells were similar to anchorage-dependent osteoblasts and behaved anomalously and became sensitive to the ECM adhesion because they were “forced” to attach to the underlayment. This study might provide new insights into rational design of scaffolds for tumor or tissue engineering.



Disclosures: *Tongmeng Jiang, None*

SAT-0197

Identification of potential mediators of bone loss in cancer Jessica Dorschner^{*}, Jennifer Westendorf, Theodore Craig, Xuwei Wang, Rajiv Kumar. Mayo Clinic, United States

Abstract: Bone loss occurs frequently in patients with breast, prostate, and lung cancer, and plasma cell dyscrasias such as multiple myeloma (MM) and is associated with considerable morbidity and reduced survival. Inhibitors of the Wnt signaling pathway such as Dkk1 are thought to contribute to bone loss of bone in MM patients, but the precise mediators of bone loss in other tumors has not been well defined. We sought to identify potential mediators of bone loss elaborated by Lewis lung cancer 1 cells (LLC1), a model of non-small cell lung cancer. Mice inoculated with LLC1 cells lost bone mass within three weeks of tumor cell injection as assessed by dual-energy x-ray absorptiometry and compared to vehicle injected mice. Micro-computed tomography of bone showed a reduction in bone trabecular volume, number and connectivity but no change in cortical bone thickness in mice injected with tumor cells. To identify modulators of bone density secreted by tumor cells, we performed whole transcriptome sequencing of LLC1 cell mRNAs and compared the information obtained from these cells with that obtained from non-tumorigenic distal respiratory epithelial cells (MLE12 cells). We identified several factors in the secretome of LLC1 cells that could alter bone formation and resorption. These factors include hedgehog interacting protein, Wnt modulators such as Dkk2, various interleukins, chemokines, and growth, differentiation factor 15 and PTH-like protein (Table 1) whose expression was significantly increased. We conclude that the “secretome” of non-small cell lung cancer cell line LLC1 encodes proteins that mediate bone remodeling. The mouse model of tumor-induced bone loss developed by us will allow the systematic examination of the role of these factors in vivo.

Table 1. Differentially Expressed mRNAs Encoding Secreted Proteins in LLC1 Compared to MLE12 Cell Is Determined by RNA-seq.

Top 10 mRNAs encoding secreted proteins whose expression is significantly increased in LLC1 cells		
Gene Name	Fold Change	FDR
Adm, adrenomedullin	989	0
Hhsp, hedgehog interacting protein	896	1.2E-214
Il27, interleukin 27	873	1.3E-64
Ngf, nerve growth factor	666	1.3E-312
Olfm1, olfactomedin	639	0
Dkk2, Dickkopf Wnt inhibitor	627	0
Col3a1, Coll Type III α 1 Chain	570	0
Fgf10, Fibroblast Growth Factor 10	502	9.4E-253
Adam3, A Disintegrin and metalloproteinase domain 3a	469	4.8E-43
Mmp3, Matrix metalloproteinase 3	450	0
Other significantly up-regulated mRNAs		
CCl2, C-C Motif Chemokine Ligand 2	61.4	0
CCl28, C-C Motif Chemokine Lig 28	138.1	2.2E-154
CCl7, C-C Motif Chemokine Lig 7	59.3	9.1E-74
Gdf15, Growth and differentiation factor 15	4.99	1.1E-30
Il11, interleukin 11	40.2	0
Il27, interleukin 27	873.1	1.3E-64
Il34, interleukin 34	119.4	7.2E-305
Pthn, PTH-like protein	32.9	1.0E-86

Disclosures: *Jessica Dorschner, None*

SAT-0198

An Incomplete Atypical Femoral Fracture Associated with Bisphosphonate Therapy and Femoral Skeletal Metastasis Pamela Taxel, Md*, Adam Lindsay, Md. UConn Health, United States

Introduction: Atypical femoral fractures (AFFs) have been associated with long-term bisphosphonate (BP) use in patients with osteoporosis. BPs are also used in the prevention of skeletal-related events (SREs) in patients with skeletal metastases and cancer. Oncology trials have reported few AFFs with limited detail, and most fractures are classified as pathologic. We report the case of a patient treated for metastatic breast cancer with an incomplete AFF in an established area of skeletal metastasis. **Case:** A 58-year-old woman was referred for opinion about anti-resorptive therapy in the setting of skeletal metastases. She was diagnosed with breast cancer 8 years ago, and received neoadjuvant chemotherapy, lumpectomy, radiation therapy and treatment with anti-estrogen therapy for 5 years. She had no history of fractures or metabolic bone disease and received adequate calcium and Vitamin D. Shortly after completing anti-estrogen treatment she was diagnosed with metastases to bone (L1, right femur) and liver. She subsequently received IV zoledronic acid, 4 mg monthly, for a year and then every 3 months, for a total of 14 doses. She did well for a year, but then developed right hip pain, and imaging confirmed multiple new areas of skeletal involvement, but low concern for impending fracture of the right femur. A month later her right hip pain progressed and she was unable to bear weight. Repeat radiographs show a nondisplaced right subtrochanteric femoral fracture with cortical thickening, consistent with an incomplete AFF. She underwent prophylactic nailing and specimens from the area confirmed rare atypical cells consistent with breast cancer. BP therapy was discontinued. Within 6 months she developed left hip pain and inability to bear weight. Xray revealed metastatic lesion of the proximal femur with erosion into the soft tissue; therefore, prophylactic nailing of left femur was performed. **Discussion:** We report an incomplete AFF in an area of established skeletal metastasis. It is important to recognize that bone pain in an area of known metastasis may be due to an impending AFF versus a pathologic one. BPs concentrate in areas of high bone resorption such as skeletal metastases, and may increase risk of AFF. Prophylactic stabilization of the femur is recommended if the patient is experiencing functional pain with incomplete AFF; however, radiation would be the initial approach if underlying malignancy was the etiology of pain and dysfunction.

Disclosures: *Pamela Taxel, Md, None*

SAT-0199

Roles of membrane bound HB-EGF and EGF-Receptor interaction on osteoblast in melanoma induced bone resorption Kenta Watanabe*, Shosei Yoshinouchi, Keita Taniguchi, Michiko Hirata, Tsukasa Tominari, Chisato Miyaura, Masaki Inada. Tokyo University of Agriculture and Technology, Japan

Prostaglandin E2 (PGE2) is associated with inflammatory bone destruction in various infectious immune responses. We have reported that the bone metastasis of malignant melanoma induced PGE2 that caused by direct interaction with melanoma and host osteoblast. Although bone metastasis of malignant melanoma is accompanied with severe bone destruction increased by bone resorption, the triggered target molecule in melanoma that induced PGE2 production in osteoblast is still not known. We have been searching the key molecules that involved cell to cell interaction between melanoma and host osteoblast. Recently, we found several candidates of these target molecules for cellular interaction that mainly found in membrane bound proteins, and some of the molecules were screened by the criteria of PGE2 production capability in osteoblast. In this study, we examined the malignant melanoma (B16) induced bone destruction focusing on heparin-binding EGF-like growth factor

(HB-EGF) which is a ligand of EGFR. The ligand HB-EGF expression was detected in both B16 and osteoblast, however, the receptor EGFR expression was only found in osteoblasts. In HB-EGF treatment, COX-2 and mPGEs-1 mRNA expression and PGE2 production were increased. Following RANKL expression was also increased that correlated the levels of PGE2 production induced by HB-EGF. Additional treatment of EGFR inhibitor clearly suppressed both PGE2 and RANKL expression that was induced by HB-EGF treatment. EGFR inhibitor also blunted EGFR and ERK phosphorylation. These data showed that cell to cell interactions between B16 and host osteoblast increased the production of PGE2 and RANKL in osteoblast, EGFR inhibitor attenuated all these of induction in osteoblast. Previous reports suggested that epidermal-mesenchymal interaction increased PGE2 production in many case of biological phenomenon. In this case, the interaction of epidermal melanoma among mesodermal osteoblast induced PGE2 production and sequentially leads to RANKL production in osteoblast that promoted following osteoclast functions. These results clearly indicated that the HB-EGF produced by melanoma activated EGFR/ERK signaling in osteoblast and increased RANKL production via PGE2 signaling. Targeting of HB-EGF/EGFR/ERK signaling is promising therapeutic candidate for the treatment of melanoma patients with bone metastasis.

Disclosures: *Kenta Watanabe, None*

SAT-0226

See Friday Plenary Number FRI-0226

SAT-0227

See Friday Plenary Number FRI-0227

SAT-0228

See Friday Plenary Number FRI-0228

SAT-0229

See Friday Plenary Number FRI-0229

SAT-0230

See Friday Plenary Number FRI-0230

SAT-0231

See Friday Plenary Number FRI-0231

SAT-0232

Runx2 Deletion in Chondrocytes Fails to Disrupt Development of TMJ David Summerford*, Haiyan Chen, Harunur Rashid, Yang Yang, Amjad Javed. University of Alabama at Birmingham, United States

The development of the orofacial structure such as palate and the temporomandibular joint (TMJ) in mammals is a highly ordered process. The TMJ is a complex structure that is essential for normal jaw function and consist of glenoid fossa of the temporal bone, the condylar head of the mandible, and a fibrocartilagenous disk. Chondrocytes and osteoblasts work in close association during the development of the TMJ. Due to unavailability of suitable mouse models, very little is known about the function of Runx2 during the development of the TMJ. To elucidate Runx2 regulatory control distinctive to chondrocyte cell population, we ablated Runx2 gene using Col2a-Cre mice. Cellular, histological and immuno-histochemical approaches were utilized to evaluate developmental progression of TMJ and orofacial bone. Runx2Ch^{-/-} mice exhibited failed endochondral ossification and die shortly after birth. The progressive differentiation of chondroprogenitors to proliferative and mature hypertrophic chondrocytes noted in long bones of wild-type mice was completely absent in the Runx2Ch^{-/-} littermates. Runx2 activity in chondrocyte also contributes to the formation of craniofacial bones derived by endochondral ossification. Unlike the wild-type littermates, the basisphenoid and occipital skull bones were absent in the Runx2Ch^{-/-} mice. Surprisingly, in spite of the loss of Runx2 in chondrocyte of Meckel cartilage, we observed normal maxilla, mandible and jaw formation, as well as odontogenesis in the Runx2Ch^{-/-} littermates. RUNX2 insufficiency in humans has been linked to the lip and/or palatal clefting. Interestingly, both the formation and fusion of palate was normal in the Runx2Ch^{-/-} littermates. However, the palate size was significantly reduced in the newborn homozygous mice. Runx2 is expressed from embryonic to adult stages of TMJ cartilage. We first confirmed, Runx2 gene deletion in developing TMJ by using both tdTomato and Rosa reporter mice. Surprisingly, development of condylar cartilage, the major component of the TMJ was unaffected in the homozygous mice. Unlike growth plate, Runx2 deficient chondrocytes in the TMJ cartilage showed progressive hypertrophic maturation, mineralization, and endochondral ossification. Together these results indicate that in chondrocytes Runx2 exerts differential

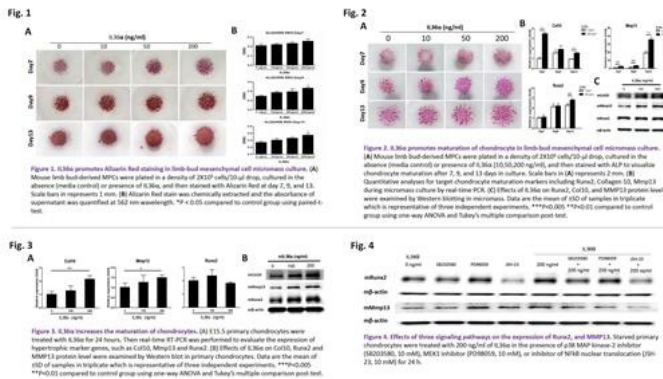
roles, where it is obligatory in hyaline cartilage of long bone but not in chondrocyte that form Meckel or TMJ cartilage.

Disclosures: *David Summerford, None*

SAT-0233

IL36 α promotes chondrocyte maturation: is this a functional role in fracture repair? Xin Jin*, Tieshi Li, Alessandra Esposito, Jie Jiang, Lai Wang, Joseph Temple, Anna Spagnoli. Rush University Medical Center, United States

Introduction: IL36 α , a proinflammatory cytokine, plays critical roles in psoriasis and osteoarthritis. However, the role of IL36 α in endochondral ossification and in fracture repair has not been evaluated. **Purpose:** To investigate the role of IL36 α in chondrocytes maturation during the endochondral ossification process and in the formation of the cartilaginous callus during fracture repair. **Methods:** 1) Fracture calluses were obtained from mice that underwent to a semi-stabilized tibia fracture and subjected to qRT-PCR and IHC analyses for IL36 α , IL36 receptor (IL36R) and IL36 receptor antagonist (IL36Ra). 2) Isolated mesenchymal limb-bud cells obtained from E11.5 mouse embryos, were cultured in micromasses and treated with IL36 α respectively for 7, 9 and 13 days, followed by Alizarin Red (AR) and Alkaline Phosphatase (AP) staining; mRNA and total protein were subjected to qRT-PCR and WB analyses. 3) Primary chondrocytes, isolated from the humerus, radius and ulna of E15.5 embryos were treated with IL36 α and respectively with inhibitors of p38 MAP kinase (SB203580), MEK1 (PD98059) and NF κ B (JSH-23) that are downstream signaling pathways of IL36 α . **Results:** mRNA expression levels of IL36 α , IL36R and IL36Ra increased in the first few days after fracture compared with D0 (tissue collected few minutes after the fracture). IL36 α and IL36R peaked at Day5 after fracture, IL36Ra peaked at Day3. IL36 α , IL36R and IL36Ra gradually reached a nadir at Day21. IHC analyses showed that at Day0, IL36 α , IL36R and IL36Ra were mainly detected in the periosteum. At Day1, Day3 and Day5, IL36 α , IL36R and IL36Ra expressing cells localized within multiple regions including hematoma, periosteal and endosteal sites. At Day7 and Day10, IL36 α , IL36R and IL36Ra were expressed in the cartilaginous callus by pre-hypertrophic and hypertrophic chondrocytes. In micromass cultures, IL36 α increased AR staining, AP staining and expression of Runx2, Collagen 10 and Mmp13. Similarly, in primary chondrocytes, IL36 α induced Runx2, Collagen 10 and Mmp13 expressions. JSH-23 significantly attenuated IL36 α stimulated Mmp13 and Runx2 expressions, suggesting that IL36 α signaling promotes chondrocyte maturation via NF κ B-Runx2-Mmp13. SB203580 and PD98059 had no effects. **Conclusions:** In the endochondral ossification process, IL36 α promotes chondrocytes hypertrophy. During fracture repair, IL36 α , IL36R and IL36Ra are temporally-regulated and expressed by hypertrophic chondrocytes. Findings are supportive for a role of IL36 α and its signaling in skeletogenesis and in fracture repair likely by regulating hypertrophy.



Disclosures: *Xin Jin, None*

SAT-0234

Role of the A2B Adenosine Receptor in Inflammatory Degradation of Cartilage Meghan Kupratis*, Lauren Mangano Drenkard, Louis Gerstenfeld, Elise Morgan. Boston University, United States

Introduction: Adenosine receptors mediate multiple pathways that lead to joint destruction in rheumatoid arthritis and are involved in inflammation through cytokine activity. The goal of this study was to assess the relationship of the A2B adenosine receptor (A2BAR) to cartilage degeneration in collagen antibody-induced arthritis (CAIA). **Methods:** A2BAR knockout (KO) mice (n=16) were bred on a C57BL/6J background, along with wild type (WT) C57BL/6J mice (n=12). At four months of age, mice were injected with collagen antibody (ArthritoMab, MDBiosciences) and lipopolysaccharide (Sigma-Aldrich) (CAIA) or saline (control). Proximal tibiae underwent contrast-enhanced microCT (CECT) with the contrast agent CA4+ to image cartilage. Quantitative real-time PCR was run in triplicate for primers for lubricin and aggrecan; expression was normalized to Rn18s. Molecular assessments of A2BAR function were carried out in ATDC5 chondrogenic cells seeded at 4.10x10⁵ cells/well and cultured for two days in DMEM with 5% fetal bovine serum (FBS) and 1% penicillin/streptomycin (P/S), followed by 21 days in α -MEM with 5% FBS,

1% P/S, and 0.5% insulin transferrin selenium. Six treatment groups were established: no A2BAR ligands \pm tumor necrosis factor (TNF; 10 ng/mL, BD Biosciences); NECA (A2BAR agonist; Tocris Bioscience) \pm TNF; and PSB-1115 (PSB; A2BAR antagonist; Tocris) \pm TNF. Cell viability was determined using a live/dead assay (Molecular Probes) and DAPI stain (Molecular Probes). **Results:** CECT attenuation (a measure of glycosaminoglycan content) in tibial cartilage decreased with CAIA at days 8 (p<0.05) and 10 (p<0.0001) in both KO and WT mice; however, there were no changes in cartilage thickness (p=0.44). Lubricin and aggrecan expression decreased four- to eight-fold with CAIA in both genotypes. The A2BAR agonist (NECA) and antagonist (PSB) had mild negative effects on chondrocyte viability; however, only the agonist combined with TNF reduced cell viability beyond the effects of TNF alone (p<0.001). **Discussion:** While loss of A2BAR in vivo leads to systemic elevation of TNF, it did not synergize the negative effects of CAIA on cartilage loss or chondrocyte function. Interestingly, activation of A2BAR in vitro increased TNF-mediated cell death while the antagonist had no effects. Taken together, these results suggest that A2BAR locally enhances actions of TNF, while systemically acting to inhibit TNF expression.

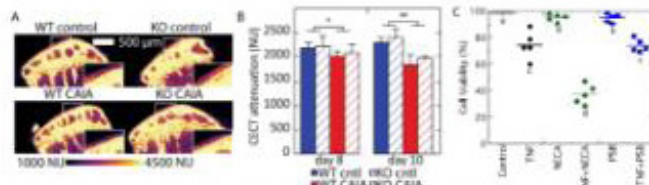


Figure 1: A) Sagittal CECT sections of the proximal tibia ("NU" = native attenuation units); B) CECT attenuation of tibia articular cartilage (*p<0.05, ** p<0.0001 CAIA vs. control); C) cell viability (live cells as a percentage of total cells) in the in vitro experiments. Non-matching letters indicate differences among groups (p<0.001).

Disclosures: *Meghan Kupratis, None*

SAT-0235

WITHDRAWN

SAT-0255

See Friday Plenary Number FRI-0255

SAT-0256

See Friday Plenary Number FRI-0256

SAT-0257

See Friday Plenary Number FRI-0257

SAT-0258

See Friday Plenary Number FRI-0258

SAT-0259

See Friday Plenary Number FRI-0259

SAT-0260

See Friday Plenary Number FRI-0260

SAT-0261

See Friday Plenary Number FRI-0261

SAT-0262

See Friday Plenary Number FRI-0262

Saturday Posters

SAT-0263

Osteocalcin Null Mice Differ From Wildtype by Sex and Genotype in Response to Prolonged High Fat Diet Patricia Buckendahl*, Saad Ahmad, Nicholas Bello, Sue Shapses. Rutgers University, United States

Osteocalcin (OC), a bone-associated gamma-carboxyglutamic acid (Gla)-containing, vitamin K dependent protein, stimulates insulin and adiponectin synthesis in mice. Gla conveys calcium-binding capability to OC and numerous other proteins. Early reports indicated that OC null mutants (KO) were obese, hyperglycemic, and insulin resistant but did not specify gender or background strain. We studied WT and KO on the C57Bl/6 background under a variety of treatments, and had not observed genotypic differences in body mass or hyperglycemia. To investigate this discrepancy, we studied male and female WT and KO mice, bred at Rutgers under approved institutional care protocols as progeny of their respective homozygous parents, thus KO had no fetal or neonatal exposure to OC. All mice were previously provided normal Lab Diet chow. We performed oral glucose tolerance tests (OGTT) in 8 month-old male (5 WT, 10 KO) and female (7 WT, 8 KO) mice. We then provided high fat diet (HFD, Research Diets) for 14 weeks and monitored weight gain. We performed another OGTT after 10 weeks on HFD. Two days before termination, we quantified body fat mass by Echo MRI. At the end of the experiment, we collected blood and placed hind limb bones into 70% EtOH for later analysis. Results: Initial body weights did not differ by genotype. OGTT did not differ significantly by genotype in males, but did differ in females (area under the curve greater in KO than WT, $p < 0.05$). Both male and female mice gained significant body mass (53% and 51% of initial body mass respectively). Relative to initial body mass, KO males gained 3% more fat mass than WT males ($p < 0.05$), but this difference was not observed in females. WT females gained 25% more fat mass than WT males ($p < 0.05$). OGTT performed after prolonged HFD indicated no genotypic difference between males; however in females, KO had an impaired tolerance compared with WT ($p < 0.05$). Analysis of femoral bone microstructure by microCT (SkyScan 1172) indicated no significant differences between male WT and KO in either trabecular or cortical parameters. Likewise, female cortical parameters did not differ by genotype; however, trabecular analysis did indicate adverse effects of diet. KO females had lower BV/TV and BS/TV than WT ($p < 0.01$), no differences in TbTh, but higher TbSp and TbN ($p < 0.01$). We conclude that HFD effects on weight gain, glucose tolerance and femoral morphology in aged osteocalcin KO mice are diet, gender and genotype specific.

Disclosures: **Patricia Buckendahl, None**

SAT-0264

Change In Body Composition And Mass In Relation To The Final Menstrual Period (FMP): Study Of Women's Health Across The Nation (SWAN) Gail Greendale*, Weijuan Han¹, Meihua Huang¹, Barbara Sternfeld², Kristine Ruppert³, Carrie Karvonen-Gutierrez⁴, Arun Karamangla¹. ¹Division of Geriatrics, David Geffen School of Medicine at UCLA, United States, ²Division of Geriatrics, Emeritus, United States, ³Epidemiology Data Center, University of Pittsburgh, United States, ⁴School of Public Health, University of Michigan, United States

Purpose: Changes in body composition and mass in mid-life women are often attributed to aging rather than to the menopause transition (MT). Small sample sizes and few women transitioning from pre-to-postmenopause in prior studies raise the possibility that an apparent absence of an MT-effect results from type-II error. We examined rates of change in body composition and weight during 8 y before and 10.5 y after the FMP, to detect and quantify any acceleration or deceleration in changes in these characteristics during this time. Methods: We measured weight, height, and body composition by DXA in women initially aged 42-52 y and pre- or early perimenopausal. We used loess plots to estimate the functional form of each outcome's trajectory in relation to # of years before or after the FMP. We used multivariable mixed effects regression to fit piecewise linear models to repeated measures of baseline-normalized values of each outcome as a function of time before or after FMP, using linear splines. Covariates were age at FMP, race, study site and time-varying hormone therapy (HT) use. Results: 356 Black, 153 Chinese, 178 Japanese and 559 White women had mean baseline age 46.7 y and age at FMP 52.2 y. Mean # of DXA's per woman was 11 (max 14). Optimum knot locations were 2 y prior to and 1.5 y after FMP for body composition and 1 y prior to and 3 y after FMP for weight and BMI. Gain in total fat mass and the proportion fat (fat mass/total mass) were evident during pre-transmenopause along with a decline in the proportion lean (lean mass/total mass). In each case, onset of transmenopause (interval bracketing FMP, defined by the change knots) saw a 2-3 fold doubling of the rate of change. Body composition parameters stabilized (slopes did not differ from 0) in postmenopause. During pre-transmenopause, weight and BMI increased; however, slopes did not change at transmenopause. In postmenopause, weight stabilized and the rate of increase in BMI slowed. Conclusion: The MT exerts unfavorable effects on fat and lean mass, characterized by accelerated, adverse changes in these parameters. These metabolic alterations are not reflected in weight and BMI, which continue on the same linear, increasing trajectory as that observed in pre-transmenopause. In postmenopause, changes in body composition and weight cease. Supported by NIH/DHHS Grants U01NR004061, U01AG012505, U01AG012535, U01AG012531, U01AG012539, U01AG012546, U01AG012553, U01AG012554, U01AG012495, R21DK107211

Average annual rates of change of body composition and weight in relation to the date of the final menstrual period (FMP) Study of Women's Health Across the Nation (SWAN) ^{a,b,c,d,e}			
	Body weight or composition slopes (% per year) during each interval before and after the FMP (95% CI)		
	Pre-Transmenopause 8 to 2 y before FMP	Transmenopause 2 y before to 1.5 y after FMP	Postmenopause 1.5 to 10.5 y after FMP
Total fat (kg)	0.95% (<.0001)	1.70% (<.0001)	0.05% (0.60)
Total lean (kg)	-0.16% (0.0002)	-0.15% (0.0073)	-0.05% (0.13)
Proportion fat	0.41% (<.0001)	1.03% (<.0001)	0.04% (0.37)
Proportion lean	-0.19% (<.0001)	-0.54% (<.0001)	0.01% (0.68)
	Body weight or composition slopes (% per year) during each interval before and after the FMP (95% CI)		
	Pre-Transmenopause 8 to 1 y before FMP	Transmenopause 1 y before to 3 y after FMP	Postmenopause 3 to 10.5 y after FMP
Weight (kg)	0.46% (<.0001)	0.34% (<.0001)	-0.03% (0.58)
BMI (kg/m ²)	0.49% (<.0001)	0.43% (<.0001)	0.11% (0.04)

^aValues in table are model-predicted slopes for the average participant, (with age at FMP, clinical site, race and HT use set at sample mean) and are presented as the percentage of baseline level that is gained per year.
^bKnots vary between body composition and anthropometric outcomes; intervals of time around the FMP which define the transmenopause are, therefore, different.
^cProportion fat = fat mass/subtotal mass; proportion lean = lean mass/subtotal mass
^dSlopes in each interval that are statistically significantly different from 0 are shown in **bold italic typeface**.
^eFor each model, slopes in each interval are statistically significantly different from each other, except for the pre-transmenopause vs. transmenopause comparison in the instances of weight and BMI.

Disclosures: **Gail Greendale, None**

SAT-0265

Hyperandrogenism is not associated with low bone mineral density in exercising women with menstrual disturbances Kristen Koltun*, Emily Southmayd, Nancy Williams, Mary Jane De Souza. Pennsylvania State University, United States

Exercise associated menstrual disturbances (EAMD) are associated with suboptimal bone health. A subset of women with EAMD also present with hyperandrogenism (HA), which may mitigate the risk for low bone mineral density (BMD). Our purpose was to determine if there were differences in BMD among exercising women with EAMD and concurrent HA (EAMD+HA, n=31), exercising women with EAMD without HA (EAMD, n=66), and exercising ovulatory controls (OV, n=45). Exercising women were recruited and menstrual status was assessed by self-reported history of menses and confirmed with daily urinary measures of estrogen and progesterone metabolites. Total testosterone (TT) and sex hormone binding globulin (SHBG) were measured in serum and used to calculate free androgen index (FAI) (FAI=TT/SHBG*100). HA was defined as FAI>2.92, representing the upper bound of the 95% confidence interval for all subjects. BMD (total body, L1-L4, femoral neck, total hip) and percent body fat (%BF) were assessed via DXA. One-way ANOVA was used to compare body composition and BMD among the groups with a Tukey post-hoc, as necessary. Subjects were 22.3±0.3 yrs old, 165.6±0.5 cm tall, had a body mass of 57.4±0.6 kg, a BMI of 21.1±0.2 kg/m², and had 25.3±0.4 %BF. Groups were similar with respect to weight, but BMI (p=0.007) and %BF (p=0.019) were elevated in EAMD+HA (21.9±0.4 kg/m²; 27.0±1.0%) compared to EAMD (20.5±0.3 kg/m²; 24.1±0.6%). Groups were similar with respect to BMD for the total body (p=0.068; 1.12±0.01 g/cm²), femoral neck (p=0.404; 1.05±0.01 g/cm²), and total hip (p=0.107; 1.05±0.01 g/cm²). There was a significant main effect for group at the lumbar spine (p=0.001). Post-hoc analyses identified that L1-L4 BMD was significantly lower in EAMD (1.09±0.02 g/cm²) compared to OV (1.19±0.02 g/cm²) (p<0.001), however, L1-L4 BMD was not different in the EAMD+HA group (1.13±0.02 g/cm²) compared to either the EAMD or OV groups (p>0.05). Women with EAMD in the absence of HA presented with a significantly lower BMD at the lumbar spine compared to ovulatory controls. This difference was not apparent in women with EAMD and evidence of HA. This cross sectional study suggests that EAMD combined with HA is not associated with the commonly observed reduction in BMD reported in women with EAMD. It is possible that HA may be protective of BMD in the face of EAMD, likely because of the higher exposure to androgens, but additional prospective studies are required.

Disclosures: **Kristen Koltun, None**

SAT-0266

Thermonutral housing exacerbates bone loss from atypical antipsychotic drugs Roni Kunst*, Megan Rue², Katherine Motyl². ¹MMCRI, Netherlands, ²MMCRI, United States

Risperidone (RIS) and olanzapine (OLA) are atypical antipsychotic (AA) drugs that are used to treat mental disorders, such as schizophrenia and bipolar disorder. AA drugs cause several metabolic side effects, such as hyperlipidemia and glucose intolerance. More recently, bone loss and increased fracture risk have been added to this list. We have previously shown that bone loss from RIS is mediated through the sympathetic nervous system (SNS) and accompanied by markers of thermogenesis in brown adipose tissue. However, room temperature housing in mice is sub-thermonutral and accelerates age-related bone loss. This complicates preclinical studies because humans are thermoneutral around room temperature. In this experiment we aimed to explore the effect of thermoneutral housing on AA drug-induced bone loss. We housed 8-week-old female C57BL/6j mice at room temperature (22 °C) or thermoneutrality (28-30 °C) to better model clinical exposure. Mice were dosed daily for four weeks with 1.5 mg/kg RIS, 10 mg/kg OLA or vehicle by oral gavage. In thermoneutral conditions, OLA, but not RIS, caused a decrease in femoral bone mineral density (BMD) by dual X-ray absorptiometry (DXA), despite an increase in lean mass in both groups. At room temperature, we observed a similar increase in lean mass (p<0.05), but only in the RIS treated mice. Both RIS and OLA-treated mice had significantly decreased trabecular bone volume fraction and trabecular number, and increased trabecular separation com-

pared to vehicle treated mice housed at thermoneutrality (all $p < 0.05$). Although, femur total cross-sectional area did not change, cortical thickness decreased due to both RIS ($p < 0.05$) and OLA ($p < 0.0001$) treatment. Expression of the osteoclast marker, Acp5, increased in tibia marrow of RIS treated mice ($p < 0.05$), whereas the marrow adipocyte marker, fatty acid binding protein Fabp4, increased after both RIS ($p < 0.01$) and OLA ($p < 0.05$) treatments. This is contrary to the decrease in marrow adiposity we have seen before in RIS treated mice at room temperature. In contrast to thermoneutral conditions, AA treated mice housed at room temperature did not exhibit changes in cortical micro-architecture. In conclusion, we found bone loss with AA treatment was more severe at thermoneutrality, suggesting room temperature housing may mask some of the deleterious bone effects of treatments involving the SNS.

Disclosures: Roni Kunst, None

SAT-0267

Metabolic, Anthropometric and Nutritional Profile of Girls with Adolescent Idiopathic Scoliosis: A Pilot Study Émilie Normand*, Anita Franco, Stefan Parent, Alain Moreau, Valérie Marclil. Centre de recherche CHU Sainte-Justine, Canada

Purpose of the study: Studies have shown that patients with adolescent idiopathic scoliosis (AIS) have anthropometrical differences compared to their peers, but results are inconsistent. While differences in energy metabolism and nutrition could explain these discrepancies, they have been poorly studied in AIS. This study aims to thoroughly characterize the metabolic profile, nutritional habits and level of physical activity of girls affected by AIS and to compare them to age-matched healthy controls. Methods: For this pilot study, 20 girls with AIS and 20 healthy controls are being enrolled. Fasting glucose, insulin and lipid profile (total cholesterol, LDL-cholesterol, HDL-cholesterol, triglycerides and apolipoprotein B) are assessed. Bone mineral density and body composition is determined by osteodensitometry scan. Anthropometric parameters (weight, standing and sitting height, body mass index (BMI), waist circumference and arm span) are measured and questionnaires are administered to assess food intake and physical activity level. Results: To this day, 13 AIS and 9 healthy girls have completed the study. The mean age for AIS girls and controls was 14.8 ± 1.8 and 14.7 ± 1.7 yrs, respectively. The AIS group had a mean Cobb angle of $27.9 \pm 9.4^\circ$ and a mean age at diagnosis of 12.6 ± 1.7 yrs. Preliminary results show that AIS girls were taller than controls and have lower weight, BMI, body fat percentage and bone mineral density, although differences were not statistically significant. Fasting glucose and insulin were not different between groups. We found a tendency for perturbed lipid profile in AIS girls with higher LDL-cholesterol (18%, $P=0.065$), apolipoprotein B (22%, $P=0.087$) and total cholesterol (12% $P=0.0763$). Calorie intake and physical activity levels were similar between groups, but AIS girls consumed more calories than their needs compare to controls. There was a tendency of higher calcium intake in AIS (28%, $P=0.1437$) and both groups had similar vitamin D intake. Conclusion: In this study, AIS girls tended to have differences in their anthropometrical features, lipid profile and energy balance when compared to age-matched controls. Increasing the number of participants might confirm these results.

Disclosures: Émilie Normand, None

SAT-0268

A rat model of steroid-associated osteonecrosis Li-Zhen Zheng*, Jia-Li Wang¹, Ling Kong¹, Le Huang¹, Li Tian¹, Qian-Qian Pang¹, Xin-Luan Wang², Ling Qin¹. ¹Musculoskeletal Research Laboratory, Department of Orthopaedics & Traumatology, The Chinese University of Hong Kong, Hong Kong SAR, PR China, Hong Kong. ²Translational Medicine R&D Center, Institute of Biomedical and Health Engineering, Shenzhen Institutes of Advanced Technology, Chinese Academy of Sciences, Shenzhen, PR China, China

It is essential to establish a preclinical disease animal models to study etiology and/or pathophysiology of the relevant diseases and to test prevention and/or treatment concept(s). This study established an induction and assessment protocol for a preclinical steroid-associated osteonecrosis (SAON) animal model in rats with pulsed injections of lipopolysaccharide (LPS) and methylprednisolone (MPS). Twenty-eight 24-week-old male Sprague-Dawley rats were included in this study. Sixteen rats were used to induce SAON by one intravenous injection of LPS (0.2 mg/kg) and three intraperitoneally injections of large dose of MPS (100 mg/kg) with a time interval of 24 hours, and then low dose of MPS (40mg/kg) were intraperitoneally injected 3 times a week from week 2 to sacrifice. Additional twelve rats were used as normal controls. 2 and 6 weeks after induction, animals were scanned by a metabolic dual energy x-ray absorptiometry (DXA) for tissue composition, serum was collected for bone turnover markers, microfil perfusion was performed for angiography, liver was collected for histopathology, and bilateral femora and bilateral tibiae were collected for histological examination. Three rats died after LPS injection, with additional three supplemented, i.e. with 15.8% (3/19) mortality. All rats from SAON group showed SAON at week 2 with 100% incidence by histological evaluation. Rats from SAON group showed significantly higher fat percent and lower lean weight at week 6 by DXA, and significantly bone degradation at proximal tibia at 6 weeks by Micro-CT. Angiography showed significantly less blood vessels in proximal tibia and significantly more leakage particles in distal tibia 2 weeks after SAON induction. For bone turnover markers, serum PINP and OC were significantly lower at both 2 and 6 weeks after SAON induction, and serum CTX was significantly lower at 6 weeks after SAON induction. Histomorphometry showed significantly lower osteoblast surface,

and higher marrow fat fraction and edema area in SAON group. Hepatic edema appeared 2 weeks after SAON induction, and lipid accumulation appeared in liver of SAON rats 6 weeks after SAON induction. This SAON rat model induced with pulsed injection of LPS and MPS, which was well simulating the clinical feature and pathology, could be a cost-effective preclinical experimental model to study body metabolism, molecular mechanism of SAON and potential drugs developed for prevention or treatment of SAON.

Disclosures: Li-Zhen Zheng, None

SAT-0295

See Friday Plenary Number FRI-0295

SAT-0296

See Friday Plenary Number FRI-0296

SAT-0297

See Friday Plenary Number FRI-0297

SAT-0298

See Friday Plenary Number FRI-0298

SAT-0299

See Friday Plenary Number FRI-0299

SAT-0300

See Friday Plenary Number FRI-0300

SAT-0301

No Indication for Increased Severity of the Sclerotic Bone Phenotype of Sost Knock-out Mice in the Presence of an Lrp4 Mutation. Eveline Boudin*, Timur Yorgan², Gretl Hendrickx², Ellen Steenackers¹, Michaela Kneissel³, Ina Kramer⁴, Geert Mortier¹, Thorsten Schinke², Wim Van Hul¹. ¹Centre of Medical Genetics, University and University Hospital of Antwerp, Belgium, ²Department of Osteology and Biomechanics, University Medical Center Hamburg, Germany, ³Musculoskeletal Disease Area, Novartis Institutes for BioMedical Research, Basel, Switzerland., Switzerland, ⁴Musculoskeletal Disease Area, Novartis Institutes for BioMedical Research, Basel, Switzerland., Belgium

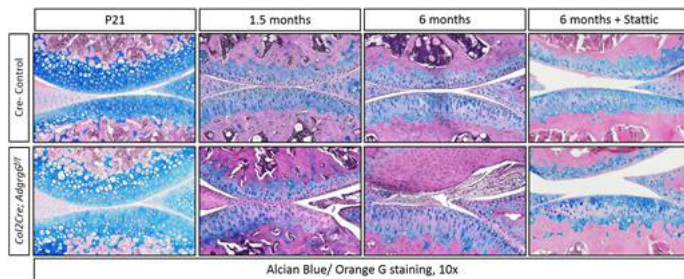
Previously we showed that loss of function of sclerostin, encoded by SOST, and hypomorphic missense mutations in LRP4 can be the genetic cause underlying sclerosteosis, a rare sclerosing bone disorder marked by an increased bone mass especially at the skull and tubular bones. Sclerostin and LRP4 are shown to interact and the interaction is impaired in the presence of the sclerosteosis causing mutations in LRP4. Furthermore, it was shown that the sclerostin-LRP4 interaction is important for the inhibition of the canonical WNT signaling, a known regulator of bone formation. In addition, not only sclerostin but also other modulators of canonical WNT signaling and bone metabolism e.g. *wisdom* and *dickkopf1* (DKK1) are reported to interact with LRP4. To investigate the importance of different binding partners of LRP4 in the regulation of bone formation, we compared the previously described *Sost* knockout mouse (*Sost*^{-/-}) with the recently described *Lrp4* p.R1170Q homozygous knockin (*Lrp4*R1170Q) mouse model (Polygene, Switzerland) and compared the bone phenotype of the double mutant mice with that of the *Sost*^{-/-} and *Lrp4*R1170Q mice. μ -CT analysis as well as structural histomorphometry data showed that the sclerotic bone phenotype of the *Lrp4*R1170Q mouse is milder compared to that of the *Sost*^{-/-} and the *Lrp4*R1170Q;*Sost*^{-/-} double mutant mice, the latter two showing no significant difference. Based on these data, it seems first that the skeletal phenotype observed in the *Lrp4*R1170Q mice is due to the impaired binding of LRP4 to sclerostin but at the same time that other binding partners of LRP4 do not contribute to the bone phenotype of the LRP4 mutant mice or that their action is not disturbed by the mutation. Measurement of DKK1 in serum of these mice demonstrated that the levels of DKK1 are, in contrast to sclerostin, not significantly increased in *Lrp4*R1170Q mice compared to wild type mice which confirms that their interaction is either not disturbed by the mutation or that LRP4 is not the main interaction partner of DKK1 in bone. Furthermore, the more severe phenotype observed in the *Sost*^{-/-} mice indicates that there is still some residual inhibitory activity of sclerostin in *Lrp4*R1170Q mice. Based on the latter one could conclude that either the binding of *Lrp4*R1170Q with sclerostin is not completely lost or that sclerostin can inhibit bone formation via LRP5/6 independent of LRP4. Finally, additional studies will be needed to further investigate the mechanism whereby sclerostin and LRP4 regulate bone formation.

Disclosures: Eveline Boudin, None

SAT-0302

Adgrg6 Is a Novel and Critical Regulator for Cartilage Homeostasis and Joint Stability Zhaoyang Liu*, Ryan Gray. University of Texas at Austin, Dell Medical School, United States

Osteoarthritis (OA) is a degenerative disease resulting in severe joint cartilage destruction and disability. Our previous studies have identified a role of Adhesion G-protein coupled receptor G6 (ADGRG6) for spine and intervertebral disc integrity. Here we identify a critical role for ADGRG6 in joint cartilage homeostasis and in the pathogenesis of OA, using a conditional Col2Cre;Adgrg6^{f/f} mutant mouse model. These mutant mice exhibit normal joint and articular cartilage morphology at P21. However, joint integrity analysis in 1.5-, 6-, and 8-month-old mutants via microCT, histology, IHC, ISH, and histomorphometry showed an early onset and progressive OA-like pathology characterized by fibrosis and degeneration of articular cartilage and meniscus, synovial tissue hyperplasia, and progressive loss of extracellular matrix (ECM) components coupled with abnormally upregulated catabolic enzyme activities. To isolate the cellular role of ADGRG6, we generated a cartilage-specific mouse model ATC;Adgrg6^{f/f} with the Acan enhancer-driven, Tetracycline-inducible Cre (ATC). Early postnatal induction (P1-P20) of these mutants recapitulate most phenotypes observed in Col2Cre;Adgrg6^{f/f} mutants at 1.5 and 8 months. To obtain insight into the biological processes affected by ADGRG6, we engineered a stable Adgrg6KO mutation in the chondrogenic ATDC5 cell line with CRISPR-Cas9, and performed RNA-seq on WT and Adgrg6KO cells. 304 differentially expressed genes have been identified, including genes involved in apoptosis, ECM composition and structural constituent. In addition, several of the upregulated genes are associated with human or animal models of OA, including Aspn, Dmp1, Clu, Ctg, Dkk-3, and RhoB. Interestingly, constitutive activation of STAT3 signaling is observed in Adgrg6KO cells and in vivo in the articular cartilage of ATC;Adgrg6^{f/f} mutants prior to histopathological changes of the knee joint. Preliminary studies showed that STAT3 inhibitor (Stat3i) treatment can partially rescue the OA-like cartilage degeneration phenotype in Col2Cre;Adgrg6^{f/f} mutant mice, and restore some of the disrupted gene expression in Adgrg6KO cell culture. Collectively, these data have identified ADGRG6 as a novel and critical regulator for cartilage homeostasis and joint integrity potentially via regulation of ECM gene expression and of the STAT3 pathway, implicating ADGRG6 as a potential therapeutic target for the treatment of OA.



Disclosures: **Zhaoyang Liu**, None

SAT-0303

Common and rare variants of WNT16, DKK1 and SOST and their relationship with bone mineral density Núria Martínez-Gil*¹, Neus Roca-Ayats¹, Anna Monistrol-Mula¹, Natàlia García-Giral², Adolfo Díez-Pérez², Xavier Nogués², Leonardo Mellibovsky², Daniel Grinberg¹, Susana Balcells¹. ¹Department of Genetics, Microbiology and Statistics, Faculty of Biology, University of Barcelona, IBUB, IRSJD, CIBERER, Spain, ²Musculoskeletal Research Group, IMIM (Hospital del Mar Medical Research Institute), Centro de Investigación Biomédica en Red de Fragilidad y Envejecimiento Saludable (CIBERFES), ISCIII, Spain

Numerous studies have highlighted the role of the Wnt pathway in bone biology. Our objective has been to study the allelic architecture of three Wnt pathway genes: WNT16, DKK1 and SOST. We have resequenced the coding and some regulatory regions of these three genes in two groups with extreme BMD (n=50, each) from the BARCOS cohort. Those predicted functional variants considered interesting have been genotyped in the full cohort (n=1490), and when appropriate (MAF>0.01), their association with BMD has been studied. We have found six variants associated with BMD. Three of them were missense (WNT16 rs2707466, WNT16 rs2908004 and SOST rs17882143) and three were putative regulatory variants (WNT16 rs55710688, in the Kozak sequence; WNT16 rs142005327, within a putative enhancer and DKK1 rs1569198 generating an alternative splice site). In addition, two rare variants in functional regions (rs190011371 in the WNT16b 3'UTR and rs570754792 in the SOST TATA box) were found only present in three women each, all with BMD below the mean of the cohort. We have carried out functional studies for the SOST variants rs17882143 and rs570754792, and WNT16 variants rs2908004 and rs2707466 to verify their association with BMD. The rs17882143 SNP is a missense change that substitutes an amino acid within the signal peptide of sclerostin. To assess whether the change might affect the subcellular localization of the mutated protein and/or its abundance, Western blot studies were performed and these showed that the amount of sclerostin excreted into the extracellular space was the same for the WT and the mutated protein. The rare variant

rs570754792 lies in the SOST extended TATA box. Reporter gene (luciferase) assays with constructs containing each of the variant alleles showed significant differences in luciferase activity between the two alleles tested, where the minor allele displayed lower transcription capacity. The WNT16 missense variants were shown to be eQTLs of CPED1 and FAM3C in artery tissue and Skin, respectively, according to GTEx. We tested whether these variants are eQTLs of these genes in primary osteoblasts (n = 45) and found an association between FAM3C RNA levels and the variant rs2908004. In conclusion, our results illustrate how functional analyses were necessary to sort out true form putative functional variants in these Wnt pathway genes.

Disclosures: **Núria Martínez-Gil**, None

SAT-0304

Genetic variability and functionality of the FLJ42280 locus, a GWAS hit for osteoporosis Neus Roca-Ayats*¹, Dario G. Lupiáñez², Núria Martínez-Gil¹, Marina Gerousi³, Mónica Cozar¹, Natàlia García-Giral⁴, Xavier Nogués⁴, Leonardo Mellibovsky⁴, Adolfo Díez-Pérez⁴, Susana Balcells¹, Daniel Grinberg¹. ¹Department of Genetics, Microbiology and Statistics, Facultat de Biologia, Universitat de Barcelona, Centro de Investigación Biomédica en Red de Enfermedades Raras (CIBERER), ISCIII, IBUB, IRSJD, Spain, ²Epigenetics and Sex Development Group, Berlin Institute for Medical Systems Biology, Max-Delbrück Center for Molecular Medicine, Germany, ³Department of Genetics, Microbiology and Statistics, Facultat de Biologia, Universitat de Barcelona, IBUB, Spain, ⁴Musculoskeletal Research Group, IMIM (Hospital del Mar Medical Research Institute), Centro de Investigación Biomédica en Red en Fragilidad y Envejecimiento Saludable (CIBERFES), ISCIII, Spain

Genome-wide association studies (GWAS) have repeatedly identified variants associated with bone mineral density (BMD) and osteoporotic fracture in intronic regions of FLJ42280, a poorly studied gene of unknown function. The aim of the present study is to analyse the variability and functionality of this locus. Firstly, we resequenced the FLJ42280 genomic region in two extreme BMD groups from the BARCOS cohort of postmenopausal women. The number and frequency of variants between the two groups were compared and 110 variants were identified, of which 59 were rare and low frequency (MAF<0.05). Overall, the number of variants was balanced between the two groups and frequency differences did not reach statistical significance. Secondly, the overlap of the variants with functional elements from ENCODE was explored and 4 of them were found to be located in putative osteoblast enhancers. Next, taking into consideration both frequency and functionality, we genotyped 8 SNPs in the complete BARCOS cohort and tested them for association with BMD and fracture. Significant differences were obtained for 2 upstream SNPs, rs4342521 and rs10085588, in lumbar spine BMD (p-values=0.0031 and 0.0036, respectively) and in osteoporotic fracture (p-values=0.0391 and 0.0355, respectively). Finally, the possible role of these 2 SNPs as cis-eQTLs in primary human osteoblasts was studied, together with SNP rs4727338 (the GWAS hit in Estrada et al Nat Genet 2012;44(5):491-501). All 3 SNPs showed a statistically significant influence on the expression of the proximal neighboring gene SLC25A13 and a tendency on SHFM1 (distal). Further functional studies of a conserved putative regulatory element 4 kb upstream of FLJ42280, which contains rs10085588, are currently underway, namely 4C-seq (circular chromosome conformation capture) and luciferase assays. We also undertook functional analysis of an enhancer present in intron 2 of FLJ42280, which has been described as an active enhancer for Dlx5 and Dlx6 in embryonic mouse branchial arches (Birbaum et al, Hum Mol Genet 21(22):4930-4938, 2012) and contains histone marks of active enhancers in osteoblasts (ENCODE data). We performed 4C-seq in mouse embryonic day (E) 12.5 developing limbs and a clear interaction between the enhancer and the Dlx5 promoter region could be detected, indicative of a role for this embryonic enhancer also in the developing bone. Further functional studies including CRISPR-Cas9 disruption in mouse are currently underway.

Disclosures: **Neus Roca-Ayats**, None

SAT-0325

See Friday Plenary Number FRI-0325

SAT-0326

See Friday Plenary Number FRI-0326

SAT-0327

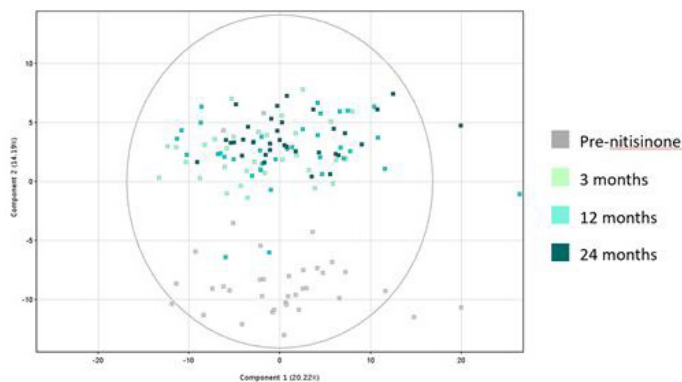
See Friday Plenary Number FRI-0327

SAT-0328

Comprehensive targeted LC-QTOF-MS metabolomics identifies novel metabolite changes associated with treatment of the rare bone disease Alkaptonuria

Brendan Norman¹, Andrew Davison², Gordon Ross³, Anna Milan², Andrew Hughes², Norman Roberts², Lakshminarayan Ranganath², James Gallagher¹. ¹Institute of Ageing & Chronic Disease, University of Liverpool, United Kingdom, ²Liverpool Clinical Laboratories, Royal Liverpool University Hospitals Trust, United Kingdom, ³Agilent Technologies UK Ltd, United Kingdom

Metabolomics involves studying the entire complement of small molecule metabolites in a biological system and is increasingly recognised as a powerful phenotyping strategy to understand the pathophysiology underlying a broad range of disease. Data processing and identification of 'unknowns' is the bottleneck in metabolomics. To resolve this an approach has been evaluated for comprehensive targeted metabolomics employing three complementary LC-QTOF-MS methods and accurate-mass retention time (AMRT) databases generated in-house from 619 metabolite standards. The strategy was then applied to Alkaptonuria (AKU), a rare inborn error of tyrosine metabolism also known as 'black bone disease'. 619 standards (mw: 45-1354 Da) covering a broad range of primary metabolism, including carbohydrates, amino and organic acids and lipids, were analysed by three chromatographic methods (two reversed-phase, one normal-phase) coupled to an Agilent 6550 LC-QTOF-MS operated in positive and negative polarity. Data from the standards formed an in-house AMRT database for each method for identifying the structures of 'unknown' chemical entities detected from metabolic profiling of AKU urine. AMRT-based targeted feature extraction was performed on data of urine samples from 25 AKU patients (19-72 years) at baseline then at 3 (2mg every other day), 12 and 24 months (2mg daily) on nitisinone. AMRT matching employed windows of ± 10 ppm (mass) and ± 0.3 minutes (retention time). Combining data from the three methods enhanced coverage of the metabolome, achieving a total of 243 unique AMRT compound identifications that passed quality control filtering. In total, 24 positively-charged AMRT matches showed significant profile differences (FDR $p < 0.05$ and fold change > 2) from the pre-treatment sampling time point; 12 decreased abundance, 12 increased abundance. The altered metabolites included changes which are known following nitisinone treatment, including homogentisic acid (decreased) and tyrosine (increased), but also some previously unreported changes: tyramine, 3-methoxytyramine, 4-hydroxyphenylacetic acid, 4-hydroxybenzaldehyde and ethylmalonic acid increased; tryptophan, kynurenine, methyl-histidine, cAMP, xanthosine and paraxanthine decreased. In conclusion, we have identified a number of novel metabolite changes in AKU urine following treatment with the promising drug nitisinone. The LC-QTOF-MS strategy will be an invaluable phenotyping tool for application to AKU and other rare bone diseases.



Principal components analysis plot from LC-QTOF-MS metabolic profiling of Alkaptonuria urine. The pre-nitisinone samples cluster separately from the post-treatment time points, showing that the profiling strategy has captured clear changes to the metabolome as a consequence of nitisinone therapy in Alkaptonuria.

Disclosures: **Brendan Norman, None**

SAT-0329

Identification of secreted factors coupling bone resorption to bone formation in humans using denosumab as a biological probe

Megan Weivoda*, David Monroe, Josh Farr, Elizabeth Atkinson, Brittany Negley, Brianne Thicke, Ming Ruan, Louise McCreedy, Matthew Drake, Merry Jo Oursler, Sundeep Khosla. Mayo Clinic, United States

Bone resorption is coupled to bone formation but the underlying mechanisms remain unclear. Anti-resorptive drugs (e.g., denosumab, DEN) are used to treat osteoporosis, but by reducing osteoclast numbers, these drugs also decrease bone formation. Thus, to identify novel coupling factors in humans, we employed DEN to eliminate osteoclasts in post-menopausal women, who were randomly assigned to placebo (PL) or DEN (N=24/group). Three months post-treatment, iliac crest bone biopsies were obtained, centrifuged to remove loosely-adherent marrow, and homogenized to obtain RNA for RNA-sequencing. DEN-treated patients showed significantly reduced serum CTX, TRAP, and PINP. In addition, centrifuged bone showed significant reductions in known resorption (ACP5, CALCR, CTSK,

MMP9, MMP13, OC-STAMP, TNFRSF11A) and formation (ALPL, BGLAP, COL1A1, COL1A2, COL2A1, COL2A2, SP7, SPP1, SPARC) genes. Of interest, the rank means of the formation and resorption genes downregulated by DEN were significantly correlated in PL patients (R=0.81, P=0.0005), demonstrating coupling of bone resorption and formation at the gene expression level. Next we used Ingenuity Pathway Analysis to identify potential secreted coupling factors, which revealed 63 suppressed and 59 upregulated secreted genes in DEN-treated patients compared to PL. The rank means of the upregulated genes showed no correlation with formation or resorption genes in PL patients; however, the suppressed secreted genes correlated significantly with bone formation (R=0.95, P<0.0001) and resorption (R=0.87, P<0.0001) genes. To determine whether any of these genes may be osteoclast-derived factors, we performed RT-QPCR to compare expression of the DEN-suppressed secreted genes in human bone-marrow-derived osteoclast cultures vs human osteoblast lineage cells. We found that several secreted genes were expressed at significantly higher levels in osteoclasts vs osteoblasts, including CREG2, DPP4, TSPEAR, and LIF. Importantly, LIF has already been identified as an osteoclast-derived coupling factor in murine models, thus both validating this approach and establishing the role of LIF as a coupling factor in humans. Collectively, these data demonstrate for the first time the coupling of bone resorption to bone formation at the gene expression level in humans. In addition, we identify several candidate coupling factors in humans, as well as independently establish LIF as a coupling factor in human bone remodeling.

Disclosures: **Megan Weivoda, None**

SAT-0330

Integrative analysis of genetic and clinical risk factors affecting bone loss

Ji Hyun Lee¹, Jooyong Park², Jung Hee Kim³, Hyung Jin Choi⁴, Eu Jeong Ku⁵, A Ram Hong⁶, Ji-Yeob Choi², Nam H. Cho⁷, Chan Soo Shin³. ¹Department of Internal Medicine, Seoul National University College of Medicine, Department of Internal Medicine, VHS Medical Center, Republic of Korea, ²Department of Biomedical Sciences, Seoul National University College of Medicine, Republic of Korea, ³Department of Internal Medicine, Seoul National University College of Medicine, Republic of Korea, ⁴Department of Anatomy, Seoul National University College of Medicine, Seoul, Republic of Korea, ⁵Department of Internal Medicine, Chungbuk National University College of Medicine, Cheongju Si, Republic of Korea, ⁶Department of Internal Medicine, Seoul National University College of Medicine, Boramae Medical Center, Republic of Korea, ⁷Department of Preventive Medicine, Ajou University School of Medicine, Republic of Korea

Objective The relative contribution of genetic and clinical risk factors for bone loss is not well known. We investigated change of total hip bone mineral density (BMD) and risk of genetic and clinical risk factors for bone loss in Korean population. Methods In a Korean prospective cohort study, we included 645 men over 50 years old and 683 postmenopausal women who repeated BMD testing between 2007 and 2013. Accelerated hip BMD loss was defined as a slope ≤ -1 standard deviation (SD) below mean at total hip BMD. We showed the relationship between the rate of change in hip BMD and clinical risk factors such as age, body mass index (BMI), and change in lean mass and fat mass, menopause in women. We investigated the association between the rate of change in hip BMD and 2,614 single-nucleotide polymorphisms from 23 known BMD-related candidate genes: AKIN, SOX9, SOX6, ZBTB40, MEF2C, ESR1, VDR, P2RX7, TNFRSF11B, TNFSF11, TNFRSF11A, FOXL1, LRP5, SOST, WNT16, WNT4, WNT5B, SP7, CTNNA1, RUNX2, DKK1, SFRP4, and BMP2. Results BMI, baseline total hip BMD and lean mass loss over 10% were independent risk factors for estimating accelerated hip BMD loss of Korean men (BMI, Odds ratio (OR) = 0.91, 95% confidence interval (CI) = 0.83-0.99; baseline total hip BMD (per 1 SD increase), OR = 0.72, 95% CI = 0.55-0.94; lean mass loss (> 10%), OR = 2.74, 95% CI = 1.51-4.99). Age, years since menopause under 3 years, fat mass loss over 7%, and TNFSF11 rs931273 minor allele homozygote are significant risk factors for accelerated hip BMD loss in Korean women (age, OR = 1.05, 95% CI = 1.01-1.10; fat mass loss (> 7%), OR = 2.02, 95% CI = 1.07-3.83; rs931273, OR = 1.99; 95% CI = 1.08-3.68). In men, LRP5 rs4988300 was associated with rate of change in hip BMD ($\beta = 0.127$, P = 0.005). In women, two TNFSF11 SNPs were associated with the rate of change in hip BMD (rs7325635 and rs931273, $\beta = 0.139$, P = 0.007, $\beta = -0.132$, P = 0.001). The areas under the ROC curve (AUC) of accelerated hip BMD loss in men and women were 0.706 (95% CI = 0.642-0.770) and 0.711 (95% CI = 0.652-0.770) respectively. Conclusion BMI, baseline total hip BMD, and lean mass loss (>10%) were independent predictors to accelerated hip BMD loss in men. In postmenopausal women, age, fat mass loss (>7%), year since menopause under 3 years, and TNFSF11 rs931273 were important risk factors to accelerated hip BMD loss. Interaction of genetic and clinical risk factors affects bone loss.

Disclosures: **Ji Hyun Lee, None**

SAT-0343

See Friday Plenary Number FRI-0343

SAT-0344

See Friday Plenary Number FRI-0344 (WITHDRAWN)

SAT-0345

See Friday Plenary Number FRI-0345

SAT-0346

See Friday Plenary Number FRI-0346

SAT-0347

See Friday Plenary Number FRI-0347

SAT-0348

See Friday Plenary Number FRI-0348 (WITHDRAWN)

SAT-0349

See Friday Plenary Number FRI-0349

SAT-0350

See Friday Plenary Number FRI-0350

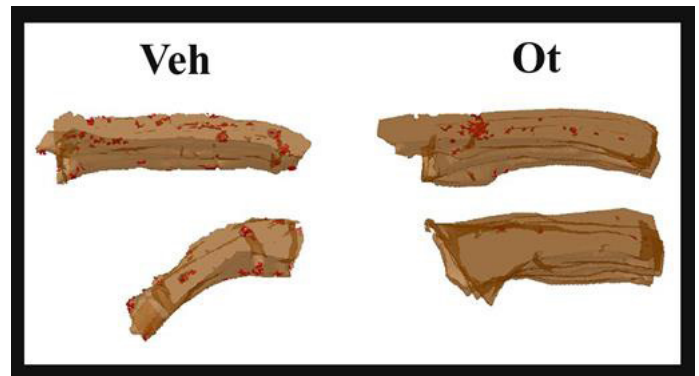
SAT-0351

See Friday Plenary Number FRI-0351

SAT-0352

Oxytocin treatment improves the femoral neck bone quality of the aging rats in periostropause Fernanda Fernandes*, Camila Tami Stringheta Garcia, Melise Jacon Peres Ueno, Angela Cristina Nicola, Fabiana Fernandes, Mário Jefferson Quirino Louzada, Antônio Hernandes Chaves-Neto, Rita Cássia Menegati Dornelles. UNESP, Brazil

Introduction: Primary osteoporosis is a disease related to the hormonal changes that occur in the female organism in the transition to the aging. Research has shown an anabolic action of oxytocin (OT) on bone homeostasis and its possible potential in osteoporosis therapy where as OT receptors have been detected in human osteoblasts and osteoclasts. Although there are results that demonstrate this performance, the action of the OT in aging organisms that are in the transition period to menopause (perimenopause) is not established, so that this action happens in a preventive way. **Objective:** The present aimed to analyze whether OT performance in the femoral neck bone metabolism of aging acyclic Wistar rats (18 months) contributes to decrease the risks of osteopenia and primary osteoporosis. **Material and method:** Wistar rats (18 months old) was distributed in the groups: 1 - Control (Veh) and 2 - Treated/OT (Ot), with eight animals each, and it was analyzed the estrous cycle from all animals to test the estrous acyclicity (periostropause). The animals received two intraperitoneal injections of NaCl (0.15 M - control group) or OT (134 µg / kg - treated group), with a 12 hour interval. After 35 days of administration of the injections, the animals were decapitated for blood collection, which was used for the biochemical assays and surgical removal of the femurs was performed for cortical bone microtomography and biomechanical assay. **Results:** In the biochemical analysis, there was statistical difference between the groups for the enzymes Alkaline Phosphatase (FAL) and Tartarate Resistant Acid Phosphatase (TRAP), and the Ot group presented the highest FAL enzymatic activity (p=0.0138) and lower enzymatic activity of TRAP (p=0.0045). In the analysis of cortical bone microtomography was observed the highest cortical bone area (Ct. Ar) (p=0.00416), lower cortical pores percentage (Ct. Po) (p=0.0102) and greater polar moment (p=0.0480), maximum polar moment (MMI-max) (p=0.0480) and minimum polar moment (MMI-maxAv) (p=0.0035) in Ot group. In the mechanical assay analysis, greater maximal strength (p=0.0003) and bone stiffness (p=0.0145) were observed in the Ot group. **Conclusion:** Therefore, we conclude that OT administration is valid anabolic strategy for the prevention of primary osteoporosis in aging rats in the periostropause period. We also emphasize the importance of these data as the basis for the direction of pre and clinical research.

Disclosures: **Fernanda Fernandes**, None**SAT-0353**

The Phosphate Hypothesis: Divergent Roles for PTH and PTHrP Robert Fredericks*. Endocrine-Associates, United States

Models developed through experience with oral calcium challenge, immersion in water, and DXA in personalization of medical care are supported by recent clarification of downstream influences of the PTH/PTHrP receptor. These findings also validate the phosphate hypothesis that proposes phosphate to be the foundational signal of metabolism leading to models that organize basic and clinical data while facilitating repurposing of available interventions. 1 alpha Vitamin D was found to suppress leptin release from cultured adipose tissue and subsequently found to resolve symptoms in 5 of 5 patients with Behcet's syndrome. Suppression of salt inducible kinases, known targets of PTH and PTHrP, by 1 alpha D, also a downstream signal, is proposed to mediate effects on BMD and inflammation. Recent clarification of PTH/PTHrP downstream signaling reveals a complex system providing protection from elevation of the Ca x PO4 product. The observations include antagonism of PTH by PTHrP signaling mediated by endosomal docking of the receptor as amplified by calcium. Partitioning of PTH signals by NHERF and Scribble are found to be cell type and cellular location specific. Incorporating the influences of FGF23 into the modeling, including modulation of distal tubular calcium and sodium, generates an interface with PTH/PTHrP and Vitamin D signaling structures in the construction of coherent models. Previous work with mouse calvarial cultures and study of patients with hyperparathyroidism or humoral hypercalcemia of malignancy, utilizing oral calcium challenge, anticipated the recent molecular observations. Discoveries made through investigation of patients with renal responses to immersion in water (gravity subtraction) has contributed to understanding of salt balance in pathogenesis of metabolic disease, including skeletal phenotypes. Modeling causal relationships through engagement of case based discovery in the context of ethical practice provides insights for appropriate transformation of metabolic disease categories. When categories are discordant with basic science discoveries, use of digital technology, including AI, for cost-effective personalization of healthcare is compromised. Modeling causal relationships in the organization of metabolism by calcitropic signals also serves the historic mission to understand their biological roles in the metabolic manifestations and skeletal phenotypes recognized in human health and disease.

Disclosures: **Robert Fredericks**, None**SAT-0354**

Estrogen Attenuates Complex I Activity and Stimulates the Mitochondrial Apoptotic Death Pathway in Osteoclast Progenitors Ha-Neui Kim*^{1,2}, Intawat Nookaew¹, Nukhet Aykin-Burns¹, Kim Krager¹, Li Han^{1,2}, Robert Jilka^{1,2}, Stavros Manolagas^{1,2}, Maria Almeida^{1,2}. ¹University of Arkansas for Medical Sciences, United States, ²Central Arkansas Veterans Healthcare System, United States

Estrogens decrease the number of osteoclasts and the resorption of cancellous bone by stimulating osteoclast apoptosis, via ERα signaling in myeloid lineage cells. However, it remains unclear whether this effect occurs in osteoclast progenitors, mature osteoclasts, or both; and the molecular mechanisms are unknown. To determine the stage of differentiation at which estrogens act, we cultured osteoclast progenitors from wild type BL/6 mice for 5-days with RANKL. 10-8 M 17β-estradiol (E2) present during only the first 24 hours decreased osteoclast number as much as it did when it was present throughout the 5 days of culture. We next cultured macrophages, pre-osteoclasts and mature osteoclasts from the bone marrow of ERαΔLysM mice and ERα^{fl/fl} littermate controls and performed microarray analysis in cells treated for 4 hours with E2. Principal-component and hierarchical clustering analysis indicated that the majority of genes affected by ERα were in osteoclast progenitors, not in mature osteoclasts. Osteoclast progenitors lacking ERα exhibited significant enrichment for the term "transmembrane electron transfer carrier". Specifically, they showed increased expression of several genes of the mitochondrial Complex I, including Ndufa1, 3, 4, 5, 6, 9, Ndufb2, 6, 8, 9, Ndufe1, 2 and Ndufs2, 6. Using extracellular flux analysis in osteoclast progenitors, we next determined that RANKL addition to cells from wild-type BL/6 mice caused an increase in basal oxygen consumption rate, maximum respiratory capacity,

and respiratory reserve, as well as ATP production. E2 had no effect in any of these mitochondrial function measures in the absence of RANKL, but it potently suppressed all the effects of RANKL. Furthermore, E2 stimulated caspase-3 activity in osteoclast progenitors by 2-fold. This effect was abrogated in cultures of progenitors lacking Bak and Bax – the two essential proteins for the mitochondrial apoptotic death pathway – isolated from Bak^{-/-};BaxΔLysM mice. Rotenone, an inhibitor of Complex I activity, also increased the apoptosis of osteoclast progenitors and decreased osteoclast number. Like estradiol, the proapoptotic effect of rotenone required Bak and Bax. Taken together, these findings suggest that the decrease of osteoclast number by estrogens is caused, in part, by a decrease in mitochondrial complex I activity in osteoclast progenitors and thereby activation of the mitochondrial apoptotic death pathway.

Disclosures: **Ha-Neui Kim**, None

SAT-0355

The impact of dietary phosphate on acute renal phosphate and calcium excretion in healthy subjects. Tom Mazzetti^{*1}, Mandy E. Turner², Laura Couture³, Jenny Munroe⁴, Rachel M. Holden⁵. ¹Queen's University School of Medicine, Canada, ²Queen's University Department of Biomedical and Molecular Sciences, Canada, ³McGill University Faculty of Health Sciences, Canada, ⁴Kingston General Hospital, Canada, ⁵Queen's University Department of Medicine, Canada

The kidney eliminates excess phosphate from the body by preventing phosphate reabsorption acutely in response to changing levels of the counter-regulatory hormone parathyroid hormone (PTH). However, PTH influences calcium (Ca) homeostasis; which affects several crucial physiologic processes. Phosphate (Pi) intake modifies Ca and Pi homeostasis in rats - those exposed to a high-Pi diet respond adaptively by increasing excretion via PTH. Here, we conduct a translational experiment in healthy humans to determine whether the acute excretion of Ca and Pi changes in response to the prevailing level of dietary phosphate. This was a 2 week randomized crossover study. 16 participants were randomly assigned to the low- or high-Pi condition and put on a fixed low-phosphate diet for 5 days. The low-Pi condition was supplemented with 500mg CaCO₃ daily and the high-Pi condition was supplemented with 500 mg CaCO₃ daily and 3000 mg of Pi daily. Participants collected their urine for 24 hours prior to presenting fasted for baseline blood and urine assessments (Pi, Ca, PTH, FGF-23, creatinine). After a 1500 mg oral Pi challenge, bloodwork and urine studies were repeated every hour for 3 hours. The mean age of participants was 23.3; 64% were female, mean creatinine was 76.5. In the high-Pi condition, had significantly higher 24h-urine Pi (49.9 mmol vs 21.5 mmol, p<0.0001), higher baseline FGF-23 (63.7 vs 55.2 pg/mL, p<0.01) and PTH (4.6 vs 3.8, p<0.05). Serum Ca and Pi were similar between conditions. Fractional excretion (FE) of Pi and urinary Pi:creatinine ratio were significantly higher in the high-Pi condition. After the oral Pi challenge, serum Pi increased in both conditions at 1h (+0.15 mM, p<0.001) and returned to baseline at 2 hours. In the low-Pi condition, the participants had no change in PTH and a significant increase in FEPI over baseline at 2 and 3 hours. In the high-Pi condition, participants had a significant decrease in PTH at 1 and 2 hours (-0.7 and +1.1 pmol/L, p<0.05), and FEPI was significantly lower at 1 hour compared to baseline. Among healthy subjects, a high level of prevailing dietary phosphate decreases the kidneys' ability to respond to an acute oral phosphate challenge. This phenomenon appears to proceed through a PTH-mediated mechanism.

Disclosures: **Tom Mazzetti**, None

SAT-0356

Relative influence of serum ionized calcium and 25-hydroxyvitamin D in regulating PTH secretion in healthy subjects: an analysis of a large cohort Federica Ferrone^{*1}, Jessica Pepe¹, Cristiana Cipriani¹, Vittoria Danese¹, Veronica Cecchetti¹, Valeria Fassino¹, Federica Biamonte¹, Luciano Colangelo¹, Frank Blocki², Salvatore Minisola³. ¹Department of Internal Medicine and Medical Disciplines, "Sapienza" University of Rome, Italy, ²diasorin inc, United States, ³Department of Internal Medicine and Medical Disciplines, "Sapienza" University of Rome, Jamaica

Purpose: To evaluate the relative influence of serum ionized calcium (Ca⁺⁺), ionized magnesium (Mg⁺⁺), 25(OH)D and 1,25(OH)₂D on PTH secretion. Methods: 2259 volunteer blood donors (1652 men and 607 women, age range 18-68 years) were enrolled. Ca⁺⁺ and Mg⁺⁺ were assayed by biochemical analyzer NOVA8; PTH, 25(OH)D and 1,25(OH)₂D by chemiluminescence-immunoassay (LIAISON XL®). Three different statistical approaches were utilized to test effects among these parameters: regression tree analysis, general linear models and Anova type III errors. Results: In the whole population, significant inverse and direct correlations [between Ca⁺⁺ and PTH (r=-0.223, p<0.001), 25(OH)D and PTH (r=-0.178, p<0.001) and between PTH and age (r=0.322, p<0.001), respectively] were found. Below or above 38 years, differential covariate effects on PTH levels were observed. For younger subjects, 25(OH)D values were the most important parameter in regulating PTH; subjects with 25(OH)D <14 ng/mL had average PTH values equal to 23 pg/mL, while subjects with 25(OH)D levels >14 ng/mL had average PTH values equal to 20. For subjects 38 years or older, both 25(OH)D and Ca⁺⁺ levels were effective in regulating PTH secretion. However, 25(OH)D values had the strongest effect, since subjects with 25(OH)D < 13 ng/mL had average PTH values equal to 29 pg/mL, while those > 13 ng/mL had average PTH

values equal to 25 pg/mL. Variations of PTH levels, in this latter group only, disclose a Ca⁺⁺ effect. Subjects with Ca⁺⁺ levels ≥ 1.30 mmol/L show an average PTH value (23 pg/mL) that is lower than that observed (26 pg/mL) in subjects with Ca⁺⁺ values < 1.30 mmol/L. Multivariate analysis using a linear model to quantitatively assess the most important parameters influencing PTH serum levels was performed. After stepwise selection, all variables retained in the model had a significant effect (p<0.001) on log transformed PTH values. Finally, Anova Type III errors contributed by 25(OH)D, Ca⁺⁺, BMI and 1,25(OH)₂D accounted for 32.1%, 18%, 14.3% and 11.1% of total PTH variance, respectively. Remaining percentages were attributable to age and sex. Conclusion: Under clinically stable conditions not challenged by acute calcium perturbation shifts, 25(OH)D plays a significant role regulating PTH secretion. Finally, under conditions of relative vitamin D sufficiency, serum Ca⁺⁺ also plays an important role.

Disclosures: **Federica Ferrone**, None

SAT-0357

Decrement of Dentin Matrix Protein 1 caused by Excessive Parathyroid hormone is one of the pathogenesis in elevating Fibroblast Growth Factor 23 expression in Bone Tissue on Primary Hyperparathyroidism Model Yuki Nagata^{*}, Yasuo Imanishi, Tomomi Maeda, Daichi Miyaoka, Noriyuki Hayashi, Masanori Emoto, Masaaki Inaba. Osaka City University Graduate School of Medicine, Department of Metabolism, Endocrinology, and Molecular Medicine, Japan

Primary hyperparathyroidism (PHPT) is the endocrine disorder characterized by hypercalcemia, accompanied with excessive secretion of parathyroid hormone (PTH) from parathyroid tumor or hyperplasia. Although it is well known that PTH acts directly on bone to increase secretion of Fibroblast growth factor 23 (FGF23), which is a phosphaturic factor, expressed in mature osteoblast and osteocyte and so patients with PHPT represent hypophosphatemia with the high level of plasma FGF23, this mechanism has not been fully elucidated. Dentin matrix protein 1 (DMP1) is non collagenous bone matrix protein of small integrin-binding ligand, N-linked glycoproteins (SIBLINGs), mainly expressed in osteocyte, to contribute bone mineralization. In addition, DMP1 may regulate phosphate metabolism to suppress FGF23 expression, resulting from hypophosphatemic osteomalacia with increment of FGF23 secretion in Dmp1 knockout mice. To determine if DMP1 play a role on FGF23 expression via PTH regulation, we examined their alterations in bone tissue on PHPT model mice, which presented with hypercalcemia, hypophosphatemia and increased serum FGF23. The FGF23 and DMP1 expressions on calvaria in PHPT mice significantly increased and decreased respectively by quantitative PCR and immunohistochemistry, compared to WT mice. We then investigated its mechanism in vitro using primary osteoblast (OB) and the mature OB cell line UMR 106. We tested if 1-34 PTH (10-7 M) treatment affects both of FGF23 and DMP1 expressions. 1-34 PTH increased fgf23 expression, while it decreased dmp1 expression in primary OB as well as UMR-106. Not only 1-34 PTH but also forskolin increased fgf23 expression and decreased dmp1 expression in UMR-106 in a dose-dependent manner. Furthermore, PKA inhibitor H89 (10-5 M) reversed elevated fgf23 and reduced dmp1 expressions by 1-34 PTH treatment, respectively. Silence of dmp1 expression, besides treating with 1-34 PTH, elevated fgf23 expression additively as same as phosphorylated form of the transcriptional factor cAMP-response element-binding protein (CREB), stimulating FGF-23 promoter activity in OB. These results demonstrated that PTH increases and decreases FGF23 and DMP1 expressions via activation of PKA signaling. Furthermore, the regulation of DMP1 expression negatively via PKA Signaling would be in part of the mechanism which PTH increases FGF23 transcription on bone tissue in PHPT.

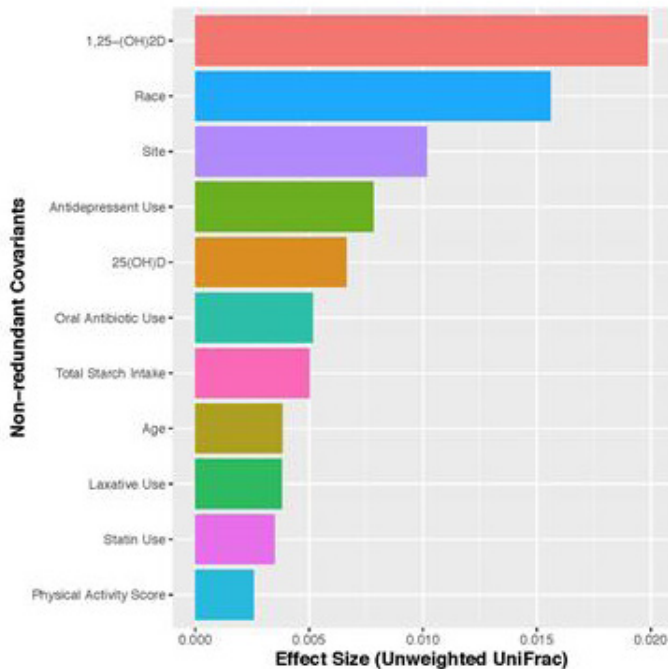
Disclosures: **Yuki Nagata**, None

SAT-0358

Vitamin D Metabolites and the Gut Microbiome in Older Men: The MrOS Study. Robert Thomas^{*1}, Lingjing Jiang¹, Zech Xu¹, Jian Shen¹, Stefan Janssen¹, Gail Ackermann¹, John Adams², Steven Pauwels³, Dirk Vanderschueren³, Rob Knight⁴, Eric Orwoll⁴, Deborah Kado¹. ¹University of California San Diego, United States, ²University of California Los Angeles, United States, ³UZ Leuven, Belgium, ⁴Oregon Health Sciences University, United States

The vitamin D receptor (VDR) is highly expressed in the gastrointestinal tract where, when activated with 1,25-(OH)₂D, it impacts local inflammation, immunity, epithelial function, and calcium/vitamin D absorption. In animal studies, gut microbiota have been shown to alter intestinal vitamin D metabolism (VDM), but human evidence is sparse. Thus, we tested the hypothesis that the human gut microbiome may interact with VDM using blood and stool samples collected from 599 U.S. MrOS men (mean age 84.2, SD = 4.1). To quantify 25(OH)D, 1,25-(OH)₂D and 24,25(OH)₂D levels, we used LC:MS:MS. From the raw 16S ribosomal RNA sequencing data, we used Deblur to define sub-Operational Taxonomic Units and Greengenes 13.8 to assign taxonomic labels; all analyses were conducted in QIIME. Men had an average BMI of 27 kg/m², their mean 25(OH)D level was 35.2 ng/mL (SD = 12.5), 75% reported taking vitamin D supplementation, and 7.2% were D deficient (≤20 ng/mL). To determine which factors were important in determining within subject differences in stool microbiota, we used Faith's Phylogenetic Diversity (PD) and non-redundant covariate analyses. We found that 1,25-(OH)₂D explained 5% of variance in α-diversity; the other non-redundant covariates of site, race, history of recent antibiotic

use, 25(OH)D and antidepressant use all combined explained another 8%. In multiple linear regression analyses adjusted for age, site, antibiotic use and antidepressant use, with higher 1,25-(OH)2D, there was greater α -diversity (standardized β -estimate 1.32, $p = 1.08 \times 10^{-6}$). Likewise, with higher levels of 24,25(OH)2D, there was greater α -diversity (standardized β -estimate 0.66, $p = 0.016$). In β -diversity analyses using unweighted UniFrac to assess between subject differences in stool microbiota, 1,25-(OH)2D was the strongest factor assessed, explaining about 2% of the variation (Figure). In older men, higher levels of the active vitamin D hormone 1,25-(OH)2D and the catabolic product 24,25(OH)2D, but not the pro-hormone 25(OH)D, were associated with greater α -diversity, concordant with numerous other studies suggesting that greater stool microbial diversity is associated with better health. Although directionality cannot be determined, our results suggest that the gut microbiota play an important role in host VDM.



Disclosures: **Robert Thomas**, None

SAT-0359

Determination of reference ranges for parathyroid hormone in healthy individuals classified by vitamin D status using the Elecsys® PTH and Vitamin D total II immunoassays Richard Ostlund*¹, Naga Yalla¹, Gabriella Bobba², Ge Guo³, Ann Stankiewicz³. ¹Washington University, St. Louis, MO, United States, ²Roche Diagnostics International Ltd, Rotkreuz, Switzerland, ³Roche Diagnostics Inc., Indianapolis, Indiana, United States

Intro/Background Parathyroid hormone (PTH) concentrations are routinely measured in the diagnosis and management of bone and mineral diseases and chronic kidney diseases. PTH secretion can be increased in individuals with vitamin D deficiency, which has an estimated prevalence of 41.6% among US adults. Reference ranges for PTH may be over-estimated if determined in a population of otherwise healthy individuals for whom vitamin D deficiency was not evaluated. We aimed to establish distinct PTH reference ranges in apparently healthy, normocalcemic, normophosphatemic individuals according to vitamin D status. **Methods** Apparently healthy individuals aged ≥ 21 years with body mass index > 18 and < 30 were enrolled at three diverse geographical sites across the US during summer (August 2015 and June 2016) and winter (December 2015 and February 2016) months. Use of drugs influencing bone and calcium/phosphorus metabolism was an exclusion criterion. Serum PTH and vitamin D concentrations were measured with the Elecsys® PTH (cobas e 601) and Elecsys® Vitamin D total II electrochemiluminescence immunoassays (cobas e 411) at one central laboratory (Washington University, MO, USA). Samples with values outside of the reference ranges for calcium, phosphorus and creatinine were excluded. PTH reference ranges were calculated using a standard nonparametric analysis (CLSI EP28-A3c guidelines). **Results** Samples were collected from 653 individuals, and 490 evaluable serum samples were analysed (56.73% female; 68.16% white/Caucasian; 28.57% African American; median age 44 yrs [range: 21–83]). Across all samples, median (2.5–97.5th percentile) serum PTH concentration was 35.46 pg/mL (17.25–76.43). A significant inverse relationship was found between PTH and vitamin D ($p < 0.001$). Median PTH concentrations decreased with increasing vitamin D concentration (Table), and all of the clinical categories of vitamin D (≤ 20 , > 20 – < 30 and ≥ 30 ng/mL) were significantly different from one another ($p < 0.01$). Any additional effects of race or season as covariates were relatively small or absent. **Conclusion** We provide reference ranges for PTH in serum from apparently healthy normocalcemic, normophosphatemic individuals, using the Elecsys® PTH and Elecsys® Vitamin D

total II assays, according to three categories of vitamin D concentration. Values for vitamin D replete individuals will support the accurate and reliable diagnosis and management of various diseases.

Table. PTH reference ranges by vitamin D class.

Median PTH concentration, pg/mL (2.5th to 97.5th percentile)	Vitamin D concentration, ng/mL			
	≤ 20	> 20 and < 30	≥ 30	Total
Summer	39.20 (16.69–74.13) n=71	37.43 (20.09–60.41) n=81	31.58 (14.32–51.86) n=94	35.12 (18.14–74.01) n=246
Winter	40.03 (19.49–86.55) n=112	33.01 (13.81–60.40) n=85	33.70 (17.66–68.33) n=47	35.78 (17.24–76.95) n=244
Total	39.78 (19.49–86.43) n=183	35.46 (16.96–60.41) n=166	31.90 (17.86–58.64) n=141	35.46 (17.25–76.43) n=490

PTH, parathyroid hormone

Disclosures: **Richard Ostlund**, Roche Diagnostics and Regeneron, Grant/Research Support

SAT-0392

See Friday Plenary Number FRI-0392

SAT-0393

See Friday Plenary Number FRI-0393

SAT-0394

See Friday Plenary Number FRI-0394

SAT-0395

See Friday Plenary Number FRI-0395

SAT-0396

See Friday Plenary Number FRI-0396

SAT-0397

Growth Hormone Effects on Bone Loss-Induced by Mild Traumatic Brain Injury and/or Hind Limb Unloading Nikita Bajwa*¹, Chandrasekhar Kesavan^{1,2}, Heather Watt¹, Subburaman Mohan^{1,2}. ¹Musculoskeletal Disease Center, VA Loma Linda Healthcare System, United States, ²Department of Medicine, Loma Linda University, United States

Disruption of the hypothalamus-pituitary axis in response to traumatic brain injury (TBI) is a key element in inducing bone loss and this effect is maximized during immobilization. To study if the skeletal consequence of mild repetitive TBI and/or hind limb unloading (UL) is rescued by growth hormone (GH) treatment, eighty-one 9-week old female C57BL/6J mice were randomly assigned to the following groups: Control-Sham-Vehicle (VH), Control-Sham-GH, Control-UL-VH, Control-UL-GH, TBI-Sham-VH, TBI-Sham-GH, TBI-UL-VH, and TBI-UL-GH. Mild TBI was induced experimentally using a weight drop model, once per day for four consecutive days. Unloading (right hind limb) and treatment (3 mg/day GH or vehicle) began two weeks after the first TBI episode and lasted for four weeks. We previously showed that TBI, UL and TBI-UL reduced tibia trabecular bone mass by 15%, 70%, and 75% respectively compared to control mice and that GH treatment significantly increased trabecular bone mass in all four (VH, TBI, UL and TBI+UL) groups. To determine if TBI and/or hind limb UL adversely affects other skeletal sites besides long bones, we evaluated the trabecular bone mass of vertebra in this study. Micro-CT analysis revealed 20% reduction in BV/TV ($P = 0.01$) at the lumbar vertebra in the vehicle treated TBI-Sham-VH mice compared to VH treated Control-Sham mice. Hind limb UL caused a small reduction (15%) in trabecular bone mass at the vertebra compared to the tibia (70%). In TBI-UL-VH mice, vertebral trabecular bone mass was reduced by 40% ($P < 0.01$) compared to VH group. While GH treatment increased trabecular bone mass of tibia in all four groups (VH, TBI, UL and TBI+UL) groups, GH treatment increased vertebral trabecular bone mass in VH and Control UL groups but not in the TBI or TBI+UL groups. **Conclusions:** 1) TBI significantly reduced trabecular bone mass at both long bone and vertebra several weeks post impact. 2) Hind limb UL reduced trabecular bone mass at the local (tibia) as well as distal (vertebra) site, suggesting involvement of both local and systemic mechanisms for

UL effects. 3) GH anabolic effect in the TBI and UL groups varied depending on the skeletal site studied.

Disclosures: *Nikita Bajwa, None*

SAT-0398

Mechanical Stress-induced Intracellular Ca²⁺ Oscillations in Human Periodontal Ligament Fibroblasts Ei Ei Hsu Hlaing^{*1}, Yoshihito Ishihara², Ziyi Wang¹, Naoya Odagaki¹, Hiroshi Kamioka¹. ¹Department of Orthodontics, Okayama University Graduate School of Medicine, Dentistry, and Pharmaceutical Sciences, Japan, ²Department of Orthodontics, Okayama University Hospital, Japan

Objective: Periodontal ligament (PDL) fibroblasts are the first cells to receive mechanical stress (MS) followed by alveolar bone remodeling in tooth movement. However, the role of intracellular calcium ([Ca²⁺]_i)-based mechanotransduction is poorly understood in PDL fibroblasts. We examined the MS-induced [Ca²⁺]_i mobilization in PDL fibroblasts to investigate its possible role in tooth movement-initiated bone remodeling as a clue to determine the optimum orthodontic force to apply to teeth. **Methods:** PDL fibroblasts were isolated from healthy donors' extracted premolars for orthodontic reasons. Static compressive force was applied to the PDL cells for 24 h. The oscillatory [Ca²⁺]_i activity was measured by a live Ca²⁺ imaging system and evaluated by a wavelet analysis in the time and frequency domains. Responsive cells were identified by their displaying a transient increase in [Ca²⁺]_i of at least 50% increase over the baseline. PDL fibroblasts were treated with various doses of the Ca²⁺-transporting ionophore A23187 for 6 and 24 h to further investigate the functional role of [Ca²⁺]_i upregulation in PDL cell behavior. Reverse transcription polymerase chain reaction was used to examine the mRNA expression. **Results:** The percentage of responsive PDL fibroblasts was significantly increased in response to MS. Individual cells responded with a sudden elevation of [Ca²⁺]_i followed by intermittent increases in the [Ca²⁺]_i. The cell response frequency, waveform length and maximum amplitude were significantly different from the control group. According to the Moran index for evaluating the influence of MS on cell-cell communication, individual cells independently responded to MS. Treatment with A23187 induced the upregulation of the RANKL/OPG ratio and SOST expression. **Conclusion:** Our findings suggest that RANKL/OPG and canonical Wnt/β-catenin signaling via augmented MS-mediated [Ca²⁺]_i oscillation may be involved as an early signaling process in tooth movement-initiated bone remodeling.

Disclosures: *Ei Ei Hsu Hlaing, None*

SAT-0399

Role of Parathyroid Hormone Receptor Type I and Primary Cilia in Bone Mechanotransduction on Osteocytes and Osteoblasts Arancha Gortazar^{*}, Irene Buendia, Eduardo Martin-Guerrero, Irene Tirado, Juan Antonio Ardura. Bone Physiopathology Laboratory, Departamento de Ciencias Médicas Básicas, Facultad de Medicina, Universidad San Pablo CEU, CEU Universities, Spain

Effects of mechanical stimulus on osteocytes and osteoblasts are determinant to bone physiopathology. Multiple mechanosensing mechanisms, including the activation of primary cilia in osteocytes and osteoblasts have been proposed as modulators of bone remodeling. Recently, we have described the mechanosensing ability of parathyroid hormone receptor type 1 (PTH1R) in bone. We hypothesize that PTH1R and primary cilia constitute a mechanosensing signalosome that regulates osteocyte- and osteoblast-mediated bone remodeling. We aim to describe the role of PTH1R and primary cilia as the molecular tools that concomitantly act as mechanosensors in osteocytes and osteoblasts. MLO-Y4 osteocytes and MC3T3-E1 pre-osteoblasts were mechanically stimulated with fluid flow (FF) [10 min, 10 dynes/cm²] or with PTHrP (1-37) [a PTH1R agonist]. PTH1R or primary cilia siRNAs and a primary cilia specific inhibitor [chloral hydrate] were used to decrease receptor or primary cilia signaling. Gene expression of bone remodeling and formation markers including OPG, RANKL, Runx2, osteocalcin, alkaline phosphatase and osterix and phosphorylation of the MAP kinase ERK 1/2 was studied in MLO-Y4 and MC3T3-E1 cells. FF increased OPG and RANKL expression and OPG/RANKL ratio and induced phosphorylation of ERK 1/2 kinase in both osteocytes and pre-osteoblasts. In addition, FF overexpressed Runx2, osteocalcin, and alkaline phosphatase in MC3T3-E1 pre-osteoblasts. These effects were partially inhibited by PTH1R silencing. Moreover, PTHrP (1-37)-dependent increase of OPG/RANKL ratio and ERK 1/2 phosphorylation in osteocytes and pre-osteoblasts and Runx2, osteocalcin, and alkaline phosphatase overexpression in MC3T3-E1 pre-osteoblasts were inhibited by primary cilia silencers or chloral hydrate. The osteogenic response of osteocytes and osteoblasts is mediated, at least in part, by a PTH1R and primary cilia combined mechanism.

Disclosures: *Arancha Gortazar, None*

SAT-0400

Adaptive Changes in Micromechanical Environment of Cancellous and Cortical Bone Following Mechanical Loading and Disuse Haisheng Yang^{*1}, Ran Liu¹, Whitney Bullock², Russell Main². ¹Beijing University of Technology, China, ²Purdue University, United States

Mechanical stimuli play an important role in bone (re)modeling for maintenance of the skeleton to resist fracture during habitual loading. It is known that extra mechanical stimuli (e.g. exercise) can increase bone mass while a reduction of mechanical stimuli (e.g. space flight or prolonged bed rest conditions) may lead to bone loss. Little is known how mechanical loading or unloading alter the micromechanical environments of cancellous and cortical bone, which may be associated with tissue-level failures. Sixteen-week-old female C57BL/6J mice were used in this study. Loading and unloading experiments were conducted. For the loading experiment, one group of mice underwent *in vivo* tibial compressive loading for two weeks with the left limb being loaded and the contralateral limb serving as nonloaded control (n=10). For the unloading experiment, a second group of mice underwent hindlimb disuse for 3 weeks via tail suspension and the third group of mice served as an age-matched control group for the disuse group and had normal cage activities for 3 weeks (n=10/group). Changes in bone mass and tissue-level mechanical environments following loading or unloading were determined using micro-computed tomography (microCT) and microCT-based finite element analysis, respectively. We found that loading or unloading significantly altered cancellous and cortical bone mass and the change in bone mass was more pronounced in the proximal metaphyseal cancellous than midshaft cortical bone of the tibia. These loading- or unloading-induced changes in cancellous and cortical bone mass and morphology were accompanied by altered bone tissue-level mechanical environments when the tibiae were virtually loaded in compression. In the metaphyseal cancellous or midshaft cortical bone, there was a shift in the amount of bone tissue from high towards low strain regions for the loaded relative to control tibiae (Fig. 1); with unloading there was a decrease in the amount of low strain tissues and an increase in the amount of high strain tissues (Fig. 1). In addition, regression analyses indicated that bone mass was a good predictor of bone tissue strain for the midshaft cortical bone but not for the metaphyseal cancellous bone. In summary, loading- or disuse-induced changes in bone mass lead to an overall reduction or increase in tissue-level strains, respectively, and micromechanics of the cancellous bone may not be correlated with bone mass.

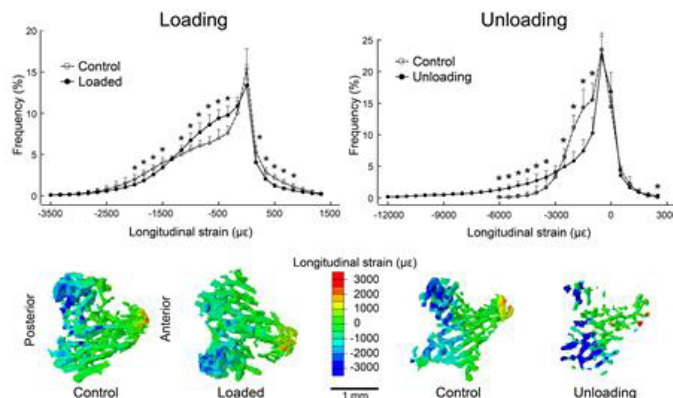


Fig. 1. Changes in tissue strain distribution of the proximal metaphyseal cancellous bone of the tibia with applied compressive loading or hindlimb unloading. * $p < 0.05$ (paired t-test for control vs. loaded tibiae or unpaired t-test for control vs. unloaded tibiae). Bars: mean±SD.

Disclosures: *Haisheng Yang, None*

SAT-0419

See Friday Plenary Number FRI-0419

SAT-0420

See Friday Plenary Number FRI-0420

SAT-0421

See Friday Plenary Number FRI-0421

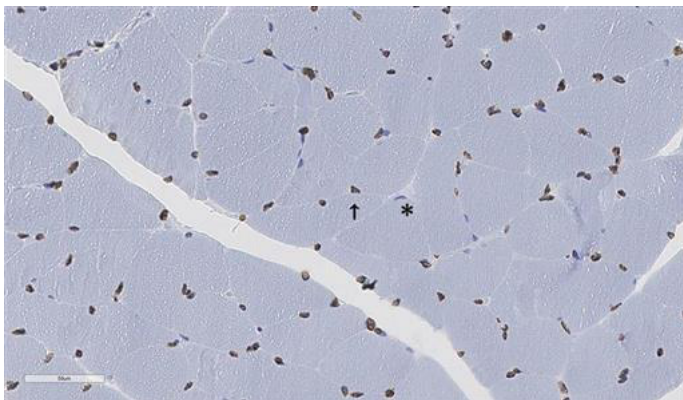
SAT-0422

See Friday Plenary Number FRI-0422

SAT-0423

The Vitamin D Receptor Expression in Skeletal Muscle of Women with Distal Radius Fracture Kahyun Kim^{*1}, Hyun Sik Gong². ¹Department of Orthopaedic Surgery, Hallym University College of Medicine, Republic of Korea, ²Department of Orthopaedic Surgery, Seoul National University College of Medicine, Republic of Korea

Introduction: We aimed to evaluate the relationship between the VDR expression in the muscle cell and the muscle mass in women with a distal radius fracture (DRF). **Methods:** We prospectively recruited 45 women over 50 years of age (mean age, 66 years) with DRF and acquired biopsy of the forearm flexor muscle. The muscle cross-sectional area (CSA) and VDR expression were measured using immunohistochemistry staining. The clinical parameters including grip strength, gait speed, body mass index (BMI), bone mineral density (BMD), and serum vitamin D levels were compared between patients grouped by appendicular lean mass index and were correlated with the VDR expression. **Results:** Twelve patients (27%) showed a decreased appendicular lean mass index, less than the cut-off value of 5.4 kg/m² which was suggested by the Asian Working Group for Sarcopenia. Patients with a low appendicular lean mass index had significantly lower muscle CSA ($p = 0.037$), but a higher VDR expression ($p = 0.045$) than those with higher indices. VDR expression was negatively correlated with BMI ($r = -0.417$, $p = 0.004$) and appendicular lean mass index ($r = -0.316$, $p = 0.044$). **Conclusions:** DRF patients with low appendicular lean mass index presented high VDR expression and low CSA in forearm muscle cells. This suggests that the VDR expression might be up-regulated in the attempt to compensate for the decreasing muscle mass. Further studies are necessary to explore the role of VDR in the progression of sarcopenia.



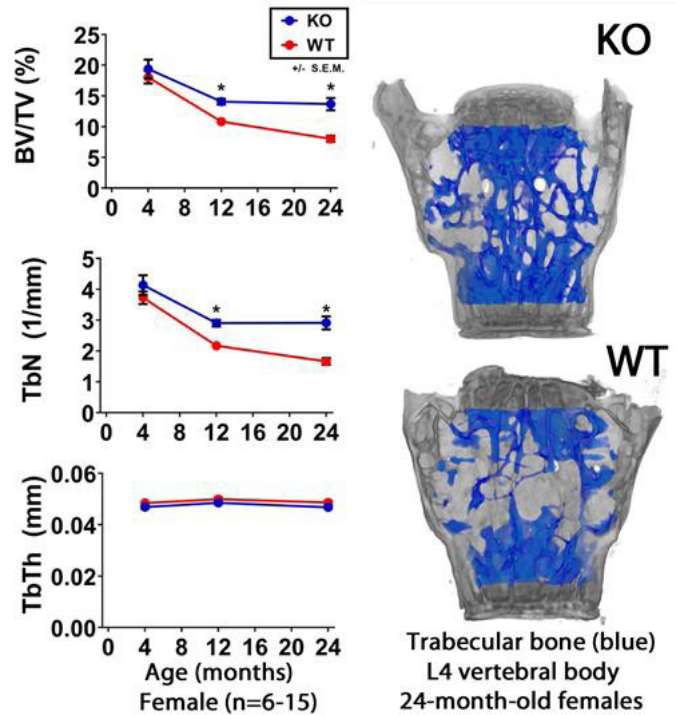
Disclosures: Kahyun Kim, None

SAT-0424

Age-related Decline of Osteogenesis Depends on Regulation of Protein Kinase A (PKA) by the Protein Kinase Inhibitor Gamma (PKI γ) Bryan S. Hausman^{*1}, Xin Chen², Hyonmin Choe³, Ozan Akkus¹, Edward M. Greenfield¹. ¹Case Western Reserve University, United States, ²University of North Carolina at Chapel Hill, United States, ³Department of Orthopaedic, Yokohama City University, Japan

Aging bone is characterized by decreased osteogenesis and increased adipogenesis resulting in bone loss and diminished repair capacity. Stimulation of the cAMP/PKA pathway in osteoblast lineage cells is responsible for increased bone formation in response to PTH therapy as well as many endogenous anabolic factors. We previously showed that PKI γ terminates PTH-induced PKA activity in the nucleus of mesenchymal precursor cells and that the termination of anabolic primary PKA-response genes (c-fos, IL-6, and LIF) by PKI γ reduces osteogenesis and enhances adipogenesis in vitro. We, therefore, generated and characterized Pkig^{-/-} mice, which were indistinguishable from wild-type littermates by body weight and fertility. μ CT analysis revealed that vertebrae of female Pkig^{-/-} mice are protected from age-related trabecular bone loss (see figure). As a result, female Pkig^{-/-} mice have 32% and 67% higher vertebral BV/TV at 12 and 24 months of age than wild-type mice (12-month, $n=15$: $13.9 \pm 0.5\%$ vs $10.5 \pm 0.4\%$, $p=0.0006$ and 24-month, $n=10$: $13.4 \pm 1.0\%$ vs $8.0 \pm 0.5\%$, $p<0.0001$). The increased vertebral BV/TV results from increased Tb.N without changes in Tb.Th (see figure). Accordingly, Tb.Sp was decreased and Connectivity Density increased with more plate-like geometry (decreased SMD). Regulation of age-related bone loss by PKI γ occurs primarily in vertebral trabecular bone of female mice as there was little or no effect in femora of female mice, in vertebrae and femora of male mice, or in younger mice. Based on the age dependence of the μ CT results, we speculated that the decline in osteogenesis with aging would also be lessened in Pkig^{-/-} mice. We, therefore, investigated intramembranous bone formation 7 days after placing a unicortical titanium implant in the distal femoral metaphysis. Biomechanical pull-out testing showed the expected age-related decline in osteogenesis in wild-type but not in Pkig^{-/-} mice. As a result, osseointegration in 12-month old Pkig^{-/-} males was significantly greater than in 12-month old wild-type males: Ultimate Force (7.6 ± 1.7 vs 3.8 ± 2.7 N, $p=0.02$) and Average Stiffness (6.7 ± 1.6 vs 3.4 ± 2.4 N/m, $p=0.005$). The increased osseointegration in femora of male Pkig^{-/-} male mice shows that inducing rapid osteogenesis reveals effects of PKI γ deletion that are obscured during

normal development and aging. Overall, our results show that preventing PKI γ regulation of PKA activity in aging bone enhances the effects of endogenous anabolic factors.



Disclosures: Bryan S. Hausman, None

SAT-0425

Lineage Tracing Studies Identify The Source Of Chondrocyte-Like Cells In Mouse Intervertebral Disc With Normal Aging Sarthak Mohanty^{*1}, Robert Pinelli¹, Chitra Dahia². ¹Hospital for Special Surgery, United States, ²Weill Cornell Medical College, United States

Intervertebral disc degeneration and associated back pain affects almost 1/7 individuals at some point in life and is a huge financial burden. Despite its high incidence, the current treatments are either palliative or surgical that are limited to taking care of the symptoms rather than treating the cause. This is due to limited understanding of the molecular mechanisms of disc growth and differentiation, and of the changes associated with its degeneration and aging. Our approach has been to use a mouse model to understand the normal postnatal growth and differentiation of the disc, and how that changes with disc degeneration and aging. One of the limitations in the development of treatment of the degenerated disc is knowledge about the cellular and molecular changes associated with physiological aging of the disc and its degeneration, this includes the morphological changes observed in the nucleus pulposus cells of aged or degenerated discs. With aging or degeneration, the disc undergoes pathological changes associated with the replacement of reticular and vacuolated notochordal/ nucleus pulposus cells with cells that resemble chondrocyte-like cells (CLCs). The presence of these CLCs in the disc space has been considered as an indication of disc degeneration. However, the source of these cells remains unknown. Identifying the lineage of the CLCs with disc aging and degeneration will provide a better understanding of the progression of disc degeneration. In normal mouse, these CLCs can be seen from 18 months of age. To understand the source of CLCs in the mouse disc with normal physiological aging, we did lineage tracing studies and identified that the reticular NP cells differentiate into CLCs with normal physiological aging. Using fate-mapping studies, we also observed that with aging all nucleus pulposus cells are lost from mouse lumbar disc as it fuses. The disc loses height and extracellular matrix as it ages and fuses. However, it is not clear that what causes the reticular nucleus pulposus to differentiate into the CLCs, and will require further studies.

Disclosures: Sarthak Mohanty, None

SAT-0438

See Friday Plenary Number FRI-0438

SAT-0439

See Friday Plenary Number FRI-0439

SAT-0440

See Friday Plenary Number FRI-0440

SAT-0441

See Friday Plenary Number FRI-0441

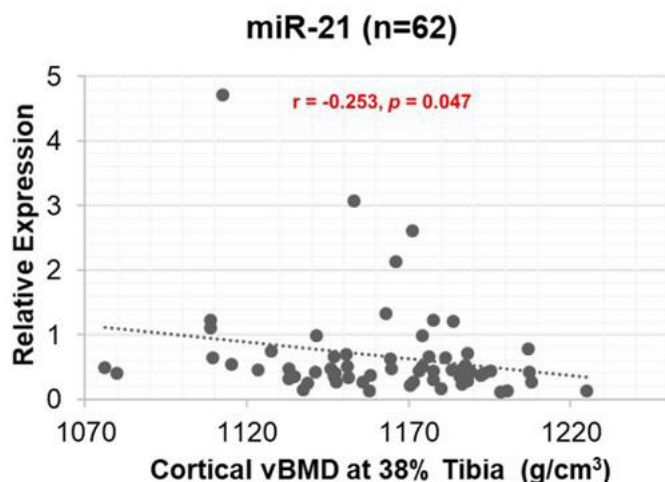
SAT-0442

See Friday Plenary Number FRI-0442

SAT-0443

Circulating MicroRNAs Are Negatively Associated with Bone Mineral Density in Postmenopausal Women Zhaojing Chen¹*, Debra Bembem², Michael Bembem². ¹California State University, San Bernardino, United States, ²University of Oklahoma, United States

MicroRNAs (miRNAs) are short, non-coding RNA molecules that fine tune posttranscriptional gene expression. Recent research has indicated that some miRNAs, such as miR-21 and miR-23a, target on genes of osteogenesis. Aging is accompanied with progressive declines in bone mineral density (BMD) and bone strength, which potentially may be regulated by these miRNAs. Additionally, miRNAs are found stable in body fluids such as blood, thus circulating miRNAs (c-miRNAs) may be useful as noninvasive biomarkers of bone metabolism. Purpose: To examine the relationships between specific c-miRNAs, BMD and bone strength in older postmenopausal women. Methods: Seventy-five postmenopausal women aged 60 to 85 years old participated in this study. Body composition and areal BMD (aBMD) at total body, lumbar spine, dual femur (total hip, femoral neck, trochanter) were measured by Dual Energy X-ray Absorptiometry (DXA). Volumetric BMD (vBMD) and bone strength at 4%, 38%, and 66% of the non-dominant tibia were measured by Peripheral Quantitative Computed Tomography (pQCT). Total RNA were extracted from serum, and relative expression levels of c-miRNAs (miR-21, -23a, -24, -100, -125b) were analyzed using miRNA assays and real-time PCR. Results: Osteopenia and osteoporosis were particularly common in this group of participants with a total percentage of 81% (n=61). MiR-21 was significantly negatively correlated with left trochanter BMC ($r = -0.252, p = 0.048$), right trochanter BMC ($r = -0.294, p = 0.020$), and cortical vBMD at tibia 38% site ($r = -0.253, p = 0.047$). There also was a trend for a significant correlation between miR-21 and lumbar spine aBMD ($r = -0.249, p = 0.051$). Conclusion: Our results suggest that a higher expression level of circulating miR-21 is associated with decreased BMD in relatively healthy postmenopausal women. Future investigations are needed to further explore circulating miRNAs in osteoporotic or fragile older adults.

Disclosures: *Zhaojing Chen, None***SAT-0444**

Comparing the epithelial-mesenchymal interaction effects in alveolar bone and long bone Chul Son^{*}, Joo-Cheol Park, Dong-Seol Lee, Yeoung Hyun Park. Laboratory for the Study of Regenerative Dental Medicine, Department of Oral Histology and Developmental Biology, School of Dentistry and Dental Research Institute, Seoul National University, Republic of Korea

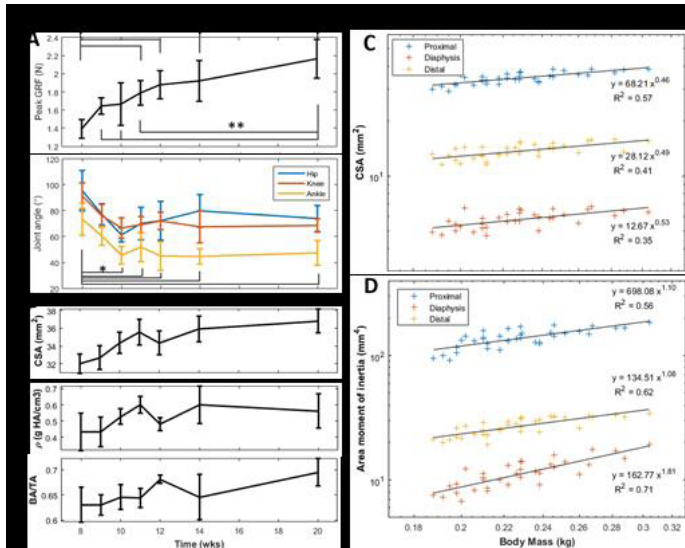
Epithelial-mesenchymal interaction (EMI) plays an essential role during the development of both alveolar bone and long bone. Especially, alveolar bone remodeling has re-

cently been reported to be affected by peripheral epithelial tissue that remains after tooth development. Remodeling occurs more actively by external stimuli in alveolar bone, making the condition of alveolar bone an important factor in various dental surgical processes. Therefore, understanding of alveolar bone development and remodeling procedure is critical. We aim to elucidate how the EMI affects alveolar bone and long bone differently during development and remodeling. We did histological analysis to elucidate alveolar bone and long bone development. We isolated cells from alveolar, femur and tibia bone tissues. The morphology of primary cultured mouse alveolar bone-derived cells (mABDC) and long bone-derived cells (mLBDC) looked similar. The expression level of Bsp was high in both types of cells. When the cells were cultured in osteogenic differentiation media, they manifested mineralized nodule formation. We focused on the difference between alveolar bone and long bone considering from cell and tissue level. The intramembranous ossification (IO) associated markers, Msx and Dlx family genes, which are also known to be involved in EMI were expressed higher in alveolar bone than in long bone. Interestingly, EMI related genes, Bmp family, Cpne7 and Nfic expression were different between alveolar bone and long bone. RNA sequencing data showed consistent results. Some other neural crest-derived cell marker and EMI related genes were also highly expressed in mABDC. When we analyzed the osteoblast marker genes, IO and EMI related genes during osteogenic differentiation, Bsp, OC and Bmp2 showed increasing expression patterns in both. Meanwhile Alp, IO and EMI related genes showed different expression patterns between mABDC and mLBDC. mLBDC showed more nodules stained during differentiation. Among the EMI related proteins we treated to each cells, BMP4 elevated the expression levels of osteoblast marker genes the most, more noticeably in mABDC than in mLBDC. Our data suggest that factors involved in EMI signaling may affect alveolar bone and long bone differently, possibly because of their different developmental origin and local environment. Especially BMP4 affects mABDC more than mLBDC; further investigation is needed to figure out the mechanism underlying the discrepancy.

Disclosures: *Chul Son, None***SAT-0445**

Gait and Scaling Effect on Bone Growth in Rat Tibia Hyunggi Song^{*}, Mariana Kersh. Department of Mechanical Science and Engineering, UIUC, United States

During growth, bones in the extremities have a preferential distribution of material and composition to sustain the loading cycles from everyday movement, but it is not clear how material and mechanical properties of bone are optimized. We aimed to understand how bone morphology and material properties change during growth, and whether they are related to gait dynamics using rats. Data was collected from 5 healthy female Sprague-Dawley rats at the age of 7 weeks. Rats were scanned using in vivo microCT (resolution = 35.8 μm) and gait analysis was performed at 8, 9, 10, 11, 12, 14, and 20 weeks. A custom walkway was created to measure ground reaction forces (GRF) with a force plate. Joint kinematics of the hindlimb were measured with two high-speed cameras. When the right foot steps on the force plate correctly, both kinematics and GRF were collected during one gait cycle at 240 Hz. The right tibia was segmented using Amira 5.6. Hounsfield unit to apparent density conversions were calculated for each scan with HA phantoms. Custom Matlab code was used to calculate cross-sectional area (CSA), density, bone area fraction (BA/TA), and polar moment of inertia (J) at distal, diaphysis, and proximal regions. Averaged peak GRF and joint angles at the time of the peak were obtained over time (Fig. 1A). The rate of increase in peak GRF decreased, but the peak GRF still increased during growth, while joint angles decreased until at ten weeks and then converged. The proximal region had a larger CSA and lower density compared to the other regions, since it has more trabecular bone (Fig. 1B). The proximal CSA kept increasing, while middle and distal CSA were stayed at a constant level, which indicated that growth in proximal CSA was affected by both GRF and joint angles during gait. Both GRF and joint angles influence density since density and BA/TA in all regions increased and converged, except for distal BA/TA. To investigate the scaling relationships, CSA and J were compared with body mass in log scale (Fig. 1CD). CSA and J in diaphysis showed higher slopes than the other regions and the slopes were close to the scaling relationships [1], implies that the diaphysis of tibia is getting stronger most to sustain the loading during growth. Bone properties change and relationships to gait properties during the growth period were investigated. How muscle forces can change bone strategies during growth remains to be understood. Spence, A. J. Current Biology, 19(2), 2009.



Disclosures: *Hyunggi Song, None*

SAT-0446

Associations of Insulin-like Growth Factor-1, Insulin-like Growth Factor Binding Protein-3, Bone and Body Composition Variables in Children 2 to 8 y Olusola Sotunde*¹, Neil Brett², Sherry Agellon¹, Catherine Vanstone¹, Hope Weiler¹. ¹School of Human Nutrition, McGill University, Canada, ²School of Nutrition Ryerson University, Canada

Musculoskeletal growth is multifaceted and influenced by several hormones including insulin like growth factor-1 (IGF-1). The majority of IGF-1 is bound by insulin-like growth factor binding protein-3 (IGFBP-3) in circulation, with IGFBP-3 serving as a circulatory reservoir for IGF-1. However, very little is known about the interactions between IGF-1, IGFBP-3, muscle and bone geometry of healthy young children. Therefore, we examined the associations between bone variables, body composition, IGF-1 and IGFBP-3 in children. Healthy children 2 to 8 y (n = 49) from Montreal Canada were studied (NCT02387892) for demographics, physical activity and standardised anthropometry. Fasting venous blood samples were collected to assess plasma IGF-1 and IGFBP-3 (enzyme-linked immunosorbent assays) and serum 25-hydroxyvitamin D (25(OH)D; Liaison, Diasorin Inc). Body composition and bone densitometry (whole body, lumbar spine and radius) were measured using dual-energy X-ray absorptiometry (Hologic 4500A: APEX version 13.3.3). Tibia geometry (4 and 66%) and muscle density (66%) were measured at the distal end of the tibia with peripheral quantitative computed tomography (pQCT, XCT-2000; Stratec). The ratio of IGF-1 to IGFBP-3 was calculated as a marker of free bioactive IGF-1. Linear regression analyses were carried out with adjustments for covariates. Participants were 4.71 ± 1.89 y with body mass index z- score of 0.65 ± 0.84 kg/m², 59.2% were boys and 46.9% were white. All participants were within the reference ranges for IGF-1 and IGFBP-3 while 18.4% were vitamin D inadequate [25(OH)D < 50 nmol/L]. IGF-1 was positively associated with whole body lean mass and pQCT parameters (muscle density, muscle cross sectional area, trabecular density, cortical cross sectional area and cortical density; Table 1), with no association to fat mass. IGF-1/IGFBP-3 ratio had a positive association with total radius densitometry, and cortical density of tibia at the 66% site. The associations of IGF-1 with tibia bone geometry; IGF-1/IGFBP-3 ratio and total radius densitometry suggests an important role of IGF-1 on long bone growth. Though IGFBP-3 had an independent positive association with cortical cross sectional area, IGF-1 appears to have stronger independent associations with bone and muscle parameters compared to IGFBP-3.

Table 1: Association between IGF1, IGFBP3 or IGF1/IGFBP3 ratio and bone and muscle quality in 2 – 8 year olds

	Body Composition and Bone parameters (DXA)															
	Whole body lean mass, g				Whole body fat mass, g				Total Radius BMC, g/cm ²				Total Radius BMC, g			
	β	SE	p	Adj R ²	β	SE	p	Adj R ²	β	SE	p	Adj R ²	β	SE	p	Adj R ²
IGF-1, ng/ml	20.20	8.830	0.03	0.360	-2.329	7.677	0.76	0.673	0.001	0.000	0.01	0.768	0.008	0.002	0.004	0.843
IGFBP-3, ng/ml	0.942	0.616	0.14	0.895	0.241	0.516	0.64	0.674	0.000	0.000	0.16	0.735	0.000	0.000	0.20	0.811
IGF-1/IGFBP-3 ratio	42326	30561	0.18	0.894	-27243	2043	0.29	0.682	1.219	0.581	0.04	0.751	16.64	6.849	0.02	0.830
Tibia bone geometry (pQCT)																
	4% Trabecular density, mg/cm ³				66% Cortical density, mg/cm ³				66% Cortical CSA, mm ²				66% Cortical thickness, mm			
	β	SE	p	Adj R ²	β	SE	p	Adj R ²	β	SE	p	Adj R ²	β	SE	p	Adj R ²
IGF-1, ng/ml	0.288	0.173	0.03	0.158	1.111	0.317	0.001	0.280	0.450	0.121	0.001	0.764	0.003	0.002	0.15	-0.020
IGFBP-3, ng/ml	0.012	0.012	0.34	0.043	0.043	0.024	0.06	0.106	0.023	0.009	0.01	0.723	0.000	0.000	0.07	0.007
IGF-1/IGFBP-3 ratio	957.2	617.5	0.13	0.080	3497.4	1123	0.004	0.239	936.8	467.0	0.05	0.705	2.265	0.002	0.78	-0.09
Muscle Density (pQCT)																
	66% Muscle density, mg/cm ³				66% Muscle CSA, mm ²											
	β	SE	p	Adj R ²	β	SE	p	Adj R ²								
IGF-1, ng/ml	0.116	0.047	0.02	0.639	0.030	0.022	0.03	0.642								
IGFBP-3, ng/ml	0.005	0.003	0.13	0.603	0.237	0.161	0.15	0.616								
IGF-1/IGFBP-3 ratio	264.6	169.6	0.13	0.604	10562	6159	0.20	0.611								

Disclosures: *Olusola Sotunde, None*

SAT-0447

Interactions between protein phosphatases and potassium channels control chondrocytes proliferation and regeneration Earnest Taylor*, Elizabeth Bradley, Xiaodong Li, Jennifer Westendorf. Mayo Clinic, United States

Osteoarthritis (OA) is the most common form of arthritis and is characterized by degeneration of articular cartilage, a shock absorbing tissue between bones, as a result of injury or aging. The protein phosphatases Phlpp1 and Phlpp2 are aberrantly expressed in articular cartilage from OA patients and limit chondrocyte proliferation in vitro. Phlpp1 deficiency and Phlpp inhibitors limit OA disease progression and pain in mice. In a candidate screen of mitogenic factors, we found that Phlpp1 depletion increased expression of a number of factors that are now in OA trials: Fgf18, Tgfb, Wnts. The Pth receptor, PthR1, was also upregulated in Phlpp1-deficient and Phlpp inhibitor treated chondrocytes. To further understand how Phlpp inhibitors increase chondrocyte proliferation and matrix production, we performed an unbiased RNA-seq experiment on human OA tissues. OA tissue explants treated with Phlpp inhibitors expressed higher levels of Girk2. Girk2 is a component of G protein-gated inwardly rectifying potassium (GIRK) channels that regulate potassium ion transport across cell membranes via specific G-protein-coupled signaling mechanisms. Various neurotransmitters, dopamine, opioids and serotonin control GIRK channels and potassium efflux by stimulating their cognate G protein coupled receptors. Our preliminary data demonstrate that Girk2 knockout (KO) and Girk3 KO mice have normal limbs and that chondrocytes from Girk2 KO or Girk3 KO mice differentiate normally in vitro. However, mice lacking both Girk2 and Girk3 have longer bones and chondrocytes from Girk2/Girk3 double KO mice produce more matrix in vitro. These data suggest that there is greater chondrocyte formation and regenerative capacity when both Girk2 and Girk3, which together comprise more than 90% of Girk channels, are absent. We have also discovered that GIRK channels bind to Phlpp1 and Phlpp2. Thus Girk2 may play a role in cytoplasmic retention and positioning of these phosphatases in close proximity to key substrates such as Akt and PKC that limit chondrocyte proliferation and matrix production. These data identify novel relationships between potassium channels and kinase signaling pathways in chondrocytes. Inhibitors of Phlpp1 and/or Girk2/3 may enhance chondrocyte regeneration by promoting anabolic pathways through secretion of growth factors and/or releasing.

Disclosures: *Earnest Taylor, None*

SAT-0464

See Friday Plenary Number FRI-0464

SAT-0465

See Friday Plenary Number FRI-0465

SAT-0466

See Friday Plenary Number FRI-0466

SAT-0467

See Friday Plenary Number FRI-0467

SAT-0468

See Friday Plenary Number FRI-0468

SAT-0469

See Friday Plenary Number FRI-0469

SAT-0470

See Friday Plenary Number FRI-0470

SAT-0471

Human mesenchymal stromal cells in adhesion to cell-derived extracellular matrix and titanium: comparative kinome profile analysis Marta Baroncelli^{*1}, Gwenny Fuhler², Jeroen Van De Peppel¹, Willian Zambuzzi³, Johannes Van Leeuwen¹, Maikel Peppelenbosch², Bram Van Der Eerden¹. ¹Internal Medicine, Erasmus MC, Netherlands, ²Gastroenterology, Erasmus MC, Netherlands, ³Chemistry and Biochemistry, Institute of Bioscience, UNESP, Brazil

The extracellular matrix (ECM) is essential to physically support cells and actively influence cell behaviour by modulating kinase-mediated signalling cascades, key regulators of signal transduction. Cell-derived ECMs have recently emerged in the context of bone regeneration, as they reproduce physiological tissue-architecture and ameliorate the promising properties of mesenchymal stromal cells (MSCs). Titanium scaffolds show good mechanical properties and porosity to facilitate cell adhesion, and thus have been routinely used for bone tissue engineering applications. The aim of this study was to analyze the kinomic signature of human MSCs in adhesion to an osteoblast-derived ECM that we have previously shown to be osteopromotive, and to compare it to MSCs on titanium. PamChip kinase array analysis revealed 63 phosphorylated peptides on ECM and 59 on titanium, with MSCs on ECM exhibiting significant higher levels of kinase activity than those on titanium (Area under curve on ECM 34.1 vs 27.6 on titanium, $P < 0.0001$). MSCs on the 2 substrates showed a substantial overlap of kinome profiles, with the activation of similar signalling pathways, such as FAK, ERK and PI3K signalling, as confirmed by immunoblot analyses. Inhibition of PI3K signalling in cells significantly reduced cell adhesion to the ECM (0.5-fold, $P < 0.001$), and increased the number of non-adherent cells, both on ECM (2.4-fold, $P < 0.001$) and on titanium (1.9-fold). The increase in non-adherent cell number in response to PI3K inhibition was not due to induction of apoptosis by PI3K inhibitors. In summary, this study comprehensively characterized the kinase activity in MSCs on cell-derived ECM and on titanium, highlighting the role of PI3K signalling in the kinomic changes regulating osteoblast viability and adhesion. Kinome profile analysis represents a powerful tool to select pathways for a better understanding of cell behaviour. Osteoblast-derived ECM could be further investigated as coating for titanium scaffolds, to improve bone tissue engineering applications.

Disclosures: *Marta Baroncelli, None***SAT-0472**

Requirement of the PDGFR-PI3K-AKT signaling axis in periosteal cells Laura Doherty^{*}, Xi Wang, Jungeun Yu, Ivo Kalajzic, Archana Sanjay. UConn Health, United States

Insufficient fracture healing remains a significant public health problem with a large economic burden and limited therapeutic options. PI3K signaling, a major pathway involved in regulation of fracture healing, promotes proliferation, migration, and differentiation of osteoprogenitors. We have recently reported that knock-in mice with a global increase in PI3K signaling (gCblYF) show enhanced femoral fracture healing characterized by an extraordinary early periosteal response. Periosteal-derived progenitors are essential during fracture repair, as they expand at the fracture site and provide a template for new bone formation. Platelet-derived growth factor (PDGF) is a potent mitogen for mesenchymal progenitors, with expression highest during the earliest phases of injury. The effects of PDGF are mediated through receptors Pdgfr- α and - β , and we have established that Pdgfr β is the predominant isoform expressed in the fracture callus. Treatment of periosteal cells with PDGF-BB, that activates all platelet derived growth factor receptors, resulted in increased proliferation and migration. By flow cytometry analysis we found that 75% of periosteal cells express Pdgfr β . Interestingly, of all the growth factor receptors involved in fracture healing, only Pdgfr β directly bind to PI3K. Given these findings, we hypothesized that PDGFR-PI3K signaling is necessary for mediating robust periosteal cell proliferation. We found that mRNA and protein expression of Pdgfr β was augmented during the proliferative phase of cell culture in gCblYF periosteal cells compared to WT. Western blots showed that relative to FGF2 or IGF1, PDGF efficiently increased AKT phosphorylation in gCblYF periosteal cells, and also augmented phosphorylation of AKT substrates containing RXXS*/T* motif. In contrast, induction of ERK phosphorylation was comparable among all treatment groups. Phosphorylation of Pdgfr β and AKT substrates was reduced in cells treated with SU16f, a Pdgfr β inhibitor, and deletion of Pdgfr β in periosteal cells using a mouse model abrogated AKT phosphorylation. Additionally, we found that treatment of periosteal cells with SC79, a small molecule activator of AKT, increased phosphorylation of AKT substrates to the same extent as treatment with PDGF. These results suggest that increased PI3K-AKT activation is necessary for Pdg-

fr β signaling in periosteal cells, and presents the PDGF-PI3K axis as a novel therapeutic target in the context of regenerative medicine.

Disclosures: *Laura Doherty, None***SAT-0473**

DPP-4-Cleaved SDF-1 β Diminishes Migration and Osteogenic Differentiation Capacities of Bone Marrow Mesenchymal Stem Cells Ahmed Elmansi^{*1}, Khaled Hussein¹, Brian Volkman², Galina Kondrikova¹, Wendy Bollag³, Sadanand Fulzele⁴, Xingming Shi⁵, Meghan Mcgee-Lawrence¹, Mark Hamrick¹, Carlos Isales⁵, William Hill¹, Sudharsan Periyasamy-Thandavan⁶. ¹Department of Cellular Biology and Anatomy, Augusta University, United States, ²Department of Biochemistry, Medical College of Wisconsin, United States, ³Department of Physiology, Augusta University, United States, ⁴Department of Orthopedic Surgery, Medical College of Georgia, United States, ⁵DEPARTMENT OF NEUROSCIENCE AND REGENERATIVE MEDICINE, Augusta University, United States, ⁶Cancer Center Pharmacy, Medical College of Georgia, Augusta University, United States

Mechanisms for age-related bone loss are poorly understood. In part it can be attributed to a decline in bone marrow mesenchymal stem cell (BMSC) osteogenic potential. Stromal cell derived factor-1 (SDF-1/CXCL12) is a chemokine responsible for activation of osteogenic differentiation pathways in BMSCs. Dipeptidyl peptidase-4 (DPP4) is a proteolytic enzyme that cleaves the two N-terminal amino acids Lysine and Proline from SDF-1. Intact SDF-1 has a very short half-life, and is cleaved by DPP4 within minutes of its release. SDF-1 cleaved by DPP4 enzyme is referred to as SDF-1(3-67) for the α splice variant, or SDF-1(3-72) for the β splice variant. Both cleaved isoforms have been thought to be inactive, and reported to have no activity through CXCR4, the primary receptor for SDF-1. However, we propose the DPP4 cleaved isoforms are not inactive but possess a separate bioactivity. We tested the effect of both intact and DPP4-cleaved SDF-1 β on inducing osteogenesis, adipogenesis, and migration in BMSCs. To be able to measure the difference in concentration between intact and cleaved SDF-1, we developed an antibody specific for cleaved SDF-1. We report the first known biological effects for DPP4 cleaved SDF-1(3-67 and 3-72) to be inhibition of osteogenesis and migration of BMSCs. Using the Alizarin Red osteogenic assay, we show that SDF-1 significantly increased BMSCs osteogenesis by 48%, while cleaved SDF-1 significantly decreased it by 22% relative to controls. Adding both cleaved and intact SDF-1 to BMSCs lead to an effect similar to that of cleaved SDF-1 alone. In terms of migration, cleaved SDF-1 shows similar outcomes in transwell assays and microfluidic migration assays in that DPP4 cleaved SDF-1 inhibits BMSCs migration to SDF-1-gradients. Further, in young human BMSCs treated with DPP4 Cleaved SDF-1 there is an increase in expression of the anti-osteogenic miRNAs 29b-1-5p and 141-3p, which are up-regulated in aged human BMSCs. In contrast intact SDF-1 reduces the expression of these miRNAs in BMSCs from aged humans. This suggests DPP4 cleaved SDF-1 modulates osteogenic gene expression potentially through epigenetic regulation, as well as more rapidly responsive signaling pathways. These results add to our understanding regarding roles of intact SDF-1 and its metabolites in bone homeostasis with age.

Disclosures: *Ahmed Elmansi, None***SAT-0474**

Assessment of a new anabolic drug, picolinic acid, in MSC cultures using in vitro live-cell confocal imaging Damian Myers^{*}, Ahmed Al Saedi, Gustavo Duque. University of Melbourne, Australia

Introduction: Mesenchymal stem cells (MSC) are pluripotent used for in vitro studies of both adipocytes and osteoblasts. Picolinic acid (PIC) has been proposed as an anabolic therapy for bone conditions and, in this study, we have utilized intracellular calcium ion ([Ca²⁺+Int]) mobilization is an indicator of cell activation. The aims of this study were to assess whether addition of PIC to MSC cultures could induce changes (Δ) in [Ca²⁺+Int] and, also, to characterise MSC cultures for both calcium ion responses and lysosomal expression in live-cell cultures. Methods: Bone marrow-derived MSC (Lonza Biosciences, Mt. Waverley, VIC, Australia) were cultured onto ϕ 18mm coverglass and, after 7 days of culture, were loaded for 30 min using Fluo-4-AM and LysoTracker-Red (Invitrogen, Thermofisher), both at 2 μ M in the medium. After washing, time-course experiments were performed using a Nikon A1Rsi CLSM (x20 lens). Fluo-4 fluorescence changes, proportional to Δ [Ca²⁺+Int], were monitored over 10-20 min to monitor cell responses to PIC (20 μ M). Ionomycin (10-8 M) was added for maximal Δ [Ca²⁺+Int] response and MnCl₂ (2 mM) was added to quench fluorescence signals for minimal fluorescence to establish dynamic range. Results: 5-10% of the cell population showed low-level transient oscillations (periodicity of 55.3 \pm 3.3 secs, mean \pm SD); in a field population of approx 220-240 cells. ROI assessment of single cells showed that MSCs expressing low levels of lysosomes exhibited a higher Δ [Ca²⁺+Int] in response to PIC (20 μ M) compared to cells with high levels of lysosomes (mean ratio change of 2.43 (range 2.0-2.8) compared to 1.50 (1.0-1.9); $p < 0.05$ by Kruskal-Wallis with Bonferroni correction; n=6 per analysis. Maximal ratio response to ionomycin was a value of 10-12. Conclusions: MSCs in culture exhibited differential expression of lysosomes and cells responded to PIC exhibiting dynamic Δ [Ca²⁺+Int]. The capacity of these cells to exhibit spontaneous [Ca²⁺+Int] oscillations is a novel finding and the fact that higher expression of lysosomes may affect induced Δ [Ca²⁺+Int] responses may be important in long-term cultures

and related bone studies. [Ca²⁺+Int] dynamics are central to many cellular processes affecting bone cell function and lysosomes have been implicated in autophagy and cell survival so further studies are justified to characterize these responses and to investigate impacts of novel therapies.

Disclosures: **Damian Myers**, None

SAT-0475

Validation of osteogenic properties of Cytochalasin D by high-resolution RNA-sequencing in mesenchymal stem cells derived from bone marrow and adipose tissues Rebekah Samsonraj*¹, Christopher Paradise¹, Amel Dudakovic¹, Buer Sen², Asha Nair¹, Allan Dietz¹, David Deyle¹, Simon Cool³, Janet Rubin², Andre Van Wijnen¹. ¹Mayo Clinic, United States, ²University of North Carolina, United States, ³Institute of Medical Biology, Singapore

Differentiation of mesenchymal stem cells involves a series of molecular signals and gene transcription events required for attaining cell lineage commitment. Modulation of the actin cytoskeleton using cytochalasin D (CytoD) drives osteogenesis at early time points in bone marrow-derived MSCs, and also initiates a robust osteogenic differentiation program in adipose-derived MSCs. To understand the molecular basis for these pronounced effects on osteogenic differentiation, we investigated global changes in gene expression in CytoD-treated murine and human MSCs by high-resolution RNA-sequencing analysis. A three-way bioinformatic comparison between human adipose-derived, human bone marrow-derived and mouse bone marrow-derived MSCs revealed significant upregulation of genes linked to extracellular matrix organization, cell adhesion and bone metabolism. As anticipated, the activation of these differentiation related genes is accompanied by a down-regulation of nuclear and cell cycle-related genes presumably reflecting cytostatic effects of CytoD. We also identified eight novel CytoD activated genes – VGLL4, ARHGAP24, KLHL24, RCBTB2, BDH2, SCARF2, ACAD10, HEPH – which are commonly upregulated across the two species and tissue sources of our MSC samples. The up-regulation of these 8 CytoD-responsive genes was confirmed via RT-qPCR. We selected the Hippo-pathway related VGLL4 gene, which encodes the transcriptional co-factor Vestigial-like 4, for further study because this pathway is linked to osteogenesis. Depletion of VGLL4 via siRNA knockdown reduced the pro-osteogenic effect of CytoD in adipose-derived MSCs upon assessment of matrix mineralization. Together, our RNA-seq analyses and subsequent in vitro experiments suggest that while the stimulatory effects of CytoD on osteogenesis are pleiotropic and depend on the biological state of the cell type, a small group of genes including VGLL4 may be central mediators controlling MSC commitment towards the bone lineage.

Disclosures: **Rebekah Samsonraj**, None

SAT-0476

Activation of Mitochondrial OxPhos Drives Osteogenesis via β -catenin Brianna Shares*, Melanie Busch, Noelle White, Laura Shum, Roman Eliseev. University of Rochester, United States

Bone marrow mesenchymal stem cells (BMSCs) can differentiate into osteoblasts (OB), adipocytes, and chondrocytes. As BMSCs undergo OB differentiation, they upregulate use of mitochondrial oxidative phosphorylation (OxPhos). Our lab is investigating mechanism(s) connecting mitochondrial OxPhos to OB differentiation. First, we showed that treating osteoinduced BMSC-like C3H10T1/2 (C3H) cells with an OxPhos inhibitor reduced their osteogenic potential with no change in cell viability, underlining the importance of OxPhos in osteogenesis. Interestingly, ATP levels were not reduced as glycolysis compensated for the decreased OxPhos. Thus, mitochondria support OB differentiation not only by supplying ATP but by some other mechanisms. To uncover such mechanisms, our strategy was to stimulate OxPhos and study downstream signaling. Replacing glucose in cell culture media with galactose is a known strategy to stimulate OxPhos. We thus replaced media glucose with galactose and observed stimulation of both OxPhos and osteogenesis in C3H cells in the absence of osteoinducers. To elucidate signaling mechanisms responsive to galactose-mediated stimulation of OxPhos, we used various promoter reporters carrying luciferase. β -catenin is regulated by acetylation, and OxPhos generates AcCoA, a substrate for acetylation. AcCoA is then converted to citrate capable of exiting mitochondria. Cytosolic citrate is next converted back into AcCoA by ACLY enzyme. We found that inhibiting the conversion of citrate to AcCoA using an ACLY inhibitor, SB204990 (SB), reversed the galactose-induced β -catenin activity and OB differentiation. This indicates that acetylation is involved in β -catenin activation after forced stimulation of OxPhos. We also detected SB-dependent β -catenin acetylation using immunoprecipitation. Both β -catenin protein and acetylation levels increased during osteoinduction, again in a SB-dependent manner, showing the importance of OxPhos-dependent β -catenin acetylation for the osteogenic program. These data suggest that active OxPhos is required for OB differentiation not only because of ATP demands but also due to its effect on β -catenin acetylation and, thus activity.

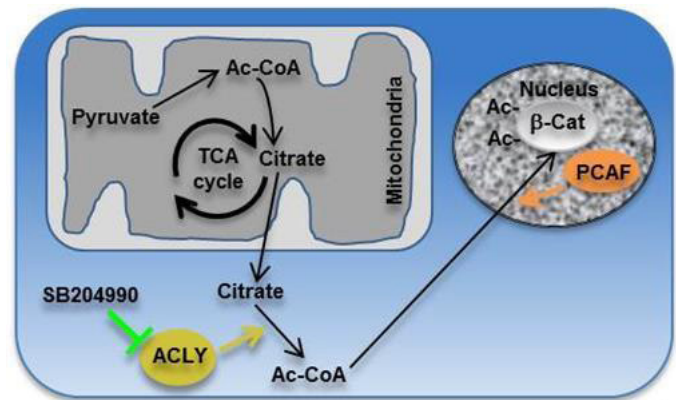


Figure 1. Citrate, derived from Ac-CoA in active mitochondria, translocates to the cytosol where it is converted back to Ac-CoA by ACLY enzyme. This ACLY-dependent cytosolic Ac-CoA is then used to acetylate and, thus activate β -catenin. ACLY is inhibited by SB204990 (SB).

Disclosures: **Brianna Shares**, None

SAT-0501

See Friday Plenary Number FRI-0501

SAT-0502

See Friday Plenary Number FRI-0502

SAT-0503

See Friday Plenary Number FRI-0503

SAT-0504

See Friday Plenary Number FRI-0504

SAT-0505

See Friday Plenary Number FRI-0505

SAT-0506

See Friday Plenary Number FRI-0506 (WITHDRAWN)

SAT-0507

Subchondral cyst number is positively associated with proximal tibia bone mineral density, alignment and joint space narrowing in individuals with OA Wadena Burnett*¹, Saija Kontulainen¹, Christine McLennan², Diane Hazel², Carl Talmo², David Wilson³, David Hunter⁴, James Johnston¹. ¹University of Saskatchewan, Canada, ²New England Baptist Hospital, United States, ³University of British Columbia, Canada, ⁴Kolling Institute of Bone & Joint Research, University of Sydney, Australia

Purpose/Background: Osteoarthritis (OA) is a debilitating joint disease marked by altered cartilage and underlying bony tissues. Subchondral cysts are a commonly observed, but poorly understood, feature of knee OA. Clinical quantitative computed tomography (QCT) has the potential to characterize cysts in vivo, but it is unclear which specific cyst parameters (e.g., number, size) are associated with clinical signs of OA. The purpose of this study was to use QCT and image-processing to explore relationships between proximal tibial subchondral cyst parameters and subchondral bone density as well as clinical characteristics of OA in patients with knee OA. **Methods:** The preoperative knee of 42 patients was scanned using QCT, scored for pain using the Western Ontario and McMaster Universities Arthritis Index (WOMAC) and classified for OA severity. We also included medial and lateral joint space narrowing (JSN) and CT-measured joint alignment in our analysis. Cysts were

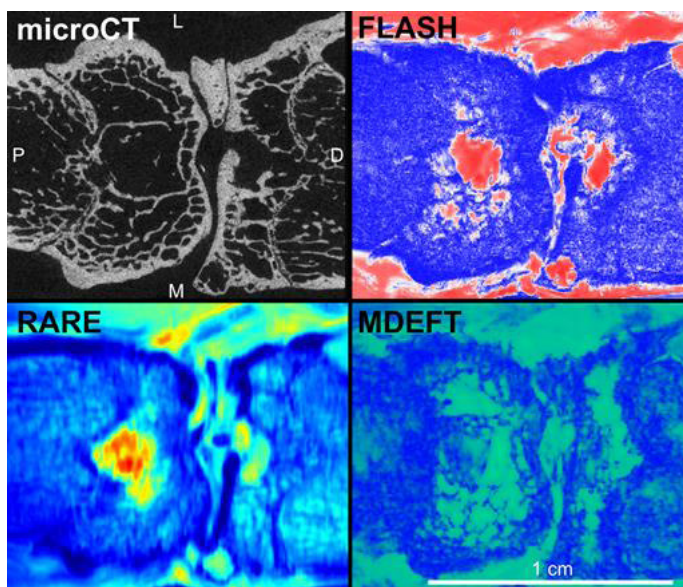
identified as approximate elliptical or spherical volumes of lower greyscale surrounded by higher greyscale through visual inspection guided by subject-specific half-maximum-height threshold values, then manually segmented. Only cysts within the subchondral region (depth of 7.5mm from the subchondral surface) were evaluated. We used a custom algorithm to measure cyst parameters (total, maximum, average, minimum, and standard deviation of cyst volume; number of cysts; cyst volume and cyst number per subchondral volume) and proximal tibial bone mineral density (BMD) excluding cysts. Cyst parameters and BMD were evaluated over total, medial, and lateral subchondral regions of the proximal tibia. Pearson's and Spearman's rank correlation were used to determine associations between cyst parameters and clinical characteristics of OA. Results: Lateral cyst number was associated with lateral BMD ($r=0.55$, $p<0.001$), valgus alignment ($r=0.60$, $p<0.001$) and lateral JSN ($r=0.66$, $p<0.001$). Although most individuals had medial OA, there were no associations for the total or medial regions, or between cyst parameters and OA severity or pain. Conclusion: To our knowledge, this is the first study to provide evidence of a positive association between subchondral cyst number and BMD, valgus alignment, and JSN in individuals with knee OA. These findings suggest that there may be disease-associated changes in tibial loading distribution leading to cyst development.

Disclosures: *Wadena Burnett, None*

SAT-0508

Establishing a Model to Investigate the Role of Non-Traumatic Bone Marrow Lesions in the Pathogenesis of Knee Osteoarthritis: 9.4T MRI and microCT in Dunkin-Hartley Guinea Pigs Alicia K Gabilondo*¹, John R Matyas², Jeffrey F Dunn¹, Sarah L Manske¹. ¹McCaig Institute for Bone and Joint Health, Department of Radiology, Cumming School of Medicine, University of Calgary, Canada, ²McCaig Institute for Bone and Joint Health, Faculty of Veterinary Medicine, University of Calgary, Canada

Purpose: Bone marrow lesions (BMLs), which appear as diffuse hyper-intense regions in the subchondral bone on fat-saturated MRI sequences, are one of few imaging findings strongly associated with pain in late-stage knee osteoarthritis (OA). However, the underlying pathogenesis of non-traumatic BMLs in knee OA is poorly understood. The Dunkin-Hartley guinea pig spontaneously develops degenerative changes with characteristics similar to human knee OA. The purpose of this study was to investigate the occurrence of subchondral BMLs and their underlying bone microarchitecture in older Dunkin-Hartley guinea pigs to establish a model of spontaneous BMLs. Methods: We extracted the left hind limbs of 4 (2F, 2M) 24-month old guinea pigs and completed scanning within 48 hours. We obtained 3 image sequences using a 9.4T MRI (Magnex and Bruker) and a cryogenic transceiver quadrature RF surface coil (CryoProbe, Bruker) to identify BMLs and cysts, as well as bony anatomy: 1) gradient echo (FLASH), 2) proton-density weighted rapid acquisition with relaxation enhancement (RARE) and 3) modified drive-equilibrium Fourier-transform (MDEFT). We also obtained microCT images (vivaCT40, Scanco Medical) and performed H&E staining. Results: All samples demonstrated diffuse hyper-intense regions in the central distal femoral epiphysis and the proximal tibial epiphysis anterior to the ACL insertion site. Hyper-intense regions were absent of trabecular bone. Three of four samples also displayed a small spherical cyst in the medial tibial condyle inferior to the calcified medial meniscus. On histological sections, these regions did not contain cells or tissue and likely corresponded with fluid-filled cavities. Conclusions: In 24-month old Dunkin-Hartley guinea pigs, we observed hyper-intense regions on MRI in anatomically similar locations. Based on the absence of cells, fibrous and bone tissue in histology and microCT, these hyper-intense regions were likely fluid-filled and may be suggestive of subchondral bone cysts. In humans, subchondral cysts form nearly exclusively in regions previously associated with BMLs. The cyst-like finding may reflect the late-stage degeneration in 24-month old guinea pig knees, as other OA-like features begin to develop at less than 12-months of age. Further comparison of these hyper-intense regions with younger guinea pigs will establish a model to investigate the role of BMLs in idiopathic knee OA.



Disclosures: *Alicia K Gabilondo, None*

SAT-0509

Accelerated Osteoarthritic-like Symptoms in a Novel Dual Injury Model Combining Destabilisation of the Medial Meniscus and Cartilage Damage Kendal Mcculloch*¹, Carmen Huesa², Lynette Dunning¹, Rob Van 'T Hof³, John Lockhart¹, Carl Goodyear⁴. ¹University of the West of Scotland, United Kingdom, ²University of Edinburgh, United Kingdom, ³University of Liverpool, United Kingdom, ⁴University of Glasgow, United Kingdom

Osteoarthritis (OA) is associated with articular cartilage damage. It is assumed OA pathogenesis can be initiated via an isolated injury, or an accumulation of joint damage over time. OA represents a major clinical challenge due to the poor regenerative capability of cartilage. Several murine models are used to study OA (e.g. destabilisation of the medial meniscus (DMM)), however, they do not combine simultaneous joint destabilisation with cartilage damage. The principle aim of this study was to investigate if combining DMM and cartilage damage could accelerate the onset of OA-like symptoms. OA was induced in C57BL/6 mice via (a) transection of the medial meniscotibial ligament (DMM), (b) microblade scratches of articular cartilage (cartilage damage) or (c) combined DMM and cartilage scratch (DCS). Seven and 14 days post-surgery, inflammation, cartilage degradation and bone changes were monitored using histology and microcomputed tomography. Dynamic weight bearing was assessed as an indirect measurement of pain at 14 days. Osteophytes were observed in all groups at days 7 and 14 post-surgery. When compared with DMM and cartilage damage models, osteophytes were visually larger and more numerous in the DCS model. Osteophyte total bone volume (BV) was greater at day 14 in both cartilage damage and DCS models; these osteophytes also encompassed a larger surface area of subchondral bone (14.12 ± 0.31 versus 12.4 ± 0.62 , 12.68 ± 0.54 , $p<0.01$ respectively). With regard to other bone changes, at day 7 there was no detectable increase in BV and osteosclerosis was absent, but by day 14 osteosclerosis was detectable in both DMM and DCS models. Assessment of cartilage at day 14, revealed that there was a significant increase in damage in the DCS model when compared with DMM and cartilage damage models ($p<0.01$). Furthermore, there was a significant increase in synovitis in the DCS model compared with the cartilage scratch model ($p<0.05$). In mice that underwent DCS surgery there was significant increase in front paw load compared with the other models. At day 14 a positive correlation was observed between osteophyte number and front paw load ($r=0.69$, $p=0.003$). Combining DMM and cartilage damage provides a robust and reproducible model for OA-associated joint changes, suggesting this novel dual injury model not only accelerates osteophytogenesis, but also includes features of OA-related pain; arguably one of the most problematic and physically limiting symptoms of OA.

Disclosures: *Kendal Mcculloch, None*

SAT-0510

LPS Induced Inflammation Pre-Injury Increases the Severity of Post-Traumatic Osteoarthritis in MRL/MpJ Superhealer Mice Melanie Mendez*¹, Deepa Muruges², Allison Hsia³, Blaine Christiansen³, Gabriela Loots³. ¹University of California-Merced, Lawrence Livermore National Laboratory, United States, ²Lawrence Livermore National Laboratory, United States, ³University of California-Davis, United States

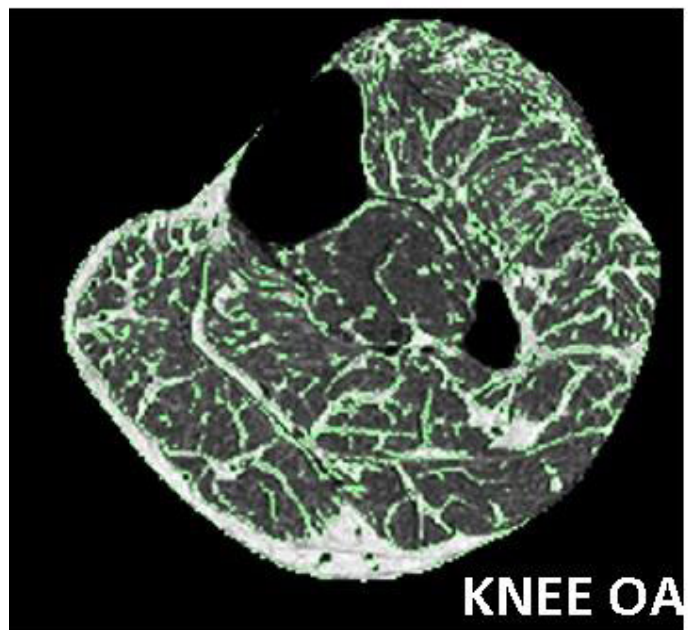
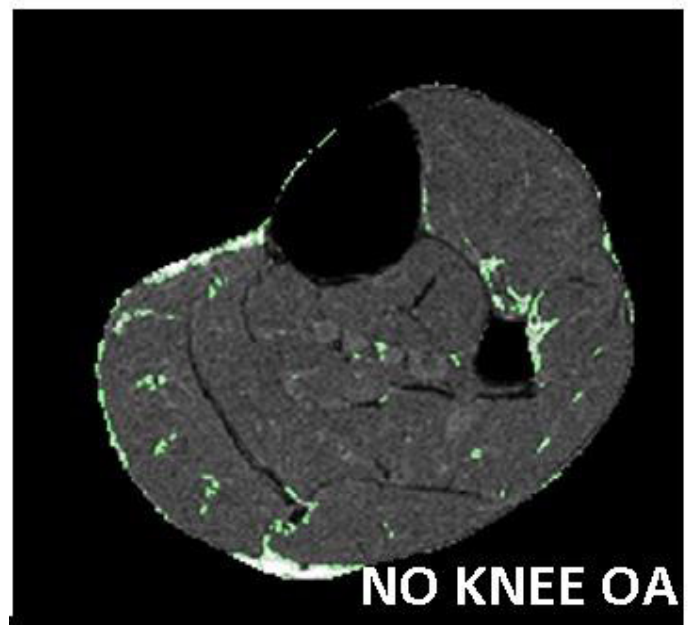
Post-traumatic osteoarthritis (PTOA) develops in ~50% of people who suffered a severe joint injury such as an anterior cruciate ligament (ACL) rupture. Inflammation could be one of the key contributing factors to the development of PTOA, therefore a state of heightened inflammation prior to injury could cause a more rapid progression of PTOA. Lipopolysaccharides (LPS) are microbial associated molecular patterns expressed in gram-negative bacteria which activate an inflammation cascade through toll-like receptor 4 (TLR4). To determine whether LPS-induced inflammation modulates PTOA after ACL rupture, we compared 3 strains of mice: 2 sensitive to LPS (C57Bl/6 and MRL/MpJ) and 1 resistant to LPS (C3H/HeJ, which carry a TLR4 mutation). In C57Bl/6 mice, a single non-invasive tibial compression overload that ruptures the ACL will result in severe PTOA within 6 weeks. MRL/MpJs subjected to the same type of injury did not display significant cartilage degradation 6-weeks post injury, but C3H/HeJ injured joints did display a more severe PTOA phenotype than C57Bl/6 at this time point. To determine if an acute state of inflammation prior to injury would increase the severity of PTOA, we induced systemic inflammation by administering a single LPS injection (1mg/kg) intraperitoneally 5 days prior to injury. As expected, LPS did not cause any changes in the PTOA phenotype of C3H/HeJ mice. Micro-computed tomography analysis of the femoral epiphysis revealed that LPS treated C57Bl/6 mice displayed a significant loss of epiphyseal trabecular bone in both the tibia and the femur in both injured and uninjured joints. Histological analysis revealed that there was a loss of mineralized surface area and a higher marrow content. The synovium was also thicker and more cellular in these mice. The LPS treated group showed a reduction in Safranin O staining and thinning of the articular cartilage suggesting loss of proteoglycan content and chondrocyte apoptosis, due to cartilage degradation. MRL/MpJ mice treated with LPS also showed a significant loss of subchondral bone, thinning of the cartilage, and loss of Safranin O staining. The PTOA phenotypes were less severe in MRL/MpJ than C57Bl/6, but significantly more severe than injured MRL/MpJs that received a PBS injection. These data suggests that LPS-induced inflammation prior to ACL rupture exacerbates the PTOA phenotype in both C57Bl/6 mice and MRL/MpJ mice and that MRL/MpJ mice are not protected from inflammation-induced PTOA.

Disclosures: *Melanie Mendez, None*

SAT-0511

Bone and Muscle Quality in Postmenopausal Women with Both Osteoarthritis and Osteoporosis – the AMBERS study Andy Kin On Wong*¹, Shannon Reitsma², Hana Gillick², Abinaa Chandrakumar³, Eva Szabo³, Justin Chee³, Angela M Cheung³, Jonathan D Adachi². ¹Joint Department of Medical Imaging, University Health Network, Canada, ²Department of Medicine, McMaster University, Canada, ³CESHA, University Health Network, Canada

Our previous study showed that knee pain in women with both osteoarthritis (OA) and osteoporosis (OP) was associated with differences in bone but not cartilage properties. However, little is known about bone and muscle properties in this overlapping subgroup versus those with only OA. Objectives: 1) To determine differences in muscle and bone quality among postmenopausal women with OP, OA, and those with both; 2) To evaluate the impact of muscle properties in knee OA (KOA) and falls. 312 women 60-85 yrs old from the Appendicular Muscle and Bone Extension Research Study (AMBERS) completed baseline imaging and annual follow-up on fractures, falls, and frailty for 3 years. This study is a cross-sectional analysis of the baseline data for women 76-85 yrs old (N=170). Peripheral QCT (pQCT) and MRI (pMRI) scans of the mid-leg (66% site) measured muscle density and % inter- and intra-muscular fat (%IMF). 4% distal tibia pQCT scans quantified bone density and micro-architecture. Total hip and lumbar spine DXA-derived BMDs were converted to T-scores for diagnosing osteoporosis. OA and KOA were self-reported. Falls over the last 2 years were captured. General linear models compared muscle and bone properties among groups, exploring interactions between disease groups. Binary logistic regression examined the effect of muscle properties on OA and falls. Among 170 women (age: 80±3yrs, BMI: 29.1±5.5kg/m²), 37.1% had OA (58.7% knee), 18.8% had OP, and 61.8% had osteopenia. Among those with OA, 19.0% also had OP and 63.5% also had osteopenia. Muscle density was 2.44 mg/cm³ lower in those with KOA versus without (p=0.011) but not all OA (p=0.130). In those with OA, concurrently having OP was associated with 48.51 mg/cm³ lower distal tibia volumetric BMD (p<0.001, interaction p<0.001), and 4.19% higher %IMF (p=0.023, interaction p=0.025). In those with OP, each standard deviation (SD) larger %IMF was associated with 4.85(1.18, 19.91)-fold odds for KOA (interaction p=0.028). This effect was not significant in those without OP. Having KOA (OR: 2.94(1.03, 8.40) or any OA (OR: 2.30(1.06, 5.00) but not OP alone was significantly associated with falls. The effect on bone and muscle properties for those with both OA and OP is significantly greater than for those with either disease alone. Having higher muscle adiposity is a risk factor for KOA among those who already have OP. While this measure is not directly a risk factor for falls, KOA itself was a prominent correlate of falls.



Disclosures: *Andy Kin On Wong, None*

SAT-0512

Intermittent PTH exerts an anabolic effect on the osteochondral tissue of the TMJ Sumit Yadav*¹, Po-Jung Chen², Mara H O'Brien², Eliane Dutra². ¹Associate Professor, United States, ²University of Connecticut Health Center, United States

Introduction: Intermittent Parathyroid Hormone (I-PTH) is the only anabolic FDA-approved drug for the treatment of bone loss due to conditions such as osteoporosis. The mechanisms of the effects of I-PTH in bone are known, however, the effects of I-PTH on the mandibular condylar cartilage (MCC) remains to be understood. In addition, it is unknown whether I-PTH could be used as an anabolic drug to treat degenerative disorders of the temporomandibular joint (TMJ). Objective: The purpose of this study was to characterize the long-term effects of I-PTH on the MCC and subchondral bone of the TMJ, in vivo and in vitro. In addition, we attempted to identify the mechanisms by which I-PTH promotes its effects in the chondrogenic lineage of the MCC. Material and Methods: For the in vivo experiments, 24 10-week-old mice (C57BL/6J) were divided into two groups: (1) I-PTH (n=12): subcutaneous daily injection of PTH; (2) Control Group (n=12): subcutaneous daily injection of saline solution. Experiments were carried out for four weeks. Mice were injected with calcein, alizarin complexone and EdU before euthanasia. The mandibular condyle of I-PTH treated and control mice were examined by microCT and histology. For the in vitro

experiments, primary chondrocyte cultures from the MCC of 6-week-old mice (C57BL/6J) were treated with I-PTH for 14 days. Gene expression from experimental and control chondrocyte cultures were analyzed by QPCR. Results: There was an anabolic response in the mandibular condyle of the I-PTH treated mice when compared to control group characterized by an increase in cartilage thickness, subchondral bone volume, mineral deposition, TRAP activity and cellular proliferation. In addition, immunohistochemistry revealed that I-PTH administration led to a significant decreased expression of SOST (negative regulator of mineralization), MMP13 and ADAMST4. QPCR analysis of the I-PTH treated chondrocytes revealed significantly increased PRG4 (lubricant and anti-inflammatory agent for the articular joints) and significantly decreased SOST, BMP2 (promoter of chondrocyte differentiation), IHH (promoter of chondrocyte hypertrophy and osteoarthritis) and Col10 (marker for chondrocyte hypertrophy and osteoarthritis). Conclusion: I-PTH exerts an anabolic effect at the MCC that may be correlated with decreased chondrocyte hypertrophy. In addition, I-PTH treatment may promote a prevent TMJ degeneration by increasing the expression of cartilage protective agents at the MCC.

Disclosures: Sumit Yadav, None

SAT-0537

See Friday Plenary Number FRI-0537

SAT-0538

See Friday Plenary Number FRI-0538

SAT-0539

See Friday Plenary Number FRI-0539

SAT-0540

See Friday Plenary Number FRI-0540

SAT-0541

See Friday Plenary Number FRI-0541

SAT-0542

See Friday Plenary Number FRI-0542

SAT-0543

See Friday Plenary Number FRI-0543

SAT-0544

See Friday Plenary Number FRI-0544

SAT-0545

See Friday Plenary Number FRI-0545

SAT-0546

See Friday Plenary Number FRI-0546

SAT-0547

See Friday Plenary Number FRI-0547

SAT-0548

See Friday Plenary Number FRI-0548

SAT-0549

See Friday Plenary Number FRI-0549

SAT-0550

See Friday Plenary Number FRI-0550

SAT-0551

See Friday Plenary Number FRI-0551

SAT-0552

Possible involvement of regulation of intracellular RANKL by a RANKL binding peptide WP9QY in osteogenesis. Yuriko Furuya*. Nagahama Institute for Biochemical Science, Oriental Yeast Co., Ltd., Japan

WP9QY (W9) peptide consisting of 9 amino acids is known to abrogate osteoclastogenesis in vitro and in vivo via blocking receptor activator of NF- κ B (RANK) ligand/RANK signaling as a RANKL antagonist. We reported that W9 exerted osteoblastic differentiative activity in mouse preosteoblastic cells and human mesenchymal stem cells (MSCs), and accelerated bone formation in vivo. We reported that RNA interference (RNAi)-mediated RANKL gene knockdown using lentivirus suppressed W9-induced calcification in mouse MSCs C3H10T1/2 cells, suggesting an important role of RANKL in osteoblastogenesis by W9. Although we have hypothesized that reverse signaling through membrane-bound RANKL regulates osteogenesis, direct evidence of participation of RANKL in osteoblasts differentiation has not been clarified. In this study we established a method detecting intracellular RANKL using human and mouse RANKL antibodies. We failed to detect membrane-bound RANKL on MSCs and preosteoblastic cells. In contrast we found strong signals of intracellular RANKL in MSCs and preosteoblastic cells. Addition of W9 decreased the signal of intracellular RANKL in MSCs, suggesting the involvement of intracellular RANKL in W9-induced osteogenesis. On the other hand W9 also enhanced chondrogenesis in mouse prechondrogenic cells, human MSCs and rabbit model of full-thickness articular cartilage defects. To clarify participation of RANKL in W9-induced chondrogenesis, we conducted RNAi-mediated RANKL gene knockdown in mouse C3H10T1/2 cells using lentivirus, followed by induction of chondrocyte differentiation. As opposed to osteogenesis, W9 stimulated chondrocyte differentiation even in the RANKL knockdown cells. The results showed that RANKL had little effect on W9-induced chondrocytes differentiation. The mechanism of W9-induced osteogenesis through intracellular RANKL and the difference of mechanism between chondrogenesis and osteogenesis by W9 should be clarified in the near future.

Disclosures: Yuriko Furuya, None

SAT-0553

Remarkable early bone-forming efficacy of bisphosphonate (alendronate, zoledronate or risedronate)-conjugated collagen sponges as a rhBMP-2 delivery carrier Soon Jung Hwang*¹, In Sook Kim². ¹Department of Oral and Maxillofacial Surgery, School of Dentistry, Seoul National University, Republic of Korea, ²Dental Research Institute, Seoul National University, Republic of Korea

Our previous study demonstrated the manufactured collagen sponge (CS) composite combined with a bisphosphonate (BP), alendronate (ALN) led to excellent outcome with less adverse effects and higher bone-forming efficacy in the treatment of high dose rhBMP-2. This study aimed to compare the early bone-forming efficacy of CS composites conjugated with various BPs including ALN, zoledronate (ZOL) or risedronate (RIS) as rhBMP-2 carrier. Alkaline phosphatase activities of rat osteoblasts in vitro showed a synergistic effect of rhBMP-2 with BPs, while proliferation was inhibited, dependently of BP-doses. Osteoclast differentiation was also inhibited by ALN, Zol and RIS, dose dependently. ALN-, ZOL-, or RIS-CS were loaded with low and high doses (5 and 40 μ g) of rhBMP-2 and analyzed for new bone formation using 8 mm-critical sized calvarial defect model of rats, compared with normal CS. Bone mass and bone density calculated from micro computed tomography reconstructions at 4 weeks were significantly greater in all BP-CS-BMP groups. Ossification at defect exterior was significantly decreased in all BP-CS-BMP groups over CS-BMP group. Notable findings are that BP-CSs at low dose BMP (5 mg) resulted in approximately 2 fold greater bone volume (BV), and only a reduction rate of less than 10 % BV at the central defect area, compared to CS and BP-CSs at high dose BMP (40 mg), respectively. Histology corroborated these findings and revealed dense spatial pattern of bone formation in all BP-CS-BMP groups. Net osteogenic efficacy for rhBMP-2 delivery was evaluated as the order of ALN-CS, ZOL-CS and RIS-CS. These results demonstrate that BP-CS composites has remarkable advantages in the rhBMP-2 delivery over CS with early dense ossification minimizing heterotopic ossification, and great efficiency at low dose, suggesting a remarkably effective carrier of rhBMP-2.

Disclosures: Soon Jung Hwang, None

SAT-0554

Gene activated-matrix (GAM) comprised of atelocollagen and plasmid DNA encoding microRNA promotes rat cranial bone augmentation Rena Shido^{*1}, Yoshinori Sumita², Masashi Hara¹, Shun Narahara¹, Izumi Asahina¹. ¹Department of Regenerative Oral Surgery, Unit of Translational Medicine, Graduate School of Biomedical Science, Nagasaki University, Japan, ²Basic and Translational Research Center for Hard Tissue Disease, Nagasaki University Graduate School of Biomedical Sciences, Japan

Therapeutic method for in vivo gene delivery has not been established on bone engineering though its potential usefulness has been suggested so far. To facilitate the clinical setting of this strategy, an effective condition should be developed to transfer the genes in vivo without any of transfection-reagents or virus-vectors. On this account, we have made a try at developing an atelocollagen-based GAM containing naked-plasmid (p) DNAs encoding osteogenic-proteins such as BMP-4 and have demonstrated the potential of such simple and probably safe strategy for bone engineering. However, a certain dose (more than 6µg/µl) of pDNA was still required for inducing the sufficient bone regeneration when pBMP4 was incorporated. Therefore, the efficient methods for generating non-viral GAM with high transgene efficacy and low toxicity should be developed further. In this study, we examined whether GAM containing pDNAs encoding microRNA (miR) 20a, which regulates the BMP2/4 expression on mesenchymal stem/progenitor cells (MSCs) during their osteoblastic differentiation via multiple pathways, facilitates the rat cranial bone regeneration. As experiments, first, to determine the biological activity of generated pDNA encoding miR20a (pmiR20a), we confirmed its functions of osteoblastic differentiation on rat bone marrow MSCs via gene transfection in culture. Then, GAMs were manufactured by mixing 0.5mg (3.3µg/µl) of AcGFP plasmid-vectors encoding miR20a with 100µl of 2% bovine atelocollagen and 20mg β-TCP granules. After that, GAM was lyophilized and transplanted to the rat cranial bone surface. After 1 to 8weeks of transplantation, new bone formation and its specific gene and protein expressions in specimens were analyzed. As results, transfection of miR20a could regulate the expression of its target genes multiply in rat BM-MSCs and induce the up-regulation of bmp4 mRNA expression. Then, when transplanted the GAMs containing pmiR20a, the newly formed bone tissues surrounded by Osteocalcin-stained area were markedly observed via up-regulation of bmp4, vegf-a and -b mRNA expressions, compared to GAMs containing pGFP without encoding osteogenic protein. We are currently carrying out the additional experiments, such as developing an appropriate matrix and verifying the safe concentration of pDNAs, for clarifying the actual usefulness of GAM encoding miR20a.

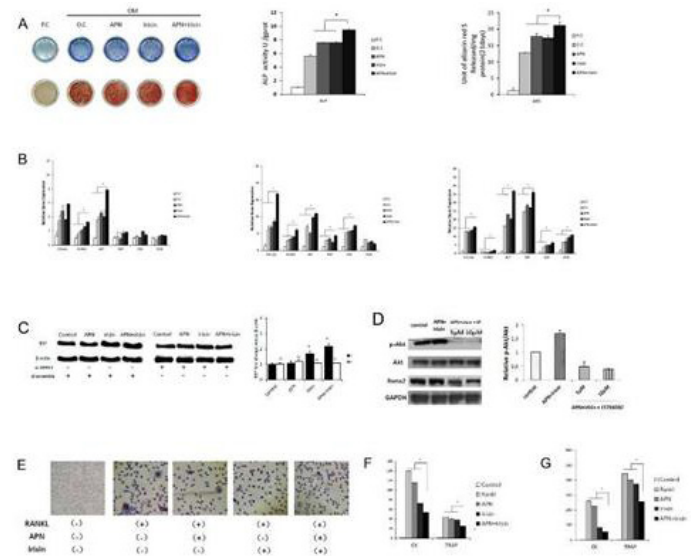
Disclosures: **Rena Shido**, None

SAT-0555

Synergistic Effects of Adiponectin and Irisin on Bone Cells Tong Chen^{*1}, Weina Zhou^{2,3}, Qisheng Tu², Jinkun Chen^{2,4}. ¹2nd Dental Center, Peking University School and Hospital of Stomatology, Beijing, China. Central Laboratory, Peking University School and Hospital of Stomatology, Beijing, China., China, ²Division of Oral Biology, Tufts University School of Dental Medicine, Boston, Massachusetts, United States, ³Jiangsu Key Laboratory of Oral Disease, Nanjing Medical University, Nanjing, China, ⁴Department of Developmental, Molecular and Chemical Biology Sackler School of Graduate Biomedical Sciences Tufts University School of Medicine, United States

Objectives:Adiponectin (APN) plays a pivotal role in glucose metabolism and energy homeostasis. Evidences suggest a positive association between APN and bone formation. Irisin is a newly discovered myokine and could increase adipocyte browning and bone formation. APN and irisin are protagonists of the muscle-fat-bone axis. This study was to investigate the synergistic effects and regulatory mechanisms of APN and irisin in bone metabolism. **Materials and Methods:**MC3T3-E1 and RAW264.7 cells were cultured in corresponding induced media with APN or irisin or both, respectively. The ALP, Alizarin Red S and TRAP staining were performed to visualize the cell differentiation. RT-PCR was performed to detect the expression of osteoblast/osteoclast differentiation markers. Signaling transduction pathways were investigated to elucidate the mechanism by western blotting. **Results:**The ALP staining and ARS staining at 7- and 14-day showed that the APN plus irisin enhanced ALP activity and increased mineralization deposition, in contrast to APN or irisin treatment alone. At 1-day osteogenic induction, the level of RUNX2 and ALP expression more significantly increased in the APN plus irisin group than in control groups. At 3 and 7-day, the levels of RUNX2, ALP, collagen type 1, BSP, OSX and OCN were significantly increased in the APN plus irisin group. Western blots revealed that the expression of BSP protein could be upregulated by APN plus irisin and this effect could be inhibited by knock-down of APPL1 with siRNA. Also, a significantly increased amount of phosphorylated Akt was detected by western blot after treatment with APN and irisin, which could be impaired by PI3K inhibitor LY294002. In osteoclasts induction of RAW264.7 cells, the cell number detected by TRAP staining decreased more significantly in the APN plus irisin group than the APN or irisin, and control groups. At 1- and 3-day after osteoclasts induction, the level of CK and TRAP mRNA significantly decreased in the APN plus irisin group compared with that the APN or irisin, and control groups. **Conclusions:**Adiponectin and irisin could synergistically enhance the osteogenic induction of preosteoblasts via upregulating of APPL1, an adaptor protein of adiponectin signaling, and subsequently mediating PI3K/Akt pathways. Additionally APN and irisin could coactively inhibit osteoclastogenesis. This

synergistic effect can be used pharmaceutically for treating bone disorders particularly in diabetic patients.



Disclosures: **Tong Chen**, None

SAT-0556

The stimulation of osteogenesis by delivery of recombinant protein of osteogenic molecular switches Woo-Jin Kim^{*}, Youngdan Cho, Hyunmo Ryoo. Seoul National University, Republic of Korea

Protein therapy, which delivers proteins into the cell to replace the dysfunctional protein, is considered the most direct and safe approach for treating bone disease. However, there are limitations include inefficient cellular uptake, degradation of protein in serum environment and damage to cells in the delivery process. Recently, researchers have introduced silk fibroin based spherical nano-particle system. Silk Fibroin protein as a natural polymer, provides useful properties including biocompatibility, biodegradability, tunable drug loading capacity and release. Using this system, we can fabricated nano-particles which loaded verified multiple recombinant proteins and introduced functional proteins directly into the cells to control bone disease. In this study, we use recombinant Pin 1 and GFP proteins to confirm cytosolic delivery of proteins and regulatory effect of osteogenesis. Pin 1 is a cis-trans isomerase which recently reported playing critical role in osteogenesis via regulation of Runx2 protein stability. Fabrication of silk Fibroin nano-particles containing recombinant Pin 1 and GFP proteins shows high loading efficacy without any assistant conjugation and control-able particle size and stability. GFP loaded fibroin nano-particle shows significantly enhanced cellular uptake compare with naive-protein treatment and maintained long-term protein activity in serum condition. In low level BMP2 stimulating C2C12 cells, Alp activity relatively increased in Alp staining by Direct-delivery of recombinant Pin 1 proteins. However, their cellular toxicity level while protein delivery was significantly lower than commercially using transfection reagent. Multiple recombinant proteins can be delivered to cells with high efficiency while maintaining protein activity and low toxicity, suggesting potential application in bone-related disease therapy.

Disclosures: **Woojin Kim**, None

SAT-0596

See Friday Plenary Number FRI-0596

SAT-0597

See Friday Plenary Number FRI-0597

SAT-0598

See Friday Plenary Number FRI-0598

SAT-0599

See Friday Plenary Number FRI-0599

SAT-0600

See Friday Plenary Number FRI-0600

SAT-0601

See Friday Plenary Number FRI-0601

SAT-0602

See Friday Plenary Number FRI-0602

SAT-0603

See Friday Plenary Number FRI-0603

SAT-0604

See Friday Plenary Number FRI-0604

SAT-0605

See Friday Plenary Number FRI-0605

SAT-0606

Osteoclastogenic cues induce both priming and assembly signals for the NLRP3 inflammasome Yael Alippe^{*1}, Chun Wang¹, Biancamaria Ricci², Jianqiu Xiao¹, Dustin Kress¹, Guillermo Blanco³, Yousef Abu-Amer², Roberto Civitelli¹, Gabriel Mbalaviele¹. ¹Division of Bone and Mineral Diseases, Washington University School of Medicine, United States, ²Department of Orthopaedic Surgery, Washington University School of Medicine, United States, ³IDEHU, University of Buenos Aires, Argentina

Events that promote the abundance of NLRP3 are referred to as NLRP3 priming signals. Upon recognition of ligands, NLRP3 recruits other proteins, such as caspase-1 to form a protein complex called the NLRP3 inflammasome. This inflammasome plays an important role in bone resorption associated with high bone turnover as Nlrp3 deficiency attenuates bone loss induced by ovariectomy or sustained exposure to PTH or RANKL in mice. However, the mechanisms through which the NLRP3 inflammasome regulates bone resorption remain unknown. Since crystalline materials activate this inflammasome, we tested the hypothesis that bone matrix degradation products, which are released during bone resorption, activate the NLRP3 inflammasome and regulate osteoclast differentiation. We found that bone particulates produced from shredded cortical bones synergized with RANKL to cause exuberant osteoclastogenesis from mouse bone marrow macrophages (BMM; approximately 10-fold from baseline), a response that was attenuated in cells lacking NLRP3. Mechanistically, treatment of BMM with RANKL resulted in a rapid rise in NLRP3 protein levels (approximately 50% over baseline levels), a response that peaked at 3 hours before returning to baseline levels 24 hours post RANKL exposure. Bone particles also increased NLRP3 protein abundance. Thus, osteoclastogenic factors are inducers of NLRP3 inflammasome priming signals. Given that RANKL-driven osteoclast differentiation is associated with the generation of reactive oxygen species (ROS), also potent activators of NLRP3 inflammasome assembly, we tested the role of RANKL and bone particles in NLRP3 inflammasome formation. RANKL stimulated ROS production by 43±7.3% in osteoclast precursors as detected by flow cytometry, as did bone particles. This response correlated with NLRP3 recruitment and activation of other of the components of the inflammasome, caspase-1, and was abolished upon NLRP3 ablation. Thus, the NLRP3 inflammasome is not only assembled in responses to osteoclastogenic cues, but it is also implicated in the maintenance of oxidative stress that is needed for efficient osteoclast differentiation. Collectively, we uncovered novel mechanisms in bone resorption whereby RANKL synergizes with signals originating from bone matrix to promote osteoclast differentiation by regulating multiple steps in the NLRP3 inflammasome pathway.

Disclosures: *Yael Alippe, None***SAT-0607**

Regulation of Membrane Localization of CD44 and Migration of Osteoclasts by ERM proteins Meenakshi Chellaiah^{*}. School of Dentistry, University of Maryland, United States

Osteopontin is a ligand for several cell surface receptors, such as $\alpha v\beta 3$, $\alpha v\beta 1$, $\alpha v\beta 5$, $\alpha 4\beta 1$, $\alpha 8\beta 1$, and $\alpha 9\beta 1$ and CD44. Both CD44 and integrin $\alpha v\beta 3$ have been implicated in osteoclast motility and bone resorption. We have previously demonstrated that a cooperativity exists between $\alpha v\beta 3$ and CD44 receptors for osteoclast motility and bone resorption. Still, the details of how CD44 is responsible for osteoclast motility and molecular mechanism

involved in CD44 trafficking remain unclear. The goal of this study was to determine the mechanism by which PtdIns4, 5 P2 (PIP2) synthesis and its binding to ERM proteins coordinate CD44 surface expression and osteoclast (OC) motility. Transduction of TAT-fused constitutively active RhoVal14 into OCs increased phosphatidylinositol 4-phosphate (PI4P) 5-kinase activity and enhanced cellular levels of PIP2. The effects of RhoVal14 transduction simulate the effects of osteopontin (OPN) in OCs. The Rho inhibitor C3 transferase and Rho kinase inhibitor Y27632 reversed OPN or RhoVal14 effect. An increase in the phosphorylation and PIP2 binding of ERM proteins augment ERM/CD44/actin interaction and surface expression of CD44. siRNA to ezrin not only blocked CD44/ERM/actin complex formation but also the surface expression of CD44. OPN or RhoVal14-induced migration and bone resorption is blocked in OCs treated with C3 transferase, Y27632, or siRNA to ezrin. The increased levels of PIP2 in OCs subjected to above-mentioned treatments can be attributed to increased activity of PI4P 5-kinase which is located downstream of the Rho/Rho-kinase-dependent pathway. ERM protein is dynamically regulated under these conditions and it may partake in CD44 surface expression. Bone resorption involves active motility of osteoclasts on bone surfaces to be resorbed. Activation of PI4P-5 kinase and interaction of PIP2 with ERM may represent a key molecular switch that aides CD44 surface expression and motility of osteoclasts. We believe ERM and signaling protein(s) that regulates the activation of ERM proteins may represent rational therapeutic targets. Although our understanding of the role of ERM proteins in the mechanisms of CD44 surface expression and osteoclast motility is limited, we believe our studies outlined above will provide new insights on these cellular processes. (Work is supported by funding from NIH-NIAMS R01-AR46292 and R01AR066044).

Disclosures: *Meenakshi Chellaiah, None***SAT-0608**

Protective effect of a novel benzamide derivative on alveolar bone erosion through suppression of NFATc1-mediated osteoclastogenesis Hye Jung Ihn^{*1}, Soomin Lim², Hong-In Shin², Eui Kyun Park². ¹Institute for Hard Tissue and Biotooth Regeneration, Kyungpook National University, Republic of Korea, ²Department of Oral Pathology and Regenerative Medicine, Kyungpook National University, Republic of Korea

Enhanced osteoclast formation and/or activity have been attributed to pathogenesis of diverse osteolytic bone diseases including periodontitis and osteoporosis. In this study, we investigate the therapeutic potential of a novel benzamide-linked molecule, KDS-070, for preventing alveolar bone loss in mice with ligature-induced experimental periodontitis. KDS-070 inhibited osteoclast formation in a dose-dependent manner, and attenuated the induction of nuclear factor of activated T-cells, cytoplasmic 1 (NFATc1) and the expression of osteoclast-specific genes. In addition, KDS-070 significantly suppressed the formation of actin rings and resorption pits. Analysis of the inhibitory action of KDS-070 showed that it markedly suppressed receptor activator of nuclear factor- κ B ligand (RANKL)-induced extracellular signal-regulated kinase (ERK) and NF- κ B signaling cascades. Moreover, KDS-070 prevented ligature-induced alveolar bone erosion in mice by suppressing osteoclast formation. These findings demonstrate that KDS-070 attenuated osteoclast differentiation and function as well as ligature-induced bone erosion by inhibiting RANKL-mediated ERK and NF- κ B signaling pathways.

Disclosures: *Hye Jung Ihn, None***SAT-0609**

Fas/S1P1 crosstalk via NF- κ B activation in osteoclasts controls subchondral bone remodeling in murine TMJ arthritis Islamy Rahma Hutami^{*}, Eiji Tanaka, Takashi Izawa. Tokushima University Graduate School, Japan

Enhanced turnover of subchondral trabecular bone is a hallmark of rheumatoid arthritis (RA) and it results from an imbalance between bone resorption and bone formation activities. To investigate the formation and activation of osteoclasts which mediate bone resorption, a Fas-deficient MRL/lpr mouse model which spontaneously develops autoimmune arthritis and exhibits decreased bone mass was studied. Various assays were performed on subchondral trabecular bone of the temporomandibular joint (TMJ) from MRL/lpr mice and MRL+/+ mice. Initially, greater osteoclast production was observed in vitro from bone marrow macrophages obtained from MRL/lpr mice due to enhanced phosphorylation of NF- κ B, as well as Akt and MAPK, to receptor activator of nuclear factor- κ B ligand (RANKL). Expression of sphingosine 1-phosphate receptor 1 (S1P1) was also significantly upregulated in the condylar cartilage. S1P1 was found to be required for S1P-induced migration of osteoclast precursor cells and downstream signaling via Rac1. When SN50, a synthetic NF- κ B-inhibitory peptide, was applied to the MRL/lpr mice, subchondral trabecular bone loss was reduced and both production of osteoclastogenesis markers and sphingosine kinase (Sphk) 1/S1P1 signaling were reduced. Thus, the present results suggest that Fas/S1P1 signaling via activation of NF- κ B in osteoclast precursor cell is a key factor in the pathogenesis of RA in the TMJ.

Disclosures: *Islamy Rahma Hutami, None*

SAT-0610

Downregulation of receptor activator NF- κ B (RANK) expression by methylation of its gene promoter Riko Kitazawa*¹, Yuki Murata², Ryuma Haraguchi², Sohei Kitazawa². ¹Division of Diagnostic Pathology, Ehime University Hospital, Japan, ²Department of Molecular Pathology, Ehime University Graduate School of Medicine, Japan

Receptor activator of NF- κ B (RANK) is a member of the tumor necrosis factor receptor (TNFR) family expressed in osteoclast precursors, and RANK-RANK ligand (RANKL) signaling plays a central role in differentiation, activation and survival of osteoclasts. The 5'-flanking region of the mouse RANK gene we had previously analyzed lacked canonical TATA-box but contained four continuous Sp-1 binding sites and CpG-islands around the transcription and translation start sites. In this study, the passage-dependent change in osteoclastogenesis and RANK expression in relation to the status of CpG methylation of its gene promoter was investigated with the use of RAW 264 pre-osteoclastic cells. Quantitative RT-PCR disclosed that the steady-state expression of RANK mRNA of the RAW cells was lower at passage 40 (P40) than at P18; also, RANKL-induced osteoclastogenesis as well as the expression of TRACP and CTSK mRNA was significantly lower at P40 than at P18. To clarify the epigenetic regulation of the RANK gene, the genomic DNA of the two subpopulations of RAW cells was analyzed. Methylation-specific PCR of CpG island region -150/+110, adjacent to transcription and translation start sites, showed a methylated pattern at P40, but not at P18; bisulfite mapping detected a higher frequency of CpG methylation of region -150/+110 at P40 than at P18. Furthermore, pre-treatment with demethylating agent 5-Aza-dC, restored significantly the expression of RANK gene and RANKL-induced osteoclastogenesis at P40. Next, examination of the CpG methylation of region -150/+110 in mono-nucleated cells of mouse spleen disclosed higher methylation in 12-month-old mice than in 10.5-week-old ones, mirroring the passage-dependent CpG methylation of the cultured RAW cells. These data suggest that the epigenetic regulation of the RANK gene promoter by DNA methylation may be one of the age-dependent regulatory mechanisms of osteoclastogenesis.

Disclosures: Riko Kitazawa, None

SAT-0611

CCR5 is required for osteoclast function through regulating lysosomal vesicle trafficking Jiwon Lee*, Yuuki Imai, Tadahiro Iimura. Ehime University, Japan

Osteoclasts resorb bone matrix through the cellular polarization event, in which the cells directionally deliver vesicles containing specific cargo carrying bone-resorptive enzymes and protons along cytoskeleton to the bone-apposed plasma membrane. However, this critical cellular event by osteoclasts remains largely undescribed. We previously reported that the deficiency of C-C chemokine receptor 5 (CCR5), a co-receptor of HIV, impaired the cellular locomotion and bone-resorptive activity, which was associated with the disarrangement of podosomes and adhesion-mediated signaling complex including integrins and Pyk2. Our current study demonstrated that Ccr5-deficient osteoclasts dampened lysosome-related pathways and vesicle trafficking. Analysis by RNA-sequencing and subsequent data mining found that Ccr5-deficient osteoclasts impaired the expression levels of lysosomal and cargo molecules as well as H+ transporters. We observed unique and distinct subcellular distribution of a lysosomal membrane protein expression, Lamp1 in Ccr5-deficient osteoclasts compared to that in wild-type cells using immunocytochemistry. In wild-type osteoclasts, clusters of Lamp1-positive vesicles were preferentially distributed around nuclei indicating a converged distribution of lysosomal vesicles, whereas these vesicles were found to be predominantly localized in periphery of Ccr5-deficient osteoclasts when cultured either on glass-bottomed dishes and dentin slices. Further analyses demonstrated that the expression of Dynein, an important minus-end-directed cargo transporter along microtubules was attenuated in Ccr5-deficient osteoclasts, thus causing the failure of the polarized vesicle trafficking. We further observed that the interaction between centrosphere (plural of centrosome) and cytoskeletal structure were crucial for maintaining the cellular polarity and directional vesicle trafficking of osteoclasts as revealed by super-resolution microscopy-based three-dimensional fluorescence morphometry. These findings together with our previous report support an idea that CCR5-mediated signal plays an important role in osteoclast function through regulating the cell polarity and directional vesicle trafficking as well as cell adhesion, thus leading to a novel insight into the functional association between cellular architecture and lysosomal organelles.

Disclosures: Jiwon Lee, None

SAT-0612

Inhibition of osteoclast differentiation and P. gingivalis lipopolysaccharide-induced alveolar bone resorption by novel Bruton's tyrosine kinase inhibitor acalabrutinib Youngkyun Lee*, Yong-Gun Kim, Jung-Hong Ha. Kyungpook National University School of Dentistry, Republic of Korea

Background: Periodontitis is not only one of the most prevalent inflammatory diseases among adults, but also commonly linked to numerous systemic conditions including cardiovascular diseases, stroke, and diabetes. Although osteoclasts are responsible for the alveolar bone resorption during periodontitis pathogenesis, the development of treatment strategies targeting these cells has not been fruitful. In the present report, the effect of a novel Bruton's

kinase inhibitor acalabrutinib on osteoclast differentiation and alveolar bone resorption was studied. For *in vitro* experiments, mouse bone marrow macrophages were cultured in the presence of macrophage-colony stimulating factor (M-CSF) and nuclear factor of activated T cells cytoplasmic 1 (NFATc1) to induce osteoclast differentiation. The effect of acalabrutinib was tested by tartrate-resistant acid phosphatase (TRAP) staining as well as real-time PCR detection of marker genes and western blot analyses of typical osteoclast proteins. The calcium oscillation characteristics of osteoclast precursors were also tested. Finally, the protective effect of acalabrutinib on alveolar bone erosion was analyzed in mice challenged with Porphyromonas gingivalis lipopolysaccharide. The inhibition of Bruton's kinase inhibitor by acalabrutinib significantly reduced the formation and function of osteoclasts, concomitant with decreased expression of osteoclast marker genes and proteins. Acalabrutinib conspicuously diminished the phosphorylation of mitogen-activated protein kinases, calcium oscillation responses, and NFATc1 nuclear localization, all of which are critical for osteoclastogenesis. Administration of acalabrutinib resulted in significantly reduced lipopolysaccharide-induced osteoclastogenesis and alveolar bone erosion in mice.

Disclosures: Youngkyun Lee, None

SAT-0613

Regulation of osteoclastogenesis by protein kinase D2 and protein kinase D3 Carina M G Meyers*, Kim Mansky, Eric Jensen. University of Minnesota, United States

Excessive bone resorption by osteoclasts contributes to bone destructive pathologies of osteoporosis, arthritis and bone malignancies. Despite having important identified functions in diverse cell types, the role of Protein Kinase D (Prkd) family of serine/threonine kinases in osteoclasts is largely unknown. The Prkdfamily consists of three related kinases: PRKD1, PRKD2 and PRKD3. Characterization of Prkdexpression in osteoclasts demonstrated predominantly Prkd2and Prkd3. We previously found that PRKD chemical inhibitors compromise fusion of mononuclear preosteoclasts into multinucleated osteoclasts. In our current work, we describe functions for PRKD2 and PRKD3 in multiple cellular processes including precursor cell migration, osteoclast fusion and maintenance of the podosome belt and resorptive function in mature osteoclasts. Toward understanding how PRKDs regulate osteoclastogenesis we are performing mass-spectrometry-based proteomic identification of PRKD phosphorylation targets and describing the skeletal phenotype of conditional knockout of Prkd2and Prkd3in osteoclast lineage cells. Together our observations suggest that antagonizing PRKD activity might represent a novel therapy in pathologies involving excessive osteoclast bone resorption.

Disclosures: Carina M G Meyers, None

SAT-0614

WITHDRAWN

SAT-0615

Lipoteichoic acid, a membrane component of gram-positive bacteria, induces PGE2-mediated inflammatory bone resorption in periodontitis. Tsukasa Tominari*, Ryota Ichimaru, Keita Taniguchi, Kenta Watanabe, Chiho Matsumoto, Michiko Hirata, Masaki Inada, Chisato Miyaura. Tokyo University of Agriculture and Technology, Japan

Toll-like receptors (TLRs) are the mold receptors play a critical role in innate immunity. Several reports indicated that TLRs regulate the host defense with inflammation against the pathogens. Lipopolysaccharide (LPS), an outer membrane component of gram-negative bacteria, induced inflammatory bone resorption with TLR4 signaling in periodontitis. We also have reported that the roles of the synthetic ligand of TLR1/2 or TLR2/6 induced prostaglandin (PG) E2-mediated osteoclast differentiation via NF κ B signaling pathway that induced alveolar bone destruction in *in vivo* mouse experimental model of periodontitis. In this study, we examined lipoteichoic acid (LTA) from gram-positive bacteria, a natural ligand of TLR2/6, induced bone destruction in the mouse model of periodontitis. In cocultures of mouse primary osteoblast (POB) and bone marrow cell, LTA dose-dependently induced osteoclast differentiation. Further treatment of LTA to purified mature osteoclast, LTA also prolonged its life span. LTA increased the bone resorbing activity in the mouse calvarial organ cultures. In osteoblasts, LTA stimulated PGE2 production and upregulated the mRNA expression of membrane bound PGE synthase (mPGES)-1, COX-2 and RANKL. When the treatment of indomethacin, a COX inhibitor, significantly blocked LTA-induced these effects. To examine LTA induced NF κ B activity, the degradation of I κ B alpha was analyzed using western blot based detection analysis. LTA promoted degradation of I κ B alpha, suggesting RANKL expression was increased by NF κ B translocation into nuclear in osteoblasts. In *ex vivo* organ cultures of mouse alveolar bone, LTA induced bone resorbing activity, and treatment of indomethacin abrogated its bone resorbing activity. In *in vivo* experiment as the mouse model of periodontitis, the local injection of LTA to mouse lower gingiva, alveolar bone destruction was clearly observed using dual energy X-ray absorptiometry (DXA) and micro-CT. These results suggested that LTA induced inflammatory bone resorption promoted RANKL expression through the pathway of COX-2 and mPGES-1 mediated PGE2 production. Recent reports indicated that LTA derived from gram-positive bacteria such as Streptococcus mutans thought to be involved augment of inflammation. LTA may prolong

inflammation in the initial stage of periodontitis, and also contribute severe bone resorption with the crosstalk between LPS in mature stage of periodontitis.

Disclosures: *Tsukasa Tominari, None*

SAT-0655

See Friday Plenary Number FRI-0655

SAT-0656

See Friday Plenary Number FRI-0656

SAT-0657

See Friday Plenary Number FRI-0657

SAT-0658

See Friday Plenary Number FRI-0658

SAT-0659

See Friday Plenary Number FRI-0659

SAT-0660

Defective Perilacunar/Canalicular Remodeling in Subchondral Bone Exacerbates Osteoarthritis Karsyn Bailey*, Jonathon Woo, Cristal Yee, Claire Acevedo, Aaron Fields, Jeffrey Lotz, Alexis Dang, Alfred Kuo, Thomas Vail, Tamara Alliston. University of California San Francisco, United States

Osteoarthritis (OA) is a debilitating joint disease characterized by articular cartilage degeneration and subchondral bone sclerosis. Although the precise contributions of articular cartilage and subchondral bone in the etiology of OA are yet to be established, mounting evidence suggests that bone-cartilage crosstalk is critical to maintain joint health. Our previous work demonstrated a role for osteocytes in osteonecrosis through perilacunar/canalicular remodeling (PLR), a process by which osteocytes maintain bone quality by dynamically acidifying their microenvironment and secreting matrix metalloproteinases (MMPs), cathepsin K, and other enzymes. Models of PLR suppression demonstrate a coordinated repression of PLR enzyme expression (MMP2, MMP13, MMP14, and cathepsin K), bone matrix hypermineralization, collagen disorganization, and disruption of canalicular networks. Similar hallmarks of hypermineralization and increased subchondral trabecular bone volume occur in OA, but the contribution of osteocytes to cartilage degeneration is unknown. We therefore hypothesize that osteocyte-mediated PLR is critical for healthy joint homeostasis and participates directly in OA development. To determine the role of osteocytic PLR in OA, we evaluated key PLR outcomes in human OA tibial plateaus and assessed arthritic changes in a mouse model of PLR deficiency. Relative to healthy cadaveric controls, tibial plateaus from patients with end-stage OA (n=5/group) exhibit hallmarks of suppressed PLR within the subchondral bone, including significantly blunted canalicular networks, disrupted collagen alignment, and decreased expression of the PLR enzyme MMP13. While these data suggest a correlation between deregulation of PLR and joint disease, in order to determine if osteocyte-mediated PLR participates causally, we evaluated cartilage in mice with osteocyte-intrinsic PLR defects. In mice with disrupted PLR due to an osteocyte-specific ablation of TGF β receptor II (T β RIIoc $^{-/-}$), OA was induced using a meniscal-ligamentous injury (MLI) model. Histological analysis of MLI-injured T β RIIoc $^{-/-}$ cartilage shows more severe cartilage degeneration with a trend toward increased OARSI score (WT+MLI = 5.4 vs. T β RIIoc $^{-/-}$ +MLI = 7.8, n=10/group, p=0.06). This work provides further evidence for the importance of healthy bone-cartilage crosstalk and suggests that osteocyte-intrinsic defects in PLR can contribute to OA progression.

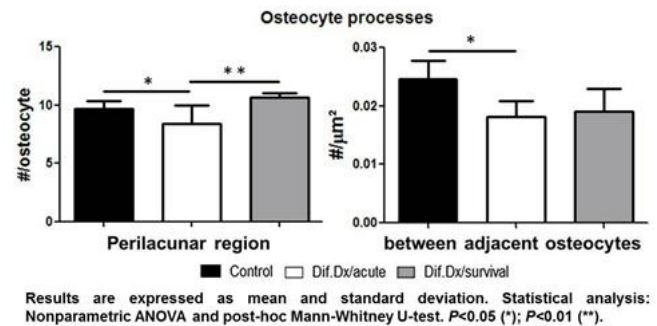
Disclosures: *Karsyn Bailey, None*

SAT-0661

Effects of in vivo Induction of Diffuse Damage in Osteocyte Network Rinaldo Florencio-Silva*, Leila Mehraban Alvandi, Dorra Frikha, Erica Teixeira, Robert Majeska, Mitchell Schaffler. The City College Of New York, United States

Linear microcracks in bone induce osteocyte apoptosis. In contrast, diffuse damage regions (Dif-Dx) do not similarly impair osteocyte viability(1). However, given the extensive array of submicron-sized crack comprising Dif-Dx regions and intimate association these small cracks with canaliculi in particular, it seems reason to posit that osteocytes perceive and react to diffuse matrix damage in bone. Diffuse damage was selectively induced in rat ulnar diaphysis in order to evaluate the effects of Dif-Dx in osteocyte network in vivo (F, SD, 17w, n=8)(2). After loading, rats were either sacrificed immediately Dif.Dx or 14 survival and control. The current study focus was on how osteocyte processes are affected by Dif.Dx

and its repair in vivo. At sacrifice, ulnae were harvested and cryosections through Dif.Dx regions were stained with Alexafluor488-Phalloidin to show F-actin in osteocyte processes; imaging was performed using SIM type super-resolution microscopy. Number of osteocyte processes were measured in the perilacunar region and between adjacent osteocytes. RESULTS Osteocyte processes declined acutely (~25%) after damage loading both immediately surrounding the cell and in bone matrix between osteocytes. Number of processes in the perilacunar zone recovered by 14 days. However, number of osteocyte processes in bone between cells did not recover. DISCUSSION: Osteocytes in Dif-Dx areas lose processes acutely after induction of diffuse damage in vivo. Acute in vivo loading during in these studies lasted less than 60 minutes, thus these data indicate that osteocytes can rapidly remodel cell process cytoskeletons in response to local mechanical stresses caused by Dif-Dx. Osteocytes processes in the perilacunar zone recovered by 14 days after loading. In contrast, processes remained diminished in between osteocytes. These data suggest that osteocytes attempt to restore connectivity to other osteocytes after the acute stress of Dif-Dx induction, but this action is ineffective. Whether the cells inability to regrow their processes is due to a cellular defect or canalicular obstruction caused by damage or infilling is not known. The latter might be similar to loss of odontoblast processes and dentinal tubule infilling during dentin repair. We speculate that this process may be important for repair of diffuse damage in bone and more globally for maintaining overall bone health. Ref: 1) Herman + Bone. 2010; 2) Seref-Ferlengez + JBMR. 2014.



Disclosures: *Rinaldo Florencio-Silva, None*

SAT-0662

A potential role for the NLRP3 inflammasome in osteocyte-mediated triggering of osteoclast differentiation Dorra Frikha-Benayed*, Maria Lapshina, Robert Majeska, Mitchell Schaffler. The City College Of New York, United States

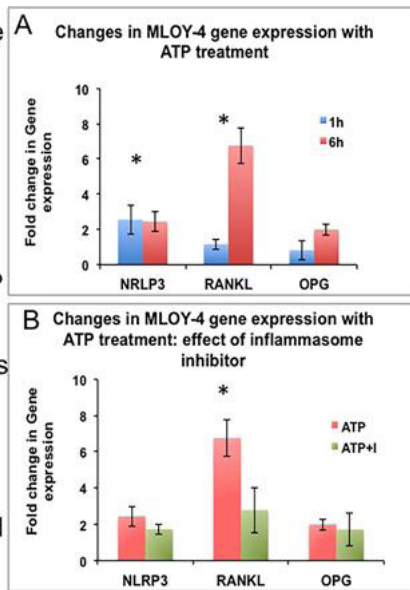
Osteocyte apoptosis activates bone remodeling by inducing neighboring surviving bystander osteocytes produce RANKL, but how apoptotic cells signal bystander cells to express RANKL is not understood. Intriguingly, mice lacking the ATP membrane channel Pannexin1 do not produce RANKL in response to osteocyte apoptosis, pointing to extracellular (e) release of ATP as a potential key signal in this process [1,2]. High levels of eATP can signal a broad range of biological responses, including activation of the NLRP3 inflammasome [3,4]. In these studies, we tested whether (1) eATP stimulates NLRP3 and RANKL expression in osteocytes and (2) if NLRP3 activation is required to trigger osteocyte RANKL expression. Methods: MLO-Y4 osteocyte cultures maintained on collagen coated plates in α -MEM with 5% FBS and 5% calf serum were treated at confluency for 1 hr with 10 μ M ATP in order to mimic a bolus-type extracellular exposure associated with nearby apoptotic cells. Cells were examined either acutely (after 1 hr ATP) or after an additional 5 hr in standard medium (no ATP). NLRP3, RANKL and OPG expression (normalized to GAPDH) were assessed by qPCR. To test whether NLRP3 triggers osteocyte RANKL expression, cells were cultured with the NLRP3-inflammasome inhibitor MCC950 (300 nM, Invivogen, [5]) prior to ATP challenge; gene expression assessed at 6 hr. Statistical test was assessed by 2-way ANOVA. Results: ATP exposure increased osteocyte NLRP3 gene expression ~3 fold after 1 hr and maintained this increase at 6 hrs. ATP also stimulated RANKL (7-fold) and OPG (2-fold) expression, but only at 6 hrs. Inhibiting NLRP3 inflammasome formation markedly suppressed the ATP-induced increase in RANKL expression. Discussion: These studies demonstrate that acute exposure of osteocytes to ATP stimulates RANKL expression, mimicking Panx1-mediated release of bolus ATP by apoptotic osteocytes [1, 2] and consistent with a driving role for ATP release in upregulation of RANKL by bystander osteocytes. Moreover, our studies reveal that this ATP-induced RANKL expression depends on the activation of the NLRP3 inflammasome, indicating a novel link between osteocyte inflammasome activation and RANKL signaling as part of the triggering mechanism for normal bone resorption. References: 1) Cheung WY et al, J Bone Miner Res, 2016; 2) Ravichandran KS et al, Nature, 2009; 3) Iyer S et al, Proc Natl Acad Sci, 2009; 4) Dongli Yang et al, Austin J Clin Ophthalmol. 2014; 5) Coll RC et al, Nature Med, 2015.

Figure 1: Fold change in MLOY-4 genes (NLRP3, RANKL, OPG) expression.

A: with 10 μ M ATP treatment 1 & 6 hrs.

B: inflammasome inhibitor effect on ATP treated cells.

Data are presented as mean \pm SE of three experiments performed in duplicate. (* $p < 0.05$ Versus ATP-untreated MLOY-4 cells)



Disclosures: Dorra Frikha-Benayed, None

SAT-0663

Scriptaid Induces Osteocyte Respiration through an HDAC5 Independent Mechanism Ningyuan Sun*¹, Ehab Azab¹, Yuhei Uda¹, Chao Shi², Paola Divieti Pajevic¹. ¹Boston University Henry M. Goldman School of Dental Medicine, United States, ²The Second Affiliated Hospital of Xi'an Jiaotong University, China

Bone undergoes continuous remodeling to maintain its structural integrity. During development, bones rely on glucose uptake for proper skeletal development. Osteoblasts take up one fifth of the glucose consumed by muscles through a Glut1/AMPK-dependent pathway independent of insulin signaling. Glucose uptake in osteoblasts is necessary for osteoblast differentiation, bone formation and glucose homeostasis. However, the role of glucose in osteocytes is still unknown. Previous studies have shown that parathyroid hormone (PTH) promotes bone anabolism, in part, by stimulating osteoblasts anaerobic glycolysis while suppressing glucose oxidation through the TCA cycle. In osteocytes, PTH suppresses Sost expression by inducing HDAC4/5 nuclear translocation and Mef2C suppression. Recently, scriptaid, an HDAC inhibitor, has been shown to induce Mef2 activation and exercise-like adaptation in skeletal muscle. In muscle cells, scriptaid disrupts the class IIa HDAC co-repressor complex comprising HDAC3, SMRT and Ncor and induces nuclear export of HDAC4/5 with increase in Mef2, Glut4, Pdk4 and ATP-5d expression. This suggested that scriptaid might upregulate Mef2 and Sost expression in osteocytes. To test this hypothesis, a clonal osteocytic cell line, Ocy454-12H was treated with scriptaid and/or PTH and gene expression was analyzed by semi-quantitative PCR. Unexpectedly, scriptaid potently suppressed Sost, whereas induced Glut4, Pdk4 and ATP-5d expression. Both scriptaid and PTH stimulated mitochondrial respiration and glucose uptake in these cells. Western blot analysis demonstrated that, in osteocytes, scriptaid induced nuclear translocation of HDAC5 whereas had no effect on HDAC4. Downregulation of HDAC5 by shRNA, increased basal Sost expression and prevented scriptaid-induced Sost suppression. However, Glut4 up-regulation by scriptaid was still present, even in the absence of HDAC5. These studies demonstrated that scriptaid induced osteocyte metabolism and glucose uptake through an HDAC5 independent mechanism. Furthermore, calvariae and long bone explants from C57/Bl6 animals treated with scriptaid showed significant increase in the expression of Glut4, Pdk4 and ATP-5d. Taken together these results suggest that scriptaid might enhance metabolism and glucose uptake in osteocytes.

Disclosures: Ningyuan Sun, None

SAT-0680

See Friday Plenary Number FRI-0680

SAT-0681

See Friday Plenary Number FRI-0681

SAT-0682

See Friday Plenary Number FRI-0682

SAT-0683

See Friday Plenary Number FRI-0683

SAT-0684

See Friday Plenary Number FRI-0684

SAT-0685

See Friday Plenary Number FRI-0685

SAT-0686

See Friday Plenary Number FRI-0686

SAT-0687

See Friday Plenary Number FRI-0687

SAT-0688

See Friday Plenary Number FRI-0688

SAT-0689

See Friday Plenary Number FRI-0689

SAT-0690

Clinical Applicability of TBS in Women with Short Stature Pedro Alvarenga*¹, Mariana Diniz², Milena Leite³, Caroline Silva⁴, Jessica Eleuterio², Maria Marta Soares⁵, Bruno Muzzi⁶, Barbara Silva⁷. ¹Alberto Cavalcanti Hospital, Brazil, ²Santa Casa de Belo Horizonte, Brazil, ³Mario Pena Hospital, Brazil, ⁴CEMA, Brazil, ⁵Felicio Rocho Hospital, Brazil, ⁶Mater Dei Hospital, Densimeter, Brazil, ⁷Felicio Rocho Hospital, Santa Casa de Belo Horizonte, Brazil

Introduction: Areal bone mineral density (aBMD) as measured by dual X-ray absorptiometry (DXA) is influenced by bone size such that true BMD is underestimated in those with smaller bones and overestimated in those with larger bones. This could overestimate the risk of fracture, leading to excessive treatment of small individuals, who have a lower fracture risk than taller subjects, particularly at the femoral neck. Trabecular bone score (TBS), a textural index evaluated by pixel gray-level variations in the lumbar spine (LS) DXA image, appears to be independent of bone size. **Objective:** We aimed to assess TBS in a group of women >50 years with short stature, compared to a control group. **Material and methods:** We retrospectively analyzed LS and femoral DXA scans of all women aged 50 to 90 years old with short stature (161cm in height, matched for age and LS BMD) with cases, selected from the same database. Site-matched LS TBS was extracted from the DXA image using the TBS iNsight software. **Results:** The study population included 171 women per group. Cases and controls were well matched in age (69.7 \pm 8.6 vs. 69.7 \pm 8.5 yrs; $p=0.91$), LS BMD (0.970 (0.880-1.090) vs. 0.970 (0.880-1.090) g/cm²; $p=0.9$), and LS BMD T-score (-1.7(-2.5; -0.7) vs. -1.7(-2.5; -0.8); $p=0.9$). Cases had a lower height ($p < 0.001$), despite being considered osteoporotic by BMD T-score. In contrast, none of the women with osteoporosis in the control group had a TBS >1.350. **Conclusion:** TBS is greater in women with short stature than in their taller counterparts. These findings suggest that TBS may offer advantages over aBMD alone to assist in treatment decisions in individuals with small bones.

Disclosures: Pedro Alvarenga, None

SAT-0691

BRIDGING THE GAP WITH FRAX: FRAX UTILITY IN PREVENTING HIP FRACTURES IN MEN Eduardo Dusty Luna*^{1,2}, Donna Davenport², John W Hinchey², Jan M Bruder^{1,2}. ¹UTHSCSA, United States, ²ALMVAH, United States

INTRODUCTION: Osteoporosis is an under-recognized issue that goes untreated in the majority of men with fractures. The National Osteoporosis Foundation (NOF) estimates that currently 1:4 men over the age of 50 years will have a fracture related to osteoporosis in their remaining lifetime. Although dual energy x-ray absorptiometry (DXA) classifies osteoporosis with a T-score < -2.5, the FRAX calculation can help provide an estimated ten-year likelihood of fracture based on clinical risk factors in a multivariable analysis without the use of DXA. To better understand the clinical utility of the FRAX tool, we reviewed the clinical risk factors in men admitted for hip fracture. **METHODS:** A retrospective chart review was conducted from January 2016 through December 2017. Seventy-seven patients

were admitted to the Veterans Administration Audie L. Murphy Hospital (ALMVAH) in San Antonio, Texas with a hip fracture. Forty-four patients were seen by endocrine in consultation for osteoporosis evaluation; four female patients were excluded. Demographic data was reviewed from the medical record during hospital stay. The FRAX® tool (version 4.0) by the University of Sheffield was individualized based on ethnicity and calculated without the use of DXA for each patient. RESULTS: The average age of the men admitted for hip fracture was 74 +/- 9 years; 75% were Caucasian and 25% Hispanic. Social risk factors including alcohol and tobacco use were most prevalent at 45% and 53% of patients, respectively. Previous osteoporotic fractures were noted in 18% of patients. Only 8% of veterans had a significant family history. Fracture risk calculation without DXA upon admission, demonstrated that 60% of the veterans had a major osteoporotic fracture (MOF) or hip fracture (HF) risk warranting therapy for osteoporosis. The average MOF risk was 10.4% while HF risk was 4.9%. Treatment for osteoporosis therapy prior to hip fracture was warranted in 90% of men over age 72 years. CONCLUSION: The awareness of preventing fractures in men is crucial as patients who suffer hip fracture develop significant disability and morbidity. Prolonged hospitalizations, multiple physician visits, chronic pain and loss of independence are only some of the most common problems that translate into a significant health care cost. The FRAX tool is a quick, inexpensive and effective resource to close the gap in treating men over age 72 years at risk for osteoporotic fracture.

Disclosures: **Eduardo Dusty Luna, None**

SAT-0692

Trabecular Bone Score (TBS) Integrating a New Correction for Soft Tissue Effects Based on Estimated Tissue Thickness François De Guio*¹, Enisa Shevroja², Franck Michelet¹, Doris Tran¹, Christophe Lelong¹, Didier Hans². ¹Medimaps, France, ²Center of Bone diseases, Bone and Joint Department, Lausanne University Hospital, Switzerland

Purpose: TBS is a textural parameter based on DXA spine scans that provides an indirect estimation of trabecular microarchitecture status, a valuable clinical information in osteoporosis. To account for soft tissue variability between individuals, current TBS insight (v3.0 and older) integrates a TBS correction based on BMI. We aimed at improving this correction by considering the tissue thickness estimated by the DXA device, which should be a better estimate of patient morphology than BMI. We evaluated the impact of this new correction in terms of in-vivo reproducibility and correlations with BMI for both GE-Lunar (GE) & Hologic (HLX) DXA manufacturers. Methods: We acquired scans of dried ex-vivo human vertebrae with several thicknesses of tissue-equivalent material and estimated the relationship between TBS and soft tissue thickness. From there, a derived specific model was defined and applied retrospectively on several datasets: one reproducibility study including 37 individuals having 2 or 3 scans each (Cohort A, GE); one reproducibility study including 27 individuals scanned 2 times each with repositioning (Cohort B, HLX); 2 population-based cohorts of women (Cohort C, HLX, N=6742, age=61±9; Cohort D, GE, N=6361, age=63±9), one population-based cohort of men (Cohort E, HLX, N=1343, age=56±11). For both current and new TBS, we computed 1) root mean square standard deviation (rms-SD) as an estimate of the reproducibility, 2) correlation coefficients with BMI. Results (see table): Overall, the new correction based on tissue thickness yield to a better in vivo reproducibility. The current TBS were negatively correlated with BMI for both manufacturers (r values ranged from -0.17 to -0.27) while the new TBS were now positively correlated which is consistent with expectations. Positive correlations between BMD and BMI were also reported (Cohort C: 0.23, Cohort D: 0.19, Cohort E: 0.26). Conclusions: With the new corrective and optimized model based on soft tissue thickness, we have a method that no longer depends on manual inputs (weight, height) and a better estimate of patient morphology enabling an improved in-vivo reproducibility. This is a promising approach to follow-up patients in longitudinal studies and to assess inter-individual variability hardly captured by BMI (for example, different morphotypes related to age). Whether clinical performance is improved with this new correction requires further studies.

Outcome	Cohort	Device	Sample size	Current TBS based on BMI	New TBS based on tissue thickness
rms-SD	A	GE	37	0.030	0.018
	B	HLX	27	0.025	0.023
TBS - BMI correlation coefficient	C	HLX	6742	-0.24	0.08
	D	GE	6361	-0.17	0.07
	E	HLX	1343	-0.27	0.08

Disclosures: **François De Guio, Medimaps, Other Financial or Material Support**

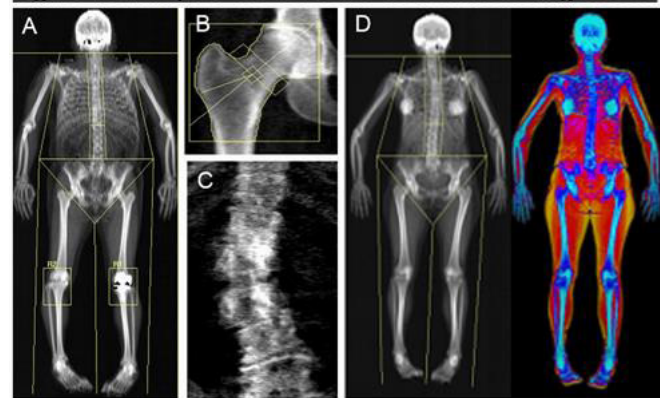
SAT-0693

Accounting for Confounding Factors Affecting Dual-Energy X-ray Absorptiometry in a Large Clinical Trial Catherine Donlon*¹, Cindy Yu¹, Sharon Chou^{1,2}, Meryl Leboff^{1,2}. ¹Division of Endocrinology, Diabetes and Hypertension, Brigham and Women's Hospital, United States, ²Harvard Medical School, United States

Dual-energy X-ray absorptiometry (DXA) is considered the gold standard for measuring bone mineral density (BMD) and body composition (fat and lean tissue). As the prevalence of joint replacements, osteoarthritis (OA), and degenerative disc disease rises with the aging U.S. population, it is necessary to account for these factors, which affect the accuracy and precision of DXA measures. In the VITamin D and Omega-3 Trial (VITAL): Effects

on Bone Structure and Architecture study, 771 participants including 411 men ≥50 years and 360 women ≥55 years completed spine, hip, and whole body DXA scans (Discovery W; APEX Version 4.2, Hologic, Bedford, MA) at baseline and 2-years post-randomization to determine whether supplemental vitamin D and/or omega-3 fatty acids have beneficial effects on bone health. To detect small changes in BMD, it was necessary to account for internal metal, OA, degenerative disc disease, and breast implants. About 12.8% of participants had internal metal artifacts at baseline including joint replacements, spinal fusions, insulin pumps, and other screws and plates. According to the International Society for Clinical Densitometry, the bone measures from the unaffected, contralateral side were used to replace the metal artifact when possible, thus preventing falsely elevated BMD results (n=62; Fig. 1A). By using the equation in Kelly et al., 2009, 2 T-scores and Z-scores were recalculated using the default sex and ethnicity-matched databases. However, if the metal adjustment was within the least significant change, no change was made to the bone data (n=11). Additionally, when there was not an unaffected contralateral side to copy (ie. spinal metal, bilateral hip/knee replacements), bone measures were excluded at the site as well as at the whole body (n=27). OA is also known to increase BMD. 3 Femoral neck measures were excluded in 11 participants with severe OA at the hip (Fig. 1B), and 51 participants who had severe degenerative disc disease and/or scoliosis whose spine measures were excluded (Fig. 1C). Lastly, the bone density and body composition analyses of 2 participants with bilateral breast implants (Fig. 1D) were excluded due to uncertain effects on bone density, fat and lean mass. Metal artifacts, OA, advanced degenerative disease and breast implants may confound DXA results. It is therefore important in clinical studies to account for these factors to detect physiologically relevant differences in bone and soft tissue measures. References: 1. ISCD Body Composition Course Syllabus. Middletown, CT. 2012. p. 1162. Kelly TL, et al. PLoS one. 2009;4(9):e70383. Glowacki J, et al. J Clin Densitom. 2010;13(1):24-8

Figure 1. Examples of DXA scans with confounding factors



A. Whole body scan with subregions around knees due to metal left knee replacement
B. Hip DXA scan with excluded femoral neck measures due to osteoarthritis
C. Spine scan with degenerative disc disease and scoliosis
D. Whole body scan of participant with breast implants

Disclosures: **Catherine Donlon, None**

SAT-0694

Can DXA-derived 3D measurements at the lumbar spine predict thoracic spine fractures? Mirella López Picazo*¹, Ludovic Humbert¹, Silvana Di Gregorio², Miguel Angel Gonzalez Ballester², Luis Del Rio³. ¹Galgo Medical, Spain, ²BCN MedTech, Universitat Pompeu Fabra, Spain, ³CETIR Grup Mèdic, Spain

Objective: Evaluate the association of DXA-derived 3D measurements at the lumbar spine with thoracic spine fractures. Method: We retrospectively analyzed a cohort of 32 post-menopausal Caucasian women collected at CETIR Grup Mèdic: 16 subjects with thoracic spine fractures (fracture group) and 16 age-matched subjects without any type of fracture (control group). Inclusion criteria for the fracture group were no prior osteoporotic fractures at baseline, and thoracic spine fracture event between one year to ten years from baseline visit. Inclusion criteria for the control group were no prior fractures at baseline and during at least 7 years from baseline visit. Spine AP DXA scans were acquired at baseline using a Prodigy scanner (GE Healthcare). Areal BMD (aBMD) at L1-L4 segment was measured using enCORE software (v14.10, GE Healthcare). DXA-derived 3D measurements at L1-L4 segment were assessed using the software 3D-SHAPER (v2.3, Galgo Medical). The software computes the 3D shape and density distribution of the lumbar spine by registering a statistical model onto the AP DXA scan. Volumetric BMD (vBMD) is computed at trabecular, cortical and integral (cortical plus trabecular) compartments. Differences in aBMD and DXA-derived 3D measurements between fracture and control groups were evaluated using unpaired t-test. Individual odds ratio (OR) and area under the receiver operating curve (AUC) were computed. Results: No significant difference between groups was found in terms of age (p = 0.74), weight (p = 0.44), height (p = 0.25), T-score (p = 0.10), aBMD (p = 0.11) and integral vBMD at the total vertebra (vertebral body plus posterior arch) (p = 0.05). However, when computed at the vertebral body, integral, trabecular and cortical vBMD showed significant differences (Table 1). Higher AUC were found for vBMD measurements at the vertebral body, compared to aBMD and integral vBMD at total vertebra.

Each incremental decrease of one standard deviation of the aBMD was associated with 1.86 the odds of presenting a fracture at dorsal vertebrae. OR for trabecular vBMD at the vertebral body was 5.42. Conclusion: This study shows that DXA-derived 3D measurements at the vertebral body could potentially be used to predict thoracic spine fracture using standard L1-L4 AP DXA scans.

Table I. Differences between measurements for fracture and control group.

L1-L4 segment		Control	Fracture	ρ	AUC	OR [95% CI]
		Mean \pm SD	Mean \pm SD			
Total Vertebra	aBMD (g/cm ²)	0.93 \pm 0.13	0.86 \pm 0.13	0.11	0.66	1.86 [0.86 - 4.02]
	Integral vBMD (mg/cm ³)	220.03 \pm 32.95	197.12 \pm 29.83	0.05	0.69	2.26 [0.96 - 5.30]
Vertebral Body	Integral vBMD (mg/cm ³)	166.16 \pm 20.21	144.03 \pm 17.04	<0.01	0.79	4.43 [1.40 - 14.00]
	Trabecular vBMD (mg/cm ³)	135.40 \pm 20.92	113.08 \pm 16.27	<0.01	0.81	5.42 [1.47 - 20.02]
	Cortical vBMD (mg/cm ³)	213.33 \pm 22.18	190.47 \pm 19.90	<0.01	0.80	3.46 [1.29 - 9.24]

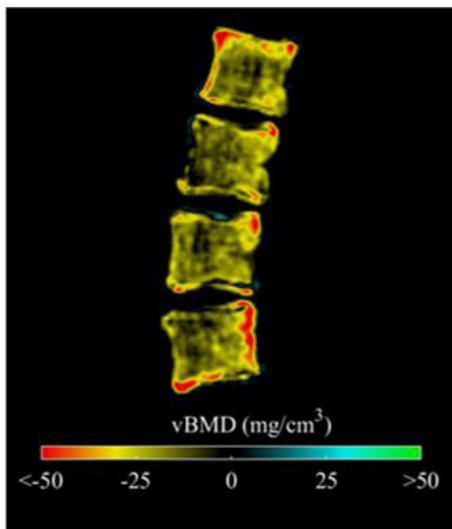


Figure 1. Differences between average vBMD of each group showed at the mid sagittal plane of the vertebral body.

Disclosures: Mirella López Picazo, None

SAT-0695

Are They Really a Different Population? Comparing Fracture Risk Factors Between Home Care Recipients and Long-Term Care Residents
Caitlin Mearthur^{*}, George Ioannidis¹, Micaela Jantzi², Jonathan Adachi³, Lora Giangregorio², John Hirdes², Alexandra Papaioannou¹. ¹McMaster University, GERAS Centre for Aging Research, Canada, ²University of Waterloo, Canada, ³McMaster University, Canada

Home care (HC) recipients have unique fracture risk factors compared to community dwelling individuals. Existing fracture risk assessment tools may not be feasible or valid. Our Fracture Risk Scale (FRS) leverages routinely collected RAI-MDS data and has been validated in the long-term care (LTC) setting but may not be applicable to the HC setting. We hypothesize that fracture rates and risk factors in HC and LTC are not the same, and that a HC-specific scale is needed. The purpose of this study is to explore the prevalence of FRS risk factors, and number of new fractures in one year among HC recipients, as compared to LTC residents. Methods: Clinical data were obtained through the Resident Assessment Instrument-HC and Minimum Data Set 2.0, and incident fractures in the Discharge Abstract Database and National Ambulatory Care Reporting System. We included Ontario HC recipients who had an admission assessment and another assessment within one year between April 1st, 2011 and March 31st, 2015 and LTC residents between April 1st, 2006 and March 31st, 2010. We excluded people who had end-stage disease, received hospice or respite care, or expected a short stay. Descriptive statistics (n, %) were used to describe clinical characteristics and proportion of individuals sustaining fracture(s) within one year. Chi-squared tests

were used to evaluate if there were statistically significant differences in the proportions of people in HC and LTC with fractures and risk factors. Results: 136868 HC recipients and 29848 LTC residents were included. The proportions of HC recipients and LTC residents with each risk factor were significantly different ($p < 0.001$). A slightly higher proportion of HC recipients experienced fractures within one year (5.6 %HC, 5.2% LTC). Of those fractures, LTC residents experienced more hip (61.8% LTC, 43.7% HC) while HC recipients had more other fractures (56.3% HC, 38.2% LTC). HC recipients were younger, more mobile, and had less cognitive impairment ($p < 0.001$). A higher proportion of HC recipients fell in the last 180 days (47.2% HC, 33.8% LTC) and experienced unintentional weight loss (HC 10.7%, LTC 5.3%). Conclusions: The proportion of people experiencing incident fractures and fracture risk factors differ between HC and LTC. HC recipients were younger, more mobile, and less cognitively impaired, but they experienced more falls, unintentional weight loss, and other fractures. The FRS may need to be tailored to the unique HC population.

Disclosures: Caitlin Mearthur, None

SAT-0696

Common mistakes in the clinical use of bone mineral density testing
Radamés Leal Freitas^{*}, José Seabra Alves-Neto², Amanda Raquel Costa Cruz², Francisco De Assis Pereira¹, Fábio De Souza Santos¹, Lúcio Moraes Lanzeri-Filho¹, Patricia Monique Vila Nova Pereira¹. ¹Universidade Federal de Sergipe, Brazil, ²Universidade Tiradentes, Brazil

Introduction: The World Health Organization considers bone densitometry (DXA) as the best technique for assessing Bone Mineral Density (BMD). DXA is used in clinical practice as the main diagnostic tool for osteoporosis and fracture risk, however, its performance may present errors that compromise not only its analysis and interpretation, but also decisions regarding the treatment of osteoporosis. Objective: Evaluate the frequency and types of errors present in the DXA. Materials and methods: It is a descriptive, observational and cross-sectional study with a quantitative approach and convenience sampling. In the analysis of the DXA exams, the demographic and anthropometric data of the patients and the evaluation of the technical quality of the exams in lumbar spine and proximal femur were evaluated. DXA was categorized as adequate and inadequate due to poor patient positioning, poor image analysis and demographic errors. Results: Of the 246 DXA, 144 (62.6%) were adequate and 92 (37.4%) were inadequate. The lumbar spine presented inadequacies in 82 (33.4%) of the exams and the proximal femur in 72 (30.9%); inadequacies in the lumbar spine or in the proximal femur were found in 16 (6.5%) and 10 (4.0%), respectively. The most common inadequacies for lumbar spine were non-centered and rectified lumbar spine and absence of vertebrae when necessary. Regarding the inadequacies found in the proximal femur densitometries, the patient's poor positioning, poor overall hip delimitation and positioning of the region of interest in the femoral neck were observed as being more frequent. Conclusion: Of the 246 DXA, 37.4% present at least one error of poor patient positioning or poor analysis of the acquired image, this demonstrates that the orientations determined by the guidelines are not widely adopted, which may contribute to the implications for monitoring of bone mass and diagnosis of osteoporosis.

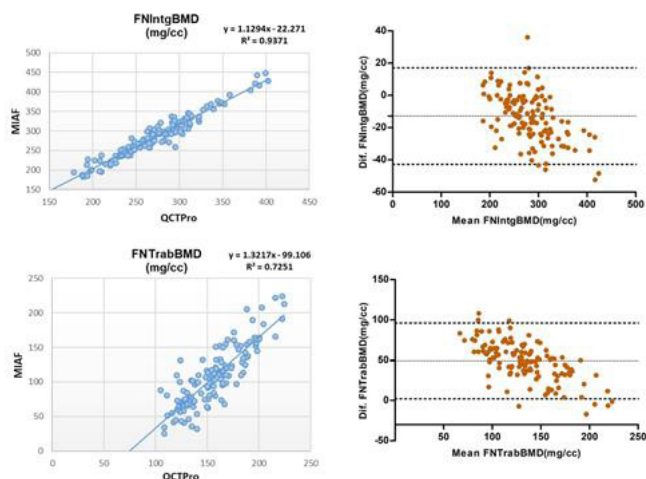
Disclosures: Radamés Leal Freitas, None

SAT-0697

QCT of the femur: Comparison between QCTPro and MIAF Femur
Ling Wang^{*}, Oleg Museyko², Klaus Engelke², Keenan Brown³, Xiaoguang Cheng¹. ¹Department of Radiology, Beijing Jishuitan Hospital, China, ²Institute of Medical Physics, University of Erlangen, Germany, ³Mindways Software Inc., United States

Introduction QCT is commonly employed in research studies and clinical trials to measure BMD and structural parameters at the proximal femur. In this study we compared two analysis software options, CTXA and MIAF-Femur, using a semi-anthropometric femur phantom and in vivo data from Chinese elderly men and women. Methods CT scans of the European Proximal Femur Phantom (EPFP) and of the hip from 130 subjects aged 60-80 years were analyzed with QCTPro CTXA Hip and MIAF-Femur. Integral(Inte), cortical(-Cort) and trabecular(Trab) vBMD, volume, and BMC of the femur neck (FN), trochanter (TR), inter-trochanter (IT), and total hip (TH) VOIs were compared. Accuracy was determined in the 5mm central portion of the femoral neck of the EPFP. Nominal values were: cross-sectional area (CSA) 4.9mm², cortical thickness (C.Th) 2mm, CortBMD 723 mg/cm³ and TrabBMD 100 mg/cm³. In MIAF the so-called peeled trabecular VOI was analyzed which excludes subcortical bone to avoid partial volume artefacts at the endocortical border that artificially increase TrabBMD. For CTXA corrected and uncorrected (so called raw cortical values unaffected by corrections of cortical volume) data were analyzed. Results For QCTPro and MIAF phantom results were: CSA 5.9 mm² versus 5.1 mm²; C.Th 1.68 mm versus 1.92 mm; CortBMD 578 mg/cm³ versus 569 mg/cm³; and TrabBMD 154 mg/cm³ versus 104 mg/cm³. In the human data correlations (R²) of integral and trabecular bone parameters ranged from 0.63 to 0.96. Bland-Altman analysis for TH and FN TrabBMD showed that lower mean values were associated with higher differences, which means that TrabBMD differences between MIAF and CTXA are larger for osteoporosis than for normal patients, which can be largely explained by the inclusion of subcortical BMD in the trabecular VOI with CTXA analysis. Correlations between QCTPro corrected CortBMD and MIAF were negative, whereas raw data correlated positively with MIAF measurements for all VOIs questioning the validity of the corrections. Conclusion The EPFP results demon-

strated higher MIAF accuracy of cortical thickness and TrabBMD. Integral and trabecular bone parameters were highly correlated between CTXA and MIAF. Partial volume artefacts at the endocortical border artificially increase trabecular BMD by CTXA, especially for osteoporosis patients. With respect to volumetric cortical measurements with QCTPro, it is recommended to use raw data, because corrected data cause a negative correlation with MIAF CortBMD.



Disclosures: **Ling Wang**, None

SAT-0698

Comparison between laser scanning confocal microscopy and traditional light microscopy in forensic histo-osteology Lelia Watamaniuk*¹, Ashley Smith², Natalie Dion³, Louis Georges Ste Marie³. ¹Department of Anthropology, McMaster University, Canada, ²Department of Anthropology, University of Toronto, Canada, ³CHUM- Centre Hospitalier de l'Université de Montreal, Canada

Traditionally, in forensic histo-osteological analysis, light microscopy is utilized as the primary mode of study. Recent advances in other modalities such as scanning electron microscopy, back scatter electron microscopy, microcomputer tomography (micro CT), and synchrotron have allowed for addition avenues of histo-osteological research. The purpose of this presentation is to demonstrate the comparison between laser scanning confocal microscopy (LSCM) and traditional light microscopy, both polarized and non-polarized. This project examined variations in bone mineral visualization, and age estimation in three populations of human individuals: clinical patients (trans iliac biopsy sections; n=16), ancient remains (rib sections from 3-5th C A.D. Apollonia; n=20), and anatomical collection donors (femoral sections; n=5). The analyses were performed using two staining protocols for undecalcified bone specimens (basic fuchsin, and toluidine blue), and 5 microscopes: Carl Zeiss® LSM800 laser scanning confocal microscope, a Carl Zeiss® LSM880 laser scanning multi-photon microscope, and an LSM880 laser scanning spinning disk microscope, Keyence® VHX1000 Digital Light Microscope and an Nikon® Eclipse E200 Light Microscope with a Nikon® DSLR7000 camera. The results of this study found that the LSCMs all provided a better three-dimensional visualization of the bone microstructure using the basic fuchsin stain versus light microscopy, and provided better visualization of osteonal mineralization variance; the LSCM modality was not as practical in the age calculations. Results of this project demonstrate that laser scanning confocal microscopy is a good tool in bone mineral visualization and research.

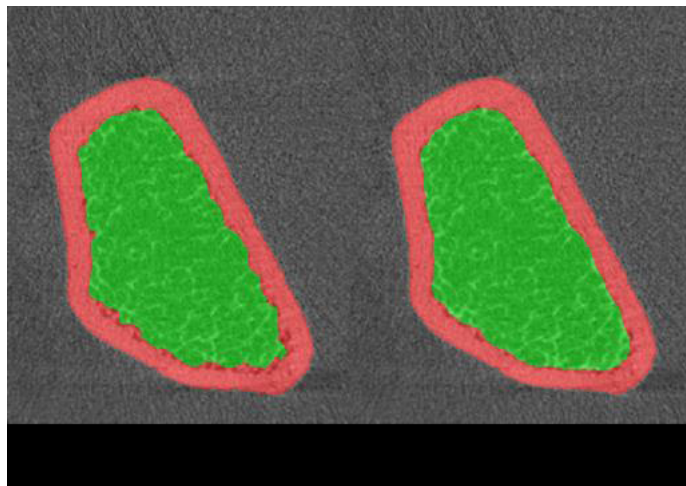
Disclosures: **Lelia Watamaniuk**, None

SAT-0699

Machine Learned Features and Classifier for Automatic HR-pQCT Cortical and Trabecular Compartment Segmentation Bryce A Besler*¹, Nils D Forkert², Lauren A Burt³, Steven K Boyd³. ¹Biomedical Engineering Graduate Program, Canada, ²Hotchkiss Brain Institute, Canada, ³McCaig Institute for Bone and Joint Health, Canada

Segmentation of the periosteal and endosteal surfaces are important for measuring clinical outcomes of bone health. Currently, a standardized algorithm is used for segmentation of the cortical and cancellous compartments in high resolution peripheral quantitative computed tomography (HR-pQCT). However, for poor quality bone, up to 50% of the segmentations need manual correction (internal data). This introduces rater variability and increases processing time. Using machine learning, a mathematical function can be trained to replace manual segmentation. Deep learning can be used to determine image features for classification. It is hypothesized that a machine can learn both the features and a classifier for periosteal and endosteal segmentation of HR-pQCT data. The radius and tibia of 155 healthy subjects

were imaged using HR-pQCT (XtremeCT II, SCANCO Medical AG, Switzerland). Average age was 62.6 years and 45.8% were female. Age- and sex-matched Tt.BMD percentiles ranged from 0.1% to 99.9% with a mean of 53.5%. The manufacturer's standard algorithm was used to generate periosteal and endosteal segmentations. All 310 segmentations were reviewed and corrected by a human rater. A deep learning model was constructed to learn both features and a classifier for cortical and trabecular segmentation. The mathematical function maps from a 1.98 mm by 1.98 mm patch to a label of either background, cortical bone, or trabecular bone. 16 learned image features are extracted from each patch. A classifier maps from the 16 image features to a label for each voxel. The model was trained end-to-end using the corrected segmentations as ground truth. Post-processing was performed to remove the ulna/fibula. Qualitatively, the machine learned model was accurate at the periosteal surface but shrank the endosteal surface (Figure). Average cortical and trabecular bone mineral density (Ct.BMD, Tb.BMD) were measured as outcomes. For the ground truth segmentation, Ct.BMD and Tb.BMD is 876.9 mg HA/ccm and 163.3 mg HA/ccm, respectively. For the machine learned segmentation, Ct.BMD and Tb.BMD is 856.7 mg HA/ccm and 150.5 mg HA/ccm, respectively. Average time to segment one HR-pQCT dataset was 62.1 seconds. A machine learned model for HR-pQCT segmentation is presented. The learned model shrinks the trabecular segmentation compared to the ground truth. The segmentations are rapid and comparable to manual segmentations.



Disclosures: **Bryce A Besler**, None

SAT-0738

See Friday Plenary Number FRI-0738

SAT-0739

See Friday Plenary Number FRI-0739

SAT-0740

See Friday Plenary Number FRI-0740

SAT-0741

See Friday Plenary Number FRI-0741

SAT-0742

See Friday Plenary Number FRI-0742

SAT-0743

See Friday Plenary Number FRI-0743

SAT-0744

See Friday Plenary Number FRI-0744

SAT-0745

See Friday Plenary Number FRI-0745

SAT-0746

See Friday Plenary Number FRI-0746

SAT-0747

See Friday Plenary Number FRI-0747

SAT-0748

See Friday Plenary Number FRI-0748

SAT-0749

Serum Estradiol, Follicle Stimulating Hormone and Sex Hormone Binding Globulin and the Risk of Fracture across the Menopausal Transition: Study of Women's Health Across the Nation (SWAN) Kristine Ruppert^{*1}, Jane Cauley¹, Yinjuan Lian¹, Joel Finkelstein², Carrie Karvonen-Gutierrez³, Sioban Harlow³, Joan Lo⁴, Sherri Burnett-Bowie², Arun Karlamangla⁵, Gail Greendale⁵. ¹University of Pittsburgh, United States, ²Massachusetts General Hospital, United States, ³University of Michigan, United States, ⁴Kaiser Permanente Northern California Division of Research, United States, ⁵University of California, United States

Sex steroid hormones have been linked to fractures in older women. It is unknown if hormones measured over the menopausal transition predict fractures. In SWAN, we studied 2960 women who had at least two repeat hormone measures and prospective information on fractures. Fasting serum was collected approximately annually for hormone assays on day 2-5 of the menstrual cycle when possible. Hormones were assayed at the SWAN Central Laboratory at the University of Michigan. Estradiol (E2) was measured with a modified immunoassay (Bayer Diagnostics Corp, Norwood MA) (inter- and intraassay Coefficient of variation(CV), 12% and 6%, respectively). Serum follicle stimulating hormone (FSH) (inter- and intraassay CV%, 10.6% and 6.4%, respectively) and sex hormone binding globulin (SHBG) (inter- and intraassay CV%, 9.9% and 6.1%, respectively) were measured with 2 site chemiluminometric immunoassays. Hormones were lagged (visit year -1) and transformed using log base 2 because they were not normally distributed. Incident fractures were ascertained at each annual visit and include high and low trauma fractures. Digit and facial fractures were excluded. The accuracy of self-report of fracture was determined by review of radiology reports. False positive rate was 4.6%. All medications including hormone therapy (HT) were time varying covariates. Discrete survival methods were used because information on incident fractures were identified only at annual interview. Data were censored after the first fracture. At baseline all women were pre- or early perimenopause with an average age of 46.4 (SD, 2.7) years. A total of 508 women experienced an incident fracture over an average follow-up of 8.8 (SD, 4.4), years. Women who experienced an incident fracture were more likely to be White, report high alcohol intake and diabetes and less likely to report premenopausal status at baseline. Each doubling of log E2 was associated with an 10% reduced risk of fracture independent of covariates and SHBG, (Table). The interaction between E2 and HT was not significant, p=0.45. In contrast, neither FSH or SHBG was associated with incident fractures. Serum E2 levels may help to identify women at higher risk of fractures over the menopausal transition. However, hormone assays must be standardized across laboratories for clinical implementation and further work is needed to define E2 thresholds.

Table: Relative Risk(RR) and 95%Confidence (CI) of Incident Fracture by doubling (Log base 2) of Estradiol, Follicle Stimulating Hormone(FSH) and Sex Hormone Binding Globulin(SHBG): SWAN

	Base Model ¹	MV Model ²
Estradiol	0.92 (0.85, 0.996)	0.90 (0.82, 0.98)
FSH	0.99 (0.92, 1.10)	1.06 (0.95, 1.17)
SHBG	1.02 (0.92, 1.11)	1.04 (0.92, 1.18)

¹ Base Model adjusted for cycle day and time of blood draw, age, race and site.

² Multivariable (MV) model adjusted for Base + corticosteroids, postmenopausal hormone therapy, selective estrogen receptor modulators, other osteoporosis medications e.g., bisphosphonates, smoking, alcohol, body mass index, vitamin D intake, physical activity and diabetes status. Estradiol and FSH models were also adjusted for SHBG.

Disclosures: *Kristine Ruppert, None***SAT-0750**

Vertebral fractures cascade: potential etiologies and risk factors Helene Che^{*1}, Veronique Breuil², Bernard Cortet³, Julien Paccou³, Thierry Thomas⁴, Laure Chapuis⁵, Francoise Debiais⁶, Nadia Mehzen Cetre⁷, Rose Marie Javier⁸, Sylvie Loiseau Peres⁹, Christian Roux¹⁰, Karine Briot¹⁰. ¹CHU Lapeyronie Montpellier, Rheumatology department, France, ²CHU L'Archet Nice, Rheumatology department, France, ³CHU Roger Salengro Lille, Rheumatology department, France, ⁴CHU Nord Saint Etienne, Rheumatology department, France, ⁵CH Simone Veil du Vitre, Rheumatology department, France, ⁶CHU La Miletrie Poitiers, Rheumatology department, France, ⁷CHU Pellegrin Bordeaux, Rheumatology department, France, ⁸CHU Hautepierre Strasbourg, Rheumatology department, France, ⁹CHR Orléans, Rheumatology department, France, ¹⁰CHU Paris Cochin, Rheumatology department, France

Background Vertebral fracture (VF) is the most common osteoporotic fracture, and a strong risk factor of subsequent vertebral fracture. Prospective studies have shown that a recent VF increases an imminent risk of a subsequent one, and attention has been paid recently to a possible cascade phenomenon i.e. the occurrence of multiples VFs in less than one year. This cascade could have severe consequences, and we prompted a study to identify potential causes of osteoporosis and risk factors. Methods Vertebral fractures cascade (VFC) observations were collected retrospectively between January 2016 and April 2017. VFC was defined as the occurrence of at least 3 vertebral fractures within one year. Patients with other etiologies than osteoporosis (i.e. malignant or traumatic VFs) were excluded. The cause of osteoporosis associated with VFC was the one retained by the physician at the time of diagnosis. Results We collected in 10 centers, a total of 113 observations of VFC (79.6% of women, median age of 73). The median number of incident VF was 5. 40.5% and 30.9% patients had a previous major fracture and a previous VF respectively and 68.6% had densitometric osteoporosis (T-Score \leq -2.5SD either at lumbar or femoral site). 18.9% patients currently received oral glucocorticoids at the time of VFC and 37.1% in the past. The main comorbidities were history of cancer (18.7%), chronic inflammatory diseases (29.7%) and diabetes mellitus (7.2%). A secondary osteoporosis associated with the VFC was diagnosed in 52 patients: glucocorticoid-induced osteoporosis (25.7%), benign hemopathies (6.2%), alcoholism (4.4%), use of aromatase inhibitors (3.6%), primary hyperparathyroidism (2.7%) and hypercorticism (2.7%), anorexia nervosa (2.7%), pregnancy and lactation-associated osteoporosis (1.8%). Thirteen cases were reported following a vertebroplasty procedure. 31.5% patients previously received an anti-osteoporotic treatment. In 6 patients, VFC occurred early (in the year) following discontinuation of an anti-osteoporotic treatment: 5 after denosumab and one after an infusion of zoledronic acid. Conclusion The results of this retrospective study show that almost half of VFC occurred in patients with secondary osteoporosis. While they suggest that a careful management has to be given to these patients in order to prevent VFC in these circumstances, prospective studies are needed to further explore the determinants of such a severe complication of osteoporosis.

Disclosures: *Helene Che, None***SAT-0751**

Trabecular Bone Score in Healthy Adult Population of India: Chandigarh Urban Bone Epidemiological Study (CUBES) Abhilasha Garg^{*1}, Ruban Dhaliwal², Anshita Aggarwal¹, Rimesh Pal¹, Priyanka Singh¹, Niranjan Khandelwal³, Naresh Sachdeva¹, Anil Bhansali¹, Sanjay Kumar Bhadada¹. ¹Department of Endocrinology, Post Graduate Institute of Medical Education and Research, India, ²Endocrinology, Diabetes and Metabolism, Department of Medicine, State University of New York Upstate Medical University, United States, ³Department of Radiodiagnosis, Post Graduate Institute of Medical Education and Research, India

Purpose: Trabecular bone score (TBS), a textural analysis of the lumbar spine image, utilized complementary to dual energy x-ray absorptiometry (DXA) has been shown to assess bone quality and capture fracture risk. As bone mineral density (BMD) varies with ethnicity, TBS is also expected to vary. Indians have lower BMD than their Western counterparts. The aim of this study was to generate normative data on TBS in healthy Indian population. Methods: Study population included 764 healthy volunteers, ages 20-80 years, recruited from Chandigarh, India. Following comprehensive biochemical evaluation, BMD was assessed in all participants by DXA. TBS (L1-L4) was calculated utilizing TBS iNsight software in 310 participants. Results: Mean age of the study population (n=310) was 43.8 \pm 12.5 years with 40.6% males and 59.3% females. Highest TBS was noted in both male and female subjects in the youngest decade (20-29 years), 1.297 \pm 0.14 and 1.265 \pm 0.15 respectively. TBS was higher in males compared to females at each decade. TBS decreased with age by 2-3 % per decade. Mean TBS in males aged >50 years (n= 39) was 1.159 \pm 0.123 and in postmenopausal females (n=85) was 1.142 \pm 0.015. Modest negative correlation was found between TBS and age (r = -0.375) and very weak negative correlation between TBS and vitamin D (r = -0.136). Significant positive correlation was found between BMD and TBS. Per TBS cut-offs proposed for western population, normal, partially degraded, and degraded micro-architecture was noted in 18.8%, 15.3% and 65.8% of postmenopausal females. Conclusion: Age and gender specific reference curves generated from this cohort can be used for osteoporosis management in India. Applying the western thresholds may lead to overestimation of fracture risk.

Disclosures: *Abhilasha Garg, None*

SAT-0752

Association between locomotive syndrome and bone mass, vertebral fractures and sarcopenia in the elderly aged 80 years and over. Jane Erika Frazao Okazaki*, Fernanda Martins Gazoni, Daniela Regina Brandao Tavares, Maria Carolyn Fonseca Batista Arbex, Lais Abreu Bastos, Flavia Kurebayashi Fonte, Maysa Seabra Cendoroglo, Fania Cristina Santos. UNIFESP, Brazil

Introduction: Musculoskeletal diseases, such as osteoarthritis and chronic pain, have been cited as causes of mobility loss and disabilities in the elderly. The Japanese Orthopedic Association (JOA) introduced the term Locomotive Syndrome (Slo) to refer to individuals who are at high risk of dependence due to disorders of the osteoarticular system. The evaluation of locomotor function can be performed using the GLFS-25 (25-Geriatric Locomotor Function Scale) developed by Seichi et al. This instrument was validated for Portuguese language in Brazil by Tavares and named GLFS 25-P. Some Japanese studies have shown association with osteoporosis, fractures and sarcopenia, but the relationship between bone health is not clear in the Brazilian population. **Objective:** Evaluate the association between Slo and bone density, sarcopenia, vertebral fractures and vitamin D levels. **METHODS:** This is an observational, analytical, cross-sectional study of locomotor syndrome in individuals aged 80 years or older, functional, and living in São Paulo. The data were collected from May 2016 to February 2017. We applied questionnaires related to Slo (GLFS 25-p), as well as anthropometric measurements. We assessed bone density and Baugartner index (IB) by densitometry of total body, and also vertebral fractures by thoracolumbar spine radiography and serum vitamin D values in the last year. The diagnosis of locomotive syndrome was defined as a score of 19 or more at the GLFS 25-P instrument. **Results:** Sample made by 102 elderly people with a mean age of 87.29 years, with a female majority (73.5%). Slo had a high prevalence in the study population (55%). It was observed that 18.3% of the participants have fracture; 47.9% were classified as osteoporotic; 51.7%, with sarcopenia and 5.3% VIT D 25OH below 20. There was no association between GLFS25-P and fracture ($p = 0.272$), Osteoporosis ($p = 0.662$) or Sarcopenia ($p = 0.239$). In addition, no differences in mean VITD 25OH (0.853) and IB ($p = 0.805$) were found comparing to the GLFS25-P. **Conclusion:** No associations were found between locomotor syndrome and osteoporosis, sarcopenia, vertebral fractures and vitamin D deficiency at this population.

Disclosures: Jane Erika Frazao Okazaki, None

SAT-0753

Involvement of lifestyle-related diseases in the development of fragility fracture of the proximal femur Takashi Iwakura*, Atsushi Sakurai, Satoru Sawamura. Awaji Medical Center, Japan

Purpose: Recently, the association between lifestyle-related diseases and osteoporosis/fragility fracture has been investigated (1-3). The purpose of this study was to examine the involvement of lifestyle-related diseases in fracture of the proximal femur. **Materials & methods:** The subjects were 1,027 patients with fragility fracture of the proximal femur (229 males, 798 females) admitted to our hospital between 2013 and 2016. We retrospectively examined the patient background and incidences of lifestyle-related diseases using medical records. Hypertension (HT), dyslipidemia (DL), diabetes mellitus (DM), chronic kidney disease (CKD), and chronic obstructive pulmonary disease (COPD) were investigated as lifestyle-related diseases. **Results:** The mean age of the subjects was 85 years (male: 83 years, female: 86 years). Patients with lifestyle-related diseases accounted for 82% (male: 80%, female: 82%). The incidences of HT, DL, DM, CKD, and COPD were 63, 17, 18, 43, and 3%, respectively (male: 54, 11, 19, 36, and 8%, respectively, female: 65, 18, 17, 44, and 1%, respectively). The incidences of HT, DL, and CKD were significantly higher in the females. That of COPD was significantly higher in the males. We also examined the presence or absence of lifestyle-related diseases and age at the time of injury. In the DM group, the age was younger than in the non-DM group (82 years vs. 86 years). This tendency was more marked in the males (male: 78 years vs. 84 years, female: 83 years vs. 86 years). Among both the males and females, the age at the time of fracture was even younger in DM patients receiving insulin (male: 71 years, female: 80 years). **Discussions:** Lifestyle-related diseases are associated with bone-quality reduction, and may increase the risk of non-bone-mineral-density-dependent fracture. In this study, most patients with fracture of the proximal femur had lifestyle-related diseases, and there were sex-related differences in their incidences. As an etiological factor for fragility fracture, the presence of lifestyle-related-disease-associated osteoporosis must be considered. Furthermore, the results showed that fracture of the proximal femur developed at a younger age in DM patients. It may be necessary to develop a more positive therapeutic intervention for osteoporosis in DM patients. **Conclusion:** Among patients with lifestyle-related diseases, fracture of the proximal femur develops at a younger age in those with DM.

Disclosures: Takashi Iwakura, None

SAT-0754

WITHDRAWN

SAT-0755

Longitudinal change of bone quality according to serum adipokine levels in Korean adults: The KoGES-ARIRANG study Jung Soo Lim*¹, Tae-Hwa Go², Dae Ryong Kang³, Sang Baek Koh⁴. ¹Department of Internal Medicine, Yonsei University Wonju College of Medicine, Republic of Korea, ²Center of Biomedical Data Science, Yonsei University Wonju College of Medicine, Republic of Korea, ³Institute of Genomic Cohort, Yonsei University Wonju College of Medicine, Republic of Korea, ⁴Department of Preventive Medicine, Yonsei University Wonju College of Medicine, Republic of Korea

Fat is the biggest endocrine organ that releases various adipokines. Previous studies have shown that adipokines are involved in bone metabolism through direct or indirect effects. However, there is a paucity of data on prospective studies regarding the association between bone health and serum adipokines. The aim of the study was to investigate the effects of serum adipokine levels on longitudinal change of bone quality in Korean adults. A total of 1,874 adults aged 40–70 years assessed in the Korean Genomic Rural Cohort Study from 2005 to 2007 were examined and followed. We divided them into four groups based on sex, age, or menopausal status. The serum concentrations of leptin and adiponectin were measured by radioimmunoassay. In addition, bone status was assessed using the calcaneal quantitative ultrasound method; longitudinal change in bone parameters was evaluated using the values of baseline and follow-up. The average follow-up period was about 2.2 years. In women, logistic regression analysis showed that the change in bone stiffness index (BSI) was not significantly associated with both adiponectin and leptin levels. However, only in men aged over 50, there was a negative correlation between the change in BSI and serum adiponectin level, but not leptin, even after adjusting for confounding factors (coefficient = -0.27, $p = 0.012$). Our results suggest that adipokines may affect bone quality differently in Korean adults depending on their characteristics. Long-term clinical research would be needed to clarify the role of various adipokines in the development of osteoporosis.

Disclosures: Jung Soo Lim, None

SAT-0756

Pain at Multiple Sites Is Associated with Prevalent and Incident Fractures in Older Adults: a 5.1-year Follow-up Study Feng Pan*¹, Jing Tian¹, Dawn Aitken¹, Flavia Cicuttini², Graeme Jones¹. ¹Menzies Institute for Medical Research, University of Tasmania, Australia, ²Department of Epidemiology and Preventive Medicine, Monash University Medical School, Australia

Purpose: Pain is common in older adults typically involving multiple sites. Pain at multiple sites has been shown to be associated with a number of adverse health outcomes; however, whether pain at multiple sites is associated with fractures, and whether this association is dependent on falls risk and/or bone mineral density (BMD) is unknown. This study aimed to describe the association between number of painful sites and fractures, and to explore whether pain at multiple sites is an independent marker for fractures. **Methods:** Data from a longitudinal population-based study of older adults (mean age 63 years, 51% female) were utilized with measurements at baseline ($n=1086$), 2.6 ($n=875$) and 5.1 years ($n=768$). Presence/absence of pain at the neck, back, hands, shoulders, hips, knees and feet was assessed by questionnaire at baseline. Fractures were self-reported at each time-point. BMD was measured by Dual-energy X-ray absorptiometry (DXA). Baseline demographic, lifestyle, and falls risk assessment were also obtained. **Results:** A total of 385 fractures were reported at the three time-points and 86 incident fractures were observed over 5.1 years. Greater number of painful sites was associated with higher fracture prevalence at any site, and fractures occurring at the vertebral, non-vertebral and major sites (including the femur, radius, ulnar, vertebrae, rib and humerus) in univariate and multivariable analyses with adjustment for age, sex, body mass index, smoking history, physical activity, pain medication, BMD and falls risk. There was a dose-response relationship between number of painful sites and fracture prevalence at these sites (all P for trend <0.05). In addition, there was a dose-response relationship between number of painful sites and the risk of incident fractures occurring at any sites (relative risk (RR) 1.4, 95% CI 1.1-1.8) and major sites (RR 1.9, 95% CI 1.2-2.9) over 5.1 years after adjustment for confounders. No significant association between number of painful sites and prevalent and incident hip fractures was observed possibly due to the small sample size (7 prevalent and 3 incident hip fractures). **Conclusions:** Pain at multiple sites is associated with a higher risk of prevalent and incident fractures, which is independent of falls risk and BMD, suggesting that widespread pain may be an independent marker of higher fracture risk.

Disclosures: Feng Pan, None

SAT-0757

Vitamin D Insufficiency and Elevated Vitamin D Metabolite Ratios (VMR) are Associated with Increased Risk of Injuries: Results from the British Army Lower Limb Injury Prevention (ALLIP) Study Jonathan Tang¹, Sarah Jackson², Rachel Izard³, Samuel Oliver⁴, Isabelle Piec¹, Christopher Washbourne¹, Neil Walsh⁵, Julie Greeves², William Fraser¹. ¹University of East Anglia, United Kingdom, ²Army Personnel and Research Capability, United Kingdom, ³Army Recruiting and Training Division, United Kingdom, ⁴University of Bangor, United Kingdom, ⁵Bangor University, United Kingdom

Introduction Up to 20.4% of British Army recruits suffer from musculoskeletal injuries (MSI) during initial training. Up to 10% suffer skeletal stress fracture (SfX) resulting in lost training days and medical attrition, which is a significant financial cost to the Army. There is evidence to suggest that vitamin D deficiency is prevalent in the army. Our aim was to determine baseline vitamin D status in recruits upon starting training and the relationships between vitamin D metabolites (VDM) and health outcomes after a 14-week training programme. Methods 2252 healthy new army recruits, mean (range) age 21.7(18-32)yrs participated in this prospective, observational study (ClinicalTrials.gov ID: NCT02416895). After exclusion of those who took calcium/vitamin D supplements, and those with prior injuries, 940 individuals were included in the analysis. Serum concentrations of 25OHD and 24,25(OH)2D(LC-MS/MS), 1,25(OH)2D(DiaSorin) and PTH(Roche) were among a panel of analytes tested across all seasons. The co-primary endpoints were subject incidence of SfX, MSI, infections and days lost in rehabilitation (DLR) in relation to VDM. Secondary outcomes were BMD and seasonal variations in analytes. Results 38% of participants identified as vitamin D insufficient (25OHD<50nmol/L) at baseline had an increased risk (OR) of SfX (1.03), medial tibial stress syndrome (MTSS) (1.26), upper limb trauma (1.02) and respiratory infections (1.13), and highly significant risk of upper limb overuse injuries (3.18) and subsequent DLR (3.49). Mean 24,25(OH)2D was 9.5-fold lower than 25OHD, and 25OHD:24,25(OH)2D VMR was significantly increased at 25OHD<50nmol/L (p<0.001). There was no significant relationship between 1,25(OH)2D and 25OHD, whereas the distribution of 1,25(OH)2D:24,25(OH)2D VMR showed an exponential negative correlation with 25OHD ($y = 1525.8x - 0.983, r_{2Exp} = 0.582, p < 0.001$). Using this model, we found that subjects with high 1,25(OH)2D:24,25(OH)2D VMR and low 25OHD have significantly higher PTH mean(SEM) 4.9(0.5) pmol/L, p>0.001 than those at the opposite end of the spectrum (PTH 3.0(0.3) pmol/L). Cosinor-fit curves revealed circannual rhythm on all VDM and VMR except for 1,25(OH)2D. PTH exhibited a low amplitude, circasemiannual rhythm. Baseline BMD was not associated with any health outcomes. Conclusion Vitamin D insufficiency is strongly associated with training-related injuries and lengthened rehabilitation. By using VMR model we demonstrated possible underlying mechanisms preceding the accelerated injury.

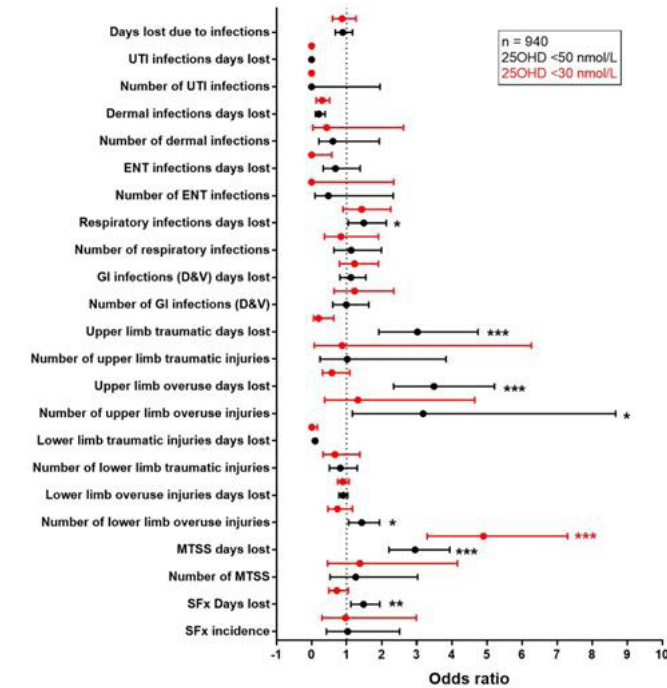


Figure showing the risk of vitamin D insufficiency and deficiency with training-related injuries and health outcomes. *Denotes (p<0.05), ** (p<0.01), *** (p<0.001)

Disclosures: Jonathan Tang, None

SAT-0758

Greater Bone Marrow Adiposity Predicts Loss of Spine Compressive Strength and Trabecular Bone in Postmenopausal Women from the AGES-Reykjavik Study Gina Woods¹, Susan Ewing², Deborah Kado¹, Trisha Hue³, Sigurdur Sigurdsson⁴, Gudny Eiriksdottir⁴, Vilundur Gudnason⁴, Eric Vittinghoff², Thomas Lang², Tamara Harris⁵, Clifford Rosen⁶, Kaipin Xu⁷, Xiaojuan Li⁷, Ann Schwartz². ¹Department of Medicine, UCSF, United States, ²Department of Epidemiology, UCSF, United States, ³Department of Epidemiology and Biostatistics, UCSF, United States, ⁴Icelandic Heart Association, Iceland, ⁵National Institute on Aging, United States, ⁶Maine Medical Center Research Institute, United States, ⁷Program of Advanced Musculoskeletal Imaging, Cleveland Clinic, United States

Greater bone marrow adipose tissue (BMAT) is associated with lower bone mineral density (BMD) and prevalent vertebral fractures in older adults, but it is uncertain whether or not greater BMAT predicts bone loss over time. If greater BMAT leads to bone loss, then targeting BMAT to prevent osteoporosis may have therapeutic potential. One previous study in 120 postmenopausal women reported that those with greater femoral neck BMAT had a non-significant trend toward femoral neck BMD loss, measured by DXA, at 4 years (r = -0.23, p = 0.14). The purpose of this study is to evaluate the associations between baseline vertebral BMAT and change in measures of bone density and strength in older adults from the Age, Gene/Environment Susceptibility (AGES) - Reykjavik study. A total of 364 participants had concurrent baseline measurements of BMAT and BMD/bone strength, and repeat BMD/bone strength measurements after a mean follow-up of 3.1 (SD 1.5) years. Those with missing BMAT measurements (n=1) and those using medications known to affect BMAT and BMD (n=65) were excluded, leaving 150 men and 148 women in the analytic sample. Mean (L1-4) BMAT (ratio of fat to water + fat, %) was measured by 1.5-T 1H magnetic resonance spectroscopy. BMD was measured by QCT and DXA of the hip and spine, and bone strength by QCT of the spine. Participants were a mean age of 81.8 (SD 4.3) years, had a mean BMI of 27.2 (SD 4.0) kg/m², a mean (L1-4) BMAT of 54.7 (SD 8.1)%, 9.7% had diabetes, and 19.5% had prevalent vertebral fractures. During an average of 3.0 years of follow-up, participants experienced statistically significant loss of trabecular bone at the spine (-7.3%, p<0.0001) and total hip (-9.5%, p<0.0001), but not cortical bone. Greater baseline BMAT was associated with loss of spine compressive strength (r = -0.26; p=0.001) and trabecular bone loss at the spine (r = -0.18, p = 0.03) and femoral neck (r = -0.19, p = 0.03), in women but not men (Table). The reason for this gender difference is unclear. No associations between baseline BMAT and cortical bone loss were observed. Further studies are needed to investigate whether BMAT predicts incident fractures in older adults.

	Men (n=150)		Women (n=148)	
	r	p	r	p
Spine trabecular vBMD, g/cm ³ /year	-0.03	0.67	-0.18	0.03
Spine integral vBMD, g/cm ³ /year	0.03	0.69	0.02	0.82
Spine compressive strength, g ² /cm ² /year	0.08	0.31	-0.26	0.001
Total hip trabecular vBMD, g/cm ³ /year	0.15	0.08	-0.05	0.56
Total hip cortical vBMD, g/cm ³ /year	-0.01	0.88	0.07	0.45
Total hip integral vBMD, g/cm ³ /year	0.03	0.75	0.02	0.86
Femoral neck trabecular vBMD, g/cm ³ /year	-0.01	0.87	-0.19	0.03
Femoral neck cortical vBMD, g/cm ³ /year	-0.02	0.85	0.05	0.54
Femoral neck integral vBMD, g/cm ³ /year	-0.02	0.80	0.04	0.66
Lumbar spine areal BMD, g/cm ² /year	0.02	0.83	0.002	0.98
Total hip areal BMD, g/cm ² /year	0.12	0.14	0.06	0.46
Femoral neck BMD, g/cm ² /year	0.11	0.17	0.001	0.99

Disclosures: Gina Woods, None

SAT-0759

Meta-analysis of Lithium use on the Risk of Fracture in Epidemiological Studies Qing Wu¹, Bowen Liu¹, Shu Zhang¹. ¹University of Nevada, Las Vegas, United States

Research findings regarding the association between lithium medication and risk of fracture are inconsistent. No related meta-analysis has been reported in the literature. Therefore, we conducted the first meta-analysis to examine the effect of lithium treatment on the risk of fracture. We performed an electronic search of Medline, Web of Science and Embase through February 1, 2018, and manual search of related references and review articles. Two researchers independently conducted study selection, study appraisal, and data abstraction via Research Electronic Data Capture tool. The disagreement was resolved by consensus. Confounder-adjusted risk ratios were pooled using a random-effects model. Each study was weighted by the reciprocal of its variance. Cochrane's Q and Higgins index I² were used to examine heterogeneity. Study quality was appraised by using the Newcastle-Ottawa Scale. We also performed several pre-specified sensitivity analysis and subgroup analyses to determine if fracture risk associated with lithium use was influenced by duration of follow-up, sex, demographic region, the sample size of the study, and controlling important confounders. Five studies including 1,130,689 subjects were eligible for the meta-analysis. The Newcastle-Ottawa study quality scores ranged from 7 to 9. The overall pooled estimate

suggests that the use of lithium is associated with 20% decrease in fracture risk (RR = 0.80, 95% CI, 0.73-0.87, p<0.01). Cochrane's Q test (p = 0.61) and Higgin index (I2 = 0) indicated that no heterogeneity was observed among the included original reports. The funnel plot and Egger's test (p=0.63) indicated that no published bias was observed. The reduced fracture risk associated with lithium medication was consistent in sensitivity analyses with different inclusion criteria, and in the subgroup analyses. Therefore, our meta-analysis results suggested that lithium use is associated with a significantly decreased risk of fracture.

Disclosures: *Qing Wu, None*

SAT-0804

See Friday Plenary Number FRI-0804

SAT-0805

See Friday Plenary Number FRI-0805

SAT-0806

See Friday Plenary Number FRI-0806

SAT-0807

HIP Mobile: A community-based Monitoring, Rehabilitation and Learning e-system for patients following a Hip Fracture Ahmed Abou-Sharkh*¹, Nancy E. Mayo¹, Michelle Wall¹, Anthony Albers², Stephane Bergeron³, Sonia Jean⁴, Pierre Berube⁵, Edward J. Harvey¹, Suzanne N. Morin¹. ¹Research Institute of McGill University Health Center, Canada, ²St-Mary's Hospital, Canada, ³Jewish General hospital, Canada, ⁴Institut national de sante publique du Quebec, Canada, ⁵Greybox Solutions, Canada

PURPOSE: Following a hip fracture, most patients do not return to pre-fracture autonomy level. e-Health solutions incorporated within homecare rehabilitation may lead to better clinical outcomes and health-related quality of life (HRQoL). Our objective is to enable recovery and improve HRQoL following a hip fracture through the implementation of the HIP Mobile e-Monitoring and Coaching system.**METHODS:** HIP Mobile comprises a wearable smart insole with a tablet based app interface including an exercise program and a secure cloud based remote monitoring dashboard. Expert educational content, exercise-tracking algorithms and patient-oriented interface have been validated. A pragmatic randomized trial to determine the effectiveness of a 4-month HIP Mobile program compared to printed educational material on mobility and patient reported outcomes in men and women >60 y, introduced 6 weeks after hip fracture repair was initiated. The primary outcome is functional mobility measured by gait speed and 30 second sit-to-stand measured at 6-months post-fracture. Baseline results from the recruited participants are presented.**RESULTS:** We have recruited 12 participants with average age 78 (SD 11) y, 50% women, within an average of 75 (SD 27) days post fracture repair. One third of participants had experienced a prior fracture; yet only 2 participants were on anti-osteoporosis medication. Median gait speed (0.9; IQR 0.69- 0.95 m/sec), median 30 second sit-to-stand (10; IQR 5-12) and mean grip strength (24; SD 9 kg) and were similar normative values for community dwelling older adults. Despite this, participants voiced serious concerns in 8 areas of HRQoL affected by their hip fracture, using the Patient Generated Index, an individualized measure of HRQoL. The most frequently mentioned areas of concern were walking and mobility (26%), endurance (16%) and fatigue (16%). The top-ranking concern at baseline was walking and mobility. (Table) Of interest, no participants mentioned pain as a concern.**CONCLUSIONS:** Despite gait speed and sit-stand metrics being similar to normative values 10-weeks post-fracture, the top-ranking concerns identified by these elderly participants were related to functional mobility, suggesting they had not yet returned to their pre-fracture autonomy and mobility levels. Our interactive HIP Mobile encourages active engagement in the rehabilitation process and has potential to improve functional mobility over an extended period.

Table: Baseline Patient Generated Index (PGI) Results

PGI areas reported by participants*	Participants Reported areas of concern- N=12	Top ranking areas of concern N=12
Mobility/walking	10	4
Endurance/strength	5	2
Fatigue	4	2
Social Activities	4	3
Independence	3	1
Working	2	0
Cooking	2	0
Driving	1	0

* Questions asked: What areas of life has been affected by hip fracture?
- Participants could report up to 5 areas of concern

Disclosures: *Ahmed Abou-Sharkh, None*

SAT-0808

Time trends among new users of osteoporosis drugs over 20 years: considerations for pharmacoepidemiologic study design Kaleen Hayes*¹, Joann Ban¹, Grace Athanasiadis¹, Andrea Burden², Suzanne Cadarette¹. ¹University of Toronto, Canada, ²ETH Zurich, Switzerland

Background: Oral bisphosphonates entered the market in 1996 and are the main osteoporosis drugs prescribed in Canada. Introduction of new therapeutic options, updates to practice guidelines, and healthcare policy changes may make studies examining new-users of bisphosphonates susceptible to time-varying biases.**Objective:** To compare characteristics of first-time bisphosphonate users in Ontario, Canada over time.**Methods:** The Ontario Drug Benefit (ODB) program covers prescription drugs listed on the ODB formulary for residents aged 65 or more years. We identified first dispensation of an oral bisphosphonate (alendronate [10 and 70 mg], etidronate [400 mg and 500 mg calcium], and risedronate [5, 35, and 150 mg]) among residents of Ontario, from 1996/04 to 2015/03. We excluded patients taking other osteoporosis drugs, with health conditions known to impact bone, and residents of long-term care facilities. We also excluded patients aged younger than 66 years to ensure at least one year of drug plan eligibility. Medical and pharmacy claims within the year prior to first bisphosphonate dispensation were used to characterize patients. Descriptive statistics were used to summarize and compare patient characteristics by fiscal year.**Results:** We identified 523,210 eligible seniors starting bisphosphonate therapy in Ontario from 1996 to 2015 (mean age 75 years; 5.0% rural). A larger proportion of men (6.2% to 29.0%) and diabetics (8.7% to 17.8%) initiated therapy over time. History of benzodiazepines decreased (26.6% to 11.5%), while prior statin use (9.5% to 42.8%), oral corticosteroid use (10.6% to 14.7%), and prior bone mineral density testing (46.7% to 68.0%) increased. A shift in prescriptions from etidronate to alendronate and risedronate was documented, consistent with drug policy changes.**Conclusions:** Characteristics of new initiators of oral bisphosphonates among Ontario seniors changed over time, reflecting changes in healthcare delivery and osteoporosis management. Consideration must be given to time-trends when designing pharmacoepidemiologic studies in this population, including those using interrupted time series analysis, matching, propensity scores, or self-controlled designs.

Disclosures: *Kaleen Hayes, None*

SAT-0809

Reasons for not-attending the FLS: a survey among non-attenders based on home visits and questionnaires Peter Van Den Berg*¹, Dave Schweitzer¹, Paul Van Haard¹, Joop Van Den Bergh², Piet Geusens³. ¹Reinier de Graaf Gasthuis, Netherlands, ²Maastricht University Medical Center, VieCuri Medical Centre Noord-Limburg, Netherlands, ³Maastricht University Medical Center, Hasselt University, Netherlands

IntroductionDeveloping an effective strategy to improve Fracture Liaison Service (FLS) attendance is a challenge. To elicit reasons for non-attendance, we visited non-attenders at home and conducted structured interviews.**Patients and Methods**We analyzed 357 patients >50 yr. with a clinical fracture that had visited the Emergency Department between August 1 and December 1 2017. After exclusion of 5 patients (1%) who had died and 83 patients (24%) because of permanent institutionalization or osteoporotic treatments already given by other hospital specialists, 269 patients were invited to the FLS. In case of no response within 12 weeks, patients were requested by telephone to consent to a home visit and/or to complete a single questionnaire. Questions concerned demographics, such as age, gender and a composite score of frailty-related issues, as well as patients' perceptions regarding instructions to attend the FLS (extrinsic motivation) and patients' ideas and opinions about fracture prevention (intrinsic motivation).**Results**Of the 269 patients invited to the FLS, 133 (49%) actually attended the FLS. Of the remaining patients, 136 (51%) did not reply to our FLS invitation (non-responders). Of these 136 non-responders, 99 could be reached by telephone. Of these, 42 patients (43%) consented to be visited at home (HV), while 24 patients (24%) agreed to complete a questionnaire but did not give permission for a home visit (Q), and 33 patients (33%) did not want any contact. Outcome results of the whole group (HV and Q) were analyzed. In the perception of the majority of HV and Q patients, no information had been provided about the necessity to attend the FLS, neither from the physician (86%) nor from the plaster nurse (94%). In 100% of patients, lack of intrinsic motivation was due to the conviction that the fracture was mainly caused by trauma and/or fall and to a lack of awareness of potential fragile bones. Moreover, 39 patients (59%) explicitly reported not to be interested in their bone health. We found 2 associations between non-attenders (HV+Q) and medical reasons hearing loss (OR 0.12; p<0.01) and vertigo (OR 0.13; p<0.01). **Conclusion**This is the first FLS-initiated survey with home visits focusing on patients who did not respond to our invitation to attend the FLS. Perceived lack of patient information is an important focus of concern (lack of extrinsic motivation). Notably, all non-responders reported lack of intrinsic motivations to attend, and hearing loss and vertigo was associated with non-attendance.

Saturday Posters

Non-attenders	Total (HV+Q)	HV	Q	No consent
N=136	66 (100%)	42 (100%)	24 (100%)	33 (100%)
Male	19 (29%)	6 (14%)	13 (54%)	9 (27%)
Female	47 (71%)	36 (86%)	11 (46%)	24 (73%)
Age; mean (yrs.)	51-101 (74)	58-101 (79)	51-88 (65)	50 - 91; (70)
Minor fracture (%)	22 (33%)	7 (17%)	15 (63%)	10 (30%)
Major fracture (%)	33 (50%)	25 (60%)	8 (33%)	15 (46%)
Hip fracture (%)	9 (14%)	8 (19%)	1 (4%)	7 (21%)
Vertebral fracture (%)	2 (3%)	2 (4%)	-	1 (3%)

Disclosures: *Peter Van Den Berg, None*

SAT-0810

Improvement in the primary and secondary prevention of osteoporosis by a Fracture Liaison Service: feedback from a single French center care pathway Arthur Vrignaud*, Simon Pelletier, Emmanuelle Dernis, Yvon Moui, Bénédicte Haettich. Le Mans General Hospital, France

Background: Osteoporosis is a major public health concern, causing significant morbidity and mortality. Care pathways, called Fracture Liaison Services, have demonstrated their utility in preventing osteoporosis-associated morbidity and mortality. The aim of this study was to analyze the activity of one such care pathway. Methods: This was a retrospective, observational, cohort study, in which 272 patients who had fragility fractures between January 2012 and December 2016 were included. Screening of the medical records and data analyses were performed to characterize the population and the medical care received related to osteoporosis, and to compare these data with those of another study carried out from January 2010 to January 2011 on 54 patients in the same Fracture Liaison Service. Results: There was no statistically significant difference between the two cohorts concerning their demographic characteristics, with 92.3% women and a mean age of 68.7 in our cohort. Secondary prevention was improved, as shown by a reduction in the number of vertebral fractures detected by systematic assessment and fewer low-energy fractures. This study also demonstrated a decline in the percentage of patients with a first-degree parental history of hip fracture and a trend towards a decline in the rate of those having vitamin D insufficiency. Conclusion: Communication with patients and healthcare professionals through the Fracture Liaison Service was beneficial for patients in terms of fracture prevention. This study supports the development of similar care pathways in other healthcare institutions.

Disclosures: *Arthur Vrignaud, None*

SAT-0824

See Friday Plenary Number FRI-0824

SAT-0825

See Friday Plenary Number FRI-0825

SAT-0826

See Friday Plenary Number FRI-0826

SAT-0827

See Friday Plenary Number FRI-0827

SAT-0828

See Friday Plenary Number FRI-0828

SAT-0829

See Friday Plenary Number FRI-0829

SAT-0830

Response of Common Genetic variants of Vitamin D Binding Protein (DBP) to vitamin D supplementation in Saudi adults Nasser Al-Daghri*. King Saud University, Saudi Arabia

Background: Genetic variations in vitamin D binding protein (DBP) gene are known to affect 25(OH)D levels in various population. However, the influence of these genetic variants on 25(OH)D levels in Saudi population is never been studied. The study aimed to determine the influence of DBP gene polymorphisms in vitamin D metabolites before and after

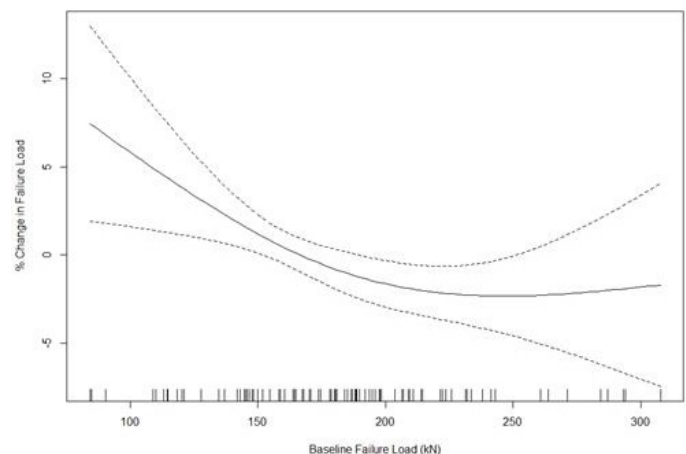
vitamin D supplementation. Methodology: A total of 235 Saudi adults were recruited, out of which 146 participants with vitamin D deficiency (25(OH)D <50nmol/l) were given 2000IU daily dose of vitamin D supplement for 12 months. Serum 25(OH)D, DBP levels were measured after year of supplementation. Two common single nucleotide polymorphisms (rs4588 and rs7041) DBP were assessed using TaqMan genotyping system. Results: Serum 25(OH)D (nmol/l) levels increased significantly post-supplementation [34.1 (24.0-46.8) to 55.3 (40.4-73.8); p<0.001] along with free 25(OH)D (nmol/l) [21.5 (11.7-33.2) to 31.6 (13.7-50.9); p<0.001] and bio available 25(OH)D (nmol/l) [17.0 (9.2-28.5) to 26.6 (11.7-42.1); p<0.001]. No significant change was observed in vitamin D binding protein, as well as in other factors including lipid profile after supplementation. Post supplementation median 25(OH)D was significantly higher [61.2 (46.3-76.8) and 66.6 (53.2-83.7)] in patients with CC genotype of rs4588 and GG genotype of rs7041 respectively than other genotypes. The increase in DBP was found in 94.4% from baseline only patients carrying TT genotype than other genotypes of both SNPs but this change was not statistically significant (p=0.069). Conclusion: The rs7041 and rs4588 variants in DBP are associated with baseline 25(OH)D levels and modifies 25(OH)D response after vitamin D supplementation Saudi adults.

Disclosures: *Nasser Al-Daghri, None*

SAT-0831

Female recruits with the lowest baseline bone strength have the greatest increases in bone strength following 8 weeks of U.S. Army Basic Combat Training Katelyn Guerriere*¹, Julie Hughes¹, Erin Gaffney-Stomberg¹, Kathryn Taylor¹, Kristin Popp², Chun Xu³, Ginu Unnikrishnan³, Mary Bouxsein², Jaques Reifman³. ¹USARIEM, United States, ²MGH, United States, ³BHSAI, United States

Mechanical loading has been demonstrated in animal studies to induce bone adaptations that result in increased bone strength. U.S. Army Basic Combat Training (BCT) is a period of unaccustomed physical activity at the beginning of military service when recruits are at high risk of skeletal stress fractures. Prior studies report variability in bone strength among Army recruits, with some recruits entering BCT with relatively weak bones and others with more robust bones. We hypothesized that recruits with the weakest bones at the beginning of BCT would experience relatively greater mechanical stimuli compared to recruits with stronger bones, and therefore, mount the greatest adaptive response as defined by change in bone strength. Accordingly, the purpose of this study was to determine if estimates of baseline bone strength influenced changes in bone strength following 8 weeks of BCT. Ninety one female BCT recruits (age = 21.5±3.3 yrs) completed the study. Failure load (F_{ult}), an index of bone strength, was estimated with finite element analysis (Scanco Medical FE software version 1.13) derived from high-resolution pQCT (XtremeCT II, Scanco Medical) scans of the distal tibia (4% of tibial length) obtained at the beginning and end of BCT. To evaluate the effects of baseline F_{ult}, we used a generalized additive model with naturalized spline with 3 degrees of freedom applied to baseline values of F_{ult}. We adjusted for age, race, and BMI prior to BCT. The relationship between baseline F_{ult} and change in F_{ult} was significantly nonlinear (p = 0.017; Figure 1). Individuals in the bottom 10% of baseline F_{ult} had the greatest change in F_{ult} (~+7%), whereas no significant changes in F_{ult} were detected in recruits with the highest F_{ult} at baseline. These results suggest that female recruits with the weakest bones at entrance to BCT will mount the greatest increases in bone anabolism during initial military training.



Disclosures: *Katelyn Guerriere, None*

SAT-0832

Effect of high impact exercise on femoral neck bone mineral density and T2 relaxation times of articular cartilage in postmenopausal women Chris Hartley^{*1}, Robert Kerslake², Jonathan Folland¹, Katherine Brooke-Wavell¹. ¹NCSEM, School of Sports and Exercise Science, Loughborough University, United Kingdom, ²Nottingham University Hospital NHS Trust, United Kingdom

Unilateral, high impact exercise has been found to increase femoral neck bone mineral density (BMD) in older men and premenopausal women. Postmenopausal women are at increased risk of osteoporotic fracture and could benefit from an intervention to increase BMD but may be reluctant to participate in high impact exercise due to concern about knee joint damage. The aim of the current study was to evaluate the effects of high-impact exercise on femoral neck BMD and knee articular cartilage properties in postmenopausal women. Postmenopausal women were recruited into a six-month, unilateral exercise intervention. This progressed to 50 multidirectional hops each day, using a randomly assigned exercise leg for comparison with the contralateral control leg. Dual energy X-ray absorptiometry provided information on the BMD of both femurs. Coronal T2 maps using a 3.0T MRI scanner provided T2 relaxation times of knee articular cartilage in 12 regions of interest (ROIs) from a single slice in the weight bearing region. Scans were taken of both legs, pre and post intervention. Repeated measures ANOVA were carried out to analyse effects of leg, time and interaction. To date, 29 of the 43 participants have completed the study (age 61.1 ± 4.4 years; BMI 24. ± 3.7 kg/m²). Of these, 4 participants withdrew due to exercise related injury or discomfort (knee pain that resolved upon cessation of exercise [n=3], Achilles tendonitis [n=1]), 2 due to other injury or illness and 2 were lost to follow up. Femoral neck BMD increased by 0.73% in the exercise leg and decreased by 0.74% in the control leg, but this difference between legs did not reach statistical significance (P=0.067). There were no significant exercise effects on T2 relaxation times of knee cartilage (0.97>P>0.18): across the 12 ROIs changes ranged from -3.2 to 2.7% in the exercise leg and -6.1 to 4.6% in the control leg. The intervention was feasible but the incidence of withdrawal due to exercise related injury or discomfort suggests that modification may be desirable for postmenopausal women. That there were no significant changes in T2 relaxation times in healthy women agrees with previous research, in women with mild osteoarthritis, that high impact exercise does not adversely affect knee articular cartilage. Although not statistically significant, this brief, high impact exercise had similar net effects on femoral neck BMD in postmenopausal women (1.5% as reported in a group of 35 older men (1.6%).

Disclosures: *Chris Hartley, None*

SAT-0833

Association of trabecular bone score and bone density with actigraphy-measured physical activity in NHANES 2005-2006 Rajesh Jain^{*1}, Meltem Zeytinoglu², Tamara Vokes². ¹Lewis Katz School of Medicine at Temple University, United States, ²University of Chicago Medicine, United States

Background: Physical activity is generally associated with good bone health and lower fracture rates. It is not clear whether this beneficial effect is due to higher bone mass or better bone structure. Recently, the trabecular bone score (TBS), a textural analysis of the lumbar spine DXA image that correlates with measures of bone microarchitecture, has been developed. In this study we examined the association between objectively measured physical activity with BMD (as a measure of bone mass) and with TBS (as a measure of bone structure). We also investigated whether the association depends on the type or intensity of activity. Methods: This is a study of NHANES 2005-2006 data. Subjects over age 20 and with BMI 15-37 were analyzed, as that is the working BMI range for TBS. Women were stratified by menopausal status. Individual physical activities were obtained by questionnaire and grouped by the 2011 Compendium of Physical Activities. Included subjects were asked to wear physical activity monitors (Actigraph 7164) for 7 days. Only subjects with at least 4 days of at least ≥10 hours of wear time were included. All analyses were done using survey weights and controlled for age, BMI, and race. Results: Among 493 postmenopausal women, those in the top half of actigraphy-measured moderate to vigorous physical activity (MVPA) had higher TBS (0.029 ± 0.011, 0.19 standard deviations (SD), p=0.02), and total hip T-score (0.30 ± 0.12, p=0.02), but not femoral neck or spine T-score. No specific activity was associated with TBS or T-score when controlling for MVPA. Among 388 pre-menopausal women, neither MVPA, nor specific activities were associated with TBS or T-scores. Among 1,126 men, men in the top half of MVPA had higher TBS (0.021 ± 0.006, 0.14 SDs, p=0.006), total hip T-score (0.28 ± 0.09, p=0.009), and femoral neck T-score (0.25 ± 0.10, p=0.03), but not spine T-score. Walking was associated with greater TBS (0.014 ± 0.006, 0.09 SDs, p=0.04), while running/jogging and sports activities were associated with higher T-scores at all sites (range 0.28-0.52, p<0.05) even when controlling for MVPA. Conclusion: Actigraphy-measured physical activity was associated with higher TBS and BMD at hip sites. While intensity of activity had a clear association with bone outcomes, the association with activity types was less striking when controlling for intensity. This suggests that activity intensity may be more important than the type of activity.

Disclosures: *Rajesh Jain, None*

SAT-0834

Dairy Intake and Its Associations with Bone Mineral Density and Trabecular Bone Score in the VITamin D and Omega-3 Trial (VITAL) Meryl Leboff^{*1,2}, Catherine Donlon¹, Nancy Cook^{2,3,4}, Sharon Chou^{1,2}, Julie Buring^{2,3,4}, Joann Manson^{2,3,4}. ¹Division of Endocrinology, Diabetes and Hypertension, Brigham and Women's Hospital, United States, ²Harvard Medical School, United States, ³Department of Epidemiology, Harvard T.H. Chan School of Public Health, United States, ⁴Division of Preventive Medicine, Brigham and Women's Hospital

Higher intakes of dairy products have been associated with greater lumbar spine bone mineral density (BMD) in adults taking vitamin D supplements. Therefore, dairy intakes may have beneficial effects on bone. In this study, we investigated whether there were similar associations in the VITamin D and Omega-3 Trial (VITAL) between dairy intake (servings/week of milk, cream, cheese, or yogurt, individually and combined) and BMD at the spine, femoral neck, total hip, and whole body. Additionally, we assessed whether dairy intake was associated with Trabecular Bone Score (TBS), a structural measure of bone. VITAL is a 2X2 factorial randomized controlled trial (RCT) investigating whether a median of 5-years of supplemental cholecalciferol (2000 IU/day) and/or omega (ω)-3 fatty acids (1 g/d) in 25,874 US men ≥50 years and women ≥55 years is of benefit in the primary prevention of cancer and cardiovascular disease. In-person assessments were completed at baseline and 2-years post-randomization in a subcohort of 771 participants (46.8% women, 53.2% men) in the VITAL: Effects on Bone Structure and Architecture ancillary study. A detailed food frequency questionnaire was used to collect dairy and vitamin/mineral supplement intakes at baseline, and BMD was determined by dual-energy X-ray absorptiometry (Discovery W; APEX Version 4.2, Hologic, Bedford, MA). TBS was derived from the lumbar spine DXA images (Medimaps Version 2.1, Geneva, Switzerland). The statistical analyses below were adjusted for age, race, sex, and BMI. At baseline, participants had a mean age of 63.79 ± 6.13 years and a mean of 11.17 ± 0.57 servings of milk, yogurt and cheese per week (Table 1). There were no significant associations at baseline between combined or separate dairy intakes and BMD at the spine, femoral neck, total hip or whole body or TBS. Analyses on the effects of dairy intakes on two-year changes in bone health outcomes are in progress and will be assessed. The RCT design of VITAL will evaluate, without bias, whether baseline intakes of dairy products modify effects of supplemental vitamin D on bone density and other structural measures. References: 1. Sahni S, et al. J Nutr. 2017 Apr; 147(4):645-6522. LeBoff MS, et al. Contemp Clin Trials. 2015 Mar; 41:259-683. Donlon CM, et al. Contemp Clin Trials. 2018 Apr; 67:56-67

Table 1. Baseline characteristics of participants in the VITAL bone density subcohort

Variable	Mean (Standard Deviation) n=771
Age (years)	63.79 (6.13)
BMI (kg/m ²)	28.31 (5.14)
Milk (servings/wk)	5.30 (7.83)
Cream (servings/wk)	4.96 (7.94)
Cheese (servings/wk)	3.71 (4.13)
Yogurt (servings/wk)	2.31 (4.88)
Milk + yogurt (servings/wk)	7.54 (10.47)
Milk + yogurt + cheese (servings/wk)	11.23 (11.56)
Femoral neck BMD (g/cm ²)	0.77 (0.13)
Total hip BMD (g/cm ²)	0.93 (0.14)
Lumbar spine BMD (g/cm ²)	1.02 (0.16)
Whole body BMD (g/cm ²)	1.15 (0.13)
Trabecular Bone Score	1.32 (0.09)

Disclosures: *Meryl Leboff, None*

SAT-0835

Vitamin D status and its associated factors in Taiwanese healthy adults Yi-Chin Lin^{*}, Yi-Wen Cheng. Department of Nutrition, Chung Shan Medical University, Taiwan

Vitamin D plays critical roles in maintaining serum calcium and phosphorus balance. According to the results of the Nutrition and Health Survey in Taiwan (NAHSIT) 2005-2008, there is more than 66% of the Taiwanese adults are deficient in vitamin D. The purposes of the current study were to explore the vitamin D status and its associated factors in Taiwanese adults. The current cross-sectional study was conducted between February and August in 2017, and a total of 60 healthy subjects aged 20-50 years were recruited in Taichung, which is the metropolis of central Taiwan. Structural questionnaires were administered to obtain data of lifestyle information and dietary intake, and a sun exposure score was generated according to the frequency and body parts exposing to sun. Skin melamins at inner and outer forearm as well as forehead were measured by a multiprobe mexameter. Body composition, including bone measurements were measured by a dual-energy x-ray absorptiometry. The venous blood samples were collected and the serum levels of 25(OH) D and PTH were measured by RIA method. The prevalence rates of vitamin D deficiency

and insufficiency were 30.33% and 34.88%, respectively. Age was significantly correlated with serum level of 25(OH)D in both genders. In men, weight, waist-circumference, waist-hip ratio were each significantly correlated with serum level of 25(OH)D. The average skin melanin index at outer forearm was significantly correlated with serum level of 25(OH)D in females. Male's serum level of phosphorus and female's serum level of calcium were significantly correlated with serum level of 25(OH)D, respectively. Positive correlations were also observed between the intake of codfish, mushroom, and golden mushroom and the level of serum 25(OH)D in females. There was also a positive correlation between the amount of dairy products consumption and serum level of 25(OH)D in males. In addition, comparing to the group of vitamin D deficiency [25(OH)D < 20 ng/mL], those who were sufficient in vitamin D had higher serum level of calcium, and higher intake of salmon as well. In conclusion, there is positive correlation between women's average skin melanin index at outer forearm and serum level of 25(OH)D. For young female adults, exposure to sunlight before 10 am and after 2 pm at least twice weekly should be encouraged to improve and/or maintain optimal vitamin D status.

Disclosures: *Y-Chin Lin, None*

SAT-0859

See Friday Plenary Number FRI-0859

SAT-0860

See Friday Plenary Number FRI-0860

SAT-0861

See Friday Plenary Number FRI-0861

SAT-0862

See Friday Plenary Number FRI-0862

SAT-0863

Bilirubin promotes down-regulation of RUNX2 and up-regulation of RANKL gene expression in bone explants and in osteoblastic and osteocytic cell lines Silvia Ruiz-Gaspà*, Albert Parés, Andrés Combalia, Pilar Peris, Ana Monegal, Núria Gunañabens. Metabolic Bone Diseases and Liver Units, Hospital Clínic, IDIBAPS, CIBERehd, University of Barcelona, Barcelona, Spain

In vitro studies have shown that the retained substances of cholestasis have deleterious effects in human osteoblasts and osteocytic cells. Bilirubin (BIL) and lithocholic acid (LCA) induce alterations in the proliferation, differentiation and apoptosis of osteoblastic and osteocytic cells. However, their effects in human bone tissue and in bone cell lines have not been deeply analysed. Aim: To investigate the effects of BIL, LCA and ursodeoxycholic acid (UDCA) in gene expression of human trabecular bone explants as well as in osteoblastic (SAOS2) and osteocytic cells (MLO-Y4/ MLO-A5). Methods: Bone tissue harvested from trabecular bone fragments, SAOS2 and MLO-Y4/ MLO-A5 cells were cultured and treated with BIL (50µM), LCA (10µM) and UDCA (10/100µM) for 24h. Gene expression of osteocalcin (BGLAP), Cbfa1 (RUNX2)/Osterix (OSX) and RANKL (TNFRSF11)/osteoprotegerin (TNFRSF11B) were quantified by real time PCR. Results: BIL diminishes RUNX2 gene expression in bone tissue (-37%), SAOS2 (-75%), MLO-Y4 (-56%) and MLO-A5 (-77%), and increases RANKL expression in 60%, 27%, 72% and 60%, respectively (p<0.02). In bone tissue and in osteoblastic and osteocytic cells, LCA increases gene expression of BGLAP (NS) and RANKL (p<0.03). UDCA 100µM increases RUNX2 and OSX expression in bone tissue (78% and 82%), MLO-Y4 (72% and 80%) and SAOS2 (75% and 70%) (p<0.03). In addition, UDCA 100µM significantly increases expression of BGLAP, OPG and RANKL in bone tissue and in osteocytic lines. UDCA 10/100µM counteracts the decrease in RUNX2 induced by BIL in bone tissue, SAOS2, MLO-A5 and MLO-Y4 cells. Conclusion: The retained substances of cholestasis, particularly bilirubin, cause noxious effects on transcription factors of osteoblast differentiation and on osteoclastic activators in bone tissue and in osteoblastic and osteocytic cells. Ursodeoxycholic acid reverses the harmful effects of bilirubin. These results provide new insights into the low bone formation and at some stages, high resorption, associated with chronic cholestasis.

Disclosures: *Silvia Ruiz-Gaspà, None*

SAT-0864

Effects of hydroxyapatite/collagen complex on bone formation at osteotomy site of proximal tibia after povidone-iodine or ethanol exposure in ovariectomized rats Itsuki Nagahata*, Naohisa Miyakoshi, Yuji Kasukawa, Yuichi Ono, Manabu Akagawa, Yusuke Yuasa, Chiaki Sato, Yoichi Shimada. Akita University graduate school of medicine, Japan

Introduction: Hydroxyapatite/collagen complex (HAp/Col) is widely used in reconstruction of bone defects after severe trauma or resection surgery for bone tumor. Povidone-iodine or ethanol is sometimes used for sterilization at trauma sites or for prevention of tumor recurrence. These agents have the possibility of impairing bone formation. However, whether HAp/Col exerts similar effects on local bone formation after povidone-iodine or ethanol exposure remains unclear. This study examined the effects of HAp/Col or hydroxyapatite (HA) on osteogenesis and chondrogenesis at osteotomy sites on the proximal tibia after povidone-iodine or ethanol exposure in ovariectomized (OVX) rats. Method: OVX was administered to 16-week-old female Sprague-Dawley rats. After 4 weeks, cancellous osteotomy was performed at the proximal tibia and soaked with 10% povidone-iodine (I), 90% ethanol (E), or vehicle for 6 min. Rats were divided into the following four groups (n = 4-6 each): 1) HAp/Col group, HAp/Col placed into the osteotomy following vehicle soaking; 2) I+HAp/Col group, HAp/Col placed following I soaking; 3) E+HAp/Col group, HAp/Col placed following E soaking; and 4) HA group, HA placed in the osteotomy site following vehicle soaking. After 2 or 4 weeks, sections of proximal tibia were decalcified, stained with hematoxylin and eosin and prepared for subsequent evaluations. Cancellous bone volume (BV/TV) was measured at the osteotomy boundary (Border) and center of artificial bone (Center). Cartilage volume (CV/TV) was measured at the same sites of proximal tibia using Safranin O-stained sections. Results: BV/TV at Border and Center did not differ significantly among groups at 2 weeks. At 4 weeks, BV/TV at Border were significantly higher in the HAp/Col and E+HAp/Col groups than in the HA group (p < 0.05). BV/TV at Center was significantly higher in the HAp/Col group than in the HA group (p < 0.05). No significant difference in BV/TV was seen in the I+HAp/Col or E+HAp/Col groups compared with the HAp/Col group. CV/TV was significantly higher in the HAp/Col group than in the HA group at 2 weeks (p < 0.05). At 4 weeks, no significant difference was evident between groups. Conclusion: With bone formation at cancellous bone osteotomy sites in OVX rat, HAp/Col promoted osteogenesis even after exposure to povidone-iodine or ethanol at the proximal tibia. Povidone-iodine and ethanol treatment delayed cartilage formation.

Disclosures: *Itsuki Nagahata, None*

SAT-0877

See Friday Plenary Number FRI-0877

SAT-0878

See Friday Plenary Number FRI-0878

SAT-0879

See Friday Plenary Number FRI-0879

SAT-0880

See Friday Plenary Number FRI-0880

SAT-0881

Absence of Alpha-Synuclein (Snca) Protects Against Ovariectomy-Induced Weight Gain and Bone Loss by Independent Mechanisms. Carolina Figueroa*¹, Clifford Rosen¹, Charles Farber², Gina Calabrese², Victoria Demambro¹. ¹Maine Medical Center Research Institute, United States, ²University of Virginia, United States

Alpha-Synuclein (Snca) intracytoplasmic aggregation known as Lewy bodies are the major hallmark of most patients with Parkinson's disease (PD). PD has been associated with high incidence of osteoporosis. Recently, we have shown that Snca is one of the majorly connected "hub" genes and its global deletion in mice leads to a 40% reduction in Ovariectomy(Ovx)-induced bone loss. These observations lead us to hypothesize that deletion of Snca may protect against bone loss caused by estrogen-deficiency in a cell-autonomous manner. Therefore, we generated a conditional knock out for Snca; Prrx1-Cre^{+/+} Snca^{-/-} female mice that were randomly assigned to Sham or Ovx surgical groups (n=3-8 per group) and euthanized at 16 weeks after surgery. Analysis of body composition of the femur by Dual-energy X-ray absorptiometry showed that ^{+/+} Snca^{-/-} mice weighed significantly more (p=.0319) after Ovx, however, this change was not significant in Prrx1Cre^{+/+} Snca^{-/-} mice. Ovx increased %body fat in both genotypes, although, Prrx1Cre^{+/+} Snca^{-/-} mice showed a tendency to acquire less body fat (23.3%^{+/+} 3.3, mean ± SE) compared to ^{+/+} Snca^{-/-} mice (31.1% ± 9.5) after Ovx. There were no differences in lean mass, whole body aBMD or aBMC. Contrary to our expectations, µCT of femoral trabecular (Tb.) bone after OVX

revealed that both genotypes showed loss of femoral BV/TV, but showed no differences in Tb.BV/TV, Tb.TMD, Tb.N and Conn.D between genotypes. Similarly, no significant difference was observed in respect to the cortical parameters. On the other hand, Inguinal white adipose depots (iWAT) from Prrx1-Cre/+Snca^{-/-} were 53.8% smaller (0.2095g ± 0.059) than in +/+ Snca^{-/-} (0.3889g ± 0.038). Analysis of H&E staining in iWAT sections from Sham and Ovx Prrx1-Cre/+Snca^{-/-} mice showed presence of small and multilocular adipocytes, meanwhile, +/+ Snca^{-/-} showed enlarged and unilocular adipocytes. iWAT gene expression showed significant increase in Pcg1a (p= 0.0267) mRNA levels in Prrx1Cre/+Snca^{-/-} after Ovx compared to +/+ Snca^{-/-}. Pparg, aP2, Prdm16 and DiO2 followed similar trends. In sum, deletion of Snca under the Prrx1 Cre promoter seems to affect iWAT capacity to store lipids, switching adipocytes phenotype from white to beige-like and protecting mice from Ovx-induced weight gain. This study provides evidence that Snca may be regulating systemically bone homeostasis and estrogen-deficiency induced bone loss, but cell-autonomous peripheral lipid accumulation.

Disclosures: *Carolina Figueroa, None*

SAT-0882

Low Bone Density and Fragility Fractures as the Initial Presentation of Hemochromatosis: Two Case Reports Yi Liu^{*1}, Joseph Lane¹, Raymond Pastore², Dorothy Fink¹. ¹Hospital for Special Surgery, United States, ²New York Presbyterian Hospital, Weill Cornell Medical College, United States

Hereditary hemochromatosis (HH) is a genetic disorder of iron metabolism. The clinical manifestations of HH are related to tissue damage from iron deposition, including liver disease, skin pigmentation, diabetes mellitus, hypopituitarism and heart disease. Patients with HH are at high risk of bone loss and low energy fractures due to underlying hypogonadism or liver disease. Here we presented two HH cases presenting with osteoporosis and fragility fractures as the initial presentation of HH in the absence of cirrhosis. A 68 year-old female presented with buttock pain after knee replacement. MRI confirmed sacral insufficiency fracture and bone density showed mild osteopenia (lowest T-score of -1.4 at right total hip). She underwent bone biopsy that revealed hemochromatosis. Abdominal ultrasound showed increased echogenicity of the liver. Genetic test revealed she carries HFE H63D genetic mutation. Patient was treated with denosumab for her fragility fracture and monthly phlebotomy. Her ferritin went down to normal after three months of treatment. A 52 year-old man presented with multiple spontaneous vertebral compression fractures. DXA showed osteopenia with lowest Z-score of -2.4 at lumbar spine. Secondary work up for osteopenia showed hypogonadotropic hypogonadism. He underwent bone biopsy and was found to have hemochromatosis. Lab tests were summarized in the table. He is managed with testosterone replacement and teriparatide for his compression fractures. With these two cases, we aim to enhance the awareness of osteoporosis and fragility fracture in patients with HH and suggest bone biopsy might be a useful diagnosis for HH.

Lab Tests	Reference Range for Case 1	Case 1	Reference Range for Case 2	Case 2
Ferritin	15-150 ng/ml	175	22-320 ng/ml	223.9
Iron	27-139 ug/dl	63	65-175 ug/dl	95
TIBC	250-450 ug/dl	313	250-425 ug/dl	429
Iron Saturation	15-55%	20	13-15%	22.1
ESR	0-40 mm/hr	59	0-20 mm/hr	<1
CRP	0.0-4.9 mg/L	4.1	<1 mg/L	<0.4
ALT	0-32 U/L	19	7-56 U/L	34
AST	0-40 U/L	18	0-40 U/L	19
TSH	0.450-4.500 uIU/ml	1.030	0.40-4.500 uIU/ml	0.93
HbA1C	4.8-5.6%	5.9	<5.7%	5.2
Hgb	11.1-15.9 g/dl	13.1	13.2-17.1 g/dl	14.2
WBC	3.4-10.8 x 10E3/ul	6.0	3.8-10.8 x 10E3/ul	5.0
Plt	150-379 x 10E3/ul	288	150-450 x 10E3/ul	291

Disclosures: *Yi Liu, None*

SAT-0883

Effect of Parathyroidectomy versus Antiresorptive Treatment on Bone Mineral Density in Osteoporotic Postmenopausal Women with Primary Hyperparathyroidism Tomaz Kocjan^{*1}, Gaj Vidmar², Andrej Janez¹, Soncka Jazbinsek³, Katarina Remec³, Mojca Jensterle Sever¹. ¹University Medical Centre Ljubljana, Slovenia, ²University Rehabilitation Institute Republic of Slovenia, Slovenia, ³Medical Faculty Ljubljana, Slovenia

Limited data suggest that surgical treatment and antiresorptive therapies increase BMD in primary hyperparathyroidism (PHPT) to a similar degree, and thus medical treatment represents a reasonable option for patients who are unwilling or unfit for the parathyroidectomy (PTX). We compared BMD changes in osteoporotic patients with PHPT after 12 – 18 months post operation versus after 12 – 18 months of antiresorptive treatment. We retrospectively analyzed 55 women (age 69 years, 20 years from menopause, BMI 28 kg/m² on average) with PHPT and osteoporosis who had been treated at our clinic from 2004 to 2016. 17 of them sustained at least one osteoporotic fracture before the study onset. They were prescribed with vitamin D3 800-1400 IU daily and instructed to ingest 1000 mg of calcium daily. PTX was performed on 23 patients, while 33 patients opted for medical treatment,

either with a bisphosphonate (alendronate (8), risedronate (7), ibandronate (3) or zoledronic acid (5 patients)) or with denosumab (9 patients) per physician's and/or patient's preference. BMD was measured at lumbar spine (LS), total hip (TH), femoral neck (FN) and distal radius (RAD) by DXA at the time of diagnosis and 12 – 18 months after intervention. No significant difference in any difference score was found between the denosumab and the bisphosphonate group, so they were pooled into one medically treated (MED) group and compared with the PTX group. As expected, serum calcium decreased significantly more in the PTX group than in the MED group (median decrease by 0.50 vs. 0.04 mmol/L, p<0.001). PTH also decreased markedly in the PTX group (median decrease by 144 ng/L) and remained unchanged (median increase by 6 ng/L) in the MED group (p<0.001 for comparison of change scores). The increase in TH BMD was higher in the PTX group than in the MED group (median 0.037 vs. 0.001 g/cm², p=0.008) and marginally so for the LS BMD (median 0.051 g/cm² vs. 0.018 g/cm², p=0.065). No difference between the PTX and the MED group was observed regarding change in FN BMD, whereby FN BMD increased significantly in the whole sample (median increase by 0.019 g/cm², p=0.046). RAD BMD did not change significantly, and its change did not differ between the groups. No new fractures occurred in either group during the observation period. In osteoporotic postmenopausal women with PHPT, PTX is superior to antiresorptive treatment with bisphosphonate or denosumab in terms of improvement of BMD, in particular of TH BMD.

Disclosures: *Tomaz Kocjan, None*

SAT-0884

Glucocorticoid-induced osteoporosis induced poor bone quality, low bone mineral density, low muscle mass and high low back pain Tomohisa Koyama^{*1}, Masayuki Miyagi¹, Sho Inoue¹, Shuichiro Tajima¹, Kosuke Murata¹, Ayumu Kawakubo¹, Yui Uekusa¹, Yuji Yokozeki¹, Hisako Fujimaki¹, Daisuke Ishi¹, Koji Ishikawa², Seiji Ohtori³, Kazuhide Inage³, Kentaro Uchida¹, Gen Inoue¹, Masashi Takaso¹. ¹Department of Orthopedic Surgery, Kitasato University, School of Medicine, Japan, ²Department of Orthopedic Surgery, Showa University, School of Medicine, Japan, ³Department of Orthopedic Surgery, Chiba University, Graduate School of Medicine, Japan

BACKGROUND: Glucocorticoid-induced osteoporosis (GIO) patients have been reported at high risk for fragility fractures as compared with primary osteoporosis patients. To better understand the characteristics of GIO and to improve treatment of GIO patients, we focused on low back pain (LBP), muscle mass, and bone quality. The aim of the current study was to compare GIO patients and primary osteoporosis patients for LBP, muscle mass, bone mineral density (BMD), and bone turnover markers. METHODS: Two hundreds and four osteoporosis over 60 years patients (35 men and 169 women) without evidence of new vertebral body fractures were included in the study. Forty two subjects with a mean age of 73.6 years were in the GIO group (G group); 162 patients with a mean age of 73.9 years composed the primary osteoporosis group (P group). We reviewed BMD of the lumbar spine (LS) and total hip (TH), and also reviewed the number of vertebral fractures. We calculated lean muscle mass and limb muscle mass (corrected by the square of height: lean mass index (LMI) and skeletal muscle mass index (SMI)) using the bio-impedance method (TANITA MC - 780A). Bone turnover markers were used to assess bone formation (BAP) and bone resorption (TRACP5b). Bone quality was assessed by evaluating pentosidine, and homocysteine. LBP was evaluated using the Oswestry disability index (ODI). These factors were compared between the two patient groups. Group comparisons for muscle mass were made in men and women separately. RESULTS: BMD of TH in the G group (0.58) was significantly lower than that in the P group (0.63). There were more vertebral fractures in the G group (2.4) than that in the P group (1.0). Homocysteine in the G group (14.7) was significantly higher than that in the P group (10.3). LMI in women in the G group (14.3) was significantly lower than those in women of the P group (14.6). ODI score in the G group (34.5) was significantly higher than that in the P group (25.2). DISCUSSION: GIO patients had lower BMD of TH, more vertebral fractures, and poorer bone quality than patients in the primary osteoporosis group. Poor bone quality might be one risk factor for osteoporotic fragility fractures in GIO patients. In addition, GIO patients had low muscle mass and high LBP. Although we could not still identify the mechanisms of these findings, exercise therapy and intervention for LBP might help to improve treatment efficacy in GIO patients.

Disclosures: *Tomohisa Koyama, None*

SAT-0885

BONE STATUS OF PATIENTS WITH CHRONIC KIDNEY DISEASE STAGE 5 (CKD5) WAIT-LISTED FOR KIDNEY TRANSPLANTATION IS POORLY EVALUATED BY DXA Vanessa Lapierre^{*1}, Martin Jannot¹, Myriam Normand¹, Pawel Szulc², Elisabeth Sornay-Rendu², Thierry Thomas¹, Christophe Mariat³, Roland Chapurlat², Marie-Hélène Lafage-Proust¹. ¹INSERM 1059, Université de Lyon, France, ²INSERM 1033, Université de Lyon, France, ³NEPHROLOGY DPT, CHU ST-ETIENNE, France

Kidney transplantation (KT) increases fracture (Fx) risk. Thus, we need to assess bone status in patients with CKD5 when they are wait-listed for KT (WKT) in order to detect patients at risk and develop preventive strategies. Our aim here, was to compare bone status evaluated by DXA and High Resolution μ CT (HR-pQCT) in this population. METHODS: We included 102 CKD5 patients, 64? and 38? at the time of KT list registration. We evaluated

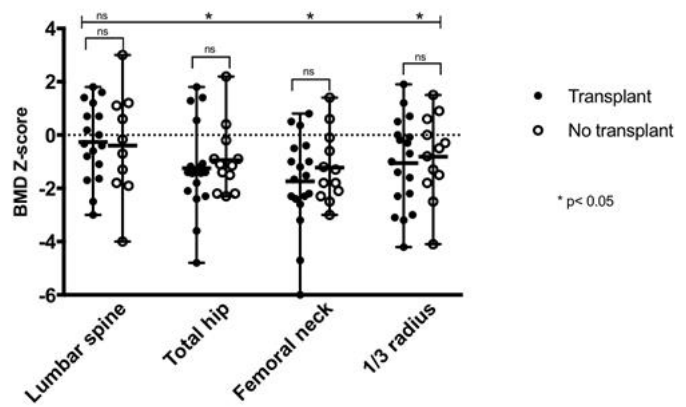
clinical risk factors for Fx, hip and vertebral areal (a) Bone Mineral Density (BMD) by DXA, FRAX score for Major Osteoporotic (MOF) and Hip (HF) Fx, radius and tibia structural parameters and volumetric (v) BMD by μ CT (Scanco). Patients were compared to age and sex-matched non uremic subjects (CT) from two cohorts, OFELY and STRAMBO, with 1 WKT/2 CT ratio. Statistics included Student t or Bivariate Wilcoxon tests. HR-pQCT data were adjusted for the FRAX-MOF without BMD score. Results are mean \pm SD or median [1st-3rd IQ]. RESULTS: In males, median age was 65 [54-69]. WKT included more patients with diabetes (28 vs 13%), hypertension (81 vs 30%) and more smokers (21 vs 8%) than CT. In WKT, hip aBMD was higher than in CT (0.85 [0.79-0.94] vs 0.81 [0.74-0.89]g/cm²) while the FRAX-MOF or HF scores were higher (4 [3-5] vs 3% [2-5]) than in CT (p<0.01). In contrast, cortical (Crt) and trabecular (Tb) vBMD were lower in WKT (Radius Total vBMD: 297 \pm 84 vs 328 \pm 57 mg/cm³ p<0.01). Tb bone was less dense and connected (p<0.01) in WKT at the radius only. In females, median age was 58 [53-63]. WKT had more prevalent osteoporotic Fx than CT (32 vs 4% p<0.01), lower BMI [24 (21-27) vs 27 (24-29), p<0.02], higher FRAX-MOF (4.8 [3.4-6.7] vs 3.6% [2.6-4.6], p=0.03) than CT. aBMD was similar in the 2 groups at both the spine and the hip. In contrast, Crt and Tb vBMD were lower in WKT than in CT (radius Total vBMD 245 \pm 81 vs 306 \pm 62 mg/cm³, p<0.03). Crt thickness at both sites was similar in the 2 groups while tibia Crt porosity was lower in WKT than in CT (6.2 [3.7-10.5] vs 8.8% [4.5-13.7] p<0.01). Tb bone Volume and Thickness were lower at both sites in WKT (Tibia BV/TV: 10 \pm 3 vs 13 \pm 3%, p<0.01). 29% WKT had a DXA Hip T-score <-2.5. Fractured WKT were older than patients with no Fx (p<0.01). Patients with KT history had worse bone status. Neither aBMD nor HR-pQCT parameters were discriminant. CONCLUSIONS: Osteoporosis in CKD5, is gender specific and combines structural trabecular bone degradation and hypomineralization of both bone compartments, not detected by DXA

Disclosures: *Vanessa Lapierre, None*

SAT-0896

Skeletal Consequences of Nephropathic Cystinosis Pablo Florenzano^{*1,2}, Carlos Ferreira³, Galina Nesterova³, Mary Scott Roberts⁴, Sri Harsha Tella⁴, Luis Fernandez De Castro⁴, Sydney M. Brown⁴, Adom Whitaker⁴, Renata C. Pereira⁵, Dorothy Bulas⁶, Rachel I. Gafni⁴, Isidro B. Salusky⁵, William A. Gahl³, Michael T. Collins⁴. ¹Skeletal Diseases and Mineral Homeostasis Section, National Institute of Dental and Craniofacial Research, NIH, United States, ²Department of Endocrinology, School of Medicine, Pontificia Universidad Catolica de Chile., United States, ³Medical Genetics Branch, National Human Genome Research Institute, NIH, United States, ⁴Skeletal Disorders and Mineral Homeostasis Section, National Institutes of Dental and Craniofacial Research, NIH, United States, ⁵Division of Nephrology, Department of Pediatrics, David Geffen School of Medicine at University of California, Los Angeles, United States, ⁶Division of Radiology, Children's National Health System, United States

Nephropathic cystinosis is a rare lysosomal storage disorder. Patients present in the first year of life with renal Fanconi syndrome that evolves to progressive chronic kidney disease (CKD). Goal: Despite the multiple risk factors for bone disease, the frequency and severity of skeletal disorders in nephropathic cystinosis have not been described. Methods: We performed systematic bone and mineral evaluations of subjects with cystinosis seen at the NIH (N=30), including history and physical examination, serum and urine biochemistries, DXA, vertebral fracture assessment, skeletal radiographs, and renal ultrasound. Additionally, histomorphometric analyses are reported on six subjects seen at the UCLA-Bone and Mineral Metabolism Clinic. Results: In NIH subjects, mean age (range) was 20 (5-44), 60% were CKD stage 1 to 4, and 40% had a renal transplant. Mean bone mineral density (BMD) Z-scores were decreased in the femoral neck, total hip and 1/3 radius (p<0.05). Low bone mass at one or more site was present in 46% of subjects. Thirteen percent of subjects reported one or more long bone fractures. Thirty-two percent of subjects had incidental vertebral fractures, which were unrelated to transplant status. Long bone deformity/bowing was present in 64%; 50% had scoliosis. Diffuse osteosclerosis was present in 22% of evaluated subjects. Risk factors included CKD, phosphate wasting, hypercalciuria, secondary hyperparathyroidism, vitamin D insufficiency, male hypogonadism, metabolic acidosis and glucocorticoid/immunosuppressive therapy. Over half of the non-transplanted subjects had ultrasonographic evidence of nephrocalcinosis or nephrolithiasis. Histomorphometric analyses showed impaired mineralization in 4 of 6 studied subjects. Conclusions: We conclude that skeletal deformities, decreased bone mass, and vertebral fractures are common and relevant complications of nephropathic cystinosis, even before renal transplantation. Efforts to minimize risk factors for skeletal disease include optimizing mineral metabolism and hormonal status, combined with monitoring for nephrocalcinosis/nephrolithiasis. Fig 1. BMD Z-scores in NIH subjects with nephropathic cystinosis. *Z-score mean values in total hip, femoral neck, and 1/3 radius are significantly lower than age-, sex-, and ethnicity- matched population (p<0.05). No statistical differences between Z-score mean values from subjects with and without a renal transplant (p=ns). BMD Z-scores have been corrected for height (HAZ) in subjects <20 years of age.



Disclosures: *Pablo Florenzano, None*

SAT-0902

See Friday Plenary Number FRI-0902

SAT-0903

See Friday Plenary Number FRI-0903

SAT-0904

See Friday Plenary Number FRI-0904

SAT-0905

See Friday Plenary Number FRI-0905

SAT-0906

See Friday Plenary Number FRI-0906

SAT-0907

See Friday Plenary Number FRI-0907

SAT-0908

See Friday Plenary Number FRI-0908

SAT-0909

See Friday Plenary Number FRI-0909

SAT-0910

See Friday Plenary Number FRI-0910

SAT-0911

See Friday Plenary Number FRI-0911

SAT-0913

Persistence with Buffered Solution of Alendronate 70mg: Prospective Observational Study Andrea Giusti^{*1}, Dennis M Black², Antonella Barone³, Josef Hruska⁴, Gerolamo Bianchi¹. ¹La Colletta Hospital, Italy, ²University of California San Francisco, United States, ³Galliera Hospital, Italy, ⁴EffRx Pharmaceuticals, Switzerland

Keywords: osteoporosis, persistence, buffered alendronate Introduction: Alendronate 70mg effervescent (ALN-EX) was developed to improve upper gastrointestinal (GI) tolerability of alendronate tablets (ALN-T)1. It is associated with a lower frequency of GI adverse

reactions (AR) than ALN-T2, potentially leading to increased persistence with ALN-EX. Objective: To evaluate persistence and reasons for discontinuation in patients treated with ALN-EX, and to compare the outcomes with a historical cohort of patients on ALN-T. Materials and Methods: Postmenopausal women (PMW) from a standardized Clinical Database with BMD T-score <-2.5, or between -2 and -2.5 and at least one vertebral fracture, starting ALN-EX between July 2015 and June 2016 were included. A historical cohort comprised of randomly selected and age-matched PMW on ALN-T was used as a control. Persistence at 6- and 12-month and reasons for discontinuation were compared between the ALN-EX and ALN-T groups. Reasons for discontinuation including occurrence of AR were recorded prospectively (ALN-EX) or retrieved from the database (ALN-T). Efficacy data (BMD and bone ALP) are reported separately. Results: 144 PMW on ALN-EX and 216 PMW on ALN-T (144 ALN, 72 ALN plus cholecalciferol) were analyzed. The two groups were comparable with respect to baseline characteristics (previous fractures, baseline BMD and use of PPIs). Persistence at 6- and 12-months was 91% and 81% in ALN-EX group vs 75% and 69% in ALN-T. The difference was significant at both time points: 6-month $P<.001$ and 12-month $P=.009$. Significantly higher % of PMW receiving ALN-T discontinued treatment due to GI AR or patient preference: GI AR, 4% ALN-EX versus 11% ALN-T ($P=.027$); patient preference, 6% ALN-EX versus 13% ALN-T ($P=.016$). Conclusion: This is the first report indicating that ALN-EX is associated with higher persistence than ALN-T. ALN-EX is a well tolerated oral bisphosphonate and a viable alternative option in the management of osteoporosis, being able to improve persistence.

Reason Discontinuation	ALN-EX N° (%)	ALN-T N° (%)	P-value
Gastro-Esophageal Adverse Event (GE AE)	6 (4%)	23 (11%)	.027
Nausea	3 (2%)	8 (4%)	.382
Gastric Pain	1 (1%)	5 (2%)	.239
Esophageal Reflux	2 (1%)	3 (1%)	>.999
Nausea & Gastric Pain	0 (0%)	4 (2%)	.101
Esophageal Reflux & Gastric Pain	0 (0%)	3 (1%)	.156
Severe GE AE	1 (1%)	7 (3%)	.108
Patient's Preference	8 (6%)	29 (13%)	.016
Inconvenient Way	1 (1%)	7 (3%)	.108
Fear Adverse Events (incl. Fear ONJ)	6 (4%)	16 (7%)	.209
Fear ONJ	5 (3%)	9 (4%)	.738
Not Specified	1 (1%)	6 (3%)	.161
Clinical Events Not Related To Treatment or Osteoporosis	13 (9%)	15 (7%)	.470

Disclosures: **Andrea Giusti**, *Labatec, Speakers' Bureau, Merck & Co, Consultant, EffRx Pharmaceuticals, Grant/Research Support, Internis Pharma, Speakers' Bureau, Chiesi, Consultant, Abiogen, Consultant*

SAT-0914

Effect of Prevalent Vertebral Fractures on Incidental Vertebral Fractures and Low Back Pain During Bisphosphonate Treatment for Osteoporosis Yuji Kasukawa^{*1}, Naohisa Miyakoshi¹, Toshihito Ebina², Michio Hongo¹, Koji Nozaka¹, Yoshinori Ishikawa¹, Hiroyuki Tsuchie¹, Daisuke Kudo¹, Yoichi Shimada¹. ¹Department of Orthopedic Surgery, Akita University Graduate School of Medicine, Japan, ²Department of Orthopedic Surgery, Kakunodate General Hospital, Japan

Introduction: Osteoporotic vertebral fractures (VFs) comprise one cause of low back pain. We prospectively determined the incidence of low back pain (LBP) and VFs during treatment with risedronate alone or risedronate and vitamin K2 in osteoporotic women over 60 years of age with and without already present VFs. Methods: Altogether, 101 osteoporotic women were randomly stratified into two groups: Ris-group (n = 51) treated with risedronate alone (17.5 mg/week) and the Ris+K2 group (n = 50) treated with risedronate and menatetranone (45 mg/day). In all, 29 women in the Ris group and 26 in the Ris+K2 group continued treatment and were included in this study. They were divided into two subgroups—with or without VF—and underwent evaluation for incidental VFs by plain radiography, bone metabolic markers including serum cross-linked N-telopeptide of type 1 collagen (NTX) and bone alkaline phosphatase, and LBP by interview before and after treatment. Results: VFs were present pretreatment in 12 patients (41%) in the Ris group and 13 (50%) in the Ris+K2 group. LBP was present pretreatment in 15 (52%) in the Ris group and 15 (58%) in the Ris+K2 group. After 1 year of treatment, incidences of VF and LBP had decreased to 4 (14%) and 8 (28%), respectively, in the Ris group and 7 (27%) and 7 (27%), respectively, in the Ris+K2 group. Among the patients who developed VF or LBP during treatment, pretreatment VFs had been present in all 4 (100%, $p = 0.01$) and in 7 of 8 patients (88%, $p = 0.002$), respectively, in the Ris group and in 6 of 7 (86%, $p = 0.02$) and in 4 of 7 (57%, NS) patients, respectively, in the Ris+K2 group. The serum NTX level in participants with pretreatment VFs was significantly higher than that in those who did not already have VFs in both the Ris ($p = 0.01$) and Ris+K2 ($p = 0.03$) groups. Conclusion: VF incidences were significantly high in participants with pretreatment VFs independent of the type of treatment for osteoporosis. Incidence of LBP was significantly high only in participants who had pretreatment VFs and who were treated with Ris monotherapy.

Disclosures: **Yuji Kasukawa**, *None*

SAT-0915

The impact of switching once-weekly teriparatide to denosumab in severe osteoporosis patients Masayuki Miyagi^{*}, Kosuke Murata, Tomohisa Koyama, Hisako Fujimaki, Koji Naruse, Gen Inoue, Masashi Takaso. Department of Orthopedic Surgery, Kitasato University School of Medicine, Japan

INTRODUCTION: Switching from daily (d) teriparatide (TPTD) to denosumab (DMAb) had been reported effective for severe osteoporosis patients. However, there have been no reports about switching from weekly (w) TPTD to DMAb in patients with osteoporosis. Once-weekly 56.5- μ g TPTD treatment increases bone mineral density (BMD) and reduces fracture events. The objective of the current retrospective study was to elucidate the impact of switching w-TPTD to DMAb in patients with severe osteoporosis. METHODS: In this study, 40 patients were treated with w-TPTD for 18 months and then switched to DMAb for 18 months. The sample included 2 men and 38 women with a mean age of 74.5 (60-85) years. Twenty-five subjects had primary osteoporosis, and 15 had secondary osteoporosis. The mean number of osteoporotic vertebral fractures was 4.1. Serum bone turnover markers and BMD were evaluated every 6 months. And we also reviewed incident vertebral fractures by X-ray every 6 months. RESULTS: Bone alkaline phosphatase (BAP) and tartrate resistant acid phosphatase 5b (TRACP5b), markers of bone formation and resorption respectively, were not significantly different in w-TPTD subjects at 18 months compared with those at baseline ($p>0.05$), but BAP and TRACP5b in subjects treated with DMAb were significantly lower at 36 months compared with those at baseline ($p<0.05$). BMD of the lumbar spine (LS), femoral neck (FN), and total hip (TH) increased by 12.3%, 2.5%, and 2.2% by 36 months with DMAb treatment, significantly higher than at baseline ($p<0.05$). Changes in BMD of LS, FN, and TH in primary osteoporosis patients were significantly higher than in secondary osteoporosis patients at 18 months (w-TPTD) and 36 months (DMAb, $p<0.05$). Incident vertebral fractures were observed in 5 cases (12.5%), four (26.7%) of which were in patients with secondary osteoporosis, one (4%) case was in patients with primary osteoporosis. DISCUSSION: This is the first study to evaluate the impact of switching from w-TPTD to DMAb in severe osteoporosis patients, including those with secondary osteoporosis. BMD significantly increased in severe osteoporosis patients switched from w-TPTD to DMAb. However, the impact of switching from w-TPTD to DMAb in secondary osteoporosis patients was not as great as in primary osteoporosis patients.

Disclosures: **Masayuki Miyagi**, *None*

SAT-0916

Effects of Intravenous Ibandronate among Patients with Insufficient Changes to Bone Resorption Markers after Oral Bisphosphonate Monotherapy Naohisa Miyakoshi^{*1}, Yuji Kasukawa¹, Michio Hongo¹, Akira Horikawa², Yoichi Shimada¹. ¹Department of Orthopedic Surgery, Akita University Graduate School of Medicine, Japan, ²Igarashi Memorial Hospital, Japan

Introduction: Among multiple therapeutic options available for pharmacotherapy against osteoporosis, bisphosphonates (BPs) are the first-line drugs and act strongly to reduce osteoclast-mediated bone resorption. However, some individuals do not adequately respond to these drugs. This study first investigated the prevalence of non-responders to oral BP monotherapy among patients with postmenopausal osteoporosis using serum N-terminal telopeptide of type I collagen (NTX) as a marker. Second, we tested the effects of intravenous ibandronate among patients with insufficient changes to NTX after oral BP monotherapy to identify true non-responders to BPs. Methods: Among 146 consecutive patients with postmenopausal osteoporosis who received oral BP monotherapy for more than 12 months, insufficient responders to oral BP monotherapy were switched to intravenous ibandronate injection. The decision on whether to switch to intravenous ibandronate was made by each patient. Patients who agreed to switch intravenous ibandronate were followed-up for more than 12 months and bone turnover markers at 6 and 12 months after switching to intravenous ibandronate were evaluated. Serum NTX and bone alkaline phosphatase (BAP) concentrations were measured. Patients who also showed insufficient response to intravenous ibandronate were defined as true BP non-responders. Insufficient response to BP therapy was evaluated based on the serum NTX reduction cut-off for minimum significant change. Results: Sixty-one patients (41.8%) were diagnosed as oral BP non-responders. Among these non-responders, 22 patients (36.1%) agreed to switch to intravenous ibandronate treatment. Fourteen patients who switched to intravenous ibandronate and had complete data available were used for final analysis. After switching to intravenous ibandronate, both NTX and BAP decreased significantly ($p<0.05$). However, at 6-12 months after switching, 57.1-64.3% of patients still showed insufficient response of NTX as compared to baseline (before oral BP monotherapy), and 21.4-35.7% of patients still showed insufficient response of NTX when compared to data immediately before switching. Conclusions: These results estimated that as few as 9-15% (i.e., 21.4-35.7% of 41.8%) or as many as 24-27% (i.e., 57.1-64.3% of 41.8%) of patients might be true BP non-responders.

Disclosures: **Naohisa Miyakoshi**, *None*

SAT-0917

The Impact of Prior Bisphosphonate Treatment on Weekly Teriparatide for Severe Osteoporosis Kosuke Murata*, Tomohisa Koyama, Sho Inoue, Masayuki Miyagi, Eiki Shirasawa, Shuichiro Tajima, Ayumu Kawakubo, Yui Uekusa, Hiroki Saito, Maho Tsuchiya, Yusuke Mimura, Masahiro Yoneda, Koji Naruse, Kentaro Uchida, Gen Inoue, Masashi Takaso. Department of Orthopedic Surgery, Kitasato University, School of Medicine, Japan

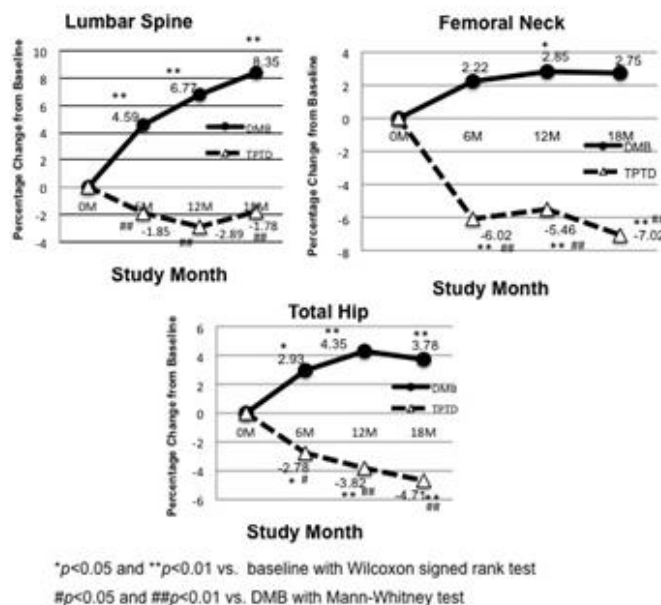
Introduction: Bisphosphonate (BP) use prior to daily teriparatide (d-TPTD) treatment may reduce the increase in bone mineral density (BMD). The impact of prior BP treatment on weekly (w) TPTD has not been reported. This study aimed to determine the effect of BP prior to w-TPTD on the efficacy of osteoporosis treatment. **Methods:** This study included 58 patients with severe osteoporosis (3 men and 55 women, mean age: 77.4 years). Of these, 32 had primary osteoporosis and 26 had secondary osteoporosis, including glucocorticoid-induced osteoporosis. The mean number of fractures was 3.3, indicating severe osteoporosis. We reviewed bone turnover markers (BAP, TRACP 5b) and BMD (lumbar spine [LS] and femoral neck [FN] using DEXA) every 6 months and calculated the ratio of change from baseline. We also reviewed medical records for new osteoporotic fragility fractures. We divided subjects into a prior BP treatment group (prior BP(+); n=18) and others (prior BP(-); n=40), and compared all reviewed factors. **Results:** BAP changes from baseline at 6, 12, and 18 months were -8.5%, -2.8%, and -4.7%, respectively. TRACP 5b changes at 6, 12, and 18 months were -8.5%, -12.9%, and -15.9%, respectively. BMD changes in the LS and FN at 6, 12, and 18 months were 2.6%, 3.7%, and 5.2%, and 0.6%, 0.5%, and 0.3%, respectively. There were 12 secondary osteoporosis patients (66.7%) in the prior BP(+) group and 14 secondary osteoporosis patients (35%) in the prior BP(-) group. BAP and TRACP 5b changes in the prior BP(+) group and prior BP(-) group at 18 months were 3.6% and -11.4%, and -8.7% and -18.1%, respectively. Changes in bone turnover markers tended to be high in the prior BP(+) group, although there was no significant difference between groups ($p>0.05$). BMD changes in the LS and FN at 18 months were 5.0% and -1.5%, respectively in the prior BP(+) group, and 5.3% and 0.7%, respectively in the prior BP(-) group. There were no significant differences between groups ($p>0.05$). However, BMD changes in the FN tended to be low in the prior BP(+) group. Of 7 cases with 9 new osteoporotic fragility fractures, the prior BP(+) group had 4 cases (22%) and 6 fractures, and the prior BP(-) group had 3 cases (7.5%) and 3 fractures. **Discussion:** The prior BP(+) group had more secondary osteoporosis cases, indicating less effect on BMD of the FN and more new osteoporotic fragile fractures. Thus, BP prior to w-TPTD treatment, especially for secondary osteoporosis, might reduce treatment efficacy.

Disclosures: Kosuke Murata, None

SAT-0918

Denosumab was superior to teriparatide to improve bone mineral density in patients with rheumatoid arthritis; 18 months of follow-up Tokutaro Okawa*, Motomi Okawa¹, Shuhei Ueno², Eri Narita², Tatsuya Koike². ¹Okawa Orthopaedic Surgery Hospital, Japan, ²Search Institute for Bone and Arthritis Disease, Shirahama Foundation for Health and Welfare, Japan

Background: Both denosumab (DMB) and teriparatide (TPTD) are well known as a great useful treatment option for OP. RA and medications for RA have been considered risk factors for fractures and bone loss, especially in the elderly. Head to head comparison between these medications for OP in RA patients in elderly has not been well addressed previously. **Object:** In this retrospective study, we compared BMD changes with DMB and TPTD treatment for OP in elderly Japanese RA patients for 18 months of follow-up. **Methods:** Subjects were patients with a diagnosis of RA according to the 2010 ACR/EULAR criteria. All patients were postmenopausal women with OP who were OP treatment naïve. The DMB dose was 60 mg every 6 months with daily native vitamin D. The treatment with TPTD included 20 µg daily or 56.5 µg weekly by subcutaneous injection. BMD was measured with DXA for lumbar spine (LS), femoral neck (FN) and total hip (TH) at baseline and months 6, 12, 18 during treatment. The statistical significance in mean values between two groups in time with Mann-Whitney U-tests. To identify difference in one group between time points, Wilcoxon signed rank test was used. **Result:** DMB (n=21) and TPTD (n=15) were enrolled. Baseline characteristics of DMB and TPTD were the mean age 72.1 and 72.8 years old, the body mass index 19.6 and 19.9, LS-BMD 0.658 and 0.662, FN-BMD 0.437 and 0.448, TH-BMD 0.573 and 0.539, respectively. There was no significant difference between two groups at baseline. The percent change of LS-BMD from baseline to 6, 12 and 18 months were each 4.59% vs -1.85% ($p<0.01$) at 6 months, 6.77% vs -2.89% ($p<0.01$) at 12 months and 8.35% vs -1.78% ($p<0.01$) at 18 months. The percent change of FN-BMD from baseline to 6, 12 and 18 months were each 2.22% vs -6.02% ($p<0.01$) at 6 months, 2.85% vs -5.46% ($p<0.01$) at 12 months and 2.75% vs -7.02% ($p<0.01$) at 18 months. The percent change of TH-BMD from baseline to 6, 12 and 18 months were each 2.93% vs -2.78% ($p<0.05$) at 6 months, 4.35% vs -3.82% ($p<0.01$) at 12 months and 3.78% vs -4.71% ($p<0.01$) at 18 months. **Conclusion:** This study shows that DMB was more effective to increase BMD than TPTD in elderly RA patients with osteoporosis.



Disclosures: Tokutaro Okawa, None

SAT-0919

Comparative Analysis of new adjacent and remote fracture after vertebroplasty: survivorship analysis of 205 patients Ye Soo Park*, Jaedong Kim¹, Jin-Sung Park², Woong Hwan Choi³. ¹Hanyang University Guri Hospital, Republic of Korea, ²Korea University Ansan Hospital, Republic of Korea, ³Hanyang University Hospital, Republic of Korea

Background: We don't know the risk factors of adjacent and remote vertebral fracture after vertebroplasty. **Objective:** The purpose of this study was to investigate the natural history of new fracture following vertebroplasty for osteoporotic vertebral compression fracture (OVCF) and to evaluate the risk factors for adjacent vertebral fracture (AVF) and remote vertebral fracture (RVF) separately. **Design:** A retrospective study of 205 consecutive patients who underwent a vertebroplasty for OVCF with a minimum follow-up of 1 year was conducted. A separate survivorship analysis of AVF and RVF was performed using the Cox proportional hazards model. **Results:** Of the 47 patients (22.9%) with new vertebral fracture, AVF developed in 21 patients (10.2%) and RVF in 26 patients (12.7%). The median survival time was 4.0 months for AVF and 14.0 months for RVF. Multivariate analyses revealed that sagittal alignment imbalance and initial vertebroplasty at the thoracolumbar junction were independent risk factors for AVF (hazard ratio=9.6 and 4.7, respectively), whereas the significant risk factor for RVF was a sagittal alignment imbalance (hazard ratio=11.5). A low bone mineral density of the spine (T-score ≤ -3) was shown to be a risk factor for AVF and RVF on univariate analyses, but not on multivariate analyses. **Conclusion:** AVF developed at a median of 4 months and RVF at a median of 14 months. An initial vertebroplasty at the thoracolumbar junction was an independent risk factor for AVF, and patients with sagittal alignment imbalance had a high risk of AVF and RVF after vertebroplasty for OVCF.

Disclosures: Ye Soo Park, None

SAT-0920

The mechanical properties of human trabecular bone accompanying one to twenty years of bisphosphonate treatment. David Pienkowski*, Constance Wood, Hartmut Molluche. University of Kentucky, United States

Bisphosphonates are widely used for treating osteoporosis, but the relationship between treatment duration and bone quality is unclear. Material properties determine bone quality, thus the present study quantifies the relationship between modulus and hardness of human bone with bisphosphonate treatment duration. **Patients and Methods:** iliac crest bone samples from a consecutive series of 86 osteoporotic Caucasian women continuously treated with oral bisphosphonates for 1.1 to 20 years were analyzed using nanoindentation. Young's modulus and hardness were measured and related to bisphosphonate treatment duration by statistical modeling. **Results:** the statistical models showed that modulus and hardness increased, peaked, and plateaued with increasing bisphosphonate treatment duration. Both quadratic and linear terms were needed to model modulus increases from 1 to 6 years of bisphosphonate treatment and plateaued from 6 to 20 years of treatment. Models also indicated that the quadratic-linear transition point in bisphosphonate treatment duration depends upon trabecular location. Hardness increased and peaked at 12.4 years of treatment; it remained constant from 12.4 to 20 years and was less sensitive to trabecular location. **Conclusions:** bone modulus increases with bisphosphonate treatment duration up to 6 years and no addi-

tional modulus gains can be expected from treatment durations exceeding 6 years. Hardness increased, peaked at 12.4 years, and remained constant up to 20 years of bisphosphonate treatment. The clinical relevance of hardness awaits further study.

Disclosures: David Pienkowski, None

SAT-0921

Effectiveness of Monthly Intravenous Ibandronate Injections in a Real-World Setting: Subgroup Analysis of a Post-Marketing Observational Study Yasuhiro Takeuchi^{*1}, Junko Hashimoto², Hiroyuki Kakihaya², Yosuke Nishida², Michiko Kumagai², Chiemi Yamagiwa². ¹Endocrine Center, Toranomon Hospital, Japan, ²Chugai Pharmaceutical Co. Ltd., Japan

Purpose: The favorable safety and consistent effectiveness of monthly intravenous (IV) ibandronate (IBN) injections was reported recently in a prospective, post-marketing, observational study in Japanese patients (pts) with osteoporosis (BON1301) [Takeuchi Y et al. Osteoporosis and Sarcopenia, 2018. In press]. Here we present subgroup analyses from the study. **Methods:** The effectiveness parameters evaluated in this large-scale, real-world study included bone mineral density (BMD) gains and the cumulative incidence of vertebral fractures. BMD gains were assessed in the following subgroups: previous bisphosphonate (BP) treatment, concomitant vs naïve osteoporosis drug treatment, younger vs older age (<75 or ≥75 years), and absence vs presence of vertebral fractures. **Results:** 1,062 pts were enrolled and 1,025 pts received monthly IV IBN 1mg for 1 year. Overall, significant increases in BMD relative to baseline were observed at the lumbar spine (LS; 4.84%, 95% CI 3.47, 6.21) at 12 months. In total, 515 pts (50.2%) had previously been treated with osteoporosis drugs; of these, 166 pts (16.1%) were treated with other BPs. The mean BMD changes at the LS were 4.15% (95% CI, 1.43, 6.87) in pts previously treated with other BPs and 6.12% (95% CI, 3.13, 9.11) in pts receiving other prior osteoporosis treatments at 12 months from baseline, compared with 4.04% (95% CI, 2.61, 5.47) in pts who had not received prior osteoporosis treatment. Among the 510 pts (49.7%) concomitantly prescribed activated vitamin D drugs, mean LS BMD changes were 5.75% (95% CI, 3.65, 7.86) at 12 months from baseline vs 3.54% (95% CI, 1.98, 5.10) in pts receiving IBN alone. In pts aged <75 or ≥75 years, LS BMD gains were 4.30% (95% CI 2.82, 5.77) and 5.24% (95% CI 3.12, 7.36), respectively. LS BMD gains were 5.75% (95% CI 3.95, 7.56) and 5.21% (95% CI 2.42, 8.00), respectively, in pts with vs without vertebral fractures. No renal-related adverse drug reactions were observed. Estimated glomerular filtration rate (eGFR) levels did not change throughout the study (mean eGFR: 67.64mL/min/1.73m² at baseline; 67.60mL/min/1.73m² at 12 months). No notable renal impairment was seen in 24 pts with eGFR levels <35mL/min/1.73m². **Conclusions:** Monthly IV IBN demonstrated comparable BMD gains in subgroups defined by prior or concomitant osteoporosis treatment, age, and presence or absence of vertebral fractures. These data suggest that IBN shows high utility and a positive benefit-risk profile in these pts.

Disclosures: Yasuhiro Takeuchi, Chugai, Daiichi-Sankyo, Teijin Pharma, Grant/Research Support, Chugai, Daiichi-Sankyo, Teijin Pharma, Asahikasei Pharma, Speakers' Bureau

SAT-0922

Pharmacogenomics study of denosumab Victoria Ho-Yee Wong^{*}, Vincent Ka-Fai Cheng, Grace Koon-Yee Lee, Ching-Lung Cheung. The University of Hong Kong, Hong Kong

Background Denosumab (Dmab) is a fully human monoclonal antibody that targets the key bone resorption mediator RANKL. RANKL is expressed in osteoblasts and stromal cells and binds to its receptor RANK that regulates bone resorption. Contrary to this, OPG is secreted endogenously to bind RANKL, thus inhibiting bone resorption. As Dmab functions by blocking the binding between RANKL and RANK, understanding the function and expression of members of RANKL-RANK-OPG axis is essential to pharmacodynamic study of Dmab. However, the genetic variation or expression of these genes remain unexplored. We aimed to study the association between serum levels of RANK/RANKL/OPG, mRNA expression levels of RANK/RANKL/OPG, and bone mineral density (BMD). **Methods** We recruited cases (N=50) who are osteoporotic patients treated with Dmab monotherapy, while controls (N=217) being participants from the Hong Kong Osteoporosis Study who had never received anti-osteoporotic treatment. BMD was measured by DEXA with 6-month period prior to Dmab monotherapy, at 12 months (+/-3 months) after 1-year Dmab monotherapy. Peripheral blood mononuclear cells (PBMC) from the cases and controls were collected and used for mRNA expression study. Circulating RANK/RANKL/OPG in serum was quantified using ELISA. Association studies were performed using linear regression. **Results** After 1-year treatment efficacy of Dmab, 20.6% of cases did not have lumbar spine BMD increased, while 27.5% of them did not have femoral neck BMD increased. We observed that circulating RANKL (R=-0.505, P=0.002) and OPG/RANKL ratio (R=-0.364, P=0.029) were significantly correlated with 1-year BMD change at the lumbar spine after Dmab monotherapy, but not with bone loss in controls. No significant association between circulating OPG/RANK/RANKL and BMD change at the hip was observed. On the other hand, mRNA expression of RANKL in PBMC was positively correlated with the circulating RANKL levels (R=0.497; P<0.001) and showed trend toward significant association with BMD change at the lumbar spine after 1-year Dmab treatment (R=-0.298, P=0.10). No significant association between mRNA expression levels of OPG/RANK/RANKL and BMD change at the hip was observed. **Conclusion** The circulating RANKL is likely to be an important determinant of Dmab treatment outcome; whereas RANKL mRNA expression in PBMC is highly cor-

related with circulating RANKL. This pharmacogenomic study provided useful insight to the evaluation of efficacy of Dmab.

Disclosures: Victoria Ho-Yee Wong, None

SAT-0962

See Friday Plenary Number FRI-0962

SAT-0963

See Friday Plenary Number FRI-0963

SAT-0964

Racially determined, serum-mediated resistance to 25-hydroxyvitamin D induced innate immune responsivity in human macrophages Rene Chun^{*1}, Carter Gottlieb¹, Kathryn Zavala¹, Albert Shieh¹, Andrea Salinas¹, Vahe Yacoubian¹, Samya Konda¹, Jefferey Wang¹, Martin Hewison², Philip Liu¹, John Adams³. ¹Department of Orthopaedic Surgery, UCLA, United States, ²Institute of Metabolism and Systems Research, University of Birmingham, United Kingdom, ³Departments of Orthopaedic Surgery and Molecular, Cell and Developmental Biology, UCLA, United States

Low serum concentrations of 25-hydroxyvitamin D (25D), not low levels of intracellularly-active hormone, 1,25-dihydroxyvitamin D (1,25D), are correlated to increased mortality and poor disease outcomes in humans. This observation indicates the importance of the linkage between substrate levels of inactive 25D and bioactivity in target cells through the functionality of CYP27B1- and CYP24A1-hydroxylases and vitamin D receptor (VDR) and the influence of factors that impinge upon their activity. An example of intracrine regulation is that of antimicrobial cathelicidin (CAMP) gene expression in human macrophages. Paired serum samples, obtained before and after vitamin D supplementation and restoration of 25D>30ng/ml, from age and sex-matched White (n=11), Black (n=11) or Hispanic (n=11) donors were used to culture non-autologous primary human adherent monocyte-macrophages. Total and free 25D-normalized serum from White, but not Black or Hispanic, subjects was associated with increased expression of CAMP (p<0.001). Thus, some 25D-independent factor(s) in serum may impose resistance to intracrine induction of CAMP in the face of normalized 25D levels. Considering that cells and platelets are absent in serum, we speculated resistance may reside in the exosome fraction of serum; exosomes are extracellular vesicles that contain non-organelle intracellular and membrane contents of its source cell. To explore this possibility, we employed chemical precipitation or ultracentrifugation to isolate exosomes from pooled human serum. The resultant exosome-containing pelleted material was re-suspended, cultured with adherent monocytes, and CAMP expression measured. Expression of CAMP was reduced while CYP27B1, VDR and TREM1 were increased. Given that increased CYP27B1 and VDR should increase CAMP expression, the observed CAMP reduction suggests the presence of a potent inhibitory component. After boiling, the bioactivity was lost revealing it to be either heat-labile protein(s) or intact exosomes. Because exosomes frequently co-purify with protein aggregates, we used sucrose density gradient to separate exosome-enriched (lower density) and protein-enriched (higher density) fractions. We found that the CAMP suppressive activity segregated with the protein-enriched fraction. These findings point to protein(s) co-migrating with isolated human serum exosomes that can inhibit 25D-dependent CAMP innate immune responses in human macrophages.

Disclosures: Rene Chun, None

SAT-0965

WITHDRAWN

SAT-0973

See Friday Plenary Number FRI-0973

SAT-0974

See Friday Plenary Number FRI-0974

SAT-0975

See Friday Plenary Number FRI-0975

SAT-0976

See Friday Plenary Number FRI-0976

SAT-0977

See Friday Plenary Number FRI-0977

SAT-0978

See Friday Plenary Number FRI-0978

SAT-0979

See Friday Plenary Number FRI-0979

SAT-0980

See Friday Plenary Number FRI-0980

SAT-0981**Allosteric or ectosteric inhibition of cathepsin K by an exosite inhibitor**
Simon Law*, Dieter Bromme. University of British Columbia, Canada

Cathepsin K (CatK) is the predominant mammalian bone-degrading protease and thus an ideal target for anti-osteoporotic drug development. NSC-13345 was previously characterized as an allosteric inhibitor of CatK binding at a site remote from the active site. However, crystallization was performed using a non-fully processed enzyme where the binding site was influenced by a remaining propeptide piece. Here we crystallized the fully processed and active protease with NSC-13345 and identified three simultaneous binding sites different from the putative allosteric site. In particular, one binding site was located in the S2-3' region of the enzyme without blocking the catalytic Cys-His diad. This binding site may explain the substrate selective inhibition of the hydrolysis of peptides and proteins by hindering the proper binding of a peptide chain C-terminally from the scissile bond. Larger substrates that occupy this region were selectively inhibited whereas substrates occupying only the Sx-S1' site were not affected. In addition, a second binding site of the inhibitor corresponded to a chondroitin sulfate-binding site that has been associated with the collagenase activity of CatK. This may contribute to the observed anticollagenase activity of the inhibitor. A third site appears to have no effect. The binding of NSC-13345 at all three sites does neither influence the geometry of the catalytic diad nor traditional substrate binding sites and thus excludes an allosteric mechanism. The previously described allosteric site was not observed and mutations of this site had no effect on any of the substrate hydrolyses. These findings suggest that NSC-13345 may function as a substrate selective ectosteric inhibitor for CatK.

Disclosures: *Simon Law, None***SAT-0982****Pharmacokinetic Models for Bisphosphonate-Conjugated Drugs** Jayesh Shah*¹, Frank H. Ebetino², Lianping Xing³, Robert Boeckman³, Shuting Sun², Parish Sedghizadeh⁴, Michael T Yin¹, Suzanne Lentzsch¹, Graham Russell⁵, Serge Cremers¹. ¹Columbia University Medical Center, United States, ²Biovinc, United States, ³University of Rochester, United States, ⁴University of Southern California, United States, ⁵University of Oxford, United Kingdom

Introduction: Bisphosphonates (BPs) can be used to target other compounds to bone. New chemical linker strategies have enabled BP-conjugated agents that deliver the drug specifically to the skeleton, and not release the active compounds until the bone has been reached (Wang 2017, Sedghizadeh 2017). BP-conjugates are in development for various therapeutic classes which include antibiotics and anti-cancer drugs. For BPs, identification of an optimal dose regimen has been challenging. The optimal dose regimens for BP-conjugated drugs will also be a challenge, especially because of the difficulties in assessing the active compound at the bone. In a first effort to help find the right dose regimen for these compounds we developed PK models for BP-Ciprofloxacin (BP-Cipro-) and BP-Bortezomib (BP-Btz)-conjugated drugs which are able to simulate the active drugs at the bone, and might be useful for drug development. **Methods:** Compartmental PK models for BPs, Cipro and Btz in humans were derived from the literature (Cremers 2002, Forrest 1993, Hanley 2017). These models were merged to multi-compartmental PK-models for the BP-conjugates with SAAM-II PK software. Using these models serum, urine and bone concentrations (concs) of the BP conjugate, the free BP and the free Cipro and Btz were simulated during various dose regimens. Simulations were also performed using PK models for free Cipro and Btz. **Results:** Our simulations suggest that the PK of free Cipro and Btz is different when the drug is administered as conjugate. Serum and bone concs of the free drugs reach C_{max} a few days rather than a few hrs after IV administration with t_{max} and C_{max} determined by the hydrolysis rate of the free drug from the conjugate. Concs of free drug at the bone are projected higher than in serum. Importantly, the serum conc of the free drug over time parallels the bone conc over time as free drug seems to be released with depot like characteristics. The model also suggests that studies into the PK of BP-conjugated drugs need to be of sufficient length to fully characterize the long term release of the drugs from bone. **Conclusion:** We developed mechanism-based PK models for BP-conjugated drugs. These models which remain to be validated and further optimized can ultimately be used to estimate free drug at bone

surfaces over time. Expanding these models with bactericidal and anti-tumor effects will be useful to determine the optimal dose regimens for these most interesting new class of drugs.

Disclosures: *Jayesh Shah, None***SAT-0983****Calcilytic, the calcium-sensing receptor antagonist, enhances bone remodeling and increases bone mineral density without increasing urinary calcium excretion** Bingzi Dong*¹, Itsuro Endo², Yukiyo Ohnishi², Zhengju Fu¹, Toshio Matsumoto³, Yangang Wang¹. ¹Department of Endocrinology and Metabolism, the Affiliated Hospital of Qingdao University, Qingdao, China, ²Department of Hematology, Endocrinology and Metabolism, Tokushima University Graduate School of Medical Sciences, Japan, ³Fujii Memorial Institute of Medical Sciences, Tokushima University, Japan

Calcium-sensing receptor (CaSR) belongs to the G-protein coupled receptor superfamily, locating on parathyroid gland, gastrointestinal tract, and kidney, and plays an important role in maintaining calcium hemostasis. CaSR is also expressed in cartilage, osteoblast and osteoclast in the bone, to regulate skeletal development and bone metabolism. Calcilytic is the antagonist of CaSR. It binds to the transmembrane domain, blocks downstream signaling, and disturbs the sensitivity of CaSR to extracellular calcium. Calcilytic mimicks hypocalcaemic environment, leading to the stimulation of endogenous parathyroid hormone (PTH) release. Thus, calcilytic may promote bone anabolic effect. In this study, we examined the effects of calcilytic (JTT-305) on bone metabolism, and compared them with calcium-vitamin D supplement and PTH(1-34) (teriparatide) administration. Calcilytic rapidly stimulated endogenous PTH release. Daily administration of calcilytic significantly increased cancellous and cortical bone mineral density (BMD) to the comparable level to teriparatide treatment. Bone histomorphometric analysis revealed that bone volume, trabecular thickness, and trabecular number was increased. Calcilytic also improved bone formation markers, serum bone-specific ALP and osteocalcin, and bone resorption markers, serum TRAP and urinary NTX. Both calcilytic and teriparatide accelerated bone turnover. Calcilytic administration slightly increased serum calcium level. However, compared with calcium-vitamin D supplement or teriparatide treatment, calcilytic did not increase urinary calcium excretion, which did not increase the risk of kidney stone formation. For the treatment and prevention of osteoporosis, calcium-vitamin D supplement is essential but not enough. Calcilytic increases BMD by stimulating endogenous PTH secretion, and shows comparable bone anabolic effect to teriparatide injection. Thus, calcilytic may become a promising anti-osteoporosis candidate.

Disclosures: *Bingzi Dong, None***SAT-0984****Influence of Vitamin D Restriction on Bone Strength, Body Composition, and Muscle in Ovariectomized Rats Fed a High-fat Diet** Kanae Nakaoka*, Asako Yamada, Seiko Noda, Masae Goseki-Sone. Japan Women's University, Japan

Vitamin D insufficiency is associated with a greater risk of osteoporosis and also influences skeletal muscle functions. Obesity is associated with metabolic syndrome, and low levels of serum 25-hydroxyvitamin D3 have been frequently observed in patients with obesity. Both obesity and vitamin D insufficiency have been recognized as major public health issues worldwide. The present study investigated the influences of vitamin D restriction on bone strength and body composition in ovariectomized (OVX) rats fed a high-fat diet. Twenty-four 13-week-old female rats were ovariectomized, and another six rats were sham-operated (Sham). The OVX rats were divided into four groups and fed experimental diets: a basic control diet (OVX-Cont.), a basic control diet with vitamin D restriction (OVX-DR), a high-fat diet (OVX-F), and a high-fat diet with vitamin D restriction (OVX-FDR). At 28 days after starting the experimental diets, the food intake, final body weight, and fat mass were significantly increased by OVX ($p < 0.001$, $p < 0.01$, and $p < 0.01$, respectively) and the cancellous bone mineral contents (BMC) of the vertebrae and femur were significantly decreased by OVX ($p < 0.05$ and $p < 0.01$, respectively). The fat mass was significantly increased in the OVX-F and OVX-FDR groups compared with OVX-Cont. group ($p < 0.001$ and $p < 0.01$, respectively), while the muscle mass was significantly decreased in the OVX-F and OVX-FDR groups compared with OVX-Cont. group ($p < 0.05$ and $p < 0.001$, respectively). The BMC of the vertebrae and femur were significantly lower in the OVX-DR and OVX-FDR groups compared with OVX-Cont. group [OVX-DR ($p < 0.01$ and $p < 0.05$, respectively) and OVX-FDR ($p < 0.001$ and $p < 0.05$, respectively)]. In addition, the cortical bone of the vertebrae was significantly thinner in the OVX-FDR group compared with OVX-F group ($p < 0.05$). Myogenin is one of the muscle-specific transcription factors. The levels of mRNA expression of myogenin of the soleus and gastrocnemius from the OVX-DR and OVX-FDR groups were reduced markedly compared with those from the OVX-Cont. group [OVX-DR ($p < 0.01$ and $p < 0.05$, respectively) and OVX-FDR ($p < 0.01$, respectively)]. In conclusion, we provide evidence that a high-fat diet with vitamin D deficiency markedly impairs bone and muscle metabolism using OVX rats. Further studies on vitamin D insufficiency in the regulation of muscle as well as bone metabolism would provide valuable data for the prevention of lifestyle-related disorders, including osteoporosis and sarcopenia.

Disclosures: *Kanae Nakaoka, None*

SAT-0985

Propranolol administration has a non-statistically significant positive effect on the osseointegration procedure of stainless steel implants. An experimental study in rats Marinos Karanassos^{*1}, Kyriakos Papavasiliou², Ioannis Mirisidis³, Ioannis Margaritis⁴, Ioannis Sarris², Pericles Papadopoulos⁵, Dimosthenis Tsitouras², Dimitrios Tsatsalis², Fares Sayegh². ¹2nd Dept. of Orthopaedics and Trauma Surgery, 424 General Military Hospital, Thessaloniki, Greece, ²3rd Orthopaedic dept., Aristotle University of Thessaloniki, Papageorgiou General Hospital, Thessaloniki, Greece, ³Dept. of Mechanical Engineering, University of Western Macedonia, Kozani, Greece, ⁴Laboratory of Physiology, Faculty of Veterinary Medicine, School of Health Sciences, Aristotle University of Thessaloniki, Greece, ⁵1st Orthopaedic dept., Aristotle University of Thessaloniki, Papanikolaou General Hospital, Thessaloniki, Greece

Purpose. Orthopaedic implants are widely used in everyday practice (especially in elderly patients), either in elective surgery or in trauma (osteoporotic or not). β -Blockers, apart from their current well-established indications, are considered as potential candidates of therapeutic drugs under investigation for enhancing fracture healing and treating osteoporosis. Fracture healing and orthopaedic implants' osseointegration procedure share common pathways, hence β -Blockers administration may enhance the latter as well. Aim of this study was to assess the potentially positive effect of the administration of β -Blocker on the osseointegration procedure of stainless steel orthopaedic implants. Methods. This experimental study (approved by our Institution's Ethical Committee) was performed in two groups (study, control), consisting of 15 adult (12-weeks old) male Wistar rats each. Their average weight was 340 ± 20 gr and there was no difference as far as the weight was concerned between groups (t-test, $p=0.989$). In the proximal metaphysis of each tibia of all animals, a specially designed stainless steel screw was implanted under sedation on day 0. All animals followed the same pharmaceutical perioperative protocol, had unrestricted access to food and water and were exposed to the same period of light (12h) on a daily basis. Starting on the first postoperative day, study group animals received 2.5mg/kg of propranolol daily intraperitoneally (Dociton Injektionslösung® 1mg/ml). Control group received saline. On day 29, all animals were euthanized, tibias were harvested and the implants' pullout strength and removal torque were assessed. Results. All animals completed the study period and all harvested tibias were suitable for evaluation. The weight of the animals of both groups increased in a statistically significant manner (study: $p=0.002$ Wilcoxon test, control: $p=0.000$ t-test). However, the difference in weight increase between groups was statistically non-significant ($p=0.299$, Mann-Whitney test). (See Table of Results for data concerning pullout strength and removal torque). Conclusions. Propranolol enhances the osseointegration of stainless steel orthopaedic implants, albeit in a non-statistically significant manner. Blocking of β -adrenergic receptors in osteoblasts and stromal cells, leading to increased bone formation and decrease of bone resorption may be its mechanism of action.

Parameter	Units	Study Group	Control Group	P (student t-test, 95% CI)
Pullout strength	Newton	104.23 \pm 21.28	90.76 \pm 18.19	0.103
Torque	N/cm	5.398 \pm 0.778	4.89 \pm 0.715	0.091

Disclosures: Marinos Karanassos, None

SAT-0986

Intra-Articular Monosodium Iodoacetate Induced Knee Osteoarthritis: Effects on Bone as Measured by Micro-Computed Tomography in Rats Jukka Vaaraniemi^{*}, Jukka Morko, Jaakko Lehtimäki, Zhiqi Peng, Jussi M Halleen. Pharmatest Services Ltd, Finland

Several experimental animal models have been developed for human osteoarthritis (OA) and used to study the preclinical efficacy of disease and symptom modifying OA drug candidates. One of these models is induced chemically by an intra-articular injection of monosodium iodoacetate (MIA) into rat knee. Intra-articular MIA disrupts chondrocyte glycolysis through the inhibition of glyceraldehyde-3-phosphate dehydrogenase resulting in chondrocyte death, joint damage, and OA symptoms. In this study, we characterized the effects of intra-articular MIA injection on bone by high-resolution micro-computed tomography (micro-CT) in the tibiofemoral and patellofemoral joints of young rats. Unilateral OA was induced by the injection of MIA at 2 mg into the knee joint of male Sprague-Dawley rats at the age of 6 weeks. Rats were terminated at 4 weeks after the MIA injection and their knee joints were fixed in 10% neutral buffered formalin. After the fixation, knee joints were scanned by high-resolution micro-CT using 8 μ m image pixel size. After the scanning, the epiphyses of femur and tibia, the weight-bearing regions of femoral condyles and tibial plateau in medial and lateral compartments, and patella were segmented using a free-hand tool, and analyzed separately. The intra-articular MIA injection decreased bone volume (BV) slightly more in the entire epiphysis of femur than in the entire epiphysis of tibia, namely by 47% in femur and 44% in tibia. In the weight-bearing region, the amount of epiphyseal bone was decreased slightly more in the medial compartment than in the lateral compartment of MIA-injected knee. Namely, BV was decreased by 34% in the medial compartment and 29% in the lateral compartment of femoral condyles, and by 44% in the medial compartment and 40% in the lateral compartment of tibial plateau. These reductions in epiphyseal BV were associated with decreased number and thickness of individual trabeculae in epiphyseal marrow cavity. In patellofemoral joint, clear erosion was observed on articular surface without significant changes in the BV of entire patella. This study demonstrated that micro-CT is a

useful tool to measure MIA-induced changes in bone when testing the preclinical efficacy of disease modifying OA drug candidates in the rat MIA model of knee OA. The follow-up of treatment effects by in vivo micro-CT both on articular cartilage and bone would improve the analysis of preclinical efficacy in the rodent models of human OA.

Disclosures: Jukka Vaaraniemi, None

SAT-0987

Effect of Age and Dietary Phosphorus Intake on Phosphorus Regulatory Hormones and Intestinal Phosphate Transporter Gene Expression Colby Vorland^{*1}, Loretta Aromeh², Pamela Lachcik¹, Sharon Moe², Neal Chen², Kathleen Hill Gallant¹. ¹Department of Nutrition Science, Purdue University, United States, ²Division of Nephrology, Department of Medicine, Indiana University School of Medicine, United States

We previously reported higher phosphorus (P) absorption efficiency in 10wk SD rats vs older rats and no effect of low P diet on net P absorption using an in situ ligated loop method (Vorland JBMR 31(S1)). To understand the mechanisms involved in these age-related changes, we evaluated the effects of age and dietary phosphorus (P) on P-regulating hormones and intestinal P transporter gene expression. N=72 male SD rats studied at 3 ages (10wk, 20wk, and 30wk of age) were fed diets of 0.6% Ca and 0.1% (LP), 0.6% (NP), or 1.2% (HP) P (n=8/group) for 14d before sacrifice. Intestinal P absorption was measured by jejunal ligated loop (5 μ Ci ³³P in 0.5 mL of 0.1 mmol/L P transport buffer) over 30min prior to sacrifice. Jejunal and duodenal mucosal tissue and blood were collected. Gene expression of intestinal P transporters NaPi2b and Pit1 were measured by RT-PCR, plasma 1,25-dihydroxyvitamin D3 (1,25D) by EIA, and intact parathyroid hormone (iPTH), intact and c-terminal fibroblast growth factor 23 (iFGF23, cFGF23) by ELISA. Data were analyzed by 2-way ANOVA for age, diet and interaction effects, with Tukey's post-hoc tests. 1,25D levels were significantly lower, and iFGF23 and iPTH levels were higher at 20 or 30wk compared with 10wk in all animals (all $p<0.05$). LP increased 1,25D, decreased both iFGF23 and cFGF23 (all $p<0.01$). There was an age x diet interaction only for iPTH ($p<0.0001$) where LP had lower iPTH vs NP and HP, but the magnitude was greatest in 10wk. 10wk rats had higher jejunal NaPi2b mRNA than 20wk and 30wk rats ($p=0.002$ & $p=0.02$), but there was no effect of diet ($p=0.14$), consistent with our previously reported increased P absorption at 10wk versus 20wk and 30wk of age. LP diet increased duodenal NaPi2b mRNA expression, but only in 10wk ($p=0.001$). There were no significant effects for age or diet in Pit1 mRNA in the duodenum ($p=0.50$). In contrast to the decrease in NaPi2b with age, there was an increase in jejunal Pit1 mRNA expression at 30 weeks compared to 10wk and 20wk ($p=0.002$). These results show that higher P absorption observed in younger normal SD rats is due to higher 1,25D and lower PTH and FGF23, resulting in upregulation of NaPi2b. Overall, LP diet caused expected changes in P-regulating hormones, but only upregulated NaPi2b at 10wk and only in the duodenum, and had no effect on Pit1. This corresponds with the lack of effect of diet P level on intestinal P absorption assessed in the jejunum in these rats.

Disclosures: Colby Vorland, None

SAT-0988

Effects of selective estrogen receptor modulator and low-intensity aerobic exercise on bone and fat parameters in ovariectomized rats Yusuke Yuasa^{*}, Naohisa Miyakoshi, Yuji Kasukawa, Itsuki Nagahata, Manabu Akagawa, Yuichi Ono, Chiaki Sato, Yoichi Shimada. Department of Orthopedic Surgery, Akita University Graduate School of Medicine, Japan

Introduction Estrogen deficiency decreased bone mineral density (BMD) and dyslipidemia. The selective estrogen receptor modulator bazedoxifene (BZA) may inhibit both diseases. However, the effects of treatment with a combination of BZA and exercise are unclear. In this study, we examined the effects of BZA and exercise on bone and fat parameters in ovariectomized (OVX) rats. Methods Sixteen-week-old Sprague Dawley female rats were OVX and randomized into the following 4 groups (n=6-9) after 8 weeks: (1) BZA group, 0.3 mg/kg/day BZA orally; (2) Ex group, exercised by treadmill at 12-15 m/min, 60 min/day, 5 days/week; (3) Combined (COMB) group, treated with BZA and exercised by treadmill; and (4) Control (CNT) group, treated with vehicle of BZA and no exercise. BZA administration and/or exercise were continued for 4 or 8 weeks. After sacrifice, BMD of the total femur and lumbar spine (L2-4, LS) as well as body fat percentage were measured by dual-energy x-ray absorptiometry (DXA). Bone histomorphometry was performed at the proximal tibia. Adipocyte volume per total bone marrow volume (AV/MV), number of adipocytes per unit area of marrow (N.A/MV), and volume of each adipocyte per number of adipocytes (AV/N.A) were evaluated in the bone marrow of the proximal tibia. Mechanical strength of the femoral shaft were measured using the three-point bending test. Results BMD of the LS was significantly higher in the BZA and COMB groups than in the Ex and CNT groups ($p < 0.05$) at 4 weeks. After 8 weeks of treatment, only the BMD of the LS in the COMB group was significantly higher than that in the Ex and CNT groups ($p < 0.05$). Body fat percentages were significantly lower in the BZA and COMB groups than in the CNT group ($p < 0.05$) at 4 and 8 weeks. AV/MV ratios were significantly lower in the Ex and COMB groups than in the CNT group ($p < 0.05$), and AV/N.A ratios were significantly lower in the Ex and COMB groups than in the BZA and CNT groups ($p < 0.05$) at 4 weeks. AV/MV and AV/N.A were significantly lower in the Ex, BZA, and COMB groups than in the CNT group ($p < 0.01$) at 8 weeks. Breaking times were significantly longer in the COMB groups than in the CNT group

($p < 0.05$) at 4 and 8 weeks. Conclusion A combination of BZA and exercise improved BMD of the LS, body fat percentage, bone marrow adipocytes, and breaking time. Combination therapy with BZA and exercise has positive effects on BMD and fat metabolism in OVX rats.

Disclosures: *Yusuke Yuasa, None*

SAT-1019

See Friday Plenary Number FRI-1019

SAT-1020

See Friday Plenary Number FRI-1020

SAT-1021

See Friday Plenary Number FRI-1021

SAT-1022

See Friday Plenary Number FRI-1022

SAT-1023

See Friday Plenary Number FRI-1023

SAT-1024

See Friday Plenary Number FRI-1024

SAT-1025

See Friday Plenary Number FRI-1025

SAT-1026

See Friday Plenary Number FRI-1026

SAT-1027

See Friday Plenary Number FRI-1027

SAT-1028

See Friday Plenary Number FRI-1028

SAT-1029

Clinical features of Sternocostoclavicular Hyperostosis: a large Single Center Dutch Cohort Ashna Ramautar*, Natasha Appelman-Dijkstra, Shannon Lakerveld, Pieter Valkema, Marieke Snel, Marielle Schroijen, Liesbeth Winter, Neveen Hamdy. LUMC, Netherlands

Sternocostoclavicular hyperostosis (SCCH) is a rare inflammatory bone disorder due to a chronic sterile osteomyelitis of unknown origin, leading to hyperostosis and sclerosis of sternum, medial end of clavicles and first ribs. Other areas of the axial skeleton such as mandible and vertebrae may also be affected. We report the clinical characteristics of a large single centre Dutch cohort of 189 patients with an established diagnosis of SCCH on the basis of characteristic clinical, scintigraphic and radiological features. Data on gender, age at first symptoms and at diagnosis, clinical manifestations, shoulder girdle function, and disease-related incapacity for work, were retrieved from medical records. The cohort consisted of 189 patients, predominantly female (88%), with a median age of 37 years (range 17-70) at first symptom. Most common first symptoms were pain in 159 patients (85%), local inflammatory changes in 77 (41%), impairment of shoulder girdle function in 63 (34%), and bone swelling in the SCC region in 54 (29%). At time of diagnosis, which occurred after a mean delay of 5 ± 5 years, main clinical manifestations were chronic pain of variable severity in the SCC region in 183 (95%), bony swelling of affected areas of the anterior chest wall in 124 (66%) and restricted shoulder girdle function in 81 patients (43%). 64 patients (35%) had palmoplantar pustulosis, and 47 (25%) had an autoimmune disease, mainly psoriasis ($n=15$, 8%). The most commonly affected sites were the medial end of the clavicles in 76% of patients, followed by medial end of first ribs in 64%. Mandible and vertebrae were less commonly affected. SCCH is a rare inflammatory bone disorder associated with variable degrees of disability leading to potential disease-related incapacity to work due to chronic pain

and impairment in shoulder girdle function. Initial symptoms may be elusive, and delayed diagnosis is common because of inability to identify the clinical features of the disorder. This may result in irreversible structural changes in the SCC region and potentially debilitating chronic symptoms. Early diagnosis and early institution of therapy may positively influence prognosis by preventing disease progression, although this remains to be established by long-term follow-up studies.

Disclosures: *Ashna Ramautar, None*

SAT-1030

Joint Replacement Procedures in Individuals with Skeletal Dysplasias Kate Citron*, Sobiah Khan, Erin Carter, Mathias Bostrom, Mark Figgie, Cathleen Raggio. Hospital for Special Surgery, United States

INTRODUCTION: Skeletal dysplasias are a heterogeneous group of more than 400 genetic disorders characterized by abnormal growth and remodeling of cartilage and bone. Many individuals experience joint pain and limitation. Epiphyseal development is affected in many of these disorders, resulting in hindered endochondral ossification. Joint replacements are usually required much earlier and survival rate of the prosthesis is shorter than in individuals without these disorders. Underlying medical conditions, including cardiovascular and pulmonary issues, are common, as are other orthopaedic issues such as atlantoaxial instability, spinal deformity, and spinal stenosis. Use of BMI to predict failure is not reliable in this short-statured population. **METHODS:** This is an IRB-approved, retrospective chart review of 19 individuals (14 women and 5 men) with a confirmed diagnosis of a skeletal dysplasia who underwent joint replacement surgery. **RESULTS:** 19 individuals enrolled had 41 surgeries: 33 hip replacements, 4 knee replacements, and 4 shoulder replacements. The average age, height, weight, and BMI were 41.5 years, 126.0 cm, 56.6 kg, and 35.1, respectively. Average follow up was 5.9 years. 43.9% of surgeries were done on individuals with an underlying cardiovascular or pulmonary condition. All individuals had decreased pain and mobility after surgery. 14.6% of surgeries required revision. 19.5% of surgeries performed on 6 individuals had serious post-operative complications, including hematoma, pulmonary embolism, effusion secondary to staph infection, deep vein thrombosis, myocardial infarction and pneumonia. 7/8 of the surgeries with a serious complication were done on individuals with an underlying cardiovascular/pulmonary condition. No individuals died in surgery. **DISCUSSION:** Our study supports existing literature that have concluded that individuals with skeletal dysplasias have decreased pain and increased function after joint replacement. Short stature skews BMI. Based on our results BMI does not seem predictive of complication risk in this population. Pre-existing cardiovascular or pulmonary disorder as a better indication of complication risk, as 7/8 surgeries (88%) that resulted in serious complication were done on individuals with a pre-existing cardiovascular and/or pulmonary condition.

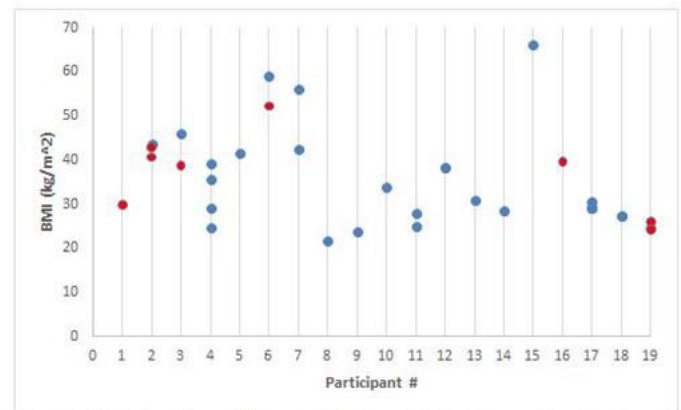


Figure 1. BMI of study participants with those with major complications in red.

Disclosures: *Kate Citron, None*

SAT-1031

Iatrogenic Osteosclerosis in Osteogenesis Imperfecta Vandana Dhiman*¹, Anshita Aggarwal², Nirmal G Raj³, Ruban Dhaliwal⁴, Sanjay Kumar Bhadada⁵, Naresh Sachdeva³, Sudhaker D Rao⁶. ¹PhD student, India, ²DM Resident, India, ³Additional Professor, India, ⁴Assistant Professor, United States, ⁵Professor, India, ⁶Professor, United States

Purpose: Bisphosphonates (BPs) are widely used for treatment of osteogenesis imperfecta (OI). However, prolonged use may be associated with suppression of bone turnover, the exact molecular mechanism of which is poorly understood. Caspase-3 activity is necessary for osteoclast differentiation. The objective of this study was to evaluate the effect of zoledronic acid (ZOL) on precursor osteoclasts by studying the caspase-3 activity. **Methods:** Total 15 children were enrolled in the study ($n = 10$ with OI, $n = 5$ controls). Out of the 10 children with OI, six had OI type IV, two had type III and two had types I & II each. Five children with OI had received a cumulative dose of ZOL < 30 mg and the other five had received ≥ 30 mg. Serum bone turnover markers (P1NP, CTX) were measured in these serum

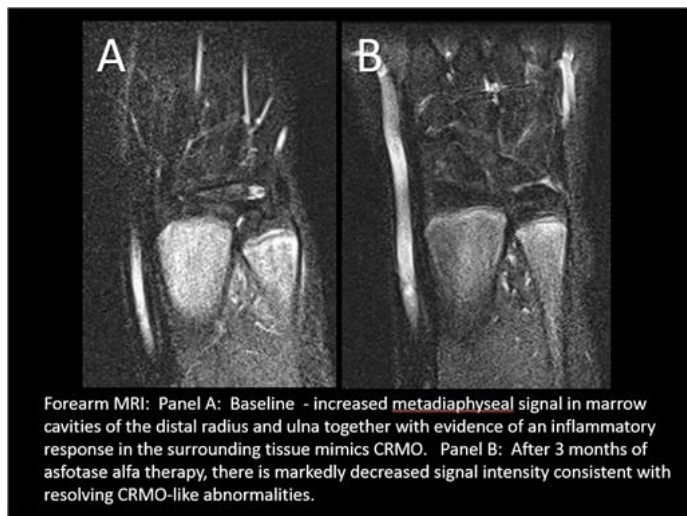
of all participants. Peripheral blood mononuclear cells were isolated from all participants and studied for caspase-3 activity. Results: The mean age of study participants was 7 ± 1.5 years. Radiographs showed "zebra stripe sign" and dense metaphyses, suggestive of acquired osteosclerosis. Bone turnover markers (BTM) were suppressed in all OI patients compared to controls. Caspase-3 activity increased in osteoclasts at higher doses of BPs (>30 mg). Conclusions: Overzealous use of ZOL in OI suppresses bone turnover markers (PINP, CTX), causes osteosclerosis and increases expression of caspase-3 activity in osteoclasts which results in adynamic bones.

Disclosures: *Vandana Dhiman, None*

SAT-1032

Childhood Hypophosphatasia: Painful Bone Marrow Edema Mimicking Chronic Recurrent Multifocal Osteomyelitis Improved After Three Months of Asfotase Alfa Enzyme Replacement Therapy Gary S Gottesman¹, Deborah Wenkert¹, William H Mcalister², Geetika Khanna², Karen Mack¹, Steven Mumm², Michael P Whyte¹. ¹Shriners Hospital for Children - St. Louis, United States, ²Washington University School of Medicine, United States

Hypophosphatasia (HPP) is the inborn-error-of-metabolism that features hypophosphatemia, tooth loss, and impaired skeletal mineralization with varying expressivity. In 2009, we reported an unrelated boy and girl with childhood HPP and recurrent periarticular soft tissue swelling and pain, primarily at the distal forearms and ankles. Radiographic, histopathologic, and MRI findings, including bone marrow edema, mimicked chronic recurrent multifocal osteomyelitis (CRMO). The pathogenesis remained unknown. Herein, we report a teenage boy with childhood HPP and 7 episodes of recurrent wrist swelling and pain (5 episodes within the preceding 3 years). At age 9 years, he reported brief morning stiffness and intermittent leg pain treated with non-steroidal medications (NSAIDs). He had no fever or mucocutaneous or gastrointestinal symptoms. Each episode occurred with minor trauma causing rapid localized swelling and was associated with point tenderness. Conservative treatment with casting, for presumed Salter-Harris I growth plate fractures, improved the pain and swelling. The NSAIDs were usually taken twice weekly for pain. At 13 years of age, our review of his interval radiographs revealed slight worsening of the changes typical of HPP at his wrists and knees. We then explored the most recent episode with an MRI of his forearms and hands, which showed metadiaphyseal signal increases consistent with CRMO. Additionally, functional testing confirmed new gross motor deficits consistent with childhood HPP. Mutational analysis of ALPL identified a novel heterozygous ~65 base pair deletion 5' of exon 4 that removed the splice site. With a worsening clinical status during his pubertal growth spurt, we started asfotase alfa enzyme replacement therapy (ERT). Three months later, pain had resolved (off NSAIDs), and follow-up MRI showed significant improvement of the metadiaphyseal bone edema (Figure). C-reactive protein and erythrocyte sedimentation rate were normal at baseline and the follow-up. Procollagen type I amino-terminal peptide, elevated at baseline, fell 3.6-fold but was still increased; collagen carboxy-terminal telopeptide also elevated at baseline, had normalized. Autoinflammatory mechanisms are considered an etiology for CRMO. Our patient's response to ERT alone suggests that CRMO-like lesions in HPP reflect a metabolic consequence of the alkaline phosphatase deficiency.



Disclosures: *Gary S Gottesman, None*

SAT-1033

A case report of the novel use of asfotase alfa to improve outcomes after spinal surgery for dystrophic scoliosis related to neurofibromatosis type 1 Tasma Harindhanavudhi¹, Takashi Takahashi¹, Anna Petryk², David Polly¹. ¹University of Minnesota, United States, ²Alexion Pharmaceuticals, United States

Dystrophic scoliosis is a rare and serious skeletal manifestation in neurofibromatosis type 1 (NF1) patients. Dystrophic curves progress rapidly and require early fusion, often complicated by poor bone healing and lack of fusion (pseudoarthrosis). Due to poor bone quality, patients may experience loosening of the spinal instrumentation with rods displacement into the surrounding soft tissue leading to serious neurological complications. Poor bone quality in NF1 is multifactorial and caused by a reduction of bone formation, increased bone resorption, and poor bone mineralization due to accumulation of a mineralization inhibitor, inorganic pyrophosphate (PPi), and impaired osteoblast differentiation with reduced alkaline phosphatase expression. There is a need to develop effective medical approaches to improve surgical outcomes. Asfotase alfa (AA, STRENSIQ®) is a recombinant human alkaline phosphatase approved for the treatment of pediatric-onset hypophosphatasia (HPP). Subcutaneous administration of AA in HPP reduces serum PPi concentration and improves bone mineralization. In a mouse model of NF1, AA also improved bone mineralization and strength. Its use in humans with NF1 has not been previously reported. We describe a case of a 54-year-old woman with NF1 who underwent 3 spinal surgeries for advanced dystrophic scoliosis over the past 7 years, complicated by advanced dural ectasia and pseudoarthrosis. She continued to have progressive loosening of the spinal instrumentation, paresthesia of the thighs, and intractable back pain. A CT scan revealed a fracture of the left vertebra at the L4 pedicle screw connection, left posterior iliac screw loosening and a periscrew fracture, necessitating the 4th spinal surgery. Given a high probability of failing, she received all available treatments, including intrasurgical bone morphogenetic proteins (BMPs) to enhance bone formation, zoledronic acid to inhibit bone resorption (5 mg IV at 3 months after surgery x1), and off-label AA to improve bone mineralization (2 mg/kg 3x/week s.c. injection from 7 to 13 months after surgery) without adverse events. A CT showed stable instrumented spinal fusion and healed fracture at the tip of the left posterior iliac screw without evidence of loosening 13 months after surgery. In conclusion, AA in combination with BMPs and a bisphosphonate resulted in solid arthrodesis and enhanced bone healing after spinal surgery in a patient with NF1-related dystrophic scoliosis.

Disclosures: *Tasma Harindhanavudhi, Alexion Pharmaceuticals, Grant/Research Support*

SAT-1034

A novel TRPS1 mutation in a patient with tricho-rhino-phalangeal syndrome provides further support for the importance of this zinc-finger transcription factor in skeletal development Anara Karaca¹, Lauren Toyomi Shumate¹, Monica Reyes¹, Isilay Taskaldiran², Tulay Omma², Nese Ersoz Gulcelik³, Murat Bastepe¹. ¹Endocrine Unit, Massachusetts General Hospital and Harvard Medical School, United States, ²Ankara Training and Research Hospital, Endocrinology, Turkey, ³University of Health Sciences, Gulhane Training Hospital, Turkey

Brachydactyly type E (BDE), inherited as an autosomal dominant trait with variable expressivity, is shortening of one or more metacarpals or metatarsals and can often involve digits. Genetic aberrations in genes that are important during maturation of growth plate chondrocytes typically lead to BDE, including PTHLH, PRKAR1A, PDE4D, HOXD13, HDAC4, and TRPS1. Depending on the mutated gene, the patient may display additional features, such as hormone resistance, facial dysmorphism, and cognitive impairment. Herein we report two unrelated Turkish females with an autosomal dominant pattern of BDE. The first patient had severe BDE and short stature, while the second had relatively milder BDE with normal height. Neither patient showed evidence of hormone resistance or cognitive impairment. We screened the patients for PTHLH, PDE4D, and TRPS1 mutations by Sanger sequencing of exons and flanking intronic regions. In the first patient, we identified a novel heterozygous missense mutation in exon 6 (c.2783A>G, p. Tyr928Cys) of TRPS1. The second patient was found to have a previously described heterozygous nonsense mutation in exon 4 (c.1870C>T, p. Arg624Ter) of the same gene. Mutations in TRPS1 cause a tricho-rhino-phalangeal syndrome (TRPS). Along with BDE, the hallmarks of the syndrome include sparse hair, a pear-shaped nose with bulbous tip, an underdeveloped alae nasi, and a long flat philtrum. These phenotypic features were largely present in our patients. While the nonsense mutation identified in the second patient is predicted to lead to nonsense-mediated decay and loss of protein, the novel Tyr928Cys variant is located in the GATA DNA-binding domain, which is critical for the function of TRPS1, a zinc-finger transcriptional repressor. Multiple other mutations have been previously identified in nearby residues of this domain. The Tyr928Cys variant is absent from the Genome Aggregation Database of control populations, and in silico tools (SIFT, MutationTaster, Polyphen-2) predict it to impact protein function. Therefore, this variant is likely pathogenic. Missense mutations, particularly within the GATA DNA-binding region, are associated with significantly more severe BDE and short stature than nonsense mutations. Thus, the novel mutation in our first patient explains her severe phenotype. Our findings emphasize the role of TRPS1 in skeletal development and highlight the GATA DNA-binding region with respect to phenotype-genotype correlation in patients with TRPS.

Disclosures: *Anara Karaca, None*

SAT-1035

Bruck Syndrome Variant Lacking Congenital Contractures Due To Novel Compound Heterozygous PLOD2 Mutations Steven Mumm^{*1}, Gary S. Gottesman², Philippe M. Campeau³, Angela Nenninger², Margaret Huskey¹, Vinieth N. Bijanki², Deborah J. Veis¹, Aileen Barnes⁴, Joan C. Marini⁴, Deborah Wenkert², William H. McAlister⁵, Michael P. Whyte². ¹Division of Bone and Mineral Diseases, Department of Internal Medicine, Washington University School of Medicine, United States, ²Center for Metabolic Bone Disease and Molecular Research, Shriners Hospital for Children, United States, ³Department of Pediatrics, University of Montreal, Canada, ⁴National Institute of Child Health and Human Development, NIH, United States, ⁵Mallinckrodt Institute of Radiology, Washington University School of Medicine at St. Louis Children's Hospital, United States

A 10-year-old girl was referred for an unidentified skeletal dysplasia featuring osteopenia with poorly-healing fragility fractures, short stature, Wormian bones in her skull, cleft soft palate and uvula, congenital fusion of cervical vertebrae, bell-shaped thorax, progressive scoliosis, restrictive and reactive pulmonary disease, blue sclera, and other dysmorphic features. Previously, chromosome 22q11 deletion analysis for velocardiofacial syndrome and COL1A1 and COL1A2 sequencing were negative. Iliac crest biopsy revealed low trabecular connectivity, abundant osteoid, and active bone formation featuring widely-spaced tetracycline labels consistent with osteogenesis imperfecta (OI). Alendronate treatment improved her bone density. Copy number microarray excluded a contiguous gene syndrome. Sanger sequencing of LRP5, PPIB, FKBP10, and IFITM5 was negative. Instead, exome sequencing revealed two novel missense variants in PLOD2 (exon 8, c.797G>T, p.Gly266Val; exon 12, c.1280A>G, p.Asn427Ser) which encodes procollagen-lysine, 2-oxoglutarate 5-dioxygenase 2 (lysyl hydroxylase 2, LH2). In ExAC, absence (Asn427Ser) and low frequency (Gly-266Val, 0.0000419) implicated both as mutations. The father carried the exon 8 mutation whereas the mother and sister carried the exon 12 defect, and all were well. Autosomal recessive (AR) PLOD2 mutations cause Bruck syndrome 2 (OMIM #609220) reported in at least 20 cases/15 families as a rare OI featuring congenital contractures of large joints, typically with pterygia, a feature not seen in our patient. Defective LH2 causes under-hydroxylated type I collagen telopeptides compromising crosslinking. Most PLOD2 missense mutations causing Bruck syndrome 2 are located in exons 17-19 (of 20 total) encoding the C-terminal domain having LH activity, but others are truncating defects (frameshift, splice site mutations) found throughout the gene. AR PLOD2 mutations causing mild or moderate OI without congenital contractures have been reported in only three cases. Our patient represents the fourth such patient. Her PLOD2 missense mutations are in the central domain of unknown function, and one (Gly266Val) is the most N-terminal missense defect to date. Hence, our patient's novel PLOD2 mutations underlie a distinctive skeletal phenotype. Atypical Bruck syndrome should be considered as a possibility in COL1A1 and COL1A2-negative OI cases

Disclosures: *Steven Mumm, None*

SAT-1036

Prevalence of Hypophosphatasia in a Reference Hospital in Granada (Spain) Manuel Muñoz-Torres^{*1}, Cristina García Fontana², Juan Miguel Villa Suarez³, Francisco Andújar-Vera², José María Gómez Vida⁴, Tomás De Haro³, Beatriz García-Fontana García-Fontana⁵. ¹Endocrinology and Nutrition Unit. University Hospital San Cecilio. Department of Medicine. University of Granada. Biomedical Research Institute of Granada. (ibs GRANADA), Spain, ²Biomedical Research Institute of Granada. (ibs GRANADA), Spain, ³Clinical Analyses Unit. University Hospital San Cecilio., Spain, ⁴Pediatric Unit. University Hospital San Cecilio, Spain, ⁵Endocrinology and Nutrition Unit. University Hospital San Cecilio. Biomedical Research Institute of Granada. (ibs GRANADA).CIBERFES. ISCIII., Spain

Hypophosphatasia (HPP) is a rare, serious and potentially mortal genetic disease caused by one or several mutations in the gene coding for the alkaline phosphatase without tissue specificity (TNSALP). A low serum total alkaline phosphatase (ALP) level is the hallmark for the diagnosis of HPP. Objective: To assess the recognition of persistent low ALP levels in a tertiary care hospital in Granada (Spain) to identify the patients affected with HPP and to provide an appropriate management of these patients. Subjects & Methods: An assessment of ALP levels was performed in 78590 patients between 1st of January and 31st of December 2016 in the Biochemistry Unit of our hospital. The database was divided into adult population and pediatric population. Ninety-eight patients (66 adults and 32 children) had several serum ALP values persistently below the reference interval. Twenty-two patients were discarded because of potential causes of secondary HPP. Twenty-four potential HPP patients were contacted to fulfill a questionnaire about clinical manifestations HPP-related. Pyridoxal-5'-phosphate (PLP) was determined by high-performance liquid chromatography (HPLC) and sequencing TNSALP gene was performed. This project was approved by Ethical Committee from Granada. Results: 0.12% of the studied patients had persistently low value of ALP (65% females). Twenty-four were contacted. Ten of them had fractures, 4 had symptomatic chondrocalcinosis and 4 had dental abnormalities. From them, 11 patients (9 adults and 2 children) presented decreased ALP and increased PLP levels, of which, 7 adults had TNSALP mutations (4 corresponding to new variants not described previously). In conclusion our study shows that there are several omitted diagnostics of HPP in a tertiary care

hospital. From 78590 patients analyzed, 7 of them presented TNSALP mutation obtaining 2 new genetic variants. These data indicate an estimated prevalence of 9/100.000 in our area.

Disclosures: *Manuel Muñoz-Torres, None*

SAT-1037

Asfotase Alfa: Interference with ALP-detection systems in immunoassays Isabelle Piec^{*}, Beatrice Thompkins, William D. Fraser. University of East Anglia, United Kingdom

Asfotase alfa (AA, STRENSIQ®, Alexion Pharmaceuticals, Inc.) is the first FDA-Approved treatment for patients with hypophosphatasia, the result of a mutation in the tissue-nonspecific alkaline phosphatase (ALPL) gene. ALP continues to be used as the measuring/signalling system in routine assays for proteins, hormones and other small molecules, albeit less and less commonly. Because it contains the ALP active site, AA is able to catalyse the substrate as the antibody-conjugated ALP would within an assay. Therefore, AA present in a patient's sample may generate a false positive or a false negative assay result. We investigated whether the presence of AA within a sample induces interference in sandwich and competitive assays using plate based assays and on a routine automated analyser that use ALP or alternative detection systems. AA was added to samples at concentrations from 0.08-5 µg/mL. Manual ELISAs and COBAS6000 assays were tested. We observed no significant change in the absorbance of ALP measured using the RayBiotech assay for ALKP1, Normetanephrine (IBL) in urine samples (hydrolysed or not) and nor adrenaline (IBL) at any AA concentration. However, AA significantly cross-reacted with an oxytocin assay (ENZO, p<0.001), in a concentration dependant manner in non-extracted samples (false negative results). Recommended extraction of the samples for this assay using a C18 column. While the ALP activity showed a significant (p<0.0001) AA concentration-dependant increase, the concentration of the analytes of interest did not change by more than 2.4% from the baseline value for assays run on the COBAS analyser (TSH, LH, FSH). Assays using a different detection system than ALP were not affected by the presence of AA in the samples. Most assays tested using ALP detection systems were sufficiently specific not to show interference with AA. Oxytocin needed to be extracted to demonstrate this specificity. The effects observed depended on the method of ALP detection used. The presence of AA must be taken into consideration when analysing blood samples using certain assay technology to avoid any risk of misinterpretation of false positive/negative results

Analyte	Assay type	Format	Manufacturer	Detection system	Interference
ALP	ELISA (Manual)	Enzyme activity	RayBiotech	HPP	YES
IL6		Sandwich	R&D systems	ALP/NADPH	No
Oxytocin		Competitive	IBL/ biosupply	ALP/PNPP	YES on non extracted samples
Adrenaline		Sandwich	IBL/ Camb. Bios	ALP/PNPP	No
Normetanephrine	Competitive	IBL/ Camb. Bios	ALP/NADPH	No	No
LH	ADVIA analyser	Direct	Siemens	acridinium ester	No
TSH		Direct		acridinium ester	No
ALP	COBAS 6000 analyser	Direct	Roche	pNPP	YES
Free T4		Competitive		ruthenium	No
TSH		Direct		ruthenium	No
LH	Architect c16000 analyser	Direct	Abbott	acridinium ester	No
FSH		Direct		acridinium ester	No

Table: Assay information and effect of asfotase alfa.

Disclosures: *Isabelle Piec, Alexion Pharmaceuticals, Inc., Grant/Research Support*

SAT-1038

Hypophosphatasia: Clinical Presentation Jay R Shapiro^{*}. Uniformed Services University of the Health Sciences, United States

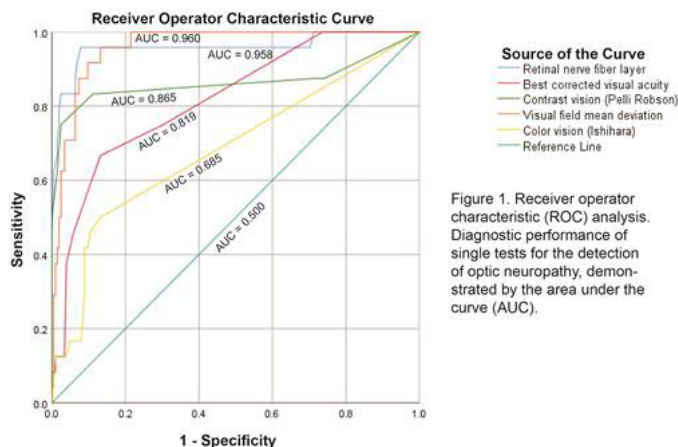
Hypophosphatasia (HPP) is a rare metabolic bone disorder inherited in either an autosomal recessive or dominant form. Approximately 500 cases are recognized in the US although the actual incidence may be several fold that number. HPP is notable for marked variability in clinical expression. A low serum tissue non-specific alkaline phosphatase (TNSALP) level is the hallmark of HPP. However, the clinical expression of that defect is highly variable over the lifespan ranging from life threatening or severe in infants, to varied clinical expression ranging from asymptomatic to severe in adults. This report describes the clinical findings in 6 patients with HPP ages 16-62 years. (Table). DXA scores vary from normal to osteoporotic regardless of age. There is no apparent genotype/phenotype correlation. Serum Vit B6 levels are elevated in most individuals. In certain patients, treatment with asfotase alfa may improve bone density and function. Conclusion: HPP is rare disorder in which the diagnosis is based on low serum TNSALP levels, This abnormal test result may frequently be overlooked or misinterpreted when a patient is evaluated for osteoporosis and/or a history of fractures.

Disclosures: *Jay R Shapiro, None*

SAT-1070

Utility of Optical Coherence Tomography in the Diagnosis of Optic Neuropathy in Fibrous Dysplasia of Bone Kristen S Pan ^{*1}, Alison M Boyce¹, Edmond J Fitzgibbon², Michael T Collins¹, Janice S Lee³. ¹Skeletal Disorders and Mineral Homeostasis Section, National Institute of Dental and Craniofacial Research, National Institutes of Health, United States, ²Laboratory of Sensorimotor Research, National Eye Institute, National Institutes of Health, United States, ³Office of the Clinical Director, National Institute of Dental and Craniofacial Research, National Institutes of Health, United States

Fibrous dysplasia (FD) is an expansile bone disorder that frequently affects the cranial base, resulting in encasement of the optic canal. Rarely, compression and/or traction of the optic nerve may result in optic neuropathy (ON). Optic nerve decompression can prevent blindness; however, surgery may also lead to vision loss. Optical coherence tomography (OCT), an imaging modality to measure retinal nerve fiber layer (RNFL) thickness, has emerged as a potential diagnostic and prognostic tool for compressive ON and visual recovery. Some clinicians have advocated using OCT to identify patients who may benefit from optic nerve decompression. The purpose of this study was to evaluate the utility of OCT findings in the management of ON. 159 neuro-ophthalmologic exams and concurrent OCTs were reviewed from 81 subjects with FD. The diagnosis of ON was defined by abnormal results on 2 of the following tests: 1) best corrected visual acuity, 2) visual fields (Humphry Visual Field Analyzer), 3) color vision (16 Ishihara plates), 4) contrast sensitivity vision (Pelli Robson chart), and 5) fundus examination. The performance of each test, including RNFL thickness, in diagnosing ON was determined using receiver operator characteristic (ROC) analyses. The following area under the curve (AUC) values, listed best to worst, were generated ($p < 0.005$, compared to $AUC = 0.5$): visual field mean deviation = 0.960 (SE 0.01, 95% CI 0.934–0.987), RNFL = 0.958 (0.29, 0.90–1.00), contrast vision = 0.865 (0.06, 0.75–0.98), best corrected visual acuity = 0.819 (0.05, 0.73–0.91), color vision = 0.684 (0.07, 0.56–0.81). Based on 95% CI, the AUC for visual field mean deviation, RNFL thickness, contrast vision, and best corrected visual acuity were not different. An RNFL thickness of $\leq 75 \mu\text{m}$ was the cutoff that yielded the greatest sensitivity and specificity (0.92 and 0.93) for diagnosing ON. These data, demonstrate that OCT measurement of RNFL thickness is not the best single test for diagnosing ON in FD. Also, RNFL thickness used as a single test for ON carries an unacceptably high false positive rate of 7%, even when optimized. Given the high morbidity of surgical ON decompression, we advocate that RNFL thickness be used in combination with additional testing, to confirm diagnosis of ON in patients with FD.



Disclosures: *Kristen S Pan, None*

SAT-1077

See Friday Plenary Number FRI-1077

SAT-1078

See Friday Plenary Number FRI-1078

SAT-1079

See Friday Plenary Number FRI-1079

SAT-1080

See Friday Plenary Number FRI-1080

SAT-1081

See Friday Plenary Number FRI-1081

SAT-1082

See Friday Plenary Number FRI-1082

SAT-1083

See Friday Plenary Number FRI-1083

SAT-1084

Microarray Expression Profile Analysis and its Clinical Implication for the Treatment of Fibrogenesis Imperfecta Ossium Sanjay Kumar Bhadada^{*1}, Vandana Dhiman², Ruban Dhaliwal³, Anil Bhansali¹, Wim Van Hul⁴, Sudhaker D Rao⁵. ¹Professor, India, ²PhD student, India, ³Assistant Professor, United States, ⁴Professor, Belgium, ⁵Professor, United States

Introduction: Fibrogenesis imperfecta ossium (FIO) is a rare bone disease manifested by generalized by bone pain, fragility fractures, progressive disability, and extensive mineralization defect on bone biopsy. The molecular pathogenesis and treatment stratification of FIO is not clearly known. Hence, the present study is designed to study to identify putatively involved genes in the pathogenesis of FIO based on their expression profile. **Methods:** Two siblings (males, 48 and 38 years) with FIO were recruited for differential gene expression and compared with healthy controls by using global microarray (Affymetrix Genechip, Human Primview) and then analyzed by Gene Spring GX 12.1 software. We explored the topological characteristics of differentially expressed genes in the context of the human interactome and furthermore analyzed for pathway annotations using reactome and NCBI gene database. **Results:** We observed downregulation of Secreted protein and acidic rich in cystine encoding osteonectin and osteocalcin respectively. The mineralization defect and clinical finding of pseudo fractures can be explained by down regulation of genes involved in mineralization, namely Secreted phosphoprotein (SPP1) and BGLAP. We found upregulation of Osteoporosis associated transmembrane protein 1 (OSTM1) involved in osteoclastogenesis. Similarly, we also observed increase in collagen expression but a decrease in expression of signalling molecules such as Matrix metalloproteinases and Intercellular adhesion molecules (MMP1 and ICAM) involved in the assembly of these collagen fibrils leading to defective collagen synthesis. **Conclusion:** Altered gene expression profile in FIO suggests the molecular mechanisms underlying the defect in mineralization and collagen synthesis in this rare bone disorder. The effect on potential therapies on these genes can be studied to identify an effective treatment for FIO.

Disclosures: *Sanjay Kumar Bhadada, None*

SAT-1085

Whole-cell proteomic profiling of osteoclasts from a mouse model for craniometaphyseal dysplasia Jitendra Kanaujiya^{*1}, Jeremy Balsbaugh², Ernst Reichenberger¹, I-Ping Chen¹. ¹University of Connecticut Health, United States, ²University of Connecticut, United States

Craniometaphyseal dysplasia, a rare genetic disorder characterized by hyperostotic craniofacial bones and flaring metaphyses of long bones, can be inherited by autosomal dominant (AD) or autosomal recessive (AR) forms. We have previously reported a knock-in (KI) mouse model expressing a F377del mutation in ANK, one of the most common mutations for AD CMD. AnkKI/KI mice replicate many features of CMD. AnkKI/KI osteoclasts are smaller in size with disrupted actin rings and resorb less bone when cultured on bone chips. Here we examine via liquid chromatography-mass spectrometry (LCMS) and bioinformatics data mining whether proteomic profiles of AnkKI/KI and Ank+/+ osteoclasts differ, and whether the differentially expressed proteins in AnkKI/KI osteoclasts can be clustered in the context of cell regulatory pathways. Bone marrow-derived macrophage (BMM) cultures were derived from 8-week-old Ank+/+ and AnkKI/KI male mice. Cell lysates were prepared from BMMs treated with MCSF and RANKL for 2.5 days using a previously published Filter-Aided Sample Preparation (FASP) protocol. After proteolysis, peptides were labeled using a Duplex Tandem Mass Tag (TMT) kit (Thermo Fisher Scientific). Equimolar amounts of samples were pooled and analyzed on a Thermo Q Exactive HF mass spectrometer. All raw data were analyzed using Proteome Discoverer 2.2 software for peptide/protein identifications and TMT reporter ion-based abundance ratios. Further classification of these proteins was analyzed by gene ontology. LCMS data of Ank+/+ and Anknull/null BMMs were compared to Ank+/+ and AnkKI/KI data. Each LCMS biological replicate identified and quantified over 3000 proteins. Approximately 100 proteins were differentially expressed between Ank+/+ and AnkKI/KI osteoclasts ($p < 0.05$) with about 90% targets down-regulated in AnkKI/KI osteoclasts. These targets were mainly involved in cellular processes and metabolic processes with binding or catalytic activity. Three major clusters of these proteins emerged: 1) signaling pathways (Wnt, FGF, Toll-like receptors); 2) cytoskeleton regulation; 3) inflammation. While ANK is undetectable in Anknull/null BMMs, ANK was found significantly decreased in AnkKI/KI osteoclasts. Targets only being affected in AnkKI/KI but not

Anknull/null BMMs suggested unique effects of CMD-mutant ANK. These results will help us to understand CMD pathogenesis and to potentially develop therapeutic targets for CMD.

Disclosures: Jitendra Kanaujiya, None

SAT-1086

Lack of mature collagen-links is associated with osteomalacia in patients with X-linked hypophosphatemia Nadja Fratzl-Zelman^{*1}, Stamatia Rokidi¹, Stéphane Blouin¹, Pia Plasenzotti², Kamilla Nawrot-Wawrzyniak¹, Katharina Roetzer³, Goekhan Uyanik³, Gabriele Haessler⁴, Klaus Klaushofer¹, Peter Fratzl⁵, Eleftherios Paschalis¹, Paul Roschger¹, Elisabeth Zwettler^{1,6}, Ludwig Boltzmann Institute of Osteology at the Hanusch Hospital of WGKK and AUVA Trauma Centre Meidling, 1st Medical Department Hanusch Hospital, Austria, ²1st Medical Department, Hanusch-Hospital, Austria, ³Center for Medical Genetics, Hanusch-Hospital, Austria, ⁴Department of Pediatrics, Medical University of Vienna, Austria, ⁵Max Planck Institute of Colloids and Interfaces, Department of Biomaterials, Germany, ⁶Medical Directorate, Hanusch-Hospital, Austria

X-linked hypophosphatemia (XLH) is caused by inactivating mutations in the PHEX gene, resulting in decreased circulating phosphate, low 1,25-dihydroxyvitamin D levels and osteomalacia. Osteopontin, a potent inhibitor of mineralization normally degraded by PHEX, was reported to accumulate within the unmineralized XLH osteoid. However, it is not clear whether bone matrix is generally modified or less mineralized. We present four adult patients (33-41 years old) with short stature and elevated FGF23 serum levels. They were prescribed oral phosphate and calcitriol supplementation but according clinical records two of them had a discontinuous treatment adherence (DTA). Transiliac bone biopsies were obtained and evaluated by histomorphometry, Fourier-transform infrared imaging (FTIR) and quantitative backscattered electron imaging (qBEI) to assess matrix composition and material properties. DTA patients had increased ALP and PTH levels, severe osteomalacia and twice the amount of mineralized trabecular bone volume as the compliant ones. In contrast, the latter had very low indices of bone formation and osteoid thickness mostly within normal range. FTIR analysis of XLH osteoid showed that while divalent collagen cross-links were evident in all patients, the mature trivalent cross-link pyridinoline (Pyd) was present only in the compliant ones. Interestingly, also in the compliant patients, the few osteoid seams that were broader than 5 µm did not have any measurable Pyd. However, Pyd was evident in the mineralized tissue in all patients. Unexpectedly, all osteoid independently of compliance exhibited considerable acidic lipid content. qBEI revealed that the average calcium content of the mineralized bone matrix was within normal range in all patients but the percentage of lowly and highly mineralized matrix were both increased, resulting in a broad heterogeneity in mineralization. In summary, the increased trabecular bone volume in DTA along with the finding that bone mineralization was not decreased in any patient is consistent with densitometric reports of elevated trabecular BMD in XLH. Differentiation of osteoid based on width and therapy compliance indicate altered collagen maturation while the abundant acidic lipids may be contributing to the delayed mineralization. The data of this study highlight additionally to the already published osteopontin accumulation, further organic matrix alterations that may contribute to the delayed mineralization in XLH.

Disclosures: Nadja Fratzl-Zelman, None

SAT-1087

Patient with resistant poliostotic Paget relapsed after discontinuing long time olpadronate oral treatment. A case-report of protracted drug exposition Claudia Gomez Acotto^{*1}, Susana Moggia¹, Emilio Roldán². ¹Maimonides Univ., Argentina, ²Scientific Direction Gador S.A., Argentina

Paget's disease of bone, or osteitis deformans, is a focal disorder of bone metabolism that is characterized by an accelerated rate of bone remodeling, resulting in bone overgrowth. It is a rare skeletal disease that remains asymptomatic for many patients most of the time. The response to bisphosphonates is usually satisfactory, but some patients become resistant and request further therapies. In Argentina, sodium olpadronate, a di-methylated amino-bisphosphonate, is available for compassionate use, therefore it is accessible to patients not responding to any other approved compound. We describe a case of an 80-year-old patient diagnosed with poliostotic Paget 20 years before having high serum bone alkaline phosphate (bone ALP) 4,258 UI/mL. He was initially medicated with disodium pamidronate orally, referring mild pain at the sacrum area. Skeletal 99mTc scintigraphy bone scan of the total skeleton showed a hyper-uptake of the pelvis and lumbar vertebrae 2, 3 and 4. In the radiography, an osteo-dense image with an osteolytic lesion in the right iliac wing was observed. At the beginning of the treatment he received 90mg of intravenous pamidronate, after which serum ALP was reduced to 3,828 UI/mL. Then with a second infusion bone ALP decayed to 1,842 UI/mL, with an elevation of PTH. No further response was achieved. Afterwards, he received 200 mg oral olpadronate per day during 12 days (Under Ministry of Health compassionate use authorization). The subsequent month bone ALP was 1,848 UI/mL, but 4 months later it was 1,379 UI/mL. After 7 months bone ALP increased again, and he repeated the 200 mg/day oral olpadronate, but this time during 4 consecutive months, until bone ALP was reduced to 488 UI/mL. During the following years up to present, the patient repeated several schedules of oral olpadronate having bone ALP remained normal with borderline values. Finally, the intervention was halted 3 years ago, after being long-term asymptomatic. But, at present he has returned to our service with a scintigraphy study

informing a similar state to the original one, bone ALP relapse to 1,248 UI/mL. According to our knowledge, this patient is the person most protractedly treated with olpadronate, at least with several schedules from 12 to 120 days each, during 17 years. The therapy was satisfactory as well as the tolerability of oral olpadronate. It is important to highlight that unlike other bisphosphonates, olpadronate solubility is much greater and so its gastrointestinal tolerability, as well as its dosing regimens, can be more flexible. Olpadronate is currently under development for different indications and this case suggests efficacy and safety in a condition not responding well to other compounds. After approximately three years, the condition relapsed, and the patient requires medical intervention again, which shows severe nature of Paget's bone disease in some subjects.

Disclosures: Claudia Gomez Acotto, None

SAT-1088

Exome sequencing identifies novel variants in GATA3 and MAFA genes associated with isolated hypoparathyroidism in Korean population Ji Hyun Lee^{*1,2}, Taekyeong Yoo³, Jung Hee Kim¹, Hyung Jin Choi⁴, Kyung Sil Chae¹, A Ram Hong⁵, Sang Wan Kim⁵, Murim Choi³, Chan Soo Shin¹. ¹Department of Internal Medicine, Seoul National University College of Medicine, Republic of Korea, ²Department of Internal Medicine, VHS Medical Center, Republic of Korea, ³Department of Biomedical Sciences, Seoul National University College of Medicine, Republic of Korea, ⁴Department of Anatomy, Seoul National University College of Medicine, Republic of Korea, ⁵Department of Internal Medicine, Seoul National University College of Medicine, Boramae Medical Center, Republic of Korea

INTRODUCTION Isolated hypoparathyroidism is a very rare disease and has been linked to several loci including CASR, GCM2, PTH and GATA3. Here, we report four rare novel variants in GATA3 and three in a novel candidate gene, MAFA (MAF bZIP transcription factor A) in isolated hypoparathyroidism. **METHODS** We enrolled 18 hypoparathyroidism patients without 22q11.2 deletion. Whole-exome sequencing was performed for all of them. We compared them with 1,055 healthy Korean individuals (Korean Variant Archive) using gene burden test. **RESULTS** The median age of onset was 33.5 years. Seizures were the most common symptom of onset, although there was one patient without symptom. Four of 7 patients presented with seizure and/or deafness had GATA3 variants. We identified three novel missense variants (p.Arg276Trp, p.Cys288Tyr, and p.Cys318Tyr), and a nonsense variant (p.Glu180*) in the GATA3 (novel variant burden P = 6.7 x 10⁻⁶). We also discovered a rare missense variant in the N-terminal region of MAFA (p.Glu114Lys). Two frameshift variants (p.His200fs and p.His201fs) were found in MAFA (novel variant burden P = 4.3 x 10⁻⁸). **CONCLUSIONS** Using whole exome sequencing, we identified four genetic variants in GATA3 and discovered three novel MAFA variants in patients with isolated hypoparathyroidism in Korean population. Identification of these novel types of GATA3 and MAFA variants has potential implications for better understanding of molecular pathogenesis of isolated hypoparathyroidism.

Disclosures: Ji Hyun Lee, None

SAT-1089

Molecular Characterization of a Complex Mosaicism in Supernumerary Ring Chromosome 6 Involving Bone-Related Factors in a Proband Yang Lou^{*1}, Lauren Hurd², John A. Wixted³, Jonathan A.R. Gordon⁴, Katrina A. Conard⁵, Micheal B. Bober², Jane B. Lian⁶. ¹University of Massachusetts Medical School, United States, ²Department of Biomedical Research, Alfred I. duPont Hospital for Children, United States, ³University of Massachusetts Medical Center School, United States, ⁴Department of Biochemistry, University of Vermont, United States, ⁵Department of Pathology, Alfred I. duPont Hospital for Children, United States, ⁶Department of Biochemistry, University of Vermont Medical School, United States

Certain chromosomal translocations, t(16;17)(q22;p13) and rearrangement of 17p13 have been associated with primary recurrent aneurysmal bone cysts. Two unrelated patients were recently reported with a small supernumerary ring chromosome 6 [sSRC (6)], a rare chromosomal abnormality characterized by a broad clinical phenotype, including normal to severe developmental delay and congenital anomalies. We characterized the phenotype of a proband (designated sSMC6) with sSRC (6) and a unique skeletal phenotype associated with decreased bone mineral density and cortical thinning, severe osteopenia, pathologic fractures and multiple aneurysmal cysts appeared with woven dysplastic bone. The duplicated region encompasses a pure 18.2 Mb gain from 6p12.3-6q12. of chromosome 6 and contained several osteogenic regulatory factors including genes promoting facial and limb development (TRAP2B, 2D) endochondral, bone formation (BMP5), and cytokines (TNFRSF21, IL-17) related to bone resorption. Nearly contiguous to the chromosomal duplication is the bone essential transcription factor Runx2 transcription factor gene. that is implicated in the skeletal abnormalities of the proband. We find that isolated skin fibroblasts from an unaffected region of the patient express very high levels of the entire family of human Runx factors (Runx1 and Runx3) and these cells undergoes ex vivo osteoblast differentiation in normal MEM media (!0% FCS without osteogenic supplements) compared to biopsied fibroblasts from a control subject. Microarray analyses revealed high levels of Runx2 and Runx2 target

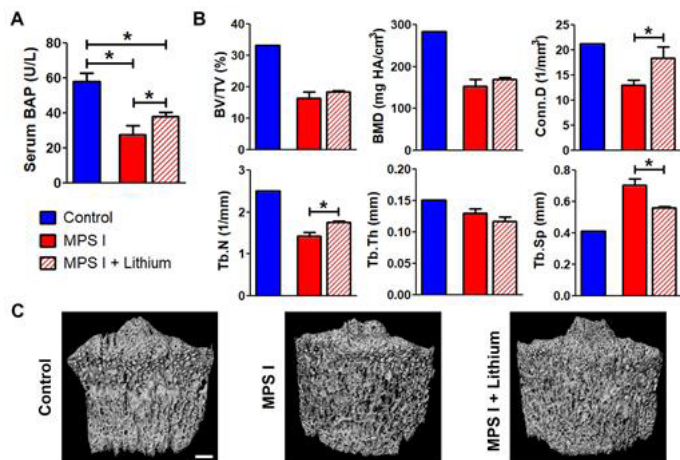
genes, ITGA1, ITGA3, TGF β 1, TGF β 3, VEGFA, EGF and the hypertrophic cartilage marker, COL10A compared to control cells. Our data suggest that genes expressed in the duplicated region of Chromosome 6 and including Runx2 can drive promiscuous osteogenic potency behavior in non-osteoblastic cells and that high RUNX 2 levels Runx2 may be the signaling molecule for induction of the bone cyst formation as well as contributing to osteopenia in this novel pathological fracture syndrome.

Disclosures: *Yang Lou, None*

SAT-1090

Lithium-mediated effects on vertebral bone formation in mucopolysaccharidosis I dogs during postnatal growth Sun Peck*, Yian Khai Lau, Justin Bendigo, Megan Lin, Toren Arginteanu, Jessica Bagel, Patricia O'Donnell, Neil Malhotra, Peter Klein, Eileen Shore, Margret Casal, Lachlan Smith. University of Pennsylvania, United States

Mucopolysaccharidosis (MPS) I is a lysosomal storage disease characterized by deficient alpha-L-iduronidase activity that leads to abnormal accumulation of glycosaminoglycans (GAGs). MPS I patients present with severe spinal deformity, due in part to impaired vertebral bone formation during postnatal growth, which decreases quality of life and increases mortality. Current treatments fail to normalize bone formation in MPS I patients. Our previous work in other MPS subtypes with similar bone manifestations showed that impaired bone formation is associated with decreased Wnt signaling, an important regulator of endochondral ossification during postnatal growth. Thus, the objective of this study was to investigate whether treatment with lithium, a Wnt pathway agonist, could enhance bone formation during postnatal growth in MPS I using the naturally-occurring canine model. MPS I dogs (n=3) were treated orally with lithium carbonate daily from 14 days to 6 months-of-age. The lithium dose was adjusted twice a week based on animal weight and serum analyses in order to maintain serum lithium levels in the putative therapeutic range (0.5-1.5 mmol/L). At 6 months-of-age, serum bone alkaline phosphatase (BAP) was measured in lithium-treated dogs along with age-matched normal (control, n=4) and untreated MPS I (n=5) dogs. Thoracic vertebrae were excised postmortem and analyzed using μ CT. While control dogs had significantly higher serum BAP than either the untreated or treated MPS I dogs, BAP levels were significantly higher in lithium-treated than untreated MPS I dogs (Fig A) suggesting increased osteoblast activity with treatment. While bone volume fraction, bone mineral density, and trabecular thickness were not significantly different in lithium-treated MPS I dogs compared to untreated MPS I dogs, connectivity density and trabecular number were significantly higher, and trabecular spacing was significantly lower, suggesting improvements in bone microarchitecture (Fig B, C). Importantly, these findings demonstrate that bone cells in MPS I are still able to respond to activating stimuli despite significant GAG storage and that Wnt pathway agonists may represent a potential therapeutic strategy for stimulating bone formation in MPS I. Ongoing work will establish the underlying cellular basis of improved bone formation with lithium treatment in MPS I dogs and if these alterations in trabecular bone architecture are associated with improved mechanical properties.



A. Serum bone-specific alkaline phosphatase (BAP) levels in control (n=4), MPS I (n=5), and MPS I lithium-treated (n=3) animals. * $p < 0.05$; one-way ANOVA with Bonferroni post-hoc test. **B.** Micro-computed tomography (μ CT) measurements of T12 vertebrae from control (representative baseline), MPS I (n=3), and MPS I lithium-treated animals (n=3). Bone volume fraction (BV/TV), bone mineral density (BMD), connectivity density (Conn.D), trabecular number (Tb.N), thickness (Tb.Th), and spacing (Tb.Sp). * $p < 0.05$; unpaired t-test between MPS I and MPS I + lithium. **C.** Representative 3D reconstructions of vertebral trabecular bone. Scale bar = 2 mm.

Disclosures: *Sun Peck, None*

SAT-1118

See Friday Plenary Number FRI-1118

SAT-1119

See Friday Plenary Number FRI-1119

SAT-1120

See Friday Plenary Number FRI-1120

SAT-1121

See Friday Plenary Number FRI-1121

SAT-1122

See Friday Plenary Number FRI-1122

SAT-1123

Associations between Educational Attainment and Operational Definitions of Sarcopenia: Data Spanning Six Years from the Tasmanian Older Adult Cohort Sharon Brennan-Olsen^{*1,2}, Sara Vogrin^{1,2}, Saliu Balogun³, David Scott⁴, Graeme Jones⁵, Alan Hayes⁵, Steven Phu¹, Gustavo Duque¹, Tania Winzenberg³. ¹University of Melbourne, Australia, ²Australian Institute for Musculoskeletal Science, Australia, ³University of Tasmania, Australia, ⁴Monash University, Australia, ⁵Victoria University, Australia

Introduction: A social gradient has been observed for osteoporosis and osteoporotic fracture. Such a gradient is also possible for sarcopenia; however, to date this is under-investigated. Thus, we aimed to examine the relationship of education with two operational definitions of sarcopenia, handgrip strength and appendicular lean mass (ALM), in community-dwelling older adults. **Methods:** ALM was measured by dual-energy X-ray absorptiometry (Hologic Corp., Massachusetts, USA) and handgrip strength measured by pneumatic dynamometer in 1,099 randomly recruited community-dwelling adults (51 % female; aged 50-80 years at baseline), and followed up twice: approximately 3 years, and 5 years after baseline. The highest level of education was self-reported at baseline and categorised according to having a tertiary education, completed secondary/high school, or not completed secondary/high school. Lifestyle variables were self-reported. Potential confounders of age, sex, smoking (ever, or current at baseline), protein intake (achieving the recommended dietary intake of 1.2g/kg/day), and history of stroke/diabetes were tested for inclusion in the final models. General estimating equations were performed separately for handgrip strength and ALM divided by body mass index (kg/m²) (ALMBMI). **Results:** Mean ALMBMI at baseline was 0.89 \pm 0.20 units. A decrease in ALMBMI was observed at first follow up (0.85 \pm 0.19) and an increase at second follow up (0.90 \pm 0.20). Similar trends were observed for handgrip strength (12 \pm 3 psi at baseline, 10 \pm 3 at 1st follow up and 11 \pm 4 at 2nd follow up). Those with a tertiary degree had \sim 0.03 units higher ALMBMI (95%CI 0.01-0.05) than those that did not complete secondary schooling ($p=0.019$); no other differences were observed between education groups. Similar associations were observed for handgrip strength, whereby those with a tertiary degree had \sim 0.5 psi greater handgrip strength compared to those with the lowest level of education (95%CI 0.1-0.9, $p=0.017$). Changes in ALMBMI and/or handgrip strength over time were not affected by education. **Conclusions:** Having a greater educational attainment were associated with small but potentially clinically significant differences in anthropometric and performance-based operational measures of sarcopenia across education groups. Further work is required to investigate change over time in these operational measures of sarcopenia, particularly in terms of other social factors such as occupation-related exposures.

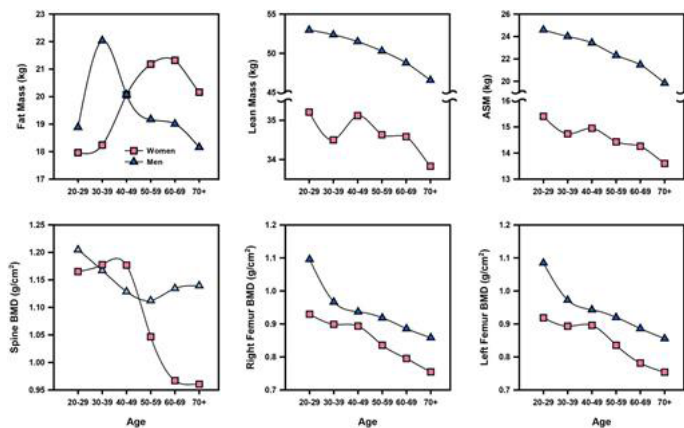
Disclosures: *Sharon Brennan-Olsen, None*

SAT-1124

Sex- and age-related changes in body composition among population-based healthy Chinese in Taiwan Yi-Chien Lu^{*1}, Wing P. Chan¹, Ying Chin Lin², Ing-Jy Tseng³. ¹Department of Radiology, Wan Fang Hospital, Taipei Medical University, Taiwan, ²Shuang Ho Hospital, Taipei Medical University, Taiwan., ³School of Gerontology Health Management, College of Nursing, Taipei Medical University, Taiwan

Background: We aimed to evaluate sex- and age-related changes in BMD, lean mass (LM), and fat mass (FM) using population-based health examinations of healthy Chinese, which have not been previously described. **Methods:** A cross-sectional study was conducted using 2256 consecutive healthy Chinese in Taiwan (1169 women) who were aged 20-89 years. Lumbar spine and bilateral femoral neck BMDs and body composition were measured using DXA. Osteoporosis was diagnosed based on WHO classification criteria using the lowest T-score from these BMD measurements. The Asian Working Group for Sarcopenia (AWGS) recommends that the cutoff for DXA-derived low muscle mass (sarcopenia) is 5.4 kg/m² and 7.0 kg/m² in women and men, respectively. This value and the reference cutoff from our data were compared in determining the prevalence of sarcopenia. Obesity cutoffs of 38% and 25% body fat were used for women and men, respectively. Participants were

grouped by sex and age using 10-year intervals except for the oldest group aged 70 years or more. For comparison, 20 participants (16 women) from community-dwelling elderly were recruited for body composition examinations. Results: In women, peak BMD (1.18 g/cm²) was reached by age 30-39 years in the lumbar spine, but it was reached by age 20-29 years in the right and left femoral necks (0.93 g/cm² and 0.92 g/cm², respectively). In men, it was reached by age 20-29 in all three areas (1.17 g/cm², 0.97 g/cm², and 0.97 g/cm², respectively). Peak mean LM was reached by age 20-29 years in both women (35.21 kg) and men (52.37 kg), whereas mean peak FM was reached in women by age 60-69 years (21.32 kg), but in men by age 20-29 years (22.04 kg). Distribution of the FM varied in the reverse way by sex and age. In men, both LM and FM declined with aging, but in women, less LM was lost than in men (-0.8% vs. -2.4% per 10-yr increment) and more fat, almost twice as much, was gained than in men (+4.7% vs. -4.4% per 10-yr increment). The prevalence of osteoporosis in individuals aged more than 50 years was 24% among women and 6% among men. The cutoffs for sarcopenia from our data in women and men were 4.25 kg/m² and 6.10 kg/m², respectively. In those considered to be elderly (age 65 or more), when the AWGS cutoff was compared to our cutoff, the prevalence of sarcopenia was greater in both sexes (23.5% vs. 0% in women and 33.0% vs. 7.0% in men), as was the prevalence of osteosarcopenia (10.6% vs. 0% in women and 10.0% vs. 2.0% in men). In comparison, using our reference value, the prevalence of sarcopenia in community-dwelling elderly people was 6% in women and 25% in men, respectively. Additionally, obesity occurred in 33.7% of the women and 59.9% of the men aged more than 60 years. Conclusion: This study provides the first data describing the body compositions of healthy adult Chinese in Taiwan. Further studies with larger sample size are needed to obtain valid cut-off points for our populations to improve diagnosis of sarcopenia.



Disclosures: **Yi-Chien Lu**, None

SAT-1125

Association of bone mineral density and appendicular lean mass with fracture risk assessed by FRAX for postmenopausal women in the north part of China. Dr Dongmei*. The Second Affiliated hospital of Inner Mongolia Medical University, China

Objective: In order to prevent osteoporotic fractures, numerous studies have shown the positive effects of bone mineral density and appendicular lean mass among the middle-aged and elderly women in the community. However, the effect of osteoporotic fracture risk on the postmenopausal women with bone mineral density and appendicular lean mass has not yet been addressed. Methods: A cross-sectional study was conducted with 369 postmenopausal women at the Second Affiliated Hospital of Inner Mongolia Medical University living in the community of Hohhot, north part of China. Subjects were included for no drug treatment for osteopenia or osteoporosis. The whole body, spine and hip bone mineral density and body composition were measured by dual-energy x-ray absorptiometry, and the fracture risk assessment was calculated using WHO FRAX risk assessment for the risk of major fractures and the hip fracture. Results: There were 369 women with a mean age of 60.7 years (range, 50 to 86 years). The fracture risk calculated in 10 years by using the FRAX for hip fracture and major fracture was 0%~27% and 1.1%~28.8%, respectively. Appendicular lean mass was significantly and positively associated with hip fracture and major fracture rates at all site even after adjustment for aBMD. Conclusions: The results of this study suggest that the implementation of the risk of major fracture or of the hip for the prevention of osteoporosis has a significant association with muscle mass in postmenopausal Chinese women.

Disclosures: **Dr Dongmei**, None

SAT-1126

Osteosarcopenia phenotype and frailty status by CHS and SOF Criteria Alberto Frisoli*, Angela Paes, Sheila Inghan, Antonio Carlos De Camargo Carvalho. Federal University of Sao Paulo, Brazil

There is a robust physiological interaction between muscle and bone. Sarcopenia and osteoporosis are risk factors for fracture and frailty. Different concepts of frailty have sub-

stantial heterogeneity in the physical phenotype. We hypothesized that Osteosarcopenia is musculoskeletal manifestations of Frailty. To test our hypothesis we evaluate the association among Osteosarcopenia (OSP), Osteoporosis only (OPON) and Sarcopenia only (SARCON) with frailty by Fried criteria and SOF criteria. Method: Cross sectional analyzes of 386 patients from SARCON study, an observational study of the epidemiology of Sarcopenia and Osteoporosis in older outpatients from Federal University of Sao Paulo-Brazil. All patients were underwent DXA of total body and bone sites. Frailty was defined by the SOF criterion (2-3 frailty, 1 pre frailty and 0 robust): Weight loss, Chair stand test; low energy; and by CHS criterion (≥ 3 frailty, 1-2 pre frailty and 0 robust): Weight loss, low walking speed, weakness, Low energy (adapted), exhaustion. Osteoporosis was diagnosed if BMD ≤ -2.5 SD at any bone site. Sarcopenia was diagnosed only by low muscle mass according to FNIIH criterion (appendicular muscle mass/ BMI < 0.567 women, < 0.723 men). Osteosarcopenia (OSP) was diagnosed if Osteoporosis and Sarcopenia were present. Results: The mean age was 78.22(7.16) yo, and 56.2% were women. OSP occurred in 14.8%, SARCON in 39.8% and OPON in 19.2% (p<0.001). Subjects with OSP were older (p<0.001), with lower fat index (p<0.001), muscle mass (p<0.001) and BMD at all bone sites (p<0.001) compared to others phenotypes. Frailty by CHS was diagnosed in 17.8% of the sample, and by SOF criterion, in 20.2%. Among subjects classified by CHS criterion, OSP occurred in 25.8% of frailty, 7.3% of pre frailty and 3.4% of robust; SARCON occurred in 41.9% of frailty, 40.6% of pre frailty and 34.5% of robust and OPON in 22.6% in frailty, 20.8% pre frailty and in 22.4% of robust (p=0.005). In the SOF Frailty phenotype, OSP occurred in 16.7% of frailty, 16.1% of pre frailty, and 12.7% of robust; SARCON in 38.5% of frailty, 39.9% of pre frailty and 40.0% of robust; OPON only in 21.8% of frailty, 17.5% of pre frailty and 19.4% of robust (p=0.937). In the adjusted (age/female) regression analysis for Frailty by CHS, OSP OR: 19.01 (CI 95%: 3.84-93.95; p<0.001), SARCON OR: 4.78 (CI 95%: 1.25-18.20; p=0.022), and OPON OR: 3.35 (CI 95%: 0.79-14.21; p=0.10). For Frailty by SOF criterion, OSP presented OR: 1.22 (CI 95%: 0.54-2.79; p=0.624), SARCON OR: 1.19 (CI 95%: 0.61-2.30; p=0.597) and OPON: 1.25 (CI 95%: 0.59-2.67, p=0.552). Conclusion: There are significantly differences in the musculoskeletal manifestations of the frailty phenotypes according by the criterion chosen. Osteosarcopenia and sarcopenia only are associated with frailty by CHS, however, Osteosarcopenia seems to be more specific of the frailty status than other musculoskeletal phenotypes.

Disclosures: **Alberto Frisoli**, None

SAT-1127

Integrated Women's Health Programme (IWHP): A cross-sectional study of prevalence & correlates for sarcopenia in midlife Singaporean women Win Pa Pa Thu*, Susan Jane Sinclair Logan¹, E.L Yong¹, Jane A. Cauley². ¹Department of Obstetrics & Gynaecology, National University of Singapore, Singapore, ²Department of Epidemiology, Graduate School of Public Health, University of Pittsburgh, United States

Purpose: Singapore is one of the countries in Asia facing a rapid demographic transition towards ageing. By 2030, one in five people will be 65 years and older. Sarcopenia, prevalent in older women, poses major healthcare and dependence costs due to associated disability. No previous studies on in midlife Singaporean women exist. This study aimed to determine the prevalence of sarcopenia and evaluate its correlates. Method: Cross-sectional study enrolling 45-69 year old women attending gynaecology for "well women" checks & symptoms, excluding cancer. Assessments included standardised questionnaires- socio-demographics, menopausal, incontinence/prolapse, health/function, depression, anxiety, sleep, physical activity & sex; biophysical measures; short physical performance battery/ grip strength & Dual-Energy X-ray Absorptiometry (DXA) scan. Sarcopenia was diagnosed using the Asian Working Group for Sarcopenia (AWGS) definition- handgrip strength < 18 kg, gait speed ≤ 0.8 m/sec and skeletal muscle mass ≤ 5.4 kg/m² using DXA. Analysis used SPSS Version 20. Results: Of 1201 women, the mean (SD) age was 56.3(6.2) years. Majority were Chinese (84%) followed by Malay (6%) & Indian (10%). Postmenopausal, peri-menopausal and pre-menopausal women constituted 72%, 16% and 12%, respectively. Diabetes and hypertension were the most commonly reported medical conditions affecting 10% and 29%, respectively. Mean (SD) body mass index was 24.1(4.4) kg/m² with 5% in underweight category (BMI < 18.5 kg/m²). Only 3% were alcohol consumers. A high prevalence of Sarcopenia (39%) was observed. Among these, 6% were also osteoporotic at either hip or spine. Chinese ethnicity (p<0.01), menopausal status (p<0.05), diabetes (p<0.01), hypertension and BMI less than 18.5 (p<0.001) were positively associated with sarcopenia. Adjusted multivariate logistic regression model reported that only women with BMI < 18.5 kg/m² were more likely to have sarcopenia (Odds Ratio=4.16, 95% Confidence Interval = 1.99-8.71). The risk of sarcopenia attributable to this BMI category was 43%. Age, physical activity, number of falls in the last 12 months and consumption of alcohol did not influence the likelihood of sarcopenia. Conclusion: The 39% prevalence rate reported is higher than previously described and needs urgent confirmation in a community-based sample. Our findings suggest that a BMI cut-off (<18.5 kg/m²) could be used to screen sarcopenia in midlife Singaporean women attending gynaecology outpatients.

Disclosures: **Win Pa Pa Thu**, None

LB SAT - 1147

Exploration of an epidemiological association between air pollutant exposure and the development of T2DM. A systematic review. Marilena Marzia*. Freelance Professional Nutritionist, Italy

Background: Type 2 diabetes (T2DM) and obesity are known to be associated with high bone mass and increased fracture risk. Environmental and life-style factors are risk factors explaining the 80% of adverse effects for communicable and not communicable diseases, including osteoporosis, Paget's disease of bone, osteoarthritis, cancer, and T2DM. The exposure to climate and high level of air, water, food, and food packaging contamination can convey infective and not infective agents. Air pollution is hypothesized to be a risk factor for diabetes and obesity. Objective: This review is exploring the existence of an epidemiological association between air pollutant and the development of T2DM. Methods: Electronic literature databases have been systematically searched (through 2017) for studies reporting the association between air pollution exposure and the T2DM. Selected studies have been synthesized. Results: 39 articles have been included; those studies have been conducted in Europe, UK, Switzerland, USA, Canada, South Israel, Latin America Asia. 20 studies were longitudinal, 7 cross-sectional, 6 time-series. Conclusions: Existing evidence indicates positive association between air pollutant exposure (PM2.5, PM10, NO2, SO2, CO, O3) and the T2DM prevalence and incidence, the T2DM-related mortality and morbidity; research has been expanded in those countries with high level of air pollution and where obesity and diabetes prevalence are increasing; to better understand this association further high quality studies assessing dose-response are needed.

Disclosures: *Marilena Marzia, None*

LB SAT - 1150

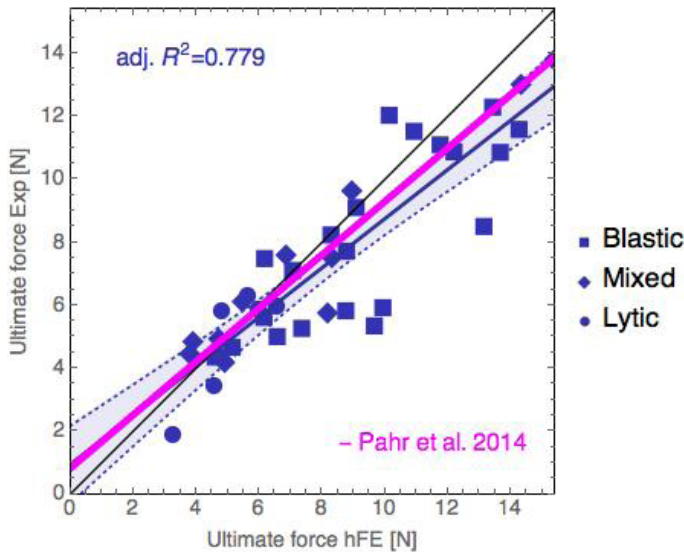
Distribution of Stress on the Distal Femur in Advanced Osteoarthritis Kwangkyoun Kim*. Konyang University, Republic of Korea

Purpose: The aim of this study is to analyse regional differences of the stress distribution on the distal femur in the advanced osteoarthritis. Design: Distal femur specimens with primary OA were obtained from ten donors composed of 10 women cadaver with OA (mean age of 65 years, ranging from 53 to 79). As controls, distal femur without OA was obtained from age and gender matched cadavers consisting of 10 women (mean age of 67 years, ranging from 58 to 81). Articular surface of distal femur was divided with anterior, middle, posterior regions on each condyle. Mechanical property and microstructure of regions were assessed with micro-CT and finite element model analysis. Results: Table 1 shows the summary of the mechanical and microstructural measures (median, interquartile range) on the 6 regions of OA and control groups. In the control group, there was regional difference of stress distribution among 6 regions on the distal femur (p=0.037), but there was no regional difference of stress distribution among 6 regions on the distal femur in the advanced osteoarthritis group (p=0.179). There was significant regional difference in BV/TV, SMI, Tb.Th, Tb.Sp, Tb.N and DOA in the control group. In the advanced OA group, BV/TV, SMI and Tb.Th showed no regional difference (p=0.132, p=0.136, 0.712), but there was significant regional difference in Tb.Sp, Tb.N and DOA (p=0.003, p=0.009, p=0.000). Conclusion: Microstructural and mechanical properties of the distal femur were changed according to the progression of osteoarthritis. No regional differences in stress distribution were detected in advanced OA. Altered loading patterns, bone remodeling and chemical composition affect changes in stress distribution.

Table 1. Summary of the mechanical and microstructural measures (median, interquartile range) on the 6 regions of OA and control groups.

	BV/TV(%)		SMI		Tb.Th (mm)		Tb.N		Tb.Sp (mm)		DOA		Yield strength (MPa)	
	(M)	(I)	(M)	(I)	(M)	(I)	(M)	(I)	(M)	(I)	(M)	(I)	(M)	(I)
OA	18.86	31.72	1.3	0.74	0.19	0.29	1.05	1.06	0.70	0.69	0.46	0.43	8.78	10.81
Ant	(13.49 to 24.82)	(0.87 to 0.71)	(0.17 to 0.25)	(0.78 to 0.99)	(0.57 to 0.86)	(0.36 to 0.39)	(7.32 to 7.83)	(10.22 to 11.27)						
Medial condyle	31.72	33.12	1.48	0.84	0.24	0.31	1.27	1.09	0.74	0.73	0.48	0.47	11.73	13.01
Mid	(21.64 to 29.43)	(0.59 to 0.39)	(0.18 to 0.25)	(1.20 to 1.11)	(0.53 to 0.58)	(0.52 to 0.49)	(4.60 to 10.06)							
Post	29.57	35.05	0.64	0.54	0.23	0.28	1.12	1.15	0.79	0.83	0.55	0.52	5.65	10.7
Ant	(13.49 to 24.82)	(0.87 to 0.71)	(0.17 to 0.25)	(0.78 to 0.99)	(0.57 to 0.86)	(0.36 to 0.39)	(7.32 to 7.83)	(10.22 to 11.27)						
Medial condyle	31.72	33.12	1.48	0.84	0.24	0.31	1.27	1.09	0.74	0.73	0.48	0.47	11.73	13.01
Mid	(21.64 to 29.43)	(0.59 to 0.39)	(0.18 to 0.25)	(1.20 to 1.11)	(0.53 to 0.58)	(0.52 to 0.49)	(4.60 to 10.06)							
Post	29.57	35.05	0.64	0.54	0.23	0.28	1.12	1.15	0.79	0.83	0.55	0.52	5.65	10.7
Ant	(13.49 to 24.82)	(0.87 to 0.71)	(0.17 to 0.25)	(0.78 to 0.99)	(0.57 to 0.86)	(0.36 to 0.39)	(7.32 to 7.83)	(10.22 to 11.27)						
Medial condyle	31.72	33.12	1.48	0.84	0.24	0.31	1.27	1.09	0.74	0.73	0.48	0.47	11.73	13.01
Mid	(21.64 to 29.43)	(0.59 to 0.39)	(0.18 to 0.25)	(1.20 to 1.11)	(0.53 to 0.58)	(0.52 to 0.49)	(4.60 to 10.06)							
Post	29.57	35.05	0.64	0.54	0.23	0.28	1.12	1.15	0.79	0.83	0.55	0.52	5.65	10.7
Ant	(13.49 to 24.82)	(0.87 to 0.71)	(0.17 to 0.25)	(0.78 to 0.99)	(0.57 to 0.86)	(0.36 to 0.39)	(7.32 to 7.83)	(10.22 to 11.27)						
Medial condyle	31.72	33.12	1.48	0.84	0.24	0.31	1.27	1.09	0.74	0.73	0.48	0.47	11.73	13.01
Mid	(21.64 to 29.43)	(0.59 to 0.39)	(0.18 to 0.25)	(1.20 to 1.11)	(0.53 to 0.58)	(0.52 to 0.49)	(4.60 to 10.06)							
Post	29.57	35.05	0.64	0.54	0.23	0.28	1.12	1.15	0.79	0.83	0.55	0.52	5.65	10.7
Ant	(13.49 to 24.82)	(0.87 to 0.71)	(0.17 to 0.25)	(0.78 to 0.99)	(0.57 to 0.86)	(0.36 to 0.39)	(7.32 to 7.83)	(10.22 to 11.27)						
Medial condyle	31.72	33.12	1.48	0.84	0.24	0.31	1.27	1.09	0.74	0.73	0.48	0.47	11.73	13.01
Mid	(21.64 to 29.43)	(0.59 to 0.39)	(0.18 to 0.25)	(1.20 to 1.11)	(0.53 to 0.58)	(0.52 to 0.49)	(4.60 to 10.06)							
Post	29.57	35.05	0.64	0.54	0.23	0.28	1.12	1.15	0.79	0.83	0.55	0.52	5.65	10.7
Ant	(13.49 to 24.82)	(0.87 to 0.71)	(0.17 to 0.25)	(0.78 to 0.99)	(0.57 to 0.86)	(0.36 to 0.39)	(7.32 to 7.83)	(10.22 to 11.27)						
Medial condyle	31.72	33.12	1.48	0.84	0.24	0.31	1.27	1.09	0.74	0.73	0.48	0.47	11.73	13.01
Mid	(21.64 to 29.43)	(0.59 to 0.39)	(0.18 to 0.25)	(1.20 to 1.11)	(0.53 to 0.58)	(0.52 to 0.49)	(4.60 to 10.06)							
Post	29.57	35.05	0.64	0.54	0.23	0.28	1.12	1.15	0.79	0.83	0.55	0.52	5.65	10.7
Ant	(13.49 to 24.82)	(0.87 to 0.71)	(0.17 to 0.25)	(0.78 to 0.99)	(0.57 to 0.86)	(0.36 to 0.39)	(7.32 to 7.83)	(10.22 to 11.27)						
Medial condyle	31.72	33.12	1.48	0.84	0.24	0.31	1.27	1.09	0.74	0.73	0.48	0.47	11.73	13.01
Mid	(21.64 to 29.43)	(0.59 to 0.39)	(0.18 to 0.25)	(1.20 to 1.11)	(0.53 to 0.58)	(0.52 to 0.49)	(4.60 to 10.06)							
Post	29.57	35.05	0.64	0.54	0.23	0.28	1.12	1.15	0.79	0.83	0.55	0.52	5.65	10.7
Ant	(13.49 to 24.82)	(0.87 to 0.71)	(0.17 to 0.25)	(0.78 to 0.99)	(0.57 to 0.86)	(0.36 to 0.39)	(7.32 to 7.83)	(10.22 to 11.27)						
Medial condyle	31.72	33.12	1.48	0.84	0.24	0.31	1.27	1.09	0.74	0.73	0.48	0.47	11.73	13.01
Mid	(21.64 to 29.43)	(0.59 to 0.39)	(0.18 to 0.25)	(1.20 to 1.11)	(0.53 to 0.58)	(0.52 to 0.49)	(4.60 to 10.06)							
Post	29.57	35.05	0.64	0.54	0.23	0.28	1.12	1.15	0.79	0.83	0.55	0.52	5.65	10.7
Ant	(13.49 to 24.82)	(0.87 to 0.71)	(0.17 to 0.25)	(0.78 to 0.99)	(0.57 to 0.86)	(0.36 to 0.39)	(7.32 to 7.83)	(10.22 to 11.27)						
Medial condyle	31.72	33.12	1.48	0.84	0.24	0.31	1.27	1.09	0.74	0.73	0.48	0.47	11.73	13.01
Mid	(21.64 to 29.43)	(0.59 to 0.39)	(0.18 to 0.25)	(1.20 to 1.11)	(0.53 to 0.58)	(0.52 to 0.49)	(4.60 to 10.06)							
Post	29.57	35.05	0.64	0.54	0.23	0.28	1.12	1.15	0.79	0.83	0.55	0.52	5.65	10.7
Ant	(13.49 to 24.82)	(0.87 to 0.71)	(0.17 to 0.25)	(0.78 to 0.99)	(0.57 to 0.86)	(0.36 to 0.39)	(7.32 to 7.83)	(10.22 to 11.27)						
Medial condyle	31.72	33.12	1.48	0.84	0.24	0.31	1.27	1.09	0.74	0.73	0.48	0.47	11.73	13.01
Mid	(21.64 to 29.43)	(0.59 to 0.39)	(0.18 to 0.25)	(1.20 to 1.11)	(0.53 to 0.58)	(0.52 to 0.49)	(4.60 to 10.06)							
Post	29.57	35.05	0.64	0.54	0.23	0.28	1.12	1.15	0.79	0.83	0.55	0.52	5.65	10.7
Ant	(13.49 to 24.82)	(0.87 to 0.71)	(0.17 to 0.25)	(0.78 to 0.99)	(0.57 to 0.86)	(0.36 to 0.39)	(7.32 to 7.83)	(10.22 to 11.27)						
Medial condyle	31.72	33.12	1.48	0.84	0.24	0.31	1.27	1.09	0.74	0.73	0.48	0.47	11.73	13.01
Mid	(21.64 to 29.43)	(0.59 to 0.39)	(0.18 to 0.25)	(1.20 to 1.11)	(0.53 to 0.58)	(0.52 to 0.49)	(4.60 to 10.06)							
Post	29.57	35.05	0.64	0.54	0.23	0.28	1.12	1.15	0.79	0.83	0.55	0.52	5.65	10.7
Ant	(13.49 to 24.82)	(0.87 to 0.71)	(0.17 to 0.25)	(0.78 to 0.99)	(0.57 to 0.86)	(0.36 to 0.39)	(7.32 to 7.83)	(10.22 to 11.27)						
Medial condyle	31.72	33.12	1.48	0.84	0.24	0.31	1.27	1.09	0.74	0.73	0.48	0.47	11.73	13.01
Mid	(21.64 to 29.43)	(0.59 to 0.39)	(0.18 to 0.25)	(1.20 to 1.11)	(0.53 to 0.58)	(0.52 to 0.49)	(4.60 to 10.06)							
Post	29.57	35.05	0.64	0.54	0.23	0.28	1.12	1.15	0.79	0.83	0.55	0.52	5.65	10.7
Ant	(13.49 to 24.82)	(0.87 to 0.71)	(0.17 to 0.25)	(0.78 to 0.99)	(0.57 to 0.86)	(0.36 to 0.39)	(7.32 to 7.83)	(10.22 to 11.27)						
Medial condyle	31.72	33.12	1.48	0.84	0.24	0.31	1.27	1.09	0.74	0.73	0.48	0.47	11.73	13.01
Mid	(21.64 to 29.43)	(0.59 to 0.39)	(0.18 to 0.25)	(1.20 to 1.11)	(0.53 to 0.58)	(0.52 to 0.49)	(4.60 to 10.06)							
Post	29.57	35.05	0.64	0.54	0.23	0.28	1.12	1.15	0.79	0.83	0.55	0.52	5.65	10.7
Ant	(13.49 to 24.82)	(0.87 to 0.71)	(0.17 to 0.25)	(0.78 to 0.99)	(0.57 to 0.86)	(0.36 to 0.39)	(7.32 to 7.83)	(10.22 to 11.27)						
Medial condyle	31.72	33.12	1.48	0.84	0.24	0.31	1.27	1.09	0.74	0.73	0.48	0.47	11.73	13.01
Mid	(21.64 to 29.43)	(0.59 to 0.39)	(0.18 to 0.25)	(1.20 to 1.11)	(0.53 to 0.58)	(0.52 to 0.49)	(4.60 to 10.06)							
Post	29.57	35.05	0.64	0.54	0.23	0.28	1.12	1.15	0.79	0.83	0.55	0.52	5.65	10.7
Ant	(13.49 to 24.82)	(0.87 to 0.71)	(0.17 to 0.25)	(0.78 to 0.99)	(0.57 to 0.86)	(0.36 to 0.39)	(7.32 to 7.83)	(10.22 to 11.27)						
Medial condyle	31.72	33.12	1.48	0.84	0.24	0.31	1.27	1.09	0.74	0.73	0.48	0.47	11.73	13.01
Mid	(21.64 to 29.43)	(0.59 to 0.39)	(0.18 to 0.25)	(1.20 to 1.11)	(0.53 to 0.58)	(0.52 to 0.49)	(4.60 to 10.06)							
Post	29.57	35.05	0.64	0.54	0.23	0.28	1.12	1.15	0.79	0.83	0.55	0.52	5.65	10.7
Ant	(13.49 to 24.82)	(0.87 to 0.71)	(0.17 to 0.25)	(0.78 to 0.99)	(0.57 to 0.86)	(0.36 to 0.39)	(7.32 to 7.83)	(10.22 to 11.27)						
Medial condyle	31.72	33.12	1.48	0.84	0.24	0.31	1.27	1.09	0.74	0.73	0.48	0.47	11.73	13.01
Mid	(21.64 to 29.43)	(0.59 to 0.39)	(0.18 to 0.25)	(1.20 to 1.11)	(0.53 to 0.58)	(0.52 to 0.49)	(4.60 to 10.06)							
Post	29.57	35.05	0.64	0.54	0.23	0.28	1.12	1.15	0.79	0.83	0.55	0.52	5.65	10.7
Ant	(13.49 to 24.82)	(0.87 to 0.71)	(0.17 to 0.25)	(0.78 to 0.99)	(0.57 to 0.86)	(0.36 to 0.39)	(7.32 to 7.83)	(10.22 to 11.27)						
Medial condyle	3													

trabecular tissue. No significant differences in any indentation properties between lytic and normal trabecular tissue were found ($p>0.05$). As shown in the figure, vertebral strength computed by FE analysis correlated linearly with the experimental values ($r=0.883$). The linear regression parameters obtained for metastatic vertebrae were not significantly different from those reported in [2] for healthy vertebrae ($p>0.05$) and the adjusted coefficients of determination were comparable ($r^2=0.779$ vs $r^2=0.768$). Discussions: The small indentation modulus difference observed between blastic and normal bone may be attributed to the woven nature of the blastic tissue in comparison to the lamellar organization of normal tissue. The bone tissue surrounding lytic lesions does not seem to be altered. Despite the lack of patient history in this ex vivo study, the results suggest that the FE method developed in osteoporosis research may also be used in the estimation of fracture risk in vertebrae with metastatic lesions. However, the influence of radiotherapy on vertebral biomechanics needs to be further investigated. We acknowledge funding from grant #165510, SNF and grant #R21AR066916, NIAMS/NIH.[1] Dall'Ara et al., J Biomech, 2010. [2] Pahr et al., J Mech Behav Biomed Mater, 2014.

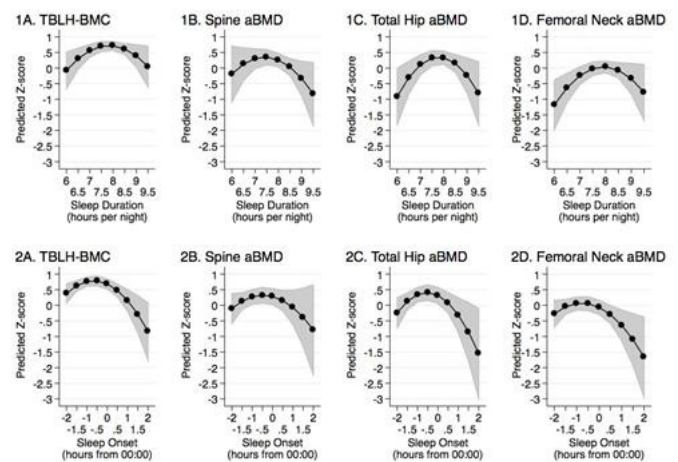


Disclosures: Marc Stadelmann, None

LB SAT - 1157

Sleep Duration and Timing Predicts Bone Mineral Density Among Adolescents Jonathan Mitchell¹, David Dinges², Knashawn Morales², Nicholas Huffnagle¹, Struan Grant¹, Babette Zemel¹. ¹Children's Hospital of Philadelphia, United States, ²University of Pennsylvania, United States

In adults, inverted U-shaped associations between sleep duration and areal bone mineral density (aBMD) have been observed and this may be a consequence of circadian misalignment. It is not known if this association replicates in the pediatric setting when bone is being accrued. We aimed to determine if sleep duration and sleep timing are associated with aBMD among 8th graders. Our sample comprised 102 adolescents enrolled in the Sleep and Growth Study (13-14y, 54% female, 72% white). From dual energy X-ray absorptiometry scans, sex and age-specific aBMD Z-scores were calculated for total hip, femoral neck, and spine. We also calculated total body less head (TBLH) bone mineral content (BMC) Z-scores. Sleep patterns were objectively estimated over a 14-day period using wrist actigraphy. Multiple linear regression was used to test for the associations between the sleep exposures with each bone Z-score, with quadratic sleep variables included to assess for inverted U-shaped associations. All models were adjusted for sex, race, body mass index Z-score, dietary calcium, physical activity and pubertal stage. Nighttime sleep duration averaged 7.85 (SD: 0.66) hours. Sleep onset timing averaged -0.64 (SD:0.86) hours from midnight (i.e., 23:22). The average bone Z-scores for TBLH, total hip, femoral neck and spine were 0.62 (SD:0.84), 0.18 (SD:1.18), -0.10 (SD:1.12) and 0.18 (SD:1.04). We observed inverted U-shaped associations between nighttime TST and each bone Z-score (Figure 1; panel 1A-D). For example, 8 hours of nighttime sleep predicted TBLH Z-score to be 0.71 (95%CI: 0.57, 0.85). This was 0.79 (95%CI: 0.14, 1.43) Z-score units higher than the 6-hour prediction, and 0.66 (95%CI: -0.03, 1.36) Z-score units higher than the 9.5-hour prediction. We also observed inverted U-shaped associations between sleep onset timing and each bone Z-score (Figure 1; panel 2A-D). For example, 23:00 sleep onset predicted TBLH-BMC Z-score to be 0.76 (95%CI: 0.61, 0.91). This was 0.61 (95%CI: 0.18, 1.04) Z-score units higher than the 1:00 sleep onset prediction. Shorter and longer sleep durations predicted lower bone Z-scores compared to moderate sleep duration among adolescents. Whereas, earlier-to-moderate timing of sleep onset predicted higher bone Z-scores, compared to later timing of onset. Follow-up investigation is needed to fully understand sleep patterns in early life and their contribution to bone accretion and risk of later life osteoporosis.



Disclosures: Jonathan Mitchell, None

LB SAT - 1160

Rescuing age-associated decline in muscle mass by inhibition of the receptor for advanced glycosylation end products, RAGE Alyson Essex^{1,2}, Hannah Davis^{1,2}, Fabrizio Pin^{2,3}, Lilian Plotkin^{1,2,4}, Andrea Bonetto^{1,2,3}. ¹Department of Anatomy & Cell Biology, Indiana University School of Medicine, ²Indiana Center for Musculoskeletal Health, United States, ³Department of Surgery, Indiana University School of Medicine, ⁴Roudebush Veterans Administration Medical Center, United States

RAGE inhibition by treatment with Azeliragon (Az), a small molecule RAGE inhibitor developed as a therapeutic for Alzheimer's Disease, suppresses bone turnover with no net effect on architecture or mechanical properties in young 5-month old (mo) and aged 16mo C57BL/6 mice. Interestingly, these studies found that treatment with 110 $\mu\text{g}/\text{d}$ Az for 28 days increases lean body mass and skeletal muscle weight in aged mice. Consistent with the previously reported Az-induced decreased mRNA expression of the E3-ubiquitin ligase atrogin-1, our studies now show that, when compared to 5mo vehicle-treated young mice, Az also prevented the age-associated increase in total protein ubiquitination. In addition to restoring the expression of the myogenesis marker myoD in aged mice to the young-vehicle treated values, as previously described, Az reversed several age-induced metabolic changes in skeletal muscle including reduced levels of the glucose transporters (GLUT1-4) and glycolysis-associated enzymes (PGK1 and LDHA). Additionally, Az increased protein levels of OPA1 and PGC1 α , associated with mitochondrial inner membrane cristae fusion and biogenesis respectively. Concurrently, Az also rescued the age-associated decrease in the levels of mitofusin-2, implicated in the fusion of mitochondrial outer membranes, and of SOD-1, an enzyme endowed with antioxidant properties. Furthermore, in studies aiming to clarify whether Az treatment rescues the decrease in muscle mass with aging through a systemic effect rather than a direct action on muscle cells, differentiated murine C2C12 myotubes exposed to 5% serum from aged mice displayed fiber atrophy when compared to cells treated with serum from young vehicle-treated counterparts, whereas serum from Az-treated aged mice did not promote atrophic effects on the myotubes. Interestingly, we found no discernable changes in diameter in C2C12 myotube cultures treated with 1nM Az for 48 hours. Altogether, our observations suggest that Az rescues aging-associated muscle wasting by counteracting skeletal muscle hypercatabolism and by restoring mitochondrial homeostasis and metabolism, thereby highlighting a novel potential therapeutic use for this drug. Future studies will aim to elucidate the Az-target cell(s) and the molecular mediators of the skeletal muscle protective effect of the drug in aging.

Disclosures: Alyson Essex, None

LB SAT - 1164

Bone metastatic growth was not inhibited by anti-PD-1 blockage in a humanized mouse model of triple-negative breast cancer – difference in responses between primary and bone metastatic tumors Tiina E Kähkönen¹, Mari I Suominen¹, Jenni Mäki-Jouppila¹, Jussi M Hallee¹, Teppo Haapaniemi², Azusa Tanaka³, Michael Seiler³, Jenni Bernoulli¹. ¹Pharmatest Services, Finland, ²BioSiteHisto Ltd, Finland, ³Taconic Biosciences, United States

Immuno-oncology (IO) has provided promising results in cancer treatment. Triple-negative breast cancer (TNBC) tumors attract immune cells, including programmed cell death 1 (PD-1) positive tumor-infiltrating lymphocytes (TILs), and high number of TILs is linked to improved survival in patients. High frequency of bone metastases is typical in TNBC. As immune regulation is different in bone than in other organs it is essential to study the efficacy of IO therapies in the metastatic bone microenvironment. The aim of this study was to assess

the efficacy of anti-PD-1 therapy (pembrolizumab, Keytruda®) in TNBC cells growing in bone of humanized mice. MDA-MB-231(SA)-luc human TNBC cells were inoculated into tibia bone marrow of female huNOG mice (Taconic Biosciences). Treatment with pembrolizumab or human IgG4 isotype control (5 mg/kg, i.p., Q5D, n=8) was started 3 days after the inoculations and continued for 18 days. Tumor-induced bone changes were monitored by X-ray imaging. At sacrifice, tumor-bearing and healthy tibias were collected for ex vivo analysis by micro-computed tomography (μ CT) and histological and immunohistochemical characterization of tumors, TILs and PD-1 expression in tumors. A group of mice inoculated orthotopically with the same cells served as a positive control for pembrolizumab treatment. Pembrolizumab had no effect in regulation of bone metastatic growth in humanized mice. No changes were observed in tumor area at endpoint, in the development of osteolytic lesions, or in any of the bone parameters studied. Also, no changes were observed in bone parameters of the healthy tibias of pembrolizumab treated mice. CD4+ cells were dominant in tumors growing in bone, and CD8 and PD-1 positive cells were rarely observed. On the contrary, orthotopic tumors responded to pembrolizumab treatment, as expected. In these tumors, CD8 and PD-1 positive TILs were observed in moderate to high quantity. Bone metastatic growth was not inhibited by the PD-1 blockage in this study, which could be explained by low infiltration of cytotoxic cells. Bone marrow has a unique microenvironment and immune cell compartment compared to any other organ, and the immune cells in bone are involved in immune surveillance and favor tumor cells to become immune evasive. Demonstration of efficacy of IO compounds in preclinical metastasis models would be important before entering clinical phases in IO drug development.

Disclosures: *Tiina E Kähkönen, None*

LB SAT - 1165

Exosomal release of L-plastin by breast cancer cells facilitates metastatic bone osteolysis Kerstin Tiedemann^{*1}, Gulzhakhan Sadvakasova¹, Nicolas Mikolajewicz¹, Michal Juhas¹, Zarina Sabirova¹, Sebastian Tabaries¹, Jan Gettemans², Peter M. Siegel¹, Svetlana V. Komarova¹. ¹McGill University, Canada, ²Gent University, Belgium

Breast and prostate carcinoma often metastasize to bone, where excessive bone degradation is mediated by bone resorbing osteoclasts. Previously we demonstrated that breast and prostate cancer cells secrete soluble factors that promote osteoclastogenesis and using proteomics identified peroxiredoxin-4 as a mediator of these effects. Here we report identification and validation of L-plastin as an osteoclastogenic factor secreted by breast cancer. Using immunoblotting and mass spectrometry, L-plastin was detected in MDA-MB-231 conditioned medium (CM). When L-plastin in MDA-MB-231 cells was silenced using siRNA, the CM ability to induce osteoclast formation was significantly reduced. L-plastin, but not PRDX4, was detected in cancer-derived exosomes, and inhibition of exosomal release significantly decreased osteoclastogenic capacity of MDA-MB-231 CM. When added to osteoclast precursors primed with RANKL for 2 days, recombinant L-plastin induced calcium oscillations, NFATc1 nuclear translocation, and osteoclastogenesis to the levels similar to continuous treatment with RANKL. Using shRNA, we generated MDA-MB-231 cells lacking L-plastin, PRDX4 or both; injected the parental and clonal cancer cells intra-tibial in CD-1 immunodeficient mice; and examined bone osteolysis two weeks after the injection. Micro-CT and histomorphometric analysis of the mouse tibial metaphyseal area demonstrated the trend for reduction in osteolysis when MDA-MB-231 cells lacking L-plastin or PRDX4 were injected, and prevention of the osteolysis when MDA-MB-231 cells lacking both L-plastin and PRDX4 were injected. A meta-analysis demonstrated an increase in L-plastin mRNA expression in carcinoma and metastatic breast tissues. This study demonstrates that secreted L-plastin and PRDX4 mediate osteoclast activation by human breast cancer cells, and may represent viable targets for the development of novel therapies for prevention of osteolytic bone metastasis.

Disclosures: *Kerstin Tiedemann, None*

LB SAT - 1172

1,25(OH)D3 abrogates palmitic acid-induced lipotoxicity in normal human osteoblasts in vitro Ahmed Al Saedi^{*}, Damian Myers, Steven Phu, Gustavo Duque. Australian Institute for Musculoskeletal Science (AIMSS), The University of Melbourne and Western Health, St. Albans, VIC, Australia

Introduction: Bone loss begins in the third decade of life and involves decreased bone formation associated with a progressive reduction in osteoblast (Ob) survival, function and number. With ageing, MSC number and differentiation potential decrease due to reduced capacity to transform into Ob, leading instead to increased adipogenesis and lipid accumulation in the bone marrow of osteoporotic bones. Adipocytes produce palmitic acid (PA), a fatty acid (FA) known to be toxic to Ob in vitro. Potential mechanisms include induction of dysfunctional autophagy and reduced differentiation. Vitamin D (1,25(OH)2D3) induces osteoblastogenesis and has an anti-apoptotic effect on Obs. We therefore hypothesised that 1,25(OH)2D3 might rescue Obs from PA-induced lipotoxicity in vitro. Methods: Initially we compared the capacity of human Obs (Lonza, CC2538) to differentiate and mineralize in the presence of PA or 1,25(OH)2D3 or in combination. Cell survival was assessed using a 3-(2,5-diphenylterazolium bromide (MTT) assay. Autophagy was assessed via LC3-II expression, confocal microscopy, and monitoring of live autophagosomes at different time points. RT-PCR was performed to test the palmitoylation process in the presence of PA and 1,25(OH)2D3. Results: As expected, PA decreased mineralisation, differentiation and

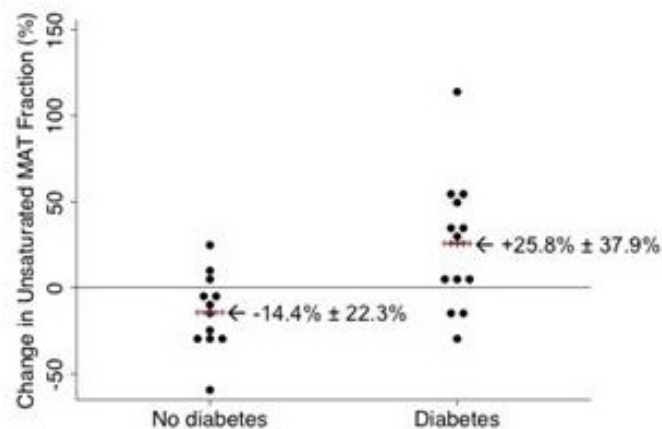
affected autophagy in human Obs. In contrast, cells treated with a combination of PA and 1,25(OH)2D3 recovered their capacity to differentiate and mineralise. 1,25(OH)2D3 increases Ob survival ($P < 0.01$) in the presence of PA. Furthermore, 1,25(OH)2D3 inhibited the autophagy process which was induced by PA at 24 and 48 hrs. Conclusion: This study has identified potential mechanisms to explain how 1,25(OH)2D3 might abrogate PA-induced lipotoxicity, including normalization of mineralization, survival and autophagy in Obs exposed to a strong lipotoxic milieu that mimics the human bone marrow environment. Future work should characterise the mechanisms of this effect as a step towards development of novel therapies to overcome lipotoxicity in the bone setting.

Disclosures: *Ahmed Al Saedi, None*

LB SAT - 1173

Changes In Bone Marrow Adipose Tissue Composition Are Associated With Metabolic Improvements After Gastric Bypass-Induced Weight Loss Tiffany Kim^{*1}, Ann Schwartz¹, Xiaojuan Li², Kaipin Xu², Galatea Kazakia¹, Carl Grunfeld¹, Robert Nissenson¹, Dolores Shoback¹, Anne Schafer¹. ¹University of California, San Francisco, United States, ²Cleveland Clinic, United States

Bone marrow adipose tissue (MAT) may interact with bone and energy metabolism. Both the quantity and composition are altered in metabolic bone disease, with higher levels of total MAT but lower levels of the unsaturated MAT fraction in those with osteoporosis and diabetes (DM). While longitudinal changes in total MAT have been studied, changes in MAT composition have not been described. Roux-en-Y gastric bypass (RYGB) surgery presents a unique opportunity for insights in MAT, given dramatic postoperative changes in bone, fat and glucose metabolism. We hypothesized the effect of RYGB-induced weight loss on MAT varies with DM status and glycemic control. We enrolled 30 morbidly obese women (14 with DM, 16 without DM) and measured vertebral MAT before and 6 months after RYGB with 3T magnetic resonance spectroscopy. Other measures included BMD by DXA and quantitative CT. Baseline characteristics were similar between those with and without DM, aside from hemoglobin A1c (HbA1c). There were no differences in baseline vertebral total MAT and the unsaturated MAT fraction (mean 66.3% and 4.9%, respectively). Six months after RYGB, women lost a mean 27 kg. BMD significantly declined at the spine and hip. Mean HbA1c decreased from 7.6% to 5.7% in women with DM. For total MAT, mean changes were $-6.1\% \pm 11.7\%$ in those with DM ($p=0.08$) and $+5.3\% \pm 9.5\%$ in those without DM ($p=0.08$; $p=0.01$ for difference between groups). For the unsaturated MAT fraction, mean changes were $+25.8\% \pm 37.9\%$ in those with DM ($p=0.03$) and $-14.4\% \pm 22.3\%$ in those without DM ($p=0.05$; $p<0.01$ for difference between groups). In the overall cohort, changes in total MAT and the unsaturated MAT fraction correlated with HbA1c improvements ($r=0.41$, $p=0.04$; $r=-0.51$, $p=0.01$, respectively). Changes in total MAT correlated with spinal volumetric BMD decline ($r=-0.41$, $p=0.04$) and femoral neck areal BMD decline ($r=-0.39$, $p=0.06$). In contrast, changes in MAT composition did not correlate with BMD declines or weight loss. Changes in MAT composition after RYGB correlated with metabolic improvements and varied by DM status. There was no relationship between changes in the unsaturated MAT fraction and declines in BMD, as was observed for changes in total MAT. Distinct MAT composition profiles are associated with marrow adipocyte subpopulation profiles. Thus, shifts in MAT composition may reflect changes in marrow adipocyte function, although how these changes affect skeletal health requires further study.



Disclosures: *Tiffany Kim, None*

LB SAT - 1178

KDM6B Regulates Estrogen-Mediated Osteogenic Differentiation of Human DMSCs Zhenqing Liu^{*1}, Chang-Ryul Lee¹, Zhongkai Cui¹, Michael Zhou², Hye-Lim Lee³, Min Lee¹, Cun-Yu Wang¹, Christine Hong¹, Tara Aghaloo¹. ¹University of California, Los Angeles, United States, ²University of California, Berkeley, United States, ³University of California, Irvine, United States

Objectives: KDM6B is a histone demethylase that removes the repressive epigenetic mark, H3K27me3 and has been previously shown to regulate the osteogenic commitment of human mesenchymal stem cells. The role of estrogen as an important medical component to preventative and therapeutic post-menopausal osteoporosis is well studied, but the epigenetic regulation of estrogen-mediated osteogenesis remains elusive. Estrogen is known to induce osteogenesis by activating the estrogen signaling pathway and upregulating osteogenic genes such as bone morphogenic proteins (BMP). This study assessed the epigenetic controls over these processes by looking at the effects of KDM6B in dental mesenchymal stem cells (DMSCs) in order to gain mechanistic insight into their potential clinical use in tissue regeneration and repair. **Methods:** Using the overexpression and knockdown of KDM6B in DMSCs, we induced cells to undergo osteogenic differentiation following estrogen treatment and investigated further mechanisms with ChIP. In vivo, the calvarial defect model was used and DMSC/ScrsH-Control, DMSC/ScrsH-E2, DMSC/shKDM6B-Control, DMSC/shKDM6B-E2 cells were loaded onto apatite-coated poly (lactic-co-glycolic acid) (Ap-PLGA) scaffolds (3 mm in diameter and 0.5 mm in height) and were transplanted. After 10 weeks, we compared new bone formation between the 4 groups. **Results:** Estrogen dramatically induced the expression of histone demethylase, KDM6B in DMSCs. When KDM6B was overexpressed, osteogenic differentiation was significantly enhanced. In contrast, KDM6B depletion by shRNA led to a significant reduction in osteogenic potential of DMSCs. Mechanistically, upon estrogen stimulation, ER α was recruited to the KDM6B promoter and enhanced KDM6B expression. Subsequently, KDM6B removed a silencing epigenetic mark, H3K27me3, from the BMP2 and HOXC6 promoters and activated the transcription of BMP2 and HOXC6, master genes of osteogenic differentiation. In vivo, micro-CT analysis demonstrated that BV/TV was increased in DMSC/ScrsH cells upon E2 treatment, however this increase was not seen in DMSC/shKDM6B even with E2 treatment. In addition, quantification of H&E staining showed the consistent results. In brief, KDM6B depletion inhibited estrogen-mediated bone formation in vivo. **Conclusion:** Our results demonstrated the critical role of KDM6B in the epigenetic regulation of estrogen-mediated osteogenic differentiation of DMSCs.

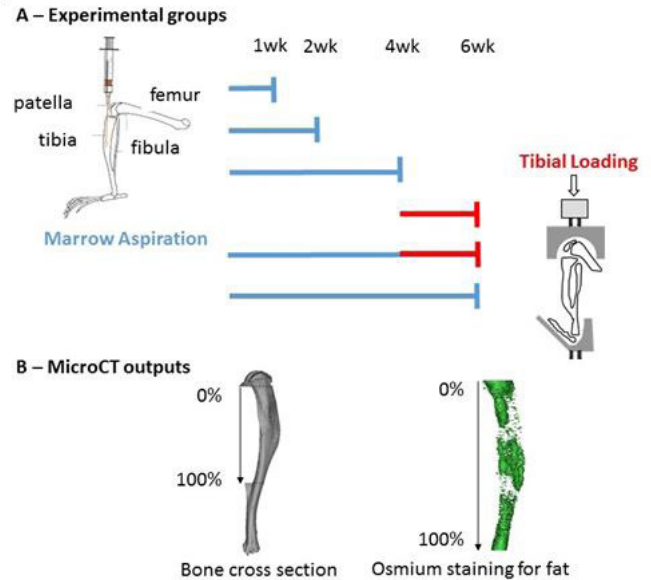
Disclosures: Zhenqing Liu, None

LB SAT - 1180

Effects of bone marrow regeneration on mechanoadaptation in aged bone Judith Piet^{*1}, Roland Baron², Sandra Shefelbine¹. ¹Northeastern University, United States, ²Harvard School of Dental Medicine, United States

Bone marrow in long bones become fatty with age, with mesenchymal stem cells differentiating into adipocytes rather than the osteoblast lineage. Previous studies have found an inverse relationship between marrow adiposity and bone volume [Justesen et al. 2001, Shen et al. 2012, Scheller et al. 2015]. This shift in marrow composition is suspected to be one of the causes for the age-related decrease in mechanoadaptation. In young mice, ablated bone marrow regenerates within 4 weeks but, to our knowledge, no study has investigated bone marrow regeneration in aged mice. We hypothesize that (1) bone marrow regeneration decreases the adipocyte composition in aged bone; (2) the response to mechanical loading in aged bone increases after bone marrow regeneration. **Material and methods:** In aged female C57BL/6 mice (22 months), we aspirated bone marrow in the right tibia with a saline-filled needle, inserted through the tibial plateau. Left legs were kept intact as internal controls. We sacrificed mice after 1, 2 and 4 weeks (Figure 1A). We imaged tibiae with micro-computed tomography to test changes in bone geometry, between the tibio-fibular junctions (from 0% at proximal junction to 100% at distal junction, see Figure 1B). We then performed Osmium staining and imaging in order to quantify marrow adipose tissue. Additionally, we examined 3 groups of aged mice: (1) axial loading at 9N for 2 weeks (100 cycles a day, 3 days a week); (2) bone marrow aspiration followed by 4 weeks recovery and 2 weeks axial loading at 9N; (3) bone marrow aspiration followed by 6 weeks recovery (Figure 1A). Left legs were kept intact as internal controls. After sacrifice, we imaged samples with micro-computed tomography. Samples were then embedded for histomorphometry. **Results:** 2 weeks following aspiration, bone cross section increased the proximal end, due to trabecular bone ($p < 0.05$). After 4 weeks, trabeculae were resorbed and the amount of bone was no different from the contralateral leg, but the adipocyte volume was increased locally (volume between 35-40%, $p < 0.05$). The location of adaptation was different in the groups that received loading only (adaptation at 50% and 70%, $p < 0.05$), or combined marrow regeneration and loading (adaptation in a more proximal site, between 30% and 50%, $p < 0.05$). **Conclusion:** Bone marrow aspiration changes the cellular environment of bone in response to loading, which alters the mechano-adaptive response in aged bone.

Figure 1



Disclosures: Judith Piet, None

LB SAT - 1184

Dietary Inflammatory Index and Cortical Bone Outcomes in Healthy Adolescent Children Lauren Coheley^{*1}, Emma Laing¹, Nitin Shivappa², James Hebert³, Richard Lewis⁴. ¹Department of Foods and Nutrition, University of Georgia, United States, ²Cancer Prevention and Control Program, University of South Carolina, United States, ³Cancer Prevention and Control Program, Epidemiology and Biostatistics, University of South Carolina, United States, ⁴Department of Foods and Nutrition, University of Georgia, United States

Chronic, low-grade inflammation is theorized to negatively affect bone strength. Dietary factors are thought to influence inflammation through pro- and anti-inflammatory processes. The Dietary Inflammatory Index (DII[®]) was developed to assess the inflammatory potential of the diet on a continuum from maximally pro-inflammatory to maximally anti-inflammatory. The primary aim of this study was to determine the relationships between DII[®] score and cortical bone in 290 healthy black and white adolescents, ages 9-13 years. The secondary aim was to assess the associations between DII[®] score and biomarkers of inflammation. The DII[®] score was calculated based on 3-day diet records and categorized into tertiles defined as low (<-1.34), medium (-1.34 to 1.41), and high (>1.41) levels of inflammation. Radius and tibia cortical bone were assessed via peripheral quantitative computed tomography (Stratec XCT 2000) at the 66% site relative to the distal growth plate. Fasting sera was measured for tumor necrosis factor-alpha (TNF- α), interleukin-6 (IL-6), vascular endothelial growth factor (VEGF), and monocyte chemoattractant protein-1 (MCP-1) using Luminex XMap system (TNF- α , VEGF, MCP-1) and Meso Scale Discovery assay (IL-6). The relationships between DII[®] score and cortical bone outcomes and biomarkers of inflammation were assessed using bivariate and multiple partial correlations adjusting for BMI-for-age-percentile, sexual maturation rating stage, and sex. ANOVA and ANCOVA models were used to compare DII[®] tertiles with cortical bone outcomes and biomarkers of inflammation. DII[®] score was negatively associated with tibia trabecular area ($r = -.141$, $P = .019$), periosteal circumference (Peri.Circ; $r = -.145$, $P = .016$), endosteal circumference ($r = -.145$, $P = .016$), strength strain index (SSI; $r = -.129$, $P = .032$), and radius Peri.Circ ($r = -.138$, $P = .027$) and SSI ($r = -.131$, $P = .036$). All relationships were nullified when adjusting for covariates. Mean tibia Peri.Circ was higher in the lower DII[®] score group compared to medium ($P = .050$) and high ($P = .046$) DII[®] score groups, but nullified when controlling for covariates. DII[®] score was not associated with TNF- α , VEGF, or IL-6, but was positively associated with MCP-1 in the unadjusted ($r = .125$, $P = .042$) and adjusted ($r = .021$, $P = .038$) models. It appears that DII[®] score is not related to bone strength in adolescents. The relationship between MCP-1 and DII[®] score should be further explored.

Disclosures: Lauren Coheley, None

LB SAT - 1185

Prickle1 is Required for Chondrocyte Polarity and Terminal Differentiation during Endochondral Ossification Yong Wan^{*}, Heather Szabo-Rogers. University of Pittsburgh, United States

The organized, polarized maturation of chondrocytes in the growth plate is necessary for the expansion and growth of the limb and cranial base. Decreased expansion of the

growth plates can result in shorter stature and midfacial hypoplasia. The molecular pathology of decreased growth plate expansion is not well described. We observed that the Prickle1Bj/Bj mutant mice develop a shorter cranial base and limbs. The Prickle1Bj mouse line has a missense mutation that results in compromised protein structure. Prickle1 is a core component of the Wnt/Planar cell polarity pathway. We hypothesized that the midfacial hypoplasia and short stature observed in Prickle1Bj/Bj mutants, resulted from loss of cell polarity and signaling during endochondral ossification. The Prickle1Bj/Bj midfacial hypoplasia results from loss of growth and expansion in the cranial base. We observed completely randomized polarity of the Prickle1Bj/Bj resting and proliferating chondrocytes. In addition, we observed prolonged and increased Wnt/ β -catenin and HH signaling resulting in the precocious maturation of chondrocytes and the stalling of terminal differentiation in the Prickle1Bj/Bj synchondroses and growth plates. Our data support the conclusion that Prickle1 acts as a rheostat in endochondral ossification by regulating chondrocyte polarity and coordinating HH and Wnt/ β -catenin signaling to control chondrocyte maturation during endochondral ossification.

Disclosures: *Yong Wan, None*

LB SAT - 1187

Circulating cells of the osteoblast lineage are increased in breast cancer patients with bone metastasis and could represent a novel biomarker for diagnosis and monitoring of tumor progression Jiarong Li*, Karine Sellin, Louis Dore Savard, Richard Kremer. Research Institute of MUHC, Canada

Circulating cells of the osteoblast lineage (cOB) have previously been identified using flow cytometry by positive selection with osteocalcin (OCN) and alkaline phosphatase (AP) antibodies. Although OCN is predominantly an intracellular protein, when secreted, it can be anchored to the cell membrane through Glu residue and bind to cell surface OCN receptors thus permitting its characterization in live cells. cOB may play a role in bone remodelling and are found in higher concentrations in peripheral blood during the pubertal growth spurt and in patients with recent bone fractures. However, the role of cOB has not yet been studied in patients with cancer and bone metastasis. We posit that cOB could be used as markers of skeletal metastases in breast cancer patients. Peripheral blood mononuclear cells (PBMC) of healthy volunteers and patients with breast cancer with and without bone metastasis were collected by apheresis and underwent further purification by Ficol-Paque density gradients. We next examined the proportion of circulating tumor cells and cOB in 5 healthy volunteers, 5 patients without bone metastasis and 8 patients with bone metastasis. PBMC were then subjected to flow cytometry using an antibody directed at the white blood cells surface marker CD45 and fixable viability dye negative selections to eliminate white blood cells and dead cells. CD 45 negative fractions were further fractionated by positive selection using monoclonal antibodies against human OCN, ALP and Cytokeratin 8/18 (for CTCs) molecular markers. Our results (Table 1) indicated that CTCs were significantly increased above baseline values (from healthy volunteers) ($p < 0.001$) in breast cancer patients with or without bone metastasis. In contrast both OCN and AP expressing cOB were found to be significantly higher than healthy volunteers only in breast cancer with bone metastasis ($p < 0.001$) but not in patients without bone metastasis. Our results suggest that cOB may represent novel biomarkers of skeletal metastasis.

Table 1

	%CD45 ⁺ CK8 ⁺	%CD45 ⁺ OCN ⁺	%CD45 ⁺ ALP ⁺	%CD45 ⁺ CXCR4 ⁺ ALP ⁺	P value
Patient with bone metastasis	Mean=0.364 SD=0.236	Mean=2.26 SD=1.70	Mean=0.715 SD=0.583	0.1925	<0.05
Patient without bone metastasis	Mean=0.664 SD=0.078	Mean=0.117 SD=0.069	Mean=0.0505 SD=0.039	N	<0.05
Healthy volunteers	Mean=0.1246 SD=0.09	Mean=0.139 SD=0.11	Mean=0.048 SD=0.0612	N	<0.05

Disclosures: *Jiarong Li, None*

LB SAT - 1191

PERK activity in osteoblast lineage does not contribute to skeletal homeostasis in mice Srividhya Iyer*, Alexander Harb, Christian Melendez-Suchi, Aaron Warren, Ha-Neui Kim, Maria Almeida. University of Arkansas for Medical Sciences, United States

The bone matrix synthesizing osteoblasts secrete large amounts of collagen and have extensive endoplasmic reticulum (ER). The ER orchestrates protein folding and secretion and the unfolded protein response (UPR) maintains ER homeostasis. The UPR is mediated by three signal transduction pathways, controlled by the proteins PERK, IRE1 α , and ATF6, that act to clear unfolded proteins from the ER. Sustained elevation of the UPR, or

its insufficient activation, contributes to the pathology of diseases such as diabetes, obesity, atherosclerosis, and cancer. Notably, humans and mice lacking functional PERK protein exhibit several metabolic defects, have low bone mass and abnormal collagen matrix. In mice, these skeletal defects are associated with a reduction in osteoblast number and bone formation. However, it remains unknown whether the skeletal defects in PERK null mice are due to a decrease in the UPR in osteoblasts or in other cell types. We found that PERK phosphorylation increases during osteoblast differentiation of bone marrow derived stromal cell cultures. To determine if PERK activity in osteoblasts contributes to skeletal homeostasis, we deleted the PERK gene from the entire osteoblast lineage using *Osx1-Cre* transgene. The body weight, lumbar and femoral BMD of CKO mice was indistinguishable from the *Osx1-Cre* littermate control males and females mice at 3 and 5 months of age. Bone marrow-derived osteoblast cultures from 6 month-old CKO mice had reduced mRNA expression of PERK, however, their ability to mineralize was comparable to similar cultures obtained from *Osx1-Cre* mice, as determined by Alizarin staining. MicroCT analysis revealed that the vertebral cancellous bone volume and femoral cortical thickness was indistinguishable between CKO and *Osx1-Cre* mice at 6 months of age. Moreover, PERK deletion did not affect vertebral compression strength. Collectively these results indicate that PERK signaling in osteoblasts is not essential for skeletal homeostasis. It is therefore likely that either the IRE1 or ATF6 axes mediate osteoblast differentiation in vivo or that there is functional redundancy between the three arms of UPR.

Disclosures: *Srividhya Iyer, None*

LB SAT - 1192

Deletion of menin early in the osteoblast lineage reduces mineralization of dense collagen gels by primary osteoblasts Ildi Troka*, Gabriele Griffanti², Showan N. Nazhat², Geoffrey N. Hendy¹. ¹Division of Experimental Medicine, McGill University, Canada, ²Department of Mining and Materials Engineering, McGill University, Canada

Background: Menin, the product of the Multiple Endocrine Neoplasia Type 1 (MEN1) gene, is a widely expressed, predominantly nuclear protein that facilitates cell proliferation and differentiation control. In vivo studies have shown the importance of menin for proper functioning of the mature osteoblast and maintenance of bone mass. Aims of the study: To use three-dimensional (3D) dense collagen hydrogel scaffolds, which mimic the physiological bone microenvironment, as a cell-culture model to investigate the differentiation and mineralization capabilities of primary osteoblasts of conditional knockout mice in which the *Men1* gene is deleted early in the osteoblast lineage. Methods: Primary calvarial osteoblasts were isolated from control, *Men1^{fl/f}*, and *Prx1-Cre;Men1^{fl/f}* mice which represent knockout of the *Men1* gene at the level of the pluripotent mesenchymal stem cell that gives rise to osteoblasts. The cells were seeded into plastic compressed dense collagen gels and cultured for 21 days in an osteogenic medium to induce differentiation. Results: The viability and mineralization activity of primary calvarial osteoblasts within the dense collagen scaffolds of knockout mice were identical to that of control. Scanning electron microscopy of day 21 samples revealed that in contrast to collagen gels seeded with control primary osteoblasts, collagen fibres of *Prx1-Cre;Men1^{fl/f}* cell-seeded gels were covered by smaller quantities of calcium phosphate based mineral, suggesting a difference in the cell mediated mineralization process carried out by knockout cells. By Fourier Transform Infrared Spectroscopy analysis, the absorption band intensities attributable to phosphate and carbonate groups were lower in collagen gels seeded with knockout primary osteoblasts. The mineral to matrix and carbonate to phosphate ratios in knockout samples were significantly lower ($p < 0.01$) and higher ($p < 0.05$), respectively, indicating impairment in the mineralization process and in the mineral crystal purity. Diffractograms obtained by X-Ray Diffraction at day 21 from knockout cell-seeded gels were characterized by the presence of lower intensity peaks attributable to hydroxyapatite, the main mineral component of bone. Conclusions: By the use of 3D dense collagen hydrogel scaffolds—a better alternative to the conventional two-dimensional system of primary cell culture—we show that expression of menin early in the osteoblast lineage is important for osteoblast mineralization

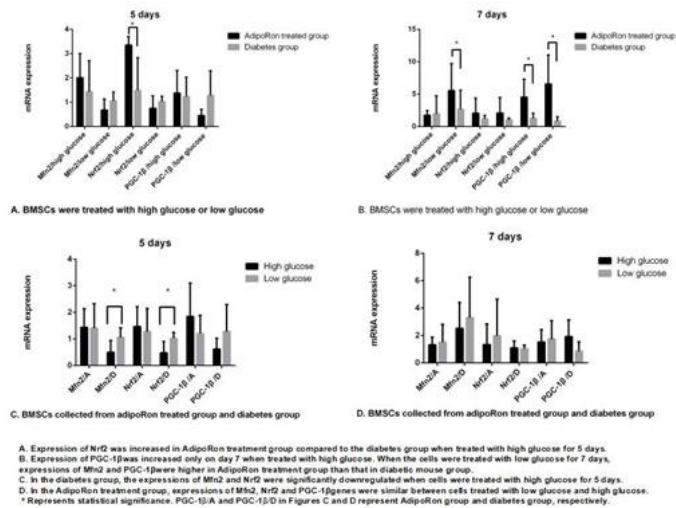
Disclosures: *Ildi Troka, None*

LB SAT - 1193

Adiponectin Receptor Agonist AdipoRon Increases Mitochondrial Fusion and Biogenesis in Diabetic Bone Cells Xiaoxuan Wang*, Xingwen Wu¹, Qisheng Tu¹, Jake Chen^{1,3}. ¹Division of Oral Biology, Tufts University School of Dental Medicine, Boston, Massachusetts, United States, ²Department of Periodontology, Peking University School of Stomatology, United States, ³Department of Developmental, Molecular and Chemical Biology Sackler School of Graduate Biomedical Sciences, Tufts University School of Medicine, Boston, Massachusetts, United States

Objective: AdipoRon is an orally active synthetic adiponectin agonist. It binds to both adiponectin receptors 1 and 2, and ameliorates diabetic complications. The dynamics and biogenesis of mitochondria were reported to be disrupted in diabetes. Mitofusin 2 (*Mfn2*), plays critical roles in mitochondrial fusion. *Nrf2* and *PGC-1 β* are related to mitochondrial biogenesis. We for the first time investigated the role of AdipoRon in mitochondrial fusion and biogenesis genes expression in type 2 diabetic (T2D) bone cells. Materials and methods: Twenty-week-old diet-induced obesity (DIO, a model for T2D) mice were divided into 2

groups: diabetes mellitus group (DIO), AdipoRon treatment group (DIO + AdipoRon). Bone marrow derived stem cells (BMSCs) were isolated from femur and tibia of mice. In each group, cells were treated respectively with low glucose (5.5mM glucose, glucose control), high glucose (25 mM glucose) for 5 days and 7 days. Expression of Mfn2, Nrf2 and PGC-1 β genes in mouse BMSCs were detected by real time PCR assays. Results: Expression of Nrf2 was increased in AdipoRon treatment group compared to the diabetes group ($p < 0.05$) when treated with high glucose for 5 days. Interestingly, expression of PGC-1 β was increased only on day 7 ($p < 0.05$). When the cells were treated with low glucose for 7 days, expressions of Mfn2 and PGC-1 β were higher in cells from AdipoRon treatment group than that from diabetic mice group ($p < 0.05$). Furthermore, in the diabetes group, the expressions of Mfn2 and Nrf2 were significantly downregulated when cells were treated with high glucose for 5 days ($p < 0.05$). The expression of PGC-1 β was also downregulated, but there was no statistical significance. In contrary, expressions of Mfn2 and PGC-1 β genes were similar between cells treated with low glucose and high glucose in the AdipoRon treatment group. Conclusion: We have previously shown that AdipoRon promotes osteoblast differentiation and bone formation. The findings of current study provide the first evidence of the mitochondrial protective effects of AdipoRon in DIO mice model suggesting that AdipoRon exerts its anabolic effect probably through increasing the critical gene expressions of mitochondrial biogenesis. It also opens new avenue to develop pharmaceutical molecules to manipulate mitochondrial biogenesis aiming to target the bone disorders particularly in the diabetic patients.



Disclosures: Xiaoxuan Wang, None

LB SAT - 1198

Osteoclasts serve as an intracellular niche for replicating Staphylococcus aureus Anna Ballard^{*1}, Jennifer L. Krauss¹, Pei Ying Ng², Linda Cox¹, Emily Goering¹, Nathan J. Pavlos², Deborah J. Veis¹. ¹Division of Bone and Mineral Diseases, Washington University School of Medicine, United States, ²School of Biomedical Sciences, University of Western Australia, Australia

Osteomyelitis (OM) is a severe bacterial infection of bone associated with an inflammatory reaction and disruption of skeletal integrity, and Staphylococcus aureus (S. aureus) is the primary causative agent. Although S. aureus is considered to be an extracellular pathogen, recent evidence indicates it can persist intracellularly in many cell types, including osteoblasts (OB). Infected OBs produce RANKL and recruit osteoclasts (OCs) to the site of bone infection, but the role of OCs in OM, and in particular their ability to become infected, is not well understood. We hypothesized that S. aureus could infect OCs to contribute to OM pathogenesis. Confocal imaging of decalcified calvaria sections from TRAP-red reporter mice injected with GFP-labeled S. aureus over the periosteum shows that S. aureus is present within OCs following infection, in vivo. We next utilized an in vitro infection protocol to assay the ability of S. aureus to reside in differentiating OCs. Primary expanded bone marrow macrophages (BMMs), cultured +/- RANKL, are infected with S. aureus for 30 min, extracellular bacteria killed with 1 hr gentamycin treatment, and cells cultured 16.5 hrs more prior to lysis; intracellular S. aureus growth is assessed by colony forming assay, comparing numbers immediately following gentamycin treatment with endpoint. We find that while BMMs cultured in M-CSF alone reduce S. aureus, the same cells stimulated with M-CSF + RANKL experience increases of ~50-fold (2 d RANKL) to ~500-fold (3 d RANKL) in intracellular bacteria. Further supporting the requirement for OC lineage differentiation, intracellular S. aureus levels are diminished to BMM levels in RANKL-treated cells lacking NFATc1 or NIK, which fail to form OC. To determine whether increased bacterial recovery in mature OCs represents intracellular S. aureus proliferation, we used a microscopy approach and observe replicating bacteria in infected OCs in vitro by transmission EM. Further, in vitro confocal imaging on both glass and bone demonstrates that S. aureus division events occur inside OC cells. While most bacteria co-localize with lysosomes 2 hrs post-infection, this occurrence decreases by 18 hrs post-infection in OCs, suggesting a possible mechanism for

lack of killing. In sum, our data indicate that OCs represent a unique niche for intracellular S. aureus proliferation, and further study of host-pathogen interactions in OCs may inform our understanding of disease progression in OM.

Disclosures: Anna Ballard, None

LB SAT - 1199

Ciliogenesis is inherent to osteoclastogenesis and IFT proteins drive osteoclast formation Vishwa Deepak*, Shuying Yang. University of Pennsylvania School of Dental Medicine, United States

Purpose: Osteoclasts are multinucleated bone resorbing cells. Primary cilia are microtubule-based organelles present on almost all vertebrate cells. IFT proteins regulate protein transport and cilia formation and their loss causes ciliopathies. Even though presence of cilia is essential for other cell types, it remains enigmatic that cilia are absent on osteoclasts and play no role in osteoclastogenesis. Hence, we performed this study to identify and delineate the exact roles of cilia and IFT proteins in osteoclasts. Methods: Myeloid-specific IFT80 or IFT20 knockout LysM-Cre transgenic mice were generated. Cilia were identified through a cilia-GFP mouse model and cilium-specific antibody staining. A detailed view of cilia was observed using electron microscopy. TRAP staining for osteoclasts was done in differentiation assays and bone histology sections. Bone mineral density was analyzed through μ CT. Inhibitors of cilia formation and PI3K, AKT, GSK3 β were used to identify molecular pathways. Gene expression, and phosphorylation of these pathways were analyzed through qPCR, western blotting and immunofluorescence. Results: Here, we report for the first time the presence of cilia on osteoclasts. The shape and physical structure represented characteristic properties of cilia. Cilium with well-defined axoneme, ciliary pocket and a 9+0 microtubule arrangement were seen through SEM and TEM respectively. Cilia number and length increased within 1 day of RANKL addition whereas they decreased at day 3 and further increased again at day 5 of osteoclastogenesis. IFT80 and 20 mRNA and protein expression modulated in same manner along with the differentiation. IFT 20 or 80 deletion caused cilia loss and growth retardation in mice. Increased osteoclast size and numbers were seen both in ex vivo assays as well as in histological sections of long bone. μ CT analysis revealed massive bone erosion in trabecular region of 1 and 3-month-old mice. Mechanistically, inhibition of cilia formation through cilia inhibitor also increased osteoclast formation. Inhibition of PI3K/AKT pathways decreased osteoclast numbers in mutant cells. Increased activation of NFATc1 and phosphorylation of Akt, GSK3 β , ERK1/2 proteins was observed in mutant cells. Conclusions: Primary cilia are present on osteoclasts and are inherent to osteoclast differentiation and bone resorption. These findings may pave the way for designing novel therapeutics against bone overgrowth or destructive disorders.

Disclosures: Vishwa Deepak, None

LB SAT - 1200

Bone Cell Effects of Mono-unsaturated Palmitoleic Acid Jian-Ming Lin*, Karen E Callon, Jillian Cornish. Department of Medicine, University of Auckland, New Zealand

We have previously demonstrated that saturated palmitic acid (C16:0) potentially inhibited osteoclast formation and function at low concentrations while some reports show that it is cytotoxic and has detrimental effect on health at higher concentrations. In the current study, we have investigated the bone cell effects of palmitoleic acid (C16:1), an omega-7 mono-unsaturated fatty acid, which is biosynthesized from palmitic acid in cells including adipocytes and is a common component in the diet. Comparing to saturated palmitic acid, mono-unsaturated palmitoleic acid has demonstrated a wide array of positive effects on health, being anti-inflammatory, cytoprotective in beta-cells and down-regulating lipogenesis. Osteoclastogenesis assays were conducted using both RAW264.7 cells and primary mouse bone marrow cells. Palmitoleic acid inhibited osteoclast formation with significant effect seen at 10 and 20 μ g/mL in RAW264.7 cells (by 29 and 52%, respectively; $P < 0.0001$, ANOVA) and in bone marrow cultures (by 27% and 33%, respectively; $P < 0.002$). The inhibition was not due to non-specific cytotoxicity, since the AlamarBlue[®] assay showed that the fatty acid stimulated the viability in both of the models. In addition, palmitoleic acid significantly stimulated the viability (by 33% at 20 μ g/mL; $P < 0.002$) and 3H-thymidine incorporation (by 12 and 14%, at 1 and 10 μ g/mL respectively; $P < 0.001$) in primary osteoblasts. Further study using real-time PCR found that palmitoleic acid reduced the expression of osteoclastic genes M-CSF, DC-STAMP, NFATc1, TNF- α and TRAP. It is likely that the inhibition of osteoclastogenesis is independent of RANKL/OPG pathway since the molecule reduced RANKL and OPG expression at the similar rates. In conclusion, palmitoleic acid is a promising factor in increasing bone health, stimulating osteoblasts and inhibiting osteoclasts.

Disclosures: Jian-Ming Lin, None

LB SAT - 1207

Fracture Risk Assessment in Patients on a Drug Holiday Michael Morkos^{*1,2}, Paul Mahrous¹, Alessandra Casagrande¹, Muriel Tania Go², Hasan Husni², Mirette Hanna¹, Sara Bedrose², Dingfeng Li², Monica Tawfic¹, Yu-Chien Cheng^{1,2}, Sanford Baim¹. ¹Rush University Medical Center, United States, ²John H. Stroger, Jr. Hospital of Cook County, United States

We aimed to describe fracture risk assessment practices among providers prescribing osteoporosis medications in a real-life setting. This is a retrospective cohort study in a tertiary academic center in Chicago, IL. Inclusion criteria involved adults (aged ≥ 18 years) who received minimum adequate therapy (bisphosphates, raloxifene, or denosumab ≥ 3 years, or Teriparatide ≥ 18 months), otherwise patients were excluded. Of 1,814 charts randomly selected and reviewed, 274 patients met the inclusion criteria. Risk stratification tools included: fragility fractures, Dual-energy X-ray Absorptiometry (DXA), and the FRAX risk assessment tool. Fracture risk assessment for the patients was assessed at the time of therapy initiation (N= 274 patients) and at the time of drug holiday (N=119 patients). High risk patients were defined as: prevalent fragility fracture, T-score ≤ -2.5 on DXA at the lumbar spine, femur neck, total hip, or distal 1/3 radius, or high risk score by FRAX defined as 10-year major osteoporotic fracture risk $\geq 20\%$ and/or hip fracture risk $\geq 3\%$; otherwise, patients were considered as low risk. Data was collected by chart review and FRAX scores were independently calculated by the research team for comparison and assessment purposes. Prior to initiation of therapy, 29.9% of patients had a baseline fragility fracture. DXA scan was performed at least once in 58.8% of the patients and 10.5% of the providers performed a FRAX risk assessment. At baseline, 71.5% of all patients would be considered at high risk for fragility fractures and as such eligible for therapy based on the aforementioned high risk categorization of patients. Drug holiday (DH) was started in 119 patients (43.4%) and 3.4% of the patients sustained a fragility fracture during therapy. At the time of initiation of a DH, 67.2% of patients had DXA performed within the previous 2 years and 10.9% of the providers performed a FRAX risk assessment. At the time of initiation of a DH, 66.4% of patients would be considered at high risk and eligible for continuation of therapy. A DXA scan was performed at least once in 95.3% of the total cohort that included the continued therapy and drug holiday groups. In conclusion, there was an under-utilization of FRAX risk stratification at the time of DH with two thirds of patients considered at high risk for future osteoporosis fractures placed on drug holiday. We recommend comprehensive fracture risk assessment utilizing history of fractures, DXA, and FRAX at therapy initiation and when considering a DH.

Fracture Risk Assessment – A Real Life Experience

	At Therapy Initiation (N=274 patients)	At Drug Holiday (N=119 patients)
DXA Scan performed	58.8%	67.2%
FRAX Score Performed	10.5%	10.9%
Fragility Fractures	29.9%	3.4%
High Risk Patients (candidates for therapy)	71.5%	66.4%

Disclosures: *Michael Morkos, None*

LB SAT - 1211

Lower total hip BMD and 25OHD levels are associated with the presence of abdominal aortic calcification in the Canadian Multicentre Osteoporosis Study (CaMos) Claudie Berger^{*1}, Alexandre Semionov², Brian C. Lentle³, Christopher S Kovacs⁴, David A Hanley⁵, Stephanie M Kaiser⁶, Robert G Josse⁷, Jerilynn C Prior³, Jonathan D Adachi⁸, Wojciech Olszynski⁹, K Shawn Davison¹⁰, Nancy Kreiger¹¹, Suzanne N Morin¹², David Goltzman¹². ¹Research Institute of the McGill University Health Centre, Canada, ²McGill University Health Centre, Canada, ³University of British Columbia, Canada, ⁴Memorial University, Canada, ⁵University of Calgary, Canada, ⁶Dalhousie University, Canada, ⁷St. Michael's Hospital, Canada, ⁸McMaster University, Canada, ⁹University of Saskatchewan, Canada, ¹⁰CaMos, Canada, ¹¹University of Toronto, Canada, ¹²McGill University, Canada

Purpose: We examined the association between risk factors (including total hip BMD and serum 25-hydroxyvitamin D (25OHD)) with cross-sectional and longitudinal 10-year measures of abdominal aortic calcification (AAC) in older CaMos participants. Methods: We scored AAC on lateral lumbar spine (L1-L4) x-rays using the Framingham method (scores 0-24) on 1930 participants aged 60+ at Year 10 follow-up (949 with 25OHD levels). We used a zero-inflated negative binomial (ZINB) model to determine cross-sectionally risk factors for presence and severity of AAC, and linear regression, for longitudinal change

in AAC from baseline to Year 10 (n=1196 with total hip BMD and n=243 with 25OHD). Additional risk factors studied: sex, age, BMI, race, education, smoking status (current, past, never), self-reported hypertension, heart attack, TIA, diabetes and kidney disease, use of calcium or vitamin D supplements and total calcium intake. Results: Presence and severity of AAC in women and men at Year 10 increased with age: 49% of those 60-69 years had AAC with mean (SD) score of 5.4 (4.6), while 87% of those 80+ years had AAC with mean score of 8.4 (5.6). Participants with AAC had mean (SD) total hip BMD and median (IQR) 25OHD levels of 0.868g/cm² (0.15) and 67nmol/L (53-82) compared to 0.904g/cm² (0.15) and 70nmol/L (58-84) in those without AAC. Being older and Caucasian, smoking, self-reported hypertension, heart attack and diabetes were associated with the presence of AAC (Table 1) in ZINB adjusted models. Lower total hip BMD was associated with higher odds of having AAC: OR=1.25 (95% C.I.: 1.04; 1.51) per SD. Age, smoking, self-reported hypertension, heart attack, TIA and diabetes were all associated with higher AAC severity while total hip BMD was not. Participants with 25OHD levels < 50nmol/L had higher odds of having AAC (OR of 1.95 (1.01; 3.76)), compared to those with levels > 50nmol/L, but lower 25OHD levels were not associated with severity of AAC. Finally, a model assessing change in AAC score from baseline to Year 10 showed self-reported heart attack and diabetes, current smoking, older age and higher baseline AAC score were associated with increasing AAC score over 10 years; but baseline total hip BMD and 25OHD levels were not. Conclusion: Lower total hip BMD and 25OHD levels are associated with the presence of AAC independently of self-reported cardiovascular disease and other risk factors, but not with severity or longitudinal change in AAC.

Table 1: Cross-sectional associations between risk factors and presence and severity of abdominal aortic calcification at CaMos Year 10 follow-up.

	PRESENCE vs. absence (ZINB, non-zero count)		SEVERITY (ZINB, count)	
	OR	95% C.I.	RR	95% C.I.
Male (ref=Female)	1.10	0.75; 1.60	0.92	0.81; 1.04
Age (per 1 year increase)	1.13	1.10; 1.16	1.03	1.02; 1.04
BMI (per 1 kg/m ² increase)	1.01	0.97; 1.04	1.00	0.99; 1.02
Non-Caucasian (ref=Caucasian)	0.52	0.28; 0.95	1.11	0.83; 1.48
Education (ref=no high school diploma)				
High school	0.82	0.54; 1.26	1.10	0.95; 1.27
Trades diploma or university w/o diploma	0.95	0.65; 1.37	1.04	0.92; 1.17
University certificate or diploma	0.72	0.49; 1.06	0.94	0.82; 1.08
Smoking status (ref=never)				
Current	8.29	3.70; 18.58	1.45	1.20; 1.76
Past	2.94	2.14; 4.02	1.25	1.13; 1.38
Hypertension (ref=no)	2.05	1.50; 2.80	1.18	1.07; 1.31
Heart attack (ref=no)	2.69	1.34; 5.42	1.32	1.14; 1.52
TIA (ref=no)	1.19	0.59; 2.39	1.20	1.03; 1.40
Kidney disease (ref=no)	0.55	0.27; 1.13	1.10	0.83; 1.45
Diabetes (ref=no)	1.72	1.04; 2.86	1.30	1.13; 1.49
Calcium or vit D supplement use (ref=none)	0.71	0.50; 1.03	0.96	0.85; 1.08
Total calcium intake (per 500mg/day increase)	0.93	0.84; 1.03	1.01	0.97; 1.04
Total hip BMD (per 1 SD increase)	0.80	0.66; 0.96	0.97	0.92; 1.03

ZINB= zero-inflated negative binomial

Disclosures: *Claudie Berger, None*

LB SAT - 1214

Determinants of Bone Microarchitecture Assessed by HR-pQCT in Adults with Long-Term HIV Infection Sarah Foreman^{*1}, Po Hung Wu¹, Ruby Kuang¹, Malcolm John², Phyllis Tien², Thomas Link¹, Roland Krug¹, Galatea Kazakia¹. ¹Department of Radiology and Biomedical Imaging, UCSF, United States, ²Department of Medicine, UCSF, United States

Purpose: In adults with long-term HIV infection, low bone density and increased fracture risk have emerged as significant comorbidities. Our aim was to assess influences of exercise, nutrition, and medications on bone microarchitecture using high-resolution peripheral QCT (HR-pQCT) in adults with long-term HIV infection. Methods: Thirty subjects with HIV (3 postmenopausal women, 27 men) were prospectively enrolled (BMI 26±4 kg/m², age 57±6 years, HIV duration 21±9 years). Questionnaires included the revised Community Healthy Activities Model Program for Seniors (CHAMPS), the Mini Nutritional Assessment (MNA), and medication assessments. Participants underwent radius and tibia HR-pQCT and dual-energy x-ray absorptiometry (DXA) of spine and hip. Multivariable linear regression models were used to evaluate effects of exercise, nutritional status, tenofovir disoproxil fumarate (TDF) and protease inhibitor (PI) use on bone macro- and microstructure, adjusting for demographic risk factors. Results: In regression models, higher nutrition scores were associated with higher radius and tibial cortical thickness (radius: R²=0.47; β =0.04; p=0.026; tibia: R²=0.46; β =0.07; p=0.005) and tibial cortical BMD (R²=0.56; β =12.77; p=0.026). Higher weekly frequency of all activities predicted higher radius and tibial trabecular number (radius: R²=0.36; β =0.01; p=0.020; tibia: R²=0.55; β =0.02; p=0.002) and less heterogeneity of tibial trabecular distribution (R²=0.46; β =-0.01; p=0.002) while higher caloric expenditure of all activities was associated with increased moment of inertia (resistance to bending and torsion) (radius: R²=0.51; β =28.91; p=0.023). TDF used in combination with a PI predicted decreased trabecular number (R²=0.35; β =-0.49; p=0.024) and increased heterogeneity of radius trabecular distribution (R²=0.35; β =-0.17; p=0.006), while TDF use without a PI did not. A secondary analysis of extent of HIV disease control, showed no significant influence of HIV viral load and CD4 count on bone microarchitecture. DXA

BMD values were not significantly associated with any evaluated determinants ($p > 0.05$). Conclusions: Cortical bone in adults with HIV is detrimentally affected by poor nutrition status, while trabecular bone is detrimentally affected by reduced physical activity. TDF use in combination with a PI is associated with deleterious effects on trabecular bone structure. DXA may be less useful for evaluating osseous changes in adults with HIV infection.

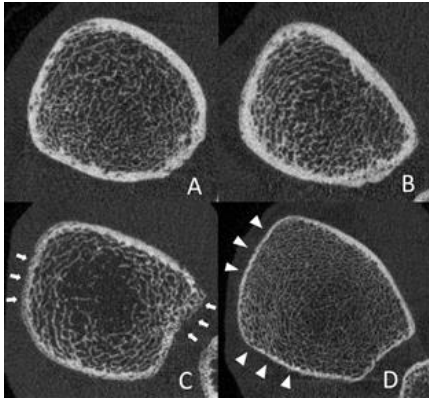


Figure 1: Ultradistal tibial HR-pQCT images of two HIV-infected subjects with high nutritional scores (A, B) and two HIV-infected subjects with low nutritional scores (C, D). Those with low nutritional scores show reduced cortical BMD with visibly increased porosity (C, white arrows) and reduced cortical thickness (D, white arrowheads).

Disclosures: *Sarah Foreman, None*

LB SAT - 1215

Definition of Vitamin D Deficiency based on Free 25OH Vitamin D Concentrations Nicolas Heuroux*. DIASource Immunoassays, Belgium

25-hydroxy Vitamin D (25OHD) is today the best marker of Vitamin D status. Since decades, the measurement of total 25OHD has been considered as the most reliable method to evaluate individual's Vitamin D deficiency and insufficiency. Recently, several publications have identified free 25OHD as a potentially better marker of Vitamin D status in multiple conditions (B. Hocher J. Steroid Biochem. Mol. Biol. 2018 181:80-87, S. Pilz J. Clin. Endocrinol. Metab. 2018 103(6):2385-2391). In this communication, we define probationary cut-off points of Vitamin D deficiency and insufficiency, based on the concentration of free 25OHD. Although the measurement of total 25OHD exists since more than 30 years, there is still no clear consensus on the cut-off points of Vitamin D deficiency and insufficiency. Severe deficiency is defined by concentrations below 10 ng/mL (25 nmol/L) and insufficiency is considered at levels between 10 and 20 or 30 ng/mL (50 or 75 nmol/L), depending on experts. One of the reason could be that the measurement of total 25OHD is not pertinent in multiple conditions. Therefore, we have established cut-off points for free 25OHD, based on a large multi-center study correlation between total 25OHD and free 25OHD. Two methods are applied: using the mean percentage of free 25OHD compared to total 25OHD, or based on the correlation parameters between both metabolites. The first method results in cut-offs of 2.0, 4.0 and 6.0 pg/mL for 25OHD severe deficiency and insufficiency. Using the correlation between free and total 25OHD leads to 1.5, 4.2 and 5.5 pg/mL. Both methods deliver similar probationary cut-off points of Vitamin D deficiency and insufficiency, based on the concentration of free 25OHD, and can be used by researchers and clinical laboratories.

Disclosures: *Nicolas Heuroux, None*

LB SAT - 1218

Mechanisms of Bone Loss Associated with Inflammatory Bowel Disease Christopher Peek*¹, Caleb Ford¹, Nicole Putnam¹, Jacob Curry², Blanca Piazuolo¹, Keith Wilson^{1,2}, Jim Cassat^{1,2}. ¹Vanderbilt University, United States, ²Vanderbilt University Medical Center, United States

Inflammatory bowel disease (IBD) is characterized by severe gastrointestinal inflammation and changes in the intestinal microbiota. Patients with IBD often experience extra-intestinal disease manifestations. Skeletal abnormalities are a frequent extra-intestinal manifestation of IBD, and patients exhibit a 40% increased fracture risk compared to that of the general population. Many factors, including malabsorptive malnutrition and glucocorticoid use, contribute to IBD-associated bone loss. Yet, nutritionally replete and glucocorticoid naive patients remain susceptible to bone loss. We used complementary mouse models of colitis-driven bone loss to test the hypothesis that IBD-associated bone loss is triggered in part by inflammatory cytokines and microbial constituents. We observed significant reductions in trabecular bone volume over total volume (BV/TV), up to 36%, and trabecular thickness in mice subjected to a chemically induced colitis with dextran sodium sulfate (DSS). Furthermore, trabecular bone loss occurs 7 days after DSS treatment and is sustained after DSS withdrawal. Using multiplexed cytokine analysis, we defined the abundance and kinetics of 32 cytokines within the skeletal microenvironment during DSS-colitis. We discovered increased abundance of several cytokines which have been implicated in multiple models of inflammatory bone loss, including TNF- α , CXCL5, and CXCL10, in the skeletal microenvironment of DSS-treated mice. Additionally, IL-12/23p40, the common subunit of IL-12 and IL-23, was found to be significantly increased. Intriguingly, IL-12 and IL-23 cytokines share a common subunit, IL-12/23p40 (p40), yet exert opposing effects on bone remodeling. IL-12 largely inhibits osteoclast differentiation, while IL-23 leads to bone

resorption through enhanced osteoclastogenesis. Co-housing experiments indicate that dysbiosis may contribute to these cytokine changes, as femur homogenates of DSS-treated mice cohoused with control mice exhibited reductions in p40 and TNF- α . We are utilizing fecal microbiome transplants, gnotobiotic mice, and skeletal specific pattern recognition receptor genetic knockout mice to test the hypothesis that the microbiome impacts skeletal homeostasis during colitis. This work will elucidate fundamental mechanisms by which systemic cytokines and circulating microbiota components impact bone biology during colitis and provide a platform to test the role of colitis-associated cytokines in pathologic bone loss.

Disclosures: *Christopher Peek, None*

LB SAT - 1221

Long-term risk of bone loss and fracture in rheumatoid arthritis and inflammatory bowel disease in the population-based Canadian Multicentre Osteoporosis Study (CaMos) Dana Blücu*¹, Thach Tran¹, Tineke Van Geel², Jonathan Adachi³, Claudie Berger⁴, Joop Van Den Bergh⁵, John Eisman¹, Piet Geusens², David Goltzman³, David Hanley⁶, Robert Josse⁷, Stephanie Kaiser⁸, Christopher Kovacs⁹, Lisa Langsetmo¹⁰, Jerilynn Prior¹¹, Tuan Nguyen¹, Jacqueline Center¹. ¹Bone Biology Garvan Institute of Medical Research, Australia, ²University of Maastricht, Netherlands, ³Department of Medicine, McMaster University, Canada, ⁴McGill University, Canada, ⁵Maastricht University, Netherlands, ⁶University of Calgary, Canada, ⁷University of Toronto, Canada, ⁸Dalhousie University, Canada, ⁹Memorial University, Canada, ¹⁰University of Minnesota, United States, ¹¹University of British Columbia, Canada

Background: This study sought to assess long-term risk of bone loss, and fracture in people with chronic inflammation such as rheumatoid arthritis (RA) and inflammatory bowel disease (IBD). Design and setting: Canadian Multicentre Osteoporosis Study, population based prospective study with 9 centres in Canada. Participants: 5527 women and 2164 men aged 50+ at baseline (1995/1997) who had been followed for an average of 10 (± 5) years until 2013. Exposure: Self-reported RA (n=483, 78% women) and IBD (n=434, 85% women) at baseline. Linear regression models were used to estimate the rate of bone loss at the site of femoral neck. Cox's proportional hazards model was used to assess the association with fracture and post-fracture mortality, after adjustment for age, physical activity, smoking, co-morbidities, education, weight and glucocorticoids use. Main outcome measure: Annual rate of bone loss (between baseline, year 3, 5 and 10), low trauma fracture (except head and digits), and all-cause mortality. Results: Participants with RA and IBD had similar baseline characteristics and both were older, had lower BMD, and a greater prevalence of cardio-vascular and respiratory diseases compared to controls. The use of glucocorticoid therapy throughout the study was low (9%, 3%, and 3% for RA, IBD and controls, respectively). Compared to controls, RA had a higher rate of bone loss [mean difference, %/year, 0.2 (95% CI, 0.8-0.31); $p < 0.0001$], and an increased risk of hip [HR 1.64 (95% CI, 1.01-2.65)], vertebral [HR 1.59 (95% CI, 0.92-2.74)] and non-hip non-vertebral fracture [HR 1.57 (1.27-1.94)] after adjusting for all confounders. Compared to controls, IBD had a similar rate of bone loss, but increased risk of hip [1.62 (95% CI, 1.00-2.63)], vertebral [2.06 (95% CI, 1.25-3.39)] and non hip non vertebral fracture [HR 1.30 (95% CI, 1.04-1.64)]. Exclusion of glucocorticoid users did not change fracture risk magnitude. Following fracture, mortality risk was increased by 2-fold in RA [HR, 2.05 (1.15-3.65)] and IBD [2.18 (95% CI, 1.09-4.37)] and by 43% in controls [1.45 (95% CI, 1.29-1.64)]. Conclusion: Patients with RA and IBD have increased risk of long-term bone loss, fractures, and increased post-fracture mortality which are not explained by glucocorticoid therapy. Further studies are needed to determine the role of inflammatory factors on bone metabolism and fracture outcomes in these conditions.

Disclosures: *Dana Blücu, None*

LB SAT - 1224

AFFs with Bisphosphonate Therapy (BP): Real Rare Side-Effect or Bad Medicine? David B. Karpf*¹, Frederick Singer², Kathleen Cody³. ¹Stanford University, United States, ²John Wayne Cancer Institute, United States, ³American Bone Health, United States

Introduction: Hypophosphatasia (HPP) is a rare disease affecting the development of bones and teeth, caused by the absence/reduced level of tissue-nonspecific alkaline phosphatase. Its severe, potentially fatal congenital form occurs in 1/100,000 births. HPP leads to increased circulating levels of inorganic pyrophosphate (iPPyP), which inhibits bone mineralization. The milder adult form usually presents in early middle age with low T-scores and sometimes metatarsal or femoral stress fractures, often with no history of premature loss of deciduous teeth. These patients usually have total alkaline phosphatase (TAP) levels ≤ 40 , and an elevated vitamin B6 level. TAP may be > 40 in some adults with HPP (JCEM 103(6):2234-2243). However, physicians unfamiliar with HPP may not note a low TAP, and these patients are often misdiagnosed with osteoporosis and inappropriately treated with a bisphosphonate (BP). As BPs are hydrolysis-resistant analogs of iPPyP, they should not be used in patients with HPP. Methods and Results: Atypical femur fractures (AFFs) have been associated with long term BP use in several case-control studies, yet no signal for AFFs was observed in the FDA review of 100,000 patient-years of data from the RCTs including 2-10 years of treatment with all 4 BPs. It is possible that this discordance results from patients with HPP being excluded from the BP trials, but occasionally, perhaps frequently, being

treated with BPs in clinical practice. One of the authors has been referred patients on BP therapy who he subsequently diagnosed as having HPP. Discussion and conclusion: Many clinical labs still lack a lower limit of normal for TAP, further hindering the proper diagnosis of milder forms of HPP in adults. Given the rarity of HPP, many practicing physicians are unaware that all adults with a TAP ≤ 40 should be screened for HPP by assessing for an elevated B6 level, even absent a stress fracture or history of premature tooth loss. It is possible that at least a portion of the patients who develop AFFs while on BP therapy may be non-diagnosed HPP patients inappropriately treated with BPs. This could explain the association of BP therapy with the rare event of AFFs in case-control studies but not in RCTs. This hypothesis could be tested by screening large hospital or HMO (eg, Kaiser) databases for adults with TAP values ≤ 40 , their association with diagnostic codes for osteoporosis, followed by chart reviews to screen for BP therapy and codes for AFFs.

Disclosures: *David B. Karpf, None*

LB SAT - 1232

Hydroxyapatite Nanoparticles Doped with Silver and Gold for Enhanced Bone Regeneration Deepak Kumar Khajuria*, David Karasik. The Musculoskeletal Genetics Laboratory, The Azrieli Faculty of Medicine, Bar-Ilan University, Safed-1311502, Israel

The repair of bone defects is one of the most challenging tasks in the orthopedic and maxillofacial surgery. Recapitulating embryological development is an attractive approach for engineering new bone at the defect site. We have investigated the osteogenic potential of hydroxyapatite (HA), silver doped HA (Ag-HA), gold doped HA (Au-HA), or silver-gold doped HA (Ag-Au-HA) nanoparticles in a zebrafish jaw bone regeneration (JBR) model. The HA, Ag-HA, Au-HA, and Ag-Au-HA nanoparticles were fabricated by the co-precipitation technique. The surface structures of HA, Ag-HA, Au-HA, and Ag-Au-HA nanoparticles were characterized by X-ray diffraction (XRD), Fourier-transform infrared spectroscopy, scanning and transmission-electron microscopy (TEM), Energy Dispersive X-Ray Spectroscopy (EDS) and elemental mapping analysis. Zebrafish JBR model was used to confirm the effect of HA, Ag-HA, Au-HA, and Ag-Au-HA nanoparticles on bone regeneration. After jaw resection surgery, ZF were divided into 9 groups of 20 fish each. Two experimental diets were designed with adding each of HA, Ag-HA, Au-HA, and Ag-Au-HA nanoparticles in concentrations of 40, and 80 mg/kg to the fish feed TetraMin, and control group without any nanoparticles, for the whole duration of the experiment. The ZF jaw bone volume after 14, 28 and 35 days post-resection (dpr) was statistically superior in the Ag-Au-HA 40 and 80 mg/kg ($p < 0.001$), HA 40 and 80 mg/kg ($p < 0.05$), Ag-HA 40 and 80 mg/kg ($p < 0.05$), and Au-HA 40 and 80 mg/kg ($p < 0.05$) treated groups as compared to the control group. Strikingly, the whole-body bone mineral density (BMD) of ZF after 14, 28 and 35 dpr was statistically superior in the Ag-Au-HA 40 and 80 mg/kg ($p < 0.001$), HA 40 and 80 mg/kg ($p < 0.05$), Ag-HA 40 and 80 mg/kg ($p < 0.05$), Au-HA 40 and 80 mg/kg ($p < 0.05$) groups as compared to the control group. Besides that, it is noteworthy to mention that both the ZF lower jaw bone volume and whole-body BMD in Ag-Au-HA (80 mg/kg) group was statistically superior to HA (40 and 80 mg/kg), Ag-HA (40 and 80 mg/kg) and Au-HA (40 and 80 mg/kg) treated groups ($p < 0.05$) after 14, 28 and 35 dpr. These observations indicate the intriguing therapeutic potential of Ag-Au-HA nanoparticles for bone repair; these nanoparticles seem especially important for bone regeneration. Finally, we showed that in-vivo Ag-Au-HA nanoparticles have the capacity to enhance BMD in ZF, suggesting their potential application as anti-osteoporotic agents. Khajuria et al. ACS Appl Mater Interfaces 2018; 13;10(23):19373-19385.

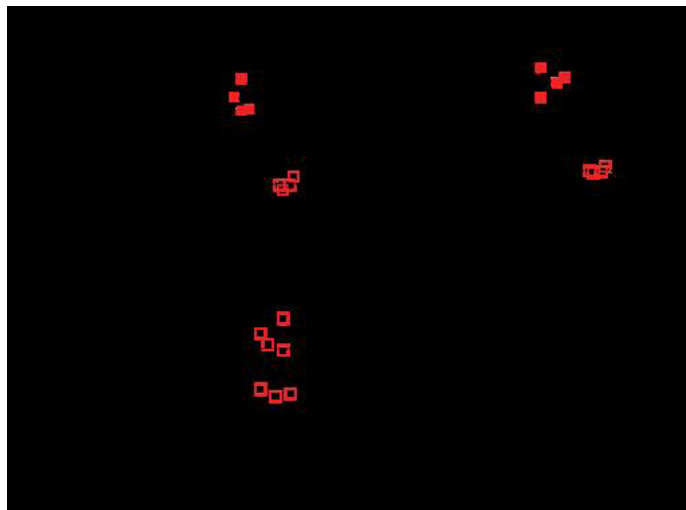
Disclosures: *Deepak Kumar Khajuria, None*

LB SAT - 1233

Activation of guanylyl cyclase-B increases long bone mass, density and strength Jerid Robinson*, Nicholas Blixt¹, Gordon Warren², Andrew Benton², Zhou Ye¹, Conrado Aparicio¹, Kim Mansky¹, Lincoln Potter¹. ¹University of Minnesota, United States, ²Georgia State University, United States

C-type natriuretic peptide (CNP) activation of guanylyl cyclase (GC)-B, also known as NPR2 or NPR-B, increases intracellular cGMP and stimulates long bone growth. However, the possible function of GC-B in maintaining bone density is relatively unknown. CNP activation requires the phosphorylation of multiple GC-B residues and dephosphorylation inactivates the receptor (1). Knock-in GC-B7E/7E mice expressing a phosphomimetic, glutamate-substituted, form of GC-B that cannot be inactivated by dephosphorylation, have increased CNP-dependent cellular cGMP concentrations and longer bones (2). Here, we show that male nine-week old GC-B7E/7E mice have greater bone mass, density, and flexural strength. Micro-computed tomography of tibiae indicated that GC-B7E/7E tibiae have 43% greater trabecular bone volume, 40% greater trabecular number and 17% less trabecular separation than wild type tibiae. GC-B7E/7E tibiae also have 10% greater cortical cross-sectional area, 9% greater cortical thickness, 6% greater periosteal diameter and a 24% greater cortical cross-sectional moment of inertia. Trabecular, but not cortical, bone mineral density was elevated 40% in tibiae from the mutant mice. Three-point bending analysis determined that mutant tibiae and femurs had 35% and 36% greater ultimate load and 35% and 49% greater stiffness compared to wild type bones, respectively. Microhardness assays revealed no differences in bone quality. Serum PINP levels were increased and CTX levels were not decreased in the GC-B7E/7E mice, consistent with increased osteoblast but not decreased osteoclast activity. In a translational study, 12-week-old male and female wild type mice

injected subcutaneously once daily for four weeks with a protease-resistant form of CNP (BMN-111) had 27%, 28% and 48% greater tibial trabecular bone volume fraction, trabecular number, and serum osteocalcin levels, respectively, with no changes in tibial length compared to bones from saline-injected control mice (Figure 1). We conclude that GC-B activation increases bone mass, density and strength possibly by elevating osteoblast activity. To our knowledge, these are the first data to show that GC-B activation results in anabolic effects in adult bone. We suggest that GC-B activators may be beneficial in the treatment of bone fractures and/or osteoporosis and warrant further study. References: 1. Potter, L. R. (1998) Phosphorylation-dependent regulation of the guanylyl cyclase-linked natriuretic peptide receptor B: dephosphorylation is a mechanism of desensitization. *Biochemistry* 37, 2422-2429. Shuhaibar, L. C., Robinson, J. W., Vigone, G., Shuhaibar, N. P., Egbert, J. R., Baena, V., Uliasz, T. F., Kaback, D., Yee, S. P., Feil, R., Fisher, M. C., Dealy, C. N., Potter, L. R., and Jaffe, L. A. (2017) Dephosphorylation of the NPR2 guanylyl cyclase contributes to inhibition of bone growth by fibroblast growth factor. *Elife*



Disclosures: *Jerid Robinson, None*

LB SAT - 1236

The A242T Mutation in the Low-density Lipoprotein Receptor-related Protein 5 Gene in Korean Family with Osteopetrosis Eunheui Kim*, Yunkyeung Jeon, Injoo Kim. Pusan National University Hospital, Republic of Korea

Objective Osteopetrosis is a heterogeneous group of disorders that characterized by a generalized increase in bone density. Type I autosomal dominant osteopetrosis results from mutation of low-density lipoprotein receptor-related protein 5 (LRP5) gene. Methods Radiographic and biochemical examinations and bone mineral density (BMD) and genetic analyses were performed in patient and her family members. Results A 22-year old woman went to dental clinic for orthodontics with asymptomatic malocclusion. She transferred to endocrinologist for the evaluation of acromegaly due to the jaw enlargement. She had normal height (161.6 cm), and weight (49.5 kg). She had a palpable torus palatinus which the patient was not aware of. Skull, humerus, femur and hand X-ray revealed thickened calvaria especially at the frontal and occipital bone, increased gonial angle of mandible and cortical thickening of long bone, metacarpal bone and phalanges. The BMD values were significantly higher than the standard age- and sex- matched adult mean reference values. The aBMD value of the hip and lumbar spine revealed 1.745 g/cm² in the left total hip (Z-score = +8.75), 1.612 g/cm² in the femoral neck (FN; Z-score = +5.6) and 1.868 g/cm² in the L1-L4 spine (Z-score = +6.1). The serum calcium level was 9.1 mg/dL (8.5-10.3 mg/dL), serum phosphate 3.6 mg/dL (2.0-4.6 mg/dL), urinary calcium 134.4 mg/24hr, serum intact parathyroid hormone 22.44 pg/mL (10-57 pg/mL), and 25-hydroxyvitamin D3 51.56 ng/mL (30-150 ng/mL). The values were serum osteocalcin 10.69 ng/mL (4-20 ng/mL), bone specific alkaline phosphate (bone ALP) 18.51 U/L (premenopausal 8.50-14.30 U/L), c-telopeptide of type 1 collagen (CTX) 0.54 ng/mL (premenopausal <0.573 ng/mL). The heterozygous missense mutation p.Ala242Thr in exon 4 of the LRP5 gene was detected in patient. And her mother, older sister and younger brother had the same missense mutation c.724G>A, but her father did not. Conclusion As far as we know, this is the first case report of A242T mutation in LRP5 gene with osteopetrosis in South Korea. The autosomal dominant gain-of-function missense mutations resulting in a high bone mass phenotype with an elongated mandible and torus palatinus. It is necessary to study the underlying mechanism of elevated bone mineral density including gene mutations. These studies might give us a clue to improve bone health.



Disclosures: *Eunheui Kim, None*

LB SAT - 1237

Asfotase Alfa in Adults – Functional Outcome in a Real World Setting Lothar Seefried*, Silke Achtziger, Franca Genest. Wuerzburg University, Germany

BACKGROUND: Hypophosphatasia (HPP) is rare metabolic disorder due to genetically determined deficient activity of the Tissue Non-specific Alkaline Phosphatase (TNAP), causing a wide range of musculoskeletal symptoms and functional disabilities. Asfotase Alfa (AA) is approved as enzyme-replacement therapy for the treatment pediatric-onset HPP. Clinical trials with AA have mainly focused on survival and functional improvements in children. Available data on AA treatment in adults is largely limited to solitary case reports. In order to add to this knowledge, we report real-world data on functional outcomes of AA treated adult HPP patients. **METHODS:** Retrospective data analysis of adult patients with pediatric-onset HPP treated with AA for bone manifestation of the disease in line with the label in Europe. Analysis focused on functional outcome data over a follow-up period of the first 12 months of treatment. Statistical analysis was conducted using non-parametrical testing procedures. **RESULTS:** Evaluation included 12 individuals (9 female) with a mean (SD) age of 51.4 (18.1) years, an average body weight of 81.5 (22.6)kg and a height of 159.6 (12.4) cm. During the course of treatment, one patient sustained a fracture not requiring surgery while three patients were subject to elective orthopedic surgeries of their lower limbs. Along with that, 4 patients could reduce their level of dependency on walking aids and still, distance covered during 6 Minute Walking Test (MWT) increased significantly from 327.6m to 354.9m ($p=0.008$). However, time required to perform the Chair Rising Test (CRT) only improved insignificantly ($p=0.125$) and average results for handgrip strength remained unchanged. In line with that, constitutional assessment using Bioimpedance Analysis (BIA) did not show any alteration of the Skeletal Muscle Index (SMI). None of the patients cancelled treatment for side effects or subjective lack of efficacy. **Discussion:** On label treatment with AA was safe and essentially enhanced patients mobility while results on other parameters of physical performance showed insignificant improvements. Importantly, functional outcome data exhibited a wide range of individual variability and was affected by numerous additional health issues like pre-existing limb deformities and concomitant illnesses. Considering the time course, functional changes were not completed at 6 months and further improvements could still be observed at 6 to 12 months.

Disclosures: *Lothar Seefried, Alexion, Grant/Research Support, Alexion, Speakers' Bureau, Alexion, Consultant*

LB SAT - 1241

An Acvr1[R258G] “Conditional On” Mouse Model of Atypical Fibrodysplasia Ossificans Progressiva (FOP) is Activin A dependent Sarah J. Hatsell*, Lily Huang, Chris Schoenherr, Lili Wang, Xialing Wen, Joyce McClain, Vincent Idone, Kalyan C. Nannuru, Andrew J. Murphy, Aris N. Economides. Regeneron Pharmaceuticals Inc, United States

FOP is an autosomal dominant disorder characterized by early onset, episodic and progressive ossification of skeletal muscle and associated connective tissue. FOP is driven by mutations in the intracellular domain of ACVR1 (ALK2), the most common of which is R206H. However, rare FOP causing mutations exist throughout the GS and the kinase domain of Acvr1. Several of these mutations result what appears to be a more severe FOP phenotype that includes significant developmental abnormalities in addition to the postnatal heterotopic bone formation. Two unrelated individuals with one such mutation, R258G, in the kinase domain of Acvr1 have a severe phenotype (Kaplan et al. 2015). We have modeled this mutation to investigate whether it results in a more severe phenotype in a mouse when present in the same genetic background as the more common R206H mutation. We engineered a Cre-regulated ‘conditional-ON’ allele of ACVR1[R258G] in the mouse, Acvr1[R258G]FlEx/+, similar to that previously used to model the R206H mutation (Hatsell, Idone et al. 2015). Body-wide activation of the FOP allele in Acvr1[R258G]FlEx/+;Gt(ROSA26)Sor-CreErt2/+ adult mice resulted in progressive ossification, evident radiographically as early as 2 weeks after dosing with tamoxifen in a similar manner to that seen with the previously published Acvr1R206HFlEx mouse. Detailed studies to determine whether this mutation has a different and more severe embryonic phenotype compared to R206H are planned. We have previously shown that HO resulting from R206H mutation is Activin A dependent and can be completely blocked with the administration of an Activin A blocking antibody. Other FOP causing mutations also render Acvr1 responsive to Activin A (Hino et al 2015) suggesting Activin A blockade would also be effective in inhibiting HO formation induced by these mutations. Here we show that HO generated by the R258G mutation is also Activin A dependent in this mouse model.

Disclosures: *Sarah J. Hatsell, None*

LB SAT - 1243

Percent total body fat is negatively associated with muscle strength and jump test performance in older men and women, independent of age, height, and muscle mass. Bethany Moore*, Harshvardhan Singh, Gary Hunter. University of Alabama at Birmingham, United States

Purpose: To assess the independent relationship between percent total body fat, muscle strength, and neuromuscular performance in older men and women. **Methods:** Dual X-ray absorptiometry (DXA) was used to measure percent total body fat and muscle mass in 60 older adults (men = 27, women = 33) between ages 55-85 (men = 64.8 ± 6.5 years, women = 62.5 ± 5.3 years). Appendicular skeletal muscle mass (ASM) was quantified as the sum of the lean soft-tissues of the arms and legs. An average of three maximum counter-movement jumps was used to calculate jump power (JPow) and jump height (JHt). Two leg press (LP) as well as the right and left side hip abduction (HipAbd) strength were assessed by 1-repetition maximum testing. The average of the right and left HipAbd values were used for analysis. JPow, LP, and HipAbd were normalized for body weight. Data normality was checked with Shapiro-Wilk test. Stepwise sequential multi-variable regression analysis was used to examine associations of percent total body fat and ASM with jump test performance and muscle strength tests. **Results:** Stepwise sequential regression analysis of percent total body fat and ASM versus jump test performance and measures of muscle strength after adjusting for age and height showed that percent total body fat negatively predicted 1) JPow ($n = 27$, $\beta = -0.583$, 95% CI = -0.289 to -0.073 , $r_{\text{partial}} = -0.586$, $P = 0.002$), 2) JHt ($n = 27$; $\beta = -0.618$, 95% CI = -0.149 to -0.538 , $r_{\text{partial}} = -0.624$, $P = 0.001$), and 3) HipAbd ($n = 27$, $\beta = -0.433$, 95% CI = -0.056 to -0.002 , $r_{\text{partial}} = -0.423$, $P = 0.035$) in men. In women, percent total body fat negatively predicted 1) JHt ($n = 33$, $\beta = -0.618$, 95% CI = -0.258 to -0.096 , $r_{\text{partial}} = -0.639$, $P < 0.001$), 2) LP ($n = 33$, $\beta = -0.542$, 95% CI = -0.128 to -0.035 , $r_{\text{partial}} = -0.556$, $P = 0.001$), and 3) HipAbd ($n = 33$, $\beta = -0.067$, 95% CI = -0.067 to -0.032 , $r_{\text{partial}} = -0.720$, $P < 0.001$). **Conclusion:** Our findings suggest that percent total body fat has an independent negative association with jump test performance and muscle strength in older men and women. This knowledge is important for evidence-based musculoskeletal rehabilitation in older adults with sarcopenia and increased adiposity as well as decisions about weight loss in overweight or obese older men and women.

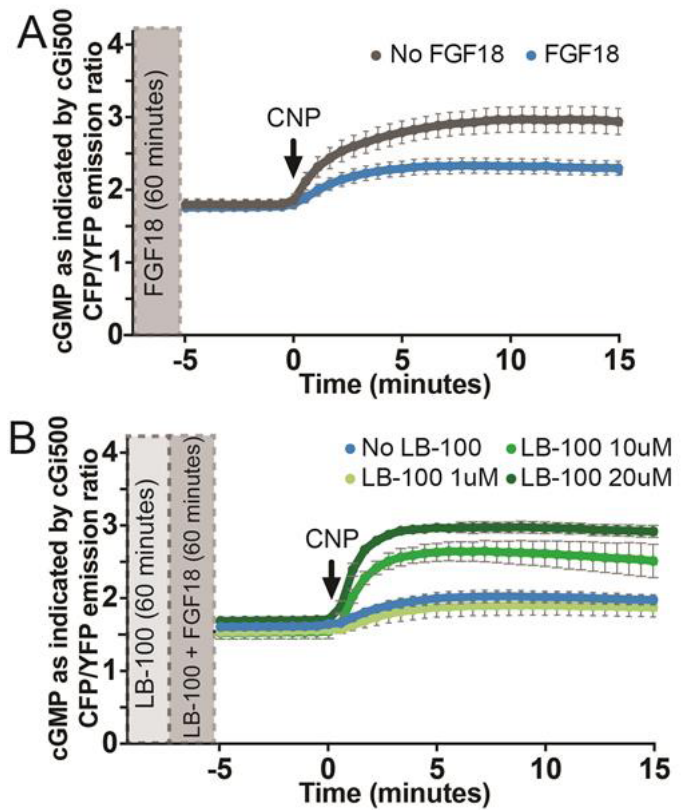
Disclosures: *Bethany Moore, None*

LB SAT-1245

FGF-inhibition of NPR2-mediated Cyclic cGMP Production in Growth Plate Chondrocytes Is Reversed by the Phosphatase Inhibitor LB-100 Leica C Shuhaibar*, Giulia Vigone, Laurinda A Jaffe. Department of Cell Biology, University of Connecticut Health Center, United States

Chondrocyte proliferation and differentiation during endochondral bone growth is controlled by multiple regulatory pathways. Activating mutations in fibroblast growth factor receptor 3 (FGFR3) and inactivating mutations in the natriuretic peptide receptor 2 (NPR2) guanylyl cyclase both cause decreased production of cyclic GMP (cGMP) and severe short

stature, causing Achondroplasia and Acrosomic Dysplasia Type Maroteaux, respectively. However, how these signaling pathways interact to regulate bone growth is poorly understood. We developed a novel ex vivo imaging system using mice expressing the cGi500 FRET sensor for cGMP and confocal microscopy to measure real-time changes in cGMP production in chondrocytes of living newborn tibias, and showed that FGF18 decreases cGMP production by NPR2 (1). Activation of NPR2 requires both C-type natriuretic peptide (CNP) binding to the extracellular domain and phosphorylation of 7 intracellular serines and threonines. Conversely, FGF-induced inactivation of NPR2 depends on the dephosphorylation of these phosphorylation sites (1, 2). These results suggested the potential use of phosphatase inhibitors to suppress the FGF-induced NPR2 dephosphorylation and inactivation, for the treatment of skeletal dysplasias such as Achondroplasia, a condition where FGFR3 is constitutively active. To investigate this possibility, we tested the effect on chondrocyte NPR2 activity of the PPP family phosphatase inhibitor LB-100, a small molecule that has been used successfully in phase one clinical trials for other diseases (3). By treating tibias from cGi500 mice with LB-100, we tested whether inhibiting PPP-family phosphatases counteracts the inhibitory effect of FGF18 on NPR2 and enhances the production of cGMP in the growth plate, thus stimulating bone growth. We show that LB-100 dose-dependently reverses the inhibition of NPR2 activity by FGF in the growth plate. Tibias treated with FGF18 for 1 hour produced 44% less cGMP when exposed CNP, as compared to control bones (Fig 1A). In contrast, when tibias were treated with 10-20 μ M LB-100 for 1 hour prior to treatment with FGF18, the production of cGMP was restored to normal levels (Fig 1B). Our results suggest that LB-100 or other phosphatase inhibitors could also be useful for treatment of skeletal dysplasias. References: 1. Shuhaibar et al., eLife. 6: e31343, 2017. Robinson et al., Cell. Signal. 40: 222, 2017. Chung et al., Clin. Cancer. Res. 23: 13, 2017



Disclosures: Leia C Shuhaibar, None

SUN-0019

High Frequency of Bone Mineral Density (BMD) Abnormalities in Women with Symptoms Typical of Thyroid Dysfunction and Normal Thyroid Hormones Georgia Antoniou^{*1}, Stelios Kasikis², Charis Chourpiliadis², Dimintra Bantouna², Panagiota Koukoutsidi², Juan Carlos Jaume³, Rodis D Paparodis⁴. ¹Agia Sofia General Pediatric Hospital, Greece, ²University of Patras Medical School, Greece, ³Division of Endocrinology, Diabetes and Metabolism and Center for Diabetes and Endocrine Research (CeDER), University of Toledo, United States, ⁴Division of Endocrinology Diabetes and Metabolism and Center for Diabetes and Endocrine Research (CeDER) University of Toledo, Greece

Background: Subclinical thyroid disease has significant negative impact on bone metabolism, both in the forms of bone accrual at the young age and bone loss after menopause. Our clinical observation suggested that this phenomenon is present in women with normal thyroid hormones as well, as long as thyroid abnormalities can be found by ultrasound or thyroid scan. We performed the present study to further delve into this topic. **Methods:** We prospectively enrolled women complaining of five or more concurrent, unexplained symptoms of potential thyroid dysfunction at our Endocrinology clinic in Patras, Greece within 3 years. Subjects with abnormal thyroid function, primary hyperparathyroidism, eGFR<60ml/min, or those on medications affecting thyroid hormones were excluded. We measured serum TSH, performed a Tc-99m thyroid scan, thyroid ultrasound and DEXA scan of the spine, hip or distal radius. We split our subjects by age (pre and post-menopausal) and BMD, [lowest T- or Z-score >-1.0 - Normal, -1.0 to -2.4 - Low Bone Mass (LBM) and <-2.4 Osteoporosis (OST)]. Fracture history was recorded as well. The non-Hispanic white female population from the NHANES database was used as a control (CON). Mann-Whitney test was used to compare TSH, T/Z scores of the hip area between our subjects and CON. **Results:** Out of 3563 subjects, 356 consecutive women met the inclusion criteria; Ultrasound findings: n=8 (2.2%) were normal; n=282(79.2%) increased vascularity; n= 91(25.6%) single thyroid nodule; n=170(47.8%) multiple nodules. Thyroid scan findings: n=273(76.7%) increased uptake; n=25(7.0%) decreased uptake; n=178(50.0%) cold nodule(s); n=40(11.4%) hot nodules; n=17(4.8%) both hot and cold nodules; n=52(14.6%) normal thyroid scan. No subjects had normal thyroid ultrasound and scan at the same time. TSH was higher in our subjects compared to the CON(p<0.001). LBM was present in 23.8% to 50.5% of our subjects, while OST prevalence increased with age. High rates of fracture were noted in all age groups and increased with age (18.2%-45.5%). **Conclusions:** Subjects with symptoms suggestive of thyroid dysfunction and TSH values within reference range, regardless their age group, tend to have low bone mass. Our findings imply that an unidentified thyroid dysfunction might strongly impact bone mass accrual and peak bone mass, leading to a high risk of OST in this population even before menopause.

Disclosures: Georgia Antoniou, None

SUN-0020

Renal Function Change in Chronic Hypoparathyroidism Patients Treated With Recombinant Human Parathyroid Hormone (1-84) (rhPTH[1-84]) and in a Historical Control Cohort Treated With Standard Therapy Kristina Chen^{*1}, Mishaela Rubin², Fan Mu³, Elyse Swallow³, Jing Zhao³, Jessie Wang³, Alan Krasner¹, Nicole Sherry¹, James Signorovitch³, Markus Kettele⁴, John Bilezikian². ¹Shire Human Genetic Therapies, Inc., United States, ²Columbia University College of Physicians and Surgeons, United States, ³Analysis Group Inc., United States, ⁴Division of Nephrology, Klinikum Coburg, Germany

Standard therapy (ST) for chronic hypoparathyroidism (HPT) includes calcium and active vitamin D supplementation, which can be associated with an increased risk of renal complications. This study compared renal function change, assessed by estimated glomerular filtration rate (eGFR) over 5 years, between HPT patients receiving rhPTH1-84 as an adjunct to ST and a historical control cohort without rhPTH1-84. rhPTH1-84-treated HPT patients were selected from 2 single-arm, long-term, open-label studies, RACE (NCT01297309) and NCT02910466. Control patients were selected from the MedMining database using similar inclusion criteria to the 2 studies. Patients were required to have ≥ 2 eGFR measures, 5 years apart, after HPT diagnosis. Index date was defined as the baseline visit in the rhPTH1-84-treated cohort and the 1st eligible eGFR measure date in the historical control cohort. eGFR change over time from baseline was compared using an adjusted multivariable model. A sensitivity analysis was conducted at 3 years for patients with ≥ 2 eGFR measures 3 years apart after HPT diagnosis. 122 patients (n=69 with and 53 without rhPTH1-84) were included in the 5-year analyses. At baseline, rhPTH1-84-treated patients compared with control patients were younger (51.7 vs 55.8 y) and had lower eGFR (75.5 vs 82.5 mL/min/1.73m²). Race and sex were similar between cohorts. A lower proportion of rhPTH1-84-treated patients had concomitant nephrotoxic drug use or a history of hypocalcemia, hypercalcemia, hypertension, diabetes mellitus, or cardiac disorders. Characteristics were similar in the 3-year sensitivity cohorts (n=75 with and 76 without rhPTH1-84). In the adjusted model, predicted eGFR change at year 5 was +5.80 vs -5.56 mL/min/1.73m² in the rhPTH-treated vs historical control cohort. Annual rate of eGFR decline over 5 years of follow-up was significantly lower in rhPTH1-84-treated patients (difference in annual eGFR change=2.13 mL/min/1.73m²; P=0.002). The trend in eGFR change over 3 years was similar in the sensitivity analysis (difference in annual eGFR change=2.96 mL/min/1.73m²; P<0.001). In this retrospective analysis, patients with chronic HPT without rhPTH1-84 treatment exhibited significantly greater decline in eGFR than patients receiving rhPTH1-84 over 5 years, with

and without adjusting for confounders. This difference was also observed over 3 years in similar cohorts. This analysis is hypothesis generating and further research is warranted.

Disclosures: Kristina Chen, Shire, Other Financial or Material Support

SUN-0021

Treatment of Tertiary Hyperparathyroidism After Renal Transplant Chee Kian Chew^{*1}, Jennifer Hill², Robert Wermers², Tricia Veglahn², Hatem Amer², Matthew Hathcock². ¹Tan Tock Seng Hospital, Singapore, ²Mayo Clinic, United States

Background: Elevated parathyroid hormone (PTH) persists in up to 70% of patients one year and 43% two years after renal transplant. Tertiary hyperparathyroidism (3HPT) occurs in an estimated 23% of patients one year after renal transplant. Although hyperparathyroidism has been identified as an independent risk factor for fractures and allograft failure, appropriate treatment remains unclear. Purpose: To evaluate if bone health and allograft function in adult patients with 3HPT is adversely affected by 3HPT and if 3HPT management provides benefit in these parameters within the first five years after renal transplant. **Methods:** A retrospective chart review of renal transplant patients 18 years of age or older at a Midwestern tertiary healthcare center who received a first time, solitary kidney transplant between January 1, 2010 - December 31, 2011 was completed. **Results:** A total of 209 patients were identified with a mean age of 53 years and of whom 128 were male (61.2%). The mean PTH at the time of transplant was 196 pg/mL. Overall, 45 patients (23%) had 3HPT during at least one time point throughout the study, and specifically was present in 32 (15%), 28 (13%), 14 (7%), and 6 patients (3%) at 4 months, 1 year, 2 years, and 5 years after renal transplant respectively. Parathyroidectomy was performed in 20 patients, 9 pre-transplant and 11 post-transplant. Those with 3HPT were noted to have longer hemodialysis duration pre-transplant (P < 0.001) and received a deceased donor transplant (P = 0.04). Resolution of 3HPT was noted in 10% of patients with 3HPT between 4 months and 12 months and 4% between 12 months and 24 months without parathyroidectomy or cinacalcet. When comparing patients with 3HPT to those without 3HPT there was no significant difference in bone mineral density at the spine or hip or fractures post-transplant. Renal function at 5 years and graft failure were also not significantly different in patients with 3HPT. **Conclusions:** A significant number of patients develop 3HPT after renal transplant especially in patients with dialysis prior to transplant or with deceased donor transplants. Although skeletal health and renal function were not adversely impacted by the presence of 3HPT, changes in the management of renal transplant (e.g. preemptive living donor transplants) likely impacted the results. Further study will be needed to clarify appropriate management of patients who develop 3HPT after renal transplant.

Disclosures: Chee Kian Chew, None

SUN-0022

Premenopausal women with idiopathic osteoporosis (PreMenIOP) and low bone formation have decreased responsiveness to teriparatide (TPTD) and evidence of IGF-1 resistance in skeletal and non-skeletal tissues Adi Cohen^{*1}, Nandini Nair¹, Stephanie Shiao¹, Robert R. Recker², Joan M. Lappe², David W. Dempster^{1,3}, Hua Zhou³, Binsheng Zhao¹, Xiaotao Guo¹, Mafo Kamanda-Kosseh¹, Mariana Bucovsky¹, Julie Stubby², Elizabeth Shane¹. ¹Columbia University Medical Center, United States, ²Creighton University, United States, ³Helen Hayes Hospital, United States

PreMenIOP have marked deficits in bone microarchitecture but variable bone remodeling. We have reported that PreMenIOP with low tissue level bone formation rate (BFR) are less responsive to TPTD and have higher serum IGF-1, a hormone anabolic for osteoblasts and other tissues. The IGF-1 data were unexpected because serum IGF-1 is low in other forms of low turnover osteoporosis: male IOP, obesity, growth hormone deficiency (GHD). We thus hypothesized that PreMenIOP with low BFR have IGF-1 resistance at the osteoblast level and this IGF-1 resistance may affect nonskeletal tissues. To investigate these hypotheses, we prospectively evaluated 39 PreMenIOP who received 12M of TPTD (20 mcg/d) in an FDA-funded RCT. The mean 12M increase in lumbar spine (LS) BMD was 8.7±5.6% but varied widely: -7% to +21%. Lower LSBMD response to TPTD was again associated with lower pre-TPTD cancellous (CAN; r=0.4, p=0.03) and endocortical (ENDO; r=0.4, p=0.01) BFR. Consistent with our hypothesis, IGF-1 Zscores correlated inversely with CAN (r=-0.5, p=0.007) and ENDO (r=-0.4, p=0.04) BFR. LSBMD response was also inversely related to IGF-1 Zscore (r=-0.3, p=0.04), with a trend for an inverse association with IGF-1 Zscore (r=-0.3, p=0.1). To assess for evidence of IGF-1 resistance in nonskeletal tissues, we asked whether PreMenIOP with low BFR/high IGF-1 resemble patients with low IGF-1 due to GHD, a clinical profile characterized by visceral adiposity, low adiponectin/high leptin, insulin resistance, high LDL/low HDL, high inflammatory CV risk markers (CRP, IL-6). We compared PreMenIOP with low and high BFR based on median CANBFR on biopsy (Table). Low BFR had lower BMD response to TPTD, higher serum IGF-1 and IGF-1 Zscores. They also had higher weight, BMI, central adiposity and leptin (all p<0.05). Lower BMD response to TPTD was associated with some clinical features of GHD: higher DXA trunk fat (r=-0.4, p=0.01), subcutaneous fat at L4 level by CT (r=-0.5, p=0.01) and leptin (LS: r=-0.3, p=0.08). Also consistent with our IGF-1 resistance hypothesis, several common features of GHD were associated with higher IGF-1 Zscores in PreMenIOP: higher DXA trunk fat (r=0.3, p=0.048), triglycerides (r=0.3, p=0.03) and leptin (r=0.4, p=0.02) and lower adiponec-

tin ($r=-0.4, p=0.02$). In conclusion, IGF-1 resistance may underlie both the skeletal phenotype and decreased responsiveness to TPTD in PreMenIOP with low bone turnover. Such women also demonstrate metabolic consequences of IGF-1 resistance in nonskeletal tissues.

Variable	Low BFR N = 16	High BFR N = 20	p-value	Reference Range (Premenopausal Adult Women)
Baseline Bone Remodeling				
CAN BFR (mm ³ /mm/yr)	0.004 \pm 0.002	0.016 \pm 0.008	N/A	
Serum CTX (pg/ml)	255 \pm 100	401 \pm 160	0.003	112-738 pg/ml
Serum P1NP (ug/ml)	33 \pm 9	41 \pm 15	0.1	19-83 ug/ml
Response to 12M of TPTD				
Lumbar Spine BMD g/cm ² (% change)	0.050 \pm 0.048 (6.7 \pm 6.3%)	0.081 \pm 0.035 (10.3 \pm 4.9%)	0.04	
Growth Hormone (ng/ml)	2.0 \pm 3.1	2.3 \pm 2.2	0.7	<10 ng/ml
GH/IGF-1 Parameters				
IGF-1 (ng/ml)	142 \pm 37	114 \pm 39	0.04	<15-447 ng/ml
IGF-1 (Z-score)	+0.2 \pm 1.1	-0.8 \pm 0.8	0.004	
IGFBP3 (mg/ml)	6.5 \pm 1.1	5.9 \pm 1.3	0.2	1.2-9.1 ug/ml
IGF-1/IGFBP3 Ratio	22.0 \pm 4.8	19.7 \pm 5.5	0.2	
Body Composition				
Weight (kg)	62.1 \pm 11.2	54.9 \pm 7.9	0.03	
BMI (kg/m ²)	24.0 \pm 3.8	20.4 \pm 2.4	0.002	
DXA Whole Body Fat (% Fat)	36.0 \pm 5.9	33.1 \pm 7.0	0.2	
DXA Trunk Fat (% Fat)	32.4 \pm 6.2	27.6 \pm 7.9	0.08	
Subcutaneous Fat (based on CT slice at L4; mm ²)	27403 \pm 21293	15771 \pm 10446	0.005	
Visceral Fat (based on CT slice at L4; mm ²)	6495 \pm 4804	4598 \pm 3323	0.06	
Serum Markers Associated with Central Adiposity				
Leptin (ng/ml)	24.0 \pm 12.5	16.1 \pm 9.9	0.045	2-11.1 ng/ml
Adiponectin (ng/ml)	9022 \pm 3083	11047 \pm 3827	0.1	559-7271 ng/ml
CRP (mg/l)	1.4 \pm 1.3	1.1 \pm 1.8	0.5	<5.0 mg/l
IL-6 (pg/ml)	2.83 \pm 4.24	1.22 \pm 1.08	0.2	0.44-9.96 pg/ml
HDL (mg/dl)	72 \pm 15	80 \pm 21	0.2	>55 mg/dl
Triglycerides (mg/dl)	85 \pm 33	69 \pm 25	0.1	<200 mg/dl
LDL (mg/dl)	98 \pm 33	90 \pm 31	0.4	<100 mg/dl
HOMA-IR (calculated measure of insulin resistance based on fasting glucose and insulin)	1.06 \pm 0.66	0.92 \pm 0.79	0.6	

Disclosures: *Adi Cohen, None*

SUN-0023

Functional outcomes of nonoperatively treated LC-1 pelvic ring fractures: a retrospective study Aidan Hadad¹, Matthew Cohn², Rehan Saiyed¹, Omer Or³, Eric Marty¹, Gülce Askin⁴, Joseph Lane¹. ¹Hospital for Special Surgery, United States, ²Rush University Medical Center, United States, ³Hebrew University Hadassah Medical Center, Israel, ⁴Weill Cornell Medical College, United States

Lateral compression type 1 (LC-1) fractures are the most common pelvic ring injury.(1) Formally standardized treatment regimens for LC-1 fractures are lacking, with symptomatic treatment, medical management, and surgical stabilization observed.(1,2) While data on short-term pain after nonoperative treatment is available, there is limited data on long-term function.(3) No study to date has compared long-term functional outcomes to age and sex matched non-injured controls. This study evaluates the effect of nonoperative treatment on functional outcomes in a consecutive cohort of patients with LC-1 pelvic ring fractures. We identified consecutive adults treated nonoperatively from 2012-2015 for an isolated LC-1 pelvic ring fracture per Young and Burgess classification.(4) Patients with additional lower extremity fracture at presentation or treatment with osteoactive medications within 6 months of injury were excluded. Those meeting inclusion/exclusion criteria, along with age and gender matched (2:1) controls with no history of lower extremity fracture, were contacted and administered the Short Musculoskeletal Function Assessment (SMFA). Associations between continuous variables were assessed with Wilcoxon rank-sum tests or t-tests and discrete variables with chi-squared tests or Fisher's exact tests. 39 of 97 (40%) identified LC-1 fracture patients were consented a median of 3 years (range 2-4 years) after injury. 15 patients (15%) were reported deceased. Non-contacted individuals were older (84 vs 80 years, $p=0.008$) and demonstrated shorter length of stay (3 vs 4 days, $p=0.004$) than those contacted. No significant difference was observed in charlson comorbidity index at time of presentation between contacted and non-contacted individuals ($p>0.05$). No significant differences were observed in SMFA scores of LC-1 fracture patients versus controls (Table 1). No patient, radiographic, or injury characteristics predicted worse functional outcome. Patients with LC-1 pelvic ring fractures appear to achieve functional outcomes comparable to healthy age and sex matched controls at least two years after injury. Such findings can be viewed in the context of heightened focus towards anti-resorptive and anabolic medications in the acute post-fracture setting. Our results suggest that such treatments, which are often costly and burdensome in their administration, may ultimately be unnecessary in this subset of pelvic ring injury.

	Case N=39	Control N=78	P
Age	80.0	77.0	NS
Gender:			NS
F	37 (94.9%)	74 (94.9%)	
M	2 (5.13%)	4 (5.13%)	
Functional Index	17.2 \pm 21.1	16.1 \pm 19.1	NS
Bothersome Index	18.5 \pm 24.4	14.6 \pm 19.8	NS
Daily Activities	18.9 \pm 24.0	21.5 \pm 23.4	NS
Emotional Status	18.6 \pm 26.6	13.2 \pm 19.1	NS
Arm & Hand Function	16.2 \pm 24.7	10.9 \pm 19.1	NS
Mobility	16.7 \pm 23.5	18.4 \pm 24.9	NS

Table 1: Demographics and SMFA Scores in LC-1 Fracture Patients and Controls. SMFA sub-scores reported as mean \pm standard deviation.

References:

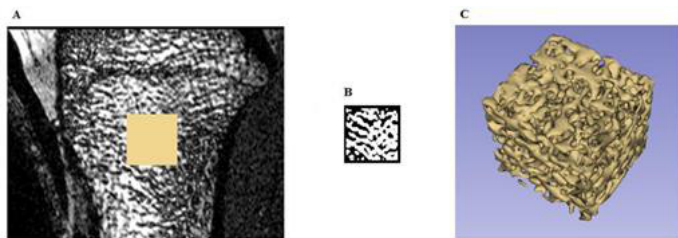
- Tosounidis T, Kanakaris N, Nikolaou V, Tan B, Giannoudis PV. Assessment of Lateral Compression type 1 pelvic ring injuries by intraoperative manipulation: which fracture pattern is unstable? *Int Orthop*. Dec 2012;36(12):2553-8. Epub 2012/10/26.
- Gaski GE, Manson TT, Castillo RC, Slobogean GP, O'Toole RV. Nonoperative treatment of intermediate severity lateral compression type 1 pelvic ring injuries with minimally displaced complete sacral fracture. *J Orthop Trauma*. Dec 2014;28(12):674-80. Epub 2014/04/18.
- Hagen J, Castillo R, Dubina A, Gaski G, Manson TT, O'Toole RV. Does Surgical Stabilization of Lateral Compression-type Pelvic Ring Fractures Decrease Patients' Pain, Reduce Narcotic Use, and Improve Mobilization? *Clin Orthop Relat Res*. Jun 2016;474(6):1422-9. Epub 2015/08/26.
- Alton TB, Gee AO. Classifications in brief: young and Burgess classification of pelvic ring injuries. *Clin Orthop Relat Res*. Aug 2014;472(8):2338-42. Epub 2014/05/29.

Disclosures: *Aidan Hadad, None*

SUN-0024

Magnetic Resonance Imaging (MRI) Evidence that Trabecular Bone Structure and Marrow Adipose Tissue (MAT) Are not Affected in Type 2 Diabetes Mellitus (T2D) Iana De Araujo¹, Carlos Salmon², Carlo Rondinoni¹, Marcello Nogueira-Barbosa¹, Francisco De Paula¹. ¹Ribeirao Preto Medical School-University of Sao Paulo, Brazil, ²Faculty of Philosophy, Sciences and Arts - University of Sao Paulo, Brazil

Introduction: The underlying mechanisms of bone fragility in T2D remain unclear. There are conflicting results using HR-pQCT to estimate bone structure (Figure 1) in T2D. MRI is a versatile technique able to measure bone structure and adipose tissue, including MAT. Objective: To evaluate bone structure and MAT by MRI in T2D, as well as the relationship between total MAT [lumbar spine (L3) and proximal tibia (pT)] and soleole intramyocellular lipids (IMCL/EMCL with BV/TV [i.e., apparent bone/total volume (appBV/TV)] in T2DM. Material and Methods: MR 1H spectroscopy was used to assess bone L3MAT, pTMAT and soleole intramyocellular lipids (IMCL/EMCL). In addition, MRI was used to quantify BV/TV. DXA was used to measure bone mass in lumbar spine (LSBMD), total hip (THBMD) and femoral neck (FNBMD). Results: 75 volunteers were evaluated: control (C: 11F/8M), overweight (Ov: 15F/7M), obese (O: 10F/6M) and type 2 diabetes (T2D: 12F/6M). The groups were matched by sex, age (C:50 \pm 11; Ov:51 \pm 13; O:47 \pm 8; T2D:52 \pm 9 years) and height (C:1.69 \pm 0.1; Ov:1.65 \pm 0.1; O:1.66 \pm 0.1; T2D:1.65 \pm 0.1m). The BMI was higher in O and T2D than in C and Ov (C:23 \pm 1.6; Ov:26.0 \pm 1.3; O:35 \pm 4.4; T2D:32 \pm 6.0Kg/m²; $p<0.05$). The LSBMD was similar in the groups (C:0.974 \pm 0.095; Ov:1.003 \pm 0.105; O:0.995 \pm 0.112; T2DM:1.057 \pm 0.117 g/cm², $p>0.05$), whereas FNBMD and THBMD was higher in T2D than the C group, respectively (C:0.750 \pm 0.139; Ov:0.801 \pm 0.116; O:0.860 \pm 0.134; T2D:0.869 \pm 0.119 g/cm²) and (C: 0.860 \pm 0.143; Ov:0.910 \pm 0.114; O:0.939 \pm 0.141 e T2D:0.991 \pm 0.117 g/cm²). The L3MAT and PTMAT were similar in the four groups, respectively (C: 40.6 \pm 9.7; Ov: 44.6 \pm 10.6. O: 46.0 \pm 16.6 and T2D:46.8 \pm 12.9%) and (C: 92 \pm 3.4; Ov: 89 \pm 7.6. O: 83 \pm 20.6 and T2D: 90 \pm 6.9%). Also, the BV/TV was similar in the 4 groups (C:0.507 \pm 0.056; Ov:0.526 \pm 0.054; O:0.516 \pm 0.047 e T2D: 0.555 \pm 0.023). There was no correlation between BV/TV and pTMAT ($r=0.03$, $p>0.05$). There was a trend of negative correlation between L3MAT and FNBMD ($r=-0.25$, $p=0.08$). Also, there was a tendency for positive correlation between IMCL/EMCL with PTMAT ($r=0.31$, $p=0.07$) and L3MAT ($r=0.26$, $p=0.1$). Conclusion: The present results indicate that there is no impairment in trabecular bone structure as determined by MRI in T2D. MAT is not increased in peripheral and axial bone in T2D, but lipids deposition in muscle and MAT seems to be related.



Disclosures: Iana De Araujo, None

SUN-0025

Bone loss in hepatitis B virus-infected patients is associated with greater osteoclastic activity independently of the retroviral use Renata Dessordi^{1*}, Rodrigo Carvalho De Santana², Elen Almeida Romão², Anderson Marliere Navarro². ¹Sao Paulo State University, Brazil, ²University of Sao Paulo, Brazil

Hepatitis B is a major public health problem worldwide and is associated with considerably high mortality rates. Oral medications, generally nucleoside/nucleotide analogs such as tenofovir, are used as long-term therapy and have possible side effects such as the reduction in bone mineral density associated with their use. Objective: to evaluate the effects of tenofovir, compared with those of other nucleoside/nucleotide analogs (entecavir and lamivudine), on the bone mineral density of hepatitis B patients. Materials and Methods: a cross-sectional study was conducted with 81 adult patients with chronic hepatitis B who were treated at the Clinical Hospital of Ribeirão Preto (University of São Paulo [USP]). Dual-energy x-ray absorptiometry (DXA) was performed to assess bone mineral density. Biochemical analyses were performed of osteocalcin, deoxypyridinoline, parathyroid hormone and anthropometric measures of weight, height, and body mass index were taken. Participants, of both sexes, were subdivided according to the use of antiretrovirals: Group 1: 27 patients who were inactive virus carriers without medication; Group 2: 27 patients on tenofovir; Group 3: 27 patients taking lamivudine or entecavir. Results: there was no difference in the mean age, body mass index, lean and fat mass between the patients in both study groups ($p > 0.05$). Osteopenia was diagnosed from the DXA readings for lumbar spine in the Group 1: 7.4%; Group 2: 15%; and Group 3: 3.7%. It was observed that the bone formation markers, osteocalcin levels as well as parathyroid hormone and insulin growth factor 1 values were within normal values for all groups. In all groups, the bone resorption marker, urinary deoxypyridinoline levels, showed an increase. Conclusion: the increase in the bone resorption marker levels indicates a high resorptive activity of bone tissue. These data point to a greater osteoclastic activity resulting in the bone loss in hepatitis B virus-infected patients both treated and not treated with antiretrovirals.

Disclosures: Renata Dessordi, None

SUN-0026

Bone Tissue Composition in Post-menopausal Women Varies with Glycemic Control Heather B. Hunt^{1*}, Nicholas A. Miller¹, Kimberly J. Hemmerling¹, Maho Koga¹, Kelsie A. Lopez¹, Kendall F. Moseley², Eve Donnelly^{1,3}. ¹Department of Materials Science and Engineering, Cornell University, United States, ²Division of Endocrinology, Johns Hopkins University School of Medicine, United States, ³Research Division, Hospital for Special Surgery, United States

Type 2 diabetes mellitus (T2DM) is associated with elevated skeletal fragility, despite patients with T2DM having normal to high bone mineral density (BMD). The observation that individuals with T2DM are at higher risk for fracture suggests that sustained glycemic derangement causes changes in bone quality independent of BMD. Therefore, the objective of this study was to assess the bone tissue composition in post-menopausal women with varying degrees of glucose tolerance. Transiliac crest biopsies were collected in three groups of postmenopausal women based on an oral glucose tolerance test or an established, insulin-requiring T2DM diagnosis: normal glucose tolerance (NGT; n=35, age=64.8±6.8), impaired glucose tolerance (IGT; n=27, age=64.5±5.4), and T2DM (n=25, age=64.2±6.1). Biochemical parameters of glucose control and bone metabolism were collected. Three cortical (c) and three trabecular (t) regions (1600µm²) on 3 sections per biopsy were scanned using Fourier transform infrared imaging. The means and widths of the pixel distributions of each image were calculated for mineral:matrix ratio (M:M), collagen maturity (XLR), mineral crystallinity (XST), and carbonate:phosphate ratio. In T2DM vs NGT cortex, the mean M:M was 7% greater, the M:M distribution was 10% narrower, and the XST distribution was 16% wider (all $p < 0.05$). In T2DM vs NGT trabeculae, the mean XLR was 5% lower and the XST distribution was 14% wider (all $p < 0.05$). The mean c-XLR and t-XLR and c-M:M distribution width were negatively correlated with HbA1c, and the distribution widths of c-XST and t-XST were positively correlated with HbA1c (Table 2). No differences between IGT and NGT or T2DM were observed. The distributions of M:M were narrower and shifted to higher mean values in T2DM vs NDM cortex, indicating that glycemic derangement is associated with increased mineral content that is more homogeneous. Because mineral content increases with tissue age (time since formation), these findings support prior observations of reduced turnover in T2DM. In contrast, the greater mean XLR values and wider XST distributions of both tissue types in T2DM suggests glucose intolerance yields

less-mature collagen with more heterogeneous crystals, a finding consistent with less mature tissue. In summary, this study demonstrates that T2DM, but not IGT, has complex effects on bone tissue composition, particularly its mineral properties, and that T2DM may affect cortical and trabecular tissue differently.

T1. Characteristics	NGT	IGT	T2DM	T2. Regression with HbA1c	R ²
n	35	27	25	c-XLR mean	0.06 *
Age (years)	64.8 ± 6.8	64.5 ± 5.4	64.2 ± 6.1	t-XLR mean	0.05 *
BMI (kg/m ²)	29.6 ± 5.6	35.0 ± 9.1	36.9 ± 6.4 †‡	c-M:M distribution width	0.10 *
HbA1c (%)	5.76 ± 0.26	6.01 ± 0.41	9.07 ± 2.07 †‡	c-XST distribution width	0.13 *
T2DM Dx (years)	--	--	14.5 ± 8.4	t-XST distribution width	0.07 *
Calcium (mg/dL)	9.19 ± 1.56	9.27 ± 1.30	9.43 ± 0.39	$p < 0.05$ indicated with *	
Phosphorus (mg/dL)	3.64 ± 0.49	3.42 ± 0.56	3.56 ± 0.66		
25(OH)D (ng/mL)	33.8 ± 9.44	33.9 ± 10.2	30.6 ± 7.63		
Creatinine (mg/dL)	0.84 ± 0.25	0.85 ± 0.12	0.85 ± 0.16		
eGFR (mL/min/1.73 m ²)	81.9 ± 15.0	80.1 ± 14.5	80.0 ± 15.9		

ANOVA with Tukey posthoc; $p < 0.05$ indicated with † IGT vs NGT ‡ T2DM vs NGT § T2DM vs IGT

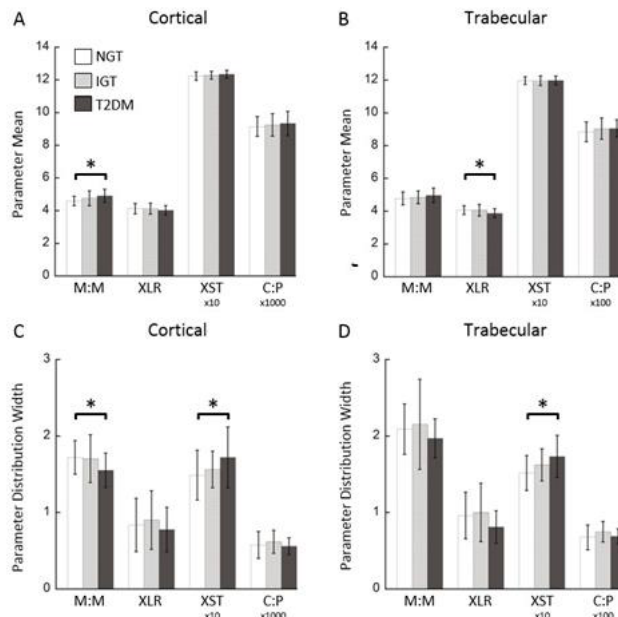


Table 1: Patient characteristics and metabolic panel measures. **Table 2:** Coefficients of determination for regressions of compositional parameters with HbA1c. **Figure 1:** FTIR image parameter means and distribution widths (full widths at half maxima) for cortical and trabecular tissue. Bar heights and error bars indicate parameter raw means and standard deviations, respectively. * $p < 0.05$ evaluated by mixed effects model to account for repeated measures. Abbreviations: NGT=normal glucose tolerance, IGT=impaired glucose tolerance, T2DM=type 2 diabetes mellitus, M:M=mineral:matrix ratio, XLR=collagen maturity, XST=mineral crystallinity, C:P=carbonate:phosphate ratio.

Disclosures: Heather B. Hunt, None

SUN-0027

The Effect of TransCon PTH on Bone Markers in a Phase 1 Trial David B. Karpf^{1*}, Susanne Pihl², Aimee Shu¹, Eva Mortensen¹, Jonathan A. Leff¹. ¹Ascendis Pharma Inc., United States, ²Ascendis Pharma A/S, Denmark

Background: Hypoparathyroidism (HP), a condition of parathyroid hormone (PTH) deficiency, leads to abnormal calcium metabolism. Standard of care (active vitamin D and calcium) does not correct decreased osteoclast activity and diminished bone turnover associated with HP. PTH replacement therapy is evolving with PTH analogues such as Natpara [PTH(1-84)] and Forteo [PTH(1-34)]. However, due to short half-lives, they incompletely control the disease and are known to be anabolic, causing an increased risk of osteosarcoma in rats. True replacement therapy would entail PTH exposure in the normal range 24 hours per day with an infusion-like profile. Horwitz et al demonstrated that continuous PTH(1-34) infusion in healthy adults led to suppression of bone formation and increased resorption markers. NIH studies in adults with HP showed continuous PTH(1-34) infusion in the normal range via an infusion pump normalized bone turnover. TransCon PTH, a sustained-release prodrug of PTH(1-34), is in development for the treatment of HP. Through auto-cleavage at physiological temperature and pH, unmodified PTH(1-34) is sustainably released. Methods: This phase 1, randomized, placebo-controlled, single and multiple ascending dose (SAD and MAD) trial evaluated safety, tolerability, pharmacodynamics (PD), and (pharmacokinetics) PK of TransCon PTH in 130 healthy adults. Cohorts of 10 subjects (8 active, 2 placebo) received

Sunday Posters

7 SAD (3.5-124 µg) or 6 MAD (3.5-24 µg) for 10 days. The PD endpoints included serum calcium and bone turnover markers (serum PINP, BSAP, CTx, and urine NTx). The primary PK endpoint was free PTH. Results: Completed SAD and MAD cohorts showed TransCon PTH was generally well-tolerated. Free PTH (and serum calcium) showed a dose-dependent response, with a half-life of approximately 60 hours and an infusion-life profile with daily administration. Similar to the Horwitz data, PINP decreased in response to TransCon PTH administration, consistent with suppression of bone formation and in contrast to increases known to occur with daily PTH(1-34) and PTH(1-84) therapies, while serum CTx levels increased. Conclusion: Interim data supports an infusion-like PTH profile with TransCon PTH, which may predict improved efficacy and long-term safety in the treatment of HP. The effect of TransCon PTH on both bone formation and bone resorption markers were consistent with a continuous infusion of PTH(1-34) and lacking an anabolic effect.

Disclosures: **David B. Karpf**, Ascendis Pharma, Other Financial or Material Support

SUN-0028

The Relationship of Trabecular Bone Score (TBS) with Vitamin D in Older African-American Women John Aloia*, Mageda Mikhail. NYU Winthrop hospital, United States

Background: Trabecular bone score (TBS) is a software program approved by the US Food and Drug Administration for post-acquisition and processing of the lumbar spine dual-energy X-ray absorptiometry images that allows assessment of bone structure as a surrogate for bone quality. Low TBS values are associated with increased risk of major osteoporotic fractures in postmenopausal women and men aged 40 years and older independent of BMD. Objective: We examined TBS in elderly African-American women, in a randomized, double-blind, placebo-controlled trial designed to examine the effect of vitamin D on bone loss and physical performance in elderly African-American women. Design: In this 3-year intervention trial, 260 healthy African-American women older than 60 years of age, were assigned to receive either placebo or vitamin D3. Initial vitamin D3 dose was determined by the baseline serum 25OHD levels. The vitamin D3 dose was further adjusted at 3-month intervals, to maintain serum 25OHD levels between 75-172 nmol/L. Subjects with baseline 25OHD <20 nmol/L or >65 nmol/L, were excluded from the study. Trabecular bone score (TBS) was measured in 217 subjects, every 6 months. Total daily calcium intake of 1200 mg was ensured. Results: No significant differences in baseline characteristics (demographics, BMD, TBS, and serum total 25OHD) were noted between the active and placebo group. Baseline serum 25OHD level was 54.8±16.8 nmol/L. Spearman correlation coefficients were calculated between TBS and all demographic and clinical variables in 217 subjects. Significant negative correlation was observed between TBS and BMI. There were highly significant positive correlations with each of the BMD measurements. None of the biochemical variables including 25OHD level, BSAP and CTX were significantly correlated with TBS. Mixed effects model for repeated measures showed that TBS significantly declined over time (P<0.001) regardless of the treatment assignment. However, this decline was not different between the treatment groups (P=0.985). Conclusion: The lack of vitamin D supplementation over a 3-year period, did not differentially diminish TBS in older African-American women compared to those treated to maintain serum 25OHD above 75 nmol/L.

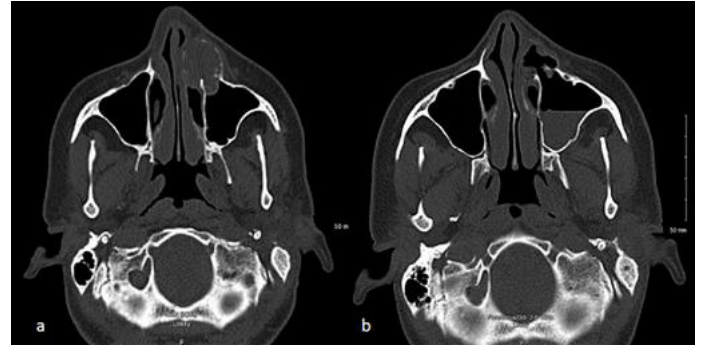
Disclosures: **John Aloia**, None

SUN-0029

A Rare Case of Bilateral Maxillary Brown Tumors in a Patient with Primary Hyperparathyroidism Sapna Patel*, Uma Gunasekaran. University of Texas Southwestern Medical Center, United States

The presentation of primary hyperthyroidism is variable with brown tumors being a rare sequelae of hyperparathyroidism. Brown tumors localize in areas of intense bone resorption with bone defect becomes filling with fibroblastic tissue. We report a rare case of primary hyperthyroidism presenting as a brown tumor of the maxillary sinus. Ms. R is a 47 year old female who presented to the ED with intermittent constipation and recent imaging showing a left maxillary mass. Four months prior to onset of symptoms, patient noted a bump on the left side of her face, which she initially thought was acne, but progressed over two months to deform the left maxillary and nasal surface. Clinical evaluation and labs revealed calcium level, 16.5 mg/dL, PTH, 555 pg/mL, low Vitamin D 25-OH (value unavailable) and a soft, non-tender, immobile lesion in the left maxillary region. CT maxillofacial showed a ~3cm mass in left maxillary region with exophytic extension to adjacent soft tissues of the face. Patient was acutely reevaluated in the ED and found to have serum calcium 16.5 mg/dL, (ionized 8.7 mg/dL). Phosphorous 2.0 mg/dL, PTH level 953.5 pg/mL, Vitamin D 25-OH 14.7 ng/mL, alkaline phosphatase 186 U/L. A parathyroid technetium scintiscan showed increased uptake posterior to the right lobe of the thyroid indicating a 4.6 x 2.7 x 2.4 cm mass. The patient underwent excision of the maxillary mass, and was noted to have a bilateral, multifocal maxillary mass. Pathology of the maxillary mass was consistent with brown tumor. Subsequently, the patient underwent right superior parathyroidectomy. Intra-operatively, patient's parathyroid hormone decreased from 671.1 pg/mL to 54.9 pg/mL. The patient's calcium decreased post-procedure as expected, and she was started on calcium carbonate and ergocalciferol with stable electrolytes on discharge. While the mandible is the most frequently involved bone in brown tumors of the head and neck region, maxillary involvement is extremely rare. Very few cases in the literature describe Brown tumor localizing in the maxillary/facial regions in primary hyperparathyroidism [1]. Furthermore, as seen in our patient, it is extremely rare for a brown tumor occurring within the facial bones to be the first

manifestation of the systemic condition.1. Heath H, Hodgson SF, Kennedy MA. Primary hyperparathyroidism. Incidence, morbidity, and potential economic impact in a community. The New England Journal of Medicine. 1980;302(4):189-193



Disclosures: **Sapna Patel**, None

SUN-0030

Effect of Renal Transplantation on Bone Microstructure and Strength Assessed by MRI Catherine Reilly*, Mary Leonard, Wenli Sun, Chamith Rajapakse, Felix Wehrli. University of Pennsylvania, United States

Abnormal vitamin D and mineral metabolism are a universal complication of advanced chronic kidney disease (CKD). Secondary hyperparathyroidism results in abnormal trabecular microarchitecture and cortical thinning. Renal transplantation (RTxp) corrects many of the risk factors for bone deficits; however, glucocorticoid therapy and persistently elevated PTH levels may further deteriorate bone. The objective of this study was to investigate the effects on bone microstructure and strength following RTxp. Sixty RTxp recipients (52% male, 32% preemptive), ages 20-60 years, were enrolled at transplantation. MRI of the distal tibia was performed on a 1.5 Tesla scanner (Siemens Tim Trio, Erlangen, Germany) using a 2-element surface coil at 0.137 mm x 0.137 mm x 0.410 mm voxel size. Microstructural bone parameters and whole-section stiffness were computed on the basis of these images using digital topological and finite element analysis, respectively, to test the hypothesis that bone quality assessed in terms of the derived structural and mechanical parameters improves upon treatment. Whole cross-section stiffness was computed by simulating compressive loading conditions along bone's axial direction. Cortical porosity was computed at each voxel retaining partial volume information and averaged over the entire cortical bone region. BV/TV was computed as the average fractional occupancy of bone over the total trabecular volume. Plate-to-rod ratio was computed to describe the relative plate and rod likeness of trabeculae. Longitudinal changes in bone parameters are summarized in Table 1. Briefly, bone deteriorated structurally and mechanically from baseline to 6 months, and to a lesser extent from 6 to 12 months of RTxp, but improving thereafter during the final 12 to 24-month period. Initial deterioration is likely a consequence of exposure to high doses of steroid.

Table 1: Changes in Parameters between Study Visits

	0-6 Month (%)	6-12 Month (%)	12-24 Month (%)
Whole Cross-Section			
Stiffness	-6.28 (p<0.0001)	-1.91 (p=0.0042)	2.69 (p=0.0029)
Area	-1.79 (p=0.17)	-2.47 (p=0.070)	-1.60 (p=0.14)
Cortical Bone			
Thickness	0.94 (p=0.33)	1.32 (p=0.33)	0.15 (p=0.90)
Porosity	4.25 (p<0.0001)	0.60 (p=0.58)	-2.10 (p=0.023)
Area	-0.16 (p=0.91)	-0.29 (p=0.80)	-0.73 (p=0.54)
Trabecular Bone			
BV/TV	-4.83 (p=0.0003)	-2.37 (p=0.02)	4.74 (p=0.0071)
Plate-to-Rod	-3.74 (p=0.050)	-2.34 (p=0.12)	6.74 (p<0.0001)
Area	-2.07 (p=0.20)	-2.78 (p=0.16)	-1.54 (p=0.16)

Disclosures: **Catherine Reilly**, None

SUN-0031

Total Alkaline Phosphatase is an unreliable marker of relapse in treated Paget's Disease of the Bone Rebecca Sagar*, Stephen Orme, Afroze Abbas. Leeds Centre for Diabetes and Endocrinology, Leeds Teaching Hospitals Trust, United Kingdom

Background: Paget's disease of bone is a disorder of increased bone remodeling. Current guidelines suggest the use of imaging and biochemistry (total alkaline phosphatase) to aid diagnosis and monitoring. The use of intravenous zoledronic acid (ZOL) has been shown to induce sustained remission in most patients. However, the utility of total alkaline phosphatase (ALP) as a means of identifying disease relapse after initial treatment remains controversial. Methods: We retrospectively evaluated the management of 100 unselected patients with Paget's disease of bone treated with ZOL over the last 5 years in a UK teaching

hospital (mean follow-up 4 years 3 months, post first infusion). Data collected included demographics, presentation, sites, biochemistry and imaging findings. Results: The majority of patients were male (56%), had polyostotic disease (64%) and had radionuclide bone imaging at baseline (84%). Prior to any treatment, 84% of patients had elevated ALP (monostotic mean ALP 462iu/L vs polyostotic mean ALP 872 iu/L, range 30-300 iu/L). Most patients required a single ZOL infusion (mean 1.81 treatments). 88% of patients had normal ALP levels at 6 months post infusion. However only 39% were below the mid-point of the reference range, as recommended per guidelines. The vast majority of these patients were patients with polyostotic disease (66%). 74% of patients had normal ALP post ZOL for the duration of the follow-up (mean 4.5 years). Of the patients who had a biochemical relapse, as evidenced by elevated ALP, 74% had polyostotic disease. 26 patients received a second IV zoledronic acid infusion. Of these, 71% did not reach an ALP below the mid-point of the reference range. 26% of patients had symptomatic relapse during follow-up, but less than half of these had elevated ALP at the time. Overall, 28 patients had repeat radionuclide bone scan during follow-up, with 64% of these demonstrating active disease on imaging. However, 72% of patients with scan-confirmed relapse had normal ALP at the time of the repeat scan. Conclusions: Our study reaffirms the efficacy of single ZOL infusion in normalizing ALP, in a large cohort of patients with Paget's disease of bone, over 4-5 years. However, the majority of patients do not reach an ALP below the mid-point of the reference range, as suggested in guidelines. Additionally, our data suggests ALP is not a reliable biochemical marker of relapse in patients who have been previously treated with ZOL.

Disclosures: *Rebecca Sagar, None*

SUN-0032

Cardiovascular Autonomic Neuropathy as a new complication of chronic hypoparathyroidism Gaia Tabacco^{*1}, Anda Mihaela Naciu¹, Roberto Cesareo², Claudio Pedone³, Gianluigi Gaspa², Assunta Santonati⁴, Daniela Bosco⁴, Daria Maggi¹, Nicola Napoli¹, Paolo Pozzilli¹, Silvia Manfrini¹, Andrea Palermo¹. ¹Unit of Endocrinology and Diabetes, Dept. of Medicine, University Campus Bio-Medico, Italy, ²Thyroid Disease Center, "S. M. Goretti" Hospital, Italy, ³Unit of Geriatrics, University Campus Bio-Medico, Italy, ⁴Department of Endocrinology, San Giovanni Addolorata Hospital, Italy

Background: calcium and vitamin D supplementation represent the conventional therapy for chronic Hypoparathyroidism (HP) but this treatment does not fully replace the functions of PTH. Several case reports revealed peripheral neuropathy and myopathy in HP subjects with or without hypocalcemia. Fatigue is a common complaint and is not related to post-surgical hypothyroidism. In most cases, symptoms diminished or disappeared when plasma calcium levels bring back to normal but their relationship to biochemical control or other aspects of the disease have been not well described. Autonomic dysfunction has been described in a broad variety of endocrine diseases but, up to now, no studies have evaluated this complication in HP subjects. Aim: to evaluate cardiovascular autonomic neuropathy (CAN) in subject with HP. Design: Monocentric, cross-sectional study comparing 44 post-surgical HP patients treated with calcium and calcitriol to 37 control subjects underwent thyroidectomy without PTH/calcium/phosphate disorders. CAN was assessed by NeuroTester (Meteda) evaluating: 1) heart rate response to deep breathing (expiratory-to-inspiratory ratio) 2) heart rate response to lying-to-stand test (30:15 ratio) 3) heart rate response to Valsalva maneuver (maximum heart rate during expiration- minimum heart rate after expiration ratio) 4) blood pressure response to standing. One pathologic test is diagnostic for early CAN, two or more identify moderate CAN. Results: The overall prevalence of CAN was 48.8%, with a marked difference between HP and control (70.5% and 23.7%, respectively, OR 7.4, 95% CI 2.8-21.1). Of the 12 patients with 2 positive tests, 11 had hypoparathyroidism. Among people with HP, we found no association between serum calcium, PTH and phosphate concentration and CAN, and the prevalence of CAN was not significantly increased in people with hypocalcemia, PTH < 10 pg/ml or hyperphosphatemia. The prevalence of moderate CAN, instead, was increased among patients with calcium < 8.5 mg/dL (n=18, 44%) compared to those with normal serum calcium concentration (n=26, 11%), with OR 5.7 (95% CI 1.3-32.3). These results were not confirmed for PTH < 10 pg/mL (N:22, prevalence of moderate CAN 31.8% vs 18.2%, OR 2.03, 95% CI 0.5-9.5) and for phosphate > 4.4 mg/dL (N:22, prevalence of moderate CAN 31.8% vs 18.2%, OR 2.03, 95% CI 0.5-9.5). Conclusion: HP is associated with CAN and hypocalcemia seems to affect its severity. However, larger and prospective studies are needed to confirm our findings.

Disclosures: *Gaia Tabacco, None*

SUN-0033

Cognitive and Emotional Deficits in Hypoparathyroidism and Their Relation to Undercarboxylated Osteocalcin Mishaela Rubin^{*}, Gaia Tabacco, Rukshana Majeed, Beatriz Omeragic, Maximo Gomez, Elzbieta Dworakowski, Christiane Hale, Adam Brickman. Columbia University, United States

Clinically, hypoparathyroid patients (HypoPT) describe poor cognitive and emotional function. SF36 tests show poor quality of life (QoL), but cognitive and emotional data do not exist. HypoPT also have low bone remodeling, with low osteocalcin (OC) levels; in mice, circulating undercarboxylated OC (uOC) binds in the hippocampus and improves learning, memory and mood. We hypothesized that HypoPT have cognitive and emotional deficits and that these are associated with uOC. 18 HypoPT (44±13 yrs, 2 men, duration 8.9±1 yrs,

median education=16 years, calcium 2.3±2 g/d, calcitriol 0.74±1 µg/d, serum calcium 8.9±1 mg/dl, PTH 5.3±5 pg/ml) were tested with the SF36 and NIH Toolbox®. The cognitive battery assesses "crystallized" (dependent upon past learning) and "fluid" (capacity for new learning and information processing) abilities and the emotional battery assesses psychological well-being. Scores are adjusted for age, sex, race/ethnicity, education and compared to census-based averages for the US population. The SF36 showed decreases in physical role, vitality, social function and general health. The Toolbox showed overall cognitive function at 42nd percentile of the US population. Crystallized abilities were at 58th percentile: general vocabulary knowledge at 52nd percentile and reading decoding skill at 66th percentile. Fluid abilities were at 27th percentile: inhibitory control and attention at 47th percentile, executive function at 68th percentile, episodic memory (acquisition and retrieval of new information) at 32nd percentile, working memory (ability to store information) at 32nd percentile and processing speed (amount of information processed within a certain time) at 7th percentile. Toolbox emotion tests showed overall psychological well-being at 30th percentile; social satisfaction at 21st percentile and negative affect at 75th percentile. SF36 measures correlated strongly with emotional measures. uOC was associated with episodic memory (r=0.50, p=0.07), psychological well-being (r=0.57, p=0.02) positive affect (r=0.52, p=0.03) and general life satisfaction (r=0.54, p=0.03). In conclusion, HypoPT have cognitive deficits primarily involving processing speed, and to a lesser extent episodic and working memory. Emotional deficits are associated with poor QoL. uOC in HypoPT relates to episodic memory and well-being, suggesting that it might cross the blood brain barrier to bind in the brain and thus provide a skeletal regulation of cognition and emotion.

Disclosures: *Mishaela Rubin, None*

SUN-0034

A Unique Longitudinal Cohort of Hypoparathyroidism Treated for 8 Continuous Years with rhPTH (1-84) Donovan Tay^{*1}, Gaia Tabacco¹, Natalie Cusano², John Williams¹, Beatriz Omeragic¹, Rukshana Majeed¹, Maximo Gomez Almonte¹, John Bilezikian¹, Mishaela Rubin¹. ¹Columbia University Medical Center, United States, ²Lenox Hill Hospital Department of Medicine, United States

Hypoparathyroidism (HypoPT) is characterized by hypocalcemia and undetectable or insufficient PTH levels. Conventional management consists of supplemental calcium, sometimes in high dosage, and active vitamin D. With the advent and approval of human recombinant parathyroid hormone [rh]PTH(1-84)], the missing hormone in this disorder can now be replaced. Since no limit has been placed on the duration of therapy by the Food and Drug Administration (FDA), and given the chronic nature of this disorder, the need for long term data of the efficacy and safety of rhPTH(1-84) is compelling. Twenty four HypoPT subjects (46±3 yrs, 75% women, disease duration 22.9±3 yrs) were studied. Causes were postsurgical (n=13), autoimmune (n=10) and DiGeorge (n=1). Baseline medications were calcium 3.0±0.3 g/d; calcitriol 0.76±0.1 µg/d; vitamin D 13932±3132 IU/d and HCTZ 36.6±9.0 mg/d. Serum calcium was 8.5±0.2 mg/dL, PTH 4.0±0.6 pg/mL, phosphate 4.5±0.2 mg/dL; Ca*P product 38±2 mg²/dL²; 24-hr urine calcium 254±29 mg/d. BMD measurements (g/cm²) were: lumbar spine (L5) 1.242±0.044; femoral neck (FN) 0.992±0.033, total hip (TH) 1.105±0.029 and distal 1/3 radius (DR) 0.735±0.011. rhPTH(1-84) was started at 100 µg every other day and changed after 3 yrs to doses ranging from 25-100 µg/d. Daily calcium supplementation fell by 57% to 1.3±0.3 g/d (p<0.01) as did calcitriol by 76% to 0.18±0.1 µg/d (p<0.001). Parent vitamin D intake decreased by 59% to 5727±3433 IU/d, p=0.02. Only 8 subjects required more than 1.5g/d of calcium supplementation and half of all subjects (n=12) eliminated calcitriol completely. Serum calcium remained stable (8.1±0.2 to 8.5±0.2 mg/dL; p=NS) while 24-hr urine calcium decreased by 38% to 157±37 mg/d (p=0.01). There were no changes in serum phosphate, Mg, creatinine, or in the Ca*P product. Total alkaline phosphatase increased (64±4 to 76±4 U/L; p=0.006). BMD increased by 2.8 ± 1.5% (p=0.06) at LS, 2.6 ± 1.1% at TH (p=0.03), unchanged at FN and fell 3.5 ± 1.1% at DR (p=0.001). Adverse events consisted of hypocalcemia in 3 patients (1-2 events/patient in yr 2); 3 episodes of hypercalcemia in 3 patients at yr 1, 4 and 7; 8 fractures in 6 patients (yr 1, elbow; yr 2, toe; yr 3 metatarsal; yr 5, wrist; yr 6, wrist, leg, yr 8, metacarpal, wrist) and a single renal stone (1 patient in yr 4). These data, the longest-term clinical experience with continuous PTH treatment for HypoPT or any condition, suggest that rhPTH(1-84) is a safe and effective long-term option in HypoPT

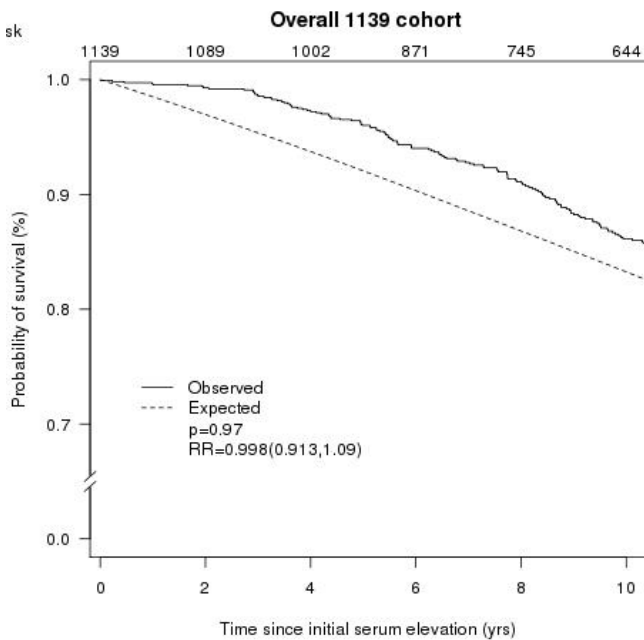
Disclosures: *Donovan Tay, None*

SUN-0035

Survival in primary hyperparathyroidism over five decades (1965-2010) Robert Wermers^{*1}, Marcio Griebeler², Euijung Ryu¹, Prabin Thapa¹, Matthew Hathcock¹, Ann Kearns¹. ¹Mayo Clinic, United States, ²Cleveland Clinic, United States

Purpose: To update survival in primary hyperparathyroidism (PHPT) in our community and determine if there has been a decrease in survival as suggested by others. Methods: Rochester, Minnesota, residents who met criteria for PHPT from 2002 through 2010 were identified through the medical records-linkage system of the Rochester Epidemiology Project and added to the historical cohort beginning in 1965. Survival was estimated using the Kaplan Meier product-limit method. Comparison of survival experience between two or more groups was done with log-rank test. The Cox proportional hazards model was used to determine associations, as relative hazards (RR) with 95% confidence intervals (CI), of

various risk factors with time to death. Results: From 1965 through 2010, we identified 1139 PHPT patients with a median age of 57.8 years and the majority were female (75.9%). The overall age and gender-adjusted survival compared to white Minnesota residents was unchanged in patients with PHPT with a relative risk of death of 0.998 (95% CI: 0.91-1.09, P=0.97) (Figure 1). In a multivariate model older age, male sex, maximum serum calcium level, and PHPT diagnosis after June 1974 were significantly associated with all-cause mortality. Survival declined with increasing quartiles of serum calcium elevation, with a significantly worse survival among patients with serum calcium levels above 10.8 mg/dL (RR 1.32, P=0.002). Parathyroid surgery was performed in 350 patients (30.7%), with more patients undergoing surgery from 1965-June 1974 (35.9%) and 1998-2010 (35.2%) compared to July 1974-1997 (26.1%). Survival among PHPT patients after parathyroidectomy was no different from expected (RR = 1.07, P = 0.465). However, in patients with a maximum serum calcium ≥ 10.8 mg/dL, parathyroidectomy was associated with a significant reduction in mortality (HR 0.47, 95% CI: 0.36-0.61, P<0.001). Conclusions: In a well-defined unselected U.S. community based cohort of PHPT subjects with predominantly asymptomatic disease and mild hypercalcemia mortality is not increased. However, a maximum serum calcium elevation of ≥ 10.8 mg/dL was associated with increased mortality and parathyroidectomy in these subjects was associated with a significant reduction in mortality, suggesting that the current recommendation for surgery in asymptomatic PHPT when serum calcium is > 1 mg/dL (0.25 mM) the upper limit of normal may warrant reconsideration.



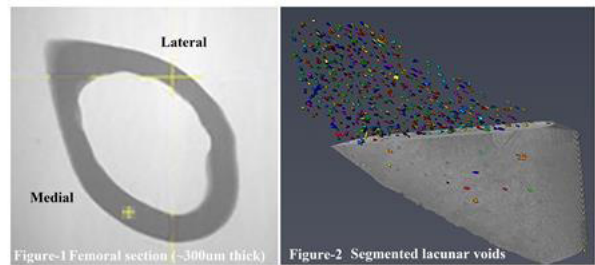
Disclosures: **Robert Wermers, None**

SUN-0072

Disuse Alters the Size of Osteocyte Lacunar Voids Mohammed Akhter*, Diane Cullen, Robert Recker. Creighton University, United States

We have shown that skeletal disuse due to the tail or hindlimb suspension caused significant decline in trabecular number and thickness for adult WT mice (Akhter et al., 2011). In this study we used MicroXCT-200 (Zeiss/Xradia) 3D imaging to quantify osteocyte lacunar void properties (void volume, surface area, density, sphericity, etc.) in mid-shaft femurs (C57BL/6Tac mice) obtained from the previous study (Akhter et al., 2011). Osteocyte lacunar void properties may influence bone mechanical properties with regards to changes in the mineralization. The aim of this study was to quantify changes in the osteocyte lacunar void properties of cortical bone with regards to disuse. Male adult (15wk-old) mice were randomized to Disuse, tail suspended (hindlimb) in individual cages for 4 weeks or Control, allowed normal ambulation. This study was approved by the Institutional Animal Care and Use Committee (IACUC). Femoral mid-shaft cortical sections (~300 micron [μ m] thick, n=6/group) were scanned in the medial and lateral regions at 0.6 micron resolution (Figure-1). Avizo (v9.4, FEI) software was used to segment the lacunar voids (Figure-2). Using the one-way ANOVA (SPSS), the treatment related (Control vs Disuse, P<0.05) differences were analyzed. A Total of 22,741 segmented lacunar voids (1,895voids/specimen, 50 to 610 μ m³ range) were analyzed. The osteocyte lacunar void volume was lower (P<0.05) and surface area tended to be lower in Disuse than Control (Table). The lacunar void sphericity (=1 for perfect sphere) was lower (P<0.05) in Disuse than Control suggesting a less spherical shape. The density of lacunar voids was similar between the two groups. These data suggest that disuse alters the lacunar properties (size, shape) and thus may have some influence on the intrinsic properties of bone tissue with regards to greater brittleness (Vennin et al., 2017). Disuse may promote osteocyte apoptosis and therefore causing micropetrosis (Bonewald

et al., 2011; Jilka et al., 2013) and shrinking of osteocyte lacunar voids. Micropetrosis may increase mineralization of the lacunar voids and thus cause changes in the intrinsic material properties of bone tissue (Mullender et al., 2005). Future studies of determining the relationship between lacunar voids and intrinsic material properties of bone tissue are important to understand their impact on bone quality.



Osteocyte Lacunar Void Properties	Volume (μ m ³)	Surface Area (μ m ²)	Density (#Voids/cm ³)	Sphericity (=1 perfect sphere)
Control	184 \pm 1.3	237 \pm 1.4	40179 \pm 1524	0.661 \pm 0.0011
Disuse	177 \pm 1.2*	234 \pm 1.3**	41542 \pm 2248	0.653 \pm 0.0010*

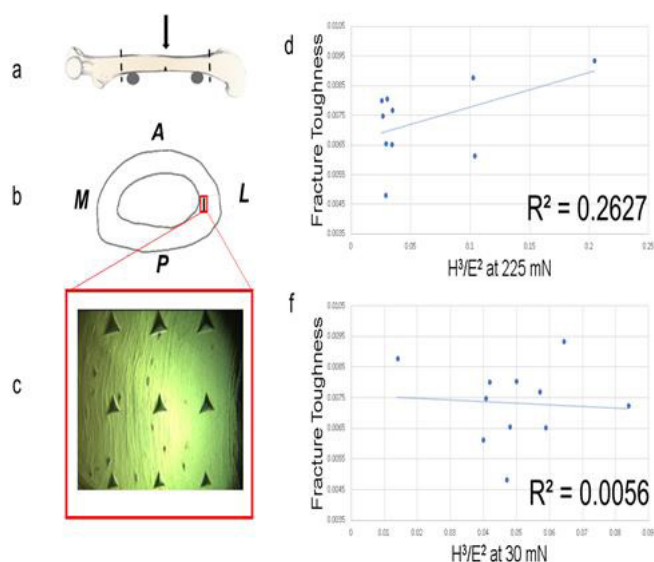
Male C57BL/6Tac mice; Mean \pm SEM; *P<0.05; ** P<0.1;
 A Total of 22,741 (1,895voids/specimen) segmented lacunar voids (50 to 610 μ m³ range) were analyzed.

Disclosures: **Mohammed Akhter, None**

SUN-0073

Assessing Correlates of Fracture Toughness using Nanoindentation Faisal Almeahimid*, Chelsea M Heveran, Bhavya Senwar, Virginia L Ferguson. University of Colorado, Boulder, United States

Introduction: Measuring fracture toughness (K_c) is conventionally achieved with whole-bone notched fracture, but a critical need exists for small-volume testing techniques to evaluate fracture toughness through less destructive methods. A brittleness parameter from nanoindentation was proposed by Labonte et al, which quantifies the degree of material brittleness using the ratio of indentation hardness to modulus (H₃/E₂). The purpose of this study was to evaluate whether microscale H₃/E₂ predict whole-bone fracture toughness in bone. Methods: Femurs from young adult male, exercised (n = 5) and sedentary (n = 5) Wistar rats fed a low fat diet were evaluated for notched fracture toughness. Femur fragments were then dehydrated, embedded with poly(methyl) methacrylate and polished to 0.1 μ m finish to expose the midshaft cortical bone near the notch. Nanoindentation arrays (Hysitron TI950, high load, berkovich tip) were placed in lamellar bone in the lateral quadrant (Figure 1). Rows of three indents each were placed at 30, 60, 100, 150, and 225 mN for each bone. At each point, H₃/E₂ and plastic work (hysteresis of load-unload curve) were evaluated. The average H₃/E₂ for each row was plotted against K_c. Results: H₃/E₂ was strongly linearly related to plastic work for every sample, r₂ = 0.98-0.99. The relationship between K_c and H₃/E₂ improved with increasing load. At 30, 60, 100, 150, and 225 mN, r₂ for K_c vs H₃/E₂ was 0.0056, 0.0544, 0.0876, 0.263, and 0.2627, respectively. A similar relationship was observed between K_c and plastic work, where r₂ increased from 0.0116 at 30 mN to 0.216 at 225 mN. Conclusion: We sought to evaluate whether fracture toughness was related to microscale indentation properties of bone material measured for the same whole bones tested in notched fracture. Here, H₃/E₂ was a proxy for plasticity, indicating that microscale plasticity is related to whole bone fracture toughness. While correlations between fracture toughness and H₃/E₂ were moderate at best and may improve in hydrated tissue, no other tool has provided insight into fracture toughness for bone at this length-scale. However, some plasticity was indeed apparent for embedded samples and was related to fracture properties. These results suggest that monitoring H₃/E₂ or plastic work at sufficient indentation load may access information about fracture toughness at the microscale.



Disclosures: *Faisal Almeahmid, None*

SUN-0074

The effects of age and sex on viscoelastic bone properties in mice Ingo Grafe^{*1}, Ian Tomkinson², Heather Haerberle², Yi-Chien Lee¹, Xiaohong Bi³, Brendan Lee¹, Catherine G. Ambrose². ¹Department of Molecular and Human Genetics, Baylor College of Medicine, United States, ²Department of Orthopaedic Surgery, UTHSC-Houston, United States, ³Department of Precision Biomedicine, UTHSC-Houston, United States

Age and sex have been shown to have significant effects on the elastic properties of bone but less is known about the effects of these variables on bone ductility and viscoelastic properties. Mouse femora from 2 strains (FVB/N and C57BL/6), 3 age groups (6 weeks, 3 months, 9 months), and both sexes were analyzed using both dynamic mechanical analyses (DMA) and quasi-static monotonic loading to failure to determine the effect of mouse strain, age and sex on elastic, plastic, and viscoelastic bone material properties. A three-point bending configuration (anterior side in compression, posterior side in tension) was used for both dynamic and quasi-static loading and, although the spans were adjusted for each group to maximize span to diameter aspect ratio, the same spans were used for both tests. DMA tests were conducted at frequencies ranging from 0.1 to 20Hz with displacements cycling between 0.01 to 0.018mm. Quasi-static loading was conducted at a rate of 0.1mm/s until failure. All tests were performed with the bones wet and at room temperature. For both strains and sexes, bone strength and modulus increased with age (average increases of 34% and 84%, respectively), while measures of ductility (post-yield displacement and energy to failure) and viscoelasticity (phase angle, reported as $\tan\delta$) decreased with age (average decrease of 71%, 44% and 17%, respectively). More significant differences were seen between the 6 week and 3 month age groups than between the 3 and 9 month age groups. Overall, FVB/N femurs were stronger ($p=0.002$) but more brittle ($p=0.01$) than those from C57BL/6J mice. Regardless of mouse strain, femurs of male mice were more ductile ($p=0.007$) but the femurs from females had higher strength ($p=0.01$) and elastic moduli values ($p=0.001$). A general linear model using strain and sex as fixed factors and age as a covariate showed that strength and ductility properties depended on all 3 variables (strain, age and sex), while modulus only depended on age and sex, and viscoelastic properties varied only by age. Future work will investigate relationships between these properties and the bone composition (from Raman spectroscopy and chemical analyses) to determine the contributions of the mineral and protein components of bone to the mechanical properties.

Disclosures: *Ingo Grafe, None*

SUN-0075

SERUM 25-HYDROXYVITAMIN D AND ITS METABOLISM IN BONE TISSUE IS ASSOCIATED WITH IMPROVED BONE QUALITY IN ELDERLY HIP FRACTURE PATIENTS Deepti Sharma^{*1}, Rebecca Sawyer¹, Roumen Stamenkov², Thomas Robertson³, Catherine Stapledon³, Gerald Atkins³, Peter Clifton¹, Lucian Solomon², Morris Howard¹, Paul Anderson¹. ¹University of South Australia, Australia, ²Royal Adelaide Hospital, Australia, ³University of Adelaide, Australia

Vitamin D and calcium supplementation significantly reduces the risk of fractures although improvement of bone mineral density (BMD) is controversial suggesting that these nutrients may act through improvement of bone quality and not by increasing BMD. We

have investigated the relationship between vitamin D status and trabecular bone quantity and quality in intertrochanteric biopsies retrieved from elderly hip fracture patients. **Material and Methods:** Intertrochanteric trabecular bone biopsies and serum samples were collected from hip fracture patients undergoing hip arthroplasty (65 females, 38 males, mean age 85 years) at Royal Adelaide Hospital. Trabecular bone was analysed by micro CT (SkyScan 1076), mean wall thickness was measured by histology and serum 25(OH)D, 1,25(OH)2D, and parathyroid hormone (PTH) by immunoassay (Diasorin Liaison). Bone mRNA levels for vitamin D metabolising enzymes CYP27B1 and CYP24A1 were measured by RT-PCR. **Results:** Serum 25(OH)D correlated negatively to the ratio of bone surface to bone volume BS/BV ($r = -0.206, p < 0.05$) and positively (trend) with trabecular thickness ($r = 0.19, p = 0.06$) both indicators of improved bone quality. Patients with higher vitamin D status had significantly higher mean wall thickness ($p < 0.001$). No correlation was found between serum 25(OH)D and any variable describing bone quantity. No bone quality or quantity variables correlated with either PTH or 1,25(OH)2D levels. Serum 25(OH)D, gender and bone CYP27B1 and CYP24A1 mRNA accounted for 19% of the variability of BS/BV ($P = 0.001$). **Conclusion:** Three measures of bone quality relate to serum 25(OH)D and support the concept that bone metabolism of 25(OH)D to 1,25(OH)2D improves bone quality through increasing plate-like trabeculae even in elderly patients. Plate-like structures improve bone strength (1). At the cellular level these structures arise from an increase in the bone formation period with osteoblasts forming bone for longer. These data support the need for maintaining adequate vitamin D status in the elderly to promote bone health and BMD is likely an inadequate measurement for vitamin D action on bone.

Disclosures: *Deepti Sharma, None*

SUN-0076

Ultra-low dose MDCT allows accurate assessment of vertebral fracture risk: a finite element study D. Anitha^{*1}, Kai Mei², Felix Kopp², Peter Noel², Thomas Baum², Karupppasamy Subburaj¹. ¹Singapore University of Technology and Design, Singapore, ²Technical University of Munich, Germany

Purpose: Assessment of osteoporotic vertebral fracture risk is insufficient using BMD measurements as the current clinical standard. A non-invasive fracture prediction tool such as finite element modelling (FEM) will be useful in identifying patients at risk for osteoporotic vertebral fractures. The goal of this study was to assess if patients with and without OVFs can be differentiated using MDCT scans at virtually reduced ultra-low doses. **Materials and Methods:** Vertebral MDCT images were retrieved from patients undergoing routine thoracic and abdominal scans. Patients with ($n=8$; age= 75 ± 11 years) and without vertebral fractures ($n=8$; age= 71 ± 11 years) were matched for sex and age and associated with the groups, Fracture and Control respectively. MDCT dose was virtually reduced to 50%, 25%, and 10% of the standard clinical dose using a simulation algorithm. Lumbar vertebrae (L1-3) were segmented from each patient. Finite element analysis was performed on all segmented vertebrae to simulate axial loading and a numerical failure load was obtained. Statistical differences within each group at individual doses and between each group at each dose was performed with Kruskal-Wallis and Mann-Whitney test respectively. Pearson correlations with standard dose were reported for all reduced doses. Receiver operating characteristic (ROC) curve analysis was performed to differentiate between Fracture and Control groups. **Results:** In both Fracture and Control groups respectively, numerical failure load obtained at standard dose was not significantly different from half ($p=0.718$ and $p=0.670$) and quarter dose ($p=0.606$ and $p=0.592$), except the tenth dose ($p=0.00198$ and $p=0.0354$). Numerical failure loads predicted at all doses, were able to differentiate patients in fracture and control groups (standard (3254 ± 909 vs. 3794 ± 984 N; $p=0.0373$), half (3390 ± 890 vs. 3860 ± 1063 N; $p=0.0305$) and quarter (3375 ± 915 vs. 3925 ± 990 N; $p=0.0233$) doses, except at the tenth dose (4513 ± 1762 vs. 4766 ± 1628 N; $p=0.458$). ROC analysis also demonstrated that standard, half, and quarter doses can significantly differentiate both groups ($p < 0.05$). **Conclusion:** With a dose reduction of up to 75%, patients can undergo regular and longitudinal MDCT examinations, which allows better monitoring of fracture risk and treatment response. Osteoporotic patients at high risk of OVFs can benefit from a non-invasive analysis on spinal stability with clinically acceptable exposure of radiation.

Disclosures: *D. Anitha, None*

SUN-0077

Alterations in Bone Matrix Composition During Estrogen-deficiency Induced Bone Loss are Influenced by Genetic Background Michael-John Beltejar^{*}, Dana A. Godfrey, Robert D. Maynard, Cheryl L. Ackert-Bicknell. Center for Musculoskeletal Research, University of Rochester Medical Center, United States

Reduction in bone mass during osteoporosis is a well-appreciated phenomenon, however concomitant alterations in bone-matrix composition are understudied. Knowing how changes in bone-matrix composition during osteoporosis results in fragile bones is critical, given that matrix composition contributes to fracture toughening mechanisms in and above what is captured by bone mass. While estrogen is known to impact bone turnover and thereby alter parameters of bone-matrix composition, it is undetermined if this interacts with genetic factors. The goal of this work was to determine if genetic variation modifies the response to estrogen deficiency with regards to bone-matrix quality. To accomplish this, we leveraged the genetic diversity of 3 inbred mouse strains: C57BL/6J (B6), NZO/HILJ (NZO) and 129S1/SvImJ (129). At 12 weeks of age, female mice were ovariectomized and humeri and

uteri were collected at 20 weeks of age (n=10 per strain and per procedure). Uterine masses, normalized to individual body mass, were used to exclude mice in which there was incomplete ovariectomy. From the humeri, the following parameters of bone-matrix quality were obtained using Fourier-Transform Infrared Spectroscopy (FTIR): mineral to matrix ratio, carbonate to phosphate ratio, collagen crosslinking/maturity, non-enzymatic crosslinking, mineral maturity and splitting factor. A two-factor ANOVA was conducted for the six aspects of bone-matrix composition to compare the main effects of strain and ovariectomy, and the interaction between these main effects (so called Gene by Environment effects). All statistical analyses were conducted using R statistical computing software with the Companion to Applied Regression (car) package. The interaction between strain and ovariectomy was significant for the mineral to matrix ratio, $F(1,58) = 4.1013$, $p=0.022$, suggesting that genetics interacts with estrogen status to influence the amount of mineral relative to collagen in compact bone. Furthermore, interactions of main effects were significant for the non-enzymatic crosslinking of collagen, $F(2,58) = 7.8304$, $p = 0.000976$. This indicates that glycation of collagen helices, is also susceptible to estrogen levels. Taken together, these results indicate that estrogen-deficiency differentially affects facets of bone-matrix composition based in part on genetic background and could potentially affect intrinsic fracture resistance beyond reductions in bone mass.

Disclosures: *Michael-John Beltejar, None*

SUN-0078

Damage under Anterior Bending is Associated with Vertebral Body Structural Organization, but not Donor Characteristics Travis D. Eliason¹, Ellen E. Quillen², Donald E. Moravits¹, Roberto J. Fajardo³, Karl J. Jepsen⁴, Todd L. Bredbenner⁵. ¹Materials Engineering, Southwest Research Institute, United States, ²Molecular Medicine, Wake Forest School of Medicine, United States, ³Clinically Applied Science Education, University of the Incarnate Word School of Osteopathic Medicine, United States, ⁴Orthopedic Surgery, University of Michigan, United States, ⁵Mechanical and Aerospace Engineering, University of Colorado Colorado Springs, United States

The structural behavior of bone is an integrative function of a multitude of complex and interrelated characteristics, including bone morphology and the spatial distribution of bone mineral density (BMD). In earlier work, composite traits, that describe independent combinations of vertebral body geometry and BMD distribution, were determined from quantitative computed tomography data of 28 L1 vertebral bodies obtained from cadavers (15 males, 13 females, age range of 25-88 years). A subset of composite traits was found to be associated with donor sex and age [1]. The objective of this work was to investigate whether there is an association between vertebral body damage and composite traits, volumetric BMD (vBMD), donor sex, age, or BMI. We loaded the same 28 L1 vertebral bodies experimentally. A damaging pulse with peak anterior bending moment of 30.6 Nm was applied, held for 60 seconds, and specimens were unloaded. After a recovery period of 300 seconds, a second loading pulse with a peak bending moment of 2.5 Nm was applied. Bending stiffness was determined from data from each loading pulse. Vertebral body damage was determined using a continuum damage mechanics approach to determine the loss of bending stiffness due to an applied anterior bending moment [2]. An unbalanced ANOVA was used to determine whether damage was associated with vertebral body composite traits and a 4-way unbalanced ANOVA was used to determine whether damage was associated with vertebral body vBMD, sex, age, or BMI. Two composite traits were significantly associated with damage ($p = 0.014$ and $p = 0.017$). These composite traits cumulatively describe 7.5% of the total variability in structural organization within the set of vertebral bodies. Vertebral body damage was not significantly associated with vBMD, sex, age, BMI, or with interactions of these characteristics ($p > 0.05$ in all cases). Furthermore, there was no overlap between the composite traits associated with sex and age and those associated with vertebral body damage. Previously published studies have related structural bone traits to vertebral fracture risk [3,4], supporting the notion that vertebral body damage is related to structural bone traits, rather than characteristics of the individual.[1] Coogan, et al. ASBMR 2015. [2] Bredbenner and Davy, J Biomech Eng, 2006. [3] Ruyssen-Witrand, et al. Osteoporos Int 2007. [4] Bruno, et al. J Bone Miner Res, 2014.

Disclosures: *Travis D. Eliason, None*

SUN-0079

Differential Effects of Zoledronic Acid and Teriparatide on Microdamage Across Bone Sites. A Study at the Femoral Diaphysis, Neck, Lumbar Vertebra and Iliac Crest in Ewes Nathalie Portero-Muzy*, Pascale Chavassieux, Roland Chapurlat. INSERM UMR 1033, Université de Lyon, France

Purpose: It has been debated whether bisphosphonates (BPs) might promote bone microdamage, in contrast to teriparatide (TPTD). No association between BPs treatment and microdamage accumulation has been observed in humans (1), but a site-specific variation of microdamage has been reported (2). Thus, the purpose of this study performed in aged ewes was to compare the cortical (Ct) and cancellous (Cn) microcrack density/tissue volume (Cr. Dn) and length (Cr.Le) in Ct bone of femoral diaphysis (FD), in Ct and Cn bone of femoral neck (FN), lumbar vertebra (LV) and iliac crest (IC). Methods: Ewes (n=8/group) received either vehicle (CTRL), or one single dose of 10 mg of zoledronic acid (ZOL) or 20µg/day of TPTD. After 3 months, microdamage was sought after bulk-staining of bone samples with

5mM xylenol orange in 70% ethanol. Results: In CTRL, Ct-Cr.Dn was significantly higher at FD than at the 3 other sites ($p=0.027$). When compared to CTRL, ZOL treatment induced significant increases in Ct-Cr.Dn at FN, FD and IC. In all treatment groups, Ct-Cr.Dn was always markedly greater at FD than at other sites (Table). ZOL also induced a significant increase in Cn-Cr.Dn at all sites and Cr.Dn was significantly greater in Cn than Ct bone at LV ($p=0.036$) and IC ($p=0.017$) but lower at FN ($p=0.018$) (Table). At the FN, it was associated with increases in Ct and Cn-Cr.Le. In contrast, TPTD did not significantly change Ct and Cn-Cr.Dn vs CTRL but decreased Cr.Le in both Ct and Cn bone in FN (Table). Conclusion: In ewes, microdamage density differs across the skeletal sites and is greater at FD than at other sites. A high dose of ZOL increases microdamage density in the short term, at all sites, especially at FD.1. Chapurlat et al. J. Bone Miner. Res. 22:1502-9, 2007. Allen MR et al. Bone. 49:56-65, 2011

		Femoral diaphysis	Femoral neck	Lumbar vertebra	Iliac crest
Ct-Cr.Dn/TV (#/mm ²)	CTRL	1.86±1.46*	0.003±0.006	0.017±0.024	0.082±0.113
	ZOL	5.86±2.71* ^b	0.023±0.023* ^{5a}	0.029±0.32 ^b	0.217±0.142* ^{5a}
	TPTD	2.71±1.50*	0.008±0.014	0.011±0.021	0.042±0.073
Cn-Cr.Dn/TV (#/mm ²)	CTRL		0.001±0.002	0.004±0.007	0
	ZOL		0.008±0.008 ^a	0.059±0.044* ^b	1.364±1.513 ^d
	TPTD		0.001±0.002	0.006±0.012	0
Ct-Cr.Le (µm)	CTRL	107.26±79.18	99.46±0.59	152.38±67.67	178.21±24.77
	ZOL	154.82±53.03	170.68±43.46 ^c	249.48±140.8	179.71±59.05
	TPTD	135.31±61.5	77.08±20.56 ^a	120.08±54.04	163.32±50.17
Cn-Cr.Le (µm)	CTRL		106.02±4.95	110.2±51.37	
	ZOL		160.31±27.64 ^b	137.53±40.38	293.19±212.01
	TPTD		75.56±6.35 ^a	133.27±15.56	

* $p<0.03$ vs other sites; ^a $p<0.04$ vs Cn at the same site; ^b $p<0.05$, ^c $p<0.005$, ^d $p<0.001$, ^e $p<0.0001$ vs CTRL

Disclosures: *Nathalie Portero-Muzy, None*

SUN-0080

Peripheral neuropathy is associated with diabetes-induced bone fragility Clarissa S Craft¹*, Madison R Mcmanus¹, Madelyn R Lorenz¹, Amy Stickland¹, Kristann Magee L¹, Natalie K Wee², Eric D Hilker¹, Sungjae Park¹, Zhaohua Wang¹, Yusuf Bekirov¹, Aaron Diantonio¹, Jeff Milbrandt¹, Erica L Scheller¹. ¹Washington University in St. Louis, United States, ²University of Connecticut, United States

Patients with type-1 and type-2 diabetes mellitus are at significantly increased risk of bone fracture. Fracture risk remains unexplained by common clinical measures including body mass index, bone mineral density by DEXA, or glycemic control. The purpose of this study was to determine whether neuropathy is predictive of diabetes-induced bone fragility. Methods: Streptozotocin (STZ) injections were used to induce type-1 (insulin dependent) diabetes in 12-week old c57BL/6J (c57) control and neuropathy-resistant SARM1-knock-out mice. Diabetes was confirmed by blood glucose and insulin measurement. Peripheral neuropathy was determined by nerve conduction studies and quantitative histomorphometry of epidermis nerve fibers within foot pads. Bone mass and architecture were determined by micro-CT. Bone quality (fragility) was characterized using 3-point bend testing. Results: STZ injections caused sustained hyperglycemia (>300mg/dL) and hypoinsulinemia in both c57 and SARM1-KO mice. The development of peripheral neuropathy was evident in STZ-treated c57 mice. Specifically, electrophysiology studies performed 12-weeks post STZ treatment showed reduced nerve depolarization (amplitude), and histomorphometry revealed a reduction in the relative abundance of CGRP+ peptidergic sensory nerve fibers within the footpads of STZ-treated c57 mice. As expected, SARM1-KO mice were resistant to STZ-induced neuropathy. Interestingly, micro-CT demonstrated that c57 and SARM1-KO mice had comparable cancellous bone mass loss in response to STZ, however, STZ-treated SARM1-KO femurs did not develop cortical thinning that was evident in STZ-treated c57 mice. Importantly, STZ-treated SARM1-KO femurs were also less susceptible to mechanical failure than STZ-treated c57 femurs; suggesting neuropathy contributes to impaired bone mechanical properties in diabetes. Conclusions: In total, this work suggests that diabetic patients with diagnosed neuropathy may be at higher risk for fracture, prompting preventive intervention with anti-resorptive or osteo-anabolic therapy.

Disclosures: *Clarissa S Craft, None*

SUN-0081

Bone Mechanical Properties (nanoindentation) and Microarchitecture (micro-CT) in Type 2 Diabetes Ruban Dhaliwal^{1*}, Jagadeesh Bose², Navin Kumar², Praveer Sihota³, Ram Naresh Yadav³, Vijay Goni⁴, Sameer Agarwal⁴, Sudhaker D. Rao⁵, Sanjay Kumar Bhadada². ¹Endocrinology, Diabetes and Metabolism, Department of Medicine, State University of New York Upstate Medical University, United States, ²Department of Endocrinology, Postgraduate Institute of Medical Education and Research, India, ³Department of Mechanical Engineering, Indian Institute of Technology Ropar, India, ⁴Department of Orthopedics, Postgraduate Institute of Medical Education and Research, India, ⁵Bone and Mineral Research Laboratory, Henry Ford Hospital, United States

Purpose: Individuals with type 2 diabetes (T2D) have a 2.8-fold greater fracture risk than non-diabetics despite normal to high BMD. Mechanisms underlying diabetic skeletal fragility are poorly understood, making it difficult for clinicians to identify those at risk for fractures. Poor bone quality has been implicated in diabetic skeletal fragility, but no data exists on biomechanical properties of bone assessed by nanoindentation in T2D. Methods: Femoral neck bone tissue specimens were collected from adults during surgery for femoral neck fractures; n=8 with T2D of duration >5 years, n=9 without diabetes. Specimens were examined using nanoindentation technique. Elastic modulus (E) and hardness (H) were calculated using the Oliver-Pharr method. Bone microarchitecture was assessed by microcomputed tomography. Linear mixed model analysis was used for comparisons and statistical significance was set to 0.05. Results: Baseline characteristics were comparable for both groups [Table 1]. Elastic modulus and hardness were significantly lower in those with T2D compared to non-diabetic controls (E= 6.76 ± 2.67 vs. 9.64 ± 2.14, p=0.026) (H=0.23 ± 0.13 vs 0.26 ± 0.10, p=0.027). No differences were observed in microarchitectural measurements between the groups. Of note, the E/H ratio was lower in T2D compared to controls (29 vs. 37), representing reduced fracture resistance. Conclusion: Our study is the first to demonstrate compromised bone mechanical strength as assessed by nanoindentation in individuals with T2D. Further studies are needed to precisely characterize the relationship between nanoindentation measures and increased fracture risk in T2D.

Table 1. Characteristics of individuals with T2D and controls

Characteristic	Type 2 Diabetes (n=8)	Control (n=9)	p-value
Demographic			
Age (yrs)	67.3 ± 5.5	67.8 ± 10.3	0.899
Gender (M/F)	2/6	7/2	
BMI (kg/m ²)	27.1 ± 1.5	24.6 ± 5.0	0.192
Duration of type 2 diabetes (yrs)	7.5 ± 2.7	n/a	n/a
Biochemical			
HbA1c	7.8 ± 2.6	5.6 ± 0.2	0.020
Parathyroid hormone (pg/ml)	39.6 ± 15.7	41.1 ± 15.8	0.843
Total 25-hydroxyvitamin D (ng/ml)	19.0 ± 8.6	24.2 ± 5.6	0.159
Bone Mineral Density(BMD)			
L ₁ -L ₄ T-score	-2.5 ± 1.0	-2.7 ± 0.8	0.623
L ₁ -L ₄ BMD(gm/cm ³)	0.758 ± 0.117	0.743 ± 0.085	0.773
Contralateral Total Hip T-score	-2.6 ± 0.7	-2.3 ± 0.7	0.429
Contralateral Total Hip BMD (gm/cm ³)	0.610 ± 0.086	0.615 ± 0.091	0.922
Nanoindentation			
Modulus (Gpa)	6.76 ± 2.67	9.64 ± 2.14	0.026
Hardness (Gpa)	0.23 ± 0.13	0.26 ± 0.10	0.027

Disclosures: *Ruban Dhaliwal, None*

SUN-0082

Local, but Not Global, CT-Based Texture Analysis Improves the Prediction of Femoral Strength Fjola Johannesdottir^{*}, Mary L. Bouxsein. Beth Israel Deaconess Medical Center and Harvard Medical School, United States

It is not clear whether evaluation of spatial distribution of bone mineral density gives additional information about bone strength beyond BMD. The purpose of this study was to determine if co-occurrence textural features (Haralick 1973) from clinical resolution CT images combined with aBMD by DXA are more strongly associated with femoral failure load than aBMD alone. We obtained 64 human cadaveric proximal femurs (41 women and 24 men; age 73 ± 8 yrs), performed imaging with DXA and QCT, and mechanically tested the femurs to failure in a sideways fall configuration at a high loading rate. Textural analysis was performed on 3D region of interests (ROIs) extracted from the trochanter, femoral neck and head. For each ROI, gray level co-occurrence matrices were calculated (distance of 1 voxel in each neighboring direction). A number of different textural features were derived from the co-occurrence matrices to quantify textural patterns (e.g. smoothness, heterogeneity). We also evaluated global textural features: skewness and kurtosis of trabecular bone density at the total hip. The prediction of femoral failure load was evaluated using multiple regression analysis. The observed mean failure load was 3805 ± 1839 N. We found that combining femoral neck aBMD and a textural feature from either the femoral head or the neck significantly improved the failure load prediction (Table 1). A textural feature assessed from the femoral head improved the adjusted r² by 2% (p<0.05, Table 1) and a textural feature from the femoral neck improved the adjusted r² by 4% (p=0.003, Table 1), whereas an assessment from the trochanter provided no additional information. The global textural features did not

improve the failure load prediction compare to FN aBMD alone (p>0.25). The localized textural feature was independent of femoral aBMD (p>0.05), whereas skewness and kurtosis were negatively correlated with FN aBMD, r = -0.84 and r = -0.49, respectively (p < 0.0001). These findings imply that increased localized heterogeneity is negatively associated with failure load. In addition, these results suggest that incorporation of localized textural features may enhance hip fracture prediction, though additional studies are needed to identify the optimal region for textural analysis.

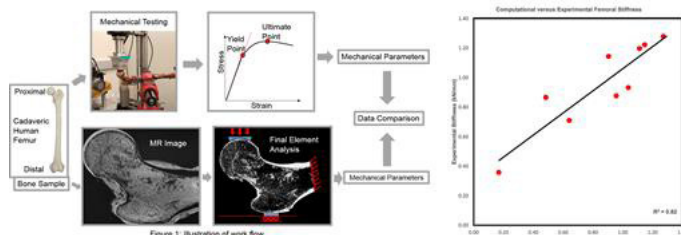
	Adjusted r ²	p-value vs aBMD alone	RMSE (N)
aBMD	0.679	-	1039
aBMD + head texture	0.695	0.047	996
aBMD + neck texture	0.717	0.003	964
aBMD + troch texture	0.675	0.428	1049

Disclosures: *Fjola Johannesdottir, None*

SUN-0083

MRI-Based Assessment of Proximal Femur Compared to Direct Mechanical Testing Daniel Kargilis^{*}, Gregory Chang², Jae Lee¹, Alexander Farid¹, Sneha Shetye¹, Michael Hast¹, Chamith Rajapakse¹. ¹University of Pennsylvania, United States, ²New York University, United States

Half of the women who sustain a hip fracture would not have qualified for osteoporosis treatment by the current criteria, which are based on bone mineral density measurements by DXA. Thus, a better approach is needed to determine if an individual is at risk for hip fracture from a fall. MRI provides an ionizing-radiation free approach for assessing proximal femur microstructure in human subjects. The objective of this study was to determine the association between MRI-derived strength compared to direct mechanical testing of cadaveric femurs. This study used human femurs obtained from 6 male and 7 female donors aged 36-99 years. Specimen storage occurred at a temperature of -30° C before experimentation. Imaging was conducted on a clinical whole-body 3 Tesla MRI scanner (Siemens Prisma, Erlangen, Germany) using a sequence (flip angle 25°, TR/TE 27/3.8 ms, and voxel size 0.242 x 0.242 x 1.5mm 3). Femora were dissected free of soft tissue and 4-120 ohm strain gauges (Omega Engineering, Norwalk, CT) were securely applied to the areas of interest on the bone with an adhesive (Figure 1). Strain gauges were arranged with 120 ohm resistors on a breadboard to form a Wheatstone bridge. The circuit was connected to custom software (Labview 2013, National Instruments, Austin, TX) capable of converting changes in resistance to changes in strain. The femora were securely fixed into a vise at a 10 degree angle relative to horizontal, similar to Keyak et al. (1998). The actuator of a universal test frame (Instron 8874, Norwood, MA) was equipped with a rigid, molded acetabular cup that conformed with the femoral head, and another rigid mold conformed to the greater trochanter. Bone strains (strain x 10 6) were recorded at a rate of 100Hz as the actuator pressed down upon the femoral head at a rate of 1.67mm/s until failure occurred. The acquired MR images were processed to generate FE models. Simulations included forces that mimicked loading conditions for a side fall condition that replicated falling directly on the hip. Computational bone stiffness showed strong correlation with experimental stiffness (R 2 = 0.82). The findings from this study support the use of MRI-based FE analysis of the hip to reliably predict the mechanical competence of the human femur in clinical settings. Further work is needed to determine if post yield measures such as yield strength and ultimate strength could be accurately predicted using the MRI-based computational biomechanics approach.



Disclosures: *Daniel Kargilis, None*

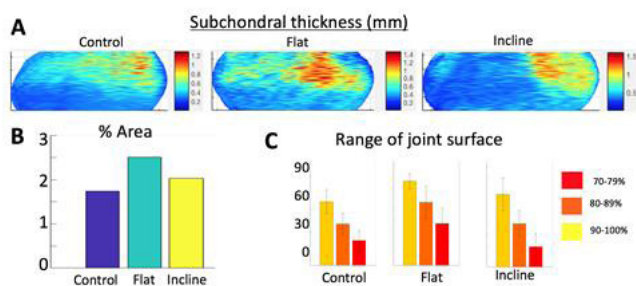
SUN-0084

Exercise driven changes in subchondral bone thickness and distribution John Polk^{*}, Munsur Rahman, Mariana Kersh. University of Illinois at Urbana-Champaign, United States

The adaptive response of bone to mechanical loading via exercise remains an opportunity to encourage bone modeling and remodeling at all stages of life[1]. However, efforts to identify specific responses that decrease bone fracture risk and influence bone stiffness have been hampered by low image resolution and small animal models that do not reflect the nature of human bone at the microstructural level. We aimed to evaluate the response of subchondral bone in an ovine exercise model. METHODS Following IACUC approval, juvenile sheep (mean age = 60 days) were divided into (i) incline treadmill (15% grade; n=5),

Sunday Posters

(ii) flat treadmill (0% grade; n=5), and (iii) control (n=4) groups. Groups (i) and (ii) were exercised twice daily at 1.12m/s for 20 min/bout for 60 days[2,3]. Joint angles were measured at mid-stance using a motion capture system (Qualisys). All subjects were euthanized humanely at day 61. Femora were microCT scanned (50µm voxel, Siemens). Images were post-processed (Amira) and binarized using a histogram-based threshold (Matlab). Thickness measurements were obtained using BoneJ (imageJ). The subchondral surface of the medial femoral condyle was analyzed and the location of maximum thickness was identified. Areas of high thickness, normalized per subject, were defined as thickness values within the highest 30%. Differences between groups were assessed using t-tests ($\alpha=0.05$). RESULTS Exercised sheep experienced ~3600 more loading cycles per day than did non-exercised sheep. On the incline walking, sheep used more flexed knees (8% increase, $p < 0.0001$) at mid-stance than on flat treadmills. There was a heterogeneous distribution of subchondral bone thickness, with the highest thickness values located on the posterior portion of the joint surface (Fig 1A). Exercise increased the maximum subchondral thickness by 22.5% for flat walking and 9.7% for inclined walking. Similarly, areas of high thickness were larger in the exercised sheep (Fig 1B). Areas of increased thickness were spread out over a larger portion of the joint surface in the exercised sheep compared to the controls (Fig 1C). CONCLUSIONS Exercise increased both the maximum thickness and the spread of increased thickness throughout the joint surface. Increased flat walking more evenly spread the distribution of increased bone thickness compared to inclined walking. These spatially specific increased areas of thickness are likely modulated by the changes in flexion angle and body posture. 1. Warden + PNAS 111(14): 5337-5342, 2014 2. Schulz+ JSES 11:174-181, 2002 3. Polk+ Anat Rec 291:293-302, 2008.



Disclosures: John Polk, None

SUN-0085

Lower Limb Geometry in Individuals With Atypical Femoral Fractures as Compared to Typical Fracture and Unfractured Controls Van Krueger^{*1}, Marjolein Van Der Meulen^{2,3}, Jeri Nieves^{4,5}, Elizabeth Foley², Eric Marty³, Amelia Ni³, Jordan Troy², Abigail Campbell³, Douglas Mintz², Jingyan Yang³, Joseph Lane³. ¹Brown University, United States, ²Cornell University, United States, ³Hospital for Special Surgery, United States, ⁴Helen Hayes Hospital, United States, ⁵Columbia University, United States

Bisphosphonates (BP) have been associated with atypical femoral fractures (AFF), but the mechanism is unknown, yet hypothesized to have a critical mechanical component. AFFs initiate on the lateral cortex, suggesting elevated stresses at this location, likely developed through geometric characteristics. We hypothesized that individuals with AFFs will have lower limb geometry differences compared to two BP control groups: hip fractures and unfractured controls. We compared 3D femoral geometry based on CT scans from AFF patients (n=21) and asymptomatic patients on long-term (>5y) BP treatment without AFF or other femoral fracture (BP-nofx, n=50); and, patients on long-term (>5y) BP treatment with femoral neck (FN) or intertrochanteric fractures without AFF (BP-hipfx, n=15). Femur structure and cortical geometry were characterized from the contralateral (nonfractured) femur by isolating contour data from thresholded CT scans and creating a 3D solid model (Materialise Mimics). We then identified relevant femoral geometric landmarks on the model (Geomagic Studio). Finally, we compared 10 anatomic measurements (MATLAB; n=2 blinded individuals): Femoral Length (FL), Femoral Head Width, Femoral Offset, Hip Axis Length, FN Axis Length, FN Shaft Angle, Cortical Thickness (at 25/50/75% FL), middiaphyseal width (at 50/75% FL), FN anteversion and FN offset. Data are presented as mean (SD). The AFF and BP-nofx were age-matched: 72y (8.1); 73y (9.2), but the BP-hipfx group was significantly older: 81y (7.7). BP use was 7.7y (4.4) in AFF, 9.2y (3.4) in BP-nofx ($p=0.03$ vs AFF) and 8.6y (2.5) in BP-hipfx. BMI was significantly higher in the AFF group, 26.0 (4.6) kg/m², than in either control group (22 kg/m² in both controls). In unadjusted analysis cortical thickness at 25%FL and 50%FL were different between AFF and BP-nofx group ($p=0.04$ for both). AFF and BP-hipfx differed in FN width ($p=0.02$), FN offset ($p=0.04$), cortical thickness at 25%FL and 50%FL ($p<0.05$) and middiaphyseal width at 75%FL ($p=0.03$). After adjusting for age, BMI and years of BP use, only FN width differed between AFF and BP-hipfx ($p=0.03$). Several geometric differences existed between AFF and other BP users, but these differences were eliminated after controlling for BMI and age (with or without BP years). Controlling for BMI eliminated the skeletal differences, raising the question as to whether higher BMI, and the associated geometric differences in the lower limb, may increase susceptibility to AFF.

Disclosures: Van Krueger, None

SUN-0086

Osseointegrated implants for trans femoral amputees: radiographic evaluation of bone remodeling Seamus Thomson^{*1}, William Lu¹, Munjed Al Muderis². ¹The University of Sydney, Australia, ²The Osseointegration Group of Australia, Australia

Background and aim(s) Osseointegration is a novel method to overcome persistent socket prosthetic issues in amputees by anchoring a transcutaneous implant directly onto the skeletal residuum. Although similar technologies have been widely applied in the area of hip and knee arthroplasty, little evidence exists in the literature reporting the bone remodeling effects of osseointegrated implants. Stress shielding results in the reduction of bone density due to the implant removing the stress that is usually exerted on the bone, which greatly reduces implant stability. This paper investigates the bone remodeling effect and quantifies it in two of the most common osseointegration implants. Method This is a prospective study of 50 patients with trans-femoral amputations, consisting of 35 males and 15 females, aged 20-73 (mean 48.2) years at surgery, with minimum two-year follow-up. Two implants, the Integral Leg Prosthesis (ILP) and Osseointegrated Prosthetic Limb (OPL), with differences in tapering, coating and bone ingrowth regions were examined. Radiographs were taken at 6 months, 1, 2 and 5-years post-surgery. The surrounding bone was defined using inverse Gruen zones and graded into 5 levels of bone growth or resorption. Result(s) Results obtained at 1 and 2 year follow-ups were compared to the 6-month follow-up values as a baseline. Significant bone growth near the proximal zones of the implant was observed on patients with the ILP implant. This was accompanied by significant resorption towards the distal end indicating the occurrence of stress shielding. The OLP implant demonstrated much more uniform bone density throughout the length of the implant. Conclusion(s) Overall, the patterns of bone remodeling after osseointegration showed similarities to those seen on hip stems with a press-fit design. Of the two osseointegration implants examined in this paper, the OLP implant exhibited less stress shielding effects and is expected to provide better long-term stability.

Disclosures: Seamus Thomson, Osseointegration International, Grant/Research Support

SUN-0087

The role of MEK1/2 and MEK5 on melatonin-mediated effects on bone microarchitecture, mechanical strength, osteogenic and metabolic protein expression in intact female Balb(c) mice Fahima Munmun^{*1}, Van Hoang², Matthew Burow², Bruce Bunnell³, Paula Witt-Enderby¹. ¹Duquesne University Division of Pharmaceutical, Administrative and Social Sciences, United States, ²Tulane University School of Medicine Department of Pharmacology, United States, ³Tulane University School of Medicine Cancer Research Center, United States

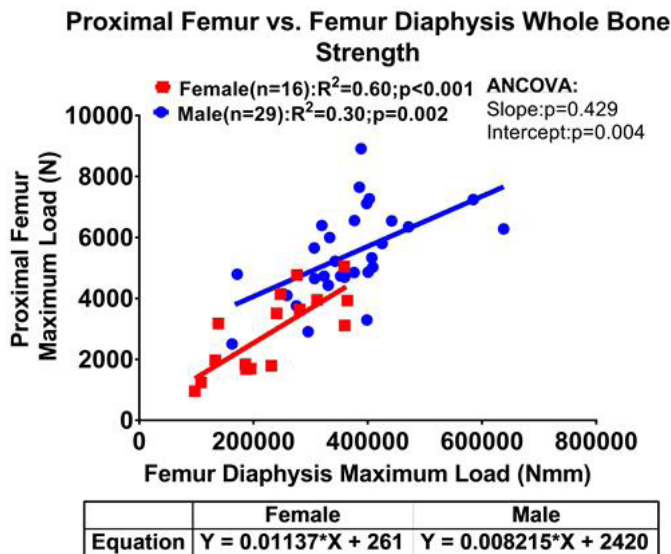
Melatonin exposure has been shown to increase bone mineral density (BMD) in intact female mice equal in efficacy to a one-year exposure to an estrogen/progesterone hormone therapy. In the Melatonin Osteoporosis Prevention Study (MOPS; NCT01152580), melatonin (3mg, p.o. nightly for 6 mos) renormalized bone marker turnover in perimenopausal women. In the MelaOst (NCT01690000) and MOTS (NCT01870115) RCTs, melatonin (3mg for MelaOst or 5mg for MOTS, p.o. nightly for one year) alone (MelaOst) or in combination with strontium citrate, vitamin K2 and vitamin D3 (MOTS) increased BMD in postmenopausal osteopenic women. Using a human bone marrow-derived mesenchymal stem cell (hMSC) and peripheral blood monocyte (hMC) co-culture model system, we have demonstrated that MT2 melatonin receptors, MEK1/2, MEK5 and perhaps PPAR γ and GLUT4 underlie melatonin's stimulating effects on osteoblast differentiation, which results in osteoprotegerin-mediated inhibition of osteoclastogenesis. We wanted to further these findings in vivo using intact female Balb(c) mice. Specifically, mice were injected with melatonin (0.166mg/kg) in the absence or presence of the selective MEK1/2 inhibitor, PD184352 (25mg/kg), MEK5 inhibitor, Bix02189 (25mg/kg), or the dual MEK1/2 and MEK5 inhibitor, SC-1-151 (25mg/kg) for 45 days. We assessed the effect of these treatments on osteogenic and metabolic protein expression in femur bone by western blot; bone microarchitecture through microCT; and bone biomechanics by the mediolateral three-point bending test. Melatonin, through MEK1/2 or MEK5, increased the expression of Runx2, Bmp-2, Fra-1 and decreased Ppar γ expression. Furthermore, melatonin in combination with Bix02189 modulated bone microarchitecture by decreasing trabecular number and connectivity density and by increasing trabecular separation. Melatonin in combination with SC-1-151 decreased ultimate breaking load of the femur bone. These in vivo studies support the findings in the hMSC:hMC co-culture model system and lend further support for a role of MEK1/2 and MEK5 in melatonin effects on bone.

Disclosures: Fahima Munmun, None

SUN-0088

The Relationship of Whole Bone Strength across Cadaveric Diaphyseal and Cortical-Cancellous Sites Daniella Patton*¹, Erin Bigelow¹, Stephen Schlecht², Todd Bredbenner³, Karl Jepsen¹. ¹Department of Orthopedic Surgery, University of Michigan, United States, ²Mechanical Engineering, University of Michigan, United States, ³Department of Mechanical and Aerospace Engineering, University of Colorado Colorado Springs, United States

Estimating the strength of fracture-prone cortico-cancellous structures like the proximal femur would benefit from knowing how well bone strength correlates across anatomical sites and whether age-related declines in strength at another site predicts strength-declines at the hip. We conducted a biomechanical evaluation of bone strength at weight and non-weight bearing sites, determined how strength correlates across anatomical sites on an absolute basis and relative to age, and tested for sex-specific effects. Cadaveric proximal femora (M: n=45, F: n=40) and femoral (M: n=34, F: n=19) and radial diaphyses (M: n=36, F: n=19) were loaded to failure in a fall-to-side and four-point bending configuration, respectively. Whole bone strength of the proximal femur correlated significantly with the strength measured for the femoral diaphysis for both sexes (M: R²=0.30, p=0.002, F: R²=0.60, p<0.001) and only for the male radial diaphysis (M: R²=0.18, p=0.029, F: R²=0.18, p=0.145). Likewise, diaphyseal strength of the radius and femur correlated significantly only for males (M: R²=0.41, p<0.001, F: R²=0.28, p=0.093). Significant sex-specific effects were observed at the proximal femur and femur diaphysis with males being 60% (~2159 N) stronger than females at matched diaphyseal strength values (Fig. 1). Residuals from the strength-age regressions were plotted across bone sites. Strength-age residuals of the proximal femur and femur diaphysis were significant for both sexes (M: R²=0.22, p=0.011, F: R²=0.50, p<0.001) and only for the male radial diaphysis (M: R²=0.19, p=0.023, F: R²<0.01, p=0.810). Strength-age residuals of the femur and radial diaphysis were only significant for males (M: R²=0.46, p<0.001, F: R²=0.01, p=0.705). Our results indicate that bone strength correlates across anatomical sites on an absolute basis and relative to age, such that individuals who were weak (or strong) for their age at one site, were also weak (or strong) for their age at other sites. In addition, females had significantly weaker proximal femurs than would be predicted from their diaphyseal strengths compared to males. These findings are clinically important because they reveal the potential to improve estimates of bone strength at fracture-prone site like the proximal femur based on strength and age effects at more simple tubular structures of the diaphysis.



Disclosures: Daniella Patton, None

SUN-0089

Comparative effect of deproteinized bovine bone, bioglass and synthetic hydroxyapatite on bone repair Andrea Mattiuzzi*¹, Miguel Angel Pellegrini¹, Macarena Gonzales-Chaves¹, Ricardo Orzuza², Susana N Zeni¹, Gretel G Pellegrini¹. ¹CONICET-Universidad de Buenos Aires. Instituto de Immunología, Genética y Metabolismo (INIGEM). Facultad de Farmacia y Bioquímica-Hospital de Clínicas "José de San Martín", Buenos Aires, Argentina., Argentina, ²Universidad de Buenos Aires, Facultad de Odontología. Cátedra de Bioquímica Gral y Bucal, Buenos Aires, Argentina., Argentina

Deproteinized bovine bone putty (BB), bioglass (BG) and synthetic hydroxyapatite (SH), (Synergy, Odontit Implant Systems, Argentina) guide bone repair because of their osteoconductive properties. The bone healing response of these bone-grafting materials was compared using a critical sized bone defect model. A bone defect of 4 mm diameter was created in rat tibiae for implantation with each biomaterial (N=30 rats). Samples for histological

and histomorphometrical analysis of new bone formation (NBF) and remaining particles of each device (RP) were collected at 2 and 4 weeks. Results: Percentage (%) of NBF (mean ± SD): 2 weeks: Control group: 6.60±3.71; BB group: 23.23±3.89*; BG group: 18.35±5.23*; SH group: 26.27±9.30*; 4 weeks: Control group: 6.69±2.38; BB group: 24.37±3.66*; BG group: 17.45±6.64*; SH group: 32.25±3.80*. Percentage (%) of RP: 2 weeks: Control group: 0±0; BB group: 5.04±1.39*; BG group: 3.03±2.31*; SH group: 4.46±2.87*; 4 weeks: Control group: 0±0; BB group: 4.45±2.35*; BG group: 2.87±1.14*; SH group: 3.78±1.68* (*p<0.05 versus control group; p= NS between BB, BG and SH groups). We did not find statistical significance among the three biomaterials, although SH exhibited a trend towards increased NBF. The three biomaterials were histologically substantially equivalent showing the expected histological stages of bone repairing: progressive inflammatory response accompanied bone healing at the implanted sites. All biomaterials were associated with trabecular bone formation. While further studies need to be done, our results indicate that BB, BG and SH exhibit similar characteristics in terms of osteoconduction.

Disclosures: Andrea Mattiuzzi, None

SUN-0090

High Resolution pQCT Micro-Architectural Parameters to Predict Bone Failure in the Case of a Forward Fall Martin Revel*, François Dubouef, François Bermond, Jean-Paul Roux, David Mitton, H el ene Follet. Univ Lyon, INSERM, UMR1033, France

The gold standard for the diagnosis of osteoporosis is the measurement of bone mineral density by Dual X-ray absorptiometry. However, the assessment of the risk of fracture is still not sufficiently discriminant. Indeed, half of the patient considered non-osteoporotic will fracture [1]. In this context, the objective of this study is to evaluate whether bone micro-architecture of distal radius assessed by high-resolution peripheral quantitative computed tomography (HR-pQCT) manage to discriminate fractured from non-fractured bones obtained in an ex vivo experimental study reproducing a forward fall under dynamic loading conditions [2]. Thirty radii from elderly donors (79 ± 12 y.o., 15 M, 15 F) were scanned using a HR-pQCT device with an isotropic 82 µm voxel size (XtremeCT, Scanco Medical AG) before being loaded at 2 m/s to mimic impact that corresponds to a fall, leading to two groups: fractured and non-fractured. Clinical standard evaluation was performed on the images in order to assess bone micro-architecture. Statistical non-parametric Spearman's and Wilcoxon's rank-sum tests were performed using R software and p-values under 0.05 were considered as significant. On the entire population, all the parameters were significantly correlated to the maximal load. Nevertheless, important differences appeared when analyzing in two groups. Indeed, the fractured group shows high significant correlation with the trabecular parameters whereas no link was found with any parameters in the other group (Table 1). Furthermore, the two groups showed in the second test a significant difference for: all trabecular parameters, the cortical thickness and the experimental load (p < 0.05) but the cortical vBMD remain non-significant. The aim of this study was to assess whether micro-architecture assessed by HR-pQCT could discriminate bone fracture obtained experimentally. The correlations showed that trabecular parameters explained the bone strength for the fractured group and showed significant difference between the two groups. The results are in accordance with an epidemiologic study where the authors conclude that the trabecular micro-architecture in the radius is a good predictor of incident fracture in postmenopausal women [3]. Finite element analysis will be performed to enhance our understanding of bone fracture during a fall.[1] E. S. Siris et al, Arch.Intern.Med. 164:10, 2004[2] E. Zapata et al, J.Biomech., 63, 2017[3] E. Sornay-Rendu et al, JBMR, 32:6, 2017

	Tt.vBMD (mg/cm ³)	Tb.vBMD (mg/cm ³)	BV/TV (%)	Tb.N (1/mm)	Tb.Th (mm)	Tb.Sp (mm)	Tb.Sp/SD (mm)	Ct.vBMD (mg/cm ³)	Ct.Th (mm)
All samples	r	0.68	0.62	0.45	0.73	-0.49	-0.47	0.39	0.51
	p-value	<.0001	0.0003	0.001	<.0001	0.006	0.008	0.03	0.004
Fractured	r	0.69	0.81	0.69	0.74	-0.72	-0.74	0.36	0.48
	p-value	0.007	0.0004	0.0004	0.006	0.003	0.003	0.02	0.08
Non Fractured	r	0.30	0.10	0.10	-0.10	0.42	0.053	0.096	0.15
	p-value	0.3	0.7	0.7	0.7	0.1	0.8	0.7	0.6

Table 1: Spearman correlation (r) between the experimental load and the micro-architectural parameters. Regarding the fractured group, the coefficient ranged between 0.69 to 0.81 for the trabecular parameters whereas the cortical ones were found as not significant. As to non-fractured group, no link was found with any cortical or trabecular parameters. Tt: Total, Tb: Trabecular, Ct: Cortical, vBMD: Volumetric Bone Mineral Density, N: number, Th: Thickness, Sp: Separation, SD: Standard Deviation.

Disclosures: Martin Revel, None

SUN-0119

Impact of Sex and Maturation on Trabecular and Cortical Microarchitecture in Children and Young Adults Tandy Aye*¹, Kyla Kent¹, Jin Long¹, Jessica Whalen¹, Ariana Strickland¹, Andrew Burghardt², Mary B. Leonard¹. ¹Stanford University School of Medicine, United States, ²University of California San Francisco, United States

The impact of sex and maturation on trabecular (Tb) and cortical (Ct) microarchitecture in children and young adults has not been well established. The new second-generation high-resolution peripheral quantitative CT (HR-pQCT) scanner (XCT II, Scanco Medical)

Sunday Posters

incorporates three important advances. First, the 61µm isotropic voxel provides greater spatial resolution to accurately determine the thickness of individual human trabeculae. Second, the device uses direct voxel-based measures of trabecular thickness and spacing with Gaussian thresholding. Third, the gantry of the scanner allows the limb to advance further into the field of view, providing measures in the cortical midshaft that are less subject to partial volume effects. The objective of this study was to identify sex and maturation effects on bone structure and strength, and to determine the impact of adjustment for leg muscle mass. This cross-sectional study included 208 healthy participants (98 females), ages 5 to 30 yrs recruited from the community and excluded from diseases or medications known to effect growth and bone health. The reference line was placed 2 mm proximal to the proximal margin of the growth plate (or growth plate remnant if fused) and scans were centered 3.5% and 30% of tibia length proximal to the reference line. Log linear regression models were adjusted for age, age², sex, tibia length and Tanner stage. The results are presented as percent differences in female vs. male, and Tanner stage (Table). Female participants had significantly lower Ct thickness, greater Ct bone mineral density (BMD), and lower Ct porosity, with lower micro-finite element analysis estimates of failure load, compared with males. Greater skeletal maturity was associated with greater Ct thickness and failure load, independent of age. Cortical porosity was markedly higher in pre-pubertal participants (averaging 5.2 and 3.5% in Tanner stage 1 males and females respectively, compared with 1.5 and 1.1% in Tanner stage 5). In the tibia metaphysis, female participants had significantly, lower bone volume fraction (BV/TV) and Tb thickness compared with males; Tb number did not differ. BV/TV and Tb number were greater in progressively mature participants, compared with pre-pubertal participants. Leg muscle mass was positively associated with Ct thickness and failure load and Tb BV/TV and Tb thickness. Adjustment for muscle mass eliminated sex and Tanner differences in these outcomes.

	Tibia Midshaft			
	Cortical Thickness	Cortical BMD	Cortical Porosity	Failure Load
	Percent Difference			
Sex (F vs. M)	-7.3**	2.6*	-33.3***	-8.2***
Tanner, vs. T1				
T2	12.2***	-2.1	10.1	11.0**
T3	11.8**	-0.0	-39.3**	14.7***
T4	23.3**	1.1	-54.3***	23.9***
T5	20.0*	1.4	-49.3**	23.8***
	Tibia Metaphysis			
	Bone Volume Fraction	Trabecular Number	Trabecular Thickness	Failure Load
	Percent Difference			
Sex (F vs. M)	-5.1*	-1.2	-4.1***	-14.1***
Tanner, vs. T1				
T2	5.7	10.0***	-3.6	7.5
T3	8.4	4.1	1.4	20.5*
T4	26.1***	11.1***	1.3	48.8***
T5	32.2***	16.4***	0.6	58.7***

All adjusted for age, age² and tibia length.

* = p < 0.05, ** = p < 0.01, *** = p < 0.001; n.s. = not significant

Disclosures: **Tandy Aye**, None

SUN-0120

Healing rickets: Lessons from the Vienna Studies 1921-1923 David Ayoub*, Southern Illinois University School of Medicine, United States

Purpose: Hans Wimberger's landmark study on the radiology of healing rickets was based upon the observations of infants who developed disease prior to or following admission to institutions in and around Vienna, Austria from 1919-1922 following WWI. I sought to reanalyze the original findings in greater detail for further characterization of healing patterns. Methods: High quality prints of radiographs from the original publication were reviewed from ten institutionalized infants (6-13 months, x̄ = 9.2 months) who underwent unilateral upper and lower limb (n=9) or upper limb only (n=1) imaging during various stages of disease. Radiographs were taken at 4 to 6 points in time in each infant, including 19 limbs, and yielded a dataset comprised of 264 individual long bones and 440 growth plates (GPs). Nine infants were treated with various combinations of either sun exposure (n=3), cod-liver oil (n=4), artificial light (n=3) or calcium (n=1). One was allowed to spontaneously heal. Results: Changes of active rickets was present in 9 of 10 infants while one presented in a state of healing. All infants demonstrated healing as manifested by mineralization above an original and distinct zone of provisional calcification (ZPC). This occurred in 39% of all GPs. During healing, a new line of mineralization often appeared above the original ZPC in all infants (range 2-7 GPs per infant). Other signs of healing included the appearance of perichondrial spurs in 100% of infants and 46% of GPs and subperiosteal new bone (SPNB) (90% of infants and x% of bones). SPNB was never during pre-rachitic or healed states. Generalized osteopenia was uncommon, seen in 30% of infants during active stages, often worsened during the healing process. The changes of both active and healing rickets commonly occurred asynchronously in time. The disease never involved all bones. Conclusions: Rickets presents as a much more diverse range of radiographic changes than widely assumed. A classification scheme of healing stages is proposed.

Disclosures: **David Ayoub**, None

SUN-0121

Irisin Levels Are Positively Associated with Bone Mineral Density and Better Glycemic Control in Healthy and Type 1 Diabetes Children Graziana Colaianni¹, Giacomina Brunetti², Maria Felicia Faienza³, Lorenzo Sanesi¹, Monica Celi⁴, Laura Piacente³, Gabriele D'Amato³, Giorgio Mori⁵, Silvia Colucci², Maria Grano¹. ¹Department of Emergency and Organ Transplantation, University of Bari, Italy, ²Department of Basic Medical Sciences, Neuroscience and Sense Organs, University of Bari, Italy, ³Department of Biomedical Science and Human Oncology, Paediatric Unit, University of Bari, Italy, ⁴Tor Vergata, University of Rome, Italy, ⁵Department of Clinical and Experimental Medicine, University of Foggia, Italy

Irisin is a myokine secreted by skeletal muscle during physical activity both in mice and humans. After its discovery, irisin raised great expectations as regulator of energy homeostasis able to promote the trans-differentiation of white into brown adipocytes, triggering non-shivering thermogenesis. Later, we demonstrated that its primary target organ was the skeleton given that a lower dose of irisin was able to increase cortical bone mineral density in healthy mice and to ameliorate bone and muscle losses in a mouse model of disuse-induced osteoporosis and muscular atrophy. Aiming to understand if these results could be translated to humans in future, we sought to determine if irisin levels were correlated with a bone healthy status in a population of children, given that bone mass reached during childhood is one of the most important determinants of lifelong skeletal health. More specifically, we investigated irisin correlation with bone status in both physiological and pathological conditions, by analyzing two subpopulations of children, healthy or diagnosed with childhood type 1 diabetes mellitus (T1DM), with the latter group characterized by decreased bone mass. 34 controls (9.82 ± 3.2 years) and 96 T1DM subjects (12.2 ± 4 years), the latter further divided in 56 children receiving multiple insulin daily injections (MDI) and in 40 children on continuous subcutaneous insulin infusion (CSII), were included in the study. Irisin and bone metabolic markers were quantified in sera and bone mineral density (BMD) was evaluated by QUS. In healthy children, we found that irisin levels were positively correlated with BMD measured as BTT-Z-score (r = 0.375; p < 0.001), and osteocalcin (r = 0.37; p < 0.001), and negatively correlated with Dickkopf WNT Signaling Pathway Inhibitor 1 (DKK1) (r = -0.27; p < 0.001) and glucose (r = -0.14; p < 0.01). Interestingly, irisin levels were higher in T1DM children respect to controls (p < 0.001). In these patients, irisin negatively correlate with HbA1c (r = -0.105; p < 0.001), years of diabetes (r = -0.07; p < 0.04), 25(OH)-Vitamin D (r = -0.175; p < 0.0001), and positively with BTT-Z-score (r = 0.088, p = 0.016) and osteocalcin (r = 0.059, p < 0.04). Moreover, we detected higher levels of irisin in CSII than MDI patients (p < 0.001), indicating a strong positive association between irisin and the better glycaemic control given by the pump device which closely mimic the behaviour of the pancreas and improves the bone health status of these patients.

Disclosures: **Graziana Colaianni**, None

SUN-0122

Safety and Effectiveness of Stoss Therapy in the Treatment of Vitamin D Deficiency. Paul Tannous¹, Melissa Fiscoletti¹, Chris Cowell¹, Nicholas Wood¹, Yvonne Zurynski², John Coakley¹, Philip Britton¹, Hasantha Gunasekera¹, Andrew Biggin¹, Craig Munns¹. ¹Children's hospital at Westmead, Australia, ²Australian Pediatric Surveillance Unit, Australia

BACKGROUND AND OBJECTIVES: Pediatric vitamin D deficiency is associated with musculoskeletal disease, most notably nutritional rickets. Vitamin D treatment can correct vitamin D status (25-hydroxyvitamin D - 25OHD), prevent nutritional rickets and its extra-skeletal complications including hypocalcaemic seizure, cardiomyopathy and rarely death. Compliance with daily oral therapy can be difficult to achieve, making high dose, short-term vitamin D (stoss) therapy a potentially valuable therapeutic tool to improve compliance and thus normalize 25OHD status. Consensus on optimal stoss dosing is lacking and concerns regarding its safety in children remain. Our objective was to compare the effectiveness and safety of stoss versus standard vitamin D therapy in treating 25OHD deficiency in children. METHODS: Children aged 2 to 16 years of age with vitamin D deficiency (25OHD < 50nmol/L) were randomized to receive either stoss (100,000 IU/ week for 4 weeks) or standard (5,000IU/day for 80 days) therapy. Participants underwent clinical and biochemical evaluation of effectiveness and safety at baseline, 4 weeks, and 12 weeks after starting therapy. Primary outcome was 25OHD status at 12 weeks. Compliance was measured by assessment of medication taken. RESULTS: 135 children were enrolled in the study; 73 received stoss therapy and 62 received standard therapy, median age of 9 years (IQR: 6, 12 years). Baseline 25OHD levels were 26 nmol/L (IQR: 19, 35 nmol/L) and 32 nmol/L (IQR: 24, 39 nmol/L) in the standard and stoss groups respectively. Change in 25OHD was 50 nmol/L (IQR: 35, 98 nmol/L) in the standard group and 35 nmol/L (IQR: 25, 46 nmol/L) in the stoss group (p = 0.0005). While the standard group achieved greater changes in the 25OHD levels over the study period, there was no significant difference in normalization of 25OHD status between the two groups. At 12 weeks, more than 80% of participants in both groups achieved sufficiency (25OHD > 50nmol/L). A similar result was seen with ALP, and PTH levels. Similarly, serum calcium and urinary calcium/creatinine ratio were largely within normal limits with no significant difference seen between the two groups. Compliance was similar in the 2 treatment groups. CONCLUSIONS: We found no difference in efficacy or safety between 100,000 IU weekly for 4 weeks and standard daily therapy of 5,000 IU in the management of vitamin D deficiency in children. Although simplifying treatment regimens

has been known to improve medication compliance, this was not evident in our study. These results add to previous data supporting stoss as an effective and safe alternative for children. Long-term studies are needed to determine optimal dosing and monitoring schedules to maintain sufficient vitamin D levels throughout childhood.

Disclosures: *Paul Tannous, None*

SUN-0123

Larger muscle area is a positive predictor of bone strength while subcutaneous fat is a negative predictor of bone strength: A pQCT and HR-pQCT study of boys and girls Saija Kontulainen*¹, Amy Bunyamin², Chantal Kawallilak², Kelsey Bjorkman², Jd Johnston². ¹University of Saskatchewan, UofS, Canada, ²UofS, Canada

Muscle and fat tissues are proposed to have clinically important site- and sex-specific roles on bone strength development in children but evidence is limited. Study purposes were to A) quantify sex-differences in bone strength estimates at the distal radius and tibia in children approaching their growth spurt; and B) assess if sex-differences in bone strength were influenced by adjustment of site-specific muscle and subcutaneous fat areas. We scanned the dominant distal radius and tibia from 138 children (mean age: 10.7, SD: 1.8 yrs) using high resolution peripheral quantitative CT (HR-pQCT) and applied finite element analysis to estimate bone strength (failure load and stiffness). We scanned the dominant forearm and lower-leg with pQCT to quantify muscle and subcutaneous fat areas. We defined biological age by calculating age from the estimated age at peak height velocity (aPHV) and included 129 children (67 girls) preceding aPHV. We compared anthropometrics, physical activity (via questionnaire), dietary intakes of protein, calcium and vitamin D (questionnaire) between sexes to identify covariates. We compared bone strength estimates between boys and girls using biological age, limb length and weight as covariates. We then entered site-specific muscle and fat areas in the linear regression models. Maturity, limb length and weight adjusted failure load and stiffness were 11% greater at the distal radius and 12% and 11% greater, respectively, at the distal tibia in boys vs. girls. After adjusting for forearm or lower-leg muscle area (with or without subcutaneous fat area), failure load and stiffness no longer differed between sexes. Inclusion of muscle area improved the fit (R2 from 0.5 to 0.6, p<0.001) of all bone strength models and was a significant positive predictor of failure load and stiffness at both the distal radius and tibia (B ranged 0.50 to 0.58, p<0.05). Subcutaneous fat area was a negative predictor of failure load and stiffness at the distal tibia only (B -0.36 to -0.37, p<0.05). Findings suggest that greater bone strength at the distal radius and tibia in boys was explained by larger forearm and lower-leg muscle areas. Results also indicated a negative role of calf subcutaneous fat on distal tibia bone strength. Interventions to improve muscle size and strength development, particularly for girls, may alleviate observed sex-differences in bone strength may contribute to life-long prevention of bone fragility fractures in both sexes.

Disclosures: *Saija Kontulainen, None*

SUN-0124

Is adiposity increased in children with achondroplasia and hypochondroplasia? Takuo Kubota*¹, Yukako Nakano¹, Kei Miyata¹, Kenichi Yamamoto¹, Shinji Takeyari¹, Hirofumi Nakayama^{1,2}, Takeshi Kimura¹, Yasuhisa Ohata^{1,3}, Taichi Kitaoka¹, Keiichi Ozono¹. ¹Department of Pediatrics, Osaka University Graduate School of Medicine, Japan, ²The Japan Environment and Children's Study, Osaka unit center, Japan, ³The 1st. Department of Oral and Maxillofacial Surgery, Osaka University Graduate School of Dentistry, Japan

Achondroplasia (ACH) and hypochondroplasia (HCH) are caused by gain-of-function mutations of FGFR3. FGF18 and FGF2 bind FGFR3 and regulate the development of chondrocytes in the growth plate. However, endocrine FGF, FGF21 and FGF23, also binds FGFR3 and plays some roles in glucose and phosphate metabolism. Obesity is one of complications of ACH and HCH, but evaluation of obesity by BMI is inappropriate in these disorders due to extreme short stature. Thus, it is required to develop appropriate measurements for ACH and HCH. In this study, dual X-ray absorptiometry (DXA) was used to evaluate the degree of obesity in children with ACH and HCH. Our objective is to assess their obesity using % body fat by DXA and body index obtained from anthropometric measurement and to examine whether any body index predicts an accurate adiposity. Thirty-one participants with ACH (14 males, 10 females) and HCH (4 males, 3 females) with p.N540K at our University Hospital were recruited in this retrospective study. The mean age of male and female was 10.7 and 10.4 years, respectively. Their anthropomorphic measurements (height, weight, hip circumference and waist circumference) were obtained from their medical records. We calculated BMI, waist height ratio and waist hip ratio. Whole body DXA scans were performed to measure % body fat (%BF) on a Hologic Discovery A DXA scanner. All statistical analyses were performed using IBM SPSS Statistics software. On basis of 'Guidelines for the management of obesity disease in children and adolescents 2017', we defined obesity as the following: boys with more than 25% BF, girls under 10 years of age with more than 30% BF and girls over 11 years with more than 35% BF. One quarter (25.8%) of ACH patients met the criteria for obesity by %BF (27.8% in boy and 23.1% in girl). On the other hand, subjects with BMI percentile over 85% accounted for 83.9% (83.3% in boy, 84.6% in girl). Moreover, as much as 45.2% of all was above 95% BMI (50% in boy, 38.5% in girl). Our data showed no age dependency to fulfill obesity criteria from the point of %BF. The prev-

alence of obesity was high in children with ACH and HCH compared to general population according to the "general" obesity criteria. No apparent age-dependence was observed. High BMI percentile did not predict increased %BF in the cohort. The relationship between obesity and insulin resistance is the next issue to be examined.

Disclosures: *Takuo Kubota, None*

SUN-0125

Racial Differences in Bone Histomorphometry within Children and Young Adults on Dialysis. Marciana Laster*¹, Renata Pereira, Isidro Salusky. UCLA, United States

Introduction: In the healthy population, Black race is associated with greater bone mineral density and decreased risk of fracture when compared to White race. Comparison of iliac crest histomorphometry in healthy children reveals greater cortical thickness and decreased cortical porosity in Black vs. White children. How these differences are reflected in the bone of children and young adults on dialysis is unknown. Methods: Using tetracycline-labeled, iliac crest bone biopsies obtained in prior research protocols in pediatric and young adult dialysis patients, we compared trabecular and cortical parameters between Black subjects and non-Hispanic White subjects matched by age, gender, disease etiology, modality and PTH. Results: The cohort consisted of 25 Black subjects and 29 White subjects with a mean age of 13.9 ± 4.7. 60.4% of subjects were male and 73.6% used PD as the primary modality. There were no differences in phosphate, PTH or Alkaline Phosphatase between the racial groups and albumin-corrected serum calcium was significantly lower in Black subjects (Table 1). Turnover, mineralization and volume parameters in trabecular bone did not show significant differences between racial groups (Table 2). Analysis of cortical bone showed greater median cortical thickness in Black subjects (Figure 1) and in linear regression analysis, Black race was associated with 37.5% higher cortical thickness (95% CI 2.1% to 85.2%, p=0.04). There was no significant difference in cortical porosity. Conclusions: Similar to findings in populations of normal children, Black race in pediatric and young adults on dialysis is associated with greater cortical thickness. Contrarily, there were no significant differences in cortical porosity or trabecular bone. These findings suggest the possibility of racial variation in the response of cortical bone to the perturbations of CKD-MBD.

Table 1: Cohort Characteristics

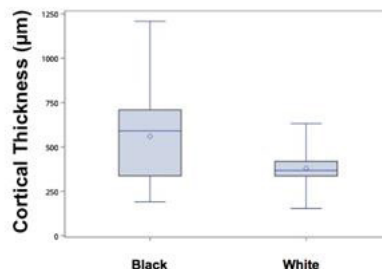
	Black	White	p
N	24	29	
Age, mean ± SD	13.7 ± 4.7	14.1 ± 4.8	0.7
Gender, n (%)			0.8
F	9 (37.5)	12 (41.4)	
M	15 (62.5)	17 (58.6)	
Modality, n (%)			0.3
HD	8 (33.3)	6 (20.7)	
PD	16 (66.7)	23 (79.3)	
Disease, n (%)			0.6
CAKUT	7 (29.2)	10 (34.5)	
GN	9 (37.5)	13 (44.8)	
Other/Unknown	8 (33.3)	6 (20.7)	
Laboratory Parameters			
Calcium (mg/dL), mean ± SD	9.06 ± 0.91	9.74 ± 0.84	0.02
Phosphorus (mg/dL), median (IQR)	6.2 (5.7, 6.7)	6.05 (5.4, 7.7)	1
PTH (pg/mL), median (IQR)	592 (329, 1189)	625 (398, 893)	1
Alkaline Phosphatase (IU/L), median (IQR)	274.5 (127, 439)	229 (166, 363)	0.7

Table 2: Bone Histomorphometry by Race and Ethnicity

	Black	White	p
Turnover			
Bone Formation Rate (µm ³ /mm ³ /year)	77.7 (51.1, 150.2)	69.9 (46.9, 131.8)	0.6
Eroded Surface (%)	9.8 ± 4.6	8.6 ± 4.1	0.3
Mineralization			
Osteoid Volume (%)	5.0 (1.8, 9.5)	8.3 (4.7, 11.7)	0.2
Osteoid Thickness (µm)	11.1 (9.3, 16.3)	11.7 (9.8, 15.5)	0.6
Osteoid Surface (%)	39.9 ± 21.2	44.3 ± 14.8	0.4
Osteoid Maturation Time (days)	9.9 (6.5, 13.2)	11.6 (8.3, 15.4)	0.2
Mineralization Lag	16.7 (8.6, 37.8)	22.9 (14.7, 55.8)	0.1
Time (days)	1.3 (1.1, 1.4)	1.1 (1, 1.1)	0.2
Mineral Apposition Rate (µm/day)	0.9 ± 0.6	0.9 ± 1.1	0.9
Adjusted Apposition Rate (µm/day)	20.5 ± 12.3	20.7 ± 11.1	1
Mineralized Surface			
Bone Surface (%)			
Volume			
Bone Volume (%)	33.31 ± 7.8	31.5 ± 8.6	0.4
Trabecular Thickness (µm)	166.7 (141.1, 162.6)	149.2 (136, 168.2)	0.1
Trabecular Number (#/mm)	2 ± 0.3	2.1 ± 0.5	0.6
Trabecular Separation (µm)	351 (263.2, 393.7)	341.79 (254.1, 388.4)	0.9
Cortical			
Cortical Thickness (µm)	590.8 (336.8, 709.2)	367.6 (336.2, 419.1)	0.04
Cortical Porosity (%)	7.2 (4.3, 15)	9.5 (3.4, 15.5)	0.3

Normally distributed variables reported as mean ± SD and non-normally distributed variables presented as median (interquartile range).

Figure 1: Median Cortical Thickness by Race



Disclosures: *Marciana Laster, None*

Sunday Posters

SUN-0126

Multimodality Study of Glucocorticoid Induced Osteoporosis in Pediatric Crohn's Disease Jin Long¹, Dale Lee², Rita Herskovitz³, Babette Zemel⁴, Mary Leonard⁵. ¹Department of Medicine, Stanford University, Stanford, United States, ²Department of Pediatrics, Seattle Children's Hospital, Seattle, WA, United States, ³Department of Pediatrics, The Children's Hospital of Philadelphia, Philadelphia, PA, United States, ⁴Division of GI, Hepatology & Nutrition, The Children's Hospital of Philadelphia, Philadelphia, PA, United States, ⁵Department of Pediatrics, Stanford University, Stanford, CA, United States

Childhood Crohn's disease (CD) is associated with multiple risk factors for impaired bone accrual. We reported the results of a 12 month double-blind, placebo-controlled trial of low magnitude mechanical stimuli on bone health in 138 children with CD, ages 8 to 21 year, followed by one year open-label extension (JBMR 2016). The trial showed a modest effect on spine quantitative CT (QCT) trabecular volumetric bone mineral density (BMD). In all participants combined, tibia pQCT trabecular vBMD and cortical area, DXA BMD at all sites, DXA leg lean mass, and spine QCT trabecular BMD Z-scores improved markedly (all p<0.001). Greater physical activity (by accelerometer) and lesser disease activity were associated with greater gains in leg lean mass. The objective of this secondary analysis was to identify correlates of changes in bone outcomes over 24 months. DXA and pQCT scans were obtained at baseline, 6, 12 and 24 months, and spine QCT at baseline, 12 and 24 months. Longitudinal multivariable mixed models were used to assess correlations of bone Z-scores (adjusted for height/tibia length) with demographics, pediatric Crohn Disease Activity Index (PCDAI), leg lean mass Z-score, physical activity, glucocorticoid exposure, and 25(OH) vitamin D. Younger age was associated with greater BMD across most sites (see Table). Glucocorticoid therapy was associated with significantly lower trabecular vBMD in the tibia and spine, and DXA BMD across all sites. Vitamin D was associated with greater trabecular vBMD in the tibia only, and greater physical activity was associated with greater tibia trabecular vBMD and femoral neck BMD. Leg lean mass Z-score was not associated with cortical vBMD but was highly and positively associated with all bone outcomes shown below (all p<0.0002 with the exception of spine QCT vBMD with p=0.02). Adjustment for leg lean mass attenuated the associations with age and physical activity. In summary, glucocorticoid therapy was associated with significant bone deficits across multiple axial and appendicular sites, independent of disease activity. The observation that glucocorticoids were associated with greater cortical vBMD is consistent with our prior reports in multiple pediatric conditions, and attributed to glucocorticoid effects to suppress bone formation with greater accumulation of older cortical bone of greater density. Greater muscle mass was associated with greater trabecular vBMD, cortical area and DXA Z-scores across all sites.

Table 1. Multivariate models for bone Z-scores

	Tibia pQCT			DXA				Spine QCT
	Trabecular vBMD	Cortical vBMD	Cortical Area	Total body BMC (without head)	Posteroanterior Spine BMD	Total Hip BMD	Femoral Neck BMD	Spine Trabecular vBMD
Age at baseline, years	β -0.05 (P-value) (0.04)	β -0.13 (P-value) (0.0006)	β -0.04 (P-value) (0.31)	β -0.07 (P-value) (0.02)	β -0.09 (P-value) (0.005)	β -0.07 (P-value) (0.01)	β -0.03 (P-value) (0.25)	β -0.16 (P-value) (0.0001)
Pediatric Crohn's Disease Activity Index								
Mild vs. Inactive	β -0.05 (0.43)	β 0.23 (0.02)	β -0.10 (0.06)	β -0.07 (0.11)	β -0.06 (0.20)	β -0.06 (0.23)	β -0.11 (0.03)	β -0.02 (0.84)
Moderate/Severe vs. Inactive	β -0.23 (0.053)	β 0.17 (0.36)	β 0.07 (0.54)	β -0.01 (0.91)	β 0.05 (0.57)	β -0.10 (0.24)	β -0.09 (0.29)	β 0.17 (0.38)
Glucocorticoid at study visit, vs. none	β -0.33 (0.002)	β 0.58 (0.0001)	β -0.09 (0.35)	β -0.14 (0.049)	β -0.27 (0.0007)	β -0.21 (0.007)	β -0.25 (0.0009)	β -0.46 (0.004)
Serum 25(OH) vitamin D, ng/mL	β 0.008 (0.002)	β 0.0009 (0.32)	β 0.003 (0.17)	β 0.001 (0.49)	β -0.0004 (0.86)	β 0.004 (0.08)	β 0.0007 (0.74)	β -0.002 (0.78)
Daily moderate-to-vigorous intensity of physical activity (per 30 minutes)	β -0.003 (0.04)	β -0.006 (0.0007)	β 0.002 (0.07)	β 0.001 (0.20)	β 0.002 (0.09)	β 0.002 (0.05)	β 0.002 (0.01)	β 0.003 (0.09)

Disclosures: Jin Long, None

SUN-0147

WITHDRAWN

SUN-0148

Measured Cortical Bone Strain during Muscle Contraction in a Mouse Model of Osteogenesis Imperfecta Alycia Berman¹, Rachel Surridge², Joseph Wallace². ¹Weldon School of Biomedical Engineering, Purdue University, United States, ²Department of Biomedical Engineering, Indiana University - Purdue University Indianapolis, United States

In many bone diseases, bone wasting is accompanied by sarcopenia. Bone responds to the strains engendered on it and since muscle contraction is one contributor to bone strain, the presence of sarcopenia may reduce the ability of muscle to engender strain on bone, leading to further bone disease progression. In this study, we used a mouse model of osteogenesis imperfecta (OI) and measured bone strain during muscle contraction to assess the ability of weakened muscle to engender strain on weakened bone. Osteogenesis imperfecta murine (OI) mice and their wildtype (WT) and heterozygous (HET) littermates underwent surgery at 16 weeks to attach a single axis strain gage to the anteromedial portion of the tibial diaphysis. After surgery, the posterior muscles (predominately gastrocnemius and soleus) were stimulated in vivo (250 Hz repeated activation over a 200-ms period) to induce isometric plantar flexion. Muscle torque and bone strain were recorded simultaneously. After the stim-

ulation protocol, mice were euthanized and their tibiae harvested. Tibiae were scanned by micro-CT (10 μm resolution) and a 1-mm midshaft region of interest was analyzed to assess cortical geometry. Data were statistically analyzed using one-way ANOVA with post-hoc Tukey tests (p<0.05). All animal procedures were performed with prior approval from IUSM IACUC. Results demonstrated that OI mice had smaller bones, with a reduced cross-sectional area as compared to WT (-24%; p=0.01) and HET (-27%; p<0.01). In addition, functional muscle testing indicated weaker muscle in OI mice, with a 78% reduction (p<0.0001) and a 76% reduction (p<0.0001) in maximum contractile torque compared to WT and HET, respectively. Interestingly, although muscle force was reduced by 78% compared to WT, the strain engendered on bone during muscle contraction was only reduced by 44% (vs WT; p=0.02). As a result, although there was a reduction in both muscle force and bone strain in OI mice, the amount of strain engendered on the bone per unit torque was significantly greater in the OI group (+486% vs WT; +700% vs HET; both p<0.0001). Thus, the OI mice required far less muscle torque to engender strain on bone. In addition, the average strain engendered on OI bone during muscle contraction was 1400 με, which is similar to levels of strain noted during other stimulation methods (e.g. axial compression) and suggests that muscle stimulation may be a viable means to induce bone formation in this OI mouse model.

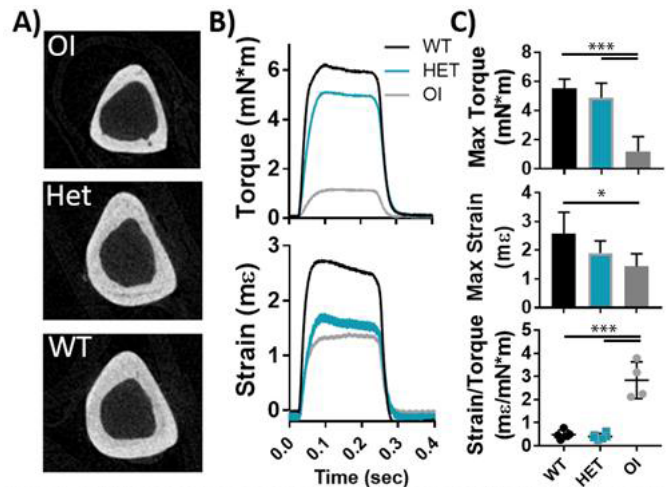


Fig. 1 - A) CT scans show a smaller overall cross-section with a thin cortex in the OI group. **(B)** Representative images and **(C)** quantification of the torque and strain curves show decreased maximum torque and strain in the OI group, but significantly increased strain per unit torque.

Disclosures: Alycia Berman, None

SUN-0149

Reactive oxygen species (ROS) accumulate in skeletal muscle with age, and ROS stimulates the release of exosomes from myoblasts that can induce senescence-like changes in bone marrow derived stem cells (BMSCs) Sadanand Fulzele^{*}, Bharati Mendhe, Carlos Isales, William Hill, Meghan Mcgee-Lawrence, Kanglun Yu, Mark Hamrick. Augusta University, United States

The molecular mechanisms underlying loss of muscle mass and strength with age are not completely understood, but reactive oxygen species (ROS)-induced injury is thought to play a role. Elevated ROS levels can increase cellular senescence, and senescent cells may negatively impact other cells and tissues in a paracrine fashion by secreting molecules referred to as the senescence-associated secretory phenotype (SASP). Here we test the hypothesis that exosomes carry SASP-related factors induced by age-associated ROS accumulation in skeletal muscle. We first assessed ROS levels in skeletal muscles of aged (22-24 mo) and young (4-6 mo) mice using Amplex Red assay for hydrogen peroxide and 4HNE staining to examine lipid peroxidation. Amplex Red data indicate that hydrogen peroxide (H2O2) levels are significantly (2-fold) increased in muscles of aged mice. The age-associated increase in ROS is further confirmed by positive 4HNE staining in muscle tissue from aged mice but not young mice. We then performed co-culture studies to determine the effects of muscle-derived exosomes on proliferation of bone marrow stromal cells (BMSCs) using MTT assay, since exit from the cell cycle and impaired proliferation are hallmarks of cellular senescence. Exosomes isolated from mouse C2C12 myoblasts significantly increased BMSC proliferation; however, exosomes isolated from C2C12 myoblasts following myoblast exposure to hydrogen peroxide had the opposite effect. That is, exosomes from H2O2-treated myoblasts significantly decreased cell proliferation. Exosomes from H2O2-treated myoblasts were found to be enriched in senescence-associated microRNAs such as miR-183, and miR-183 was also significantly elevated in aged skeletal muscle. These findings suggest that ROS-induced senescence in skeletal muscle cells can stimulate the production of extracellular vesicles that may have detrimental effects on bone cells, ultimately contributing to age-related bone loss.

Disclosures: Sadanand Fulzele, None

SUN-0150

Prx1-derived muscle interstitial cells contribute to bone repair and cause fibrosis in musculoskeletal trauma Anais Julien^{*1}, Anuya Kanagalingam¹, Oriane Duchamp De Lageneste¹, Jerome Megret², Frédéric Relaix³, Céline Colnot¹. ¹INSERM U1163, Imagine Institute, Paris Descartes University, France, ²INSERM US24 - CNRS UMS3633 Cytometry Platform, Paris Descartes University, France, ³INSERM IMRB U955, Paris Est-Créteil University, France

Skeletal muscle and bone exhibit great capacities to regenerate due to tissue-specific stem cells, i.e. satellite cells and skeletal stem cells from periosteum(1,2). However, bone fails to heal properly in 10% of bone injuries and delayed healing is increased to 40% in patients with soft tissue damage. The role of muscle in bone repair is well recognized clinically but the underlying cellular and molecular mechanisms are poorly understood. Muscle regulates the inflammatory environment of fracture and muscle satellite cells are providing a source of growth factors for bone repair(3, 4). Here we characterized the impact of muscle injury on bone regeneration in a new musculoskeletal trauma model. Under ethical approval, tibial fractures were induced in adult mice with or without injury to skeletal muscles surrounding the tibia. Histomorphometric analyses show that muscle injury delays callus, cartilage and bone formation. This is accompanied by abnormal callus organization with the presence of unresorbed cartilage and fibrosis leading to non-union. Using cell lineage tracing in genetic mouse models and tissue grafting, we show that osteochondro progenitors are actively recruited from muscle during bone repair and are derived from the Prx1 mesenchymal lineage also giving rise to periosteal cells[2]. In fractures combined with muscle injury, the contribution of muscle and periosteal cells to cartilage is decreased. Moreover, in the traumatic environment, Prx1-derived muscle cells but not periosteal cells are the source of fibrosis in the fracture callus. FACS and molecular analyses indicate that the Prx1-derived muscle cells are muscle interstitial cells distinct from endothelial, hematopoietic and myogenic cells, and express CD29, Sca1 and Cxcl12. This Prx1-derived muscle cell population overlaps with the muscle fibro/adipogenic progenitor population marked by PDGFR α . In conclusion, we identified a critical cell population within muscle that participates directly in cartilage and bone formation during fracture repair, but fails to do so after traumatic injury and becomes the source of fibrosis causing fracture non-union. This study provides a cellular basis for delayed bone regeneration in severe musculoskeletal injuries.[1] Lepper C, et al, Development, 138(17): 3639–3646, 2011[2] Duchamp de Lageneste O, et al, Nature Communications, 22;9(1):773, 2018[3] Abou-Khalil R, et al, JBM, 29(2):304-15, 2014[4] Abou-Khalil R, et al, Stem cell 33(5):1501-11, 2015

Disclosures: *Anais Julien, None*

SUN-0151

The bone anabolic effects of irisin are through preferential stimulation of aerobic glycolysis Sung Kil Lim^{*}. College of Medicine, Yonsei University, Republic of Korea

Irisin, a recently identified hormone secreted by skeletal muscle in response to exercise, displays anabolic actions on the skeleton primarily through the stimulation of bone formation. However, the mechanism underlying the irisin-stimulated anabolic response remains largely unknown. To uncover the underlying mechanism, we biosynthesized recombinant irisin (r-irisin) using *Escherichia coli* expression system and used it to treat several types of osteoblast cell. Our synthesized r-irisin could promote proliferation and differentiation of osteoblasts as evidenced by enhanced expression of osteoblast-specific transcriptional factors, including Runt-related transcription factor-2 (Runx2) and Osterix (Ox), along with transcriptional activating transcription factor 4 (Atf4); and osteoblastic early differentiation markers, such as alkaline phosphatase (Alp) and collagen type I alpha 1 (Colla1). Furthermore, we showed that the promotion of r-irisin on the proliferation and differentiation of osteoblast lineage cells are preferentially through aerobic glycolysis, as indicated by the enhancement on the abundance of its representative enzymes lactate dehydrogenase A (LDHA) and pyruvate dehydrogenase kinase 1 (PDK1), together with increased lactate levels. The favorite of the aerobic glycolysis after r-irisin treatment was then confirmed in the primary cultured calvarial cells by metabolic analysis using gas chromatography-mass spectrometry. Thus, our results suggest that the anabolic actions of r-irisin on the regulation of osteoblast lineage cells are preferentially through aerobic glycolysis, which may help us to develop new irisin based bone anabolic agents.

Disclosures: *Sung Kil Lim, None*

SUN-0152

Risedronate could rescue podocyte injury in Pit-1 overexpressing transgenic rats Atsushi Masuda^{*1}, Takeshi Takayanagi¹, Yohei Asada¹, Shogo Nakayama¹, Eisuke Tomatsu¹, Yasumasa Yoshino¹, Sahoko Sekiguchi-Ueda¹, Megumi Shibata¹, Eishin Yaoita², Atsushi Suzuki¹. ¹Department of Endocrinology and Metabolism, Fujita Health University, Japan, ²Department of Structural Pathology, Institute of Nephrology, Niigata University Graduate School of Medical and Dental Sciences, Japan

Hyperphosphatemia is known to be one of prognostic factors in chronic kidney disease - mineral and bone disorder (CKD-MBD). We have previously reported type III Pi

transporter(Pit-1)-overexpressing transgenic(TG) rats increased proteinuria via podocyte injury and glomerular basement membrane (GBM) thickening. We have also revealed that risedronate could improve proteinuria and reduce GBM thickening. In the present study, we investigated the effect of risedronate on podocyte injury in Pit-1 TG rats. Methods: Pit-1TG rats and control rats are randomly divided into 4 groups; I: control rat without risedronate administration(C-C), II: control rat with risedronate administration(C-R), III: Pit-1TG rat without risedronate administration (TG-C), and IV: Pit-1TG rat with risedronate administration (TG-R). The protocol of risedronate administration was 5 μ g/kg weight s.c. twice a week starting at 5 weeks old through 12 weeks old. Tissues for histological analysis were performed at 12 weeks of age. For immunofluorescence microscopy, the sections were immunostained with murine monoclonal anti-nephrin antibody as a podocyte constituent protein marker, and murine monoclonal anti-desmin antibody and rabbit anti-connexin 43 antibody as podocyte injury markers. Results: TG-C group rats showed GBM thickening, and risedronate could keep the width of GBM and its three-layers structure in TG-R rats. Immunostaining for podocyte injury markers such as desmin and connexin 43 exhibited focally and segmentally conspicuous staining in TG-C rats. When the TG rats were treated with risedronate, podocytes showed less changes than TG-C rats. On the other hand, localization or staining intensity of nephrin were same in all groups. In conclusion, these findings suggest us that risedronate could improve injury of podocyte and keeps barrier function of the glomerulus in the kidney.

Disclosures: *Atsushi Masuda, None*

SUN-0153

A Direct LC-MS/MS Method for the Simultaneous Quantification of Isomeric Aminobutyric Acids in Biological Fluids and Its Application in Bone-Muscle Studies Chenglin Mo^{*1}, Zhiying Wang¹, Liangqiao Bian², Janalee Isaacson³, Robert Recker⁴, Joan Lappe⁵, Lynda Bonewald⁶, Marco Brotto¹. ¹College of Nursing and Health Innovation, the University of Texas-Arlington, Arlington, TX, United States, ²Shimadzu Center for Advanced Analytical Chemistry, the University of Texas at Arlington, Arlington, TX, United States, ³School of Nursing & Human Physiology, Gonzaga University, Spokane, WA, United States, ⁴School of Medicine Osteoporosis Research Center, Creighton University, Omaha, NE, United States, ⁵School of Nursing, Creighton University, Omaha, NE, United States, ⁶Department of Anatomy, Cell Biology and Orthopedics, Indiana Center for Musculoskeletal Health, School of Medicine, Indiana University, IN, United States

Isomeric aminobutyric acids, especially β -aminoisobutyric acid (BAIBA) and γ -aminobutyric acid (GABA), are PGC-1 α -dependent myokine-like signaling molecules released from skeletal muscle during exercise. We demonstrated that BAIBA plays an important role in bone-muscle crosstalk through protecting osteocytes against oxidative stress. Quantification of BAIBA and GABA in biological samples is a huge challenge due to the nature of their ultra-low molecular weight and extreme similarity in structure. All methods to date are indirect and require long sample preparation i.e. derivatization. In this study, by developing a fast and sensitive LC-MS/MS method, we were able to quantify simultaneously five major aminobutyric acid enantiomers BAIBA (D-, L-), GABA, and α -aminobutyric acid (AABA, D-, L-) in biological fluids from humans and rodents. This newly developed LC-MS/MS methodology enables baseline separation for underivatized aminobutyric acid isomers, and is sensitive for the detection of these isomers in the minimal sample amount (10 μ L) of mouse serum/plasma and human serum/cerebrospinal fluid. Accuracy (85%–115%) and precision (\pm 15%) of the method met assay acceptance criteria as required in FDA guidance. The predominant configuration of BAIBA in human serum is the R-enantiomer (D-BAIBA), with an average concentration of 0.34 ± 0.02 μ M in pooled healthy human serum. This result was confirmed in serum samples from 22 individual human subjects, with the ratio of L:D less than 1:10. In contrast, L-BAIBA is the dominating form in mouse circulation, with the D being not detected. Difference in diet (protein sources) and metabolism between mice and humans possibly accounts for these differences in D vs L levels. We measured the serum concentration of BAIBA and GABA in females 50-60 and 66-75 years old with or without osteoporotic fractures (OF). D-BAIBA was lower in the 50-60 OF group but not in the 66-75 OF group. GABA levels were significantly lower ($P = 0.024$) in the 66-75 OF group. Our findings reinforce the concept of muscle-bone crosstalk and indicate that BAIBA and GABA might be necessary for optimal bone function. This fast and sensitive quantification method, first developed by our group, will facilitate the study of mechanisms underlying biological activities of BAIBA, GABA, and other aminobutyric acids in bone-muscle crosstalk, which will further promote the development of new methods in the diagnosis and treatments for musculoskeletal diseases.

Disclosures: *Chenglin Mo, None*

SUN-0154

Anti-Nerve Growth Factor Therapy Attenuates Cutaneous Hypersensitivity and Musculoskeletal Discomfort in Mice with Osteoporosis Miyako Suzuki^{1*}, Magali Millecamps¹, Seiji Ohtori², Laura S. Stone¹. ¹The Alan Edwards Centre for Research on Pain, Faculty of Dentistry, McGill University, Canada, ²Department of Orthopaedic Surgery, Graduate School of Medicine Chiba University, Japan

Introduction. The prevalence of osteoporosis is increasing with the aging global population. In addition to increased risk of fracture, osteoporosis is associated with chronic pain. We previously reported that improvement in bone mineral density is not sufficient to reduce osteoporotic pain in an ovariectomy (OVX)-induced mouse model of osteoporosis, highlighting the need for new treatments. Targeting of Nerve Growth Factor (NGF) with sequestering antibodies is a promising new direction for the treatment of musculoskeletal pain including low back pain and arthritis. Its efficacy is currently unknown for osteoporotic pain. The aim of this study was to examine the efficacy of anti-NGF antibody therapy against behavioural indices of osteoporotic pain and on sensory neuron plasticity in a mouse model of OVX-induced osteoporosis. **Methods.** Ovariectomy (OVX, n=20) - and sham-operated (n=10) female C57BL/6 mice at 5-7 week of age were assigned to receive either anti-NGF antibody or vehicle (OVX/anti-NGF, OVX/Vehicle, and Sham/Vehicle; n=10 per group) at 8 weeks after surgery. Evaluation of the vertebral and femoral bone mineral density (BMD) were performed prior to the behavioral testing and after anti-NGF treatment. Animals received 2 injections of anti-NGF antibody (Exalpa Biologicals Inc., Shirley, MA, USA, 10mg/kg, i.p) or vehicle (0.01 mL/g, i.p sterile saline), 2 weeks apart. Behaviors were monitored at baseline, and for a maximum of 2 months after the initial treatment. Behavior included measures of cutaneous hindpaw hypersensitivity (von Frey, acetone-evoked behavior, cold plate test and heat test), deep musculoskeletal discomfort (grip test assay) and physical function (rotarod and open-field tests). Sensory nervous system plasticity was evaluated by quantification of the sensory neuropeptide calcitonin gene-related peptide (CGRP)- and neurotrophin-1 immunoreactivity (-ir) in dorsal root ganglia. Results. There was a significant loss in vertebral and femoral BMD of the OVX mice compared to the sham-operated controls. Anti-NGF treatment had no adverse effect on the vertebral or femoral BMD. Furthermore, anti-NGF treatment attenuated OVX-induced hypersensitivity to mechanical, cold and heat stimuli on the plantar surface of the hindpaw. The OVX-induced impairment in grip force strength, used here as a measure of deep musculoskeletal discomfort, was partially reversed by anti-NGF therapy. No changes were observed in the rotarod or open field tests for overall motor function and activity. Finally, anti-NGF treatment attenuated the increase in CGRP-immunoreactive dorsal root ganglia neurons observed in OVX mice. **Discussion.** We demonstrated anti-NGF efficacy in the OVX mouse model of osteoporosis-related pain. These data implicate NGF as a driver of long-term osteoporotic pain and suggest that anti-NGF treatment may be a useful therapy for this population.

Disclosures: Miyako Suzuki, None

SUN-0155

Advanced Age Leads to Aberrant Wnt Pathway Expression and Bone Turnover in a Murine Model of Chronic Kidney Disease Elizabeth Terhune*, Ryan Clark, William Schroeder, Karen King. Department of Orthopedics, University of Colorado Anschutz Medical Campus, United States

Chronic kidney disease-mineral and bone disorder (CKD-MBD) is a common complication of CKD that includes disrupted serum mineral homeostasis, low bone density, vascular calcifications and increased fracture risk. Over half of individuals age >65 meet the clinical definition for CKD, and elderly individuals undergoing dialysis experience four times as many hip fractures as expected for their age. We investigated whether bone responds distinctly to CKD at older ages, and hypothesized that age may be an aggravating factor for CKD-MBD. To explore this hypothesis, we conducted a 5/6th nephrectomy or sham procedure in three age groups of male C57BL/6 mice. Groups were Young CKD (3 months, n= 7), Young Control (n= 7), Adult CKD (15 months, n= 12), Adult Control (n= 10), Geriatric CKD (21 months, n= 14) and Geriatric Control (n= 10). Twelve weeks later, at study completion, we analyzed serum mineral and protein concentrations, and we measured gene expression in cleaned, femoral diaphyseal bone. Nephrectomized mice were determined to have mild to moderate CKD as defined by increased serum levels of urea, calcium, phosphorus, FGF23 and PTH (parathyroid hormone). Geriatric CKD mice showed increases in serum type I collagen propeptides (PINP) (p= 0.012) and type I collagen fragments (CTX-I) (p= 0.035), indicating high bone turnover. Young and Adult CKD mice showed modest increases in CTX-I, but not PINP. Gene expression of several mineralization markers were altered in the Young and Geriatric groups (Table 1). Geriatric CKD mice showed decreased levels of the Wnt inhibitor genes Sost (sclerostin) (p= 0.0046, Fold Change= 0.29 compared to age-matched control) and Dkk1 (p= 0.0233, Fold Change= 0.40) as well as Tnfrsf11b (osteoprotegerin) (p= 0.1531, Fold Change= 0.53). Geriatric CKD mice also showed increased levels of Ager (RAGE) (p= 0.0021, Fold Change= 2.14). These changes were not significant in Young CKD mice. The Wnt ligands Wnt10 and Wnt16 differed between Young and Geriatric mice, but not CKD groups. Genes encoding major structural proteins of bone, including Colla1 and Ibsp, did not differ between cohorts. Our results suggest that the bone of geriatric individuals may respond more severely to CKD. Understanding the cellular mechanisms underlying the bone's response to CKD in the elderly will aid in the development of clinical treatments for individuals experiencing increased rates of bone fractures and CKD-induced osteoporosis.

Gene	Age	Treatment	$\Delta Cq \pm StDev$	$\Delta \Delta Cq \pm StDev$	$2^{-\Delta \Delta Cq}$ (Fold Change)	Factor Significance (Two-Way ANOVA)
Dkk1	Young	Control	4.31 ± 0.85	0.00 ± 0.85	N/A	CKD (p= 0.0092)
		CKD	4.99 ± 0.84	0.68 ± 0.84	0.71	
	Geriatric	Control	4.45 ± 1.08	0.14 ± 1.08	1.12	
		CKD	5.66 ± 0.35	1.34 ± 0.35	0.4 (p=0.0233)	
Wnt10a	Young	Control	7.14 ± 1.00	0.00 ± 1.00	N/A	Age (p= 0.0101)
		CKD	7.27 ± 0.64	0.13 ± 0.64	1	
	Geriatric	Control	5.78 ± 1.17	-1.36 ± 1.17	3.40	
		CKD	3.37 ± 1.01	-0.80 ± 1.01	2.16	
Wnt16	Young	Control	3.39 ± 0.89	0.00 ± 0.89	N/A	Age (p= 0.0213)
		CKD	3.78 ± 0.85	0.39 ± 0.85	0.89	
	Geriatric	Control	4.23 ± 0.68	0.84 ± 0.68	0.61	
		CKD	4.50 ± 0.5	1.11 ± 0.57	0.5	
Sost	Young	Control	-0.86 ± 1.10	0.00 ± 1.10	N/A	Age (p= 0.0097), CKD (p= 0.0342)
		CKD	-0.86 ± 0.92	0.31 ± 0.92	0.98	
	Geriatric	Control	-0.33 ± 0.88	0.52 ± 0.88	0.81	
		CKD	1.04 ± 0.68	1.90 ± 0.68	0.29 (p= 0.0046)	
Ager	Young	Control	2.89 ± 0.37	0.00 ± 0.37	N/A	Age (p= 0.0136), CKD (p= 0.0087)
		CKD	2.39 ± 0.66	-0.51 ± 0.66	1.56	
	Geriatric	Control	2.42 ± 0.21	-0.47 ± 0.21	1.39	
		CKD	1.84 ± 0.37	-1.06 ± 0.37	2.14 (p= 0.0021)	
Tnfrsf11b	Young	Control	2.74 ± 0.87	0.00 ± 0.87	N/A	CKD (p= 0.0428)
		CKD	3.35 ± 1.00	0.61 ± 1.00	0.81	
	Geriatric	Control	2.79 ± 1.07	0.05 ± 1.07	1.19	
		CKD	3.73 ± 0.48	0.99 ± 0.48	0.53	

Dkk1= Dickkopf1; Wnt10a= WNT Family Member 10a; Wnt16= WNT Family Member 16; Sost= Sclerostin; Ager= Advanced Glycosylation End-Product Specific Receptor 2/ RAGE; Tnfrsf11b= Osteoprotegerin.

Disclosures: Elizabeth Terhune, None

SUN-0156

Oncostatin M is a key effector of heterotopic ossification following spinal cord injuries Hsu-Wen Tseng^{1*}, Kylie Alexander¹, Irina Kulina¹, Marjorie Salga^{2,3}, Beulah Jose¹, François Genet^{2,3}, Frédéric Torossian⁴, Bernadette Guerton⁴, Adrienne Anginot⁴, Whitney Fleming¹, Susan Millard¹, Allison Pettit¹, Natalie Sims⁵, Jean-Jacques Lataillade^{4,6}, Marie-Caroline Le Bousse-Kerdiles⁴, Jean Pierre Levesque¹. ¹Mater Research Institute-The University of Queensland, Brisbane, Queensland, Australia, ²Service de Médecine Physique et de Réadaptation, Raymond Poincaré Hospital, Garches, France, ³END:ICAP U1179 INSERM, UFR des Sciences de la Santé-Simone Veil, Université Versailles Saint Quentin en Yvelines, Montigny le Bretonneux, France, ⁴Inserm UMR-S-MD1197, Paris 11 University, Paul Brousse Hospital, Villejuif, France., France, ⁵St. Vincent's Institute of Medical Research and Department of Medicine, St. Vincent's Hospital, The University of Melbourne, Fitzroy, Victoria, Australia, ⁶Centre de Transfusion Sanguine des Armées, L'Institut de Recherche Biomédicale des Armées, Clamart, France

Neurogenic heterotopic ossification (NHO) is traumatic brain injury or spinal cord injuries (SCI)-associated abnormal ectopic bones in soft tissues. NHO leads to reduction of joint movement and complication associated with blood vessel and nerve compression. There is no effective pharmaceutical treatment to prevent NHO due to poor understating of NHO etiology, and surgical resection might only be temporary as it can reoccur. To identify the pathogenic factors, we established a NHO mouse model, in which NHO is induced in genetically unmodified mice following a combination of SCI and cardiotoxin-induced muscle injury. While cardiotoxin-triggered inflammatory and muscle injury gradually repaired in the absence of SCI, macrophages remained abundant in damaged muscle and intercalated with ectopic bone foci three weeks post SCI. Macrophage depletion abolished NHO formation suggesting macrophages are required in NHO pathogenesis. Comparing mRNA expression of injured muscle from SCI and sham-operated mice showed an upregulation of several macrophage-related proinflammatory cytokines in SCI group, such as Tnf, Ccl2, Csf1 and Osm. Osm encodes Oncostatin M, which also regulates osteoblast activity and hematopoietic stem cell mobilisation, is expressed by macrophages and osteoblasts around NHO and highly accumulated in the injured muscle. Phosphorylation of STAT3, one downstream signalling pathway, was significantly higher in injured muscle of the SCI group than sham group. Moreover, OSM receptor deficiency significantly reduced NHO volume by 2.5 fold compared to WT mice. Likewise, treatment with inhibitor of JAK/STAT signalling significantly reduced NHO volumes. In agreement with NHO murine model, OSM concentration was significantly higher in patients developing NHO compared to healthy volunteers. Furthermore, conditioned media from macrophages isolated from patients' NHOs promoted mineralisation of patient muscle-derived stromal cells in vitro and this effect was inhibited by addition of neutralising anti-OSM antibody. In conclusion, we identified OSM as a key mediator of NHO pathogenesis; therefore, blocking OSM signalling pathway might prevent or retard NHO formation.

Disclosures: Hsu-Wen Tseng, None

SUN-0157

Osteocyte markers and vascular health in kidney transplantation Yue Pei Wang*, Aboubacar James Sidibé, Roth-Visal Ung, Karine Marquis, Mohsen Agharazii, Fabrice Mac-Way. CHU de Québec Research Center, L'Hôtel-Dieu de Québec Hospital, Endocrinology and Nephrology Unit, Faculty and Department of Medicine, Université Laval, Canada

Introduction: New bone and vascular markers such as sclerostin, dickkopf-related protein 1 (DKK1), fibroblast growth factor 23 (FGF23) and α -klotho have been suggested to contribute to kidney transplant (KTx)-related bone and vascular disorders. We aimed to evaluate the evolution of these markers after kidney transplantation and whether they are associated with arterial stiffness. **Methods:** Longitudinal observational cohort study of all eligible patients for vascular assessment who underwent KTx at CHU de Québec between 2007 to 2011. Comorbidities and biochemical parameters were collected from patients' electronic records. Bone markers levels were measured by ELISA on plasma collected on the day of KTx, at 3 (M3) and 6 months (M6) where hemodynamic parameters, carotid-femoral (CFpwv) and carotid-radial (CRpwv) pulse-wave velocity were assessed using a Complior device. Associations between arterial stiffness (adjusted for mean blood pressure and/or heart rate) and bone markers were analyzed with generalized estimating equations in univariate and multivariate models (baseline arterial stiffness parameter, age, sex, smoking, diabetes and cardiovascular disease) using SPSS 20.0. **Results:** This study included 79 patients (69.6% male with a mean age of 50.2 ± 13.7). All bone markers decreased significantly after KTx compared to baseline (Figure 1). The changes in sclerostin levels (M3 and M6) correlated with changes in DKK1 ($R=0.523$ and 0.424 , $p<0.01$) and FGF23 ($R=0.301$ and 0.334 , $p<0.01$). Sclerostin levels were associated with CFpwv in univariate model and with pulse pressure (PP) amplification both in univariate ($\beta=-0.259$; CI95 [-0.412, -0.105]) and multivariate models ($\beta=-0.180$; CI95 [-0.330, -0.030]) at M3. Baseline sclerostin levels also predicted CFpwv at M3 ($\beta=0.346$; CI95 [0.080, 0.613]) and M6 ($\beta=0.334$; CI95 [0.082, 0.586]) in univariate analyses while sclerostin levels at M3 predicted CFpwv ($\beta=1.850$; CI95 [0.263, 3.437]) at M6. Furthermore, sclerostin levels at M6 were associated with central PP in all models (multivariate: $\beta=9.717$; CI95 [0.887, 18.547]) at M24. Sclerostin, DKK1 and FGF23 levels were associated with parathyroid hormone levels at baseline but not after KTx. **Conclusion:** Sclerostin, DKK1, FGF23 and α -klotho levels significantly decrease after kidney transplant. Sclerostin levels seem to be associated with arterial stiffness parameters and may therefore play a role in regulation of vascular health in this population.

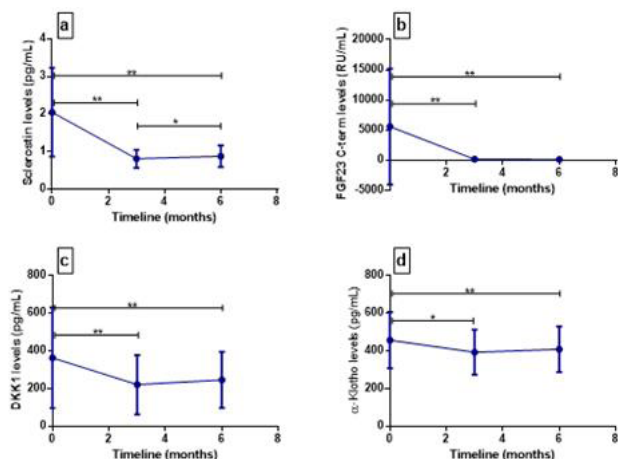


Figure 1. Sclerostin, DKK1, FGF23 and α -klotho After Kidney Transplantation

** refers to p-value ≤ 0.001 ; * refers to p-value ≤ 0.05

a. Sclerostin decreased from $2.05 \text{ pg/mL} \pm 1.18 \text{ (M0)}$ to $0.81 \text{ pg/mL} \pm 0.24 \text{ (M3)}$ to $0.88 \text{ pg/mL} \pm 0.29 \text{ (M6)}$ | b. FGF23 decreased from $5594.80 \text{ RU/mL} \pm 9602.73 \text{ (M0)}$ to $168.46 \text{ RU/mL} \pm 288.24 \text{ (M3)}$ to $137.45 \text{ RU/mL} \pm 77.80 \text{ (M6)}$ | c. DKK1 decreased from $363.96 \text{ pg/mL} \pm 266.66 \text{ (M0)}$ to $221.35 \text{ pg/mL} \pm 157.59 \text{ (M3)}$ to $246.66 \text{ pg/mL} \pm 149.11 \text{ (M6)}$ | d. α -klotho decreased from $457.63 \text{ pg/mL} \pm 148.60 \text{ (M0)}$ to $393.38 \text{ pg/mL} \pm 119.42 \text{ (M3)}$ to $409.79 \text{ pg/mL} \pm 120.74 \text{ (M6)}$

Disclosures: Yue Pei Wang, None

SUN-0175

Enhanced bone growth with lipoxinA4 Amy Koh*, Justin Do, Hernan Roca, Laurie Mccauley. University of Michigan, United States

LipoxinA4 (LXA4) is an eicosanoid lipid mediator derived from arachidonic acid metabolism and is one of the most abundant lipoxin molecules. LXA4 binds to its receptor ALX, a G protein coupled receptor expressed in a variety of cells, and mediates resolution of inflammation and wound healing. Bone is a dynamic tissue serving as a vital supply and disseminator of bone marrow cells. Macrophages (F4/80+) comprise ~15% of bone marrow cells, mediate bone formation, and facilitate anabolic actions of parathyroid hormone (PTH). PTH increases lipoxins in the bone marrow and studies of lipoxin action in bone are

of recent interest. The purpose of this study was to investigate LXA4 effects on growing bone, a phase of high bone activity that mimics an inflammatory state. **METHODS:** In vivo, C57Bl/6 mouse pups (5d old) were treated daily for 17 days with LXA4 (10ng/g, IP; n=7) or vehicle control (VEH; n=5) and sacrificed 24h after the last injection. Bone turnover markers TRAcP5b and PINP were determined in serum and microCT analyses of tibiae performed. In vitro, an LXA4 dose response was investigated on M-CSF-1 and RANKL induced osteoclastogenesis in primary bone marrow cultures. **RESULTS:** After 17 days of LXA4 administration, microCT analyses revealed significantly increased bone volume/total volume ($0.21 \pm 0.02 \text{ VEH}$ vs. $0.28 \pm 0.02 \text{ LXA4}$; $p<0.02$). There was a significant increase in trabecular number ($5.96 \pm 0.22 \text{ VEH}$ vs. $7.15 \pm 0.34 \text{ LXA4}$; $p<0.02$) and BMD ($124.29 \pm 6.60 \text{ VEH}$ vs. $155.18 \pm 9.99 \text{ LXA4}$; $p=0.03$) and a trend of increased trabecular thickness and decreased trabecular spacing. With LXA4 administration, serum TRAcP5b, an indicator of osteoclast numbers, was decreased ($13.12 \pm 1.49 \text{ VEH}$ vs. $9.71 \pm 0.88 \text{ LXA4}$; $p=0.07$) while PINP, an indicator of bone formation, was unchanged ($p=0.13$). In vitro, LXA4 dose dependently inhibited osteoclastic differentiation of primary bone marrow cell cultures, confirming a report previously shown with the RAW264.7 macrophage cell line. These data reveal the pro-resolving mediator, LXA4, increases bone growth at least in part via an inhibition of bone resorption.

Disclosures: Amy Koh, None

SUN-0176

In vivo Intramedullary Pressure Measurements and Femoral Bone Microarchitecture and Cortical Thickness in Young and Old Male Fischer-344 Rats David Lee*¹, Sunggi Noh¹, Jeong-Bong Lee², Rhonda Prisyb¹. ¹University of Texas, Arlington, United States, ²University of Texas, Dallas, United States

Previous studies have demonstrated that increased and decreased bone intramedullary pressure (IMP) augments and diminishes bone mass, respectively. Since advancing age corresponds with declines in bone mass, we theorized that bone IMP would also be reduced. The purpose of the study was to examine in vivo IMP in the femoral canal of young and old male Fischer-344 rats in relation to bone volume. We hypothesized that IMP and bone volume would be reduced in the older vs. younger rats. **Experiment 1:** young (6 months; n=5) and old (24 months; n=6) male Fischer-344 rats were anesthetized (2% isoflurane to O₂ balance) and the femoral shafts were catheterized. Following 1-hour of recovery, the catheter was connected to a pressure transducer and in vivo IMP (mmHg) was recorded (PowerLab, AD Instruments) for 15 minutes in conscious animals. The last 5 minutes of data were averaged and reported. **Experiment 2:** Left femora from young (6 months; n=5) and old (24 months; n=5) male Fischer-344 rats were dissected, fixed and scanned using an inspeXio SMX-100CT Micro-Focus X-Ray Computed Tomography System (Shimadzu, Japan) to determine trabecular bone microarchitecture (i.e., bone-volume to total-volume ratio [BV/TV;%], trabecular thickness [Tb.Th, μm], trabecular number [Tb.N /mm], and trabecular separation [Tb.Sp, μm]) in the distal femoral metaphysis and cortical thickness (Ct.Th, μm) at the midshaft. One-way ANOVAs were performed. Alpha level was set at $p<0.05$ a priori. Values represent Means \pm S.E. Intramedullary pressure did not differ between groups (young, $16 \pm 3 \text{ mmHg}$ vs. old, $13 \pm 3 \text{ mmHg}$). Trabecular BV/TV ($21 \pm 2\%$ vs. $18 \pm 3\%$, respectively) did not differ between young and old rats; however, Tb.N ($3.0 \pm 0.2 / \text{mm}$ vs. $2.3 \pm 0.3 / \text{mm}$, respectively) and Tb.Sp ($273 \pm 24 \mu\text{m}$ vs. $375 \pm 41 \mu\text{m}$, respectively) tended ($p=0.08$ and $p=0.07$, respectively) to differ. In addition, cortical thickness was higher ($p<0.05$) in old ($820 \pm 24 \mu\text{m}$) vs. young ($652 \pm 10 \mu\text{m}$) rats. No differences in IMP and trabecular bone volume were observed between the young and old rats; however, additional work is warranted.

Disclosures: David Lee, None

SUN-0177

Primary Perturbations in the Myeloid Lineage, Including Neutrophils and the OsteoMac, Contribute to Cystic Fibrosis-Related Bone Disease John Stabley*¹, Jessica Hook², Shadaan Abid¹, Li Li¹, Megan Mead¹, Abraham Behrmann¹, Jessica Moreland², Dwight Towler¹, Raksha Jain¹. ¹Department of Internal Medicine, UT Southwestern Medical Center, United States, ²Department of Pediatrics, UT Southwestern Medical Center, United States

The increase in lifespan of our patients living with cystic fibrosis (CF) has revealed new challenges to bone health management. The elevated prevalence of osteopenia and osteoporosis in this setting – and potentially avascular necrosis – is collectively denoted as cystic fibrosis-related bone disease (CFBD). Flow cytometry of circulating polymorphonuclear leukocytes (PMN) reveals an elevated number of activated PMNs (reduced L-selectin) from CF patients with low bone mineral density (T-score < -2.0), accompanied by an increased RANKL/OPG ratio, thus suggesting a role for the myeloid lineage in driving CFBD. To better understand the role of the cystic fibrosis transmembrane conductance regulator (CFTR) in bone homeostasis, we assessed female Cfrt^{+/+} and Cfrt^{-/-} mice possessing an intestinal epithelial human CFTR transgene to mitigate the contribution of nutritional malabsorption to skeletal homeostasis. Immunohistochemistry and immunofluorescence demonstrate increased myeloid (neutrophil elastase) and osteoclastic (RANKL) markers in the tibial bone marrow of Cfrt^{-/-} mice vs. Cfrt^{+/+} controls. MicroCT analysis of bone indicates a geometrically disadvantaged cortical phenotype in the tibiae of Cfrt^{-/-} mice when compared to Cfrt^{+/+} sibling controls (Ps.Pm: 3.56 ± 0.16 vs. $3.91 \pm 0.24 \text{ mm}$, $p<0.05$; Tt.Ar: 0.79 ± 0.08 vs.

0.87±0.03 mm², p=0.06). Volumetric bone mineral density was unaltered. Primary calvarial osteoblast cultures from Cfr^{-/-} mice, maintained under mineralization conditions, exhibit reductions in tissue-nonspecific alkaline phosphatase mRNA accumulation (80.6±4.3% decrease, p<0.01) and enzyme activity (54.5±0.01% decrease, p=0.06) vs. Cfr^{+/-} controls as noted by others, along with other markers of osteogenic differentiation and significantly reduced Vegf expression. Intriguingly, Cfr^{-/-} calvarial osteoblast cultures exhibit increased OsteoMac accumulation compared to Cfr^{+/-} controls, first revealed by RT-qPCR analyses (% increases, F4/80: 3453±78%, p<0.0001; Cd11c: 2763±97%, p<0.001; Csf1r: 1225±369%, p<0.01). This was confirmed by increased numbers of F4/80 – positive cells in the tibial bone marrow of Cfr^{-/-} vs. Cfr^{+/-} mice, and in primary calvarial cell cultures (Cfr^{-/-} vs. Cfr^{+/-}; 17.7±1.7% vs. 4.7±0.3% of cells; p<0.01). These data point to a novel and primary role of marrow-derived neutrophils and OsteoMacs in the pathogenesis of CFBD, beyond the cell-autonomous synthetic deficiencies in the osteoblast lineage.

Disclosures: *John Stabley, None*

SUN-0178

Human obesity is associated with enhanced insulin signaling and accelerated differentiation of bone marrow stromal stem cell leading to premature skeletal aging Michaela Tencerova^{1,2}, Morten Frost¹, Florence Figeac¹, Anders Kristian Haakonsson¹, Jens-Jacob Lauterlein¹, Tina Kamilla Nielsen¹, Dalia Ayesh Hafez Ali¹, Kurt Højlund^{1,2}, Moustapha Kassem^{1,2}. ¹Department of Molecular Endocrinology, KMEB, University of Southern Denmark and Odense University Hospital, DK-5000 Odense C, Denmark, ²Danish Diabetes Academy supported by the Novo Nordisk Foundation, Denmark

The effects of obesity and type 2 diabetes (T2D) on bone are paradoxical as these patients usually exhibit higher bone mineral density but increased risk of bone fragility fractures. Since obesity increases with aging, we hypothesized that bone fragility is caused by a premature aging phenotype of bone marrow (BM) microenvironment. Thus, we investigated in a case-control study of 54 men subdivided into lean (n=19), overweight (n=15) and obese (n=20) groups based on their body mass index, the metabolic and senescence phenotype of BM stromal (skeletal) stem cells (BM-MSC). We found accelerated differentiation of primary BM-MSC obtained from obese participants. This was supported by global RNA sequencing analyses demonstrating a shift of molecular phenotype of BM-MSC towards committed adipocytic and osteoblastic progenitors. Genes differently expressed encompassed many metabolic genes, particularly of the glycolytic pathway, and genes encoding enzymes with oxidoreductase activity. Interestingly, in paired samples of BM-MSC and peripheral adipose tissue (AT-MSC) insulin signaling measured by insulin-stimulated pAKT/totalAKT was impaired in AT-MSC but up-regulated in BM-MSC of obese individuals. In addition, analysis of cellular composition of BM-MSC of obese participants revealed a unique pattern of increased number of insulin receptor (IR+) and leptin receptor (LepR+) positive cells that exhibited ex vivo enhanced adipogenic differentiation and hyper-activated metabolic phenotype. Our data provide a potential molecular explanation to the “bone fragility paradox” of obese patients as it shows enhanced insulin signaling in BM microenvironment leading to a premature aging phenotype of BM-MSC, and to creation of senescent microenvironment conducive to bone fragility. Also this clinical study highlights the differences between the metabolic responses of bone and peripheral AT, which is an important factor to be considered in designing tailored treatment of obesity-associated metabolic bone disease.

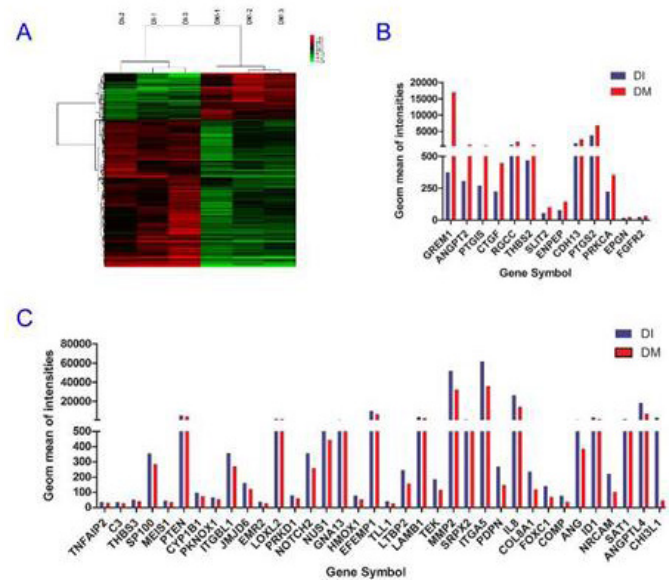
Disclosures: *Michaela Tencerova, None*

SUN-0179

Gene Expression Profiles Associated with Angiogenesis in Human Site-Specific Bone Marrow Stromal Cells (hBMSCs) Yifei Du^{1*}, Weina Zhou^{2,3}, Hongbin Jiang¹, Qisheng Tu², Jinkun Chen^{2,4}. ¹Jiangsu Key Laboratory of Oral Diseases, Nanjing Medical University, Department of Oral and Maxillofacial Surgery, Affiliated Hospital of Stomatology, Nanjing Medical University, Nanjing, China, ²Division of Oral Biology, Tufts University School of Dental Medicine, Boston, Massachusetts, United States, ³Jiangsu Key Laboratory of Oral Disease, Nanjing Medical University, Nanjing, China, ⁴Department of Developmental, Molecular and Chemical Biology Sackler School of Graduate Biomedical Sciences Tufts University School of Medicine, United States

Objectives: Bone marrow stromal cells (BMSCs) from iliac crest and craniofacial regions are candidate seeding cells with site-specific characteristics and bone regenerative properties. Previous studies suggested that craniofacial BMSCs might possess stronger potentials and osteogenic capabilities than that isolated from iliac crest. BMSCs have the ability to regulate new blood vessel formation, maintain its stability and functions via secreting angiogenic growth factors and cytokines in a paracrine fashion. This study was to characterize the changes of gene expression profiles associated with angiogenesis in these two kinds of human BMSCs (hBMSCs). **Materials and Methods:** Bone samples were obtained from the same individuals undergoing alveolar bone grafting using iliac bone. The samples were cultured and hBMSCs of iliac crest (I-hBMSCs) and maxillae (M-hBMSCs) were isolated, respectively. Total mRNA of the paired I-hBMSCs and M-hBMSCs was extracted, and reversely transcribed into cDNA. The expression profiles of angiogenesis marker genes were determined by a gene expression profile chip. **Results:** Among all the differential-

ly expressed genes, 49 genes were found to be related to angiogenesis. In I-hBMSCs, a total of 13 angiogenesis-related genes was significantly down-regulated comparing with that in M-hBMSCs. The most pronouncedly decreased genes were gremlin 1 (GREM1), angiopoietin 2 (ANGPT2) and prostaglandin I2 synthase (PTGIS), with a more than 50% reduction of expression (Figure 1 B). Besides, the expression of 36 angiogenesis-related genes was significantly higher in I-hBMSC than that in M-hBMSCs. The most up-regulated genes were tumor necrosis factor alpha-induced protein 2 (TNFAIP2), complement component 3 (C3) and thrombospondin 3 (THBS3). All these three genes were increasingly expressed two times than that in M-hBMSCs (Figure 1 C). **Conclusions:** The site-specific hBMSCs exhibit distinct expression profiles of angiogenesis-related genes, which could attribute to the angiogenic variations between I-hBMSC and M-hBMSCs. Among these differentially expressed genes, GREM1, ANGPT2, PTGIS, TNFAIP2, C3 and THBS3 are the most profound and significant. Their roles in the angiogenic variations between I-hBMSC and M-hBMSCs need to be further clarified. The gene chip technique was useful to detect the multi-gene different expression profile and features.



Disclosures: *Yifei Du, None*

SUN-0180

Osteal Macrophage Regulation of the Plasminogen System in Bone Laura Zweifler*, Amy Koh, Benjamin Sinder, Megan Michalski, Hernan Roca, Yuji Mishina, Laurie Meccauley. University of Michigan, United States

Macrophage phagocytosis of dead or dying cells is termed efferocytosis. This process plays an important role in development, homeostasis, and repair of the skeletal system. Apoptotic cell clearance occurs rapidly and at a high rate in the bone given the large turnover of marrow cells; however, it is unclear how macrophages respond specifically to apoptotic osteoblasts. The goal of this project is to address this question by studying the unique macrophage gene expression profile during uptake of apoptotic bone cells. Macrophages (Macs) were derived from 6-8 week-old primary murine bone marrow stimulated with macrophage-colony stimulating factor (M-CSF) for 1 week. Macs were then co-cultured with apoptotic bone marrow stromal cells (apBMSCs) to model a skeletal pre-osteoblastic cell and simulate efferocytosis in bone. We also used apoptotic thymocytes (apThym) as a control to simulate efferocytosis of non-skeletal cells. To understand mechanisms of skeletal tissue-specific efferocytosis, RNA was isolated and gene expression analyzed with an Affymetrix Mouse Gene 2.1 ST Array. Efferocytic co-cultures with non-skeletal apThym resulted in 101 differentially regulated genes compared to Macs alone. However, efferocytosis co-cultures with skeletal apBMSC's revealed 1219 significantly up- or down-regulated genes, suggesting efferocytosis of skeletal cells may be particularly impactful. Plasminogen activator inhibitor 2 (PAI2) was 9.69 fold higher in Macs+apBMSCs co-cultures compared to Macs alone, and was not increased in Macs+apThym co-cultures. This finding was confirmed with quantitative reverse-transcribed polymerase chain reaction (qRT-PCR). Additionally, PAI2 was not upregulated when Macs were co-cultured with apBMSCs at 4°C, which is a condition known to inhibit efferocytosis. Western blot analysis has shown that Macs+apBMSCs secreted significantly higher PAI2 compared to macrophages alone. PAI2 is a serine protease inhibitor that can bind to plasminogen activators, reducing plasmin concentrations. In bone, plasmin has been implicated in mechanisms to degrade the osteoid layer covering the bone surface, providing osteoclasts with access to bone for resorption. Given the roles of the fibrinolytic system in the bone microenvironment, PAI2 upregulation suggests that osteal macrophages are mediating a decrease in bone resorption. These data support a critical role for efferocytosis in bone cell signaling and regulation.

Disclosures: *Laura Zweifler, None*

SUN-0200

The Extracellular Matrix Protein Spondin-2 Induces Osteomimicry in Prostate Tumor Cells via Primary Cilia Activation Juan Ardura*, Bethan Kitchen, Irene Gutierrez-Rojas, Luis Álvarez-Carrión, Arancha R Gortazar, Verónica Alonso. Bone Physiopathology Laboratory, Departamento de Ciencias Médicas Básicas, Universidad San Pablo CEU. CEU Universities, Madrid (Spain)

Prostate cancer cells preferentially metastasize to bone in part by acquiring a bone phenotype based on ectopic expression of bone-related genes. This process, known as osteomimicry, allows cancer cells to colonize and proliferate in the bone microenvironment. Primary cilia loss is associated to prostate tumor progression causing over activation of the bone modulating protein β -catenin. The extracellular matrix protein spondin-2 is a member of a β -catenin-activating family that has recently been described as an inductor of osteomimicry and is overexpressed in prostate tumors that metastasize to bone. We hypothesize that spondin-2 induces osteomimicry in prostate tumor cells via a primary cilia-dependent pathway. A C57BL/6 mouse model of prostate cancer induction by orthotopic injection of adenocarcinoma TRAMP-C1 cells was used. TRAMP-C1 cells in the in vivo model and for in vitro experiments were silenced or not with 3 specific siRNAs targeted to spondin-2. We evaluated the presence of primary cilia and the expression of the primary cilia marker IFT88 and ectopic bone-related markers in the prostates of the mouse model and in TRAMP-C1 cells. TRAMP-C1 cell adhesion to collagen-coated surfaces was also assessed. TRAMP-C1-induced tumors showed overexpression of spondin-2, decreased number of primary cilia and downregulation of IFT88 gene expression in association to osteomimicry changes in the prostate tissue, namely overexpression of RANKL, OPG, Runx2 and osterix. In vitro, stimulation with spondin-2 decreased the percentage of primary cilia-presenting cells. Moreover, IFT88 silencing further promoted spondin-2-induced changes on the aforementioned bone-related genes in TRAMP-C1 cells. Both spondin-2 stimulation and IFT88 silencing enhanced TRAMP-C1 cell adhesion to collagen-coated plates. We propose that spondin-2 induces prostate tumor cell osteomimicry and adhesion by decreasing primary cilia expression.

Disclosures: **Juan Ardura, None**

SUN-0201

LIGHT/TNFSF14 and RANKL: biomarkers and therapeutic targets of bone disease in multiple myeloma patients experiencing therapeutic regimens Giacomina Brunetti*¹, Rita Rizzi², Giuseppina Storlino³, Sara Bortolotti³, Graziana Colaianni³, Lorenzo Sanesi³, Luciana Lippo³, Maria Grano³, Silvia Colucci¹. ¹Department of Basic and Medical Sciences, Neurosciences and Sense Organs, Section of Human Anatomy and Histology, University of Bari, Bari, Italy, ²Department of Emergency and Organ Transplantation, Section of Hematology with Transplantation, University of Bari, Bari, Italy, ³Department of Emergency and Organ Transplantation, Section of Human Anatomy and Histology, University of Bari, Bari, Italy

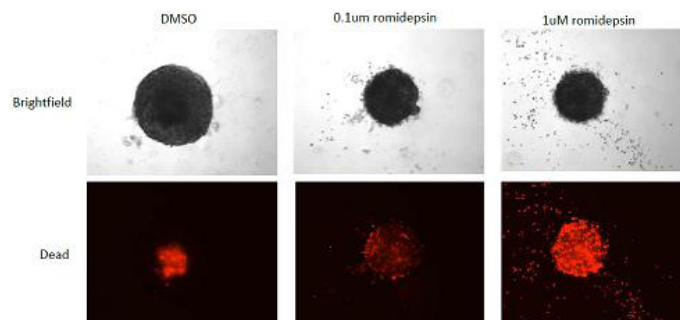
The two members of TNF superfamily, LIGHT and RANKL, are involved in physiological and pathological bone remodeling and implicated in newly diagnosed Multiple Myeloma (MM)-bone disease. Bone disease occurs in about 80% of MM patients at diagnosis, and up to 90% at relapse. Despite improvements in the depth and the duration of response, most patients eventually relapse, with the duration of response decreasing with each line of therapy. Patients with relapsed, or refractory, or progressive MM and active bone disease represent a therapeutic challenge to identify both new pharmacological approaches and biomarkers. Herein, we investigated whether LIGHT and RANKL have also a role in Multiple Myeloma (MM)-bone disease patients experiencing therapeutic regimens. We found that LIGHT is over-expressed by CD14⁺ monocytes of peripheral blood from MM-bone disease patient responders, at relapses, and in progressive disease similarly to newly diagnosed MM-bone disease (NDMM) patients. Moreover, T-cells isolated from the same patients also over-express the pro-osteoclastogenic cytokine RANKL. Additionally, we found that in all the patients the percentage of osteoclast progenitors CD14⁺CD16⁺ monocytes is higher than the controls, irrespective of the bone disease. Consistently with all these findings, we also demonstrated that spontaneous osteoclastogenesis only occurs in cultures derived from PBMCs of MM-bone disease patient responders, at relapses, and in progressive disease as demonstrated in NDMM patients. Finally, we proved that increasing doses of RANK-Fc or anti-LIGHT neutralizing antibody induce a dose-dependent reduction of spontaneous osteoclastogenesis of MM-bone disease patients' responders, relapses and in progressive disease, supporting the involvement of RANKL and LIGHT in the spontaneous osteoclast formation. These ex-vivo and in vitro findings are supported by the high serum levels of TRAP5b and CTX, two markers of osteoclast activity, in MM-bone disease patients' responders, relapses and in progressive disease. In conclusion, our study points out the key role of LIGHT in osteoclast and immune cell crosstalk in the pathophysiology of MM-bone disease, suggesting that LIGHT could be a new therapeutic target in the active bone disease of MM.

Disclosures: **Giacomina Brunetti, None**

SUN-0202

HDAC Inhibitors Synergize with Standard-of-Care MAP Chemotherapeutics to Block Growth of Osteosarcoma Sarcospheres Leah Everitt*, Christopher Collier, Gabrielle Knafler, Deep Gandhi, James Buschbach, Patrick Getty, Edward Greenfield. Case Western Reserve University Department of Orthopaedics, United States

Standard-of-care for osteosarcoma patients has remained largely unchanged in the last thirty years due to scarcity of clinical trials and prohibitive costs of traditional drug discovery. Our goal is to repurpose drugs to block the growth of osteosarcoma lung metastases, the lethal disease process. We therefore screened the NCI-panel of 114 FDA-approved oncology drugs to identify agents that potentially reduce growth of osteosarcoma spheroids (sarcospheres). We first developed a system to routinely generate large numbers of highly-uniform spherical sarcospheres with a 400um diameter (1/well), by a centrifugation-based method, using highly metastatic human cell lines (143B, MG63.3, and LM7). Sarcospheres most closely simulate micrometastases of the lungs in vivo. Our primary drug screen (Z' -factor=0.70+0.10) measured effects of FDA approved oncology drugs on reazurin reduction by sarcospheres in the presence and absence of MAP chemotherapy (methotrexate, doxorubicin, and cisplatin). Dose-response experiments with 13 of the most effective drugs confirmed initial results and allowed comparison with each drug's toxicity on normal human osteoblasts and normal small airway epithelial cells. Romidepsin, a HDACi (histone deacetylase inhibitor), had the most favorable toxicity/efficacy ratios (TD50/IC50=57-580, depending on cell line). The only other HDACi in the panel of FDA-approved drugs (vorinostat) also ranked highly in the primary screen. Since newer HDACi's may have improved toxicity/efficacy ratios, we compared romidepsin and vorinostat with the three other HDACi's that are FDA-approved (belinostat, panobinostat, and valproic acid) plus one that is in clinical trials (entinostat). Romidepsin (Cmax/IC50=36-360) and belinostat (Cmax/IC50=14-20) reduced sarcosphere growth at clinically-achievable levels, in the presence or absence of MAP. Importantly, both romidepsin and belinostat were synergistic with MAP (BLISS scores=5-15). Propidium iodide staining showed that romidepsin substantially induced cell death throughout the sarcospheres. Our results strongly support future studies to determine effects of romidepsin and belinostat on growth of lung metastases in vivo.



143B sarcospheres were treated with DMSO control or romidepsin for 48 hours then stained with propidium iodide for 2 hours to show dead cells. Images obtained using Leica DM16000, top images are brightfield and lower images obtained with a TRITC/RFP filter set (535/617 nm). Each set of images is 1 representative sarcosphere of 3 replicates.

Disclosures: **Leah Everitt, None**

SUN-0203

Estrogen receptor alpha is a novel tumor suppressor in osteosarcoma Susan Krum*, Gustavo Miranda-Carboni, Maria Angeles Lillo Osuna. UTHSC, United States

Osteosarcoma is a malignant tumor in the bone that originates from normal osteoblasts or osteoblast precursors. Normal osteoblasts express estrogen receptor alpha (ER α); however, osteosarcomas do not due to promoter DNA methylation. Treatment of 143B osteosarcoma cells with Decitabine (DAC, 5-Aza-2'-deoxycytidine) induced expression of ER α , leading to a decrease in proliferation and a concurrent induction of osteoblast differentiation, as marked by alkaline phosphatase expression and activity and expression of bone sialoprotein (BSP). 17 β -estradiol (E2) further decreases the DAC-induced reduction in proliferation. Over-expression of ER α also inhibits proliferation and induces osteoblast differentiation and silencing of ER α prevents the effects of DAC, demonstrating that ER α is both necessary and sufficient for DAC-mediated suppression of osteosarcoma. In an orthotopic model of osteosarcoma in vivo, 143B cells were injected into the tibia of NSG mice and DAC inhibited tumor growth and metastasis. Together, these experiments suggest that the FDA-approved DNA methylation inhibitor DAC can be used to treat osteosarcoma patients to decrease proliferation and induce osteoblast differentiation.

Disclosures: **Susan Krum, None**

SUN-0204

Parathyroid hormone-related protein (PTHrP) regulates CSC/EMT in a human breast cancer model and administration of anti-PTHrP therapeutic monoclonal antibodies reduces tumor burden in bone Jiarong Li*, Louis Dore Savard, Guoming Xiong, Richard Kremer. RI MUHC, Canada

Parathyroid hormone-related protein (PTHrP) is dysregulated in advanced cancers where it causes malignancy-associated hypercalcemia and plays a major role in the progression of bone metastases. We have shown previously that PTHrP ablation delays tumor initiation and that it is preferentially expressed in triple negative breast cancer (TNBC). Here we investigated whether PTHrP can influence the phenotype of the human TNBC cell line MDA-MB231 in vitro and can be targeted in vivo with anti-PTHrP monoclonal antibodies (mAbs). First we used CRISPR/Cas9 to construct a U6G RNA-Cas9-2A-red fluorescence protein (RFP) vector with a human PTHrP specific guide RNA directed to exon 4 (knockout/KO) or an empty vector as control. Single clones of PTHrP KO cells (RFP+) were isolated and several clonal cell lines with over 95% PTHrP ablation were used in the studies. In vitro cancer stem cell (CSC) characterization showed a 60% reduction in mammosphere formation and a significant reduction in CSC markers (ALDH1, CXCR4 and CD44^{high}/CD24^{low}) in KO cells. Furthermore, cell morphology and cell surface markers of epithelial mesenchymal transition (EMT) including E-cadherin, CK8, CK18, N-cadherin, CK14 and vimentin showed a shift from a mesenchymal phenotype towards an epithelial phenotype in KO cells. Next, we examined the potential of therapeutic mAbs against PTHrP in an intra-tibial model of skeletal metastasis in female nude mice (n=10/group) transplanted with 1x10⁵ MD-AMB-231 cells. Two hundred micrograms of mAbs were administered 3 times/week intra-peritoneally two weeks post tumor transplantation and treated for three weeks. Bone imaging performed by PET scan and MRI showed a 40% reduction in tumor burden (P=0.012) in mAbs treated animals compared to controls. Overall our data show that PTHrP regulates TNBC towards a more aggressive phenotype and demonstrate the therapeutic efficacy of anti-PTHrP mAbs in vivo.

Disclosures: Jiarong Li, None

SUN-0205

Runx2 promotes autophagy through enhancing cytoskeletal stability in bone metastatic breast cancer cells. Ahmad Othman*, Manish Tandon², Jitesh Pratap¹. ¹Rush University Medical Center, United States, ²KBI Biopharma, United States

Bone metastasis of breast cancer causes significant patient mortality. Recent studies suggest that metastatic cancer cells induce autophagy to survive metabolic and hypoxic stress. During autophagy, cytoplasmic components and damaged organelles are captured by autophagosomes followed by lysosomal fusion and degradation, releasing metabolites as energy sources to meet metabolic demands. Although the components of autophagy have been well characterized, the regulatory mechanism of autophagy in metastatic cancer cells in the bone microenvironment is still unknown. To examine autophagy during bone metastasis, we used a bone metastatic isogenic variant of breast cancer MDA-MB-231 cells isolated from a xenograft tumor mouse model of metastasis. Previously, we and others have shown that Runx2-related transcription factor-2 (Runx2) promotes cell survival, cell migration and invasion, and tumor growth associated osteolysis. Therefore, we examined whether Runx2 regulates autophagy for increased cell survival in the bone microenvironment. Our results show that Runx2 enhances autophagy in metastatic breast cancer cells. Silencing of Runx2 causes accumulation of autophagic vesicles due to reduced turnover of autophagosomes. Live cell confocal microscopy and biochemical studies show that Runx2 enhances trafficking of autophagic vesicles and increases acetylation of α -tubulin (Ac- α Tub) subunit of microtubules. Similar to cancer-related functions of Runx2, elevated levels of Ac- α Tub have been linked with an invasive, migratory, and metastatic phenotype in cancer cells. Ac- α Tub is a marker of the stable fraction of the tubulin cytoskeleton which is utilized for vesicle trafficking. Our studies in Runx2 knockdown cells and treatments with microtubule depolymerizing agents such as Nocodazole and vinblastine showed that depolymerization of stable microtubule fraction decreases autophagic flux and that Runx2 is required for stable fraction of microtubules. These results suggest that Runx2 enhances autophagy through maintaining cytoskeletal stability which is critical for autophagosome trafficking. Furthermore, immunohistochemical analysis of an autophagy marker LC3B protein in clinical breast cancer specimens showed significant association between high Runx2 and low LC3B protein levels. Taken together, our studies reveal a novel function of Runx2 in cytostructure and provide molecular insights into the role of autophagy in bone metastatic cancer cells.

Disclosures: Ahmad Othman, None

SUN-0206

The JNKs/XBP1s Signaling Cascade Regulates Bone Microenvironmental Support to the Progression of Myeloma Bone Disease Risheng Chen*, Guoshuang Xu¹, Wissam Beaino¹, Kai Liu¹, Xuemei Zeng¹, Nathan Yates¹, Rong Chong¹, Konostas Verdelis¹, G Roodman², Denise Toscani³, Nicola Giuliani³, Yan Lin¹, Carolyn Anderson¹, Hongjiao Ouyang⁴. ¹University of Pittsburgh, United States, ²Indiana University School of Medicine, United States, ³University of Parma, Italy, ⁴Texas A&M University, United States

Spliced X-box binding protein-1 (XBP1s) is an endoplasmic reticulum (ER) stress signaling molecule and implicated in pathogenesis and drug resistance of cancer, e.g. multiple myeloma and breast cancer. However, very little is known as to its roles in regulating the tumor bone microenvironment properties in tumor bone diseases. In addition, while its mRNA splicing has been widely studied, it remains largely elusive as to how its post-translational modification occurs and whether and/or how XBP1s' post-translational modification impacts its pathophysiological functions. We previously reported that human XBP1s (hXBP1s) in bone marrow stromal cells is required for the bone marrow stromal support of the growth multiple myeloma bone disease (MMBD), the most prevalent and severe tumor-induced bone disease. Here we report that human XBP1s (hXBP1s) is a physiological and direct phosphorylation substrate of JNKs. This phosphorylation promotes hXBP1s protein degradation via enhancing its physical interaction with the E3 ubiquitin ligase, β -TrCP, resulting in the enhanced ubiquitination and 26S proteasome-mediated degradation of hXBP1s. Mutation of the JNK phosphorylation site of hXBP1s to alanine largely prevents JNK phosphorylation of hXBP1s and JNK-induced protein degradation of hXBP1s. Further, we found that bone marrow stromal cells (BMSCs) harboring the hXBP1s mutant resistant to JNK phosphorylation provided significantly greater support of MM growth and MM-induced osteoclastogenesis and bone destruction both in vitro and in vivo, compared with the counterparts expressing wild type (WT) hXBP1s. Finally, we, utilizing a custom-made antibody that specifically recognizes JNKs' phosphorylation of hXBP1s, observed that JNK-mediated phosphorylation of hXBP1s is associated with favorable therapeutic outcome of MM patients in response to a combination treatment of bortezomib, dexamethasone, thalidomide (and/or their derivatives), three MM drugs known to stimulate the JNKs activities. These results suggest p-hXBP1s/JNK as a potential predictive biomarker for MM patients' response to the drug treatment. Taken together, our study provides the first evidence that hXBP1s is a novel physiological and direct target of JNK phosphorylation and demonstrates that the JNKs/XBP1s signaling cascade plays an essential role in mediating MM drug therapeutic effects on repressing bone microenvironment support of MM growth and MM-induced bone destruction.

Disclosures: Risheng Chen, None

SUN-0207

Effect of Extracellular Vesicles Derived from Osteotropic Tumors on Bone Resident Cells Riccardo Paone*, Alexander Loftus¹, Christopher George¹, Kirsty Shefferd¹, Argia Ucci¹, Simona Delle Monache¹, Alfredo Cappariello^{1,2}, Maurizio Muraca³, Anna Maria Teti¹, Nadia Rucci¹. ¹Department of Biotechnological and Applied Clinical Sciences, University of L'Aquila, Italy, ²Bambino Gesù Children Hospital, Rome, Italy, ³Department of Women's and Children's Health, University of Padua, Italy

Extracellular vesicles (EVs) are membrane-bound cargos of biologically active molecules shed by cells, which are emerging as mediators of a range of pathological processes, including cancer. Their role in both primary and metastatic cancers of the bone has been poorly explored. We investigated EV-mediated effect of osteosarcoma cells (MNGG-HOS) or osteotropic breast cancer cells (MDA-MB-231) on bone resident cells, including osteoblasts, osteoclasts and endothelial cells. In mouse primary osteoblasts, HOS- and MDA-EVs inhibited the mRNA expression of Cyclin D1 (-75%, p=0.02) and of the osteoblast-related genes *Alp* (-35%, p=0.002) and *Osx* (-40%, p=0.06), whereas they enhanced the expression of *Nos2* (15-fold, p=0.015), *Lcn2* (4-fold, p=0.01) and *Serp1b2* (22-fold, p=0.049). An increase of IL-1 β (12-fold, p<0.001), IL-6 (10-fold, p=0.05) and *Rankl* (1.5-fold, p=0.02) was also observed in tumour cell-EVs-treated osteoblasts, which was confirmed at protein level. ELISA and cytokine array assays on conditioned media (CM) from osteoblasts treated with HOS-EVs showed an increase of Pentraxin-3 (2-fold, p=0.045), a positive modulator of tumour-associated inflammation. Moreover, the chemokines CCL-2 and -5, CXCL-1 and -2 and LIX, which were undetectable in untreated osteoblasts, were expressed by HOS EV-treated osteoblasts. Similarly, MDA-EVs-treated osteoblasts presented with an increase of CCL-3, CXCL-2 and -11, and of the cytokines IL-5, -12p40, -13, -15 and -17. HOS-EV transcriptional profile showed the expression of genes involved in bone metabolism, such as Cathepsin K, CLCN7, CD40 and VEGFA. In line with this molecular profile, HOS-EVs significantly increased in vitro osteoclastogenesis (7fold, p=0.012) performed in the presence of suboptimal concentrations of RANKL. Moreover, HOS-EVs significantly increased endothelial cell chemotaxis (p=0.02, AUC) and in vitro tube formation (3-fold, p=0.007), evaluated by scratch assay and number of branching formed in HUVEC cell cultures. Consistently, in vivo angiogenesis, evaluated by the matrigel plug assay, was significantly enhanced by HOS-EVs (3.5fold, p=0.001; n.mice/group=5). In conclusion, these data elucidated i) the transcriptional profile of osteosarcoma and breast cancer derived EVs and ii) their impact on bone cells and endothelial physiology.

Disclosures: Riccardo Paone, None

SUN-0208

RANKL Increases Resistance to TRAIL Induced Cell Death in Oral Squamous Cell Carcinoma Tumor Cells Purushoth Ethiraj*, Yuvaraj Sambandam, Jessica Hathaway-Schrader, Azizul Haque, Chad Novince, Sakamuri Reddy. Medical University of South Carolina, United States

Oral squamous cell carcinoma (OSCC) is the most common malignancy among oral cancers. OSCC has potent osteolytic activity, resulting in local bone invasion. Tumor necrosis factor (TNF) family member, RANK ligand (RANKL) is a critical osteoclastogenic factor that resorb bone. We have recently shown that OSCC tumor cells express RANKL and the RANK receptor. We have also identified that RANKL expression is autoregulated in OSCC tumor cells. Furthermore, RANKL significantly increases OSCC tumor cell proliferation. TNF-related apoptosis inducing ligand (TRAIL) has been shown to induce apoptosis in a variety of tumor cells. However, OSCC cells are relatively resistant to TRAIL-induced apoptosis. Therefore, we hypothesized that RANKL increases resistance to TRAIL-induced cell death in OSCC tumor cells. TRAIL interacts with receptors DR4, DR5, DcR1 and DcR2. Real-time RT-PCR analysis showed high-level of DR4, DR5 and relatively low levels of DcR1 and DcR2 mRNA expression in OSCC cells. Further, SCC1 and SCC74A tumor cells stimulated with TRAIL (100 ng/ml) for 24 h showed increased levels of RANKL expression. In addition, we analyzed apoptosis in OSCC cells by labeling DNA strand breaks (TUNEL assay) by fluorescence microscopy. Interestingly, RANKL stimulation of SCC1 tumor cells treated with TRAIL showed increased resistance to TRAIL induced cell death. We further confirmed these results by analyzing apoptotic marker protein expression in OSCC tumor cells. These data suggest that blockade of RANKL expression in OSCC tumor cells may enhance the therapeutic potential of TRAIL to control OSCC tumor growth/progression.

Disclosures: Purushoth Ethiraj, None

SUN-0209

CD44 Intracellular Domain interaction with RUNX2 regulates metastasis of prostate cancer cells to the bone. Linda T. Senbanjo*, Meenakshi A. Chellaiah. University of Maryland Dental School, United States

Prostate cancer (PCa) is the second leading cause of death in males in the western world. It is characterized by extensive metastasis leading to secondary lesions in the bone, lymph node, and brain. Bone is the most common site for PCa metastasis and it targets bone with osteoclastic and/or osteoblastic lesions due to the activity of osteoclasts (OC) or osteoblasts (OB), respectively. The goal of this study was to investigate the role of two key proteins involved in bone metastasis, CD44, a receptor that has been shown to increase the metastatic potential of cancer cells and RUNX2, a transcription factor required for bone formation in osteoblasts. CD44 and RUNX2 have roles in the expression of RANKL, a key protein involved in osteoclast (OC) differentiation and activation. In this study, we used prostate cancer cell lines derived from bone (PC3 and PCa2b) and lymph node (LNCaP) metastases along with control cell lines (HPR1 and BPH). We used semi-quantitative PCR, immunoblotting, and immunostaining analyses in our study. Our findings revealed the following: 1) CD44 is variably expressed in different PCa cell lines. A significant increase in the expression of CD44 was observed in PC3 cells derived from bone metastasis of a Caucasian patient. Neither PCa2b (derived from an African American patient) nor LNCaP demonstrated the expression of CD44. 2) CD44 is cleaved by γ -secretase to generate CD44-Intracellular Domain (ICD). Co-localization of CD44-ICD with RUNX2 was observed in the nucleus of PC3 cells. 3) Expression of serial deletion constructs of CD44-ICD in PC3 cells demonstrated more interaction of CD44-ICD fragment with RUNX2 between amino acid sequences 671 and 706. 4) Knockdown (KD) of CD44 in PC3 cells decreased RUNX2 expression and RANKL expression. Hence conditioned medium from these cells failed to support osteoclast differentiation *in vitro*. Our results indicate that CD44 can be one of the key biological factors which contribute to prostate cancer health disparity. Future investigation of the differences in the expression of CD44 in PC3 and PCa2b will ultimately pave way for future studies to understand the role of this protein and its downstream targets in bone metastasis and metastasis-related events (osteolytic vs. osteoblastic).

Disclosures: Linda T. Senbanjo, None

SUN-0210

Paracrine Actions of FGF23 on Bone-Metastatic Prostate Cancer Attaya Suvannasankha*, Douglas Tompkins, Colin Crean, John Chirgwin. Indiana University School of Medicine, United States

Osteocytes are the major source of circulating endocrine FGF23. Feng et al (Oncotarget, 2015) reported that FGF23 is also made by prostate cancers (PCs), functioning as an autocrine growth factor. We previously reported that intact FGF23 was not elevated in the serum of PC patients, a result confirmed by Vlot et al (Clin Chim Acta, 2018). These results do not address whether osteocyte FGF23 contributes to PC growth in bone. We found that PC cell lines secreted physiologically insignificant amounts of FGF23, while responding to exogenous factor by increasing EGR1 transcription factor and its target gene heparanase, which contributes to tumor colonization of bone. Responses to FGF23 were blocked with FGFR kinase inhibitor BGJ398, which has IC50s of ~1nM for FGFRs 1, 2 and 3. PC-3 and LNCaP PC cell lines were assayed for secretion of intact FGF23 (Kainos ELISA) in 48hr conditioned media of confluent cells. LNCaPs made 1.5 pg/ml, less than the level in normal

serum, and PC-3s were below the limit of detection. Cleaved C-terminal FGF23 was undetectable. Treatment of LNCaP and PC3 with 100ng/ml FGF23 significantly increased mRNA for EGR1 at 1hr, followed by heparanase mRNA at 8 & 24hrs - responses that were blocked by BGJ398. When 14d mouse calvariae were incubated with BGJ398, markers of osteoblasts (alkaline phosphatase & type 1 collagen) and osteocytes (PHEX, MEPE, & FGF23) were increased 2-5 fold & 3-8 fold, respectively; the osteoclast marker TRAP was increased less than 2-fold, while RANKL mRNA was unchanged. Changes were consistent with anabolic responses in mice treated with BGJ398 (Wöhrle et al, JBMR, 2013). When human PC cells were grown on mouse calvariae *in vivo* organ co-culture assays (EVOCA), 25nM BGJ398 effectively blocked growth of both LNCaP & PC-3 cell lines, while 100X higher concentrations of BGJ398 only marginally decreased growth of the cells *in vitro*. The results suggest that osteocyte-derived FGF23 contributes to PC growth in bone, independent of the intracrine growth role of the PC-expressed factor found by Feng et al. Blockade of FGFR signaling could effectively suppress growth of metastatic PC in bone, but not primary prostate cancer. Agents with bone-anabolic effects, such as BGJ398, which is in Phase II clinical trials for cancers with activated FGFR signaling, could be effective in prostate cancer patients with osteosclerotic bone metastases.

Disclosures: Attaya Suvannasankha, None

SUN-0211

Targeting the Wnt/beta-catenin pathway in human osteosarcoma cells Jianning Tao^{1,2}, Fang Fang¹, Ashley Vanleave¹, Ralph Helmuth¹, Jing Zhao¹, Kirby Rickel¹, Erliang Zeng². ¹Sanford Research, United States, ²University of South Dakota, United States

Osteosarcoma (OS) is the most common primary malignancy of bone in adolescents and young adults. The five-year survival rate for localized osteosarcoma is about 70% while patients with metastatic or recurrent disease suffer poorly with the rate approximately 30%. However, the outcome for either group of patients with OS has not changed in more than four decades. This highlights the need for the second-line treatment options for patients. Aberrant activation of Wnt signaling has been implicated in human OS, which provides a genetic vulnerability in OS treatment. Using deposited data from Next Generation Sequencing (NGS) studies, we analyzed somatic mutations and gene expression of components of Wnt/ β -catenin pathway. To prove a principle that Wnt activation is necessary for osteosarcoma growth, colony formation, invasion, and metastasis, we treated human OS cells with a small molecule inhibitor of Wnt/ β -catenin, PRI-724 (an ICG-001 derivative), which suppresses Wnt/ β -catenin-mediated transcription. We found that constitutive Wnt/ β -catenin signal activation is common in human osteosarcoma while activating genetic mutations of Wnt pathway components in osteosarcoma are rare. We also found that increased protein levels of both active- β -catenin and CyclinD1 in five human OS cell lines. Treatment with PRI-724 was sufficient to inhibit 143B and SJS1 cell proliferation. Suppressed Wnt signaling was confirmed by decreased protein levels of CyclinD1, the Wnt target. Moreover, we revealed significant inhibitory effects on cell migration, invasion and colony formation in those human OS cells. Taken together, our results illustrate the critical role of Wnt/ β -catenin signaling in human osteosarcoma pathogenesis and growth, and Wnt inhibitors represent potential therapeutic agents for the treatment of human osteosarcoma.

Disclosures: Jianning Tao, None

SUN-0212

Remineralization of Bone Lytic Lesions in high risk myeloma patients enrolled on total therapy five protocol (TT5); the Arkansas experience. Maurizio Zangari¹, Shivang Desai¹, Meera Mohan¹, Frits Van Rhee¹, Sharmilan Thanendrarajan¹, Carolina Schinke¹, Faith Davies¹, Gareth Morgan¹, Larry Suva², Donghoon Yoon¹, Leo Rasche¹, Niels Weinhold¹, Shobhit Sharma¹, Manoj Kumar¹. ¹University of Arkansas for Medical Sciences, United States, ²College of Veterinary Medicine and Biomedical Sciences Texas A&M University, United States

We have previously reported treatment associated remineralization of lytic pelvic lesions in a subset of low risk multiple myeloma (MM) patients who experience median progression free survival of eight years. In this study, the effect of total therapy five protocol (TT5) on bone lytic lesions in patients with high risk disease and a median progression free survival of two years was assessed. The TT5 protocol enrolled high risk myeloma patients (GEP 70 Gene Expression Profile ≥ 0.66 or lactate dehydrogenase (LDH) ≥ 360) or other high risk clinical features. Treatment included induction, stem cell collection, and tandem autologous transplant followed by velcade revlimid / melphalan dexamethasone maintenance therapy for three years along with monthly bisphosphonate therapy. The single largest lytic lesion measuring more than 1 cm was identified on the baseline PET CT and serially followed. Remineralization of the lesion was defined as sclerotic changes within the identified lytic lesion from baseline, using the largest diameter on the axial plane. Percent healing was defined as 100 (initial lesion size - final lesion size) / initial lesion size and categorized to 26-50%, 51-75%, 76-99% and 100% complete healing. Lesions with $\leq 25\%$ remineralization were not considered in this analysis. Among the 95 patients enrolled, 66 presented with a lesion ≥ 1 cm and appropriate imaging (median follow-up 36 months; 58% male; median age 60 years, IgG disease 51%, IgA 24% light chain 23%). The average size of the lytic lesion was 3.21 cm (range of 1 to 9 cm). Pelvic bone lesions were observed in 50% of the patients.

One third of patient presented with more than 100 lytic lesions at the baseline PET-CT. Any grade of remineralization > than 25% from baseline was observed in 48 subjects (72.7%), sixteen patients (33%) achieved complete remineralization(100% healing), 25% of subjects achieved > 75% healing and 41% of patient lesions achieved 25-50% reduction. In a cohort of patients with cervical vertebral lytic lesions, 33% (6/18) demonstrated complete remineralization during treatment. One important limitation is that the analysis focused only on the single largest lytic lesion in these patients. Ongoing efforts are examining treatment efficacy of the entire lytic compartment to ascertain if the repair process is affected by tumor heterogeneity. This retrospective analysis documents the first evidence of significant bone healing at lytic sites in high risk myeloma patients, with a significantly shorter survival compared to the overall myeloma population.

Disclosures: **Maurizio Zangari, None**

SUN-0236

BMP2 signaling is required for postnatal maintenance of osteochondral tissues of the temporomandibular joint and knee Eliane Dutra*, Mara O'Brien, Po-Jung Chen, Sumit Yadav. University of Connecticut Health, United States

Introduction: Osteoarthritis (OA) of knee and temporomandibular joint (TMJ) is a growing epidemic that afflicts aging men and women not only in United States but across the globe. The osteochondral tissues of TMJ and knee have distinct developmental origins, and are made up of different types of cartilage, with matrices that differ in molecular composition, structure and mineral content. Bone Morphogenic Protein 2 (BMP2) plays an important role in cartilage growth and development. Chondrocyte differentiation and remodeling of the osteochondral tissue are the major functions regulated by BMP2. **Objective:** In this study, we sought to better identify the role of BMP2 in cartilage health, matrix synthesis and its ability to form calcified cartilage. Our aim was to compare and contrast the effects of BMP2 loss of function on the cartilage and subchondral bone of the TMJ and the knee. **Methods:** In vitro studies: The chondrocytes of TMJ from triple transgenic reporter mice (Col1a1XCol2a1XCol10a1) were treated with BMP2 and noggin for over a period of 2 weeks in a chondrogenic medium. In vivo studies: Three-week-old mice with floxed BMP2 and Cre-expression specific to the aggrecan (ACAN) promoter, and their Cre-negative littermates, were injected with tamoxifen (75 µg/kg body weight) for 5 days. The animals were euthanized after 1, 3 and 6 months following treatment with tamoxifen. Mice were injected with alizarin complexone and calcein before euthanization. EdU was injected at 2 days and 1 day before euthanization. **Results:** In vitro: In the TMJ cartilage cultures, BMP2 enhanced proliferation, differentiation and mineralization; whereas noggin decreased proliferation and differentiation of the chondrocytes. In vivo: Conditional deletion of BMP2 in the cartilage of TMJ from mice of all age groups examined led to a decrease in TRAP activity, decreased proliferation (EdU) and decreased differentiation. However, there was no appreciable difference in the proliferation and differentiation between the control and BMP2 deleted mice. We also observed an altered cellular morphology (loss of zonal architecture) and decrease in matrix synthesis with the conditional deletion of BMP2 in the cartilage of TMJ and knee. **Conclusion:** In summary, conditional deletion of BMP2 in ACAN-expressing cells can lead to cartilage breakdown and early development of osteoarthritis of the TMJ cartilage, whereas the effects observed in the articular cartilage of knee were not severe.

Disclosures: **Eliane Dutra, None**

SUN-0237

Novel TNFR2 Signaling in Osteoarthritis Wenyu Fu*, Young-Su Yi, Jyoti Joshi Mundra, Aubryanna Hettinghouse, Chuanju Liu. New York University Medical Center, United States

Purpose: TNFR1 primarily mediates inflammatory activity of TNF α and is responsible for cartilage degeneration and bone erosion in various diseases/conditions, particularly under inflammatory conditions. Growing evidences indicate that TNFR2 plays a protective and anti-inflammatory role in various disorders; however, the role of the TNFR2 pathway in the pathogenesis of osteoarthritis (OA) remains largely unknown. The current study aims to determine the role of anabolic TNFR2 pathway in cartilage homeostasis and OA. **Materials & Methods:** Both Rosa26-CreERT2 and Agc1CreERT2 strains were obtained from Jackson Laboratory. 14-3-3e F/F mouse was obtained from Dr. Wynshaw-Boris at UCSF. Mass spectrometry and microarray analysis was employed to identify the binding partners and downstream mediators. CRISPR/Cas9 technology was used to knockout 14-3-3e in human chondrocytes. Signaling pathways, anabolic and catabolic reactions, as well as characterization and analysis of OA phenotypes were performed with either chondrocytes or OA animal models, accordingly. **Results:** Our previous genetic screen isolated TNFR2 as the PGRN-binding receptor (Tang, et al, Science, 2011). Remarkably, PGRN exhibits an approximately 600-fold higher binding affinity to TNFR2 than does TNF α . Additionally, PGRN-mediated protective effects against post traumatic osteoarthritis (PTOA) was also largely lost in TNFR2 $^{-/-}$ mice (Zhao, et al, ARD, 2015), indicating that the PGRN/TNFR2 pathway plays a critical role in PGRN-stimulated chondro-protective effects. Interestingly, 14-3-3e was identified as a novel component of TNFR2 receptor complex in response to PGRN stimulation in a proteomics screen (Fig1A-C). PGRN-activated signaling and anabolic activity was abolished in 14-3-3e knockout human chondrocytes and PGRN-mediated protective effects was also largely lost in inducible 14-3-3e knockout PTOA mouse model (Fig 1D-F). Further, Tgfb1 and Tgfb2 were isolated as the downstream mediators of PGRN

in a whole genome microarray (Fig1G,H), and blocking these receptors with their specific inhibitors also abolished PGRN's anabolic activity (Fig1I). **Conclusions:** Our results indicate that the PGRN/TNFR2/14-3-3e/Erk-Akt/Tgfb axis plays a pivotal role in chondrocyte metabolism and OA. These findings not only advance our understanding of the TNFR2 pathway in cartilage homeostasis and degeneration, but may also lead to the development of novel interventions for OA.

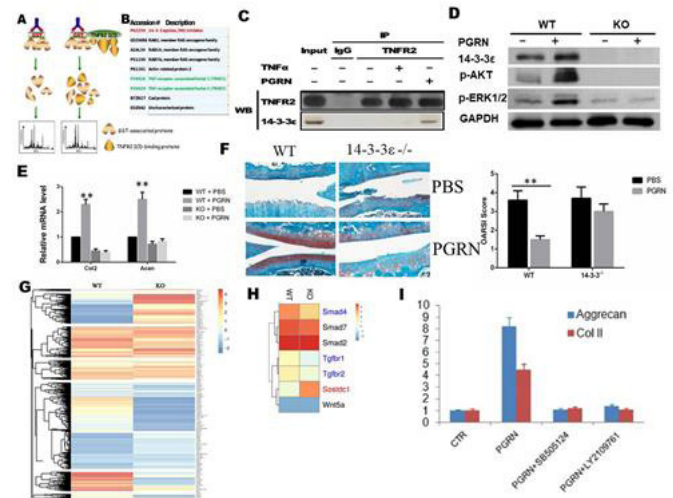


Fig1. PGRN/TNFR2/14-3-3e/Erk-Akt/Tgfb axis plays a pivotal role in chondrocytes and OA. (A) Scheme used to identify potential molecules binding to TNFR2 intracellular domains in response to PGRN stimulation. (B) Summary of the hits that were specifically recruited to TNFR2 complexes after treating chondrocytes with PGRN. (C) Co-IP assay showed 14-3-3e binds to TNFR2 in chondrocytes. (D-E) WT or 14-3-3e deficient human chondrocytes were treated with or without PGRN, western blot was used to determine the activation of signal molecules (D) and qPCR was performed to determine the mRNA level of Col2 and Acan (E). (F) Safranin O staining of knee joint obtained from ACLT WT or 14-3-3e $^{-/-}$ mice treated with or without PGRN. n=8 (G) Genome microarray analysis of WT and PGRN KO mice. Differentially hierarchical clustering of the top 300 differentially expressed genes in KO as compared to WT. (H) DAVID gene ontology analyses identify the genes which are up-regulated (red) or down-regulated (blue) genes in KO mice. (I) PGRN-stimulated expressions of Collagen II and Acan in the absence or presence of specific inhibitor for Tgfb1 (5µM, SB505124) or for Tgfb2 (5µM, LY2109761), assayed by real-time PCR.

Disclosures: **Wenyu Fu, None**

SUN-0238

Lin28a overexpression promotes chondrocyte reprogramming and protects from osteoarthritis in mice Yohan Jouan*^{1,2}, Joanna Sanna^{1,2}, Augustin Latourte^{1,2,3}, Pascal Richette^{1,2,3}, Hang-Korng Ea^{1,2,3}, Martine Cohen-Solal^{1,2}, Eric Hay^{1,2,3}. ¹Paris Diderot University, Paris, France, ²Inserm 1132, Paris, France, ³Hopital Lariboisière, Paris, France

Purpose: Osteoarthritis (OA) affects all joint tissues including bone (osteophyte, subchondral bone sclerosis) in addition to cartilage degradation. In OA, activated chondrocytes have a reduced anabolism, whereas catabolism and apoptosis are increased. Cartilage matrix lesions are irreversible due to the poor regeneration abilities. Lin28a is a RNA binding protein involved in tissue repairing processes. Here we asked if Lin28a overexpression in cartilage could promote dedifferentiation of osteoarthritic chondrocytes and regenerate cartilage matrix. **Methods:** Ex vivo assays were performed using explant cultures of femoral head of 10 week-old transgenic CreCol2ERLin28ac(Tg) mice. Lin28a overexpression was induced by hydroxyl tamoxifen. After 24 hours, chondrocyte activation was induced by Wnt3a for 48 hours. Supernatant was collected for western blot analysis. Samples were processed for mRNA extraction or for histological analysis. In vivo assay, OA was induced by meniscus destabilization (DMM) in CreCol2ERLin28ac(Tg) or Lin28ac(Tg) as controls. Recombination was induced 1 week before DMM (preventive assay) or 4 weeks after DMM (regenerative assay). Left knee was sham-operated. Cartilage and bone were analyzed 4 and 8 weeks after surgery. **Results:** Ex vivo Wnt3a induces a decrease in Col2, Aggrecan, Sox9, PRG4 expression and a reduced matrix proteoglycan content, thereby increased MMP3-13 expressions. Lin28a overexpression totally abolished this effect. Moreover, Lin28a overexpressing-explants revealed reduced apoptosis and increased cell proliferation, concomitantly with an increase stem cell marker mRNA. In regenerative assay, chondrocyte activation led to cartilage lesions (increased MMP and reduced PRG4 expression) at 4 weeks post DMM. At bone level, osteophytes and bone sclerosis are already detectable. At 8 weeks, cartilage breakdown is more severe and PRG4 protein is totally absent in control mice, but stabilized in CreCol2ERLin28ac(Tg) to same level than week 4. At 8 weeks, PRG4 expression is reactivated, suggesting reprogramming of mature chondrocytes towards progenitors. Moreover, osteophyte size is remarkably increased without subchondral bone changes compared to controls. In preventive assay, Lin28a overexpression has the same protective effect. **Conclusion:** Our data suggest that targeting Lin28a could enhance cell reprogramming, thus reversing chondrocyte activation. This promotes the preservation of remaining osteoarthritic cartilage.

Disclosures: **Yohan Jouan, None**

SUN-0239

NFI-C is Required for Chondrocyte Proliferation in Growth Plate during Postnatal Cartilage Development Joo-Cheol Park*, Dong-Seol Lee, Yeoung-Hyun Park, Chul Son. Seoul National University, Republic of Korea

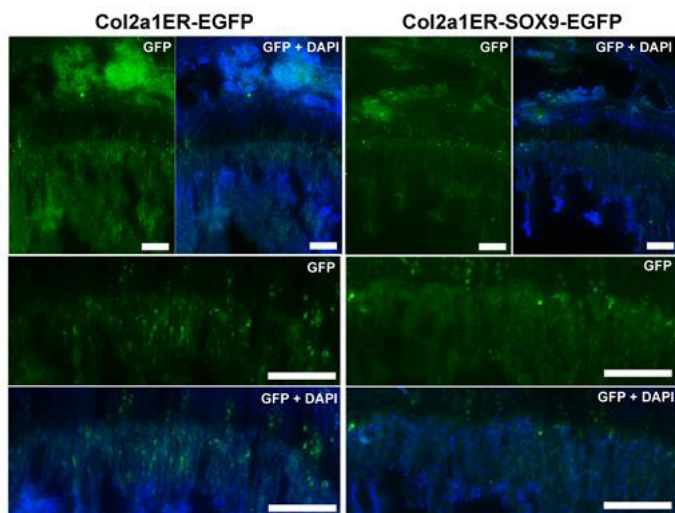
The nuclear factor I (NFI) gene family encodes site-specific transcription factors essential for the development of a number of organ systems. Our previous studies indicate that NFI-C is required for tooth root development and bone formation, but the exact function of NFI-C in cartilage development remains unknown. In this study, *Nfic*^{-/-} mice revealed decreased growth-plate lengths compared to WT. In particular, the width of the proliferating and hypertrophic zone in the growth plate was dramatically reduced in *Nfic*^{-/-} mice compared to WT. However, NFI-C disruption has no influence on prenatal cartilage development. In addition, cell proliferation rates of *Nfic*^{-/-} chondrocytes were decreased approximately 40% at 3 days and 70% at 5 days compared to WT, respectively. PCNA-positive cells were significantly diminished in the proliferating zone of *Nfic*^{-/-} mice compared to WT. In contrast, chondrocyte apoptosis was increased in the hypertrophic zone of *Nfic*^{-/-} mice compared to WT. *Nfic*^{-/-} chondrocytes exhibited increased p21 expression but decreased Cyclin D1 expression, strongly suggesting cell growth arrest due to the lack of Nfic activity. Further, *Nfic*^{-/-} chondrocytes exhibited increased caspase-3 activation. These results indicate that NFI-C disruption results in decreased femur length caused by reduction in the width of the growth plate, decreased chondrocyte proliferation, and increased chondrocyte apoptosis.

Disclosures: Joo-Cheol Park, None

SUN-0240

Downregulation of Sox9 in growth plate hypertrophic zone promotes chondrocyte-osteoblast transdifferentiation Julian Lui*, Shanna Yue, Audrey Lee, Kevin Barnes, Jeffrey Baron. Section on Growth and Development, United States

Longitudinal bone growth is driven by endochondral ossification, a process in which cartilage tissue is generated by growth plate chondrocytes and then remodeled into bone by osteoblasts. In the postnatal growth plate, as hypertrophic chondrocytes approach the chondro-osseous junction, they either undergo apoptosis, or as recent findings suggest, transdifferentiate into osteoblasts. The molecular mechanisms governing this switch in cell lineage is poorly understood. In the current study, laser capture microdissection followed by real-time PCR demonstrated that Sox9 was downregulated as growth plate chondrocytes underwent hypertrophic differentiation whereas osteoblast-associated genes (*Mmp9*, *Mmp13*, *Col1a1*, *Sp7*, and *Ibsp*) were modestly upregulated in the hypertrophic chondrocytes, even before they enter the metaphyseal bone. In transgenic mice that continue to express Sox9 at physiological levels in the hypertrophic zone, upregulation of these osteoblast-associated genes failed to occur ($P < 0.05$). In these transgenic mice, we performed lineage tracing experiments. GFP expression was induced in chondrocytes (using a tamoxifen-inducible *Col2a1-Cre* transgene) at 4 days of age, and then the number of GFP-expressing osteoblasts were counted in a defined region of metaphyseal bone below the growth plate at 2 and 4 weeks of age. In transgenic mice expressing Sox9, the number of cells transdifferentiating from chondrocytes to osteoblasts was suppressed (4.3 vs 1.5 at age 2 wks; 6.9 vs 2.4 at age 4 wks; wild-type versus Sox9 transgenic, $P < 0.01$ at both time points). Collectively, our findings suggest that Sox9 downregulation in hypertrophic chondrocytes promotes subsequent transdifferentiation into osteoblasts.



Disclosures: Julian Lui, None

SUN-0241

Glutamine and Glucose Metabolism Controls Chondrocyte Function during Endochondral Ossification Steve Stegen*, Kjell Laperre¹, Guy Eelen², Gianmarco Rinaldi³, Sophie Torrekens¹, Sarah-Maria Fendt³, Peter Carmeliet², Geert Carmeliet¹. ¹Clinical and Experimental Endocrinology, KU Leuven, Belgium, ²Angiogenesis and Vascular Metabolism, Vesalius Research Center, VIB/KU Leuven, Belgium, ³Cellular Metabolism and Metabolic Regulation, Vesalius Research Center, VIB/KU Leuven, Belgium

Endochondral ossification highly depends on proliferation and matrix deposition by growth plate chondrocytes, two energy-dependent anabolic processes. The avascularity of the growth plate requires controlled activity of hypoxia-inducible transcription factor HIF-1 α that may alter chondrocyte metabolism. However, the type of metabolic adaptations and their importance for bone development are largely unknown. Here, we identify the HIF prolyl hydroxylase 2 (PHD2) oxygen sensor as a central gatekeeper of chondrocyte metabolism and cartilage matrix. Prolonged HIF-1 α signaling in PHD2-deficient chondrocytes (Phd2chon⁻) leads to skeletal dysplasia by interfering with cellular bioenergetics and biosynthesis. Decreased glucose oxidation results in an energy deficit, which limits proliferation and reduces collagen synthesis. However, enhanced glutamine anaplerosis increases α -ketoglutarate (α KG) levels, which in turn increases collagen proline and lysine hydroxylation. This metabolically regulated collagen modification renders the cartilaginous matrix more resistant to protease-mediated degradation and thereby increases bone mass. To prove the specific contribution of the altered glutamine and glucose metabolism, we pharmacologically blocked the rate-limiting enzymes. Normalization of glucose oxidation in Phd2chon⁻ mice with dichloroacetic acid (DCA), a blocker of pyruvate dehydrogenase kinase (PDK), corrects the hypometabolic state and, consequently, matrix synthesis. DCA-treated Phd2chon⁻ mice display a further accumulation of cartilage remnants and bone mass, likely because the high glutamine-derived α KG levels stimulate collagen modification. Accordingly, blocking glutaminase (GLS) in DCA-treated mice decreases α KG levels and thereby normalizes completely the cartilage and bone phenotype to the level of wild-type mice. Thus, chondrocytic HIF-1 α signaling metabolically controls extracellular matrix properties and thereby regulates bone mass.

Disclosures: Steve Stegen, None

SUN-0242

Salmon calcitonin exerts more preventive effects than celecoxib on cartilage degeneration, subchondral bone microarchitecture deterioration and tactile allodynia in a rat model of lumbar facet joint osteoarthritis Faming Tian*, Yu Gou², Liu Zhang². ¹Medical Research Center, North China University of Science and Technology, China, ²Department of Orthopedic Surgery, Hebei Medical University, China

Objective: To evaluate and compare the effects of salmon calcitonin (sCT) and celecoxib (CLX) on cartilage, subchondral bone and tactile allodynia in a rat model of lumbar facet joint (FJ) osteoarthritis (OA). Method: Forty 3-month-old male Sprague-Dawley rats were randomly divided into four groups: 30 received surgical collagenase (type II) injections in the right L3-L6 facet joints followed by 8 weeks of treatment with normal saline, CLX or sCT, and the other 10 received sham surgery. Tactile allodynia was evaluated using von Frey filaments. All rats were euthanized after completing treatment, and changes of the cartilage and subchondral bone of the L4-L5 FJs and serum biomarkers were analyzed. Results: sCT ameliorated cartilage lesions and significantly increased aggrecan expression and decreased caspase-3 and ADAMTS-4 expression, whereas CLX only significantly decreased caspase-3 expression. According to the micro-computed tomography (micro-CT) analysis, sCT significantly increased the BMD, BV/TV, and Tb.Th; decreased the Tb.Sp, SMI and micro-CT score; and inhibited articular process hypertrophy. sCT possessed a better analgesic effect than CLX on days 42 and 56 postoperatively. The sCT treatment reduced the elevated COMP concentration in rats injected with collagenase (type II). Additionally, the serum COMP concentration was significantly correlated with the histological and micro-CT scores. Conclusions: Both sCT and CLX exerted preventive effects on FJ OA caused by collagenase (type II), but sCT showed more protective effects, particularly on maintaining cartilage metabolism, restraining the deterioration of the subchondral bone microarchitecture and tactile allodynia, and reducing serum COMP concentrations.

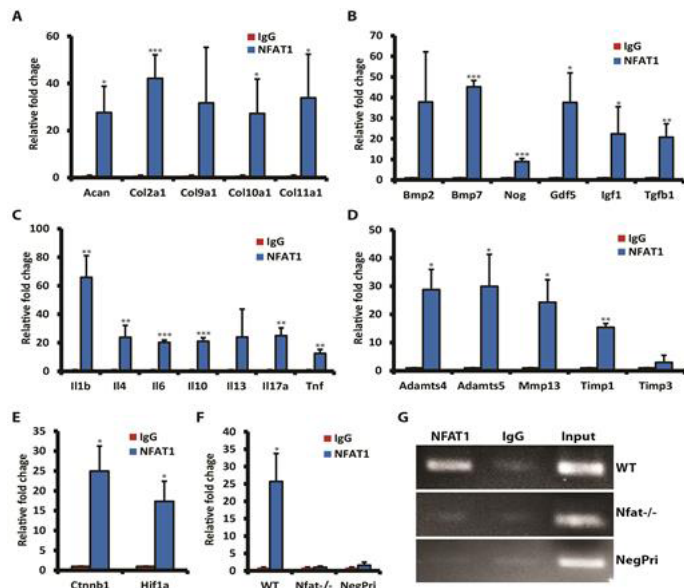
Disclosures: Faming Tian, None

SUN-0243

NFAT1 Protects Articular Cartilage Against Osteoarthritis by Directly Regulating Transcription of Specific Anabolic and Catabolic Genes Mingcai Zhang*, Qinghua Lu, Theodore Budden, Jinxi Wang. Harrington Laboratory for Molecular Orthopedics, Department of Orthopedic Surgery, University of Kansas Medical Center, United States

Purpose: Mice lacking NFAT1, a member of the nuclear factor of activated T cells (NFAT) family of transcription factors, exhibit osteoarthritis (OA). The precise molecular mechanism for NFAT1 deficiency-induced osteoarthritic cartilage degradation remains to be elucidated. This study aimed to investigate if NFAT1 protects articular cartilage (AC)

against OA by directly regulating the transcription of specific catabolic and anabolic genes in articular chondrocytes. **Methods:** Through a combined approach of gene expression analysis and web-based searching of NFAT1 binding consensus DNA sequences, 25 candidate target genes that displayed aberrant expression in *Nfat1*^{-/-} AC at the initiation stage of OA and possessed at least 4 NFAT1 binding sites in each promoter were selected and tested for NFAT1 transcriptional activities by chromatin immunoprecipitation (ChIP) and luciferase reporter assays using chromatin and chondrocytes isolated from AC of 3 to 4-month-old wild-type mice or *Nfat1*^{-/-} mice with early OA phenotype. Normal mouse IgG and a pair of primers without NFAT1 binding sequences served as negative controls to verify the ChIP specificity. **Results:** ChIP assays revealed that NFAT1 directly bound to the promoter of 21 of the 25 tested genes encoding cartilage-matrix proteins, growth factors, inflammatory cytokines, matrix-degrading proteinases, and specific transcription factors (Figure 1). Luciferase reporter assays of representative anabolic and catabolic genes demonstrated that NFAT1-DNA binding functionally regulated the promoter activity of specific target genes in wild-type chondrocytes, but not in *Nfat1*^{-/-} chondrocytes lacking functional NFAT1 protein. **Conclusions:** These results suggest that NFAT1 protects AC against OA by directly regulating the transcription of numerous target genes in articular chondrocytes. NFAT1 deficiency causes defective transcriptions of specific anabolic and catabolic genes in articular chondrocytes, leading to increased matrix catabolism and osteoarthritic cartilage degradation.



Disclosures: Mingcai Zhang, None

SUN-0244

Effect of Doxycycline on Osteochondral Graft Chondrocyte Viability Ex Vivo Brett Owens*, Li Yue. Brown University Alpert Medical School, United States

The surgical transplantation of fresh osteochondral (OC) grafts is an increasingly common procedure used to treat articular cartilage lesions. Fresh OC grafts have a limited window for transplantation, as chondrocyte viability significantly decreases after 14 days based on the current graft storage practices. Thus, it is critical to preserve fresh OC grafts without significant chondrocyte death. The antibiotic doxycycline has been shown to promote cartilage growth, disrupt chondrocyte differentiation, and improve chondrogenesis of human bone marrow-derived mesenchymal stem cells. This suggests the potential use of doxycycline to improve cartilage repair and delay the onset of osteoarthritis. However, it is unknown whether doxycycline delays chondrocyte death in OC grafts. We hypothesized that doxycycline prolongs fresh OC graft chondrocyte viability. To test this hypothesis, the calf cartilages purchased from local slaughter were aseptically harvested within 4 hours of death, and were punched into the plugs with a diameter of 4 mm. The plugs were cultured in 48-well plates at 37°C or 40°C in the presence or absence of doxycycline (10, 2 or 1 µg/ml) for 9 weeks, while the medium was changed weekly. Chondrocyte viability in plugs was examined using the LIVE/DEAD Viability/Cytotoxicity kit with calcein acetoxymethyl for live cells and ethidium homodimer-1 for dead cells, respectively. We found that 1 µg/ml of doxycycline is the optimized concentration to increase chondrocyte viability. When cultured at 37°C, the chondrocyte viability was 82%, 65%, 62%, 54%, 53%, and 29% at d0, d14, d28, d48, d56, and d63, respectively. However, the viability of chondrocytes was 16%, 0.32% and 0% when the plugs were cultured at 40°C for 14, 28, and 48 days, respectively. Treatment of doxycycline caused a significant increase in the viability of chondrocytes, which was demonstrated by an increase of 17% on d14 and d48, 11% on d56, and 27.6% on d63 in OC plugs at 37°C culture. In addition, doxycycline treatment (1 µg/ml) at 37°C attenuated decreased glycosaminoglycan content and reduced increased empty lacunae through immunohistochemical staining in plugs during the culture duration. In conclusion, doxycycline at a concentration of 1 µg/ml under 37°C delays OC graft chondrocyte death. These findings

provide a potential approach to preserve fresh OC grafts for patients with articular cartilage lesions who wait for OC graft transplantation.

Disclosures: Brett Owens, None

SUN-0245

Hajdu Cheney Syndrome Mutants are Susceptible to Osteoarthritis Stefano Zanotti*, Jennifer Wolf², David Bridgewater¹, Ernesto Canalis¹. ¹UConn Health, United States, ²University of Chicago, United States

Osteoarthritis is a degenerative disease of the joint characterized by compromised cartilage integrity, altered gene expression in articular chondrocytes and inflammation. NOTCH1 and NOTCH2 receptors and their ligand JAGGED1 are expressed by chondrocytes, and Notch plays a fundamental role in chondrocyte maturation. However, the role of Notch and its target genes in osteoarthritis has been controversial. Hajdu Cheney Syndrome (HCS) is a rare genetic disorder associated with NOTCH2 mutations in exon 34 that lead to the translation of a truncated and stable protein and NOTCH2 gain-of-function. Subjects afflicted by HCS have osteoporosis with fractures and inflammatory lesions of the distal phalanges that result in osteolysis. We created a mouse model (*Notch2tm1.1Ecan*) that reproduces the HCS mutation and manifests many aspects of the human disease. The availability of *Notch2tm1.1Ecan* mutants allowed us to determine whether HCS is associated with osteoarthritis. For this purpose, we destabilized the medial meniscus of 3-month-old *Notch2tm1.1Ecan* male mice and sex- and age-matched wild type littermates by resecting the medial meniscotibial ligament. Destabilized and sham-operated knees were analyzed for joint degeneration 2 months after the intervention. The expression of Notch target genes (*Hey1*, *Hey2* and *HeyL*) was increased in the femoral heads of *Notch2tm1.1Ecan* mice, verifying enhanced NOTCH2 signaling. Microcomputed tomography and histological analysis of medial tibial plateaus revealed modest differences in periarticular bone structures and articular cartilage integrity between *Notch2tm1.1Ecan* mutants and control littermates subjected to sham interventions. Following destabilization of the medial meniscus, *Notch2tm1.1Ecan* mutants had a significant increase in osteophyte volume and thickened subchondral bone compared to wild type littermates. Moreover, *Notch2tm1.1Ecan* mutants, exhibited histological signs of moderate to severe cartilage degeneration, demonstrating that joints of *Notch2tm1.1Ecan* mutants are sensitized to osteoarthritis progression. Primary chondrocytes from *Notch2tm1.1Ecan* mutants cultured on JAGGED1-coated substrates expressed increased IL6 transcripts, possibly explaining the susceptibility of *Notch2tm1.1Ecan* mice to osteoarthritis. In conclusion, *Notch2tm1.1Ecan* mutant mice are sensitized to the development of osteoarthritis and NOTCH2 activation may play a role in the pathogenesis of the disease.

Disclosures: Stefano Zanotti, None

SUN-0269

Associations between Circulating Osteoprogenitor (COP) cells, Parathyroid Hormone, Vitamin D and function in older adults Ahmed Al Saedi*, Steven Phu², Gustavo Duque¹. ¹Australian Institute for Musculoskeletal Science (AIMSS), The University of Melbourne and Western Health, St. Albans, VIC, Australia, ²Department of Medicine-Western Health, Melbourne Medical School, The University of Melbourne, Australia

Associations between Circulating Osteoprogenitor (COP) cells, Parathyroid Hormone, Vitamin D and function in older adults. **Authors:** Ahmed Al Saedi^{1,2}, Steven Phu^{1,2}, Piumali Gunawardene³, Sara Vogrin^{1,2}, Damian Myers^{1,2}, Gustavo Duque^{1,3} **Affiliations:** 1 Australian Institute for Musculoskeletal Science (AIMSS), The University of Melbourne and Western Health, St. Albans, VIC, Australia 2 Department of Medicine-Western Health, Melbourne Medical School, The University of Melbourne, St. Albans, VIC, Australia 3 Sydney Medical School Nepean, The University of Sydney, Penrith, NSW, Australia **Introduction:** Circulating osteoprogenitor (COP) cells have been linked to bone formation and osteogenesis during the initial stages of fracture healing. Recent studies have shown a strong association between low percentages of COP cells (%COP) and frailty and disability. Additionally, increased levels of COP cells have been associated to low bone mineral density. However, the association between serum levels of Parathyroid hormone (PTH) and vitamin D remain unknown. In this study we aimed to identify the potential associations between COP cells, parathyroid hormone, vitamin D and their clinical significance in older adults. **Methods:** A random sample of community-dwelling individuals aged 65 and older enrolled in the Nepean Osteoporosis and Frailty (NOF) Study (mean age 82.8; N = 77; 70% female). COP cells were identified by flow cytometry using selective gating of CD45/OCN+ cells and by Mean Fluorescence Intensity (MFI). Logistic regression models estimated the relationship between the percentage of COP cells and prevalent disability and frailty. **Results:** There was a positive correlation between PTH levels and COP cells (p=0.003). A trend towards a negative correlation for vitamin D and COP cells was also evident (p=0.060). No correlations were found between COP cells and bone mineral density at the heel. **Conclusions:** COP cells were positively correlated with PTH levels in older adults. This may suggest involvement of COP cells in bone turnover in particular the formation and mineralisation of bone. Whether pathological states such as hyperparathyroidism and vitamin D deficiency are also associated with significant changes in %COP remains to be determined.

Disclosures: Ahmed Al Saedi, None

SUN-0270

Total adiposity as reflected in body weight, rather than specific fat compartments, predicts incident low-trauma fractures in healthy non-osteoporotic post-menopausal women Emmanuel Biver*, Jessica Pepe, Alessandro De Sire, Thierry Chevalley, René Rizzoli, Serge Ferrari. Division of Bone Diseases, Geneva University Hospitals and Faculty of Medicine, University of Geneva, Switzerland

Purpose: Despite higher bone mineral density (BMD), individuals with high fat mass have an increased fracture risk. Cortical microstructure at non-weight bearing bone sites has been suggested to be inversely associated with visceral fat. It remains however unknown whether higher fracture risk is specifically associated with fat mass compartments, such as android or visceral fat, independent of body mass index (BMI) or body weight. We investigated whether incident low-trauma major osteoporotic fractures (MOF) would be associated with levels of a specific fat mass compartment in a cohort of community-dwelling healthy non-osteoporotic postmenopausal women. Methods: Six hundred and forty-four non-osteoporotic (T-score spine or hip >2.5SD) postmenopausal women (age 65.1 ± 1.5 yrs (mean ± SD), 15% with obesity defined as BMI <30kg/m²), enrolled in the Geneva Retirees Cohort, were prospectively evaluated over 5.7 ± 1.5 yrs for the occurrence of low-trauma MOF. At baseline, areal BMD and body composition were assessed by DXA, and FRAX fracture probability was calculated. Results: Thirty eight incident MOF (humerus n=13, wrist n=13, clinical and morphometric vertebral fractures n=9 and hip n=3) occurred in 34 women, while 534 women had no fracture. In Cox's proportional hazard models, MOF were positively associated with body weight, whole body fat mass, trunk and android fat compartments, and abdominal subcutaneous adipose tissue (HR per one SD increase of fat variable from 1.41 to 1.51, p<0.05 for all). Most associations with fat mass remained significant after adjustment for BMI, femoral neck BMD (Table) and FRAX (with BMD). However, they disappeared after adjustment for body weight (adjusted HR 0.87 to 1.19, p≥0.634 for all). In subgroups analyses, the associations were of higher magnitude in non-obese than in obese women [HR (95%CI) for trunk fat 1.99 (1.25, 3.17), p=0.004 vs 1.32 (0.34, 5.13), p=0.686, respectively]. Conclusion: Whole body fat mass and trunk fat predict incident MOF independently of BMI, BMD and FRAX, but not of body weight, in non-osteoporotic women. These data do not support the hypothesis of a metabolic deleterious impact of a specific visceral fat compartment on bone fragility but suggest that total adiposity, as reflected in body weight, is the main contributor to fracture risk. These findings need however to be confirmed in larger populations including men and more hip fractures before generalization.

Table: Associations between fat mass compartments and the risk of incident low-trauma major osteoporotic fractures in healthy non-osteoporotic postmenopausal women.

	Crude associations		Adjusted for BMI		Adjusted for femoral neck BMD	
	HR (95%CI)	P-value	HR (95%CI)	P-value	HR (95%CI)	P-value
Bodyweight	1.51 (1.07, 2.14)	0.019	NA		1.67 (1.16, 2.40)	0.006
BMI	1.27 (0.90, 1.78)	0.176	NA		1.34 (0.94, 1.90)	0.106
Whole bodyfat	1.43 (1.04, 1.98)	0.029	2.65 (1.17, 6.03)	0.020	1.53 (1.10, 2.14)	0.012
Trunk fat	1.48 (1.06, 2.05)	0.020	2.72 (1.25, 5.92)	0.012	1.58 (1.12, 2.21)	0.009
Android fat	1.42 (1.02, 1.97)	0.036	2.08 (1.00, 4.34)	0.051	1.50 (1.07, 2.09)	0.017
VAT	1.40 (1.00, 1.95)	0.050	1.61 (0.86, 3.01)	0.134	1.48 (1.05, 2.08)	0.024
SAT	1.41 (1.01, 1.97)	0.046	1.91 (0.91, 4.00)	0.085	1.48 (1.05, 2.09)	0.025
Gynoid fat	1.33 (0.96, 1.84)	0.086	1.34 (0.76, 2.34)	0.313	1.40 (1.00, 1.95)	0.049

BMI, body mass index; VAT, visceral adipose tissue; SAT, subcutaneous adipose tissue; NA, not applicable

Disclosures: **Emmanuel Biver, None**

SUN-0271

Overexpression of MitoNEET in osteoblasts leads to impaired bone mass and energy metabolism in mice Phuong Le*, Sheila Bornstein, Victoria Demambro, Clifford Rosen, Anyonya Guntur. MCCR, United States

Osteoblasts during in vitro differentiation increase glycolytic ATP production rates in response to exogenous glucose supply. To study the role of the two major ATP generating pathways in vivo in osteoblasts we overexpressed MitoNEET a mitochondrial membrane protein generating a novel osteoblast specific overexpression mouse model. Previous work shows that overexpression of MitoNEET in adipocytes leads to decreased oxidative phosphorylation and a concomitant increase in glycolysis. In our overexpression model, mice containing the tetracycline responsive element fused to the MitoNEET ORF were crossed to Runx2 rTA to generate osteoblast specific overexpression. Two groups of 4 week old male mice were generated and Doxycycline+Saccharin (Dox), and Saccharin (controls) were introduced through drinking water for 12 weeks. Tibiae from mice were isolated and qRT-PCR analysis performed showing a significant increase in MitoNEET expression in bone. Furthermore, we did not find any increases in MitoNEET gene expression in WAT, BAT or liver suggesting that the overexpression was specific for bone. Trabecular bone microarchitecture was assessed in the distal femoral metaphysis, whereas cortical bone morphology was assessed at the femoral mid-shaft with μ CT analysis at 16 weeks of age. Dox treated male mice had significantly lower trabecular bone mineral density and trabecular thickness, along with lower cortical tissue mineral density (Ct.TMD, -0.7%), medullary area (Ma.Ar, -11.8%), total area (Tt.Ar, -10.7%), and minimum moment of inertia (Imin, -22%) compared to controls. Next, we performed indirect calorimetry to obtain energy expenditure (EE) and respiratory quotient (RQ) data. We found a significant increase in day time ener-

gy expenditure suggesting modulation in circadian rhythms. Interestingly, 24 hour RQ was significantly lower in the MitoNEET overexpressing animals, suggesting oxidation of fat (n=8-10, p=0.03). There was no difference in food consumption with the Dox group drinking significantly less amount of water (n=8-10, p=0.009). We also performed additional control experiments in metabolic cages on mice fed Saccharin and Saccharin+Dox and identified that the metabolic changes we observed were specific for MitoNEET overexpression. In sum, manipulating MitoNEET expression specifically in the osteoblast impairs bone mass and leads to decreased, energy expenditure and respiratory quotient in male mice potentially affecting whole body energy metabolism.

Disclosures: **Phuong Le, None**

SUN-0272

Energy metabolism in the bone is associated with histomorphometric changes in rats with hyperthyroidism Liao Cui*, Zhuoqing Hu, Minqun Du, Yajun Yang. Department of pharmacology, Guangdong Medical University, China

Hyperthyroidism led to a higher frequency of bone remodelling and net bone loss. With the development of proteomics, the molecular mechanisms of osteoblast and osteoclast biology have been identified through several proteomic analyses. Nevertheless, the underlying histological consequence of hyperthyroidism remains to be elucidated by bone proteomic analysis. Therefore, we assessed histomorphometric changes induced by thyroxine (T₄, 250 μ g/kg/day) in 3-month-old hyperthyroid male rats and examined whether the potential mechanism of these changes is related to bone changes by using isobaric tags for relative and absolute quantification (iTRAQ). Compared with the control rats (n=8), hyperthyroid rats (n=8) showed a reduction in the fifth lumbar vertebral BMD as well as in the entire femoral BMD (p=0.033 and 0.026, respectively). Histomorphometric analysis of the proximal tibial metaphysis showed that the percentage of the trabecular area, trabecular number, and percentage of the cortical bone area in the hyperthyroid rats significantly decreased compared with those of the control rats. Conversely, bone formation rate (per unit of bone surface and bone volume), percentage of the osteoclast perimeter, trabecular separation, and endosteal mineral apposition rate in the hyperthyroid rats significantly increased compared with the control rats (all p<0.05). Micro-CT three-dimensional structural changes in the proximal tibial metaphysis: compared with CON group, the connective density, volumetric bone density, bone volume fraction, number of trabecular bones and trabecular thickness were decreased in hyperthyroid group, but structural model index increased (all P<0.05). Except for stiffness, all bone biomechanical properties of the femur showed a significant decreasing trend in the hyperthyroid rats versus the control rats (all p<0.05). Serum levels of osteocalcin, alkaline phosphatase, terminal telopeptides of type β collagen, and tartrate-resistant acid phosphatase were higher in the hyperthyroid rats than in the control rats (all p<0.05). Using iTRAQ, the expression levels of 1,310 proteins in left femurs were found to be significantly different between the hyperthyroid and control rats (711 proteins were upregulated and 599 were downregulated in hyperthyroid rats). Gene Ontology and Kyoto Encyclopedia of Genes and Genomes pathway enrichment analyses showed that most of the enzymes in the glycolysis-tricarboxylic acid (TCA) cycle-oxidative phosphorylation signalling pathway were upregulated in hyperthyroid rats, and seven differentially expressed proteins were selected to verify the iTRAQ results using western blotting. Energy metabolism via the glycolysis-TCA cycle-oxidative phosphorylation pathway is positively associated with T₄-induced bone histomorphometric changes in rats.

Disclosures: **Liao Cui, None**

SUN-0273

Deficiency of Long Non-Coding RNA ADPC Impairs Bone and Adipose Tissue Metabolism Yao Liu*^{1,2}, En Luo², Junxiang Lian^{1,2}, Qisheng Tu¹, Zoe(Xiaofang) Zhu^{1,3}, Jake(Jinkun) Chen^{1,4}. ¹Division of Oral Biology Tufts University School of Dental Medicine, Boston, MA, United States, ²State Key Laboratory of Oral Diseases, National Clinical Research Center for Oral Diseases, West China Hospital of Stomatology, Sichuan University, Chengdu, China, ³Shanghai Jiaotong University, China, ⁴Department of Developmental, Molecular and Chemical Biology Sackler School of Graduate Biomedical Sciences Tufts University School of Medicine, Boston, MA, United States

Objectives. The long non-coding (lnc) RNA ANRIL is a 58-kilobase (kb) interval on human chromosome 9p21 and associated with coronary artery disease, periodontitis, diabetes mellitus and cancers. In mouse genome there is an orthologous lncRNA of ANRIL on the chromosome 4 known as AK148321, temporarily termed lncRNA ADPC. We hypothesized that ADPC has the similar biological functions as ANRIL playing important regulatory roles in bone and adipose tissue metabolism. We planned to use AK148321 knockout mice to study the roles and mechanism of ADPC in vitro and in vivo. Materials and Methods. Mice were genotypically separated into 3 groups as AK148321-KO (homozygous, hm), heterozygous (ht) and wild type (WT). Bone marrow stem cells (BMSCs) were isolated and cultured with osteo/adipo- genesis-inducing medium, respectively. In vitro studies included CCK8 cell proliferation assay, scratch migration assay, quantitative RT-PCR, Alizarin Red staining (ARS), ALP staining and oil red O staining. Bone and adipose tissues were analyzed by Micro CT scanning and histological examination. Osteo/adipo- genetic markers (osteogenesis: Runx2, OCN, BMP-2, ALP; adipogenesis: FAS, aP2, C/EBP α), and metabolic and

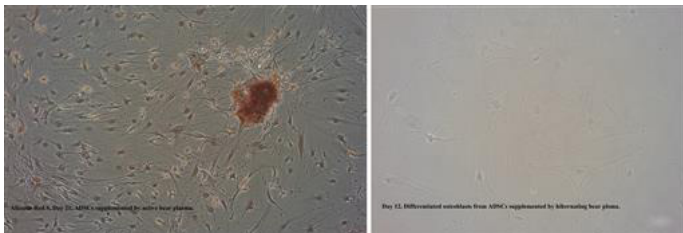
inflammatory markers (PPAR γ , CXCR4, APN, IL-6 and TGF β) were also tested. Results. The expression of AK148321 in BMSCs increased during the early stage of osteogenesis, while decreasing in adipogenesis. The enhancement of migration and proliferation in hm group were observed comparing with ht and WT groups in vitro. The expression of SDF-1 and MMP9 were upregulated in hm group. The reducing of osteogenesis and mild enhancing of adipogenesis were found by qPCR and staining analysis, while the expression of inflammation markers mildly increasing in hm group. The obvious phenotyping differences of bone and white adipose tissue (WAT) appeared until 8 weeks with the osteogenic markers downregulated and reduced bone mineralization in hm. Upregulation of adipogenic markers appeared in hm comparing with ht and WT groups. There was a slight increasing of inflammation markers in hm group. Conclusions. Deletion of lncRNA ADPC in mice impaired bone formation and enhanced inflammation. At the meantime ADPC deficiency promoted adipogenesis. ADPC represents an important regulatory element in bone and fat tissue metabolism. Currently we are further studying the epigenetic mechanism and molecular signaling pathway of how ADPC exerts its effects in metabolism of a variety of tissues.

Disclosures: **Yao Liu**, None

SUN-0274

Differentiation of Japanese Black Bears' Adipose-Derived Stem Cells to Osteoblasts Alireza Nasoori^{*1}, Yuko Okamatsu-Ogura², Woongchul Shin², Michito Shimozuru¹, Mohamed Abdallah Mohamed Moustafa¹, Toshio Tsubota¹. ¹Laboratory of Wildlife Biology and Medicine, Department of Environmental Veterinary Science, Graduate School of Veterinary Medicine, Hokkaido University, Japan, ²Department of Biomedical Sciences, Graduate School of Veterinary Medicine, Hokkaido University, Japan

Background: Bears are resistant to disuse bone loss in 5 months of hibernation. Therefore, understanding bears' bone cell response would enable bone biologists to develop therapeutic measures for osteoporosis. Accordingly, here we report our methodology by which we recruited bears' adipose derived stem cells (ADSCs) to be differentiated to osteoblasts. Methods: Adipose tissue was obtained from 4 mature male Japanese black bears in active season (September). The animals – based on our institutional rules for handling wild animals – were anesthetized by medetomidin and tiletamine/zolazepam. The samples, which were obtained from the inguinal and intrascapular areas, were delivered to lab within 72 hours at room temperature. The tissues were digested by collagenase with BSA and DMEM for 90 min at 37°C. After twice filtrations (200 and 20 μ m) and centrifugations (1000 rpm/5min), the ADSCs were isolated, and then preserved at -80°C. After 4 months, the ADSCs were cultured on dish with DMEM with 10% FCS. After 2 subcultures, the cells were treated with 50 mM ascorbic acid, 10 mM beta glycerophosphate, 100 nM dexamethasone in α -MEM for 21 days. The cells were supplemented by 10% FCS, or 10% active bear plasma (ABP) or hibernating bear plasma (HBP), and were incubated at 37°C with 5% CO₂. The cells were assessed by observation and Alizarin Red S staining. Results: After 4 months of preservation, bears' ADSCs proliferated well. The cells supplemented by FCS and ABP both could differentiate well. Whereas, HBP-supplemented cells showed poor differentiation. Differentiated cells were trigonal or polygonal after 21 days. Cell size by FCS and ABP supplementations were rather similar, and appeared larger than HBP-supplemented cells. Alizarin Red S showed mineralization in all groups. However, FCS and ABP-cultured cells had more calcium accumulation than HBP. Conclusions: We observed that Japanese black bears' ADSCs differentiated to osteoblasts. The differentiation was affected by cell supplementations; the use of active bear plasma in cell culture resulted in more differentiation and mineralization than the use of hibernating bear plasma. The use of bear plasma in this study showed its effectiveness for bear ADSCs differentiation. Further investigations are required to check gene expression for bears' osteoblasts proliferation and differentiation when cells are treated with different supplementations.



Disclosures: **Alireza Nasoori**, None

SUN-0275

Uc-dpMGP is associated with body composition and BMD in type 2 diabetes mellitus Natascha Schweighofer^{*1}, Christoph Haudum¹, Michaela Goschnik², Ewald Kolesnik³, Ines Mursic¹, Albrecht Schmidt³, Thomas R Pieber¹, Barbara Obermayer-Pietsch¹. ¹Div. Endocrinology and Diabetology, Medical University Graz, Austria, ²Endocrinology Lab Platform, Medical University Graz, Austria, ³Div. Cardiology, Medical University Graz, Austria

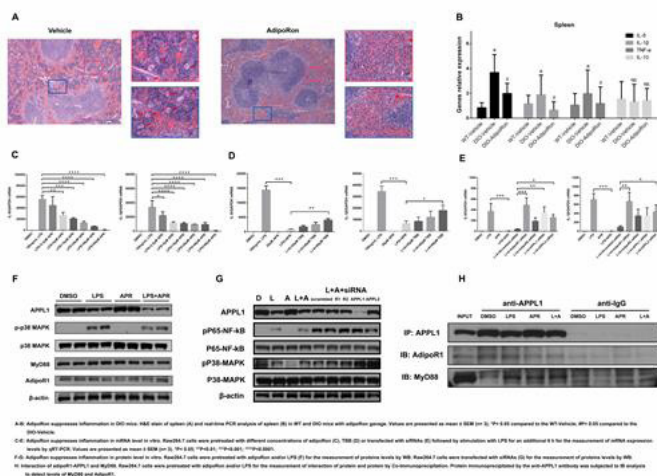
Body composition significantly influences the development of type 2 diabetes mellitus (T2DM) which affects bone metabolism and strength. Matrix gla protein (MGP) has been associated with bone parameters, but also with cardiovascular risk in patients with and without T2DM. We investigated whether uncarboxylated, dephosphorylated MGP (uc-dpMGP) is associated with parameters of body composition, bone density and clinical parameters, and whether these associations change during diabetes progression in lean and obese subjects. We analysed data from the BioPersMed cohort (n=966, 531 females and 435 males, mean age 58 +/- 9 years), a prospective cohort study of asymptomatic patients at cardiovascular risk with broad clinical and lab phenotyping. T2DM, prediabetic and non T2DM patients were defined according to ADA criteria. Uc-dpMGP was measured with IDS-iSYS InaKtif MGP Kit. Body composition and bone mineral density were determined by Lunar iDXA. Uc-dpMGP correlated in T2DM with tissue and overall mass negatively in lean (both r=-0.78; p=0.039) and positively in obese patients (both r=0.27; p=0.047 and p=0.044, respectively) and with lean and fat free mass in obese pre-diabetes patients (both -0.30; p=0.007). A correlation of regional fat distribution with uc-dpMGP was seen in non-diabetic (both lean and obese) and obese prediabetic patients. Furthermore, uc-dpMGP and total fat mass correlated positively in both lean (r=0.26; p=0.004) and obese (r=0.18; p=0.046) non-diabetic patients, but only in obese prediabetic (r=0.43; p<0.0001) and obese diabetic (r=0.30; p=0.025) patients. Total bone mass and uc-dpMGP correlated differentially in obese prediabetic patients and T2DM. As MGP is expressed in fat tissue, uc-dp MGP might have a potential role as a modulator of body composition and fat distribution which changes during diabetes progression. Our data implicate an association of uc-dp MGP depending on differentially carboxylated and phosphorylated forms of MGP.

Disclosures: **Natascha Schweighofer**, None

SUN-0276

AdipoRon Alleviates Diabetic Bone Disorders via Suppressing Inflammation Wei Qiu^{*1}, Jake Chen², Qisheng Tu², Xingwen Wu², Xuedong Zhou¹, Junxiang Lian². ¹West China School of Stomatology, Sichuan University, China, ²Tufts Univ. School of Dental Medicine, United States

Objectives: Diabetic bone disorders including osteoporosis, arthritis and periodontitis cause an increase in bone fractures, delay healing of fractures, and affect the quality of life of patients. AdipoRon, a recently found orally active small molecule, binds and activates both adiponectin receptors (AdipoR1, R2), with potent effects of anti-diabetes and prolonging shortened life of diabetic mice. However, its effects and underlie mechanisms of anti-inflammation on diabetic bone disorders are unknown. In this study, we investigated whether AdipoRon could suppress inflammation in diet-induced obesity (DIO) mice and explored the molecular mechanisms of signal transduction in the process. Our findings suggest a promising approach for the treatment of bone diseases via suppressing inflammation particularly in diabetes patients. Materials, Methods and Results: DIO mice with AdipoRon gavage showed an decreased number of multinucleated giant cells in spleen by histomorphometry analysis (Fig. A). Real-time PCR analysis exhibited that the increased mRNA expressions of inflammation-associated cytokines (IL-6, IL-1 β , TNF- α and IL-10) were reversed in DIO mice with AdipoRon treatment in spleen (Fig. B), bone marrow and white adipose tissues (data not shown). In vitro experiments, bone marrow-derived macrophages (BMMs) (data not shown) and RAW264.7 cells were stimulated by AdipoRon and Lipopolysaccharides (LPS) separately or synergistically. Results of Real-time PCR and Western blot analysis showed that AdipoRon suppressed LPS-stimulated inflammatory environment (Figs. C, F). Functional inhibition experiments (Pharmacological inhibitor TBB and siRNA knockdown) demonstrated the involvement of AdipoR1, APPL1/2 and CK2 axis in signal pathway (Figs. D, E, G). Co-immunoprecipitation assays indicated that the interaction of AdipoR1-APPL1 and MyD88 blocked the signal transduction in macrophages stimulated by LPS (Fig. H). Conclusions: AdipoRon suppresses diabetes-induced systemic inflammation in DIO mice and reverses LPS-stimulated inflammatory environment in the early phase of differentiation of BMMs and RAW264.7 cells via the interaction with AdipoR1-APPL1 and MyD88. In summary, AdipoRon represents a potential molecule for the treatment of diabetic bone disorders via strongly suppressing inflammation.



Disclosures: **Wei Qiu**, None

SUN-0277

Lipid Droplets Contribute to the Bioenergetic Capacity of Osteoblasts by Supplying Endogenous Fatty Acids for Mitochondrial Respiration Elizabeth Rendina-Ruedy^{*1}, Ron Helderman¹, Michael Czech², Clifford Rosen¹. ¹Maine Medical Center Research Institute, United States, ²Program in Molecular Medicine, University of Massachusetts Medical School, United States

Bone formation by the osteoblast has been described as an energy-demanding process which requires various substrates to generate cellular energy or adenosine triphosphate (ATP). As such, much of the interest surrounding osteoblast substrate utilization has been focused on these cells unique ability to metabolize glucose via aerobic glycolysis. In addition to glucose osteoblasts also require fatty acids (FAs) which can undergo β -oxidation and subsequent oxidative phosphorylation for energy generation. Until recently the source of these fatty acids had remained somewhat illusive and presumed to primarily be supplied from exogenous sources, however, we now know that FAs can also be mobilized from endogenous, lipid droplets. Therefore, we aimed to further characterize lipid droplet function in osteoblasts throughout their differentiation by determining their contribution to overall bioenergetic capacity. The dependency of primary bone marrow stromal cells (Day 0 osteogenic differentiation), osteoprogenitor (Day 2 osteogenic differentiation), or mature osteoblasts (Day 7 osteogenic differentiation) on endogenous FAs for mitochondrial respiration was determined by first inhibiting FA (etomoxir) utilization and measuring the change in oxygen consumption rate (OCAR). Afterwards, glutamine (BPTES) and glucose/ pyruvate (UK5099) utilization was inhibited and dependency was calculated based on any further change in OCAR. Alternatively, the capacity of the cells to utilize endogenous FAs was measured by directing the cells to utilize FAs by inhibiting glutamine and glucose/ pyruvate while measuring OCAR, and then subsequently blocking FAs. Interestingly, our results demonstrate bone marrow stromal cells depend more on endogenous FAs vs. glucose or glutamine, while maintaining a similar capacity to use FAs and glucose when exogenous substrates are limited. Osteoprogenitor cells and mature osteoblasts were equally dependent on endogenous glucose and FAs and have a similar capacity to use these substrates. Cells throughout osteoblast differentiation demonstrated a lower capacity to use endogenous glutamine, and the cells did not rely on this substrate for mitochondrial respiration. While studies are ongoing to further delineate the role of lipid droplets in osteoblasts, these results suggest that lipid droplets supply a considerable amount of FAs for mitochondrial respiration during osteoblast differentiation.

Disclosures: **Elizabeth Rendina-Ruedy**, None

SUN-0278

Complex Role for PPAR γ in Bone, Inflammation and Immune function in Aging Animals Raysa Rosario^{*}, Ashwin Ajith, Ke-Hong Ding, Ranya Elsayed, Yun Su, Anatolij Horuzsko, Mohammed Elsalanty, Meghan Mcgee Lawrence, Carlos Isales, Xing-Ming Shi. Medical College of Georgia, United States

Aging is a state of chronic low-grade inflammation, and is accompanied by bone loss, marrow fat accumulation, and decline of immune function. Peroxisome proliferator-activated receptor gamma (PPAR γ) is a key transcription factor regulating adipocyte differentiation and function. The adipose tissues produce many factors including adipokines, inflammatory cytokines and chemokines that may contribute significantly to the aging process. In the present study, we hypothesized that inhibition of PPAR γ would reduce fat-generated inflammatory responses, improve immune function, and decrease age related bone loss. To test this hypothesis, we treated young (6mo) and old (23mo) female C57BL/6 mice with a PPAR γ antagonist GW9662 (1mg/kg body weight, daily IP injection for 6 weeks) and examined the effects on bone mass, lymphoid to myeloid cell lineage skewing, and the expression profiles

of inflammation related genes. micro-CT analysis showed that GW treatment significantly increased Tb.Th, but also the Tb.Sp in old mice. GW treatment increased BV/TV and Tb.N in young mice, although these increases were not statistically significant. These results suggested that inhibition of PPAR γ has limited beneficial effect on bone mass in old mice. FACS analysis data showed that in the bone marrow, GW treatment significantly increased lymphoid and decreased myeloid lineage cells in young mice, as indicated by large increases in CD3/CD11b and CD4/CD8 ratios, and decreased the Ly6C/Ly6G ratio. GW treatment increased CD4/CD8 ratio significantly only in the old mice. In the spleen, GW significantly increased the CD3/CD11b ratio in young, and CD4/CD8 ratio in old mice. GW treatment significantly decreased Ly6C/Ly6G ratio in both young and old mice. Similar to that seen in bone marrow and spleen, in peripheral blood, GW treatment increased CD4/CD8 ratio in the old, but only decreased Ly6C/Ly6G ratio in the young mice. These data indicate that inhibition of PPAR γ can significantly improve immune functions of the old mice by increasing the numbers of CD4+CD8+ T cells in blood, spleen, and bone marrow. Interestingly, NanoString profiling of inflammation related genes in bone cells revealed opposite effects of GW treatment in young vs. old mice; i.e., genes whose expression are downregulated by GW in bone cells of the young mice are upregulated in the old mice. Taken together, these data demonstrate that while inhibiting PPAR γ can improve immune function in older animals, it may actually exacerbate the inflamm-aging. Thus, tissue or site-specific approaches should be considered when PPAR γ is targeted for therapeutic interventions.

Disclosures: **Raysa Rosario**, None

SUN-0279

Mouse Model of Severe Osteogenesis Imperfecta is Protected Against High-Fat Diet Induced Obesity but not against High-Fat Diet Induced Insulin Resistance Josephine T. Tauer^{*}, Iris Boraschi-Diaz, Svetlana Komarova. Shriners Hospital for Children and Faculty of Dentistry, McGill University, Canada

Objective: Osteogenesis imperfecta (OI) is a genetic disorder mainly caused by mutations in collagen type I, and characterised by high bone turnover leading to low bone mass and high fracture rates. Recently, we have shown that young Col1a1Jrt/+ mice - mouse model of severe OI - exhibit beside high bone turnover, altered glucose/insulin metabolism, and energy expenditure, due to elevated levels of undercarboxylated osteocalcin, a novel bone-derived hormone that affects insulin production and sensitivity. Here we examined the effect of long-term high-fat diet on weight gain, glucose metabolism, and bone properties in Col1a1Jrt/+ mice. Methods: Starting at an age of 4 weeks, male and female wild-type (WT) and OI mice were fed with either high-fat diet (60%, HFD) or a matched low-fat diet (10%, LFD) for 26 weeks. Body weight was measured weekly and glucose metabolism by glucose tolerance test every 4 weeks. Long bone properties were examined by MicroCT and 3-point-bending test at the end of the study. Results: At 4-weeks of age, male and female OI mice had 20% lower body mass than WT littermates. WT male and female mice on LFD gained 0.65 \pm 0.03 g/week and 0.39 \pm 0.02 g/week, respectively, while on HFD males gained 1.00 \pm 0.05 g/week and females 1.10 \pm 0.06 g/week. Compared to WT mice, male and female OI mice showed significantly lower increase in body mass. Female OI mice gained about 0.28 \pm 0.02 g/week on LFD and 0.62 \pm 0.04 g/week on HFD. Male OI mice were protected from HFD-induced weight gain and showed a gain in body mass of 0.44 \pm 0.02 g/week on LFD and 0.46 \pm 0.02 g/week on HFD. In WT mice, HFD-induced gain of body mass coincided with an increase in white adipose tissue and liver weight, whereas in OI white adipose tissue and liver weight was not affected. No diet-induced changes in brown adipose tissue, heart, spleen, or pancreas weight was observed in WT or OI mice. Glucose tolerance test demonstrated HFD-induced diabetic changes in glucose metabolism in both WT and OI mice. Trabecular structure as well as mechanical properties of long bones were significantly different between WT and OI but were not affected by LFD or HFD. Conclusion: Here we show for the first time that mice with a severe form of OI, in particular males, are protected against HFD-induced weight gain, but not from HFD-induced insulin resistance disclosing an altered fat and energy metabolism in OI.

Disclosures: **Josephine T. Tauer**, None

SUN-0280

FSH is Positively Associated with Vertebral Bone Marrow Adiposity in Postmenopausal Women from the AGES-Reykjavik Cohort Annegreet G. Veldhuis-Vlug^{*1}, Gina N. Woods², Sigurdur Sigurdsson³, Susan K Ewing⁴, Phuong T. Le⁵, Trisha F. Hue⁴, Eric Vittinghoff⁴, Kaipin Xu⁶, Vilundur Gudnason⁷, Gunnar Sigurdsson⁷, Deborah M. Kado⁹, Gudny Eiriksdottir³, Tamara Harris⁸, Xiaojuan Li⁶, Clifford J Rosen⁵, Ann V. Schwartz¹. ¹Academic Medical Center dept of Endocrinology and Center for Clinical and Translational Research, Maine Medical Center Research Institute, Netherlands, ²Dept. Medicine, University of California San Diego and VA San Diego Healthcare System, United States, ³Icelandic Heart Association, Iceland, ⁴Department of Epidemiology and Biostatistics, University of California San Francisco, United States, ⁵Center for Clinical and Translational Research, Maine Medical Center Research Institute, United States, ⁶Program of Advanced Musculoskeletal Imaging (PAMI), Cleveland Clinic, United States, ⁷Icelandic Heart Association Faculty of Medicine, University of Iceland, Iceland, ⁸National Institute on Aging, National Institutes of Health (NIA, NIH), United States, ⁹Dept of Medicine and Department of Family Medicine and Public Health, University of California, United States

Purpose Bone marrow adiposity increases with age, particularly in women around menopause when estradiol levels decrease and follicle stimulating hormone (FSH) levels increase. Increased bone marrow adiposity is associated with osteoporosis and vertebral fractures. Understanding the factors that regulate bone marrow adiposity in older adults may lead to novel mechanisms for combating age-related bone loss. Postmenopausal hormonal replacement therapy, increasing estradiol and decreasing FSH levels, decreases bone marrow adiposity. A recent study in mice showed that blocking FSH signaling with an antibody also decreases bone marrow adiposity following ovariectomy. The association between FSH and bone marrow adiposity in humans has not been previously reported. Methods We hypothesized that in humans higher FSH levels are associated with greater bone marrow adiposity. To test this hypothesis, we performed a cross-sectional, observational study in the AGES-Reykjavik cohort. In 237 women and 245 men, we measured vertebral (L1-L4) bone marrow adipose tissue (BMAT, %) by magnetic resonance spectroscopy and serum FSH concentration by ELISA. Results In older women (mean age 80.6 years) with a mean FSH of 71.5 IU/L and a mean vertebral BMAT of 55%, mean vertebral BMAT was 0.65% greater for each 10 IU/L increment of FSH (95% CI: 0.19, 1.10, p=0.006) in linear regression models adjusted for age, BMI and estradiol. In older men (mean age 82.4 years) with a mean FSH of 19.0 IU/L and a mean vertebral BMAT of 54%, there was no evidence of an association between vertebral BMAT and FSH in unadjusted (beta 0.23, 95% CI: -0.42, 0.87, p=0.49) or adjusted (beta -0.25, 95% CI: -0.94, 0.45, p=0.48) models. Conclusion Higher FSH is associated with greater vertebral bone marrow adiposity in older women but not in men. Longitudinal studies are needed to determine whether higher FSH levels predict increases in bone marrow adiposity in older adults.

Disclosures: *Annegreet G. Veldhuis-Vlug, None*

SUN-0281

Network analysis of skeletal muscle during spaceflight in male mice David Waning^{*1}, Paul Childress², Raina Kumar³, George Dimitrov³, Bintu Sowe⁴, Aarti Gautam⁵, Nabanur Chakraborty⁶, Rasha Hammamieh⁵, Melissa Kacena². ¹Penn State College of Medicine, United States, ²Indiana University School of Medicine, United States, ³Advanced Biomedical Computing Center, NCI, United States, ⁴ORISE, US Army Center for Environmental Health Research, United States, ⁵Integrative Systems Biology, US Army Center for Environmental Health Research, United States, ⁶Geneva Foundation, US Army Center for Environmental Health Research, United States

The unloading associated with spaceflight results in the rapid loss of bone and muscle tissue thereby affecting functionality. These are two of the most concerning physiologic changes that occur in space and could limit long-term occupation in space. Thus, a better understanding of the mechanisms of changes to bone and muscle could lead to development of improved therapies to counteract both spaceflight and terrestrial-based bone and muscle dysfunction. Here we used a non-biased, stringent, deep sequencing (96 million paired end reads targeting 100 bp read length) assay to examine genomic networks altered by spaceflight in the quadriceps (n=4/group). Specifically, 9-week-old C57BL/6 male mice were housed on the International Space Station or at Kennedy Space Center for approximately four weeks (n=10/group). 14,228 genes (70% of whole mouse genome) met the cut-off criteria and the data sets were mapped to an average of ~76% of the whole mouse genome. Of these, 840 genes met the t-test criteria, p < 0.05. Canonical networks linked to EIF2 signaling, mTOR signaling, calcium ion signaling, and oxidative stress response were significantly enriched by the differentially expressed genes. A comprehensive energy deprivation was indicated as functions related to protein synthesis and degradation, lipid synthesis and oxidation, and ATP hydrolysis were inhibited, and mitochondrial dysfunction was activated. This is the first time that skeletal muscle changes have been studied in male mice during spaceflight, and these mice were euthanized in space to avoid rehabilitation to earth's gravity. These data add important new findings to changes that occur to the musculoskeletal system in male mice during spaceflight. Disclaimer: Research was conducted in compliance with the Animal Wel-

fare Act, and all other Federal requirements. The views expressed are those of the authors and do not constitute endorsement by the U.S. Army.

Disclosures: *David Waning, None*

SUN-0305

High Fidelity of Mouse Models Mimicking Human Genetic Skeletal Disorders Resulting from Mutations in 316 Genes (Skeletal Dysplasia Society 2015 Nosology Update) Robert Brommage^{*}, Claes Ohlsson. Centre for Bone and Arthritis Research, Sahlgrenska Academy, University of Gothenburg, Sweden

The 2015 Human Genetic Skeletal Disorders Nosology update (Bonafe L, Am J Med Genet A 167A:2869-2892; 2015) summarizes knowledge of human skeletal disorders with Mendelian inheritance. The 316 genes identified code for enzymes (33%), signal transduction proteins (17%), transcription factors (16%), scaffolding proteins (15%), cilia proteins (7%), extracellular matrix proteins (6%) and membrane transporters (5%). The goal of this analysis was to determine the extent to which mutant mouse models (spontaneous and chemical-induced mutants, global and conditional gene knockout mice, and transgenic mice with gene overexpression or specific base-pair substitutions) show skeletal phenotypes similar to those observed in homologous human gene disorders. The human X-linked gene ARSE (Arylsulfatase E) and small nuclear RNA U4ATAC, a component of the minor spliceosome, do not have mouse homologues. Mutations in seven (3%) mouse genes (Fgf10, Flna, Hlxb9, Lmd3, Nsd1, Smarcc1, Wisp3) do not result in similar skeletal phenotypes observed with mutations of the homologous human genes. These discrepancies can result from failure of mouse models to mimic the exact human gene mutations. Skeletal phenotypes resulting from mutations in 200 mouse genes (63%) are similar to those observed in homologous human skeletal disorders. Mutant mice are not presently available for 56 (17%) of genes. For 52 mouse mutants (16%) possible bone phenotypes have not been investigated. Global gene knockouts of several of these genes result in early embryonic lethality, precluding skeletal analyses. Since many human disorders involve gain-of-function or dominant-negative mutations, future studies will undoubtedly utilize CRISPR/Cas9 technology to examine transgenic mice having genes modified to exactly mimic variant human sequences. These comparisons indicate that homologous mutations in 97% of mouse genes examined (200 of 207) result in skeletal phenotypes mimicking human skeletal disorders. Mutant mice provide excellent models for drug development, with examples including Acvr1 (Fibrodysplasia Ossificans Progressiva), Casr (Familial Hypocalcemic Hypercalcemia), Notch2 (Hajdu-Cheney Osteolysis Syndrome) and PheX (Hypophosphatemic Rickets). The International Skeletal Dysplasia Society met during September 2017 and an updated Nosology summary is anticipated during 2018.

Disclosures: *Robert Brommage, None*

SUN-0306

Spontaneous Knee Osteoarthritis Caused by 1,25(OH)2D Deficiency Is Corrected by Overexpression of Sirt1 in Mesenchymal Stem Cells Jie Chen^{*1}, Na Lu¹, Lulu Chen¹, David Goltzman², Dengshun Miao¹. ¹Nanjing Medical University, China, ²McGill University, Canada

Vitamin D deficiency is associated with an increased risk of developing osteoarthritis (OA), however, the mechanisms are unclear. We compared the knee phenotypes of 6-month-old 1 α (OH)ase^{-/-} mice fed a high calcium/phosphate diet after weaning with age- and diet-matched wild-type mice. We found that serum calcium, phosphorus and PTH were normalized by the diet but serum 1,25(OH)2D3 was undetectable. In these mice, safranin O staining and type II collagen immunostaining of the articular cartilage of the medial femoral condyle and the tibial plateau were reduced compared to WT mice. In contrast, the summed tibial and femoral OARSI (Osteoarthritis Research Society International) score, the percentages of chondrocytes positive for type X collagen, MMP-3/13, β -galactosidase and p16, and inflammatory factors, including TNF α , IL-1 α/β and IL-6 gene expression levels were all increased significantly in 1 α (OH)ase^{-/-} mice compared to WT mice. Furthermore, these OA phenotypes in 1 α (OH)ase^{-/-} mice became more severe with anterior cruciate ligament transection and with age, however, they were rescued by supplementation with exogenous 1,25(OH)2D3 or with antioxidant N-acetyl-L-cysteine. We then examined the expression of the NAD-dependent deacetylase, Sirt1 (Sirtuin1), which has previously been reported to exert a preventive role against the development of OA. The expression levels of Sirt1 were down-regulated significantly in 1 α (OH)ase^{-/-} chondrocytes compared to WT chondrocytes. By using a chromatin immunoprecipitation approach and luciferase assays, we then demonstrated that 1,25(OH)2D3 directly regulates Sirt1 expression at a transcriptional level, mediated via VDR. Since disruption of Sirt1 in chondrocytes can accelerate development of osteoarthritis, we crossed Prx1-Sirt1 transgenic mice with 1 α (OH)ase^{-/-} mice to generate 1 α (OH)ase^{-/-} mice with Sirt1 overexpression in mesenchymal stem cells (MSCs). Overexpression of Sirt1 in 1 α (OH)ase^{-/-} mouse MSCs rescued all OA phenotypes observed in 6- and 12-month-old 1 α (OH)ase^{-/-} mice. These studies therefore indicate that 1,25(OH)2D deficiency can induce the development of spontaneous knee OA by transcriptional down-regulation of Sirt1, inducing chondrocyte senescence and production of inflammatory factors, whereas overexpression of Sirt1 in MSCs can prevent the development of OA caused by 1,25(OH)2D deficiency.

Disclosures: *Jie Chen, None*

SUN-0307

Effects of Alzheimer's Disease and high-fat diet on bone quality and quantity in mice Ryanne Chitjian¹, Anthony Capellino², Lisa S Robison³, Olivia J Gannon³, Abigail E Salinero³, Kristen L Zuloaga³, David E Komatsu². ¹Stony Brook University, Department of Biomedical Engineering, United States, ²Stony Brook University, Department of Orthopaedics, United States, ³Albany Medical College, Department of Neuroscience & Experimental Therapeutics, United States

Clinical observations have noted that patients with Alzheimer's Disease (AD) have a concomitantly higher incidence of osteoporosis and the data suggest that the two diseases share common antecedents. In addition, high-fat diets are known to exacerbate both AD and osteoporosis. Therefore, we sought to evaluate the interplay of AD and dietary fat intake on bone quality and quantity. 3xTg-AD mice containing three human mutant genes that result in familial AD, Psen1tm1Mpm, APPSwe, and tauP301L, on a mixed background and wild-type controls were utilized. At 2.5 months of age, the mice were randomized into groups and fed either a high-fat diet or a low-fat diet for the next 4.5 months and they were then euthanized at 7 months of age. Left femurs were subjected to μ CT evaluation (μ CT40, Scanco) at 10 μ m resolution to assess morphometric properties. Among female mice fed a low-fat diet, μ CT analysis of the distal femoral metaphysis revealed significant increases in BV/TV (315%), trabecular thickness (141%), trabecular number (224%), and BMD (134%), as well as decreases in BS/BV (61%) and SMI (85%) and for the 3xTg-AD mice compared to wild-type controls ($p < 0.05$). Similarly, analysis of the femoral mid-diaphysis in female mice fed a low-fat diet identified significant increases in bone volume (125%) and cortical thickness (129%) for the 3xTg-AD compared to wild-type controls ($p < 0.05$), as well as a trend toward decreased BMD. These morphometric data suggest that 3xTg-AD mice may have increased bone quantity compared to wild-type mice both in trabecular and cortical. However, as the wild-type controls were not littermates it is too early to determine if these findings are fully attributable to the genotype. Regardless, these data suggest that the interplay between AD, osteoporosis, and dietary fat is more complex than expected. We are currently performing additional morphometric and biomechanical analysis in these mice, as well as female mice subjected to high-fat diets and male mice subjected to low- and high-fat diets. As this study did not identify the concomitant development of AD and osteoporosis in this strain of mice, it suggests that we have only begun to elucidate the interactions between these two devastating and widespread diseases.

Disclosures: *Ryanne Chitjian, None*

SUN-0308

Investigating Zbtb40 as a Determinant of Osteoblast Function and Commitment Madison Doolittle¹, Robert Maynard¹, Gina Calabrese², Charles Farber², Cheryl Ackert-Bicknell¹. ¹University of Rochester, United States, ²University of Virginia, United States

Osteoporosis is a polygenic disorder that occurs due to an imbalance between bone formation and resorption rates. Focusing our genetic studies on bone formation, we previously identified a genomic locus on Chromosome 4 associated with mouse osteoblast mineralization, which lies upstream of the uncharacterized gene Zinc Finger and BTB Domain-Containing 40 (Zbtb40). A locus for bone mineral density (BMD) at the homologous region in humans has been identified in multiple previous genome wide association studies. This gene has no known function; however, proteins from the same family are transcription factors that regulate cell differentiation and maturational commitment. Our studies indicate that Zbtb40 has its highest expression in the initial days of *in vitro* differentiation of both MC3T3-E1 preosteoblasts and primary calvarial osteoblasts, with expression tapering as these cells mature. Using siRNA-mediated gene silencing, we found that knocking down Zbtb40 expression in differentiating MC3T3-E1 cells drastically decreased alkaline phosphatase activity (a marker of osteoblast differentiation) and inhibited mineralization by mature osteoblast-like cells. Furthermore, silencing of Zbtb40 decreased expression of early osteoblast markers Col1a1, Runx2, and Sp7. Zbtb40 knockdown also inhibited expression of Mx2, a transcription factor that stimulates commitment of mesenchymal progenitors to the osteoblast over adipocyte lineage. Moreover, we found that expression of Pparg, an adipocyte marker, was markedly increased in these cells, suggesting Zbtb40 loss-of-function down-regulates osteoblast commitment and up-regulates adipogenesis. We constructed a CRISPR mutant mouse line with a germline mutation causing systemic production of a truncated form of the ZBTB40 protein to study loss-of-function *in vivo*. Female mice from this line exhibit decreased BMD (WT=0.052 g/cm² Zbtb40mut=0.049g/cm² $p=0.035$) and bone mineral content (WT=0.43 g Zbtb40mut=0.39 g $p=0.024$) at 16 weeks of age. In summary, we demonstrate that Zbtb40 has a role in bone metabolism whereby reduced expression leads to decreased osteoblast differentiation and mineralization *in vitro*, and decreased bone mass *in vivo*. These data strongly support the hypothesis that Zbtb40 is the gene underlying these mouse and human genetic loci and that this gene represents a novel regulator of bone mass, possibly through regulation of mesenchymal cell fate commitment down the osteoblast lineage.

Disclosures: *Madison Doolittle, None*

SUN-0309

Short Truncation of the C-terminus Tail of Connexin43 in Mice Causes Metaphyseal Dysplasia, Stunted Growth and Low Bone Mass Francesca Fontana^{*}, Marcus Watkns, Roberto Civitelli. Washington University School of Medicine, United States

Connexin43 (Cx43) forms trans-cellular channels that allow direct gap junctional inter-cellular communication (GJIC) between apposing cells. Recent data indicate that the C-terminus tail of Cx43 also serves as a scaffold for components of signaling pathways important for osteogenic cells, independent of channel function. We have previously reported that mice with either conditional deletion of Gja1 or with one Gja1G138R mutant allele, found in patients with oculodentodigital dysplasia (ODDD), develop abnormally expanded long bones with thinner cortices, secondary to increased osteoclastogenic support by mutant osteoblastic cells. As the G138R Cx43 mutant abrogates gap junction channel function, these data corroborate the notion that GJIC is important for Cx43 action on bone remodeling. To further define the role of Cx43 signaling scaffold function *in vivo*, we generated mice carrying one Gja1 allele truncated of the last 5 aminoacids at the C-terminus, Gja1D378STOP/+;Tw2-cre (cDel5CTw2), thus removing the ZO1 binding site. In the heart, such mutation causes fatal arrhythmias, despite conserved gap junction channel function. Strikingly, young cDel5C mice exhibit stunted growth and 40% lower body weight at 4 weeks of age relative to WT littermates. They also have 20% lower whole-body bone mass by DXA at 6 weeks of age compared to control littermates, in both genders. Plane radiography reveals misshapen diaphysis and a flaring of the metaphyses of long bones reminiscent of the Erlenmeyer flask deformity typical of metaphyseal dysplasia. Consistently, Gja1D378STOP/+;Oxsc-cre (c5CdelOxsc) mice exhibit similar delays in skeletal growth and juvenile phenotype, with low bone mass and Erlenmeyer flask deformity at 6 weeks of age. In cDel5CTw2 mice, the modeling defects slowly improve with aging, but the diaphyses become tubular, taking a shape observed in mice lacking Cx43 in osteolineage cells. Mechanistically, bone marrow stromal cells from cDel5C mice retain GJIC capacity but induce higher osteoclast numbers when co-cultured with bone marrow monocytes. Intriguingly, a mutation in the C-terminus tail of Cx43 has been recently identified in families with a rare recessive form of craniometaphyseal dysplasia (rCMD). Thus, both the gap junction and scaffolding/signaling functions are important for Cx43 modulation of bone modeling and osteoclastogenesis, offering pathogenetic mechanisms for the spectrum of Cx43 diseases, including ODDD and rCMD.

Disclosures: *Francesca Fontana, None*

SUN-0310

Aberrant Endo-lysosomal-mitochondrial System in Skeletal Progenitors Causes Inordinate Bone Growth Xianpeng Ge¹, Lizhi He², Haibo Liu³, Guangchuan Yu⁴, Bradford Tremblay³, Ben Zhang⁵, Cole Haynes³, Jaehyuck Shim¹. ¹Department of Medicine, Division of Rheumatology, University of Massachusetts Medical School, United States, ²Department of Biological Chemistry and Molecular Pharmacology, Harvard Medical School, United States, ³Department of Molecular, Cell and Cancer Biology, University of Massachusetts Medical School, United States, ⁴State Key Laboratory of Emerging Infectious Diseases, School of Public Health, The University of Hong Kong, China, ⁵Department of Orthopedics, University of Massachusetts Medical School, United States

The intracellular endo-lysosomal pathway is critical in keeping protein and metabolic homeostasis. A broad interaction between this pathway and mitochondria is being increasingly appreciated, thereby constituting an integrated endo-lysosomal-mitochondrial system. Dysfunction of this system can cause complex human diseases like lysosomal storage diseases which may manifest severe musculoskeletal abnormalities. Previously we discovered that the ESCRT protein CHMP5 is essential for lysosomal degradation in embryonic fibroblasts during development. To explore the role of CHMP5 in skeletal biology, we deleted this gene in periosteal/periarticular progenitors and endosteal/bone marrow DMP1-expressing bone lineage cells by generating Chmp5Ctsk and Chmp5Dmp1 mouse strains. Ablation of Chmp5 in these skeletal progenitors caused significant bone overgrowth including extended cortical bone, ectopic bone formation at entheses, progressive joint stiffness and craniofacial suture patency. Fate mapping using the Chmp5Ctsk;Rosa26-mTmGfl/+ mouse line showed that both Chmp5 knockout and wild type cells were involved in the abnormal bone growth. Chmp5 knockout cells displayed decreased proliferation and enhanced mineralization when induced toward osteogenesis *in vitro*, while wild type GFP- cells showed both enhanced proliferation and osteogenesis. Mechanistic analyses revealed that Chmp5 depletion induced cellular senescence and elevated the secretory activity of skeletal progenitors. As observed in Chmp5 knockout mouse embryonic fibroblasts, the endo-lysosomal pathway was disrupted in Chmp5 depleted skeletal progenitors. Moreover, these progenitors demonstrated accumulation of mitochondria and elevated levels of extracellular acidification rate, mitochondrial respiration and reactive oxidative species. The increased oxidative stress may contribute to cellular senescence of Chmp5 knockout cells. Overall, our data revealed that CHMP5 is essential for normal function of the endo-lysosomal-mitochondrial system in skeletal progenitors. Mutation or loss of function of this gene can disrupt this intracellular quality control system, activate the aging process of skeletal progenitors and ultimately lead to multiple skeletal abnormalities. The Chmp5Ctsk and Chmp5Dmp1 mouse models recapitulate musculoskeletal pathologies in multiple human complex diseases and thus may

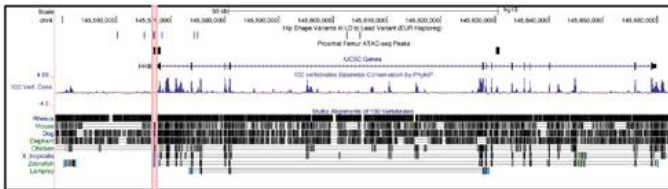
represent valuable animal models to explore the underlying mechanism and develop potential novel therapeutics.

Disclosures: *Xianpeng Ge, None*

SUN-0311

Identification of putative variants underlying human hip bone geometry using murine functional epigenomics data Terence D. Capellini^{1*}, Yi-Hsiang Hsu², Mariel Young¹, Douglas P. Kiel², David Karasik². ¹Human Evolutionary Biology, Harvard University, United States, ²Institute for Aging Research Hebrew SeniorLife, United States

Hip geometry (HG) is an important predictor of bone fracture. We performed a meta-analysis of GWAS studies to identify genetic variants associated with proximal femur geometry. The Discovery stage included 18,719 adult men and women; in-silico replication included 8,334 men and women. We analyzed four geometry phenotypes measured from DXA scans: 1) Femoral neck length (FNL); 2) Neck-shaft angle (NSA); 3) Femoral neck width, and 4) Femoral neck section modulus (NNZ). In the top 13 genome-wide significant loci ($p \leq 5 \times 10^{-8}$), for the lead SNP in each locus we identified all hg19 variants in LD with the conditionally independent lead SNP ($r^2 \geq 0.4$, 1000G build hg19). This yielded 880 SNPs in LD with HG variants. To whittle this variant list down to putative functional variants, the Assay for Transposase-Accessible Chromatin followed by sequencing (ATAC-seq) was performed genome wide using E15.5 embryonic mouse proximal femora to derive two datasets consisting of: (A) 24,804 proximal head+neck+femur growth plate ATAC-seq peaks; and (B) 22,727 femoral head-specific peaks. After mapping the peaks in mice to the human genome, we used BED intersection tools and the UCSC Genome Browser to detect and visualize overlaps between a HG variant and an ATAC-seq (open chromatin) peak. Strikingly, our intersections with the complete proximal femur dataset (A) revealed 9 HG variants from 4 loci that overlapped an ATAC-seq peak. At the HHPH locus (Chr. 4) associated with NNZ, rs13106087 ($r^2 = 0.9$ with the lead variant) resided within an ATAC-seq peak marking the promoter region (Figure 1). At the IRX1/ADAMTS16 locus (Chr. 5) associated with FNL, four variants fell within the same cis-acting ATAC-seq peak, whereas at the GDF5/UQC1 locus (Chr. 20) three variants associated with NNZ fell in separate ATAC-seq peaks. Intersections with the femoral head-specific dataset (B) yielded two variants in an intronic peak in the C8orf34 locus (Chr. 8) associated with NSA. The remaining loci did not yield intersections with either dataset. In conclusion, we found associations between HG measures and several genes belonging to biological pathways relevant to body size. Associated HG proxy SNPs were identified through intersections with epigenomic datasets relevant to proximal femoral morphology. Integration of GWAS with molecular data from bone development underscores the significance of non-coding variants and aids in understanding the biology underlying normal human bone geometry.



Disclosures: *Terence D. Capellini, None*

SUN-0312

Distinct subsets of non-coding RNAs, including miRNAs, are associated with BMD in stressed and unstressed bone Kaare M. Gautvik^{1*}, Clara-Cecilie Günther², Mazyar Yazdani³, Einar Lindalen¹, Haldor Valland⁴, Vigdis T. Gautvik¹, Ole K. Olstad³, Marit Holden², Tor P. Utheim³, Sjur Reppe¹. ¹Lovisenberg Diakonale Hospital, Norway, ²Norwegian Computing Center, Norway, ³Oslo University Hospital, Norway, ⁴Diakonhjemmet Hospital, Norway

The causes and molecular pathogenesis of postmenopausal osteoporosis (PMO) are far from understood even though osteoporotic fractures affect almost 50% of women above 50 years of age, resulting in e.g. femoral neck fractures imposing high risk to normal life. We addressed this issue by characterizing the global non-coding RNA (ncRNA) transcriptomes in non-weight bearing (unstressed) iliac and weight bearing (stressed) femoral postmenopausal bone across BMDs varying from normal (T-score > -1.0) to osteoporotic (T-score ≤ -2.5). The analyses were performed on transiliacal (84) and femoral trochanter (18) bone biopsies. Nearly 700 iliac bone ncRNAs were determined by a PCR based method and more than 6600 femoral ncRNAs were accessed by Affymetrix microchip analysis. BMD associations were calculated by linear regression and validated by Lasso analysis. DIANA TOOLS – mirPath v.3 software was used to identify overrepresented signaling pathways among the BMD associated transcripts at the two different sites. In iliac bone 36 or 75 ncRNAs were associated with age and body mass index (BMI) adjusted total hip BMD at 1% or 10% FDR, respectively. Lasso analysis involving cross validations identified nine iliac bone ncRNAs explaining 41% of the BMD variation. In trochanter, we identified 89 ncRNAs correlated to total hip, age and BMI adjusted BMD at 0.1% FDR. Several miRNAs, including hsa-miR-484, hsa-miR-378a-5p, and hsa-miR-409-3p, correlated positively to BMD in femoral

bone, but inversely to BMD in iliac bone. Furthermore, several ncRNAs correlating to BMD in iliac bone were not correlated in femoral bone, and vice versa. Several small ncRNAs were correlated to BMD in both stressed and unstressed bone. Using mirPath v.3 with conservative statistics, the “Extracellular matrix-receptor interaction” pathway came out as the topmost, involving KEGG pathway in both stressed and unstressed bone with same $p = 1 \times 10^{-325}$. “Fatty acid biosynthesis” and “Fatty acid metabolism” were significant only in unstressed bone ($p = 1 \times 10^{-325}$ and $p = 8 \times 10^{-8}$, respectively). In conclusion, we have performed a comprehensive mapping of ncRNAs in stressed and unstressed bone from postmenopausal women with greatly varying BMDs and identified striking differences in the expression pattern between the two tissues. The differences may reflect a requirement for higher turnover in stressed bone, e.g. due to repair of microfractures and demonstrate a remarkable functional adaptability of bone tissue.

Disclosures: *Kaare M. Gautvik, None*

SUN-0313

An evolving classification system for the range of skeletal phenotypes encountered in IMPC mice. David Rowe^{1*}, Douglas Adams², Hong Seung-Hyun³, Caibin Zhang⁴, Shin Dong-Guk³, Sundberg John⁵, Cheryl Ackert-Bicknell⁶. ¹School of Dental Medicine, University of Connecticut, United States, ²School of Medicine, University of Connecticut Health, United States, ³School of Engineering, University of Connecticut, United States, ⁴School of Dental Medicine, University of Connecticut Health, United States, ⁵The Jackson Laboratory, United States, ⁶University of Rochester School of Medicine, United States

The International Mouse Phenotyping Consortium (IMPC) lists >10,000 gene-inactivated mouse lines. We have examined 220 unselected KO lines by μ CT and bone cryohistomorphometry and find that about 12.5% have significant variation in bone mass (trabecular or cortical) that is exceptionally dimorphic for both sex and site (appendicular vs axial). Our data and that of others indicate the ~2,500 homozygous viable KO genes contribute to variance in bone mass. The number will be even greater when mice heterozygous for a perinatal lethal homozygous mutation are examined. Thus the magnitude of the genetic influence on skeletal health is overwhelming. We are exploring how to present this broad array of KO mice that is reliable, informative and organized in a manner that recognizes similar patterns of bone architecture, body size and osteoclast (Oc) number and osteoblast (Ob) activity as interpreted by bone cryohistomorphometry. Two well-characterized KO lines, Irf8 and Spp1, were encountered that provide a comparison of data produced by individual research laboratories and our screening program. Based on this experience, two levels of classification have been developed. (1) Bone architecture and body weight: Low and high trabecular bone volume can be subdivided by the presence of a corresponding normal, low or high bone size and body weight. The latter two groups have an overall phenotype of frailty and fitness. Bone size can also vary without a change in trabecular bone volume. (2) Dynamic cellular activity of bone: KO lines with a low bone mass (low trabecular volume and/or bone size) can be classified as having high turnover or remodeling (high Oc number and Ob activity), adynamic bone or low remodeling (low Oc number and Ob activity), Oc/Ob uncoupling or low modeling (normal Oc number and low Ob activity) and ineffective Ob function (low Oc number and high Ob activity). KO lines with a high bone mass (high trabecular volume and/or bone size) can be classified as low remodeling (low Oc number with normal Ob activity), ineffective remodeling (high Oc number without an increase Ob activity) and continued modeling activity (low Oc number and high Ob activity). These classification patterns are likely to be expanded as more KO lines are encountered and additional phenotyping criteria are developed. As this basic fund of knowledge grows, it will contribute to the interpretation of genomic sequencing of human subjects with disorders of the bony skeleton.

Disclosures: *David Rowe, None*

SUN-0314

Male specific low bone mass phenotype in Down Syndrome humans and mouse models Diarra Williams^{1*}, Alexis Mitchell¹, Alyssa Falck¹, Shannon Huggins¹, Kent Mckelvey², Dana Gaddy¹, Larry Suva¹. ¹Texas A&M University, United States, ²University of Arkansas for Medical Sciences, United States

Low BMD in people with Down syndrome (DS) is associated with impairments in skeletal maturation and bone-mass accrual that predispose patients to fracture. We previously identified that low BMD and low bone turnover was common in healthy, euthyroid, calcium-replete, community dwelling adults with DS. Indeed, serum bone turnover markers were significantly decreased in the face of profound hypogonadism, a situation that is usually associated with high bone turnover. Moreover, the low bone mass condition was more pronounced in DS men and osteopenia appeared earlier in males than females; although bone deficits progressed with age in each group. In order to investigate this apparent sex difference, we have characterized the skeletal phenotypes of 3 of the most commonly used murine DS models, Ts65Dn, Tc-1, and DP16(Yey1). Human chromosome 21 (Hsa21) contains ~300 genes of which 166 orthologs are present in mice and carried on three murine chromosomes (Mmu10, 16, 17). Ts65Dn mice are trisomic for 152 genes of Mmu16, Tc-1 are transchromosomal for Hsa21 (trisomic for 152 genes) and Dp(16)Yey1 are trisomic for the entire syntenic region of Mmu16 and contain 110 genes orthologous to Hsa21. These murine models manifest as DS and recapitulate many, but not, all of the phenotypic characteristics

of human DS and have been used extensively to investigate the pathology of DS behavioral, cardiac and metabolic phenotypes. We previously reported that Ts65Dn male mice phenotype the low bone mass phenotype of human DS. However, in comparison with Ts65Dn mice, Tc-1 mice that model many of the behavioral aspects of DS lack any discernible bone phenotype. Female Ts65Dn mice are unavailable for study. However, we have analyzed the bone phenotype of both male and female 3 month old Dp(16)1Yey mice, and identified that just as in humans, the low bone mass phenotype in Dp16(Yey1) is also more pronounced in males. Male Dp(16)1Yey mice display low total body BMD, tibial trabecular BV/TV and number, decreased total cross-sectional area, periosteal and endosteal perimeters, with significantly diminished mineral apposition rates. These data demonstrate that both Ts65Dn and Dp(16)1Yey DS mice have low bone mass more consistently in males than females that appears to be the result of decreased bone accrual. In sum, these animals have the potential to provide a more detailed understanding of the genetic and cellular basis for the altered bone development of people with DS.

Disclosures: *Diarra Williams, None*

SUN-0331

Metabonomic signatures of high fruit and vegetable intake and reduced prevalence of osteoporosis: The Boston Puerto Rican Osteoporosis Study Kelsey Mangano¹*, Sabrina Noel¹, Chao Qiang Lai², Laurence Parnell², Jose Ordovas², Katherine Tucker¹. ¹University of Massachusetts, Lowell, United States, ²Nutrition and Genomics Laboratory, Jean Mayer U.S. Department of Agriculture Human Nutrition Research Center on Aging, Tufts University, Boston, MA, United States

There is evidence that fruit and vegetable [FV] intake is important for bone health, but the mechanisms underpinning this link remain unclear. The purpose of the current study was to examine associations between FV intake and metabolomic profiles in 586 older adults, aged 47-77y, from the Boston Puerto Rican Osteoporosis Study (BPROS), an ancillary study to the Boston Puerto Rican Health Study (BPRHS). Bone mineral density was measured using dual-energy X-ray absorptiometry and osteoporosis (OS) at the femoral neck or the lumbar spine was defined as T-score, ≤ 2.5 (2.5 SD or more below peak bone mass of a 30 y/o reference group). Usual dietary intakes were assessed with a food frequency questionnaire, adapted and validated for use in this population. The association between total FV intake and odds of OS was assessed by logistic regression. Metabonomic analyses were conducted to determine associations between FV intake, metabolites and OS. Enriched metabolic pathways related to FV-associated metabolites were examined for enzyme inhibition among participants with and without OS. Covariates included age (y), sex, education, menopause, smoking status, alcohol status, physical activity score, total energy intake, height and body mass index. Greater FV intake was associated with lower prevalence of OS ($P=0.031$). Among participants without OS, 66 metabolites were associated with high FV intake. In men without OS, FV intake was related to 38 metabolites, vs. 66 metabolites in women without OS. In both men and women, 30 metabolites were associated with OS, without correction for multiple testing. Of these metabolites, 10 were overrepresented in the branched chain amino acid (BCAA) metabolic pathway ($P \leq 5.65 \times 10^{-15}$) in men; and 10 were overrepresented in the steroid hormone pathway ($P \leq 8.49 \times 10^{-21}$) in postmenopausal women not taking estrogen. Hence, these results suggest that sex-specific metabolic pathways are linked to OS with FV-associated metabolite enrichment. Of the 66 identified metabolites associated with FV intake, five were observed as inhibitors of enzymes in the steroid hormone pathway in women and one inhibitor of L-amino-acid oxidase, encoded by the IL4I1 gene, in the BCAA pathway in men. We hypothesize that high FV consumption is associated with reduced risk of OS through regulation of the steroid hormone pathway in women; data in men are less clear. Future research should elucidate downstream effects of modulated metabolic pathways by FV metabolites.

Disclosures: *Kelsey Mangano, None*

SUN-0332

Exercise preconditioning promotes bone anabolism in hind-limb suspended mice via miR-152-3p-TFAM signaling dependent mitochondrial DNA replication Jyotirmaya Behera^{*}, Suresh C Tyagi, Kimberly E Kelly, Neetu Tyagi, Nicholas Theilen. University of Louisville, United States

Aims: Exercise exerts a wide range of biological actions in the body, especially in the promotion of bone mass. However, critical process of mitochondrial DNA (mtDNA) replication that regulates mitochondrial biogenesis and bone formation during exercise is largely unknown. Therefore, we aimed to investigate whether exercise affects mtDNA replication to promote bone anabolism in a hind-limb suspension (HLS) induced bone loss model. We hypothesize that exercise enhances mtDNA copy number via inhibition of DNA methyltransferase 1 (Dnmt1) transcription and TFAM promoter demethylation. Methods: To test this hypothesis, 12-week-old female mice were underwent preconditioning treadmill exercise (5 day/week@7-11 m/min) for 4 weeks followed by HLS for another 3 weeks. Results: Here, we demonstrated that trabecular bone phenotype (BV/TV; 34% in the femur) was significantly increased upon exercise treadmill test in comparison with HLS group, as assessed by *In vivo*, μ CT measurements. *In vitro* study also confirmed BMMSC derived osteoblast mineralization was increased upon exercise administration. MicroRNA analysis using qRT2-PCR array demonstrated a significant reduction in the transcript expression of

microRNA-152-3p (miR-152-3p) in the BMMSCs of HLS mice as compared to wild-type controls. The sequence matching tools also validated miR-152 targets the Dnmt1 transcriptional activity by binding to its 3'UTR of Dnmt1 mRNA. It was demonstrated that hyperhomocysteinemia (HHcy) phenotype was observed in HLS mice group. The mechanistic study revealed that HHcy reduced miR-152 transcriptionally upregulates the Dnmt1 expression. Bisulfite sequencing PCR (BSP) and methylation-specific PCR (MSP) confirmed that HLS enhanced TFAM promoter hyper-methylation leads to reduced mtDNA copy number and oxidative phosphorylation. Administration of miRNA mimics (agomiR) or Dnmt1 knockdown diminished the HLS obliterated mtDNA replication, and BMMSCs mediated osteogenesis. In addition, TFAM knockdown diminished exercise-enhanced *in vivo* bone formation. We further found that exercise was able to reverse the plasma level of Hcy which caused to upregulate the transcript level of microRNA-152-3p and decreases the Dnmt1 transcription. Conclusion: Our data provide the evidence that exercise administration contributes to mtDNA replication and bone formation via epigenetic mechanism miRNA-TFAM signaling and provides a novel therapeutic avenue against osteoporosis.

Disclosures: *Jyotirmaya Behera, None*

SUN-0333

Transcriptional Profiling of Two Mechanisms of Bone Fracture Repair Brandon Coates^{*}, Jennifer Mckenzie, Evan Buettmann, Matthew Silva. Washington University in St. Louis, United States

Bone fracture is a debilitating orthopedic injury. Depending on the severity of the injury, fractures heal through either endochondral ossification, which has a cartilaginous intermediate state, or intramembranous ossification, which is direct bone formation. While these bone repair types have been well studied separately, the specific molecular cues that govern their similarities and differences have not been documented. Twelve-week old C57BL/6J female mice underwent either a full femur fracture (Fx) to induce endochondral bone repair, or an ulnar stress fracture (Sfx) to induce intramembranous bone repair. Post fracture time points were selected to coincide with periods of inflammation, angiogenesis, and osteogenesis which are characteristic for endochondral (4 hrs, 1, 3, 7, & 14 days) and intramembranous (4 hrs, 1, 3, 5, & 7 days) repair. RNA-seq analysis (n=5 mice/group; N=50 total) was performed on bilateral bone segments including bone and callus tissue. Segments were pulverized, RNA was extracted, and RINs were measured to assure quality (RIN > 6). All samples were processed by using Illumina HiSeq, 50 bp single end reads and mapped to mouse genome mm10. Injured samples in each time point were compared to pooled non-fractured controls (n=10/fracture type) for differential expressed genes (DEGs) (FDR<0.05 and fold-change >2). Fx resulted in immediate and robust differential expression that continued through all time points and peaked at 7 days post-fracture. Sfx had little change in expression at 4 hrs and 1 day with more robust differential expression for the remaining time points and a peak at day 5 post-fracture. Tracking the fold change of genes with annotations of inflammation, angiogenesis, cartilage development, and ossification revealed some differences between fracture types (Fig 1). Fx induced a higher upregulation of inflammatory and angiogenic genes, especially at early time points. Contrastingly, Sfx repair displayed an earlier and more prolonged upregulation of ossification related genes. This works represents a valuable source of data that can illuminate many unanswered questions about endochondral and intramembranous fracture healing. With these data we can probe the expression of single genes, gene families, and signaling pathways in two distinct types of bone formation across several time points, providing useful insight into the complex biological process of fracture repair.

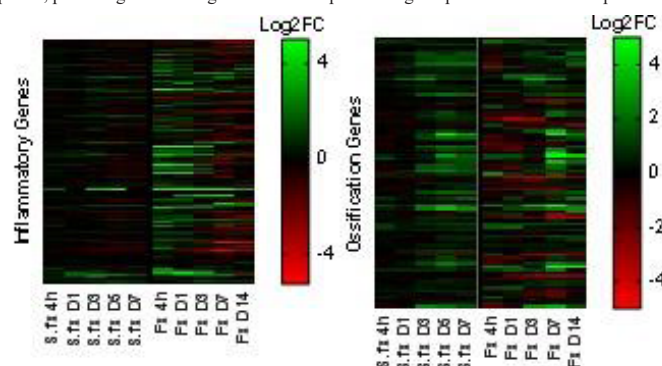


Figure 1. Heat maps of the Log₂ fold change (over contralateral controls) for each time point of fracture repair for gene lists with annotations of "Inflammatory Response" and "Ossification" generated using AmiGO2. Fx has a strong upregulation of inflammatory genes at early time points, while Sfx has a much more subdued reaction to injury. Both injuries show robust upregulation of ossification related genes, especially at later time points, with Sfx turning on these genes earlier than Fx.

Disclosures: *Brandon Coates, None*

SUN-0334

Using Co-expression Network Analysis to Inform GWAS for Bone Mineral Density Olivia Sabik^{*1}, Gina Calabrese¹, Cheryl Ackert-Bicknell², Charles Farber¹. ¹University of Virginia, United States, ²University of Rochester Medical Center, United States

Genome-wide association studies (GWASs) have identified over 200 genomic loci associated with bone mineral density (BMD); however, the causal genes are known for the majority of loci. Here, we hypothesized that causal genes underlying a subset of BMD GWAS loci could be identified by integrating GWAS data with an osteoblast specific co-expression network. Our approach was based on the idea that a subgroup of causal genes are likely to influence BMD via osteoblast-mediated bone formation and genes involved in specific biological processes are often co-expressed. To test this hypothesis, we applied weighted gene co-expression network analysis (WGCNA) to genome-wide gene expression profiles of mineralizing calvarial osteoblasts from a population of genetically diverse mice and identified 65 modules of co-expressed genes. Of these, one module was significantly enriched for genes located within BMD GWAS loci (odds ratio (OR) = 3.4, $P = 4 \times 10^{-9}$) and its expression was significantly correlated with *in vitro* levels of mineralization ($r = 0.49$; $FDR = 0.012$). This module was also enriched for skeletal development genes (OR = 8.58; $P < 2.2 \times 10^{-16}$), and for genes that result in a bone phenotype when knocked-out (OR = 4.06; $P = 2.14 \times 10^{-9}$). Genes in this module were expressed in two distinct patterns, either early or late in osteoblast differentiation, and the enrichments listed above were increased in the late differentiation group. Additionally, we observed that the mean connectivity of GWAS-implicated genes was significantly higher than non-GWAS genes, leading us to prioritize genes based on their degree of connectivity within the module. Of the 30 most highly connected genes in the late differentiation subset, 13 had not been previously linked to bone formation, and three (Beta-1,4-N-Acetyl-Galactosaminyltransferase 3 (B4galnt3), Cell Adhesion Molecule 1 (Cadm1), and Solute Carrier Family 8 Member A3 (Slc8a3)) were located within BMD GWAS loci. For all three genes, their expression in humans was regulated by local expression quantitative trait loci (eQTL) that colocalized with the BMD GWAS associations. Furthermore, B4galnt3 and Cadm1 knockout mice had decreased whole-body BMD and Slc8a3 knockout mice exhibited increased vertebral trabecular bone volume fraction. Through the integration of mouse co-expression network analysis and GWAS data, we have identified the genes responsible for three BMD GWAS associations and improved our understanding of the genetics of BMD.

Disclosures: *Olivia Sabik, None*

SUN-0335

WITHDRAWN

SUN-0336

Genetic Variants Associated with Circulating Parathyroid Hormone among Patients with Chronic Kidney Disease Cassianne Robinson-Cohen^{*1}, Farzana Perwad², Myles S. Wolf³, Ian H. De Boer⁴, Bryan Kestenbaum⁴, Loren Lipworth¹, Adriana Hung¹, T. Alp Ikizler¹. ¹Vanderbilt University Medical Center, United States, ²University of California San Francisco, United States, ³Duke University, United States, ⁴University of Washington, United States

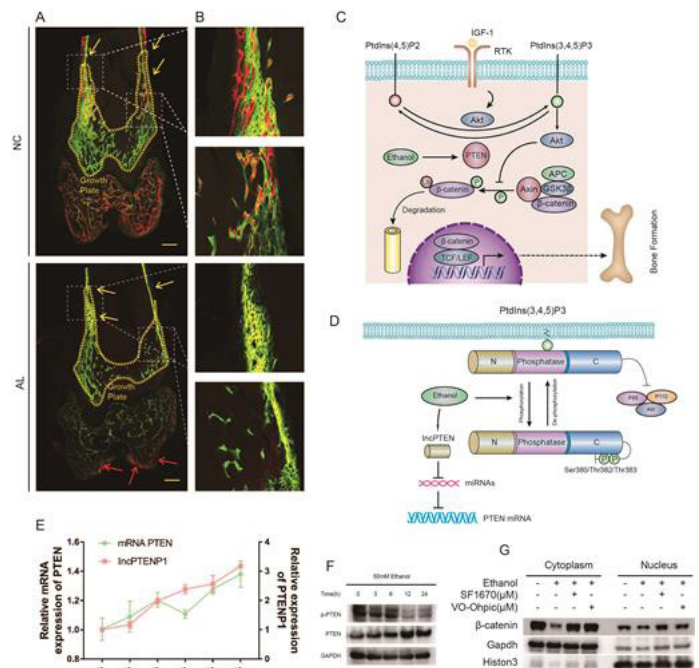
Recent genome-wide association studies (GWAS) identified loci associated with differences in parathyroid hormone (PTH) concentrations, near genes involved in vitamin D metabolism and calcium and renal phosphate transport. These studies were conducted among individuals with preserved kidney function. It is possible that genetic contributions to circulating PTH may differ among individuals with mineral metabolism disturbances, such as those with chronic kidney disease (CKD), in whom the biologic implications and potential treatment options are most relevant. We examined 5 SNPs previously identified in GWAS of PTH (index SNPs) and 53 putatively functional SNPs in the surrounding regions (± 250 kb) among unrelated individuals of European ancestry ($n = 1,666$) who participated in the Chronic Renal Insufficiency Cohort (CRIC) Study. We additionally tested for interactions of eGFR on the SNP-PTH association. Two index SNPs were associated with PTH, after adjustment for age, sex, eGFR and BMI: rs6127099 at 20q13.2/CYP24A1 (beta coefficient for the T allele: 4.5% higher PTH, 95% CI: 0.28, 8.83, $p = 0.036$) and rs4074995 at 5q35.3/RGS14 (beta for the G allele: 5.7% higher PTH, 95% CI: 1.19, 10.42, $p = 0.013$). All 5 SNPs were directionality-consistent with the previously published results. When we expanded to surrounding functional variants, 21 SNPs were associated with PTH (false discovery rate ≤ 0.05), all within the 5q35.3 region. The strongest association was for rs3812035 in SLC34A1 (NaPi-IIa) (beta for the A allele: 7.8% lower PTH, 95% CI: -11.6, -3.9, $p = 1 \times 10^{-4}$). Statistically significant interaction by eGFR was noted for the association of rs1801725 at 3q13.33/CASR ($p < 0.05$). Our findings provide evidence that some genetic variants associated with PTH under normal conditions are also associated with PTH in the setting of CKD. Larger, more comprehensive studies are needed to fully assess the generalizability of published GWAS findings and to identify potential novel associations in CKD. Both replication and lack of replication of published GWAS findings in CKD provides important information on the genetic etiology and the importance of pathways influencing mineral metabolism disorders.

Disclosures: *Cassianne Robinson-Cohen, None*

SUN-0360

PTEN REGULATION ALLEVIATES THE ALCOHOL-INDUCED OSTEOPENIA IN RAT VIA AKT/GSK-3B/B-CATENIN PATHWAY IN BMSCS Yi-Xuan Chen^{*}, You-Shui Gao, Chang-Qing Zhang. Shanghai Sixth People hospital, China

Background: Alcohol is regarded as a leading risk factor of osteopenia. Our previous works indicated Akt/GSK-3 β /catenin pathway plays crucial role in the ethanol-induced anti-osteogenic effect in bone mesenchymal stem cells (BMSCs). It was acknowledged that PI3K/Akt is negatively regulated by the phosphatase and tensin homologue (PTEN) phosphatase. PTEN expression was reported to be upregulated in ethanol-administrated animals. Objectives: In this study, we explored the molecular mechanisms underlying alcohol-induced osteopenia and investigated the role of PTEN and Akt/GSK-3 β /catenin axis in this pathological process. Methods: *In vitro*, Western blotting, separation of nucleus and cytosolic extracts, confocal scanning, RT-PCR were used to investigate the inhibition of ethanol on Akt/GSK3 β -catenin signaling pathway via upregulation of PTEN in hBMSCs. *In vivo*, micro-computerized tomography, hematoxylin & eosin (H&E) staining, Van Gieson staining, Masson's trichrome and fluorochrome labeling were employed to reveal that PTEN inhibition provided protective effects against ethanol on bone tissue. Results: We found that ethanol increased PTEN expression both in BMSCs and in bone tissue of ethanol-administrated rats. PTEN upregulation impaired the recruitment of Akt to the plasma membrane, and suppressed Akt phosphorylation at Ser473, there by inhibiting the Akt/GSK3 β /catenin signaling pathway in BMSCs and inhibited the expression of osteogenic genes COL1 and OCN both *in vitro* and *in vivo*. To counteract the inhibitory effect of ethanol, two selective PTEN inhibitors were introduced. The result of micro-computerized tomography, hematoxylin & eosin (H&E) staining, Van Gieson staining, Masson's trichrome and fluorochrome labeling indicated PTEN inhibition provided protective effects against ethanol on bone tissue. Interestingly, our data revealed that the mRNA of PTEN, paralleled with PTENP1, was increased in a time-dependent manner upon ethanol stimulation, which resulted in increasing PTEN protein level. In addition, ethanol increased PTEN expression while decreased p-PTEN expression in a time-dependent manner, which indicated the generation of more functional PTEN.



Disclosures: *Yi-Xuan Chen, None*

SUN-0361

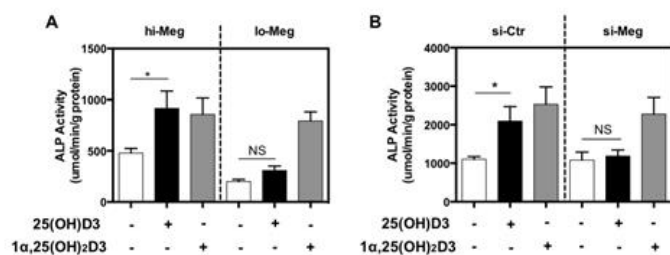
WITHDRAWN

SUN-0362

Megalyn-Mediated 25-hydroxyvitamin D Actions in Human Mesenchymal Stem Cells Yuan Gao^{*}, Simon Luu, Shuanhu Zhou, Julie Glowacki. Brigham and Women's Hospital, United States

Between 85-90% of circulating 25-hydroxyvitamin D [25(OH)D] is bound to D-binding protein (DBP), but implications of free and bound 25(OH)D are not known. Megalin is a cellular receptor for DBP in renal tubular epithelial cells, but nothing is reported about

megalyn in human Mesenchymal Stem Cells (hMSCs). We tested the hypotheses that (i) megalin is expressed in hMSCs, (ii) megalin is required for 25(OH)D but not 1 α ,25-dihydroxyvitamin D(1,25)-induced osteoblastogenesis, and (iii) megalin is required for DBP-dependent 25(OH)D action. hMSCs from surgically discarded marrow were used for gene expression by RT-PCR and alkaline phosphatase (ALP) enzyme activity for osteoblastogenesis. Transient transfection of siRNA for megalin (si-Meg) and control (si-Ctr) was performed with the Human MSC Nucleofector Kit (Lonza). Because constitutive megalin was variably expressed in 15 specimens, hMSCs with high (hi-Meg) or low (lo-Meg) megalin were studied first. Both 1,25 (10nM) and 25(OH)D3 (100nM) induced osteoblast signature genes Runx2 and ALP (3d), and stimulated ALP activity (Panel A, 7d in osteogenic medium, p<0.05) in hi-Meg hMSCs, but only 1,25 did so in lo-Meg hMSCs. The amount of extra-renal 1,25 biosynthesized from 25(OH)D3 by si-Meg hMSCs was only 26% of that for si-Ctr cells (p<0.05). Both 1,25 and 25(OH)D3 increased expression of Runx2, ALP, and BSP, and stimulated ALP activity (Panel B, p<0.05) in si-Ctr cells, but only 25(OH)D failed to do so in si-Meg cells. In 10% fetal bovine serum (FBS), 25(OH)D3 induced target gene CYP24A1 in hi-Meg and si-Ctr cells, but was blocked in lo-Meg and si-Meg cells. In contrast, 1,25 induction of CYP24A1 was equivalent in MSCs between hi-Meg and lo-Meg or between si-Meg and si-Ctr. In serum-free medium however, 25(OH)D3 stimulated CYP24A1 in all hi-Meg, lo-Meg, si-Meg, and si-Ctr hMSCs. Addition of 0.02 g/L rhDBP to serum-free medium blocked 25(OH)D3's induction of CYP24A1 in lo-Meg and si-Meg hMSCs, but not in hi-Meg and si-Ctr hMSCs; thus megalin was required for CYP24A1 activation by the DBP-dependent 25(OH)D3, but not for free 25(OH)D. In conclusion, to our knowledge, this is the first study showing that megalin is expressed in hMSCs and is required for extra-renal hydroxylation of 25(OH)D and production of 1,25 and for the 25(OH)D/DBP complex to stimulate VDR targets and osteoblastogenesis in hMSC.



Disclosures: *Yuan Gao, None*

SUN-0363

Phosphorylation of S122 in ER α is Dispensable for the Physiological Regulation of the Skeleton in Female Mice Karin Gustafsson^{*1}, Helen Farman¹, Petra Henning¹, Vikte Lionikaite¹, Sofia Movérare-Skrtic¹, Klara Sjögren¹, Pierre Chambon², Claes Ohlsson¹, Marie Lagerquist¹. ¹Centre for Bone and Arthritis Research at the Institute of Medicine, Sahlgrenska Academy at University of Gothenburg, Sweden, ²Institut de Génétique et de Biologie Moléculaire et Cellulaire Centre National de la Recherche Scientifique, National de la Santé et de la Recherche Médicale, ULP, Collège de France, Illkirch-Strasbourg, France

Estrogen signaling leads to cellular responses, not only in reproductive tissues, but also in several other tissues, including the skeleton. Loss of estrogen leads to increased risk of postmenopausal osteoporosis and fracture. It is therefore important to increase our knowledge regarding estrogen signaling in the skeleton. ER α , the main mediator of estrogen effects in the skeleton, is widely subjected to posttranslational modifications (PTMs). PTMs can affect cellular responses to estrogen in a tissue specific manner by influencing the function of ER α and its interactions with other proteins. Phosphorylation of S122 has been shown, in vitro, to affect the transcriptional activity of ER α , but the role in vivo is still unknown. Our aim was to investigate if phosphorylation of S122 in ER α is involved in the physiological regulation of the skeleton in vivo. Female mice with a point mutation in S122 (S122A) were compared to wild-type (WT) littermates and analyzed using DXA at 3, 6, 9, 12 and 15 months of age, and high resolution micro CT at 3 and 15 months of age. S122A mice had normal levels of estradiol and testosterone compared to WT mice, as measured using GC-MS/MS, demonstrating a normal sex steroid feedback. DXA analysis showed no difference in total body bone mineral density between S122A and WT mice at any time point. Furthermore, analysis using micro CT demonstrated that the trabecular bone fraction (BV/TV) in long bones and vertebrae, as well as cortical thickness in long bones were similar between S122A and WT mice at both 3 and 15 months of age. Interestingly, S122A mice displayed significantly increased fat content, as analyzed by DXA, at 6, 9, 12 and 15 months of age. In conclusion, we demonstrate that phosphorylation of S122 in ER α might have a role in the regulation of fat mass in older mice, but that it is dispensable for the physiological regulation of the skeleton in female mice.

Disclosures: *Karin Gustafsson, None*

SUN-0364

Glucocorticoid receptor dimerization is deleterious in trauma-induced compromised fracture healing Yasmine Hachemi^{*1}, Anna E. Rapp², Ann-Kristin Pickel¹, Anita Ignatus³, Jan Tuckermann¹. ¹Institute of Comparative Molecular Endocrinology, Ulm University, Germany, ²German Rheumatism Research Centre, Germany, ³Institute of Orthopedic Research and Biomechanics, Center for trauma research, Ulm University Medical Center, Germany

After severe trauma, fracture healing is impaired. Glucocorticoids (GCs), acting via the glucocorticoid receptor (GR) influence fracture healing by modulating the trauma-induced local and systemic inflammation. Our previous study revealed an important role of the GR in endochondral ossification by promoting cartilage to bone transition. GR dimerization dependent gene regulation is essential for the anti-inflammatory effects of GC. In a murine model of trauma, combining femur osteotomy and blunt thorax trauma, resembling human trauma situations such as a car accident, we aim to investigate how GR dimerization affects trauma response towards fracture. Therefore we used male BALB/C mice with a point mutation impairing GR dimerization capacity (GRdim) and wildtype littermate control mice (WT). We performed a femur osteotomy stabilized by an external fixator and challenged the mice with an additional thorax trauma. Subsequently, healing phase was analysed by histomorphometry, μ CT, and biomechanics. As expected, in WT mice the thoracic trauma compromised fracture healing. Bone formation in the fracture callus was strongly reduced in comparison to WT mice with fracture only (-47%, p=0.003), resulting in poor mechanical properties of the healed bone and reduced bending stiffness (-68%, p=0.001). In contrast, fracture healing was not impaired in GRdim mice after additional trauma. Furthermore, 23 days after osteotomy, residual cartilage was increased in calli of WT compared to GRdim mice after thorax trauma (+167%, p=0.0009). Collectively, our data show that intact GR dimerization critically contributes to trauma-induced compromised bone repair.

Disclosures: *Yasmine Hachemi, None*

SUN-0365

Relaxin Accelerates Rat Midpalatal Suture Expansion and Subsequent Bone Formation Hiroyuki Kamimoto^{*}, Yukiho Kobayashi, Keiji Moriyama. Department of Maxillofacial Orthognathics, Division of Maxillofacial and Neck Reconstruction, Graduate School of Medical and Dental Sciences, Tokyo Medical and Dental University, Japan

Objectives: Relaxin (RLN) is an insulin-like peptide hormone that enables softening and lengthening of the pubic symphysis and uterine cervix. This study analyzed the effect of RLN2 on the expansion of rat midpalatal suture (MPS) using a magnetically controlled liposome-based drug delivery system. Materials and Methods: Thirty-six male SD rats were divided into three groups: the control (MPS was not expanded), lipo (MPS expanded for 1 week, treated with liposome only), and RLN-lipo groups (MPS expanded for 1 week, treated with liposomes encapsulating RLN2 [100 ng/kg], ferric oxide, and fluorescent Cy5.5 dye). Each group was subdivided into two groups: the expansion group, sacrificed after the 1-week expansion, and the retention group, sacrificed after a 2-week retention period following expansion. MPS expansion was performed using a helical spring of 0.014-inch orthodontic stainless-steel wire. To accumulate RLN2-liposome, a magnetic sheet was fixed to the palatal mucosa, just above the MPS. Either liposomes or RLN2-liposome mixture were injected into the MPS every 48 h. Bone histomorphometric analysis was performed by bone double-labeling method with calcein and tetracycline. Accumulation of liposomes was tracked in vivo using IVIS imaging system. Morphological analysis of skeletal tissue was performed by micro-CT, HE, and alkaline phosphatase (ALP) staining. Expressions of RLN2, Rln receptor (Rxfp) 1 and 2, periostin (Postn), inducible NO synthase (iNos), and matrix metalloproteinase-1 (Mmp-1) in the MPS were analyzed by immunohistochemical (IHC) staining. Results: In vivo imaging showed magnetically controlled accumulation of liposomes in the MPS area for 72 h. IHC staining revealed the existence of applied RLN2 in the MPS after the expansion, and Rxfp2 expression at the osteogenic front (OF) in the RLN-lipo group alone, while all groups expressed Rxfp1 in the MPS. Micro-CT, bone double-labeling, and ALP staining showed significantly accelerated MPS expansion and bone formation at the OF in RLN-lipo group as compared to other groups. In the RLN-lipo group, HE staining revealed sinuous bone deposition at the OF, while IHC staining showed increased expression of iNos and Mmp-1 in the MPS and Postn at the OF. Discussion and Conclusions: These results suggested that RLN promoted MPS expansion through secretion of iNos and Mmp-1 by fibroblasts in the MPS, and it could enhance subsequent bone formation by Postn at the OF during the MPS expansion via Rxfp2.

Disclosures: *Hiroyuki Kamimoto, None*

SUN-0366

Skeletal Effects of Non-Genomic Thyroid Hormone Receptor (TR) β 1 Signaling in Mice Richard Lindsey^{*1,2}, Catrina Godwin¹, Subburaman Mohan^{1,2}. ¹Musculoskeletal Disease Center, VA Loma Linda Healthcare System, United States, ²Department of Medicine, Loma Linda University, United States

Thyroid hormone (TH) levels increase rapidly during the prepubertal growth period in mice, and studies have shown that this change is necessary for endochondral ossification of

the epiphyses. Recent studies have suggested that the effect of TH on epiphyseal chondrocyte hypertrophy involves TR β 1-mediated activation of Indian hedgehog (IHH) signaling. In addition to its traditional genomic signaling role as a transcription factor, TR β 1 can also exert non-genomic effects by interacting with other signaling molecules such as PI3K. To investigate the role of non-genomic TR β 1 signaling in endochondral ossification, we evaluated the skeletal phenotype of TR β 147F mutant mice in which a tyrosine residue which is essential for interaction with PI3K is replaced with phenylalanine. These TR β 147F mice exhibit a normal genomic response of TR β 1 to TH, but the non-genomic response through the PI3K pathway is impaired. Using microCT, we found that 13-week-old TR β 147F mice had significantly less trabecular bone mass in the distal femoral secondary spongiosa compared to littermate control mice, and trabecular BV/TV at the tibial epiphyses was also decreased. The mutants' reduced trabecular bone mass was primarily due to decreased trabecular thickness. Histomorphometric analyses of distal femoral secondary spongiosa revealed that labeled surface to bone surface and BFR/BS were reduced in the mutant mice. To explore the mechanisms of these TR β 1 effects in osteoblasts, we measured changes in mRNA expression caused by TR β -specific agonist GC-1 in calvarial osteoblasts of mutant and control mice. We found that GC-1 increased Alp expression in control osteoblasts (1.55-fold, $P = 0.01$) but not TR β 147F mutant osteoblasts. Since canonical β -catenin signaling has been implicated in mediating PI3K non-genomic signaling in other cell types, we evaluated the GC-1 effect on β -catenin protein levels in MC3T3-E1 pre-osteoblasts. GC-1 treatment, however, did not significantly alter β -catenin levels, suggesting that PI3K non-genomic TR β 1 pathway modulation of β -catenin signaling is not likely involved in mediating GC-1 effects on osteoblast differentiation. Together, these results suggest that TH acting through TR β 1 regulates endochondral ossification in part via non-genomic signaling in mice. Further investigation of this non-genomic mechanism of TR β 1 signaling could lead to novel therapeutic targets for promoting endochondral ossification.

Disclosures: **Richard Lindsey**, None

SUN-0367

Parathyroid Hormone is Anabolic for Bone due to Progenitor Recruitment and Adipogenic Lipolysis David Maridas^{*1}, Elizabeth Rendina-Ruedy², Ron Helderman², Victoria Demambro², Daniel Brooks³, Anyonya Guntur¹, Vicki Rosen¹, Beate Lanske¹, Mary Bouxsein³, Clifford Rosen². ¹Harvard School of Dental Medicine, United States, ²Maine Medical Center Research Institute, United States, ³Center for Advanced Orthopaedic Studies, Beth Israel Deaconess Medical Center, United States

Parathyroid hormone (PTH) prevents adipogenesis of bone marrow stromal cells in vitro, and in vivo, suppresses bone marrow adipose volume in both mice and humans. Furthermore, genetic deletion of the PTH receptor in mice results in an excess of bone marrow adipose tissue (BMAT). Thus, we postulated that PTH could prevent the increase of BMAT in calorie-restricted mice that recapitulates the marrow phenotype in anorexia nervosa. 8-week-old female C57BL/6J mice were fed the AIN93M control diet (CTRL) or calorie restricted at 30% (CR). At 12 weeks of age, CR and CTRL mice were injected daily with PTH (CR/PTH or CTRL/PTH) or vehicle (CR/Veh or CTRL/Veh) for 4 weeks. 2 other cohorts of 8-week-old mice were calorie-restricted and simultaneously injected (CR+PTH or CR+Veh) for 4 weeks. CR mice had markedly reduced bone mass and histological sections revealed an accumulation of BMAT in the proximal tibiae. Intermittent PTH injections significantly increased aBMD and aBMC in both CR/PTH and CTRL/PTH mice as well as in CR+PTH mice when compared with their respective controls. Intermittent PTH significantly increased femoral and vertebral BV/TV in all cohorts despite calorie reduction in the experimental group. Cortical bone fraction was considerably decreased with calorie restriction but PTH injections only increased it in the CR+PTH but not in the CR/PTH cohort. Adipocyte density and size were markedly increased with calorie restriction. PTH significantly reduced adipocyte numbers in CR+PTH mice while adipocyte size was reduced in CR/PTH mice. Bone marrow stromal cells cultured differentiated into adipocytes and treated with PTH showed increased concentration of glycerol, a byproduct of lipolysis, in their conditioned media. In summary, our results suggest that when PTH injections start simultaneously with CR, PTH affects the number of adipocytes indicating an inhibition of adipogenesis. However, when PTH treatment occurs after CR has started, a lipolytic effect is observed with a significant reduction in adipocyte size. Thus, PTH can partially rescue both bone loss and MAT expansion in CR mice by affecting progenitor recruitment and lipolysis of marrow adipocytes. PTH induction of lipolysis in BMAT may provide a synergistic mechanism to provide fuel for osteoblasts during anabolic therapy.

Disclosures: **David Maridas**, None

SUN-0368

Propranolol treatment reduced sympathetic tone and prevented PTH-induced resorption in C57BL/6J mice Annika Treyball^{*1}, Hina Hashmi¹, Daniel Brooks², Kenichi Nagano³, Deborah Barlow⁴, Karen Houseknecht⁴, Roland Baron³, Mary Bouxsein², Anyonya Guntur¹, Katherine Motyl¹. ¹Maine Medical Center Research Institute, United States, ²Beth Israel Deaconess Medical Center, United States, ³Harvard School of Dental Medicine, United States, ⁴University of New England, United States

Previous studies have demonstrated that the β 2-adrenergic receptor (β 2AR) is required for the anabolic effect of intermittent parathyroid hormone (PTH). Conversely, the non-selective β AR blocker, propranolol (PRO) improves bone parameters with PTH in ovariectomized (OVX) mice. This suggests that there are differences in the mechanisms of action of the β 2AR deletion and the β AR blocker. In order to better understand this phenomenon, we wanted to determine whether the positive effects of combined treatment could also be observed in intact mice. We treated 16-wk-old C57BL/6J female, intact mice with vehicle (VEH), PTH (80 μ g/kg, 5 days/wk), PRO (5 mg/mL), or a combination of PTH and PRO for 4 wks. We hypothesized that PRO would enhance the anabolic effect of PTH. Interestingly, PTH and PRO had additive effects on trabecular bone volume fraction in the vertebrae ($p < 0.001$), but PTH improved trabecular and cortical parameters to the same extent with or without PRO in the femur. PTH+PRO mice had higher serum PINP ($p = 0.012$) and lower CTX ($p < 0.001$) levels than those treated with PTH alone, suggesting PRO improved bone formation and reduced PTH-induced resorption. While PTH alone caused a significant increase in osteoclast number/total area in the vertebrae ($p = 0.001$), this was completely blocked in the PTH-PRO group. In contrast, PRO did not improve static or dynamic osteoblast parameters beyond that of PTH in vertebrae. However, the combination significantly reduced cortical porosity in both the tibia ($p = 0.019$) and femur ($p = 0.007$) while neither PTH nor PRO had a significant impact on porosity alone. We found no differences in femur cortical bone PTH-induced Rankl or Opg expression when PRO was present, but extracellular matrix genes Osteomodulin ($p = 0.003$) and Dmp1 ($p < 0.001$) were increased by PTH+PRO, suggesting osteocytes may play a role in the improved cortical porosity distinctive to combination treatment. Finally, we determined that PTH+PRO also reduced serum norepinephrine (as measured by mass spectrometry) by 38% ($p = 0.014$), suggesting that combined treatment uniquely reduced sympathetic tone. In light of the current literature, our data suggest that suppression, but not complete loss, of β AR signaling improves bone parameters from PTH treatment, and we hypothesize that the site- and compartment- specificity may be related to localized differences in sympathetic nervous system activity.

Disclosures: **Annika Treyball**, None

SUN-0369

WITHDRAWN

SUN-0370

A Novel Long-Acting PTH(1-34) Analog Containing a Palmitoylated C-Terminal Tag Hiroshi Noda^{*}, Ashok Khatri, Thomas J Gardella. Massachusetts General Hospital and Harvard Medical School, United States

PTH analogs with prolonged actions have potential therapeutic applications, particularly for hypoparathyroidism. Unmodified PTH(1-34) clears rapidly from the circulation (t_{1/2} ~ 30'), in part via renal filtration, and thus has a limited duration of action. Addition of bulky polyethylene glycol (PEG) chains to the peptide's C-terminus can impede renal filtration and result in a prolonged circulation half-time, but such PEGylated peptides are difficult to produce in pure form, in part due to the non-mono-dispersed nature of the PEG precursors. Zorzi et al. (Nat Comm. 2017) developed a palmitoylated heptapeptide tag sequence [EYEK(palmitoyl)EYE] that is optimized for binding albumin, which has a half-life in the serum of ~20 days, and thus can be used to extend the pharmacokinetic (PK) profile of a target peptide in vivo. We explored this approach for PTH by synthesizing a PTH(1-34) analog containing the [EYEK(palmitoyl)EYE] tag at the C-terminal position and assessing the peptide, called palm-PTH(1-34) in cells and in mice. In human osteoblast-derived SaOS-2 cells, palm-PTH(1-34) stimulated cAMP formation with the same potency as PTH(1-34) (pEC50 = 9.65 ± 0.1 vs. 9.60 ± 0.1, respectively). After injection into mice, palm-PTH(1-34) (10 nmol/kg, s.c.) increased blood Ca⁺⁺ levels for at least 24 hours, whereas an equal dose of PTH(1-34) increased blood Ca⁺⁺ for no longer than 7 hours. Palm-PTH(1-34) also induced more prolonged hypophosphatemia. Consistent with these prolonged pharmacodynamic (PD) actions, palm-PTH(1-34) exhibited a markedly prolonged PK profile, as it persisted in the plasma following a single injection (10 nmol/kg, s.c.) for longer times, and attained a significantly greater maximum concentration than did PTH(1-34) (t_{1/2} = 1.9 h vs. 0.2 h; C_{max} = 28.1 vs. 0.65 nM; detection by PTH(1-34) ELISA, Quidel Inc.). Evaluation of renal filtration using TMR-labeled derivative peptides and tracking TMR fluorescence in the urine at times after injection, revealed that TMR-palm-PTH(1-34) was excreted into the urine at a greatly reduced rate, as compared to TMR-PTH(1-34). The findings overall show that palm-PTH(1-34) mediates prolonged PK/PD actions in vivo via a mechanism that involves reduced renal filtration, as presumably mediated by binding to serum albumin. The tagged peptide maintains adequate affinity for the PTH receptor and effectively activates down-stream signaling responses in bone and kidney target cells. Further study of such PTH

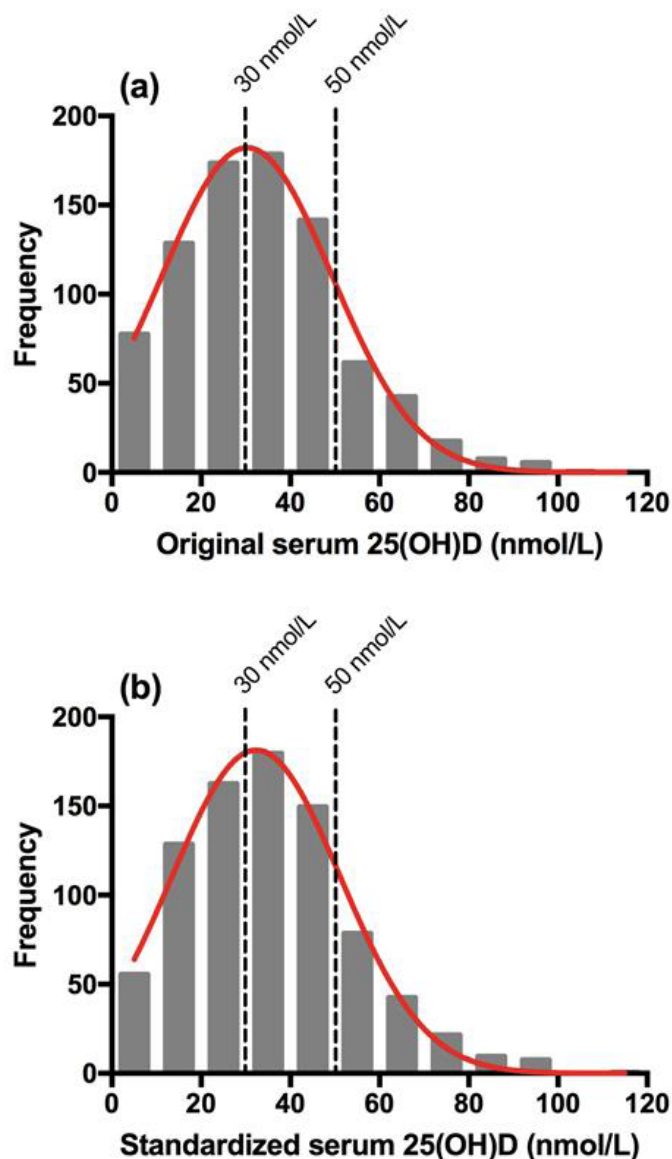
analogs may lead to new treatment options for hypoparathyroidism and potentially other PTH-related disorders.

Disclosures: *Hiroshi Noda, Chugai Pharmaceutical Co., Ltd., Other Financial or Material Support*

SUN-0371

Standardizing 25-Hydroxyvitamin D Concentrations Does Not Change the Number of Infants Classified as Vitamin D Deficient Sharina Patel*¹, Sherry Agellon¹, Paula Lavery¹, Catherine A. Vanstone¹, Nora Shero¹, Nathalie Gharibeh¹, Maryam Razaghi¹, Shuqin Wei², Hope A. Weiler¹. ¹School of Human Nutrition, McGill University, Canada, ²Department of Obstetrics and Gynecology, Sainte Justine Hospital, University of Montreal, Canada

Immunoassays are commonly used to measure total 25-hydroxyvitamin D (25(OH)D) concentrations in research and clinical settings due to their low cost and high-throughput. Large assay variability in measuring serum 25(OH)D impedes the ability of researchers to effectively make comparisons across studies and draw conclusions about potential deficiencies. Even within a laboratory, assay drift can occur over time despite the use of external quality control programs. The Vitamin D Standardization Program (VDSP) was organized to address these issues and has developed protocols to standardize laboratory 25(OH)D measurements to gold-standard reference measurement procedures (RMPs). Our objective was to standardize total serum 25(OH)D values of infants from a newborn vitamin D screening program to RMPs. Capillary blood samples taken from 849 neonates 24-36 h after birth (March 2016 through March 2018) were analyzed for total serum 25(OH)D using a chemiluminescent immunoassay (Liaison, Diasorin). Across this period, 142 quality control samples with 25(OH)D values assigned by the National Institute for Standards and Technology (NIST) were measured using the same immunoassay: 50 NIST 972a Level 1-4 samples and 92 Vitamin D External Quality Assessment Scheme (DEQAS) samples. The NIST and Liaison 25(OH)D concentrations of quality control samples were used to establish a weighted Deming regression equation to standardize infant serum 25(OH)D concentrations to RMPs. Fisher's exact test was used to compare proportions before and after standardization. The inter-assay coefficient of variation for NIST and DEQAS samples was 6% at 47.3 nmol/L and 7% at 116.2 nmol/L 25(OH)D, with a mean accuracy of 92%. The weighted Deming regression equation was: $y = 1.002x - 2.449$. After standardization, mean infant serum 25(OH)D increased from 43.0 ± 18.8 to 45.3 ± 18.8 nmol/L (mean \pm SD). The median and inter-quartile range increased from 41.9 (29.7, 54.0) to 44.3 nmol/L (32.1, 56.3). Proportions of infants with serum 25(OH)D < 30, 30-49.9 and ≥ 50 nmol/L were originally 25%, 42% and 33%, and were 23%, 40% and 37% after standardization ($p > 0.05$; Figure 1). Standardizing original measurements to RMPs led to small increases in 25(OH)D concentrations yet no difference in rates of deficiency (< 30 nmol/L), inadequacy (30-49.9 nmol/L) or sufficiency (≥ 50 nmol/L). Standardization of infant serum 25(OH)D concentrations will enable comparisons of this data to other studies as well as national data.



Disclosures: *Sharina Patel, None*

SUN-0372

Hypocalcemia from Hypoparathyroidism after Harvoni treatment for Hepatitis C Puspalatha Sajja*, Catherine Anastasopoulou, Nissa Blocher. Einstein Medical Center, United States

Background: Harvoni (Ledipasvir and Sofosbuvir) is one of the treatment options for Hepatitis C infection. We report a case of hypocalcemia from hypoparathyroidism precipitated by Harvoni therapy. **Case Presentation:** A 64-year old African American man with Hepatitis C was treated with 12 weeks course of Harvoni. He had no previous history of hypocalcemia prior to the therapy. Patient was first noted to have corrected calcium of 8.4 mg/dl during the last week of Harvoni treatment with repeat calcium level of 8.2 mg/dl two months later. Another two months later he presented to Emergency Department with numbness, palpitations, and muscle cramping. His blood work showed calcium 6.6 mg/dl, albumin 4.3 mg/dl, PTH 18 pg/ml, 25-hydroxy vitamin D 11 ng/ml, magnesium 2.2 mg/dl, phosphorus 3.8 mg/dl and 24-hour urine calcium was less than 2. Oral calcitriol, ergocalciferol and calcium carbonate were initiated at that point and his calcium normalized on treatment within four weeks. Five months later repeat labs showed 25(OH)vit D 37.2 ng/ml and PTH 18 pg/ml. His calcium remained normal on calcitriol and calcium carbonate, but because of the persistently low PTH intact levels, patient was considered for parathyroid hormone injections. **Discussion:** Harvoni is a combination medication of Ledipasvir and Sofosbuvir which are hepatitis C virus NS5A protein and NS5B RNA polymerase inhibitors blocking viral replication. There have been no case reports of hypoparathyroidism in the literature from Harvoni treatment. In our patient, the absence of other potential causes of hypoparathyroidism, including lack of autoimmune background, or any history of neck surgery or radiation exposure, as well as the sudden onset of hypocalcemia right at the end of Harvoni treatment,

makes Harvoni the most likely cause of his hypoparathyroidism. More long term data on this drug is needed to find out if hypoparathyroidism is one of the potential complications of Harvoni therapy. Conclusion: Hypoparathyroidism leading to hypocalcemia could be a potential complication of Harvoni treatment. Monitoring calcium and parathyroid hormone levels prior to initiation and periodically after completion of Harvoni treatment should be recommended for all patients.

	Calcium mg/dl	Albumin mg/dl	PTH pg/dl	25(OH)vit D	Phosphorous mg/dl	Magnesium mg/dl	HCV RNA PCR IU/ml
3/23/2016	9.9	4.3			2.8		1,481,500
7/5/2016	8.4	3.9					< 12
9/30/2016	8.2	4.4					
12/1/2016	6.6	4.3					
12/16/2016	7.0	3.9	18	11	3.8	1.8	
12/27/2016	9.3						
2/2/2017	9.0	3.8			3.5	1.7	
5/12/2017	8.5		18	37.2	3.8		

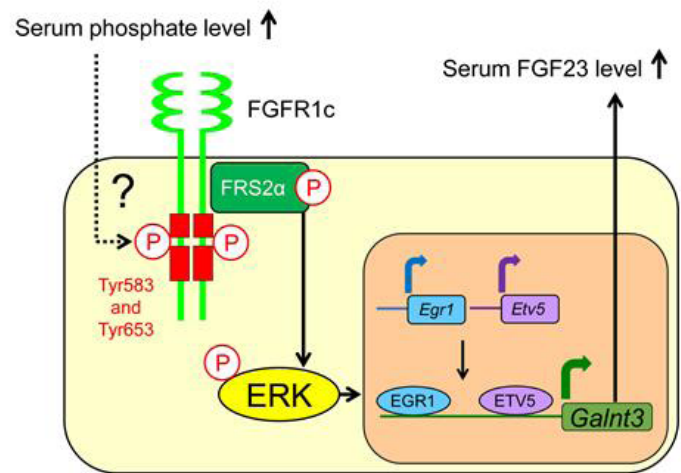
Harvoni therapy from 4/12/2016 to 7/15/2016.

Disclosures: Puspalatha Sajja, None

SUN-0373

FGF Receptor 1c Works as a Phosphate-Sensor to Regulate FGF23 Production Yuichi Takashi*¹, Yuka Kinoshita², Nobuaki Ito², Shun Sawatsubashi¹, Hidetaka Kosako¹, Masahiro Abe¹, Munehide Matsuhisa¹, Toshio Matsumoto¹, Seiji Fukumoto¹. ¹Tokushima University, Japan, ²The University of Tokyo Hospital, Japan

Phosphate is essential for proper functions of all cells. Serum phosphate level is maintained within a narrow range indicating that there is a machinery to monitor changes of this mineral concentration. Fibroblast growth factor (FGF) 23 produced by bone especially osteocytes is a hormone that decreases serum phosphate level. However, it has been unclear how changes of phosphate level modify serum FGF23 concentration. FGF23 level can be regulated by both its expression in osteocytes and posttranslational cleavage into inactive fragments. Galnt3 gene product initiates the attachment of mucin-type O-glycan to FGF23 and prevents this cleavage. High phosphate diet increased serum phosphate and FGF23, and enhanced the expression of Galnt3 in bone without changing that of Fgf23 in mice. These results suggest that posttranslational modification via Galnt3 gene product is the main mechanism to regulate serum FGF23 level at least in this model. Then, transcriptomic analysis was employed to identify regulatory factors of Galnt3 expression using UMR106 cells. High extracellular phosphate upregulated expression of several transcription factors and signaling components of ERK pathway. Subsequent functional analysis identified early growth response 1 (EGR1) and ETS variant 5 (ETV5) are required to enhance transcription of Galnt3 by phosphate. We further explored how UMR106 cells sense extracellular phosphate to activate ERK. We focused on receptor tyrosine kinases (RTKs) which can activate the ERK pathway. LC-MS/MS analysis of immunoprecipitated cell extract using anti-phosphotyrosine antibody identified Tyr583 and Tyr 653 of FGF receptor (FGFR) 1c as phosphorylated residues by high extracellular phosphate. Western blotting indicated that high extracellular phosphate induced phosphorylation of FGFR substrate 2 α (FRS2 α) and ERK. Inhibitors of FGFR and ERK pathway abolished the stimulatory effect of phosphate on Galnt3 expression. In addition, an inhibitor of FGFR also abolished the effect of high phosphate diet on Galnt3 expression in mice. Together, we have shown that phosphate activates FGFR1c to phosphorylate FRS2 α , leading to activation of the ERK pathway that induces Galnt3 expression via two transcription activators. These findings uncover an unrecognized facet of FGFR1c function and provide a molecular basis of phosphate-sensing in regulated FGF23 production.



Disclosures: Yuichi Takashi, None

SUN-0374

Effects of Biliopancreatic Diversion on Bone Turnover Markers and Association with Hormonal Factors in Patients with Severe Obesity Anne-Frederique Turcotte*¹, Thomas Grenier-Larouche², Roth-Visal Ung¹, David Simonyan³, Anne-Marie Carreau², André Carpentier², Fabrice Mac-Way¹, Claudia Gagnon¹. ¹Laval University, Canada, ²Sherbrooke University, Canada, ³Chu de Quebec, Canada

Context: No study has assessed the early impact of biliopancreatic diversion with duodenal switch (BPD-DS) on bone remodeling and whether it is influenced by hormonal factors. Objectives: To evaluate the early, mid- and longer-term changes in serum bone turnover markers and its regulators as well as their associations with hormonal factors after BPD-DS in patients with severe obesity. Methods: Ancillary study using fasting frozen plasma from 16 individuals with severe obesity (11F/5M, 69% with type 2 diabetes, mean BMI 49.4 kg/m²) assessed before (T0), 3 days (T1), 3 months (T2) and 12 months (T3) after BPD-DS. Serum bone turnover markers (C-terminal telopeptide (CTX), intact osteocalcin (OC)), regulators of bone turnover (sclerostin, osteoprotegerin (OPG)) and hormonal factors (GLP-1, GIP, insulin, glucagon, leptin, high molecular weight adiponectin, PTH and 25-hydroxyvitamin D) were analyzed at each visit. Changes between baseline and each timepoint in bone turnover markers and its regulators were correlated with changes in hormonal factors using Pearson partial correlations adjusted for weight loss. Results: Weight did not change at T1 but decreased by 33±27 kg at T2 and 59±12 kg at T3. CTX increased significantly at T1 (+66%), T2 (+219%) and T3 (+295%). OC decreased significantly at T1 (-19%) then increased at T2 (+69%) and T3 (+164%) (Figure 1). Change in sclerostin was modest overall and only significant between T1-T2 (+13%) while change in OPG was only significant between T0-T1 (+48%) and T0-T3 (+45%). All changes were similar between participants with or without diabetes. The increase in CTX correlated with weight loss at T2 (r=-0.63, p=0.009) and T3 (r=-0.58, p=0.039). Changes in sclerostin correlated with changes in insulin at T3 (r=-0.60, p=0.040) and adiponectin at T2 (r=-0.62, p=0.013). Changes in adiponectin also correlated with changes in OC at T1 (r=0.54, p=0.039) and OPG at T1 (r=-0.61, p=0.017). No other hormonal factor correlated significantly with bone turnover markers or its regulators. Conclusions: BPD-DS causes an earlier and greater increase in bone resorption over bone formation, potentially favouring bone loss. Sclerostin did not increase as expected following massive weight loss, suggesting an altered osteocyte response to mechanical unloading. Changes in adiponectin and insulin seem to play a role independent of weight loss in bone remodeling after BPD-DS.



Disclosures: Anne-Frederique Turcotte, None

SUN-0375

The Kruppel-like transcription factor 6 (KLF6/CPBP) plays a critical role in Colony Stimulating Factor 1-dependent transcriptional activation of the SPHK1 gene Gang Qing Yao*, Karl Insogna. Yale university, United States

Intermittent activation of the PTH receptor stimulates bone formation. CSF1 is the principal colony stimulating activity released by osteoblasts constitutively and in response to PTH treatment and its receptor, c-fms, is more highly expressed on osteoclasts than any other cell in bone. We have found that deleting c-fms in osteoclasts attenuates the anabolic response to PTH, suggesting that PTH-induced CSF1 from osteoblasts may stimulate the release of anabolic cytokines from osteoclasts. Sphingosine kinase 1 (SPHK1) is the rate-limiting enzyme required for the synthesis of sphingosine-1-phosphate (S-1-P), a phospholipid with known anabolic effects in bone and we have previously reported that CSF1 increases SPHK1 expression by transcriptional activation of the SPHK1 gene. To study the mechanism of CSF1-induced SPHK1 gene expression, we cloned a 2,608 bp fragment of the murine SPHK1 gene (-2497 to +111 bp relative to the transcription start site) into the pGL3-basic vector and transfected it into P-zen cells (murine fibroblasts engineered to express c-fms). SPHK1 promoter activity was assessed using the Dual-Luciferase reporter assay system, which employs the pGL4.73 vector (Promega®). By analyzing a series of 5'-deletions, we identified a CSF1-responsive region located in the region -1250 to -1016 bp. To define putative DNA binding site(s) in this fragment, we generated two biotin-labeled fragments, one 163 bp in length (-1302 to -1139) and one 169 bp in length (-1158 to -989) that completely overlap this region. EMSAs revealed the 163 bp fragment as the target for protein binding. Using EMSAs, we further narrowed the binding region to an 83 bp fragment, (-1222 to -1139). By querying the TRANSFAC database, we identified a cis element consensus sequence for the transcription factor CPBP/KLF6 in this region. Cold competitor fragments for use in an EMSA were engineered based on this sequence, a wild type sequence and a CPBP-mutated sequence. We found that a shifted band, which was induced by CSF1, was completely competed using the wild type oligo but not the mutated oligo. Full-length wild type and CPBP/KLF6-mutated promoters were introduced into the pGL3 expression vector and transfected into P-zen cells. Mutating the CPBP site nearly completely abrogated the ability of CSF1 to activate the promoter. We conclude that the CPBP/KLF6 cis-element plays an important role in mediating CSF1-dependent transcriptional activation of the SPHK1 gene.

Disclosures: Gang Qing Yao, None

SUN-0401

Specific modulation of vertebral marrow adipose tissue by physical activity Daniel Belavy*¹, Matthew Quittner¹, Nicola Ridgers¹, Adnan Shiekh², Timo Rantalainen³, Guy Trudel². ¹Deakin University, Australia, ²University of Ottawa, Canada, ³University of Jyväskylä, Finland

BACKGROUND: Marrow adipose tissue (MAT) accumulation with normal aging impacts the bone, hemopoiesis and metabolic pathways. Hormonal and nutritional factors have been reported to accelerate the process. There is also evidence that reduced physical activity (spinal cord injury, experimental bed-rest) leads to accelerated MAT accumulation. It is unknown whether increased physical activity, or specific types of physical activity, may reduce MAT. We investigated whether exercise was associated with lower MAT, as measured by vertebral marrow fat fraction (VFF) on magnetic resonance imaging. **METHODS:** 101 healthy individuals (54 females) aged 25-35 yrs without spine or bone disease but with distinct exercise histories were studied. We examined 25 long-distance runners, 30 habitual joggers, 22 high-volume road cyclists and 24 non-sporting referents. VFF was quantified in

lower thoracic (T10, T11, T12) and lumbar (L1 to L5) vertebrae via mDIXON sequence on magnetic resonance imaging. All participants wore a 3D accelerometer (ActiGraph) at their hip for 8d after scanning. In 10 additional individuals, accelerometry data were collected in to associate acceleration profiles with specific physical activities. **RESULTS:** Long-distance runners exhibited lower mean lumbar VFF (27.9[8.6]% vs. 33.5[6.0]%; $p=0.0048$) than non-sporting referents. In habitual joggers, mean lumbar VFF was 31.3(9.0)% ($p=0.22$ versus referents) and 6.0 percentage points lower than referents at vertebrae T10, T11 and T12 ($p\leq 0.023$). Regression analysis showed a 0.7 percentage point reduction in mean lumbar VFF with every 9.4km/week run ($p=0.002$). Mean VFF of high-volume road cyclists was comparable to non-sporting referents. 3D accelerations corresponding to faster walking, slow jogging and high-impact activities correlated with lower VFF while low-impact activities and sedentary time correlated with higher mean lumbar VFF (all $p\leq 0.05$). **CONCLUSIONS:** This study presents the first evidence in humans or animals that specific volumes and types of exercise may influence the age-determined adipose marrow conversion and result in low MAT. There is an estimated adipose bone marrow conversion of 7% per decade of life. In comparison to this, long distance runners, with 5.6 percentage points lower VFF, showed an estimated 8-year younger vertebral marrow adipose tissue phenotype. Running, but not high volume road cycling, may impact MAT.

Disclosures: Daniel Belavy, None

SUN-0402

The role of acetylcholine receptor signaling in bone mechanotransduction Karl J Lewis*, Alexander G Robling. Indiana University School of Medicine, United States

Decades ago, Rubin and Lanyon showed that disuse-induced bone loss could be mitigated by short bouts of daily loading[1]. Cytokine signaling changes among bone cells related to mechanical loading are well studied, however the role of neurotransmitters is not well understood. Our group recently found that transcripts for the nicotinic acetylcholine (ACh) receptor subunit CHRNA1 are significantly down regulated in cortical bone after mechanical loading, suggesting ACh signaling may be important for osteocyte mechanotransduction. The present studies interrogate the role of ACh signaling in bone mechanotransduction. Botulinum toxin (BTX), a potent inhibitor of ACh release, has been used as a model for limb disuse in rodents previously[2,3]. Here we use this method as both a model of disuse and means of exposing bone to BTX locally. We injected BTX into the major muscle groups surrounding the tibia and femur of 15wk old female B6 mice ($n=10$), followed by 3 tibial loading bouts per week for 2 weeks (2700 μ ?, 120 cycles, 2Hz). Saline injected ($n=6$), non-injected ($n=6$), and BTX injected/non-loaded ($n=10$) groups were included as controls. DEXA scans were collected at 15 (experiment start) and 18 wks (experiment termination) wks of age, and μ CT analysis was performed after sacrifice at 18 weeks. Additionally, a CHRNA1 floxed loss-of-function mouse was generated, crossed to the Dmp1-Cre driver, and characterized with μ CT following 2wks of tibial loading. Statistical analyses by Student's t-test, $p<0.05$. Loading resulted in a significant increase in DEXA properties among the saline-injected mice. BTX treatment resulted in bone loss in the treated limb, whether the limb was loaded or not, though more severe bone loss was found in the mice that were not loaded. μ CT data taken from the tibial midshaft, however, showed cortical BV/TV and BMC decreased in only the non-loaded BTX group. CHRNA1 mutants showed no statistically significant differences from wild-type B6 controls. The lack of response to loading in BTX-treated limbs suggests that either ACh signaling is required for osteocytes but was prevented by local BTX injection around the nearby bone, that in order for bone to respond to mechanical stimuli a tonic myokine originating from nonparalyzed muscle is required, or some combination of the two. These data suggest that either CHRNA1 can be compensated for by some other subunit, or that the effect of ACh signaling in bone is mediated through some other receptor. [1] C.T. Rubin, L.E. Lanyon, J Bone Joint Surg Am. 66 (1984) 397-402. [2] S.E. Warner et al, Bone. 38 (2006) 257-264. [3] S.L. Manske et al, Calcif Tissue Int. 87 (2010) 541-549.

Disclosures: Karl J Lewis, None

SUN-0403

Expression pattern of the mechanoresponsive piezo2 ion channel during skeletal development and growth Jerahme Martinez*, Ashutosh Parajuli, Sucharitha Parthasarathy, Padma Srinivasan, Catherine Kim-Safran, Liyun Wang. University of Delaware, United States

Piezo2, a recently discovered stretch-activated cation channel, plays an important role in mediating mechanosensation and proprioceptive. Mutations in the piezo2 gene have been associated with the human musculoskeletal disorder Gordon syndrome (GS; MIM #1143000), characterized by impaired mobility, congenital contractures of the limbs, and shortened stature. The ability of piezo2 to sense mechanical stimuli and its role in musculoskeletal development prompted us to explore its role in bone. The widespread expression of piezo2 in mechanosensitive tissues suggests a distinct physiological role for mechanotransduction. We hypothesize piezo2 acts as a mechanosensor in bone and plays an important role in maintaining overall skeletal health and bone adaptation. To gain insight into its function within the skeletal system we examined piezo2 transcript levels in murine bone under in vivo mechanical loading, and characterized protein spatial and temporal expression patterns bone tissue, via quantitative real-time PCR (qPCR) and immunohistochemistry (IHC), respectively. Piezo2 mRNA levels were elevated in murine bone when subjected to 7 days of axial tibia loading relative to the non-loaded control limbs, whereas no change was observed follow-

ing one bout of loading. We demonstrated *piezo2* is present during the early stages of murine embryonic development, particularly in mesenchyme tissue undergoing endochondral bone formation, and was found to be expressed by bone cells (e.g. osteoblasts and osteocytes), bone marrow cells, and chondrocytes of adult bone. These studies implicate the *piezo2* gene in the adaptive response of bone when subjected to dynamic loading and unloading. At the protein level, *piezo2* is present within bone tissue throughout all stages of development and growth. Additionally, we found *piezo2* is expressed by key cells involved in the bone remodeling process, and is present in regions that are subjected to high levels of mechanical load. It is possible that *piezo2* serves as a key contributor of bone adaptation process and may function as a viable target to orchestrate bone formation.

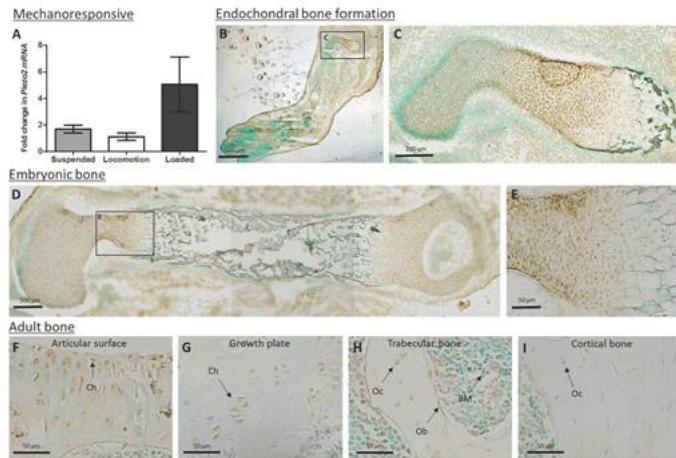


Figure 1. Piezo2 transcript levels in response to mechanical stimulation and protein expression during skeletal growth. (A) Piezo2 transcript levels were elevated in bone under both unloaded and loaded conditions, using the hind limb suspension/unloading and axial tilt loading models respectively. Piezo2 levels were determined by qPCR analysis. (B-E) Immunohistochemistry analysis of piezo2 protein accumulation in embryonic and adult tissue. (B-C) Piezo2 is expressed in E 14.5 in mesenchymal/precartilage tissue undergoing endochondral ossification. (D-E) As bone continues to develop piezo2 expression is found along the proximal and distal ends of the femur, particularly at the growth plate region. (F-I) In adult bone (81 weeks), piezo2 is expressed by chondrocytes of articular cartilage (F) and the growth plate (G), bone marrow cells (H), osteoblasts (H), and osteocytes (H).

Disclosures: **Jerahme Martinez, None**

SUN-0404

Substantial Repair of Diffuse Damage in Bone In-Vitro Can Occur Through Physicochemical Mechanisms. Leila Mehraban Alvandi*, Donna Chen, Samuel Stephen, Zeynep Seref-Ferlengez, Robert J Majeska, Mitchell B. Schaffler. Department of Biomedical Engineering, City College of New York, United States

Linear microcracks (50-100 μm long) and diffuse damage (Dif-Dx) (sub-micron size cracks) are the major microdamage types resulting from wear and tear in bone. Recently, we discovered that Dif-Dx repairs without remodeling, pointing to a direct healing mechanism for these cracks (1). Here we tested the hypothesis that repair of Dif-Dx regions in bone, as assessed functionally by recovery of mechanical properties, can occur in vitro in the absence of viable osteocytes. Methods: Diffuse damage was selectively introduced into the ulnar diaphysis of rats (SD, Female, 19w, n=8) in vivo. The loading used for these studies (~15% stiffness loss in creep) selectively creates a discrete Dif-Dx region in the mid diaphysis (1, 2). Ulnae were harvested after loading and frozen in PBS at -20°C until tissue testing. One mm thick cross sections from diaphyseal damage zones were mounted on small plastic slides and incubated in saline buffer either with or without supplemental Ca^{2+} at plasma concentration (2mmol/L) for 5 days at 37°C . This solution has been shown to remineralize small enamel defects. Samples from acutely damaged and non-damaged control bones as well as baseline bone slices were tested using microindentation to determine tissue level Elastic modulus (E) and Dif-Dx area was measured by histomorphometry. Comparisons: Nonparametric ANOVA with post-hoc Mann-Whitney U-test. Results: Elastic modulus in Dif-Dx zones (acute loaded ulnae, time=0) was reduced significantly (15%) compared to non-damaged control bone. Modulus of Dif-Dx region was recovered to 95% of control level after 5 days incubation in saline+ Ca^{2+} . In addition, Dif-Dx area was reduced by 55% after 5 days incubation in saline+ Ca^{2+} vs acute diffuse damage levels (Fig 1). Discussion: In the current study Dif-Dx in compact bone repaired through purely physicochemical processes and without live osteocytes, as evidenced by recovery of tissue mechanical properties and reduction in damage content. Dif-Dx occurs entirely within cortical bone. The principal exchange surface within cortex is the osteocyte lacunar-canalicular space (LCS). We posit that the Ca^{2+} source responsible for healing Dif-Dx in vivo is the fluid contained within the LCS. How this repair occurs is not yet known but may include growth of existing mineral crystals and/or infilling of crack spaces with new mineral deposition analogous to enamel repair (3). Ref.:1) Seref-Ferlengez+ JBMR 2104; 2) Vashishth + Bone 2000; 3) Simmer + Oral Biol 1995.

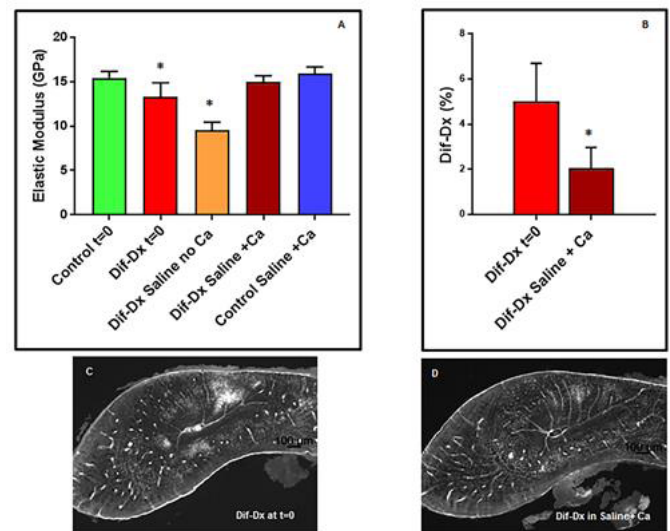


Figure 1. A. Elastic Modulus(GPa) (* p<0.05) B. Dif-Dx Area (%) (* p<0.05) C. Dif-Dx at t=0 D. Dif-Dx in Saline+Ca

Disclosures: **Leila Mehraban Alvandi, None**

SUN-0405

Bone Properties and the Endocannabinoid System Observed with Neurectomy and Hibernation in Marmots (*Marmota flaviventris*) Emily Mulawa*, Rebecca Packer, Jay Kirkwood, Lisa Wolfé, Samantha Wojda, Jessica Prenni, Gregory Florant, Seth Donahue. Colorado State University, United States

Hibernators have adapted a physiological mechanism allowing them to undergo long periods of inactivity without experiencing bone loss from disuse. A previous study of the bone proteome in marmots found monoacylglycerol lipase to be 98-fold higher during hibernation. Monoacylglycerol lipase is responsible for degrading the endocannabinoid ligand 2-arachidonoyl glycerol and endocannabinoid-like ligands N-palmitoylethanolamide (PEA) and N-oleoylethanolamide (OEA). The primary cannabinoid receptors (CB) have divergent localization in bone. CB1 is predominately found on sympathetic nerve terminals, while CB2 is found on bone cells and their progenitors. This study determined the contribution of neural innervation on endocannabinoid regulation of bone remodeling. Neurectomy for forced disuse was performed on the right leg sciatic nerve perineal branch, with the left leg serving as a control, in both hibernating and active groups of marmots. Endocannabinoid and endocannabinoid-like ligand concentrations were measured from the fourth metatarsals using microflow chromatography coupled with tandem quadrupole mass spectrometry (LC-QQQ-MS). In addition, trabecular bone properties of the fifth metatarsals were evaluated using micro-computed tomography to quantify bone loss. The endocannabinoid anandamide, as well as PEA and OEA, significantly increased with neurectomy in bone marrow in active, but not hibernating, marmots. Ligand concentrations in bone did not change significantly with neurectomy regardless of state. There were no significant changes with neurectomy in trabecular bone properties of active and hibernating marmots, indicating that bone loss did not occur. Elucidating the mechanism hibernators use to maintain bone architecture and density could help guide development of novel bone loss prevention therapies in humans.

Disclosures: **Emily Mulawa, None**

SUN-0406

The Role of Panx1 and P2X7R in Inflammation-induced Diabetic Bone Dysfunction Zeynep Seref-Ferlengez*¹, Marcia Urban-Maldonado¹, Herb Sun¹, Mitchell Schaffler², Sylvia Suadcani¹, Mia Thi¹. ¹Albert Einstein College of Medicine, United States, ²City College of New York, United States

Bone loss is a complication in diabetes that is often overlooked. Despite growing clinical and epidemiological evidence that supports the association of Type 1 diabetes (T1D) with low bone mass and fractures, the mechanisms underlying diabetic osteopenia are still not completely understood. We propose that diabetic bone becomes insensitive to mechanical loading due to dysregulation of the osteocyte Panx1-P2X7R mechanosignaling complex that not only disrupts proper load-induced bone adaptation but also triggers local load-induced inflammation, which in combination ultimately lead to bone loss in T1D. To test this hypothesis we used the Akita (C57BL/6J-Ins2Akita) mouse model of T1D and age-matched wildtype (WT) mice (8 wk old, male, n=7/group) that were submitted to mechanical loading by treadmill running (2 or 4 wks; 5 days/wk, 300 m/day) or to normal cage control activity. All animals were euthanized immediately after the last running bout. Right hindlimbs were used for histomorphometry, lefts were used for Western blotting and forelimbs were used for qPCR analysis. All experiments were performed under IACUC approval. We found that the anabolic response to mechanical loading is impaired in Akita mice when compared to

age-matched WT mice. We also observed that mechanical loading regulates both Panx1 and P2X7R expression in the bone (Fig.1). In WT mice, Panx1 and P2X7R expression changed in response and adapted to different loading durations; expression peaked at 2 wks loading time and returned to basal levels at 4 wks loading time when compared to non-loaded WT bones (blue traces). This adaptive response was not lost in diabetic bone, but was dysregulated (red and green traces; Panx1 and P2X7R remain at higher levels at 4 wks loading time), indicating that diabetic mice are unable to properly adapt to mechanical loading. Remarkably, this dysregulation of Panx1-P2X7R was accompanied by a significant inflammatory response in diabetic bone, as evidenced by upregulation of the NLRP3 inflammasome and IL-1 β (Fig. 2). Because Panx1 and P2X7R can mediate NLRP3 inflammasome activation, it is likely that Panx1-P2X7R dysregulation is the major driver of this load-induced inflammatory response. Such dysregulation of Panx1-P2X7R signaling, fueling the inflammasome activation in response to mechanical loading, may thus be a key factor in the events leading to the lack of load-induced anabolic response and increased bone loss observed in T1D mice.

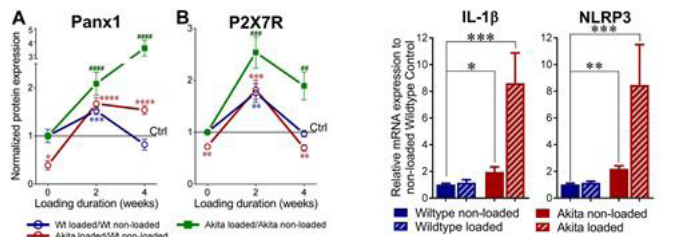


Figure 1. Panx1-P2X7R mechanosignaling complex responds differently to mechanical loading in wildtype and T1D Akita mice. Panx1 and P2X7R in loaded wildtype (WT) and Akita mice compared to their age-matched non-loaded WT before (0 week) and after 2 or 4 weeks of loading (treadmill running). Protein levels normalized by β -actin then by age-matched non-loaded WT levels or non-loaded Akita levels. * P <0.05, *** P <0.001, non-loaded WT vs. age-matched loaded Akita and wildtype (blue and red traces), ** P <0.01, *** P <0.001, non-loaded Akita vs. age-matched loaded Akita (green trace), one-way ANOVA followed by Tukey's multiple comparison test. Loading group: n = 4-6 (0 weeks), n = 7-9 (2 weeks), n = 9 (4 weeks). Data presented as means \pm SEM.

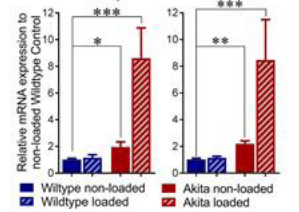


Figure 2. Mechanical loading upregulates IL-1 β and NLRP3 in Akita bones. IL-1 β and NLRP3 mRNA levels in non-loaded and in 2-week loaded WT and Akita bones compared to non-loaded age-matched WT controls. Note already higher IL-1 β and NLRP3 in non-loaded Akita that are further increased by loading. * P <0.05, ** P <0.01, *** P <0.001, non-loaded WT vs. loaded WT and Akita, one-way ANOVA followed by Tukey's multiple comparison test. Means \pm SEM, 3/group

Disclosures: Zeynep Seref-Ferlengez, None

SUN-0407

Exercise in Calorie Restricted Mice fails to Increase Bone Quantity, despite suppression of Marrow Adipose Tissue (MAT) Cody Mcgrath^{1*}, Jeyant Sankaran¹, Negin Misaghian-Xanthos¹, Buer Sen¹, Zhihui Xie¹, Martin A Styner², Xiaopeng Zong³, Maya Styner¹. ¹Division of Endocrinology and Metabolism, Department of Medicine, UNC-Chapel Hill, United States, ²Departments of Computer Science and Psychiatry, UNC, United States, ³Biomedical Research Imaging Center, UNC, United States

Marrow adipose tissue (MAT) and its physiologic relevance to skeletal health in the setting of anorexia or calorie restriction (CR) is unknown. We hypothesized that MAT of CR differs from the calorie-replete state. Ten-week-old female B6 mice fed a regular (RD) or 30% CR-diet were allocated to sedentary (RD n =10, CR n =10) and running exercise groups (RD-E n =7, CR-E n =7). After 6 weeks, CR mice weighed 20% less than RD, p <0.001; exercise did not affect weight. Femoral bone volume (BV) quantified by 3D-MRI/9.4T scanner was 20% lower in CR and CR-E compared to RD and RD-E (p <0.0001). CR associated with decreased bone by μ CT: Tb.Th was 15% less in CR vs RD p <0.03, and cortical bone fraction was 4% less, p <0.01. Similarly, in CR-E, trabecular bone was 27% less than RD-E, p <0.0001. Exercise associated with increased trabecular bone quantity (+18% RD-E vs RD p <0.0001) but failed to in CR. Furthermore, cortical porosity, which was similar between RD and RD-E- increased in CR-E vs CR (+33%, p =0.04), suggesting the combination of CR and exercise is deleterious to bone, particularly the cortex. Metaphyseal MAT/BV quantified by 3D-MRI/9.4T scanner increased by 159% in CR vs RD, p =0.003. As expected, exercise lessened MAT/BV by 52% in RD, p <0.05, Fig 1. Notably, exercise also suppressed CR MAT by 47%, p <0.05. Histologic analysis of marrow adipocytes correlated with MRI findings, Fig 2. Tibial mRNA demonstrated an increase in PLIN1 in CR (+100% CR vs RD, p =0.065), confirming an increase in adipocytes. Unexpectedly, SOST mRNA negatively associated with MAT in CR (r 2=0.49, p =0.06), indicating that increased SOST was not responsible for increase in MAT in CR; as well, a significant decrease in osteoclasts (Fig 2) in CR was consistent with decreased SOST. Intriguingly, the repressed SOST in CR rose with exercise, and may underlie the failure of CR-bone to increase due to exercise. In sum, our study shows that CR is associated with a robust increase in MAT. While CR-MAT decreases with exercise, exercise fails to increase bone in CR, perhaps due to impaired bone formation.

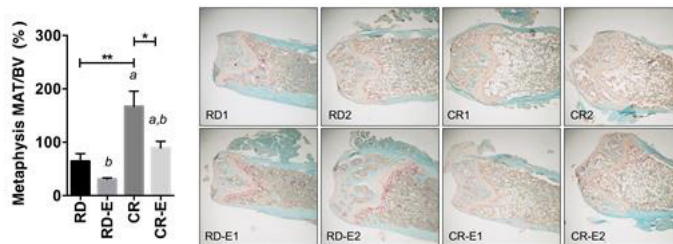


Figure 1. MAT quantified by 3D-MRI/9.4T scanner in CR mice reduced by exercise in CR.

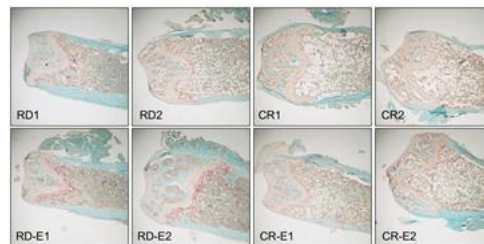


Figure 2. Representative sections of mouse femurs (n =2 per group), stained with TRAP.

Disclosures: Cody Mcgrath, None

SUN-0408

Mechanical signals activate YAP and TAZ in part via Piezo 1 Xuehua Li^{*}, Charles O'Brien, Jinhu Xiong. University of Arkansas for Medical Sciences, United States

YAP (Yes associated protein) and TAZ (transcriptional co-activator with PDZ-binding motif) are related transcription cofactors that are thought to mediate cellular responses to mechanical signals. Specifically, in vitro studies show that mechanical signals emanating from extracellular matrix or fluid flow enhance YAP/TAZ activity by promoting their nuclear translocation, suggesting that YAP/TAZ are mediators of transcriptional changes induced by mechanical signals. Previous studies have examined the role of YAP/TAZ in mature osteoblasts and osteocytes by deleting them from mice using the Dmp1-Cre transgene. These mice exhibited decreased bone mass associated with decreased bone formation and increased bone resorption, consistent with loss of mechanical signals in bone. However, the underlying molecular mechanisms remain unknown. To determine whether YAP/TAZ are regulated by mechanical signals in osteoblast-lineage cells, the MLO-Y4 cell line or primary calvaria cells were cultured under either static or fluid shear stress and gene expression was examined by Taqman assay. Fluid flow significantly increased the activity of YAP/TAZ as measured by the expression of their target gene Ctgf. Moreover, deletion of YAP/TAZ in calvaria cells significantly blunted the effect of fluid flow as measured by expression of Cox-2, a gene well-known to be responsive to fluid flow. To examine the mechanisms by which YAP/TAZ are activated by mechanical signals in osteoblast-lineage cells, we focused on Piezo1, a mechanical activated ion channel that has been reported to be critical for fluid shear stress induced calcium signaling and nitric oxide synthase expression. Besides fluid shear stress, matrix stiffness also regulates Piezo1 activity, as it does YAP/TAZ. Therefore, we determined whether Piezo1 regulates YAP/TAZ activity in osteoblastic cells by responding to mechanical signals. Piezo1 expression increased significantly with fluid flow in osteoblastic cells, and this is associated with increased expression of Cox-2 and Ctgf. More importantly, deletion of Piezo1 in osteoblastic cells blunted the increase of Cox-2 and Ctgf expression induced by fluid flow. Taken together, these results indicate that YAP/TAZ are mediators of mechanotransduction in bone cells and that Piezo1 activates YAP/TAZ by responding to fluid shear stress. Thus, loss of YAP/TAZ mediated mechanical response may contribute to the skeletal phenotype of mice lacking YAP/TAZ in osteocytes.

Disclosures: Xuehua Li, None

SUN-0409

Disruption of Nucleo-Cytoskeletal Connectivity Impairs Mechanical Competence of MDA-MB-231 Cells and Regulates Responses to Low Magnitude Mechanical Forces Xin Yi^{*}, Laura Wright¹, Gabriel Pagnotti¹, Gunes Uzer², Clinton Rubin³, Uma Sankar¹, Katherine Powell¹, Joseph Wallace¹, Khalid Mohammad¹, Theresa Guise¹, William Thompson¹. ¹Indiana University, United States, ²Boise State University, United States, ³Stony Brook University, United States

Low intensity vibrational (LIV) forces are capable of stimulating bone formation. Additionally, LIV restricts bone loss and tumor progression in models of ovarian cancer and myeloma. The mechanisms by which mechanical forces influence cancer are unknown. Transmission of LIV requires connection between the actin cytoskeleton and the nucleus via the Linker of Nucleoskeleton and Cytoskeleton (LINC) complex. This study examined the mechanisms by which the LINC complex regulates LIV effects on MDA-MB-231 cells. Human MDA-MB-231 breast cancer cells, which induce osteolysis in mice, were exposed to LIV (90Hz, 0.3g) in twenty-minute bouts, twice a day. LIV had no direct effect on cell death; however, LIV upregulated expression of the death receptor Fas (3-fold, p <0.05), suggesting that MDA-MB-231 cells may be more susceptible to Fas-ligand (FasL)-mediated death after LIV. Compared to static controls, treatment with recombinant FasL, after LIV, resulted in a 2-fold increase (p <0.05) in apoptosis. Using trans-well assays, a 4-fold (p <0.05) decrease in cell invasion was observed following LIV. Reductions in Mmp1 (4-fold, p <0.01) and Mmp3 (3-fold, p <0.05) mRNA were seen with LIV. To determine if exposure of MDA-MB-231 cells to LIV influences osteoclast formation, conditioned media from MDA-MB-231 cells, exposed to LIV, was added to RAW 264.7 macrophages. Conditioned media from LIV treated cells reduced osteoclast formation by 3-fold (p <0.0001). Disruption of nucleo-cy-

toskeletal connectivity, by siRNA knock-down of LINC genes Sun1 and Sun2 blocked the beneficial effects of LIV on cell invasion and osteoclastogenesis. Furthermore, as assessed by atomic force microscopy, LIV treatment increased cell stiffness by 1.2-fold ($p<0.05$) and enhanced actin stress fiber formation. siRNA knockdown of Sun1 and Sun2 negated the increases in actin formation and cellular stiffness. Expression of LINC genes Syne1 (2-fold, $p<0.001$), Syne2 (3-fold, $p<0.05$), Sun1 (2-fold, $p<0.001$), and Sun2 (4-fold, $p<0.05$) were increased with LIV treatment. These data demonstrate that the beneficial effects of LIV in human breast cancer cells requires nucleo-cytoskeletal connectivity. As a decline in cell stiffness is associated with increased metastatic potential and expression of LINC genes are suppressed in breast tumors, LIV may serve as a non-invasive intervention to suppress breast cancer metastasis and osteolysis by increasing physical connections between the nucleus and actin cytoskeleton.

Disclosures: *Xin Yi, None*

SUN-0426

Defining the Role of BMP Signaling in the Development of Degenerative Disc Disease Avionna Baldwin¹, Roman Eliseev¹, Addisu Mesfin¹, Noriaki Yokogawa², Alex Hollenberg¹. ¹University of Rochester School of Medicine and Dentistry, United States, ²Kanazawa University, Japan

Purpose: Degenerative disc disease (DDD) has become an increasing burden on society as the population ages with 80% of the population complaining of back and neck pain at a certain point. The intervertebral disc is composed of two cartilage endplates, nucleus pulposus cells, and annulus fibrosus. Pain associated with DDD can be secondary to dysfunction of all of these parts of the intervertebral disc. This current study sought to determine if up-regulation of the BMP-SMAD pathway leads to the development of DDD. **Methods:** Human DDD and control intervertebral disc samples were collected and analyzed by immunohistochemistry for expression phosphorylated (active) SMAD1/5/8 (p-SMAD), BMP-2, and Alk3(BMP-2 receptor). Slides were photographed and analyzed for positive and total cell count using OsteoMeasure software. **In vitro**, chondrocyte-like ATDC5 cells were transfected with SMAD1. After 24 hrs media was changed, and 24 or 48 hrs later cells were analyzed for SMAD activity using a luciferase promoter reporter and collected for RNA and protein. RT-PCR was used to assess expression of inflammatory markers (IL6 and TNF α). Western blot was used to assess expression of SMAD, p-SMAD, and Bax (apoptosis). **Results:** BMP-2 and p-SMAD expression was significantly higher in patient samples with DDD while Alk3 did not change. **In vitro** we observed that after transfection of ATDC5 cells with SMAD1, SMAD activity significantly increased, protein levels of SMAD, p-SMAD and Bax were elevated, and RNA levels of inflammatory cytokines IL6 and TNF α were upregulated. **Conclusion:** These results suggest that BMP-SMAD pathway plays a role in DDD pathogenesis by upregulating inflammatory cytokines and apoptotic factor Bax. Future studies will focus on a mouse model of DDD using Alk3 gain of function mice. Currently there are no targeted treatment options for patients with DDD as there is a limited role for spine fusion for back or neck symptoms only. Therefore, understanding which pathway results in DDD can help in the development of future targeted treatment. Importantly this study challenges the current dogma about the role of BMP-2 in treatment for DDD.

Disclosures: *Avionna Baldwin, None*

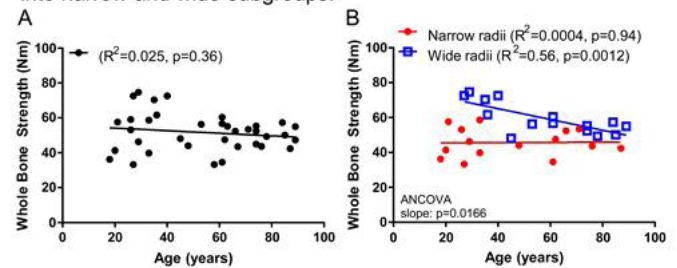
SUN-0427

Age-related changes in bone strength of male radii depend on outer bone size Erin M.R. Bigelow¹, Daniella M. Patton¹, Gurjit Mandair¹, Ferrous S. Ward¹, Stephen H. Schlecht¹, Michael D. Morris¹, David Kohn¹, Todd L. Bredbenner², Karl J. Jepsen¹. ¹University of Michigan, United States, ²University of Colorado Colorado Springs, United States

Intracortical remodeling was shown to be greater in wide compared to narrow bones. As remodeling is central to age-related declines in bone mass and strength, we hypothesized whole bone strength would decline faster with age in wide compared to narrow bones. Cadaveric male radii ($n=36$, 18-89 years) were imaged with pQCT to measure mid-shaft cross-sectional morphology and loaded to failure in 4-point bending to assess strength. Porosity, ash content, mineral/matrix ratio (MMR), and tissue-level mechanical properties were assessed using contralateral radii. Bones were sorted into narrow and wide subgroups using height-adjusted robustness (total area/bone length). When using all the data, bone strength did not decline with age ($R^2=0.025$, $p=0.36$). However, when split by subgroup, bone strength declined significantly with age for wide ($R^2=0.56$, $p=0.0012$) but not narrow radii ($R^2=0.0004$, $p=0.94$) (Fig 1). Significant positive correlations between age and robustness ($R^2=0.27$, $p=0.05$), cortical area (CtAr) ($R^2=0.36$, $p=0.02$), ash content ($R^2=0.37$, $p=0.02$), and MMR ($R^2=0.32$, $p=0.03$) were seen for narrow but not wide radii (robustness, $R^2=0.02$, $p=0.65$; CtAr: $R^2=0.1$, $p=0.25$; Ash: $R^2=0.03$, $p=0.54$; MMR ($R^2=0.06$, $p=0.35$)). A new porosity measure called Cortical Pore Score (CPS) was quantified as $CPS = S Ap d2$ by summing over all pores in nanoCT cross-sections (Ap =pore area, d =distance from the geometric centroid). Porosity increased with age for narrow ($R^2=0.42$, $p=0.01$) and wide ($R^2=0.22$, $p=0.06$) radii, but a significantly greater elevation in the CPS-porosity regression for wide compared to narrow radii ($p=0.003$, ANCOVA) showed that pores had a more deleterious effect on strength for wide radii. The data together provided insight into novel biomechanical mechanisms that explain the different strength-decline trajectories. Narrow radii had a lower baseline strength, which was maintained with aging by increases in outer bone size, CtAr, and ash content that mechanically offset an increase in porosity. Wide radii had a greater

baseline strength, much of which was lost with aging as the effects of porosity and pore location were not offset by changes in morphology or ash content. Subgroup analysis provided evidence of different strength-decline trajectories among individuals that arise through different biomechanical mechanisms. Consideration of inter-individual strength declines could greatly advance our understanding of the biomechanical pathways underlying fracture risk.

Figure 1. Linear regression between whole bone strength and age when A) using all the data and B) when samples were segregated into narrow and wide subgroups.



Disclosures: *Erin M.R. Bigelow, None*

SUN-0428

Adult vs. Middle-Aged Bone Responses to Hindlimb Unloading in Males and Females Rihana Bokhari¹, Corinne Metzger¹, Alexandra Marich¹, Emily Sturgell¹, Matthew Allen², Alyssa Flack¹, Larry Suva¹, Susan Bloomfield¹. ¹Texas A&M University, United States, ²Indiana University of Medicine, United States

Pre-clinically, skeletally mature rodents are used to model the adult human skeleton. In C57Bl6/J mice 16 weeks of age is considered skeletally mature. A recent study suggested that both male and female C57Bl6/J mice experience age-related declines in bone volume throughout life, starting at 6-8 wks of age (Glatt 2009). Indeed, the greatest decline in BV/TV occurred after 20 months, but a steady decline was observed between 4 and 20 months. To this end, the response of male and female C57Bl6/J mice to 28 days of hindlimb unloading (HU) was examined in both adult skeletally mature mice (ASM; 16 wks) and older skeletally mature mice (OSM; 44 wks). HU is a well-accepted model of disuse that has been used to measure the impact of disuse primarily in adult or aged animals. Age matched controls ($n=10$ /group) were compared, by t-test, to HU mice at each age ($n=10$ /group/sex). Dual x-ray absorptiometry revealed ASM female total body bone mineral density (BMD) was 7%, lean mass was 5% lower and fat mass was 30% lower with HU. In ASM males, there were no differences in BMD, but lean mass was 7% and fat mass was 39% lower with HU. In ASM females, HU resulted in 26% lower bone volume (BV/TV), 10% lower trabecular thickness (Tb. Th) and 17% lower trabecular number at the distal femur with similar significant declines in cancellous bone microarchitecture in ASM males. OSM females had no differences in BMD or in distal femur cancellous bone microarchitecture; however, lean mass was 7% and fat mass was 71% lower with HU. OSM males were lower with HU by 10% in BMD, 11% in lean mass, 70% in fat mass, 25% in BV/TV and 15% in Tb. Th. Together these results suggest that the impact of disuse on the appendicular skeleton is not uniform in all skeletally mature rodents. Additionally, these data highlight an interesting age- and sex-dependent response to disuse where OSM females are largely resistant to the effects of HU whereas OSM male mice remain sensitive and have significant decreases in bone architecture. Since the majority of studies assessing disuse effects on bone have been conducted in either young (<5 mo) rodents or old (>20 mo) rodents, these data demonstrate that disuse-induced bone loss varies by both sex and age. Importantly, the spectrum of what constitutes so-called "skeletally mature rodents" should be challenged and the idea that ASM rodents are representative of middle-aged humans, such as those embarking on spaceflight missions, should be carefully considered.

Disclosures: *Rihana Bokhari, None*

SUN-0429

Tomographic and biomechanical differences in trabecular bone in the early stage of male osteoporosis Ruci-Ming Chen^{*}, Wei-Hua Chang. Taipei Medical University, Taiwan

Osteoporosis, also called a silent disease, is an age-related continuous process of bone demineralization. Compared to women, osteoporotic fracture in men is associated with greater morbidity and mortality. This study was aimed to elucidate tomographic and mechanistic differences in trabecular and cortical bone in the early stage of male osteoporosis. Male Wistar rats were divided into sham-operated and orchietomy groups. After surgery for 4 weeks, the animals were sacrificed and their femurs and tibias were collected. Scanning the distal femurs with micro-computed tomography revealed that orchietomy decreased the trabecular bone number and the trabecular separation, but increased the trabecular pattern factor. Separately, mechanistic analyses of trabecular bone using a reduced-plate-compression test further showed that orchietomy diminished the maximum loading force, the displacement at maximum load, the energy at maximum force, and the ultimate stress. In contrast, orchietomy did not influence tomographic structures and mechanistic strength of

cortical bone in the early stage of male osteoporosis. Moreover, statistical analyses demonstrated that the alterations in the maximum loading force measure in osteoporotic trabecular bone meaningfully correlated with the changes in the trabecular bone number, the trabecular separation, and the trabecular pattern factor. Taken together, this study shows the significant trabecular demineralization in the early stage of male osteoporosis.

Disclosures: Rwei-Ming Chen, None

SUN-0430

The Decline of Osteoprogenitor Number and Loss of Bone Mass with Old Age in Mice is Attenuated by Repleting NAD⁺ with Nicotinamide Riboside Administration Ha-Neui Kim^{*1,2}, Li Han^{1,2}, Srividhya Iyer¹, Jianhui Chang¹, Aaron Warren^{1,2}, Julie Crawford^{1,2}, Daohong Zhou¹, Stavros Manolagas^{1,2}, Maria Almeida^{1,2}. ¹University of Arkansas for Medical Sciences, United States, ²Central Arkansas Veterans Healthcare System, United States

The forkhead box O (FoxO) transcription factors attenuate Wnt signaling and the proliferation of osteoprogenitors, and thereby decrease bone formation. The NAD⁺ dependent Sirtuin1 (Sirt1) deacetylates FoxOs and inhibits their binding to β -catenin; and it also deacetylates β -catenin. Via these mechanisms Sirt1 in osteoblast progenitors increases bone mass. A decline in NAD⁺ levels with age occurs in many species, from yeast to humans. NAD⁺ repletion with precursors such as nicotinamide riboside (NR) attenuates the loss of muscle function with old age and prolongs lifespan in mice. Here, we examined whether the NAD⁺/Sirt1/FoxO signaling pathway plays a role in the age-related bone loss. The levels of NAD⁺ were decreased in bone marrow stromal cell cultures from 22 month-old as compared to 6 month-old C57BL/6 mice. Acetylation of FoxO1 was also increased in cells from old mice, while the levels of Sirt1 were unaltered. Addition of NR to the cultures increased NAD⁺ levels in cells from both young and old mice. NR also decreased the acetylation of both FoxO1 and β -catenin and increased the total levels β -catenin in cells from old mice. In addition, NR decreased several marker of senescence including p21, GATA4 and the senescence associated secretory phenotype. Consistent with these effects, NR increased the osteoblastogenic capacity of cells from old mice, but had no effect in cells from young mice, as determined by Alizarin Red staining. We next administered NR (via the drinking water) to 12 month-old C57BL/6 female mice or TdRFP;Oxsl-Cre mice, to achieve a dose of 400 mg/kg of body weight/day, for 8 months. NR administration increased the levels of NAD⁺ in liver and fat, and in cultured bone marrow-derived stromal cells. The number of TdRFP;Oxsl osteoprogenitors, present in the bone marrow, was also increased as determined by flow cytometry. Furthermore, NR attenuated the loss of both cortical and cancellous bone as determined by micro-CT in femur and vertebrae. The bone mass phenotype was associated with increased osteoblast differentiation in bone marrow cultures. These findings suggest that the decrease in bone formation with old age is due to a decrease in NAD⁺ and inhibition of Sirt1 activity in osteoblast progenitors. NAD⁺ repletion, therefore, represents a rational therapeutic approach to skeletal involution, in addition to other aging associated pathologies.

Disclosures: Ha-Neui Kim, None

SUN-0431

Microstructural analysis of human whole spine vertebrae by using HR-pQCT Narihiro Okazaki^{*1}, Shuta Yamada¹, Ko Chiba¹, Toshiyuki Tsurumoto², Makoto Osaki¹. ¹Department of Orthopaedic Surgery, Nagasaki University Hospital, Japan, ²Department of Macroscopic Anatomy, Nagasaki University Graduate School of Biomedical Sciences, Japan

Introduction: Vertebral fracture is the most frequent osteoporotic fracture, and various factors are involved in its occurrence. Although bone microstructure is an important factor contributing to the bone strength, there are no studies that have analyzed the microstructure of human whole spine vertebrae. In this study, we analyzed the microstructure of human spine vertebrae by using high-resolution peripheral quantitative computed tomography (HR-pQCT), and investigated the differences between their vertebral levels. **Methods:** Three formalin-fixed cadavers were investigated (average age: 80.3 years, women). A total of 63 vertebrae (21 vertebrae of C3-L4, each cadaver) were scanned using HR-pQCT (XtremeCT II; Scanco Medical, Switzerland) with a voxel size of 60.7 μ m. After excluding the upper and lower endplates and posterior elements, the trabecular and cortical bone microstructure were analyzed for each vertebra: trabecular volumetric bone mineral density (Tb.vBMD), bone volume fraction (BV/TV), trabecular number (Tb.N), trabecular thickness (Tb.Th), trabecular separation (Tb.Sp), structure model index (SMI), connectivity density (Conn.D), and degree of anisotropy (DA), cortical thickness (Ct.Th), and cortical porosity (Ct.Po). We divided the spine into 4 regions: cervical region (C3-7), thoracic region (T1-12), thoracolumbar junction (T12-L1) and lumbar region (L2-4), and analyzed the differences of the microstructure parameters between 4 regions. **Results:** Tb.vBMD, BV/TV, Tb.N, and Conn.D of cervical region were significantly higher, and Tb.Sp, SMI, DA, and Ct.Po of cervical region were significantly lower compared with the other regions. In addition, Ct.Th of cervical region was significantly higher than that of the thoracic region. Meanwhile, there were no statistical differences between thoracic region, thoracolumbar junction, and lumbar region. **Conclusions:** The cervical spine had higher Tb.vBMD, well-connected plate-like trabecular bone, thickened cortical bone with lower cortical porosity, compared with the other sites.

In addition to the lower mechanical loads, it might be one of the reasons that osteoporotic vertebral fracture is uncommon in the cervical spine.

Disclosures: Narihiro Okazaki, None

SUN-0448

Role of Discoidin Domain Receptor 2 in Bone Regeneration Abdulaziz Binrayes^{*}, Renny Franceschi. University of Michigan, United States

Study Goals: Bone is a dynamic tissue with self-healing capabilities that allow the repair of defects and fractures with restoration of original architecture. Bone regeneration requires differentiation of mesenchymal stem cells to osteoblasts and remodeling of the bone extracellular matrix (ECM). Discoidin domain receptor 2 (DDR2) is a bone-associated collagen-activated receptor tyrosine kinase that is required for normal bone development and homeostasis. The purpose of this study is to investigate the role of DDR2 in bone regeneration using a Ddr2-null mouse model (Ddr2slie/slie mice, which contain a spontaneous 150 kb deletion in the Ddr2 locus to create an effective null). **Methods:** Two bone sites were evaluated for bone regeneration, calvaria and tibia. For calvarial bone regeneration, a 0.5 mm subcritical size defect (SSD) was created in 8 week wild-type (WT), Ddr2slie/slie, and Ddr2+/lacZ mice (contain a LacZ knock-in in one Ddr2 allele) in the parietal lobe of the calvaria. Four weeks post-surgery, bone regeneration of the SSD was compared between WT and Ddr2slie/slie mice. For the tibial fracture model, a tibial fracture was generated in WT, Ddr2slie/slie, Ddr2+/lacZ mice. Three weeks post-surgery, bone healing was compared between WT and Ddr2-/- mice. **Results:** For calvarial bone regeneration, Ddr2slie/slie mice showed delayed bone regeneration of the SSD with significant lower BV/TV compared to the WT mice. Furthermore, Ddr2slie/slie female mice exhibited lower BV/TV of the SSD than Ddr2slie/slie male mice. In addition, immunohistochemistry showed less GlI1 positive cells in the sagittal suture of Ddr2slie/slie mice when compared with WT. The Ddr2+/lacZ mice showed that Ddr2 is highly expressed in the defect area. For the tibial fracture model, Ddr2slie/slie mice had a lower Radiographic Union Score Tibia (mRUST) than WT. In addition Ddr2slie/slie mice had a larger callus volume compared with the WT. **Conclusion:** These results indicate that Ddr2 is required for normal intramembranous and endochondral bone regeneration.

Disclosures: Abdulaziz Binrayes, None

SUN-0449

Cartilage-like microfiber/hydrogel composite scaffold for articular cartilage therapy and regeneration Young Hun Jeong^{*}, Cheol Woo Park, Gyu Man Kim, Moon Kyu Kwak. Kyungpook National University, Republic of Korea

Cartilage, an important tissue related to the stability of joint motion in human body, has limited life and repair capability. Therefore, the damaged cartilage is difficult to heal or regenerate and it leads to swelling, function impairment, and instable motion with severe pains. There are various surgical and medicinal therapeutic methods that help to postpone the total replacement of joint. Recently, tissue engineering to regenerate new cartilage is being developed using scaffold and stem cells. Particularly, hydrogel receives a lot of attention because of its advantages as tissue engineering scaffold. However, it has low mechanical strength and toughness, which are troublesome limitations in cartilage tissue engineering. Here, we present a cell-laden microfibers/hydrogel construct for cartilage regeneration. The construct is composed of melt-electrospun microfibers, cell-laden hydrogel, and solution-electrospun thin nanofibers. Microfibers provide a higher pore size for cell/hydrogel infiltration and higher mechanical properties. Thin nanofibers were deposited on the microfibers, which could help to prevent washing-out cells and hydrogels by synovial fluid flow. The hydrogel can encapsulate the cells and provide cartilage ECM-like environment to the cells. We used two types of hydrogels; alginate and hyaluronic acid. The cells for this study were human bone marrow-derived mesenchymal stem cells. The transforming growth factor (TGF)- β was loaded into the each type of hydrogel to accelerate cartilage differentiation and maturation. After the fabrication, we investigated morphological properties of nano- and microfibers using scanning electron microscopy. Also, the mechanical properties of the constructs with different hydrogels were identified using compression tests. We carried out the in-vitro cell tests to evaluate cell proliferation, differentiation, and maturation. Consequently, we demonstrated that the mechanical properties of constructs could be controlled and close to real cartilage. Furthermore, the cells in the construct exhibited excellent differentiation into a cartilage phenotype and secretion of cartilage-related ECM as well as high cell viability and proliferation. This work was supported by the NRF funded by the Korea government (MSIT) (No. 2018R1A2B2009540, 2016R1A2B4007858, 2017R1A2B2005515) and "Project of Advanced Technology Center (10077414, 2017)" funded by the Korean Government (MOTIE).

Disclosures: Young Hun Jeong, None

SUN-0450

Pin1 suppression rescued impaired endochondral ossification in Fgfr2 S252W/+ Apert mouse model Bong-Soo Kim*, Hye-Rim Shin, Han-Sol Bae, Woo-Jin Kim, Hee-In Yoon, Won-Jun Yoon, Hyun-Mo Ryoo. Seoul National University, Republic of Korea

Apert syndrome is a genetic disease showing craniosynostosis and midface hypoplasia, which is caused mainly by activating mutations on FGFR2. Compare to premature fusion of cranial sutures, impaired endochondral ossification has been poorly understood. In this study, we observed abnormal growth of cranial base and long bone development in Apert syndrome mouse. Furthermore, to rescue Apert phenotypes, we modulated peptidyl-prolyl cis/trans isomerase (Pin1) that is a modifying enzyme of FGF signal transduction by genetic or pharmacological way. Newborn and three-week old mice were analyzed by microCT and histological examination. RNA isolated from cartilage, primary cultured cells and chondrogenic cell line, ATDC5 were assessed for gene expression profiles. For the genetic modulation of Pin1, mice carrying the Fgfr2 S252W/+; Pin1 +/- were generated. To test the effect of Pin1 inhibition on cartilage development, isolated cranial base and tibia from P0 mice were cultured for three weeks with or without Pin1 inhibitor, juglone. Apert syndrome mouse showed early fusion of cranial sutures and midface hypoplasia with high neonatal lethality. Synchondrosis of cranial base was significantly shortened and cranial base was bent in a 10° angle in Apert mouse compare to normal. Severer phenotypes were showed in three-week old mouse including absence of matrix ossification, hypoplasia of cranial base and shortened cranial length. The similar phenotype was observed on tibia. Osteogenic and chondrogenic marker expression was reduced, while proliferation and apoptosis were increased. Interestingly, these abnormal cranial phenotypes were partially rescued in Pin1-deficient Apert mice at P0 stage. Likewise, upon Pin1 inhibitor treatment during organ culture, reduced chondrocyte maturation and cartilage development were restored. Increased chondrogenesis by Pin1 inhibition was also confirmed in vitro. We closely investigated abnormal endochondral ossification in Apert mouse model. Especially, decreased maturation and hypertrophy of chondrocyte caused by activating mutation of Fgfr2 led to under-development of cranial base and long bone. Inhibition of FGF signal by modulating Pin1 resulted rescue of chondrocyte hypertrophy and relieved abnormal craniofacial phenotype in Fgfr2 S252W/+ mice. So far, we briefly showed the possibility of Pin1 inhibition as a therapeutic method on impaired chondrocyte and cartilage development, further studies need to be performed.

Disclosures: **Bong-Soo Kim, None**

SUN-0451

Adult Ece1 Ablation in Mice Causes Pulmonary Dysfunction and Pectus Excavatum Jasmin Kristianto*, Michael Johnson², Abigail Radcliff², Robert D Blank¹. ¹Medical College of Wisconsin, United States, ²University of Wisconsin Madison, United States

Endothelin (ET) signaling has been shown to mediate the development of osteoblastic lesions in cancer. Endothelin converting enzyme-1 (Ece1) catalyzes the production of mature ET peptides. Previous gene targeting studies in mice showed that homozygous Ece1 deletion had an embryonic lethal phenotype arising from failure of multiple neural crest-derived lineages, characterized by craniofacial malformations, cardiovascular system defects, and colonic aganglionosis. To study the role of Ece1 in post-natal physiology, our lab generated an inducible Ece1 knockout (KO) mouse model using tamoxifen-Cre-ERT2 recombinase. We crossed Ece1^{flox/flox} and Cre-ERT2 Ece1^{Δ/+} mice and studied male and female offspring of all resulting genotypes. We treated the Cre-ERT2 Ece1^{Δ/flox} mice with either tamoxifen or vehicle, and treated all other genotypes with tamoxifen at 8-9 weeks of age. The adult Ece1 KO mice started to develop respiratory distress about ~4 weeks after tamoxifen injection, accompanied by kyphosis and reduction of activity. They also lost weight (p<0.001) and reached endpoint criteria by 16-20 weeks of age. Pulse oximetry prior to euthanasia showed 10%-20% reduction in SpO₂ (Males, p=0.003; Females, p=0.005), and isolated right heart failure (Ejection fraction, p=0.001). At necropsy, pectus excavatum, which is typically seen in restrictive lung disease, was found in all the Ece1 KO mice and none was observed in the control groups. Histology of the lungs showed mild emphysematous changes in the Ece1 KO mice, but not of sufficient severity to account for the degree of respiratory disease. There was no evidence of pulmonary fibrosis or other restrictive lung disease, as determined by picrosirius red histology or collagen quantification (p=0.46) of lung tissue. This combination of findings indicates that impaired pulmonary function in the Ece1 KO mice is primarily musculoskeletal in origin, and demonstrates that Ece1 function is essential in normal physiology as well as in development. Severe cases of pectus excavatum and kyphosis are known to reduce pulmonary function. It is also worth noting that severe forms of osteogenesis imperfecta and hypophosphatasia also cause lethality because of the skeleton inability to support breathing.



Disclosures: **Jasmin Kristianto, None**

SUN-0452

A Survey of Skeletal Adaptations in Young Male Mice after Four Weeks of Microgravity Aboard the International Space Station Kevin Maupin*, Paul Childress¹, Riley Gorden¹, Alexander Brinker¹, Elliott Beckner¹, Rachel Mannfeld¹, Faisal Khan¹, Matthew Allen^{1,2}, Nabarun Chakraborty³, Aarti Gautam⁴, Rasha Hammamieh⁴, Melissa Kacena^{1,2}. ¹Indiana University School of Medicine, United States, ²Richard L. Roudebush VA Medical Center, United States, ³Geneva Foundation, US Army Center for Environmental Health Research, United States, ⁴US Army Center for Environmental Health Research, United States

Rapid loss of both bone mass and strength is a serious complication experienced by extended exposure to microgravity. Without the skeletal loading that bone is subjected to by Earth's gravity, bone has less stress placed on it, and consequently, bone mass significantly decreases. Astronauts lose a staggering ~1-3% of their bone mass per month while in space, compared to osteoporosis patients who lose ~1% of their bone mass per year. The loss of bone mass in space is not equally distributed across the skeleton and tends to be worse in load bearing bones such as the femur. Characterizing how multiple skeletal compartments change in response to microgravity will lead to better countermeasures to preserve skeletal health for successful long-term spaceflight. To better understand the effects of microgravity on skeletal health, we characterized the skeletal phenotype of young male C57BL/6J mice after four weeks aboard the International Space Station and compared them to identically housed ground controls. Ten-week-old cohabitated male mice (n = 10; 5 mice per cage) were flown on SpaceX-10, launched February 19, 2017. From these mice we analyzed the calvarial parietal bone, mandible, incisor, humerus, tibia, rib, sternum, and L5 vertebra via microcomputed tomography. We observed several significant differences (p < 0.05) between flight and ground mice. There was a decrease in the bone volume fraction (BV/TV) of the incisor, driven by increased expansion of the dental pulp. BV/TV was also decreased in the L5 vertebra due to a reduction in bone volume. There was an overall reduction in rib size including tissue area (T.Ar), bone area (B.Ar), and marrow area (M.Ar). Although there was a trend toward increased calvarial BV/TV (p = 0.1), this was not due to increased bone volume, but reduced tissue volume. Surprisingly, no significant differences were observed in the humerus, which is a weight-bearing bone in mice. Unique to our study was the use of young-adult males and increased mouse density per cage. The colonization of space may require the migration of individuals of healthy reproductive age. Our study increases our knowledge of detrimental effects of unloading/microgravity on the skeleton, and brings mankind one paw closer to Mars...and beyond. Disclaimer: Research was conducted in compliance with the Animal Welfare Act, and all other Federal requirements. The views expressed are those of the authors and do not constitute endorsement by the U.S. Army.

Disclosures: **Kevin Maupin, None**

SUN-0453

Beginning Maternal Vitamin D Supplementation Before Pregnancy is Associated with Higher Serum Vitamin D Status in Neonates Maryam Razaghi*, Sharina Patel¹, Nathalie Gharibeh¹, Nora Shero¹, Sherry Agellon¹, Catherine Vanstone¹, Shugin Wei², Hope Weiler¹. ¹McGill University, Canada, ²Hôpital Sainte-Justine (Montréal), Canada

Adequate vitamin D intake during pregnancy may improve pregnancy and neonatal health outcomes. Approximately 24% of neonates in Quebec City are born with inadequate serum 25-hydroxyvitamin D (25(OH)D) concentrations. This preliminary analysis aimed to

explore the association of maternal vitamin D supplementation before and/or during pregnancy with neonatal serum 25(OH)D concentrations. Healthy mother-infant pairs (n=849) were recruited at the Lakeshore General Hospital, Montreal, from March 2016 through March 2018. Within 36 h of delivery, maternal demographic and lifestyle factors were surveyed and newborn capillary blood samples were taken to assess vitamin D status using total serum 25(OH)D (Liaison, Diasorin). Data were analyzed descriptively (mean±SD or n (%)) and using mixed model ANOVA with Tukey post hoc tests accounting for effects of neonatal sex, season of delivery, maternal prepregnancy body mass index, family income and maternal race. Mothers were classified into 3 groups according to supplement intake, those taking supplements: during the 3 mo before and during pregnancy (group 1), only during pregnancy (group 2) and not at all (group 3). Differences among groups were tested using ANOVA with Tukey's post hoc tests. Proportions were tested using Chi square analyses. As many as 329 (39%) mothers reported taking a vitamin D supplement before and during pregnancy, while 459 (54%) took it only during pregnancy. Overall, 310 (37%) mothers before pregnancy and 724 (85%) mothers during pregnancy took a supplement at least 4 days per week. Infants born to mothers in group 1 (45.7±18.9 nmol/L) had a higher serum 25(OH)D than those in group 2 (42.1±18.4 nmol/L; p=0.0290) and group 3 (34.0±18.8 nmol/L; p=0.0001); group 2 was higher than group 3 (p=0.0114). More neonates had healthy serum 25(OH)D (≥ 50 nmol/L) in group 1 (37%) than in group 2 (30%) or group 3 (18%; Table 1). Beginning vitamin D supplementation 3 months prior to gestation is associated with higher neonatal vitamin D status than beginning during pregnancy. Considering that low vitamin D status is common among pregnant women, prenatal vitamin D supplementation may be important to establish vitamin D stores in the developing fetus and subsequently improve neonatal status. Public health policy and healthcare professionals should consider recommendations to encourage vitamin D supplementation prior to pregnancy and to reinforce the importance of supplementation during pregnancy.

Table 1. Frequency of infant serum 25(OH)D concentrations by group*

	Group 1	Group 2	Group 3
Overall	329 (39%)	459 (54%)	60 (7%)
≤ 29.9 nmol/L	59 (18%)	127 (28%)	29 (48%)
30.0 – 49.9 nmol/L	143 (43%)	190 (41%)	20 (33%)
≥ 50.0 nmol/L	127 (37%)	142 (30%)	11 (18%)

*Chi square, p<0.05, adjusted for the effect of neonatal sex, season of delivery, maternal prepregnancy body mass index, family income and maternal race. Data is presented as n (%)

Disclosures: *Maryam Razaghi, None*

SUN-0454

Effect of extracellular high phosphate on myogenesis of C2C12 myoblasts
Eisuke Tomatsu¹, Hidehito Inagaki², Tsukasa Kawakami¹, Yohei Asada¹, Shogo Nakayama¹, Izumi Hiratsuka¹, Yasumasa Yoshino¹, Sahoko Sekiguchi-Ueda¹, Megumi Shibata¹, Takeshi Takayanagi¹, Yoshihisa Sugimura¹, Hiroki Kurahashi², Atsushi Suzuki¹. ¹Department of Endocrinology and Metabolism, Fujita Health University, Japan, ²Division of Molecular Genetics, Institute for Comprehensive Medical Science, Fujita Health University, Japan

Background: Our previous study shows that the vascular smooth muscle cells survive by changing osteoblast-like cells and promoting extracellular matrix calcification in mild high phosphate (Pi) medium. However, the higher Pi concentration lead apoptosis in the vascular smooth muscle cells. On the contrary, osteoblasts and chondrocytes can survive at higher Pi concentration. Therefore, the impact of hyperphosphatemia seems to depend on cellular phenotype. The purpose of our study is identifying how the skeletal muscle cell lineage behaves under high Pi milieu. Methods: We cultured the C2C12 myoblasts, skeletal muscle cell lines of mouse derived muscle satellite cells, for 7 days in 1 to 10 mM Pi concentration. The cell number was counted with Cell Counter, and their myotube formation was observed with light microscopy. RNA expression levels of Runx2, MyoD1, Myogenin, ACTA2 at each Pi concentration were quantified by RT-PCR on day = 1, 4 and 7. Result: The C2C12 myoblasts survived for 7 days under higher Pi concentration up to 5 mM Pi. However, 10 mM Pi induced cell apoptosis in these cells. The gene expression of Runx2 temporarily increased in high Pi medium (x 2.27 in 2 mM, x 3.03 in 3 mM, x 1.48 in 5 mM, x 2.50 in 10 mM at 8 h incubation), and then decreased for 24 hours. When the cells were cultured in high Pi medium for 7 days, high Pi milieu up to 5 mM did not affect the Runx2 expression but suppressed the MyoD1 expression. On the other hand, the gene expression of Myogenin and ACTA2 was not affected by high Pi milieu. C2C12 cells in high Pi milieu up to 5 mM showed myotube differentiation as well as in normal Pi concentration. Conclusion: High Pi milieu temporarily enhances osteoblastogenesis and reduces myogenesis in C2C12 myoblast, but does not affect final differentiation to myotubes.

Disclosures: *Eisuke Tomatsu, None*

SUN-0455

Delayed tooth eruption in Runx2+/- mice is rescued by HDAC inhibitors.
Heein Yoon*, Han-Sol Bae, Hye-Rim Shin, Bong-Soo Kim, Jeong-Hwa Baek, Yun-Sil Lee, Kyung-Mi Woo, Hyun-Mo Ryoo. Seoul National University, Republic of Korea

Cleidocranial dysplasia (CCD) is an autosomal dominant skeletal dysplasia caused by loss-of-function mutations in RUNX2. The distinct symptoms of CCD include premature closure of cranial sutures, poorly developed clavicles and dental anomalies. The latter include retention of deciduous teeth, delayed or unerupted permanent teeth and supernumerary teeth and the treatment at present would be very painful surgical and expensive orthodontic intervention. The objective of this study is to elucidate the mechanism of the tooth eruption problems in CCD patients and to develop easier and cheaper therapeutic avenues. We found that Runx2+/- mice have delayed tooth eruption by micro CT and histological analysis. Runx2+/- mice have shown decreased TRAP-positive multinucleated osteoclasts in histological analysis. The combinations of co-cultures of bone marrow-derived macrophage / osteoblast from WT and Runx2+/-, respectively, indicated that Runx2+/- primary osteoblast is responsible for the decreased osteoclast differentiation. RNA sequencing analysis of mRNAs from Runx2+/- calvarial tissue and primary osteoblasts indicated that the mRNA expression of Csf-1 in primary osteoblast was significantly and consistently lower in Runx2+/- than in WT. As our previous reports indicated several histone deacetylase (HDAC) inhibitors can reverse genetic Runx2 deficiency through both epigenetic regulation of Runx2 expression and posttranslational modification of Runx2 activity. HDAC inhibitors treated group recovered decreased Runx2 mRNA level in Runx2+/- primary osteoblasts. Previous papers suggested that decreased osteoclast differentiation in Runx2+/- mice is caused by decreased Rankl/Opg. Interestingly, the Rankl/Opg ratio was neither changed significantly nor increased by HDAC inhibitors treatment in Runx2+/- primary osteoblasts culture system. Importantly, administration of a HDAC inhibitor, accelerated delayed tooth eruption of Runx2+/- mice significantly. These results indicated that attenuated expression of Csf-1 in Runx2+/- osteoblast could be the major target for recovery of down-regulated osteoclast differentiation and consequently of delayed tooth eruption in Runx2+/- mice. Taken together, our work establishes a suggestion that a HDAC inhibitor could be a potential therapeutic reagent of dental anomalies in CCD patients.

Disclosures: *Heein Yoon, None*

SUN-0477

Toll-like Receptors 3 and 4 are Critical Regulators of Bone Formation even in the Absence of Infection Alan Davis*. Baylor College of Medicine, United States

Toll-like Receptors 3 and 4 are Critical Regulators of Bone Formation even in the Absence of Infection Toll-like receptor pathways TLR3 and 4 play a critical role in innate immunity because they are upstream regulators of the NFκB pathway. These receptors are present on macrophages and activated by binding of dsRNA (TLR3) or LPS (TLR4) as a rapid defense mechanism that leads to both Cox2 formation as well as interferon release. Surprisingly, both receptors have been recently linked to cancer because of the production of myeloid-derived suppressor cells that prevent adaptive immunity and support tissue growth, which in the case of TLR4 includes the production of osteoclasts. We recently noted that cells within peripheral nerves begin to express TLR3, which is normally absent, after induction of heterotopic ossification (HO). Since nerves are normally protected by a blood-nerve barrier, its presence inside such nerves led us to hypothesize that it plays an additional function in HO beyond immune surveillance. In support of this finding, studies of HO in mice lacking TLR3, show a four-fold reduction in bone volume as assessed by microCT compared to their wild type counterparts (p less than 0.001), whereas mice lacking TLR4 show an increase in bone volume. Further, while our studies show that TLR3 is expressed, after HO induction, in the endoneurium of peripheral nerves, both TLR3 and 4 are also expressed in a key regulatory population of cells, which are also present in humans during HO, that we have termed transient brown fat (tBAT). Finally, mice lacking TLR3 have an altered vasculature and during induction of HO undergo substantial hemorrhaging at the site of new bone formation. Since we have previously shown that cells within the endoneurium respond to BMP2 signaling and rapidly exit the nerve to contribute directly to bone formation, we hypothesize that TLR3 may play a key role in this process. Since we observe the presence of osterix expression in cells present in the endoneurium, we hypothesize that activation of TLR3 in the presence of BMP2 signaling may be capable of driving trans-differentiation of nonmyelinating Schwann cells, to a cell type with the characteristics of neural crest. Since the TLR3 pathway has been shown to be essential for the formation of induced pluripotent stem cells (IPS cells), we hypothesize that this is a key component in this process. To further confirm this, we are analyzing TLR3 KO mice for the presence of the neural-derived osteogenic cells. We are also characterizing the additional early molecular and cellular stages of HO in both the TLR3 and TLR4 KO mice and highlighting differences between HO in these mice and their wild type counterparts

Disclosures: *Alan Davis, None*

SUN-0478

Discoidin Domain Receptor 2 Controls Skeletal Stem Cell Lineage Chunxi Ge^{*1}, Fatma Mohamed², Yi Tang³, Stephan Weiss³, Renny Franceschi¹. ¹Dept of Periodontics & Oral Medicine, University of Michigan School of Dentistry, United States, ²Dept of Periodontics & Oral Medicine, Univ. of Michigan School of Dentistry, United States, ³Life Sciences Institute, University of Michigan, United States

Discoidin domain receptor 2 (DDR2), a receptor tyrosine kinase activated by fibrillar collagens, is essential for skeletal development. In humans, mutations in DDR2 cause spondylo-meta-epiphyseal dysplasia (SMED), an autosomal recessive disorder characterized by abnormal skeletal development, short stature, craniofacial and dental anomalies. Ddr2-deficient mice phenocopy SMED and have defects in bone formation and osteoblast differentiation accompanied by increased marrow adipogenesis (Ge et al. JBMR 31:2391, 2016). This study examines whether these changes are explained by a possible requirement for DDR2 in skeletal stem cell (SSC) function. Ddr2 expression, measured using Ddr2^{+/lacZ} mice, localized Ddr2 to most skeletal structures including regions known to harbor SSCs (cranial sutures, resting zone cartilage and marrow). In addition, FACS-purified LacZ⁺ marrow cells were enriched in SSC marker mRNAs (Scal and LepR). Likewise, purified SSCs (PDGFRa+CD51+) were enriched in Ddr2 mRNA when compared with unsorted nucleated cells. To determine if Ddr2 is necessary for SCC lineage allocation, PDGFRa+CD51+ SSCs were purified from Ddr2loxP/loxP mice and treated with control (AdLacZ) or Cre-expressing adenovirus (AdCre). Ddr2 knockout reduced CFU-OB and osteoblast differentiation while increasing CFU-Adipo and adipocyte differentiation without altering CFU-F. The basis for Ddr2-dependent changes in SSC lineage is currently being explored, but may be related to possible functions of Ddr2 in ECM remodeling in that Ddr2 deficient mice have low bone levels of MT1-MMP (MMP14), a matrix metalloproteinase with known effects on SSC osteoblast/adipocyte lineage commitment (Tang et al Dev Cell 2013;25:402-16). Indeed, MT1-MMP induction during osteoblast differentiation is decreased in BMSCs from Ddr2-deficient mice. Together, these studies identify an important function of Ddr2 in SSCs that is likely related to its ability to remodel the SSC ECM niche.

Disclosures: **Chunxi Ge, None**

SUN-0479

Sost KO mice cannot rescue the conditional knockout of the Bmp2 gene Using the Osterix-CreERT2 or aSMA-CreERT2 model Stephen E Harris^{*1}, Jelica Gluhak-Heinrich¹, Marie A Harris¹, Jian Feng², Yong Cui¹, Ivo Kalajzic³. ¹uthcsa, United States, ²texas a and m Dental School, United States, ³Uconn Health, United States

We have deleted the Bmp2 gene in stem/progenitor cells in the bone marrow and periodontium, using the aSMA-CreERT2 and Osterix-CreERT2 models starting at 6 day and assayed up to 3 months. As in previous studies, the major defects in the spine, long bones, and periodontium is on the periosteum progenitors and vascular associated mesenchymal stem/progenitor cells in the bone marrow and periodontium, as assayed in vivo with CD146, aSMA, and CD31 immunocytochemistry. Using EdU labeling, we have found that one of the functions of Bmp2 is to allow expansion and growth of the stem cells, as well as drive their differentiation to osteoblast, -cytes, alveolar bone and cementums of the mandible. In vivo and in vitro studies have demonstrated that one of the major enhancers of the Bmp2 regulator region contains, an estrogen receptor response element, and is stimulate by estradiol 17beta. This same region of the Bmp2 gene enhancer, also contains a TCF/b-catenin response region and has been shown to respond to Wnt3a in vitro. In vivo the Bmp2 gene expression is increased in the Axin2 deletion model, where Axin2 normally acts to inhibit or restrain Wnt activity. Our hypothesis is that Bmp2 gene is a critical downstream component of Wnt activity on long bones/spine and bones of the craniofacial region. To test this hypothesis, we crossed the Bmp2cKO mouse models, in which the Bmp2 gene is removed in stem/progenitor cells in the bone marrow or periodontium (aSMA+ or Osterix+), with the global SostKO. SostKO has been established to increase both alveolar bone in the mandible and increase bone mass in the long bones and spine, due to the increased canonical Wnt signaling in the absence of the Sost gene. We found that deletion of the Sost gene increases bone mass, as expected. However, the bone and mandible bone defects are not rescued in Bmp2 cKO with deletion of the Sost gene. Thus, the Bmp2 gene is a critical downstream component and node of canonical Wnt activity on both, long bones, spine and mandibular alveolar bone.

Disclosures: **Stephen E Harris, None**

SUN-0480

Exposure of Nutrient-stressed Bone-derived Mesenchymal Stem Cells to the Tryptophan Metabolite Kynurenine Inhibits Autophagy and Promotes Cell Death Robert Bragg^{*1}, Thomas Barrett², Ahmed Elmansi², Khaled Hussein², Tanner Mobley¹, Wendy Bollag³, Sadanand Fulzele⁴, Xingming Shi⁵, Meghan Mcgee-Lawrence², Mark Hamrick², Carlos Isales⁶, William Hill⁷. ¹Medical College of Georgia, Augusta University, United States, ²Dept Cellular Biology & Anatomy, Medical College of Georgia, Augusta University, United States, ³Department of Physiology and Endocrinology, Medical College of Georgia, Augusta University, United States, ⁴Department of Orthopedic Surgery, Medical College of Georgia, Augusta University, United States, ⁵Dept of Neuroscience and Regenerative Medicine, Medical College of Georgia, Augusta University, United States, ⁶Dept of Medicine Endocrinology, Medical College of Georgia, Augusta University, United States, ⁷Charlie Norwood VAMC, United States

Autophagy is increasingly understood to be critical in promoting cell survival in response to stressors. Bone-derived mesenchymal stem cells (BMSCs) differentiate into osteoblasts and osteocytes driving formation of new bone. BMSC survival and capacity to differentiate declines with age, correlating with impaired autophagy in aged BMSCs. A proposed reason for such deterioration is chronic exposure to a hostile microenvironment brought on by age-associated changes within the bone marrow niche, such as an increase in free radicals and reactive oxygen species (ROS). A recently identified change in bone and bone marrow is a relative increase in the metabolism of the essential amino acid tryptophan (TRP) to kynurenine (KYN), catalyzed by indoleamine 2,3-dioxygenase (IDO) or free-radical oxidation of TRP to KYN. IDO activity increases with age, and could be a promising therapeutic target for age-related osteopenia and osteoporosis. To further investigate this link, our group has shown that serum levels of KYN are elevated with age and correlate with bone loss in vivo. Furthermore, direct administration of KYN in the diet decreases bone mass in vivo and in vitro murine BMSCs treated with KYN show decreased osteogenesis. Here we determined the effects of KYN on autophagy as a modulator of both BMSC survival and function. BMSCs were treated with KYN (200uM) in the presence or absence of 100uM chloroquine (CQ) to assess autophagic flux under serum starvation. LC3-II, a prominent marker of autophagy, showed disruption of autophagic flux by 12 through 24 hours post KYN treatment relative to controls under normoxic (21% oxygen) culture conditions. Further, under more physiologically representative long-term 3% oxygen culturing conditions found in the bone marrow BMSC niche microenvironment LC3-II was markedly lower across all time points (4, 12, and 24 hours) following kynurenine treatment. Again showing disruption of autophagic flux as well as overall reduction in LC3-II levels. Additionally, markers for apoptosis (e.g. cleaved PARP) were also lost with kynurenine treatment suggesting a more rapid rate of cell death and switching of the cell death mechanism to necrosis. Overall, these data indicate that kynurenine enhances cell death in BMSCs during prolonged stress, in part by blocking autophagy

Disclosures: **Robert Bragg, None**

SUN-0481

The role of the RhoGTPase cdc42 in the differentiation of mesenchymal stromal cells to osteoblasts and adipocytes Katrin Huck^{*1}, Carla Sens-Albert², Inaam Nakhbandi¹. ¹Max-Planck Institute for Medical Research, Germany, ²University of Heidelberg, Germany

Mesenchymal stromal cells (MSCs) in the bone marrow either differentiate to osteoblasts or adipocytes. Despite major advances in understanding how cell fate decisions are made much remains to be understood. Integrins are receptors on cell surfaces that transmit cues from the microenvironment and control vital functions such as cell differentiation. Integrins and Rho family GTPases interact to affect cell behavior. Our aim was to evaluate the role of integrins and integrin signaling in determining whether mesenchymal stromal cells differentiate to osteoblasts or adipocytes. As MSCs differentiate to osteoblasts integrin expression changes with a decrease in $\beta 3$, suggesting that integrins play a role in differentiation. Inhibiting FAK, an early mediator of integrin signaling decreased PPAR γ mRNA expression, the master regulator of adipogenesis in MSCs. Either culturing on or adding tenascin C decreased PPAR γ mRNA expression (30% and 50% of CT respectively). Since tenascin C engages, among others, $\beta 3$ integrins, we deleted $\beta 3$ integrin genetically. This increased PPAR γ expression in MSCs in line with a possible inhibitory effect on adipogenesis mediated by a $\beta 3$ integrin. Calvarial osteoblasts from knockout mice also showed decreased nodule formation and stimulation of $\beta 3$ integrin mediated signaling increased nodule formation. Thus, stimulating $\beta 3$ integrin increases osteogenic differentiation in parallel to inhibiting adipogenesis. We then evaluated two key RhoGTPases cdc42 and rac1, because of their role in mediating integrin signaling. Chemically inhibiting either molecules diminished osteoblast differentiation and increased mainly the number of preadipocytes in newborn calvarial osteoblast cultures. The inhibition of cdc42 or rac1 increased PPAR γ mRNA expression in MSCs (3-fold increase; $p < 0.05$). While cdc42 affected PPAR γ by stimulating MAP kinase (ERK and p38) signaling, rac1 effects were modest. In line with this, deletion of cdc42 in stromal cells led to an increase in adipocytes in the bone marrow (Osx-cre_cdc42fl/fl vs. Osx-cre: 2-fold increase, $p < 0.05$), while deletion of rac1 failed to show an effect. Taken together, our data suggest that integrin signaling in mesenchymal stromal cells, at least partially through $\beta 3$ integrin, enhances osteoblast differentiation while inhibiting adipocyte

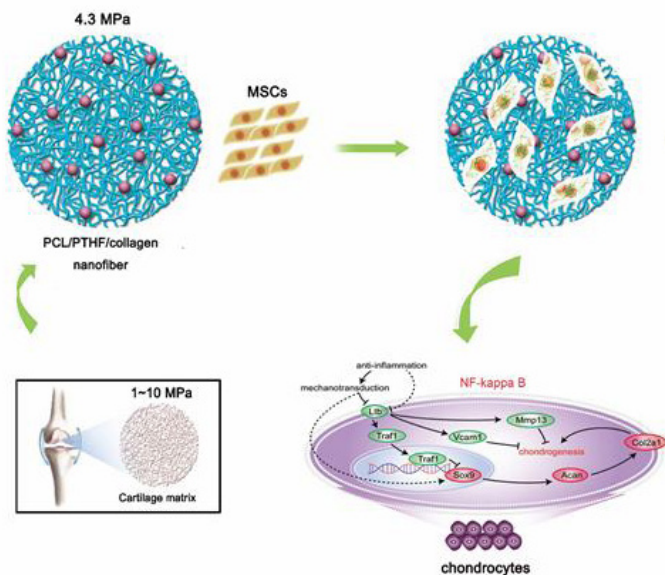
differentiation molecules in the bone marrow. Furthermore, the RhoGTPase cdc42 in MSCs mediates the crosstalk between osteogenic and adipogenic differentiation pathways.

Disclosures: Katrin Huck, None

SUN-0482

Cartilage tissue engineering using poly(PCL/PTHF urethane)/collagen nanofibers via blocking NF- κ B signaling pathway Tongmeng Jiang*, Xianyuan Huang, Shujun Heng, Li Zheng, Jinmin Zhao. Guangxi Engineering Center in Biomedical Materials for Tissue and Organ Regeneration & Guangxi Collaborative Innovation Center for Biomedicine, The First Affiliated Hospital of Guangxi Medical University, China

Cartilage tissue engineering is one of the most promising methods for cartilage repair. We carried out nanofibers made of poly(ϵ -caprolactone)/polytetrahydrofuran (PCL/PTHF) and collagen I from calf skin using electrospinning technology, and further effects of chondrogenesis of mesenchymal stem cells (MSCs) and the cartilage regeneration in vivo were evaluated. PCL/PTHF nanofibers had a modulus of 4.3 Mpa and PCL/PTHF/collagen nanofibers had a modulus of 6.8 Mpa are within the range of the modulus of natural cartilage (1 to 10 MPa). Intriguingly, the softer PCL/PTHF/collagen nanofibers induced the chondrogenesis in vitro and cartilage regeneration in vivo more efficiently than the stiffer PCL/PTHF nanofibers without additional chondrogenesis inducers. Transcriptional profiles showed that the PCL/PTHF/collagen nanofibers prior to PCL/PTHF/collagen nanofibers in inducing chondrogenesis by suppressing inflammation via specifically blocking the NF- κ B signaling pathway. This study indicates that the PCL/PTHF/collagen nanofibers can serve as building blocks of new scaffolds and provides new insights on the effect of the mechanical properties of the nanofibers on the cartilage tissue engineering.



Disclosures: Tongmeng Jiang, None

SUN-0483

A Long Intergenic Noncoding RNA in Macrophages and Mesenchymal Stem Cells Regulates in vivo Trabecular Bone Formation Coralee E. Tye*, Jonathan A.R. Gordon¹, Kristiaan Finstad¹, Roland Elling², Kate A. Fitzgerald², Janet L. Stein¹, Gary S. Stein¹, Jane B. Lian¹. ¹Department of Biochemistry, University of Vermont Larner College of Medicine, United States, ²Department of Medicine, University of Massachusetts Medical School, United States

Long non-coding RNAs (lncRNAs) are critical for organ development, sex determination and lineage commitment through multiple mechanisms. Among their functional activities are regulating RNA splicing, forming interactomes with transcription factors, acting as sponges to inhibit miRNAs and mediating chromatin interactions – all contributing to a cell's phenotype. Thousands of lncRNAs are found within any genome; however, in vivo functional characterization of lncRNAs for all tissues and disease states is limited. We have identified lncRNAs associated with specific stages of osteoblastogenesis by global RNA-Seq using human and mouse primary mesenchymal stromal cells (hMSC; mMSC) during osteoblast differentiation (days 0-proliferation, 7-commitment, 14-ECM deposition, 21-mineralization). In contrast to expressed genes and miRNAs, only 22% of mouse lncRNA genes had conserved expression with human. Focusing on these common lncRNAs, subsets of lncRNAs were expressed at distinct stages. Guilt-by association analyses correlated the expression patterns of lncRNAs with mRNAs, and mRNA clusters were associated with differ-

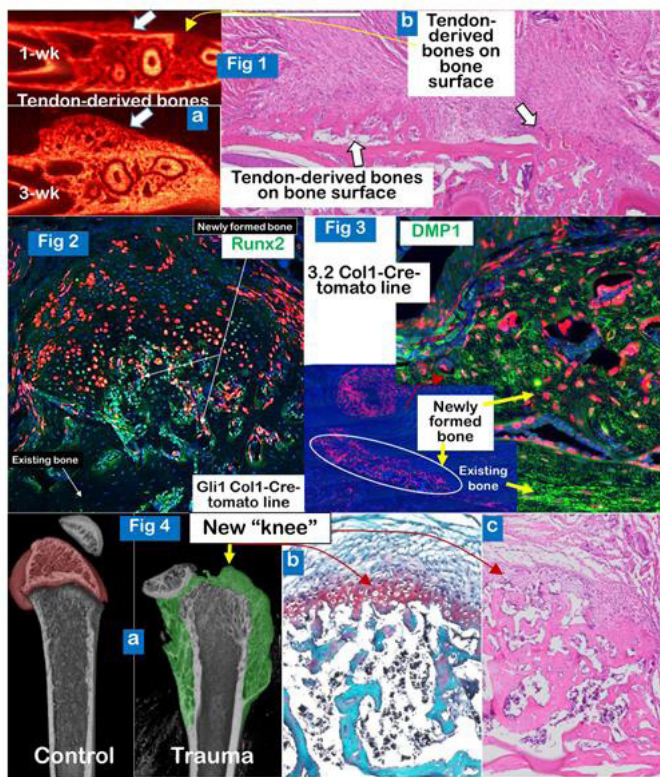
ent functional activities (GO terms). Biological categories were related to skeletal development, ossification, mineralization, proteins located at the cell periphery, G-protein receptor signaling and metabolism. We have characterized a lncRNA expressed during proliferation to identify the presence of a bone phenotype in an available KO mouse of the lncRNA, lincRNA-Cox2 (ptgs2os2). This lncRNA is responsible for NF- κ B signaling in macrophages and is a broad-acting regulator of the inflammatory response. The lincRNA-Cox2 is located proximal to the prostaglandin synthase gene, Pgts. Crosstalk between osteoblasts and macrophages has been well documented in the literature. We found that female KO mice exhibit a 2.5-3.7 fold increase in trabecular bone (TB) formation by 2 month and was sustained at 4 and 6 month compared to WT bone (Scanco CT analyses, n=12 KO and WT, 4 HET/ group) with no effect on cortical bone. However male mice exhibited 1.6-2.1 fold increase at 2 month in TB which was not sustained at 4 months. This sexual dimorphism is currently being addressed in vitro. These findings open novel dimensions for exploring this linc-COX2 in contributing to skeletal disorders, resulting from inflammation and for many other lncRNAs with potential and critical roles in bone formation.

Disclosures: Coralee E. Tye, None

SUN-0484

Autograft ligament-tendon tissues formed a “new knee” in the damaged knee surface Chi Ma^{*1}, Chuanju Liu², Lei Zhang¹, Hu Zhao³, Xiaohua Liu³, Yan Jing³, Jian Q. Feng². ¹Postdoctoral Fellow, United States, ²Professor, United States, ³Assistant Professor, United States

Although a great progress has been made in last decades in improving skeletal trauma repairing, cartilage trauma or diseases cannot be repaired by their own cells, and common procedures for restoration of joint function are the replacement with metal prostheses. The aim of this study is to develop a new strategy for cartilage and bone repairing by the detached ligament/tendon. To achieve this goal we firstly carried out the surgery at the mandible of a young adult mice in the line of Gli1-CreERT2 and 3.2 Col 1-CreERT2, where a bone trauma was created at the mandible, and the tendon from lateral masseter was cut and fixed on the defective bone surface. The mice were given injection of tamoxifen to activate the tdTomato signal simultaneously. These mice were separately collected at weeks-1, -2 and -3. There were ectopic bones formed on the bone surface by m-CT (Fig.1a). Histological analyses showed the newly formed tissue with the typical articular structure (cartilage & subchondral bone) (Fig.1b). The cell lineage tracing studies showed that 1) there were a gradual increase in the Gli1+ bone & cartilage cells in neo-tissue during 3 weeks (Fig 2); 2) the new formed “subchondral bone” strongly expressed markers of tendon, cartilage and bone (vimentin, periostin, aggrecan, Col X and DMP1) compared to the existed bone. Importantly, in the 3.2 Col 1 tracing line, there were much more tdTomato+ bone cells in the early repairing (Fig 3), supporting the notion that the terminate tendon cells react to trauma first and the Gli1+ progenitor-derived cells add new tenocytes, which take much long time. Next, we created a trauma sites in the knee joint of mice (including removal of the articular cartilage) under the background of the the Gli1-CreERT2 mice. Following the same strategy as described above, the results showed the great increase of the ectopic calcified mass. By 3-weeks, there were astonishing amount of new bone formed on the bone surface and a “new knee” on the articular cartilage surface (Fig 4a). Histology data revealed an articular-subchondral bone-like structure on the articular trauma area (Fig 4b), and a clear view of the tendon-derived bone cells in the damaged bone surface (Fig 4c). These finding suggest that 1) the cells from ligament and tendon can directly transdifferentiate into either cartilage or bone cells based on the local factors released from trauma sites; and 2) the newly formed “knee” or bone are robust in speed and quantity.



Disclosures: *Chi Ma, None*

SUN-0485

Characterizing Osteogenic Deficiency in Neurofibromatosis Type 1 at Single-Cell Resolution Nandina Paria^{*1}, Jinyan Chan², Jingya Gu², Carol Wise¹, Jonathan Rios¹. ¹Texas Scottish Rite Hospital for Children, United States, ²Baylor Research Institute, United States

Neurofibromatosis Type 1 (NF1) is a cancer-predisposing syndrome caused by haploinsufficiency of the NF1 gene. Some children with NF1 present at birth with significant tibia deformity that has a high risk of fracture and subsequent persistent healing defects (pseudarthrosis, PA) often requiring amputation. The goal of this study is to characterize the molecular mechanisms leading to fracture healing defects in children with NF1. Studies in multiple mouse models suggest that loss of NF1 in mesenchymal progenitors leads to a failure in osteogenic differentiation, and thus skeletal defects. We previously demonstrated that tibia PA is associated with NF1-deficiency caused by somatic mutation of the remaining NF1 allele. However, mechanistic studies of osteogenic differentiation defects have been limited by the mosaic nature of somatically-mutated PA cells in culture. We recently established that upregulation of EREG, encoding Epregrulin, is a biomarker for NF1-deficient patient-derived stromal cells from the PA site that, for the first time, allows study of NF1-deficient cells from a mixed population in culture. Here we report a new study in which single-cell mRNA-sequencing (sc-mRNAseq) was performed on patient-derived stromal cells from the affected PA and unaffected iliac crest bones cultured through a time-course of osteogenic differentiation. Single-cell expression results were used to organize cells along an "osteogenic trajectory" that proceeds from undifferentiated cell to osteoblast cell populations. For the first time, we show that osteogenic differentiation is a dynamic process during which cells progress through multiple transition states. As expected, patient-derived EREGLOW haploinsufficient cells from PA bone display an osteogenic trajectory consistent with proper differentiation, similar to iliac crest cells. Surprisingly, EREGHIGHNF1-deficient PA cells upregulate ALPL (encoding Alkaline Phosphatase), a marker of osteogenic differentiation, independent of differentiation state, a phenomenon not observed in mouse stromal cells. Furthermore, EREGHIGHNF1-deficient cells show a scattered osteogenic trajectory suggestive of cell-autonomous defects throughout differentiation. Coupling sc-mRNAseq with a novel biomarker, our approach allows for a mechanistic investigation of the osteogenic defects associated with NF1-deficiency leading, at least in part, to persistent fracture healing defects in children with NF1.

Disclosures: *Nandina Paria, None*

SUN-0486

β catenin preserves stem state of MSC through activation of EZH2 Buer Sen^{*1}, Zhihui Xie¹, Jeyant S Sankaran¹, Amel Dudakovic², Gunes Uzer³, Maya Styner¹, Mark B Meyer⁴, Andre J Van Wijnen², Janet Rubin¹. ¹University of North Carolina, United States, ²Mayo Clinic, United States, ³Boise State University, United States, ⁴University of Wisconsin, United States

The contribution of β catenin to Wnt's downstream osteogenic effect is a significant but poorly understood area. While β catenin promotes expansion of the osteoprogenitor clone, it does not, alone, cause osteoblast differentiation. While β catenin directly inhibits MSC adipogenesis through inhibition of PPAR γ activity, it also inhibits PPAR γ expression via unknown mechanisms. We postulated that β catenin might regulate the switch between osteoblast and adipocyte differentiation through co-modulation of cytoskeletal cues known to affect lineage selection. We thus set out to find if β catenin inhibition of adipogenesis was dependent on cytoskeletal context, overexpressing β catenin resistant to proteolysis ("mut β cat") in marrow derived mouse MSC. The anti-adipogenic effect of mut β cat (\downarrow >50%) persisted when the actin cytoskeleton was either enhanced (LPA) or depleted (ROCK inhibition). siRNA silencing of β catenin promoted adipogenesis (\uparrow >50%) was also cytoskeleton independent. We next asked if β catenin's anti-adipogenic effect was at the expense of enhanced osteogenesis. Mut β cat overexpression did not promote osteogenesis, but rather significantly inhibited osteoblast gene expression by >50% (Sp7, Bglap, Alpl). siRNA against β catenin significantly enhanced osteogenesis; all effects were independent of cytoskeletal context. A clue to the mechanism by which β catenin prevented both adipogenesis and osteogenesis was found in ChIPseq of LiCl-treated MSC: β catenin associated with the Ezh2 promoter. Ezh2, a key component of the PRC2 complex, is inhibits osteogenesis by promoting stemness and proliferation through genome methylation. This led us to hypothesize that β catenin might alter Ezh2 activity. Indeed, overexpression of mut β cat increased Ezh2 expression and H3K27 methylation, and silencing β catenin decreased Ezh2 expression and activity. Critically, inhibition of Ezh2 genome methylation with GSK126 blocked β catenin's inhibition of both osteogenic and adipogenic differentiation. Taken together, our results suggest that β catenin is not a primary effector of Wnt-induced osteogenesis. Instead, β catenin serves to preserve MSC stemness and prevent differentiation, independent of but additive to cytoskeletal context. Most importantly, this fundamental effect of β catenin requires direct control of Ezh2 activity, indicating that β catenin regulation of MSC fate involves alterations in chromatin state.

Disclosures: *Buer Sen, None*

SUN-0487

Extracellular lipid availability determines skeletal progenitor cell fate Nick Van Gestel^{*1,2,3}, Steve Stegen^{1,2}, Guy Eelen^{4,5}, Sandra Schoors^{5,6}, Aurelie Carlier^{2,6,7}, Veerle Daniels⁴, Maarten Depypere^{8,9}, Pieter-Jan Stiers^{1,2}, Riet Van Looveren¹, Sophie Torrekens¹, Patrizia Agostinis¹⁰, Frederik Maes^{8,9}, Johan Swinnen⁴, Liesbet Geris^{2,6,7}, Hans Van Oosterwyck^{2,6}, Peter Carmeliet^{4,5}, David Scadden^{3,11}, Geert Carmeliet^{1,2}. ¹Department of chronic diseases, metabolism and ageing, KU Leuven, Belgium, ²Prometheus, Division of Skeletal Tissue Engineering, KU Leuven, Belgium, ³Department of Stem Cell and Regenerative Biology, Harvard University, Cambridge, MA, United States, ⁴Department of Oncology, KU Leuven, Belgium, ⁵Center for Cancer Biology, VIB, Belgium, ⁶Department of Mechanical Engineering, KU Leuven, Belgium, ⁷Biomechanics Research Unit, GIGA In Silico Medicine, University of Liege, Belgium, Netherlands, ⁸Medical Imaging Research Center, KU Leuven, Belgium, ⁹Department of Electrical Engineering, KU Leuven, Belgium, ¹⁰Department of Cellular and Molecular Medicine, KU Leuven, Belgium, ¹¹Center for Regenerative Medicine, Massachusetts General Hospital, Boston, MA, United States

The avascular nature of cartilage makes it a unique tissue in the human body, but whether and how the absence of blood vessels regulates chondrogenesis remains unknown. In this study, we show that obstruction of vascular invasion during bone healing favors chondrogenic over osteogenic differentiation of skeletal progenitor cells. Unexpectedly, we found that this process was linked to a decreased availability of extracellular lipids. When lipids are scarce, skeletal progenitors increase intracellular lipid droplet turnover to temporarily maintain fatty acid oxidation (FAO). At the same time, lipid deprivation increases the levels of the master chondrogenic transcription factor SOX9, which acts as a regulator of cellular metabolism by suppressing FAO. In accordance, mature chondrocytes exhibit low rates of FAO compared to skeletal progenitors and mature osteoblasts. Together, our results define lipid scarcity as an important determinant of chondrogenic commitment, and identify SOX9 as a critical metabolic mediator.

Disclosures: *Nick Van Gestel, None*

SUN-0488**Nestin+ Mesenchymal Stem/Progenitor Cells essential for Type H Vessels Formation in Coupling Osteogenesis**

Liang Xie^{*1}, Xiao Wang², Manman Gao², Changjun Li², Hui Xie², Lingling Xian⁴, Mei Wan³, Qianming Chen¹, Xu Cao². ¹State Key Laboratory of Oral Diseases, West China Hospital of Stomatology, Sichuan University, China, ²Department of Orthopedic Surgery, School of Medicine, Johns Hopkins University, United States, ³Department of Sports Medicine, Xiangya Hospital, Central South University, China, ⁴Division of Hematology, Department of Medicine, The Johns Hopkins University School of Medicine, United States, ⁵Department of Orthopaedic Surgery, Johns Hopkins University School of Medicine, United States

Bone remodeling is a lifelong process depending on two dynamic and balanced activities. Specifically, mature bone is removed by osteoclasts, which are phagocytic cells generated by the fusion of monocytes, and new bone is formed by osteoblasts, which are differentiated by bone marrow mesenchymal stem/progenitor cells (MSPCs). Nestin was recognized as an MSPCs' marker, while recent studies suggested nestin+ cells are heterozygous populations providing the precursors to both mesenchymal and endothelial lineages. Clarification of the nestin+ cell fate is necessary for the understand the mechanism of bone remodeling. The coupling of bone resorption by osteoclasts and bone formation by osteoblasts during bone remodeling may be regulated by the vascular system. Cumulative evidence demonstrated that angiogenesis not only establishes local circulation in the newly formed bone, but also directly promotes osteogenesis. Particularly, a subset of smallest vessels highly expressed CD31 and endomucin (Emcn), termed CD31hiEmcnhi type H vessel, has recently been shown to promote bone formation, presumably by optimizing efficiency of blood flow and nutrient exchange. However, the cellular origin of type H vessel is unknown. In this study, we sought to characterize cell origin of type H vessels, particularly during bone pathophysiological changes such as in PDGF-BB signaling deficient mice or after PTH stimulation. We found that bone marrow nestin+ cells located in metaphysis gave rise to type H vessel formation and subsequent osteogenesis during bone remodeling in different animal models. A subset of nestin+ MSCs enriched in metaphysis are essential for type H vessels formation during bone remodeling. Deletion of nestin+ cells caused less vessels formation. PDGF-BB could bind to its receptor PDGF- β on nestin+ cells, thereby affect type H vessels angiogenesis. PTH accelerated bone remodeling through induced type H vessels formation by increasing nestin+ cells. Our finding fully characterizes this sub-population of MSCs and help to understand the physiological function of nestin+ cells in angiogenesis during bone remodeling.

Disclosures: *Liang Xie, None*

SUN-0513**RNA-Seq Based Comparative Transcriptome Profiling To Decipher The Role Of Glycogen Synthase Kinase 3 Signaling In Cartilage Biology**

Supinder Kour Bali^{*1}, Lauren Solomon², Dawn Bryce¹, Frank Beier¹. ¹Department of Physiology and Pharmacology, The University of Western Ontario, Canada, ²Department of Pathology and Laboratory Medicine, The University of Western Ontario, Canada

Osteoarthritis is the most common degenerative disease of diarthrodial joints, which is classically characterized by the breakdown of articular cartilage. However, increasing scientific evidence support involvement of other tissues in the affected joint, contributing to disease pathophysiology and progression. It is, therefore, crucial to identify molecular pathways that regulate regenerative potential of cartilage and other joint tissues, with the long-term goal to design strategies to regenerate damaged joint tissues and to prevent or reverse disease progression. Studies have shown glycogen synthase kinase (GSK) 3 alpha and beta to be key regulators of cartilage development, but their roles in cartilage homeostasis and disease are not well understood. In this study, we aim to investigate key GSK-3 dependent processes and functions by comparative differential transcriptome profiling of normal mouse articular chondrocytes and those treated with a pharmacological inhibitor of GSK-3. Immature murine articular chondrocytes were treated with GSK3 inhibitor SB216763 for 24 hours, followed by RNA-Seq. GTF 'mm10' was used to map alignment of query sequence reads on mouse genome. Two publically available databases – UCSC and Ensembl - were used to analyze RNA-Seq data; and only included the transcripts represented and annotated in both the databases for enrichment analyses. RNA-Seq results were further validated by gene expression studies using real-time PCR. Bioinformatics analyses for comparative differential gene expression profiling between the two experimental groups highlighted 324 genes involved in various biological, cellular and molecular processes, as well as skeletal abnormalities associated with reported human phenotypes. For further validation of results, we performed gene expression analysis by real-time PCR using a subset of these 324 genes, which are involved in important biological processes as well as in musculoskeletal health and disease. Gene expression of molecules important in maintenance of cartilage such as Acan, Comp, Matn1, Col2a1, Col10a1 and Frzb were significantly downregulated upon pharmacological or genetic inhibition of GSK-3 in immature mouse articular chondrocytes, supporting our RNA-Seq results. These results suggest significant involvement of GSK-3 signaling in cartilage health and disease, and highlight potential molecular targets involved in various developmental skeletal defects as well as in maintenance of cartilage health.

Disclosures: *Supinder Kour Bali, None*

SUN-0514**The Rare Disease, Alkaptonuria, Reveals New Mechanisms of Joint Destruction, Subchondral Cracking and HDMP Formation, that may be Prevalent in Osteoarthritis**

J A Gallagher^{*1}, N P Thomas¹, N Jeffery¹, L R Ranganath¹, A Boyde². ¹University of Liverpool, United Kingdom, ²Queen Mary University of London, United Kingdom

Osteoarthritis (OA) is a major cause of disability, yet, despite major research efforts, the pathogenesis has not been elucidated and there are no therapies. Studying extreme phenotypes of Mendelian disorders can reveal pathological mechanisms present in more common diseases. The purpose of our research was to investigate the early onset, severe arthropathy in the ultra-rare disorder, alkaptonuria (AKU), to better understand the pathogenesis of OA. We investigated joints obtained at surgery from AKU patients, by correlated ex vivo MRI, microCT, BSE-SEM and LM. Subsequently we extended the investigation to OA joints obtained at surgery or from donated cadavers. We also analysed clinical DESS MRI knee scans from patients in the Osteoarthritis Initiative Progression Cohort from five annual visits. Finally we surveyed MR, microCT and histological images from public data bases and publications. In AKU joint samples studied ex vivo using microCT and BS-SEM, we identified cracks in the subchondral plate which ran through bone and articular calcified cartilage. In some cases cracks had healed by intercalation of a highly mineralised infill material. This material also extruded into hyaline articular cartilage as High Density Mineralised Protrusions (HDMPs), which could be detected by microCT, DESS MRI, BSE-SEM and LM. Subsequently we identified HDMPs in ex vivo OA joints from surgery and cadavers by DESS MRI, corroborated by microCT. We identified homologous features in >80% of images acquired from the Osteoarthritis Initiative. Our search of online CT and MR databases revealed that putative HDMPs were widely identifiable in joints including vertebral joints. We also detected evidence of previously unrecognised HDMPs in histological images of joints from OA mice in published papers, despite their destruction by decalcification during processing. Our results from these parallel studies reveal a high incidence of HDMPs in joints and suggest that they constitute a major but previously unrecognised cause of joint destruction, not only in rare diseases, such as AKU, but also in common OA. HDMPs are hard and may fragment to produce an abrasive cutting and grinding agent, damaging HAC from within. They appear to form prior to the detection of symptomatic OA and could provide a useful imaging biomarker to monitor disease progression. The identification of widespread prevalence of this mechanism of joint destruction provides a new paradigm for joint destruction in OA.

Disclosures: *J A Gallagher, None*

SUN-0515**Porous Tantalum Rods Implantation for Osteonecrosis of Femoral Head:**

Longitudinal Follow-up of 40 hips Mincong He^{*1}, Qiushi Wei², Wei He², Yi-Xian Qin³. ¹First School of Clinical Medicine, Guangzhou University of Chinese Medicine, China, ²Department of Orthopaedics Surgery, The First Affiliated Hospital of Guangzhou University of Chinese Medicine, China, ³Department of Biomedical Engineering, Stony Brook University, United States

The objective of this study was aimed to evaluate the clinical and radiographic outcomes, and the hip survivorship of osteonecrosis of femoral head (ONFH) patients accepting a surgery implantation for femoral head fixation with a porous tantalum rods surgery (PTRS). Total of 38 subjects (40 hips) were included in this retrospective study, surgeries performed between January 2008 and December 2011. All the subjects were evaluated prior to the surgery using the Association Research Circulation Osseous (ARCO) classification, the Japanese Institute Committee (JIC) classification and Harris hip Score (HHS). The end point of hip survivorship analysis was set as the time of failure of the hip preservation with the total hip arthroplasty (THA) revision surgery. The mean time for following up was up to 75.5 months; and the overall survival rate reached to 70% after 72 months (ARCO stage 2: 81.5%; stage 3: 46.2%; JIC type B: 100%; C1: 78.3%; C2: 30%. The average HHS in the preoperation of PTRS was 75.8 \pm 8.0, contrast to 93.0 \pm 4.8 of the postoperative on (P<0.05). Twelve hips required for secondary THA were followed for 65.3 \pm 18.2 months; and the control group underwent primary THA were followed for 55.6 \pm 15.7 months. HHS in revision group was at a mean of 90.1 \pm 6.4, and primary THA was 93.0 \pm 5.2 (P>0.05). Secondary THA had poorer clinical outcome when compared to the primary THA patients, but the difference was not significant. The results suggested the outcome of porous tantalum implant in the mid-term follow-up showed an encouraging survival rate in symptomatic patients with ONFH in early stages or limited necrotic lesion. Patients with necrotic area involving large area or in late stage THA are not suitable for the tantalum rods implantation but THA can be a considerable remedy once the tantalum rods are failed.



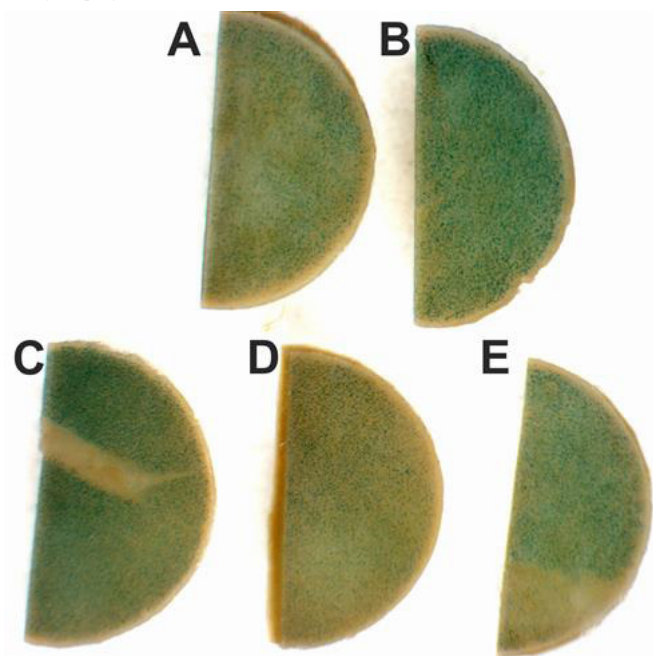
Disclosures: **Mincong He**, None

SUN-0516

TGF- β Signaling Plays an Important Role in Chondrocyte Senescence after Oxidative Stress Jie Jiang*, Tieshi Li, Alessandra Esposito, Lai Wang, Xin Jin, Joseph Temple, Arnava Hakimiyan, Susan Chubinskaya, Anna Spagnoli. Department of Pediatrics, Rush University medical Center, United States

Senescence is associated with much different age-related pathology. A recent study has shown new evidence for the causative role of senescent cells (SnCs) in the development of osteoarthritis (OA). A key characteristic of SnCs is their senescence-associated secretory phenotype (SAPS) that includes many different inflammatory cytokines. Our previous study of *Tgfr2* conditional knockout mice resulted in undeveloped joints and a change in the expression of inflammatory cytokines. Additionally, TGF- β signaling has been shown to accelerate senescence in many different cell types including mesenchymal stem cells. The overall goal of this study was to examine the role of TGF- β signaling in chondrocyte senescence during both development and osteoarthritis. This abstract presents data on the effect

of up- and down-regulation of TGF- β signaling in vitro after oxidative stress. Oxidative stress is a contributing factor to various diseases, and more recently in OA. Human articular cartilage plugs (4mm diameter) were cored out from cadavers with healthy articular cartilage (Collins grade 0 or 1). Cartilage explants were cultured in vitro and then stimulated with H₂O₂ (200 μ M) for 3 hours in ITS media. After induction of oxidative stress, the cartilage explants were then treated with recombinant TGF- β 1 (10ng/mL) to activate TGF- β signaling or with TGF- β inhibitor SB505124 (10 μ M) and ITD1 (5 μ M) to block TGF- β signaling for up to 48 hours. Cartilage explants was harvested and whole-mount senescence associated β -galactosidase staining was performed. We found that oxidative stress with H₂O₂ resulted in an increase in senescence associated β -galactosidase (SA- β -gal) staining. TGF- β treatment resulted in further increase in staining intensity while blocking TGF- β signaling with SB505124 and ITD1 resulted in reduced staining. These data indicate that articular cartilage chondrocytes are susceptible to oxidative stress and that TGF- β signaling can further exacerbate cellular senescence. To examine the role of TGF- β signaling and senescence during the development of musculoskeletal system, we examined the conditional knockout mice where *Tgfr2* was knocked-out with *Prx1Cre*. In these mice, the joint cavity between the phalanges fails to form. The formation of the joint cavity requires the clearance of cells that reside in the cavity either through apoptosis or senescence. When the SA- β -gal staining was compared, a marked decrease in *Tgfr2* knockout mice was found. Taken together, we found that TGF- β signaling may play a significant role in modulating senescence during both development of joint cavity and disease progression in articular cartilage. Future studies will focus on the mechanism by which TGF- β signaling modulate cellular senescence and using in vivo OA model to further confirm the role of TGF- β signaling in cellular senescence during the progression of OA.



Senescence associated β -galactosidase staining after 48hours of treatment in human articular cartilage explant. A) no-treatment; B) H₂O₂ treatment; C) H₂O₂ with TGF- β 1 treatment; D) H₂O₂ with SB505124 treatment; E) H₂O₂ with ITD1 treatment. Oxidative stress cause by H₂O₂ treatment resulted in increased senescence in cartilage explant and TGF- β inhibitor reduced senescence in the cartilage explant after oxidative stress.

Disclosures: **Jie Jiang**, None

SUN-0517

Clinical symptoms, quality of life (QOL), function and gait in community dwelling Seniors: Comparing those with and without osteoarthritic (OA) knee pain. Angela Juby*¹, Christopher Davis¹, Justin Lewicke². ¹University of Alberta, Canada, ²Glenrose Rehabilitation Hospital, Canada

BackgroundKnee pain is a common symptom in Seniors. The Western Ontario and McMaster Universities Osteoarthritis Index (WOMAC) is the most widely used validated tool for assessing knee and hip osteoarthritis. It assesses pain, stiffness and function. The EuroQol 5D (EQ-5D) is a validated self administered QOL scale. The functional assessments in this study are validated tests recommended by the OA Research Society International (OARSI) as objective performance-based tests for knee OA evaluation. PurposeTo assess whether knee pain will measurably affect symptoms, quality of life, functional performance and gait. MethodsCommunity dwelling Seniors were invited to participate. Evaluations included demographics, medical history, clinical knee examination, Romberg test, peripheral

neuropathy evaluation, symptom questionnaires (WOMAC, KOOS), Quality of Life (EQ-5D), 30s chair stand, 40m walk test, stair climb, Timed up and go (TUG), 6 minute walk test, pedobarographic assessment, and motion capture gait analysis. Here we present the clinical and functional results. Results 30 participants completed the study, 11 men and 19 women, with an average age of 77 years (69-89). 9 reported no pain, and 21 reported knee pain. Most with knee pain had some knee X-ray abnormalities, but 2 with no knee pain had osteoarthritic X-ray changes. The average WOMAC score was not significantly different between those with pain versus those without (27.9 vs 32.3), in fact it was higher in the no knee pain group because 3 of the subjects had other pathologies affecting lower limb function (peripheral neuropathy, chronic Achilles tendonitis, plantar fasciitis). QOL using EQ 5D was not statistically significant between the two groups, however the KOOS QOL subscale did discriminate between those with and without pain. Similarly, timed functional evaluations were no different. There was a clinical difference in distance walked in the 6 minute walk test (pain vs no pain: 388m vs 500m), but this was not statistically significant. Conclusions The results were not what was hypothesised. This study did not show any significant symptomatic, overall QOL or functional differences between these community dwelling Seniors with and without knee pain. All reported high QOL. The WOMAC was not discriminatory, and was also elevated in those with other causes of lower limb dysfunction. The KOOS scale, being highly specific for knee symptoms, better discriminated between those with and without knee pain.

Disclosures: *Angela Jubly, None*

SUN-0518

Biochemical Profiling of MRI-detected Bone Marrow Lesions in Knee Osteoarthritis Patients: Altered Mineralization of the Subchondral Bone Matrix Julia Kuliwaba*, Yea-Rin Lee, Dzenita Muratovic, David Findlay. Adelaide Medical School, The University of Adelaide, Australia

Purpose: The osteochondral degenerative changes in human osteoarthritis (OA) are most prominent in MRI-detected subchondral bone marrow lesion (BML) zones [Muratovic et al. 2016]. Given that BMLs associate with pain and structural progression, emerging treatment approaches for OA (eg. anti-resorptives) are now targeting BMLs. However, the molecular basis for the distinctive pathology of BMLs remains unclear. Thus, the study aim was to examine the biochemical composition of BMLs for human knee OA. Methods: Tibial plateaus (TP) collected from 24 knee OA arthroplasty patients (11 men, 13 women; aged 52-77 years) and from 8 non-OA control cadavers (5 men, 3 women; aged 44-80 years) were MRI scanned (PDFS and T1) to identify BMLs. Four groups, each n=8, were assessed: OA-noBML, OA-BML1 (PDFS detected in medial-TP), OA-BML2 (PDFS+T1 detected in medial-TP), control. For each TP, subchondral trabecular bone was sampled from the medial (BML zone/noBML) and lateral compartment for Raman spectroscopy analysis and quantitative backscattered electron imaging (qBEI). Results: The mineral-organic matrix ratios of phosphate/amide I, phosphate/proline and phosphate/amide III, were similar between OA-noBML and control subchondral bone (for medial and lateral). In contrast, phosphate/amide I was reduced in the medial BML zones, for both OA-BML1 (p=0.02) and OA-BML2 (p=0.004), compared to control. Also, phosphate/proline was lower for OA-BML1, compared to control (p=0.02). Within the OA-BML1 and OA-BML2 groups, phosphate/amide I (BML1:p<0.0001; BML2:p=0.009) and phosphate/amide III (BML1:p=0.006; BML2:p=0.0005) were lower in medial vs lateral. The qBEI bone mineralization density distribution (BMDD) for both OA-BML1 and OA-BML2 was shifted to low mineralization density (p<0.03) combined with an increased peak width (p<0.04), compared to control. There were no differences for mineral crystallinity, type-B carbonation, relative proteoglycan content, or hydroxyproline/proline. Conclusions: Raman spectra of subchondral bone from knee OA patients without tibial BMLs and non-OA controls demonstrated a similar mineral-organic bone matrix composition. However, medial-tibial BML tissue from knee OA patients showed an altered Raman spectral bone signature, characterized by reduced mineralization with increased heterogeneity. These data support the concept of BMLs representing localized areas of active bone remodeling in response to microdamage accumulation [Muratovic et al. 2018].

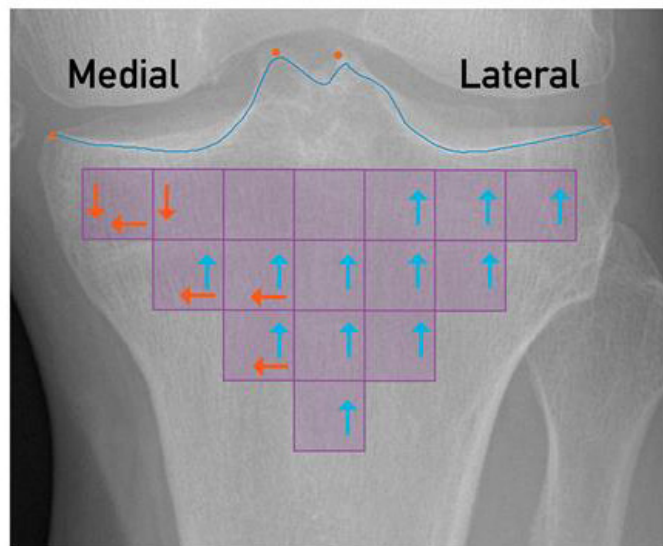
Disclosures: *Julia Kuliwaba, None*

SUN-0519

Subchondral tibial bone texture is related with knee replacement surgery Thomas Janvier*¹, Guillaume Odri², Rachid Jennane¹, Hechmi Toumi¹, Eric Lespessailles³. ¹University of Orléans, I3MTO Laboratory, France, ²Hospital Lariboisière, Orthopedics, France, ³Hospital of Orléans, Rhumatology, France

Purpose: Examine the association between subchondral bone changes reflected by trabecular bone texture (TBT) analyses on computed radiograph, and knee replacement surgery (KRS). Methods: Data were obtained from the osteoarthritis initiative (OAI) public use data set. In this preliminary study 1304 patients were included based on: at least one symptomatic knee, 48 months radiographic follow-up and baseline digital radiographs. These patients correspond to the pooling of two previous studies focused on the prediction of knee osteoarthritis incidence and progression [1,2]. Cases were defined as patient-reported KRS and adjudicated confirmed status on subsequent radiograph between baseline and the 108 month follow-up visit. Baseline radiographs were semi-automatically segmented into a patchwork of 16-squared region of interest (ROI) covering the whole proximal tibial epiphysis (Figure). Each ROI was characterized using fractal descriptors (FD) computed along the vertical and horizontal axis for two observation scales (short range: [100µm, 400µm], long range:

[600µm, 2mm]). Non-parametric Mann-Whitney test was used to compare patients with and without KRS for both WOMAC, BMI, age and TBT markers. Odds ratio (OR) were computed for lower and upper quartiles with each ROI and TBT markers. Results: From the 2497 analyzed knees, 39 underwent KRS within 108 months. No differences in the age, BMI nor gender were found between the groups whereas WOMAC scores for pain (P<0.001) and stiffness (P = 0.006) were significantly higher in the KRS group. TBT analysis along the vertical axis for short range (blue arrows in Figure) showed significantly higher FD for the KRS group in the distal and lateral ROIs (P<0.05). Such differences were confirmed by the higher prevalence of KRS for patients with FD in the lower quartile (OR > 2). In the medial compartment, horizontal and vertical FD at long range (red arrows in Figure) was lower in the KRS group (P<0.05). Conclusions: These results suggest that the TBT of the subchondral proximal tibia assessed at baseline on computed radiographs is related to KRS as well as WOMAC pain and stiffness score. This preliminary study provides a proof of concept for a future comprehensive study of the full longitudinal OAI cohort. [1] Janvier T, Jennane R, Valery A, et al. Subchondral tibial bone texture analysis predicts knee osteoarthritis progression: data from the Osteoarthritis Initiative. *Osteoarthr Cartil.* 2017 [2] Janvier T, Jennane R, Toumi H, Lespessailles E. Subchondral tibial bone texture predicts the incidence of radiographic knee osteoarthritis: data from the Osteoarthritis Initiative. *Osteoarthr Cartil.* 2017



Disclosures: *Thomas Janvier, None*

SUN-0520

Older adults with greater severity of lumbar disc height narrowing and facet joint osteoarthritis have higher lumbar volumetric BMD, independently of body weight: Framingham QCT Study Elizabeth Samelson*¹, Mohamed Jarraya², Michelle Yau³, Elise Morgan⁴, Brett Allaire⁵, Mary Bouxsein⁵, Marian Hannan³, Douglas Kiel³, Thomas Trivison³, Pradeep Suri⁶, Ali Guermazi⁷. ¹Institute for Aging Research, Hebrew SeniorLife, Harvard Medical School, United States, ²Mercy Catholic Medical Center, United States, ³Institute for Aging Research, Hebrew SeniorLife, United States, ⁴Boston University, United States, ⁵Beth Israel Deaconess Medical Center, United States, ⁶University of Washington, United States, ⁷Boston Medical Center, United States

Spinal degeneration is a major public health problem, causing pain, disability, and high health care costs. Despite its importance, the etiology of spinal degeneration is not well-established. Individuals with osteoarthritis (OA) are observed to have elevated BMD, however, it is unknown whether this is due to alterations in mechanical loading and bone remodeling, increased body weight, or an artifact of DXA measures of areal BMD. Therefore, we conducted a cross-sectional study of spinal degeneration and BMD, based on QCT imaging measures, in the community-based Framingham Study. Further, in order to tightly control for weight, which is associated with OA and high BMD, we stratified our analysis by BMI and additionally adjusted for weight. We used QCT scans to evaluate L3 trabecular volumetric BMD (Tb vBMD) and disc height narrowing (DHN) and facet joint OA (FOA) from L1/L2-L4/L5. DHN and FOA were scored at each level as 0=normal, 1=mild, 2=moderate, or 3=severe, based on standardized criteria. Briefly, DHN for a selected level was compared (>, =, <) to the height of the disc immediately superior. FOA was scored based on the presence and severity of joint space narrowing, osteophytes, hypertrophy of articular process, subarticular bone erosions, subchondral cysts, and vacuum phenomenon in the joints. We created summary indexes for DHN and FOA by summing scores across the 4 levels (bilaterally for FOA) and categorized each into quartiles. Participants included 1,130 individuals: 616 women, 514 men, mean age 60 ± 8 years. Mean summary index was 2.4 ± 2.3 for DHN (range, 0-12) and 7.1 ± 5.0 for FOA (range, 0-24). Mean L3 Tb vBMD increased with increasing quartile of DHN and FOA, adjusted for age, sex, height, and weight, and a positive trend was observed in those with low and high BMI (TABLE). Results were similar when additionally

adjusted for vertebral fracture and when women and men were analyzed separately. We found individuals with more severe spinal degeneration had higher trabecular volumetric BMD, independent of weight. These results suggest that alterations in bone remodeling and biomechanical factors from FOA may increase bone density, or conversely, increased BMD may accelerate FOA. Longitudinal assessments will allow us in the future to more clearly determine the pathway between spinal degeneration and increased BMD, and this knowledge may have important implications for prevention.

Association between severity of lumbar spine disc height narrowing (DHN) and facet joint osteoarthritis (FOA) and L3 trabecular volumetric bone mineral density (vBMD), stratified by body mass index (BMI)			
	Trabecular L3 vBMD (g/cm ³)		
	Low BMI ¹ (N=562)	High BMI ¹ (N=568)	
	Mean (SE) ²		
DHN Summary Index³			
Quartile 1 (low)	0.1208 (0.0026)	0.1204 (0.0033)	
Quartile 2	0.1187 (0.0038)	0.1270 (0.0042)	
Quartile 3	0.1226 (0.0026)	0.1245 (0.0030)	
Quartile 4 (high)	0.1345 (0.0029)	0.1434 (0.0030)	
Trend	p=0.0017		p<.0001
FOA Summary Index³			
Quartile 1 (low)	0.1182 (0.0028)	0.1232 (0.0036)	
Quartile 2	0.1220 (0.0028)	0.1275 (0.0035)	
Quartile 3	0.1294 (0.0028)	0.1356 (0.0030)	
Quartile 4 (high)	0.1303 (0.0033)	0.1295 (0.0034)	
Trend	p=0.0175		p=0.0742

¹ Categorized by sex-specific median values (< vs > 26.5 kg/m² in women and < vs > 27.9 kg/m² in men)
² Adjusted for age, sex, height, and weight
³ Calculated as sum of severity scores for L1/L2-L4/L5

Disclosures: Elizabeth Samelson, None

SUN-0521

Postmenopausal Women Have Increased Risk of Periprosthetic Fracture After Total Knee Arthroplasty Blossom Samuels^{*}, Josue Santana², Alexander Dash¹, Yi Liu¹, Alana Serota¹, David Mayman¹, Kaitlin Carroll¹, Michael Pitta¹, Timothy Wright¹, Emily Stein¹. ¹Hospital for Special Surgery, United States, ²Cornell University, United States

The number of total knee arthroplasty (TKA) procedures is burgeoning due to the increasing population of older adults. As a result, the number of complications after TKA is also rising. Periprosthetic fractures (PPFXs), while relatively rare, are a devastating and costly complication that necessitate revision surgery. Whether these fractures relate to poor bone quality is not known. In this study, we investigated risk factors for periprosthetic knee fracture using a large prospective registry at a single institution. We hypothesized that patients with PPFXs would have similar characteristics to patients with classic osteoporotic fractures, namely postmenopausal status, older age, and low BMI. Our registry captured a total of 18,065 primary total knee arthroplasties (TKA), performed in 16,083 patients over 5 years (2007-2012). In follow-up (2007-2016), 405 primary TKAs in 400 patients failed, resulting in revision surgery. The vast majority (93%) of patients had primary surgery for osteoarthritis. A retrospective review of patient medical records and radiographic data was performed to determine a cause of failure (Pitta et al., J Arthroplasty). As menopausal status was not easily ascertained from the medical records, a classification of >60 years was used as a conservative definition. DXA data were available on only a few patients. Of 400 patients with failed TKAs, the most common reasons for revision were infection (26%) and instability (24%). Fourteen (3.5%) patients required revision because of PPFX. Baseline factors were compared in patients with PPFXs and those with revisions for other reasons (Table). Patients with PPFXs were older and were more likely to be postmenopausal women. No differences in BMI, or time to failure were found. In summary, the availability of a large, well classified cohort with close follow-up enabled us to investigate risk factors for PPFX, a rare but devastating complication of TKA. In this study, in the absence of DXA data, we used postmenopausal status as a surrogate for skeletal fragility. Our finding that older patients and in particular postmenopausal women were at greatest risk for PPFX suggests that poor bone quality may be a risk factor for this complication. Future studies are needed to confirm these findings. Further evidence linking PPFXs with poor bone quality would support development of strategies for early identification and therapeutic intervention for patients at greatest risk.

Characteristics of Patients Requiring Revision After TKA (mean ± SD)

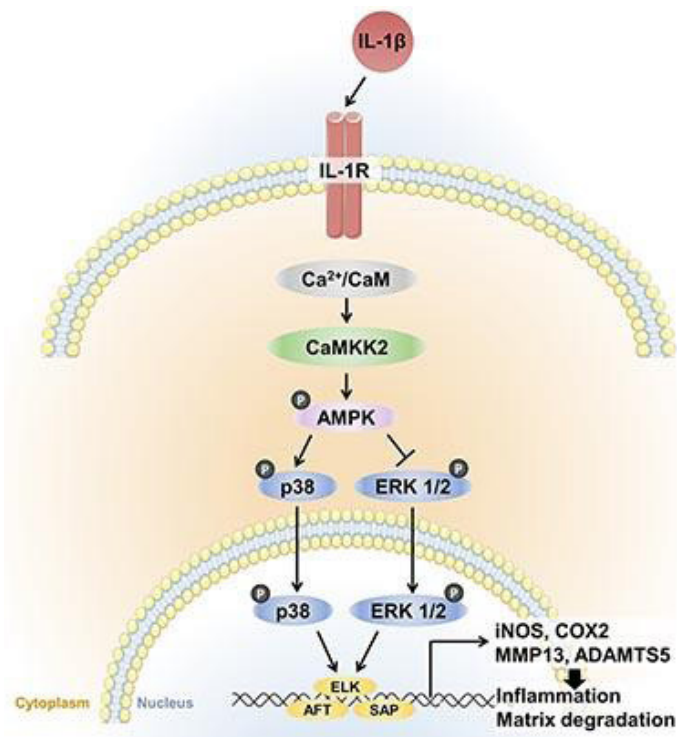
Characteristic	PPFX (n=14)	Other revision (n=391)	p-value
Mean Age (years)	68±10	62±10	<0.03
Postmenopausal Female (%)	64%	36%	<0.04
BMI (kg/m ²)	32±9	31±7	0.54
Unilateral TKA (%)	86%	21%	0.12
Time of implantation (months)	29±27	25±21	0.55
Early failure, <1 yr (%)	43%	28%	0.47
Intermediate failure, 1-3 yr (%)	35%	48%	
Late failure >3 yr (%)	23%	24%	

Disclosures: Blossom Samuels, None

SUN-0522

CaMKK2-AMPK-p38MAPK Axis Regulates the Onset of Post-Traumatic Osteoarthritis Uma Sankar^{*}, Elsa Mevel¹, Yong Li¹, Ushashi Dadwal¹, William Thompson¹, Diane Wagner², Stephen Trippel¹, Matthew Allen², David Burr¹. ¹Indiana University School of Medicine, United States, ²Indiana University Purdue University of Indianapolis, United States

Osteoarthritis (OA) is a severely debilitating degenerative joint disease that is the leading cause of adult disability worldwide. The disease is characterized by the progressive loss of articular cartilage, remodeling and sclerosis of the subchondral bone and inflammation of the synovial tissue. Patients experience debilitating pain, stiffness of joints and lack of mobility. Unfortunately, no curative treatments exist in the clinic, leaving pain management and/or joint replacement as the only therapeutic options. Calcium/calmodulin-dependent kinase kinase 2 (CaMKK2) is a multifunctional serine/threonine protein kinase activated by Ca²⁺-bound calmodulin (CaM). In addition to its substrates within the CaMK cascade, CaMKK2 phosphorylates adenosine mono phosphate-dependent protein kinase (AMPK) to regulate cell-metabolic responses to stress. We previously reported roles for CaMKK2 in bone remodeling and inflammation, two key mechanisms in OA. In this study, we investigated the role of CaMKK2 in the onset of post-traumatic OA (PTOA) surgically induced by destabilizing the medial meniscus (DMM). CaMKK2 is expressed by murine articular chondrocytes and its levels in chondrocytes within the superficial zone significantly increase following OA induction at 8 weeks post-surgery. These data informed our hypothesis that targeting CaMKK2 will protect against PTOA. We observed that the genetic deletion or pharmacological inhibition of CaMKK2 in 10-week old male C57BL6 mice prevents the occurrence of the three major joint pathologies associated with PTOA viz., cartilage destruction, subchondral bone alteration and synovial inflammation. When challenged with interleukin-1 β (IL-1 β), primary chondrocytes lacking CaMKK2 display attenuated inflammatory and cartilage catabolic responses. Moreover, Camkk2^{-/-} chondrocytes expressed enhanced levels of type II collagen (Col2) and glycosaminoglycan (GAG) in response to IL-1 β , indicating an anabolic response when challenged with the inflammatory cytokine. Mechanistic investigations reveal that CaMKK2 acts as a "molecular hub" coordinating catabolic and inflammatory responses in chondrocytes through its regulation of the AMPK-p38 mitogen activated protein kinase (p38MAPK) and extracellular receptor kinase (ERK) signaling cascades. Our findings reveal a novel function for CaMKK2 in chondrocytes and identify this kinase as an attractive therapeutic target in the prevention of OA.



Disclosures: Uma Sankar, None

SUN-0523

Targeting the IGF-1 Signaling Pathway for the Prevention of Post-Traumatic Osteoarthritis (PTOA) Yongmei Wang¹, Long Le², Tianlu Wang¹, Tejal Desai², Daniel Bikle¹. ¹Endocrine Unit, University of California, San Francisco and San Francisco VA Health Care System, United States, ²Department of Bioengineering and Therapeutic Sciences, University of California, San Francisco, United States

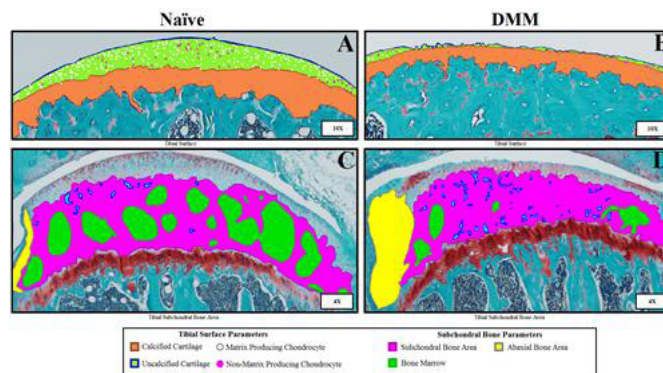
Our previous studies showed that ablation of the insulin-like growth factor-1 receptor (IGF1R) in chondrocytes prevented the development of PTOA suggesting a potential means for its prevention. Here, we investigated the therapeutic role of the IGF1R inhibitor (NVP-AEW541) in PTOA development. NVP-AEW541 (IGF1Ri) was incorporated into the polyethylene glycol dimethacrylate (PEG-DMA) hydrogel carriers (microrods) for prolonged local delivery in the joint space following ACL rupture (ACLR). ACLR was achieved with a single bout of tibial compression overload (TCO) at 12 N of the right knee in 12 wks old C57BL/6 mice. The left knee served as the control (CON). 1 day after the TCO, vehicle (Veh) or microrods loaded with inhibitor (IGF1Ri/rod) was injected into the injured knee. The CON and ACLR knees were analyzed 2wks later. Immunohistochemistry (IHC) demonstrated that ACLR induced phosphorylation of Erk in the Veh-treated injured knee, but the effect was blocked in the IGF1Ri-treated injured knee, verifying inhibition of IGF1 signaling. As determined by μ CT, compared with the CON knee, ACLR decreased BV/TV (24%) in the subchondral bone, while the IGF1Ri/rod treatment (Tx) prevented the bone loss. Safranin O /Fast Green staining revealed erosion of the articular cartilage and formation of osteophytes in the Veh-treated injured knee, but these effects were not observed in the CON or IGF1Ri-treated injured knee. As indicated by IHC, ACLR increased the number of PCNA positive articular chondrocytes and MMP-13 production in the Veh-treated injured knee, but these effects were blunted in the IGF1Ri-treated knee. Moreover, ACLR increased the production of VEGF, resulting in vessel formation within articular cartilage (as indicated by CD31) in the Veh-treated knee, but these effects were blocked in the IGF1Ri-treated knee. To test the effects of IGF1Ri/microrods in chondrocytes in vitro, ATDC5 cells were treated by DMSO or IGF1Ri/microrod (4,000 microrods/ 0.5 ml), then further treated with PBS or IGF1. QPCR showed that delivery of the inhibitor blocked IGF1 stimulated expression of MMP-13 (65%) in chondrocytes. Our data indicate that IGF1 signaling plays deleterious roles in the development of PTOA by promoting abnormal articular chondrocyte proliferation and vascular invasion, while increasing matrix metalloproteinase production to damage articular cartilage and subchondral bone. Inhibition of this pathway may lead to therapy that can prevent and/or treat PTOA.

Disclosures: Yongmei Wang, None

SUN-0524

A Standardized Approach to Quantifying Pathological Parameters of Osteoarthritis in a Preclinical Model Gregory Young^{*}, Fadia Kamal, Vengadesh Karrupagounder, William Pinamont, Reyad Elbarbary. Department of Orthopedics and Rehabilitation, Penn State University, College of Medicine, Hershey PA., United States

Gregory M. Young, Vengadesh Karrupagounder, William Pinamont, Reyad Elbarbary, Fadia Kamal. Department of Orthopedics and Rehabilitation, Penn State University, College of Medicine, Hershey PA. Objective: Measuring OA severity is essential to exploring potential disease pathways and novel therapies. Currently, OA is measured largely using OARSI scoring system, which limits statistical rigor and introduces observer bias. So far, cartilage area has been the most commonly reported quantitative measure of OA severity, however, pathological changes observed in OA also include other joint compartments. The purpose of this study was to discern critical parameters which can be measured quantitatively using an established system to define OA progression and severity. Method: Safranin-O Fast green stained knee sections were obtained from naïve mice and mice with surgically induced OA (12 weeks following DMM, Destabilization of the medial meniscus). OA induced histopathological changes were examined quantitatively using the OsteoMeasure™ system. After these changes were well defined, measurements were performed by several observers independently following a short training session. Results: Nine parameters proved to be statistically significant in determining OA severity. These factors include changes in articular cartilage (Fig. 1 A&B: reduced uncalcified cartilage area, increased cartilage surface fibrillation, reduced normal chondrocyte number and increased number of chondrocytes with pathological phenotype in OA vs naïve), changes in subchondral bone (Fig. 1 C&D: increased osteophyte formation and reduced marrow area in OA vs naïve), and changes in the synovium (increased thickness, inflammation and fibrosis in OA vs naïve). Conclusion: Measuring parameters which change during OA can clearly quantify OA development and progression. By measuring these parameters quantitatively, we can determine the reach and scale of potential novel signaling pathways and drug therapies, which may exert a selective effect on some or all of these pathological changes in OA. In conclusion, we are able to establish a system that allows us to quantify pathological changes in OA in a sensitive, highly reproducible and unbiased manner.



Disclosures: Gregory Young, None

SUN-0557

Pro-Osteoporotic mir-320a Induces Oxidative Stress and Impairs Osteoblast Function Natalia Garcia-Giralt¹, Laura De-Ugarte², Susana Balcells³, Xavier Nogues¹, Daniel Grinberg³, Adolfo Diez-Perez¹. ¹IMIM (Hospital del Mar Medical Research Institute), CIBERFES, Spain, ²IMIM (Hospital del Mar Medical Research Institute), Spain, ³Universitat de Barcelona, CIBERER, Spain

MicroRNAs (miRNAs) are important regulators of many cellular processes, including the differentiation and activity of osteoblasts. Hence, their alteration may provoke an impaired functioning of these cells that lastly might affect bone turnover. In this regard, miR-320a was previously found overexpressed in osteoporotic bone tissue but its role in osteoblasts is still unknown. In the present study, functional assays were performed with the aim to elucidate the mechanism of action of miR-320a in osteoblastic cells. For this purpose miR-320a was either overexpressed or inhibited in human primary osteoblasts (hOB) and gene expression changes were evaluated through microarray analysis. In addition, the effect of miR-320a on cell proliferation, viability and oxidative stress of hOB and osteosarcoma cell lines (MG-63 and U2OS) was evaluated. Finally, osteoblast functionality was also evaluated by assessing matrix mineralization and alkaline phosphatase activity. Microarray results showed a number of key osteoblast genes, together with genes involved in oxidative stress, which were regulated by miR-320a. Regulation of osteoblast differentiation and ossification appeared as best significant biological processes (PANTHER P value=3.74E-05; and P value=3.06E-04, respectively). The other enriched pathway was that of the cellular response to cadmium and zinc ions, mostly by the overexpression of metallothioneins. In hOBs, overexpression of miR-320a increased proliferation and oxidative stress levels whereas mineralization capacity was reduced. In osteosarcoma cells, miRNA-320a also in-

duced oxidative stress leading to reduced cell viability and mineralization capacity. In conclusion, overexpression of miR-320a produces an increase in stress oxidation levels and a reduced osteoblastic functionality that could trigger an osteoporotic phenotype.

Disclosures: *Natalia Garcia-Giralt, None*

SUN-0558

Role of Methylsulfonylmethane (MSM) as an osteoinductive material in the osteogenesis of stem cells from human exfoliated deciduous teeth (SHED) Hanan Aljohani*, Meenakshi A. Chellaiiah. University of Maryland- Dental School, United States

In the field of dentistry, there is always a necessity for new advancement in bone restoration therapy. Methylsulfonylmethane (MSM) showed the ability to induce osteogenic differentiation of stem cells from human exfoliated deciduous teeth (SHED). It serves as a cost-effective adjunct to available bone augmentation techniques. Objectives: 1. To show the ability of SHED cells to differentiate into osteoblast. 2. To determine a dose and time dependent effect of MSM on SHED cells to induce osteogenic differentiation as an alternative to the commonly used osteogenic medium. 3. To demonstrate the combination effect of MSM and bone particles on osteogenesis of SHED cells. Methods: MSM was used to induce osteoblast differentiation in stem cells from human exfoliated deciduous teeth (SHED). The expression of osteogenic markers in SHED cells was examined using immunoblotting and real-time PCR analysis for protein and mRNA expression, respectively. Alizarin red and Calcein blue mineralization assays were used to assess osteogenic differentiation. Results: Our findings revealed the following: 1) SHED cells express osteogenic markers: Ostrix, OPN, Runx2, and OCN at protein and mRNA, respectively. 2) SHED cells have the ability to express alkaline phosphates and produce mineralization nodules under osteogenic medium. 3) MSM induces osteogenesis of SHED cells by expressing osteogenic markers: Ostrix, OPN, Runx2, and OCN at protein and mRNA, respectively. 4) MSM induces osteogenesis of SHED cells by increasing ALP activity and mineralization nodules. 5) Combination of MSM and bone particles induce osteogenesis and mineralization of SHED cells. Conclusion: Methylsulfonylmethane (MSM) is a potential cost-effective osteoinductive material. It has the capability to induce dental stem cells to differentiate into osteoblast by enhancing the expression of mineralization markers, resulting in bone formation.

Disclosures: *Hanan Aljohani, None*

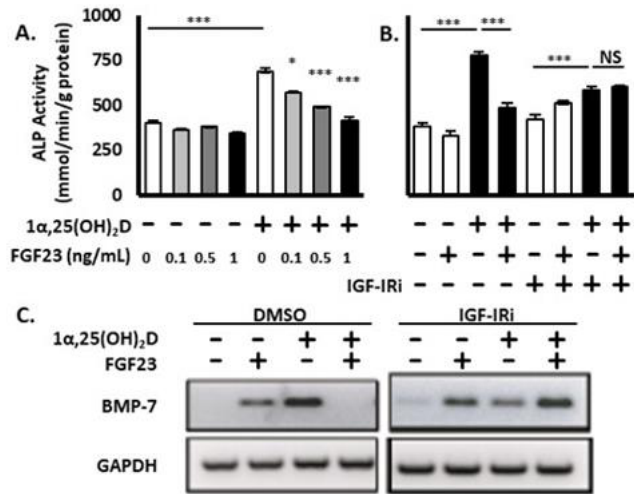
SUN-0559

FGF23 Counters Osteoblast Differentiation in Human Mesenchymal Stem Cells by Inhibiting Vitamin D Signaling and Metabolism Christopher Bertucci*, Fangang Meng, Shuanhu Zhou, Julie Glowacki. Brigham and Women's Hospital, United States

Chronic kidney disease (CKD) is associated with vitamin D deficiency, decreased BMD, and increased risk of hip fractures. Circulating FGF23 is elevated in CKD and reduces renal biosynthesis of 1 α ,25-dihydroxyvitamin D₃ (1,25) by inhibiting renal 1 α -hydroxylase/CYP27B1 gene expression and activity. With human mesenchymal stem cells (hMSCs), we tested the hypotheses that 1) rhFGF23 inhibits 1,25-stimulated osteoblast differentiation and 2) rhFGF23 inhibition occurs through specific signaling pathways; 3) because hMSCs express CYP27B1 and 1 α -hydroxylase 25(OH)D, we also tested the effects of rhFGF23 on 25(OH)D actions and metabolism. Human MSCs were isolated from discarded orthopedic surgical tissue. Upon confluence, hMSCs (passage 2-5) were cultured \pm treatments \pm pathway inhibitors for 1 day (RT-PCR) or 7 days (ALP activity, osteogenic medium, n=4). Group data were analyzed non-parametrically and are presented as mean \pm SEM. rhFGF23 (0.1-1 ng/mL) dose-dependently inhibited osteoblastogenesis (ALP activity) stimulated by 1,25 (10 nM) (Panel A). The mechanism by which rhFGF23 inhibited MSCs was investigated. First, 1,25 induced BMP-7 and IGF-1 expression; rhBMP-7 (50-100 ng/mL) dose-dependently stimulated osteoblastogenesis. BMP-7 inhibitor (10 μ M LDN214117) blocked 1,25 stimulation of ALP activity. rhFGF23 (1 ng/mL) or VDR siRNA blocked 1,25 upregulation of BMP-7; IGF-IR inhibitor (3 μ M AG1024) blocked rhFGF23 inhibition of 1,25's stimulation of ALP activity (Panel B) and of BMP-7 gene expression (Panel C). rhFGF23 also reduced constitutive expression of VDR and CYP27B1; FGFR1 inhibitor (0.5 μ M BGJ398) blocked this action. Similar experiments with 25(OH)D (100 nM) showed rhFGF23 inhibited stimulation of ALP activity and reduced BMP-7, VDR, and CYP27B1 gene expression. These data indicate that FGF23 inhibits 1,25 stimulation of osteoblastogenesis through VDR, IGF-IR, and BMP-7 signaling pathways. FGF23's downregulation of CYP27B1 expression in hMSCs is evidence of similarity to the effects of CKD on vitamin D metabolism in renal cells. These findings highlight the importance of exogenous and endogenous 1,25 in osteoblast differentiation and how elevated serum FGF23 levels in CKD could contribute to poor skeletal status. Studies with hMSCs can provide better understanding of extra-renal D metabolism in hMSCs and mechanisms of FGF23 impairment of osteoblastogenesis; they may indicate new approaches to improve bone quality in CKD.

Effects of rhFGF23 on 1 α ,25(OH)₂D action and signaling in hMSCs.

(A) Osteoblastogenesis (ALP activity) stimulated by 1 α ,25(OH)₂D (10nM) was dose-dependently inhibited by rhFGF23. (B) rhFGF23 (1 ng/mL) inhibition of 1 α ,25(OH)₂D-stimulated ALP activity was blocked by IGF-IR inhibitor (3 μ M AG1024). (C) IGF-IRi blocked rhFGF23 inhibition of 1 α ,25(OH)₂D-stimulated BMP-7 expression. (*p<0.05, ***p<0.001, n=4, ANOVA)



Disclosures: *Christopher Bertucci, None*

SUN-0560

Developmental contribution of growth plate-derived hedgehog signal-responsive cells in growing bone Ryuma Haraguchi*¹, Riko Kitazawa², Yuuki Imai³, Sohei Kitazawa¹. ¹Department of Molecular Pathology, Ehime University Graduate School of Medicine, Japan, ²Department of Diagnostic Pathology, Ehime University Hospital, Japan, ³Proteo-Science Center, Ehime University, Japan

Background: Longitudinal bone growth progresses by continuous bone replacement of epiphyseal cartilaginous tissue, known as "growth plate", produced by columnar proliferated- and differentiated-epiphyseal chondrocytes. The endochondral ossification process at the growth plate is governed by paracrine signals secreted from terminally differentiated chondrocytes (hypertrophic chondrocytes), and hedgehog signaling is one of the best known regulatory signaling pathways in this process. Here, to investigate the developmental relationship between longitudinal endochondral bone formation and osteogenic progenitors under the influence of hedgehog signaling at the growth plate, genetic lineage tracing was carried out with the use of Gli1CreERT2 mice line in order to follow the fate of hedgehog signal-responsive cells during endochondral bone formation. Finding: Gli1CreERT2 genetically labeled cells are detected in hypertrophic chondrocytes and osteo-progenitors at the chondro-osseous junction (COJ); these progeny then commit to the osteogenic lineage in periosteum, trabecular and cortical bone along the developing longitudinal axis. Furthermore, in ageing bone, where longitudinal bone growth ceases, hedgehog signal responsiveness and its implication in osteogenic lineage commitment is significantly weakened. Conclusion: Our results show, for the first time, evidence of the developmental contribution of endochondral progenitors under the influence of epiphyseal chondrocyte-derived secretory signals in longitudinally growing bone. This study provides a precise outline for assessing the skeletal lineage commitment of osteo-progenitors in response to growth plate-derived regulatory signals during endochondral bone formation. We are currently conducting a mouse genetically conditional gene mutation analysis with the use of the Gli1CreERT2 line for understanding growth plate-derived regulatory signals during endochondral bone formation within hedgehog signal-responsive cell lineages.

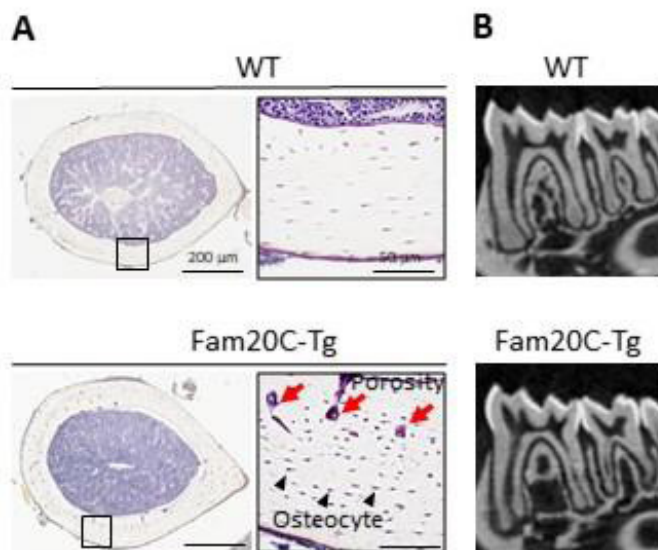
Disclosures: *Ryuma Haraguchi, None*

SUN-0561

The role of Fam20C on the bone and tooth formation Katsutoshi Hirose*¹, Yu Usami¹, Kaori Oya¹, Sunao Sato¹, Toshihisa Komori², Satoru Toyosawa¹. ¹Osaka University Graduate School of Dentistry, Japan, ²Nagasaki University Graduate School of Biomedical Sciences, Japan

[Background] Family with sequence similarity 20-C (Fam20C) is Golgi-localized protein kinase, which phosphorylates secretory proteins with S-X-E/pS motifs, including SIBLINGs family proteins. Fam20C is highly expressed in the bone and tooth. In vitro studies demonstrated that recombinant Fam20C can phosphorylate Dmp1 and osteopontin, which are important for mineralized tissue formation. However, the role of Fam20C on these mineralized tissues is still unclear. In this study, we investigated the role of Fam20C on the min-

eralized tissue using osteoblast-specific Fam20C overexpressing mice (Fam20C-Tg). [Materials and methods] We generated the transgenic mice that Fam20C is driven by a 2.3-kb pro- $\alpha 1(I)$ collagen promoter, leading to osteoblast-specific Fam20C overexpression. Skeletal samples were analyzed in vivo and in vitro. [Results and Discussion] In Fam20C-Tg, exogenous Fam20C produced by osteoblasts actually had a kinase activity. Phosphoproteomic analysis of the cortical bone revealed that various proteins including SIBLINGs, were highly phosphorylated. Fam20C-Tg had significantly higher cortical MAR and BFR/BS than wild type mice (WT), which may lead to an increased cortical bone volume of Fam20C-Tg (Fig. A). Moreover, porosity had increased in the cortical bone of Fam20C-Tg compare to that of WT, indicating an increase in bone resorption (Fig. A, arrows). The number of osteocyte in the Fam20C-Tg cortical bone was also increased (Fig. A, arrowheads). Gene expression analyses of cortical bone revealed that there was no significant difference in type I collagen (osteoblast marker) mRNA expression between Fam20C-Tg and WT. However, osteocalcin (mature osteoblast marker) and Dmp1 (osteocyte marker) mRNA expression in Fam20C-Tg mice were significantly increased compared to those in WT. These findings were consistent with the increased osteocyte number in cortical bone of Fam20C-Tg. On the other hand, Fam20C-Tg had significantly lesser trabecular bone volume than those of WT, which may be caused by an increased number of osteoclasts in trabecular bone of Fam20C-Tg. Fam20C protein was also overexpressed in the odontoblast, cementoblast and periodontal ligament cell. Fam20C-Tg had porous jawbone and decreased dentin and cementum formation of the dental root whereas there was no significant change in the dental crown (Fig. B). We have in vivo findings that Fam20C is associated with regulation of bone and tooth formation by phosphorylating secretory proteins.



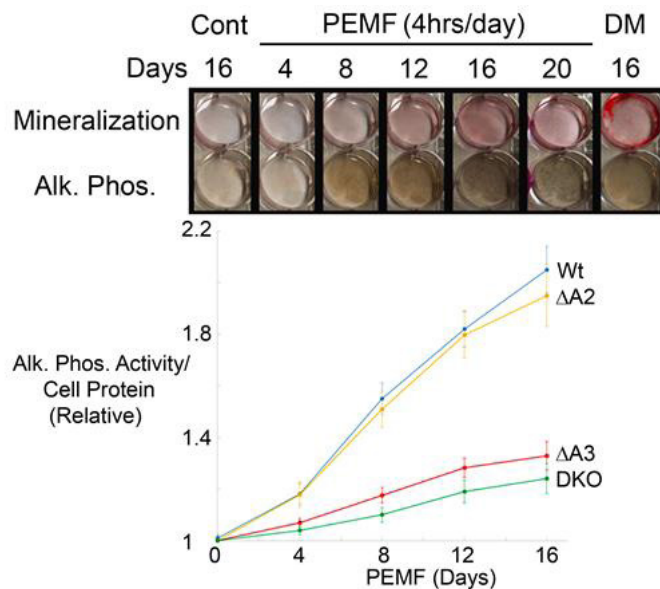
Disclosures: *Katsutoshi Hirose, None*

SUN-0562

Adenosine Receptors A2A and A3 are crucial in Pulsed-Electromagnetic-Field Induced Pre-Osteoblast Cell Differentiation Niladri S. Kar^{*1}, Daniel Ferguson², Nianli Zhang³, Erik I. Waldorff³, James T. Ryaby³, Joseph A. Didonato¹. ¹Cleveland Clinic, United States, ²Washington University in St. Louis, United States, ³Orthofix, United States

Though for years Pulsed Electromagnetic Field (PEMF) is known to effectively augment the healing process of non-union fracture, the upstream biochemical and signaling processes leading to such effects have not been studied extensively, and thus deserve further attention. PEMF treatment has been shown to enhance migration of Adenosine class A Receptors A2A and A3 (Adora2A and Adora3) to the plasma membrane, and to modulate cAMP levels leading to anti-inflammatory responses in various cell types. Here we report that a four-hour daily PEMF stimulation enhances cellular differentiation of the mouse preosteoblast, MC3T3-E1, to osteoblast as a model response for the fracture healing observed with PhysioStim™ (Orthofix, Inc., Lewisville, TX). Alpl, cFos, Pth1 and Runx2 are the primary genes that are found to be overexpressed in the PEMF-mediated osteoblast differentiation process in the wildtype preosteoblast cells. The two Adenosine Receptors, A2A and A3 were functionally impaired by biochemical inhibitors or CRISPR-Cas9-mediated gene disruption, and the effects were studied in the context of the PEMF-mediated osteoblast differentiation as measured by alkaline phosphatase enzymatic activity and cell alkaline phosphatase staining, collagen staining, mineralization staining, and quantitative RT-PCR for expression of the differentiation-associated genes. We observed that, while the disruption of Adora2A resulted in a delayed Alpl mRNA expression, but alkaline phosphatase activity and cell staining were nearly equal to the wild type; Adora3 disruption as well as simultaneous disruption of both receptors resulted in significantly reduced responses at both the mRNA and protein levels for the alkaline phosphatase activity throughout the PEMF stimulation period.

Moreover, in the cells with Adora2A disruption, gene expression profile showed a blunted response of cFos and Pth1 to PEMF treatment, whereas as in the cells with Adora3 disruption, the responses of those genes were mostly unaltered. To demonstrate specificity for A3 function to PEMF, further experiments are being performed to rescue PEMF responsiveness in Adora3 disrupted cells by a CRISPR-Cas9 based inducible knock-in of Adora3 into the ROSA26 locus. Thus, in the PEMF-enhanced osteoblastic differentiation in bone healing, we propose complementary positive roles for Adenosine Receptor A2A and A3 in regulating cFos and Pth1 PEMF-mediated gene overexpression and alkaline phosphatase-mediated signaling pathways, respectively.



Disclosures: *Niladri S. Kar, None*

SUN-0563

The epigenetic regulator and H3K9me2 demethylase encoded by the Hairless (Hr) gene controls osteoblast differentiation Farzaneh Khani^{*}, Roman Thaler, Christopher Paradise, Amel Dudakovic, Andre Vanwijnen. Department of Orthopedic Surgery, Mayo Clinic, United States

The Hairless gene (Hr) has key functions in skin and hair development and genetic mutations in the Hr gene lead to a bald mouse phenotype. Specific mutations in the human HR gene have been associated with delayed bone development during childhood. Furthermore, Hr has been recently shown to act as a histone H3 lysine 9 demethylase (H3K9me2). Because epigenetic modifications at the histone level and chromatin organization control osteogenic lineage commitment and progression, we addressed the role of Hr during osteoblast maturation. Using RNA-seq analysis and our RT-qPCR platform for epigenetic regulators, we show that Hr is expressed at a low basal level in bone marrow derived mouse and human mesenchymal stem cells (BMSCs), mouse MC3T3 osteoblasts and MLO-A5 osteocytes, as well as human bone outgrowth cells. However, Hr expression steadily increases during differentiation of MC3T3-E1 osteoblasts, as well as primary mouse BMSCs and human bone outgrowth cells. In contrast, Hr is only transiently expressed during differentiation of MLO-A5 osteocytes where it is initially increased during the initial stages of differentiation but declines at later stages of differentiation. Loss of function analysis by depletion of Hr through shRNA mediated stable knock down in MC3T3-E1 osteoblasts and MLO-A5 osteocytes compromises differentiation, as reflected by decreased extra cellular matrix (ECM) deposition and mineralization, reduced ALPL activity and suppressed expression of several primary osteoblastic genes like Sp7, Sparc (osteonectin), Phex, Ibsp (bone sialoprotein), Ifitm5 and several members of the Wnt family. Strikingly, CRISPR-dCas9 mediated inducible overexpression of Hr in MC3T3-E1 cells also inhibits osteoblast differentiation by suppressing Alpl activity, ECM deposition and mineralization. This suppression of osteoblastogenesis is associated with decreased expression of primary osteoblastic factors like Runx2, Bglap, Phospho1 and others. The inhibition of osteoblastogenesis by either loss or gain of function of Hr indicates that its balanced and carefully regulated expression is critical for its normal function as H3K9me2 demethylase during bone cell differentiation. Because H3K9me2 demethylase activity removes H3K9me3 marks necessary for heterochromatin formation, it appears that fidelity of heterochromatinization is important for late stages of osteoblast maturation.

Disclosures: *Farzaneh Khani, None*

SUN-0564

Salt-inducible kinase 1 regulates bone metabolism by affecting proliferation of osteoblast precursors and differentiation of osteoblasts Min Kyung Kim*, Hong-Hee Kim. Department of Cell and Developmental Biology, Seoul National University, Republic of Korea

A good understanding of the molecular mechanisms that regulate the various stages in bone metabolism is crucial to the development of therapeutic agents to prevention and treatment of bone diseases. In present study, we demonstrate the potential of Salt-inducible kinase 1 (SIK1) as a candidate for therapeutic agents. SIK1 previously known to be important for various reactions including myogenesis, hepatogenesis. However, the role of SIK1 in bone metabolism has not been known. Especially, SIK1 expression was sharply downregulated among SIK isoforms during osteogenesis. Knockdown or overexpression of SIK1 affected osteogenic process including expansion of osteoblast precursors and differentiation of osteoblast. And, its kinase activity modulated osteogenesis through CREB/Id1 axis by phosphorylating Transducer of regulated CREB activity 1 (TORC1). Calvariae transfected SIK1siRNA showed a phenotype of increased osteoblast number and ALP activity. In addition, enhanced bone mass and bone parameters were revealed in SIK1 knockout mice. Osteoblast differentiation and mineralization were increased in calvarial osteoblasts of SIK1 KO mice, but osteoclast formation and marker genes were not altered in SIK1 KO BMMs compared with WT. Taken together, our results demonstrate that SIK1 is a novel role in osteoblast precursors proliferation and differentiation stage via CREB/Id1 axis during osteogenesis and is a possible therapeutic drug target in bone disease.

Disclosures: *Min Kyung Kim, None*

SUN-0565

Osteoblast-Specific Cell-Surface Antigen Regulating Osteoclastogenesis and Calcification: A Possible Unique Modulator of Bone Remodeling Tamer Badawy*, Yukari Kyumoto-Nakamura¹, Norihisa Uehara¹, Akiko Kukita², Toshio Kukita¹. ¹Molecular Cell Biology & Oral Anatomy, Faculty of Dental Science, Kyushu University, Japan, ²Microbiology, Faculty of Medicine, Saga University, Japan

(Background & Purpose) Bone remodeling is a continuous process characterized by highly coordinated cell-cell interaction in distinct multi-cellular units. Osteoclasts play a central role in bone remodeling. Although RANKL/RANK axis is considered to determine the gross number of osteoclasts present in bone tissues, detailed molecular events regulating frequency and efficiency of bone remodeling are still ambiguous. We hypothesized that osteoblast-specific cell-surface molecules could contribute to the fine regulation of bone remodeling. Therefore, we searched for cell-surface regulatory molecules expressed in osteoblasts. In the course of such survey, we found a unique cell-surface antigen (A7 antigen) highly specific to cells in the osteoblast-lineage. Here we report on the expression pattern and possible unique function of A7 antigen in bone remodeling. (Methods) Osteoblastic cell line ROS17/2.8 cell clone was utilized for BALB/c mice immunization. Splenocytes were fused with murine myeloma cell line. A panel of monoclonal antibodies was established according to the standard protocol. Antibody screening was performed by staining rat bone marrow cultures, mesenchymal stem cells, and osteoblastic cell lines. Bioassay was performed using calvaria-derived primary osteoblasts to form calcified matrices and osteoclastogenesis using bone marrow cultures. (Results and Discussion) In vitro, A7 antigen was expressed on cell-surface of osteoblasts and bone marrow stromal cells. In vivo, A7 antigen was detected in a subset of bone surface osteoblasts and in osteocytes, with a typical membrane expression pattern. Tissue array analysis showed only a limited expression of A7 antigen in osteocytes just close to the bone surface. Immunoblotting and immunoprecipitation analysis showed that A7 antigen is a lineage-specific cell-surface protein with approximate molecular weight of 45 KDa. Cross-linking of cell-surface A7 antigen in cultures of osteoclastogenesis showed limited stimulation of osteoclast formation. Marked suppression of calcification was observed when A7 antigen was cross-linked by A7 MAb in cultures of primary osteoblasts. These data suggest that A7 antigen is a key cell-surface molecule involved in the fine regulation of osteoclast recruitment as well as in the critical regulation of osteoblast maturation especially in calcification. A7 antigen could be a therapeutic molecular target in pathological bone diseases.

Disclosures: *Tamer Badawy, None*

SUN-0566

Osteoblast-specific overexpression of Gas or Ga11 leads to differential fracture healing responses. Kathy Kyungeun Lee*, Jane Mitchell¹, Marc Grynpas². ¹University of Toronto, Canada, ²Lunenfeld-Tanenbaum Research Institute, Canada

Bone exhibits a remarkable ability for self-repair; however, the normal process of healing is sometimes compromised resulting in non-union that requires additional interventions that are costly and have long-term adverse impact on quality of life and productivity. Thus, advances in our understanding of the regulatory pathways underlying bone repair, which may be therapeutically targetable, have clinical and economical potential. G protein-coupled receptor signaling in osteoblasts has a regulatory role in skeletal development and homeostasis. Aberrant expression of Gas and Gaq/11 leads to profound changes in bone mass,

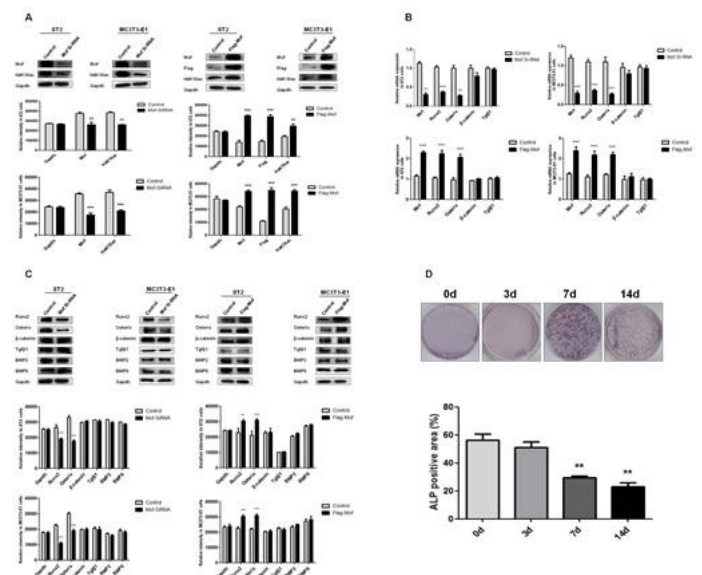
quality, and rate of bone turnover. Here we have examined the effects of Gas and Ga11 overexpression in osteoblasts on bone healing from stabilized transverse osteotomy of tibiae using wild-type and two transgenic mouse models previously developed in our lab, Gs-Tg that has increased bone and G11-Tg that has osteopenia. The progression of fracture healing was evaluated by Micro-CT analysis and histomorphometry at 2 and 3 weeks post-fracture. Our Micro-CT analyses revealed that increased Gas signaling in osteoblasts leads to rapid fracture healing with enhanced callus mineralization at 2 weeks and new bone formation at 3 weeks in Gs-Tg mice. On the contrary, increased Ga11 signaling in osteoblasts leads to delayed fracture healing with reduced bone formation but early transition into the remodeling phase at 3 weeks. Histologically, Safranin-O/Fast Green staining demonstrated a large amount of newly formed woven bone containing residual cartilage matrix at 2 weeks and persistence of irregular morphology of woven bone at 3 weeks in Gs-Tg mice. Interestingly, despite high basal osteoclast activity in G11-Tg mice, residual cartilage islands were still evident at the fracture site at 2 weeks similar to WT mice. However, no obvious difference in the remodeling of woven bone into a lamellar bone structure was observed between WT and G11-Tg mice at 3 weeks. Altogether, our results indicate that osteoblast-specific overexpression of Gas and Ga11 lead to different fracture healing responses.

Disclosures: *Kathy Kyungeun Lee, None*

SUN-0567

Analysis of osteoblast-specific histone-modifying enzymes Mof reveals novel epigenetic basis of osteoblast differentiation Xiangzhi Li*, Jianmei Chen¹, Di Liu², Minqi Li³, Yang Yang¹, Shuang Gao¹, Meng Wang¹, Shiguo Yan⁴. ¹Department of Cell Biology, Shandong University School of Basic Medical Sciences, China, ²Department of Prosthodontics, Shandong Provincial Key Laboratory of Oral Tissue Regeneration, School of Stomatology Shandong University, China, ³Department of Bone Metabolism, School of Stomatology Shandong University, China, ⁴Department of Periodontology, School of Stomatology Shandong University, China

Translational histone modification and accompanying histone-modifying enzymes form the largest and most complex regulatory entity, which is an important epigenetic modification that contributes to specific functions of different cell types. However, available information is lacking regarding the changes in the specific epigenetic program that may directly interfere with the differentiation process. To study the function of histone H4K16 acetyltransferase Mof in osteoblast differentiation for 3, 7 and 14 days, protein expression of Mof and the H4K16 acetylation level were gradually elevated according to time course of induction measured by Western blot, quantitative reverse transcription-polymerase chain reaction (RT-qPCR), alkaline phosphatase (ALP) and Alizarin Red stain assays. Small interfering RNA targeting Mof and Flag-Mof plasmid were constructed and transfected into ST2 and MC3T3-E1 cells to silent and overexpress Mof in both of cell types were determined by measuring expression changes of key markers of osteoblast differentiation; these markers include runt-related transcription growth factor 2 (Runx2), Osterix (Osx), Bone Morphogenetic Protein-2 (BMP-2), B-catenin, transforming growth factor (Tgf) B1, and BMP9 by using Western blot, RT-qPCR, ALP stain and co-immunoprecipitation technique. Results showed that Runx2 and Osx expression declining dramatically at mRNA and protein levels during Mof knock-down. No significant changes were observed in BMP2, B-catenin, TgfB1, and BMP9. Altogether, these results strongly indicate that Mof plays an important role in proper osteoblast differentiation.



Disclosures: *Xiangzhi Li, None*

SUN-0568

Plasticizer Di(2-ethylhexyl)phthalate Interferes with Osteoblastogenesis and Adipogenesis *in vitro* and *in vivo* Rong-Sen Yang*, Chen-Yuan Chiu, Ding-Cheng Chan, Shing-Hwa Liu. National Taiwan University, Taiwan

Introduction: Plasticizer di(2-ethylhexyl)phthalate (DEHP) can leach from medical devices. Epidemiological studies showed that phthalate metabolites levels in the urine are associated with low bone mineral density (BMD) in older women. The effect and mechanism of DEHP on bone loss remain to be clarified. Here, we investigated the effect and mechanism of DEHP and its active metabolite mono(2-ethylhexyl)phthalate (MEHP) on osteoblastogenesis and adipogenesis from bone marrow stromal cells (BMSCs) *in vitro* and BMD and microstructure in mice. **Methods:** The primary BMSCs were isolated from mice for osteoblastogenesis or adipogenesis. Both alkaline phosphatase (ALP) activity and mineralized nodule formation stained by Alizarin red S were determined for osteoblastogenesis. Adipocyte staining by Oil Red O was determined for adipogenesis. The protein expressions were determined by Western blotting. Moreover, mice were randomly divided into four groups (12 animals/group): 0 (corn oil), 1, 10, and 100 mg/kg DEHP (oral administration for 8 weeks). Bone mass and microarchitecture analysis in mice were determined by a micro-computed tomography (μ CT). **Results:** The osteoblast differentiation of BMSCs was significantly and dose-dependently decreased by DEHP and MEHP (10-100 μ M) without cytotoxicity to BMSCs (Figure 1-A; n=5, p<0.05). The mRNA expressions of alkaline phosphatase, Runx2, osteocalcin, Wnt1, and β -catenin were significantly decreased in DEHP- and MEHP-treated BMSCs during differentiation (Figure 1-C; n=3, p<0.05). MEHP significantly increased the adipocyte differentiation of BMSCs and PPAR γ mRNA expression (Figure 1-B and D; n=5, p<0.05). DEHP did not promote the adipogenesis (n=5, p<0.05). Both DEHP and MEHP significantly increased the ratios of phosphorylated β -catenin/ β -catenin and inhibited osteoblastogenesis, which could be reversed by Wnt activator lithium chloride (n=3, p<0.05) and PPAR γ inhibitor T007097 (Figure 1-E; n=3, p<0.05). Moreover, exposure of mice to DEHP (1, 10, and 100 mg/kg) for 8 weeks altered BMD and microstructure (Figure 1-F; n=12, p<0.05). In BMSCs isolated from DEHP-treated mice, osteoblastogenesis and Runx2, Wnt1, and β -catenin expression were decreased, but adipogenesis and PPAR γ expression were increased (n=3, p<0.05). **Conclusion:** DEHP and its metabolite MEHP exposure may inhibit osteoblastogenesis and promote adipogenesis of BMSCs through the Wnt/ β -catenin-regulated signals and thus triggering bone loss.

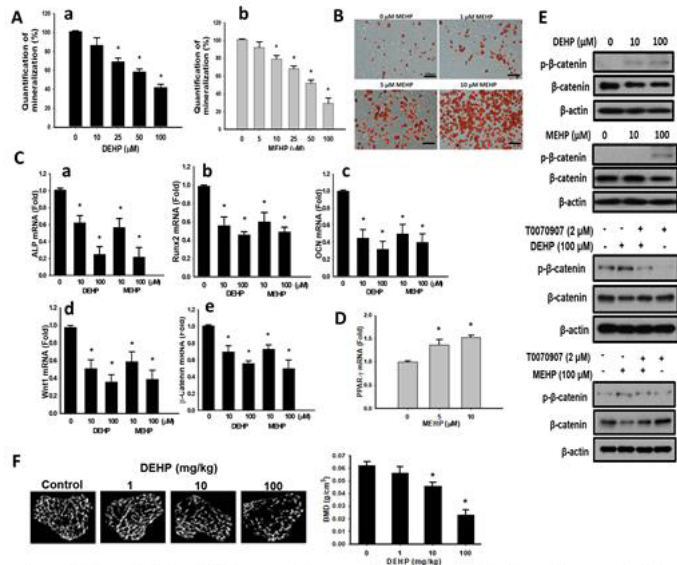


Figure 1. Effects of DEHP and MEHP on osteoblastogenesis and adipogenesis *in vitro* and bone mass *in vivo*. BMSCs were cultured in osteogenic differentiation medium (A, C, E) or adipogenic differentiation medium (B, D) with or without DEHP (10-100 μ M) and MEHP (1-100 μ M) for 7 or 16 days, respectively. In *in vivo* experiments, mice were orally administered with corn oil (vehicle control) or DEHP (1, 10, and 100 mg/kg) daily for 8 weeks (F). The excised tibia specimens were used for μ CT analysis. Data are presented as mean \pm SEM of at least three independent experiments performed in triplicates. * P < 0.05 compared to the control.

Disclosures: Rong-Sen Yang, None

SUN-0569

TRAPPC9 Regulates BMP2-mediated Osteoblast Differentiation and Bone Regeneration through Down-Regulation of NF- κ B Activation Thomas Mbimba*, Gregory Sondag¹, Fouad Moussa¹, Fayed Safadi². ¹Musculoskeletal Research Group, NEOMED, United States, ²Musculoskeletal Research Group, NEOMED, Akron Children Hospital, United States

Intellectual disability (ID) is a serious disorder of the central nervous system with a prevalence of 1-3% in the general population. Recent studies identified different nonsense mutations in the trafficking protein particle complex (TRAPPC9) gene in consanguineous and nonconsanguineous families with autosomal-recessive non syndromic mental retardation.

These patients exhibit severe skeletal phenotypes such as short stature, polydactyly, craniofacial deformity and microcephaly. TRAPPC9 is known to bind Nfkb inducing kinase (NIK) and Ikb kinase-beta (IKKbeta) and enhances cytokine-induced Nfkb activation by increasing the kinase activities of IKK2 (IKKbeta) and NIK. It thus plays a role in the canonical and non-canonical Nfkb signaling. Recent studies have identified NF- κ B as a major negative regulator of osteoblast (OB) proliferation and differentiation that binds and suppresses Runx2 activation in response to BMP2. Here we hypothesize that TRAPPC9 regulates BMP2-mediated activation of NF- κ B through Samd/p38/MAPK activation. We first examined TRAPPC9 expression and localization in bone by qPCR, Western blot and immunoprecipitation, which confirmed its expression in both OC and OB. Co-immunoprecipitation studies confirmed TRAPPC9 binding to both NIK and IKK2 in OB. To examine TRAPPC9 role during OB differentiation, we performed loss- and gain-of-function studies in both MC3T3 and Bone marrow-derived MSCs using shRNA viral system. TRAPPC9 down-regulation showed a marked increase in all osteogenic markers such Runx2, Osx, Ocn, ALP, ColA1A. TRAPPC9 down-regulation increases matrix maturation and mineralization shown by an increase in ALP staining and activity, Von Kossa and Alizarin red staining. Next, we showed that TRAPPC9 down-regulation mediates an increase in Smad1,5,8 and p38 MAPK activation associated with NF- κ B down-regulation. Next, we assessed the effects of TRAPPC9 downregulation on bone regeneration *in vivo* using calvarial defect model and found that MSC engineered with shRNA for TRAPPC9 incudes bone regeneration compared to control cells. Taken together, these data suggest that inhibition of TRAPPC9 enhances OB differentiation through Smad1,5,8 and P38 activation and bone regeneration, at least in part, by suppressing of NF- κ B signaling.

Disclosures: Thomas Mbimba, None

SUN-0570

Role of Hp1 family proteins Cbx1, Cbx3, and Cbx5 during osteoblastic differentiation Christopher R. Paradise*, Pengfei Zan¹, Roman Thaler¹, Farzaneh Khani¹, Merel O. Mol², Esther Liu¹, Guodong Li³, Peter Kloen², Marianna Kruithof-De Julio⁴, Simon M. Cool⁵, David R. Deyle¹, Amel Dudakovic¹, Andre J. Van Wijnen¹. ¹Mayo Clinic, United States, ²University of Amsterdam, Netherlands, ³Tongji University, China, ⁴University of Bern, Switzerland, ⁵Agency for Science, Technology and Research, A(*)STAR, Singapore

Bone development and homeostasis are tightly regulated by several cellular mechanisms, including epigenetic control of gene expression. Post-translational modifications of histone tails are critical in this process as they induce chromatin compaction and/or relaxation to control access to regulatory sequences and genes packaged into nucleosomes. Heterochromatin-associated Chromobox (Cbx) proteins play a crucial role in chromatin compaction by binding the repressive marks tri-methylated histone 3 lysine 9 (H3K9Me3) and tri-methylated histone 3 lysine 27 (H3K27Me3). Analysis of our comprehensive musculoskeletal RNA-seq dataset revealed that among the family of 8 Cbx genes, all three isoforms of the heterochromatin protein 1 (HP1) subfamily (Cbx1, Cbx3, and Cbx5) which bind and compact H3K9Me3 are highly expressed in bone and osteoblastic cells. Loss of function analysis of these CBX proteins was carried out by siRNA mediated knockdown. Depletion of Cbx1 and Cbx3 promotes osteogenic differentiation of pre-osteoblasts as shown by the enhanced expression of key osteogenic transcription factors Runx2 and Sp7 (Osx) and ECM-maturation associated genes Alpl, Ibsp, Bglap, and Col1a1. Furthermore, knockdown of these genes increases extracellular matrix mineralization during an osteogenic differentiation time course. In contrast, knockdown of Cbx5 reduces matrix mineralization and does not affect expression levels of osteoblast-specific gene. We also note a compensatory effect within the Hp1 family members as knockdown of one member induces expression of the remaining two. Simultaneous siRNA mediated knockdown of two or three Hp1 family members no longer enhanced osteoblastic differentiation as observed previously with the single knockdown of Cbx1 or Cbx3. We also noted an increase in nuclear size after knockdown of the Hp1 proteins, suggesting relaxation of chromatin condensation. Interestingly, we observe a major reduction in global H3K9Me3 levels upon knockdown of all three Hp1 related Cbx proteins but not with single or double knockdown. Taken together, our results indicate that Cbx1, Cbx3 and Cbx5 collectively protect H3K9Me3 heterochromatin marks and that these HP1 family proteins have novel roles in regulating osteoblast differentiation.

Disclosures: Christopher R. Paradise, None

SUN-0571

Role of Pre-proenkephalin 1 in the response of bone to mechanical unloading and in osteoblast differentiation Nadia Rucci*, Antonio Maurizi, Isabella Baldini, Mattia Capulli, Anna Teti. University of L'Aquila, Italy

Pre-proenkephalin 1 (Penk1) belongs to the family of the typical opioid peptides. The Penk1 gene encodes for a pro-peptide that is proteolytically processed to generate 4 copies of Met-enkephalin, 2 copies of Met-enkephalin extended sequence and 1 copy of Leu-enkephalin. These pentapeptide opioids modulate the response to stimuli such as the perception of pain. Interestingly, we found Penk1 to be the most down-regulated gene in a microarray analysis performed in osteoblasts subjected to microgravity (0.008 g) as a model of *in-vitro* mechanical unloading. Penk1 mRNA downregulation was confirmed in the bones of two *in-vivo* models of mechanical unloading: tail suspended mice (-30%, p=0.023) and mice

injected with botulin toxin A (-40%, $p=0.057$). Consistently, in human sera from healthy volunteers subjected to bed rest, we observed an inverse correlation between PENK1 levels and duration of bed rest ($p=0.0006$, $R=0.6$). These results prompted us to investigate a role for PENK1 in bone metabolism. We found Penk1 to be highly expressed in the marrow flushed-out bone, and its expression progressively increased during in vitro osteoblast differentiation in osteogenic medium. Accordingly, the stimulation of osteoblast differentiation by the c-Src inhibitor PPI increased Penk1 mRNA (1.8-fold, $p=0.03$). Silencing osteoblast Penk1 by siRNAs decreased Alp (-37%, $p=0.018$) and Runx2 (-40%, $p=0.019$), while it increased Sclerostin (7.5-fold, $p=0.035$) compared to osteoblasts treated with scrambled siRNA. Consistently, overexpression of Penk1 by Amara nucleofection increased osteocalcin expression (6-fold $p=0.02$). Moreover, primary osteoblasts isolated from Penk1 KO mice showed lower formation of mineralization nodules (-60%) and ALP activity (-70%) compared to the WT mice. Interestingly, mouse primary osteoblasts expressed all the known opioid receptors, thus suggesting that osteoblasts could respond to the enkephalin treatment. Indeed, osteoblast cultures treated with Met- and Leu- enkephalins showed an increased osteocalcin expression (4-fold, $p=0.03$), together with an increased mineralization (1.5-fold). Accordingly, the type I collagen release in the medium was higher in both Met- and Leu-enkephalin treated osteoblasts compared to control. Taken together, these results highlight a role for PENK1 in osteoblast differentiation and in the regulation of the response of the bone to mechanical unloading.

Disclosures: **Nadia Rucci**, None

SUN-0572

Iron Involves in the Regulatory Effect of High Static Magnetic Field on Osteoblasts and Osteoclasts Jiancheng Yang^{*1,2}, Jian Zhang^{1,2}, Dandan Dong^{1,2}, Shenghang Wang^{1,2}, Peng Shang^{2,3}. ¹School of Life Sciences, Northwestern Polytechnical University, China, ²Key Laboratory for Space Bioscience and Biotechnology, Institute of Special Environment Biophysics, Northwestern Polytechnical University, China, ³Research & Development Institute in Shenzhen, China

High static magnetic fields (HiSMF) are usually defined as those static fields with intensities $\geq 1T$. Although many studies have indicated that static magnetic fields have positive effects on bone tissue, there were limited studies investigate the effects of HiSMF on bone system. Evaluating the effects of HiSMF on osteoblasts and osteoclasts, which is critical for understanding the possible risks or benefits from HiSMF to the balance of bone remodeling. Iron and magnetic fields have the natural relationship, and iron is an essential element for normal bone remodeling. Iron overload or deficiency can cause severe bone disorders including osteoporosis. In this study, HiSMF of 16T were used to investigate how osteoblasts (MC3T3-E1 cells) and osteoclasts (Raw264.7 cells) response to HiSMF and the changes of intracellular iron levels under HiSMF. The results showed that HiSMF promoted osteoblast proliferation with an increased iron content. One possible explanation for this finding is that elemental iron is essential for cell growth and crucial to many fundamental cellular processes, including DNA synthesis, respiration, cell cycle regulation and the function of proteins. During osteoblast differentiation, HiSMF reduced the initial stage of osteogenic differentiation and cellular iron, but accelerated matrix maturation, ultimately enhancing osteogenic mineralization and iron levels in osteoblasts. Osteoblast mineralization is a process that mineral crystals of hydroxyapatite were embedded into type I collagen fibers. And iron is a cofactor for the prolyl- and lysyl-hydroxylases in collagen synthesis and plays a crucial role in collagen maturation. As for osteoclasts, osteoclast differentiation and bone resorption activity was inhibited by HiSMF and was accompanied by a decrease of iron content in osteoclasts. Mature osteoclasts highly express tartrate-resistant acid phosphatase (TRAP) that they release upon active bone resorption. It is important that TRAP contains 2 iron atoms/molecule, and its activity is rapidly inhibited by the iron chelators. In conclusion, our results showed that HiSMF have positive effects on osteoblasticgenesis with altered iron levels, meanwhile, osteoclastogenesis was suppressed with decreased iron content under HiSMF. These results will improve our further understandings of the exact mechanisms of HiSMF on bone remodeling and have potential application value in treating or preventing human bone metabolism disorders.

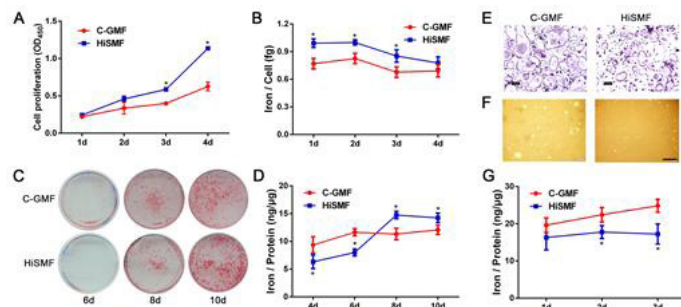


Figure 1. Iron involves in the regulatory effect of HiSMF on osteoblasts and osteoclasts. A. The proliferation of MC3T3-E1 cells were examined by CCK8 assay. B. Iron levels of osteoblasts during proliferation was detected by graphite furnace AAS. C. Osteogenic differentiation was confirmed by alizarin red S staining. D. Iron content of osteoblasts during differentiation. E. TRAP staining of osteoclasts generated by RAW264.7 cells. F. Bone resorption ability in osteoclast was determined by pit formation assay. G. Iron content of osteoclasts during differentiation. All HiSMF groups were compared with the geomagnetic field (GMF). Data shown are mean \pm SD. * $p < 0.05$.

Disclosures: **Jiancheng Yang**, None

SUN-0573

The sulforaphane-sensitive Tet2 enzyme controls osteoblast differentiation and bone homeostasis by regulating active DNA demethylation Roman Thaler*, Farzaneh Khani, Chris Paradise, Oksana Pichurin, Amel Dudakovic, Andre J Van Wijnen. Mayo Clinic, United States

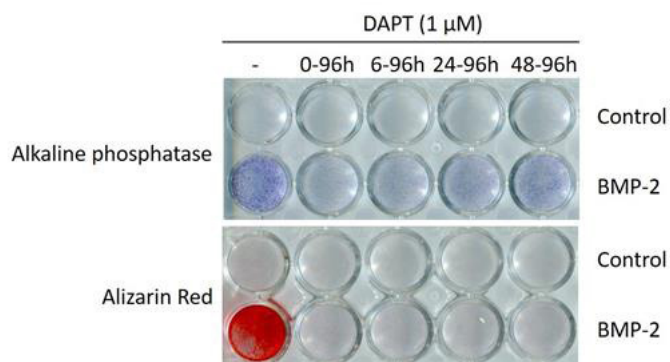
Proper osteoblastic differentiation is essential for normal bone development and homeostasis. We have previously shown that small molecules like Sulforaphane (SFN) or DMSO strongly promote osteoblastic differentiation by active DNA demethylation via Tet enzymes (Ten-eleven translocation methylcytosine dioxygenases). Specifically, because sulforaphane induces Tet1/Tet2-mediated active DNA demethylation, we addressed the molecular and physiological contribution of Tet enzymes to osteoblast differentiation in culture and bone in vivo. Using in vitro shRNA-mediated gene knock-down and CRISPR-dCas9 mediated gene activation paired with a conditional knock-out mouse model, we investigated the biological roles of the Tet1 and Tet2 enzymes in osteoblast differentiation and bone physiology. In mesenchymal stem cells, in osteoblasts as well as in primary bone tissue, Tet1 is expressed at low levels, but Tet2 expression is about 4-6 fold higher and appears to control active DNA demethylation during osteoblastic differentiation. We find that Tet2 but not Tet1 is required for global active DNA demethylation as measured by cytosine hydroxymethylation levels in MC3T3-E1 and MLO-A5 cells. However, both enzymes are necessary for osteoblast maturation as measured by ALPL activity, extra cellular matrix (ECM) deposition, ECM mineralization as well as expression of several osteoblastic genes. Conversely, forced expression of Tet1 and Tet2 reveals that a global increase of active DNA demethylation is achieved by Tet2, but not Tet1. Moreover, only Tet2 overexpression results in enhanced osteoblast function. We further confirmed the role of Tet2 in bone homeostasis using conditional Tet2 knock-out mice driven by an osteoblast specific *Osx-Cre* recombinase. Although these mice do not show apparent effects on general bone morphology, the overall bone quality and strength may be compromised as compared to their littermate controls. Collectively, our results establish Tet2 as a central epigenetic driver of osteoblast differentiation in vitro and in vivo and that active hydroxymethylation is causally linked to normal bone development and maintenance of bone health.

Disclosures: **Roman Thaler**, None

SUN-0574

Notch activation augments bone morphogenetic protein mediated human osteoblast differentiation Yadav Wagley^{*1}, Matthew Johnson², Sumei Lu², Andrew Wells^{2,3}, Alessandra Ches², Struan F.A. Grant^{2,4}, Kurt Hankenson¹. ¹Department of Orthopaedic Surgery, University of Michigan Medical School, United States, ²Center for Spatial and Functional Genetics and Division of Human Genetics, The Children's Hospital of Philadelphia, United States, ³Department of Pathology and Laboratory Medicine, University of Pennsylvania Perelman School of Medicine, United States, ⁴Department of Pediatrics, Perelman School of Medicine, University of Pennsylvania, United States

Bone morphogenetic proteins (BMP) play a well-established role in osteoblastogenesis, while the role of canonical Notch signaling in osteoblastogenesis is less-understood. To determine common regulatory mechanisms between Notch-mediated and BMP-mediated human osteoblast differentiation, three independent primary human donor mesenchymal progenitor cell isolates were stimulated in parallel with either the Notch ligand Jagged-1 or BMP2. Both treatments similarly increased terminal osteoblast differentiation as determined by alkaline phosphatase (ALPL) activity and Alizarin red S staining. RNA was harvested three days post-treatment and subjected to RNA-seq on the Illumina NovaSeq platform. Data was analyzed with the PORT pipeline and differential expression analysis was performed with the R-package limma. At $FDR < 10\%$, 4477 and 370 genes were differentially expressed in the BMP2 and the Jagged-1 treated cells, respectively. Genes associated with osteoblast differentiation, such as SPP1, SOST, DKK1, Osterix (SP7) and DMP1 were induced in BMP2-treated cells, but not in Jagged-1-treated cells. 45 genes were commonly upregulated, and 69 genes were commonly downregulated ($FC > 1.5$). ALPL and genes involved in extracellular matrix synthesis (eg. ACAN, ADAMTS10, ADAMTS2, HAPLN3, and HAS3) were upregulated with both treatments. Ingenuity pathway analysis of commonly upregulated genes showed increases in Notch signaling; Regulation of the Epithelial-Mesenchymal Transition Pathway; Osteoarthritis Pathway; RhoA signaling; and Epithelial Adherens Junction Signaling. Common downregulated pathways were NF- κ B signaling; Hepatic Fibrosis/ Hepatic Stellate Cell Activation; LXR/RXR Activation; Uracil Reduction II (Reductive); and Thymine Degradation. Notably, two of the top 5 commonly upregulated genes belonged to the Notch signaling pathway (Hey2 and Hes4), and additionally both induction protocols induced Jagged-1 and Notch 3. Interestingly, inhibiting Notch signaling with the gamma-secretase inhibitor DAPT during BMP-mediated human osteoblast differentiation abolished terminal osteoblastogenesis. Taken together, these data advance our current understanding of the basic mechanisms regulating bone formation, and suggest that Notch signaling is required for BMP-mediated osteoblastogenesis. These findings highlight the role of aberrant Notch signaling associated with human skeletal disorders, such as those seen in Alagille syndrome.



Disclosures: *Yadav Wagley, None*

SUN-0575

Gi signaling regulates the fate of murine bone marrow mesenchymal progenitor cells Liping Wang*, Linh Ho, Theresa Roth, Robert Nissenson. Endocrine Research Unit, San Francisco VA Medical Center, and Departments of Medicine and Physiology, University of California, United States

Signaling through Gs-G protein coupled receptors (GPCRs) is known to regulate the fate of bone marrow mesenchymal progenitor cells (MPCs). Stimulating Gs activity in MPCs enhances osteoblast differentiation and suppresses adipocyte differentiation. In contrast, little is known about the role of inhibitory G α protein (Gi) signaling in determining the fate of MPCs. We have previously shown that constitutive activation of Gi signaling in committed osteoblasts restrains bone formation and leads to osteopenia. We hypothesized that enhancing Gi signaling in MPCs would suppress osteoblast differentiation and promote bone marrow adipogenesis, thereby reducing bone mass. To test this hypothesis, we generated a mouse line (Ro1 mice) in which an engineered, constitutively active Gi-activating receptor (Ro1) is expressed in MPCs, driven by an osterix promoter. The tet-off system was used to delay the expression of Ro1 in MPCs until approximately the time of birth. Firstly, μ CT assessment of distal femurs of 10-week-old Ro1 mice demonstrated that constitutive Gi activation in MPCs decreased bone fractional volume by almost 50% ($p < 0.05$) in female (F) mice and by about 21% ($p > 0.05$) in male (M) mice, compared to age and sex matched littermate control mice. The decreased bone volume in Ro1 mice was mainly associated with decreased trabecular number (M vs. F: 38% vs. 46%) and increased trabecular separation (M vs. F: 66% vs. 75%). Secondly, bone marrow stromal cells (BMSCs) from Ro1 mice were cultured. Under osteogenic conditions, activating Gi signaling by expression of Ro1 decreased mRNA levels of alkaline phosphatase (1.6 fold, $p < 0.05$), osteocalcin (3 fold, $p < 0.01$), and type 1 collagen (1.5 fold, $p < 0.01$). By contrast, under adipogenic conditions, expression of Ro1 led to a 1.6 fold increase in adipogenesis, assessed by Oil Red O staining ($p < 0.01$). Thirdly, 6-week-old Ro1 mice were fed a high fat diet (HFD, 60% of kcal from fat) for 4 weeks. Activation of Gi signaling by expression of Ro1 in mice on a control diet significantly increased (by 2.4-fold, $p < 0.05$) the number of adipocytes in the bone marrow, compared to littermate controls. HFD led to a 2.3-fold ($p < 0.05$) increase in marrow adipocytes in Ro1 mice vs. the HFD-fed littermate control mice. The MPCs from Ro1 mice fed with HFD were harvested. HFD significantly increased the expression of oxidative stress response genes in MPCs, including Hif-1 α (2.5 fold, $p < 0.01$) and SOD1 (1.7 fold, $p < 0.01$). Strikingly, the expression of the gene encoding, Gai2 was increased by 10 fold. In conclusion, endogenous Gi signaling regulates the fate of MPCs. Excessive Gi activity in MPCs drives adipocyte differentiation at the expense of osteoblast differentiation. Metabolic stress such as HFD enhances the expression of oxidative stress genes in MPCs and this together with upregulation of Gi signaling may serve to increase marrow adipogenesis at the expense of osteogenesis.

Disclosures: *Liping Wang, None*

SUN-0576

Calmodulin dependent protein kinase kinase-2 (CamKK2) activates AMPK at an early stage which is required for osteoblast differentiation Susan D'Costa*, Gang Xi, David Clemmons. University of North Carolina at Chapel Hill, United States

Our previous studies showed that activation of AMPK at an early stage (day 1-9) is required for osteoblast differentiation. However, that study did not determine the upstream kinase which is directly responsible for AMPK activation during osteoblast differentiation. LKB1 is the traditional upstream kinase that activates AMPK but an LKB1 inhibitor had no effect thereby excluding it as a candidate kinase in this context. Previous studies have shown that calmodulin dependent protein kinase kinase-2 (CamKK2) is an alternative upstream kinase for AMPK activation. Our *in vitro* data clearly showed that addition of STO609, a CamKK2 inhibitor, at the early stage of differentiation inhibited AMPK activation in a dose dependent manner. Alizarin red staining and osteocalcin immunoblotting results showed that STO609 treatment early in the differentiation cycle attenuated osteoblast differentiation but

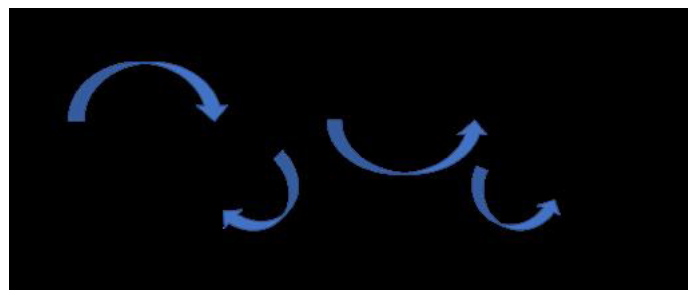
it was without effect if added at the later stages of differentiation, such as after day 11. This time frame was similar to the timeframe of AMPK activation during osteoblast differentiation. *In vitro* kinase assays showed that commercially available pure CamKK2 or CamKK2 immunoprecipitated from lysates obtained from cells that had been exposed to differentiation medium phosphorylated a substrate peptide AMPK homologue containing the T172 site activation site and STO609 inhibited this phosphorylation. This supports the hypothesis that CamKK2 is active during differentiation and phosphorylates AMPK T172. Furthermore, immunoprecipitation studies demonstrated that AMPK bound to CamKK2 during the early phase of differentiation. In addition, knock down of CamKK2 using a siRNA suppressed both basal and IGF-1-stimulated AMPK activation. Consistent with the inhibitor data, silencing CamKK2 was also able to inhibit osteoblast differentiation but only if the siRNA was added early in the differentiation cycle and no inhibition was detected if it was added after day 11. We conclude CamKK2 is activated early in the differentiation cycle, it directly phosphorylates AMPK and that CamKK2-mediated AMPK activation at an early stage is required for osteoblast differentiation.

Disclosures: *Susan D'Costa, None*

SUN-0616

Snx10 and PIKfyve are Required for Lysosome Formation in Osteoclasts Weimin Liu¹*, Gabriela Picotto², Leslie Morse³, Megan Summers³, Ricardo Battaglini¹. ¹UC Denver, United States, ²U de Cordoba, Argentina, ³Craig Hospital, United States

Osteoclasts rely on intracellular trafficking and organelle homeostasis for normal function. Snx10 is a PI3P-binding protein which localizes to osteoclastic early endosomes. Snx10-deficient osteoclasts show impaired endocytosis, extracellular acidification, ruffled border formation and bone resorption, suggesting that Snx10 regulates vesicular trafficking in endosome/lysosome formation. In order to elucidate the cellular mechanisms by which Snx10 regulates vesicular transport to control osteoclastic resorption we studied PIKfyve, another PI3P-binding kinase, which phosphorylates PI3P to PI(3,5)P₂. PI(3,5)P₂ is required for the biogenesis of lysosomes. Genetic or pharmacological inhibition of PIKfyve (and diminished PI(3,5)P₂ synthesis) causes endosome enlargement and cytoplasmic vacuolation. Overexpression of SNX10 also induces accumulation of early endosomes. These changes in the number and size of endosomes and lysosomes suggests that both Snx10 and PIKfyve are involved in membrane traffic between these organelles. Apilimod, a small molecule with cytotoxic activity used for the treatment of inflammatory diseases, inhibits PIKfyve with nanomolar specificity. Intriguingly, expression of CLCN7, OSTM1, and SNX10 is essential for sensitivity to apilimod which suggests that endosome/lysosome dysfunction mediates apilimod's cytotoxic effect. Snx10 and PIKfyve co-localize to early endosomes in osteoclasts, as determined by subcellular fractionation studies and immunofluorescent staining. Treatment with 10nM Apilimod results in accumulation of early endosomes, inhibition of RANKL-induced osteoclast formation, inhibition of lysosome formation and secretion of TRAP from differentiated osteoclasts. Apilimod, on the other hand, does not inhibit lysosome biogenesis in Snx10-deficient osteoclasts. Taken together, these results suggest that Snx10 and PIKfyve are involved in the regulation of endosome/lysosome homeostasis via the synthesis of PI(3,5)P₂. These findings may suggest novel therapeutic approaches targeting the secretory pathway in osteoclasts.



Disclosures: *Weimin Liu, None*

SUN-0617

Biodegradable Polymeric Nanoparticles Encapsulated with Small Molecular Weight L-Plastin Peptides Reduces Resorption Activity of Osteoclasts Sunipa Majumdar¹*, Aniket Wadajkar², Anthony Kim², Meenakshi Chellaiiah¹. ¹Department of Oncology and Diagnostics, University of Maryland, School of Dentistry, United States, ²Departments of Neurosurgery and Pharmacology, University of Maryland School of Medicine, United States

Background: Tumor necrosis factor alpha (TNF- α) was shown to stimulate the resorptive activity of osteoclasts (OCs) independent of integrin α v β 3. The actual target of TNF- α signaling is unclear. We have shown the vital role of an actin-bundling protein L-plastin (LPL) previously, in the assembly of nascent sealing zones (NSZs) at the early phase of sealing ring formation. TNF- α signaling regulates the phosphorylation of LPL at Ser-5 and -7 residues and the assembly of NSZs. These studies prompted us to gain more insight into

the role of LPL phosphorylation on OC bone resorption. Materials: To test the hypothesis that reducing the phosphorylation of LPL will attenuate the formation of NSZs and resorption, we used TAT-fused small molecular weight LPL peptides (P1 and P2) containing unmutated (P1-TAT-MARGSVSDEF) and mutated (P2-TAT-MARGADEF) serine residues. Poly(lactide-co-glycolic acid) (PLGA) is an FDA approved polymer and a commonly used delivery system in bone tissue engineering. To deliver the peptides in a controlled and sustained fashion in vivo in mice, we formulated P1 or P2-loaded PLGA nanoparticles. Prior to injecting into mice, we characterized the P1 or P2-loaded PLGA nanoparticles (~150 nm) and analyzed their effects on OCs in vitro. Results: Transduction of TAT-fused P1 into OCs reduces the formation of both NSZs and bone resorption which is due to the selective inhibition of cellular LPL phosphorylation. Characterization of the peptide (P1 and P2) loaded nanoparticles demonstrated the following: a) Transmission electron microscopy (TEM) images showed well-dispersed spherical shaped nanoparticles. b) The release of peptides over three weeks period due to slow hydrolysis of biodegradable polymer over time. c) both P1 and P2 nanoparticles had nearly neutral surface charge of -3.6 mV and -3.1 mV, respectively. d) Incubation of OCs with peptide-loaded PLGA nanoparticles for 4h substantiates the significance of the inhibitory effect of the P1 peptide on LPL phosphorylation and NSZs formation. Discussion and conclusion: Attenuation of NSZs formation and bone resorption in OCs transduced with TAT-fused P1 and not with P2 peptide documents the importance of phosphorylation of LPL in OC function. Small molecular weight peptide-based manipulations of OC bone resorption have the potential for pharmacological manipulations. Inhibition of endogenous LPL phosphorylation and NSZs formation by P1-loaded PLGA nanoparticles suggests the entry of these particles into OCs in vitro. These observations provide a 'stepping stone' to evaluating the effects of loaded nanoparticles in mouse models in vivo. (Patent pending for peptides; Equal contribution by 1st and 2nd authors; Work is supported by funding from NIH-NIAMS R01-AR46292 and R01AR066044 to MAC)

Disclosures: *Sunipa Majumdar, None*

SUN-0618

HDAC4-ERK Crosstalk Regulates Osteoclast Function Bora Faulkner*, Nicholas Blixt, Rajaram Gopalakrishnan, Eric Jensen, Kim Mansky. University of Minnesota, United States

Bone-resorbing osteoclasts are important for physiological bone remodeling process; however, their dysregulation contributes to development of skeletal diseases such as osteoporosis and cancer-induced bone disease. Histone deacetylases (HDACs) are well known repressors of gene transcription and have been shown to induce specific changes in gene transcription. Studies have shown that HDACs can influence skeletal development by affecting bone formation and resorption. These observations imply roles of HDACs in skeletal diseases such as osteoporosis and suggest these molecules could represent unique therapeutic targets. Here, we examined the consequence of genetic disruption of HDAC4, a class IIA deacetylase, in osteoclastogenesis using both in vitro cellular and molecular analyses associated to in vivo characterization of conditional HDAC4-knockout (HDAC4cKO). Thus, we mated Hdac4^{fl/fl} mice with those expressing c-Fms-Cre to target osteoclast lineage cells. We found that male HDAC4cKO mice at 3 months of age exhibit increased bone volume by micro-CT and decreased bone resorption. This result was unexpected given previous work on other class IIA deacetylases by our lab and others that had demonstrated that loss of HDAC7 or HDAC9 expression in osteoclasts resulted in mice with osteopenia. Analysis of the in vitro phenotype of osteoclasts from the HDAC4cKO mice demonstrate osteoclasts from the HDAC4cKO were larger than wild-type during early stages of osteoclast differentiation but had less demineralizing activity. Mechanistically, we show that in the absence of HDAC4, ERK1/2 activation is reduced independent of changes in MEK1/2 phosphorylation status. This data suggests that HDAC4 might target a MAP kinase phosphatase (MKP) to regulate ERK1/2 phosphorylation. ERK1/2 signaling has been shown to promote osteoclast survival, so this may represent a mechanism to explain the osteopetrotic phenotype of the HDAC4cKO mice. Moreover, these data support the hypothesis that HDAC4 could be involved in bone disease, and provide a rationale for the development of novel HDAC4-specific inhibitors as potential therapies for excessive osteoclast activity.

Disclosures: *Bora Faulkner, None*

SUN-0619

MEF2C positively regulates osteoclastogenesis by controlling c-Fos expression Takayuki Fujii*, Lionel Ivashkiv, Kyung Parkmin, Ye Ji Lee, Seyon Bae, Sehwan Mun, Kaichi Kaneko, Carmen Chai, Eric Sohn. Arthritis and Tissue Degeneration Program, David Z. Rosensweig Genomics Research Center, Hospital for Special Surgery, United States

Hypoxia augments osteoclastogenesis and can contribute to bone resorption at hypoxic sites such as bone marrow and the synovium of rheumatoid arthritis (RA) patients. We previously identified that hypoxia enhances osteoclast formation by suppressing COMMD1, a negative regulator of osteoclastogenesis. However, the mechanism which hypoxia increases osteoclastogenesis is complicated and remains unclear. In this study, we used transcriptomic and bioinformatics approaches to discover a positive regulator important for osteoclastogenesis under hypoxia conditions. We treated human osteoclast precursors (OCPs) with RANKL in either normoxia or hypoxia (2% of O₂) conditions. RNA sequencing analysis identified that MEF2 family members are significantly enriched in the RANKL-inducible and hypoxia-enhanced genes, in addition to HIF family proteins. In human CD14⁺ cells,

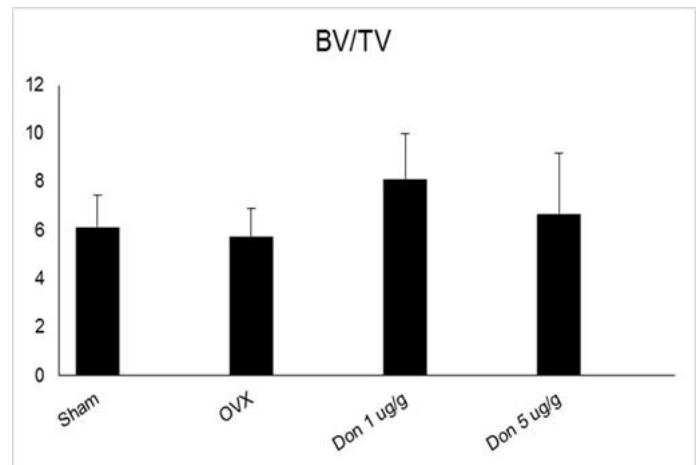
MEF2C gene silencing using siRNA dramatically suppressed osteoclast formation in hypoxia conditions and inhibited osteoclast marker genes such as NFATC1, CTSK and ITGB3. Consistently, the gain-of function approach using adenovirus encoding human MEF2C enhances osteoclastogenesis in normoxia and phenocopied hypoxia mediated enhancement of osteoclastogenesis. We found that c-FOS is a downstream mediator of MEF2C and c-FOS target genes are significantly enriched in MEF2C-regulated genes. RANKL-induced c-FOS expression is correlated with MEF2C expression in human osteoclasts. To further investigate the function of MEF2C in vivo, we deleted Mef2c in mice using Mx-cre inducible system and evaluated the bone phenotype. Mef2c deficient mice revealed increased bone mass. Mef2c-deleted bone marrow-derived macrophages showed inhibition of osteoclast formation with low expression of c-FOS. These findings identify MEF2C as a positive regulator of osteoclastogenesis in physiological and pathological conditions. Taken together, MEF2C positively regulates osteoclastogenesis and works by enhancing c-FOS expression that is important for osteoclastogenesis. Our results provide insight into mechanisms by which hypoxia promotes osteoclastogenesis by enhancing a positive regulator MEF2C as well as suppressing a negative regulator COMMD1.

Disclosures: *Takayuki Fujii, None*

SUN-0620

Osteoporosis and dementia common pathways and targets: Investigating the effect of acetylcholine esterase inhibitors on bone. A Mouse Model. Charles Inderjeeth¹, Dian Teguh², Warren Raymond¹, Jennifer Tickner², Jiak Xu². ¹Sir Charles Gairdner Hospital and University of WA, Australia, ²University of WA, Australia

Purpose: Previous research has shown that low bone mass density (BMD) appears to be related to increased risk of Alzheimer's disease. A recent study by Tamimi and colleagues in 2012 suggests cholinesterase inhibitors to treat dementia may reduce fracture risk. We previously reported that in vitro cholinesterase inhibitor Donepezil reduces osteoclast activity. We aimed to establish the therapeutic effects of Donepezil, on bone loss in ovariectomised (OVX) mouse model. Methods: In healthy mice we compared sham OVX (4) and OVX (4) against low (4) and high dose (5) Donepezil. MicroCT scanning was utilised to assess femur and Tibia bone quality parameters including BV/TV, TbSp, TbTh, TbN, cortical bone area, cortical thickness and marrow area. Results: At both femur and tibia as expected OVX mice showed deterioration in most parameters compared to sham. Donepezil treated mice showed trend to maintenance or improvement in these parameters. This was not dose dependent. As an example BV/TV changes are illustrated in Figure 1. Conclusions: Osteoporosis and dementia may share some common pathogenesis and potential therapeutic targets. Acknowledgements: Dr Shangfu Li; Grant: RAC Grant #2015-16_047



Disclosures: *Charles Inderjeeth, None*

SUN-0621

Ion-doped hydroxyapatite nanoparticles designed for bone regeneration affect osteoclastogenesis in vitro Carina Kamplleitner¹, Montserrat Espanol², Maria-Pau Ginebra², Michelle Epstein³, Oskar Hoffmann¹. ¹Dept. Pharmacology and Toxicology, University of Vienna, Austria, ²Universitat Politècnica de Catalunya, Spain, ³Dept. Dermatology, Medical University of Vienna, Austria

Nanosized hydroxyapatite (HA), chemically similar to the mineral phase of hard tissue, is a promising biomaterial for the treatment of large bone lesions. A novel strategy to enhance its osteoconductive and osteoinductive properties is ionic substitution (doping) into the HA nanocrystal structure. Locally applied, HA nanoparticles (NPs) can interact with bone cells and modulate cell behavior. However, HA-NP features as size, composition, morphology, surface charge and dose can differently affect bone cell responses and finally treatment outcomes. We sought to investigate the effect of non-doped and ion-doped HA-NPs for

bone tissue engineering on bone cell viability and osteoclast (OC) development and activity in vitro. Four recently developed HA-NPs formulations were evaluated: 1) non-doped HA (HA), 2) carbonate-doped HA (10 wt%, cHA), 3) strontium-doped HA (6 wt%, srHA) and 4) silicon-doped HA (2 wt%, siHA). To determine the cytocompatibility of HA-, cHA-, srHA-, and siHA-NPs, primary mouse osteoblasts (OBs) and OBs co-cultured with mouse bone marrow-derived OC precursors were incubated with NPs (250 µg/ml) for 24 hours and tested in WST-1 cell viability assays. We observed that non-doped and ion-doped HA-NPs were well tolerated at the concentrations tested without evidence of adverse or cytotoxic effects due to ionic substitution. To assess OC development and activity, we used a mouse OB-OC co-culture and added NPs at 50, 100 and 250 µg/ml. After 6 days, multinucleated OCs were stained for tartrate-resistant acid phosphatase, quantified by counting, and cathepsin K, a marker for OC activity, was measured. We found that non-doped and ion-doped NPs dose-dependently (250 > 100 > 50 µg/ml) reduced OC differentiation and activity in a similar manner. The different HA-NPs decreased RANKL levels in cell lysates, whereas RANKL added to NPs-treated co-cultures was able to stimulate OC development suggesting that OB-mediated OC development might be impaired. In summary, these data show that NPs can modulate OC differentiation and behavior, which might affect bone metabolism, and indicate more in-depth investigations on the mechanisms involved. Although HA-NPs are potential candidates for bone regeneration, pre-clinical in vitro evaluation of novel NPs elucidating effects on cells within the bone microenvironment should be considered before their clinical use.

Disclosures: *Carina Kampléitner, None*

SUN-0622

Estrogen-Related Receptor Gamma Negatively Regulates Osteoclastogenesis and Protects Against Inflammatory Bone Loss Hyun-Ju Kim*, Hye-Jin Yoon, Woo Youl Kang, Sook Jin Seong, Young-Ran Yoon. Kyungpook National University, Republic of Korea

Estrogen-related receptor gamma (ERR-gamma) is an orphan nuclear receptor that plays an important role in various metabolic processes under physiological and pathophysiological conditions. Here, we report that ERR-gamma functions as a negative regulator in RANKL-induced osteoclast differentiation. We observed that ERR-gamma was strongly expressed in osteoclast precursors, bone marrow-derived macrophages (BMMs) while its expression was significantly reduced by RANKL during osteoclastogenesis. Overexpression of ERR-gamma in BMMs suppressed the formation of multinucleated osteoclasts and attenuated the induction of c-Fos and NFATc1, which are critical modulators in osteoclastogenesis. Similarly, the treatment of ERR-gamma agonists, DY131 or GSK4716, also inhibited osteoclast generation and the expression of these key modulators. On the other hand, shRNA-mediated knockdown of ERR-gamma accelerated the formation of bone resorbing cells and the expression of osteoclastogenic markers. Forced expression of ERR-gamma blocked RANKL-stimulated phosphorylation of the NF-κB inhibitor IκBα and suppressed NF-κB transcriptional activity induced by RANKL or the NF-κB subunit p65. Furthermore, by employing a pharmacological approach, we showed that the ERR-gamma agonist DY131 protected against inflammatory bone loss induced by lipopolysaccharide in vivo. Together, our findings reveal that ERR-gamma is a pivotal regulator in RANKL-mediated osteoclastogenesis and suggest that ERR-gamma may have potential as a therapeutic target for pathological bone loss.

Disclosures: *Hyun-Ju Kim, None*

SUN-0623

G Protein-Coupled Receptor 120 Signaling Inhibited Osteoclast Formation and Bone Resorption Akiko Kishikawa*, Keisuke Kimura¹, Masahiko Ishida¹, Kazuhiro Shima¹, Saika Ogawa¹, Jiawei Qi¹, Wei-Ren Shen², Fumitoshi Ohori¹, Takahiro Noguchi¹, Aseel Marahleh¹, Hideki Kitaura¹. ¹Division of Orthodontics and Dentofacial Orthopedics, Department of Translational Medicine, Tohoku University Graduate School of Dentistry, Japan, ²Division of Orthodontics and Dentofacial Orthopedics, Tohoku University Graduate School of Dentistry, 4-1 Seiryomachi, Aoba-ku, Sendai 980-8575, Japan

In recent years, obesity has been regarded as one of lifestyle-related diseases. Recent studies have shown that when a high fat diet is given to mice deficient in G-protein coupled receptor 120 (GPR 120), obesity was occurred. GPR120 can be activated by free fatty acids. Therefore, GPR120 was found to be related to obesity. Also, it was newly discovered that osteoclast formation is suppressed by signaling from GPR120. In this study, we investigated the effects of docosahexaenoic acid (DHA), which is one of the free fatty acids and agonist of GPR120, on LPS-induced osteoclast formation and bone resorption. LPS with or without DHA was administered to mouse calvariae by daily subcutaneous injection for 5 days. After sacrifice, the number of osteoclasts, the area of bone resorption, and the level of C-terminal telopeptide fragments of type I collagen cross-links (CTX) were significantly decreased in LPS and DHA co-administrated mice compared to LPS alone administrated mice. Furthermore, the effect was eliminated by administering of AH7614 which is inhibitor of GPR120. In vitro experiment, bone marrow macrophages were cultured in a medium containing M-CSF and RANKL or TNF-α with or without DHA. The results showed direct inhibitory effects of DHA on RANKL-induced osteoclast formation and TNF-α-induced osteoclast formation. Expression levels of both RANKL and TNF-α mRNA were also reduced

in the DHA and LPS co-administrated group than LPS administrated group in vivo. These results suggest that DHA inhibits LPS-induced osteoclast formation and bone resorption in vivo by decreased LPS-induced osteoclast related cytokines TNF-α and RANKL production and directly inhibits osteoclast formation via GPR120 stimulation.

Disclosures: *Akiko Kishikawa, None*

SUN-0624

Local Regulator Del1 Inhibits Bone-resorption via Suppression of Wnt5a-Ror2 Signaling Axis Tomoki Maekawa¹, Yasuhiro Kobayashi², Hisanori Doman¹, Hikaru Tamura¹, Takumi Hiyoshi¹, Takeyasu Maeda¹, Yutaka Terao¹, George Hajishengallis³. ¹Niigata University, Japan, ²Matsumoto Dental University, Japan, ³University of Pennsylvania, United States

Objectives: The endothelial cell-secreted protein Del1 works homeostatically to regulate neutrophil transmigration and local inflammation. Our preliminary studies suggest that Del1 also regulates osteoclasts via Wnt5a-Ror2 axis. Therefore, the multifunctional Del1 can potentially act as a gatekeeper of inflammation and may be a candidate therapeutic target. The overall objective is to investigate how Del1 expression is regulated at the molecular signaling level, define novel Del1 functions, and identify key functional sites within the Wnt5a-Ror2 signaling that could be exploited as anti-inflammatory drugs. Methods: The expression of osteoclast-related molecules was examined in bone marrow cell cultures from Del1-KO and Ror2-KO mice using immunoblotting and qPCR. To determine interactions between Del1 and Wnt5a-Ror2 axis, all recombinant (r) proteins were subjected to pull-down assay. Binding kinetics and affinity of rDel-1, rWnt5a and rRor2 was calculated by Surface Plasmon Resonance. To evaluate Del1 and Ror2 function, intervention study was performed in periodontitis model in mice. To understand the mechanisms whereby Del1 regulates osteoclastogenesis and test its capacity to block inflammatory bone loss, three adult cynomolgus monkeys were used for local (intraingival) administration of Del1-Fc or Fc control. Therapeutic treatments were performed two times per week, starting 3 days after study initiation. Effect of daily injection of srRor2, Del1 or DHEA in arthritis were evaluated in collagen antibody induced arthritis (CAIA)-Del-1 WT or CAIA-Del-1 KO mice on arthritis scores and microcomputed tomography analysis. Results: Del1 suppressed Wnt5a-Ror2 axis in osteoclast precursors, which, in turn, decreased osteoclast formation and their bone-resorbing activity. Moreover, Del1 competitively antagonize Wnt5a to Ror2. Administration of Del1 in mice inhibits inflammation and bone loss by CAIA mice and periodontitis, suggesting that Del-1 suppresses bone destruction through the inhibition of Wnt5a-Ror2 axis. Conclusions: In the present study, Del1 is suggested to be a functionally versatile molecule which homeostatically regulates critical upstream (inflammatory cell recruitment) and downstream (osteoclastogenesis – suppression of Wnt5a-Ror2 axis) events during inflammatory bone loss.

Disclosures: *Tomoki Maekawa, None*

SUN-0625

Fine tuning of calcium oscillations by ITAM receptors regulates RANKL-induced osteoclast differentiation Hiroyuki Okada*, Hiroshi Kajijiya², Jun Hirose¹, Takumi Matsumoto¹, Koji Okabe², Takeshi Miyamoto³, Sakae Tanaka¹. ¹Department of Orthopaedic Surgery, The University of Tokyo, Japan, ²Department of Physiological Science and Molecular Biology, Fukuoka Dental College, Japan, ³Department of Orthopaedic Surgery, Keio University School of Medicine, Japan

[Introduction] Costimulatory signals mediated by ITAM (immunoreceptor tyrosine-based activation motif) receptors play critical roles in RANKL-induced osteoclastogenesis. Although Ca oscillations are considered essential for RANKL-induced osteoclastogenesis downstream of ITAM receptors, accurate monitoring of Ca oscillations in osteoclast precursor cells (OCPs) has been challenging because of the difficulty in detecting oscillation waves in OCPs. Previous studies demonstrated that at least 24 hours of RANKL treatment was necessary to detect oscillation waves in osteoclasts. In the present study, we developed a novel method to analyze the frequency of oscillations in OCPs, and demonstrated that each ITAM receptor regulates different types of Ca oscillations. [Methods] OCPs obtained from mice with four different phenotypes were subjected to experiments: wild type, FcRgamma KO, DAP12 KO, and FcRgamma & DAP12 double KO (ITAMs DKO). To obtain OCPs, adherent bone marrow macrophages cultured on glass cover slips were incubated with M-CSF and RANKL for 24 or 48 hours. Prepared coverslips stained with a fluorescent calcium indicator fura-2 were placed in a chamber of a fluorescent microscope, and ratio of fluorescence emission was measured at an interval of approximately two seconds. Software R version 3.4.3 was used for statistical analysis. [Results] We detected two distinguished types of Ca oscillations, oscillations in high frequency range (HFR) and low frequency range (LFR), at early stages of osteoclast differentiation. In wild type and FcRgamma KO-derived OCPs, HFR oscillations appeared after 48 hours of RANKL stimulation, while HFR oscillations were detected by 24 hours with RANKL stimulation, and disappeared after 48 hours in DAP12 KO-derived cells. Interestingly, HFR oscillations were observed in OCPs from ITAMs DKO mice even before RANKL stimulation, and the HFR oscillations continued after RANKL stimulation. In contrast, LFR oscillations were detected in DAP12 KO and ITAMs DKO OCPs but not in wild type or FcRgamma KO OCPs. [Discussion] Previous studies have demonstrated the critical role of ITAM receptor-mediated Ca oscillations in

osteoclast differentiation although the exact role remains elusive. In the present study, we found that 2 different types of Ca oscillations, HFR and LFR oscillations, were induced by RANKL in OCPs. Using ITAM receptor-deficient cells, we found that the induction of HFR and LFR oscillations was different depending on the types of ITAM receptor deficiency. These results, in combination with the observation that osteoclast differentiation was defective in DAP12 KO and ITAMs DKO OCPs, indicate a distinguished and crucial role of two types of RANKL-induced Ca oscillations in osteoclast differentiation, and the fine tuning of Ca oscillations is necessary for RANKL-induced osteoclast differentiation.

Disclosures: *Hiroyuki Okada, None*

SUN-0626

Molecular and cellular analyses of BMP-dependent coupling signals between osteoclasts and osteoblasts during bone remodeling Maiko Omi^{*1}, Ce Shi², Yuji Mishina¹. ¹Department of Biologic and Materials Sciences, University of Michigan, School of Dentistry, United States, ²Department of Oral Pathology, School and Hospital of Stomatology, Jilin University, China

The balance between bone formation and bone resorption is regulated by a cellular mechanism called coupling that includes communication from osteoclasts (OCs) to osteoblasts (OBs) in a direct or an indirect manner. We previously reported that osteoclast (OC)-specific disruption of *Bmpr1a* using a cathepsin K-Cre mouse line (*Ctsk-Cre/+; Bmpr1a flox/flox*) results in an increase of OB-mediated bone formation. These findings allow us to generate a novel hypothesis that BMPs regulate OB function through altering OC function. We hypothesize that BMP signaling mediated by BMPRI1A in OCs regulates OB function through paracrine or direct cell contact mechanisms. To address this hypothesis, we applied conditioned media (CM) from mature OCs into OB cultures to examine if OC-secreting factors affect OB activity. To further elucidate the direct cell-cell contact mechanism, we focus on a new route of cell-cell communication called tunneling nanotubes (TNTs). TNT is a recently recognized distinct type of intercellular communication device. OC precursors form TNTs in prior to cell-cell fusion, which is an essential process during osteoclastogenesis. We hypothesize that OCs communicate with OBs through TNTs that regulate OB function. We found that (1) OC-secreting factors increased OB mineralization in vitro, and (2) secreted factors from *Bmpr1a* mutant OCs further increased OB mineralization. These results suggest that BMP signaling mediated by BMPRI1A in OCs regulates OB differentiation by paracrine mechanisms. In contrast, (3) OCs inhibited OB differentiation in the direct OC-OB culture system, suggesting that other means of cell-cell communication occur when cells are in physical contact with each other. We found that (4) OCs communicated with OBs via TNTs. Furthermore, (5) *Bmpr1a* mutant OCs had less ability to form TNTs than controls and (6) the communication from *Bmpr1a* mutant OCs to OBs was less than that from control OCs. This result suggests that the communication via TNTs is critical for OC-OB coupling and this communication is one of the downstream events of BMP signaling. Overall, our data strongly suggest that secreted factors from OCs enhance OB activity and the direct communication between OCs and OBs negatively regulates OB function. Our data also suggest that loss of BMPRI1A-mediated BMP signaling in OCs promotes enhancing activity in secreted fractions and reduces TNT formation that results in reduction of suppressive activity toward OB differentiation.

Disclosures: *Maiko Omi, None*

SUN-0627

The Effect of Retention Period and an Anti-c-Fms Antibody On Orthodontic Relapse In a Mouse Model Jiawei Qi^{*}, Keisuke Kimura, Masahiko Ishida, Akiko Kishikawa, Kazuhiro Shima, Saika Ogawa, Wei-Ren Shen, Fumitoshi Ohori, Takahiro Noguchi, Aseel Marahleh, Hideki Kitaura. Division of Orthodontics and Dentofacial Orthopedics, Department of Translational Medicine, Tohoku University Graduate School of Dentistry, Japan

Orthodontic relapse has been a major clinical issue troubled orthodontic dentist and patient. Therefore, it is important to prevent orthodontic relapse. However, the mechanism of relapse is still unknown because there are few reports about relapse in mouse model. Orthodontic force induces osteoclastogenesis in vivo. Macrophage-colony-stimulating factor (M-CSF) is essential factor for osteoclast formation. It has recently been reported that administration of an antibody against the macrophage-colony-stimulating factor (M-CSF) receptor c-Fms inhibited mechanical loading-induced osteoclastogenesis and osteolysis in an orthodontic tooth movement model in mice. This study aimed to establish orthodontic relapse mouse model and examine the effect of an anti-c-Fms antibody on orthodontic relapse in mouse model. The Ni-Ti closed-coil spring was fixed between the upper incisors and the upper-left first molar to move first molar to mesial direction in 10-week-old wild type mice. After 12 days the tension appliance was removed. Mice were randomly divided into without-retention group (R0), retention for keeping space 2-weeks group (R2) and retention for keeping space 4-weeks group (R4). In R2 and R4, light-cured resin was put into the space between first and second molar and solidified through LED light to keep the moved space for 2 or 4 weeks. After 2 or 4 weeks the resin was removed, then the relapse check was started in R2 and R4 for 15 days. R4 group showed the smallest relapse distance in all groups. Only R4 group showed bone resorption by osteoclast. Therefore, we decided R4 group is a suitable model for our experiment. We injected anti-c-Fms antibody into a local site during relapse after 4 weeks retention. The anti-c-Fms antibody inhibited orthodontic relapse. The

findings suggested that M-CSF and/or its receptor are potential therapeutic targets in orthodontic relapse, and that injection of an anti-c-Fms antibody might be useful for inhibition of orthodontic relapse.

Disclosures: *Jiawei Qi, None*

SUN-0628

DPP-4 Inhibitor Inhibits LPS-induced Osteoclast Formation and Bone Resorption In Vivo Through Downregulating TNF- α Expression of Macrophages Wei-Ren Shen^{*}, Masahiko Ishida, Keisuke Kimura, Akiko Kishikawa, Kazuhiro Shima, Saika Ogawa, Jiawei Qi, Fumitoshi Ohori, Takahiro Noguchi, Aseel Marahleh, Hideki Kitaura. Division of Orthodontics and Dentofacial Orthopedics, Department of Translational Medicine, Tohoku University Graduate School of Dentistry, Japan

Recently, patients with metabolic syndrome have increased as a result of the global trends in population aging. Diabetes is one of the major diseases developed from metabolic syndrome. Dipeptidyl peptidase 4 (DPP-4) inhibition is a new therapeutic strategy for type 2 diabetic patients. DPP-4 has been reported to enhance inflammation. However, the effect of DPP-4 inhibition on inflammation remains unknown. Lipopolysaccharide (LPS) is a strong inducer of inflammation and osteoclast formation. To investigate in vivo effects of DPP-4 inhibition on LPS-induced osteoclast formation and bone resorption, LPS with or without a DPP-4 inhibitor was subcutaneously injected into mouse calvaria for 5 days. Osteoclast number and bone resorption were significantly lower in mice underwent LPS and DPP-4 inhibitor co-administration than that of LPS administration alone. Moreover, RANKL and TNF- α expression also reduced in the LPS and DPP-4 inhibitor co-administration group. In vitro, there were no direct effects of DPP-4 inhibitor or DPP-4 on RANKL- and TNF- α -induced osteoclast formation, or LPS-induced RANKL expression in stromal cells. Nevertheless, macrophages from LPS and DPP-4 inhibitor co-administrated mice exhibited lower TNF- α mRNA expression than macrophages from LPS-only mice. However, TNF- α mRNA expression was not reduced in LPS and DPP-4 inhibitor co-treated macrophages in vitro, compared with macrophages treated with LPS alone. These results indicate that DPP-4 inhibition may inhibit LPS-induced osteoclast formation and bone resorption in vivo by down-regulating LPS-induced TNF- α production by macrophages.

Disclosures: *Wei-Ren Shen, None*

SUN-0629

Deletion of the gene encoding Nupr1/p8, a regulator of autophagy, attenuates osteoclastogenesis but increases trabecular bone mass by enhancing osteoblast differentiation Makoto Shiraki^{*1}, Hirohito Hirata², Asana Kamohara², Juan Iovanna³, Toshio Kukita⁴, Masaaki Mawatari¹, Akiko Kukita². ¹Department of Orthopaedic Surgery, Faculty of Medicine, Saga University, Japan, ²Department of Pathology and Microbiology, Faculty of Medicine, Saga University, Japan, ³Center de Recherche en Cancérologie de Marseille, INSERM U1068, France, ⁴Department of Molecular Cell Biology & Oral Anatomy, Faculty of Dentistry, Kyushu University, Japan

Backgrounds: Nuclear protein1 (Nupr1)/p8 is a nuclear protein induced by multiple stress stimuli, that is involved in tumor progression and pathological conditions by regulating cell growth, apoptosis and autophagy. However, its normal function remains poorly understood. We have shown that Nupr1 regulate autophagy and apoptosis of osteoclast (OC) under serum-starved condition. Recent reports show that autophagy has an important role in long-lived cells such as osteoblasts (OB) and osteocytes in bone. Herein, we analyzed role of Nupr1 in bone homeostasis using Nupr1 KO mice. Methods and Results: MicroCT analysis revealed that trabecular bone volume and trabecular number were significantly increased in the femur of Nupr1 KO mice compared to wild-type (WT). Bone histomorphometry of trabecular bone indicated that the number of OC and preosteoclasts (pOC), and eroded surface were decreased in Nupr1 KO mice. In contrast, the number of OB and mineral apposition rate were increased to about 2-fold in Nupr1 KO mice. Using calvarial primary OB, expression of OB-related genes and bone formation were assessed. Alizarin red staining of primary OB showed calcification was enhanced in Nupr1 KO mice. The mRNA levels of osteocalcin, type I collagen, Runx2 and Osterix were also upregulated in specifically early phase of OB differentiation in Nupr1 KO. Interestingly, SOST mRNA expression was significantly reduced in Nupr1 KO. Expression analysis of autophagy-related genes, Foxo3 and Bnip3 which are targets of Nupr1 and Western analysis of LC3, p62 and ATG5 indicated that autophagy is upregulated in OB of Nupr1 KO. Defect of autophagy in osteoblasts is known to cause bone loss and increase the number of empty lacunae which is an indicator of osteocyte death. Analysis of osteocytes showed the number of empty lacunae was reduced in Nupr1 KO mice. We analyzed OC differentiation from bone marrow macrophages in more detail. The data showed that expression of OC-specific genes were reduced in Nupr1 KO mice. In addition, FACS analysis showed surface expression of RANK was decreased in bone marrow macrophage of Nupr1 KO mice, suggesting Nupr1 KO has defect in pOC. Conclusion: In summary, our data show inhibition of Nupr1 increase bone mass by enhancing differentiation and autophagy of OB but attenuating early OC differentiation. Nupr1 could be a new drug target to increase bone mass.

Disclosures: *Makoto Shiraki, None*

SUN-0630

Carbon Monoxide Releasing Molecule 3 Inhibits Osteoclastogenic Differentiation of RAW264.7 Cells by Heme Oxygenase 1 Hui Song*, Fenghe Zhang, School of Dentistry Shandong University, China

Increased osteoclastogenic differentiation may disrupt the balance of bone resorption and formation, giving rise to bone defective disease. The study aimed to investigate the influence of carbon monoxide releasing molecule 3 on osteoclastogenic differentiation of RAW264.7 cells, and explore the possible mechanism underlying the regulatory effect. Influence of CORM-3 on the proliferation of RAW264.7 cells was determined by CCK-8 assay. RAW264.7 cells were divided into four groups: Control group; Osteoclastogenic differentiation group, in which cells were induced osteoclastogenic differentiation in medium supplemented with 100 μ g/L RANKL and 50 μ g/L M-CSF; Degassed CORM-3-osteoclastogenic differentiation group, in which cells were pretreated with 200 μ mol/L degassed CORM-3 for 6hrs, and then induced osteoclastogenic differentiation; CORM-3-osteoclastogenic differentiation group, in which cells were pretreated with 200 μ mol/L CORM-3, and then induced osteoclastogenic differentiation. The mRNA and protein expression of RANK, TRAP, MMP-9, Cathepsin K and HO-1 of the cells during the osteoclastogenic differentiation was checked by RT-qPCR and Western blot. The induced osteoclasts were identified by TRAP staining. The HO-1 expression of the RAW264.7 cells was silenced by lentivirus transfection, and the expression of RANK, TRAP, MMP-9 and Cathepsin K was examined by RT-qPCR and Western blot. CORM-3 promoted the proliferation of RAW264.7 cells at the concentration of 200 μ mol/L. Pretreatment with CORM-3, but not degassed CORM-3, significantly decreased the mRNA and protein expression of osteoclast-specific marker TRAP, RANK, MMP-9 and Cathepsin K induced by RANKL and M-CSF on day 5, 7 and 9 during the osteoclastogenic differentiation ($P < 0.05$). After HO-1 was silenced by lentivirus transfection, the mRNA and protein expression of TRAP, RANK, MMP-9 and Cathepsin K in group with CORM-3 pretreatment maintained the same level as in osteoclastogenic differentiation group. CORM-3 inhibits osteoclastogenic differentiation of RAW264.7 cells via releasing CO. The inhibitory effect is mediated partially by HO-1 pathway. The results suggest the potential application of CORM-3 on some bone defective diseases.

Disclosures: *Hui Song, None*

SUN-0631

The Role of G alpha 12 In Osteoclast Min-Kyoung Song*, Hong-Hee Kim, Department of Cell and Developmental Biology, BK21 Program and Dental Research Institute, Seoul National University, Republic of Korea

The G12 family of G protein alpha subunits has been shown to participate in the regulation of various physiological processes. However, the role of G α 12 in bone physiology has not been well described. Here, by micro-CT analysis, we discovered that G α 12-knockout mice have an osteopetrotic phenotype. Histological examination showed lower osteoclast number in femoral tissue of G α 12-knockout mice compared to wild-type mice. Additionally, in vitro osteoclastic differentiation of precursor cells with receptor activator of nuclear factor- κ B ligand (RANKL) showed that G α 12 deficiency decreased the number of osteoclast generated and the bone resorption activity. The induction of nuclear factor of activated T-cell c1 (NFATc1), the key transcription factor of osteoclastogenesis, and the activation of RhoA by RANKL was also significantly suppressed by G α 12 deficiency. We further found that the RANKL induction of NFATc1 was not dependent on RhoA signaling, while osteoclast precursor migration and bone resorption required RhoA in the G α 12-mediated regulation of osteoclasts. Therefore, G α 12 plays a role in differentiation through NFATc1 and in cell migration and resorption activity through RhoA during osteoclastogenesis.

Disclosures: *Min-Kyoung Song, None*

SUN-0632

Fusion and Hemagglutinin Proteins of Canine Distemper Virus Support Osteoclast Formation Through NF- κ B Dependent and Independent Mechanisms in Paget's disease Wei Wang*, Dongfang Li, Minqi Li, Department of Bone Metabolism, School of Stomatology Shandong University, Shandong Provincial Key Laboratory of Oral Tissue Regeneration, Jinan, China

Paget's disease (PD) features abnormal osteoclasts which sharply increase in number and size and then intensely induce bone resorption. The purpose of this study was to determine the direct effects of canine distemper virus (CDV) and its fusion and hemagglutinin proteins (FH) on receptor activator of nuclear factor kappa-B ligand (RANKL) induced osteoclast formation in vitro. Here, CDV promoted osteoclast formation in RAW 264.7 mouse monocyte cell line and human peripheral blood mononuclear cells, and the effect of FH have been detected on the former by lentiviral vectors. We applied immunofluorescence assay to prove the infectious effects of CDV and FH lentiviral vectors; tartrate-resistant acid phosphatase (TRAP) staining and bone resorption pit formation assay to detect the function of osteoclast; western blot analysis to observe the alteration of osteoclastic transcription factors and the phosphorylation of intracellular signaling pathway transduction proteins; RT-PCR analysis to test the alteration of osteoclastic marker genes and inflammatory cytokine marker genes. As results, immunofluorescence assay provided the first conclusive proof that CDV can infect and replicate in primary human osteoclast precursor cells. Both of CDV and FH significantly promoted osteoclast formation and bone resorption induced by RANKL. Mean-

while high level expression of osteoclastic marker genes and transcription factors confirmed differential regulation of RANKL-induced osteoclastogenesis by CDV and FH stimulation. TRAP, Cathepsin K and matrix metalloproteinase 9 levels mainly depended on nuclear factor kappa-light-chain-enhancer of activated B cells (NF- κ B) activation and interleukin-6 levels principally depended on p38 mitogen-activated protein kinase (MAPK) activation after the same stimulation. Intracellular signaling transduction analysis revealed CDV and FH specifically upregulated the phosphorylation of NF- κ B and MAPKs induced by RANKL, respectively. Moreover, without RANKL stimulation, both of CDV and FH slightly induced osteoclast-like cells formation in RAW 264.7 cell line even in the presence of NF- κ B inhibitor. Taken together, our findings demonstrated that FH regulate osteoclast differentiation and activity through modulation of NF- κ B signaling pathway and induce osteoclast precursor cells merging dependent on the function of protein themselves. These results meant that FH play a pivotal role in CDV supporting osteoclast formation during PD happening.

Disclosures: *Wei Wang, None*

SUN-0633

Mutual restriction between p38/NFATc1 and p38/Pax6 axis during osteoclastogenesis Ziang Xie*, Shunwu Fan, Sir Run Run Shaw Hospital, School of Medicine, Zhejiang University, China

Balance of osteoclast formation is regulated by receptor activator of NF- κ B ligand (RANKL) and extracellular negative regulator such as interferon- γ (IFN- γ) and interferon- β (IFN- β), which can suppress excessive bone destruction. However, poor knowledge is known about intrinsic negative regulatory factors in RANKL-mediated osteoclast differentiation. Recently, paired-box homeodomain transcription factor Pax6 is shown to act as a negative regulator of RANKL-mediated osteoclast differentiation, but the crosstalk related to the other signaling pathway is still unclear. Here, we show a novel p38 inhibitor (VX-745) upregulates the expression of Pax6 during osteoclastogenesis. Subsequently, we found that β -catenin was binded to the proximal region of Pax6 promoter and promotes the transcription of Pax6, which was impaired by VX-745 through enhancing the ubiquitination degradation of β -catenin. These results suggest that Pax6 is positively regulated by p38/ β -catenin signaling pathway, which maintains the balance of osteoclast formation with the classical p38/c-Fos/NFATc1 signaling pathway. Our study demonstrates that the p38/ β -catenin/Pax6 signaling pathway contributes a new aspect of the negative regulatory in osteoclastogenesis and the novel p38 inhibitor VX-745 and the blocking of Pax6 might provide additional approaches to treat osteoclast-related diseases.

Disclosures: *Ziang Xie, None*

SUN-0634

LRP1 suppresses bone resorption in mice by inhibiting the RANKL-stimulated NF κ B and p38 pathways during osteoclastogenesis Di Lu*, Jianshuang Li, Huadie Liu, Gabrielle Foxa, Bart Williams, Tao Yang, Van Andel Research Institute, United States

Single nucleotide polymorphisms in the LRP1 gene coding sequence are associated with low bone mass, and cell culture studies suggest that LRP1 plays a role in osteoblast proliferation and osteoblast-mediated osteoclastogenesis. However, the in vivo function of LRP1 in bone homeostasis has not been explored. In this work, we studied the osteoclast-specific role of LRP1 in bone homeostasis using a Ctsk-Cre;Lrp1f/f mouse model on the C57BL/6J background. These mice had a dramatically decreased trabecular bone mass with markedly more osteoclasts, while the osteoblast activity was unaffected or slightly increased. The cortical bone parameters were largely unaltered. Upon RANKL treatment, Lrp1-deficient bone marrow monocytes more efficiently differentiated into osteoclasts and showed elevated p65 NF κ B and p38 signaling. Consistently, Lrp1-overexpressing Raw264.7 cells were desensitized to RANKL-induced p38 and p65 activation and osteoclastogenesis. Moreover, RANKL treatment led to a sharp decrease of LRP1 protein and RNA in BMs. Overall, our data suggest that osteoclast-expressed LRP1 is a crucial regulator of bone mass. It inhibits the NF κ B and p38 pathways and lessens the efficiency of RANKL-induced osteoclastogenesis.

Disclosures: *Di Lu, None*

SUN-0635

Nuclear Factor of Activated T Cells 2 Is Required for Osteoclast Differentiation and Function in vitro Jungeun Yu*, Stefano Zanotti, Lauren Schilling, Ernesto Canalis, UConn Health, United States

Nuclear factor of activated T cells (NFATc) 2 is important for the immune response and its activation in the osteoclast lineage can compensate for the downregulation of NFATc1 and promote osteoclastogenesis. However, the role of NFATc2 in the osteoclast lineage is uncertain because studies interrogating its function in the skeleton have used mouse models of global Nfatc2 gene inactivation. Nfatc2 null mice have a generalized inflammatory phenotype, limiting their usefulness. To study the direct effect of NFATc2 in osteoclasts, Nfatc2loxP/loxP mice, where the Nfatc2 exon2 is flanked by loxP sequences, were created and mated with mice expressing Cre under the control of the Ly22 promoter. Nfatc2 mRNA was downregulated by 50-80% in bone marrow-derived macrophages (BMMs) and in in-

tact bones and NFATc2 protein was not detectable in BMMs from *Lyz2Cre*/*WT*;*Nfatc2* Δ/Δ mice by immunoblotting, documenting downregulation of *Nfatc2*. Cultured BMMs from *Lyz2Cre*/*WT*;*Nfatc2* Δ/Δ mice exhibited a 30% decrease in osteoclast number in comparison to cells from littermate controls. *Lyz2Cre*/*WT*;*Nfatc2* Δ/Δ osteoclasts exhibited a 50% decrease in total bone resorption area. When corrected for osteoclast number, bone resorption area was 30% lower in *Lyz2Cre*/*WT*;*Nfatc2* Δ/Δ than controls, indicating decreased osteoclast resorptive activity. Actin staining of osteoclasts from *Lyz2Cre*/*WT*;*Nfatc2* Δ/Δ mice cultured on bovine bone slices revealed smaller cells with smaller sealing zones than littermate controls. These findings demonstrate that NFATc2 is necessary for optimal osteoclast maturation and function in vitro. *Lyz2Cre*/*WT*;*Nfatc2* Δ/Δ mice did not exhibit an obvious skeletal phenotype in vivo by microcomputed tomography (μ CT) at either 1 or 4 months of age when compared to *Nfatc2**loxP/loxP* littermates. Bone histomorphometry confirmed the μ CT results, and conditional *Lyz2Cre*/*WT*;*Nfatc2* Δ/Δ mice did not exhibit changes in parameters of bone formation or resorption compared to controls. The absence of an in vivo phenotype is likely because of compensation by NFATc1. In conclusion, NFATc2 is necessary for optimal osteoclast differentiation and function in vitro, but its downregulation in osteoclast precursors does not alter skeletal remodeling in vivo.

Disclosures: **Jungeun Yu**, None

SUN-0664

Osteocytes Are the Major Source of Circulating FGF23 During Acute Inflammation

Guillaume Courbon*¹, Claire Gerber¹, Samantha Neuburg¹, Maralee Capella¹, Xueyan Wang¹, Corey Dussold¹, Lixin Qi¹, Wenhan Chang², Myles Wolf³, Aline Martin¹, Valentin David¹. ¹Division of Nephrology and Hypertension, Department of Medicine, and Center for Translational Metabolism and Health, Institute for Public Health and Medicine, Northwestern University Feinberg School of Medicine, Chicago, IL, United States, ²Division of Endocrinology and Metabolism, UCSF, San Francisco, CA, United States, ³Division of Nephrology and Hypertension, Duke University, Durham, NC, United States

Background: Inflammation is a novel mechanism that stimulates fibroblast growth factor (FGF) 23 production in bone cells and extrasosseous tissues, however the contribution of osteocytes to circulating FGF23 levels during acute inflammation is unknown. Methods: To investigate the effects of inflammation on FGF23 production, wild-type (WT) mice and mice with a conditional deletion (cKO) of *Fgf23* in osteocytes (*Fgf23*^{fl/fl};*DMP1-Cre*⁺) received a single injection of interleukin-1 β (IL-1 β) or saline (Ctr). We measured FGF23 mRNA and circulating intact and total protein (cFGF23 which includes intact and cleaved proteins) up to 6 hours post injection. Results: In WT mice, injection of IL-1 β increased circulating levels of intact and total FGF23 (12-fold and 62-fold, respectively, $p < 0.001$ vs Ctr). IL-1 β increased *Fgf23* mRNA expression by 60 fold in bone, 7 fold in spleen and 300 fold in kidney ($p < 0.05$ vs. Ctr), suggesting that extrasosseous production of FGF23 may contribute to circulating FGF23 levels. In line with these findings, cKO-Ctr mice did not show a significant reduction in circulating FGF23 compared to WT-Ctr mice, suggesting that extrasosseous FGF23 production is sufficient to maintain relatively normal circulating FGF23 levels. However, cKO mice showed a markedly reduced FGF23 secretion in response to IL-1 β injection compared to WT-IL-1 β mice for both intact (~80%) and total FGF23 (~92%, $p < 0.001$). Consistent with these data, bone *Fgf23* mRNA and protein expression levels were also dramatically reduced by 80% ($p < 0.01$) in cKO-IL-1 β mice compared to WT-IL-1 β . Finally, IL-1 β treatment of primary osteocytes cultures from WT and cKO animals increased *Fgf23* mRNA expression and protein secretion by 10 fold in WT mice ($p < 0.05$ vs. Ctr) but failed to increase FGF23 in cKO cultures. Conclusions: These results suggest that *Fgf23* expression is increased in bone and extraskeletal tissues during acute inflammation, however osteocytes are the major secretory source for the circulating FGF23 protein.

Disclosures: **Guillaume Courbon**, None

SUN-0665

Sclerostin regulates adipocyte fate and mediates paracrine and endocrine signaling between osteocytes and fat.

Jessica H. Nelson*¹, Hannah M. Davis², Kevin Mcandrews², Meloney D. Gregor², William R. Thompson³, Lillian I. Pltokin², Alexander G. Robling², Teresita Bellido², Jesus Delgado-Calle¹. ¹Indiana University School of Medicine, Dept. of Medicine, Hematology/Oncology, United States, ²Indiana University School of Medicine, Dept. of Anatomy and Cell Biology, United States, ³School of Health and Rehabilitation Sciences, Dept. of Physical Therapy, United States

Osteocyte (Ot)-derived sclerostin (Scl) acts on osteoblastic cells by binding to its chaperone LDL receptor related protein (LRP) 4 and to the Wnt co-receptors LRP5/6 to antagonize Wnt/ β -catenin signaling, inhibiting bone formation and stimulating bone resorption. Emerging evidence suggests that Scl also regulates adipose tissue (AT), however conflicting results have been reported. We examined the effects of Scl on AT of the bone marrow (BMAT) and peripheral fat depots using mice with activated β -catenin in Ots (*da β catOt*), a mouse model characterized by high bone remodeling with bone gain and elevated Scl expression in bone. *da β catOt* mice display a marked increase in BMAT volume, a 3-4 fold increase in BM adipocyte number, and elevated mRNA expression of the adipocyte marker

Fabp4 in bone/BM. In addition, *da β catOt* mice exhibit a 3-fold increase in mRNA expression of the brown adipocyte markers *Ucp1*, *Pgc1 α* , and *Zic1*, without changes in the white adipocyte markers *Cidec*, *HoxC9*, or *Tbx1*, in bone/BM. *da β catOt* mice also show a 3-fold increase in serum Scl, which is accompanied by increased body fat mass, elevated peripheral inguinal white AT (iWAT; 50%), and increased interscapular brown AT mass (BAT; 15%). Similar to the findings in BMAT, mRNA expression of the brown adipocyte markers *Pgc1 α* and *Zic1* is also increased by 2-3-fold in iWAT from *da β catOt* mice. Remarkably, mice with *LRP4* deletion in Ots, another high bone mass model exhibiting high serum Scl, also display increased body-fat mass and elevated BAT mass compared to control mice; although, iWAT mass is decreased. Further, treatment of mesenchymal stem cells (MSCs) with recombinant (r)Scl or conditioned media from *da β catOt* bones increased by 15-20% their differentiation into adipocytes, an effect that was fully blocked by an anti-Scl antibody. Moreover, rScl increased the expression of *Fabp4* and adiponectin and the brown adipocyte marker *Ucp1* in MSCs undergoing adipogenic differentiation; and also increased *Ucp1* expression when added to MSCs fully differentiated into mature adipocytes. Thus, Scl stimulates adipogenesis in the BM and in both white/brown peripheral fat depots, regulates MSC differentiation, and alters adipocyte fate favoring brown versus white adipocyte identity. These findings demonstrate paracrine and endocrine signaling between Ot-derived Scl and adipocytes, and reveal a novel paradigm of high adipocyte number together with high osteoblast number and elevated bone formation.

Disclosures: **Jessica H. Nelson**, None

SUN-0666

Connexin 43 Hemichannels Protect Bone Loss during Estrogen Deficiency

Rui Hua*¹, Liang Ma¹, Hongyun Cheng¹, Roberto Fajardo², Joseph Pearson³, Teja Guda³, Daniel Shropshire¹, Sumin Gu¹, Jean X. Jiang¹. ¹Department of Biochemistry, UT Health San Antonio, United States, ²Department of Orthopaedics, UT Health San Antonio, United States, ³Department of Biomechanical Engineering, University of Texas at San Antonio, United States

Estrogen deficiency in post-menopausal women is a major cause of bone loss resulting in osteopenia, osteoporosis and a high risk for bone fracture. Connexin 43 (Cx43) forms gap junctions that mediate osteocyte coupling and are critical for maintaining proper bone physiology. Hemichannels (HCs), unpaired gap junction channels, are extensively involved in the communication between osteocytes and their extracellular environment, and play important roles in osteocyte viability and bone remodeling. Here we show that estrogen deficiency reduced Cx43 expression and Cx43 hemichannel activity in vitro. To determine if functional HCs protect osteocytes and bone loss during estrogen deficiency in vivo, we adopted an ovariectomy (OVX) model in wild type (WT) and two transgenic Cx43 mice: R76W (dominant-negative mutant affecting only gap junction channels) and Δ 130-136 (dominant-negative mutant compromising both gap junction channels and HCs). The bone mineral density (BMD), bone structure and histomorphometric changes of cortical and trabecular bones after OVX were investigated. Our results showed that the extent of bone loss in trabecular and cortical bones in R76W was similar to those in WT control mice. However, the Δ 130-136 transgenic cohort had a greater decrease in trabecular bone than WT and R76W mice, associated with a significant increase in numbers of apoptotic osteocyte and empty lacunae. Interestingly, osteoclast surfaces in trabecular and cortical bones were increased after OVX in the WT and R76W but not in Δ 130-136 mice. Furthermore, biomechanical properties were analyzed using three-point bending flexural evaluation of the femurs. OVX significantly reduced bone stiffness in Δ 130-136 mice while no significant changes were observed in WT and R76W groups, and there was a significant decrease shown in the percentage of yield force change between the Δ 130-136 and R76W groups. Additionally, ablation of HCs may render osteocytes more vulnerable to oxidative stress, indicated by the increased 4-hydroxynoneanal (4-HNE) positive osteocytes, which is a biomarker for lipid peroxidation. Taken together, given the functional differences of R76W and Δ 130-136 on gap junctions and gap junctions/HCs, respectively, these data demonstrate that impairment of Cx43 HCs in osteocytes accelerates bone loss and increases osteocyte apoptosis after OVX, and further suggest that Cx43 HCs in osteocytes protect bone fragility against catabolic effects due to estrogen deficiency.

Disclosures: **Rui Hua**, None

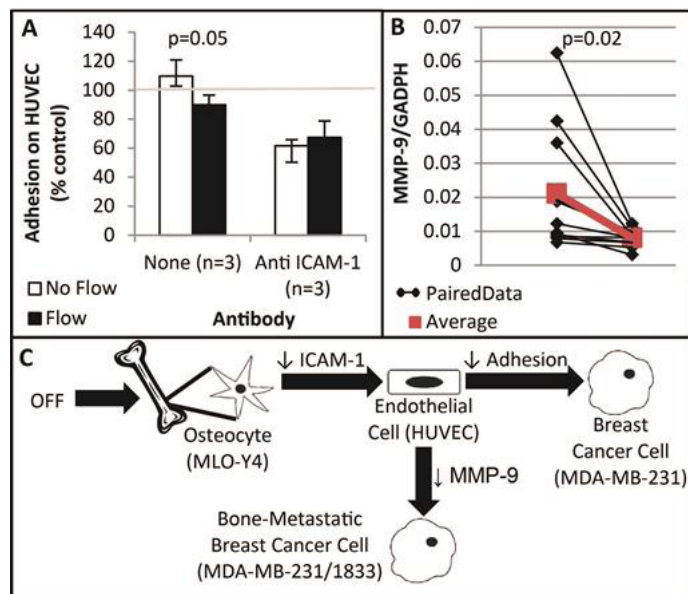
SUN-0667

Mechanical Regulation of Breast Cancer Bone Metastasis via Osteocytes' Signaling to Endothelial Cells

Yu-Heng Vivian Ma*, Liangchen Xu, Xueting Mei, Lidan You. University of Toronto, Canada

Introduction: Bone metastases occur in 65-75% of patients with advanced breast cancer and significantly increase their morbidity and mortality. Bone mechanical loading during exercise, commonly suggested for patients, stimulate osteocytes, the major cell population in the bone. We previously showed that mechanically stimulated osteocytes affect breast cancer cell apoptosis and migration both directly and indirectly through osteoclasts and endothelial cells. Since endothelial cells respond to osteocyte signaling and exist in large number and close proximity to metastasizing cells in blood vessels, we hypothesize that their response to mechanically stimulated osteocytes affect breast cancer cell activity during bone metastasis. Methods: To simulate the mechanical stimulation osteocytes experience physiologically, MLO-Y4 osteocyte-like cells (gift of Dr. Bonewald, Indiana University) were placed in flow chambers and subjected to oscillatory fluid flow (OFF; 1Pa; 1Hz; 2 hours).

Controls were MLO-Y4 cells not placed in flow chambers. Human umbilical vein endothelial cells (HUVECs; gift of Dr. Young, University of Toronto) were conditioned in medium extracted (conditioned medium; CM) from MLO-Y4 cells. The strength of MDA-MB-231 breast cancer cells' adhesion to HUVECs was tested by applying 30 minutes of OFF (1Pa; 1Hz) after 30 minutes of adhesion. Gene expression of MDA-MB-231/1833 bone-metastatic breast cancer cells (gift of Dr. Seth, University of Toronto) conditioned in HUVEC CM was determined with qPCR. Results: CM from OFF-stimulated MLO-Y4 cells reduces the adhesion of MDA-MB-231 cells (by 18%) to HUVECs by lowering HUVECs' expression of ICAM-1 (intercellular adhesion molecule 1) (Fig. A). This aligns with our previous result demonstrating MDA-MB-231 cells' lower extravasation towards CM from OFF-stimulated MLO-Y4 cells. Furthermore, CM from HUVECs conditioned in CM from OFF-stimulated MLO-Y4 cells lowered the expression of MMP-9 (matrix metalloproteinase 9; important for cancer cells to degrade matrix during invasion into the bone) by MDA-MB-231/1833 cells (by 54%) (Fig. B). Conclusion: We demonstrated that endothelial-mediated signaling from mechanically stimulated osteocytes reduced the ability of breast cancer cells to adhere to endothelial cells and degrade the bone (Fig. C). This provides insights into the impact of exercise on bone metastases, and will assist in designing exercise or bone loading regimens that lower the risk for bone metastases.



Disclosures: Yu-Heng Vivian Ma, None

SUN-0668

Stretch-stimulus activates the mechano-signaling via opening of the mechano-sensitive channel, Piezo1 and the subsequent calcium influx in osteocyte-like cells. Takuya Notomi¹, Akiko Hiyama¹, Tadashige Nozaki¹, Masaki Noda². ¹Osaka Dental University, Japan, ²Yokohama City Minato Red Cross Hospital, Japan

The bone mechano-signaling is related to membrane-bound molecules and the subsequent intracellular signaling. We have focused on one of membrane proteins, Piezo channels (Piezo) and investigated their role on mechano-signaling in bone cells. The Piezo are mechano-sensitive cation channel and two subtypes (Piezo1, Piezo2) are reported. The expression of mRNA levels of Piezo1 was abundant and Piezo2 was background levels in osteocyte-like cells (MLO-Y4) and calvaria primary osteoblasts. The phosphorylated ERK/total ERK (ERK ratio) was quantified as the indicator for activation of mechano-signaling. The ERK ratio was increased at 10min after application of stretch-stimulus but this increment was decreased by the addition of Piezo inhibitor. Addition of Piezo agonist increased the ERK ratio without stretch-stimulus. Next, we generated Piezo1-deficient MLO-Y4 (Piezo1-KO) by CSIPR/CAS9. The stretch-stimulus increased the ERK ratio in Piezo1-wild type (Piezo1-WT) but not in Piezo1-KO cells. To investigate intracellular mechano-signaling, intracellular Ca²⁺ levels were measured. The cells which exhibit Ca²⁺ oscillation in response to stretch-stimulus were identified as Ca²⁺ oscillation-positive cells. The stretch-stimulus occurred the Ca²⁺ oscillation in Piezo1-WT cells, but the number of Ca²⁺ oscillation-positive cells were decreased with Piezo channel inhibitor. In Piezo1-KO cells, the number of Ca²⁺ oscillation-positive cells were decreased in comparison to Piezo1-WT cells. The generation of Ca²⁺ oscillation was diminished by exclusion of extracellular Ca²⁺. These results suggested that the stretch-stimulus induced Ca²⁺ oscillation via activation of Piezo1 and the subsequent Ca²⁺ inflow. Then the relationships between voltage-gated Ca²⁺ channel (VGCC) and Piezo were investigated. We focused on L-type VGCC which is highly expressed in osteocyte and osteoblasts. Addition of inhibitors for L-type VGCC decreased the number of Ca²⁺ oscillation-positive cells while inhibition of both L-type VGCC and Piezo further decreased the number of Ca²⁺ oscillation-positive cells. In addition, the Piezo agonists-induced Ca²⁺ oscillation was decreased by addition of L-type VGCC inhibitors. These

results indicate that Piezo1 channel activates mechano-signaling via intracellular Ca²⁺ pathway. Our findings suggest that the mechano-channels and the related membrane molecules might give the cue for elucidating bone mechano-signaling.

Disclosures: Takuya Notomi, None

SUN-0669

Nfat Transcription Factors are Key Regulators of Osteocyte Function Independent of c-fos Matt Prideaux^{*}, Lynda Bonewald. Indiana University, United States

We have previously shown that during lactation, osteocytes remove mineral from their perilacunar matrix. This is mediated through the receptor PTH1R in response to PTHrP, which is elevated during lactation. Genes normally associated with osteoclasts, such as Atp6v0d2, Ctsk, Acp5/Trap and Mmp13 were also increased in osteocytes with lactation. As Nfatc1 is a transcription factor known to regulate the differentiation and activity of osteoclasts, we sought to determine if it plays a role in osteocyte perilacunar remodeling. We utilized the MLO-Y4 osteocyte-like and the IDG-SW3 mature osteocyte-like cell lines. MLO-Y4 cells were treated with 40μM INCA6, an inhibitor of Nfat/calcieneurin activity, for 72 hrs and the expression of key osteocyte genes examined by qRT-PCR. INCA6 decreased the expression of Atp6v0d2 by 53% (p<0.01), Rankl by 50% (p<0.001) and Acp5/Trap by 30% (p<0.05). Treatment of differentiated, mature IDG-SW3 cells with INCA6 downregulated Sost (44%, p<0.05), Rankl (57%, p<0.001) and Mepe (57%, p<0.01) and upregulated the mineralization-associated genes Dmp1 (95%, p<0.001) and Ocn (58%, p<0.01). To determine whether Nfats play a role in PTHrP signaling, mature IDG-SW3 cells were treated with 100nM PTHrP in the presence or absence of INCA6 for 72 hrs. The expression of Nfatc1 was increased by PTHrP treatment (3-fold, p<0.001). Atp6v0d2 mRNA expression was increased by PTHrP (15-fold, p<0.001), which was attenuated 46% (p<0.01) by co-incubation with INCA6. Rankl was strongly induced by PTHrP (35-fold, p<0.001) and attenuated 55% (p<0.001) by INCA6. INCA6 also decreased Mmp13 (30%, p<0.001) and Car2 (46%, p<0.01) mRNA expression. As Nfatc1 activity in osteoclasts is downstream of c-fos, we next investigated the effects of blocking c-fos in osteocytes using the inhibitor T-5224. T-5224 did not block the PTHrP-induced increase in Atp6v0d2 and Rankl in IDG-SW3 cells. Furthermore, T-5224 failed to decrease Sost expression, suggesting that in osteocytes Nfat activity is independent of c-fos. Together, these results suggest that Nfats may be essential regulators of bone remodeling by targeting genes such as Sost and Rankl in osteocytes. Furthermore, Nfats may function in a similar manner in osteocytes as in osteoclasts, by inducing factors that promote resorption such as Atp6v0d2. Ongoing studies targeting deletion of Nfatc1 in osteocytes in vivo, will further elucidate the role of Nfat activity in osteocyte perilacunar remodeling and bone homeostasis.

Disclosures: Matt Prideaux, None

SUN-0670

PINCH regulates bone homeostasis through its expression in osteocytes Yishu Wang^{*1}, Qinnan Yan¹, Yiran Zhao¹, Yiming Lei¹, Liting Ma¹, Simin Lin¹, Yumei Lai², Huiling Cao¹, Chuanyue Wu¹, Guozhi Xiao¹. ¹Department of Biology and Guangdong Provincial Key Laboratory of Cell Microenvironment and Disease Research, Southern University of Science and Technology, China, ²Department of Orthopedic Surgery, Rush University Medical Center, United States

Pinch is a LIM-domain-only adaptor that plays an important role in integrin activation and extracellular matrix adhesion and migration. Mammalian cells have two functional Pinch proteins, Pinch1 and Pinch2. To investigate the role of Pinch in bone, we deleted Pinch1 expression selectively in osteocytes by the Dmp1-Cre transgene and Pinch2 globally in mice (Pinch1^{f/f}; Dmp1-Cre; Pinch2^{-/-} mice, referred to as P1D1/P2KO hereafter). P1D1/P2KO mice displayed a severe osteopenic phenotype. Both trabecular and cortical bone parameters such as the bone volume fraction (BV/TV), trabecular number (Tb.N), cortical thickness (Cort.Th) and bone mineral density (BMD) were dramatically reduced and trabecular separation (Tb.Sp) was increased in P1D1/P2KO mice compared to age- and sex-matched control littermates. Results from calcein double labelling experiments revealed significant reductions in mineralization apposition rate (MAR), mineralizing surface per bone surface (MS/BS), and bone formation rate (BFR) in the femoral metaphyseal cancellous bones in P1D1/P2KO mice compared control littermates. In contrast, osteoclast formation and bone resorption were not altered in P1D1/P2KO relative to control littermates. Interestingly, neither osteocyte-specific Pinch1 knockout nor global Pinch2 knockout mice displayed any marked bone phenotypes, suggesting a functional redundancy between the two Pinch proteins in control of bone mass. In vitro studies revealed that the osteoblast differentiation was severely impaired in primary bone marrow stromal cultures from P1D1/P2KO mice. These results demonstrate a critical new role for Pinch proteins through its expression in osteocytes in regulation of bone homeostasis.

Disclosures: Yishu Wang, None

SUN-0671

Validated analyses of osteocyte-mediated bone remodeling using in vivo and in vitro methods Cristal S. Yee*, Tamara Alliston. UCSF, United States

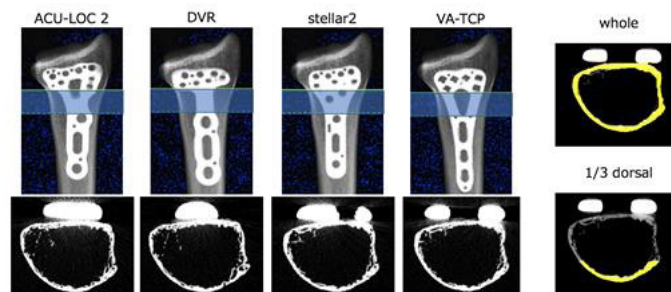
Perilacunar/canalicular remodeling (PLR) is a dynamic process by which osteocytes resorb and replace local bone extracellular matrix (ECM). During PLR, osteocytes secrete matrix metalloproteinases (MMPs) and enzymes like cathepsin K and carbonic anhydrases to resorb organic and mineral components of the perilacunar ECM. PLR maintains systemic mineral homeostasis, lacunocanalicular networks (LCN), and bone quality. As with osteoblasts and osteoclasts, deregulation of osteocyte PLR can be a product or a driver of skeletal disease. Therefore, there is a need to elucidate the regulation and role of PLR in skeletal health. However, the methods to study PLR are rapidly evolving and are not yet used or interpreted consistently. For example, quantification of lacunar size by 3D radiographic detection of perilacunar mineral may yield different outcomes from 2D histomorphometric analysis of demineralized sections. Therefore, standardization and validation of methods to evaluate PLR would improve efforts to understand this cellular process. Ideally, a robust analysis would include qualitative and quantitative in vivo and in vitro outcomes for PLR that are validated, reproducible, simple, and cost-effective. We have streamlined the analysis of PLR by developing and validating in vivo and in vitro outcome measures to investigate the effect of physiologic, pathologic, or pharmacologic interventions on PLR. As MMP13 is a key PLR enzyme, we used an osteocyte specific MMP13 knockout mice (MMP13oc^{-/-}) that had PLR deficiency and validated in vivo PLR outcomes using a 'gold standard' model of lactation-induced PLR. In vitro PLR outcomes were tested in MLOY4 or OCY454 osteocyte-like cell lines. We prioritized outcomes with the sensitivity and reproducibility to consistently reveal qualitative and quantitative significant differences in PLR between virgin and lactating cohorts of WT and MMP13oc^{-/-} mice. Based on this process, we developed a protocol for quantifying LCN integrity, as well as a PLR gene profile to gain molecular insight. For in vitro outcomes apart from the PLR gene profile, we monitored PLR function by measuring osteocyte intracellular acidification. These in vitro outcomes efficiently corroborate our in vivo findings. By presenting the validation and methodologic details for these protocols, our work will support the efforts of this research community to investigate and better understand the role of PLR in skeletal health and diseases.

Disclosures: *Cristal S. Yee, None*

SUN-0700

In Vivo Analysis of Fracture Healing by HR-pQCT: The Effect of Osteosynthesis Plate on Image Quality Ko Chiba*, Makoto Era, Yuichiro Nishino, Takashi Miyamoto, Narihiro Okazaki, Makoto Osaki. Department of Orthopedic Surgery, Nagasaki University Graduate School of Biomedical Sciences, Japan

Introduction: It has been difficult to study fracture healing in living patients at the micro level. HR-pQCT is a high-resolution clinical CT for human peripheral sites, which enables us to analyze the bone microstructure of living humans non-invasively. In this study, we validate the accuracy and reproducibility of HR-pQCT analysis of distal radius with metal plate in order to establish in vivo analysis of fracture healing treated by osteosynthesis plate. Methods: (Study-1 SNR) Four metal plates for distal radius fracture (VA-LCP, Synthes, Switzerland / DVR, Biomet inc., USA / Acu-Loc2, Acumed, USA / Stellar, HOYA, Japan) were put on a rubber bag filled with water. The middle region of the metal plate was scanned by HR-pQCT at the voxel size of 61 μm (XtremeCT II, Scanco Medical, Switzerland). Signal to noise ratio (SNR) was calculated in the water region under the metal plate. (Study-2 Accuracy) 12 cadaveric radii (age: 72 years, 60-80 years) were scanned by HR-pQCT under conditions with and without the metal plates. Cortical bone mineral density (Ct.BMD) and cortical thickness (Ct.Th) were measured at the whole circumference and dorsal 1/3 cortical regions (TRI/3D-BON, Ratoc System Engineering). Percentage changes in the conditions with and without metal plates were analyzed. (Study-3 Reproducibility) 10 patients with distal radius fractures (54 years, 21-74 years) were treated with VA-LCP plates. Two scans were performed using HR-pQCT. Ct.BMD and Ct.Th were measured at the dorsal 1/3 cortical region, and the root mean square percent coefficient of variance (RMS%CV) was analyzed. Results: (Study-1 SNR) There was no great difference in the SNR of the control (49.9), VA-LCP (45.6), DVR (47.6), Acu-Loc2 (43.6), and Stellar (47.7). (Study-2 Accuracy) When the whole circumference of the cortical region was measured, percentage changes with and without a metal plate were 1.4-3.2% in Ct.BMD and 7.2-9.8% in Ct.Th. When the dorsal 1/3 region was measured, percentage changes with and without metal plate were 0.4-1.7% in Ct.BMD and 1.7-2.7% in Ct.Th. (Study-3 Reproducibility) RMS%CV were 1.1% in Ct.BMD and 4.2% in Ct.Th. Conclusion: The accuracy and reproducibility of HR-pQCT analysis of distal radius with osteosynthesis plate are acceptable when the dorsal 1/3 region is analyzed. This method would be useful for the research of fracture healing.

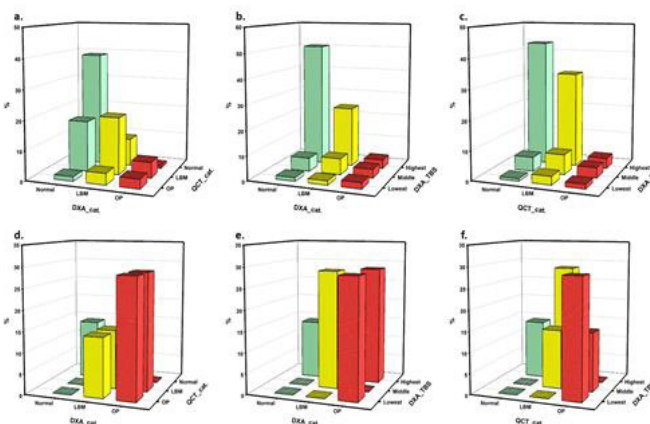


Disclosures: *Ko Chiba, None*

SUN-0701

Opportunistic screening for osteoporosis using abdominopelvic CT: Direct comparison of asynchronous QCT with DXA and TBS in older healthy Chinese Wing P. Chan*¹, Yi-Chien Lu¹, Ying Chin Lin². ¹Department of Radiology, Wan Fang Hospital, Taipei Medical University, Taiwan, ²Shuang Ho Hospital, Taipei Medical University, Taiwan

Background: It has recently been reported that abdominopelvic CT scans obtained for other indications can be used to assess bone mineral density (BMD) in the spine for opportunistic screening for osteoporosis. Asynchronous calibration quantitative computed tomography (QCT) is a new tool that allows quantification of BMD without the use of a calibration phantom during routine CT scanning. Use of the trabecular bone score (TBS) has been suggested to improve the diagnostic performance of DXA of the lumbar spine for patients with low bone mass (LBM). This study aimed to compare BMDs obtained using asynchronous QCT during abdominopelvic CT for health screening with DXA and TBS in older Chinese adults. Methods: Consecutive patients who underwent a CT examination of the abdominopelvic region and who also received a DXA during health examinations were retrospectively included. This cohort included 494 adults (men aged at least 50 years and postmenopausal women) who underwent standard non-contrast CT assessments at 120 kVp as well as DXAs for BMD assessment within 3 months. The 3D spine function QCT pro software (Mindways Software Inc., TX) was used to perform L1-L4 BMD analysis using the asynchronous calibration module, and TBS was analyzed using iN Sight software (Med-Imaps, Pessac, France). Lumbar spine BMD was measured by DXA. Diagnosis of osteoporosis was based on T-score according to WHO classification. Vertebral fractures were identified on sagittal-reformed standard CT images of the lumbar spine using Genant's semi-quantitative method. Results: In this sample, 48 individuals (9.7%) had osteoporosis according to DXA, and 7 (1.4%) had vertebral fractures. The correlation between DXA and QCT was good ($R^2 = 0.611$, $p < 0.001$); it was fair between DXA and TBS ($R^2 = 0.470$, $p < 0.001$) and between QCT and TBS ($R^2 = 0.405$, $p < 0.001$). In 17.3% of the sample, QCT found a more degraded BMD to be LBM, whereas DXA reflected normal BMD for these individuals. On the other hand, in 9.4%, DXA identified a more degraded BMD to be LBM compared to QCT. Likewise, TBS classified the highest percentage in this way compared to QCT (32.7%) and to DXA (24.5%). Conclusion: For spine BMD screening during routine abdominopelvic CT, asynchronous QCT performs as well as DXA. Also, TBS provides information that is independent of spinal BMD. Spinal TBS reclassifies LMB as osteoporosis less often than DXA but yields similar results compared to QCT.



Disclosures: *Wing P. Chan, None*

SUN-0702

Trabecular Bone Score in aged postmenopausal women with type 2 diabetes without fragility fracture history Dong Jin Chung*, Jin Ook Chung, Dong Hyeok Cho, Min Young Chung. Chonnam National University Medical School, Republic of Korea

Type 2 diabetic patients are at increased risk for osteoporotic fracture regardless of BMD status. In addition to many falling risks factors, deterioration of bone quality such as bone microstructure may be one of the important underlying mechanism. Trabecular bone score (TBS) is a novel texture index that evaluates the pixel gray-level variations in lumbar spine dual-energy X-ray absorptiometry images and is related to bone microarchitecture independent of bone mineral density (BMD). We investigated lumbar spine TBS as an indicator for skeletal microarchitectural deterioration in type 2 diabetes. We included 52 type 2 diabetic (71.6±6.5 years) and 77 non-diabetic (71.1±4.2 years) aged postmenopausal Korean women without fragility fracture history who visited the outpatient clinic of Chonnam National University Hospital. Serum 25OHD, CTX, osteocalcin and other laboratory data were acquired after overnight fasting. BMD was measured at the lumbar spine using dual energy X-ray absorptiometry (Hologic Discovery-Wi). All TBS measurements were performed retrospectively using the TBS iNsite Software, ver. 3.0.2.0 (Med-Imaps) using spine DXA files from the database. Lumbar spine BMD was higher in type 2 diabetic women (0.834 ± 0.129 vs 0.771 ± 0.095 g/cm², P<0.05) than in nondiabetic women, whereas lumbar spine TBS was not significantly different between two groups (1.341 ± 0.086 vs 1.332 ± 0.074). Serum 25OHD level was lower in diabetic women than in nondiabetic women (21.0 ± 10.4 vs 25.1 ± 11.4, P<0.05). Serum CTX and osteocalcin levels were not significantly different between two groups. Unlike from previous studies which showing lower TBS in diabetic patients, lumbar TBS was not lower in aged diabetic women in this study. It may still suggest deterioration of bone microarchitecture in diabetic women when considering higher BMD status. Otherwise, it may be due to small sample size of participants. Larger studies considering many confounding factors such as onset, duration of diabetes, glycemic control status, diabetic complications, or the use of antidiabetic drugs which are known to be affect on bone metabolism are needed.

Disclosures: **Dong Jin Chung, None**

SUN-0703

TBS VALUE IN POSTMENOPAUSAL WOMEN WITH AND WITHOUT FRACTURES Edward Czerwinski*¹, Maja Warzecha², Malgorzata Berwecka², Anna Kumorek³, Jaroslaw Amarowicz², Didier Hans⁴. ¹Krakow Medical Centre, Poland, ²Department of Bone and Joint Diseases Jagiellonian University Medical College, Poland, ³Healthy Statistic, Poland, ⁴Center of Bone Diseases Bone and Joint Department, Switzerland

Determining the risk of fracture is a key problem in osteoporosis. The threshold of -2.5 BMD T-score has been used as a criterion for diagnosing osteoporosis (OP), majority of fractures are sustained by patients above this threshold. However, bone structure quality is more important in assessing fracture risk than bone density alone. A major advance in osteoporosis diagnostics is Trabecular Bone Score (TBS), a method to indirectly assess bone structure based on lumbar spine DXA in clinical routine. TBS was assessed from lumbar spine DXA image in Lausanne, blinded from clinical outcome in a group 1045 postmenopausal women (mean age 65 ± 7 SD), patients of Krakow Medical Centre. All statistics were performed in Krakow. Low-energy fractures were diagnosed in a group of 244 women, while the group without fractures was 761 women. In non-fractured group (mean age 64 ± 7.2 SD) the mean TBS was 1.238± 0.09 SD (partly degraded). In the group with prevalent low energy fractures of spinal and non-spinal (mean age 67± 7.6 SD), TBS equaled 1.202± 0.09 SD (p<0.0001 after age and BMI adjustment). The mean TBS in the group with prevalent non-spinal fractures only was 1.213± 0.09 SD and in the group of women with spinal fractures 1.166± 0.08 SD (fully degraded) (p<0.01 after age and BMI adjustment). Conclusions: The mean TBS in non-fractured women showed a partial bone structure degradation, whereas in patients with prevalent fractures of any kind the mean was within the scope of degraded structure.

Disclosures: **Edward Czerwinski, None**

SUN-0704

Trabecular Bone Score (TBS) ex-vivo performance study for the GE Healthcare ARIA system Franck Michelet*, François De Guio, Christophe Lelong. Medimaps, France

Aim: Trabecular Bone Score (TBS) is compatible with multiple DXA systems from different manufacturers. Technical requirements, like image resolution and noise level, are a prerequisite for TBS compatibility with a given DXA system. Then, pre-clinical and clinical performance can be evaluated to further assess compatibility with TBS. The goal of this study is to assess the TBS ex-vivo performance of General Electrics Healthcare (GE) Aria DXA system. Results from the GE Aria device are compared to those of GE Prodigy devices. Material and methods: We used 15 dry ex-vivo human vertebrae, set in AP position. Soft tissues were simulated by a mix of homogeneous layers of HDPE and PVC, achieving an equivalent thickness of 16.7cm with 29.4% fat content. We scanned these vertebrae 3 times each without repositioning on a GE Aria device and on 3 different GE Prodigy devices. For each device model, we computed the ex-vivo reproducibility of TBS as the root mean square

standard deviation (rms-SD). We also computed the coefficient of determination (r²) between the 15 TBS values obtained on GE Aria and the 15 average TBS values obtained on the 3 GE Prodigy devices. Results: TBS ex-vivo reproducibility was measured at rms-SD = 0.025 for GE Aria and rms-SD = 0.019 for GE Prodigy. The coefficient of determination between GE Aria and the average of GE Prodigy devices was r² = 98.8%. By comparison, the average coefficient of determination between GE Prodigy devices, was r² = 99.4%. Conclusion: The strong correlation between TBS values on GE Aria and GE Prodigy devices validates the first step for having TBS compatibility with GE Aria devices. As expected, TBS ex-vivo reproducibility appears to be better on GE Prodigy than on GE Aria, but this trend will have to be confirmed with an in-vivo reproducibility study.

Disclosures: **Franck Michelet, Medimaps, Other Financial or Material Support**

SUN-0705

Trabecular microstructure is influenced by race and sex in young adults Julie Hughes*¹, Kristin Popp², Chun Xu³, Amy Yuan², Ginu Unnikrishnan³, Jaques Reifman³, Mary Bouxsein². ¹USARIEM, United States, ²MGH, United States, ³BHSAI, United States

Lower rates of fracture in Black men and women compared to their White counterparts, may, in part, be explained by enhanced cortical bone microstructure. Using individual trabecular segmentation (ITS) analysis of high-resolution peripheral quantitative computed tomography (HR-pQCT) may allow better understanding of the contribution of the trabecular bone compartment to bone strength and fracture risk. A prior study using ITS technology suggests that among older Black and White women, Black women had more plate-like trabecular morphology and higher axial alignment of the trabeculae compared to White women. However, it is not known whether these racial differences are established in young adulthood or developed during aging, nor whether they exist among men. Therefore, the purpose of this study was to determined differences in trabecular bone microarchitecture, connectivity and alignment according to race and sex. We analyzed HR-pQCT scans of 184 young adult (24.2±3.4 yrs) women (n=51 Black, n=50 White) and men (n= 34 Black, n=49 White) from a prior cross-sectional study. We used two-way ANOVA to compare bone outcomes, adjusted for age, height, and weight. Overall, the effect of race on bone outcomes did not differ by sex, and the effect of sex on bone outcomes did not differ by race. After adjusting for covariates, Blacks and men had significantly greater trabecular plate volume fraction, plate thickness, plate number density, and plate surface area in addition to greater axial alignment of trabeculae compared to Whites and women (Table 1, p<0.05 for all). These findings demonstrate that more favorable bone microarchitecture in Blacks compared to Whites and in men compared to women is not unique to the cortical bone compartment. Enhanced plate-like morphology and greater axial alignment of trabeculae, established as early as young adulthood, may contribute to the improve bone strength and lower lifetime fracture risk among Blacks and men compared to their White and female counterparts.

Table 1. Individual trabecular segmentation analyses at the distal tibia (4%) among Black and White men and women adjusted for height, weight, and age.

	Caucasian Women n=50	Black Women n=51	Caucasian Men n=49	Black Men n=34	p race/sex interaction	*p race	*p sex
Total BV/TV	0.323 (0.007)	0.330 (0.007)	0.361 (0.007)	0.349 (0.007)	0.13	0.69	0.001
Plate BV/TV	0.131 (0.007)	0.162 (0.007)	0.187 (0.007)	0.212 (0.008)	0.6	<0.001	<0.001
Rod BV/TV	0.192 (0.006)	0.168 (0.006)	0.174 (0.006)	0.137 (0.007)	0.2	<0.001	0.001
Axial BV/TV	0.125 (0.005)	0.147 (0.005)	0.161 (0.005)	0.181 (0.006)	0.9	<0.001	<0.001
Plate BV/BV	0.403 (0.017)	0.491 (0.016)	0.513 (0.017)	0.609 (0.019)	0.8	<0.001	<0.001
Rod BV/BV	0.597 (0.017)	0.509 (0.016)	0.487 (0.017)	0.391 (0.020)	0.8	<0.001	<0.001
Plate to Rod Ratio	0.721 (0.081)	1.043 (0.076)	1.189 (0.081)	1.671 (0.090)	0.2	<0.001	<0.001
Plate Number (1/mm)	1.53 (0.02)	1.61 (0.02)	1.63 (0.02)	1.64 (0.02)	0.3	0.002	0.003
Rod Number (1/mm)	1.95 (0.02)	1.85 (0.02)	1.85 (0.02)	1.70 (0.03)	0.2	<0.001	<0.001
Plate Thickness (mm)	0.227 (0.003)	0.229 (0.003)	0.242 (0.004)	0.241 (0.004)	0.7	0.9	0.002
Rod Thickness (mm)	0.216 (0.007)	0.217 (0.007)	0.217 (0.007)	0.219 (0.008)	0.4	0.1	0.02
Plate Surface (mm ²)	0.161 (0.003)	0.169 (0.002)	0.178 (0.003)	0.189 (0.003)	0.5	<0.001	<0.001
Rod Length (mm ³)	0.637 (0.003)	0.645 (0.003)	0.647 (0.003)	0.659 (0.004)	0.6	0.001	0.002
Plt-plt junction (1/mm ²)	2.68 (0.09)	2.95 (0.09)	3.24 (0.09)	3.09 (0.11)	0.02	0.5	0.003
Rod-rod junction (1/mm ²)	3.49 (0.15)	2.77 (0.15)	2.87 (0.16)	1.92 (0.18)	0.5	<0.001	<0.001
Rod-plt junction (1/mm ²)	5.25 (0.17)	5.28 (0.16)	5.68 (0.17)	4.84 (0.19)	<0.007	0.01	0.9

Values are adjusted mean (SE). BV = Bone Volume, TV = Total Volume, Plt = Plate

Disclosures: **Julie Hughes, None**

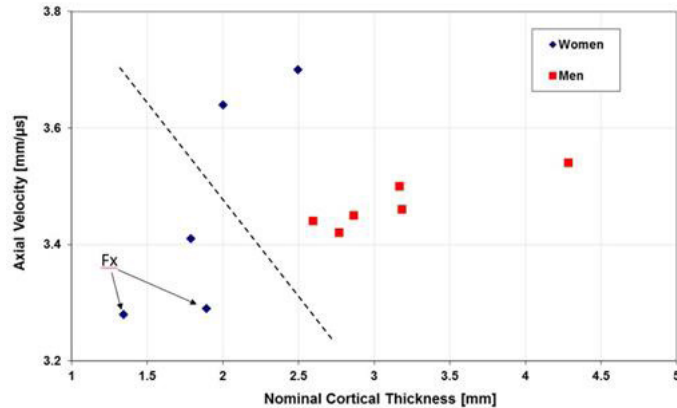
SUN-0706

A Novel Dual-Mode Ultrasonic Method for Assessing Tibial Cortical Bone Quality Jonathan Kaufman*^{1,2}, Gangming Luo¹. ¹CyberLogic, Inc., United States, ²The Mount Sinai School of Medicine, United States

Osteoporotic fractures are a major public health problem; diagnosis is based on x-ray densitometry (DXA). However DXA is not able to accurately predict who will and will not suffer a fracture. An alternative to DXA is ultrasound, which is viewed as having the potential to better characterize fracture risk. Our approach is based on "dual-mode" ultrasound in which two distinct modes of propagation are used together. In particular, measurements are made at the mid-shaft tibia in both axial-transmission and pulse-echo modes. Axial transit time (τA) and pulse-echo transit time (τP/E) are obtained at the same tibial site. The potential for the dual-mode's approach to assess bone quality is rooted in the facts that (i) the pulse-echo mode measurement is dependent on cortical bone quality (as reflected in radial ultrasound velocity (UV) as well as on cortical thickness; and (ii) the axial transit time measurement is dependent on cortical bone quality (as reflected in axial UV) and on cortical thickness as well. Therefore, the measurement of both ultrasonic parameters (that is, the pulse-echo and axial transmission times) allows for identification of both bone quality (as reflected in ultrasound velocity) and cortical thickness (a structural parameter), both of

Sunday Posters

which are related to bone strength and fracture risk. These 2 transit times can be used in a classification scheme to identify individuals at greatest risk of fragility fracture. The two transit times can also be converted to axial UV ($UV_a=d/\tau A$, where d is the separation of two ultrasound receivers), and nominal cortical thickness ($CTN = VR \cdot \tau P/E/2$, where VR is the radial UV). A pilot set of measurements on 11 individuals has been carried out to demonstrate the feasibility of the proposed technology. For the 11 subjects, each subject data point was found to be located in a distinct region (i.e., a hypothesized distinct bone quality-bone structural state) of the quadrant associated with axial UV and nominal CT. Because the 2 parameters are each affected in distinct fashions by a variety of bone quality factors (such as degree of mineralization, porosity, cortical thickness, biomechanical stiffness), the bivariate feature has the potential to more accurately identify those individuals at increased risk of fracture. The figure shows the data for the 11 subjects ("Fx" indicates two subjects with fragility fractures). Future studies will elucidate the capabilities of the new dual-mode ultrasound technology.

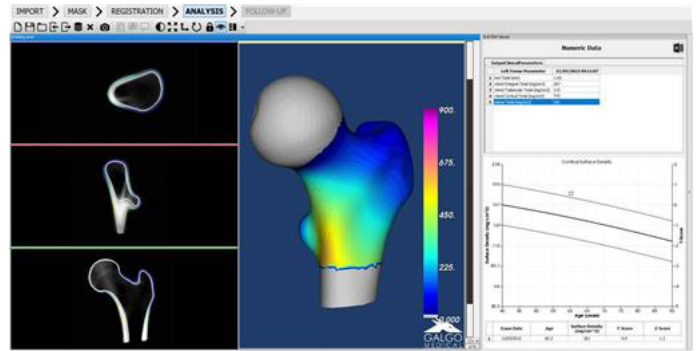


Disclosures: Jonathan Kaufman, CyberLogic, Inc., Major Stock Shareholder, CyberLogic, Inc., Grant/Research Support

SUN-0707

3D Modelling of hip DXA indicates cortical vBMD superior efficacy of denosumab versus alendronate Mohammed Almohaya*¹, Naveen Sami², Renaud Winzenrieth³, David Kendler⁴. ¹King Fahad Medical City, Saudi Arabia, ²Prohealth Clinical Research, Canada, ³Galgo Medical, Spain, ⁴University of British Columbia, Canada

Evaluation of the cortical compartment of bone may be valuable in determining risk of nonvertebral fracture and treatment effects of therapies which may benefit cortical bone. Clinical evaluation of cortical bone at the hip has been restricted to high-resolution CT techniques requiring high dose radiation and high cost. More recently, modelling algorithms have been developed to estimate cortical bone parameters from hip DXA scans. We retrospectively reviewed 252 consecutive male and female patients referred for osteoporosis consultation at a specialist clinic in Vancouver Canada. All patients had baseline and follow-up hip DXA scans on the same equipment, which were subjected to DXA-based 3D modeling (3D-SHAPER v2.7, Galgo Medical, Spain) for cortical bone parameters. Patients' average age was 71±9 years; there were 225 females and 27 males. Patients were divided into groups according to their treatment prior to and subsequent to baseline: treatment naïve to bisphosphonate (tnBP, N = 56), treatment naïve to denosumab (tnDmab, N = 92), or prior bisphosphonate to denosumab (switch, N = 104). Using 3D-SHAPER, volumetric trabecular and volumetric cortical BMD as well as average cortical thickness (CTh) were evaluated (Figure 1). Cortical vBMD increased in both tnDmab (+13.8 mg/cm³, +1.9%, p=0.0002) and Switch groups (+11.1 mg/cm³, +1.53%, p=0.0005); in the tnBP group, cortical vBMD was stable (+3.17 mg/cm³, +0.44%, p=0.34). Cortical vBMD increased significantly more in the tnDmab (p=0.026) and the Switch group (p=0.036) compared to the tnBP group. CTh increased significantly more after denosumab, either tnDmab (1.02%, p=0.02) or Switch (1.35%, p=0.0009) as compared to tnBP (0.47%, p=0.68). There were positive correlations between cortical vBMD and femoral neck DXA aBMD (r=0.64) and trochanter DXA aBMD (r=0.79). These data provide the first observational evidence of hip cortical volumetric bone density improvements after denosumab and differentiation from bisphosphonate therapy. This may be supportive of observations of long-term progressive increases in BMD on denosumab with greater non-vertebral fracture prevention associated with longer duration of denosumab therapy. This information may aid clinicians with treatment decisions where non-vertebral fracture prevention is important.



Disclosures: Mohammed Almohaya, None

SUN-0708

Structural analysis at the female femoral neck for a clinically useful predictor of future hip fracture risk Ling Wang*¹, Benjamin Cc Khoo², Joshua Lewis³, Keenan Brown⁴, Xiaoguang Cheng¹, Richard Prince⁵. ¹Beijing Jishuitan Hospital, China, ²Medical Technology & Physics, Australia, ³Edith Cowan University, Australia, ⁴Mindways Software, United States, ⁵University of Western Australia, Australia

Age, gender and two dimensional (2D) DXA imaging of proximal femur areal bone mineral density (aBMD), are the established and commonly used predictors of hip fracture risk. To improve prediction we have been exploring the use of structural information present in the DXA image in addition to aBMD, these are bone width (BW), standard deviation of a normalised mineral-mass projection profile distribution (σ) and displacement between centre-of-mineral-mass and geometric centre-of-mineral-mass of projection profile (δ) [1]. We report the differences in these measurements in hip fracture cases and controls in a large Chinese data set. Participants were 447 Chinese females who sustained trochanter or femoral neck fractures and 528 community controls. The four femoral neck (FN) structural variables were calculated from DXA equivalent 2D images obtained from QCT scans of non-fractured hips analysed using BIT QCT software (Mindways Software, Texas, USA) [1]. Comparison of the mean (SD) of age, and the structural data in the fracture and control participants are shown in the Table. Compared to controls fracture participants were older, had lower values for aBMD, similar FNbw but higher values for the other structural variables previously associated with increased fracture propensity [2]. Stepwise logistic regression modelling was used to select the most parsimonious model from these 6 variables, the final model included FN aBMD, FN σ and FN δ . To assess hip fracture prediction the area under the ROC for the final model was found to be significantly larger than for the base model ROC of age and THaBMD (0.876 and 0.834 respectively, P<0.001). A risk model including FN aBMD together with FN σ and FN δ suggest that extra information from the DXA equivalent image provided a substantially better hip fracture risk prediction than the gold standard of THaBMD and age, and thus may be a useful additional analysis in older women. [1] Khoo et al. J Clin Densitom. 2014;17(1):38-46. [2] Khoo et al. Osteoporos Int. 2016;27(1):241-8.

	Age (years)*	THaBMD (g/cm ²)*	FN aBMD (g/cm ²)*	FNbw (cm)	FN σ (cm)*	FN δ (cm)*
Hip fracture	74.8(9.2)	0.56(0.11)	0.48(0.09)	2.58(0.28)	0.91(0.11)	0.41(0.10)
Controls	68.1(8.8)	0.73(0.14)	0.64(0.12)	2.60(0.30)	0.88(0.09)	0.33(0.09)

* P< 0.05; results are mean (± SD)

Disclosures: Ling Wang, None

SUN-0709

Resorbed and Formed Bone Mass in Osteoporosis Treatment Were Correlated with the Values of the DXA and Bone Turnover Markers Measurements: by Bone Morphometry Using Multiple Detector Computed Tomography (MDCT) Images Nobuhito Nango*¹, Shogo Kubota¹, Kazutaka Nomura¹, Yusuke Horiguchi¹, Ko Chiba², Masafumi Machida³. ¹Ratoc System Engineering Co., LTD., Japan, ²Department of Orthopedic Surgery, Nagasaki University Graduate School of Biomedical Sciences, Japan, ³Department of Spine and Spinal Cord Surgery, Yokohama Brain and Spine Center, Japan

1. Introduction Bone metabolism markers can be used to evaluate the state of bone turnover and are applied in the treatment of osteoporosis. However, how the values for these markers correlate with increases or decreases in bone remains unclear. Measuring the resorbed bone mass and formed bone mass to controlling the medication efficacy are thought to be important in enhancing the therapeutic effects. In this study, using the computed to-

mography (CT) images, we investigated bone volume fractions and resorbed bone mass are correlated with DXA bone density and bone resorption markers in each other. 2. Cases The subjects were (A) using MDCT images, 12 women (mean age: 71 years) undergoing osteoporosis treatment with denosumab and teriparatide and (B) using HR-pQCT images, 10 volunteers (mean age: 65 years; 9 women and 1 man) undergoing osteoporosis treatment with denosumab, teriparatide and other protocols. 3. Methods (1) The MDCT images of lumbar vertebrae were measured. For bone extraction, we set the TMD value to ≥ 80 mg/cm³. When bone with a TMD value of ≥ 80 mg/cm³ decreased to < 60 mg/cm³ after 6 months, the bone was determined to be resorbed. Conversely, after 6 months, when the tissues of < 60 mg/cm³ reached a bone density of ≥ 80 mg/cm³, bone was determined to be formed. (2) Using HR-pQCT, the distal tibia and the distal radius were scanned. The TMD value for bone extraction was 300 mg/cm³. Used software was TRI/3D-BON-FCS V.10.0 (RATOC, Tokyo, Japan). Also, the DXA bone density (mg/cm²) in patients were measured. (3) Serum marker measurement The bone resorption marker TRACP-5b and bone formation marker PINP were measured. 4. Results (1) The tibial bone mass BV/TV measured by HR-pQCT correlated with the femoral areal BMD evaluated by DXA ($r > 0.7$; $p < 0.00$). (2) A correlation was noted between bone resorption mass and resorption markers. In the lumbar vertebrae assessed by MDCT, the resorbed bone mass and value for the pre-administration resorption marker (TRACP-5b) after 6 months of osteoporosis drug administration were correlated ($r_2 = 0.8$; $p < 0.00$). In contrast, in the case of distal tibia evaluated by HR-pQCT, we observed a correlation ($r_2 = 0.41$; $p < 0.00$). (3) The correlation between the formed bone mass and formation markers was weak. In the lumbar vertebrae assessed by MDCT, the formed bone mass 6 months after was correlated with the bone formation marker PINP after starting medication, $r_2 = 0.46$. Correlation was $r_2 = 0.11$ in the tibia as measured by HR-pQCT. 5. Discussion (1) These results suggested that a period close to 6 months is required to determine the efficacy of the resorption marker values. (2) The weak correlation of formation markers with the new bone suggested that bone could be resorbed without becoming hypercalcified. 6. Conclusions (1) From CT images, it is possible to know the detailed mechanism of calcified bone modification as a result of drug treatment. (2) Although the voxel resolution of MDCT is 0.5 mm, it will be feasible to measure the trends in bone metabolism by reconfiguring the resolution to 0.2 mm.

Disclosures: **Nobuhito Nango**, None

SUN-0710

Trabecular Bone Score in Thais with or without Type 2 Diabetes. Hataikarn Nimitphong^{*1}, Sasima Srisukh¹, Jintanan Jangsiripornpakorn¹, Nantaporn Siwasaranond¹, Sirimon Reutrakul^{1,2}, Sunee Saetung¹, Suchawadee Musikarat³, Chanika Sritara³, Piyamitr Sritara¹, Boonsong Ongphiphadhanakul¹. ¹Department of Medicine, Faculty of Medicine, Ramathibodi Hospital, Mahidol University, Bangkok, Thailand, ²Division of Diabetes, Endocrinology and Metabolism, University of Illinois College of Medicine at Chicago, Chicago, Illinois, United States, ³Department of Diagnostic and Therapeutic Radiology, Faculty of Medicine, Ramathibodi Hospital, Mahidol University, Bangkok, Thailand

Background When compared with non-diabetic subjects, patients with type 2 diabetes mellitus (T2DM) have an increase in fracture risk at most skeletal sites despite having higher bone mineral density (BMD). Lumbar spine trabecular bone score (TBS) provides skeletal microarchitecture information not captured by BMD measurement and is associated with fracture risk in Caucasians. Previous studies, mostly in Caucasians, demonstrated that TBS is lower in T2DM subjects than non-diabetic subjects and associated with poor glycemic control. The utility of TBS as a fracture risk assessment tool in Asians with T2DM is currently unclear. We compared lumbar spine BMD and TBS in Thai subjects with or without T2DM. The correlation between TBS and glycemic control in subjects with T2DM was also investigated. Methods This is a cross-sectional study of 104 T2DM subjects and 342 non-diabetic controls. Lumbar spine (L1-L4) BMD was measured by dual-emission x-ray absorptiometry (DXA) and TBS was calculated using TBS iNspire software. Results Subjects with T2DM were older and had higher body mass index (BMI) than non-diabetic subjects. When compared with non-diabetic subject, higher BMD was demonstrated in T2DM subjects in both unadjusted model ($p=0.001$) and adjusted model for age, gender and BMI ($p<0.001$). Lumbar spine TBS was significantly lower in T2DM ($p<0.001$) in both unadjusted model and adjusted model for age and gender. However, after further adjustment for BMI, there were no differences among the two groups ($p=0.808$). There was no correlation between TBS and hemoglobin A1c (HbA1c; $p=0.863$). Conclusion Subjects with T2DM have higher lumbar BMD than those without. Contrary from the previous report in Caucasians, lumbar spine TBS in Thai T2DM was not different from non-diabetic subjects after controlling for BMI. There was no association between TBS and glycemic control in this study.

Disclosures: **Hataikarn Nimitphong**, None

SUN-0711

Optimal Bone Mineral Density Testing Intervals in Korean Women Seung Shin Park^{*1}, Jung Hee Kim¹, Hyung Jin Choi², Eu Jeong Ku³, Seo Young Lee¹, A Ram Hong¹, Nam H. Cho⁴, Chan Soo Shin¹. ¹Department of Internal Medicine, Seoul National University College of Medicine, Republic of Korea, ²Department of Anatomy, Seoul National University College of Medicine, Republic of Korea, ³Department of Internal Medicine, Chungbuk National University College of Medicine, Republic of Korea, ⁴Department of Preventive Medicine, Ajou University School of Medicine, Suwon, Republic of Korea

Background: Low bone mineral density (BMD) is a major predictor of fragility fracture. BMD testing is recommended for screening for osteoporosis, but there were a few studies regarding the appropriate BMD testing intervals in normal or osteopenic subjects. Therefore, we aimed to elucidate the optimal BMD testing intervals according to baseline BMD and clinical risk factors in Korean postmenopausal women. Methods: In a Korean prospective cohort study, we included 938 postmenopausal women who underwent repeated BMD testing during a median follow-up period of 7.2 years. We classified study subjects into four groups according to baseline BMD T-score. The duration of transition to osteoporosis was assessed using the parametric estimation of cumulative incidence functions for interval-censored competing risk data. After adjusted for age and body mass index (BMI), the estimated time for 10% of subjects to transit to osteoporosis were calculated for each group. Fracture events were treated as a competing risk. Results: The prevalence of normal BMD (T score ≥ -1.00), mild (T score, -1.01 to -1.49), moderate (T score, -1.50 to -1.99), and severe osteopenia (T score, -2.00 to -2.49) based on baseline BMD T-score were 48.5%, 17.7%, 20.5%, and 13.3%. The mean age and BMI of study subjects were 62.9 (± 7.6) years and 25.0 (± 3.3) kg/m². Women with lower BMD T-score tended to be older and had lower BMI (all p for trend < 0.001). During a median follow-up duration of 7.2 years, 10.3% (97/938) of subjects made transition to osteoporosis. The rate of transition to osteoporosis in women increased with lower BMD T-score (2.6%, 3.6%, 12.0%, 44.8% respectively, $p < 0.001$). The time for 10% of subjects to make the transition to osteoporosis was 10.6 years (95% confidence interval [CI], 7.6 to 14.8) for subjects with mild osteopenia, 8.3 years (95% CI, 6.7 to 10.2) for subjects with moderate osteopenia, and 3.8 years (95% CI, 2.9 to 5) for subjects with severe osteopenia. In subjects with normal BMD, the time for 10% of subjects to transit to osteoporosis was not estimated due to the low incidence of osteoporosis. Conclusions: Approximately 10 years, 8 years, and 3 years may be an appropriate interval of BMD screening for subjects with mild osteopenia, moderate osteopenia, and severe osteopenia respectively. There is very low likelihood of a transition to osteoporosis in subjects with normal BMD.

Disclosures: **Seung Shin Park**, None

SUN-0712

Active Young Women with Current Tibial Stress Fracture have Reduced Cortical and Total Bone Area Kristin Popp^{*1}, Sara Rudolph¹, Amy Yuan¹, Julie Hughes², Chun Xu³, Ginu Unnikrishnan³, Jaques Reifman³, Mary Bouxsein⁴. ¹Massachusetts General Hospital, United States, ²United States Army Research Institute of Environmental Medicine, United States, ³Department of Defense Biotechnology High Performance Computing Software Applications Institute, United States, ⁴Massachusetts General Hospital and Center for Advanced Orthopedic Studies, Beth Israel Deaconess Medical Center, United States

Stress fractures are common overuse injuries, particularly among young women participating in repetitive physical activity. These partial or complete bone fractures occur most often in the tibia and require significant healing time that can hinder or terminate sports and military training. While numerous risk factors for stress fracture have been identified, few studies have quantified measures of bone microarchitecture and strength that discriminate women with a current stress fracture from healthy active women. Purpose: We aimed to determine differences in bone density, microarchitecture and strength among active young women with a current tibial stress fracture compared to those without. Methods: We enrolled 30 women within 3 weeks of an MRI diagnosed tibial stress fracture and 47 healthy controls. All participants were 18-35 years old and reported ≥ 4 hours of weight-bearing exercise weekly. We used dual-energy X-ray absorptiometry (DXA) to assess areal bone mineral density (aBMD) of the hip and spine, and high-resolution pQCT (HR-pQCT; 82 mm³ voxel size) to assess cortical and trabecular bone density, microarchitecture and strength by micro-finite element analysis (mFEA) at the distal tibia (4% of tibia length). We compared the uninjured tibia in those with a current stress fracture to the non-dominant tibia among controls. We used ANCOVA to compare bone outcomes, adjusting for age, height, weight, menstrual status and age of menarche. Results: Mean age was 25.0 \pm 4.0 and BMI 22.7 \pm 2.7 kg/m². Groups were comparable for age, height, weight, menstrual status, age of menarche, aBMD, and most bone parameters. However, women with a current stress fracture had smaller total area (-5.6%, $p < 0.05$) by HR-pQCT compared to healthy controls. Total volumetric bone mineral density (vBMD; +7.4%), trabecular thickness (+8.7%) and trabecular vBMD (+10.56%) were higher among women with a stress fracture compared to controls ($p < 0.05$ for all), though there were no differences in cortical microstructure or estimated strength and stiffness between groups. Conclusion: These data indicate that while microarchitecture is largely similar between groups, women with a current stress fracture have higher bone density and trabecular thickness compared to controls but smaller bone size. Smaller, more consolidated

bones may be at greater risk for stress fracture compared to larger, less dense bones, although this remains to be verified.

Disclosures: *Kristin Popp, None*

SUN-0713

Postmenopausal Women with Isolated Osteoporosis at the 1/3 Radius Have Generalized Abnormalities in Microarchitecture and Stiffness Emily Stein^{*1}, Alexander Dash¹, Mariana Bucovsky², Sanchita Agarwal², X. Edward Guo², Elizabeth Shane². ¹Hospital for Special Surgery, United States, ²Columbia University Medical Center, United States

Postmenopausal women with osteoporosis only at the 1/3 radius (1/3RO), but not the spine or hip, present a therapeutic dilemma because little is known about whether they have focal cortical bone deficits or generalized skeletal fragility. It is therefore often unclear whether to initiate treatment in these patients, particularly as most available medications do not significantly improve BMD at this site. In this study, we used high resolution peripheral QCT (HRpQCT) to measure volumetric BMD (vBMD), microarchitecture, and stiffness in women with 1/3RO. We hypothesized that compared to controls, women with 1/3RO have smaller bone size and cortical deficits at the radius that contribute to low areal BMD by DXA, but preserved trabecular bone, and few abnormalities at the tibia. We enrolled 285 postmenopausal women; all had BMD of lumbar spine (LS), total hip (TH), femoral neck (FN) and 1/3 radius (1/3R) measured by DXA, trabecular (Tb) and cortical (Ct) vBMD and microarchitecture measured by HRpQCT (voxel size ~82 μm) of the distal radius (RAD) and tibia (TIB) and whole bone stiffness estimated by finite element analysis. Women were grouped by their densitometric pattern: isolated osteoporosis (T<-2.5) at the 1/3 radius (1/3RO, n=30), classical osteoporosis at the spine or hip (PMO, n=85) and controls without osteoporosis at any site (C, n=170). Mean age of subjects was 70±8, 75% were Caucasian. 1/3RO tended to be older than C (p=0.06) but similar in age to PMO. BMI did not differ among groups. Mean DXA T-scores were, in 1/3RO: -1.2±0.7 at LS, -1.5±0.5 at TH, -1.9±0.4 at FN, -3.0±0.5 at 1/3R, in PMO: -2.6±1.0 at LS, -2.1±0.6 at TH, -2.4±0.6 at FN, -2.3±1.2 at 1/3R. While bone size did not differ, 1/3RO had lower total, Ct and Tb density at RAD and TIB than C (Table). At RAD, 1/3RO also had lower Ct thickness and Tb number, higher Tb separation and heterogeneity. Whole bone stiffness was lower at both sites. There were no significant differences in vBMD, microarchitecture and stiffness between 1/3RO and PMO. In summary, women with isolated osteoporosis at the 1/3 radius by DXA have abnormal Ct and Tb microarchitecture and low stiffness by HRpQCT at both radius and tibia. Our results suggest that although aBMD appears relatively preserved at the spine and hip by DXA, postmenopausal women with osteoporosis only at the 1/3R site have comparable deficits in vBMD, microarchitecture and stiffness to postmenopausal women with osteoporosis at the spine and hip.

Microarchitecture in Postmenopausal Women with 1/3O and PMO: % Difference from Postmenopausal Controls

	1/3RO RADIUS	1/3RO TIBIA	PMO RADIUS	PMO TIBIA
Total Density (mgHA/cm ³)	-17 ³	-15 ³	-17 ³	-14 ³
Ct Density (mgHA/cm ³)	-6 ³	-6 ¹	-6 ³	-6 ³
Ct Thickness (mm)	-14 ²	-10	-19 ³	-18
Tb Density (mgHA/cm ³)	-23 ³	-16 ²	-20 ³	-15 ³
Tb Number (1/mm)	-21 ³	-15	-17 ³	-15
Tb Thickness (mm)	-1	-2	-4	-1
Tb Separation (mm)	+47 ³	+22	+38 ³	+22
Tb heterogeneity (mm)	+78 ²	+45	+86 ³	+46
Stiffness (N/mm)	-14 ²	-15 ³	-22 ³	-18 ³

* 1 p<0.05, 2 p<0.01, 3 p<0.001 versus Controls

Disclosures: *Emily Stein, None*

SUN-0714

Peripheral Artery Calcification on HR-pQCT Scans and Cardiovascular Risk in Men Pawel Szulc^{*}, Catherine Plankaert, Roland Chapurlat. INSERM UMR 1033, University of Lyon, Hôpital Edouard Herriot, France

Data on the link between severity of peripheral artery calcification and cardiovascular risk are limited and focused on patients with chronic kidney disease and peripheral artery disease. Our aim was to study the association between severity of peripheral artery calcification found on the scans of distal forearm and distal leg obtained by high resolution peripheral quantitative computed tomography (HR-pQCT) and the prospectively assessed cardiovascular risk in community-dwelling older men. In a cohort of 819 men aged 60-87, calcification was assessed at baseline on HR-pQCT scans at the level of the arteries of distal leg (ante-

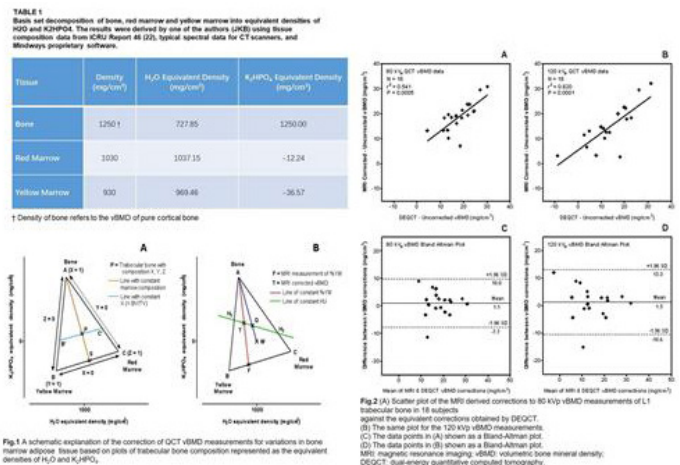
rior and posterior tibial artery [a.], intraosseous aa.) and distal forearm (ulnar a., radial a., intraosseous aa.). For each artery calcification was scored 0 to 2 yielding a global score of 0 to 12. During the prospective 8-year follow-up, 164 men died (55 cardiovascular deaths) and 53 men had acute coronary syndrome confirmed by troponin assay, electrocardiogram or coronarography. Peripheral artery calcification score increased with age. After adjustment for age, the score was higher in men with obesity, diabetes mellitus, ischemic heart disease or hypertension and in men taking vitamin K antagonists (p<0.005). In 43 men with severe calcification (score >5), all-cause mortality was higher compared to men with lower calcification score (0-5): HR=1.68, 95%CI: 1.01 – 2.82, p<0.05 after adjustment for age, BMI, lifestyle, co-morbidities, treatments, biological measures and abdominal aortic calcification. In this group, cardiovascular mortality was significantly increased: HR=2.60 vs. men with the score 0-5, 95%CI: 1.19 – 5.66, p<0.05 after adjustment for confounders. Finally, severe peripheral artery calcification was associated with higher risk of acute coronary syndrome: HR=5.58 vs. men with the score 0-5, 95%CI: 2.49 – 12.54, p<0.001 after adjustment for relevant confounders. In conclusion, in older community-dwelling men followed up prospectively, severe peripheral artery calcification observed on the HR-pQCT scans is associated with a significantly higher risk of cardiovascular death and acute coronary syndrome. Severe peripheral artery calcification found fortuitously on a medical imaging scan performed for other reasons can provide clinically relevant information on the cardiovascular risk.

Disclosures: *Pawel Szulc, None*

SUN-0715

The Correction of Quantitative Computed Tomography Measurements of Vertebral Bone Mineral Density for Marrow Fat using Magnetic Resonance Imaging Ling Wang^{*1}, Xiaoguang Cheng¹, Glen Blake², Keenan Brown³, Li Xu¹, Zhe Guo¹. ¹Department of Radiology, Beijing Jishuitan Hospital, China, ²King's College London Osteoporosis Research Unit, United Kingdom, ³Mindways Software Inc., United States

Purpose: Single-energy quantitative computed tomography (SEQCT) measurements of volumetric bone mineral density (vBMD) are subject to errors due to variations in bone marrow composition. We describe a method of using chemical shift-encoded magnetic resonance imaging (CSE-MRI) measurements of marrow fat to correct these errors, together with a validation study in which CSE-MRI corrections to SEQCT vBMD measurements of L1 trabecular bone were compared with the same corrections derived from dual-energy QCT (DEQCT) scans. Methods: We describe a method based on the H2O and K2HPO4 equivalent densities of bone, red and yellow bone marrow to correct SEQCT vBMD measurements for marrow fat using CSE-MRI measurements of proton density fat fraction (PDFF). Using data from earlier studies, we show that PDFF measurements provide a reliable estimate of the yellow marrow content of bone marrow. The resulting corrections to spine SEQCT vBMD measurements were compared with similar corrections obtained by performing DEQCT scans in 18 subjects enrolled as healthy controls in the China Action on Spine and Hip Status study. Results: Plots of the MRI vBMD corrections against the DEQCT corrections showed statistically significant correlations for 80 kVp (r² = 0.541; P < 0.001) and 120 kVp vBMD data (r² = 0.620; P < 0.001). Bland-Altman plots showed a bias of 1.1 (95% LOA: -7.7 to 10.0) mg/cm³ at 80 kVp and 1.5 (95% LOA: -10.3 to 13.3) mg/cm³ at 120 kVp. Conclusions: We have validated a method of using CSE-MRI measurements of PDFF to correct the accuracy errors in SEQCT vBMD measurements.



Disclosures: *Ling Wang, None*

SUN-0716

Cortical and trabecular bone of patients with prevalent major osteoporotic fracture: a case-control study using DXA-based 3D modelling Renaud Winzenrieth^{*1}, Ludovic Humbert¹, Edward Leib². ¹Galgo Medical SL, Spain, ²Dept. of Medicine, University of Vermont College of Medicine, United States

Purpose: The aim of this study was to assess the differences at the cortical and trabecular bone between subjects with and without prevalent osteoporotic fractures in a large cohort of non-Hispanic white women from USA, using DXA-based 3D modelling. **Method:** This retrospective case-control study involved 1746 women aged 50 and older. Eligibility was determined through a thorough review of records of patients having had a DXA scan between 2002 and 2008. Individuals suffering from illness or taking medications known to affect bone metabolism were excluded. Individuals in the fracture group (n=105) had at least one low-energy major osteoporotic fracture (MOF). Areal BMD (aBMD) was measured at lumbar spine (aBMDLS) and total femur (aBMDTot). A software algorithm was used to derive 3D models from the hip DXA scans and compute the following measurements: trabecular volumetric BMD (TrabvBMD) and cortical surface BMD (CortsBMD). Descriptive statistics and inferential tests for difference between groups were used. Univariate and multivariate logistic regression models were used to investigate possible association between independent variables and the presence of fracture. Odds ratios per standard deviation decrease (OR) and areas under the ROC curve (AUC) were evaluated. **Results:** Mean age, aBMDTot, TrabvBMD, smoking (all p<0.001), as well as CortsBMD (p=0.02) and aBMDLS (p=0.03) were significantly different between control and fracture groups, whereas no difference was noted for BMI, weight, height, menopause status, family history of osteoporosis (FHO) and parental history of hip fracture (ParFx). After adjustment for age and smoking, aBMDTot (p=0.037) and TrabvBMD (p=0.021) remained significantly lower in individuals with MOF while aBMDLS and CortsBMD were not. AUC of aBMDTot and TrabvBMD were 0.60 [0.54-0.65] and 0.61 [0.55-0.66] respectively. Using multivariate analysis, TrabvBMD, age and smoking were the three co-factors included in the model to explain presence of MOF, while aBMDLS, aBMDTot, CortsBMD, FHO, and ParFx were excluded from the model (p>0.1). Trabecular vBMD remained associated with the presence of prevalent fracture after adjustment for age and smoking with an OR of 1.28 [1.03-1.60] (1.52 [1.22-1.89] before adjustment). **Conclusion:** This study demonstrates the potential of DXA-based 3D measurements to discriminate between subjects with and without MOF. TrabvBMD was the measurement exhibiting the strongest association with the presence of fragility fracture, which is consistent with results in the literature obtained in similar studies using quantitative computed tomography.

Disclosures: Renaud Winzenrieth, Galgo Medical, Other Financial or Material Support

SUN-0717

The Design and Validation of a New Algorithm to Identify Initial Incident and Recurrent Incident Fragility Fractures in Administrative Claims Data Nicole Wright^{*1}, Shanette Daigle², Mary Melton², Elizabeth Delzell¹, Akhila Balasubramanian¹, Jeffrey Curtis². ¹Department of Epidemiology, University of Alabama at Birmingham, United States, ²Division of Clinical Immunology and Rheumatology, University of Alabama at Birmingham, United States, ³Center for Observational Research, Amgen Inc, United States

Purpose: Administrative databases offer an avenue for clinical research on osteoporotic fractures. The procedure codes of the Ray et al fracture identification algorithms have been updated, potentially affecting algorithm validity. We validated new claims-based algorithms to identify incident and recurrent fractures in administrative claims data. **Methods:** We used 2005-2014 Medicare claims linked to the Reasons for Geographic and Racial Differences in Stroke (REGARDS) study, a prospective cohort of Black and White adults ≥45 years. "Case qualifying (CQ)" incident fractures (defined in Table footnote) were identified among participants (≥65 years) having ≥12 months of traditional fee-for-service coverage prior to first fracture claim, and ≥6 months after. A recurrent fracture was defined as the first CQ event to occur after a clean period (≥90 days) before the preceding incident fracture episode. We used medical record content (discharge summary, imaging and/or surgical report) to adjudicate fractures, and ensured the claim event was correctly matched to the fracture site. We calculated positive predictive values (PPV) as the number of confirmed fractures divided by the total number of claims-identified fractures. **Results:** We identified 2,049 potential incident fractures in claims among 1,650 participants, and attempted record retrieval for 728 (35.5%) suspected incident fracture events (prioritizing recent CQ fractures associated with osteoporosis). Our final sample included 520 claims-identified CQ incident fractures having medical records; 502 (96.5%) were confirmed. The PPVs of the hip, radius/ulna, humerus, and clinical vertebral all exceeded 95% (Table). We identified 117 beneficiaries with 292 ≥2 CQ fracture episodes at the same skeletal site, and attempted retrieval for 105 (36.0%) episodes. Our analytic sample included 72 (68.5%) CQ episodes from 33 participants. The PPVs for identifying recurrent clinical vertebral, hip/femur, and non-vertebral fractures with a clean period ≥90 days exceeded 95%. **Conclusions:** Our fracture identification algorithms had high validity, even for clinical vertebral fractures and recurrent fractures of the same site (not previously evaluated by Ray et al). While medical record review and clinical adjudication remains a gold standard, our claims-based algorithms provide valid fracture outcome ascertainment, particularly for research questions focusing on high specificity such as comparative effectiveness and safety.

Table. Validation of Case-Qualifying Claims-based Algorithm to Identify Initial Incident and Recurrent Incident Fragility Fractures

	Episodes Identified by Claims	Medical Record Confirmed	PPV (95% CI)
Incident Fractures			
All Clinical CQ Fractures*	520	502	96.5 (94.6, 97.8)
Hip	107	102	95.3 (89.5, 98.0)
Radius/Ulna	90	87	96.7 (90.7, 98.9)
Humerus or Scapula	54	53	98.1 (90.2, 99.7)
Clinical Vertebral	148	146	98.6 (95.2, 99.6)
Recurrent Fractures*			
All clinical fractures**	72	70	97.2 (90.4, 99.2)
Clinical Vertebral	40	39	97.5 (87.1, 99.6)
Hip/Femur	22	21	95.5 (78.2, 99.2)
All Non-V-vertebral**	32	31	96.9 (84.3, 99.4)

PPV = Positive Predictive Value, CI = Confidence Interval, CQ = Case Qualifying
Case qualifying fractures were identified on the basis of meeting any of the following criteria:
(1) fracture diagnosis code was in the primary position on an hospitalized claim, or
(2) fracture diagnosis code was in secondary (i.e. non-primary) position on an hospitalized claim, or
(3) fracture diagnosis code was on an outpatient claim and paired with surgical fracture repair procedure, or
(4) for clinical vertebral fractures, fracture diagnosis code was on a physician claim and paired with spine imaging code (≤10 days)

*All clinical fractures include hip, pelvis, femur, tibia/fibula or ankle, radius/ulna, humerus or scapula, clavicle, and clinical vertebral fractures
**All non-vertebral fractures include hip, pelvis, femur, tibia/fibula or ankle, radius/ulna, humerus or scapula, and clavicle fractures

*90 day clean-period in which no fracture claims were observed during the 90-days

Disclosures: Nicole Wright, Pfizer, Consultant, Amgen, Grant/Research Support

SUN-0718

Serum Circulating MicroRNAs as a Novel Biomarker for Osteoporotic Vertebral Fractures Patryk Zarecki^{*1}, Matthias Hackl², Johannes Grillari³, Miguel Debono¹, Richard Eastell¹. ¹University of Sheffield, United Kingdom, ²TAmiRNA GmbH, Austria, ³TAmiRNA GmbH, Christian Doppler Laboratory on Biotechnology of Skin Aging, Austria

Vertebral fractures are the hallmark of osteoporosis. Some microRNAs (miRNAs) can affect bone homeostasis, including bone remodelling and fracture healing by altering the gene expression in osteoblasts, osteoclasts and osteocytes. We hypothesise that miRNAs affect bone metabolism and their levels should differ between osteoporotic patients and healthy controls. We compared the levels of circulating miRNAs in older women with osteoporotic vertebral fractures, women with low bone mineral density (BMD) and healthy controls. We correlated miRNAs expression levels with currently-used bone turnover markers (BTMs) and osteoporosis-related hormones. The set of 20 circulating miRNAs was selected based on the literature and our previous studies. The serum levels of selected miRNAs were measured by a RT-qPCR in 4 groups of older women: healthy controls (n=40, group 1); low BMD and no fractures (n=35, group 2); vertebral fractures and low BMD without a treatment (n=24, group 3); or receiving a treatment against osteoporosis (n=17, group 4). The data quality was monitored using spike-in and hemolysis controls and was normalized to the RNA spike-in control. Statistical analysis was performed by a two-way ANOVA with Tukey post hoc test with statistical significance of P-value < 0.05. The correlation between miRNAs and BTMs was performed in SPSS Statistics software by regression analysis. We found 7 miRNAs (miR-375, miR-532-3p, miR-19b-3p, miR-152-3p, miR-23a-3p, miR-335-5p, miR-21-5p) which were upregulated (P<0.05) in patients with vertebral fractures/low BMD against patients with low BMD/no fractures (2-fold) and against healthy controls (1.5-fold), regardless of osteoporosis treatment. There were no significant differences in any miRNA level between low BMD/no fracture group and healthy controls. We found 39 significant correlations (P<0.05) of measured miRNAs with: CTX, PTH, PINP, OC, Bone ALP, cortisol, estrone and 25-OH vit D. There was no correlation between any of measured miRNAs with: IGF-1 and estradiol. These data suggest that some miRNA levels reflect the presence of osteoporotic vertebral fractures. They are unlikely to reflect low BMD, and more likely changes in bone quality or fracture healing. Bisphosphonate treatments do not appear to have a large influence on miRNA levels in this cohort. The correlation between miRNAs and BTMs suggest that miRNAs may be involved in bone turnover or fracture healing.

Disclosures: Patryk Zarecki, None

SUN-0760

Multiple missed opportunities to reduce key fragility fractures: can we afford to continue to ignore the facts? Emese Toth^{*1}, Jonas Banefelt², Kristina Akesson³, Anna Spangues⁴, Gustaf Orstater², Cesar Libanati¹. ¹UCB Pharma, Belgium, ²Quantify Research, Sweden, ³Lund University, Skåne University Hospital, Department of Orthopaedics, Sweden, ⁴Department of Endocrinology/Department of Medical and Health Sciences, Linköping University Hospital, Sweden

The ageing population in most countries will precipitate a healthcare crisis if the increasing burden of fragility fractures (Fxs) is not addressed. Despite the well-recognized increase in imminent Fx risk after a first fragility Fx, worldwide, most patients remain undiagnosed and untreated. While we must continue to prevent first Fx, this requires the identification of patients who are very often asymptomatic. In contrast, identifying patients at risk

of secondary Fx requires less effort, as they become known to healthcare systems during their Fx episode. Here, we report on missed opportunities to reduce secondary hip, clinical vertebral (clin vert), and humerus fragility Fxs in postmenopausal women in Sweden. Women aged 55–90 years with a hip, clin vert, or humerus fragility Fx in 2013 (index Fx) were identified from Swedish national registries. For each woman, we calculated the number of previous Fx from their medical history (earliest available date 2001) as well as exposure to osteoporosis therapies (OP Tx). The cumulative incidences of hip, clin vert and humerus Fx within 24 months following index Fx were also assessed in order to evaluate the association between index Fx type and subsequent Fx incidence. The analysis included 14,971 women (index Fx type: 7,180 hip; 2,831 clin vert; 4,960 humerus). Mean age at index date was 77 years (range, 55–90 years). The percentage of patients with a prior Fx, by their index-Fx type were: 38% hip; 37% clin vert; 28% humerus. The proportion of women with a history of Fx prior to the index Fx increased with age (Table 1A). Cumulative incidences of new Fx over 24 months are shown by index-Fx type in Table 1B. The Fx event (index Fx) had little effect on the initiation of OP Tx. At the time of index Fx, only 23% of women had any prior OP Tx; during the 2 years following the index Fx this proportion increased slightly to 27%. In conclusion, more than a third of women with an index hip, humerus, or clin vert Fx were found to have ≥ 1 previous Fx, suggesting an association between Fx, in particular clin vert Fxs, and subsequent Fx. Of note, most women were not receiving OP Tx and most had no OP Tx during the 2-year follow up. Specific treatment pathways and guidelines, with clear metrics and performance assessments, are needed to ensure timely identification and intervention in patients at risk of Fx. These findings indicate that opportunities are being missed to improve a current and future healthcare problem.

Table 1.

A: Prevalence (%) of prior Fx by index-Fx type and age (years)					
Index Fx type	55–59	60–69	70–79	80–89	90
All	14.7	27.1	32.3	40.2	44.4
Hip	24.2	35.2	34.9	39.5	44.2
Clin vert	15.2	30.3	33.5	43.6	46.3
Humerus	12.0	22.5	28.5	38.9	43.4
B: Incidence (%) of subsequent fractures after the index Fx by index-Fx type					
Index Fx type	Subsequent fracture type within 24 months				
	Hip	Humerus	Clin vert	Any	
Hip	4.0	2.6	1.7	13.7	
Humerus	4.0	0.6	1.5	11.4	
Clin vert	5.9	2.0	4.6	17.6	
Any	4.4	1.8	2.2	8.0	

*Any' Fx refers to either hip, humerus or clin vert Fx for both index and subsequent Fx.

Disclosures: **Emese Toth**, UCB Pharma, Other Financial or Material Support, UCB Pharma, Major Stock Shareholder

SUN-0761

Women and Men with Diabetic Complications have a Greater Risk for Hip Fracture Shreyasee Amin*, Elizabeth Atkinson, Sundeep Khosla. Mayo Clinic, United States

Impaired bone quality contributes to increased fracture risk in diabetics, which may be related to poor blood glucose control. Complications related to diabetes mellitus, which reflects poor long-term disease control, may be a relevant clinical marker of bone fragility and increased fracture risk. We examined the association between diabetes, with and without complications, and hip fractures, in both women and men. Using administrative claims data from a large US commercial insurance database (OptumLabs Data Warehouse), we identified women and men aged ≥ 50 yrs who had a hip fracture between Jan 1, 2006-Dec 31, 2016, and who had at least 1 yr health plan coverage pre-fracture. Control subjects without known hip fracture were matched to cases exactly on sex, age, race, year, US region, and insurance; they were also required to have at least 1 yr of health plan coverage pre-index date. Diagnostic codes related to diabetes with or without complication and medications were captured for the year prior to fracture/index date. We categorized subjects into 3 groups (no diabetes, diabetes without complications, and diabetes with complications) and used conditional logistic regression to examine the association with hip fracture. Women and men were analyzed separately and also by race, focusing on those identified as white, black or Asian. We studied 50,136 white/5,770 black/1,130 Asian women (median age [IQR], yrs: 79 [72, 83]/78 [71, 83]/79 [71, 83], respectively) and 22,329 white/2,419 black/451 Asian men (median age [IQR], yrs: 77 [66, 82]/75 [66, 81]/78 [67, 83], respectively) who had hip fractures and an equal number of matched controls. Compared to the referent group (no diabetes), we found that both women and men with diabetic complications had an increased risk for hip fracture, while diabetics without complications had no association with hip fractures (Table). Findings were similar in women and men across races studied (Table) and when subset to diabetics not on insulin (data not shown). Diabetics who have no complications may not be at imminent risk for hip fracture. On the other hand, diabetics who do have complications should have further evaluation of their bone health and be considered for preventive therapy. Further work is indicated on determining whether poor glucose control, generally, or specific complications have a greater impact on hip fracture risk among diabetics.

Odds Ratio (OR) and 95% Confidence Interval (95% CI) for Hip Fractures by Diabetes Mellitus Status and Complications

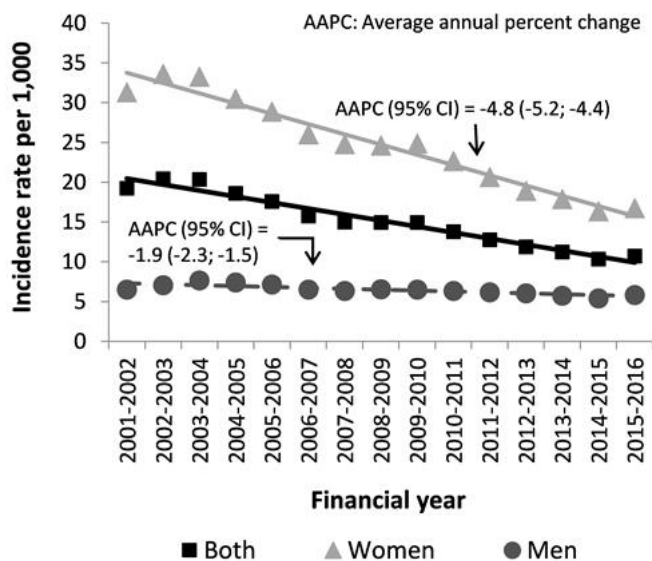
	White			Black			Asian		
	Hip Fracture No	Hip Fracture Yes	OR (95% CI)	Hip Fracture No	Hip Fracture Yes	OR (95% CI)	Hip Fracture No	Hip Fracture Yes	OR (95% CI)
Women									
N	50,136	50,136		5,770	5,770		1,130	1,130	
Diabetes Status									
No diabetes	77.1%	74.6%	referent	66.6%	64.5%	referent	68.3%	63.5%	referent
Diabetes, no complications	15.1%	14.4%	0.99 (0.95, 1.02)	20.1%	18.5%	0.95 (0.87-1.05)	20.4%	21.3%	1.13 (0.92-1.39)
Diabetes, with complications	7.9%	11.0%	1.45 (1.39-1.52)	13.3%	17.0%	1.32 (1.19-1.47)	11.2%	15.1%	1.44 (1.12-1.85)
Men									
N	22,329	22,329		2,419	2,419		451	451	
Diabetes Status									
No diabetes	74.0%	69.4%	referent	65.6%	62.4%	referent	65.2%	60.5%	referent
Diabetes, no complications	17.4%	16.1%	0.99 (0.94-1.04)	20.5%	18.7%	0.96 (0.83-1.11)	23.9%	22.0%	1.02 (0.73-1.42)
Diabetes, with complications	8.6%	14.5%	1.83 (1.72-1.94)	13.9%	18.9%	1.44 (1.23-1.69)	10.9%	17.5%	1.74 (1.17-2.60)

Disclosures: **Shreyasee Amin**, None

SUN-0762

Temporal Trends in Prevalence and Incidence of Diagnosed Osteoporosis in Quebec, Canada Claudia Beaudoin*, Philippe Gamache¹, Suzanne N. Morin³, Jacques P. Brown⁴, Louis Bessette⁴, Sonia Jean¹. ¹Institut national de santé publique du Québec, Canada, ³McGill University, Canada, ⁴CHU de Québec Research Center, Canada

Background: Osteoporosis (OP) and related fractures are associated with increased mortality, morbidity and medical costs. Given the major consequences of OP, its monitoring is an important part of a chronic disease surveillance system. Objective: The objective of this study is to describe temporal trends in the prevalence and incidence rate of diagnosed OP in individuals aged ≥ 45 years from the province of Quebec, Canada. Method: This study was performed using four linked provincial administrative databases (health insurance, hospitalizations, physician claims, and pharmaceutical services). Individuals were considered to have OP diagnosis if they had one or more: (i) physician claims with an OP diagnosis code (ICD-9-CM: 733.0, 733.9), (ii) hospital discharges with an OP diagnosis code (ICD-9-CM: 733.0, 733.9; ICD-10-CA: M80, M81), or (iii) prescription claims for an OP medication. The sensitivity of this case-definition was 0.65 and the positive predictive value was 0.73 in a previous validation study. To identify incident cases, a “run-in” period of 5 years (from 1996-97 to 2000-01) was used to exclude prevalent cases. Crude prevalence and incidence rates were calculated annually between 2001-02 and 2015-16. Prevalence and incidence rates standardized to the 2001 age structure of the Quebec population were also calculated. Negative binomial regression was used to test for linear change in standardized incidence rates. Results: In 2015-16, the crude prevalence of diagnosed OP was 15.7%. The prevalence was higher in women (25.0%) than in men (5.6%) and increased with age (45-54y: 2.1%, 55-64y: 9.2%, 65-74y: 23.7%, 75-84y: 38.1%, $\geq 85y$: 50.6%). The age-standardized prevalence increased slightly from 13.8% in 2001-02 to 14.4% in 2011-12, and remained stable afterwards. The age-standardized incidence rate decreased significantly from 19.3 cases per 1,000 adults in 2001-02 to 10.7 cases per 1,000 adults in 2015-16 ($p < 0.001$, Figure 1). Average annual percent changes were -4.8 (95% CI -5.2, -4.4) and -1.9 (95% CI -2.3, -1.5) in women and men, respectively. Conclusion: In Quebec, the age-standardized prevalence of diagnosed OP remains around 14% since 2011-12. A significant decrease in the rate of individuals newly diagnosed with OP has been observed between 2001-02 and 2015-16. This may be attributable to a decrease in the management of OP, fracture rate, use of OP diagnosis codes, prescriptions for an OP medication, or OP risk factors over time.



Disclosures: Claudia Beaudoin, None

SUN-0763

Social deprivation is associated with poor health outcomes following hospital admission for hip fracture in England Arti Gauvri Bhimjiyani¹*, Jenny Neuburger², Yoav Ben-Shlomo³, Celia L Gregson¹. ¹Translational Health Sciences, Bristol Medical School, University of Bristol, United Kingdom, ²Department of Health Services Research and Policy, London School of Hygiene and Tropical Medicine, United Kingdom, ³Population Health Sciences, Bristol Medical School, University of Bristol, United Kingdom

Social deprivation predicts a range of adverse health outcomes; however, its impact post hip fracture is not established. We examined the effect of area-level social deprivation on outcomes after hospital admissions for hip fracture in England. We used English Hospital Episodes Statistics linked to the National Hip Fracture Database (04/2011-03/2015) and National Statistics mortality data to identify patients admitted with hip fracture aged 60+ years. Deprivation was measured by quintiles of the Index of Multiple Deprivation; Q1-least deprived; Q5-most deprived. Charlson score quantified comorbidities. Associations with 30-day mortality and emergency readmissions were assessed by logistic regression, adjusted for age and gender. Mean length of stay (LOS) in acute plus rehabilitation hospitals ('super-spell') and total bed occupancy within 1-year post-fracture were calculated; their associations with deprivation were estimated using linear regression. We identified 218,907 hospital admissions with an index hip fracture over 4 years. Mean [SD] age 82.8 [8.4] years; 72.6% female, 75.9% had ≥1 comorbidity. Overall 30-day mortality was 7.8% (n=17,072/218,907). Among survivors, mean superspell was 23.6 [21.6] days; 15.6% were re-admitted within 30 days (n=31,072/199,564), mean 1-year bed occupancy 33.4 [32.7] days. Greater deprivation was associated with higher 30-day mortality (Q5: 8.4% [n=3,229/38,434] vs. Q1: 7.2% [n=3,143/43,866]), age/gender-adjusted OR 1.32 (95% CI [1.25,1.39], p<0.001); partly explained by further comorbidity adjustment (OR 1.18 [1.12,1.25], p<0.001). Among survivors, age/gender-adjusted mean superspell was longer in those most deprived (Q5: 18.5 95% CI [17.6,19.4] days, Q1: 16.7 [16.1,17.2], p<0.001). 30-day readmissions were higher in those most deprived 17.5% (Q5: n=6,062/34,693) vs. those least deprived 14.2% (Q1: n=5,744/40,377), age/gender-adjusted OR 1.32 [1.27,1.38], p<0.001; this was not explained by comorbidity (OR 1.24 [1.20,1.29], p<0.001). A similar trend was seen for mean 1-year hospital bed occupancy (Q5: 28.1 [26.8,29.4] days; Q1: 24.8 [24.0,25.6], p<0.001). Greater deprivation predicts reduced 30-day survival and, among survivors, longer hospital stays and a greater need to be re-admitted once discharged. Whilst deprivation-related comorbidity explains part of these apparent health inequalities, the role of other patient factors and the configuration of hospital services remains to be determined.

Disclosures: Arti Gauvri Bhimjiyani, None

SUN-0764

Performance of FRAX and FRAX-Based Treatment Thresholds in Women aged 40 and Older: The Manitoba BMD Registry Carolyn Crandall¹*, John Schousboe², Suzanne Morin³, Lisa Lix⁴, William Leslie⁴. ¹University of California, Los Angeles, United States, ²Park Nicollet Institute, United States, ³McGill University, Canada, ⁴University of Manitoba, Canada

Objective. To examine among women aged ≥40 years the performance of the Fracture Risk Assessment Tool (FRAX) and FRAX-based osteoporosis treatment thresholds under

the U.S. National Osteoporosis Foundation (NOF) and U.K. National Osteoporosis Guideline Group (NOGG) guidelines. Methods. We used registry data for all women aged ≥40 years in Manitoba, Canada with baseline bone mineral density (BMD) testing (n = 54,459). The Canadian FRAX was used to calculate 10-year risk of hip or major osteoporotic fracture (MOF). Incident MOF, hip fracture, and any fracture (excluding head, neck, hand, foot, and ankle) were assessed from population-based health services data (mean follow-up 10.5 years). Age-stratified hazard ratios (HR) were estimated from Cox regression models, with interaction terms for age decade. We assessed the sensitivity, specificity, positive predictive value (PPV), and number needed to treat (NNT) to prevent a fracture (assuming 40% relative risk reduction on Rx) for osteoporosis treatment thresholds under the NOF and NOGG guidelines. Results. Femoral neck T-score and FRAX (with and without BMD) predicted all fracture outcomes at all ages. Age interactions, where detected, were modest. There was good calibration in FRAX-predicted vs observed 10-year MOF and hip fracture probability. The sensitivity (PPV) for incident MOF was: 25.7% (24.0%) for femoral neck T-score ≤ -2.5, 20.3% (26.3%) for FRAX-predicted 10-year MOF risk ≥ 20% (NOF threshold), 27.3% (22.0%) for FRAX-predicted 10-year MOF risk ≥ age-dependent cutoff (NOGG threshold), 59.4% (19.0%) for the full NOF algorithm, and 28.5% (18.4%) for the full NOGG algorithm. The sensitivity of the strategies for incident MOF varied markedly by age, often being lowest in women 40-49 years-old (range 0.0%- 26.3%). The strategies with the lowest NNT for MOF were femoral neck BMD T-score ≤ -2.5 and FRAX-predicted risk of MOF ≥ 20% (NNT = 10 overall, maximum NNT = 15 age 40-49 years-old, minimum NNT = 9 age 80+ years-old). NNTs were similar for the full NOF (=13 overall) and full NOGG (=14 overall) guidelines. Conclusion. The gradient of risk for fracture prediction from femoral neck T-score and FRAX (with and without BMD) as continuous measures was strong across the age spectrum. The sensitivity and PPV of the strategies examined based upon dichotomous cutoffs were low, especially among women aged 40-49 years where the incidence rates are the lowest, but the NNT is reasonable at all ages.

Table. Association of Fracture Risk Assessment Tool (FRAX)-Predicted Risk with Incident Fracture, Stratified by Age Group*

Incident Major Osteoporotic Fracture (MOF)	Incidence	FRAX MOF risk ≥ 20%							
		HR per SD (CI)	Sens	Spec	PPV	NPV	Acc	NNTS	NNT (PPV, 40% RRRI)
Age 40-49 (N=5324)	5.6%	1.67 (1.44-1.95)	0.0%	99.9%	0.0%	94.4%	94.2%	783	Calculation not possible
Age 50-59 (N=15,466)	7.1%	2.06 (1.89-2.23)	1.5%	99.4%	17.5%	92.0%	92.4%	159	14
Age 60-69 (N=16,620)	10.2%	2.65 (1.91-2.21)	6.7%	97.3%	20.8%	90.1%	87.8%	30	12
Age 70-79 (N=12,492)	16.6%	1.98 (1.86-2.12)	23.6%	89.9%	26.5%	85.0%	76.4%	7	9
Age 80+ (N=5,151)	21.9%	2.66 (1.85-2.29)	58.9%	58.6%	27.8%	83.3%	58.6%	2	9
All ages (N=54,459)	11.4%	2.14 (2.08-2.20)	20.3%	92.7%	26.3%	89.0%	81.4%	11	10

Incident Hip Fracture	Incidence	FRAX hip fracture risk ≥ 2%							
		HR per SD (CI)	Sens	Spec	PPV	NPV	Acc	NNTS	NNT (PPV, 40% RRRI)
Age 40-49 (N=5324)	0.6%	3.93 (2.60-5.96)	6.7%	99.2%	7.7%	99.9%	98.8%	137	33
Age 50-59 (N=15,466)	1.0%	4.13 (3.33-5.12)	12.0%	98.1%	5.8%	99.1%	97.2%	50	43
Age 60-69 (N=16,620)	2.3%	3.33 (2.99-4.60)	31.7%	89.7%	6.9%	98.2%	88.3%	9	36
Age 70-79 (N=12,492)	6.0%	3.01 (2.64-3.43)	66.1%	55.9%	9.4%	95.0%	56.2%	2	26
Age 80+ (N=5,151)	13.0%	3.26 (2.65-4.01)	94.0%	15.9%	11.8%	95.7%	24.2%	1	21
All ages (N=54,459)	3.9%	4.59 (4.30-4.89)	62.2%	70.2%	8.0%	98.3%	78.9%	4	25

Incident any fracture	Incidence	FRAX any fracture risk ≥ 30%							
		HR per SD (CI)	Sens	Spec	PPV	NPV	Acc	NNTS	NNT (PPV, 40% RRRI)
Age 40-49 (N=5324)	8.7%	1.67 (1.47-1.89)	0.2%	99.0%	14.3%	91.3%	91.2%	783	18
Age 50-59 (N=15,466)	10.4%	1.92 (1.79-2.06)	1.7%	99.5%	28.0%	89.8%	89.4%	159	9
Age 60-69 (N=16,620)	13.0%	1.98 (1.85-2.11)	6.4%	97.2%	35.0%	87.3%	85.0%	30	10
Age 70-79 (N=12,492)	20.6%	1.97 (1.85-2.08)	27.8%	87.2%	31.4%	81.3%	74.0%	7	8
Age 80+ (N=5,151)	25.9%	2.64 (1.85-2.25)	57.9%	59.1%	32.4%	80.2%	58.7%	2	8
All ages (N=54,459)	14.0%	1.98 (1.94-2.03)	18.6%	92.9%	31.3%	86.7%	81.8%	11	9

* Fracture risk assessment tool with bone mineral density information
 † HR per SD (CI), hazard ratio per standard deviation in FRAX score with 95% confidence interval. Sens=sensitivity, Spec=specificity, PPV=positive predictive value, NPV=negative predictive value, NNTS=number needed to screen, NNT=number needed to treat (from PPV, 40% relative risk reduction), Acc=accuracy.

Disclosures: Carolyn Crandall, None

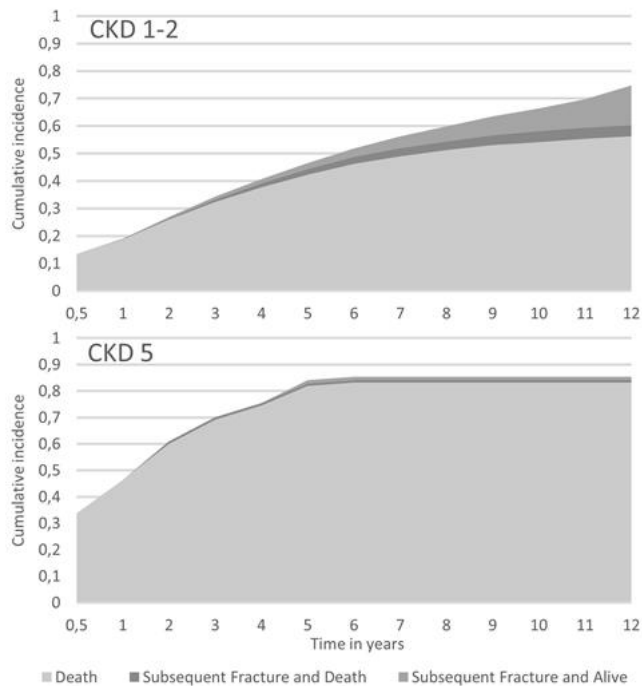
SUN-0765

Increased mortality risk, but no increased subsequent fracture risk following hip fracture in elderly patients with chronic kidney disease Irma Ja De Bruin¹*, Caroline E Wyers¹, Patrick C Souverein², Tjeerd P Van Staa^{2,3,4}, Piet M Geusens^{5,6}, Joop Pw Van Den Bergh^{1,6}, Frank De Vries^{2,5}, Johanna H Driessen^{2,5}. ¹VieCuri Medical Center, Department of Internal Medicine; Maastricht UMC+, NUTRIM School for Nutrition and Translational Research in Metabolism, Department of Internal Medicine, Netherlands, ²Utrecht University, Utrecht Institute of Pharmaceutical Sciences, Division of Pharmacoepidemiology and Clinical Pharmacology, Netherlands, ³London School of Hygiene & Tropical Medicine, ⁴University of Manchester, Farr Institute for Health Informatics Research, ⁵Maastricht UMC+, CAPHRI Care and Public Health Research Institute, Department of Internal Medicine subdivision of Rheumatology, Netherlands, ⁶Hasselt University, Netherlands

Purpose: To evaluate the association between chronic kidney disease (CKD, stages G3-G5 versus G1-G2) and the risk of a subsequent non-hip major fragility fracture (humerus, distal forearm and vertebral fracture) following a hip fracture. Methods: A retrospective cohort study using data from the UK Clinical Practice Research Datalink (CPRD) (2004-2016) was conducted. All patients with a first hip fracture, aged 50 years or older were included. Kidney function (eGFR) was assessed time-dependently and the eGFR was used to determine the KDIGO CKD stage. Cox proportional hazard analyses adjusted for lifestyle variables, comorbidities and concomitant drug use, were used to estimate cause specific (cs)-hazard ratio (HR) of the association between kidney function (CKD G3-5 vs CKD G1-2) and subsequent non-hip major fragility fracture risk. CKD G3-5 was further stratified by CKD 3, 4 and 5 stages. To explore the potential competing risk of mortality, a cause-specific HR for

Sunday Posters

mortality was estimated. In addition, the cumulative incidence of different outcomes after the initial hip fracture was calculated. Results: We included 37,820 patients with a first hip fracture during the study period. Patients with CKD stage G1-G2 were younger than patients with CKD stage G3-G5 (79.2 vs. 84.2 years). CKD G3-G5 was not associated with risk of subsequent major fragility fractures (adjusted cs-HR: 0.89, 95%CI 0.79-1.00). Stratification of kidney function by CKD resulted in a cs-HR of 0.89 (95%CI 0.79-1.01) for CKD G3, 0.88 (95%CI 0.64-1.20) for CKD G4 and 0.56 (95%CI 0.20-1.56) for CKD G5. CKD G3-G5 was associated with a small increased risk of mortality (cs-HR 1.05 (95%CI 1.01-1.09)). Stratification by CKD stage resulted in a 1.5 and 3-fold increased mortality risk for CKD G4 and CKD G5, respectively (cs-HR CKD G4 1.50, 95%CI 1.38-1.62; CKD G5 2.93, 95% CI 2.48-3.46). The cumulative incidence of fracture and mortality outcomes after the initial hip fracture is shown in figure 1. Conclusion: This study did not demonstrate an increased risk of subsequent fractures following a hip fracture in patients with CKD G3-G5 compared to CKD G1-2. However, mortality risk was increased in patients with CKD G4 and G5 as compared to CKD G1-2. The higher mortality risk may, as competing risk, explain our main finding of no increased subsequent fracture risk with CKD stage 3-5.



Disclosures: **Irma Ja De Bruin**, Sanofi, Grant/Research Support, Pfizer, Novartis, Speakers' Bureau

SUN-0766

Long-term impact of body mass index in childhood on adult bone mineral density Hongbo Dong*, Yinkun Yan, Junting Liu, Dongqing Hou, Jie Mi. Capital Institute of Pediatrics, China

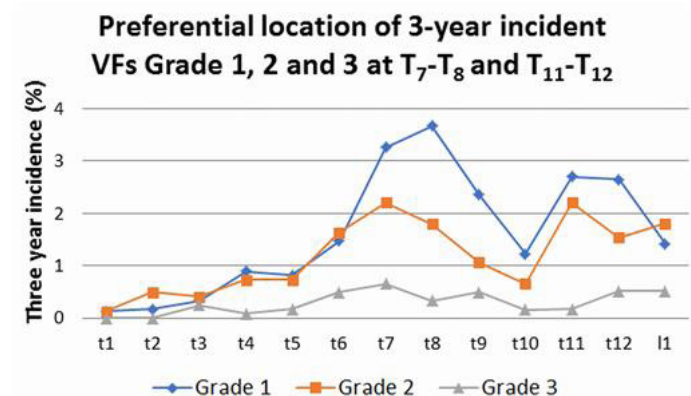
OBJECTIVES This study aimed to examine the association of long-term burden and trajectory patterns of childhood body mass index (BMI) with adult bone mineral density (BMD) and the mediation effect of adult BMI on these association. **METHODS** The longitudinal study consisted of 397 adults (54.4% males), who had been examined for BMI 4-8 times during childhood (6-19 years) and BMD in adulthood (29-37 years). Adult BMD was assessed via dual-energy x-ray absorptiometry. Childhood BMI growth curves were constructed using a random-effects mixed model. The area under the curve (AUC) was calculated to represent the long-term burden of childhood BMI. **RESULTS** From age around 10-years onwards, men with normal BMD had significantly higher BMI than those with low BMD at femoral neck, and similar trend was observed for spine BMD in females. In both sexes, childhood BMI measures (BMI at the first exam and total AUC) were all significantly and positively associated with adult BMD of whole body, spine, and femoral neck. Mediation effects of adult BMI were significant for the association of childhood BMI measures with adult femoral neck BMD (63.4% to 87.0%) in both sexes and childhood BMI at the last exam with adult spine BMD (74.6%) in males, but not significant for childhood BMI measures and whole body BMD in either sex. **CONCLUSIONS** These findings suggest that the impact of body weight on adult BMD originated partly from childhood, which differs by sex and skeletal sites. Maintaining an adequate weight from childhood is important for achievement of higher subsequent bone density. **KEYWORDS** child, bone density, body mass index, longitudinal study

Disclosures: **Hongbo Dong**, None

SUN-0767

The distribution of prevalent and short-term incident vertebral fractures on chest CT scans according to fracture severity in smokers with and without COPD Johanna Driessen^{*1}, Mayke Van Dort², Piet Geusens³, Frank De Vries^{4,5}, Emiel Wouters⁶, Joop Van Den Bergh^{7,8}. ¹CAPHRI Care and Public Health Research Institute, NUTRIM School for Nutrition and Translational Research in Metabolism, Department of Clinical Pharmacy and Toxicology, Maastricht University Medical Centre+ (MUMC+), Netherlands, ²NUTRIM School of Nutrition and Translational Research in Metabolism, Maastricht University Medical Centre+ (MUMC+), Netherlands, ³Department of Internal Medicine, Rheumatology, Maastricht University Medical Centre+ (MUMC+), the Netherlands, Netherlands, ⁴Department of Clinical Pharmacy and Toxicology, Maastricht University Medical Centre+ (MUMC+), Netherlands, ⁵CAPHRI Care and Public Health Research Institute, Netherlands, ⁶Department of Respiratory Diseases, Maastricht University Medical Centre+ (MUMC+), the Netherlands, ⁷Department of Internal Medicine, VieCuri Medical Centre, Venlo, Netherlands, ⁸Department of Internal Medicine, NUTRIM School of Nutrition and Translational Research in Metabolism, Maastricht University Medical Centre+ (MUMC+), Netherlands

Background: Biomechanical analyses indicate that compressive load is heterogeneous throughout the thoraco-lumbar spine, with maximal loads during daily activities in T7-T8 and T11-L1 (Bruno, 2017). At population level, studies have shown a bimodal spinal distribution of prevalent and incident VFs. However, prevalence and short-term incidence of individual VFs according to both their location and severity has not been reported. Therefore, the aim of this study was to analyse the distribution of prevalent and 3-year incident VFs according to severity on chest CT scans. **Methods:** The ECLIPSE study included current and former heavy smokers without (n=240) and with chronic obstructive pulmonary disease (COPD) (n=998), mean age 61.3 years, 61% men. VFs were scored according to Genant (grade (Gr) 0, 1, 2 or 3). Vertebrae with Schmorl's nodules, Scheuermann's disease and platyspondyly were excluded. All vertebrae which were evaluable at baseline and at 3 years were included (n=14,974). Incident VFs were defined as a new or a worsening VF. The proportion of VFs at preferential locations versus other locations were compared by McNemer's test for dependent proportions. **Results:** Clinical chest CT scans were available at baseline and 3 years for 1238 patients. At patient level, VF prevalence was 20.4% and the 3-year VF incidence was 24.0%. According to the individual vertebrae analysis, we identified 461 (3.1%) prevalent VFs and 473 (3.2%) incident VFs within 3 years. Prevalent VFs (n=239 Gr1, 179 Gr2 and 43 Gr3) showed bimodal distributions over the spine region T1-L1, for each of the VF grades 1-3. Prevalent VFs were preferentially located at T7-T8 and T11-T12. The proportion of prevalent VF fractures located at T7, T8, T11 or T12 was 5.7%, as compared to 1.8% for all other locations (p<0.01). A similar bimodal distribution at T7-8 and T11-12 was found for incident VFs (n=250 Gr1, 179 Gr2 and 44 Gr3) (Figure). The proportion of incident VF fractures located at T7, T8, T11 or T12 was 5.4%, as compared to 2.1% for all other locations (p<0.01). **Conclusion:** These results indicate that the prevalence and short term incidence of VFs is high in current and former heavy smokers with and without COPD. Prevalent VFs as well as incident VFs, regardless of VF severity, are preferentially located at T7-T8 and T11-T12 on chest CT scans. These regions have been documented to be at highest compressive load during daily activities.



Disclosures: **Johanna Driessen**, None

SUN-0768

Lower limb muscle force is negatively associated with hip fracture risk in community-dwelling older women April Hartley*¹, Yunhua Luo², Andrew Goertzen³, Kimberly Hannam¹, Ahmed Elhakeem¹, Emma M Clark¹, William D Leslie⁴, Jon H Tobias¹. ¹Bristol Medical School, University of Bristol, United Kingdom, ²Faculty of Engineering, University of Manitoba, Canada, ³Department of Radiology, University of Manitoba, Canada, ⁴Rady Faculty of Health Sciences, University of Manitoba, Canada

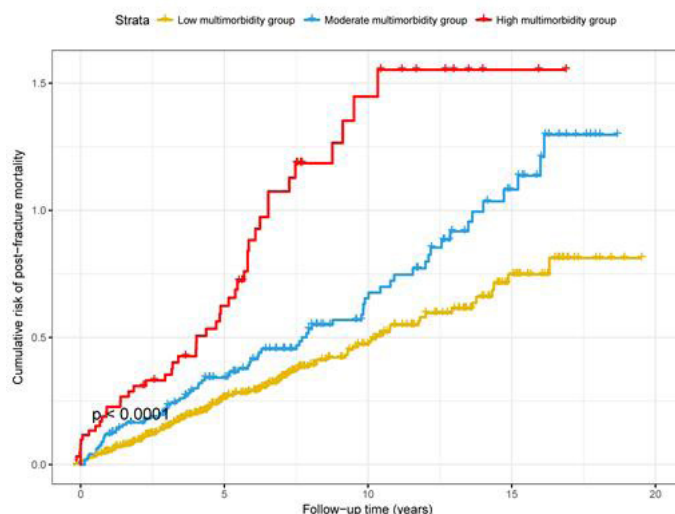
Background: Reduced muscle mass, a hallmark of sarcopenia, is associated with increased hip fracture risk. However, it is less clear whether directly measured lower limb muscle function also relates to hip fracture risk. Dual X-ray Absorptiometry (DXA)-based finite element analysis (FEA) is a novel method designed to determine fracture risk from 2D hip DXA images. **Aims:** (i) determine whether peak lower limb muscle force and/or power, assessed by Jumping Mechanography (JM), are related to hip bone mineral density (BMD) in older women; (2) establish whether equivalent relationships are seen for risk of hip fracture as determined by FEA. **Methods:** Community-dwelling women aged 71-88 attended an assessment clinic where total hip BMD, fat and lean mass were assessed by DXA. Fracture risk indices (FRI) at the femoral neck, intertrochanteric and subtrochanteric sites were calculated using FEA of hip DXA images. A two-footed jump was performed to assess lower limb peak muscle power and a one-legged hop used to assess peak muscle force. We analysed cross-sectional associations between total body lean mass (TBLM), peak force and power as exposures, and hip BMD and FRI as outcomes, using multivariable linear regression. Results are shown adjusted for age, height, weight (fat mass for models including TBLM) and comorbidities (self-reported by questionnaire). **Results:** 266 women had complete JM, hip DXA and covariate data, mean age 76.4 [SD 2.6] years. TBLM was strongly associated with total hip BMD ($\beta=0.31$ [0.14, 0.47] $p=4 \times 10^{-4}$) (β represents an SD change in outcome per SD change in exposure). TBLM was also inversely associated with fracture risk, estimated by FRI, at the femoral neck and intertrochanteric regions (-0.19 [-0.37, -0.01] and -0.13 [-0.23, -0.04] respectively, both $p<0.05$). Peak muscle force was strongly associated with total hip BMD (0.28 [0.14, 0.41] $p=8 \times 10^{-5}$). Peak force was also inversely related with FRI estimated at the femoral neck, intertrochanteric and subtrochanteric hip regions (-0.17 [-0.31, -0.03], -0.07 [-0.12, -0.01] and -0.18 [-0.32, -0.04] respectively, all $p<0.05$). There was some evidence for an inverse association between peak power and intertrochanteric and subtrochanteric FRI, but confidence intervals were wide. **Conclusions:** Lower limb peak muscle force is inversely related to hip fracture risk, estimated by FEA in older women, supporting the use of leg muscle strengthening exercises to reduce hip fracture risk in this population.

Disclosures: April Hartley, None

SUN-0769

Contribution of Multimorbidity to Post-Fracture Mortality: Result of a Long Term Population Based Study Thao P. Ho-Le*¹, Thach S. Tran², Jacqueline R. Center^{2,3}, John A. Eisman^{2,3,4}, Tuan V. Nguyen^{1,4,5,6}. ¹School of Biomedical Engineering, University of Technology, Sydney, Australia, ²Bone Biology Division, Garvan Institute of Medical Research, Australia, ³St Vincent Clinical School, UNSW Australia, Australia, ⁴School of Medicine, Notre Dame University, Australia, ⁵Bone Biology Division, lia, Australia, ⁶School of Public Health and Community Medicine, UNSW Australia, Australia

Aims: Osteoporosis frequently coexists with other chronic diseases. Multimorbidity is defined as the co-occurrence of two or more chronic diseases. The present study sought to define the pattern of multimorbidity and its impact on the risk of post-fracture mortality. **Methods:** This is a prospective, population-based study that involved 890 women and 244 men with a fracture. Health status of the individuals had been monitored for over 20 years. Osteoporosis was defined as femoral neck bone mineral density T-score ≤ -2.5 . Seven broad diseases were considered: osteoarthritis, cardiovascular disease, type II diabetes, cancer, rheumatoid arthritis, neurological illnesses, and mental illnesses. The diseases were self-report ascertained at baseline. A latent class analysis (LCA) was used to define the pattern of co-occurrence of diseases within an individual. The relationship between the LCA-derived clusters of diseases and post-fracture mortality was assessed by the Cox's proportional hazard model. **Results:** During the follow-up period (1989 to 2009), the mortality rate for men was 54%, approximately two-fold higher than that for women (30%). The prevalence of multimorbidity was 38% in women and 35% in men. Multimorbidity was associated with increased risk of post-fracture mortality (HR 2.4, 95%CI: 1.68-3.38). The LCA identified 3 clusters of patients: low multimorbidity group (68%), moderate multimorbidity group (20%), and high multimorbidity group (12%). The 5-year risk of post-fracture mortality among the high multimorbidity group was 45%, which was 1.64-fold higher than the moderate multimorbidity group, and 2.3-fold higher than the low multimorbidity group. The increased risk of death was mainly seen among individuals with cardiovascular disease (HR 1.6, 95%CI: 1.2-2.3), type II diabetes (HR 1.8, 95%CI: 1.0-3.2), rheumatoid arthritis (HR 1.8, 95%CI: 1.1-2.9) and neurological illnesses (HR 2.74, 95%CI: 1.2-6.3). The proportion of post-fracture mortality attributable to multimorbidity in women and men was 33% and 28%, respectively. **Conclusions:** These prospective data suggest that more than one-third of men and women with a fracture have multimorbidity, and that the coexistence of morbidities account for one-third of post-fracture mortality. The data emphasize the need for a wholistic management of patients with a fracture.



Disclosures: Thao P. Ho-Le, None

SUN-0770

Decreased Physical Health-Related Quality of Life – a Persisting State for Older Women Living with Clinical Vertebral Fracture Lisa Johansson*¹, Daniel Sundh¹, Hilda Svensson², Jon Karlsson³, Lars-Eric Olsson², Dan Mellstrom¹, Mattias Lorentzon¹. ¹Geriatric Medicine, Department of Internal Medicine and Clinical Nutrition, Institute of Medicine, University of Gothenburg, Gothenburg, Sweden, ²Institute of Health and Care Sciences/ Centre for Person-Centred Care (GPCC) Sahlgrenska academy Gothenburg university, Sweden, ³Sahlgrenska Academy, University of Gothenburg, Gothenburg, Sweden

Introduction: Vertebral fractures are often associated with back pain and reduced physical function, which might result in isolation and depression. As a result, women with vertebral fractures often have lower health-related quality of life (HRQoL), but during what time frame the decrease lingers is unclear. Therefore, the aim of this study was to investigate if clinical vertebral fracture was associated with lower HRQoL and to determine whether the association remained over time. **Methods:** Vertebral fracture assessment (VFA) was performed using dual-energy X-ray absorptiometry. Data regarding prior fractures, medications, medical history, and physical activity was collected using a questionnaire. Self-rated physical HRQoL was assessed using the 12-Item Short-Form Health Survey (SF-12). Women with clinical vertebral fractures were divided into tertiles according to time since fracture and their HRQoL was compared with non-fractured women. **Results:** In a population-based study of 3028 women aged 77.8 \pm 1.63 (mean \pm SD), a total of 130 (4.3%) women reported at least one clinical vertebral fracture. Women with a clinical vertebral fracture, divided into tertiles (T1-T3) depending on time since the fracture occurred, had lower physical HRQoL (T1: 36.3 \pm 10.8; T2: 41.0 \pm 9.94; and T3: 41.6 \pm 11.4) than women without fracture (46.2 \pm 10.6; $p<0.001$) (Figure 1A), whereas no differences were seen for mental HRQoL. Physical HRQoL in women with hip fracture showed a similar pattern (T1: 40.7 \pm 11.8; T2: 42.7 \pm 11.6; T3: 42.4 \pm 10.6) compared to women without fracture (46.2 \pm 10.6; $p=0.02$) (Figure 1B). Using linear regression analysis, clinical vertebral fracture was associated with reduced physical HRQoL for up to 18.9 years, independently of covariates (age, height, weight, smoking, prior stroke, mental HRQoL, and grip strength). **Conclusion:** Clinical vertebral fracture was associated with lower self-rated physical HRQoL, for up to 18.9 years after time of fracture independently of covariates. Our results indicate that clinical vertebral fracture affects physical HRQoL, with a persisting decline which resembles the reduction following hip fracture, indicating that vertebral fracture patients deserve the same attention and rehabilitation as hip fracture patients.

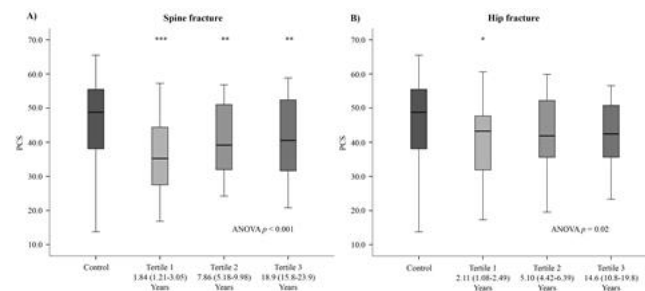


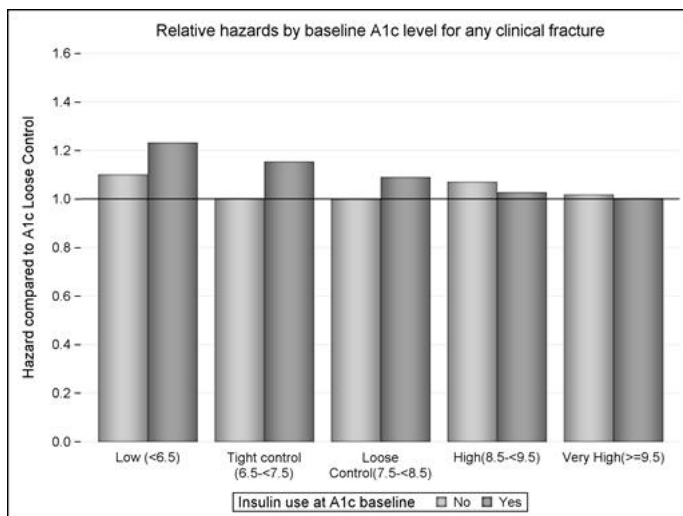
Figure 1 Physical component summary (PCS), obtained from the SF-12 questionnaire. Comparison between controls (without any fractures) and women with a clinical vertebral fracture (A) and hip fracture (B) according to tertiles of time since fracture. Differences were compared with ANOVA and following post hoc analysis were performed with least significant difference (LSD) and significance levels are presented as: * $p<0.05$, ** $p<0.01$, *** $p<0.001$.

Disclosures: Lisa Johansson, None

SUN-0771

Effect of hemoglobin A1c and treatment regimen on fracture risk among older men with diabetes mellitus Richard Lee^{*1}, Richard Sloane¹, Carl Pieper¹, Cathleen Colon-Emeric². ¹Duke University, United States, ²Durham VAMC, United States

Introduction: Type 2 diabetes mellitus among older men has been associated with increased bone mineral density, but paradoxically increased fracture risk. Prior studies have not examined the relative contribution of and interaction between treatment regimen and glycemic control. **Methods:** Retrospective study of male Veterans age ≥ 65 years who received primary care in the Veterans Health Administration (VHA) from 2000 to 2010, using administrative data from all 146 VHA medical centers, linked to Medicare fee-for-service data. Sample was limited to those with diagnosis of diabetes and baseline Hemoglobin A1c (HbA1c) value. Prescription data for diabetes medications were obtained from pharmacy database 1 year prior to baseline HbA1c value. Hazard ratios were calculated, using competing risk hazards models, adjusted for fracture risk factors including age, race/ethnicity, BMI, and medical comorbidities including alcohol and tobacco use, rheumatoid arthritis, corticosteroid use, cardiovascular disease, chronic kidney disease, and peripheral neuropathy. **Results:** During the study period, there were 900,402 males with a diagnosis of diabetes, of whom 652,901 (72.5%) had a baseline HbA1c value. After adjusting for fracture risk factors, the risk of any clinical fracture associated with HbA1c $< 6.5\%$ was 1.08 (95%CI: 1.06–1.11), compared to those with HbA1c of 7.5–8.5%. Fracture risk was not increased among those with A1c $\geq 8.5\%$, nor among those with A1c 6.5–7.5%. Independent of HbA1c level, use of insulin was associated with greater risk of fracture (HR 1.10, 95% CI: 1.07–1.12). There was significant interaction between insulin use and HbA1c level, ($P < 0.001$), such that those using insulin with HbA1c $< 6.5\%$ had HR 1.23 and those with HbA1c 6.5–7.5% had HR 1.15. Metformin use was associated with decreased fracture risk (HR 0.88, 95% CI: 0.87–0.90). **Conclusions:** Among older men with diabetes, those with HbA1c lower than 6.5% are at increased risk for clinical fracture. Insulin use is associated with higher fracture risk, especially among those with tight glycemic control. Our findings demonstrate the importance of the treatment regimen and avoiding hypoglycemia for fracture prevention in older men with diabetes.



Disclosures: Richard Lee, None

SUN-0772

Non-trauma rib fracture in the elderly: risk factors and mortality consequence Ha Mai^{*}, Thach Tran, Thuy Pham, Jacqueline Center, John Eisman, Tuan Nguyen. Garvan institute of medical research, Australia

Objectives: To define the epidemiology of rib fractures and the association between rib fracture and mortality in men and women aged 60 years and older. **Methods:** The study was part of the Dubbo Osteoporosis Epidemiology Study (DOES) which was designed as a population-based prospective study. The study consisted of 2,041 participants (1,132 women and 909 men) whose average age was ~ 70 years at baseline. The incidence of minimal trauma rib fractures was ascertained from X-ray reports and clinical details during the follow-up (1989–2016). Femoral neck bone mineral density (FNBMD) was measured by dual-energy X-ray absorptiometry (GE-LUNAR Prodigy). Data on anthropometry, clinical history and lifestyle were ascertained by a structured questionnaire at baseline and subsequent visits. The association between risk factor and rib fracture was analyzed by Cox's proportional hazards model, and population attributable risk was assessed to determine the contribution of risk factors to fracture. The time-dependent Cox's model was used to access the relationship between rib fracture and mortality. **Results:** Fifty nine men and 78 women sustained a rib fracture, making the cumulative incidence $\sim 7\%$. Each 5-year advancing age was associated with a 37% and 47% ($P < 0.001$) increase in the hazard of fracture in men and women, respectively. In addition, lower FNBMD was associated with increased risk of fracture in

men (HR 1.9; 95% CI, 1.4 to 2.6) and women (HR 2.1; 95% CI, 1.6 to 2.8). A prior fracture increased the risk of fracture by 8.5-fold (95%CI, 3.6 to 20.1) in men and 3.8-fold (95%CI, 1.5 to 9.6) in women. Approximately 45% and 50% of rib fractures in men and women, respectively, were attributable to advancing age and osteoporosis. Rib fracture was associated with an increased risk of death in the first 2.5 years post-fracture, after adjusting for age and co-morbidities. The risk of death was highest within the first 12 months (HR 7.75; 95%CI 2.7 to 22.5 in men and HR 4.9; 95%CI 2.0 to 11.8 in women). **Conclusions:** Advancing age, reduced bone mineral density, prior fall (in men) and prior fracture were risk factors for rib fracture, and rib fracture signaled an increased mortality risk.

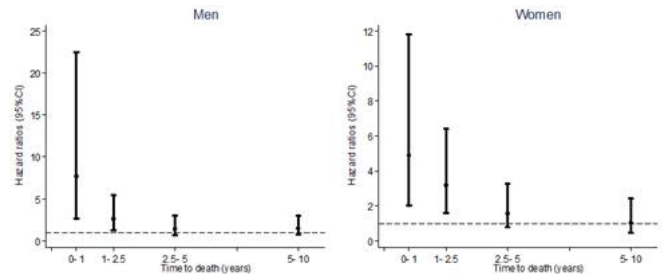


Figure 1: Hazard ratio of mortality associated with rib fracture by time, adjusted for age and co-morbidity in men (left panel) and women (right panel)

Disclosures: Ha Mai, None

SUN-0773

Is Type II Diabetes a Clinical Risk Factor for Atypical Femur Fractures? (The View from South Texas) Kenneth Mensch^{*1}, Roberto Fajardo², Todd Bredbenner³, Khang Dang¹, Rose Huynh¹, Sean Catlett¹, Mitchell Hymowitz¹, Patrick Ryan¹, Ventrice Shillingford-Cole¹, Sara Sprecher¹. ¹UT Health San Antonio, United States, ²University of Incarnate Word School of Osteopathic Medicine, United States, ³University of Colorado -Colorado Springs, United States

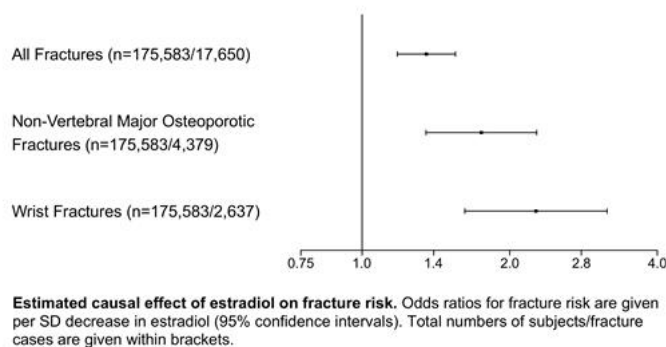
Although clinical guidelines report that bisphosphonate (BP) use and type 2 diabetes (T2D) are independent risk factors for atypical femur fractures (AFFs), there has been little evidence to support a relationship between T2D and atypical fractures. The objective of this study is to determine the relationship between T2D, as well as use of BPs, and AFFs in a clinical sample of femur fracture patients from South Texas, where the T2D prevalence is over 25% among elderly residents. **Methods:** We performed a retrospective analyses of University Hospital patients (aged 50–89) presenting with a closed femur fracture during 2007 - 2017. Trauma cases were excluded. Demographic data, fracture dates, bisphosphonate and glucocorticoid use, menopausal and diabetic status were recorded. Fracture type, cortical thickness, and AFF status were determined by two physicians using the ASBMR Task Force Case Definition. Matched case-control conditional logistic regressions were used to calculate odds ratios and 95% confidence intervals of risk factors for Subtrochanteric/Femoral Shaft (ST/FS) fractures matched to intertrochanteric fracture controls. A binary logistic regression was used to identify risk factors for typical and atypical ST/FS fractures. **Results:** The sample size equaled 236 subjects, 19.5% of the cases were ST/FS and 36.9% intertrochanteric fractures. In this sample, 43% of the subjects were diabetic and 10% had a history of bisphosphonate use. Seven AFFs were identified among the ST/FS cases; all cases were female. The prevalence of AFFs in the entire sample was 3.0% and 15.2% among all ST/FS fractures. Results indicate minor differences between ST/FS and matched intertrochanteric fractures. Diabetes trended strongly in the AFF group (71.4%) compared to the typical ST/FS fracture group (40.5%, $p=0.220$). BP use also trended higher among the AFF cases (42.9%) compared to typical ST/FS cases (8.1%, $p=0.146$). Cortical thickness trended higher in the ST/FS group ($p=0.064$) compared to the IT group but was similar in all ST/FS cases ($p=0.928$). **Discussion:** The prevalence of AFFs (3%) in our study was over two-fold greater than previously reported by Guisti et al. We also found strong trends in our results: all AFFs were female, and bisphosphonates and diabetes were independently associated with AFFs, although significant differences have not been observed yet. It is still unclear whether AFFs are associated with BP use or diabetes and merit further study.

Disclosures: Kenneth Mensch, None

SUN-0774

Evidence of a Causal Effect of Estradiol on Fracture Risk in Men Maria Nethander^{*1,2}, Liesbeth Vandenput¹, Anna Eriksson¹, Sara Windahl¹, Thomas Funck-Brentano¹, Claes Ohlsson¹. ¹Centre for Bone and Arthritis Research, Department of Internal Medicine and Clinical Nutrition, Institute of Medicine, Sahlgrenska Academy, University of Gothenburg, Sweden, ²Bioinformatics Core Facility, Sahlgrenska Academy, University of Gothenburg, Sweden

Observational association studies indicate that serum estradiol (E2) is more strongly associated with bone mineral density (BMD) than serum testosterone (T) while both E2 and T associate with fracture risk in men. The possible causal effect of E2 and/or T levels on fracture risk in men is unknown. It is possible that endocrine therapies for prostate cancer may have differential skeletal side-effects depending on whether they affect both E2 and T levels or only androgen receptor action. To evaluate the causal effect of E2 and T primarily on fracture risk but also on estimated BMD (eBMD) of the heel using ultrasound, a Mendelian Randomization (MR) approach was undertaken using individual-level data of genotypes, eBMD, fractures (n=17,650), and relevant covariates from 175,583 unrelated men (mean age 57 ± 7 years) of European origin. This research has been conducted using the UK Biobank Resource. The genetic instruments for serum E2 and T were taken from the most recent large scale GWAS meta-analyses on these hormones in men. MR analyses demonstrated a causal effect of serum E2 on eBMD and fracture risk. A 1 SD (or 9.6 pg/ml) genetically instrumented decrease in serum E2 was associated with a 0.38 SD decrease in eBMD (p-value 9.7 × 10⁻⁷⁴) and an increased risk of any fracture (OR 1.35, 95% CI, 1.18-1.55), non-vertebral major osteoporosis fractures (OR 1.75, 95% CI, 1.35-2.27) and wrist fractures (OR 2.27, 95% CI, 1.62-3.16) (see figure). These causal effects of serum E2 on fracture risk were robust in sensitivity analyses and remained unchanged in stratified analyses for age (divided by median age), BMI (overweight yes/no), eBMD (divided by median), smoking status (current smoking yes/no), and physical activity (vigorous activity yes/no). MR analyses revealed no evidence of a causal effect of T levels on fracture risk. In this study, we provide the first evidence of a robust causal effect of serum E2, but not T, on fracture risk in men. Our findings may have direct clinical implications for prostate cancer patients when comparing the possible skeletal side-effects of endocrine treatments affecting both E2 and T levels with those only modulating androgen receptor action.



Disclosures: **Maria Nethander, None**

SUN-0775

WITHDRAWN

SUN-0776

Mechanisms of Injury Associated with Non-Traumatic Vertebral Fractures in Older Adults Sara E. Rudolph^{*1}, Signe Caksa¹, Dennis E. Anderson^{2,3}, Mary L. Bouxsein^{1,2,3}. ¹Endocrine Unit, Massachusetts General Hospital, United States, ²Harvard Medical School, Boston, MA, United States, ³Center for Advanced Orthopedic Studies, Beth Israel Deaconess Medical Center, United States

Vertebral fractures (VF) contribute to morbidity and decreased quality of life in older adults. Few studies have examined the precipitating events leading to VF. To address this knowledge gap, we determined the mechanism of injury associated with clinical VF by sex and spinal region. We reviewed medical records of 65 men and 65 women aged ≥60 years diagnosed with a VF via radiology report in 2013-2017 at Partners HealthCare hospitals. VF involving pathologic vertebrae, transverse or posterior elements, spinal cord injury, or a history of spinal surgery with hardware were excluded. Data were extracted regarding mechanism of injury, medical/lifestyle history and region of VF: upper thoracic (T1-T5), mid-thoracic (T6-T10), thoracolumbar (T11-L1), or lumbar (L2-L5). Here we report on 159 events involving 228 VF by sex and region of VF. Fractures occurred most commonly in the thoracolumbar region (42.1%), followed by lumbar (27.0%), and upper and mid-thoracic (6.3% each). Men with VF were more likely to have a history of smoking (50.0% vs. 24.7%, p=0.005) and Parkinson's disease (6.8% vs. 0.0%) than women with VF, but lower prevalence of osteoporosis (14.9% vs 63.5%), chronic back pain (5.4% vs. 31.8%), and hy-

pothyroidism (6.8% vs. 20.0%) (p<0.05 for all). Multiple VF occurred in 28.9% of events, and concomitant injury in 20.1% of events. The mechanisms of injury were fall from standing height or less (34.6%), falls on steps or from greater than standing height (8.8%), other minimal trauma (4.4%), other severe trauma (5.0%), or unknown (47.2%). More men reported falls than women (52.7% vs. 35.3% of events, trending towards significance, p=0.08). Among reported falls, the direction of the fall was backwards (36.2%), sideways (7.2%), forwards (7.2%) or unknown (49.3%), and the site of fall impact was buttocks (24.6%), back (11.6%), head (8.7%), extremity (4.4%) or unknown (50.7%). Thoracolumbar VF were more likely to have occurred with a backwards fall (42.5%) and with impact on the back or buttocks (52.5%) compared to other regions. Consistent with prior reports, our results indicate that falls contribute to many VF. Falling backwards and impacting the buttocks may be an important mechanism of injury. However, the mechanisms of injury associated with VF remain unknown in about half of cases, warranting further investigation in prospective studies.

Disclosures: **Sara E. Rudolph, None**

SUN-0777

A Preliminary Study of the Association Between Bone Material Properties and Clinical Risk Factors for Fracture Pamela Rufus^{*1}, Kara L Holloway-Kew¹, Adolfo Diez-Perez², Mark A Kotowicz¹, Julie A Pasco¹. ¹Deakin University, Australia, ²Department of Internal Medicine, Hospital del Mar-IMIM, Autonomous University of Barcelona and CIBERFES, Instituto Carlos III., Spain

Purpose Impact microindentation is an emerging technique which measures bone material strength index (BMSi) in vivo. However, it is unclear how well the technique predicts bone fragility. The aim of this study was to evaluate the association between BMSi and clinical risk factors for fracture. Methods BMSi was measured using the OsteoProbe for the first 266 men (ages 33-92yr) assessed in the current phase of the Geelong Osteoporosis Study, a population-based cohort study in Australia. Associations between BMSi values and clinical risk factors from the FRAX were identified using Pearson's correlation for continuous variables and 2-sample t-tests for categorical variables. Risk factors included: BMD at the femoral neck, age, height, weight, prior fracture, parental hip fracture, smoking, alcohol consumption, glucocorticoid use, rheumatoid arthritis and secondary osteoporosis. Multiple regression models were used to determine whether identified differences in BMSi were independent of other factors. Results There were 26(9.9%) men with prior fracture, 31(11.7%) with parental hip fracture, 20(7.6%) smokers, 4(1.5%) glucocorticoids users, 7(2.7%) with rheumatoid arthritis, 3(1.1%) with secondary osteoporosis and 133(50%) alcohol consumers. Mean (±SD) for BMD, age, weight and height were 0.967±0.122g/cm², 63.7±12.5yr, 81.3±10.9kg and 174.3±6.8cm respectively. No correlations were detected between BMSi and BMD (r=0.001, p=0.99), age (r=-0.082, p=0.18), weight (r=-0.051, p=0.18) and height (r=0.083, p=0.18). Mean BMSi for men with and without risk factors were: prior fracture (80.5±5.5 vs 83.1±5.6, p=0.02); parental hip fracture (81.8±5.1 vs 83.0±5.7, p=0.25); smoking (83.7±5.5 vs 82.8±5.7, p=0.41); alcohol consumption (82.8±5.7 vs 82.9±5.7, p=0.95). The lower BMSi for men with prior fracture persisted after adjustment for BMD, age, weight and height (p=0.02). The numbers of glucocorticoid users, and those with rheumatoid arthritis or secondary osteoporosis were too small for further analyses. Conclusions With the exception of smoking, mean BMSi values were lower in the presence of risk factors; however, this difference was significant only for prior fracture. We acknowledge that small numbers may have limited our ability to detect differences in BMSi and further work is in progress. Taken together, these data support the notion that impact microindentation may be a useful technique for identifying men with bone fragility.

Disclosures: **Pamela Rufus, None**

SUN-0778

Urban-Rural Differences In Hip Fracture Mortality. A NOREPOS Study Siri Marie Solbakken^{*1}, Jeanette H. Magnus², Haakon E. Meyer^{1,3}, Anne Johanne Sogaard⁴, Grethe S. Tell^{5,6}, Nina Emaus⁷, Kristin Holvik⁴, Siri Forsmo⁸, Clara G. Gjesdal⁹, Berit Schei^{10,11}, Peter Vestergaard¹², Tone K. Omsland¹. ¹Department of Community Medicine and Global Health, Institute of Health and Society, University of Oslo, Norway, ²Section for Leadership, Faculty of Medicine, University of Oslo, Norway, ³Division of Mental and Physical Health, Norwegian Institute of Public Health, Norway, ⁴Division of Mental and Physical Health, Norwegian Institute of Public Health, Norway, ⁵Department of Global Public Health and Primary Care, University of Bergen, Norway, ⁶Division of Mental and Physical Health, Norwegian Institute of Public Health, Norway, ⁷Department of Health and Care Sciences, UiT The Arctic University of Norway, Norway, ⁸Department of Public Health and Nursing, NTNU, Norwegian University of Science and Technology, Norway, ⁹Department of Clinical Science, University of Bergen and Department of Rheumatology, Haukeland University Hospital, Norway, ¹⁰Department of Public Health and Nursing, Faculty of Medicine and Health Sciences, University of Science and Technology, Norway, ¹¹Department of Obstetrics and Gynaecology, St. Olav's hospital, Trondheim University Hospital, Norway, ¹²Department of Endocrinology, Aalborg University Hospital and Department of Clinical Medicine, Aalborg University, Denmark

Purpose: To study urban-rural differences in mortality 30 days and 1 year post hip fracture, and to explore whether possible differences were associated with level of education. **Methods:** The study was based on the NOREPOS hip fracture database (NORHip) using hip fractures sustained during 2002-2013. The first registered hip fracture was included in the study. Dates on death and emigration were obtained from the National Registry. Information on education and municipality of residence was obtained from the 2001 Population and Housing Census, Statistics Norway. The degree of urbanization was based on the proportion of inhabitants living in densely populated areas (rural: <1/3, semi-rural: 1/3-2/3 and urban: >2/3). Mortality in hip fracture patients living in urban and semi-rural municipalities was compared to mortality in patients living in rural municipalities using a negative binomial model. Analyses on 30-day mortality and 1-year mortality were adjusted for age, and analyses of 1-year mortality were additionally adjusted for education. In the current abstract we have chosen to focus on differences between rural and urban areas only. **Results:** In 27 748 male and 65 527 female hip fracture patients aged 50-100 years there was no statistically significant urban-rural difference in 30-day hip fracture mortality (incidence rate ratio (IRR) 1.00 (95% CI 0.84, 1.18) in men and 1.03 (95% CI 0.88, 1.22) in women). Among women, 1-year mortality was higher in hip fracture patients living in urban compared to rural municipalities (IRR 1.16 (95% CI 1.01, 1.32)), with similar results in men (IRR 1.15, (95% CI 0.98, 1.35)). Differences in 1-year mortality were even more pronounced when adjusting for education (IRR 1.24, (95% CI 1.05, 1.45) in men and 1.21 (95% CI 1.06, 1.37) in women). **Conclusions:** One-year post hip fracture mortality was 16% higher in women in urban compared to rural municipalities, and similar estimates were found in men. There were no significant differences in 30-day mortality, suggesting that the immediate post-fracture quality of healthcare does not differ substantially between urban and rural areas. On the other hand, the differences in 1-year mortality could possibly be explained by inequalities in follow-up health care services or by differences in general health status between urban and rural hip fracture patients, but this requires further investigations.

Disclosures: *Siri Marie Solbakken, None*

SUN-0779

Factors associated with delayed wound healing longer than 8 weeks after tooth extraction in Japanese patients >60 years of age Akira Taguchi^{*1}, Mikio Kamimura², Shigeharu Uchiyama³, Hiroyuki Kato⁴. ¹Department of Oral and Maxillofacial Radiology, School of Dentistry, Matsumoto Dental University, Japan, ²Center for Osteoporosis and Spinal Disorders, Kamimura Orthopedic Clinic, Japan, ³Department of Orthopedic Surgery, Okaya City Hospital, Japan, ⁴Department of Orthopedic Surgery, Shinshu University School of Medicine, Japan

Little is known about whether osteoporosis, use of antiresorptive medication, or duration before tooth extraction is a main risk factor for osteonecrosis of the jaw. We evaluated whether use of bisphosphonate (BP) and/or denosumab (Dmab), self-reported kyphosis, or duration before tooth extraction were associated with an incidence in delayed wound healing beyond 8 weeks after tooth extraction during the past year in Japanese men and women 60 years of age and older. Among the 586 patients who responded to the structured questionnaire survey, 426 patients (151 men and 275 women) aged 60-96 years participated in this study. Subjects who had waited >2 months for tooth extraction had a significantly higher risk of delayed wound healing compared with those whose tooth was extracted within 1 month (Odds ratio [OR] 7.23; 95% confidence interval [CI] 2.19-23.85). The presence of self-reported kyphosis was significantly associated with an increased risk of delayed wound healing (OR 5.08; 95%CI 1.11-23.32). BP and/or Dmab use was not significantly associated with delayed wound healing (p=0.17). A long waiting time before tooth extraction

and self-reported kyphosis but not use of antiresorptive medication may be risk factors for delayed wound healing beyond 8 weeks after extraction.

Disclosures: *Akira Taguchi, None*

SUN-0780

Prevalence of Morphometric Vertebral Fractures Does Not Differ in Patients With and Without Clinical Fractures in a Fracture Liaison Service Open Model Francisco Torres-Naranjo^{*1}, Alejandro Gaytán-González¹, Roberto González-Mendoza³, Noé Albino González-Gallegos⁴, Pilar De La Peña-Rodríguez⁵, Hugo Gutiérrez-Hermosillo⁶, Pedro García-Hernández⁷, Claudia Flores-Moreno⁷, Jorge Alberto Morales-Torres⁸, Juan López-Taylor⁹. ¹Centro de Investigación Ósea, Universidad de Guadalajara., Mexico, ³Instituto de Ciencias Aplicadas a la Actividad Física y del Deporte, Universidad de Guadalajara, Mexico, ⁴Departamento de Bienestar y Desarrollo Sustentable, Centro Universitario del Norte, Universidad de Guadalajara, Colotlán, Mexico, ⁵Servicios Médicos De la Peña, Mexico, ⁶Universidad de Guanajuato Hospital Aranda de la Parra, Mexico, ⁷Endocrinología/Centro de Osteoporosis, Hospital Universitario de Monterrey, Mexico, ⁸Hospital Aranda de la Parra y CMOVA, Mexico, ⁹Instituto de Ciencias Aplicadas a la Actividad Física y del Deporte, Mexico

Vertebral fractures are associated with a high risk of new vertebral and non-vertebral fractures and with increased morbidity and mortality. Fracture Liaison Service (FLS), as proposed by the International Osteoporosis Foundation (IOF), focuses in clinical vertebral and non-vertebral fractures as trigger for the search of radiographic vertebral fractures. Since vertebral fractures are generally asymptomatic and occur early in the course of the disease, the lack of a systematic approach for the early detection of morphometric vertebral fractures (MVF) in patients without clinical fractures can lead to a large number of patients with vertebral fractures being undiagnosed. **Purpose:** To compare the prevalence of MVF in patients with and without clinical fractures at a center with a FLS open model. **Methods:** From August to December of 2017, 126 Mexican patients aged 50 to 80 years visited our osteoporosis center, 35 patients with clinical fracture where evaluated according to the IOF Capture the Fracture Program Best Practice Framework, and 91 patients with low bone mineral density (BMD) and without clinical fracture were evaluated at primary prevention unit (PPU). For detection of vertebral fractures, a vertebral morphometry was performed in all patients utilizing the High Definition Instant Vertebral Assessment (Hologic) on images obtained from DXA scans. MVF were defined according to the Genant's semiquantitative method. For analysis, sample was stratified in decenniums. We compared the prevalence of MVF and BMD at three sites between groups using X2 and ANCOVA, respectively, both with a significant level of p<0.05. **Results:** The overall prevalence of MVF was of 46.8% (IC95% 38.0 - 55.6). For the FLS group we observed a prevalence of 51.4% (IC95% 34.0 - 68.9), and 45.1% (IC95% 34.7 - 55.5) for the PPU group. The prevalence per decennium was extended from 18.4% to 66.7% in both groups. No significant differences were observed in prevalence between groups (Table 1). There were significant differences in BMD between the patients with and without MVF. We observed significantly lower BMD at lumbar spine, total hip and femoral neck in patients with MVF. **Conclusions:** Prevalence of MVF were similar independently of presence or absence of clinical fracture at the moment of initial evaluation. Our findings suggest that evaluating for vertebral fracture is necessary in patients with low BMD with or without clinical fractures at the moment of initial evaluation.

Age		FLS		PPU		p
		n	%	n	%	
50-60	(n = 45)	7	28.6	38	18.4	0.28
60-70	(n = 53)	16	50.0	37	64.9	0.16
>70	(n = 28)	12	66.7	16	62.5	0.8
Total	(n = 126)	35	51.4	91	45.1	0.26

FLS= Fracture Liaison Service (patient with clinical fracture)

PPU= Primary Prevention Unit (patients without clinical fracture)

Disclosures: *Francisco Torres-Naranjo, None*

SUN-0781

Increase in Bone Mineral Density in Transwomen and Transmen During the First Ten Years of Gender-affirming Hormonal Treatment Chantal Wiepjes^{*}, Christel De Blok, Mariska Vlot, Paul Lips, Renate De Jongh, Martin Den Heijer. VU University Medical Center, Netherlands

Purpose: Concerns about the effects of gender-affirming hormonal treatment (HT) on BMD exist, particularly regarding the decrease in estrogen concentrations in transmen. HT in transgender people affects BMD on short term, but long-term follow-up studies are lacking. Therefore this study aimed to investigate the change in BMD during the first 10 years of HT in transwomen and transmen, in order to determine whether it is necessary to assess BMD during HT. **Methods:** A retrospective cohort study was performed in adult transgender

people receiving HT at the VU University Medical Center Amsterdam between 1998 and 2015. People were included for analyses if they were HT naïve and had a DXA scan at the start of HT. Follow-up DXA scans performed after 2, 5, or 10 years of HT were used for analyses. The change in Z-scores of the lumbar spine during the first 10 years of HT were analyzed using multilevel analyses. Furthermore, the influence of serum sex hormone concentrations during HT were analyzed. Results: 711 transwomen (median age 35 years, IQR 26-46 years) and 543 transmen (median age 25 years, IQR 21-34) were included for analyses. Prior to the start of HT, 22% of transwomen and 4% of transmen had a low BMD, defined as a Z-score below -2.0. In transwomen, mean baseline Z-score was -0.93 (SD±1.32), which increased with +0.22 (95%CI 0.12-0.32) after 10 years of HT. Transmen had a mean baseline Z-score of +0.01 (SD±1.14), which increased with +0.34 (95%CI 0.23-0.45) after 10 years of HT. In transwomen, higher estradiol concentrations were associated with a larger increase in Z-score, but LH and testosterone concentrations were not associated with a change in Z-score. In transmen, estradiol and testosterone concentrations were not associated with a change in Z-score, but lower LH concentrations were associated with a larger increase in Z-score. Conclusion: This study showed that HT does not have negative effects on BMD in transgender people, which indicates that regularly assessing BMD during HT does not seem necessary. However, as even prior to start of HT a high percentage of low BMD is found, especially in transwomen, evaluation of bone health prior to start of HT may be considered. Higher estradiol concentrations in transwomen and lower LH concentrations in transmen were associated with a larger increase in Z-score, which indicates that adequate hormone substitution and therapy compliance should be stimulated, particularly in those with low baseline Z-scores.

Disclosures: *Chantal Wiegjes, None*

SUN-0811

More Frequent and More Sustain Osteoporosis Treatment After Fragility Vertebral Fractures When Introduced Early in Inpatients Than Delayed in Outpatients: A Controlled Study Thierry Chevalley¹, Herve Spechbach², Isabelle Fabreguet¹, Emilie Saule¹, Magaly Hars¹, Jerome Stirnemann³, Serge Ferrari¹, Rene Rizzoli¹. ¹Division of Bone Diseases, University Hospitals and Faculty of Medicine, Switzerland, ²Division of General Internal Medicine, University Hospitals and Faculty of Medicine, Switzerland, ³Division of General Internal Medicine, University Hospitals of Geneva and Faculty of Medicine, Switzerland

Objective: After a fragility fracture, fracture liaison service (FLS) allow the identification of patients at risk and secondary prevention of fragility fracture. In general, osteoporosis treatment appears more frequent and more adequate when introduced in the hospital phase of FLS than upon recommendation to primary care physician (PCP). Whether this is true regarding prevalent vertebral fractures detected on routine X-rays during hospitalization in general internal medicine for other causes however remains unknown. We tested whether in-hospital management of patients with newly identified vertebral fractures leads to a higher percentage of patients with osteoporosis medication at 3 and 6 months than delayed management by PCP in outpatients. Methods: In-hospital patients over 60 years systematically searched for vertebral fractures by semi-quantitative visual grading on lateral chest and/or spinal radiographs were included either in phase 1 (outpatients care - recommendations to PCP on assessments and osteoporosis medications to be prescribed) or phase 2 (inpatients care - assessments and osteoporosis medication initiated in hospital). The percentage of patients under specific osteoporosis treatment was evaluated by telephone-interview at 3 and 6 months. Results: Patients included as outpatients (84 with fracture out of 407 assessed, 21%; 75.7±7.7 years) and as inpatients (100/524, 19%; 77.8±9.4 years) were similar for gender, mean age, prevalence of vertebral fractures of grade 1 or grade 2 and more, prevalence of prior fractures as well as for FRAX scores and Charlson comorbidity index. A specific osteoporosis medication was more often prescribed in inpatients than in outpatients at 3 (67 vs 19%, p<0.001) and 6 months (69 vs 27%, p<0.001). Percentage of patients still under treatment was higher in inpatients than in outpatients at 3 (52 vs 19%, p<0.001) and 6 months (54 vs 22%, p<0.001). Similar results were observed in patients with grade ≥ 2 vertebral fracture only. Length of stay and destination after discharge were not different between both groups. Conclusion: This controlled study highlights that, in a FLS, early patient assessment and osteoporosis treatment initiation during hospital stay rather than delayed management in outpatients, is a more efficacious strategy of secondary fracture prevention for oldest olds with newly detected vertebral fragility fractures, and that without difference in length of stay.

Disclosures: *Thierry Chevalley, None*

SUN-0812

Self-reported fracture history compared to fracture codes from an electronic health record dataset Maria I. Danila¹, Amy Mudano¹, Elizabeth Rahn¹, Andrea Lacroix², Jeffrey Curtis¹, Kenneth Saag¹. ¹University of Alabama at Birmingham, United States, ²University of California, San Diego, United States

Purpose: Self-reported fracture (fx) history data is frequently used in epidemiological studies of osteoporosis. Self-reported fx data may differ from fx history coded in electronic health records (EHR) due to imperfect patient recall, incomplete communication with clinicians, or lack of a universal EHR. Because both self-reported fx history and EHR data can define phenotypes for clinical research studies, it is important to understand how these 2 data

sources compare. Our objective was to compare self-reported fx history using survey data with fx codes from an available EHR dataset. Methods: Self-reported fx data was derived from the Activating Patients at Risk for Osteoporosis (APROPOS) trial, which recruited participants from the Global Longitudinal study of Osteoporosis in Women (GLOW) cohort. Prior fx data was collected using a survey deployed June - August 2015. Women were asked if they ever had a fx and for each fx type the date of the most recent one. Data on fx recorded in the EHR September 2011 - June 2015 was obtained from Kaiser Permanente Washington Health Research Institute. We excluded skull, toes and fingers fxs. We defined concordance between the EHR and self-reported data if the location of fx was reported to be the same and if the reported dates were within 1 year of each other. Kappa (κ) statistic described the concordance between the 2 sources of fx history. Descriptive statistics evaluated potential factors associated with discordance between the self-reported and EHR-coded fx history. Results: A total of 133 fxs from 360 women (91% white, mean[SD] age 74.5(7.5) years, 82% had some college education) were included. There were 35 fxs reported on the survey but not in the EHR and 39 fxs coded in the EHR but not in the survey. Agreement between self-reported and EHR fxs was κ=0.48. Of the discordant fxs, we were more likely to find claims for fxs in EHR referent to self-report among whites (OR=5.5, 95%CI 1.1-27.9), for major osteoporotic fxs (OR=2.8, 95%CI 1.1-7.1), and for fragility fxs that typically require hospitalization (vertebral, hip, femur, pelvis) (OR=3.8, 95%CI 1.3-10.7). Discordance between EHR codes and self-reported fxs did not vary by age, formal education, or health literacy. Conclusion: There was only modest correlation between self-reported fx history and EHR fx codes. This discrepancy may have implications for clinical and epidemiological studies of fxs suggesting that combining both types of data may be optimal.

Disclosures: *Maria I. Danila, None*

SUN-0813

Radiological Validation of Fracture Definitions from Administrative Data: The Manitoba Bone Mineral Density Database Riley Epp^{*}, Mashael Alhribi, Linda Ward, William Leslie. University of Manitoba, Canada

BACKGROUND: Health care services / administrative data used for studying the epidemiology of osteoporosis-related fractures typically rely on fracture ascertainment from hospitalization and medical claims diagnoses. Fracture definitions used for national surveillance by the Public Health Agency of Canada (PHAC) show sex- and age-specific fracture rates in Manitoba comparable to radiologically confirmed fractures in a national population-based cohort but have not been directly validated against x-rays. PURPOSE: To determine the level of agreement between fractures ascertained from administrative data and radiological imaging. METHODS: We selected all patients in the Manitoba Bone Mineral Density Database (MBMDD) with a Winnipeg postal code who underwent bone mineral density (BMD) testing March 1- 31, 2016. This population was enriched with fractures by including patients undergoing BMD testing January 1- February 28, 2016, who were coded as having a prior fracture in the BMD report. For each patient we reviewed all relevant imaging and reports on province-wide Picture Archiving and Communication System (PACS) for the presence and date of fractures affecting the hip, vertebrae, forearm or humerus preceding the BMD test. We restricted analysis to fractures that occurred since 2011, the year PACS was expanded to include images and reports for all imaging modalities. We excluded fractures that were not reported, and where x-ray review and the BMD report for fracture were inconsistent. These radiologically confirmed fractures were then compared with fractures in the prior 5 years as determined from administrative data using the PHAC case definitions. Negative predictive values (NPV) and positive predictive values (PPV) were calculated overall and for each fracture site. RESULTS: The final study population included 480 patients, 148 with a radiologically confirmed fracture in the last 5 years. For any fracture, administrative case definitions gave PPV of 94.6% and NPV of 88.9% (see TABLE). PPV and NPV were high for non-vertebral fractures (range 88.2 to 100.0%, 98.5 to 100.0%, respectively), but were slightly lower for vertebral fracture (81.8% and 96.4%, respectively). CONCLUSIONS: Administrative case definitions from fracture ascertainment show acceptably high PPV and NPV for identifying radiologically-confirmed fracture of the hip, forearm, humerus and vertebrae supporting their role in epidemiological research and surveillance.

TABLE: Positive and negative predictive values (PPV and NPV) for radiological confirmation of fracture from administrative data.

	Number of fractures	PPV*	NPV**
Hip fracture	23	100.0%	100.0%
Vertebral fracture	42	81.8%	99.4%
Forearm fracture	74	90.0%	99.4%
Humerus fracture	22	88.2%	99.2%
Any of the above	148	94.6%	95.6%

* Jan 1- Mar 31, 2016. ** Mar 1 - Mar 31 2016.

Disclosures: *Riley Epp, None*

SUN-0814

Defining Alendronate Drug Holidays and Re-initiation in US Medicare Data Ayesha Jaleel^{1*}, Jeffrey Curtis², Rui Chen², Huifeng Yun², Tarun Arora², Suzanne Cadarette³, Nicole Wright², Amy Mudano², Phillip Foster², Kenneth Saag². ¹Brookwood Baptist Hospital, United States, ²University of Alabama at Birmingham, United States, ³University of Toronto, Canada

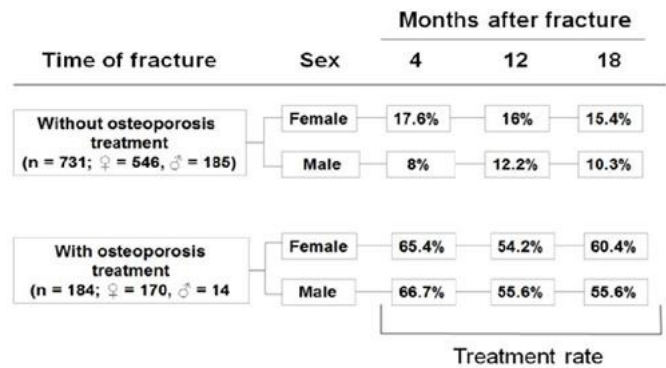
Introduction: Given alendronate's (ALN) prolonged skeletal retention and emerging safety concerns, the ASBMR task force recommended consideration of a "drug holiday" after 5 years of use. Distinguishing a prolonged gap in intended treatment vs. an intentional drug holiday is often unclear. We sought to estimate the prevalence of potential ALN holidays using two definitions of drug discontinuation, and to evaluate the characteristics of those who restart osteoporosis (OP) therapy after an ALN treatment gap. **Methods:** We included only women ALN users (n = 81,287) with a treatment gap in the 2006-2015 US Medicare data, with medical and pharmacy coverage (Medicare parts A, B, and D), and who were at least 80% adherent (MPR) with ALN for ≥ 3 years prior to the gap. We excluded patients with history of cancer, Pagets, Osteogenesis Imperfecta, or systemic hormone therapy. We evaluated the proportion of women with a treatment gap (no prescription claims) for ≥ 6 months and/or ≥ 1 year at which time follow-up began (day 184 and day 366) (index date) until restarting of any OP medication (study end). We used descriptive statistics to characterize women restarting vs. not restarting therapy after a gap of >1 year. **Result:** Using the 6-month gap definition, we identified 35,239 women (43.3% of previously adherent long-term ALN users) who discontinued ALN, of which 6172 (17.5%) restarted on any OP therapy. The median time to restart was 162 days (58, 413.5; 25th and 75th percentile). Half (50%) of the women restarted therapy within a year of stopping, suggesting that a 6-month gap may not truly represent an intended drug holiday. Using a ≥ 1 year gap definition, we identified 27,436 (33.8%) women with a possible drug holiday, of which 2978 (10.9%) restarted OP therapy. The median time to restart was 259 days (92, 512; 25th and 75th percentile). Using the ≥ 1 year definition, restarters and non-restarters differed significantly (p < 0.001) by fracture history (6.9% vs 5.1%), history of previous DXA (21.6% vs. 15.0%), and ≥ 1 rheumatologist or endocrinologist visit (13.8% vs. 8.6%). **Conclusion:** Given the large proportion of rapid restarters, a drug holiday gap of only 6-months may not accurately reflect a true drug holiday; a minimum of a 1-year gap appeared more appropriate for defining a likely drug holiday. Increased OP care and history of fractures were associated with OP therapy restart.

Disclosures: Ayesha Jaleel, None

SUN-0815

TREATMENT GAP AFTER FRACTURE IN OSTEOPOROSIS PATIENTS – RESULTS OF THE AUSTRIAN ARM OF THE INTERNATIONAL COSTS AND UTILITIES RELATED TO OSTEOPOROTIC FRACTURES STUDY (ICUROS) Oliver Malle*, Hans Peter Dimai. Medical University of Graz, Dpt. of Internal Medicine, Div. of Endocrinology and Diabetology, Austria

Objective Despite availability of effective treatment options proven to prevent osteoporotic fractures, a huge gap in osteoporosis treatment exists. Reasons for this gap include underdiagnosis of osteoporosis, lack of adequate patient management, and concerns of adverse events. The aim of the present study was to evaluate the treatment rate after osteoporotic fracture in Austria, one of the 25 wealthiest countries worldwide by measure of gross domestic product at purchasing power parity (PPP) per capita. **Material and Methods** The ICUROS is a prospective observational study aimed to describe costs and Quality of Life (QoL) consequences of osteoporotic fractures. An amendment to the protocol of the Austrian arm of the ICUROS aimed at assessing the treatment rate after fracture without a concomitant awareness program, thus providing data from the "real world". Patients who had sustained a major osteoporotic fracture were interviewed at the time of the index fracture, and 4, 12, and 18 months thereafter. **Results** A total of 915 patients with a recent fracture were recruited at 8 different trauma centers throughout Austria. 78.3% of these patients were female. Mean age at the time of fracture was 75.5 + 10.2 yrs. Female and male patients were stratified into 2 groups, depending on whether she or he received an osteoporosis treatment at the time of fracture or not (Fig.). At the time of fracture, some 20% of the patients were receiving anti-osteoporotic treatment. In this group, follow-up analysis after 4, 12 and 18 months revealed a treatment rate of 65%, 54% and 60%, respectively, in female patients. Comparable results were detected in male patients. The treatment rate in the female group without osteoporosis medication at the time of the fracture was 18%, 16%, and 15%, after 4, 12, and 18 months, respectively, and the treatment rate in the respective male group was 8%, 12%, and 10%. Among the different fracture types, no significant differences were found in the treatment rate. **Conclusion** Only 1 in 10 men, and less than 2 in 10 women who do not receive an osteoporosis treatment at the time of fracture is prescribed an adequate osteoporosis treatment in Austria. Even worse, roughly every second patient who receives an osteoporosis treatment at the time of fracture will be deprived of his/her treatment after the fracture.

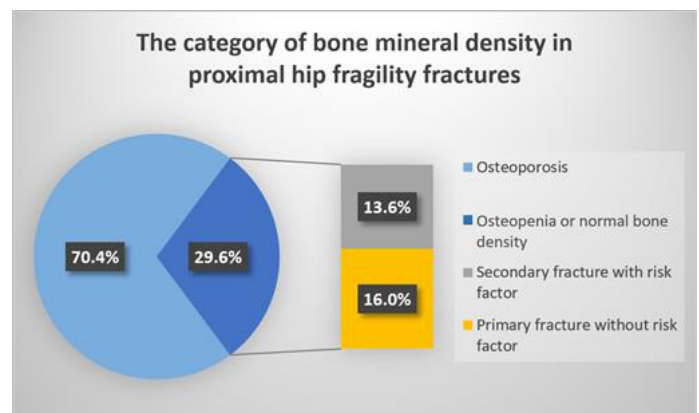


Disclosures: Oliver Malle, None

SUN-0816

The category of non-osteoporotic bone mineral density in proximal hip fragility fracture cases: Preliminary data from a tertiary care hospital Hyun Uk Moon*, Yong Jun Choi¹, Jung-Taek Kim², Ye-Yeon Won², Yoon-Sok Chung¹. ¹Department of Endocrinology and Metabolism, Ajou University School of Medicine, Suwon, South Korea, Republic of Korea, ²Department of Orthopedic Surgery, Ajou University School of Medicine, Suwon, South Korea, Republic of Korea

There is a discrepancy between low bone mineral density (BMD) and fracture risk, as many fractures are observed in elderly people who are not in the osteoporotic range. We investigated the proportion of the non-osteoporotic patients among the patients with proximal femur fracture aged over 50 and their risk factors for fragility fracture. A total of 81 fragility hip-fracture (neck or trochanter) patients (mean age of 75.3) were included (72.8% female) in this prospective real-world setting study. Consultations and BMD measurements (GE Lunar DXA) were performed with collaboration among responsible departments including Endocrinology and Orthopedics in a tertiary care academic hospital (Ajou University Hospital) in South Korea, from April 27th, 2017 to March 14th, 2018. From all the fracture cases, the percentages of osteoporosis and normal or osteopenia were 70.4% (n=57) and 29.6% (n=24), respectively. Analyzing the normal or osteopenia group, 54.2% (n=13) had no specific risk factors. Some of them had been exposed to only chronic heavy alcohol intake. Specific risk factors involved in non-osteoporotic group were suspected in 11 subjects as bone metastasis (n=3), previous osteoporotic fracture (n=4), chronic renal failure (n=3), liver cirrhosis (n=1), glucocorticoids exposure (n=1), rheumatoid arthritis (n=1). Two subjects had two risk factors concomitantly. Subsequently, we assessed the ten-year fracture risk for each normal or osteopenia subject using FRAX scoring system. The mean (range) risk of ten-year major osteoporotic fracture was 6.4% (2.9%~18%), and that of ten-year hip fracture was 2.6% (0.3%~6.3%). These FRAX scores were below the general guideline of intervention threshold. Although osteoporosis was still the dominant category in hip fracture patients, normal or osteopenia in BMD also accounted for considerable proportion of hip fractures in this study. In addition, even osteopenia patients without known risk factors were not free from hip fracture risk. The study emphasizes that we need more attention to patients with normal or osteopenic BMD but no osteoporosis to prevent fractures.



Disclosures: Hyun Uk Moon, None

SUN-0817

Improving Access to Osteoporosis Specialists through Electronic Consultations Christopher Tran*, Krista Rostom, Clare Liddy, Erin Keely. University of Ottawa, Canada

Purpose: Ensuring timely access to specialist care in Canada remains challenging. Electronic consultations (eConsults) can help address long wait times by allowing primary care providers (PCPs) to access specialist advice in lieu of face-to-face office visits. The purpose of this study is to describe the impact of eConsult advice provided by osteoporosis specialists. **Methods:** We performed a cross-sectional study of osteoporosis-related eConsults submitted to endocrinologists and rheumatologists between April 2011 and January 2015. Each eConsult was coded according to clinical topic and question type through consensus between two authors. eConsult usage data and PCP survey responses were analyzed to determine response times, PCP practice behavior, and referral outcomes. **Results:** A total of 74 PCPs submitted 119 osteoporosis-related eConsults during the study period. Osteoporosis cases comprised of 22% and 15% of all eConsults submitted to rheumatology and endocrinology, respectively. Patients were mainly female (86%). Median age was 70.4 years. Fragility fractures were present in 38 (32%) of cases; 20 of these were vertebral fractures. Median response time was 0.8 days, with 75% of responses occurring within 3 days. More than half of PCPs received a new or additional course of action as a result of an eConsult. A face-to-face referral was avoided in 67% of cases where the PCP initially contemplated requesting a referral. Among the 85 eConsults pertaining to pharmacotherapy, common questions included when to start therapy (24%), how to coordinate a drug holiday (14%), drug of choice (14%) and side effects (13%). Other eConsults included 9 cases on how to define a fragility fracture and 8 cases on how to interpret a bone mineral density report. **Conclusion:** The clinical content of osteoporosis-related eConsults is comparable to face-to-face referrals. By providing timely, practice-changing advice while avoiding unnecessary face-to-face office visits, eConsults can improve access to osteoporosis specialists.

Disclosures: Christopher Tran, None

SUN-0836

Three months of vitamin D3 supplementation, 2,800 IU/d, improves trabecular bone microarchitecture and bone strength in vitamin D insufficient, hyperparathyroid women – a randomized placebo controlled trial Lise Sofie Bislev*, Lene Langagergaard Roedbro¹, Lars Rolighed², Tanja Sikjaer¹, Lars Rejnmark¹. ¹Department of Endocrinology and Internal Medicine, Denmark, ²Department of Surgery, Denmark

Introduction: Vitamin D supplementation has historically been associated with improved bone health, but lately, the role of vitamin D without calcium supplementation has been questioned. **Methods:** In a double-blinded placebo controlled randomized trial, we aimed to investigate the effect of vitamin D3 supplementation (2800 IU/d vs. placebo) for three months during wintertime in 81 healthy postmenopausal women with low 25(OH)D (<20 ng/mL) and high PTH levels. We assessed bone health by bone turnover markers, DXA (spine L1-L4, hip, forearm, and total body), HRpQCT (tibia and radius) and QCT (spine L1-L2 and hip) scans. **Results:** Median age was 65 (range 60-76) years. Baseline levels of p-25(OH)D was 13±3.7 ng/mL and p-PTH 58.4±13.5 ng/mL. None used daily supplements with calcium and/or vitamin D. The median estimated dietary calcium intake was 800 mg and 22% have had fractured during adulthood. Compared with placebo, vitamin D3 supplementation increased levels of 25(OH)D and 1,25(OH)2D by 230% (95% CI: 189% to 272%, p<0.0001) and 58% (95% CI: 190% to 271%, p<0.0001) respectively. PTH was reduced by 17% (-23% to -11%, p<0.0001). Vitamin D3 supplementation had no effect on bone turnover markers, except from borderline (p=0.07) increased osteocalcin levels. Nor were there any effect on aBMD at any site measured by DXA. HRpQCT showed no changes in radius, but in tibia, vitamin D3 increased trabecular number (1.2% vs -0.2%, p=0.04), trabecular thickness (1.8% vs -3.2%, p<0.01) and reduced trabecular separation (0.0% vs -0.1%, p=0.05) compared with placebo. Finite element analysis revealed a highly significant improvement in bone strength in the vitamin D3 group compared with placebo, assessed by failure load (1.0% vs -1.4%, p=0.001) and stiffness (1.3 vs. -1.7%, p=0.002). Trabecular vBMD measured by QCT increased in the trochanter region (0.4% vs -0.6%, p=0.02) and tended to increase vBMD at the total hip (p=0.10) and femoral neck (p=0.07). Changes in 25(OH)D correlated with failure load (r=0.33, p=0.01), stiffness (r=0.20, p=0.07) and tended to correlate with trabecular thickness (r=0.30, p=0.07) in tibia, whereas changes in PTH did not correlate with any of the stated measurements. **Conclusion:** Compared with placebo, three months of treatment with vitamin D3, 2,800 IU/d improved trabecular microarchitecture and bone strength without affecting BMD. Our data suggest beneficial bone effects of improving vitamin D status in postmenopausal women with low 25(OH)D levels.

Disclosures: Lise Sofie Bislev, None

SUN-0837

Trunk Muscle Endurance in Women with Osteoporotic Vertebral Fractures: an Exploratory Analysis from a Pilot Randomized Controlled Trial Caitlin Mearthur*^{1,2}, Jenna C. Gibbs³, Jonathan Adachi¹, Maureen C. Ashe⁴, Robert Bleakney⁵, Angela M. Cheung⁵, Keith D. Hill⁶, David L. Kendler⁴, Aliyah Khan¹, Sandra Kim⁷, Judi Laprade⁵, Nicole Mittman⁵, Alexandra Papaioannou^{1,2}, Sadhana Prasad⁸, Samuel C. Scherer⁹, Lehana Thabane¹, John D. Wark¹⁰, Lora Giangregorio³. ¹McMaster University, Canada, ²GERAS Centre for Aging Research, Canada, ³University of Waterloo, Canada, ⁴University of British Columbia, Canada, ⁵University of Toronto, Canada, ⁶Curtin University, Australia, ⁷Women's College Hospital, Canada, ⁸Centre for Bone Health, Canada, ⁹Northern Health, Australia, ¹⁰University of Melbourne, Australia

Purpose: To explore (1) the relationships between trunk muscle endurance, balance, and falls self-efficacy for woman with vertebral fractures, and (2) the effect of a 1-year home exercise program on trunk muscle endurance. **Methods:** This is an exploratory, secondary analysis of a pilot randomized controlled trial of a 1-year home exercise program including strength, balance, aerobic and postural exercises compared with equal attention control. Trunk muscle endurance was assessed with the Timed Loaded Standing (TLS) test, standing balance with the Balance Outcome Measure for Elder Rehabilitation (BOOMER), and falls self-efficacy with the Falls Efficacy Scale International (FES-I). The associations between TLS, balance and falls self-efficacy were tested via linear regression models adjusted for age, pain with movement, and occiput to wall distance. The models for the BOOMER and FES-I were also adjusted for the FES-I total score, and the models for the FES-I were adjusted for the BOOMER total score. Linear models were constructed for the total score of the BOOMER and FES-I, and for each of the components of both tests. Associations with p < 0.05 were considered statistically significant. Differences in mean change of TLS from baseline were compared between groups using general linear models adjusted for baseline measures (analysis of covariance). **Results:** Thirty-one women, with a mean age of 75.5 years (standard deviation (SD) 6.9), an average of 3.0 (SD 2.1) vertebral fractures, and a mean history of 0.6 falls (SD 1.3) in the previous year were included in the analyses. The mean baseline TLS holding time was 85.6 seconds (SD 39.8) for the intervention group (n=17), and 84.3 (SD 41.2) for the control group (n=14). Trunk muscle endurance was associated with better balance performance, specifically static standing with eyes closed (parameter=0.005, standard error (SE)=0.003, p=0.02), and with reported self-efficacy of the ability to get out of a chair without falling (parameter=0.005, SE 0.002, p=0.04). There was no improvement in trunk muscle endurance at 12 months for women who participated in the home exercise program as compared with the control group (mean between group difference -0.5, 95% CI -24.3 to 23.3, p=0.96). **Conclusions:** Our study contributes to the growing literature surrounding trunk muscle endurance for people with osteoporosis, and suggests a positive relationship between standing balance, falls self-efficacy, and trunk muscle endurance.

Disclosures: Caitlin Mearthur, None

SUN-0838

Different Association of Dietary Fat Intake with Femoral Neck Strength According to Gender in Korean Population (KNHANES 2008-2010) Hyeonmok Kim*, Sun Hee Beom, Tae Ho Kim. Seoul Medical Center, Republic of Korea

Introduction: Despite the general belief that higher fat intake may be harmful for bone homeostasis, its associations with human bone health, mainly focused on bone mass, have been inconsistent. Furthermore, the role of dietary fat intake in bone strength, which can predict fracture risk independently of bone mineral density (BMD), has not been thoroughly studied. We here investigated the association between dietary fat intake and composite indices of femoral neck (FN) strength reflecting the risk of hip fracture. **Methods:** This population-based cross-sectional study examined data from Korea National Health and Nutrition Examination Surveys. After serial selection of subjects according to the exclusion criteria, 2595 subjects were included in our analysis. Usual dietary intake and bone mineral density (BMD) was assessed, and composite indices of FN strength, such as compression strength index (CSI), bending strength index (BSI), and impact strength index (ISI) were calculated. **Results:** After adjustment for confounders, daily fat intake (%) meaning fat energy intake divided by total energy intake negatively correlated with CSI and ISI in men (P = 0.010 and 0.046, respectively), but not in women. For further analysis, we categorized our participants into quintiles according to daily fat intake (%). In men, compared with subjects in the lowest fat intake quintile, those in the third, fourth and highest quintiles had significantly lower FN BMD, CSI and ISI values (P = 0.003 – 0.026), except for CSI in the highest quintile. In contrast to men, CSI and ISI values were significantly lower in women in lowest and highest quintile both than in those in the third quintile group (P = 0.005 – 0.044). We additionally divided our participants into three groups [<15% (low), 15% to 25% (appropriate), <25% (high)] according to recommended dietary reference intake of fat for Korean population. After adjustment for confounding variables, men with low fat intake group had higher ISI, and women with appropriate fat intake group was associated with higher all composite indices of FN strength. **Conclusion:** These results demonstrate that the effect of dietary fat intake on FN strength may be different according to gender, therefore appropriate amount of fat intake may be assessed based on gender, at least in bone health.

Disclosures: Hyeonmok Kim, None

SUN-0839

Prevalence of Vitamin D Deficiency in Postmenopausal Fracture Patient Ji Wan Kim^{*1}, Jun Sung Lee², Kwang Hwan Jung³, Jai Hyung Park⁴, Hyun Chul Shon⁵, Jae Suk Chang¹. ¹Asan Medical Center, Republic of Korea, ²Haeundae Paik Hospital, Republic of Korea, ³Ulsan University Hospital, Republic of Korea, ⁴Kangbuk Samsung Hospital, Republic of Korea, ⁵Chungbuk National University Hospital, Republic of Korea

Objective: The goal of this study was to investigate prevalence of vitamin D deficiency in post-menopausal women with fracture and to determine if there is any association between injury mechanism and serum vitamin D level. **Methods:** This study is a retrospective cohort study. The medical records of patients who presented with a fracture from March 2010 to October 2017 were retrospectively obtained. Inclusion criteria were following: 1) long bone fracture or pelvis fracture, 2) post-menopausal women aged 50years or older, 3) patients who had data of serum vitamin D level. Exclusion criteria were 1) pathologic fracture, 2) metabolic bone disease like Paget's disease, hyperparathyroidism, 3) isolated hand and foot fracture. One hundred and thirty-six patients were enrolled, and divided two groups according to injury mechanism; low-energy (107 patients) and high energy (29 patients). Serum vitamin D levels, bone turnover markers including serum osteocalcin, PTH, C-telopeptide and calcium, phosphorus, alkaline phosphatase, albumin, body mass index, bone mineral density, history of previous osteoporosis medications, vitamin D supplement and postoperative prescription rate were compared between two groups. **Results:** The rate of Vitamin D deficiency was 62%, and the rate of insufficiency was 14%, while only 24% of patient showed normal. The average level of Vitamin D level was 24.1ng/ml in low-energy group, and 21.1ng/ml in high energy group, respectively (p=0.889). The rate of Vitamin D deficiency rate was 61% and 66% in low-energy and high energy group (p=0.673). There was no difference in age between low and high energy groups. No seasonal variation of Vitamin D deficiency rate was observed. BMI, serum Ca, P, PTH, Osteocalcin, C-telopeptide, ALP, albumin were similar between two groups. BMD was evaluated in 85% of low energy group, and 77% of high energy group (p=0.441). The rate of osteoporosis (≤ -2.5 of T-score) was higher in low energy group (62.6% vs 37.5%, p=0.024). BMD in spine and femoral neck were similar between two groups (p=0.368, p=0.067), but BMD in total femur was lower in low-energy group (p=0.005). Postoperative Ca and Vitamin D supplement was taken in 91% of low energy injury and 59% of high energy injury (p = 0.003). Osteoporosis medication was prescribed more frequently in low energy group (74% vs 48%, p=0.009). In both groups, the prescription rate of calcium & Vitamin D supplement and osteoporosis medication was increased after fracture. **Conclusion:** Post-menopausal women with fracture have high incidence of Vitamin D deficiency in both high and low-energy injury group. Therefore physician should pay attention to Vitamin D deficiency in high energy injury group, as well as low energy group.

Disclosures: Ji Wan Kim, None

SUN-0840

Prevalence of Hypovitaminosis D in Patients from a Private Hospital in Leon, Mexico Jorge L A Morales Torres^{*1,2}, Hugo Gutierrez-Hermosillo³, Gilberto Aguilar-Orozco⁴, Jaime Romero-Ibarra², Enrique Diaz De Leon-Gonzalez⁴, Francisco Torres-Naranjo⁵. ¹Hospital Aranda de la Parra, Mexico, ²Morales Vargas Centro de Investigacion, Mexico, ³Medicina y Nutricion, Universidad de Guanajuato, Mexico, ⁴Instituto Mexicano del Seguro Social, Mexico, ⁵Centro de Investigacion Osea, U. de Guadalajara, Mexico

Hypovitaminosis D is extremely common worldwide. There is limited information in Latin America, but existing reports suggest a high prevalence linked to important health impacts. Attempts to improve our knowledge on hypovitaminosis D may come from many sources. **Objective:** To establish the frequency of Vitamin D deficiency and insufficiency in patients studied in a private hospital in Leon, Mexico. **Methods:** This observational, descriptive study included all the 25-OH-Vitamin D measurements performed at the laboratory of Hospital Aranda de la Parra from June 19, 2012 to September 19, 2017 by chemiluminescent microparticle immunoassay (Abbott Diagnostics, USA). We considered Vitamin D insufficiency in those below 30 ng/ml and deficiency below 20 ng/ml. **Results:** We identified 2165 measurements (1795 in women, 370 in men), of whom 1538 (71%) were Vitamin D insufficient and 559 (25.8%) were deficient. Mean age according to the levels of Vitamin D are: <10 ng 62±23 years; 10-30 ng/ml, 56±18 and >30 ng, 57±17 (p=0.658). Table 1 shows the distribution of values across decades of age. **Conclusions:** Hypovitaminosis D is highly prevalent in all age groups in this sample of population. This prevalence tends to be higher in the extremes of age Table 1. Levels of Hypovitaminosis D across decades of age (years) n (%) <20 ng/ml (%) <30 ng/ml (%) 0-10 59 (2.7) 14 (23.7) 44 (74.5) 11-20 48 (2.2) 9 (18.7) 37 (77.2) 21-30 87 (4) 29 (33.3) 66 (75.8) 31-40 170 (7.8) 40 (23.5) 123 (72.3) 41-50 271 (12.5) 70 (26.1) 203 (74.9) 51-60 581 (26.8) 132 (22.7) 404 (69.5) 61-70 495 (22.8) 107 (21.6) 328 (66.2) 71-80 342 (15.9) 106 (30.9) 245 (71.6) 81-90 100 (4.6) 44 (44) 76 (76) 91-100 12 (0.5) 7 (58.3) 12 (100) TOTAL 2165 (100) 559 (25.8) 1538 (71)

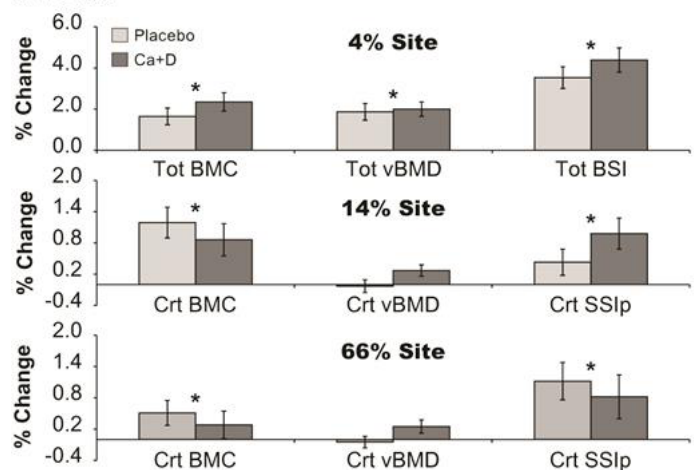
Disclosures: Jorge L A Morales Torres, None

SUN-0841

Effects of Vitamin D Intake and Status on Changes in Distal Tibia Strength in Marine Recruits Undergoing Training Anna Nakayama^{*1}, Katelyn Guerriere², Laura Lutz², Leila Walker², Jonathan Scott³, Heath Gasier³, James McClung², Erin Gaffney-Stomberg². ¹Oak Ridge Institute for Science and Education, United States, ²US Army Research Institute of Environmental Medicine, United States, ³Uniformed Services University of Health Sciences, United States

Bone health is a concern during initial military training (IMT) due to a high incidence of stress fracture, particularly in the lower extremities. Studies in Army recruits demonstrated that supplemental Ca and vitamin D above reference intakes throughout 8 weeks of IMT increased tibia vBMD and maintained parathyroid hormone (PTH) compared to placebo. The objective of this study was to assess the effects of the same dose of Ca (2000 mg/day) and vitamin D (1000 IU/day), provided as a twice daily fortified food product, on bone changes after 12 weeks of IMT. Marine recruits were enrolled during two seasons (summer and winter) and block randomized by sex (male=69, female=77) and race (69% white, 24% black, 7% other) to receive either two Ca and vitamin D fortified (Ca+D) or placebo food bars (130 kcal/each) daily throughout IMT. Serum bone turnover markers, nutritional status indicators, and pQCT scans of the tibia at the 4%, 14%, and 66% sites were collected at the start and end of IMT. Data were analyzed using linear mixed modeling evaluating time, group, and the time-by-group interaction, with race, sex, and BMI as covariates (SPSS v21). There were no differences in dietary Ca (1201 ± 620 mg, 1157 ± 678 mg) nor vitamin D (288 ± 194 IU, 264 ± 190 IU) when comparing supplemented and placebo groups, respectively at baseline. Mean bar consumption was >96% in both groups. IMT resulted in significant changes in BMC and strength at all 3 sites (Figure, p<0.05, all such), as well as vBMD at the 4% site. Those receiving the food product, Ca+D, compared to placebo, demonstrated greater increases in some pQCT measures, but none reached significance. When volunteers were divided into tertiles according to percent change in 4% BSI, change in 25OHD was greater in tertile 3 (+3.9 ± 25.7 ng/ml) as compared to tertile 1 (-9.9 ± 31.3 ng/ml, p<0.05) and this change exhibited a linear trend (r=0.21, p<0.05). Greater body fat loss and lower baseline 25OHD were also observed in those who exhibited the greatest change in BSI and change in body fat was negatively correlated with change in 25OHD (r=-0.21, p<0.01). In addition, a greater proportion of volunteers in tertile 3 entered training in the winter months (62%) as compared to volunteers in tertile 1 (42%). In conclusion, baseline 25OHD, as well as change in 25OHD due to shifts in body composition and season, may be important regulators of the skeletal responses to IMT.

Figure. Percent change of bone indices at the 4%, 14%, and 66% sites of the tibia



* indicates variable significantly increased after IMT (p<0.05); analyzed using linear mixed modeling evaluating time, group, and the time-by-group interaction; covariates include race, sex, and BMI.

Disclosures: Anna Nakayama, None

SUN-0842

Meal Phosphate Bioavailability Alters Hormonal Response in Healthy Humans Kathryn Neville^{*}, Mandy Turner, Cynthia Pruss, Laura Couture, Michael Adams, Rachel Holden. Queen's University, Canada

Background: Chronic kidney disease (CKD) patients have impaired phosphate (PO₄) excretion, leading to chronically elevated parathyroid hormone (PTH) and eventually hyperphosphatemia. Elevated PO₄ and PTH contribute to mineral-bone disorders and cardiovascular disease. Dietary PO₄ contributes to the elevation of these markers, therefore CKD patients are often prescribed phosphate-restricted diets. Current kidney disease guidelines stress reducing PO₄ intake, however, there is little emphasis on the composition of the source. PO₄ sources vary greatly in their bioavailability, with plant-derived sources being less bioavailable, and inorganic PO₄ additives being ~100% bioavailable. PO₄ salts are add-

ed to a large number of processed foods, which are consumed in excess in North America, particularly in lower socioeconomic status groups. Methods: Healthy individuals (N=18) were recruited to participate. Two meals with identical PO₄ amounts, but different compositions were selected; one healthy meal that contained organic sources of PO₄, such as fruits and whole grains, and a second convenience-style meal with inorganic PO₄ sources, such as additives. Fasted participants were randomized to one of the two meals. Baseline urine and blood samples were taken, and participants consumed the meal in 15 minutes. Post-prandial blood and urine samples were taken over three hours. Participants returned to consume the second meal, with at least a week separating visits. Results: The two meals resulted in vastly different circulating mineral and hormonal responses and resultant altered urinary appearance of phosphate. Compared to the convenience meal, the healthy meal displayed significantly lower serum PO₄ after 30 minutes (-0.053mM, p<0.05), had significantly less urinary PO₄ appearance after 120 minutes (-22.6%, p<0.001), significantly increased serum Ca after 60 minutes (-0.07mM, p<0.001), and significantly decreased serum PTH after 90 minutes (-0.073mM, p<0.05). No significant difference was seen between the meals in respect to urinary Ca. Preliminary results in CKD patients (N=2) show a similar trend. Conclusions: Differences in the mineral and hormonal responses between meals can likely be attributed to the meal bioavailabilities, although insulin response could also have a role. We expect the distinction between meals to be exacerbated in CKD. These data suggest that dietary restrictions should emphasize PO₄ composition, in addition to amount.

Disclosures: *Kathryn Neville, None*

SUN-0843

Systematic Screening For Environmental And Behavioral Determinants Identifies Factors Detrimental to Skeletal Health Ling Oei^{1*}, Joy Wu², Edwin Oei³, Fernando Rivadeneira¹, Andre Uitterlinden¹, John Ioannidis⁴, Michael Snyder², Chirag Patel⁵. ¹Erasmus MC, Dept. Internal Medicine, Netherlands, ²Stanford School of Medicine, United States, ³Erasmus MC Dept. Radiology, Netherlands, ⁴Stanford School of Medicine, Netherlands, ⁵Harvard Medical School, United States

Objective: An increasing amount of biomedical data is becoming available, and methods are needed to tackle these "big data". We performed a systematic evaluation of 138 environmental and behavioral factors in relation to bone mineral density (BMD) in the National Health and Nutrition Examination Survey (NHANES). Methods: Dual energy X-ray absorptiometry (DXA) scans were available for total body, head, pelvis and lumbar spine for 27,259 participants from NHANES surveys 1999-2000 (A), 2001-2002 (B), 2003-2004 (C) and 2005-2006 (D). After the Bonferroni correction for multiple testing (P<0.00036) in the discovery random effects meta-analysis of surveys B and D, there were seven unique environmental factors that replicated in the joint analysis of surveys A and C. Results: Higher serum levels of α -tocopherol and of γ -tocopherol, forms of vitamin E, were associated with decreased BMD (per SD β =-.369% and β =-.150% for lumbar spine). In contrast, retinol serum levels were related to higher BMD (per SD β =+11.6% for total body). Serum lead levels had a negative relationship to BMD of the lumbar spine (per SD β =-1.2%) and head (per SD β =-2.2%). Higher levels of physical activity were associated with higher BMD (total body: per MET +1.2%). Being a current or past smoker was associated with decreased BMD of the total body, pelvis and head. Summary and Conclusions: In conclusion, our study demonstrates consistently that several behavioral traits and fat-soluble vitamins may have detrimental effects on BMD, while reinforcing the benefit of physical activity for skeletal health.

Disclosures: *Ling Oei, None*

SUN-0844

Association Between Fermented Milk Product Intake and Bone Health In Postmenopausal Women: A Systematic Review Angel Ong^{1*}, Hope Weiler¹, Suzanne Morin², Kai Kang¹. ¹School of Human Nutrition, McGill University, Canada, ²McGill University, Canada

Purpose: Emerging evidence suggests that fermented milk products (FMPs) may have more favorable effects on bone health than non-fermented milk. The present systematic review aimed to summarize the evidence on the association of FMP intake with bone health indicators including bone mineral density (BMD), incident fractures, and bone turnover markers in postmenopausal women. Methods: This review followed the Preferred Reporting Items for Systematic Review and Meta-Analyses (PRISMA) guidelines. The protocol was registered at PROSPERO (CRD42018085232). We searched CENTRAL (Cochrane), EMBASE, MEDLINE, PubMed, and CINAHL up to January 2018 without language restrictions. Randomized controlled trials (RCTs), cohort studies and case-control studies examining the association between FMP intake, including cheese and yogurt, and bone health outcomes were included. Two reviewers independently screened articles for inclusion, performed data extraction, and assessed risk of bias of included studies. Results: Of the 468 retrieved citations, 11 articles met the inclusion criteria (3 RCTs, 5 prospective cohort studies, 3 case-control studies). Association between bone health outcomes and cheese intake was examined in 9 studies, whereas the association with yogurt intake was evaluated in 7 studies. One short-term yogurt-based RCT reported a reduction in bone resorption and 1 cohort study suggested an inverse association between yogurt/sour milk intake and hip fracture rates; 4 other cohort studies and 1 case-control study reported no association between yogurt intake and bone health outcomes. A trial of cheese fortified with vitamin D and calcium reported a reduction

in bone resorption, but no effect on bone formation was observed in an RCT of non-fortified cheese. Two case-control studies suggested that regular cheese consumption is a protective factor for osteoporosis, whereas evidence from cohort studies examining cheese intake is less clear. No association was found between hip fractures and cheese intake. Some concerns for bias from the randomization process were identified in 2 RCTs. The methodological quality of all observational studies was high, except for 2 case-control studies with moderate quality. Conclusion: It remains unclear whether FMP intake is a protective factor for bone health in postmenopausal women, owing to the paucity of literature examining its effect. Larger and higher quality RCTs are required to further examine the role of FMP in skeletal health.

Disclosures: *Angel Ong, None*

SUN-0845

Milk and Alternatives Intervention Improves Total Hip and Whole Body Bone Mineral Accretion in 14- to 18-year Postmenarcheal Females: Results at 12 Months From a 2-year Randomized Controlled Trial May Slim^{*}, Catherine Vanstone, Suzanne Morin, Elham Rahme, Hope Weiler. McGill University, Canada

Purpose: The role of milk and alternatives intake (MILK) in optimizing peak bone mass during skeletal growth has been widely recognized. However, average intakes for Canadians 9 y and older fall below Canada's Food Guide (CFG) recommendations for MILK. The objective was to examine bone mineral accretion from baseline to 12 months (mo) in postmenarcheal females with usual intake of < 2 servings of MILK per day who are participating in a 2-year trial (NCT02236871, August 2014-December 2018). Methods: Healthy girls 14- to 18-y (n=64) from Montreal, Canada were randomized to control [no intervention], improved [3 MILK servings/d] or recommended [4 or more MILK/d] intervention groups. Bone mineral content (BMC, g), bone mineral density (BMD, g/cm²) and BMD z-scores (BMDZ) of the whole body (WB), lumbar spine 1-4 (LS), 33% radius (R), femoral neck (FN) and total hip (TH) were measured at baseline and at 12 mo using DXA (Hologic Discovery APEX version 13.3.3). Differences among trial groups were tested using mixed model ANOVA with post-hoc Tukey adjustment; data are mean \pm SD. Results: At baseline, mean age was 16.3 \pm 1.4 y and BMI was 22.3 \pm 3.5 kg/m². BMC, BMD and BMDZ were not different among groups at R, TH and FN, but were higher in the recommended group compared to the improved group at LS and WB (p<0.005). Compared to baseline, all groups showed no change over time in any of the bone parameters at LS, R, and FN, whereas only the recommended group increased BMC, BMD and BMDZ at WB and TH at 12 months (p<0.02). At 12 mo, all WB bone parameters were significantly higher in the recommended group compared with the other 2 groups (p<0.02). Furthermore, BMD and BMDZ were higher in the recommended group compared with the control at the TH (p<0.05). Compared with the improved and control groups, the recommended group had greater increases of WB BMC (5.6%) vs the improved group (3.2%, p=0.03) and control group (2.6%, p=0.03), and greater increases in WB BMD (3.0%) vs the improved group (1.5%, p=0.01) and the control group (1.4%, p=0.03). Moreover, TH BMD increased significantly in the recommended compared with the control group only (2.6% vs 0.7%, p=0.01) (Figure). Conclusions: These results suggest that increasing MILK intake to meet CFG's recommendation for this age group favors bone mineral acquisition in postmenarcheal females particularly at the whole body and total hip.

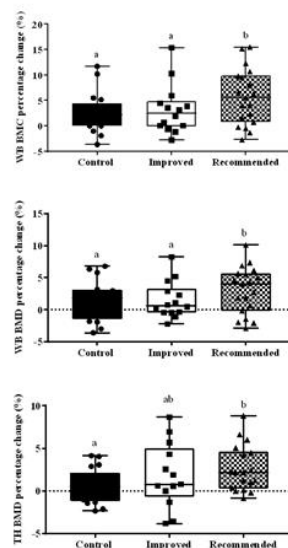
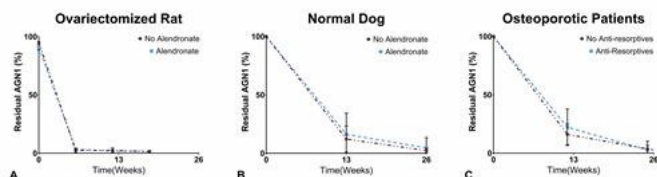


Figure: Percent change in whole body BMC and BMD, and total hip BMD over 12 mo in adolescent females 14 to 18 y participating in a trial to improve milk and alternatives intakes.
a, b Groups with different superscripts are significantly different from each other using a mixed model ANOVA, adjusted for height, weight and skin color (p<0.05). Data are represented in a box and whisker plot format showing median and interquartile range along with the actual values of a sample of 64 participants.
WB: Whole body; TH: total hip; BMD: bone mineral density; BMC: bone mineral content.

Disclosures: *May Slim, None*

were not possible clinically, the analogous results across species suggest that bone formed in patients would also be healthy, normal bone.



Disclosures: **James Howe**, AgNovos Healthcare, Other Financial or Material Support

SUN-0867

Central Acetylcholine Signaling Contributes to Age-related Bone Loss Yun Ma*, Florent Elefteriou. Baylor College of Medicine, United States

Bone loss begins in the third decade of life and continues after menopause/andropause, thus mechanisms additional to gonadal deficiency contribute to age-related bone loss. Studies in both humans and rodents have shown that parasympathetic cholinergic tone decreases, while sympathetic outflow increases with aging. Although reports have illustrated effects of cholinergic receptors global embryonic genetic ablation on bone, mechanisms whereby cholinergic signaling impacts bone homeostasis in adults and during aging remain unknown. To address this question, we chronically raised acetylcholine (ACh) levels in WT mice at time of peak bone mass and before bone loss associated with aging (14 weeks of age), by using blood brain barrier (BBB) permeable and non-permeable acetylcholinesterase inhibitors (AChEIs). Mice were sacrificed 6 weeks later and were analyzed by microcomputed tomographic and histomorphometric analyses. These analyses revealed that only AChEIs able to pass blood brain barrier (BBB), thereby elevating central ACh level, increased bone mass. The bone anabolic effect of centrally-acting AChEIs was associated with an increase in both osteoblast and osteoclast number/surface. Unexpectedly, the bone anabolic effect of AChEIs was observed only in females. Bone marrow stromal cells (BMSCs) isolated from long bones of vehicle or AChEIs-treated females and differentiated in osteogenic conditions formed a similar number of colony-forming unit (cfu)-AP/-Ob. AChEIs treatment of WT BMSCs at 3 different doses (0.1, 1 and 10 μ M) during 5 days did not have any stimulatory effect on BMSC number, and upon growth in osteogenic medium did not increase differentiation, as measured by alkaline phosphatase (ALP) staining. No major effect of treatments was detected either on osteoclast differentiation, measured by tartrate-resistant acid phosphatase (TRAP) staining of spleen monocytes in the presence of MCSF and RANKL. These results thus are in line with a mechanism of action whereby ACh signaling in the central nervous system prevents bone loss after peak bone acquisition, consistent with previously published data related to the bone phenotype of M3r-deficient mice. They also suggest that the beneficial effect of centrally-acting AChEIs on cognition in patients with Alzheimer disease (AD) may be associated with positive effects on bone health, which is supported by the recent observation of reduced fracture risk in AD patients taking AChEIs.

Disclosures: **Yun Ma**, None

SUN-0868

The Chemotherapeutic Trabectedin Negatively Impacts Osteal Macrophages and Bone Healing Benjamin Sinder*¹, Justin Do², Amy Koh², Hernan Roca², Laurie Mccauley². ¹UConn Health, United States, ²University of Michigan, United States

Osteal macrophages have emerged as vital regulators of bone mass and inhibition of macrophages compromises bone formation. A key function of macrophages is to efferocytose apoptotic cells, a normal process which is ramped up during wound healing. Trabectedin is an FDA approved chemotherapeutic that induces apoptosis in macrophages and certain types of cancer cells and reduces macrophage efferocytosis. The purpose of this study was to investigate the role of macrophages and trabectedin on bone healing. A stress fracture (sFx) was created in the ulna of 16 wk old C57BL/6 male mice using 2Hz cyclic fatigue loading at 80% of ultimate force until a total displacement of 0.55mm was achieved. After stress fracture, mice were immediately treated with trabectedin or vehicle (0.15mg/kg i.v, n=8-10/gp). Stress fractures were allowed to heal for 3 days (n=20) or 1wk (n=16) followed by flow cytometric analyses, histology for macrophage immunostaining, and microCT outcomes. After 3 days of healing, trabectedin significantly reduced F4/80+ (-35%) and CD11b+ (-33%) macrophages and monocytes in non-sFx (unloaded) bone marrow as assessed by flow cytometry. Correspondingly, spleen weight was also reduced (-28%), suggesting systemic disruption of the myeloid system. Histologic analysis of total callus sFx area at the 3day time point revealed trabectedin significantly reduced (-45%) early callus size. Total callus F4/80+ macrophages were significantly reduced (-55%) with trabectedin and F4/80+ macrophages per sFx callus area trended towards a decrease (-25%, p=0.16). After 1wk of healing, the early impact of trabectedin persisted and microCT analysis revealed significantly reduced total callus size (-52%) as well as callus bone volume (-57%) with trabectedin treatment (p<0.01). Histologic immunostaining for macrophages with the F4/80+ marker showed a significant reduction in the total number of callus macrophages after 1wk (-60%), but no significant reduction in F4/80+ cells in the callus normalized to sFx callus area. In conclusion, trabectedin significantly compromises osteal macrophages and has a negative impact

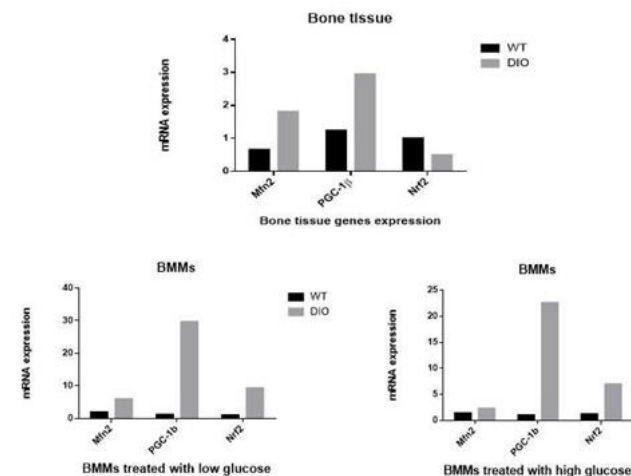
on bone healing. Results of this study highlight the regenerative role that macrophages play in osseous wound healing and may have immediate clinical relevance for patients receiving trabectedin treatment.

Disclosures: **Benjamin Sinder**, None

SUN-0869

Evidence of Mitochondrial Fusion and Biogenesis Altering in Diabetic Bones Xiaoxuan Wang*^{1,2}, Zhekai Hu¹, Xingwen Wu¹, Qisheng Tu¹, Jinkun Chen^{1,3}. ¹Division of Oral Biology Tufts University School of Dental Medicine., United States, ²Department of Periodontology, Peking University School and Hospital of Stomatology, Beijing, China, ³Department of Developmental, Molecular and Chemical Biology Sackler School of Graduate Biomedical Sciences Tufts University School of Medicine, United States

Objective: Diabetes mellitus (DM) is one of the most common metabolic diseases worldwide. Diabetes has been reported to disrupt the dynamics and biogenesis of mitochondria. Mitofusin 2 (Mfn2), plays critical roles in mitochondrial fusion. PGC-1 β and Nrf2 are related to mitochondrial biogenesis. Expression of Mfn2, PGC-1 β and Nrf2 changed in brains, heart, muscles of diabetic rodents while not clear in bone of diabetic rodents. This study is to investigate the expression of Mfn2, PGC-1 β and Nrf2 genes in bone of type 2 diabetes mellitus (T2DM) mouse model. Materials and methods: Twenty-week-old diet-induced obesity (DIO) mice model of T2DM and wild type mice were used for the animal experiments. Femur and tibia of mice were isolated and RNA was extracted. Bone marrow derived stem cells (BMSCs) were isolated from femur and tibia of mice. Mice bone marrow-derived macrophages (BMMs) were isolated and cultured in medium supplemented with soluble receptor activator of NF- κ B ligand and macrophage colony-stimulating factor. Cells were treated respectively with low glucose (5mM glucose, glucose control), high glucose (25 mM glucose). Expression of Mfn2, PGC-1 β and Nrf2 genes were detected by real time PCR assays in mouse bone, BMMs and BMSCs. Results: Expression of Mfn2, PGC-1 β were increased in the bone of DIO mice compared to the WT mice while expression of Nrf2 was decreased (p<0.05). Expression levels of all the three genes were higher in the BMMs isolated from DIO mice than that from WT mice when treated with high glucose or not. Interestingly, expression levels of Mfn2 and PGC-1 β were decreased while the expression of Nrf2 increased in BMSCs when treated with high glucose or not. Furthermore, in the DIO mice group, the alterations of genes expression were opposite in the BMSCs and BMMs when the cells were treated with high glucose. Expression of Mfn2 was upregulated and PGC-1 β downregulated in BMMs. In contrary, expression of Mfn2 was downregulated and PGC-1 β upregulated in BMSCs. In the WT mice group, the alterations of genes expression in BMMs and BMSCs were similar with the DIO mice group when treated with high glucose. Conclusion: This study represents the first report exploring the gene expression profiles in diabetic bone tissues, BMMs and BMSCs. These data suggest that Mfn2, PGC-1 β and Nrf2 may participate in the bone metabolism in T2DM mouse model and the alteration of these genes expression may contribute to the T2DM osteoporosis.



Disclosures: **Xiaoxuan Wang**, None

SUN-0870

Microbiota Regulates Bone Loss in Sickle Cell Disease Male Mice Liping Xiao*, Kavita Rana, Kimberly Pantojia. UConn Health, United States

Bone loss is a common complication in sickle cell disease (SCD) subjects. The mechanism(s) of bone loss in SCD patients has not been fully investigated. Studies showed increased circulating aged neutrophils that are regulated by the intestinal microbiota and depletion of gut microbiota significantly reduced the number of aged neutrophil and dramatically improved the inflammation-related organ damages in SCD mice. Since neutrophils

are abundantly present in bone marrow (BM) and regulate bone cells, we examined whether bone loss in SCD mice is due to microbiota-regulated accumulation of aged neutrophils in BM. We treated control and SCD male mice with a broad-spectrum antibiotic to deplete gut microbiota. Antibiotic treatment significantly improved splenomegaly and improved decreased body weight, leg bone mineral density, leg bone mineral content, bone formation parameters of the femur, and Runx2 and Igf1 mRNA in tibia from SCD mice. Antibiotic treatment rescued accumulation of BM aged neutrophils. Decreased osteoblast functions co-cultured with BM neutrophils from SCD mice were rescued when co-cultured with BM neutrophils from antibiotic treated mice. We conclude that increased gut bacteria load may contribute to bone loss in SCD male mice. Furthermore gut microbiota-regulated BM neutrophil ageing may contribute to impaired osteoblast function in SCD mice.

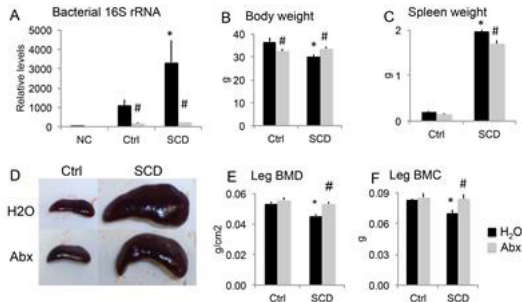


Figure 1. Microbiota depletion improved splenomegaly and leg BMD and BMC in SCD male mice. Mice were housed by genotype after weaning. Ctrl and SCD male mice were singly housed to avoid cage effects on microbiota at 4 months of age and randomly assigned to H₂O or Abx treatment groups. After 7 weeks of treatment at 6 months of age, feces were collected, body weight was measured, and in vivo DEXA was performed. Then mice were euthanized for sample collection. (A) Increased gut bacteria load in SCD mice and bacterial depletion after Abx treatment in both Ctrl and SCD mice. Genomic DNA was isolated from equal amounts of fecal material of Ctrl and SCD mice with and without Abx treatment. Relative quantification of 16S rRNA gene copies of total bacteria was determined by real time PCR using universal 16S rRNA primers. NC: negative control, every step is same as real samples except no feces were collected in the collecting tube. n=4 mice/group. (B) Body weight. n=4 mice/group. (C) Spleen weight. n=4 mice/group. (D) Representative images of spleen. (E) Leg BMD and (F) BMC were significantly decreased in SCD-H₂O mice compared with Ctrl-H₂O mice and Abx treatment significantly increased leg BMD and BMC in SCD mice. n=4 mice/group. Data are mean±SE. *, compared with Ctrl-H₂O p<0.05, #, compared with corresponding H₂O group p<0.05 by two-way ANOVA.

Disclosures: *Liping Xiao, None*

SUN-0886

Cross sectional study of severity of bone disease in liver transplant from pre-transplant to one year post transplant and potential factors associated with bone loss Ejigayehu Abate*. Mayo Clinic Florida, United States

Background: The liver plays an important role in bone and mineral metabolism. The rate of bone loss is highest in the first 6-12 months after transplant. We evaluated rate of bone loss in 1st year of transplant and potential factors contributing to bone loss. Methods: This is a retrospective study of 296 patients with liver transplant at Mayo Clinic Florida in 2009 to 2013 and 19 patients had combined kidney/liver transplant analyzed separately. Results: An unadjusted annual rate of bone loss from pre-transplant to 1 year post transplant was an increase of 0.78% in the spine (0.78%, 95% CI 0.07% to 1.49%), a decrease of 5.67% in the total hip (-5.67%, 95% CI -7.79% to -3.5%), decrease of 3.67% in femoral neck (-3.67%, 95% CI -4.23% to -3.11%). Worsening BMD at all site (spine, hip and femoral neck) was associated with a lower MELD score at the time of transplant (P<0.001). In addition, worsening BMD of the total hip and femoral neck were associated with lower body mass index prior to transplant (P=0.003) and the number of days between pre-transplant BMD test and transplant (P=0.035). There was no association of prednisone dose after transplant and the annual percent change in BMD at the spine, hip, or femoral neck. Among those with fracture within the first year of transplant, history of fracture before transplant and annual total hip BMD change of -3.5% or higher was associated with higher rate of fracture after transplant. Although not statistically significant, we noticed that 26% those who had a combined liver and kidney transplant had a fracture within the 1st year vs. 14% of the liver transplant alone (P=0.14). Prednisone dose of >1.2grams was associated with increased risk of fracture (P=0.24). Among those who had prednisone prior to transplant, 25.0% had a fracture within 1 year post transplant compared to 14.2% of those who did not have any prednisone before transplant (P=0.24). Conclusion: This study shows a significant bone loss in the hip and femoral neck within 1 year of transplant. Higher MELD scores and low BMI at the time of transplant are the main risk factor to bone loss. We did not find a significant correlation between prednisone dosage and rate of bone loss although higher dose was associated with increased risk of fracture. Prior fracture regardless of bone density changes was a main predictor of fracture risk within the first year of transplant. Findings signify the importance of utilizing other modalities for assessment of fracture in these patients rather than relying on bone mineral density testing alone.

Disclosures: *Ejigayehu Abate, None*

SUN-0887

Prevalence and Risk factors for Low Bone Mineral Density in Transfusion Dependent Anemia Rahul Agarwal*¹, Farzana Sayani², Mohammad El Sibai¹, Mona Al Mukaddam¹. ¹Perelman School of Medicine at the University of Pennsylvania, Division of Endocrinology, Diabetes and Metabolism, United States, ²Perelman School of Medicine at the University of Pennsylvania, Division of Hematology and Oncology, United States

Purpose: Osteoporosis and fractures are increasingly reported complications in transfusion dependent anemia (TDA). This retrospective study reports on the prevalence of low bone mineral density (BMD; defined as Z-Score ≤ -2.0) and its association to risk factors in adult patients with TDA. Methods: We performed a retrospective review of the electronic medical record for adult patients (age 18 or above) with confirmed TDA seen at the Penn Comprehensive Adult Thalassemia Program between July 2012 and June 2017. Only patients who underwent at least one dual-energy x-ray absorptiometry (DXA) scan were included in the analysis. Results: A total of 38 patient charts were reviewed and 33 patients who had a DXA measurement (28 with Beta Thalassemia, 5 with Diamond Blackfan Anemia) were included in the final analysis. 17 patients were males, 20 Caucasians, 10 Asians, and 3 African Americans with average age of 37 years at time of DXA measurement (Table 1). 23 patients (69.7%) had low BMD and 11 patients (33%) had a fracture. The most commonly associated endocrinopathy was hypogonadism in 22 (67%) patients. Patients with low BMD were more likely to be males, had prior history of steroid use, osteoporosis treatment, delayed puberty, hypogonadism, hypothyroidism, and diabetes. There was no difference in ferritin level and liver and cardiac iron deposition between the two groups. Only 13 patients had a 24-hour urine collection for calcium and creatinine and 12 (92%) of these patients had hypercalciuria as defined by >4mg/kg/24 hours. 5 of the 12 hypercalciuric patients (42%) had kidney stones and all 12 patients were taking the iron chelating drug deferasirox. Patients who were followed by endocrinology were more likely to have serial DXA measurements (18/21(86%) vs. 8/12(67%)) and 24-hour urine calcium measurement (13/21(62%) vs. none) compared to patients not followed by endocrinology. Conclusions: This study on racially diverse adults with TDA living in the US demonstrates a high prevalence of low bone mineral density, fractures, endocrinopathies and hypercalciuria. Routine endocrinology referral is recommended and further research in the pathogenesis and treatment of low bone mineral density in this patient population is required.

	All Patients	Z-Score ≤ -2.0	Z-Score > -2.0
	N (%)	N (%)	N (%)
Total Patients	33	23	10
Beta Thalassemia	28 (85)	18 (78%)	10 (100)
DBA	5 (15)	5 (22%)	0
Male	17 (52)	14 (61)	3 (30)
Female	16 (48)	9 (39)	7 (70)
Caucasian	20 (61)	15 (65)	5 (50)
Asian	10 (30)	6 (26)	4 (40)
African American	3 (9)	2 (9)	1 (10)
Age at Last DXA Measurement	37.7 (18-63)	38.8 (18-63)	35.1 (24-50)
Years (range)			
Average DXA Z-score by Site			
Lumbar Spine	-2.4	-2.8	-1.5
Total Hip	-1.5	-2.0	-0.6
Femoral Neck	-1.3	-1.7	-0.8
Kidney Stone	6 (18)	4 (17)	2 (20)
Steroid Exposure	6 (18)	6 (26)	0
Prior Osteoporosis Treatment	6 (18)	6 (26)	0
Delayed Puberty	7 (43)	6 (46)	1 (10)
Hypogonadism	22 (67)	17 (74)	5 (50)
Growth Hormone Replacement	6 (18)	4 (13)	2 (20)
Adrenal Insufficiency	0	0	0
Thyroid Disease (Hypothyroid)	6 (18)	6 (26)	0
Diabetes	6 (18)	6 (26)	0
Any Fracture	11 (33)	8 (35)	3 (30)
Traumatic	5 (45)	3 (38)	2 (67)
Fragility	5 (45)	5 (63)	0
Unknown	1 (9)	0	1 (33)
Hypercalciuria	12/13 (92)	9/10 (90)	3/3 (100)
Ferritin	2389	2150	2937
Last Liver Iron Content (LIC)	11.8	10.1	15.65
Cardiac T2*	28.76	29.28	30.61
Iron Chelating Agent			
Deferasirox only	19 (58)	14 (61)	5 (60)
Deferasirox + Deferoxamine	4 (12)	4 (17)	0
Deferasirox + Deferiprone	8 (24)	4 (17)	4 (40)
Deferiprone only	2 (6)	1 (4)	1 (10)

Disclosures: *Rahul Agarwal, None*

SUN-0888

The Effects of Cortisol and Adrenal Androgen on Bone Mass in Asian Patients with and without Subclinical Hypercortisolism Seong Hee Ahn^{*1}, Jae Hyeon Kim², Mihye Jung¹, Yoon Young Cho³, Sunghwan Suh⁴, Beom-Jun Kim⁵, Seongbin Hong¹, Seung Hun Lee⁵, Jung-Min Koh³, Kee-Ho Song⁶. ¹Department of Endocrinology and Metabolism, Inha University Hospital, Inha University School of Medicine, Republic of Korea, ²Division of Endocrinology and Metabolism, Department of Medicine, Samsung Medical Center, Sungkyunkwan University School of Medicine, Republic of Korea, ³Division of Endocrinology and Metabolism, Department of Medicine, Gyeongsang National University Hospital, Gyeongsang National University School of Medicine, Republic of Korea, ⁴Division of Endocrinology and Metabolism, Department of Medicine, Dong-A University Medical Center, Dong-A University College of Medicine, Republic of Korea, ⁵Division of Endocrinology and Metabolism, Asan Medical Center, University of Ulsan College of Medicine, Republic of Korea, ⁶Division of Endocrinology and Metabolism, Department of Medicine, Konkuk University Medical Center, Konkuk University School of Medicine, Republic of Korea

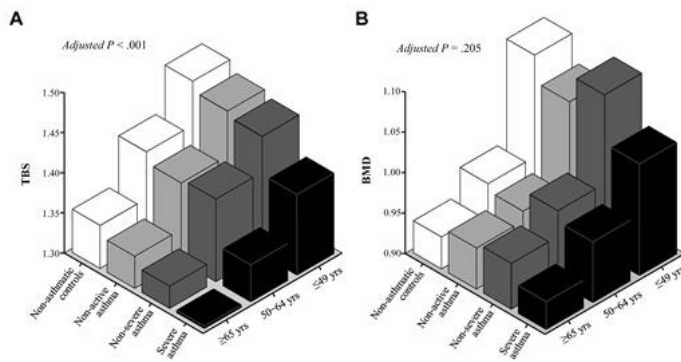
Purpose: Despite ethnic differences in cortisol sensitivity between Caucasians and Asians, scanty reports evaluated bone metabolism in Asian patients with subclinical hypercortisolism (SH). We investigated associations of both cortisol and dehydroepiandrosterone-sulfate (DHEA-S), an adrenal androgen, with bone mineral density (BMD) and bone turnover makers (BTMs) in Asian adrenal incidentaloma (AI) patients with and without SH. **Methods:** We measured BMD, BTMs, cortisol levels after 1 mg-dexamethasone suppression test (1 mg-DST), and cortisol to DHEA-S ratio (cort/DHEA-S) in 109 AI patients with SH (56 women and 53 men) and 686 with non-functional AI (NFAI) from a large Korean cohort. **Results:** Women but not men with SH had lower BMDs at lumbar spine (LS), femoral neck, and total femur than patients with NFAI ($P < 0.001$ to 0.015). After adjusting for confounders, higher 1 mg-DST was associated with lower BMDs at all skeletal sites in women ($\beta = -0.021$ to -0.032 , $P = 0.010$ to 0.023), but not in men. Higher cort/DHEA-S was associated with lower LS BMD in both women ($\beta = -0.035$, $P < 0.001$) and men ($\beta = -0.029$, $P = 0.011$). The inverse association of cort/DHEA-S with LS BMD remained significant even after adjusting for 1 mg-DST ($\beta = -0.031$, $P < 0.004$ for women; $\beta = -0.026$, $P < 0.029$ for men). In women, the odd ratio for lower BMD by cort/DHEA-S was 1.54 (95% confidence interval, 1.02–2.31). **Conclusion:** Subtle cortisol excess in women and reduced DHEA-S in both genders may contribute to BMD reduction in Asian patients with SH.

Disclosures: Seong Hee Ahn, None

SUN-0889

Severe asthma and high doses of corticosteroid impair trabecular bone score more than bone mineral density Yong Jun Choi^{*1}, Hyun-Young Lee², Sihoon Lee³, Yoon-Sok Chung¹, Young-Min Ye⁴. ¹Department of Endocrinology and Metabolism, Ajou University School of Medicine, Republic of Korea, ²Clinical Trial Center, Ajou University Medical Center, Republic of Korea, ³Gachon University School of Medicine, Republic of Korea, ⁴Department of Allergy and Clinical Immunology, Ajou University School of Medicine, Republic of Korea

BACKGROUND: In asthmatic patients, treatment with corticosteroids, in addition to conventional risk factors for osteoporosis, may lead to bone loss. Trabecular bone score (TBS) is a new, indirect parameter of bone quality. Studies have yet to evaluate TBS in asthmatic patients in relation to disease severity and corticosteroid use. **OBJECTIVE:** This study aimed to evaluate TBS in asthmatics in comparison to propensity score-matched controls and to investigate correlations between TBS and cumulative systemic and inhaled corticosteroid doses 1 year prior to bone mineral density measurement in patients with asthma. **METHODS:** In total, 627 patients with asthma and the same number of non-asthmatic controls matched for sex and age were included in this retrospective cohort study. TBS was calculated in the lumbar region, based on two dimensional projections of dual-energy X-ray absorptiometry. **RESULTS:** Patients with severe asthma exhibited lower vertebral TBS values (1.33 ± 0.11) than those with non-severe asthma (1.37 ± 0.10 , $P = .004$), with non-active asthma (1.38 ± 0.10 , $P < 0.001$), and without asthma (1.39 ± 0.10 , $P < 0.001$). No significant differences in BMD were noted among the study groups (0.96 ± 0.18 vs 0.98 ± 0.25 vs 0.97 ± 0.17 vs 0.97 ± 0.18 , all P -values $> .05$). A TBS of 1.42 was determined as a cut-off for osteoporosis. TBS was significantly associated with cumulative systemic and inhaled corticosteroid doses, as well as lung function and airway hyper-responsiveness. **Conclusion:** TBS can be used as an early indicator of altered bone quality stemming from glucocorticoid therapy or, possibly, more severe asthma.



Disclosures: Yong Jun Choi, None

SUN-0890

The effects TSH suppressive therapy on changes of TBS and BMD in menopausal women with differentiated thyroid cancer Yun Kyung Jeon^{*1}, Keunyoung Kim², In Joo Kim¹, Kyoung Min Kim³, Kyoungjune Pak², Seong-Jang Kim⁴. ¹Endocrinology and metabolism, Pusan National University Hospital, Republic of Korea, ²Department of Nuclear Medicine and Biomedical Research Institute, Pusan National University Hospital, Republic of Korea, ³Seoul National University College of Medicine and Seoul National University Bundang Hospital, Republic of Korea, ⁴Department of Nuclear Medicine and Biomedical Research Institute, Yang San Pusan National University Hospital, Republic of Korea

This study aimed to examine the changes of trabecular bone score (TBS), areal bone mineral density (aBMD) and diagnosis in postmenopausal women who were undergoing thyrotropin (TSH) suppressive therapy for treatment of papillary thyroid cancer (PTC) after total thyroidectomy. **Methods:** We enrolled a total of 36 postmenopausal patients (mean age: 60.5 ± 5.5 years) undergoing TSH suppressive therapy with levothyroxine after receiving total thyroidectomy for papillary thyroid cancer. Ninety-four postmenopausal women (mean age: 60.8 ± 5.3 years) matched for age and body mass index were recruited as healthy control group. Dual-energy X-ray absorptiometry (DXA) was performed for the evaluation of BMD status. The BMD and TBS of the lumbar spine were generated from DXA at the baseline and after mean 4.92 year. **Results:** The proportion of both osteopenia and osteoporosis was not significantly different between TSH suppression group and control group at the first DXA evaluation, (11.2% vs. 21.2%, $p = 0.350$), however, progression rate of normal to osteopenia or osteopenia to osteoporosis was more common in a group of TSH suppression (77.8% vs 38.5%, $p < 0.001$). The incidence of osteoporosis is more common at the time of followed DXA evaluation (27.8% vs. 10.6%, $p < 0.001$). The TBS was not significantly different between initial DXA and follow up DXA images. There was slightly decreasing trend in TBS and BMD among the patients and control groups, however, there was no statistical significance. The median degradation ratio of TBS was significantly higher in PTC group (median 0.054; IQR: 1.18–1.47) than in control group (median: 0.020; IQR: 1.18–1.47, $p = 0.039$), however, BMD did not show significant median changing ratio ($p = 0.215$). The number of patients who showed $TBS < 1.3$ was significantly higher in the group of PTC than in the group of normal control group at the time of the first DXA evaluation (28.5% vs. 12.8%, $p = 0.027$). In total 132 patients, if the initial TBS was higher than 1.3, more participants stay at the same BMD status, whereas, if the initial TBS was lower than 1.3, more patients have trend of deteriorating BMD status without statistical significance. Even TBS of the participant was higher than 1.3, the patients who were under TSH suppression were more tend to progress to osteopenia or osteoporosis (85.2% vs. 52.4%, $p = 0.003$). **Conclusions:** BMD and TBS were not significantly changed during short-term follow up period in both groups of PTC and control. The degradation ratio of TBS was minimal but significantly decreased and the incidence of progression to deteriorating BMD was higher in PTC group despite of normal TBS value. Therefore, dedicated management and evaluation including TBS should be considered in the postmenopausal patients undergoing long-term TSH suppressive therapy.

Disclosures: Yun Kyung Jeon, None

SUN-0891

Bone Mineral Density and Trabecular Bone Score Associations with Hypertension and Diabetes in the VITamin D and Omega-3 Trial (VITAL): Effects on Bone Structure and Architecture Study Meryl LeBoff^{*1,2}, Catherine Donlon¹, Nancy Cook^{2,3,4}, Julie Buring^{2,3,4}, Joann Manson^{2,3,4}. ¹Division of Endocrinology, Diabetes and Hypertension, Brigham and Women's Hospital, United States, ²Harvard Medical School, United States, ³Division of Preventive Medicine, Brigham and Women's Hospital, United States, ⁴Department of Epidemiology, Harvard T.H. Chan School of Public Health, United States

Previous studies have shown associations between hypertension and low bone mineral density (BMD) and increased fracture risk. Both cardiovascular disease (CVD) and osteoporosis share similar risk factors, including older age, diabetes, smoking, and low physical activity levels. In this study, we investigated whether Trabecular Bone Score (TBS) and BMD at the spine, femoral neck, total hip, and whole body were associated with a history of hypertension, diabetes, and/or use of anti-hypertensive, anti-diabetic, or cholesterol-lowering medications in VITamin D and Omega-3 Trial (VITAL). The parent VITAL study is a 2x2 factorial randomized controlled trial (RCT) investigating effects of supplemental cholecalciferol (2000 IU/d) and/or omega (ω)-3 fatty acids (1 g/d) for the primary prevention of cancer and CVD. The study had a median of 5-yrs of treatment in 25,874 US men ≥50 yrs and women ≥55 yrs. In our ancillary study, VITAL: Effects on Bone Structure and Architecture, 1,2 in-person assessments were completed in a subcohort of 771 participants (46.8% women, 53.2% men). Medical histories were obtained by annual questionnaires, and BMD was determined by dual-energy X-ray absorptiometry (Discovery W; APEX Software Version 4.2, Hologic, Bedford, MA). TBS, a measure of bone structure, was derived from the spine DXA images (Medimaps Version 2.1, Geneva, Switzerland). All analyses were adjusted for age, race, sex, and BMI. Overall, higher BMD at the spine was associated with ever use of anti-hypertensive medications (p=0.049) and history of diabetes (p=0.031). When anti-hypertensive medications were broken down by type (ie. beta-blockers, calcium-blockers, diuretics, ACE-inhibitors, angiotensin-receptor blockers, or alpha-blockers), there were no associations with spine BMD, possibly due to smaller sample sizes. TBS was not significantly associated with hypertension or anti-hypertensive medications but was lower in participants with a history of diabetes (p=0.003) and those currently using anti-diabetic medication (p<0.001). There were no associations between total hip, femoral neck, or whole body BMD and hypertension, diabetes, or anti-hypertensive, anti-diabetic, or cholesterol-lowering medications. In future analyses in the VITAL RCT, we will assess whether hypertension and diabetes are associated with incident fractures and changes in bone structure and whether these co-morbidities modify effects of supplemental vitamin D and/or ω-3 fatty acids on bone health. References: 1. LeBoff MS, et al. Contemp Clin Trials. 2015 Mar;41:259-682. Donlon CM, et al. Contemp Clin Trials. 2018 Apr;67:56-67

Table 1. Baseline associations of spine BMD and TBS with hypertension and diabetes in participants in the VITAL: Effects on Bone Structure and Architecture Study, adjusted for age, sex, race and BMI

Description	Category	N (%)	Spine BMD		TBS	
			Mean (95% CL)	P-value	Mean (95% CL)	P-value
Hypertension History	No	415 (54.3%)	1.013 (0.998-1.027)	0.069	1.325 (1.316-1.334)	0.37
	Yes	349 (45.7%)	1.034 (1.018-1.051)		1.319 (1.308-1.329)	
Ever use of anti-hypertensive medication	No	434 (56.5%)	1.012 (0.998-1.027)	0.049	1.325 (1.317-1.334)	0.23
	Yes	334 (43.5%)	1.036 (1.019-1.053)		1.317 (1.307-1.328)	
Current use of cholesterol-lowering medication	No	501 (65.7%)	1.017 (1.004-1.031)	0.29	1.323 (1.315-1.332)	0.43
	Yes	262 (34.3%)	1.030 (1.011-1.048)		1.318 (1.306-1.329)	
Diabetes History	No	686 (89.9%)	1.017 (1.006-1.028)	0.031	1.325 (1.318-1.331)	0.003
	Yes	77 (10.1%)	1.056 (1.022-1.090)		1.290 (1.268-1.312)	
Current use of anti-diabetic medication	No	711 (92.2%)	1.020 (1.009-1.031)	0.18	1.325 (1.318-1.332)	<0.001
	Yes	60 (7.8%)	1.047 (1.009-1.086)		1.281 (1.256-1.306)	

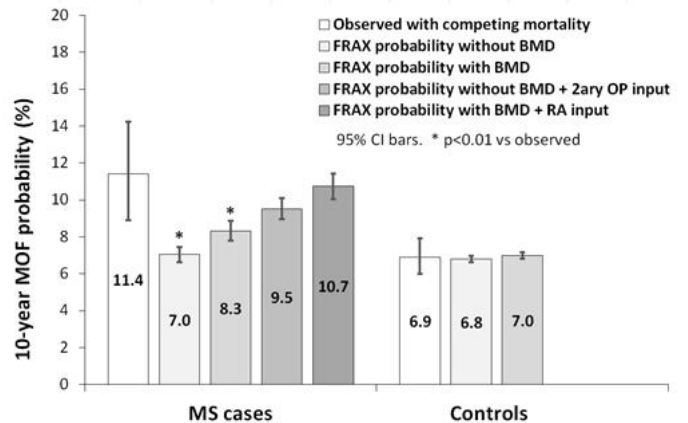
Disclosures: Meryl LeBoff, None

SUN-0892

Accuracy of FRAX® in People with Multiple Sclerosis: A Manitoba BMD Registry-Based Cohort Study Etienne J. Bisson^{*1}, Marcia Finlayson¹, Okechukwu Ekuma², Ruth Ann Marrie², William D Leslie². ¹Faculty of Health Sciences, Queen's University, Canada, ²Rady Faculty of Health Sciences, University of Manitoba, Canada

People with multiple sclerosis (MS) have a higher risk of low bone mineral density (BMD) and osteoporotic fractures as compared to healthy adults. The fracture risk assessment tool (FRAX®) has been reported to underestimate fracture risk in people with MS when BMD is unknown. AIM: To test the performance of FRAX BMD for people with MS, and determine if MS is a risk factor for fracture independent of FRAX score. METHODS: Using population-based data for Manitoba Canada, we identified MS cases with BMD screening after diagnosis (n=744) and controls matched on age, sex and BMD screening date (n=3721). We calculated FRAX 10-year probabilities and ascertained subsequent major osteoporotic fractures (MOF). Cox proportional hazards models were used to assess the effect of MS on the risk of MOF, after accounting for baseline risk. Calibration (predicted vs observed 10-year MOF probability with competing mortality) was compared in people

with MS with/without use of secondary osteoporosis (2ary OP) as an input to FRAX without BMD, and with/without use of rheumatoid arthritis (RA) as a proxy for MS in FRAX with BMD. RESULTS: MS cases had higher mean FRAX MOF probability calculated with BMD than controls (8.32% vs 6.98%; p<0.01) and lower femoral neck T-score (1.42 vs 1.07; p<0.01). MS cases had a higher cumulative incidence of MOF (n=77; 10.4%) compared to controls (n=238; 6.4%; p<0.001). FRAX stratified risk for incident MOF in people with MS (HR=2.08, 95% CI 1.67-2.61 without BMD; HR=1.99, 95% CI 1.60-2.47 with BMD) similar to those without MS (HR=1.62, 95% CI 1.42-1.85 without BMD; HR=1.77, 95% CI 1.56-2.01 with BMD). MS was a predictor of MOF after controlling for FRAX without BMD (HR=1.67, 95% CI 1.29-2.16). FRAX with BMD (HR=1.48, 95% CI 1.14-1.92), and individual risk factors including BMD (HR=1.45, 95% CI 1.12-1.89). FRAX was well-calibrated in the controls but underestimated observed MOF risk in MS cases (by 4.4% without BMD, by 3.1% with BMD; both p<0.01). Calibration improved when 2ary OP was used to calculate FRAX without BMD, and was best when RA was used to calculate FRAX probability with BMD. CONCLUSION: MS is a FRAX-independent risk factor for MOF but FRAX still stratifies fracture risk in people with MS. Using secondary osteoporosis or RA as proxies for MS improves performance of FRAX and accurately predicts MOF outcomes in those with MS. This provides clinicians with a readily available approach to improve the accuracy of fracture prediction in MS.



Disclosures: Etienne J. Bisson, None

SUN-0893

Smaller but Denser Bones in Older Women with Type 2 Diabetes Anna Nilsson^{*1,2}, Daniel Sundh¹, Mattias Lorentzon^{1,3}. ¹Geriatric unit, Institute of Medicine, Sahlgrenska Academy, University of Gothenburg, Sweden, ²Dept Endocrinology, Internal Medicine, Sahlgrenska University Hospital, Sweden, ³Geriatric Medicine Clinic, Sahlgrenska University Hospital, Sweden

Background: Type 2 diabetes mellitus (T2DM) is associated with an increased risk of fractures, despite higher bone mineral density (BMD) compared to controls, which may be due to higher body mass index (BMI). There are conflicting results in the literature regarding bone microstructure. Objective: The objective of the present study was to evaluate bone microstructure and bone geometry in older women with T2DM. Methods: 293 women with T2DM were identified in a population-based study on 3,028 women between 75-80 years, performed in Gothenburg 2013-2016. After exclusion of 20 women with T1DM, propensity score matching for age, BMI, family history of fractures, smoking, alcohol habits, rheumatoid arthritis, and glucocorticoid usage, was performed to select 3 controls per subject with T2DM. Volumetric BMD (vBMD) and bone microarchitectural indices were assessed at two sites in radius and tibia (standard site and at 14% of bone length) with high-resolution peripheral quantitative computed tomography. Physical function (Timed Up and Go (TUG), one-leg standing (OLS), number of chair-stands, grip strength, and walking velocity), was tested in all women by physiotherapists. Results: After matching, mean (±SD) age was 77.7±1.6 years in both groups, and BMI was 29.0±5.1 kg/m² in women with T2DM and 28.9±4.8 kg/m² in controls (n=879). Despite highly similar BMI, women with T2DM had generally better values with higher total vBMD (e.g., standard site tibia 248±52 vs. 232±45 mg/cm³, p<0.001), cortical vBMD (e.g., 14% site tibia 930±41 vs. 914±40 mg/cm³, p<0.001) and trabecular bone volume fraction (e.g., standard site tibia 13.3±2.9 vs. 12.5±2.7%) than controls. However, the total area of the bone sections was significantly smaller (e.g., 14% tibia 429±57 vs 442±59 mm², p=0.001) despite a clearly greater cortical area (e.g., 14% tibia 156±24 vs 152±24 mm², p=0.007) in T2DM (Fig.1). Cortical porosity was lower at 14% tibia (4.8±2.4 vs 5.3±2.4%, p=0.001) in T2DM. All tests showed a significantly worse physical function (TUG +10%, OLS -8.6%, chair-stands -6.4%, grip strength -7.3%, walk speed -4.9%) in women with T2DM compared to controls. Conclusion: Elderly women with T2DM had smaller but denser bones and performed worse in physical function tests than controls matched for BMI. Whether reduced bone size and poorer physical function explain an increased fracture risk in T2DM, despite higher bone density, remains to be elucidated.

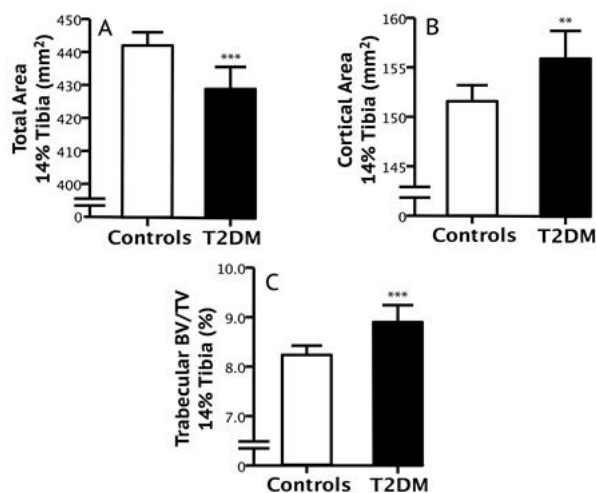


Figure 1. Total (A) and cortical (B) area and trabecular bone volume fraction (C) at the 14 % tibia site in women with type 2 diabetes (n=293) and in BMI-matched controls (n=879). ** p<0.01, *** p=0.001

Disclosures: Anna Nilsson, None

SUN-0894

Bone Biomarkers Do Not Differ in Older Men With and Without Severe Nocturnal Hypoxemia Christine Swanson^{*1}, Steven Shea², Sheila Markwardt³, Orfeu Buxton⁴, Katie Stone⁵, Thuy-Tien Dam⁶, Nancy Lane⁷, Susan Redline⁸, Jane Cauley⁹, Douglas Bauer¹⁰, Eric Orwoll¹¹. ¹University of Colorado, Division of Endocrinology, Metabolism and Diabetes, United States, ²Oregon Institute of Occupational Health Sciences, Oregon Health and Science University, United States, ³OHSU-PSU School of Public Health, United States, ⁴Department of Biobehavioral Health, Pennsylvania State University, United States, ⁵California Pacific Medical Center Research Institute and San Francisco Coordinating Center, United States, ⁶Columbia University, United States, ⁷Center for Musculoskeletal Health, University of California, Davis Medical Center, United States, ⁸Department of Medicine, Brigham and Women's Hospital and Beth Israel Deaconess Medical Center, Harvard Medical School, United States, ⁹Department of Epidemiology, Graduate School of Public Health, University of Pittsburgh, United States, ¹⁰University of California Medical Center, United States, ¹¹Division of Endocrinology Bone and Mineral Unit, Oregon Health and Science University, United States

Obstructive sleep apnea (OSA) is a risk factor for many endocrine disorders but has been variably linked with alterations in bone metabolism. The inconsistent associations between OSA and bone health may be due to the complex OSA phenotype and spectrum of sleep disruption seen in OSA sufferers (e.g., nocturnal hypoxemia, sleep fragmentation, sleep loss, etc.). We used the Osteoporotic Fractures in Men (MrOS) study to investigate the association between nocturnal hypoxemia and biomarkers of bone metabolism. Biomarkers of bone formation (P1NP), resorption (CTX), and osteocyte function (sclerostin, FGF-23) were obtained in older men with polysomnography recordings from the MrOS ancillary sleep study. Men were excluded if they had other sleep disorders, were on treatment for OSA or osteoporosis, had daytime hypoxemia at rest (SaO₂ < 90%), were current smokers, had excess alcohol use, a fracture within three months of their blood draw, were using glucocorticoids, or had a condition known to affect bone metabolism (hyper/hypothyroid, diabetes mellitus, or eGFR < 30 mL/min/1.73 m²). Polysomnography was used to determine the severity of nocturnal hypoxemia based on percent (%) sleep time with oxygen saturation (SaO₂) less than 90% and the apnea hypopnea index (AHI) which was defined as all events with a ≥ 4% desaturation. Bone biomarker levels were compared between a subgroup of men with severe nocturnal hypoxemia (defined as ≥ 10% sleep time with SaO₂ < 90% and AHI ≥ 15) and age/BMI/race-matched men with normal nocturnal oxygenation (defined as < 1% sleep time with SaO₂ < 90% and AHI < 5) using a paired t-test. In total, 36 pairs of men met inclusion/exclusion criteria and had sufficient serum available for this analysis. On average, men were 78 ± 4.6 years old, had a BMI of 28.4 ± 3.0 kg/m², and all were Caucasian. Levels of 25OHD, testosterone, and eGFR were similar between the two groups. CTX tended to be lower in men with severe nocturnal hypoxemia compared to age/BMI/race-matched men with normal nocturnal oxygenation but this was not statistically significant (Table 1). Levels of P1NP, FGF-23, and sclerostin were not significantly different in men with severe nocturnal hypoxemia compared to those with normal nocturnal oxygenation (Table 1). In conclusion, severe nocturnal hypoxemia is not associated with bone biomarkers in older men. This should be confirmed in larger studies.

Table 1: Bone biomarker levels in men with and without severe nocturnal hypoxemia

	Severe Nocturnal Hypoxemia (Mean ± SE)	Normal Nocturnal Oxygenation (Mean ± SE)	Difference (95% CI)	p-value
CTX (ng/mL)	0.38 ± 0.03	0.44 ± 0.03	-0.06 (-0.13, 0.01)	0.12
P1NP (mcg/L)	39.87 ± 2.67	43.05 ± 2.67	-3.18 (-10.60, 4.24)	0.39
FGF-23 (pg/mL)	54.71 ± 2.66	52.35 ± 2.66	2.36 (-4.89, 9.61)	0.51
Sclerostin (pmol/L)	71.33 ± 4.06	72.07 ± 4.06	-0.74 (-12.20, 10.72)	0.90

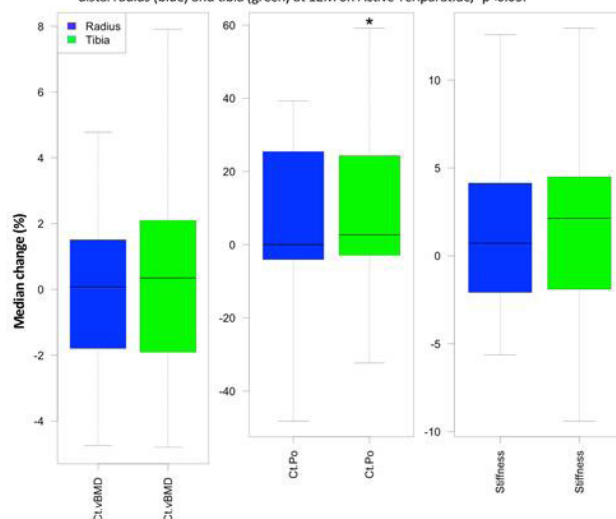
Disclosures: Christine Swanson, None

SUN-0923

Effects of Teriparatide on Bone Microarchitecture and Stiffness Assessed by High Resolution Peripheral Computed Tomography (HR-pQCT) in Premenopausal Idiopathic Osteoporosis (IOP) Sanchita Agarwal^{*1}, Adi Cohen¹, Stephanie Shiau², Mafo Kamanda-Kosseh¹, Mariana Bucovsky¹, X Edward Guo³, Elizabeth Shane¹. ¹Division of Endocrinology, Department of Medicine, Columbia University, United States, ²Gertrude H. Sergievsky Center, Columbia University Medical Center, United States, ³Bone Bioengineering Laboratory, Department of Biomedical Engineering, Columbia University, United States

Pre-menopausal women with IOP (PreMenIOP) have marked deficits in bone mass, microarchitecture and stiffness. In a pilot study of teriparatide (TPTD) in 21 PreMenIOP, we observed increases in BMD by DXA at the spine and hip and no change at the 1/3 radius. After 18M of TPTD, HR-pQCT revealed significant 2.5% increases in trabecular (Tb) density and estimated stiffness, at both radius (RAD) and tibia (TIB), and in cortical (Ct) porosity at RAD only. In a double-blind, placebo-controlled, single-switchover study of TPTD (20mcg SC QD), 41 PreMenIOP were randomized to ActiveTPTD or Placebo pens. At 6M, those randomized to ActiveTPTD continued for 18M and those randomized to Placebo began ActiveTPTD and continued for 24M. A subset (n=34; age=37±8 yrs) had HR-pQCT performed at baseline and after 6M on ActiveTPTD (n=25) or Placebo (n=9) injections. All 34 subjects were scanned after 12M of ActiveTPTD. 22 of 34 had baseline scans on the first-generation HR-pQCT scanner (XCT1) and follow-up scans on the second-generation HR-pQCT (XCT2). To compare subjects with scans on different scanners, XCT2 data were calibrated to XCT1 with regression equations developed in our lab. After excluding 3 radius scans with motion score >3, 6 subjects in the Placebo group had paired 6M scans. Data were analyzed as percent change from baseline. Independent and paired t-tests were performed with p<0.05 considered significant. At baseline, there were no between-group differences at the RAD. TIB Tb thickness was 7 microns lower in the Placebo group (p=0.034). There were no significant between- or within-group differences in Total, Ct or Tb volumetric density, Ct porosity or estimated stiffness after 6M of ActiveTPTD or Placebo at the RAD or TIB. After 12M of ActiveTPTD, TIB Ct porosity increased significantly (+16%, p=0.04), with a trend towards an increase at the RAD (+14%, p=0.06). There were no significant increases in Total, Ct or Tb volumetric density, or estimated stiffness at either site. In summary, we did not detect significant between- or within-groups differences in volumetric density, Ct porosity or stiffness after 6M of ActiveTPTD or Placebo, although the small number of Placebo subjects renders this analysis unreliable. After 12M of ActiveTPTD, we did not detect significant changes in volumetric density or microstructure at either RAD or TIB. We conclude that the increase in Ct porosity with TPTD does not adversely affect Ct volumetric BMD and stiffness in PreMenIOP.

Figure: Median percentage changes and interquartile range (box) for measurements at distal radius (blue) and tibia (green) at 12M on Active Teriparatide, *p<0.05.



Disclosures: Sanchita Agarwal, None

SUN-0924

Effects Of Two Years Of Teriparatide Treatment Followed By Two Years Of Bisphosphonates In Reduction In Fracture Rate And Back Pain At Patients With Multiple Pre-Existing Vertebral Fractures. Corina Galesanu^{*1}, Iulian Pascariu², Veronica Mocanu³, Mihail Romeo Galesanu⁴. ¹University of Medicine and Pharmacy "Grigore T.Popa", Romania, ²Sf.Spiridon Emergency Clinical Hospital, Romania, ³Grigore T. Popa University of Medicine and Pharmacy, Romania, ⁴Romanian Academy of Medical Sciences, Iasi, Romania

Background: Teriparatide (TPTD) is a therapeutic agent that increases the formation of new bone tissue and provide some remediation of the architectural defects in the osteoporotic skeleton. It is unclear which treatment should be given after stopping teriparatide therapy for severe osteoporosis. Bisphosphonate therapy can maintain bone mineral density (BMD) gains after medication cessation. **Objectives:** To evaluate the effect of prior teriparatide exposure and after that the bisphosphonate response, and to compare BMD effects of follow-up treatments. **Methods:** Ten osteoporotic naïve-patients (7 postmenopausal women and 3 men) are treated with teriparatide 20 µg/day for 24 months, followed by risedronate 75 mg/mo for other 24 months. All patients received calcium and vitamin D supplementation. Changes in BMD from baseline to 24 mo, 48 mo were analyzed. Fasting serum was collected for baseline PTH, 25 hydroxyvitamin D, and baseline and treatment 24,48 mo, P1NP, CTX, bone ALP, osteocalcin, serum calcium. **Results:** Daily teriparatide treatment for 2 yr significantly increased spine BMD by 16.6%, total hip and femoral neck, 7.5% and 11.9% respectively. Under the risedronate the year 2 nd have had an increase of BMD at the lumbar by 6.7%, and 4.0% at the total hip and -1.6% at femoral neck. Markers of bone formation (P1NP, bone ALP, osteocalcin) increased early during teriparatide therapy. Under the risedronate markers in bone resorption (CTX) decreased. **Conclusions:** BMD increases progressively over 2 yr of teriparatide therapy in patients with severe osteoporosis. After discontinuation of teriparatide, risedronate 75 mg increases spine and total hip BMD. This confirms the need an antiresorptive treatment to prevent bone loss after teriparatide.

Disclosures: Corina Galesanu, None

SUN-0925

Effect of Buffered Solution of Alendronate 70mg on Bone Mineral Density and Bone ALP: Prospective Observational Study Andrea Giusti^{*1}, Dennis M Black², Antonella Barone³, Josef Hruska⁴, Gerolamo Bianchi¹. ¹La Colletta Hospital, Italy, ²University of California San Francisco, United States, ³Galliera Hospital, Italy, ⁴EffRx Pharmaceuticals, Switzerland

Keywords: osteoporosis, bone mineral density, buffered alendronate **Introduction:** Alendronate 70mg effervescent (ALN-EX) is administered as buffered solution of fully dissolved ALN1. While registration studies have demonstrated bioequivalence of ALN-EX to ALN tablets (ALN-T), BMD and BTM data are lacking. **Objective:** To evaluate the effect of ALN-EX on BMD and bone-ALP (b-ALP), and to compare the outcomes with a historical cohort of patients on ALN-T. **Materials and Methods:** A standardized Clinical Database has been used for the study. 42 postmenopausal women (PMW), presenting with BMD T-score <-2.5, or between -2 and -2.5 and at least one vertebral fracture, starting ALN-EX between July 2015 and June 2016 were enrolled. BMD at femoral neck (FN-BMD), total hip (TH-BMD), and b-ALP were measured at baseline and after 12-month. 54 PMW on ALN-T were randomly selected for the historical cohort. Mean % changes (±SD) of FN-BMD, TH-BMD and b-ALP from baseline to 12-month were compared between the two groups (ALN-EX and ALN-T). **Results:** The two groups were comparable at baseline, including previous history of vertebral/femoral fractures, and baseline BMD. The two groups had comparable mean % increases in FN-BMD and TH-BMD after 12-month of treatment: in ALN-EX group by 1.5%±2.8% (FN-BMD) and 2.1%±2.6% (TH-BMD), in ALN-T group by 1.4%±3.3% (FN-BMD) and 2.2%±3.5% (TH-BMD). Also the absolute decrease (mean U/L±SD) of b-ALP was comparable between ALN-EX group (-6.0±2.8 U/L) and the ALN-T group (-6.9±4.4 U/L). There was no significant difference in BMD or BTM change between ALN-EX and ALN-T. **Conclusion:** To the best of our knowledge, this is the first report comparing BMD and a marker of bone turnover between PMW treated with ALN-EX and PMW treated with ALN-T. Given the limits of the trial design (e.g., lack of randomization), the results of our study demonstrated that ALN-EX is as effective as traditional ALN-T on surrogate anti-fracture efficacy outcomes.

Variable	ALN-EX	P	ALN-T	P
Number of Patients	33		34	
TH-BMD (mean g/cm ² ± SD)	Baseline 0.710 ± 0.092	<.001	Baseline 0.715 ± 0.078	<.001
	12-month 0.725 ± 0.095		12-month 0.730 ± 0.078	
FN-BMD (mean g/cm ² ± SD)	Baseline 0.562 ± 0.058	.001	Baseline 0.560 ± 0.053	.005
	12-month 0.569 ± 0.059		12-month 0.567 ± 0.049	
LN (b-ALP) [†] (mean U/L ± SD)	Baseline 2.9 ± 0.4	<.001	Baseline 3.0 ± 0.4	<.001
	12-month 2.6 ± 0.5		12-month 2.6 ± 0.4	

[†] b-ALP values were transformed in their natural logarithm.

Disclosures: Andrea Giusti, Merck & Co, Consultant, Internis Pharma, Speakers' Bureau, Abiogen, Consultant, Labatec, Speakers' Bureau, EffRx Pharmaceuticals, Grant/Research Support, Chiesi, Consultant

SUN-0926

Patient Characteristics and Fracture Outcomes in Patients Previously Treated With Bisphosphonates or Treatment-naïve in the Teriparatide versus Risedronate VERO Clinical Trial Peyman Hadji^{*1}, Fernando Marin², David Kendler³, Piet Geusens⁴, Luis Russo⁵, Jorge Malouf⁶, Peter Lakatos⁷, Salvatore Minisola⁸, Pedro López-Romero², Astrid Fahrleitner-Pammer⁹. ¹Krankenhaus Nordwest GHMB, Germany, ²Lilly Research Center Europe, Spain, ³University of British Columbia, Canada, ⁴Maastricht University Medical Center, Netherlands, ⁵Centro de Analises e Pesquisas Clinicas LTDA, Brazil, ⁶Hospital Sant Pau, Spain, ⁷Semmelweis University Medical School, Hungary, ⁸Sapienza Rome University, Italy, ⁹Division of Endocrinology, Medical University of Graz, Austria

Background: The fracture results after switching osteoporosis drugs have not been adequately addressed in randomized clinical trials. We previously reported a significant reduction in the risk of new vertebral (VFX) and clinical fractures in patients treated with teriparatide (TPTD) compared to risedronate (RIS), similar in both prior bisphosphonate (BP) users, and in osteoporosis treatment naïve patients. Incident fracture rates were also similar regardless of prior BP treatment. Here, we report a post-hoc analysis comparing the baseline patient characteristics by prior BP therapy. **Patients & Methods:** 1360 postmenopausal women with at least 2 moderate or 1 severe VFX and low bone mass (BMD T-score ≤-1.5) were randomized and treated with SC daily TPTD 20 µg or oral weekly RIS (35 mg) in a double-blind, double-dummy 2-year trial. Patients were considered prior BP users if they had received ≥3 months of any oral, im or iv BPs (ibandronate or pamidronate), or ≥1 dose of iv zoledronic acid. The osteoporosis treatment-naïve group included patients who received none or <3 months of any osteoporosis drugs. Calcium and vitamin D supplements were not considered osteoporosis medications. Data from 57 (4.2%) patients who had received non-BP drugs are not shown. **Results:** 728 (53.5%) patients were prior BP users and 575 (42.3%) were treatment-naïve (full analysis set). Prior BP users were older, had a lower body mass index, more frequently reported a history of a non-vertebral fracture, and were more frequently enrolled in Europe and North America (Table). Fewer prior BP users had a history of a recent clinical vertebral fracture (32.0% vs 43.0%; p<0.0001). Baseline mean serum 25OH-vit D levels were higher in BP users (33.3 vs 29.7 ng/mL; p<0.01). The number and severity of prevalent vertebral fractures and baseline BMD T-scores were similar in the two groups (Table). **Conclusion:** The baseline characteristics of postmenopausal women enrolled in the VERO trial are relatively similar with regard to fracture risk in both women with prior BP use or treatment-naïve. The lower frequency of prior recent spine fracture in the prior BP users was balanced with a higher frequency of prevalent non-vertebral fractures in this group. Differences in baseline characteristics between prior BP users and treatment naïve women are unlikely to have impacted on the fracture risk reduction observed in women randomized to TPTD or RIS. 1Geusens P et al. JBMR (2018);DOI:10.1002/jbmr.3384

Table: Baseline Characteristics

	Treatment naïve (N=575) ^a	Bisphosphonate pre-treated (N=728) ^b	p-value
Age (yrs), mean (SD)	71.2 (9.3)	72.9 (8.1)	<0.001
Body mass index (kg/m ²), mean (SD)	27.4 (4.8)	26.7 (4.5)	<0.01
Geographical region, n (%)			<0.0001
North America	60 (10.4)	122 (16.8)	
South America	178 (31.0)	117 (16.1)	
Europe	337 (58.6)	489 (67.2)	
Bone mineral density, mean (SD)			
Lumbar spine T-score	-2.32 (1.27)	-2.25 (1.19)	0.319
Femoral neck T-score	-2.22 (0.77)	-2.28 (0.73)	0.118
Total hip T-score	-1.93 (0.84)	-1.95 (0.83)	0.576
Patients with ≥1 recent clinical VFX ^c , n (%)	247 (43.0)	233 (32.0)	<0.0001
Number of prevalent VFX, mean (SD)	2.6 (1.9)	2.8 (2.1)	0.053
Grade of the most severe VFX fracture, n (%)			
SQ2	62 (10.8)	68 (9.3)	0.388
SQ3	512 (89.0)	659 (90.5)	0.380
Patients with ≥1 non-VFX >40 yrs of age, n (%)	196 (34.1)	357 (49.0)	<0.0001
Patients with ≥1 hip Fx >40 yrs of age, n (%)	12 (2.1)	29 (4.0)	0.051
Patients on glucocorticoid therapy, n (%) ^d	49 (8.5)	72 (9.9)	0.398
25-OH-vitamin D baseline (ng/mL), mean (SD)	29.7 (24.3)	33.3 (22.6)	<0.01

SD = standard deviation; SQ = semiquantitative grading; VFX = Vertebral fracture

^a Teriparatide=289; Risedronate=286

^b Teriparatide=365; Risedronate=363

^c Within the last 12 months prior to screening.

^d Prednisone-equivalent doses of ≥5 mg/day at the baseline or any post-baseline visit.

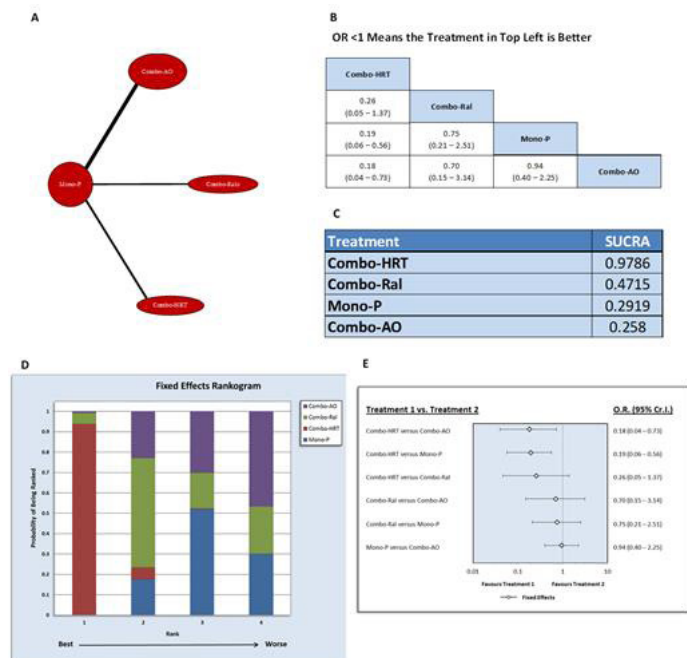
For the comparison of continuous variables t-tests were calculated, for categorical variables χ^2 -tests were used.

Disclosures: Peyman Hadji, Eli Lilly, UCB, Amgen, Gedeon Richter, Meda, Novartis, Hexal, Pfizer and Dr. Kade/Besins, Speakers' Bureau

SUN-0927

Combination therapies for the treatment of osteoporotic fractures are not created equal: A network meta-analysis study Osama Haji Ahmed*¹, Paula Karabelas², Abdulhafez Selim³. ¹Mouwasat Hospitals, Saudi Arabia, ²Independent Investigator, United States, ³PCOM, United States

Background: According to the mechanisms of action, combination therapy may produce more effect for the treatment of osteoporosis. This study aims to assess the effect of 4 interventions: (1) anabolic monotherapy of parathyroid hormone (PTH); (2) combination therapies of anabolic (PTH) and other treatment modalities including anti-osteoclast (AO) agents (Bisphosphonates or Denosumab); (3) hormone replacement therapy (HRT); or (4) Raloxifene (Ral) in adults with osteoporosis. Methods: We searched Medline, EMBASE, and The Cochrane Library from January 1, 1980 to March 1, 2018 for randomized controlled trials of adults with osteoporosis treated in combination therapy compared with monotherapy. The outcome was the incidence of osteoporotic fractures. A total of 11 trials were analyzed with a total of 1,130 patients. The analysis included 4 interventions: monotherapy of PTH (Mono-P), PTH with HRT (Combo-HRT), PTH with Raloxifene (Combo-Ral), and PTH with anti-osteoclast agents (Combo-AO). The meta-analysis was performed using a fixed-effects model. The data were expressed as odds ratio (OR) and 95% CI. Results: Combo-HRT was the only combination that demonstrated a statistically significant reduction of fracture risk compared to Mono-P (OR of 0.18, CI: 0.04-0.73). A significant difference in risk reduction was also observed in the Combo-HRT group when compared to the Combo-AO group (OR of 0.19, CI: 0.06-0.56). Overall ranking demonstrated that Combo-HRT is the most effective treatment (SUCRA score of 94.0%), followed by Combo-Ral (SUCRA score of 47.0%). The Mono-P and Combo-AO groups had low SUCRA scores of 29.0% and 26.0% respectively. Additional data are presented in Figure 1. Conclusion: This is the first network meta-analysis study to evaluate various modalities of the combination therapies. Moderate-quality evidence shows that the combination therapy of PTH and HRT, followed by the combination of PTH and Raloxifene are superior to PTH monotherapy. These differences may be clinically meaningful, particularly for patients at highest risk for hip fractures, including those who have had a recent hip fracture, multiple prevalent fractures, or extremely low hip BMD. Significant differences in effectiveness may be attributed to the variability among mechanisms of action. Further, properly designed, high methodological quality studies are needed to determine the anti-fracture efficacy, cost-effectiveness, and safety of this strategy of combination therapy.



A: Network diagram. B: League table. C: SUCRA scores. D: Rankogram. E: Forest Plot. Combo-HRT: Combination of PTH and HRT. Combo-Ral: combination of PTH, and Raloxifene. Mono-P: PTH only. Combo-AO: combination of PTH, and anti-osteoclast agents (bisphosphonates or Denosumab). SUCRA is a numeric presentation of the overall ranking and presents a single number associated with each treatment. SUCRA values range from 0 to 100%. The higher the SUCRA value, and the closer to 100%, the higher the likelihood that a therapy is in the top rank or one of the top ranks.

Disclosures: Osama Haji Ahmed, None

SUN-0928

Goal-Directed Treatment of Osteoporosis in Patients with Rheumatoid Arthritis Using Daily Teriparatide for Two Years Followed by Antiresorptive Drugs for Three Years (Results in Five Years in Total) Yuji Hirano*, Daisuke Kihira. Department of Rheumatology, Toyohashi Municipal Hospital, Japan

Background: Osteoporosis (OP) is frequently concomitant with rheumatoid arthritis (RA). Effective treatment have to be performed in RA patients with OP (RAOP). We reported results of treatment with 2-year daily teriparatide (dTP) followed by either denosumab (DMB) or minodronate (MIN: a bisphosphonate developed in Japan) with eldcalcitol (ELD: activated vitamin D developed in Japan) in RAOP at ASBMR 2015, 2016 and 2017. It was shown that both treatment strategy has similar efficacy in RAOP. Recently treatment goal of OP was reported from ASBMR-NOF working group (Goal-Directed Treatment, JBMR2017). This progress report advocated that the goal of treatment is a T-score > -2.5 at femoral neck (FN), total hip (TH) or lumbar spine (LS) by DXA if the primary reason for starting treatment was T-score < -2.5 at that skeletal site. The aim of this retrospective study is to evaluate whether 2-year dTP followed by "DMB" or "MIN with ELD" for 3 years can achieve treatment goal of OP reported recently. Methods: This study used 24 female RAOP patients from Toyohashi RA database (TRAD). All patients completed 2-year dTP treatment followed by 3-year either antiresorptive drug treatment shown in background part (DMB: n=10, MIN+ELD: n=14). Treatment goal was set as T-score > -2.5 at five years in patients whose T-score is below -2.5 at the same skeletal site at the initiation of OP treatment in this study. Bone mineral density (BMD) was measured by DXA. As was in clinical setting in Japan, dTP was prescribe as daily self-injection agent. 60mg DMB was administered every 6 months with native vitamin D3 agent. 50mg MIN was administered every 4 weeks and 0.75 µg ELD was administered every day. Results: Baseline characteristics of 24 patients: Mean age was 70 years. RA duration was 18 years. Prednisolone use was 67%. Number of patients with T-score < -2.5 in LS, TH and FN at baseline was 14, 18 and 16, respectively. Proportion of patients with T-score > -2.5 at 5 years was 57.1% in LS-BMD, 22.2% in TH-BMD and 25.0% in FN-BMD (Fig1). Cut-off values at baseline for achievement of treatment goal calculated using receiver operating characteristic (ROC) analysis was -3.4 in LS-BMD, -3.0 in THBMD and -2.9 in FN-BMD. Conclusions: This study suggested that achievement of treatment goal in RAOP is possible in LS-BMD but difficult in TH-BMD and FN-BMD when 2-year dTP followed by antiresorptive drugs for 3 years was used as treatment for RAOP. ROC analysis revealed that early intervention is necessary when treating RAOP aiming treatment goal especially in treating THBMD and FNBMd.

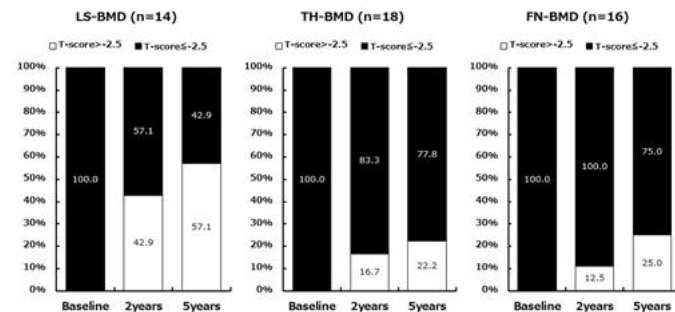


Fig1. Change of percentage of patients with T-score > 2.5. Daily teriparatide treatment was performed from baseline to 2 years. Either denosumab treatment or monodronate with eldcalcitol was performed from 2 years to 5 years.

Disclosures: Yuji Hirano, None

SUN-0929

Determinants of Oral Bisphosphonate Therapy Beyond Five Years Monika Izano*¹, Bonnie Li², Fang Niu³, Romain Neugebauer¹, Bruce Ettinger¹, Susan Ott⁴, Joan Lo¹, Annette Adams². ¹Division of Research, Kaiser Permanente Northern California, United States, ²Department of Research & Evaluation, Kaiser Permanente Southern California, United States, ³Pharmacy Outcomes Research Group, Kaiser Permanente California, United States, ⁴Department of Medicine, University of Washington, United States

Purpose: In this cohort study of women receiving osteoporosis treatment with oral bisphosphonate (BP) within Kaiser Permanente Southern California, we investigated factors that were associated with BP continuation. Methods: Women who received 5 consecutive years of BP treatment entered the cohort during 2002-2010 and were followed for up to 5 additional years. A woman was considered on treatment in each 90-day interval of follow-up if she received BP for more than a 0.6 proportion of days covered based on pharmacy days' supply. We used multivariable logistic regression with robust standard errors (Generalized Estimating Equations) to evaluate the possible association of (1) demographic factors, (2) period of cohort entry, (3) predictors of fracture risk, and (4) elements of medical history with continuation of BP treatment. Results: The study cohort included 19481 women, mean age 72 years (interquartile range: 65-79 years); 58% were white, 5% black, 16% Hispanic, and 17% Asian; 25% entered the study between 2002-2007, and 75% entered between 2008-

Sunday Posters

2010; 43% were overweight/obese, 40% had a Charlson Comorbidity Index (CCI) ≥ 1 , and 10% had diabetes mellitus. Of the 13302 women with available bone mineral density (BMD) measured in the 2 years prior to BP initiation, 55% had a BMD t-score ≤ -2.5 (lowest of hip, femur, spine). Factors significantly associated with increased odds of BP continuation were: (a) cohort entry on or before 2007 (Odds Ratio (OR)=1.38, 95% Confidence Interval 1.32–1.44), (b) most recent BMD t-score (referent t-score > -2 ; OR=1.50, 1.42–1.58 for $-2.5 < t < -2$; OR=1.49, 1.38–1.61 for $-2.5 \leq t < -3$; OR=1.70, 1.57–1.85 for $t \leq -3.0$), and (c) longer BP use (OR ranging 1.2–1.3 from 1–5 years, compared to < 6 months). In contrast, factors significantly associated with decreased odds of continued BP use were: (a) a recent hip (OR=0.64, 0.55–0.75) or non-major osteoporotic fracture (OR=0.86, 0.80–0.93), (b) CCI > 2 (OR=0.92, 0.85–0.99), (c) Hispanic (OR=0.91, 0.86–0.96) or Asian (OR=0.94, 0.89–0.99) race, (d) proton-pump inhibitor (OR=0.59, 0.38–0.91), glucocorticoid (OR=0.82, 0.72–0.95), and aromatase-inhibitor (OR=0.44, 0.39–0.50) use. Age, smoking, estimated low income/education, body mass index, chronic kidney disease, and fracture prior to BP initiation were not associated with BP continuation. Conclusions: Factors that predict continued BP treatment beyond 5 years include recent fracture, low BMD t-score, medication exposure and era of treatment.

Disclosures: *Monika Izano, None*

SUN-0930

Increased iliac crest bone hardness under Denosumab treatment is accompanied by a low number of viable osteocytes Katharina Jähn^{*1}, Björn Jobke², Eva Maria Wölfel¹, Tobias Barth¹, Christoph Riedel¹, Maya Hellmich³, Mathias Werner⁴, Björn Busse¹. ¹University Medical Center Hamburg-Eppendorf, Germany, ²Telemedicine Clinic, Spain, ³Immanuel Krankenhaus Berlin, Germany, ⁴Helios Klinikum Emil von Behring, Germany

Antiresorptives are among the first treatment options for osteoporosis. Denosumab is the latest approved potent osteoclast inhibitor. Recent data identified the risk of vertebral fractures during drug-holiday from Denosumab osteoporosis therapy. In bone health, the spatiotemporal activation of bone remodeling is guided by the mechanosensitive osteocyte network. One hallmark of osteoporosis progression is the death of osteocytes with weakening of their network connectivity and regulatory functionality. We have identified iliac crest biopsies (n=25 during Denosumab - duration: 26±13 months, n=10 on drug-holiday from Denosumab - holiday duration: 15±12 months, n=11 age-matched osteoporotic controls; 67±14yrs) that underwent previous clinical histopathological assessment. We performed structural and cellular histomorphometry according to ASBMR guidelines. Histological sections were stained with toluidine blue and von Kossa van Gieson and analyzed with Osteomeasure. Biomechanical properties of the bone tissue were tested with nano-indentation. The local degree of tissue mineralization was assessed by backscattered electron microscopy. Statistics were performed by ANOVA and Turkey post-hoc test. Bone tissue exposed to Denosumab treatment had a higher tissue hardness compared to osteoporotic controls (0.62±0.05 to 0.52±0.09 GPa; p=0.0042). The tissue mineralization, expressed by calcium weight percentages, was not significantly higher in the Denosumab group compared to untreated (22.2±1.3 to 21.2±2.0 wt%; p=0.074). However, the percentage of micropetrotic, mineralized lacunae was higher in the Denosumab group (8.1±4.1, compared to control: 3.3±1.6 %; p=0.0067). Trabecular BV/TV was lowest during drug-holiday compared to Denosumab (10.48±3.41 vs. 15.93±6.45; p=0.036). As expected, osteoclast numbers were significantly lower with treatment in comparison to untreated individuals (0.12±0.23 vs. 0.72±0.8 /mm; p=0.003). Interestingly, the number of empty osteocyte lacunae in trabecular bone was higher with Denosumab treatment compared to osteoporotic controls (35.1±10.5 vs. 23.3±5.7 %; p=0.011) and remained elevated (35.8±13.4) during drug-holiday (p=0.039 to control). Our results imply that Denosumab treatment results in harder bone tissue accompanied by a lower number of viable osteocytes at the iliac crest.

Disclosures: *Katharina Jähn, None*

SUN-0931

Influence of glucocorticoids on effect of denosumab on osteoporosis in patients with Japanese rheumatoid arthritis; 36 months of follow-up ~a Multicenter Registry Study~ Yasuhide Kanayama^{*1}, Yuji Hirano², Nobunori Takahashi³, Naoki Ishiguro³, Toshihisa Kojima³. ¹Toyota Kosei Hospital, Japan, ²Toyohashi Municipal Hospital, Japan, ³Nagoya University Graduate school of Medicine, Japan

[Objectives] To investigate the efficacy of DMB for 36 months on glucocorticoid-induced OP in Japanese RA patients. [Methods] Patients with a diagnosis of RA according to the 2010 ACR/EULAR criteria who had been prescribed DMB from Tsurumi Biologics Communication Registry (TBCR)-BONE between October 2013 and February 2015 were enrolled. The final study cohort of 65 patients received continuous DMB therapy more than 36 months. The DMB dose was 60mg at once every 6 months. In all cases native or activated vitamin D has been used. We reviewed the results for 36 months about the increase and decrease of bone mineral density (BMD) of lumbar spine (LS) and total hip (TH) by DEXA and bone turnover markers, intact n-terminal propeptide type I procollagen (PINP) and tartrate-resistant acid phosphatase form 5b (TRACP-5b). [Results] In the patients receiving oral prednisolone group (n=24, GC+) and not receiving group (n=41, GC-), the number of female was each 22 (92%) and 39 (95%) cases (p=0.576). The mean age was 69.9 ± 6.8 and 70.8 ± 7.2 years old (p=0.749); disease duration was 15.4 ± 9.1 and 15.5 ± 12.6 years (p=0.859);

the body mass index was 20.8 ± 3.5 and 19.7 ± 3.0 (p=0.226) and the FRAX was 34.3 ± 18.7 and 23.6 ± 13.4 (p=0.013). Clinical findings related to RA and OP at baseline were as follows; CRP 1.2 ± 1.4 and 0.4 ± 1.0 mg/dl (p=0.006); DAS-CRP 3.09 ± 1.20 and 2.48 ± 1.23 (p=0.032); HAQ-DI 1.19 ± 0.91 and 0.80 ± 0.81 (p=0.098); PINP 60.8 ± 37.9 and 55.3 ± 31.8 µg/l (p=0.471); TRACP-5b 521 ± 255 and 504 ± 201 mU/dL (p=0.870); LS-BMD 0.87 ± 0.18 and 0.80 ± 0.14 g/cm² (p=0.091) and TH-BMD 0.60 ± 0.11 and 0.60 ± 0.08 g/cm² (p=0.674). The rate of decreased PINP from baseline to 6, 12, 24 and 36 months were each -27.8% vs -39.8% (p=0.237) at 6 month, -11.1% vs -44.1% (p=0.047) at 12 month, -16.8% vs -35.8% (p=0.172) at 24 month and -15.0% vs -33.4% (p=0.298) at 36 month and TRACP-5b were -28.6% vs -35.6% (p=0.994) at 6 month, -24.5% vs -36.7% (p=0.273) at 12 month, -23.0% vs -30.7% (p=0.613) at 24 month and -23.0% vs -30.7% (p=0.613) at 36 month in the GC+ group vs GC- group. The rate of increased LS-BMD from baseline to 6, 12, 24 and 36 months were each 4.1% vs 4.6% (p=0.682) at 6 month, 5.2% vs 7.1% (p=0.221) at 12 month, 9.9% vs 7.9% (p=0.119) at 24 month and 11.1% vs 9.9% (p=0.151) at 36 month and TH-BMD were 3.5% vs 2.4% (p=0.408) at 6 month, 1.6% vs 3.8% (p=0.842) at 12 month, 5.9% vs 4.8% (p=0.954) at 24 month and 7.8% vs 4.7% (p=0.873) at 36 month in the GC+ group vs GC- group (Fig.1). [Conclusion] DMB was effective in OP of RA patients. Glucocorticoids use did not influence the efficacy of DMB for 36 months.

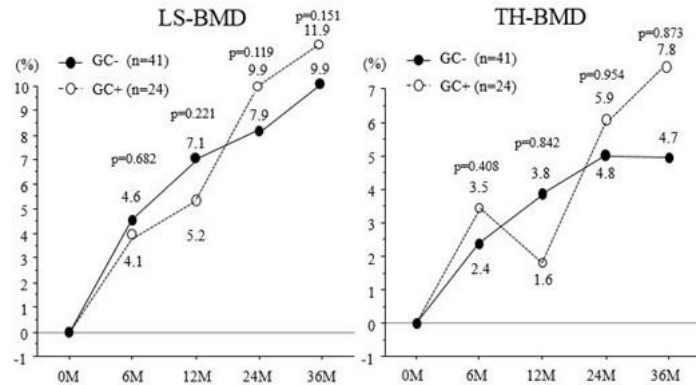


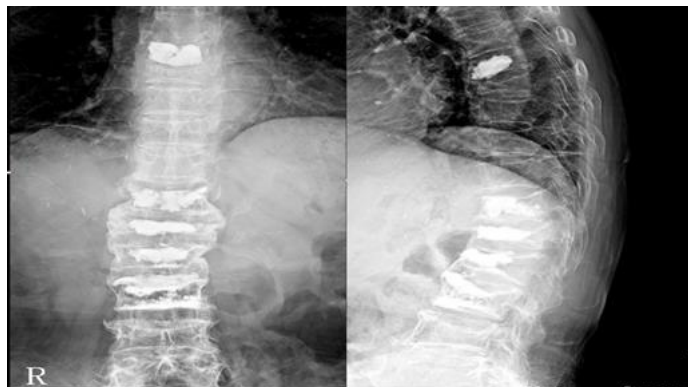
Figure 1: The rate of increased LS-BMD and TH-BMD from baseline to 36 month

Disclosures: *Yasuhide Kanayama, None*

SUN-0932

Spontaneous Fusion after Vertebroplasty and Kyphoplasty in Painful Osteoporotic Compression Fracture Jin Hwan Kim^{*1}, Jae Hyup Lee², Young Kyu Kim¹. ¹Inje University, Ilsanpaik Hospital, Republic of Korea, ²Seoul National University, College of Medicine, Republic of Korea

Purpose : We found a spontaneous fusion at adjacent vertebrae after percutaneous vertebroplasty (PVP) or kyphoplasty in painful osteoporotic compression fractures and analyze the radiologic & clinical characteristics. Materials & Methods : Between January 2002 and December 2015, 555 patients were treated with PVP or kyphoplasty for osteoporotic compression fracture in our department. We classified the spontaneous fusion as two groups. One is solid spontaneous fusion group with at least three cortical continuity to adjacent vertebrae, the other is partially fusion group which progressed fusion compared to previous radiologic finding. We reviewed the plain film and analyzed the radiologic characteristics of those patients with duration of fusion, location and extent of fused segments. A clinical characteristic by visual analogue score (VAS) compared to our previous report was checked. Results : Among them, 54 patients (9.7%) had an solid spontaneous fusion and 43 patients (7.7%) had partially fused on plane image. In solid fusion group, the average duration of fusion was 19 months ranged of 3 to 48 months. Forty six cases (85%) of solid fusion patients had occurred with proximal adjacent vertebrae and 7 cases (13%) had proximal with distal adjacent vertebrae. Forty one cases (76%) of spontaneous fusion occurred within 1 segment and 13 cases within multiple segments. The most cases of solid fusion group were occurred at thoracolumbar junction (40 patients, 74%). Mean VAS score of solid fusion group was 2.0 at final follow-up and were analyzed relatively low score compared to mean VAS of our previous report (2.0, 2.8 respectively). Conclusion : After percutaneous vertebroplasty or kyphoplasty in painful osteoporotic compression fracture, unpredictable spontaneous fusion could develop more than 10% rate, especially with proximal vertebra within 1 segment at thoracolumbar junction in radiologic aspect. Clinically, patients with spontaneous fusion had a tendency of more reduced pain than others.

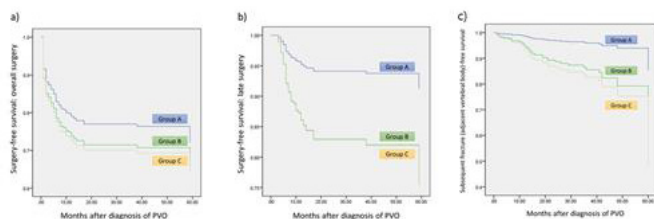


Disclosures: *Jin Hwan Kim, None*

SUN-0933

Is early bisphosphonate treatment safe or effective for pyogenic vertebral osteomyelitis with osteoporosis? Jihye Kim^{*1}, Tae-Hwan Kim². ¹Kangdong Sacred Heart Hospital, Hallym University College of Medicine, Republic of Korea, ²Hallym University Sacred Heart Hospital, Hallym University College of Medicine, Republic of Korea

Background. Patients with pyogenic vertebral osteomyelitis (PVO) have greatly increased risk of bone loss because of rapid destruction of vertebral structure by the causative organism, delay in diagnosis, bed rest and immobilization by rigid brace for three to four months, and limited sunlight exposure by long hospitalization for long-term intravenous antibiotic administration. Such bone loss could be fatal on bone health of elderly PVO patients with several medical comorbidities. In this respect, early bisphosphonate therapy would be clinically effective for PVO patients with osteoporosis. **Methods.** A retrospective case review was performed on PVO patients who received bisphosphonate treatment for osteoporosis. PVO patients were divided into three groups: 1) group A (initiation of bisphosphonate within 6 weeks after PVO diagnosis); 2) group B (initiation of bisphosphonate between 6 weeks and 3 months after PVO diagnosis), and group C (initiation of bisphosphonate between 3 and 6 months after PVO diagnosis). Long-term effectiveness and safety of bisphosphonate on bone loss after PVO was analyzed by Cox proportional hazard model. **Results.** A total of 405 PVO patients with osteoporosis were evaluated for following four endpoints. Group A PVO patients had significantly lower hazard ratio for undergoing late surgery than either group B or C PVO patients ($p=0.020$). There was no difference in the rate of recurrence among the three groups ($p=0.602$). Significant difference was observed in the occurrence of subsequent fractures at adjacent vertebral bodies among the three groups ($p=0.020$), and group A PVO patients had significantly lower hazard ratio for subsequent fracture than either group B ($p=0.032$) or group C ($p=0.004$) PVO patients. Hazard ratios were not significantly different among the three groups for either overall death ($p=0.133$) or later death ($p=0.127$). **Conclusions.** Early bisphosphonate treatment in PVO patients with osteoporosis was associated with lower occurrence of subsequent vertebral fracture at adjacent vertebral bodies, and lower occurrence of late surgery.



Disclosures: *Jihye Kim, None*

SUN-0934

Effect of Medications on Secondary Prevention of Osteoporotic Vertebral Compression Fracture: a Meta-analysis of Randomized Controlled Trials Yuan-Zhe Jin^{*1}, Jae Hyup Lee¹, Jin-Hwan Kim². ¹Seoul National University, College of Medicine, Republic of Korea, ²Inje University, College of Medicine, Republic of Korea

Bone loss with aging and menopause increases the risk of fragile vertebral fracture, osteoporotic vertebral compression fracture (OVCF). The fracture causes severe pain, impedes respiratory function, lower the quality of life, and increases the risk of new fractures and deaths. Various medications have been prescribed to prevent a secondary fracture, but few study summarized their effects. Therefore, we investigated the effects of medications on preventing subsequent OVCF via meta-analyses of randomized controlled trials. Elec-

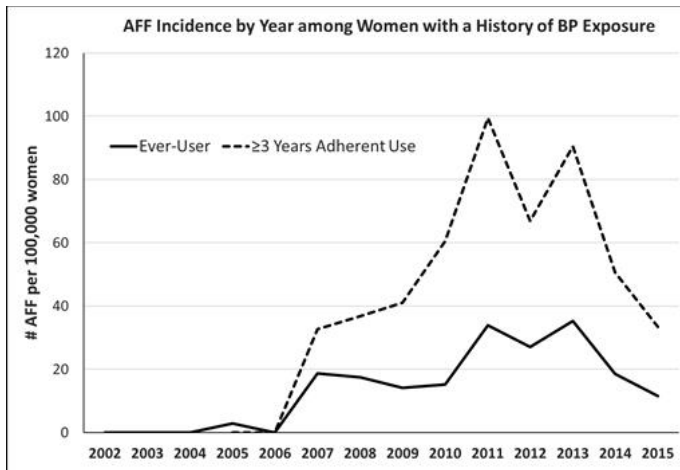
tronic databases, including MEDLINE, EMBASE, CENTRAL, and Web of Science were searched for published randomized controlled trials until December 2017. The trials that recruited participants with at least one OVCF were included. We assessed the risk of bias of every study, estimated relative risk ratio of secondary OVCF, non-vertebral fracture, gastrointestinal complaints and discontinuation due to adverse events. Finally, we evaluated the quality of evidence. Thirty-nine articles were included. Moderate to high quality evidence proved the effectiveness of alendronate (Relative Risk, RR: 0.54), risedronate (RR: 0.52), ibandronate (RR: 0.52), parathyroid hormone (RR: 0.30), and selective estrogen receptor modulators (Raloxifene, RR: 0.58; Bazedoxifene, RR: 0.66) in preventing secondary fractures. Moderate quality evidence proved romosozumab had better effect than alendronate (Romosozumab vs. alendronate, RR: 0.64) and high quality evidence proved that teriparatide had better effect than risedronate (risedronate vs. teriparatide, RR: 1.67). Zoledronic acid, alendronate, risedronate, ibandronate, parathyroid hormone, denosumab and selective estrogen receptor modulators had significant secondary prevention effects on OVCF. Moderate quality evidence proved romosozumab had better effect than alendronate. High quality evidence proved parathyroid hormone had better effect than risedronate, but with higher risk of adverse events.

Disclosures: *Yuan-Zhe Jin, None*

SUN-0935

Incidence of Complete Atypical Femur Fracture among Women with Oral Bisphosphonate Exposure in an Integrated Healthcare System Joan Lo^{*1}, Christopher Grimsrud², Susan Ott³, Malini Chandra¹, Rita Hui⁴, Monika Izano¹, Annette Adams⁵, Bruce Ettinger¹. ¹Division of Research, Kaiser Permanente Northern California, United States, ²Department of Orthopedic Surgery, Kaiser Permanente Oakland Medical Center, United States, ³Department of Medicine, University of Washington, United States, ⁴Pharmacy Outcomes Research Group, Kaiser Permanente California, United States, ⁵Research and Evaluation, Kaiser Permanente Southern California, United States

PURPOSE: This study provides annual estimates of the incidence of atypical femur fracture (AFF) among older women with a history of oral bisphosphonate (BP) exposure, a measure for which few recent population-level estimates are currently available. **METHODS:** The study population included 94,553 Kaiser Permanente Northern California (KPNC) female members age 45-89 years who initiated oral BP between 2002-2014 and had at least 2 years prior health plan membership. We excluded women who received intravenous BP, teriparatide, or denosumab or who had metastatic cancer, skeletal disorders, or advanced chronic kidney disease prior to the start of follow-up. Among this group ("ever-users"), follow-up started at BP initiation and ended at disenrollment, death, age 90 years, or development of an aforementioned exclusion indication. We searched for ICD-9 codes for hospitalized diaphyseal femur fractures and reviewed radiographs to identify complete AFF using the 2013 ASBMR criteria, ascertaining the first AFF per person. The annual incidence of AFF (2002-2015) was calculated as the ratio of AFF events that year to the number of women with BP exposure; this number included women initiating BP in that year or in prior years (BP exposure could have varied from <1 and up to 14 years). We additionally estimated AFF incidence (2005-2015) among women who received at least 3 consecutive years of treatment (adherence 60%) after BP initiation. **RESULTS:** The cumulative number of women with AFF in the KPNC cohort increased dramatically over the years 2002-2015; there were <10 women with AFF in the first 6 years of observation and >100 women with AFF by the end of the 14-year period. The number of BP ever-users increased more than 3-fold during this same observation period; in 2007, there were >40,000 women, and by 2015, there were >60,000 women. The number of women who had adherent BP treatment for at least 3 years after BP initiation increased more than 2-fold during 2005-2015; in 2007, there were >9,000 women, and by 2015, there were >14,000. AFF incidence for ever-users averaged 21.3 per 100,000 during 2007-2015. In marked contrast, AFF incidence for those with at least 3 years of BP use was more than double that of ever-users in the same time period, averaging 56.9 per 100,000 during 2007-2015. **CONCLUSION:** The duration of BP exposure is important when examining the incidence of AFF.



Disclosures: **Joan Lo, Sanofi, Grant/Research Support**

SUN-0936

Compliance, Adverse Effects, Bone-related Mineral and Vitamin D Status, and Literature Review of Denosumab Therapy for Osteoporosis in Japan Yukio Nakamura*, Takako Suzuki, Hiroyuki Kato. Shinshu University School of Medicine, Japan

Background: Denosumab is a first-line drug both for primary and secondary osteoporosis. In our clinical setting, denosumab use on patients ranging from 2 to 110 years of age have reached over 2500 osteoporosis cases to date for analysis of bone turnover markers, bone mineral density of the lumbar 1-4 vertebrae and bilateral total hips, calcium, and vitamin D metabolism (ClinicalTrials: #NCT02156960). Over the last few years, more than 15 English reports have been published regarding the usefulness and efficacy of denosumab (generally 60 mg subcutaneously every 6 months with adjustment according to body weight for children) for osteoporosis related to such conditions as congenital skeletal diseases (TJEM. 2017; MR. in press), glucocorticoid-induced osteoporosis with collagen diseases (JCM. 2018; MR. 2018; Ther Clin Risk Manag. 2018), early pregnancy (JNDT. 2017), and others including atypical femoral fracture caused by long-term bisphosphonate (BP) therapy (MR. 2017; MR. 2018). Of particular note was the rarity of serious adverse effects, such as hypocalcaemia or osteonecrosis of the jaw. However, real-world data on denosumab use remain insufficient. **Methods:** We present novel findings concerning: 1) the compliance, discontinuation rate, and fracture incidence of 143 primary osteoporotic postmenopausal Japanese women (average age: 76.4 ± 0.9 years) and 96 osteoporotic women with RA (average age: 70.0 ± 0.8 years) after 2 years of denosumab treatment, and 2) serum bone-related minerals (zinc, iron, and magnesium) and 25-hydroxyvitamin D (25OHD) status in female osteoporosis with RA of low-to-moderate disease activity in 26 cases with BP pre-treatment (mean age: 69.8 ± 1.3 years) and 26 cases without (mean age: 70.6 ± 1.9 years) after 3 years of denosumab treatment. **Results and Conclusions:** We observed that: 1) discontinuation rate was low over 2 years of treatment in primary osteoporotic patients, with high persistence at 24 months (65.0%) and no occurrence of fracture. In RA patients, discontinuation was found to increase due to economic reasons from 1 to 2 years of therapy, but overall persistence remained high at 24 months (70.8%), with 2 reports of fracture, and 2) among bone-related minerals, serum zinc and iron levels were significantly improved at 12 months and serum 25OHD remained high after denosumab therapy. Taken together, denosumab treatment was successful, thus validating its use as a first-line drug for primary and secondary osteoporosis.

Disclosures: **Yukio Nakamura, None**

SUN-0937

Subgroup Analysis of the Effect of Denosumab Compared With Risedronate on Percentage Change in Lumbar Spine Bone Mineral Density at 24 Months in Glucocorticoid-treated Individuals Ken Saag*¹, Nico Pannacciuoli², Piet Geusens³, Jonathan Adachi⁴, Eric Lespessailles⁵, Jorge Malouf-Sierra⁶, Bente Langdahl⁷, Peter W. Butler², Xiang Yin², Willem F. Lems⁸. ¹University of Alabama, Birmingham, United States, ²Amgen Inc., United States, ³Maastricht University Medical Center, Netherlands, ⁴McMaster University, Canada, ⁵University Hospital Orleans, France, ⁶Hospital San Pablo, Spain, ⁷Aarhus University Hospital, Denmark, ⁸VU University Medical Centre, Netherlands

Purpose: We previously demonstrated that denosumab (DMAb) increased lumbar spine (LS) and total hip (TH) BMD significantly more than risedronate (RIS) at 12 and 24 months (mos) in glucocorticoid (GC)-treated individuals (Saag ACR 2016; Saag ECTS 2018). Pre-specified subgroup analyses of LS BMD at 12 mos indicated that DMAb was superior to RIS across 7 subgroups of GC-treated individuals (Saag ASBMR 2017). This analysis explored the effects of DMAb and RIS on LS BMD in the same subgroups of GC-treated

individuals at 24 mos. **Methods:** The phase 3, randomized, double-blind, double-dummy, active-controlled study enrolled women and men age ≥18 years receiving ≥7.5 mg prednisone or equivalent daily for <3 mos (GC-initiating [GC-I]) or ≥3 mos (GC-continuing [GC-C]) before screening. All subjects age <50 years were required to have a history of osteoporotic fracture. GC-C subjects age ≥50 years were required to have LS, TH, or femoral neck BMD T-score ≤-2.0; or ≤-1.0 with a history of osteoporotic fracture. Subjects were randomized 1:1 to DMAb 60 mg SC every 6 mos or RIS 5 mg PO daily for 24 mos. All subjects were to receive daily calcium (≥1000 mg) and vitamin D (≥800 IU). The treatment difference (DMAB - RIS) for percentage change from baseline in LS BMD at 24 mos was estimated in the GC-I and GC-C subpopulations, both overall and in 7 prespecified subgroups where treatment effect might differ (sex, race, age, baseline BMD T-score, geographic region, menopausal status, and baseline GC daily dose). **Results:** The study enrolled 795 subjects (290 GC-I, 505 GC-C). Baseline characteristics were balanced between treatment groups within each subpopulation. DMAb was superior to RIS for gains in LS BMD at 24 mos in both the GC-I and GC-C subpopulations. Within each subgroup (Table), DMAb was consistently associated with a greater increase in LS BMD at 24 mos compared with RIS. Significant quantitative interactions were observed only in the sex and race subgroups in the GC-I subpopulation. However, qualitative tests indicated the direction of the DMAb effect did not differ significantly by sex or race in this subpopulation. **Conclusion:** DMAb consistently increased LS BMD more than RIS at 24 mos in both GC-I and GC-C subpopulations, with no evidence of directional heterogeneity in treatment effect across 7 prespecified subgroups of GC-treated individuals. DMAb may be a useful addition to the osteoporosis armamentarium in the common clinical setting of GC use.

Table. Treatment Difference (DMAB - RIS) in Lumbar Spine BMD Percentage Change From Baseline at Month 24

	Glucocorticoid-Initiating Subpopulation (N = 133 RIS / 128 DMAB)				Glucocorticoid-continuing Subpopulation (N = 230 RIS / 228 DMAB)			
	DMAB (n)	RIS (n)	Least Square Mean Estimate of Difference (95% CI)	Interaction P value Quantitative (Qualitative)	DMAB (n)	RIS (n)	Least Square Mean Estimate of Difference (95% CI)	Interaction P value Quantitative
Overall subpopulation	107	113	4.5 (3.2, 5.8)*	-	183	174	3.2 (2.0, 4.3)*	-
Sex								
Female	69	72	5.7 (4.0, 7.5)*	0.013	141	131	3.7 (2.4, 5.0)*	0.13
Male	38	41	2.1 (0.1, 4.1) [†]	(0.50) [†]	42	43	1.4 (-1.1, 4.0)	
Race								
Caucasian	92	97	3.9 (2.4, 5.3)*	0.024	166	158	3.3 (2.1, 4.5)*	0.63
Not Caucasian	15	16	7.6 (3.8, 11.4)*	(0.50) [†]	17	16	1.9 (-1.6, 5.4)	
Age								
< 60 years	28	41	2.9 (0.1, 5.8) [†]	0.089	79	86	2.9 (1.2, 4.6) [†]	0.72
≥ 60 years	79	72	5.1 (3.6, 6.6)*		104	88	3.4 (1.9, 5.0)*	
Baseline LS T-score								
≤ -2.5	17	21	4.6 (1.0, 8.1) [†]	0.066	66	68	3.4 (1.1, 5.6) [†]	0.44
> -2.5	90	92	3.9 (2.5, 5.2)*		117	106	2.9 (1.6, 4.2)*	
Baseline LS T-score								
≤ -1.0	55	60	5.4 (3.6, 7.3)*	0.13	142	141	3.2 (1.8, 4.5)*	0.89
> -1.0	52	53	2.8 (1.0, 4.6) [†]		41	33	2.9 (1.0, 4.8) [†]	
Geographic region								
Europe	65	73	4.0 (2.4, 5.6)*	0.24	135	122	3.2 (1.8, 4.6)*	0.90
Non-Europe	42	40	5.3 (2.9, 7.8)*		48	52	2.6 (0.8, 4.5) [†]	
Menopausal status								
Premenopausal	9	3	11.4 (1.2, 21.7) [†]	0.77	20	20	3.9 (0.2, 7.6) [†]	0.98
Postmenopausal	59	67	5.7 (3.9, 7.6)*		119	109	3.7 (2.3, 5.1)*	
Baseline GC dose[‡]								
≤ 7.5 to < 10 mg	20	28	6.3 (2.8, 9.7)*	0.57	61	67	3.4 (1.6, 5.2)*	0.88
≥ 10 mg	85	85	4.3 (2.8, 5.8)*		121	107	3.2 (1.7, 4.7)*	

CI = confidence interval; N = Number of randomized subjects with a baseline measurement and ≥ 1 postbaseline measurement for the lumbar spine BMD; n = number of subjects with observed value. *p<0.001, DMAb vs RIS. [†]p<0.05, DMAb vs RIS. [‡]Qualitative p-values >0.05 support consistent directionality of treatment effect within the subgroups. [†]In prednisone equivalents.

Disclosures: **Ken Saag, Amgen, Lilly, Merck, Radius, Consultant, Amgen, Merck, Grant/Research Support**

SUN-0938

Teriparatide re-activates bone metabolism of the patients with bisphosphonates treatment failures. Shinya Tanaka*¹, Katsuya Kanesaki², Yoichi Kishikawa³, Sathoshi Ikeda⁴, Masato Nagashima⁵, Tsuyoshi Miyajima¹, Hiromi Oda¹. ¹Saitama medical university, Japan, ²Nagat orthopedic hospital, Japan, ³Kishikawa orthopedic surgery, Japan, ⁴Ken-ai memorial hospital, Japan, ⁵Katsuki brain and orthopedic surgery, Japan

In the practice of the goal-directed treatment of osteoporosis, physicians must change treatments when treatment failures, no increase in bone mineral density (BMD) or occurrences of vulnerable fracture, happen. Once treatment failure occurs during osteoporosis treatment with bisphosphonate, it is reasonable to re-activate bone metabolism. In this retrospective cohort study, we tested whether teriparatide can re-activate the bone metabolism of the patients with bisphosphonates treatment failures. **Patients and Methods:** Menopausal osteoporosis patients whose BMD had not increased or who had had vulnerable fractures during bisphosphonate treatment were included in this study. Daily teriparatide was used for 28 patients for 2 years (dTPD group) and weekly teriparatide was used for 34 patients for 1.5 years (wTPD group). After teriparatide therapy, patients were treated by anti-bone resorption drugs, bisphosphonates or anti-RANKL-antibody, and were measured BMD periodically by 1 year after the end of teriparatide therapy. We investigated changes of BMD during those therapies. **Results:** There were 11.9% increase in lumbar vertebral BMD and 2.7% increase

in femoral neck BMD of dTPD group during teriparatide therapy. Anti-bone resorption therapy after teriparatide brought 2.0% increase in the vertebral BMD. There was 3.2% increase in lumbar vertebral BMD of wTPD group. Anti-bone resorption therapy after weekly teriparatide brought 5.6% increase in the vertebral BMD and 3.1% increase in femoral neck BMD. Discussion; In spite of after bisphosphonate therapy, teriparatide therapy and following anti-resorption therapy partially brought increase in BMD. Teriparatide causes re-activation of metabolism and increase in bone mass to the metabolism suppressed bone and following anti-resorption therapy accelerated the calcification of the bone mass, and BMD increased. Conclusion; Teriparatide re-activates bone metabolism of the patients with bisphosphonates treatment failures.

Disclosures: *Shinya Tanaka, None*

SUN-0939

Two-year persistence with Teriparatide improves significantly after extension of an educational and motivational support program Maud Van Maren^{*1}, Caroline E Wyers^{1,2}, Johanna Hm Driessen³, Jonathan V Visser⁴, Frank De Vries⁵, Katrien Van De Wijdeven⁴, Sonja Gevers⁴, Willem F Lems⁶, Marielle H Emmelot-Vonk⁷, Joop Pw Van Den Bergh^{1,2,8}. ¹VieCuri Medical Center, Department of Internal Medicine, Netherlands, ²Maastricht University Medical Center (Maastricht UMC+), NUTRIM School for Nutrition and Translational Research in Metabolism, Department of Internal Medicine, Netherlands, ³Maastricht UMC+, CAPHRI Care and Public Health Research Institute, NUTRIM School for Nutrition and Translational Research in Metabolism, Department of Clinical Pharmacy and Toxicology, Netherlands, ⁴ApotheekZorg (Pharmacy), Netherlands, ⁵Maastricht UMC+, Department of Clinical Pharmacy and Toxicology, Netherlands, ⁶VU Medical Centre, Amsterdam Rheumatology and Immunology Center, Netherlands, ⁷University Medical Center Utrecht, Department of Geriatric Medicine, Netherlands, ⁸Hasselt University, Netherlands

Purpose: To determine whether an educational and motivational support program increases treatment persistence with teriparatide (TPTD) in the Netherlands. Methods: In the Netherlands, one central pharmacy provides TPTD, enabling us to study persistence in all patients who were prescribed TPTD from January 2013 - January 2018. TPTD was dispensed as a pre-filled pen containing 750mcg TPTD intended to be used as daily subcutaneous injection of 20mcg TPTD for 28 consecutive days. A max. of 26 pens was dispensed during the 24-month treatment period. From January 2013 - April 2015, all patients were instructed and followed according to a basic care program (BCP) consisting of an intake, educational home visit by a nurse, TPTD home delivery, phone calls at 1 week, 2.5 weeks and 8 weeks after treatment initiation. Since May 2015, the BCP was extended with an educational and motivational support program (EMP) including the Morisky scoring system (MSS) during phone calls, an extra phone call at 12 months and motivational letters at 9 and 14 months. The MSS was aimed at identifying potential non-persistent patients and providing them an additional phone call or home visit to enhance the awareness of the importance of treatment completion. Persistence was defined as the act of continuing the treatment for the prescribed duration, without exceeding the permissible gap (discontinuation up to 28 days). Patients were classified as persistent if 24-26 pens were delivered. The potential 24-month treatment period was evaluated using age and sex adjusted Cox proportional hazard analyses. Results: TPTD treatment was initiated in 1162 patients: 766 received BCP (88% women, mean age 72yrs), and 396 received EMP (84% women, mean age 72yrs). In the BCP group, 2-year persistence was 59% vs. 73% in the EMP group (p<0.001). Reasons for treatment discontinuation were comparable between both groups, except for discontinuation due to side effects, which was lower in the EMP group (18% vs 8% respectively, p<0.001). Adjusted analyses showed a reduction of 40% for being non-persistent with the EMP compared to the BCP (HR:0.58 95%CI:0.46-0.72)(Fig.1). Conclusion: Persistence with TPTD significantly improved by the EMP including the MSS. The MSS was able to identify patients who were at risk of treatment discontinuation mainly due to side effects and allowed targeted interventions by a trained nurse resulting in a significant reduction of non-persistence during the 24-month treatment course.

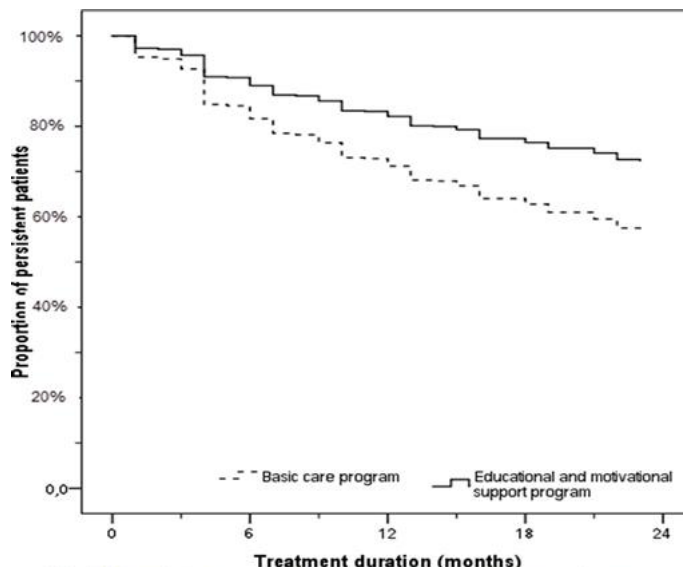


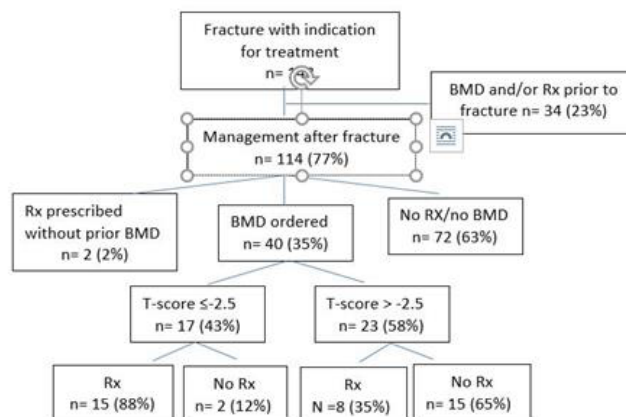
Fig 1. Persistence with Teriparatide per support program

Disclosures: *Maud Van Maren, None*

SUN-0940

Treatment Patterns in the Management of Osteoporotic Fractures in Older Adults Lagari Violet^{*1}, Levis Silvina¹, Naomi Leonore¹, Berger Hara², Rodriguez Graciela¹. ¹Miami VA Healthcare System, United States, ²Reproductive Health Physicians, United States

After the first fracture, the risk of subsequent fractures is significantly increased, with the highest risk following hip (RR, 9.97) and vertebral (RR, 15.12) fractures. Independence, mobility and quality of life decrease with recurrent fractures, while morbidity and mortality increase. Although medical treatment can reduce the risk of a second fracture by about 50%, many older adults do not receive osteoporosis medication following their first fracture. This observational study aimed to understand treatment patterns in the initiation of anti-osteoporosis therapy in older adults who sustain osteoporotic fractures at the Miami Veterans Affairs (VA) Healthcare System. Over a 12-month period, reports from VA's electronic medical records identified patients with a new ICD-10 fracture code in the prior month. After excluding traumatic fractures and fractures in nursing homes residents, a total of 148 cases who had an indication for osteoporosis treatment were identified; 89% men, 67 ± 9 years, 57% non-Hispanic white, 22% non-Hispanic black, 18% Hispanic white, and 3% unknown. The Figure describes our findings. Chart review indicated that 34 (23%) had had a bone density (BMD) or medical treatment prior to the fracture. After the fracture, most patients, 72/114 (63%), did not have a BMD or medical treatment. Only 25/114 (20%) patients were started on an osteoporosis medication by their primary care physician. While a clinical diagnosis of osteoporosis may be made based on a low trauma fracture, this study demonstrates that physicians may not equate low trauma fractures with a diagnosis of osteoporosis. Along with our previous findings, this study suggests that physicians are more likely to prescribe osteoporosis therapy based on a BMD T-score diagnosis of osteoporosis, rather than a clinical diagnosis of osteoporosis based on a low trauma fracture. There was no correlation between treatment initiation and gender or type of fracture. Continuous education in the primary care setting is necessary to improve the medical treatment of osteoporotic fractures.



Disclosures: *Lagari Violet, None*

Sunday Posters

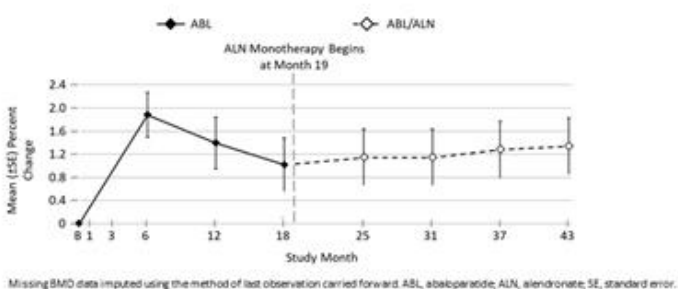
SUN-0941

Forearm Bone Mineral Density and Fracture Incidence in Postmenopausal Women with Osteoporosis: Results from the ACTIVEExtend Phase 3 Trial

Nelson B. Watts¹, Robin K. Dore², Sanford Baim³, Gary Hattersley⁴, Greg Williams⁴, Yamei Wang⁴, Tamara D. Rozental⁵, Meryl S. Leboff⁶. ¹Mercy Health Osteoporosis and Bone Health Services, United States, ²Robin K Dore M.D., Inc., United States, ³Rush University Medical Center, United States, ⁴Radius Health, Inc., United States, ⁵Beth Israel Deaconess Medical Center, United States, ⁶Brigham and Women's Hospital, United States

Wrist fractures are the most common fracture of the upper extremity and are associated with increased subsequent fracture risk in women with postmenopausal osteoporosis. Most wrist fractures occur at the ultradistal (UD) radius. Abaloparatide (ABL) is a selective activator of the PTH1 receptor signaling pathway that stimulates bone formation. In the ACTIVE phase 3 study, 18 months of ABL significantly increased bone mineral density (BMD) at the UD radius and maintained BMD at the 1/3 distal radius vs placebo (PBO) and teriparatide (TPD). BMD effects were associated with a trend for numerically lower wrist fracture incidence for ABL vs TPD (P=0.052). Women receiving ABL or PBO in ACTIVE were offered enrollment in the ACTIVEExtend extension study in which both groups received 24 months of open-label alendronate (ALN) 70 mg/wk for a total of 43 months (18 months ABL or PBO, 1 month for re-consent, 24 months ALN). Our objective was to determine the efficacy of ABL followed by ALN (ABL/ALN) vs PBO/ALN on BMD at the UD radius over 43 months. Forearm BMD data (ACTIVE baseline and month 43) were measured for 213 and 233 women in ABL/ALN and PBO/ALN groups, respectively. BMD was centrally analyzed and adjusted for machine differences. DXA scanner and baseline BMD were included as covariates. Wrist fracture event rates were estimated for the ACTIVEExtend ITT population (558 ABL/ALN; 581 PBO/ALN) by KM method. Over the 18 months of the ACTIVE trial, BMD of the UD radius decreased in the placebo group but increased with ABL; these increases were maintained over the ALN extension (Figure). There were 15 women with wrist fractures in the ABL/ALN group (KM estimate: 2.8%) and 20 in the PBO/ALN group (3.6%). Although the number of wrist fractures was low, these fractures were numerically lower with ABL/ALN vs PBO/ALN (HR=0.77, 95% CI [0.39, 1.50], P=NS). In conclusion, the BMD gains at the UD radius following treatment with ABL were maintained over the subsequent 24 months of treatment with ALN. Wrist fracture risk was numerically lower with ABL/ALN vs PBO/ALN. These results, together with previous ACTIVE analyses, suggest that BMD of the UD radius, which is rich in trabecular bone, may be a better predictor of wrist fracture than the 1/3 distal radius.

Figure. Mean (±SE) Percent Change in Ultradistal Radius BMD from Baseline Through Month 43



Disclosures: Nelson B. Watts, Abbvie, Consultant, Amgen, Speakers' Bureau, Janssen, Consultant, Sanofi, Consultant, Amgen, Consultant, Radius Health, Consultant, Shire, Speakers' Bureau

SUN-0942

Eldecalcitol Increases BMD More Than Alfacalcidol in Chinese Osteoporotic Patients without Vitamin D or Calcium Supplementation

Yan Jiang¹, Hai Tang², Xinlong Ma³, Qun Cheng⁴, Hua Lin⁵, Xiaolan Jin⁶, Zhenlin Zhang⁷, Wei Yu¹, Tsuyoshi Kobayashi⁸, Satomi Uehara⁸, Toshio Matsumoto⁹, Weibo Xia¹. ¹Beijing Union Medical College Hospital, China, ²Beijing Friendship Hospital, Capital Medical University, China, ³Tianjin Hospital, China, ⁴Huadong Hospital affiliated to Fudan University, China, ⁵Nangjing Drum Tower Hospital Affiliated of Nanjing University Medical School, China, ⁶Chengdu Military Central Hospital, China, ⁷Shanghai Sixth People Hospital, China, ⁸Chugai Pharmaceutical Co., Ltd., Japan, ⁹okushima University, Fujii Memorial Institute of Medical Sciences, Japan

Eldecalcitol was shown to prevent vertebral fractures and increase bone mineral density (BMD) who received vitamin D supplementation to keep serum 25(OH)D over 20 ng/mL. In the current study, 265 Chinese patients with osteoporosis were randomly assigned to receive 1.0 µg/day alfacalcidol or 0.75 µg/day eldecalcitol for 12 months without vitamin D or calcium supplementation. Lumbar BMD increased by 2.51% with eldecalcitol treatment for 12 months, while the increase was 0.46% in the alfacalcidol group (LS mean difference, 2.05%; 95% confidence interval, 0.96-3.15; p<0.001). Total hip and femoral neck BMD

also increased with eldecalcitol, by 1.50% and 1.95% respectively, but were not increased with alfacalcidol. Baseline serum 25(OH)D levels were 15.6 ± 6.3 ng/mL (mean ± SD) in the eldecalcitol-treated group and 17.0 ± 8.3 ng/mL in the alfacalcidol treated group, and remained almost constant throughout the study in both groups. Baseline calcium intake was 500 ± 268 mg/day (mean ± SD) in the eldecalcitol group and 549 ± 271 mg/day in the alfacalcidol group. The eldecalcitol group was further analyzed by stratifying into subgroups by baseline serum 25(OH)D and calcium intake. Lumbar spine BMD increased by 2.60% from baseline in the subgroup with baseline serum 25(OH)D < 20 ng/mL and by 2.17% in the subgroup with serum 25(OH)D ≥ 20 ng/mL. Lumbar spine BMD increased by 2.81% in the subgroup with calcium intake < 400 mg/day and 2.28% in the subgroup with calcium intake ≥ 400 mg/day. Serum calcium exceeded 10.4 mg/dL in 8 of 136 patients (5.9%) in the eldecalcitol group and 11 of 127 patients (8.7%) in the alfacalcidol group. Urinary Ca/creatinine ratio exceeded 0.4 in 5 patients (3.7%) in the eldecalcitol group and 3 (2.4%) in the alfacalcidol group. These results demonstrate that eldecalcitol increases both lumbar and hip BMD in Chinese osteoporotic patients more than alfacalcidol without sustained hypercalcemia or hypercalciuria, and that eldecalcitol increases BMD in osteoporotic patients regardless of serum 25(OH)D level or calcium intake.

Disclosures: Yan Jiang, None

SUN-0966

Gender Differences in Tibial Fracture Healing in Normal and Muscular Dystrophic Mouse Models

Zhenhan Deng¹, Xueqin Gao, Xuying Sun, Yan Cui, Sara Amara, Walter R. Lowe, Johnny Huard. University of Texas Health Science Center at Houston, United States

Introduction: Duchenne muscular dystrophy (DMD) patients have high fracture risk and poor fracture healing. The mdx mice is a mouse model for study of human DMD and exhibits delayed bone fracture healing due to chronic inflammation. Previous work in our lab has shown that male muscle-derived stem cells (MDSCs) are more osteogenic and chondrogenic in vitro and regenerate more bone and cartilage in vivo. However, whether there are gender differences in fracture healing in normal and mdx mice is not known. The objective of this study was to explore gender differences in fracture healing, and their mechanistic basis, in normal and mdx mice. Methods: Two-month-old wild-type C57BL/10J (WT) and mdx mice underwent tibial fracture surgery. MicroCT live scanning was performed at the fracture site at 2, 4, and 6 weeks after surgery. The callus was manually segmented from the host bone, and bone histomorphometric parameters were measured. The mice were sacrificed at 6 weeks and 10 days post-surgery for the purpose of characterization and mechanistic studies, respectively. The callus was collected for histology. RNA was extracted from the 10-day callus, and several osteogenesis-related gene markers were detected with RT-qPCR. Gene expression was expressed as fold change versus the male control or mdx groups. Results: 1. The fracture site was healed in both groups at the 6 weeks after surgery. The callus size was larger in both male normal and male mdx mice, but showed less remodeling, than in the female groups. The callus bone density was higher in females. More osteoclasts (OCs) were detected in the female callus, but no gender differences were observed in osteoblast (OB) number. 2. At 10 days after surgery, males formed larger calli composed of more mesenchyme, whereas females formed well-remodeled calli with greater bone percentage. More OBs were detected in the male groups. There were no gender differences in the number of pSMAD1/5-positive cells in both groups. Higher IGF-1 expression was seen in male mdx mice, whereas female mdx and WT mice showed a trend toward higher osterix (OSX) expression. Conclusions: Male mice form larger bone calli during tibial fracture healing in both groups; this may be attributed to higher IGF-1 expression and greater OB number during callus formation. Female mice achieve better morphology in the healed fractured bone with higher bone quality, due to the greater number of OCs and higher OSX levels in the female callus.

Disclosures: Zhenhan Deng, None

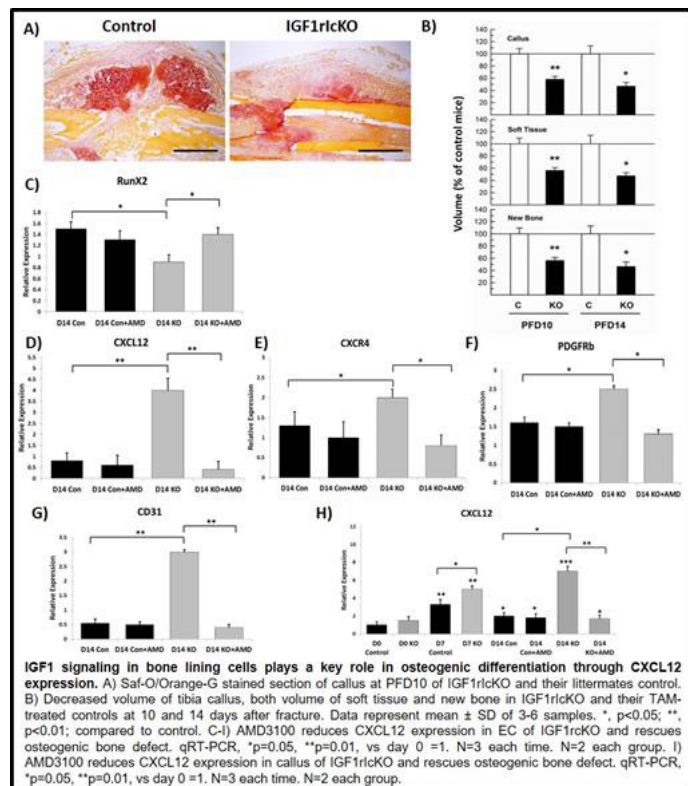
SUN-0967

IGF1 Signaling Regulation of Bone Lining Cells Osteogenic Differentiation Through CXCL12 Expression is Critical in Fracture Repair and Bone Homeostasis

Alessandra Esposito¹, Jie Jiang, Lai Wang, Tieshi Li, Xin Jin, Anna Spagnoli. Rush University Medical Center, United States

IGF signaling through IGF1/IGF1r plays a key anabolic role in postnatal skeletal development. We previously reported that C-X-C-motif-chemokine-ligand-12 (CXCL12) plays a critical role in fracture repair. Here we test the hypothesis that IGF1 signaling regulates CXCL12's expression to maintain bone homeostasis and to promote fracture repair. To this purpose, we generated conditional IGF1rCKO mice by crossing Prx1Cre+ with IGF1r-floxed mice. In IGF1rCKO mice, we found impaired bone formation and abnormal cortical bone neo-angiogenesis, associated with an increase of bone lining CXCL12+/CXCR4+ cells surrounding endothelial CD31+ cells. To evaluate the role of IGF1/CXCL12 interplay in fracture repair, we generated inducible IGF1rCKO mice. To this purpose, adult mice received 4OHTam 3 days before and 2 days post fracture (PFD). Calluses from IGF1rCKO and controls were collected and analyzed at different PFDs. µCT analyses at PDF14 showed that IGF1rCKO mice have reduced total callus, soft tissue and new bone volumes compared to controls (Fig). mRNA expression analyses of IGF1rCKO PDF14 calluses showed an increase of CXCL12, CXCR4, CD31 and pericytes markers, as well as a decrease of osteo-chondrogenic markers, compared to controls (Fig). To further evaluate the IGF1r-CX-

CL12 axis, we isolated endosteal cells from the hind-limb long bones of IGF1rCKO mice and controls. IGF1rCKO endosteal cells showed an increase in pericyte markers, and a decrease in osteogenic markers and Alizarin-Red (AR) staining (Fig). Furthermore, in IGF1rCKO endosteal cells CXCL12, CXCR4 and CD31 mRNA expressions were respectively 5-, 2- and 4-fold higher than controls (Fig). Next, we treated IGF1rCKO endosteal cells with AMD3100, an inhibitor of CXCL12 signaling. AMD3100 rescued the osteogenic differentiation defect of IGF1rCKO endosteal cells, as shown by an increase in osteogenic marker and AR-staining (Fig). We then evaluated the effect of AMD3100 in vivo. IGF1rCKO mice and controls were treated with AMD3100 (2.5 µg/g by intraperitoneal injection given twice a day from PFD2 through PFD7). Analyses of calluses obtained respectively at PDF7 and PDF14, showed that in IGF1rCKO, AMD3100 treatment normalized mRNA levels of CXCL12, CXCR4, CD31, pericyte and osteochondrogenic markers. µCT and histological analyses are in progress. Findings unveil a novel role of IGF1 signaling in regulating CXCL12 expression in bone lining cells that is critical to promote fracture healing.



Disclosures: Alessandra Esposito, None

SUN-0968

The C-terminal domain of PTHrP limits PTH receptor-mediated changes in gene expression in osteocytes Yao Sun^{*}, Patricia W M Ho¹, Rachelle W Johnson², T John Martin¹, Natalie A Sims¹. ¹St. Vincent's Institute of Medical Research, Australia, ²Vanderbilt University, United States

Parathyroid hormone-related protein (PTHrP) promotes skeletal development and maintains bone mass. PTHrP and PTH share a common receptor (PTH1R) and both promote bone formation, as indicated by the anabolic effects of their N-terminal domains. However, PTHrP contains additional protein domains, with intracellular and nuclear activities, that are independent of the PTH1R; these could be exploited to improve anabolic activity. To determine the effects of PTHrP's unique domains in osteocytes, Ocy454 cells expressing the following PTHrP isoforms were generated: PTHrP-FL = full length PTHrP(1-139); PTHrP-ΔNLS = PTHrP lacking the nuclear localization sequence (NLS); and PTHrP-67 = PTHrP(1-67) lacking both the NLS and C-terminal regions. Stable expression of each isoform was validated by qPCR, RIA and bioassay. Gene expression changes induced by each PTHrP isoform compared to vector control were analysed by RNA-Seq. When compared to vector control, cells expressing PTHrP-67 regulated a greater number of genes (4463, FDR < 0.05) than cells expressing either full length, or NLS-deficient constructs (1413 and 1741 genes, respectively). This suggests that the PTHrP C-terminal domain has intracellular functions that suppress gene responses to PTHrP. To test whether the C-terminus suppresses the extent of gene responses to endogenous full length PTHrP in osteocytes, we compared genes regulated by both PTHrP-67 and PTHrP-FL (n=1154). The magnitude of change (increased and decreased) in these genes was significantly greater in cells expressing PTHrP-67 than those expressing PTHrP-FL (p=0.0008). In contrast, a similar comparison of common genes regulated by both PTHrP-FL and PTHrP-ΔNLS (n=515) found no difference in the magnitude of response (P=0.5592). This indicates that the PTHrP C-terminus, but not the NLS, restricts the amplitude of gene responses to PTHrP in osteocytes. To determine whether

this action suppresses PTH1R-mediated action, we assessed a panel of 32 known CREB responsive genes in each cell line, since PTH1R signals through cAMP/CREB. PTHrP-67 regulated more than double the number of CREB responsive genes than PTHrP-FL (21/32 compared to 8/32), indicating that absence of the C-terminal domain increases PTH1R-CREB signalling. Deciphering these suppressive activities of C-terminal PTHrP may lead to ways to improve the bone formation response to PTH1R activation and thereby optimize anabolic effects of PTHrP-based therapies in bone.

Disclosures: Yao Sun, None

SUN-0969

Myeloid Wnts control cortical and trabecular bone formation through paracrine and autocrine production of recruitment and differentiation factors Megan Weivoda^{*}1, Ming Ruan¹, Glenda Evans¹, Christine Hachfeld¹, Jean Vacher², Bart Williams³, Sundeeep Khosla¹, Jennifer Westendorf¹, Merry Jo Oursler¹. ¹Mayo Clinic, United States, ²McGill University, Canada, ³Van Andel Institute, United States

Eighty percent of age-related fractures involve cortical bone, yet current therapies are not highly effective at preventing cortical fractures. Because of this, there is a need to understand the mechanisms that support cortical, as well as trabecular, bone formation. CD11b+ myeloid cells are located in cortical and trabecular regions and express the canonical Wnt co-receptors Lrp5/6, suggesting that myeloid cells are Wnt responsive. While the positive influences of Wnts on bone formation are well known, whether there are influences of myeloid Wnt responses on bone metabolism remains unexplored. We employed CD11b-Cre mice to delete Lrp5/6 in myeloid cells (Lrp cKO mice) and observed trabecular osteopenia and decreased cortical thickness. There were significant reductions in osteoblasts and bone formation in Lrp cKO bones, supporting myeloid cell production of osteogenic factors in response to canonical Wnt signaling. We examined monocytes isolated from control and Lrp cKO mice without intervening culture to provide a "snapshot" of cell responses to altered myeloid canonical Wnt signaling in the in vivo microenvironment. Loss of canonical Wnt signaling reduced expression of several osteogenic genes including BMPs and Wnts as well as numerous chemokines. These data indicate that myeloid cells are likely pro-osteogenic mediators of the positive influences of Wnts on bone metabolism. We next sought to determine possible sources of Wnts that could influence myeloid cells. Wnt hydrophobicity reduces diffusion, thus Wnt sources within bone are local. Our studies revealed that myeloid cells expressed several canonical and noncanonical Wnts and we therefore conjectured that myeloid Wnts could act in an autocrine manner. To examine this, we conditionally deleted Wntless (Wls) using the CD11b-Cre mice (Wls cKO mice). Consistent with Lrp cKO mice, femurs from the Wls cKO mice exhibit trabecular osteopenia, decreased cortical thickness, and reduced osteoblast numbers. There was a striking 78% reduction in periosteal mineral apposition rate in the cortical bone. Our data support that myeloid canonical Wnts directly promote bone formation and act in an autocrine manner to stimulate production of chemotactic and osteogenic factors. These studies have elucidated an important Wnt source in bone and revealed potential mechanisms by which myeloid cell Wnt responses influence cortical and trabecular bone metabolism.

Disclosures: Megan Weivoda, None

SUN-0989

Phytic acid, a phosphate store in plants, inhibits osteogenic differentiation in ectopic calcifications but not in bone. Faisal Ahmed^{*}, Tomoko Minamizaki, Masaaki Toshishige, Yuji Yoshiko. Department of Calcified Tissue Biology, Hiroshima University Graduate School of Biomedical and Health Sciences, Japan

Ectopic calcification is defined as abnormal biomineralization occurring in soft tissues including arteries, skins and joints age- and disease-dependently (for example, arteriosclerosis, diabetes, and chronic kidney disease). An active process is implicated in ectopic calcifications via a variety of the mechanisms underlying impairments in the production of pyrophosphate, an endogenous inhibitor of mineralization, BMP2 signaling, inorganic phosphate transport. Plants store phosphate as phytic acid (myo-inositol-1,2,3,4,5,6- hexaphosphate, IP6). In humans, dietary intake of grains increases serum IP6 levels. IP6 is known to act as an antioxidant via metal ion chelation and suppression of hydroxyl radical formation and used as pharmaceutical and food ingredients. We hypothesized the clinical benefits of IP6 for ectopic calcification. First, we found that IP6 inhibited matrix mineralization but not osteogenic cell proliferation and development in fetal rat calvaria and mouse MC3T3-E1 cell cultures. The anti-mineralization effect of IP6 appears to be involved in its calcium chelating activity. We also tested mouse aorta organ cultures under conditions at high phosphate levels; IP6 inhibited not only matrix mineralization but also expression of osteoblast marker genes and proteins. Using osmotic pumps, we injected IP6 intravenously into three different rodent ectopic calcification models: mice intramuscularly implanted with collagen sponges including BMP2 and TGFβ (Fibrodysplasia Ossificans Progressiva), rats treated with warfarin (aortic calcification induced by dysfunction of MGP), and the Enpp1 mutant mice as models of generalized arterial calcification of infancy. In all three independent rodent models, IP6 significantly suppressed ectopic calcification with inhibition of osteogenic differentiation, while it showed no obvious effects on bone parameters and serum Ca and Pi levels. Given the finding of unique gene clusters in the mouse aorta organ culture model as

above, these data suggest that IP6 may act on osteogenic fate conversion in ectopic calcification processes. Our results indicate that IP6 may strongly suppress ectopic calcification by inhibiting heterotopic osteogenesis. Thus, IP6 may represent a new class of anti-ectopic calcification agents.

Disclosures: Faisal Ahmed, None

SUN-0990

Doses of 1,25-Dihydroxyvitamin D Supplementation in CKD Rats Influence Bone Mineralisation and Vascular Calcification Sarah-Kim Bisson*, Roth-Visal Ung, Sylvain Picard, Mohsen Agharazii, Richard Larivière, Fabrice MacWay. Centre de recherche de l'Hôtel-Dieu de Québec, Canada

Background: Active vitamin D is widely used for the treatment of secondary hyperparathyroidism in CKD. Recent animal studies in CKD suggest that high doses of active vitamin D (calcitriol) also induce bone mineralisation defects. The objective of this study was to assess the effects of high vs low doses of calcitriol on hemodynamic, biochemical, bone parameters and vascular calcification in CKD rats. **Methods:** CKD was induced in rats by a 5/6 nephrectomy. Animals were then fed with an enriched calcium (1.2%) and phosphate (1.2 %) diet (Ca/P), and were given either 0.1 µg/kg or 0.5 µg/kg of calcitriol 3 times/week and compared to controls for a month. Hemodynamic parameters were measured prior to sacrifices where tibias, femur and aortas were harvested for bone histomorphometry, micro-CT analysis and quantification of vascular calcification. **Results:** Rats treated with Ca/P + 0.1 µg/kg or 0.5 µg/kg calcitriol had similar systolic, diastolic and mean arterial pressure. However, animals treated with 0.5 µg/kg calcitriol had higher pulse pressure and pulse wave velocity while vascular calcification occurred only in rats treated with the high dose of calcitriol. Serum biochemical parameters also revealed lower creatinine clearance and higher renal excretion of Ca and P in these animals. While micro-CT analysis did not reveal notable differences in the tibia bone volume and size between the two groups, bone mineral density was decreased in the high calcitriol group only, suggesting decreased mineralisation. Finally, histomorphometry analysis confirmed a bone mineralisation defect in the high but not in the low calcitriol treated group of animals. **Conclusion:** In CKD rats fed with enriched Ca/P diet, a higher dose of calcitriol induces vascular calcification, further deterioration of kidney function and bone mineralisation anomalies. Further studies regarding the safe dose of calcitriol should be conducted in CKD patients.

Disclosures: Sarah-Kim Bisson, None

SUN-0991

A cysteine peptidase inhibitor from the Orange tree (*Citrus sinensis*) inhibits periodontitis-induced bone loss by retaining osteoclasts at the macrophage stage. Natalia Da Ponte Leguizamón*, Glaucia Coletto-Nunes², Daniela Morilha Néo-Justino³, Vanessa Karine Schneider³, Andressa Vilas Boas Nogueira⁴, Rafael Scaf Molon⁴, Flavio Henrique Da Silva³, Andrea Soares Da Costa Fuentes³, Ulf Holger Lerner⁵, Joni Augusto Cirelli⁴, Pedro Paulo Chaves Souza². ¹Department of Diagnosis and Surgery, School of Dentistry at Araraquara, Sao Paulo State University, Brazil, ²Department of Physiology and Pathology, School of Dentistry at Araraquara, Sao Paulo State University-UNESP, Brazil, ³Department of Genetics and Evolution, Federal University of São Carlos, Brazil, ⁴Department of Diagnosis and Surgery, School of Dentistry at Araraquara, Sao Paulo State University-UNESP, Brazil, ⁵Centre for Bone and Arthritis Research at the Sahlgrenska Academy, University of Gothenburg, Sweden

During the course of periodontitis, bone resorption by osteoclasts causes loss of alveolar bone and loosened teeth. Thus, targeting osteoclastogenesis and osteoclast activity is a strategy to block the progression of this bone destructive disease. In humans, cystatins or cysteine peptidase inhibitors are responsible for regulation of physiological processes, which are limited by overexpression of cysteine peptidases. The lack of regulation of cathepsins-like activity can result in bone loss process. The cDNA from a cysteine peptidase inhibitor (CsinCPI-2) from *Citrus sinensis* was cloned and expressed in *Escherichia coli*. This protein was purified by affinity chromatography and its ability to inhibit human cathepsins was tested. The activity of human cathepsins was efficiently inhibited by CsinCPI-2, with Ki in nanomolar order. CsinCPI-2 was capable to inhibit RANKL-induced TRAP⁺ multinucleated osteoclast formation in mouse bone marrow macrophage (BMM) cultures in a concentration-dependent manner, with maximal effect at 20 µM and with IC50 at approximately 2.7 µM. This effect was not due to cytotoxicity, as demonstrated by MTT assay in BMMs and osteoclasts cultured for 4 days. CsinCPI-2 was capable to inhibit RANKL-induced mRNA expression of the osteoclast phenotypical markers *Acp5*, *Ctr* and *Ctsk*, but not mRNA expression for the receptor RANK, encoded by the *Tnfrsf11a* gene. Down-regulation of the mRNA expression for the macrophage marker *Irf8* by RANKL was partially prevented by CsinCPI-2. The RANKL-induced up-regulation of *Nfatc1* mRNA and protein, a crucial transcription factor for RANKL-induced osteoclast differentiation downstream to RANK, was also inhibited by CsinCPI-2. In vivo, using the ligature-induced periodontitis model, we demonstrated, using microCT analyses, that treatment with CsinCPI-2 (0.82Ug/Kg) prevented the loss of alveolar bone mass (BV/TV) and the decrease of bone height (assessed by measuring the distance between the cementum-enamel junction and alveolar bone crest), caused by periodontal dis-

ease. In conclusion, CsinCPI-2 has the potential to prevent bone loss induced by periodontal disease, by retaining osteoclast precursors at the macrophage stage.

Disclosures: Natalia Da Ponte Leguizamón, None

SUN-0992

Compositional Heterogeneity in Lumbar Vertebral Trabecular Bone as a Function of Disease and Treatment Isabel Colon-Bernal*, Phillip Yang², Taeyong Ahn³, Le Duong⁴, Brenda Pennypacker⁵, Meagan Cauble⁶, Sriram Vaidyanathan⁷, Kenneth Kozloff⁸, Bradford Orr⁹, Mark Banaszak Holl¹⁰. ¹Chemistry Department, University of Michigan, United States, ²Biomedical Engineering, University of Michigan, United States, ³Macromolecular Science and Engineering, University of Michigan, United States, ⁴Merck & Co, Inc (Retired), United States, ⁵Merck & Co, Inc, United States, ⁶Department of Orthopaedic Surgery, University of Connecticut Health Center, United States, ⁷Department of Pediatrics, Stanford University, United States, ⁸Department of Orthopaedic Surgery and Biomedical Engineering, University of Michigan, United States, ⁹Physics Department, University of Michigan, United States, ¹⁰Department of Chemical Engineering, Monash University, Australia

Osteoporosis is a degenerative bone disease characterized by a loss of bone density and quality. Recent studies have demonstrated that compositional heterogeneity plays an important role in fracture prevention for osteoporotic bone. In this study, we seek to understand compositional changes linked to disease and treatment in lumbar vertebral trabecular bone using a treatment animal model. A group of cynomolgus monkeys were either ovariectomized (OVX) or submitted to sham surgery. Two years post-surgery, OVX animals were treated in rescue mode with vehicle (VEH), ALN (0.03 mg/kg weekly), or CatKi MK-0674 (0.6 mg/kg daily) for two years and compared to a control Sham surgery group. Baseline BMD values taken prior to drug treatment show a significant decrease in BMD for all OVX animals (10-15% decrease in BMD) indicating the animals became osteoporotic. To understand compositional changes, atomic force microscopy with infrared spectroscopy (AFM-IR) was used to obtain topographical information coupled to chemical composition for cross-section of lumbar vertebrae 4 (LV4). A total of 16 locations were imaged per sample, a 10 by 10 µm and two 3.5 by 3.5 µm images were obtained as well as a localized IR spectrum per 3.5 by 3.5 µm image. The average organic matrix and mineral content for each group was evaluated. Average mineral (1200-900 cm⁻¹) to matrix (1800-1500 cm⁻¹) ratios obtained for Sham, ALN, and CatKi groups were 0.31, 0.34 and 0.38 respectively (p < 0.05), which all differ from the 0.22 value for the OVX group. These results indicate an average bone composition recovery for both the ALN and CatKi treatments. Our presentation will link these average compositional changes to previous micro-CT and mechanical measurements as well as the full distribution of composition results from across the entire LV4 cross-section.

Disclosures: Isabel Colon-Bernal, None

SUN-0993

Comparison of Calcitonin Receptor Fragment Peptide to Teriparatide for the Prevention of Ovariectomy-Induced Bone Loss David E Komatsu*, Anthony Cappellino¹, Ryanne Chitjian², Anne Savitt³, Sardar Mz Uddin¹, Suresh Anaganti³, Srinivas Pentyala⁴. ¹Stony Brook University, Department of Orthopaedics, United States, ²Stony Brook University, Department of Biomedical Engineering, United States, ³AJES Lifesciences, United States, ⁴Stony Brook University, Department of Anesthesiology, United States

Osteoporosis is the most widespread musculoskeletal disorders in the US with a prevalence of >10 million. Moreover, ~2 million osteoporotic fractures occur annually, which result in pain, immobility, and loss of independent living, as well as increased morbidity and mortality. While there is widespread clinical availability of several classes of antiresorptive drugs, such drugs merely reduce disease progression and do not induce new bone formation. One anabolic agent, teriparatide, is available, but it has not garnered widespread utilization. As such, there is a clear need for new skeletally anabolic treatments. We previously reported on the development and characterization of Calcitonin Receptor Fragment Peptide (CRFP), a short peptide with homology to the C-terminus of the calcitonin receptor. In this study, we directly compared the efficacy of CRFP to teriparatide in improving rat bone quality and quantity following ovariectomy (OVX). Twenty-four Sprague Dawley rats underwent OVX surgery at 6 months of age and were randomly assigned to 4 groups (N=6/group) by body weight. The first group was immediately sacrificed to serve as baseline controls. The remaining rats were treated with vehicle, teriparatide (10ug/kg), or CRFP (150ug/kg) 5 days/week for 5 weeks via subcutaneous injections. They were then euthanized, and femora were collected for analyses. In addition, serum was collected weekly and at the time of euthanasia. The femora were analyzed by microCT at the midshaft and distal metaphysis followed by 3-point bending tests. Serum samples were used for antibody analyses. MicroCT analyses revealed a trend towards increased bone mineral density (BMD) in the mid-diaphysis in both the teriparatide and CRFP treated rats as compared to baseline and vehicle. In the distal metaphysis, trabecular bone volume fraction (BV/TV) and BMD in CRFP treated rats trended higher in comparison to all other groups. Subsequent mechanical testing identified trends toward increased yield force and ultimate force for both teriparatide and CRFP treated rats as compared to baseline and vehicle controls. Serum analysis of CRFP treated rats showed

no production of CRFP binding antibodies. Serum biomarker analyses, as well as dynamic histomorphometry and vertebral analyses are ongoing. The relative efficacy of CRFP compared to teriparatide in the treatment of ovariectomy-induced bone loss cannot be conclusively determined given the limited sample size for this study. Future longitudinal *in vivo* bone morphometry studies with a larger number of animals are being planned to validate the osteogenic potential of CRFP. In summary, the data from this study demonstrates that CRFP administration to OVX rats is safe and results in changes in bone density, structure, and mechanical characteristics similar to teriparatide.

Disclosures: *David E Komatsu, None*

SUN-0994

Biological Effects of Abaloparatide on Bone Mass and Bone Turnover in Mice, a Comparison with Teriparatide. Akito Makino^{*1}, Tomoka Hasegawa², Norio Amizuka². ¹Pharmacology Research Department, Teijin Pharma Limited, Japan, ²Developmental Biology of Hard Tissue, Graduate School of Dental Medicine, Hokkaido University, Japan

Background: Abaloparatide (ABL), an analog of parathyroid hormone-related protein, has been recently approved by Food and Drug Administration as a drug for severe osteoporosis. In the phase 3 ACTIVE clinical trial, daily administration of ABL induced a robust increase in BMD and reduction of fracture rate. It also increased total hip and femoral neck BMD to a greater extent than daily administration of teriparatide (TPTD, PTH[1-34]). In this study, therefore, we have examined the bone mass and bone turnover between ABL- or TPTD-treated mice. **Methods:** Six-week-old male C57BL/6J mice received subcutaneous injection of ABL or TPTD for 28 days. The dosage of these peptides was fixed to 30 mcg/kg daily. Taking the different activation frequency (rate of bone turnover) between human and rodents into account, the dosing frequency was once daily (30 mcg/kg every 24 hrs), twice daily (15 mcg/kg every 12 hrs) or three times a day (10 mcg/kg every 8 hrs). BMD of femur and lumbar was measured under anesthesia on the day before the last injection. Next day of the last injection of the drug, blood and femurs were collected after euthanasia. The femurs were then analyzed with micro-CT, or embedded in paraffin for histological analysis. **Results and Discussion:** Both ABL and TPTD administration increased the BMD of femurs and lumbar depending on the dosing frequency. There was no significant difference in BMD between the two peptides when administered once daily. However, when the dosing frequency was twice daily or more, a significant increase in BMD was found in ABL group when compared with TPTD group. Micro-CT analysis showed a significant increase in trabecular and cortical bone when administered with ABL rather than TPTD. The index of serum PINP was significantly higher in ABL-treated group compared with TPTD group in the regimens of two or three times a day administration. However, regardless of the administration frequency, there seems no significant difference in the indices of serum CTx and urine DPD/Cr between the two peptides. Histological analysis demonstrated abundant alkaline phosphatase-positive osteoblasts and trabecular bone in femoral metaphysis with injections of ABL three times a day. Taken together, it seems likely that ABL potentially stimulates anabolic activities in bone with limited elevation of catabolic activity that consequently brings robust BMD increase in mice.

Disclosures: *Akito Makino, Teijin Pharma Limited, Grant/Research Support*

SUN-0995

Analgesic Effects of Morphine on Knee Osteoarthritis Induced by Intra-Articular Monosodium Iodoacetate in Rats Jukka Morko^{*}, Jukka Vaaranemi, Jaakko Lehtimäki, Zhiqi Peng, Jussi M Halleen. Pharmatest Services Ltd, Finland

Several experimental animal models have been developed for human osteoarthritis (OA) and used to study the preclinical efficacy of symptom and disease modifying OA drug candidates. One of these models is induced chemically by an intra-articular injection of monosodium iodoacetate (MIA) into rat knee. Intra-articular MIA disrupts chondrocyte glycolysis through the inhibition of glyceraldehyde-3-phosphate dehydrogenase leading to chondrocyte death, joint damage, and OA symptoms. In this study, we characterized the effects of intra-articular MIA injection on knee joint discomfort and pain and evaluated the analgesic effects of opioid morphine both at rest and during movement in young rats. Unilateral OA was induced by the injection of MIA at 2 mg into the knee joint of male Sprague-Dawley rats at 6 weeks of age. The effects of MIA and the analgesic effects of morphine (3 mg/kg s.c.) were analyzed at 2 days and at 1, 2, 3 and 4 weeks after the MIA injection. Knee joint discomfort was determined as static weight bearing and measured as hind paw weight distribution (HPWD) using Incapacitance Tester. Knee joint pain was determined as static mechanical allodynia and analyzed as paw withdrawal threshold (PWT) using von Frey monofilaments. Changes in gait were used as an index of knee joint discomfort and pain during movement. The gait was analyzed using CatWalk XT computer-assisted method of locomotor analysis. The analgesic effects of morphine were studied by von Frey monofilaments at 1 hour, by CatWalk at 1.5 hours and by Incapacitance Tester at 2 hours after treatment. Intra-articular MIA injection decreased static HPWD and PWT during the entire study period indicating knee joint discomfort, static mechanical allodynia and neuropathic pain in MIA-injected hind limb. The MIA injection decreased dynamic weight bearing and slowed down and impaired movement during the entire study period as well. This was demonstrated by changes in various gait parameters including decreased paw weight distribution, stride length and swing speed. Treatment with morphine reversed the reduction in PWT completely and improved gait during the entire study period as well as reversed the reduction in HPWD

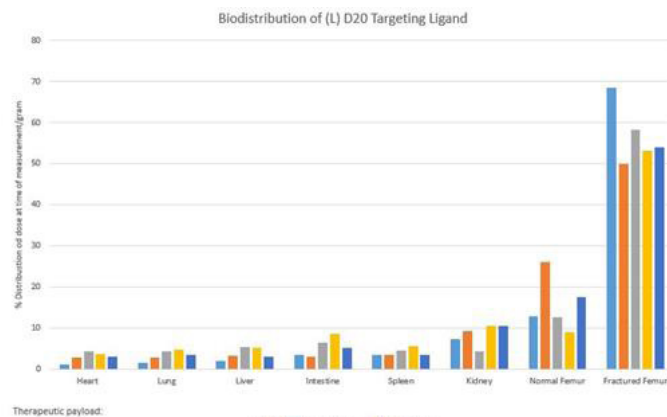
partly during the first 3 weeks. This rat MIA model of OA-related joint pain and these assessments of static weight bearing, static mechanical allodynia and gait can be used to study the preclinical efficacy of symptom modifying OA drug candidates at rest and during movement.

Disclosures: *Jukka Morko, None*

SUN-0996

Targeted Delivery of Peptide Therapeutics to Bone Fractures Jeffery Nielsen^{*}, Philip Low, Stewart Low. Purdue University, United States

Background: We sought to develop a drug delivery system that can safely and effectively be used to deliver therapeutics to the site of a bone fracture. Bone homing oligopeptide drug conjugates are one of the most promising strategies to increase the efficacy and safety of drugs used to treat bone-related diseases. Targeting also opens the door for new methods of administering drugs. Traditionally, use of bone anabolic agents to treat bone fractures has relied entirely on local surgical application. However, because these methods are so invasive, their use and development has been limited. By conjugating bone anabolic agents to bone homing molecules, bone fracture treatment can be performed through minimally invasive subcutaneous administration. The exposure of raw hydroxyapatite that occurs at the bone fracture site allows hydroxyapatite-binding molecules to concentrate on the fracture surface and stimulate bone deposition at the fracture site. Many bone-homing molecules (such as bisphosphonates and tetracycline targeting) have been developed to treat osteoporosis. However, several of these have toxicity associated with them. **Methods/ Results:** We have found that certain short oligopeptides can localize to bone fractures with high selectivity and have very low toxicity compared to bisphosphonates and tetracyclines. We have also demonstrated the ability of these oligopeptides to target bone with numerous payloads of small molecules linked via labile linkers with high selectivity. We have also established that the same targeting peptides can be used to deliver drugs of all chemical classes: hydrophobic, neutral, cationic, anionic, large, and small. This is particularly useful as many bone anabolics are peptidic in nature and have better persistence at the site of the fracture than bisphosphonate-targeted therapeutics. We have also seen that the increased size of the targeting ligand has increased the selectivity for the fracture site over that of the healthy bone in comparison with bisphosphonate targeting. This method allows for a systemic administration of bone anabolics to treat bone fractures, which it achieves by accumulating the bone anabolic agent at the fracture site. This method opens the door for a new way of treating the prevalent afflictions of broken bones and associated deaths.



Disclosures: *Jeffery Nielsen, None*

SUN-0997

In Vitro and In Vivo Assessment of Poloxamers as a Drug Delivery System for Bone Regeneration Young-Eun Park^{*1}, Kaushik Chandramouli², Maureen Watson³, Karen Callon³, Mark Zhu⁴, Donna Tuari³, Dorit Naot⁴, David Musson⁴, Darren Svirskis⁴, Manisha Sharma⁴, Jillian Cornish⁵. ¹Miss, New Zealand, ²Mr, New Zealand, ³Ms, New Zealand, ⁴Dr, New Zealand, ⁵Professor, New Zealand

Numerous hydrogels have been tested for delivery of growth factors or cells into areas of bone injury. Although the general approach is promising, there is a need for better hydrogel formulations and a great scope for the development of novel drug delivery systems for bone repair. Poloxamers are copolymer hydrogels used for a wide range of applications, including drug delivery in cancer treatment. The aim of this study was to determine the potential of poloxamers as a delivery system for the bone anabolic factor lactoferrin (LF). The release profile of LF from poloxamers was measured by HPLC over a 72 hour period. To assess poloxamers' cytocompatibility, LF-loaded poloxamers (LF/poloxamers) were placed in tissue culture inserts suspended above cultures of primary rat osteoblasts, and viability assessed after 72 hours using alamarBlue[®] assay. Immune response was assessed in THP-1 human macrophage-like cells. Cells were collected after 24 and 48 hours with LF/poloxamers and gene expression of proinflammatory cytokines evaluated by real-time PCR. To study bone regeneration *in vivo*, 5 mm critical-size defects were created over the parietal bone in

43 Sprague–Dawley rats. The rats were randomized into three groups of: Control (n=20); Defects grafted with LF/poloxamers (40 ug/gel, n=20); and Sham surgeries (n=3). The rats were sacrificed at 4 or 12 weeks post-operation, calvariae were dissected and bone regeneration determined by microCT (Skyscan1172). The study of the release profile found that 50% of the LF was released from the poloxamers during the first 8 hours, with the remaining released over 72 hours. Cell viability assays demonstrated that poloxamers, with and without LF, increased alamarBlue reading at 72 hours (p<0.001). LF/poloxamers had no effects on the levels of expression of IL1b and IL8 genes in THP-1 cells, whereas TNF gene expression was higher than the controls group at 24 hours, but was back to control levels at 48 hours. MicroCT analysis of bone regeneration showed that the LF/poloxamers had no effect on bone volume (BV) and tissue mineral density (TMD) at the defect site at 4 weeks post-operation, however at 12 weeks the LF/poloxamers group had lower BV than the controls. TMD was similar in the two groups. LF/poloxamers are cytocompatible and support cell viability in vitro, and are not likely to induce an unfavourable immune response. However, the current formulation of LF/poloxamers did not improve bone regeneration in vivo.

Disclosures: *Young-Eun Park, None*

SUN-0998

Distinct mechanisms regulate the response of female and male skeletons to sex steroid deficiency and to the bone protective effects of blueberry containing diets. Amy Y Sato^{*1}, Gretel G Pellegrini², Meloney Cregor¹, Kevin Mcandrews¹, Emily Atkinson¹, Roy B Choi¹, Maria Maiz³, Lilian I Plotkin¹, Linda D Mccabe⁴, George P Mccabe⁴, Munro Peacock⁵, Connie Weaver³, David Burr⁶, Teresita Bellido⁷. ¹Department of Anatomy & Cell Biology, Indiana University School of Medicine, United States, ²CONICET-Universidad de Buenos Aires. Instituto de Inmunología, Genética y Metabolismo (INIGEM). Facultad de Farmacia y Bioquímica-Hospital de Clínicas, Universidad de Buenos Aires, Facultad de Odontología. Cátedra de Bioquímica Gral y Bucal, Argentina, ³Department of Nutrition Science, Purdue University, United States, ⁴Department of Statistics, Purdue University, United States, ⁵Department of Medicine, Division of Endocrinology, Indiana University School of Medicine, United States, ⁶Department of Anatomy & Cell Biology, Department of Biomedical Engineering, Indiana University School of Medicine, United States, ⁷Department of Anatomy & Cell Biology, Department of Medicine, Division of Endocrinology, Indiana University School of Medicine, Roudebush Veterans Administration Medical Center, United States

There is an unmet need for non-sex steroid interventions that prevent bone loss induced by sex steroid deficiency with better compliance and lower side effects than current approaches. Loss of sex steroids causes accumulation of reactive oxygen species (ROS) in bone. ROS, in turn, activate the transcription factor Nrf2 and increase the endogenous antioxidant response (EAR), in an attempt to mitigate damaging oxidative effects. We investigated the ability to prevent bone loss due to sex steroid deficiency of diets containing 10% of 3 types of blueberries rich in antioxidant metabolites fed to 4 mo-old female (F) or male (M) WT and Nrf2 KO littermate mice (N=19-26). In mice fed control diet, ovariectomy (OVX) or orchidectomy (ORX) induced the expected bone loss, which was similar in WT and KO mice, as quantified by % change BMD/month or final BMD. Only the diet with Montgomery berries decreased the rate of bone loss, either fully in F or partially in M. Whereas the berry diet prevented bone loss in both WT and KO F, it only prevented bone loss in WT M. OVX decreased expression of the estrogen response element (ERE)-containing gene C3 and ORX decreased expression of the androgen ARE-containing gene Rhox5 in bone, in WT and KO mice fed control diet. And, C3 or Rhox5 expression remained low in OVX or ORX mice fed the berry diet, indicating that bone protection is not due to estrogenic/androgenic actions of the diet. OVX increased the EAR in bone, but ORX did not. Moreover, the berry diet prevented the increase in EAR induced by OVX in both WT and KO mice, but it did not alter EAR in ORX mice. In summary, (1) bone loss induced by estrogen/androgen deficiency is independent of Nrf2; (2) only Montgomery berry diet decreased bone loss rate; (3) berry diet-induced skeletal protection depends on sex (full in F vs partial in M) and is exerted by a mechanism independent of canonical ERE or ARE signaling; and (4) bone EAR in sex steroid deficiency (OVX-increased vs ORX-not altered) or in response to the berry diet (prevention of OVX-induced increases vs not altered-ORX) also depends on sex. We conclude that distinct mechanisms underlie the response of the F and M skeletons to (a) sex steroid deficiency, as bone EAR is increased in F but not M, or to (b) bone protection by the berry diet, as Nrf2 is required in M but not in F. Thus, optimal skeletal benefits might be achieved by tailoring antioxidant-rich diets to patients of either sex.

Disclosures: *Amy Y Sato, None*

SUN-0999

Pasteurized Akkermansia muciniphila reduces fat mass accumulation after ovariectomy but induces bone-loss in the femur of gonadal intact mice Lina Lawenius^{*1}, Julia Scheffler¹, Petra Henning¹, Karin Gustafsson¹, Karin Nilsson¹, Hannah Collén¹, Ulrika Islander¹, Willem M De Vos², Patrice Cani³, Hubert Plovier³, Claes Ohlsson¹, Klara Sjögren¹. ¹Centre for Bone and Arthritis Research, Institute of Medicine, Sahlgrenska Academy at University of Gothenburg, Sweden, ²Laboratory of Microbiology, Wageningen University, Netherlands, ³Université catholique de Louvain, Louvain Drug Research Institute, WELBIO (Walloon Excellence in Life sciences and BIOTEchnology), Metabolism and Nutrition Research Group, Belgium

The gut microbiota affects the metabolism and immune system of its host. Ovariectomy (ovx) leads to bone loss, altered immune status and intestinal permeability. Different strains of Lactobacillus protect from ovx-induced osteoporosis associated with effects on gut permeability. Pasteurized Akkermansia muciniphila increases the mucus layer in the intestine and contributes to the gut barrier. The aim of the study was to determine if treatment with A. muciniphila protects from ovx-induced bone loss. Mice were treated with pasteurized A. muciniphila or vehicle (veh) by oral gavage for 28 days, starting 3 days before sham or ovx surgery. The percentage of retroperitoneal fat was reduced when treating both gonadal intact mice (-36%, p<0.05) and ovx-mice (-34%; p<0.05) with pasteurized A. muciniphila compared to veh treated ovx mice. Pasteurized A. muciniphila treatment decreased bone mineral density (BMD) measured by DXA in femur in gonadal intact mice (-9%, p<0.01). As expected, ovx decreased BMD in femur in veh treated mice (-9%, p<0.01). However, ovx did not further decrease the already low femur BMD in pasteurized A. muciniphila treated mice. Pasteurized A. muciniphila treatment did not significantly affect BMD in vertebra (L5) in gonadal intact mice. OvX reduced vertebrae BMD in both veh treated (-15%, p<0.01) and pasteurized A. muciniphila treated mice (-10%, p<0.05), indicating no protective effect of pasteurized A. muciniphila on ovx-induced bone loss in vertebra. Regulatory T cells (Tregs) can be protective of bone and the frequency of Tregs in bone marrow was measured by flow cytometry to evaluate the effect of pasteurized A. muciniphila. The frequency of Tregs was decreased in veh treated ovx-mice compared to veh treated gonadal intact mice (-29%, p<0.01). Tregs was also decreased for pasteurized A. muciniphila treated gonadal intact mice compared to veh treated gonadal intact mice (-29%, p<0.01). Tregs was further decreased for pasteurized A. muciniphila treated ovx-mice compared to pasteurized A. muciniphila treated gonadal intact mice (-21%, p<0.01). In conclusion, pasteurized A. muciniphila reduced BMD in femur but not in vertebrae in gonadal intact mice. In addition, pasteurized A. muciniphila reduced the frequency of Tregs in bone marrow. This study does not support a beneficial effect of pasteurized A. muciniphila in ovx-induced osteoporosis.

Disclosures: *Lina Lawenius, None*

SUN-1000

Assessing the effects of a ketogenic diet on the development of osteoarthritis in obese mice Thomas Solé^{*1}, Thierry Thomas², Laurence Vico¹, Maura Strigini¹. ¹INSERM, U1059 and University of Lyon, UJM Saint-Etienne, France, ²INSERM, U1059 and University of Lyon, University Hospital Saint-Etienne, France

Osteoarthritis (OA) is a disease of joints defined by multi-tissue degradation including cartilage, subchondral bone and synovial membrane. OA is particularly prevalent in the obese population, where weight-related joint overload is accompanied by a chronic, low-grade metabolic inflammation and a damaging adipokine-related profile. beta-hydroxy-butyrate (BHB) is a ketone body whose plasma levels increase during fasting or following a ketogenic diet (KD) - a low carb/high fat regime inducing a metabolic state known as ketosis. BHB affects histone modifications and gene expression in vitro and in vivo possibly also by interfering with the activity of histone deacetylases (HDAC). HDAC inhibitors downregulate the expression of Runx2 and proteases in chondrocytes from OA patients in vitro, suggesting that lowering HDAC activity could slow down OA progression. A KD should simultaneously induce weight-loss, decrease metabolic inflammation and increase BHB circulating levels, all of which would be beneficial in obesity-linked OA. To directly test this hypothesis, we set up a protocol to evaluate the impact of a KD in a murine OA model combining obesity and osteoarthritis (Cleret et al., ASBMR 2016). The first step of our project was to validate the animal model. CB57B16 male mice were fed an obesogenic high fat diet (HFD) from age 6 weeks. We bilaterally destabilized the medial meniscus of the knee at week 16 to induce OA. Then obese mice were fed one of three diets for 8 weeks ad libitum: HFD; KD; standard Control Diet (CD). Weight, fat/lean body composition, glycemia and BHB levels, and muscle strength (Kondziela test) were monitored. At 8 weeks after surgery (week 24) we collected joints for determination of disease severity (OARS1 score) and bone analysis by micro-CT; we dissected tibia epiphysis and bones for biomolecular analysis. Serum, muscle, fat, renal and hepatic tissues were also collected. BHB levels increased tenfold in KD group only. Glycemia remained high in HFD group, but it decreased in CD group and even more in KD group. HFD mice continued to gain weight, while both CD and KD lost weight. Kondziela test showed no variation in muscle strength over the 8-week treatment in CD and KD groups and lower performance in HFD group. We have validated the efficacy of our KD protocol to induce a raise in BHB levels and a loss of weight

in obese OA mice, without a negative impact on muscle function. We can now appraise the effects of KD on OA in this model.

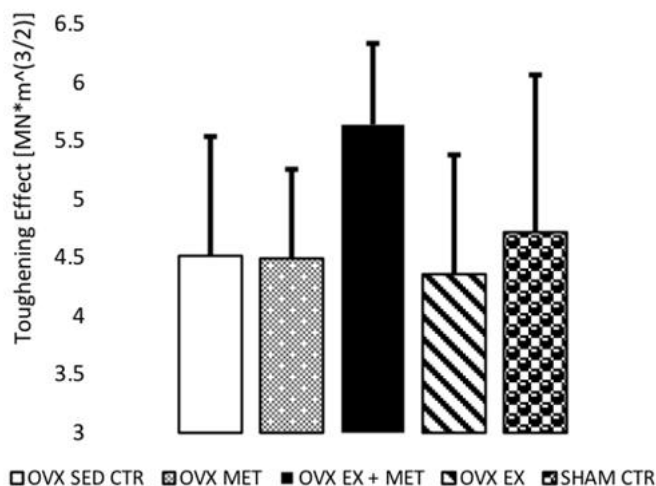
Disclosures: **Thomas Solé**, None

SUN-1001

Effects of Metformin and Exercise on Material Properties of Ovariectomized Rat Femurs Matthew Tice^{*1}, Mats Mosti², Astrid Kamilla Stunes², Unni Syversen², Deepak Vashishth¹. ¹Rensselaer Polytechnic Institute, United States, ²Norwegian University of Science and Technology, Norway

Bone fragility fractures, caused by estrogen deficiency and type 2 diabetes, represent a significant economic burden with increased morbidity. As such, a better understanding of these conditions and the effectiveness of its treatment is crucial to alleviating the burden of bone fractures. Metformin, an oral antidiabetic drug, provides a promising solution. However, its interaction with other anabolic stimuli, such as exercise, is not well established. Here we explore the interaction of metformin with exercise under control condition. An ovariectomy (OVX) was performed in 15-week-old rats to mimic the estrogen drop characteristic of the postmenopausal state. The rats were divided into 5 groups: OVX sedentary control (n=11), OVX sedentary + metformin (n=11), OVX exercise + metformin (n=9), OVX exercise control (n=11), and sham control (n=12). An exercise regimen was mimicked by 6 jumps in 3 sets thrice a week. Metformin-treatment was delivered in dissolved water at a dosage of 100 mg/kg/day. Both regimens began 4 weeks after OVX and were conducted for 8 weeks. One femur per rat had a notch was placed mid-shaft with a diamond-tipped saw blade. The femurs then underwent microcomputed tomography imaging for measurement of bone cross-sectional parameters (cortical area, radii and bone mineral density) as well as notch angle (Viva CT40, Scanco). Following imaging, fracture toughness testing was performed on the notched femurs; samples were loaded in 3-point bending testing until failure at 0.001 mm/s (Instron System). All statistical analyses were done using one-way ANOVA (LSD Post-Hoc test, IBM SPSS). There were no significant differences between the geometric parameters and bone mineral density between groups (p>0.05). However, the metformin + exercise group exhibited a distinctive toughening effect (ΔK , difference of propagation and initiation toughness) when compared to other OVX groups (p<.05), reaching higher levels than those in the SHAM control group. ΔK is representative of bone's ability to sustain loading without fracturing when a microcrack is already present in bone. Reduced ΔK is hallmark of brittle materials and a decreased ability to resist crack propagation. These results suggest beneficial effects of metformin on bone fragility can be enhanced through exercise.

7 Effect of Treatment on Toughening Effect



Disclosures: **Matthew Tice**, NIH, Grant/Research Support

SUN-1002

Effect of Kidney Disease Progression on Intestinal Phosphorus Absorption in Male Cy/+ Chronic Kidney Disease Rats Colby Vorland^{*1}, Pamela Lachcik¹, Sharon Moe², Neal Chen², Kathleen Hill Gallant¹. ¹Department of Nutrition Science, Purdue University, United States, ²Department of Medicine, Indiana University School of Medicine, United States

The Cy/+ rat has been characterized as a progressive model of chronic kidney disease-mineral bone disorder (CKD-MBD). We aimed to determine the effect of kidney disease progression on intestinal phosphorus (P) absorption and whole-body P balance in this model. N=48 Cy/+ (CKD) and N=48 normal littermates (WT) rats were studied at two ages: 20wk and 30wk, to model early (~50% loss of kidney function) and moderate-late CKD

(~75% loss of kidney function), respectively. All rats were placed on a 0.7% Ca, 0.7% P casein-based diet to promote disease progression in the CKD rats. Intestinal P absorption efficiency was measured by ligated loops using ~5 μ Ci ³³P in 0.5mL transport buffer (0.1 mmol/L KH₂PO₄, with or without sodium (Na)) injected into a ~5cm jejunal segment while rats were anesthetized. The 2 different transport buffers assessed Na-dependent and Na-independent components of P absorption (n=12/genotype/age/test). ³³P activity was measured in the excised, digested loop by liquid scintillation counting. Absorption was determined by disappearance from the loop at 30min post-injection. P balance was determined over 4d prior to sacrifice. Diet, urine, and fecal P were measured by ICP-OES. Two-way ANOVA was used to determine genotype and age effects and interaction, with Tukey's post-hoc comparisons. There was a significant genotype x age interaction (p<0.05) for Na-dependent absorption with decreased absorption from 20wk to 30wk in the CKD rats (13 to 5%, p < 0.01) and no difference in WT rats. However, there were no differences for genotype, age, or interaction observed for Na-independent absorption efficiency (overall p=0.36). CKD rats had marginally lower P balance compared to WT (-10 vs -2 mg/day, p=0.06). There was a significant effect of age where 30wk rats had lower P balance compared to 20wk rats, regardless of genotype (-13 vs 1 mg/day, p<0.001). There was no significant genotype x age interaction. These results demonstrate decreasing Na-dependent P absorption with progression of CKD when assessed by an in situ ligated loop test.

Disclosures: **Colby Vorland**, None

SUN-1003

EXD Chinese Herbal Formula Did Not Alter the Bone Protective Effects of SERMs in Mature Ovariectomized Rats Liping Zhou^{*1}, Ka Ying Wong¹, Christina Chui Wa Poon¹, Wenxuan Yu¹, Chi-On Chan¹, Daniel Kam-Wah Mok¹, Hui-Hui Xiao², Man-Sau Wong¹. ¹The Hong Kong Polytechnic University, Hong Kong, ²The Hong Kong Polytechnic University Shenzhen Research Institute, China

Er Xian decoction (EXD), a popular Chinese herbal formula containing Herba epimedii (HEP) and Curculigo orchioides Gaertn (XM), has been prescribed in China for management of postmenopausal osteoporosis over the past 60 years. Previous study demonstrated that EXD stimulated cell proliferation in rat osteoblastic-like UMR106 cells via estrogen receptors (ERs). The present study aimed to determine if the use of EXD will interfere with the bone protective effects of Selective Estrogen Receptor Modulators (SERMs, tamoxifen and raloxifene), which also exert their effects via ERs. Six month-old Sprague Dawley rats were randomly assigned to the following treatments for 12 weeks: 1) sham-operated control group with vehicle (sham), 2) ovariectomized group with vehicle (OVX), 3) OVX with 17 β -estradiol 17 β -estradiol (E2, 2.0mg/kg.day), 4) OVX with tamoxifen (Tamo, 1.0mg/kg.day), 5) OVX with Raloxifene (Ralo, 3.0mg/kg.day), 6) OVX with EXD (EXD, 1.6g/kg.day), 7) OVX with EXD+Tamoxifen (EXD+Tamo) and 8) OVX with EXD+Raloxifene (EXD+Ralo). EXD, tamoxifen, raloxifene and their combinations significantly increased bone mineral density (BMD) and improved micro-architectural bone properties, including bone volume/total volume (BV/TV), trabecular bone number (Tb.N) and trabecular bone separation (Tb.Sp) at distal femur, proximal tibia and lumbar vertebra in OVX rats. In particular, the optimal effects of EXD in improving BMD and bone properties appeared at lumbar vertebra, indicating the bone protective effects of EXD might be site-specific. Co-treatment with EXD did not alter the bone protective effects of either tamoxifen or raloxifene at all the three bone sites in OVX rats. In addition, SERMs, but not EXD, significantly increased uterus index in OVX rats. Our results indicate EXD alone exerted site-specific bone protective effects in OVX rats and did not alter the bone protective effects of SERMs in vivo.

Disclosures: None

Disclosures: **Liping Zhou**, None

SUN-1039

Efficacy and Safety of Denosumab Treatment in Bisphosphonate-resistant Fibrous Dysplasia: a Case Series Natasha M. Appelman-Dijkstra^{*1}, Bas C.J. Majoor², P.D.Sander Dijkstra², Socrates E. Papapoulos¹, Neveen A.T. Hamdy¹. ¹Leiden University Medical Center; Center for Bone Quality; Department of Medicine; Division Endocrinology, Netherlands, ²Leiden University Medical Center; Center for Bone Quality; Department of Orthopedic Surgery, Netherlands

Fibrous dysplasia (FD) is a rare bone disorder due to a postzygotic activating mutation of theGNAS gene. In FD, skeletal lesions show increased bone turnover and upregulation of RANKL expression in GNAS-mutated skeletal progenitor cells leading to increased cAMP production. Exposure of GNAS mutation-harboring bone marrow stromal cells to a RANKL-antibody was associated with a decrease in cAMP production, suggesting that treatment with the monoclonal antibody to RANKL Denosumab may be beneficial in FD. Individual Case Studies have recently reported the effectiveness of Denosumab in FD. We present a case series of 12 FD patients (9 female), treated with denosumab for at least one year at the Leiden Center for Bone Quality between May 2013 and May 2016. All patients had been previously treated with bisphosphonates at high cumulative doses for a mean period of 8.8 years. One patient had monostotic craniofacial FD, 7 polyostotic FD and 4 McCune-Albright syndrome, 2 with growth hormone excess. Median Skeletal Burden Score was 20.8 (range 0.3–64.7). Denosumab was administered at a dose of 60 mg at 3 or 6-monthly intervals for a median of 14.5months (range 13–29M) on the basis of increased bone

turnover markers (BTM) and pain. At baseline, mean serum ALP was 226 ±152 U/L and PINP was 369 ±385 ng/mL. Patients receiving Denosumab at 3-monthly intervals demonstrated sustained and more significant decreases in BTMs than those treated at 6-monthly intervals: ALP ($p = 0.007$) and PINP ($p = 0.025$). BTMs normalized in 8 of the 12 treated patients after a median time of 4.7 months (range 2.1–24.0), in 5 of whom BTMs had not normalised after long-term treatment with bisphosphonates. Treatment was associated with decreases in bone pain. Denosumab was well tolerated and no side effects were reported, particularly no hypocalcaemia, for the duration of treatment. Our data show that Denosumab at a dose of 60 mg three-monthly is effective in decreasing BTMs and pain in FD. We also show that treatment was well-tolerated and safe in this selected group of FD patients with severe symptomatic FD despite long-term treatment with bisphosphonates, suggesting that Denosumab may represent a promising therapeutic option in FD patients refractory to treatment with bisphosphonates. Long-term studies in larger number of patients are warranted to confirm these findings.

Disclosures: *Natasha M. Appelman-Dijkstra, None*

SUN-1040

Long-term complications of patients with hypophosphatemic rickets treated in a public institution Julia Oberger*, Tatiana Lemos Costa, Carolina Moreira, Victoria Borba. Serviço de Endocrinologia e Metabologia do Hospital de Clinicas da Universidade Federal do Paraná, Brazil

Objectives: describe clinical complications of patients with the diagnosis of hypophosphatemic rickets (HR) treated in a tertiary public care service. Methods: All patients diagnosed with rickets treated at Endocrinology Unit at the Universidade Federal do Paraná (SEMPR) were selected, and those with the diagnosis of HR were included. Patient's files were reviewed seeking for demographic and clinical data (etiology, age at diagnosis, results of initial laboratory tests, progression and of bone densitometry (BMD), radiographs and presence of complications). Results: 35 patients with rickets were selected, 13 excluded by hypocalcemic rickets and 22 (15 (69%) women) with HR were included. The mean follow up was 11 years (1 month - 27 y), with a mean age at the diagnosis of 8.75 (1.1 – 32 y). The first evaluation showed bone deformity in lower limbs in all patients, 11 (50%) had genu varum, 10 (45%) genu valgum and 1 patient varum and valgum (4%). Initial X ray showed in 12 (54%) deformities characteristic of rickets, 3 (13%) reduction of BMD and 2 (9%) presented fractures. Initial laboratory tests showed a normal calcium (Ca) 9.1 mg / dL (8.3-9.9 mg / dL), low phosphorus (P) 2.18 mg / dL (1.3-3.0 mg / dL) and phosphorus reabsorption rate 43% (9-82%), high alkaline phosphatase (ALP) 848 U / L (19.26-2109 U / L) and parathyroid hormone (PTH) 122 pg / mL (6-523 pg / mL). Treatment consisted of phosphate replacement in 14 (63%) patients [1.7 g / d (0.6-3.0 g)], calcitriol in 13 (59%) [0.32 mcg / day (0.125 -0.5mcg)] and in 9 (40%) combined treatment with phosphate and calcitriol. After treatment was observed a 76% (from 884 to 236 U / L) decrease in ALP, a 37% (0.5 to 0.8 mg / dL) increase in creatinine, and no change in PTH, P or Ca values. The complications present at the follow-up period of 6.8 years (3-14 years) were: fractures in 8 (36%) patients, mean of 2.12 (1-4) fractures / patient (femur 7 (41%) and tibia 4 (23%)); the delayed bone age was evaluated in 9 (40%) and present in all [mean delay of 19 (12 - 84 months)]; renal complication was evaluated in 17 (77%) patients by ultrasound and was positive in 7 (41%), 3 (17%) had nephrocalcinosis and nephrolithiasis and 4 (23%) had renal parenchymal disease, 1 (4%) patient had hyperparathyroidism. Conclusion: We observed a high prevalence of clinical complications mainly fractures and kidney abnormalities in a relatively young population, which alerts for the need of better care of these patients.

Disclosures: *Julia Oberger, None*

SUN-1041

Low Bone Mineral Density and Increased Bone Resorption in Loeys-Dietz Syndrome Alison Boyce*, Caeden Dempsey, Samara Levin, Marjohn Rasooly, Pamela Guerrero. National Institutes of Health, United States

Loeys-Dietz syndrome (LDS) is a rare connective tissue disorder resulting from dysregulation of TGF- β pathway signaling, leading to a wide phenotypic spectrum involving the vascular, gastrointestinal (GI), and skeletal systems. While an association between LDS and osteoporosis has been reported, the skeletal phenotype has not been well-characterized, and the etiology of low bone mineral density (BMD) has not been established. The purpose of this study was to investigate bone metabolism in a large cohort of patients with LDS. Clinical, radiographic, and biochemical data from 51 subjects in an LDS natural history study were reviewed (median age 14, range 2-58). Mean DXA Z-scores were significantly decreased in all skeletal compartments compared to the reference population: lumbar spine -1.47 (± 1.17 , range -3.33-0.8)($p < 0.001$), 1/3 radius -1.54 (± 1.78 , -7.35-2.3), total hip -1.82 (± 1.21 , -4.27-0.34)($p < 0.001$), total body -1.89, (± 1.49 , -5.1.9)($p < 0.001$); 70% of subjects had low BMD (Z-score ≤ -2) in at least one site. Subjects with a history of inflammatory or eosinophilic GI disease had significantly reduced BMD in the lumbar spine in comparison to subjects without GI disease: median Z-score -2.57 (-3.33-0.3) vs -1.13 (-3.33-0.9), $p = 0.03$. There were no differences in BMD between groups of patients with different pathogenic mutations, TGFBR1 (n=17), TGFBR2 (n=21), SMAD3 (n=8), and TGFBR2 (n=5). 19 subjects (37%) reported at least one long bone or vertebral fracture; 4 of 17 subjects (24%) who underwent screening lateral spine films had vertebral compression fractures. Mean serum procollagen 1-propeptide age-adjusted Z-scores were within normal limits (0.125, ± 1.16 , -1.81-2.5)($p = 0.67$), while serum C-telopeptide was increased compared to the reference

population (0.71, ± 1.18 , -1.36-3.45)($p = 0.01$). Two subjects, ages 11 and 17, were treated with zoledronate, which was well-tolerated and associated with an increase in BMD at all sites. Conclusion: LDS is associated with low BMD and fragility fractures, particularly in patients with co-morbid GI disease. There does not appear to be a correlation between genotype and BMD. Bone resorption markers are elevated, suggesting that anti-resorptives may be an effective treatment strategy.

Disclosures: *Alison Boyce, None*

SUN-1042

Bone Mineral Status in Adults X-Linked Hypophosphatemia Rickets Rosa Arboiro Pinel*, Manuel Díaz Curiel¹, Natalia Bravo Martín², Manuel Quesada Gómez³, Miguel Torralbo García¹. ¹Bone Mineral Department. Fundación Jiménez Díaz. Quirónsalud, Spain, ²Internal Medicine Department. Fundación Jiménez Díaz. Quirónsalud, Spain, ³Endocrinology Department. Hospital Reina Sofía., Spain

Introduction: X-linked hypophosphatemia (XLH) is the most common inherited form of rickets, and it is characterized by hypophosphatemia with renal phosphate wasting, and inadequate skeletal mineralization, usually accompanied by short stature and radiological signs of rickets. There are few reports on bone mineral measurements in adults with XLH, which are controversial. Several studies have shown that most patients have normal bone mineral densities, but others authors found some bone strength alteration related with the underlying mineralization defect. Objective: The aim of this study was to assess bone mineral status in XLH using dual-energy X-ray absorptiometry (DXA), Trabecular Bone Score and Tridimensional-DXA software. Methods: Seven adult patients (age 29 to 67 years; 7 female) with clinical (short stature, leg deformities) and biochemical diagnosis of XLH were evaluated on its bone mineral densities (BMD) and bone quality. All patients were on treatment with calcitriol and phosphate supplementation. The BMD of the lumbar spine and femoral neck were determined by dual-energy X-ray absorptiometry scans (DXA), using Hologic QDR 4500C. Trabecular Bone Score (TBS), a texture parameter related to bone microarchitecture that may provide skeletal information that is not captured from the standard BMD measurement, was also determined in lumbar spine using TBS iNsite software. We analysed the standard hip DXA scan with the tridimensional-DXA algorithm (3D - SHAPER software) that quantifies the trabecular volumetric Bone Mineral Density (vBMD) and the Cortical Surface Density (sDens) both reflecting trabecular and cortical bone strength respectively. Results: All 7 female patients showed a normal BMD in lumbar spine with also normal TBS. With respects hip evaluation, 2 patients showed diminished femoral neck BMD with normal Trabecular vBMD but Cortical sDens below normal range (-1.7 and -2.4 T-score). Conclusions: All patients included in this study showed normal lumbar spine BMD and normal TBS. Most patients showed normal femoral neck BMD with vBMD and sDens at normal range which correlate with normal strength. With this data we can not affirm that TBS and 3-D DXA values are different in the evaluation of bone status at least in patients with XLH.

	BMD L2-L4 g/cm2	T-score BMD L2-L4	TBS L2-L4	BMD FN g/cm2	T-score FN	Trabecular vBMD mg/cm3	T-score vBMD	Cortical sDens mg/cm2	T-score sDens
1	1.051	-0.3	1,548	0.775	-0.7	194	-0.0	162	-0.2
2	1.027	-0.5	1,546	0.657	-1.7	180	-0.4	131	-1.7
3	1.254	1.6	1,519	0.946	0.9	246	1.4	168	0.1
4	1.390	2.8	1,528	0.981	1.2	314	3.2	196	1.4
5	1.278	1.8	1,638	0.774	-0.7	205	0.3	153	-0.6
6	1.113	0.3	1,522	0.635	-1.9	161	-1.2	117	-2.4
7	1.138	0.5	1,477	0.793	-0.5	195	0.0	139	-0.2

Disclosures: *Rosa Arboiro Pinel, None*

SUN-1043

Hypophosphatasia among patients presenting for osteoporosis evaluation Roger Fan*, Ananya Kondapalli, John Poindexter, Naim Maalouf, Khashayar Sakhaee. University of Texas Southwestern Medical Center, United States

Introduction: Hypophosphatasia is a rare heritable disorder characterized by deficiency of tissue non-specific alkaline phosphatase leading to accumulation of phosphorylated molecules, including inorganic pyrophosphate, which causes impaired bone mineralization and fractures. Hypophosphatasia may be overlooked among adults diagnosed with osteoporosis. The distinction is important because bisphosphonate use is associated with atypical femoral fractures (AFF) in hypophosphatasia. A low serum alkaline phosphatase level (ALP) is the hallmark of hypophosphatasia. We sought to characterize patients presenting to an osteoporosis clinic with a low ALP and assess for features of hypophosphatasia. Methods: Our population included all patients presenting to a single university specialty clinic for osteoporosis from 7/1/2006-6/30/2016 with initial ALP ≤ 40 IU/L. We collected information on fracture history, bone mineral density (BMD), laboratory studies, medications, and secondary causes of low ALP. These patients were compared to controls matched for age, gender, race, and date of initial visit. We further compared features of patients with persistently vs. transiently low ALP, and patients in whom hypophosphatasia was suspected (based on clinic notes). Results: Of 2810 patients presenting to clinic for osteoporosis, 159 patients had initial ALP ≤ 40 IU/L (5.66%). Compared to matched controls, low ALP patients had significantly lower BMI ($p < 0.001$) and lower BMD Z-score at the femoral neck and total hip ($p < 0.05$) but not

at the lumbar spine. Only 23 patients (14.5%) had a persistently low ALP, defined by ≥ 2 ALP values, with all values ≤ 40 IU/L. There was no significant difference in 24-hour urine calcium excretion between patients with persistently vs. transiently low ALP (226 ± 134 vs. 222 ± 188 mg/day, $p=0.90$). Of 10 patients suspected of having hypophosphatasia, vitamin B6 was checked in 9 patients, and was only elevated in one patient with hypophosphatasia confirmed by genetic analysis. Compared with the 149 patients not suspected of having hypophosphatasia, the 10 patients with suspected hypophosphatasia had significantly higher prevalence of AFF (20% vs. 0.67%), foot fractures (40% vs. 12.1%) and a history of unusual tooth loss/decay (20% vs. 1.34%). Conclusions: Even among patients with persistently low ALP, the diagnosis of HPP was rarely suspected. Patients suspected of having hypophosphatasia had higher rates of AFF, foot fractures and unusual dental history.

Table 2: Persistently low ALP versus transiently low ALP

	Persistently low ALP	Transiently low ALP	p-value
# of patients	23	107	
Average ALP (mean \pm sd)	32.9 ± 4.3	45.0 ± 7.8	< 0.001
Urine calcium (mg/d)	226 ± 134	222 ± 188	0.9
Urine DPD/Cr ⁺	3.8 ± 1.2	4.1 ± 1.7	0.6
History of fractures (n, %)	8 (35.8%)	48 (44.9%)	0.4
Atypical femoral fractures	0 (0%)	3 (2.8%)	0.4
Foot fractures	5 (21.7%)	11 (10.3%)	0.08
Vitamin B-6 checked	4 (17.4%)	5 (4.7%)	0.03
HPP suspected	4 (17.4%)	4 (3.7%)	0.01
Bone agent [†]	12 (52.2%)	74 (69.2%)	0.1

Disclosures: **Roger Fan**, None

SUN-1044

High Prevalence of Nephrolithiasis and Hypercalciuria in Women with Osteogenesis Imperfecta Vivian Rf Simoes*, Adriana M Fernandes, Manuela Gm Rocha-Braz, Regina M Martin, Bruno Ferraz-De-Souza. Endocrinology/LIM-25, Hospital das Clinicas, University of Sao Paulo School of Medicine, Brazil

Increased risk of nephrolithiasis has been reported in children with osteogenesis imperfecta (OI), but studies in adults are scarce. The frequent finding of hypercalciuria in OI suggests a pathophysiologic association, but the mechanisms of hypercalciuria or nephrolithiasis in OI are not well understood. Hypercalciuria, and its potential link to nephrolithiasis, may hamper Ca and VitD supplementation in OI, with possible detriment to the bone. In this context, our objective was to assess the prevalence of nephrolithiasis and hypercalciuria in individuals with OI in relation to clinical, laboratory, imaging and molecular parameters. We have performed a retrospective analysis of OI patients followed in our institution. Sixty-five patients with OI were identified: 40 F, 25 M; 22 mild OI, 19 moderate, 24 severe; 16 to 71 yo, median 29 yo, 56 adults. Molecular diagnosis was available for 49 individuals, and 40 had COL1A1/COL1A2 defects. All patients were actively questioned about previous history of kidney stones and had 24-h urinary Ca (24-h uCa) determinations in at least 3 occasions; renal ultrasound was available for 82% of the cohort. Nephrolithiasis was found in 29% of the cohort (19/65), being more prevalent in females (15/40, 38%) than males (4/25, 16%) with OI. Twenty-six individuals (40%) had 24-h uCa excretion > 4 mg/kg, and 42% of these had nephrolithiasis. There was no association between hypercalciuria and OI severity, use of Ca or VitD supplementation or molecular etiology. Amongst individuals with nephrolithiasis, 58% had hypercalciuria; in particular, amongst women with nephrolithiasis, 73% had hypercalciuria. Institution of low sodium diet and adjustment of Ca intake were sufficient to normalize 24-h uCa in half of hypercalciuric patients, and for those that required thiazides, a complete response was seen in half. In conclusion, we have found a high prevalence of nephrolithiasis in adult women with OI (38% vs 9% in the general population), and high prevalence of hypercalciuria in these women (73%). Elevated 24-h uCa was seen in 40% of the cohort, but it was not associated with OI severity or underlying molecular defect, nor with Ca or vitamin D supplementation. Considering the bone health benefits of Ca and VitD adequacy, our data suggests that supplementation can be safely advised in adults with OI. Nevertheless, periodic monitoring of 24-h uCa and renal ultrasound emerge as important follow-up strategies, particularly in women with OI.

Disclosures: **Vivian Rf Simoes**, None

SUN-1045

A Comprehensive Study of Bone Manifestations in Adult Patients with Gaucher Disease type 1 Beatriz Oliveri*¹, Diana Gonzalez², Felisa Quiroga³, Claudio Silva³, Paula Rozenfeld⁴, Camilo Lis³, Omar Riemersma⁵, Martin Kot⁵. ¹Conicet UBA Hospital de Clinicas, Argentina, ²Mautalen Salud e Investigacion, Argentina, ³Diagnostico Maipu, Argentina, ⁴IIFP, Universidad Nacional de La Plata, CONICET, Facultad de Ciencias Exactas, Departamento de Ciencias Biológicas, Argentina, ⁵Shire Argentina, Argentina

Gaucher disease (GD) is the most prevalent lysosomal storage disease and bone involvement is the most disabling condition. Purpose: Evaluate bone involvement in adult patients with GD and its relationship with parameters of bone mass, quality and remodeling

markers. Methods: observational, transversal and prospective analysis. Skeletal involvement was evaluated by X-rays (spine and lower limbs) bone densitometry (BMD) and magnetic resonance imaging (MRI) of lumbar spine (LS) and femur(F). Trabecular bone score (TBS) was calculated at LS and Bone Marrow infiltration (BMB) by MRI. Laboratory: hemogram, ferritin (FT), chitotriosidase (CHIT), β cross laps (CTX), N terminal procollagen type1 (PINP) and bone alkaline phosphatase (BAP). Results: 32 Type 1GD patients were included (19 females; age: 40 ± 16 years; range 20-77). 9 patients referred history of long fractures. Patients have been receiving velaglucerase for 2.7 ± 1.4 years, 19/32 were previously treated with imiglucerase. Ninety four % of the subjects met therapeutic goals (TG) for hematological parameters, 8 were splenectomized (SPX) and only one patient did not reach TG for visceromegalies. 19/32 patients had bone irreversible lesions (IL): avascular necrosis (n=14), bone infarction (n=16) and vertebral fractures (n=7). Bone MRI showed positive BMB in 71% of the patients in F and 22% in LS. Patients with IL had BMB higher than patients without IL ($p=0.001$). All splenectomized patients have IL, higher prevalence of bone marrow edema ($p=0.02$) and lower TBS ($p=0.03$) compared with those with preserved spleen. Only 18.7% of the patients had abnormal BMD without correlation with fractures (FX). TBS values were < 1350 in 53% of the patients and a tendency to lower TBS was observed in those with FX ($p=0.06$). Patients with PINP in the lower quartile had lower TBS ($p=0.03$) and a higher prevalence of bone marrow edema compared to those in the higher quartiles. TBS correlated moderately but without reaching statistical significance with PINP ($r=0.32$) and with BMB ($r=-0.44$). Conclusions: Even after reaching hematological and visceral TG, a high prevalence of irreversible bone lesions was documented. Bone quality, evaluated by TBS, was more affected than BMD in fractured patients. Low bone formation active bone marrow infiltration and splenectomy might be implicated in IL.

Disclosures: **Beatriz Oliveri**, Shire, Speakers' Bureau

SUN-1046

6 years experience of a multidisciplinary approach to Osteogenesis Imperfecta in a Swiss Tertiary Health Center: bone management and quality of life Bérengère Aubry-Rozier*¹, Céline Richard², Sheila Unger³, Didier Hans⁴, Belinda Campos-Xavier³, Luisa Bonafe³, Aline Bregou⁵. ¹Rheumatology and Centre of Bone Diseases, Lausanne University Hospital, Switzerland, ²ENT, Head and Neck Surgery Department, Lausanne University Hospital, Switzerland, ³Service of Genetic Medicine, Lausanne University Hospital, Switzerland, ⁴Centre of Bone Diseases, Lausanne University Hospital, Switzerland, ⁵Orthopaedic Surgery UPCOT, Lausanne University Hospital, Switzerland

Osteogenesis imperfecta (OI) is a rare genetic connective tissue disorder with wide phenotypic and molecular heterogeneity, causing risk of fractures in early life, progressive bone deformity, tooth and hearing alterations, and poor quality of life. In rare diseases, there is a real lack of patient information and recognition. Starting in 2012, we have employed a multidisciplinary approach for OI in our tertiary hospital, the Centre Hospitalier Universitaire Vaudois (CHUV), and created the CHUV OI group. The purpose of the present study is to evaluate the efficiency of this approach after 6 years. An OI day is organized annually, and patients are invited to attend an individualized medical checkup, depending on their own situation and needs. Each patient receives a physiotherapeutic evaluation with a proposition of physical therapy or counselling in physical activity and sport. In the same day, a clinical and scientific information session about the latest updates of the disease is organized, open to families and professional caregivers. 50 patients have received a personalized medical evaluation since the beginning. 12 children (age 1 to 17 years, mean 8.5) and 38 adults (age 18 to 69 years, mean 43.5) participated. All adults, except 1 without any site measurable, had at least one DXA measurement, with a mean spine T score of -2.55 ($-5.6; +0.6$), hip T score -1.4 ($-3.3; +1.6$), neck T score -1.58 ($-3.5; +1.3$). 34 patients had a bone texture measurement by TBS with a mean spine TBS of 1.259 ($1.003; 1.501$). Genetic evaluation was performed in 39 cases, and revealed mutation in 34 cases (table). The majority of patients experienced multiple fractures in childhood, and 12 had never received any bone active drug, apart from calcium/vitamin D substitution. The mean EQ5D at the beginning of the management was 0.74. It increased to 0.78 after the multidisciplinary management ($p=0.11$). The multidisciplinary approach, including the DXA and genetic evaluation resulted in personalized treatment adaptation/new treatment/ for all patients. The CHUV OI group multidisciplinary approach is efficient, resulting in better diagnosis, management and satisfaction of patients and their families as well as facilitating continuing education for the team members. Since 2012, the number of new patients has increased annually, with more patients benefiting of quality management including bone treatment and physical activity.

Number of patients	phenotype	genotype
4	V	IFITM5
1	IV	proline substitution in COL1A1
5	III	glycine substitution in COL1A2
1	III	proline substitution in COL1A1
1	III	alanine substitution in COL1A1
3	I	glycine substitution in COL1A2
1	I	aspartate substitution in COL1A2
17	I	haploinsufficiency mutations in COL1A1
1	osteoporosis pseudoglioma	LRPS

Table. Phenotype and genotype.

Disclosures: *Béregère Aubry-Rozier, None*

SUN-1047

EFFECTS OF BUROSUMAB, AN ANTI-FGF23 ANTIBODY, IN PATIENTS WITH TUMOR-INDUCED OSTEOMALACIA: RESULTS FROM AN ONGOING PHASE 2 STUDY Nobuaki Ito^{*1}, Yasuo Imanishi², Yasuhiro Takeuchi³, Yutaka Takahashi⁴, Yumie Rhee⁵, Chan Soo Shin⁶, Hironori Kanda⁷, Seiji Fukumoto⁸. ¹University of Tokyo Hospital Division of Nephrology and Endocrinology, Japan, ²Osaka City University Graduate School of Medicine, Department of Metabolism, Endocrinology and Molecular Medicine, Japan, ³Toranomon Hospital Endocrine Center, Japan, ⁴Division of Diabetes and Endocrinology, Department of Internal Medicine, Kobe University Graduate School of Medicine, Japan, ⁵Department of Internal Medicine, Yonsei University College of Medicine, Democratic People's Republic of Korea, ⁶Department of Internal Medicine, Seoul National University Hospital, Democratic People's Republic of Korea, ⁷Kyowa Hakko Kirin Co., Ltd., Japan, ⁸Department of Molecular Endocrinology, Fujii Memorial Institute of Medical Sciences, Institute of Advanced Medical Sciences, Tokushima University, Japan

Burosomab, a fully human monoclonal antibody targeting FGF23, is under development for treatment of FGF23-related hypophosphatemia. The aim was to evaluate the efficacy and safety of burosomab on serum phosphorus (Pi) and osteomalacia in adults with tumor-induced osteomalacia (TIO) with unresectable or unidentifiable tumors. In an ongoing open-label, single-arm, Phase 2 study conducted in Japan and Korea, subjects receive subcutaneous burosomab (0.1-2.0 mg/kg) every 4 weeks, dose adjusted according to individual serum Pi concentration. Interim data were obtained for subjects who have completed 72 weeks of therapy. Thirteen subjects with TIO (9 in Japan, 4 in Korea) were enrolled and 12 subjects completed 72 weeks. Mean age at entry was 60.5 years and all subjects had received prior oral phosphate and/or active vitamin D therapy with 2 weeks drug holiday before burosomab. At baseline (BL), serum levels of intact FGF23 ranged from 106-5150 pg/mL (median: 320) and mean (SD) BL serum Pi was 1.62 (0.49) mg/dL. Mean (SD) serum Pi substantially increased to 2.52 (0.68) mg/dL at Week (W) 16 and 2.73 (0.39) mg/dL at W72; this was accompanied by increases in TmP/GFR (BL=1.15 [0.43] mg/dL, W72=2.35 [0.56] mg/dL) and serum 1,25(OH)2D (BL=22.58 [11.87] pg/mL, W72=41.34 [8.53] pg/mL). Bone turnover markers increased at initial phase and then decreased. At BL, as assessed by bone scan, 13 subjects presented with 133 active fractures and 22 active pseudofractures. After 48 weeks of treatment, 15.0% of fractures and 17.4% of pseudofractures were healed. Bone histomorphometric findings related to osteomalacia assessed by paired bone biopsy samples also improved at W48. Mean (SD) distance walked in 6 minutes increased from 295.8 (96.0) meters at BL to 353.7 (115.8) meters at W48. Adverse events (AEs) were observed in 12 subjects. Two subjects had serious AEs, but none were drug-related. There were no meaningful changes in serum calcium or iPTH. In summary, burosomab treatment was well tolerated, increased serum Pi and 1,25(OH)2D in subjects with TIO and showed evidence of improvement of bone quality and fracture healing over 48 weeks, suggesting improvement in osteomalacia in subjects with TIO.

Disclosures: *Nobuaki Ito, Kyowa Hakko Kirin, Grant/Research Support*

SUN-1048

Effectiveness of asfotase alpha in an 18-year-old prenatal benign hypophosphatasia patient with prolonged tibial pseudofracture. Minae Koga^{*}, Yuko Kinoshita, Nobuaki Ito. Division of Nephrology and Endocrinology, The University of Tokyo, Japan

Background: Hypophosphatasia (HPP) is a rare inherited disorder caused by loss-of-function mutation in ALPL (alkaline phosphatase, liver/bone/kidney type) gene with

a reduction in TNSALP (alkaline phosphatase, tissue-nonspecific isozyme) activity. Disability in TNSALP inhibits dissociation of local PPi into phosphate, which subsequently cause hypocalcification in the bone. As a result, symptoms including pathological fracture/pseudofracture, tooth loss and soft tissue calcification represent HPP. Recently, Asfotase Alpha: an enzyme replacement therapy has been introduced for the treatment of HPP. Case presentation: The patient was an 18 years old girl genetically diagnosed as HPP with compound heterozygous mutation in ALPL (c.979T>C/c.1559delT). At birth, her serum ALP was 89 IU/L and her left femur was severely bent. The gap in the length between legs increased as she grew up. At the age of 10, she was referred to our hospital and underwent epiphyseodesis in her right knee. She went through left humerus fracture at the age of twelve while exercising. At 18 years old, as she was suffering the pain with a pseudofracture in her left tibia for more than one year, we finally decided to use Asfotase alpha on her. On admission, serum ALP was 74 U/L [106-322] and urine phosphoethanolamine (PEA) was 559.1 mmol/L [5.9-76.6]. X-ray revealed pseudofracture in her left tibia and bone scintigraphy accumulated in that lesion. Clinical course: Asfotase alpha was initiated at 80 mg (2 mg/Kg), three times a week. Her left tibia became painless in four and a half months, and she recovered and could do exercise in six months. Her urine PEA decreased to 89.8 nmol/L in 6 months and bone scintigraphy presented obvious improvement. Therapy related adverse events includes slight fever, fatigue and skin induration at the injection sites. However, these adverse events subsided and became tolerable. Discussion: While Asfotase alpha showed unarguable life-saving effect in perinatal and infantile HPP, the use of this drug in adult HPP or prenatal benign HPP with mild symptoms remains a matter of dispute. In a review article, there is a suggested indication of Asfotase alpha in adult HPP, for example, with pathological fracture or prolonged healing process of fracture. At least, we witnessed the invaluable effect of Asfotase Alpha in an 18 year old HPP patient who suffered prolonged tibial pain and anxiety for future fracture risk.

Disclosures: *Minae Koga, None*

SUN-1049

A Unique Case of Chronic Hypocalcemia and Ectopic Cushing Syndrome Lima Lawrence^{*}, Susan Williams, Peng Zhang, Humberto Choi, Usman Ahmad, Vinni Makin. Cleveland Clinic, United States

BACKGROUND Mutations in the calcium-sensing receptor (CaSR) and G-proteins involved in signaling pathways that regulate PTH synthesis, secretion and action are implicated in hyper and hypocalcemia (hypoCa). These disorders may be familial or acquired due to CaSR antibodies. We present a patient with suspected, life-long asymptomatic hypoCa who developed an ACTH-secreting thymic neuroendocrine tumor causing ectopic Cushing syndrome. CLINICAL CASE A 54 year old man presented to Endocrinology for evaluation of asymptomatic hypoCa diagnosed at age 19. He had no Ca-related complications including renal stones, renal dysfunction or fractures. Exam was consistent with a normal adult male phenotype. He had no family history of Ca or endocrine abnormalities. Lab studies over 8 years revealed baseline Ca around 6.0 (8.4 - 10.2 mg/dL) with normal albumin. With a serum Ca of 6.1 mg/dL and 25 OH-Vitamin D of 28.1, his PTH was inappropriately normal 17.1 pg/mL, with elevated Phos 6.0 mg/dL and normal Mg 1.8 mg/dL. Twenty-four hour urine studies revealed hypocalciuria 14.3 mg/24 hours. DEXA scan revealed osteopenia and brain MRI noted dystrophic calcifications within the basal ganglia. He limited intake of Ca and Mg supplements due to muscle cramping and was eventually lost to follow-up. Six years later, he presented to the hospital with oral thrush, severe metabolic abnormalities including hypokalemia, metabolic alkalosis and hypoCa of 4.1 mg/dL. Extensive workup revealed a large mediastinal mass, found to be a thymic neuroendocrine tumor secreting ACTH causing ectopic Cushing syndrome. Patient underwent successful surgical resection of the mass and is receiving steroids until adrenal recovery. CONCLUSION Although we do not yet have genetic confirmation, we hypothesize that our patient has autosomal dominant hypoCa type 2 due to abnormalities in the Gα11 subunit from mutations in the GNA11 gene. CaSR signals via G-proteins including Gα11, and gain-of-function mutations in GNA11 lead to increased cell sensitivity to extracellular Ca. As he has no family history of hypoCa, it is likely that he has a de-novo mutation or variable penetrance. Additionally, GNA11 gain-of-function mutations are also implicated in the pathogenesis of uveal melanoma. As melanocytes and thymic cells have a common embryonic neural crest origin, it is important to consider the possible implications of GNA11 mutations that may underlie hypoCa and development of malignancy in later life.

Disclosures: *Lima Lawrence, None*

SUN-1050

Long term health-related quality of life in patients with achondroplasia and hypochondroplasia Masaki Matsushita^{*1}, Hiroshi Kitoh¹, Kenichi Mishima¹, Naoki Ishiguro¹, Sayaka Fujiwara², Nobuhiko Haga², Taichi Kitaoka³, Takuo Kubota³, Keiichi Ozono³. ¹Department of Orthopaedic Surgery, Nagoya University Graduate School of Medicine, Japan, ²Department of Rehabilitation Medicine, The University of Tokyo, Japan, ³Department of Pediatrics, Osaka University Graduate School of Medicine, Japan

Achondroplasia (ACH) and hypochondroplasia (HCH) are the most common short-limbed skeletal dysplasias caused by activating mutations in the FGFR3 gene. Patients with ACH/HCH often need orthopaedic procedures for their disproportionate short stature or spinal involvement such as spinal canal stenosis and foramen magnum stenosis. Quality of life

(QoL) measures have gained recognition as essential tools for assessment of the impacts of diseases and therapeutic interventions, but only a few reports examined the QoL in individuals with ACH/HCH. In the current study, we assessed the health-related QoL (HRQoL) in adolescents and adults with ACH/HCH. Data for this cross-sectional study were collected from July 2016 to March 2018. Patients were recruited based on either a history of treatment to our institutions or registration to the patients' association of ACH in Japan. The HRQoL was assessed with the Short Form-36 as well as a disease-specific questionnaire, including presence or absence of growth hormone administration and surgical interventions for short stature or neurological impairments. The Physical Component Summary (PCS) and Mental Component Summary (MCS) from the patients were compared with those of the Japanese norm data by age groups and height groups. 201 patients with an average age of 25.6 years (10 to 67 years) were included in this study. The average MCS of the patients was similar to that of healthy subjects in all age groups. The average PCS of the patients, on the other hand, was significantly lower in all age groups than that of healthy subjects, and deteriorated with age. The physical QoL was rated poorly in the patients with a height of less than 140 cm, while favorable PCS scores were observed in the patients with a height of 140 cm or more, who are likely to be attributable to currently standard medical interventions such as growth hormone administration and limb lengthening surgeries. Neurological impairments that required surgical interventions, which was increased with age, seem to be one of the factors associated with decreased PCS in elderly patients. Physical QoL appears to be impaired in adult patients with ACH/HCH especially in elderly populations. Treatment for short stature in ACH/HCH patients should be planned so that they can acquire a final height of 140 cm or more. In order to maintain the QoL of elderly patients, we should take care for neurological complications such as spinal canal stenosis in this specific disorder.

PCS and surgical intervention of spine for each age group

Age Group, y	PCS	P Value vs History of Spine	
		Norm Data	Surgery, %
10-19 (n = 80)	44.22 ± 13.68	NA	5.0
20-29 (n = 51)	46.37 ± 16.19	<0.005	19.6
30-39 (n = 38)	41.32 ± 19.19	<0.005	31.6
40-49 (n = 16)	32.38 ± 18.03	<0.005	50.0
50-59 (n = 8)	29.74 ± 15.01	<0.005	87.5
60-69 (n = 5)	20.31 ± 15.54	<0.005	20.0

NA; not available

PCS and surgical intervention of limb lengthening For each height group

Height Group, cm	PCS	History of Limb	
		P Value vs Norm Data	Lengthening Surgery, %
100-109 (n = 10)	35.46 ± 13.93	<0.005	10.0
110-119 (n = 33)	35.88 ± 18.05	<0.005	18.2
120-129 (n = 52)	39.50 ± 17.09	<0.005	38.5
130-139 (n = 46)	39.05 ± 17.96	<0.005	65.2
140-149 (n = 38)	50.39 ± 11.20	NS	84.2
150-159 (n = 15)	50.55 ± 17.26	NS	93.3

NS; not significant

Disclosures: *Masaki Matsushita, None*

SUN-1051

Congenital Hypophosphatemia in Adults: Determinants of Bone Turnover Markers and Changes Following Total Parathyroidectomy Malachi Mckenna*, Rachel Crowley, Julie Grace-Martin, Patrick Twomey, Mark Kilbane. St. Vincent's University Hospital, Ireland

Introduction: Congenital hypophosphatemia (CH) results in defective mineralisation of bone that manifests as rickets in childhood; in adulthood osteomalacia prevails with residual disabling consequences. Bone turnover markers (BTMs) are a means of estimating disease severity and of guiding efficacy of therapy but published data on BTMs in CH in adults is limited. This is pertinent in view of the advent of KRN23, which is a recombinant human monoclonal antibody that binds to carboxy-terminal fibroblast growth factor 23 (FGF23) blocking its activity, as a treatment of CH in adults. We sought to review our experience of BTMs and their determinants in adults with CH. **Methods:** We studied 27 patients with CH, all presenting in childhood with rickets and all having reduction in the maximum renal threshold for phosphate reabsorption (TmP/GFR): 23 had X-linked hypophosphatemia (XLH) of whom 2 were hypoparathyroid post total parathyroidectomy; 2 had autosomal dominant hypophosphatemic rickets (ADHR), and 2 had unknown mutations. We measured TmP/GFR, fibroblast growth factor (FGF23), parathyroid hormone (PTH) ionised calcium, 25-hydroxyvitamin D (25OHD), 1,25-dihydroxyvitamin D (1,25D), and a panel of BTMs including: serum bone-specific alkaline phosphatase (bone ALP), osteocalcin (Oc), and total procollagen type I amino-terminal propeptide (PINP), and carboxy-terminal telopeptide of

type I collagen (CTX); and urinary N-terminal telopeptides of type I collagen (uNTX). Results: TmP/GFR varied widely with the principal determinant being FGF23 and to a lesser extent ionised calcium and PTH. After excluding the two patients with XLH and total parathyroidectomy, BTMs (n=25) varied in sensitivity as follows: bone ALP (96%); CTX (72%); PINP (38%); uNTX (48%); Oc (32%). The strongest association with bone ALP was PTH. Those on phosphate supplements had significant elevation in CTX. The 2 patients with XLH and complete hypoparathyroidism had normalization of TmP/GFR and near normalisation of BTMs despite marked elevation in FGF23: 10.015 RU/ml and 4310 RU/ml. Conclusions: The clinical management of CH in adulthood continues to be challenging with most patients still manifesting with abnormalities in BTMs that indicates ongoing osteomalacia. The primacy of PTH over FGF23 in renal phosphate handling is suggested by the 2 cases with XLH and hypoparathyroidism, as suggested by our group in an earlier case report. Reference: Crowley RK et al. J Med Case Rep 2014; 8: 84.

Disclosures: *Malachi Mckenna, None*

SUN-1052

Comprehensive Genetic Analysis by Targeted Next Generation Sequencing and Genotype-phenotype Correlation of 47 Japanese Patients with Osteogenesis Imperfecta Yasuhisa Ohata*^{1,2}, Shinji Takeyari¹, Taichi Kitaoka¹, Hirofumi Nakayama^{1,3}, Varoona Bizaoui^{1,4}, Yukako Nakano¹, Kenichi Yamamoto^{1,5}, Kei Miyata¹, Keiko Yamamoto^{1,6}, Takuo Kubota¹, Katsusuke Yamamoto⁷, Toshimi Michigami⁸, Takehisa Yamamoto⁹, Keiichi Ozono¹. ¹Department of Pediatrics Osaka University Graduate School of Medicine, Japan, ²The 1st. Department of Oral and Maxillofacial Surgery Osaka University Graduate School of Dentistry, Japan, ³The Japan Environment and Children's Study Osaka unit center, Japan, ⁴Department of Medical Genetics Reference Center for Skeletal Dysplasia Hôpital Necker - Enfants Malades, Japan, ⁵Department of Statistical Genetics Osaka University Graduate School of Medicine, Japan, ⁶Department of Bone and Mineral Metabolism Osaka Women's and Children's Hospital, Japan, ⁷Department of Pediatric Nephrology and Metabolism Osaka Women's and Children's Hospital, Japan, ⁸Department of Bone and Mineral Metabolism Osaka Women's and Children's Hospital, Japan, ⁹Department of Pediatrics Minoh City Hospital, Japan

Osteogenesis imperfecta (OI) is a genetic disorder characterized by fragile bones and increased susceptibility to fracture. Currently, 20 genes have been identified as the causative candidate genes of OI. Since little is known about genotype-phenotype correlation in Japanese OI, we developed a novel panel of genes targeting OI for next generation sequencing (NGS) and analyzed Japanese patients. We enrolled 47 Japanese OI patients from 45 unrelated families. The panel was designed to include 15 OI candidate genes (COL1A1, COL1A2, FKBP10, SERPINH1, IFTIM5, SERPINF1, CRTAP, P3H1, PPIB, SP7, PLOD2, BMP1, CREB3L1, TMEM38B, and WNT1) and 19 genes (LRP5, LRP6, TNFRSF11A, TNFRSF11B, CBS, MTHFR, MTR, WNT4, CTNBI, WNT16, DKK1, LRP4, SOST, WLS, SFRP4, WNT5B, AXIN1, RSO3, and TNFSF11) associated with bone fragility or Wnt signaling. After detecting mutations by NGS, we confirmed them by Sanger sequencing. We identified mutations in 36 out of 47 patients: 19 had reported mutations, 8 had mutations which were located in same codon with reported mutation but resulted in other amino acid change, and 9 had novel mutations. We also performed whole exome sequencing in 3 patients in whom we could not detect mutations by the panel, and identified 1 reported and 1 novel mutations. Twenty-seven, 10, and 1 patients had mutations in COL1A1, COL1A2, and IFITM5 gene, respectively, and all of them were heterozygous. In COL1A1, we identified 9 missense mutations including 8 glycine substitutions, 7 nonsense mutations, 6 splice site mutations, 4 frameshift mutations, and 1 intron mutation. In COL1A2, 6 missense mutations including 5 glycine substitutions, 1 splice site mutation, 1 intron mutation, and 2 duplications were detected. The IFITM5 mutation was the reported one (c.-14C>T). We classified these COL1A1 and COL1A2 mutations into 4 groups (glycine substitutions; nonsense and frameshift mutations as non-functional allele; splice site and duplication mutations; other missense mutations) and analyzed them for genotype-phenotype correlation. As a result, patients with glycine substitution had severer symptoms than other patients, since more patients were diagnosed as type III OI in Silencence classification, and the numbers of fractures before treatment were significantly higher than in other groups. In bone mineral density (BMD), however, there was no significant difference among these groups, implicating that the bone fragility in OI could not be evaluated by BMD.

Disclosures: *Yasuhisa Ohata, None*

SUN-1053

Aortic Measurements in Children with Osteogenesis Imperfecta Remain Stable At Short Term Surveillance Interval Eric Rush*¹, Shelby Kutty², Rose Kreikemeier³, Ling Li², Mary Craft², David Danford². ¹Children's Mercy Hospital, United States, ²University of Nebraska Medical Center, United States, ³Children's Hospital and Medical Center, United States

Background: Osteogenesis imperfecta (OI) is a rare skeletal disorder that causes bone fragility, fractures, and short stature. There has been recent interest in the cardiopulmonary pathology of OI, however the onset and progression of cardiovascular disease is not well

known. Changes in left ventricular and aortic dimensions have been observed in young patients with OI. We report follow-up echocardiographic findings in 49 patients with OI derived from an inception cohort of 100 who had baseline echocardiography. Methods: This was a single-center prospective investigation from 2014 to 2016. Patients were phenotyped using modified Silience criteria published in the Nosology and Classification of Genetic Skeletal disorders: 2015 Revision. Ventricular, valvular and aortic measurements were performed according to American Society of Echocardiography guidelines. Aortic measurements were made at end-diastole in parasternal long-axis view at annulus, sinuses of Valsalva, sinotubular junction, and ascending aorta 2 cm from annulus. Z-score and percentile based comparisons were made between the baseline and follow-up measurements using paired t-test of corresponding data sets. Results: 49 patients were evaluated in this study, with a mean age of 12.1 years. 22 patients were male and 27 female. 26 patients had Type I OI, 16 had Type IV OI, and 7 had Type III OI. The mean time between studies was 2.3 years with range between 1.8 and 3.2 years. Raw aortic dimensions at each measurement site increased commensurate with somatic growth. Z-score comparisons did not show statistically significant increase in aortic dimensions at the annulus ($p=0.32$), the sinus of Valsalva ($p=0.11$), or the proximal ascending aorta ($p=0.92$). There was statistically significant increase in aortic diameter at the sinotubular junction ($p=0.047$). Analysis of patients by OI type also revealed no statistically significant increases at any aortic location, with p value between 0.12 and 0.98. Conclusion: This study confirms higher incidence of mild aortic dilation in patients with OI. There was no significant progression of aortic size over the short time frame of the study, indicating stable or slowly progressive changes. An ideal time interval for echocardiographic surveillance in the asymptomatic OI patient is not established based on these findings.

Disclosures: *Eric Rush, None*

SUN-1054

Twelve Chinese Patients with Primary Hypertrophic Osteoarthropathy: Mutation Identification and Clinical Features Yang Xu*, Zhen-Lin Zhang. Department of Osteoporosis and Bone Diseases, Metabolic Bone Disease and Genetics Research Unit, Shanghai Jiao Tong University Affiliated Sixth People's Hospital, China

Objective: Primary hypertrophic osteoarthropathy (PHO) is a rare inherited disease characterized by clubbing fingers, periostosis and pachydermia. Mutations in HPGD cause autosomal recessive 1 (PHOAR1) and mutations in SLCO2A1 cause autosomal recessive 2 (PHOAR2). This study analyzed and compared pathogenic genes and clinical manifestations of two types of PHO to improve clinical knowledge. Methods: Clinical data of 12 patients with PHO were collected and radiographs of hands, the right tibia and fibula, and the right knees were taken. Sanger sequencing was used to identify the pathogenic genes. Results: 6 patients were caused by SLCO2A1 mutations and 3 were caused by HPGD mutations, and no mutations in SLCO2A1 or HPGD were detected in the remaining 3. Two novel mutations were identified in SLCO2A1 (c.1375T>C, p.Cys459Arg; c.1657A>G, p.Ile533Val), and one novel mutation was identified in HPGD (c.1A>T, p.Met1Leu). The mutation, c.310_311delCT (p.Leu104AlafsX3) in HPGD may be a common mutation, for 3 patients with PHOAR1 carried the same one. The 6 patients with PHOAR2 were all male, and the onset was during puberty. 2 of them had swelling knees and ankles which caused limited movement, and they also had progressive pachydermia in faces and heads and severe clubbing fingers which were accompanied with anemia, diarrhea, gastrointestinal ulcers. However, the other 4 only had clubbing fingers, and other symptoms including pachydermia and swelling joints were not obvious. 3 patients with PHOAR1 had clubbing fingers since childhood and they also had swelling knees and ankles, while the pachydermia in face was not significant. 1 of them was female and had pain of ankles with menstrual cycle. 3 patients with undetected mutations were all male and 2 of them were from one family. The onset was from puberty, and pachydermia in faces and heads was the earliest symptom, followed by clubbing fingers and swelling knees and ankles. All of them had severe gastrointestinal ulcers and anemia. Radiographs of both patients with PHOAR1 and PHOAR2 showed periostosis in long bones, and patients with PHOAR1 also had dissolution of the extremities. Conclusion: PHO is a disease with genetic and clinical heterogeneity, clinical manifestations contribute to clinical classification, and molecular diagnosis ultimately depends on genetic detection. Further study in cases with undetected mutations may be significant to determine the exact mechanism of PHO and figure out related pathways.



Disclosures: *Yang Xu, None*

SUN-1055

Loss of Gassignaling induces osteoblast differentiation in soft tissues of POH patients and during normal cranial bone development by activating Hedgehog signal Yingzi Yang^{*1}, Ruoshi Xu², Xuedong Zhou³, Eileen Shore⁴, Fred Kaplan⁵. ¹Harvard University, United States, ²Harvard School of Dental Medicine and West China Hospital of Stomatology, United States, ³West China Hospital of Stomatology, China, ⁴University of Pennsylvania School of Medicine, United Kingdom, ⁵University of Pennsylvania School of Medicine, United States

How osteoblast cells are induced during bone development is a central question for understanding the organizational principles underpinning a functional skeletal system. Abnormal osteoblast differentiation leads to a broad range of devastating diseases such as craniosynostosis (premature suture fusion), heterotopic ossification (HO) and osteoporosis. Molecular analyses of skeletal genetic diseases with abnormal osteoblast differentiation have provided important insights in the regulation of osteoblast induction. Progressive osseous heteroplasia (POH) (OMIM#166350) and Albright's hereditary osteodystrophy (AHO, OMIM 103580) are caused by loss function mutations in the GNAS gene, which encodes the stimulatory alpha subunit, Gas, of heterotrimeric G protein that transduces signals from G protein coupled receptors (GPCRs). POH and AHO are characterized by progressive extra-skeletal bone formation through an intramembranous process. We have demonstrated that Gas restricts bone formation to the skeleton by inhibiting Hedgehog (Hh) signaling in mesenchymal progenitor cells. More recently, we have investigated intramembranous ossification during cranial bone development in mouse models of POH. We find here while Hh ligand-dependent Hh signaling is essential for endochondral ossification, it is dispensable for intramembranous ossification, where Gas regulates Hh signaling in a ligand-independent manner. We further show that Gas controls intramembranous ossification during cranial bone development by regulating both Hh and Wnt signaling. In addition, sustained Gas activation in the developing cranial bone leads to reduced ossification, but increased cartilage presence due to reduced cartilage dissolution, not cell fate switch. Small molecule inhibitors of Hh signaling can effectively ameliorate cranial bone phenotypes in mice caused by loss of Gnas function mutations. Our work shows that studies of genetic diseases provide invaluable insights in normal bone development and understanding both leads to better diagnosis and therapeutic treatment of bone diseases.

Disclosures: *Yingzi Yang, None*

SUN-1056

Hypoparathyroidism, real life experience in 55 patients Maria Belen Zanchetta^{*1}, Damian Robbiani¹, Fernando Silveira², Jose Ruben Zanchetta¹. ¹IDIM, Universidad del Salvador, Argentina, ²IDIM, Argentina

Hypoparathyroidism (HPT) is a rare disorder characterized by hypocalcemia and absent or deficient PTH. It is associated with an increased risk of various complications, but only few data is available on the natural history and correct management of this disease. Aim: Describe clinical characteristics, treatment and complications in a group of patients with hypoparathyroidism followed in our Bone Clinic under routine clinical care. Secondary, describe how many patients reached guidelines recommendations for rHPTH(1-84) treatment (Brandi ML. JCEM. 2016). Materials and Methods: Patients with a diagnosis of HPT of ≥ 6 months seen between June 2013 and December 2017 were eligible for inclusion. Demographics, HPT etiology, HPT management, fractures, DXA values, biochemical values, including renal function; renal and cardiovascular events; soft tissue calcification and hospitalizations were collected via electronic data capture. Results: 55 HPT patients were included; mean age was 49.1 ± 16.3 years, 46/55 were women. Treatment regimens were determined by the patients' physician, per usual clinical practice, and all were receiving calcium supplementation and calcitriol. Regarding etiology 48/55 (87.2%) was post-surgical, 3/55 DiGeorge Syndrome, one autoimmune, one pseudo-hypoparathyroidism and two unknown. Biochemical and DXA values at diagnosis are shown in table 1. 9/55 (16.3%) had history of hypocalcemia requiring hospitalization. 3/55 had fracture history (wrist, hip and tibia, last two fractures in patients with DiGeorge Syndrome). 3/55 has history of seizures. Only 14/55 (25.4%) had renal ultrasound done and 3 of them (21, 4%) had kidney stones. 65% (36/55) had 24-hour urine calcium excretion measured and half of them had hypercalciuria confirmed. Only 4/55 patients had central nervous system imaging performed, and two of them had basal ganglia calcification confirmed. Finally, 19/55 met criteria to rHPTH (1-84) treatment according to the guideline; most of them (13) because their oral calcium requirements exceed 2.5 g of calcium. Conclusion. Although these patients were followed by specialists, clinical management and monitoring was heterogeneous and probably insufficient to assess all the potential complications of this chronic disease. rHPTH (1-84) is not yet available in Argentina, but 34.5% of our patients met criteria for this new treatment. Being aware of this situation is the first step to improve our medical management of HPT in the future.

	All (n=55)	Women (n=46)	Men (n=9)	P
Age (years)	49.1 ± 16.3 (n=54)	49.6 ± 15.7 (n=45)	46.7 ± 20.1	
Age at diagnosis	40.7 ± 17.3 (n=48)	40.5 ± 17.1 (n=39)	41.8 ± 19.1	
Calcium	8.5 ± 0.7 (n=53)	8.6 ± 0.7 (n=44)	8.1 ± 0.7	0.02
Ionic Calcium	4.1 ± 0.5 (n=28)	4.3 ± 0.3 (n=23)	3.5 ± 0.5 (n=5)	
Phosphate	4.9 ± 1.0 (n=47)	4.8 ± 1.0 (n=39)	5.0 ± 1.4 (n=8)	
PTH	15.4 ± 7.2 (n=25)	14.6 ± 6.7 (n=19)	17.9 ± 8.9 (n=6)	
VitD	35.2 ± 12.8 (n=37)	35.3 ± 13.3 (n=30)	34.8 ± 10.8 (n=7)	
Magnesium	1.8 ± 0.2 (n=28)	1.8 ± 0.2 (n=24)	1.8 ± 0.1 (n=4)	
Creatinine	0.88 ± 0.19 (n=15)	0.85 ± 0.18 (n=13)	1.05 ± 0.25 (n=2)	
24 hs Calcitriol	229.7 ± 175.0 (n=22)	245.3 ± 190.9	176.8 ± 102.1	0.33*
Crosslaps	329.3 ± 276.0 (n=15)	239.9 ± 120.4	508.2 ± 417.2	
Osteocalcin	13.5 ± 6.0 (n=8)	13.2 ± 5.6 (n=6)	14.5 ± 9.8 (n=2)	
DXA				
Lumbar S Ts	0.4 ± 2.3 (n=9)	-0.5 ± 1.7 (n=7)	3.6 ± 0.6 (n=2)	
Femoral neck Ts	0.5 ± 1.3 (n=9)	0.2 ± 1.2 (n=7)	1.3 ± 1.6 (n=2)	
Total Hip Ts	-0.4 ± 1.2 (n=6)	-0.3 ± 1.3 (n=5)		

Disclosures: Maria Belen Zanchetta, None

SUN-1057

Novel Mutation in the P4HB Gene in Chinese Patient of Osteogenesis Imperfecta with Cole-Carpenter Syndrome Hao Zhang*, Yangjia Cao, Zhenlin Zhang, Shanghai Jiao Tong University Affiliated Sixth People's Hospital, China

Purpose: Cole-Carpenter syndrome (CCS) is commonly regarded as a rare osteogenesis imperfecta (OI) characterized by bone fragility, ocular proptosis, craniosynostosis, hydrocephalus, and distinctive facial features. CCS can be caused by homozygous mutations in CRTAP gene and heterozygous mutation in P4HB gene. To date, only one heterozygous missense mutation in exon 9 of P4HB (c.1178A>G [p.Tyr393Cys]) and one heterozygous deletion variation in exons 5 to 8 of the P4HB gene have been found to cause CCS. We sought to characterize the phenotypes and to identify the P4HB gene mutation associated with Chinese patient with CCS. Methods: Using whole-exome sequencing in 1 CCS patient, we identified 1 novel heterozygous missense mutation of P4HB gene. The patient was a 54-year-old female; she had recurrent limb fractures from 2.5 years old to 13 years old. At the age of 36, she suffered a fracture of the left elbow due to sprain. At age 54, she suffered fractures of her left calf and left knee due to a fall and a sprain. The patient showed severe scoliosis and both legs were short and with bent deformity. She was unable to walk, and used two benches in place of wheelchair. She had ocular proptosis and protuberant forehead. But X-ray of the skull showed normal. Results: We identified 1 novel heterozygous missense mutation of P4HB (c.1198T>C, [p.Cys400Arg]). The protein structure shows that the site is located in the center of the reaction of the gene encoding protein disulfide isomerase. Conclusions: We discovered 1 novel heterozygous missense mutation of P4HB gene of Chinese CCS patient. Our study extended both the phenotypic and the genotypic spectrum of the CCS patient with P4HB mutation.

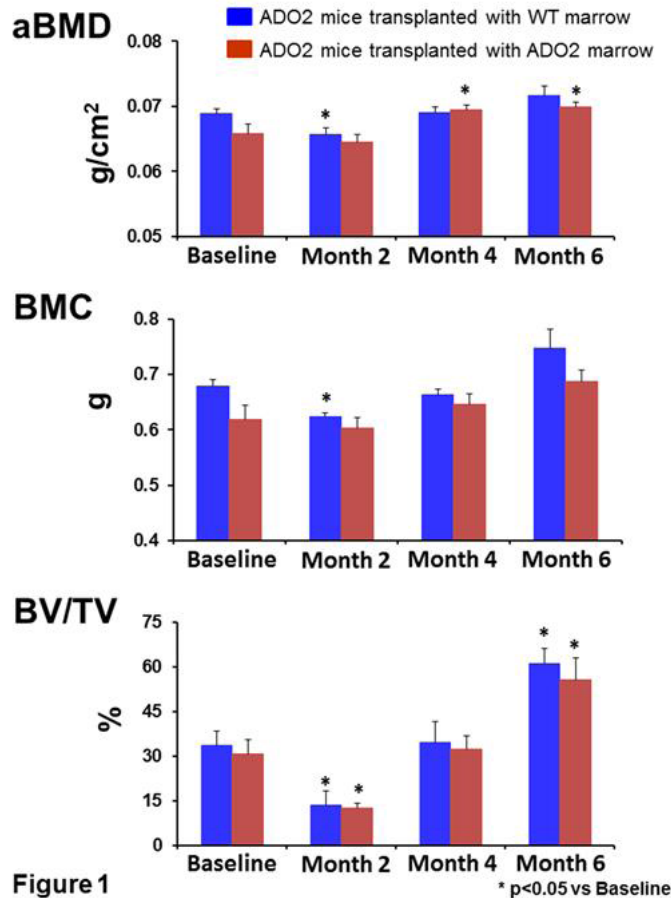
Disclosures: Hao Zhang, None

SUN-1091

Bone Marrow Transplantation as a Therapy for Autosomal Dominant Osteopetrosis Type II in Mice Imranul Alam*, Erik Imel, Rita Gerard-O'Riley, Dena Acton, Dana Oakes, Marta Alvarez, Melissa Kacena, Michael Econs, Indiana University School of Medicine, United States

Autosomal dominant osteopetrosis type II (ADO2) is a heritable osteosclerotic bone disorder caused by missense mutations in the chloride channel 7 (CLCN7) gene. Clinical features of ADO2 include fractures, osteomyelitis, vision loss, and in severe cases, bone marrow failure. Currently, there is no effective therapy for ADO2. Theoretically, bone marrow transplantation (BMT) could be used to treat ADO2, although mortality from the procedure is high. Two of our severely affected ADO2 patients (females ages 16 and 41 years) recently underwent BMT and neither engrafted (one died shortly after BMT and the second died shortly after a second BMT). Recently, we created an ADO2 knock-in mouse model on the 129S1 background, which phenocopies human ADO2. To test whether BMT could restore osteoclast function and rescue the bone defect in ADO2 mice we transplanted bone marrow cells from 6-week-old male WT or ADO2 donor mice into 9-month-old (a model of the adult patient) recipient female ADO2 mice through tail vein injections after irradiation (1100 cGy split dose). Donor chimerism was determined using Y chromosome contribution. ADO2 recipient mice had more than 80% engraftment up to 6 months post-transplantation. DXA results demonstrated that compared to the ADO2 mice that received bone marrow from ADO2 mice (control group), ADO2 recipient mice with bone marrow from WT mice (experimental group) displayed greater % decreases of aBMD and BMC at 2 months post-transplantation (Figure 1). At 4 months post-transplantation, both control and experimental groups regained bone mass closer to the baseline, although experimental mice gained significantly lesser bone mass compared to the control mice. However, at 6-month post-transplantation percent bone mass gained from baseline was similar in both control and experimental groups (Figure 1). MicroCT results demonstrated that trabecular BV/TV at the distal femur decreased significantly in both groups at 2 months post-transplantation but returned to the baseline level by 4 months (Figure 1). In addition, serum CTX and CTX/TRAP ratio were increased in the experimental mice at 2 months post-transplantation and then returned to baseline levels afterwards. Our results suggest that BMT does not provide long-term beneficial effect in older

ADO2 mice; however, the outcome in younger mice remains to be determined. Studies in younger mice should be performed before attempting BMT in ADO2 patients.



Disclosures: Imranul Alam, None

SUN-1092

Cystinosis Deficiency Primarily Affects Bone Remodeling In Cystinosis Giulia Battafarano¹, Michela Rossi¹, Laura Rita Rega², Gianna Di Giovamberardino³, Anna Pastore⁴, Matteo D'Agostini⁵, Ottavia Porzio⁵, Francesco Emma², Anna Taranta², Andrea Del Fattore¹. ¹Bone Physiopathology Group, Multifactorial Disease and Complex Phenotype Research Area, Bambino Gesù Children's Hospital, IRCCS, Italy, ²Department of Nephrology and Urology, Division of Nephrology, Bambino Gesù Children's Hospital, IRCCS, Italy, ³Laboratory of Metabolomics and Proteomics, Bambino Gesù Children's Hospital, IRCCS, Italy, ⁴Laboratory of Metabolomics and Proteomics, Bambino Gesù Children's Hospital, IRCCS, Italy, ⁵Clinical Laboratory, Bambino Gesù Children's Hospital, IRCCS, Italy

Purpose: Cystinosis is a rare disease caused by loss-of-function mutation of CTNS gene, encoding for cystinosis lysosomal transporter. It is characterized by cystine accumulation into the lysosomes leading to crystals formation and cellular damage. Cystinosis patients develop nephropathic Fanconi syndrome, bone deformity and fragility, osteomalacia and rickets. Skeletal alterations in cystinosis patients have been considered until now as a consequence of renal impairment. To understand if cystinosis deficiency primarily affects the skeleton, we studied ctns^{-/-} (KO) male mice that develop skeletal alterations without Fanconi syndrome up to 9 months of age. Methods: The nephropathy was excluded by histological evaluation of kidney and biochemical analysis. Intra-lysosomal cystine accumulation in KO tissues was evaluated by HPLC. In vivo bone phenotype was studied by μ CT, histomorphometry and bone turnover markers analysis. In vitro experiments were performed to identify alterations of osteoblasts and osteoclasts isolated from WT and KO animals. Results: HPLC analysis revealed that KO mice accumulate intra-lysosomal cystine in bones reaching higher levels than those observed in kidney. μ CT analysis of 1-month-old KO femurs displayed a reduction of trabecular bone volume and bone mineral density (BMD mgHA/cm³, WT: 188.6±4.13; KO: 162.8±4.11, p<0.005) with a decrease of trabecular number and thickness and increased trabecular separation. Histomorphometric analysis revealed a reduction of osteoclasts (Oc.S/BS %, WT: 22.45±6.62; KO: 12.91±4.85, p<0.05) and osteoblast parameters (Ob.S/BS %, WT: 20.87±3.26; KO: 12.08±6.69, p<0.05) in KO animals compared to WT. These alterations were confirmed by reduced TRAcP and P1NP

levels in KO sera. In vitro analysis revealed intra-lysosomal cystine accumulation in KO osteoclasts and osteoblasts with a perinuclear engulfment of lysosomes. Cultures from bone marrow of *ctns*^{-/-} mice displayed reduced number of osteoclasts (Osteoclast number %, WT: 100.70±4.59; KO: 75.34±26.44. *p*<0.05). Moreover a defect of differentiation (ALP+ cells %, WT: 99.67±0.58; KO: 59.63±20.65. *p*<0.05) with reduced *runx2*, *sp7*, *alp* and *coll1a2* expression was observed in KO osteoblasts compared to WT cells. Conclusion: All together these data reveal that the absence of cystinosis primarily affects bone cell differentiation leading to osteopenic phenotype in *ctns*^{-/-} mice.

Disclosures: **Giulia Battafarano**, None

SUN-1093

Enhanced activation of Rac1/Cdc42 and MITF as a possible mechanism of augmented osteoclastogenesis in autosomal dominant osteopetrosis type II with G215R mutation of chloride channel 7 gene Gun-Woo Kim^{*1}, Youn-Kwan Jung², Ji-Ae Jang², Min-Su Han², Seungwoo Han³. ¹Laboratory for arthritis and bone biology, Fatima Research Institute, Department of Internal medicine, Daegu Fatima Hospital, Republic of Korea, ²Laboratory for arthritis and bone biology, Fatima Research Institute, Daegu Fatima Hospital, Republic of Korea, ³Department of Internal medicine, Kyungpook National University Hospital, Republic of Korea

The autosomal dominant osteopetrosis type II (ADOII) caused by the mutation of chloride channel 7 (CIC-7) gene is the most common form of adult-onset osteopetrosis. Despite of dysfunctional bone resorption, an augmented osteoclast differentiation was reported recently in ADOII patients. DNA sequencing analysis of patient's CIC-7 gene identified a known heterozygous ADO II mutation, c.643G>A in exon 7, encoding p.Gly215Arg. In vitro osteoclast differentiation from ADOII patient's peripheral blood mononuclear cells (PB-MCs) increased compared to control despite of their dysfunctional bone resorbing capacity. Osteoclasts from ADOII patient's PBMCs and CIC-7 knockdown bone marrow monocytes (BMMs) showed an enhanced Ser-71 phosphorylation of Rac1/Cdc42 and increase of the microphthalmia-associated transcription factor (MITF) and receptor activator of nuclear factor κB (RANK) that can be responsible for the enhanced osteoclast differentiation.

Disclosures: **Gun-Woo Kim**, None

SUN-1094

Antioxidant and anti-inflammatories dampen the PSACH chondrocyte pathology Karen Posey^{*}, Jacqueline Hecht. McGovern Medical School at UTHealth, United States

Karen Posey¹, Francoise Coustry¹, Alka Veerisetty¹, Mohammad Housain¹ and Jacqueline T. Hecht^{1,2} McGovern Medical School and ²School of Dentistry at UTHealth Mutations in the cartilage oligomeric matrix protein (COMP) gene cause pseudoachondroplasia (PSACH), a severe dwarfing condition associated with limb shortening, joint laxity and early onset osteoarthritis. Using our MT-COMP mouse that recapitulates PSACH, we defined the underlying mechanism resulting from massive mutant COMP chondrocyte retention, wherein intense cellular stress is activated through CHOP arm of the UPR culminating in an unrelenting inflammatory and oxidative stress environment, and ultimately chondrocyte death. By eliminating CHOP, there was a reduction in mutant COMP retention, alleviation of the devastating cellular inflammation and oxidative stresses and reduction in chondrocyte death. Based on these observations, we tested anti-inflammatories (aspirin and ibuprofen) and antioxidants (resveratrol, grape seed extract (GSE), turmeric, CoQ10, vitamin E) therapeutics to determine whether they reduced the chondrocyte stress cycle. Aspirin, ibuprofen, resveratrol, GSE, or vitamin E treatments decreased mutant COMP intracellular retention and chondrocyte death, and restored chondrocyte proliferation. Inflammatory markers associated with cartilage degradation and eosinophils were undetectable in treated mice. While, turmeric and CoQ10 reduced retention and chondrocyte death, they did not reduce all inflammation markers. We have recently identified a treatment window wherein aspirin and resveratrol treatments can be started as late as 2 wks of age in MT-COMP mice and still reduce the chondrocyte stress burden. Given that human skeletal growth spans 16-20 years and murine skeletal growth is 8-10 weeks, one week in mice growth approximates 2 years in human growth. This suggests that PSACH aspirin or resveratrol therapy would be most beneficial if started by 4 years of age. These are important therapeutic approaches that mitigate both the chondrocyte and long bone pathology in our PSACH mouse model and will be tested in human clinical trials.

Disclosures: **Karen Posey**, None

SUN-1095

Upregulated Transforming Growth Factor Beta (TGFβ) Signaling in Osteoblast-like cells from Osteogenesis Imperfecta Patients Nathalie Bravenboer^{*}, Elise Riesebos, Huib Van Essen, Marelise Eekhoff, Gerard Pals, Dimitra Micha. VU University Medical Center, Netherlands

Osteogenesis Imperfecta (OI) is primarily characterized by bone fragility as a result of mutations in genes responsible for collagen regulation. Recently excessive TGFβ signaling

has been demonstrated to underlie the mechanism of OI in *Crtp*^{-/-} and *Col1a2tm1.1Mcb* mouse models of the disease. This has introduced fresolimumab, an inactivating antibody against TGFβ, to clinical trials for OI. However, the effect of TGFβ in OI patient osteoblast cells has not yet been investigated. The objective of this study was to examine TGFβ signaling in transdifferentiated osteoblasts of OI patients. For this primary dermal fibroblasts from 2 patients with a CRTAP mutation, 2 patients with a COL1A2 mutation and 2 healthy donors were subjected to osteogenic transdifferentiation with human platelet lysate. The transdifferentiated osteoblasts were then stimulated with TGFβ1 and phosphorylated SMAD3 expression was analysed by western blotting. We also used immunohistochemistry to stain for phosphorylated SMAD3 in bone biopsies of OI patients. We observed increased expression of phosphorylated SMAD3 in transdifferentiated osteoblasts of OI patients with pathogenic CRTAP and COL1A2 mutations compared to the healthy controls following TGFβ stimulation. This difference was found to be less in the primary fibroblasts. Immunohistochemistry confirmed positive nuclear staining of phosphorylated SMAD3 in trabecular bone cells of OI patients. This study shows excessive TGFβ signaling in OI patient-derived transdifferentiated osteoblasts which is in line with the findings in the respective OI mouse models. This was also reflected in the bone tissue of OI patients. TGFβ signaling appears to be crucial in recessive and dominant OI pathogenesis; the outcome of the current clinical trials will determine its therapeutic potential.

Disclosures: **Nathalie Bravenboer**, None

SUN-1096

Igfl Derived from Osteoclasts in Paget's Disease Increases Bone Formation via Signaling through EphrinB2/EphB4 Kazuaki Miyagawa^{*1}, Yasuhisa Ohata¹, Jolene J. Windle², G. David Roodman^{1,3}, Noriyoshi Kurihara¹. ¹Medicine/Hematology-Oncology; Indiana University, United States, ²Human and Molecular Genetics, Virginia Commonwealth University, United States, ³Roudebush VA Medical Center, United States

We reported that Igfl derived from osteoclasts (OCLs) increased EphrinB2 on OCLs, which bound EphB4 on osteoblasts (OBs) to enhance bone formation. Further, OCLs expressing measles virus nucleocapsid protein (MVNP), a model of Paget's Disease (PD), expressed higher levels of Igfl than normal OCLs. However, the role of OCL-derived Igfl in PD in vivo is unclear. Therefore, we conditionally deleted Igfl in OCLs expressing MVNP by crossing *Trap-MVNP* (MV) mice to *Trap-Cre* (TC) and *Igfl1* flox/flox mice to generate mice of the following four genotypes: *MV+/TC+/Igfl1* flox/flox (*MV/Igfl1*-), *MV+/TC-/Igfl1* flox/flox (*MV/Igfl1*+), *TC(+)/Igfl1* flox/flox (*Igfl1*-) mice, *TC(-)/Igfl1* flox/flox (*Igfl1*+ = WT). At 6 months of age, body weight and serum Igfl and IGFBP3 levels were similar among the 4 genotypes. μCT analysis of 12 month old male mice showed that BV/TV of the distal femur in *MV/Igfl1*- mice was significantly decreased by 55% compared to *MV/Igfl1*+ mice (*p*<0.05). BV/TV of *Igfl1*- mice was similar to *MV/Igfl1*- mice. OCL number and surface, and OB number and surface in *MV/Igfl1*- and *Igfl1*- mice were decreased by 40% compared to *MV/Igfl1*+ and *Igfl1*+ mice (*p*<0.01) respectively. We then measured Igfl levels in media conditioned (CM) for 48 hours by purified OCLs from the 4 genotypes. Igfl levels in *MV/Igfl1*+ OCL CM were 250±23 pg/ml, while Igfl in CM from the other genotypes were < 50 pg/ml (*p*<0.01). Igfl-receptor expression on OCLs was similar in all genotypes. OCL formation in RANKL treated bone marrow cultures of *MV/Igfl1*- mice was decreased by 50% vs *MVNP/Igfl1*+ mice, and the OCLs in *MV/Igfl1*- marrow cultures were smaller and had ~20 nuclei/OCL compared to 50 nuclei/OCL in *MV/Igfl1*+ cultures. Further, bone resorption capacity/OCL on bone slices in *MV/Igfl1*- and *Igfl1*- cultures was significantly decreased by 60% compared with *MV/Igfl1*+ and *Igfl1*+ cultures respectively. As expected, EphrinB2 levels on purified OCLs from *MV/Igfl1*- and *Igfl1*- mice were much lower compared to *MV/Igfl1*+ and *Igfl1*+ mice. *MV/Igfl1*- and *Igfl1*- OCLs also expressed lower NFATc-1 and cathepsinK levels vs *MV/Igfl1*+ and *Igfl1*+ OCLs. Finally, osterix, EphB4 and Col-1A levels in OBs from *MV/Igfl1*- and *Igfl1*- mice were also significantly decreased compared to *MV/Igfl1*+ and *Igfl1*+ OBs, respectively (*p*<0.05). These results suggest that Igfl derived from PD OCLs contributes to the increased bone formation in PD by enhancing bidirectional signaling through EphrinB2/EphB4 in vivo.

Disclosures: **Kazuaki Miyagawa**, None

SUN-1097

Kyphosis, moderate restrictive lung disease and sleep apnea of X-linked hypophosphatemia: a case study. Gregory Newman^{*}, Carolyn Macica. Frank H. Netter School of Medicine Quinnipiac University, United States

X-linked hypophosphatemia (XLH) is the most common heritable renal phosphate-wasting disorder. Adults with XLH exhibit degenerative osteoarthritis and ossification of fibrocartilaginous tendons/ligaments that are not improved by standard therapy. Significant thoracic skeletal deformity can occur and may include kyphosis, scoliosis, ossification of spinal ligaments, vertebral body fusion by syndesmophytes and limited range of motion of costovertebral joints. We previously reported a case series of mild restrictive lung disease in 3 patients with XLH with radiographic evidence of kyphosis (ASBMR 2017). Here, we present an XLH case study of a 64 yo female with ossification of the cervical and thoracic spinal ligaments. The patient displayed severe kyphosis of the thoracic spine without scoliosis, had minimal expansion of the chest wall on inspiration and had chronic bibasilar atelectasis. Kyphosis and scoliosis were evaluated by Cobb angle; kyphosis > 40° and scoliosis ≥ 10° were considered abnormal. Spirometry measurements included forced

vital capacity (FVC), forced expiratory volume in 1 second (FEV1), the ratio of forced expiratory volume in 1 second to forced vital capacity (FEV1/FVC), total lung capacity (TLC), reserve volume (RV), functional residual capacity (FRC), and diffusing capacity (DLCO). A six-minute walk test (6MWT) was also used as a performance-based measure of functional exercise capacity. PFT data was read as restrictive lung disease, with decreased TLC, RV, FRC and DLCO. Oxygen desaturation was assessed by pulse oximetry and declined from 98% to 90% following 6MWT. Split-night polysomnography was also performed to evaluate suspected sleep disordered breathing. The patient was found to have mild obstructive sleep apnea and a score of 9 on the Epworth Sleepiness Scale, indicative of higher-normal range of sleep propensity in daily life. Use of continuous positive airway pressure (CPAP) therapy, indicated for obstructive sleep apnea, resulted in an increase in total sleep time of 37.5% to 100%. Bilevel CPAP with humidification was implemented with dual settings to facilitate increased inspiration and expiration and to reduce airway resistance and improve tolerance to CPAP therapy. We conclude that kyphosis secondary to spinal fusion and enthesopathy in XLH can give rise to restrictive lung disease and obstructive sleep apnea and that this patient population may benefit from CPAP therapy as an intervention.

Disclosures: *Gregory Newman, None*

SUN-1098

A Mutation in Cx43(R239Q) Causes Craniometaphyseal Dysplasia (CMD)-like Phenotype in Knock-in Mice Ichihiro Okabe*, Jitendra Kanaujiya, Nelson Monteiro, Ernst Reichenberger, I-Ping Chen. University of Connecticut Health, United States

Craniometaphyseal dysplasia (CMD) is a rare craniofacial disorder characterized by hyperostosis of craniofacial bones and flaring metaphyses in long bones. A missense mutation (R239Q) in Connexin43 (Cx43), a major gap junction protein in bone cells, causes the autosomal recessive (AR) form of CMD. CMD pathogenesis remains largely unknown and treatment is limited to repetitive surgeries. We have generated knock-in (KI) mice expressing mutant Cx43(R239Q) protein by CRISPR/Cas and characterized their bone phenotype. Cx43KI/KI mice appear normal in size and are fertile. Skulls, femurs and mandibles from 3-month-old male and female Cx43^{+/+} and Cx43KI/KI mice (n=8/group) were analyzed by radiographs, microCT and histomorphometry. Cx43KI/KI mice showed CMD-like features, such as hyperostotic calvariae and cranial base; increased bone volume of jawbones; narrowing of cranial neural foramina; club-shaped femurs with increased diaphyseal cortical thickness. Although serum levels for calcium, phosphate, N-terminal procollagen type I (P1NP) propeptide and type I collagen cross-linked C-terminal telopeptide (CTX) were normal, Cx43KI/KI mice had increased osteoclast-like cells (shown by increased TRAP staining) on endosteal surfaces, active bone formation (shown by mineralization labeling) on periosteal surfaces and decreased density of osteocytes with reduced apoptosis in cortical bone of femurs. To study the Cx43 mutational effects in vitro, we derived mouse calvarial osteoblast (COB) and bone marrow macrophage (BMMs) cultures. Total Cx43 mRNA and protein levels were comparable between Cx43^{+/+} and Cx43KI/KI cultures shown by qPCR and immunoblotting. Increased proliferation and decreased apoptosis were found in Cx43KI/KI COB cultures by EdU and TUNEL assays, respectively. Cx43KI/KI BMM cultures showed delayed formation of TRAP⁺ multinucleated osteoclasts (nuclei ≥ 3) and significantly decreased resorption pits on bone chips. We previously published a CMD mouse model (AnkKI/KI) with a ANK Phe377del mutation for the autosomal dominant form of CMD. In contrast to AnkKI/KI mice which die at age of 6 months, Cx43KI/KI have normal life span and do not develop joint stiffness. In summary, Cx43KI/KI mice phenocopy human AR CMD. CMD-mutant Cx43 acts on osteoblasts, osteoclasts and osteocytes leading to disturbed bone remodeling. Studying both AnkKI/KI and Cx43KI/KI mouse models will help our understanding of the pathogenesis of CMD.

Disclosures: *Ichihiro Okabe, None*

SUN-1099

Macrophages and TNF α Regulate Fibroproliferation and Muscle Degradation Preceding Heterotopic Ossification in an ALK2R206H Model of Fibrodysplasia Ossificans Progressiva Chuanmin Cheng*, Michael R Convente², Nicole Fleming¹, Yueqi Zhang¹, Amisha Kalra¹, Cody M Elkins¹, Eileen M Shore², Daniel S Perrien¹. ¹Vanderbilt University Medical Center, United States, ²University of Pennsylvania, United States

Fibrodysplasia Ossificans Progressiva (FOP) is a rare and currently untreatable disease characterized by heterotopic ossification (HO) in skeletal muscle. FOP is caused by mutations in ACVR1, encoding the Type 1 BMP Receptor ALK2, but little is known about the mechanisms that redirect muscle repair toward ectopic bone formation. FOP "flares" begin as hyperinflammatory, fibroproliferative swellings that transition to endochondral bone. Depletion of phagocytic macrophages (M Φ) from mast cell deficient FOP mice substantially reduces HO, but how these cells influence FOP are unknown. We hypothesized that inflammatory M Φ (iM Φ) cytokines are key regulators of muscle turnover and fibroblasts in FOP. Following muscle injury, flow cytometry confirmed elevation of intramuscular CD206-iM Φ s, but not CD206⁺ anti-inflammatory M Φ s (aM Φ s) in ALK2R206H_FIEX (FOP) mice vs wildtype (WT) at 2 and 4 days post-injury (pi) (p<0.05). Significantly more muscle degradation occurred in FOP vs WT muscles, peaking at d4 pi (p<0.01). Fsp1+ fibroblasts were significantly greater (p<0.01) in FOP than WT mice at d7 and d14. IHC revealed iM Φ s (F4/80+;CD206- or pStat1+) primarily localized to degrading muscle fibers at all timepoints.

aM Φ s (F4/80+;CD206+ or Stat6+) were only in areas of fibroproliferation at days 4, 7, and 14. The expression of polarization markers in WT and FOP M Φ s was measured by qRT-PCR. iM Φ markers Nos2, Tnfa, and Inhba were increased by LPS and IFN γ , while aM Φ markers Ym1 and Arg1 were increased by IL-4 in both genotypes, however, levels were not significantly different between WT and FOP cells. Treatment with BMP4, BMP6, or ActA did not influence M Φ polarization in either genotype. Since iM Φ s are a major source of TNF α , its role in fibroproliferation and HO was tested in FOP mice. Injection of rTNF α into injured muscles of FOP mice significantly increased the volume of HO vs Veh injection (μ CT; p<0.01). In contrast, inhibiting TNF α with 2mg/kg or 4mg/kg anti-TNF α (etanercept) twice-weekly from injury until sacrifice did not significantly alter HO volume. Interestingly, etanercept treatment significantly increased fibroproliferation in FOP muscles (p<0.05). These data indicate that the role of M Φ s in FOP may be dependent on the abundance and balance of polarized M Φ s rather than altered gene expression within each phenotype. Additionally, TNF α may have a dual role to promote HO but suppress fibroproliferation, likely via different, time-dependent mechanisms.

Disclosures: *Chuanmin Cheng, None*

SUN-1100

Cell-Autonomous And Systemic Alterations In Gorham-Stout Disease Michela Rossi*, Giulia Battafarano¹, Eda Mariani¹, Paola Sabrina Buonomo², Ippolita Rana³, Alessandro Jenkner⁴, Rita De Vito⁵, Simone Pelle⁶, Matteo D'Agostini⁷, Andrea Bartuli², Andrea Del Fattore¹. ¹Bone Physiopathology Group Multifactorial Disease and Complex Phenotype Research Area Bambino Gesù Children's Hospital, IRCCS, Italy, ²Rare Disease and Medical Genetic Unit, Bambino Gesù Children's Hospital, IRCCS, Italy, ³UO Rare Diseases, Bambino Gesù Children's Hospital, IRCCS, Italy, ⁴Division of Immunology and Infectious Diseases Department of Pediatrics, Bambino Gesù Children's Hospital, IRCCS, Italy, ⁵Histopathology Unit, Bambino Gesù Children's Hospital, IRCCS, Italy, ⁶Casa di Cura Villa Aurora-San Feliciano, Italy, ⁷Clinical Laboratory, Bambino Gesù Children's Hospital, IRCCS, Italy

PurposeGorham-Stout disease (GSD) is a very rare disorder characterized by progressive osteolysis and angiomatous proliferation. The most common symptoms are swelling, fractures, pain and impairment of affected regions. The etiology of GSD is unknown and diagnosis is performed by exclusion criteria. Unfortunately, there are no set therapeutic approaches for patients. We aim to investigate the bone phenotype and to identify molecular and cellular defects in GSD patients. MethodsBone biopsy analysis was performed. Bone turnover markers were measured by ELISA. In vitro osteoclast and osteoblast cultures were performed to evaluate alterations of differentiation, morphology, and activity. Gene expression was evaluated by transcriptomic and Real-Time RT-PCR analysis. ResultsBone biopsy analysis revealed, in patients, fibrous tissue, increase of osteoclasts number, vessels and osteocyte lacunae area. In patient sera high levels of ICTP, VEGF-A, IL-6 and Sclerostin were revealed. Patient's osteoclast precursors showed a 2-fold increased ability to differentiate into osteoclasts, with more nuclei per cell. About 75% of GSD osteoclasts displayed a more motile phenotype. A 2-fold increased ability to resorb bone was observed in GSD osteoclast cultures compared to control. Transcriptome analysis revealed an enrichment of PI3 kinase, EGF receptor and beta-arrestin pathways. To investigate the involvement of systemic factors in GSD, Healthy Donor (HD)-PBMC were treated with GSD sera and showed increased osteoclastogenesis compared to control sera-treated cells (Osteoclast number/field, HD: 17.24 \pm 2.38; GSD: 26.27 \pm 2.43, p<0.02). Bone Marrow Mesenchymal Stem Cells isolated from a patient revealed a defect of osteogenic differentiation, as shown by reduced ALP activity and expression compared to HD-MS-C. Affected osteoblasts displayed reduced ability to form mineralized nodules. Transcriptome analysis revealed in GSD osteoblasts a modulation of pathways involved in bone morphogenesis and ossification and an increase of osteoclastogenic potential. Moreover, mature HD-osteoblasts treated with GSD sera showed decreased expression of ALP and COL1a2 and increased RANKL/OPG ratio. Conclusion- These results suggest that in GSD the bone remodeling defect could be related to bone cell autonomous defects and to involvement of systemic factors. Understanding the mechanisms leading to the progressive osteolysis could open the way for the identification of new therapeutic approaches.

Disclosures: *Michela Rossi, None*

SUN-1101

Osteoclast formation is inhibited by Activin-A in healthy controls and fibrodysplasia ossificans progressiva patients Ton Schoenmaker*¹, Fenne Wouters¹, Dimitra Micha², Coen Netelenbos³, Marelise Eekhoff³, Nathalie Bravenboer⁴, Teun De Vries¹. ¹Department of Periodontology, Academic Centre for Dentistry Amsterdam (ACTA), University of Amsterdam and Vrije Universiteit, Netherlands, ²Department of Clinical Genetics, VU University Medical Center, Amsterdam Movement Sciences, The Netherlands, Netherlands, ³Internal Medicine, Endocrinology Section, VU University Medical Center, Netherlands, ⁴Department of Clinical Chemistry, VU University Medical Center, Netherlands

Fibrodysplasia Ossificans Progressiva (FOP) is a genetic disease characterized by heterotopic ossification (HO) that occurs in muscle tissue, tendons and ligaments. The disease is caused by a mutation in the Activin receptor type 1 (ACVR1) gene, resulting in highly enhanced responsiveness to ligands including Activin-A. Binding of Activin-A to the mutated ACVR1 receptor induces osteogenic differentiation in osteoblast-like cells. The metabolism and composition of heterotopic bone formed in FOP patients appears to be comparable to skeletal bone in healthy subjects. Normal bone remodelling requires the coupled action of both osteoblast and osteoclast activity. In this study we investigated the effect of the FOP mutation and Activin-A on osteoclast formation. Firstly, the effect on the osteoclastogenic-inducing potential of periodontal ligament fibroblasts (PLF) was studied by coculturing CD14 positive osteoclast precursor cells from healthy donors with PLFs from healthy controls and FOP patients. Secondly, the effect on M-CSF and RANK-L induced osteoclast differentiation was investigated in a monoculture of CD14 positive precursors from healthy donors and FOP patients. Osteoclast differentiation was assessed by counting the number of TRACP positive multinuclear cells. qPCR was performed to study gene expression. Cell proliferation was assessed by DNA measurement. Activin-A inhibited osteoclast formation induced by control and FOP PLFs. This inhibition was only significant in the cocultures with FOP PLFs. In these cultures Activin-A downregulated M-CSF and DC-STAMP expression, genes important for osteoclastogenesis. Similarly Activin-A inhibited osteoclastogenesis in M-CSF and RANKL stimulated monocultures from control and FOP CD14 positive cells. This inhibition was probably due to a decreased proliferation of the CD14 cells. Our study shows that Activin-A can inhibit osteoclast formation both in a PLF induced coculture system as well as in a M-CSF and RANKL induced CD14 positive monoculture. This inhibition seems to be mediated via a direct effect on the osteoclast precursors regardless of the presence of the FOP mutation. This study provides new insight into the pathophysiology of FOP; while Activin-A is known to evoke enhanced heterotopic bone formation this study shows that Activin-A may also inhibit osteoclast formation, favouring the bone remodelling balance towards HO formation even more.

Disclosures: **Ton Schoenmaker, None**

SUN-1102

In Vitro and In Vivo Treatment Response of Osteogenesis Imperfecta Bone Tissue to Bone Forming Sclerostin Antibody Rachel Surowiec*¹, Lauren Battle², Stephen Schlecht³, Michelle Caird², Kenneth Kozloff¹. ¹Departments of Biomedical Engineering and Orthopaedic Surgery, University of Michigan, United States, ²Department of Orthopaedic Surgery, University of Michigan, United States, ³Departments of Mechanical Engineering and Orthopaedic Surgery, University of Michigan, United States

Osteogenesis Imperfecta (OI) is a rare, severe and highly variable heritable collagen-related bone dysplasia. Genotypic patient diversity may not only contribute to the heterogeneity of the disease but also impact individual patient response to therapy. We aim to determine the impact of baseline gene expression and morphological bone phenotype on response to bone forming sclerostin antibody (SclAb) therapy in vitro and in a novel xenograft model using OI patient-derived bone isolates. Cortical and trabecular bone samples (~2mm³) typically discarded as surgical waste (OI, n=5; non-OI control, n=5) were collected to media, randomly assigned to an untreated (UN), low-dose SclAb (TRL, 2.5 µg/mL), or high-dose SclAb (TRH, 25 µg/mL) group and maintained (37°C). TR occurred on day 2 and 4 and removed on day 5 for RNA extraction (Fig1A). Genes related to the canonical and non-canonical Wnt pathways (TWIST1, WISP1, DKK1, SOST, RANKL, OPG, SP7, RUNX2, BGLAP, COL1A1) were analyzed. Fold changes >1.5 were considered statistically significant (p < 0.05) via a Student's (baseline phenotypic comparison) and paired (treatment effect) t-test. A subset of bone was implanted s.c. into a nude mouse and TR (25 mg/kg s.c. 2x/wk for 2/4wks). Pre and post-µCT and dynamic histomorphometry was obtained. One sample per patient was formalin fixed at baseline for morphology (H&E). OI bone generally demonstrated lower baseline expression of downstream Wnt targets, variable-to-increased expression of inhibitory regulators, lower osteoblast markers and variable expression of progenitor markers compared to non-OI bone (Fig1C-D). SclAb induced an upregulation (compensatory response) in downstream and associated Wnt targets (SOST, DKK1, WISP1, TWIST1) with the greatest magnitude from OI cortical bone (OI2, 3) (Fig1E). OI bone demonstrated an upregulation of osteoblast activity with TR (except OI 3 whose low baseline expression had the greatest upregulation in TRH TWIST1, DKK1, RANKL and SP7). When implanted, OI4 demonstrated increased bone surface, corroborated by histomorphometry, and an upregulation in Wnt targets with concurrent in vitro TR (Fig1B,E). Heterogeneous baseline gene expression and TR response was observed in patient-derived OI bone tissue. Clinical

heterogeneity is a hallmark of OI; understanding a patient's genetic, cellular and morphological bone phenotype may play a crucial role in predicting treatment response and could help guide clinical decision making.

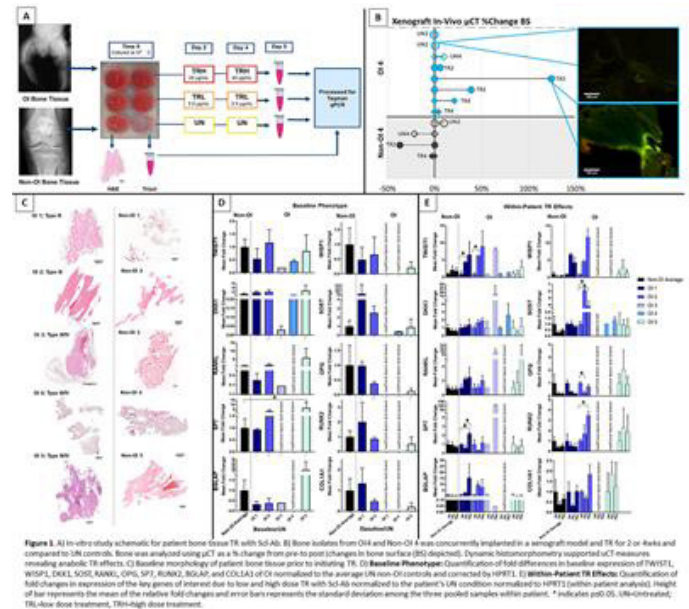


Figure 8. All in vitro study schematic for patient bone tissue TR with SclAb. **B:** Bone isolates from OI4 and Non-OI4 were concurrently implanted in a xenograft model and TR for 2 or 4wks and compared to UN controls. Bone was analyzed using µCT as a % change from pre to post (changes in bone surface [BS] depicted). Dynamic histomorphometry supported µCT measurements regarding analysis. **TR effects:** **C:** Baseline morphology of patient bone tissue prior to releasing. **TR:** **D:** Baseline Phenotype: Quantification of fold changes in baseline expression of TWIST1, WISP1, DKK1, SOST, RANKL, OPG, SP7, RUNX2, BGLAP, and COL1A1 of OI normalized to the average UN non-OI controls and corrected by HPRT1. **E:** Within-Patient TR Effects: Quantification of fold changes in expression of the key genes of interest due to low and high dose TR with SclAb normalized to the patient's UN condition normalized to HPRT1 (within patient analysis). Height of bar represents the mean of the relative fold changes and error bars represents the standard deviation among the three pooled samples within patient. * indicates p < 0.05, SclAb control, TR-Low dose treatment, TR-High dose treatment.

Disclosures: **Rachel Surowiec, None**

SUN-1103

Hyperphosphatemia in Hypophosphatasia of Childhood is Associated with Decreased FGF7 and Normal FGF23 Levels in the Circulation Michael P. Whyte*¹, Fan Zhang¹, Gary S. Gottesman¹, Steven Mumm², Rajiv Kumar³.

¹Center for Metabolic Bone Disease and Molecular Research, Shriners Hospital for Children, United States, ²Division of Bone and Mineral Diseases, Department of Internal Medicine, Washington University School of Medicine, United States, ³Division of Nephrology and Hypertension, Departments of Medicine and Biochemistry & Molecular Biology, Mayo Clinic College of Medicine, United States

Hypophosphatasia (HPP) is the inborn-error-of-metabolism caused by loss-of-function mutation(s) of the gene ALPL that encodes the tissue-nonspecific isoenzyme of alkaline phosphatase (TNSALP). The disorder is characterized enzymatically by low serum ALP activity (hypophosphatasemia). TNSALP is a cell-surface phosphohydrolase abundantly expressed in bone, liver, and kidney. Inorganic pyrophosphate, pyridoxal 5'-phosphate, and phosphoethanolamine, its natural substrates, accumulate extracellularly. Our clinical experience indicates that hyperphosphatemia, from increased tubular maximum for phosphate (TmP/GFR), is common in HPP. Furthermore, treatment with asfotase alfa enzyme replacement does not correct elevated circulating phosphate levels. Herein, we verified this hyperphosphatemia of HPP in our study of 41 children representing the broad-ranging severity of pediatric HPP while also quantitating by batch assay fasting serum levels of the phosphatonins FGF23, FGF7, and FRP4. Data were obtained prospectively also from 73 children with XLH receiving standard-of-care [1,25(OH)2D3 and Pi] therapy and 15 healthy pediatric controls (PC). For the three subject groups, including their subgroup comprising exclusively the pre-teenage children, serum Pi was significantly elevated in HPP (P < 0.0001) and low in XLH (P < 0.0001) compared to the PCs (Table). No differences were observed in total or ionized calcium or intact PTH (P > 0.10) among the three groups. Serum creatinine levels for the HPP and XLH groups were low (P < 0.001) compared to the PCs. In XLH, serum FGF23 was, as expected, elevated (P < 0.002) and serum FGF7 concentrations were low (P < 0.04) while FRP4 levels were normal (P > 0.2). In HPP, serum FGF7 was distinctly low (P < 0.007) and FGF23 and FRP4 normal (P > 0.8). The decreased circulating FGF7 level in the hyperphosphatemia of HPP is intriguing, but its pathogenesis requires further investigation.

Serum	Mean (SD)		
	Pediatric Controls (n=15)	XLH (n=73)	HPP (n=41)
Phosphorus	4.6 (0.6)	3.0 (0.4)****	6.1 (0.6)****
ALP	282 (106)	448 (135)***	57 (29)***
Creatinine	0.7 (0.1)	0.5 (0.2)**	0.5 (0.2)**
Total Calcium	9.5 (0.4)	9.5 (0.4)††	9.6 (0.4)††
Ionized Calcium	5.0 (0.2)	5.0 (0.4)††	5.0 (0.1)††
PTH	29 (11)	36 (24)††	20 (9)††
FGF23	42.7 (20.5)	345.4 (319.7)**	38.3 (14.3)†
FGF7	38.4 (3.0)	30.5 (9.6)*	27.0 (7.7)**
FRP4	781 (461)	937 (1204)††	830 (899)†

Compared to healthy controls: *Ps<0.04, **Ps<0.007, ***Ps<0.0006, ****Ps<0.0001; †Ps>0.8, ††Ps>0.1

Disclosures: Michael P. Whyte, None

SUN-1104

Plasma microRNA as novel biomarker for curve progression in Adolescent Idiopathic Scoliosis (AIS) – a 6 years longitudinal follow up study Jia Jun Zhang*^{1,2}, Yu Jia Wang^{1,2}, Ka Yee Cheuk^{1,2}, Carol Cheng^{1,2}, Tsz Ping Lam^{1,2}, Bobby Kin-Wah Ng^{2,3}, Yong Qiu^{2,4}, Jack Chun Yiu Cheng^{1,2}, Wayne Yuk-Wai Lee^{1,2}. ¹Department of Orthopaedics and Traumatology, SH Ho Scoliosis Research Laboratory, The Chinese University of Hong Kong, Hong Kong, ²Joint Scoliosis Research Center of the Chinese University of Hong Kong and Nanjing University, The Chinese University of Hong Kong, Hong Kong, ³Department of Orthopaedics and Traumatology, The Chinese University of Hong Kong, Hong Kong, ⁴Spine Surgery, The Affiliated Drum Tower Hospital of Nanjing University Medical School, Nanjing, China

Purpose: AIS is a three-dimensional spinal deformity without clear etiopathogenesis. The outstanding clinical question is to develop effective prognostication for timely treatment. Low bone mass and cortical thickness are reported prognostic factors for curve progression. Last year, we reported overexpression of miR-145-5p in AIS osteoblasts impairing osteocytogenic differentiation (2017 ASBMR MO0570). Our bioinformatic analysis has identified a differential miRNA profile in AIS iliac crest bone biopsies. We hypothesized that circulating miRNA(s) could be a new biomarker in predicting curve progression in AIS. Method: Fifty-two AIS girls were sequentially recruited from local Scoliosis Research Clinic at their first presentation and followed up longitudinally for 6 years. In addition to blood taking, anthropometry and curve severity were measured at first visit. The subjects were followed up clinically every 6 months with standard protocols. The subjects were subclassified into progressive or non-progressive stable group based on changes in the Cobb angle according to SRS criteria (> 6 degrees or <6 degrees respectively) after completing the 6 years follow-up and reaching skeletal maturity. miRNA candidates were selected from bioinformatics analysis. miRNA expression was detected in plasma. Bone formation (PINP) and resorption (CTX) markers were measured in serum. Mann-Whitney, Spearman's rank correlation test, area under ROC curve (AUC) and stepwise logistic regression were used for statistical analysis. Results: Twenty-two progressive and thirty stable AIS subjects were identified at the end of 6 years (Table 1). AIS girls with progressive spinal deformity had significantly higher PINP (p=0.007) level. A lower plasma level of miR-145-5p (p=0.052) and miR-96-5p (p=0.017) were found in the progressive group. Plasma level of miR-224-3p was negatively correlated with serum PINP and plasma miR-145-5p level in progressive group. In progressive AIS, the diagnostic efficacy of miR-96 (AUC=0.702, 95%IC=0.559-0.845) and PINP (AUC=0.719, 95%IC=0.58-0.858) was markedly higher than other miRs. Logit model including miR-96, miR-145 and PINP had higher predicted probability. Conclusion: This is the first study to demonstrate prognostic potential of serological markers for curve progression of AIS in a longitudinal cohort. Result of the study shed light on potential of novel biomarkers in addition to bone quality parameters, which may improve prognostic power to AIS.

Table 1. Anthropometric and radiological assessment in AIS subjects

	Age (1 st visit)	Cobb angle (1 st visit)	Cobb angle (after 6 yrs)	Treatment	
				Observation	Bracing
Progressive	12.77± 0.93	24.29± 7.18	35.43± 8.20	1	21
Stable	13.16±0.734	25.22±9.02	27.50±10.64	12	18

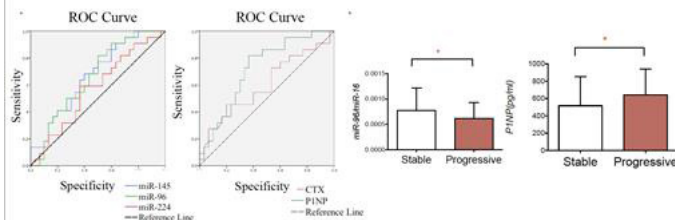


Figure (a) ROC analysis of candidate miRNAs and serum bone markers (b) Expression of plasma miR-96 and serum P1NP in stable AIS and progressive AIS

Disclosures: Jia Jun Zhang, None

SUN-1128

Prospective Associations of Osteosarcopenia and Osteodyspnea with Incident Fracture and Mortality over 10 years in Community-dwelling Older Adults Saliu Balogun*¹, Tania Winzenberg¹, Karen Wills¹, David Scott^{2,3}, Michele Callisaya¹, Flavia Cicuttini⁴, Graeme Jones¹, Dawn Aitken¹. ¹Menzies Institute for Medical Research, University of Tasmania, Australia, ²Department of Medicine, School of Clinical Sciences at Monash Health, Australia, ³Faculty of Medicine, Nursing and Health Sciences, & Peninsula Clinical School, Central Clinical School, Monash University, Australia, ⁴Department of Epidemiology and Preventive Medicine, Monash University, Australia

Aim: To determine whether older adults with low muscle mass (sarcopenia) and strength (dynapenia), in the presence of osteoporosis/osteopenia, have an increased risk of fracture and mortality over 10 years, compared to those with low muscle or low bone mass alone or with neither condition. Methods: 1032 participants (52% women; mean age 62.9±7.4 years) were studied at baseline, 2.5, 5 and 10 years. Mortality was ascertained from the death registry and fractures were self-reported. Baseline appendicular lean mass (ALM) was assessed using dual-energy X-ray absorptiometry and normalised to body mass index (BMI). Hand grip strength (HGS) was assessed by dynamometer. Osteosarcopenia and osteodyspnea were defined as having T-scores of the total hip and/or lumbar spine bone mineral density (BMD) <-1 combined with being in the lowest 20% of the sex-specific distribution for ALM/BMI or HGS respectively. Results: Incident fracture risk was significantly higher in participants who were osteodyspnetic (RR=2.07, 95% CI: 1.26-3.39), dynapenic alone (RR=1.74, 95% CI: 1.05-2.87), and osteopenic alone (RR=1.63, 95% CI: 1.15-2.31), compared to those without dynapenia or osteopenia. Mortality risk was significantly higher only in participants with osteosarcopenia (RR=1.49, 95% CI: 1.01-2.21) compared to those without sarcopenia or osteopenia. However, osteosarcopenia and osteodyspnea did not lead to a significantly greater fracture or mortality risk compared to having these conditions on their own. Conclusion: Osteopenia combined with low muscle mass or strength does not significantly increase the risk of fracture or mortality compared to having osteopenia or sarcopenia/dynapenia alone, suggesting that combined assessments may not add additional risk for fracture and mortality.

Disclosures: Saliu Balogun, None

SUN-1129

Associations between home environmental modifications and falls from the Women's Health Initiative Daniel Beavers*¹, Laura Welti², Annie Mampieri², Stephen Rapp¹, Kristen Beavers², Edward Ip¹, Sally Shumaker¹. ¹Wake Forest School of Medicine, United States, ²Wake Forest University, United States

Purpose: Home environmental modifications (HEMs) are commonly used by older adults at risk of or in the presence of aging-related functional limitations. Adverse events such as a history of falls and fractures are often associated with HEM usage strategies. However, given the diversity of types of HEMs, it is unclear what are the patterns of HEM usage as relates to falls and major bone health events. Methods: Utilization of 9 types of HEMs were collected from 71,257 women currently active in the Women's Health Initiative (WHI) [78.6±6.3 years, 88.7% Caucasian] from a questionnaire administered Oct 2013 - Dec 2014. In addition to demographic and health data, information was collected regarding usage of hand rails, grab bars, ramps, non-slip surfaces, tacking down carpets/rugs, decreasing clutter,

increasing lighting, raised sink/counter heights, and other HEMs. Health event-related function measures included history of recent falls and broken hip. Odds ratios were estimated based on overall HEM use as well as for latent classes of HEM strategies adjusted for age, marital status, race/ethnicity, education, depression, and obesity. Results: Overall, 53% of women reported use of any HEM, and latent class analyses grouped HEM usage strategies into low utilization (56%), increased lighting and decluttering (18%), adding rails and grab bars to home (20%), and multiple combined HEM strategies (5%). Furthermore, 22.7% of women reported a fall at home in the past year, and 1.8% had history of a broken hip. Women with falls (OR 1.8; 95% CI 1.7, 1.9) and hip fracture (OR 1.7; 95% CI 1.5, 2.0) reported higher use of any HEM strategy. Women who experienced falls reported multiple HEM strategies (OR 3.2; 95% CI 2.9, 3.5), railings/grab bars (OR 2.6; 95% CI 2.5, 2.8), and lighting/declutter use (2.0; 95% CI 1.9, 2.2) compared to low HEM users; likewise, women with history of broken hip reported railing/grab bar use latent class (OR 2.89; 95% CI 2.4, 3.5), and multiple HEM strategies (OR 2.3; 95% CI 1.8, 3.1). Discussion: In this large, cross-sectional study, women with function-related health events such as falls and broken hip reported HEM use more frequently than women without such events. These women have likely adopted these strategies to help prevent future events or to maintain function in the presence of health insult. Given that we cannot directly measure risk, future research should explore whether HEMs are effective for the prevention of distal health outcomes.

Latent Class Models: Association between latent HEM classes and disease/health status.

Variable	Model	Low HEM Use (reference)	Railings/Grab Bars	High HEM Use	Lighting/Declutter
Fall at home	Unadjusted	1.00 (-, -)	2.62 (2.46, 2.78)	3.16 (2.90, 3.46)	2.01 (1.87, 2.15)
	Adjusted*	1.00 (-, -)	2.32 (2.18, 2.48)	2.89 (2.64, 3.16)	1.93 (1.79, 2.08)
Broken Hip	Unadjusted	1.00 (-, -)	3.48 (2.93, 4.14)	2.68 (2.04, 3.5)	1.30 (0.99, 1.71)
	Adjusted*	1.00 (-, -)	2.89 (2.39, 3.50)	2.33 (1.75, 3.11)	1.21 (0.88, 1.65)

Adjusted for age, marital status, race, education, ethnicity, depression, & obesity status.

Disclosures: **Daniel Beavers, None**

SUN-1130

Dynapenia and Muscle Loss in Older-Aged Women Francisco Torres-Naranjo¹, Roberto González-Mendoza², Alejandro Gaytán-González³, Hugo Gutiérrez-Hermosillo⁴, Noé Albino González-Gallegos⁵, Claudia Flores-Moreno⁶, Pilar De La Peña-Rodríguez⁷, Pedro Alberto García-Hernández⁸, Juan López-Taylor². ¹Centro de Investigación Ósea, Universidad de Guadalajara, Mexico, ²Instituto de Ciencias Aplicadas a la Actividad Física y del Deporte, Universidad de Guadalajara, Mexico, ³Universidad de Guadalajara, Mexico, ⁴Universidad de Guanajuato, Hospital Aranda de la Parra, Mexico, ⁵Departamento de Bienestar y Desarrollo Sustentable, Centro Universitario del Norte, Universidad de Guadalajara, Colotlán, Mexico, ⁶Endocrinología/Centro de Osteoporosis, Hospital Universitario de Monterrey, Mexico, ⁷Servicios Médicos De la Peña, Mexico, ⁸Servicio de Endocrinología, Hospital Universitario, UANL, Mexico

Low skeletal muscle mass (LSMM) is associated with strength loss and disability. Epidemiological findings suggest that LSMM and dynapenia are associated with both mortality and physical disability. The association of muscle mass loss and dynapenia is still controversial. Purpose: This study aimed to examine the association between dynapenia and LSMM defined by several operational definitions in older-aged women. Methods: We evaluated a sample of 107 women 65 years of age and older from western of México. A whole body DXA scanning (Hologic QDR 4500) was performed to evaluate the body composition. The indicators and cut points used to diagnose LSMM were: 1) appendicular lean soft tissue absolute kilograms (ALSTKG) ≤ 15.02 ; 2) appendicular lean soft tissue corrected by body mass index (ALST/BMI) < 0.512 , both according to The Foundation for National Institutes of Health Sarcopenia Project (FNHISP); and 3) appendicular lean soft tissue corrected by squared height (ALST/HT²) ≤ 5.45 as established by The European Working Group on Sarcopenia in Older People (EWGSPOP). The criteria of dynapenia was a maximum isometric strength (MIS) of the hand and forearm muscles equal or lower the 20 kg evaluated by hand-grip dynamometry (Jamar Handgrip Dynamometer). Results: Overall prevalence of dynapenia was 71.3%. The prevalences of LSMM and their respective prevalence of dynapenia are showed in Table 1. The probability for dynapenia was significant for women with LSMM defined by ALSTKG and ALST/BMI. No statistical probability was observed with ALST/HT². Conclusions: We observed a high prevalence in both loss of muscle mass and dynapenia in our sample. Prevalence of dynapenia is higher in women with LSMM defined by FNHISP criteria. Our findings suggest that several indicators should be taken in consideration in order to properly assess the impact of LSMM.

Loss of muscle mass criteria	Prevalence of LSMM	Prevalence of dynapenia	Odds ratio (*P<0.05)	95% confidence interval
ALSTKG	60.75	84.62	5.5*	2.22 - 13.6
ALST/BMI	38.32	90.24	6.4*	2.04 - 20.08
ALST/HT ²	42.06	77.78	1.8	0.75 - 4.31

Disclosures: **Francisco Torres-Naranjo, None**

SUN-1131

Insulin-like growth factor-I is required to maintain muscle volume in adult mice Satoshi Nakamura*, Arihiko Kanaji, Takeshi Miyamoto, Morio Matsumoto, Masaya Nakamura. Department of Orthopedic Surgery, Keio University School of Medicine, Japan

[Background & purpose] Sarcopenia is defined as mass reduction and dysfunction of skeletal muscle in elderly, and is a big concern causing a fall followed by fractures. Sarcopenia is developed with various factors such as aging, endocrine, nutrition and disuse, however, precise pathogenesis of sarcopenia were remained to be elucidated. Insulin-like growth factor-I (IGF-I) is a peptide protein, which has diverse functions including regulating embryonic development and bone homeostasis. Serum IGF-I levels decline in the elderly; however, IGF-I function in adults has not been clearly defined. Here, we show that IGF-I is required to maintain muscle mass in adults. [Methods] We crossed IGF-I flox mice with Mx1 Cre mice to yield Mx1 Cre/IGF1flox/IGF1 cKO mice. 8-week-old female mice were treated with polyIpolyC to delete IGF-I gene and sacrificed at 18-weeks-old. Serum IGF-I levels were measured by ELISA, and blood glucose levels were monitored. Expressions of Eif4e, p70S6K, MuRF1 and Atrogin-1 mRNA were analyzed by qRT-PCR, accumulations of proteins were detected by Western blot, and bone mineral densities were analyzed by dual-energy X-ray absorptiometry (DEXA) measurements. [Results] We demonstrate that, although serum IGF-I levels significantly decreased in IGF-I cKO mice after polyIpolyC injection relative to controls, serum glucose levels were unchanged. We show that muscle mass and cross-sectional area decreased significantly, while bone mass did not after IGF-I down-regulation in after IGF-I cKO mice. In IGF-I cKO muscle, expression of anabolic factors such as Eif4e and p70S6K significantly decreased, while expression of catabolic factors MuRF1 and Atrogin-1 was normal and down-regulated, respectively, suggesting that observed muscle mass reduction was due to perturbed muscle metabolism. [Conclusion] Our data demonstrate a specific role for IGF-I in maintaining muscle homeostasis in adults. Our model, reducing serum IGF-I levels, may recapitulate age-related muscle atrophy in adults.

Disclosures: **Satoshi Nakamura, None**

SUN-1132

The body composition changes in elderly people which relations with dysmobility syndrome Woong Hwan Choi¹, Sang Mo Hong², Ye Soo Park³. ¹College of medicine, Hanyang University, Republic of Korea, ²College of medicine, Hanleem University, Republic of Korea, ³Hanyang university hospital, Republic of Korea

Background: The total volume of bone and muscle are decreased in the elderly. These changes are risk factors for fracture and other metabolic disease. Recently, the prevalence of osteoporosis and sarcopenia in the elderly has dramatically increased along with bone fracture and metabolic syndrome. However the relationship between these disease is not clear. Objective: We aimed to determine the independent relations of muscle mass to osteoporosis (femur neck) in relation to body weight, fat mass, and other confounders. Design: We analyzed body composition and BMD data of 570 Male and 734 female who are older than 65 years. Body composition and bone mineral density (BMD) of femur neck were measured by DXA (Hologic QDR 4000). Sarcopenia was defined as the appendicular skeletal muscle mass (ASM) divided by height squared (Ht)² (kg/m²) of < -1 SD below the sex-specific mean for 20 - 39 years adults. Results: ASM/(Ht)² and BMD were positive correlated with body fat mass/(Ht)². Protein & fat, carbohydrate, calcium, phosphate, calories intake were also positive correlated with BMD. Exercise also had positive correlation with ASM/(Ht)² and BMD. However Vitamin D only positively related with ASM/(Ht)². With compounding factors adjusting, ASM/(Ht)² had also positive relation with BMS in men (R²=0.171, B=0.027, p<0.001) and in women (R²=0.226, B=0.016, p=0.002). The adjusted odds ratios (95% CIs) of osteoporosis in sarcopenia patients were 1.24 (95%CI; 1.47-8.15) in men and not significant in women. Conclusions: BMD were decreased with the increase of insulin resistance in normal fasting glucose. And with the increase fasting glucose, these relations were weakening (IFG) and disappeared (DM). Bone mineral density was independently associated with muscle mass. Sarcopenia was independent risk factor for osteoporosis in men but not women.

Disclosures: **Woong Hwan Choi, None**

SUN-1133

Appendicular Lean Mass Adjusted for Body Mass Index: Reference Data for Australian Men and Women Julie Pasco*, Kara Holloway-Kew, Monica Tembo, Sophia Sui, Kara Anderson, Pamela Rufus, Natalie Hyde, Mark Kotowicz. Deakin University, Australia

Purpose Recommendations from the Foundation for the National Institutes of Health (FNIH) Sarcopenia Project are that appendicular lean mass (ALM, kg) adjusted for body mass index (BMI, kg/m²) be used for identifying low lean mass that discriminates the presence or absence of weakness; ALM/BMI cutpoints of < 0.789 for men and < 0.512 for women were proposed. Although cutpoints were derived by pooling data from multinational studies, Australian data were absent. Our primary aim was to report ALM/BMI reference ranges for men and women in Australia. Our secondary aim was to compare the prevalence of low lean mass by our definition, based on T-scores for BMI/ALM < -2.0 , with those from the FNIH.

Methods Body composition was measured by DXA (Lunar) for 1411 men and 960 women aged 20-93yr enrolled in the Geelong Osteoporosis Study (GOS), a population-based cohort study set in south-eastern Australia. Mean values were calculated for DXA-derived ALM (sum of lean mass for arms and legs) adjusted for BMI. Data are provided for men and women for each age decade, and cutpoints equivalent to T-scores of -2.0 for each sex were derived using reference data for 374 men and 308 women aged 20-39 years. Agreement between low lean mass estimates using our criteria in comparison with FNHI criteria were evaluated using the kappa statistic. Results For men, mean±SD values for weight and height were 82.0±12.4 kg and 1.75±0.07 m; for women, 69.4±12.9 kg and 1.62±0.07 m, respectively. Mean ALM/BMI values were greater for men than for women, and decreased with age in both sexes (Table). Mean±SD values for ALM/BMI for GOS men and women aged 20-39yr were for men, 1.108±0.141 and for women 0.759±0.121. Cutpoints for ALM/BMI equivalent to T-scores of -2.0 were <0.827 for men and <0.518 for women. The overall agreement for identifying low lean mass using our criteria compared with FNHI criteria was 0.73 for men and 0.89 for women. For men aged 20+, the crude prevalence of low lean mass was 13.9% (95%CI 12.1-15.8) using our cutpoints and 8.5% (7.1-10.1) using FNHI cutpoints (p for difference 0.001); corresponding figures for women were 5.5% (4.2-7.2) and 4.5% (3.3-6.0), respectively, (p=0.3). Conclusion Use of cutpoints from our population corresponding to T-scores of -2 identified more individuals with low ALM/BMI than using FNHI criteria, but the difference was significant for men only. These data emphasise the importance of using universal criteria for identifying low lean mass.

Table: Mean±SD values for ALM/BMI by age and sex.

Age (yr)	Men		Women	
	n	ALM/BMI	n	ALM/BMI
20-29	180	1.138 ± 0.136	176	0.775 ± 0.118
30-39	194	1.081 ± 0.140	132	0.737 ± 0.121
40-49	203	1.032 ± 0.122	161	0.700 ± 0.090
50-59	215	0.984 ± 0.116	159	0.670 ± 0.107
60-69	206	0.935 ± 0.124	146	0.643 ± 0.092
70-79	225	0.899 ± 0.111	121	0.619 ± 0.093
80+	188	0.868 ± 0.113	65	0.617 ± 0.099

Disclosures: *Julie Pasco, None*

SUN-1134

Phenotypic Features of Sarcopenic Older Adults According to Current Operational Definitions: Data from the GERICO Study Mélanie Hars*, Emmanuel Biver, Thierry Chevalley, René Rizzoli, Serge Ferrari, Andrea Trombetti. Division of Bone Diseases, Department of Internal Medicine Specialties, Geneva University Hospitals and Faculty of Medicine, Switzerland

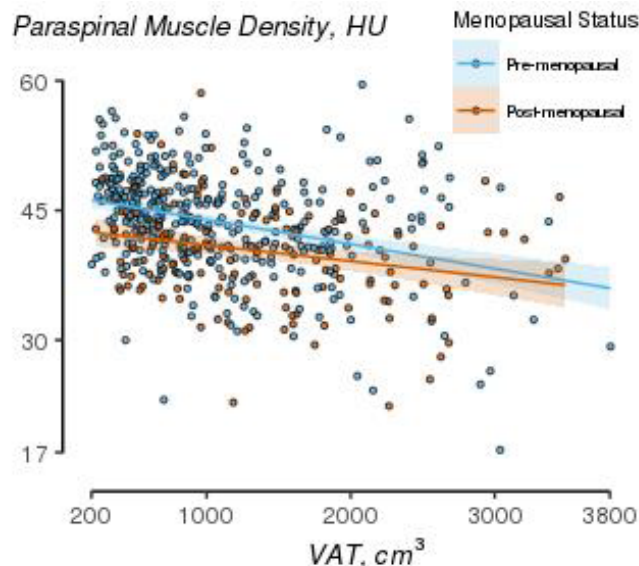
Controversies regarding how best to define sarcopenia have impeded epidemiological and interventional research, and hindered efforts to elucidate whether sarcopenia overlap with other disease states. In order to contribute to the knowledge base on candidate sarcopenia criteria, we aimed to i) report and compare the prevalence of sarcopenia according to different current operational definitions in a large Swiss cohort of early-old aged community-dwelling healthy adults, and ii) compare the phenotypic features of sarcopenic individuals, with a focus on conditions typically associated with increased risk of fall and fracture, including osteoporosis, frailty, and obesity. Seven hundred sixty-seven participants (608 women; 67.9±1.5 years) enrolled in the ongoing Geneva Retirees Cohort (GERICO) were studied. Appendicular lean mass (ALM) was determined by dual-energy X-ray absorptiometry. Gait speed was measured over 4-m and grip strength using a handheld dynamometer. Six definitions were applied, among which three were based on low muscle mass alone (Baumgartner, Delmonico 1 and 2), and three required both low muscle mass and low muscle function (EWGSOP, IWG, FNHI). Degree of agreement was assessed using kappa statistics, and phenotypic features of sarcopenic individuals were compared, based on regression analyses. Low lean mass prevalence varied from 3.8% to 19.9% depending on the cutoff. Prevalence of low lean mass combined with either weakness or slowness was the lowest for FNHI (0.3%) compared with IWG (1.2%) and EWGSOP (1.6%), with higher prevalence found in women across all definitions. There was poor agreement between the groups identified according to the different criteria and definitions (all kappa values below 0.3). Individuals who met the low ALM/BMI criterion in comparison to those meeting the ALM/height² or ALM criteria, were more likely to be obese (51.7% vs 0% vs 1.4%, respectively; p<0.001) and pre-frail or frail (44.8% vs 21.1% vs 20.7%, respectively; p<0.030), but were less likely to be osteopenic or osteoporotic (58.6% vs 85.3% vs 84.8%, respectively; p<0.001). Our results in a large Swiss cohort of 68-year old participants suggest that sarcopenia widely vary depending on the low muscle mass and low muscle function criteria applied, with poor agreement between classifications and with different phenotypes captured across definitions. The FNHI low ALM cutoff adjusted for BMI tends to capture sarcopenic obese and less robust individuals.

Disclosures: *Mélanie Hars, None*

SUN-1135

Greater visceral adiposity is associated with lower paraspinal muscle density: the Framingham Study Timothy Tsai^{*1}, Brett Allaire², Ilean Isaza¹, Marian Hannan^{1,2,3}, Mary Bouxsein², Douglas Kiel^{1,2,3}, Thomas Trivison^{1,2,3}. ¹Hebrew SeniorLife Institute for Aging Research, United States, ²Beth Israel Deaconess Medical Center, United States, ³Harvard Medical School, United States

Obesity is a significant contributor to premature death and disability. While its influence on cardiometabolic outcomes has been well-studied, less is known concerning its relation to musculoskeletal health and particularly muscle quality. In this analysis, we investigated the relationship between visceral adipose tissue and the density of the paraspinal muscle groups among 1,158 members of the Framingham Study Generation 3 cohort. Data were obtained from 645 men, 358 premenopausal women, and 155 postmenopausal women enrolled in the FHS multidetector CT substudy, selected for muscle morphology analysis on the basis of having QCT measurements at baseline examination occurring from 2002 to 2005. Fifty-seven participants lacking VAT measures were excluded. Abdominal CT scans from an 8-slice multidetector CT scanner (LightSpeed Ultra; General Electric, Milwaukee, WI) were used to assess visceral adipose tissue (VAT, cm³) and density (Hounsfield units, HU) of the paraspinal muscles in the lumbar region (bilateral erector spinae, transversospinalis, psoas major, and quadratus lumborum muscles). Multiple linear regression was used to quantify the cross-sectional relationship between VAT and muscle density. VAT volume was scaled such that slope estimates represent average differences in muscle density corresponding to 100 cm³ cross-sectional increases in VAT. Linear models adjusted for age, height, diabetes status, and menopausal status. Mean (standard deviation) VAT volume was 937 (858), 1061 (688), and 1377 (780) cm³ in men (ages 31 to 68 y), premenopausal women (33 to 55 y) and postmenopausal women (40 to 70 y), respectively. There was an inverse association between VAT volume and paraspinal muscle density which was nonsignificant in men (-0.042 HU, 95% confidence interval: -0.093 to 0.01 HU), but more evident among women irrespective of menopausal status. Among women, each 100 cm³ greater VAT volume was associated with 0.221 HU (95% confidence interval: 0.152 to 0.290 HU) lower paraspinal muscle density. Additional adjustment for physical activity yielded no difference in slope estimates. These data suggest that visceral adiposity may lead to lower trunk muscle density with possible implications for trunk stability, postural sway and falls; however longitudinal studies and underlying mechanistic investigations are needed to confirm these findings.



Disclosures: *Timothy Tsai, None*

SUN-1136

Serum DHEA and its Sulfate Are Associated with Incident Fall Risk in Older Men - the MrOS Sweden Study Liesbeth Vandenput^{*1}, Maria Nethander^{1,2}, Magnus Karlsson³, Björn Rosengren³, Eva Ribom⁴, Dan Mellström⁵, Claes Ohlsson¹. ¹Centre for Bone and Arthritis Research, Department of Internal Medicine and Clinical Nutrition, Institute of Medicine, Sahlgrenska Academy, University of Gothenburg, Sweden, ²Bioinformatics Core Facility, Sahlgrenska Academy, University of Gothenburg, Sweden, ³Clinical and Molecular Osteoporosis Research Unit, Department of Clinical Sciences, Lund University, and Department of Orthopaedics, Skåne University Hospital, Sweden, ⁴Department of Surgical Sciences, University of Uppsala, Sweden, ⁵Centre for Bone and Arthritis Research and Department of Geriatric Medicine, Institute of Medicine, Sahlgrenska Academy, University of Gothenburg, Sweden

The adrenal-derived hormones dehydroepiandrosterone (DHEA) and its sulfate (DHEAS) are the most abundant circulating hormones and their levels decline substantially with age. Many of the actions of DHEA are considered to be mediated through metabolism into androgens and estrogens in peripheral target tissues. The predictive value of serum DHEA and DHEAS for the likelihood of falling is unknown. The aim of this study was, therefore, to assess the associations between baseline DHEA and DHEAS levels and incident fall risk in a large cohort of older men. Serum DHEA and DHEAS levels were analyzed with mass spectrometry in the population-based Osteoporotic Fractures in Men study in Sweden (n=2516, age 69-81 years). Falls were ascertained every 4 months by mailed questionnaires. Associations between steroid hormones and falls were estimated by generalized estimating equations. During a mean follow-up of 2.7 years, 968 (38.5%) participants experienced a fall. High serum levels of both DHEA (odds ratio [OR] per SD increase 0.85, 95% CI 0.78-0.92) and DHEAS (OR 0.88, 95% CI 0.81-0.95) were associated with a lower incident fall risk in models adjusted for age, BMI and prevalent falls. Further adjustment for serum sex steroids or age-related comorbidities only marginally attenuated the associations between DHEA or DHEAS and the likelihood of falling. Moreover, the point estimates for DHEA and DHEAS were only slightly reduced after adjustment for lean mass and/or grip strength. Also, the addition of the narrow walk test did not substantially alter the associations between serum DHEA or DHEAS and fall risk. Finally, the association with incident fall risk remained significant for DHEA but not for DHEAS after simultaneous adjustment for lean mass, grip strength, and the narrow walk test. This suggests that the associations between DHEA and DHEAS and falls are only partially mediated via muscle mass, muscle strength, and/or balance. In conclusion, older men with high DHEA or DHEAS levels have a lesser likelihood of a fall.

Disclosures: *Liesbeth Vandenput, None*

SUN-1137

Regucalcin Signaling Is Involved in Advanced Glycation End Products-induced Muscle Cell Senescence and Atrophy Rong-Sen Yang^{*}, Chen-Yuan Chiu, Ding-Cheng Chan, Shing-Hwa Liu. National Taiwan University, Taiwan

Introduction: Advanced glycation end products (AGEs) may contribute to aging-induced functional decline of cells and tissues. Elderly men with AGEs accumulation had lower muscle mass and strength. The fundamental mechanism of action of AGEs in sarcopenia still remains unclear. Regucalcin, also known as senescence marker protein-30 (SMP30), is involved in regulation of aging and metabolic disorders. Here, we investigated the molecular mechanism of action of AGEs in sarcopenia and assessed the therapeutic potential of AGEs inhibitors on sarcopenia in vitro. **Methods:** Human tissue sampling of the present study was approved by the Institutional Review Board and written informed consent from all participating subjects. Human skeletal muscle-derived progenitor cells (HSMPCs) isolated from rectus muscles of orthopedic surgery patients and mouse myoblast cell line (C2C12) were cultured to test the in vitro effects of AGEs (10-200 µg/mL) on the myotube formation and atrophy with or without AGEs inhibitors. The protein expressions were determined by Western blotting. Morphological and senescent examinations were performed by H&E staining and senescence-associated β -galactosidase (SA- β -Gal) staining, respectively. **Results:** AGEs significantly induced cellular senescence by measuring SA- β -Gal activity (about 66% increase, n=5, p<0.01; Figure 1A-a) in HSMPCs under growth medium. The protein expressions of progerin, another senescent biomarker, and regucalcin (SMP30) were up-regulated in AGEs-treated HSMPCs (n=5, p<0.01; Figure 1A-b and 1A-c). In addition, in C2C12 myoblasts and its differentiated myotubes, AGEs significantly reduced the myotube formation (about 52%, 97%, and 100% decreases in 2-5, 6-10, and over 10 nuclei myotubes, n=3, p<0.01; Figure 1B-a) and the myotube size (about 74% decrease in 20 µm diameter myotubes, n=3, p<0.01; detailed in Figure 1C-a) with a down-regulated protein expression of MHC (n=5, p<0.01; Figure 1B-b) and up-regulated protein expressions of Atrogin-1 (n=4, p<0.01; Figure 1C-b) and SMP30 (n=4, p<0.01; Figure 1B-c and 1C-c). Moreover, Alagebrium chloride (Ala-Cl, an AGEs cross-link breaker) and the receptor for AGE neutralizing antibody could efficiently protect against aforementioned injury induced by AGEs. **Conclusion:** These findings suggest that SMP30 may be as an etiological target in sarcopenic skeletal muscles with AGEs accumulation and AGEs inhibitors may be a therapeutic potential in sarcopenia.

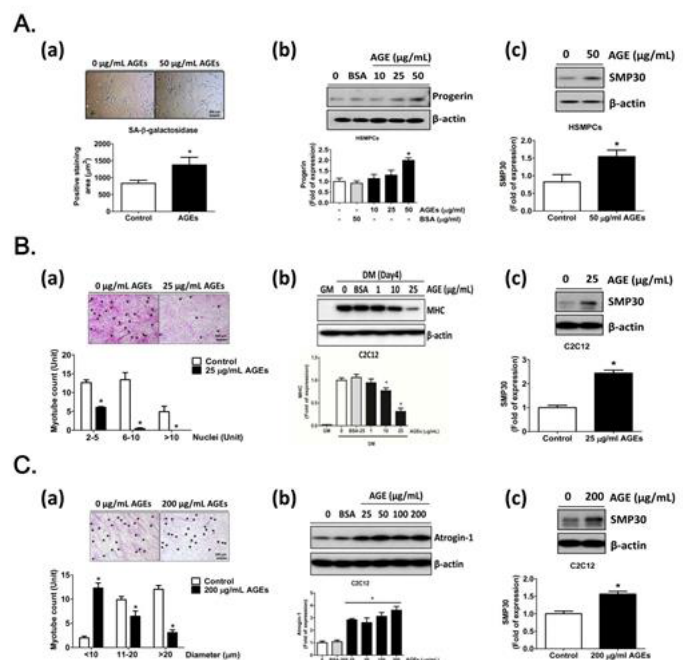


Figure 1. Advanced glycation end products (AGEs) significantly suppressed myotube formation and hypertrophic myotubes via regucalcin (SMP30) activation under the cellular senescence process. Human skeletal muscle progenitor cells (HSMPCs) were cultured in growth medium with 50 µg/mL AGEs for 48 h (A). C2C12 myoblasts and myotubes were cultured in differentiation medium (DM) with AGEs (25 and 200 µg/mL) for 96 h (B) and 48 h (C), respectively. (a) The cellular senescence and cell morphology examined by SA- β -Gal and H&E stain; arrows indicate multinucleated myotube formation; quantification of senescent area and myotubes with different nuclei. (b, c) Western blot analysis of protein expressions of progerin, myosin heavy chain (MHC), Atrogin-1, and SMP30. Scale bar = 100 µm. All data are present as means \pm SEM for at least three independent experiments. *, p<0.05 as compared with control group.

Disclosures: *Rong-Sen Yang, None*

LB SUN - 1148

Circulating miRNAs are associated with higher tibial cortical porosity in postmenopausal women with history of osteoporotic fractures Ursula Heilmeyer^{*1}, Matthias Hackl², Susanna Skalicky², Janina Patsch³, Thomas Baum⁴, Fabian Schröder⁵, Klemens Vierlinger⁵, Andrew Burghardt⁶, Ann Schwartz⁷, Johannes Grillari⁸, Thomas Link⁹. ¹Department of Radiology & Biomedical Imaging, United States, ²TamiRNA GmbH, Austria, ³Department of Biomedical Imaging and Image-Guided Therapy, Medical University of Vienna, Austria, ⁴Department of Neuroradiology, Technical University Munich, Germany, ⁵Department of Molecular Diagnostics, Austrian Institute of Technology (AIT), Austria, ⁶Musculoskeletal Quantitative Imaging Research Group, Department of Radiology & Biomedical Imaging, University of California San Francisco, United States, ⁷Department of Epidemiology and Biostatistics, University of California San Francisco, United States, ⁸Department of Biotechnology, University of Natural Resources and Life Sciences, Austria, ⁹Musculoskeletal Quantitative Imaging Research Group, Department of Radiology & Biomedical Imaging, University of California San Francisco, United States

Cortical bone porosity (Ct.Po.) has been shown to substantially impact bone strength, bone stiffness and fracture toughness and is therefore regarded as a key determinant of the bone fragility underlying fracture risk. Ct.Po. is defined as the fraction of non-mineralized tissues within cortical bone, and is routinely measured in vivo at peripheral skeletal sites in humans via high resolution peripheral quantitative computed tomography (HR-pQCT). However, the mechanisms driving increased cortical porosity are still not understood. MicroRNAs (miRNAs) are small non-coding RNA molecules that regulate gene expression at a posttranscriptional level. They are secreted from various cells into the blood where they can be accessed by venipuncture and can be taken up by recipient cells while altering the

recipient cell's gene expression and mediating functional effects. Recently, miRNAs were found to be crucial players in bone homeostasis/remodeling as well as in bone diseases such as osteoporosis. Here, we aimed to explore potential pathomechanisms underlying Ct.Po. in osteoporosis. Thus, we tested the correlation between serum miRNA levels and tibial Ct.Po measured by HR-pQCT in a cohort of postmenopausal women with and without history of osteoporotic fractures. Postmenopausal women with (Fx, n=19) and without history of osteoporotic fractures (Co, n=17) underwent HR-pQCT scanning of the ultradistal tibia. All women were mobile and otherwise free of bone affecting diseases or medications. Serum was collected from each subject and serum miRNA levels were quantified by qPCR-arrays for 20 miRNAs that were previously identified as promising discriminators of osteoporotic fractures. Spearman's rank-order correlations were employed. Women were on average 61.6 ± 6.3 years old with a mean BMI of 25.8 ± 3.9 kg/m². We found that in the postmenopausal women with history of fragility fractures miRNA expression levels of four out of 20 miRNAs were positively correlated with the extent of Ct.Po.: these were miR-19b-1-5p (R₂=0.560, p=0.013), miR323a-3p (R₂=0.519, p=0.023), miR-32-3p (R₂=0.439, p=0.060), and miR-143-5p (R₂=0.504, p=0.028). Our findings suggest for the first time potential pathomechanistic links between miRNAs and cortical porosity. Further bone analyses are needed to validate our findings in vitro.

Disclosures: Ursula Heilmeier, None

LB SUN - 1153

Serum Free Testosterone-Estradiol Ratio and Dehydroepiandrosterone Sulfate Levels Are Associated With Muscle Strength Independent of Muscle Mass in the Elderly Sung Hye Kong^{*1}, Jung Hee Kim¹, Ji Hyun Lee¹, A Ram Hong¹, Chan Soo Shin¹, Nam H. Cho². ¹Seoul National University College of Medicine, Republic of Korea, ²Aju University College of Medicine, Republic of Korea

Purpose: Sex steroids including free testosterone (FT), estradiol (E2), and dehydroepiandrosterone sulfate (DHEA-S) is known to decrease over age, and has been suggested to be related with sarcopenia. However, the relationship between FT/E2 or DHEA-S levels and muscle strength has rarely been studied in a community-dwelling population. We aimed to evaluate whether serum FT/E2, and DHEA-S levels are associated with muscle mass and strength in a community-dwelling elderly population. **Method:** We analyzed 923 men over 60 years and 1,224 postmenopausal women from Ansong cohort study, which is a community-based cohort study in Korea. Body composition, and hand grip strength were measured by dual-energy X-ray absorptiometry, and hydraulic dynamometer, respectively. Weak muscle strength was defined as hand grip strength <26 for men, and <18 kg for women according to the Asian Working Group of Sarcopenia. **Result:** Subjects within higher FT/E2 tertiles tended to be younger and more physically active. Also, women within higher FT/E2 tertiles had higher BMI. Subjects within higher DHEA-S tertiles were likely to be younger, and men within higher DHEA-S tertiles had higher BMI. In correlation analyses, hand grip strength has a positive correlation with FT/E2 (r=0.278, p<0.001 in men, r=0.142, p<0.001 in women), and DHEAS (r=0.239, p<0.001 in men, r=0.157, p<0.001 in women). Correlation of hand grip strength with FT/E2 remained significant (B=0.081, p=0.002 in men, B=0.078, p=0.006 in women) after adjustments for age and appendicular muscle mass (ASM)/height², physical activity, drinking, smoking, diabetes, and hypertension. In logistic regression models of FT/E2 for weak muscle strength, the odds ratio (OR), (95% confidence interval [CI]) of the 3rd tertile was 0.447 (0.260-0.769) in men, and 0.660 (0.473-0.922) in women compared with the 1st tertile after adjustments for all covariates. Also, comparing with the 1st tertile of DHEA-S, the OR (95% CI) was 0.558 (0.335-0.931) in men within 3rd tertile after adjustment for age and ASM/height². Women within the 3rd tertile harbored a lower risk for weak muscle strength (OR [95% CI], 0.703[0.503-0.983]) than those within the 1st tertile after adjustments for all covariates. **Conclusion:** In a community-dwelling Korean population, serum FT/E2 and DHEA-S levels could be related with muscle strength independent of muscle mass in both genders. Therefore, FT/E2 or DHEA-S may have an independent role in muscle strength in the elderly.

Disclosures: Sung Hye Kong, None

LB SUN - 1154

Organic Matrix Quality discriminates between Age- and BMD-matched Fracturing versus Non-Fracturing Postmenopausal Women Eleftherios Paschalis^{*1}, Stamatia Rokidi¹, Klaus Klaushofer¹, Severin Vennin², Anastasia Desyatova², Joseph Turner², P Watson³, Joan Lappe³, Mohammed Akhter³, Robert Recker³. ¹Ludwig Boltzmann Institute of Osteology at the Hanusch Hospital of WGKK and AUA Trauma Centre Meidling, 1st Medical Department, Hanusch Hospital, Austria, ²University of Nebraska, United States, ³Osteoporosis Research Center, Creighton University, United States

Women with similar areal Bone Mineral Densities (BMD) may show divergent fracture incidence due to differences in bone quality. The hypothesis tested here is that postmenopausal (PM) women who have sustained osteoporotic fractures have altered organic matrix bone quality compared to those who have not. We used Raman microspectroscopy to analyze epoxy resin embedded transiliac biopsies (N=12) collected from fracturing (n=6, mean age 62.5 ± 7.4 yrs; Cases) and non-fracturing PM women (n=6, age- and BMD-matched; mean age 62.2 ± 7.3 yrs; Controls). Previous results show significant differences

in intrinsic material properties by nanoindentation that are more homogeneously distributed and could propagate microcracks more easily in Cases, along with lower mineral carbonate/phosphate ratio by Fourier transform infrared spectroscopic imaging (FTIRI), and no differences in bone tissue mineralization by digitized microradiography (DM). No differences between groups were seen by conventional histomorphometry. Spectra were acquired 2 μm away from previously performed nanoindentations, in cortical and cancellous compartments. Twenty such anatomical areas per biopsy per compartment were analyzed, the results averaged and the mean value treated as a single statistical unit for the biopsy compartment. The determined parameters were: mineral to matrix ratio (MM; positive correlation with bone stiffness), and tissue water (TW; positive correlation with bone strength), glycosaminoglycan (GAG; negative modulators of bone mineral homeostasis; responsible for keeping the canalicular network mineral-free), lipid, pyridinoline (Pyd; trivalent enzymatic collagen cross-link; strongly associates with fracture incidence), N(6)-Carboxymethyllysine (CML; advanced glycation endproduct; negative correlation with bone strength), and pentosidine (PEN; advanced glycation endproduct; negative correlation with bone strength) content. The results showed no changes in MM in either cortical or cancellous compartments in general agreement with previous FTIRI and DM results. Cases had significantly lower TW and GAG content and significantly elevated Pyd, CML, and PEN content in both anatomical compartments analyzed compared to Controls. In conclusion, the results of the present study indicate significant differences in organic matrix quality in PM women that sustain fragility fractures versus age- and BMD-matched controls, and highlight its importance as an independent determinant of fracture incidence.

Disclosures: Eleftherios Paschalis, None

LB SUN - 1158

The Influence of Maternal Diet on Offspring Bone Acquisition at Birth among Samoan Infants Rachel L Duckham^{*1}, Kendall J Arslanian², Ulai Fidow³, Theresa Atanoa⁴, Folla Unasa-Apelu³, Abigail I Wetzel³, Alysya Pomer⁶, Take Naseri⁷, Natalie Hyde⁸, Nicola L Hawley⁶. ¹Institute for Physical Activity and Nutrition, Deakin University, Australia, ²Department of Anthropology, Yale University, United States, ³Yale-Ministry of Health Research Center, Samoa, ⁴Community Studies Program, University of California-Santa Cruz, United States, ⁵International Health Institute, Brown University, United States, ⁶Department of Chronic Disease Epidemiology, Yale School of Public Health, United States, ⁷Ministry of Health, Samoa, ⁸Epi-Centre for Healthy Ageing, Deakin University, Australia

Purpose: Osteoporosis and obesity share many genetic and environmental factors and are suggested to have origins early in life. There are growing data indicating that maternal nutrition may play an important role in predisposing infants to both conditions. However, very few studies with a focus on maternal diet have been conducted in the Polynesian populations, who are known to differ in body composition from other ethnic populations. Furthermore, little is known about the role of maternal diet on offspring skeletal acquisition at birth in this population. The aim of this study was to determine the association between qualities of maternal dietary consumption and total skeletal bone content at birth. **Methods:** Subjects were 111 mother-infant pairs. Maternal dietary intake was assessed with a 115-item food frequency questionnaire to quantify intakes of total calories, fat, carbohydrate and bone-specific nutrients protein, calcium and potassium between 35-weeks gestation. At birth, trained personnel assessed infant weight and length. Dual-energy X-ray Absorptiometry (DXA) (GE iDXA, Madison, WI, USA) quantified total body bone mineral content less head (BMC-LH), in full-term Samoan newborns (mean ± SD, 6.2 ± 6.7 days old). **Results:** Mean maternal age was (mean ± SD) 27.9 ± 5.6 years, and body mass index (BMI) was 34.3 ± 6.9 kg/m². Mean offspring birth weight was 3.5 ± 0.5 kg and percent body fat (total fat mass/total lean + total fat mass) was 17.8 ± 3.5%. BMC-LH was positively correlated with all measured nutrients (r=0.19-0.25; all p<0.05), except for protein, fat and calcium. Multivariable linear regression models adjusted for maternal calorie intake, height and age, and offspring weight and height, revealed a positive association between maternal potassium intake and offspring total BMC-LH (β0.003, 95%CI 0.001-0.005, p<0.05), but not other bone-promoting nutrients of protein (β0.000, 95%CI -0.009-0.010, p>0.05) or calcium (β-0.005, 95%CI -0.092-0.083, p>0.05). No further associations between maternal diet and offspring BMC-LH were detected. **Conclusion:** These preliminary data suggest that maternal dietary intake of potassium, but not protein or calcium; in Samoans play an integral role in positive bone acquisition at birth. Therefore, encouraging pregnant women to consume healthy potassium-rich foods such as bananas, rather than potassium-rich foods high in sodium, may optimize infant bone health within this population.

Disclosures: Rachel L Duckham, None

LB SUN - 1161

FGF23 induces ventricular arrhythmias in mouse hearts mediated through the phospholipase C pathway Jonah M. Graves^{*}, Julian A. Vallejo, Chelsea Hamill, Michael J. Wacker. University of Missouri-Kansas City School of Medicine, United States

Fibroblast growth factor 23 (FGF23) is a phosphate regulating peptide hormone released by osteocytes. It becomes markedly elevated in chronic kidney disease (CKD), for which the leading cause of death is cardiovascular disease, particularly sudden cardiac death.

Previously, we found that FGF23 increases intracellular calcium in cardiac myocytes and alters cardiac contractility in mouse ventricles *ex vivo*. We have since observed that FGF23 induces contractile dysrhythmias and hypothesize that these aberrant rhythms are due to ventricular muscle hyperexcitability. Since FGF23 has been shown to induce cardiac effects via fibroblast growth factor receptor 4 (FGFR4) and phospholipase C (PLC), we hypothesize that these arrhythmias are mediated through the PLC signal transduction pathway. To test this hypothesis, isolated ventricles from CD1 mouse hearts were perfused *ex vivo* in a modified Langendorff model and paced at 1.8 Hz. Ventricular contractility and rhythm were analyzed by assessing isometric force during treatment with vehicle or FGF23 with and without pretreatment with a PLC blocker (U73122) or an IP3 receptor antagonist (2-aminoethoxydiphenyl borate, 2-APB). Ectopic contractile events were categorized using criteria from an adjunct on the Lambeth conventions on animal arrhythmias. In order to confirm our mechanical categorizations, we measured electrocardiographic (ECG) activity and intraventricular pressure via a balloon catheter inserted in the ventricle of isolated hearts. We found that hearts perfused with FGF23 displayed increased mechanical arrhythmias in the form of ventricular premature beats (VPBs), which increased in frequency from 0.2/min at baseline to 1.8/min ($p < 0.001$, $n=11$). Additionally, FGF23 induced runs of bigeminy in 4 of 11 animals and tachycardia in 6 of 11 animals. Arrhythmias were prevented when hearts were pretreated with a PLC blocker ($p < 0.05$, $n=5$) or an IP3 receptor antagonist ($p < 0.05$, $n=5$). ECG recordings of FGF23 treated mouse hearts ($n=5$) confirmed that the contractile abnormalities corresponded to premature ventricular contractions (PVCs), PVCs in bigeminy, and ventricular tachycardia. Our results show that in Langendorff perfused mouse hearts, FGF23 induces ventricular arrhythmias that are prevented by blockade of PLC and IP3 receptor signaling. Since ventricular arrhythmias represent a leading cause of morbidity and mortality in CKD patients, this pathway may represent an important therapeutic target.

Disclosures: **Jonah M. Graves, None**

LB SUN - 1166

Identification of Novel Notch1 Interacting Partners in Osteosarcoma Cells Haydee Torres^{*1,2}, Fang Fang¹, Danielle May¹, Kyle Roux^{1,2,3}, Jianing Tao^{1,2,3}. ¹Sanford Research, United States, ²South Dakota State University, United States, ³The University of South Dakota, United States

Skeletal Notch proteins regulate embryogenesis and play a critical role in skeletal development and homeostasis. Pathological Notch gain of function has emerged as a major disease mechanism for skeletal disorders and bone cancer. Human osteosarcoma is a major malignant bone tumor found predominantly in children, and the clinical outcomes for osteosarcoma patients with recurrence and metastasis are devastating. Recently, our and other studies suggest that hyperactivation of Notch1 signaling contributes to the pathogenesis of human and murine osteosarcoma and its inhibition may be a therapeutic approach for the treatment of osteosarcoma. As protein-protein interactions are essential for most proteins function including Notch1 nuclear complexes, targeting these interactions represents a broad range of targets and potential therapeutics. Canonical Notch pathway regulates its downstream targets through a transcription complex composed of Notch Intracellular Domain (NICD), Recombination Signal Binding Protein for Immunoglobulin Kappa J Region (Rbpj), Mastermind-Like Transcriptional Coactivator 1 (MAML1), and other unknown interacting proteins in a cell type specific manner. The objective of these studies is to identify Notch1 nuclear interactome using the proximity-based labeling method, BioID, to understand key regulators of its transcriptional activity and oncogenic function in osteoblast and osteosarcoma cells. We have generated and functionally verified a BioID construct for NICD, called Myc-BioID2-NICD, in which a Myc-tag and a new version of the promiscuous biotin ligase (BirA or BioID2) was cloned in frame to the N-terminus of NICD. We have completed a BioID proteomics study and found a large set of proteins (more than 214 highly confident genes) associated with NICD, including transcriptional regulators and protein modifiers. Moreover, we found that 47 potential interacting proteins are enzymes, which are easily druggable. 14 of them also overlapped with a total of 114 proteins recently identified by a Flag-tagged N1-ICD pull-down proteomics study. Functional analysis of Notch1 potential interacting proteins with enzymatic activity are being carried out in osteosarcoma cells. This study of interaction of Notch and its partners will improve our understanding of the molecular mechanism(s) underlying cancer stem cell self-renewal and maintenance, as well as identifying new druggable candidates for molecularly targeted therapeutics in precision treatment for cancer.

Disclosures: **Haydee Torres, None**

LB SUN - 1167

The Runt domain of RUNX2 induces the migration of melanoma cells to bone Maria Teresa Valenti^{*1}, Michela Deiana¹, Michela Serena¹, Samuele Cheri¹, Francesca Parolini¹, Giulia Marchetto¹, Mihaela Mina¹, Antonio Mori¹, Alberto Gandini¹, Franco Antoniazzi¹, Natascia Tiso², Giovanni Malerba¹, Luigi Gennari³, Monica Mottes¹, Donato Zipeto¹, Luca Dalle Carbonare¹. ¹University of Verona, Italy, ²University of Padova, Italy, ³University of Siena, Italy

The mortality rate for malignant melanoma (MM) is very high since it is highly invasive and genetically resistant to chemotherapeutic treatments. Some transcription factors modulate and affect cellular processes influencing gene expression in MM. In particular, a higher expression of the osteogenic master gene RUNX2 in melanoma cells than in normal melanocytes has been reported. To better understand the role of RUNX2 in melanoma development

and to evaluate a therapeutic target, we applied the CRISPR/Cas9 technique to explore the role of the RUNT domain of RUNX2 in a melanoma cell line. A web-based interrogation of public databases for recurrent RUNX2 genetic and epigenetic modifications in melanoma showed that the transcript upregulation is the most common RUNX2 genetic alteration, followed by genomic amplification, mutation, and, finally, by multiple changes. Additionally, altered RUNX2 is involved in dis-regulated pathways promoting tumor progression, Epithelial Mesenchymal Transition (EMT) and metastasis. The RUNT-deleted clone harboring the deletion showed reduced proliferation, reduced EMT features and reduced migration ability in zebrafish model, suggesting the involvement of the RUNT domain in different pathways. In particular, RUNT KO cells showed a reduced relative migration distance to bone as well as the expression of bone specific genes associated to tumor invasiveness. All these findings suggest that the RUNT domain may represent an important oncotarget to prevent bone metastases in Malignant Melanoma.

Disclosures: **Maria Teresa Valenti, None**

LB SUN - 1168

Activation of PI3K in the Myeloid Lineage Results in Myeloproliferative Neoplasm, Increase in Myeloid-Derived Suppressor Cells and Bone Loss Jungeun Yu^{*1}, Laura Doherty¹, Evan Jellison², Ernesto Canalis¹, Archana Sanjay¹. ¹UConn Musculoskeletal Institute, UConn Health, Farmington, CT 06030, United States, ²Department of Immunology, UConn Health, Farmington, CT 06030, United States

Subjects with myeloproliferative neoplasms (MPN), which are characterized by increased expansion of the myeloid lineage, are at an increased risk of osteoporotic fractures although the underlying mechanisms are unknown. Phosphoinositide 3-kinase (PI3K) is required for osteoclast differentiation and function, and plays a role in tumorigenesis. However, its role in the pathogenesis of MPN is not known. Here we report that PI3K activation in the myeloid lineage not only confers MPN but also results in bone loss. To activate PI3K in the myeloid lineage, we crossed R26StopFLP110* conditional mice, where the ROSA26 allele harbors sequences expressing constitutively active P110 alpha (P110*) preceded by a loxP flanked STOP cassette, with *Lyz2Cre*/WT mice. P110* mice had splenomegaly, hepatomegaly, increased number of granulocytes in peripheral blood and accumulation of erythrocytes under the skin which worsened with age. Flow cytometry of 10-week-old P110* mice revealed enhanced myelopoiesis as documented by an increase in monocytes, macrophages in the bone marrow and an increase in macrophages, neutrophils, eosinophils in spleen-derived myeloid populations. Moreover, osteoclast precursors (OCP) were increased in both cell compartments. Micro-CT and bone histomorphometry showed that 10-week-old P110* mice had osteopenia due to an increase in osteoclast number and bone resorption. Myeloid-derived suppressor cells (MDSC) are T cell suppressors that increase in number during tumor progression and recently found to be OCP in cancer and arthritis. P110* mice harbored a 1.4-2-fold increase in CD11b+Ly6G-Ly6Chigh monocytic-MDSCs in the bone marrow and spleen, and a 3.5-fold increase in CD11b+Ly6G+Ly6Cl_o polymorphonuclear-MDSCs in the spleen compared to control littermates. There was a 30% decrease in CD3+ T cells of P110* mice *in vivo*. Supporting these observations, sorted MDSCs from the bone marrow of P110* mice, and not from control mice, reduced T cell proliferation by 40% and MDSCs differentiated into functional osteoclasts *in vitro*. These results show that PI3K activation in the myeloid lineage causes MPN, and accumulation of MDSCs with the capacity to differentiate into osteoclasts and resorb bone.

Disclosures: **Jungeun Yu, None**

LB SUN - 1174

PGC1 α deficiency negatively regulates bone mass and strength Graziana Colaianni^{*1}, Luciana Lippo¹, Lorenzo Sanesi¹, Giacomina Brunetti², Monica Celi³, Nunzio Cirulli², Giovanni Passeri⁴, Janne Reseland⁵, Ernestina Schipani⁶, Maria Felicia Faienza⁷, Umberto Tarantino³, Silvia Colucci², Maria Grano¹. ¹Department of Emergency and Organ Transplantation, University of Bari, Italy, ²Department of Basic Medical Science, Neuroscience and Sense Organs, University of Bari, Italy, ³Department of Orthopedics and Traumatology, Tor Vergata University of Rome, Italy, ⁴Department of Clinical and Experimental Medicine, University of Parma, Italy, ⁵Department of Biomaterials, Institute for Clinical Dentistry, University of Oslo, Norway, ⁶Departments of Medicine and Orthopaedic Surgery, University of Michigan, United States, ⁷Department of Biomedical Science and Human Oncology, Pediatric Unit, University of Bari, Italy

Peroxisome proliferator-activated receptor- γ coactivator 1- α (PGC1 α) is a transcription factor regulating adaptive thermogenesis, glucose metabolism and skeletal muscle fiber type specialization. Here we show that PGC1 α plays a role in skeletal homeostasis since PGC1 α -deficient mice (PGC1 α -/-) display impaired bone structure and increased fragility. Micro-CT of the tibial mid-shaft showed a marked decrease of cortical thickness in PGC1 α -/- (-8.4%, $p < 0.05$) and PGC-1 α -/- (-11.9%, $p < 0.05$) mice compared to wild type littermates. Trabecular bone was also impaired in knock out mice which displayed lower trabecular thickness (Tb.Th) (-5.9% Vs PGC1 α +/-, $p < 0.05$), whereas trabecular number (Tb.N) was higher than wild type mice (+72% Vs PGC-1 α +/-, $p < 0.05$), thus resulting in

increased (+31.7% Vs PGC-1 α +/+, $p < 0.05$) degree of anisotropy (DA), despite unchanged bone volume fraction (BV/TV). Notably, the impairment of cortical and trabecular bone in PGC-1 α knock out mice led to a dramatic -48.4% decrease in bending strength ($p < 0.01$). Bone defects were paralleled by a significant increase in osteoclast number at the cortical bone surface and in serum levels of the bone resorption marker, namely C-terminal cross-linked telopeptides of type I collagen (CTX-I) (+42% Vs PGC-1 α +/+, $p < 0.05$), whereas no difference was observed in serum levels of N-terminal propeptide of type I procollagen (PINP) among the genotypes. In PGC-1 α -/-, we also found a lower expression of mRNAs codifying for Osteocalcin (Ocn) in cortical bone and for Collagen I in bone marrow stromal cells. Moreover, we found that PGC-1 α -/- mice displayed a lower ratio of inguinal WAT (iWAT)/body weight and histological analysis of iWAT revealed profound ~75% decrease in adipocyte area and a lower expression of Adiponectin (AdipoQ) mRNA, whereas Leptin mRNA was several folds higher than wild type mice. Overall, results presented herein suggest for the first time that PGC-1 α may play a key role in bone metabolism.

Disclosures: *Graziana Colaianni, None*

LB SUN – 1175

Metabolic Fuel Selection During the Osteoblast to Osteocyte Transition

Thomas O'Connell*, Matt Prideaux, Yukiko Kitase, Lynda Bonewald. Indiana University, United States

Osteocytes are the most abundant bone cells in the body and play key roles in regulating bone homeostasis. However, despite the importance of these cells, we still know relatively little regarding osteoblast to osteocyte transition and how energy metabolism may change during this process. To investigate metabolism changes during osteocyte differentiation, we used the IDG-SW3 cell line, which differentiate into mature osteocyte-like cells in culture. An untargeted NMR-based metabolomics approach was applied on cells and media taken at days representing the early osteoblast (day 4), osteoid osteocyte (day 9), mineralizing osteocyte (day 18) and mature osteocyte (day 28). Metabolic profiles of both cell media and cell extracts were obtained to monitor the consumption and release of metabolites and the metabolic processes within the cells. This profiling revealed novel features of fuel selection and cellular biosynthesis that develop during differentiation. Glucose consumption is relatively stable through day 9 with little production of lactate. At day 18, there is a nearly 3 fold increase in glucose consumption along with a nearly 10 fold increase in the production of lactate suggesting a dramatic switch to aerobic glycolysis. At day 28, glucose consumption is reduced and lactate production drops to about four fold higher than at day 9 indicating a return to oxidative metabolism. A consistently high level of glycerol is produced by the cells and excreted into the media, suggesting a sustained level of lipolysis and utilization of fatty acid oxidation throughout the differentiation process. Initial qPCR analyses show elevations in some lipase and fatty acid receptor genes, consistent with increased fatty acid utilization in the mature osteocyte. Increased production of acetate by the cells is also consistent with fatty acid utilization. A distinct spike in citrate production was observed at day 9 as the cells initiate hydroxyapatite deposition within the collagenous matrix. Citrate is critical for stabilization of the apatite nanocrystals in bone and may function to stabilize the mineral surrounding the newly embedded cell. Citrate is also known to be reduced in osteoporosis, a time of osteocyte death and reduced function. These studies have identified novel changes in metabolic pathways during osteocyte differentiation, which may maintain osteocyte function while depositing and then residing within their mineralized matrix.

Disclosures: *Thomas O'Connell, None*

LB SUN - 1181

Mechanically-stimulated ATP release from murine bone cells is regulated

by a balance of injury and repair Nicholas Mikolajewicz*, Elizabeth Zimmermann², Bettina Willie¹, Svetlana Komarova¹. ¹McGill University, Canada, ²Shriners Hospital for Children-Canada, Canada

Mechanical environment is an important determinant of bone health. ATP release is one of the first events induced by mechanical stimulation of bone-forming osteoblasts and bone-resident osteocytes; however, the dominant pathways of ATP release remain disputed. We examined the mechanism of ATP release from mechanically-stimulated compact bone or bone marrow-derived osteoblasts. We demonstrated that 70 ± 24 amol ATP/cell were released in response to single cell membrane deformation and 21 ± 11 to 422 ± 97 amol ATP/cell in response to turbulent fluid shear stress. Mechanical stimulation induced exocytosis of quinine-positive ATP-containing vesicles. Pharmacological activation of protein kinase C (PKC) potentiated vesicular exocytosis, while PKC inhibition reduced exocytosis. Unexpectedly, increase in vesicular release coincided with a significant decrease in released ATP, and vice versa. To examine the contribution of injury to ATP release, we evaluated membrane integrity during and after mechanical stimulation using membrane impermeable markers. We demonstrated that in vitro or in vivo mechanical stimuli induced magnitude-dependent repairable cell membrane injury. Ca²⁺/PLC/PKC-dependent vesicular release was critical for successful repair of membrane damage, suggesting that rather than delivering ATP to extracellular space, vesicular exocytosis limits the much larger efflux of intracellular ATP through damaged membranes. Prior activation of PKC/vesicular signaling improved membrane integrity and limited ATP release induced by subsequent mechanical stimulation. Our study suggests a new model of biological adaptation to mechanical forces that combines

graded perception of mechanical environment through membrane injury and an ability to effectively counteract the destructive potential of mechanical forces through membrane repair.

Disclosures: *Nicholas Mikolajewicz, None*

LB SUN - 1182

Association of osteosarcopenia and cognitive impairment in a community dwelling older population: The Bushehr Elderly Health (BEH) program

Bagher Larijani^{*1}, Gita Shafiee², Afshin Ostovar³, Ramin Heshmat⁴, Farshad Sharifi⁵, Iraj Nabipour⁶. ¹Endocrinology and Metabolism Research Center, Endocrinology and Metabolism Clinical Sciences Institute, Tehran University of Medical Sciences, Tehran, Iran, Islamic Republic of Iran, ²Chronic Diseases Research Center, Endocrinology and Metabolism Population Sciences Institute, Tehran University of Medical Sciences, Tehran, Iran, Islamic Republic of Iran, ³Osteoporosis Research Center, Endocrinology and Metabolism Clinical Sciences Institute, Tehran University of Medical Sciences, Tehran, Iran, Islamic Republic of Iran, ⁴Chronic Diseases Research Center, Endocrinology and Metabolism Population Sciences Institute, Tehran University of Medical Sciences, Tehran, Iran, Islamic Republic of Iran, ⁵Elderly Health Research Center, Endocrinology and Metabolism Population Sciences Institute, Tehran University of Medical Sciences, Tehran, Iran, Islamic Republic of Iran, ⁶The Persian Gulf Tropical Medicine Research Center, Bushehr University of Medical Sciences, Bushehr, Iran, Islamic Republic of Iran

Background: The combination of sarcopenia and osteopenia/osteoporosis (Osteosarcopenia) shows a high prevalence and further adverse outcomes in elderly. Also, the prevalence of cognitive impairment increases after 60 years old. The aim of this study is to investigate the relationship between Osteosarcopenia (OS) and cognitive impairment in a large sample of older adults in Iran. Methods: A total of 2426 Iranian adults aged ≥ 60 years, participating in the stage II of Bushehr Elderly Health (BEH) program, a population-based prospective cohort study; were included in this study. Sarcopenia was defined as having low muscle index (< 7.0 in men and < 5.4 Kg/m² in women) with low handgrip strength (< 26 Kg in men, < 18 Kg in women) or low usual gait speed (< 0.8 m/s). Body composition was measured by dual X-ray absorptiometry (DXA). Subjects were divided into 3 groups: 1) nonsarcopenia - nonosteopenia (normal), 2) sarcopenia /osteopenia (BMD < -1.0 SD or sarcopenia), 3) sarcopenia + osteopenia (OS). Cognitive status was assessed by Mini Mental State Examination (MMSE), Category Fluency Test (animals naming), Functional Assessment (FAST) and history of dementia. Everybody who had problem at least in one of these tests were considered as subjects with cognitive impairment and those with normal condition in all tests were assumed as normal cognition. The multivariable logistic regression was used to investigate the association between OS and cognitive impairment. Results: Of the total participants, 484 (21.8%) of subjects were normal, 51.4% of subjects had sarcopenia /osteopenia and 26.8% of participants had OS. In univariate logistic analysis, sarcopenia/osteopenia and OS increased risk of cognitive impairment to OR=1.70(1.37-2.11) and 2.68(2.09-3.43), respectively. After adjustment for age and sex, the association remained statistically significant [OR=1.27(1.01-1.60) and OR=1.47(1.12-1.91), for sarcopenia/osteopenia and OS, respectively]. The association remained statistically significant only between OS and cognitive impairment [OR= 1.37(1.04-1.80)] in the full model (adjusted for age, sex, physical activity and smoking). Conclusions: This study provides evidence that the presence of osteopenia with sarcopenia (OS) independently increases risk of cognitive impairment. Common pathways, such as mitochondrial dysfunction, may have a role in both conditions.

Disclosures: *Bagher Larijani, None*

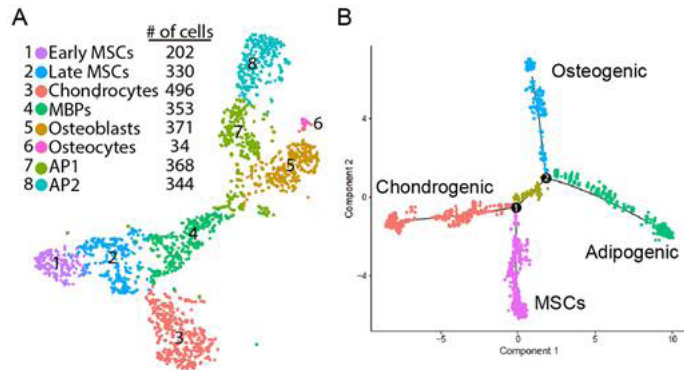
LB SUN - 1188

Building a single-cell transcriptome atlas of mouse bone marrow mesenchymal lineage cells for analyzing MSC heterogeneity

Robert Tower*, Leilei Zhong, Jihwan Park, Luqiang Wang, Rojesh Shrestha, Katalin Susztak, Ling Qin. University of Pennsylvania, United States

Stem cell heterogeneity and plasticity are common features of mammalian tissues. However, owing to a lack of investigative tools, whether bone marrow MSCs are made of heterogenic subpopulations has long been suspected, but never proven. The Col2-Cre Rosa-tdTomato (Col2/Td) specifically labels all mesenchymal lineage (MLin) cells, thus providing a perfect system to comprehensively analyze subpopulations of MLin cells in vivo. In this project, we enzymatically digested endosteal bone marrow from 1-month-old Col2/Td mice and sorted for the top 1% Td+ cells, which contained all the CFU-F forming cells found in unsorted cells. Cells were subjected to single-cell RNA sequencing using the 10X Genomics drop-seq platform. After rigorous quality control and exclusion of contaminating hematopoietic and endothelial cells, we identified 2,489 MLin cells expressing ~2500 sequenced genes per cell. Unsupervised clustering with Seurat divided those cells into 8 clusters (Fig. 1A). According to known markers, they are early MSCs (Sca1, CD34), late MSCs, chondrocytes (Col2a1, Col10a1), mesenchymal bi-potent progenitors (MBPs), osteoblasts (osteocalcin, Col1a1), osteocytes (SOST), adipoprogenitor (AP) 1, and AP2 (adiponectin, Lpl, Pparg). Interestingly, plots suggest that these cells exist in a continuum, rather than in discrete states. Cell cycle analysis based on the expression levels of >90 cell cycle-related genes revealed that early MSCs are quiescent; osteocytes are the least proliferative cells;

AP1 and late MSCs are the most proliferative cells. Monocle trajectory analysis generated three differentiation directions with the first branch separating chondrocytes from MBPs and the second branch bi-pronged into osteoblasts and APs (Fig. 1B). Cells in AP clusters, particularly those in AP2, highly and specifically express *Cxcl12* and *LepR*, resembling the previously identified CAR/LepR+ MSC population. Fluorescence imaging confirmed that in Col2/Td mice, Td+ stromal cells have reticular shape and that almost all LepR+ bone marrow cells were Td+. Interestingly, sequencing data suggests that these AP cells are a major source of cytokines and chemokines such as *Scl*, *RANKL*, *VEGFs*, *Il6*, *Cxcl12*, etc, indicating that they play important roles in regulating the bone marrow environment. Taken together, our work demonstrates the heterogeneity of bone marrow MSCs by identifying their novel subpopulations and delineating their relative positions along the MSC tri-differentiation axes.



Disclosures: **Robert Tower**, None

LB SUN - 1194

Investigating the Dose-Dependent Response of Black Tea Polyphenols in SaOS-2 Cells Riley Cleverdon*, Michael D. Mcalpine, William Gittings, Wendy E. Ward. Brock University, Canada

Many epidemiological studies suggest that the consumption of black tea is associated with reduced risk of several diseases, as well as higher bone mineral density. Polyphenols present in black tea, due to their potent antioxidant capacity, may mediate potential beneficial effects. Recently, our lab has shown increased mineral deposition with supplementation of black tea polyphenols (1 µg/mL) in an osteoblast cell model (SaOS-2 cells). The purpose of this study was to determine if a dose-dependent response exists between supplementation with black tea polyphenols and mineral deposition in SaOS-2 cells. SaOS-2 cells were cultured and differentiated for 8 days at 37°C in 5% CO₂. Mineralization was induced for 5 days in the presence or absence of 0.1, 0.5, 0.75, 1, 2, 5, or 10 µg/mL of black tea polyphenols. Black loose-leaf tea (English Breakfast) was steeped in accordance to manufacturer's recommendations. Total polyphenol content (TPC) of black tea was determined using Folin-Ciocalteu's reagent with a gallic acid standard. Alizarin red staining was utilized to quantify mineral deposition (n=6, each 'n' corresponds to 4 averaged biological replicates). Cells treated with concentrations of black tea polyphenols at or greater than 0.75 µg/mL resulted in a significantly greater (p<0.05) mineral deposition relative to control (% of control, 0.75 µg/mL: 240% ± 0.44, 1 µg/mL: 300% ± 0.36, 2 µg/mL: 351% ± 0.57, 5 µg/mL: 358% ± 0.81, 10 µg/mL: 354% ± 0.96). Supplementation with 1, 2, 5, and 10 µg/mL of black tea polyphenols did not significantly differ in mineral deposition from one another. Intriguingly, this data exhibits a positive dose-dependent response which peaks at approximately 1 µg/mL of black tea polyphenols and higher concentrations resulted in negligible increases in mineral deposition, indicating that at higher concentrations of black tea polyphenols, the positive dose-dependent relationship is lost. These findings suggest that there is a dose-dependent response between black tea polyphenols and mineral deposition. The studied doses represent dietary through to supplemental levels of black tea polyphenols. Key cell signaling pathways are currently being analyzed to determine how black tea polyphenols mediates its effect in SaOS-2 cells.

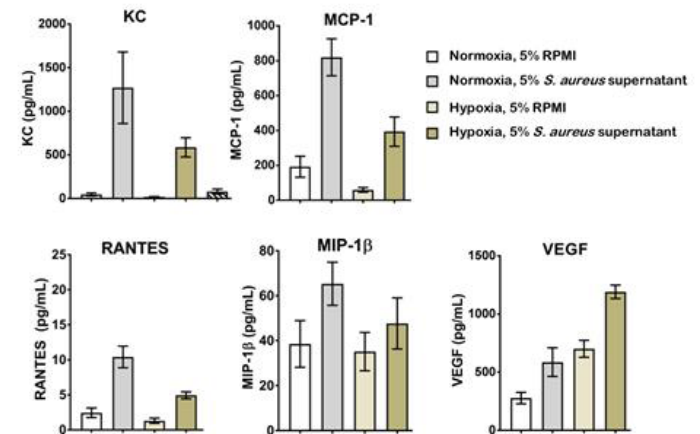
Disclosures: **Riley Cleverdon**, None

LB SUN - 1195

The impact of tissue oxygenation on antibacterial immunity during Staphylococcus aureus osteomyelitis Caleb Ford*, Aimee Wilde¹, Nicole Putnam¹, Jacob Curry², Jim Cassat^{1,2}. ¹Vanderbilt University, United States, ²Vanderbilt University Medical Center, United States

Osteomyelitis is a highly morbid inflammatory state of bone most commonly triggered by *Staphylococcus aureus* infection. During osteomyelitis, the structural matrix and vascular architecture of bone is damaged, resulting in regions of necrotic, avascular tissue that increase risk of chronic infection. Extreme hypoxia occurs during osteomyelitis due to a disrupted vascular supply, inflammation, and the metabolism of invasive *S. aureus*. The host responds to hypoxia by initiating hypoxia-inducible factor (HIF) signaling, which is implicated in the regulation of bone development, bone healing, and antibacterial immunity.

However, the role of hypoxia and HIF signaling during osteomyelitis is unknown and may serve as an important clinical target to combat invasive infection. Using a murine model of post-traumatic *S. aureus* osteomyelitis, we found intense hypoxyprobe staining at the infectious focus that is out of proportion to hypoxyprobe staining of non-infectious fracture healing. Furthermore, cytokine profiling of infected femur homogenates demonstrates that VEGF, a well-characterized target of HIF signaling, is increased *in vivo* during osteomyelitis relative to mock-infected bone, consistent with the notion that HIF signaling is activated during invasive infection of bone. Via western blot, we found that stimulation with bacterial supernatants induces HIF-1 α accumulation in primary osteoblasts not only under 1% O₂ (hypoxia), but also when grown in 21% O₂ (normoxia). These *in vitro* data led to the hypothesis that tissue oxygenation influences antibacterial immunity during *S. aureus* osteomyelitis. To begin testing this hypothesis, cytokine abundance was tested in conditioned media from primary murine osteoblasts that were grown in normoxia and hypoxia and stimulated with bacterial supernatants. The data indicate that osteoblasts sense and respond to both bacterial stimulation as well as environmental hypoxia. While bacterial supernatant stimulation almost universally induces cytokine production in osteoblasts compared to vehicle, hypoxia significantly altered the inflammatory profile of *S. aureus*-stimulated osteoblasts. Hypoxia augments bacterially induced VEGF production and inhibits production of important neutrophil-chemotactic cytokines such as KC, MCP-1, MIP-1 β , and RANTES. These data and future *in vivo* experiments will further elucidate how oxygenation impacts skeletal cell biology and the innate immune responses to bacterial pathogens.



Disclosures: **Caleb Ford**, None

LB SUN - 1196

Antagonism between Bone Morphogenetic Protein and Activin signaling pathways in osteoprogenitor cells Madeline Totten*, Sydni Yates, Kelli Jestes, Sylvia Chlebek, Jordan Newby, Jon Arthur, Jonathan Lowery. Division of Biomedical Science, Marian University College of Osteopathic Medicine, United States

Osteoporosis is a disease characterized by low bone mineral density due to the rate of bone resorption exceeding that of bone formation. Substantial evidence indicates the Bone Morphogenetic Protein (BMP) pathway promotes bone formation through action of the effectors SMAD1/5/8 while the Activin pathway negatively influences bone mass through action of the effectors SMAD2/3. Recent studies suggest that BMPs and Activins regulate bone mass in a see-saw-like mechanism. Here, we seek to test this hypothesis *in vitro* via signaling responsiveness assays using pathway-specific western blot analyses in the osteogenic murine bone marrow stromal cell line W-20-17. We first confirmed that W-20-17 cells exhibit basal activation of SMAD1/5/8 and SMAD2/3 under serum-restricted conditions. Moreover, treatment with Follistatin, which sequesters Activin ligands in the extracellular environment, leads to an increase in BMP pathway activation. To determine the molecular mechanism allowing for this relationship, we treated W-20-17 cells with SB431542, which is an intracellular inhibitor of Activin signaling that functions downstream of receptor engagement, and found no effect on BMP pathway activation. In contrast, treatment of W-20-17 cells with BMP pathway inhibitor Noggin had no effect on Activin pathway activation despite robust inhibition of BMP signaling. Collectively, our results suggest Activin-mediated repression of BMP signaling in these cells is ligand-dependent but occurs upstream of SMAD2/3 activation. Gene expression analyses indicate that W-20-17 cells express Activin A and its receptors ALK4, ACVR2A, and ACVR2B. Given that ACVR2A and ACVR2B also have high affinity for BMP ligands, this raises the possibility that Activin-mediated repression of BMP signaling may occur via competition for a shared pool of receptors. Over-expression studies coupled with osteoblast activity assays are currently underway to examine this hypothesis. Collectively, our work seeks to elucidate the mechanism(s) that regulate antagonism of BMP and Activin signaling pathways in the osteoblast lineage to identify novel opportunities for treating low bone mass in humans.

Disclosures: **Madeline Totten**, None

LB SUN - 1201

Pattern recognition and IL-1 receptor signaling drive host immunity and altered bone homeostasis during Staphylococcus aureus osteomyelitis Nicole Putnam*, Laura Fulbright, Jacob Curry, Jenna Petronglo, Jim Cassat. Vanderbilt University Medical Center, United States

Osteomyelitis is an invasive and debilitating infection of bone, most frequently caused by the Gram positive pathogen *Staphylococcus aureus*. Treatment of osteomyelitis is difficult, in part due to pathogen-induced bone destruction that limits antibiotic penetration to the infectious focus. Understanding the mechanisms by which bacteria alter bone homeostasis is therefore a critical step in deciphering the pathogenesis of osteomyelitis. The objectives of this study were to define critical immune responses during osteomyelitis, and to understand how bone homeostasis is altered by innate sensing of bacteria. We hypothesized that pattern recognition receptor (PRR) signaling pathways are necessary for antibacterial defenses during osteomyelitis, but may contribute to pathogen-associated bone loss. To test this hypothesis, we used both *in vitro* assays and a murine osteomyelitis model to determine how *S. aureus* alters osteoclastogenesis and triggers bone loss *in vivo*. We discovered that *S. aureus* dramatically enhances osteoclastogenesis of bone marrow macrophage (BMM)-derived pre-osteoclasts. *In vivo*, *S. aureus* triggers profound cortical bone destruction locally, but also increases the number of osteoclasts at trabecular sites distant to the infectious focus. To define how PRR signaling contributes to these processes, we used mice lacking the critical PRR signaling adaptor MyD88 or the Gram positive-sensing PRRs TLR2 and TLR9. Staphylococcal enhancement of osteoclastogenesis *in vitro* was found to be dependent on both MyD88 and TLR2. However, TLR2 was dispensable for both antibacterial defenses and pathogen-induced bone destruction *in vivo*. In contrast, both MyD88- and TLR9-deficient mice sustained significantly increased bacterial burdens during osteomyelitis. Since TLR9-deficiency also failed to impact bone destruction *in vivo*, we subsequently investigated the role of IL-1R signaling during osteomyelitis. Mice lacking the IL-1R were highly susceptible to *S. aureus* proliferation during osteomyelitis, yet had significantly greater new bone formation and a smaller increase in trabecular osteoclast number. Collectively, these data suggest divergent roles of IL-1 signaling in antibacterial host defense and pathologic bone remodeling during osteomyelitis. Additionally, MyD88-dependent PRR signaling significantly impacts osteoclastogenesis *in vitro*, but these effects may be masked *in vivo* by innate immune responses and inflammatory cytokines such as IL-1.

Disclosures: *Nicole Putnam, None*

LB SUN - 1202

AP-002: A novel inhibitor of osteoclast differentiation and function without disruption of osteogenesis Yongqiang Wang*, Yixue Mei¹, Yushan Song¹, Carly Bachus¹, Chunxiang Sun¹, Hooshmand Sheshbaradaran², Michael Glogauer¹. ¹University of Toronto, Canada, ²Altum Pharmaceuticals Inc, Canada

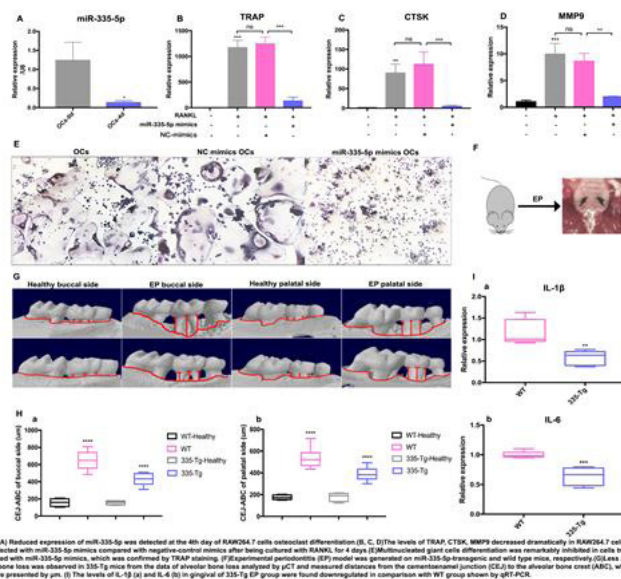
AP-002 is a novel clinical stage oral gallium based compound. In this study we examined the effects of AP-002 on osteoclastogenesis, fusion and osteoclast function, as well as its effects on osteoblastogenesis. The early stages of osteoclast differentiation were impaired by AP-002, as evidenced by the significant down-regulation of TRAP and cathepsin K mRNA expression in murine osteoclast precursor cells RAW264.7 treated with AP-002 in the presence of RANKL. AP-002 (1 μ M) was also found to block fusion of osteoclasts in these cultures. Importantly, AP-002 caused these inhibitory effects without causing osteoclast cell death in these cultures, which was in contrast to zoledronic acid (ZA) controls, where osteoclastogenesis inhibition and cell death overlapped. AP-002 is further differentiated from ZA in that it did not inhibit small GTPase Rac1 activation in these cultures. AP-002 had a similar inhibitory effect on RANKL-induced mouse primary bone marrow monocytes (BMMs) fusion. Similarly, human blood monocytes treated with AP-002 failed to form TRAP-positive cells. Furthermore, mouse BMMs-derived mature osteoclasts seeded on dentine slices and treated with AP-002 exhibited dramatically reduced numbers of resorption pits and resorption area. Analysis of AP-002 impact on RANKL-induced osteoclastogenesis related gene expression (in RAW264.7 cells) by gene microarrays, showed that AP-002 significantly reverses the effect of RANKL on 115 genes. These include several key osteoclast-differentiation/function associated genes such as: scinderin, Ocstamp, Atp6v0d2, Oscar, Rhou, Usp18, MMP9 and Trim30. Microarray data were confirmed by RT-qPCR. AP-002 is however not just a RANKL inhibitor, as for at least 50 genes, AP-002 effect adds to RANKL effect. Furthermore, AP-002 has no effect on NFATc1 mRNA levels, the master RANKL induced transcription regulator. The difference between AP-002 and ZA is also seen in its effects on osteoblastogenesis. Osteoblast mineralization was promoted by AP-002 (0.01-3.0 μ M), whereas ZA showed toxicity to osteoblasts at the concentration >0.5 μ M. ZA therefore has no therapeutic window in its toxic effect on osteoclasts and osteoblasts, while AP-002 has a therapeutic window, and in fact AP-002 promotes osteogenesis in this therapeutic window. We conclude therefore that AP-002 is a promising new anti-bone resorption agent, with a mechanism of action different from other currently marketed anti-bone resorption agents.

Disclosures: *Yongqiang Wang, None*

LB SUN - 1203

MicroRNA-335-5p Inhibits Alveolar Bone Resorption and Inflammation in Periodontitis Junxiang Lian*^{1,2}, Qisheng Tu¹, Jake Chen^{1,3}. ¹Division of Oral Biology, Tufts University School of Dental Medicine, United States, ²State Key Laboratory of Oral Diseases, West China School of Stomatology, Sichuan University, United States, ³Department of Cellular, Molecular, Developmental Biology, United States

Objectives: Bone homeostasis is delicately maintained by osteoblasts and osteoclasts (OCs). Our laboratory has identified and characterized miR-335-5p that promotes osteoblast differentiation and bone regeneration in miR-335-5p transgenic (335-Tg) mice via inhibiting Wnt antagonist DKK1. This study was to investigate, for the first time, the effects of miR-335-5p constitutive overexpression on OC activity and experimental periodontitis (EP). Materials and Methods: OC differentiation of RAW264.7 cells were induced by RANKL, and miR-335-5p mimics and inhibitor were transfected into RAW264.7 separately under the same culture condition. The level of miR-335-5p was detected via qRT-PCR. Expression of TRAP, Cathepsin K and MMP9 were examined and TRAP staining was performed to observe OC formation. To examine the effect of miR-335-5p on periodontitis, EP model was constructed by ligature on both sides of maxillary second molar in 8-week old male 335-Tg mice and C57BL/6 wild type (WT) mice. After 2 weeks of ligation, mice were sacrificed. For alveolar bone morphology observation and analysis, samples were scanned with 3-dimensional μ CT, and the CEJ-ABC distance (cemento-enamel junction to the alveolar bone crest) was measured at 6 predetermined points on buccal and palatal sides of treated molars. The levels of IL-1 β and IL-6 in EP gingival were detected by qRT-PCR. Results: Expression level of miR-335-5p declined remarkably at the day 4 of osteoclastogenesis when OCs were fully developed. RAW264.7 cells transfected with miR-335-5p mimics hardly developed into mature OCs, which was demonstrated by the reduced level of TRAP, Cathepsin K, MMP9 and weakened TRAP staining. MiR-335-5p overexpression reduced alveolar bone loss and osteoclast activity, and attenuated gingival inflammation level (IL-1 β and IL-6) compared with WT group. Conclusion We found that while miR-335-5p level decreased during OC differentiation, exogenous overexpression of miR-335-5p could significantly suppress this process. As a result, periodontitis in 335-Tg mice were less severe than that in WT mice due to the inhibiting effect on OCs and anti-inflammatory effect of miR-335-5p. Taken together, our results for the first time demonstrate that constitutive overexpression of miR-335-5p inhibits osteoclast differentiation and suppresses periodontitis in mice suggesting a promising and potent role of miR-335-5p in treating bone-loss disorders including periodontitis.



Disclosures: *Junxiang Lian, None*

LB SUN - 1206

PPAR γ : A Molecular Brake for Osteocyte Energy Metabolism and Bone Mass Sudipta Baroi*¹, Lance Stechschulte¹, Amit Chougule¹, Patrick Griffin², Beata Lecka-Czernik¹. ¹University of Toledo College of Medicine, United States, ²Scripps Research Institute, United States

Diabetes impairs systemic energy metabolism and affects bone which is reflected in low material quality and susceptibility to fractures. The etiology of diabetic bone disease is unclear, however it includes attenuation of bone remodeling. Plethora of evidence indicate that bone and energy metabolism share the same regulatory mechanisms including an activity of PPAR γ , which simultaneously regulates cellular and systemic energy metabolism and is a key regulator of bone remodeling process. We hypothesized that, PPAR γ plays an important role in regulation of energy metabolism in osteocytes (OT), which comprise 95% of bone

cells and play an essential role in regulation of bone remodeling. To test this hypothesis, we developed osteocyte specific PPAR γ knock out animals (γ OTf/f mice) using Cre-LoxP technology. We monitored these mice from 2 to 6 months of age for bone mineral density (BMD), body composition using NMR, and energy expenditure using indirect calorimetry. In addition, the PPAR γ transcriptome in OT was analyzed using next generation sequencing (NGS). In a separate set of experiments, PPAR γ effect on cellular energy metabolism was measured using Seahorse technology in OT-like MLO-A5 cells with PPAR γ KD with lentiviral expression of shRNA. As compared to WT, male γ OTf/f mice had higher oxygen consumption, carbon dioxide production, heat generation and increased locomotion at all analyzed ages. Females have opposite metabolic phenotype up to 5 mo of age, which at 6 mo shifts to that observed in males. γ OTf/f mice have higher lean mass and higher BMD, but are insulin intolerant, as compared to age-matched WT. Activation of PPAR γ in OT upregulates genes associated with lipid and carbohydrate metabolism. Surprisingly, PPAR γ KD in MLO-A5 cells increases oxidative phosphorylation and ATP production. We conclude that PPAR γ in OT acts as a molecular brake that regulates the extent of energy production and utilization, and OT function. When this brake is no longer active, as in γ OTf/f mice, there is an increase in energy demand by OT which is reflected in elevated systemic energy metabolism. In support to this conclusion, another group has recently reported increased glucose uptake in bone of mice with PPAR γ KO in OT. It is unclear at this point whether increased BMD is a result of increased energy metabolism or it results from different, but PPAR γ -specific, mechanism in OT. These specific questions and relationships are currently under study.

Disclosures: *Sudipta Baroi, None*

LB SUN - 1208

Assessment of bone density using QCT on single and dual energy CT data. An Ex-vivo Study on Human Femur Philippe P Wagner^{#1}, Jean-Paul Roux¹, Quentin Chuzel², Francois Duboeuf¹, Roland Chapurlat^{1,2}, Helene Follet¹, Jean-Baptiste Pialat¹. ¹Univ Lyon, Université Claude Bernard Lyon 1, INSERM, Lyons UMR1033, Lyon, France, ²Hospices Civils de Lyon, Lyon, France

Introduction: Opportunistic diagnosis of osteoporosis during routine computed tomography (CT) may allow for earlier recognition of undiagnosed fracture. Mono energy multi-slice CT (MSCT) allows accurate assessment of bone density using calibration phantom and post-processing convolution kernel. Dual-energy CT (DECT) can produce a mono-energetic reconstruction from two different energy spectra. Depending on the convolution kernel selected (bone or standard), the ability to obtain accurate and reliable areal bone mineral density (aBMD) or bone mineral content (BMC) values has been questioned. The objective of this study was to quantify image inter-reliability filtering measurements of human ex-vivo femurs. **Methods:** Forty femurs from elderly donors were analysed for aBMD and BMC with the Dual x-ray absorptiometry (DXA) method. Two acquisitions (MSCT and DECT) were performed (Revolution CTTM, GE Healthcare, USA) and reconstructed using either sharp kernel ("bone" for spatial resolution) or a smooth kernel ("standard" for contrast resolution). Density assessment was performed with a dedicated software (QCT PRO[®], Mindways Software Inc., Austin, TX, USA). **Statistics:** Inter-reliability's ICC was assessed with a single measurement, absolute agreement, 2-way mixed-effects model. 95% confidence intervals were obtained by bootstrapping. Pearson coefficients were used to assess linear correlation. **Results** (see Table): With DXA, comparing kernels and MSCT, a significant correlation was found for aBMD and BMC: $r=0.83-0.92$ ($p<0.001$); a good to excellent agreement: ICC= $0.83-0.92$ and a negligible random measurement bias ($<5\%$). With DXA, comparing kernels and DECT acquisition, a significant correlation was found for aBMD and BMC: $r=0.84-0.94$ ($p<0.001$); a good to excellent agreement: ICC= $0.84-0.93$; and a negligible random measurement bias ($<5\%$). Comparing MSCT to DECT, a significant correlation was found for aBMD and BMC: $r=0.93-0.99$ ($p<0.001$); a good to excellent agreement: ICC= $0.93-0.99$; and a negligible random measurement bias ($<2\%$). **Conclusion** Compared with DXA, we showed that aBMD and BMC assessment could be measured ex-vivo on femurs with a high inter-reliability regardless of the convolution kernel for both DECT and MSCT acquisitions. The mono-energetic reconstruction from a DECT do not disturb the ability to evaluate aBMD and BMC, independently of the convolution kernel filtering.

Tableau 1: Femoral neck parameters according imagery techniques and kernel types

Variables	Mean of differences	Pearson correlation coefficient	Intra Class Correlation	95% confidence Interval	
				Lower bound	Higher Bound
MSCT vs DXA parameters with a bone filter					
BMC (g)	0.04 (0.70%)	0.85 *	0.84	0.73	0.92
aBMD (g/cm ²)	0.00 (0.96%)	0.92 *	0.92	0.86	0.96
MSCT vs DXA parameters with a contrast filter					
BMC (g)	0.15 (4.60%)	0.83 *	0.83	0.70	0.91
aBMD (g/cm ²)	0.02 (3.70%)	0.91 *	0.90	0.83	0.95
DECT vs DXA parameters with a bone filter					
BMC (g)	0.06 (1.96%)	0.85 *	0.85	0.73	0.92
aBMD (g/cm ²)	0.02 (2.87%)	0.94 *	0.93	0.87	0.97
DECT vs DXA parameters with a contrast filter					
BMC (g)	0.10 (2.93%)	0.84 *	0.84	0.73	0.91
aBMD (g/cm ²)	0.03 (4.70%)	0.92 *	0.91	0.90	0.96
DECT vs MSCT parameters with a bone filter					
BMC (g)	0.03 (0.82%)	0.96 *	0.96	0.93	0.98
aBMD (g/cm ²)	0.01 (1.84%)	0.99 *	0.99	0.97	0.99
DECT vs MSCT parameters with a contrast filter					
BMC (g)	-0.04 (1.47%)	0.93 *	0.93	0.87	0.96
aBMD (g/cm ²)	0.01 (0.92%)	0.95 *	0.95	0.92	0.98

p: * <0.001

Disclosures: *Philippe P Wagner, None*

LB SUN - 1212

High Levels of Abdominal Aortic Calcification Predict Higher Health Care Costs John Schousboe^{*1,2}, Tien Vo², Lisa Langsetmo², Brent Taylor², Allyson Kats², Susan Diem², Pawel Szulc³, Joshua Lewis⁴, Kristine Ensrud². ¹HealthPartners Institute, United States, ²University of Minnesota, United States, ³INSERM UMR 1033, University of Lyon, Hospices Civils de Lyon, France, ⁴University of Western Australia, Australia

Purpose: Greater abdominal aortic calcification (AAC) assessed on lateral spine radiographs or densitometric images obtained at the time of bone densitometry is associated with increased risks of cardiovascular disease and all-cause mortality. However, to date no studies have assessed whether or not greater AAC is associated with higher health care burden and utilization. Our purpose was to estimate the associations of AAC with subsequent total and outpatient health care costs acute hospitalization, and post-hospital skilled nursing facility (SNF) care, before and after adjusting for known cardiovascular disease (CVD) risk factors. **Methods:** AAC was scored on lateral lumbar spine x-rays obtained at the baseline visit of the Osteoporotic Fractures in Men (MrOS) study, using a validated 24-point scale. Total and outpatient health care costs, acute hospital stays, and SNF stays were identified from Medicare Fee for Service claims over the 36 months following the baseline visit. The associations of AAC with total and outpatient health care costs were estimated with generalized linear models using gamma distribution and log link, and with hospital and SNF stays with logistic models. **Results:** Among 5994 men aged 65 and older enrolled in MrOS at baseline, 5083 had lateral spine x-rays interpretable for AAC and complete data for covariates; 2340 men (mean age 73.5 years) were also enrolled in Medicare FFS for 36 months after the baseline visit. Annualized median (IQR) total health care costs (2017 dollars) were \$2209 (961-5960), \$2932 (1112-8060), \$3231 (1335-8774), and \$4613 (1675-10881) for those with, respectively, AAC scores of 0-1, 2-4, 5-8, and ≥ 9 . After consideration of CVD risk factors and diagnoses (Table), men with AAC level ≥ 9 compared with those with AAC level 0-1 had 29% and 43% higher total and outpatient costs, and 1.5- and 2.5-fold higher odds of ≥ 1 hospital stay and ≥ 1 SNF stay. **Conclusion:** Greater levels of AAC assessed using lateral spine radiographs performed for vertebral fracture detection are a marker of individuals with higher health care costs and utilization, even after accounting for clinical CVD risk factors and diagnoses. Further studies of clinical potentially modifiable characteristics associated with AAC that are driving health care utilization) are needed.

Table: Association of AAC with Health Care Utilization over 36 Months

AAC Level	Total Health Care Cost Ratio (95% C.I.)	Outpatient Care Cost Ratio (95% C.I.)	Hospital Stays OR (95% C.I.)	SNF Stays OR (95% C.I.)
Base Model^a				
0 to 1 (n=670)	Reference	Reference	Reference	Reference
2 to 4 (n=635)	1.05 (0.89-1.24)	1.10 (0.90-1.34)	1.46 (1.16-1.85)	1.31 (0.71-2.43)
5 to 8 (n=534)	1.17 (0.98-1.39)	1.10 (0.89-1.35)	1.40 (1.10-1.80)	1.05 (0.55-2.00)
9 or more (n=501)	1.49 (1.25-1.78)	1.55 (1.25-1.92)	1.78 (1.39-2.30)	2.48 (1.40-4.39)
Multivariable Model^b				
0 to 1	Reference	Reference	Reference	Reference
2 to 4	1.02 (0.87-1.20)	1.07 (0.89-1.29)	1.33 (1.04-1.71)	1.41 (0.71-2.80)
5 to 8	1.06 (0.89-1.27)	1.06 (0.87-1.31)	1.25 (0.96-1.64)	1.09 (0.53-2.24)
9 or more	1.29 (1.07-1.55)	1.43 (1.15-1.77)	1.51 (1.15-1.99)	2.47 (1.29-4.73)

^a adjusted for age and study enrollment site

^b adjusted for age, study enrollment site, race, education, systolic blood pressure, HDL cholesterol, LDL cholesterol, triglycerides, smoking status, angina, prior myocardial infarction, prior stroke, congestive heart failure, and diabetes mellitus

Disclosures: *John Schousboe, None*

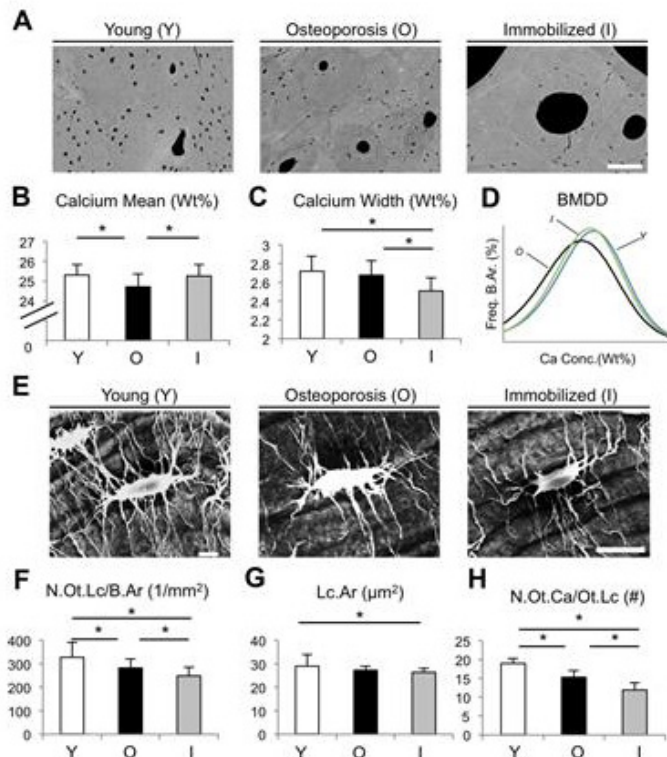
LB SUN - 1216

WITHDRAWN

LB SUN - 1219

Long-term immobilization is associated with increased cortical porosity, osteocyte deficiency and high matrix mineralization Tim Rolvien*¹, Petar Milovanovic², Felix N. Schmidt¹, Matthias Krause¹, Klaus Püschel³, Robert O. Ritchie⁴, Michael Amling¹, Björn Busse¹. ¹Department of Osteology and Biomechanics, University Medical Center Hamburg-Eppendorf, Germany, ²Laboratory for Anthropology, Institute of Anatomy, Faculty of Medicine, University of Belgrade, Serbia, ³Department of Legal Medicine, University Medical Center Hamburg-Eppendorf, Germany, ⁴Materials Sciences Division, Lawrence Berkeley National Laboratory, United States

Immobilization as a result of long-term bed rest can lead to pronounced bone loss. Due to their distribution throughout the bone matrix and remarkable interconnectivity, osteocytes are the major mechanosensors in bone and translate mechanical into biochemical signals to trigger bone remodeling. To test whether immobilization affects the characteristics of the osteocyte network in human bone, femoral diaphyseal cortical bone specimens were analyzed in 20 aged formerly bedridden immobilized female patients and compared to eleven primary osteoporosis cases as well as seven young patients. Cortical porosity, osteocyte number and lacunar area, the frequency of hypermineralized lacunae (N.Mn.Lc/B.Ar), as well as cortical bone calcium content (CaMean) were assessed using bone histomorphometry and quantitative backscattered electron imaging. Bone quality characteristics and local mechanical competence were further assessed by Fourier transform infrared (FTIR) spectroscopy and reference point indentation, respectively. In immobilization cases, the cortical porosity was drastically reduced, while the overall matrix mineralization was significantly increased compared to osteoporotic bone ($p=0.027$, $p=0.021$, respectively) (Fig. 1 A-D), which was associated with a lower indentation distance increase. The number of osteocytes, osteocyte lacunar size and canaliculi showed a declining pattern from young to osteoporotic cases with further diminishment in immobilization cases (Fig. 1 E-H), whereas the number of hypermineralized lacunae changed in an opposing pattern reaching 71% more mineralized lacunae in immobilization. In conclusion, reduced osteocyte numbers and impaired connectivity in immobilization are associated with a dramatic bone loss pattern, reflecting a phenotype clearly distinguishable from postmenopausal osteoporosis. Immobilization periods may lead to loss of survival signals for osteocytes, provoking bone loss that is even higher than in osteoporosis states, while osteocytic osteolysis remains absent in immobilization.

Disclosures: **Tim Rolvien**, None

LB SUN - 1222

Fragility Fracture Risk Reduction in Women with Breast Cancer on Aromatase Inhibitors Treated with Anti-Osteoporosis Therapy Yu-Chien Cheng*, Cydney Bullock, Shriya Gandhi, Andrea Sterenstein, Megan Randall, Sara Ahmad, Samarthkumar Thakkar, Michael Morkos, Garnet Meier, Sanford Baim. Rush University Medical Center, United States

The use of aromatase inhibitors (AI) for treatment of breast cancer is associated with significant loss of bone mineral density (BMD) and increased fracture risk. We aimed to determine whether concurrent AI and anti-osteoporosis therapy (anti-OP) is associated with reduced risk in fragility fractures in an oncology referral center spanning April 2011 to October 2017. Inclusion criteria included women with breast cancer diagnosis and AI use. Exclusion criteria included bone metastasis, AI use < 12 months, and inadequate clinical information. Longitudinal data on the use of AI and anti-OP therapies, fragility fractures, and baseline BMD were chart reviewed. Eligible women were grouped according to whether an anti-OP agent was used for a minimum duration of 12 months during AI or not. Hazard ratios of various anti-OP agents for fragility fractures were assessed using Cox regression analysis. Of 1519 eligible women, 64% were Caucasians. The mean age at AI initiation was 63 ± 10 years. The group treated with anti-OP agents (N=346) had greater number of fragility fractures prior to AI initiation compared to the untreated group (10% vs 6%, $P<0.05$) and greater number of women diagnosed with osteopenia (41% vs 27%, $P<0.05$), and osteoporosis (24% vs 4%, $P<0.05$) at baseline. Anti-OP regimens consisted of oral bisphosphonates (BP) (N=183) for a median of 37 months (interquartile range [IQR] 24, 60), i.v. BP including zoledronate 4 mg every 6 months (N=10) and 5 mg every 12 months (N=30) for 30 months (IQR 17, 45), and denosumab 60 mg every 6 months (N=122) for 22 months (IQR 17, 28). Thirty-one fragility fractures (9%) occurred in women on anti-OP agents, compared to 98 (8%) in the untreated group ($P>0.05$). Time to first fragility fractures was 7.5 (±3.0) years in women on anti-OP agents vs 6.9 (±3.6) years in women without anti-OP agents ($P>0.05$). Incidence rates of fragility fractures were similar: 1.5 per 100 person-years (95% CI: 1.1-2.2) in the anti-OP treated women vs 1.7 per 100 person-years (95% CI: 1.4-2.0) in the untreated group ($P>0.05$). Among various anti-OP therapies, lower incidence rate of fragility fractures was observed in women on denosumab: 0.5 per 100 person-years (95% CI: 0.2-1.7) vs 1.7 per 100 person-years (95% CI: 1.4-2.0) in the untreated group ($P<0.05$). Hazard ratio for fragility fractures was 0.3 (95% CI: 0.10-0.95, $P<0.05$) with denosumab therapy but non-significant with BP after multivariable regression adjusting for age at AI initiation, baseline BMD, and presence of fragility fractures prior to AI. In conclusion, denosumab therapy during AI was associated with a lower incidence rate of fragility fractures and 70% fracture risk reduction. No significant fragility fracture reduction was observed with oral or i.v. BP treatment. In patients at high risk for fracture, denosumab should be considered as the preferred therapy prior to initiation of AI therapy.

Disclosures: **Yu-Chien Cheng**, None

LB SUN - 1223

Impact of Thyroid Hormone Therapy on Bone Health in Older Adults with Subclinical Hypothyroidism: a Randomized Clinical Trial Elena Gonzalez Rodriguez*^{1,2}, Axel Lennart Löwe^{3,4}, Cinzia Del Giovane³, Martin Feller^{3,4}, Patricia Kearney⁵, Jacobijn Gussekloo⁶, Simon P. Mooijaart⁶, Rudi GJ Westendorp⁷, David J Stott⁸, Daniel Aeberli⁹, Doug Bauer¹⁰, Didier Hans¹, Nicolas Rodondi^{2,3}. ¹Center of Bone Diseases, Rheumatology Unit, Bone and Joint Department, CHUV, Switzerland, ²Endocrinology, Diabetology and Metabolism Unit, Internal Medicine Department, CHUV, Switzerland, ³Institute of Primary Health Care (BIHAM), University of Bern, Switzerland, ⁴Department of General Internal Medicine, Inselspital, Bern University Hospital, University of Bern, Switzerland, ⁵Department of Epidemiology and Public Health University College Cork, Ireland, ⁶Departments of Gerontology and Geriatrics Leiden University Medical Center, Netherlands, ⁷Department of Public Health and Center for Healthy Aging, University of Copenhagen, Denmark, ⁸Institute of Cardiovascular and Medical Sciences, University of Glasgow, United Kingdom, ⁹Department of Rheumatology and Clinical Immunology/Allergy, Bern University Hospital, Switzerland, ¹⁰Departments of Medicine, Epidemiology and Biostatistics, University of California, United States

Introduction: The deleterious effect of high thyroid function on bone even at high-normal levels is well established. While subclinical hypothyroidism does not appear to impact on bone health, little evidence exists on the effect, if any, of levothyroxine therapy in subclinical hypothyroidism. The only data are conflicting results from 4 small randomized clinical trials (N= 17 to 73), from which only one showed a significant decrease of spine bone mineral density (BMD) accompanied by an increase in bone turnover markers (BTMs). **Aim:** To assess the effect of levothyroxine treatment on BMD, and crosslaps (CTX) and PINP BTMs, in older adults with subclinical hypothyroidism. **Methods:** Randomized, double-blind, placebo-controlled trial, bone substudy of the TRUST trial on levothyroxine substitution in community-dwelling adults over 65 years with subclinical hypothyroidism, with a TSH target range 0.40 to 4.59 mIU/L. Participants from TRUST study centers in Switzerland were included without any additional exclusion criteria. Linear regression analysis on BMD (measured by dual-energy X-ray absorptiometry, n=117) and BTMs (measured by automated assays, Roche Elecsys, n=190) changes from baseline to 1-year follow-up, adjust-

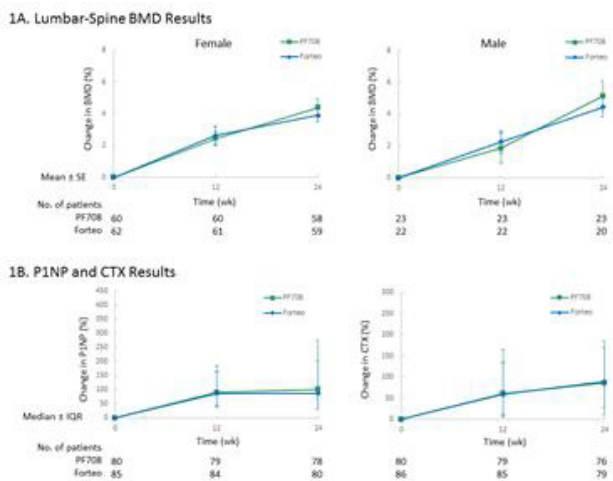
ed for gender, were conducted. Results: All 117 participants completed the study (levothyroxine n=59); after application of ISCD guidelines, 105 and 114 DXA images for lumbar spine and hip respectively were included. At baseline, participants mean±SD values were: age, 74.1±5.6 years; BMI, 27.0±4.7 kg/m²; TSH, 6.4±2.0 mIU/l; free T4, 13.58±1.88 pmol/l; 43% were women. Baseline mean BMD: spine, 1.128±0.179 g/cm²; total hip, 0.969±0.168 g/cm²; and hip neck, 0.897±0.147 g/cm². Baseline characteristics were balanced between groups. At 1 year, lumbar BMD change was similar in levothyroxine treated participants as compared to placebo in non-adjusted and gender-adjusted analysis (adjusted: +0.015 g/cm², 95%CI [-0.0007 to 0.03], p=0.062). There was no difference between the two groups in either analysis in total hip BMD change (lowest p-value=0.984) or hip neck BMD change (lowest p-value= 0.8059). BTMs changes were also similar in both groups (levothyroxine vs. placebo, adjusted): CTX +9.96 ng/l, 95%CI [-21.75 to 41.67], p=0.536, and PINP +2.35 µg/l, 95%CI [-3.08 to 7.77], p=0.394. Conclusion: These data provide no evidence of a negative impact of levothyroxine treatment in subclinical hypothyroidism on bone density after one year of treatment.

Disclosures: *Elena Gonzalez Rodriguez, None*

LB SUN - 1225

PF708, a Therapeutic Equivalent/Biosimilar Teriparatide Candidate, Demonstrates Comparable Clinical Profiles Relative to Forteo in Osteoporosis Patients Hubert Chen^{*1}, Michael Noss², Jonathan Lee¹, Hongfan Jin¹, Carrie Schneider¹, Christine Thai¹. ¹Pfenex Inc, United States, ²Synexus, United States

PF708 is a teriparatide drug candidate being developed as a therapeutic equivalent/biosimilar to Forteo, which is approved for the treatment of osteoporosis patients at high risk of fracture. PF708 was previously shown to be bioequivalent to Forteo in healthy subjects (NCT02656810). In this study (NCT03002428), we compared the long-term effects of PF708 and Forteo in a 24-week, randomized, open-label, parallel-arm study in male and postmenopausal female osteoporosis patients in the US. We enrolled 181 patients: 90 (65 female/25 male) received PF708 and 91 (66 female/25 male) received Forteo. 82 patients completed the study in the PF708 group vs. 81 in the Forteo group. The primary endpoint was anti-drug antibody (ADA) incidence. Secondary endpoints included mean percentage changes in lumbar-spine bone mineral density (BMD), median percentage changes in bone turnover markers (BTM) and pharmacokinetic (PK) parameters after the first dose. Safety endpoints were incidences of adverse events (AE) and serious adverse events (SAE). Two PF708-treated patients (2.3%) and two Forteo-treated patients (2.2%) developed ADA during the study. These low rates of immunogenicity are consistent with historical Forteo results (~3%). At Week 24, there were two ADA-positive findings for PF708 vs. none for Forteo, but the difference was not statistically significant (P=0.50, Fisher's exact test). All PF708 ADA findings were low in titer (1:1) and returned to nondetectable during follow-up measurements. One PF708 patient had in vitro neutralizing activity transiently detected at Week 4, however this finding did not correlate with a loss of pharmacological activity. There were no apparent safety issues related to ADA or neutralizing activity findings. PF708 and Forteo demonstrated comparable effects on lumbar-spine BMD (Figure 1A) and two BTM (Figure 1B): N-terminal propeptide of type 1 procollagen (PINP), a marker of bone formation, and cross-linked C-terminal telopeptide of type 1 collagen (CTX), a marker of bone resorption. There were no statistically significant differences between PF708 and Forteo in BMD and BTM. PK profiles after PF708 or Forteo injection were comparable. There were no significant imbalances in AE incidences or severity profiles between PF708 and Forteo. These results indicate that PF708 and Forteo have comparable profiles in osteoporosis patients and support the development of PF708 as a therapeutic equivalent/biosimilar candidate to Forteo.

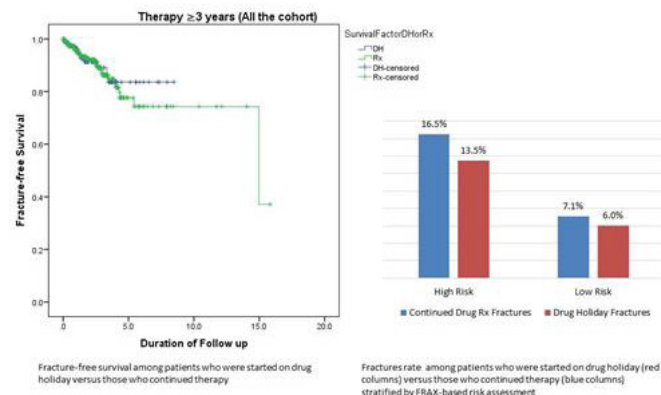


Disclosures: *Hubert Chen, Pfenex, Other Financial or Material Support*

LB SUN - 1226

Fragility Fractures after Initiation of a Drug Holiday in a Real Life Setting Michael Morkos^{*1,2}, Alessandra Casagrande¹, Paul Mahrous¹, Muriel Tania Go², Hasan Husni², Mirette Hanna¹, Sara Bedrose², Dingfeng Li², Yu-Chien Cheng^{1,2}, Sanford Baim¹. ¹Rush University Medical Center, United States, ²John H. Stroger, Jr. Hospital of Cook County, United States

We aimed to assess the difference in fractures rate between patients who were placed on drug holiday (DH) after minimum adequate therapy versus those who continued therapy (CT) in a real-life setting. This is a retrospective cohort study in a tertiary academic center in Chicago, IL. Inclusion criteria involved adults (aged ≥18 years) who received minimum adequate therapy (bisphosphates, raloxifene, or denosumab ≥ 3 years, or teriparatide ≥ 18 months), otherwise, patients were excluded. Of 1,814 charts randomly selected and reviewed, 274 patients met the inclusion criteria. In our cohort, females were 90.9%, White 50.0%, African American 40.5%, and Latino 8.0%. A DH was initiated in 43.4% of the total cohort. In the DH versus CT cohorts, mean duration of therapy was 5.7±2.3 vs 6.0±2.6 years (P<0.01), total duration of follow up 7.8±2.7 vs 6.1±2.9 years, and fractures occurred in 9.2% vs 11.7% respectively, not statistically significant. Further fracture risk stratification was used, high risk patients were defined as having a dual energy X-ray absorptiometry (DXA) with T-score ≤-2.5 at the lumbar spine, femur neck, total hip, or distal 1/3 radius (DXA HR), history of fragility fracture, and/or FRAX risk assessment with probability of major osteoporotic fractures ≥20% or hip fractures ≥3% (FRAX HR). Fragility fractures in high risk versus lower risk patients in the DH cohort based on FRAX HR was 13.5% versus 6.0% (P=0.14), combined FRAX HR and DXA HR was 11.3% versus 6.3% (P=0.28), and based on the presence of fragility fractures during therapy was 14.3% versus 8.2% (P=0.30), respectively. Fragility fractures in high risk versus lower risk patients in the CT cohort based on FRAX HR were 16.5% versus 7.1% (P=0.01), combined FRAX HR and DXA HR was 13.2% versus 9.0% (P=0.20), and based on fragility fractures during first three years of therapy was 0.0% versus 13.2% (P=0.02) respectively. Fragility fractures in the DH versus CT cohorts among high risk patients were not statistically significant. The greater the duration of a DH, the higher the risk of fragility fractures: 0.0% in the first year, 6.7% in the second, 12.5% in the third, 5.0% in the fourth, and 26.3% for five years or more (P=0.04). In conclusion, based on the results from our cohort study, continued drug therapy did not provide additional protective benefit beyond the minimum adequate duration of therapy. However, the longer the drug holiday, the higher the risk of fractures emphasizing the importance of routine fracture risk assessment during drug holiday.



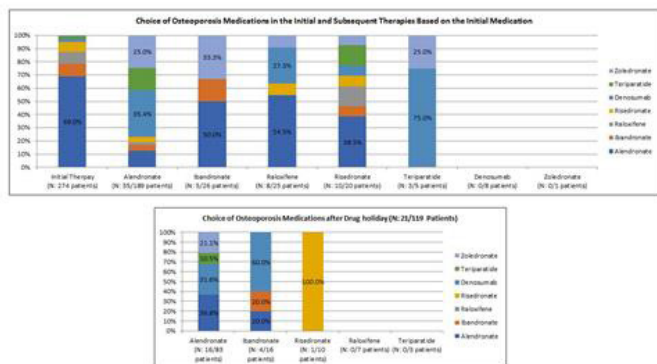
Disclosures: *Michael Morkos, None*

LB SUN - 1227

Patterns of Osteoporosis Medications Selection after Drug Holiday or Continued Therapy: A Real World Experience Michael Morkos^{*1,2}, Alessandra Casagrande¹, Paul Mahrous¹, Muriel Tania Go², Hasan Husni², Mirette Hanna¹, Dingfeng Li², Sara Bedrose², Mishita Goel¹, Yu-Chien Cheng^{1,2}, Sanford Baim¹. ¹Rush University Medical Center, United States, ²John H. Stroger, Jr. Hospital of Cook County, United States

We aimed to assess the pattern of medication selection for treatment of osteoporosis at the initiation of therapy (Rx), any subsequent changes, and re-initiation after drug holiday (DH) in a real-life setting. This is a retrospective cohort study in a tertiary academic center in Chicago, IL. Inclusion criteria involved adults (aged ≥18 years) who received a minimum adequate Rx (bisphosphates, raloxifene, or denosumab ≥ 3 years, or teriparatide ≥ 18 months), otherwise, patients (pts) were excluded. 1,814 charts were randomly selected and reviewed, 274 pts met the inclusion criteria. 61 pts received subsequent Rx before any interruption, 119 pts were placed on drug DH, and 21 pts were restarted on Rx after the DH. Among the 274 patients, Alendronate was the most common initial Rx (percentage, mean duration of Rx ± standard deviation in years): 69.0%, 5.4±2.4y. This was followed by ibandronate (9.5%, 4.9±2.1y), raloxifene (9.1%, 5.2±1.6y), risedronate (7.3%, 4.2±2.0y), denosumab (2.9%, 4.1±0.8y), teriparatide (1.8%, 2.1±0.1y), and zoledronate (0.4%, 7.8 years). Among

189 pts who received alendronate as the initial Rx, 35 patients were transitioned to subsequent therapies at different time points before going into any DH. Denosumab was the most common subsequent Rx prescribed accounting for 35.4% of the total 48 subsequent Rx, followed by zoledronate (25.0%), teriparatide (16.7%), alendronate (12.5%), ibandronate (4.2%), risedronate (4.2%), and raloxifene (2.1%). Among 25 pts who received raloxifene as initial Rx, eight pts received 11 subsequent Rx: Alendronate (54.5%), denosumab (27.3%), risedronate (9.1%), and zoledronate (9.1%). In 26 patients who received ibandronate as initial therapy, five pts received six subsequent Rx: Alendronate (50.0%), zoledronate (33.3%), and ibandronate (16.7%). Among 20 patients who received risedronate as initial Rx, ten pts received 13 subsequent therapies: Alendronate (38.5%), raloxifene (15.4%), teriparatide (15.4%), ibandronate, risedronate, denosumab, and zoledronate (7.7% each). Among five patients who received teriparatide as initial Rx, three pts received four subsequent therapies: Denosumab (75.0%) and zoledronate (25.0%). Eight pts received denosumab and one pt received zoledronate as initial therapies with no subsequent Rx. In this cohort, denosumab was the most commonly prescribed subsequent therapy (29.3%) followed by alendronate (24.4%), zoledronate (20.7%), and teriparatide (12.2%). Among the 21 pts who restarted Rx after DH, 10 pts (40.0%) received denosumab, eight pts (32.0%) received alendronate, four pts (16.0%) received zoledronate, two pts (8.0%) received teriparatide, and one pt (4.0%) received ibandronate. In conclusion, oral bisphosphonates constituted most of the initial therapy in our cohort. Denosumab was the most common subsequent therapy followed by Alendronate, Zoledronate, and Teriparatide in both continued therapy and drug holiday cohorts



Disclosures: Michael Morkos, None

LB SUN - 1228

Apparent Response Rate by PINP to Oral Bisphosphonates in Clinical Practice and Clinical Trial Settings Antonia Ugur*¹, Fatma Gossiel¹, Kim Naylor¹, Jennifer Walsh¹, Nicola Peel², Eugene McCloskey¹, Richard Eastell^{1,3}. ¹Academic Unit of Bone Metabolism, Oncology and Metabolism, University of Sheffield, United Kingdom, ²Metabolic Bone Centre, Sheffield Teaching Hospitals, United Kingdom, ³Mellanby Centre for Bone Research, United Kingdom

Background: Guidelines recommend bone turnover markers to monitor anti-resorptive treatments; to identify those not responding or non-adherent to oral bisphosphonates (BPs). In clinical practice, we use serum PINP as it is relatively unaffected by food intake or time of day. We wished to compare apparent response rates in serum PINP when using the geometric mean of a healthy premenopausal reference interval as the target, and associated changes in total hip BMD, between women recruited to a trial of oral BPs (the TRIO study) and an unselected cohort of patients receiving oral BPs in our clinic. Methods: A cohort of 92 unselected clinic-based patients (17 male; 75 female all postmenopausal), with osteoporosis on an oral BP for at least 3 months were matched to 92 untreated matched subjects as controls and compared to 135 postmenopausal women who had participated in TRIO, from whom pre-treatment serum provided same-subject controls. On a single serum sample from the treated and untreated clinical subjects, and TRIO baseline and week 48 serum samples, we measured Intact PINP using the IDS-iSYS assay, to calculate apparent response rates and perform ROC curve analysis. Implication for change in total hip BMD was examined in a subset of subjects where comparable baseline and follow up (TRIO 1-year n=128, Clinical 1-5 years n=30) DXA was available. Results: The demographics of the clinical cohort and TRIO were comparable with a mean age of 70.2 and 67.2 years, and total hip T-score of -1.66 and -1.35, respectively. Comorbidities that affect bone metabolism were exclusion criteria in TRIO but were recorded in 51% of the treated clinical subjects, including fracture within 12 months (5%), significant glucocorticoid use (25%), thyroid disorder (15%) and diabetes mellitus (11%). Adherence was high in the TRIO cohort but unrecorded in the clinical cohort. The apparent response rate in the clinical cohort was high (75%) but lower than in the TRIO study (96%); the AUC was also lower in the clinical cohort as in table 1. Hip BMD improved to a greater extent in responders versus non-responders in both cohorts. Conclusions: Apparent response rates to oral BPs are lower in clinic patients than in clinical trial participants with poor adherence and secondary osteoporosis being possible contributory factors. Nonetheless, detection of an apparent positive biochemical response is associated with beneficial changes in BMD comparable to that seen in clinical trial settings.

		TRIO Oral Bisphosphonates n=135	CLINICAL Oral Bisphosphonates n=92
Apparent Responders by PINP Threshold Level %		96	75
AUC (95% CI)		0.98 (0.95-0.99)	0.77 (0.71-0.83)
BMD Mean % change Total Hip	Responder	2.06 n=124	2.96 n=26
	Non-responder	0.61 n=4	-1.64 n=4

Table 1. AUC for PINP by IDS iSYS automated assay to detect treatment response to oral bisphosphonate and percent of apparent responders when PINP is set at a female premenopausal geometric mean (threshold level). Mean percentage change in BMD of the total hip is given by biochemical "threshold" response.

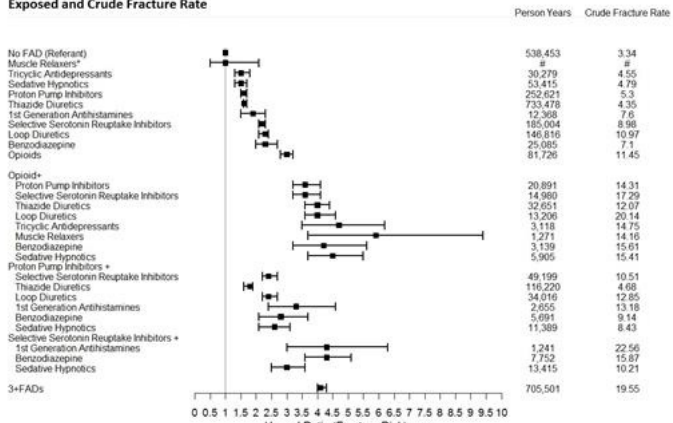
Disclosures: Antonia Ugur, None

LB SUN - 1234

Additive Adverse Effects: Use of Multiple Fracture Associated Drugs and Hip Fracture Risk Rebecca Emeny*¹, Chiang-Hua Chang¹, Jonathan Skinner¹, A. James O'Malley¹, Jeremy Smith¹, Gouri Chakraborti¹, Clifford J. Rosen², Nancy E. Morden¹. ¹The Dartmouth Institute for Health Policy & Clinical Practice, The Geisel School of Medicine at Dartmouth, United States, ²Maine Medical Center Research Institute, United States

Background: Many commonly used prescription drugs are known to increase fracture risk which raises concern for patients receiving two or more such drugs concurrently. The combined risk of taking multiple fracture-associated drugs (FADs) is unknown and may be additive, or worse, supra-additive - when risk exceeds the sum of the component risks. Methods: We used a 20% sample of Medicare fee-for-service data, 2004-2014, to study hip fractures among beneficiaries receiving zero, one, two or three-or-more of 21 FADs. Data were structured at the person-day level. We used Cox regression models adjusting for patient age, sociodemographics, receipt of fracture protective drugs and morbidities. Preliminary analyses estimated the incremental hip fracture risk associated with current receipt of any one, two or three-or-more FADs. Our main analysis then explored risk associated with exposure to each specific single FAD and each two-way FAD combination, versus no FAD. All analyses were sex stratified. Results: Mean cohort age was 77 (SD 7.3) years. Of 11.3 million person years, 25.1% involved one FAD, 11.7% two FADs and 8.5% three-or-more FADs. In fully adjusted models, among women, risk associated with one, two and three-or-more FADs, versus no FAD, was Hazard Ratio (HR) 1.9 (95% CI 1.9, 2.0), HR 2.6 (95% CI 2.5, 2.7), HR 4.1 (95% CI 3.9, 4.2), respectively. Risks in men were slightly higher. Exposure-specific models revealed combinations conferring additive risk, including: opioids HR 3.0 (95% CI 2.8, 3.2), sedatives HR 1.5 (95% CI 1.4, 1.7), opioids plus sedatives HR 4.5 (95% CI 3.7, 5.5). Over thirty supra-additive pairs included: proton-pump-inhibitors plus sedatives, HR 2.6 (95% CI 2.1, 3.1) serotonergic-antidepressants plus antihistamines HR 4.3 (CI 3.0, 6.3), opioids plus muscle relaxers HR 5.9 (95% CI 3.7, 9.4) See Figure 1. Male risks were similar but with wider confidence intervals. Conclusion: Combination FAD use is common. Many drug pairs are associated with additive risks and some with supra-additive risks, suggesting synergistic adverse effects. Our results suggest judicious prescribing and caution in combining FADs when use is discretionary, alternatives exist, or fracture risk is high.

Figure 1: Select Results from the Cox Regression Model for Women: Hazard Ratio of Hip Fracture Associated with Fracture Associated Drugs and Two-Way Combinations of These Drugs, Total Observed Person Years Exposed and Crude Fracture Rate



Legend Figure 1. Selective Serotonin Reuptake Inhibitors + combined drug group of selective serotonin reuptake inhibitors and selective norepinephrine reuptake inhibitors. Sedative Hypnotics include only non-benzodiazepine drugs. # indicates cell value suppressed in compliance with Centers for Medicare & Medicaid reporting requirements. These cells all reflect exposure > 100 person years but fracture count < 11.

Disclosures: **Rebecca Emery, None**

LB SUN - 1238

Bone Mineral Density and fracture risk in adult Hypophosphatasia
 Franca Genest*, Lena Clausen, Silke Achtziger, Lothar Seefried. University of Wuerzburg, Germany

Introduction: Hypophosphatasia is a rare inherited metabolic disorder caused by inactivating mutations in the ALPL gene. Adult patients with HPP exhibit a wide spectrum of clinical symptoms including an increased fracture risk. Despite this awareness, data on clinical significance of DXA measurement in adult HPP is very limited. Accordingly, this evaluation aims at providing a systematic overview of technically consistent Bone Mineral Density (BMD) results from a large cohort of adult HPP patients in order to identify fundamental patterns of BMD values in HPP and potential associations of BMD results with fracture risk, ALP values and the prevailing genetic background. **Methods:** Retrospective single-center analysis of DXA-Scans conducted in adult HPP patients with confirmed ALPL-gene mutations, HPP-associated clinical symptoms and low alkaline phosphatase levels. All measurements were performed on the same Scanner (Hologic Discovery A). Further data evaluation included lab values (ALP, PLP, PEA), fracture type, medical history and childhood symptoms. **Results:** Analysis included data of 110 patients (84 female, mean age 46.2y) of whom 36.4% (n=40) were harboring two mutations. Average T-Score levels were -0.1 (SD 1.9) and -1.1 (SD 1.2) at the lumbar spine and total hip, respectively. Both lower ALP activity as well as higher substrate levels (PLP/PEA) were significantly correlated with higher BMD levels at the lumbar spine but not at the hip. Nearly half of the patients (n=53, 48.2%) had sustained at least one fracture in the past. Total hip BMD was sig. lower in patients with previous fractures while lumbar spine BMD was not associated with overall fracture incidence. Patients with two mutations had significantly higher lumbar spine BMD (p<0.001) which were in turn sig. associated with HPP specific metatarsal and diaphyseal long bone fractures (p=0,001). **Discussion:** Increased fracture risk in HPP patients is not universally associated with decreased BMD. Conversely, lumbar spine BMD appears to be particularly high in patients with lower ALP activity, higher substrate levels and compound heterozygous mutational status. Accordingly, high lumbar spine BMD might be a hallmark of severe disease and an indicator for an increased risk of HPP-specific fractures. Otherwise, overall fracture prevalence and the risk for non-HPP specific fractures appears to be higher in patients with lower hip BMD, i.e. hip BMD appears to be a valuable tool to predict vertebral and femoral neck fracture in HPP patients.

Disclosures: **Franca Genest, Alexion, Speakers' Bureau**

LB SUN - 1239

Asfotase Alfa Therapy in Adults with Pediatric-Onset Hypophosphatasia: Compassionate Use Results Michaël Laurent*¹, David Alster², Evelien Gielen¹, David Cassiman¹, Franz Jakob³, Lothar Seefried³. ¹University Hospitals Leuven, Belgium, ²Tucson Endocrine, United States, ³University of Würzburg, Germany

BACKGROUND: Hypophosphatasia (HPP) is a metabolic bone disorder caused by mutations in the liver-bone-kidney isoform of alkaline phosphatase (ALPL). Asfotase alpha (AA, Strensiq®) is an enzyme-replacement therapy approved for the treatment of skeletal symptoms of severe (i.e. perinatal, infantile and childhood-onset) forms of HPP. Clinical trials with AA have been performed mostly in children, while reports in adults remain anecdotal. Here, we report outcomes in adults with pediatric-onset HPP treated in the global AA compassionate use program. **METHODS:** Treating clinicians of n=5/7 adults consented to aggregate data (3F/2M; age 33-69 years). **RESULTS:** Four patients had infantile-onset HPP and biallelic ALPL mutations, whereas one had childhood-onset HPP and a single mu-

tation. Follow-up ranged 2-6 years. Weekly AA dose was 6 mg/kg (n=3) or 3 mg/kg (n=2). All patients had rickety bone deformities and a history of (atypical) femoral fracture(s). Four patients had a history of multiple fractures, whereas during follow-up only one patient experienced 4 new fractures in 6 years, at times when dosing was temporarily reduced. Two patients had baseline pseudofractures and two had femoral non-unions, which healed within 1 year of AA treatment. All patients were wheelchair users at baseline; after 1 year, n=2 were walking unassisted and n=2 used mostly crutches. During longer follow-up, one could eventually use a rolling walker. Patients reported improvements in SF36-physical functioning (n=5/5) and SF36-health change (n=4/4). Six minute walking distance improved in n=4/4 patients. One patient required nocturnal oxygen support, which could be discontinued after 6 months. Pyridoxal-5-phosphate (n=4/4), inorganic pyrophosphate (=4/4) and urinary phosphoethanolamine (n=3/3) decreased, and PTH(1-84) increased (n=3/3). Bone mineral density improved in n=3/4 patients. Adverse events were mild injection-site reactions (n=5/5) and serious adverse events considered unrelated to AA (n=5/5); one patient developed symptomatic urolithiasis possibly attributable to AA. No AA-neutralizing antibodies were detected. Limitations of this report include lack of a control group and missing data. **CONCLUSIONS:** Compassionate-use AA was safe, and associated with decreased fracture burden, improved mobility/physical functioning, and biochemical and radiographic improvements in adults with pediatric (particularly infantile-onset) HPP. Further clinical trials in this population are warranted.

Disclosures: **Michaël Laurent, Alexion, Consultant**

LB SUN - 1240

Successful treatment of osteoporosis with intermittent parathyroid hormone related peptide (Tymlos) injections in patients with Ehlers-Danlos syndrome
 Julianna Barsony*. Georgetown University Medical Center, United States

Intermittent administration of parathyroid hormone related peptide (PTHrP) in rodent models of osteoporosis increased osteoblast formation, and PTHrP increased type I collagen production by osteoblasts in culture. PTHrP (Tymlos) has recently been approved for the treatment of severe osteoporosis in postmenopausal women and early experience is highly valuable. Ehlers-Danlos Syndrome (EDS) is a group of inherited disorders of connective tissue that frequently causes osteoporosis due to defects in collagen synthesis and low bone formation. Clinical manifestations of EDS are variable and clinical diagnosis is made based on family history and combination of symptoms affecting bone, joints, skin, blood vessels, ligaments, gut, and brain (anxiety and chronic pain). We report results from four postmenopausal women with severe treatment resistant osteoporosis and EDS receiving Tymlos injections 80 mcg daily for one year. They also continued vitamin D supplement. Serum calcium and phosphorus and bone turnover markers were assessed before treatment and twice during treatment. Tymlos improved symptoms, markedly increased bone formation marker levels (PINP 7-11-fold and osteocalcin 4-7-fold), and mildly increased bone resorption (urine NTX up to 2-fold), without increasing serum calcium. Bone density measurements of the hip/spine and vertebral fracture assessments were completed before and after this treatment and demonstrated improved bone mineral density 3-5% at the spine, 2.7-5.1% at the hip and 2.9-7.2% at the femoral neck. No new fractures noted. These findings suggest that Tymlos treatment should be considered for patients presenting with EDS and osteoporosis.

Disclosures: **Julianna Barsony, None**

LB SUN - 1242

Homozygous knock-in Gly682Arg mutation in mouse Col27a1 gene phenocopies human steel syndrome with osteochondrodysplasia Kalyan Nannuru*¹, Claudia Gonzaga-Jauregui², Harikiran Nistala², Johanna Jimenez¹, Silvia Smaldone¹, Saathyaki Rajamani¹, Johnathon Walls¹, Chia-Jen Siao¹, Andrew Murphy¹, Sarah Hatsell¹, Aris N Economides¹. ¹Regeneron Pharmaceutical Inc, United States, ²Regeneron Genetic Center, United States

Homozygous rare missense variant p.Gly697Arg in collagen type XXVII alpha 1 (COL27A1) results in Steel syndrome (STLS, MIM #615155). This mutation arose as a founder mutation in Puerto Rican population. Steel syndrome is a rare osteochondrodysplasia characterized by short stature, congenital bilateral hip dysplasia, carpal coalitions, and scoliosis. To determine the pathogenicity and functional effect of the p.Gly697Arg variant, we developed a mouse model with the mutation at orthologous location (Gly682) in the murine Col27a1 gene. Embryonic and post-natal phenotyping of these mice revealed skeletal abnormalities similar to those observed in Steel Syndrome individuals including dwarfism, kyphosis, scoliosis, and a rounded skull shape. Significant post-natal lethality before day 7 was observed in homozygous knock-in mice. Analysis of E18.5 embryos reveal cranio-facial abnormalities and poorly developed alveolar space in lungs. Characterization of the phenotype revealed it is likely the result of abnormal collagen deposition in the extracellular matrix leading to the disorganization of the proliferative zone of the growth plate in long bones. Heterozygous mice were viable and did not display any gross skeletal abnormalities. Our study delineates the important role of Col27a1 in growth plate organization for endochondral bone formation during skeletal development.

Disclosures: **Kalyan Nannuru, Regeneron Pharmaceuticals Inc, Other Financial or Material Support**

MON-0036

Vitamin D and bone turnover markers dynamics during the first year after liver transplantation. Gonzalo Allo Miguel^{1*}, Soledad Librizzi¹, Mercedes Aramendi Ramos², Carlos Jiménez³, Federico Hawkins¹, Guillermo Martínez Díaz-Guerra¹. ¹Endocrinology Service, 12 de Octubre University Hospital, Spain, ²Laboratory Service, 12 de Octubre University Hospital, Spain, ³General Surgery Service, 12 de Octubre University Hospital, Spain

INTRODUCTION: In spite of the substantial morbidity (such as increased risk of fracture and low bone mineral density) caused by impaired bone health among patients after liver transplantation (LT), data on bone metabolism changes are limited. So, the aim of our study is to evaluate the evolution of vitamin D [25(OH)D] and several bone markers during the first year after LT. **METHODS:** 96 patients with LT were included in this study. We used prospectively collected samples for measurements of 25(OH)D and different serum turnover markers: sclerostin (SCL), β -Crosslaps (CTX), osteocalcin (OC) and bone alkaline phosphatase (BAP), at time of transplantation, 3, 6 and 12 months after the procedure. **Statistics:** Data are expressed as mean \pm s.d. for continuous variables. Student's t-test was used to compare 25(OH)D and bone markers levels (from baseline to 12 months). A p-value <0.05 was considered as statistically significant. **RESULTS:** 66:30 (male/female) patients were included in the study. Mean age was 57.3 \pm 10.4 years. At time of transplantation most of the LT recipients showed 25(OH)D deficiency [25(OH)D<20.60.4%]. At the end of the study the number of 25(OH)D deficient patients dropped (45.9%), but deficiency remained a common finding. Bone markers levels at baseline were: SCL:0.77 \pm 0.34ng/ml; CTX:0.57 \pm 0.12ng/ml; OC:17.09 \pm 10.23ng/ml; BAP:34.86 \pm 17.79ng/ml. SCL levels decreased significantly during the study (3rd month: 0.62 \pm 0.22, p<0.001; 6th month 0.60 \pm 0.26, p<0.001; 12th month: 0.56 \pm 0.1, p=0.01). CTX levels increased significantly between measurement at transplantation and 3 (0.69 \pm 0.39 p<0.001) and 6 months (0.63 \pm 0.36 p<0.001), but there was a non-significant decrease after 12 months (0.50 \pm 0.32). OC increased significantly (doubling its value) throughout the study (3rd month: 31.11 \pm 18.1, p<0.001; 6th month: 37.21 \pm 17.08, p<0.001; 12th month: 39.13 \pm 27.9, p<0.001). BAP remained stable after 3 months (33.72 \pm 13.08) compared to baseline, which persisted after 6 months (36.04 \pm 10.30). There were no significant differences in bone markers levels between patients with 25(OH)D deficiency and sufficiency. **CONCLUSIONS:** Our study shows high prevalence of 25(OH)D deficiency before and one year after liver transplantation. Also, our results showed that SCL decreased significantly during the study, which contrasts with the increase of other bone markers (such as OC and CTX). Based on our results, supplementation with vitamin D should be considered in liver transplantation recipients.

Disclosures: Gonzalo Allo Miguel, None

MON-0037

Persistently elevated PTH after parathyroidectomy at one year: experience in a tertiary referral center Marie Caldwell^{1*}, Marshall Clark², Lawrence Kim², Janet Rubin². ¹University of North Carolina Hospitals, United States, ²University of North Carolina, United States

The availability of effective minimally invasive outpatient parathyroid surgery, along with guidelines recommending surgery for patients with bone density T scores \leq -2.5, and data suggesting improved bone quality after surgery, has led to increased parathyroidectomy for treatment of primary hyperparathyroidism (PHPT). Several small reviews have noted that, despite correction of hypercalcemia, 8-43% of patients will have persistently elevated PTH post-surgery. We set out to determine if clinical factors could identify this patient group. We queried a 12 year retrospective cohort who underwent parathyroidectomy at UNC-associated hospitals. We captured age, sex, race, BMI, PTH, calcium, vitamin D, creatinine and urinary calcium prior and up to 15 months post-surgery (Table 1). After excluding patients with creatinine \geq 2, pre-surgical data was available for 411 patients, and 1y (9-15 month) data for 69 patients. Loss of data at 1y reflected our referral base: the pre-surgical characteristics of patients with and without 1y follow up did not differ with respect to age, F/M, calcium, PTH, Ucalcium or vitD. Pre-op calcium averaged 11 with PTH 157 \pm 7 (nl 12-72 pg/mL). In patients with 1y data, 25% had persistently elevated PTH ("1y-highPTH"), despite correction of hypercalcemia, with average PTH 94 \pm 6. Elevated PTH was apparent in the 1y-highPTH group at 6 months post-surgery (95 \pm 8, p<0.001). Post-op calcium levels did not significantly differ between groups at any time. Pre-surgery, PTH in what would become the 1y-highPTH group was significantly higher than in the 1y PTH-normal group (208 vs 129, p<0.0001) and pre-op urinary calcium lower (208 vs 292, p<0.0001). Pre-op calcium, age, sex, and vitamin D were not significantly different. Our experience suggests that, despite success of surgery to normalize calcium, PTH remains elevated in large number of patients. At presentation, this group had higher PTH and lower calcium excretion. The physiology that results in persistently elevated PTH after successful correction of hypercalcemia is not well understood, but may be consistent with a higher calcium set point directing PTH secretion. This retrospective study did not address whether symptom relief was less successful in the PTH high group. Importantly, whether bone quality is equally improved in patients with persistently elevated PTH is unknown; such data will be important to guide recommendations for surgery aimed at improving bone density in PHPT patients.

Table

	Cohort (n= 411)	Lost to f/u at 1y (n=341)	1y-nl PTH (n= 52)	1y-High PTH (n= 17)
Pre-op Calcium	11.09 (\pm 0.03)	11.09 (\pm 0.03)	11.07 (\pm 0.05)	11.0 (\pm 0.12)
Pre-op PTH	156.4 (\pm 7.2)	158.3 (\pm 8.3)	129.2 (\pm 13.6)	207.5 (\pm 30.0)*
Post-op Calcium	9.4 (\pm 0.03)	9.4 (\pm 0.03)	9.5 (\pm 0.05)	9.6 (\pm 0.11)
Post-op PTH 0-6 mon	56.31 (\pm 2.33)	55.64 (\pm 2.65)	48.13 (\pm 4.34)	94.76 (\pm 8.11)*
Post-op Ca 0-6 mon	9.45 (\pm 0.03)	9.41 (\pm 0.03)	9.58 (\pm 0.08)	9.69 (\pm 0.15)
Post-op PTH 9-15 mon	55.21 (\pm 1.64)	N/A	40.25 (\pm 2.18)	93.52 (\pm 5.81)*
Post-op Ca 9-15 mon	9.50 (\pm 0.02)	N/A	9.54 (\pm 0.07)	9.48 (\pm 0.17)
Pre-op 24-hr U _{Ca}	301.3 (\pm 15.3) N = 115	310.3 (\pm 17.4) N = 85	292.4 (\pm 37.9) N = 24	208 (\pm 45.7)* N = 6
Pre-op Vitamin D	29.2 (\pm 1.1) N = 131	28.1 (\pm 1.2) N = 100	33.8 (\pm 2.5) N = 23	29.75 (\pm 7.1) N = 8
Post-op Vitamin D	34.7 (\pm 0.9) N = 185	34.6 (\pm 1.1) N = 138	36.3 (\pm 1.9) N = 38	30.7 (\pm 5.0) N = 9
Age	57 (0.69)	57.5 (0.76)	55.2 (2.02)	60.1 (2.50)
BMI	30.26 (\pm 0.38)	30.63 (\pm 0.43)	28.43 (\pm 0.83)	29.32 (\pm 1.71)
Sex %female	79%	60%	78%	82%

Table. Data from prior to parathyroidectomy until 1 year out from surgery; Ave \pm SEM. * = p<0.0001

Disclosures: Marie Caldwell, None

MON-0038

A Novel Mutation in the Calcium Sensing Receptor Gene in an Italian Family Affected by Autosomal Dominant Hypocalcemia Filomena Cetani^{1*}, Simona Borsari², Federica Saponaro³, Elena Pardi², Chiara Banti², Laura Mazoni², Matteo Apicella², Claudio Marcocci². ¹University Hospital of Pisa, Endocrine Unit 2, Italy, ²Department of Clinical and Experimental Medicine, University of Pisa, Italy, ³Department of Surgical, Medical, Molecular Pathology and Clinical Area, University of Pisa, Italy

The G protein-coupled calcium sensing receptor (CaSR), widely expressed on the surface of parathyroid chief cells and in the kidney, plays a central role in calcium homeostasis. Activating mutations of CaSR gene are responsible for autosomal dominant hypocalcemia (ADH), a rare disorder caused by hypocalcemia, hyperphosphatemia, hypercalciuria and inadequately low concentration of parathyroid hormone (PTH). In this study, we report a family affected by ADH. The proband, a 26 year-old Italian woman, was referred to our Department in 2011 for a mild asymptomatic hypocalcemia detected in 2009 during routine blood tests. Biochemical evaluation confirmed a mild hypocalcemia (mean value: 8 \pm 0.26 mg/dl, normal range: 8.6-10.2), normal serum PTH (mean value 22 \pm 5.57 pg/ml, normal range 8-40) and relative 24h urinary calcium excretion (mean value: 171 \pm 30.3 mg/24h, normal range: <250). Instrumental evaluation excluded intracranial calcifications, kidney stones and nephrocalcinosis. Serum calcium of first-degree relatives showed hypocalcemia in her father (8.1 mg/dl) and brother (8.2 mg/dl), and normocalcemia in her mother (9.6 mg/dl). Genomic DNA of the proband and her family members was isolated from peripheral blood leukocytes and the entire coding region and exon-intron boundaries of the CaSR gene were directly sequenced. Mutational analysis revealed a novel heterozygous variant of the CaSR gene in the proband, leading to the substitution of serine to proline at codon 591 in exon 7 (S591P), localized in the CaSR extracellular domain where >85% of activating mutations occurs. All affected relatives carried the same alteration that was absent in her mother and in 100 chromosomes of unrelated healthy subjects. In silico tests, using Mutation Taster software that integrates data from different databases, predicted a probably deleterious effect of the detected variant. In conclusion, we identified a novel missense variant in the CaSR gene co-segregating with hypocalcemia.

Disclosures: Filomena Cetani, None

MON-0039

Burden of Illness Among Patients With Chronic Hypoparathyroidism Not Adequately Controlled With Standard Therapy by Self-Perception Heide Siggekkow^{1*}, Bart L. Clarke², Helen Dahl-Hansen³, Elizabeth Glenister⁴, Davneet Judge⁵, Nawal Bent-Ennakhlil⁵, Katie Gibson⁵, John Germak⁶, Kristina Chen⁷, Claudio Marelli⁶, Jens Bollerslev⁸. ¹Department of Gastroenterology and Endocrinology, University of Göttingen, Germany, ²Mayo Clinic Division of Endocrinology, Diabetes, Metabolism, and Nutrition, United States, ³Nordic hypoPARA Organisation, Norway, ⁴Hypopara UK, United Kingdom, ⁵Adelphi Real-World, United Kingdom, ⁶Shire International GmbH, Switzerland, ⁷Shire Human Genetic Therapies, Inc., United States, ⁸Section of Specialized Endocrinology, Oslo University Hospital, Norway

Significant knowledge gaps exist regarding the humanistic effects of chronic hypoparathyroidism (HPT). We provide interim results from a global survey conducted to characterize the burden associated with chronic HPT from the patient perspective. An anonymous, self-reported survey was conducted in patients with chronic HPT, not adequately controlled with standard therapy by self-perception, from 12 countries through physicians or patient

associations. Symptoms and impact of HPT were assessed via HPT Symptom Diary, a disease-specific, patient-reported outcome tool that recorded severity of symptoms experienced in the last 7 days. Health-related quality of life (HRQoL) was evaluated by the SF-36 v2 and EQ-5D-5L. Patient demographics and clinical characteristics were also captured. Of 226 patients (mean age, 51.6 years; 77% women; mean time since diagnosis, 7.8 years; surgery as main cause of HPT, 81%), 94% had persistent symptoms despite treatment and 63% were told by a physician that their calcium levels were poorly controlled. Most patients received oral calcium (77%) and/or activated vitamin D (74%). Self-perceived overall symptom severity was reported as mild, moderate, or severe in 56 (25%), 138 (61%), and 30 (13%) patients, respectively. Per symptom diary, 98% of patients reported physical fatigue (symptom severity: mild, 22%; moderate, 42%; severe, 26%; very severe, 9%), 90% reported muscle cramps (symptom severity: mild, 31%; moderate, 42%; severe, 13%; very severe, 4%), and 90% reported heaviness in limbs (symptom severity: mild, 24%; moderate, 46%; severe, 16%; very severe, 4%). An impact on daily life, rated as 'somewhat' or 'very much', was reported by 89% of patients for ability to exercise, 85% for sleep, 80% for ability to work, and 72% for family relationships. The correlation of higher symptom severity level and inferior HRQoL status was observed. Mean SF-36 summary scores were 44.3/36.6/28.2 (physical component summary) and 44.4/33.9/31.4 (mental health component summary) for patients reporting mild/moderate/severe HPT symptoms, respectively. Mean EQ-5D scores were 0.8/0.7/0.3 for patients reporting mild/moderate/severe HPT symptoms [n=132]. Findings from this analysis demonstrated a spectrum of symptom severity within a cohort of patients self-reporting inadequately-controlled HPT on standard therapy. The magnitude of patient-reported symptom severity appeared to correlate with extent of impact on daily life and reduction in HRQoL.

Disclosures: Heide Siggelkow, Shire, Consultant, Shire, Speakers' Bureau

MON-0041

Adults With Hypophosphatasia Enrolled in the Global HPP Registry Have Delayed Diagnosis and Systemic Manifestations of the Disease

Lothar Seefried*¹, Wolfgang Högl², Hugo Gomes Da Silva³, Anna Petryk³, Shona Fang³, Agnes Linglart⁴, Keiichi Ozono⁴, Cheryl Rockman-Greenberg⁵, Craig Langman⁶, Priya Kishnani⁷. ¹Orthopaedic Clinic King-Ludwig-Haus, University of Würzburg, Germany, ²Department of Endocrinology and Diabetes, Birmingham Children's Hospital, and Institute of Metabolism and Systems Research, University of Birmingham, United Kingdom, ³Alexion Pharmaceuticals, Inc., United States, ⁴APHP, Bicêtre Paris-Sud, University Paris Saclay, France, ⁵University of Manitoba, Rady Faculty of Health Sciences, Max Rady College of Medicine, and Children's Hospital Research Institute of Manitoba, Canada, ⁶Feinberg School of Medicine, Northwestern University, and Lurie Children's Hospital of Chicago, United States, ⁷Department of Pediatrics, Duke University Medical Center, United States

Purpose: Hypophosphatasia (HPP), a rare, inherited, systemic disease caused by mutation(s) within the ALPL gene, resulting in low activity of tissue-nonspecific alkaline phosphatase (ALP), has a poorly understood natural history in adults. Asfotase alfa, an enzyme replacement therapy, has been approved for treatment of patients with pediatric-onset HPP. The HPP Registry is collecting real world data on the epidemiology and clinical course of HPP in patients of all ages, regardless of treatment status. **Methods:** The HPP Registry is an observational, prospective, multinational study (NCT02306720; EUPAS13514). We report demographics, characteristics, and medical history of adults (age ≥18 y) at enrollment in the Registry. Patients included in this analysis had low serum ALP activity and/or ALPL mutation(s). **Results:** Of the 269 patients with pediatric- or adult-onset HPP from 11 countries who were enrolled in the Registry from January 2015 through September 2017, 148 were adults. Median (min, max) age of the adults at enrollment was 51.4 (18.5, 78.9) years; most adults were female (73.0%) and white (90.0%). Age at earliest HPP manifestation was 37.6 (0.2, 75.2) years, whereas age at diagnosis was 47.5 (0.2, 75.2) years, representing ~10-year delay in diagnosis. Common (>10%) HPP-related disease history included rheumatic symptoms (83.9%); pain: 74.5%), skeletal symptoms (48.2%); recurrent and poorly healing fractures: 36.5%), orthopedic procedures and therapies (44.6%), muscular symptoms (37.2%); muscle weakness: 30.7%), premature loss of deciduous teeth (24.8%), renal symptoms (16.1%); kidney stones: 5.1%) and neurologic symptoms (11.7%); seizures: 8.8%). Bone-related medication histories included bisphosphonates (17.6%) and/or parathyroid (PTH) hormone analog (13.5%). At enrollment, 26 (17.6%) adults were receiving asfotase alfa. Of the treated adults, all had pediatric-onset HPP; 11 were previously asfotase alfa clinical study participants. **Conclusion:** The delay in diagnosing HPP in symptomatic adults was substantial. Medical histories highlight the systemic nature of HPP in this population. The data also show that mostly ineffective therapies (PTH) or those currently considered inappropriate (bisphosphonates) were prescribed to patients with HPP. At present, the small proportion of adults receiving treatment with asfotase alfa may reflect differences in availability of asfotase alfa in various countries.

Disclosures: Lothar Seefried, Alexion Pharmaceuticals, Inc., Grant/Research Support, Alexion Pharmaceuticals, Inc., Other Financial or Material Support

MON-0042

Value of periostin and tartrate-resistant acid phosphatase 5b as biochemical markers of activity in Paget's disease of bone

Nuria Guanabens*¹, Xavier Filella², Silvia Ruiz-Gaspa³, Helena Florez¹, Arantxa Conesa⁴, Pilar Peris¹, Ana Monegal¹, Ferran Torres⁵. ¹Metabolic Bone Diseases Unit, Hospital Clinic, IDIBAPS, CIBERehd, University of Barcelona, Spain, ²Biochemistry and Molecular Genetics Department, Hospital Clinic, Spain, ³Hospital Clinic, CIBERehd, Spain, ⁴Rheumatology Department, Hospital General Universitario, Spain, ⁵Biostatistics and Data Management Platform, Hospital Clinic, IDIBAPS, Spain

Periostin is a matricellular protein with a preferential location in cortical bone and periosteal tissue, and tartrate-resistant acid phosphatase 5b (TRAP5b) is a marker of osteoclast numbers. In Paget's disease of bone (PDB) there is increased cortical thickening, periosteal apposition and increased osteoclast numbers. **Aim:** To analyse if circulating periostin is a biomarker for PDB and if it is associated with disease activity, as well as whether TRAP5b is useful in the assessment of PDB. **Patients and Methods:** We recruited 41 patients with PDB (13F/28M; 71.1±11.8 yrs). 70.7% had active disease, defined as total alkaline phosphatase higher than the upper normal range. Blood and urine samples were taken between 8:00 and 10:00 am after an overnight fast. Periostin and TRAP5b were measured in serum using commercial ELISA assays (Biomedica and IDS, respectively). Serum PINP, CTX, bone ALP and urinary NTX were measured. Reference values for periostin and TRAP5b were obtained from 38 healthy subjects. **Results:** Serum periostin did not differ between patients and controls (966±210 vs 992±175 pmol/L, p=0.553), between patients with and without active disease (967±171 vs 1052±176 pmol/L, p=0.160), involvement or not of long bones (1022±146 vs 952±204 pmol/L, p=0.209), monostotic or polyostotic disease (990±982 vs 988±143 pmol/L, p=0.897) and previous bisphosphonate treatment (964±199 vs 1007±163 pmol/L, p=0.471). There were no significant correlations between periostin and any of the assessed bone turnover markers, except for TRAP5b (r=0.312, p=0.047). TRAP5b was significantly higher in patients than in controls (4.41±1.77 vs 3.24±0.95 U/L, p=0.0005), significantly correlated with PINP, CTX, bone ALP and NTX, and showed a high predictive capacity for PDB (ROC:0.715 [95%CI:0.600-0.829]), particularly when combined with age and gender (ROC:0.919 [95%CI 0.858-0.979]). **Conclusions:** Serum periostin is not useful for assessing Paget's disease. By contrast, TRAP5b may be a useful marker in Paget's disease assessment.

Disclosures: Nuria Guanabens, None

MON-0043

A Highly Sensitive Fluorescence Immunoassay for the Biomarker NOGGIN FluoBolt™: A New Tool for Bone Research

Gerhard Hawa*¹, Linda Sonnleitner¹, Albert Missbichler. FIANOSTICS GmbH, Austria

Objective: NOGGIN is a potent inhibitor of bone morphogenetic proteins and involved in bone/cartilage regeneration, limb development and fracture repair (1,2). We developed a fluorescence immunoassay for this molecule by using a new technology based on plasmonic microtiter plates (3) that allows quantification of NOGGIN with prior unprecedented sensitivity and reliability. The assay has been proven useful in monitoring Denosumab therapy in patients with thalassemic osteoporosis (4). We hereby present a thorough analytical validation and reference values in a blood donor cohort. **Methods:** Microtiter plates, capable of metal enhanced fluorescence (MEF-MTPs) were coated with anti-NOGGIN capture antibody and blocked of unspecific binding o.n. at room temperature. 25µl of anti-NOGGIN antibody labeled with AlexaFluor 680 together with 20µl of human serum samples were incubated over night in the dark. Signals were read using a standard fluorescence microplate reader. **Results:** The detection limit of this MEF-FIA for NOGGIN (0 pM + 3xSD) was determined as 1,0 pmol/l. Intra- and inter-assay CVs (n=12) ranged from 2-5% and 3-7% respectively. Average recovery in human serum samples (n=4) was 87% (79-108%) and linearity of dilution was 104% (93-114%). Comparison of sensitivity with commercially available ELISA systems for NOGGIN revealed a 2 orders of magnitude higher sensitivity of the MEF-FIA. Titration experiments with BMP-2, -4 and -7 proved that the assay is highly specific for free, biological active circulating human NOGGIN. Analysis of NOGGIN in 100 serum samples of randomly selected blood donors (aged 18-60 years) showed no differences in sex and no dependency on age. **Conclusion:** We successfully demonstrated superior performance of our new MEF-MTP assay platform (FluoBolt™) to conventional NOGGIN-ELISA. It is fully compatible to standard fluorescence microplate reader technology, works with all fluorescence labels and will become a valuable new tool for bone research. (1) "Noggin", Krause C, Guzman A, Knaus P. Int J Biochem Cell Biol. 2011 Apr;43(4):478-81. (2) "Noggin suppression enhances in vitro osteogenesis and accelerates in vivo bone formation" Wan DC, et al. J Biol Chem. 2007 Sep 7;282(36): 2.(3) "Single step, direct fluorescence immunoassays based on metal enhanced fluorescence (MEF-FIA) applicable as micro plate-, array-, multiplexing- or point of care-format" Hawa G. et al. Analytical Biochemistry (549) May 2018, Pages 39-44(4) "Denosumab Effects on Serum Levels of the Bone Morphogenic Proteins Antagonist NOGGIN in Patients with Beta-thalassemia Major and Osteoporosis" Voskaridou E. et al, submitted to the annual meeting 2018 of the European Hematology Association

Disclosures: Gerhard Hawa, None

MON-0044

Evaluation of a Radiophosphorus Method for Intestinal Phosphorus Absorption Assessment in Humans Kathleen M. Hill Gallant^{*1}, Mun Sun Choi¹, Elizabeth R. Stremke¹, George P. McCabe¹, Munro Peacock², Meryl E. Wastney³. ¹Purdue University, United States, ²Indiana University School of Medicine, United States, ³Purdue University, New Zealand

Phosphorus(P) absorption is understudied in humans because methods applicable for clinical studies have not been promoted. Our aim was to test a radiophosphorus absorption test that can be used in studies in healthy subjects (HS) and patients with chronic kidney disease (CKD). 33P clearance from IV injection was obtained in 14 HS and 10 CKD patients from published studies (Farrington, 1981). Four HS (19-29y, 1 male, 3 females, all non-Hispanic white) underwent 2 oral 33P absorption tests with different stable P loads separated by ≥ 1 week. Ten μ Ci 33P was given in 4oz juice containing a P carrier load of 50 or 100 mg in crossover randomized order. Twelve serial blood draws occurred pre-dose through 24-hours post-dose. All urine was collected over 24-hours with specified collection end times. Subjects stayed on the research unit until 6-hours post-dose, then returned the next day for a 24-hour post-dose blood draw & urine collection. 33P activity in serum and urine was analyzed by liquid scintillation counting, serum P was measured by a Cobas Mira analyzer, and urine P was determined by inductively-coupled plasma spectrophotometry. 33P blood and urine curves were analysed by compartmental modelling with WinSAAM software. Fractional absorption was calculated from the 24-hour period and compared with 4-hours. Additionally, a comparison was made between fractional absorption calculated using IV tracer clearance data from HS and CKD subjects to determine the effects of reduced renal function on absorption estimates. A repeated-measures ANOVA model was used to compare mean differences using SAS 9.3, and significance set at $\alpha=0.05$. No statistically significant difference in fractional absorption was observed between carrier loads of 50 mg and 100 mg (mean \pm SE:0.68 \pm 0.02,0.69 \pm 0.02, $p=0.82$). There was no significant difference observed in fractional absorption calculated from the full 24-hours of data versus only 4 hours (0.68 \pm 0.01,0.67 \pm 0.01, $p=0.59$). However, calculating fractional absorption from CKD patient IV data resulted in significantly lower values than HS IV data (0.31 \pm 0.04,0.68 \pm 0.04, $p<0.0001$). We conclude that an oral 33P dose with 50 or 100 mg P carrier load and 4 hours sampling post-dose are sufficient for measuring fractional P absorption in HS. The significant difference in estimated absorption using IV data from HS versus CKD indicates that IV clearance of a tracer should be directly measured in subjects with known or suspected reduced kidney function.

Disclosures: *Kathleen M. Hill Gallant, Chugai Pharmaceutical, Grant/Research Support*

MON-0045

The Design and Results of a Phase 1 TransCon PTH Trial in Healthy Volunteers David B. Karpf^{*1}, Susanne Pihl², Eva Mortensen¹, Kennett Sprogøe², Jonathan A. Leff¹. ¹Ascendis Pharma Inc., United States, ²Ascendis Pharma A/S, Denmark

Background: Hypoparathyroidism (HP), a condition of parathyroid hormone (PTH) deficiency, leads to abnormal calcium and phosphate metabolism. Standard of care (SOC), ie, large amounts of calcium and active vitamin D, causes hypercalciuria and increased calcium x phosphate product. Daily Natpara [PTH(1-84)] injections reduce calcium and active vitamin D doses but not 24-hour urinary calcium (uCa) excretion or incidence of hypo- and hypercalcemia, likely due to its 3-hour half-life (Natpara label). NIH studies of PTH(1-34) in patients with HP have shown that a single subcutaneous (SC) injection is superior to SOC, twice daily injections are superior to once daily, and continuous SC infusion normalizes serum calcium (sCa), serum phosphate (sP), and uCa. Ascendis Pharma is developing TransCon PTH, a sustained-release prodrug of PTH(1-34), for the treatment of HP. In its pro-drug form, PTH is transiently bound to the TransCon carrier via a TransCon linker. Through autocleavage at physiological temperature and pH, unmodified PTH is released, providing free PTH at steady state with an infusion-like profile in the physiological range over 24 hours. Methods: This phase 1, randomized, placebo-controlled, single and multiple ascending dose (SAD and MAD) trial evaluated safety, tolerability, pharmacodynamics (PD), and pharmacokinetics (PK) of TransCon PTH in up to 130 healthy adults. Cohorts consisted of 10 subjects (8 active, 2 placebo) who received 7 SAD (3.5, 12, 32, 48, 72, 100, and 124 μ g) or 6 MAD (3.5, 7.0, 12, 16, 20, and 24 μ g) for 10 days. The primary PD endpoints included sCa, uCa, sP, bone turnover markers, and PTH(1-84). The primary PK endpoint was free PTH. Results: TransCon PTH was generally well tolerated. The PK showed dose-dependent increases in exposure, with T_{1/2} of ~60 hours. Single injections up to 124 μ g showed dose-dependent increases in albumin-adjusted sCa sustained for ≥ 72 hours associated with reductions in PTH(1-84) but without change in urinary fractional excretion of Ca (FE_{Ca}) and no evidence of anabolic activity with metabolic doses. The trial is ongoing; 7 SAD cohorts and 6 MAD cohorts, including relevant phase 3 doses, will be presented. Conclusion: TransCon PTH is being developed for HP as a once-daily SC injection. Interim data supports an infusion-like PTH profile, with a PTH T_{1/2} of ~60 hours and sustained increases in sCa without change in FE_{Ca} or anabolic activity, potentially addressing limitations of available HP therapies.

Disclosures: *David B. Karpf, Ascendis Pharma, Other Financial or Material Support*

MON-0046

Does Cerebral Vascular Stiffness Contribute to Altered Cognition in Primary Hyperparathyroidism? Minghao Liu^{*1}, Yunling Gazes¹, Ivelisse Colon¹, Mariana Bucovsky¹, Kevin Slane¹, John Williams¹, Randolph Marshall¹, Ronald Laker², James Lee¹, Jennifer H. Kuo¹, Shonni Silverberg¹, Marcella Walker¹. ¹Columbia University Medical Center, United States, ²University of Alabama at Birmingham, United States

We have reported cognitive changes in primary hyperparathyroidism (PHPT) that improved with parathyroidectomy (PTX) as well as an association between PTH and vascular stiffness. We hypothesized that PTH-dependent vascular stiffness impairs cerebral blood flow and cognition in PHPT. We compared cognition, vasomotor reactivity (VMR) by transcranial Doppler and neural activation by functional magnetic resonance imaging (fMRI) in postmenopausal women with hypercalcemic PHPT (calcium 10.7 \pm 0.5mg/dL, PTH 87 \pm 43pg/mL, n=28), normocalcemic PHPT (Ca 9.5 \pm 0.4mg/dL, PTH 120 \pm 43pg/mL, n=7), and non-PHPT ctrls (n=6). Women with PHPT having PTX were re-tested 6-mos post-PTX (n=21). VMR in PHPT was normal and not different from normocalcemic or non-PHPT controls (4.0 \pm 2.1 vs. 5.1 \pm 3.1 vs. 3.5 \pm 3.3% mmHgPCO₂, $p=0.09$). VMR did not correlate with calcium or PTH. Depressive symptoms, verbal/visual memory, fluency, attention, and motor skills were normal and did not differ by group. VMR did not correlate with cognition. On fMRI, neural activation was lower during pattern recognition (k=152, $p<0.005$) only in the cerebellum in PHPT vs. non-PHPT ctrls (n=18). During verbal memory tasks, greater activation in the left precentral gyrus and insula correlated with higher PTH ($r=0.72$) while activation in the bilateral anterior cingulate gyrus ($r=0.71$) and left insula ($r=0.69$) correlated with higher calcium (all $p\leq 0.0005$). Post-PTX, 2 verbal fluency tests and motor skills improved (Z-score change 0.31-0.55; all $p<0.05$), but verbal recognition worsened. Depressive symptoms improved by 45% ($p=0.007$). There was no change in VMR ($p=0.53$). Post-PTX, activation during verbal memory tasks declined in some brain regions where activation correlated with higher calcium and PTH pre-PTX: the insula and cingulate gyrus (k=745 voxels, $p<0.005$). There was also a decrease in activation in other brain regions associated with language, motor skills and attention (all k>100 voxels, $p<0.005$). In summary, in PHPT, cognition and vascular function were normal and not associated with one another. Cortical activation correlated with biochemical severity of PHPT. Mood and some aspects of cognition improved after PTX while neural activation in areas associated with language, motor control, and attention decreased. Further work is needed to determine if post-PTX cognitive improvement and activation changes are due to cure of PHPT, learning and/or an improvement in mood.

Disclosures: *Minghao Liu, None*

MON-0047

A microRNA approach to diagnosing renal osteodystrophy Thomas Nickolas^{*1}, Neal Chen², Donald McMahon¹, David Dempster³, Hua Zhou³, Sharon Moe². ¹Columbia University, United States, ²Indiana University, United States, ³Helen Hayes Hospital Regional Bone Center, United States

Background: A main impediment to the diagnosis and management of renal osteodystrophy (ROD) is the non-invasive identification of underlying bone turnover-type (low, normal or high). Bone biopsy, the gold standard method to diagnose ROD turnover-type is painful, invasive, expensive and not widely available in clinical practice, and the non-invasive biomarkers in current clinical use provide only mild to moderate diagnostic accuracy. We hypothesized that four circulating microRNAs (miRs) that regulate osteoblast (miR-30b, 30c, 125b) and osteoclast development (miR-155) would provide superior discrimination of low turnover from normal or high turnover than the biomarkers that are currently used for ROD diagnosis and management. Methods: In twenty-four patients with chronic kidney disease (CKD) Stages 3-5D, we obtained tetracycline double-labeled transiliac crest bone biopsy and measured levels of the current ROD biomarkers, parathyroid hormone (PTH) and bone specific alkaline phosphatase (BSAP), and circulating levels of miR-30b, 30c, 125b and 155. Spearman correlations assessed relationships between miRs and dynamic parameters of histomorphometry and PTH and BSAP. Low, normal and high turnover ROD were based on local reference ranges for bone formation rate/bone surface (BFR/BS) and adjusted apposition rate from quantitative histomorphometry. Diagnostic test characteristics for discriminating low or high turnover were determined by receiver operator curve analysis; areas under curve (AUC) were compared by χ^2 -test. Results: Circulating levels of miRs moderately correlated with BFR/BS and adjusted apposition rate at the endo- and intra-cortical envelopes (p 0.43-0.51; $p<0.05$). The AUCs and 95% confidence intervals for discrimination of ROD turnover-type for miRs, PTH and BSAP are in Table 1. miRs and BSAP but not PTH discriminated low versus non-low turnover ROD: AUCs 0.875, 0.825, 0.800 and 0.767 for miR-30b, 30c, 125b and 155 respectively, and 0.781 for BSAP. For all four miRs combined, the AUC was 0.983, which was superior to that of BSAP alone ($p < 0.05$). BSAP and all four miRs combined but neither the individual miRs nor PTH discriminated high versus non-high turnover. Conclusions: These data suggest that circulating miRs provide accurate non-invasive identification of bone turnover. Future work will discover and validate additional miR biomarkers of both high and low turnover and determine their impact on clinical decision making and outcomes.

Table 1: Area under the curve (AUC): Parathyroid Hormone (PTH), Bone Specific Alkaline Phosphatase (BSAP) and miRNAs for the diagnosis of turnover

	Low vs. Non-Low		High vs. Non-High	
	AUC	95% CI	AUC	95% CI
PTH	0.476	0.209-0.763	0.593	0.294-0.921
BSAP	0.781	0.571-0.991	0.956	0.862-1.000
miR-30b	0.875	0.733-1.000	0.650	0.408-0.892
miR-30c	0.825	0.645-1.000	0.608	0.362-0.856
miR-125b	0.800	0.613-0.987	0.658	0.369-0.951
miR-155	0.767	0.559-0.974	0.558	0.310-0.807
miR Panel	0.943	0.944-1.000	0.800	0.576-1.000

Disclosures: **Thomas Nickolas, None**

MON-0048

Incidence of fracture in Kidney Transplantation: A population-based Healthcare administrative study Aboubacar Sidibé¹, Sonia Jean², Philippe Gamache³, Lynne Moore⁴, Fabrice Mac-Way⁵. ¹Chu de Québec-Université Laval, Institut National de Santé Publique de Québec, Canada, ²Université Laval, Institut National de Santé de Publique, Canada, ³Université Laval, Institut National de Santé Publique de Québec, Canada, ⁴Chu de Québec-Université Laval Research center, Enfant-Jésus Hospital, Traumatology Axis, Canada, ⁵Chu de Québec-Université Laval, Hotel-Dieu de Québec Hospital, Canada

Administrative databases have been widely used to assess fracture risk in kidney transplant (KT). In the province of Quebec (Canada), there is a knowledge gap on whether fracture risk for KT patients is different from the general population. We therefore aimed to derive and validate a case definition for the identification of KT patients in physician claims database and measure the incidence of fracture in this population. Methods: Multiple algorithms combining diagnostic (ICD), surgical, hospitalization follow-up or immunotherapy billing codes related to KT were applied in physician claims database to identify all new cases of adult patients from 1996 to 2015. Algorithms were validated against the hospital discharge database. We linked cases identified in the hospital discharged database to those identified by the algorithms, using a unique identifier, and estimated sensitivity (Sen), specificity (Spe), positive (PPV) and negative predictive value (NPV) to assess the accuracy of each algorithm. Incidence of all first fracture after KT were identified with a validated algorithm and compared to a control group composed of adult Quebec patients, hospitalized in the same period and hospital, with similar age and sex (matching 3 controls /case) and to the Quebec general adult population of the same period, using a Poisson regression model (SAS Enterprise Guide 7.1). Results: Twelve algorithms were derived. The validity of each algorithm is presented in Table 1. Sen ranged from 51.74% to 99.49%. Spe and NPV were close to 100% for all algorithms. PPV ranged from 37.66% to 90.91%. Based on Sen and PPV, algorithm 4 and 7 are the most accurate with Sen at 98.92 and 95.28, and PPV at 86.53% and 90.91%, respectively. Incidence of first fracture was 15.78% in 5,407 KT patients, 12.69% in 14,723 controls and 8.70% in 8,514,424 Quebec adults. Using algorithm 7, the risk of all fractures and hip fractures were significantly higher in KT patients as compared to the control group (RR: 1.24 (95% CI: 1.15 to 1.34) and 2.60 (95% CI: 1.93, 3.50) respectively) and to general population (RR: 1.79 (95% CI: 1.69, 1.91) and 1.46 (95% CI: 1.18, 1.80)). Conclusion: Our results demonstrate that algorithms using physician-claims database are accurate and reliable for identifying new cases of KT. Fracture risk in KT patients is higher than that observed in general population or in matched control group. Further studies should address some modifiable factors to reduce fracture risk in KT.

Table 1: Definition and Validation of Case definition of kidney transplantation in Physician-Claim database

N	Case Definition of algorithm	Medical service Billing or diagnosis Codes	Sen	Spe	PPV	NPV	Pre	Res
1	IP with a billing code for kidney transplantation	I-(06221 or 06222 or 06223)	93.85	100	98.23	100	✓	
2	IP with a billing code for diagnostic, therapeutic act before and after kidney transplantation, or IP with a billing code for immunosuppressive therapy	B-(00699 or 00771 or 00773 or 00774 or 00775 or 00776 or 09489)	91.09	100	87.85	100	✓	
3	IP with ICD-9 or ICD-10 diagnostic code for kidney transplantation	III-(5320 or 5340)	51.74	100	37.66	100	✓	†
4	Algorithm 1 or algorithm 2	IV-(1 or II)	98.92	100	86.53	100	✓	†
5	Algorithm 1 or IP with ICD-9 or ICD-10 diagnostic code for kidney transplantation	V-(I or II)	95.58	100	68.41	100	✓	†
6	Algorithm 2 or IP with ICD-9 or ICD-10 diagnostic code for kidney transplantation	VI-(I or II)	94.56	100	66.71	100	✓	†
7	Algorithm 1 or IP with a billing code for hospitalization for kidney transplantation	VII-(I or 1543E)	95.28	100	90.91	100	✓	†
8	Algorithm 2 or IP with a billing code for hospitalization for kidney transplantation	VIII-(I or 1543E)	91.91	100	90.10	100	✓	†
9	Algorithm 4 or IP with a billing code for hospitalization for kidney transplantation	IX-(V or 1543E)	99.20	100	80.42	100	✓	†
10	Algorithm 4 or IP with ICD-9 or ICD-10 diagnostic code for kidney transplantation	X-(V or II)	99.69	100	67.57	100	✓	†
11	Algorithm 4 or IP with ICD-9 diagnostic code for kidney transplantation and a billing code for hospitalization for kidney transplantation	XI-(V or III and 1543E)	99.16	100	84.41	100	✓	†
12	Algorithm 4 or IP with ICD-9 diagnostic code for kidney transplantation and a billing code for hospitalization for kidney transplantation or for visit during the first year post transplantation	XII-(V or III and 1543E)	99.16	100	83.44	100	✓	†

Cases in the gold standard database (Hospital Discharge) were identified using information codes related to KT (ICD-9: ICD-9 code 570 or ICD-10 codes U0A52X, U0A53X, U0A54X). N: Number of Algorithms, P: Physician class, Sen: Sensitivity, Spe: Specificity, PPV: Positive Predictive Value, NPV: Negative Predictive Value, Pre: Prevalence, Res: Resection.

† A second transplantation is considered if physician class codes separated by at least 361 days. † Only the first diagnostic code is considered. † Only the first code for hospitalization for kidney transplantation is considered.

Disclosures: **Aboubacar Sidibé, None**

MON-0049

TBK1 expression and activity in OCL lineage cells generates a pagetic-like bone disease in mice Quanhong Sun¹, Peng Zhang², Juraj Adamik², Mark A. Subler³, Noriyoshi Kurihara⁴, Laëtitia Michou⁵, Jacques P. Brown⁵, G. David Roodman^{4,6}, Philip E Auron⁷, David W. Dempster^{8,9}, Jolene J. Windle³, Kostas Verdellis¹⁰, Hua Zhou⁸, Deborah L. Galsou¹. ¹Department of Medicine, Hematology-Oncology Division, University of Pittsburgh, UPMC Hillman Cancer Center, Pittsburgh, PA, United States, ²Department of Medicine, Hem-Onc Division, UPCI, University of Pittsburgh, United States, ³Department of Human and Molecular Genetics, Virginia Commonwealth University, Richmond, VA, United States, ⁴Department of Medicine, Hem-Onc Division, Indiana University, Indianapolis, IN, United States, ⁵Department of Medicine, Laval University, CHU de Quebec Research Center and Department of Rheumatology, CHU de Quebec, Quebec City, Canada, ⁶Veterans Administration Medical Center, Indianapolis, IN, United States, ⁷Department of Biological Sciences, Duquesne University, Pittsburgh, PA, United States, ⁸Regional Bone Center, Helen Hayes Hospital, Route 9W, West Haverstraw, NY 10993, United States, ⁹Department of Pathology, College of Physician and Surgeons, Columbia University, New York, NY 10993, United States, ¹⁰The Center for Craniofacial Regeneration, University of Pittsburgh, Pittsburgh, PA, United States

Paget's disease of bone (PDB) is a very common late-onset metabolic bone disease affecting 1 million Americans. Measles virus nucleocapsid protein (MVNP) expression in osteoclast (OCL) precursors contributes to the development of abnormally active OCL in Paget's disease in concert with aberrant excess woven bone formation. In addition, MVNP expression targeted to OCL in transgenic mice induces pagetic-like lesions in vivo and OCL with a pagetic phenotype in vitro. We reported that MVNP activation of TBK1, an IKK family member, plays a critical role in mediating the effects of MVNP on OCL differentiation. Further, MVNP expression up-regulated TBK1 protein in BMM. Importantly, over-expression of TBK1 in BMM by lentiviral transduction generated pagetic-like OCL. Therefore, to assess if over-expression of TBK1 was sufficient to phenocopy the effects of MVNP in mice, we generated a new mouse model with TBK1 targeted to the OCL lineage (TgTBK1). Analysis of all three founder lines (F1, F3, F4) compared to WT mice revealed that TgTBK1 BMM form increased OCL numbers with increased nuclei/OCL that were capable of resorbing bone at significantly higher rates (resorbing a greater pit area/OCL), had elevated Taf12 and Atf7, decreased Sirt1, and produced more IL-6 mRNA. Thus, indicating that the BMM isolated from TgTBK1 mice generated pagetic OCL in vitro. The TgTBK1-F4 bones had both increased OCL surface, and increased MS/BS and BFR (MAR trended up) when compared to WT at both 10 and 16 month. These led to a decrease in the trabecular number along with increased trabecular width at 10 month in TgTBK1 vs WT. These data indicate that increased expression and activity of TBK1 in OCL-lineage cells is sufficient to generate both increased OCL formation and increased bone formation characteristic of PDB. No lesions were found in the 4-month TgTBK1-F4 or WT mice. A combination of microCT and histologic analyses of vertebrae identified 2 pagetic bone lesions in 10-month TgTBK1-F4 mice (n=17), but none were found in 10-month WT mice (n=16). Similar analysis identified 3 pagetic lesions in 16-month TgTBK1-F4 mice (n=17) and in 2 pagetic lesions in 16-month WT mice (n=14). Thus, overall, vertebral pagetic lesions were found in 15% of TgTBK1-F4 mice and 7% of WT mice. Together these data indicate that increased TBK1 expression and activity in OCL lineage cells generates a pagetic-like bone disease in mice, with both increased osteoclast activity and increased bone formation.

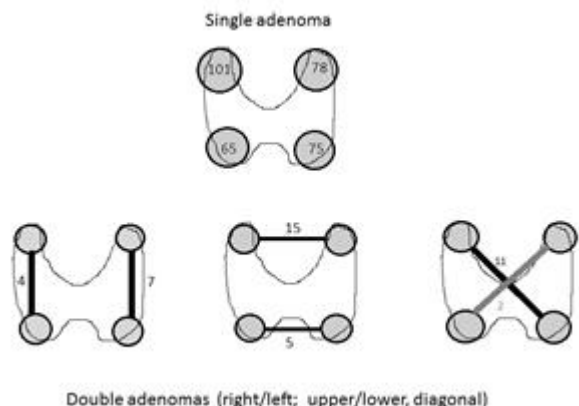
Disclosures: **Quanhong Sun, None**

MON-0050

Anatomic distribution of single and multiple parathyroid adenomas in primary hyperparathyroidism Gaia Tabacco¹, Randy Yeh², Donovan Tay Yu-Kwang¹, Laurent Dercle², Jennifer Kuo³, Leonardo Bandeira¹, Catherine Mcmanus⁴, James Lee³, John Bilezikian¹. ¹Department of Medicine, Division of Endocrinology, College of Physicians & Surgeons, Columbia University, United States, ²Department of Radiology Columbia University, New York, United States, ³Department of Surgery GI/Endo, Columbia University, United States, ⁴Columbia University, United States

Primary hyperparathyroidism is caused by a single adenoma in more than 85% of the cases. The remaining cases are due to double adenomas, hyperplasia and, rarely, parathyroid carcinoma. Adenomas occur in every parathyroid gland. In this study, a retrospective review of 400 consecutive patients with primary hyperparathyroidism (PHPT), we evaluated the anatomic distribution of parathyroid adenomas. All subjects underwent surgery and met Miami Criteria for post-operative reduction in PTH (intra-operative PTH levels falling by 50% or more in comparison to the higher of 2 pre-excision values). The reference standard for correct localization was the location of the gland(s) based on surgical reports, with pathological confirmation of resected glands as parathyroid adenoma or hyperplasia. 363 (90.7% of the total) had a pathological diagnosis of adenoma, the subject of this report. Of the patients with adenomatous disease, 319 (87.9%) had a single adenoma and 44 had double adenomas (12.1%). The distribution of single adenoma showed that LUQ and LLQ locations occurred with equivalent frequency (n=78 and n=75, respectively). RUQ location of a single adenoma was significantly more frequent (n=101, p=0.004 and the RLQ location of single adenoma

was significantly less frequent (n=65, p=0.031), than expected if equivalent frequency is expected at all sites. Double adenomas were more frequent in the upper quadrants (n=15 p=0.004). The right (n=4), left (n=7), lower (n=5) and diagonal RU-LL (n=11) and RL-LU (n=2) double adenomas showed similar distribution. Furthermore, also in the double adenomas, RUQ localization for 1 of the 2 glands was significantly more frequent (n=30, p=0.02) and RLQ localization was significantly less frequent (n=11, p=0.001). This study demonstrates that single and double adenomas are more frequent in the right upper quadrant and less frequent in the right lower quadrant. Furthermore, double adenomas showed a preferential distribution in upper quadrants (fourth pouch origin). Double adenomas most likely affect both sides of the neck, thus suggesting that when removal of a single adenoma does not lead to successful lowering of the PTH level, a contralateral adenoma is more likely than an ipsilateral one. These results may also be helpful in planning for surgery of patients who are suspected of multiglandular, adenomatous PHPT.



Disclosures: Gaia Tabacco, None

MON-0051

Estrogen Decreases Bone Turnover and Increases Bone Mineral Density in Transwomen: a Prospective Study Mariska Vlot*, Chantal Wiepjes, Annemieke Heijboer, Martin Den Heijer. VU University Medical Center, Netherlands

Purpose: Sex steroids play a key role in bone turnover, bone remodeling and preserving bone mineral density (BMD). Gender-affirming hormonal treatment (HT) therefore affects bone metabolism in transgender people. Yet, studies looking into the effect of HT on bone turnover are scarce. As a result, the aim of this study is to investigate the changes in bone turnover markers (BTMs) and BMD in transgender people during the first year of HT. Methods: This prospective cohort study was conducted in HT-naïve adult transgender people. Sclerostin, the bone resorption marker CTX and bone formation markers PINP and total alkaline phosphatase (ALP) were measured. A DXA scan was performed of lumbar spine (LS) and total hip (TH). BTMs and DXA scans were evaluated at baseline and after 1 year of HT. All analyses were performed separately for transwomen and transmen and stratified for age and sex steroid concentrations. Changes were described as mean percentage changes with corresponding 95% confidence interval (CI). Correlations were calculated between changes in BMD and BTMs. Results: 121 transwomen (median age 30 years, IQR 24-41) and 132 transmen (median age 24 years, IQR 21-33) were included. In transwomen, CTX, sclerostin and ALP decreased with 11% (95% CI -18 ; -4.0), 8% (95% CI -13 ; -4) and 19% (95% CI -21 ; -16) after 1 year of HT. PINP did not change. In contrast, in transmen PINP, ALP and sclerostin increased with 33% (95% CI 24 ; 42), 16% (95% CI 12 ; 20) and 15% (95% CI 10 ; 20) after 1 year of HT. CTX did not change. Furthermore, regarding age, transmen in the highest quartile (age 50 years or older) showed a decrease of all BTMs in contrast to the other quartiles, while this age difference was not seen in transwomen. Regarding BMD, the LS BMD increased with 3.9% (95% CI 3.1 ; 4.6) and TH with 1.0% (0.5 ; 1.5) in transwomen respectively, whereas in transmen an increase of LS BMD of 1.0% (0.4 ; 1.7) and 0.9% (0.4 ; 1.4) was seen after 1 year of HT. Conclusion: One year of HT resulted in decreased bone turnover in transwomen and an increased bone turnover in transmen. BMD LS and TH increased after 1 year of HT in both transwomen and transmen. This study supports previous data that estrogen plays a major role in preserving BMD, most likely due to inhibition of osteoclast activity during 1 year of HT.

Disclosures: Mariska Vlot, None

MON-0052

WITHDRAWN

MON-0091

Regional Analysis of Cortical Bone Using Second-generation High-resolution Peripheral Quantitative Computed Tomography (HR-pQCT) Sanchita Agarwal*, Fernando R Rosete, Ivelisse Colon, Mariana Bucovsky, Kyle K Nishiyama, Elizabeth Shane. Division of Endocrinology, Department of Medicine, Columbia University, United States

HR-pQCT permits 3D measurement of bone density and microstructure and can be combined with finite element (FE) analysis to estimate bone strength. The advent of 2nd-generation HR-pQCT, with its isotropic voxel size of 61 µm and direct measurements of cortical (Ct) and trabecular (Tb) compartments, has stimulated interest in studying Ct bone parameters. Conventional global analysis of the entire cortex obscures regional variation in the cortical structure, which may be important in assessing some clinical conditions and effects of therapeutic interventions. We assessed variation in Ct measurements (porosity, density, thickness) by regional analysis of the Ct compartment. Healthy adults (N=30, 20F/10M, age 42±15) were scanned at standard distal and contiguous proximal sites. After segmenting and analyzing the whole cortex for global measurements, it was divided into 6 regions: anterior (A), posterior (P), medial (M), lateral (L), endosteal (En), and periosteal (Pe); each region was analyzed separately. Regional were compared to global measurements by repeated measures ANOVA (RMANOVA) and Tukey's post-hoc test (Table). At the distal radius (RAD), Ct porosity (Ct.Po) is markedly lower (-78%) in Region A but does not appear to affect Ct.vBMD. It is highest (+32%) in Region M, with larger pore diameter (Ct.Po.Dm) and lower Ct.vBMD (-3%). Ct thickness (Ct.Th) is highest in Region P (+8%) and lowest in Region L. At the proximal RAD, differences are concentrated in Region A with markedly fewer (-90%) and smaller (-17%) pores, lower Ct.Th (-18%) and density (-4%). At the distal tibia (TIB), differences are also concentrated in Region A with fewer (-53%) and smaller (-19%) pores, lower Ct.Th (-12%) but higher density (+3%). At the proximal TIB, only Ct.Th was below global in Regions A and P. At all 4 measurement sites, Ct.Po and Ct.Po.Dm were higher in the En than the Pe Region; density followed the reverse pattern. In summary, we found significant heterogeneity in cortical porosity, pore diameter and thickness, most prominent in the Anterior Regions of the distal and proximal RAD and distal TIB. However, the differences did not consistently affect cortical density. Higher porosity and larger pores in the Endosteal Region likely reflect endocortical trabecularization. Our results resemble prior studies with 1st-generation HR-pQCT. Measuring regional variation could provide more insight into effects of diseases and therapeutic interventions on cortical bone.

Table: Percent difference between global and regional cortical measurements at distal and proximal radius and tibia with *p<0.05, **p<0.01 and ***p<0.001 compared to global.

Parameter	Mean ± SD	Distal Radius					
		Posterior	Anterior	Medial	Lateral	Endosteal	Periosteal
Ct.vBMD	910 ± 59	3***	1	-3*	-1	-2*	2*
Ct.Po	0.51 ± 0.4	11	-78***	32**	-14	32**	-39*
Ct.Po.Dm	0.155 ± 0.029	10**	-5	11**	9*	5	-1
Ct.Th	1.00 ± 0.17	8***	-3	-5	-17***	NA	NA
Ct.TMD	950 ± 45	2***	0	-1	-1	-1	0
Parameter	Mean ± SD	Distal Tibia					
		Posterior	Anterior	Medial	Lateral	Endosteal	Periosteal
Ct.vBMD	918 ± 75	-3***	3***	-1	0	-3*	3**
Ct.Po	2.09 ± 1.2	17	-53**	8	6	28*	-34
Ct.Po.Dm	0.228 ± 0.039	-4	-19***	-4	6	-1	1**
Ct.Th	1.53 ± 0.28	-9*	-12***	-5	9*	NA	NA
Ct.TMD	965 ± 58	-3***	2**	1	0	-1	1
Parameter	Mean ± SD	Proximal Radius					
		Posterior	Anterior	Medial	Lateral	Endosteal	Periosteal
Ct.vBMD	1030 ± 46	1*	-4***	0	1	-2***	2***
Ct.Po	1.20 ± 0.5	3	-90***	15	9	65**	-158*
Ct.Po.Dm	0.170 ± 0.033	-1	-17*	4	-3	2	-36***
Ct.Th	1.61 ± 0.20	4	-18**	2	-10***	NA	NA
Ct.TMD	1048 ± 37	2**	-4***	1	1	-1***	1*
Parameter	Mean ± SD	Proximal Tibia					
		Posterior	Anterior	Medial	Lateral	Endosteal	Periosteal
Ct.vBMD	980 ± 57	-1	1	0	-1	-4***	4***
Ct.Po	1.43 ± 0.9	-10	-4	19	-4	42***	-58*
Ct.Po.Dm	0.218 ± 0.042	-10	-4	2	-1	9	-29**
Ct.Th	2.02 ± 0.39	-12***	-8*	4	2	NA	NA
Ct.TMD	1011 ± 45	-1	1*	1**	-1***	-2***	2***

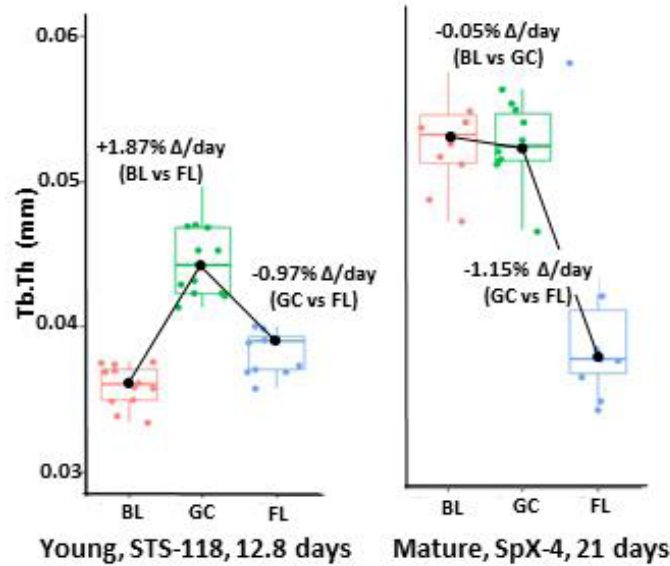
Disclosures: Sanchita Agarwal, None

MON-0092

Microgravity exposure diminishes trabecular microarchitecture and cortical bone structure differently in growing and skeletally mature mice Jennifer C. Coulombe¹, Eric W. Livingston², Alicia M. Ortega¹, Ted A. Bateman², Eric A. Vance³, Louis S. Stodieck⁴, Virginia L. Ferguson¹.

¹Department of Mechanical Engineering, University of Colorado, Boulder CO, United States, ²Department of Biomedical Engineering, University of North Carolina, Chapel Hill, NC, United States, ³Department of Applied Mathematics, University of Colorado, Boulder CO, United States, ⁴BioServe Space Technologies, University of Colorado, Boulder, CO, United States

Microgravity causes extreme disuse and disrupts the rates of bone formation and resorption. Yet, the differential influence of microgravity and skeletal growth on net bone mass is not known, and outcomes vary greatly with animal age and flight duration. Here, we compare bone microarchitectural alterations in growing and skeletally mature mice following microgravity exposure. Female C57Bl/6 flight mice (FL) aged 9 (Young) and 32 wks (Mature) were flown on STS-118 (Space Shuttle; n = 12/group) and SpaceX-4 (SpX-4, International Space Station; 10/group) missions for 12.8 and 21 days, respectively. Equal group sizes were assigned to baseline (BL; at day 0) and ground controls (GC; at 12.8 and 21 days). Cortical and trabecular bone at the proximal tibia were evaluated using microcomputed tomography (μ CT; 10 μ m; Scanco μ CT80). SpX-4 μ CT outcomes were pooled from wild-type and MURF-1 knockouts showing no differences between genotypes. One-way ANOVA and Tukey's HSD evaluated for age and flight differences. To compare across missions data are presented as growth rates (comparing BL vs. GC or FL) by determining the % change, for each parameter per study day (%/day). Significance is reported for p<0.01. In Young mice, growth (BL vs. GC) was marked by increasing Tb.BV/TV (+4.01%/day) and Tb.Th (+1.87%/day), with no change in Tb.Sp; microgravity exposure (GC vs. FL) reduced Tb.BV/TV (-2.97%/day), Tb.Th (-1.05%/day), and Tb.Sp (+0.88%/day). Similarly, in cortical bone, Ct.Th increased (+2.15%/day) and Ct.Po decreased (-2.26%/day) with growth, whereas microgravity reduced Ct.Th (-0.84%/day) but not Ct.Po. In contrast, Mature mice showed no growth effects vs. BL. However, microgravity exposure reduced Tb.BV/TV (-2.02%/day), Tb.Th (-1.15%/day), and Ct.Th (-0.76%/day), while Ct.Po (+1.29%/day) increased. Highly significant interactions (p<0.001) were found comparing growth rates across missions for age and flight. Young mice exhibited a net +0.73%/day increase for Tb.BV/TV, +0.18% Tb.Th, +0.54% Ct.Po, and +0.02% Ct.Th. vs. Mature mice. Bone loss observed with microgravity exposure (BL vs. FL) in growing mice was dominated by both diminished formation and elevated resorption and through elevated resorption only in Mature mice. Overall, it appears that mature bone may be at greater risk of the deleterious microarchitectural changes from microgravity disuse than growing bone.



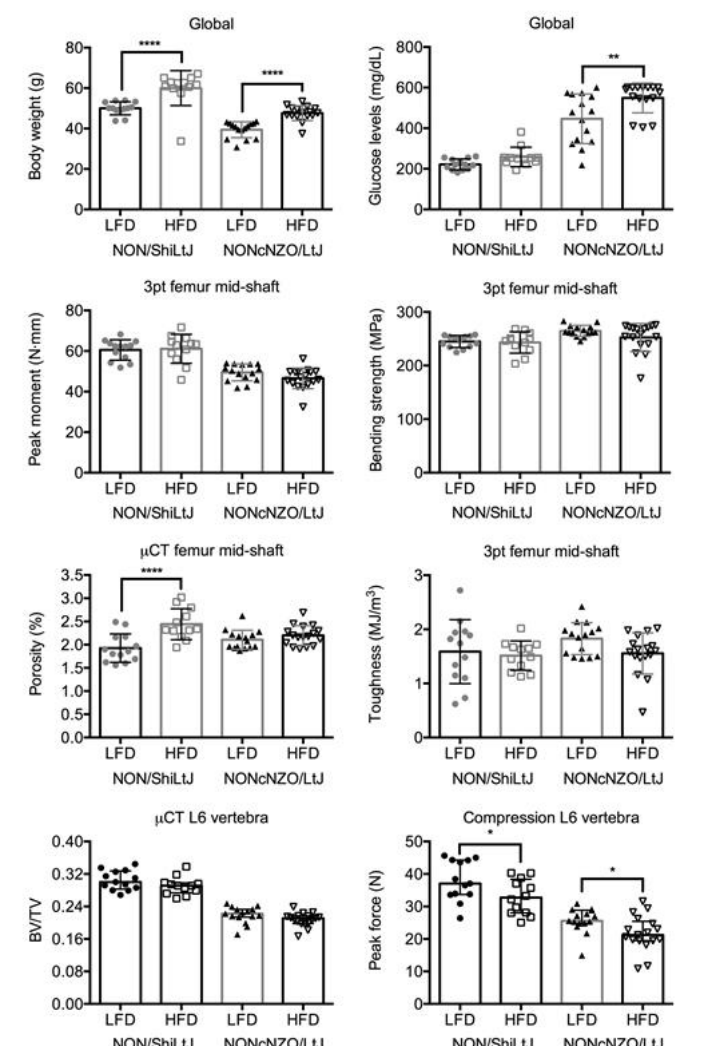
Disclosures: Jennifer C. Coulombe, None

MON-0093

Effect of High Fat Diet on the Fracture Resistance of Bone in Mice with and without Type 2 Diabetes Amy Creecy¹, Sasidhar Uppuganti², Alyssa Merkel², Deanna Bradley¹, Daniel Fernandes¹, Jeffrey Nyman². ¹Vanderbilt University, United States, ²Vanderbilt University Medical Center, United States

Individuals with type 2 diabetes (T2D) have a greater likelihood of suffering a fragility fracture at multiple sites than age-matched individuals without the disease. Obesity is also a risk factor of fragility fractures at certain sites, and a high fat diet (HFD) is thought to negatively affect bone. We hypothesized that HFD independently lowers fracture resis-

tance in both non-diabetic and diabetic adult mice. At 16-wks, male NONcNZO10/LtJ, a new model of T2D, and male NON/ShiLtJ mice, the recommended control, were switched from standard chow to either low fat diet (LFD; 10%kcal from fat) or HFD (45%kcal from fat). Non-fasting blood glucose levels and body mass were monitored weekly and then biweekly after maturity. Except for 11 mice euthanized early (lost body mass) or prematurely died (infection), the left femur and L6 vertebra (VB) were harvested at 37-wks (n \ge 12/group). Following μ CT evaluations of each femur diaphysis (1.8 mm at mid-point) and VB (between endplates) to determine structural/architectural properties and tissue mineral density (TMD), each hydrated femur and VB was loaded-to-failure in three-point bending and in compression, respectively, to assess fracture resistance. Mice on HFD weighed more, irrespective of strain. The HFD significantly increased average blood glucose levels only in the diabetic strain, but HFD did not affect HbA1c at 37-wks (9% for NONcNZO10/LtJ and 5% for NON/ShiLtJ across diets). For the femur, HFD did not affect Imin, peak moment, bending strength, or toughness in either strain (Fig). Neither did HFD affect Ct/Tb.TMD (p=0.222). However, in the control strain, mice on the HFD had a higher cortical porosity. For the VB, HFD did not affect BV/TV in either strain. Interestingly, the peak force of the VB was lower for mice on HFD, suggesting bone quality was affected by diet. There were a number of differences in bone between NONcNZO10/LtJ and NON/ShiLtJ mice indicating that T2D weakens bone, but these mice are not littermate controls making it difficult to ascertain if the effect is strain- or T2D-related. In preliminary studies, many of the same strain-related differences existed at 15-wks (before persistent hyperglycemia). In contrast to prior HFD studies that feed growing mice a HFD, our study investigated the effect of HFD on bone after primary growth. HFD for 21-wks did not cause many changes to cortical bone, even when the mice were diabetic, but it did lower VB strength in non-diabetic and diabetic adult mice.



Disclosures: Amy Creecy, None

MON-0094

Finite Element Modelling based Prediction of Vertebral Bone Strength using Statistical Iterative Reconstruction (SIR) Anitha D.^{*1}, Kai Mei², Felix Kopp², Peter Noel², Thomas Baum³, Subburaj Karupppasamy¹. ¹Singapore University of Technology and Design, Singapore, ²Technical University of Munich, Germany, ³Technical University of Munich, Dominican Republic

Purpose: Regular monitoring of patients with a risk for osteoporotic vertebral fractures is limited due to radiation exposure concerns. Advances in image reconstruction methods beyond the current standard, filtered back projection (FBP), can reduce radiation dose, while maintaining image quality. The goal of this study is to compare FBP and a novel Statistical Iterative Reconstruction (SIR) algorithm to access the clinical feasibility of SIR for assessing bone strength using multidetector computed tomography (MDCT) scans. **Materials and Methods:** Human vertebral specimens (n = 10) were retrieved MDCT imaging at clinical radiation dose, was performed and reconstructed with both FBP and SIR methods. Mechanical testing was performed to obtain experimental failure loads. Apart from image noise, contrast-to-noise ratio (CNR), and signal-to-noise ratio (SNR), bone mineral density (BMD) was also calculated from the images. Finite element (FE) analysis was performed on each specimen and the FE-predicted failure load was obtained. Pearson correlations were reported between experimental failure loads, FE-predicted failure load, and MDCT-based BMD values. Student's t-test was used to analyze differences between the two reconstruction techniques. **Results:** SIR produced significantly lower image noise (30.39 vs. 56.72; p<0.0001), better SNR (5.03 vs. 2.80; p<0.0001), and CNR (5.23 vs. 2.73; p<0.0001) than FBP. Experimentally-determined failure load (Fexp) significantly correlated with FE-predicted failure load derived from FBP (FFBP) (R = 0.89, p=0.0002), and SIR (FSIR) (R = 0.92, p<0.0001). FFBP had a significant correlation with FSIR (R = 0.97, p<0.0001). A statistically significant correlation was also observed between BMDFFBP and BMDSIR (R = 0.98, p<0.0001). **Conclusion:** SIR can produce better quality images, whilst maintaining accuracy in terms of FE analysis. Since FBP has a trade-off in reducing image noise and increasing image quality, SIR could be a better alternative in the clinical scenario. Reduction in radiation doses will go a long way in ensuring regular patient monitoring of skeletal conditions such as osteoporosis.

Disclosures: Anitha D., None

MON-0095

Supervised Machine Learning Techniques for Hip Fracture Prediction from DXA-based 3D Patient-Specific Femur Model Fall Simulations. Sara Guardiola^{*1}, Carlos Ruiz², Jérôme Noailly², Jordi Moretón¹, Silvana Di Gregorio³, Ludovic Humbert⁴, Luis Del Rio³. ¹CETIR Fundació Privada, Spain, ²BCN MedTech, Universitat Pompeu Fabra, Spain, ³CETIR Medical Centre, Spain, ⁴Galgo Medical, Spain

Hip fracture risk prediction can be improved by enhancing anatomical and bone mineral density (BMD) descriptions from DXA with biomechanical information derived through DXA-based 3D modeling methods and patient-specific finite elements (FE) simulations. The variable Major Principal Stress (MPS) is the best descriptor for a robust classification of fracture and non-fracture cases. The objective of this work is to obtain a MPS estimation model and a hip fracture classifier using supervised machine learning techniques trained with estimated biomechanical variables obtained with FE simulation of hip fracture. **Method:** 156 DXA images from osteoporotic patients were collected: 85 fracture and 71 non-fracture cases. Patient-specific FE femur models were created by combining DXA-based 3D modeling method (3D-SHAPER, Galgo Medical) and mesh morphing algorithm. Models included volumetric BMD distribution, translated into element properties and linked to local Young's modulus values. Lateral fall simulations consisted in approaching the femur to a fixed plate. Movement velocity depended on gravity and patient's height. MPS regression models (multiple linear regression, regression tree and support vector machines) were fitted and cross-validated (10 folds). As a measure of comparison of the predictive capacity of the models obtained, the root mean square error (RMSE) was used. Finally, hip fracture/no-fracture predictive classification models (logistic regression, random forest, support vector machines and naïve Bayes) were fitted and cross-validated (10 folds). The area under the curve (AUC) was used to compare the predictive capacity of the models. **Results:** Fall simulations allowed identifying critical regions for fracture risk assessment. ROC-AUC analyses in these regions showed that MPS best discriminated fracture and non-fracture cases. The MPS model with the smallest root mean square error was the multiple linear regression, which also indicates that vBMD, weight and gender are significant and should be included in the regression model (R²=0.79). Finally, a first approach to get a hip fracture predictive classification tool obtained an AUC of 0.80 using a logistic regression. **Conclusion:** Though the sample size was small, results suggested that fracture can be predicted from virtually enhanced DXA 3D data, using biomechanical parameters that can be reasonably estimated using supervised learning techniques, bypassing the need to do simulations in each new patient.

Disclosures: Sara Guardiola, None

MON-0096

Load Sharing of Cancellous and Cortical Bone in Rat Vertebrae Under Uniaxial Compression Determined Using Finite Element Analysis (FEA) Madeleine G. Driver^{*1}, W. Brent Liewers², A. Keith Pilkey¹. ¹Department of Mechanical and Materials Engineering, Queen's University, Canada, ²Bharti School of Engineering, Laurentian University, Canada

Uniaxial testing of rat vertebrae is often performed in drug treatment studies to evaluate the response of healthy versus osteoporotic tissue. However, a recent experimental study by Morton² found that the large vascular apertures in the cortical shell of rat vertebra have a strong influence on the observed failure behaviour, suggesting this model may have limitations. The relative importance of the vertebral cortical shell during loading may be another important difference. The objective of the present study is to use specimen-specific FEA models to investigate the load sharing of cortical versus cancellous bone of healthy and osteoporotic rat L4 vertebral bodies in order to better understand the challenges of extrapolating rat model results to human vertebral behaviour. Morton² examined healthy (SHAM), osteoporotic (OVX) and treated osteoporotic (OVX+E) rat vertebrae (n = 31) under uniaxial compression while synchronously imaged with a micro-CT scanner. For the present study, these same images were converted into 3D finite element models using a voxel-based meshing procedure. The images were also processed using a separation algorithm³ to create another set of FE models, with the trabecular network removed from the vertebral body, to enable loading of just the cortical shell (Fig. 1). Assuming isotropic linear elastic behaviour, the models were subjected to a 2% uniaxial compressive strain. The relative load sharing of the cortical shell was determined as the ratio of cortical shell apparent stiffness to the whole vertebral body apparent stiffness. The cortical shell load contribution across all models (Tab. 1) was 70%, which is higher than the 52% reported for human vertebrae⁴. These mechanical differences are important to consider when extrapolating results from rat studies to humans. A confounding issue is the presence of large vascular apertures in the cortical surface of rat vertebrae; without their presence the proportional load bearing of the cortical shell might be even higher. Future work will study the effect of these vascular apertures on load distribution in the rat vertebral body. **References:** 1. Rhee Y et al. Clin Orthop Surg. 2009;1(1):40. doi:10.4055/cios.2009.1.1.40. 2. Morton, JJ. [MASc Thesis]. Queen's University, 2013.3. Buie HR et al. Bone. 2007;41:505-515. doi:10.1016/j.bone.2007.07.007.4. Eswaran SK et al. Comput Methods Appl Mech Eng. 2007;196:3025-3032. doi:10.1016/j.cma.2006.06.017.

Table 1: Average Relative Cortical Shell Load Contribution for all Models

	N	Average Relative Cortical Load Contribution (%)
SHAM	10	71.0 ± 4.5
OVX	11	68.5 ± 5.6
OVX+E	10	69.9 ± 2.3
Total Average	31	70.0 ± 4.5



Figure 1: Micro-CT Image (left), Processed image with removed cancellous bone (right)

Disclosures: Madeleine G. Driver, None

MON-0097

Voluntary Jumping Exercise in Rats Produces a Greater Anabolic Response in the Forelimbs than the Hindlimbs Jon Elizondo^{*1}, Corinne Metzger², Scott Lenfest¹, Jessica Brezicha¹, Amelia Looper³, Nicholas Igbini², Peter Phan², Susan Bloomfield², Harry Hogan⁴. ¹Department of Mechanical Engineering, Texas A&M University, United States, ²Department of Health & Kinesiology, Texas A&M University, United States, ³College of Veterinary Medicine, Texas A&M University, United States, ⁴Departments of Mechanical Engineering and Biomedical Engineering, Texas A&M University, United States

To better understand exercise's effect on bone, we employed a novel rat jumping model for resistance exercise that uses positive reinforcement instead of negative. The goal of this study is to assess the effect of our jumping protocol on the forelimbs and hindlimbs of adult male rats, as there are apparent differences in loading on each set of limbs: rats jump exclusively with their hindlimbs, resulting in high muscular contractions, while the forelimbs

absorb most of the impact loading of the landing. Over 5 weeks, sucrose pellet rewards were used to condition adult male Sprague Dawley rats (5 mo.) to jump onto and down from a 10" high platform. After training, rats were assigned to ambulatory control (AC, n=10) or exercise (JE, n=10). JE animals performed 30 jumps/d, 5 d/wk, for 4 weeks. Vertical ground reaction forces (GRFs) were measured with a custom force plate and analyzed with a mixed-model ANOVA and Tukey HSD. Peak GRFs were significantly higher than body-weight during both hindlimb jumps (1.6-3.5x BW) and forelimb landings (2.1-3.3x). GRFs were not different between forelimbs and hindlimbs. Ex vivo data collected after 4 weeks of exercise were analyzed with a paired t-test. pQCT scans of the distal femur metaphysis (DFM) and proximal humerus (PH) revealed significantly higher total vBMD in JE compared to AC at the DFM (+10.1%) and the PH (+12.0%). At both sites, the increase was due to higher cortical vBMD with no differences in cancellous vBMD. Histomorphometry at the proximal tibia metaphysis (PTM) and PH demonstrated significantly higher %BV/TV in JE compared to AC at the PTM (+29.5%) and at the PH (+80.3%). Exercise produced significantly higher osteoid surface and lower osteoclast surface at the PTM (+52.8% and -35.7%, resp.) and at the PH (+166% and -56.3%). Bone formation rate was significantly higher in JE compared to AC at the PTM (+36.8%) and PH (+70.5%). These data indicate that our new exercise protocol induces an anabolic bone response in both the hind- and forelimbs. Larger percent differences at the PH suggest the protocol has more pronounced anabolic effects in the forelimbs than hindlimbs. Since mean peak GRFs were not different between sites, other factors, such as differences in load transmission, loading rate, and bone strain distribution characteristics, should be further studied. Better understanding the relationship between loading and bone anabolism could help to focus future exercise interventions for improving bone mass.

Disclosures: *Jon Elizondo, None*

MON-0098

Alterations in Gut Microbiome Secreted Vitamin K are Associated with Impaired Bone Quality Christopher J. Hernandez¹, Jason D. Guss¹, Erik A. Taylor¹, C. Hazel Higgins¹, Eve Donnelly¹, M. Kyla Shea², Sarah L. Booth³, Rodrigo C. Bicañho¹. ¹Cornell University, United States, ²Jean Mayer USDA Human Nutrition Research Center on Aging, Tufts University, United States, ³Jean Mayer USDA Health Nutrition Research Center on Aging, Tufts University, United States

Introduction: Poor bone quality impairs bone strength beyond what can be explained by bone density. Recently we found that altering the gut microbiome in mice can cause impaired bone quality (Fig. 1A), but the mechanism remains unknown. The gut microbiome a major source of vitamin K, a molecule required for the proper function of matrix proteins that influence bone strength². To test the idea that microbiome-derived vitamin K explains the observed effects on bone quality we determined: 1) tissue vitamin K concentrations; 2) changes in the functional capacity of the gut microbiome (metagenomics); and 3) bone tissue quality determined with Raman spectroscopy. Methods: We examined tissue from a prior study¹ (Fig. 1A, n = 7-10/group). C57Bl/6 WT mice and Toll-like receptor 5 deficient mice (TLR5KO, a strain with distinct gut microbiota) were either untreated or exposed to antimicrobials from 4-16 weeks of age to disrupt the gut microbiota (Δ Microbiota). Samples were collected at 16 weeks of age. Shotgun metagenomics was used to determine the functional capacity of the microbiota. Cecal contents and liver and kidney were submitted to biochemical analysis using LC/MS. Raman spectroscopy was used to assess mineral quality (crystallinity, mineral-matrix and carbonate-phosphate ratio) in the tibial cortex. Results: Disruption of the gut microbiota was associated with changes in total vitamin K concentrations, primarily due to changes in microbiome-derived forms of vitamin K (menaquinones MK 5-12, Fig 1B). Disruption of the gut microbiota altered the abundance of microbial genes in both mouse strains, and large changes in the abundance of microbial genes involved in vitamin K synthesis (Fig. 1C). Δ Microbiota also led to changes in mineral crystallinity that mirrored the changes in vitamin K concentrations. Discussion: Vitamin K has long been associated with fracture risk². Vitamin K dependent proteins in bone matrix that influence bone strength include matrix Gla protein, and osteocalcin. Interestingly, alterations in matrix crystallinity like those observed here are present in osteocalcin deficient mice³. Impaired bone quality has been implicated in many patient populations that also have altered gut microbiota (obesity, diabetes, inflammatory bowel disease). Microbiome-derived vitamins may help explain increases in fracture risk not explained by BMD. 1Guss et al J Bone Miner Res 2017;22:1232-1240. 2Gundberg et al. Adv Nutr 2012;3:123-130. 3Boskey et al. Bone 1998.

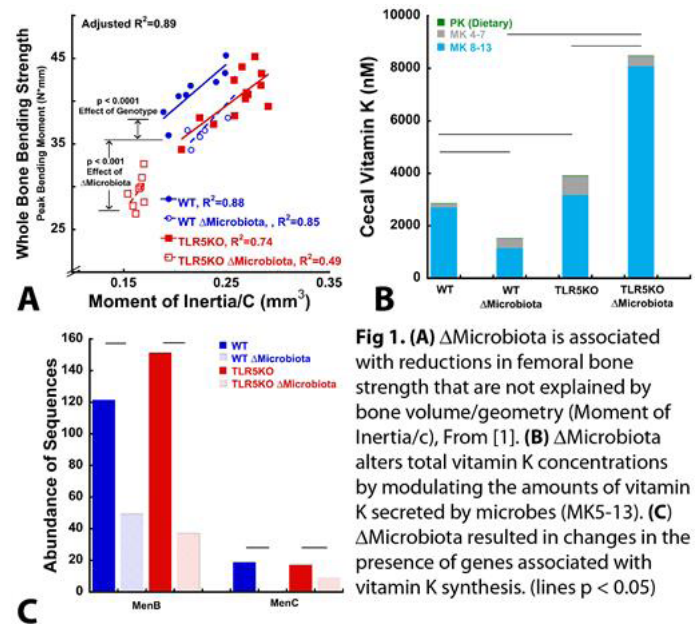


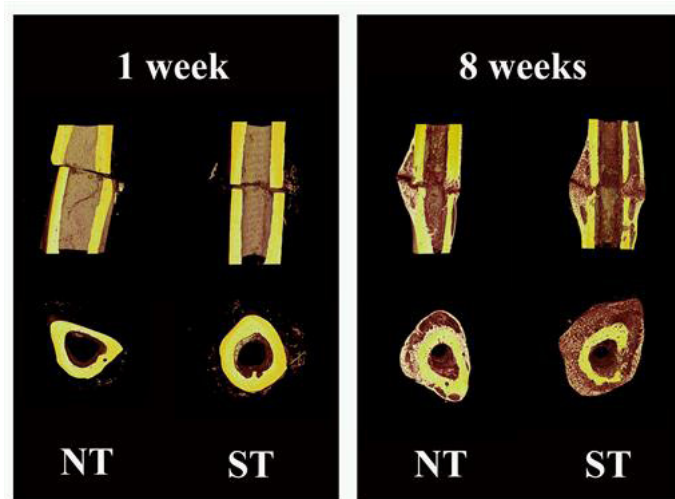
Fig 1. (A) Δ Microbiota is associated with reductions in femoral bone strength that are not explained by bone volume/geometry (Moment of Inertia/c), From [1]. **(B)** Δ Microbiota alters total vitamin K concentrations by modulating the amounts of vitamin K secreted by microbes (MK5-13). **(C)** Δ Microbiota resulted in changes in the presence of genes associated with vitamin K synthesis. (lines p < 0.05)

Disclosures: *Christopher J. Hernandez, None*

MON-0099

Strength training performed prior to fracture improves oxidative profile and fracture healing in aging female rats Melise Jacon Peres Ueno*, Fernanda Fernandes, Amanda Pinatti, Camila Stringheta Garcia, Angela Cristina Nicola, Mário Jefferson Quirino Louzada, Paulo Cesar Ciarlini, Rita Cássia Menegati Dornelles. UNESP, Brazil

Introduction: the incidence of bone fracture is high in the senile population and although there is evidence on the efficacy of physical exercise in improving bone quality, it is not yet clear whether physical exercise performed prior to fracture may improve oxidative stress and accelerate bone repair, especially in peri- or postmenopausal women. Therefore, the present study aimed to analyze the influence of strength training (ST) on oxidative stress and healing fracture in aging female rats during peri-estropause after total tibial osteotomy. Methods: Eighty wistar female rats were distributed in: NT (untrained) and ST (strength training). For a total of 120 days, aging female rats at 18-21 months of age performed ST on a ladder three times per week and the overload used was equivalent to 80% of the maximal strength test. After the experimental period, unilateral total osteotomy was performed on the left tibia in all animals that were euthanized at two experimental times, 1 week and 8 weeks after the osteotomy, to evaluate the response to the initial fracture stage and healing fracture. For this, was evaluated the biochemical and oxidative profile (spectrophotometry) and analysis of soft (1 and 8 weeks) and hard (8 weeks) callus microarchitecture (micro-ct). Anova (two-way) with Tukey's post-test (GraphPad Prism 6.0) were used. Results: The results show that 1 week after the osteotomy, there was a important decrease of malondialdehyde (MDA) in the animals that performed ST. Eight weeks after the osteotomy, ST was able to improve the oxidative profile, increasing the formation of the ferric reducing antioxidant potential (FRAP) and reducing the total oxidizing capacity (TOS), culminating with the action in favor of bone formation, increasing the plasma concentration of alkaline phosphatase. This ST action in the oxidative and biochemical profile resulted in a significant increase in the bone volume of soft and hard callus (BV/TV), trabecular number (Tb.N), decreases of trabecular separation (Tb.Sp) as well the increases of the soft and hard callus resistance shown by the polar moment (MMII polar) compared to those animals that did not perform strength training. Conclusion: According to these results, it can be suggested that strength training performed during the premenopausal phase improves the oxidative profile and interferes in the process of bone callus formation, improving healing fracture and increasing resistance to the bone stresses.

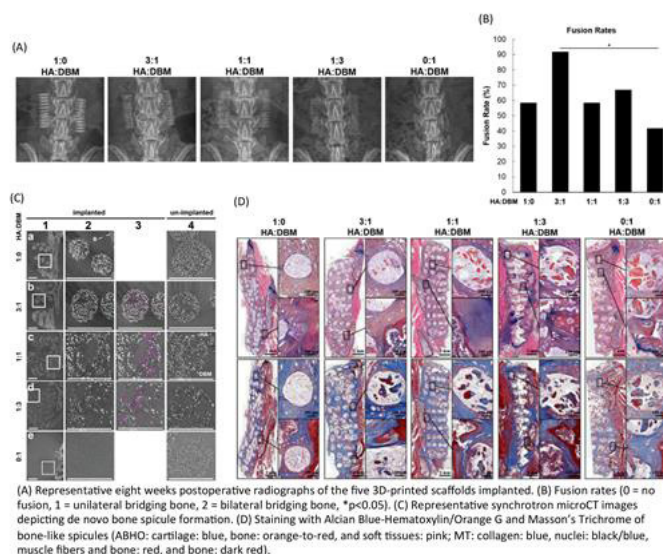


Disclosures: *Melise Jacou Peres Ueno, None*

MON-0100

Composition of Hyperelastic Bone Composite Scaffolds Affects De Novo Bone formation Soyeon Jeong^{*1}, Adam Jakus^{2,3}, Chawon Yun¹, Ryan J. Lubbe¹, Adam Driscoll¹, Meraaj S. Haleem¹, Kevin Y. Chang¹, Wellington K. Hsu¹, Ramille Shah², Stuart R. Stock⁴, Erin L. Hsu¹. ¹Northwestern University Department of Orthopaedic Surgery, United States, ²Northwestern University Department of Materials Science and Engineering, United States, ³Simpson Querrey Institute for BioNanotechnology, United States, ⁴Northwestern University Department of Cell and Molecular Biology, United States

BACKGROUND Bone graft extenders for spine fusion include demineralized bone matrix (DBM) and ceramic-based products, but their efficacy is insufficient to qualify them as bona fide bone graft substitutes (BGS). We previously developed a novel 3D-printed composite scaffold containing synthetic hydroxyapatite particles (HA), osteoinductive DBM particles, and a poly lactic-co-glycolic acid (PLGA) binder to create hyperelastic "bone" composites (HBC). The current study evaluated the ability of various iterations of these HBC scaffolds to promote bone regeneration and spine fusion in a rat posterolateral spine fusion (PLF) model. **METHODS** Sixty female Sprague-Dawley rats underwent PLF at the L4-L5 intertransverse space utilizing HBC scaffolds composed of 30 vol.% PLGA and 70 vol.% particles (N=12/group). For each group, the particle components consisted of the following ratios of HA:DBM: 1:0, 3:1, 1:1, 1:3, and 0:1. Eight weeks postoperatively, spine fusion was evaluated via radiography and manual palpation, and bone formation was assessed using both laboratory and synchrotron microCT imaging. Histology [Alcian blue-Hematoxylin/Orange G (ABHO) and Masson's Trichrome (MT)] was also used to visualize the bone-scaffold interface. **RESULTS** 3:1 HA:DBM HBC scaffolds had the highest fusion rate (92%), although this was only significantly higher than the 0:1 group (42% fusion). The 1:0, 1:1, and 1:3 scaffolds achieved fusion rates of 58%, 58%, and 67%, respectively. De novo spicule formation was only seen in scaffold that had both the HA and the DBM components, while the 1:0 and 0:1 scaffolds elicited none. Staining with ABHO and MT showed evidence of bone where bone-like spicules were seen in synchrotron microCT imaging. **CONCLUSION**—This study evaluated the combination of HA and DBM particles within this novel 3D-printed composite material and its potential to overcome the limitations of currently used BGS in spine fusion procedures. Varying the proportions of HA:DBM within each scaffold resulted in only slight differences in fusion rates. However, microCT showed that de novo bone spicule formation was only present within scaffold struts that contained both HA and DBM particles. This study suggests that 1) the presence of osteoinductive DBM is key to de novo bone formation, and 2) the hydroxyapatite provides the calcium and phosphate necessary to re-mineralize the DBM particles.



(A) Representative eight weeks postoperative radiographs of the five 3D-printed scaffolds implanted. (B) Fusion rates (0 = no fusion, 1 = unilateral bridging bone, 2 = bilateral bridging bone, * $p < 0.05$). (C) Representative synchrotron microCT images depicting de novo bone spicule formation. (D) Staining with Alcian Blue-Hematoxylin/Orange G and Masson's Trichrome of bone-like spicules (ABHO: cartilage: blue, bone: orange-to-red, and soft tissues: pink; MT: collagen: blue, nuclei: black/blue, muscle fibers and bone: red, and bone: dark red).

Disclosures: *Soyeon Jeong, None*

MON-0101

Panx3 is important for tibial morphogenesis during skeletal development and bone homeostasis Xian Jin^{*1}, Xiangguo Che¹, Na-Rae Park¹, Yu-Min Hong¹, Clara Park², Yu-Ra Choi¹, Je-Yong Choi¹. ¹Department of Biochemistry and Cell Biology, Cell and Matrix Research Institute, BK21 Plus KNU Biomedical Convergence Program, Korea Mouse Phenotyping Center, School of Medicine, Kyungpook National University, Daegu, South Korea., Republic of Korea, ²Division of Food and Nutrition Chonnam National University 77 Yongbong-ro, Buk-gu, Gwangju, Korea, Republic of Korea

Although Panxexin 3 (Panx3) has been known as a channel for ATP in chondrocytes, the function of Panx3 in bone formation and mineralization remains poorly understood. We addressed the role of Panx3 during skeletal development using Panx3 knockout (KO) mice. Panx3 KO mice had shorter femurs, tibia curvature defects and delayed endochondral ossification during the embryo stage. Microcomputed tomography (μ CT) analysis resulted in greater femoral bone volume to tissue volume ratio (BV/TV), bone mineral density (BMD) and trabecular number (Tb.N) in Panx3 KO mice compared to wild type (WT) mice at 12 weeks. Lower tibial osteoclast surface to bone surface (Oc.S/BS) was observed in Panx3 KO mice compared to WT mice at 12 weeks through TRAP staining. By quantitative real-time PCR analyses, Panx3 KO mice showed less expression of osteogenic markers such as Runx2, Osterix and Osteocalcin compared with WT mice. Osteoclast differentiation and resorption activity were lower in osteoclasts derived from Panx3 KO than WT when bone marrow monocytes were cultured with M-CSF and RANKL. Collectively, the positive role of Panx3 on both osteoblast and osteoclast differentiation and morphological change during skeletal development suggests that Panx3 may play an important role in bone homeostasis as well as skeletal morphogenesis.

Disclosures: *Xian Jin, None*

MON-0102

Guided Bone Regeneration with rhBMP-2 Improves Bone Quality Surrounding Dental Implants Trenton Johnson^{*1}, Jung-Suk Han², Toru Deguchi¹, Frank Beck¹, Do-Gyoon Kim¹. ¹Ohio State University, United States, ²Seoul National University, Republic of Korea

Guided bone regeneration (GBR) has been used to promote osteogenesis in a bone defect surrounding a dental implant. While bone quantity at the implant interface has been investigated to evaluate stability of the implant system, bone quality is also responsible for determining mechanical response of bone around the implant. The objective of this study is to examine the nanoindentation based elastic modulus (E) and plastic hardness (H) at different bone regions adjacent to titanium dental implants with GBR treated with demineralized bone matrix (DBM) and bone morphogenetic protein (BMP) during different post-implantation periods. Following IACUC approval, six adult male beagle dogs were used to create circumferential defects (Ø6.3 mm x 4 mm) with buccal bone removal at each implantation site of mandibles following 3 months post-extraction healing periods (Fig. 1a). Four titanium dental implants were bilaterally placed in each dog mandible. The implant systems were randomly assigned to only GBR (control), GBR with DBM (DBM), and GBR with DBM+rhBMP-2 (BMP) groups. Three animals were sacrificed at each 4 and 8 weeks of post-implantation healing periods. The bone-implant constructs were buccolingually dissected for nanoindentation. The E and H values were assessed by 980 indentations at the defects (Defect),

interfacial bone tissue adjacent to the implant (Interface), and pre-existing bone tissue away from the implant (Pre-existing) (Fig. 1b). A mixed model ANOVA with the Tukey-Kramer procedure was performed. Pearson's correlation was tested between E and H. Significance was at $p < 0.05$. The E and H values of BMP group had significantly higher than control and DBM groups for interface and defect regions at 4 weeks of post-implantation period and for the defect region at 8 weeks ($p < 0.043$) (Fig. 1c). The DBM group had higher E and H values than control group only for the defect region at 4 weeks ($p < 0.001$). Significant strong positive correlations of H with E were found ($p < 0.001$). The correlation slope of the defect region was significantly steeper than those of other regions ($p < 0.011$) (Fig. 1d). The current results indicate that treatment of rhBMP-2 with GBR accelerates bone tissue mineralization, which enhances bone quality of the defect region during early post-implantation healing and maintain it for longer healing period. The GBR likely facilitate a microenvironment to provide more metabolites with the open space of the defect region adjacent the titanium implant.

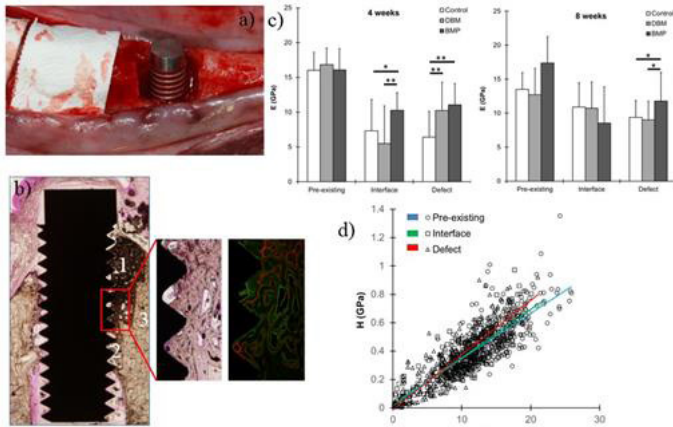


Fig. 1 a) The implant placement procedure for GBR placement, b) effects of treatment on regional variation of E at 4 and 8 weeks of post-implantation periods (*, $p < 0.045$, **, $p < 0.001$), c) representative histological image of the indent locations as 1) defect, 2) interface, and 3) pre-existing bone areas with fluorescence new bone labeling, and d) significantly different correlation slopes of E vs H between areas ($p = 0.01$).

Disclosures: **Trenton Johnson, None**

MON-0103

Morphology of bird bone during egg-laying Leeann Louis*. University of California, Berkeley, United States

Introduction Female birds require a large calcium load to create an eggshell. A typical chicken eggshell requires 2.4 g of calcium, or about 20% of the calcium present in their body. To prepare, birds create a mineralized tissue, medullary bone, inside their bones. We know that medullary bone is used as a calcium resource during egg-laying² and that its formation is initialized by high levels of estrogen³. Here, we explore the relationship between estrogen and whole-bone structure. Methods Avian endosteal cells form medullary bone when androgens and estrogen are present³. Therefore, we created a model of medullary bone formation by implanting adult male zebra finches (*Taeniopygia guttata*) with an empty silastic tube (SH, $n = 4$) or one filled with β -estradiol (ES, $n = 6$). After 3 weeks, we performed micro-computed tomography (μ CT35; Scanco Medical AG) on one humerus per bird. We analyzed the midshaft for cortical bone microarchitecture (Ct), and the proximal humerus for trabecular bone (Tb). We also measured bone mass (Sartorius Research R200D). For each bone parameter, we report the p-value of a Welch's t-test between groups. Results Estrogen-treated males grew medullary bone along endosteal surfaces (see Fig. 1). In the cortex, this treatment did not change total area (CtTtAr $p = 0.784$) or cortical thickness (CtTh $p = 0.821$), but did reduce marrow area (CtMaAr $p = 0.031$). This resulted in a slight increase in polar moment of inertia (pMOI $p = 0.186$) and bone mass (BoneMass $p = 0.474$). In the trabecular region, medullary bone growth increased bone volume fraction (TbBVTV $p < 0.001$) and trabecular number (TbN $p = 0.010$), and increased trabecular thickness (TbTH $p = 0.025$). Discussion Continuous treatment with estrogen resulted in osteogenesis in the male zebra finch. This process reduced marrow area due to encroaching medullary bone, and slightly increased pMOI and bone mass. These findings suggest that medullary bone may improve resistance to torsion and offset the reduction in whole-bone mechanical properties that occurs when a bird mobilizes calcium to lay an egg. Work is underway to use mechanical testing to confirm whether these changes result in whole-bone mechanical effects. References 1. Dumont, E.R., (2010). Proc. R. Soc. B, 277 p2193. 2. Candlish, J.K. & Taylor, T.G., (1970). J. Endocrinol., 48, p143. 3. Miller, S.C. & Bowman, B.M., (1981). Dev. Biol., 87, p52.

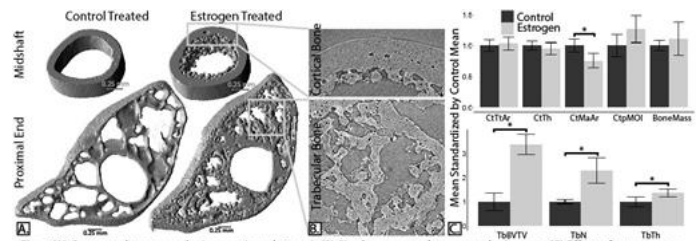


Fig. 1 (A) Computed tomography images (voxel=6 μ m). (B) Single computed tomography images. (C) Effect of estrogen on cortical & trabecular morphology and bone mass. See text for meanings of abbreviations. * = $p < 0.05$ under Welch's t-test.

Disclosures: **Leeann Louis, None**

MON-0104

Influence of Age, Sex, and Anatomical Location on Human Cortical Bone Microarchitecture: A Synchrotron Radiation Micro-CT Study Lindsay Loundagin¹, David Cooper², W. Brent Edwards¹. ¹Human Performance Laboratory, Faculty of Kinesiology, University of Calgary, Canada, ²Department of Anatomy and Cell Biology, College of Medicine, University of Saskatchewan, Canada

Microarchitecture is a function of bone remodeling, which is heavily determined by age, sex, and loading environment. Advanced age has been associated with increased porosity and larger canal sizes (1,2), while the shape and spatial distribution of osteocyte lacunae is thought to reflect local loading conditions (3). Although variations in microarchitecture have been observed, the relative influence of age, sex or loading is unknown. The purpose of this study was to determine the influence of age, sex and anatomical location on microarchitectural parameters. Cadaveric femoral and tibial shafts were obtained from 2 females (71 and 99 years old, $n = 26$) and 1 male (77 years old, $n = 15$). Cylindrical cores were extracted from the cortex of the femur ($n = 28$) and tibia ($n = 13$) and machined into a waisted geometry. A region 2.8x2.25mm was imaged using synchrotron x-ray microCT (BMIT, Canadian Light Source) with a resolution of 1.8 μ m. Within a cylindrical volume of interest (1.77mm³), pores were segmented using hysteresis thresholding, and Fiji software (NIH, Bethesda, MD) was used to quantify porosity, mean canal diameter (Ca.Dm) and osteocyte lacunar density (Ocy.Den). Three univariate ANCOVAs were performed to assess the effect of sex, anatomical location (fixed) and age (covariate) on each microarchitectural parameter ($p \leq 0.05$). Microarchitectural measures are summarized in Table 1. Sex explained 46% ($p \leq 0.001$) of the variation in porosity while 17% was accounted for by age ($p = 0.01$). Ca.Dm was significantly affected by sex ($p = 0.001$, partial $\eta^2 = 0.27$) but not age ($p = 0.36$, partial $\eta^2 = 0.023$). Anatomical location did not affect any parameter, but an interaction between location and sex was observed for Ocy.Den ($p = 0.018$). In females, Ocy.Den was higher in the femur when compared to the tibia, whereas the opposite trend was observed in the male. Although several studies report an age-dependent increase in porosity and canal size, the current results suggest that sex is more influential on these measures than age alone. Despite a 30-year age difference, both females demonstrated a more porous bone with larger canals compared to the male. Assuming Ocy.Den is indicative of the mechanical loading environment, an interaction of sex and location may indicate sex-specific loading conditions. Multiple samples were analyzed from a limited number of subjects, so these findings should be replicated with independent samples from a larger population. 1.Cooper. (2007). Bone. 40: 957-965. 2.Chen. (2010). Osteoporos Int.21: 627-636. 3.Carter. (2013). Bone.52: 126-132.

	Porosity (%)	Ca.Dm (µm)	Ocy.Den (mm ⁻³)
71	11.72 ± 5.44	65.59 ± 26.75	17660.54 ± 2394.50
	3.62 ± 1.07 ^{a,b}	35.37 ± 4.49 ^{a,b}	18604.09 ± 3823.86 ^b
77	7.86 ± 4.42	57.86 ± 26.42	14580.46 ± 3701.64
	3.62 ± 1.07	35.37 ± 4.49	18604.09 ± 3823.86
Female	9.79 ± 5.24 ^c	61.77 ± 26.35 ^c	16170.50 ± 3434.49 ^c
	3.62 ± 1.07	35.37 ± 4.49	18604.09 ± 3823.86
Femur	7.61 ± 5.24	54.60 ± 26.11	16893.14 ± 2859.99
	7.37 ± 5.19	46.65 ± 20.96	17322.03 ± 5289.86
Tibia	7.37 ± 5.19	46.65 ± 20.96	17322.03 ± 5289.86
	7.37 ± 5.19	46.65 ± 20.96	17322.03 ± 5289.86

Disclosures: Lindsay Loundagin, None

MON-0105

Zoledronate and Raloxifene Combination Therapy Enhances Architecture and Mechanical Properties Katherine Powell^{*1}, Joseph Wallace¹, Alexis Pulliam¹, Alycia Berman², Matt Allen³. ¹IUPUI Department of Biomedical Engineering, United States, ²Purdue University Weldon School of Biomedical Engineering, United States, ³IU School of Medicine Department of Anatomy and Cell Biology, United States

Bisphosphonates (BPs) are used to treat osteoporosis and other bone disorders, including Osteogenesis Imperfecta (OI). BPs increase BMD and bone mass in OI, but do not effectively enhance bone quality. Alternatively, Raloxifene (RAL) increases tissue hydration, leading to increased bone toughness with modest changes in BMD. We hypothesized that a combination of RAL and Zoledronate (ZOL) would improve mechanical and material properties of normal and OI bone better than either monotherapy. Heterozygous males from the OI mouse model (Het; n=19) and wildtype littermates (WT; n=22) were treated starting at 8 weeks of age (4-6/group). RAL was given 5x/week in RAL and RAL+ZOL groups (0.5 mg/kg). ZOL and RAL+ZOL groups were treated with 80 µg/kg ZOL at 8 and 12 weeks of age. An untreated control group (CON) was included. Mice were euthanized at 16 weeks. Right femurs were scanned by micro-CT (10 µm resolution) and cancellous and cortical regions were analyzed. Bones underwent 3-point bending to obtain mechanical properties. One Way ANOVA with posthoc Dunnett's tests statistically analyzed effects of treatment versus control in each genotype. WT cancellous properties were enhanced in all treatment groups. Tissue mineral density (TMD) increased with RAL (+6.6%, p=0.037) and RAL+ZOL (+13.2%, p<0.001) versus CON. Bone volume fraction (BV/TV) dramatically increased by 178% with ZOL and 191% with RAL+ZOL compared with CON (both p<0.001). Trabecular thickness (Tb.Th) increased in both RAL (+14.1%, p=0.0485) and ZOL (+8.6%, p=ns) with a greater than additive effect in RAL+ZOL (+36.4%, p<0.0001). In Het, TMD in RAL+ZOL increased (+6.1%, p=0.0058), but RAL and ZOL groups did not change significantly. BV/TV increased 127% with ZOL and 139% with RAL+ZOL (both p<0.001). RAL+ZOL was the only treatment to increase Tb.Th (+16.6%, p=.0058). The only significant effect on cortical geometry was increased cortical thickness in the WT RAL+ZOL group versus CON (+17.3%, p=0.018). Minimal cortical effects confirm that changes in mechanical properties were driven by tissue level quality changes. Ultimate stress trended up with all treatments but only changed significantly in WT RAL+ZOL (+27.8%, p=0.017) and Het RAL (+37.5%, p=.004) when compared to their respective controls. Overall, this study demonstrates compelling changes with the use of combination therapies which both increase bone mass and enhance bone quality.

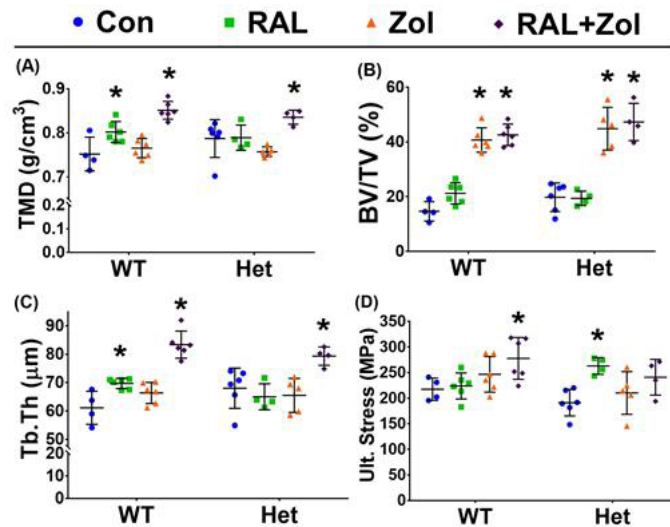


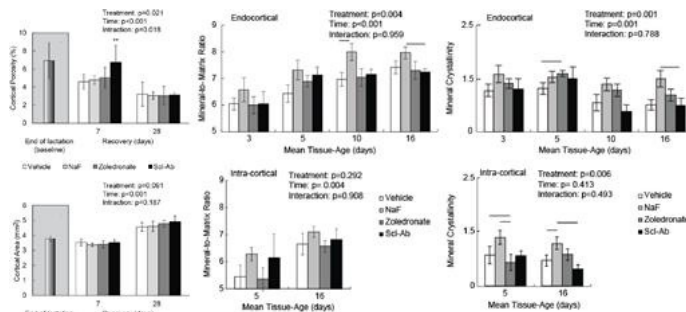
Figure 1: Cancellous architecture in distal femur (A-C) and whole bone strength (D), as bar (mean) and whiskers (standard deviation). * indicates p<0.05 vs. control group within genotype.

Disclosures: Katherine Powell, None

MON-0106

Investigating pharmaceutical-induced alterations to matrix maturation using the lactation during low calcium model. Ryan Ross^{*}, Matthew Meagher, Rick Sumner. Rush University Medical Center, United States

Matrix maturation is a critical, yet oft-neglected component of bone remodeling. Our laboratory has recently demonstrated the utility of a low calcium during lactation model to study bone matrix maturation in cortical bone (1). In the current study we used the model to compare the effects of pharmaceutical agents on matrix maturation independent of their effects on bone remodeling. At parturition (13 weeks of age) 72 female Sprague-Dawley rats were fed a low calcium diet (0.01% Ca) for a 23-day lactation period. At weaning a cohort of 8 animals was sacrificed to establish baseline cortical structure. The remaining animals were fed a normal calcium diet (0.6%) and equally distributed into one of four treatment groups, control (saline weekly), sodium fluoride (NaF, 100 mg/L, drinking water), zoledronic acid (ZA, 1.5 µg/kg weekly), or sclerostin antibody (Scl-Ab, 5 mg/kg weekly). Fluorochrome labels were given to identify bone tissue-age. 8 animals per group were sacrificed at either 7 or 28 days. Cortical geometry and porosity at the distal femoral diaphysis were assessed using micro-computed tomography. Bone matrix composition (mineralization and crystallinity) was assessed at various tissue-ages within the endocortical and intra-cortical compartments using Fourier transform infrared imaging. Treatment and time effects were assessed using two-way analyses of variance. Both cortical area and porosity had significant time effects as all groups recovered lost bone mass by 28 days. There was no treatment effect for cortical area, but was in porosity. The normalization of cortical porosity was slightly delayed in the Scl-Ab group, but all groups showed similar levels by 28 days. Mineralization and crystallinity had significant time effects, consistent with matrix maturation. There was a significant treatment effect for mineralization. NaF treatment increased mineralization at each time point, while Scl-Ab treatment increased mineralization at the early time points compared to controls. Treatment effects were also noted in crystallinity with NaF and ZA treatment increasing crystallinity compared to controls. The results demonstrate the utility of the lactation during low calcium model and could help to identify matrix-related concerns with new osteoporosis treatments, such as those previously seen following NaF. (1) Ross and Sumner. Calcif Tissue Int 2017, 101[2], 193-203. Scl-Ab provided by Amgen Inc, Thousand Oaks, CA and UCB, Brussels, Belgium.



Disclosures: Ryan Ross, None

Monday Posters

MON-0107

Local and Global Microarchitecture Control Different Features of Bone Biomechanics Jean-Paul Roux^{*1}, Stephanie Boutroy¹, Mary L Bouxsein², Roland Chapurlat¹, Julien Wegrzyn^{1,3}. ¹INSERM UMR 1033, Université de Lyon, France, ²Center for Advanced Orthopedics Studies, Harvard Medical School - Beth Israel Deaconess Medical Center, United States, ³Department of Orthopedic Surgery, Pavillon T, Hôpital Edouard Herriot, France

Purpose: Beside aBMD assessment, most previous in-vivo and ex-vivo studies evaluating the fragility fracture risk relied on measurement of whole bone specimen microarchitecture. The trabecular bone, however, is not a uniform network, especially in vertebrae. Therefore, this study aimed to: 1) evaluate local microarchitectural weakness inside the vertebral body, 2) compare the parameters of local weakness to those of global trabecular microarchitecture and 3) demonstrate which features of bone biomechanics the local and global trabecular microarchitecture controlled. Methods: Twenty-one L3 vertebrae were harvested from human donors (76±10 years). Microarchitecture was measured using HR-pQCT (XtremeCT, Scanco) with an 82µm nominal isotropic voxel size. The following global parameters of trabecular microarchitecture were measured: Tb.BV/TV (%), Tb.N (1/mm), Structure Model Index and connectivity density (Conn.D, 1/mm³). The image stack oriented along the cranio-caudal mechanical was extracted from the µCT images using Dataviewer and CTan software (Skyscan) to identify the minimal value of trabecular 2D-Tb.BV/TV for each vertebral body. The “local weakness” was therefore defined as Tb.BV/TV_{min} (Fig1). Uniaxial compression mechanical testing was performed in 3 phases with the initial compression phase until mild vertebral fracture, a 30-minute unloaded period of relaxation, and a second compressive phase until failure. Results: Initial and post fracture mechanics were significantly correlated with bone mass, global and local trabecular microarchitecture (table1). Notably, the correlation between Tb.BV/TV_{min} with initial and post failure load remained significant after adjustment for BMD or global Tb.BV/TV (p=0.014 and 0.038 respectively). The combination of the most pertinent parameters of bone mass, global microarchitecture and local microarchitecture expressed by the equation “mechanical behavior= Tb.BV/TV + ConnD + Tb.BV/TV_{min}” demonstrated that global microarchitecture was most strongly correlated with initial and post-failure stiffnesses, while only local microarchitecture expressed by Tb.BV/TV_{min} explained initial and secondary failure loads. Conclusion: This study evaluated the effect of global and local microarchitecture on the initial and post mechanical testing behavior. The pre- and post-failure stiffnesses were controlled by global microarchitecture while the pre- and post-failure loads were controlled by local microarchitecture.

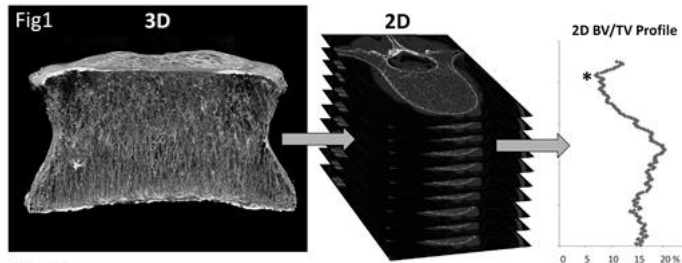


Table 1

	BMD	BV/TV	ConnD	SMI	TbN	BV/TV _{min}
Failure load	0.66***	0.73***	0.70***	-0.81***	0.51*	0.81***
stiffness	0.54*	0.65***	0.69***	-0.66***	0.58***	0.66***
Post failure load	0.72***	0.86***	0.80***	-0.85***	0.67***	0.89***
Post stiffness	0.58**	0.84***	0.86***	-0.78***	0.79***	0.79***

Pearson correlation coefficients * p<0.05; ** p<0.01; *** p<0.001

Disclosures: Jean-Paul Roux, None

MON-0108

BMP-2 Revealed Enhanced Healing in Fractured Mouse Tibia using Micro-CT and Torsion Test Sotcheadt Sim^{*1}, Theresa Farhat², Martin Pellicelli², Martin Garon¹, Eric Quenneville¹, René St-Arnaud². ¹Biomomentum Inc., Canada, ²Shriners Hospital for Children, Canada

The purpose of this study was to investigate the ability of torsion tests to monitor the mechanical properties of fractured mouse tibias after treatment with BMP-2. An intramedullary rodged surgical fracture repair model was performed on 3-month old wild type female C57BL/6 mice. Two groups were defined: a vehicle group receiving water-loaded absorbable collagen sponge (ABS) and a treatment group receiving 10µg of recombinant human BMP-2 (rhBMP-2)-loaded ABS at the fracture site. The healing bones were collected and assessed through micro-CT and torsional testing at day 15 and 21 post-fracture. Tibiae were scanned, and reconstruction was performed to determine callus total volume (TVCallus), callus bone volume (BVCallus) and callus mineralized volume fraction (BV/TVCallus). Subsequently, torsional testing was performed using the mechanical tester Mach-1 model v500et (Biomomentum) with a 70N multi-axial load cell. Specimens were kept hydrated during sample preparation and mounting, then subjected to a torsion test with a loading rate of 5 deg/s. The ultimate torque and torsional stiffness were extracted from the torque-rotational displacement curves. At 15 days post-fracture (Fig.1), mice that received BMP-2 displayed significant higher TVCallus (50±1mm³ vs 23±6mm³;p<0.0001), BVCallus

(9±1mm³ vs 5±1mm³;p<0.0001), ultimate torque (12±3N·mm vs 7±1N·mm;p=0.01) and torsional stiffness (0.5±0.1N·mm/deg vs 0.3±0.1N·mm/deg;p=0.008) than the vehicle group. However, the callus mineralized volume fraction was significantly lower in BMP-2 treated group (17±1% vs 20±1%;p=0.01). At 21 days post-fracture (Fig.1), significant higher TV-Callus (44±7mm³ vs 17±3mm³;p<0.0001) and BVCallus (5±1mm³ vs 3±1mm³;p=0.003) were still observed in the treated group while the mineralized volume fraction (12±1% vs 16±4%;p=0.06), the ultimate torque (11±3N·mm vs 13±3N·mm;p=0.9) and torsional stiffness (0.4±0.1N·mm/deg vs 0.6±0.04N·mm/deg;p=0.17) were similar in both groups. This suggests that mechanical competence of the bone (forces required to disrupt the callus), mechanical strength and elasticity of bone of the callus has been reached faster in the BMP-2 treated group. The present study is a first step toward the establishment of torsion testing as a means of understanding the mechanical behavior of callus tissues and their role in reestablishment of stiffness and strength during the fracture healing of bone.

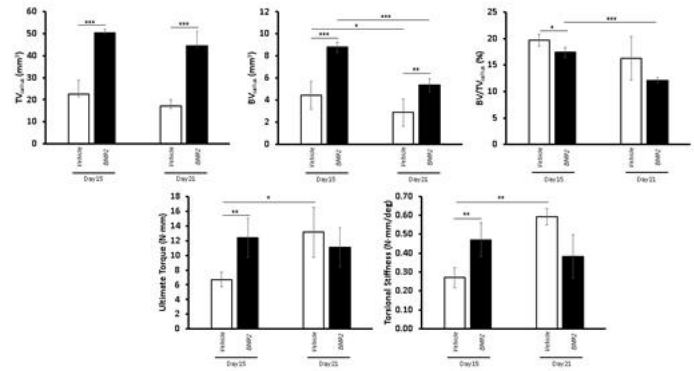


Figure 1. The effects of BMP-2 on bone healing in mouse tibial fracture. Quantification of callus total volume, callus bone volume and callus mineralized volume fraction using micro-CT analysis and ultimate torque and torsional stiffness through torsional testing. Data are expressed as means ± SD. * p≤0.05; ** p≤0.01; *** p≤0.001

Disclosures: Sotcheadt Sim, Biomomentum Inc., Grant/Research Support

MON-0109

Effects of Carboxymethyl-lysine on Bone Matrix Deepak Vashishth^{*}, Grazyna Sroga, Ondrej Nikel. RPI, United States

CML, a non-fluorescent AGE crosslink, is 10-100 times more prevalent than PEN and accumulates in various tissues like skin, intervertebral discs, and arteries with age and diabetes. More CML is present in serum of T2D patients and recently, serum levels of CML were shown to be associated with hip fracture [1]. Here we demonstrate, for the first time, formation of CML in bone and show that, similar to skin, CML is 40-100 times PEN in human bone and is highly correlated to bone toughness [2]. Unlike PEN and fAGES that form intramolecular crosslinks, CML is present as a side chain. Thus, it is likely that through molecular conformational changes CML modifies the collagen I-hydroxyapatite (HA) interface and alters energy dissipation in bone at the level of HA crystal. To this end we developed a technique using the C-13{P-31} rotational echo double resonance (REDOR) NMR pulse sequence that identifies carbon atoms that are spatially close to the phosphorus atoms of the mineral in the collagen-HA interface region by quantifying percent dephasing. Results obtained showed that REDOR dephasing was highly correlated to AGEs in bone (R-square = 0.89). In order to investigate the mechanistic aspects of this correlation, we developed an in vitro technique to form CML in fully mineralized bone and use it to successfully demonstrate the effects of CML on collagen-HA distance in bone. [1] Barzilay et al, JBMR (2015) [2] Thomas et al, Bone (2018)

Disclosures: Deepak Vashishth, None

MON-0127

Comparison of Zoledronate and Pamidronate in Children with Skeletal Disorders: Short Term Safety Experience from a Single Institution Alison M. Boyce^{*1,2}, Andrea Estrada^{2,3}, Marianne Floor², Mirini Kim², Lindsay Weigley², Elizabeth Carlson⁴, Christina Dollar², Austin Gillies², Mary Scott Roberts², Rachel I. Gafni^{1,2}, Laura L. Tosi². ¹Skeletal Disorders and Mineral Homeostasis Section, National Institute of Dental and Craniofacial Research, NIH, United States, ²Bone Health Program, Division of Orthopaedics and Sports Medicine, Children’s National Health System, United States, ³Division of Endocrinology and Diabetes, Children’s National Health System, United States, ⁴Children’s National Health System, United States

Background: Bisphosphonates are frequently used in children with skeletal disorders, however optimal dosing and regimens are unknown. Early treatment focused on pamidro-

nate (PAM), a second-generation formulation, however use of zoledronate (ZOL), a more potent third-generation bisphosphonate, has recently increased due to shorter and less frequent infusions. The objective of this study is to compare short-term safety of ZOL and PAM in a pediatric population. Methods: Retrospective chart review including demographics, indications, and formulations. Adverse events (AEs) for 7 days post-infusion were categorized: 1) Acute phase reactions (APR): fever, bone pain, myalgia, decreased oral intake, and/or fatigue; 2) nausea/vomiting; 3) hypocalcemia (serum calcium <8.5 mg/dL); 4) seizures; 5) respiratory distress; 6) anaphylaxis; 7) emergency department evaluations and hospital admissions. Results: 119 patients (median age 8.6y, range 0.1-23.4) received 782 infusions (46 ZOL, 736 PAM) between June 2007 and August 2017. The most common diagnoses were osteogenesis imperfecta (31%), cerebral palsy (22%), and muscular dystrophy (12%). AEs were more common after ZOL than PAM: 50% vs 23.1% for initial infusions, $p=0.03$; and 18.8% vs 4.5% for subsequent infusions, $p=0.0004$. APRs occurred after 6/46 total ZOL infusions (13.0%) vs 28/736 total PAM infusions (3.8%) ($p=0.003$). Nausea/vomiting occurred after 4/46 ZOL (8.7%) vs 20/736 PAM infusions (2.7%) ($p=0.02$). Hypocalcemia occurred after 5/46 ZOL (10.8%) vs 4/736 PAM infusions (0.5%) ($p<0.0001$), and was managed with oral calcium and calcitriol. An increase over baseline seizure activity was reported after 2/46 ZOL (4.3%) vs 1/736 PAM infusions ($p<0.0001$). Respiratory distress occurred after 0/46 ZOL and 2/736 PAM infusions ($p=0.72$). There were no cases of anaphylaxis. Emergency department evaluations and/or admissions occurred after 2/46 ZOL (4.3%) and 4/736 PAM infusions (0.5%) ($p=0.04$). Conclusions: ZOL treatment is associated with a higher incidence of AE's compared to PAM, consistent with the increased potency of this formulation. While AEs following both ZOL and PAM are common, they are generally mild and treatable. Additional research regarding long-term safety, efficacy, and costs are needed to determine if ZOL's convenience justifies its routine use over PAM.

Disclosures: *Alison M. Boyce, None*

MON-0128

Diagnosis of recurrent fracture in a pediatric cohort Melissa Fisceletti^{*1}, Craig Peter Coorey², Julie Briody², Andrew Biggin², David Little², Aaron Schindler³, Craig Munns². ¹Children's hospital at Westmead, Canada, ²Children's hospital at Westmead, Australia, ³University of Sydney, Australia

Significant fracture history in children is defined as having at least one vertebral fracture, at least 2 fractures by age 10, or at least 3 fractures by age 19. Between September 2011 and December 2014, clinical data were collected on children with a significant fracture history that attended a major Australian children's hospital. Fifty-six patients were identified as having 305 fractures in total, including 44 vertebral fractures. 18% of patients (10/56) were diagnosed with osteogenesis imperfecta (OI) by a bone health expert, molecular testing or both, and they sustained 23% of all fractures (71/305). Analysis of serum bone biochemistry showed all median values to be within a normal range and no clinically significant differences between patients with and without OI. The DXA and pQCT derived bone mineral density (BMD) and bone mineral content (BMC) Z-scores were reduced overall. DXA derived total body and lumbar spine areal BMD-for-age and BMC-for-age Z-scores were significantly lower in children who had vertebral fractures or who were later diagnosed with OI. Similarly, pQCT performed on radii and tibiae showed Z-scores significantly less than zero. In conclusion, this study describes the bone phenotype of children referred to a tertiary hospital clinic for recurrent fractures and highlights a subset of children with previously undiagnosed OI, but a larger cohort without classic OI. Thus it can be clinically challenging to differentiate between children with OI type 1 (mild phenotype) and non-OI children without bone densitometry and genetic testing. We conclude that recurrent fractures in children should prompt a comprehensive bone and systemic health assessment to eliminate an underlying pathology.

Disclosures: *Melissa Fisceletti, None*

MON-0129

Three Patient Kindred with Novel Phenotype of Osteogenesis Imperfecta due to a Mutation in the COL1A1 gene Nidhi Gupta^{*1}, Seth Gregory², David Deyle³, Peter Tebben³. ¹Vanderbilt University Medical Center, United States, ²Mayo Clinic Health System, United States, ³Mayo Clinic, United States

Objective: Osteogenesis Imperfecta (OI) is a heterogeneous disorder characterized primarily by fractures and progressive bone deformities. We report a novel phenotype of a mutation in the COL1A1 gene in three members of a non-consanguineous family of European descent. Methods: Data were collected from the patients' and their medical records. Results: The first affected member (M1) was a 37-year-old female with nine non-traumatic long bone fractures (primarily femoral) before 5 months of age. Prenatal ultrasound findings were unknown. She did not receive bisphosphonate treatment, despite which she suffered no additional non-traumatic fractures. The second affected member (M2) was the son of M1. There was prenatal evidence of bowing of long bones. He sustained 10 fractures (femoral and humeral) within his first 4 weeks of life. He was treated with IV pamidronate every 2 months between 6 weeks to 18 months of age. No further fractures were noted after 4 weeks of age. He is now 15 years old and has normal ambulation. Both M1 and M2 were clinically diagnosed as OI type IV. During a subsequent pregnancy of M1, the third affected member (M3) was noted to have bowed proximal femurs bilaterally. After birth, he had multiple rib, femoral and tibial fractures. His last fracture occurred at 4.5 months of age. He was treated with IV zoledronic acid every 3 months between 3 weeks to 12 months of age. Extraskelatal

findings were not present in any of the three members (normal sclerae, hearing and dentition). There were no spinal or cranial deformities, no cardiovascular complications, and no joint hypermobility. Both M1 and M2 were of normal stature (25th and 75th percentile for height, respectively), while M3 is tracking along <2nd percentile for length-for-age. There was an unaffected 17-year-old daughter of M1. Conformation sensitive gel electrophoresis revealed that both M1 and M2 were heterozygous for C>T substitution (p.Pro1005Leu) in exon 49 of the COL1A1 gene. Conclusions: We described a previously unreported phenotype of OI due to a pathogenic dominant mutation in the COL1A1 gene. Affected members followed a pattern of congenital bone deformities with multiple fractures in long bones within the first few months of life followed by paucity of non-traumatic fractures thereafter. Proline to leucine substitution has been implicated in defects in collagen folding. The potential role of this substitution in explaining the phenotype of our patients remains unclear.

Disclosures: *Nidhi Gupta, None*

MON-0130

Calcemia and inflammatory markers in neonatal sepsis Stepan Kutilek^{*1}, Martina Vracovska¹, Kamila Pecenkova¹, Zlata Fejfarikova², Richard Pikner², Hana Brozikova¹. ¹Dept. of Pediatrics, Klatovy Hospital, Czech Republic, ²Dept. of Clinical Biochemistry, Klatovy Hospital, Czech Republic

Hypocalcemia, in particular low level of Ca²⁺, has been repeatedly described in neonates with sepsis. Ionised hypocalcemia (S-Ca²⁺) is considered a negative prognostic factor in the neonatal sepsis, together with calcitoninemia and serum levels of parathyroid hormone (S-PTH). Our aim was to retrospectively evaluate total calcemia (S-Ca) and its relationship to laboratory markers of sepsis/infection (C-reactive protein - CRP; procalcitonin - PCT) in neonates. Between the years 2012 and 2016, 3441 neonates were hospitalized at our neonatology ward. S-Ca was assessed in 988 samples drawn from 828 babies. Out of those, neonatal sepsis/infection was diagnosed in 29 children. The control assessments of inflammatory markers and S-Ca were based on the clinical situation of the patients. The children were treated by intravenously administered gentamicin and ampicillin for seven days. S-Ca, S-CRP, S-PCT were assessed on days 1, 2, 3 of the infection. The mean values of S-Ca in neonates with sepsis were always significantly lower when compared to 799 children without infection (i.e. controls) ($p<0.0001$). There were no correlations between S-Ca and S-CRP or S-PCT on days 1, 2 and 3, nor between S-Ca on day 1 and S-CRP or S-PCT on days 2 and 3, respectively. The pooled values of S-Ca and S-PCT showed weak inverse correlation approaching statistical significance ($r=-0.22$; $p=0.06$). There also was a poor negative correlation between pooled values of S-Ca and S-CRP ($r=-0.19$; $p=0.09$). In conclusion, total S-Ca was decreased in neonates with infection/sepsis and did not show any strong or significant correlation with S-CRP and S-PCT. We are aware of the limitations of our paper as S-Ca²⁺, albumin-adjusted-Ca, S-25-OH-vitamin D and S-PTH were not measured. However, pediatricians should be aware of the fact, that even low total S-Ca should alert their attention to the risk of neonatal sepsis.

Disclosures: *Stepan Kutilek, None*

MON-0131

The effect of growth hormone treatment in a child with a novel TRPS1 gene mutation Yael Levy-Shraga^{*1}, Shlomo Wientroub², Leonid Zeitlin². ¹Pediatric Endocrinology Unit, The Edmond and Lily Safra Children's Hospital, Chaim Sheba Medical Center, Tel-Hashomer, Israel, ²Pediatric Orthopaedics, Dana Children's Hospital, Israel

Background: Tricho-rhino-phalangeal syndrome (TRPS) is an autosomal dominant disorder characterized by craniofacial and skeletal malformations including short stature, cone shaped phalangeal epiphyses of the hand and Perthes-like changes of the hip. We report a case of a boy with TRPS type 1 and severe growth hormone deficiency. Case presentation: The patient presented at age 4 years for evaluation of short stature (87cm, -3.7 SD). On physical examination characteristic phenotype of TRPS was found: sparse thin hair, lateral rarefaction of the eyebrows, a pear-shaped nose, a long philtrum and a thin upper lip. Radiographs of the left hand at a chronological age of 4.8 years revealed a bone age of 2.8 years. Furthermore, cone-shaped epiphyses were identified. Two growth hormone stimulation tests revealed severe growth hormone (GH) deficiency (pick GH after stimulation of 3.3 and 1.7mcg/l) with low IGF1 (30.1ng/ml, normal 35-217). Further work up revealed bilateral Perthes-like changes of the hips on pelvis radiographs. GH treatment was initiated (0.03 mg/kg/day). Genetic analysis: Sanger sequencing of the TRPS1 gene was performed identified a heterozygous sequence variant, c.3698G > A, in exon 7. This missense mutation leads to an amino acid change at codon 1233, (p.Cys1233Tyr). To the best of our knowledge, this mutation was not described previously. Two prediction programs (PolyPhen, SIFT) rat this mutation as disease causing. Both his parents did not carry this mutation. Follow up: Growth velocity improved under GH treatment (8-9 cm/year). His current height at the age of 7.5 years is 116.4cm (-1.6 SD). Furthermore, marked improvement of the femoral epiphysis was shown on sequential pelvis radiographs. Conclusion: Our observations may suggest the benefits of growth hormone treatment on both height and epiphyses status in TRPS. Further studies are needed to support this observation.

Disclosures: *Yael Levy-Shraga, None*

MON-0132

Prevalence of Low BMD in Pediatric Cancer Survivors When Z Scores are Height Adjusted Chanthu Pillai^{*1}, Avni Shah¹, Anita Ying², Steven Waguespack². ¹McGovern Medical School, United States, ²The University of Texas MD Anderson Cancer Center, United States

Background: Pediatric cancer survivors are at higher risk of poor bone mineral deposition than the general population. There is a high degree of variability to the exact prevalence of low bone mineral density (BMD) in pediatric cancer survivors. It has been reported as low as 8% and high as 60%. Because of concern for increased fracture risk and its associated morbidities, pediatric cancer survivors are often screened for low bone mineral density with dual-energy X-ray absorptiometry (DXA). In DXA by current clinical guidelines, low BMD is defined as Z score ≤ -2.0 . Currently, the International Society of Clinical Densitometry recommends that DXA scan Z scores be adjusted for height in children with short stature or growth delay. Children's Oncology Group Long-Term Follow-Up (COG-LTFU) Guidelines do not specifically recommend adjusting Z scores based on height. This study assessed the change in prevalence of low BMD in pediatric cancer survivors when DXA results were height adjusted. **Methods:** We retrospectively reviewed medical records of 91 pediatric cancer survivors at MD Anderson Cancer Center who underwent DXA between January 1, 2000 and October 31, 2010. We used the calculator from the Bone Mineral Density Childhood Study to height adjust Z scores. **Results:** Based on raw Z scores, seventeen cancer survivors (18%) had low lumbar spine BMD (raw z score ≤ -2.0) after completion of cancer treatment. When Z scores were height adjusted, only five patients (5%) had low lumbar spine BMD (modified z score ≤ -2.0). **Conclusion:** In pediatric cancer survivors, low bone mineral density is less prevalent when DXA Z scores are corrected for height. Ninety five percent of pediatric cancer survivors screened by DXA scan, did not have low bone mineral density. DXA Z scores should be height adjusted in pediatric cancer survivors to provide more accurate diagnosis of low bone mineral density. Current clinical practice may be over diagnosing low bone mineral density and perhaps increasing parental concern and medical cost.

Disclosures: Chanthu Pillai, None

MON-0133

Vitamin D level of toddlers with "physiologic" genu varum is lower than that of control toddlers: 1:2 case-control study Yuko Sakamoto^{*1}, Satoshi Nakano², Mitsuyoshi Suzuki², Akifumi Tokita³, Ayaka Kaneko⁴, Eri Maeda-Murohara⁴, Masashi Nagao⁴, Toshiaki Shimizu², Kazuo Kaneko⁴, Masahiko Nozawa¹, Muneaki Ishijima⁴. ¹Department of Orthopaedics, Juntendo University Nerima Hospital, Japan, ²Department of Pediatrics, Juntendo University Graduate School of Medicine, Japan, ³Clinic Bambini, Japan, ⁴Department of Medicine for Orthopaedics and Motor Organ, Juntendo University Graduate School of Medicine, Japan

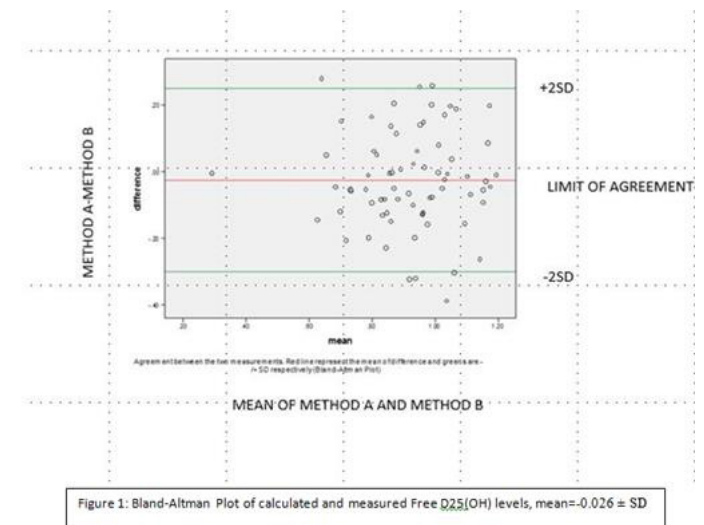
When children around 2 yo show leg bowing, and diseases are ruled out based on radiograph without conducting blood tests, the bowing is classified as "physiologic" genu varum. "Physiologic" is named for physician's experiences that toddler's genu varum without radiographic abnormality usually resolves by itself. Recently we revealed that genu varum severity in toddlers was correlated with serum alkaline phosphatase (ALP) levels, suggesting that genu varum is not a physiologic condition in toddlers (J Bone Miner Metab, 2017). The present 1:2 case-control study was conducted to compare the bone metabolic conditions of toddlers with "physiologic" genu varum and those with normal alignment of lower limb. During 2013 to 2016, blood samples were obtained from 33 of toddlers with genu varum and 66 age and gender-matched subjects among toddlers in our previous study, which examined the vitamin D status in healthy Japanese children (J Nutr Sci Vitaminol 2018). Serum levels of ALP, intact parathyroid hormone (iPTH), 25-hydroxy vitamin D [s25(OH)D], calcium (Ca), and inorganic phosphorus (P) were measured in a postprandial state. The mean age of the control and genu varum groups were 17.1 and 17.8 months old, respectively, while the mean body weight of them were 10.2 and 10.1 kg, respectively. No difference for the frequency of summer born from spring was observed between them. The s25(OH)D levels of the subjects with genu varum (24.8 ng/mL) was significantly lower than those of the control subjects (33.6 ng/mL) ($p < 0.001$). The frequency of vitamin D insufficiency (< 20 ng/mL) of the subjects with genu varum (39%) was significantly higher than that in control subjects (14%) ($p = 0.004$). The odds ratio of the vitamin D insufficiency was 4.12 (95%CI: 1.5-11.1) in subjects with genu varum compared with those with control ($p = 0.004$). sCa levels of the subjects with genu varum (10.2 ng/mL) was significantly higher than those of the control subjects (9.8 ng/mL) ($p < 0.001$), although no difference of sP levels was observed between them ($p = 0.18$). sALP (1057 IU/L) and siPTH (28.4 pg/ml) levels of the subjects with genu varum were significantly higher than those of the control subjects (740 IU/L, 8.8 pg/ml), respectively ($p < 0.001$). siPTH levels were associated with s25(OH)D levels in subjects with genu varum ($r = -0.57$, $p < 0.001$), while the association was not observed in the control subjects ($r = 0.11$, $p = 0.36$). As siPTH levels were associated with s25(OH)D levels, vitamin D insufficiency may increase siPTH levels in toddlers with genu varum, which may also increase sCa levels. Based on these results, we should not treat these toddlers as "physiologic" genu varum, but should recommend them to take vitamin D. In conclusion, toddlers with genu varum showed vitamin D insufficiency and hyper-ALP activity with relatively hypercalcemia within reference range than healthy toddlers without genu varum.

Disclosures: Yuko Sakamoto, None

MON-0134

Measured Versus Calculated Free serum 25(OH)-Vitamin D Level: which one is better? Judith Vansickle^{*}, Tarak Srivastava, Uttam Garg, Uri Alon. Division of Pediatric Nephrology, Children's Mercy Hospital, University of Missouri Kansas City, United States

Background: Serum 25(OH)D is mainly bound to Vitamin D Binding Protein (VDBP) (~85%) and to albumin (~15%) with only a minute amount circulating as free 25(OH)D. A stronger association of free 25(OH)D than total 25(OH)D was observed with serum calcium, PTH, bone mineral density, and vascular outcomes. Free 25(OH)D can be calculated from the concentrations of total 25(OH)D, VDBP, and albumin by a mathematical method or may be directly measured by ELISA. Previous studies questioned the accuracy of calculated vs. measured free 25(OH)D. **Objective:** To compare the validity of the mathematically calculated versus measured free 25(OH)-Vitamin D. **Method:** We collected blood samples from 74 children (ages 1-19 years old) and simultaneously measured total 25(OH)D on Tandem Mass Spectrometer, serum albumin by bromocresol green dye on COBAS chemistry analyzer, VDBP and free 25(OH)D by ELISA. Free 25(OH)D was calculated as follows: $\text{Calculated free 25(OH)D} = (\text{Total 25(OH)D}) / (1 + (6 * 10,000 * [\text{albumin}]) + (7 * 10,000,000 * [\text{VDBP}]))$ **Pearson correlation analysis and Bland-Altman Plot** were used to examine the true agreement between the two methods. **Results:** The mean age was 9.03 ± 5.07 years with 55% males and 76% Caucasians and 24% African-Americans. The mean \pm SD for Total 25(OH)D was 37.12 ± 11.33 ng/mL, calculated free 25(OH)D 8.87 ± 3.66 pg/mL and measured free 25(OH)D 8.59 ± 3.41 pg/mL. Pearson correlation reflected a significant correlation between calculated and measured free 25(OH)D ($r = 0.66$, $p < 0.0005$) (Figure 1). Bland-Altman Plot reflected a tight agreement with in a 95% limit of agreement (mean = $-0.026 \pm 2SD$) (Figure 2). **Conclusion:** The measured and calculated values of free 25(OH)D are in agreement and seem interchangeable. Depending on the availability of instruments and methods, free 25(OH)D can be either measured or calculated.



Disclosures: Judith Vansickle, None

MON-0158

Critical sex- and age-dependent role of osteocytic pannexin1 on bone and muscle mass and strength Alexandra Aguilar-Perez^{*1}, Lilian Plotkin¹, Hannah Davis¹, Emily Atkinson¹, Matthew Allen¹, Leland Gomez², Padmini Deosthale¹, Carmen Herrera², Julian Dilley¹, Angela Bruzzaniti³, Teresa Zimmers¹, Ziyue Liu², Rafael Pacheco⁴, Joseph Rupert¹. ¹Indiana University School of Medicine, United States, ²Indiana University, United States, ³Indiana University School of Dentistry, United States, ⁴Brazil, Brazil

Deletion of Pannexin1 (Px1) channels in osteocytes (Ot) in young 4mo female Px1^{f/f};8kb-DMP1 (Px1^{Δot}) mice results in higher cancellous bone and bone formation compared to Px1^{f/f} littermates. We now report the increased bone mass in female but not male mice with Ot Px1 deletion up to 13m of age. Px1^{f/f} (n=9) control mice showed the expected age-induced bone geometry deterioration and reduced strength vs 4mo Px1^{f/f} mice. Bone formation was low, with reduced PINP (-54%) and ALP (-16%) in serum, osteoblast (Ob) activity (MAR; 45%, BFR/BS; 43%) and number/surface (N.OB/B.P; 39%, OB.S/BS; 38%) in 13mo vs 4mo Px1^{f/f} mice. Ot Px1 deletion prevented these aging effects. Further, femoral and spinal BMD were higher (5% and 13%) in Px1^{Δot} (n=12) vs 13mo Px1^{f/f} mice. Also, femoral cortical bone area (6%) and thickness (11%) were higher in aged Px1^{Δot} mice vs Px1^{f/f} at the same age. Vertebral osteoclast (Oc) number (-16%) was low in aged Px1^{Δot} mice, whereas Obs were unchanged. Oc gene (TRAP, RANKL, NFATC1) levels in bone increased in aged Px1^{f/f} and were lower in Px1^{Δot} mice, suggesting that Ot Px1 is required for Oc differentiation in old female mice. Further, pre-yield mechanical properties (yield

force; +49%) were improved in femur of 13mo PxlΔot mice, with values similar to those of 4mo Pxl1f/f. This suggests that Pxl1 in Ot controls Obs and Ocs resulting in sustained increase in bone mass and mechanical properties. Surprisingly, in addition to a bone phenotype, female but not male Pxl1Δot mice showed transient increase in lean body mass and decrease in fat mass (2-5mo), although Pxl1 levels were decreased in bone and unchanged in skeletal muscle. Ot Pxl1 deletion result in higher soleus (SOL) weight (21%) and cross-sectional area (38%) only in female mice. Ex vivo SOL and extensor digitorum longus (EDL) contractility properties did not change with Ot Pxl1 deletion in either sex. EDL fatigue at a higher rate and in vivo maximum plantarflexion torque was lower in male Pxl1Δot (-11%) compared to Pxl1f/f, but muscle strength was unchanged in female mice. In summary, Ot Pxl1 deletion differentially increases bone mass in young and old and muscle in young female mice, but has deleterious effects on muscle strength only in males. Our studies suggest that Pxl1-mediated release of Ot factors affect bone and muscle cell generation/function. Thus, Pxl1 plays a critical role in Ot, regulating bone formation and resorption and muscle mass/strength in sex- and age-dependent manners.

Disclosures: *Alexandra Aguilar-Perez, None*

MON-0159

Soft-tough cartilage scaffold with a patterned nanofibrous frame Haider Ali*, Kyung Won Kim, Moon Kyu Kwak, Young Hun Jeong, Gyu Man Kim, Cheol Woo Park. Kyungpook National University, Republic of Korea

Here, we presented a unique nanofiber/hydrogel composite mimicking native connective tissue, especially cartilage, which gains much attention in tissue engineering and regenerative medicine because of its limited-life but complicated mechanical properties such as soft-tough stiffness behavior induced by selective engagement of load carrying components. In order to mimic its mechanical properties, a patterned nanofibrous 3D frame with regular pores, which was fabricated using an improved electrospinning, was introduced to cell-laden hydrogel matrix as a reinforcement component. Particularly, we designed the composite with cell culture medium playing the role of physical separation between nanofibers and hydrogel in load carrying. Three types of nanofiber/hydrogel composites with different properties were prepared and their mechanical properties for compressive load were experimentally identified. Consequently, it was demonstrated that the proposed composite had sufficient biocompatibility as well as cartilage-like soft-tough properties. **KEYWORDS:** nanofiber, cartilage, cell-laden hydrogel, engagement, property **ACKNOWLEDGMENTS:** This study was supported by the National Research Foundation of Korea (NRF) grant funded by the Korea government (MSIP) (No. 2017R1A2B2005515, 2018R1A2B2009540).

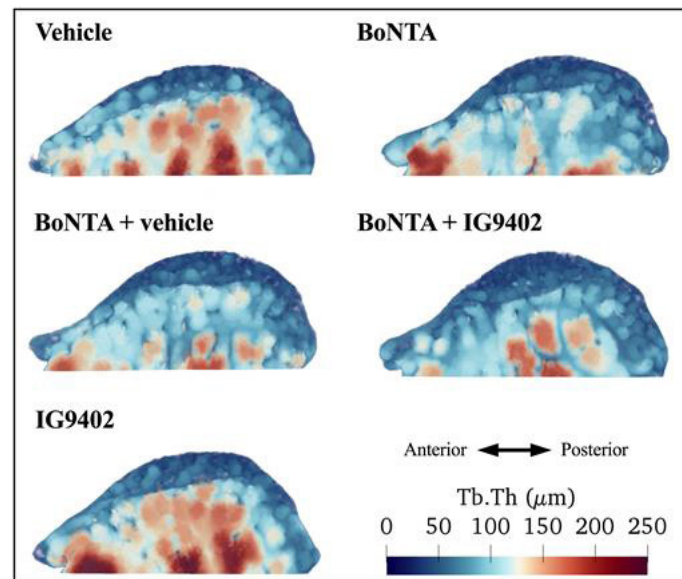
Disclosures: *Haider Ali, None*

MON-0160

The osteocyte apoptosis inhibitor IG9402 prevents bone loss of the mouse mandibular condyle during masseter muscle atrophy Sonja Buvinic*, Julián Balanta-Melo², Viviana Toro-Ibacache³, María Angélica Torres-Quintana⁴, Kornelius Kupczik⁵, Lilian Plotkin⁶. ¹Institute for Research in Dental Sciences, Faculty of Dentistry; CEMC, Faculty of Medicine; Universidad de Chile, Chile, ²Institute for Research in Dental Sciences, Faculty of Dentistry, Universidad de Chile, Chile; School of Dentistry, Universidad del Valle, Colombia; Max Planck Weizmann Center, Max Planck Institute for Evolutionary Anthropology, Germany, Chile, ³Institute for Research in Dental Sciences, Center for Quantitative Analysis in Dental Anthropology, Faculty of Dentistry, Universidad de Chile, Chile; Department of Human Evolution, Max Planck Institute for Evolutionary Anthropology, Germany, Chile, ⁴Department of Pathology and Oral Medicine, Faculty of Dentistry, Universidad de Chile, Chile, ⁵Max Planck Weizmann Center, Max Planck Institute for Evolutionary Anthropology, Germany, ⁶Department of Anatomy and Cell Biology, Indiana University School of Medicine, Roudebush Veterans Administration Medical Center, and Indiana Center for Musculoskeletal Health, United States

Background: The masseter muscle atrophy induced by botulinum toxin type A (BoNTA) results in altered loading of the temporomandibular joint and bone loss of the mandibular condyle in mice. Osteocytes are the most abundant bone cells and specifically their apoptosis is correlated with bone resorption during excessive mechanical stress. Thus, the inhibition of osteocyte apoptosis may prevent bone loss. Here we investigate whether a bisphosphonate analog that does not inhibit osteoclast activity but prevents osteocyte apoptosis (IG9402) preserves bone mass in the mouse mandibular condyle after BoNTA intervention. **Methods:** Random assignment of 24 adult BALB/c mice as follows: BoNTA(n=8); BoNTA + vehicle(n=6), BoNTA + IG9402(n=5), and IG9402-only (n=5). Mice from BoNTA groups received BoNTA injection once in the right masseter muscle at the beginning of the experiment, and saline solution in the contralateral side. IG9402 (0.6 mg/kg/day) or the vehicle were administered daily during the whole study. All animals were euthanized after 14 d and mandibles were dissected and scanned with high-resolution X-Ray Microtomography (microCT). Bone volume fraction (BV/TV), trabecular thickness (Tb.Th) and trabecular separation (Tb.Sp) were quantified from the resulting microCT scans of the mandibular condyles. Non-parametric analysis was performed to determine the differences between the groups.

All procedures were approved by the local ethical committee. **Results:** Both BV/TV and Tb.Th were significantly reduced in mandibular condyles from BoNTA-injected sides in the BoNTA ($p < 0.05$ and $p < 0.001$, respectively) and BoNTA + vehicle (both $p < 0.05$) groups as shown for Tb.Th in Figure 1. IG9402 prevented the loss of BV/TV by $36 \pm 6\%$ ($p < 0.05$) but not for Tb.Th ($p > 0.05$) in samples from BoNTA-injected sides. In addition, BV/TV and Tb.Th were both increased by 3% in samples from both sides of IG9402-only group when compared with condyles from saline-injected sides. No difference in Tb.Sp was found among groups. **Conclusions:** In this study, IG9402 prevented bone loss in the samples from BoNTA-injected sides. Also, an increase of BV/TV and Tb.Th in animals without BoNTA intervention may be evidence for the role of osteocyte apoptosis in the mature mandibular condyle remodeling. Taken together, these results suggest that IG9402 could prevent bone loss in the mouse mandibular condyle during masseter muscle atrophy induced by BoNTA.



Disclosures: *Sonja Buvinic, None*

MON-0161

Gut microbiota manipulation promotes bone formation mediated through regulatory T-Cell differentiation in obese mice Jyotirmaya Behera*, Suresh C Tyagi, Kimberly E Kelly, Nandan K Mondal, Neetu Tyagi. University of Louisville, United States

Aim: Probiotics are viable bacterial components that exert beneficial effects on the host, have been shown to prevent multiple comorbidities. However, the effects of probiotics in the pathological setting like obesity-induced osteoporotic bone phenotype via immune homeostasis are largely unknown. Therefore, we aimed to investigate the effect of probiotics on the gut microbiota eubiosis via epigenetic mechanism in the regulatory T-Cells (Tregs) function and bone formation using high-fat diet (HFD) induced obese mice. To test this hypothesis, 10-week-old female mice were fed on the high-fat diet (HFD; 42%) for 12 weeks. Probiotics (GSL#5) were given at the dose of 1×10^9 total bacteria 5 times/week through intragastric administration. **Results:** In vivo, μ CT measurements revealed that probiotics induced a significant increase of trabecular bone phenotype (BV/TV; 30% in the femur) as compared to HFD condition. In vitro study also showed that mouse BMSC derived osteoblast mineralization was indeed increased in probiotics treated HFD condition. Mechanistic studies revealed that probiotics epigenetically regulates immune homeostasis by up-regulating bone marrow (BM) regulatory T cells (Tregs CD4+Foxp3hi) differentiation via demethylation of Foxp3, as assessed by bisulfite sequencing PCR (BSP) and methylation-specific PCR (MSP). Additional studies revealed that probiotics administration attenuates the phosphorylation of S276 on RelA/p65 subunit of NF- κ B is required for RelA/p65-DNMT-1 interactions, chromatin loading of DNMT-1. Thereby DNMT-1 mediated hyper-methylation of CpG islands of the FoxP3 promoter was abolished and subsequent Tregs-specific Foxp3 hypomethylation and Tregs differentiation. Small molecule inhibitor PTD-RelA/p65 (38-47 amino acid) peptide/5-azacytidine blocked the RelA/p65-DNMT-1 interactions and abrogated FoxP3 hyper-methylation and Tregs differentiation. In vivo blockade of Tregs expansion by treatment with anti CD25 Ab or silencing of Foxp3 by shRNA based RNA interference in mice prevented the bone anabolic activity of probiotics. Further, Tregs induced the release of the IL10 and TGF- β , leading to inhibit bone resorption assessed by TRAP+ staining in vitro, while increased bone formation (PINP expression) under probiotics treatment. **Conclusion:** Collectively, our data provide the evidence that probiotics administration maintain the gut microbiome/eubiosis dependent bone formation via immune homeostasis in HFD induced obese female mice.

Disclosures: *Jyotirmaya Behera, None*

MON-0162**Elucidation of mechanisms governing the activity of SOXC-inflammatory cytokine molecular axis in synovial fibroblasts** Kyle Jones*, Veronique Lefebvre, Pallavi Bhattaram. Cleveland Clinic, United States

Purpose: Sox4, Sox11, and Sox12 encode the SOXC group of Sry-related HMG box (SOX) transcription factors. We recently identified a novel SOXC-inflammatory cytokine molecular axis that operates in synovial fibroblasts and plays a critical role in joint degeneration due to arthritis. The goal of this study is to identify the mechanism underlying the activation of the SOX-inflammatory cytokine axis. **Methods:** We used mouse primary synovial fibroblasts to study the effect of the pro-inflammatory cytokine, Tumor necrosis factor- α (TNF) on SOXC proteins. Proteomics assay was used to identify TNF-induced modifications in SOX11 protein. ENCODE chromatin immunoprecipitation-sequencing (ChIP-seq) data and reporter gene assays are being used to understand the relation between SOXC proteins and inflammation. **Results:** We previously showed that inactivation of the SOXC genes in the synovial and articular surfaces hampered the development of synovitis and cartilage degeneration in a mouse model of TNF-induced arthritis. We also showed that SOXC genes significantly contribute to the TNF-mediated upregulation of several inflammation-associated genes. TNF in turn stabilized SOX4 and 11 proteins. Here, we report that TNF induces the phosphorylation of SOX4 and 11. The C-terminal half of SOX11, which contains 7 of the 13 newly identified phosphorylation sites, is needed for protein stabilization. We also investigated the mechanism underlying the SOXC-dependent upregulation of TNF target genes. We hypothesized that RELA (TNF signaling transcription factor) and SOXC proteins bind to closely located regulatory domains of TNF-target genes. This notion is supported by ChIP-seq profiles available in the ENCODE database, which show that RELA is bound to the upstream genomic regions of the SOXC-TNF co-regulated genes, such as VCAM1 and EZH2 in multiple cell lines. RELA binding domains also contained putative SOX binding sites. The TNF-dependent activity of luciferase reporter genes encompassing the RELA binding sequences of VCAM1 and EZH2 was also enhanced by SOX11. **Conclusions:** Our study strongly suggests that the SOXC-inflammatory cytokine axis is regulated by SOXC protein phosphorylation. It also suggests that the SOXC proteins and RELA may bind to adjacent regulatory DNA sequences, leading to the enhanced expression of several inflammation-associated genes. This data will likely aid in the development of SOXC-targeted therapies for inflammatory joint diseases.

Disclosures: Kyle Jones, None

MON-0163**CARNITINE PALMITOYL TRANSFERASE-1A VARIANT 2: A NEW METABOLIC TARGET IN OSTEOPOROSIS RELATED SARCOPENIA?** Umberto Tarantino*, Monica Celi, Chiara Greggi, Elena Gasbarra, Sabina Pucci. university of rome tor vergata, Italy

Introduction. Carnitine palmitoyl transferase-1A (CPT1A), a protein belonging to the carnitine / choline acetyltransferase family, transports long chain fatty acids into the mitochondria for β -oxidation and for the synthesis of ATP. CPT1A, whose classical form, (CPT1A v1), is involved in the metabolism and resides in the mitochondrion. Recently we have identified a variant of this enzyme, CPT1A variant 2 (CPT1A v2), found only in tumors and which resides in the nucleus, is involved in the epigenetic regulation of DNA. The main purpose of the present study is to investigate the regulation of muscle's energy metabolism in osteoporoticOP and osteoarthriticOA, characterizing the expression of the two variants (v1 and v2) of CPT1A and their role in these pathologies. **Methods:** To this end, 40 female patients (80.58 \pm 6.3 years) were enrolled, 20 of whom underwent partial or total prosthetic replacement of the hip following femoral neck fragility fracture, and 20 patients (67.63 \pm 8 years) undergoing the same type of surgery for hip osteoarthritis. The muscle tissue of 6 patients (19 \pm 9 years) who underwent hip arthroplasty following a fracture (CTRL) was also taken. The bone mineral density of these patients was also evaluated by Lunar iDXA. Muscle biopsies were used for: mRNA extraction to evaluate the expression of CPT1A variants, proteins extraction, for the purpose of carrying out tests of enzymatic activity, and finally they were fixed in 4% paraformaldehyde for 24 hours and included in paraffin. Serial sections were used for morphometric and immunohistochemical evaluation. **Results:** Immunohistochemical analysis of muscle tissue showed that CPT1A protein appears to have a "polarized" expression in the muscle tissue of OP patients, as opposed to OA and CTRL patients, in which its expression is homogeneous. The mRNA expression analysis for CPT1A, showed a greater expression of the metabolic form (CPT1A v1), in the muscle tissue of OA patients; the same result was also obtained and in CTRL patients. In contrast, OP patients showed a strong expression of CPT1A v2. CPT1A metabolic activity assay on protein extracts from muscular tissue, confirmed a significant reduction in activity of this enzyme in OP patients as compared to OA. In addition, immunohistochemical data confirm that the presence of CPT1A v2 correlates with the histone H4 acetylation pattern in OP patients, in which a strong expression of acetyl histone H4 was found predominantly at nuclear level, as opposed to the OA patients, in which only a few cell nuclei are positive. Moreover quantification rates of intracellular ATP have shown that there are significant differences between the two experimental groups, confirming the result obtained through the enzymatic activity test of CPT1A protein. These data suggest an important role of CPT1A variant 2 as a new marker and potential therapeutic target in osteoporotic pathology

Disclosures: Umberto Tarantino, None

MON-0164**Fibroblast Growth Factor 9 (FGF9) Acts as an Inhibitory Osteokine in Mouse C2C12 and Human Skeletal Muscle Cells** Jian Huang*¹, Kun Wang², Lora Shiflett², Leticia Brotto¹, Lynda Bonewald³, Sarah Dallas², Marco Brotto¹. ¹Bone-Muscle Collaborative Sciences, College of Nursing and Health Innovation, University of Texas at Arlington, United States, ²Department of Oral and Craniofacial Sciences, School of Dentistry, University of Missouri-Kansas City, United States, ³Department of Anatomy, Cell Biology and Orthopedics, Indiana Center for Musculoskeletal Health, School of Medicine, Indiana University, United States

Osteoporosis and sarcopenia occur together and evidence is accumulating for molecular crosstalk between muscle and bone that may play a role in these age-related diseases. We have identified positive mediators of crosstalk from bone to muscle, including PGE2 and WNT3a, and from muscle to bone, including β -aminoisobutyric acid (BAIBA). We have previously shown that FGF9 is an early osteocyte factor that prevents differentiation. Recently we have identified FGF9 as an osteocyte-produced factor that may negatively regulate myogenesis in C2C12 myoblasts. Here, we sought to elucidate the molecular mechanisms for FGF9 regulation of myogenesis and confirm whether it has a similar regulatory role in human primary myoblasts. In C2C12 myoblasts treated with FGF9, smaller and fewer myotubes were seen and the fusion index (FI) was significantly reduced compared to control (FI values: control = 47.6% \pm 2.6; 2ng/ml FGF9 = 38.2 \pm 4.8, $p > 0.05$; 10ng/ml FGF9 = 34.6% \pm 6.99, $p < 0.05$; 50ng/ml = 17.0% \pm 2.1, $p < 0.0001$). Although myotube differentiation was inhibited, FGF9 treatment strongly stimulated myoblast proliferation. FGF9 (10-50ng/ml) significantly decreased mRNA expression of myogenesis markers MyoG and Mhc while increasing expression of the myogenic inhibitor, Myostatin. Measurements of intracellular Ca²⁺ using Fura-2 revealed that FGF9-treated myotubes showed a lower Ca²⁺ peak and a shortened relaxation phase in response to caffeine, suggesting that FGF9 disrupts Ca²⁺ homeostasis in myotubes. RT-qPCR array revealed that FGF9 (10ng/ml) treated C2C12 cells, increased expression of Icam1 by 2.8-fold, while Hey1, Wnt1 and Wnt6 were decreased 3.1, 3.5 and 4.2 fold, respectively. Although human skeletal muscle cells were less sensitive than C2C12 muscle cells, both myotube formation and FI were significantly inhibited at 200ng/ml FGF9. These findings suggest that FGF9 may act as an inhibitory osteokine with the intrinsic capacity to modulate myogenic differentiation via a complex signaling mechanism that seems to involve the orchestration of myostatin with key regulators of muscle development (MyoG, Mhc, Hey1, Wnt1, Wnt6), cell proliferation (Icam1 and myostatin), and differentiation (Hey1, Wnt1, Wnt6). The fine-tuning of bone-muscle crosstalk mechanisms likely requires both stimulatory and inhibitory myokines and osteokines. Deciphering 'kines' mechanisms and their actions in bones and muscles could lead to a new era in the treatment of musculoskeletal disorders.

Disclosures: Jian Huang, None

MON-0165**Muscle-Derived IGF-1 Affects Bone Elongation in a Gender-Specific Manner** Gisele Martins*¹, Vitor Torres¹, Bianca Neofiti-Papi¹, Joao Silvestre¹, William Silva¹, Antonio Musarò², Anselmo Moriscot¹, Cecilia Gouveia¹. ¹Institute of Biomedical Sciences, University of São Paulo, Brazil, ²Sapienza Università di Roma, Italy

There is growing evidence that paracrine interactions between bone and muscle tissue contribute to the regulation of bone and muscle mass, independently of the mechanical interaction. One putative factor to have a role in a non-mechanical muscle-bone interaction is insulin-like growth factor 1 (IGF-1), which is secreted by skeletal and muscle cells and plays important roles in both bone and muscle development, in addition to promote anabolic effects in both bone and muscle mass. The purpose of this study was to investigate whether muscle-derived IGF-1 affects bone growth and bone mass in female and male mice. We studied MLC/mIGF-1 transgenic mice (IGF-1TG) that overexpress mIGF-1 (a isoform synthesized in skeletal and cardiac muscle) in skeletal muscle fibers by means of a rat mIGF-1 cDNA driven by skeletal muscle specific regulatory elements from the rat myosin light chain (MLC)-1/3 locus. We characterized the bone and muscle mass phenotypes of IGF-1TG mice and their wild-type (WT) controls, at 1, 3, 5, 7, 9, 11 and 13 months of age. IGF-1TG females showed significant increases in body mass (BM), quadriceps muscle mass (QM) and tibialis anterior muscle mass (TAM) at 3,5,9 and 11 months of age when compared to WT controls. On the other hand, the lengths of the body, femur, tibia, humerus and radius (BL, FL, TL, HL and RL, respectively) were normal in IGF-1TG females. By X-ray microtomography analysis (μ CT) of the femur, we detected increases in trabecular bone volume and trabecular number, and decreases in trabecular separation and trabecular porosity in IGF-1TG females at 3 and 5 months of age. In IGF-1TG male mice, BM, QM and TAM were increased from 3 to 13 months of age. Differently from females, IGF-1TG males showed increased BL (at 9 months), FL (at 5,7 and 13 months), TL (at 5,7 and 13 months) and HL (at 11 and 13 months), but normal trabecular bone mCT parameters in the femur, when compared to WT control. In conclusion, muscle-derived IGF-1 does not affect trabecular bone in male mice. At this point, it is not possible to discriminate if the improvements in trabecular bone parameters observed in IGF-1TG female mice are due to IGF-1 overexpression or to the increased muscle mass. Interestingly, the data of the present study suggest that muscle-derived IGF-1 does not affect bone linear growth in female mice but has a positive effect in this process in male mice, revealing that paracrine interactions between bone and muscle may depend on sex factors.

Disclosures: Gisele Martins, None

MON-0166

Mechanisms Responsible for Pamidronate Rescue of Post-Burn Muscle Loss in Children Fabrizio Pin^{*1}, David Herndon², Andrea Bonetto¹, Celeste Finnerty², Christopher Nieten², Lynda Bonewald¹, Gordon Klein². ¹Indiana University Medical Center, United States, ²University of Texas Medical Branch, Shriners Burns Hospital, United States

Pamidronate has been shown to prevent inflammation-associated bone resorption following burn injury. We reported that burned children who received pamidronate also had reduced protein breakdown and positive protein balance in muscle (Borsheim et al JBMR 2014). The aim of this study was to identify the molecular mechanisms responsible for muscle mass rescue in pamidronate vs placebo/standard of care-treated patients. Mature myotubes generated by differentiating murine C2C12 myoblasts were exposed for 48h to 1 or 5% serum obtained from 3 groups of children: normal unburned (N), burned receiving placebo/standard of care after 30d (B), burned receiving pamidronate and standard of care (BP) after 30d. Exposure to B serum caused dose-dependent myotube atrophy compared to N serum (-13 or -40%, p<0.01), reproducing muscle atrophy induced by burn injury in humans and animals (Quintana et al Inflamm Res, 2015; Song et al, Shock 2015). When the C2C12 myotubes were treated with BP serum, their size was partially rescued compared to myotubes exposed to B serum (+9 and 15%, p<0.05). At the molecular level, atrophy induced by B serum was associated with reduced phosphorylation of AKT (-34%, p<0.05) and its downstream target mTOR (-51%, p<0.01), suggesting that muscle anabolism was down-regulated. In addition, muscle protein catabolism appeared to be greater in myotubes exposed to B serum, as shown by increased STAT3 activation (+100%, p<0.001) and reduced phosphorylation of FOXO3a (-53%, p<0.01). In accordance with the effects on fiber size, BP serum was able to restore the phosphorylation of AKT (+46%, p<0.05) and mTOR (+83%, p<0.05), as well as the protein ubiquitination (-58%, p<0.05) when compared to B serum alone. No differences were observed relative to STAT3 or FOXO3a activation. Of note, the exposure to ACVR2B/Fc had no effects suggesting that the TGFbeta signaling is not responsible for the effects of B serum on muscle. These data show that the rescue effect of serum from BP patients appears related to the reactivation of the anabolic AKT-mTOR pathway. The reduction of protein ubiquitination associated with BP serum is also consistent with previously-reported retrospective findings of stable isotope studies showing less muscle protein breakdown in the pamidronate-treated patients. These data suggest that bisphosphonate protection of bones from resorption prevents the release of muscle pro-catabolic factors into the circulation.

Disclosures: *Fabrizio Pin, None*

MON-0167

Electrical Stimulation of Hindlimb Skeletal Muscle has a Beneficial Effect on Sublesional Muscle and Bone in a Rat Model of Spinal Cord Injury. Wei Zhao^{*1}, Yuanzhen Peng², Yizhong Hu³, Edward X. Guo³, William A Bauman^{1,2}, Weiping Qin^{1,2}. ¹Icahn School of Medicine at Mount Sinai, United States, ²James J. Peters VA Medical Center, United States, ³Columbia University, United States

Spinal cord injury (SCI) causes severe skeletal muscle atrophy and bone loss below the lesion. In this study, we evaluated the effect of a prolonged course of electrical stimulation (ES) on muscle mass and bone formation. In addition, we also tested whether the combination of ES and testosterone (TE) will have a synergistic effect on these musculoskeletal endpoints. Implantation of the electrical stimulators towards the bifurcation of the sciatic nerve of the left leg was performed immediately after neurologically complete spinal cord transection at T3-4; ES was initiated 2 weeks after SCI and continued daily for 4 weeks. Compared to sham-transected animals, significant reduction of the soleus, plantaris and EDL muscle mass was observed in animals 6 weeks post-SCI. Notably, ES or ES+TE combination resulted in a +13% increase of the EDL muscle mass, as well as a marginal increase of the plantaris and soleus muscles. ES or ES/TE significantly decreased expression of markers of muscle atrophy (e.g., the muscle-specific ubiquitin ligases MAFbx and MurF1 mRNA) in the EDL. Expression of secreted frizzled-related protein (sFRP) 1, a Wnt antagonist, also increased after SCI, and was drastically reduced by TE, ES or ES+TE treatment. In parallel, SCI for 6 weeks resulted in significant decreases in BMD (-27%) and trabecular bone volume (-49.3%) at the distal femur; notably, TE, ES and ES+TE treatment significantly increased the BMD and BV/TV% by +6.4% and +22.2%, +5.4% and +56.2%, and +8.5% and +60.2%, respectively. The larger magnitude of changes of bone mass in sublesional skeleton in ES+TE animals suggested potential synergistic effect of TE and ES on bone. Osteoblastogenesis was evaluated by colony-forming unit-fibroblastic (CFU-F) staining using bone marrow mesenchymal stem cells obtained from the femur. SCI decreased the CFU-F+ cells by -56.8% compared to sham animals. Excitingly, TE or ES+TE treatment after SCI increased osteoblastogenesis by +74.6% and +67.2%, respectively. An osteoclastogenesis assay revealed significantly increased TRAP+ multinucleated cells by +34.8% in SCI animals compared to sham animals. Both TE and TE+ES treatment following SCI markedly decreased TRAP+ cells by -51.3% and -40.3%, respectively. Collectively, our findings demonstrate that after neurologically complete paralysis, ES generated sufficient contractile force to initiate muscle hypertrophy, downregulate genes involved in muscle atrophy, and restored mechanical loading to sublesional bone to a degree that allowed for preservation of bone, either by inhibition of bone resorption and/or by facilitating bone formation.

Disclosures: *Wei Zhao, None*

MON-0168

Osteocytic Connexin Channels Regulate Skeletal Muscle Structure and Function Guo Bin Li^{*1}, Lan Zhang¹, Peng Shang², Jean X. Jiang³, Huiyun Xu¹. ¹Key Laboratory for Space Bioscience and Biotechnology, School of Life Sciences, Northwestern Polytechnical University, Youyi Xilu 127, 710072, Xi'an, Shaanxi, China, ²Key Laboratory for Space Bioscience and Biotechnology, Research & Development Institute in Shenzhen, Northwestern Polytechnical University, Gaoxin Fourth South Road 19, 518057, Shenzhen, Guangdong, China, ³Department of Biochemistry and Structural Biology, University of Texas Health Science Center, San Antonio, TX, United States

Bone and muscle are connected as a functional unit and show synchronization throughout lifespan. The mechanical coupling of bone and muscle is readily appreciated, with bone providing the attachment sites and muscle loading the bone for locomotion. Recently, it has been shown that the two tissues bi-directionally communicate through secreted factors. Given that osteocytes compose 90-95% of total bone cells compared to other bone cell types in adult, these cells are a likely source that secretes majority of circulating factors. Connexin (Cx) 43, a protein richly present in osteocytes, forms functional gap junctions and hemichannels that mediate cell-cell and cell-extracellular communication, respectively, in osteocytes. To test if these channels are functionally involved in bone-muscle crosstalk, we used two Cx43 dominant negative mutant transgenic mouse models: R76W, a dominant negative mutant that blocks only gap junction channels; and Δ130-136, a dominant negative mutant that inhibits both gap junctions and hemichannels. The muscle mass and contractile function were determined *in vivo*, and the effects of primary osteocytes secreted factors on myogenesis of C2C12 myoblast were measured. Hematoxylin and eosin (H&E) stain on paraffin sections of gastrocnemius (GS) showed a decrease (10.6%) of muscle mass only in Δ130-136 compared to that of WT mice, but not in R76W mice. qPCR showed significant down-regulation of important myogenic markers Mrf4 and Myf5 in GS of both Δ130-136 and R76W mice. Isometric force of GS in Δ130-136 and R76W was decreased by 43% and 36%, respectively compared to WT mice. A significant reduction of fiber number of soleus (SOL) was seen in both types of transgenic mice. Conditioned media (CM) were collected from primary osteocytes isolated from 3-month-old Δ130-136, R76W and WT mice, respectively, and were used to culture C2C12 myoblast. Interestingly, treatment of CM from osteocytes of Δ130-136 significantly inhibited the differentiation of C2C12, with a reduction of myotube number/diameter and fusion index, while this difference was not shown with CM from R76W-expressed osteocytes. Collectively, these findings reveal the important roles of osteocytic gap junctions and hemichannels in modulating skeletal muscle structure and function; hemichannels in maintaining of muscle mass and regulation on myogenesis, while gap junctions in regulating muscle force and myofiber number.

Disclosures: *Guo Bin Li, None*

MON-0181

Effects of Sclerostin Depletion on Hematopoietic Stem Cells in the Bone Marrow and Spleen Cristine Donham^{*1}, Jennifer Manilay¹, Gabriela Loots², Aris Edonomides³. ¹University of California Merced, United States, ²University of California Merced, Lawrence Livermore National Laboratory, United States, ³Regeneron Pharmaceuticals, United States

The interactions between long-term hematopoietic stem cells (LT-HSCs) and cells in the bone microenvironment result in changes in stem cell behavior that are incompletely understood. Our overall goal is to define the molecular mechanisms that guide the behavior of LT-HSCs after exposure to an irregular bone marrow (BM) niche. Sclerostin (Sost) is a secreted Wnt antagonist protein that is important for bone homeostasis. We hypothesized that that loss of Sost would influence LT-HSC maintenance and self-renewal due to increased Wnt signaling in the bone. We performed transplantation of wild-type (WT) B6 hematopoietic progenitors into sclerostin-knockout mice (KO), and we have observed increased frequencies of LT-HSCs in WT → KO recipients, indicating that SostKO microenvironment enhances LT-HSC self-renewal. This increase was also observed in WT mice treated with anti-sclerostin antibodies. This suggests that even relatively short-term depletion of Sost can have effects on LT-HSCs. As the SostKO mice age, we have observed evidence of extramedullary hematopoiesis (EMH) in the spleen; whether EMH is induced simply by physical occlusion in the bone marrow cavity, or a change in signaling or migration patterns of BM LT-HSCs to mobilize them to the spleen is not yet clear. To test if LT-HSCs from the spleens and bone marrow of SostKO mice have similar reconstitution potentials, we performed transplantation of lineage negative (Lin-) cells isolated from KO spleen, KO BM, and WT BM into WT hosts. Donor hematopoietic chimerism in recipients of KO splenic LT-HSCs was significantly lower compared to recipients of KO BM. Reduction in the frequencies of LT-HSCs, multipotent progenitors, and differentiated hematopoietic lineages was also observed from KO splenic LT-HSCs. Our data suggest that splenic HSCs lose self-renewal and differentiation capabilities when they leave the bone marrow. We are currently investigating whether estrogen can influence the extent of EMH in the SostKO mice by comparing transplants of splenic KO LT-HSCs from male and female donors into sex-matched recipients. Taken together, our data indicate that depletion of Sost in the bone regulates LT-HSC migration, self-renewal, and differentiation. Our results could have significant impact on the tracking of hematopoietic function in human patients treated with sclerostin-depleting antibodies for bone diseases.

Disclosures: *Cristine Donham, None*

MON-0182

MicroRNA-17-5p Facilitates Bone Remodeling in Periapical Periodontitis

Daimo Guo*, Xinyu He, Ruoshi Xu, Xin Zhou, Liwei Zheng, Xuedong Zhou. State Key Laboratory of Oral Diseases; West China School of Stomatology, Sichuan University, China

Aims: Periapical periodontitis is an acute or chronic inflammatory disease of the periradicular tissue which can destroy the alveolar bone surrounding the tooth root apex. In current study, we tried to identify the miRNAs expression profile in periradicular lesions. Furthermore, we tried to promote bone remodeling by modulating the local concentration of miRNAs. **Methods:** Periapical lesions were induced in rats mandibular first molars. Small RNAs were isolated from the total RNA of bone surrounding the tooth root apex and underwent a rat miRNA Microarray. AgomiR-17-5p, antagomiR-17-5p, and their respective negative controls were sealed in root canal. Micro-CT, histological and immunohistochemical analyses were performed to evaluate the presence of bone remodeling. Bioinformatic analysis was performed to further identify pathways related to the bone remodeling under the influence of selected miRNAs. Isolation and culture of BMSCs, miRNA mimic were used to suppress the expression of target gene. Quantitative RT-PCR was used to measure the expression of related genes in RNA level. Expression of the target proteins was detected using western blot assay. **Results:** We identified 49 differentially expressed miRNAs in periradicular bone tissue, including 28 upregulated miRNAs and 21 downregulated miRNAs. We validated miRNAs differentially expressed in microarray analysis by q-PCR and found that the expressing level of miR-17-5p was lower in periradicular bone tissue of periapical periodontitis. Locally elevated miR-17-5p level had less bone loss in periradicular tissue relative to control. Also we identified zinc finger FYVE-type containing 9 (ZFYVE9) as the direct targets of miR-17-5p in TGF- β signaling pathway. **Conclusions:** The current findings supported the view that miR-17-5p could directly target ZFYVE9 in TGF- β signaling pathway. And locally elevated miR-17-5p level could reduce bone defect of periapical disease. These result may provide potential targets for future treatment of periradicular bone defect.

Disclosures: Daimo Guo, None

MON-0183

SINGLE-CELL RNA SEQUENCING ANALYSIS OF FRESHLY ISOLATED HUMAN SKELETAL STEM/PROGENITOR CELLS FROM HUMAN BONE MARROW

Randall Merling*, Joseph Featherall, Danielle Bonfim, Natasha Cherman, Sergei Kuznetsov, Pamela Robey. Skeletal Biology Section, National Institute of Dental and Craniofacial Research, National Institutes of Health, United States

Multipotential human skeletal stem cells (SSCs) are a subpopulation of bone marrow stromal cells (BMSCs) and are considered to be central mediators of skeletal homeostasis and support hematopoiesis. In order to better understand the character of BMSCs/SSCs, analysis of freshly isolated uncultured cells is needed. For enrichment of the SSCs, we used magnetic separation: RBC depletion followed by CD45+/CD31+ cell depletion. FACS sorting was then used to isolate CD146+/CD271+ double positive cells. There was a 220 to 720-fold increase in CFU-Fs, a close approximation of multipotent SSCs, from the CD146+/CD271+ enriched fraction compared to unpurified cells. Single-cell RNA sequencing analysis (10X Genomics Chromium) of this fraction revealed two distinct osteogenic populations: one subpopulation with over-representation of mature osteogenic markers (RUNX2, SPP1, IBSP, BGLAP, COL1A1, IFITM5), another subpopulation with over-representation of pericyte/BMSC markers (CXCL12, LEPR, FRZB, VCAN, IGFBP4, TAGLN, FRZB). All genes indicated are in the top 20 differentially expressed genes for each cluster group (P-Value < 10⁻⁶). Seurat, an R toolkit for single cell genomics was used to combine our data sets from CD146+/CD271+ enriched cells with publically available data sets from total bone marrow mononuclear cells. The double positive cells localize specifically to the osteogenic cluster of cells and distinctly away from non-osteogenic bone marrow mononuclear cell lineages represented by tSNE plots. Additional transcriptome network analyses of the mature osteogenic and pericyte/BMSC markers suggest a regulatory role of the SMAD pathway differentiating the subpopulations within the double positive population. Future work will entail targeting unique candidate genes from the single-cell analysis findings for knockdown in BMSCs/SSCs for evaluation by in vitro and in vivo assays to provide a better understanding of the hierarchy, biological nature and function in the bone/marrow microenvironment.

Disclosures: Randall Merling, None

MON-0184

Novel function of BMP-2 in inhibiting bone formation in marrow environment

Ha Nguyen Thi ^{*1}, Mitsuaki Ono ², Yasutaka Oida¹, Emilio Satoshi Hara³, Taishi Komori¹, Kentaro Akiyama¹, Ha Nguyen Thi Thu ¹, Hai Thanh Pham ¹, Kyawthu Aung¹, Toshitaka Oohashi², Takuo Kuboki ¹. ¹Department of Oral Rehabilitation and Regenerative Medicine, Okayama University Graduate School of Medicine, Dentistry and Pharmaceutical Sciences, Japan, ²Department of Molecular Biology and Biochemistry, Okayama University Graduate School of Medicine, Dentistry and Pharmaceutical Sciences, Japan, ³Department of Biomaterials, Okayama University Graduate School of Medicine, Dentistry and Pharmaceutical Sciences, Japan

Bone morphogenetic protein 2 (BMP-2) is widely known as a potent growth factor in promoting bone formation. In some clinical cases, it is necessary to induce bone formation in marrow area; however, the efficacy of BMP-2 in the marrow environment has not been thoroughly investigated. This study aimed to investigate the BMP-2 function in the marrow environment. At first, defects were made in mouse femur and calvaria, then transplanted with freeze-dried collagen pellet containing 10 μ g BMP-2 or distilled water (control) for 5 days and 14 days. Bone formation was evaluated by micro-CT and histological analysis. BMP-2 significantly enhanced bone formation in calvarial bone but dramatically inhibited bone formation in marrow-containing femur. Next, to investigate the effect of marrow cells on BMP-2 function, BMP-2/collagen pellet was transplanted into ablated femur with the confirmed decrease in the number of marrow cells. As expected, the capability of BMP-2 to induce bone formation was then recovered in the absence of marrow cells. Next, in an attempt to understand whether the marrow inhibits BMP-2-induced osteoblast differentiation, the appearance of osteoblasts was investigated in Col1a1-GFP mice. In control group, a high number of osteoblasts was observed in the surrounding of the pellet in marrow space after 5 days, and gradually decreased after 14 days. In BMP-2 group, the osteoblasts were detected markedly less in marrow space both at 5 days and 14 days after transplantation. To further analyze the effect of marrow on the inhibition of BMP-2-induced osteoblast differentiation, we investigated luciferase activity of C2C12 cells with BMP-responsive element (BRE) and ALP activity of MC3T3-E1 cells co-cultured with marrow or marrow components (cells and plasma). Similar to the in vivo findings, BMP-2 induced luciferase activity and ALP activity was significantly suppressed when marrow cells were co-cultured in direct contact with C2C12 or MC3T3-E1 cells. Marrow plasma only, blood cells (as the reference) or indirect co-culture did not affect BMP-2 function. Taken together, these results revealed that BMP-2-induced bone formation was significantly suppressed in marrow environment, and was associated with the depletion of osteoblasts. Marrow cells inhibited BMP-2-induced osteoblast differentiation as demonstrated by the repression of BMP-responsive luciferase activity and osteogenesis in a direct cell-cell contact manner.

Disclosures: Ha Nguyen Thi, None

MON-0185

The Effects of Interleukin-1 Receptor Antagonism on Endothelium-Dependent and Endothelium-Independent Vasodilation of Femoral Principal Nutrient Artery and Femoral Bone Parameters in Young Male Fischer-344 Rats Sunggi Noh*, Seungyong Lee, David Lee, Rhonda Prisby. University of Texas at Arlington, United States

We previously reported impaired endothelium-dependent vasodilation of the femoral principal nutrient artery (PNA; the primary conduit for blood flow to long bones) in the presence of marrow. The declines in vasodilator capacity were associated with augmented production of the pro-inflammatory cytokines interleukin-1 α and -1 β from the marrow cells. Thus, we surmised that treatment with an interleukin-1 receptor antagonist (IL-1RA) may blunt the production of marrow-derived IL-1 α and IL-1 β , serving to protect endothelium-dependent vasodilation. Young (5 months) male Fischer-344 rats were randomized to a control (CON; n=5) or IL-1RA (n=5) group and underwent surgery to create a small bone defect in the right femur. Following recovery from surgery, rats were injected intraperitoneally with IL-1RA (3 μ g/kg, 3 days/week) or phosphate buffered saline as a vehicle (100 μ l/day, 3 days/week) for 3 weeks. At sacrifice, right femoral PNAs were isolated, cannulated, and pressurized to 60 cmH₂O (44 mmHg) to assess vasodilator function. Endothelium-dependent (ACh; 10⁻⁹ - 10⁻⁴ M) and endothelium-independent (DEA NONOate; 10⁻¹⁰ - 10⁻⁴ M) vasodilation were determined in the absence and presence of marrow. In addition, bone microarchitectural properties (BV/TV, %; Tb.N, /mm; Tb.Th, μ m; Tb.Sp, μ m and Conn.D, /mm³) in the distal femoral metaphysis were determined by micro-computed tomography. The presence of marrow reduced (p<0.05) endothelium-dependent vasodilation in CON rats; i.e., vasodilation in CON+Marrow was impaired vs. CON and IL-1RA). Three weeks of IL-1RA treatment improved endothelium-dependent vasodilator capacity such that responses were similar between IL-1RA and IL-1RA+Marrow. In addition, vasodilation in IL-1RA was higher (p<0.05) vs. CON+Marrow. Endothelium-independent vasodilation did not differ between CON and CON+Marrow but responses in IL-1RA+Marrow were reduced (p<0.05) in comparison to CON. Further, vasodilator responses were higher (p<0.05) in IL-1RA vs. CON+Marrow and IL-1RA+Marrow. Bone volume did not differ between the CON (13 \pm 6%) and IL-1RA (15 \pm 4%) groups; however, Tb.N (2.4 \pm 0.1 /mm vs. 2.9 \pm 0.2 /mm, respectively) and Conn.D (41 \pm 2 /mm³ vs. 51 \pm 2 /mm³, respectively) were higher (p<0.05) in IL-1RA vs. CON. In this context, Tb.Sp was lower (p<0.05) in IL-1RA (345 \pm 22 mm) vs. CON (427 \pm 20 mm). IL-1RA treatment improved endothelium-dependent vasodilation in

the presence of marrow; however it may have served to impair endothelium-independent vasodilation.

Disclosures: *Sunggi Noh, None*

MON-0186

Mitochondrial Function in Mesenchymal Stem Cells and New Bone Formation During Spinal Fusion Laura Shum*, Avionna Baldwin, Addisu Mesfin, Roman Eliseev. University of Rochester, United States

Iliac crest autografts are often used in spine surgery, and bone marrow-derived mesenchymal stem cells (MSCs) are believed to be responsible for new bone formation during spinal fusion. We have previously shown the importance of mitochondrial function in MSCs, and thus we designed the current study to determine the impact of mitochondrial function in MSCs on spinal fusion surgery outcomes. Iliac crest bone marrow samples were obtained from patients undergoing spinal fusion surgery (9 male, 4 female, average age 48.3, age range 16-73). Aliquots of whole bone marrow were reserved for CMXRos staining (mitochondrial function), and the remainder was spun, treated with Red Blood Cell Lysis Buffer, strained, and plated at either CFU density (25,000 cells per cm²) or at 20 million cells per 15 cm cell culture dish for expansion. CFU plates were grown for 14 days, then stained with crystal violet for CFU-fibroblastic (CFU-F) or with ALP-specific stain for CFU-osteoblastic (CFU-O). Surface markers were detected with fluorescently-labeled anti-human antibodies against CD105, CD31, and CD45 (BD Bioscience) using flow cytometry and 12-color FACS Canto II machine. At 6 months following spinal fusion surgery, surgeons assessed patient spinal healing by radiographic assessment (Lenke grading). A grade of A (best) – D (worst) was given. Human patient colony forming unit assay did not correlate with patient age or spinal fusion outcomes; and spinal fusion outcomes did not decrease with age within the studied age range. Additionally, we found that mitochondrial function of MSCs did not decrease with age. However, we found that higher mitochondrial function in freshly isolated MSCs correlated with better spinal fusion outcomes. Our study revealed a correlation between mitochondrial function assessed in isolated MSCs and spinal fusion outcomes. This information could be used as a predictor of the need for additional modalities to improve surgical outcomes. Importantly, this study opens new research questions regarding whether improving mitochondrial function of MSCs prior to grafting would improve surgical outcomes for more patients.

Disclosures: *Laura Shum, None*

MON-0213

Aplidin (Plitidepsin) is a Novel Anti-Myeloma Drug with Potent Anti-Resorptive Activity Mediated by Direct Effects on Osteoclasts. Jesus Delgado-Calle*¹, Noriyoshi Kurihara¹, Jessica H. Nelson¹, Emily G. Atkinson², Carlos Galmarini³, G. David Roodman¹, Teresita Bellido². ¹Indiana University School of Medicine, Dept. of Medicine, Hematology/Oncology, United States, ²Indiana University School of Medicine, Dept. of Anatomy and Cell Biology, United States, ³PharmaMar S.A., Spain

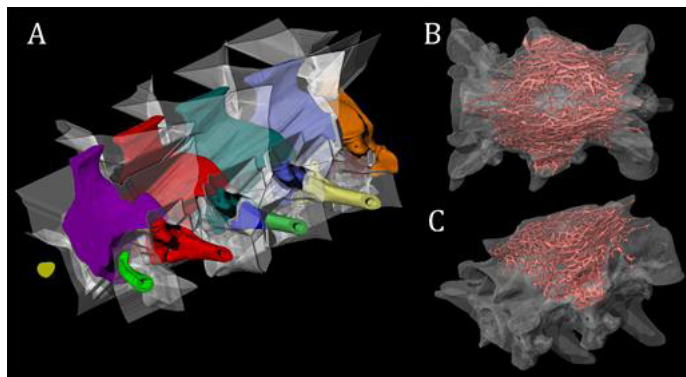
Despite recent progress in its treatment, Multiple Myeloma (MM) remains incurable and the associated bone disease persists even after complete remission. Thus, identification of new drugs that simultaneously suppress MM growth and protect bone is an unmet need. We examined the effects of Aplidin, a novel anti-cancer marine-derived agent isolated from *Aplidium albicans*, on MM and bone cells using in vitro and ex vivo approaches. Aplidin ≥ 1 nM decreased human JJN3 and murine 5TGM1 MM cell numbers in a dose- and time-dependent manner (EC₅₀~10nM), accompanied by increased cell death. The other anti-MM agents dexamethasone (Dex; 10-5M) or bortezomib (Btz; 3nM) also decreased MM cell numbers and significantly enhanced the effect of Aplidin by 1.6-fold and 2.5-fold, respectively. Aplidin ≥ 10 nM also increased osteocyte and osteoblast cell death to 15%, and reduced osteoblast mineralization by 20%. These effects were enhanced by Dex, but partially prevented by Btz. Osteoclastic cells (Ocl) exhibited high sensitivity to Aplidin, as nM doses induced massive Ocl death. When tested at pM doses, Aplidin decreased GM-CSF colony formation by 15%, reduced M-CSF-mediated Ocl precursor expansion, and decreased RANKL-mediated Ocl differentiation by blunting ERK but not P38 kinase activation. In contrast, Dex increased Ocl numbers by 3.3-fold, while Btz decreased Ocls by ~50%. Co-treatment with Aplidin 0.1pM reduced Dex-induced Ocl numbers by 25% and further decreased Ocls when combined with Btz. Aplidin also decreased mature Ocl numbers, and either alone or in combination with Dex or Btz, markedly reduced the number of resorption pits formed by mature Ocls on bone slices. Lastly, we examined the effects of Aplidin on MM cell growth (IgG2b) and bone resorption (CTX) in conditioned media (CM) from ex vivo bone organ cultures that reproduce the 3D-organization and the cellular diversity of the MM/bone marrow niche. CM from bones bearing 5TGM1 MM cells exhibited increased CTX and IgG2b levels compared to bones without MM. Aplidin (10nM) decreased IgG2b and CTX levels by 80% and 50% respectively after 3d, and reduced IgG2b and CTX levels to control levels after 12d. Suboptimal doses of Aplidin alone (1nM, x3d) were ineffective; but combined with Dex or Btz, Aplidin significantly decreased IgG2b and CTX levels in bones with MM. Thus, Aplidin exhibits potent anti-myeloma and anti-resorptive activities, and enhances proteasome inhibitor blockade of MM growth and bone destruction.

Disclosures: *Jesus Delgado-Calle, PharmaMar, Grant/Research Support*

MON-0214

Automatic Bone Measurement from X-Ray Computed Tomography and New Snake Osteosarcoma Alexander Hall*. Thermo Fisher Scientific, United States

Analyzing three-dimensional data often requires slow and tedious manual decision making by a trained user. Traditionally, decisions about what belongs to a material are made layer-by-layer for every single image in a z-stack of hundreds or thousands of images. For example, digitally extracting one single bone from a complete skeleton is often the most time consuming portion of comparative morphology projects. Using X-ray computed tomography data with sufficient information about biologically real boundaries (sutures, joints, etc.), one can use Thermo Scientific™ Amira-Avizo™ Software to automatically segment skeletons. In this project, I achieved a new workflow using an object separation process within the software (Fig. 1A). After optimizing the object separation parameters, individual bones were isolated and measured with only a fraction of the work required by manually selecting bones layer by layer. I will present a use case where I studied several snake skeletons at the single-bone level leading to the discovery of a neoplasm, currently thought to be an osteosarcoma (Figs. 1B and 1C). This process can be quite useful for studies of non-human systems, including mammals and reptiles. Anyone with this software or similar image analysis tools can implement this method, given some experimentation with optimizing for your data.



Disclosures: *Alexander Hall, None*

MON-0215

The effects of castration on prostate cancer tumor growth in bone Tiina E Kähkönen*¹, Mari I Suominen¹, Jenni Mäki-Jouppila¹, Jussi M Halleen¹, Jenni Bernoulli¹, Pascale Lejeune². ¹Pharmatest Services, Finland, ²Bayer AG, Germany

Advanced prostate cancer tumors typically lose their dependence on endogenous androgens, leading to aggressive growth and development of metastatic castration resistant prostate cancer (mCRPC). High incidence of bone metastases is typical for mCRPC patients and causes high morbidity. The aims of this study were to evaluate the effects of castration on tumor growth and tumor-induced changes in bone, and to establish a preclinical model that could be used for evaluation of efficacy of new therapies against mCRPC. NOD.Scid male mice aged 5-6 weeks were divided into three groups. One group was left intact and two groups were castrated either before or 4 weeks after inoculation of 2x10⁶ VCaP human prostate cancer cells to proximal tibia. Tumor-induced bone changes (lesions) were followed by X-ray imaging during the study, and imaged by micro-computed tomography (μ CT) at endpoint. Tumor growth was followed by measuring serum PSA levels, and evaluated by histology and immunohistochemical staining for androgen receptor (AR) and AR variant 7 (AR-V7) at endpoint. Castration decreased the weight of androgen-dependent organs, indicating decreased androgen levels. VCaP cells induced osteoblastic-mixed bone lesions and castration did not affect the lesion type. Bone lesion growth was similar in all study groups, but a trend towards decreased lesion area was observed in the mice castrated before cancer cell inoculation. μ CT imaging showed less changes in cortical bone of the mice castrated before cancer cell inoculation. Castration was associated with a trend towards increased cortical bone area in healthy tibias. PSA levels were similar in intact mice and in the mice castrated 4 weeks after the cancer cell inoculation, and lower in the mice castrated before the cancer cell inoculation. Castration strongly induced AR and AR-V7 expression in the tumors, and decreased tumor take rate from 60% to 40 - 50% based on evaluation of X-ray images, PSA levels and histological findings. These results demonstrate that castration alters tumor growth rate, and suggest that early phases of tumor development into the bone are androgen-regulated. Castration may have direct effects on bone, and it may induce changes in marker expression in the tumor cells. Careful validation of preclinical models is essential in selecting most predictive models for evaluation of efficacy of new therapies against mCRPC.

Disclosures: *Tiina E Kähkönen, None*

MON-0216

$\alpha 4\beta 1$ Integrin and vascular cell adhesion molecule (VCAM) 1 interactions regulate myeloid-derived suppressor cells (MDSC) mobilization from the bone metastatic tumor hosts Kyung Jin Lee*¹, Eun Jeong Lee¹, Bo Yeon Seo¹, Sun Wook Cho², Serk In Park¹. ¹Korea University College of Medicine, Republic of Korea, ²Seoul National University Hospital, Republic of Korea

MDSCs are a subset of immature bone marrow-derived cells that play diverse pro-tumorigenic roles such as suppressing T cell-mediated anti-tumoral immunity. We have previously reported that tumor-derived parathyroid hormone-related peptide (PTHrP) increased MDSC recruitment in tumor tissue. In contrast, little is known about how MDSCs are mobilized from the bone marrow of tumor hosts. In this study, we investigated whether interactions between $\alpha 4\beta 1$ integrin expression in MDSCs and VCAM 1 expression in the bone marrow stromal cells (BMSC) regulate retention and release of MDSCs in the bone marrow. CD11b+Gr1+ cells (commonly defined as murine MDSCs) were isolated from the femurs by flow cytometry, and in vitro cell binding assays were performed. Briefly, MDSCs were carboxyfluorescein succinimidyl ester (CFSE)-stained and co-cultured with MC3T3E1 pre-osteoblastic cells in the presence of anti-VCAM 1 and/or anti- $\beta 1$ integrin neutralizing antibodies (0.5 to 2 $\mu\text{g}/\text{mL}$). After washing unbound cells, fluorescence intensity was measured to quantify MDSC-BMSC binding. VCAM-1 and/or $\beta 1$ integrin neutralizing antibodies dose-dependently decreased MDSC-BMSC binding, suggesting that MDSCs bind to BMSC via VCAM-1 and $\beta 1$ integrin. We further examined whether tumor-derived PTHrP disrupts the VCAM-1 and $\beta 1$ integrin axis of MDSC-BMSC. PTHrP (1-34) administration rapidly increased MDSCs in the peripheral blood in vivo. In addition, PTHrP conditioned-media from calvarial osteoblasts reduced MDSC-BMSC binding in vitro compared with control conditioned media, and the effects were reversed by anti-interleukin (IL)-6 or anti-vascular endothelial growth factor (VEGF)-A antibodies, suggesting that PTHrP-induced IL-6 and VEGF-A expression in osteoblasts mobilize MDSCs. In addition, recombinant IL-6 and VEGF-A reduced MDSC-BMSC binding in vitro. Lastly, immunohistological analyses of the bones of tumor-bearing mice showed that CD11b+Gr1+ cells localized adjacent to trabecular osteoblasts. In summary, our data demonstrate that bone marrow stromal cells regulate MDSC trafficking from the bone marrow to the peripheral blood, and also that VCAM-1 (expressed in BMSC) and $\alpha 4\beta 1$ integrin (expressed in MDSC) interactions regulate MDSC retention and mobilization. Further studies on the PTHrP-induced expression of proteinases such as matrix metalloproteinases and A Disintegrin and Metalloproteinase (ADAM) in bone will elucidate the mechanism of MDSC mobilization in the bone marrow of tumor hosts.

Disclosures: *Kyung Jin Lee, None*

MON-0217

WITHDRAWN

MON-0218

Microfluidic Platform for Investigation of Mechanoregulation of Breast Cancer Bone Metastasis Xueting Mei*¹, Kevin Middleton², Yu-Heng Ma², Liangcheng Xu², Noosheen Walji¹, Edmond Young^{1,2}, Lidan You^{1,2}. ¹Department of Mechanical and Industrial Engineering, University of Toronto, Canada, ²Institute of Biomaterials and Biomedical Engineering, University of Toronto, Canada

Introduction: Approximately 70% of advanced breast cancer patients experience bone metastasis (1). Breast cancer cells (BCC) that invade across the endothelium to the bone reduce bone quality by altering normal osteoclast activity. Exercise, a common cancer intervention strategy, can regulate bone remodeling, thus potentially affect BCC metastasis to bone through mechanotransduction of osteocytes. Our recent in vitro studies showed that mechanically stimulated osteocytes can regulate BCC migration and modify endothelial cells (2). However, a more physiologically relevant platform is needed to better investigate the mechanisms leading to interactions between BCC and bone microenvironment under mechanical loading. We present here a novel in vitro microfluidic tri-culture lumen model for studying mechanical regulation of breast cancer metastasis. **Methods:** Highly metastatic MDA-MB-231 human BCCs were cultured inside a lumen lined with human umbilical vein endothelial cells (HUVECs) (3), which is adjacent to a population of either static or mechanically-stimulated osteocyte-like MLO-Y4 cells (Figure 1A). Soluble factors were diffused through hydrogel-filled side channels to instigate intercellular communication between MLO-Y4 cells and BCCs over 3 days. BCC transendothelial invasion distances were measured and normalized to the control without MLO-Y4 cells and osteoclast conditioned media (CM). Mechanical stimulation of osteocytes was validated by measuring intracellular calcium fluctuation under flow. **Results:** Photolithography and soft lithography were used to fabricate silicon SU-8 master and PDMS replicates. An HUVEC lumen was successfully cultured in the PDMS microfluidic device (Figure 1B). Experiments showed that BCCs invaded 37% ($p < 0.05$) further for static osteocytes cultured in osteoclast CM comparing to no osteoclast CM (Figure 1C & D), likely due to osteoclast support of cancer cell growth (4). **Discussion:** We developed a novel microfluidic platform allowing the integration of physiological relevant fluid stimulation and real-time intercellular signaling between different cell populations in vitro. Future work with this platform will elucidate the effects of bone mechanical loading on BCC transendothelial invasion and determine the key mechanisms

involved in osteocyte regulation of BCC metastasis. References: (1) Hagberg. Cancer Epidemiol. 2013. (2) Ma. J. Cell. Biochem. 2018. (3) Bischel. Biomaterials. 2013. (4) Yaccoby. Cancer Res. 2004.

Figure 1A

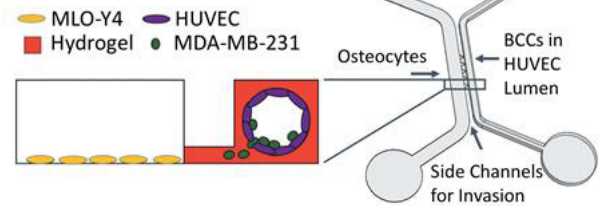


Figure 1B

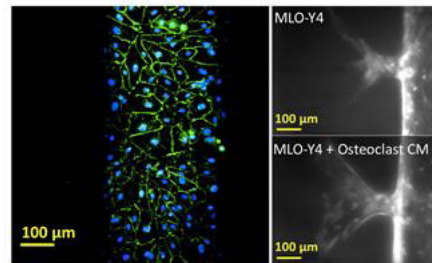
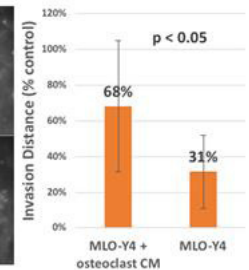


Figure 1C

Figure 1D



Disclosures: *Xueting Mei, None*

MON-0219

IL-6 family cytokines and receptors regulate breast cancer bone colonization and tumor progression Tolu Omokehinde*¹, Miranda Sowder¹, Rachelle Johnson². ¹Vanderbilt Center for Bone Biology, Vanderbilt University Medical Center, United States, ²Vanderbilt Center for Bone Biology, Department of Medicine, Division of Clinical Pharmacology, Vanderbilt University Medical Center, United States

Breast cancer cells commonly metastasize to bone, where they may induce osteolysis, leading to increased fracture risk. Through mechanisms that remain unclear, bone-disseminated breast cancer cells may also enter a period of quiescence prior to inducing bone destruction. The interleukin-6 (IL-6) cytokine family includes IL-6, leukemia inhibitory factor (LIF), and oncostatin M (OSM), among others, and has known roles in bone colonization. Our lab has previously shown that LIF receptor (LIFR) expression on breast cancer cells promotes tumor cell dormancy in the bone marrow, but since LIF, OSM, and several other IL-6 cytokines are able to complex with LIFR, it remains unclear which ligand, if any, induces pro-dormancy signals through LIFR. To examine this, we performed qPCR analysis for OSM, LIF, OSMR and LIFR mRNA levels across a panel of breast cancer cell lines, including parental (MCF7, SUM159, D2.0R, MDA-MB-231, 4T1) and bone-metastatic variants (MCF7, MDA-MB-231, 4T1). Our goal was to identify patterns of expression of the ligands and receptors. LIFR and OSMR showed a similar pattern of expression and were highest in cell lines with low metastatic potential (MCF7, SUM159, and D2.0R). LIF and OSM expression did not correspond with metastatic potential but were detectable at the mRNA level across all breast cancer cell lines. Interestingly, LIFR, but not OSMR mRNA levels, were lower in the bone metastatic variants of MDA-MB-231 (70% lower) and 4T1 cells (86% lower, $p < 0.01$) compared to parental cells, which already have low LIFR function. OSM had a similar expression profile, with decreases in expression for bone metastatic variants of MDA-MB-231 (90% lower, $p < 0.05$) and 4T1 cells (85% lower), suggesting that OSM signaling through LIFR may prevent bone homing. In support of our in vitro data, breast cancer patient data from Kaplan-Meier (KM) Plotter indicates that patients with high OSM and OSMR levels experience significantly greater relapse free survival ($p < 0.05$ - $p < 0.0001$), and we have previously shown that loss of LIFR corresponds with reduced patient survival. These data suggest that OSM signaling through LIFR or OSMR in breast cancer cells may confer tumor dormancy and prevent breast cancer bone dissemination. In future studies we will determine the effects of OSM and LIF in tumor dissemination to bone using CRISPR/Cas9 to knockout OSM, LIF, and OSMR in breast cancer cell lines and evaluate their ability to disseminate to and colonize the bone marrow.

Disclosures: *Tolu Omokehinde, None*

MON-0220

Extracellular ATP Reduces Osteosarcoma Single and Collective Migration Through the P2X7 Receptor Daniel Shropshire*, Manuel Riquelme, Jean Jiang. UT Health Science Center San Antonio, United States

Osteosarcoma (OS) is the most common primary bone cancer and primarily affects adolescents. Metastasis is a usually fatal complication and responsible for the majority of mortality due to the disease. The primary tumor microenvironment is a crucial regulator of the metastatic process, which requires cancer cell motility and invasion. OS most commonly arises on long bone endosteum, an environment influenced by osteocyte connexin 43 hemichannels that release ATP and other paracrine signaling factors. Activation of the P2X7 ATP receptor drives differentiation in normal osteoblastic precursors and osteosarcoma, which is correlated with better prognosis. We therefore hypothesized that osteocytic connexin 43 hemichannels play a role in osteosarcoma progression. We found that extracellular ATP (200 μ M) and P2X7R-specific agonist BzATP reduce single and collective migration in OS-17 cells, an osteoblastic OS cell line that robustly expresses the receptor. Chondroblastic MOS-J OS cells do not express P2X7R but have an even greater migratory inhibition due to extracellular ATP, with chemotaxis inhibition at 10 μ M. In neither cell line did ATP metabolite adenosine (200 μ M) significantly alter cell migration. These findings point to osteocytic connexin 43 hemichannels as potential regulators in osteosarcoma metastasis through purinergic signaling.

Disclosures: Daniel Shropshire, None

MON-0221

A role for immunoglobulins in the osteolytic bone disease of multiple myeloma Marita Westhrin*, Vlado Kovacic¹, Albert Bondt², Stephanie Holst², Zejian Zhang³, Tobias Slordahl⁴, Anders Sundan⁴, Anders Waage⁴, Manfred Wuhrer², Therese Standal¹. ¹Department of Clinical and Molecular Medicine/Centre of Molecular Inflammation Research, Norwegian University of Science and Technology (NTNU), Norway, ²Leiden University Medical Center, Leiden University, Netherlands, ³Key Laboratory of Glycoconjugate Research Ministry of Public Health, School of Basic Medical Sciences, Fudan University, China, ⁴Department of Clinical and Molecular Medicine, Norwegian University of Science and Technology (NTNU), Norway

Most patients with multiple myeloma develop a severe osteolytic bone disease causing pain and fractures. The myeloma cells secrete immunoglobulins and the presence of monoclonal immunoglobulins in the patients' sera is the main diagnostic criteria. Immunoglobulins play a role in bone loss in rheumatoid arthritis, but have not, surprisingly perhaps, been linked with the bone disease in multiple myeloma. In this work, we isolated immunoglobulins from serum of myeloma patients using protein G coupled magnetic beads and columns. We found that immunoglobulins from patients with bone disease (n=18) promoted osteoclast differentiation when added to human monocyte-derived pre-osteoclasts in vitro, whereas immunoglobulins from patients without bone disease (n=13) did not. The effect was mediated, at least partly, by Fc γ R2, since inhibiting Fc γ R2 reduced the effect of the immunoglobulins on osteoclastogenesis. Fc γ R2 is known to bind primarily immune-complexes. Indeed, when we fractionated the immunoglobulin samples by size-exclusion chromatography we found that the "osteoclast promoting activity" was in the high-molecular weight fractions, suggesting that they are in complexes. Since extent of complex formation may be determined by immunoglobulin glycosylation, we next examined whether there is a difference in immunoglobulin glycosylation between healthy controls and patients, and whether it changes during disease progression. To this end we analysed IgG glycosylation in serum samples from patients (n=72) and age and sex matched controls (n=51). These analyses showed that patient IgG was less galactosylated (p=0.02) and less sialylated (p=0.04) compared with control IgG. Moreover, patients with bone disease (n=43) had significantly less galactose on IgG compared with patients without bone disease (p=0.02, n=29). Further, the glycosyltransferases ST6GAL1 and B4GALT1, which adds sialic acid and galactose to the sugar chain, respectively, are less expressed in plasma cells obtained from patients with bone disease (n=137) compared with those without (n=36, p<0.002, p<0.001). Importantly, we observed a significant reduction of IgG glycosylation (p=0.02, n=8) in serum samples obtained from individual patients before and after the onset of bone disease. Taken together, our data support that immunoglobulins may directly promote bone loss in multiple myeloma.

Disclosures: Marita Westhrin, None

MON-0222

HIF-2 α is Sufficient to Cause Aggressive Fibroproliferative Lesions in the Developing Limb Zachary Tata*, Christophe Merceron, Mohd Parvez Khan, Ernestina Schipani. Department of Orthopedic Surgery, School of Medicine, University of Michigan, United States

The Hypoxia Inducible Factors 1 α and 2 α (HIF-1 α and HIF-2 α) are critical mediators of the cellular response to low oxygen tension (hypoxia). In normoxia, the HIFs are ubiquitinated by the E3-ubiquitin ligase von Hippel Lindau (VHL) and targeted to the proteasome for degradation. However, in hypoxia, they are stabilized and translocate to the nucleus where they regulate transcription of numerous genes. The HIFs are also implicated in pathological

states such as fibrosis and tumor initiation. We have previously established that loss of VHL in the limb bud mesenchyme produces fibroblastic tumors in proximity to the synovial joints. The onset of these tumors is HIF-1 α dependent. Moreover, their frequency is reduced by the concomitant loss of HIF-2 α . Our findings, in addition to the knowledge that VHL possesses both HIF dependent and independent functions, led us to question if the HIFs are sufficient to initiate fibroblastic tumors. Mice expressing a stabilized form of HIF-1 α or HIF-2 α in the limb bud mesenchyme (PRX;HIF-1dPAf/f and PRX;HIF-2dPAf/+) were generated. Both mutant proteins are constitutively active regardless of oxygen tension. Mutant mice were grown for 12 weeks and screened for the presence of fibroproliferative lesions by nanoCT and histology. PRX;HIF-1dPAf/f mice (n=30) did not show any lesion development up to 12 weeks of age. 35% of PRX;HIF-2dPAf/+ mice (n=30) developed masses, primarily in proximity to the radiocarpal joint. Similarly to the tumors observed in VHL mutant mice, these lesions were characterized by fibroproliferation, a core of amorphous, and most likely necrotic, material, and the ability to invade and destroy adjoining tissues. However, they developed more slowly and in different locations. Work is currently in progress to establish a PRX;HIF-2dPAf/+ xenograft model to determine the degree of malignancy of these fibroproliferative lesions and to conduct a microarray to compare their molecular signature to that of the VHL tumors. HIF2 overexpression is sufficient to generate discrete fibroproliferative lesions in proximity to synovial joints up to 12 weeks of age. These lesions share characteristics of the VHL tumors, yet differences render each unique. The significance of this study is twofold. It contributes to our understanding of the function of the hypoxia signaling pathway in mesenchymal cell biology in addition to offering insight into potential roles it may play in the development of human sporadic fibrosarcomas.

Disclosures: Zachary Tata, None

MON-0223

Opposite effects of TRAIL on the Sp1-c-FLIP survival pathway in myeloma cells and osteoclasts. Hirofumi Tenshin*, Jumpei Teramachi², Masahiro Hiasa¹, Asuka Oda³, Mohannad Ashtar¹, Kotaro Tanimoto¹, Iwasa Masami³, Ariunzaya Bat-Erdene³, Takeshi Harada³, Singen Nakamura³, Hirokazu Miki⁴, Itsuro Endo³, Eiji Tanaka¹, Toshio Matsumoto⁵, Masahiro Abe³. ¹Department of Orthodontics and Dentofacial Orthopedics, Institute of Biomedical Sciences, Tokushima University Graduate School, Japan, ²Department of Tissue Regeneration, Institute of Biomedical Sciences, Tokushima University Graduate School, Japan, ³Department of Hematology, Endocrinology and Metabolism, Institute of Biomedical Sciences, Tokushima University Graduate School, Japan, ⁴Division of Transfusion Medicine and Cell Therapy, Tokushima University Hospital, Japan, ⁵Fujii Memorial Institute of Medical Sciences, Tokushima University, Japan

Multiple myeloma (MM), a malignancy of plasma cells, induces receptor activator of nuclear factor kappa-B ligand (RANKL)-mediated osteoclastogenesis; thus activated osteoclasts (OCs) in turn enhance MM growth, thereby forming a vicious cycle between MM tumor expansion and osteoclastic bone destruction. Although TNF-related apoptosis-inducing ligand (TRAIL) induces apoptosis in MM cells, we reported that TRAIL enhances OC differentiation and activity. The present study was undertaken to dissect the underlying mechanism of this cell type-specific effects of TRAIL, focusing on regulation of the critical survival mediator c-FLIP. Intriguingly, TRAIL substantially reduced c-FLIP expression at mRNA and protein levels in MM cells, whereas further upregulating it in OCs. Because c-FLIP is a target gene of the transcription factor Sp1, we next looked at the role of Sp1 in c-FLIP expression in these cells. TRAIL was found to form complex II but not DISC to activate the TAK1-NF- κ B-Sp1 signaling pathway in OCs; however, inhibition of Sp1 abrogated their upregulation of c-FLIP by TRAIL, indicating a critical role of Sp1. In contrast, TRAIL was able to activate caspase-8 and reduce Sp1 at protein but not mRNA levels in MM cells. The caspase-8 inhibitor Z-IETD-FMK restored Sp1 protein levels in parallel with resumption of c-FLIP mRNA expression in MM cells, suggesting caspase-8-dependent enzymatic degradation of Sp1 protein to reduce c-FLIP. In OCs, the TAK1 inhibitor LLZ1640-2 inhibited NF- κ B activation to reduce Sp1 expression in the presence of TRAIL while inducing caspase-8 activation to trigger Sp1 protein degradation and cell death. In addition, cocultures with OCs upregulated c-FLIP expression to blunt TRAIL-induced cell death in MM cells. However, LLZ1640-2 substantially reduced c-FLIP expression to restore the TRAIL-induced caspase-8 activation and cell death in MM cells in the cocultures with OCs. These results demonstrate that c-FLIP levels are regulated in an Sp1-dependent manner by TRAIL in MM cells and OCs in the downward and upward directions, respectively, and suggest that TAK1 inhibition triggers TRAIL-induced apoptosis in OCs while potentiating its anti-MM action.

Disclosures: Hirofumi Tenshin, None

MON-0224

Disruption of a progressive vicious cycle between myeloma tumor growth and bone destruction by TAK1 inhibition Jumpei Teramachi^{*1}, Hirofumi Tenshin¹, Masahiro Hiasa¹, Asuka Oda¹, Ariunzaya Bat-Erdene¹, Takeshi Harada¹, Shingen Nakamura¹, Hirokazu Miki², Itsuro Endo¹, Toshio Matsumoto¹, Masahiro Abe¹. ¹Tokushima University, Japan, ²Tokushima University Hospital, Japan

Multiple myeloma (MM) has a unique propensity to develop and expand almost exclusively in the bone marrow and generates destructive bone disease. MM cell interaction to bone marrow stromal cells (BMSCs) confers cell adhesion-mediated drug resistance (CAM-DR) or secreted factor mediated drug resistance (SFM-DR) along with induction of bone destruction. We have reported that PIM2 is upregulated in MM cells and their surrounding cells in bone lesions, and that treatment with PIM inhibitors suppressed MM tumor growth and bone destruction. We subsequently identified TGF- β -activated kinase-1 (TAK1) as an upstream mediator responsible for PIM2 up-regulation in these cells. Here, we therefore aimed to clarify TAK1 activation status in MM-bone marrow interaction and the therapeutic impact of TAK1 inhibition. TAK1 was constitutively overexpressed and phosphorylated in all MM cell lines tested; the TAK1 inhibitor LLZ1640-2 suppressed NF- κ B activation and thereby PIM2 expression to induce apoptosis in MM cells. Interestingly, treatment with LLZ1640-2 reduced the expression of TAK1 and Sp1 in MM cells. Although Sp1, a transcription factor for TAK1 gene expression, is upregulated in MM cells, inhibition of NF- κ B as well as TAK1 reduced Sp1 levels in MM cells. The Sp1 inhibitor terameprocol reduced TAK1 levels in MM cells, suggesting a progressive amplification loop in TAK1- NF- κ B-Sp1 signaling. When BMSCs were co-cultured with MM cells, TAK1 phosphorylation was also induced in parallel with upregulation of VCAM-1, IL-6 production and the critical osteoclastogenic mediator RANKL in BMSCs; however, the TAK1 inhibition reduced the VCAM-1 and RANKL expression and IL-6 production by BMSCs and impaired MM cell adhesion onto BMSCs and CAM-DR to doxorubicin. Furthermore, treatment with LLZ1640-2 substantially suppressed osteoclastogenesis in cocultures of bone marrow cells with MM cells. The TAK1 inhibition also suppressed VEGF production and the expression of BCMA and TACI, receptors for BAFF and APRIL. These results collectively demonstrate that TAK1 plays a pivotal role in MM cell-bone marrow interaction to enhance tumor progression and bone destruction in MM. Therefore, TAK1 inhibition may become a unique anti-MM therapeutic option with bone-modifying activity.

Disclosures: **Jumpei Teramachi**, None

MON-0225

In Situ Imaging of Collagen Degradation May Assess Myeloma Bone Disease Activity Donghoon Yoon^{*1}, Ikjae Shin¹, Juchan Lim¹, Carol Morris¹, Lucas Bennink², S. Michael Yu², Gareth Morgan¹, Maurizio Zangari¹. ¹University of Arkansas for Medical Sciences, United States, ²University of Utah Department of Bioengineering, United States

Collagen is the most abundant protein in bone matrix and continuously remodeled. Aberrant collagen remodeling are often found in pathological conditions including multiple myeloma (MM). Myeloma lytic bone disease (MBD) is associated with patient morbidity and mortality. The recently developed collagen hybridizing peptide (CHP) selectively binds to denatured collagen in vitro in conjunction and with near-infrared fluorescence (NIRF) dye indicates detection of the collagen degradation activity in vivo. We transplanted 1x10⁶ Luciferase expressing 5TGM1 cells (5TGM1-Luc) into 8 ~ 12 week old non-obese diabetic-acid IL2rg^{-/-} (NSG) mice via tail vein. Myeloma progression was monitored weekly by bioluminescence (BL) imaging using IVIS-200 (PerkinElmer). The median post-transplant animal survival was 40 days. When the mouse developed endpoint symptoms (i.e. >109 BL signals, hind limb paralysis, significant weight loss), 1nM of NIRF conjugated CHP was intravenously injected. NIRF imaging was taken using IVIS-200. At postmortem, spine and femur/tibia were surgically removed ex vivo images were obtained for BL and NIRF images. Extracted bones were scanned by micro-computer tomography (microCT400, Scano medical Inc) and prepared for the bone histomorphometric analysis. In vivo BL image analysis showed that myeloma cells initially appears at spine level at 4th week and subsequently spread on 5th and 6th week. Micro-CT analysis confirmed osteolytic lesions at the lumbar spine. In vivo, NIRF signals significantly increased in MM mouse compare to control mouse (P<0.0001) and showed a positive correlation to BL signal. In the ex vivo analysis, NIRF signals were found located in lumbar spine and joint areas of the femur/tibia. The area with high NIRF signal does not matched with areas of previous bone reabsorption indicated by micro-CT. This finding indicate that NIRF signal is specifically expressed in active bone osteolytic sites while micro-CT image shows previous location of osteolysis. Our data demonstrate that NIRF-CHP signals can detect extensive collagen degradation activity associated to MM growth and indicate active areas of Myeloma osteolysis. Since NIRF-CHP areas may show early active osteolytic site at much, NIRF-CHP imaging can be a promising non-invasive diagnostic method to indicate the osteolytic forming sites in MM.

Disclosures: **Donghoon Yoon**, None

MON-0246

Postnatal Chondrocyte-Specific RUNX2 Overexpression Results in Accelerated Development of Osteoarthritis Following Traumatic Knee Joint Injury Sarah Catheline^{*}, Elizabeth Botto, Christopher Dean, Martin Chang, Jennifer Jonason. University of Rochester, United States

Osteoarthritis (OA) is a debilitating joint disease causing irreversible loss of cartilage within synovial joints. Studies show roughly 50% of patients with an ACL or meniscus tear will eventually develop knee OA. Despite the high prevalence of OA, molecular mechanisms underlying onset are unclear. RUNX2 is a transcription factor that promotes chondrocyte hypertrophy and expression of factors catabolic to the cartilage extracellular matrix. It is also known to regulate apoptosis in osteoblasts. Importantly, enhanced RUNX2 expression is seen in early stages of human OA and in murine models of injury-induced OA. Our preliminary data surprisingly show, however, that postnatal chondrocyte-specific RUNX2 overexpression alone is insufficient to induce OA. Here, we investigate whether cartilage-specific RUNX2 overexpression can accelerate OA progression following joint injury. At 2 months of age, Acan-Cre^{+/+}-ERT2; ROSA-Runx2^{f/+} (RUNX2 GOF) and littermate Cre-negative control mice received tamoxifen (100 μ g/g body weight) daily for 5 days (N = 6 per genotype). At 10 weeks of age, mice received meniscal-ligamentous injury (MLI) on the right hindlimb or a sham injury on the left hindlimb and were harvested 1 or 2 months post injury. Histology reveals that RUNX2 GOF mice have enhanced cartilage damage and Safranin-O staining loss compared to controls; these findings were confirmed by significantly increased modified OARSI scores and significantly decreased total tibial cartilage areas in RUNX2 GOF mice 2 months post-MLI (Figure 1A, 1C). RUNX2 GOF sham joints show no changes relative to controls. RUNX2 GOF mice also show significantly increased TUNEL-positive cells and MMP13 expression 1 month post-MLI in the articular cartilage (Figure 1B, 1D, 1E). Preliminary in vitro studies suggest that oxidative stress may promote RUNX2 activity, which could provide an explanation as to why RUNX2 GOF accelerates OA development following injury, but has no effect at homeostasis. Specifically, RUNX2 transcriptional activity measured by luciferase reporter assays is increased in ATDC5 cells overexpressing RUNX2 after treatment with oxidant tBHP. Overall, our results suggest chondrocyte-specific RUNX2 overexpression accelerates OA development after joint injury. These results highlight the contribution of genetic variability to the development of OA and suggest that genetic alterations affecting RUNX2 expression levels may in part predetermine the rate of OA onset following injury.

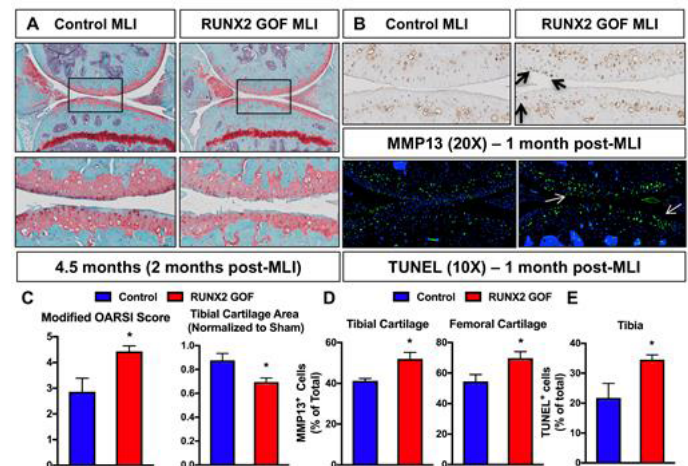


Figure 1. Postnatal RUNX2 overexpression accelerates articular cartilage degeneration following MLI. (A) Safranin-O/Alcian Blue staining of knee joint sections from Acan-Cre^{+/+}-ERT2; ROSA-Runx2^{f/+} (RUNX2 GOF) and littermate Cre-negative control mice injected with tamoxifen (100 μ g/g) daily for 5 days at 2 months of age, given MLI at 2.5 months, and sacrificed 2 months later (upper panel, 5X, lower panel 20X). (B) MMP13 immunohistochemistry (top, 20X) and TUNEL staining (bottom, 10X) from control and RUNX2 GOF mice as described in (A), but sacrificed 1 month post-MLI. (C) Modified OARSI and quantification of total cartilage area from control and RUNX2 GOF mice ($p < 0.05$, unpaired t-test, N = 6). (D) Quantification of MMP13⁺ and (E) TUNEL⁺ cells ($p < 0.05$, unpaired t-test, N = 4).

Disclosures: **Sarah Catheline**, None

MON-0247

Fibroblast Growth Factor 1 (FGF-1) impinges on Chondrocyte Degradation in OA through Matrix Metalloproteinase 13 (MMP-13) and Connective Tissue Growth Factor (CCN2) Abdellatif Elseoudi*¹, Tarek Abd El Kader², Takashi Nishida¹, Eriko Aoyama³, Takanori Eguchi⁴, Masaharu Takigawa³, Satoshi Kubota¹. ¹Biochemistry and Molecular Dentistry, Okayama University Graduate School of Medicine, Dentistry and Pharmaceutical Sciences., Japan, ²Assistant professor, Health and Social Sciences Cluster Singapore Institute of Technology (SIT), Singapore, ³Advanced Research Center for Oral and Craniofacial Sciences, Okayama University Graduate School of Medicine, Dentistry and Pharmaceutical Sciences., Japan, ⁴Dental Pharmacology, Okayama University Graduate School of Medicine, Dentistry and Pharmaceutical Sciences., Japan

PurposeOsteoarthritis (OA) involves the degradation of cartilage tissue with an overall shift toward catabolism over anabolism. CCN (Connective tissue growth factor/CCN2, Cysteine rich protein 61/CCN1, and Nephroblastoma overexpressed gene/CCN3) family proteins play critical roles in osteo/chondrogenesis and vasculo/angiogenesis. Particularly, CCN2 plays a crucial role in embryogenesis and skeletogenesis to promote proliferation, differentiation and chondrocyte maturation as well as matrix remodeling during chondrogenesis. CCN2 interacts with several growth factors involved in endochondral ossification, which include fibroblast growth factor 1 (FGF-1) showing a specific binding with this CCN2. Therefore, this study elucidates, the effect of FGF-1 on cartilage degradation through CCN2 and matrix metalloproteinase-13 (MMP-13) genes in vivo as well as in vitro in relation to OA.MethodsEffect of FGF-1 on CCN2 was evaluated in vitro with human chondrocytic HCS-2/8 cells. The cellular phenotype was estimated by the gene expression of chondrocytic metabolism markers (ACAN, COL2A1, and MMP13). Effect of FGF-1 on CCN2 mRNA and protein levels was evaluated by quantitative RT-PCR analysis and enzyme-linked immunosorbent assay (ELISA) respectively. Reporter gene assay was used to examine if CCN2 is regulated by FGF-1 through a particular genetic element involved in the proximal promoter. Involvement of FGF-1 and MMP-13 in OA development was evaluated in vivo by using immunohistochemistry.ResultsAn interesting finding was manifested through the analysis of FGF-1 addition to the chondrocytic cell culture. FGF-1 restrained the mRNA levels of the anabolic genes (ACAN and COL2A1) in chondrocytic HCS-2/8 cells; however, a catabolic gene (MMP13) was dramatically induced in those cells. FGF-1 drastically repressed the mRNA and protein levels of CCN2 in HCS-2/8 cells. Reporter gene assay suggested that FGF-1 down-regulated CCN2 gene expression at a transcriptional level. It is important to note that both FGF-1 and MMP-13 were produced in articular cartilage upon OA induction, which was evaluated in vivo by using a rat model.ConclusionsThese results suggest a critical effect of FGF-1 via MMP-13 on the balance of chondrocytic metabolism; with a remarkable shift toward catabolism over anabolism. Furthermore, their effect on CCN2 may lead to further degradation of cartilage tissue in OA.

Disclosures: *Abdellatif Elseoudi, None*

MON-0248

Role of IL36 α signaling in human chondrocyte homeostasis Tieshi Li*, Xin Jin, Arnava Hakimiyani, Susan Chubinskaya, Jie Jiang, Lai Wang, Alessandra Esposito, Joseph Temple, Anna Spagnoli. Rush University Medical Center, United States

Chondrocyte homeostasis is maintained via the balance between cartilage anabolism and catabolism. Disrupted balance in articular cartilage induces joint disease like osteoarthritis. Our previous studies and other reports showed that IL36 α signaling might be involved in the catabolic and inflammatory response in chondrocytes. OA chondrocytes, treated with IL-36 α , showed significant increase in the expression of MMP-13. IL-36 α stimulated cells showed NF κ B and p38 MAPK activated pathways. The present study is aimed at determining whether IL36 α signaling also regulate anabolic factors, the other catabolic factors, inflammatory cytokines as well as the mechanism of how IL36 α signaling does this. Healthy human primary chondrocyte harvested from human cadaver, (Collins Grade 0/1 Ankle articular cartilage) at passage 0 (cultured 5-6 days) were starved for 24 hours followed with different doses of IL36 α treatment for 24 hours. Cells were harvested for mRNA extraction and RT-PCR. Conditioned media was also harvested for western blot. We found that IL36 α treatment induced a dose-dependent increase in Adamts4, Mmp3, IL1 β , IL6 and IL8 expression levels but dose-dependent decrease in Sox9, Collagen2 and Aggrecan expression levels suggesting that IL36 α might play essential role for chondrocyte homeostasis as a catabolic factor. Furthermore, primary chondrocytes were cultured with the p38 MAPK kinase inhibitor (SB203580, 10 μ M), the MEK1/Erk inhibitor (PD98059, 10 μ M) or the inhibitor of NF κ B nuclear translocation (JSH23, 10 μ M) in the presence or absence of IL36 α for 24 h. Treatment with SB203580 but not PD98059 and JSH23 significantly attenuated the inductions of Mmp13, Adamts4 and Mmp3 by IL36 α . Western blot analysis of Mmp13 further confirmed this result. PD98059 and JSH23 but not SB203580 significantly attenuated the induction of IL1 β . SB203580 and PD98059 but not JSH-23 significantly attenuated the induction of IL8. All three inhibitors significantly attenuated the induction of IL6. These results suggest the involvement of P38 MAPK kinase signaling in IL36 α -mediated catabolic factors induction and mainly involvement of MEK1 kinase and NF κ B signaling in IL36 α -mediated inflammatory cytokine induction. Additionally, none of the inhibitors treatment significantly attenuated the suppression of Sox9, Collagen2 and Aggrecan expression levels with high dose of IL36 α .

In conclusion, IL36 α regulate chondrocyte homeostasis as a catabolic factor suggesting the viability of therapeutically intervening in the OA process by inhibiting IL36 α signaling.

Disclosures: *Tieshi Li, None*

MON-0249

Targeted Deletion of Claudin (Cldn)-11 Gene Promotes Chondrocyte Differentiation and Reduces Articular Cartilage Thickness in Mice Richard Lindsey*^{1,2}, Weirong Xing^{1,2}, Catrina Godwin¹, Sheila Pourteymoor¹, Subburaman Mohan^{1,2}. ¹Musculoskeletal Disease Center, VA Loma Linda Healthcare System, United States, ²Department of Medicine, Loma Linda University, United States

The claudin (Cldn) family comprises 24 members of 20–34 kDa tetraspan transmembrane proteins of tight junctions. In addition to their established canonical role as barriers controlling the flow of molecules in the intercellular space between cells, a distinct non-canonical role for Cldns is now emerging in which they serve as mediators of cell signaling. In our studies evaluating expression of all 24 Cldn family members during osteoblast (OB) differentiation, Cldn-11 showed the largest changes during in vitro OB differentiation. In previous studies, we showed that mice with targeted deletion of Cldn-11 gene exhibited reduced trabecular bone mass. During our immunohistochemistry (IHC) studies of Cldn-11 expression in bone, we found high levels of Cldn-11 expression in articular chondrocytes. Therefore, we evaluated the articular cartilage phenotype in 12-week-old Cldn-11 knockout (KO) mice. Quantitation of articular cartilage revealed a 27% and 40% reduction in the thickness and area ($P < 0.05$), respectively, in the Cldn-11 KO mice. In contrast, growth plate cartilage thickness was not affected. IHC showed increased expression of differentiation marker Col10a1 and decreased expression of articular chondrocyte marker lubricin in the articular cartilage of KO mice. Overexpression of Cldn-11 using a lentiviral vector in ATDC5 chondrocytes increased mRNA expression of articular markers Col2 and lubricin by 75% and 160%, respectively ($P < 0.01$). Since Cldn-11 overexpression increased Notch signaling target Hey1 by 62% ($P < 0.01$), we evaluated whether inhibition of Notch signaling blocked the Cldn-11 effect on expression of articular cartilage markers. We found that treatment with DAPT, a Notch inhibitor, blocked Cldn-11-induced lubricin expression in ATDC5 chondrocytes. Based on these data, we propose a novel role for Cldn-11 in regulating articular chondrocyte differentiation and articular cartilage thickness in part via manipulating Notch signaling. Further confirmation of this role would make manipulation of Cldn-11 signaling in articular chondrocytes an effective therapeutic means to treat osteoarthritis.

Disclosures: *Richard Lindsey, None*

MON-0250

SMPD3 Deficiency in Chondrocytes and Osteoblasts Affects Fracture Healing Garthiga Manickam*¹, Pierre Moffatt^{2,3}, Monzur Murshed^{1,2,4}. ¹Faculty of Dentistry, McGill University, Montreal, Quebec, Canada, ²Shriners Hospital for Children, McGill University, Montreal, Quebec, Canada, ³Department of Human Genetics, McGill University, Montreal, Quebec, Canada, ⁴Department of Medicine, McGill University, Montreal, Quebec, Canada

Traumatic bone fractures can be a serious and frequent problem for patients suffering from osteoporosis, metastatic bone cancer and congenital bone disorders. The promotion of new bone formation and mineralization at the fracture site can shorten the time of healing and yield stronger union. We recently demonstrated that sphingomyelin phosphodiesterase 3 (SMPD3), a lipid-metabolizing enzyme, plays a critical role during skeletal development. We generated Smpd3^{flox/flox};Osx-Cre (Smpd3^{ChOb}) mice to ablate Smpd3 in both chondrocytes and osteoblasts in the embryonic skeleton. Our data showed that SMPD3 activity in both these cell types is required for the initiation of extracellular matrix (ECM) mineralization and apoptosis of hypertrophic chondrocytes. Interestingly, the function of SMPD3 in adult bones appears to be less critical as only mild bone mineralization defects were observed in 3 month-old Smpd3^{ChOb} mice. Next, we performed rodent immobilized fracture surgeries on 2 month-old Smpd3^{ChOb} and control mice. We observed an induction of SMPD3 expression at the fracture site of wild type mice, 2 weeks post-surgery. Although micro-CT analyses did not show any differences in callus size and the amount of mineralized tissues, histomorphometric analyses showed that there was a marked increase of unmineralized osteoid in the fractured bones of Smpd3^{ChOb} mice in comparison to the control mice. As was the case in the embryonic bones, we also observed impaired chondrocyte apoptosis at the fracture sites of Smpd3^{ChOb} mice. Considering the induction of Smpd3 expression at the fracture site, we next examined how Smpd3 expression is regulated in cultured chondrocytes. To address this aim, we looked at two major regulators of chondrogenesis, BMP-2 and PTHrP. Our data showed that BMP-2 positively regulates Smpd3 expression in ATDC5 chondrogenic cells via p38 MAPK and Sox9. On the other hand, PTHrP downregulates Smpd3 expression by suppressing the BMP-2 signaling pathway. This suggests that BMP-2 and PTHrP have opposing effects on the regulation of Smpd3 expression. Taken together, our data provides compelling evidence that SMPD3 plays an important role during fracture healing. The novel insight generated through this study will add to the current understanding of SMPD3 regulation in skeletal tissue regeneration and has potential to pave the way for the development of therapeutic approaches to expedite ECM mineralization and healing of fractured bones.

Disclosures: *Garthiga Manickam, None*

MON-0251

PTHrP+ Chondrocytes in the Resting Zone Maintain the Growth Plate Integrity Koji Mizuhashi*, Noriaki Ono. University of Michigan School of Dentistry, United States

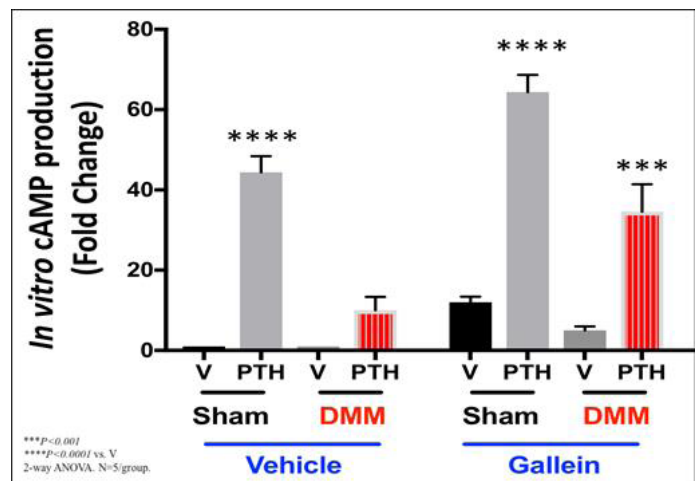
The resting zone is a critical component of the postnatal growth plate that contains precursor cells for differentiated columnar chondrocytes and releases morphogens to maintain the tissue architecture. In vivo lineage-tracing experiments demonstrate that resting chondrocytes expressing parathyroid hormone-related protein (PTHrP) encompass skeletal stem cells that can populate columnar chondrocytes for a long period. However, the functional significance of PTHrP+ resting chondrocytes in maintaining the growth plate architecture is unknown. In this study, we set out to reveal such significance by specifically ablating PTHrP+ chondrocytes from the resting zone. To achieve this goal, we took advantage of a resting-chondrocyte specific tamoxifen-inducible PTHrP-creER line, a Rosa26-iDTA allele and a Rosa26-tdTomato reporter allele. In this system, PTHrP+ chondrocytes exposed to an active form of tamoxifen will undergo recombination in the Rosa26 locus and result in rapid cell death. PTHrP-creER; Rosa26ls1-tdTomato/lsl-tdTomato mice were mated with Rosa26ls1-DTA/+ mice to generate PTHrP-creER; R26RtdTomato/+ (Cont) and PTHrP-creER; R26RtdTomato/iDTA (DTA) littermate mice. These mice were pulsed with a single dose of tamoxifen at P6 (0.5mg), when PTHrP+ chondrocytes are actively formed within the resting zone, and subsequently analyzed at P21. Initial fluorescence microscopy analysis revealed that PTHrP+ cells were only partially ablated from the resting zone in the DTA mice, as the number of tdTomato+ cells only moderately decreased (Cont: 1329±505 vs. DTA: 927±406 cells), while the number of tdTomato+ columns was significantly reduced (Cont: 64±23 vs. DTA: 32±17 columns). Although the bone length was unchanged, the height of each layer of the growth plate was significantly altered in the DTA mice; the proliferating layer was significantly reduced associated with significant expansion of the resting and hypertrophic layers (Cont vs. DTA; resting: 63±16 vs. 83±10 µm, proliferating: 127±10 vs. 91±12 µm, hypertrophic: 116±11 vs. 162±25 µm). Therefore, partial loss of PTHrP+ chondrocytes in the resting zone is sufficient to alter the integrity of the growth plate by inducing premature hypertrophic differentiation of chondrocytes in the proliferating zone. This leads us to speculate that PTHrP+ skeletal stem cells in the resting zone can maintain the integrity of the growth plate by sending a forward signal (PTHrP) for their progeny.

Disclosures: Koji Mizuhashi, None

MON-0252

Small molecule G-protein $\beta\gamma$ subunit inhibition potentiates parathyroid hormone chondroprotection in osteoarthritis William Pinamont*, Fadia Kamal, Elijah Carlson. Penn State College of Medicine, United States

Osteoarthritis (OA) is a debilitating joint disease with no curative therapy. Chondrocyte hypertrophy (CH) is a hallmark sign of OA, leading to cartilage degeneration. Parathyroid hormone (PTH) is chondroprotective in OA, however the mechanism of action is unknown. Chondrocytes are rich in PTH type-1 receptor (PTH1R), a G-protein coupled receptor (GPCR). Ligand stimulation of a GPCR promotes physiological $G\alpha$ signaling. Pathologically elevated $G\beta\gamma$ signaling leads to GPCR desensitization and $G\alpha$ uncoupling in disease states. We previously showed that gallein, a small molecule $G\beta\gamma$ inhibitor, prevents GPCR desensitization and recovers normal $G\alpha$ signaling in heart disease. However, the role of GPCR $G\beta\gamma$ signaling in OA is unknown. Thus we hypothesize that, in OA, elevated $G\beta\gamma$ signaling leads to PTH1R desensitization and loss of PTH chondroprotection. Destabilization of the medial meniscus (DMM) was used as the surgical OA mouse model to simulate clinical meniscal injury induced OA. Sham or DMM mice were treated with gallein or vehicle, knee cartilage was harvested, cultured ex vivo and stimulated with PTH. PTH1R-Gas signal activation was quantified by measuring cAMP production. To confirm this pathway in human OA, articular cartilage was collected from knee arthroplasty patients and cultured ex vivo. Cultures were treated with vehicle, G, PTH, or in combination and cAMP production was quantified. Immunofluorescent staining for CH markers MMP-13 and ADAMTS-5 was used to determine the antihypertrophic effects of the treatments. DMM impaired PTH-PTH1R-Gas-cAMP production in murine chondrocytes, suggesting PTH1R desensitization occurs in OA. $G\beta\gamma$ inhibition by gallein potentiated baseline chondrocyte cAMP production and recovered PTH1R-Gas-cAMP production in DMM cartilage (Figure 1). In human OA cartilage, both gallein and PTH attenuated CH with a synergistic effect of their combination. Similar to mouse OA cartilage, gallein increased baseline cAMP production in human OA chondrocytes and recovered PTH1R-Gas-cAMP production following PTH treatment. In conclusion, our data supports our hypothesis that $G\beta\gamma$ promotes PTH1R desensitization in OA. $G\beta\gamma$ inhibition by gallein prevents PTH1R desensitization and recovers its chondroprotective effects, suggesting a novel synergistic therapy for OA. Future experiments using knockout mouse models, and combination therapy in DMM mice will further elucidate the role of $G\beta\gamma$ signaling in PTH1R chondroprotection in OA.



primary cultures of epiphyseal chondrocytes. As expected, expression of Vegf, a HIF-1 α target, is increased in IOX-2 treated and Phd2 shRNA knockdown cultures. To establish if PHD2 effect on glycolysis is mediated via increased HIF-1 α levels, we used lentiviral Hif-1 α shRNA to knockdown Hif-1 α expression in epiphyseal chondrocytes. Hif-1 α shRNA reduced expression of Hif-1 α by 92% (P<0.002) compared to control shRNA treatment. Accordingly, expression of Vegf was reduced by 75% (P<0.01). Knockdown of Hif-1 α expression reduced expression levels of markers of glycolysis, Glut1 and Pkg1 by 41% and 56% respectively (both P<0.05). While expression levels of markers of immature chondrocytes (Col2, tenascin C) were unaffected, Col10 and Mmp13 expression was reduced by 50% (P<0.05). Furthermore, IOX-2 treatment increased expression levels of Glut1, Pkg1 and Col10 (2.5-3-fold, all P<0.01) in control shRNA but not in lentiviral Hif-1 α shRNA treated cultures. To determine the role of glycolysis in mediating PHD2/HIF-1 α effects on chondrocyte differentiation, we inhibited glycolysis using 2-deoxy glucose (2-DG) and found that 2-DG treatment did not block increased expression of Col10 in IOX-2 treated cultures. Based on our data, we conclude that PHD2/HIF-1 α regulates chondrocyte hypertrophy via both glycolysis-dependent and -independent pathways.

Disclosures: *Aruni Wilsonsanthoshkumar, None*

MON-0282

The Age-Dependent Decrease of Insulin Sensitivity in Mice is Unaffected by the Deletion of PPAR γ in Mesenchymal Lineage Cells of the Appendicular and Craniofacial Skeleton and of Subcutaneous Fat Elena Ambrogini*, Michela Palmieri, Stavros C Manolagas, Robert L Jilka, Maria Almeida. Center for Osteoporosis and Metabolic Bone Diseases, University of Arkansas for Medical Sciences and the Central Arkansas Veterans Healthcare System, United States

Peroxisome proliferator-activated receptor γ (PPAR γ) is a master regulator of energy metabolism and may also influence bone homeostasis. Previous studies in mice have suggested that osteocytes are involved in glucose homeostasis through a PPAR γ -dependent mechanism. Like humans, mice exhibit an age dependent decline in insulin sensitivity. We therefore examined the effects of PPAR γ deletion on glucose metabolism in 22 month old female mice. To do this, we deleted PPAR γ in Prx1-Cre targeted cells (PPAR γ Δ Prx1 mice), which include pluripotent mesenchymal progenitors, osteoblasts, and osteocytes of the appendicular and craniofacial skeleton as well as mesenchymal progenitors that give rise to subcutaneous white adipose tissue (WAT). Female PPAR γ -fl/fl littermates were used as controls. All mice were on a C57BL/6J background. Deletion of PPAR γ in bone was confirmed by qPCR of DNA from cortical bone. Consistently, and in contrast to cells from control mice, rosiglitazone failed to stimulate adipocyte differentiation or to inhibit osteoblast differentiation in ex-vivo bone marrow cultures of 22 mo old PPAR γ Δ Prx1 mice. PPAR γ Δ Prx1 mice also exhibited a dramatic reduction in subcutaneous WAT whereas interscapular brown fat and visceral WAT were unaffected. Nonetheless, the age-associated gain in body weight and total body fat between 3 and 22 months of age was unaffected by the PPAR γ deletion. Furthermore, fasting glucose levels were indistinguishable among 22 mo-old control mice, 22 mo-old PPAR γ Δ Prx1 mice, and 6 mo-old female C57BL/6J mice. Glucose tolerance was tested by administration of 2 g glucose /kg body weight i.p. to mice fasted for 16 h; and blood glucose was measured immediately prior to glucose administration, and at 15, 30, 60, 90, and 120 min afterwards. Glucose levels were significantly lower at 60, 90 and 120 min in 6-mo old mice, compared to either 22-mo-old control or PPAR γ Δ Prx1 mice. There was no difference in glucose levels between aged control and PPAR γ Δ Prx1 mice. These findings indicate that the PPAR γ expressed in osteoblasts and osteocytes of the appendicular and craniofacial skeleton, or in subcutaneous WAT, plays no role in the age-dependent decline in insulin sensitivity in mice.

Disclosures: *Elena Ambrogini, None*

MON-0283

A Greater Proportion of the Variance in Body Fat and Bone Mineral Content is accounted for by Serum Estradiol than Follicle Stimulating Hormone (FSH), and Estradiol not FSH Contributed to the Variance in Cortical and Trabecular Microarchitecture Camilla Andreassen*^{1,2}, Ann Kristin Hansen^{1,2}, Ken Sikaris³, Clifford J Rosen⁴, Åshild Bjørnerem^{1,5}. ¹Department of Clinical Medicine, UiT The Arctic University of Norway, Tromsø, Norway, ²Department of Orthopaedic Surgery, University Hospital of North Norway, Tromsø, Norway, ³Melbourne Pathology, Melbourne, Australia, ⁴Maine Medical Center Research Institute, Scarborough, Maine 04074, United States, ⁵Department of Obstetrics and Gynecology, University Hospital of North Norway, Tromsø, Norway

At menopause bone remodeling becomes unbalanced, microarchitecture deteriorated, and bone loss and visceral adiposity increases. The important role of estrogen for bone health is well known, and serum estradiol (E2) is inversely associated with cortical porosity in elderly men not women. In rodents, a blocking antibody to follicle-stimulating hormone (FSH) increased bone mass and reduced adipose tissue. Human studies are yet controversial, but if such an effect exist in humans, novel treatment possibilities for bone fragility and adiposity may be developed. We hypothesized that serum E2 and FSH will be independently associated with body mass index (BMI), total body fat mass, lean mass and bone mineral content (BMC), and distal tibial microarchitecture and medullary adiposity index (MAI) in

postmenopausal women. Images of distal tibia were acquired using high-resolution peripheral quantitative computed tomography in 131 postmenopausal women aged 49-77 years in Melbourne, Australia. Bone microstructure and MAI were quantified using StrAx software. The women had a mean age of 58.5 \pm 15.7 years, BMI 26.2 \pm 4.9 kg/m², total body fat mass 26.7 \pm 9.8 kg, lean mass 39.0 \pm 4.9 kg, and BMC 2.4 \pm 0.4 kg, serum E2 46.4 \pm 14.7 pmol/L and FSH 67.4 \pm 21.4 IU/L. Each SD higher serum E2 was associated with 0.47 SD higher BMI, 0.47 SD higher fat mass, 0.28 SD higher lean mass, 0.30 SD higher BMC of the total body and 0.35 SD higher trabecular number, 0.25 SD higher trabecular volumetric bone mineral density (vBMD) and 0.27 SD lower MAI at distal tibia (all p<0.01). Serum E2 was associated with 0.18 SD lower porosity of the inner transitional zone (p=0.044) and with 0.19 SD higher total vBMD (p=0.034). Each SD higher serum FSH was associated with 0.20 SD lower BMI, 0.18 SD lower fat mass, 0.17 SD lower lean mass, and 0.17 SD lower BMC of the total body (all p<0.05). FSH was not associated with microarchitecture at distal tibia. All results are adjusted for age and physical activity and mutually adjusted for E2 and FSH. Serum E2 explained 19-21%, and FSH explained 3-4% of the variance in BMI and total body fat mass. We infer that E2 contributes to a five-fold greater proportion of the variance in body fat than FSH, and E2 contributes to increased body fat, lean mass, bone mass and more robust microarchitecture. The independent contribution made by FSH to less body fat but not to the variance in bone traits, lends support to the possibility that humans are different from mice.

Disclosures: *Camilla Andreassen, None*

MON-0284

The consequences of postnatal androgenization in bone markers, micro and macro-architecture in a rodent model of polycystic ovary syndrome Fabio Comim*, Lady Serrano Mujica, Alfredo Antoniazzi, Paulo Gonçalves, Melissa Premaor. Federal University of Santa Maria, Brazil

Background: Polycystic ovary syndrome (PCOS) is a common health problem affecting 8-10% of all women during the menarche. The presence of reproductive and metabolic disorders characteristics of a majority of PCOS patients may have considered as potential factors with a role in bone metabolism. Animal models replicate many disruptions observed in women with PCOS and are widely employed for the study of the mechanisms related to the development of abnormalities. Therefore, the aim of this study was to investigate the role of androgens in bone metabolism and micro and macro-architecture in a rodent model of PCOS. Methods: Wistar female rats (n=7) were androgenized through the injection of 1.25 mg of testosterone propionate (TP) s.c. at postnatal day 5; controls (n=8) received the same amount of volume of corn oil. CT and micro-CT were performed in the rat femur, respectively, to define the dimensions of the bone, and the bone microarchitecture at the distal portion. The analysis of micro-CT was blind and performed at SCANCO, Co (USA). The length of the femur was compared by the use of Osirix X lite software. P1NP and CTX in plasma were determined by a specific rat ELISA kit assay. Results: Androgenized animals exhibited a typical phenotype of PCOS (PCOS rats). The length of the femur was similar between PCOS rats and controls. However, PCOS rats exhibited at the midline, higher diameter (mean \pm SEM) 3.55 \pm 0.03 mm versus controls 3.35 \pm 0.08 (p=0.04) at the expenses of an increased cortical area (mean \pm SEM) 9.79 \pm 0.27 mm against control rats 8.98 \pm 0.19 (p=0.03). Results of de Micro-Ct from the distal femur indicated an increased Cortical Bone Volume VOX-BV in androgenized animals (mean \pm SEM) of 3.28 \pm 0.09mm³ versus 2.89 \pm 0.07mm³ than in controls (p=0.015). BV/TV (T) was also increased in androgenized rats (mean \pm SEM) of 0.41 \pm 0.04 in comparison to non-androgenized rats 0.27 \pm 0.01 (p=0.01). Cortical thickness and Conn-Dens in this segment were also similar between the two groups. Finally, we observed a similar trabecular thickness, but an increased trabecular number (p=0.048) and decreased trabecular separation (p=0.049) in PCOS rats. CTX and P1NP levels were detectable and higher at day 60 than 100 of life, but no differences could be identified between androgenized rats and controls. Conclusion: As a whole, postnatal androgenization in young female rats had a positive influence on bone micro and macro-architecture.

Disclosures: *Fabio Comim, None*

MON-0285

Exercise increases UCP1 expression but decreases trabecular bone acquisition in mice during cold exposure and at thermoneutrality Amy Robbins*, Christina Tom, Rebecca Tutino, Miranda Cosman, Taylor Spencer, Cleo Moursi, Rachel Hurwitz, Maureen Devlin. University of Michigan, United States

Chronic cold exposure induces bone loss via increased sympathetic outflow to osteoblast beta-adrenergic receptors. Brown adipose tissue (BAT) can protect against such bone loss by inducing nonshivering thermogenesis (NST) and increasing body temperature, thereby reducing sympathetic tone. Exercise reportedly stimulates BAT, suggesting exercise during cold stress could have osteoprotective effects by increasing NST. To test this hypothesis, wildtype C57BL/6J male mice were housed at 26C (thermoneutrality), 22C (standard housing temperature), and 16C (moderate cold stress) from 3-6 wks of age with food and water ad libitum. Half of the mice at each temperature were housed with running wheels (exercise, EX) and half without (control, CON). Outcomes at 6 wks of age included body mass, food intake, leptin, uncoupling protein (UCP1) expression in BAT, whole body bone mineral density (BMD, g/cm²) and percent body fat (%) via PIXImus, and cortical and trabecular bone architecture at the midshaft and distal femur via μ CT. Results indicate that body mass,

BMD, and percent fat did not differ in response to temperature or exercise, but mice at 16C ate more compared to mice at 22C or 26C. Serum leptin was lower in EX vs. CON mice at 16C and 22C but not 26C. Exercise led to lower trabecular bone volume fraction (BV/TV), connectivity density (Conn. D), and trabecular number (Tb.N) vs. controls at 16C and 26C (BV/TV -28% and -28%, Tb.N -7% and -8%, Conn.D -18% and -24%, $p < 0.05$ for all). Cold stress decreased BV/TV in EX mice at 16C and 22C (-24% and -24%), and decreased Tb.N (-8% and -8%) and Conn.D (-25% and -35%) in both CON and EX mice ($p < 0.05$ for all). There were no differences among groups in trabecular thickness or spacing, nor in midshaft femur cortical bone cross-sectional geometry. At 16C and 26C, both CON and EX mice had higher UCPI mRNA (+43%, +50%, $p < 0.007$ for both) and higher UCPI protein expression (+52%, +31%, $p < 0.006$ for both). Within each temperature, EX mice had higher UCPI protein expression compared to CON (+32% at 16C, +91% at 26C, $p < 0.03$ for both). These results indicate that both cold stress and exercise upregulated UCPI mRNA and protein levels, but both exercise and cold also decreased trabecular BV/TV, Tb.N, and Conn.D. These data indicate increased NST as reflected in UCPI expression does not protect trabecular bone mass during cold exposure. This unexpected result could reflect energetic tradeoffs between thermogenesis and skeletal acquisition.

Disclosures: *Amy Robbins, None*

MON-0286

Estrogen deficiency: the only cause behind senile osteoporosis? Deeksha Malhan^{*1}, Sabine Stoetzel¹, Diaa Eldin S Daghma¹, Fathi Hassan¹, Stefanie Kern¹, Markus Rupp², Christian Heiss², Thaqif El Khassawna¹. ¹Institute for Experimental Trauma Surgery, Faculty of Medicine, Justus Liebig University of Giessen, Germany, ²Department of Trauma, Hand, and Reconstructive Surgery, University Hospital of Giessen and Marburg, Germany

Estrogen deficiency results in both early and late osteoporosis in postmenopausal women. Higher osteoclast mediated resorption due to estrogen deficiency leads to an increase in pro-inflammatory cytokines and alters bone metabolism. This study aimed to gain an insight into the discrepancies in bone metabolism because of estrogen deficiency alone and/or in combination with deficient diet in a senile rat model. 46 Sprague-Dawley rats (age = 12 months) were randomly divided into: 1) Control group (M=Months) at 0M, 2) Sham (3M), 3) bilaterally ovariectomized (OVX, 3M), 4) Sham combined with deficient diet (Diet, 3M), and 5) OVX combined with deficient diet (OVXD, 3M). Bone mineral density (BMD) were measured using Dual X-ray absorptiometry (DXA). Lumbar vertebral samples were collected after euthanasia and histological analysis & serum analysis were carried out. Imbalanced bone metabolism and deteriorated bone quality is the hallmark of osteoporosis. DXA revealed lower BMD in OVXD group post-treatment and higher Fat% in Sham, OVX, Diet, and OVXD when compared with Control ($p \leq 0.05$). This reflects on diminished bone quality in OVXD group. Further, increase in Fat% directs to disturbed bone metabolism after 3M. Therefore, histological analysis of bone formation (osteocalcin) and resorption (TRAP) markers were carried out. This study showed lower osteoblast and higher osteoclast activity in both OVX and OVXD group which directs to the prominent effect of estrogen deficiency. Our results correlates with the previous reports that suggested increased osteoclast mediated resorption in osteoporosis due to estrogen deficiency. Serum analysis of bone metabolic markers showed severe effect of treatments. Parathyroid hormone (PTH) serum level was higher in Diet when compared with OVXD, OVX, and Sham. PTH inversely affects Vitamin D which is important for bone mineralization. The higher PTH level in Diet group point to severe effect of diet deficiency alone. Another marker linked to Vitamin D deficiency is Adrenocorticotropic (ACTH), which was lower in Diet and higher in OVX group. This inverse link between PTH and ACTH directs towards the bone loss due to Vitamin D deficiency. Bone homeostasis is also maintained by osteocytes activity. Therefore, investigation of morphological changes in osteocytes using Silver Nitrate stain are being carried out. Moreover, higher amount of inflammatory cells were seen in OVX and OVXD groups after 3M. Therefore, histological analysis of inflammatory markers will be carried out.

Disclosures: *Deeksha Malhan, None*

MON-0287

Butyrate enhances myogenesis and muscle function through modulation of intracellular calcium and bioactive lipid mediators Chenglin Mo^{*1}, Zhiying Wang¹, Xuejun Li², Jianxun Yi², Leticia Brotto¹, Marco Brotto¹, Jingsong Zhou². ¹College of Nursing and Health Innovation, the University of Texas-Arlington, Arlington, TX, United States, ²Department of Physiology, Kansas City University of Medicine and Bioscience, Kansas City, MO, United States

Butyrate is a short-chain fatty acid synthesized by intestinal microbiota. Previous studies have shown that butyrate is important in the regulation of intestinal functions and anti-inflammation. In bone and muscle, butyrate can improve metabolism in both tissues, and reduce muscle atrophy during aging and pathological bone loss, respectively. Recently, Treatment with butyrate was found to significantly delay the progression of amyotrophic lateral sclerosis (ALS), a neuromuscular disease, in mice. To date, the knowledge concerned with the effect of butyrate in muscle, which could have significant impact on bone, is limited. In this study, we used C2C12 cells, isolated intact muscles, and the ALS mouse model to study the mechanisms behind the function of butyrate in myogenesis and muscle-related diseases. Our results indicated that treatment with 10 μ M butyrate significantly enhanced C2C12 myo-

genesis. Fusion index increased from 30% to 42% ($p < 0.05$). Moreover, ex vivo treatment with 2mM butyrate for 30 min increased the contractile force of soleus muscle by 27 \pm 4% ($p < 0.03$) at 20Hz of stimulation. Normal and functional calcium homeostasis is critical for myogenesis and muscle function. Treatment with 10 μ M butyrate for 2 h induced a significant increase in calcium release from the sarcoplasmic reticulum after caffeine stimulation in C2C12 myotubes. It is therefore possible that modulating intracellular calcium homeostasis might underlie the effects of butyrate on myogenesis and muscle function. To seek a deeper understanding of ALS muscle metabolism, we used the ALS mouse model (G93A mice) with or without butyrate supplement. Skeletal muscles from these mice were analyzed with our new-targeted lipidomics method to determine how ALS and butyrate could affect the metabolism of lipid mediators (LMs). Compared with control, the levels of six LMs belonging to the arachidonic acid pathway and eight LMs in the DHA pathway were significantly higher in G93A mice, suggesting higher levels of inflammation and oxidative stress. When these mice were treated with butyrate for one-month (2% in drinking water), the levels of these LMs returned to the levels observed in the control mice. Overall, our data suggest that butyrate could play an important role in muscle regeneration and muscle function via mechanisms associated with the signaling of calcium and LMs. Further studies will provide new insights for potential clinical application of butyrate in musculoskeletal diseases.

Disclosures: *Chenglin Mo, None*

MON-0288

Lysosomal Acid Lipase and Its Role in Osteoblast Differentiation Elizabeth Rendina-Ruedy^{*1}, Madalina-Cristina Duta-Mare², Dagmar Kratky³, Clifford Rosen¹. ¹Maine Medical Center Research Institute, United States, ²Gerot Lannach Pharma, Medical University of Graz, Austria, ³Gottfried Schatz Research Center for Cell Signaling, Metabolism and Aging Molecular Biology and Biochemistry Medical University of Graz, Austria

Lysosomal acid lipase (LAL) is an enzyme essential for cholesterol ester (CE) and triacylglycerol (TAG) hydrolysis, mediated by low density lipoprotein (LDL)-receptor endocytosis, as well as lipid droplet lipolysis via lipophagy. Clinical LAL deficiency is a rare, autosomal recessive disease that results from a mutation in the LIPA gene and presents as either Wolman disease (WD) or cholesterol ester storage disease (CESD). While both conditions are a result of the same genetic cause, WD is much more severe (i.e., hepatosplenomegaly, steatorrhea, abdominal distention, adrenal calcification) and often results in death < 1 yr of age. Conversely, the milder CESD is often described to be later-onset and manifests with variable CE and TAG accumulation in the liver, adrenal gland, and small intestine. Additionally CESD patients display premature atherosclerosis and hypercholesterolemia. However, to date, there has been no mention of the bone phenotype in CESD patients or within the LAL^{-/-} mouse model. Therefore, given this gap in knowledge, along with the recently identified importance of lipolysis in osteoblast function, we sought to characterize the bone phenotype in 16-wk old, male and female LAL^{-/-} mice. Structural analyses of the distal femur metaphysis revealed that male LAL^{-/-} mice had a lower trabecular BV/TV (12%) compared to wild type (WT) mice (21%), which was primarily due to decreased trabecular number and increased trabecular separation. Interestingly, there was no change in BV/TV from the female LAL^{-/-} compared to WT. While both the male and female LAL^{-/-} mice displayed a decrease in cortical bone thickness and polar moment of inertia compared to WT, only the female LAL^{-/-} mice had increased cortical porosity. Due to the previously characterized systemic derangements in LAL^{-/-} mice, including lipodystrophy, malabsorption, and ectopic lipid deposition in the liver, spleen, and lymph nodes, primary calvaria osteoblasts (cOb) were isolated to determine the cell-autonomous role of LAL. Consistent with the low bone mass phenotype, cOb from LAL^{-/-} mice demonstrated impaired osteoblastogenesis. Moreover, despite the ectopic lipid accumulation and reduced BV/TV in the LAL^{-/-} mice, initial histological evaluation of the tibia revealed no differences in marrow adipocytes compared to WT mice. Collectively, these data suggest a cell autonomous role for LAL in osteoblasts, which may be related to impaired fuel utilization and altered bioenergetics.

Disclosures: *Elizabeth Rendina-Ruedy, None*

MON-0289

Roles of macrophages and plasminogen activator inhibitor-1 in delayed bone repair induced by diabetic state in female mice Takeshi Shimoide^{*1}, Naoyuki Kawao¹, Yukinori Tamura², Kiyotaka Okada¹, Katsumi Okumoto³, Shinji Kurashimo³, Yoshitaka Horiuchi³, Kohei Tatsumi¹, Osamu Matsuo¹, Hiroshi Kaji¹. ¹Department of Physiology and Regenerative Medicine, Kindai University Faculty of Medicine., Japan, ²Kobe Gakuin University, Faculty of Nutrition., Japan, ³Life Science Research Institute, Kindai University., Japan

Diabetic patients suffer from various complications. It has been recently recognized that fracture risk is increased and its' repair process is delayed in diabetic patients. However, details in the mechanisms of diabetic delayed bone repair still remain unclear. It has been recently noted about the roles of macrophages in bone formation, however, there has been no reports available about the roles of macrophages in the delayed bone repair associated with diabetes. Here, we investigated the roles of macrophages and hematopoietic stem cells in diabetic delayed bone repair after femoral bone defect using streptozotocin (STZ)-treated or plasminogen activator inhibitor-1 (PAI-1)-deficient female mice. STZ treatment significantly decreased the numbers of F4/80-positive cells (macrophages), but not Gr-1-positive cells

(neutrophils), at the damaged site on day 2 after femoral bone injury in mice. It significantly decreased the mRNA levels of macrophage colony-stimulating factor, inducible nitric oxide synthase (iNOS), interleukin (IL)-6 and CD206 at the damaged site on day 2 after bone injury. Moreover, STZ treatment attenuated a decrease in the number of hematopoietic stem cells in bone marrow from damaged femurs induced by bone injury. Next, we investigated the involvement of PAI-1 in the decreased accumulation of macrophages at the damaged site during bone repair, since our previous studies revealed that PAI-1 is involved in delayed bone repair and osteopenia induced by STZ-treated diabetic state in female mice. PAI-1 deficiency significantly attenuated a decrease in the number of F4/80+ cells induced by STZ treatment at the damaged site on day 2 after bone injury in mice. Moreover, it significantly attenuated the phagocytosis of macrophages at the damaged site suppressed by diabetic state, when analyzed with a transmission electron microscope. On the other hand, PAI-1 deficiency did not affect the mRNA levels of iNOS and IL-6 in F4/80- and CD11b-double positive cells sorted by FACS from the bone marrow of the damaged femurs decreased by diabetic state. In conclusion, we demonstrated that diabetic state decreases the accumulation and phagocytosis of macrophages at the damaged site during the early stage of bone repair after femoral bone injury partly through PAI-1 related mechanism in female mice. These findings will give a novel insight that macrophages might be the potential target for the treatment of delayed bone repair in diabetic patients.

Disclosures: *Takeshi Shimoide, None*

MON-0290

Inducible Sirt1 Knockout Mice Exhibit Increased Bone Mineral Density, Uphill Sprint Capacity, and Open Field Activity Ramkumar Thiyagarajan*, Kenneth Seldeen, Merced Leiker, Yonas Redae, Bruce Troen. University at Buffalo and VA Western New York Healthcare System, United States

Background: Age related chronic diseases are the major health and economic burden in the United States. Sirtuin 1 (Sirt1), an NAD-dependent deacetylase, regulates muscle mass and function, bone and energy metabolism, and mitochondrial biogenesis. Sirt1 expression declines with aging and overexpression in some organisms increases longevity. Endurance exercise increases Sirt1 expression in rats and further, constitutive muscle specific Sirt1 knockout (KO) in young sedentary mice results in reduced endurance capacity. Aim: To determine whether inducing whole-body Sirt1 knockout in adult mice will reduce their overall physical performance and bone mineral density (BMD), and whether the absence of active Sirt1 will decrease the response to exercise. Methods: We have crossed a ubiquitin promoter-CRE-ERT2 mouse with a loxP-Sirt1(exon4)-loxP mouse to create an inducible whole body Sirt1KO mouse line. A total of 60 mice (6-month-old C57BL/6J mice) were divided into Sirt1 (WT) or Sirt1KO (KO) groups. Both WT and KO groups were further divided into groups that were either sedentary (WT+SED and KO+SED) or treadmill exercised 30 minutes a day for 5 days a week over a 6 month period (WT+EX and KO+EX). We longitudinally assessed body weight and food consumption, body composition (lean and fat), and BMD. We also evaluated a battery of physical performance tests, including, voluntary wheel running, gait speed, treadmill endurance, uphill sprint, open field test, rotarod, grip hang time and grip strength. Results: Sirt1KO did not alter body composition in either exercised or sedentary mice. Exercise training increased endurance and uphill sprint capacity in both the WT+EX and KO+EX mice. The KO+SED mice had greater BMD (KO+SED: 51.4 ± 2.6 g/cm² vs WT+SED: 49.3 ± 1.6 g/cm², p=0.009), increased uphill sprint endurance (KO+SED: 143 ± 43.6 meters vs WT+SED: 111.1 ± 39.2 meters, p=0.024), and covered more distance in open field test (KO+SED: 51.2 ± 19.0 meters vs WT+SED: 39.8 ± 14.9 meters, p=0.043). The KO+EX mice exhibited better grip strength than KO+SED (KO+EX: 2.4 ± 0.2 N vs KO+SED: 2.2 ± 0.2 N, p=0.003). Conclusion: Inducing whole-body Sirt1KO in adult mice did not affect body composition, but unexpectedly increased bone mineral density, uphill sprint capacity and open field activity over a 6-month period. Additionally, the absence of Sirt1 did not attenuate the response to exercise training in these mice.

Disclosures: *Ramkumar Thiyagarajan, None*

MON-0291

Association Between Changes in Bone Remodeling and Glucose Homeostasis After Biliopancreatic Diversion in Patients with Severe Obesity Anne-Frederique Turcotte*, Thomas Grenier-Larouche², Roth-Visal Ung¹, David Simonyan³, Anne-Marie Carreau², André Carpentier², Fabrice Mac-Way¹, Claudia Gagnon¹. ¹Laval University, Canada, ²Sherbrooke University, Canada, ³CHU de Quebec, Canada

Context: Preclinical studies revealed that bone regulates glucose homeostasis. Whether changes in bone remodeling contribute to the improvement in glucose homeostasis after biliopancreatic diversion with duodenal switch (BPD-DS) remains unknown. Objectives: To determine whether the increase in bone remodeling seen early, in the mid- and longer-term following BPD-DS is associated with glucose homeostasis markers in patients with severe obesity, independently of weight loss and high molecular weight adiponectin. Methods: Ancillary study using fasting frozen plasma from 16 individuals with severe obesity (11F/5M, 69% with type 2 diabetes, mean BMI 49.4 kg/m²) assessed before, 3 days, 3 months and 12 months after BPD-DS. Serum bone turnover markers (C-terminal telopeptide (CTX), intact osteocalcin (OC) and its regulators (sclerostin, osteoprotegerin (OPG)) were analyzed at each visit. Glucose homeostasis markers including insulin resistance indices (HOMA-IR, adipose tissue insulin resistance index (ADIPO-IR), insulin sensitivity index (Si)), insulin

secretion rate (ISR) and insulin disposition index (DI) were also assessed. Changes between baseline and each timepoint in bone turnover markers and its regulators were correlated with changes in glucose homeostasis markers using Pearson partial correlations adjusted for weight loss and adiponectin. Results: Weight did not change at 3 days but decreased by 33±27 kg at 3 months and 59±12 kg at 12 months. CTX was the only bone marker correlating with weight loss (r=-0.63, p=0.009 at 3 months and r=-0.58, p=0.039 at 12 months). The increase in CTX correlated with the reduction in HOMA-IR (r=-0.56, p=0.036) and the increase in Si (r=0.58, p=0.026) at 3 months and the reduction in ADIPO-IR (r=-0.70, p=0.013) at 12 months (Table 1). The increase in OPG also correlated with the decrease in ADIPO-IR (r=-0.62, p=0.039) at 12 months as well as with the increase in Si (r=0.54, p=0.046) at 3 days. The increase in OC correlated with the improvement in Si at 3 days (r=0.56, p=0.025), but adjustment for weight loss and adiponectin weakened this association (r=0.48, p=0.082). Change in sclerostin did not correlate with any marker of glucose homeostasis. None of the bone turnover markers or its regulators correlated with ISR or DI. Conclusions: The early and longer term increase in bone remodeling (mainly CTX) after BPD-DS potentially contributes to the improvement in insulin resistance independently of weight loss and adiponectin.

	0.26	0.339	-0.50	0.049*	-0.51	0.076
	0.24	0.426	-0.56	0.036*	-0.30	0.384
	0.13	0.658	-0.45	0.091	-0.59	0.044*
	0.16	0.548	0.41	0.112	0.15	0.616
	0.02	0.959	0.58	0.026*	0.11	0.756
	0.35	0.200	0.34	0.217	-0.57	0.054
	0.30	0.2641	0.28	0.291	-0.69	0.009*
	0.31	0.303	0.25	0.393	-0.62	0.039*
	-0.51	0.053	-0.46	0.082	-0.19	0.557
	-0.24	0.3656	-0.25	0.351	-0.00	0.999
	-0.22	0.453	-0.19	0.519	-0.23	0.506
	-0.34	0.216	-0.17	0.545	0.05	0.883
	0.56	0.025*	0.19	0.493	0.03	0.909
	0.48	0.082	0.21	0.485	-0.04	0.902

*p<0.05
Adj. Weight: After adjustment for weight loss
Adj. Weight and adiponectin: After adjustment for weight loss and change in adiponectin

Disclosures: *Anne-Frederique Turcotte, None*

MON-0292

Effect of Abaloparatide and Teriparatide on marrow adipose tissue in postmenopausal osteoporosis Annegreet G. Veldhuis-Vlug*, Rob J Van 'T Hof², Roland Baron³, Dennis M. Black⁴, Clifford J Rosen⁵. ¹Academic Medical Center Amsterdam and Center for Clinical and Translational Research, Maine Medical Center Research Institute, Netherlands, ²Institute of Ageing & Chronic Disease, University of Liverpool, United Kingdom, ³Department of Oral Medicine, Infection and Immunity, Harvard School of Dental Medicine, Harvard Medical School, United States, ⁴Department of Epidemiology and Biostatistics, University of California San Francisco, United States, ⁵Center for Clinical and Translational Research, Maine Medical Center Research Institute, United States

Purpose Increased marrow adipose tissue (MAT) is associated with decreased bone mass, osteoporosis and fractures in humans. In mice, treatment with parathyroid hormone (PTH) decreases MAT and increases bone mass. Abaloparatide, a recently developed PTH-related peptide (PTHrP) analog, and Teriparatide, a recombinant PTH protein, both increase bone mass and reduce fracture risk in patients with osteoporosis. We investigated the effect of Abaloparatide and Teriparatide compared to placebo treatment on MAT in women with osteoporosis from the Abaloparatide-SC Comparator Trial In Vertebral End-

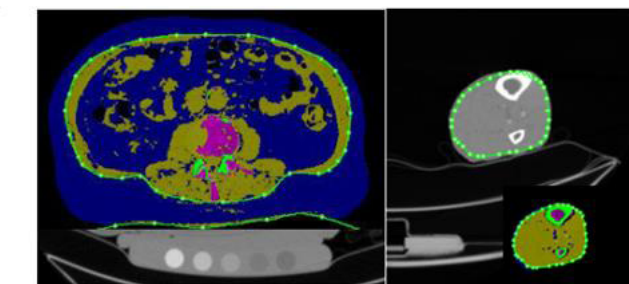
points (ACTIVE) trial and we hypothesized that both treatment with Abaloparotide and Teriparatide would decrease MAT. Methods In this cross-sectional study, we measured MAT and bone volume in Goldner's trichrome stained transiliac crest bone biopsies obtained after 18 months of treatment from 74 (26 Abaloparotide, 21 Teriparatide and 27 placebo treated) women with osteoporosis included in the histology study of the ACTIVE trial. Histomorphometric analysis was performed using FatHisto, a newly developed, open-source, semi-automated image analysis software based on Image J. We measured adipocyte volume per tissue volume (Ad.V/TV, %), adipocyte volume per marrow volume (Ad.V/Ma.V, %), and bone volume per tissue volume (BV/TV, %). We compared the combined active treatment groups versus placebo using T-tests. Results Overall, there was a trend towards lower MAT (Ad.V/TV) of 28.8% in the combined active treatment groups versus 31.6% in the placebo group ($p=0.20$). As observed previously using Bioquant Osteo for histology image analysis, active treatment increased bone volume (BV/TV) compared to placebo (21.2% versus 17.7%, $p=0.02$). There was no difference between the Abaloparotide and Teriparatide groups for both parameters. In addition, bone volume (BV/TV) and MAT (Ad.V/TV) were inversely correlated ($r=-0.378$, $p=0.0007$) as expected from previous studies using DEXA and MRI to measure bone volume and MAT in humans. Conclusion In this study we found a trend towards lower MAT after 18 months of treatment with Abaloparotide or Teriparatide compared to placebo in women with osteoporosis. Larger studies with a longitudinal design are needed to confirm these results. In addition, we observed the inverse relation between MAT and bone volume in both treated and untreated individuals. Ongoing studies will investigate the effect of active treatment on individual adipocyte size and number.

Disclosures: *Annegreet G. Veldhuis-Vlug, None*

MON-0293

Characterization of Bone Marrow Adiposity with Computed-Tomography (CT) scan in Relation to Mineral and Bone Disorders in Dialysis Patients
Yue Pei Wang*, Cyrille De Halleux, Roth-Visal Ung, Nada Khelifi, Claudia Gagnon, Fabrice Mac-Way. CHU de Québec Research Center, Endocrinology and Nephrology Unit, Faculty and Department of Medicine, Université Laval, Canada

Introduction: Fractures and cardiovascular events are among the complications that characterize the Chronic Kidney Disease-Mineral and Bone Disorders (CKD-MBD). Recent studies suggest the potential role of bone marrow adipose tissue (MAT) in the development of bone loss in aging population. The optimal characterization of MAT in CKD is currently unknown. We conducted a pilot study to determine the feasibility of characterizing MAT, bone mineral density (BMD), visceral and subcutaneous adipose tissue in one acquisition by computed-tomography scan (CT-scan). Methods: CT-scan (Philips iCT256) slices were acquired at L3 and L5 vertebrae, at 1/3 and 2/3 non-dominant distal tibia using 80 kVp and 140kVp levels of energy and at the hip using 120 kVp. Cortical and trabecular bone parameters, visceral adipose tissue (VAT) and subcutaneous adipose tissue (SAT) area as well as yellow marrow (YM) fraction were calculated with QCT-Pro software (Mindways, Austin, TX, USA). Spearman's correlations were performed between YM fraction and BMD, VAT, SAT using SPSS, version 20.0. Results: We recruited and imaged 15 hemodialysis patients (74.0 ± 9.2 years old, dialysis vintage 47.0 ± 27.9 months, 80% male) from CHU de Québec, Hôtel-Dieu de Québec hospital. MAT, VAT, SAT, cortical and trabecular volumetric BMD, as well as tibia cortical thickness can be evaluated with a five-minute CT-scan acquisition (Figure 1). Our analyses showed correlations between L3 and L5 yellow marrow (YM) fraction ($R = 0.529$, $p = 0.043$). On one hand, inverse correlations have been obtained between L3 YM fraction and L3 Z-score ($R = -0.621$, $p = 0.013$) and between L5 YM fraction and tibia BMD ($R = -0.650$, $p = 0.009$). On the other hand, positive correlations have been found between proximal tibia YM fraction and L3 BMD ($R = 0.613$, $p = 0.020$), L5 BMD ($R = 0.556$, $p = 0.039$) as well as tibia cortical thickness ($R = 0.697$, $p = 0.006$). Conclusion: CT-scan allows simultaneous evaluation of MAT, BMD, VAT, SAT in dialysis patients. A better characterization of MAT and its interrelation with bone components may help to understand the mineral and bone complications in CKD.



140 kVp images
Figure 1. Representative Images of Lumbar Spine and Distal Tibia Acquisition With a Calibration Phantom

■ Fat tissue
■ Lean tissue
■ Bone tissue
--- Subcutaneous delimitation

Disclosures: *Yue Pei Wang, None*

MON-0294

Bone Quality Analyses in Cases with Type 2 Diabetes Mellitus Reflect Patterns of Femoral Cortical Bone Reorganization Along with High Porosity

Eva Maria Wölfel*¹, Petar Milovanovic¹, Katharina Jähn¹, Felix N. Schmidt¹, Birgit Wulff², Michael Amling¹, Klaus Püschel², Graeme M. Campbell³, Björn Busse¹. ¹Department of Osteology and Biomechanics, University Medical Center Hamburg, Germany, ²Department of Forensic Medicine, University Medical Center Hamburg, Germany, ³Institute of Biomechanics, Hamburg University of Technology, Germany

Diabetes mellitus is a chronic systemic disease with increasing prevalence worldwide. Despite usually presenting with a high bone mineral density, type 2 diabetes mellitus (T2DM) patients suffer from an increased fracture risk. In the literature, clinical data on cortical porosity has been displayed with a high variability in the diabetes group. In our study we focus on human cortical bone obtained at autopsy on multiple length scales to understand the underlying mechanism affecting bone microstructure of patients with T2DM. In an ongoing collection of mid-diaphyseal femoral cortices of T2DM-diagnosed cases ($n = 12$) and age-matched controls ($n = 11$) we investigate geometrical parameters with contact radiography to identify resorption patterns. Here, the anterior quadrant of the cross-section was further analyzed with micro-computed tomography to assess cortical porosity and tissue mineral density. Static histomorphometry was performed on toluidine-blue and modified silver nitrate stained histological sections. Finally, mechanical properties were determined via nanoindentation, Fourier-transfer infrared imaging and material testing. Contact radiography data revealed a high variability in the T2DM group. Quantification with 3D micro-computed tomography showed a higher cortical porosity in the subgroup of the diabetic cases compared to control cases and T2DM cases without increased porosity (44.36 ± 16.2 vs. 9.96 ± 5.61 vs. 10.93 %, $p < 0.05$). Image processing revealed a larger inner diameter in T2DM with high porosity leading to a larger buckling ratio compared to the non-diabetic control group ($p < 0.05$). Osteonal density was lower in the endocortical region in T2DM group with high porosity compared to control and diabetic individuals ($p < 0.005$ and $p < 0.05$, respectively). Osteoclast activity was more pronounced, although not statistically significant, in the diabetes groups while the lowest Young's modulus value was measured in the endocortical region of the T2DM group with high porosity (18.12 ± 1.73 GPa). Overall these results suggest the presence of two morphological patterns of bone reorganization in T2DM cases. In the T2DM group with high porosity mainly changes at the endocortical site were observed proposing pronounced endocortical reorganization. These results provide new insights into the possible mechanisms affecting the microstructure of bone and leading to an increased fracture risk in T2DM patients.

Disclosures: *Eva Maria Wölfel, None*

MON-0315

Cranial Neural Crest-Targeted Deletion of Cdc73 Results in Embryonic Lethality Jessica Costa-Guda*¹, Lilia Shen², Wade Berry¹, Robert Romano¹, Haeyoung Yi¹, Justin Bellizzi¹, Andrew Arnold¹. ¹UConn SDM, United States, ²UConn, United States

Loss-of-function mutations of the CDC73 tumor suppressor gene (previously HRPT2) and aberrant expression of its encoded protein, parafibromin, contribute to the pathogenesis of a variety of tumor types. Germline mutations of CDC73 cause Hyperparathyroidism-Jaw Tumor Syndrome, an autosomal dominant disorder consisting of benign and/or malignant parathyroid tumors, (cemento-)ossifying fibromas of the mandible and/or maxilla and, a variety of kidney, renal and uterine tumors. Somatic (and sometimes germline) mutations of CDC73 are common in sporadic ossifying fibromas (OF) and parathyroid carcinomas. Little is known about the molecular pathogenesis of OF, a benign neoplasm virtually exclusive to the craniofacial skeleton, beyond the involvement of CDC73/parafibromin. The precise mechanism of tumor formation secondary to CDC73/parafibromin loss is unknown. Parafibromin is an essential component of the RNA polymerase II-associated Paf1 transcriptional regulatory complex, which functions in maintenance of stem cell pluripotency and may contribute to lineage commitment during development. Parafibromin can bind β -catenin and may function in canonical Wnt/ β -catenin signaling but parafibromin's role in Wnt/ β -catenin signaling is unclear. We sought to investigate the mechanisms through which CDC73/parafibromin loss contributes to tumorigenesis and model ossifying fibroma in mice. Cdc73-floxed mice were crossed with Wnt1-Cre mice, thereby targeting Cdc73 loss to craniofacial bone progenitors without significantly affecting parafibromin expression in long bone. Homozygous Cdc73 deletion in the Wnt1 expression domain was embryonic lethal by embryonic day 13, with increased apoptosis noted in the region of the developing mandible and midbrain. Heterozygous null mice were viable and healthy. Followed to 15 months, they exhibited no evidence of OF development or any other craniofacial abnormalities. Our results provide further evidence of a role for parafibromin in development: expression of Cdc73 is required for development. Tumorigenesis appears to require biallelic inactivation of Cdc73 in post-natal life; that the second allele did not become somatically inactivated in heterozygous null mice, resulting to tumor formation, is likely a reflection of the time required to acquire such genetic alterations. Further studies are required to elucidate the mechanisms through which CDC73/parafibromin loss contributes to tumorigenesis.

Disclosures: *Jessica Costa-Guda, None*

MON-0316

Enpp1-Fc treatment reduces renal calcifications in Npt2anull mice Jonathan Fetene*, Daniel Caballero, Xiaofeng Li, Dillon Kavanagh, Demetrios Braddock, Clemens Bergwitz. Yale School of Medicine, United States

Nephrocalcinosis (NC) is a condition caused by calcium phosphate (hydroxyapatite) deposits in the kidneys. The condition is a frequent complication of inherited renal phosphate (Pi) wasting disorders, such as infantile idiopathic hypercalcemia (IH) and hereditary hypophosphatemic rickets with hypercalciuria (HHRH). These conditions can be caused by loss-of-function of the sodium-Pi cotransporter NPT2a and the related transporter NPT2c, respectively. In addition, calcium-Pi nidus formation is thought to be the initial event in the formation of Randall's plaques, which are thought to underlie most forms of NC and nephrolithiasis (NL) including idiopathic hypercalciuria (IH), although much about the pathophysiology is unclear. We used Npt2a^{-/-} mice to model the renal calcifications observed in these disorders. We previously reported elevated urinary excretion of PPi in Npt2a^{-/-} mice when compared to WT mice. Reduced levels of Extracellular nucleotide pyrophosphatase phosphodiesterase 1 (Enpp1), an enzyme that generates the mineralization inhibitor pyrophosphate (PPi), in Npt2a^{-/-};Enpp1^{asj/asj} double mutant mice further worsens the NC and the intraperitoneal administration of sodium PPi reduces NC in Npt2a^{-/-} mice. These findings suggest that mechanisms which can be blocked by supplemental PPi contribute to its pathogenesis. We here report that also once-daily subcutaneous injections of the fully bioactive Enpp1 enzyme linked to the immunoglobulin Fc domain (Enpp1-Fc) is able to prevent the NC observed in Npt2a^{-/-} mice. Enpp1-Fc from postnatal day (P) 15 through P30 days reduces the number, but not the size, of these deposits. Enpp1-Fc administered from P3 through P15 reduces mineral deposit size, but, in contrast to later treatment or treatment with PPi, the number of mineral deposits remains unchanged. This result suggests that Enpp1-Fc has an effect on mineral growth and nidus formation. More importantly, the effect on mineral growth may be independent of PPi and may reveal, previously unrecognized novel activities of Enpp1-Fc, which are currently under investigation in the lab. Because Ca-Pi deposits (Randall's plaques) are the common precursor of many forms of renal calcifications, if successful, treatment with Enpp1-Fc has the potential to be a game-changing therapy for preventing and/or reversing NC in IH and HHRH and other rare genetic conditions such as primary hyperoxaluria or cystinuria which can lead to kidney failure and for which currently no cure exists, or for the most common form of NL/NC due to formation of renal Ca-oxalate mineral deposits.

Disclosures: Jonathan Fetene, None

MON-0317

Skeletal muscle mitochondrial dysfunction in the osteogenesis imperfecta murine (oim) mouse model of Osteogenesis imperfecta (OI) Victoria L. Gremminger*¹, Youngjae Jeong¹, Rory Cunningham^{2,3}, Grace Meers^{2,3}, R. Scott Rector^{2,3}, Charlotte L. Phillips⁴. ¹Department of Biochemistry, University of Missouri, United States, ²Departments of Nutrition and Exercise Physiology and Medicine-GI, University of Missouri, United States, ³Research Service-Harry S Truman Memorial VA Hospital, United States, ⁴Departments of Biochemistry and Child Health, University of Missouri, United States

Osteogenesis imperfecta (OI), also referred to as brittle bone disease, is a heritable connective tissue disorder characterized by skeletal fragility, short stature, and more recently, muscle weakness. Homozygous oim/oim (osteogenesis imperfecta murine) mice model moderately severe human type III OI, as the result of non-functional $\alpha 2(I)$ collagen chains and the production of homotrimeric type I collagen, $\alpha 1(I)3$. In addition to marked skeletal fragility, the oim/oim mice exhibit pronounced muscle weakness with reduced relative muscle mass and contractile function relative to age and sex-matched wildtype (WT) littermates. To further investigate the cause of this muscle weakness, we examined citrate synthase activity, an indirect measure of mitochondrial content, in oim/oim and WT mixed gastrocnemius muscle and found oim/oim mice had increased citrate synthase activity suggesting increased mitochondrial content. This was unexpected in light of poor oim/oim muscle contractile function and led us to further investigate mitochondrial content, turnover, and function. We evaluated mitochondrial content and gross morphology by and relative mitochondrial to nuclear DNA levels by qPCR and transmission electron microscopy (TEM). We examined known markers of mitochondrial biogenesis and mitophagy. oim/oim mice had elevated markers of mitochondrial biogenesis, including PGC1 α and TFAM and decreased levels of mitophagy markers, specifically LC3. Protein content of complex IV of the electron transport chain was decreased in oim/oim compared to WT. In addition, state 2, state 3 and maximal uncoupled skeletal muscle mitochondrial respiration was severely decreased (>50% reduction) in oim/oim compared to age and sex-matched WT littermates. These findings suggest that skeletal muscle mitochondrial dysfunction likely contributes directly or indirectly to reported muscle weakness in the oim/oim mouse. Further studies to discern the pathogenic mechanisms responsible for the mitochondrial dysfunction in the oim/oim mouse model of osteogenesis imperfecta are warranted.

Disclosures: Victoria L. Gremminger, None

MON-0318

The 839(C/A) Polymorphism in the ECE1 Isoform b Promoter Associates with Hip Bone Mineral Density in Postmenopausal Women Karen Hansen*¹, Michael Johnson², Tonia Carter³, Nicholas Keuler¹, Robert Blank⁴. ¹University of Wisconsin-Madison, United States, ²Lucigen, United States, ³Marshfield Clinic, United States, ⁴Medical College of Wisconsin, United States

Secretion of the vasoactive peptide endothelin-1 (ET1) promotes breast and prostate cancer bone metastases by activating the Wnt signaling system. We found that variation in a QTL containing the murine gene encoding endothelin converting enzyme (Ece1) affected bone size, accounting for 40% of the variance in bone biomechanics and bone mineral density (BMD). We tested the hypothesis that polymorphisms within the human endothelin converting enzyme (ECE1) isoform b promoters, located at ECE1 b -338 (G/T) and ECE1 b -839 (C/A) that are known to affect transcription, would associate with BMD and fractures in postmenopausal women. We analyzed data from 3,564 postmenopausal women with banked DNA in the Marshfield Clinical Personalized Medicine Research Project (PMRP) and at least one BMD test at ≥ 60 years of age at Marshfield Clinic. Personnel at the University of Wisconsin-Madison Biotechnology Center genotyped DNA for the ECE1 -338(G/T) and -839(A/C) single-nucleotide polymorphisms (SNPs). We evaluated relationships between genotype and BMD using linear regression models, and between genotype and clinical fractures using logistic regression models. Women with the -839 C allele had lower femoral neck BMD than those with the A allele (0.856 ± 0.145 g/cm² vs 0.872 ± 0.140 g/cm², $p=0.015$). In single linear models predicting hip T-scores, the AC polymorphism was inversely associated with the lowest hip T-score (C allele, $R=-0.106$, $p=0.036$). We found no relationship between the ECE1b -338 (G/T) and BMD or fracture. In multivariate models, neither polymorphism was significant in models predicting osteoporosis, fracture after age 50, fracture at any age, spine or hip T-score. In summary, the C allele of the ECE1 b -839 (C/A) promoter was associated with lower hip BMD in univariate models. However multivariate models found no association between the C allele and hip BMD. Our small sample size, largely Caucasian cohort, and exclusion of men are study limitations. Confirmation of our findings is needed in other, larger databases.

Disclosures: Karen Hansen, None

MON-0319

Understanding the Role of Protein Gamma-Carboxylation in Craniofacial Development Jane Hendrickson-Rebizant*¹, Juliana Marulanda Montoya¹, Omar Al Rifai², Genevieve Chiasson¹, Mathieu Ferron², Monzur Murshed^{3,4}. ¹Faculty of Dentistry, McGill University, Canada, ²Institut de Recherches Cliniques de Montreal, Canada, ³Faculty of Dentistry and Department of Medicine, McGill University, Canada, ⁴Shriners Hospital for Children, Canada

Congenital anomalies are a major cause of perinatal lethality, affecting 2-3% of all newborns. A significant number (1 in 3000) of these infants present with abnormal craniofacial development, such as midface hypoplasia. Midface hypoplasia is caused by impaired growth of the nasal, zygomatic, and maxillary bones. This trait is observed in many human disorders, including Keutel Syndrome, which is caused by autosomal recessive mutations in matrix Gla protein (MGP). MGP, a potent mineralization inhibitor, is expressed by chondrocytes. We recently demonstrated that MGP-deficient (Mgp^{-/-}) mice showed shorter antero-posterior measurements of the skull (cranial, maxillary and palatine lengths), causing midface hypoplasia. Both the nasal septum and sphenoccipital synchondrosis (SOS) are abnormally calcified in Mgp^{-/-} mice. Although cephalometry on Mgp^{-/-} heads suggested a critical role for nasal septum in midface development, it is currently unknown whether calcification of the SOS, alone, is sufficient to cause midface hypoplasia. To study the relative contributions of the nasal septum and the SOS to midface development, we generated a unique mouse model (referred to as Ggexch^{-/-} in this application) in which only chondrocytes lack the enzyme gamma-glutamyl carboxylase (GGCX). GGCX modifies specific glutamic acid (Glu) residues of MGP and other Gla proteins to carboxylated glutamic acid (Gla) residues. Cephalometric analyses were performed on micro-CT scans of the heads from our experimental Ggexch^{-/-} mice and control mice at ages 2 and 3 weeks and 6 months. The Ggexch^{-/-} mice showed ectopic calcification of the SOS, which was first detected by 2 weeks of age, however nasal septum calcification was not observed at any age. Interestingly, cephalometric analyses demonstrated a complete absence of midface hypoplasia. Our findings suggest that GGCX activity is required for the prevention of SOS, but not nasal septum, calcification. Comparing the craniofacial phenotypes of Ggexch^{-/-} and Mgp^{-/-} mice, we demonstrated that nasal septum calcification, not SOS calcification, is the primary cause of midface hypoplasia in the latter model. Our work provides information on the role of protein gamma-carboxylation and abnormal calcification of cartilaginous tissues in midface hypoplasia. Ongoing studies on various mouse models will be important in understanding the causes, onset, progression, and possible treatments for patients with craniofacial dysplasias.

Disclosures: Jane Hendrickson-Rebizant, None

MON-0320

Biomechanical evaluation of enthesopathy in a murine model of X-linked hypophosphatemia Jack Luo^{*1}, Steven Tommasini², Carolyn Macica¹. ¹Frank H. Netter, M.D., School of Medicine at Quinnipiac University, United States, ²Yale School of Medicine, United States

X-linked hypophosphatemia (XLH) is the most common heritable phosphate-wasting disorder, resulting in both rickets and osteomalacia. Although osteomalacia, growth, and skeletal deformities have been the primary clinical focus of XLH, patients typically develop severe paradoxical mineralization of fibrocartilaginous tendon/ligament insertion sites (enthesophytes) in their second and third decades. We have previously demonstrated the hyperplastic expansion of mineralizing fibrochondrocytes in the insertion sites of Hyp mice. Here, we test the hypothesis that hyperplasia of mineralized fibrocartilage is a compensatory mechanism to accommodate the abnormal transmission of mechanical forces that arise due to insertion into a hypomineralized bone matrix substrate. Tensile testing of the left Achilles enthesis from 6-month-old female HYP (n=9) and wild-type mice (n= 8) was performed using a pneumatic grip, gripping as close to the Achilles insertion site as technically possible, and pulled at a constant rate of 10 mm/min until failure. Stiffness, strain, and strength (max stress) were measured. There were no significant differences in stiffness (7.9±4.4 v. 7.3±3.2 N/mm), strain (58±22 v. 69±30%), or strength (116.3±65.2 v. 113.6±61.2 N/mm²) of the tendinous insertion site between HYP and wild-type mice, although there was a 27.8% decrease (p < 0.05) in the tendon width in HYP mice. The contralateral Achilles insertion was used for histological validation of mineralizing fibrocartilaginous hyperplasia by alkaline phosphatase staining and von Kossa staining to evaluate the degree of mineralization of the insertion and the subchondral calcaneus matrix. Relative to controls, staining confirmed a significant increase in alkaline phosphatase-positive fibrochondrocytes embedded in mineral matrix and osteomalacia in subchondral bone. Thus, the mineralizing enthesopathy in XLH provides a biomechanical compensatory mechanism that strengthens the Achilles insertion despite the compromised bone material properties at the calcaneus. Future studies are aimed at unloading the enthesis to evaluate if the compensatory fibrochondrocyte hyperplasia occurs in the absence of tensile forces on the insertion site.

Disclosures: Jack Luo, None

MON-0321

Type 1 diabetes (T1DM) impacts bone phenotype and fracture healing in Akita mice Pei Hu^{*}, Jennifer Mckenzie, Evan Buettmann, Nicole Migotsky, Matthew Silva. Washington University in St. Louis, United States

Type 1 diabetes (T1DM) impairs bone formation and delays fracture healing in human patients. Around 5 wks, male Akita mice become spontaneously diabetic, with high blood glucose levels, due to a mutation in one allele of the insulin-2 (Ins2) gene. We hypothesized that T1DM in Akita mice is associated with decreased bone mass, mechanical properties and impaired fracture healing. We used 18 wk old male Akita mice (Ins2Akita, Jax) and compared them to wildtype littermates (WT). Both Akita and WT mice gained weight from 3 to 18 wks of age, but Akita mice weighed less starting at 5 wks (-5.20%, p = 0.04). Akita mice were hyperglycemic by 6 wks, which continued at 18 wks (fasting glucose > 450 mg/dL; WT mice < 200 mg/dL). Phenotyping: Non-fractured left femurs were analyzed by microCT (cortical and cancellous bone) and mechanically tested (3-point bending/torsion). At 20 wks Akita mice had a shorter femur than WT (-1.9%, p<0.001) with reduced cortical bone total area (-6.5%, p<0.05), bone area (-16%, p<0.001), and cortical thickness (-17%, p<0.001). After adjusting for body mass, the cortical differences remained significant. Cancellous bone was largely unaffected by T1DM. Mechanical testing of non-fractured femurs showed decreases in structural and material properties of Akita bones. Terminal blood was collected and Akita mice had a serum insulin deficiency (-94%, p<0.01), lower osteocalcin (OCN, -44%, p<0.01) and higher C-telopeptide (CTX-1, 75%, p<0.05) on D14 after fracture. Fracture Healing: A closed, transverse diaphyseal right femur fracture was made in Akita and WT mice at 18 wks. Using CT on D14 Akita mice had a significantly smaller callus (-32%, p<0.01) with a significantly higher callus bone mineral density (BMD, 24%, p<0.05). D21 CT Akita mice had a significantly smaller callus volume (-26%, p<0.05) while BV/TV and callus BMD showed no differences between groups. D21 torsion tests showed a weaker callus in Akita femurs with lower stiffness (-42%, p<0.01), maximum torque (-44%, p<0.05) and work to fracture (-44%, p<0.05). In summary, cortical bone size was reduced in Akita mice, which is consistent with lower serum OCN levels and smaller fracture callus, suggesting a bone impairment. The higher callus BMD and higher serum CTX level found in D14 Akita mice might demonstrate an early remodeling after fracture, which needs further examination. Consistent with clinical features and bone changes in human T1DM patients, Akita mouse is a good T1DM model.

Disclosures: Pei Hu, None

MON-0322

Generation and Characterization of a Conditional Mouse Model for Atypical Type VI Osteogenesis Imperfecta Samantha Robinson^{*}, Frank Rauch, Pierre Moffatt. Shriners Hospitals for Children - Canada, Canada

Osteogenesis imperfecta (OI) is a rare heritable disorder that affects bones and leads to overall skeletal fragility, reduced height, and fractures. The majority of mutations in OI

affect type I collagens. Atypical type VI OI, however, is inherited in an autosomal dominant fashion and caused by a heterozygous mutation in the BRIL gene (also called IFITM5), introducing a single amino acid change at position 40 (S40L). Atypical type VI is clinically extremely severe with bowed and hypomineralized bones. A patient bone biopsy revealed accumulation of un-mineralized osteoid extracellular matrix, similarly to OI type VI caused by mutations in Serpinf1. We have generated a transgenic conditional mouse model expressing the human (h)S40L-BRIL protein under the tTA response element (TRE). Two founders were bred with the tTA-Osx-GFP-Cre mice and expression was induced by putting mice on regular diet ('on'), or repressed ('off') by administration of doxycycline-containing food. When hS40L-BRIL was expressed from conception, the skeletal phenotype was extremely severe with accompanied neonatal lethality. As assessed by alizarin red/alcan blue staining and μ CT, all long bones were shorter, hypomineralized, and bowed. RT-qPCR indicated significant reduction in the expression of bone specific markers (Bglap, Ibsp, Col1a1) in E18.5 calvaria. Histological assessment showed that humeri were filled with hypertrophic chondrocytes and presented with Osx:GFP+ cells at a wedge like structure at the midshaft. The mRNA and protein levels for hS40L-BRIL were also itself attenuated in mutant embryonic calvaria, suggesting feedforward deleterious effects. When hS40L was induced postnatally from 8 to 12 weeks of age, mouse body length was reduced. Strikingly, visual appearance of the mutant mice femur, tibia, vertebrae, and mandible were bulky and white. μ CT imaging revealed massive expansion of the periosteal and trabecular compartment reminiscent of mouse models for fibrous dysplasia. Ongoing studies will provide further clues as to the histological features and molecular mechanisms at play and perhaps serve as a platform for more directed therapies.

Disclosures: Samantha Robinson, None

MON-0323

Sexual Dimorphism in Skeletal Abnormalities in Down Syndrome Mice Jared Thomas^{*1}, Adam Knox¹, Randall Roper¹, Elizabeth Fisher², Victor Tybulewicz³, Joseph Wallace¹. ¹Indiana University-Purdue University Indianapolis, United States, ²UCL Institute of Neurology, United Kingdom, ³The Francis Crick Institute, United Kingdom

Down syndrome (DS), caused by three copies of human chromosome 21 (Hsa21), is characterized by a spectrum of phenotypes including cognitive and skeletal deficits. Sexual dimorphism in skeletal deficits has been hypothesized in individuals with DS, however, differences in age, methodology and tissue have impacted interpretation of these results. The Ts65Dn DS mouse model exhibits similar skeletal phenotypes as those associated with DS. Ts65Dn mice have some limitations including limited genetic composition (~104 human orthologs on Mmu16) and exclusion of female mice in previous studies because of fertility issues. Another model of DS, Dp1Tyb, was developed to contain three copies of all the Hsa21-orthologous regions on Mmu16 (~148 genes). Due to the presence of more orthologous genes at a dosage imbalance and, because both trisomic males and females are fertile Dp1Tyb mice may be a better model to study DS phenotypes. We hypothesized that there would be a difference in the skeletal deficits between trisomic Dp1Tyb male and female mice. Right femurs from both male and female mice at 6- and 16-weeks were imaged using microCT, resolution of 6 μ m, to determine trabecular microarchitecture (distal metaphysis) and cortical geometry (midshaft). The left femurs were subjected to three point bending test to determine bone mechanical integrity. ANOVA was used to determine the main and interactive effects of genotype, sex, and age. There was a sexual dimorphism in the effect of trisomy on the trabecular microarchitecture including percent bone volume, trabecular thickness and trabecular number. For cortical bone, there was a sexual dimorphism for the effect of trisomy on total cross sectional area in 6- and 16-week old but differing main and interactive effects at 6- and 16-weeks for other cortical measures. There was a main effect of sex and genotype on whole bone and material-level properties. In addition, there was an interaction of age and genotype for Dp1Tyb mice for both pre-yield and post-yield properties. These data suggest that with an increase in age, trisomic Dp1Tyb mice have weaker bones compared to their euploid counterparts. Overall, it appears that male mice have stronger bones in comparison to female mice across age and genotype. These results may be important to humans with DS because disruption in bone homeostasis appears during adolescence and continues throughout adulthood, and females have weaker bones than males with DS.

Disclosures: Jared Thomas, None

MON-0324

Knockout and Human Transgenic Mouse Models Reveal a Role for the Cathelicidin Antimicrobial Peptide (Camp/CAMP) Gene in Bone Metabolism Yang Zhang^{*1}, Carmen P. Wong², Richard L. Gallo³, Amanda R. Gamboa², Dawn A. Olson², Malcolm B. Lowry⁴, Mary L. Fantacone⁵, Claudia S. Maier⁶, Jan F. Stevens⁷, Russell T. Turner², Urszula T. Iwaniec², Adrian F. Gombart⁸. ¹School of Biological and Population Health Sciences, Linus Pauling Institute, Oregon State University, United States, ²School of Biological and Population Health Sciences, Oregon State University, United States, ³Department of Dermatology, University of California San Diego, United States, ⁴Department of Microbiology, Oregon State University, United States, ⁵Linus Pauling Institute, Oregon State University, United States, ⁶Department of Chemistry, Oregon State University, United States, ⁷Linus Pauling Institute, Department of Pharmaceutical Sciences, Oregon State University, United States, ⁸School of Biological and Population Health Sciences, Linus Pauling Institute, Department of Integrative Biology, College of Science, Oregon State University, United States

The cathelicidin antimicrobial peptide (CAMP/Camp) genes in humans and mice encode the hCAP18 and CRAMP pro-proteins, respectively. Both pro-proteins are processed into peptides (LL-37 in humans) that mediate their well-established antimicrobial properties. These peptides also modulate inflammation, cell proliferation, and wound healing, making them important in innate immunity. Expression of the gene is regulated by vitamin D in humans but not in mice. Both the human and mouse genes are highly expressed in bone marrow and in vitro studies suggest that CRAMP, the mouse peptide, is produced by osteoblasts and suppresses differentiation of osteoclasts. Furthermore, monocytes differentiated by LL-37 treatment appear to develop novel bone forming properties. While these in vitro studies suggest a role for CRAMP/LL-37 in bone metabolism, in vivo studies are lacking. To address this gap in knowledge, we evaluated the architecture of the cortical bone in the femur diaphysis and cancellous bone in the distal femur metaphysis using microcomputed tomography in skeletally mature 6-month-old male C57BL/6J mice. We compared wild type (WT/WT, n = 5), Camp knockout (KO/KO, n = 8), and human CAMP transgenic mice on the Camp knockout background (Tg+/Tg+;KO/KO, n = 8). Differences between genotypes were determined using Kruskal Wallis ANOVA followed by a Dunn's posthoc test. We did not observe significant differences between genotypes in cortical bone architecture (cross-sectional volume, cortical volume, marrow volume, cortical thickness, polar moment of inertia). In contrast, cancellous bone volume fraction tended to be lower (p = 0.1), trabecular number was lower (p = 0.03), and trabecular spacing was higher (p = 0.03) in KO/KO compared to WT/WT mice. Furthermore, KO/KO mice exhibited lower cancellous bone volume fraction (p = 0.0029), trabecular number (p = 0.0001) and connectivity density (p = 0.0006), and higher trabecular spacing (p = 0.0001) compared to Tg+/Tg+;KO/KO mice. Significant differences between Tg+/Tg+; KO/KO and WT/WT mice were not detected for any of the cancellous endpoints evaluated. Our findings suggest that Camp plays a role in the regulation of cancellous bone mass and architecture and that the human CAMP gene can substitute for the loss of the mouse gene. Future studies will focus on the molecular and cellular mechanisms responsible for the changes in bone architecture.

Disclosures: *Yang Zhang, None*

MON-0337

Circulating MicroRNA Expression is Upregulated after 30 Days of Head-Down Bed Rest Debra Bemben^{*1}, Breanne Baker¹, Samuel Buchanan¹, Carl Ade². ¹University of Oklahoma, United States, ²Kansas State University, United States

MicroRNAs (miRNAs) are short, non-coding RNA molecules that are negative regulators of gene expression. Recently, miRNAs have been identified that target on genes of osteogenesis (Lian et al. 2012) and/or muscle atrophy (Wada et al. 2011). Circulating miRNAs (c-miRNAs) can be measured in the blood as biomarkers of cellular activity, and they may play a role in cell to cell communication. Large decreases in BMD and muscle mass during prolonged exposure to microgravity are well-documented, but c-miRNA responses have not been examined. C-miRNAs have potential to be useful biomarkers of physiological changes during spaceflight. The purpose of this study was to examine c-miRNA and bone marker responses to a 30 day six-degree head-down bed rest protocol at an ambient 0.5% CO₂. The study protocol was conducted at the bed rest facility located at the Institute for Aerospace Medicine in Germany. Eleven participants had fasting blood draws taken 3 days before and on the last day of the 30 day bed rest protocol. Serum levels of miRNAs associated with bone and muscle function (miR-21, -100, -125b, -126) were analyzed using real-time PCR. Sclerostin and TRAP5b concentrations were assayed using commercial ELISA kits. The normalized c-miRNA expression values and bone marker responses were analyzed by paired t-tests. TRAP 5b significantly increased (p=0.018) post bedrest but sclerostin was unchanged. MiR-21 was significantly upregulated (p = 0.019) from pre to post bed rest. MiR-125b showed a trend (p = 0.11) for upregulation with 10 participants showing increased expression and 1 showing decreased expression post bed rest. MiR-21 regulates bone cell activity; it is highly expressed in osteoclast precursors during osteoclastogenesis and it is upregulated in patients with osteoporotic fractures. The upregulation of miR-21 in this study may reflect an increase in osteoclast activity after 30 days of bed rest, which is corroborated by the increase in TRAP 5b. In conclusion, these findings suggest that c-miR-21 has potential as a biomarker of bone resorption and bone loss in an unloading condition.

Table 1. Circulating MiRNA Expression Pre and Post 30 days of Head-down Bed Rest (means ± SE)

Time Point	Expression (n=11)			
	MiR-21	MiR-100	MiR-125b	MiR-126
Pre bed rest	-0.536 ± 0.147	-8.926 ± 0.315	-5.666 ± 0.231	-0.901 ± 0.124
Post bed rest	-0.065 ± 0.107*	-8.487 ± 0.310	-5.342 ± 0.186	-0.608 ± 0.158

* p = 0.019 vs. pre

Disclosures: *Debra Bemben, None*

MON-0338

Novel genetic variants of OFD1 gene are associated with a familial form of stress fractures of long bones and a sporadic case of atypical femur fracture associated with bisphosphonate use Marie-Eve Boisvert^{*1}, Jacques P Brown^{1,2}, Rachel Laframboise³, Maxime Vallée¹, Frédéric Fournier¹, Suzanne N Morin⁴, Edith Gagnon¹, Arnaud Droit¹, Laetitia Michou^{1,5}. ¹CHU de Québec-Université Laval Research Centre, Canada, ²Department of medicine, Université Laval, Canada, ³Department of Genetics, CHU de Québec-Université Laval, Canada, ⁴Department of Medicine, McGill University, Canada, ⁵Department of medicine, CHU de Québec-Université Laval, Canada

Purpose - The pathogenesis of atypical femur fractures (AFFs), an insufficiency fracture of the subtrochanteric or diaphyseal region of femur, is incompletely understood. They are thought to be associated with long-term use of bisphosphonates but also occur in patients who are naive to pharmacological therapy or have genetic disorders such as hypophosphatasia and osteogenesis imperfecta. Here, we report the genetic analysis of a French-Canadian family in which eleven relatives have X-linked osteoporosis and/or dental and facial hypoplasia and/or adult-onset multiple stress fractures of long bones, with a radiological aspect akin to AFF. We also performed resequencing in a cohort of 49 individuals with AFF associated with bisphosphonate use. **Methods** - After having ruled out mutations in all exons of the Plastin3 gene by Sanger sequencing, we performed a whole exome sequencing to identify a causal genetic variant in relatives of this family. Data were analyzed by a first bioinformatic filtering and intrafamilial segregation analysis with emphasis on X chromosome genetic variants. The resequencing of the OFD1 gene was further performed in 49 patients from the Quebec AFF Registry, all exposed to bisphosphonates. **Results** - A novel variant, p.A642D, of the OFD1 gene, was our only candidate on the X chromosome perfectly segregating with the phenotype within the family. In the literature, mutations of OFD1 gene were reported to be associated with the oral-facial-digital syndrome, which belongs to the group of ciliopathies. Ciliopathies are genetic disorders of the cellular cilia or the anchoring structure of the cilia or cilia dysfunction. Oral-facial-digital syndrome is characterized by malformations of the face, oral cavity and digits, and is transmitted in an X-linked pattern of inheritance with lethality in males. Interestingly, the resequencing of OFD1 gene allowed us to detect another novel variant, p.K668N, of this gene in one woman with AFF who used bisphosphonate. **Conclusions** - This family demonstrates that such insufficiency fractures of long bones may occur in patients with oral-facial-digital syndromes. It may also contribute to a better understanding of the pathophysiology of these fractures and their association with dental and facial hypoplasia. Further studies are needed to increase improve our knowledge on the functional effects of these genetic variants on bone modeling and remodeling, and their contributions to bisphosphonate-associated AFF.

Disclosures: *Marie-Eve Boisvert, None*

MON-0339

Is serum free DNA methylation a bone biomarker? Alvaro Del Real^{*1}, Carolina Sañudo¹, Carmen Garcia Ibarbia¹, Carmen Valero¹, Mario F. Fraga², Agustin F. Fernandez², Flor M. Perez-Campo⁴, Maria Isabel Perez-Nuñez⁵, Esther Laguna⁵, Jose A. Riancho¹. ¹Department of Internal Medicine, Hospital Universitario Marqués de Valdecilla-IDIVAL, University of Cantabria, Spain, ²Nanomaterials & Nanotechnology Research Center (CINN-CSIC), University of Oviedo, Spain, ³Cancer Epigenetics Laboratory, Institute of Oncology of Asturias (IUOPA), HUCA, University of Oviedo, Spain, ⁴Department of molecular biology, University of Cantabria-IDIVAL, Santander, Spain, ⁵Department of Traumatology/Hospital U M Valdecilla, University of Cantabria, Santander, Spain

Cell-free DNA (cfDNA) is present in fluids, such as urine and serum. It is an appealing molecular biomarker because it is easy to obtain without using invasive procedures. DNA methylation regulates gene expression and has specific profiles according to the tissue of origin. We have previously shown that methylation of SOST (gene encoding sclerostin) contributes to the regulation of sclerostin synthesis. In fact, there is an inverse correlation

between SOST methylation and expression (Delgado-Calle et al, JBMR 2012). The aim of this study was to determine the methylation of the SOST promoter in cfDNA, in comparison with the methylation pattern in DNA from blood and bone cells. For this study, 30 patients with osteoporotic hip fractures undergoing replacement surgery were included. From each patient, bone tissue, blood and serum samples were obtained. A second group of 28 osteoporotic patients was also included. Serum samples were obtained at baseline and after 6-months therapy with alendronate, teriparatide or denosumab. DNA was analysed by pyrosequencing that allowed the interrogation of 3 CpGs of the SOST promoter. Sclerostin levels in serum were measured with ELISA. The methylation level of the sclerostin promoter was very similar in serum cfDNA (84±11%) and bone-derived DNA (86±3%), but lower than in blood cells DNA (94±3%). Pairwise comparisons revealed statistically significant differences between blood and serum ($p=0.0001$), and between blood and bone ($p=0.007$). However, there were no difference between serum and bone ($p=0.21$). Moreover, there was a positive correlation between DNA methylation in serum and DNA methylation in bone ($r=0.56$; $p=0.000002$). We did not find differences in sclerostin serum levels nor in cfDNA methylation before and after anti-osteoporosis therapy. In conclusion, methylation of the SOST promoter in serum cfDNA is lower than in blood cell DNA and similar to bone DNA, suggesting that serum cfDNA might originate in bone cells. However, since we did not find significant changes in either serum sclerostin or SOST methylation after therapy with bone-active drugs, the role of cfDNA as a bone biomarker cannot be confirmed yet.

Disclosures: *Alvaro Del Real, None*

MON-0340

Search for modifier genes by whole exome sequencing in familial form of Paget's disease of bone linked to the SQSTM1/P392L mutation Mariam Dessay*¹, Maxime Vallée¹, Frédéric Fournier¹, Arnaud Droit¹, Edith Gagnon¹, Jacques P. Brown^{1,2}, Laetitia Michou^{1,2,3}. ¹CHU de Québec-Université Laval Research Centre, Québec, Canada, ²Department of Medicine, Division of Rheumatology, Université Laval, Québec, Canada, ³Department of Rheumatology, CHU de Québec-Université Laval, Québec, Canada

Purpose: Paget's disease of bone (PDB) is a chronic disorder characterized by increased bone remodeling. Although the pathogenesis is still poorly understood, genetic and environmental factors are involved. The SQSTM1/P392L mutation was reported in 46% of familial forms of PDB with a high penetrance $\geq 80\%$ after 60 years old. In our cohort, we identified families in which relatives with PDB carrying or not the SQSTM1/P392L mutation coexist, suggesting the presence of a modifier gene. In this study, we performed a whole exome analysis (30 Mb) in two familial forms of PDB linked to the SQSTM1 gene to search for modifier genes. Methods: Whole exome sequencing (WES) was performed using a HiSeq 2500 with the Agilent XT protocol at 3 µg on four patients with PDB not carrier of any SQSTM1 mutation. These patients came from two different families (2 in each family) in which at least one other sibling with PDB was carrier of a SQSTM1/P392L mutation. The bioinformatic analysis relied on filtering on minor allele frequency <0.01 and on in silico predictions of any damaging effect of the variants, followed by the intra-familial segregation analysis within the two families. Targeted resequencing was performed using the same technology in four extended pedigrees (18 patients) linked to SQSTM1, including the two families studied by whole exome sequencing. Results: The intra-familial segregation analysis and filtering of the WES data identified 242 variants in 191 different genes. Interestingly, in silico prediction showed interaction of some of these genes with SQSTM1 gene such as: MPRIP and MAP3K5 (genetic interaction), TTN and PEX5 (same signaling), SH3TC1 and HLA-A (co-expression). After filtering variants shared by the four studied patients based on rarity (allele frequency <0.01) and expected deleteriousness, five shared variants were found in the following genes: PPIAL4G, FDF1, KRT18, MPRIP and DOCK6. Therefore, amongst the 191 genes, 106 genes of interest were further selected for targeted resequencing. The resequencing identified relevant candidate genes which would be involved in bone metabolism such as: ZNF141 and VEZF1 (transcription factor), PEX5 and MTMR3 (autophagy), POSTN and BMP7 (bone formation), to name a few. Conclusions: This whole exome analysis allowed us to detect variants of interest in different candidate genes. The modifier effect of these variants on the SQSTM1/P392L mutation and the pagetic phenotypes needs to be further investigated.

Disclosures: *Mariam Dessay, None*

MON-0341

Associations Between Single Nucleotide Polymorphisms in the Vitamin D Receptor and Vitamin D Binding Protein Genes and Tibia Bone Mineral Content, Density and Strength in Young Adults Entering Initial Military Training Erin Gaffney-Stomberg*¹, Laura Lutz¹, Anna Nakayama¹, Philip Fremont-Smith², Darrell Ricke², Martha Petrovick², James McClung¹. ¹US Army Research Institute of Environmental Medicine, United States, ²MIT Lincoln Laboratory, United States

Single nucleotide polymorphisms (SNPs) in vitamin D-related genes have been associated with risk of stress fracture as well as vitamin D status and 25-hydroxyvitamin D (25OHD) response to vitamin D supplementation during initial military training (IMT). The purpose of this study was to determine whether these previously identified SNPs are associated with measures of tibial bone density, content and strength collected using peripheral

quantitative computed tomography (pQCT) in young adults entering IMT. Baseline associations between SNPs (vitamin D receptor (VDR; n=2, FokI and BsmI)) and vitamin D binding protein (DBP; n=2, GC1S and GC2), as well as a genetic risk score (GRS; calculated as the number of 25OHD lowering alleles in the DBP [GC1S] and VDR [BsmI] SNPs) and vBMD, bone mineral content (BMC) and strength (either BSI or SSIp) at three bone sites (4, 14, and 66% of the tibia length) were evaluated in volunteers starting IMT (n=445; 220 male and 225 female, 64.5% Caucasian, age 24 ± 3 yr). Gene-bone parameter associations were analyzed by univariate ANOVA (SPSSv21) while controlling for race, sex, age, and body mass index. There were no associations between the GRS or VDR BsmI SNP and any bone parameter at any site. Several 3-way interactions were observed between race, sex and each DBP SNP, but sample sizes were too small to make meaningful post hoc comparisons. However, the VDR FokI SNP, which was previously associated with greater fracture risk, was associated with strength at the 4% site (BSI; $p<0.001$) with those homozygous for the minor allele having 16.3 ± 6.5 mg/mm⁴ lower BSI as compared to those homozygous for the major allele ($p<0.05$). This relationship differed by race ($p<0.05$) with the minor allele resulting in lower BSI in Caucasians, and higher BSI in African Americans. This study demonstrated an association between the VDR SNP and baseline bone strength at the distal tibia which differed by race. Whether SNPs in VDR affect bone responses to training and whether these SNPs would be useful in predicting stress fracture risk in military trainees remains to be determined. The views expressed in this abstract are those of the authors and do not reflect the official policy of the Department of Army, Department of Defense, or the U.S. Government. Research supported by: USAMRMC and DHP.

Disclosures: *Erin Gaffney-Stomberg, None*

MON-0342

Differential prevalence of CYP2R1 variants across populations reveals pathway selection for vitamin D homeostasis. Alex Casella*¹, Jingman Zhou², Lauren O'Leary², Caella Long², Zahra Tara², Ilana Caplan², Meizan Lai², Michael Levine², Jeffrey Roizen². ¹University of Maryland, United States, ²The Children's Hospital of Philadelphia, United States

When human populations moved away from the equator there was an associated loss of pigmentation; this pervasive pattern has been attributed to a need for increased vitamin D synthesis in the context of decreased sun exposure. Equally pervasive is the persistence of pigmentation in those close to the equator. We hypothesized that this persistence might indicate an evolutionary strategy to protect against vitamin D excess. To examine this hypothesis we measured the activity of all of the non-synonymous variants in CYP2R1, which encodes the principal 25-hydroxylase required for initial activation of vitamin D, reported in the 1000 genomes project as well as any variants occurring in the publically available databases more than once. We determined the effect of 41 non-synonymous polymorphisms in CYP2R1 on expression and function of the recombinant enzyme in HEK293T cells. Twenty-one of 41 amino acid replacements led to significantly decreased activity relative to wild-type CYP2R1 protein, while two variants have significantly increased activity. Three mutations led to frame shifts and truncated proteins. The combined prevalence of CYP2R1 alleles that encode enzymes with decreased 25-hydroxylase activity is three in every 1,000 Caucasians and seven in every 1,000 African-Americans, while in populations closer to the equator, where exposure to sunlight is high, hypomorphic alleles occur at frequencies as high as 7%. To further test our hypothesis, we theorized that there would also be similar patterns of variation in other proteins in the vitamin D pathway. To examine this possibility we examined the geographic prevalence of hypomorphic variation in the GC protein (the vitamin D binding protein). We observed a similar geographic prevalence with variants associated with decreased vitamin D being more prevalent in populations close to the equator. We conclude that CYP2R1 polymorphisms have important effects on vitamin D homeostasis, and that the geographic variability of CYP2R1 alleles represents an adaptation to differential exposures to UVB irradiation from sunlight.

Disclosures: *Alex Casella, None*

MON-0376

Inhibition of FGF23 signaling corrects LPS-induced hypoferrremia through the erythropoiesis-inflammation axis Rafiou Agoro*¹, Anna Montagna¹, Moosa Mohammadi², Despina Sitara¹. ¹New York University, United States, ²New York University School of Medicine, United States

Inflammation and iron deficiency have been described to stimulate the synthesis of the osteocyte-secreted protein FGF23. Activation of toll-like receptors (TLRs), the key sensors of the innate immune system, induces the hepatic expression and secretion of the iron-regulating hormone hepcidin. Hepcidin acts by causing degradation of the iron exporter ferroportin, resulting in hypoferrremia and anemia during inflammation. Conversely, stimulation of erythropoiesis suppresses hepcidin expression via induction of the erythropoietin-responsive hormone erythroferrone. Here, we used the C-terminal tail of FGF23 to impair endogenous full-length FGF23 signaling in wild-type mice, and investigated its impact on hypoferrremia induced by lipopolysaccharide (LPS), a TLR 4 agonist. Our data show that LPS-induced expression of the liver pro-inflammatory cytokines Tnf- α and Lipocalin-2 was significantly attenuated by inhibition of FGF23 signaling. Similarly, LPS-induced liver hepcidin expression was significantly reduced by FGF23 signaling disruption, consistent with upregulation of spleen erythroferrone. Accordingly, the increase in liver and spleen iron content caused by TLR4 activation was completely abrogated by inhibition of FGF23 signaling. Interest-

ingly, inhibition of FGF-23 signaling selectively upregulated spleen ferroportin expression, and increased serum iron and transferrin saturation. Moreover, we show that LPS-induced acute inflammation leading to hypoferrremia upregulated bone Fgf23 expression. In addition, LPS-treated mice showed a decrease in serum phosphate associated with a decrease in renal phosphate reabsorption as demonstrated by significant downregulation of renal NaPi2a/2c expression. Importantly, inhibition of FGF23 signaling induced hyperphosphatemia and upregulated renal NaPi2a/2c expression. Finally, our findings show that LPS induced a significant downregulation of Erythropoietin (Epo) and its receptor (EpoR) in kidney, liver, and spleen. Interestingly, inhibition of FGF23 signaling increased significantly the expression of renal and extra-renal Epo and EpoR when the mice were challenged with LPS. Taken together, our studies highlight for the first time that inhibition of FGF23 signaling attenuates LPS-induced inflammation and hypoferrremia, while promoting erythropoiesis by increasing erythropoietin and erythroferrone expression.

Disclosures: *Rafiu Agoro, None*

MON-0377

Hypoxia enhances EPO-mediated FGF23 expression in hematopoietic cells Erica Clinkenbeard*¹, Maegan Capitano¹, Megan Noonan¹, Pu Ni¹, Mark Hanudel², Kenneth White¹. ¹Indiana University School of Medicine, United States, ²David Geffen School of Medicine at UCLA, United States

Fibroblast growth factor (FGF) 23 is a crucial phosphaturic hormone. Interestingly, FGF23 has been found to undergo regulation by factors outside of the normal phosphate, vitamin D, parathyroid hormone feedback loops. This was underscored by the fact that autosomal dominant hypophosphatemic rickets phenotype could be induced in FGF23-R176Q mutant mice with a low iron diet and in ADHR patients during anemia. In addition to possible localized tissue hypoxia, low iron elicits a renal induction of erythropoietin (EPO) which acts to induce red blood cell production by stimulating bone marrow hematopoietic cells. In accord with previous studies, and compared to saline controls, infusion with patient equivalent doses of recombinant EPO significantly induced circulating total FGF23 protein (274.8±33.3 vs 4514.6±1128; p<0.05) as well as full-length intact FGF23 (324.6±29.3 vs 556.8±57.2; p<0.05). In addition to osteoblast/osteocyte induction of Fgf23 mRNA expression with EPO administration (10-fold; p<0.01), Fgf23 mRNA was also significantly induced within the flushed bone marrow of the EPO treated mice compared to controls (26-fold; p<0.01), a novel site of FGF23 production. To better understand the mechanisms controlling FGF23, flushed marrow from wild-type (WT) mice were plated ex vivo and treated with 100 U/mL recombinant EPO. After 4 hours, EPO treatment only increased Fgf23 mRNA levels 2-fold compared to control treated cells in conjunction with a 4-fold increase in the EPO responsive factor erythroferrone (ERFE). It was shown that the bone marrow niche remains moderately hypoxic and cells collected under similar conditions retain their stem cell phenotype which improves grafting during bone marrow transplant. Therefore, we hypothesized isolating and culturing bone marrow cells under hypoxia will improve responses to exogenous EPO. Bone marrow cells were isolated in a hypoxia chamber (3% O₂) from WT mice and lysed of red blood cells. Incubation under low oxygen tension with 1-10 U/mL EPO elicited a maximal response of a 4-fold increase in Fgf23 mRNA (p<0.01) and an 11-fold induction of ERFE mRNA (p<0.01), equating a 40- to 110-fold improvement in sensitivity, respectively. Stem cell factor (SCF), a normal supplement for culturing hematopoietic cells, did not further enhance EPO-mediated Fgf23 mRNA induction. In summary, hematopoietic cell production of FGF23 in response to EPO is enhanced under low oxygen tension which simulates in vivo conditions.

Disclosures: *Erica Clinkenbeard, None*

MON-0378

FGF23 impairs osteocyte maturation by inhibition of Wnt/b-catenin pathway and is associated with bone alterations in early CKD Juan Miguel Diaz Tocados*¹, Maria Encarnacion Rodriguez Ortiz¹, Yolanda Almaden², Julio Manuel Martinez Moreno¹, Carmen Herencia Bellido¹, Noemi Vergara Segura¹, Antonio Casado Diaz¹, Catarina Carvalho³, João Miguel Frazão⁴, Mariano Rodriguez Portillo¹, Juan Rafael Muñoz Castañeda¹. ¹Maimonides Institute for Biomedical Research (IMIBIC), Reina Sofia University Hospital, University of Cordoba, Spain, ²Maimonides Institute for Biomedical Research (IMIBIC), ³Internal Medicine Service, Reina Sofia University Hospital, Spanish Biomedical Research Networking Centre consortium for the area of Physiopathology of Obesity and Nutrition (CIBEROBN), Spain, ⁴Braga Hospital, Department of Nephrology, Institute of Investigation and Innovation in Health (I3S), National Institute of Biomedical Engineer (INEB), University of Porto, Portugal, ⁵Department of Nephrology, São João Hospital Center, Institute of Investigation and Innovation in Health (I3S), National Institute of Biomedical Engineer (INEB), University of Porto, Portugal

Chronic kidney disease patients commonly develop mineral metabolism abnormalities associated with reduction of bone mineral density and fractures. In these patients Fibroblast Growth Factor 23 (FGF23) is markedly increased. The direct effects of FGF23 on bone cells is not clear. In this study, the effects of high FGF23 on bone were investigated in vivo in an experimental model of heminephrectomized rats fed on a moderately high phosphate diet

(1/2Nx-HP) and compared with Sham rats on the same diet. Additionally, in vitro studies were performed to evaluate the effect of recombinant FGF23 (rFGF23) on osteocytes and osteoclasts formation. In vivo, our results showed that serum FGF23 levels were significantly increased in Nx1/2-HP as compared with sham animals after 21 days, while other parameters of mineral metabolism such as PTH, phosphate or calcitriol remains similar between both groups. Bone histomorphometric analysis revealed that animals with high FGF23 had a decreased bone volume and a high bone turnover. RNA analysis of bones revealed a decrease in the expression of specific osteogenic genes such as Runx2, Osterix or DMP1 and an increase of SOST expression that was also detected in plasma. In vitro, high rFGF23 was added during maturation of mesenchymal stem cells into mature osteoblasts or for 24 hours once mature. Alkaline phosphatase activity and osteoblast master genes expression were decreased in rFGF23-treated cells. In mature osteocytes, high rFGF23 downregulated osteoblast gene expression: Osterix, Osteocalcin, DMP1 and RANKL. Furthermore, high FGF23 levels decreased the nuclear translocation of β-catenin after 24 hours. With respect to osteoclasts formation, the presence of FGF23 enhanced TRAP staining, the number of nuclei and osteoclasts and cathepsin K expression. In conclusion, high FGF23 concentration decreases osteocyte maturation through inhibition of the canonical Wnt signaling and increases osteoclast differentiation.

Table 1. Bone histomorphometry

	Sham 1.2%P n=8	Uni-Nx 1.2%P n=8	P value
BV/TV (%)	27.6±2.02	21.4±1.77	<0.05
OV/BV (%)	0.83±0.109	2.39±0.727	<0.05
OS/BS (%)	6.6±0.95	14.0±2.74	<0.05
Ob.S/BS (%)	1.14±0.184	4.89±0.803	<0.01
Oc.S/BS (%)	1.86±0.487	3.68±0.435	<0.05
ES/BS (%)	6.84±1.74	9.50±2.28	n.s
Tb.Th (µm)	85.6±3.93	73.6±2.52	<0.05
O.Th (µm)	5.27±0.481	5.13±0.525	n.s
N.Ob/B.Pm (µm)	0.98±0.225	3.61±0.650	<0.01
N.Oc/B.Pm (µm)	0.52±0.109	0.94±0.121	<0.05
Tb.Sp (µm)	229±14.6	302±27.5	<0.05
Tb.N (mm)	3.01±0.129	2.9±0.183	n.s

Disclosures: *Juan Miguel Diaz Tocados, None*

MON-0379

Estrogen Receptor-α Knockout Affects Femoral Cortical Geometry and Trabecular Microarchitecture, but not Osteocyte Sclerostin Expression, in Aged Male Mice Rebecca Dirkes*¹, Nathan Winn¹, Thomas Jurrisen¹, Dennis Lubahn², Victoria Vieira-Potter¹, Jaume Padilla¹, Pamela Hinton¹. ¹Department of Nutrition and Exercise Physiology, University of Missouri, Columbia MO, United States, ²Department of Biochemistry, University of Missouri, Columbia MO, United States

Estrogen plays an important role in skeletal growth and maintenance throughout the lifespan, with differential effects on cortical and cancellous bone due to differences in the relative distribution of estrogen receptor-α (ERα) and ERβ. Hypoestrogenemia results in bone loss associated with increased osteocyte sclerostin expression and reduced bone formation. Here, we examined the effects of global ERα-knockout (ERKO) on femoral cortical geometry and trabecular microarchitecture and on osteocyte sclerostin expression in cortical and cancellous bone in male mice. In a longitudinal study, ERKO (n=6) and wild-type (WT) littermates (n=6) were allowed ad libitum access to a standard rodent diet from weaning until 16 months of age, at which time body composition was assessed via EchoMRI and hind limbs and blood collected. Circulating estradiol concentrations were measured via radioimmunoassay. Cortical geometry of the mid-diaphysis and trabecular microarchitecture of the distal right femur were assessed via mCT, and osteocyte sclerostin expression in these regions was assessed via immunohistochemistry. ANCOVA was used to test the effects of ERKO on cortical geometry with body weight as a covariate; t-tests were used to compare ERKO and WT for other outcomes. ERKO mice had 36% higher estradiol concentrations than WT, but this difference was not significant (p=0.286). ERKO mice had greater body fat percentage (p=0.026) than WT controls. ERKO mice had greater bone volume (p=0.005) and trabecular number (p=0.001) and decreased trabecular separation (p=0.002) of the distal femur compared to WT controls. Femur length did not differ between groups. ERKO had lower total area (p=0.042), cortical area (p=0.018), and cortical thickness (p=0.047) of the mid-diaphysis compared to WT controls. Robustness tended to be lower in ERKO than WT (p=0.075); cortical area to total area did not differ between groups. The percentage of sclerostin+ osteocytes was not altered by ERKO. In conclusion, estrogen receptor-α knockout

affects femoral cortical geometry and trabecular microarchitecture, but not osteocyte sclerostin expression, in aged male mice.

Disclosures: *Rebecca Dirkes, None*

MON-0380

Effects of Sodium Glucose Cotransporter 2 Deletion on Bone and Mineral Metabolism Claire Gerber*, Nicolae Valentin David, Susan Quaggin, Aline Martin, Tamara Isakova. Northwestern University, United States

Background: Type 2 diabetes mellitus (T2DM) and chronic kidney disease are associated with an increased risk of developing bone and mineral metabolism abnormalities. A new class of glucose-lowering agents, sodium-glucose cotransporter 2 (SGLT2) inhibitors, promotes urinary glucose excretion and improves renal and cardiovascular outcomes in patients with T2DM. However, SGLT2 inhibitors are associated with increased risk of bone fractures. Because loss of SGLT2 function may decrease urinary phosphate, we hypothesize that inhibition of SGLT2 induces mineral metabolism alterations that could contribute to increased bone fragility. Design: Slc5a2 nonsense mutation in Sweet Pee (SP) mice results in total loss of SGLT2 function in proximal tubules. To understand the effects of loss of SGLT2 function on mineral metabolism, urine and serum was collected from fasted wild type (WT) and SP mice. Levels of fractional excretion of calcium and phosphate; serum phosphate, calcium, PTH, 1,25(OH)2D, and FGF23 were evaluated at 15 and 25 weeks. To determine the longitudinal impact of loss of SGLT2 function on bone metabolism, bone architecture, remodeling, and mineralization was assessed in SP mice and WT mice at 15 and 25 weeks of age. Results: At 25 weeks, SP mice showed significantly decreased body weight compared to WT mice (21.6±3.8 vs 25.1±2.9 g, p<0.05). Consistently, femoral length was significantly shorter in SP mice compared to WT mice (14.1±0.4 vs 14.5±0.2 mm, p<0.05). Overall renal function was not impaired in SP mice compared to WT mice (blood urea nitrogen: 18±4 vs 21±5 mg/dL, NS). Fasted SP mice did not show modification of fractional excretion of calcium. Serum calcium, PTH, and 1,25(OH)2D levels were similar between WT and SP mice at 15 and 25 weeks. Fractional excretion of phosphate was significantly higher at 25 weeks in SP mice compared to WT (5.5±2.0 vs 2.5±1.9 %, p<0.05), despite unchanged levels of FGF23. SP mice had reduced cortical bone mineral density, compared to WT mice at 25 weeks (1240±16 vs 1264±14 mg/cm³, p<0.05). Conclusion: These results suggest that loss of SGLT2 function in the absence of T2DM may contribute to bone fragility. Future studies are required to determine how loss of SGLT2 function impacts bone fragility in T2DM.

Disclosures: *Claire Gerber, None*

MON-0381

Estrogens Suppress the Senescence-Accelerated Secretory Phenotype (SASP) in Osteoprogenitors by Restraining NF-κB Activation, but not GATA4 Expression or Transcriptional Activity Ha-Neui Kim^{1,2}, Li Han^{1,2}, Srividhya Iyer¹, Aaron Warren^{1,2}, Maria Almeida^{1,2}, Stavros Manolagas^{1,2}. ¹University of Arkansas for Medical Sciences, United States, ²Central Arkansas Veterans Healthcare System, United States

Estrogen deficiency and old age are the two most critical factors for the development of osteoporosis in both women and men. However, it is unknown whether the pathogenic cellular and molecular changes responsible for the imbalance between resorption and formation in sex steroid deficiency versus old age are similar or distinct; or whether and how sex steroid deficiency influences the age-dependent involution of the skeleton. Nonetheless, in mice the protective effects of estrogens against cortical bone loss result from actions mediated via ERα signaling on mesenchymal cells (targeted by Prx1 or Osx1-Cre); and in both females and males, estrogens alone protect against the resorption of cortical bone, via actions on osteoprogenitors. Moreover, the age-dependent decrease of cortical thickness is associated with increased osteoclast numbers in the endosteal surface and classical features of osteoprogenitor senescence and the SASP, including some of the same osteoclastogenic cytokines that are upregulated acutely by estrogen deficiency in young and adult mice. Accumulation of the transcription factor GATA4 and the resulting activation of the canonical IKKβ/NFκB pathway play a seminal role in SASP. We examined the effects of 17β-estradiol (E2) on GATA4-stimulated SASP in primary calvaria cell cultures infected with a pMX vector containing a GATA4 expressing plasmid. GATA4-dependent transcription was determined by luciferase activity in C2C12 cells co-transfected with the GATA4 plasmid and a GATA4 3x-Luc promoter. GATA4 stimulated NF-κB as measured by the phosphorylation of the p65 subunit. E2 (10⁻⁸M) had no effect on the transcriptional activity of GATA4 or its protein levels. E2, on the other hand, potentially suppressed NF-κB activation, in agreement with long standing evidence that ERα attenuates NF-κB. More importantly, E2 suppressed the GATA4-induced SASP, including IL-1α, IL-1β, TNFα, GM-CSF, and MMP-13. These results support the working hypothesis that in the aged skeleton, senescence of mesenchymal lineage cells and the SASP, driven by NF-κB activation, is the predominant mechanism of the increased osteoclast number and resorption in the endosteal surface. Because NF-κB is also upregulated by estrogen deficiency, NF-κB is the key molecular nexus where the two pathologies intersect and as a result estrogen deficiency accelerates the adverse effects of aging on cortical bone in both sexes.

Disclosures: *Ha-Neui Kim, None*

MON-0382

Intestinal calcium absorption increases markedly during pregnancy and lactation despite absence of the vitamin D receptor (VDR) or calcitriol Beth J. Kirby^{*1}, Brittany A. Ryan¹, K. Berit Sellars¹, René St-Arnaud², Christopher S. Kovacs¹. ¹Memorial University of Newfoundland, Canada, ²Shriner's Hospital and McGill University, Canada

Intestinal calcium absorption (CaAbs) and calcitriol both increase during pregnancy and lactation. Does calcitriol stimulate the increase in CaAbs? Vdrnull mice increase CaAbs >2-fold during pregnancy (lactation was not studied), but have very high levels of calcitriol that may act on an alternate receptor. We investigated whether calcitriol is required for CaAbs during pregnancy and lactation, by comparing the effects of absence of calcitriol (Cyp27b1nulls) to absence of its receptor (Vdrnulls). WT and null sisters in both colonies were raised on a calcium and lactose-enriched "rescue" diet. Time points were pre-pregnancy, day 18.5 of pregnancy, and day 10 of lactation. Using DeLuca and Fleet's methodology, mice were fasted overnight and 0.5 microCi 45Ca was administered by oral gavage. After 10 min, blood was collected by cardiac puncture. Duodena were snap frozen for gene expression analysis by qPCR. Radioactivity in sera was adjusted for total blood volume, and expressed as percent of administered dose. Compared to pre-pregnancy, Vdrnull mice showed a 2.5-fold increase (p<0.05) of CaAbs during pregnancy that remained 2.1-fold increased during lactation; Vdrnull values were not different than corresponding WT at all time points. Cyp27b1nulls showed a marked 9.2-fold increase in CaAbs during pregnancy with no difference from corresponding WT value; lactation has not yet been assessed. Duodenal expression of Trpv6 and S100g increased 4-fold (p<0.01) and 2.4-fold (p<0.01) respectively in WT during pregnancy but did not change in Vdrnulls; pregnancy values were 6 and 5-fold fold higher in WT than respective Vdrnull (p<0.01). Pmca1 showed no differences between time points or genotypes. Ncx did not change in WT but decreased 0.35-fold during pregnancy in Vdrnulls (p<0.01). In summary, CaAbs increased over 2-fold during pregnancy and lactation in Vdrnulls, and 9-fold during pregnancy in Cyp27b1nulls, with all values being equivalent to respective WT. But WT and Vdrnull mice differed in duodenal gene expression patterns, with none of the observed changes explaining the increased CaAbs in Vdrnulls. In conclusion, CaAbs upregulates during pregnancy without calcitriol, since neither absence of VDR nor absence of calcitriol affect the achieved peak value in CaAbs. The persistence of increased CaAbs during lactation indicates that placental factors cannot explain it. The mechanisms that explain this reproductive increase in CaAbs remain to be elucidated.

Disclosures: *Beth J. Kirby, None*

MON-0383

Regulation of IGF-1- and Mechano-responsive Signaling by the RhoGAP MYO9B Monica Sun^{*1}, Emma Hassell¹, Benjamin Scandling², Beth Lee¹. ¹The Ohio State University College of Medicine, United States, ²The Ohio State University College of Engineering, United States

Purpose: Anabolic signaling in bone by IGF-1 and mechanical stimuli are closely intertwined due to interactions between IGF-1 receptors and integrins that perceive mechano-stimulation at the cellular level. By regulating both hormonal and mechanical pathways, the small G protein RhoA is likely to be central to this functional interaction. Previous studies demonstrated that a regulator of RhoA, the RhoGAP MYO9B, is required for normal skeletal growth in mice since the absence of MYO9B resulted in decreased growth and bone formation. Further, osteoblasts lacking MYO9B showed poor spreading and chemotactic responses to IGF-1, but not to other growth factors. Preliminary studies indicated this may be due to defects in IGF-1 receptor (IGF1R) localization. The goal of this study was to further characterize how IGF-1 signaling is affected in MYO9B-deficient cells and to determine their ability to respond to mechanical strain. Methods: Primary mouse osteoblasts and MC3T3-E1 cells expressing or lacking MYO9B were assessed for integrity of the IGF-1 signaling pathway by cell fractionation, western blot, and confocal microscopy. For measuring responses to mechanical stimuli, cells were subjected to uniaxial stretch on a Flexcell tension system, and the orientations of stress fibers were measured using FibrilTool software. Results: Osteoblasts deficient in MYO9B demonstrated abnormal trafficking, expression, and activation of IGF1R. These cells showed high levels of total and activated IGF1R in the nucleus, rather than in its normal distribution in focal adhesions and along stress fibers. Cells lacking MYO9B were also unable to undergo a normal downregulation of IGF1R following IGF-1 stimulation, leading to prolonged activation and probable desensitization of the signaling pathway. Further, cells lacking MYO9B were unable to align themselves appropriately to uniaxial mechanical strain. Conclusions: These results reveal that the RhoGAP MYO9B lies at the intersection of IGF-1- and mechanical-mediated signaling by regulating the function of the IGF1 receptor and the ability of cells to respond to mechanical stimuli. Because this RhoGAP plays a key role in mediating not only hormonal, but mechanical based signaling, these studies help elucidate the RhoA-mediated mechanisms that play key roles in bone growth.

Disclosures: *Monica Sun, None*

MON-0384

Acute Calcitriol-Mediated PTH Suppression Attenuated by High Dietary Phosphate Intervention in Experimental Model of CKD Lok Hang Lee*, Mandy Turner, Cynthia Pruss, Kim Laverty, Rachel Holden, Michael Adams. Queen's University Department of Biomedical and Molecular Sciences, Canada

Chronic kidney disease (CKD) patients have impaired phosphate and calcium excretion. Vitamin D deficiency is also prevalent, due to a decline in functional kidney mass and reduction in renal CYP27B1 conversion of calcitriol, which exacerbates secondary hyperparathyroidism (SHPT). SHPT leads to increased bone resorption and is a risk factor for vascular calcification and cardiovascular disease in the CKD population. Vitamin D is commonly prescribed to bypass this deficiency and reduce SHPT, however resistance to suppression often occurs. Resistance may be due to parathyroid hyperplasia and downregulation of receptors. This pathology is exacerbated by high dietary phosphate. The purpose of this study is to characterize the capability of single doses of calcitriol to acutely suppress parathyroid hormone (PTH) as kidney function declines and dietary phosphate is increased. In a dietary adenine rat model of CKD (N=10) Adenine was removed at 4.5 weeks and stable CKD was generated. An oral dose of calcitriol (160ng/kg) was given at baseline, 1, 3, and 5 weeks as CKD progressed on low (0.5%) dietary phosphate, and at 7 and 8 weeks following a high (1.0%) dietary phosphate intervention. At each dose, calcium, phosphate and PTH was assessed over a 24-hour period prior to and a 48-hour period after dosing. Serum creatinine elevated by one week of dietary adenine (p<0.01) and stabilized at ~300uM. Despite the alterations in dietary phosphate, at no point in the experiment were serum phosphate elevated above baseline. Throughout CKD generation (baseline to 5 weeks), the single dose of calcitriol consistently induced a PTH reduction by 24 hours. The responsiveness was maintained despite elevations in PTH from 79.6±/25.8 pg/mL to 221.4±/66.7 by week 5. Following the increase in dietary phosphate, PTH increased to 1207±/176 pg/mL to 1342±/310, at 7 and 14 days post-intervention, respectively. PTH was no longer reduced at 24 hours following the dose of calcitriol at both of these time points, despite causing an elevation in serum calcium at 48 hours. The response mediated by PTH and FGF-23 was independent of serum of phosphate and was not a result of daily fluctuations in the hormone. The suppression of PTH by an acute dose of calcitriol was attenuated by dietary phosphate in the setting of stable experimental CKD. This suggests that limiting dietary phosphate in the CKD population is critical to limiting mineral bone disease in this population.

Disclosures: Lok Hang Lee, None

MON-0385

Attenuated parathyroid megalin expression contributes to the pathogenesis in hyperfunctioning parathyroid tumors Daichi Miyaoka*¹, Yasuo Imanishi¹, Masayo Yamagata², Ikue Kobayashi¹, Noriyuki Hayashi¹, Masaya Ohara¹, Yuki Nagata¹, Katsuhito Mori¹, Masanori Emoto¹, Toshimi Michigami³, Masaaki Inaba¹. ¹Osaka City University Graduate School of Medicine, Japan, ²Osaka Ohtani University, Japan, ³Osaka Women's and Children's Hospital, Japan

Insufficient vitamin D status, measured as 25-hydroxyvitamin D (25OHD) in plasma, is associated a higher circulating parathyroid hormone (PTH) level in general population. PTH secretion from parathyroid cells is directly suppressed by 1,25-dihydroxyvitamin D (1,25(OH)2D), however, little is known about mechanisms of 25OHD on secretory PTH suppression. In addition, decrement of vitamin D receptor (VDR) expression and/or calcium-sensing receptor (CaSR) enhances PTH secretion from parathyroid tumors in primary hyperparathyroidism (PHPT) and secondary hyperparathyroidism of uremia (SHPT), however, these factors do not totally account for the role of 25OHD on PTH secretion. Megalin is a multiligand endocytotic receptor involving in the reabsorption of 25OHD and vitamin D binding protein in renal proximal tubules, and we attempted to determine the expression of megalin in the hyperfunctioning parathyroid tumors, and the roles of megalin and 1 α -hydroxylase (CYP27B1) in PTH expression in parathyroid cells. Megalin expression was determined by immunohistochemistry in parathyroid tumors, obtained from PHPT and SHPT patients, and in normal parathyroid glands from thyroid carcinoma patients. To assess the role of megalin in incorporation of 25OHD, histidine-tagged soluble receptor-associated protein (His-sRAP) which binds and accelerates internalization of megalin, was administered to primary cultured parathyroid cells obtained by therapeutic parathyroidectomies from PHPT patients. The distributions of megalin and His-sRAP were analyzed by immunofluorescence. PTH expression was analyzed by real-time PCR. The megalin expressions decreased in tumors with PHPT and SHPT. In cultured cells, the megalin localized at the membrane, and added His-RAP is rapidly internalized in cytosol. 25OHD significantly reduced PTH mRNA, which was completely reversed by His-sRAP. CYP27B1 siRNA also reversed attenuated PTH mRNA by 25OHD. CYP27B1 siRNA, however, failed to reverse attenuated PTH mRNA by 1,25(OH)2D. To conclude, megalin has a crucial role in endocytosis of 25OHD in parathyroid cells. Incorporated 25OHD is converted to 1,25(OH)2D, which suppress PTH expression. These results highlight the direct inhibitory effect of 25OHD in PTH secretion. Reduced megalin expression is assumed to enhance PTH secretion in addition to reduced VDR and CaSR in hyperfunctioning parathyroid tumors. Megalin-CYP27B1 axis would be a next therapeutic target in PHPT and SHPT.

Disclosures: Daichi Miyaoka, None

MON-0386

Directly targeting HIF activity controls FGF23 expression and has implications for translational outcomes Megan L. Noonan*¹, Erica L. Clinkenbeard¹, Pu Ni¹, Mircea Ivan¹, Matthew Prideaux¹, Gerald J. Atkins², William R. Thompson¹, Mark R. Hanudel³, Kenneth E. White¹. ¹Indiana University School of Medicine, United States, ²The University of Adelaide, Australia, ³David Geffen School of Medicine at UCLA, United States

Fibroblast growth factor-23 (FGF23) is a bone-derived hormone that regulates systemic phosphate homeostasis. In the common disorder chronic kidney disease (CKD), there is progressive anemia with concurrent elevation of FGF23 that continues to increase as kidney function declines. FGF23 has been shown to be markedly stimulated by anemia and hypoxia, and recently, by erythropoietin (EPO); however, the molecular mechanisms driving FGF23 in the context of CKD are not well understood. A new class of drugs, hypoxia-inducible factor prolyl hydroxylase inhibitors (HIF-PHI), stabilize HIFs to increase endogenous EPO production to correct anemia. The purpose of this study was to assess in vitro how FGF23 expression is potentially controlled by HIF-PHI. To address this, we used a novel murine mesenchymal progenitor cell line clone 2 (MPC-2) that when differentiated in osteogenic media expresses Fgf23. MPC-2 cells treated with 20 μ M or 50 μ M of HIF-PHI FG-4592 (Roxadustat) for 24 hours had an 8.8 and 15-fold upregulation of FGF23 mRNA, respectively (p<0.01), with concurrent upregulation of Hif-1 α target gene Transferrin receptor (TfRc1) mRNA (2.8 and 3.9-fold respectively; p<0.05). These cells were also found to secrete (C-term) FGF23 protein when treated with 100 μ M HIF activator AG490 (2.8-fold). Additionally, after 4-hour treatment with FG-4592, MPC-2 cells showed Hif-1 α stabilization at both doses via immunoblot. For translational relevance, FG-4592 was also tested in the human U2OS osteoblast/osteocyte cell line, showing a significant induction of FGF23 mRNA with treatment at both doses (10 and 11-fold, respectively; p<0.05) after 24 hours, also coinciding with increased TfRc1 mRNA expression at each dose. U2OS cells were also shown to stabilize Hif-1 α protein after FG-4592 treatment. These data demonstrate expression of FGF23 in a novel cell line, likely via HIF stabilization, and highlight in vitro systems that can be used to elucidate the molecular mechanisms related to FGF23 expressional control during anemia and its treatment.

Disclosures: Megan L. Noonan, None

MON-0387

Interference with atrophy signaling prevents GC actions on bone and muscle in vitro and ex vivo. Amy Y Sato*¹, Lilian I Plotkin¹, Teresita Bellido². ¹Department of Anatomy & Cell Biology, Indiana University School of Medicine, United States, ²Department of Anatomy & Cell Biology, Indiana University School of Medicine, Roudebush Veterans Administration Medical Center, United States

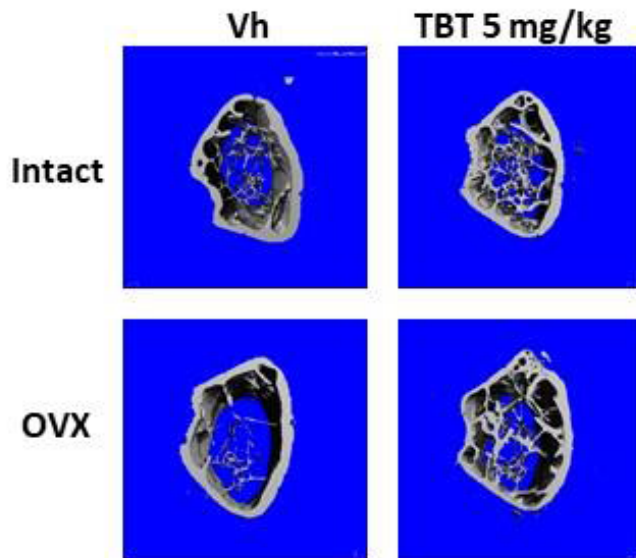
Fracture risk induced by excess glucocorticoids (GC) is largely accounted for by decreased bone mass and skeletal deterioration combined with loss of muscle mass and strength leading to higher incidence of falls. Therefore, therapeutic approaches that interfere with GC actions in both tissues are needed. Earlier work demonstrated that GC increase the expression in both bone and muscle of the proteasomal degradation inducers E3 ubiquitin ligases atrogin1, MuRF1, and MUSA1 (named atrophy-related genes or atrogenes), which were traditionally considered muscle-specific. We examined here the role of this pathway in GC action. We found that blockade of proteasomal activity with bortezomib (Bor, 3nM) prevented the effects of GC on osteoblast function. Thus, the GC dexamethasone (dex, 10-6M, 24-72 h) increased apoptosis of OB-6 osteoblastic cells (~50%), and this effect was blocked by Bor at all times examined. Dex also inhibited (26-70%) matrix mineral production by OB-6 cells in a dose-dependent manner (10-9M-10-6M), quantified by alizarin red staining, and Bor blunted this effect, increasing mineralization to veh control levels. Further, dex failed to inhibit mineralization of cultured OB-6 silenced for MuRF1 using pGFP-C-shLenti vectors, whereas significantly reduced it in scrambled control cells. These results suggest that GC action on osteoblasts is controlled by proteasomal-mediated events that depend on MuRF1. Because the active metabolite of Vitamin D (1,25D3) has beneficial musculoskeletal effects and might prevent falls by acting directly on muscle, we examined its effect on GC action. We found that the increased mRNA expression of atrogin1, MuRF1, MUSA1 induced by dex (10-6M) was fully prevented by co-treatment with 1,25D3 (10-8M) in ex vivo organ cultures of bone as well as muscle (N=8-10). In addition, dex increased mRNA expression of Sost (200%) in bone organ cultures, which was prevented by 1,25D3. 1,25D3 also prevented the ~20% reduction in the diameter of C2C12 myotubes induced by dex (10-6M, 24h, N=6), quantified by OsteoMetrics (100 myotubes scored/well). Collectively, these findings support the notion that atrogenes upregulation is a common mechanism underlying GC actions in bone and muscle, and suggest that therapeutic genetic and pharmacological approaches interfering with atrophy signaling will simultaneously prevent harmful actions of GC in both tissues.

Disclosures: Amy Y Sato, None

MON-0388

Tributyltin Increases Trabecular Bone in Female C57BL/6J Mice and Protects Against Ovariectomy-Induced Trabecular Bone Loss Jennifer Schlezinger^{*1}, Rachel Fried¹, Amira Hussein Ali², James Watt¹, Paola Divieti Pajevic², Elise Morgan³, Louis Gerstenfeld². ¹Boston University School of Public Health, United States, ²Boston University School of Medicine, United States, ³Boston University College of Engineering, United States

Bone mass and quality are determined by genetic and environmental factors. Risk factors for poor bone quality include estrogen loss at menopause and exposures to drugs/chemicals that activate peroxisome proliferator activated receptor gamma (PPAR γ). We unexpectedly observed that the environmental PPAR γ and retinoid X receptor (RXR) ligand, tributyltin (TBT), represses periosteal bone formation but enhances trabecular bone formation in young, female C57BL/6J mice. This is in contrast to TBT's known ability to suppress osteogenesis in vitro and the greater sensitivity of female-derived, versus male-derived, bone marrow multipotent mesenchymal stromal cells (BM-MSCs) to suppression of osteogenesis by TBT. In vivo, oral gavage of 12 week old female, C57BL/6J mice with 10 mg/kg TBT 3x per week for 10 weeks resulted in femurs with a smaller cross-sectional area and thinner cortex. Surprisingly, TBT induced significant increases in trabecular thickness, number, and bone volume fraction. TBT marginally inhibited the number of osteoclasts that differentiated, in spite of significantly suppressing expression of osteoclast markers Nfatc1, Acp5 and Ctsk. In contrast, expression of Ctf1, an osteoblastogenic cytokine secreted by osteoclasts, increased. TBT induced expression of RXR- and LXR-dependent genes in whole bone and in vitro mouse primary osteoclast cultures. However, only an RXR antagonist, but not a liver X receptor antagonist, significantly inhibited TBT's ability to suppress osteoclast differentiation. Next, we examined the interaction of estrogen loss and TBT exposure in C57BL/6J mice. Mice underwent either sham surgery or ovariectomy (OVX) at 10 weeks of age. At 12 weeks of age, mice were treated by oral gavage 3x per week with TBT (1 or 5 mg/kg) for 14 weeks. TBT treatment protected against OVX-induced trabecular bone loss. Serum CTX was significantly reduced in TBT-treated, OVX mice, while serum PINP and osteocalcin were not significantly affected. Gene expression analyses on cortical bone and bone marrow are being conducted and will provide information on TBT's disparate effect in the cortical and trabecular compartments. These results suggest that TBT has a distinct effect on cortical versus trabecular bone, likely resulting from independent effects on osteoblast and osteoclast differentiation that are mediated via RXR. Our novel observations will provide new information on basic bone biology, potential therapeutic targets and toxicological pathways.



Disclosures: Jennifer Schlezinger, None

MON-0389

Dynamics of Vitamin D Metabolism in the Maternal-Fetal Dyad in Response to Vitamin D Supplementation Inez Schoenmakers^{*1}, Kerry Jones², Shima Assar², Stefania D'Angelo³, Ann Prentice², Nick Bishop⁴, Stephen Kennedy⁵, Aris Papageorgiou⁵, Robert Fraser⁵, Saurabh Gandhi⁵, Elisabeth Curtis³, Sarah Crozier³, Rebecca Moon³, Keith Godfrey³, Hazel Inskip³, Elaine Dennison³, Richard Eastell⁷, Kassim Javaid⁸, Cyrus Cooper³, Nick Harvey³, The Mavidos Study Group (Arden, Carr, Mughal, Reid, Robinson)³. ¹Department of Medicine, University of East Anglia and MRC Elsie Widdowson Laboratory, United Kingdom, ²MRC Elsie Widdowson Laboratory, United Kingdom, ³MRC Lifecourse Epidemiology Unit, University of Southampton, United Kingdom, ⁴Academic Unit of Child Health, Sheffield Children's Hospital, University of Sheffield, United Kingdom, ⁵Nuffield Department of Women's & Reproductive Health, John Radcliffe Hospital, University of Oxford, United Kingdom, ⁷Academic Unit of Bone Metabolism, University of Sheffield, United Kingdom, ⁸NIHR Oxford Biomedical Research Centre, University of Oxford, United Kingdom

Fetal vitamin D supply is dependent on maternal status. It is unclear whether the relationships between maternal and cord blood vitamin D metabolite concentrations are linear over a wide range of maternal vitamin D supplies and status and whether the maternal free or total 25(OH)D concentration best reflects fetal 25(OH)D availability. We investigated the effect of maternal vitamin D supplementation on maternal and cord concentrations of total and free 25(OH)D, 3-epi-25(OH)D3 and 24,25(OH)2D3 and their interrelationships. This study utilised a subset of maternal (34 weeks gestation) and cord (umbilical vein) bloods from the MAVIDOS study, a UK-based double-blind, placebo-controlled vitamin D supplementation (1000IU/d) trial in pregnancy (n=100 pairs; 1:1:1:1 from the supplementation/placebo group and winter/summer births). Vitamin D metabolites were quantified by UPLC-MS/MS and free 25(OH)D by ELISA (Diasource). Maternal and cord concentrations of all vitamin D metabolites (mean(SD)) were significantly higher with supplementation (all P < 0.001). Total 25(OH)D and 24,25(OH)2D3 concentrations were lower, 3-epi-25(OH)D3 comparable and free 25(OH)D higher in cord blood than in maternal blood. The maternal free: total 25(OH)D ratio was lower than in cord. Maternal and cord concentrations of individual metabolites were highly correlated. In multiple regression models, concentrations of total 25(OH)D strongly predicted those of free 25(OH)D, 3-epi-25(OH)D3 and 24,25(OH)2D3 within and between the maternal and cord compartments. There were significant interactions between total 25(OH)D and supplementation group and season for all these metabolites when relationships were assessed within the maternal compartment and between maternal and fetal compartments but not within cord plasma. In conclusion, although cord vitamin D metabolite concentrations were highly dependent on those in maternal plasma, differences in absolute and relative concentrations between compartments suggest that: (1) maternal total and free 25(OH)D concentrations may not fully reflect availability to the fetus; (2) an active transport mechanism for 25(OH)D and (3) partial autonomy of fetal vitamin D metabolism.

	Maternal		Cord	
	placebo	1000 IU/d	placebo	1000 IU/d
Total 25(OH)D (nmol/l)	62(28)	95(24)	36(17)	54(21)
Free 25(OH)D (pmol/l)	7.1(2.9)	11.1(3.0)	9.6(5.3)	15.0(6.7)
3-epi-25(OH)D (nmol/l)	3.8(1.9)	6.1(2.5)	3.6(2.1)	5.5(2.5)
24,25(OH) ₂ D (nmol/l)	3.8(2.2)	7.3(2.8)	2.3(1.3)	4.1(1.9)

Disclosures: Inez Schoenmakers, None

MON-0390

IN PGE1 BONE ANABOLIC PREDOMINATES MODELING-BASED FORMATION WITHOUT HYPERCALCEMIA Francisco Velasquez-Forero^{*}, Mariela Esparza, Pedro Valencia Mayoral. Hospital Infantil de México Federico Gómez, Mexico

Purpose: to evaluate the PGE1 bone anabolism and to test our hypothesis that PGE1 primarily elicited modeling bone formation while decreasing resorption. Methods: to evaluate the PGE1 anabolic bone effects and its mechanism of formation-based on the rabbit orthodontic palate disjunction, 30 rabbits were divided into 3 groups: ten control, ten sham and ten PGE1 subjects. Basal Rx, repeated days 3 and 22. Using an orthodontic appliance in the sham and the PGE1 groups were submitted to palate disjunction for five days, after it was fixed with a steel bar. All received double tetracycline bone labeling. Control and sham groups a daily IV vehicle solution, and the third group, vehicle with 50 µg of PGE1. On day 22 blood and urine samples were taken, to analyze bone formation biochemical markers (Ca, Mg, P, calcitropic hormones, calciuria and N-telopeptides) and then they were killed. Bone palate samples were processed undecalcified. The sutural bone (sB) was histomorphometrically evaluated using a Osteomeasure software, following the ASBMR recommendations.

Remodeling and modeling bone formation were analyzed on the mineralization front stained with toluidine blue. The scalloped lines reflect initial resorption phase (remodeling formation), whereas modeling cycle are associated with smoother lines (modeling formation). Data were statistically analyzed. Results: radiology verified the suture palate disjunction. The PGE1 group, exhibited significant calcitriol and calciuric increments. The other calciotropic hormones, calcemia and N-telopeptides were normal (Table 1). Histomorphometric the PGE1 the sBV/TV, sBAr and sBTb (structural parameters) exhibited a significant increased when compared with the sham. Remodeling bone formation (RBF) in the sham group was 20% ± 6.1 and the modeling bone formation (MBF) was 6% ± 2.5. In the PGE1 group the results were significantly inverted (RBF was of 8.6% ± 1.3 and the MBF was of 17% ± 4.4). So the PGE1 bone anabolism was mainly through MBF. Table 1. The PGE 1 group exhibited accelerated mineralization parameters (Omt, MLT). On the contrary, the resorption indexes (ES/BS and OcS/BS) showed mild decreased activity which may explain the normocalcemia. Table 1. Conclusions: this model confirmed that PGE1 is an important osseous anabolic molecule by predominated MBF with scanty resorption and no hypercalcemia. Hopefully this finding could guide researchers to investigate options for osteopenic treatments.

Table 1. BLOOD AND URINE BIOCHEMICAL AND HISTOMORPHOMETRIC BONE RABBITS RESULTS

Abbr	Group A (control)	Group B (sham)	Group C (with PGE ₁)	p
Blood				
Ca (mg/dL)	11.55 ± 0.72	11.55 ± 0.68	11.85 ± 0.42	0.1
PTHi (pg/mL)	28.1 ± 15.6	30.2 ± 26.0	27.4 ± 10.1	0.1
Calcitriol (pg/mL)	50.5 ± 13.15	48.0 ± 13.8	82.1 ± 13.5**	0.002
Urinary				
Ca (mg/dL)	186 ± 66.5	178 ± 53.3*	376 ± 102.2*	0.001
N-telopeptides (nMBCE/liter)	32 ± 4.1	38 ± 16.5	30 ± 12.0	0.1
Bone Structural				
sBAr mm ²	0.29 ± 0.12	0.36 ± 0.09	0.53 ± 0.08	0.014
sB.Th μ	452.47 ± 86.14	810.03 ± 373.80	1007.83 ± 246.40*	0.001
sB.V/TV %	35.62 ± 11.10	42.23 ± 11.25	57.20 ± 8.12	0.007
Bone Static				
Oth μm	14.05 ± 1.85	13.65 ± 2.02	7.98 ± 2.79	0.004
RBF%	13.81 ± 2.85	19.7 ± 6.12	8.64 ± 1.34	0.001
MBF%	3.36 ± 0.74	5.98 ± 2.53	16.68 ± 4.42	0.001
Bone Dynamic				
MS/BS%	67.67 ± 13.56	281.85 ± 56.37	273.07 ± 54.61	0.1
MAR μ/day	2.85 ± 0.49	4.73 ± 1.13	4.81 ± 0.77	0.983
Omt day	5.11 ± 1.35	3.00 ± 0.69	1.72 ± 0.77	0.009
MLT day	23.30 ± 4.03	22.21 ± 3.18	10.38 ± 2.95	0.001
Bone Resorption				
OcPm/sBS%	1.12 ± 0.52	1.34 ± 0.98	0.87 ± 0.38	0.388
ES/sBS%	3.63 ± 1.44	4.04 ± 3.15	3.18 ± 1.62	0.742

The biochemical and histomorphometric markers abbreviation are: PTHi pg/mL=parathyroid hormone molecule integral; cross-linked N-telopeptide of type 1 collagen. sBArmm²=structural bone area; sB.Thμ= satural bone thickness; sBV/TV%= satural bone volume/tissue volume; Othμ= osteoid thickness; RBF%=remodeling-base formation; MBF%=modeling-base formation; MS/BS%=mineralizing surface/bone surface; MARμ/day=mineral apposition rate; Omt/day=osteoid maturation time; MLT/day=mineralization lag time; OcPm/sBS%=osteoclast perimeter/satural bone surface and ES/sBS%=eroded surface/satural bone surface. One way ANOVA, allowed the comparison between groups by p values sham vs PGE₁.

Disclosures: **Francisco Velasquez-Forero, None**

MON-0391

Salt inducible kinases control responses to parathyroid hormone in the renal proximal tubule Maureen Omeara¹, Han Xie¹, Alexandra Clifford¹, Jinhua Gray², Nathanael Gray², Kei Sakamoto², Michael Mannstadt¹, Marc Wein¹. ¹MGH Endocrine Unit, United States, ²Dana Farber Cancer Institute, United States

Background: We recently described a central role for salt inducible kinase 2 (SIK2) in parathyroid hormone (PTH) signaling in osteocytes. PTH-induced cyclic AMP signaling, via protein kinase A, leads to inhibitory SIK2 phosphorylation. Therefore, small molecule SIK inhibitors mimic the skeletal actions of PTH. However, role of SIKs in other PTH-responsive organs remains to be determined. PTH signaling in the renal proximal tubule plays a central role in controlling blood phosphate and 1,25-(OH)₂-vitamin D levels. Here, we tested the hypotheses that (1) renal PTH signaling involves PKA-mediated SIK phosphorylation, and that (2) small molecule SIK inhibitors mimic the renal actions of PTH. Methods: Opossum kidney (OK) cells were treated with PTH and small molecule SIK inhibitors (YKL-05-099, crenolanib, and AZD-7762). Effects on CYP27B1 gene expression were measured by RT-qPCR, and effects on phosphate uptake were measured by 32P uptake assays. C57B6 mice were treated with YKL-05-099 (18 mg/kg) or PTH (300 mcg/kg) for 1, 2, and 4 hours. Serum was collected at all time points, and 1,25-(OH)₂-vitamin D, phosphate,

PTH, and calcium were measured. Kidney RNA was collected from mice after one hour treatment (n=8/group) with vehicle, PTH, or YKL-05-099 for RNA-seq analysis. Results: PTH signaling in OK cells leads to rapid (within 5 minutes) SIK3 phosphorylation at T469, a known PKA target site. Both PTH and SIK inhibitor treatment up-regulate CYP27B1 expression in OK cells. Both PTH and SIK inhibitors block 32P uptake in OK cells in a dose dependent manner. In vivo, both PTH and YKL-05-099 acutely reduce serum phosphate levels (veh 9.38 ± 1.37 mg/dl, PTH 7.81 ± 1.49, YKL 7.38 ± 1.68, p<0.05) and increase serum 1,25-(OH)₂-vitamin D (veh 90.3 ± 39.9 pM, PTH 157.9 ± 37.0, YKL ± 188.9 ± 61.6, p<0.05) after 2 hours. Importantly, YKL-05-099 accomplishes these changes in mineral metabolism without affecting levels of serum PTH, serum calcium, or urinary cAMP. RNA-seq profiling 1 hour after acute treatment reveals a remarkable concordance between the global effects of PTH and YKL-05-099. Of the 157 genes whose expression is significantly (>2-fold, FDR<0.05) up-regulated by PTH, 63 (40.2%) are co-upregulated by YKL-05-099 (including CYP27B1). Conclusions: SIK inhibition is a key component of PTH signaling in the renal proximal tubule, with respect to both the ability of this hormone to promote phosphaturia and to drive 1,25-(OH)₂-vitamin D synthesis.

Disclosures: **Maureen Omeara, None**

MON-0410

Loss of Bone Volume and Bone Strength from Unloading is Mouse Strain-Dependent Michael Friedman¹, Yue Zhang¹, Jennifer Wayne¹, Charles Farber², Henry Donahue¹. ¹Virginia Commonwealth University, United States, ²University of Virginia, United States

Astronauts in space and patients experiencing prolonged bed rest are exposed to mechanical unloading of bones, decreasing bone volume and strength by up to 3% per month. Similar levels of bone loss result from aging and lead to increased risk of fragility fracture. It is well known that variability in accretion of bone mass and risk of osteoporosis is influenced by genetics. However, it remains unclear how genetic variation affects bone's response to unloading or the efficacy of countermeasures. Diversity Outbred (DO) mice are highly diverse outbred mice derived from 8 inbred founder strains. As a first step towards examining the genetic basis of the unloading response in bone, we examined unloading in DO founder strains. We hypothesized that there would be differential, strain-dependent effects of unloading on mice of the founder strains C57Bl/6J, PWK/PhJ and WSB/EiJ after 3 weeks of unloading using single limb immobilization (SLI). At 16 weeks old, 6 male mice of each strain had the left limb immobilized in a cast for 3 weeks. The unaltered right limb was used as a control. Bone geometry was analyzed by micro-CT. Mechanical properties were tested by 3-point bending. One-way ANOVAs with Tukey's tests were used to test for significant group differences, and paired t-tests for significant effects of immobilization (p<0.05). All strains had significantly decreased BV/TV in immobilized versus control limbs (Fig. 1). The magnitude of bone loss was significantly greater in the B6 and WSB strains compared to the PWK strain. Losses of cortical area fraction and Young's modulus were significantly greater in the B6 strain compared to the WSB strain. The PWK strain was most resistant to bone loss. This occurred despite the B6 strain having greater body weight, and the WSB strain having lesser body weight than the PWK strain. These results indicate that different strains respond to unloading from SLI differently, and this could be explained by genetic differences. Future studies examining gene expression differences between strains may provide clues as to the molecular basis of bone loss in response to unloading. More importantly, these results suggest that DO mice will be a useful model for examining the genetics of differential, strain-dependent bone response to unloading. References: 1. Lang T et al. J Bone Miner Res 19, 2004. 2. Svenson KL et al. Genetics 190:2, 2012.

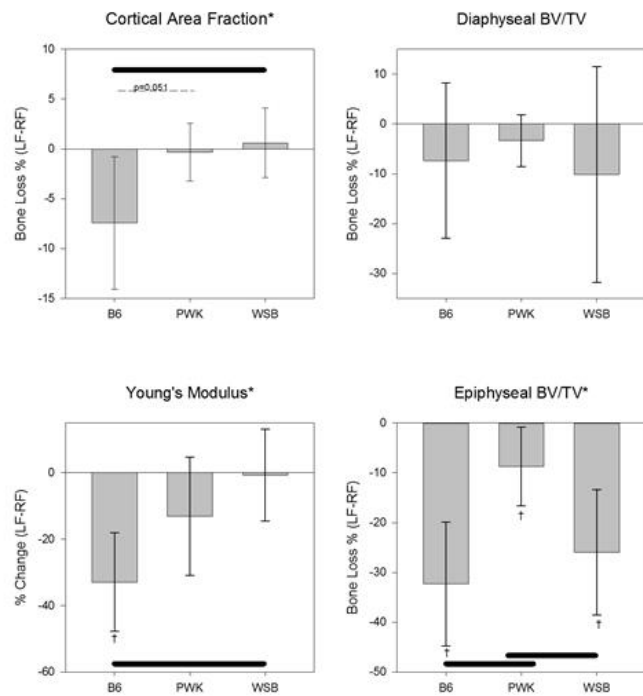


Figure 1. Percent loss (immobilized – control) of cortical area fraction, trabecular bone volume fraction, and Young's modulus of the mouse femurs after 3 weeks of immobilization.
 *p < 0.05 Main effect (One-way ANOVA)
 †p < 0.05 Group differences (Tukey's test)
 ‡p < 0.05 Immobilized vs Control limbs (paired t-test)

Disclosures: Michael Friedman, None

MON-0411

CLINICALLY RELEVANT DOSES OF VITAMIN A DECREASES THE ANABOLIC BONE RESPONSE TO MECHANICAL LOADING BY INHIBITING BONE FORMATION Vikte Lionikaite*, Petra Henning, Christina Drevinge, Sara Windahl, Ulf Lerner. Centre for Bone and Arthritis Research, Institute for Medicine, Sahlgrenska Academy at University of Gothenburg, Sweden

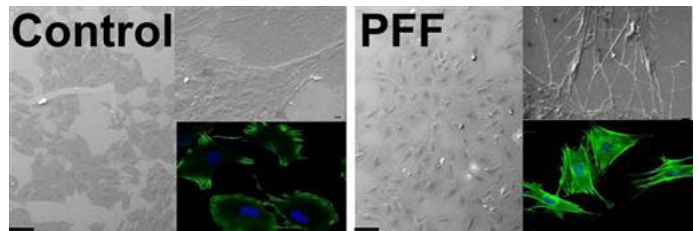
Increased vitamin A consumption has been associated with decreased cortical bone thickness and increased fracture risk in humans. With increasing intake of supplements in the population as well as fortification of foods, excess vitamin A may affect many individuals. Rodent studies have shown that increased osteoclastogenesis and resorption of cortical bone at the periosteal surface are important mechanisms leading to bone fragility in hypervitaminosis A. We have recently shown that also clinically relevant doses of vitamin A given to mice during a longer period of time have a negative impact on cortical bone mass. The effect could be blocked by simultaneous treatment with bisphosphonates, indicating that osteoclasts are important for the response. The in vivo effects of vitamin A on osteoblasts and bone formation have been less studied. The aim of the present study was to investigate if clinically relevant doses of vitamin A affect loading-induced bone formation. C57BL/6 female mice were fed control (4.5µg retinyl acetate/g chow) or vitamin A supplemented (60µg retinyl acetate/g chow) diets for 4 weeks, after which the right tibiae were subjected to axial loading three times per week for 2 weeks (40 cycles, peak strain 2250 µε), whilst continuing on the diets. Left limbs were used as internal controls. Bone architecture was analyzed by micro-CT. Micro-CT analysis showed that vitamin A decreased the loading-induced increase in trabecular bone volume. Vitamin A treated mice also had decreased cortical bone area compared to controls and the loading-induced increase in bone area was robustly reduced in mice treated with supplemented dose of vitamin A. Dynamic histomorphometry demonstrated that vitamin A suppressed the loading induced increase in periosteal and endocortical bone formation due to decreased osteoblast activity. Vitamin A treatment inhibited the loading-induced increase in the expression of the osteoblast genes Sp7, Alpl, and Col1a1 in cortical bone. To conclude, using a model of induced bone formation, we show that clinically relevant doses of vitamin A for long duration can suppress the anabolic bone response to mechanical loading. This results in less bone formed, an effect that can be attributed to decreased osteoblast activity.

Disclosures: Vikte Lionikaite, None

MON-0412

Fluid Shear Stress Affects Morphology and Osteogenic Differentiation of Pre-osteoblasts Jianfeng Jin^{1*}, Richard T. Jaspers², Astrid D. Bakker¹, Gang Wu³, Johanna F.M. Verstappen¹, Mohammad Haroon², Joannes A.M. Korfa⁴, Behrouz Zandieh-Doulabi¹, Jenneke Klein-Nulend¹. ¹Dept Oral Cell Biology, Academic Centre for Dentistry Amsterdam (ACTA), University of Amsterdam and Vrije Universiteit Amsterdam, Amsterdam Movement Sciences, Netherlands, ²Laboratory for Myology, Faculty of Behavioral and Movement Sciences, Vrije Universiteit Amsterdam, Amsterdam Movement Sciences, Netherlands, ³Dept Oral Implantology and Prosthetic Dentistry, Academic Centre for Dentistry Amsterdam (ACTA), University of Amsterdam and Vrije Universiteit Amsterdam, Amsterdam Movement Sciences, Netherlands, ⁴Dept Functional Anatomy, Academic Centre for Dentistry Amsterdam (ACTA), University of Amsterdam and Vrije Universiteit Amsterdam, Amsterdam Movement Sciences, Netherlands

Introduction: Mechanical stimuli, e.g. fluid shear stress, are known to affect osteogenic differentiation of osteogenic precursor cells through hereto unknown mechanisms. Interestingly, mechanical stimuli are also known to influence cell morphology, while the morphology of a cell (spread vs. round) determines osteogenic differentiation of osteogenic precursor cells. We hypothesized that the enhancing effect of mechanical stimulation on osteogenic differentiation of osteogenic precursor cells is determined by its' effect on precursor cell morphology. Therefore, we first aimed to determine bone cell responses to fluid shear stress in terms of osteogenic differentiation state and precisely determined cell morphology. **Methods:** MC3T3-E1 pre-osteoblasts were stimulated for 1 h by pulsating fluid flow (PFF; peak shear stress rate: 6.5 Pa/s, amplitude: 1.0 Pa, 1 Hz) or kept under static conditions (control). The cell mechanoresponse was quantified as nitric oxide (NO) release. F-actin was visualized using phalloidin, and cell nuclei by DAPI. Cell morphology and orientation were assessed using scanning electron microscopy and confocal microscopy, respectively. Osteogenic differentiation was assessed in static and PFF-stimulated cells post-incubated for 3 weeks by quantifying alkaline phosphatase (ALP) activity, collagen protein (Sirius Red), and matrix mineralization (Alizarin Red). Expression of osteogenic genes (RUNX2, BMP2, FGF2), proliferation (Ki67), and angiogenesis-related gene (FGF2) was analyzed (qPCR). **Results:** PFF rapidly increased NO production (4-fold) at 10 min. PFF also increased actin cytoskeletal (green) and nuclear DAPI staining (blue). Static control cells were more oval-shaped, while PFF-treated cells seemed more polygonal-shaped (Fig. 1). PFF also affected cell orientation, reduced cell spreading, and increased number and length of pseudopodia. PFF stimulated collagen protein (1.8-fold), and slightly (n.s.) increased ALP activity (1.2-fold) and mineralization (1.3-fold). Finally, PFF strongly increased BMP2 (9.3-fold), and slightly Ki67 (1.3-fold), and FGF2 (1.4-fold) expression, but decreased (n.s.) RUNX2 expression (0.7-fold). **Conclusion:** Our results indicate that mechanical stimuli in the form of fluid shear stress affect cell morphology and osteogenic differentiation of MC3T3-E1 pre-osteoblasts. Future studies will determine whether, and which morphology changes drive osteogenic differentiation, and try to unravel the underlying mechanism.



Disclosures: Jianfeng Jin, None

MON-0413

Bone (Re)modeling in Response to Load is Targeted to Mechanically Advantageous Structures and Further Enhanced with PTH Treatment Samuel Robinson*, Yizhong Hu, X. Edward Guo. Bone Bioengineering Lab, Columbia University, United States

Bone modeling and remodeling are distinct biochemical regimes that may hold unique opportunities for optimizing bone mass (remodeling being coupled resorption followed by formation on bone surfaces, and modeling being uncoupled instances of these events). Mechanical loading and intermittent parathyroid hormone (PTH) are both known to enhance total bone mass, though the regime(s) through which these ends are achieved remain less clear. Dynamic in vivo morphometry utilizing high resolution micro-CT and image registration has only recently become feasible and thus holds an untapped and expanding potential for analyzing bone metabolism through quantifying and localizing formation/resorption and thus modeling/remodeling events. C57Bl/6 mice 16 weeks of age were given 2 weeks of baseline weekly micro-CT scans of both tibiae prior to the initiation of daily treatment with PTH and/or unilateral tibia loading. The contralateral tibia served as a nonloaded control. Weekly scanning and daily treatment continued for 5 weeks. Registered images for each mouse in a global coordinate system revealed the time course of each voxel, allowing for changes in bone mass to be quantified as modeling or remodeling starting at the onset of

treatment. In cortical bone, after an initial response to treatment in both anabolic modeling and remodeling, modeling developed as the dominant response. Differences between groups were starkest in areas of mechanical significance. For example, anabolic modeling on the periosteal surface on the half of the tibia in compression under axial load presents a strong effect of treatment, whereas the same measure on the endosteal surface in the area in tension showed no differences between groups (Fig 1A). Similarly, in trabecular bone anabolic modeling was significantly increased with loading on trabecular plates, the major contributor to trabecular bone strength, but not rods (Fig 1B). In both bone types, PTH tended to enhance the effects of both modeling and remodeling but without bias towards these mechanically relevant locations. Curiously, the catabolic modeling response on the endosteal surface showed a remarkable transition over time. Loading initially suppressed catabolic modeling, but over time increased it to levels significantly beyond that of nonloaded controls, with and without PTH (Fig 1C). In total our data demonstrate strong independent and combined effects of PTH and load, with load directing the response to favorable locations.

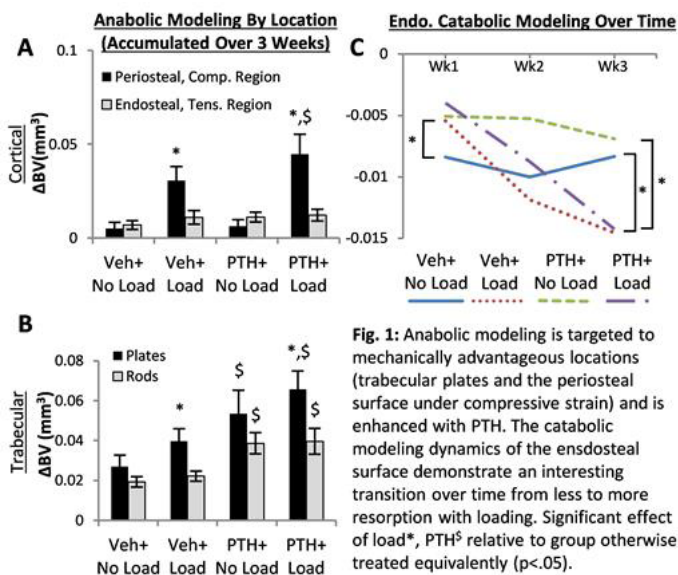


Fig. 1: Anabolic modeling is targeted to mechanically advantageous locations (trabecular plates and the periosteal surface under compressive strain) and is enhanced with PTH. The catabolic modeling dynamics of the endosteal surface demonstrate an interesting transition over time from less to more resorption with loading. Significant effect of load*, PTH relative to group otherwise treated equivalently ($p < .05$).

Disclosures: Samuel Robinson, None

MON-0414

Cyclosporin A Enhances Loading Induced Trabecular and Cortical Bone Formation at Senescence Sundar Srinivasan*, Dwayne Threet, Philip Hubber, Ted Gross, Steven Bain. University of Washington, United States

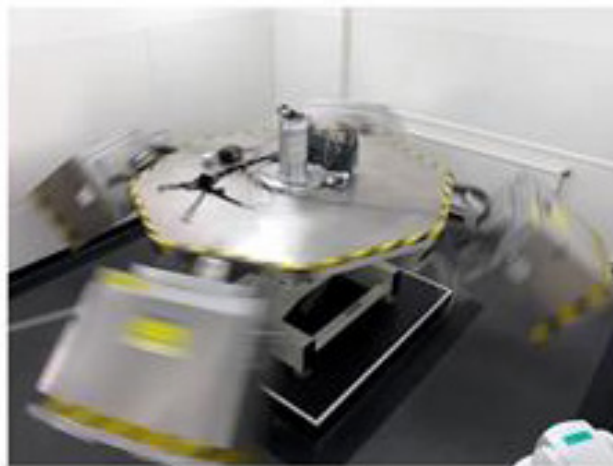
Age-related degradation in bone mechanotransduction markedly reduces the efficacy of exercise in augmenting bone mass in the elderly. In previous studies exploring underlying mechanisms, we identified specific age-related deficits in bone mechanotransduction that could be counteracted by low-dose Cyclosporin A treatment (CsA). In follow-up studies, we observed that loading supplemented with low-dose CsA restored cortical bone formation in senescent animals to the robust levels observed in young. Given the significant age-related loss of trabecular bone mass and its contribution to fracture risk, we proposed that CsA supplementation could also serve as a means to augment bone mass in this compartment. However, considering the differences in structure, cell populations and bone remodeling dynamics between bone compartments, we hypothesized that distinct dosages of CsA supplementation will be required to enhance trabecular and cortical bone formation induced by loading at senescence. To examine our hypothesis, the right tibiae of three groups of senescent female C57BL/6 mice (19 Mo, $n = 4$ /grp) were subject to dynamic loading (off-axial compression, -0.01 N static preload, -3.6 N dynamic loading at 1-Hz, 50 cycles/d, 3 days/week, 3-weeks) either without (0.0 mg/kg) or with CsA supplementation (0.1 or 3.0 mg/kg s.c.). Upon sacrifice, trabecular adaptation was assessed via μ CT (d 22) and mid-shaft cortical bone formation via dynamic histomorphometry (Calcein d 10, 19). In trabecular bone, we found that loading without or with 0.1 mg/kg CsA did not significantly enhance BV or BV/TV vs contralateral. In contrast, loading supplemented with 3.0 mg/kg CsA significantly enhanced BV (0.08 ± 0.01 vs 0.06 ± 0.01 mm³) and BV/TV (3.8 ± 0.8 vs $2.7 \pm 0.3\%$; $p < 0.05$). In cortical bone, loading without or with 0.1 mg/kg CsA did not influence MAR, MS or BFR vs contralateral bone. However, loading supplemented with 3.0 mg/kg CsA significantly enhanced MAR (0.47 ± 0.07 vs 0.37 ± 0.05 μ m/d), MS (22 ± 5 vs $12 \pm 4\%$) and BFR (0.11 ± 0.03 vs 0.05 ± 0.02 μ m³/ μ m²/d) vs contralateral bone ($p < 0.05$). Unexpectedly, we found that the same dose of CsA that enhanced loading induced cortical bone formation also enhanced trabecular adaptation in senescent animals. While preliminary, use of this low-cost, approved drug as a supplement that augments loading-induced bone formation at senescence holds potential as a novel countermeasure against skeletal fragility across bone compartments.

Disclosures: Sundar Srinivasan, None

MON-0415

Is Chronic Hypergravity Able to Protect the Musculoskeletal System in a Murine Model of Knee Osteoarthritis? Benoit Dechaumet*, Damien Cleret, Norbert Laroche, Arnaud Vanden-Bossche, Marie-Hélène Lafage-Proust, Laurence Vico. INSERM, U1059, University of Lyon, UJM Saint-Etienne, France

Osteoarthritis (OA) patients do little physical activity, which is known to maintain musculoskeletal health although its role on OA remains a matter of debate. Hypergravity was shown to act as endurance training on muscle (Bojados and Jamon, 2014) and to improve bone (Gnyubkin et al., 2015) in growing mice. Here, we tested the effects of acceleration at 2g during 8 weeks in mature mice with or without OA on the musculoskeletal system and OA progression. Male C57BL/6J were randomized in centrifuged (2g) and non-centrifuged (1g) group, after destabilization of the medial meniscus of the right knee in half of them, giving 4 groups: 1g, OA-1g, 2g and OA-2g ($n=16$ /group). 2g mice, housed in gondolas hanging at the periphery of the 1.4 m radius centrifuge were provided with food and water for 4 weeks. The centrifuge was stopped once at mid-time for animal husbandry and at 7 and 2 days before the end of the experiment for fluorochrome labelling. Tibias (nanoCT, bone and vascular histomorphometry), calf muscles (typing, fiber size) and molecular markers (tibia and gastrocnemius muscle), right side, were analyzed. OA-1g mice had increased OARSI score, subchondral bone sclerosis and thinning of articular cartilage; all were still present in OA-2g mice. In the tibia proximal metaphysis, trabecular bone loss (-28%) and increased resorption activity were observed in OA-1g vs 1g. Hypergravity in OA prevented trabecular bone loss, increased mineralization rate (+18%), but decreased cortical thickness (-9%). Bone marrow vascular density decreased in 2g groups but less in OA than non OA. OA increased bone (Runx2, 149%), adipocyte (C-EBP α , 98%) and inflammatory (TNF α , 175%) markers; these increases being prevented in OA-2g. Soleus and gastrocnemius mass increased in 2g groups. OA-2g soleus had greater fiber area (+43%) with increases in type I fibers and decreases in type II fibers compared to OA-1g. Soleus vascular density decreased in 2g groups (-37%, vs 1g or OA-1g). In the gastrocnemius 2g (with or without OA) increased the expression of myostatin, FNDC5 and visfatin. Further, hypergravity in OA prevented increases of serum inflammatory markers observed in OA-1g. Thus, if 2g has no bone effect in intact mice, it prevents trabecular bone loss but reduces cortical thickness in OA mice. In all cases, hypergravity improves muscle parameters, as does endurance exercise. In conclusion, chronic 2g reinforces muscles and prevents trabecular bone loss and inflammation in OA.



1.4 m radius centrifuge (COMAT Aerospace, Flourens, France)

Disclosures: Benoit Dechaumet, None

MON-0416

The contribution of TRPV4-dependent calcium influx and purinergic calcium oscillations to the regulation of sclerostin during osteocyte mechano-sensing Katrina Williams*, Derek Jones, Christopher Ward, Joseph Stains. University of Maryland, United States

Skeletal remodeling is driven in part by the osteocyte's ability to respond to its mechanical environment and regulate sclerostin (a negative regulator of bone mass) abundance. We have recently shown that the osteocyte responds to fluid shear stress (FSS) via the microtubule network-dependent activation of NADPH oxidase 2-generated reactive oxygen species and subsequent opening of TRPV4 cation channels, thus leading to calcium influx, activation of CAMKII, and rapid sclerostin protein downregulation. In addition to the initial calcium influx, purinergic receptor signaling and calcium oscillations have been observed downstream from mechanical load; however, the role of TRPV4 and the initial calcium influx versus downstream calcium oscillations in the rapid sclerostin protein downregulation remains unclear. Here, using pharmacologic gain (GSK1016790A, 15 μ M, 30 minutes) and

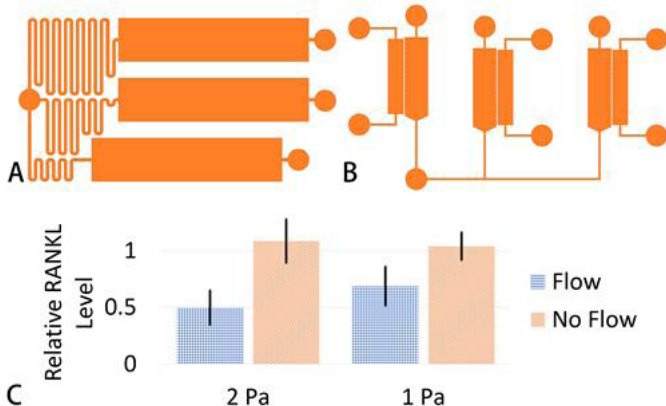
loss (GSK2193874, 15 μ M, 30 minutes) of function approaches, we confirm that activation of the TRPV4 channel is required for the initial calcium influx, CaMKII activation, and rapid loss of sclerostin protein following FSS. TRPV4 antagonist significantly reduces downstream oscillations (% cells oscillating, intensity of calcium signal, and number of oscillations per cell) following FSS; however, TRPV4 agonist does not induce high levels of oscillations (% cells oscillating) as seen with ATP (100nM), demonstrating that TRPV4 is necessary, but not sufficient, for the downstream calcium oscillations seen in these osteocytes using live cell calcium imaging with Fluo-4 AM calcium indicator dye. Furthermore, inducing calcium oscillations alone with ATP in Ocy454 cells is not sufficient to induce rapid sclerostin protein downregulation, although oscillations can activate CaMKII. This suggests that pathways downstream of TRPV4 and parallel to CaMKII activation are obligated for sclerostin downregulation. In total, our data suggest that activation of the TRPV4 channel is the primary response required for CAMKII phosphorylation and rapid sclerostin protein downregulation, whereas the calcium oscillations downstream from TRPV4 likely serve independent roles in tuning osteocyte function.

Disclosures: *Katrina Williams, None*

MON-0417

Novel in vitro Microfluidic Platforms for Osteocyte Mechanotransduction Studies Liangcheng Xu^{*1}, Lilia Fuller-Thomson², Lidan You^{1,2}. ¹Institute of Biomaterials and Biomedical Engineering, University of Toronto, Canada, ²Department of Mechanical and Industrial Engineering, University of Toronto, Canada

Osteocytes are the major mechanosensing cells in bone remodelling [1]. Current bone mechanotransduction research use macro-scale devices, however in vitro microfluidic devices provide an optimal tool to better understand this biological process with its flexible design, physiologically-relevant dimensions, and high-throughput capabilities. Our recent work on co-culture platform has demonstrated the feasibility of building more complex microfluidic devices for osteocyte mechanotransduction studies [2]. However, there still lacks a robust system where multi-physiological flow conditions are applied to bone cells to study their intercellular communication. **OBJECTIVE:** This project aims to design and fabricate a multi-shear stress, co-culture platform to study interaction between osteocytes and other bone cells under varying flow conditions. **METHODS AND RESULTS:** Standard microfluidic principles utilize changing geometric parameters to induce different flow rates that are directly proportional to the levels of shear stress. All channels within the same device will share a common inlet, while adjusting the resistance of each individual channel will result in a different flow rate (Figure A). Devices are fabricated using PDMS and bonded to glass slides of equal sizes. MLO-Y4 osteocyte-like cells seeded in the device are stimulated with oscillatory fluid flow with a custom in-house pump. Significant differences in RANKL levels are observed between channels (Figure B), demonstrating that proper cellular response to flow can be elicited from each distinct shear stress channels as designed. Furthermore, we paired these multi-shear stress channels with corresponding culturing chambers connected through perfusion pores (Figure C). Through perfusion between the multi-shear stress channels and culturing chambers, different cell population can communicate to each other as they are stimulated by varying levels of shear stress. **DISCUSSION:** Using this platform, we will be able to mimic the interaction between osteocytes and other bone cells in vitro. Future integration with on-chip analytical methods will allow for detection of molecular factors, leading to better understanding of bone cell intercellular communication under physiologically relevant conditions, and ultimately, discovery of novel therapeutic targets. [1] Santos. Osteoporos Int. 2009. [2] Middleton. J. Biomech. 2017.



A) Layout design for multi-shear device, each chamber containing osteocytes stimulated by shear stress levels 0.5 Pa, 1 Pa, 2Pa, from top to bottom, respectively. **B)** Layout design for multi-shear co-culture device, with each flow chamber paired with an osteoclast growth chamber. Scale bar for A and B equals 4.5 mm. **C)** RANKL expression level measured in multi-shear device normalized to the 0.5 Pa channel levels in each device.

Disclosures: *Liangcheng Xu, None*

MON-0418

Mechanical loading regulates Hippo signaling in a three-dimensional osteocyte culture model Mylène Zarka^{*1}, François Etienne², Morgane Bourmaud¹, Christophe Helary³, François Rannou², Eric Haÿ¹, Martine Cohen-Solal¹. ¹Inserm UMR1132, Hôpital Lariboisière; Univ Paris Diderot, Sorbonne Paris Cité, Paris France, France, ²Inserm UMR-S1124, Université Paris Descartes, Sorbonne Paris Cité, Paris France, France, ³Sorbonne Universités UPMC Univ Paris 06, CNRS, Collège de France, Laboratoire Chimie de la Matière Condensée de Paris UMR7574, France

Purpose: Osteocytes are mechanosensitive cells that control bone remodeling in response to mechanical loading. To date, signaling pathways modulated by mechanical loading in osteocytes are not clearly described. Since YAP/TAZ, the main effectors of the Hippo pathway, mediate the mechanotransduction process, we hypothesized that they also induce osteocyte response to mechanotransduction. In addition, YAP/TAZ interacts with several signaling pathways regulated during osteoblastogenesis. The objective of our study is to define the response of osteocytes in response to mechanical loading and identify the mechanism of cell activation via the Hippo pathway. **Methods:** MLO-Y4 osteocyte cell lines were cultured in concentrated collagen hydrogels for 14 days. Osteocytes were submitted to mechanical loading using the Flexcell Compression Plus System® with a regimen of sinusoidal compression at 1 Hz, 40 kPa during 9 hours. RNA sequencing was performed to determine gene expression modifications. Immunofluorescence and Western blot analysis were carried on, respectively, from paraffin embedded hydrogel sections and total protein lysate. **Results:** Mechanical loading induced an increase of the expression of mechanosensitive target genes, permitting us to validate our experimental model (E11GP38 and COX2, x3 fold increase p<0.05). Mechanical compression induced a large increase in the expression of osteoprotegerin (OPG, x4 fold increase p<0.05) associated with a decrease in the expression of RANK ligand (RANKL, 25% of decrease p<0.05), suggesting a negative role for osteoclastogenesis. RNA sequencing results indicates that 83% of YAP/TAZ target genes modulated by compression in osteocytes were up-regulated, this being confirmed by RTqPCR regarding gene expression analysis of YAP/TAZ target genes (ANKRD1, x3 fold increase p<0.05). We also observed that mechanical compression increase nuclear translocation of YAP/TAZ by immunofluorescence, and increase total protein level of YAP/TAZ as shown by western blot. In addition, mechanical compression reduced osteocyte apoptosis (50% decreased apoptosis). **Conclusion:** our model allowed highlighting the activation of Hippo signaling in osteocytes in response to mechanical loading. These results show the contribution of YAP/TAZ signaling in the mediation of mechanical loading through osteocytes and in the regulation of bone remodeling.

Disclosures: *Mylène Zarka, None*

MON-0432

A WINDOW OF OPPORTUNITY: IDENTIFICATION OF MEDICALLY HOSPITALIZED PATIENTS WITH FRAGILITY FRACTURE RISK Vafa Tabatabaie^{*}, Wanda Horn, Brandon Tauberg, Gabriel Lopez Vega, Mikhail Bekarev, Paul Levin, Sara Merwin. Montefiore Medical Center, United States

Background: Despite increasing prevalence, osteoporosis is widely undiagnosed and undermanaged with fragility fracture risk (FFR) under-documented. 90% of fragility fractures (FF) occur in people >60 years. Fracture Risk Assessment Tool (FRAX) is a validated instrument to predict FFR in ensuing 10 years. **Objective:** To increase FFR awareness in providers. Inpatient admission offers an opportunity to intervene with human alert methodology previously demonstrated as effective. We hypothesized increased surveillance, documentation and referral to outpatient services to prevent FF in at-risk patients identified as a result of the intervention. **Methods:** IRB-approved educational intervention via alerts to providers of at-risk patients identified by concurrent chart review on medical units at an urban tertiary care teaching hospital. Study instruments were FRAX calculator and script for provider encounters. **Patient inclusion:** females \geq 65 years, males \geq 70 years, and known osteoporosis risk factors. **Exclusion:** age <18 or >100 years, current consult with endocrine service, admission to orthopaedic or palliative service, predicted survival <6 months, current/previous antiresorptive or anabolic agents. **Primary outcome measure** was FFR documentation or initiation of treatment. **Results:** Pre-intervention chart review revealed 0% documentation for FFR. During the initial 8 weeks of the intervention, 36 of 118 screened charts met inclusion criteria. Mean age 85 \pm SD 6.5 years, female 53% (N=19), most prevalent admitting diagnosis was pneumonia (16%). Mean FRAX: 13% major osteoporotic fracture (MOF), 6.5% hip fracture (HF). Eight patients (22%) had FFR documentation on discharge summary: mean age 85 \pm SD 6.7 years, mean FRAX: 17.1% MOF, 8.4% HF. **Conclusion:** To our knowledge and confirmed by preliminary data, documentation of FFR of medically hospitalized patients is uncommon. With our intervention we have verified an increase in documentation as hypothesized, suggesting that medical providers recognize the importance of enhanced prevention measures to offset the risk of fragility fractures. This study lays groundwork for the integration of a systems-based approach using electronic alerts to complement human alert methodology to enhance communication and support continuity across transitions of care.

Disclosures: *Vafa Tabatabaie, None*

MON-0433

Trends towards Decreased Cortical Thickness and Increased Cortical Porosity in a One-Year Pilot Study of Premenopausal BRCA Mutation Carriers Undergoing Prophylactic Salpingo-Oophorectomy Angela Cheung^{*1,2}, Madeline Dwyer², Jeevitha Srighanthan¹, Joan Murphy³, Amy Finch⁴, Joanne Kotsopoulos⁵, Marcus Bernardini¹, Michelle Jacobson⁵, Gabrielle E.V. Ene¹, Irene Ho¹, Suzanne Cohen¹, Paula Harvey³, Barry Rosen¹, Steven Narod⁵. ¹University Health Network, Canada, ²University of Toronto, Canada, ³Trillium Health Partners, Canada, ⁴Sunnybrook Health Sciences Centre, Canada, ⁵Women's College Hospital, Canada

Introduction: Women who carry a mutation in the BRCA1 or BRCA2 genes are at increased risk for breast and ovarian cancer. Prophylactic salpingo-oophorectomy (PSO) has been shown to effectively reduce the risk of breast and ovarian cancer by 50% and 90%, respectively. However, this leads to an abrupt decrease in circulating estrogen levels among premenopausal women, which can cause BMD loss and increase fracture risk. **Objectives:** This pilot study aims to assess the effects of PSO on bone structure and strength using high resolution peripheral quantitative computed tomography (HRpQCT). **Materials and Methods:** This pilot 1-year cohort study assesses bone structure and strength in pre-menopausal women who are BRCA mutation carriers undergoing PSO compared to pre-menopausal age-matched women who are not oophorectomized and are non-carriers. All women were scanned at the distal radius and tibia on the Xtreme CT (Scanco, Switzerland) at baseline and 1 year. Standard HRpQCT parameters, such as volumetric BMD, cortical thickness, trabecular BV/TV, were obtained. In addition, scans were analyzed for cortical porosity as well as bone stiffness, ultimate stress and failure load using finite element analysis. The percent change from baseline to one year post-surgery was calculated for all parameters for both BRCA carriers and non-carriers. Depending on data distribution, t-tests or Wilcoxon rank-sum tests were used to assess differences between BRCA carriers who underwent PSO and non-oophorectomized non-carriers. **Results:** A total of 21 PSO BRCA carriers (mean age (SD): 41.8 (5.32) years) and 12 non-oophorectomized non-carriers (mean age (SD): 46.6 (3.77) years) were included in this analysis. 85% of the study population are Caucasian. Our preliminary analyses showed no differences in total, cortical and trabecular vBMD, trabecular BV/TV, trabecular thickness, separation or number at the distal radius or tibia ($p > 0.1$). There were trends of decreased cortical thickness and increased cortical porosity at the distal radius and tibia ($p = 0.045$ to 0.09). No statistically significant differences in estimated bone strength were observed. **Conclusions:** This preliminary analysis of bone structure and strength in premenopausal women with BRCA mutations undergoing PSO showed trends towards decreased cortical thickness and increased cortical porosity at 1 year. Our pilot study was limited by small sample size and short duration. Larger sample sizes and longer follow-up duration are required to clarify these findings.

Disclosures: *Angela Cheung, Clementia, Grant/Research Support, Amgen, Grant/Research Support, Mereo, Grant/Research Support, Amgen, Consultant, Gilead, Consultant*

MON-0434

Hyperkyphosis and Self-reported and Objectively Measured Sleep Quality in Older Men Christopher Kaufmann^{*1}, Jian Shen¹, Katie Stone², Deborah Kado¹. ¹University of California San Diego, United States, ²California Pacific Medical Center Research Institute, United States

Hyperkyphosis (HK), or increased thoracic curvature, is associated with restricted pulmonary function and posture, potentially contributing to poor sleep. A previous study reported that older women with HK had worse self-reported sleep quality, but it is unknown if such an association exists in men. Thus, we studied 754 U.S. MrOs men, average age of 78.1 (SD = 4.8), who had kyphosis measured during the 3rd clinic visit (2007-2009) and future subjective and objective sleep quality assessed between 2009-2012, an average of 2.9 years later. To measure kyphosis, 1.7 cm thick blocks were placed under the participant's head to achieve a neutral spine position while lying supine on a DXA table. We collected data on both subjective (Pittsburgh Sleep Quality Index [PSQI]), and Epworth Sleepiness Scale [ESS]) and objective (based upon wrist actigraphy: Total Sleep Time [TST], Wake After Sleep Onset [WASO], Sleep Efficiency [SE], Sleep Onset Latency [SOL]) sleep measurements. Based upon a previously used definition of HK in MrOs, those requiring ≥ 4 blocks were considered hyperkyphotic ($n=145$ or 19.2%). In simple and multivariable linear regression analyses, men with HK did not report having worse self-reported sleep characteristics in unadjusted or age and site adjusted models with the PSQI Global Score: $\beta=0.26$, 95% CI=-0.29, 0.81 and ESS: $\beta=0.50$, 95% CI=-0.22, 1.22. Similarly, there were no significant associations between HK and objective sleep measures including TST: $\beta=4.78$, 95% CI=-7.25, 16.80; WASO: $\beta=0.90$, 95% CI=-4.84, 6.64; SE: $\beta=-0.19$, 95% CI=-1.45, 1.07 or SOL: $\beta=3.21$, 95% CI=-3.30, 9.73. When examined as a continuous predictor (blocks ranging from 0-8), there was no difference in the results. Although it would seem that worse fixed posture might interfere with sleep, in this sample of older men, worse kyphosis was not associated with self-reported or objectively measured poor sleep quality.

Disclosures: *Christopher Kaufmann, None*

MON-0435

The Role of Megakaryocytes and Osteomacs in Skeletal Homeostasis and Aging Kevin Maupin^{*1}, Safa Mohamad¹, Alexandra Aguilar-Perez², Artur Plett¹, Hui Lin Chua¹, Paul Childress¹, Marta Alvarez¹, Joydeep Ghosh¹, Irushi Abeysekera¹, Evan Himes¹, Chi Zhang¹, Jung Min Hong², Louis Pelus¹, Christie Orschell¹, Angela Bruzzaniti², Melissa Kacena¹. ¹Indiana University School of Medicine, United States, ²Indiana University School of Dentistry, United States

Aging is associated with many debilitating bone degenerative diseases, including osteoporosis. A growing body of evidence shows that megakaryocytes (MKs) stimulate bone formation by increasing osteoblast (OB) and osteomac (OM) proliferation. Our studies also suggest that age-associated bone degeneration is due to a decrease in the ability of MKs to regulate skeletal homeostasis, despite an increase in total MK number in aged mice. In support of this, transplantation of cells enriched for MKs from young donor C57BL/6 mice increased BV/TV and Tb.N in age-matched recipients by 60% and 49%, respectively. However, similar graft cells from old donor mice did not change BV/TV in young recipients, confirming the reduced efficacy of old MKs to stimulate bone formation. Our studies also show that MKs from young mice (3-4 month) were 1.5-fold more active than MKs from old mice (22-25 month) in stimulating the proliferation of neonatal calvarial cells (which are 95% OB lineage and 5% OM cells), with the predominant effect being the stimulation of OM proliferation (3.6-fold increase). In contrast, neither MKs from young nor old mice were able to increase the proliferation of bone marrow macrophages (BMMs). We found that OMs and BMMs can undergo differentiation into mature osteoclasts (OCs) capable of bone resorption, whereas MK conditioned medium robustly inhibits this process. Moreover, osteoclastogenesis was higher with OM populations from both young (150% increase) and old mice (87% increase), compared to age-matched BMMs, further demonstrating that OMs are functionally distinct from BMMs. To examine the mechanisms behind the functional differences between OMs and BMMs, freshly isolated OMs and BMMs from young and old mice were subjected to single cell RNAseq. Non-biased, bioinformatics analyses identified the oxidative phosphorylation pathway as being the predominant pathway upregulated in old versus young OMs ($p=7.3e-5$). Likewise, the oxidative phosphorylation pathway was significantly enriched in young OMs compared to young BMMs ($p=0.001$), providing a possible mechanism for the increased osteoclastogenesis of OMs compared to BMMs. Taken together, these findings suggest that MKs increase OB and OM populations, while simultaneously inhibiting OC development, leading to a net increase in bone mass. However, aging decreases the ability of MKs to stimulate bone formation, as well as increases the ability of OMs to undergo osteoclastogenesis.

Disclosures: *Kevin Maupin, None*

MON-0436

Comparing CT bone density values of middle-aged daughters with their elderly fall-prone mothers confirms heritability of BMD except in cases of maternal hip fracture Kenneth Poole^{*}, Monika Kondratowicz, Karen Blesic, Daniel Chappell. University of Cambridge, United Kingdom

If a mother fractures her hip before the age of 80, her daughters are more than twice as likely to fracture their own hips from the age of 65 onward. Surprisingly, this increased risk appears independent of the daughters' femoral neck bone mineral density (BMD) score at age 65. We further explored the familial determinants of daughters' hip BMD, focusing on the influence of maternal hip BMD. 20 older women were recruited who had sustained fragility hip fractures (mean age 77.8 \pm 9.5), along with 25 of their daughters (51.4yrs \pm 9.9). Also recruited were 25 mothers (72.5yrs \pm 6.2), who had sustained falls (but not hip fracture) and 32 of their daughters (44.9yrs \pm 6.8). BMD of the femoral neck was measured using CTXA by Quantitative Computed Tomography. Mothers with hip fracture had lower femoral neck BMD than mothers without. In the absence of hip fracture, fall-prone mothers and their daughters had positively correlated age-adjusted femoral neck BMD ($r=0.30$, $p=0.0007$) indicating familial inheritance. However, the bone density of mothers with hip fracture did not correlate with their daughters' BMD ($r=0.06$, $p=0.24$), irrespective of whether the mothers were aged > 80 years at the time of injury. Age-related differences among the daughters' BMD values (-0.5% per annum across the sample aged 32-72 years) did not point to excessive post-menopausal bone loss in daughters of mothers with hip fracture. Heights were strongly correlated between mother and daughter in all groups. Studying these mother-daughter pairs indicated heritability of BMD only in daughters of fall-prone women without hip fracture. Apparently, a maternal hip fracture did not confer low BMD onto her daughters and neither was there an apparent acceleration of BMD loss around the menopause. The aetiology of hip fracture inheritance remains elusive, but may relate to musculoskeletal attributes other than bone density.

Disclosures: *Kenneth Poole, None*

MON-0437**Increased Cortical Porosity and Reduced Trabecular Density are Not Necessarily Synonymous With Bone Loss and Microstructural Deterioration**

Roger Zebaze^{*1,2}, Elizabeth J. Atkinson³, Yu Peng², Ali Ghasem-Zadeh¹, Sundeep Khosla⁴, Ego Seeman^{1,2,4}. ¹Depts. Medicine and Endocrinology, Austin Health, University of Melbourne, Australia, ²Straxcorp Pty Ltd, Australia, ³Mayo Clinic, United States, ⁴Australian Catholic University, Australia

Measurements of cortical porosity and trabecular density are used to estimate fracture risk. However, absolute values of these traits are the net result of their growth-related assembly and age-related deterioration. As bone loss affects both cortical and trabecular compartments, we hypothesized that the desirable characteristic of a surrogate of bone fragility is a measure of the deterioration of both compartments relatively free of growth-related determinants of bone strength. Accordingly, we developed a Structural Fragility Score (SFS) which quantifies the coexisting age-related bone loss dependent increment in cortical porosity and decrement in trabecular density relative to their premenopausal mean values. We compared ultra-distal radial microstructure in 99 postmenopausal women with forearm fractures and 105 controls using high resolution peripheral computed tomography. Results are presented as Odds Ratio (95% confidence intervals CI). Cortical porosity was associated with fractures before excluding women with deteriorated trabecular density (2.30, 1.30 – 4.05, $p = 0.004$), not after (0.96, 0.50 – 1.86; $p = 0.91$). Trabecular density was associated with fractures before excluding women with high cortical porosity (3.35, 1.85 – 6.07, $p < 0.0001$), not after (1.60, 0.78 – 3.28, $p = 0.20$). By contrast, the SFS, capturing coexisting deterioration in cortical porosity and trabecular density, was associated with fractures (4.52, 2.17 – 9.45, $p < 0.0001$). BMD was associated with fracture before accounting for the contribution of the SFS (5.79, 1.24 – 27.1, $p = 0.026$), not after (4.38, 0.48 – 39.9, $p = 0.19$). The SFS was associated with fracture before (4.67, 2.21 – 9.88) and after (3.94, 1.80 – 8.6, both $p < 0.0001$) accounting for BMD. Measurement of the coexisting cortical and trabecular deterioration is likely to identify women at risk for fracture more robustly than absolute values of cortical porosity, trabecular density, or BMD.

Disclosures: **Roger Zebaze**, *StrAx Corp, Major Stock Shareholder*

MON-0456**Impaired tooth development and mineralization in Slc20a2-deficient mice**

Laure Merametdjian^{*1}, Céline Gaucher², Nina Bon¹, Sophie Sourice¹, Jérôme Guicheux¹, Sarah Beck-Cormier¹, Laurent Beck¹. ¹INSERM UMR 1229, France, ²EA 2496, France

The importance of phosphate (Pi) in hydroxyapatite crystals suggests a role for membrane proteins controlling Pi uptake during tooth mineralization. Accordingly, we recently identified the Slc20a2 Pi transporter as a potential important player of tooth mineralization (Merametdjian et al. JDR 2017). Slc20a2 was expressed 2- to 10-fold higher in teeth than the other Pi transporters, and was predominantly expressed in the stratum intermedium and the subodontoblastic cell layer. Interestingly, Slc20a2 knockout mice showed a disrupted dentin mineralization. Here, we extended these initial observations by performing quantitative morphometric and histological analyses. Micro-CT analysis demonstrated decreased incisor and molar volumes in 1-month-old Slc20a2^{-/-} mice ($p < 0.0001$). Dentin and enamel volumes were also reduced, and accompanied by an increased pulp volume ($p < 0.0001$). Similar abnormalities were also present in incisors from 8-month-old mutants. Movat's pentachrome staining demonstrated normal organization of odontoblast and ameloblast palisades in Slc20a2^{-/-} mice. Nevertheless, there was a marked increase in the unmineralized predentin layer and reduction of the mineralized dentin layer in mutant mice ($p < 0.05$), indicating a mineralization defect consistent with the increased pulp volume. Consistent with these data, we illustrated a severe dental fragility of 4-month-old Slc20a2^{-/-} mice evidenced by a high incidence of incisor fractures. At 8 months, Slc20a2^{-/-} incisors exhibited an irregular yellow-brown discoloration and chipping that further illustrated increased fragility. Energy Dispersive X-Ray Spectroscopy revealed an increased Ca/Pi ratio in Slc20a2^{-/-} mice in incisor enamel and mantle dentin at 1 month, and in incisor mantle and circum-pulpal dentin at 8 months ($p < 0.01$). Consistent with our histological studies, Scanning Electron Microscopy analysis showed that dentin matrix morphology was abnormal in mutant mice, with irregular intertubular dentin, unfused calcospherites and increased interglobular spaces. Interestingly, these latter features being shared with the hypophosphatemic HYP and DMP1 mice, immunohistochemistry analyses revealed that PHEX and DMP1 expression were strongly increased in the predentin of Slc20a2^{-/-} mice. In summary, we illustrated the role of Slc20a2 in dentin mineralization, morphology and fractures, a finding that arise in absence of hypophosphatemia and may involve the role of local regulators of teeth mineralization.

Disclosures: **Laure Merametdjian**, *None*

MON-0457**Gestational exposure to nicotine administered by e-cig juice accelerates osteogenesis and bone formation in dams, but suppresses bone growth and development in the pups.** Alyssa Falck^{*}, Marcus Orzabal, Raine Lunde, Shannon Huggins, Alexis Mitchell, Josue Ramirez, Vishal Naik, Jayanth Ramadoss, Dana Gaddy, Larry Suva. Texas A&M University, United States

Electronic cigarette (e-cig) use is gaining favor with pregnant women, as it is considered a safer alternative to smoking since e-cig smoke delivers nicotine as aerosol without tobacco or the burning process. However, studies of the effects of e-cig vaping on the adult and developing skeleton are sorely lacking. Therefore, we sought to determine whether maternal exposure during gestation to a conventional vaping base medium with or without nicotine, at levels approximating adult human maternal and neonatal exposure, affected the skeleton of the dams and/or pups. Bred virgin female rats were housed individually in modified chambers and pair-fed. Controls and nicotine-exposed (NIC) dams of similar weight were pair-fed throughout the duration of the study to control for caloric intake. E-cig juice dams (JUICE) were exposed for 2hr to a 1 second puff, every 20 seconds of a vaping base medium (80:20 propylene glycol:vegetable glycerin blend) and matched by weight with NIC dams and pair-fed accordingly. In the NIC group, dams were exposed to an identical duration of the same vaping medium with nicotine added. Rats were acclimatized with a nicotine exposure of 50 mg/ml from gestational days (GD) 5-10 and continued a 100 mg/ml dose from GD 11-21, 5 days/wk. Dams and pups were exposed for postnatal days (PND) 4-10 for a total number of 34 GD exposed hrs and 14 PND exposed hrs prior to tissue collection. Proximal tibia microCT showed that BV/TV and TbN of dams (PND10) was unchanged by JUICE. However, NIC significantly increased tibial BV/TV and TbN, which was associated with an increase in serum PINP. Ex vivo bone marrow cultures demonstrated that exposure to JUICE or NIC suppressed recruitment of cells into the osteoblast lineage (% AP⁺ CFU-F). However, further osteoblast differentiation into bone nodules was unaffected by JUICE but significantly increased by NIC. Neonatal measurements on PND10 demonstrated that NIC exposure, but not JUICE, significantly inhibited skeletal element development. Together, these findings demonstrate that gestational nicotine exposure either through conventional tobacco products or e-cig vaping significantly suppresses osteoblast recruitment into the lineage and accelerates osteoblast development and bone formation in vivo. Exposure of pregnant dams to e-cig NIC vaping significantly suppressed fetal growth and skeletal development. It is thus highly likely that e-cig smoke is hazardous to both the dam and the developing fetal skeleton.

Disclosures: **Alyssa Falck**, *None*

MON-0458**Deletion of the Auxiliary Voltage Sensitive Calcium Channel Subunit and Gabapentin Receptor $\alpha 2\delta 1$ Results in Impaired Skeletal Density, Mass, and Strength**

Madison Kelly^{*1}, Karan Sharma¹, Xin Yi², Christian Wright², Megan Noonan², Taylor Gorrell², Aaron Gegg², Brandon Chenoweth², Uma Sankar², Julia Hum¹, Alexander Robling², Mary Farach-Carson³, William Thompson². ¹Marian University, United States, ²Indiana University, United States, ³University of Texas Health Science Center at Houston, United States

Voltage sensitive calcium channels (VSCCs) tightly control Ca²⁺ signaling. The mechanisms by which the pore-forming ($\alpha 1$) subunit of VSCCs regulates skeletal formation has been well-defined; however, little is known about how the auxiliary subunits, which influence VSCC activity, regulate skeletal health. As $\alpha 2\delta 1$ is the only known receptor for the antiepileptic and neuropathic pain drug gabapentin, which has deleterious skeletal effects, we examined how $\alpha 2\delta 1$ regulates bone formation and strength in vivo. Targeted deletion of exon 2 of *Ca_v2d1*, the gene encoding $\alpha 2\delta 1$, resulted in global peptide loss, with no compensation of other $\alpha 2\delta$ variants. DXA analyses were carried out at 6, 9, 12, 15, and 18 weeks of age. Body weight of *Ca_v2d1^{-/-}* mice was reduced by an average of 11% over the ages examined. BMD in *Ca_v2d1^{-/-}* mice (n=10) was reduced starting at 6 weeks of age (17% femur, 10% spine, and 7% total BMD) compared to *Ca_v2d1^{+/+}* littermate controls (n=18). BMC changes were similar, with decreases of 22%-femur and -spine, and 20%-total in *Ca_v2d1^{-/-}* mice (n=10) compared to controls (n=18). Femoral μ CT analysis showed decreased trabecular BV/TV (31%, $p < 0.01$), BMC (38%, $p < 0.05$), and TbTh (12%, $p < 0.05$). Reductions in cortical thickness (6%, $p < 0.05$), BMC (9%, $p < 0.01$), and polar moment of inertia (29%, $p < 0.01$) were observed with no changes in cortical BMD. Vertebral μ CT showed *Ca_v2d1^{-/-}* mice had decreases in trabecular BV/TV (16%, $p < 0.05$), BMC (25%, $p < 0.05$), and connectivity (23%, $p < 0.01$) compared to control mice. Additionally, trabecular spacing was increased by 12% in *Ca_v2d1^{-/-}* mice. Reductions in endosteal MS/BS (82%, $p < 0.05$), MAR (83%, $p < 0.05$), and BFR (85%, $p < 0.05$) were observed at the midshaft femur, showing impaired bone formation. No changes in serum CTX concentration was observed between *Ca_v2d1^{-/-}* and control (*Ca_v2d1^{+/+}*) mice. Femurs were tested in three-point bending to failure where *Ca_v2d1^{-/-}* mice (n=13) had reductions in stiffness (28%, $p < 0.01$) and ultimate force (20%, $p < 0.01$) compared to controls (n=8). Our results suggest that deletion of the $\alpha 2\delta 1$ subunit results in reduced trabecular and cortical bone, likely due to impaired bone formation, leading to compromised strength. We propose that $\alpha 2\delta 1$ is a critical regulator of VSCC activity to control bone formation. As $\alpha 2\delta 1$ is the receptor for gabapentin, these studies reveal and potential mechanism to understand how this antiepileptic and neuropathic pain drug influences skeletal health.

Disclosures: **Madison Kelly**, *None*

MON-0459

Global and Conditional Disruption of the Igf-I Gene in Osteoblasts and/or Chondrocytes Reveals Cell Type- and Compartment-Specific Effects of IGF-I in Bone Chandrasekhar Kesavan¹, Jon Wergedal², Catrina Godwin², Subburaman Mohan¹. ¹VA Loma Linda Healthcare System, Loma Linda University, United States, ²VA Loma Linda Healthcare System, United States

Recent studies have established that the increase in thyroid hormone levels during the prepubertal growth period is essential for the endochondral ossification that occurs at the epiphyses and secondary spongiosa (SS) of long bones. Thyroid hormone effects on endochondral bone formation are predicted to be mediated via activation of a number of growth factor signaling pathways. One such mediator of TH effects is IGF-I which acts as an endocrine hormone as well as a local autocrine/paracrine regulator in different bone cell types. To establish the relative importance of IGF-I expression in various cell types for endochondral ossification, we used microCT to evaluate the trabecular bone phenotypes at the distal femoral epiphysis and SS of 8-12-week-old male mice with a global knockout (KO) of the Igf-I gene as well conditional KO (cKO) of the Igf-I gene in osteoblasts (OBs) and/or chondrocytes (CCs), and their corresponding control wild type (WT) littermates (n = 6-9 per genotype). OB- and/or CC-specific Igf-I cKO mice were generated by crossing Igf-I floxed mice with transgenic Cre mice in which Cre expression is under the control of regulatory regions of Col1 α 2 (OB) or Col2 α 1 (CC) genes, respectively. The reduced trabecular bone mass at the SS in OB- and/or CC-specific Igf-I cKO mice is caused by reduced trabecular number and increased trabecular separation. Immunohistochemistry studies revealed that expression levels of CC (COL10, MMP13) and OB (BSP) markers were reduced in the SS and epiphyses of global Igf-I KO mice. Summary: 1) Disruption of the Igf-I gene globally reduces bone size (TV) to a much greater extent than conditional disruption in OBs. 2) Trabecular bone mass is similarly reduced in the SS of all four genotypes studied. 3) Global Igf-I KO but not cKO of Igf-I locally reduces trabecular bone mass in the epiphysis. Conclusion: Local and endocrine IGF-I actions in bone are pleiotropic and dependent on cell type as well as the bone compartment where IGF-I acts.

Genotype	SS - TV	SS - BV/TV	Epiphysis - TV	Epiphysis - BV/TV
Global KO	19.7*	78.5*	31.5*	76.6*
OB-specific cKO	73.8*	81.8*	75.3*	101.6
CC-specific cKO	109.1	83.4*	98.5	105.5
OB/CC double cKO	68.9	81.9*	76.3*	101.5

Values are the % of littermate WT control; * = p < 0.05 vs. control; TV, tissue volume; BV, bone volume

Disclosures: Chandrasekhar Kesavan, None

MON-0460

Vertebrate Lonesome Kinase is Required in Early Stages of Skeletogenesis David Maridas*, Laura Gamer, Leila Revollo, Malcom Whitman, Vicki Rosen. Harvard School of Dental Medicine, United States

Vertebrate Lonesome Kinase (VLK) is a novel secreted tyrosine kinase capable of phosphorylating extracellular proteins. Human mutations of Vlk have recently been identified to cause skeletal abnormalities. Accordingly, Vlk^{-/-} mice showed remarkable shortening of their long bones caused by a failure of transition from proliferative to hypertrophic chondrocytes. However, whether the chondrogenic phenotype was caused by loss of Vlk specifically in bone or due to a general loss of Vlk was unknown. Therefore, we investigated the effects of conditional loss of Vlk during development in mice. Using a Prx1-CRE deleter strain with Vlk^{fl/fl} mice, Vlk was removed in the limb bud mesenchyme of the progeny (cKO). At E13.5, we observed a delayed initiation of the primary ossification center in mutant hindlimbs. This lack of primary ossification center persists to E15.5 when the mutant limbs are shorter with absence of mineralization. Interestingly, we noted that the ulna and tibia are both curved with deletion of Vlk. At birth, limbs of cKO mice had developed primary ossification centers but the long bones remain markedly shorter. Unlike Vlk^{-/-} mice, cKO mice survive postnatally. At 1 week of age, the long bones remain shorter and the tibias remain curved. Interestingly, we observe an accumulation of marrow fat at the curvature of the tibia. At 10 days of age, the marrow fat expanded in the tibias. 4 days later, the long bones of cKO mice appear straight but still 8% shorter than the littermate controls. mCT analysis revealed that cortical fraction and thickness are markedly reduced in 2-week-old cKO femurs. Trabecular parameters are also decreased but only trabecular number and separation reached statistical significance. Our data indicates that Vlk is required for embryonic bone development. Prx1-specific deletion of Vlk is sufficient to recapitulate the skeletal growth retardation reported in the Vlk^{-/-} mice. However, the cKO mice are able to survive after birth with shorter limbs. Postnatal bone acquisition appears to be altered with targeted loss of Vlk. So, in addition to its role during bone development, it is possible that VLK is necessary to achieve peak bone mass acquisition. Phosphorylated targets of VLK have also yet to be confirmed but our results suggest that VLK regulates proteins essential for the proper timing of skeletogenesis. Ongoing experiments attempt to resolve those questions and to test if VLK is important during fracture repair.

Disclosures: David Maridas, None

MON-0461

High Bone Mass Phenotype is Present as Early as 8 weeks in CFW Mice Meghan Moran¹, Kelsey Carpenter¹, Brittany Wilson¹, Abraham Palmer², D. Rick Sumner¹. ¹Rush University Medical Center, United States, ²University of California San Diego, United States

Some Carworth Farms White (CFW) mice have abnormally high aBMD1; 2. This commercially available outbred strain can be stratified into distinct high (HBM) and normal bone mass (NBM) groups using either radiography or microcomputed tomography (μ CT) measurements of trabecular BV/TV or vBMD2. In the current study we sought to characterize the anatomic distribution of the phenotype, the timing of its appearance and its relationship to bone resorption and formation. Right femora, tibiae, humeri and vertebral columns of 48 CFW mice equally divided among males and females at 8 and 16 weeks of age were surveyed. Contact radiography showed the presence of the HBM phenotype, as evidenced by greatly enhanced radio-opacity (Fig. 1A), in the distal metaphysis in 13 of 48 femora. Of these 13 mice, 10 were HBM positive in the proximal tibia and 6 of these 10 mice were also HBM positive in the proximal humerus. The HBM phenotype was unaffected by sex (χ^2 , p=0.653) or age (χ^2 , p=0.512). The HBM phenotype was not observed in the vertebrae. Histology showed more trabecular bone in HBM mice with no difference in osteoblasts or osteoclasts and no evidence of pathology (Fig. 1B). μ CT showed a bimodal distribution of distal femoral metaphyseal BV/TV and vBMD (Fig. 1C, 1D), consistent with our previous findings. μ CT measurements, body weight, femur length and bone remodeling markers were subjected to ANOVAs with radiographic classification for HBM, age and sex as the main factors (Table 1). Distal femoral metaphyseal BV/TV and vBMD were significantly higher in the HBM group regardless of sex or age (Fig. 1E, 1F). Midshaft femoral cortical area (Ct.Ar) was greater in males compared to females, greater in the HBM group and the greatest between-group difference was present at 16 weeks (Fig. 1G). Body weight, femoral length and the bone remodeling biomarkers, CTX-1 and PINP did not vary as a function of HBM phenotype (Fig. 1H, 1I). The prevalence of the radiographic HBM phenotype was ~30% in the surveyed mice, did not differ between males and females and was not associated with variance in either bone length or body size. The lack of difference in the bone remodeling markers suggests that any differences in bone resorption or formation responsible for the phenotype had equilibrated by 8 weeks. Thus, the HBM phenotype in CFW mice is first evident before the cessation of longitudinal bone growth, is stable through the acquisition of peak bone mass and has a site-specific distribution.

Acknowledgements: The authors thank Dr. Matti Kiupel of the Michigan State University Veterinary Diagnostic Laboratory for histology.

References:

1. Parker CC, Gopalakrishnan S, Carbonetto P, et al. 2016. Genome-wide association study of behavioral, physiological and gene expression traits in outbred CFW mice. Nat Genet 48:919-926.
2. Moran M, Sumner DR, Palmer A, et al. 2017. Outbred CFW mice exhibit a bimodal bone mass distribution. American Society for Bone and Mineral Research Annual Meeting. Denver, CO.

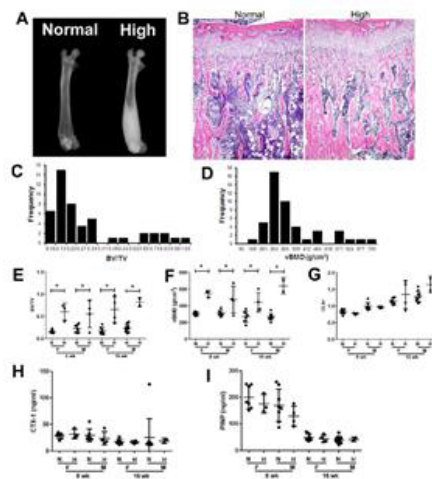


Figure 1. CFW mice phenotyping (n = 48). (A) Radiograph of femurs from CFW mice with normal and high bone mass. (B) Decalcified, H&E stained proximal tibial sections. (C-D) Frequency distributions for distal femoral BV/TV and vBMD. (E-G) BV/TV, vBMD and Ct.Ar in mice with normal (N) or high (H) bone mass (identified by plane film radiography) as a function of sex (F v M) and age (individual data points, means and SDs, see also Table 1). (H-I) Bone remodeling biomarkers CTX-1 and PINP (individual data points, means and SDs, see also Table 1).

Variable	Radiographic		Age	Sex	HBM*Age	HBM*Sex	Age*Sex	H*A*S	
	HBM								
BV/TV	<0.001		0.079	0.210	0.136	0.994	0.260	0.260	
vBMD	<0.001		0.855	0.148	0.125	0.178	0.007	0.005	
Ct.Ar	0.031		<0.001	0.001	0.004	0.384	0.678	0.540	
Body Weight			0.354	<0.001	<0.001	0.139	0.169	0.924	0.623
Femoral Length			0.588	<0.001	0.005	0.386	0.327	0.014	0.686
CTX-1			0.706	0.174	0.890	0.832	0.571	0.486	0.892
PINP			0.157	<0.001	0.073	0.193	0.861	0.172	0.645

Table 1. Results of 3-way analyses of variance (n = 12 males and females each at 8 and 16 weeks). p-values for each factor and interaction term. Bold=significance, p<0.05.

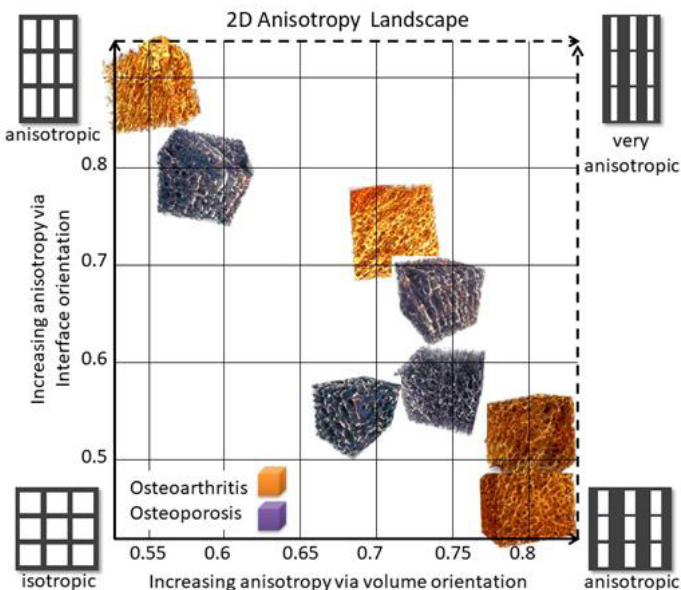
Disclosures: Meghan Moran, None

Monday Posters

MON-0462

Trajectories of Human Trabecular Bone Adaptation within a 4D Landscape of Tissue Anisotropy Nicolas Piche*¹, Natalie Reznikov², Ievgeniia Morozova³, Iskandar Tamimi⁴, Jun Song², Faleh Tamimi². ¹Objects Research Systems Inc., Canada, ²McGill University, Canada, ³Trikon Technologies Inc, Canada, ⁴Hospital Carlos Haya, Spain

Anisotropy of trabecular bone is a result of life-long functional adaptation. Anisotropy physiologically increases from infancy to adulthood, and it is more pronounced where mechanical loading is predictable, consistent and strenuous. There are conflicting reports in the literature regarding anisotropy in the context of bone pathology. For example, increased anisotropy accompanies decreased bone mineral density in osteoporosis (causing fragility), whereas in osteoarthritis, increased anisotropy leads to joint degeneration attributable to excessive subchondral bone stiffness. The reason for these inconsistent effects of anisotropy on bone biomechanics is that there are several independent pathways that lead to bone anisotropy. Such pathways include enhanced preferred orientation of the bone-marrow interface, and enhanced volume orientation which can be achieved either by coarsening of certain trabecular elements and/or by thinning of other elements. We present a machine-learning algorithm for identification of salient characteristics of trabecular bone. Samples were imaged by μ CT and analyzed using a set of independent parameters, such as interface orientation, volume moment of inertia and network connectivity orientation (all of which contribute to net mechanical anisotropy), and trabecular thickness distribution that accounts for volume fraction. We present these parameters as “coordinate axes” in a 4D landscape. Normal and pathologic bone samples characterized by these coordinates were mapped onto the 4D landscape. We used 20 μ CT volumes of human bones unaffected by pathology (proximal femur, distal femur and calcaneus), and more than 80 μ CT volumes of pathologic bone samples (hip osteoarthritis, osteoporotic femoral neck fracture, talar joint ankylosis and clubfoot). Mapping the specimens onto the 4D landscape allows principal component analysis to be conducted for identification of the trabecular bone adaptation trajectories in both health and disease. This illustrates how continuous bone adaptation can result in its over-adaptation, which is an exaggerated narrow specialization to monotonous, repetitive loading. Thus, over-adaptation undermines the biomechanical fitness of bone to accidental, non-stereotypical loading. We explain the endpoints of trabecular bone adaptation trajectories as disuse, overuse or abuse in the context of common and rare skeletal pathologies.



Disclosures: *Nicolas Piche, Object Research Systems Inc, Major Stock Shareholder*

MON-0463

Forward-genetic ENU screen identifies genes regulating skeletal development in mice Jonathan Rios*¹, Carol Wise¹, Bruce Beutler². ¹Texas Scottish Rite Hospital for Children, United States, ²University of Texas Southwestern Medical Center, United States

Embryonic and post-natal skeletal development is a highly regulated and dynamic process that is impacted by numerous genetic and non-genetic factors. Genome-wide association studies have identified numerous loci associated with variation in bone quality (bone mineral density, BMD). However despite these efforts, the current catalogue of genes regulating proper skeletal development is far from complete. To discover additional genes regulating proper skeletal development, we initiated live-animal skeletal screening as part of a high-throughput N-ethyl-N-nitrosourea (ENU) forward-genetic screen in mice. Briefly, pups from inbred (C57BL/6J) ENU-mutagenized mice are back-crossed to produce ~600 G3

mice weekly that undergo dual-energy X-ray absorptiometry (DEXA) and X-ray imaging. Images are evaluated for tibia and femur lengths and BMD, and ENU-induced mutations tested for statistical association with dominant, additive, and recessive phenotypes. As proof-of-concept, we present preliminary results from G3 mice harboring ENU-induced damaging mutations cumulatively targeting ~1% of all genes in the mouse genome. First, the ‘bone-loss’ mouse harbors a recessive ApsaF261 mutation associated with a ~20% reduction in tibia and femur BMD. Mutations in human ASPA, encoding Aspartoacylase, cause Canavan disease. Second, the ‘cooper’ mouse carries a recessive IduaD202 mutation associated with a ~20% increase in tibia and femur BMD. Recessive loss-of-function mutations in human IDUA, encoding Alpha-L-Iduronidase, cause Hurler syndrome. Skeletal development is also subject to hormonal regulation. The ‘ito4’ mouse harbors a recessive Tgl1352K mutation in Thyroglobulin that results in a dwarf mouse with significant reductions in tibia, femur, and pelvis lengths, as well as changes in fat deposition. In contrast to other large-scale mouse knockout efforts, the ENU-induced forward screen is capable of detecting significant association with gain-of-function missense mutations. We detected significant association of a Bicc1T469M mutation in the ‘Pebbles’ mouse with a dominant increase in tibia and femur BMD. Interestingly Bicaudal C Homolog 1, the protein encoded by Bicc1, positively regulates osteogenesis and was recently associated with BMD in humans. Our results show the feasibility of an unbiased high-throughput ENU forward-genetic approach to discover genes relevant in human skeletal development and disease.

Disclosures: *Jonathan Rios, None*

MON-0489

NF- κ B Activation in BMSC’s Drives Bone Loss Via Cell Intrinsic and Extrinsic Effects Manoj Arra*, Gaurav Swarnkar, Gabriel Mbalaviele, Yousef Abu-Amer. Washington University in St. Louis School of Medicine, United States

The skeletal system undergoes constant turnover due to an interplay between osteoclast and osteoblast activity, with bone loss occurring due to an imbalance between these two cell types. However, there exist many other cells that affect bone quality by regulating the number and function of osteoclasts and osteoblasts. BMSC’s are a numerically minor population in the marrow but play an extremely critical role by acting as the precursors for osteoblasts and marrow adipocytes, thus requiring great attention for understanding the physiology of bone loss. One of the most studied and recognized drivers of bone loss is inflammation, which has been shown extensively to promote osteoclastogenesis by activating the NF- κ B pathway, the key signaling pathway of the inflammatory response. However, the effect of inflammation and NF- κ B signaling on osteoblasts and their precursor BMSC’s is less clear and somewhat controversial. Here, we describe the use of genetic models to study the effect of chronic inflammation on BMSC differentiation and function. We use a constitutively active form of IKK2 (IKK2ca), which is an essential kinase required for activating NF- κ B transcription factor, which we have previously shown is a model of chronic inflammation that consistently activates NF- κ B in the absence of inflammatory stimuli while sparing the pleiotropic effects of these exogenous stimuli. IKK2ca was expressed under the control of the PRX1-cre to target BMSC’s in vivo, resulting in a profound phenotype when activated in utero, including severe runting and low bone mass. Further, the bone marrow was found to be extremely dense and filled predominantly with inflammatory cells, and lacked the presence of marrow adipocytes. Histology showed elevated osteoclast activity and decreased osteoblast activity, likely contributing to the severe bone loss. In vitro studies supported these in vivo findings and displayed that IKK2ca inhibits BMSC differentiation, while also increasing their ability to support myeloid cell survival and differentiation into osteoclasts through the secretion of extracellular factors. These results highlight the response of BMSC’s to inflammation and their ability to drive an inflammatory phenotype in vivo to cause bone loss. This work identifies BMSC’s as a critical cell type for promoting bone loss. Future work involves studying the effect of IKK2ca activation in BMSC’s in adult mice as well as the mechanisms of differentiation inhibition.

Disclosures: *Manoj Arra, None*

MON-0490

Loss of the histone methyltransferase Ezh2 induces cellular senescence in mesenchymal stem cells Amel Dudakovic*, Catalina Galeano-Garces, Christopher Paradise, Daniela Galeano-Garces, Farzaneh Khani, Roman Thaler, Andre Van Wijnen. Mayo Clinic, United States

Ezh2, a histone 3 lysine 27 (H3K27) methyltransferase, plays a critical role during skeletal development and osteoblast differentiation. We previously showed that pharmacological inhibition of Ezh2 enhances osteogenesis, stimulates bone formation, and mitigates bone-loss associated with estrogen depletion. However, conditional genetic loss of Ezh2 early in the mesenchymal lineage (Ezh2 cKOPrx1, Ezh2flox/flox; Prx1-Cre) causes skeletal abnormalities as a result of patterning defects. Interestingly, Ezh2 cKOPrx1 animals exhibit enhanced marrow adiposity and premature suture fusion. These observations suggest that Ezh2 may protect mesenchymal stem cells from premature aging and senescence. Here, we examined the impact of mesenchymal loss of Ezh2 on cellular senescence in vitro and in vivo. Treatment of adipose-derived mesenchymal stem cells (AMSCs) with GSK126, a specific Ezh2 inhibitor, up-regulates the expression of many senescence-associated secretory phenotype (SASP) genes (e.g., IGFBP2, ICAM, IL6) as measured by mRNA-Seq analysis. Similarly, Ezh2 inhibition up-regulates the expression of the CDKN2A, a key marker of

cellular senescence that encodes the cell cycle inhibitor p16/INK4A and the p53 related p19/ARF protein. Immunofluorescence (IF) microscopy demonstrates enhanced staining of several senescence-related markers including p16, phosphorylated p53 (p-Ser15), and γ H2AX (p-Ser139) in GSK126-treated AMSCs. Prolonged exposure of AMSCs to GSK126 significantly increases senescence-associated β -galactosidase (β -gal) staining. Similar to AMSCs, mRNA-Seq assessment of primary calvaria derived from control (CON) and Ezh2 cKOPrx1 demonstrates that several SASP genes and Cdkn2a are up-regulated with the loss Ezh2 in the mesenchyme. Indeed, IF results show enhanced p16 staining in proximal tibias derived from Ezh2 cKOPrx1 three-week old animals. Additional assessment reveals enriched detection of lipofucin (Sudan-Black-B staining), an established hallmark of senescent cells, in mouse tibias that lack Ezh2 expression in mesenchymal cells. Taken together, Ezh2 loss in the mesenchymal compartment induces cellular senescence. Thus, while Ezh2 serves as a critical inhibitor of osteogenic differentiation as seen in previous studies, our current study shows that this epigenetic regulator also protects mesenchymal stem cells from undergoing premature senescence.

Disclosures: Amel Dudakovic, None

MON-0491

The Effect of Ascorbic Acid on BMP-2 Treated C3H10T1/2 Mesenchymal Stem Cells in Phosphate Deficient Conditions Matthew Bui*, Amira Hussein, Louis Gerstenfeld. Boston University School of Medicine, United States

Introduction: Our prior in vivo studies showed that dietary phosphate deficiency impairs oxidative phosphorylation and decreased BMP-2 signaling that promoted MSC chondrogenic differentiation during fracture healing. In this study we examine the molecular relationship between BMP-2 mediated chondrogenic differentiation and energy consumption. We further assessed the extent to which collagen hydroxylation that increases during chondrocyte differentiation contributes to energy use. Methods: C3H10T1/2 murine cells were expanded in growth medium DMEM with 10% FBS. At 60% confluence (day 0), cells were switched to differentiating media (α -MEM with 5% FBS and 1X insulin-transferrin-selenium) containing either 100% (1mM) or 25% (0.25mM) inorganic phosphate (Pi), \pm 200ng/mL BMP-2 (BMP), and \pm 0.2 mM L-ascorbic acid (AA; to facilitate collagen hydroxylation). Cells grown in α -MEM with 10% FBS were used as a baseline control. At day 8, total DNA, protein, and hydroxyproline (HP) content were examined. Chondrocyte and adipocyte gene expression were measured. Results: The +BMP media groups contained less DNA and more protein than the -BMP differentiation media groups ($p < 0.001$). There was a significant interaction between Pi and AA treatment ($p = 0.030$), with 25% Pi +AA groups producing more protein than 100% Pi +AA groups. Hydroxyproline production was greater in +BMP, +AA, and 25% Pi groups ($p < 0.001$). Col2a1, Acan, and ColXa1 expression were increased in +BMP groups. AA treated groups expressed significantly more Col2a1 and Acan than -AA groups. 100% Pi media had greater Acan expression than 25% Pi groups ($p = 0.001$) while 25% Pi media tended to lead to greater ColXa1 expression over 100% Pi groups ($p = 0.073$). Pparg and Plin1 expression were increased in the 25% Pi mediums. There were no differences in Ucp1 expression. Discussion: BMP-2 promoted both chondrogenic and adipogenic differentiation while Pi deficiency in the presence of BMP-2 increased adipogenesis while diminishing chondrocyte maturation. Hypertrophic chondrocyte expression was decreased in Pi deficient media, which coincides with increased protein and hydroxyproline production observed in low Pi conditions. AA increased HP production in all BMP-2 treated samples independent of Pi levels however HP levels were the highest in low Pi +BMP +AA cultures. Together, the results indicate that increased energy consumption is related to BMP-2 mediated differentiation and promotion of collagen hydroxylation.

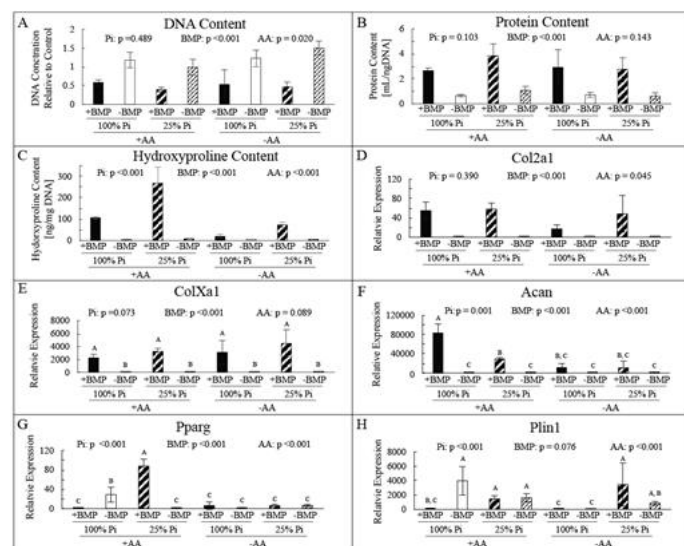


Figure 1. Relative to Day 8 controls: (A) DNA content; (B) total protein; (C) hydroxyproline content; (D-H) Gene expression. If Pi*BMP*AA $p < 0.05$, different letters indicate statistically significant differences between groups.

Disclosures: Matthew Bui, None

MON-0492

Notch and Wnt Signaling Crosstalk Regulates Skeletal Stem/Progenitor Cell Behavior during the Early Stages of Fracture Repair Sooyeon Lee^{*1}, Anna Josephson², Philipp Leucht¹. ¹Dept. of Orthopaedic Surgery, NYU Langone Orthopedic Hospital, United States, ²Dept. of Cell Biology, NYU School of Medicine, United States

Bone regeneration is a complex process that requires the coordinated efforts from multiple different cell types and tissues. When bone healing fails, patients are often left with painful disability and deformity. During fracture healing, recruitment of skeletal stem/progenitor cells (SSPCs) to the injury site is one of the first steps. Once SSPCs have migrated to the fracture site, they begin to divide in an effort to provide a sufficient number that then can undergo osteogenic differentiation to form a bony callus. There is evidence that the Notch and Wnt signaling pathways are essential for bone regeneration after injury, and preliminary data point towards a regulated interplay between the two pathways. We hypothesize that Notch signaling predominates in the initial fracture callus to support the expansion of the SSPC pool; this is followed by an increase in Wnt responsiveness, indicating onset of differentiation. The coordinated activity between Notch and Wnt signaling shapes the initial repair process of a skeletal injury site. We first focused our attention to the temporal expression profile of members of the Notch and Wnt signaling family within the injury site. Using qPCR, we detected that Notch target genes are significantly up-regulated in the early phase of fracture healing, while Wnt downstream targets were upregulated at a later stage during fracture repair. This switch from Notch to Wnt occurred around 7 days post-injury, a time when osteogenic differentiation dominates within the injury site. We then used immunofluorescence to characterize the spatial signaling profile and demonstrated that Notch pathway components were expressed during the early proliferative phase of fracture healing. Using a Wnt reporter mouse, we showed that Wnt-responsive cell appeared during the early differentiation phase (day 7) and that these cells were also osterix-positive, indicating their osteogenic lineage commitment. Transcriptional analysis of SSPCs isolated by flow cytometry during early fracture healing revealed a temporal expression of Notch and Wnt downstream targets consistent with the previous immunostaining. Finally, in vitro studies provided evidence that Notch and Wnt signaling regulate each other, e.g. inhibition of Wnt signaling leads to an enhanced/prolonged Notch activation. Taken together, we provide evidence that SSPC proliferation and differentiation is tightly regulated by Notch and Wnt signaling during healing.

Disclosures: Sooyeon Lee, None

MON-0493

Differences in osteoprogenitor populations between bone compartments Brya Matthews^{*1}, Francesca Sbrana², Sanja Novak³, Danka Grcevic³, Ivo Kalajic². ¹Department of Molecular Medicine and Pathology, University of Auckland, New Zealand, ²School of Dental Medicine, University of Connecticut, United States, ³Department of Physiology and Immunology, University of Zagreb, Croatia

The aim of our study is to evaluate the frequency of mesenchymal stem/progenitor cells in different bone compartments. Studies often consider bone as whole without dissecting periosteum versus endosteum or bone marrow (BM). Flow cytometry is a proven technique to identify stem/progenitor cells, and has recently been applied to the skeletal system. Populations of 'skeletal stem cells' (SSC, CD51+CD90-Ly51-CD105-) and 'bone, cartilage and stromal progenitors' (BCSP, CD51+CD90-Ly51-CD105+) were identified in whole bone of neonatal mice (Cell 160:285, 2015). These results were not validated in adult animals. We identified long term progenitors as label retaining cells (LRC) by doxycycline-inducible H2B-GFP, with labelling from P10-P45, then 13+ weeks chase. Col2.3-GFP reporter mice were used to identify osteoblasts. Analyses were done on the 'mesenchymal' fraction, CD45/Ter119/CD31- (CD45- cells). Periosteal CD45- cells are enriched for Sca1, PDGFR α , CD51 and CD90. Sca1 and PDGFR α are present on ~15% of periosteum, 1% of endosteum and 0.1% BM cells. In contrast, endosteal cells are CD105+ (~50%) compared to 10% in periosteum. CFU-F assays indicate that CD45- cells from periosteum form 20x more colonies than endosteal cells. 1% of cells in periosteum and endosteum had a BCSP phenotype, and <0.1% in the BM. SSC were more common, representing 11% periosteum, 2.5% endosteum and 2% BM. The endosteum contains Col2.3GFP+ osteoblasts that do not express Sca1, PDGFR α and CD90, but are CD51+ (31.5%) and CD105+ (13.8%). A large proportion of osteoblasts have BCSP or SSC phenotype, and over 30% of BCSP and SSC in the endosteum are osteoblasts. LRCs identified by H2B-GFP were present in all tissue compartments, and showed enrichment of Sca1, CD51 and CD90, but reduced CD105. Periosteal LRCs formed more CFU-F than negative cells, although greater enrichment for CFU-F was achieved sorting for Sca1+ or CD90+ cells. LRCs also contributed to in vivo bone formation, as did Sca1+ cells. Our results show that BCSP and SSC do not specifically identify stem cells in adult bone as many mature osteoblasts express these marker panels. However, the periosteum of adult mice is enriched for skeletal stem/progenitor cells compared to endosteum and BM. Label retention along with Sca1, CD51, CD90 and PDGFR α , but not CD105, are useful for identifying these populations. In conclusion, developmental stem cell biology cannot be simply translated to adult stem cells.

Disclosures: Brya Matthews, None

MON-0494

Cartilage is Derived from Nerve in Trauma-Induced Heterotopic Ossification

Elizabeth Olmsted-Davis*¹, Elizabeth Salisbury². ¹Baylor College of Medicine, United States, ²UTMB, United States

Our studies suggest that cartilage forms at exactly the same time as bone in heterotopic ossification (HO) and not before bone as would be expected for an endochondral process. Its formation is a direct result of the hypoxic microenvironment established by transient brown adipocytes (tBAT). We have previously shown that tBAT is derived from perineurial fibroblasts associated with peripheral nerves. However, the cartilage progenitor in this model has yet to be elucidated. Previous data suggests that it's derived from a macrophage-like cell, and here we present that it is a subset of tBAT. A murine model of HO that involves the delivery of low levels of BMP2 was used in these studies. This model has been shown to match the early stages of human HO. Preliminary studies using the tamoxifen-inducible Wnt1-cre: R26RTdTomato red system, suggest the presence of the red reporter in some of the chondrocytes. However, it is unclear whether the lack of more of the red reporter is due to the pulse-lineage tracing methodology, where an intermediate such as the labeled perineurial fibroblasts, are more delayed in their appearance. To address this we have employed other lineage tracing models including the tamoxifen-regulated GLASTcre: R26RTomato red and the UCP1Cre-R26TdTomato red reporter mice. We selected lineage tracing with GLAST, since it appears in a small subset of our perineurial cells on peripheral nerves, after induction of HO. These cells appear to migrate and expand at the site of bone formation. Previously it was reported that GLAST was expressed in the chondrocytes made during HO. Lineage-tracing studies do show the presence of GLAST in chondrocytes. Cartilage formation correlates with perineurial cells using the UCP1 lineage-tracing model. However, surprisingly, UCP1 is quickly down regulated in the cells prior to chondrogenesis. Only a subset of these cells appeared to contribute directly to cartilage. Additional analysis of these cells supports the idea that they also express key macrophage markers. The data collectively suggests that these perineurial cells function similarly to astrocytes in the central nervous system, in that they display a large amount of heterogeneity and have a variety of functions. Recent data suggests that astrocytes express a large number of cartilage matrix proteins and may function as cartilage under specific conditions. Thus the cartilage formed during HO may be unique in that it forms from perineurial progenitors.

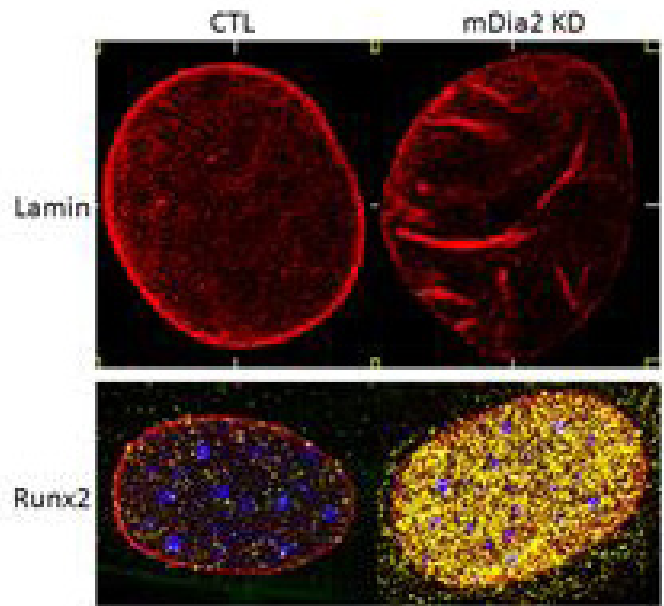
Disclosures: *Elizabeth Olmsted-Davis, None*

MON-0495

Nucleoskeletal Actin-Lamin Architecture Regulates MSC Runx2 Directed Osteogenesis

Jeyantt S. Sankaran*¹, Buer Sen¹, Zhihui Xie¹, Cody McGrath¹, Maya Styner¹, Amel Dudakovic², Andre J. Van Wijnen², Janet Rubin¹. ¹UNC Chapel Hill, United States, ²Mayo Clinic, United States

Nucleoskeletal lamin scaffolds genetic material critical to mesenchymal stem cell (MSC) fate. A dynamic actin cytoskeletal network, comprised of monomeric and polymeric actin, interacts with this scaffold, regulating its shape and structure. We previously showed that actin transfer into the nucleus profoundly promoted MSC differentiation; further, structural changes in internal nuclear actin structure were crucial to MSC lineage. Here we wished to understand how intranuclear actin structure epigenetically specified osteogenic differentiation. Specifically, we aimed to alter internal nuclear actin structure without changing the cytosolic actin network in murine MSC. We first found that the diaphanous formins, which regulate actin polymerization, are compartmentalized: mDia1 is cytoplasmic while mDia2 is almost exclusively intranuclear. Thus, we knocked down nuclear mDia2 using siRNA. Compared to MSC treated with control siRNA, mDia2 KD robustly and rapidly stimulated osteogenesis: at 3d, osterix (Sp7) and osteocalcin (Bglap) gene expression increased by 4-fold, and alkaline phosphatase activity (at 5d) was upregulated 3 fold ($p < 0.05$). Upregulation of multiple other osteogenic genes was confirmed by unbiased mRNAseq. Importantly, mDia2 KD did not promote adipogenic differentiation. We thus hypothesized that nuclear F-actin might support a nucleoskeletal architecture that silences the osteogenic genome. Confocal microscopy showed that F-actin ring co-localizes with laminB on the inner surface of the MSC nuclear envelope. After mDia2 KD, structural changes were prominent: 67% of mDia2 KD cells showed >2 lamin folds extending into the nucleus whereas only 7% control cells had lamin folding. On average, mDia2 KD cells had 4x lamin folds extending 3x longer than in control cells ($p < 0.05$). LaminB staining was decreased by 22% (cf control, $p < 0.05$) and pixel intensity was more variable in mDia2 KD nuclei cf to control (75% vs 58%, $p < 0.05$) indicating a non-uniform distribution of the nuclear envelope. LaminB folding due to mDia2 KD was accompanied by intense nuclear staining with Runx2 Ab. In sum, our findings indicate that actin polymers provide structure to the nucleoskeleton. Inhibiting F-actin polymerization by nuclear mDia2 knockdown leads to a profound alteration in laminB structure that activates nucleoskeletal bound Runx2. This suggests that the actin-lamin interface dynamically silences the osteogenic Runx2 cistrome.



Disclosures: *Jeyantt S. Sankaran, None*

MON-0496

Oxidized Phospholipids Are Ligands for LRP6 in Bone Marrow MSCs

Lei Wang*, Weiping Su, Xiaonan Liu, Janet Crane, Xu Cao, Mei Wan. Johns Hopkins University School of Medicine, United States

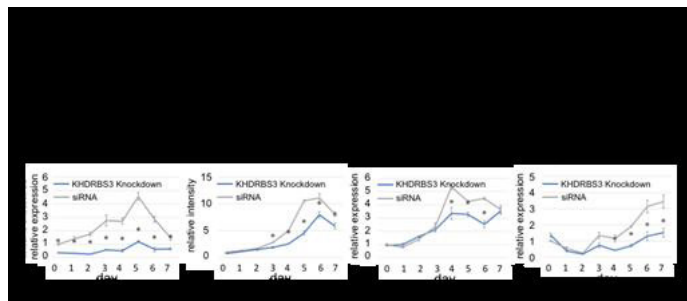
Human mutations in Low-density lipoprotein receptor-related protein 6 (LRP6), a known positive regulator of osteoblast bone formation, have been linked to early onset hyperlipidemia, atherosclerosis, and osteoporosis. Our objective is to define whether and how LRP6 is involved in hyperlipidemia/atherosclerosis-associated bone loss. LRP6 is a co-receptor for Wnt and can be recruited by multiple growth factors/hormones, such as PTH, PDGF-BB, TGF β and BMP, to their receptors facilitating intracellular signaling activation. However, these factors are not actual ligands of LRP6 as their direct binding to LRP6 has not been recognized. Here, we report that oxidized phospholipids (oxPLs) are native ligands of LRP6. oxPLs are bioactive components in oxidized LDL particle (oxLDL), which serves as a hallmark for hyperlipidemia and atherosclerosis. We detected high levels of oxPLs in bone marrow in mice fed a Western high fat diet. Importantly, bone marrow mesenchymal stromal cells (MSCs) had a reduced cell surface LRP6 expression with an impaired osteogenic differentiation capacity. Consistently, direct treatment of MSCs with oxLDL and individual biologically active oxPLs, including POVPC and PGPC, caused a rapid decrease in cell surface LRP6. Thus, MSC surface LRP6 may act as a specific sensor of oxPLs in bone marrow. By employing multiple approaches, including flow cytometry analysis, fluorescence spectra-based ligand-receptor binding assays, biotin-precipitation assays, protein-lipid overlay assays, and subcellular localization assays, we showed that LRP6 directly bound and mediated the uptake of oxPLs by MSCs. The binding of oxPLs and LRP6 led to endocytosis of LRP6 through a clathrin-mediated pathway, decreasing the responses of MSCs to osteogenic factors such as Wnt, PTH, and BMP. As a result, osteoblast differentiation of MSCs was diminished. We also tested whether increasing cell surface LRP6 expression could restore the impaired MSC function. A specific inhibitor of clathrin-dependent endocytosis pathway elevated cell surface LRP6 level, and almost restored the blunted response of MSCs to osteogenic factors by oxPLs. Similarly, expression of Mesd, an ER chaperone protein specifically targeting LRP6 on cell surface, increased oxPL-impaired osteogenic differentiation of MSCs. Thus, LRP6 functions as a receptor and molecular target of oxPLs for their adverse effect on MSCs. Our study reveals a potential mechanism underlying hyperlipidemia-associated bone loss.

Disclosures: *Lei Wang, None*

MON-0497

The Power and Potential of Alternative Splicing to Dictate Stem Cell Fates in Bone Yuanyuan Wang*¹, Rene Chun², Emad Bahrami-Samani³, Lan Lin³, Yi Xing³, John Adams⁴. ¹Bioinformatics Interdepartmental Graduate Program, University of California, Los Angeles, United States, ²Department of Orthopaedic Surgery, University of California, Los Angeles, United States, ³Department of Microbiology, Immunology and Molecular Genetics, University of California, Los Angeles, United States, ⁴Department of Orthopaedic Surgery, Department of Molecular, Cell & Developmental Biology, University of California, Los Angeles, United States

Almost all multi-exonic genes in human genome are subject to alternative splicing (AS) under the regulation of RNA binding proteins (RBPs). Despite the critical role of AS in the establishment of tissue identity and development, there has been no unbiased, transcriptome-wide analysis of AS of human mesenchymal stem cells (hMSC) that reside in the human skeletal niche. As such, the primary goal of this study is to comprehensively evaluate how AS, under control of RBPs, affect the differentiation fates of hMSCs. Initially, pair-wise comparisons between hMSC and its terminally differentiated progeny in the osteoblast and adipocyte lineage were performed using RNA-seq data from the ENCODE consortium; these studies revealed widespread changes in AS between the MSC and the two derivative cell types. We then provoked osteogenic differentiation of human bone marrow-derived MSC (hbmMSC) and performed RNA-seq in triplicate wells of cells on day 0-to-12. Transcriptome-wide analysis identified temporal coordination of numerous significantly differential exon-skipping (SE) events and significantly differentially expressed RBPs during stepwise differentiation. By co-expression-splicing analysis, we identified 5304 correlative temporal patterns in expression of a specific RBP and a specific SE event ($r2>0.5$), some of which reside in known osteogenesis-related genes and others in transcription factors (TFs) known to shape the MSC-to-osteoblast pathway. Six RBPs with the following characteristics were identified as key drivers of AS during this differentiation: i) differentially expressed; ii) temporally correlated with differential SE events; and iii) cognate RNA binding motifs enriched within the alternative exon or its adjacent flanking introns. Perturbation RBP expression was then performed to ascertain if those RBPs impact differentiation trajectories. Robust siRNA knockdown of one of these six candidate RBPs, KHDRBS3, significantly inhibited osteoblastogenesis and bone formation in vitro, as indicated by both alkaline phosphatase staining and maturation-dependent gene expression (see Figure). Our findings support the hypothesis that creation of developmentally-regulated AS isoforms, especially of TFs, is controlled, at least in part, by differential expression of key RBPs. Delineating time-dependent, coordinate AS and RBP expression-action changes are crucial to understanding the molecular mechanisms underlying the hbmMSC-to-osteoblast differentiation program.

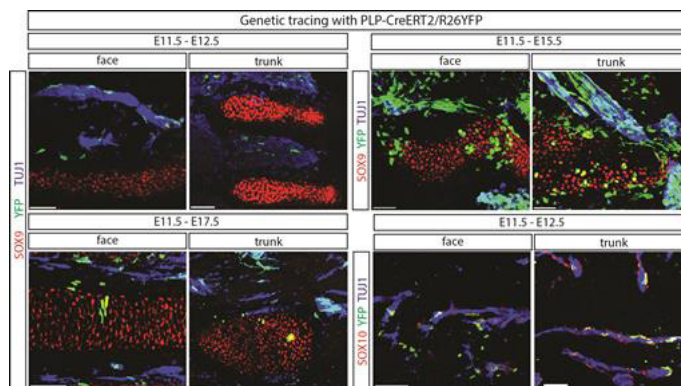


Disclosures: Yuanyuan Wang, None

MON-0498

Multipotent Schwann cell precursors contribute to chondro- and osteo-progenitors during embryogenesis Meng Xie*¹, Dmitrii Kamenev², Baoyi Zhou¹, Maria Eleni Kastriiti¹, Kaj Fried², Igor Adameyko¹, Viacheslav Dyachuk², Andrei Chagin¹. ¹Department of Physiology and Pharmacology, Karolinska Institutet, Stockholm SE-171 77, Sweden., Sweden, ²Department of Neuroscience, Karolinska Institutet, Stockholm SE-171 77, Sweden., Sweden

The Schwann Cell Precursors (SCPs) are emerging as a new type of multipotent stem cells. Their contribution to melanocytes, parasympathetic nerves, tooth mesenchymal cells and adrenal cells has recently been shown. The cellular and developmental origin of osterix (Osx) positive chondro- and osteo-progenitors has long been debated. Here, employing genetic tracing we show that a number of Osx-positive progenitor cells is originated from the SCs. Additionally, we revealed that SCs differentiate into chondrocytes and osteocytes during mouse embryonic development. The process seems to be evolutionary conservative since such a contribution was also observed in zebrafish. Our findings expand the multipotent potential of the SCs by revealing their connective tissue fate and provide a novel link between the nervous and skeletal systems.

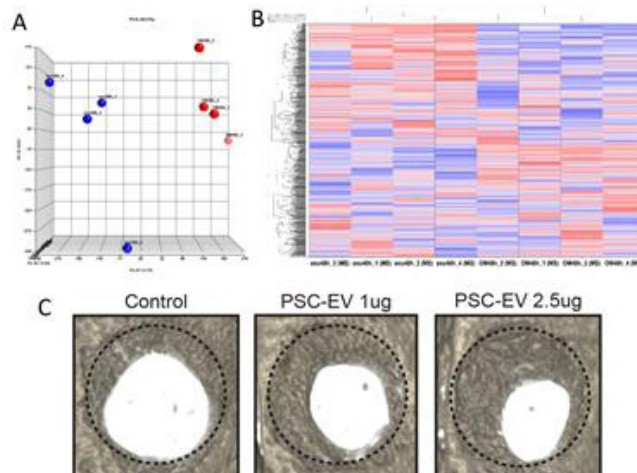


Disclosures: Meng Xie, None

MON-0499

The perivascular progenitor cell vesicular secretome incites bone repair via pleiotropic effects on endogenous skeletal progenitor cells Jiajia Xu*¹, Carolyn Meyers¹, Leslie Chang¹, Leitia Zhang¹, Yiyun Wang¹, Kristen Broderick¹, Bruno Peault², Aaron James¹. ¹Johns Hopkins University, United States, ²University of California, Los Angeles, United States

Human perivascular progenitors are known to incite bone defect healing, predominantly via paracrine means. Adipose resident perivascular progenitors (perivascular stem cells, PSC) may be derived by fluorescence activated cell sorting. Here, we detail how extracellular vesicles obtained from the perivascular incite bone healing via modulation of endogenous skeletal stem cell (SSC) behavior. Methods: Human white adipose tissue was processed using previously established protocols to isolate PSC, including CD146+CD34-CD45-CD31- pericytes and CD34+C146-CD45-CD31- adventitial cells. PSC were first examined in non-contact co-culture with human bone marrow, culture derived SSC. Next, PSC derived extracellular vesicles (PSC-EV) were obtained by ultracentrifugation. Validation was performed based on ISEV minimal experimental requirements, including Western blot and electron microscopy. The effects of PSC-EV were either examined in vitro on human SSC, or in vivo in a mouse calvarial defect. For in vitro studies, SSC proliferation, migration and osteogenic differentiation were assessed (1, 2.5, and 5 ug/mL). Affymetrix microarray examined the SSC transcriptome before and after PSC-EV treatment. For in vivo studies, PSC-EV were applied by injection to mouse calvarial bone defects, and healing was assessed by microCT and histology. Results: Human PSC induced significant changes in SSC behavior in non-contact co-culture, including an increase in proliferation, migration, and osteogenic differentiation. These in vitro effects were accompanied by release of PSC-derived, fluorescently labelled extracellular vesicles (PSC-EV), which fused with recipient cells. These findings were replicated by addition of PSC-EV to SSC cultures. Transcriptomic analysis of PSC-EV treated SSC demonstrated a robust change in key signaling pathways, as observed by principal component analysis, gene ontology, and ingenuity pathway analysis (Fig. 1A,B). When applied to a calvarial defect model, PSC-EV led to a marked increase in bone healing overtime (up to 70.0% increase in healing), accompanied by increased SSC proliferation, migration, and in situ osteogenic differentiation (Fig. 1C). Our data suggest that PSC derived extracellular vesicles (PSC-EV) induce marked changes in SSC behavior that converge to yield successful bone defect repair. Identifying the essential cargo delivered by PSC-EV that dictates the bone forming effects is the ongoing focus of study.



Disclosures: Jiajia Xu, None

MON-0500

Specific Knockout of *Gsa* in Murine Osteoblast Precursors Leads to Blunted Response to Intermittent PTH Administration in vivo Mingxin Xu*, Deepak H. Balani, Sophia Trinh, Henry M. Kronenberg. Endocrine Unit, Massachusetts General Hospital, Harvard Medical School, United States

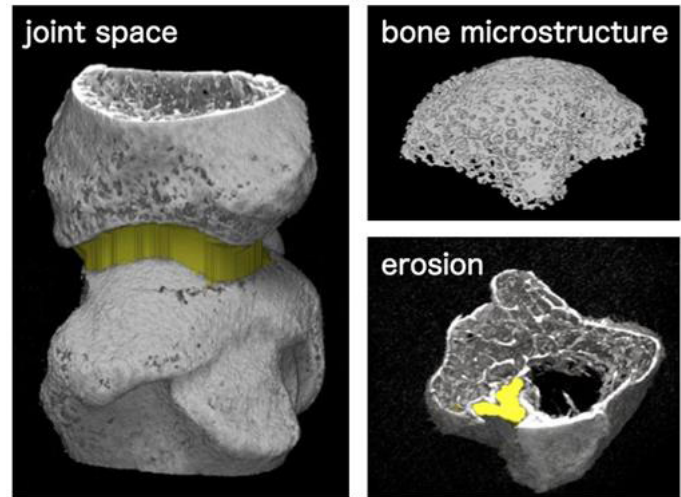
A lineage-tracing strategy, using a tamoxifen-dependent, promoter-driven cre system, has identified Sox9-expressing cells as a group of early osteoblast precursors. Intermittent PTH administration can significantly increase the number of these precursors through direct action on the PTH receptor. As a G protein-coupled receptor, PTH receptor can activate multiple G proteins, including *Gsa*. To assess whether *Gsa* has a role in the PTH-mediated increase of Sox9-expressing precursors, Sox9-creERT2; R26RTomato; *Gsafi/fl* triple-transgenic mice (called floxed mice here) and Sox9-creERT2; R26RTomato; *Gsa*WT/WT mice (called WT mice here) received 2 mg tamoxifen intraperitoneally at P42 and received vehicle or PTH (100ng/g body weight) administration daily for 7 days. Knockdown of transcripts encoding *Gsa* was confirmed by FACS-sorted tdTomato+ cells from floxed mice 2 days after tamoxifen injection. TdTomato+ cells were counted blindly in pre-determined boxes in 12 sections from each of three tibiae per condition. In WT mice, PTH treatment significantly ($P < 0.05$) increased the number of tdTomato+ cells in metaphyseal (105.09 ± 15.61 vs. 23.09 ± 9.45) and cortical (39.95 ± 12.82 vs. 17.77 ± 4.30) bone of tibia when compared to vehicle. However, PTH could only increase the number of tdTomato+ cells in metaphyseal (58.29 ± 14.19 vs. 10.39 ± 0.59 , $P < 0.05$), but not in cortical bone (10.07 ± 8.50 vs. 12.20 ± 2.55), in mice with specific knockout of *Gsa*. The increase in tdTomato+ cells in the metaphysis of floxed mice was lower than the increase in the metaphysis of WT mice ($105.23.09 \pm 15.61$ vs. 58.29 ± 14.19 , $P < 0.05$). These findings indicate a role for *Gsa*-PKA-cAMP signaling in the PTH-mediated increase of Sox9-expressing osteoblast precursors.

Disclosures: *Mingxin Xu, None*

MON-0525

Quantitative analysis of juxta-articular osteoporosis by HR-pQCT in patients with rheumatoid arthritis Ko Chiba*¹, Kounosuke Watanabe¹, Oki Nozomi², Naoki Iwamoto³, Narihiro Okazaki¹, Atsushi Kawakami², Makoto Osaki¹. ¹Department of Orthopedic Surgery, Nagasaki University Graduate School of Biomedical Sciences, Japan, ²Department of Radiological Sciences, Nagasaki University Graduate School of Biomedical Sciences, Japan, ³naoki_iwa@hotmail.com, Japan

[PURPOSE] HR-pQCT is a high-resolution CT dedicated to human extremities with a voxel size of 61 μ m. It has been used for the study of osteoporosis and rheumatoid arthritis (RA) as well, enabling quantitative analysis of bone microstructure, bone erosion, and joint space. The purpose of this study is to investigate a correlation between bone deterioration (juxta-articular osteoporosis and erosion) and cartilage loss in patients with RA by HR-pQCT. [METHOD AND MATERIALS] Twenty patients with RA (70 \pm 8 years, 15 female, 5 male) participated in this study. The second and third MCP joints were scanned by HR-pQCT (XtremeCT II, Scanco Medical, Switzerland) at the voxel size of 61 μ m. The following parameters were measured semiautomatically using dedicated software (TRI/3D-BON, Ratoc System Engineering, Tokyo) based on previous studies (Burghardt AJ, et al. Ann Biomed Eng. 2013 / Yang H, et al. Int J Rheum Dis. 2017 / Chiba K, et al. Eular 2017). 1) bone microstructure of metacarpal head: volumetric bone mineral density (vBMD), trabecular thickness (Tb.Th), trabecular number (Tb.N), and structure model index (SMI), 2) total volume of erosions (ER-volume) on the metacarpal head, 3) Average joint space width (ave-JSW) of MCP joints [RESULTS] vBMD of the metacarpal head was 131.4 (54.3-263.5) mg/cm³, Tb.Th was 213.1 (166-329.3) μ m, Tb.N was 0.95 (0.69-1.50) /mm, and SMI was 1.68 (0.65-2.52). The total number of erosions was 31, and an average number of erosions on each metacarpal head was 0.9 (0-4). Total ER-volume on the metacarpal head was 1.96 (0-16.7) mm³. Ave-JSW of MCP joints was 1.47 (1.00-1.89) mm. Ave-JSW had significant correlations with vBMD, SMI and ER-volume ($R = 0.37, -0.40, -0.42, P < 0.05$). [CONCLUSION] Juxta-articular osteoporosis and bone erosion was correlated with cartilage loss in RA patients. Quantitative evaluation of total joint structure (joint space, bone microstructure, and erosion) by HR-pQCT would be useful for the pathophysiological research and drug development of RA.



Disclosures: *Ko Chiba, None*

MON-0526

The Therapeutic Effect of GPNMB in a Traumatically-Induced Osteoarthritic Model Bryson Cook*¹, Asaad Aladlaan¹, Matthew Desanto², Fayeza Safadi^{1,3}. ¹Musculoskeletal Research Group, NEOMED, United States, ²Musculoskeletal Research Group, United States, ³Akron Children's Hospital Research Institute, United States

Osteoarthritis is a severe joint disease that affects millions of people. At this time, the current treatment for osteoarthritis is total joint reconstruction surgery. GPNMB plays a key role in bone remodeling and bone growth. Data from our lab suggested that GPNMB is positive regulator of osteoblastogenesis and a negative regulator of osteoclastogenesis. Furthermore, the role of GPNMB in cartilage has not been investigated before. Here we present that damaged human cartilage has significantly higher levels of GPNMB compared to undamaged cartilage. In addition, human osteoarthritic chondrocytes treated with GPNMB showed a protective response to inflammation induced by IL1-beta. In this study, we examined whether recombinant GPNMB has an anti-inflammatory effect in a model of post-traumatic osteoarthritis. The destabilization of the medial meniscus (DMM) surgery in mice has been found to be an excellent model for studying post-traumatic osteoarthritis. We performed the DMM surgery on 21 C57/BL6 mice. These mice were divided into three intra-articular injection treatment groups consisting of a control, low dose GPNMB, and high dose GPNMB. Moderate to severe osteoarthritis develops around six to eight weeks with this model. Based on studies performed in our lab, we expected cartilage degeneration to be dramatically decreased in response to the therapeutic effects of GPNMB. A protective factor against osteoarthritis progression, GPNMB-injected mice had significantly reduced cartilage damage and OARS1 scores in comparison to the control group, proving GPNMB a promising therapy in lieu of total joint reconstruction. GPNMB-injected mice also had reduced expression of IL-6 and MMP13 but significantly increased expression of aggrecan in comparison to control mice. We also tested the effects of rGPNMB on chondrocytes pre-treated with IL1b and found that rGPNMB has anti-inflammatory effects over IL-1b response. The GPNMB response was mediated by the CD44 receptor. Taken together, GPNMB has a significant, therapeutic potential as anti-inflammatory, repair response for osteoarthritis.

Disclosures: *Bryson Cook, None*

MON-0527

CCL21 Promotes Post Knee Injury Inflammation and Osteoarthritis Progression In part via Inducing T-Cell Recruitment Bouchra Edderkouki*¹, Neha Mohindroo², Salma Khan³, Mohan Subburaman¹. ¹VALLHCS, LLU, United States, ²VALLHCS, United States, ³Loma Linda University, United States

Osteoarthritis (OA) is characterized by progressive cartilage loss, with resultant joint pain that worsens over time. T cells are responsible for activating cells of the monocytic lineage and have been predicted to play a key role in OA development since more than 50% of patients with OA have mononuclear cell infiltrates consisting of CD3+ T, CD4+ and CD8+ cells in the synovial membrane. In terms of molecular pathways involved in the pathogenesis of OA, a recent study has reported an increased expression of CCL21 in the destabilized joints of both young and old mice that went through medial meniscectomy destabilization (MMD). Furthermore, the findings that CCL21 and CXCL13, ligands for CCR7 and CXCR5, which are known markers of CD4+ and CD8+ cells, respectively, suggest CCL21 and CXCL13 may be involved in attracting these two T cell sub-populations to the injury site. To test a role for CCL21 and CXCL13 on OA development, we first evaluated the expression profile of these two chemokines in response to partial MMD in a rat knee injury model. Expression levels for both chemokines were increased by 6-fold compared sham

operated knees at 3 days post-surgery ($P < 0.01$). However, only Ccl21 mRNA levels were significantly elevated (3.5-fold) in MMD knees compared to sham operated knees at 4 weeks post-surgery ($P = 0.04$). These data suggest that CXCL13 is only involved in the first stages of OA development, while CCL21 is involved in both the early inflammation and the later stages of OA. We next assessed the infiltration of inflammatory cells post-MMD. A significant increase in the infiltration of CD4+ and CD8+ cells in the MMD knees was observed at 1 and 3 days post-surgery. MMD knees treated with the CCL21 neutralizing antibody caused a significant reduction in post-surgery inflammation. This was reflected by a reduction in the expression of the major inflammatory cytokine IL-6 as well as both T cell and B cell makers at three days post-surgery. In addition, there was a significant reduction in the expression of matrix metalloproteinase 13 (MMP13) but not MMP3. Based on our data, we conclude that chemokines such as CCL21 play an important role in mediating injury-induced inflammatory response and progression of OA by recruiting T-cells and promoting MMP13 expression.

Disclosures: Bouchra Edderkaoui, None

MON-0528

Cell Death and IL-1 β Release Induced by TI Particles Depends on Lysosomal Membrane Disruption Brian Fort*, Edward Greenfield, Givenchy Manzano, Alexander Rascoe, Matthew Hoffa, George DUBYAK. Case Western Reserve University, United States

Aseptic loosening is the major cause of revision surgeries and occurs when osteolysis is stimulated around the implant by pro-inflammatory cytokines including IL-1 β . Production of active IL-1 β in response to orthopedic wear particles depends on processing by the NLRP3 inflammasome which requires priming followed by activation. We found that pathogen associated molecular patterns (PAMPs) adherent to wear particles are necessary to prime the NLRP3 inflammasome. In contrast, in pre-primed macrophages, particles themselves are sufficient to activate the NLRP3 inflammasome and induce secretion of active IL-1 β . Particles themselves also induce cell death, kinetically preceding the release of active IL-1 β . Phagocytosis of particles is required to initiate both responses as the phagocytosis inhibitor cytochalasin blocks cell death and IL-1 β release. Lysosomal membrane destabilization is also critical as inhibition of lysosomal function with bafilomycin or chloroquine significantly abrogated the release of active IL-1 β and cell death in response to wear particles. The pan-cathepsin inhibitors Ca-074-Me or K777 also inhibit cell death and IL-1 β release indicating that cathepsin release from lysosomes is also a necessary step in the particle-induced response. Our results open the possibility of clinical intervention with lysosomal or cathepsin inhibitors to treat aseptic loosening as these drugs have better specificity and less in vivo toxicity than the phagocytosis inhibitors. Testing of these inhibitors in vivo in models of particle induced osteolysis is a key future direction.

Disclosures: Brian Fort, None

MON-0529

Circulating sclerostin is associated with preserved joint space in non-weight bearing joints in a population enriched for high Bone Mineral Density April Hartley*, Lavinia Paternoster, Aaron Murphy, Sarah Hardcastle, Jon H Tobias, Celia L Gregson. Bristol Medical School, University of Bristol, United Kingdom

Animal studies suggest Wnt signaling is a risk factor for osteoarthritis (OA) and that sclerostin, a Wnt inhibitor, may protect against cartilage degeneration. Hence we aimed to determine the association between plasma sclerostin levels and OA endophenotypes, ie. osteophytosis, joint space narrowing (JSN), in different joints. We analysed adults with unexplained generalized high BMD (Z -score > 3.2) and their unaffected relatives/spouses. Sclerostin levels were measured by ELISA immunoassay. Pelvis, bilateral knee and dominant hand radiographs were graded for osteophyte and JSN severity using an established atlas. Binary variables were generated for any osteophyte and JSN at four sites: either hip, either knee, the index distal interphalangeal (DIP) and the first carpometacarpal (CMC) joints. Associations between sclerostin and OA endophenotypes were assessed by logistic regression using generalized estimating equations to account for within-family correlation. Models were adjusted a priori for age & sex, then height & weight. 360 adults (231 with high BMD; 129 unaffected relatives/spouses) had hand radiographs (mean age 59.6 [SD 14.7] years; mean plasma sclerostin 83.1 [41.0] pmol/L [standard range 0–80 pmol/L]); 334 had knee and 295 hip radiographs. Before adjustment, sclerostin was positively associated with osteophytes in all joints assessed; age & sex adjustment attenuated associations, although sclerostin remained weakly associated with knee osteophytes (OR per SD increase in sclerostin = 1.28 [95%CI 0.99, 1.66], $p = 0.06$); however 95% CIs widened with further adjustment for height/weight. Regarding JSN, a strong inverse association was observed between sclerostin and CMC JSN (age & sex-adjusted OR = 0.68 [0.53, 0.87], $p = 0.002$) which persisted after adjustment for height/weight. A similar pattern was seen between sclerostin and bilateral hip JSN (0.65 [0.43, 0.98], $p = 0.042$), even after adjusting for height/weight. Associations between sclerostin and JSN measured at the knee and DIP joints were consistent, although 95% CIs were wider. In a population augmented by individuals with high BMD, we identified an inverse association between sclerostin and a measure of cartilage loss at the hips and thumb base; a common site for hand OA. Our findings highlight the importance of stratifying by endophenotypes in studies of OA, as these may be explained by differential aetiologies. Whether sclerostin is protective against cartilage loss warrants longitudinal evaluation.

Disclosures: April Hartley, None

MON-0530

Blood-Induced Bone Loss In A Mouse Model Of Hemophilic Arthropathy Is Prevented By Blocking The iRhom2/ADAM17/TNF α Pathway Coline Haxaire*¹, Narine Hakobyan², Tania Panellini¹, Camila Carballo¹, David McIlwain³, Tak W. Mak⁴, Suchitra Acharya⁵, Dan Li¹, Jackie Szymonifka¹, Scott Rodeo¹, Xiangqian Song⁵, Sébastien Monette⁶, Alok Srivastava⁷, Jane Salmon¹, Carl Blobel¹. ¹Hospital for Special Surgery at Weill Cornell Medicine, United States, ²Pediatric Hematology/Oncology, Rush University Medical Center, United States, ³Baxter Laboratory in Stem Cell Biology, Department of Microbiology and Immunology, Stanford University, United States, ⁴Campbell Family Institute for Breast Cancer Research, Princess Margaret Cancer Center, University Health Network, Canada, ⁵Pediatric Hematology/Oncology, Northwell Health, United States, ⁶Laboratory of Comparative Pathology, Memorial Sloan Kettering Cancer Center, The Rockefeller University, Weill Cornell Medicine, United States, ⁷Department of Hematology, Christian Medical College, India

A major manifestation of Hemophilia A, an X-linked bleeding disorder, is hemophilic arthropathy (HA), a debilitating degenerative joint disease that is caused by intraarticular bleeding. HA typically begins with hypertrophy of synovocytes with inflammation of the synovium and neovascularization, ultimately leading to arthropathy with cartilage destruction and erosion of the underlying bone. HA has features in common with inflammatory arthritides such as Rheumatoid arthritis (RA). The pro-inflammatory cytokine tumor necrosis factor α (TNF α) is a major target for treatment of RA, TNF α is synthesized as a membrane-anchored precursor that is released by the TNF α convertase (TACE, also referred to as ADAM17). We have recently uncovered a crucial role for TACE and its regulator, iRhom2, in the pathogenesis of inflammatory arthritis in mice. Since RA is caused, at least in part, by inappropriate release of TNF α , we hypothesized that iRhom2/TACE/TNF α also have pivotal roles in promoting HA. Here, we show that addition of blood or its components to macrophages activates iRhom2/ADAM17-dependent TNF α shedding, providing the premise to study the activation of this pathway by blood in the joint in vivo. For this, we studied hemophilic FVIII-deficient mice (F8-/- mice), which develop a hemarthrosis following needle puncture injury with synovial inflammation and significant osteopenia adjacent to the affected joint. Needle puncture-induced bleeding led to increased TNF α levels in the affected joint of F8-/- mice. Interestingly, treatment of punctured F8-/- mice with etanercept to block TNF α , or genetic inactivation of Tnfa (F8-/-/TNF α -/-) or iRhom2 (F8-/-/iRhom2-/-) reduced synovial inflammation after 2 weeks. Moreover, μ CT analysis showed that inactivation of TNF α and iRhom2 prevented the severe osteopenia observed in F8-/- mice punctured knee. TRAP staining and gene expression demonstrated that the bone loss in F8-/- mice was mainly due to a significant local increase in osteoclasts, absent in etanercept-treated F8-/-, TNF α -/-/F8-/- and iRhom2-/-/F8-/- mice. Taken together, our results suggest that blood entering the joint activates the iRhom2/ADAM17/TNF α pathway, thereby contributing to osteopenia and synovitis in mice. Therefore, this proinflammatory signaling pathway may provide an attractive new target to prevent osteoporosis and joint damage in HA patients.

Disclosures: Coline Haxaire, None

MON-0531

Vitamin D Status in Patients with Hip Dysplasia Undergoing Periacetabular Osteotomy and Its Influence on the Postoperative Results Taro Mawatari*¹, Kazuki Kitade¹, Shinya Kawahara¹, Satoshi Ikemura², Gen Matsui¹, Takahiro Iguchi¹, Hiroaki Mitsuyasu¹, Reima Sueda¹. ¹Hamanomachi Hospital, Japan, ²Kyushu University, Japan

Purpose: Vitamin D is widely known as an important factor for bone health and mineralization, while high prevalence of vitamin D deficiency is reported worldwide. Periacetabular osteotomy (PAO) is accepted as an effective treatment for hip dysplasia in young to middle-aged patients. The purpose of our study was to clarify the relationships between vitamin D levels and postoperative complications including ischio-pubic stress fracture or delayed union of the osteotomy sites. Methods: PAO was performed of 46 hips in 39 patients with symptomatic hip dysplasia and followed for more than 8 months after surgery. There were 3 men and 36 women, and the mean age of the patients at operation was 41.0 (16-59) and the mean body mass index (BMI) was 21.5 (15.8-29.3). All surgeries were performed by a transtrochanteric approach. Partial and full weight-bearing started two and five weeks after operation, respectively. Diagnosis of postoperative ischio-pubic stress fracture or delayed union of the osteotomy sites were evaluated by symptoms and radiographs. A correlation between postoperative complications and age at surgery, BMI, smoking, preoperative center-edge angle, and serum 25-hydroxyvitamin D (25(OH)D) levels were explored. This study was approved by institutional review board. Results: Ischio-pubic stress fracture and delayed union of the greater trochanter osteotomy site occurred in 3 (6.5%) and 5 (10.9%) patients, respectively, while no delayed union were seen at pelvic osteotomy site. Average serum 25(OH)D concentrations was very low (11.9 ng/mL, 6-23) and most of the patients were vitamin D deficient (serum 25(OH)D < 20 ng/mL, 92.3%), and none of them were sufficient. A multivariate analysis demonstrated that serum 25(OH)D < 9 ng/mL and smoking were significantly associated with ischio-pubic stress fracture, and only serum 25(OH)D < 11 ng/mL with delayed union of greater trochanter. Conclusions: A very high prevalence of vitamin D deficiency was revealed in these relatively young patients undergoing PAO. Although development of nonunion or fatigue fracture may be multifactorial complications, our study suggests that severe vitamin D deficiency such as serum 25(OH)D < 11 ng/mL

may have negative impact on bone remodeling and healing and result in worse outcomes in patients undergoing PAO although it is still unclear whether vitamin D supplementation may improve the results of not.

Disclosures: Taro Mawatari, None

MON-0532

Chronic Antibiotic Use Pre-Injury Reduces Severity of Post-Traumatic Osteoarthritis on ACL rupture STR/ort Mouse Models Melanie Mendez^{*1}, Deepa Muruges², Jillian Mccool¹, Edward Kuhn², Allison Hsia³, Blaine Christiansen³, Gabriela Loots⁴. ¹University of California-Merced, Lawrence Livermore National Laboratory, United States, ²Lawrence Livermore National Laboratory, United States, ³University of California-Davis, United States, ⁴Lawrence Livermore National Laboratory, University of California-Merced, United States

The gut microbiota has a key role in human physiology, one of its most important functions involves immunoregulation. It gives positive protective activation to the immune system by constantly releasing microbial associated molecular patterns (MAMPs) that help naïve immune cells mature. Perturbations to the gut microbiome are linked to changes in bone mass, fracture healing, and susceptibility to inflammation. Post-traumatic osteoarthritis (PTOA) develops in ~50% of people who suffered a severe joint injury such as anterior cruciate ligament (ACL) rupture. Although PTOA is not classified as an inflammatory disease, it has been suggested that inflammation could be one of the contributing factors to the initiation and progression of PTOA. To determine the role of the gut microbiome on the severity of PTOA we examined post-injury joint degeneration in STR/ort mice, a strain known to develop OA spontaneously due to systemic high levels of inflammatory cytokines. We treated mice with oral antibiotics [ampicillin (1000mg/L); neomycin (500mg/L)] in the drinking water starting at 4 weeks of age, continuously for a six week period prior to injury at 10 weeks of age. Antibiotic treatment efficacy was monitored by qualitatively using the Lawrence Livermore Microbial Detection array and quantitatively via 16s ribosomal RNA (rRNA) sequencing which combined assessed bacterial diversity and abundance in fecal samples, collected weekly. Antibiotic treatment was stopped immediately prior to injury. The right knee of each mouse was injured using a single non-invasive tibial compression overload to induce ACL rupture. Injured and contralateral joints were analyzed at 6 weeks post injury using micro-computed tomography and histology. Both uninjured and injured STR/ort mice treated with antibiotics had thicker articular cartilage than the untreated groups, suggesting lower chondrocyte apoptosis in the antibiotic treated mice. Treated mice also showed reduced cellular infiltration in the synovium than untreated groups, indicative of a reduced inflammatory response in the mice treated with antibiotics. There was also a statistically significant reduction in osteophyte formation in these mice. These data suggest that the gut biome composition can dramatically impact PTOA outcomes, and that antibiotic treatment prior to injury reduces the overall systemic inflammation in STR/ort mice and improves PTOA outcomes.

Disclosures: Melanie Mendez, None

MON-0533

An ectosteric tanshinone inhibitor of cathepsin K prevents the progression of joint inflammation and destruction in an arthritis mouse model Preety Panwar^{*}, Dieter Bromme. University of British Columbia, Canada

Cathepsin K (CatK) is a validated drug target for musculoskeletal diseases. Active site-directed inhibitors of CatK have demonstrated efficacy in osteoporosis and osteoarthritis human clinical trials but were never approved due to significant safety concerns. Side effects were likely caused by on-target effects due to the inhibition of the entire activity of this multifunctional protease. To avoid side effects, we developed the ectosteric inhibitor concept that specifically allows blocking the disease relevant collagenase activity of CatK. Using the collagen-induced arthritis (CIA) mouse model, we demonstrated that the orally applied ectosteric CatK inhibitor tanshinone IIA sulfonate (T06) effectively reduced joint inflammation and erosion. T06 markedly inhibited cartilage degradation and also had significant effects on bone destruction and pannus formation. Serum biochemical assays confirmed that T06 reduced collagen I and II degradation markers and prevented the expression of various inflammatory markers such as TNF α , IL-6, and IL-1 β . No systemic toxicological effects were observed. In contrast, odanacatib, a highly potent active site-directed CatK inhibitor, had a weaker effect on inflammation and joint preservation. Moreover, odanacatib had no significant effect on the inflammatory cytokines and careful histological tissue examination revealed fibrotic alterations in several organs, which also reflected some of the safety issue in the clinical trials. The T06 treatment did not show any of these adverse effects. These data support that T06 inhibits immune-receptor signalling, has direct anti-resorptive activity, and suggest that T06 might represent a promising therapeutic drug for patients with rheumatoid arthritis and warrants further investigation.

Disclosures: Preety Panwar, None

MON-0534

Synovial B-cell infiltration as a novel candidate mediator of OA in obese mice and humans Eric Schott^{*1}, Jacquelyn Lillis¹, Christopher Farnsworth², Javier Rangel-Moreno¹, John Ketz¹, Douglas Adams³, Jennifer Anolik¹, Cheryl Ackert-Bicknell¹, Robert Mooney¹, Michael Zuscik¹. ¹University of Rochester School of Medicine and Dentistry, United States, ²Washington University in St. Louis, United States, ³University of Connecticut, United States

Obesity is a major risk factor for osteoarthritis (OA), a disease that currently afflicts 31M Americans and has no accepted disease modifying treatment. Recent studies implicate a primary role for immune cell infiltration and corresponding inflammation of the synovial membrane in disease pathogenesis. These findings led us to hypothesize that in the OA of obesity, the synovium is the primary driver of accelerated cartilage and joint degeneration. To test this hypothesis, we performed a transcriptomic analysis of synovial tissue from lean and obese mice at a time point that precedes any evidence of cartilage degeneration. Starting at 5 weeks of age, male C57BL/6J mice were fed a low fat or high fat diet for 16 weeks, at which point the synovial membrane was removed for RNA isolation and sequencing. Significantly differentially expressed genes were then analyzed using CTen and Ingenuity Pathway Analysis (IPA) to identify enriched cell types, canonical pathways, and diseases and functions. These analysis tools identified a significant induction of inflammation in the obese synovium compared to lean, despite an absence of histologic evidence of joint pathology under either condition. Cell type enrichment analysis identified the macrophage as a significant mediator of early synovial pathobiology, correlating with pathway analysis identifying significant induction of inflammatory pathways including NF- κ B, macrophage activation, and joint inflammation. Notably, the RNAseq identified the B-cell as a candidate mediator of early disease. Cell type enrichment analysis revealed a significant B-cell signature in the obese synovium, correlating with activation of canonical pathways and diseases and functions related to the B-cell. Flow cytometric analysis revealed increased abundance of B-cells in the obese synovium, confirming the RNAseq results. Suggesting that this B-cell phenotype is present in obese humans, synovium from low (<27, N=6) and high (>27, N=10) BMI total knee replacement patients revealed significant increases in the number (p<0.0001) and size (p<0.001) of ectopic lymphoid structures that contained B20+ cells in the high BMI group. In conclusion, synovial pathobiological change occurs well before evidence of joint degeneration is discernable, with both murine and human data supporting a potentially pathogenic role of the B-cell in the OA of obesity.

Disclosures: Eric Schott, None

MON-0535

Blocking Transforming Growth Factor- β 1 By Oral Intake Of Losartan Can Improve Microfracture-Mediated Cartilage Healing- A Rabbit Model Hajime Utsunomiya^{*1}, Xueqin Gao², Zhenhan Deng², Gilberto Nakama¹, Haizi Cheng², Sudheer Ravuri¹, Julia Goldman², Tamara Alliston³, Walter Lowe², William Rodkey¹, Marc J Philippon¹, Johnny Huard¹. ¹Steadman Philippon Research Institute, United States, ²University of Texas Health, United States, ³University of California San Francisco, United States

Background: Microfracture is often the first choice for clinical treatment of cartilage injuries; however, fibrocartilage, not pure hyaline cartilage, has been reported to develop after microfracture surgery. Transforming growth factor (TGF)- β 1, which can result in fibrosis, can be inhibited by losartan. Hypothesis: We hypothesized that blocking TGF- β 1 would improve cartilage healing in a rabbit knee microfracture model by decreasing the amount of fibrocartilage formation and increasing hyaline-like cartilage formation. Study Design: Controlled laboratory study. Methods: An osteochondral defect (diameter: 5 mm, depth: 2 mm) was made in the patellar groove of 21 New Zealand White rabbits. The rabbits were divided into three groups (N=7/group) randomly, a control group (defect only, group 1), a microfracture group (osteochondral defect + microfracture, group 2), and a losartan-treated group (osteochondral defect + microfracture + losartan, group 3). Microfracture was performed using a 0.7-mm burr with a 2-mm depth. For the rabbits in group 3, losartan was administered orally from the day after surgery through the day of euthanasia. Rabbits were sacrificed 6 week postoperatively. Macroscopic appearance, microcomputed tomography (microCT) and histological assessment were evaluated. Results: At 6 weeks after surgery, group 3 scored highest in the International Cartilage Repair Society (ICRS) macroscopic assessment (mean[SD], group 1: 7.9 [1.9], group 2: 6.9 [2.7], group 3: 9.0 [1.0], p < 0.05). MicroCT showed healing of the bony defect in group 3, in comparison to no healing in group 1 and partial healing in group 2. Histologically, the results obtained using the Modified O'Driscoll ICRS grading system yielded significantly superior scores in group 3 compared to both group 1 and 2 (group 1: 23.3 [7.2], group 2: 28.0 [1.4], group 3: 33.0 [2.0]). Conclusion: On blocking TGF- β 1 with losartan, the healed tissue after microfracture was more similar to that of normal hyaline cartilage than that obtained without blocking TGF- β 1. These results are encouraging for the clinical application of losartan in microfracture for the repair of chondral defects. Clinical relevance: TGF- β 1 has been believed to be essential for the homeostasis of the articular cartilage. The current results demonstrate that an optimal expression of TGF- β 1 is also required for the healthy joint cartilage, and losartan can provide a less fibrotic healing of cartilage after microfracture surgery.

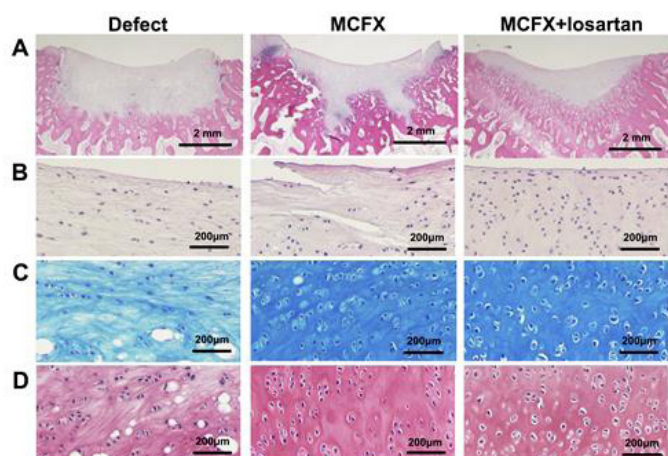


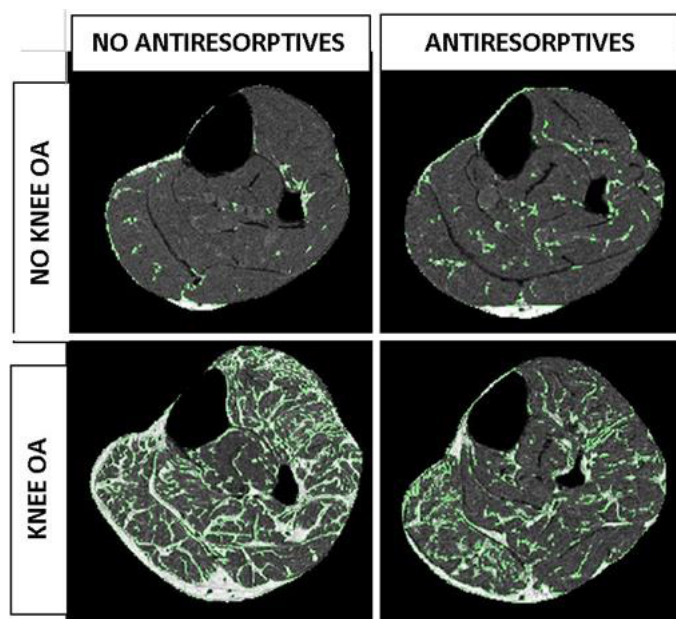
Figure: Histology findings at 6 weeks after surgery. A: Hematoxylin&Eosin (HE) staining (20x). B: HE staining (100x). C: Alcian blue staining. D: Safranin O staining. The defect only group showed poor quality of repaired cartilage. Repaired cartilage in the microfracture (MCFX) group revealed fibrocartilage healing. The MCFX + losartan group showed hyaline-like cartilage healing with plenty of collagen matrix.

Disclosures: Hajime Utsunomiya, None

MON-0536

Conditional Bone and Muscle Correlates of Osteoarthritis Influenced by Use of Antiresorptive Therapy in Postmenopausal Women– the AMBERS study Andy Kin On Wong^{*1}, Shannon Reitsma², Hana Gillick², Abinaa Chandrakumar³, Eva Szabo³, Justin Chee³, Angela M Cheung³, Jonathan D Adachi². ¹Joint Department of Medical Imaging, University Health Network, Canada, ²Department of Medicine, McMaster University, Canada, ³CESHA, University Health Network, Canada

Previous trials have shown mixed effects of antiresorptive therapy on osteoarthritis (OA). Understanding ways antiresorptives could influence bone and muscle properties in OA could help delineate pathways or patient groups to target. Objective: to determine the effect of bone and muscle properties on knee OA (KOA) in those who have or have not used antiresorptives. 312 women 60-85 yrs old from the Appendicular Muscle and Bone Extension Research Study (AMBERS) completed baseline imaging and annual follow-up of fractures, falls, and frailty for 3 years. This study is a cross-sectional analysis of baseline data for women 76-85 yrs old (N=170). Peripheral QCT (pQCT) and MRI scans of the mid-leg (66% site) measured muscle density and % inter- and intramuscular fat (%IMF). 4% distal tibia pQCT scans quantified bone density and microarchitecture. Total hip and lumbar spine DXAs were converted to T-scores. OA and KOA were self-reported. Antiresorptive use over the last 5 years was captured. General linear models compared muscle and bone properties between antiresorptive users and non-users among those with OA or KOA. Binary logistic regression examined the effect of bone and muscle properties on OA or KOA conditional on use of antiresorptive therapy. Among 170 women (age: 80±3yrs, BMI: 29.1±5.5kg/m²) in whom 63 had OA and 37 KOA, 39.7% and 32.4% used antiresorptives within the last 5 years, respectively. Antiresorptive use was associated with thinner trabeculae after adjusting for lowest BMD T-score (p=0.048) among those with OA, and lower BV/TV (p=0.004), vBMDtr (p=0.050), and larger Tb.Sp (p=0.005) in those with KOA. Antiresorptive therapy showed marginally significant interaction effects with Tb.Sp (p=0.063) and BV/TV (p=0.085) on associations with KOA, with apparent associations shown only when antiresorptives were not used. Conversely in models examining muscle interaction effects (p-interaction=0.041), having a higher %IMF was associated with KOA when antiresorptives were used (OR: 4.10(1.26,13.37)) but was not associated with KOA when not used (OR: 0.95(0.53,1.70)). Use of antiresorptive therapy is associated with less dense and thinner trabeculae in OA patients after accounting for confounding by indication. The differential effects of bone and muscle on OA conditional on antiresorptive therapy could be explained by potential resolution of bone abnormalities in OA, but exposing a residual impact of muscle adiposity on OA.



Disclosures: Andy Kin On Wong, None

MON-0577

Dephosphorylation of NACA by PP1A enhances c-JUN transcriptional activity William N. Addison^{*}, Martin Pellicelli, René St-Arnaud. Shriners Hospitals for Children - Canada, Canada

The transcriptional cofactor NACA (nascent polypeptide-associated complex and co-regulator alpha, α NAC) is a critical regulator of osteoblast maturation and activity. NACA functions, at least in part, by binding to the AP-1 transcription factor c-JUN and potentiating the transactivation of AP-1 targets such as Osteocalcin and Mmp9. Knock-in mice deficient in nuclear NACA exhibit a significant reduction in bone formation leading to a marked reduction in bone mass. The activity of NACA is mediated by multiple post-translational modifications including phosphorylation. Although several kinases have been shown to phosphorylate NACA, a phosphatase capable of dephosphorylating NACA has not yet been identified. In this study, we utilized an affinity purification approach combined with mass spectrometry to purify NACA protein complexes from HEK293T cells and identified the serine-threonine protein phosphatase PP1A as a novel NACA-associated phosphatase. Notably, we found that NACA was associated with multiple components of the PP1A holoenzyme complex including the catalytic subunit, PPP1CA as well as the regulatory subunits PPP1R9B, PPP1R12A and PPP1R18. Independent immunoprecipitation assays confirmed that NACA interacts with endogenous PPP1CA in MC3T3-E1 osteoblast cells. Consistent with this, in vitro dephosphorylation of NACA with recombinant PP1A resulted in a faster migrating hypo-phosphorylated form of NACA. By mass spectrometry analysis, we also demonstrated that co-expression of NACA with PPP1CA in HEK293T cells leads to dephosphorylation of NACA at residues Thr89, Ser151, Ser166 and Thr174. Moreover, NACA dephosphorylation was correlated with the recruitment of novel NACA interactants. PP1A-dephosphorylated NACA, but not phosphorylated NACA, interacts with the basic transcription factor BTF3 and its homologue BTF3L4. In addition, promoter studies showed that NACA and PP1A could synergistically potentiate c-JUN transcriptional activity on the AP-1-responsive Mmp9-luciferase reporter. This synergy was abolished when Thr89, Ser151 or Ser166 were mutated into phosphatase-resistant phosphomimetic aspartate residues. Collectively, these data suggest that PP1A dephosphorylates NACA at specific residues, which leads to recruitment of novel NACA interactants such as BTF3 to ultimately regulate c-JUN transcriptional activity. This unique transcriptional regulatory mechanism advances our understanding of NACA in the regulation of osteoblast gene expression.

Disclosures: William N. Addison, None

MON-0578

miR-219a-5p Regulates Ror β During Osteoblast Differentiation and in Age-related Bone Loss Ruben Aquino-Martinez^{*}, David Monroe. MAYO CLINIC, United States

Osteoporosis and increased fracture risk in the aging population is correlated with deterioration in quality of life and loss of autonomy. To improve upon the limited efficacy of current clinical therapies, we investigated new molecular targets to stimulate bone accrual. We have reported that retinoic acid receptor-related orphan receptor beta (Ror β) is upregulated in bone marrow-derived osteoprogenitor cells and in osteocytic bone fractions isolated from aged mice and humans, that Ror β expression is inhibited during osteoblastic differentiation,

and that deletion of *Rorb* in mice results in preservation of bone during aging. Collectively, these data suggest that *Rorb* is an inhibitor of osteogenesis and that proper control of *Rorb* expression is essential for bone homeostasis. Here, we investigated the interaction between *Rorb* and a specific subset of microRNAs (miRs) to establish their roles in osteoblast differentiation and in the context of aging. We used the miR target prediction database TargetScan to identify a subset of miRs as potentially *Rorb*-regulating. To determine any potential involvement of these miRs in the regulation of *Rorb* levels, MC3T3-E1 mouse osteoblastic cells were differentiated and assayed for *Rorb* and miR expression. As *Rorb* levels declined with differentiation, the expression of multiple miRs was upregulated, suggesting possible involvement in the suppression of *Rorb*. We also demonstrated that miR-219a-5p was down-regulated ($p < 0.001$) in osteocytic bone fractions from old mice, concomitant with increased *Rorb* expression. We further showed that miR-219a-5p directly suppressed *Rorb* and that miR-219a-5p inhibition using a lentiviral antagomir vector in MC3T3 cells (resulting in ~90% inhibition) led to increased *Rorb* expression and impairment in osteoblastic differentiation. RNA sequencing analysis further confirmed that pathways involved in osteoblast function (i.e. extracellular matrix, calcium signaling, adhesion and Wnt signaling) were dys-regulated in miR-219a-5p inhibited cells. Our findings thus demonstrate that miR-219a-5p is involved in the regulation of both *Rorb* and differentiation-related pathway in osteoblasts, suggesting that miR-219a-5p mimics may be useful tools to stimulate bone formation.

Disclosures: *Ruben Aquino-Martinez, None*

MON-0579

Blastema formation and periosteal ossification in the regenerating adult mouse digit. Lindsay A. Dawson*, Connor Dolan, Felisha Imholt, Osama Qureshi, Katherine Zimmel, Ken Muneoka. Texas A&M University, United States

Purpose: Mammalian regeneration in response to amputation is restricted to the distal digit tip, the terminal phalanx (P3). Successful regeneration in the mouse is amputation-level dependent; amputations nearing the epiphysis of P3 fail to stimulate regeneration, instead culminating in bone truncation and associated scar formation. What distinguishes regeneration from scar formation is the formation of the blastema, defined as a heterogeneous population of proliferating cells that function to regenerate the amputated structures. We used the amputation-level dependent regeneration response to investigate blastema formation and associated bone regeneration. We report that blastema cells associated with the periosteum and endosteal/marrow regions are stimulated to undergo ossification in endogenous regeneration, and the periosteum is required for bone regeneration distal to the amputation plane. Methods: Regenerative (distal) and non-regenerative (proximal) amputations were performed on adult, female, 8-week-old CD-1 mice. The periosteal tissue was surgically removed prior to amputation, with sham operated digits analyzed in parallel. Bone regeneration was quantified using Micro-computed tomography (μ CT) and digits were assayed via histology and immunohistochemistry. Results: In response to distal amputation, sequential μ CT analysis demonstrated P3 regeneration is characterized by restoration of amputated skeletal length and enhanced bone volume associated with the periosteal compartment. Conversely, proximal amputation does not induce bone length regeneration but intriguingly results in enhanced bone volume associated with the endosteal/marrow compartment. Analysis of distal amputations revealed blastema formation is characterized by proliferation and osteogenesis initially compartmentalized to the periosteal and endosteal/marrow regions. In contrast, proximal amputation induces proliferating osteoblasts restricted to the endosteal/marrow region, and distal fibrotic tissue formation. P3 digits lacking periosteum showed attenuated bone length and volume regeneration compared to sham operated control digits. Discussion: The non-regenerative proximal amputation is associated with a blastema-like structure restricted to the endosteal/marrow region. These findings identify the periosteum as a therapeutic target for designing strategies to enhance mammalian regeneration.

Disclosures: *Lindsay A. Dawson, None*

MON-0580

CALM1 and GARS: novel biomarkers to diagnose Pseudarthrosis Thaqif El Khassawna*, Stefanie Kern¹, Deeksha Malhan¹, Markus Rupp², Christian Heiss². ¹Institute for Experimental Trauma Surgery, Faculty of Medicine, Justus Liebig University of Giessen, Germany, ²Department of Trauma, Hand, and Reconstructive Surgery, University Hospital of Giessen and Marburg, Germany

Fracture non-union (or pseudarthrosis) is a critical problem in pre-clinical as well as clinical research. Decreased osteoblasts, increased fibroblasts, impaired vascularization, and bone matrix alterations results in the pathogenesis of pseudarthrosis. Bone morphogenetic proteins (BMP) are commonly used in clinic to treat pseudarthrosis. But BMP's also increase fibroblast cell types along with osteoblasts resulting in severe complications. Our study aimed to identify the potential biomarkers using Mass spectrometry (MS) approach to diagnose pseudarthrosis. Human reaming debris were used to harvest mesenchymal stem cells (MSCs) and fibroblasts and then osteogenic differentiation were carried out using BMP-2 stimulation. Nano-HPLC-ESI-MS/MS were carried out to extract, digest, and purify proteins. Post-normalization and analysis, differentially expressed proteins were obtained using fold change (FC) = |2| and $p \leq 0.01$. Additionally, RNA was isolated from obtained cells and relative gene expression were measured. Immunostainings of biomarkers on human pseudarthrotic samples and previously established NfI Prx1 mouse model were carried out for validation. MS analysis showed 193 common proteins between

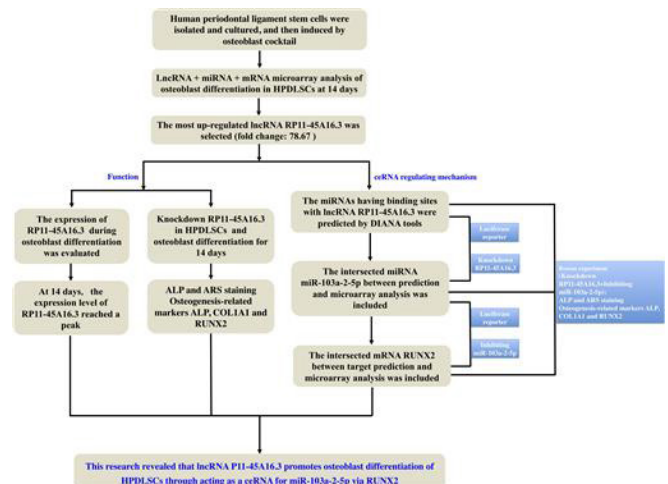
osteogenic differentiated MSCs and fibroblasts out of 2470 total proteins prior to filtering. Collagen-alpha-2(I)-chain, Calmodulin-1 (CALM1) and Glycine-tRNA-synthetase (GARS) were significantly down-regulated in osteogenic differentiated fibroblasts when compared with differentiated MSCs. This downregulation indicates the pathogenesis of Pseudarthrosis. Previous studies reported the incidence of metastasis and cell cycle abnormalities in GARS knock-down model. Bone mass is maintained by CALM1 and its downregulation directs to the impaired healing. Intriguingly, relative gene expression showed similar downregulation of CALM1 and GARS. Further, immunostainings of CALM1 and GARS showed relatively lower signal in human and NfI Prx1 samples. Taken together, MS-based approach showed higher potential in disease diagnosis and biomarker discovery. Further, targeted upregulation of CALM1 and GARS can help in the treatment of pseudarthrosis. Establishing a correlation between biomarkers discrepancies in the tissue and their serum level concentration can provide information about the healing status of surgically revised non-unions. Cell-specific molecular analysis of pseudarthrotic tissue is the main outlook of the study.

Disclosures: *Thaqif El Khassawna, None*

MON-0581

Long Non-coding RNA RP11-45A16.3 Promotes Osteoblast Differentiation of Human Periodontal Ligament Stem Cells via Runt-Related Transcription Factor 2 by Sponging miR-103a-2-5p Fuchun Fang*^{1,2}, Jianjia Li², Qisheng Tu¹, Jake Chen^{1,3}. ¹Division of Oral Biology, Tufts University School of Dental Medicine, Boston, MA 02111, USA, American Samoa, ²Department of Stomatology of Nanfang Hospital, Southern Medical University, Guangzhou 510515, China, ³Department of Cellular, Molecular and Developmental Biology, Tufts University School of Medicine, Boston, MA 02111, USA, American Samoa

Background: The great potential for differentiation into osteoblasts showed in human periodontal ligament stem cells (HPDLSCs) might make them a promising therapeutic option for periodontal tissue regeneration. Recently, long non-coding RNAs (lncRNAs) were reported to function as a competitive endogenous RNAs (ceRNAs) to regulate the effect of microRNAs (miRNAs) on their target genes. However, the molecular mechanism how (whether) lncRNAs regulates the osteoblast differentiation of HPDLSCs still remains poorly understood. Materials and Methods: Expression patterns of lncRNA, miRNA and messenger RNA (mRNA) during osteoblast differentiation of HPDLSCs at 14 days were profiled using microarray analysis. The function and regulating mechanism of RP11-45A16.3, as the most up-regulated lncRNA (fold change: 78.67), were investigated. First, the expression of lncRNA RP11-45A16.3 and miR-103a-2-5p in HPDLSCs cultured with or without an osteoblast inductive cocktail was explored using qRT-PCR. The recombinant lentiviral vectors knocking down RP11-45A16.3 or inhibiting miR-103a-2-5p were constructed and transfected into HPDLSCs to regulate their endogenous expression. The mineralized nodules formation and the expressions of ALP, COL1A1, RUNX2 expressions were used as specific markers for osteogenesis. Results: RP11-45A16.3 was up-regulated during osteoblast differentiation of HPDLSCs. Knockdown of RP11-45A16.3 suppressed osteoblast differentiation of HPDLSCs. The expression level of miR-103a-2-5p decreased during osteoblast process and inhibiting miR-103a-2-5p promoted osteoblast differentiation. Luciferase reporter assays revealed that RP11-45A16.3 had binding sites with miR-103a-2-5p, and RP11-45A16.3 knockdown increased miR-103a-2-5p expression level, demonstrating that RP11-45A16.3 may act as a ceRNA for miR-103a-2-5p. Luciferase reporter assays also demonstrated that miR-103a-2-5p could target RUNX2. Inhibiting miR-103a-2-5p led to an increased RUNX2 expression during osteoblast differentiation. Moreover, RP11-45A16.3 knockdown resulted in a decreased RUNX2 expression, which could be partly rescued by inhibiting miR-103a-2-5p. In addition, reduced osteoblastogenesis resulting from RP11-45A16.3 knockdown was partly rescued by miR-103a-2-5p inhibition. Conclusions: This research revealed that lncRNA P11-45A16.3 promotes osteoblast differentiation of HPDLSCs through acting as a ceRNA to sponge miR-103a-2-5p molecules enhancing RUNX2 signal pathway.



Disclosures: *Fuchun Fang, None*

MON-0582

Grainyhead-like 3 Mediates BMP and Wnt Signaling in Skeletal Stem Cells during Bone Formation and Repair

Laura Gamer*, Valerie Salazar, David Maridas, Vicki Rosen. Harvard School of Dental Medicine, United States

While there is general agreement that BMPs and Wnts are fundamental regulators of bone formation and bone repair, aspects of osteoblast specification and function controlled by either pathway remain largely undefined. Previously, we identified Grainyhead-like 3 (Grhl3), a transcription factor with critical roles in epithelial tissues, as a new mediator of both BMP and Wnt signaling during osteoblast differentiation using bone marrow stromal cells. To examine the connection between Grhl3 and signaling pathways that mediate osteoblast physiology, we first defined Grhl3 expression during limb development using *in situ* hybridization. Grhl3 transcripts are present in the perichondrium of nascent bones at E14.5, where the Grhl3 expression domain overlaps with Lrp5 and Bmp2. At E16.5, Grhl3 is expressed by hypertrophic chondrocytes, bone collar cells and subchondral bone. After birth, Grhl3 localizes to the periosteum and nascent trabecular bone. To verify a connection between Grhl3 expression and function, we obtained mice carrying a conditional allele for Grhl3 and crossed them with the Prx1-cre deleter mice to remove Grhl3 from skeletal stem cells. Grhl3 cKO mice have normal skeletons at birth with no obvious defects in size or shape of individual limb skeletal elements. Strikingly, at 2 weeks of age, Grhl3 cKO mice have a profound deficit in postnatal bone formation that affects both the cancellous and cortical bone compartments and results in Grhl3 cKO mice lagging behind control littermates in the acquisition of bone mass. To gain information on the potential importance of Grhl3 in the adult skeleton, we looked for Grhl3 expression after femur fracture and found a substantial increase 5 days after fracture, consistent with a regulatory function for this factor in skeletal stem cell differentiation. Our findings suggest a potential role for Grhl3 as a node that coordinates inputs from the BMP and Wnt pathways on cells of the osteoblast lineage. Future studies are aimed at understanding if Grhl3 is a key determinant of bone mass acquisition and fracture repair in the postnatal skeleton.

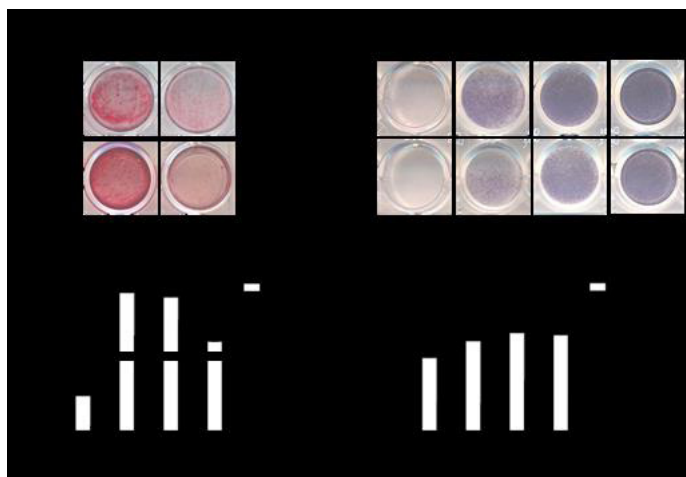
Disclosures: *Laura Gamer, None*

MON-0583

MACF1 Promotes Osteoblast Differentiation by Sequestering Repressors of Wnt Signaling

Lifang Hu*, Chong Yin, Zixiang Wu, Zizhan Huang, Airong Qian. Laboratory for Bone Metabolism, Key Laboratory for Space Biosciences and Biotechnology, School of Life Sciences, Northwestern Polytechnical University, China

Microtubule actin crosslinking factor 1 (MACF1), a versatile cytoskeletal crosslinker, has been shown to promote osteoblast differentiation by our previous study. The underlying mechanism of MACF1 promoting osteoblast differentiation is still unclear. Here we aimed to clarify the mechanism of MACF1 regulating osteoblast differentiation by adopting MACF1-knockdown (MACF1-KD) MC3T3-E1 cells, based on the previous study. We found that MACF1 knockdown suppressed mineralization and ALP activity, and impaired the osteogenic genes³ expression during osteoblast differentiation (Figure 1). RNA sequencing (RNA-seq) and gene ontology analyses revealed that MACF1 knockdown affected the expression of genes that linked to the Wnt, Hippo, or PI3K-AKT pathways, all involved in osteoblast differentiation. Further cluster analysis demonstrated that MACF1 knockdown significantly downregulated key transcription factors of Wnt signaling, especially T-cell factor 7 (TCF7) and lymphoid enhancer-binding factor 1 (LEF1). Real time PCR and western blot confirmed the decrease in both expressions and activities of TCF7 and LEF1 in MACF1-KD cells. As the activation of Wnt signaling promotes osteoblast differentiation via TCF7 and LEF1, we further investigated how MACF1 regulated the expression of the transcription factors. Chromatin immunoprecipitation sequencing (ChIP-seq) analyses displayed the enrichment of MACF1 binding at the promoter sites in MACF1-KD cells and gene ontology analyses revealed that Wnt signaling pathway was highly affected. In addition, two transcription factors, TCF12 and E2F6, were identified to be regulated by MACF1. The functional analyses showed that knockdown of TCF12 and E2F6 promoted osteoblast differentiation and Wnt signaling, indicating them as repressors of Wnt signaling. Thus, we proposed that MACF1 promoted osteoblast differentiation through sequestering TCF12 and E2F6, and preventing them translocate into nucleus, thus enhancing the expression of active transcription factors of Wnt signaling (e.g. TCF7). The luciferase reporter assay further confirmed that MACF1 regulated the balance between active (TCF7) and repressive transcription factors (TCF12) to regulate the Wnt signaling and osteoblast differentiation. Taken together, these findings suggest that MACF1 promotes osteoblast differentiation by sequestering repressors of Wnt signaling. This study uncovers a new mechanistic insight of MACF1 regulating osteoblast differentiation.



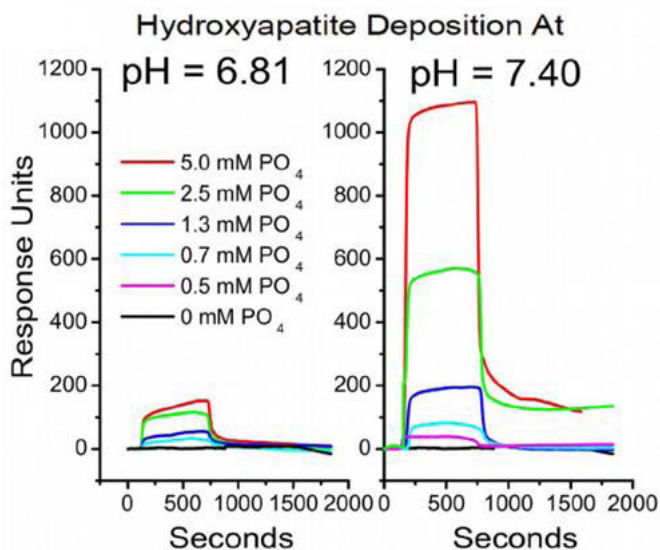
Disclosures: *Lifang Hu, None*

MON-0584

How Acid Transport Supports Formation of Dense Bone Mineral

Quitterie C Larrouette*, Harry C Blair², Irina L Tourkova³, Jing H Bian³, Li Liu³, Donna Beer Stolz⁴, Deborah J Nelson⁵, Paul H Schlesinger⁶. ¹Nuffield Department of Orthopaedics, Rheumatology and Musculoskeletal Sciences, Botnar Research Centre, Oxford University, United Kingdom, ²Veteran's Affairs Medical Center and Department of Pathology, University of Pittsburgh, United States, ³Department of Pathology, University of Pittsburgh, United States, ⁴Department of Cell Biology, University of Pittsburgh, United States, ⁵Department of Pharmacological and Physiological Sciences, University of Chicago, United States, ⁶Department of Cell Biology, Washington University, United States

Osteoblasts secrete collagen I and isolate the bone-matrix from extracellular space. In the matrix, alkaline phosphatase generates phosphate that combines with available calcium to form bone mineral. Amorphous calcium phosphate crystals form on the collagen template, but must be matured into a stable hydroxyapatite-collagen composite, this process liberates eight protons for each ten calcium atoms deposited. This proton load must be removed from the mineralizing bone matrix. However, pH dependent hydroxyapatite deposition in bone collagen had not been demonstrated. Directly to address this, we determined pH and phosphate dependency of hydroxyapatite deposition on type I collagen by surface plasmon resonance in 0-5 mM phosphate with 1 mM calcium at pH 6.94-7.6. Mineral deposition was sensitive to phosphate concentration but was saturated by <1 mM Ca⁺⁺. Initial mineral deposition was rapidly reversible consistent with amorphous precipitation but more stable deposition appeared with time and required EDTA removal. Importantly, at pH 6.94 little hydroxyapatite deposited on collagen, but mineral accumulation increased 10 fold at pH 7.4 (Figure). Previously we demonstrated NHE1, NHE6, CIC-3, and CIC-5 to be highly expressed. We hypothesized that in combination these proteins, transcellularly, move protons across the osteoblast cell layer to the general extracellular space. Directly to determine whether osteoblast membranes mediate proton transport consistent with this model, we made membrane vesicles from human osteoblasts by nitrogen cavitation. With these vesicles, we used acridine orange quenching to characterize proton transport. We found H⁺ transport dependent on gradients of chloride or sodium, consistent with CIC-family Cl⁻/H⁺ antiporters at apical surfaces and NHE-family Na⁺/H⁺ exchangers in basolateral surfaces of osteoblasts. In contrast to osteoclast membranes, little, if any, active H⁺ transport, supported by ATP or other energy sources, occurred. We conclude that mineral deposition in bone collagen is pH dependent, in keeping with a model of H⁺ removal by Cl⁻/H⁺ antiporters and Na⁺/H⁺ exchangers on the apical and basolateral faces of osteoblasts. Periodic orientation hydroxyapatite is organized on type I collagen coiled-coils, in keeping with earlier extensive work on organization of mineral during initial amorphous crystallization.



Disclosures: *Quitterie C Larrouture, None*

MON-0585

Bone formation in osteoblast cell culture Elena Makareeva*, Edward Mertz, Anna Roberts-Pilgrim, Sergey Leikin. NICHD, NIH, United States

Cell culture is widely used for mechanistic studies of osteoblast biology, testing osteogenic potential of progenitor cells, and tissue engineering. Formation of nodules or extended regions of mineralized extracellular matrix (ECM) in osteogenic media containing β -glycerophosphate (bGP) is commonly used as a proxy for bone formation. However, it is still unclear how well these assays characterize osteogenic potential of the cells. It is known that artificial mineralization can be induced by alkaline phosphatase expressing cells that hydrolyze bGP, producing mineralized ECM with different structure and appearance from bone. Cell culture and in vivo observations are often inconsistent; and many researchers believe that bone formation in culture is impossible. Here, we reevaluated bone formation by cultured osteoblasts in the absence of bGP. To characterize cell differentiation, we combined imaging of cells expressing osterix with analysis of different osteoblast and osteocyte marker genes in the whole culture and individual cells. We imaged mineral deposition by fluorescent labeling and examined ECM and cell structure, ultrastructure, and morphology by light and electron microscopy. We measured mineral composition and orientation relative to collagen fibers by Raman micro-spectroscopy. In the absence of bGP, both primary mouse calvarial osteoblasts and MC3T3 cells formed mineralized matrix that had the appearance, ECM structure and ultrastructure, and mineral composition and organization consistent with bone. Embedded cells had the morphology, ultrastructure and gene expression consistent with mature osteocytes. Without bGP, ECM mineralization started around embedded osteoblasts transitioning into osteocytes and gradually extended throughout the matrix, similar to bone formation in vivo. In the presence of bGP, ECM mineralization was more diffuse and did not produce large, contiguous bone-like regions. The resulting mineralized ECM had lower density and abnormal ultrastructure of collagen fibers as well as random hydroxyapatite orientation. Nevertheless, expression of genes marking different stages in osteoblast differentiation was qualitatively similar with and without bGP. Overall, we concluded that cultured osteoblasts can produce ECM that has the same appearance and properties as bone. While accelerating osteoblastic differentiation, bGP induces artificial mineralization and inhibits more physiological bone matrix formation and mineralization.

Disclosures: *Elena Makareeva, None*

MON-0586

Opposing Effects of Inorganic Phosphate and Trps1 Transcription Factor on Expression of SerpinB2 in Bone and Tooth Mairobys Socorro*, Daisy Monier, Sana Khalid, Victoria Smethurst, Dobra Napierala. Center for Craniofacial Regeneration, Dept. of Oral Biology, McGowan Institute for Regenerative Medicine, University of Pittsburgh School of Dental Medicine, United States

Inorganic Phosphate (Pi) is essential for normal skeletal and dental mineralization. This function is accomplished, in part, by regulating expression of genes involved in this process. In our interest to study the Pi-regulated mineralization process, we use 17IIA11 osteogenic cells, which undergo rapid mineralization in standard osteogenic conditions. Pi-regulated gene expression was analyzed by RNA-sequencing after exposing the cells to 5mM Pi for 24h. Besides the classic Pi-responsive genes to be upregulated in osteogenic cells (Spp1, Dmp1, Ank and Slc20a1), we identified SerpinB2 as one of the novel genes highly upregulated by Pi. Interestingly, this gene has never been implicated in formation nor homeostasis

of mineralized tissues. SerpinB2 gene codes for plasminogen activator inhibitor-2 (PAI-2), a protein that is widely studied in the context of immunity and cancer. Moreover, SerpinB2 is considered a stress protein, which under physiological conditions is highly expressed only in endothelial cells, but becomes highly expressed in response to stress. Encouraged by this novel observation, we analyzed in vivo expression of SerpinB2, in bone and tooth. Additionally, we compared expression of SerpinB2 in WT and transgenic mice overexpressing Trps1 specifically in osteoblasts and odontoblasts (Colla1-Trps1 mice). To accomplish this, skeletal and dental tissues were analyzed at different developmental stages. Immunohistochemical detection of SerpinB2 in alveolar bone and tooth uncovered that this protein is highly expressed not only in endothelial cells, but also in cells producing mineralized ECM. Specifically, osteoblasts lining alveolar bone, odontoblasts and ameloblasts were highly positive for SerpinB2. Of note, osteocytes express very low levels of SerpinB2. Furthermore, we determined that overexpression of Trps1 leads to decreased expression of SerpinB2. In summary, we identified that SerpinB2 is highly and specifically expressed by cells producing mineralized ECM, and showed that SerpinB2 is upregulated by Pi and repressed by Trps1.

Disclosures: *Mairobys Socorro, None*

MON-0587

PTHrP (1-36) and Abaloparatide: Weaker Modulators of SIK2/CRTC2-CRTC3 Signaling Axis Compared with PTH (1-34) Florante Ricarte*¹, Carole Le Henaff², Nicola Partridge². ¹New York University School of Medicine, United States, ²New York University College of Dentistry, United States

In 2017, abaloparatide (ABL), an analog of parathyroid hormone-related protein (PTHrP 1-34), was approved by the FDA and became the second osteoanabolic after teriparatide (PTH 1-34). This study aims to elucidate the mechanisms that underlie the actions of PTH (1-34), PTHrP (1-36), and ABL in the osteoblast. Previously, we have shown that in primary murine calvarial osteoblasts, PTHrP (1-36) and ABL resulted in a significantly reduced cAMP response compared with PTH (1-34). Similarly, activation of protein kinase A (PKA) was observed at 1-2.5min and dose response analyses showed 1/2 max values of 1nM, 13nM, and 30nM for PTH (1-34), PTHrP (1-36), and ABL, respectively. Additionally, CREB activation by all three peptides reflected the relative differences in time and dose-dependent effects observed in the cAMP/PKA responses. qRT-PCR of osteoblastic genes showed that while all three peptides similarly regulate a subset of genes (e.g., SOST, ALPL, RUNX2), two genes, the transcription factor, c-Fos and RANKL, are differentially modulated. PTH (1-34) results in 2-fold greater c-Fos expression and 3-fold greater RANKL expression compared with PTHrP (1-36) and ABL (n=9, p<0.05). Co-treatment with the PKA agonist, 8-bromo-cAMP, increased RANKL mRNA and was decreased by the PKA-specific inhibitor, myristoylated protein kinase inhibitor. Recently, others have shown that in the osteocyte, PTH, through PKA, negatively regulates Sik2 and Sik3 (salt inducible kinases), which allows the nuclear translocation of the transcriptional cofactor, Crtc2, and transcription of RANKL. To determine the downstream signaling axes utilized by these peptides in the osteoblast, knockdown of reported effectors, Mef2c, Hdac4, Sik2, Sik3, Crtc2, Crtc3, and Creb were performed. While knockdown of Mef2c, Hdac4, Sik3, Crtc2, and Creb did not affect RANKL mRNA, Sik2 knockdown increased the effects of all three peptides, while Crtc3 knockdown decreased their effects. Confocal microscopy demonstrated that PTH (1-34) induces greater nuclear localization of CRTC2 and CRTC3 compared with PTHrP (1-36) and ABL. Knockdown of SIK2 mimics the effects of PTH (1-34) on CRTC2 localization, but does not affect CRTC3, suggesting that alternative mechanisms are employed by PTH (1-34) to exert its effects on CRTC3. Taken together, these data show that in the osteoblast, the effects of PTH (1-34), PTHrP (1-36), and ABL on RANKL are governed by differential regulation of the cAMP/PKA/SIK2/CRTC3 signaling axis.

Disclosures: *Florante Ricarte, None*

MON-0588

A Comparison Between Osteoactivin and Bone Morphogenetic Protein-2 in Rat Spinal Fusion Model Jeremy Robinson*¹, Scott McDermott¹, Kevin Budge², Nazar Hussein², Fatima Jaber², Omar Azem³, Matt Desanto⁴, Adnan Raslan⁴, Maleck Saleh⁵, Bradley Inkrott¹, Faye Safadi¹. ¹Department of Orthopedic Surgery, SUMMA Health, United States, ²School of Biomedical Sciences, Kent State University, United States, ³Musculoskeletal Research Group, Northeast Ohio Medical University, United States, ⁴Musculoskeletal Research Group, NEOMED, United States, ⁵Musculoskeletal Research, NEOMED, United States

The search for osteoinductive therapeutic compounds remains critical to help accelerate bone healing in orthopaedic procedures including bony trauma and fusion surgeries. Osteoactivin/GPNMB (OA) is an osteoinductive compound that has previously been shown by our group to stimulate bone regeneration in vivo in the rat and sheep models without any deleterious side effects. Our goal is to compare OA to a currently accepted osteoinductive therapeutic compound, namely bone morphogenetic protein-2 (BMP-2). Specifically, the goal of this project is to compare BMP-2, which is widely accepted in the spine community for its role in spinal fusion, to OA n using a rat model for spinal fusion. The surgical protocol for posterolateral fusion was performed according to Yamaguchi et al. This method has already been accepted for spinal fusion results and allows for high standardization processes across each animal. Seventy male Sprague-Dawley rats were utilized and randomly divided

into seven groups with 10 rats in each group. Group 1: OA treated, Group 2: OA treated with autologous bone graft, Group 3: BMP-2 treated, Group 4: BMP-2 treated with autologous bone graft, Group 5: OA and BMP-2 treated with autologous bone graft, Group 6: no treatment with autologous bone graft, Group 7: no treatment without bone grafting. We analyzed fusion using μ CT assessment, along with histological comparison of tissues for toxicity. Serum analysis using ELISA to detect OA protein levels was also investigated. Quantitative data from Avizo 3D software shows that BMP-2 has a greater amount of osteogenesis at the site of spinal fusion when compared to OA. Samples with BMP-2 show a larger amount of grossly disorganized bone growth and ossification of surrounding soft tissues. OA without graft shows bone growth with a well distributed bony fusion at the spinal transverse processes. The addition of graft enhanced osteogenesis in both BMP2 and OA treated groups. Histologic analysis of BMP-2 treated groups showed increased indicators of soft tissue inflammation, especially in lung tissue, when compared to OA treated groups. Dermal, cardiac, and neural soft tissue samples lacked any apparent difference between treatment groups. ELISA for OA protein levels did not show any difference in serum levels of OA. Overall, it appears OA has no systemic soft tissue inflammatory effects and has more organized bony fusion compared to BMP-2 when used in spinal fusion.

Disclosures: *Jeremy Robinson, None*

MON-0589

Global Gene Expression Analysis Identifies *Mef2c* as a *Wnt16* Target in Osteoblasts Aimy Sebastian*, Nicholas Hum, Cesar Morfin, Deepa Muruges, Gabriela Loots. Lawrence Livermore National Laboratory, United States

Wnt16 is a major *Wnt* ligand involved in the regulation of postnatal bone homeostasis. Genome-wide association studies (GWAS) identified *WNT16* as a key gene associated with low bone mineral density, reduced cortical thickness and high fracture risk. Studies in animal models and in vitro systems have shown that *Wnt16* promotes bone formation and inhibits osteoclastogenesis, suggesting that this molecule could be targeted for therapeutic interventions to treat bone thinning disorders such as osteoporosis. It has also been suggested that *Wnt16* signals via both canonical and non-canonical *Wnt* signaling pathways to perform its function. To better understand the molecular mechanisms by which *Wnt16* promotes bone formation and to identify genes regulated by *Wnt16* in osteoblasts (OBs), we treated calvarial OBs purified from C57Bl/6 mice with recombinant *Wnt16* and profiled the gene expression changes by RNA-seq at 24h post-treatment. We also compared gene expression profiles of *Wnt16*-treated OBs to gene expression profiles of canonical *Wnt3a*- and non-canonical *Wnt5a*-treated OBs. We found 576 genes differentially expressed in *Wnt16*-treated OBs; these included several members of *Wnt* signaling pathway (*Wnt2b*, *Wnt7b*, *Wnt11*, *Axin2*, *Sfrp2*, *Sfrp4*, *Fzd5*, *Rspo2* etc.) and TGF- β /BMP signaling pathway (*Bmp7*, *Inhba*, *Inhbb*, *Tgfb2* etc.). We also found that about 37% (215/576) of the *Wnt16* targets overlapped with *Wnt3a* targets and ~15% (86/576) overlapped with *Wnt5a* targets, suggesting that *Wnt16* activates both canonical and non-canonical *Wnt* signaling targets in OBs. Only ten genes including *Cxcl14*, *Kcnj15*, *Prg4* and *Aqp5* were differentially expressed in response to treatment with all three *Wnts*. Transcription factor binding motif enrichment analysis in the promoter regions of *Wnt16* targets identified *Wnt/JNK* pathway activated transcription factors *Fos1* and *Fos2* as significantly enriched transcription factors associated with genes activated by *Wnt16* while *Mef2c* was the most significantly enriched transcription factor associated with genes repressed by *Wnt16*. We also found that *Wnt16* transcriptionally down-regulates *Mef2c*, suggesting that a subset of genes repressed by *Wnt16* treatment are normally activated by *Mef2c*. This is consistent with the negative feedback loop involving *Mef2c* and sclerostin where *Mef2c* deletion is anabolic by transcriptionally repressing *Sost* expression. *Wnt16* also up-regulated *FtL3*, a mediator of exercise-driven bone formation.

Disclosures: *Aimy Sebastian, None*

MON-0590

Potential usefulness of osteogenic exosomes as a therapeutic agent for bone engineering Takaki Sugihara¹, Yoshinori Sumita², Myumi Iwatake², Naomi Sakashita², Izumi Asahina¹. ¹Department of Regenerative Oral Surgery, Unit of Translational Medicine, Graduate School of Biomedical Science, Nagasaki University, Nagasaki, Japan, ²Basic and Translational Research Center for Hard Tissue Disease, Nagasaki University Graduate School of Biomedical Sciences, Nagasaki, Japan

Exosomes are extracellular vesicles with a diameter of 50 to 150 nm, contain miRNAs and proteins in its membrane structure, transport them without damage even in plasma or serum rich in degrading enzymes, it is thought that it contributes to intercellular communication. In this study, we focused on the exosomes secreted from bone marrow-mesenchymal stem cells (BM-MSCs) that received the osteoblastic differentiation stimulus by bone morphogenic protein (BMP) 2 and investigated the usefulness for applying them for bone engineering. As experiments, the osteogenic exosomes (O-EVs) were firstly obtained from the rat BM-MSCs after induced to the osteoblastic differentiation by exposing to recombinant human (rh) BMP2. Then, O-EVs were analyzed for their character via gene or protein expressions and evaluated further for their osteoblastic inducibility in BM-MSC culture. Lastly, O-EVs were transplanted to the rat cranial bone defects with alloplastic substitutes, and then the histological and immunohistological analyses were performed to observe the new bone formation in harvested specimens. Exosomes (EVs) obtained from non-induced BM-MSCs were employed as an experimental control. As results, mRNA expressions of osteo-

genic genes such as *runx2*, *alp*, or *bmp2* in O-EVs were up-regulated compared with those of EVs. Moreover, some of microRNAs (miRNAs) related to the regulation of osteoblastic differentiation on MSCs were significantly up- or down-regulated in O-EVs. Then, when BM-MSCs were treated by O-EVs or EVs in culture, O-EVs could promote the osteogenic gene expressions in cells compared to EVs. We are currently carrying out an in vivo experiment to clarify the actual usefulness of O-EVs as an alternative option for bone engineering.

Disclosures: *Takaki Sugihara, None*

MON-0591

Bone Morphometric and Immunohistological Study on Mechanism of Longitudinal Overgrowth of Femur of Developing Rat Following Circumferential Periosteal Division Shinjiro Takata*. Tokushima National Hospital, National Hospital Organization, Japan

Here we report the mechanisms of longitudinal overgrowth of femur after CPD. Twenty-four Wistar rats aged 8 weeks were used for this study. Periosteum of diaphysis of the right femur was divided circumferentially (CPD group), and the left femur was control (Control group). Longitudinal length of CPD and Control groups 4 weeks after CPD were 39.43 \pm 1.2 and 38.48 \pm 0.75 mm ($p=0.0086$, $n=6$), respectively, indicating that overgrowth of longitudinal length reached to approximately 2.5% of Control group. Distal growth plate is responsible for approximately 91.5% of longitudinal overgrowth ($n=6$). Bone histomorphometry showed that CPD increased longitudinal growth rate, mineral apposition rate, bone volume, osteoid volume, trabecular number and thickness of femur ($n=6$). Analysis of three-dimensional trabecular microarchitecture and bone mass measurement by micro-computed tomography showed that trabecular number of CPD group was significantly greater than that of Control group ($p=0.0116$). Trabecular separation and trabecular spacing of CPD group were significantly smaller than those of Control group ($p=0.0332$, $p=0.0261$). Histological findings showed that the width of distal growth plate and the number of hypertrophic chondrocytes of CPD group were greater than those of Control group 4 weeks after CPD. Immunohistological expression of *Runx2* and *IHH* of CPD group in the growth plate was higher than that of Control group. HE and AB staining analysis in distal growth plate of rat femur showed an increased number of hypertrophic chondrocytes and width of hypertrophic zone of the distal growth plate of rat femur of CPD group compared with Control group. These results showed that CPD stimulates endochondral ossification of growth plate to produce longitudinal overgrowth of femur of developing rat. These facts suggest that periosteum plays an important role to regulate endochondral ossification of growth plate, and that CPD might become promising treatment to lengthen tubular bone of pediatric patients with leg length discrepancy.

Disclosures: *Shinjiro Takata, None*

MON-0592

Lnc-OIF, A newly identified Long noncoding RNA, Inhibits Osteoblast Differentiation and Bone Formation Ye Tian*, Chong Yin, Xue Wang, Chaofei Yang, Zixiang Wu, Xiaoli Ma, Zizhan Huang, Aironq Qian. Northwestern Polytechnical University, China

Long non-coding RNAs (lncRNAs) correlates with multiple physiological and pathology processes including development, carcinogenesis and osteogenesis. However, reports on lncRNAs regulating bone formation were relatively limited. The maintenance of bone formation relies on the activity and differentiation of osteoblast. It has been proved that lncRNAs participate in the regulating of osteoblast differentiation. Previously, we identified MACF1 with ossification-promoting properties. MACF1, a cytoskeletal protein, enhances osteoblast differentiation by mediating translocation of β -catenin into nuclear. We assume MACF1 may be a regulator of osteogenic non-coding RNAs as well. In this study, we screened osteogenic lncRNAs through mRNA/lncRNA-microarray in MACF1 low/normal expressed MC3T3-E1 cell line combined with gene coexpression analysis. The lncRNAs with most significant average coexpression levels (<0.85) were selected. While, only lnc-OIF was enriched in skeletal tissues of mice. And it progressively decreased in bone-derived mesenchymal stem cells (MSCs) isolated from 12 to 24 month mice of age. In addition, the expression level of lnc-OIF decreased with the progress of osteoblastic differentiation in MC3T3-E1 cells. The biological function of the screened lnc-OIF was assessed both in vitro and in vivo. Down-regulating lnc-OIF by siRNA in MC3T3-E1 cells up regulated osteogenic gene ALP and Col-I expression, and augmented ALP activity and calcium nodules. Administering si-lnc-OIF with EntransterTM In Vivo Transfection nanoparticles subcutaneously over the calvarial surface, increased 21.7% ($p<0.001$) of average calvarial thickness, 99.6% ($p<0.001$) of mineral apposition rate and protein levels for osteogenic marker genes (OCN and OPG) compared to negative control. To further clarify the regulation mechanism of lnc-OIF to ossification, we evaluated the expression and activity of osteogenic transcription factors after si-lnc-OIF transfection both in vitro and in vivo. Interference of lnc-DA2 expression increased *RUNX2*, *LEF1* and *TCF7* mRNA level, *RUNX2* protein expression in mouse cranium, and *LEF1/TCF7* transcriptional activity. In conclusion, we have revealed lnc-OIF as a novel osteogenic regulator. lnc-DA2 inhibits osteoblast differentiation and bone formation through suppressing osteogenic transcription factors. This newly identified lncRNA has provided a fresh mechanism of osteogenic differentiation and target for treatment of skeletal disorders.

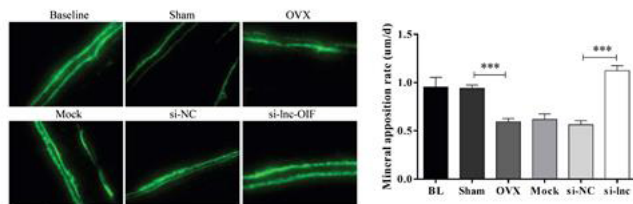


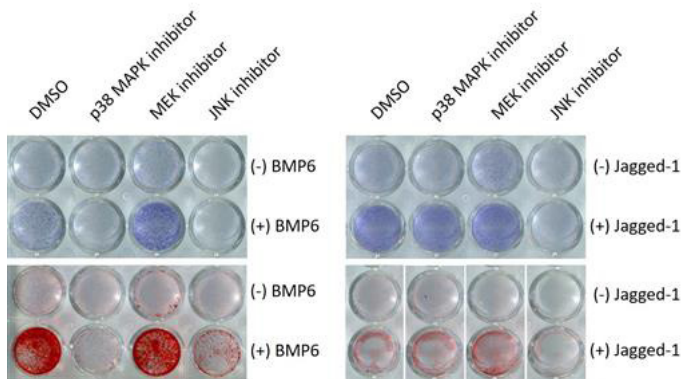
Fig.1 Rescue effect of Inc-OIF siRNA on calvarial bone formation in OVX mice. Representative images showing calvarial mineral apposition rate of C57BL/6 mice after OVX treatment and siRNA-Inc-OIF transfection.

Disclosures: *Ye Tian, None*

MON-0593

JNK MAP Kinase is required for both BMP and Notch induced Human Osteoblast Differentiation Yadav Wagley*, Kurt D. Hankenson. Department of Orthopaedic Surgery, University of Michigan, United States

Earlier studies from our laboratory have shown that human mesenchymal stem cells (hMSCs) undergo osteoblast differentiation in response to BMP-6 stimulation or by culturing them in presence of immobilized Jagged-1. However, the converging point of these different signaling cascades on osteoblast differentiation of hMSCs has not been identified. Since mitogen activated protein kinase (MAPK) components are known to affect gene expression in response to various stimuli, and ERK has been previously shown to intersect with Runx2, we examined the role of MAPK pathways during both BMP-6 and Jagged-1 mediated osteoblastogenesis in three independent donor cell lines. Histochemical staining for ALP expression and extracellular matrix mineralization using Alizarin red S in the presence of MAPK inhibitors showed that only c-jun N-terminal kinase (JNK) activity was required for immobilized Jagged-1 mediated osteoblastic differentiation whereas both p38 MAPK and JNK activity were required for BMP-6. Interestingly, inhibiting ERK increased ALP expression and accelerated mineralization in response to both stimuli. Gene expression analysis revealed that disruption of the p38 MAPK and JNK in BMP-6 stimulated cells resulted in decreased expression of Osterix, although Runx2 expression remained variable. However, in response to Jagged-1, the protein levels of both Runx2 and Osterix remained unaffected suggesting a different mode of osteoblast differentiation. Finally, to examine if BMP-6 signaling utilized MAPK signals to couple to Notch activation, immunoblot analyses were carried out, which showed that abolishing both p38 MAPK or JNK activity affected Notch-2 processing and expression of full length Notch-3 protein. Collectively, these results suggest that MAPK activity may integrate BMP and Notch signaling pathway to augment human osteoblast differentiation.



Disclosures: *Yadav Wagley, None*

MON-0594

The Regulatory Actions of TRPC3 Channels in the Differentiation and Functions of Osteoblastic Cells Yu-Mi Yang*, Dong Min Shin. Department of Oral Biology, Yonsei University College of Dentistry, Republic of Korea

Mechanical stress plays an important role in bone remodelling and maintenance. However, the mechanism of intracellular Ca²⁺ entry by canonical transient receptor potential 3 (TRPC3) channels and mechanical stress in bone cells is not well known. This study investigated the role of TRPC3 channels for the Ca²⁺ signal transduction in the osteoblastogenesis using TRPC3 knockout (KO) mice. The deletion of TRPC3 markedly increased of the bone density of the femur (~1.39-fold in 4-week old) in an age-dependent manner. After treatment with RANKL, TRPC3 KO bone marrow-derived monocytes/macrophages (BMMs) significantly reduced NFATc1 translocation to the nucleus, bone resorption activity, and multinucleated cells formation. The potency of osteoblastic differentiation in TRPC3 KO mice showed enhanced effects compared to wild-type mice by the methods of alkaline

phosphatase and alizarin red staining. Mechanical stress induces extracellular ATP release. TRPC3 contributed to an ATP-induced increases of intracellular Ca²⁺ in osteoblast cells (~2.33-fold), providing a pathway for receptor-operated Ca²⁺ entry in osteoblastic cells of TRPC3 KO mice. These results suggest that TRPC3 channels play an important regulatory action in the activation of receptor-operated Ca²⁺ entry and differentiation and functions of osteoblasts.

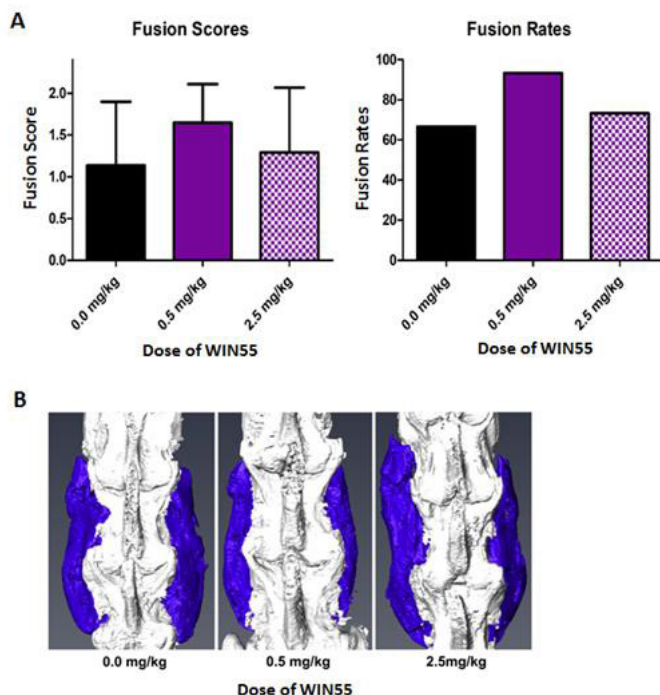
Disclosures: *Yu-Mi Yang, None*

MON-0595

Effect of Cannabinoid Receptor Ligands on Osteogenic Differentiation Chawon Yun*¹, Adam Driscoll¹, Ryan Lubbe¹, Soyeon Jeong¹, Kevin Chang¹, Meraaj Harleem¹, Richard Pahapill¹, Mark Oyer¹, Stuart Stock², Wellington Hsu³, Erin Hsu³. ¹Northwestern University Department of Orthopaedic Surgery, Chicago, IL, United States, ²Northwestern University Cell and Molecular Biology, United States, ³Northwestern University Feinberg School of Medicine Department of Orthopaedic Surgery, United States

BACKGROUND CONTENTS : After spine surgery, most patients receive opioids for pain, but controversy exists because of widespread abuse. The endocannabinoid system has been shown to have anti-nociceptive activity in animal models of acute tissue and nerve injury, and is thought to be important to bone homeostasis via activity at the CB1 and CB2 receptors. In this study, we explore the potential for the use of WIN55 as an alternative post-operative analgesic. **METHODS:** In vitro: Rat bone marrow stromal cells (BMSC) were cultured under standard or osteogenic media and subsequently exposed to either the vehicle control (DMSO) or the cannabinoid receptor agonist, WIN55,212-2 (WIN55). Expression of Runx2 and Alkaline phosphatase were quantified via qPCR. ALP activity and bone matrix mineralization were also measured. In vivo: Female Sprague Dawley rats underwent L4-L5 posterolateral spine fusion (PLF) with bilateral placement of absorbable collagen sponge (ACS) pre-loaded with 0.5 µg of recombinant bone morphogenetic protein-2. Animals (n=15/group) received DMSO, low-, or high-dose WIN55 via intraperitoneal injection for 5 days post-operatively. All animals received routine post-operative pain control. Bone regeneration was assessed using radiography, manual palpation-based fusion scoring, and microCT imaging. For fusion scoring, an established scoring system was used whereby 0 = no bridging bone, 1 = unilateral bridging, and 2 = bilateral bridging between the L4-L5 transverse processes. **RESULTS:** In vitro: mRNA expression of Alp and Runx2 was similar between DMSO and WIN55 treated cells. Exposure to WIN55 did not inhibit ALP activity or bone matrix mineralization. In vivo: No significant differences were found among groups in regards to mean fusion scores or fusion rates, (Fig. 1A), or in the volume of newly formed bone (representative fused specimens shown, Fig. 1B). Histological sections show bridging bone in fused specimens from each group. **CONCLUSION:** Here, we present pre-clinical evidence that WIN55, a dual cannabinoid receptor agonist, does not adversely affect osteogenic differentiation in vitro or bone regeneration and spine fusion in vivo. These results support the notion that cannabinoid receptor agonists should be further pursued as a potential alternative approach for post-operative analgesia following spine surgery and other orthopaedic procedures requiring bone healing.

Figure 1



Disclosures: Chawon Yun, None

MON-0636

WITHDRAWN

MON-0637

Phlpp1 controls osteoclastogenesis and bone resorption Dana Begun*, David Molstad, Jennifer Westendorf, Merry Jo Oursler, Elizabeth Bradley. Mayo Clinic, United States

Bone remodeling processes are disrupted in many diseases, including osteoporosis, periodontitis, tumor-induced bone disease and arthritis. Decreased bone mineral density in these conditions is often caused by enhanced osteoclast function. Phlpp1 is a protein phosphatase that is poised to be a critical regulator of bone mineral density because it dephosphorylates and inactivates numerous pathways (e.g., Akt, PKC, MAPK) that regulate osteoclast differentiation and function. Previous results demonstrate that Phlpp1 germline deficiency reduces bone volume, but the cell-type specific functions of Phlpp1 remained to be elucidated. To evaluate the function of Phlpp1 in bone resorbing osteoclasts, we generated Phlpp1^{fl/fl} mice via a TALEN-based approach. Phlpp1^{fl/fl} mice were then crossed with Ctsk-Cre expressing mice to conditionally delete Phlpp1 in mature osteoclasts. MicroCT analyses of 12-week-old mice demonstrated that female Phlpp1 cKO^{ctsk} mice exhibit increased femoral bone volume, BV/TV, BMD and trabecular number with a corresponding decrease in trabecular spacing. Vertebral body trabecular parameters were also enhanced in Phlpp1 cKO^{ctsk} female mice. No changes in bone parameters of male Phlpp1 cKO^{ctsk} male mice were observed via microCT. Histomorphometric analyses confirmed increased BV/TV, but also revealed increased osteoclast numbers in Phlpp1 cKO^{ctsk} female mice. Phlpp1 deficiency elevated osteoclast number and osteoclast size in ex vivo osteoclastogenesis assays, but reduced Alizarin red staining of calvarial osteoblast cultures. This was accompanied by enhanced bone marrow macrophage expression of c-fms and hyper-responsiveness to M-CSF. Western blotting demonstrated that Phlpp1 deficient osteoclasts have enhanced activation of Mekk1/2, Erk1/2 and Akt2 in response to M-CSF, but activation of conventional PKC α/β isoforms was unchanged. In addition to regulating the activity and stability of conventional PKC isoforms, Phlpp1 also inactivates the atypical PKC ζ isoform to establish cell polarity. We observed increased PKC ζ activity and diminished actin ring formation in Phlpp1 deficient osteoclast cultures. Likewise, serum markers of bone resorption (CTX-1) were not elevated in Phlpp1 cKO^{ctsk} despite enhanced osteoclast numbers. In contrast, serum PINP levels were elevated by 35% in Phlpp1 cKO^{ctsk} mice. These results suggest that Phlpp1 deficiency enhances osteoclast number, but diminishes bone resorption by disrupting osteoclast polarity.

Disclosures: Dana Begun, None

MON-0638

Trpm8 Knockout causes compartment-specific bone loss and altered osteoclast number and activity Adriana Carvalho*, Trevor Morin, Katherine Motyl. MMCRI, United States

Trpm8 (transient receptor potential melastatin 8) is a cold-sensing channel expressed by pain- and temperature-sensing neurons known to be the principal detector of environmental cold. Recent data suggest environmental temperature impacts bone density. Our aim was to investigate the role of these sensory neurons in regulating bone turnover using the Trpm8 knockout (KO) mice. Bones were collected from 8-week-old male wild-type (WT) and Trpm8KO mice. Bone mineral density (aBMD) and body composition were measured by DXA. Trabecular and cortical bone were evaluated by micro-computed tomography (μ CT). Trpm8KO mice had lower body mass compared to WT due mostly to fat mass loss. aBMD was similar between groups. However, Trpm8KO mice had reduced trabecular BV/TV in the femur compared to WT (WT=28.22 \pm 1.59%vs.Trpm8KO=23.29 \pm 2.45;p<0.05). Similarly, trabecular BV/TV (WT=38 \pm 2%vs.Trpm8KO=33 \pm 3%;p<0.05) was also reduced in the vertebrae of Trpm8KO mice with significantly lower connectivity density (Conn.D) and trabecular thickness (Tb.Th) compared to WT. Cortical bone was similar between groups. We previously found that Trpm8 deletion increases Rankl expression and suppresses osteoblast differentiation. To determine if Trpm8 deletion directly impacts bone resorption, we differentiated WT and Trpm8KO bone marrow stromal cells to osteoclasts (OCL). TRAP positive OCL numbers were decreased in Trpm8KO cultures compared to WT; however, Trpm8KO OCL resorbed more synthetic calcium phosphate surface compared to WT OCL. OCL markers (Acp5 and Ctsk) had increased expression throughout differentiation, but no differences existed between groups. Despite these differences in vitro, there was no convincing Trpm8 expression in OCL at any stage of differentiation. Interestingly, brain-derived neurotrophic factor (BDNF) and nerve growth factor (NGF) were significantly elevated in the Trpm8KO group at day 7, which may explain increased resorption as both have direct effects on OCL. In summary, male Trpm8KO mice had low trabecular BV/TV. Although Trpm8 showed little to no expression in OCL, the deletion affected the number and functionality of the cells ex vivo. BDNF and NGF data suggest that deletion of Trpm8 may influence bone density by altering neurotrophic factor-receptor signaling in OCL in vivo. Our future directions will be to investigate and sensory neuron crosstalk and whether the Trpm8 deletion specifically in sensory neurons triggers uncoupled bone remodeling.

Disclosures: Adriana Carvalho, None

MON-0639

Models of Elevated Cortical Bone Remodeling in the Rabbit: Platforms for Longitudinal Imaging of Basic Multicellular Units Beverly Hiebert*¹, Kim Harrison¹, Arash Panahifar², Amir Ashique¹, Terra Arnason¹, Janna Andronowski³, Kurtis Swekla¹, David Cooper¹. ¹University of Saskatchewan, Canada, ²Canadian Light Source, Canada, ³University of Akron, United States

Background: Regulation of Basic Multicellular Units (BMUs) in cortical bone remodeling has been the subject of a great deal of theoretical and/or in silico research due to a lack of direct empirical evidence. Synchrotron-based imaging combined with an appropriate animal model has the potential of tracking individual cortical bone remodeling events and thereby directly testing hypotheses related to BMU spatio-temporal regulation. The rabbit is the smallest model system which exhibits cortical remodeling that, like humans, creates secondary osteons; however, this process is slow and experimental approaches to elevate remodeling in rabbits have primarily focused on trabecular bone. Objective: Our objective is to develop model systems of elevated cortical remodeling in rabbits to optimize 4D synchrotron-based imaging of BMUs in vivo. Methods: Four mechanisms for elevating remodeling were explored in groups (n=7) of skeletally mature New Zealand White Rabbits – primary osteoporosis (ovariectomy; OVX), secondary osteoporosis (glucocorticoid; GC), a combination of OVX and GC (OVXGC) and finally, parathyroid hormone (PTH), a potent regulator of remodeling. The OVX groups (OVX and OVXGC) and control (SHAM) were operated upon eight weeks prior to the commencement of pharmaceutical treatments. GC (1.5 mg/kg/day), PTH (30 μ g/kg/day), or vehicle (1 mL saline/day) dosing were carried out for four weeks with two day calcein labels administered at two and four weeks. Cortical microarchitecture was assessed by micro-CT (cortical porosity) at 10 μ m voxel size and histomorphometry (resorption space and labelled osteon numbers). Results: Cortical porosity on the scale of resorption spaces was higher than SHAM for only the PTH group (p<0.01). Within all groups, pores on this scale included classic cutting cone configurations as well as more complex clustered resorption spaces particularly for the PTH group. Resorption space number was greater than SHAM for both PTH and OVXGC (p<0.01) while a combined measure of remodeling activity (resorption spaces plus labelled osteons) was greater than SHAM for OVX (p<0.05) and PTH (p<0.01). Conclusions: While variance within the groups limited the number of parameters which were significantly different from the SHAM group, all groups demonstrated trends towards increased remodeling activity. This suggests they may all be good targets for longitudinal synchrotron-based imaging and comparative analysis of four dimensional BMU behavior.

TABLE 1: Comparison of Bone Remodeling Parameters in Rabbit Tibia

Parameter	SHAM	OVX	OVXGC	GC	PTH
Cortical Porosity (%)	0.13	0.75	1.38	0.60	3.75 ^b
Resorption Space Number (resorption spaces/mm ²)	0.046	0.493	0.804 ^a	0.466	1.031 ^b
Remodeling Activity (resorption spaces + labelled osteons/mm ²)	0.301	2.098 ^a	1.071	0.916	3.878 ^b

Data expressed as mean for seven rabbits per group.

^ap < 0.05 vs. SHAM.^bp < 0.01 vs. SHAM.Disclosures: *Beverly Hiebert, None*

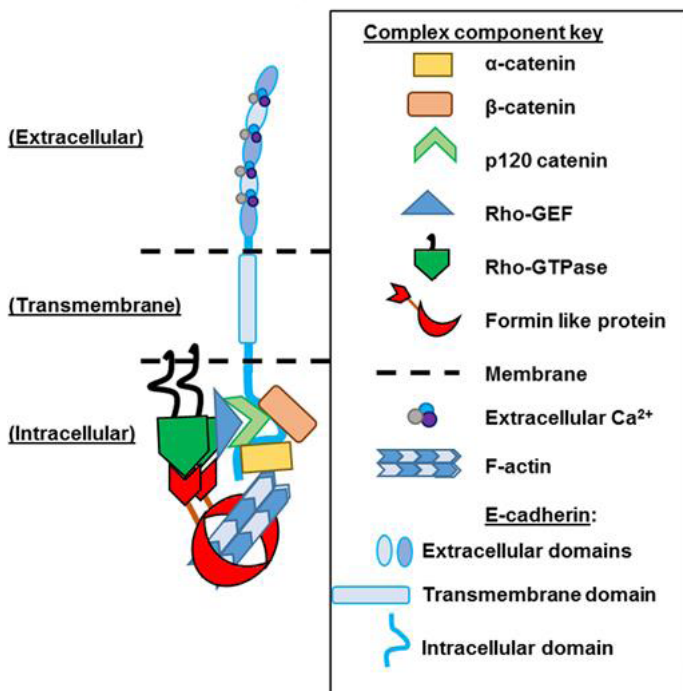
MON-0640

miR-29 Targets E-cadherin Complex Members in the Osteoclast Lineage

Henry Hrdlicka*, Sun-Kyeong Lee, Anne Delany. UConn Health, United States

miR-29 is a positive regulator of osteoclastogenesis; miR-29 inhibition decreases pre-osteoclast motility, and causes the formation of smaller and fewer osteoclasts in vitro. Two members of the Rho-GTPase family are validated direct (Cdc42) or indirect (Rac1 via srGAP2) miR-29 targets. These molecules positively regulate actin remodeling needed for osteoclast formation and function. Rac1 and Cdc42 also contribute to the E-cadherin signaling complex (see Figure). E-cadherin is a transmembrane protein that promotes strong cell-cell interactions, including those important for pre-osteoclast fusion. The E-cadherin complex is composed of α -, β -, and p120-catenins, actin remodeling proteins (i.e. Formin-like 2; Fmn12), Rho-GTPases, and GTPase regulatory proteins. Of these complex members, E-cadherin, Fmn12, and β - and p120-catenins are predicted to be novel miR-29 targets. We investigated the E-cadherin complex and the impact of miR-29 on E-cadherin complex members in osteoclasts. qPCR showed that E-cadherin and Fmn12 mRNA were well expressed in osteoclast progenitors isolated from whole mouse bone marrow, but their expression decreased >80% as progenitors were differentiated toward osteoclasts with RANKL. This inversely correlated with the increase in miR-29 during osteoclastogenesis. To validate miR-29 regulation of E-cadherin complex members, we cloned the E-cadherin, Fmn12, and β -catenin 3'-UTRs into the pMIR-REPORT luciferase construct. RAW264.7 cells were transfected with luciferase constructs, in the presence of either miR-29b inhibitor or a non-targeting control. For each luciferase construct, we observed a 2 fold increase in luciferase activity upon inhibition of miR-29b (p<0.01; n=5-6), indicating that E-cadherin, Fmn12, and β -catenin are indeed miR-29 targets. To evaluate the regulation of the E-cadherin complex by miR-29 in primary cells, osteoclast progenitors were isolated from mice globally expressing a miR-29 competitive inhibitor (tough decoy) from the ROSA26 locus. In osteoclast precursors from miR-29 decoy mice, E-cadherin and Fmn12 mRNA were increased more than 2 fold (p<0.05; n=3-4). In summary, we identified novel miR-29 targets in the osteoclast lineage: E-cadherin, Fmn12, and β -catenin. The E-cadherin complex facilitates cell-cell interactions necessary for pre-osteoclast fusion, and the fine tuning of these complex members by miR-29 may be necessary to ensure the formation of appropriately sized osteoclasts.

E-cadherin signaling complex

Disclosures: *Henry Hrdlicka, None*

MON-0641

WITHDRAWN

MON-0642

IgG complex with protein A of Staphylococcus aureus enhances osteoclastogenesis and bone resorption.

Asana Kamohara*¹, Xianghe Xu¹, Makoto Shiraki², Hirohito Hirata¹, Toshio Kukita³, Akiko Kukita¹. ¹Department of Microbiology, Faculty of Medicine, Saga University, Japan, ²Department of Orthopedic Surgery, Faculty of Medicine, Saga University, Japan, ³Department of Molecular Cell Biology & Oral Anatomy, Faculty of Dentistry, Kyushu University, Japan

Staphylococcus aureus is a main pathogen of osteomyelitis which is associated with inflammation and bone destruction. S. aureus protein A (SpA) is a virulence factor which has highly affinity for IgG. Recent reports demonstrated that immune complexes produced in pathogenetic condition regulate not only inflammation but also osteoclastogenesis. In vivo, IgG complex with S. aureus may play a role in bone resorption caused by bacterial infection. In this study, we investigated whether S. aureus has effect on differentiation and bone resorption of osteoclasts through IgG binding capacity of SpA. While addition of S. aureus to POC induced osteoclast (Oc) differentiation moderately, S. aureus pretreated with mouse serum dramatically increased OC differentiation to 2-10 fold from POC in mouse bone marrow culture. Serum pretreated S. aureus also strongly induced the expression of cathepsin K whereas SpA deficient mutant S. aureus did not increase the expression of cathepsin K. In addition, S. aureus but not SpA deficient mutant induced bone resorptive Ocs. Instead of mouse serum, S. aureus pretreated with IgG polyclonal, IgG1 or IgG2a monoclonal antibodies strongly induced Oc differentiation, demonstrating that IgG is responsible for osteoclastogenesis. Because IgG complex may bind to Fc receptor on POC, we analyzed the effect of blocking of Fc receptor using CD16/32 antibody and found that Oc differentiation induced by S. aureus was strongly inhibited. Although SpA is also released from bacterial surface, SpA alone did not induce significant number of Ocs even if it was pretreated with mouse serum. To analyze the contribution of cell wall components and mechanism, we analyzed whether S. aureus stimulate OC differentiation from POC of TLR2 and Myd88 KO mice. Oc differentiation induced by S. aureus was markedly decreased in comparison with WT mice, suggesting TLR2 signaling is involved. Consistently, stimulation of POC with both of serum pretreated SpA and TLR2 ligand Pam3CSK4 enhanced Oc differentiation in comparison with Pam3CSK4 alone. In addition, NFATc1 and NFkB but not p38 MAPK inhibitors suppressed Oc differentiation induced by S. aureus. Finally, local injection of S. aureus but not SpA deficient mutant into mouse calvaria formed erosion of bone surface. Taken together, we show here that IgG complex with SpA formed on cell surface of S. aureus play a new role in bone destruction, which is mediated by both Fc receptor and TLR2 in POC.

Disclosures: *Asana Kamohara, None*

MON-0643

Effect of C-X-C Motif Chemokine 12 in Lipopolysaccharide-induced Osteoclast Formation and Bone Resorption

Hideki Kitaura*, Kazuhiro Shima, Keisuke Kimura, Masahiko Ishida, Akiko Kishikawa, Saika Ogawa, Jiawei Qi, Wei-Ren Shen, Fumitoshi Ohori, Takahiro Noguchi, Aseel Marahleh. Division of Orthodontics and Dentofacial Orthopedics, Department of Translational Medicine, Tohoku University Graduate School of Dentistry, Japan

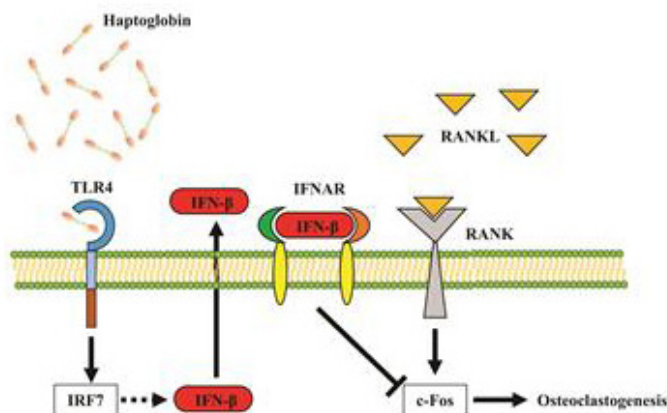
C-X-C motif chemokine 12 (CXCL12), also known as stromal cell-derived factor 1 (SDF1), belongs to the family of CXC chemokines. In recent years, it has been reported that CXCL12 has been associated with survival of osteoclast progenitor cells, differentiation, fusion, and functions. Therefore, it is important to investigate the relationship between osteoclast formation and CXCL12 to elucidate mechanisms of diseases that induce bone resorption. Lipopolysaccharide (LPS) is a major component of cell wall of gram-negative bacteria that is able to induce osteoclast formation and pathological bone resorption. In the present study, we investigated the effects of CXCL12 on LPS-induced osteoclast formation and bone resorption. LPS with or without CXCL12 was administered to mouse calvariae by daily subcutaneous injection. The number of osteoclasts and bone resorption were significantly higher in LPS and CXCL12-co-administered mice than in mice administered LPS alone. Receptor activator of NF- κ B ligand (RANKL) and tumor necrosis factor- α (TNF- α) mRNA expression levels were higher in the CXCL12 and LPS-co-administered group than in the LPS-administered group. Our in vitro results also showed direct stimulatory effects of CXCL12 on RANKL- and TNF- α -induced osteoclast formation. Furthermore, TNF- α mRNA expression was enhanced in CXCL12 and LPS-co-treated macrophages compared with cells treated with LPS alone in vitro. However, there was no effect of CXCL12 on LPS-induced RANKL expression in stromal cells in vitro. These results suggest that CXCL12 enhances LPS-induced osteoclast formation and bone resorption in vivo by increasing LPS-induced TNF- α production in macrophages and directly enhancing osteoclast formation.

Disclosures: *Hideki Kitaura, None*

MON-0644

Haptoglobin acts as a novel ligand for TLR4, suppressing osteoclastogenesis via activation of TLR4 - INF- β signaling pathway Zang Hee Lee*, Hong-Hee Kim, Jun-Oh Kwon. Department of Cell and Developmental Biology, Dental Research Institute, School of Dentistry, Seoul National University, Republic of Korea

Inflammatory molecules such as cytokines and small molecules are well known to play a major role in the regulation of bone homeostasis, but the effects of anti-inflammatory molecules among inflammatory molecules on osteoclasts are not fully unveiled. Haptoglobin (Hp), a kind of acute protein, is known to play as an anti-inflammatory function systematically and to modulate inflammation by directly affecting immune cells such as T cells, dendritic cells, and macrophages. However, the effect of Hp on osteoclast differentiation is not well studied, even though osteoclast precursor cells belong to macrophage-monocyte lineage. Here, we confirmed that the bone volume of the Hp-deficient mice was reduced and observed an increase in the number of osteoclasts. Besides, in vitro studies, we have shown that Hp inhibits osteoclastogenesis by suppressing post-translation of c-Fos at the early phase of osteoclast differentiation. We found that Hp-induced suppression of c-Fos was mediated by an increase of interferon beta (INF- β) levels, a well-known to inhibit post-translation of c-Fos. Further, Hp stimulates INF- β via toll-like receptor 4 (TLR4) dependently. Taken together, these results demonstrate that Hp plays a protective role against excessive osteoclastogenesis via the Hp-TLR4-INF- β signaling pathway.



Disclosures: Zang Hee Lee, None

MON-0645

RANK PVQEEET560-565 and PVQEQG604-609 Motifs play important roles in Porphyromonas gingivalis-mediated regulation of osteoclastogenesis Yuyu Li*, Shenyuan Chen², Zhenqu Shi³, Xu Feng³, Ping Zhang⁴. ¹Sichuan University, China, ²Stomatological Hospital of Chongqing Medical University, Chongqing Key Laboratory of Oral Diseases and Biomedical Sciences, Chongqing Municipal Key Laboratory of Oral Biomedical Engineering of Higher Education, Chongqing, 400015, China, ³Department of Pathology, University of Alabama at Birmingham, AL35284, United States, ⁴Department of Pediatric Dentistry, University of Alabama at Birmingham, AL35294, United States

Porphyromonas gingivalis (Pg) is a major pathogen of periodontitis, an inflammatory osteolytic disease characterized by the damage of tissues surrounding the teeth, including alveolar bone. The receptor activator of NF- κ B ligand (RANKL) and its receptor RANK are crucial regulators for the differentiation and activation of osteoclasts. Our previous studies have shown that Pg was able to potentiate RANKL-induced osteoclastogenesis in RANKL-committed osteoclast precursors. In addition, we have identified two functional motifs in the RANK cytoplasmic domain: PVQEEET560-565 (Motif 2) and PVQEQG604-609 (Motif 3) that are critical for RANKL-mediated osteoclast differentiation. In this study, we aimed to clarify whether Motif 2&3 are involved in Pg-mediated regulation of RANKL-induced osteoclastogenesis. Bone marrow macrophages (BMMs) were isolated from 6- to 8-week old wild type (WT) mice and homozygous knockout (KI) mice bearing inactivating mutations in Motif 2&3 (RANKmut/mut). Cells were maintained with macrophage colony-stimulating factor (M-CSF), pretreated with RANKL for 24h, and then stimulated with Pg. Pg induced the formation of tartrate-resistant acidic phosphatase (TRAP)-positive multinucleated cells in WT BMMs after 4-day culturing, while Pg failed to induce osteoclast differentiation in RANKmut/mut BMMs. We also examined osteoclast formation on bone slices by assessing the presence of multinucleation and actin ring, both of which are important features of mature osteoclasts. Similarly, osteoclast formation was only detected in WT but not RANKmut/mut BMMs treated with Pg. To understand the underlying mechanism, we examined the effect of Pg on RANKL-induced expression of osteoclast genes, as well as the activation of transcription factors important in osteoclast differentiation. Our results showed that 24h treatment of RANKL-pretreated WT BMMs with Pg significantly increased the expression of osteoclast genes including carbonic anhydrase II (Car2), cathepsin K (Ctsk), matrix metal-

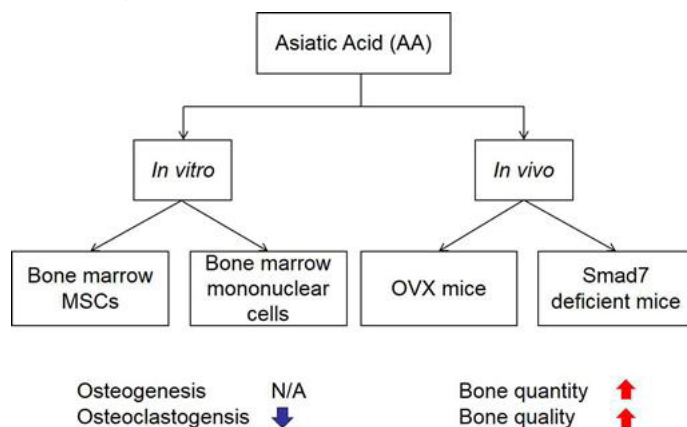
lopeptidase 9 (MMP9), and TRAP, whereas no up-regulation of these genes was observed in RANKmut/mut BMMs following Pg treatment. Furthermore, Pg increased the activation of c-fos and NFATc1 in WT BMMs but not in RANKmut/mut BMMs. Taken together, our results suggest that RANK Motif 2 and 3 are critical in Pg-mediated regulation of osteoclastogenesis. These motifs may represent potential therapeutic targets for periodontitis.

Disclosures: Yuyu Li, None

MON-0646

Asiatic Acid Attenuates Bone Loss by Regulating Smad7/TAK1/NF- κ B Signaling Pathway in Osteoclastogenesis Sien Lin*, Haixing Wang¹, Bo Wei², Yuk Wai Lee¹, Liao Cui², Gang Li¹. ¹The Chinese University of Hong Kong, Hong Kong, ²Guangdong Medical University, China

Objective Recently we have demonstrated that partial loss of Smad7 in mice leads to compromised bone quality. This study is to examine the role of Asiatic acid (AA), an activator of Smad7, in the regulation of osteogenesis and osteoclastogenesis, and further to investigate its effect on bone quality in ovariectomized (OVX) mice and Smad7-deficient mice model. Methods For in vitro studies, the effects of AA at different doses on mice bone marrow derived mesenchymal stem cells (MSCs) proliferation and osteogenic differentiation potentials were tested. The effects of AA on bone marrow derived mononuclear cells (BM-MNCs) osteoclastogenic differentiation were also tested by TRAP stain and bone resorption activity in HA-coated plates. Real time-PCR and western blot were performed to measure the changes of key markers including Smad7, Smad2/3, pSmad2/3, TAK1, pTAK1, NF- κ B, and RANK involved in osteoclastogenesis. For in vivo studies, female ICR mice were subjected to either OVX or sham operation. The OVX animals were treated with saline, AA, Alendronate (ALN), or a combination of AA and ALN. Another in vivo study was performed to verify the effect of AA on Smad7 deficient mice using the same approach. Micro-computed tomography (μ CT) examinations, four-point bending test, and histomorphometric analysis were performed at the endpoint. Result Result shown that AA exhibited no cytotoxic effect on MSCs and no significant effect on osteogenesis. Interestingly, AA significantly inhibited osteoclastogenesis of MNCs at a dose-dependent manner. Results also shown that Smad7 was upregulated, and pSmad2/3, pTAK1, NF- κ B, and RANK were downregulated by AA in MNCs during osteoclastogenesis. In the animal study, AA significantly restored trabecular bone and increased bone mechanical properties in the two animal models. Histomorphometry and TRAP stain revealed that the activity of osteoclasts was significantly inhibited by AA. However, a combination of AA and ALN didn't show any synergistic effect on bone quantity and quality. Conclusion AA shown significant inhibition effect on osteoclastogenesis dose-dependently by upregulating the expression of Smad7, and then inhibiting the phosphorylation of TAK1 and activation of NF- κ B. AA also attenuated bone loss by inhibiting activity of osteoclasts in both the OVX mice and Smad7-deficient mice. In a word, we found that AA effectively prevented osteoporosis by regulating Smad7/TAK1/NF- κ B pathway in the osteoclastogenesis.



Disclosures: Sien Lin, None

MON-0647

Protease Activated Receptor 2 (PAR2): A Novel Regulator of Osteoclastogenesis Sarah Mcgrath*, Leif Hultin², John C Lockhart³, Carl S. Goodyear¹. ¹Institute of Infection, Immunity, and Inflammation, University of Glasgow, United Kingdom, ²Respiratory, Inflammation and Autoimmunity, Innovative Medicines and Early Development, AstraZeneca, Sweden, ³Institute of Biomedical & Environmental Health Research, University of the West of Scotland, Paisley, United Kingdom

Protease activated receptor 2 (PAR2) is a G protein coupled receptor responsive to serine proteases, which plays a key role in inflammation and pain perception. We have previously demonstrated that Par2^{-/-} mice are protected from Freund's Complete Adjuvant (FCA) induced arthritis. Moreover, rheumatoid arthritis (RA) patients have up-regulated

surface expression of PAR2 in circulating monocytes, and the level of expression correlates with disease activity. Monocytes play a dual role in the progression of RA, through their capacity to differentiate into both inflammatory monocyte-derived macrophages and bone resorbing osteoclasts (OCs). In order to investigate the role of PAR2 in osteoclastogenesis we investigated the impact of loss of PAR2 on both the non-adherent bone marrow compartment and osteoblasts. Non-adherent bone marrow (BM) cells from 6-10 week old Par2^{-/-} and control C57BL/6 mice were cultured in pro-osteoclastogenic media for 5 days and mature OCs, identified as tartrate-resistant acid phosphatase positive (TRAP) multinucleated cells, counted. The resorption potential of these cells was assessed using osteolytic plates and the total osteo-resorption quantified after 7-14 days of culture. Transcript levels of osteoclast associated genes were analysed. Pre-osteoblasts (pOBs) were digested from calvaria of 3-5 day old pups from WT and Par2^{-/-} genotypes and matured in cell culture. Transcript of OB associated genes were analysed in mature OBs and their potential to initiate osteoclastogenesis was assessed in a prostaglandin E2 (PGE) and vitamin D supplemented co-culture with BM monocytes. In vitro osteoclastogenesis assays exhibited increased numbers of mature OCs generated from Par2^{-/-} non-adherent BM compared to WT, which corresponded with elevated levels of resorption. Transcript levels of OC-associated genes (i.e. NFATc1, Cathepsin K, TRAP, and DC-STAMP) were all increased compared to WT comparators. Co-culture of monocytes with mature OB revealed Par2^{-/-} OB had the capacity to increase osteoclastogenesis in both WT and Par2^{-/-} monocytes. This seems to be in part due to diminished production of the regulatory factor osteoprotegerin, found in Par2^{-/-} OB transcript. In conclusion, we propose that PAR2 contributes to the regulation of osteoclastogenesis via the mesenchymal arm of the bone remodelling unit; suggesting a potential regulatory role for protease activity and sensing via PAR2 in bone remodelling and osteoclastogenesis.

Disclosures: *Sarah McGrath, None*

MON-0648

Targeted Deletion of TAF12 in Osteoclasts Decreases Osteoclast Activity in Vivo Kazuaki Miyagawa^{*1}, Yasuhisa Ohata¹, Jolene J. Windle², G. David Roodman^{1,3}, Noriyoshi Kurihara¹. ¹Medicine/Hematology-Oncology; Indiana University, United States, ²Human and Molecular Genetics, Virginia Commonwealth University, United States, ³Roudebush VA Medical Center, United States

We previously reported that TAF12, a member of the TFIID transcription family, also acts as a coactivator of VDR-mediated gene expression, by forming a complex with ATF7 and TAF4 that binds VDR via TAF12. TAF12 is upregulated in osteoclasts (OCL) from Paget's Disease (PD) patients and the increased TAF12 levels enhance the 1,25-Dihydroxyvitamin D3 (1,25-D3) responsiveness of PD OCL-precursors. This allows OCL formation at physiologic levels (10-11M) of 1,25-D3. However, the role of TAF12 in normal OCL activity in vivo is unclear. Therefore, we generated Taf12^{flx/flx} mice using CRISPR/Cas9 technology and bred them to TRAP-Cre (TC+) mice to develop TRAP-Cre/Taf12^{flx/flx} (TC+/Taf12) mice with targeted deletion of TAF12 in OCL. Purified OCL from TC+/Taf12 mice expressed 60-75% less TAF12 than OCL from TC-/Taf12 mice. TAF12 expression in osteoblasts and bone marrow stromal cells was similar in both genotypes. μ CT analysis at 8 month old mice showed a 1.3 fold increase in BV/TV in TC+/Taf12 vs. TC-/Taf12 mice ($p < 0.05$). Histomorphometric analysis revealed that OCL number and surface were decreased by 40% in TC+/Taf12 mice vs. TC-/Taf12 ($p < 0.01$), while osteoblast numbers and surface were similar. These findings suggest that increased bone mass results from decreased OCL activity. To further characterize the OCL defect in TC+/Taf12 mice, OCL formation and activity in bone marrow cultures of purified OCL precursors from TC+/Taf12 mice treated with 1,25-D3 (10-8 M) were determined. OCL numbers, CY-P24A1, VDR, cathepsinK and IL-6 expression in OCL and bone resorption capacity/OCL on bone slices were significantly decreased in TC+/Taf12 compared to TC-/Taf12 cultures. Although OCL formation with RANKL (50 ng/ml) treatment was similar in TC+/Taf12 and TC-/Taf12 marrow cultures, bone resorption capacity/OCL remained greatly decreased in TC+/Taf12 cultures. Since autophagy regulates bone resorption and 1,25-D3 may induce Syntaxin17 expression, we then measured LC3 and Syntaxin17 levels in OCL. LC3-II and Syntaxin17 were decreased in TC+/Taf12 OCL regardless if the OCL were induced by 1,25-D3 or RANKL. Syntaxin17 immunostaining of bone sections confirmed decreased Syntaxin17 expression in OCL of TC+/Taf12 vs. TC-/TAF12 mice. Thus, these data suggest that TAF12 is an important contributor to OCL activity in vivo, in part through its effects on autophagy in OCL.

Disclosures: *Kazuaki Miyagawa, None*

MON-0649

Effects of advanced glycation end products on bone cells Hyung-Moo Park^{*1}, Ho-Yeon Chung², In-Jin Cho², You Cheol Hwang², In-Kyung Jeong², Kyu Jeung Ahn². ¹Grace woman's Hospital, Republic of Korea, ²Kyung Hee University, Republic of Korea

Diabetes mellitus adversely affects the skeleton and is associated with an increased risk of fragility fractures in dependent of BMD. In diabetes mellitus, high glucose and advanced glycation end products (AGEs) may be involved in bone quality deterioration. Here, we examined the effects of high glucose and AGE on osteoclast formation using bone marrow-derived macrophage and osteoblast function using MC3T3-E1 cells. AGE significantly inhibited RANKL-induced TRAP-positive multinucleated cell formation in bone mar-

row-derived macrophages cultures in a dose-dependent manner. The suppression of JNK, p38 mitogen-activated protein kinases engaged by RANK were observed in Western blotting after AGE treatment in mouse marrow cells. AGE also suppressed ICAM-1 and LFA-1 expression in mouse marrow cells in RT-PCT assay. Furthermore, AGE suppressed osteoblastic specific genes such as RUNX2, osterix in RT-PCR. The expressions of lysine hydroxylase (LH) and lysyl oxidase (LOX) genes were decreased by AGE treatment in MC3T3-E1 cells. These results demonstrate that AGE may affect bone quality through low bone turnover and the changes of collagen crosslink activity.

Disclosures: *Hyung-Moo Park, None*

MON-0650

SLIT2 inhibits osteoclastogenesis and bone resorption via the suppression of Cdc42 activity So Jeong Park^{*1}, Beom-Jun Kim², Mi Kyung Kwak³, Seung Hun Lee³, Jung-Min Koh³. ¹ASAN Institute for Life Sciences, Republic of Korea, ²ASAN MEDICAL CENTER, Republic of Korea, ³Division of Endocrinology and Metabolism, Asan Medical Center, University of Ulsan College of Medicine, Republic of Korea

Axon-guidance molecules including neurotrophins, semaphorins, and netrins have been receiving great attention due to their critical roles to regulate the coupling process linking bone resorption to formation. Recently, the axon-guidance molecule SLIT3 was identified as a novel cytokine that influences bone formation and resorption by promoting osteoblast migration and suppressing osteoclast differentiation. By the extension of these backgrounds, we investigated the effects of SLIT2, one of SLIT proteins, on osteoclastic differentiation and bone resorption. Quantitative RT-PCR revealed that Slit2 was comparably expressed in both pre-osteoclasts and mature osteoclasts. SLIT2 suppressed RANKL-stimulated osteoclast differentiation, mainly in the early-stage of osteoclastogenesis, and in vitro bone resorption using dentine discs. Consistently, the expression of osteoclastic differentiation markers, such as tartrate-resistant acid phosphatase (Trap) and calcitonin receptor (Ctr), was significantly decreased by SLIT2. Pre-osteoclast fusion was decreased in the presence of SLIT2, whereas pre-osteoclast viability was unaffected. Western blot showed that SLIT2 suppressed Cdc42 expression among small GTPases, although the expression of RANKL-dependent signals was not changed by SLIT2. Importantly, Cdc42 overexpression almost completely reversed the SLIT2-mediated suppression of osteoclast differentiation. Among ROBO1-4, the SLIT receptors, ROBO1 and ROBO3 were known to be predominantly expressed in osteoclast lineages. A binding ELISA experiment in mouse bone marrow-derived macrophages showed that ROBO1, rather than ROBO3, was directly associated with SLIT2, and gene silencing with Robo1 siRNA blocked the SLIT2-mediated suppression of osteoclastogenesis. Finally, SLIT2 injection in mouse calvaria markedly reduced LPS-induced inflammatory bone destruction. Taken together, our results indicate that SLIT2, one of axon-guidance molecules, inhibits osteoclastogenesis and the resultant bone resorption by decreasing Cdc42 activity, and thus plays an osteoprotective role in bone metabolism.

Disclosures: *So Jeong Park, None*

MON-0651

CD55 is a negative regulator of inflammation induced osteoclastogenesis Bongjin Shin^{*}, Sun-Kyeong Lee. University of Connecticut Health Center, United States

CD55 is a glycosylphosphatidylinositol (GPI)-anchored protein, which regulates complement-mediated as well as innate and adaptive immune responses. We have found that CD55 is expressed in multiple cells in bone marrow and mediates the survival and bone-resorption activity of osteoclasts by regulating Rac activity. CD55KO female mice have increased trabecular bone volume compared to WT and are reported to have a reduced severity of inflammatory arthritis with K/BxN serum transfer or collagen injection. In the current study we examined how an inflammatory stimulus, produced by local TNF α treatment, affected bones in CD55KO mice and their osteoclast precursor (OCP) pools. WT and CD55KO female mice were injected with TNF α for 4 days over their calvariae and examined 1 day later. We found that TNF α treatment augmented osteoclast formation in calvaria of CD55KO mice in vivo (3.8 fold) compared to WT. This was associated with an increase in the RANKL/OPG ratio (6.5 fold) and the expression of the inflammatory cytokines (IL-1 and IL-6) and chemokines (CCL2 and CCL3) in the calvariae. We also found that a differential response to TNF α was observed in the spleen compared to bone marrow. CD55KO mice had an increase in the weight and number of cells in the spleen (by 57% and 68%, respectively) in response to TNF α treatment while WT mice did not. In the bone marrow, the most efficient OCP (CD45R- CD3- CD11b-/lo CD115+ CD117hi) was increased (26%) in response to TNF α in both WT and CD55KO mice. Further, TNF α treatment increased the absolute number of peripheral OCP in spleen from both WT and CD55KO mice (2.3 fold and 8.4 fold, respectively). In vitro spleen cells from CD55KO mice formed more TRAP(+) OCL while bone marrow cells from CD55KO mice formed fewer, indicating that there were more peripheral and fewer bone marrow OCP available. We speculate that because the size and cell number in the spleen of CD55KO mice was significantly larger than WT, there were more OCP available for recruitment to the inflammatory site, in the calvariae, resulting in an enhancement of osteoclast formation. These results indicate that CD55 is an inhibitor of the osteoclastic response to the acute inflammatory stimulus, TNF α . TNF α specifically augmented available peripheral OCP in CD55KO mice while decreasing bone marrow OCP.

Unlike previous studies that examined the role of CD55 in an arthritic mouse model, we report an important role for CD55 in inflammatory bone disease.

Disclosures: Bongjin Shin, None

MON-0652

Sialic acid-binding immunoglobulin-like lectin 15 (Siglec-15) plays important roles in the induction of both bone-resorbing activity of osteoclasts and osteoblast differentiation Nobuyuki Udagawa^{*1}, Masanori Koide², Shunsuke Uehara³, Atsushi Arai², Toshihide Mizoguchi², Teruhito Yamashita², Midori Nakamura⁴, Yasuhiro Kobayashi², Naoyuki Takahashi², Seiichiro Kumakura⁵, Chie Fukuda⁵, Eisuke Tsuda⁵. ¹Department of Biochemistry, Institute for Oral Science, Matsumoto Dental University, Japan, ²Institute for Oral Science, Matsumoto Dental University, Japan, ³Department of Biochemistry, Matsumoto Dental University, Japan, ⁴Department of Biochemistry, Institute for Oral Science, Matsumoto Dental University, Japan, ⁵Rare Disease & LCM Laboratories, R&D Division, Daiichi Sankyo Co., Ltd., Japan

We previously reported sialic acid-binding immunoglobulin-like lectin 15 (Siglec-15) as a gene product expressed in giant cell tumor of bone. The expression of Siglec-15 was increased with osteoclast formation in mouse bone marrow cultures. Treatment of bone marrow macrophage cultures with anti-Siglec-15 antibody (Siglec-15 Ab) inhibited TRAP-positive multinucleated cell formation induced by RANKL and M-CSF. However, Siglec-15 Ab failed to suppress TRAP-positive mononuclear cell (mononuclear osteoclast) differentiation. We then examined the effects of Siglec-15 Ab on the appearance of osteoclast precursors, which express RANK and c-Fms but not TRAP, in mouse co-cultures of osteoblasts and bone marrow cells. Siglec-15 Ab showed no effects on the appearance of osteoclast precursors in the co-culture. Osteoclasts prepared from mouse co-cultures were further cultured on dentin slices in the presence or absence of Siglec-15 Ab. Pit-forming activity of osteoclasts was inhibited by Siglec-15 Ab. The actin rings in osteoclasts on dentin slices completely disappeared within 8 hours in the presence of Siglec-15 Ab. In contrast, treatment of alendronate for 1 hour completely disrupted actin rings of mature osteoclasts. Treatment of Siglec-15 Ab for 24 hours decreased the number of multinucleated osteoclasts, but alendronate treatment did not. We next examined effects of Siglec-15 Ab on sclerostin expression in UMR106 rat osteosarcoma cells. Sclerostin, an antagonist of Wnt/beta-catenin signaling, is secreted from osteocytes and inhibits bone formation. We previously reported that conditioned medium from osteoclast cultures suppressed sclerostin expression in UMR106 cells. In vitro experiments revealed that osteoclasts secreted leukemia inhibitory factor (LIF), which in turn inhibited sclerostin expression. Interestingly, conditioned medium from osteoclasts treated with Siglec-15 Ab for 48 hours also inhibited sclerostin expression in UMR106 cells. Siglec-15 Ab did not inhibit LIF expression in osteoclasts. These results indicate the possibility that maintenance of LIF expression may be involved in promoting bone formation in osteoclasts treated with Siglec-15 Ab. We previously showed that osteoblasts derived from Wnt5a-deficient mice had decreased alkaline phosphatase activity and Wnt5a produced by osteoclasts acted on osteoblasts leading to promotion of their differentiation. In this study, Wnt5a expression was increased in osteoclasts by treatment with Siglec-15 Ab, suggesting that Wnt5a induced by Siglec-15 Ab is involved in osteoblast differentiation. Our findings suggest that Siglec-15 plays important roles in the induction of both bone-resorbing activity of osteoclasts and osteoblast differentiation.

Disclosures: Nobuyuki Udagawa, Daiichi Sankyo Co., Ltd., Grant/Research Support

MON-0653

IL-3 inhibits osteoclastogenesis by upregulating the cytoprotective enzymes and diverts the cells toward M2 macrophages Suhas Mhaske^{*1}, Anil Kumar¹, Mohan Wani¹. ¹National Centre for Cell Science, India

IL-3, a cytokine secreted by activated T lymphocytes is a haematopoietic regulatory protein that stimulates the proliferation, differentiation and survival of haematopoietic stem cells. IL-3 is known to inhibit both RANKL- and TNF α - induced osteoclast differentiation in vitro. However, the molecular mechanism(s) for the inhibitory role of IL-3 on osteoclastogenesis is not yet delineated. In present study, we used iTRAQ-based quantitative proteomics approach to analyze the differential regulation of proteins in mouse bone marrow-derived osteoclast precursors treated with RANKL and IL-3. We observed that IL-3 significantly upregulates the expression of cytoprotective enzymes such as heme oxygenase-1, NQO2, G6PD, glutathione peroxidases, glutathione S transferase and catalase; and also downregulates the expression of NF κ B1 (p50) and NF κ B2 (p52). The cytoprotective enzymes are known to be involved in scavenging and detoxification of reactive oxygen species (ROS). RANKL generated ROS are crucial for activation of NF κ B pathway and expression of NFATc1, a master regulator of osteoclast differentiation. Our results suggest that IL-3 inhibits osteoclast differentiation by masking ROS and inhibition of NF κ B signaling. It was also observed that IL-3 upregulates the expression of arginase-1, a known negative regulator of osteoclast differentiation and a competitor of nitric oxide synthase. Moreover, IL-3 upregulates the expression of macrophage galactose-type C-type lectin 2 (CD301b), platelet glycoprotein 4 (CD36) and macrophage mannose receptor 1 (Mrc1), which are the phenotypic markers of anti-inflammatory M2 macrophages. Thus, our results suggest that

IL-3 inhibits osteoclast differentiation by regulating the cytoprotective enzymes and diverts the cells toward M2 macrophages.

Disclosures: Suhas Mhaske, None

MON-0654

Zscan10 Suppresses Osteoclast Differentiation through Expression of Haptoglobin. Yuta Yanagihara^{*1}, Kazuki Inoue¹, Noritaka Saeki¹, Yuichiro Sawada², Jiwon Lee³, Tadahiro Iimura³, Yuuki Imai¹. ¹Division of Integrative Pathophysiology, Proteo-Science Center, Ehime University, Japan, ²Department of Urology, Ehime University Graduate School of Medicine, Japan, ³Division of Bio-Imaging, Proteo-Science Center, Ehime University, Japan

Zscan10 (zinc finger and SCAN domain containing 10) was identified as a novel transcription factor in osteoclast differentiation by our genome-wide chromatin structure remodeling analysis, DNase-seq (JBMR 2014). However, the biological functions of Zscan10 have not been fully understood except its role in maintenance of genome stability and pluripotency in embryonic stem cells. Therefore, the aim of this study is clarification of Zscan10 function in osteoclastogenesis. First, Zscan10 KO RAW264 (KO) cells was established using CRISPR/Cas9 system and single cell sorting. Then, Control (Ctrl) and KO cells were differentiated into osteoclast by RANKL stimulation. TRAP activity, mRNA expression of differentiation markers such as Nfatc1 and inhibitory factors such as Irf8 were determined. As a result, TRAP activity and the marker genes expression were significantly increased and the expression of inhibitory factors was decreased in KO cells as compared to Ctrl cells. Furthermore, Zscan10 overexpression successfully suppressed increased TRAP activity of KO cells to the same extent as Ctrl cells. These results suggested that Zscan10 might regulate transcription of the genes which negatively control osteoclastogenesis. To understand the transcriptomes controlled by Zscan10, RNA-seq were performed and stringent analyses identified down-regulated 35 genes and up-regulated 18 genes in KO cells. GO analyses displayed that defense and immune response genes were enriched among down-regulated genes. To investigate direct target gene of Zscan10, integrative genome-wide analyses were performed using RNA-seq data, Zscan10 binding sequence motif and DNase-seq data. In consequence, Haptoglobin (Hp) was identified as a possible direct target gene because its expression was significantly decreased in Zscan10 KO cells, the Zscan10 binding motif was located near the genomic region of Hp gene locus, and chromatin structure of its gene locus was remodeled by RANKL stimulation. To examine the effect of Hp under Zscan10 mediated osteoclastogenesis, recombinant Hp was administered into KO cells. As a result, Hp treatment could suppress the elevated TRAP activity in KO cells without affecting cell proliferation. In addition, it has been reported that Hp KO mice exhibited decreased bone mass and increased number of osteoclasts. These results reveal that Zscan10 negatively regulates osteoclastogenesis through transcription of Hp.

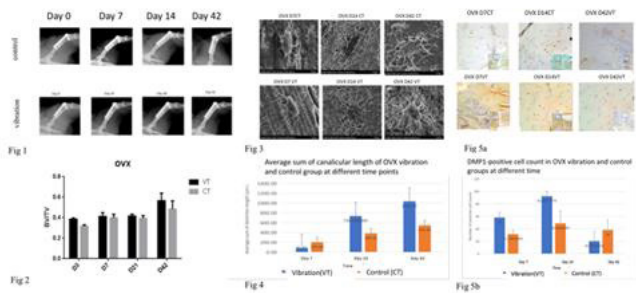
Disclosures: Yuta Yanagihara, None

MON-0672

Enhancement of Morphological and Functional Changes of Osteocyte in Osteoporotic Metaphyseal Fracture Healing Model with Low-Magnitude High-Frequency Vibration Man Huen Victoria Choy^{*1}, Ronald Man Yeung Wong¹, Simon Kwoon Ho Chow², Meng Chen Li², Jack Chun Yiu Cheng¹, Wing-Hoi Cheung¹. ¹Department of Orthopaedics and Traumatology, Faculty of Medicine, The Chinese University of Hong Kong, Prince of Wales Hospital, Shatin, NT, Hong Kong, ²Department of Orthopaedics and Traumatology, The Chinese University of Hong Kong, Shatin, NT, Hong Kong SAR, China, Hong Kong

INTRODUCTION Osteoporotic fracture is mostly occurring in the metaphyseal region. It is considered a prevailing challenge for clinicians due to its impaired healing process and limited treatment options. Previous studies have reported low-magnitude high-frequency vibration (LMHFV) as a non-invasive biophysical intervention in promoting osteoporotic fracture healing [1]. Osteocytes has been shown to be responsible for mechano-sensing in initiating bone healing processes [2]. We hypothesize that LMHFV can enhance fracture healing in ovariectomized metaphyseal fracture through morphological and functional changes in the osteocyte and osteocyte lacuno-canalicular Network (LCN). **METHODS** A total of 72 six-month old female Sprague-Dawley rats (n=72) underwent bilateral ovariectomy (OVX) and kept for 3 months for osteoporosis development (animal ethical approval ref: 16-037-MIS). Metaphyseal fracture on left distal femur was performed and fixed. Rats were then randomized to (1) OVX+LMHFV (20 mins/day and 5 days/week with 35 Hz, 0.3g), (2) OVX without LMHFV. Assessments of healing (X-ray, MicroCT), morphological changes of the LCN and osteocytic functional expression (Scanning Electron Microscopy, FITC-Imaris, immunohistochemistry) were performed at week 1, 2 and 6 post-fracture. **RESULTS**-Significant enhancement of fracture healing was found in the OVX+LMHFV group with MicroCT evidence of increase in bone density and 26% increase in canalicular length at week 2. At week 6, the osteocytes in OVX+LMHFV group exhibited densely-branched canalliculi, with a 50% increase in length. In addition to the morphological changes, DMP1 expressions were significantly enhanced after week 1 and 2 (p<0.05) in OVX+LMHFV group. Sclerostin expressions were dramatically reduced in OVX+LMHFV group at early stage followed by a gradual increase at week 6. **DISCUSSION** Our findings supported the hypothesis that LMHFV can enhance the osteoporotic fracture healing through morphological and functional

changes in osteocyte and the LCN. Additionally, expressions of DMP1 and sclerostin increased after vibration at early and late phase, respectively which could imply that osteocyte might play an important role through the regulation of DMP1 and sclerostin. This could stimulate further mechanistic investigation with significant potential clinical implications. REFERENCES: Shi, H.F., et al., Bone, 2010; Sapir-Koren, et al, Osteoporosis Int, 2014



Disclosures: *Man Huen Victoria Choy, None*

MON-0673

Osteocyte regulates osteoclasts formation through Neuropilin1 Ehab Azab¹, Kevin Chandler², Yuhei Uda¹, Amira Hussein³, Raghad Shuwaikan¹, Ningyuan Sun¹, Mark McComb², Paola Divieti Pajevic¹. ¹Molecular and Cell Biology, Boston University, United States, ²Department of Biochemistry, Boston University, United States, ³Department of Orthopedics, Boston University, United States

Osteocytes control bone modeling and remodeling through direct contact with adjacent cells and via secreted factors that can reach cells in the bone marrow microenvironment. Osteocytes express several receptors including G protein-coupled receptors (GPCRs). Previous studies have shown that Gsa-signaling in osteocytes controls myelopoiesis. Myeloid cells give rise to macrophages and osteoclasts, suggesting that osteocytes might regulate both macrophages and osteoclasts through Gsa mediated mechanisms. To investigate the cross-talk between osteocytes and osteoclasts, CRISPR/Cas9 was used to knockout, in vitro, Gsa expression in the Ocy454 osteocytic cell line. Conditioned media (CM) from Ocy-GsaControl Ocy-GsaKO cells were used to treat bone marrow mononuclear cells (BMNCs) isolated from long bones of C57/Bl6 mice. BMNCs were treated with M-CSF(50ng/ml) for 48 hr. and with RANKL(50ng/ml) for additional 3-5 days. CM from Ocy-GsaControl and Ocy-GsaKO (50/50 vol/vol) was added at the beginning of the culture and maintained during the whole culture period. TRAP activity, resorption pits, F-actin ring and mRNA expression were used to evaluate osteoclasts differentiation and function after 3 and 5 days of RANKL treatment. BMNCs treated with CM from Ocy-GsaControl or Ocy-GsaKO showed a significant increase in proliferation as compared to untreated BMNCs. Both the numbers and activities of osteoclasts were significantly suppressed by treatment with CM from Ocy-GsaControl and further suppressed by CM from Ocy-GsaKO compared to non-treated cells. Proteomic analysis of CM from Ocy-GsaControl and Ocy-GsaKO identified several proteins differentially expressed in KO compared to controls, including neuropilin1 (NRP-1) and semaphorin3A (Sema3A), two axon guidance proteins. NRP-1 expression was significantly increased in Ocy-GsaKO cells compared to control whereas Sema3A was significantly suppressed. Next we investigate if Nrp-1 was responsible for the osteoclasts inhibition seen in BMNCs treated with CM from Ocy-GsaKO cells. Treatment of BMNCs with Nrp-1, in the presence of CM from Ocy-GsaControl significantly suppressed osteoclastogenesis, compared to CM treated control. This data demonstrates, that osteocytes control osteoclast formation and function, in part through secreted NRP-1. Sema3A binds to Nrp-1 and suppress osteoclast formation. Sema3A and Nrp-1 are both expressed in osteocytes suggesting an important role of these proteins in these cells.

Disclosures: *Ehab Azab, None*

MON-0674

MLO-Y4 osteocyte response to simulated microgravity in a 3D scaffolding Roxanne Fournier^{*}, Rene Harrison. University of Toronto, Scarborough, Canada

The negative effects of spaceflight on astronaut bone homeostasis is currently limiting our ability to undergo long-term manned missions beyond low-Earth orbit. Here, we studied an osteocyte cell line, MLO-Y4, under simulated microgravity achieved with the Synthecon Rotary Cell Culture System (RCCS) to investigate how the lack of mechanical forces influences the transcriptome and morphology of these bone cells. The study also aimed to validate the RCCS with a novel 3D physiologically relevant collagen and mineral scaffolding for the cells and compare their gene expression and morphology to studies conducted in true microgravity. This work will lead to a better understanding of the osteocyte's role in astronaut osteoporosis and provide a more 3D-relevant platform for studying bone

cells in a ground-based microgravity simulator. Gel scaffolds composed of collagen I and calcium phosphate were used to produce a bone-like environment for the cells. The gel was inoculated with a cell suspension and mixed to ensure homogenous cell distribution. The mixture was then formed into droplets to allow compatibility with the RCCS. Our results of cell distribution in the scaffolding indicate that cell viability is maintained in the core of the droplets. We also show that the droplets coalesce in the RCCS and achieve stable free-fall in the culture media. Quantitative Real-Time PCR data from cells exposed to free-fall for 3 days in the scaffolding will determine if MLO-Y4 cells are being mechanically loaded or unloaded. Once an optimized simulated microgravity environment is achieved, a transcriptome analysis will be performed. The data obtained will be used to determine novel genes affected by mechanical unloading in osteocytes which can be further studied as potential therapeutic targets to combat astronaut bone loss. We will also observe the changes in morphology between cells in simulated microgravity and static control conditions to better inform the mechanisms responsible for osteocyte dysregulation in unloaded environments.

Disclosures: *Roxanne Fournier, None*

MON-0675

WITHDRAWN

MON-0676

Exogenous Irisin Treatment Ameliorates Inflammatory Changes in Osteocyte Proteins and Altered Bone Turnover in Chronic DSS-induced Inflammatory Bowel Disease Corinne E Metzger^{*1}, S Anand Narayanan², Anne Michal Anderson¹, David C Zawejja², Susan A Bloomfield¹. ¹Texas A&M University, United States, ²Texas A&M University Health Science Center, United States

Inflammatory bowel disease (IBD) patients incur bone loss resulting in a 40% greater fracture incidence than the average population. Treatments for IBD often have negative side effects, such as greater loss of bone (corticosteroids) or increased risk of serious infections (anti-TNF therapies). We previously discovered treatment with exogenous irisin, a protein derived from skeletal muscle FNDC5, resolved inflammatory changes in the colon, lymphatics and bone in chronic TNBS-induced IBD (Narayanan, Metzger, FASEB J, 2018). In this current study, we aimed to study the impact of irisin treatment in chronic DSS-induced IBD that exhibits greater disease severity compared to TNBS. We hypothesized that irisin treatment would mitigate bone loss, decrease osteoclast surfaces (% Oc.S), and increase bone formation rate (BFR). Male Sprague Dawley rats were either given standard drinking water (CON) or 2% dextran sulfate sodium in drinking water (DSS) for 4 weeks. Beginning in the second week, half of each group (CON+Irisin and DSS+Irisin) received intraperitoneal injections of irisin twice weekly for 3 weeks. n=8/group. At the end of 4 weeks, standard histomorphometry of the proximal tibia revealed 50% lower bone volume (%BV/TV), 2x higher Oc.S, and 65% lower BFR in DSS compared to CON. DSS+Irisin had 50% lower Oc.S and 55% greater BFR compared with DSS alone, though the %BV/TV values were not different. DSS+Irisin had restored Oc.S back to CON levels while BFR was 24% lower than CON. Immunohistochemical analysis of the distal femur cancellous bone demonstrated an elevation of osteocytes positive for pro-inflammatory factors in DSS (8-fold higher TNF- α and 3-fold higher IL-6 vs. CON). These values in DSS+Irisin were comparable to that of CON. Similarly, the DSS-induced increases in osteocytes positive for RANKL, OPG, and sclerostin were reduced in the DSS+Irisin group back to CON levels. While treatment with exogenous irisin did not mitigate the DSS-induced bone loss, it did resolve the pro-inflammatory changes in osteocytes and restored osteocyte regulators of bone turnover back to control levels. These changes in osteocyte proteins corresponded with lower osteoclast surface and increases in bone formation rate. We hypothesize these changes in bone turnover would result in improvements in bone mass at later time points than those examined here. These data corroborate our TNBS data demonstrating irisin as a potential anti-inflammatory treatment for inflammatory diseases impacting bone.

Disclosures: *Corinne E Metzger, None*

MON-0677

Osteocytes Maintain Mechanosensing Following Long-Term Dosing with Sclerostin Antibody Andrea Morrell^{*1}, Samuel Robinson¹, Jingyi Wang², Gill Holdsworth³, Hua Zhu Ke³, X. Edward Guo¹. ¹Columbia University, United States, ²Southern University of Science and Technology, China, ³UCB Pharma, United Kingdom

Despite continuous and progressive increase in BMD with long-term administration of antibodies to sclerostin (Scl-Ab), the response of bone formation markers such as P1NP are attenuated after repeat dosing of Scl-Ab. Recent work has demonstrated an up-regulation of other Wnt antagonists following multiple doses of Scl-Ab, which may contribute to self-regulation of the bone formation response. Here, we investigate whether this attenuation is associated with changes in osteocyte mechanosensitivity as measured by real-time Ca²⁺ signaling *ex vivo*. Scl-Ab or PBS vehicle was administered weekly to 12-week-old female Balb/c mice at 25 mg/kg/week s.c. per the following groups: vehicle (PBS), short-term (2 doses of Scl-Ab), or long-term treatment (8 doses of Scl-Ab) (Fig.1). Serum was collected

immediately before and 4 days following the 1st, 7th, and 8th treatment doses and P1NP measured using competitive EIA. At the conclusion of treatment, tibiae were explanted, maintained in cell culture media, and dyed with Fluo-8 AM. Tibiae were secured in a custom mechanical loader used with a confocal microscope for simultaneous loading and imaging of osteocyte Ca²⁺ signaling, where cyclic loading was applied at a peak load of 12N to tibiae from all groups. Pre-dose P1NP levels in Scl-Ab treated groups were comparable to those of vehicle and a significant increase in P1NP was observed 4 days following the first Scl-Ab dose administered to both long-term and short-term groups. This peak in P1NP was absent following the 7th and 8th doses of Scl-Ab, confirming a reduced bone formation marker response with long-term dosing, despite a significant increase in BMD. However, osteocytes exhibited robust load-induced intracellular Ca²⁺ responses with no differences in percentage of responsive cells or number of Ca²⁺ peaks per cell between vehicle and long-term treated mice. Osteocyte Ca²⁺ responses provide a measure of mechanosensitivity to whole bone loading. Our data suggests that osteocytes maintain mechanosensing after long-term Scl-Ab treatment whilst the bone formation effect was attenuated. This study uses real-time Ca²⁺ signaling to demonstrate for the first time osteocyte mechanosensitivity was maintained after long-term Scl-Ab treatment.

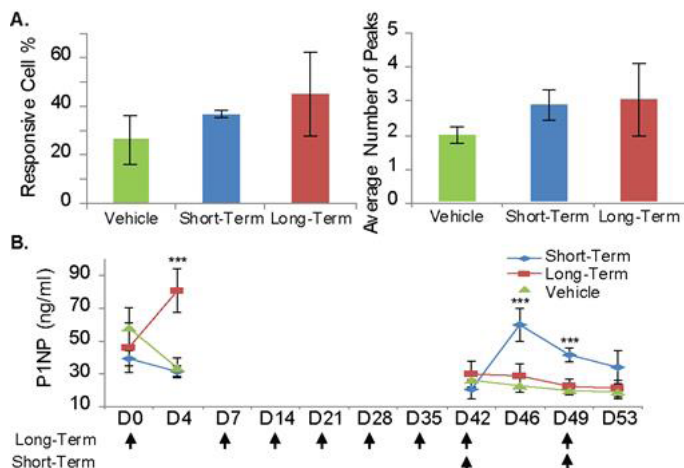


Fig. 1. Ex vivo osteocytes exhibit load-induced Ca²⁺ oscillations and dampened P1NP response with long-term Scl-Ab treatment. A. Ca²⁺ signaling parameters for osteocytes in vehicle and Scl-Ab treated mice. B. Serum P1NP levels immediately before and 4 days following treatment doses. *P<0.001 compared with vehicle control (t-test); N=2-4/group. Values are mean ± SD.**

Disclosures: *Andrea Morrell, UCB Pharma, Grant/Research Support*

MON-0678

Voluntary Wheel Running Exercise Maintains Osteocyte Connectivity and Muscle-Secreted Osteocyte Protective Factors in Aged C57BL/6 Mice Leann Tiede-Lewis¹, Yukiko Kitase², Kaitlyn Tom¹, Mark Dallas¹, Hong Zhao², Yixia Xie¹, Michael Wacker¹, Marco Brotto³, Lynda Bonewald², Sarah Dallas¹. ¹University of Missouri, Kansas City, United States, ²Indiana University, United States, ³University of Texas, Arlington, United States

Age-related osteoporosis and sarcopenia occur together and evidence suggests that molecular crosstalk between muscle and bone may regulate the function of the other tissue. Using an aged mouse model, we have shown that aging is associated with decreased osteocyte connectivity due to a linear decline in dendrite number, followed by reduced osteocyte number. We also showed that factors secreted by contracted muscle from young 5-6mo C57BL/6 mice protected osteocytes from oxidative stress-induced cell death and that this ability is lost in muscle from aged 22-24mo mice. As exercise has beneficial effects on both muscle and bone, we sought to determine if exercise, in the form of voluntary wheel running (VWR), can protect against osteocyte degenerative changes in aged mice. 12mo female C57BL/6 mice (n=8) were given access to VWR for 6 or 10mo, with daily running activity recorded electronically. Controls were singly housed without wheel access. The 6mo VWR mice ran an average of 3.4km/day and 10mo VWR mice ran 3.9km/day. In both groups, running activity was maximal in the first 8-10wks then plateaued to ~2.5km/day. Although there was no significant difference in body weight, the heart weight and heart to body weight ratio were significantly increased in VWR mice vs. controls. 6mo of VWR (harvest age 18mo) significantly increased osteocyte dendrite number by 27% vs. controls with no significant change in osteocyte number/mm³. This increased osteocyte dendricity was not maintained in the 10mo VWR group (harvest age 22mo). Trabecular BV/TV and cortical BV/TV, perimeter, thickness and porosity were not significantly different in VWR mice vs. control and plotting the mean distance run by individual mice against osteocyte or μ CT parameters did not reveal statistical correlations. VWR for both 6mo and 10mo restored the ability of conditioned media from static and contracted soleus and EDL muscles to protect MLO-Y4 osteocytes from oxidative stress-induced cell death, similar to effects with muscles from 5mo old mice. These results suggest that voluntary exercise has beneficial effects even when initiated in 12mo old

mice by slowing the degeneration of osteocyte connectivity, which may be mediated in part by maintaining muscle secretion of osteocyte protective factors. Although no significant differences in bone mass/structural properties were observed, maintenance of osteocyte connectivity may enhance bone function, strength and/or preserve crosstalk with other tissues.

Disclosures: *Leann Tiede-Lewis, None*

MON-0679

The Role of Osteocyte Estrogen Receptor β in Bone Turnover and Skeletal Mechanotransduction Differs in Male and Female Mice. Xiaoyu Xu¹, Haisheng Yang², Rachel Embry³, Whitney Bullock⁴, Teresita Bellido⁴, Russell Main³. ¹Weldon School of Biomedical Engineering Purdue University, United States, ²Beijing University of Technology, China, ³Musculoskeletal Biology and Mechanics Lab, Department of Basic Medical Sciences, Purdue University, United States, ⁴Department of Anatomy and Cell Biology, Indiana University School of Medicine, United States

Estrogen receptors (ER α , ER β) have long been recognized as regulators of bone physiology and bone's anabolic response to mechanical load. While previous studies have largely focused on the role of ER α in the skeleton, recent studies suggest that ER α may play a minor role in osteocyte-regulated bone turnover and mechanotransduction. Therefore, ER β may be the primary ER isoform regulating estrogen-related and ligand-independent ER actions in osteocytes. Targeted deletion of ER β in osteocytes was achieved by crossing Dmp-8kb1-Cre⁺-ER β lox/flox mice with ER β lox/flox mice to produce Cre⁺-ER β lox/flox (ER β KO) and Cre⁻-ER β lox/flox (WT) mice. DXA was performed on male and female WT and ER β KO mice from 4- to 52wks of age for femur and lumbar spine BMD measures (n=5-10/group/age). MicroCT analysis of L5 was conducted in 30wk old mice. Two-week tibial loading studies were conducted in 10- and 28wk-old male and female WT and ER β KO mice (n=9-10/group). Loaded and non-loaded tibiae were scanned by microCT for analysis of cortical bone morphology. Between 32- and 48wks of age, male ER β KO mice showed greater spine BMD (+13%) and femur BMD (+8%, 32wks only) than WT. There was not a consistent BMD phenotype in female ER β KO mice. By microCT, 30wk old male ER β KO mice showed a trend for greater L5 cancellous BV/TV (+28%, p=0.10), increased Tb.N (+18%, p=0.01) and decreased Tb.Sp (-18%, p=0.01) compared to WT, while 30wk old female ER β KO mice showed reduced L5 cancellous BV/TV (-29%, p=0.01), decreased Tb.N (-22%, p=0.01) and increased Tb.Sp (+28%, p=0.01). These results demonstrate that ER β in osteocytes may exacerbate age-related cancellous bone loss in male mice but may be protective in females. Tibial loading induced greater cortical bone mass in ER β KO and WT mice of both sexes at 10wks and 28wks of age. At 28wks of age, the response to load was similar in ER β KO and WT mice. However, 10wk-old female ER β KO mice showed an attenuated cortical bone response to load for the minimum moment of inertia relative to WT mice (KO +21%, WT +35%, p=0.005). A similar (non-significant) trend was found in 10wk male ER β KO and WT mice. These results suggest that osteocyte ER β may enhance the load-induced cortical adaptive response in younger female mice but does not affect cortical bone adaptation in adult mice. Future work will examine the role of osteocyte ER β in regulating the cancellous bone response to mechanical load and its role in sex hormone regulation of adult bone turnover.

Disclosures: *Xiaoyu Xu, None*

MON-0719

IMMINENT RISK OF NEW VERTEBRAL FRACTURE IN PATIENTS WITH RECENT CLINICAL VERTEBRAL FRACTURE Enrique Casado¹, Silvia García-Cirera¹, Marta Arévalo¹, Luis Del Río², Joan Carles Oliva³, Jordi Gratacós¹. ¹Rheumatology Dpt. University Hospital Parc Taulí (UAB), Spain, ²CETIR Centre Med. Spain, ³Statistics Dpt. University Hospital Parc Taulí (UAB), Spain

INTRODUCTION The risk of vertebral fracture in patients who have already had a previous vertebral fracture is high, especially in the first year after the fracture. However, it is unknown if this risk is greater in the first months and what clinical factors may be associated. **PURPOSE** To evaluate the radiological progression in patients who present a recent clinical vertebral fracture and to analyze what clinical factors are associated with the appearance of a new fracture or the radiographic progression of some previous one. **PATIENTS AND METHODS** All patients from a rapid Rheumatology Clinic who had been referred for a recent clinical vertebral fracture in the last 3 years (January 2015-December 2017) were systematically evaluated for inclusion. We excluded cases of intense trauma such as falling down the stairs or accidents, pathological fractures or patients with vertebroplasty. At baseline we collected demographic data, a VAS Pain score, fracture risk was assessment according to FRAX, biochemical parameters of bone metabolism in all patients. A bone densitometry (DXA, Lunar GE Prodigy) and a spine X-ray were also performed, using the semi-quantitative scale of Genant to establish the severity of the fracture. At 2 and 6 months, a clinical and radiological control was performed in all patients. **RESULTS** We included 83 patients (57 women and 26 men), of which 33 patients had 2 or more vertebral fractures. Age 72 ± 9.8 years. The most frequent cause was postmenopausal osteoporosis (39 patients), while 37 patients had secondary osteoporosis, mainly early menopause, diabetes and glucocorticoid-induced osteoporosis. 31% of the patients had at least one severe vertebral fracture. The absolute risk of major and hip fracture at 10 years according to FRAX was 15.7±12.3% and 8.3±10.7%,

respectively. The baseline VAS Pain score was 9.2 ± 1.2 . The 25OHD and PTH levels were 23.6 ± 17.6 and 66.0 ± 42.6 respectively, with 54% of patients having values of 25OHD < 20 ng/ml. 67% of patients had osteoporosis by DXA. 18% and 26% of patients had at least one new vertebral fracture at 2 and 6 months; and 54% and 68% showed radiographic progression in at least one degree over an existing fracture. Only FRAX for major fracture and hip fracture was associated with the incidence of a new fracture in our population. CONCLUSION The risk of new vertebral fracture in patients with a recent clinical vertebral fracture is very high, even at 2 months after the fracture and increases at 6 months, being especially significant in patients with a high fracture risk according to FRAX.

Disclosures: **Enrique Casado**, None

MON-0720

High bone marrow fat in osteopenic older adults may cause overestimation of DXA-measured BMD: A quantitative MRI study Wing P. Chan^{*1}, Shiou-Ping Lee¹, Yi-Chien Lu¹, Hou-Ting Yang², Yi-Jui Liu³. ¹Department of Radiology, Wan Fang Hospital, Taipei Medical University, Taiwan, ²Department of Nuclear Medicine, Chang Gung Memorial Hospital, Taiwan, ³Department of Automatic Control Engineering, Feng Chia University, Taiwan

Purpose: It is well known that a shift of differentiation of mesenchymal stem cells to adipocytes rather than osteoblasts partly contributes to osteoporosis. Whether bone marrow fat has a protective role for fractures and bone loss in older adults is still debated. Yet more than 40% subjects with vertebral compression fractures are not classified in osteoporosis category as defined by T-score. DXA precision declines with increasing BMI due to an obesity artifact. This study aimed to investigate bone marrow fat relating to vertebral BMD in older adults using quantitative MRI. Methods: We prospectively recruited 135 participants (88 women, 47 men), age > 50 years men and postmenopausal women, who underwent MRI and DXA scans in this study. MRI and DXA were performed within 1 week. All subjects were categorized into three groups: normal (T-score ≥ 1), low bone mass (LBM) ($-1 < \text{T-score} < -2.5$) and osteoporosis (T-score ≤ -2.5) as examined by DXA scan. All subjects received 1.5-T MRI of lumbar spine (center at L1 & L2) using axial gradient-echo sequential acquisitions at six TEs for 6-point IDEAL reconstruction. The initial 85 subjects (47 females, 38 males) were also received STEAM 1H-MRS sequence without water suppression. The fat fraction ratio was calculated as $\text{Ifat}/(\text{Ifat} + \text{Hwater}) \times 100\%$ (I = signal intensity). A P value < 0.05 was considered as statistically significant. For comparison, 27 patients with compression fractures were prospectively enrolled, with use of the same protocols. Results: Excellent linear correlation was shown for 6-pt IDEAL and MRS ($R^2 = 0.758$, $P < 0.001$), indicating accurate fat quantification by Dixon technique. In postmenopausal women, the results showed no significant correlation between regional fat fraction and BMD ($p = 0.170$) (Table 1), but fat fraction differences of normal vs LBM ($p < 0.01$) and normal vs. osteoporosis ($p < 0.01$) reached statistical significance. In men, the results showed no significant correlation between regional fat fraction and BMD ($p = 0.053$), fat fraction differences of normal vs LBM ($p = 0.276$) and normal vs. osteoporosis ($p = 0.696$). For comparison, nine (33.3%) and 18 subjects (66.6%) with vertebral compression fractures were classified as LBM and osteoporosis, respectively. Of these, fat fraction differences of LBM vs osteoporosis were not significant ($p = 0.639$). Conclusion: Our results revealed that high marrow fat in LBM group, comparable to osteoporosis group, in both non-fractured and fractured subjects, and that BMD of LBM group could be overestimated by DXA due to marrow 'obesity' artifact.

Table 1. Fat ratio and BMD of non-fractured patients among three groups

	Normal N=9	LBM n=46	Osteoporosis n=33
Female			
Fat_ratio	0.41 ± 0.11	$0.50 \pm 0.03^{**}$	$0.49 \pm 0.05^{**}$
BMD	1.16 ± 0.09	$1.04 \pm 0.13^*$	$0.87 \pm 0.11^{**}$
Male			
Fat_ratio	0.44 ± 0.08	0.47 ± 0.04	0.45 ± 0.05
BMD	1.35 ± 0.15	$1.12 \pm 0.15^{**}$	$0.97 \pm 0.19^{**}$

LBM, low bone mass. * $p < 0.05$, ** $p < 0.01$

Table 2. Fat ratio and BMD of fractured patients between two groups

	LBM n=9	Osteoporosis n=18
Fat_ratio	0.47 ± 0.05	0.48 ± 0.05
BMD	1.03 ± 0.13	$0.86 \pm 0.22^*$

LBM, low bone mass. * $p < 0.05$, ** $p < 0.01$

Disclosures: **Wing P. Chan**, None

MON-0721

Trabecular Bone Score in Conditions of Extremely High BMD. Does it have any utility? Manju Chandran^{*1}, Ann Kerwen Kwee², Matthew Bingfeng Chuah². ¹Osteoporosis and Bone Metabolism Unit, Singapore General Hospital, Singapore, ²Department of Endocrinology, Singapore General Hospital, Singapore

Purpose: TBS quantifies grey-level texture variations between adjacent pixels in raw DXA images. Conceptually, a dense trabecular network produces many grey-level texture variations of small amplitude and therefore a steep variogram slope with a high TBS value. In contrast, a sparse network produces fewer variations of larger amplitude with resultant low TBS value. It's utility in assessing bone microarchitecture in patients with extremely high BMD due to genetic and non-genetic causes has not been explored. Method: 2 cases are presented 1) A 32-year old Chinese woman presented with persistent headaches. A cervical spine X-ray showed occipital bone scalloping. Brain MRI showed Arnold Chiari malformation with minimal cerebellar tonsillar descent. X rays showed rugger jersey spine appearance with sclerosis of the superior and inferior vertebral end plates. Physical examination was normal. Hematological parameters and bone turnover markers were normal. Hepatitis panel was negative. The patient herself had no fractures so far but her sibling had a history of vertebral fractures. DXA scan showed Z-scores of +6.6, +5.7 and +4.4 at the femoral neck (NOF), total hip and lumbar spine (LS) respectively. TBS (L1-L4) was 1.829 and that of an age matched normal control was 1.471. Next Generation Sequencing revealed a pathogenic c.643G>A transition in exon 7 of the CLCN7 gene associated with autosomal dominant Osteopetrosis. 2) A 67-year old Chinese man presented for bone health evaluation after renal transplantation. He had sustained a NOF fragility fracture, 2 years prior to the transplant. A DXA scan done at the time of transplant showed Z-scores of +4.8, +4.3 and +5.6 at the NOF, total hip and LS respectively. TBS (L1-L4) was 1.692. That of a matched control was 1.418. X-ray showed superior and inferior vertebral end plate sclerosis and a rugger jersey spine appearance. He had biochemical evidence of low bone turnover with levels of Serum Osteocalcin 8 mcg/l (12-51) and Bone Specific Alkaline Phosphatase (6.7 mcg/l (7.1-28.4). Conclusion: TBS may not be a good index of skeletal microarchitecture in conditions causing diffuse osteosclerosis and complete absence of grey-level texture variation. High values obtained in such situations may erroneously overestimate the structural integrity of bone. Modalities such as micro indentation that can evaluate bone material strength may be preferable in diseases that cause fragility fractures despite having extremely high BMD.

Disclosures: **Manju Chandran**, None

MON-0722

The association between muscle mass deficits estimated from bioelectrical impedance analysis and osteoporosis in elderly people Hee-Jeong Choi^{*1}, Han-Jin Oh¹, Hyeok-Jung Kweon². ¹Department of Family Medicine, Eulji University School of Medicine, Republic of Korea, ²Department of Family Medicine, Konkuk University School of Medicine, Republic of Korea

Background: Osteoporosis is a global public health problem that affects an enormous number of people and its prevalence will increase as the population ages. Throughout life, bone mineral density (BMD) is influenced by many factors and body weight is an important determinant of BMD. Muscle mass affects the body weight and may contribute to BMD because bone functions with muscle as a musculoskeletal unit and adapts to the load and strain exerted by muscle. The aim of this study was to investigate the association between muscle mass deficits (MMD) estimated from bioelectrical impedance analysis (BIA) and BMD in elderly aged between 50 and 75. Methods: Data was gathered from 2661 males and females who visited a health promotion center. Lumbar spinal BMD was measured by dual-energy absorptiometry. Body composition analysis was performed using BIA. MMD is the difference between ideal fat-free mass and real fat-free mass of the subject and is expressed as the muscle control (kg) on the result sheet. The subjects were divided into three groups according to the tertile of MMD in each gender. Multivariate linear regression analysis was done to identify the major predictors of the BMD. A logistic regression analysis was used to estimate the odds ratios for osteoporosis in the MMD groups. Results: The mean age of the 1471 males and 1190 females was 56 years old. The mean MMD of the males and females were 2.0 ± 2.7 kg and 2.0 ± 2.2 kg, respectively (NS). MMD had the strongest influence on the lumbar spine BMD when age and all other variables were included in the regression models in both the males and females. MMD, weight, and height explain up to 9.1% of the variation in the lumbar spine BMD in males. In females, MMD, weight, waist circumference, and age explain up to 23.7% of the variation in the lumbar spine BMD. In males, the adjusted odds ratio of Group 2 ($0 \text{ kg} < \text{MMD} \leq 3.05 \text{ kg}$) and Group 3 ($\text{MMD} > 3.05 \text{ kg}$) for osteoporosis were 3.58 (95% CI, 1.62-7.91) and 4.30 (95% CI, 1.98-9.35), respectively. This association was similar after adjusting for other covariates including lifestyle-related variables. In females, the adjusted odds ratio of Group 3 ($\text{MMD} > 2.7 \text{ kg}$) was 2.07 (95% CI, 1.04-4.14) after adjusting for all covariates. Conclusion: MMD estimated by BIA showed a significant association with lumbar spine BMD and could be regarded as an independent risk factor for osteoporosis in males and females aged 50-75.

Disclosures: **Hee-Jeong Choi**, None

MON-0723

Cortical and Trabecular Bone Response in Proximal Femur from Women with Osteoporosis Treated with Denosumab or Zoledronic Acid using 3D Modelling Techniques obtained from DXA. Fidencio Cons Molina^{*1}, Mario Feuchter¹, Luis Ernesto Bejarano¹, Diana Wiluzanski², Carla Altieri², Edison Edgardo Romero Galvan², Jose Luis Mansur³, Yves Martelli⁴, Ludovic Humbert⁴. ¹Centro de Investigacion Artritis & Osteoporosis, Mexico, ²CENTROSEO, Uruguay, ³Centro de Endocrinología y Osteoporosis, Argentina, ⁴Galgo Medical, Spain

Purpose: Assess changes that occur after 2 years with denosumab(DMAb) or zoledronic acid(ZOL) treatment in areal bone mineral density (aBMD) obtained by DXA and in volumetric BMD(vBMD) evaluating 3 bone compartments (trabecular,cortical & integral) assessed with 3D modelling techniques from a standard proximal femur DXA(hip-DXA). **Methods:** We retrospectively analysed 160 patients with postmenopausal osteoporosis. The cohort was stratified by treatments: DMAb naïve n=50; DMAb Pretreated n=50; Naïve treatment n=30, Zoledronic Acid(ZOL) n=30 for comparison purposes. Patients came from Mexico,Uruguay & Argentina. From a hip-DXA acquisition in addition to aBMD,volumetric trabecular total(vBMDTrab), cortical surface density(CSD) and volumetric BMD Integral(vBMDInt) were assessed, using a 3D-Shaper software 2.6ver (Galgo Medical,Spain). The changes observed at 2 years were evaluated in terms of (%) of change in vBMD. A paired T-student test were used to compare parameters from baseline. All hip-DXA were acquired using GE-Prodigy devices.**Results:** After 2years, in the naïve treatment group, a significant decrease was observed in all 3D parameters when compared to baseline,additionally to decreasing aDMO. In ZOLgroup only a significant increase was observed in CSD(2.3%) and in vBMDInt(2.4%). A greater trabecular response was observed in DMAb naïve group vBMDTrab(6.9%) vs.DMAb Pretreated(2.4%). The response to treatment was analyzed in both DMAb groups dividing in tertiles vBMD at baseline (low,medium,high) for all 3D parameters showing only in DMAb naïve group a greater response in those from lowest tertile vs. medium and high (vBMDTrab 13.3%,4.0%,0.2%), CSD 6.2%,2.2%,1.3%), vBMDInt (5.7%,2.5%,0.1%). On the other hand, DMAb Pretreated group showed no differences between tertiles in response to treatment.**Conclusions:** Significant vBMD increases were observed in cortical & trabecular compartments in both ZOL group and both DMAb groups. The finding of a more pronounced response to treatment for patients with vBMD in the lower tertile in the group with naïve DMAb (trabecular vBMD & cortical surface density), suggests that identification of those patients using 3D-SHAPER may provide a personalized treatment in this subgroup of patients at high risk of fracture. 3D modelling techniques are a promising new technology for identification/monitoring of vBMD changes in patients with osteoporosis. More studies are required to confirm our results.

Table 1	Treatments			
	Naive (n=30)	Zol (n=30)	DMAb Naive (n=50)	DMAb Pre Treat (n=50)
Age (years)	65.5	67.3	63.6	66.1
Body Mass Index	28.3	28.3	25.4	26.2
<i>Observed changes after 2 years expressed in % ± SEM</i>				
vBMD Trabecular Total (mg/cm ³)	-7.7 ± 1.0 *	2.8 ± 1.5	6.9 ± 1.3 *	2.4 ± 0.7 **
Cortical Surface Density (mg/cm ²)	-3.1 ± 0.4 *	2.3 ± 0.8 ***	2.6 ± 0.5 *	2.8 ± 0.4 *
vBMD Integral Total (mg/cm ³)	-4.9 ± 0.6 *	2.4 ± 0.7 ***	3.2 ± 0.6 *	2.9 ± 0.4 *
aBMD Total Femur (mg/cm ²)	-3.2 ± 0.4 *	1.3 ± 0.5	2.5 ± 0.4 *	2.0 ± 0.3 *

Significant difference from baseline: * p< 0.001 ** p< 0.01 *** p< 0.05

Disclosures: Fidencio Cons Molina, None

MON-0724

Sandwich Immunoassay for the Specific Detection of Circulating Bioactive Sclerostin in comparison with other Sclerostin ELISA Jacqueline Wallwitz*, Elisabeth Gadermaier, Gabriela Berg, Gottfried Himmler. The Antibody Lab GmbH, Austria

Purpose: Sclerostin is a glycoprotein of the DAN/Cerberus protein family and is mainly secreted by osteocytes. It has long highly flexible N- and C-terminal arms and the core consists of a cystine-knot with three loops. The bioactive function of sclerostin is the regulation of bone formation as an antagonist of the osteoanabolic Wnt signaling pathway by binding with its second loop to the LRP5/6 complex. In a clinical setting, blocking sclerostin by therapeutic antibodies is an important approach to decrease bone resorption. There are some ELISAs on the market, but they neither specifically detect bioactive sclerostin, nor specify the epitopes of their antibodies. Therefore it is not clear which forms or fragments of sclerostin are detected. Our ELISA specifically detects the bioactive sclerostin in human serum and plasma samples.**Methods:** We have developed an immunoassay for the detection of bioactive sclerostin in human samples. The ELISA contains a monoclonal capture and a horseradish-peroxidase conjugated affinity-purified polyclonal detection antibody. Both antibodies were characterized regarding their epitopes, affinities and kinetics. The assay performance was validated according to ICH and EMEA guidelines. Measured bioactive sclerostin con-

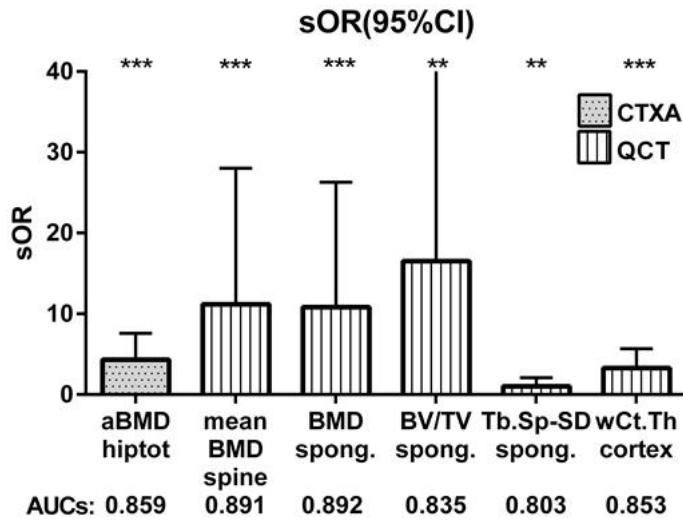
centrations in apparently healthy individuals as well as in diseased patients were compared with other commercially available ELISA (Biomedica, Teco and R&D Systems).**Results:** Epitope mapping revealed a distinct epitope within the bioactive site of sclerostin for the monoclonal capture antibody and five linear epitopes distributed throughout sclerostin for the detection antibody. Both antibodies have good binding kinetics of kdiss of <1.0E-07 s⁻¹ for the monoclonal antibody and 1.19E-05 s⁻¹ for the polyclonal goat antibody, respectively. All validation parameters were within the standard of acceptance demonstrating the robustness, accuracy and precision of the assay. The correlation between the assays was dependent on the sample type and disease state of the patients.**Conclusion:** This validated ELISA is a tool for the defined detection of bioactive Sclerostin in human samples and may be helpful to further investigate sclerostin as a biomarker in the diagnosis of bone remodeling disorders and in the assessment of therapeutic effectiveness.

Disclosures: Jacqueline Wallwitz, None

MON-0725

Combined model of QCT derived bone mass and microarchitecture parameters for improved vertebral fracture discrimination Lukas Maximilian Huber^{*1}, Timo Damm¹, Stefan Reinhold², Wolfram Timm³, Jan Borggrefe⁴, Julian Ramin Andresen⁵, Claus-Christian Glüer¹, Reimer Andresen⁶. ¹Section Biomedical Imaging, Department of Radiology and Neuroradiology, UKSH, Christian-Albrechts-Universität zu Kiel, Germany, ²Department of Computer Science, Multimedia Information Processing Group, Christian-Albrechts-Universität zu Kiel, Germany, ³MINDWAYS CT, United States, ⁴Department of Diagnostic and Interventional Neuroradiology, University Hospital Cologne, Germany, ⁵Medical School, Sigmund Freud University, Austria, ⁶Institute of Diagnostic and Interventional Radiology/Neuroradiology, Westkuestenlinikum Heide, Academic Teaching Hospital of the Universities of Kiel, Luebeck and Hamburg, Germany

Objectives We compared the performance of multiparameter quantitative computed tomography (QCT) and CTXA based areal bone mineral density (aBMD) in discriminating patients with and without vertebral fractures. Automatic segmentation was applied for detailed analyses of bone density and microarchitecture.**Methods** 135 female patients (mean age 69[40-89] years) were examined for osteoporosis, 67 with at least one fractured vertebral body (cases) and 68 without fractures (controls). Clinical QCT images of the spine (120kVp,90-420mAs,st 0.8mm,reconstructed increment 0.4mm,in-plane px size 0.5-0.7mm) and CTXA of the hip were evaluated using standard QCT software (Mindways). Simultaneous calibration to mg/cc K2HPO4 and additional analysis of the spinal images was performed using StructuralInsight (SI), our in-house CT software. Segmentation process: cortical ridge surface is modeled by a statistical shape model (automatically constructed meshes extracted from pre-segmented images (EuroGIOPs)). Following automated landmark generation and alignment process, model parameters are optimized to maximize BMD along the surface. After manual correction to improve accuracy, the detected ridge surface is used to generate the final mask. Fracture status was evaluated by an experienced radiologist (RA). Fracture discrimination was assessed in age-adjusted logistic regression models (per SD) and ROC analysis (AUC) using JMP and MedCalc. Investigated parameters: mean BMD (typically L1-3; meanBMDspine) and aBMD of total proximal femur (aBMDDhptot). Using SI we calculated bone volume fraction (BV/TV), BMD and SD of trabecular separation (Tb.Sp-SD) of the spongiosa along with weighted cortical thickness (whole cortex, wCt.Th). Combined models (CM) were constructed.**Results** CM1: BMDspongiosa (p=0.0001)&Tb.Sp-SDspongiosa (p=0.002)&wCt.Thcortex (p=0.02) with AUC=0.920; CM2: BV/TVspongiosa (p=0.513)&Tb.Sp-SDspongiosa (p=0.002)&wCt.Thcortex (p=0.02) with AUC=0.892. AUC of CM1 was significantly larger than for aBMD (DeLong p=0.04) but not versus QCT based BMD (p=0.1).**Conclusion** All parameters investigated were found to discriminate patients with and without vertebral fractures. Combined analyses of bone mass and microarchitecture yield numerically highest AUCs but statistical improvement was only achieved compared to CTXA based aBMD, not versus QCT based BMD. Semiautomatic model based segmentation facilitates image analysis and is helpful for standardized QCT based fracture risk assessment.



Disclosures: Lukas Maximilian Huber, None

MON-0726

Prevalence of Diabetes in Patients with Osteoporotic Hip Fractures: A tertiary Care Center Fracture Consultation Service Experience Sabrina Huq*, Lakshmi Das, Arti Bhan, Mahalakshi Honasoge, Sudhaker D. Rao. Henry Ford Hospital, United States

Osteoporotic fractures are a major cause of disability, morbidity and mortality. Both diabetes mellitus (DM) and hip fractures contribute to morbidity and mortality. Although DM is a known risk factor for osteoporotic fractures and the risk of hip fracture is increased 1.3-2.1 folds in DM, little is known about the prevalence of DM in patients admitted to hospital for hip fractures. The aim of our study was to determine the prevalence of DM among patients admitted to hospital with acute proximal femur fractures over a five year period (January 1st, 2011 to December 31st 2016). The electronic health records of 163 patients with acute hip fractures in our tertiary care setting were reviewed to determine the prevalence of DM in patients with hip fractures. There were 72 Caucasians (44%), 52 African Americans (32%), 4 Hispanics (2%), 1 Asian, 1 Arab and 33 patients (20%) who had no race documented. The prevalence of DM was 36%, four fold higher than in the general population, and the majority (93%) were Typ 2 DM. Both serum 25-hydroxyvitamin D and PTH levels were numerically lower in DM patients compared to non-DM patients (19.3 ± 12.2 Vs. 22.3 ± 12.9 ng/ml, and 62.3 ± 38.2 Vs. 87 ± 103 pg/ml, respectively). It is postulated that fracture risk is increased in patients with DM most likely due to increased glycation of collagen leading to decreased plasticity and bone strength without necessarily affecting bone density. In addition lower PTH levels in DM imply a low bone turnover state resulting in "aged" bone, which compromises bone strength. Further studies are needed to confirm our finding of very high prevalence of DM in hip fracture patients. References: <https://www.ncbi.nlm.nih.gov/pubmed/29502187> Saito M, Fujii K, Mori Y, Marumo K. Role of collagen enzymatic and glycation induced cross-links as a determinant of bone quality in spontaneously diabetic WBN/Kob rats. Osteoporos Int. 2006;17(10):1514-1523. doi: 10.1007/s00198-006-0155-5.

Disclosures: Sabrina Huq, None

MON-0727

Peripheral Quantitative Computed Tomography Based Finite Element Modeling (pQCT-FE) in the Classification of Fracture Patients Hongyuan Jiang*, Dale Robinson¹, Peter Lee¹, Christopher Yates², John Wark¹. ¹The University of Melbourne, Australia, ²The Royal Melbourne Hospital, Australia

PURPOSE Dual energy x-ray absorptiometry (DXA) has limitations in identifying individuals with increased fracture risk. Volumetric data and density distribution acquired by peripheral quantitative computed tomography (pQCT) can be used to generate finite element models providing bone strength assessment. The current study aimed to assess the ability of this FE modeling framework in the classification of fracture patients and aged-matched healthy controls. METHODS Seventy-eight patients (61 females, 17 males) with recent low-trauma fracture and 85 aged-matched healthy controls (66 females, 19 males) were recruited. Participants underwent DXA scans of the hip and lumbar spine, and pQCT scans of the radius and tibia at 4% and 66% sites. Peripheral QCT images were used to establish a cross-sectional FE model. Stiffness and strength of four loading cases (compression, torsion, shear, bending) were obtained from the FE models. Area under the receiver operating curve (AUC) was calculated to assess the ability of each variable to classify fracture patients and controls. RESULTS No difference was observed in DXA, standard pQCT radius, and pQCT-FE radius variables between groups for both males and females (p<0.05). Differences in most standard pQCT tibia measures were observed in males, while only vBMD at 4%

tibia was significantly different between groups in females (p<0.05). Most pQCT-FE tibia variables at the 4% site were significantly different between groups in both females and males, while most pQCT-FE variables at the 66% site were significantly different only in males (p<0.05). In females, vBMD, compression stiffness and strength, shear stiffness and strength, bending strength at 4% tibia had higher AUC than DXA measures (0.80-0.84 vs 0.79), while no variables of radius or 66% tibia out-performed DXA measures. In males, the highest AUC was 0.94 observed for torsion strength at 4% radius compared to 0.89 for DXA hip BMD. Various variables from standard radius (0.90-0.93) and tibia (0.91-0.93) pQCT analysis, radius (0.90-0.94) and tibia (0.90-0.91) pQCT-FE out-performed DXA measures (0.88-0.89) in the classification between groups. CONCLUSION FE modeling of single pQCT cross sections of trabecular-dominant tibial epiphysis had highest ability to classify fracture patients and healthy controls. In combination with our recent validation study, this FE modeling framework has the potential to enhance fracture risk assessment and may be useful in clinical settings.

Table 1. Comparison in DXA, standard pQCT analysis and pQCT-FE between fractures and control in females and males (only variables with significant difference displayed)

DXA	Fracture (n=172)	Control (n=172)	Female		Male	
			p	p	p	p
DXA: lumbar spine aBMD	0.985	0.969	0.2	1.096	1.385	0.3
DXA: total hip aBMD	0.958	0.979	0.1	0.982	1.047	0.07
DXA: femoral neck aBMD	0.934	0.939	0.5	0.944	0.950	0.99
DXA: femoral neck vBMD	0.099	0.120	0.2	0.805	0.841	0.4
DXA: total hip vBMD	0.109	0.144	0.001	0.109	0.179	0.001
DXA: total hip Ct.Th	212.53	207.53	0.4	214.62	192.72	0.04
DXA: total hip Tb.Th	182.03	190.49	0.001	186.96	185.08	0.001
DXA: total hip Tb.Sp	268.82	286.20	0.8	263.11	282.99	0.02
DXA: total hip Tb.N	183.39	186.27	0.3	173.50	182.08	0.03
DXA: total hip BV/TV	426.54	407.79	0.5	478.76	386.27	0.03
DXA: total hip Ct.Th	293.45	320.86	0.001	282.28	336.05	0.001
DXA: total hip Tb.Th	213.02	215.96	0.3	216.21	208.54	0.001
DXA: total hip Tb.Sp	76.54	64.53	0.001	70.73	117.05	0.001
DXA: total hip Tb.N	963.97	1018.37	0.1	1475.35	1508.52	0.05
DXA: total hip vBMD	213.87	147.87	0.1	189.38	106.79	0.001
DXA: total hip Ct.Th	1403.81	1447.29	0.4	1404.88	1308.84	0.01
DXA: total hip Tb.Th	795.81	795.64	0.99	795.02	717.02	0.001
DXA: total hip Tb.Sp	2031.72	2128.41	0.2	2029.58	1976.32	0.01
DXA: total hip Tb.N	401.28	454.77	0.001	414.54	438.05	0.001
DXA: total hip vBMD	925.24	1228.19	<0.001	1051.08	1754.84	0.01
DXA: total hip Ct.Th	289.24	302.40	0.001	278.97	409.14	0.001
DXA: total hip Tb.Th	4.89	6.40	<0.001	6.00	13.41	<0.001
DXA: total hip Tb.Sp	2.76	3.64	0.001	3.86	4.97	0.001
DXA: total hip Tb.N	215.54	205.81	<0.001	217.91	208.01	0.001
DXA: total hip vBMD	40.62	46.22	<0.001	40.82	326.06	0.01
DXA: total hip Ct.Th	2.02	3.01	<0.001	3.09	4.85	0.01
DXA: total hip Tb.Th	0.79	0.88	0.001	0.81	1.01	0.001
DXA: total hip Tb.Sp	1123.80	1232.04	0.1	1232.90	1250.13	0.03
DXA: total hip Tb.N	98.72	117.02	0.001	100.02	100.08	0.001
DXA: total hip vBMD	14.07	14.01	0.88	14.31	74.53	<0.001
DXA: total hip Ct.Th	17.22	16.94	0.99	18.65	20.20	0.02
DXA: total hip Tb.Th	19.20	19.86	0.001	19.67	18.47	0.001
DXA: total hip Tb.Sp	18.15	17.80	0.88	18.66	19.39	0.03
DXA: total hip Tb.N	2405.39	1920.74	0.2	1704.51	4013.82	0.01
DXA: total hip vBMD	613.79	168.99	0.001	679.73	1385.51	0.001
DXA: total hip Ct.Th	102.02	118.85	<0.001	117.91	176.51	0.01
DXA: total hip Tb.Th	28.38	28.38	0.99	27.79	46.02	0.001
DXA: total hip Tb.Sp	223.80	230.99	0.2	218.26	4296.25	0.04
DXA: total hip Tb.N	107.86	107.86	0.99	107.86	110.13	0.01
DXA: total hip vBMD	83.58	86.97	0.3	125.12	138.58	0.03
DXA: total hip Ct.Th	17.11	17.28	0.88	18.01	20.19	0.01

Table 2. AUCs for each variable in females and males (only variables with higher AUC than DXA measures displayed)

DXA	Fracture (n=172)	Control (n=172)	Female		Male	
			AUC	AUC	AUC	AUC
DXA: LS aBMD	0.78	0.88	0.78	0.88	0.77	0.89
DXA: TH aBMD	0.77	0.89	0.77	0.89	0.79	0.88
DXA: FN aBMD	0.79	0.88	0.79	0.88	0.74	0.90
DXA: FN vBMD	0.74	0.89	0.74	0.92	0.75	0.93
DXA: FN Ct.Th	0.74	0.92	0.74	0.92	0.74	0.91
DXA: FN Tb.Th	0.74	0.91	0.74	0.91	0.74	0.91
DXA: FN Tb.Sp	0.74	0.91	0.74	0.91	0.74	0.91
DXA: FN Tb.N	0.74	0.91	0.74	0.91	0.74	0.91
DXA: FN vBMD	0.74	0.91	0.74	0.91	0.74	0.91
DXA: FN Ct.Th	0.74	0.91	0.74	0.91	0.74	0.91
DXA: FN Tb.Th	0.74	0.91	0.74	0.91	0.74	0.91
DXA: FN Tb.Sp	0.74	0.91	0.74	0.91	0.74	0.91
DXA: FN Tb.N	0.74	0.91	0.74	0.91	0.74	0.91
DXA: FN vBMD	0.74	0.91	0.74	0.91	0.74	0.91
DXA: FN Ct.Th	0.74	0.91	0.74	0.91	0.74	0.91
DXA: FN Tb.Th	0.74	0.91	0.74	0.91	0.74	0.91
DXA: FN Tb.Sp	0.74	0.91	0.74	0.91	0.74	0.91
DXA: FN Tb.N	0.74	0.91	0.74	0.91	0.74	0.91
DXA: FN vBMD	0.74	0.91	0.74	0.91	0.74	0.91
DXA: FN Ct.Th	0.74	0.91	0.74	0.91	0.74	0.91
DXA: FN Tb.Th	0.74	0.91	0.74	0.91	0.74	0.91
DXA: FN Tb.Sp	0.74	0.91	0.74	0.91	0.74	0.91
DXA: FN Tb.N	0.74	0.91	0.74	0.91	0.74	0.91
DXA: FN vBMD	0.74	0.91	0.74	0.91	0.74	0.91
DXA: FN Ct.Th	0.74	0.91	0.74	0.91	0.74	0.91
DXA: FN Tb.Th	0.74	0.91	0.74	0.91	0.74	0.91
DXA: FN Tb.Sp	0.74	0.91	0.74	0.91	0.74	0.91
DXA: FN Tb.N	0.74	0.91	0.74	0.91	0.74	0.91
DXA: FN vBMD	0.74	0.91	0.74	0.91	0.74	0.91
DXA: FN Ct.Th	0.74	0.91	0.74	0.91	0.74	0.91
DXA: FN Tb.Th	0.74	0.91	0.74	0.91	0.74	0.91
DXA: FN Tb.Sp	0.74	0.91	0.74	0.91	0.74	0.91
DXA: FN Tb.N	0.74	0.91	0.74	0.91	0.74	0.91
DXA: FN vBMD	0.74	0.91	0.74	0.91	0.74	0.91
DXA: FN Ct.Th	0.74	0.91	0.74	0.91	0.74	0.91
DXA: FN Tb.Th	0.74	0.91	0.74	0.91	0.74	0.91
DXA: FN Tb.Sp	0.74	0.91	0.74	0.91	0.74	0.91
DXA: FN Tb.N	0.74	0.91	0.74	0.91	0.74	0.91
DXA: FN vBMD	0.74	0.91	0.74	0.91	0.74	0.91
DXA: FN Ct.Th	0.74	0.91	0.74	0.91	0.74	0.91
DXA: FN Tb.Th	0.74	0.91	0.74	0.91	0.74	0.91
DXA: FN Tb.Sp	0.74	0.91	0.74	0.91	0.74	0.91
DXA: FN Tb.N	0.74	0.91	0.74	0.91	0.74	0.91
DXA: FN vBMD	0.74	0.91	0.74	0.91	0.74	0.91
DXA: FN Ct.Th	0.74	0.91	0.74	0.91	0.74	0.91
DXA: FN Tb.Th	0.74	0.91	0.74	0.91	0.74	0.91
DXA: FN Tb.Sp	0.74	0.91	0.74	0.91	0.74	0.91
DXA: FN Tb.N	0.74	0.91	0.74	0.91	0.74	0.91
DXA: FN vBMD	0.74	0.91	0.74	0.91	0.74	0.91
DXA: FN Ct.Th	0.74	0.91	0.74	0.91	0.74	0.91
DXA: FN Tb.Th	0.74	0.91	0.74	0.91	0.74	0.91
DXA: FN Tb.Sp	0.74	0.91	0.74	0.91	0.74	0.91
DXA: FN Tb.N	0.74	0.91	0.74	0.91	0.74	0.91
DXA: FN vBMD	0.74	0.91	0.74	0.91	0.74	0.91
DXA: FN Ct.Th	0.74	0.91	0.74	0.91	0.74	0.91
DXA: FN Tb.Th	0.74	0.91	0.74	0.91	0.74	0.91
DXA: FN Tb.Sp	0.74	0.91	0.74	0.91	0.74	0.91
DXA: FN Tb.N	0.74	0.91	0.74	0.91	0.74	0.91
DXA: FN vBMD	0.74	0.91	0.74	0.91	0.74	0.91
DXA: FN Ct.Th	0.74	0.91	0.74	0.91	0.74	0.91
DXA: FN Tb.Th	0.74	0.91	0.74	0.91	0.74	0.91
DXA: FN Tb.Sp	0.74	0.91	0.74	0.91	0.74	0.91
DXA: FN Tb.N	0.74	0.91	0.74	0.91	0.74	0.91
DXA: FN vBMD	0.74	0.91	0.74	0.91	0.74	0.91
DXA: FN Ct.Th	0.74	0.91	0.74	0.91	0.74	0.91
DXA: FN Tb.Th	0.74	0.91	0.74	0.91	0.74	0.91
DXA: FN Tb.Sp	0.74	0.91	0.74	0.91	0.74	0.91
DXA: FN Tb.N	0.74	0.91	0.74	0.91	0.74	0.91
DXA: FN vBMD	0.74	0.91	0.74	0.91	0.74	0.91
DXA: FN Ct.Th	0.74	0.91	0.74	0.91	0.74	0.91
DXA: FN Tb.Th	0.74	0.91	0.74	0.91	0.74	0.91
DXA: FN Tb.Sp	0.74	0.91	0.74	0.91	0.74	0.91
DXA: FN Tb.N	0.74	0.91	0.74	0.91	0.74	0.91
DXA: FN vBMD	0.74	0.91	0.74	0.91	0.74	0.91
DXA: FN Ct.Th	0.74	0.91	0.74	0.91	0.74	0.91
DXA: FN Tb.Th	0.74	0.91	0.74	0.91	0.74	0.91
DXA: FN Tb.Sp	0.74	0.91	0.74	0.91	0.74	

Table 1. Interrelationships of bone properties at the proximal femur.

A	B	FF	R2*	Tb.vBMD	Ct.Th	Ct.vBMD	EndoTb.vBMD	f-BVF	Tb.Th	Tb.Sp	Tb.N
FF											
R2*											
Tb.vBMD											
Ct.Th											
Ct.vBMD											
EndoTb.vBMD											
f-BVF											
Tb.Th											
Tb.Sp											
Tb.N											

The linear dependence of parameter A on parameter B was tested as:
 $A = \beta_0 + \beta_1 \cdot B + \beta_2 \cdot \text{Age} + \beta_3 \cdot \text{Height} + \beta_4 \cdot \text{Weight}$
 The nonlinear dependence of parameter A on parameter B was tested as:
 $A = \beta_0 + \beta_1 \cdot B + \beta_2 \cdot B^2 + \beta_3 \cdot \text{Age} + \beta_4 \cdot \text{Height} + \beta_5 \cdot \text{Weight}$

Significant (p<0.05) linear association of A and B in: TH FH FN TR
 Significant (p<0.05) quadratic association of A and B in: TH FH FN TR

Abbreviations: FF=fat fraction; Tb.vBMD=trabecular volumetric bone mineral density; Ct.Th=cortical bone thickness; Ct.vBMD=cortical vBMD; EndoTb.vBMD=vBMD adjacent to the endosteal surface; f-BVF=fuzzy bone volume fraction; Tb.Th=trabecular bone thickness; Tb.Sp=trabecular bone spacing; Tb.N= trabecular bone number; TH=total hip; FH=femoral head; FN=femoral neck; TR=trochanter; + = positive association; - = negative association.

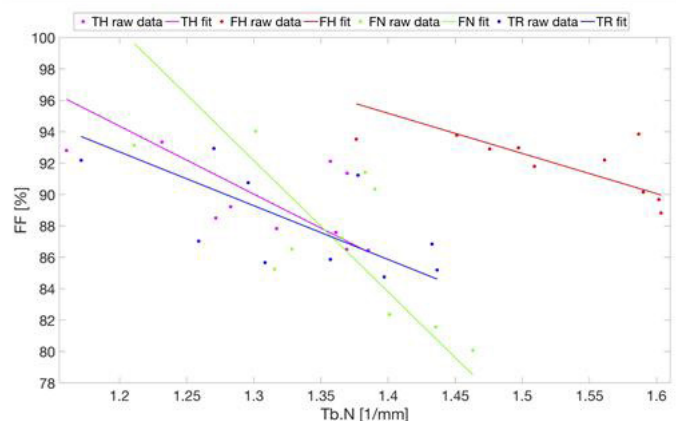


Fig. 1 Plots representing the linear associations of bone marrow fat fraction (FF) with trabecular bone number (Tb.N) at four different volumes of interest in the proximal femur of postmenopausal women without fragility fractures.

Disclosures: Roland Krug, None

MON-0729

Low-grade morphometric vertebral deformities result from historical events and are unlikely to be primarily osteoporotic in provenance Brian C Lentle^{*1}, Jacques P Brown², Linda Probyn³, Ian Hammond⁴, Jeffrey Hu¹, Ben Fine³, Kevin Lian¹, Arvind Shergill³, Jacques Trollip¹, Claudie Berger⁵, William D Leslie⁶, Jerilynn C Prior¹, David A Hanley⁷, Jonathan D Adachi⁸, Robert G Josse³, Angela M Cheung³, K Shawn Davison⁹, Stephanie M Kaiser¹⁰, Tanveer Towheed¹¹, Christopher S Kovacs¹², Andy Ko Wong³, David Goltzman¹³. ¹University of British Columbia, Canada, ²Université Laval, Canada, ³University of Toronto, Canada, ⁴University of Ottawa, Canada, ⁵Research Institute of the McGill University Health Centre, Canada, ⁶University of Manitoba, Canada, ⁷University of Calgary, Canada, ⁸McMaster University, Canada, ⁹A Priori Medical Sciences Inc, Canada, ¹⁰Dalhousie University, Canada, ¹¹Queen's University, Canada, ¹²Memorial University, Canada, ¹³McGill University, Canada

We have previously reported on the radiology of vertebral fractures (VFs) from the Canadian Multicentre Osteoporosis Study (CaMos). We compared two diagnostic methods: identifying fractures by morphometric and morphologic criteria respectively. Suspecting a difference in the natural history of these two types of "fracture" we have re-evaluated serial radiographs performed every 5 years in a sub-set of 595 from the 4465 women and 1771 men aged 50 or more years entered into the CaMos Study. These subjects were from three of the nine CaMos centres, chosen randomly, who have available radiographic images of the spine at baseline and for 15 or 16 years of follow-up. Of the 595 subjects, 170 (38.6%) had incident spinal abnormalities: 121 women had 246 such events and 49 men had 123. The ratio of morphologic to morphometric findings was 1.93 in women and 1.20 in men, indicating that

morphometric deformities were proportionately more common in men. At study entry (age 50 or more), 165 subjects had grade 1 and 22 subjects had grade 2 morphometric deformities; 5 and 10 years later only 5 and 3 subjects respectively had sustained new grades 1 or 2 morphometric deformities. Contrastingly, 34 subjects had grade 1 and 72 subjects had grade 2 morphologic fractures at entry but 5 and 10 years later, 46 and 47 subjects respectively had new grades 1 or 2 fractures, 11-times as many in total. Thus incident morphometric deformities were common at study entry (age 50) but rarely occurred thereafter, with most of the incident fractures being of the morphologic type. This extended analysis of our data adds to the body of evidence to suggest that morphometric deformities and morphologic fractures constitute relatively distinct entities with the latter conforming much more closely to our clinical understanding of OVF. In addition to the differences already reported, these two types of abnormalities evolve differently in time, differ in prevalence between the sexes, and have different radiological characteristics and prognoses.

Disclosures: Brian C Lentle, None

MON-0730

Feasibility of QCT internal density calibration for site-specific osteoporosis assessment Andrew Michalski^{*}, Bryce Besler, Geoff Michalak, Steven Boyd. University of Calgary, Canada

Quantitative computed tomography (QCT) is a well-defined method to assess skeletal health for osteoporosis. Volumetric bone mineral density (BMD) is a primary QCT outcome. To measure density, CT numbers are converted to equivalent densities by phantom-based or asynchronous density calibration. However, the inclusion of a density calibration phantom in clinical CT scans is limited to specific scanning protocols. Therefore, internal density calibration has been proposed for retrospective clinical scan analysis, but there is insufficient evidence supporting its use at major osteoporotic fracture sites. We designed our study to establish the feasibility of internal calibration, as compared with phantom-based and asynchronous scans, at the lumbar spine and proximal femur. Additionally, we evaluated intra- and inter-operator reanalysis precision for each site. The lumbar spine and pelvis from intact fresh-frozen cadavers (N=10) were imaged with clinical CT (Revolutions CT, GE Healthcare) to derive integral BMD. Density calibration was performed for each scan using phantom-based, asynchronous and internal calibration. Our internal density calibration method, based upon fundamental X-ray imaging physics, used five regions of interest within each scan to derive a relationship between CT number and equivalent density. Phantom-based and internal calibration BMD results were compared using linear regression, where a slope of 1 signifies agreement. For both the spine (Figure 1A) and pelvis (Figure 1B), the slope of the regression was not different than 1 (spine p=0.99, pelvis p=0.08). Similarly, comparing asynchronous and internal calibration resulted in a regression slope that was not different than 1 (spine p=0.93, pelvis p=0.08) at both the spine and pelvis. Precision measures for internal calibration were determined by performing measurements in triplicate and by three independent operators. Intra-operator root mean square coefficient of variation was 2.66% at the spine and 3.42% at the pelvis. Inter-operator coefficient of variation was 4.93% at the spine and 5.44% at the pelvis. These data demonstrate that our internal density calibration is feasible for accurate QCT BMD assessment at both the spine and the pelvis. However, due to large precision outcomes, our method needs to be further refined before application to clinical monitoring. With further work, internal calibration is a promising technique for opportunistic CT assessment of skeletal health.

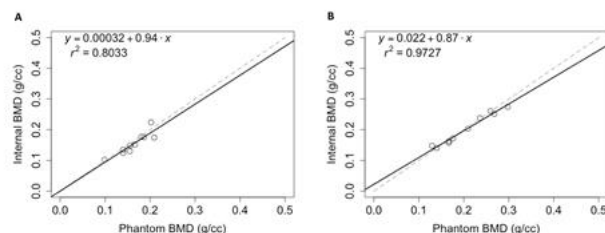


Figure 1: Linear regression plots comparing internal calibration and phantom-based calibration in the spine (A) and the pelvis (B).

Disclosures: Andrew Michalski, None

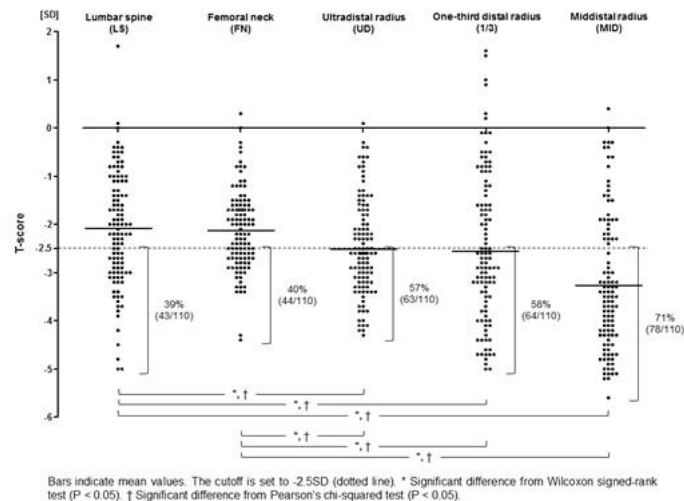
MON-0731

Utility of the Forearm Dual X-ray Absorptiometry (DXA) as a Screening Tool for Early Osteoporosis Diagnosis in Postmenopausal Women with Primary Fragility Fractures at Distal Radius Satoshi Miyamura^{*1}, Kosuke Ebina¹, Kohji Kuriyama², Kunihiro Oka¹, Hiroyuki Tanaka¹, Tsuyoshi Murase¹. ¹Department of Orthopaedic Surgery, Osaka University, Graduate School of Medicine, Japan, ²Department of Orthopaedic Surgery, Japan Community Health Care Organization Hoshigaoka Medical Center, Japan

Purpose: Previous reports have demonstrated that primary osteoporotic fragility fractures in postmenopausal women frequently occur at distal radius. Nevertheless, the guidelines of osteoporosis recommend assessment of bone mineral density (BMD) by dual x-ray

Monday Posters

absorptiometry (DXA) at either spine or hip as a screening for osteoporosis. The purpose of this single center, retrospective study was to verify which part of the BMD measurements is most sensitive as a screening tool for early osteoporosis diagnosis. Methods: One hundred and ten postmenopausal women with primary fragility fractures at distal radius, who had no past history of osteoporotic fractures and osteoporosis treatment were recruited. Spine, hip and forearm DXA (Hologic Discovery Wi; Hologic Inc., Waltham, MA, USA) and spinal radiograph were performed at the time of injury. BMD measurements with T-score were recorded for the lumbar spine (LS; L2-4 with exclusion of degenerated lesions), femoral neck (FN), and unfractured distal forearm (DF) [ultradistal end (UD), middistal (MID), and one-third distal (1/3) of the radius]. T-scores and patients with T-score ≤ -2.5 SD according to the WHO definition of osteoporosis, were compared between those in LS, FN, and DF, by using Wilcoxon signed-rank test and Pearson's chi-squared test, respectively. Results: The mean age of the study participants were 69.5 years (range, 42 to 88 years). T-scores (mean \pm SD) and proportions of patient with T-score ≤ -2.5 SD were LS $[-2.1 \pm 1.2; 39\% (43/110)]$, FN $[-2.1 \pm 0.8; 40\% (44/110)]$, UD $[-2.5 \pm 1.0; 57\% (63/110)]$, 1/3 $[-2.6 \pm 1.5; 58\% (64/110)]$, and MID $[-3.3 \pm 1.4; 71\% (78/110)]$, respectively. Compared with LS and FN, T-scores of UD (vs LS: $P = 0.012$; vs FN: $P < 0.001$), 1/3 (vs LS: $P = 0.036$; vs FN: $P = 0.024$), and MID (vs LS: $P < 0.001$; vs FN: $P < 0.001$) were significantly lower, and proportions of patient with T-score ≤ -2.5 SD in the UD (vs LS: $P = 0.007$; vs FN: $P = 0.010$), 1/3 (vs LS: $P = 0.005$; vs FN: $P = 0.007$), and MID (vs LS: $P < 0.001$; vs FN: $P < 0.001$) were significantly higher. Conclusion: In postmenopausal women with primary fragility fractures at distal radius, BMD measurements of unfractured DF, especially in MID of the radius, hold promise as a screening tool for early osteoporosis diagnosis.



Disclosures: Satoshi Miyamura, None

MON-0732

Opportunistic Screening of FDG-PET/CT Reveals Undiagnosed Low Bone Mass in Patients Being Evaluated for Oncology Purposes Fernando Kay¹, Edmund Dosunmu², Keenan Brown³, Orhan Oz². ¹UT Southwestern Medical Center, United States, ²UT Southwestern Medical Center - Radiology, United States, ³Mindways Software, United States

Purpose To assess the prevalence of undetected low bone mineral density (BMD) with quantitative computed tomography (QCT) in a cohort of potentially at risk patients undergoing PET/CT. Methods A retrospective survey was conducted in a high complexity US county hospital to identify PET/CT studies obtained between Oct/2015 and Jan/2016 in a Biograph 64 scanner (Siemens). Images were processed with the QCT Pro software (Mindways). A calibration CT scan was obtained in the same PET/CT scanner using the asynchronous Model 4 QCT Phantom. Two radiologists (one a certified clinical densitometrist) and a trained research technician performed the analyses of trabecular BMD at vertebral bodies L1 and L2. The American College of Radiology (ACR) criteria was used for diagnosing low BMD. Total BMD of femoral necks were measured on DXA-equivalent images (CTXA) of the hips and used to generate FRAX-scores for calculating absolute fracture risks. We obtained clinical data from institutional medical records. Requirement for signed informed consent was waived by the IRB. Results Sixty-nine studies were identified, two studies excluded due to severe scoliosis and one excluded due to Schmorl node affecting the analysis. The final cohort comprised 66 subjects (20F/46M, mean age: 53.8, SD: 12.1). Mean coefficient of variation (CV) for trabecular BMD in L1-2 between the 3 readers was 1.2%. Distribution of subjects according to ACR category is shown in Table 1. Thirty-two percent (21/66) of subjects showed low lumbar spine BMD on QCT. Twenty-four percent (5/21) of subjects with low BMD on QCT had a prior DXA scan, all of which showing low BMD. None of the subjects with normal BMD on QCT had a prior DXA scan. Femoral neck BMD was assessed with CXTA in 20 of 66 subjects by one radiologist and the research technician. Mean CV between the readers was 6.1%. Fifteen percent (3/20) of the subjects had at least a 3% risk of hip fracture within 10 years. Only 33.3% (1/3) of these subjects had a prior diagnosis of low BMD. Conclusion Low BMD was an under recognized condition in our sample. PET/

CT provides a unique opportunity to assess for occult low BMD in unscreened populations by leveraging the quantitative capabilities of CT. Identification of subjects at risk for future osteoporotic fractures may not only improve outcomes, but also decrease downstream costs. Future analysis will correlate metabolic activity (FDGuptake) with bone mass.

ACR Category	N	Trabecular BMD - L1	Trabecular BMD - L2
Osteoporosis (< 80 mg/cc)	6 (9%)	65.1 \pm 12.5	65.7 \pm 16.3
Osteopenia (80-120 mg/cc)	15 (23%)	103.4 \pm 13.6	100.5 \pm 12.7
Normal (> 120 mg/cc)	45 (68%)	166.8 \pm 39.1	163.0 \pm 40.1
Total	66 (100%)	143.1 \pm 49.0	140.0 \pm 48.8

Disclosures: Fernando Kay, None

MON-0733

Lower Trabecular Bone Score is Associated with the Use of Proton Pump Inhibitors Young Ho Shin¹, Hyun Sik Gong². ¹Department of Orthopedic Surgery, Asan Medical Center, Republic of Korea, ²Department of Orthopedic Surgery, Seoul National University Bundang Hospital, Seoul National University College of Medicine, Republic of Korea

Purpose: Trabecular bone score (TBS) provides indirect indices of trabecular microarchitecture and bone quality. Several studies have evaluated the influence of PPIs on bone mass and geometry parameters, but no studies have evaluated the influence of proton pump inhibitors (PPIs) on TBS. The purpose of this study was to determine whether TBS is associated with the use of PPIs. Methods: We reviewed 1505 women aged 40-89 years who had bone mineral density (BMD) examination as a part of the medical diagnosis and disease prevention program and did not have osteoporotic fractures or conditions that could affect bone metabolism. Among these, we identified 223 women with exposure to PPIs and selected the same number of age- and body mass index (BMI)-matched control patients. We compared TBS and BMD between the PPI exposure group and the control group and performed multivariate regression analyses to determine whether TBS is associated with age, BMI, and PPIs exposure. We also examined whether TBS is associated with PPIs exposure timing (current, recent, and past). Results: TBS and BMDs were significantly lower in the PPI exposure group than the control group. In a multivariable linear regression analysis, TBS was significantly associated with age ($p < 0.001$) and PPI exposure ($p = 0.02$). Lower TBS was associated with current PPIs use ($p = 0.005$), and not with recent or past PPIs usage. Conclusions: This study found that TBS is lower in subjects with PPIs exposure than in controls. The association of lower TBS with current PPIs use suggests that trabecular bone quality could be affected early by PPIs and the effect might be reversible.

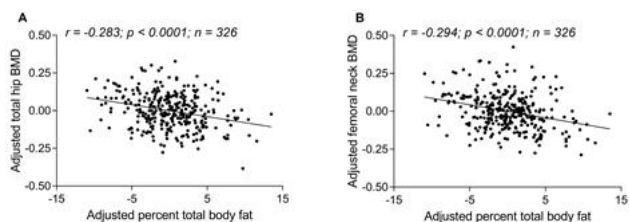
Disclosures: Young Ho Shin, None

MON-0734

Percent total body fat, independent of muscle mass, is negatively associated with bone mineral density in women Harshvardhan Singh¹, Roshita Rathore², Gary Hunter³, Debra Bembien⁴, Zhaojing Chen⁵, Kenneth Saag⁶. ¹Department of Physical Therapy, University of Alabama at Birmingham, United States, ²Department of Physical Therapy, Temple University, United States, ³Nutrition and Obesity Research Core, University of Alabama at Birmingham, United States, ⁴Department of Health and Exercise Science, University of Oklahoma, United States, ⁵Department of Kinesiology, California State University San Bernardino, United States, ⁶School of Medicine, University of Alabama at Birmingham, United States

Background: Obesity and osteoporosis are two of the most common chronic conditions associated with aging. Although obesity has been positively associated with bone mineral density (BMD), recent evidence suggests that obesity, when defined by percent total body fat, is negatively associated with BMD in Korean and South American adolescents. Notably, relationship between percent total body fat and BMD is unknown in American women across pre- to post-menopausal stages. Methods: Data from two separate studies with identical data collection methodologies are presented in this abstract. Dual energy X-ray absorptiometry (DXA) was used to measure the total hip BMD, femoral neck BMD, and body composition (percent total body fat) in 326 women (age range = 21 - 85 years; percent total body fat range = 24.7 - 55.9). Appendicular skeletal muscle mass (ASM) was quantified as the sum of the lean soft-tissues of the arms and legs. Relative skeletal muscle mass index (RSMI) was quantified as RSMI = ASM (kg) relative to body height² (m²). Data normality was checked with Shapiro-Wilk test. We used multi-variable regression analysis to examine associations of body fat with BMD. Results: Out of 326 women, there were 218 premenopausal (age range = 21.3 - 48.7 years; average age = 34.2 \pm 6.2 years; percent total body fat range = 33 - 54.2; average percent total body fat = 43.4 \pm 3.9) and 108 postmenopausal women (age range = 55.2 - 85.8 years; average age = 67.4 \pm 6.5 years; percent total body fat range = 24.7 - 55.9; average percent total body fat = 39.9 \pm 6.6). Regression analysis after adjusting for age, race, body weight, and RSMI showed that percent total body fat negatively predicted the 1) total hip BMD in premenopausal women ($\beta = -0.290$, 95% CI = -0.014 to -0.005, $P < 0.0001$) and postmenopausal women ($\beta = -0.358$, 95% CI = -0.010 to -0.001, $P = 0.016$), and 2) femoral neck BMD in premenopausal women ($\beta = -0.235$, 95% CI = -0.013 to -0.004, $P < 0.0001$) and postmenopausal women ($\beta = -0.504$, 95% CI = -0.011 to -0.003,

P = 0.001). Conclusion: Our findings suggest that, irrespective of muscle mass, total percent total body fat has an independent negative association with the total hip and femoral neck BMD in women across pre- to post-menopausal stages. This knowledge is important for musculoskeletal rehabilitation and decisions about weight loss in overweight/obese women.

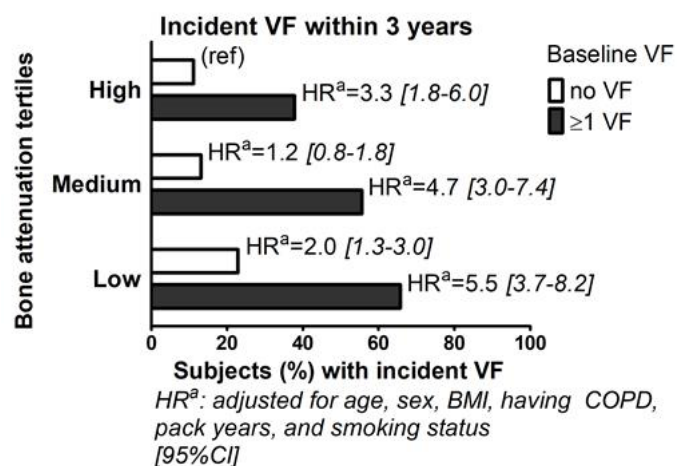


Disclosures: Harshvardhan Singh, None

MON-0735

The risk of incident vertebral fractures in current or former heavy smokers with and without COPD is associated with baseline vertebral bone attenuation and prevalent vertebral fractures: a 3-year chest-CT follow-up study Mayke Van Dort*¹, Johanna Driessen^{1,2,3}, Piet Geusens⁴, Elisabeth Romme⁵, Frank Smeenk⁵, Emiel Wouters⁶, Joop Van Den Bergh⁷. ¹NUTRIM School of Nutrition and Translational Research in Metabolism, Maastricht University Medical Centre+ (MUMC+), Netherlands, ²CAPHRI Care and Public Health Research Institute, Netherlands, ³Department of Clinical Pharmacy and Toxicology; Maastricht University Medical Centre+ (MUMC+), Netherlands, ⁴Department of Internal Medicine, Rheumatology, Maastricht University Medical Centre+ (MUMC+), Netherlands, ⁵Department of Respiratory Medicine, Catharina Hospital, Eindhoven, Netherlands, ⁶Department of Respiratory Diseases, Maastricht University Medical Centre+ (MUMC+), Netherlands, ⁷Department of Internal Medicine, VieCuri Medical Centre, Venlo; and Department of Internal Medicine, NUTRIM School of Nutrition and Translational Research in Metabolism, Maastricht University Medical Centre+ (MUMC+), Netherlands

Background Patients with chronic obstructive pulmonary disease (COPD) have increased risk of osteoporosis and vertebral fractures (VFs). Bone attenuation (BA) on CT scans, which are often made for pulmonary evaluation in COPD patients, is associated with bone mineral density on DXA and prevalent VFs. The association with incident (vertebral) fractures is largely unknown. Therefore our aim was to evaluate the association of BA on chest CT scans with prevalent and incident VFs in current or former smokers with and without COPD. Methods Participants of the ECLIPSE study with baseline, one and three year follow-up CT scans were included. BA was measured semi-automatically using 3D cubic areas of approximately 275mm³ each in vertebrae T4-T12. Prevalent and incident VFs within one and three years were evaluated on superposed sagittal reconstructions of the CT scans. VFs were scored according to the grading system proposed by Genant. Logistic regression and Cox proportional hazard models were used to assess relationships between clinical parameters and prevalent or incident VFs resp. Additionally, subjects were divided into three groups based on BA tertiles, to assess the effect of low or middle BA on incident VFs compared to high BA. Results 1239 subjects were included (mean age 61.3 ± 8.0, 61.1% men, 999 COPD patients, mean baseline BA 155.6 ± 47.5 Hounsfield Units (HU)). In multivariate models, lower BA (per -10HU OR=1.21 [95%CI 1.16-1.27]) and male sex (OR=1.89 [1.35-2.64]) were significantly associated with prevalent VFs. Baseline BA and prevalent VFs were significantly associated with incident VFs within one (BA per -10HU HR=1.08 [1.02-1.13]; VF HR=3.99 [2.67-5.93]) and three years (BA per -10HU HR=1.05 [1.02-1.08]; VF HR=3.12 [2.43-4.01]). In subjects without prevalent VFs, baseline BA was significantly associated with incident VFs (one year: per -10HU HR=1.09 [1.01-1.18]; and three years per -10HU HR=1.07 [1.02-1.12]). In addition, in absence of prevalent VFs the lowest BA tertile was significantly associated with three year VF incidence (low vs. high group HR=2.0 [1.3-3.0], figure 1) but not with one year incidence (low vs. high group HR=1.7 [0.8-3.3]). Conclusion Baseline BA was an independent determinant for prevalent and incident VFs in (former) smokers with and without COPD, but a prevalent VF was a stronger determinant. This indicates that BA measurements combined with VF assessment on CT are useful for VF risk assessment.



Disclosures: Mayke Van Dort, None

MON-0736

Investigation of Second-Generation HR-pQCT to Improve Assessment of Hip Fracture Risk in Women Danielle E Whittier*, Lauren A Burt, Prism S Schneider, Steven K Boyd. McCaig Institute for Bone & Joint Health, Cumming School of Medicine, University of Calgary, Canada

Areal bone mineral density (aBMD) measured using dual-energy X-ray absorptiometry (DXA) is a reasonable predictor of bone strength, but it has limitations. Most people who have had a fragility fracture of the hip are not considered osteoporotic (T-Scores above -2.5). High-resolution peripheral quantitative computed tomography (HR-pQCT) offers a promising approach to improve assessment of fracture risk, as it allows for the evaluation of bone microarchitecture, which has been shown to be independently correlated with fracture risk. The objective of this study was to determine what measurable bone microarchitecture properties differentiate women with and without hip fractures, but who would not be captured using current clinical tools for assessing fracture risk. Six women (aged 78.4 ± 5.0 years) who have had a hip fracture in the past 6 months and sixteen healthy women (aged 75.1 ± 5.7 years) with no prior history of fragility fractures had their distal radius and tibia scanned using the second-generation HR-pQCT (XtremeCT II, Scanco Medical, 61 µm). Standard bone density and microarchitecture parameters obtained from HR-pQCT were assessed, in addition to DXA-based total hip (TH) aBMD. Differences in measured bone parameters between women with and without a hip fracture are described using two-sided t-tests, and the association between measured bone parameters and fracture status was determined using univariate logistic regression expressed as odds ratios (OR) per standard deviation (SD) change (with 95% CI). Women with hip fractures had an average T-Score of -1.8 (range -3.0 to -0.8), with only one below -2.5. TH aBMD, total BMD (TtBMD), and cortical BMD (CtBMD) at the tibia were significantly (p<0.05) lower in women with hip fractures, and each SD decrease in these parameters was associated with a significant increase in fracture risk (ORs between 4.78 to 6.04). Significant differences in trabecular number (TbN), and trabecular separation (TbSp) at the distal tibia were also observed, but were not associated with fracture risk. No significant differences were observed at the distal radius. Overall, women who had a hip fracture had lower bone density and lower quality trabecular microarchitecture at the tibia. These initial results suggest density and trabecular microarchitecture at the tibia may provide a basis to identify those at risk of a hip fracture, not previously captured using DXA-based measures alone.

Table 1: Mean and SD of TH aBMD and HR-pQCT parameters measured at the distal tibia for women with hip fractures and controls. Percent difference between group means, and association between parameters and fracture status, expressed as ORs per SD change are provided.

Parameter	Controls (N = 16)	Hip Fractures (N = 6)	Difference (Hip Fracture vs Control)	OR (95% CI)
TH aBMD [g/cm ²]	0.93 ± 0.13	0.78 ± 0.10	-16%*	5.93 (1.43 – 58.7)*
TtBMD [mgHA/cm ³]	278.7 ± 48.3	216.5 ± 40.7	-22%*	6.04 (1.57 – 40.9)*
CtBMD [mgHA/cm ³]	787.8 ± 69.9	676.1 ± 110.7	-14%*	4.78 (1.39 – 36.8)*
TbBMD [mgHA/cm ³]	179.6 ± 40.1	142.4 ± 51.2	-21%	2.77 (0.93 – 12.7)
TbN [1/mm]	1.37 ± 0.17	1.15 ± 0.30	-16%*	2.99 (1.04 – 13.8)
TbSp [mm]	0.71 ± 0.11	0.91 ± 0.31	28%*	3.12 (1.04 – 18.3)
TbTh [mm]	0.26 ± 0.02	0.26 ± 0.02	0%	1.38 (0.52 – 4.32)
CtTh [mm]	1.30 ± 0.26	1.12 ± 0.49	-14%	1.80 (0.67 – 6.18)
CtPo [%]	3.7 ± 1.5	3.6 ± 2.5	-3%	0.93 (0.30 – 2.42)

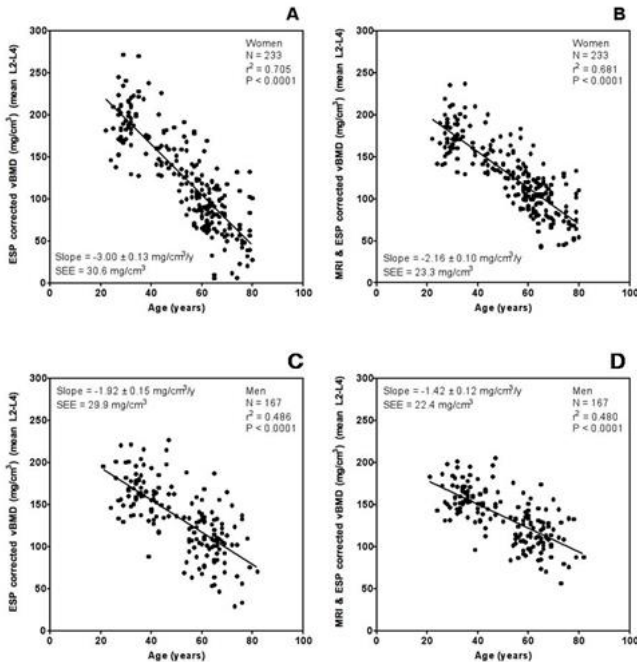
*p<0.05

Disclosures: Danielle E Whittier, None

MON-0737

The true relationship between bone marrow adipose tissue and volumetric BMD in the human spine Xiaoguang Cheng*¹, Kai Li¹, Yong Zhang¹, Ling Wang¹, Li Xu¹, Yangyang Duanmu¹, Cliff J Rosen², Glen M Blake³. ¹Department of Radiology, Beijing Jishuitan Hospital, China, ²Center for Clinical & Translational Research, Maine Medical Center Research Institute, United States, ³Biomedical Engineering Department, King's College London, United Kingdom

Objectives: In osteoporosis, a reduced level of bone formation associated with a reduction in the number and activity of osteoblasts is coupled with a corresponding increase in bone marrow adipose tissue (BMAT). Chemical shift-encoded magnetic resonance imaging (CSE-MRI) and single-energy quantitative computed tomography (SEQCT) offer precise ways of measuring BMAT and volumetric bone mineral density (vBMD) and studying their relationship. However, SEQCT vBMD measurements are subject to errors due to variations in the fat content of bone marrow. We have developed a novel method of using BMAT measurements to correct these errors and hence investigate the true relationship between vBMD and bone marrow composition. **Materials and Methods:** Four hundred healthy Chinese subjects (233 females, 167 males) aged between 21 and 82 years were enrolled in the study and had QCT and CSE-MRI scans of the L2-L4 vertebrae. Care was taken to ensure that matching regions of interest were used in both scans. Raw vBMD measurements were standardized to the European Spine Phantom (ESP) and then further corrected for the errors caused by the variations in BMAT. Scatter plots were drawn of BMAT, ESP adjusted vBMD and BMAT corrected vBMD against age and analyzed by linear regression to determine the rate of change with age between age 20 and 80 years and the standard error of the estimate (SEE) (Figure 1). **Results:** BMAT in the L2-L4 vertebral bodies increased progressively with age in both sexes, with a statistically significantly faster rate of change in women compared to with men (0.54%/y vs. 0.27%/y, P < 0.0001). In women there was a statistically significant change in the slope of the regression line with age after the vBMD measurements were corrected for BMAT (-3.00 ± 0.13 mg/cm³/y before correction vs. -2.16 ± 0.10 mg/cm³/y after correction, P < 0.0001). In addition, there was a statistically significant decrease in the SEE (30.6 mg/cm³ vs. 23.3 mg/cm³, P < 0.0001). There were similar findings in the men. **Conclusions:** Our approach reveals the true relationship between BMAT and vBMD, and provides a new tool for study of the interaction between marrow adipose tissue and bone.



Disclosures: Xiaoguang Cheng, None

MON-0782

Fall Risk Is a Predictor of Fracture Independent of Bone Mineral Density and Bone Strength: Results from the FOCUS study Annette L. Adams*¹, Heidi Fischer¹, David L. Kopperdahl², David C. Lee², Tony M. Keaveny³. ¹Kaiser Permanente Southern California, United States, ²O.N. Diagnostics, United States, ³University of California, Berkeley, United States

Fall risk remains a poorly quantified etiological factor in hip fractures, in part because of the difficulty in obtaining robust clinical metrics for fall risk. Addressing this issue, we assessed for both sexes the association between incident hip fracture and a fall risk metric that was characterized by the widely available Fall Risk Assessment Tool (FRAT), com-

monly used in geriatric evaluations and adapted here for use with electronic health record (EHR) data. We also accounted for other major risk factors, including hip BMD T-score and finite element-derived femoral strength from CT scans, as well as age, body mass index, race/ethnicity, prior history of fracture, and use of bisphosphonates and/or glucocorticoids. Our study population consisted of over 110,000 Kaiser Permanente Southern California (KPSC) patients aged ≥65 years with a pre-existing abdominal or pelvic CT exam between 01/01/2006 and 12/31/2014, who had no fragility hip fracture before the CT, and a DXA within three years of the CT. From that population, we identified a sex-stratified, randomly sampled subcohort and all incident hip fracture cases with available EHR data. The control group (without fracture) was randomly selected in approximately equal numbers to the cases. DXA-equivalent hip BMD T-scores and femoral strength were measured by analysis of the CT scans. The FRAT metric (0–4 point scale) included elements on falls within the previous year, number of medications used daily, diagnoses of stroke or Parkinson's disease, and evidence of gait or balance problems (1 point per category). Data are presented for 1019 women (645 cases) and 482 men (284 cases) with complete data at 5 years of follow-up. We found that, compared to women with a FRAT score of 0 or 1, women with a score of 2 (21.4% of the cohort) were nearly twice as likely to sustain a hip fracture, after adjustment for all other risk factors including the BMD T-score or bone strength; and women with a FRAT score of 3 or 4 (7.7% of the cohort) were approximately 5 times as likely to have a hip fracture (Table 1). The effect was stronger for men, with those with a FRAT score of 2 (23.4% of the cohort) being nearly 3 times as likely to have a hip fracture, and those with a score of 3 or 4 (7.1% of the cohort) being 10–12 times as likely (Table 1). These findings demonstrate that the FRAT score is a potent and independent risk factor for hip fracture. As such, its use may improve clinical assessment of hip fracture risk.

Table 1. Cox proportional hazard ratios per SD change (or binary change) for incident hip fracture, for univariate and multivariate (MV) models.

Characteristic	Women N=645			Men N=482		
	Univariate Model	Hip BMD MV Model	Bone Strength MV Model	Univariate Model	Hip BMD MV Model	Bone Strength MV Model
FRAT, 2 vs. 0 or 1	2.6 (1.7-3.3)	1.8 (1.2-2.6)	1.8 (1.2-2.6)	3.0 (1.9-4.9)	2.9 (1.6-5.7)	2.9 (1.6-5.2)
FRAT, 3 vs. 0 or 1	6.7 (3.3-14.1)	4.9 (2.2-10.8)	5.2 (2.3-11.4)	16.1 (3.8-68.7)	10.4 (2.5-47.4)	10.7 (2.4-48.5)
Hip BMD T-score	2.6 (2.2-3.0)	1.9 (1.6-2.3)	---	3.3 (2.5-4.4)	2.6 (1.8-3.7)	---
Bone Strength	3.3 (2.7-4.0)	---	2.4 (1.9-3.0)	3.3 (2.5-4.2)	---	2.6 (1.9-3.6)

All multivariate models also adjusted for age, body mass index, race/ethnicity, prior history of fracture, and use of bisphosphonates and/or glucocorticoids.

Disclosures: Annette L. Adams, Merck, Grant/Research Support, Amgen, Grant/Research Support

MON-0783

Cognitive Decline Is Associated with an Accelerated Rate of Bone Loss and Increased Fracture Risk in Women 65 years or Older in the Population-based Canadian Multicentre Osteoporosis Study (CaMos) Dana Bluc*¹, Thach Tran¹, Tineke Van Geel², Jonathan Adachi³, Claudie Berger⁴, Joop Van Den Bergh², John Eisman¹, Piet Geusens², David Goltzman⁵, David Hanley⁶, Robert Josse⁷, Stephanie Kaiser⁸, Christopher Kovacs⁹, Lisa Langsetmo¹⁰, Jerilynn Prior¹¹, Tuan Nguyen¹, Jacqueline Center¹. ¹Bone Biology Group, Garvan Institute of Medical Research, Australia, ²Maastricht University Medical Center, Netherlands, ³Department of Medicine, McMaster University, Canada, ⁴CaMos National Coordinating Centre, McGill University, Canada, ⁵Department of Medicine, McGill University, Canada, ⁶Department of Medicine, University of Calgary, Canada, ⁷Department of Medicine, University of Toronto, Canada, ⁸Department of Medicine, Dalhousie University, Canada, ⁹Faculty of Medicine, Memorial University, Canada, ¹⁰School of Public Health, University of Minnesota, Twin cities, United States, ¹¹Department of Medicine and Endocrinology, University of British Columbia, Canada

Background: Cognitive deficit is prevalent among older people with fractures; some evidence suggests recent bone loss predicts it. However, it is not clear whether this association is independent of ageing. Longitudinal studies that assess the complex relationships among cognitive decline, loss of areal bone mineral density (BMD) and fracture risk are lacking. **Objective:** To determine the association between: 1) change in cognitive function and BMD loss, and 2) cognitive decline of ≥3 points on MMSE between baseline (Y0) and Year 5 (Y5) and incident fracture risk (between Ys 5 and 15). **Design and setting:** CaMos population based study with 9 centres across Canada. Participants: 2443 women and 844 men aged ≥65 years, mean 73±6 years at baseline (1995/97) followed for an average of 10 years (±5) until 2013. **Exposure:** Annual % change in Mini Mental State Examination (MMSE) (Y0, 5 and 10), and cognitive decline of ≥ 3 points loss on MMSE. **Cox proportional hazards models** were adjusted for age, BMD, education, co-morbidities, weight, falls, and smoking. **Main outcome measures:** Annual % change in femoral neck BMD (Y0, Ys-3, 5 and 10); incident fragility fractures (except skull and digits) assessed from Ys 5 to 15. **Results:** Over 95% of participants had normal cognition at baseline (MMSE≥24). The annual % change in MMSE was similar for both genders [women -0.33 (IQR:-1.00 to +0.02) and men -0.33 (IQR:-0.72 to 0.00)]. Similarly, the rate of BMD loss was similar for both genders [women -0.32 (IQR: -0.81 to +0.14) and men -0.36 (IQR: -0.91 to +0.19)]. After confounder adjustment, cognitive decline was significantly associated with BMD loss (p=0.0008) in women but not in men (p=0.29). Approximately 13% of participants lost ≥3 MMSE points by Y 5. Women with cognitive decline were older, had lower weight and had increased fracture risk [HR,

1.45 (95% CI, 1.00-2.10)]. After adjusting for bone loss, the magnitude of fracture risk decreased only slightly but was no longer significant [HR, 1.39 (95% CI, 0.93-2.06)]. Men with cognitive decline did not have an increased fracture risk [HR, 0.60 (0.20-1.59)]. Conclusion: Cognitive decline is associated with bone loss in older women but not in men. Cognitive decline was also associated with fracture risk, although this was not independent of bone loss. These findings suggest a close link between bone loss and cognitive decline, at least in women. Further studies are needed to determine mechanisms that link these common conditions.

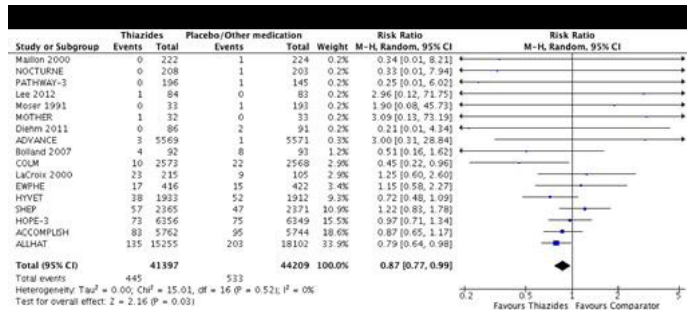
Disclosures: *Dana Bliuc, None*

MON-0784

Thiazide Diuretics and Fracture Risk: A Systematic Review and Meta-Analysis of Randomized Clinical Trials

Louis-Charles Desbiens*, Nada Khelifi, Yue-Pei Wang, Aboubacar Sidibe, Alexis F-Turgeon, Fabrice Mac-Way. CHU de Québec - Université Laval, Canada

Introduction: Thiazide diuretics are commonly prescribed for the treatment of high blood pressure and have been associated with decreased fracture risk in observational studies. We aimed to conduct a systematic review and meta-analysis of randomized clinical trials to evaluate the effect of thiazides on fractures and bone mineral density. **Methods:** We searched MEDLINE, EMBASE, CENTRAL and the WHO's International Clinical Trials Registry Platform databases from inception to March 2018. Two independent reviewers assessed studies for eligibility criteria: 1) randomized clinical trials; 2) comparing thiazide diuretics, alone or in combination; 3) to placebo or another medication; 4) in adults; and 5) reporting fracture as outcome or adverse events and/or bone mineral density (BMD) measurements. Studies comparing diuretics to anti-resorptive or anabolic bone therapy were excluded. Primary outcome was total fractures (any reported anatomical site or not). Secondary outcomes were osteoporotic, hip fractures and bone mineral density at the femoral neck, lumbar spine and/or total hip. Risk of bias was assessed with the Cochrane risk of bias tool. Meta-analysis was conducted with random-effects models. **Results:** From 14 611 unique citations retrieved, 19 trials including 85 772 patients have been included. All, but two trials were at high risk of bias, notably due to fracture assessment, pharmaceutical funding and incomplete outcome data. Thiazide diuretics were associated with a significant reduction in total fractures (RR= 0.87 [0.77, 0.99]; I2= 0%, 17 trials; Figure 1) and osteoporotic fractures (RR= 0.82 [0.70, 0.97]; I2= 0%, 10 trials) but not hip fractures (RR= 0.91 [0.51, 1.64]; I2= 0%, 3 trials). In subgroup analyses, thiazides were also associated with a significant reduction of total fractures in trials with patients over 65 years, baseline blood pressure between 140/90 and 160/100 mmHg, where antihypertensives were used as comparator and fractures measured as an outcome. Four trials reported BMD at different anatomical sites and units. A meta-analysis could not be conducted for this outcome. **Conclusion:** Thiazide diuretics are associated with decreased total and osteoporotic but not hip fractures compared to placebo or other antihypertensives. BMD was insufficiently and inconsistently reported. Further studies specifically designed to investigate the impact of thiazide diuretics on fractures are required. Registration: CRD42018078083



Disclosures: *Louis-Charles Desbiens, None*

MON-0785

The association between prevalent vertebral fractures and coronary artery calcification on chest CT in smokers with and without COPD

Johanna Driessen*¹, Mayke Van Dort², Piet Geusens³, Elisabeth Romme⁴, Frank Smeenk⁴, Braim Rahel⁵, Emiel Wouters⁶, Joop Van Den Bergh⁷. ¹CAPHRI Care and Public Health Research Institute, NUTRIM School for Nutrition and Translational Research in Metabolism, Department of Clinical Pharmacy and Toxicology, Maastricht University Medical Centre+ (MUMC+), Netherlands, ²NUTRIM School of Nutrition and Translational Research in Metabolism, Maastricht University Medical Centre+ (MUMC+), Netherlands, ³Department of Internal Medicine, Rheumatology, Maastricht University Medical Centre+ (MUMC+), the Netherlands, Netherlands, ⁴Department of Respiratory Medicine, Catharina Hospital, Eindhoven, the Netherlands, Netherlands, ⁵Department of Cardiology, VieCuri Medical Centre, Venlo, the Netherlands, Netherlands, ⁶Department of Respiratory Diseases, Maastricht University Medical Centre+ (MUMC+), the Netherlands, Netherlands, ⁷Department of Internal Medicine, VieCuri Medical Centre, Venlo and Department of Internal Medicine, NUTRIM School of Nutrition and Translational Research in Metabolism, Maastricht University Medical Centre+ (MUMC+), the Netherlands, Netherlands

Background Patients with chronic obstructive pulmonary disease (COPD) have increased risk of osteoporosis and vertebral fractures (VFs), and have more often coronary artery disease and higher coronary artery calcification (Agatston) scores as compared to controls without COPD. Bone attenuation (BA) on chest CT scans has been shown to correlate with Agatston score, but it is unknown whether VFs are associated with Agatston score in COPD patients. Therefore our aim was to investigate the association between prevalent VFs and Agatston score in (former) smokers and COPD patients. **Methods** Current and former smokers with and without COPD from the ECLIPSE study with baseline, one and three year follow up CT scans were included. Agatston score was measured on baseline CT in a subset of the ECLIPSE study. Subjects were divided into three groups based on Agatston units (AU): low (0 AU), medium (1-400 AU), or high (>400 AU). Prevalent VFs were assessed on superposed sagittal reconstructions containing the spine. Bone attenuation was measured semi-automatically in 3D areas in vertebrae T4-T12. Logistic regression models were used to assess the relationship between VFs and Agatston score. **Results** 586 subjects were included (mean age 59.8 ± 8.3, 62.3% men, 70.1% with COPD). There were 196 subjects in the low Agatston group, 266 in the medium, and 124 in the high group (table 1). Subjects with ≥1 prevalent VF had significantly more often medium (OR=2.62 [95%CI 1.52-4.51]) or high Agatston scores (OR=4.51 [2.49-8.16]) than subjects without prevalent VFs. After adjustment for age, sex, BMI, smoking status (current or former), pack years and presence of COPD, subjects with one or more prevalent VF had significantly more often medium or high Agatston scores (OR=1.83 [1.01-3.31] and OR=3.04 [1.43-6.45] resp.) than subjects without prevalent VFs. After additional adjustment for BA the result remained significant (OR=1.58 [0.86-2.90] and OR=2.47 [1.12-5.42], for medium and high Agatston scores respectively). **Conclusion** In smokers with and without COPD, the presence of ≥1 prevalent VF was associated with higher coronary artery calcium (Agatston) scores.

	Low Agatston group n = 196	Medium Agatston group n = 266	High Agatston group n = 124
Age (years: mean, sd)	55 7.6	60.8 7.7	65.3 6.1
Sex (M: n, %)	93 47.4	176 66.2	96 77.4
BMI (kg/m2: mean, sd)	26 4.6	26.2 4.0	26 4.2
With COPD (n, %)	106 54.1	200 75.2	105 84.7
Smoking status			
Current (n, %)	111 56.6	115 43.2	49 39.5
Former (n, %)	85 43.4	151 56.8	75 60.5
Pack years (mean, sd)	32.8 18.8	44.1 24.8	47.6 26.2
Bone attenuation (HU: mean, sd)	174.9 43.4	154 42.6	141.5 51.2
≥1 prevalent VF	20 10.2	61 22.9	42 33.9

Table 1: Baseline characteristics per Agatston group

Abbreviations: BMI = body mass index; COPD = chronic obstructive pulmonary disease; HU= Hounsfield Units; VF = vertebral fracture

Disclosures: *Johanna Driessen, None*

MON-0786

Impact of Comorbidity and Prognosis on Hip Fracture and Mortality Incidence Among Women in Late Life

Kristine Ensrud*^{1,2}, Allyson Kats¹, Cynthia Boyd², Susan Diem^{1,2}, John Schousboe², Brent Taylor^{1,2}, Douglas Bauer⁴, Katie Stone⁴, Lisa Langsetmo¹. ¹University of Minnesota, United States, ²Johns Hopkins University, United States, ³HealthPartners Institute / University of Minnesota, United States, ⁴University of California - San Francisco, United States

Concerns about comorbidity burden and limited life expectancy increase the complexity of managing osteoporosis (OP) in late life. To determine the effects of comorbidity burden

Monday Posters

and prognostic information on cumulative incidence of hip fracture in women in late life who might be considered candidates for drug treatment, we studied 1556 community-dwelling treatment-naïve women (mean age 84.1 years, SD 3.4) with OP (BMD T-score ≤ -2.5 , history of hip or vertebral fracture, $n=761$) or without OP at high fracture risk (BMD T-score > -2.5 , 10-year FRAX + BMD fracture probabilities \geq NOF intervention thresholds, $n=795$). Comorbidity burden was assessed by self-report of 14 medical conditions. Prognosis was estimated using a validated mortality prediction index incorporating demographics, functional status and medical diagnoses. Women were contacted every 4 months to ascertain vital status and hip fracture. 5-year hip fracture probability was calculated for each of the two distinct groups accounting for the competing risk of mortality. During follow-up, 125 (8.0%) experienced a hip fracture and 292 (18.8%) died before experiencing this event. Mortality incidence increased with greater comorbidity burden and worsening prognosis and was similar among osteoporotic women and those without OP at high fracture risk (Table). Hip fracture incidence also generally increased with greater comorbidity burden and worsening prognosis in both groups, but the probability was markedly higher among osteoporotic women. Among women with the highest comorbidity burden (≥ 3 conditions), hip fracture probability at 5 years was 18.1% among osteoporotic women vs. 2.4% among women without OP at high fracture risk. Among women with the worst prognosis (≥ 14 points), hip fracture probability was 25.3% among osteoporotic women vs. 4.5% among women without OP at high fracture risk. In summary, osteoporotic community-dwelling women in late life with greater comorbidities or poorer prognosis have a high 5-year hip fracture probability despite accounting for their competing risk of mortality and may still be candidates for drug treatment to prevent hip fracture. Data regarding efficacy and safety of drug treatment in this patient population is needed. The absolute benefit of drug treatment is likely to be less among women without OP at high fracture risk who have greater comorbidities or poorer prognosis as the probability of mortality far outweighs the probability of hip fracture.

Table: 5-Year Probability (95% CI) of Mortality and Hip Fracture by category of Comorbidity Burden and Prognostic Index

	Osteoporotic Women (n=761)*		Women without Osteoporosis at High Fracture Risk (n=795)†	
	All-cause Mortality	Hip Fracture‡	All-cause Mortality	Hip Fracture‡
Comorbid Medical Conditions				
None	19.7 (15.2-24.7)	13.0 (9.4-17.1)	12.5 (9.6-15.8)	1.9 (1.2-2.9)
1 condition	20.4 (16.1-25.1)	12.7 (9.4-16.5)	15.9 (12.7-19.4)	4.9 (3.1-7.4)
2 conditions	29.4 (22.1-37.1)	8.0 (5.4-11.3)	23.4 (17.3-30.0)	6.2 (3.0-11.0)
≥ 3 conditions	36.1 (28.2-44.0)	18.1 (12.3-24.9)	34.7 (26.3-43.2)	2.4 (1.3-4.2)
Prognostic Index				
4-5 points	11.6 (7.5-16.7)	7.0 (4.5-10.3)	8.7 (6.4-11.4)	2.5 (1.7-3.6)
6-7 points	16.2 (12.2-20.8)	11.6 (8.5-15.2)	13.3 (10.4-16.6)	1.2 (0.9-1.6)
8-9 points	25.2 (20.0-30.8)	13.0 (9.9-16.6)	21.7 (16.8-27.1)	4.0 (2.7-5.8)
10-13 points	34.1 (27.4-41.0)	14.2 (10.5-18.5)	36.4 (28.3-44.5)	10.1 (5.7-15.8)
≥ 14 points	46.7 (31.4-60.6)	25.3 (13.4-39.0)	37.6 (17.4-57.9)	4.5 (1.0-12.3)

*95 (12.5%) of the 761 osteoporotic women experienced a hip fracture and 150 (19.7%) died before experiencing this event

†30 (3.8%) of the 795 women without osteoporosis at high fracture risk experienced a hip fracture and 142 (17.9%) died before experiencing this event

‡calculated using cumulative incidence function accounting for competing risk of mortality

Disclosures: *Kristine Ensrud, None*

MON-0787

High Prevalence of Vertebral Fractures in Healthy Community-Dwelling Oldest Old: Longevity Study Fernanda Gazoni^{*1}, Jane Erika Frazão Okazaki², Daniela Regina Brandão Tavares¹, Lais Abreu Bastos³, Flavia Kurebayashi⁴, Fania Cristina Santos⁵. ¹Doctorate Student at São Paulo Federal University, Brazil, ²Associated Physician at São Paulo Federal University, Brazil, ³Affiliated physician at São Paulo Federal University, Brazil, ⁴Pos-graduate student at São Paulo Federal University, Brazil, ⁵Professor at São Paulo Federal University, Brazil

Introduction: Vertebral fractures (VFs) are associated with elevated morbimortality in aging and remain as the main risk factor for new fractures in the same site or in others. Although, they are still underdiagnosed in the very elderly population. VFs can be identified by X-ray image or by dual-emission x-ray absorptiometry (DXA), known as vertebral fracture assessment (VFA). **Objectives:** To evaluate VFs in elderly patients using two methods, VFA and conventional radiography (x-ray), and to describe their prevalences, characteristics and associated factors. **Methods:** This is a subanalysis of an observational study with elderly people of 80 years of age or older who were enrolled at the "Longevity Study" which take place at São Paulo, Brazil. This subanalysis included patients recruited from July 2014 to May 2016 and who were admitted at the Geriatrics outpatient of São Paulo Federal University. The VFs were diagnosed by VFA and X-ray, using the semi-quantitative technique of Genant applied by two trained physicians. Only moderate and severe VFs comprised between T4-L4 were included. FVs detected by VFA were analysed by demographic, anthropometric, clinical, laboratory and densitometric data. The correlation analyzes were performed according to the x2 and ANOVA tests, and a logistic regression model was applied. **Results:** This subanalysis was composed of 125 individuals with mean age of 86.7 years, with majority of females (71.2%). According to DXA, osteopenia were diagnosed in 47.6% of the participants and osteoporosis in 35.5%. Prevalence of FVs were 30.4% by VFA method ($p < 0.001$) and 20.8% by x-ray ($p < 0.001$). There were statistically significant correlations of VFs with: bone mineral density (BMD) and T-score of the total femur ($p = 0.04$ and $p = 0.05$, respectively) and creatinine clearance ($p = 0.01$). For other variables such as demographic, anthropometric, clinical and laboratory data there were not a statistically significant correlations of VFs in this population. **Conclusion:** High prevalence of VFs was observed in this population, regardless of the methods used. Also, the low total femoral t score (or BMD) and

creatinine clearance were important risk factors for VF in longevous people. The applicability of VFA in the diagnosis of VF in our routine practice could be an important way to a wide stratification of fracture risk in longevous.

Disclosures: *Fernanda Gazoni, None*

MON-0788

Impact Microindentation in Impaired Fasting Glucose and Diabetes Kara Holloway-Kew^{*1}, Pamela Rufus¹, Adolfo Diez-Perez², Lelia De Abreu¹, Mark Kotowicz³, Muhammad Sajjad¹, Julie Pasco¹. ¹Deakin University, Australia, ²Autonomous University of Barcelona, Spain

Background: Individuals with diabetes are at increased fracture risk with BMD measurements underestimating risk. Impact microindentation, a novel technique that measures bone microindentation distances, expressed as bone material strength index (BMSi), may improve fracture risk estimation in individuals with diabetes. This study describes the relationship between BMSi, femoral neck BMD (FNBM), lumbar spine BMD (LSBMD) and dysglycaemia in men. **Material and Methods:** Participants were 211 men aged 33-92yr from the Geelong Osteoporosis Study. Impaired fasting glucose (IFG) was defined as fasting plasma glucose (FPG) 5.5-6.9 mmol/L and diabetes as FPG ≥ 7.0 mmol/L, use of antihyperglycemic medication and/or self-report. BMSi was measured using the OsteoProbe[®] at the mid-tibia following international standardized procedure. FNBM and LSBMD were assessed using DXA (Lunar Prodigy Pro GE). Using linear regression techniques, the relationship between dysglycaemia and BMSi and BMD was evaluated, adjusting for age, BMI, smoking, alcohol, physical activity, medication use and prior fracture. **Results:** There were 140 (66.4%) men with normoglycaemia, 37 (17.5%) with IFG and 34 (16.1%) with diabetes. Duration of diabetes ranged from 2.8-28.0yr (median 11.1yr) and age of onset 42-91yr (median 65yr). FNBM values were not different between normoglycaemia and IFG or diabetes (adjusted mean values 0.959 g/cm² (95%CI 0.938-0.979), 0.951(0.912-0.990; $p=0.7$) and 0.965(0.923-1.007; $p=0.8$), respectively). LSBMD was also not different between the three dysglycaemia groups (1.305(1.273-1.337), 1.326(1.265-1.387; $p=0.6$) and 1.335(1.269-1.401; $p=0.4$, respectively). Adjusted BMSi values were 83.4(82.4-84.4), 83.6(81.7-85.6) and 80.6(78.9-82.9) for normoglycaemia, IFG and diabetes, respectively. Compared to normoglycaemia, there was no difference in BMSi for IFG ($p=0.8$), however, men with diabetes had a lower BMSi ($p=0.03$). **Conclusions:** Men with diabetes had lower BMSi whereas no differences in FNBM or LSBMD were detected between the glycaemia groups. The OsteoProbe[®] may be useful for improving fracture risk prediction in individuals with diabetes.

Disclosures: *Kara Holloway-Kew, None*

MON-0789

Comparing Utility Loss Due to Fractures, in Cohorts With and Without a Previous Fracture Helena Johansson^{*1}, John A Kanis², Anders Odén³, Nicholas C Harvey⁴, Vilmondur Gudnason⁵, Kerrie Sanders⁶, Gunnar Sigurdsson⁷, Kristin Siggeirsdottir⁸, Lorraine Fitzpatrick⁷, Mattias Lorentzon⁸, Fredrik Borgström⁹, Eugene McCloskey¹⁰. ¹Institute for Health and Aging, Australian Catholic University, Melbourne, Australia, Sweden, ²Institute for Health and Aging, Catholic University of Australia, Melbourne, Australia, Austria, ³Centre for Metabolic Bone Diseases, University of Sheffield, Sheffield, United Kingdom, ⁴MRC Lifecourse Epidemiology Unit, University of Southampton, Southampton, United Kingdom, ⁵Icelandic Heart Association Research Institute, Kopavogur, Iceland, ⁶Department of Medicine, The University of Melbourne and Western Health, Sunshine hospital, Melbourne, VIC, Australia, ⁷Radius Health, Waltham, MA, United States, ⁸Centre for Bone and Arthritis Research, Geriatric Medicine, Department of Internal Medicine and Clinical Nutrition, Institute of Medicine, Sahlgrenska Academy, University of Gothenburg, Gothenburg, Sweden., Sweden, ⁹LIME/MMC, Karolinska Institutet, Stockholm, Sweden, ¹⁰Mellanby Centre for bone research, Department of Oncology and Metabolism, University of Sheffield, Sheffield, United Kingdom

Purpose: With the ageing population, osteoporotic fractures are increasingly a major public health issue as well as impacting on an individual's quality of life. We wished to examine the mean utility loss in the 10 years in a cohort of patients following a sentinel fracture of the hip, clinical spine, forearm or humerus, compared to the mean utility loss from the whole population (fractured and unfractured). **Method:** The study comprised a population-based cohort of 18,872 persons born between 1907 and 1935 in the Reykjavik Area. Cumulative loss of utilities was calculated using utility multipliers derived from the EQ-5D 3 Levels descriptive system for osteoporotic fracture sites. Multipliers were applied to health state values published for the UK general population for each subsequent osteoporotic fracture that occurred during 10 years of follow up. The cumulative loss of utility and mean utility loss was calculated for the whole population, and also for the sub-cohort followed from the occurrence of a sentinel major osteoporotic fracture. **Results:** 18,872 individuals (52% female), aged on average 52.8 years (range 33-81) were included. Sentinel hip fractures were sustained in 2074 men and women; for clinical spine, forearm and humerus fractures, the respective numbers were 1365, 2364 and 1092, respectively. Utility loss over 10 years was much greater in sentinel fracture cases than in the whole cohort, when adjusted for age and gender. Loss was greatest following a vertebral fracture (0.92; 95% CI: 0.89-0.95), followed

by hip (0.63; 95% CI: 0.61-0.65), humeral (0.51 (95% CI: 0.49-0.53) and forearm fracture (0.32; 95% CI: 0.31-0.33). The utility loss during the first 10 years after a sentinel fracture was greater in women, and decreased with age. In women at the age of 70 years, the mean utility loss due to fractures in the population was 0.081 whereas this was 12-fold greater in women with a sentinel hip fracture, and was increased 15-fold for spine fracture, 4-fold for forearm fracture and 8-fold for humeral fracture. Conclusions: Sentinel major osteoporotic fractures are associated with significantly greater utility losses in the subsequent 10 years than in the population as a whole. These data can inform health economic models examining the impact of therapies to prevent major osteoporotic fractures and subsequent fracture-related utility loss.

Disclosures: *Helena Johansson, None*

MON-0790

Impact of a personal history of breast cancer on bone mineral density among women with a BRCA1 or BRCA2 mutation undergoing prophylactic bilateral salpingo-oophorectomy Joanne Kotsopoulos*¹, Elizabeth Hall², Amy Finch¹, Barry Rosen³, Joan Murphy⁴, Steven A. Narod¹, Angela M. Cheung⁵. ¹Women's College Research Institute, Women's College Hospital, Canada, ²University of Toronto, Canada, ³Beaumont Health, United States, ⁴Trillium Health Partners, Canada, ⁵University Health Network, Canada

Background: Surgical removal of the ovaries and fallopian tubes (prophylactic bilateral salpingo-oophorectomy; PBSO) is recommended to women with a BRCA1 or BRCA2 mutation to reduce their risk of developing ovarian cancer. The impact of early, surgical menopause and the ensuing endogenous hormone deficiencies on bone health in this high-risk population is unclear. Thus, we evaluated the impact of PBSO, as well as a personal history of breast cancer, on bone mineral density (BMD) among BRCA mutation carriers enrolled in a longitudinal study. Methods: The study population included women who underwent PBSO at the University Health Network (Toronto, Canada) between January 2000 and May 2013. Eligibility criteria included having a BRCA mutation, at least one ovary intact prior to surgery, and no personal cancer history other than breast cancer. Information regarding medical history, medication use, and lifestyle factors was collected via questionnaire. BMD measurements using dual energy x-ray absorptiometry were collected at baseline (prior to surgery) and at a follow-up visit (>1 year following surgery). The % change in BMD from baseline to follow-up was calculated for the lumbar spine, femoral neck, and total hip. The analysis was stratified by a personal history of breast cancer. Results: There was a total of 98 women included in the analysis: 56% were premenopausal at the time of surgery and 44% were postmenopausal. Mean age at PBSO was 47 years (range 35-75). Mean time to first follow-up was 1.8 years (range 0.4 - 6.5). Among women with a history of breast cancer (n = 43), there was a significant decrease in BMD from baseline to first follow-up across the lumbar spine (-1.95%; 95%CI -0.14 to -3.76), femoral neck (-1.91%; 95%CI, -0.33 to -3.49), and total hip (-1.77%; 95%CI, -0.43 to -3.10), respectively. Among women without a history of breast cancer (n = 55), there was a significant decrease in BMD across the lumbar spine (-5.84%; 95% CI, -4.00 to -7.68), and femoral neck (-4.87%; 95% CI, -2.99 to -6.75), and for total hip (-3.16%; 95% CI, -1.73, -4.59). Conclusions: Although preliminary, these findings suggest that PBSO is associated with a significant decline in BMD. Of interest is that the decrease in BMD was stronger among women without a personal history of breast cancer. This data adds to the emerging literature indicating that clinical guidelines should integrate the routine monitoring of BMD in this unique population.

Disclosures: *Joanne Kotsopoulos, None*

MON-0791

Calcaneal Quantitative Ultrasonography Measures and Cardiovascular and All-Cause Mortality in Older Women: a Prospective Study Joshua Lewis*¹, Kun Zhu², Wai Lim³, Richard Prince⁴. ¹School of Medical and Health Sciences, Edith Cowan University, Australia, ²University of Western Australia, Australia, ³Sir Charles Gairdner Hospital, Australia, ⁴Medical School, University of Western Australia, Australia

Background: To further progress previous studies on the importance of bone for mortality outcomes, especially cardiovascular mortality, we evaluated the relationship between calcaneal broadband ultrasound attenuation (BUA) with all-cause and cardiovascular (CV) mortality. We also investigated the modifying effects of measured covariates on the strength of the relationship. Methods: 1404 older women over 70 years (mean age 75.2±2.7 years) were recruited into the Perth Longitudinal Study of Ageing Women in 1998. Calcaneal BUA was measured at baseline using a Hologic Sahara machine (Hologic, Waltham, USA). Complete mortality and primary cause of death data were ascertained from linked mortality records. Results: Over 15 years (17,955 person years) of follow up there were 584 deaths (223 CV, 158 cancer, 200 other causes of death, 3 cases where cause of death remained under investigation). For every SD decrease in calcaneal BUA there was a 16-19% increase in the relative hazards of 15-year total mortality (HR 1.16 95%CI 1.06-1.26, P=0.002) and CV mortality (HR 1.19 95%CI 1.03-1.37, P=0.020) after adjusting for other measures of cardiovascular and mortality risk including age, BMI, smoking history, diabetes, systolic blood pressure, prescription of anti-hypertensive medications, prevalent myocardial infarction, stroke or revascularization, prevalent cancer, prevalent fractures and prevalent chronic obstructive pulmonary disease. These associations also remained significant after the addition

of total hip BMD to the multivariable-adjusted analyses (all-cause mortality HR 1.19 95%CI 1.06-1.33, P=0.002 and CV mortality HR 1.26 95%CI 1.05-1.52, P=0.016, respectively). Interaction testing between calcaneal BUA and baseline risk factors identified BMI as a potential effect-modifier of the relationship between calcaneal BUA and CV mortality (P=0.020) and all-cause mortality (P=0.009). In women with a BMI of 25-29 kg/m² per SD reduction in calcaneal BUA was associated with a 29% higher relative hazard for all-cause and CV mortality (HR 1.29 95%CI 1.12-1.48, P=0.001 and HR 1.29 95%CI 1.01-1.64, P=0.038, respectively). Conclusion: Calcaneal BUA, independent of total hip aBMD, appears to reflect a novel aspect ageing not captured by conventional cardiovascular and mortality risk factors. Further studies are required to identify other potential pathways of relationship including chronic inflammation and cell senescence.

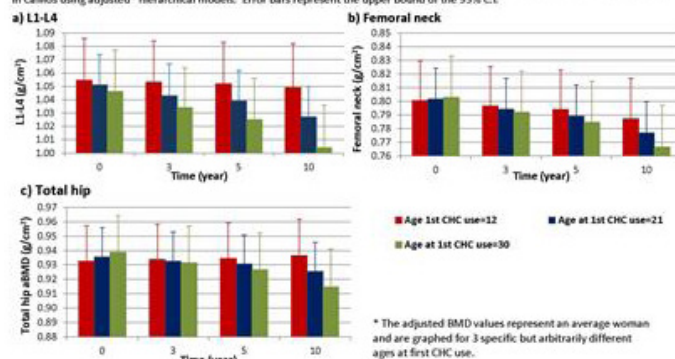
Disclosures: *Joshua Lewis, None*

MON-0792

Influence of combined hormonal contraception on 10-year areal bone mineral density change in premenopausal women in the population-based Canadian Multicentre Osteoporosis Study (CaMos) Heather Macdonald*¹, Claudie Berger², Suzanne Morin³, Christopher Kovacs³, David Hanley⁴, Tassos Anastassiades⁵, Stephanie Kaiser⁶, David Goltzman², Jerilynn Prior¹. ¹University of British Columbia, Canada, ²McGill University, Canada, ³Memorial University of Newfoundland, Canada, ⁴University of Calgary, Canada, ⁵Queen's University, Canada, ⁶Dalhousie University, Canada

Combined hormonal oral contraceptives (CHC) are the most common method of contraception for women and are also used to treat menstruation-related problems such as cramps and acne. Supra-physiological estrogen in CHC may impact women's bone health and fracture risk. However, the nature of this relationship is unclear due, in part, to a lack of prospective population-based data. Thus in CaMos data we examined the influence of CHC use, stratified by never (N-CHC) or ever (E-CHC, ≥3 months) lifetime use, on areal bone mineral density (aBMD) at baseline and aBMD change in a population-based sample of premenopausal women (recruited 1995-7) ages 25+ years (y). We identified 915 premenopausal women at baseline (42.9 ± 8.2 y), 356 at Y3, 513 at Y5 and 311 at Y10 of follow up. We fit hierarchical models using up to 10 years of longitudinal data to determine the association of CHC use with lumbar spine (L1-L4), total hip (TH) and femoral neck (FN) aBMD at baseline and changes over time. Secondly, in E-CHC, we fit hierarchical models to examine associations between aBMD (baseline and change) and: a) self-reported reason for first CHC use (contraception or therapy); and b) age at first CHC use (continuous). All models were adjusted for age, height, BMI, study centre, current smoking (yes/no), calcium intake, calcium and vitamin D supplement use, number of live births, sedentary time (hours/day), alcoholic drinks/week and physical activity (kcal/week). At baseline most women reported ever use of CHC (781, 85%). Among E-CHC, 88% of women used CHC for contraception; mean age at first CHC use was 21.5 ± 4.3 (range 12-48) y. Average follow-up was 5 ± 4 y. At baseline, CHC use was not associated with aBMD at any site. Over time E-CHC demonstrated less FN aBMD loss than N-CHC (0.002 g/cm²/y [95% CI: 0.0007; 0.0032]). In E-CHC, women who first used CHC for therapeutic reasons had lower baseline FN aBMD compared with women who started using CHC for contraception (adjusted difference of 0.03 g/cm²; 95% CI: 0.003; 0.056). Reason for first CHC use was not associated with aBMD change. Age at first CHC use was not associated with aBMD at baseline but women who started using CHC later in life demonstrated significantly greater loss over time in L1-L4, FN and TH aBMD (Figure). In summary, these population-based, prospective data suggest that CHC ever use may attenuate femoral neck aBMD loss in premenopausal women, particularly when CHC use is initiated earlier in life.

Figure 1: Modeled aBMD over 3, 5 and 10 years, for an average woman, by age at first use of Combined Hormonal Contraceptives (CHC) in CaMos using adjusted* hierarchical models. Error bars represent the upper bound of the 95% CI.



Disclosures: *Heather Macdonald, None*

MON-0793

Osteoporosis risk factors in elder Chinese and Caucasian Canadians: the Canadian Multicentre Osteoporosis Study Suzanne N Morin^{*1}, Claudie Berger², David A Hanley³, Steven K Boyd³, Jerilynn C Prior⁴, Andy Ko Wong⁵, Angela M Cheung⁵, Alexandra Papaioannou⁶, Elham Rahme¹, David Goltzman¹. ¹McGill University, Canada, ²Research Institute of the McGill University Health Centre, Canada, ³University of Calgary, Canada, ⁴University of British Columbia, Canada, ⁵University of Toronto, Canada, ⁶McMaster University, Canada

Purpose: Ethnicity is an important factor that influences the prevalence of osteoporosis, associated risk factors and fractures. The Chinese population is the second largest visible minority group in Canada, and is projected to double over 20 years. To date, there have been no Canadian studies on osteoporosis and risk factors for fractures in the Chinese Canadian population. We aimed to compare risk factors for osteoporosis between Chinese and Caucasian Canadians. Methods: We used the baseline data (1995-1997) from the population-based longitudinal Canadian Multicentre Osteoporosis Study (CaMos). We included participants aged ≥ 65 years who reported Chinese or Caucasian ethnicity. Chi-square tests of independence and T-tests were used to compare categorical and continuous variables, respectively. Linear regressions were used to examine the association of calcium intake, SF-36 domains and bone mineral density (BMD) with ethnicity. All regressions were adjusted for body mass index (BMI), height, age and history of previous low trauma fractures. Results: We studied 78 Chinese (37 women and 41 men; mean age 73.2 [6.0] y) and 4400 Caucasian (3220 women and 1180 men; mean age 73.1 [6.1] y) Canadians. Chinese participants had a lower prevalence of low trauma fractures than Caucasians (5.4% vs 32.9% in women and 12.2% vs 24.1% in men). They also differed on important risk factors such as BMI, height, dairy calcium intake and tea consumption (Table 1). Chinese participants had significantly lower femoral neck BMD than Caucasians with a T-score of -2.1 (1.1) vs -1.7 (0.9) in women and -1.8 (0.8) vs -1.2 (1.0) in men. In adjusted models, these differences were no longer significant but dairy calcium intake was lower in Chinese by 277 mg/day (95% CI: 74-480) in women and by 369 mg/day (95% CI: 216-521) in men compared to Caucasians. In adjusted models, SF-36 physical and mental component summaries did not differ between groups; however, Chinese participants had better bodily pain and mental health scores but lower social functioning scores than Caucasians. Conclusion: Predictors of fracture risk differ across populations of different origins in Canada. This supports the importance of characterizing bone health predictors in Chinese Canadians and the development of population-specific fracture prevention strategies.

Table 1: Comparison of osteoporosis risk factors and fractures between elder CaMos Chinese and Caucasian participants.

	Women		Men	
	Chinese	Caucasian	Chinese	Caucasian
Family history of osteoporosis	0.0%	6.7%	0.0%	4.0%
University Education	13.5%	11.5%	19.5%	23.0%
Living alone	24.3%	49.4%	17.1%	28.1%
History of low trauma fracture	5.4%	32.9%	12.2%	24.1%
Never smoker	91.9%	54.7%	36.6%	25.9%
Age (yrs)	72.7 (6.3)	73.1 (6.1)	73.7 (5.6)	73.1 (6.0)
BMI (kg/cm ²)	23.2 (3.6)	26.9 (5.0)	22.8 (3.2)	26.9 (3.9)
Height (cm)	152.6 (5.4)	158.2 (6.4)	164.7 (5.1)	172.1 (7.1)
Dairy Calcium intake (mg/day)	280 (280)	685 (464)	259 (267)	700 (496)
Tea (6oz/day)	1.31 (1.7)	1.60 (2.0)	1.97 (2.0)	1.39 (1.8)
L1-L4 BMD (g/cm ²)	0.833 (0.18)	0.890 (0.17)	0.973 (0.18)	1.065 (0.20)
Femoral neck BMD (g/cm ²)	0.609 (0.13)	0.654 (0.11)	0.693 (0.11)	0.772 (0.13)
Femoral neck T-score	-2.07 (1.09)	-1.70 (0.93)	-1.76 (0.8)	-1.18 (1.0)
Total hip BMD (g/cm ²)	0.739 (0.14)	0.799 (0.14)	0.871 (0.14)	0.980 (0.16)
SF-36 physical component	47.1 (8.9)	43.6 (10.7)	47.9 (10.1)	45.9 (9.7)
SF-36 mental component	54.3 (9.1)	53.9 (8.7)	54.3 (6.7)	55.3 (7.5)
Length of Residency in Canada (yrs)	20.6 (23.5)	68.3 (13.0)	21.6 (20.4)	67.1 (13.9)

Bold numbers indicate significant differences.
Continuous variables expressed as mean (SD).

Disclosures: *Suzanne N Morin, None*

MON-0794

Prospective Study of Body Mass Index, Waist Circumference and Risk of Clinical Vertebral Fracture in Women Julie M Paik^{*1}, Harold N Rosen², Jeffrey N Katz¹, Bernard A Rosner¹, Catherine M Gordon³, Gary C Curhan¹. ¹Brigham and Women's Hospital, Harvard Medical School, United States, ²Beth Israel Deaconess Medical Center, Harvard Medical School, United States, ³Cincinnati Children's Hospital Medical Center, University of Cincinnati College of Medicine, United States

Background: Recent evidence suggests that the relation between obesity and fracture risk may be site-specific. Previous studies on the association between body mass index (BMI) and risk of vertebral fracture (VF) have been inconsistent, and there have been no prospective studies to date on the relation between waist circumference, a measure of central obesity, and vertebral fracture risk. Methods: We conducted a prospective study in 54,940

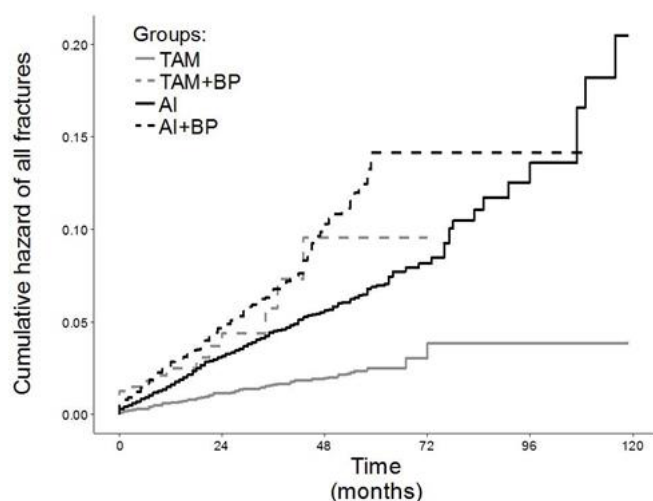
women participating in the Nurses' Health Study without prior history of any fracture. BMI was assessed from biennial questionnaires. Waist circumference was assessed in the year 2000. Self-reports of vertebral fracture were confirmed by medical record review. Cox proportional-hazards models were used to simultaneously adjust for potential confounders. When BMI and waist circumference are included in the same model, BMI reflects lean body and waist circumference reflects abdominal adiposity. Results: Our analysis included 536 incident vertebral fracture cases (2002-2014). Compared with women with BMI 21.0-24.0 kg/m², the multivariable-adjusted relative risk (MVRR) of VF for women with BMI ≥ 32.0 kg/m² was 0.84 (95% CI 0.61, 1.14). The p value for trend across all five BMI categories = 0.09. After further adjusting for waist circumference, the MVRR of VF for women with BMI ≥ 32.0 kg/m² was 0.70 (95% CI 0.49, 0.98; ptrend=0.004). Compared with women with waist circumference < 71.0 cm, the MVRR of VF for women with waist circumference ≥ 108.0 cm was 1.77 (95% CI 1.06, 2.93; ptrend=0.02), and after further adjusting for BMI was 2.50 (95% CI 1.44, 4.34; ptrend<0.001). Conclusion: Larger waist circumference, a measure of central obesity, was independently associated with higher risk of VF in women. Greater lean body mass was independently associated with lower risk of VF in women. These findings suggest that the distribution of fat is an important predictor of vertebral fracture, and that avoiding central adiposity, as well as maintaining muscle strength, may potentially reduce the risk of vertebral fracture in older women. Further research is warranted on body composition, particularly central adiposity, lean body mass, and vertebral fracture risk.

Disclosures: *Julie M Paik, None*

MON-0795

Long-Term Effect of Aromatase Inhibitors on Fracture Risk Compared to Tamoxifen: a "Real World" Cohort Study of Continued Treatment Up to Ten Years of Follow-Up Marta Pineda-Moncusí^{*1}, Natalia Garcia-Giralt¹, Adolfo Diez-Perez¹, Ignasi Tusquets², Sonia Servitja², Joan Albanell^{2,3}, Daniel Prieto-Alhambra⁴, Xavier Nogues¹. ¹IMIM (Hospital del Mar Research Institute), Centro de Investigación Biomédica en Red de Fragilidad y Envejecimiento Saludable (CIBERFES), Spain, ²Cancer Research Program, IMIM (Hospital del Mar Research Institute), Spain, ³Medical Oncology Department of Hospital del Mar- CIBERONC, Spain, ⁴Nuffield Department of Orthopaedics, Rheumatology and Musculoskeletal Sciences, University of Oxford, and NIHR Oxford Biomedical Research Centre, United Kingdom

Recommended adjuvant treatments for estrogen receptor positive breast cancer include aromatase inhibitors (AI) and tamoxifen (TAM). AI therapy has been associated with increased bone loss and excess fracture risk in pivotal RCTs. Bisphosphonates (BP) are recommended in clinical guidelines to minimize bone loss. We conducted an observational cohort study to assess fracture risk during long-term AI therapy compared with tamoxifen, and to study the association with BP use. Data on 27,695 breast cancer women on either AI or TAM were obtained from primary care records in Catalonia (SIDIP database) between 2006 and 2015. Patients were included from the first day of TAM or AI treatment until the earliest of: AI/TAM or BP (if applicable) cessation, death or migration, end of data availability, or fracture event. BP use was introduced as a time-varying exposure, with patients considered non-users at first, but contributing to the BP user cohort from BP therapy initiation. Survival analyses were performed by a) Kaplan-Meier to estimate cumulative probability plots, and b) Cox proportional hazards models accounting for competing risk of death (Fine and Gray models) adjusted for propensity scores to calculate event-specific hazard ratios (SHR [95%CI]) according to exposure and using TAM as reference group. A total of 9,233 TAM, 564 TAM+BP, 17,028 AI, and 3,914 AI+BP records were included, with fracture incidence rates [95%CI] of 5.45/1,000 person-years [4.49 to 6.56], 24.95 [15.02 to 39.14], 15.08 [13.88 to 16.36], and 25.71 [22.02 to 29.85] respectively (Fig. 1). TAM-treated patients had the lowest fracture risk: propensity-adjusted SHR 2.15 [1.26 to 3.68] in TAM+BP, 1.77 [1.43 to 2.21] in AI, and 2.42 [1.86 to 3.15] in AI+BP. Significant higher risk was observed in AI+BP (SHR 1.33 [1.10 to 1.61]) compared to AI users. AI therapy is associated with substantial increase in fracture risk compared to TAM, where the BP users manifested the worst outcomes. Monitoring fracture risk factors in AI patients is recommended. More data are needed on the protective efficacy of BP therapy in AI-induced bone fragility.

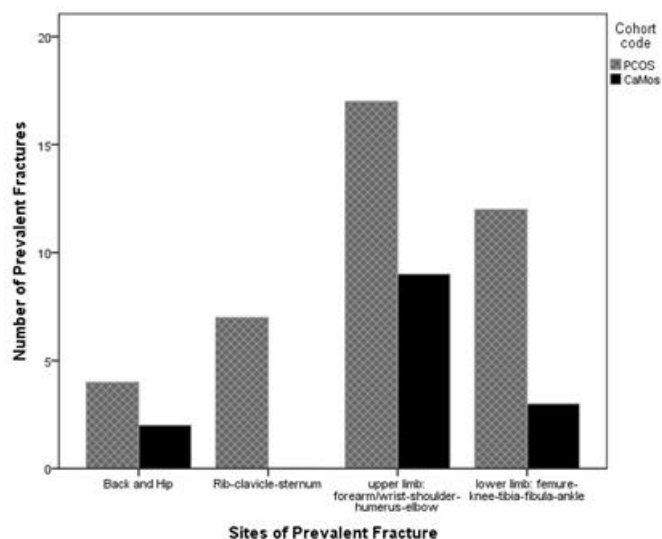


Disclosures: *Marta Pineda-Moncusí, None*

MON-0796

Community dwelling Premenopausal Women with Polycystic Ovary Syndrome/Anovulatory Androgen Excess (PCOS/AEE) Experience more Prevalent Fractures than Regional Population-based Control Women from the BC Centre of the Canadian Multicentre Osteoporosis Study (CaMos)
Azita Gostasebi *, Shirin Kalyan, Bernice Liang, Jerilynn Prior. University of British Columbia, Canada

PCOS has many known health risks; low bone mineral density (BMD) or fracture risk have not been included. We recently showed that AAE related to lower pQCT strength-strain index of the radius ($R^2=0.25$, $P=0.018$); a Japanese administrative study documented increased fractures in PCOS2 (androgen excess unclear). Our cross-sectional aim was to determine the prevalent fracture rate, age and sites in women with androgenic excess PCOS versus (vs) age-similar, population-based controls. Community premenopausal women diagnosed with PCOS enrolled in two local studies ($n=136$); diagnosis by AE/PCOS criteria3 was confirmed. All completed interviewer-administered CaMos questionnaires including prevalent fracture (fragility plus higher trauma, age, site minus skull, hands and feet)4, plus height and weight measures. A local control group included women in regional Adult ($n=72$) and Youth ($n=38$) CaMos cohorts. Eligibility = spontaneously menstruating, no PCOS diagnosis, on no steroids or osteoporosis drugs. All control and 22 PCOS women had total hip (TH) and femoral neck (FN) BMD data. Statistical analysis used descriptive, T and Chi square tests, ANOVA for menarche age vs BMI and binary regression to assess contributors to prevalent fracture. The 246 women averaged 36.8 ± 11 years (y), BMI 27.7 and height 164.5 cm with menarche at 12.8 y. The 136 PCOS and 110 CaMos controls did not differ in age at menarche, FN or TH BMD but the former were slightly younger (35.1 y), significantly taller (165.4) with higher BMI (29.6). In PCOS, younger menarche age related significantly to higher BMI ($F=4$, $p=0.001$) but not in controls ($F=1.96$, $p=0.081$). More women with PCOS had experienced a prevalent fracture—29% vs 13% ($\chi^2=10.5$, $p=0.01$). The mean age at prevalent fracture was similar (15.4 y), but there were multiple fractures in PCOS: two—PCOS 7, CaMos 3; three—PCOS 2, CaMos 0. Sites of prevalent fracture didn't differ (Figure) $\chi^2=3.92$, $p=0.27$. Binary regression analysis for prevalent fracture ($n=246$) including age, BMI, height, age at menarche and PCOS diagnosis showed that PCOS diagnosis (OR 2.77; 1.27, 6.03) and height (OR 1.07; 1.01, 1.13) made important contributions. In conclusion, this is the first study to our knowledge showing increased prevalent fractures in premenopausal women with PCOS/AEE vs population-based controls. References: 1Kalyan S Scientific Reports 2017; 2Yang HY J Bone Miner Metab 2017; 3Azziz R Fertil Steril 2009; 4Kreiger N Can J Aging 1999.



Disclosures: *Azita Gostasebi, None*

MON-0797

Why does low self-rated health increase the risk of hip fractures? Hans Ranch Lundin*, Helena Salminen. Karolinska Institutet, Sweden

From the Study of Osteoporotic Fractures, Cummings and colleagues showed in 1998 that low self-rated health (SRH) was a risk factor for hip fractures independent of previous fracture and bone mineral density (BMD). Since then, no further studies on SRH and fracture risk seems to have been published. The aim of this study was to investigate which known risk factors for hip fractures, could be responsible for the increased fracture risk in persons with low SRH. Our population-based prospective cohort study included 350 Swedish women, aged 69-79 years. At inclusion they rated their global health between "worst imaginable health" and "best imaginable health" by putting an "x" on a line drawn between these two extremes. The distance from "worst imaginable health" to the "x" was measured in millimeters so that the range of observations was 0-100. Maximum gait speed was measured over 30 meters with a 180 degree turn halfway. One-leg standing time was measured with eyes open as the best result from two attempts on each leg. The FRAX calculations included a measure of femoral neck T-score. Follow-up ten years later was based on data on incident fractures and mortality from Swedish medical records. The main outcome was a hip fracture. No participant was lost to follow up. During 10 years follow-up, 40 participants (11%) had a hip fracture. Women with a SRH below 50 had an age-adjusted HR of 2.00 (1.06-3.80) for a hip fracture compared to women with a SRH between 50 and 100. This HR was even higher after adjustment for femoral neck BMD (HR 2.33, 1.19-4.54) or FRAX-estimated hip fracture risk (2.35, 1.24-4.44). Adjustment for the maximum time to stand on one leg (OLST) or maximum gait-speed made the HR non-significant. Analyses of mediated effect showed that after adjustment for age and OLST, 36% of the effect of SRH on hip fracture risk, was mediated by gait speed. The effect mediated by OLST was non-significant after adjustment for gait speed. It seems that the increased risk of hip fractures associated with low SRH could be more related to balance and muscle strength, than to BMD and the risk factors included in FRAX.

Disclosures: *Hans Ranch Lundin, None*

MON-0798

Differences in Geometric Strength at the Contralateral Hip between Men with Hip Fracture and Non-Fractured Comparators Alan Rathbun*¹, Jay Magaziner¹, Michelle Shardell², Thomas Beck³, Laura Yerges-Armstrong⁴, Denise Orwig¹, Gregory Hicks⁵, Shabnam Salimi¹, Alice Ryan¹, Marc Hochberg¹. ¹University of Maryland School of Medicine, United States, ²National Institute on Aging, United States, ³Beck Radiological Innovations, United States, ⁴GlaxoSmithKline, United States, ⁵University of Delaware, United States

Older men who sustain hip fracture experience accelerated bone mineral density (BMD) declines and are at an increased risk of secondary fractures. However, BMD is a surrogate marker of mechanical strength and not a geometric property of bone tissue. Thus, our objective was to compare changes in bone geometry between older men after hip fracture and community-dwelling older men using two existing cohorts: the Baltimore Hip Studies 7th Cohort (BHS-7) and the Baltimore Men's Osteoporosis Study (MOST). BHS-7 was conducted from 2006 to 2011 and recruited older adults who fractured a hip ($N=339$) and had assessments at baseline (within 15 days of hospitalization) and 2, 6, and 12 months follow-up. MOST was conducted from 2000 to 2003 and enrolled community-dwelling older men ($N=694$) and collected data at baseline and a second visit between 10 to 31 months later.

The combined sample (n=170) comprised Caucasian men from BHS-7 and MOST with ≥ 2 DXA scans that were read using Hip Structural Analysis (HSA) and were propensity score matched (1:1) on baseline variables: age, height, weight, smoking, alcohol consumption, comorbidities, use of bone-active drugs, and BMD. HSA was used to derive metrics of bone geometry at the narrow neck (NN), intertrochanteric (IT), and femoral shaft (FS): surface area (cross sectional area [CSA]), bending strength (section modulus [SM]), and cortical stability (buckling ratio [BR]). Mixed-effects models estimated individual rates of change in geometric parameters, and annual percent changes were calculated. Robust regression models adjusted for covariates evaluated between-cohort differences in change. BHS-7 participants had greater declines (Table 1) in NN CSA (-2.81%; 95% CI: -3.29, -2.33) and NN SM (-1.89%; 95% CI: -2.71, -1.08) and larger increases in NN BR (3.45%; 95% CI: 2.91, 4.00). Between-group differences in change in IT geometric parameters were similar to NN estimates. Conversely, BHS-7 participants had larger increases in FS CSA (2.06%; 95% CI: 1.93, 2.19) and FS SM (2.74%; 95% CI: 2.43, 3.05) and greater declines in FS BR (-1.91%; 95% CI: -2.57, -1.25). Hip fracture in older men is associated with geometric changes at the contralateral hip characterized by declines in bone tissue, strength, and cortical stability at the distal portions of the proximal femur and increases in these parameters at the diaphyseal region. Better medical management is needed for older men after hip fracture to reduce the risk of future fractures.

Table 1. Adjusted Annual Changes and Differences in Change in Geometric Parameters between BHS-7 and MOST participants

Site	Parameter	BHS-7		MOST		Δ ^b
		(% Change, 95% CI)	(% Change, 95% CI)	(% Change, 95% CI)	(% Change, 95% CI)	
NN	CSA	-2.64 (-2.28, -2.46)	0.17 (-0.01, 0.35)	-2.81 (-3.29, -2.33)		
IT	CSA	-0.90 (-0.93, -0.86)	0.01 (-0.03, 0.04)	-0.91 (-1.03, -0.79)		
FS	CSA	2.04 (1.99, 2.08)	-0.02 (-0.06, 0.02)	2.06 (1.93, 2.19)		
NN	SM	-1.46 (-1.83, -1.09)	0.43 (0.05, 0.90)	-1.89 (-2.71, -1.08)		
IT	SM	-2.49 (-2.59, -2.39)	0.05 (-0.04, 0.15)	-2.54 (-2.82, -2.27)		
FS	SM	2.58 (2.46, 2.69)	-0.16 (-0.28, -0.04)	2.74 (2.43, 3.05)		
NN	BR	3.70 (3.38, 4.02)	0.25 (-0.07, 0.56)	3.45 (2.90, 4.00)		
IT	BR	4.24 (4.08, 4.40)	0.22 (0.07, 0.38)	4.02 (3.62, 4.42)		
FS	BR	-2.05 (-2.42, -1.69)	-0.14 (-0.50, 0.21)	-1.91 (-2.56, -1.25)		

BHS-7 = Baltimore Hip Studies 7th Cohort; BR = Buckling Ratio; CI = Confidence Interval; CSA = Cross Sectional Area; FS = Femoral Shaft; IT = Intertrochanteric; MOST = Baltimore Men's Osteoporosis Study; NN = Narrow Neck; SM = Section Modulus.

^aCohort-specific annual change holding model covariates at their sample mean.

^bAdjusted for age, height, weight, smoking status, alcohol consumption, glucocorticoids, hormone therapy, bisphosphonates, calcium supplements, comorbidity count, and baseline arial BMD.

Disclosures: Alan Rathbun, None

MON-0799

The Impact of a Beta Trabecular Bone Score (TBS) Algorithm Accounting for Soft Tissue Thickness Correction on the Prediction of Incident Major Osteoporotic Fracture (MOF) Risk in Postmenopausal Women: The OsteoLaus Study Enisa Shevroja*, Olivier Lamy, Berengere Aubry-Rozier, Gabriel Hans, Elena Gonzalez Rodriguez, Delphine Stoll, Didier Hans. Center of Bone Diseases, Bone and Joint Department, Lausanne University Hospital, Switzerland

Introduction: TBS is a texture measurement extracted from lumbar spine (LS) DXA scans reflecting bone microarchitecture. Current versions of the TBS software account for soft tissue variability by integrating a correction for body mass index (BMI) in the TBS algorithm (TBSBMI). A residual negative correlation has been reported between TBS and BMI. To address this issue, a new correction of the TBS algorithm, based on the tissue thickness as estimated by the DXA machine (TBSTH), is currently being tested. We aimed to compare the validity of TBSTH and TBSBMI in MOF prediction. **Methods:** This study was embedded in the OsteoLaus Study, a prospective population-based cohort of 1,500 women living in Lausanne, Switzerland. All women had data on LS and hip BMD, TBS, incident MOF and FRAX. The correlation between BMI and TBSBMI or TBSTH was studied using Pearson's correlation coefficient. Binary logistic regression models were used to obtain the risk estimates for MOF per standard deviation decrease in TBSBMI or TBSTH in three different models (M): M1: adjusted for age and osteoporotic (OP) treatment; M2: adjusted for M1 and LS-BMD; M3: adjusted for M2 and FRAXFN-BMD-MOF. To evaluate the prediction models and the performance of both TBSBMI and TBSTH, the area under the receiver-operating-characteristic curve (AUC) was calculated for M, M+TBSBMI, and M+TBSTH. **Results:** This analysis included 1,331 women (mean age=64.6±7.5 y; mean BMI=25.9±4.5 kg/m²). During the mean follow-up period of 5 years, 199 women sustained a MOF. BMI correlated negatively with the standard TBSBMI (r = -0.21) and positively with TBSTH (r=+0.26). In overall, lower TBS scores were significantly associated with an increased risk for incident MOF, but TBSTH was shown to be a better predictor of fracture risk than TBSBMI (Table). The AUC (95% CI) for M1 was 0.59 (0.54;0.63), M1+TBSBMI 0.62 (0.58;0.66), and M1+TBSTH 0.63 (0.58;0.67); for M2 was 0.59 (0.54;0.63), M2+TBSBMI 0.62 (0.58;0.67), and M2+TBSTH 0.63 (0.59;0.67); M3 was 0.60 (0.56;0.65); M3+TBSBMI 0.63 (0.59;0.67); and M3+TBSTH 0.64 (0.59;0.68). **Conclusion:** The residual negative correlation between BMI and TBSBMI disappeared with the new TBSTH. Furthermore, the superiority of TBSTH versus TBSBMI in MOF risk prediction was demonstrated. This study contributes to the validation of the newly tested TBS algorithm in osteoporotic fractures prediction, aiding in the improvement of the osteoporosis management.

Table. The results of the logistic regression analysis

	Model 1		Model 2		Model 3	
	TBSBMI	TBSTH	TBSBMI	TBSTH	TBSBMI	TBSTH
OR / SD	1.38	1.41	1.44	1.65	1.37	1.53
(95% CI)	(1.17;1.62)	(1.19; 1.70)	(1.20; 1.72)	(1.34; 2.04)	(1.14; 1.64)	(1.23; 1.92)

Model 1: adjusted for age, osteoporotic treatment; Model 2: adjusted for age, osteoporotic treatment, lumbar spine BMD; Model 3: adjusted for osteoporotic treatment, FRAX_{SMO} of MOF, and lumbar spine BMD; OR / SD odds ratio per standard deviation decrease; CI confidence interval; TBSBMI trabecular bone score corrected for body mass index; TBSTH TBS corrected for the soft tissue thickness.

Disclosures: Enisa Shevroja, None

MON-0800

WITHDRAWN

MON-0801

Weight Gain is Associated with Increased Bone Mineral Density (BMD) Even in Postmenopausal Women Sikarin Upala*, Amber Olson, Tamara Vokes. University of Chicago, United States

Background: In population studies, body weight is positively associated with BMD. While it is well known that weight loss causes bone loss, it is less clear that weight gain in adults leads to an increase in BMD. In this study, we examined whether the BMD changes in response to weight changes are bidirectional and whether the association between BMD and weight changes differs by age and sex. **Methods:** This is a retrospective cohort study of 2,067 patients who had repeated BMD testing as a part of their clinical care at the University of Chicago between 2006-2017. We performed regression analyses with %change in BMD at the lumbar spine (LS), femoral neck (FN) and total hip (TH) as an outcome variable and %change in weight as a predictor stratified by age (under 50 and over 50) and sex. Subjects with BMD change of less than 3% and/or weight change of less than 2% were excluded from the analysis. **Results:** The results of the regression analyses are shown in the Table. We found a bidirectional association between change in weight and change in BMD in all subgroups except men over 50, possibly due to small sample size and presence of other medical problems. **Conclusion:** The effect of weight change on BMD is bidirectional even in postmenopausal women suggesting that weight manipulation may be considered as a novel approach to improving bone health.

Table: % change in BMD (p-value) per 10% change in weight (WT) in Male (M) and Female (F) over and under age of 50 years

	F >50 (n=1570)		F <50 (n=214)		M >50 (n=178)		M <50 (n=105)	
	WT ↓	WT ↑	WT ↓	WT ↑	WT ↓	WT ↑	WT ↓	WT ↑
LS	↓ 1.1 (p<0.01)	↑ 0.8 (p<0.01)	↓ 2.0 (p<0.01)	↑ 3.7 (p<0.001)	NS	NS	↓ 4.1 (p<0.01)	↑ 2.5 (p<0.01)
FN	↓ 2.9 (p<0.001)	↑ 1.7 (p<0.001)	↓ 2.1 (p<0.01)	↑ 2.8 (p<0.001)	NS	NS	↓ 5.1 (p<0.001)	↑ 2.2 (p<0.03)
TH	↓ 0.4 (p<0.001)	↑ 2.8 (p<0.001)	NS	↑ 2.8 (p<0.001)	↓ 2.3 (p<0.03)	NS	↓ 4.6 (p<0.001)	NS

Disclosures: Sikarin Upala, None

MON-0802

Fracture Risk is not Increased in Transwomen and Transmen Receiving Long-term Gender-affirming Hormonal Treatment: a Nationwide Cohort Study Chantal Wiepjes*, Christel De Blok, Renate De Jongh, Martin Den Heijer. VU University Medical Center, Netherlands

Purpose: Gender-affirming hormonal treatment (HT) in transgender people can influence bone mineral density (BMD). Earlier studies found an increase in BMD in transwomen, and a maintenance or increase in BMD in transmen. However, the effects of HT on fracture risk are not known. Therefore, we aimed to investigate the fracture incidence in transwomen and transmen using long-term HT and to compare this with an age-matched male and female control population. **Methods:** All adult transgender people who started with HT before 2013 at the VU University Medical Center, Amsterdam, the Netherlands were included. This population was linked to a Dutch random control sample of 5 age-matched males and 5 age-matched females per person. Fracture occurrence in 2013 and 2014 was provided by Statistics Netherlands (CBS), which stores all diagnoses from visits to the hospital emergency rooms nationwide. The occurrence of fractures is expressed as percentages. Relative risks (RR) with 95% confidence intervals (CI) were calculated separately for transwomen and transmen. **Results:** A total of 1,725 transwomen (mean age 50 years, standard deviation (SD) 13 years) who used HT for median 15 years (inter quartile range (IQR) 8 – 23 years) were included. Fractures occurred in 2.5% of the transwomen (n=43), while 1.9% of the age-matched control men (RR 1.33, 95% CI 0.94 – 1.86) and 2.2% of age-matched control women (RR 1.14, 95% CI 0.82 – 1.60) had a fracture. A total of 729 transmen (mean age 44 years, SD 12 years) who used HT for median 14 years (IQR 6 – 23 years) were included. Fractures occurred in 1.4% of the transmen (n=10), while 1.6% of the age-matched control men (RR 0.85, 95% CI 0.43 – 1.66) and 2.0% of age-matched control women (RR 0.69, 95% CI 0.35 – 1.34) had a fracture. **Conclusion:** This large population of both transwomen and transmen using long-term HT does not demonstrate an increased fracture risk compared

with an age-matched control population. This increases the evidence that HT in transgender people does not negatively affect bone health.

Disclosures: *Chantal Wiepjes, None*

MON-0803

Decreased mortality risk, but unchanged subsequent fracture risk after introduction of a fracture liaison service: a 3 year follow-up survey

Caroline E Wyers^{*1,2}, Johanna Hm Driessen², Lisanne Vranken^{3,4}, Irma Ja De Bruin^{3,4}, Piet P Geusens⁵, Robert Y Van Der Velde^{3,4}, Heinrich M Janzing⁶, Sjoerd Kaarsemaker⁷, Jacqueline Center^{8,9}, Dana Bliuc⁸, John A Eisman¹⁰, Joop Pw Van Den Bergh^{3,4}. ¹Department of Internal Medicine, VieCuri Medical Center, Netherlands, ²Maastricht UMC+, CAPHRI Care and Public Health Research Institute, NUTRIM School for Nutrition and Translational Research in Metabolism, Department of Clinical Pharmacy and Toxicology, Netherlands, ³VieCuri Medical Center, Department of Internal Medicine, Netherlands, ⁴Maastricht UMC+, NUTRIM School for Nutrition and Translational Research in Metabolism, Department of Internal Medicine, Netherlands, ⁵Maastricht UMC+, CAPHRI Care and Public Health Research Institute, Department of Internal Medicine subdivision of Rheumatology; Hasselt University, Netherlands, ⁶VieCuri Medical Center, Department of Surgery, Netherlands, ⁷VieCuri Medical Center, Department of Orthopedic Surgery, Netherlands, ⁸Osteoporosis and Bone Biology Program, Garvan Institute of Medical Research, Australia, ⁹Clinical School St Vincent's Hospital, Faculty of Medicine, UNSW Australia, Australia, ¹⁰Osteoporosis and Bone Biology Department, Clinical Translation and Advanced Education, Garvan Institute, Clinical School, St Vincent's Hospital, Faculty of Medicine UNSW Australia, School of Medicine, University of Notre Dame, Australia

Purpose: Our aim was to evaluate the risk of a first subsequent fracture within 3 years after a fracture, before and after the introduction of a Fracture Liaison Service (FLS). **Methods:** Historical cohort study of all consecutive patients aged 50-90yrs with a fracture presenting at the Emergency Department. From 2005-2007, only acute fracture treatment was performed (pre-FLS). From 2008-2013 (post-FLS), a nurse screened medical records and invited patients to the FLS for evaluating fracture risk and underlying disorders that contribute to bone loss and treatment according to Dutch guidelines. Patients with finger, toe or skull fracture, osteomyelitis, metastasis, periprosthetic fracture, Paget's disease or multiple myeloma were excluded at baseline and follow up. All fractures were radiographically confirmed and categorized into hip, major (pelvis, proximal humerus or tibia, vertebral, multiple rib, distal femur) and minor (all other). Cox Proportional Hazard analyses adjusted for age, sex and baseline fracture were used. To adjust for mortality, the subdistribution hazard approach (SHR) by Fine and Gray was applied. **Results:** In the pre-FLS group 2,653 patients were included (72% women, mean age 69yrs, 56% minor, 28% major, 16% hip). Post-FLS, 6,415 were included (69% women, mean age 69yrs, 54% minor, 32% major, 14% hip), 47% attended of which around 50% were indicated for anti-osteoporosis treatment. In total, 950 patients sustained a subsequent fracture (10.2% pre-FLS vs. 10.6% post-FLS, $p=ns$), 16.6% died pre-FLS vs. 14.6% post-FLS ($p=0.15$), see figure. Mortality risk was lower after introduction of the FLS (HR:0.82 95%CI:0.70-0.95), subsequent fracture risk, also when adjusted for mortality, was not different (HR:1.02 95%CI:0.89-1.18; SHR:1.03 95%CI:0.90-1.19, resp.). Only in men, lower subsequent fracture risk was observed (SHR:0.61 95%CI:0.52-0.73). Elderly and those with a major fracture had a higher subsequent fracture risk compared to younger patients (50-59yrs) and those with a minor fracture (SHR:1.04 95%CI:1.03-1.04; SHR:1.21 95%CI:1.04-1.40, resp.). **Conclusion:** Overall, mortality risk was 18% lower while subsequent fracture risk was comparable in the first 3 years after introduction of the FLS. The limited effect of the introduction of the FLS on subsequent fractures needs exploration of the effect of decreased mortality, unchanged fall risk, low number of treatment indications and lack of information on adherence to treatment.

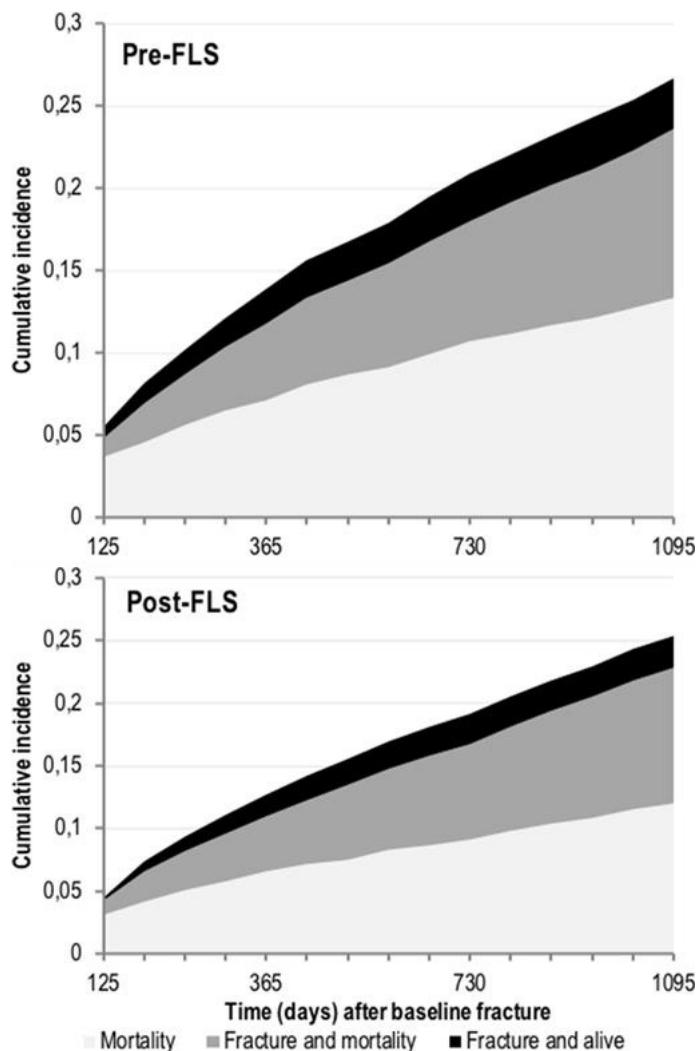


Fig 1. Cumulative incidence of subsequent fracture, subsequent fracture and mortality, and mortality outcomes within 3 yrs after a fracture Pre-FLS and Post-FLS

Disclosures: *Caroline E Wyers, None*

MON-0818

Health Literacy and Readiness to Initiate Treatment for Osteoporosis in an At-risk Sample of US Women Michael Miller*, Maria I. Danila, Amy Mudano, Ryan Outman, Elizabeth Rahn, Kenneth Saag. University of Alabama at Birmingham, United States

Objective: Many women at high risk for fragility fractures do not initiate or stop osteoporosis treatment. Contributing factors may include perceived fracture risk, knowledge and lack of trust in medications, and perceived unfavorable risk-benefit profiles of osteoporosis therapies. Understanding health literacy and its relationships with other factors affecting osteoporosis treatment initiation may assist in the design of targeted patient activation interventions. **Methods:** Women ($n=1,759$) with self-reported fracture and no current osteoporosis medication use reported at screening were derived from the Activating Patients at Risk for OsteoPorosis trial, which recruited participants from the Global Longitudinal Study of Osteoporosis in Women (GLOW) cohort. Path models with fixed relationships were used to evaluate associations among sociodemographics, health literacy, perceived fracture risk, receipt of osteoporosis medication information, distrust in osteoporosis medications, and readiness to initiate osteoporosis treatment. Multiple models were evaluated to ascertain the best fit. Criteria for optimal model fit were: nonsignificant model χ^2 test, a standardized root mean residual (SRMR) <0.08 , root mean square error of approximation (RMSEA) <0.05 , and the Bentler comparative fit index (BCFI) >0.95 . Model significance criterion = alpha of 0.01. **Results:** Age, education, health literacy, distrust in medications, perceived fracture risk, and having received medication information within the past year were associated with readiness to initiate osteoporosis therapy ($p<0.01$). Age, race, and education were also associated with health literacy ($p<0.01$). Age was associated with perceived fracture risk ($p<0.01$). In turn, perceived fracture risk was associated with medication distrust ($p<0.01$). Health literacy was not associated with perceived fracture risk or distrust for medications. A model approaching optimization was identified (SRMR=0.02, RMSEA=0.09, BCFI=0.94, $\chi^2=33.43$,

$p < 0.0001$). The significant model χ^2 likely resulted from the large sample. Conclusions: Health literacy contributes to a patient's readiness to initiate osteoporosis medication. Effective patient activation intervention design should be sensitive to age, education level, and health literacy needs. Interventional strategies should raise awareness and understanding of fracture risk, mitigate distrust in medications, and ensure medication information is derived from credible and trusted sources.

Disclosures: *Michael Miller, None*

MON-0819

The Burden of Recurrent Fragility Fractures in a Regional Hospital in Singapore

Linsey Gani*, Nicholas Tan, Vivien Tan, Joan Khoo, Thomas King, Changi General Hospital, Singapore

Background: There remains a significant treatment gap in osteoporosis management globally. Following an initial fragility fracture, the risk of subsequent fracture increases by 1.6 to 4.3 fold at any given age. We aim to assess the burden of recurrent fractures in our Asian population in the Eastern Region of Singapore. Methods: Retrospective analysis of patients presenting to Changi General Hospital, Singapore with fragility fracture. Data were extracted from all admissions during the period of 2009 – 2015 using ICD 10 codes. Patient demographics, frequency and location of prior fractures, calcium, vitamin D and anti-resorptive treatment initiation status 1-year post admission, and bone mineral density (BMD) evaluation were recorded. Results: During the period of 2009-2015, there were 8,771 admissions for fragility fractures, median age 73.0 (50-105) years, 65% female. Of these, 1686 (19.2%) admissions were recurrent fractures (1-3 recurrent fractures). Average time to 1st recurrent fracture was 696 days (1 year 11 months). The most frequent sites of these 783 second fractures were hip and vertebrae at 37.9% (n=297) and 16.2% (n=127) respectively. Of these 297 second fractures that were hip fractures, 52.1% (n=153) patients had initially presented with a 1st hip fracture. Initiation of anti-resorptive treatment was low in both first and recurrent fracture population at 2.6% and 6.6%; as was BMD testing at 18.8% and 16.2% respectively in both populations. Conclusion: Nearly one fifth of all fragility fracture admissions between 2009-2015 in the eastern region of Singapore were recurrent fractures with an average time to next fracture of less than two years. The majority of second fractures were hip fractures and more than half had initially presented with a first hip fracture. Diagnosing osteoporosis with a first fragility fracture is critical to prevent recurrent fractures. A fracture liaison service may reduce fracture recurrence by timely initiation of anti-resorptive therapy and BMD testing.

Disclosures: *Linsey Gani, None*

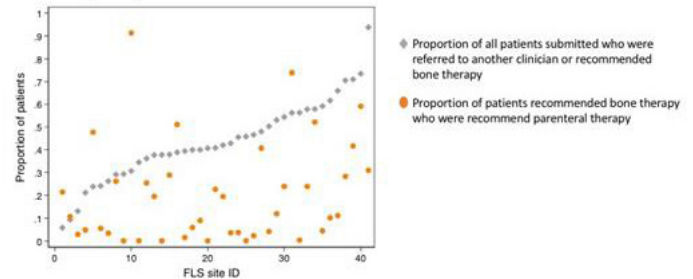
MON-0820

Service level predictors of bone treatment recommendations after a fragility fracture: Baseline findings from the first UK patient level Fracture Liaison Service Audit Muhammad Javaid*, Xavier Griffin¹, David Stephens², Tim Jones³, Sonya Stephenson³, Michael Stone⁴, Clare Cockill⁵, Alison Smith⁶, Iona Price⁶, Celia Gregson⁷, Frances Dockery⁸, Rachel Bradley⁹, Neil Gittoes¹⁰, Daniel Prieto-Alhambra¹, Cyrus Cooper¹¹, Catherine Gallagher¹², Naomi Vasilakis¹². ¹NDORMS, University of Oxford, United Kingdom, ²NHS West Kent CCG, United Kingdom, ³National Osteoporosis Society, United Kingdom, ⁴Bone Research Unit, University Hospital Llandough, United Kingdom, ⁵Rheumatology Department, Yeovil Hospital, United Kingdom, ⁶Patient representative, Royal College of Physicians, United Kingdom, ⁷School of Clinical Sciences, University of Bristol, United Kingdom, ⁸Ageing and Health Services, Guy's and St Thomas' NHS Foundation Trust, United Kingdom, ⁹Geriatric Medicine, University Hospitals Bristol NHS Foundation Trust, United Kingdom, ¹⁰Centre for Endocrinology, Diabetes and Metabolism, University of Birmingham, United Kingdom, ¹¹MRC Lifecourse Epidemiology Unit, University of Southampton, United Kingdom, ¹²Royal College of Physicians, United Kingdom

Background: Fracture Liaison Services (FLSs) are recommended nationally to provide effective secondary fracture prevention after a fragility fracture. Bone therapies vary in cost, adherence and effectiveness. The United Kingdom Department of Health has produced NICE guidance to define first, second and third line treatment choices. Objective: We wished to identify the proportion, type and service level determinants of bone protection therapy recommendations by FLSs. Methods: Each FLS in the United Kingdom was required to submit data on all patients they managed aged 50 or over and who had sustained a fragility fracture diagnosed between 1st January and 30th December 2016. Part of the audit focused on the treatments recommended by the FLS. Outcomes included treatment clinically inappropriate, patient declined, referred to primary care physician or another clinician, specific anti-osteoporotic medication, don't know and missing. We excluded FLS with less than 50 patients submitted. Where more than one drug was recommended by the FLS, the following hierarchy was used to select the one drug: oral bisphosphonate > denosumab > zoledronate, then teriparatide or raloxifene or strontium or activated vitamin D or oestrogen therapy. Results: 50 FLS submitted data on 44,139 patient records. Overall, the mean age of patients was 73 years, and 78% were women. Eighteen percent had an index hip fracture, 3.8% spine fracture and 72.9% non-hip non-spine fracture. Nine FLSs had more than 50% missing treatment data. 40% of patients submitted were recommended a specific medication or referred to

another clinician. However, there was considerable variation between individual FLSs: the decision to treat (10% to 94%), the proportion referred to another clinician (0.3 to 69%) and the proportion recommended a parenteral therapy (0 to 33%). Neither the volume of patients or proportion of patients recommended therapy predicted type of therapy. Conclusions: This audit has demonstrated marked variation between FLSs in the decision to treat and the type of bone therapy recommended despite national recommendations. A better understanding of the contributory factors for this variation will inform quality improvement for FLSs to provide more effective and efficient secondary fracture prevention.

Proportion of patients recommended parenteral therapy by the FLS



Disclosures: *Muhammad Javaid, UCB, Speakers' Bureau, UCB, Amgen, Consultant, Amgen, Grant/Research Support*

MON-0821

Cost-effectiveness Evaluation of a Screening Programme for Fracture Risk in UK Fredrik Borgström*, Emma Jonsson¹, Nick Harvey², Lee Shepstone³, Elizabeth Lenaghan³, Shane Clarke⁴, Neil Gittoes⁵, Ian Harvey⁶, Richard Holland³, Alison Heawood⁷, Niamh Redmond⁸, Amanda Howe³, Tanya Marshall¹⁰, Tim Peters⁷, David Torgerson¹¹, Terence O'Neill⁹, Eugene McCloskey¹², Cyrus Cooper², John Kanis¹². ¹Quantify Research, Sweden, ²MRC Lifecourse Epidemiology Unit, University of Southampton, United Kingdom, ³University of East Anglia, School of Medicine, United Kingdom, ⁴University Hospitals Bristol BS2 8HW, United Kingdom, ⁵University Hospital Birmingham, Endocrinology, United Kingdom, ⁶University of East Anglia, School of Medicine, Health Policy and Practice, United Kingdom, ⁷Bristol Medical School, University of Bristol, United Kingdom, ⁸University of Bristol, United Kingdom, ⁹University of Manchester, United Kingdom, ¹⁰Norfolk and Norwich University Hospital, Department of Rheumatology, United Kingdom, ¹¹York University, York Trials Unit, United Kingdom, ¹²University of Sheffield, United Kingdom

Objective To estimate the cost-effectiveness of screening for fracture risk in a UK primary care setting, based on a randomised controlled trial in women aged 70–85 comparing a screening programme using the FRAX risk assessment tool versus usual management of osteoporosis (the SCOOP study). Material and Methods The design of the SCOOP study is described elsewhere [1]. A health economic Markov model was used to predict the lifetime consequences in terms of costs and quality of life of the screening programme. The model was populated with drug, administration and screening intervention costs derived from SCOOP. Fracture costs, quality of life-weights and general population fracture risks and mortality were derived from the literature. Fracture risk reduction in the screening arm compared with the usual management arm were derived from SCOOP. Modelled fracture risk corresponded to the observed risk in SCOOP. The main outcome measures were quality-adjusted life years (QALY), costs and incremental cost/QALY. Results Fracture-related costs were £551 lower/patient in the screening arm compared with the usual management arm (Table 1). Drug and intervention costs were £265 higher in the screening arm. In total, the screening arm saved costs (£286) and gained 0.015 QALYs/patient in comparison with usual management arm. Screening saved 9 hip fractures and 20 non-hip fractures over the remaining life-time (average 14 years) of 1,000 patients, compared with usual management. Conclusion This analysis suggests that a screening programme of fracture risk in older women in the UK could gain quality of life and life years, and additionally, reduce fracture costs offsetting the cost of running the programme. References [1] Shepstone L, et al. A Randomised Controlled Trial of Screening in the Community to Reduce Fractures in Older Women: the SCOOP Study. Lancet. 2017 Dec 15.

Table 1. Cost-effectiveness results

	Usual management	Screening	Screening vs. usual management
Costs			
Hospitalisations	3,059	2,934	-125
Nursing home	6,056	5,645	-410
Outpatient	378	363	-15
Total morbidity cost	9,493	8,942	-551
Drugs	12	43	31
Treatment management	92	326	234
Total intervention cost	104	369	265
Total cost	9,596	9,310	-286
Effects			
Life years	10.485	10.487	0.002
QALYs	7.359	7.374	0.015
Cost-effectiveness ratios			
Cost/Life year			Cost-saving
Cost/QALY			Cost-saving

Disclosures: *Fredrik Borgström, None*

MON-0822

Understanding the Patient Experience and Challenges to Osteoporosis Care Delivered Virtually by Telemedicine Patricia Palcu*¹, Sarah Munce², Susan B. Jaglal³, Sonya Allin¹, Arlene Silverstein⁴, Sandra Kim⁵. ¹University of Toronto, Canada, ²Toronto Rehabilitation Institute, University Health Network, Canada, ³University of Toronto, Department of Physical Therapy, Canada, ⁴Women's College Hospital, Canada, ⁵University of Toronto, Women's College Hospital, Canada

Background: Evidence in support of telemedicine (TM) for chronic conditions in rural populations has been well described. There is limited research on the role of TM in the assessment and management of osteoporosis. In 2005, a multidisciplinary osteoporosis TM program, based on an existing outpatient program, was developed at Women's College Hospital, to provide specialized osteoporosis care to underserved areas of Ontario, Canada. We previously reported the high-risk patient characteristics of those serviced by TM. These patients had a higher prevalence of fragility fractures, comorbidities, and need for allied health resources than those serviced by the outpatient clinic. **Purpose:** To understand the patient experience, and benefits and challenges associated with receiving osteoporosis care by TM. **Methods:** This study adopted a qualitative descriptive approach. Semi-structured interviews lasting an average of 30 minutes were conducted by telephone on 16 patients of the TM program. Descriptive themes were identified from interview notes; thematic analysis as described by Braun and Clarke will be applied to full transcripts. **Results:** The majority of participants were comfortable with virtual technology and perceived that quality of care was equivalent to being seen in-person. The main benefits expressed were the convenience and ease of timely care close to home, reduced burden of travel and costs, and improved sense of reassurance and confidence associated with being assessed by an osteoporosis expert. Patients seen by allied health team members by TM indicated increased confidence in self-management; however, many patients were dissatisfied by the coordination of referral to allied health members in the TM program (eg. physiotherapist and dietician). Some patients reported never hearing back on referred appointments to the allied health team. Another perceived challenge was the coordination of investigations such as lab and bone density tests. Many participants indicated interest in a self-management program designed specifically for osteoporosis. **Conclusions:** Our study contributes to an area of limited research on patient perspectives on osteoporosis care delivered by TM. We identified the need to improve our existing processes by better coordinating access to allied health team members and arrangements for investigations. Future research will involve developing and implementing self-management initiatives for osteoporosis patients receiving care by TM.

Disclosures: *Patricia Palcu, None*

MON-0823

Knowledge Translation: Implementation of Recommendations for Fracture Prevention in Long-Term Care Alexandra Papaioannou*¹, George Ioannidis¹, Mary-Lou Van Der Horst², Caitlin McArthur², Loretta M. Hillier², Ravi Jain³, Susan Jaglal⁴, Jonathan D. Adachi¹, Lora Giangregorio⁴. ¹McMaster University, Canada, ²Geriatric Education and Research In Aging Sciences (GERAS) Centre, Canada, ³Osteoporosis Canada, Canada, ⁴University of Toronto, Canada

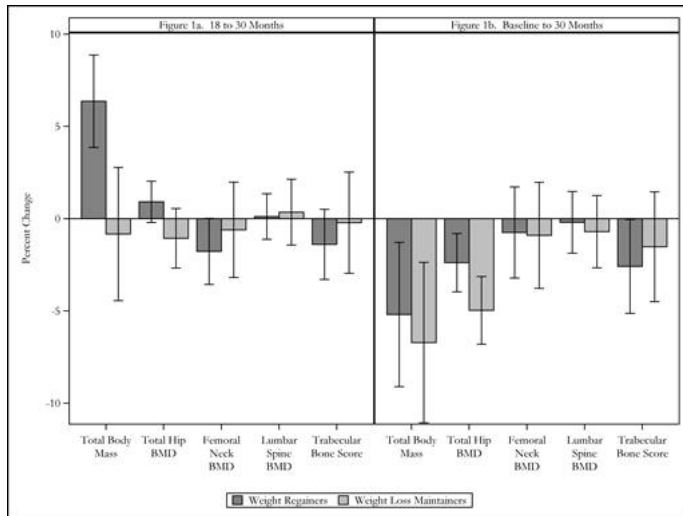
Purpose: For long-term care (LTC) residents, fractures can have life-changing and debilitating consequences. Recommendations for preventing fractures in LTC were published in 2015, aiming to reduce immobility, pain, hospital transfers and improve quality of life of residents. However, there is much research demonstrating large gaps between the development of clinical guidelines and application to practice in LTC. Aligned with the Canadian Institute of Health Research Knowledge Translation (KT) model, we describe the KT activities developed by the Ontario Osteoporosis Strategy for LTC to mobilize the fracture prevention guidelines, and present key tools to support implementation. **Methods:** KT activities were guided by the Knowledge to Action Cycle, informed by a program of research that has identified that fractures are a significant source of morbidity in LTC, with significant gaps in fracture risk assessment and treatment. Our previous work identified barriers and facilitators to fracture prevention efforts in LTC. Engagement with resident and family councils have highlighted their knowledge needs for fracture prevention. Various interventions, including education, audit and feedback and team based action planning, were developed to address identified barriers and leverage facilitators to support the implementation of fracture prevention guidelines. **Results:** KT interventions have demonstrated improvements in prescribing of osteoporosis medication, calcium, and vitamin D. Clinical support tools include: an assessment algorithm for management, an order set for managing fracture risk, and a safe administration therapy tool. The Fracture Risk Scale was created for LTC to fill the knowledge/ do gap and address the identified barriers and facilitators to fracture risk assessment. The scale will be integrated into the Resident Assessment Instrument Minimum Data Set, a standardized assessment used in LTC. A series of videos instruct staff on safe resident movement to prevent falls and fractures. Knowledge tools for residents and family councils aim to increase awareness of fracture risk and prevention. All tools are available as part of an easily accessible on-line fracture prevention toolkit. **Conclusion:** Multifaceted approaches to knowledge translation (KT) can improve the uptake of clinical recommendations. The use of these tools may help close the gap between recommendations of clinical guidelines and application to clinical practice in LTC.

Disclosures: *Alexandra Papaioannou, None*

MON-0848

Hip Bone Loss Persists One Year Following an Intentional Weight Loss Intervention in Older Adults Kristen Beavers*¹, Michael Walkup², Walter Ambrosius², Leon Lenchik², Sue Shapses³, Barbara Nicklas², Anthony Marsh¹, Jack Rejeski¹. ¹Wake Forest University, United States, ²Wake Forest School of Medicine, United States, ³Rutgers University, United States

Purpose: To evaluate change in bone mineral density (BMD) and trabecular bone score (TBS) in the year following an 18 month weight loss intervention in older weight regainers (WR) or weight loss maintainers (WLM). **Methods:** Data come from a longitudinal, non-randomized comparison of 77 older adults (67±5 years, 69% women, 74% Caucasian) with obesity (BMI: 33.6±3.7 kg/m²) who lost weight during an 18 month diet and exercise intervention (randomization groups: weight loss, weight loss + aerobic training, weight loss + resistance training). We assessed baseline, 18, and 30 month total body mass; total hip, femoral neck, and lumbar spine BMD; and TBS data. WR (n=52) and WLM (n=25) categories were defined as a ≥ or < 2 kg weight gain from 18 to 30 months, respectively. **Results:** In models adjusted for randomization group, baseline outcome value, recruitment wave, age, race, and gender, WRs lost more total body mass than WLMs during the 18 month intervention period [WR: -11.5 (-15.5, -7.7) % vs WLM: -5.9 (-10.2, -1.5) %; group p<0.01]; however, by 30 months, total body mass was similarly reduced from baseline in both groups [WR: -5.2 (-9.1, -1.3) % vs WLM: -6.7 (-11.0, -2.4) %; group p=0.44]. Of bone outcomes, only total hip BMD was reduced during the 18 month intervention period, with similar reductions observed for WRs [-3.5 (-5.3, -1.6) %] and WLMs [-2.5 (-4.6, -0.4) %], group p=0.09. After further adjustment for total body mass lost during the intervention, a differential group effect (p<0.05) was observed for change in total hip BMD from 18 to 30 months, with a modest increase in WRs [0.9 (-0.2, 2.0) %] relative to WLMs [-1.1 (-2.7, 0.5) %]. By 30 months, WRs presented with half the loss in total hip BMD from baseline, compared to WLMs [WR: -2.4 (-4.0, -0.8) % vs WLM: -5.0 (-6.8, -3.1) %; group p<0.01]. Femoral neck and lumbar spine BMD were unchanged over the intervention and follow up periods. By 30 months, TBS was modestly reduced from baseline in WRs, but not differently from WLMs [WR: -2.5 (-5.1, -0.0) % vs WLM: -1.5 (-4.5, 1.5) %; group p=0.41]. Figure 1 presents (a) 18 to 30 month and (b) baseline to 30 month percent change in total body mass, BMD, and TBS. **Conclusion:** In the year following an intentional weight loss intervention in older adults with obesity, loss in total hip BMD was partially recovered with WR, while WLM was associated with continued BMD loss. Future work will address categorization of WR and WLM and predictors of hip BMD change.



Disclosures: *Kristen Beavers, None*

MON-0849

Effective exercise for osteoporosis in the real world: Three year observations from The Bone Clinic Belinda Beck^{*1}, Lisa Weis². ¹Griffith University, Australia, ²The Bone Clinic, Australia

Introduction: Our recent work showed high intensity resistance and impact training (HiRIT) was safe and improved bone, muscle and function in postmenopausal women with low bone mass under strict RCT conditions. We then established a translational research Clinic to examine effectiveness, feasibility and acceptability of supervised HiRIT as a legitimate osteoporosis intervention in the 'real world' when delivered on a user-pays basis, with systematic longitudinal monitoring of bone, muscle, function, falls and fractures. The aim of the current work was to determine outcomes from the first 3 years of operation of the Clinic. **Methods:** Clinic clients undergo comprehensive testing for height, weight, lumbar spine (LS), total hip (TH) and femoral neck (FN) bone mineral density (BMD), lean and fat mass, kyphosis angle, back extensor strength (BES), functional performance, falls and fracture, at their baseline visit to the Clinic, and annually thereafter. Twice-weekly supervised HiRIT with balance training is undertaken on a voluntary basis. Compliance and injuries are recorded. Clients with >30% HiRIT compliance were included in the current analyses. In the absence of a control group in this real world sample, training effects were examined using one-sample T-tests of percent change in outcome measures. **Results:** We report outcomes from 121 Clinic clients (64.2±10.1yrs, 161.0±11.1cm, 60.8±14.8kg, LS T-score -2.39±0.94, FN T-score -2.37±0.65; average training compliance 85.1±29.8%, 6.7% men). Improvement was observed in every measured parameter and reached significance for LS (4.0±4.1%, P<0.0001), TH (1.5±3.4%, P<0.0001) and FN BMD (2.4±4.5%, P<0.0001), lean mass (1.8±4.1%, P<0.0001), functional reach (8.1±12.0%, P<0.0001), timed up and go (12.0±12.8%, P<0.0001), tandem walk (20.5±28.8%, P<0.0001), sit to stand (10.7±17.6%, P<0.0001), and BES (27.8±49.1%, P<0.0001). Previous 12 month falls decreased 45% (from 45 to 25, P<0.053) and fractures decreased 91.7% (from 24 to 2, P<0.0001). Twenty minor injuries were sustained in a combined total of 27,840 training sessions. **Conclusions:** Supervised, bone-targeted high intensity resistance and impact training is safe and reduces risk for osteoporotic fracture in postmenopausal women with low to very low bone mass in a 'real world' clinical setting. Ongoing monitoring of this unique translational dataset will provide insight into the long term feasibility of exercise as a first line intervention for osteoporosis.

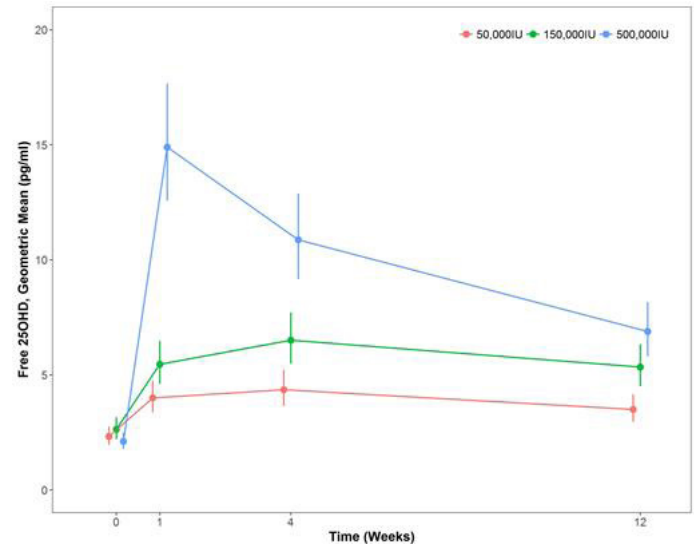
Disclosures: *Belinda Beck, The Bone Clinic, Other Financial or Material Support*

MON-0850

Effect of high dose vitamin D on free 25(OH)D and ionised calcium in vitamin D-deficient postmenopausal women Simon Bowles^{*1}, Jennifer Walsh¹, Richard Jacques¹, Eastell Richard¹, Thomas Hill². ¹University of Sheffield, United Kingdom, ²Newcastle University, United Kingdom

Several studies have shown an increase in the rate of falls and fractures after high dose vitamin D supplementation, but the mechanism for the increase in falls is yet to be elucidated. Vitamin D and its metabolites are bound to proteins in the circulation: around 85-90% of 25-hydroxylated vitamin D (25(OH)D) is bound to vitamin D binding protein (DBP), 10-15% is bound to albumin, and less than 1% is in the free form. Administration of a large bolus dose of vitamin D (e.g. 500 000IU) may saturate the binding capacity of DBP, leading to high free 25(OH)D, vitamin D toxicity and falls. We tested the clinically important hypothesis that a disproportionate rise in free 25(OH)D and hypercalcaemia could cause the increase in falls and fractures after high dose vitamin D (cholecalciferol). We recruited 33 vitamin D deficient (25(OH)D <30nmol/l) post-menopausal women who

were randomized to a bolus dose of either 50 000IU, 150 000IU or 500 000IU of orally administered cholecalciferol. We also recruited 28 postmenopausal women who were vitamin D sufficient (25(OH)D >50nmol/l) as a concurrent control group. Participants attended five study visits, over a three-month period. We made a range of biochemical measurements, including 25(OH)D₃, free 25(OH)D, parathyroid hormone (PTH) and ionized calcium. We assessed muscle strength and function with grip strength and a Short Physical Performance Battery (SPPB). 25(OH)D₃ and free 25(OH)D increased in a dose-dependent manner at 1 week and remained significantly different between treatment groups at 4 weeks and 12 weeks after administration. Peak 25(OH)D₃ was at 1 week for all doses (46.7nmol/l, 69.6nmol/l and 153.7nmol/l, respectively). Peak free 25(OH)D was at 1 week in the 500 000IU group (14.90pg/ml) and 4 weeks in the 50 000IU (4.00pg/ml) and 150 000IU (5.46pg/ml) groups. There were proportionally similar increases in 25(OH)D₃ (x=7.09 (95% CI: 5.73, 8.88)) and free 25(OH)D (x=7.21 (95% CI: 6.34, 8.19)) at 1 week in the 500 000IU treatment group. There were no within-group changes over time and no between-group effects of vitamin D dose on serum ionized calcium, PTH, SPPB scores or grip strength at any timepoint. In conclusion, the large increase in 25(OH)D₃ and free 25(OH)D in response to a high dose bolus of vitamin D is not associated with hypercalcaemia. A 500 000IU dose does not appear to have adverse effects in vitamin D deficient, but otherwise healthy postmenopausal women.



Disclosures: *Simon Bowles, None*

MON-0851

Effect of Home Exercise on Functional Performance, Posture, Quality of Life and Pain in Older Women with Vertebral Fractures: A Pilot Feasibility Trial Jenna C. Gibbs^{*1}, Jonathan D. Adachi², Maureen C. Ashe³, Robert Bleakney⁴, Angela M. Cheung⁴, Keith D. Hill⁵, David L. Kendler³, Aliya Khan², Sandra Kim⁶, Judi Laprade⁴, Caitlin Mearthar⁷, Nicole Mittmann⁸, Alexandra Papaioannou², Sadhana Prasad², Samuel C. Scherer⁹, Lehana Thabane², John D. Wark⁹, Lora M. Giangregorio¹. ¹University of Waterloo, Canada, ²McMaster University, Canada, ³University of British Columbia, Canada, ⁴University of Toronto, Canada, ⁵Curtin University, Australia, ⁶Women's College Hospital, Canada, ⁷GERAS Centre for Aging Research, Canada, ⁸Cancer Care Ontario, Canada, ⁹University of Melbourne, Australia

Guidelines for osteoporosis management advocate for regular exercise to prevent falls and fractures, but there is limited evidence on the safety and efficacy of exercise in individuals at high risk of fracture. Purpose: We conducted a pilot randomized controlled trial to evaluate the feasibility of recruitment, retention and adherence to 12 months of home exercise compared to control among older women with vertebral fractures. Herein we present an exploratory analysis of the effect of the home exercise program on secondary outcomes, including functional performance, posture, quality of life and pain. Methods: Community-dwelling women aged 65 years and older with at least one radiographically-confirmed Genant Grade 2 vertebral compression fracture were recruited at seven sites in Canada and Australia. We randomized participants in a 1:1 ratio to a 12-month home exercise program (n=71) or equal attention control group (n=70), both delivered by a physical therapist over six home visits and monthly phone calls. The exercise program included progressive strength, posture, balance and endurance training and behavioral counseling. Adherence was defined as the completion of strength or balance exercises at least three days per each seven-day period in daily diaries. Functional performance tests, occiput-to-wall distance, health-related quality of life questionnaires and pain scales were performed at baseline and 12 months by a blinded research assistant. T-tests explored between-group mean differences (MD) in change from baseline in intention-to-treat (ITT) and per-protocol analyses. Results: There was a positive effect of exercise on five times sit-to-stand test time versus control (MD: -1.58 seconds, 95% CI: -3.09, -0.07, ITT; MD: -1.49 seconds, 95% CI: -3.12, 0.16,

per-protocol). There were no other significant between-group differences for functional mobility, balance, posture, quality of life and pain. Average adherence to the exercise program over months 1 to 11 was 73%; yet, adherence declined from 68% at month 6 to 59% at month 11. Conclusions: The effect of home exercise on functional leg muscle strength was consistent in direction and magnitude to the effects of exercise on mobility outcomes in other trials in individuals with vertebral fractures. Declining adherence to home exercise suggests that strategies to enhance long-term adherence or more supervision might be important in future exercise trials in older women with vertebral fractures.

Disclosures: *Jenna C. Gibbs, None*

MON-0852

Changes in Vascular Calcification and Bone Mineral Density in Calcium Supplement Users from the Canadian Multi-center Osteoporosis Study (CaMOS). Maggie Hulbert*¹, Rachel Holden². ¹Queen's University, Canada, ²Kingston General Hospital, Canada

Background: Calcium supplements are widely used to prevent osteoporosis and fragility fractures. Recently, epidemiological data has shown a concerning association between calcium supplement use and cardiovascular events. Calcium deposition in the vasculature has been proposed as an underlying mechanism. Objectives: To determine the association between calcium supplement use and change in the Framingham vascular calcification score and bone mineral density T-scores in participants of CaMOS. Methods: We identified post-menopausal women and older men (n=296) who had completed facilitated health history questionnaires and had lateral spine X-rays and DEXA bone mineral density scans at two time points with a 5 year interval. Abdominal aortic calcification (AAC) was assessed on lateral spine X-ray by the Framingham Method. The change in BMD T-scores at L1-L4 (lumbar), total hip, and femoral neck sites measured by DXA (Hologic, Inc.) was calculated during the same 5 year interval. The association between calcium supplement use and AAC change was assessed using t-tests and multi-variable logistic regression models. Results: AAC significantly increased over 5 years (mean increase 1.86, SD 3.238). AAC progression was significantly greater in calcium supplement users as compared to non-users (p=0.033), and female calcium supplement users had the most significant amount of AAC progression (mean 2.61 p=0.018). Amount (mg/day) of calcium supplement taken positively correlated to AAC progression (r=0.16, p=0.006). In the multi-variable model, calcium supplement use and amount remained significantly associated with AAC progression after adjustment for age, hypertension, diabetes and smoking history in women only (r=2.16, p=0.032). Calcium supplement use was not associated with preservation of BMD at any site, and was associated with a significantly greater BMD loss at all three sites in men only. Conclusion: Calcium supplement users have significantly higher AAC progression over 5 years. This effect is seen most significantly in post-menopausal women. Calcium supplement users did not have any significant preservation of BMD. These results suggest that vascular calcification may contribute to the increased cardiovascular events observed in calcium supplement users, and that calcium supplement use may have a negative risk-benefit ratio.

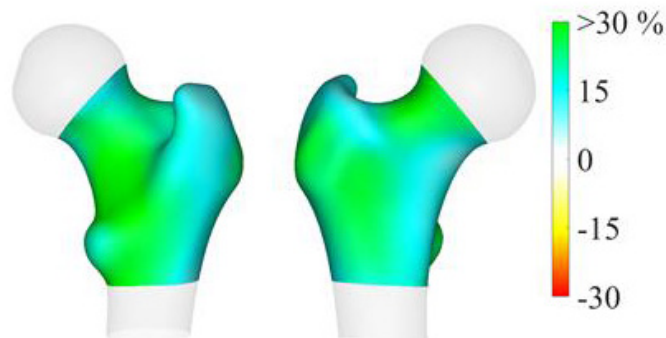
Disclosures: *Maggie Hulbert, None*

MON-0853

3D analysis of the cortical and trabecular bone of elite female athletes involved in high- and low-impact sports Ludovic Humbert*¹, Luis Del Río², Antonia Lizarraga³, Montserrat Bellver⁴, Renaud Winzenrieth¹, Amineh Amani², Franckek Drobnic³. ¹Galgo Medical, Spain, ²CETIR Centre Medic, Spain, ³Football Club Barcelona, Spain, ⁴Centro de alto Rendimiento, Spain

Purpose: To assess and compare the cortical and trabecular bone of the proximal femur of athletes involved in high-impact sports (football and volleyball) and low-impact sports (swimming, synchronised swimming and water polo) using DXA-derived 3D analysis. Methods: Elite female athletes from the football first team of FC Barcelona and from the Spanish national team of volleyball, swimming, synchronised swimming and water polo were included in this study. Hip DXA scans were performed at the Medical Services of FC Barcelona (Barcelona, Spain) using a Lunar iDXA scanner (GE Healthcare, Madison, WI). Areal BMD (aBMD) were calculated at total femur. The 3D-SHAPER software (v2.7, Galgo Medical, Barcelona, Spain) was used to provide 3D analysis of the cortical and trabecular bone from hip DXA scans. Trabecular volumetric BMD (vBMD) and cortical surface BMD (sBMD) were calculated at total femur. DXA and DXA-derived 3D measurements calculated for every groups were compared using Student's t-test. Results: The number and mean age (±SD) of the female athletes involved in this study was N=60, 22±4 years (football); N=26, 23±6 years (volleyball); N=18, 19±4 years (swimming); N=25, 21±5 years (synchronised swimming); and N=14, 24±4 years (water polo). No difference in aBMD, trabecular vBMD and cortical sBMD was found between athletes involved in high-impact sports (football and volleyball). Among the groups involved in low-impact sports, water polo athletes had 10% higher aBMD, trabecular vBMD and cortical sBMD (p<0.05 for all measurements), compared to swimmers. They showed 7% higher cortical sBMD (p<0.05), compared to synchronised swimmers, while no significant differences were found for aBMD and trabecular vBMD. Athletes involved in high-impact sports had higher aBMD (12% to 21%), trabecular vBMD (17% to 34%) and cortical sBMD (11% to 27%), compared to low-impact sports. Distribution of the mean differences in cortical sBMD between football and swimming athletes are shown in Figure 1. Conclusions: Athletes involved in high-impact sports exhibited higher densities in both cortical and trabecular compartments, compared to

low-impact sports. Interestingly, water polo athletes have higher cortical density compared with other swimming athletes which could be explained by higher workout.



Disclosures: *Ludovic Humbert, Galgo Medical, Major Stock Shareholder*

MON-0854

Yoga-related bony spine injuries Melody Lee*, Mehrsheed Sinaki. Mayo Clinic, United States

Background: Yoga has gained great popularity in recent years, being touted as a safe and gentle form of exercise. However, injuries can occur despite the perceived benign nature of yoga. The purpose of this case series is to describe vertebral anterior wedging and compression fractures that were directly linked to the practice of yoga. Methods: The study population consisted of 25 patients who were treated in the musculoskeletal clinic of the physical medicine and rehabilitation department. All of the patients had identified yoga as the primary cause of their injury and pain. Their charts were reviewed and analyzed retrospectively. Results: All 25 patients had radiographically confirmed vertebral body anterior wedging (18 patients) and/or compression fractures (14 patients). Mean age: 64, height: 162.8cm, and weight: 62.4kg. Average T-score: -2.46. Patients were able to identify the poses that induced their injuries. The most commonly identified poses were: bridge pose in 13(52%), seated forward fold in 12(48%), and plow pose in 9(36%). Conclusion: To our knowledge, this is by far the largest case series of yoga-related vertebral anterior wedging and compression fractures to date. While yoga potentially has many health benefits, it still carries some risks. Patients who have osteopenia or osteoporosis may be at higher risk of compression fractures or deformities, particularly when performing extreme spinal flexion. Practitioners should address this when counseling patients on yoga as exercise.

Disclosures: *Melody Lee, None*

MON-0855

Relationships between high sodium intake and trabecular bone score as well as fracture in postmenopausal women Kiyoko Nawata*¹, Mika Yamauchi², Masahiro Yamamoto², Toshitsugu Sugimoto². ¹Health and Nutrition, The University of Shimane, Faculty of Nursing and Nutrition, Japan, ²Internal Medicine 1, Shimane University Faculty of Medicine, Japan

Objective: Some earlier studies suggest that excessive dietary sodium (Na) intake is associated with a higher prevalence of osteoporosis. However, the role of high Na intake on bone fragility has not been yet fully elucidated. On the other hands, a decrease in trabecular bone score (TBS), which is an indicator of the cancellous bone microstructure, is recognized as a risk factor for fracture, independent of bone mineral density (BMD). Therefore, the present study investigated the influence of Na intake on TBS and Fx risk. Methods: The subjects were 213 healthy postmenopausal women who had undergone osteoporosis screening. Serum levels of PTH, 25-hydroxyvitamin D [25(OH)D], P1NP, CTX, urinary Ca (uCa) and Cr(uCr) were measured. The BMD of the lumbar (L) and femoral neck (FN) was measured using DXA, and TBS (L1-4) was calculated. Nutrient intake was calculated using a food frequency questionnaire. Results: The mean age of subjects was 63±8 years. The mean values of measured variables were: L-BMD 0.84±0.15g/cm², FN-BMD 0.62±0.09g/cm², and TBS 1.31±0.07. Na intake was 5211±1697mg. Vertebral (VFX) and non-vertebral (non-VFX) fractures were observed in 49 and 36 subjects, respectively. Na intake was not correlated with BMD, bone metabolic markers and uCa/uCr. In an analysis of TBS by quartile of Na intake, the highest Na intake group (highest Na) showed a value significantly lower than each other groups. While the presence or absence of VFX showed significant differences in TBS, no such difference was observed between the Na intake and VFX in quartile analyses. On the other hand, while the presence or absence of non-VFX did not show differences in TBS and Na intake, the proportion of the presence of non-VFX in the highest Na (7561±1035 mg) was significantly higher as compared with the other groups. Logistic regression analysis revealed that the highest Na was a significant risk factor for non-VFX even after adjustments for TBS, in addition to age, BMI, PTH, 25(OH)D, CTX, FN-BMD, uCa/uCr, other nutritional intake, and presence or absence of hypertension [odds ratio 3.01 (95%CI: 1.05-8.60), p<0.05]. Conclusion: Excessive Na intake may be associated with deteriorating cancellous bone microstructure in postmenopausal women. Excessive Na intake is also a risk factor

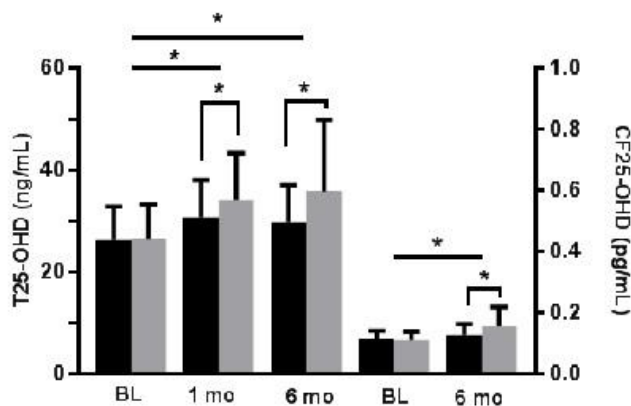
for non-VFx. However, the association between excessive Na intake and non-VFx was independent of the deterioration of the cancellous bone microstructure as well as BMD and urinary Ca excretion.

Disclosures: *Kiyoko Nawata, None*

MON-0856

A Randomized Trial of Vitamin D Supplementation in Healthy Inner-city Children Christine Simpson^{*1}, Jane Zhang², Dirk Vanderschueren³, Lei Fu⁴, Teresita Pennestri¹, Roger Bouillon³, David Cole⁴, Thomas Carpenter¹. ¹Yale University School of Medicine, United States, ²VA Connecticut Healthcare System, United States, ³Katholieke Universiteit Leuven, Belgium, ⁴University of Toronto, Canada

Determinants of vitamin D (vitD) status in children include ethnic/genetic background and vitD binding protein (DBP) haplotype. We therefore performed a trial of vitD supplementation in 2-10 yr-old children of predominantly Hispanic background to determine effects of vitD dose and DBP haplotype on the response to supplementation. Subjects were randomized to receive low (2800 IU weekly) (LD) or higher dose (HD) vitamin D₃ (7000 IU weekly) for 6 months (mos), and stratified to one of the 6 commonly occurring DBP haplotypes. Total 25-hydroxyvitamin D (T25-OHD) increased by 1 mo of supplementation, with a 31% increase in HD subjects (mean $\Delta=7.7$ ng/mL) which differed from the 22% increase in LD subjects (mean $\Delta=4.7$ ng/mL) ($P=0.003$). Increases differed slightly by DBP haplotype ($P=0.034$) with the least change occurring in the Gc1f/Gc1s (DETT) group. The difference in dose response persisted at 6 mos ($\Delta=10.4$ ng/mL in HD, a 43% increase, vs. $\Delta=3.4$ ng/mL in LD, a 17% increase; $P=0.040$). DBP haplotype effects were no longer evident ($P=0.29$) at 6 mos. Differences between doses were similar across all DBP haplotypes (interaction of dose and haplotype, $P=0.26$). 1,25-dihydroxyvitamin D (1,25D) increased after 1 and 6 mos ($P<0.001$). Change from baseline did not differ between dose groups at either 1 mo ($P=0.13$) or 6 mos ($P=0.59$). DBP haplotype did not affect 1,25D at either 1 mo ($P=0.62$) or 6 mos ($P=0.37$). No significant change from baseline occurred in circulating DBP levels (measured only at 6 mos) in either treatment group ($P=0.96$), however calculated free (CF) 25-OHD at 6 mos increased by 13% and 40% in LD and HD groups respectively ($P<0.001$), changes comparable to those observed for T25-OHD. Circulating 25-OHD levels in healthy inner-city children can be enhanced by doses of vitamin D₃ equivalent to 400 IU and 1000 IU daily without toxicity. T25-OHD levels increase by 1 mo of supplementation and dose differences are sustained at 6 mos. CF25-OHD levels increase comparably to T25-OHD. 1,25D levels increase within 1 mo of vitamin D₃ supplementation and persist through 6 mos, suggesting a sustained substrate effect contributing to circulating levels of this metabolite. Although small changes may transiently occur across DBP haplotypes, vitD supplementation does not require targeting to a patient's specific DBP haplotype.



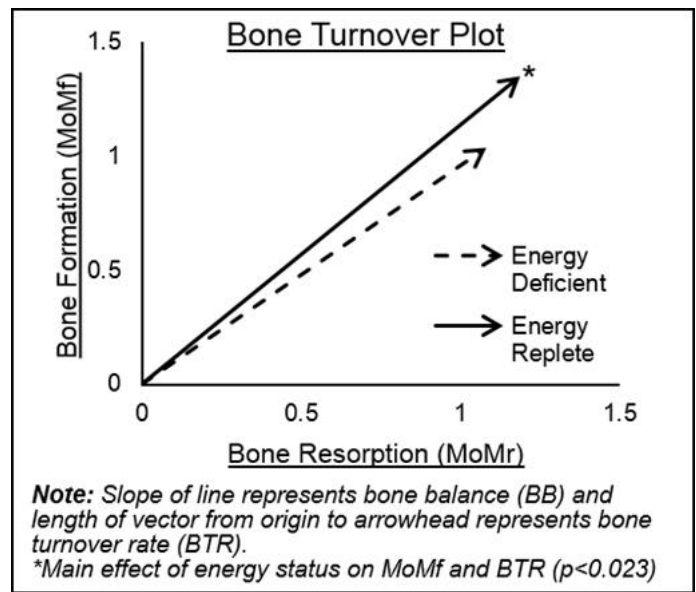
Low dose groups are shown in black and higher dose groups in gray. BL=baseline, mo=month. The 6 bars on the left of figure represent Total 25-OHD (left axis) and the 4 bars on the right represent Calculated Free 25-OHD (right axis). * $p<0.05$

Disclosures: *Christine Simpson, None*

MON-0857

Low T3 is Associated with Decreased Bone Turnover Rate in Exercising Women with Eumenorrhea and Amenorrhea Emily Southmayd^{*}, Andrew Oneglia, Rebecca Mallinson, Nancy Williams, Mary Jane De Souza. The Pennsylvania State University, United States

INTRODUCTION: Energy and estrogen deficiency are detrimental to bone health in young exercising women, increasing the risk for impaired bone density and geometry. While bone formation and resorption have been reported in isolation as a result of menstrual dysfunction, such as amenorrhea, or acute energy deficiency via caloric restriction, the effect of energy and estrogen deficiency in isolation or in combination on bone turnover dynamics, which might have implications for fracture risk, have not been established. The purpose of this study was to assess the independent and interactive effects of energy and estrogen deficiency on bone formation, resorption, net bone balance, and bone turnover rate. **METHODS:** Exercising women age 18-30yr with amenorrhea (estrogen deficient, E2D, n=48) or ovulatory eumenorrhic cycles (estrogen replete, E2R, n=31) were recruited. Menstrual status was assessed by self-reported history of menses corroborated with daily urinary measures of estrogen and progesterone metabolites for one menstrual cycle (if eumenorrhic) or one 28d monitoring period (if amenorrhic). Energy status was assessed via serum triiodothyronine (T3) concentration. Women were grouped as energy deficient (EnD, n=40) or energy replete (EnR, n=39) based on a median split of T3 concentrations (83.85 ng/dl cutoff). Bone formation (MoMf) and resorption (MoMr) scores were calculated relative to healthy, ovulatory reference data (MoMf=[P1NP]i/median[P1NP]ov; MoMr=[CTX]i/median[CTX]ov). Bone balance (BB) and Bone Turnover Rate (BTR) were calculated (BB=MoMf/MoMr; BTR=sqrt(MoMf+MoMr²)). 2-way ANOVA was used to assess main and interactive effects of energy and estrogen status on P1NP (MoMf), CTX (MoMr), BB, and BTR. **RESULTS:** There was a main effect of energy status on bone formation (P1NP, MoMf, $p=0.007$) and BTR ($p=0.023$), such that women that were energy replete based on higher T3 concentrations had greater bone formation and faster bone turnover. There were no main effects of estrogen status on bone turnover dynamics, and there were no interactive effects of energy and estrogen status. **CONCLUSION:** Energy status drives indicators of bone turnover. Thus, adequate nutrition, which may also promote menstrual health, should be a priority to optimize bone health in exercising women. Bone turnover rate is a novel measurement that should be explored with respect to bone density and fracture risk.



Disclosures: *Emily Southmayd, None*

MON-0858

Supervised high intensity resistance and impact training does not cause vertebral crush fractures and improves thoracic kyphosis in postmenopausal women with low to very low bone mass: The LIFTMOR Trial Steven Watson^{*1}, Benjamin Weeks¹, Lisa Weis², Amy Harding¹, Sean Horan¹, Belinda Beck¹. ¹School of Allied Health Sciences, Griffith University, Gold Coast, Australia, ²The Bone Clinic, Brisbane, Queensland, Australia

Introduction: The recent LIFTMOR trial demonstrated that supervised high intensity resistance and impact training (HiRIT) improves BMD and functional performance in postmenopausal women with low to very low bone mass to a greater degree than other forms of exercise. Concerns have been raised, however, that such high intensity loading may increase the risk of vertebral crush fracture in this high risk population. The aim of the current work was to assess vertebral morphology and kyphosis for evidence of fracture before

and after 8 months of HiRIT in the LIFTMOR cohort. Methods: Postmenopausal women with low bone mass (T-score <-1.0) were recruited and randomized to either 8 months of twice-weekly, 30-minute, supervised HiRIT, or a home-based, low intensity exercise program (CON). At baseline and 8 months, lateral spine DXA scans were performed (Medix DR, Medilink, France) on which lateral vertebral assessments were conducted, based on the Genant method. Clinical kyphosis measures were also performed (degree of deformity from inclinometer [Plurimeter, AMTI, Australia] and kyphosis index [unitless] from Flexicurve [Flexible curve, Staedler, Germany]), in both relaxed standing and standing tall postures. Changes in vertebral morphology and posture were tested using repeated measures ANOVA (ITT). Results: Fifty-one participants (64±4 years, 161.5±5.9cm, 63.6±10.4kg) were included in the analysis. At baseline, 17 participants (33%) had a vertebral deformity (CON=11; HiRIT=6), with wedge deformities being most common (n=12/18). No changes in vertebral morphology were observed following HiRIT. One new vertebral deformity was identified after CON. The HiRIT group exhibited greater improvement in degree of thoracic kyphosis in the standing tall position compared to CON (-6.7±8.2° vs -1.6±8.1°, p=0.031). In relaxed standing, both HiRIT and CON groups had within-group improvements in kyphosis degree (HiRIT: -6.0±6.9°, p<0.001; CON: -4.0±6.9°, p=0.005) and kyphosis index (HiRIT: -2.4±2.5, p<0.001; CON: -2.0±2.4, p<0.001), but no between-group difference could be detected. Conclusion: Contrary to concerns regarding the risk of crush fracture during heavy lifting in postmenopausal women with low bone mass, our supervised HiRIT program was not associated with changes in vertebral morphology. Indeed, HiRIT improved thoracic kyphosis. We thus conclude that supervised HiRIT not only improves BMD and posture, but is safe for postmenopausal women with low bone mass.

Disclosures: *Steven Watson, None*

MON-0871

Kynurenine Regulates Osteogenesis in Aging Through miRNAs 29b-1-5p and 141-3p Khaled Hussein*, Ahmed Elmansi¹, Sudhansu Periyasamy-Thandavan², Galina Kondrikova¹, Wendy Bollag³, Sadanand Fulzele⁴, Xingming Shi⁵, Meghan Mcgee-Lawrence¹, Mark Hamrick¹, Carlos Isales⁵, William Hill².

¹Department of Cellular Biology and Anatomy, Augusta University, United States, ²Department of Cellular Biology and Anatomy, Augusta University, Georgia, ³Department of Physiology, Augusta University, United States, ⁴Department of Orthopedic Surgery, Medical College of Georgia, United States, ⁵Department of Neuroscience and Regenerative Medicine, Augusta University, United States

We propose that age-related osteoporosis is in part due to increased levels of kynurenine (KYN), a Tryptophan (TRP) metabolite that goes up with aging and is generated by Indoleamine-(2,3)-dioxygenase as well as reactive oxygen species oxidation. miRNAs are small non-coding RNA molecules involved in post-transcriptional regulation of gene expression. Of interest, we identified miRNAs 29b-1-5p and 141-3p to target a number of osteogenic genes (Runx2, BMP-2, Col1) including stromal cell-derived factor-1 (SDF-1/CXCL12), and its receptor CXCR4, while increasing adipogenic markers such as c/BEP. We hypothesized that KYN increases both miRNAs 29b-1-5p and 141-3p leading to inhibition of osteogenic genes, including the SDF-1 axis, leading to reduced BMSC osteogenesis. We show that in BMSCs KYN increases both miRNAs in a dose-dependent fashion rapidly within 6 hours, then declining, and leads to a sustained significant reduction of both mRNA and protein levels of SDF-1 and CXCR4 over 48 hours in human and murine bone marrow mesenchymal stem cells. To test whether SDF-1 concentration is dependent on changes in miRNAs, we show that using antagonists to miRNAs with KYN co-treatment rescued SDF-1 gene expression and protein levels. KYN is known to have a cytoplasmic receptor, the aryl hydrocarbon receptor (AhR), which translocates to the nucleus to regulate gene expression as part of a xenogen transcription complex. Using a AhR blocker CH223191 with KYN only partly rescued SDF-1 expression levels, suggesting that Kynurenine could be working through the AhR pathway and potentially another mechanism as well. We also show that miR-29b-1-5p also targets Hdac3, which plays a role in determining BMSCs osteogenic or adipogenic cell fate. KYN up-regulates age associated miRNAs, decreases SDF-1 levels, and inhibits osteogenic differentiation, while at the same time upregulating adipogenic pathways. This work suggests mechanisms linking KYN directly to age-associated changes in bone homeostasis and osteoporosis.

Disclosures: *Khaled Hussein, None*

MON-0872

Exome sequencing and functional follow-up identifies KIF26B as a novel genetic determinant of familial osteoporosis Melissa M Formosa*¹, Robert Formosa², Herma C Van Der Linde³, Juriaan R Metz⁴, Gert Flik⁴, Deepak Kumar Khajuria⁵, David Karasik⁵, M Carola Zillikens⁶, Rob Willemsen³, Andre G Uitterlinden⁶, Tjakko J Van Ham³, Fernando Rivadeneira⁶, Annemieke Jmh Verkerk⁶, Angela Xuereb-Anastasi¹. ¹Department of Applied Biomedical Science, Faculty of Health Sciences, University of Malta, Msida, Malta, ²Department of Medicine, Faculty of Medicine and Surgery, University of Malta, Msida, Malta, ³Department of Clinical Genetics, Erasmus University Medical Center, Rotterdam, Netherlands, ⁴Department of Animal Physiology, Institute for Water and Wetland Research, Faculty of Science, Radboud University Nijmegen, Nijmegen, Netherlands, ⁵The Musculoskeletal Genetics Laboratory, Azrieli Faculty of Medicine, Bar-Ilan University, Safed 1311502, Israel, ⁶Department of Internal Medicine, Erasmus University Medical Center, Rotterdam, Netherlands

Objective: Osteoporosis is a skeletal disease under strong genetic control. The aim of the study was to identify the genetic determinants of primary osteoporosis in a Maltese family and investigate the function of identified novel genes and variants. Methods: A 2-generation family of 12 recruited relatives (including 7 siblings) with ages ranging from 34-77 years was tested. Osteoporosis was defined using DXA scans of the lumbar spine (LS) and hip. The proband had a LS T-score of -4.0. Exome sequencing was performed on 6 well-phenotyped relatives and replication of shortlisted variants was sought in a case-control collection of Maltese postmenopausal women (n=1012). In vitro protein expression was analyzed by transfecting in COS-7 cells and western blotting, whereas consequences of gene knockdown was studied in a zebrafish model. BMD was assessed with micro-computed tomography; mineralization rate with Alizarin red staining of the whole fish skeleton; and resorption activity with TRAcP staining of regenerating scales. Results: Comprehensive exome variant filtering according to dominant inheritance identified in all affected individuals a novel nonsense variant p.Q287X (c.C859T) within the Kinesin family member 26B (KIF26B) gene. Screening of the variant identified two heterozygous carriers of the T allele (MAF=0.001) presenting with low LS BMD (average T-score: -2.3). The variant is located within a highly conserved region of the protein, upstream of the kinesin motor domain. In silico modeling predicted the T allele to result in nonsense mediated mRNA decay. Western blotting confirmed a complete absence of the protein in the presence of the T allele. As compared to wild-type (WT) fish matched for age and length, kif26b knockout fish had lower numbers of mineralized vertebrae until 1 month post fertilization (mpf). Notorious decrease in BMD (-23%, p=0.01) and bone volume/tissue volume (-40%; p=0.01) was observed at 3mpf. At 4mpf, knockout fish presented higher osteoclast activity in regenerating scales at 6-day (p=0.04) and 14-day (p=0.03) recovery set-points. Conclusion: Our findings postulate KIF26B as a novel factor playing a role in bone biology and susceptibility to familial osteoporosis. KIF26B is involved in intracellular transport and cell division, linked to Wnt5a-Ror signaling in morphogenesis, including limb development. Further elucidation of the underlying cellular processes may identify novel therapeutic targets for osteoporosis treatment.

Disclosures: *Melissa M Formosa, None*

MON-0873

MIR4697HG knockdown prevents ovariectomy-induced osteoporosis in mice Chanyuan Jin*, Yongsheng Zhou. Peking University School and Hospital of Stomatology, China

Osteoporosis is believed to have a strong correlation with reduced osteogenic potential of bone marrow mesenchymal stem cells (BMMSCs). However, the underlying mechanism of osteogenesis of BMMSCs remains elusive. Recent studies have found long non-coding RNAs (lncRNAs) play important roles in osteogenesis of BMMSCs. In this study, we found lncRNA MIR4697HG was upregulated in BMMSCs of osteoporotic mice (OVX) compared with control group. Additionally, we found MIR4697HG was downregulated during the osteogenic differentiation of BMMSCs. Moreover, we demonstrated that knockdown of MIR4697HG promoted osteogenic differentiation of BMMSCs in vitro and in vivo, whereas overexpression of MIR4697HG inhibited osteogenesis of BMMSCs in vitro and in vivo. Finally, we found bone loss was attenuated in OVX injected with MIR4697HG siRNA. Taken together, these results suggest MIR4697HG plays an important role in osteogenesis of BMMSCs and may have a potential use in treating osteoporosis.

Disclosures: *Chanyuan Jin, None*

MON-0874

Age related changes in bone microstructure, bone turnover markers, and serum pentosidine levels: HR-pQCT study in healthy Japanese men Narihiro Okazaki*, Ko Chiba, Mitsuru Doi, Kazuaki Yokota, Makoto Osaki. Department of Orthopaedic Surgery, Nagasaki University Hospital, Japan

Introduction: Many studies on osteoporosis have been conducted in women. However, its pathogenesis in men remains unclear. In this study, we analyzed age-related changes in the bone microstructure, bone turnover markers, and serum pentosidine levels cross-sectionally to investigate the pathogenesis of osteoporosis in men. Methods: A total of 78 Japanese

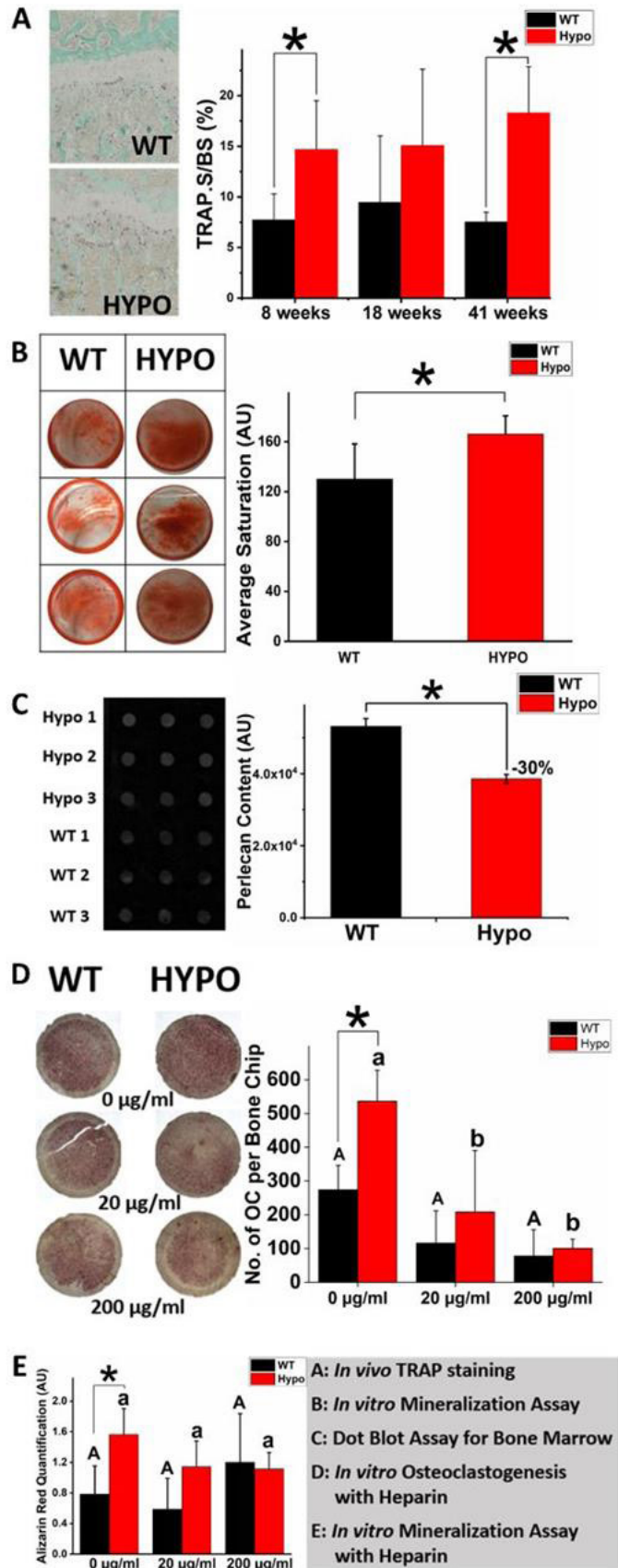
men (mean age 42 ± 14; range, 21-75 years) from the J-CaraT study (Japanese study of bone microstructure and mineral density in a non-randomized cohort measured by HR-pQCT) in Nagasaki University were included as study subjects. The distal radius and tibia were scanned using high-resolution peripheral quantitative computed tomography (XtremeCT II; Scanco Medical, Switzerland) with a voxel size of 60.7 μm, and the volumetric bone mineral density (vBMD) and bone microstructure parameters were analyzed. The serum levels of tartrate-resistant acid phosphatase-5b (TRACP-5b), total procollagen type I N-terminal propeptide (PINP), and pentosidine were also evaluated. Results: Age was negatively correlated with trabecular vBMD, bone volume fraction, and number (radius, r = -0.45, -0.47, and -0.36; tibia, -0.49, -0.49, and -0.29, respectively); positively correlated with cortical porosity (radius, r = 0.46; tibia, r = 0.30); but not correlated with cortical vBMD or cortical thickness. Furthermore, age was also negatively correlated with total PINP levels (r = 0.55), positively correlated with pentosidine levels (r = 0.51), but not correlated with TRACP-5b levels. Conclusions: In men, the bone resorption markers did not change, whereas the bone formation markers decreased with age. Furthermore, pentosidine levels increased with age; the trabecular bone decreased and cortical porosity increased; however, the cortical thickness was relatively maintained.

Disclosures: Narihiro Okazaki, None

MON-0875

Upregulated osteoclastogenesis and accelerated mineralization associated with perlecan deficiency were rescued by exogenous heparin treatment in vitro Ashutosh Parajuli*, Ping Li, Jerahme Martinez, Catherine Kirm-Safran, Liyun Wang, University of Delaware, United States

Perlecan/HSPG2, a large multifunctional heparin sulfate proteoglycan is found in basement membranes and the pericellular matrices of cartilage and bone [1]. Perlecan deficiency is also a risk factor of osteoporosis [1]. We found cortical hypermineralization [2], trabecular osteopenia [3] in perlecan deficient (Hypo) mice, upregulated osteoclastogenesis and accelerated mineralization of progenitor cells from the hypo bone marrow (Figs. A,B) [4]. The purpose of this study was to examine if exogenous treatment with Heparin (hyper-sulfated GAG) can rescue the above impairments associated with perlecan deficiency. Dot blot assay: Soluble protein were extracted from bone marrow. Perlecan content was determined using dot blot with anti-perlecan A7L6 antibody. Osteoclastogenesis assay: Freshly harvested marrow from long bones was cultured in media supplemented with M-CSF (25 ng/ml) for 2 days. The non-adherent cells were cultured 9 more days in media with M-CSF (25 ng/ml) & RANKL (20ng/ml) on dentin slices in 96-well plates, followed by TRAP staining. Osteogenesis mineralization assay: The adherent MSCs from fresh bone marrow were cultured in osteogenic media for 19 days and stained with 2% Alizarin red [2]. Mineralization was quantified. Heparin treatments: Both assays were carried out on WT and Hypo samples with 3 different concentrations of Heparin: 0, 20 and 200 μg/ml with at least three repeats. Dot blot showed significantly lower perlecan content (-30%) in Hypo bone marrow than WT (Fig. C), agreeing with the reduced perlecan gene expression in Hypo [5]. Similar to in vivo (Fig. A), the # of multinucleated TRAP+ osteoclasts was nearly doubled in Hypo without exogenous Heparin (Fig. D), while this significant difference (p < 0.05, Hypo vs. WT) was diminished with Heparin treatment at 20 and 200 μg/ml (Fig. D). Similarly, the higher mineralization seen in non-treated cultures (Hypo vs. WT, p < 0.05) appeared to be diminished with Heparin treatment (Fig. E). Our results indicate that addition of Heparin can rescue the adverse effects of perlecan-deficiency on bone progenitor cells, by slowing down mineralization and osteoclastogenesis. This result, if translated in vivo, could help develop therapeutics to treat bone impairment/osteoporosis associated with perlecan deficiency. References: [1] Farach-Carson+ 2014, Matrix Biol. [2] Lowe+ 2014, Calcified Tissue Int. [3] Parajuli+, ORS 2015 (#146). [4] Parajuli+, ORS 2017 (#0710). [5] Rodgers+ 2007, Human Mol Genetics.



Disclosures: Ashutosh Parajuli, None

MON-0876**Atrophic Non-union Fracture is Caused by Severe Damage on Periosteal Mesenchymal Progenitors and Fibrosis Derived from Non-osseous Tissue.**

Luqiang Wang*¹, Robert Tower¹, Abhishek Chandra², Yejia Zhang¹, Xiaowei Liu¹, Joel Boerckel¹, Xiaodong Guo³, Jaimo Ahn⁴, Ling Qin¹. ¹Department of Orthopaedic Surgery, Perelman School of Medicine, University of Pennsylvania, United States, ²Department of Physiology and Biomedical Engineering, Division of Geriatric Medicine & Gerontology, Mayo Clinic, United States, ³Department of Orthopaedics, Union Hospital, Tongji Medical college, Huazhong University of science and Technology, China, ⁴Orthopaedic Trauma and Fracture Reconstruction, Perelman School of Medicine, University of Pennsylvania, United States

Fractures represent a substantial economic burden to our society. The atrophic non-union of a fracture is especially challenging, as it often requires additional surgeries to overcome the lack of inherent biology in a regenerative healing process gone awry. Using a focal irradiator for rodents, we reproducibly created a nonsurgical atrophic non-union model in mice. 2-month-old male mice received radiation (8 Gy, day 1 and 3) at the mid-shaft of right tibiae (5 mm long) followed by bilateral, transverse tibial fractures on day 15. MicroCT and mechanical testing at day 57 (n=9) revealed that, in sharp contrast to bone healing in contralateral tibiae, fractures in irradiated tibiae did not show any bony bridging, resulting in 100% non-union. Histology at days 22, 29, 43, and 57 (n=6-9/time point) revealed that irradiated tibiae show less robust endochondral healing at the proximal side (region close to the knee) and a clear biologic non-union response on the distal side (region close to the ankle) with exclusive fibrotic cells and type I collagen matrix. These fibrotic cells did not stain for osteogenic (osterix and osteocalcin) and chondrogenic (Sox9 and type II collagen) markers, nor did they express VEGF. Thus, histology and microfil perfusion showed no vessel infiltration in this region. Characterization of tissues from clinical human atrophic non-union paralleled our mouse findings. Mechanistically, radiation blunted the injury response of periosteal mesenchymal progenitors at 3 days post fracture, resulting in a 67% reduction in their proliferation rate and an 83% reduction in periosteum thickness (n=6). In vitro, radiation hindered osteogenic differentiation of periosteal mesenchymal progenitors but did not affect hypoxia-induced chondrogenesis of these cells. Lineage tracing using mouse models that specifically labeled bone mesenchymal cells (Col2-Cre, aSMA-CreER, and Gli1-CreER in combination with Rosa-Td) revealed that non-union fibrotic cells did not originate from periosteal progenitors but from progenitors residing in non-osseous tissues. In addition, we surgically removed periosteum at either side or both sides of the mouse tibial fracture site and found that it eventually leads to atrophic non-union with fibrosis formation only at the surgery side(s). In summary, we demonstrate that atrophic non-union fracture is caused by severe damage to the periosteal mesenchymal progenitors with fibrosis formation that is derived from non-osseous tissue.

Disclosures: *Luqiang Wang, None*

MON-0895**Bone mass of bariatric patients may recalibrate to new body weight**

Andrew Froehle*¹, Richard Sherwood², Richard Laughlin³, Dana Duren². ¹Wright State University, United States, ²University of Missouri, United States, ³University of Cincinnati, United States

Bariatric weight loss surgery is an effective treatment for reducing excess body weight (EBW). One common procedure, Roux-en-Y gastric bypass (RYGB), results in the loss of 60-80% of EBW in the first year following surgery, with concomitant benefits for metabolic health. Despite these benefits, the malabsorptive conditions generated by the procedure may have negative effects on the musculoskeletal system in the form of significant loss of bone mass. Bone loss in general is associated with negative long-term consequences, including osteopenia, osteoporosis and fractures. However, it is unclear whether post-RYGB bone loss represents a true deficit, or whether it is instead a recalibration of bone mass to a new, lower body weight. To address this question, we assessed bone health (areal bone density; aBMD) in women 5 years after RYGB weight loss surgery and compared them to a non-surgical female reference sample matched for current age and body mass index (BMI). The present study of women who underwent RYGB bariatric surgery found that, five years after surgery, bone density was slightly lower than a non-surgical reference sample matched for current age and BMI. The Bariatric and reference samples were similar for mean age, height, weight, BMI, waist circumference, ideal body weight, EBW, and body composition. The Bariatric sample had slightly lower median aBMD values compared to the controls in each body region examined, but none of these differences reached significance. Femoral neck and total hip T-scores within the osteopenic range occurred in 56% and 44% of Bariatric participants and 34% and 24% of controls, respectively. Post hoc sub-analysis of the Bariatric sample suggests that the key explanatory factors for post-surgical osteopenia, osteoporosis, and fracture risk were not the effects of the surgery itself on digestion or body composition, but rather vitamin D and menopause status prior to surgery. The results overall indicate that RYGB patients are at greater risk for osteopenia than their non-surgical counterparts, but that this risk may be related to pre-surgical hormonal and metabolic conditions more than the effects of the surgery itself. Such factors should be taken into consideration when planning post-surgical treatment and follow-up.

Disclosures: *Andrew Froehle, None*

MON-0897**Evaluation of bone indices by DXA and HR-pQCT in newly diagnosed hyperthyroidism due to Graves' Disease and associations with disease severity.** Diana Grove-Laugesen*¹, Klavs Würgler Hansen², Eva Ebbeløe¹, Torquil Watt³, Lars Rejnmark¹. ¹Aarhus University Hospital, Denmark, ²Regionshospitalet Silkeborg, Denmark, ³Rigshospitalet, Denmark

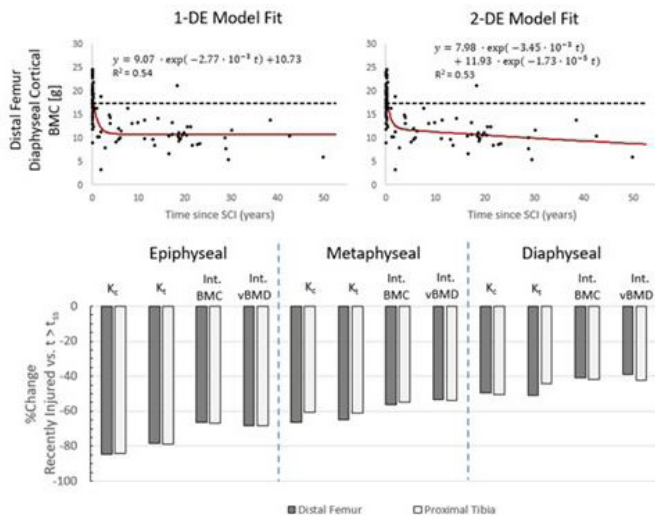
Hyperthyroidism increases bone turnover and decreases areal BMD. Risk of fracture is increased. High-resolution peripheral quantitative computed tomography (HR-pQCT) is a technique used to assess bone microarchitecture and volumetric BMD in vivo. The bone micro architectural changes in hyperthyroidism are sparsely described. A frequent cause of hyperthyroidism is Graves' Disease (GD) characterized by Thyrotropin receptor antibodies (TRAb) that correlates to the severity of the disease. We aimed to investigate the association between severity of hyperthyroidism and bone mineralization, bone geometry, and strength in the early state of hyperthyroidism due to GD. Methods. Eighty-six newly diagnosed adult patients with GD referred to our outpatient clinic were included. Patients were hyperthyroid and treated with antithyroid drug for less than 14 days. Areal BMD was assessed based on DXA scans of forearm, femoral neck, and lumbar spine. Lumbar spine trabecular bone score (TBS) was calculated. Based on HR-pQCT scans volumetric BMD and bone microarchitecture was assessed, and stiffness, failure load, and cortical porosity were calculated. Morning blood samples were collected after 8 hours of fasting. In a multiple regression analysis, associations between severity of hyperthyroidism and bone indices were estimated adjusted for age, gender, BMI, level of vitamin D, and parathyroid hormone. Results. Patient characteristics were: female (86%), age 39.4 years (interquartile range (IQR) 31.5-51.1), TRAb 9.2 iu/L (IQR 4.7-15.4), and triiodothyronine 15.6 pmol/L (IQR 7.9-14.3). TRAb was inversely associated with stiffness (-0.32 (CI 95%:-0.51;-0.13), p=0.001) and failure load (-0.14 (CI 95%:-0.022;-0.0051), p=0.002) in tibia. TRAb was associated with cortical porosity in tibia (0.02 (CI 95%:0.0037;0.036), p=0.017. There were no association with TRAb or thyroid hormones and areal or volumetric BMD, TBS, or indices of microarchitecture. Age was significantly associated with bone indices in all analysis. Conclusion. Despite abundant evidence of reduced BMD in hyperthyroidism we did not find association between areal or volumetric BMD and degree of hyperthyroidism in newly diagnosed patients with GD. However, we did find association between disease severity and increased cortical porosity and reduced stiffness and strength in tibia. These data suggests that cortical areas in weight bearing extremities are affected in early state of hyperthyroidism.

Disclosures: *Diana Grove-Laugesen, None*

MON-0898**Bone Fragility after Spinal Cord Injury: Reductions in Stiffness and Bone Mineral at the Distal Femur and Proximal Tibia as a Function of Time.**

Ifaz Haider*¹, Stacey Lobos¹, Narina Simonian², Thomas Schnitzer², W Brent Edwards¹. ¹University of Calgary, Canada, ²Northwestern University, United States

Introduction Spinal cord injury (SCI) is associated with bone loss and skeletal fragility at the knee. Understanding the temporal patterns of bone loss after SCI may help develop more effective interventions. The purpose of this investigation was to expand on our previous research [1,2] and more thoroughly quantify temporal changes at the distal femur and proximal tibia in people after SCI. We used patient-specific finite element (FE) modelling to measure stiffness and computed tomography (CT) to measure changes in bone mineral. Methods CT scans of the distal femur and proximal tibia were collected from 101 patients (ages 18-72 yrs, 80 males) with SCI between 1 month and 50 years prior to participation. We computed bone mineral density (vBMD), bone volume (BV) and bone mineral content (BMC) at integral, cortical, and trabecular compartments of the epiphyseal, metaphyseal, and diaphyseal regions. We also generated patient-specific FE models of the same three regions to estimate stiffness under axial compression (Kc) and torsion (Kt). Finally, we fit all measures as a function of time since injury using a single decaying exponential (1-DE) and a superposition of two decaying exponential functions (2-DE). Results Bone mineral and stiffness decreased exponentially over time ($R^2 \geq 0.47$; Figure 1, TOP), but the more complex 2-DE model did not explain more variation than the 1-DE model ($p \geq 0.67$). All measures reached steady-state by 3.5 years after SCI. After this time, patients had significantly decreased stiffness (40-85%; $p < 0.005$) and bone mineral (12-107%; $p < 0.005$), compared to recently injured patients ($t \leq 47$ days; Figure 1, BOTTOM). Discussion Bone loss at the knee after SCI was rapid and profound, with rates of loss greatest immediately after injury. We observed significant reductions to both torsional and axial stiffness, suggesting that both failure modes may be clinically relevant. Changes over time were described by the 1-DE model, which predicts rapid loss within 3.5 year after SCI and negligible change after this time. It is plausible that moderate bone loss occurs after this period, as predicted by the 2-DE model, but the rate of loss is likely small with respect to patient-to-patient variation and could not be detected. References [1] Edwards et al. J Bone Miner Res. 30:8, 2015. [2] Edwards et al. Osteoporos Int. 24:9, 2013. Figure 1: Sample results from model fits (TOP) and percent change in select measures (BOTTOM)



Disclosures: Ifaz Haider, None

MON-0899

EFFECT OF TNF INHIBITORS ON BONE MICROARCHITECTURE IN PATIENTS WITH ANKYLOSING SPONDYLITIS: A LONGITUDINAL STUDY BASED ON HIGH-RESOLUTION PERIPHERAL QUANTITATIVE BASED (HRPQCT) Nisha Nigil Haroon^{*1}, Angela Cheung², Robert Inman². ¹NOSM, Canada, ²University of Toronto, Canada

Background: Ankylosing spondylitis (AS) is associated with high risk of fractures. BMD, bone microarchitecture and strength are negatively affected in AS. TNF inhibitors such as etanercept, adalimumab, golimumab and infliximab are the mainstay of treatment in AS. However no data is available on the effect of TNF inhibitors on bone microarchitecture and strength. This study aimed to assess the effect of TNF inhibitors on bone microarchitecture in patients with AS. Methods: AS was defined by Modified New York criteria. Areal BMD was measured by DXA. Volumetric BMD (vBMD) and bone microarchitecture were measured using high-resolution peripheral quantitative CT (HRpQCT) at the radius and tibia at baseline and after one year of treatment with TNF inhibitors. Intake of calcium and vitamin D were optimized. Results: There were 31 subjects (58% men). Mean (+SD) age and BASDAI were 40+14 years and 4.1+ 2.1 respectively. Median duration of disease was 14 (IQ: 6.5-25.5) years. Mean duration of follow-up was 15 months. Areal BMD (n=22) at lumbar spine (1.053+0.235 vs. 1.049+ 0.202, p=0.89), total hip (0.944+ 0.152 vs. 0.912+0.164, p=0.5), and femoral neck (0.955+ 0.151 vs. 0.954+ 0.191, p=0.2) did not change significantly. HRpQCT (n=31) on follow-up demonstrated that total, trabecular and cortical volumetric BMD were unchanged at both radius and tibia. Also, HRpQCT based trabecular parameters such as trabecular number, thickness and separation, BV/TV and cortical parameters such as cortical porosity and thickness remained stable. FEA estimates of bone stiffness and stress tended to be lower at the radius on follow-up however these parameters were not significantly different at the tibia. Conclusions: This is the first study to document the changes in bone strength in AS patients with the use of TNF inhibitors. Treatment with TNF inhibitors might maintain bone microarchitecture at cortical and trabecular sites in patients with AS.

Disclosures: Nisha Nigil Haroon, AMGEN, Grant/Research Support

MON-0900

Bone Mass, Geometry and Strength in Postmenopausal Women with Type 1 Diabetes Viral Shah^{*}, Prakriti Joshee, Rachel Sippl, Dana Carpenter, Wendy Kohrt, Janet Snell-Bergeon. University of Colorado Denver, United States

Purpose: Fracture risk is increased in patients with type 1 diabetes (T1D) and cannot be explained based on areal bone mineral density (aBMD) alone. Therefore, this study examined the association between T1D and volumetric bone density (vBMD), geometry and estimated bone strength at distal radius and tibia in postmenopausal women. Methods: 24 postmenopausal women with T1D (mean age: 60.9 years, years post menopause: 11.6, T1D duration: 41 years, HbA1c: 7.8%) and 22 age, sex and BMI- frequency matched controls (mean age: 63.2, years post menopause: 16.9, HbA1c: 5.5%) were analyzed for vBMD, geometry and estimated strength at distal radius (4% and 33%) and distal tibia (4%, 38%, and 66%) using peripheral quantitative computed tomography (pQCT). Results: Prevalent fracture was higher among T1D patients compared to controls (79% vs 45%, p=0.02). Age, BMI, and use of hormone replacement therapy was similar between the groups. HbA1c and lean body mass was higher in T1D compared to controls (P<0.01). There was no difference in aBMD at lumbar spine, femoral neck and total hip, vitamin D levels, and bone

turnover markers (PINP, CTX, OC) between the groups. However, aBMD at distal radius was lower in T1D patients (0.61±0.09 vs 0.66±0.08, P=0.01). After adjusting for age, race, menopause duration, BMI and bone length, only distal radius trabecular vBMD was lower among patients with T1D compared to controls (165.9±32.6 vs 196.8±32.4, p<0.01). There was no difference in vBMD, endosteal and periosteal circumference, cortical thickness and estimated strength between the groups. BMI was associated with higher vBMD and cortical thickness at tibia and higher HbA1c and albumin excretion rate was associated with lower trabecular vBMD at distal radius. Conclusion: Areal BMD and trabecular vBMD are lower at distal radius in postmenopausal women with T1D compared to postmenopausal women without diabetes. Bone mass, geometry and estimated strength are not different by diabetes status in postmenopausal women despite higher prevalence of fracture in postmenopausal women with T1D.

	T1D (n=24)	Control (n=22)
Radius 4%		
Total vBMD (mg/cm ³)	300.1±47.0	313.5±46.8
Trabecular vBMD* (mg/cm ³)	165.9±32.6	196.8±32.4
Total area (mm ²)	310.3±34.1	335.1±33.9
Trabecular area (mm ²)	211.6±30.2	226.8±29.9
Radius 33%		
Cortical vBMD (mg/cm ³)	1231.8±39.1	1230.8±38.8
Cortical thickness (mm)	2.9±0.4	3.2±0.4
Tibia 4%		
Total vBMD (mg/cm ³)	245.2±37.3	249.3±36.7
Trabecular vBMD (mg/cm ³)	209.1±33.7	219.1±33.3
Total area (mm ²)	1134.5±103.7	1189.7±102.2
Trabecular area (mm ²)	946.3±96.1	992.5±94.7
Tibia 38%		
Cortical vBMD (mg/cm ³)	1192.7±27.3	1167.1±26.9
Cortical thickness (mm)	4.5±0.5	4.3±0.4
Tibia 66%		
Cortical vBMD (mg/cm ³)	1138.9±31.1	1124.1±30.6
Cortical thickness (mm)	3.6±0.4	3.8±0.4
Strength strain index (mm ³)	1390.3±135.7	1470.5±133.8

Disclosures: Viral Shah, None

MON-0901

Longitudinal Analysis of the Association between Glycemic Control and Sclerostin in Male Patients with Type 2 Diabetes Reiko Watanabe^{*}, Nobuyuki Tai, Junko Hirano, Yoshiyuki Ban, Daisuke Inoue, Ryo Okazaki. Teikyo University Chiba Medical Center, Japan

Background & Aim: Type 2 diabetes (T2DM) confers fracture risk. However, the mechanism is not completely understood. Serum levels of sclerostin (Scl), an inhibitor of bone formation, have been shown to be elevated in T2DM, but dependence of Scl levels on glycemic controls is still controversial. We previously reported that obesity, pioglitazone use and systemic inflammation were associated with decreased Trabecular Bone Score (TBS) in a cross-sectional study of 91 Japanese male subjects with T2DM. We present here one-year follow-up data of the same cohort, focusing on Scl. Particularly, we tested a hypothesis that impact of glycemic controls on Scl expression by osteocytes would require a long period of time, at least longer than a few months sufficient for stabilizing HbA1c. Subject & Method: In this longitudinal study, we recruited 60 Japanese male subjects with T2DM (71.7±27.3 years old, duration: 12.6±9.3 years, BMI: 24.8±3.8 kg/m²) and measured bone mineral density (BMD), TBS, bone turnover markers, and Scl, inflammatory cytokines at baseline and after one year. Result: HbA1c and Scl levels at baseline were 7.14±1.60%, 53.5±19.5 pmol/L, respectively. Scl levels were significantly decreased (49.3±23.0 pmol/ml, p=0.024) and HbA1c levels tended to be decreased (6.77±1.19%) after one year. There was no correlation between each other at either point, although Scl levels positively correlated with BMD as previously reported. Interestingly, however, percent changes in HbA1c significantly correlated with percent changes in Scl levels (r=-0.429, p=0.001), probably because individual variations were canceled out in percent changes. And weighted mean (wm) HbA1c for 1 year showed a marginally significant correlation with post Scl levels. Moreover, in multivariate linear regression analysis, wmHbA1c was an independent determinant of post Scl levels besides BMD after adjustment for age and PTH. As for bone parameters, femoral neck BMD T-score was -0.82±0.83 (osteoporosis: 3.3%, osteopenia: 33.3%) and TBS was 1.345±0.086 at baseline. And both remained virtually unchanged for 1 year. We found that the negative correlation of high sensitivity (hs) CRP with TBS at baseline became clearer after 1 year. We also observed positive correlations of wmHbA1c with post TNF-α and hsCRP (p=0.297, r=0.021; r=0.369, p=0.004). Conclusion: The current study demonstrated for the first time that serum Scl levels depend on glycemic controls during a relatively long period of time in T2DM. It may reflect inflammation and other time-requiring processes causing gradually accumulating changes in osteocytes, but further studies will be necessary to establish regulatory mechanism of Scl and its role in bone metabolism in T2DM.

Disclosures: Reiko Watanabe, None

MON-0943

Improvement of the functional status after CT-guided radiofrequency sacroplasty (RFS) and cement sacroplasty (CSP) in patients with insufficiency fractures of the sacrum – a prospective randomised comparison of methods Reimer Andresen^{*1}, Sebastian Radmer², Julian Ramin Andresen³, Mathias Wollny⁴, Urs Nissen⁵, Hans-Christof Schober⁶. ¹Institute of Diagnostic and Interventional Radiology/Neuroradiology, Westkuestenlinikum Heide, Academic Teaching Hospital of the Universities of Kiel, Luebeck and Hamburg, Heide, Germany, ²Centre of Orthopaedics, Germany, ³Sigmund Freud University, Medical School, Austria, ⁴Medimbursement, Germany, ⁵Department of Neurosurgery and Spine Surgery, Westkuestenlinikum Heide, Academic Teaching Hospital of the Universities of Kiel, Luebeck and Hamburg, Heide, Germany, ⁶Department of Internal Medicine I, Municipal Hospital Suedstadt Rostock, Academic Teaching Hospital of the University of Rostock, Germany

Introduction:The objective of this study was a comparative analysis of RFS and CSP with regard to pain reduction, change in quality of life and possible complications. **Material and method:**In 100 patients with 32 unilateral and 68 bilateral non-dislocated insufficiency fractures, RFS or CSP was performed after random allocation in 50 patients each. For RFS, the spongy space in the fracture zone was extended using a flexible osteotome. The viscous PMMA, activated by radiofrequency, was then inserted into the fracture zone. Cement augmentation was performed discontinuously with instrumental guidance under CT monitoring. For CSP, the spongy space was extended analogously to RFS. The viscous PMMA was then inserted discontinuously using a pressure gauge. Cement leakages were detected by CT on the first postoperative day. Pain intensity was determined on a VAS before the intervention, on the second day, and 6, 12, 18 and 24 months after the intervention. The patients' self-sufficiency was assessed using the Hamburger-Barthel index. Additionally occurring complications were recorded and the patients were asked to state their satisfaction. **Results:**RFS and CSP were technically fully feasible in all patients. The average amount of PMMA inserted per fracture was 5.8 ml in the RFS- and 5.2 ml in the CSP group. A leakage was ruled out for the RFS group with 82 fractures treated, 7 leakages were found among 86 fractures treated in the CSP group, while none of the leakages were symptomatic. An inter-ventually related bleeding or infection was ruled out for all patients. The mean value for pain on the VAS before intervention was 8.8 in the RFS- and 8.7 in the CSP group. On the second postoperative day, there was a significant pain reduction ($p < 0.0005$) with an average value of 2.4 for both groups. After 6 (12; 18; 24) months, these values were stable at 2.3 (2.2; 2.0; 2.3) for the RFS- and 2.4 (2.3; 2.2; 2.4) for the CSP group. The Hamburger-Barthel index increased significantly ($p < 0.001$) from an average of 30 points before the intervention to 80 points on the fourth postoperative day and 70 points 24 months after the intervention. No differences were found between the two procedures with regard to pain reduction, improvement in functional status and satisfaction. **Discussion:**RFS and CSP are minimally invasive procedures that enable equally good and sustained pain reduction which leads to a marked improvement in the patients' self-sufficiency.

Disclosures: Reimer Andresen, None

MON-0944

Abaloparatide Increases Bone Formation and Mass in Orchiectomized Male Rats with No Effect on Bone Resorption Heidi Chandler^{*1}, Daniel Brooks², Kenichi Nagano³, Dorothy Hu³, Mary Bouxsein², Roland Baron³, Gary Hattersley¹, Beate Lanske¹. ¹Radius Health Inc, United States, ²Beth Israel Hospital, Harvard Medical School, United States, ³Harvard School of Dental Medicine and Harvard Medical School, United States

Male osteoporosis can occur with advanced aging and hypogonadism, which can lead to lower bone formation and higher bone resorption resulting in bone loss and increased fracture risk. Abaloparatide (ABL), a selective PTH1 receptor agonist, increases bone mass and formation with minimal effects on bone resorption. Here we assessed the effects of ABL in orchiectomized (ORX) rats as a model of male osteoporosis. Male Sprague-Dawley rats underwent ORX or sham surgery at 4 months of age. After an 8-week bone depletion period, ORX rats were injected daily (s.c.) with vehicle (Veh) or ABL at 5 (ABL5) or 25 µg/kg/d (ABL25) ($n=10$ /group) for 8 weeks. Sham controls received s.c. vehicle ($n=10$). Dual-energy X-ray absorptiometry showed that between the pre-treatment baseline (BL) and week 8 of treatment, whole body aBMD increased by 13.8% and 17.3% in the ABL5 and ABL25 groups, respectively, versus 6.3% in Veh controls (both $P < 0.001$ vs Veh). Lumbar spine aBMD increased by 24.5% and 29.1% in the ABL5 and ABL25 groups, versus 7.6% in Veh controls (both $P < 0.001$ vs Veh) during the 8 weeks treatment period. ABL5 had lower urine deoxyypyridinoline (DPD) levels (-27%, $p < 0.05$) than ORX-Veh rats. ABL25 presented trends for increases in serum osteocalcin levels (+38%) and similar urine DPD levels as ORX-Veh. Micro-CT analyses of distal femurs and vertebrae (L4) showed a significant increase in trabecular bone volume, trabecular number and thickness with a marked decrease in trabecular spacing at both skeletal sites when compared to vehicle ($P < 0.05$ for all). Moreover, cortical thickness and cortical bone area fraction were both significantly higher in ABL25 than in ORX-Veh ($p < 0.05$). Static and dynamic histomorphometry of vertebrae (L5) demonstrated a marked increase in bone formation rate, osteoblast number, and mineralizing surface compared to ORX-Veh. Interestingly, however, osteoclast number was not increased with ABL treatment confirming previous observations that ABL has less bone

resorbing activity in comparison to its effects on bone formation. Our findings suggest that ABL may have therapeutic benefits in men with osteoporosis.

Disclosures: Heidi Chandler, Radius Health Inc, Other Financial or Material Support

MON-0945

A Bisphosphonate with Low HA-Binding Affinity Prevents Bone Loss after Estrogen Loss and Reverses Rapidly when Treatment Ceases Abigail Coffman^{*1}, Robert J. Majeska¹, Jelena Basta-Pljakic¹, Mark W. Lundy², Frank H. Ebetino³, Mitchell B. Schaffler¹. ¹City College of New York, United States, ²Indiana University School of Medicine, United States, ³University of Rochester, United States

PURPOSE: Bisphosphonate (BPs) are a mainstay of osteoporosis treatment; however, concerns about bone health due to over-suppression of remodeling remain. While the concept of a "drug holiday" to restore bone remodeling and improve bone quality seems reasonable, clinical BPs have long half-lives (> 1 yr.) due to high hydroxyapatite (HA) binding affinity. This imposes a practical limit to effective drug holiday. Several BPs with low HA affinity (thus rapid biological clearance) and strong FPPS inhibition have not been pursued for clinical use, but offer potential advantages with regard to reversibility. In this study, we tested this concept using NE-580253, a BP with low HA affinity. **METHODS:** Young adult female C57Bl/6 mice (15 w.o., JAX, $n=10$ /group, IACUC approved) were ovariectomized (OVX) and treated with either NE-580253 (NE-025, 200 µg/kg daily, s.c.), Risedronate (RIS, 2.4 µg/kg 3x/wk, s.c.) or PBS vehicle. NE-025 has much lower HA binding than RIS but comparable FPPS-inhibition. At 3 mo post-OVX+treatment, half the mice in each group were euthanized. For others, BP therapy was stopped and animals were sacrificed 1 mo later. Femurs were examined by µCT (6.7 µm voxel resolution). We focused on mid-diaphyseal cortex to provide a consistent anatomical location for comparison. Sham, baseline and age matched cage controls were also examined. Comparisons: ANOVA and post-hoc Tukey test; data shown as mean±SD. **RESULTS:** Total cross-sectional area (T.Ar) was unchanged in all groups. At 3 mo, marrow cavity area (Ma.Ar) in OVX mice increased and cortical thickness decreased by ~10% from baseline. Cortical bone loss was prevented by NE-025 and RIS. At 1 mo after ending treatment, Ma.Ar was unchanged in RIS mice; however, bone loss resumed in NE-025 mice and Ma.Ar was similar to OVX mice at 1 mo. **DISCUSSION:** Studies revealed that NE-025, a BP with low HA, suppressed OVX-induced cortical bone loss similar to RIS. However, NE-025 suppression of bone loss reversed rapidly after treatment ceased. NE-025 required daily dosing at high concentration to prevent bone loss. While no adverse effects were noted, these studies were of short duration and require follow up. Nevertheless, these proof-of-concept studies reveal that low HA affinity BPs can suppress bone loss and may prove useful as reversible anti-resorptive agents. **REFERENCES:** 1) Allen, M.R., Bone. 39:872,2006; 2) Acevedo, C., Bone 81:352, 2015; 3) Ebetino, F.H., Osteoporosis. 14, 990; 4) Fuchs, R., JBMR 23:1689,2008

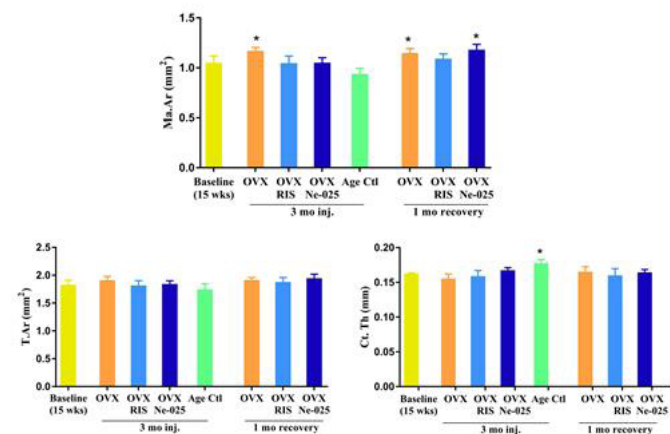


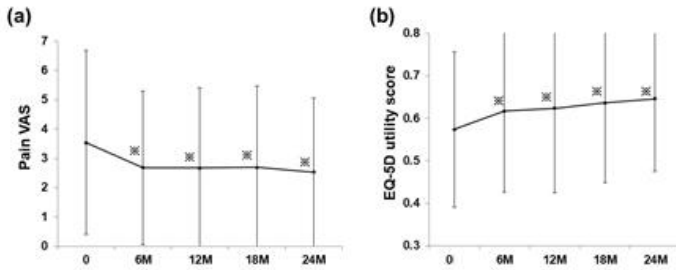
Figure: Cortical Bone microarchitecture after 3 mo. BP treatment (inj) and 1 mo. after BP cessation (recovery). * $p < 0.05$ vs baseline

Disclosures: Abigail Coffman, None

MON-0946

Denosumab treatment improves health related quality of life in patients with osteoporosis Koji Fukuda*, Shinya Hayashi, Hanako Nishimoto, Yoshitada Sakai, Yasushi Miura, Ryosuke Kuroda, Tomoyuki Matsumoto, Koji Takayama, Shingo Hashimoto. Kobe University Graduate School of Medicine, Japan

Introduction: Improving quality of life (QOL) and prevention of bone fracture are fundamental goals of the treatment for osteoporosis. Several studies have reported the therapeutic benefit of increasing bone mass, via inhibition of bone resorption, in preventing fracture, improving low back pain and QOL among patients with osteoporosis. The purpose of our study was to clarify the therapeutic effect of denosumab treatment in improving the QOL of patients with osteoporosis. **Methods:** We evaluated 332 patients with osteoporosis over a 24-month period. All patients received a 60-mg dose of denosumab, subcutaneously, every 6 months. Bone mineral density (BMD) of the distal radius was assessed in all patients, with serum concentrations of calcium, phosphate, PINP, and TRACP5b measured in 152 patients. QOL was evaluated using self-reported pain (visual analogue scale) and the EQ-5D questionnaire. **Results:** Denosumab treatment produced a 3.4% increase, from baseline, in the BMD of the distal radius, at 24 months. Serum levels of TRACP5b and PINP were significantly lower at 6 months, with no effect on calcium and phosphate levels. The average VAS pain score decreased at 6 months, from a score of 3.5 at baseline to 2.7 at 6 months ($p < 0.001$; Figure a). The average EQ-5D utility score increased from 0.57 at baseline to 0.61 at 6 months ($p = 0.007$; Figure b). The correlation between BMD values and the EQ-5D utility score at all time-points of measurements are reported, with a positive significant correlation identified at all time-points, with the exception of 12 months. **Conclusions:** We demonstrated that denosumab treatment was effective in increasing the BMD of the distal radius and improved the health-related QOL, with the improvement in QOL being associated with increase in BMD. Our findings support the feasibility of using denosumab for the treatment of osteoporosis. Comparative studies against other osteoporosis treatments are needed to identify optimal treatment strategies for osteoporosis.



Disclosures: Koji Fukuda, None

MON-0947

Multiple spontaneous vertebral fractures only 2 months after a missed dose of Denosumab Sonaina Imtiaz*, Tamara Vokes. University of Chicago, United States

Case Presentation: An 81 year old female presented with sudden onset of back pain and was found to have vertebral fractures at L4, L3, L2, T12 and T11. She had been on denosumab every 6 months for 7 years during which her BMD increased by 14.3% at the lumbar spine and 11.6% at the total hip. At the time of her last denosumab dose, 8 months earlier her T-scores were -2.3 at the lumbar spine, -2.7 at the femoral neck and -2.0 at the total hip. In addition to denosumab she was taking Vitamin D3 5000 IU daily and 1000- 1200mg of calcium through diet and calcium supplements. She had a history of thyroid cancer post total thyroidectomy more than 60 years ago and was on stable dose of levothyroxine 100 mcg daily for years. She reported no recent weight changes and had not been on steroids. She had no prior history of any fractures and had not received bisphosphonates prior to initiating denosumab. At the time of her presentation with the new vertebral fractures, a marker of bone resorption, serum c-telopeptide (CTx) was remarkably elevated at 1909 pg/ml, serum calcium was elevated at 11.5 mg/dl (previously normal), with normal serum albumin of 4.3 mg/dl, and intact PTH of 25 pg/ml (nl 15- 75 pg/ml). 11 days after receiving the dose of denosumab CTx decreased to 601pg/ml, serum calcium decreased to 9.2 mg/dl and PTH increased to 167 pg/ml. **Discussion:** Bone loss after discontinuation of denosumab has been well documented in the literature, as has the occurrence of the new vertebral fractures. Our case is interesting as it demonstrates that vertebral fractures can occur as early as 2 months after the missed dose. This finding should prompt a greater attention to educating patients and physicians prescribing this medication about the risks of discontinuing denosumab and the importance of timely administration. The other interesting finding in our case is the dramatic increase in bone resorption leading to hypercalcemia with return to normal only 11 days after the administration of the next dose of denosumab and even development of secondary hyperparathyroidism.

Disclosures: Sonaina Imtiaz, None

MON-0948

Assessing the Ability of Baseline Bone Turnover Markers to Predict the BMD Response for Denosumab Treatment in Patients with Osteoporosis: A Multicenter, Retrospective, Observational Study. Koji Ishikawa*¹, Takashi Nagai¹, Yusuke Oshita², Msayuki Miyagi³, Gen Inoue³, Takeshi Eguro⁴, Kazuaki Handa¹, Tomoaki Toyone¹, Katsunori Inagaki¹. ¹Department of Orthopaedic Surgery, Showa University School of Medicine, Japan, ²Department of Orthopaedic Surgery, Showa University Northern Yokohama Hospital, Japan, ³Department of Orthopedic Surgery, Kitasato University, School of Medicine, Japan, ⁴Department of Orthopaedic Surgery, Yamanashi Red Cross Hospital, Japan

INTRODUCTION: Several factors including bone turnover markers (BTMs) associated with BMD increase are reported with denosumab treatment. Although BTMs were affected by the prior treatment, there has been no systematic analysis to summarize these associations. The purpose of this study was to investigate the clinical determinants associated with BMD increase to denosumab treatment. **METHODS:** In total, 1822 patients with osteoporosis treatment were screened from multicenter database. 231 patients with denosumab treatment and complete 12 months follow-up were enrolled. Patients were eligible for the study if they were postmenopausal osteoporosis and BTMs (BAP and TRACP-5b) were evaluated at baseline. Of the initial cohort, 141 of 231 patients (61.0%) were eligible for this study. To determine the response variables of BMD changes, we investigated the clinical determinants using univariate and multivariate analyses. **Results:** The LS BMD after 12 months of denosumab therapy showed a 7.0 ± 6.5 (%) increase. The effect of baseline data on LS BMD increase were evaluated by univariate analysis. Baseline ALP, BAP, and TRACP concentration were significantly associated with percent LS BMD response, and strongest with TRACP ($r = 0.41, P < 0.01$). In the multivariate regression analyses (which included age, BMI, baseline LS BMD), patients with higher baseline TRACP concentration were significantly more likely to have greater percent LS BMD increase (std $\beta = 0.436, P < 0.001$). To analyze the effect of prior treatment, we examined the relationship between LS BMD increase and BTMs in categorized by prior treatment subgroups. In Naïve group (N=82), positive correlations were observed between BTMs and LS BMD increase [(BAP: $r = 0.22, P < 0.05$), (TRACP: $r = 0.38, P < 0.01$)]. Interestingly, in Prior Bis group (N=23), positive correlations were observed only between BAP and LS BMD increase. In Prior PTH group (N=36), positive correlations were observed only between TRACP and LS BMD increase. **CONCLUSIONS:** This study examined the relationship between various baseline determinants and LS BMD increase in response to denosumab treatment. Our results showed BTMs were a strong predictor of LS BMD increase. In addition, the present study is the first report to summarize that a bone turnover marker which we should mention at baseline was different according to the prior treatment. We recommend that physicians should keep these results in mind in clinical practice.

<Correlations of BTMs and Spine-BMD change categorized by prior treatment subgroups>

	All (N = 141)		Naive (N = 82)		Prior-Bis (N = 23)		Prior-PTH (N = 36)									
	Percentage change	Absolute change	Percentage change	Absolute change	Percentage change	Absolute change	Percentage change	Absolute change								
TRACP-5b	r 0.42	p <0.01**	r 0.41	p <0.01**	r 0.38	p <0.01**	r 0.36	p <0.01**	r 0.05	p 0.82	r 0.06	p 0.80	r 0.47	p <0.01**	r 0.46	p <0.01**
BAP	r 0.25	p <0.01**	r 0.26	p <0.01**	r 0.22	p <0.05*	r 0.21	p 0.06	r 0.31	p 0.14	r 0.26	p 0.24	r 0.18	p 0.28	r 0.26	p 0.14

Spearman's rank correlations are shown as r values. * P < 0.05 ** P < 0.01

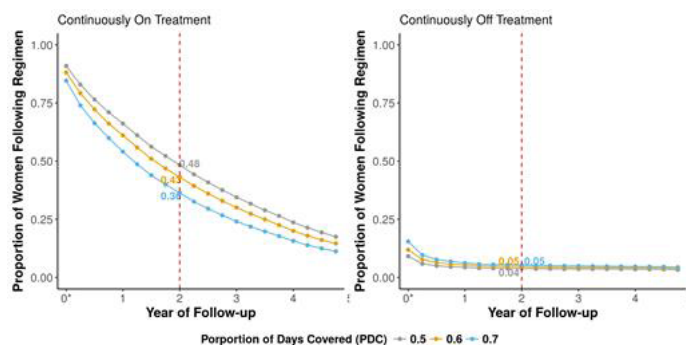
Disclosures: Koji Ishikawa, None

MON-0949

An Approach to Defining Bisphosphonate Exposure in Observational Studies Using Pharmacy Databases Monika Izano*¹, Romain Neugebauer¹, Bruce Ettinger¹, Rita Hui², Malini Chandra¹, Annette Adams³, Fang Niu², Susan Ott⁴, Joan Lo¹. ¹Division of Research, Kaiser Permanente Northern California, United States, ²Pharmacy Outcomes Research Group, Kaiser Permanente California, United States, ³Department of Research & Evaluation, Kaiser Permanente Southern California, United States, ⁴Department of Medicine, University of Washington, United States

Purpose: Assigning drug exposure is a necessary first step in examining oral bisphosphonate (BP) treatment in observational studies that use pharmacy data. One approach for assigning drug exposure in each quarter of follow-up is to determine whether drug was received for more than a specified portion of that period, referred to as the proportion of days covered (PDC). In this study we evaluated the extent to which the choice of PDC affects ongoing BP exposure assignment in a population of women who received long-term treatment. **Methods:** We identified 10,381 Kaiser Permanente Northern California female members who initiated oral BP treatment between 2002-2010 and who received 5 consecutive years of treatment. Women were subsequently followed each quarter for up to five additional years.

A woman was considered "on treatment" in each quarter if she received drug for more than a predetermined PDC based on pharmacy days' supply. Conversely, a woman was considered off treatment if she received drug for less than the PDC. We evaluated the extent to which the choice of three PDC cutoffs (≥ 0.5 , ≥ 0.6 , and ≥ 0.7) impacts the proportion of women classified as "continuously on" or "continuously off" BP treatment during follow-up. Women in the "continuously off treatment" group were off treatment in the first quarter of follow-up and were followed to see if they remained off treatment in subsequent quarters. Results: Under the 0.5, 0.6, and 0.7 PDC cutoffs, 48%, 43%, and 36%, respectively, were categorized as being continuously on treatment at year 2 of follow-up. Under these same PDC cutoffs, 18%, 14%, and 12% were categorized as continuously on treatment by the end of follow-up (Figure 1). Women who were categorized as continuously off treatment were highly likely to remain off therapy under the same 3 PDC cutoffs: 4%, 5%, 5% were classified as continuously off therapy at year 2 of follow-up, and 4% of women were classified as continuously off treatment by the end of follow-up. Conclusions: In a cohort of women with long-term BP exposure, using various PDC cutoffs somewhat altered the proportions of women considered continuously on, but not off treatment.



Disclosures: *Monika Izano, None*

MON-0950

Denosumab therapy improved bone mineral density in Japanese geriatric osteoporotic patients previously treated with bisphosphonates Jiro Kato*, Shusuke Ota, Takanobu Doi, Daiki Yonezu, Yasuyoshi Okamoto, Yuji Joyo. Department of Orthopaedic Surgery, Shizuoka Medical Center, National Hospital Organization, Japan

Background: Denosumab (DMB), a human monoclonal antibody to receptor activator of nuclear factor kappa B ligand, was approved in 2013 in Japan for osteoporosis. DMB increased bone mineral density (BMD) by inhibition of bone resorption in postmenopausal women with osteoporosis. OBJECTIVE: The aim of this study was to compare the DMB-induced efficacy in BMD and bone turnover markers (BTM) between Japanese geriatric osteoporotic patients who were previously treated with or without bisphosphonates (BP). METHODS: A retrospective chart review was conducted of Japanese elderly osteoporotic patients who start DMB administration (60mg subcutaneously every 6 months) over 2 years. A total of 75 patients were identified (12 males and 63 females; mean age, 80.0±8.1 years) and were measured BMD of lumbar spine (L-BMD) and femoral neck (F-BMD) and BTMs (serum intact type I procollagen N-propeptide (P1NP), serum undercarboxylated osteocalcin (ucOC) and serum tartrate-resistant acid phosphatase-5b (TRACP5b)) every 6 months during the DMB treatments. We divided the patients into 2 groups; naïve group (defined as who were not previously treated for osteoporosis) and post-BP group (defined as who were previously treated with BP), and compare the DMB-induced change in BMD and BTMs. RESULTS: Percent change from baseline of L-BMD significantly increased at 6 months after the treatment in both groups (naïve group; 2.9±5.3%, post-BP group; 2.0±4.0%, P<0.01). F-BMD was delayed in increase at 18 months in both groups (naïve group; 3.2±8.3%, post-BP group; 3.0±4.5%, P<0.05). BTMs were significantly higher levels at baseline in the naïve group than in post-BP group (P<0.05). However, BTMs were significantly reduced at 6 months in naïve group (TRACP5b; 333±150 at 0 month and 285±139MU/dl at 6 month, P1NP; 111±56 and 40±22ng/ml, ucOC; 7.2±8.3 and 3.0±2.7ng/ml at 6 month, respectively, P<0.01) and maintain the suppressive effect until 24 months in both groups. CONCLUSION: DMB treatment was effective in increase of BMD and maintain of BTMs' suppression despite of pre-BP treatment.

Disclosures: *Jiro Kato, None*

MON-0951

Osteoporosis Treatment Rate Following Hip Fracture in a Community Hospital Farhan Tariq*, Moin Khan¹, Madiha Tauqir¹, Paul Zalzal¹, Sacha Dubois², Rafik El Werfalli¹, Simona Abid¹, Bradley Weening¹, Mark Ginty¹, Hajar Abu Alrob¹, Aliya Khan¹. ¹McMaster University, Canada, ²Lakehead University, Canada

Introduction: Hip fractures are associated with significant morbidity and mortality and increase future fracture risk (1). A significant care gap exists with low treatment rates post

hip fracture (1). Meta-analyses evaluated models of care and confirmed their effectiveness in reducing the care gap (2,3). An Orthogeriatric team (OGT) was developed at Halton Healthcare Services in 1992 designed to enable early ambulation, evaluate skeletal health and implement effective therapy for osteoporosis. Study Objectives: Evaluate the effectiveness of the OGT in initiating osteoporosis therapy pre-discharge in comparison to the usual care by the hospitalist. Methods: A retrospective chart review of all patients over the age of 59 admitted with a hip fracture to HHS from 1 January 2016 to February 1, 2017 was undertaken. Patients with a history of cancer were excluded. A standardized audit form was used to extract patient data. Results and Discussion: 196 patients were admitted to HHS following a hip fracture during the study period. The majority of the hip fractures occurred at the femoral neck (43.7%) or intertrochanteric site (35.5%) with 6 atypical femoral fractures (AFF). All AFF patients had been on amino-bisphosphonates (ABP) duration (7yrs- 20yrs). One AFF patient was on ABP for 10 years followed denosumab for 3 years. Of the 196 patients, 134 were seen by the OGT (68.3%). Therapy rates for osteoporosis prior to discharge were 73.1% (98/134) – 21 were referred to the complex osteoporosis clinic for further evaluation (renal osteodystrophy, parathyroid disease or other metabolic bone disease). Definitive therapy was initiated in the complex osteoporosis clinic in all of these patients within 3 months of discharge increasing the treatment rate to 88.8% within 3 months of the hip fracture. 62 patients were seen by the hospitalist (31.6%) 1 patient was treated with an ABP pre-discharge – Two patients had low vitamin D levels and started supplementation. Treatment rates pre-discharge were 3/62 (4.8%). AFF were uncommon (6/196) at 3% of all hip fractures seen and ABP use was noted in all patients. All AFF patients had thigh or groin pain prior to developing the AFF. Conclusion: OGT intervention was associated with high treatment rates for the underlying osteoporosis of 73.2% pre discharge and 88.8% at 3 months post discharge. Usual care was associated with a low rate of treatment of 4.8% of patients pre-discharge. Impending AFF may be identified with early imaging of the full femurs in patients on antiresorptive therapy in the presence of thigh or groin pain (4). This study demonstrates the benefit of an OGT in implementing treatment for osteoporosis. References: 1 - Khan, A, et al. Osteoporosis in menopause. SOGC Clinical Practice Guideline 2014;36(9)2 - Haentjens, P, et al. Ann Int Med. 2010;152(6)3 - K. Ganda, et al. Osteoporos Int 20134 - Khan AA et al CARJ 2014 Atypical Femoral Fractures – A teaching perspective

Disclosures: *Farhan Tariq, None*

MON-0952

Improvement of anti-osteoporosis medication after multimodal intervention in patients with hip fracture: prospective multicenter study Deog-Yoon Kim*¹, Hyoung Moo P², Yong-Chan Ha³. ¹Kyung Hee University Hospital, Republic of Korea, ²Grace Women's Hospital, Republic of Korea, ³Chung-Ang University, Republic of Korea

Purpose: Previously, from 2008 to 2011, the authors conducted a retrospective cohort study in Jeju Island, where it was found that hip fracture occurred in 945 patients who were over 50 years of age. Among these 945 patients, 344 patients (36.4%) had their bone mineral density tested and 218 patients (23.1%) received osteoporosis medication. The purpose of this study was to determine whether a patient's education program could improve osteoporosis management after hip fracture using the data of this previous study for comparative purpose. Methods: From November 1, 2014 to September 30, 2015, 190 patients with hip fracture who were over 50 years of age who were admitted for hip fractures at six hospitals were enrolled in the present study. During the hospitalization periods, patients underwent education sessions and provided brochures. Patients were evaluated the rate of diagnosis and treatment of osteoporosis at six months after discharge and were followed-up for at least a year. Results: Of 222 hip fractures, 190 patients (37 in men and 153 women) were enrolled at the six hospitals in 2015. Dual-energy X-ray absorptiometry (DXA) was performed on 115 patients (60.5%) and 92 patients (48.4%) were prescribed medication for osteoporosis at time of discharge. Anti-osteoporosis medication was maintained in 43.7% of patients at 6 months follow-up and 40.2% of patients at 12 months follow-up. Conclusion: This interventional multicenter study demonstrates that patients education program in patients with hip fracture can improve anti-osteoporosis medication and well maintained up to 12 months follow-up.

Disclosures: *Deog-Yoon Kim, None*

MON-0953

A retrospective review of initial bisphosphonate infusion in an inpatient vs. outpatient setting for bisphosphonate naïve patients. Rose Kreikemeier*, Eric Rush, Lisa Halbur, Heather Gosnell. Childrens Hospital & Medical Center, United States

BACKGROUND: The purpose of this study was to evaluate the safety and convenience of initial bisphosphonate infusion therapy in inpatient and outpatient settings for patients with low bone mineral density. METHODS: All data were collected from retrospective chart reviews of heterogeneous groups of patients. Abnormal findings prior to the infusion and side effects during the infusion were documented. Patients were contacted following the infusion to discuss post-infusion adverse events. RESULTS: The majority of both outpatients (80%, n=44) and inpatients (50%, n=27) did not experience any adverse events related to the infusion. Some patients reported minor adverse events that were expected. Only one of the inpatients had a severe adverse event (SAE) after the infusion. CONCLUSIONS: For patients at low risk for severe reactions to treatment, the infusion center appears to be a safe and

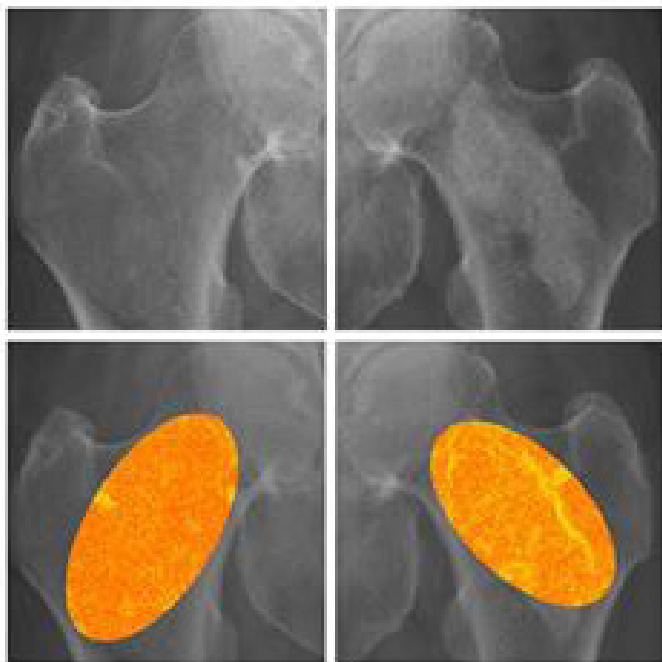
possibly more convenient treatment setting for both the patient and the hospital, although more expensive for the patient at our institution.

Disclosures: *Rose Kreikemeier, None*

MON-0954

Local Osteo-Enhancement Procedure Increases Femoral Raw Trabecular Bone Score (rTBS) at 5-7 Year Follow-up in Osteoporotic Patients Christophe Lelong^{*1}, John Stroncek², James Howe², Bryan Huber³, Ronald Hill², Didier Hans⁴. ¹Medimaps Group Plan-les-Ouates, Switzerland, ²AgNovos Healthcare, United States, ³Copley Hospital, United States, ⁴Lausanne University Hospital, Switzerland

Osteoporosis is characterized by low bone mass and deterioration of bone microarchitecture leading to increased fracture risk. Trabecular bone scoring (TBS) is correlated with changes in bone microarchitecture and is independent of bone mineral density [Silva BC et al, J. Bone Miner. Res. 2014;29:518]. The AGN1 local osteo-enhancement procedure (LOEP) is a novel, minimally invasive approach intended to strengthen the femur by addressing local osteoporotic bone loss. A triphasic calcium sulfate/calcium phosphate implant material (AGN1) is injected into the proximal femur to be resorbed and replaced with new bone. The purpose of this IRB approved study was to evaluate long-term effects of AGN1 femoral LOEP on hip microarchitecture using TBS. An IRB-approved clinical study enrolled 12 post-menopausal osteoporotic women (mean age 71, range: 59-86 years). The left proximal femur was treated with AGN1 LOEP and the right was the untreated control. Ten patients were available for imaging at 5-7 year follow-up. TRIP software v1.0 (Medimaps) used to analyze the texture of AP x-rays computes a raw TBS (rTBS), similar to the TBS iNsight computes, but with parameters adapted to x-rays. The ellipse-shaped region of interest included the trabecular space from the lateral subtrochanteric region to the femoral neck (Figure 1). There was no significant difference at baseline between treated and control femoral neck aBMD or rTBS. At 5-7 years, AGN1 was completely resorbed and femoral neck aBMD had increased 57.4% in treated compared to control femurs (0.828 ± 0.125 vs. 0.526 ± 0.039 g/cm²; $p < 0.001$). Similarly, rTBS was 48.6% greater in treated compared to control femurs (0.398 ± 0.067 vs. 0.268 ± 0.067 ; $p < 0.001$) and each individual patient had a higher treated compared to control rTBS. AGN1 LOEP improved femoral neck aBMD with a concomitant increase in femoral rTBS suggesting improved trabecular microarchitecture of the proximal femur. These differences between treated and control femurs suggest that AGN1 LOEP treatment results in bone less prone to fracture and supports performing further analyses during additional clinical use of AGN1 LOEP to reduce osteoporotic hip fracture risk.



Disclosures: *Christophe Lelong, Medimaps, Other Financial or Material Support*

MON-0955

Global Development of Bone Health TeleECHO to Improve the Care of Patients with Skeletal Diseases E. Michael Lewiecki^{*1}, Rachele Rochelle², Matthew F. Bouchonville¹, Avery Jackson³, Anne Lake⁴, John Carey⁵, Zhanna Belaya⁶, Varta Babalyan⁷, Diana Wiluzanski⁸. ¹New Mexico Clinical Research & Osteoporosis Center, United States, ²UNM Health Sciences Center, United States, ³Michigan Neurosurgical Institute, United States, ⁴Wake Forest University, United States, ⁵NUI Galway, Ireland, ⁶National Centre for Endocrinology, Russian Federation, ⁷Armenian Osteoporosis Association, Armenia, ⁸Centroseo - Densitometria Osea, Uruguay

Background. Bone Health TeleECHO (Extension for Community Healthcare Outcomes) was established at the University of New Mexico Health Sciences Center (UNM HSC) through collaboration of the ECHO Institute and the Osteoporosis Foundation of New Mexico. It is a strategy for improving the level of knowledge of healthcare professionals in the care of patients with skeletal diseases. The ECHO model of learning uses videoconferencing to link participants located anywhere there is an electronic connection. Interactive case-based discussions recapitulate familiar learning strategies of postgraduate medical training programs. Since the launch of the first Bone Health TeleECHO, additional programs have been started in other US states and other countries. Purpose. To report progress and challenges in the worldwide development of Bone Health TeleECHO. Methods. Registration of UNM HSC Bone Health TeleECHO participants is processed at the ECHO Institute. Demographic information is collected and participation is logged for each session attended. Other Bone Health TeleECHO programs collect data independently through a variety of methods. Sharing of ECHO experiences occurs through web-based postings, personal communications, quarterly collaborative teleconferences, and periodic live ECHO congresses. Results. The proof-of-concept Bone Health TeleECHO program at UNM HSC was launched on October 5, 2015. Weekly (excluding holidays) videoconferences have been held since that time. Other Bone Health TeleECHO programs are based at locations that include Grand Blanc, Michigan; Washington, DC; Galway, Ireland; and Moscow, Russia. More are anticipated. Challenges for initiating and maintaining these include funding, staffing, recruitment of participants, and bureaucratic barriers. Summary. Bone Health TeleECHO uses state-of-the-art communication technologies to connect participants to a collegial learning environment to advance their level of knowledge, with the goal of making them better equipped to manage patients with bone diseases. It offers educational opportunities with minimal disruption to office routines and relieves professional isolation that commonly occurs in a wide range of practice settings. Through replication and innovation in many global locations, Bone Health TeleECHO leverages scarce resources and expands capacity to provide better bone health care for more patients closer to home, with greater convenience and lower cost than referral to a specialty center.

ECHO Hub	Location	Starting Date	Frequency
UNM Health Sciences Center	Albuquerque, NM, USA	October 5, 2015	Weekly
MNI Great Lakes ECHO	Grand Blanc, MI, USA	February 24, 2017	Monthly
National Bone Health Alliance	Washington, DC, USA	September 21, 2017	Monthly
National Centre for Endocrinology	Moscow, Russia	October 20, 2017	To be determined
Galway University Hospitals	Galway, Ireland	March 15, 2018	Monthly

Disclosures: *E. Michael Lewiecki, None*

MON-0956

The Effects of Bisphosphonate at the Nanoscale: Effects on Bone Collagen, Mineral Strain and Collagen-Mineral Interaction Shaoheng Ma^{*1}, En Lin Goh², Angelo Karunaratne³, Crispin Wiles⁴, Yong Wu⁴, Oliver Boughton⁵, Tabitha Tay⁴, John Churchwell⁶, Rajarshi Bhattacharya⁷, Nick Terrill⁸, Justin Cobb⁹, Ulrich Hansen⁸, Richard Abel⁸. ¹MEng, United Kingdom, ²BSc, United Kingdom, ³PhD, MEng, Sri Lanka, ⁴MSc, United Kingdom, ⁵MBBS, MRCS, BSc, United Kingdom, ⁶PhD, MSc, United Kingdom, ⁷MBBS, MRCS, MRCSGlas, MSc, FRCS, United Kingdom, ⁸PhD, United Kingdom, ⁹MBBS, MRCS, FRCS, United Kingdom

Introduction Osteoporosis is a metabolic bone disorder characterized by the loss of bone mass. This condition affects 200 million individuals worldwide. Bisphosphonates (BPs) are potent anti-resorptive agents used as the first-line treatment of osteoporosis. In order to further understand the effect of BP on bone mechanical properties, especially at the nano-scale level, the present study aims to investigate and compare the mechanical behaviour of the collagen-mineral matrix under tensile loading between the BP treated bone and controls, using synchrotron small angle X-ray scattering (SAXS) and wide angle X-ray diffraction (WAXD) techniques. Methods Sample Preparation The tissue samples from patients treated with BP were compared with patients who had not received any treatment for bone osteoporotic disease. Non-fractured cadaveric femoral from individuals with no history of bone metabolic disease were also used as controls. Trabecular bone specimens were sectioned out from a tensile region in each femoral head using a diamond blade cutting saw. The dimension of the rectangular specimens was 12mm in length, 2.8mm in width and 1mm in thickness. In-Situ Tensile Testing The specimens' SAXS and WAXD spectra were collected while the specimens underwent tensile loading. All specimens were scanned in real-time during tensile testing at 2.5 second intervals. SAXS and WAXD spectra were then used to resolve the structural properties of the collagen fibrils and mineral platelets at the nanoscale. Results The bisphosphonate therapy group exhibited the lowest yield stress point across all

groups, followed by the fracture control and non-fracture control groups, all of which were statistically significant. Correspondingly, the bisphosphonate therapy group demonstrated the lowest fibril and mineral strain, followed by the fracture and non-fracture control groups (Figure 1). Discussion and Conclusion The present study showed the reduced elasticity and deformability within the collagen-mineral matrix at the nanoscale level in BP treated and untreated fracture groups. Osteoporotic bone has a lower ratio of cross-linked fibrils and mineral content compared to healthy bone. Cross-linking of collagen fibrils provides the viscoelasticity necessary for effective stress distribution. Thus, the structural changes that occur in the organic matrix as part of the osteoporotic process reduce elasticity, increasing risk of fracture.

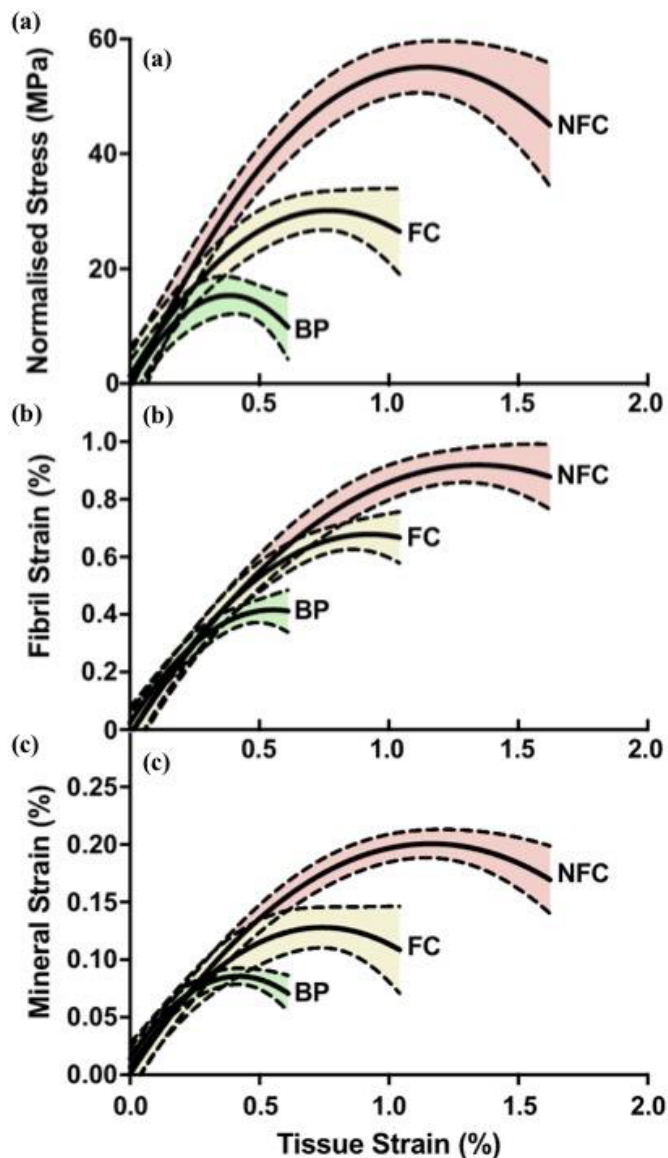


Figure 1. Overall mechanical characteristics. (a) Overall normalised stress-strain curves are shown for the non-fracture control (NFC), fracture control (FC) and bisphosphonate therapy (BP) groups. (b) Overall fibril-tissue strain curves are shown for the NFC, FC and BP groups. (c) Overall mineral-tissue strain curves are shown for the NFC, FC and BP groups. The shaded area represents the 95% confidence intervals for each group.

Disclosures: *Shaocheng Ma, None*

MON-0957

A multicenter, randomized, open label, parallel group study to evaluate the efficacy of loxoprofen on acute-phase reactions in Japanese primary osteoporosis patients treated with zoledronic acid Akinori Sakai¹, Satoshi Ikeda², Hidehiro Matsumoto³, Nobukazu Okimoto⁴, Kunitaka Menuki¹, Tomohiro Kobayashi⁵, Toru Yoshioka⁵, Toru Ishikura⁶, Saeko Fujiwara⁷. ¹Department of Orthopedic surgery, School of Medicine, University of Occupational and Environmental Health, Fukuoka, Japan, ²Department of Orthopedic Surgery, Ken-Ai Memorial Hospital, Japan, ³Department of Orthopedic Surgery, Sanzai Hospital, Japan, ⁴Okimoto Clinic, Japan, ⁵Department of Orthopedic surgery, Shimura Hospital, Japan, ⁶Department of Orthopedics, Youmeikai Obase Hospital, Japan, ⁷Faculty of Pharmacy, Yasuda Women's University, Japan

Background/Purpose: The bisphosphonate zoledronic acid (ZOL) significantly increases bone mineral density and suppresses the incidence of fractures. However, ZOL causes acute-phase responses (APRs) like other bisphosphonates. A very recent 2-year phase III study (ZOledroNate treatment in Efficacy to osteoporosis; ZONE study) carried out in Japan has shown that the incidence rate of drug-related adverse events (AEs) within 3 days after administration of ZOL was 57.4% and that of placebo was 11.7%, whereas APRs were reported in 31.6% of patients treated with ZOL in the Health Outcomes and Reduced Incidence with Zoledronic Acid Once Yearly Pivotal Fracture Trial (HORIZON-PFT). These results indicate that the incidence of APRs is higher in the Japanese populations, compared to other populations. And a sub-analysis of the HORIZON-PFT showed that the incidences of pyrexia and arthralgia in the Chinese population were higher than those in the multinational population, of which 14.2% were Asians. The highest risk of developing APRs was reported even in the non-Japanese Asians and Pacific Islanders. These results indicate that the incidence of APRs is higher in the Asian populations, including Japanese, compared to non-Asian populations. Previous studies have shown that APRs can be managed by treating patients with antipyretic and anti-inflammatory drugs such as acetaminophen and ibuprofen. **Methods:** A total of 400 patients aged 60 or older were randomly allocated to a ZOL plus loxoprofen group (Z+L group) or ZOL group (Z group) on a 1:1 basis. After the treatment, patients were observed for 7 days, during which patients will record APRs for the first 3 days, and body temperature and drugs taken for 7 days. Primary endpoints are incidence of APRs and increase in body temperature, and secondary endpoints are relationship between prior treatment for osteoporosis in the past 3 years versus incidence of APRs, and that versus a change in body temperature. **Results:** APRs occurred at a rate of 34.4% in the Z+L group and 47.8% in the Z group ($p=0.0109$). And the incidence of APRs in patients with prior history of treatment with bisphosphonate is lower than that in naïve patients. **Conclusion:** Higher incidence of APRs was observed after zoledronic acid infusion in Japanese patients. However, the incidence of APRs decreased treating with loxoprofen after the zoledronic acid infusion, and less occurrence in patients with prior bisphosphonate use. The majority of APRs was also mild, and appeared to be transient.

Disclosures: *Akinori Sakai, None*

MON-0958

Anti-sclerostin Antibodies for the Treatment of Osteoporosis: A Systematic Review and Meta-analysis Xerxes Pundole*, Maria Lopez-Olivo, Maria Suarez-Almazor, Huifang Lu. Department of General Internal Medicine, Section of Rheumatology and Clinical Immunology, The University of Texas MD Anderson Cancer Center, United States

Background: Anti-sclerostin antibodies are newer humanized monoclonal antibodies that inhibit sclerostin, with a dual effect on bone, resulting in increased bone formation and reduced bone resorption. We conducted this systematic review and meta-analysis of randomized controlled trials to evaluate the benefits and harms of anti-sclerostin antibodies in the treatment of postmenopausal osteoporosis. **Methods:** A comprehensive search was conducted in electronic databases of MEDLINE, EMBASE, Web of Science, PubMed, The Cochrane Library, clinical trials registries, and web sites of regulatory agencies until March 26th 2018. Study selection, quality assessment and data collection were done independently by two reviewers. We assessed changes in bone mineral density (BMD), incidence of fractures, and adverse events. We primarily evaluated romosozumab 210 mg every month and blososumab 270 mg every 2 weeks compared to placebo, other doses and comparisons to other therapies were considered secondary. **Results:** We included seven studies with 12,745 patients. Six of the included studies evaluated the anti-sclerostin antibody romosozumab and one study evaluated blososumab. In general, all included trials had a low risk of bias. At 12 months, romosozumab 210 mg every month resulted in significant increases in BMD at the lumbar spine (weighted mean difference (WMD) 12.95; 95% confidence interval (CI) 10.24-15.65), femoral neck (WMD 4.21; 95% CI, 3.32-5.10), and total hip (WMD 4.37; 95% CI, 3.27-5.47) compared to placebo. Similar results were seen at 12 months with blososumab 270 mg every two weeks at the lumbar spine (WMD 19.30; 95% CI, 16.65-21.95), femoral neck (WMD 5.70; 95% CI, 4.04-7.36), and total hip (WMD 7.40; 95% CI 5.46-9.34) compared to placebo. Romosozumab resulted in lower risk of new or worsening vertebral fractures (risk ratio (RR) 0.29; 95% CI 0.17-0.49), and major osteoporotic fractures (RR 0.60; 95% CI 0.40-0.90) compared with placebo or in comparison to alendronate at 12 months. There were no significant differences in adverse events in patients receiving romosozumab or blososumab compared to placebo within the 12 month follow-up period. **Conclusion:** Romosozumab and blososumab resulted in significant increases in BMD in postmenopausal women with

osteoporosis. Romosozumab also reduced new or worsening fractures and major osteoporotic fractures in comparison to other therapies. Both anti-sclerostin antibodies were generally well tolerated.

Disclosures: *Xerxes Pundole, None*

MON-0959

Effectiveness of Intravenous Ibandronate on Bone Mineral Density in Patient with Osteoporosis Treated with Oral Bisphosphonate Low-responders -MOVEMENT Study- Hiroshi Hagino^{*1}, Akinori Sakai², Satoshi Ikeda³, Yasuo Imanishi⁴, Hiroshi Tsurukami⁵, Satoru Nakajo⁶, Naohisa Miyakoshi⁷. ¹Tottori University, Japan, ²University of Occupational and Environmental Health, Japan, ³Ken-Ai Memorial Hospital, Japan, ⁴Osaka City University Graduate School of Medicine, Japan, ⁵Tsurukami Clinic of Orthopedics and Rheumatology, Japan, ⁶Nakajou Orthopaedic Clinic, Japan, ⁷Akita University Graduate School of Medicine, Japan

Objective: Bisphosphonates (BPs) have favorable efficacy in increasing bone mineral density (BMD). In some patients, however, increase in BMD may be poor, presumably in part due to interindividual variability in the bioavailability of oral BPs. We evaluated the effectiveness of intravenous (IV) ibandronate (IBN) on BMD in primary osteoporotic patients with no increase in lumbar spine BMD despite oral BPs therapy for 1-3 years. Methods: The MOVEMENT Study (the effect of Monthly IBN iV injected on the low-responders to pre-existing oral BP treatment for osteoporosis patients) is multicenter, interventional, prospective study. This study has two treatment groups as patients treated with IV IBN monthly and oral BPs. Since the dosage form differed between the treatment groups, patients were not randomized to treatment but were allowed to select their preferred dosage form (ie, intravenous or oral), for better patient accrual and prevention of dropouts due to assignment to an undesired dosage form. Patients aged 50 years or older with osteoporosis with no increase in lumbar spine BMD despite oral BPs therapy (with adherence 75% or above) for 1-3 years were eligible. In the IV IBN group, patients received IV IBN monthly. In the BPs group, patients either continued their oral BPs or were switched to another oral BPs. The primary effectiveness endpoint was the percent change in lumbar spine BMD from baseline to 12 months of IV IBN group, and the treatment period was 1-year. The safety endpoint was adverse event and calcium-related laboratory data. Results: Of 381 patients enrolled from August 2015 to March 2017, 240 and 141 patients treated with IV IBN and oral BPs, respectively. Baseline characteristics were similar between the groups (IV IBN vs BPs: mean age, 74.8±7.6 vs 74.4±7.8 years; female, 95.8% vs 97.2%; and proportion with prior fractures, 44.1% vs 52.5%, respectively). Data from 271 patients (IV IBN, n=164; oral BPs, n=107) who completed the dual-energy X-ray absorptiometry assessment by December 2017 had been locked and tabulated. Positive change has been observed in the interim tabulation of lumbar spine BMD in the IV IBN group. No new concerns on safety profiles in both groups were found. Conclusion: Switching to IV IBN (ie, a change in administration route) was suggested to be effective in low-responders to oral BPs. These results support the treatment as one of the new strategy that is expected to be beneficial for BMD as well as for treatment adherence.

Disclosures: *Hiroshi Hagino, Mitsubishi Tanabe Pharma Corp., Grant/Research Support, Ono Pharmaceutical Co., Ltd., Speakers' Bureau, Astellas Pharma Inc., Speakers' Bureau, Takeda Pharmaceutical Co., Ltd., Speakers' Bureau, Daiichi Sankyo Co., Ltd., Speakers' Bureau, Eli Lilly Japan K.K., Speakers' Bureau, Asahi Kasei Pharma Corp., Speakers' Bureau, MSD, Speakers' Bureau, Pfizer Inc., Grant/Research Support, Teijin Pharma Co., Ltd., Speakers' Bureau, Chugai Pharmaceutical Co., Ltd., Speakers' Bureau, Eisai Co., Ltd., Speakers' Bureau*

MON-0960

A fracture liaison in an orthopaedic office did not improve adherence to treatment for patients with osteoporosis Patricia Seuffert^{*1}, Carlos A. Sagebein², Dorene O' Hara². ¹University Orthopaedic Associates, LLC, United States, ²UOA, LLC, United States

Introduction: A fracture liaison service has been shown as the most effective intervention for secondary fracture prevention and osteoporosis management. In our orthopaedic practice, we have employed a dedicated fracture liaison to increase patient adherence by arranging for same day DXA scanning at the time of initial evaluation and an endocrinology consult within 14 days. Furthermore, we identified a cohort of patients with osteoporosis or fragility fracture that agreed to endocrinology consultation and adherence to treatment at the time of their initial diagnosis. Our hypothesis was that the patients who specifically agreed to treatment would show a significantly higher adherence rate for treatment. Methods: A total of 443 office patients underwent a DXA scan in our office in 2017. From this group, 42 patients consented to see an endocrinologist within 2 weeks as arranged by the fracture liaison. Patient follow-up continued during the year and adherence to osteoporosis therapy was assessed. Basic demographic data, incidence of fractures and T scores were collected for all patients. For the 42 patients, treatment recommendations and patient decisions regarding treatment were also collected. All data between groups were compared using Student's T test, with a p level of 0.05 considered significant. Results: Of the 443 patients studied in 2017, there were 72 males and 371 females. For the subset of 42 patients studied, there were 8 males and 34 females. Overall, the males were significantly older than the females (72.75

+/- 8.60 vs 69.44 +/- 9.03, p = 0.0085). T scores for the 443 patients were not significantly different overall, -2.11 +/- 1.02 for males, and -2.30 +/- 1.26 for females. Of these patients, 29 did consult with a physician for osteoporosis treatment. Data for the 42 patients is summarized in table 1. Ultimately, only 23 of these patients were adherent with medication treatment recommendations. Reasons stated for non-adherence included planned dental work, apprehension about the medication, advice from friends, and dementia. Conclusion: Despite the implementation of a dedicated fracture liaison, same day in office DXA screening and prompt endocrinology referral, our orthopaedic practice initiative was unsuccessful in optimal patient adherence to osteoporosis treatment. There continues to be significant barriers to treatment despite improved commitment and management of osteoporotic patients in an orthopaedic office.

Table 1 - Referral Group Medication Adherence

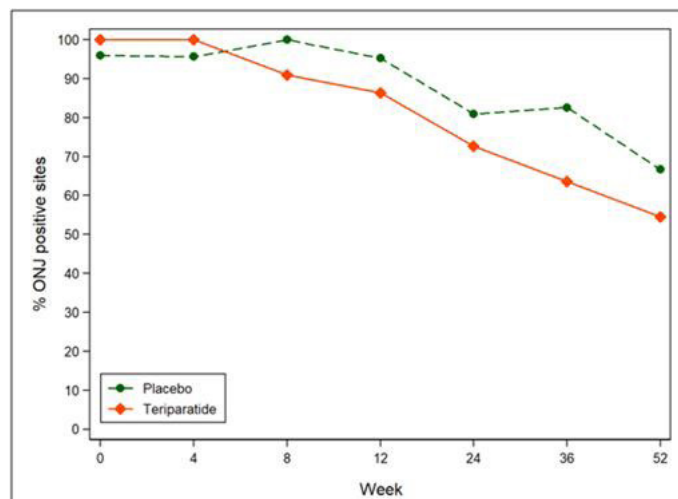
Number	Percent	Details
29	74%	Completed referral consultation
29	74%	Medication ordered
11	26%	Did not complete referral consultation
23 of 29	79%	Patients referred, saw physician, taking medication
23 of 42	55%	Those in referral group overall, taking medication

Disclosures: *Patricia Seuffert, None*

MON-0961

Teriparatide improves healing of medication-related osteonecrosis of the jaw: a placebo-controlled, randomized trial Ie-Wen Sim^{*1}, Gelsomina Borromeo², John Seymour³, Peter Ebeling⁴. ¹Melbourne Medical School, University of Melbourne, Australia, ²Eastern Health Clinical School, Monash University, Australia, ³Department of Haematology, Peter MacCallum Cancer Centre, Australia, ⁴Department of Medicine, Monash University, Australia

Medication-related osteonecrosis of the jaw (MRONJ) is an infrequent, but potentially debilitating, condition associated with antiresorptive therapy. Whereas MRONJ incidence can be reduced by optimising oral health, management of established cases remains challenging. We conducted a prospective double-blind, placebo-controlled, randomised trial (ACTRN12612000950864) investigating the efficacy of 8 weeks teriparatide (20µg/day) treatment in 34 participants, with a total of 47 MRONJ lesions. Ten participants had multiple lesions. Most participants had at least moderate severity MRONJ, with 61.8% being stage 2 or 3, ie exposed bone associated with infection and/or complications such as fistulae or fracture. Participants were followed up for 12 months, with primary outcomes including the clinical and radiological resolution of MRONJ lesions. The Oral Health Impact Profile-14 (OHIP-14) questionnaire was used to assess quality of life. Baseline characteristics were similar between groups, with the mean time from MRONJ diagnosis being 12 months. Antiresorptive therapy was indicated for treatment of skeletal-related events in the setting of malignancy in the majority of participants (79.4%). In the teriparatide arm, P1NP increased by 47% (p < 0.001) and fluoride-PET tracer uptake increased by 24% (p = 0.008). 10 of 22 (45.4%) MRONJ lesions in the teriparatide group resolved by 52 weeks compared with 8 of 24 (33.3%) lesions in the placebo group, with a greater rate of resolution of MRONJ sites with teriparatide (OR = 0.15 vs OR 0.40, p = 0.013) (Figure). Bone mineral density and OHIP-14 scores were similar between groups. The incidence of adverse events was low and balanced between groups. Adverse events were mild in severity, including nausea, anorexia and musculoskeletal pain. Therefore, teriparatide improves the rate of resolution of established MRONJ lesions, and represents an efficacious and safe treatment for MRONJ.



Disclosures: *Ie-Wen Sim, None*

MON-0970

Sex and Diet Specific Differences In Bone Mass of 4 Mouse Strains: Can Mice Tell Us What to Eat for Bone Health? Rihana Bokhari*, Peter Schneider, William Barrington, Alyssa Falck, Alexis Mitchell, Shannon Huggins, Diarra Williams, Larry Suva, David Threadgill, Dana Gaddy. Texas A&M University, United States

Diet-induced obesity increases the risk of metabolic disorders and chronic conditions, yet little is known regarding the effects of diet on the skeleton. This study investigated how genetic differences in mice influence skeletal responses to several diets. Starting at 4 wks of age, males and females of 4 genetically distinct inbred mouse strains (A/J (A), C57BL/6J (B6), FVB/NJ (FVB), and NOD/ShiLJ (NOD)) were fed one of 4 diets (Japanese, ketogenic, Mediterranean, and standard mouse chow) ad libitum for 6 months. The diets closely recapitulate human diets, matching macronutrient ratio, fiber content, types of ingredients and fatty acid ratios. At sacrifice tibias were analyzed by microCT. No change was observed in daily activity level across diet within any strain, but sex differences across diets were observed. B6 male mice had at 50-70% greater ($p < 0.05$) BV/TV than females on all diets. However, A female mice had 35% greater BV/TV than males, but only on the Mediterranean diet. Dietary differences in BV/TV in males were only observed in B6 mice, where BV/TV was 30-40% greater ($p < 0.05$) on the Japanese and Mediterranean diets compared to the standard chow diet. In females, BV/TV was significantly greater (85-90%) in B6 and A mice on the Mediterranean diet compared to those on standard diet. In FVB females, BV/TV was significantly lower (33%; $p < 0.05$) on the Japanese diet; no significant differences in BV/TV were observed in NOD females on any diet. Interestingly, both sexes of B6 mice also demonstrated a significant increase in body weight as well as both lean and fat body mass. Collectively, the Mediterranean diet consistently and significantly increased BV/TV, as did the Japanese diet, whereas the ketogenic diet did not increase BV/TV in any strain compared to standard diet. B6 mice of either sex are the most sensitive to dietary changes. Skeletons of NOD mice are the least sensitive to dietary changes, despite the Mediterranean diet inducing significant increases in overall body weight, lean and fat mass. These data indicate that although some strains are more sensitive to dietary interventions, the skeletal response is not uniform between the sexes, demonstrating that care is required in diet selection. Indeed, if similar genetic- and sex-dependent dietary responses exist in humans, then a personalized, or "precision dietetics," approach to dietary recommendations may yield better health outcomes than the traditional one-size-fits-all approach.

Disclosures: Rihana Bokhari, None

MON-0971

Immune system, bone and fat axis: the role of LIGHT/TNFSF14 Giacomina Brunetti¹, Graziana Colaianni², Sara Bortolotti², Giuseppina Storlino², Adriana Di Benedetto³, Maria Felicia Faienza⁴, Carl Ware⁵, Silvia Colucci¹, Maria Grano². ¹Department of Basic and Medical Sciences, Neurosciences and Sense Organs, Section of Human Anatomy and Histology, University of Bari, Italy, ²Department of Emergency and Organ Transplantation, Section of Human Anatomy and Histology, University of Bari, Italy, ³Department of Clinical and Experimental Medicine, University of Foggia, Foggia, Italy, ⁴Department of Biomedical Sciences and Human Oncology, Section of Pediatrics University of Bari, Bari, Italy, ⁵Infectious and Inflammatory Disease Center, Sanford Burnham Prebys Medical Discovery Institute, La Jolla, CA, United States

LIGHT/TNFSF14 is a cytokine produced by immune cells. We demonstrated its role in regulating basal and pathological bone remodeling whereas other authors showed its pro-adipogenic role. Based on the cross-talk among immune system, bone and fat, here we investigated whether LIGHT could be a new linker of this interaction. In *Tnfsf14*^{-/-} mice (KO), in which we proved the reduced trabecular bone, we firstly detected a reduced expression of PPAR γ and PCG1 α , key pro-adipogenic transcription factors, in bone marrow cell extracts. Consistently we detected a lower weight of visceral and inguinal white adipose (iWAT) tissues respect to the WT, suggesting an impairment of adipocyte precursors. Moreover, in the iWAT of KO mice, we detected a lower number of brown adipocytes and lower mRNA levels of *Wnt10b*, involved in browning response, respect to WT, indicating that LIGHT-deficiency alters the adipose phenotype in addition to the bone one. These effects are mediated by immune cells, indeed, by using *Rag*^{-/-}/*Tnfsf14*^{-/-} mice lacking mature B/T-cells and LIGHT expression, the levels of PPAR γ and PCG1 α in bone marrow extracts and the number of brown adipocytes in iWAT are rescued respect to KO mice. Consistently, obese children showed higher levels of LIGHT in sera compared to sex and age-matched controls (520 \pm 265 ng/ml vs 240 \pm 156, $p < 0.01$ ng/ml; $n = 30$ /group). These findings indicate LIGHT as new linker in immune system/bone/fat cross-talk and a potential target in obesity.

Disclosures: Giacomina Brunetti, None

MON-0972

Deletion of CXCL12 in Osteoblasts and Osteocytes Results in Lower Trabecular Bone Volume Chao Liu*, Pamela Cabahug, Shahar Qureshi, Olivia Patton, Cinyee Cai, Alesha Castillo. New York University, United States

The CXC Motif Chemokine Ligand 12 (CXCL12) is a cytokine expressed in stromal cells [1]. Though it has been shown to be secreted by osteocytes (OCs) and is a potential control mechanism for bone remodeling [2], whether CXCL12 regulates bone quality and quantity is unclear. Based on the role of CXCL12 in stem cell recruitment and osteogenic differentiation [3], we hypothesized that its deletion in mature osteoblasts (OBs) and OCs would alter bone structure and whole bone mechanical strength. Adult mice (16-week-old) with a CXCL12 conditional knockout (cKO) in OBs, and consequently OCs, (CXCL12 Δ OB) and OCs only (CXCL12 Δ OCY) were generated by crossing CXCL12 floxed mice with 2.3 kb *Col1a1*-Cre transgenic mice or 10kb *DMP-1* Cre transgenic mice. CXCL12 deletion was confirmed by qRT-PCR, Western blot and IHC. MicroCT imaging (6 μ m voxel) was used to analyze trabecular (Tb) bone structure under the proximal tibial growth plate. Cortical (Ct) bone structure was assessed at mid-length. Biomechanical properties of the femur were measured by 3-point bending. CXCL12 Δ OB and CXCL12 Δ OCY mice exhibited reduced CXCL12 mRNA (-400%) and protein (-30%). CXCL12 deletion did not affect animal weight. CXCL12 Δ OB mice exhibited significantly reduced Tb BV/TV (-31%), Tb.Th (-14%), and resulted in a decreasing trend in Tb.N in female, but not male, mice. CXCL12 Δ OCY mice exhibited significantly reduced Tb BV/TV in females (-19%) and males (-23%). Tb.N was lower in CXCL12 Δ OCY females (-19%), but not males, while Tb.Th was reduced in males (-10%) but not females. Ct geometry and bone strength were unaffected by CXCL12 deletion. Considering the high turnover rate of trabecular bone, a reduction in trabecular bone volume in cKO mice under homeostatic conditions suggests that osteoblast- and osteocyte-specific CXCL12 expression plays a role in bone remodeling. This corresponds with previously published work showing that CXCL12 regulates osteogenic differentiation [3]. Though highly expressed in OCs, *DMP-1* is also expressed in stem cells, OBs, and cells in other organs [4], which could cause disparate responses from our two CXCL12 cKO models. Sex-based differences in Tb microarchitecture in both models were unexpected, and additional work is required to examine potential cross-talk between hormonal and CXCL12 signaling. [1] Nagasawa, T. et al., PNAS, 1996 [2] Leucht, P. et al., JOR, 2013 [3] Shahnazari, M. et al., FASEB, 2013 [4] Terasawa, M. et al., 2004.

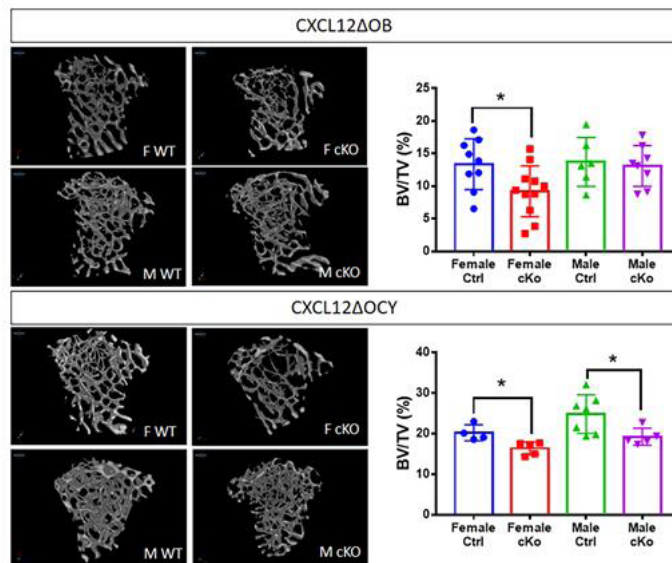


Figure 1. Trabecular structure in CXCL12 Δ OB and CXCL12 Δ OCY mice. 3D volumes were reconstructed from microCT images and assessed for bone volume (BV/TV) in a VOI of 1.5 mm under the proximal tibial growth plate. * $P < 0.05$.

Disclosures: Chao Liu, None

MON-1004

Intra-articular Parathyroid Hormone (1-34) Improved Knee function in Aging-related Osteoarthritis without Affecting Subchondral Bone Chung-Hwan Chen¹, Ling-Hua Chang¹, Sung-Yen Lin¹, Lin Kang², Yi-Shan Lin¹, Shun-Cheng Wu¹, Je-Ken Chang¹, Mei-Ling Ho¹, Shih-Tse Chen¹. ¹Kaohsiung Medical University, Taiwan, ²National Cheng Kung University, Taiwan, ³National Taiwan University Hospital Hsin-Chu Branch, Taiwan

Osteoarthritis (OA) is prevalent in geriatrics and incurable. Intra-articular parathyroid hormone (1-34) improved OA in papain-induced OA model. Subcutaneous PTH (1-34) is a potent agent for osteoporosis treatment and high dose of subcutaneous PTH (1-34) can alleviate OA progression. Thus, we examined the roles of PTH treatment on aging-related OA. The purposes of this study were to study whether PTH can alleviate OA progression

in an aging-related knee OA in Dunkin Hartley (DH) strain guinea pigs. Specifically we set out to determine (1) whether PTH improves knee function; (2) PTH can alleviate OA progression in histological study; and (3) the effects of PTH is related to subchondral bone change or not. Fifteen 6-month-old male guinea pigs were divided into the 9M group (n=7) and the 9M+PTH group (n=8) and twelve 7-month-old male guinea pigs were divided into the 11M group (n=6) and the 11M+PTH group (n=6). The treatment right knees were intra-articular injected with 40µl of 10nM PTH (1-34) or vehicle once weekly for 3 months until 9 month-old at both 9M and the 9M+PTH groups and till 10 month-old at both 11M and the 11M+PTH groups. Another eight 6-month-old guinea pigs and 7-month-old guinea pigs were served as young control groups, 6M and 7M respectively. The time of the guinea pigs can withstand in the treadmill were evaluated before sacrifice. The bone mass of tibia plateaus were analysis by µCT and histological study. PTH (1-34) increased the endurance in the treadmill test and GAG stain. In addition, PTH (1-34) decreased OARSI score and chondrocyte apoptosis rate. In µCT, there was no difference in subchondral plate bone density and trabecular bone volume at metaphysis between control and treatment group both at 9 and 11 months. In this study, we further found PTH (1-34) could improve aging-related OA in guinea pig in histology by increasing GAG and decreasing OARSI score and knee function by increasing the endurance in the treadmill test. Subchondral bone plays a crucial role in the initiation and progression of OA. Previous study showed subcutaneous PTH (1-34) improved knee OA via improving subchondral and metaphyseal bone mass. In this study, we demonstrated low dose intra-articular injection PTH (1-34) improved spontaneous OA via direct cartilage effect rather than subchondral and metaphyseal bone effect.

Disclosures: *Chung-Hwan Chen, None*

MON-1005

Bariatric Surgery in mice leads to decreased bone mass over time Katrien Corbeels*, Lieve Verlinden, Matthias Lannoo, Ann Mertens, Christophe Matthys, Annemieke Verstuyf, Ann Meulemans, Geert Carmeliet, Bart Van Der Schueren. KU Leuven, Department of Chronic Diseases, Metabolism & Ageing (CHROMETA), Clinical and Experimental Endocrinology, Leuven, Belgium

Background Bariatric surgery has proven to be a valuable treatment option for morbid obesity. However, Sleeve gastrectomy (SG) and Roux-en-Y Gastric Bypass (RYGB) can lead to impaired intestinal absorption of calcium and vitamin D, which may challenge calcium homeostasis and contribute to bone loss. To better understand the alterations in calcium homeostasis and bone metabolism, mouse models of bariatric surgery are used. Methods C57Bl/6J mice were fed a high-fat diet (60 kcal% fat) for 14 weeks. Subsequently, sham or bariatric surgery was performed and the diet was switched to a standard diet (5 kcal% fat). Calcium and bone homeostasis was assessed 2 and 8 weeks after surgery. Data are expressed as mean ± SEM. Results Micro-CT analysis at 2 weeks after surgery showed no bone loss in SG or RYGB, compared to sham-operated mice. However, 8 weeks after surgery, strong cortical thinning and loss of trabecular bone mass was observed after both SG (0.129 ± 0.003 µm; 2.61 ± 0.29%) and RYGB (0.112 ± 0.004 µm; 2.94 ± 0.42%) compared to sham (0.162 ± 0.003 µm; p<0.0001; 5.22 ± 0.27%; p<0.0001). Examination of dynamic histological parameters of the tibia after 8 weeks, showed a manifest increase in bone formation rate for both SG (0.043 ± 0.010%; p<0.001) and RYGB (0.045 ± 0.004%; p<0.001) compared to sham (0.005 ± 0.002%) Consistently, serum osteocalcin levels were significantly increased 8 weeks after SG (35.4 ± 3.0 ng/ml; p<0.01) and especially after RYGB (60.5 ± 5.4 ng/ml; p<0.0001), compared to sham (22.9 ± 2.1 ng/ml), whereas serum levels for C-terminal telopeptide (CTX) showed no differences between groups. Unexpectedly, no differences in serum levels of parathyroid hormone (PTH) at 2 and 8 weeks or 1,25(OH)2vitaminD3 levels at 8 weeks were found. Nonetheless, gene expression of the calcium transporter calbindin D9K, showed a trend to be increased in jejunum (p=0.08) and kidneys (p=0.05) after RYGB compared to sham. Moreover, after SG, fractional calcium clearance was decreased (p<0.05) compared to sham. Conclusion After SG and RYGB, bone mass decreased over time, accentuating the long-term implications of bariatric surgeries. Likely, bone resorption increased early after bariatric surgery and was followed by increased bone formation, which was however, not sufficient to restore bone mass. The unchanged PTH levels further indicate that other mechanisms contribute to bone loss after bariatric surgery.

Disclosures: *Katrien Corbeels, None*

MON-1006

High Dose Calcitriol Induces Vascular Calcification in Non-CKD Rats Corey Forster*¹, Kimberly Laverty¹, Cynthia Pruss¹, Mandy Turner¹, Rachel Holden², Michael Adams¹. ¹Queen's University Department of Biomedical and Molecular Sciences, Canada, ²Queen's University Department of Medicine, Canada

Premature mortality in chronic kidney disease (CKD) patients is linked to the progression of cardiovascular disease (CVD). In CKD, marked reductions in the kidneys' ability to excrete excess phosphate and calcium results in extra-osseous mineral deposition, particularly vascular calcification (VC), causing a significant decline in vascular health. Regulation of circulating calcium and phosphate is dependent, in part, on 1,25-dihydroxyvitamin D3 (calcitriol), as well as the signalling molecules parathyroid hormone (PTH) and fibroblast growth factor 23 (FGF-23). Calcitriol, the active form of vitamin D, is made primarily in the kidneys. In CKD, calcitriol production declines generating secondary hyperparathyroidism, a condition which is managed by administering calcitriol or other vitamin D mimetics. However, activation of vitamin D receptors can also lead directly and/or indirectly to the de-

velopment of VC. This study was designed to assess the temporal basis of calcitriol-induced VC in the absence of CKD, as the complex CKD phenotype can confound the profile of VC pathophysiology in the adenine-induced CKD model. The study, in male Sprague-Dawley rats, aged 15-16 weeks, was approved by the Queen's Animal Care Committee in accordance with the guidelines from the Canadian Council on Animal Care. After acclimation, rats were randomly sorted into either a subcutaneous (n=8) or an intraperitoneal injection group (n=5). Of these rats, one group received 1.0% dietary phosphate (n=10) while a second group received a 0.5% phosphate diet (n=3). After 72 hours on their diets, calcitriol was administered daily (0.5 or 1µg/kg dose) for 8 days. Daily blood samples were taken to monitor changes in biomarker profiles. At the end of the treatments, all animals were sacrificed and tissues were collected to determine vascular mineral content, serum hormone levels and vascular histology. Animals who received 8 doses, regardless of injection method, dose, or dietary phosphate all developed VC. The development of VC was associated with hypercalcemia, however, elevations in serum phosphate did not occur in these animals. Animals who received fewer than 8 doses did not develop VC, but were found to be hypercalcemic. The mechanisms responsible for the development of VC have not been fully elucidated. Characterizing calcitriol-induced VC in the absence of CKD will enable insight into the mechanisms involved as well as provide the basis for improved therapeutic strategies.

Disclosures: *Corey Forster, None*

MON-1007

Treatment with LpPLA2 inhibitor reduces osteopenic bone loss in diabetic and hypercholesterolemic pig model. Theresa Freeman*. Thomas Jefferson University, United States

Diabetes mellitus type 2 (DM II) affects 18.2 million Americans and can cause several chronic and morbid adverse effects on patient health. Further complication occurs when this disease is accompanied with high cholesterol. Diabetes and high cholesterol results in the oxidation of the low density lipoprotein (LDL) on "bad" cholesterol. Oxidized LDL is the hydrolyzed by lipoprotein-associated phospholipase A2 (Lp-PLA2) to produce lysophosphatidylcholine (LysoPC) and oxidized nonesterified fatty acids. Lp-PLA2 is associated with coronary heart disease. Interestingly vascular calcification is inversely related to bone loss. Inhibition of Lp-PLA2 reduces vascular calcification in a diabetic and hypercholesterolemic (DM-HC) pig model so the aim of our study was to determine if treatment with an Lp-PLA2 inhibitor would also rescue the bone loss observed in this model. Male Yorkshire domestic farm pigs were induced to develop diabetes with a single intravenous injection of 125 mg kg⁻¹ of streptozotocin and fed a hyperlipidemic diet to achieve hypercholesterolemia. One month after DM-HC induction, one group was orally with Lp-PLA2 inhibitor darapladib. After 28 weeks, the pigs were sacrificed and whole knee joints were collected according to IACUC approved procedures. MicroCT, histology and immunohistochemistry were performed. Bone loss was observed in the microCT analysis of trabecular bone of the femur from the DM-HC pigs when compared to non-diabetic, normal chow fed control pigs. Treatment with the Lp-PLA2 inhibitor, darapladib significantly reduced the amount of bone loss. Histology showed abnormal pathology in the bone marrow surrounding the trabeculae, and this was also reduced in the treated pigs. TUNEL analysis of the histology sections revealed increased apoptosis in the trabecular osteoblasts was decreased in the treated pigs. In vitro, in the presence of LysoPC osteogenesis resulted in decreased alizarin red staining. Taken together these results show DM-HC has an osteopenic effect on trabecular bone which may be rescued to some extent by treatment Lp-PLA2 inhibitor. An increase in LysoPC can slow bone mineralization, increase osteoblast apoptosis and alter the bone marrow niche. Chronic diabetes is known to cause multiorgan failure via microvascular and macrovascular damage and may possibly exacerbate this problem. Our laboratory has launched an extensive series of experiments to delineate the potential cellular mechanism for these phenomena.

Disclosures: *Theresa Freeman, None*

MON-1008

Combined Caloric and Dietary Protein Restriction Has a Synergistic Negative Impact on Bone Mass Ke-Hong Ding*¹, Tianyang Guo¹, Jianrui Xu¹, Qing Zhong¹, Wendy Bollag^{1,2}, Meghan Mcgee-Lawrence¹, William Hill^{1,2}, Xing-Ming Shi¹, Mohammed Elsalanty³, Sadanand Fulzele¹, Beom-Jun Kim⁴, Mark Hamrick¹, Carlos Isales¹. ¹Medical College of Georgia, United States, ²Charlie Norwood VA Medical Center, United States, ³School of Dental Medicine, United States, ⁴University of Ulsan College of Medicine, Republic of Korea

Both caloric restriction (CR) and dietary protein restriction (PR) have health benefits including lifespan extension in animal models. However, there is concern that dietary restrictions may lead to bone and muscle loss in the elderly. We recently published that selective amino acid supplementation, particularly with aromatic amino acids (phenylalanine, tyrosine and tryptophan; PTT) prevents bone loss in mice fed a PR diet. Previous studies however have not examined the impact of a combined CR and PR diet on bone health. This dietary combination occurs regularly in the institutionalized elderly patient resulting in frailty. The present IACUC-approved study compared the effects of restricted (8%) vs. standard (18%) dietary protein with or without added caloric restriction (25% total caloric intake reduction) and selected amino acid supplementation on bone mass. To test this, we fed mice (6-month-old male C57BL/6 mice N=8/group) specified diets for eight weeks. Bone was analyzed by densitometry (DXA) and serum markers of bone turnover (PYD). Histology and microCT studies are ongoing. Groups were: (1) standard dietary protein (PS); (2) 18% dietary pro-

tein + CR (PS+CR); (3) restricted (8%) protein (PR); (4) PR+CR; (5) PR+CR+amino acids PTT. All data are presented as Mean±SD below. We found that CR, but not PR, resulted in decreased body weight: (31.8±3.2 PS vs. 26.9±1.5 PS+CR, $p<0.002$, and 32.2±2.9 PR vs. 24.2±1.9 g PR+CR, $p<0.0001$; grams). Neither CR nor PR itself decreased total BMD: 0.055±0.002 PS vs. 0.055±0.001 PS+CR vs. 0.055±0.001 PR, g/cm^2). However, the combination of CR and PR resulted in a significant drop in total BMD: 0.055±0.002 PS vs. 0.053±0.002 PR+CR; $p<0.0027$; g/cm^2). In contrast, the addition of aromatic amino acids to the PR+CR group prevented the drop in total BMD: 0.053±0.002 PR+CR vs. 0.054±0.001 PR+CR+PTT, g/cm^2). Markers of bone breakdown (PYD) were highest in mice on a low protein diet; the combination of CR and PR suppressed resorption activity, but PTT restored resorption activity (1.72±0.23 PS vs. 2.10±0.28 PR vs. 1.55±0.41 PR+CR vs. 2.17±0.39 PR+CR+PTT; $p<0.01$ PS vs. PR; $p<0.007$ PR vs PR+CR; $p<0.008$ PR+CR vs PR+CR+PTT; nmol/L). Taken together these data suggest that the combination of CR+PR has a detrimental effect on bone health by suppressing bone turnover, but selective amino acid supplementation can prevent the negative impact CR and PR have on bone health.

Disclosures: **Ke-Hong Ding**, None

MON-1009

Repurposing PDE5 Inhibitors for Osteoporosis – Erecting Bone Se-Min Kim*, Li Sun, Lubna Munshi, Tony Yuen, Mone Zaidi. Icahn School of Medicine at Mount Sinai, United States

Purpose Nitric oxide (NO) plays an important role in skeletal homeostasis. NO-cGMP-PKG pathway mediate anabolic effects of mechanical stimuli and estradiol. In vivo studies using direct NO donor and soluble guanylate cyclase demonstrated therapeutic potential for osteoporosis. However, the role of cGMP-specific phosphodiesterase (PDE) in skeletal health is not clear. In this study, we hypothesize that widely used cGMP specific PDE5 inhibitors – tadalafil and vardenafil – have anabolic skeletal effect. Methods 14-week-old C57BL/6 mice were treated with DMSO (vehicle), tadalafil (48 μ g/day), or vardenafil (240 μ g/day) intraperitoneally for 6 weeks. This dose corresponds to 10 mg tadalafil and vardenafil in human. aBMD was measured using DXA (Piximus, Lunar-GE). Microtomography (Desktop CT40, SCANCO) and dynamic histomorphometry (Zeiss Observer) were performed. Affymetrix gene chip array was carried out to examine the expression of cGMP-specific PDE5, PDE6 and PDE9 in non-transformed mineralizing osteoblasts, human CD14+ cells, and osteoclasts. Comparisons used 1-way ANOVA with Bonferroni's correction or 2-tailed Student's t-tests. Results aBMD at all sites was significantly increased in tadalafil- and vardenafil-treated mice compared with vehicle-treated group. vBMD was also significantly increased in drug-treated mice, especially with tadalafil (~4 fold). Vardenafil-treated mice showed modest vBMD gain. Dynamic histomorphometry demonstrated increased mineralizing surface (MS) and bone formation rate (BFR) in both groups, while osteoclast surface was decreased in tadalafil-treated mice only. Microarray data showed selective expression of PDE5A in non-transformed human osteoblasts. PDE6D, but not PDE6A, the main subunit of holoenzyme PDE6, was expressed in osteoblasts and osteoclasts. Conclusions Our findings suggest that blocking cGMP-specific PDE5 have anabolic effect in bone. The additional bone gain in tadalafil over vardenafil could be the result of additional anti-osteoclastic effects. Since we did not find PDE5 expression in osteoclasts, we postulate that the specificity of PDE inhibition of tadalafil (PDE5 and PDE11) and vardenafil (PDE5 and PDE6) may explain the finding. Furthermore, widely expressed PDE6D, unlike the other PDE6 subunits, regulates prenylated-protein, and may play a role in osteoclast activation independent of the NO-cGMP-PKG pathway.

Disclosures: **Se-Min Kim**, None

MON-1010

Apolipoprotein A-I Prevents Osteoporosis and Promotes Osteogenesis of Mesenchymal Stem Cells via STAT3 and CXCL6/8 Yu-Chuan Liu*, Jean Lu. Genomic Research Center, Academia Sinica, Taiwan

Objectives Bone integrity is maintained by continuous remodeling, which consists of bone formation by osteoblasts and bone resorption by osteoclasts. Osteoporosis, a severe public issue, resulting from bone resorption predominates over bone formation. Currently, most of osteoporosis treatments function by suppressing bone resorption; on the contrary, fewer drugs are designed to promote bone formation. In addition, these treatments may have several side effects, like increasing risks in cancer or cardiovascular disease. Therefore, we want to identify potential new drug for osteoporosis. Methods We utilized high throughput screening in human bone-marrow mesenchymal stem cells with 12380 human open reading frame (ORF) clones and identified novel regulators in promoting osteogenesis by means of increasing alkaline phosphatase activity and matrix mineralization. Moreover, we also performed ovariectomy surgery to define the function of candidate genes in mouse osteoporotic model. Results By gain-of-function screen, we demonstrated that apolipoprotein A-I (ApoA-I), the major protein component of high-density lipoprotein (HDL), could promote osteogenesis of mesenchymal stem cells. Overexpression ApoA-I in the transgenic mice could prevent bone loss in ovariectomy-induced osteoporosis through increasing osteoblast numbers and decreasing osteoclast numbers concurrently, while ApoA-I induced by bromodomain inhibitor I-BET151 in ovariectomized mice could also cure bone loss as well. Interestingly, two chemokines, chemokine (C-X-C motif) ligand (CXCL) 6, and 8 are significantly enhanced by ApoA-I through STAT3 activation. In addition, the inhibition in STAT3 activation or CXCL6/CXCL8 expression blocked ApoA-I-mediated osteogenesis, while

overexpression of CXCL6 promoted osteogenesis. Summary & Conclusion Our results indicate that ApoA-I promotes osteogenesis as a positive regulator in bone formation and offer anabolic and catabolic effect on bone remodeling through increasing osteoblast numbers and decreasing osteoclast numbers simultaneously. Importantly, ApoA-I was reported to block tumor formation and treat cardiovascular diseases. Thus, our findings may support ApoA-I as a potential target to prevent or treat osteoporosis with fewer side effects in the future.

Disclosures: **Yu-Chuan Liu**, None

MON-1011

Butyrate Mediates The Bone Anabolic Activity Of The Probiotic L. rhamnosus GG Via A Regulatory T Cell Mediated Pathway Abdul Malik Tyagi*, Mingcan Yu, Trevor M. Darby, Chiara Vaccaro, Jau-Yi Li, Joshua A. Owens, Emory Hsu, Jonathan Adams, Rheinallt M. Jones, Roberto Pacifici. Emory University, United States

Probiotics are defined as viable microorganisms that confer health benefits. The most common genus of bacteria with probiotic activities are lactobacilli. Lactobacilli prevent ovariectomy induced bone loss by decreasing bone resorption, but the effects of probiotics in eugonadic conditions and their mechanism of action are largely unknown. To investigate this, 10-week-old conventionally raised (Conv.R) mice were treated for 4 weeks with vehicle or the probiotic L. rhamnosus GG (LGG) at a dose of 1×10^9 total bacteria 5 times/week. In vivo and in vitro μ CT measurements revealed that LGG markedly increased bone volume (BV/TV) by stimulating bone formation. By contrast, LGG was ineffective in germ-free mice, demonstrating that LGG acted in cooperation with the gut microbiota. LGG produces lactate, which expands clostridia, a genus which produces bone active short-chain fatty acids (SCFAs). Accordingly, LGG supplementation increased intestinal and serum levels of the main SCFA butyrate. Attesting to the mechanistic role of butyrate, direct feeding of butyrate increased BV/TV and bone formation as potentially as LGG. Neither LGG nor butyrate affected bone resorption. SCFAs are potent inducers of regulatory T cells (Tregs). Accordingly, both LGG and butyrate increased the differentiation of naive CD4+ T cells into Tregs in the bone marrow (BM). In turn, Tregs induced the release of the osteogenic Wnt ligand Wnt10b by BM CD8+ T cells. Wnt10b caused the activation of Wnt signaling in osteoblastic cells, leading to increased bone formation. Attesting to the relevance of Wnt10b, LGG and butyrate were ineffective in mice lacking CD8+ T cells production of Wnt10b. Demonstrating the role of Tregs, blockade of Treg expansion in two established in vivo models prevented the bone anabolic activity of LGG and butyrate. Mechanistically, LGG and butyrate increased Treg TGF β expression, which activates SMAD signaling in CD8+ T cells. Moreover, Tregs activated NFAT signaling and blocked AP-1 activation in BM CD8+ cells, thus favoring the binding of NFAT/SMAD dimers to a critical NFAT/SMAD-activated promoter site that stimulates Wnt10b gene expression in CD8+ T cells. In summary, the probiotic LGG is a potent bone anabolic agent that stimulates bone formation via a butyrate/Treg/Wnt10b dependent pathway. Nutritional supplementation with butyrate may provide a novel therapeutic strategy for increasing bone mass and preventing osteoporosis.

Disclosures: **Abdul Malik Tyagi**, None

MON-1012

Influence of a 17 β -hydroxysteroid dehydrogenase type 2 (17 β -HSD2) selective inhibition on ovariectomy induced bone loss in Wistar rats Sebastian T. Müller^{*1}, Sophie Pählig¹, Ahmed Merabet², Chris Van Koppen³, Sandrine Marchais-Oberwinkler², Rolf W. Hartmann³, Oliver Zierau¹, Günter Vollmer¹. ¹Technische Universität Dresden, Molecular Cell Physiology and Endocrinology, Institute for Zoology, Dresden, Germany, ²Institute for Pharmaceutical Chemistry, Philipps University Marburg, 35032 Marburg, Germany, ³Pharmaceutical and Medicinal Chemistry, Saarland University, Campus E8.1, 66123 Saarbrücken, Germany

Osteoporosis is a major healthcare factor with an important socio-economical impact. Direct costs of osteoporosis related fractures increase up to ~76.7 billion Euros in Europe in 2050. Estrogens, most notably estradiol (E2), play a major role in bone health. Therefore, postmenopausal women are a high-risk group because of their hypoestrogenemia. Hormone replacement therapy (HRT) is the “Gold Standard” for bone protection. However, side effects (e.g. increased risk of breast cancer or thrombosis) are controversially debated. Other currently available therapies like bisphosphonates or selective estrogen receptor modulators (SERMs) show a reasonable efficacy, but all have limitations and side-effects. Consequently, additional therapeutic approaches to treat osteoporosis are needed. The 17 β Hydroxysteroid dehydrogenase type 2 (17 β HSD2) is expressed in a variety of tissues (e.g bone) and catalyzes the oxidation of E2 into the less potent estron (E1). Inhibition of 17 β HSD2 should ideally increase E2 levels in tissues expressing the enzyme but impact on systemic E2 levels. Currently, only one animal experimental study about 17 β HSD2 inhibition and bone protection is available. However, the inhibitor used in this study was less potent and more limited in bio-availability than the inhibitor available to us. Within our study, we test for the first time the 17 β HSD2 inhibition in the rat model of ovariectomy induced bone loss. In order to identify bone sparing effects, we analyzed several bone parameters (e.g. BV/TV, Tb.N., Tb.Th. and, Tb.Sp. based on μ CT and histology of the tibia). To evaluate the safety of a 17 β HSD2 inhibition we analyzed uterine parameters on tissue, protein and mRNA level. Regarding bone, three out of four μ CT parameters (BV/TV, Tb.N. and, Tb.Sp.) showed a significant bone

protective effect by 17 β HSD2 inhibition compared to the ovx control. No significant effects could be observed for the other bone parameters. For the uterus no significant estrogenicity caused by the 17 β HSD2 inhibition could be observed. As a proof of principle evaluation, our data indicates that 17 β HSD2 inhibition might be a new and promising approach to prevent osteoporosis.

Disclosures: **Sebastian T. Müller**, None

MON-1013

Bilateral Distal Femoral Epiphyseal Defect Models for Safety Testing: A 5-Week Rat Bone Healing Study Luis Fernando Negro Silva^{*1}, Julius Haruna¹, Pritpal Malhi¹, Simon Authier¹, Yannick Trudel², Raluca Kubaszkyl¹, Michel Assad². ¹Citoxlab North America, Canada, ²AccelLAB Inc., Canada

Low trauma fractures represent clinical complications from our aging society. Most fractural injuries are known to occur in long bones with inevitable consequences such as pseudoarthrosis and relatively high non-union rates. In the last 20 years, substantial efforts in the field of biomechanical and biomaterials research have been devoted to the development of synthetic osteoconductive graft substitutes for tissue engineering in presence (or not) of drug-eluting therapeutic agents with osteoinductive and antimicrobial properties to respectively improve bone healing and prevent iatrogenic infections. In toxicology, the rat is the most frequently selected rodent model to investigate drug safety, but scarce data is available relative to the use of this murine species in orthopedic models. Following an IACUC-approved protocol from an AAALAC-accredited institution, eighteen (18) female Sprague-Dawley rats were used to evaluate if 2-mm critical-size defects in distal femoral condyles were adequate for toxicology evaluation of drugs with potential impact on bone remodeling. Under anesthesia, both hindlimbs were prepped and draped in sterile fashion. Then, bilateral cylindrical defects of 2x5mm (DxL) were created in distal femoral condyles. Per-op and terminal digital radiography was performed on all femurs. Then, at 5 weeks post-op, all femoral defect sites were harvested, decalcified, and embedded in paraffin. Central longitudinal histological sections were then taken from the bone defect site and prepared for microscopic examination following H&E and Goldner's Trichrome staining. Histopathology scoring was performed on the quality of new bone formation, while the extent of new bone formation was quantified by histomorphometry (Table 1). Regardless of treatment, all defect sections demonstrated significant bone remodeling characterized by the repair of the cortical bone and an ingrowth of bony trabeculae consisting of a mixture of woven and lamellar bone. These results demonstrate that creating a 2-mm long-bone defect enables evaluation of potential drug effects on bone healing in toxicology. In contrast, a 2-mm femoral epiphyseal defect will not be considered a critical-size defect in the rat long bone, but larger defects (ex. \geq 3mm) may further be explored for this purpose. When this is met, this murine femoral defect model may then represent a promising one to evaluate the superiority of new bone substitutes with osteoconductivity and osteoinductivity properties.

Table 1: Quantification of bone ingrowth

	New Bone Formation Sham Defect Right Femur (%)	New Bone Formation Saline/Defect Left Femur (%)	Soft Tissue Formation Sham Defect Right Femur (%)	Soft Tissue Formation Saline/Defect Left Femur (%)
Mean	95.66	95.50	4.34	4.50
SD	3.65	4.37	3.65	4.37
N	9	9	9	9

No significant differences between sham and saline-treated groups

Disclosures: **Luis Fernando Negro Silva**, None

MON-1014

Prevention of spaceflight-induced Osteoarthritis: a potential dietary countermeasure Elizabeth Blaber^{*}, Ann-Sofie Schreurs. NASA USRA, United States

Current treatments against spaceflight-induced bone loss provided to Astronauts are not without limitations. Most of the current treatments against osteoporosis are anti-resorptive, but few act to prevent resorption and increase bone formation simultaneously. Spaceflight is a combination of multiple factors including microgravity, in addition to space radiation. Therefore, we conducted studies to determine if our potential dietary countermeasure could prevent simulated spaceflight (simulated microgravity and radiation combined) bone loss. Mice were exposed to gamma (TBI, 137Cs, 2 Gy), simulated microgravity (using the hind-limb unloading system, HU) or TBI+HU. While we observed bone loss in mice fed the control diet due to both treatments (TBI=14%, HU=20%), and a worse effect with combined treatments (TBI+HU=25%), mice fed the countermeasure diet did not sustain significant bone loss relative to untreated controls. The countermeasure prevented microarchitectural decrements in both appendicular bone (tibia) and axial bone (vertebrae). In parallel, space-flow mice exhibited a novel and severe disruption of the epiphyseal boundary, resulting in

endochondral ossification of the femoral head and perforation of articular cartilage by bone. This suggests that spaceflight in microgravity may cause rapid induction of an aging-like phenotype with signs of osteoarthritic disease in the hip joint. Taken together, femurs from mice exposed to spaceflight onset of an accelerated aging-like phenotype with signs of osteoarthritic disease shown by disruption of the epiphyseal boundary and endochondral ossification. We plan to determine if the countermeasure also prevents the OA phenotype observed in the mice exposed to simulated spaceflight (HU+IR).

Disclosures: **Elizabeth Blaber**, None

MON-1015

Anatomic Deconvolution of Vascular and Osteoanabolic Responses in Osseointegration Kathleen Turajane^{*1}, Ed Purdue¹, Gang Ji¹, Ugur Ayturk¹, Matthew Greenblatt², Xu Yang¹, Mathias Bostrom¹. ¹Hospital for Special Surgery, United States, ²Weill Cornell Medical College, United States

Purpose: The number of total joint replacements (TJR) performed in the United States is over 1 million per year. Cementless TJRs provide better long-term fixation than conventional cemented implants. Higher failure rates in total knee replacement caused by implant loosening due to deficient osseointegration between bone and implant remains a major clinical problem. To address this problem, we need a better understanding of the molecular mechanisms of osseointegration. Here, we have performed gene expression analysis of tissues in different anatomic subdomains at the bone-implant interface in our mouse model of tibial implant osseointegration (Yang et al., 2015). Method: A titanium implant (Fig 1B) was inserted into the right proximal tibia of 16-week female mice. At 1 week post-surgery, the implant (with attached tissue) was removed from the tibia. Then, the tibia was centrifuged to isolate bone marrow. Cancellous bone was separated from the cortical bone using a 1mm biopsy punch. Bone and implant samples were homogenized separately (Kelly et al., 2014). Following total RNA extraction, samples were evaluated for RNA yield and quality. Subsequently, transcripts associated with osteoblasts (Runx2 and Col1a1), bone marrow cells (Hbb-b1 for erythrocytes and S100a8 for immune cells), and endothelial cells (Emcn and Cd31) were examined with real-time RT-PCR. Results: The RNA integrity assessment confirmed the feasibility of obtaining high quality RNA from the implant-bone interface for mRNA expression analysis. The real-time PCR analyses revealed that our approach was successful in separating bone marrow from the bone and implant (Fig 1A). Importantly, the abundance of osteoblast-associated genes (Runx2 and Col1a1) transcripts on the implant surface suggested the presence of osteoblasts. Intriguingly, the enrichment of endothelial cell markers in multiple anatomic regions demonstrated that active angiogenesis occurs in both bone and the implant interface simultaneously. Conclusion: We have developed a reproducible method to evaluate important subanatomical locations of osseointegration. Preliminary gene expression analyses support the involvement of angiogenesis and osteoblast activity directly at the bone-implant interface in total knee replacements. These findings demonstrated that our mouse implant model will be a viable platform for studying the molecular mechanisms of implant osseointegration.

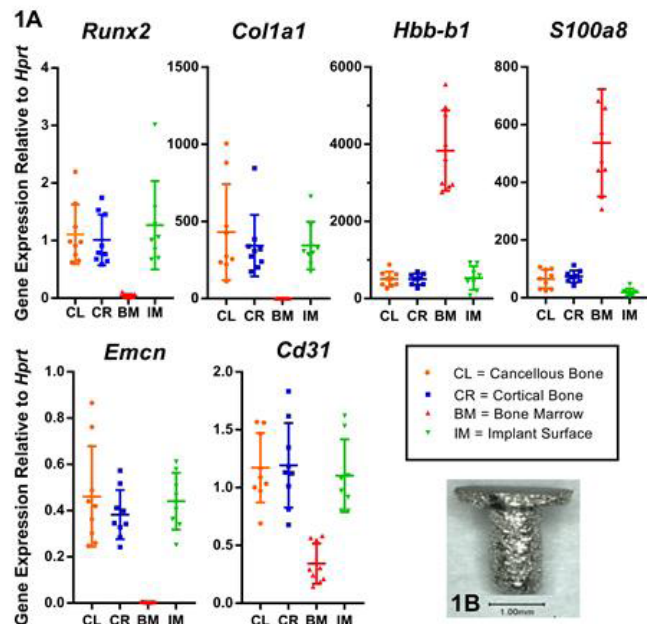


Figure 1A: The real-time RT-PCR analysis of transcripts associated with osteoblasts (Runx2, Col1a1), red blood cells and marrow cells (Hbb-b1, S100a8), and endothelial cells (Emcn, Cd31) in cancellous bone (CL), cortical bone (CR), bone marrow (BM), and bone implant surface (IM). Figure 1B: Titanium implant (1.5mm x 2mm x 2mm).

Disclosures: **Kathleen Turajane**, None

MON-1016

Measurement of lipid metabolites in a mouse model of breast cancer using imaging mass spectrometry shows specific signals linked to CYP27B1 gene ablation Mengdi Xing^{*1}, Jiarong Li¹, Ethan Yang², Pierre Chaurand², Richard Kremer¹. ¹RI MUHC, Canada, ²University Montreal, Canada

Vitamin D is known as an essential regulator of bone metabolism through the regulation of calcium and phosphate homeostasis. However, it has become clear that vitamin D and its active metabolite 1,25(OH)₂D have many extra skeletal actions such as the regulation of glycemic control and lipid metabolism. The most abundant circulating form of vitamin D, 25(OH)D, is converted to its metabolically active form 1,25(OH)₂D in both kidney and extrarenal tissues such as breast by the enzyme 1- α -hydroxylase, which is encoded by gene CYP27B1. Previous study in our group has shown that vitamin D can control fat distribution, and fat accumulation in breast promotes breast cancer. Thus, a PyMT mouse model of breast cancer has been established with the conditional knockout of CYP27B1 that could locally inhibit the production of 1,25(OH)₂D in breast. The purpose of this study is to investigate the effect of locally produced 1,25(OH)₂D in mammary glands on breast tumor progression by comparing the lipid profile and phospholipid expression in breast tumor tissues with/without 1,25(OH)₂D production by imaging mass spectrometry (IMS). A PyMT mice model has been used with the conditionally knockout of CYP27B1, which produces knockout breast tumor (without 1,25(OH)₂D production) and wild type breast tumor (with 1,25(OH)₂D production). Tumors were collected at different time points, which are hyperplasia (32-34 days), adenoma (7 weeks), and late stage (11 weeks) respectively (n=8 at each time point). Lipid profiles and images were compared across cohorts and time points. Serial sections were cut and stained to validate histology and align with IMS results and to ensure tissue quality. Segmentation of the IMS results allowed to accurately define the different histologies present with the tumors (hyperplasia, tumors, and adipose stroma) at the various time points. Interestingly, several lipid signals (for example, m/z 942.8, m/z 650.83, m/z 884.1, etc) absent (or expressed in lower abundance) in hyperplasia and adenoma stages have been found differently expressed in late stage tumorous tissues. However, the relative abundance of these appeared significantly higher in KO tumorous tissue. In contrast, there are lipid signals (such as m/z 1071.4) have been found abundant in hyperplasia and down regulated with tumor progression. Our study suggests a mechanistic link between vitamin D activation in breast tissue, lipid signals and tumor progression.

Disclosures: *Mengdi Xing, None*

MON-1017

Calcium absorption is positively affected by feeding a yogurt containing GOS obtained from enzymatic action on milk lactose. Experimental study. M Seijo^{*1}, C Vénica², Ml Pita Martin De Portela³, C Bergamini², I Wolf², Mc Perotti², Sn Zeni¹. ¹Laboratorio de Enfermedades Metabólicas Óseas, Instituto de Inmunología, Genética y Metabolismo (INIGEM). Facultad de Farmacia y Bioquímica. Hospital de Clínicas, CONICET- UBA, Argentina, ²Instituto de Lactología Industrial (INLAIN) –Universidad Nacional del Litoral/CONICET, Facultad de Ingeniería Química, Santa Fe, Argentina, Argentina, ³Cátedra de Nutrición. Facultad de Farmacia y Bioquímica – UBA, Argentina

The galactooligosaccharides (GOS) are bioactive carbohydrates present in human milk. GOS could be incorporated in dairy products, such as yogurt, from enzymatic action of β -galactosidase on the milk lactose. Its consumption changes the gut microbiota composition which release several metabolites that could improve calcium absorption (CaAbs) and bone health. We evaluated the prebiotic effect on CaAbs of a yogurt containing GOS during normal growth. Male weaning Wistar rats (n=10 per group) received during 30 days AIN⁹³-G control diet (CD) or diet based on the yogurt containing GOS (ED), and calcium (Ca) and protein according to AIN⁹³-G. Food consumption was evaluated three times per week; body weight (BW) and faecal Lactobacilli (LB) colonies weekly; CaAbs during the last 3 days of the experience and caecal pH and short-chain fatty acid (SCFAs) at the end of the study. Result as mean \pm SD. No differences in food consumption and BW were found (16.6 \pm 2.7 vs. 16.4 \pm 0.6 g and 229 \pm 13 vs. 214 \pm 5 g, respectively). ED compared to CD group showed an increased in faecal LB colonies (p

Disclosures: *M Seijo, None*

MON-1018

Engineering Dual-Specific M-CSF Antagonists That Inhibit c-FMS And α v β 3 Integrin As Anti Resorptive Compounds Yuval Zur^{*1}, Lior Rosenfeld¹, Gali Guterman-Ram², Niv Papo¹, Noam Levaot². ¹Department of Biotechnology Engineering and the National Institute of Biotechnology in the Negev, Ben-Gurion University of the Negev, Beer-Sheva, Israel, ²Department of Physiology and Cell Biology, Ben-Gurion University of the Negev, Beer-Sheva, Israel

Excessive and uncontrolled bone resorption by osteoclasts is a hallmark of many bone diseases, including osteoporosis. Therefore, controlled and specific inhibition of osteoclast activity is a desired outcome in treatments of bone diseases. Osteoclast differentiation and function are coordinated by cell surface receptors, including c-FMS and α v β 3 integrin, which cross talk with each other to drive signals that are essential for osteoclast functions. Using

functional FACS-based screening assays of random mutagenesis M-CSF libraries against c-FMS and α v β 3 integrin, we engineered dual-specific M-CSF mutants with high affinity to both receptors. We showed by SPR and cell surface binding assays that the engineered dual-specific M-CSF proteins can bind both α v β 3 integrin and c-FMS receptors, leading to antagonism of immediate signaling events (c-FMS and Akt phosphorylation) and downstream biochemical events regulating osteoclast differentiation. Moreover, the dual-specific mutants had enhanced osteoclast inhibitory capabilities compared to inhibitors that target only one of the pathways, thereby highlighting the effects of the dual functionality that we engineered into these proteins. In the presence of the dual-specific inhibitors osteoclasts were unable to form a solid actin belt and were not able to differentiate properly in a dose dependent manner. Finally, we show that injection of the bispecific c-FMS and α v β 3 integrin proteins significantly inhibited bone resorption by osteoclasts in ovariectomized mice providing proof of concept for their utilization as anti resorptive drugs.

Disclosures: *Yuval Zur, None*

MON-1058

Novel mutations in fibronectin associated with metaphyseal fractures – Expanding the phenotype of patients with a subtype of spondylometaphyseal dysplasia with “corner fractures” Jessica J. Alm^{*1}, Alice Costantini¹, Helena Valta², Nissan Vida Baratang³, Patrick Yap⁴, Débora Bertola⁵, Guilherme Yamamoto⁵, Chong A. Kim⁵, Jiani Chen⁶, Klaas J. Wierenga⁶, Elizabeth A Fanning⁶, Luis Escobar⁷, Kirsty Mcwalter⁸, Heather McLaughlin⁸, Rebecca Willaert⁸, Amber Begtrup⁸, Dieter P. Reinhardt⁹, Outi Mäkitie¹⁰, Philippe M Campeau^{3,11}. ¹Clinical Genetics, Center for Molecular Medicine, Karolinska Institutet, Sweden, ²Children’s Hospital, University of Helsinki and Helsinki University Hospital, Finland, ³CHU Sainte Justine Research Centre, University of Montr, Canada, ⁴Genetic Health Service New Zealand (Northern Hub), New Zealand, ⁵Clinical Genetics Unit, Instituto da Criança HC-FMUSP and Instituto de Biociências- Universidade de São Paulo, Brazil, ⁶University of Oklahoma Health Sciences Center, United States, ⁷Medical Genetics and Neurodevelopmental Pediatrics, St Vincent Children’s Hospital, Indianapolis, United States, ⁸GeneDx, United States, ⁹Department of Anatomy and Cell Biology, McGill University, Montreal, Canada, ¹⁰Children’s Hospital, University of Helsinki and Helsinki University Hospital, Finland, ¹¹Department of pediatrics, University of Montreal, Canada

Spondylometaphyseal dysplasias (SMD) comprise a group of genetically and phenotypically heterogeneous bone dysplasias that affect the growth plates and the spine. Metaphyseal fractures, so called “corner fractures”, are typical features in a type of SMD. The most striking feature in SMD is irregular metaphyses and the presence of atypical “corner fractures”. Only recently, mutations in the FN1 gene, encoding fibronectin (FN), were found in a fraction of individuals with this novel form of SMD. Fibronectin is an important extracellular matrix component for bone and cartilage development, but less is known about the role of FN in bone strength. So far, only ten patients in seven families with FN1 mutation-related SMD have been described, and the complete genetic and phenotypic spectrum of the disease needs more deeply characterization. In our ongoing research on genetic determinants of skeletal dysplasias we identified 5 new patients with SMD with “corner fractures” caused by five novel missense mutations in FN1. The study was approved by Institutional Ethics Boards and participants provided written informed consent. Clinical and radiographic evaluations were part of the clinical care. Genomic DNA was extracted from peripheral blood using standard procedures. Whole-exome sequencing or whole-genome sequencing was used to identify cause of disease in four patients, while targeted Sanger sequencing was applied in one case. The obvious metaphyseal bone changes and “corner fracture” appearances were the most extensive clinical feature in these patients. In addition, low trauma bilateral femoral fractures in one patient represent a novel finding in SMD with “corner fractures”. Osteopenia and increased serum N-telopeptide suggesting increased bone turnover were noted in some patients. All individuals had cysteine mutations, disrupting disulphide bonds in the fibronectin type-I assembly domain (NM_212482.2: p.Cys213Tyr, p.Cys123Tyr, p.Cys169Tyr, p.Cys231Trp and p.Cys258Tyr). These novel findings extend the clinical spectrum and genotype of SMD with “corner fractures” and indicate metaphyseal fractures as a hallmark for diagnosis of FN1-related SMD. The high frequency of metaphyseal “corner fractures” in all patients with FN1 mutations indicates altered bone tissue, causing decreased bone strength especially during childhood. This emphasizes the importance of FN not only in bone formation, but possibly also in maintenance of bone strength and fracture resistance.

Disclosures: *Jessica J. Alm, None*

MON-1059

Quality Of Life is Not Impaired In Patients With Isolated Craniofacial Fibrous Dysplasia Marlous Rotman^{*}, Natasha Appelman-Dijkstra, Stijn Genders, Sander Dijkstra, Neveen Hamdy. LUMC, Netherlands

In craniofacial fibrous dysplasia (CFD) quality of life may be impaired due to pain, disfigurement and dysfunction caused by cranial nerve entrapment, but data on predictive factors affecting quality of life (QoL) are scarce in these patients. In this study we used the Short Form-36 (SF-36) questionnaire to evaluate QoL in 97 out of 138 eligible FD/MAS pa-

tients. Twenty-two patients had CFD: 9 had isolated CFD, 13 had CFD associated with other skeletal localizations. Seventy-five patients had no CFD: 50 with monostotic FD (MFD) and 25 with polyostotic FD/McCune Albright syndrome (PFD/MAS). Data on age, gender, age at diagnosis of FD, clinical characteristics, relevant serum biochemistry and Skeletal Burden Scores (SBS) were retrieved from medical records. The SF-36 questionnaire was completed by predominantly female patients (68%). Mean age of respondents at FD diagnosis was 27.0 (0-77 years), and mean SBS was 11.6 (range 0.1-64.7). CFD patients (64% female) had a mean age at FD diagnosis of 22.8 years (0-60 years), a mean total SBS of 6.2 (range 0.1-64.7) and a mean skull SBS of 19.5 (range 2.5-75.0). Patients with isolated CFD had a lower skull SBS than those with CFD/PFD/MAS (mean 15.0 vs. 25.6). Main clinical features in CFD patients were facial deformity (48%), headache (27%), vision loss (12%) and nerve entrapment (9%). Patients with isolated CFD, who had the least complaints and the lower skull SBS, reported no impairment in any QoL domain compared to MFD and PFD/MAS patients and to the more severe and symptomatic CFD associated with PFD/MAS, who had the most bodily pain and impairment in several other SF-36 domains including physical and social function. Our data suggest that aspects of QoL as evaluated by the SF-36 appear to be unaffected in patients with isolated CFD. In contrast we show that several aspects of QoL are severely impaired when CFD is associated with PFD/MAS.

Disclosures: Marlous Rotman, None

MON-1060

High prevalence of enthesopathies in patients with X-Linked Hypophosphatemia Axelle Salcion^{*1}, Louis Lassalle², Valérie Merzoug³, Alessia Usardi⁴, Anya Rothenbuhler⁴, Peter Kamenicky⁵, Christian Roux⁶, Agnès Lingart⁷, Karine Briot⁶. ¹French Reference Center for Genetic Bone Diseases, Cochin Hospital, Assistance Publique- Hôpitaux de Paris, Paris, France, ²Department of Radiology, Cochin Hospital, Assistance Publique- Hôpitaux de Paris, France, ³Kremlin Bicêtre, France, ⁴Department of Pediatric Endocrinology, Reference Center for Rare Disorders of Calcium and Phosphate, Kremlin Bicêtre Hospital Assistance, France, ⁵Department of Endocrinology, Kremlin Bicêtre Hospital, Assistance, France, ⁶Department of Rheumatology, French Reference Center for Genetic Bone Diseases, Cochin Hospital, Assistance Publique- Hôpitaux de Paris, France, ⁷Department of Pediatric Endocrinology, Reference Center for Rare Disorders of Calcium and Phosphate, France

X-linked hypophosphatemia (XLH) is a rare genetic disease characterized by impaired renal phosphate reabsorption which leads to vitamin D resistant rickets in children. In adulthood, the burden of disease is related to musculoskeletal symptoms due to osteomalacia, osteoarthritis, and muscle weakness but also ossifications of entheses (enthesopathies), this latter feature being a strong determinant of alteration in quality of life in this population. These enthesopathies localized to the spine, peripheral joints and Achilles tendons are responsible for chronic pain, joint limitations, stiffness and disability. In the literature, these ossifications may be referred to enthesopathies or osteophytes with a different anatomical structure involved. The aim of this study was to describe the prevalence and the type of ossifications (enthesophytes and osteophytes) in a large cohort of adult patients with XLH. This retrospective study was conducted in adult patients followed in the rheumatology department, part of the French Reference Center for Rare Disorders of Calcium and Phosphate Metabolism. Full body X-rays were performed using the EOS® low-dose radiation system between June 2011 and December 2017. X-rays were interpreted independently by two trained physicians specialized in rare bone diseases. Eighty one patients were included in this study (68% women, mean age 42.4 ± 13.6 years). Sixty-three (78%) patients had been treated during childhood with phosphate and/or vitamin D analogs. At the time of the study, 41 (50.6%) were still receiving on phosphate supplements and/or vitamin D analogs, and 65 (80%) suffered from pain of multifactorial origin. 58 (72%) enthesopathies of spine, pelvis and heels. 44 (63%) had spine enthesopathies with a mean of 4.1 ± 2.6 per patient, mostly found in the cervical spine (82%) or in the lumbar spine (62%). 86% of patients had thin ossifications (similar to syndesmophyte observed in spondyloarthritis), 61% had coarse ossifications (hyperostosis-like disease), and 50% had an association of both. Calcanei were visible on 52 radiographs, showing coarse ossifications in 22 cases (42%). Overall, 90% of patients had hip osteophytes with a narrowed hip joint space in 65%. We did not observe any peri-articular and spinal enthesopathies in patients under 30 years of age. This study showed that 72% of adult patients with XLH have at least one enthesopathy of spine, pelvis and heels. We did not observe any enthesopathies in subjects below 30 years old. In most cases this enthesopathy is similar to a syndesmophyte, usually observed in SpA. Aware that this disease can be long misunderstood and finally diagnosed in adulthood, attention must be paid to ossification of the entheses. The mechanisms of formation of these enthesopathies remain to be determined.

Disclosures: Axelle Salcion, None

MON-1061

Homozygous Calcium-sensing Receptor Polymorphism R544Q Presents as Hypocalcemic Hypoparathyroidism Lucie Canaff^{*1}, Branca M. Cavaco², Alexis Nolin-Lapalme¹, Margarida Vieira², Tiago Silva², Ana Saramago², Rita Domingues², Valeriano Leite², Geoffrey N. Hendy¹. ¹Metabolic Disorders and Complications, McGill University Health Centre Research Institute, Canada, ²Instituto Português de Oncologia de Lisboa Francisco Gentil, Portugal

Background: Autosomal dominant hypocalcemia type 1 is caused by heterozygous activating mutations in the calcium-sensing receptor gene (CASR). Whether polymorphisms that are benign in the heterozygous state pathologically alter receptor function in the homozygous state is not known. Purpose: To identify the genetic defect in an adolescent female with a past history of surgery for bilateral cataracts and seizures. The patient has hypocalcemia, hyperphosphatemia and low serum parathyroid hormone (PTH) levels. The parents of the proband are healthy. Methods: Mutation testing of PTH, GNA11, GCM2 and CASR genes was done on leukocyte DNA of family members. Functional analysis in transfected cells was conducted on the gene variant identified. Public single-nucleotide polymorphism (SNP) databases were interrogated for the presence of the variant allele. Results: No mutations were identified in PTH, GNA11 and GCM2 genes in the proband. However, a germline homozygous variant (c.1631G>A; p.R544Q) in exon 6 of the CASR gene was identified. Both parents are heterozygous for the variant. The variant allele frequency was near 0.1 % in SNP databases. By in vitro functional analysis the variant was significantly more potent in stimulating both the Ca²⁺ and ERK/MAPK signaling pathways than wild-type CaSR when transfected alone (p<0.05) but not when transfected together with wild-type CaSR. The overactivity of the mutant CaSR is due to loss of a critical structural cation-π interaction. Conclusions: The patient's hypoparathyroidism is due to homozygosity of a variant in the CASR that normally has weak or no phenotypic expression in heterozygosity. Although rare, this has important implications for genetic counseling and clinical management.

Disclosures: Lucie Canaff, None

MON-1062

Cardiopulmonary Outcomes in Adults with Osteogenesis Imperfecta Sobiah Khan^{*1}, Erin Carter¹, Robert Sandhaus², Cathleen Raggio¹. ¹Hospital for Special Surgery, United States, ²National Jewish Health, United States

Introduction: OI is a type I collagen deficiency resulting in disordered connective tissue. Respiratory insufficiency is the leading cause of death in people with OI. It has been suggested that decreased pulmonary function may be an intrinsic component of OI, rather than a secondary effect of scoliosis. Hypothesis: Reduced pulmonary function in individuals with OI is intrinsic to the connective tissue disorder, not curve magnitude. Results: 14 individuals with a diagnosis of OI were enrolled in this IRB-approved prospective study. Anteroposterior radiographs were evaluated for scoliosis (curve >10°). If more than one curve was present, the largest curve was used for analysis. Pulmonary function was defined by FEV1/FVC ratio, with restrictive disease defined as FEV1/FVC >80%, while obstructive disease was defined as FEV1/FVC <70%. Chest CTs were qualitatively evaluated for evidence of lung disease. Echocardiograms and EKG were obtained to assess cardiac health. QOL was evaluated via SF-36. Individuals that complained of disordered sleep underwent polysomnography. Bivariate correlation analysis was performed, using Spearman's rho correlation coefficient as well as point-biserial correlation analysis (p<0.05). 71% of participants were female. Mean age was 35 ± 15 years. 36% had OI Type 3, 36% Type 4, and 29% Type 1. 57% presented with scoliosis. 14% had cardiac comorbidities and 7% pulmonary comorbidities. Abnormalities (parenchyma scarring, glass-ground opacities, air trapping) were seen on 23% of chest CTs. 50% EKGs showed abnormal results (tachycardia or non-specific wave abnormalities). 93% had trace mitral, tricuspid, or aortic regurgitation. Correlation between curve magnitude and pulmonary function was weak (R=0.1154) and not statistically significant (p=0.308). Conclusions: Pulmonary function is weakly correlated with curve magnitude. Therefore, decreased pulmonary function is likely an intrinsic factor of OI. We suggest that there be a reevaluation of clinical practice in evaluating cardiopulmonary health in individuals diagnosed with OI. We recommend that at least baseline echocardiograms and EKGs be obtained for all adults diagnosed with OI.

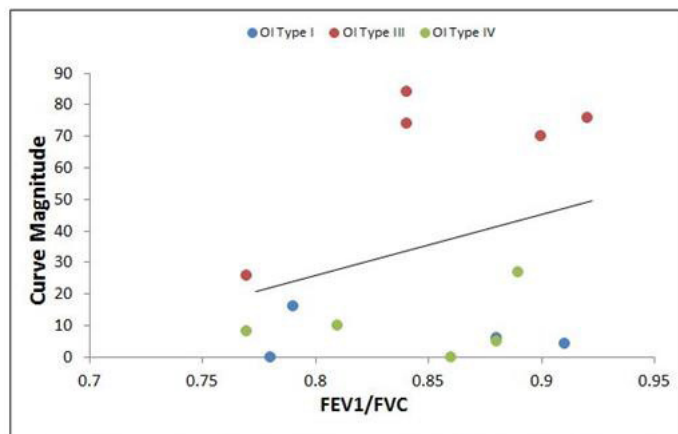


Figure 1 Weak and non-significant correlation between scoliosis curve magnitude and FEV1/FVC ($r=0.1154$; $p=0.308$).

Disclosures: *Sobiah Khan, None*

MON-1063

Asymmetric metaphyseal dysplasia due to COL2A1 mutation with mosaicism Lisa Cruz-Aviles, Md^{*}1, Thomas O. Carpenter, Md¹, Allen E. Bale, Md², Cemre Robinson, Md¹. ¹Yale University School of Medicine, Department of Pediatrics, Section of Endocrinology, United States, ²Department of Genetics, Yale School of Medicine, United States

Background: Heterozygous mutations in COL2A1 cause skeletal dysplasia syndromes involving epiphyses of the long bones and vertebral bodies. The phenotypic spectrum ranges from mild skeletal abnormalities in utero to lethal dwarfism, without clear phenotype-genotype correlation. We describe the clinical, radiological and molecular features in a patient with striking asymmetrical metaphyseal dysplasia due to a mosaic COL2A1 mutation. **Case:** This now-10-year-old girl presented at birth with skeletal asymmetry, with right arm and leg shorter than the left, and disproportionately short legs with the right femur being the most severely affected limb segment. Epiphyseal fraying of long bones and dysplastic metaphyses (Fig. 1a, arrowhead) and leg-length discrepancy (Fig. 1b, arrow) were present. Other prominent clinical findings included mild craniofacial asymmetry, facial muscle hypotonia, asymmetric chest wall, bilateral clinodactyly, and short stature, but no ocular findings. Family history was unremarkable. A right femoral/tibial lengthening procedure performed at age 3 provided near-approximation of leg-length symmetry, but asymmetry recurred by age 8. Coincidentally, she developed central precocious puberty around age 7. Whole exome sequencing revealed a pathogenic missense variant in exon 24 of COL2A1 c.G1537A:p.G513S. A reference to alternative allele ratio of 36:17 suggested mosaicism. **Conclusions:** We describe a non-lethal collagenopathy due to a mosaic glycine substitution in COL2A1, presenting as an asymmetrical metaphyseal dysplasia. Though rare, asymmetric limb shortening with marked metaphyseal dysplasia has been reported with other mutations in COL2A1. The identified G->S variant in our patient has not been observed in the general healthy population, but has been reported in a sporadic patient with lethal hypochondrogenesis1 and is predicted to have a severe phenotype. This mutation, which is likely somatic in view of both the mosaicism and the non-lethality, may explain the asymmetrical feature of the skeletal dysplasia. This case highlights the consideration of COL2A1 mutation analysis in the clinical setting of asymmetric limb skeletal dysplasias. 1. Mortier GR, Weis M, Nuytinck L, et al. Report of five novel and one recurrent COL2A1 mutations with analysis of genotype-phenotype correlation in patients with a lethal type II collagen disorder. *Journal of medical genetics.* 2000;37(4):263-271.



Disclosures: *Lisa Cruz-Aviles, Md, None*

MON-1064

Multiple Endocrine Neoplasia, type 4 - a Novel CDKN1B Mutation with High Penetrance of Primary Hyperparathyroidism Anja Lisbeth Frederiksen^{*}1, Maria Rossing², Anne Pernille Hermann³, Charlotte Ejersted⁴, Morten Frost⁵. ¹Dept. of Clinical Genetics, Odense University Hospital, Denmark, ²Center of Genomic Medicine, Copenhagen University Hospital, Denmark, ³Dept. of Endocrinology M, Odense University Hospital, Denmark, ⁴Department of Endocrinology M, Odense University Hospital, Denmark, ⁵Steno Diabetes Centre, Odense, Dept. of Endocrinology M and KMEB, Odense University Hospital, Denmark

Background: Mutations in CDKN1B have recently been associated with Multiple Endocrine Neoplasia, type 4 (MEN4). The MEN syndromes are characterized by tumors in two or more endocrine organs including parathyroid, pituitary, adrenocortical glands and gastro-enteropancreatic neuroendocrine and carcinoid tumors. These present with a dominant pattern of inheritance with heterogeneous phenotypes. Similar to MEN1, caused by mutations in the tumor suppressor gene MEN1, MEN4 appear to present with hypercalcemia. There are however, only few cases reported on CDKN1B and the clinical phenotype including penetrance and genotype/phenotype associations remains to be further illuminated. We report a novel variant in CDKN1B identified in a 38 years old woman who presented with Mb.Cushing. Further, we describe the clinical, biochemical and radiological findings in 12 mutation-positive family member including the pathological findings of five tumors. **Methods:** Genetic screening of CDKN1B was performed on DNA from whole blood (MiSeq, Illumina, CA, USA) to an average depth of at least 100X. We assessed the family history of the proband and predictive genetic testing of family members. Clinical assessment of mutation positive subjects included physical examination, biochemical evaluation, MRI of cerebrum, CT scans of thorax and abdomen. In addition, we studied "loss-of-heterozygosity" (LOH) of CDKN1B in tumor tissues on DNA extracted from paraffin embedded (FFPE) tumor samples analyzed on OncoScan assay (Affymetrix, CA, USA). **Results:** Genetic screening of the proband identified a novel heterozygous pathogenic frame-shift variant in CDKN1B (c.121_122delTT, p.Leu41Asnfs*83). The mutation segregated with the MEN4 associated diseases in two generations including two branches of the family. All 13 carriers had hypercalcemia (age of debut: 29-69 years), 12 had primary hyperparathyroidism (PHPT). The proband had Mb.Cushing with an ACTH-producing pituitary tumor while three carriers had non-functioning pituitary adenoma, and one had carcinoid tumor in pancreas. Two of five tumors had LOH. **Conclusion:** We present a novel CDKN1B and the clinical phenotypes in, to the best of our knowledge, the largest family of patients with MEN4 reported. There was a high penetrance of asymptomatic hypercalcemia and PHPT, and a high proportion of pituitary adenomas while additional MEN4 associated diseases were less frequent. The present case delineates the knowledge about MEN4.

Disclosures: *Anja Lisbeth Frederiksen, None*

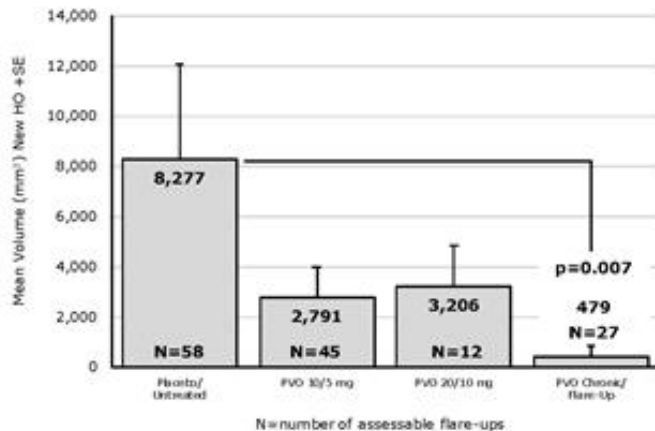
MON-1065

WITHDRAWN

MON-1066

Palovarotene Reduces New Heterotopic Ossification in Fibrodysplasia Ossificans Progressiva (FOP) Frederick S. Kaplan^{*1}, Edward C. Hsiao², Geneviève Baujat³, Richard Keen⁴, Carmen De Cunto⁵, Maja Di Rocco⁶, Matthew A. Brown⁷, Mona M. Al Mukaddam⁸, Donna R. Grogan⁹, Robert J. Pignolo¹⁰. ¹Perelman School of Medicine, The University of Pennsylvania, United States, ²Division of Endocrinology and Metabolism, University of California, San Francisco, United States, ³Groupe Hospitalier Necker Enfants Malades, France, ⁴Royal National Orthopaedic Hospital, Brockley Hill, United Kingdom, ⁵Affiliation Department of Pediatrics/Hospital Italiano de Buenos Aires, Argentina, ⁶Unit of Rare Diseases, Department of Pediatrics, Gaslini Institute, Italy, ⁷Institute of Health and Biomedical Innovation, Queensland University of Technology, Australia, ⁸The University of Pennsylvania, Center for Research in FOP and Related Disorders, United States, ⁹Clementia Pharmaceuticals Inc., United States, ¹⁰Mayo Clinic College Of Medicine, Division of Geriatric Medicine & Gerontology, United States

FOP is a rare, severely disabling disease characterized by episodic flare-ups and accumulation of heterotopic ossification (HO) that leads to restricted movement, physical disability, and early death. This preliminary analysis evaluated the ability of three palovarotene (PVO) dosing regimens to prevent HO following a flare-up using data from two Phase 2 interventional studies and one natural history study (NHS). The volume of new HO was assessed by CT of the flare-up body site at baseline and 12 weeks post-baseline. Regimens included: PVO 10 mg for 2 weeks followed by 5 mg for 4 weeks (10/5 mg [45 flare-ups/27 subjects/ages 9-44yrs]); PVO 20 mg for 4 weeks followed by 10 mg for 8 weeks or longer (20/10 mg [12 flare-ups/10 subjects/7-18yrs]); or chronic PVO 5 mg daily with increased dosing during a flare-up to 20 mg for 4 weeks followed by 10 mg for 8 weeks or longer (chronic/flare-up [27 flare-ups/18 subjects/13-46yrs]). These were compared to a pooled population of placebo-treated (9 flare-ups/9 subjects/9-53yrs) and untreated flare-ups (49 flare-ups/38 subjects/4-39yrs) from the NHS. All flare-ups were assessed using pre-specified imaging procedures by a central imaging laboratory blinded to treatment or study. The average difference in the volume of new HO at Week 12 between the chronic/flare-up regimen and placebo/untreated flare-ups was -7,798 mm³ (95% CI = -17,383 mm³, -1,764 mm³; p=0.007; ANOVA with BCa bootstrap), representing a 94% reduction in new HO (see figure). The adverse event profile was similar across the PVO groups; the majority were mild or moderate mucocutaneous events. Three subjects had four serious adverse events possibly related to treatment. No subject required dose reduction with PVO 10/5 mg. Nine of 28 subjects (32%) who received PVO 20/10 mg for at least one flare-up had at least one dose reduction; the majority (75%) during the 20-mg dose. No subject discontinued the study due to adverse events. These data demonstrated a statistically significant decrease in new HO volume with the chronic/flare-up palovarotene regimen as compared to the placebo/untreated control, and support further evaluation of this regimen in the ongoing Phase 3 MOVE study. Palovarotene was tolerated at the doses administered. Acknowledgments: the authors wish to thank the FOP patient community and the clinical research teams for their participation and support of this study.



Disclosures: **Frederick S. Kaplan, None**

MON-1067

Melorheostosis: a case series of different imaging phenotypes Anupam Kotwal^{*1}, Bart Clarke¹, Jane Matsumoto². ¹Division of Endocrinology, Diabetes, Metabolism, and Nutrition, Mayo Clinic, United States, ²Department of Radiology, Mayo Clinic, United States

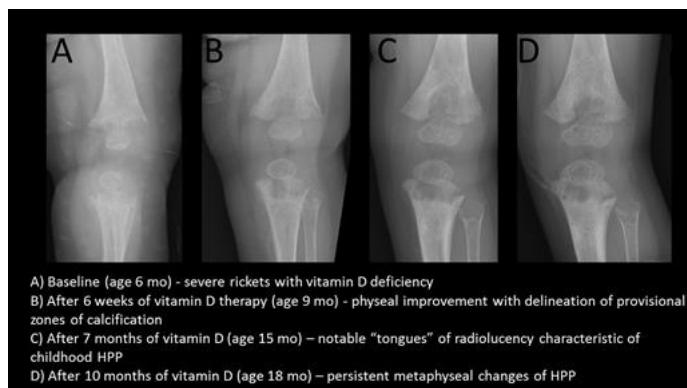
Background: Melorheostosis is a rare sclerosing bone dysplasia that affects both cortical bone and adjacent soft tissue structures in a sclerotomal distribution. The exact etiology remains unknown, with possible causes being somatic LEMD3 mutations, BMP/TGF- β pathway, or non-genetic causes. Histopathology studies have shown increased osteoid formation in a disorganized manner, and increased angiogenesis in the affected bones. Methods: Here we describe 4 cases of melorheostosis with differing radiological features. All the patients presented with pain in the affected area prior to diagnosis. Results: The 1st case is of 43 year old male whose plain radiography showed extensive hyperostosis of the left tibia shaft in the classic "flowing candle wax" pattern of melorheostosis. Bone scan demonstrated multifocal increased uptake in left tibia, left radius and lumbar spine. Management included stripping of the periosteum from the left tibia, intravenous zoledronic acid until he developed ONJ, calcitonin nasal spray, external beam radiation to tibia, but without much improvement in pain over the years. This was managed subsequently with opioids and physical therapy. The 2nd case is of a 39 year old female diagnosed with monostotic classic "flowing candle wax" cortical hyperostosis in an L3-L4 sclerotomal distribution. The 3rd case is of a 56 year old female with melorheostosis since childhood who subsequently developed postmenopausal osteoporosis. Plain radiography showed "osteopathia striata-like" hyperostosis and bone scan showed increased uptake in the left tibia, left fibula and talar dome. She received 6 infusions of zoledronic acid yearly for osteoporosis which also improved pain from melorheostosis. The 4th case is of a 22 year old female, diagnosed to have inactivating LEMD3 mutation and felt to have an overlap syndrome of melorheostosis and osteopoikilosis involving left knee, left foot and ankle. Biochemical bone and mineral parameters were normal. Left lower extremity pain due to syringomyelia was managed with gabapentin. Conclusions: Melorheostosis may present as mixed or atypical osseous involvement as opposed to the classically described "dripping candle wax" appearance of hyperostosis. The morbidity of melorheostosis appears to be mostly due to pain, contractures, limitation of joint motion, limb length discrepancies, and osseous deformities. Multidisciplinary care utilizing medical, surgical and rehabilitative techniques with an individualized approach provides the best outcomes for these patients. In recent years, bisphosphonates have demonstrated reduction in pain. Better characterization of genetic and developmental factors predisposing to this condition may lead to development of targeted therapy for this condition, as well as more commonly encountered skeletal abnormalities.

Disclosures: **Anupam Kotwal, None**

MON-1068

Vitamin D Deficiency Rickets Complicating Severe Childhood Hypophosphatasia: Response to Sequential Therapy with Vitamin D then Asfotase Alfa Elizabeth L. Lin^{*1}, Gary S. Gottesman², William H. Mcalister³, Steven Mumm¹, Michael P. Whyte². ¹Division of Bone and Mineral Diseases, Department of Internal Medicine, Washington University School of Medicine, United States, ²Center for Metabolic Bone Disease and Molecular Research, Shriners Hospital for Children, United States, ³Mallinckrodt Institute of Radiology, Washington University School of Medicine at St. Louis Children's Hospital, United States

Hypophosphatasia (HPP) is an inborn-error-of-metabolism that involves skeletal disease in the perinatal, infantile, severe and mild childhood, and adult forms. HPP is caused by loss-of-function mutation(s) in the ALPL gene that encodes the cell-surface tissue non-specific isoenzyme of alkaline phosphatase (TNSALP). Extracellular accumulation of inorganic pyrophosphate, an inhibitor of mineralization, often leads to rickets or osteomalacia. Severe childhood HPP also features muscle weakness, limb pain, and a waddling gait. Studies of mineral homeostasis show hypophosphatasemia, often hyperphosphatemia, and sometimes mild hypercalcemia with normal or suppressed circulating PTH. A 6-month-old girl presented with failure-to-thrive. Biochemical investigation was notable for 25(OH)D of 8 ng/mL (NI: 30 - 100), calcium 10.1 mg/dL (NI: 8.5 - 10.1), phosphorus 6.4 mg/dl (NI: 2.5 - 4.9), PTH 21 pg/mL (NI 14-72), and serum ALP of 55 U/L (NI: 124-341). She could not roll or sit. Radiographs revealed metaphyseal fraying consistent with rickets. Thus, she started vitamin D 1000 IU p.o. daily. We first evaluated her at age 9 months, after 6 weeks of vitamin D, when she could now roll and sit. There was thoraco-lumbar kyphosis. 25(OH)D was 86 ng/mL, but ALP remained at 55 U/L (NI: 91 - 388). Radiograph review showed marked improvement in her rickets [Figure]. Vitamin D supplementation continued at 600 IU daily. At age 15 months, she started walking. At age 18 months, her kyphosis had resolved yet her waddling gait persisted with a positive Gower's sign. Serum 25(OH)D was 55 ng/mL. Follow-up radiographs now showed "tongues" of radiolucency characteristic of pediatric HPP. Mutation analysis of ALPL revealed biallelic missense mutations. Due to persisting skeletal disease and muscle weakness, she started asfotase alfa enzyme replacement therapy with follow-up planned in 3-months. Thus, our patient highlights the importance of identifying and treating vitamin D deficiency prior to further assessing and managing severe childhood HPP. Sequential treatment with vitamin D resolved the most common type of rickets, and established a baseline for monitoring asfotase alfa therapy.



Disclosures: *Elizabeth L. Lin, None*

MON-1069

Early Diagnosis of Gaucher Disease with Focus in Bone Affection (BIG Project)Argentinian Experience Beatriz Oliveri*¹, Diana Gonzalez², Paula Rozenfeld³, Camilo Lis⁴, Omar Riemersma⁴, Martin Kot⁴. ¹Laboratorio de Osteoporosis y Enfermedades Metabólicas Óseas. Instituto de inmunología, Genética y Metabolismo (INIGEM) CONICET-UBA Hospital de Clínicas., Argentina, ²Mautalen, Salud e Investigación, Argentina, ³IIFP, Universidad Nacional de La Plata, CONICET, Facultad de Ciencias Exactas, Departamento de Ciencias Biológicas, Argentina, ⁴Shire, Argentina

Gaucher disease (GD, OMIM#230800) the most frequent lysosomal disease, is caused by a deficient activity of glucocerebrosidase (GCase) that leads to excessive storage of glucocerebroside in the liver, spleen, bone and bone marrow. The clinical suspicion of GD is traditionally associated to hepato/splenomegaly and cytopenias and available algorithms for the diagnosis are based on those signs and employed more frequently by hemathologists. However bone symptoms have been recognized in 30 % of patients at the time of diagnosis, isolated or associated with other hemathological alterations. Notably, due to a lack of awareness, long diagnostic delays are described leading to serious complications. Early diagnosis and enzyme replacement therapy (ERT) are extremely important for reversing splenomegaly and citopenias, and preventing irreversible skeleton damage. Purpose: to enhance early GD diagnosis in patients whose first manifestations are bone symptoms we designed a program of medical educational meetings in GD and proposed a novel screening algorithm for GD with focus in bone affection. The algorithm was based on the following consulting diseases: 1- osteomyelitis of unknown etiology and Perthes disease in patients below 18 years old (yo) 2- recurrent fragility Fx, bone pain, AVN, hip arthroplasty (of uncertain etiology) in patients below 50 yo. 3-Low bone density (Z score < - 2.0) and bone pain without known causality associated with abnormal ferritin levels and/or platelet count. The first step in the screening is by assaying in dried blood filter paper (DBS). Pathological results must be confirmed by measuring GCase in leukocytes. Results: From April 2017 this project has been presented in 7 hospitals of different argentinian provinces in meetings ad hoc with an overall attendance of 250 physicians with different related specialities and in two Bone Metabolism Meetings (2016 and 2017) (with 300 attendants). Until today 26 samples had been submitted (ages from 1 to 47 y) originated in: bone crisis (n= 8), AVN (n=2), recurrent fractures (n=8), bone pain (n=2), a painful bone lesion (n=1), and visceromegalies or cytopenias (n= 5). DBS was pathological in three patients, and the diagnosis of GD was confirmed in two of them. Conclusion: These results encourage to continue in implementing the educational program designed to improve the awareness in GD facilitating the early diagnoses and treatment to avoid morbidity and complications.

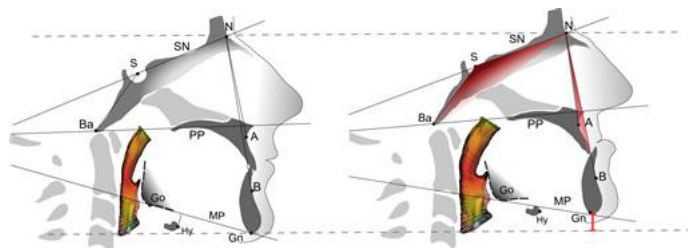
Disclosures: *Beatriz Oliveri, shire, Speakers' Bureau*

MON-1071

Cone-Beam Computed Tomography of Osteogenesis Imperfecta Types III and IV: Three-Dimensional Evaluation of Craniofacial Features and Upper Airways Natalie Reznikov*, Didem Dagdeviren, Faleh Tamimi, Francis Glorieux, Frank Rauch, Jean-Marc Retrouvey. McGill University, Canada

Osteogenesis Imperfecta (OI) is a rare genetic disease of connective tissues resulting in fractures and bone deformities. The more severe forms of OI (OI types III and IV) often affect the craniofacial skeleton but these craniofacial manifestations have not been investigated with three-dimensional (3D) imaging. In the present study, we obtained 3D craniofacial measurements by cone-beam computed tomography (CBCT) in a cohort of 41 individuals (age 11 to 35 years; 28 females) with OI type III (N = 13) or IV (N = 28). Angular and linear craniofacial measurements, facial proportions and airways assessments were compared between the type III and type IV groups, and in relation to reference data for the general population. The results showed that craniofacial deformities varied widely and overlapped between OI type III and IV with regard to most of the measured parameters. Many of the aberrant craniofacial features were associated with an increased cranial base angle. The max-

illa was retrognathic and was a significant contributor to the observed malocclusion. The total face height was significantly reduced due to counter-clockwise rotation of the mandible. Both maxilla and mandible were narrower, and together with an increased bi-temporal width, produced the characteristic triangular face appearance. Face asymmetry was common, and cranial asymmetry was often severe. Craniofacial deformities in OI patients were not associated with reduced patency of the upper airways. In conclusion, a combination of several parameters, in particular cranial base angle, cranial asymmetry and the 3D position of the maxilla and mandible should be used to assess the severity of craniofacial involvement in OI and be collectively considered for treatment planning in neurologic, orthodontic, and otorhinolaryngologic practice.



Disclosures: *Natalie Reznikov, None*

MON-1072

A Novel Case of Human Osteopetrosis Associated with Glanzmann's Thrombasthenia Due to a Homozygous Pathogenic Mutation in ITGB3 Jennifer Sarhis Avigdor*, Gary M Kupfer, Allen Bale, Thomas O Carpenter. Yale University School of Medicine, United States

Osteopetrosis, a sclerotic disorder of bone, is due to mutations in a variety of genes critical for osteoclast differentiation, recruitment, or function. We describe a novel case of osteopetrosis and Glanzmann's thrombasthenia caused by a homozygous pathogenic mutation in ITGB3, encoding a member of the integrin family. Although described in murine models, there are no reported cases of osteopetrosis and Glanzmann's thrombasthenia in humans caused by ITGB3 mutations. A 2-month old infant presented with respiratory failure due to pulmonary hemorrhage and petechiae. MRI suggested a left subdural hematoma, and radiographs identified "bone in bone" appearance of the ulnae and phalanges of the hands and feet. Serum calcium, magnesium, phosphorus, PTH and alkaline phosphatase were normal (see table). Serum 25-OHD level was low, and creatine kinase BB isoenzyme fraction was elevated (6%, nl: 0). Serum CTX was 809 pg/mL (low-normal for this age) and PINP was 1010 ug/dL (high normal for young children). Areal BMD of the lumbar spine (0.252 g/cm²) was >2 SDs above mean for age (Kalkwarf H, JBMR 28:206, 2013). Decreased hemoglobin content, hematocrit and platelet count as well as a prolonged prothrombin time were evident. Whole exome sequencing revealed a homozygous missense mutation of the ITGB3 gene (Asp145Tyr; G->T), which alters the function of the encoded protein (Loftus J, Science 249:915, 1990). α V β 3 integrin, a member of the cell adhesion receptor family, mediates an interaction between osteoclasts and the extracellular bone matrix, allowing for resorption. Integrin α IIb β 3, located on platelet membranes, is critical for clot formation, and mediates platelet adherence to fibrinogen. Defective integrin disrupts osteoclast and platelet function in β 3 knockout mice; mutations in this subunit have not been described in human osteopetrosis (McHugh K, J Clin Invest 105:433, 2000). At age 17 months the patient is healthy with intact hearing and vision, although has been hospitalized twice for observation of bleeding incidents. Platelet count has normalized since initial presentation. Computed tomography scanning performed at 6-month intervals has shown normal caliber of the optic foramina and persistent, but mild diffuse sclerosis of the skull base. Bone marrow aspirate is normal. Continued monitoring will be important in order to establish the long-term course of this novel form of osteopetrosis, which appears to present with a relatively mild phenotype in infancy.

	Patient	Reference Range
Calcium (mg/dl)	10.4	8.8-10.2
Magnesium (mg/dl)	1.9	1.7-2.6
Phosphorus (mg/dl)	5.6	3.0-7.5
PTH (pg/ml)	23	10-69
Alkaline Phosphatase (U/L)	197	80-380
25-OHD (ng/ml)	19	20-50
CK-BB (%)	6	0
CTX (pg/ml)	809	500-3,000
P1NP (ug/dl)	1010	277-824
Hemoglobin (g/dl)	7.1	13-20
Hematocrit (%)	20.9	37-60
Platelet (x1000 U/L)	96	140-165
PT (seconds)	12.4	10.1-12.1

Disclosures: *Jennifer Sarhis Avigdor, None*

MON-1073

Complications in patients with autosomal dominant hypocalcemia compared with non-surgical hypoparathyroidism Line Underbjerg*¹, Tanja Sikjaer¹, Lars Rejnmark². ¹MD, PhD, Denmark, ²Professor, senior consultant, Denmark

Only few data are available on biochemical markers and complications in terms of cardiovascular findings, bone indices and quality of life (QoL) in autosomal dominant hypocalcemia (ADH). We aimed to assess the biochemistry and complications in patients with genetically verified ADH (N=20) compared to age- and gender-matched patients with non-surgical hypoparathyroidism (Ns-HypoPT) (N=20). Patients had an average age of 44 years (75% females). Significantly fewer patients with ADH received treatment with alfacalcidol (p=0.04), however daily doses of calcium supplements did not differ between groups (p=0.16). Biochemical findings showed no difference in levels of ionized calcium, phosphate, magnesium or creatinine (p>0.05). Prevalence of renal impairment did not differ between groups with none having a GFR<30 mL/min. TSH levels were lower in patients with ADH (p=0.03), even though no differences were seen in the number of thyroid hormone supplement users (p=0.61). Renal calcium excretion did not differ between groups, and no correlations were seen between urinary calcium (mmol/24h) and total daily calcium intake. Cardiovascular findings, showed no difference in ambulatory or 24-hour blood pressure measurements. Assessing arterial stiffness in terms of pulse wave velocity (PWV) showed no difference between group in crude analyses, however, after adjustment for mean arterial pressure, BMI, age and gender, patients with ADH had a significantly higher PWV compared with Ns-HypoPT (p<0.01). Bone indices showed no difference in Z-scores as measured by DXA. Using QCT-scans, patients with ADH had a lower cortical vBMD at the total hip (p=0.04) and at the trochanter (p=0.02). No differences were seen in cortical parameters using HRpQCT. QoL was measured using SF-36v5 and WHO-5 Well-Being Index, showed a similar QoL between groups. In conclusion, for most of studied indices, patients with ADH did not differ from patients with Ns-HypoPT, including urinary calcium which wasn't increased in ADH compared with Ns-HypoPT. However, ADH was associated with an increased arterial stiffness and a lower vBMD. Further studies should aim to investigate whether ADH is associated with increased risk of fractures and cardiovascular diseases.

Disclosures: *Line Underbjerg, None*

MON-1074

Identification and Molecular Analysis of a Potential Disease-causing Mutation in ZMAT2 in Congenital Radioulnar Synostosis Takako Suzuki*¹, Yukio Nakamura¹, Tatsuya Kobayashi², Hiroyuki Kato¹. ¹Shinshu University School of Medicine, Japan, ²Endocrine Unit, Massachusetts General Hospital and Harvard Medical School, United States

Background: Congenital radioulnar synostosis (RUS) is a skeletal disorder resulting in fusion of the radius and ulna. Since the etiology of RUS is largely unknown, treatment options are limited. Elucidation of pathophysiology of RUS is needed for development of better treatment. Methods: We collected DNA samples of 10 trios (an affected patient and his or her biological parents) and performed whole exome-sequencing (WES). We identified mutations in several candidate genes including the zinc finger matrin-type 2 gene (ZMAT2) in a patient. The WES identified the following potential disease-causing de novo heterozygous missense mutation in a patient; human hg19 chr5:g.140084124T>A, c.424T>A, p.

F142I. The patient was born in the year 2000 and had bilateral RUS. His left and right arms were surgically treated at the ages of 5 and 6, respectively. Results: To date, there has been no report of mutations in the ZMAT2 gene that is evolutionarily conserved. The homology of ZMAT2 at the amino acid level is 100% between humans and mice, and 91% between humans and zebrafish. We first cloned the human and zebrafish orthologs of ZMAT2 cDNA and introduced the potential allelic mutation. We performed whole-mount in situ hybridization (ISH) in zebrafish. ISH showed specific expression of ZMAT2 in pectoral fins, which correspond to human upper limbs, and in craniofacial regions. ZMAT2 knockdown in zebrafish caused defects in pectoral fins and dorso-ventral patterning, which are likely caused by inhibitory effects of bone morphogenetic protein (BMP) action. These abnormalities were partially rescued by bmp2b RNA overexpression. In addition, the skeletal defects caused by ZMAT2 knockdown was rescued by simultaneous overexpression of ZMAT2, whereas the mutant ZMAT2 overexpression did not rescue the dorso-ventral patterning defect. Furthermore, ZMAT2 inhibited Bmp2 signaling as demonstrated by the downregulation of alkaline phosphatase activities in mouse C3H/10T1/2 cells treated with Bmp2. These findings suggest that ZMAT2 regulates skeletal development via BMP signaling. Importantly, we demonstrate that the ZMAT2 mutation, associated with RUS, leads to a loss or reduction of its biological activity in zebrafish. Conclusion: We identified ZMAT2 of which mutation potentially plays a causal role in RUS through deregulation of BMP signaling. Our zebrafish studies will provide insights into the mechanism by which ZMAT2 regulates limb and fin patterning in vertebrates.

Disclosures: *Takako Suzuki, None*

MON-1075

Follow-up After Discontinuation of Bisphosphonate Treatment in Osteogenesis Imperfecta When Skeletal Maturity is Complete Pamela Trejo*¹, Telma Palomo², Francis Glorieux², Frank Rauch². ¹Clinica Alemana Santiago, Chile, ²Shriners Hospital for Children Canada, Canada

Little is known about the follow up in osteogenesis imperfecta (OI) during adulthood. We performed a retrospective chart review of patients with OI caused by an identified collagen mutation, who received bisphosphonate treatment for at least 2 years while growing until they reached final height, and had at least 2 years of follow up after treatment discontinuation. Fifty-five patients were identified, (26 males); 30 had a mutation in COL1A1, and 25 in COL1A2; 19 were classified as OI type I, 12 as OI type III and 24 as OI type IV. We found that the number of long bone fractures decreased from a mean of 0.7 (SD 1.1; range 0 to 6) in the last two years of treatment, to a mean of 0.3 (SD 0.8; range 0 to 4) in the last two years of follow up, p = 0.01. Vertebral deformities were evaluated in 32 patients with available x-rays of the spine at the time they stopped bisphosphonate treatment and at the last follow up, with a median time in between x-rays of 3.0 years (range 0.8 - 13.9), the percentage of compressed vertebrae went from 7.1% (range 0.0% to 92.9%) to 3.6% (range 0.0% to 90.9%; p = 0.938), the severity of fractures (spine deformity index) remained stable at a median of 0.1 (ranges 0.0 to 1.9 and 0.0 to 1.8; p = 0.493). In a subgroup of 31 individuals with BMD measurements at discontinuing treatment and after 2 and 5 years, areal BMD at the lumbar spine remained stable from 0.791 g/cm² (SD 0.094) to 0.813 g/cm² (SD 0.102) after two years and 0.814 g/cm² (SD 0.090) after five years (p = 0.188). But a decrease in the lumbar spine areal BMD z score was observed from -1.8 (SD 1.1) to -2.0 (SD 1.1) at 2 years and -2.2 (SD 0.9) at 5 years, p = 0.028. Trabecular density at the distal radius (4% site) remained without significant changes from 188.2 mg/cm³ (SD 103.0), to 164.1 mg/cm³ (SD 77.9) and 168.7 mg/cm³ (SD 97.2) at 2 and 5 years respectively, p = 0.468. Cortical density at the proximal radius (65% site) increased from 1,133.0 mg/cm³ (SD 69.8) to 1,162.3 mg/cm³ (SD 58.2) at 2 years and 1,172.5 mg/cm³ (SD 45.9) at 5 years, p < 0.01. In conclusion in patients with OI after discontinuation of bisphosphonate treatment lumbar spine BMD and trabecular BMD remained stable, and cortical BMD increased after 2 and 5 years, which correlated with a decrease in long bone fractures and stability of spine deformities. However, the decrease in lumbar spine BMD z scores should continue to be monitored regularly in such patients in case re-treatment would be considered.

Disclosures: *Pamela Trejo, None*

MON-1076

Lifelong Hyperphosphatasemia Without Low Plasma Pyridoxal 5'-Phosphate In A Healthy Boy With Uniquely Aberrant Bone Alkaline Phosphatase Yet Normal ALPL Gene Structure Michael P. Whyte*¹, Nina S. Ma², Gary S. Gottesman¹, Pamela S. Smith³, Vinieth N. Bijanki¹, Steven Mumm⁴, Per Magnusson⁵. ¹Center for Metabolic Bone Disease and Molecular Research, Shriners Hospital for Children, United States, ²Division of Endocrinology, Boston Children's Hospital, United States, ³Division of Pediatric Endocrinology and Diabetes, Washington University School of Medicine, United States, ⁴Division of Bone and Mineral Diseases, Department of Internal Medicine, Washington University School of Medicine at Barnes-Jewish Hospital, United States, ⁵Department of Clinical Chemistry, Linköping University, Sweden

Alkaline phosphatase (ALP) refers to a family of homodimeric phosphohydrolases routinely assayed in the clinical and research laboratory using non-physiological conditions, including alkaline pH. In humans, three genes encode tissue-specific ALPs, whereas a fourth (ALPL) encodes the tissue non-specific ALP isoenzyme (TNSALP) expressed richly in bone

and liver. TNSALP has five putative N-linked glycosylation sites, and post-translational modifications account for the different physicochemical properties among the TNSALPs. In health, the skeleton liberates three bone ALP (BAP) isoforms into the circulation (B1, B1, and B2), and a fourth BAP isoform (B1x) can circulate in chronic kidney disease. We report an extensively studied 7-year-old healthy boy with lifelong enigmatic hyperphosphatasemia (recent ALP activity 1088 U/L, reference interval 196-449 U/L) featuring serum BAP elevated 2- to 3-fold the upper reference limit in both the routine MicroVue™ and Ostase® assays. Renal function and skeletal assessments were unremarkable except for elevated PINP and CTX. Our HPLC, electrophoretic, heat inactivation, inhibition, and polyethylene glycol precipitation findings confirmed high circulating levels of all three BAP isoforms, but no macro-ALP in his blood. His BAP profile on HPLC was different compared with other high circulating BAP conditions (e.g., Paget's bone disease, skeletal metastases, chronic kidney disease). Most remarkably, B1 had ~23-fold higher activity compared to healthy age-matched children. Despite his marked hyperphosphatasemia, plasma pyridoxal 5'-phosphate (PLP), a natural substrate for TNSALP, was not decreased, suggesting compromised catalytic activity of his BAP endogenously. In both non-consanguineous parents, total ALP was normal but BAP was twice the upper limit of normal in the commercial assays, suggesting a genetic disorder, yet ALPL sequencing of the patient was negative. In the inborn error hypophosphatasia (HPP), circulating TNSALP activity including BAP is decreased, and plasma PLP is consequently elevated. In extremely rare "pseudo-HPP" featuring severe rickets, circulating TNSALP activity is normal or increased but plasma PLP is elevated. Both HPP and pseudo-HPP involve ALPL mutations that directly impair TNSALP activity endogenously. Our patient, lacking an ALPL mutation, perhaps has a defect of a gene involved in post-translational modification of TNSALP, and could be considered the first example of "pseudo-pseudo-HPP".

Disclosures: **Michael P. Whyte**, None

MON-1105

Controlling Periodontitis Prevents Medication-related Osteonecrosis of the Jaw-like Lesions in Rice Rats (*Oryzomys palustris*) Evelyn Castillo*¹, Abel Abraham¹, Jessica Jiron¹, Jonathan Messer¹, Joshua Yarrow², Donald Kimmel¹, Jose Aguirre¹. ¹University of Florida, United States, ²Malcolm Randall VAMC; University of Florida, United States

Medication-related osteonecrosis of the jaw (MRONJ) is a potentially serious adverse event seen in patients taking powerful anti-resorptive (pAR) agents. Multiple recent pre-clinical experiments indicate that combined local factors [e.g., periodontitis (PD)] and systemic factors (e.g., pARs, etc.) are required to cause MRONJ. Although various means have been proposed to minimize risk of MRONJ in pAR patients, few prospective preclinical studies have focused on this issue. Rice rats (*Oryzomys palustris*) consuming standard (STD) rat chow develop a high prevalence of spontaneous maxillary (Mx) localized PD lesions characterized by food impaction. These lesions appear to evolve into MRONJ when these rats are also treated with a pAR (e.g., zoledronic acid [ZOL]). We hypothesize that preventing localized PD lesions by feeding rats a diet free of insoluble fiber, or controlling PD lesions with periodic mechanical cleaning will reduce MRONJ. 4-wk old rats were randomized into five groups (N=15) that received: 1) STD+vehicle (VEH; saline IV q4wks); 2) STD+ZOL (80µg/kg IV q4wks); 3) high soluble fiber (HSF) diet (7.5% inulin and 10% fructo-oligosaccharides to replace insoluble fiber)+VEH; 4) HSF+ZOL; and 5) STD+ZOL+biweekly mechanical cleaning (STD+ZOL+CL). Biweekly oral exams were conducted between ages 4-22 weeks with binocular loupes (4X). At each exam, oral condition was scored using an integral 0-4 severity scale (0=normal; 4=marked gingival recession with exposed bone [MRONJ-like lesion]). Any impacted materials were removed with a #23 dental explorer in STD+ZOL+CL rats. At the end of study, rats were euthanized, high resolution photographs of the four jaw quadrants were obtained and graded 0-4. Oral tissues were processed for MicroCT and histopathologic assessment. 40% of STD+VEH rats developed low severity focal PD lesions (1-1.5), but there were no PD lesions in any HSF+VEH rats. 25% of STD+ZOL rats had high severity (3-4. MRONJ-like) lesions. In contrast, no HSF+ZOL or STD+ZOL+CL rats developed MRONJ. In vivo oral exam data concurred with the post mortem oral analyses. Our ongoing data suggest that controlling the initiation or progression of focal PD by diet or periodic mechanical cleaning prevents development of MRONJ in rats treated with ZOL. The HSF diet is a practical method to prevent PD in rice rats. The cleaning data provide direct evidence to support current guidelines concerning maintenance of good oral hygiene in pAR patients.

Disclosures: **Evelyn Castillo**, None

MON-1106

Pyrophosphate regulators, ANK and ENPP1, regulate cementogenesis and extracellular matrix protein expression Emily Chu*¹, Atsuhiko Nagasaki¹, Michael Chavez², Daniel Leigh¹, Tammy Vo¹, Alyssa Coulter¹, Vivek Thumbigere-Math³, Demetrios Braddock⁴, Martha Somerman¹, Brian Foster². ¹NIAMS/NIH, United States, ²College of Dentistry, The Ohio State University, United States, ³University of Maryland School of Dentistry, United States, ⁴Yale School of Medicine, United States

Purpose: Regulation of pyrophosphate (PPi), a mineralization inhibitor, is critical for development of bones and teeth. Progressive ankylosis protein (ANK) and ectonucleotide

pyrophosphatase/phosphodiesterase-1 (ENPP1) increase PPi levels; ANK or ENPP1 loss results in ectopic calcifications and a striking hypercementosis phenotype in humans and mice. ENPP1 mutations are associated with generalized arterial calcification of infancy (GACI). Crosstalk between PPi regulators and SIBLING (small integrin-binding ligand- N-linked glycoprotein) members, e.g. osteopontin (OPN), dentin matrix protein (DMP1) has been proposed, however, specific mechanisms remain elusive. We propose that ANK and ENPP1 have critical, non-redundant roles in modulating PPi via different signaling pathways and downstream genes/proteins. Methods: Exfoliated primary teeth from individuals with GACI were analyzed by micro-computed tomography (microCT) and histology. Mandibles from wild-type (WT), Ank, Enpp1, and double knockout mice (dKO) were evaluated by microCT, histology, immunohistochemistry (IHC), tartrate resistant acid phosphatase (TRAP), and qPCR. Efficacy of an Enpp1-fusion protein (ENPP1-Fc) was assessed in Enpp1 KO mice. Results: GACI individuals demonstrated hypercementosis similar to Enpp1 KO mice (4 fold higher versus controls). Compared to WTs, with higher values in dKOs, increased acellular cementum width/volume (3-5 fold) were found in 60dpn Ank, Enpp1 KOs and dKOs. Ank KO cellular cementum volume was 30% higher compared to WTs. dKOs exhibited a 10% increase in cementum mineral density versus WTs and morphological characteristics of both single KOs. TRAP staining showed a trend toward increased osteoclast numbers in KOs and dKOs, and dKOs featured a further 15% decrease in alveolar bone volume compared to WTs. Distinct differences in gene/protein expression within periodontium of Ank, Enpp1 KOs and dKOs were detected, including 3-5 fold Spp1/OPN and Dmp1/DMP1 increases in Enpp1 KOs and dKOs absent in Ank KOs. Hypercementosis was attenuated in Enpp1 KO mice injected with ENPP1-Fc. Conclusions: Hypercementosis in GACI individuals validates clinical relevance of PPi regulators in dentoalveolar tissues. In alveolar bone and cementum, ANK and ENPP1 appear to have additive roles, possibly involving SIBLING regulation. Systemic ENPP1 manipulation altered cementum apposition, suggesting that factors decreasing local PPi levels are potential targets for periodontal therapies.

Disclosures: **Emily Chu**, None

MON-1107

Health Burden of Hypophosphatasia in Adults: Results from a Self-Reported Study in the United Kingdom Sara Jenkins-Jones*¹, Laura Scott¹, Robert Desborough², Ioannis Tomazos³, Richard Eastell². ¹Global Epidemiology and Medical Statistics, Pharmatelligence, United Kingdom, ²University of Sheffield, United Kingdom, ³Alexion Pharmaceuticals, Inc., United States

Background: Hypophosphatasia (HPP) is a rare, systemic, metabolic disease characterized by poor skeletal mineralization, muscular weakness and ambulatory difficulties due to tissue-nonspecific alkaline phosphatase deficiency. Diagnosis of adults with HPP is challenging owing to broad manifestations, which can result in delayed diagnosis, misdiagnosis and inappropriate treatment. To evaluate the disease burden, we interviewed adults with HPP who visited a metabolic bone clinic in Sheffield, UK. Methods: In semi-structured, face-to-face interviews carried out by a specialist registrar between December 2016 and December 2017, in total, 28 consenting adults with HPP were asked to report their experience of HPP, including history of symptoms and healthcare resources used. Results: Of the 28 patients, 18 (64%) were female. Twenty-seven patients reported age at occurrence of their first HPP symptom: two (7%) experienced initial symptoms between 0-7 years of age, five (19%) between 8-18 years, 15 (56%) between 19-40 years and five (19%) between 41-70 years. Mean (median, interquartile range [IQR]) age at initial symptom presentation was 31.8 (32.5, 19.3-40.0) years. All patients reported being diagnosed between 19-40 years of age (n=12, 43%) or 41-70 years (n=16, 57%). Mean (median, IQR) age at diagnosis was 43.8 (44.0, 36.5-51.3) years. Mean (median, IQR) delay in diagnosis was 13.4 (10.0, 1.0-20.0) years. The main initial clinical symptoms reported by patients were musculoskeletal (MSK) conditions or pain (n=11, 39%), dental problems (n=7, 25%) and fractures (n=8, 29%). Patients reported experiencing the following over the course of their disease: MSK pain (n=20, 71%), weakness (n=9, 32%), dental problems (n=12, 43%) and mobility difficulties (n=7, 25%). Twenty patients (71%) reported ≥ 1 fracture and 14 patients (50%) reported mental health problems (with 10 patients [36%] reporting symptoms of depression). Before HPP diagnosis, patients reported multiple (mean 15.3, median 8.0, IQR 3.8-19.5) outpatient contacts with different secondary care specialties, mainly radiology (82%), accident and emergency (46%) and metabolic bone clinics (46%). Mean (median, IQR) number of diagnostic tests reported was 6.9 (6.0, 4.0-8.5). Conclusion: Although our findings may be affected by incomplete recall, these data suggest a substantial delay in diagnosis for adults with HPP, even though their clinical history conveys high disease burden and healthcare resource use.

Disclosures: **Sara Jenkins-Jones**, Alexion Pharmaceuticals, Inc, Other Financial or Material Support

MON-1108

Activation of the RANKL/OPG pathway is central to the pathophysiology of fibrous dysplasia and is associated with disease burden and pain

Luis Fernandez De Castro Diaz^{*1}, Andrea B Burke¹, Howard Wang¹, Pablo Florenzano¹, Jeffrey Tsai², Kristen Pan¹, Bhattacharyya Nisan¹, Alison M Boyce¹, Rachel I Gafni¹, Alfredo Molinolo³, Pamela G Robey², Michael Collins². ¹Section on Skeletal Disorders and Mineral Homeostasis, National Institute of Dental and Craniofacial Research, National Institutes of Health, United States, ²National Institutes of Health, United States, ³University of California, San Diego, United States

Fibrous dysplasia of bone (FD) is a debilitating, often painful, mosaic disease caused by mutations of GNAS. The constitutive activation of the GNAS transcript, *Gas*, leads to an uncontrolled proliferation of bone marrow stromal cells (BMSCs), generating fibrotic tissue and abnormal immature bone that replaces marrow-resident hematopoietic cells and adipocytes. Increased FD BMSC RANKL expression has been previously demonstrated, suggesting a role for FD BMSCs in mediating lesion expansion. Treatment with denosumab, a RANKL neutralizing antibody, has been shown to decrease FD-associated pain. However, activation of the RANKL/OPG pathway is not fully characterized in FD. Methods: Serum levels of RANKL, OPG and inactive RANKL-OPG complexes in FD patients and healthy volunteers (HVs) were measured. Skeletal burden score (a validated measure of FD burden), and the presence or absence of pain was determined at the time of blood collection. FD tissue sections were assessed by immunohistochemistry for RANK, RANKL, and Ki67. BMSCs from FD lesions and HVs were cultured, and media levels of secreted RANKL and OPG were measured. FD-induced osteoclastogenesis was assessed by co-culturing FD and HV BMSCs with HV peripheral monocytes. Results: FD patients showed a 30-fold increase in serum RANKL compared to HVs, however there were no differences in OPG levels between the 2 groups. The serum RANKL/OPG ratio was 20-fold higher in FD patients than in HVs, however no differences in levels of serum RANKL-OPG complex were observed. RANKL, OPG and the RANKL/OPG ratio were positively correlated with skeletal disease burden. Serum levels of OPG, but not RANKL, were higher in patients reporting bone pain ($p=0.053$), resulting in a lower RANKL/OPG ratio in these patients. FD tissue showed RANKL+ Ki67+ fibroblastic cells co-localized to RANK+ multinucleated giant cells. RANKL levels were high in media from FD BMSC cultures, and undetectable in HV cultures. Less OPG was detected in FD BMSC cultures than in HV cultures. FD, but not HV BMSCs, induced cell fusion when co-cultured with peripheral monocytes. Conclusions: These data are consistent with the role of RANKL as a driver in FD-induced osteoclastogenesis. OPG serum levels correlate with FD burden, but on average are similar between FD and HV sera, and lower in FD BMSC cultures.

Disclosures: Luis Fernandez De Castro Diaz, None

MON-1109

When bone collagen cross-linking fails: how abnormal collagen post-translational chemistry and cross-linking causes bone fragility in Bruck syndrome caused by PLOD2 mutations. Charlotte Gistelinc^{*}, Maryann Weis, Jyoti Rai, Peter H. Byers, David R. Eyre. University of Washington, United States

Bruck syndrome (BS) is a congenital disorder characterized by joint flexion contractures, skeletal dysplasia and increased bone fragility, showing strong clinical overlap with Osteogenesis Imperfecta (OI). On a genetic level, BS is caused by biallelic mutations in either the FKBP10 or the PLOD2 gene. PLOD2 encodes the lysyl hydroxylase 2 (LH2) enzyme which is responsible for the hydroxylation of lysyl residues in fibrillar collagen telopeptides. This modification is essential for allowing collagens to form stable intermolecular cross-links in the extracellular-matrix. Bone collagen has a unique pattern of cross-linking that is required for bone strength, resistance to microdamage and crack propagation and also a normal ordered pattern of mineral nanocrystals in the collagen fibrils. To date, no direct studies of human bone from BS caused by PLOD2 mutations have been reported. We present here results from a case of BS in a 4-year-old Caucasian patient, caused by compound heterozygous mutations in PLOD2. Bone tissue was collected during surgery, and bone collagen was biochemically characterized using SDS-PAGE, cross-link analysis and peptide mass-spectrometry. The patient's bone showed diminished hydroxylation of type I collagen telopeptide lysines, while hydroxylation at helical sites was unaltered. Consequently, mature trivalent cross-links, which depend on the presence of telopeptide hydroxylysines, were shown to be greatly reduced. Mass-spectrometry identified abundant allysine aldol dimeric cross-links in the patient's bone, which are not normally present in bone but are a feature skin collagen. SDS-PAGE further illustrated a skin-like migration pattern of the patient's extracted bone collagen, with more prevalent b-dimers and g-trimers. Type II collagen cross-linked peptides from the patient's urine were also analyzed. In contrast to bone type I collagen, the results showed a normal telopeptide lysine hydroxylation of cartilage type II collagen. Taken together these findings shed light on the complex mechanisms that control the unique posttranslational chemistry and cross-linking of bone collagen, and that when defective can cause a brittle bone disorder.

Disclosures: Charlotte Gistelinc, None

MON-1110

Inhibition of tyrosine kinase receptor C-ROS-1 as a novel treatment for patients with TWIST haploinsufficiency induced craniosynostosis

Esther Camp^{*1}, Peter Anderson², Andrew Zannettino³, Stan Gronthos¹. ¹Mesenchymal Stem Cell Laboratory, Adelaide Medical School, Faculty of Health and Medical Sciences, The University of Adelaide, Australia, ²Australian Craniofacial Unit Women's & Children's Hospital, Australia, ³Myeloma Research Laboratory, Adelaide Medical School, Faculty of Health and Medical Sciences, The University of Adelaide, Australia

The *c-ros-oncogene 1* (C-ROS-1) gene encodes a receptor, which belongs to the sevenless subfamily of tyrosine kinase insulin receptors and is conserved among vertebrates [1,2]. We have, for the first time, identified C-ROS-1 expression in human bone marrow derived mesenchymal stem cells (BMSC) and cranial bone cells. Knock-down of C-ROS-1 in human BMSC and cranial bone cells resulted in a decreased capacity for osteogenic differentiation in vitro [3]. Expression of C-ROS-1 is upregulated during osteogenic differentiation, but is suppressed by the basic helix loop helix transcription factor, Twist-1 (TWIST) [3]. TWIST is important in skeletal and cranial development, where Twist-1 mutant heterozygote mice display abnormal craniofacial and skeletal structures. These abnormalities are replicated in a human childhood disorder known as Saethre-Chotzen syndrome (SCS) which is caused by a mutation in the TWIST gene. In both mice and humans, Twist-1 haploinsufficient results in the premature bony bridging between apposed skull plates in the cranium due to excessive intramembranous and endochondral ossification, leading to craniosynostosis. TWIST haploinsufficient human and mouse cranial bone cells express higher levels of C-ROS-1 when compared to wild type cells. Knock-down of C-ROS-1 transcript using siRNA, or inhibition of C-ROS-1 function using the drug Crizotinib in Twist-1 haploinsufficient cranial cells resulted in a decreased capacity for osteogenic differentiation. Furthermore, treatment of Twist-1 mouse cranial bone explants cultures with Crizotinib induced a decrease in mineral deposition compared to untreated cranial explants. We have identified C-ROS-1 as a possible novel target in the treatment of SCS. Currently, the only treatment option available is major invasive cranial surgery. This procedure is potentially life-threatening and traumatic for the children and their families, requiring substantial hospitalization and resources. The development of new approaches with therapeutic agents to prevent or minimize fusion could have a profound impact on an affected child's management resulting in reduced cranial surgery. References: [1]. Chen, J.M, et al., *Oncogene*. 6: 257-64, 1991. [2]. Acquaviva, J., R, et al., *Biochim Biophys Acta*. 1795 : 37-52, 2009. [3]. Camp E., et al. *Bone* 2017.

Disclosures: Esther Camp, None

MON-1111

Identifying Molecular Pathways in Autosomal Recessive Hypophosphatemic Rickets Type 2 (ARHR2) by Mapping Genetic Changes Associated with ENPP1 Loss of Function

Nathan Maulding^{*1}, Kristin Zimmerman², Dillon Kavanagh², Mark Horowitz², Thomas Carpenter², Demetrios Braddock². ¹Yale University, United States, ²Yale, United States

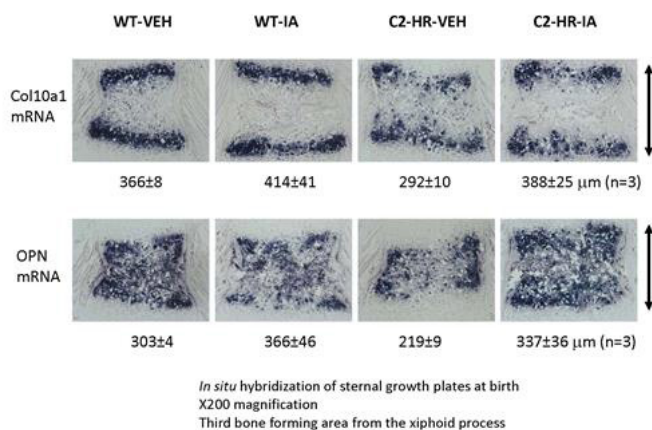
Humans with homozygous loss of function (LOF) mutations in ENPP1 develop Autosomal Recessive Hypophosphatemic Rickets Type 2 (ARHR2), a rare disease clinically indistinguishable from X-linked Hypophosphatemia (XLH), a hypophosphatemic rickets induced by mutations in the neutral endopeptidase PHEX. Characteristic findings in both humans with PHEX and ENPP1 mutations include elevated FGF23, hypophosphatemia secondary to increased urinary phosphate loss, and rickets. Impaired growth, fractures of the long bones, and skeletal deformities occur in both ARHR2 and XLH. The histologic hallmark of both human conditions is osteomalacia responsive to phosphate replacement therapy. In contrast, while mice with PHEX mutations closely parallel the human phenotype, mice with ENPP1 mutations primarily demonstrate low bone mineral density and increased bone fragility more characteristic of an osteopenic phenotype. To map genetic pathways associated with ENPP1 LOF, we performed RNAseq and qPCR in liver, kidney and cortical bone from lower limbs of 10 and 23 wk old ENPP1^{asj/asj} mice, which are characterized by an inactivating mutation near the enzymatic active site. Genetic changes were correlated with uCT and biomechanical parameters. The expression of the Wnt signaling components LRP6 (-2.2 fold, $P=0.021$), Wnt5a (-2.8 fold, $P=0.044$), and β -catenin (-2.3 fold, $P=0.0069$) are decreased in the bones of ENPP1^{asj/asj} mice, while expression of two inhibitors of Wnt signaling – SFRP1, a soluble decoy produced in liver (+2.1 fold, $P=0.037$) and WIF1, a soluble decoy produced in kidney (+11.7 fold, $P=0.0173$) – are both increased. Bone expression of osteoblastic markers (osteocalcin, osterix, and bone sialoprotein) were decreased in ENPP1^{asj/asj} mice (-2.5 to -1.8 fold, $P<0.02$). Finally, genetic evidence of increased bone resorption via decreased OPG in bone (-3.3 fold, $P=0.0067$) is also present in ENPP1^{asj/asj} mice. uCT and biomechanical findings in ENPP1^{asj/asj} mice demonstrated decreased cortical and trabecular bone mineral density and increased bone fragility. The constellation of findings suggests that ENPP1 LOF uncouples bone turnover via downregulating anabolic Wnt pathway activation while promoting bone resorption by increasing osteoclastic activity through decreased OPG. The pathways associated with ENPP1 LOF suggest mechanisms of osteopenia induced by ENPP1 loss and demonstrates ENPP1's role in balancing bone formation and resorption to maintain bone mineral density.

Disclosures: Nathan Maulding, None

MON-1112

Continuous infusion of PTHrP(7-36) Inverse Agonist Ameliorates the Delay in Endochondral Bone Formation in a Mouse Model of Jansen's Metaphyseal Chondrodysplasia Shigeki Nishimori*¹, Hiroshi Noda¹, Ernestina Schipani², Jun Guo¹, Thomas Gardella¹, Harald Jueppner¹. ¹Massachusetts General Hospital, United States, ²University of Michigan, United States

Background: Jansen's metaphyseal chondrodysplasia (JMC) is a rare genetic disease caused by heterozygous activating mutations in the parathyroid hormone receptor-1 (PTHr1). The mutations cause a delay in endochondral bone formation, which leads to short stature and limb deformities. Currently, there is no effective treatment option. PTH(7-34) and PTHrP(7-36) analogs containing a D-tryptophan-12 substitution function as inverse agonists at mutant PTHr1s of JMC, such as PTHr1-H223R, and thus suppress their basal signaling activities in cell-based cAMP assays. Furthermore, transgenic mice expressing the H223R mutation under control of the Col2-promoter (C2-HR mice: Schipani, PNAS 1997) show delayed hypertrophic differentiation of growth plate chondrocytes. Here, we report the effects of a PTHrP-based inverse agonist (IA) in this mouse model of JMC. **Methods:** Heterozygous C2-HR males were mated with WT females. From day 6 of pregnancy, these females were infused with either IA or vehicle via Alzet mini pump at 0.25 mL/hour (0.4 nmol of IA/hour). The pups were sacrificed at birth for analyses. Residual IA in the pumps exhibited the same potency as the initial peptide, as determined by cAMP bioassay using HEK293/GloSensor/PTHr1-H223R stable cells, confirming peptide stability. **Results:** Body weight, long bone length and long bone growth plates were not different between WT and C2-HR pups, either treated with IA or vehicle (WT: veh. and IA, n=6; C2-HR: veh., n=7; IA, n=4). Sternal growth plates of C2-HR mice exhibited the previously observed delay in endochondral bone formation. The distance between the two areas expressing Col10a1 was significantly reduced in C2-HR pups compared to WT pups (292±10 vs. 366±8 µm; p=0.001). The length of the areas expressing osteopontin was significantly shorter in C2-HR pups than in WT pups (219±9 vs. 303±4 µm; p=0.0006). Treatment with IA significantly expanded the areas of Col10a1 expression in C2-HR pups (292±10 vs. 388±25 µm; p=0.001), but not in WT pups (366±8 vs. 414±41 µm; p=0.08). Furthermore, IA treatment increased the area of osteopontin expression in C2-HR (219±9 vs. 337±36 µm; p=0.01), but not in WT pups (303±4 vs. 366±46 µm; p=0.15). **Conclusion:** Our studies suggest that a PTHrP(7-36)-based inverse agonist can access the growth plates and at least partially reverse the delay in endochondral bone formation that is caused by the constitutively active PTHr1-H223R allele of JMC.



Disclosures: Shigeki Nishimori, None

MON-1113

X-Linked Hypophosphatemia: PHEX 3'UTR c.*231A>G Causes a Uniquely Mild Phenotype Including Three Large American Kindreds (A Retrospective, Case-Control Study) Pamela S. Smith*¹, Gary S. Gottesman², Fan Zhang², William H. Mcalister³, Fiona Cook⁴, Valerie Wollberg², Margaret Huskey⁵, Steven Mumm⁵, Michael P. Whyte². ¹Division of Pediatric Endocrinology and Diabetes, Washington University School of Medicine, United States, ²Center for Metabolic Bone Disease and Molecular Research, Shriners Hospital for Children, United States, ³Mallinckrodt Institute of Radiology, Washington University School of Medicine at St. Louis Children's Hospital, United States, ⁴Division of Endocrinology, Brody School of Medicine, United States, ⁵Division of Bone and Mineral Diseases, Department of Internal Medicine, Washington University School of Medicine at Barnes-Jewish Hospital, United States

X-linked hypophosphatemia (XLH) accounts for ~80% of heritable hypophosphatemic rickets. Over 330 causal PHEX mutations lead to increased circulating FGF23 levels with significant renal phosphate wasting. In 2014, we reported 6 seemingly sporadic, mildly affected children and their mothers who carried the PHEX 3'UTR c.*231A>G (UTR) mutation. UTR is not listed as a normal gene variant in ExAC, gnomAD, or ClinVar. Subsequent investigation revealed three large American kindreds and additional individuals harboring this defect. The three kindreds comprised, thus far, 13, 9, and 6 members who were UTR mutation-positive. Thus, we conducted a retrospective, age/sex-matched, case-control study to delineate the phenotype of 30 UTR subjects (UTRs) versus 30 classic XLH patients (XLHs). Clinical and biochemical data were assessed using the two-sample T-test and Fischer's exact test. For the UTRs and XLHs, the mean ages were 23.4 years, with each group including 17 children (2-17 years) and 13 adults (23-63 years). There were 10 women and 3 girls in each group. UTRs versus XLHs mean (SD) fasting serum phosphorus was 3.0 (0.5) vs. 2.5 (0.7), FGF23 was 158 (61) vs. 278 (93), and TmP/GFR was 2.5 (0.5) vs. 1.9 (0.7); Ps < 0.01 (Table). Mean (SD) height Z-scores of UTRs versus XLHs were -1.03 (1.0) and -2.07 (1.4); p=0.003, whereas mean differences of arm span Z-scores and height Z-scores (AHD) were 0.1 (0.6) and 0.7 (1.0), respectively (p=0.014). Thus, UTRs were more proportionate than XLHs. The AHD of male UTRs versus male XLHs was 0.2 (0.5) and 0.8 (0.9); p=0.026. No significant difference for AHD was found between female UTRs and female XLHs (p=0.238). Notably, 43% of UTRs versus 90% of XLHs had received standard of care therapy (SOC). No female UTRs but 85% of female XLHs had received SOC. Also, 24% of male UTRs and 94% of male XLHs had received SOC (Ps < 0.0001). Thus, individuals, especially females, with UTR compared to classic XLH are mildly affected and are frequently of normal height, more proportionate, and have a better biochemical profile, even untreated. While UTR males have mild features of XLH, females have often-unrecognized subtle signs, such as genu varum/valgum, dental abnormalities, etc. UTRs with minor features may not require medical therapy, thereby avoiding potential complications. However, a correct diagnosis is important for understanding the inheritance pattern, sex-dependent expression of the UTR phenotype, and counseling for this population.

Table

	UTRs		XLHs		p-value
	N	Mean (SD)	N	Mean (SD)	
Serum Pi	30	3.0 (0.5)	30	2.5 (0.7)	0.0009
<i>female</i>	13	2.9 (0.5)	13	2.3 (0.4)	0.0022
<i>male</i>	17	3.1 (0.4)	17	2.6 (0.8)	0.0456
	<i>p</i> =0.2852		<i>p</i> =0.1833		
PTH	30	51.9 (25.1)	30	39.9 (18.5)	0.0390
FGF23	10	158.1 (60.8)	7	277.6 (93.0)	0.0055
Urine Pi/Cr	29	1.3 (0.8)	30	1.7 (1.0)	0.1502
TmP/GFR	26	2.5 (0.5)	27	1.9 (0.7)	0.0028
<i>female</i>	12	2.6 (0.5)	12	1.8 (0.4)	0.0003
<i>male</i>	14	2.4 (0.6)	15	2.0 (0.8)	0.2102
	<i>p</i> =0.3746		<i>p</i> =0.4288		
TRP	26	82.3 (11.0)	27	76.7 (9.5)	0.0369
<i>female</i>	12	88 (6.7)	12	81.3 (6.6)	0.0282
<i>male</i>	14	77.7 (12.1)	15	73.1 (6.7)	0.2209
	<i>p</i> =0.0174		<i>p</i> =0.0042		

Disclosures: *Pamela S. Smith, None*

MON-1114

Novel c.G630A TCIRG1 Mutation Causes Aberrant Splicing Resulting in Unusually Mild Form of Osteopetrosis Ralph Zirngibl¹*, Andrew Wang¹, Yeqi Yao¹, Morris Manolson¹, Joerg Krueger², Roberto Mendoza-Londono², Irina Voronov¹. ¹University of Toronto, Canada, ²Hospital for Sick Children, Canada

Infant malignant autosomal recessive osteopetrosis (ARO) is a severe genetic bone disease characterized by high bone density. This disease is caused by mutations that affect formation or function of osteoclasts, the bone resorbing cells. Mutations in the $\alpha 3$ subunit of the vacuolar type H⁺-ATPase (encoded by TCIRG1 gene) are responsible for almost 50% of all ARO cases. We identified a novel TCIRG1 mutation (c.G630A) responsible for an unusually mild form of the disease. To characterize this mutation, osteoclasts were differentiated using the peripheral blood monocytes from the patient (homozygous for the mutation, c.G630A/c.G630A), unaffected male sibling (non-carrier, +/+), unaffected female sibling (carrier, heterozygous for the mutation, +/c.G630A), and unaffected parent (carrier, heterozygous for the mutation, +/c.G630A). Osteoclast formation (tartrate resistant acid phosphatase (TRAP) staining), bone resorbing function (Osteoclast plates), TCIRG1 protein and mRNA expression levels were assessed. The c.G630A mutation did not affect osteoclast differentiation; however, the resorption of the bone-like substrate was decreased in the patient compared to the unaffected controls. Both TCIRG1 protein and full-length TCIRG1 mRNA expression levels were also diminished in the patient's sample. Next, we tested for exon skipping. We analyzed the TCIRG1 sequence between exons 4 and 8 and detected deletions of exons 5 ($\Delta E5$), $\Delta E6$, $\Delta E7$, and $\Delta E5-6$ (sequencing of the PCR products confirmed the results). These deletions were only detected in c.G630A/c.G630A and +/c.G630A samples, but not in +/+ controls. The $\Delta E5-6$ maintains the reading frame and is predicted to generate a 85 kDa protein. Exons 5-6 encode an uncharacterized portion of cytoplasmic N-terminal domain of $\alpha 3$, the domain not involved in proton translocation. To investigate the effect of $\Delta E5-6$ on V-ATPase function, we transformed yeast with full-length Vph1p, the yeast ortholog of $\alpha 3$, or Vph1p with a truncation mimicking human $\Delta E5-6$. Both proteins were expressed; however, $\Delta E5-6$ -Vph1p transfected yeast failed to grow on Zn²⁺-containing plates, a growth assay dependent on V-ATPase-mediated vacuolar acidification. In conclusion, our results so far suggest that mild ARO phenotype observed in the patient was due to the residual full-length protein expression, since the $\Delta E5-6$ truncated protein does not appear to be functional.

Disclosures: *Ralph Zirngibl, None*

MON-1115

Development and characterization of a hypophosphatasia (HPP) tooth and muscle phenotype in sheep to model disease in an index HPP patient Diarra Williams¹*, Shannon Huggins¹, Alexis Mitchell¹, Alyssa Falck¹, Jane Pryor¹, Cassandra Skenandore¹, Grant Read¹, Hays Boyd¹, Sierra Long¹, Brian Foster², Mark Westhusin¹, Charles Long¹, Larry Suva¹, Dana Gaddy¹. ¹Texas A&M University, United States, ²Ohio State University, United States

Hypophosphatasia (HPP) is a rare inherited disorder of mineral metabolism that affects the development of bones and teeth. The disease is the result of mutations in the tissue-nonspecific alkaline phosphatase (TNSALP) gene (ALPL) often accompanied by a highly variable clinical presentation. Our identification of an index patient later confirmed as a compound heterozygote with an Alanine \rightarrow Threonine (c.346 G>A) mutation in exon 5 and an Isoleucine \rightarrow Methionine (c.1077 C>G) mutation in exon 10 of ALPL led us to initiate efforts to develop a model in which to understand the biology of the myasthenia and premature teeth loss in this patient. The patient experienced rhizomelia, waddling gait, and premature tooth loss that was associated with a significantly decreased alkaline phosphatase activity at 2 years of age (29 U/L (age-adjusted); NR 1-3 yrs. 125 U/L), normal serum calcium and high normal phosphate levels. MicroCT examination of prematurely erupted teeth demonstrated marked hypomineralized dentin and evidence of bone resorption. Since sheep and humans are diphyodont (two sets of teeth), including primary and secondary sets and mice are monophyodont (one set of teeth), we developed a novel sheep platform to model the tooth, muscle and bone pathophysiology of HPP. Using CRISPR/Cas9 the index patient ALPL gene mutations in exon 5 and exon 10 of the ALPL gene were introduced individually into the sheep genome. Compared to wild-type (WT) controls mutant HPP sheep have significantly reduced serum alkaline phosphatase activity. The exon 10 sheep have decreased tail vertebral bone size, enhanced metaphyseal flaring consistent with the mineralization deficits observed in human HPP as well as an altered gait and force distribution during locomotion. Oral radiographs and computed tomography revealed thin dentin and wide pulp chambers in incisors, and radiolucency of jaws in HPP vs. WT sheep at 2 months and 7 months of age. Skeletal muscle biopsies (2 months) identified aberrant fiber size and mitochondrial cristae structure in exon 10 HPP vs. WT sheep. Since there is still much to learn regarding HPP pathophysiology, we hypothesize that the HPP sheep presented here provide a unique opportunity to address fundamental HPP questions regarding muscle, bone and tooth development that this index patient and others currently struggle to manage.

Disclosures: *Diarra Williams, None*

MON-1116

Continued development of hiPSCs as an in vivo platform for exploring heritable disorders of the human skeleton Xiaonan Xin^{*}, Kronenberg Mark, Alexander Lichtler, David Rowe. School of Dental Medicine, University of Connecticut Health, United States

Induced pluripotent stem cells derived from human subjects (hiPSCs) provide the opportunity to study gene mutations that impact osteoblasts and chondrocytes at a level that cannot be achieved with primary cells or mouse models. Specifically, the heterogeneity of disease severity of the same gene mutation in different subjects is a consequence of the genetic background of the individual, and that important effect can only be modeled in hiPSCs. We have previously demonstrated that progenitor cells derived from embryoid bodies and grown in an endothelial growth medium under a low oxygen environment produce cryohistologically recognizable human cartilage and bone in a mouse calvarial defect. Furthermore the RNA profile of laser captured tissue sections shows the expected gene expression pattern of cartilage and osseous tissues. This platform can demonstrate that CRISPR/Cas correction of a COL1A1 mutation of a subject with type III OI reverses the mutant phenotype, in which adipocytic tissue predominates, back to production of cartilage and bone. However an unanticipated feature of the cartilage and bone from all donors is the lack of osteoclast remodeling of the bone and hypertrophic cartilage matrix, and the absence of bone marrow spaces. Thus the model does not replicate the indirect effects of a type I collagen mutation on the myeloid/osteoclast lineage. Postulating that the human RANKL lacks sufficient interaction with mouse RANK in vivo to initiate osteoclast invasion, we utilized a previously described strategy to convert the extracellular domain of RANKL from human to mouse. The CRISPR/Cas strategy worked exceptionally well converting exon 5 in both alleles from human to mouse. When implanted in the calvarial defect, more mineralized osseous tissue formed and contained osteoclasts within bone marrow islands. In an unrelated experiment, we observed that human outgrowth cells from the human implant tissue can be retransplanted into a second mouse. In this case only a bone matrix without cartilage is formed, replicating the in vivo outcome of human bone marrow stromal cells, including a human bone matrix that is not remodeled by mouse osteoclasts. These advances in manipulating hiPSCs to replicate the characteristics of chondrocytes and osteoblasts in a mouse transplantation platform will hasten their application for studying heritable disease in their native genetic background and developing cell therapies utilizing mutation-corrected progenitor cells.

Disclosures: *Xiaonan Xin, None*

MON-1117

Clinical characteristics and pathogenic gene mutations identification of Paget's disease of bone in Chinese population Hua Yue*, Zhenlin Zhang. Metabolic Bone Disease and Genetic Research Unit, Department of Osteoporosis and Bone Diseases, Shanghai Jiao Tong University Affiliated Sixth People's Hospital, China

INTRODUCTION: Paget's disease of bone (PDB) is characterized by highly localized areas of increased bone resorption and disorganized bone remodeling. It is common in western descent. However, it is rare in Chinese. Genetic factors play an important role in the pathogenesis of the disease [1]. The purpose of the study was to characterize the clinical features and identify genetic mutations in Chinese PDB patients. **METHODS:** 37 clinically diagnosed PDB patients (two were father and son, the rest were sporadic) and 250 healthy donors were recruited. The clinical features were characterized and the whole-exome sequencing (WES) was carried out in patients to detect gene mutation and then confirmed in donors by Sanger sequencing. PolyPhen-2 and CADD analyses were performed to predict the damaging effect of the mutation. Mutant protein structure was constructed as well. **RESULTS:** The father and son were early-onset (onset age <30 years). The onset age of sporadic PDB patients (53.2±19.1 years) was younger than that of western patients. One of them was PDB combined with giant cell tumor (GC), had even earlier onset age (23 years) with mild symptoms. The most common lesion sites were the pelvis, femur, and skull. Most patients had high serum alkaline phosphatase (ALP) level and intravenous bisphosphonates was effective to relieve bone pain and reduce ALP level. Vitamin D receptor (VDR) gene mutation was identified in a 25-year-old male, who harbored a heterozygous G-to-A transversion at position 424 in exon 4 (c.G424A), which resulted in a glutamate-to-lysine (GAG >AAG) substitution at codon 142 (E142K). No SQSTM1 gene mutation was detected in all 37 patients, which was different from the western patients. VDRE142K was predicted to be damaging with PolyPhen-2 score of 1 and CADD score of 37. Meanwhile, the amino acid residues at p.142 is highly conserved across 9 different biological species. By constructing the mutant protein structure, it was found that the mutation site located in the VDR protein DNA binding region, and which would significantly enhance DNA interaction. **DISCUSSION:** Vitamin D regulates osteoclast function by binding to VDR [2]. Therefore, VDR dysfunction directly affects the osteoclasts status. **CONCLUSION:** Our study described the clinical features and reported that VDR gene mutation contributes to the pathogenesis of PDB in Chinese patients. **REFERENCES:** 1. Albagha OM. Genetics of Paget's disease of bone Bonekey Rep. 4: 756, 2015. 2. Shibata T, Shira-Ishi A, Sato T, et al. Vitamin D hormone inhibits osteoclastogenesis in vivo by decreasing the pool of osteoclast precursors in bone marrow. J Bone Miner Res. 17(4): 622-629, 2002.

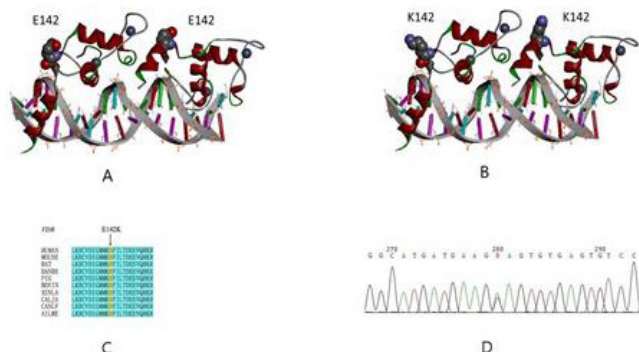


Fig.1 (A) Wild type protein spatial conformation. (B) Mutant protein spatial conformation. (C) Partial amino acid sequences of the VDR gene from 10 species. The amino acids at p.142 in exon 4 highly conserved in 10 different species. (D) VDR gene mutation sequencing diagram. A missense mutation c.G424A in exon 4 was detected.

Disclosures: Hua Yue, None

MON-1138

Prospective Associations of Sarcopenic obesity and dynapenic obesity with joint replacement over 13 years in Community-dwelling Older Adults Saliu Balogun*¹, David Scott², Stephen Graves³, Michelle Lorimer⁴, Flavia Cicuttini⁵, Graeme Jones¹, Dawn Aitken¹. ¹Menzies Institute for Medical Research, University of Tasmania, Australia, ²Department of Medicine, School of Clinical Sciences at Monash Health, Faculty of Medicine, Nursing and Health Sciences, & Peninsula Clinical School, Central Clinical School, Monash University, Australia, ³Australian Orthopaedic Association, University of Melbourne, Parkville, Australia, ⁴South Australian Health and Medical Research Institute (SAHMRI), Australia, ⁵Department of Epidemiology and Preventive Medicine, Monash University, Australia

Purpose: This study aims to determine whether older adults with low muscle mass (sarcopenia) or strength (dynapenia), in the presence of obesity, have an increased risk of total knee and hip replacement surgery over 13 years. **Methods:** 995 community-dwelling older adults (51% women; mean age 62.8±7.4 years) were studied at baseline and multiple time points over 13 years. The incidence of knee and hip joint replacement was determined by data linkage to the Orthopaedic Association National Joint Replacement Registry. Total body fat mass and appendicular lean mass were measured using dual energy X-ray absorptiometry (DXA). Lower-limb muscle strength was assessed using dynamometer. Sarcopenic obesity and dynapenic obesity were defined as the lowest sex-specific tertiles for appendicular lean mass (adjusted for height and total body fat mass) or lower-limb strength, respectively, and the highest sex-specific tertile for total body fat mass. Competing risk regression models were used to estimate the sub-distribution hazard ratio (SHR) for knee and hip joint replacement over 13 years in unadjusted and adjusted analysis. **Results:** Over 13 years of follow-up, 74 (7.4%) participants had a knee replacement and 63 (6.4%) had a hip replacement. The risk of having a knee replacement was significantly higher in participants who were dynapenic obese (SHR=5.46, 95% CI 2.50, 11.94), dynapenic non-obese (SHR=4.09, 95% CI: 1.93, 8.69), and non-dynapenic obese (SHR=3.92, 95% CI: 1.86, 8.26) compared to those without dynapenia or obesity. However, dynapenic obesity did not lead to a significantly greater risk of knee replacement compared to having dynapenia or obesity alone. The risk of having a knee replacement was significantly higher only in participants who were non-sarcopenic obese (SHR=2.28, 95% CI: 1.26, 4.13) compared to those without sarcopenia or obesity. There was no evidence for an association between sarcopenic or dynapenic obesity and hip joint replacement (all P>0.05). **Conclusions:** In the presence of obesity, dynapenia but not sarcopenia increased the risk of knee joint replacement. Notably, the combination of low muscle strength and obesity did not lead to a significantly greater risk of knee replacement compared to having these conditions on their own. This finding suggests that combining muscle and fat assessments to predict the future risk of joint replacement is no better than each individual condition on its own.

Disclosures: Saliu Balogun, None

MON-1139

Secular Trends in Mortality Due to Falls and Hip Fracture in the US Jane Cauley*, Kendra Jean Bobby, Elsa Strotmeyer, Jeanine Buchanich. University of Pittsburgh, United States

Declines in hip fracture incidence rates in the US from 2002-2012 have stopped with rates for 2013-2015 higher than expected (Lewiecky EM. Osteo Int 2017). To test whether secular changes in mortality from hip fractures or falls follow similar patterns, we used the Mortality Informatics and Research Analytics (MOIRA) database, a repository and retrieval system for US death data from the National Center for Health Statistics (NCHS) developed at the University of Pittsburgh. The MOIRA database contains individual demographic information plus the underlying and contributory cause of death for 120 million+ decedents. Age-adjusted death rates for falls from 1962 to 2014 (ICD-9th revision: 880-888; ICD 10th revision, W00-W19 (1999 on) and hip fractures from 1990-2015 (ICD 9th revision: 820.xy; ICD-10: S72.xy) were calculated. The NCHS comparability ratio of 0.84 was used for interpreting trends in fall mortality from the ICD-9 to ICD-10. No comparability ratio was available for the hip fracture mortality. Fall deaths were counted as underlying cause. Hip fractures were counted as either the contributing or underlying cause of death. Pathologic hip fractures (733.14) were excluded. We restricted our analysis to age groups 50+. Joinpoint regression was used to detect significant changes in trends. Fall death rates show a continued decline from 1962-1981; plateau in mortality rates 1981-1996 and a continued increase in fall death rates from 2000-2014, all changes in trends were significant at p<0.05, (Figure 1). Patterns were similar in men and women with fall death rates higher in men than women. Examination of age-specific fall death rates show the steepest increase in those age 85+. Hip fracture death rates have declined from 1989-2015, Figure 2, p<0.05. The slight increase in death rates from 1998 to 2001 is likely an artifact of the ICD revision change. Consistent with previous literature, age adjusted hip fracture mortality rates were higher in men than women from 1999-2005. However more recently, a different pattern emerged from 2010-2015 where hip fracture mortality rates were higher in women than men. Understanding the factors contributing to the increase in fall death rates and the differential pattern overtime by sex in hip fracture mortality is critical with the concurrent population increase of the oldest old cohorts.

Figure 1 Age-adjusted US mortality rates from falls: 1992-2014

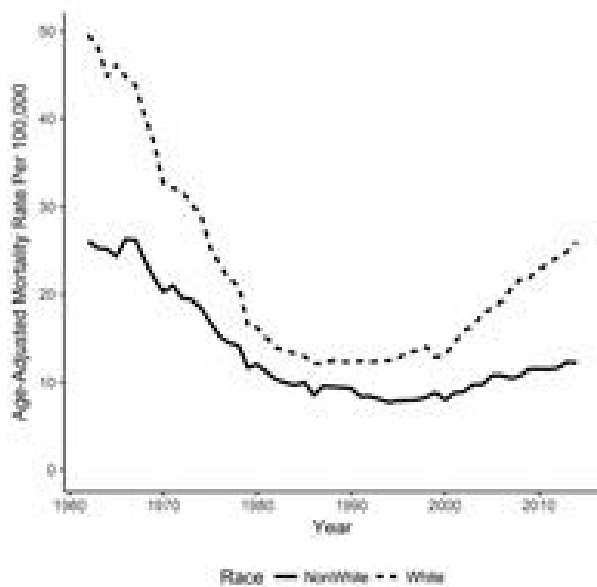
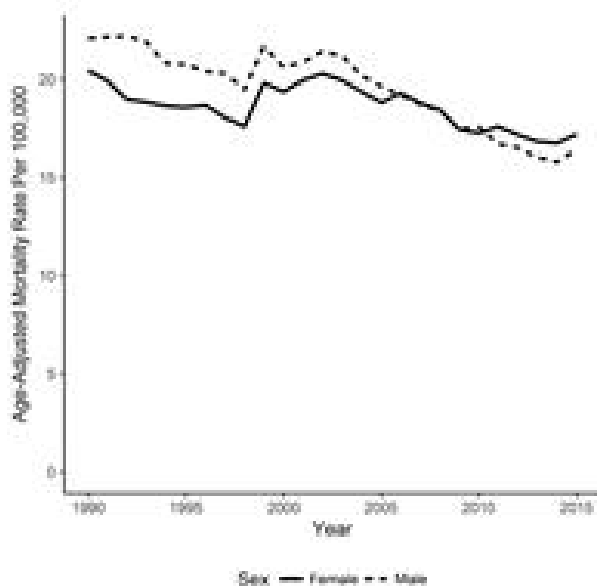


Figure 2 Age-adjusted US mortality rates from hip fracture: 1990-2015



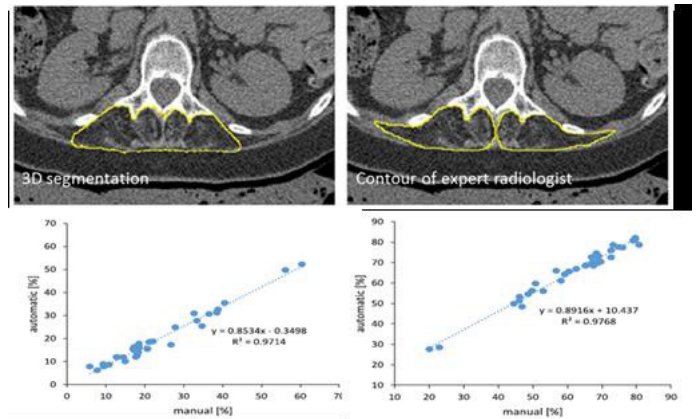
Disclosures: *Jane Cauley, None*

MON-1140

A new CT based approach to quantify adipose tissue in paraspinous muscle
 Klaus Engelke¹, Oleg Museyko², Daniel Günzel¹, Andreas Meier³, Jean-Denis Laredo⁴. ¹Inst. of Medical Physics, University of Erlangen-Nuremberg, Germany, ²Inst. of Medical Physics, Univ. of Erlangen, Germany, ³Inst. of Informatics, University of Erlangen-Nuremberg, Germany, ⁴Radiologie Ostéo-Articulaire, Hôpital Lariboisière, AP-HP, CNRS UMR 7052, France

Introduction: Adipose tissue infiltration in paraspinous muscle decreases muscle quality and may be associated with back pain, structural abnormalities of the lumbar spine and perhaps even vertebral fracture. Here a new approach for segmentation and determination of adipose tissue infiltration of paraspinous muscle using CT images is presented **Methods:** Accurate muscle segmentation in CT images is difficult due to low soft tissue contrast. We developed a new approach primarily aiming at high precision at the expense of accuracy of muscle volume. Based on a global VOI and three orthogonal clipping planes the resulting segmentation captured about 80-90% of the paraspinous muscle at the expense of the outer

parts. The clipping planes were determined automatically based on a vertebral coordinate system (VCS) and a number of landmarks such as the ends of the transverse processes, the center of the VCS and the width of the vertebral body. The resulting segmentation, implemented in the Medical Image Analysis Framework (MIAF), was compared with a manual segmentation of an expert radiologist, which served as gold standard. Within the segmented paraspinous muscle VOI, pure adipose tissue was automatically determined using a threshold obtained from subcutaneous adipose tissue. The remaining muscle tissue was further divided into 5 compartments according to the CT-value. A low muscle density indicated a higher portion of adipose tissue. Pure muscle was defined as a muscle density > 25 HU determined from young elite athletes. Automated and manual segmentations were compared in 13 elderly osteoporotic subjects. **Results:** The figure shows results of the automated segmentation of the paraspinous muscle compared to the radiological gold standard segmentation. The correlation of relative % volume of pure adipose tissue and of muscle between the automated and the manual segmentation was very high (r² > 0.97). Intra- and interoperator reanalysis precision errors were below 2%. **Conclusion:** The new segmentation approach showed excellent precision, which is highly important in longitudinal studies. The compromise on muscle volume accuracy seems justified as % adipose and muscle volume obtained from the automated approach correlated extremely high with the gold standard technique. Thus the method provides an excellent basis for further research in the field of vertebral fractures.



Disclosures: *Klaus Engelke, None*

MON-1141

Neither Sarcopenia, Body Composition Parameters, nor Salivary Cortisol Circadian Rhythm are Associated to Increased Risk of Falls in Women 50 to 80 Years. The OsteoLaus Cohort Elena Gonzalez Rodriguez^{1,2}, Didier Hans¹, Georgios Papadakis³, Peter Vollenweider⁴, Martin Preisig⁵, Gerard Waeber¹, Pedro-Manuel Marques-Vidal¹, Olivier Lamy^{1,6}. ¹Center of Bone Diseases, Rheumatology Unit, Bone and Joint Department, CHUV, Switzerland, ²Endocrinology, Diabetology and Metabolism Unit, Internal Medicine Department, CHUV, Switzerland, ³Endocrinology, Diabetology and Metabolism Unit, Internal Medicine Department, CHUV, Switzerland, ⁴Internal Medicine Unit, Internal Medicine Department, CHUV, Switzerland, ⁵Epidemiology and Psychopathology Research Unit, Psychiatric Department, CHUV, Switzerland, ⁶Internal Medicine Unit, Internal Medicine Department, CHUV, Switzerland

Introduction: Muscle weakness is an important risk factor for falls. There are increasingly efforts to identify measurable parameters related to muscle weakness that could be clinically relevant. Sarcopenia is defined as the loss of muscle mass and function, and is associated with aging, but its link to risk of falls has not been consistently found. Muscle weakness and sarcopenia are present in hypercortisolism. We wanted to determine whether these parameters were associated to an increased risk of falls the previous year. **Material and Methods:** Cross-sectional study including 815 women >50 years (mean age 63.2±7.7) from the OsteoLaus cohort. Included participants had: lean mass body composition assessment by DXA, salivary cortisol circadian rhythm measures (awakening, 30 minutes thereafter, 11 AM and 8 PM) and measurement of handgrip. All participants were asked whether they sustained a fall on the previous year. **Results:** 227 participants (27.9%) reported at least one fall, without differences in the in the 3 tertiles of age (25.6%, 31.4% and 26.6% for participants 54.9±2.6, 62.6±2.2, and 72.1±4.2 years respectively). Gynoid region lean mass, but no other lean mass measures, was inversely associated to 8 PM salivary cortisol values after adjustment to BMI (p=0.025), and to BMI and age (p=0.052). Handgrip was inversely associated to both 11AM and 8 PM salivary cortisol values (p= 0.010 and 0.014), without influence of BMI. After adjustment to age and BMI, only association to salivary cortisol at 8 PM was significant (p=0.041). There was no significant association between any body composition parameter, salivary circadian cortisol value, handgrip measure or sarcopenia diagnosis according to EWGSOP criteria (ALMI < 5.5 kg/m² and muscle strength < 20 kg), and prevalence of falls in the previous year, either in the whole participants cohort or in the oldest tertile. **Conclusions:** In our cohort of healthy post-menopausal women 50 to 80 years old, neither body lean mass measures nor muscle function (handgrip), or any of their

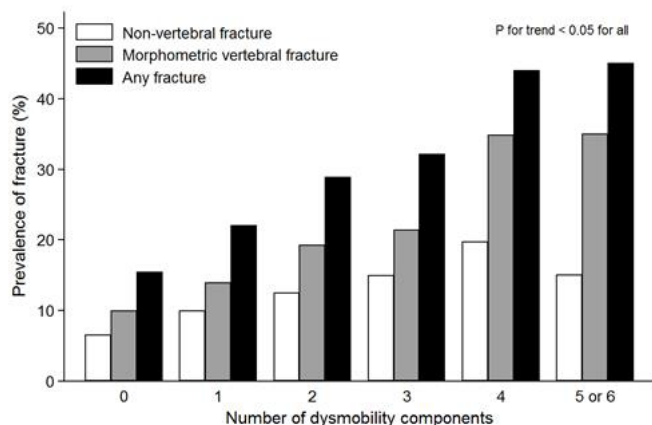
determinants (age, BMI or increased nadir salivary cortisol) were associated to increased risk of falls.

Disclosures: *Elena Gonzalez Rodriguez, None*

MON-1142

Dysmobility syndrome is associated with prevalent morphometric vertebral fracture in older adults: The Korean Urban-Rural Elderly (KURE) study
Namki Hong*, Chang Oh Kim, Yoosik Youm, Jin-Young Choi, Hyeon Chang Kim, Yumie Rhee. Yonsei University College of Medicine, Republic of Korea

The term "dysmobility syndrome" was coined to encompass the comprehensive risk factors affecting fractures. However, data on the association of dysmobility syndrome and its components with prevalent morphometric vertebral fracture (VF) in elderly persons are limited. In this prospective cohort study, a total of 1369 community-dwelling elderly subjects (mean age, 71.6 years; women, 66%) were analyzed. Dysmobility syndrome was defined as the presence of ≥ 3 of the following 6 factors: falls in the preceding year, low grip strength (<30 kg in men, <20 kg in women), osteoporosis (T-score ≤ -2.5 at any site in the lumbar spine, femoral neck, or total proximal femur), low timed get-up-and-go performance (12 s or longer), low lean mass (appendicular skeletal muscle mass/height² <7.0 kg/m² in men and <5.7 kg/m² in women in bioimpedance analysis), and high fat mass ($>30\%$ for men and $>40\%$ for women). VF was defined as a $\geq 25\%$ reduction in the height of vertebral bodies assessed using plain radiographs. Non-VF was assessed using interviewer-assisted questionnaires. The prevalence of dysmobility syndrome was 20% (n = 273). Subjects with dysmobility syndrome were older (73.5 vs. 71.1 years), malnourished (35% vs. 17%), and physically inactive (30% vs. 18%) and had more hospitalizations during the preceding year (17% vs. 10%, p < 0.001 for all). The prevalence of VF and any fracture composite of VF and non-VF was 16% and 25%, respectively, increasing from subjects with 0 dysmobility components to those with ≥ 5 (VF, 10-35%; any fracture, 16-45%, p for trend < 0.001 for all). Dysmobility syndrome and its components were associated with elevated odds of VF (crude odds ratio [OR] 2.14, p < 0.001; adjusted OR [aOR] 1.43, p = 0.047) or any fracture (OR 2.05, p < 0.001; aOR 1.39, p = 0.037); however, the association with non-VF (OR 1.16, p = 0.048; aOR 1.29, p = 0.217) was attenuated after adjustment for covariates. When subjects were stratified by bone mineral density levels, the relative odds of VF and non-VF increased in a stepwise fashion as the number of dysmobility syndrome increased in both osteoporosis group (VF, aOR 2.3 to 5.1; non-VF, aOR 4.9 to 6.7) and osteopenia group (VF, aOR 1.7 to 2.4; non-VF, aOR 3.9 to 6.8). In conclusion, dysmobility syndrome and its components were associated with elevated odds of morphometric vertebral fracture, independent of age and covariate, suggesting potential clinical utility of this concept in identifying persons with a high fracture risk.



Disclosures: *Namki Hong, None*

MON-1143

Alteration in Skeletal Muscle Mass in Women with Primary Aldosteronism
Mi Kyung Kwak*¹, Jae Hyeon Kim², So Jeong Park³, Seong Hee Ahn⁴, Hyeonmok Kim⁵, Yoon Young Cho⁶, Sunghwan Suh⁷, Beom-Jun Kim⁸, Kee-Ho Song⁹, Seung Hun Lee⁸, Jung-Min Koh⁸. ¹Division of Endocrinology and Metabolism, Asan Medical Center, University of Ulsan College of Medicine, Republic of Korea, ²Division of Endocrinology and Metabolism, Department of Medicine, Samsung Medical Center, Sungkyunkwan University School of Medicine, Republic of Korea, ³Asan Institute for Life Sciences, Republic of Korea, ⁴Department of Endocrinology, Inha University School of Medicine, Republic of Korea, ⁵Division of Endocrinology and Metabolism, Department of Internal Medicine, Seoul Medical Center, Republic of Korea, ⁶Division of Endocrinology and Metabolism, Department of Medicine, Gyeongsang National University School of Medicine, Republic of Korea, ⁷Division of Endocrinology and Metabolism, Department of Medicine, Dong-A University Medical Center, Dong-A University School of Medicine, Republic of Korea, ⁸Division of Endocrinology and Metabolism, Department of Medicine, Asan Medical Center, University of Ulsan College of Medicine, Republic of Korea, ⁹Division of Endocrinology and Metabolism, Department of Medicine, Konkuk University Medical Center, Konkuk University School of Medicine, Republic of Korea

Purpose: Despite the potential detrimental effects of aldosterone excess on skeletal muscle, whether aldosterone excess in primary aldosteronism (PA) affects skeletal muscle mass is unknown. Our objective was to understand the effects of the aldosterone level on skeletal muscle mass in patients with PA. Methods: We compared skeletal muscle mass and fat mass (FM) between 62 patients with PA (29 women and 33 men) and 247 controls (76 women and 171 men) with nonfunctioning adrenal incidentaloma (NFAI). Medical records were reviewed, and we measured body composition parameters using bioelectrical impedance analysis and serum aldosterone levels. Results: After adjusting for confounding factors, plasma aldosterone levels were inversely correlated with appendicular skeletal muscle mass (ASM) ($\beta = -0.194$, $P = 0.017$) and appendicular skeletal muscle index (ASMI) ($\beta = -0.208$, $P = 0.009$) in all women, but not men. ASMI was significantly lower by 4.6% ($P = 0.034$) in women with PA compared with those with NFAI, but not men. In women, the odds for lower skeletal muscle mass with the plasma aldosterone concentration (PAC) were 1.17-fold higher ($P = 0.030$), and with the presence of PA were 10.90-fold higher with marginal significance ($P = 0.066$) after adjustment for potential confounders. Conclusions: This study showed that women with PA had lower skeletal muscle mass, and suggested that aldosterone excess also has adverse effects on skeletal muscle metabolism.

Disclosures: *Mi Kyung Kwak, None*

MON-1144

Leisure-time aerobic physical activity and vitamin D concentrations in U.S. older adults Carlos Orces*¹, Daniella Orces². ¹Laredo Medical Center, United States, ²Southwestern University, United States

Purpose: Although leisure-time physical activity (LTPA) has been associated with increased 25(OH)D levels, previous studies among older adults have reported conflicting results between the duration or intensity of LTPA and 25(OH)D levels. Thus, this study aimed to examine the relationship between self-reported moderate and vigorous LTPA and 25(OH)D and 25(OH)D3 concentrations among U.S. older adults. Methods: The present analysis was based on participants aged 60 years and older in the The National Health and Nutrition Examination Survey 2007-2012. According to the 2008 physical activity guidelines for Americans, three levels of physical activity were created: 1) participants who engaged in ≥ 150 min/week of moderate activity, or ≥ 75 min/week of vigorous activity, or ≥ 150 min/week of an equivalent combination were defined as physically active; 2) insufficiently active were considered those who reported some physical activity, but not enough to meet the active definition (> 0 to < 150 min/week); 3) inactive if they reported no physical activity. Similarly, metabolic equivalent task (MET) scores per minutes/week were calculated. Those with < 750 MET-min/week or ≥ 750 MET-min/week were defined as insufficiently or sufficiently active, respectively. General linear models adjusted for potential confounders were created to examine mean 25(OH)D and 25(OH)D3 across physical activity levels. Results: A total of 4,764 adults with a mean age of 69.7 (SE 0.1) years comprised the study sample, representing an estimate 46 million U.S. older adults during the study period. Overall, 57.5%, 14.8%, and 27.7% of participants were defined as physically inactive, insufficiently active, and physically active, respectively. The mean 25(OH)D and 25(OH)D3 concentrations were 75.0 (SE 0.9) and 68.8 (SE 0.9) nmol/L, respectively. As shown in Table 1, after controlling for confounders, those considered physically active had 9.9 and 9.0 nmol/L higher concentrations of 25(OH)D and 25(OH)D3 than those physically inactive, respectively. Similarly, participants defined as physically active according to the intensity of LTPA had 10.4 and 9.8 higher mean 25(OH)D and 25(OH)D3 levels than their physically inactive counterparts, respectively. Conclusion: Recreational physical activity is significantly associated with higher 25(OH)D concentrations in older adults. Despite this evidence, a considerable proportion of U.S. older adults are physically inactive.

Table 1. Association between leisure-time physical activity and 25(OH)D and 25(OH)₂ concentrations (nmol/L) among U.S. older adults

Physical activity	25(OH)D		25(OH) ₂	
	Model 1	Model 2	Model 1	Model 2
Minutes/week				
Inactive (reference)	70.8 (1.0)	71.5 (0.9)	65.2 (0.9)	66.0 (0.9)
Insufficiently active	78.7 (1.8)*	78.2 (1.6)	68.1 (1.6)	67.6 (1.6)
Sufficiently active	82.7 (1.6)**	81.4 (1.4)**	76.3 (1.7)**	75.0 (1.7)**
MET-min/week				
Inactive (reference)	70.8 (1.0)	71.5 (0.9)	65.2 (0.9)	66.0 (0.9)
Insufficiently active	77.8 (1.5)	77.1 (1.3)*	69.4 (1.4)*	68.7 (1.3)
Sufficiently active	83.2 (1.5)	81.9 (1.7)**	77.1 (2.1)**	75.8 (2.0)**

Model 1: Sex-time period, age, gender, race, BMI, education, ratio family income to poverty

Model 2: Model 1 and smoking status, self-reported health, and total daily vitamin D intake

* P < .05

** P < .0001

Disclosures: *Carlos Orces, None*

MON-1145

Alterations in Body Composition and Appendicular Lean Mass Assessed Using Whole-Body Dual-Energy X-ray Absorptiometry in BRCA Carriers Undergoing Prophylactic Salpingo-oophorectomy Jeevitha Srighanthan^{*1}, Joan Murphy², Joanne Kotsopoulos³, Gabrielle E. V. Enc¹, Marcus Q. Bernardini¹, Queenie Wong¹, Diana Yau¹, Paula Harvey³, Steven Narod³, Barry Rosen¹, Amy Finch⁴, Angela M. Cheung¹. ¹University Health Network, Canada, ²Trillium Health Partners, Canada, ³Women's College Hospital, Canada, ⁴Sunnybrook Hospital, Canada

Purpose: Prophylactic salpingo-oophorectomy (removal of the fallopian tubes and ovaries) is uniformly recommended to BRCA1/2 carriers at age 35 or once childbearing is complete. However, such surgically-induced menopause can induce bone and muscle loss, among other side effects. The long-term effect of this surgery on body composition is unknown. We compared differences in whole body composition and appendicular lean mass among women undergoing prophylactic salpingo-oophorectomy (PSO) as compared to non-oophorectomized women. **Methods:** This pilot one-year study examines musculo-skeletal outcomes among pre-menopausal women with a BRCA1/2 mutation undergoing PSO compared to pre-menopausal non-oophorectomized non-carrier women. Participants undergo a whole body dual-energy x-ray absorptiometry (DXA) scan at baseline (prior to surgery) and one year following PSO (or equivalent time frame for non-oophorectomized women). Percent changes in body mass index (BMI), whole body bone mineral density (BMD), bone mineral content, total mass, total lean mass, total fat mass, and percent fat mass from baseline to one-year were obtained from DXA scans using standard analysis protocols, as well as appendicular lean mass index (ALM/height²), lean mass index (LM/height²), and fat mass index (FM/height²). Differences between groups were statistically assessed using t-tests. **Results:** To date, 22 PSO BRCA carriers and 13 non-oophorectomized non-carriers have completed their one-year visit. Mean age of PSO BRCA carriers and non-oophorectomized women was 42.41 (SD 5.24) and 45.86 (SD 3.99) years, respectively. PSO BRCA carriers had a mean BMI of 26.19 (SD 4.10), as compared to a mean BMI of 26.64 (SD 3.01) in non-oophorectomized women. Participants were mostly Caucasian (83%). The table below demonstrates changes in bone, muscle and fat parameters for PSO BRCA carriers and non-carriers. **Conclusions:** Our preliminary findings demonstrate significant decreases in whole body BMD one-year after PSO when compared to non-oophorectomized women. Elevated percent fat mass among PSO patients also demonstrates a trend towards significance. Other muscle and fat parameters were not significantly different between groups, however almost all outcomes were numerically poorer among PSO BRCA carriers. Further research with larger sample sizes and longer follow-up durations are required to understand the effects of this preventive surgery on musculoskeletal health.

One-Year Percent Change in BMI & Body Composition

	PSO BRCA carriers (n=22) % change (SD)	Non-oophorectomized non-carriers (n=13) % change (SD)	p-value
BMI (kg/m ²)	0.11 (4.40)	0.30 (3.12)	0.89
Whole Body BMD (g/cm ³)	-2.16 (2.68)	-0.10 (2.07)	0.024*
Bone Mineral Content (g)	-2.47 (3.78)	-1.33 (3.16)	0.37
Fat Mass (g)	3.48 (11.29)	-1.00 (7.74)	0.22
Percent Fat Mass	3.26 (7.50)	-0.36 (3.97)	0.072
Total Mass (g)	-0.0010 (4.68)	-0.76 (4.47)	0.64
Total Lean Mass (g)	-1.74 (3.26)	-0.67 (3.29)	0.36
Lean Mass Index (LMI) (kg/m ²)	-1.73 (3.45)	-0.65 (3.49)	0.38
Appendicular Lean Mass Index (ALMI) (kg/m ²)	-2.46 (5.12)	-1.72 (5.82)	0.70
Fat mass index (FMI) (kg/m ²)	3.46 (11.36)	-1.02 (7.78)	0.22

*p<0.05

Disclosures: *Jeevitha Srighanthan, None*

MON-1146

Falls are the most frequent provocative factor for subsequent clinical fractures during 1-year follow-up in patients with a recent clinical fracture evaluated and treated according to current osteoporosis guideline at a Fracture Liaison Service Lisanne Vranken^{*1,2}, Caroline E Wyers^{1,2}, Robert Y Van Der Velde^{1,2}, Irma Ja De Bruin^{1,2}, Heinrich Mj Janzing⁴, Sjoerd Kaarsmaker⁵, Piet Pm Geusens^{3,4}, Joop Pw Van Den Bergh^{1,2,3}. ¹VieCuri Medical Center, Department of Internal Medicine, Netherlands, ²Maastricht UMC+, NUTRIM School for Nutrition and Translational Research in Metabolism, Department of Internal Medicine, Netherlands, ³Hasselt University, Netherlands, ⁴VieCuri Medical Center, Department of Surgery, Netherlands, ⁵VieCuri Medical Center, Department of Orthopaedic Surgery, Netherlands

Purpose: Our aim was to investigate the association between falls and fractures (fx) and to identify predictors for these adverse events in patients aged 50-90yrs with a recent clinical fx who were evaluated and treated according to current osteoporosis guidelines at a Fracture Liaison Service (FLS). **Methods:** Prospective observational cohort study in 486 consecutive FLS patients willing and able to participate. Patients with skull fx, high-energetic trauma or peri-prosthetic fx, osteomyelitis, metastasis, Paget's disease or multiple myeloma were excluded. Baseline assessment included evaluation of comorbidities and medication, BMD measurement and lateral spine imaging by DXA, and physical performance tests (chair stand test (CST), timed-up-and-go test and 6-minutes walking test (6-MWT)). At 1-year, self-reported falls using a weekly report and radiologically confirmed subsequent clinical fx were evaluated. Participants were categorized as non-faller or faller (subdivided in once and recurrent fallers). Logistic regression analyses were adjusted for age, gender, height, weight, baseline fx type and time between baseline fx and fx risk evaluation. **Results:** Of 468 participants (72% women, mean age 65yrs, 34% treated with anti-osteoporosis drugs), 182 (39%) fell at least once, 98 (21%) fell once and 84 (18%) recurrently. Subsequent fx were observed in 20 (4%) participants, 4 in non-fallers (2%) and 16 in fallers (9%) (OR:6.9 95%CI:2.3-21.0). Thus, 80% of all subsequent fx occurred after a fall. Most subsequent fx in fallers (69%) occurred after the first fall. After adjustments, at least one fall was associated with a fall in the past year (OR:2.5 95%CI:1.7-3.9), low CST score (OR:3.4 95%CI:1.2-10.1), 6-MWT <450m (OR:1.6 95%CI:1.0-2.6) and depression (OR:3.1 95%CI:1.2-7.8). A single fall was associated with a fall in the past year (OR:2.90 95%CI:1.76-4.78) and recurrent falls with a fall in the past year (OR:2.04 95%CI:1.19-3.50), low CST score (OR:6.1 95%CI:1.8-21.1), arthritis (OR:3.82 95%CI:1.2-12.1) and depression (OR:5.3 95%CI:1.9-14.6). **Conclusions:** In patients with a recent clinical fx who were evaluated and treated according to current osteoporosis guidelines at the FLS, 39% fell at least once and 4% sustained a subsequent clinical fx during 1-year follow-up. Of all subsequent fx, 80% occurred after a fall, indicating that fall risk evaluation and prevention are important for immediate secondary fx prevention in addition to anti-osteoporosis treatment.

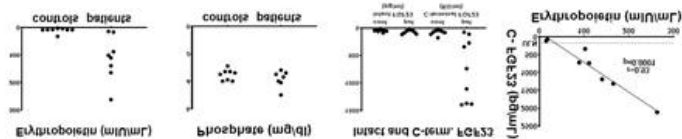
Disclosures: *Lisanne Vranken, None*

LB MON - 1149

Evidence for a direct role of Erythropoietin in the Regulation of FGF23 in Humans Kelly Roszko^{*}, Sydney Brown, Ying Pang, Thanh Huynh, Karel Pacak, Michael Collins. NIDCR, NIH, United States

FGF23 increases urinary phosphate excretion, and decreases blood phosphate and 1,25-dihydroxyvitamin D. Posttranslational regulation of FGF23 involves glycosylation by the galactosyl transferase GALNT3. Glycosylation prevents degradation of intact FGF23 into biologically inactive C- and N-terminal fragments by a proprotein convertase, probably furin. Posttranslational regulation is poorly understood, but recent, although conflicting, evidence suggests a role of the hypoxia/iron/erythropoietin (EPO) pathway. The preponderance of the data suggests that activation of the hypoxia pathway leads to increased transcription and translation of FGF23, with some models showing increased posttranslational processing to C- and N-terminal fragments with maintenance of euphosphatemia, but others

showing increased intact FGF23 and hypophosphatemia. To better understand this aspect of FGF23 physiology, we studied eight patients with a rare syndrome of paragangliomas and somatostatinomas caused by somatic, gain-of-function mutations in HIF2a that result in increased tumor-derived EPO levels with polycythemia. Intact and C-terminal FGF23 levels were assessed in relationship to blood phosphate, iron, and EPO levels in eight patients with HIF2a mutations and compared to matched controls. HIF2a patients had markedly elevated and highly correlated EPO and C-terminal FGF23 levels. Iron levels were normal and not correlated with EPO and/or FGF23. While more study is needed to better understand the cellular and molecular mechanisms underlying the observed phenomenon, these data represent the clearest evidence to date in humans for a direct role of EPO in FGF23 transcriptional, translational and posttranslational regulation. Normal blood phosphate and intact FGF23 levels in the setting of C-terminal FGF23 levels up to 20 times above normal demonstrate that posttranslational modification and processing is an exquisitely regulated process.



Disclosures: Kelly Roszko, None

LB MON - 1155

Gene expression changes are associated with severe bone loss and delayed fracture healing in paraplegic rats Mariana Butezloff*, Kelly Astolpho¹, Vitor Correlo², Rui Reis², João Paulo Ximenez¹, João Paulo Issa¹, Raquel Assed Silva¹, Antonio Carlos Shimano¹, José Batista Volpon¹, Ariane Zamarioli¹. ¹University of Sao Paulo, Brazil, ²University of Minho, Portugal

Spinal cord injury (SCI) is well known to induce severe bone loss thus increasing fracture risk. Bone fracture healing in SCI individuals can be either normal or impaired, whence such impairment may be either accelerated or delayed. The aim of this study was to investigate SCI-induced bone loss and the callus formation in rats sustaining a bone fracture. Thirty six-week-old male Wistar rats were divided into two experimental groups: (1) CON: control rats with bone fracture; (2) SCI: SCI rats with bone fracture. SCI was performed as previously described (1). Ten days after SCI, the femoral diaphysis was fractured by a closed method (2). Immediately after fracturing the bone, an incision was made parallel in the proximal extremity of the femur and a 1-mm-diameter Kirschner wire was introduced into the medullary canal in order to stabilize the bone fragments. Bone callus formation was observed for 14 days post-fracture. At the end of the experiment, animals were euthanized, femurs and tibias were harvested and analyzed by morphometric measurements, μCT, DXA, mechanical test, histomorphometry, immunohistochemistry and gene expression at the femoral bone callus and intact tibia. Gene expression in non-fractured bones was downregulated by SCI, resulting in several phenotypic changes related to severe bone loss (Fig 1A-F). Our data showed that SCI decreased bone mass in 21%, length in 6%, shaft perimeter in 14%, bone mineral density in 43% and severe microarchitecture deterioration at both trabecular and cortical bone (i.e. reduction in bone volume, trabeculae volume, number, thickness, density and connectivity, decrease in cortical volume and density and, increase in trabeculae separation), resulting in lesser mechanical strength (45% reduction in maximal load and 50% in stiffness). Although no difference was seen in gene expression at bone callus, SCI impaired fracture healing by reducing its density (-41% in BMD) and formation (decrease in newly formed trabeculae number and thickness, associated with increased porosity). Our histological data evidenced the healing delay in SCI rats by showing callus mainly formed by an unorganized non-bony structure and with an impairment in bone resorption regulation due to decreased OPG expression. As a result, bone callus was weaker in the SCI rats than in control (44% reduction in torque and 62% in failure angle). In conclusion, SCI resulted in severe deleterious changes in bone metabolism, delaying fracture callus formation.

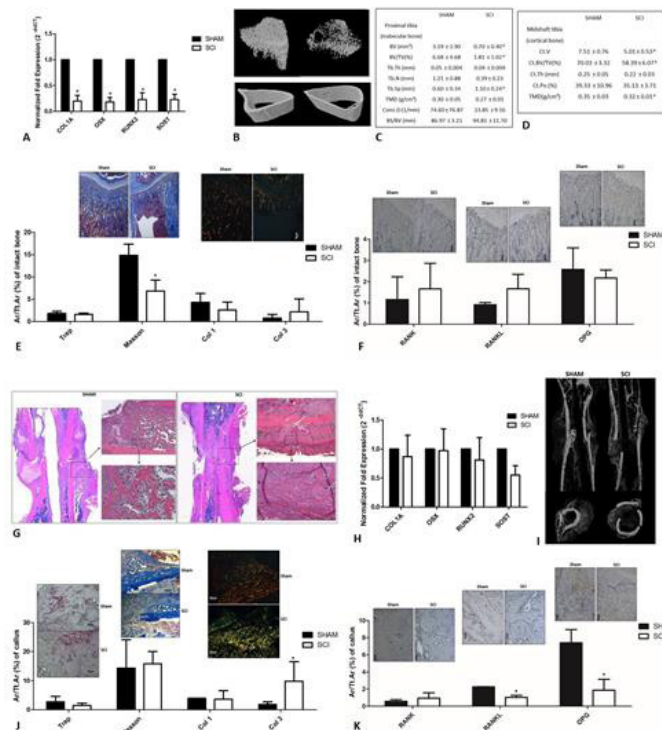


Figure 1. (A-F) analysis of the non-fractured tibia; (A) gene expression was downregulated by SCI; (B) μCT images showing trabecular and cortical loss in SCI rats; (C) μCT data of trabecular bone; (D) μCT data of cortical bone; (E) histomorphometry resorption area (TRAP staining, 100x), newly formed bone (Masson staining, 50x) and types 1 and 3 collagen deposition (50x); (F) immunohistochemistry showing the expression of RANK, RANKL and OPG (200x); (G-I) analysis of the fractured femur; (G) Histological slides stained with HE (12.5x, 50x and 200x); (H) gene expression of μPCR; (I) μCT images of bone callus; (J) histomorphometry; resorption area (TRAP staining, 100x), newly formed bone (Masson staining, 50x) and types 1 and 3 collagen deposition (50x) and; (K) immunohistochemistry (RANK, RANKL and OPG, 200x). Asterisks indicate p<0.05.

Disclosures: Mariana Butezloff, None

LB MON - 1156

Age and Gender Effects on Architectural, Biomechanical and Muscle Performance in C57BL/6 Mice Hammad Mumtaz*, Julian Vallejo, Mark Dallas, Nuria Lara-Castillo, Joanna Scott, Michael Wacker, Mark Johnson, Thiagarajan Ganesh. University of Missouri Kansas City, United States

The biomechanical performance with aging of femur, ulna and tibia were determined in C57BL/6 mice. Three groups of mice 6, 12, and 22 mo old female (n=5-7 per age) and male (n=6-7 per age) were analyzed using microCT and three point bending. We calculated the ultimate load to failure (UL), elastic stiffness (K), modulus of elasticity (E) and the moment of inertia about bending axis (MOI) for each bone. Linear regression models with robust standard errors were used to determine differences in the all parameters with age in each bone and sex. MicroCT scans of all the bones were analyzed to determine cortical BV/TV, trabecular BV/TV and cortical bone area (B.Ar) and tested for correlation with the biomechanical parameters. EDL and Soleus contractile properties were determined ex vivo. The significance level was set to p < 0.05. In femur and tibia, UL was significantly reduced at 22 mo compared to 6 mo in both sexes. In male femur and tibia, K reduced significantly from 6 to 12 mo and 22 mo of age. In female tibia K was significantly lower at 22 months. In ulna, K increased significantly at 22 mo in females, but did not change in males. In both male and female femurs E was reduced significantly at 22 mo. In female ulna, E increased significantly at 12 and 22 mo of age, while no change was detected in male ulna. Female femur showed significant increase in MOI at the age of 12 mo, while no change was observed in males. MOI was reduced significantly in male tibia from 6 to 12 mo and 22 mo of age with no change detected in females. MicroCT analysis showed that cortical BV/TV is significantly correlated with UL and K of male and female femur, E of female femur, and K of female ulna. Trabecular BV/TV is significantly correlated with UL and K of male femur, UL of male tibia, and MOI of female femur. B.Ar was significantly correlated with MOI of male femur, with K and UL of both male and female femurs, and with UL of male tibia and ulna. On average, EDL and Soleus weight to body weight and maximum force reduced across aging. EDL contractile properties were positively correlated with B.Ar in females only. Soleus contractile properties showed no correlations with structural properties. In conclusion, aging effects on the skeleton need to be evaluated in a site-specific fashion and global conclusions extrapolated from one bone to another may not be valid. Significant differences between sexes occur acro

Disclosures: Hammad Mumtaz, None

Monday Posters

LB MON - 1159

Quantifying Bone Marrow Adiposity Using T1-weighted Magnetic Resonance Images in Children With Typical Development and in Children With Cerebral Palsy Chuan Zhang^{*1}, Freeman Miller², Christopher Modlesky¹.
¹University of Georgia, United States, ²AI duPont Hospital for Children, United States

Background: Bone marrow contains mesenchymal stem cells which have the potential to promote both osteogenesis and adipogenesis at the expense of one another. Thus, quantifying adipose tissue in bone marrow may shed new light on bone growth and development status. Chemical shift magnetic resonance imaging (MRI) has been suggested to have good accuracy in assessing bone marrow adipose tissue (BMAT) in vivo. Some studies have also used standard T1-weighted magnetic resonance images to assess BMAT, but the accuracy has not been determined in children. The aim of this study was to determine whether a method using T1-weighted images provides an accurate estimate of BMAT in children who are typically developing, or in those with elevated BMAT infiltration, such as children with cerebral palsy (CP). **Methods:** Fifteen ambulatory children with spastic CP and 15 typically developing children (age range 4-11 y; 11 boys and 4 girls/group) participated in the study. Axial images (0.5 cm thick with 0.5 cm spacing) were collected from the tibia using an MRI scanner (GE, 1.5 T, Milwaukee, WI) and two different protocols. The first protocol (fast spin echo, TR = 650, TE = 14, FOV = 12, NEX = 3, BW = 15.63, frequency = 512, phase = 256) yielded standard T1-weighted images. The second protocol (IDEAL: fast-spin-echo, TR = 600, TE = min full, FOV = 12, NEX = 2, BW = 31.25, frequency = 320, phase = 224) yielded fat and water images. Images representing the mid-third of the tibia (i.e., midtibia) were processed. Bone marrow volume was determined using the standard T1-weighted images. BMAT volume was determined using the standard T1-weighted images (BMATVT1) and the fat and water images (BMATVIDEAL). BMAT fraction was calculated as the ratio of BMATVT1 to bone marrow volume (BMATFT1) and as the ratio of BMATVIDEAL to bone marrow volume (BMATFIDEAL). Results: BMATVT1 and BMATVIDEAL were highly correlated ($r > 0.99$, $p < 0.001$) and BMATFT1 and BMATFIDEAL were moderately correlated ($r > 0.7$, $p < 0.01$) in both groups of children. There were no group differences in BMATVT1 or BMATVIDEAL (both $p < 0.05$). BMATFIDEAL was higher in children with CP than in typically developing children ($p < 0.05$), but there was no significant group difference in BMATFT1 ($p > 0.05$). **Conclusion:** Standard T1-weighted magnetic resonance images can produce estimates of BMAT volume similar to estimates from chemical shift imaging in children. However, they are less sensitive to variation in AT concentration in the bone marrow.

Disclosures: Chuan Zhang, None

LB MON - 1162

Late adulthood skeletal muscle weakness and atrophy in osteoporotic OPG null mice Dounia Hamoudi^{*1}, Laetitia Marcadet¹, Louis-Benedict Landry², Antoine Boulanger-Piette¹, Françoise Morin³, Anteneh Agraw⁴, Jérôme Frenette⁵.
¹PhD student, Canada, ²Trainee, Canada, ³Professional Research, Canada, ⁴PhD, Canada, ⁵Professor, Canada

Bone and muscle are tightly coupled under normal conditions forming the functional muscle-bone unit. Cumulative evidence supports the existence of bidirectional muscle-bone molecular interactions. Osteoprotegerin (OPG) is a soluble decoy receptor and a key regulator of bone homeostasis and the lack of OPG causes an early onset osteoporosis in mice and human. In addition to bone cells, stimulated muscle cells can secrete OPG but, the role of OPG on muscle physiopathology remains poorly understood. **Methods:** Muscle function was evaluated in OPG null mice (OPG^{-/-}), a model of juvenile Paget disease, and age-matched C57BL/6J (C57) mice were used as controls. To access the functional performances, four-limb grip strength and 12-h voluntary activity in open field, recorded using a video tracking system, were measured at 1, 3 and 5-month-old in OPG^{-/-} and C57 mice. Ex vivo contractile properties followed by immunohistological staining were then performed on the fast-twitch extensor digitorum longus (EDL) muscles. Three-point bending tests, at the femur mid-diaphysis, were completed to confirm that OPG^{-/-} mice were osteoporotic. **Results:** Contractile properties of EDL muscles and functional performances showed that OPG deletion did not affect muscle function and integrity in 1 and 3-month-old mice. Interestingly, 5-month-old OPG^{-/-} and C57 mice had similar locomotor activity in open field but absolute (P0; g) and specific force production (sP0; N/cm²) of EDL muscles and normalized grip strength (gF/g) were significantly diminished in OPG^{-/-} mice. Moreover, muscle mass and myofiber area were significantly smaller in OPG^{-/-} compared to C57 mice at 5 months of age. **Conclusion:** Functional and contractile properties showed that the absence of OPG did not affect muscle function of young mice but caused, regardless of locomotor activity, muscle atrophy and weakness later in life.

Disclosures: Dounia Hamoudi, None

LB MON - 1169

Heterozygous ZNF687 P937R mutation underlies giant cell tumors arising from Paget's disease of bone also in non-Caucasian patients Fernando Gianfrancesco^{*1}, Giuseppina Divisato¹, Deborah J Veis^{2,3}, Yasmine Abbes¹, Federica Scotto Di Carlo¹, Teresa Esposito^{1,4}, Michael P Whyte^{5,6}.
¹Institute of Genetics and Biophysics, National Research Council of Italy, Italy, ²Division of Bone and Mineral Diseases, Department of Internal Medicine, Washington University School of Medicine at Barnes-Jewish Hospital, United States, ³Department of Pathology, Washington University School of Medicine at Barnes-Jewish Hospital, United States, ⁴IRCCS INM Neuromed, Italy, ⁵Department of Internal Medicine, and Department of Pathology, Washington University School of Medicine at Barnes-Jewish Hospital, United States, ⁶Center for Metabolic Bone Disease and Molecular Research, Shriners Hospital for Children, United States

Giant cell tumor of bone (GCTB) is a rare but severe complication of Paget's disease of bone (PDB). It typically occurs in polyostotic PDB. The prognosis for GCTB/PDB is poor, with ~ fifty percent of patients surviving 5 years. Recently, a founder germline mutation P937R in the ZNF687 gene was identified to underlie GCTB/PDB (all of 15 cases), but the study population was exclusively of Italian descent, all sharing the same haplotype. GCTB/PDB patients of different ethnic origin(s) were not studied. To fill this information gap, we performed mutation analysis of ZNF687 using DNA we extracted from a paraffin-embedded tumor of a deceased 45-yr-old black American woman with polyostotic PDB, neurofibromatosis type I, and remarkable extraskeletal osteoclastomas (JCEM 82: 3826-34, 1997). She had widespread PDB (skull, clavicles, ribs, pelvis, femurs and tibias) and developed two large extraskeletal tumors at the right iliac crest (15x10 cm) and left paraspinal (6x6 cm) regions as well as five smaller masses in the abdomen and pelvis. The ZNF687 P937R mutation was found in her osteoclastomas, but she did not have the ancestral haplotype that characterizes the Italian GCTB/PDB patients. We also explored the specificity of this ZNF687 mutation for GCTB/PDB, identifying a different ZNF687 mutation (R331W) in 1/28 pagetic osteosarcomas and the P937R mutation in 1/8 pagetic undifferentiated sarcomas; while no ZNF687 mutations were detected in other PDB neoplastic transformations (1 fibrosarcoma and 1 chondrosarcoma). Therefore, our results indicate that GCTB/PDB pathogenesis is globally caused by mutation in the ZNF687 gene that is involved in the DNA damage machinery to detect and repair lesions by homologous recombination. Conversely, the non-pagetic GCTB is due to alterations in the H3F3A gene, resulting in disrupted methylation of the H3.3 histone tail. Although the etiologies and pathological mechanisms are different, they give rise to histologically similar tumors, and misdiagnosis sometimes occurs. Thus, we report that combined analysis of ZNF687 and H3F3A mutations allows one to distinguish pagetic and conventional GCTBs, respectively. In fact, we identified the H3F3A mutation in a GCTB biopsy of a pagetic patient published as GCTB/PDB (Ann Rheum Dis 51: 1335-37, 1992), demonstrating here that a conventional GCTB can accompany PDB.

Disclosures: Fernando Gianfrancesco, None

LB MON - 1170

Ultra-Fast Na18F Whole Body Dynamic Using Digital PET/CT in a Preclinical Phase I Study Maria Menendez^{*}, Richard Moore, Katherine Binzel, Zhang Jun, Rebecca Jackson, Michael Knopp. The Ohio State University, United States

Na18F enables in vivo assessment of bone physiology and pathophysiology as well as its biodistribution. Whole Body (WB) Dynamic (DYN) PET imaging enables the acquisition of real time spatio-temporal activity concentration of the whole skeleton tracer uptake. DYN PET acquisitions have been primarily performed in single-bed axial field-of-views (FOVs). There is an important unmet clinical need to translate static single FOV PET into DYN WB PET. The aim of this study was to assess the ultra-fast Na18F WB DYN protocol feasibility using digital PET/CT (dPET/CT) for systemic bone imaging in a healthy canine model, and to compare it with the single bed dynamic. Twelve healthy, adult male Beagles (weight (kg) mean \pm SD; 15 \pm 1.54) were scanned. Two different doses of 3 mCi and 50 μ Ci Na18F were administered at different days. For the single FOV, imaging was initiated at the time of injection, covered 1 bed position covering the pelvis and knees, acquiring 120 seconds/bed position, lasting 30 minutes. Ultra-fast WB DYN imaging was initiated at the time of injection, covered 10 bed positions, acquiring 12 seconds/bed position for 6 consecutive WB runs, lasting 12 minutes. All imaging was performed on a digital photon counting PET/CT system. PET listmode data were reconstructed using a 576x576 matrix, producing a 1mm³ isotropic voxel size; using point spread function and Gaussian filtering. Three iterations with three subsets were used for reconstructions. Standardized uptake values (SUVmean) were assessed in the following regions of interest (ROI) including distal femur, wrist, tarsal joint, first lumbar vertebra, and liver. Blinded experienced reviewers evaluated dynamic acquisitions via visual assessment of image quality. Ultra-fast WB DYN acquisitions were shown to be feasible and resulting in excellent image quality as scored during blinded review (Fig.1). Qualitatively and quantitative assessment provided detailed insight into skeleton perfusion and bio-distribution characteristics. Quantitative outcome measurements were highly consistent among ROIs in all subjects. Ultra-fast Na18F WB DYN using a dPET/CT showed a 10x reduction in acquisition time (120 to 12 seconds per bed), in addition to increasing the FOV from 1 bed (16.4 cm) to 10 beds (? 100 cm including overlap), allowing for whole skeleton assessment. The use of this methodology in a healthy dog provided feasi-

bility to increase Na¹⁸F dPET/CT diagnostic capabilities by providing a real time ultra-fast Na¹⁸F WB DYN PET, in addition to the WB static PET/CT acquired a posteriori in a standard dPET/CT examination. The Na¹⁸F dPET/CT canine imaging is a capable translational model that may advance bone imaging by providing a sensitive tool to visualize and quantify bone pathophysiology on both specific organs as well as at a systemic (whole-body) level.

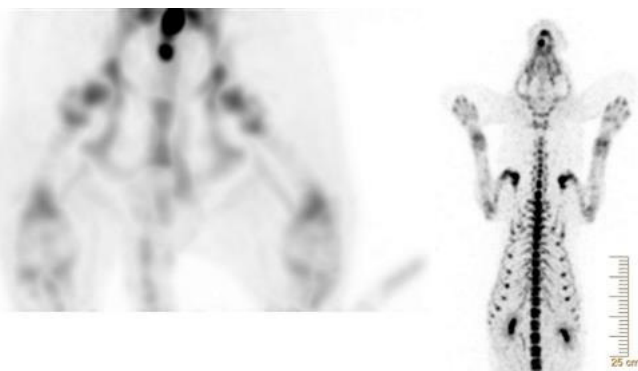


Figure 1: Representative Dynamic Na¹⁸F PET images acquired 12 minutes after Na¹⁸F administration. Showing a single FOV (top) and an Ultra-fast Na¹⁸F Whole Body Dynamic (right) using digital PET/CT in a canine model. Despite a 10X reduction in acquisition time (120 to 12 seconds/bed), in addition to an increased FOV from 1 bed (16.4 cm) to 10 beds (\approx 100 cm including overlap), the whole body DYN PET showed excellent image quality, and fast systemic Na¹⁸F biodistribution, providing additional whole skeleton tracer biodistribution.

Disclosures: *Maria Menendez, None*

LB MON - 1171

Heat Increases IGF-I Uptake in Growth Plate and Perichondrium Measured by in vivo Multiphoton Imaging Maria A Serrat*, Gabriela Ion, Dominic Thomas. Marshall University School of Medicine, United States

Introduction: Research into the molecular regulation of bone elongation has led to development of promising drug therapies for many growth plate disorders. However, delivering therapeutics to avascular cartilage remains a significant challenge. We previously combined a limb heating model with the growth-stimulating drug IGF-I to demonstrate that low dose IGF-I augments bone-lengthening effects of targeted, intermittent heat in mice. Here, we use in vivo multiphoton microscopy to directly measure uptake of IGF-I in growth plate and surrounding perichondrium at temperatures within a physiological range of healthy human knees. We tested the hypothesis that heat increases uptake of IGF-I in cartilage using fluorescently labeled, biologically active IGF-I measured in and around proximal tibial growth plates of live mice. **Methods:** Procedures were approved by our IACUC. 5-week old male and female C57BL/6 mice (N=9) were obtained from an in-house breeding colony. Purified human IGF-I (PeproTech) was conjugated with Alexa Fluor 488 (Life Technologies) and assessed for biological activity following our published protocols. The hindlimb was cooled (22C) or warmed (36C) and fluorescent IGF-I (\sim 6 μ g/g body wt) was visualized in the proximal tibial growth plate and perichondrium by multiphoton imaging at consistent depths and times as we have previously described. Data were collected in standardized regions. Statistical analysis was performed using independent samples t-tests in SPSS. **Results:** Warm temperature increased uptake of fluorescently labeled IGF-I in growth plate and perichondrium within 60 min after injection (Fig. 1). There was >1.5 times more IGF-I in the superficial perichondrium at 36C relative to 22C ($t=1.8$, $p<0.05$), and more than twice as much at the deepest edge of the perichondrium immediately adjacent to the growth plate ($t=2.12$, $p<0.05$), as well as in the growth plate itself ($t=2.05$, $p<0.05$). These data complement our prior results showing that IGF-I enhances bone lengthening effects of targeted heat, likely by increasing its uptake in the growth plate. **Conclusion:** These data support the hypothesis that heat increases IGF-I uptake in the proximal tibial growth plate and perichondrium of young mice. Our results using physiological knee temperatures suggest that mild limb heating could be a novel, noninvasive approach for modulating and targeting delivery of therapeutics such as IGF-I to enhance bone elongation in impaired growth plates of children.

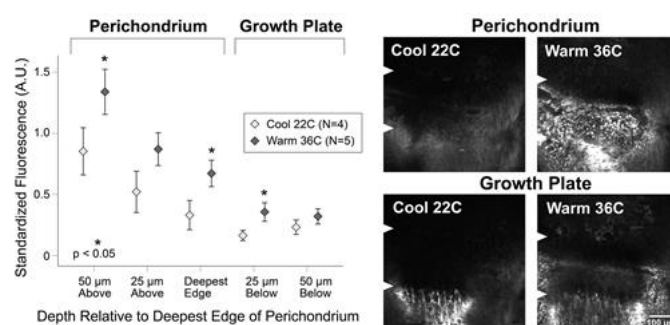


Fig 1. Heat increases IGF-I uptake in growth plate and surrounding perichondrium. Error bar plot (left) shows IGF-I fluorescence in regions of growth plate and perichondrium measured in 25 μ m optical sections from superficial to deep 60 minutes after injection. Images (right) show IGF-I accumulation in deepest edge of the perichondrium (top panel) and 25 μ m below in the growth plate (bottom panel). Growth plate is between arrowheads. Metaphyseal bone is at the bottom. There was over twice as much IGF-I in the perichondrium and growth plate in these regions at 36C compared to 22C. Mean \pm 1 SE plotted; * $p<0.05$, denotes significant increase at 36C by independent samples t-test.

Disclosures: *Maria A Serrat, None*

LB MON - 1176

Differentiated Osteocytes Synthesize Taurine Which Reduces Sclerostin Expression and Prevents Osteocyte Cell Death Matt Prideaux*, Yukiko Kitase, Morris Kimble, Thomas O'Connell, Lynda Bonewald. Indiana University, United States

Taurine is a ubiquitous metabolite, known to be important in a number of metabolic processes. It has been shown that taurine protects against bone loss in osteoporotic rats. Taurine is synthesized by the liver, whereas the major source is absorbed through the diet. An untargeted NMR-based metabolomics approach was used on IDG-SW3 cells taken at days representing the early osteoblast (day 4), osteoid osteocyte (day 9), mineralizing osteocyte (day 18) and mature osteocyte (day 28). While performing metabolomic analysis, a two-fold elevation of taurine was observed in differentiating cells, peaking at 1 mM at day 18 and remaining elevated at day 28 ($p<0.001$). Interestingly, methionine consumption increased with cell differentiation, with a commensurate production of taurine only within the cell lysate but not in the media. The mRNA expression of Cysteine Dioxygenase (Cdo1), the rate-limiting enzyme of the taurine biosynthesis pathway, was highly expressed in these cells and increased greater than two-fold at day 18 compared to day 4 of differentiation ($p<0.001$). Similarly, Cdo1 mRNA expression was 6.5 fold higher in osteocyte-enriched bone chips compared to osteoblasts taken from the long bones of C57Bl6 mice ($p<0.001$). To determine if taurine may have an autocrine function in osteocytes, exogenous taurine (1-50 mM) was tested on day 28 IDG-SW3 cells. Taurine dose-dependently inhibited Sost mRNA expression by 60-70% in IDG-SW3 cells after 24 hrs ($p<0.01$), suggesting a potential mechanism for the beneficial effects of taurine on bone. As osteocytes are long lived cells subjected to the effects of aging and generation of elevated reactive oxygen species (ROS), the MLO-Y4 osteocyte-like cells were pretreated with taurine before exposure to H₂O₂. Taurine at 1-50 mM reduced H₂O₂ induced cell death by 30-60% ($p<0.001$). These studies show that osteocytes, like liver, have the capacity to synthesize taurine, but unlike liver, do not secrete taurine. Some of the beneficial effects of exogenous taurine on bone may be mediated through osteocytes. The synthesis of taurine by these cells may serve a protective function by preserving cell viability when exposed to elevated levels of ROS and utilized by osteocytes to survive under the demanding conditions within the lacuno-canalicular environment.

Disclosures: *Matt Prideaux, None*

LB MON - 1177

A Novel Mouse Model to Elucidate the Role of Gdf5 in Postnatal Joints Steven Pregizer*¹, Vicki Rosen*². ¹Boston Children's Hospital, United States, ²Harvard School of Dental Medicine, United States

Growth and Differentiation Factor 5 (Gdf5) is expressed in all developing joints and plays a key role in joint morphogenesis. There is also a strong genetic association between Gdf5 and osteoarthritis (OA); however, it is unclear if the influence of Gdf5 in OA is due to altered joint development or to a specific role for Gdf5 in the maturation and/or subsequent maintenance of joints in postnatal life. To address this fundamental question, we developed a novel mouse model that allows us both to monitor Gdf5 expression and to inactivate Gdf5 in postnatal joints. First, we obtained embryonic stem (ES) cells containing a targeted "knock-out first" Gdf5 allele from the International Knockout Mouse Consortium repository. This allele contains a gene-trapping reporter cassette expressing LacZ instead of Gdf5, thus rendering the allele non-functional, yet useful for monitoring transcriptional activity of the locus. Next, we established a mouse line harboring this allele via microinjection of the ES cells into blastocysts and propagation of the resulting founder chimeras. Animals with a single copy of the modified allele (Gdf5LacZ/+) had a joint-restricted pattern of LacZ expression during embryogenesis, perfectly recapitulating that of the native Gdf5 allele. Interestingly, LacZ expression persisted in articular cartilage until birth, but diminished rapidly thereafter. Animals with two copies of the modified allele (Gdf5LacZ/LacZ) had shortened skeletal elements, missing joints in the wrists, ankles, and digits, missing or hypoplastic fibulas, and

dysmorphic knees lacking cruciate ligaments, perfectly recapitulating the limb phenotype of homozygous Gdf5-null mice. Next, we derived from these mice a conditional Gdf5 mouse line by outcrossing to a Flp-expressing strain. From this intercross we obtained progeny in which the LacZ reporter was excised from the germline, owing to a pair of FRT sites flanking the reporter cassette. Animals with two copies of the derived allele (Gdf5^{lox/lox}) exhibited no overt differences in limb length compared to wild-type littermates; moreover, the fibula and cruciate ligaments were present, indicating restoration of Gdf5 expression to the allele. Importantly, a pair of loxP sites flanking a critical exon can recombine in the presence of Cre, excising the exon and disrupting Gdf5 expression. This novel mouse model provides temporal control over Gdf5 levels and can be used to provide a framework for understanding how changes in Gdf5 availability correlate with joint homeostasis and the development of OA.

Disclosures: **Steven Pregizer, None**

LB MON - 1179

Bone is a major contributor of plasma FGF23 elevation in a model of chronic kidney disease in wildtype mice and mice lacking the extra-large G protein α -subunit (XLAs) Julia Matthias^{*1}, Lauren Shumate¹, Antonius Plagge², Harald Jüppner¹, Qing He¹, Murat Bastepe¹. ¹Endocrine Unit, Massachusetts General Hospital, Harvard Medical School, United States, ²Institute of Translational Medicine, University of Liverpool, United Kingdom

FGF23 is a phosphaturic hormone, whose levels rise in renal failure to maintain normal phosphate levels and prevent soft tissue mineralization. The FGF23 elevation contributes greatly to the morbidity and mortality in patients with chronic kidney disease (CKD). Mechanisms causing kidney injury-induced FGF23 elevation are poorly defined. Inflammatory mediators, which are systemically increased in CKD, can induce FGF23 expression, and bone marrow (BM) has recently been shown to contribute significantly to FGF23 production in acute kidney injury or upon bleeding. The origin of FGF23 in CKD remains uncertain. We have found that the extra-large G protein α -subunit (XLAs), which is expressed in bone, mediates FGF23 synthesis in early postnatal life. To investigate whether XLAs is involved in FGF23 synthesis in CKD, we fed XLAs knockout (XLKO) and wildtype (WT) littermates a 0.2% adenine-containing diet. This led to the expected renal tubulopathy, as confirmed by histological analyses. Plasma C-terminal FGF23 levels were 136±102 and 273±116 pg/ml at baseline in XLKO and WT mice, respectively, and rose significantly one week after starting the diet in both groups (2,444±2,387 and 1,950±637 pg/ml, respectively). At 6 weeks, FGF23 levels were markedly elevated, with higher levels in XLKO than WT (96,000 vs. 22,000 pg/ml; p<0.01). XLKO mice also showed higher BUN levels at 6 weeks (96.6±30.6 vs. 57.5±22.6 mg/dl; p<0.01), indicating more pronounced kidney impairment. Analysis of inflammation markers in bone and BM revealed a tendency of IL-1 β mRNA levels to rise in XLKO but not WT mice (bone: 1.7±0.8-fold; p=0.10; BM: 1.8±0.9-fold; p=0.06), suggesting greater inflammation in XLKO. Interestingly, XLKO bones displayed higher HIF1 α mRNA levels than WT bones at baseline (1.4±0.2-fold; p=0.01). Regardless of the genotype, FGF23 mRNA levels rose in both bone and BM, but the bone levels were 203±152 or 42±55.1 times higher than BM levels at baseline and at 6 weeks, respectively. Moreover, a direct relationship was observed between plasma FGF23 and bone FGF23 mRNA levels (r=0.9; p<0.00001), while no significant correlation could be detected between plasma FGF23 and BM FGF23 mRNA levels (r=0.32; p=0.13). Our findings suggest that XLAs ablation increases susceptibility to adenine-induced renal failure, and that bone, rather than BM, is an important contributor to plasma FGF23 levels in this CKD model.

Disclosures: **Julia Matthias, None**

LB MON - 1183

Associations of Joint Trajectories of Appendicular Lean Mass and Grip Strength with Risk of Non-Spine Fractures Rodrigo Valderrabano^{*1}, Neeta Parimi², Peggy M. Cawthon³, Jennifer S. Lee^{3,4}, Joy Y. Wu³, Andrew R. Hoffman^{3,4}, Marcia L. Stefanick⁵. ¹Division of Endocrinology, University of Miami Miller School of Medicine, Miami, FL, United States, ²California Pacific Medical Center, San Francisco, CA and Department Epidemiology and Biostatistics, UCSF, SF, United States, ³Division of Endocrinology, Stanford University School of Medicine, Stanford, CA, United States, ⁴Palo Alto Veteran Affairs Health Care System, Palo Alto, CA, United States, ⁵Stanford University School of Medicine, Stanford, CA, United States

Muscle strength and appendicular lean mass (ALM) are interrelated and may jointly influence fracture risk. Patterns of change in muscle strength and mass may be important. We hypothesized that combined trajectories of change in grip strength (GS) and ALM/ht2 would be associated with fractures independent of values at the beginning or end of the change period. The Osteoporotic Fractures in Men (MrOS) study prospectively evaluated men ages 65 years or older with grip strength by hand dynamometry and ALM/ht2 by DXA at up to four visits from 2000-2009 and subsequently adjudicated incident fractures after 2009. We analyzed 3501 men after excluding those missing covariate or DXA data. Group based trajectory models identified 3 trajectory groups for both ALM/ht2 and grip strength, which declined at roughly parallel rates within measures. Groups were classified as "high", "intermediate" and "low" based on their starting and ending values, which reflected relative performance levels. The nine combined trajectories represented different musculoskeletal phenotypes (i.e. Low ALM/ht2 / High GS) and were used as predictors. The (Intermediate

ALM/ht2 / Intermediate grip strength) group served as the referent. Cox proportional-hazards models estimated the hazards ratio (HR) and 95% confidence interval (CI) of subsequent non-spine fracture (after the trajectory period). We adjusted for: age, BMD, race, study site, and potential confounders, and then subsequently adjusted for the last visit value for ALM/ht2 or grip strength. 569 first incident non-spine fractures occurred during follow up. Men in the low ALM/ht2 / high GS group had reduced risk of non-spine fracture (HR 0.48; 95% CI 0.26-0.90) relative to the referent group (Table). This association remained after adjustment for LV ALM (HR 0.48; 95% CI 0.25-0.90) but was attenuated after consideration of LV GS (HR 0.61; 95% CI 0.32-1.16) and no longer significant. None of the other trajectory groups were associated with fracture risk. Combined trajectories in strength and lean mass were not robustly associated with fracture risk. However, older men with consistently high grip strength and low lean mass had reduced fracture risk, which was in part explained by higher grip strength value at the last visit. The reason for the association with reduced fracture in this group is not clear. Our findings do not support using these trajectories over single measurements of musculoskeletal parameters for fracture risk stratification.

Table. Association of Combined ALM and Grip Strength Trajectories with Risk of Non-Spine Fracture (HR [95% CI])

		Grip trajectory		
		Low	Intermediate	High
ALM/ht ² trajectory	Low	0.99 (0.75-1.31)	1.08 (0.84-1.38)	0.48 (0.26-0.90)
	Intermediate	1.28 (0.96-1.71)	Referent	0.97 (0.73-1.30)
	High	1.11 (0.60-2.10)	1.21 (0.80-1.83)	1.23 (0.80-1.90)

*age, race and study enrollment site, total hip BMD, BMI, alcoholic drinks, osteoporosis medications, activity score, fall history, fracture after age 50, self-rated health
ALM: appendicular lean mass, Grip: Grip Strength by hand dynamometry, CI: confidence intervals

Disclosures: **Rodrigo Valderrabano, None**

LB MON - 1186

Qsox1 is a novel genetic determinant of bone size in mice Basel Al-Barghouti^{*1,2}, Gina Calabrese¹, Larry Mesner¹, Kevin Nguyen¹, Mary Bouxsein³, Daniel Brooks³, Mark Horowitz⁴, Clifford Rosen⁵, Steve Tommasini⁶, Petr Simecek⁷, Gary Churchill⁷, Cheryl Ackert-Bicknell⁸, Daniel Pomp⁹, Charles Farber¹⁰. ¹Center for Public Health Genomics, University of Virginia, Charlottesville, VA 22911, United States, ²Department of Biochemistry and Molecular Genetics, University of Virginia, Charlottesville, VA 22911, United States, ³Center for Advanced Orthopedic Studies, Beth Israel Deaconess Medical Center, Department of Orthopedic Surgery, Harvard Medical School, Boston, MA 02215, United States, ⁴Department of Orthopaedics and Rehabilitation, Yale School of Medicine, New Haven, CT 06520, United States, ⁵Maine Medical Center Research Institute, 81 Research Drive, Scarborough, ME 04074, United States, ⁶Department of Orthopaedics and Rehabilitation, Yale School of Medicine, New Haven, CT 06520, United States, ⁷The Jackson Laboratory, Bar Harbor, Maine 06409, United States, ⁸Center for Musculoskeletal Research and Department of Orthopaedics & Rehabilitation, University of Rochester Medical Center, Rochester, NY, 14627, United States, ⁹Department of Genetics, University of North Carolina Medical School, Chapel Hill, NC 27599, United States, ¹⁰Departments of Public Health Sciences and Biochemistry and Molecular Genetics, University of Virginia, Charlottesville, VA 22911, United States

Osteoporosis is a complex disease of reduced bone strength and increased risk of fracture. Many characteristics of bone contribute to its strength; however, other than bone mineral density (BMD), which has been interrogated using genome-wide association studies (GWAS) in humans, we know little of the genetics of other strength-related traits such as bone size. To identify novel genetic factors affecting bone size, we used a powerful new murine resource, the Diversity Outbred (DO). The DO is an outbred population derived from eight genetically diverse inbred founder strains. We measured femoral size (femoral length (FL) and medial-lateral (ML)/anterior-posterior (AP) femoral widths) in a cohort of 12-16 week-old DO mice of both sexes (N=602). A significant (LOD=9.5; permutation P<0.05) quantitative trait locus (QTL) affecting ML was identified on Chr1@155Mbp. The QTL mapped to a confidence interval of ~2.8 Mbp and explained 6.6% of the variance in ML. We replicated the ML QTL in an independent cohort of 12 week-old DO mice of both sexes (N=312). To identify the gene(s) responsible, we queried the locus for non-synonymous mutations and expression QTLs (eQTLs). We imputed a complete list of variants from whole genome sequences of DO founder strains within the DO cohort and performed single variant association tests. None of the most significant variants were non-synonymous. We next identified eQTL for all genes in proximity of the ML QTL using tibial RNA-seq profiles from 192 DO mice. Of the 14 genes with eQTL, Quiescin Sulfhydryl Oxidase 1 (Qsox1) was the only one in which the ML QTL and eQTL founder haplotype effects were concordant, with the WSB/EiJ founder haplotype being associated with increased ML and decreased Qsox1

levels. QSOX1 is a secreted catalyst of disulfide bond formation that has not been previously linked to the regulation of bone size. Using CRISPR/Cas9, we generated five Qsox1 mutant lines with mutations ranging from a 1 bp frameshift to a ~1300 bp deletion encompassing the first exon of Qsox1. QSOX1 activity in serum was abolished in mutant mice from all lines. Across the five lines, we observed significantly ($P < 4.1 \times 10^{-6}$) increased ML as a function of the number of Qsox1 mutant alleles. These data identify Qsox1 as a genetic determinant of bone size and highlight the power of the DO for the genetic analysis of complex traits.

Disclosures: Basel Al-Barghouthi, None

LB MON - 1189

Deletion of the auxiliary $\alpha 2\delta 1$ voltage sensitive calcium channel subunit regulates adipogenesis Christian S. Wright*, Xin Yi, Madison M. Kelly, Karan Sharma, William R. Thompson. Department of Physical Therapy, School of Health and Rehabilitation Sciences, Indiana University, United States

Bone loss, due to disuse or the consequences of aging, is accompanied by increased bone marrow adiposity, further impairing bone quality. Given bone marrow progenitors contribute to bone and fat formation, understanding the signaling events which control mesenchymal stem cell (MSC) fate can inform the design of interventions to enhance bone quality. Calcium influx is the first measurable response of bone cells to mechanical stimuli, which is tightly regulated by voltage sensitive calcium channels (VSCCs). Inhibition of VSCCs impairs osteogenesis, decreasing bone formation and mechanosensitivity, and stimulates adipogenesis. In addition to the pore-forming ($\alpha 1$) subunit, VSCC complexes contain auxiliary subunits like $\alpha 2\delta 1$. $\alpha 2\delta 1$ regulates the gating kinetics of the channel pore and facilitates trafficking of the channel pore to the cell membrane. We hypothesized that the $\alpha 2\delta 1$ subunit is necessary for the regulation of MSC fate lineage by influencing VSCC activity. Mice (C57BL/6) with global deletion of *Cacna2d1*, the gene encoding $\alpha 2\delta 1$, displayed increased whole-body adiposity longitudinally ($p=0.0038$) with a 22% increase in whole body fat (compared to WT) at 9 weeks of age by DXA. qPCR of RNA from whole tibiae showed a 4-fold increase in adiponectin (APN, $p=0.0111$) and a 2-fold increase in PPAR γ ($p=0.0259$) expression. To determine whether the adipogenic phenotype was a result of increased MSC adipogenesis, primary murine MSCs were exposed to adipogenic media following siRNA knockdown of $\alpha 2\delta 1$. Knockdown of $\alpha 2\delta 1$ increased the expression of adipogenic markers APN, PPAR γ , and perilipin by Western blotting, suggesting the $\alpha 2\delta 1$ subunit of VSCCs influences MSC fate. Furthermore, exposure of primary MSCs to adipogenic media decreased $\alpha 2\delta 1$ expression (-30% , $p < 0.05$) while exposure to osteogenic media increased $\alpha 2\delta 1$ expression ($+20\%$, $p=0.055$) by Western blotting. Coupled with our previous work showing $\alpha 2\delta 1$ regulates bone cell mechanosensitivity, these data suggest that $\alpha 2\delta 1$ is upregulated during osteogenic differentiation, potentially enhancing mechanosensitive responses; a feature not present in cells of adipogenic lineage. As the $\alpha 2\delta 1$ subunit is the exclusive binding site for the antiepileptic and neuropathic pain drug Gabapentin (GBP), where chronic use is associated with increased fracture risk and decreased bone quantity, these data provide mechanistic insights into how GBP may influence bone development.

Disclosures: Christian S. Wright, None

LB MON - 1190

Risk of Osteoarthritis by Bone Mineral Density Status in US and Korean Older Adults: NHANES 2005-2010 & 2013-2014 and KNHANES 2008-2011 Han-Saem Park*, Seung-Hee Kim, Clara Yongjoo Park. Dept of Food and Nutrition, Chonnam National University, Republic of Korea

The association between bone mineral density (BMD) and osteoarthritis (OA) has been investigated in small studies, but the results are inconclusive. We examined the risk of OA by BMD status using two nationally representative databases of the US and Korea, the National Health and Nutrition Examination Survey (NHANES) and Korea NHANES (KNHANES), respectively. Postmenopausal women ≥ 40 years and men ≥ 50 years participating in NHANES ($n=4,551$ and $4,244$, respectively) and men and women ≥ 50 years of KNHANES ($n=2,824$ and $3,357$, respectively) with data on BMD, self-reported OA and covariates were included. Participants consuming osteoporosis medications were excluded in both populations. BMD was assessed by DXA. Bone measures were classified according to T-score following the WHO guidelines for osteoporosis or in tertiles. Femur T-scores were used to determine osteoporosis for NHANES subjects. Of KNHANES participants, the number of subjects with both OA and osteoporosis, which was determined by the lowest T-score of the hip, spine, or femur, were few, thereby the risk of OA was assessed by BMD tertiles in this population. Logistic regression was performed to calculate odds ratio (OR). In US post-menopausal women, those with osteoporosis had a 72% greater risk for OA compared to those with healthy bones (95% CI: 1.158-2.552; $p=0.03$). A similar trend was found in males [OR: 1.61 (95%CI: 1.005-2.568); $p=0.092$]. In Koreans, risk of self-reported OA was not associated with BMD in men, but women in the lowest tertile for lumbar spine BMD or whole body BMD had lower ORs for OA compared to those in the highest tertile [0.51 (95% CI: 0.37-0.71) and 0.59 (95% CI: 0.43-0.82), respectively; both $p < 0.01$], and a similar trend was observed with femoral neck BMD [OR: 0.69 (95% CI: 0.48-0.99); $p=0.07$]. The risk of OA was associated with BMD in both US and Korean women when assessed with nationally representative samples, though the direction was opposite. US post-menopausal women with osteoporosis have higher risk of OA, whereas Korean women with lower BMD had lower risk of OA.

Disclosures: Han-Saem Park, None

LB MON - 1197

Zika virus infection perturbs osteoblast function Bram Van Der Eerden*¹, Noreen Mumtaz², Marijke Schreuders-Koedam¹, Marion Koopmans², Barry Rockx², Johannes Van Leeuwen¹. ¹Erasmus MC, Internal Medicine, Netherlands, ²Erasmus MC, Viroscience, Netherlands

Zika virus (ZIKV) infection is typically characterized by a mild self-limiting disease presenting with fever, rash, myalgia and arthralgia. Virus-induced arthralgia due to perturbed osteoblast function has been described for other arboviruses. In case of ZIKV infection, the role of osteoblasts in ZIKV pathogenesis and bone-related pathology remains unknown. Here, we study the effect of ZIKV infection on osteoblast differentiation, and function by quantifying activity and gene expression of key biomarkers, using human bone marrow derived mesenchymal stem cells (MSCs) from 2 independent male healthy donors. We found that MSCs were highly susceptible to ZIKV infection. The Tissue Culture Infection Dose (TCID₅₀) exceeded 10 million particles within 48 h post-infection, which remained above 10 thousand in up to 20 days of culture. While infection did not cause a cytopathic effect, a delay in MSC-derived osteoblast differentiation and function was observed as compared to uninfected controls. Gene expression of the key osteoblast transcription factor RUNX2 was 30-50% reduced ($p < 0.05$) in MSC-derived osteoblasts at day 7 of differentiation. Alkaline phosphatase (ALP) mRNA was 40% reduced ($p < 0.05$) at day 7 of osteoblast differentiation as well, which corresponded with 30% less ALP activity ($p < 0.05$) at day 11 of culture. Finally, osteoblast mineralization measured by a calcium deposition assay, was severely affected as evidenced by 60-80% reduced calcium incorporation at day 18 and 21 of culture ($p < 0.05$). All effects observed were similar between the 2 donors. In conclusion, we have developed and characterized a new in vitro model to study the pathogenesis of ZIKV-induced arthralgia. This will help to identify possible new targets for developing therapeutic and preventive measures against the skeletal consequences of ZIKV infections.

Disclosures: Bram Van Der Eerden, None

LB MON - 1204

Role of fibrillin-1 fragments in bone resorption Muthu Lakshmi Muthu*, Kerstin Tiedemann, Svetlana Komarova, Dieter Reinhardt. McGill University, Canada

Marfan syndrome, caused by mutations in the fibrillin-1 gene, is a common type-I fibrillinopathy characterized by severe skeletal complications, including osteopenia and long bone overgrowth. How fibrillin-1 mutations lead to the skeletal problems is poorly understood. N-terminal sub-fragments of fibrillin-1 were identified as strong inhibitors of osteoclastogenesis in cell culture and in healthy animals. To identify potent osteoclast inhibitory sub-fragments of fibrillin-1, we produced several smaller fibrillin-1 N-terminal fragments. The purified proteins were tested for their function in osteoclastogenesis using primary osteoclasts. We observed reduced numbers and size of the differentiated osteoclasts. We plan to examine if these fibrillin-1 fragments exhibit sufficient anti-resorptive activity in a Marfan syndrome mouse model (Fbn1mgR/mgR). To understand the baseline bone parameters, we analyzed bones of Fbn1mgR/mgR mice at 4, 8, 12 and 16 weeks after birth. Compared to wild type littermates, young Fbn1mgR/mgR mice showed a trend of increased long bone length, increased body length and decreased bone mineral density which becomes significant at later time points. In osteoclastogenesis experiments, we found no significant difference in osteoclast number between the two groups. The expression of receptor activator of nuclear factor kappa-B ligand (RANKL) and osteoprotegerin (OPG) was increased in Fbn1mgR/mgR mice of both sexes, however the RANKL/OPG ratio was affected differently – it was higher in Fbn1mgR/mgR males compared to wild type, but lower in females. In conclusion, we have identified small fibrillin-1 fragments that exhibit osteoclast-inhibitory activity. Bone phenotype development in Fbn1mgR/mgR mice suggests that treatment with these fibrillin-1 fragments can be started at 4 week old animals.

Disclosures: Muthu Lakshmi Muthu, None

LB MON - 1205

Fluid flow shear stress alters interactions of osteoclasts to migratory tumor cells Yao Fan*¹, Aydin Jalali¹, Andy Chen¹, Bai-Yan Li², Ping Zhang³, Hiroki Yokota¹. ¹Indiana University, United States, ²Harbin Medical University, United States, ³Tianjin Medical University, China

Osteoclasts are multinucleated cells responsible for dissolving and absorbing mineralized bone tissue. Since bone loss in many diseases is linked to enhanced bone-resorbing activity, suppression of osteoclast activity is one of the primary therapeutic strategies, especially for patients with osteoporosis and osteolytic bone metastasis. While many lines of evidence demonstrate the effect of mechanical stimulation to mechano-sensing osteocytes, its effect to osteoclasts is not fully characterized. In this study, we addressed a question: does fluid flow shear stress to osteoclasts affect their interactions with migratory tumor cells in the bone microenvironment? It is reported that tumor-osteocyte interactions are affected by fluid flow-driven shear stress. Our hypothesis is that osteoclasts are sensitive to fluid flow shear stress, and they alter the migratory and proliferative behaviors of adjacent tumor cells. Using monolayer cultures and 3-dimensional spheroids, tumor cell lines (clones from MDA-MB-231 human breast cancer cells, and 4T1 mammary tumor cells) were cultured in the conditioned medium isolated from RAW264.7 osteoclast cells (CM), and fluid flow-treated

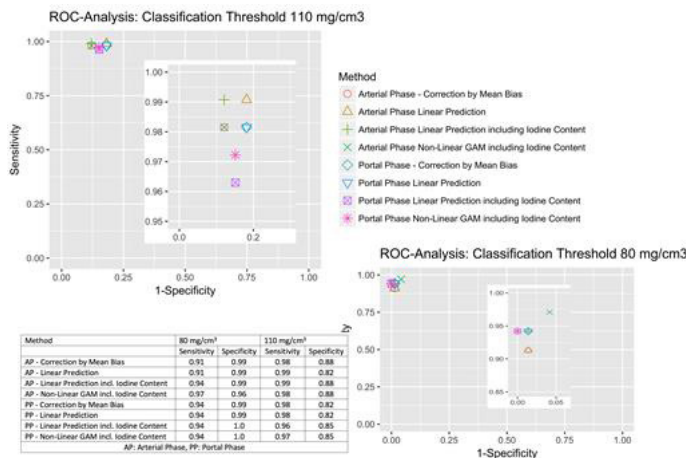
conditioned medium (FFCM; oscillatory fluid flow with 0.8 Pa shear stress at 1 Hz for 1 h). We conducted a tumor spheroid assay for evaluating proliferation of tumor cells, as well as a wound healing assay for examining their migratory capability. Furthermore, we evaluated expression of Snail, a transcription factor involved in epithelial-to-mesenchymal transition, as well as Src, a proto-oncogene tyrosine kinase. The results revealed that CM and FFCM induced opposing effects on cellular migration, proliferation, and expression of Snail and Src. While CM stimulated migration and upregulated Snail and Src, FFCM inhibited migration and downregulated Snail and Src. This study demonstrates the critical role of mechanical stimulation in tumor-osteoclast interactions. In response to mechanical stimulation, osteoclasts alter their influence to tumor cells and fluid flow-treated osteoclasts contribute to altering tumor cells less migratory in the bone microenvironment. Further analysis is needed to evaluate effects of mechanical stimulation, including other types of bone cells such as bone-forming osteoblasts and mechano-sensing osteocytes, and determine the risks and benefits of mechanical loading to bone.

Disclosures: **Yao Fan**, None

LB MON - 1209

Including Iodine based IV-Contrast Enhanced CT-Images into Screening Techniques for Osteoporosis Wolfram Timm^{*1}, J. Keenan Brown², Reimer Andresen³. ¹Mindways Software, Inc., Kiel, Germany, ²Mindways Software, Inc., Austin, TX, United States, ³Institute of Diagnostic and Interventional Radiology/Neuroradiology, Westkuestenlinikum Heide, Academic Teaching Hospital of the Universities of Kiel, Luebeck and Hamburg, Heide, Germany

Calibrated, phantomless asynchronous QCT makes feasible no-dose screening for osteoporosis from existing CT images acquired without IV contrast. Here we report results from studies including both native and IV-contrast enhanced CT-images and multiple methods for predicting native bone mineral density from contrast enhanced CT scans. Within clinical routine, 47 patients underwent native as well as IV-contrast (Imeron 350, Bracco Imaging Deutschland GmbH, Konstanz, Germany) enhanced CT scans (GE Revolution EVO, Waukesha, WI, USA) over three vertebrae, resulting in 141 native, arterial and portal phase estimates of bone mineral density (CliniQCT, Mindways Software, Inc., Austin, TX, USA) as well as iodine content calculated from aortic blood using a basis material composition scheme. In both arterial and portal phases, simple subtraction of the respective mean biases was compared to linear predictive models as well as non-linear Generalized Additive Models (GAM), with and without including the aortic iodine content into the models, resulting in eight different techniques of prediction. Two alternative thresholds, 80 and 110mg/cm³ were applied to identify the group of patients to screen for osteoporosis and to generate reference classifications based on the native BMD data. Within all pairings of classifiers, a significant difference was found with respect to the arterial phase of the GAM models compared to the simple subtraction of the bias and the linear prediction respectively, while all other pairings in both phases were not significantly different. For the threshold 80mg/cm³, sensitivity and specificity for the GAM models were 97% and 96% (arterial phase), 94% and 100% (portal phase), while for the threshold of 110mg/cm³ the GAM models showed 98% and 88% (arterial phase) as well as 97% and 85% (portal phase) in sensitivity and specificity. On the same data, Generalized Additive Models were identified elsewhere as the technique associated with the lowest residual error during prediction of native BMD data. The IV-contrast enabled classification schemes provide a universal screening technique. A clinical context might benefit from a threshold of 80mg/cm³, while an emphasis on early detection of fracture risk might favor a threshold of 110mg/cm³. The results require confirmation on an independent test data set and need to cover different CT brands before they can be used in a clinical context for screening.



Disclosures: **Wolfram Timm**, Mindways Software, Inc., Other Financial or Material Support

LB MON - 1210

Differences in Bone Mineral Density and Trabecular Bone Score in Hip Fracture Patients with Type 2 Diabetes Linsey Gani^{*}, Thomas King, K. Reddy Saripalli, Karen Fernandes, Carmen Kam, Le Roy Chong. Changi General Hospital, Singapore

Purpose: The risk of fragility fracture is higher in type 2 diabetes (DM) patients, despite higher bone mineral density (BMD) readings. Trabecular Bone Score (TBS) has been shown to improve fracture risk predictions in diabetes patients, however studies within the South East Asian population have been limited. We aimed to measure BMD and TBS in patients with fragility fracture to assess for differences in those with and without type 2 DM. Methods: We conducted a retrospective analysis of all subjects admitted with low trauma hip fracture to a regional hospital in Singapore over a 6 month period. All BMD scans were performed on a single densitometer (Hologic QDR Discovery Wi, USA) and BMD files were analysed with the TBS iNsight software programme (Med-Imaps, France). Electronic patient records were reviewed; laboratory results and anthropomorphic data from the time of DXA were collected. Subjects were classified as having diabetes according to the WHO 2011 criteria, or current treatment by oral antidiabetic drugs or insulin. Results: There were 288 fragility hip fracture admissions from January to July 2017, and 227 had BMD performed. Of these 227 patients, 73 (32%) had type 2 DM and median DM duration was 11 (1-12) years. 7 (9.6%) were diet controlled, 65 (89%) were taking oral antidiabetic drugs and 12 (16.4%) were taking insulin. There was no difference in age or body mass index (BMI) between DM and non-DM patients (79 vs 79 years; 22.3 vs 21.4 Kg/m², p=0.247), and mean HbA1c was (7.3 vs 5.9%, p<0.001). There was a greater prevalence of chronic kidney disease (CKD) in the DM vs non-DM group (45.2% vs 32.5% of subjects with eGFR <60ml/min, p=0.022). BMD was significantly higher in the DM than the non-DM group (T-score L-spine -1.4 vs -2.1, p=0.001; femoral neck -3.0 vs -3.2, p=0.034), and mean TBS was similar (1.25 vs 1.23, p=0.255). Spearman correlation between duration of diabetes and TBS was 0.17, p=0.153. In a multivariable regression, after adjusting for age, gender, BMI, CKD and race, only higher BMD in L-spine was significantly associated with DM. Conclusion: In a population with hip fracture, type 2 DM is independently associated with higher L-spine BMD after adjustment for age, gender, weight and eGFR. There was no significant difference in TBS between DM and non-DM patients. Further studies are needed to determine the relationship between DM, BMD, TBS and fractures

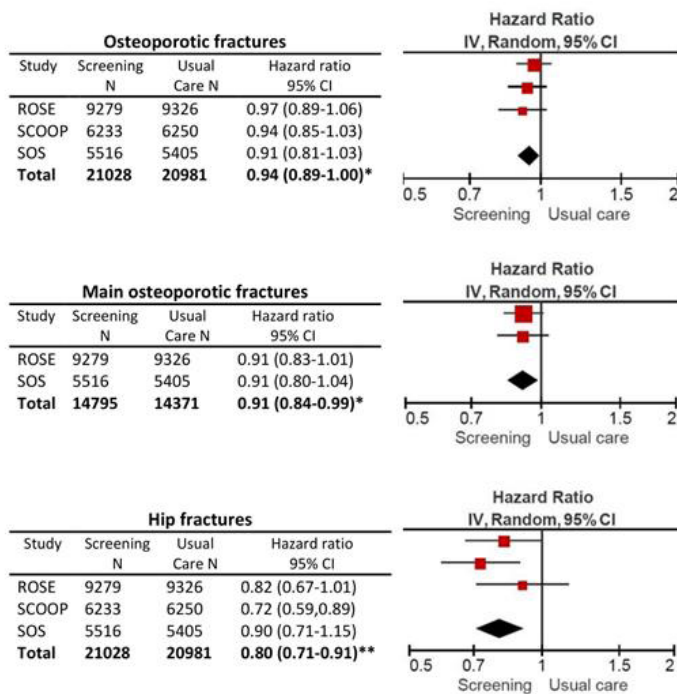
Disclosures: **Linsey Gani**, None

LB MON - 1213

The effect of screening of high fracture risk and subsequent treatment on osteoporotic fractures: a systematic review and meta-analysis Thomas Merlijn^{*1}, Karin Swart¹, Coen Netelenbos², Petra Elders¹. ¹Department of General Practice and Elderly Care Medicine, VU University Medical Center, Netherlands, ²Department of Internal Medicine, Endocrine Section, VU University Medical Center, Netherlands

Objective: To study whether screening of high fracture risk and subsequent treatment in primary care can reduce osteoporotic fractures in comparison to usual care. Method: We performed a systematic literature search in Pubmed and Embase to identify all randomized trials that compared screening on high fracture risk with usual care. Only studies with verified fractures as outcome were selected. Furthermore, the Salt Osteoporosis Study (SOS) was selected, of which the results are to be published. Two reviewers independently considered the relevance and eligibility of the studies. The risk of bias of the selected articles was assessed with the Cochrane Collaboration's Risk of Bias Tool. Aggregate data were pooled using random effect models. Results: In addition to the SOS we identified two studies that met our criteria, the ROSE and SCOOP study. The design and strategy of the three studies was similar: a primary care population of older women (mean age 70-75), preselection of high fracture risk with a questionnaire followed by bone densitometry in the women with increased risk in the intervention group. There were small differences in risk selection and treatment thresholds, but all studies used FRAX in risk selection or in treatment thresholds. In all studies there was dilution: in the intervention group 13-25% had a treatment indication and 11-17% started anti-osteoporotic drugs. All three studies had low risk for bias except from the fact that the nature of the studies made blinding impossible, this increased the risk of contamination in the control group leading to a reduction of the contrast. Follow-up was complete in 94-100% of the participants. The heterogeneity between the three studies was low (I²=0%). The pooled data (figure 1) indicated a significant effect on all osteoporotic fractures (HR=0.91 95%CI=0.81 to 1.00), the main osteoporotic fractures (HR=0.91, 95%CI=0.84 to 0.99, ROSE and SOS only) and hip fractures (HR=0.80, 95%CI=0.71 to 0.91). Conclusion: This meta-analysis of three large trials demonstrated that in older women in primary care preselection of high fracture risk followed by bone densitometry and subsequent treatment is effective in reducing all osteoporotic fractures, main osteoporotic, and hip fractures. Taking into account the dilution of the treatment effect in the intervention group and the contamination of the control group, we conclude that the effect on osteoporotic fracture reduction is substantial, especially on hip fractures reduction.

Figure 1. Forest plots with hazard ratios of the fracture outcomes



* P < 0.05 ** P < 0.001

Disclosures: *Thomas Merlijn, None*

LB MON - 1217

Time-dependent enhancement of osteoblast mineral deposition by green and black tea polyphenols originates during mineralization and not the differentiation phase William Gittings*, Michael D. Mcalpine, Adam J. Macneil, Wendy E. Ward. Brock University, Canada

There is growing interest in characterizing the effect of dietary bioactives that promote positive outcomes in musculoskeletal health, and the investigation of their interaction with tissue maintenance during aging as well as chronic inflammatory signalling. Previous results from our lab and others have demonstrated that whole tea preparations and their constituent polyphenols augment mineral deposition in osteoblasts in vitro. These findings are generally consistent with the beneficial effects of tea consumption on bone outcomes (i.e., BMD) in preclinical rodent models and associations reported in observational human studies. The objective of this study was to examine the effect(s) of green and black tea treatment in osteoblasts throughout the cell lifespan to describe the timing of modulation to cell function in a systematic fashion. SaOS-2 cells were cultured under standard conditions (37°C, 5% CO₂) and control (CC) responses were compared to three tea treatment conditions, including; tea treatment during differentiation only (TC), during mineralization only (CT), or throughout both phases of the cell lifecycle (TT). Tea treatment consisted of supplementing the control cell media with freshly prepared green or black tea at a standardized polyphenol content (1 µg/ml) determined using Folin-Ciocalteu's reagent (gallic acid equivalents). End-point mineral deposition quantified using Alizarin red staining at Day 3, 5, and 7 of mineralization determined that tea treatments during differentiation only (TC) did not enhance mineralization above control (CC) levels. In contrast, when green or black tea treatment occurred during mineralization (CT, TT), there was significant enhancement of nodule formation in both tea types at Day 3 (to ~1.4 of control values) and Day 5 (to ~2.0 of control values) (n=6, P < 0.05); a time-dependent effect which dissipated by Day 7 for both tea types. Transcriptional analysis using RT-qPCR of the principal mechanisms that regulate mineralization via the inorganic pyrophosphate (PPi) to phosphate (Pi) ratio (i.e., TNAP, ENPP1, ANKH, PHOSPHO1) did not explain the observed differences with green or black tea treatment. Our preliminary results suggest that a time-dependent enhancement of SaOS-2 mineral deposition by tea polyphenols occurs independent of modulation during the differentiation phase, and current investigation of post-translational mechanisms will accompany the primary findings.

Disclosures: *William Gittings, None*

LB MON - 1220

Microglial Progranulin Promotes Age-Related Bone Loss in Female Mice Liping Wang^{*1}, Jiasheng Zhang², Eric Huang², Robert Nissenson¹. ¹San Francisco VA Medical Center, United States, ²University of California San Francisco, United States

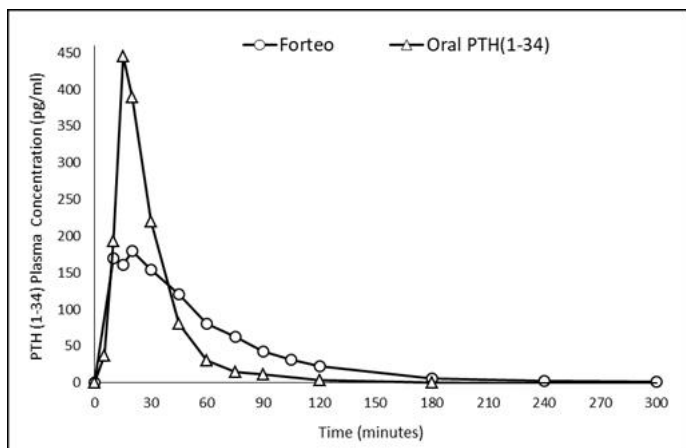
Progranulin (PGRN) is best known as a glial factor that is deficient in a subset of patients with frontotemporal dementia. PGRN has also been identified as an adipokine that regulates glucose metabolism as well as a factor that affects bone. We recently found that global deletion of PGRN in female (F) (but not male (M)) mice was protective against age-related bone loss, implicating PGRN as a negative regulator of bone in aging females. In the present study, we hypothesized that PGRN expression by adipocytes is responsible for these negative skeletal effects. To test this notion, we characterized the bones of mice that were generated by specifically deleting PGRN expression in adipocytes using adiponectin-Cre. We found that deleting PGRN in adipocytes did not result in a change in distal femoral fractional bone volume (BV/TV, %) at 3 mo (M: WT vs. KO: 21% vs. 20%; F: 7.5% vs. 6.8%) or 6 mo (M: WT vs. KO: 17% vs. 15%; F: 3.7% vs. 3.7%), but slightly decreased lean mass and body weight and significantly decreased mRNA encoding adipocyte marker genes Pparg (2.9-fold, p<0.05) and Emr1 (2-fold, p<0.05) in white adipose tissue of 3 mo male mice only. These data indicate that adipocyte-derived PGRN serves as a regulator of adipocyte metabolism, but does not account for the female skeletal effects of PGRN. We then asked whether microglial production of PGRN would inhibit bone formation since microglial PGRN contributes to the cognitive effects of PGRN. We studied the bones of female mice in which expression of the PGRN gene was deleted in microglial cells using Cx3cr1-Cre. µCT assessment of the L4 vertebra showed that deletion of PGRN in microglial cells led to a 27% (p<0.05) increase in BV/TV at 9 mo and a 86% (p<0.01) increase at 16 mo. The increase in BV/TV was associated with a significant increase in trabecular number (9 vs. 16 mo: 23%, p<0.05 vs. 58%, p<0.01) and a significant decrease in trabecular separation (9 vs. 16 mo: 20%, p<0.05 vs. 38%, p<0.001). These changes are similar to those seen in global PGRN knockout mice, suggesting that microglial PGRN negatively regulates bone mass in aging females. However, Cx3cr1-cre is also expressed in peripheral macrophages and further work will be necessary to determine if macrophage-derived PGRN contributes to the bone phenotype. We speculate that PGRN acts by modulating the central mechanisms that control bone mass. Therapies aimed at blocking these mechanisms may prevent female age-related bone loss.

Disclosures: *Liping Wang, None*

LB MON - 1229

An oral PTH 1-34 formulation with a pharmacokinetic profile optimized for the treatment of osteoporosis Gregory Burshtien^{*1}, Hillel Galitzer¹, Ariel Rothner¹, Phillip Schwartz¹, Eric Lang², Roger Garceau², Jonathan C.Y. Tang³, William D. Fraser³, Yoseph Caraco⁴. ¹Entera Bio Ltd., Israel, ²Entera Bio Ltd., United States, ³University of East Anglia, United Kingdom, ⁴Hadassah Clinical Research Center, Israel

An orally administered PTH 1-34 may be a novel treatment of Osteoporosis. It is well established that the duration of the drug exposure is critical in determining the balance between the anabolic and catabolic effects of PTH. In comparison to the commercially available PTH injections, we present clinical results of a novel oral PTH 1-34 formulation, characterized by a shorter systemic exposure, which is expected to be not only a more convenient treatment but may even have an improved anabolic effect. Methods: A Phase I, open label crossover study to assess the safety and PK of oral PTH 1-34 in ten healthy male adult volunteers was conducted. The PK profile of 1.5 mg oral PTH 1-34 was compared to that of the SC Forteo® injection. PTH 1-34 plasma levels were analyzed by immunoassay (IDS;UK). Results: The PK profile of oral PTH 1-34 was characterized by a rapid absorption and elimination. The average maximal plasma concentration (C_{max}), time to maximal exposure (T_{max}), systemic exposure (AUC) and elimination half-life of the oral drug VS. Forteo injection were 481pg/mL, 14.4 min, 190 pg*hour/mL, 16.5min VS. 207 pg/ml, 17.5 min, 197 pg*hour/mL and 36.2min. The duration of the systemic exposure above the upper limit of the endogenous PTH level was about 1 hr for the oral PTH 1-34 and about 2 hrs for Forteo. Significantly higher increase in serum calcium concentrations was observed following the SC injection, including 3 cases of transient hypercalcemia. Discussion: It is recognized that continuous administration of PTH primarily contributes to bone resorption, whereas intermittent administration promotes bone formation. It has been reported that the optimal duration of PTH exposure to promote the anabolic effect is 1 hr, as was achieved with the oral PTH 1-34 formulation. With this unique PK profile, characterized by a shorter duration of systemic drug exposure in comparison to the existing commercially available injectable formulations, we may anticipate that the oral PTH 1-34 formulation will provide not only better compliance, but also greater efficacy and a potentially improved safety profile in the treatment of osteoporosis. Additional clinical studies in patients with osteoporosis are required to confirm this hypothesis.



Disclosures: Gregory Burshtien, None

LB MON - 1230

Patient Engagement in Clinical Guidelines Development: Input from > 1000 Members of the Canadian Osteoporosis Patient Network Larry Funnel¹, Marija Djekic-Ivankovic², Rachel Chepesiuk¹, Lora Giangregorio³, Isabel Braganca Rodrigues³, Rowena Ridout⁴, Sidney Feldman⁴, Sandra Kim⁴, Heather McDonald-Blumer⁴, Gregory Kline⁵, Wendy E Ward⁶, Nancy Santesso⁷, William D Leslie⁸, Suzanne N Morin⁹. ¹Osteoporosis Canada, Canada, ²Research Institute of the McGill University Health Center, Canada, ³University of Waterloo, Canada, ⁴University of Toronto, Canada, ⁵University of Calgary, Canada, ⁶Brock University, Canada, ⁷McMaster University, Canada, ⁸University of Manitoba, Canada, ⁹McGill University, Canada

PURPOSE:Engagement of patients is essential in the development of high quality and relevant guidelines for the management of osteoporosis. Osteoporosis Canada (OC) is updating its national clinical practice guidelines using the GRADE approach, and is ensuring active patient involvement throughout the entire process.**METHODS:**Using electronic mail, we contacted 6937 members of the Canadian Osteoporosis Patient Network (COPN) to provide input in the selection of clinical questions and relevant outcomes via a self-administered on-line survey. Questions were developed by a working group that included clinicians, patients and researchers.Closed-ended questions were analyzed using descriptive statistics, and content analysis was conducted for the open-ended question. **RESULTS:**A total of 1108 individuals (16% participation rate) completed the survey (97% were women, 86% stated they lived with osteoporosis and most reported they were knowledgeable [61%] or very knowledgeable [24%] about osteoporosis). Most considered it to be very important to have recommendations on pharmacotherapy (83%), exercise (74%), nutrition (68%), fall prevention (68%), and how to discuss risks and benefits of medications (65%). Respondents stated that preventing fractures, preserving quality of life and ability to perform daily activities, preventing admission to long term care and fracture-related death, and avoiding serious harms from medications were very important outcomes (average scores ≥ 4.7 on a 5-point Likert scale). Discussion with a physician (51%) or other healthcare professional (41%), or access to material posted on the OC website (41%), were determined to be critical in ensuring a good understanding of the risks and consequences of fractures. Seven key issues emerged from the content analysis of the open-ended question (498 respondents with 960 references): “Provide up to three questions you would like to see addressed in the next Guidelines” (Table). In addition to the key issues mentioned in the closed-ended questions, pain management following fractures and alternative therapies for prevention or treatment of osteoporosis were also identified as important questions to address (48 references).**CONCLUSIONS:**This survey has identified issues important to people living with osteoporosis that will inform the search strategy for knowledge syntheses, and the development of OC clinical guidelines recommendations.

Table Content analysis of the open-ended question

Provide up to three specific questions you would like to see addressed in the next Canadian Osteoporosis Clinical Practice Guidelines.	References* N = 960
Pharmacotherapy	325
Benefits and harms	182
New medications / the best medication	58
Duration of therapy/drug holiday	54
Other (cost, medication choice etc.)	31
Screening- Monitoring -Evaluation	193
BMD tests/ response to treatment	88
Prevention	65
Early screening	30
Other (access to specialists, clinics etc.)	10
Nutrition and Supplements	140
Dietary recommendations	59
Supplements recommendations	52
Dietary sources of Calcium	22
Other (Vitamin K, protein)	7
Exercise - Physical activity	121
Recommendations	80
Safety and Benefits	31
Other (trainers, cost etc.)	10
Knowledge-Education-Advocacy	133
Patients / families/ caregivers	72
Health care professionals	20
Advocacy / support groups	17
General public	13
Other (list of specialists, funding, etc.)	11
Alternative Therapies	30
Naturopathy/natural products	28
Other	2
Pain	18
Pain management	17
Other (Osteoporosis pain vs. Arthritis pain)	1

* N= the number of references among the 498 participants who answered the open-ended question

Disclosures: Larry Funnel, None

LB MON - 1231

Osteoporosis Treatment In Patients With Atypical Femur Fractures Denise Van De Laarschot¹, Malachi Mckenna², M Carola Zillikens¹. ¹Erasmus Medical Centre, Netherlands, ²St. Vincent’s University Hospital, Ireland

Atypical femur fractures (AFFs) are related to the use of bisphosphonates and often show delayed or non-healing. After an AFF, bisphosphonates are usually discontinued. It is unclear if certain osteoporosis drugs can promote AFF healing, while there is no guideline on how patients with high risk of fragility fractures should be treated after an AFF. We performed a systematic literature review to evaluate the effect of teriparatide, raloxifene and denosumab both on healing and occurrence of AFF in order to advice on treatment after AFF. We considered complete and incomplete forms separately. Our search retrieved 910 references and we reviewed 46 papers. The effect of teriparatide in AFF patients was described in 28 case reports, 7 retrospective cohorts and 3 prospective trials; the latter included 3 retrospective cohort studies on incomplete, 3 on complete and one on combined AFF. Although use of teriparatide showed a favorable trend towards shorter time to bone union after surgery in some studies, non-healing AFFs and development of contralateral AFFs occurred even after 11 months of teriparatide. With denosumab, 2 cases of AFF were reported in the Freedom extension study. Additionally, 8 cases of AFF were documented on denosumab, of which 6 cases were preceded by long-term bisphosphonate use. Additionally, 14 AFF cases are reported when denosumab was prescribed for treatment of metastatic bone disease. Nine patients were reported with continued use of denosumab after the AFF, of which 2 patients had delayed healing, one a second complete AFF, and one recurrent bilateral incomplete AFFs whilst on denosumab. Eight patients used raloxifene before the occurrence of AFF, including one case of AFF after only one year of raloxifene without prior bisphosphonates. No data are available on the outcome of raloxifene treatment started after the occurrence of AFF. In conclusion, all current antiresorptive drugs appear to be associated with AFF, and teriparatide does not seem to prevent AFF nor ensure fracture healing. These results need to be interpreted with caution due to heterogeneity of the reported studies and due to a lack of prospective, adequately powered, controlled trials. Based on these findings, we have for-

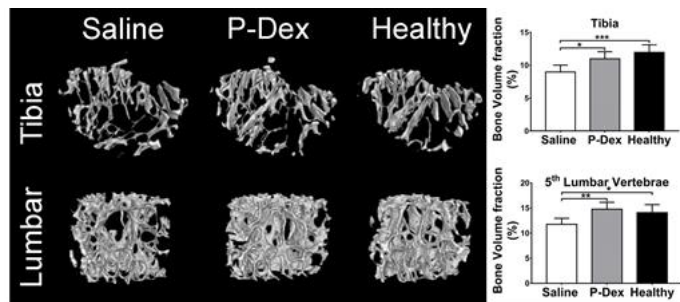
mulated treatment advise for patients who have sustained an AFF that considers the healing of both complete and incomplete forms, risk of worsening or new AFFs, and prevention of fragility fractures in those with high fracture risk due to osteoporosis.

Disclosures: *Denise Van De Laarschot, None*

LB MON - 1235

Macromolecular Dexamethasone Prodrug Ameliorates Neuroinflammation and Prevents Bone Loss Associated with Traumatic Brain Injury Gang Zhao^{*1}, Xin Wei¹, Rongguo Ren¹, Zhifeng Zhao¹, Yuanyuan Sun¹, Ningrong Chen¹, Dexuan Kong², Dong Wang¹. ¹University of Nebraska Medical Center, United States, ²China Pharmaceutical University, China

Traumatic brain injury (TBI) is a leading cause of death and disability, particularly among young adults. In addition to neurologic damage and disfunction, TBI has also been found to induce bone loss in patients and animal models. The TBI associated osteopenia not only affects the patients' quality life but also can be life threatening. The combination of balance disorder and osteopenia will put the TBI patients at a higher risk of fall and bone fracture. Neurologic injury from TBI is largely attributed to the deleterious effects of the direct mechanical impact as well as secondary cerebral swelling and edema, which will increase intracranial pressure, leading to ischemic injuries. While glucocorticoids (GC) have been used extensively in treating TBI, the clinical outcome has been controversial. To further improve the therapeutic efficacy and safety of the GC therapy, we proposed to use a macromolecular dexamethasone prodrug (P-Dex) to treat TBI. Mice (C57BL/6, 9 weeks old, female) were randomly assigned to 3 groups (10/group, P-Dex, saline and healthy control). TBI was induced by controlled cortical impact (CCI) with 2.5 mm depth at 5.25 m/s. Mice from each group were sacrificed at 6 weeks post TBI. Brains were harvested to evaluate P-Dex' therapeutic efficacy on TBI. IRDye® 800CW labeled P-Dex were administrated to evaluate P-Dex' biodistribution at 1, 3 and 7 days post i.v. administration. Tibias and lumbar vertebrae (L5) were harvested for evaluation of bone quality. Optical imaging results suggested that P-Dex targeted to the injured cortex with sustained presence for up to 7 days. Immunohistochemistry results indicated that P-Dex had inhibited the activation of microglia with reduced lipid peroxidation. Brain edema in P-Dex treated group was also reduced as evident by the inhibition of Aquaporin 4 expression. Fluoro-Jade C staining indicated P-Dex could preserve neurons from degeneration after injury. Micro-CT analysis of tibias and L5 vertebrae confirmed the post TBI trabecular bone loss at 6 weeks. BV/TV in saline group was reduced to ~75% in proximal tibia and ~85% in L5 lumbar vertebrae of the healthy mice. BV/TV of the P-Dex group showed no statistically significant difference from the healthy mice but was significantly higher than saline group. Based upon these preliminary findings, we believe P-Dex treatment may attenuate brain injury induced by TBI and systematically preserved the skeletal quality of the mice with TBI.



Representative micro-CT images and quantitative analysis of the L5 Lumbar vertebrae and tibia of TBI mice from different groups. * $P < 0.05$; ** $P < 0.01$; *** $P < 0.001$.

Disclosures: *Gang Zhao, None*

LB MON - 1244

Association between nutritional status and sarcopenia in a community dwelling older population: The Bushehr Elderly Health (BEH) Program Bagher Larijani^{*1}, Gita Shafiee², Zhaleh Shadman¹, Afshin Ostovar³, Ramin Heshmat², Ehsaneh Taheri³, Farshad Sharifi⁴, Iraj Nabipour⁵. ¹Endocrinology and Metabolism Research Center, Endocrinology and Metabolism Clinical Sciences Institute, Tehran University of Medical Sciences, Tehran, Iran, Islamic Republic of Iran, ²Chronic Diseases Research Center, Endocrinology and Metabolism Population Sciences Institute, Tehran University of Medical Sciences, Tehran, Iran, Islamic Republic of Iran, ³Osteoporosis Research Center, Endocrinology and Metabolism Clinical Sciences Institute, Tehran University of Medical Sciences, Tehran, Iran., Islamic Republic of Iran, ⁴Elderly Health Research Center, Endocrinology and Metabolism Population Sciences Institute, Tehran University of Medical Sciences, Tehran, Iran, Islamic Republic of Iran, ⁵The Persian Gulf Tropical Medicine Research Center, Bushehr University of Medical Sciences, Bushehr, Iran, Islamic Republic of Iran

Background & aim: Maintenance of skeletal muscle in older age is critical to reducing frailty and the risk of falls and fractures. Nutrition has established importance for muscle health in general, however, the relationship between specific micronutrients intake and sarcopenia has not been well established in older adults. The objective of this study was to assess the relationship between daily nutritional intake and sarcopenia. **Methods:** A total of 2426 Iranian adults aged ≥ 60 years, participating in the stage II of Bushehr Elderly Health (BEH) program, a population-based prospective cohort study; were included in this study. According to European Working Group on Sarcopenia in Older People (EWGSOP) definition, a person who had low muscle mass as well as low muscle strength and/or low physical performance (usual walking speed) was identified as having sarcopenia. Skeletal muscle mass index (SMI) less than < 7.0 kg/m² and < 5.4 kg/m² were considered as low muscle mass among men and women, respectively. Low muscle strength was defined as grip strength < 26 kg or < 18 kg for men and women, respectively, and a usual walking speed ≤ 0.8 m/s was defined as low physical performance for both genders. Body composition was measured by the dual x-ray absorptiometry (DXA) method. Dietary nutrient intakes were estimated from a 24-hour recall method. Daily nutrients intake based on the consumption of each food item was calculated. Multivariate regression was used to investigate the association of sarcopenia with tertiles of daily nutrients intake groups. **Results:** Participants with sarcopenia consumed less dietary intakes of total calories, protein, and carbohydrates ($P < 0.001$). Also, sarcopenia showed a strong inverse association with minerals such as Calcium, Iron, Magnesium, Phosphorus, Potassium, Zinc and vitamins (A, E, C, Biotin, B2, B3 and B6). When the odds ratios for sarcopenia according to daily nutrients intake tertile were analyzed, the risk for sarcopenia decreased as daily minerals and vitamins intake increased from the first to the third tertile, even after correction for confounding variables. Participants in the higher tertiles of daily protein intake, carbohydrate and total calories showed the significantly decreased risk of sarcopenia [OR=0.641(0.519-0.791); P for trend =0.002], [OR=0.731(0.593-0.901); P for trend =0.010] [OR=0.780(0.633-0.9631); P for trend =0.05], respectively. The associations remained statistically significant after adjustment for age, sex, BMI, physical activity and smoking. **Conclusions:** Our results suggest a strong inverse association between daily nutrients intake and sarcopenia in older Iranian adults.

Disclosures: *Bagher Larijani, None*

Author Index

- A**
- Abate, Ejigayehu 282
- Abbas, Afroze 202
- Abbes, Yasmine 432
- Abdel-Wahab, Omar 71
- Abe, Masahiro . 132, 234, 341, 342
- Abel, Richard 410
- Abeysekera, Irushi 361
- Abid, Shadaan 215
- Abid, Simona 409
- Abou-Sharkh, Ahmed 169
- Abraham, Abel 33, 423
- Abrahamsen, Bo. 7, 105, 110
- Abreu, Lelia De 392
- Abribat, Thierry. 117, 118
- Abu-Amer, Yousef. . . 137, 159, 364
- Acevedo, Claire 1, 65, 161
- Acharya, Suchitra 369
- Achenbach, Sara 17
- Achtziger, Silke 196, 320
- Ackermann, Gail 147
- Ackert-Bicknell, Cheryl. 105, 117, 227, 228, 230, 370, 434
- Ackert-Bicknell, Cheryl L. . . 205
- Acotto, Claudia Gomez 184
- Acton, Dena 56, 303
- Adachi, Jonathan 36, 164, 194, 277, 290, 390
- Adachi, Jonathan D 107, 156, 193, 371, 387
- Adachi, Jonathan D. . . . 399, 400
- Adameyko, Igor 367
- Adamik, Juraj 138, 324
- Adams, Annette 287, 289, 408
- Adams, Annette L. 2, 2, 103, 390
- Adams, David 105
- Adams, Douglas 117, 228, 370
- Adams, Douglas J 87
- Adams, John 147, 177, 367
- Adams, Jonathan 35, 415
- Adams, Judith 280
- Adams, Michael 278, 355, 414
- Adaway, Michele 136
- Addison, William N. 371
- Ade, Carl. 351
- Adesina, Oyebinpe 112
- Adhikari, Anish 21
- Adoum, Anne-Tounsia 105
- Aeberli, Daniel. 317
- Agarwal, Rahul 282
- Agarwal, Sameer 207
- Agarwal, Sanchita. . . 61, 131, 266, 285, 325
- Agellon, Sherry 152, 233, 240
- Aggarwal, Anshita. 166, 180
- Aghaloo, Tara 190
- Agharazii, Mohsen 215, 294
- Agnew, Amanda 133
- Agoro, Rafiou 352
- Agostinis, Patrizia. 244
- Agraw, Anteneh 432
- Aguiar-Orozco, Gilberto 278
- Aguiar-Perez, Alexandra. 83, 334, 361
- Aguirre, J Ignacio 33
- Aguirre, Jose 423
- Ahmad, Saad 142
- Ahmad, Sara. 317
- Ahmad, Usman 300
- Ahmed, Faisal 293
- Ahmed, Osama Haji. 287
- Ahn, Jaimo. 405
- Ahn, Jiyoung. 95
- Ahn, Kyu Jeung 380
- Ahn, Seong Hee 283, 429
- Ahn, Taeyong 294
- Aibibula, Zulipiya 97
- Aitken, Dawn 167, 307, 427
- Ajith, Ashwin 225
- Akagawa, Manabu 172, 179
- Akesson, Kristina 267
- Akhter, Mohammed. . . . 204, 311
- Akiyama, Kentaro. 338
- Akkus, Ozan 150
- Alade, Adekemi 121
- Aladlaan, Asaad 368
- Alam, Imranul. 303
- Alavi, Abass 101
- Al-Azazi, Saeed 103
- Albanell, Joan 394
- Al-Barghouthi, Basel 434
- Albers, Anthony 169
- Al-Daghri, Nasser 170
- Alexih, Austin. 101
- Alexander, Kylie. 214
- Alharbi, Mohammed 74
- Alhashemi, Nada 127
- Alhrbi, Mashaal 8, 38, 275
- Ali, Abdullah. 71
- Ali, Amira Hussein 356
- Ali, Dalia Ayesh Hafez 216
- Ali, Haider 335
- Ali, Sara Akhtar 134
- Alippe, Yael 159
- Alix-Panabieres, Catherine. . . 72
- Aljohani, Hanan 250
- Alkalay, Ron 139, 187
- Allaire, Brett. 247, 309
- Allen, Matt. 331
- Allen, Matthew 238, 240, 248, 334
- Allen, Matthew R. 83, 98
- Allin, Sonya 399
- Alliston, Tamara. . . 1, 65, 161, 262, 370
- Alm, Jessica J. 417
- Almaden, Yolanda 353
- Almarza, Alejandro 30
- Almehaimid, Faisal 204
- Almeida, Maria 12, 23, 26, 53, 146, 191, 239, 345, 354
- Almohaya, Mohammed 264
- Almonte, Maximo Gomez 129, 130, 203
- Aloia, John. 202
- Alon, Uri 334
- Alonso, Veronica. 217
- Alos, Nathalie 135
- Alrob, Hajar Abu 409
- Alruwaili, Seham 53
- Alshalawy, Faisal 30
- Alster, David 320
- Altieri, Carla 385
- Alvandi, Leila Mehraban 161, 236
- Alvarenga, Pedro 162
- Alvarez, Marta 303, 361
- Álvarez-Carrión, Luis. 217
- Alves-Neto, José Seabra. 164
- Amadio, Peter C. 10
- Amani, Amineh 401
- Amara, Sara 292
- Amariti, Julia 110
- Amarowicz, Jaroslaw 263
- Ambrogini, Elena 23, 345
- Ambrose, Catherine G 78
- Ambrose, Catherine G. 205
- Ambrosius, Walter 399
- Amer, Hatem. 199
- Amin, Shreyasee. 36, 268
- Amizuka, Norio 34, 295
- Amling, Michael. 4, 5, 317, 348
- Amra, Sarah 136
- An, Zhiqiang. 73
- Anaei, Carmen M 3
- Anaganti, Suresh 294
- Anastasopoulou, Catherine. . . 233
- Anastasiades, Tassos 393
- Anderson, Anne Michal. 382
- Anderson, Carolyn 218
- Anderson, Dennis E. 273
- Anderson, Kara 99, 308
- Anderson, Paul 205
- Anderson, Peter 424
- Andreasen, Camilla 54, 345
- Andresen, Julian Ramin .385, 407
- Andresen, Reimer 385, 407, 436
- Andronowski, Janna 377
- Andújar-Vera, Francisco 182
- Angermann, Alexandra 4
- Anginot, Adrienne. 214
- Anitha, D. 205
- Anolik, Jennifer 370
- Antoniazzi, Alfredo 345
- Antoniazzi, Franco 312
- Antonioni, Georgia. 199
- Aobulikasimu, Aikebaier 97
- Aoyama, Eriko. 343
- Aparicio, Conrado. 195
- Apicella, Matteo 321
- Appelman-Dijkstra, Natasha . .51, 180, 417
- Appelman-Dijkstra, Natasha M. . 297
- Aquino-Martinez, Ruben 371
- Arai, Atsushi 381
- Arai, Yoshinori 136
- Araujo, Iana De 200
- Arbex, Maria Carolyna Fonseca Batista 167
- Arden. 356
- Ardura, Juan 217
- Ardura, Juan Antonio. 149
- Aref, Mohammad W. 83, 98
- Arévalo, Marta 383
- Arginteanu, Toren. 185
- Arista, Luca 58
- Arjan, Ronak 45
- Arnason, Terra 377
- Arnold, Andrew 348
- Aromeh, Loretta. 179
- Arora, Tarun. 2, 106, 276
- Arra, Manoj 137, 364
- Arslianian, Kendall J 311
- Arthur, Jon 314
- Arts, J.J. 66
- Asada, Yohei 213, 241
- Asahina, Izumi. 158, 375
- Ashe, Maureen C. 277, 400
- Ashique, Amir 377
- Ashtar, Mohannad 341
- Askin, Gülce 200
- Asou, Yoshinori 97
- Aspden, Richard. 12
- Aspelund, Thor 11, 37
- Assad, Michel 416
- Assar, Shima 356
- Asterholm, Ingrid Wernstedt. . 69
- Astolpho, Kelly 431
- Atanoa, Theresa 311
- Athanasiadis, Grace. 169
- Atkins, Gerald. 205
- Atkins, Gerald J. 355
- Atkinson, Elizabeth . . 17, 36, 145, 268
- Atkinson, Elizabeth J. 362
- Atkinson, Emily 296, 334
- Atkinson, Emily G. 80, 98, 339
- Atkinson, John. 48
- Aubin, Jane 72
- Aubry-Rozier, Berengere . . . 3, 396
- Aubry-Rozier, Bérengère . . . 299
- Aung, Kyawthu 338
- Auron, Philip E 138, 324
- Ausk, Brandon. 117
- Authier, Simon. 416
- Avigdor, Jennifer Sarhis 421
- Awad, Mohamed. 22
- Axelsson, Kristian 99
- Axelsson, Kristian F. 46
- Aye, Tandy 209
- Aykin-Burns, Nukhet 146
- Ayoub, Akram 12
- Ayoub, David 210
- Ayturk, Ugur. 416
- Azab, Ehab. 162, 382
- Azem, Omar 374
- B**
- Babalyan, Varta 410
- Bachus, Carly 315
- Badawy, Tamer 252
- Bae, Han-Sol. 79, 240, 241
- Bae, Seyeon 95
- Bae, Seyon 256
- Bae, Yangjin 73
- Baek, Jeong-Hwa 42, 75, 79, 241
- Baek, Kyunghwa 75
- Bagel, Jessica 185
- Bahrami-Samani, Emad 367
- Baht, Gurpreet 9
- Bai, Jie 132
- Bai, Xiaochun 31
- Baierl, Andreas 116
- Bailey, Karsyn 161
- Bailey, Stacyann 139
- Baim, Sanford . 193, 292, 317, 318, 318
- Bain, Steve 117
- Bain, Steven 359
- Baird, Denis 12
- Bajwa, Nikita 30, 148
- Baker, Breanne 351
- Bakker, Astrid D. 358
- Bakker, Chantal De 16, 35
- Balani, Deepak H. 368
- Balanta-Melo, Julián 335

- Balasubramanian, Akhila . . . 267
 Balcells, Susana144, 249
 Balcells, Susanna 144
 Baldini, Isabella 253
 Baldock, Paul 105
 Baldock, Paul A. 64
 Baldwin, Avionna238, 339
 Bale, Allen 421
 Bale, Allen E. 419
 Bali, Supinder Kour. 245
 Balic, Marija 55
 Baliga, Uday 124
 Ballard, Anna 192
 Ballestas, Samir 68
 Ballester, Miguel Angel Gonzalez
 163
 Balogun, Salu185, 307, 427
 Balsbaugh, Jeremy 183
 Bamberg, Keith R 64
 Ban, Joann 169
 Ban, Yoshiyuki 406
 Bandeira, Leonardo . . . 63, 63, 324
 Banefelt, Jonas. 267
 Banti, Chiara 321
 Bantouna, Dimintra 199
 Banu, Arshiya 46
 Baratang, Nissan Vida 417
 Barker, Geoff 24
 Barker, Karen 21
 Barlow, Deborah 232
 Barnes, Aileen 182
 Barnes, Kevin 221
 Baroi, Sudipta 315
 Baron, Jeffrey 221
 Baron, Roland . . . 1, 29, 29, 87, 94,
 190, 232, 347, 407
 Baroncelli, Marta 153
 Barone, Antonella174, 286
 Barralet, Jake 64
 Barrett, Thomas 242
 Barrington, William 413
 Barruet, Emilie 51
 Barsony, Julianna112, 320
 Barth, Tobias 288
 Bartuli, Andrea 305
 Baryawno, Ninib 71
 Bashur, Lindsay 30
 Bassett, Duncan 105
 Bassett, J. H. Duncan 64
 Basta-Pljakic, Jelena 34, 407
 Bastepe, Murat84, 181, 434
 Bastin, Sonja 54
 Bastos, Lais Abreu.167, 392
 Bateman, Ted 65
 Bateman, Ted A. 326
 Bat-Erdene, Ariunzaya . .341, 342
 Batkovskyte, Dominyka 78
 Batoon, Lena 72
 Battafarano, Giulia303, 305
 Battaglini, Ricardo 255
 Battle, Lauren124, 306
 Batzdorf, Alexandra 101
 Bauer, Doug 317
 Bauer, Douglas20, 24, 285, 391
 Bauer, Douglas C. 114
 Baujat, Geneviève 420
 Baum, Thomas205, 310, 327
 Bauman, William A 337
 Beaino, Wissam 218
 Bean, Kellen 18
 Beaudoin, Claudia 268
 Beavers, Daniel 307
 Beavers, Kristen307, 399
 Beck, Belinda400, 402
 Beck, Frank 329
 Beck, Laurent 64, 362
 Beck, Thomas 395
 Beck-Cormier, Sarah 64, 362
 Becker, Kathleen A 90
 Beckner, Elliott 240
 Bedrose, Sara193, 318, 318
 Begtrup, Amber 417
 Begun, Dana 96, 377
 Behera, Jyotirmaya229, 335
 Behrmann, Abraham 215
 Beier, Frank 245
 Beil, Conor 77
 Bejarano, Luis Ernesto 385
 Bekarev, Mikhail 360
 Bekirov, Yusuf 206
 Belavy, Daniel 235
 Belaya, Zhanna 410
 Bellido, Carmen Herencia . . 353
 Bellido, Teresita . . . 80, 82, 260, 296,
 339, 355, 383
 Bellido, Teresita M. 98
 Bellizzi, Justin 348
 Bello, Nicholas 142
 Bellver, Montserrat 401
 Beltejar, Michael-John 205
 Bemben, Debra151, 351, 388
 Bemben, Michael 151
 Bendigo, Justin 185
 Benedetto, Adriana Di 413
 Benetollo, Claire 72
 Benevenia, Joseph 118
 Benkusky, Nancy 19
 Bennink, Lucas 342
 Bensamoun, Sabine 76
 Ben-Shlomo, Yoav 269
 Bent-Ennakhil, Nawal 321
 Benton, Andrew 195
 Beom, Sun Hee 277
 Berdeaux, Rebecca 74
 Berengué, Arnau Manasanch. 112
 Berg, Gabriela280, 385
 Berg, Peter Van Den. 169
 Bergamini, C. 417
 Berger, Claudie . .36, 107, 193, 194,
 387, 390, 393, 394
 Berger, Julian 69
 Bergeron, Stephane 169
 Bergh, J.P. Van Den 66
 Bergh, Jonas 55
 Bergh, Joop Pw Van Den 114, 269,
 291, 397, 430
 Bergh, Joop Van Den 169, 194, 270,
 389, 390, 391
 Bergwitz, Clemens 77, 349
 Berman, Alycia212, 331
 Bermond, François 209
 Bernardini, Marcus 361
 Bernardini, Marcus Q. 430
 Bernoulli, Jenni188, 339
 Berry, Sarah 54
 Berry, Wade 348
 Bertola, Débora 417
 Bertucci, Christopher 250
 Berube, Pierre 169
 Berwecka, Malgorzata 263
 Besler, Bryce 387
 Besler, Bryce A. 165
 Bessette, Louis 268
 Beur, Suzanne Jan De 50, 56
 Beutler, Bruce 364
 Bhadada, Sanjay Kumar 166, 180,
 183, 207
 Bhan, Arti 66, 99, 386
 Bhansali, Anil166, 183
 Bhaskaran, Manoj 81
 Bhatnagar, Sahir 39
 Bhattacharya, Rajarshi 410
 Bhattacharyya, Timothy 16
 Bhattaram, Pallavi 336
 Bhimjiyani, Arti Gauvri 269
 Bi, Xiaohong 205
 Biamonte, Federica 61, 147
 Bian, Jing H 373
 Bian, Liangqiao 213
 Bianchi, Gerolamo174, 286
 Bichahlo, Rodrigo C. 328
 Bidwell, Joseph 136
 Bieche, Ivan 72
 Bierhals, Andy 130
 Bigelow, Erin 209
 Bigelow, Erin M.R. 238
 Biggin, Andrew210, 333
 Bijanki, Vinieth N.57, 182, 422
 Bikle, Daniel 82, 249
 Bilezikian, John . . . 61, 63, 129, 130,
 199, 203, 324
 Bilezikian, John P. 128
 Billings, Paul 124
 Billington, Emma O. 21, 108
 Binkley, Neil 21, 24
 Binrayes, Abdulaziz 239
 Binzel, Katherine 432
 Bischoff-Ferrari, Heike A. . . . 109
 Bishop, Nicholas 109
 Bishop, Nick 356
 Bislev, Lise Sofie47, 125, 277
 Bisson, Etienne J. 284
 Bisson, Sarah-Kim 294
 Bittner, Ann-Kathrin 72
 Biver, Emmanuel 17, 36, 102, 223,
 309
 Bizaoui, Varoona 301
 Bjelic-Radisic, Vesna 55
 Bjorkman, Kelsey 211
 Björkman, Kelsey 28
 Bjørnerem, Åshild. 54, 345
 Blaber, Elizabeth 416
 Black, Dennis 20, 24, 106
 Black, Dennis M.174, 286
 Black, Dennis M. 2, 2, 103, 114, 347
 Blair, Harry C. 373
 Blake, Glen 46, 266
 Blake, Glen M. 390
 Blanco, Guillermo 159
 Blanco-Sánchez, Bernardo . . . 78
 Blank, Robert 349
 Blank, Robert D. 240
 Bleakney, Robert38, 277, 400
 Blesic, Karen. 361
 Bliuc, Dana194, 390, 397
 Blixt, Nicholas195, 256
 Blobel, Carl 369
 Blocher, Nissa 233
 Blocki, Frank 147
 Blok, Christel De274, 396
 Bloomfield, Susan238, 327
 Bloomfield, Susan A. 382
 Blouin, Stéphane 184
 Bobba, Gabriella 148
 Bobby, Kendra Jean. 427
 Bober, Michael. 121
 Bober, Micheal B. 184
 Bockman, Richard 129
 Body, Jean-Jacques 113
 Boeckman, Robert 45, 178
 Boer, Ian H. De 230
 Boerckel, Joel 405
 Boeyer, Melanie 67
 Bogdanov, Jacob. 88
 Boisvert, Marie-Eve. 351
 Boivin, Georges 132
 Bokhari, Rihana238, 413
 Bolamperti, Simona 31
 Bollag, Wendy . . . 153, 242, 403, 414
 Bolland, Mark 54
 Bollerslev, Jens 321
 Bon, Nina 64, 362
 Bonafe, Luisa 299
 Bondt, Albert 341
 Bone, Henry 128
 Bonetto, Andrea188, 337
 Bonewald, Lynda . . . 1, 69, 213, 261,
 313, 336, 337, 383, 433
 Bonfim, Danielle 338
 Bonnelye, Edith 72
 Bonnet, Nicolas17, 58, 75
 Bons, J.A.P. 66
 Bont, Jeroen De 54
 Boot, Annemieke 120
 Booth, Sarah L. 328
 Boraschi, Iris 123
 Boraschi-Diaz, Iris 225
 Borba, Victoria 298
 Borggreffe, Jan 385
 Borgström, Fredrik . . . 115, 392, 398
 Borhan, Asm 107
 Bornstein, Sheila 71, 223
 Borromeo, Gelsomina. 412
 Borsari, Simona 321
 Bortolotti, Sara217, 413
 Bosco, Daniela 203
 Bose, Jagadeesh 207
 Bostrom, Mathias180, 416
 Botman, Esmée 120
 Botto, Elizabeth 342
 Bouchard, Keith 26
 Bouchet, Mathilde 72
 Boudin, Eveline 143
 Boughton, Oliver 410
 Bouguillaud, Fanny 43
 Bouillon, Roger 402
 Boukpepsi, Tchilalo 1
 Boulanger-Piette, Antoine . . . 432
 Bourgain, Lucie17, 75
 Bournaud, Morgane 360
 Bousse-Kerdilès, Marie-Caroline
 Le. 214
 Boutroy, Stephanie 332
 Boussein, Mary 1, 20, 20, 24,
 29, 29, 36, 106, 170, 232, 232,
 247, 263, 265, 309, 407, 434
 Boussein, Mary L. 90, 332
 Boussein, Mary L.207, 273
 Bovee, Judith 51
 Bowles, Simon 400
 Boyce, Alison 298
 Boyce, Alison M.121, 183, 424
 Boyce, Alison M. 332
 Boyce, Brendan12, 45, 45
 Boyd, Cynthia 391
 Boyd, Hays 426
 Boyd, Josech R. 49
 Boyd, Joseph 86

- Boyd, Steven 36, 100, 387
 Boyd, Steven K 21, 108, 165, 389, 394
 Boyde, A 245
 Brachvogel, Bent 136
 Braddock, Demetrios 349, 423, 424
 Bradley, Deanna 326
 Bradley, Elizabeth 152, 377
 Bradley, Rachel 398
 Braga, Manoela 122
 Bragg, Robert 242
 Branco, Jaime Cunha 102
 Braulke, Thomas 4
 Bravenboer, Bert 52
 Bravenboer, Nathalie 304, 306
 Breault, David 6
 Bredbenner, Todd 209, 272
 Bredbenner, Todd L. 206, 238
 Bregou, Aline 299
 Brennan-Olsen, Sharon 185
 Brestoff, Jonathan 48
 Brett, Neil 152
 Breuil, Veronique 166
 Brewer, Niambi 22, 79
 Brezicha, Jessica 327
 Brickman, Adam 203
 Bridgewater, David 222
 Briley, Karen 133
 Brillante, Beth A. 131
 Brinker, Alexander 240
 Briody, Julie 333
 Briot, Karine 56, 166, 418
 Britton, Philip 210
 Broderick, Kristen 367
 Brodt, Michael 83
 Brommage, Robert 226
 Bromme, Dieter 178, 370
 Brooijmans, Natasja 26
 Brooke-Wavell, Katherine 171
 Brooks, Daniel 29, 232, 232, 407, 434
 Brooks, Daniel J. 90
 Brotto, Leticia 336, 346
 Brotto, Marco 213, 336, 346, 383
 Brown, J. Keenan 436
 Brown, Jacques 7
 Brown, Jacques P. 351, 387
 Brown, Jacques P. 268, 324, 352
 Brown, Keenan 164, 264, 266, 388
 Brown, Matthew A. 420
 Brown, Sydney 430
 Brown, Sydney M. 121
 Brown, Sydney M. 174
 Brozikova, Hana 333
 Bruder, Jan M. 162
 Bruin, Irma Ja De 269, 397, 430
 Brunetti, Giacomina 210, 217, 312, 413
 Brunjes, Danielle 126
 Bruzzaniti, Angela 95, 334, 361
 Bryanton, Mark 8, 38
 Bryce, Dawn 245
 Buchanan, Samuel 351
 Buchanich, Jeanine 427
 Buckendahl, Patricia 142
 Bucovksy 320
 Bucovsky, Mariana 121, 126, 131, 199, 266, 285, 323, 325
 Bucs, Gabor 24
 Budden, Theodore 221
 Budge, Kevin 374
 Buendia, Irene 149
 Buettmann, Evan 91, 229, 350
 Bui, Matthew 365
 Bui, Minh 38
 Bulas, Dorothy 174
 Bullock, Cydney 317
 Bullock, Whitney 149, 383
 Bunnell, Bruce 208
 Bunting, Sorrel 46
 Bunyamin, Amy 28, 211
 Buonomo, Paola Sabrina 305
 Burden, Andrea 169
 Burghardt, Andrew 40, 106, 209, 310
 Buring, Julie 171, 284
 Burke, Andrea B. 424
 Burkov, Ilya 90
 Burnett, Wadena 154
 Burnett-Bowie, Sherri 166
 Burow, Matthew 208
 Burr, David 111, 248, 280, 296
 Burrage, Lindsay C. 78
 Burshtien, Gregory 437
 Burt, Lauren 36, 100
 Burt, Lauren A. 21, 108, 165, 389
 Burt, Patience Meo 124
 Busch, Melanie 154
 Buschbach, James 217
 Busija, Lucy 20
 Buss, Daniel J 1
 Busse, Björn 288, 317, 348
 Butezloff, Mariana 431
 Butler, Katherine 54
 Butler, Peter W 21
 Butler, Peter W 290
 Butterfield, Natalie 105
 Butterfield, Natalie C. 64
 Buvinic, Sonja 335
 Buxton, Orfeu 285
 Byers, Peter H. 424
- C**
- Cabahug, Pamela 413
 Cabahug-Zuckerman, Pamela 15
 Caballero, Daniel 349
 Cabral, Joaquim 138
 Cabral, Wayne A. 16
 Cadarette, Suzanne 169, 276
 Caetano-Lopes, Joana 102
 Cai, Cinyee 413
 Cain, Corey J 51
 Caird, Michelle 306
 Caird, Michelle S. 124
 Caire, Robin 3
 Caksa, Signe 29, 273
 Calabrese, Gina 172, 227, 230, 434
 Caldwell, Marie 321
 Callisaya, Michele 307
 Callon, Karen 295
 Callon, Karen E 192
 Camerino, Claudia 136
 Camp, Esther 424
 Campbell, Abigail 208
 Campbell, Graeme M. 348
 Campbell, Phil G 138
 Campeau, Philippe 135
 Campeau, Philippe M. 417
 Campeau, Philippe M. 182
 Campos, Lydia 3
 Campos, Maysa S 67
 Campos-Xavier, Belinda 299
 Canaff, Lucie 418
 Canalis, Ernesto 31, 44, 222, 259, 312
 Canhão, Helena 102
 Cani, Patrice 296
 Cao, Huiling 31, 261
 Cao, Xu 245, 366
 Cao, Yangjia 303
 Capella, Maralee 260
 Capellini, Terence D. 228
 Capellino, Anthony 227
 Capitano, Maegan 353
 Caplan, Ilana 352
 Capozza, Ricardo Francisco 137
 Cappariello, Alfredo 218
 Cappellino, Anthony 294
 Capulli, Mattia 45, 123, 253
 Caraco, Yoseph 437
 Carballo, Camila 369
 Carbonare, Luca Dalle 312
 Carey, Heather A. 95
 Carey, John 410
 Cariou, Bertrand 17
 Carlier, Aurelie 244
 Carlier, Marie Christine 17
 Carlo, Federica Scotto Di 432
 Carlone, Diana 6
 Carlson, Brandon 129
 Carlson, Elijah 344
 Carlson, Elizabeth 332
 Carmeliet, Geert 221, 244, 414
 Carmeliet, Peter 221, 244
 Carpenter, Dana 406
 Carpenter, Kelsey 363
 Carpenter, Thomas 402, 424
 Carpenter, Thomas O. 421
 Carpenter, Thomas O. 50, 51, 56, 120, 419
 Carpentier, André 234, 347
 Carr 356
 Carratù, Maria Rosaria 136
 Carreau, Anne-Marie 234, 347
 Carrino, John 129
 Carroll, Kaitlin 248
 Carter, Erin 180, 418
 Carter, Tonia 349
 Carvalho, Adriana 377
 Carvalho, Aluizio B. 62
 Carvalho, Antonio Carlos De Camargo 186
 Carvalho, Catarina 353
 Carvalho, Marta 138
 Carys, Kashmala 45
 Casado, Enrique 113, 383
 Casagrande, Alessandra 193, 318, 318
 Casal, Margret 185
 Casella, Alex 29, 352
 Cassat, Jim 194, 314, 315
 Cassiman, David 320
 Castañeda, Juan Rafael Muñoz 353
 Castano, Daniel 64
 Castellon, Alexis 26
 Castillo, Alesha 15, 413
 Castillo, Evelyn 33, 423
 Castro, Luis Fernandez De 121, 174
 Catheline, Sarah 74, 342
 Catlett, Sean 272
 Cauble, Meagan 294
 Cauley, Jane 8, 14, 20, 24, 40, 40, 84, 166, 285, 427
 Cauley, Jane A. 186
 Cavaco, Branca M. 418
 Cawley, Keisha 12
 Cawthon, Peggy 13, 14, 40, 84
 Cawthon, Peggy M. 434
 Cayrefourcq, Laure 72
 Cecchetti, Veronica 147
 Celi, Monica 210, 312, 336
 Celis, Esteban 22
 Cendoroglo, Maysa Seabra 167
 Center, Jacqueline 194, 272, 390, 397
 Center, Jacqueline R. 79, 271
 Cesaro, Roberto 203
 Cetani, Filomena 321
 Cetre, Nadia Mehsen 166
 Chae, Byongsoo 92
 Chae, Kyung Sil 184
 Chagin, Andrei 367
 Chai, Carmen 256
 Chai, Ryan 105
 Chakraborti, Gouri 319
 Chakraborty, Nabanarun 226, 240
 Chambon, Pierre 231
 Chan, Chi-On 297
 Chan, Ding-Cheng 253, 310
 Chan, Esther 113
 Chan, Jinyan 244
 Chan, Ricky 19
 Chan, Tea V 51
 Chan, Wing P. 185, 262, 384
 Chande, Sampada 77
 Chandler, Heidi 407
 Chandler, Kevin 382
 Chandra, Abhishek 111, 405
 Chandra, Malini 289, 408
 Chandrakumar, Abinaa 156, 371
 Chandramouli, Kaushik 295
 Chandran, Manju 384
 Chang, Chiang-Hua 319
 Chang, Gregory 207
 Chang, Jae Suk 278
 Chang, Je-Ken 413
 Chang, Jianhui 26, 239
 Chang, Kevin 376
 Chang, Kevin Y. 329
 Chang, Leslie 367
 Chang, Ling-Hua 413
 Chang, Martin 342
 Chang, Po-Yin 103
 Chang, Wei-Hua 238
 Chang, Wenhan 260
 Chanpaisaeng, Krittikarn 84
 Chappell, Daniel 361
 Chapuis, Laure 166
 Chapurlat, Roland 36, 38, 61, 102, 114, 173, 206, 266, 316, 332
 Charles, Julia F. 95
 Chastek, Benjamin 104
 Chatterjee, Shilpak 124
 Chaurand, Pierre 417
 Chaussain, Catherine 1
 Chavassieux, Pascale 206
 Chaves-Neto, Antônio Hernandez 146
 Chavez, Michael 423
 Che, Helene 166
 Che, Hui 82
 Che, Xiangguo 329
 Chee, Justin 156, 371
 Chellaiah, Meenakshi 159, 255
 Chellaiah, Meenakshi A. 219, 250

- Chemaitilly, Wassim 112
 Chen, Andy 435
 Chen, Chao-Yin 55
 Chen, Chia-Yen 39
 Chen, Chung-Hwan 413
 Chen, Di 31
 Chen, Donna 236
 Chen, Haiyan 140
 Chen, Hubert 318
 Chen, I-Ping 183, 305
 Chen, Jake . 41, 111, 191, 224, 315, 372
 Chen, Jake (Jinkun) 36
 Chen, Jake(Jinkun) 223
 Chen, Jiani 417
 Chen, Jianmei 252
 Chen, Jie 226
 Chen, Jinkun 158, 216, 281
 Chen, Jin-Ran 10
 Chen, Kristina 199, 321
 Chen, Kun 94
 Chen, Lin 84
 Chen, Lo-Wei 63
 Chen, Lulu 81, 226
 Chen, Neal 179, 297, 323
 Chen, Ningrong 439
 Chen, Po-Jung 156, 220
 Chen, Qianming 245
 Chen, Shih-Tse 218
 Chen, Ruei-Ming 238
 Chen, Rui 2, 106, 276
 Chen, Shan 78
 Chen, Shenyuan 379
 Chen, Shih-Tse 413
 Chen, Tong 158
 Chen, Xiaomin 96
 Chen, Xin 150
 Chen, Yi-Xuan 230
 Chen, Yuechuan 30, 94
 Chen, Yufan 18
 Chen, Yuqing 26, 44, 78
 Chen, Zhaojing 151, 388
 Cheng, Carol 27, 307
 Cheng, Chuanmin 59, 305
 Cheng, Haizi 10, 136, 370
 Cheng, Hongyun 260
 Cheng, Jack Chun Yiu 307, 381
 Cheng, Jack Chun-Yiu 27
 Cheng, Jack Cy 68
 Cheng, Qun 292
 Cheng, Vincent Ka-Fai 177
 Cheng, Xiaoguang . 164, 264, 266, 390
 Cheng, Yi-Wen 171
 Cheng, Yu-Chien 193, 317, 318, 318
 Chenoweth, Brandon 362
 Cheong, Hae I 55, 56
 Chepesiuk, Rachel 438
 Cheri, Samuele 312
 Cherian, Philip 22
 Cherman, Natasha 338
 Chesi, Alessandra . 28, 79, 91, 254
 Cheuk, Ka Yee 68, 307
 Cheung, Angela 38, 361, 406
 Cheung, Angela M. . 107, 156, 371, 387, 394
 Cheung, Angela M. . 277, 393, 400, 430
 Cheung, Ching-Lung 113, 177
 Cheung, Elaine 113
 Cheung, Tommy 113
 Cheung, Wing-Hoi 381
 Chevalley, Thierry 17, 36, 102, 223, 275, 309
 Chew, Chee Kian 199
 Chiasson, Genevieve 349
 Chiba, Ko . 68, 239, 262, 264, 368, 403
 Childress, Paul 226, 240, 361
 Chim, Shek Man 44
 Chirgwin, John 219
 Chitjian, Rynne 227, 294
 Chiu, Chen-Yuan 253, 310
 Chlebek, Sylvia 314
 Cho, Dong Hyeok 263
 Cho, In-Jin 380
 Cho, Nam H. 145, 265, 311
 Cho, Sun Wook 45, 340
 Cho, Yoon Young 283, 429
 Cho, Youngdan 158
 Cho, Young-Dan 79
 Choe, Hyonmin 150
 Choi, Ally 137
 Choi, Hee-Jeong 384
 Choi, Humberto 300
 Choi, Hyung Jin 145, 184, 265
 Choi, Je-Yong 329
 Choi, Jin-Young 429
 Choi, Ji-Yeob 145
 Choi, Kang Young 79
 Choi, Mun Sun 323
 Choi, Murim 184
 Choi, Roy B 296
 Choi, Woong Hwan 176, 308
 Choi, Yong Jun 276, 283
 Choi, Yu-Ra 329
 Chong, Le Roy 436
 Chong, Rong 218
 Chou, Joshua 29
 Chou, Sharon 163, 171
 Choudhary, Shilpa 35
 Chougule, Amit 98, 315
 Chourpiliadis, Charis 199
 Chow, Simon Kwoon Ho 381
 Choy, Man Huen Victoria 381
 Christiansen, Blaine 156, 370
 Christina, Vrahnas 64
 Chu, Emily 423
 Chu, Tzu-Hui 63
 Chua, Hui Lin 361
 Chuah, Matthew Bingfeng 384
 Chubinskaya, Susan 246, 343
 Chun, Hyelim 6
 Chun, Rene 177, 367
 Chung, Dong Jin 263
 Chung, Ho-Yeon 380
 Chung, Jin Ook 263
 Chung, Junho 72
 Chung, Min Young 263
 Chung, Yoon-Sok 276, 283
 Churchill, Gary 434
 Churchwell, John 410
 Chuzel, Quentin 316
 Ciarlini, Paulo Cesar 328
 Cicuttini, Flavia 167, 307, 427
 Cipriani, Cristiana 61, 147
 Cirelli, Joni Augusto 294
 Cirulli, Nunzio 312
 Citron, Kate 180
 Civitelli, Roberto . 41, 44, 91, 159, 227
 Claessens, Frank 23
 Clark, Emma M 271
 Clark, Marshall 321
 Clark, Ryan 214
 Clarke, Bart 420
 Clarke, Bart L. 128, 321
 Clarke, Shane 398
 Clausen, Lena 320
 Clemens, Thomas 10, 94
 Clément, Aurélie 78
 Clementelli, Carolina 61
 Clemmons, David 81, 255
 Clemmons, David R. 117, 118
 Cleret, Damien 359
 Cleverdon, Riley 314
 Clezardin, Philippe 72
 Clifford, Alexandra 357
 Clifford, Susan 68
 Clifton, Peter 205
 Clinkenbeard, Erica 81, 353
 Clinkenbeard, Erica L. 355
 Coakley, John 210
 Coates, Brandon 229
 Coban, Daniel 118
 Cobb, Justin 410
 Cockill, Clare 398
 Cody, Kathleen 194
 Coelho, Pedro Simões 102
 Coffman, Abigail 34, 407
 Coffman, Melissa 56
 Coheley, Lauren 190
 Cohen, Adi 121, 199, 285
 Cohen, Suzanne 361
 Cohen-Solal, Martine 220, 360
 Cohn, Matthew 13, 200
 COUNTRY, Gustavo Roberto 137
 Colaianni, Graziana 210, 217, 312, 413
 Colangelo, Luciano 61, 147
 Cole, David 402
 Coleman, Robert 46
 Coletto-Nunes, Glauca 294
 Colldén, Hannah 296
 Collier, Christopher 217
 Collins, Michael 424, 430
 Collins, Michael T. 121, 183
 Collins, Michael T. 131, 174
 Colnot, Céline 213
 Colon, Ivelisse 126, 323, 325
 Colon-Bernal, Isabel 294
 Colon-Emeric, Cathleen 272
 Colucci, Silvia 210, 217, 312, 413
 Combalia, Andrés 172
 Comeau-Gauthier, Marianne 64
 Comim, Fabio 345
 Compston, Juliet 108
 Conard, Katrina A. 184
 Condon, Keith 111
 Conesa, Arantxa 322
 Confavreux, Cyrille 17
 Conrad, Bogdan 94
 Conte, Elena 136
 Convente, Michael R 305
 Cook, Bryson 368
 Cook, Fiona 425
 Cook, Nancy 171, 284
 Cool, Simon 154
 Cool, Simon M. 253
 Cooper, Cyrus 13, 21, 54, 89, 105, 105, 107, 108, 109, 356, 398, 398
 Cooper, David 330, 377
 Cooper, Herbert John 89
 Cooper, Rachel 280
 Coorey, Craig Peter 333
 Corbeels, Katrien 414
 Cornish, Jillian 137, 192, 295
 Correlo, Vitor 431
 Cortet, Bernard 105, 166
 Cosman, Felicia 25, 113, 115
 Cosman, Miranda 345
 Costa, Samantha 77
 Costa, Tatiana Lemos 298
 Costa-Guda, Jessica 348
 Costantini, Alice 417
 Cottrell, Jessica 118
 Coulombe, Jennifer C. 98, 326
 Coulter, Alyssa 423
 Courbon, Guillaume 260
 Courties, Gabriel 71
 Coudry, Fabienne 43
 Cousminer, Diana 28
 Couture, Laura 147, 278
 Cowell, Chris 210
 Cowen, Edward W. 16
 Cox, Linda 192
 Cozar, Mónica 144
 Craft, Clarissa S. 9, 206
 Craft, Mary 301
 Craig, Theodore 139
 Cramer, Martin 81
 Crandall, Carolyn 8, 40, 269
 Crane, Janet 366
 Crawford, Julie 239
 Crean, Colin 219
 Creecy, Amy 326
 Creemers, John 80
 Gregor, Meloney 296
 Gregor, Meloney D. 260
 Cremers, Serge 178
 Cresswell, Erin 134
 Crittenden, D Barry 21
 Crittenden, Daria B. 25
 Crosset, Martine 72
 Croucher, Peter 105
 Croucher, Peter I. 64
 Crowley, Rachel 301
 Crozier, Sarah 109, 356
 Cruz, Amanda Raquel Costa . 164
 Cruz-Aviles, Lisa 419
 Cuesta-Dominguez, Álvaro 71
 Cui, Liao 223, 379
 Cui, Yan 136, 292
 Cui, Yong 242
 Cui, Zhongkai 190
 Cullen, Diane 204
 Cummings, Steven 14
 Cummings, Steven R. 114, 115
 Cunningham, Matthew 129
 Cunningham, Rory 349
 Cunto, Carmen De 420
 Curhan, Gary C. 394
 Curia, Dan 24
 Curiel, Manuel Diaz 298
 Curle, Anna 123
 Curry, Jacob 194, 314, 315
 Curry, Katharine 105
 Curtis, Elisabeth 356
 Curtis, Elizabeth 109
 Curtis, Jeffrey 2, 54, 106, 267, 275, 276
 Curtis, Jeffrey R. 104
 Cusano, Natalie . 61, 129, 130, 203
 Cutler, Christopher 22
 Cuzick, Jack 46, 102
 Czaykowski, Piotr 103
 Czech, Michael 225

- Czerwinski, Edward 263
- D**
- D., Anitha 327
- D'Agostini, Matteo 303, 305
- D'Amato, Gabriele 210
- D'Angelo, Stefania 109, 356
- D'Costa, Susan 81, 255
- Da, Hao. 10
- Dadwal, Ushashi. 248
- Dagdeviren, Didem 421
- Daghma, Diaa Eldin S. 346
- Dahia, Chitra 150
- Dahl-Hansen, Helen. 321
- Dai, Jiannong 53
- Daiello, Lori 54
- Daigle, Shanette 2, 106, 267
- Dallas, Mark. 383, 431
- Dallas, Sarah. 336, 383
- Daly, Robin 20
- Dam, Thuy-Tien. 285
- Damm, Timo. 385
- Danese, Vittoria 147
- Danford, David 301
- Dang, Alexis 161
- Dang, Khang. 272
- Dang, Lei. 119
- Daniel, Ashley L. 80
- Danielpour, David. 30
- Daniels, Veerle. 244
- Danila, Maria I. 275, 397
- Dann, Pamela 18
- Dar, Ainnie. 97
- Darakananda, Karin 48
- Darby, Trevor M. 415
- Das, Lakshmi 386
- Dash, Alexander 129, 248, 266
- Datta, Mrirul 8
- Davenport, Donna. 162
- David, Dana 135
- David, Natalie 20, 25
- David, Nicolae Valentin 354
- David, Valentin 18, 260
- Davidson, J Michael. 100
- Davies, Faith. 219
- Davis, Alan. 241
- Davis, Alison 26
- Davis, Christopher 246
- Davis, Hannah. 188, 334
- Davis, Hannah M. 83, 95, 98, 260
- Davison, Andrew 145
- Davison, Erin M. 108
- Davison, K Shawn. 193, 387
- Dawson, Brian 26, 44
- Dawson, Brian C 78
- Dawson, Lindsay 85
- Dawson, Lindsay A. 372
- Day, Felix 125
- Deal, Chad 115
- Dean, Christopher. 342
- Debiais, Françoise. 130, 166
- Debnath, Shawon 3
- Debono, Miguel 267
- Decallonne, Brigitte 23
- Dechaumet, Benoit 359
- Deepak, Vishwa 192
- Deguchi, Shinji 119
- Deguchi, Toru 329
- Deiana, Michela 312
- Dekkers, Olaf 51
- Delale, Thomas 117, 118
- Delany, Anne. 92, 378
- Delgado-Calle, Jesus 80, 260, 339
- Dell, Richard M. 2, 2, 103
- Delzell, Elizabeth 2, 106, 267
- Demambro, Victoria 71, 76, 77, 81, 117, 172, 223, 232
- Demaras, Alice. 38
- Demay, Marie 36, 77
- Demirtas, Ahmet 65
- Demissie, Serkalem 36
- Dempsey, Caeden 298
- Dempster, David. 113, 121, 323
- Dempster, David W. 199, 324
- Deng, Hong-Wen 80
- Deng, Peng. 48
- Deng, Zhenhan 136, 292, 370
- Deng, Zhonghao 18
- Deng, Zuoming 16
- Denham, Douglas 128
- Dennison, Elaine. 107, 356
- Deosthale, Padmini 83, 98, 334
- Depypere, Maarten 244
- Dercle, Laurent 63, 324
- Derkatch, Sheldon. 8, 38, 100
- Dernis, Emmanuelle. 170
- Derzko, Christine 127
- Desai, Shivang 219
- Desai, Tejal. 249
- Desanto, Matt 374
- Desanto, Matthew 368
- Desbiens, Louis-Charles 391
- Desborough, Robert. 423
- Dessay, Mariam 352
- Dessordi, Renata 201
- Desvergne, Beatrice 75
- Desyatova, Anastasia 311
- De-Ugarte, Laura 249
- Devin, Maureen 345
- Dewhurst, Hannah 105
- Deyle, David 154, 333
- Deyle, David R. 253
- Dhaliwal, Ruban 166, 180, 183, 207
- Dhiman, Vandana 180, 183
- Dhole, Atharva. 118
- Diantonio, Aaron 206
- Diaz, Antonio Casado 353
- Diaz, Luis Fernandez De Castro 424
- Díaz-Guerra, Guillermo Martínez 321
- Didonato, Joseph A. 251
- Diem, Susan 316, 391
- Dietz, Allan. 154
- Diez-Perez, Adolfo. 249, 273, 392, 394
- Díez-Pérez, Adolfo. 144, 144
- Dijkstra, P.D.Sander 297
- Dijkstra, Sander. 51, 417
- Dilley, Julian. 334
- Dilley, Julian E. 98
- Dimai, Hans Peter. 276
- Dimitrov, George 226
- Ding, Ke-Hong. 93, 225, 414
- Dinges, David 188
- Diniz, Mariana. 162
- Dion, Natalie. 165
- Dirkes, Rebecca 353
- Dite, Toby 64
- Divine, George. 66, 99
- Divisato, Giuseppina 432
- Dixon, S. Jeffrey 57
- Djekic-Ivankovic, Marija 438
- Do, Justin 215, 281
- Dockery, Frances 398
- Doherty, Laura 153, 312
- Doi, Mitsuru 403
- Doi, Takanobu 409
- Dolan, Connor 372
- Dole, Neha S. 1
- Dollar, Christina. 332
- Domingues, Rita. 418
- Dominguez, Wagner V. 62
- Domon, Hisanori 257
- Donahue, Henry 357
- Donahue, Seth 236
- Dong, Bingzi 132, 178
- Dong, Dandan 254
- Dong, Hongbo 270
- Dong-Guk, Shin 228
- Dongmei, Dr 186
- Donham, Cristine 337
- Donlon, Catherine. 163, 171, 284
- Donnelly, Eve 13, 65, 201, 328
- Doolittle, Madison. 227
- Dooyema, Samuel 73
- Dore, Robin K. 292
- Dornelles, Rita Cássia Menegati 146, 328
- Dorsch, Marion 26
- Dorschner, Jessica 139
- Dort, Mayke Van 270, 389, 391
- Doshi, Krupa 125
- Dosunmu, Edmund 388
- Douni, Eleni 58
- Dowthwaite, Jodi N 135
- Doyle, Daniel. 57
- Drager, Justin 64
- Drake, Matthew 17, 123, 127, 145
- Drenkard, Lauren Mangano 141
- Drevinge, Christina 358
- Driessen, Johanna 270, 389, 391
- Driessen, Johanna H 269
- Driessen, Johanna Hm 291, 397
- Driouch, Keltouma 72
- Driscoll, Adam. 329, 376
- Drissi, Hicham 44
- Driver, Madeleine G. 327
- Drobnic, Franchek 401
- Droit, Arnaud 351, 352
- Du, Minqun 223
- Du, Xiaolan 84
- Du, Yifei 216
- Duan, Rong 45
- Duan, Shenghui 57
- Duanmu, Yangyang 390
- Duarte-Salles, Talita. 54
- Duboeuf, Francois. 61, 316
- Duboeuf, François. 43, 209
- Dubois, Sacha 409
- Dubyak, George 369
- Duckham, Rachel 20
- Duckham, Rachel L. 311
- Dudakovic, Amel 154, 244, 251, 253, 254, 364, 366
- Dudenkov, Daniel 39
- Dumuid, Dorothea. 68
- Dunn, Jeffrey F 155
- Dunning, Lynette 155
- Duong, Le 294
- Duque, Gustavo 153, 185, 189, 222
- Durai, Heather. 59
- Durand, Audrey 39
- Duren, Dana 67, 405
- Dussold, Corey. 18, 260
- Duta-Mare, Madalina-Cristina 346
- Dutra, Eliane 156, 220
- Dworakowski, Elzbieta 203
- Dwyer, Madeline. 361
- Dwyer, Terry. 109
- Dyachuk, Viacheslav 367
- Dyment, Nathaniel 4
- E**
- Ea, Hang-Korng 220
- Eastell, Richard 20, 24, 25, 46, 109, 115, 129, 267, 319, 356, 423
- Ebbehoj, Eva 405
- Ebeling, Peter 110, 412
- Ebeling, Peter R. 25
- Ebetino, Frank. 45
- Ebetino, Frank H. 34, 80, 178, 407
- Ebetino, Frank H. (Hal). 22
- Ebina, Kosuke 387
- Ebina, Toshihito 175
- Economides, Aris N 320
- Economides, Aris N. 196
- Econs, Michael. 56, 303
- Edderkaoui, Bouchra 368
- Edonomides, Aris 337
- Edwards, Beatrice. 103
- Edwards, Mark 107
- Edwards, W Brent. 405
- Edwards, W. Brent 330
- Eekhoff, Marelise 120, 304, 306
- Eelen, Guy 221, 244
- Eerden, Bram Van Der 153, 435
- Egle, Daniel 55
- Egli, Andreas. 109
- Eguchi, Takanori 343
- Egunsola, Adetutu. 73
- Eguro, Takeshi. 408
- Ehrlich, Melanie. 80
- Ehrlich, Michael. 19, 88
- Eira, Margareth 112
- Eiriksdottir, Gudny 11, 37, 168, 226
- Eisman, John 194, 272, 390
- Eisman, John A 397
- Eisman, John A. 79, 271
- Ejersted, Charlotte 419
- Ejlsmark-Svensson, Henriette 47
- Ekuma, Okechukwu 284
- Elashiry, Mahmoud 22
- Elbarbary, Reyad 249
- Elders, Petra 8, 436
- Elefterio, Florent. 281
- Eleuterio, Jessica 162
- Elhakeem, Ahmed 271, 280
- Eliason, Travis D. 206
- Eliseev, Roman 43, 74, 154, 238, 339
- Elizabeth, Bradley. 96
- Elizondo, Jon 327
- Elkins, Cody M 305
- Elkins, Cody M. 59
- Elling, Roland 243
- Ellis, James 133
- Elmans, Ahmed 153, 242, 403
- Elsalanty, Mohammed 22, 225, 414
- Elsayed, Ranya 22, 225
- Elseoudi, Abdellatif 343
- Emaus, Nina 274
- Embry, Rachel. 383
- Emeny, Rebecca 319
- Emma, Francesco 303
- Emmelot-Vonk, Marielle H. 291

- Emoto, Masanori147, 355
 Endo, Itsuro178, 341, 342
 Endo, Itsuto132
 Ene, Gabrielle E. V.430
 Ene, Gabrielle E.V.361
 Engelke, Klaus.164, 280, 428
 English, Dallas.110
 Enishi, Tetsuya.14
 Ensrud, Kris84
 Ensrud, Kristine 8, 13, 14, 40, 106, 316, 391
 Eom, Je-Hyun42
 Epp, Riley275
 Epstein, Michelle256
 Era, Makoto262
 Eriksson, Anna273
 Ernst, Martin105
 Escalera-Rivera, Katherine.74
 Escobar, Luis417
 Espanol, Montserrat256
 Esparza, Mariela356
 Esposito, Alessandra49, 53, 141, 246, 292, 343
 Esposito, Teresa432
 Essalmani, Rachid.80
 Essen, Huib Van304
 Essex, Alyson188
 Essex, Alyson L.83, 98
 Estrada, Andrea332
 Ethiraj, Purushoth219
 Etienne, François360
 Ettinger, Bruce287, 289, 408
 Eusébio, Mónica102
 Evangelou, Evangelos105
 Evans, Dave39
 Evans, David.105
 Evans, Glenda293
 Evans, William14
 Evans-Molina, Carmella136
 Everitt, Leah.217
 Evseenko, Denis88
 Ewing, Susan168
 Ewing, Susan K226
 Exner, Ruth55
 Eyre, David78
 Eyre, David R.424
 Ezura, Yoichi.136
- F**
- Fabreguet, Isabelle275
 Faccio, Roberta44
 Fahrleitner-Pammer, Astrid101, 113, 286
 Faienza, Maria Felicia210, 312, 413
 Failla, Antonio Virgilio31
 Fairfield, Heather77
 Fajardo, Roberto260, 272
 Fajardo, Roberto J.206
 Falck, Alyssa228, 362, 413, 426
 Falzon, Rebecca124
 Fan, Roger298
 Fan, Shunwu.259
 Fan, Yao435
 Fang, Emily15
 Fang, Fang219, 312
 Fang, Fuchun372
 Fang, Shona322
 Fanning, Elizabeth A417
 Fantacone, Mary L.351
 Farach-Carson, Mary.362
 Farber, Charles .94, 172, 227, 230, 357, 434
 Farhat, Theresa332
 Farid, Alexander.207
 Farlay, Delphine.132
 Farman, Helen.231
 Farnsworth, Christopher370
 Farr, Josh145
 Farr, Joshua17, 26, 111
 Fassino, Valeria61, 147
 Fattore, Andrea Del303, 305
 Faugere, Marie-Claude94
 Faulkner, Bora.256
 Faulkner-Filosa, Chad41
 Featherall, Joseph338
 Feichtinger, Xaver.116
 Fejfarkova, Zlata333
 Feldman, Sidney.438
 Feller, Martin317
 Fendt, Sarah-Maria221
 Feng, Jian70, 242
 Feng, Jian Q18
 Feng, Jian Q..31, 75, 243
 Feng, Xu379
 Fentene, Jonathan77
 Ferguson, Daniel251
 Ferguson, Virginia L.65, 204
 Ferguson, Virginia L.98, 326
 Fernandes, Adriana M299
 Fernandes, Daniel326
 Fernandes, Fabiana146
 Fernandes, Fernanda146, 328
 Fernandes, Karen436
 Fernandez, Agustin F.351
 Fernandez, Natalia126
 Ferrari, Serge17, 21, 25, 33, 36, 58, 102, 223, 275, 309
 Ferraz-De-Souza, Bruno299
 Ferreira, Carlos174
 Ferretti, Jose Luis137
 Ferris, David.126
 Ferron, Mathieu80, 349
 Ferrone, Federica147
 Fesl, Christian55
 Fetene, Jonathan349
 Feuchter, Mario385
 Fialka, Christian116
 Ficheur, Grégoire105
 Fidow, Ulai.311
 Fields, Aaron.161
 Figeac, Florence216
 Figgie, Mark180
 Figueroa, Carolina172
 Filella, Xavier322
 Finch, Amy.361, 393, 430
 Findlay, David247
 Fine, Ben387
 Fink, Dorothy173
 Finkelstein, Joel48, 166
 Finlayson, Marcia284
 Finnerty, Celeste.337
 Finstad, Kristiaan243
 Fiscaletti, Melissa135, 210, 333
 Fischer, Heidi390
 Fisher, Elizabeth.350
 Fitzal, Florian55
 Fitzgerald, Kate A.243
 Fitzgibbon, Edmond J183
 Fitzpatrick, Lorraine392
 Fitzpatrick, Lorraine A.104
 Flack, Alyssa238
 Flammier, Sacha43
 Fleet, James84
 Fleming, Nicole305
 Fleming, Paul26
 Fleming, Whitney214
 Flemming, Poul101
 Flik, Gert.403
 Floor, Marianne332
 Florant, Gregory236
 Florencio-Silva, Rinaldo161
 Florenzano, Pablo121, 174, 424
 Flores-Moreno, Claudia.274, 308
 Florez, Helena121, 322
 Foley, Elizabeth208
 Folland, Jonathan171
 Follet, Helene132, 316
 Follet, Hélène209
 Fong, John T.22
 Fonseca, João Eurico102
 Fontana, Cristina Garcia182
 Fontana, Francesca 41, 44, 91, 227
 Fonte, Flavia Kurebayashi167
 Fonzino, Adriano136
 Ford, Caleb194, 314
 Foreman, Sarah193
 Forest, Marie39
 Foretz, Marc74
 Forgetta, Vincenzo39, 105
 Forkert, Nils D.165
 Formosa, Melissa M.403
 Formosa, Robert403
 Forsmo, Siri274
 Forster, Corey414
 Fort, Brian369
 Forwood, Mark R.64
 Foster, Brian423, 426
 Foster, Phillip276
 Fournier, Frédéric.351, 352
 Fournier, Roxanne382
 Foa, Gabrielle259
 Fraga, Mario F.351
 Franceschi, Renny.239, 242
 Francis, Connor18
 Franco, Anita143
 Frantal, Sophie55
 Fraser, Daniel26
 Fraser, Robert109, 356
 Fraser, William168
 Fraser, William D.182, 437
 Fratzl, Peter184
 Fratzl-Zelman, Nadja16, 184
 Frazão, João Miguel.353
 Fredericks, Robert146
 Frederiksen, Anja Lisbeth419
 Freeman, Theresa414
 Freitas, Radamés Leal164
 Fremont-Smith, Philip352
 Frenette, Jérôme.432
 Fretz, Jackie53
 Fried, Kaj367
 Fried, Rachel356
 Friedman, Michael357
 Friedman, Richard A.71
 Frikha, Dorra161
 Frikha-Benayed, Dorra161
 Frisoli, Alberto.186
 Froehle, Andrew.405
 Frost, Morten40, 216, 419
 Frysz, Monika12
 F-Turgeon, Alexis391
 Fu, Lei402
 Fu, Wenyu220
 Fu, Zhengu178
 Fuentes, Andrea Soares Da Costa 294
 Fuhler, Gwenny153
 Fujii, Takayuki256
 Fujimaki, Hisako173, 175
 Fujita, Ryo.34
 Fujiwara, Makoto71, 76
 Fujiwara, Saeko411
 Fujiwara, Sayaka300
 Fukuda, Chie34, 381
 Fukuda, Koji.408
 Fukumoto, Seiji132, 234, 300
 Fulbright, Laura315
 Fuller-Thomson, Lilia.360
 Fulzele, Sadanand153, 212, 242, 403, 414
 Funck-Brentano, Thomas. 14, 273
 Funnel, Larry438
 Furniss, Dominic54
 Furukawa, Luzia112
 Furuya, Yuriko157
- G**
- Gabel, Leigh100
 Gabilondo, Alicia K.155
 Gaddy, Dana.228, 362, 413, 426
 Gadermaier, Elisabeth280, 385
 Gaffney-Stomberg, Erin 170, 278, 280, 352
 Gafni, Rachel I424
 Gafni, Rachel I.131, 174, 332
 Gagnon, Claudia234, 347, 348
 Gagnon, Edith351, 352
 Gahl, William A.174
 Gajic-Veljanoski, Olga107
 Galan-Diez, Marta71
 Galeano-Garces, Catalina364
 Galeano-Garces, Daniela364
 Galesanu, Corina286
 Galesanu, Mihail Romeo286
 Galitzer, Hillel437
 Gallagher, Catherine398
 Gallagher, J A245
 Gallagher, James145
 Gallant, Kathleen Hill.179, 297
 Gallant, Kathleen M. Hill.323
 Gallo, Richard L.351
 Galmardini, Carlos339
 Galson, Deborah L138
 Galson, Deborah L.324
 Galvan, Edison Edgardo Romero 385
 Galvão, J.112
 Gamache, Philippe268, 324
 Gamble, Greg54
 Gamboa, Amanda R.351
 Gamer, Laura44, 363, 373
 Gamsjaeger, Sonja111
 Gandhi, Deep217
 Gandhi, Saurabh109, 356
 Gandhi, Shriya317
 Gandhi, Varsha21
 Gandini, Alberto.312
 Ganesh, Thiagarajan431
 Gani, Linsey398, 436
 Gannon, Olivia J227
 Gao, Huanqing31
 Gao, Manman245
 Gao, Shuang252
 Gao, Xueqin10, 136, 292, 370
 Gao, You-Shui230

- Gao, Yuan 230
 Garceau, Roger 437
 Garcia, Camila Stringhetta . . . 328
 Garcia, Camila Tami Stringhetta
 146
 Garcia, Miguel Torralbo 298
 García-Cirera, Silvia 383
 García-Fontana, Beatriz García-
 Fontana 182
 Garcia-Giralt, Natalia 249, 394
 Garcia-Giralt, Natàlia 144
 García-Giralt, Natàlia 144
 García-Hernández, Pedro . . . 274
 García-Hernández, Pedro Alberto
 308
 Garcia-Hoyos, Marta 122
 Garcia-Unzueta, Maite 122
 Gardella, Thomas 425
 Gardella, Thomas J 232
 Gardiner, Edith 117
 Gardinier, Joseph 44
 Garg, Abhilasha 166
 Garg, Uttam 334
 Garner, Andrew 26
 Garon, Martin 332
 Gasbarra, Elena 336
 Gasier, Heath 278
 Gaspa, Gianluigi 203
 Gasparini, Sylvia J 9
 Gastel, Nick Van 244
 Gaucher, Céline 362
 Gaudet, Sharon 108
 Gaudier-Lintia, Alina 64
 Gautam, Aarti 226, 240
 Gautvik, Kaare M. 228
 Gautvik, Vigdis T. 228
 Gaytán-González, Alejandro . 274,
 308
 Gazes, Yunghlin 323
 Gazoni, Fernanda 392
 Gazoni, Fernanda Martins . . . 167
 Ge, Chunxi 242
 Ge, Xianpeng 227
 Gee, Andrew 90
 Geel, Tineke Van 194, 390
 Gegg, Aaron 362
 Geiger, Erik J. 2, 2, 103
 Geisler, Jennifer A. 95
 Gell, Grace 68
 Geller, Jeffrey Albert 89
 Genant, Harry 90, 280
 Genders, Stijn 417
 Genest, Franca 196, 320
 Genet, François 214
 Geng, Qinghe 80
 Geng, Sinong 47
 Gennari, Luigi 312
 Gentile, Emily 48
 George, Christopher 218
 Georgia, Senta 134
 Gerard, Karsenty 69
 Gerard-O'Riley, Rita 303
 Gerbaix, Maude 33
 Gerber, Claire 18, 260, 354
 Geris, Liesbet 244
 Germak, John 321
 Gerousi, Marina 144
 Gerstenfeld, Louis 141, 356, 365
 Gettemans, Jan 189
 Getty, Patrick 217
 Geusens, P.P. 66
 Geusens, Piet 113, 114, 169, 194,
 270, 286, 290, 389, 390, 391
 Geusens, Piet P 397
 Geusens, Piet Pm 269, 430
 Gevers, Sonja 291
 Gharibeh, Nathalie 233, 240
 Ghasem-Zadeh, Ali 68, 362
 Ghirardello, Elena 105
 Ghosh, Joydeep 361
 Gianfrancesco, Fernando . . . 432
 Giangregorio, Lora 164, 277, 399,
 438
 Giangregorio, Lora M. 400
 Giannopoulou, Eugenia 18
 Gibbs, Jenna C. 277, 400
 Gibson, Katie 321
 Gielen, Evelien 320
 Giles, Graham 110
 Gillick, Hana 156, 371
 Gillies, Austin 332
 Gilmore, Alyssa 93
 Gilsanz, Vicente 28
 Ginebra, Maria-Pau 256
 Gingery, Anne 10
 Ginty, Mark 409
 Giovamberardino, Gianna Di . 303
 Giovane, Cinzia Del 317
 Gistelinc, Charlotte 424
 Gittings, William 314, 437
 Gittoes, Neil 398, 398
 Giuliani, Nicola 218
 Giusti, Andrea 174, 286
 Gjesdal, Clara G. 274
 Glenister, Elizabeth 321
 Glimcher, Laurie 3
 Glogauer, Michael 315
 Glorieux, Francis 55, 421, 422
 Glowacki, Julie 230, 250
 Gludovatz, Bernd 13
 Glüer, Claus-Christian 385
 Gluhak-Heinrich, Jelica 242
 Gnant, Michael 55
 Go, Muriel Tania 193, 318, 318
 Go, Tae-Hwa 167
 Göbel, Andy 72
 Godfrey, Dana 117
 Godfrey, Dana A. 205
 Godfrey, Keith 109, 356
 Godfrey, Tanner 30, 94
 Godwin, Catrina 42, 231, 343, 363
 Goel, Mishita 318
 Goemaere, Stefan 114
 Goering, Emily 192
 Goertzen, Andrew 271
 Goh, En Lin 410
 Gold, Gabriel 126
 Goldman, Julia 370
 Goltzman, David
 36, 70, 81, 107, 193, 194, 226,
 387, 390, 393, 394
 Gombart, Adrian F. 351
 Gomez, Leland 334
 Gomez, Leland J. 95
 Gómez, Manuel Quesada 298
 Gomez, Maximo 63, 203
 Gómez, Néstor Más 93
 Gonçalves, Paulo 345
 Gong, Hyun Sik 150, 388
 Gong, Shiaoching 18
 Gong, Yanqing 117
 Goni, Vijay 207
 Gonzaga-Jauregui, Claudia . . 320
 Gonzales-Chaves, Macarena . . 209
 Gonzalez, Diana 299, 421
 Gonzalez, Eva 121
 González-Gallegos, Noé Albino . .
 274, 308
 González-Mendoza, Roberto . 274,
 308
 Gonzalez-Rodriguez, Elena 3
 Goodyear, Carl 155
 Goodyear, Carl S. 379
 Gopalakrishnan, Rajaram . . . 256
 Gorden, Riley 240
 Gordon, Catherine M. 394
 Gordon, Jonathan 49, 86
 Gordon, Jonathan A.R. 184, 243
 Gordon, Rebecca 57
 Gori, Francesca 29, 29, 94
 Gorrell, Taylor 362
 Gortazar, Arancha 149
 Gortazar, Arancha R 217
 Goschnik, Michaela 224
 Goseki-Sone, Masae 178
 Gosnell, Heather 409
 Gossiel, Fatma 109, 319
 Gostasebi, Azita 395
 Gottesman, Gary S 181
 Gottesman, Gary S 51, 57, 120,
 182, 306, 420, 422, 425
 Gottlieb, Carter 177
 Gou, Yu 221
 Goudy, Steven 68
 Gourrier, Aurelien 132
 Gouveia, Cecilia 336
 Govea, Nicolas 14
 Grace-Martin, Julie 301
 Gracielen, Rodriguez 291
 Grafe, Ingo 26, 78, 205
 Grahemo, Louise 69
 Grano, Maria 210, 217, 312, 413
 Grant, Struan 28, 188
 Grant, Struan F.A. 79, 91, 254
 Gratacós, Jordi 383
 Grauer, Andreas 20, 24, 108
 Graul, Chris 26
 Gravallese, Ellen 78
 Graves, Dana 74
 Graves, Jonah M. 311
 Graves, Stephen 427
 Gray, Jinhua 357
 Gray, Nathanael 357
 Gray, Ryan 144
 Grevic, Danka 88, 365
 Greenblatt, Elliot 26
 Greenblatt, Matthew 3, 18, 416
 Greendale, Gail 40, 142, 166
 Greenfield, Edward 217, 369
 Greenfield, Edward M. 150
 Greenspan, Susan 115
 Greenwood, Celia M T 39
 Greeves, Julie 168
 Greggi, Chiara 336
 Gregorio, Silvana Di 163, 327
 Gregory, Jenny 12
 Gregory, Seth 333
 Gregson, Celia 105, 398
 Gregson, Celia L. 269, 369
 Greil, Richard 55
 Gremminger, Victoria L. 349
 Grenier-Larouche, Thomas . . 234,
 347
 Griebeler, Marcio 203
 Griffanti, Gabriele 191
 Griffin, Lanny 66
 Griffin, Patrick 315
 Griffin, Xavier 398
 Grigoriadis, Agamemnon 46
 Grillari, Johannes 267, 310
 Grimsrud, Christopher 289
 Grinberg, Daniel 144, 144, 249
 Grogan, Donna R. 420
 Gronthos, Stan 424
 Gross, Ted 117, 359
 Group, The Camos Research . . . 107
 Grove-Laugesen, Diana 405
 Grover, Monica 44
 Grunfeld, Carl 189
 Grynepas, Marc 5, 118, 252
 Gu, Jingua 244
 Gu, Sumin 73, 260
 Guanabens, Nuria 322
 Guañabens, Núria 121, 172
 Guardiola, Sara 327
 Guda, Teja 260
 Gudnason, Vilmundur 11, 37, 90,
 168, 226, 392
 Guermazi, Ali 247
 Guerrero, Pamela 298
 Guerriere, Katelyn 170, 278
 Guerton, Bernadette 214
 Guicheux, Jérôme 64, 362
 Guio, François De 163, 263
 Guise, Theresa 237
 Guise, Theresa A. 42
 Gulcelik, Nese Ersoz 181
 Gunasekaran, Uma 202
 Gunasekera, Hasantha 210
 Günther, Clara-Cecilie 228
 Guntin, Jonathan 101
 Guntur, Anyonya 71, 76, 223, 232,
 232
 Günzel, Daniel 428
 Guo, Daimo 338
 Guo, Edward X. 337
 Guo, Ge 148
 Guo, Jun 29, 425
 Guo, Tianyang 414
 Guo, X Edward 68, 131, 285
 Guo, X. Edward 89, 266, 358, 382
 Guo, Xiaodong 405
 Guo, Xiaotao 199
 Guo, Yuchen 43, 48
 Guo, Yuqi 76
 Guo, Yuxi 31
 Guo, Zhe 266
 Gupta, Nidhi 333
 Gurney, James 112
 Guss, Jason D. 328
 Gussekloo, Jacobijn 317
 Gustafsson, Karin 71, 231, 296
 Gustafsson, Karin L. 69
 Guterman-Ram, Gali 417
 Guth-Gundel, Sabine 58
 Guthrie, Lori C 121
 Guthrie, Lori C. 131
 Gutierrez-Hermosillo, Hugo . 278
 Gutiérrez-Hermosillo, Hugo . 274,
 308
 Gutierrez-Rojas, Irene 217
 Guzi, Timothy 26
 Guzzo, Rosa M. 74
 H
 Ha, Jung-Hong 160

- Ha, Yong-Chan 409
 Haakonsson, Anders Kristian 216
 Haapaniemi, Teppo 188
 Haard, Paul Van 169
 Hachemi, Yasmine 231
 Hachfeld, Christine 293
 Hackl, Matthias 267, 310
 Hackney, David 139
 Hadad, Aidan 200
 Hadji, Peyman 286
 Haeberle, Heather 205
 Haettich, Bénédicte 170
 Haeusler, Gabriele 184
 Haga, Nobuhiko 300
 Hagino, Hiroshi 412
 Haider, Ifaz 405
 Haider, Marie-Therese 25
 Hajishengallis, George 257
 Hakami, Yasser 122
 Hakimiyan, Arnavaz 246, 343
 Hakobyan, Narine 369
 Hakonarson, Hakon 29
 Haks, Mariëlle C. 51
 Halbur, Lisa 409
 Hale, Christiane 203
 Haleem, Meraaj S. 329
 Hall, Alexander 339
 Hall, Deborah 280
 Hall, Elizabeth 393
 Halleen, Jussi M 179, 188, 295, 339
 Halleux, Cyrille De 348
 Ham, Tjakko J Van 403
 Hamada, Nobushiro 119
 Hamano, Hiroki 34
 Hamdy, Neveen 51, 180, 417
 Hamdy, Neveen A.T. 297
 Hamill, Chelsea 311
 Hammamieh, Rasha 226, 240
 Hammond, Ian 387
 Hammond, James 57
 Hamoudi, Dounia 432
 Hamrick, Mark 93, 153, 212, 242, 403, 414
 Han, Jung-Suk 329
 Han, Li 23, 23, 26, 53, 146, 239, 354
 Han, Min-Su 304
 Han, Qi 30
 Han, Seungwoo 304
 Han, Weijuan 142
 Han, Yujiao 32
 Handa, Kazuaki 408
 Handel, Ben Van 88
 Hankenson, Kurt 254
 Hankenson, Kurt D. 79, 91, 376
 Hankins, Jane 112
 Hanley, David 36, 100, 194, 390, 393
 Hanley, David A 21, 107, 108, 193, 387, 394
 Hanna, Mirette 193, 318, 318
 Hanna, Patrick 40
 Hannam, Kimberly 271
 Hannan, Marian 36, 247, 309
 Hans, Didier 3, 100, 163, 263, 299, 317, 396, 410, 428
 Hans, Gabriel 396
 Hansen, Ann Kristin 345
 Hansen, Karen 47, 110, 349
 Hansen, Klavs Würgler 405
 Hansen, Ulrich 410
 Hanson, Eric P. 16
 Hanudel, Mark 353
 Hanudel, Mark R. 355
 Hao, Duan 117
 Haque, Azizul 219
 Hara, Berger 291
 Hara, Dorene O' 412
 Hara, Emilio Satoshi 338
 Hara, Masashi 158
 Hara, Yannis 6
 Harada, Takeshi 341, 342
 Haraguchi, Ryuma 160, 250
 Harb, Alexander 191
 Hardcastle, Sarah 369
 Harding, Amy 402
 Harhaji, Vladimir 24
 Hari, Nikash 59
 Harindhanavudhi, Tasma 181
 Harleem, Meraaj 376
 Harlow, Sioban 166
 Harmon, Amanda L. 108
 Haro, Tomás De 182
 Haroon, Mohammad 358
 Haroon, Nisha Nilg 406
 Harrington, Anne 90
 Harris, Charles 48
 Harris, Charles A 9
 Harris, Marie A 242
 Harris, Stephen E 242
 Harris, Tamara 90, 168, 226
 Harris, Tamara B 11, 37
 Harrison, Kim 377
 Harrison, Rene 382
 Hars, Magaly 275
 Hars, Melany 17
 Hars, Mélyany 126, 309
 Harsløf, Torben 47
 Hart, Olivia 117
 Hartley, April 271, 369
 Hartley, Chris 171
 Hartmann, Rolf W. 415
 Haruna, Julius 416
 Harvey, Edward 64
 Harvey, Edward J. 169
 Harvey, Ian 398
 Harvey, Nicholas 13, 39, 47, 105, 108, 109
 Harvey, Nicholas C 115, 392
 Harvey, Nicholas C. 115
 Harvey, Nick 356, 398
 Harvey, Paula 361, 430
 Haschka, Judith 116
 Hasegawa, Jun 123
 Hasegawa, Tomoka 34, 295
 Hashimoto, Junko 177
 Hashimoto, Shingo 408
 Hashmi, Hina 232
 Hashmi, Syed 121
 Haslbauer, Ferdinand 55
 Hassan, Fathi 346
 Hassan, Quamarul 30, 94
 Hassell, Emma 354
 Hast, Michael 207
 Hatch, Nan 92
 Hathaway-Schrader, Jessica 31, 219
 Hathcock, Matthew 199, 203
 Hatsell, Sarah 320
 Hatsell, Sarah J. 196
 Hattersley, Gary 292, 407
 Haudum, Christoph 224
 Hauet, Thierry 130
 Hausman, Bryan S. 150
 Hausner, Thomas 116
 Hawa, Gerhard 322
 Hawkins, Federico 321
 Hawley, Nicola L. 311
 Hawse, John 76
 Haxaire, Coline 369
 Hay, Eric 220
 Haÿ, Eric 360
 Hayashi, Noriyuki 147, 355
 Hayashi, Shinya 408
 Hayball, John 96
 Hayes, Alan 185
 Hayes, Kaleen 169
 Haynes, Cole 227
 Hazel, Diane 154
 He, Lizhi 227
 He, Mincong 245
 He, Qing 84, 434
 He, Wei 245
 He, Xinyu 338
 He, Yaowu 72
 He, Yonghan 23
 He, Zhenqiang 117
 He, Zhiguo 3
 He, Zhiming 5, 118
 Head, Victoria 58
 Heaney, Jason D. 78
 Heawood, Alison 398
 Hebert, James 190
 Hecht, Jacqueline 121, 304
 Heijboer, Annemieke 325
 Heijde, Désirée Van Der 90
 Heijer, Martin Den 274, 325, 396
 Heilmeier, Ursula 109, 310
 Heiss, Christian 346, 372
 Helary, Christophe 360
 Helderman, Ron 225, 232
 Heller, Matthew Scott 89
 Hellman, Judith 51
 Hellmich, Maya 288
 Helmuth, Ralph 219
 Hemmerling, Kimberly J. 201
 Henaff, Carole Le 5, 118, 374
 Hendrickson-Rebizant, Jane 349
 Hendrickx, Gretl 4, 143
 Hendy, Geoffrey N. 191, 418
 Heng, Shujun 243
 Henneicke, Holger 9
 Henning, Petra 14, 69, 231, 296, 358
 Hermann, Anne Pernille 40, 419
 Hernandez, Fabiana R. 62
 Hernandez, Christopher 134
 Hernandez, Christopher J. 328
 Herndon, David 337
 Herrera, Carmen 98, 334
 Herrmann, François 126
 Herskovitz, Rita 212
 Heshmat, Ramin 313, 439
 Hesse, Eric 25, 25, 31, 49, 73
 Hettinghouse, Aubryanna 220
 Heureux, Nicolas 194
 Heveran, Chelsea M. 65, 204
 Hewison, Martin 177
 Heyer, F.L. 66
 Hiasa, Masahiro 132, 341, 342
 Hicks, Gregory 395
 Hidaka, Kouki 119
 Hiebert, Beverly 377
 Higgins, C. Hazel 328
 Hilker, Eric 9
 Hilker, Eric D 206
 Hill, Jennifer 199
 Hill, Keith 20
 Hill, Keith D. 277, 400
 Hill, Ronald 280, 410
 Hill, Thomas 400
 Hill, William 93, 153, 212, 242, 403, 414
 Hillier, Loretta M. 399
 Hillman, Charles 66
 Hilton, Matthew 86
 Himes, Evan 361
 Himmler, Gottfried 280, 385
 Hinchey, John W 162
 Hinds, David 105
 Hinton, Pamela 353
 Hirano, Junko 406
 Hirano, Yuji 287, 288
 Hirata, Hirohito 258, 378
 Hirata, Michiko 140, 160
 Hiratsuka, Izumi 241
 Hiratsuka, Sigeto 34
 Hirdes, John 164
 Hirose, Jun 257
 Hirose, Katsutoshi 250
 Hirsch, Sarah 48
 Hiyama, Akiko 261
 Hiyoshi, Takumi 257
 Hlaing, Ei Ei Hsu 149
 Ho, Bryan 77
 Ho, Irene 361
 Ho, Linh 255
 Ho, Mei-Ling 413
 Ho, Patricia W M 293
 Hoac, Betty 1
 Hoang, Van 208
 Hochberg, Marc 395
 Hodge, Allison 110
 Hodge, Kenyaita M. 79, 91
 Hodges, Jason 112
 Hodous, Brian 26
 Hof, Rob J Van 'T. 347
 Hof, Rob Van 'T. 155
 Hofbauer, Lorenz 72
 Hoff, William Van 'T. 120
 Hoffa, Matthew 369
 Hoffman, Andrew 14
 Hoffman, Andrew R. 434
 Hoffmann, Oliver 72
 Hoffmann, Oskar 256
 Hogan, Harry 327
 Högler, Wolfgang 120, 322
 Højlund, Kurt 40, 216
 Hojo, Hironori 14
 Hokugo, Akishige 22
 Holden, Marit 228
 Holden, Rachel 278, 355, 401, 414
 Holden, Rachel M. 147
 Holdsworth, Gill 382
 Ho-Le, Thao P. 79, 271
 Holguin, Nilsson 53
 Holl, Mark Banaszak 294
 Holland, Richard 398
 Hollenberg, Alex 238
 Holloway-Kew, Kara 99, 308, 392
 Holloway-Kew, Kara L 273
 Holst, Stephanie 341
 Holte, Molly Nelson 76
 Holtstander, Lauren 73
 Holvik, Kristin 274
 Holzer, Markus 116
 Homer, Ken 24
 Honasoge, Mahalakshi 66, 99, 386
 Hong, A Ram 145, 184, 265, 311

- Hong, Christine 190
 Hong, Jung Min 361
 Hong, Namki 127, 429
 Hong, Sang Mo 308
 Hong, Seongbin 283
 Hong, Yu-Min 329
 Hongo, Michio 175, 175
 Hook, Jessica 215
 Hooper, John 72
 Hoover-Fong, Julie 121
 Hopman, Wilma 107
 Horan, Sean 402
 Horiguchi, Yusuke 264
 Horikawa, Akira 175
 Horiuchi, Yoshitaka 346
 Horn, Wanda 360
 Horne, Anne 54
 Hornyak, Julia 101
 Horowitz, Mark 41, 76, 424, 434
 Horst, Mary-Lou Van Der 399
 Horuzsko, Anatolij 225
 Hosseinatababaei, Seyedmahdi 28
 Hou, Dongqing 270
 Houseknecht, Karen 232
 Howard, Morris 205
 Howe, Amanda 398
 Howe, James 280, 410
 Hrdlicka, Henry 92, 378
 Hristova, Dayana 45
 Hruska, Josef 174, 286
 Hsia, Allison 156, 370
 Hsiao, Cheng-Yuan 63
 Hsiao, Edward 79
 Hsiao, Edward C 51
 Hsiao, Edward C 420
 Hsu, Emory 415
 Hsu, Erin 376
 Hsu, Erin L 329
 Hsu, Wellington 376
 Hsu, Wellington K 329
 Hsu, Yi-Hsiang 39, 105, 228
 Hu, Dorothy 29, 94, 407
 Hu, Jeffrey 387
 Hu, Lifang 85, 93, 373
 Hu, Pei 91, 350
 Hu, Tiffany 131
 Hu, Xiaoqing 80
 Hu, Yifang 64
 Hu, Yizhong 89, 337, 358
 Hu, Zhekai 111, 281
 Hu, Zhuoqing 223
 Hua, Phuong 82
 Hua, Rui 132, 260
 Huang, Eric 437
 Huang, Jiahui 19, 88
 Huang, Jian 336
 Huang, Le 143
 Huang, Lily 196
 Huang, Meihua 142
 Huang, Shuang 21
 Huang, Xianyuan 243
 Huang, Zizhan 373, 375
 Huard, Charles 136
 Huard, Johnny 10, 136, 292, 370
 Hubber, Philip 359
 Huber, Bryan 280, 410
 Huber, Lukas Maximilian 385
 Huber, Philippe 117
 Huck, Katrin 138, 242
 Hue, Trisha 168
 Hue, Trisha F 226
 Huesa, Carmen 155
 Huffnagle, Nicholas 188
 Huggins, Shannon 228, 362, 413, 426
 Hughes, Alexander 129
 Hughes, Andrew 145
 Hughes, Julie 170, 263, 265
 Hui, Rita 289, 408
 Hul, Wim Van 143, 183
 Hulbert, Maggie 401
 Hultin, Leif 379
 Hum, Julia 81, 362
 Hum, Nicholas 375
 Humbert, Ludovic 112, 163, 267, 327, 385, 401
 Hung, Adriana 230
 Hung, Vivian Wy 68
 Hunt, Heather 13
 Hunt, Heather B 201
 Hunter, David 154
 Hunter, Gary 196, 388
 Hunter, Jeffrey 26
 Hunter, Randee 133
 Huq, Sabrina 386
 Hurd, Lauren 184
 Hurley, Marja 124
 Hurwitz, Rachel 345
 Huskey, Margaret 57, 182, 425
 Husni, Hasan 193, 318, 318
 Hussein, Amira 365, 382
 Hussein, Khaled 153, 242, 403
 Hussein, Nazar 374
 Hutami, Islamy Rahma 159
 Huynh, Rose 272
 Huynh, Thanh 430
 Hwang, Soon Jung 157
 Hwang, You Cheol 380
 Hyde, Natalie 99, 308, 311
 Hymowitz, Mtchell 272
- I**
- Ibarbia, Carmen Garcia 351
 Ichimaru, Ryota 160
 Ideno, Hisashi 136
 Idone, Vincent 196
 Igbini, Nicholas 327
 Ignatus, Anita 231
 Iguchi, Takahiro 369
 Ihn, Hye Jung 159
 Ii, Matthew F. Bouchonville 410
 Iii, Blake E. Hildreth 95
 Imura, Tadahiro 160, 381
 Iio, Hiroyuki 86
 Ikeda, Sathoshi 290
 Ikeda, Satoshi 411, 412
 Ikemura, Satoshi 369
 Ikizler, T. Alp 230
 Imai, Yuuki 86, 160, 250, 381
 Imanishi, Yasuo 56, 147, 300, 355, 412
 Imel, Erik 51, 55, 56, 56, 120, 303
 Imholt, Felisha 372
 Imtiaz, Sonaina 408
 Inaba, Masaaki 147, 355
 Inada, Masaki 140, 160
 Inagaki, Hidehito 241
 Inagaki, Katsunori 408
 Inage, Kazuhide 173
 Inderjeeth, Charles 256
 Inghan, Sheila 186
 Inkrott, Bradley 374
 Inman, Robert 406
 Inoue, Daisuke 406
 Inoue, Gen 173, 175, 176, 408
 Inoue, Kazuki 3, 18, 381
 Inoue, Sho 173, 176
 Inskip, Hazel 89, 109, 356
 Insogna, Karl 97, 235
 Insogna, Karl L 50, 56, 122
 Ioannidis, George 107, 164, 399
 Ioannidis, John 279
 Ion, Gabriela 433
 Iovanna, Juan 258
 Ip, Edward 307
 Ireland, Alex 137
 Irizarry-Roman, Moises 24
 Isaacson, Janalee 213
 Isakova, Tamara 354
 Isales, Carlos 93, 153, 212, 225, 242, 403, 414
 Isaza, Ilean 309
 Ishi, Daisuke 173
 Ishida, Masahiko 257, 258, 258, 378
 Ishiguro, Naoki 288, 300
 Ishihara, Yoshihito 149
 Ishijima, Muneaki 334
 Ishikawa, Koji 173, 408
 Ishikawa, Yoshinori 175
 Ishikawa, Toru 411
 Islander, Ulrika 296
 Isobe, Yusaku 68
 Issa, João Paulo 431
 Ito, Keita 102
 Ito, Nobuaki 56, 122, 234, 300, 300
 Ito, Teppei 133
 Ivan, Mircea 98, 355
 Ivashkiv, Lionel 256
 Iovic, Aleksandra 16
 Iwakura, Takashi 167
 Iwamoto, Naoki 368
 Iwaniec, Urszula T 351
 Iwasaki, Nrimasa 34
 Iwatake, Myumi 375
 Iyer, Srividhya 26, 191, 239, 354
 Izano, Monika 287, 289, 408
 Izard, Rachel 168
 Izawa, Takashi 159
- J**
- Jaber, Fatima 374
 Jackson, Avery 410
 Jackson, Rebecca 432
 Jackson, Sarah 168
 Jacobson, Michelle 361
 Jacot, William 72
 Jacques, Richard 129, 400
 Jaffe, Laurinda A 196
 Jafri, Syed 100
 Jaglal, Susan 7, 399
 Jaglal, Susan B 399
 Jähn, Katharina 288, 348
 Jain, Mahim 78
 Jain, Rajesh 171
 Jain, Raksha 215
 Jain, Ravi 399
 Jakesz, Raimund 55
 Jakob, Franz 320
 Jakus, Adam 329
 Jalali, Aydin 435
 Jaleel, Ayesha 106, 276
 James, Aaron 367
 James, Robert 131
 Janez, Andrej 173
 Jang, Ji-Ae 304
 Jangsiripornpakorn, Jintanan 265
 Jankelovits, Amanda 101
 Jannot, Martin 173
 Janssen, Stefan 147
 Jansson, Per-Anders 24
 Jantzi, Micaela 164
 Janvier, Thomas 247
 Janzing, Heinrich M 397
 Janzing, Heinrich Mj 430
 Jardi, Ferran 23
 Jarraya, Mohamed 247
 Jaspers, Richard T 358
 Jastrzebski, Sandra 44
 Jaume, Juan Carlos 199
 Javaid, Kassim 356
 Javaid, M Kassim 54, 105, 109
 Javaid, Muhammad 21, 398
 Javed, Amjad 140
 Javier, Rose Marie 166
 Jazbinssek, Soncka 173
 Jean, Sonia 7, 169, 268, 324
 Jeffery, N 245
 Jellison, Evan 312
 Jenkins-Jones, Sara 423
 Jenkner, Alessandro 305
 Jennane, Rachid 247
 Jensen, Alexandria 11, 37
 Jensen, Eric 160, 256
 Jeon, Yun Kyung 283
 Jeon, Yunkyung 195
 Jeong, In-Kyung 380
 Jeong, Jong Ju 127
 Jeong, Soyeon 329, 376
 Jeong, Young Hun 239, 335
 Jeong, Youngjae 349
 Jepsen, Karl 209
 Jepsen, Karl J 206, 238
 Jerrhag, Daniel 27
 Jeschke, Anke 4
 Jestes, Kelli 314
 Jha, Smita 16
 Ji, Gang 416
 Jiang, Carrie 26
 Jiang, Hongbin 216
 Jiang, Hongyuan 386
 Jiang, Jean 73, 341
 Jiang, Jean X 132, 260, 337
 Jiang, Jie 49, 53, 141, 246, 292, 343
 Jiang, Lijie 6
 Jiang, Lingjing 147
 Jiang, Ming-Ming 26, 44, 73, 78
 Jiang, Tongmeng 139, 243
 Jiang, Xi 4
 Jiang, Yan 292
 Jiang, Yizhou 48
 Jilka, Robert 23, 146
 Jilka, Robert L 23, 345
 Jiménez, Carlos 321
 Jimenez, Johanna 320
 Jimi, Eijiro 42
 Jin, Chanyuan 403
 Jin, Hongfan 318
 Jin, Jianfeng 358
 Jin, Jianliang 81
 Jin, Xian 329
 Jin, Xiaolan 292
 Jin, Xin 49, 53, 141, 246, 292, 343
 Jin, Yuan-Zhe 289
 Jin, Zixue 44, 78
 Jing, Yan 70, 75, 243
 Jiron, Jessica 33, 423

- Jobke, Björn 288
 Joeng, Kyu-Sang 78
 Johannesdottir, Fjola 90, 207
 Johansson, Helena. 13, 39, 47, 108, 115, 392
 Johansson, Lisa 271
 John, Malcolm 193
 John, Sundberg 228
 John, Sutha K. 42
 Johnson, Joshua 5, 118
 Johnson, Mark 431
 Johnson, Matthew 254
 Johnson, Matthew E. 79, 91
 Johnson, Michael 240, 349
 Johnson, Rachele 340
 Johnson, Rachele W 293
 Johnson, Rachele W. 73
 Johnson, Robert 81
 Johnson, Trenton 329
 Johnston, James 28, 133, 154
 Johnston, Jd 211
 Jonason, Jennifer 74, 342
 Jones, Derek 359
 Jones, Glenville 19
 Jones, Graeme . 109, 134, 167, 185, 307, 427
 Jones, Kerry 356
 Jones, Kyle 336
 Jones, Rheinalt M. 35, 415
 Jones, Tim 398
 Jong, J.J.A. De 66
 Jongh, Renate De 274, 396
 Jonsson, Emma 398
 Jonsson, Helgi 90
 Jorgetti, Vanda 62, 112
 Jose, Beulah 214
 Josephson, Anna 365
 Joshee, Prakriti 406
 Josse, Robert 107, 194, 390
 Josse, Robert G 193, 387
 Jouan, Yohan 220
 Joy, Tsai 25
 Joyner, Michael 17
 Joyo, Yuji 409
 Jozani, Mohammad Jafari 100
 Jr, Carl G Simon 344
 Jr, Robert K. Boeckman 80
 Jr. 104
 Juby, Angela 246
 Judge, Andy 89
 Judge, Davneet 321
 Jueppner, Harald 425
 Juhas, Michal 189
 Julien, Anais 213
 Julio, Marianna Kruithof-De. 253
 Jun, Zhang 432
 Jung, Kwang Hwan 278
 Jung, Mihye 283
 Jung, Youn-Kwan 304
 Jüppner, Harald 40, 52, 434
 Jurrissen, Thomas 353
- K**
 Kaarsemaker, Sjoerd 397, 430
 Kacena, Melissa 226, 240, 303, 361
 Kadambi, Vivek 26
 Kader, Tarek Abd El 343
 Kado, Deborah 84, 147, 168, 361
 Kado, Deborah M. 226
 Kähkönen, Tiina E 188, 339
 Kaiser, Stephanie 194, 390, 393
 Kaiser, Stephanie M. 107, 193, 387
 Kaji, Hiroshi 346
 Kajiya, Hiroshi 257
 Kakihaya, Hiroyuki 177
 Kalajzic, Ivo 77, 87, 88, 153, 242, 365
 Kalinowski, Judy 44
 Kalkwarf, Heidi 28
 Kalra, Amisha 305
 Kalyan, Shirin 395
 Kam, Carmen 436
 Kamal, Fadia 249, 344
 Kamalakar, Archana 68
 Kamanda-Kosseh, Mafo 121, 199, 285
 Kamenev, Dmitrii 367
 Kamenicky, Peter 418
 Kamenický, Peter 56, 122
 Kamimoto, Hiroyuki 231
 Kamimura, Mikio 274
 Kamioka, Hiroshi 149
 Kammoun, Malek 76
 Kamohara, Asana 258, 378
 Kampleitner, Carina 256
 Kan, Casina 72
 Kan, Michelle 108
 Kanagalingam, Anuya 213
 Kanaji, Arihiko 308
 Kanaujiya, Jitendra 183, 305
 Kanayama, Yasuhide 288
 Kanazawa, Ippei 62, 70
 Kanda, Hironori 300
 Kaneko, Ayaka 334
 Kaneko, Kaichi 95, 256
 Kaneko, Kazuo 334
 Kanesaki, Katsuya 290
 Kang, Dae Ryong 167
 Kang, Guolian 112
 Kang, Heeseog 16
 Kang, Inhong 124
 Kang, Kai 279
 Kang, Keunsoo 95
 Kang, Lin 413
 Kang, Woo Youl 257
 Kanis, John 13, 39, 47, 108, 115, 398
 Kanis, John A 392
 Kaplan, Fred. 79, 302
 Kaplan, Frederick S. 22
 Kaplan, Frederick S. 420
 Kapral, Moira 38
 Kaptoge, Stephen 105
 Kar, Niladri S. 251
 Karabacak, Murat 71
 Karabelas, Paula 287
 Karaca, Anara 181
 Karanassos, Marinos 179
 Karasik, David. 105, 195, 228, 403
 Kargilis, Daniel 207
 Karki, Sangita 74
 Karlamangla, Arun 40, 142, 166
 Karlsson, Jon 271
 Karlsson, Magnus 13, 27, 310
 Karner, Courtney 86
 Karpf, David B. 194, 201, 323
 Karrupagounder, Vengadesh. 249
 Karunaratne, Angelo 410
 Karupppasamy, Subburaj 327
 Karvonen-Gutierrez, Carrie 142, 166
 Karvonen-Gutierrez, Carrie 40
 Kasikis, Stelios 199
 Kasimir-Bauer, Sabine 72
 Kassem, Moustapha. 40, 216
 Kaste, Sue 112
 Kastriti, Maria Eleni 367
 Kasukawa, Yuji 172, 175, 175, 179
 Katagiri, Takenobu 42, 123
 Kato, Hiroyuki. 274, 290, 422
 Kato, Jiro 409
 Kats, Allyson. 316, 391
 Katz, James 16
 Katz, Jeffrey N. 394
 Kaufman, Jonathan 263
 Kaufman, Randal 30
 Kaufmann, Christopher 361
 Kaufmann, Martin 19
 Kaur, Simran 72
 Kavanagh, Dillon 349, 424
 Kawaguchi, Yoshihiro. 123
 Kawahara, Shinya. 369
 Kawakami, Atsushi 368
 Kawakami, Tsukasa 241
 Kawakubo, Ayumu 173, 176
 Kawalilak, Chantal 28, 211
 Kawamata, Ryota 119
 Kawao, Naoyuki 346
 Kawata, Akira 119
 Kay, Fernando 388
 Kazakia, Galateia 189, 193
 Ke, Hua Zhu 382
 Ke, Ke 137
 Kearney, Patricia 317
 Kearns, Ann 203
 Keaveny, Tony M. 390
 Keely, Erin 277
 Keen, Richard 420
 Keller-Baruch, Julyan 39
 Kelly, Andrea 28
 Kelly, Kimberly E. 229, 335
 Kelly, Madison 362
 Kelly, Madison M. 435
 Kemp, John 39, 105
 Kendler, David. 113, 264, 286
 Kendler, David L 21
 Kendler, David L. 277, 400
 Kennedy, Courtney 107
 Kennedy, Stephen 109, 356
 Kennel, Kurt 123
 Kent, Kyla 209
 Kern, Stefanie 346, 372
 Kersh, Mariana 151, 207
 Kerslake, Robert 171
 Kesavan, Chandrasekhar. 30, 148, 363
 Kestenbaum, Bryan 230
 Ketteler, Markus 199
 Ketz, John 370
 Keuler, Nicholas 349
 Kfoury, Youmna 71
 Khajuria, Deepak Kumar 195, 403
 Khalid, Aysha 6
 Khalid, Sana 92, 374
 Khalil, Rougin 23
 Khan, Aliya 122, 400, 409
 Khan, Aliyah. 277
 Khan, Belal 110
 Khan, Faisal 240
 Khan, Mohd Parvez. 5, 341
 Khan, Moin 409
 Khan, Naiman 66
 Khan, Salma 368
 Khan, Sobiah 180, 418
 Khandelwal, Niranjana 166
 Khani, Farzaneh 251, 253, 254, 364
 Khanna, Geetika 181
 Khassawna, Thaqif El. 346, 372
 Khatiri, Ashok 232
 Khelifi, Nada. 348, 391
 Kho, Jordan 44
 Khoo, Benjamin Cc 264
 Khoo, Joan 398
 Khosla, Sundeep 17, 20, 24, 26, 36, 111, 145, 268, 293, 362
 Khrimian, Lori 69
 Kiel, Douglas. 36, 39, 39, 54, 105, 113, 247, 309
 Kiel, Douglas P. 228
 Kihira, Daisuke 287
 Kikugawa, Tadahiko 86
 Kilbane, Mark 301
 Kilgore, Meredith 2
 Kiltz, Tina 97
 Kiltz, Tina M. 344
 Kim, Anthony 255
 Kim, Beom-Jun 283, 380, 414, 429
 Kim, Bongjun 93
 Kim, Bong-Soo. 240, 241
 Kim, Bong-Su 79
 Kim, Byung Moon. 127
 Kim, Chang Oh 429
 Kim, Chong A. 417
 Kim, Deog-Yoon 409
 Kim, Do-Gyoon 329
 Kim, Dong Joon 127
 Kim, Eunheui 195
 Kim, Gun-Woo 304
 Kim, Gyu Man 239, 335
 Kim, Haemin 72
 Kim, Han Jo 129
 Kim, Ha-Neui 23, 53, 146, 191, 239, 354
 Kim, Hong-Hee 72, 93, 252, 259, 379
 Kim, Hyeon Chang 429
 Kim, Hyeonmok 277, 429
 Kim, Hyeonwoo 1
 Kim, Hyung Joon 72
 Kim, Hyun-Ju 257
 Kim, In Joo 283
 Kim, In Sook 157
 Kim, Injoo 195
 Kim, Jae Hyeon 283, 429
 Kim, Jaedong 176
 Kim, Ji Wan 278
 Kim, Jihye 289
 Kim, Jin Hwan 288
 Kim, Jin-Hwan 289
 Kim, Joseph 26
 Kim, Jung Hee. 145, 184, 265, 311
 Kim, Jung-Eun 96
 Kim, Jung-Min 3
 Kim, Jung-Taek 276
 Kim, Justin. 101
 Kim, Kahyun 150
 Kim, Keunyoung 283
 Kim, Kwangkyoun 187
 Kim, Kyoung Min 283
 Kim, Kyung Won 335
 Kim, Lawrence 321
 Kim, Min Kyung 252
 Kim, Mirini 332
 Kim, Na Ri 23
 Kim, Na-Kyung 42
 Kim, Sandra 277, 399, 400, 438
 Kim, Sang Il 72

- Kim, Sang Wan 184
Kim, Sarah 9
Kim, Sean 26
Kim, Se-Min 415
Kim, Seong-Jang 283
Kim, Seung-Hee 435
Kim, Soohyun 10
Kim, Soon-Young 96
Kim, Tae Ho 277
Kim, Tae-Hwan 289
Kim, Tiffany 189
Kim, Woo-Jin 79, 158, 240
Kim, Young-Gun 160
Kim, Yong Kyu 288
Kim,, Ha-Neui 26
Kimble, Morris 433
Kimelman, Douglas 100
Kimmel, Don 33
Kimmel, Donald 423
Kimmig, Rainer 72
Kimura, Keisuke 257, 258, 258, 378
Kimura, Takeshi 211
Kimura-Suda, Hiromi 133
King, Karen 214
King, Karen B 65
King, Thomas 398, 436
Kinoshita, Yuka 234, 300
Kirby, Beth J 354
Kirby, Christopher 100
Kirkland, James 26
Kirkland, James C 10
Kirkwood, Jay 236
Kirn-Safran, Catherine 235, 404
Kirsch, David G. 18
Kirschner, Lawrence 5
Kishikawa, Akiko 257, 258, 258, 378
Kishikawa, Yoichi 290
Kishnani, Priya 322
Kitade, Kazuki 369
Kitajima, Michio 68
Kitajima, Yuriko 68
Kitaoka, Taichi 211, 300, 301
Kitase, Yukiko 69, 313, 383, 433
Kitaura, Hideki 257, 258, 258, 378
Kitazawa, Riko 160, 250
Kitazawa, Sohei 160, 250
Kitchen, Bethan 217
Kitoh, Hiroshi 300
Klaushofer, Klaus 16, 111, 184, 311
Klein, Gordon 337
Klein, Peter 185
Kleinman, Aaron 105
Klein-Nulend, Jenneke 358
Kliethermes, Stephanie A 135
Kline, Gregory 438
Kloen, Peter 253
Knafler, Gabrielle 217
Kneissel, Michaela 58, 143
Knight, Rob 147
Knopp, Michael 432
Knox, Adam 350
Kobayashi, Ikue 355
Kobayashi, Tatsuya 422
Kobayashi, Tomohiro 411
Kobayashi, Tsuyoshi 292
Kobayashi, Yasuhiro 257, 381
Kobayashi, Yukiho 231
Kocijan, Roland 116
Kocjan, Tomaz 173
Koga, Maho 201
Koga, Minae 300
Koh, Amy 215, 216, 281
Koh, Jung-Min 283, 380, 429
Koh, Sang Baek 167
Kohara, Yukihiko 92
Kohn, David 238
Kohrt, Wendy 406
Koide, Masanori 381
Koike, Tatsuya 176
Kojima, Toshihisa 288
Kolesnik, Ewald 224
Koltun, Kristen 142
Komarova, Svetlana 123, 225, 313, 435
Komarova, Svetlana V 189
Komatsu, David E 227, 294
Komatsu, Koichiro 136
Komatsu, Koichiro 136
Komla-Ebri, Davide 105
Komori, Taishi 338
Komori, Toshihisa 250
Konda, Samya 177
Kondapalli, Ananya 298
Kondiboyina, Vineel 66
Kondratowicz, Monika 361
Kondrikova, Galina 153, 403
Kong, Dexuan 439
Kong, Ling 143
Kong, Sung Hye 311
Kontulainen, Saija 28, 133, 154, 211
Koopmans, Marion 435
Kopp, Felix 205, 327
Koppen, Chris Van 415
Kopperdahl, David L. 390
Korfage, Joannes A.M. 358
Kosako, Hidetaka 234
Koskela, Antti 14, 69
Kot, Martin 299, 421
Kotowicz, Mark 99, 308, 392
Kotowicz, Mark A 273
Kotsopoulos, Joanne 361, 393, 430
Kotwal, Anupam 127, 420
Koukoutsidi, Panagiota 199
Kousteni, Stavroula 71, 71
Kovacs, Christopher 194, 390, 393
Kovacs, Christopher S 107, 193, 387
Kovacs, Christopher S 354
Kovacic, Vlado 341
Koyama, Tomohisa 173, 175, 176
Kozloff, Kenneth 294, 306
Kozloff, Kenneth M. 124
Kragar, Kim 146
Kram, Vardit 97, 344
Kramer, Arthur 66
Kramer, Ina 58, 143
Krasner, Alan 199
Kratky, Dagmar 346
Krause, Matthias 317
Krauss, Jennifer L 192
Kreiger, Nancy 193
Kreikemeier, Rose 301, 409
Kremer, Richard 191, 218, 417
Kress, Dustin 159
Kristianto, Jasmin 240
Krivicich, Laura 48
Kronenberg, Henry 5, 29, 74
Kronenberg, Henry M 14, 368
Krueger, Joerg 426
Krueger, Van 208
Krug, Roland 193, 386
Krum, Susan 217
Ku, Eu Jeong 145, 265
Kuang, Ruby 193
Kuang, Zhaobin 47
Kubaszky, Raluca 416
Kuboki, Takuo 338
Kubota, Satoshi 343
Kubota, Shogo 264
Kubota, Takuo. 122, 211, 300, 301
Kudo, Daisuke 175
Kuh, Diana 280
Kuhn, Edward 370
Kuijk, S.M.J. Van 66
Kukita, Akiko 252, 258, 378
Kukita, Toshio 252, 258, 378
Kulina, Irina 214
Kuliwaba, Julia 247
Kuljanin, Miljan 57
Kumagai, Michiko 177
Kumakura, Seiichiro 381
Kumar, Anil 381
Kumar, Manoj 219
Kumar, Navin 207
Kumar, Raina 226
Kumar, Rajiv 50, 139, 306
Kumorek, Anna 263
Kumpati, Jerusha 6
Kung, Annie 113
Kunst, Roni 142
Kuo, Alfred 161
Kuo, Jennifer 63, 324
Kuo, Jennifer H. 323
Kupczik, Kornelius 335
Kupfer, Gary M 421
Kupratis, Meghan 141
Kurago, Zoya 22
Kurahashi, Hiroki 241
Kurahashi, Kiyoe 132
Kurashimo, Shinji 346
Kuratani, Mai 42, 123
Kurebayashi, Flavia 392
Kurihara, Noriyoshi. 80, 304, 324, 339, 380
Kuriyama, Kohji 387
Kuroda, Ryosuke 408
Kuroda, Yukiko 15
Kushwaha, Priyanka 10, 77
Kutilek, Stepan 333
Kutty, Shelby 301
Kuzawa, Cole 78
Kuznetsov, Sergei 338
Kwak, Mi Kyung 380, 429
Kwak, Moon Kyu 239, 335
Kwee, Ann Kerwen 384
Kweon, Hyeok-Jung 384
Kwok, Timothy 13
Kwon, Jun-Oh 379
Kwon, Ron 117
Kwon, Ye-Won 75
Kyumoto-Nakamura, Yukari. 252
L
L, Kristann Magee 206
Laarschot, Denise Van De 438
Laberge-Malot, Marie 135
Labranche, Timothy 26
Lachcik, Pamela 179, 297
Lachmann, Robin 56
Lacroix, Andrea 8, 275
Lafage-Proust, Marie-Hélène 3, 173, 359
Lafont, David T 64
Laframboise, Rachel 351
Lageneste, Oriane Duchamp De 213
Lagerquist, Marie 231
Lagerquist, Marie K 69
Laguna, Esther 351
Lai, Chao Qiang 229
Lai, Liangxue 75
Lai, Meizan 29, 352
Lai, Yumei 31, 261
Laing, Emma 190
Lajlev, Siv 47
Lajoie, Gilles 57
Lakatos, Peter 286
Lake, Anne 410
Lakerveld, Shannon 180
Lakra, Akshay 89
Lam, Joanne 113
Lam, Tsz Ping 27, 68, 307
Lamb, Sarah 21
Lammertsma, Adriaan 120
Lampl, Kathy 50
Lamy, Olivier 3, 396, 428
Landry, Louis-Benedict 432
Lane, Jennifer 54
Lane, Joseph 13, 173, 200, 208
Lane, Nancy 40, 106, 114, 285
Lang, Eric 437
Lang, Thomas 168
Lang, Thomas F 11, 37
Langdahl, Bente 290
Lange, Eileen 16
Langman, Craig 322
Langs, Georg 116
Langsetmo, Lisa 40, 84, 194, 316, 390, 391
Lannoo, Matthias 414
Lanske, Beate 87, 232, 407
Lanza, Denise 78
Lanzieri-Filho, Lúcio Moraes 164
Laperre, Kjell 221
Lapierre, Vanessa 173
Lappe, Joan 28, 121, 213, 311
Lappe, Joan M 199
Laprade, Judi 277, 400
Lapshina, Maria 161
Lapunzina, Pablo 122
Lara-Castillo, Nuria 431
Laredo, Jean-Denis 428
Larijani, Bagher 313, 439
Larivière, Richard 294
Laroche, Norbert 359
Larrouture, Quitterie C 373
Larson, Joseph 8
Larsson, Berit 104
Laslett, Laura 134
Lassalle, Louis 418
Laster, Marciana 211
Lataillade, Jean-Jacques 214
Latourte, Augustin 220
Lau, Yian Khai 185
Laughlin, Richard 405
Laurent, Laetitia 105
Laurent, Michaël 320
Lauterlein, Jens-Jacob 216
Lauterlein, Jens-Jacob
 Lindgaard 40
Laverty, Kim 355
Laverty, Kimberly 414
Lavery, Paula 233
Law, Simon 178
Law, Susan 111
Lawenius, Lina 296

- Lawrence, Lima 300
 Lawrence, Meghan Mcgee 225
 Lawson, Lisa 83
 Lazar, Ronald 323
 Lazarenko, Oxana P. 10
 Le, Long 249
 Le, Phuong 76, 87, 223
 Le, Phuong T. 226
 Leader, Deane 104
 Leal, Jose. 21
 Leanza, Giulia 41, 91
 Leary, Emily 67
 Leboff, Meryl 163, 171, 284
 Leboff, Meryl S. 292
 Lecanda, Fernando 46
 Lecka-Czernik, Beata 98, 315
 Leder, Benjamin 20, 25, 48
 Lee, Audrey 221
 Lee, Beth 354
 Lee, Brendan 6
 Lee, Brendan 26, 44, 73, 78, 205
 Lee, Chang-Ryul 190
 Lee, Dale 212
 Lee, David 215, 338
 Lee, David C. 390
 Lee, Dong-Seol 151, 221
 Lee, Eun Jeong 340
 Lee, Eun-Hye 96
 Lee, Grace Koon-Yee 177
 Lee, Hak-Myung 128
 Lee, Hang 20, 25, 48
 Lee, Hye-Lim 190
 Lee, Hyun-Young 283
 Lee, Jae 207
 Lee, Jae Hyup 288, 289
 Lee, James 63, 323, 324
 Lee, Janice S. 183
 Lee, Jennifer S. 103, 434
 Lee, Jeong-Bong 215
 Lee, Ji Hyun 145, 184, 311
 Lee, Jiwon 160, 381
 Lee, Jonathan 318
 Lee, Jooyeon 127
 Lee, Jun Sung 278
 Lee, Kathy Kyungeun 252
 Lee, Kyoung Jin 45
 Lee, Kyung Jin 340
 Lee, Kyung-Hun 45
 Lee, Lok Hang 355
 Lee, Melody 401
 Lee, Min 190
 Lee, Min Joon 95
 Lee, Peter 386
 Lee, Richard 272
 Lee, Se-Jin 42
 Lee, Seo Young 265
 Lee, Seong Min 19
 Lee, Seung Hun 283, 380, 429
 Lee, Seung-Hoon 96
 Lee, Seungyong 58, 338
 Lee, Shiou-Ping 384
 Lee, Sihoon 283
 Lee, Sooyeon 365
 Lee, Sujin 127
 Lee, Suk-Hee 96
 Lee, Sun-Kyeong 44, 92, 378, 380
 Lee, Tien-Jung 16
 Lee, Wayne Yuk-Wai 27, 307
 Lee, Wayne Yw 68
 Lee, Wonsae 16
 Lee, Ye Ji 256
 Lee, Yea-Rin 247
 Lee, Ye-Ji 95
 Lee, Yeon-Ju 96
 Lee, Yi-Chien 78, 205
 Lee, Yoojin 54
 Lee, Youngkyun 160
 Lee, Yuk Wai 379
 Lee, Yun-Sil 42, 79, 241
 Lee, Zang Hee 72, 93, 379
 Leeuwen, Johannes Van 153, 435
 Lefebvre, Veronique 336
 Leff, Jonathan A. 201, 323
 Legare, Janet 121
 Leguizamon, Natalia Da Ponte 294
 Lehtimaki, Jaakko 179, 295
 Lei, Kevin 6
 Lei, Wei 45
 Lei, Yimin 31
 Lei, Yiming 261
 Leib, Edward 112, 267
 Leigh, Daniel 423
 Leiker, Merced 347
 Leikin, Sergey 374
 Leitch, Victoria 105
 Leitch, Victoria D. 64
 Leite, Milena 162
 Leite, Valeriano 418
 Lejeune, Pascale 339
 Lelliott, Christopher 105
 Lelliott, Christopher J. 64
 Lelong, Christophe 163, 263, 410
 Lems, Willem F 291
 Lems, Willem F. 290
 Lenaghan, Elizabeth 398
 Lenchik, Leon 399
 Lenfest, Scott 327
 Lengauer, Christoph 26
 Lenherr, Christopher 187
 Lentle, Brian C 387
 Lentle, Brian C. 193
 Lentzsch, Suzanne 178
 Leonard, Mary 202, 212
 Leonard, Mary B. 209
 Leonard, Michelle E. 79, 91
 Leon-Gonzalez, Enrique Diaz De 278
 Leonore, Naomi 291
 Lerner, Ulf 14, 358
 Lerner, Ulf Holger 294
 Leslie, William 8, 8, 38, 39, 47, 100, 103, 269, 275
 Leslie, William D 7, 12, 271, 284, 387, 438
 Leslie, William D. 100
 Lespessailles, Eric 38, 105, 113, 114, 247, 290
 Leucht, Philipp 365
 Levaot, Noam 417
 Levesque, Jean Pierre 214
 Levi, Benjamin 5
 Levi, Moshe 65
 Levin, Paul 360
 Levin, Samara 298
 Levine, Michael 29, 57, 352
 Levine, Michael A. 128
 Levy, Shiri 66, 99
 Levy-Shraga, Yael 135, 333
 Lewicke, Justin 246
 Lewiecki, E Michael 21
 Lewiecki, E. Michael 25, 104, 108, 410
 Lewis, Joshua 110, 264, 316, 393
 Lewis, Karl J. 235
 Lewis, Richard 190
 Leyland, Kirsten 89
 Li, Bai-Yan 435
 Li, Bonnie 287
 Li, Bonnie H. 2, 2, 103
 Li, Changjun 245
 Li, Chaoyuan 18
 Li, Ching-Ti 39
 Li, Dan 369
 Li, Daofeng 50
 Li, Dingfeng 193, 318, 318
 Li, Dongfang 259
 Li, Gang 379
 Li, Guo Bin 337
 Li, Guodong 253
 Li, Hui 75
 Li, Jau-Yi 35, 415
 Li, Jianjia 372
 Li, Jianshuang 259
 Li, Jiarong 191, 218, 417
 Li, Jie 34
 Li, Jinbo 12
 Li, Jing 48
 Li, Kai 390
 Li, Li 97, 215
 Li, Ling 301
 Li, Meng Chen 381
 Li, Minqi 252, 259
 Li, Ping 404
 Li, Qiaoli 78
 Li, Tieshi 49, 53, 141, 246, 292, 343
 Li, Troy 82
 Li, Weiwei 96
 Li, Wen 23
 Li, Xiangzhi 252
 Li, Xiaodong 152
 Li, Xiaofeng 349
 Li, Xiaohui 78
 Li, Xiaojuan 168, 189, 226
 Li, Xin 76
 Li, Xinle 34
 Li, Xuehua 237
 Li, Xuejun 346
 Li, Yihan 16, 35
 Li, Yi-Ping 93
 Li, Yong 248
 Li, Yongjia 48
 Li, Yuyu 379
 Li, Zhanjun 75
 Li, Zhu 10
 Li, Ziqing 93
 Li, Zixu 2
 Lian, Brian 24
 Lian, Jane 49, 86
 Lian, Jane B. 184, 243
 Lian, Junxiang 41, 223, 224, 315
 Lian, Kevin 387
 Lian, Yinjuan 166
 Liang, Bernice 395
 Liaw, Lucy 90
 Libanati, Cesar 25, 105, 267
 Librizzi, Soledad 321
 Lichtler, Alexander 426
 Liddy, Clare 277
 Lievers, W. Brent 327
 Lillis, Jacquelyn 370
 Lim, Jormay 74
 Lim, Juchan 342
 Lim, Jung Soo 167
 Lim, Seock-Ah 45
 Lim, Soomin 159
 Lim, Sung Kil 213
 Lim, Wai 393
 Lin, Anthony 118
 Lin, David 48
 Lin, Elizabeth L. 57, 420
 Lin, Hua 292
 Lin, Jian-Ming 192
 Lin, Lan 367
 Lin, Megan 185
 Lin, Sheldon 118
 Lin, Shuibin 48
 Lin, Sien 379
 Lin, Simin 31, 261
 Lin, Sung-Yen 413
 Lin, Yan 218
 Lin, Yi-Chin 171
 Lin, Yi-Jun 63
 Lin, Ying Chin 185, 262
 Lin, Yi-Shan 413
 Lindalen, Einar 228
 Linde, Herma C Van Der 403
 Lindsay, Adam 140
 Lindsey, Richard 231, 343
 Lindskog, Dieter 41
 Linglart, Agnes 322
 Linglart, Agnès 40, 120, 418
 Link, Thomas 193, 310
 Lionikaite, Vikte 69, 231, 358
 Lippo, Luciana 217, 312
 Lips, Paul 274
 Lipworth, Loren 230
 Lis, Camilo 299, 421
 Little, David 333
 Little, Mary Ellen 121
 Liu, Bowen 168
 Liu, Chao 15, 413
 Liu, Ching-Ti 36
 Liu, Chuanju 31, 220, 243
 Liu, Daquan 34
 Liu, Di 252
 Liu, Esther 253
 Liu, Eva 36
 Liu, Haibo 227
 Liu, Huadie 259
 Liu, Jin 119
 Liu, Junting 270
 Liu, Kai 30, 218
 Liu, Li 373
 Liu, Min 74
 Liu, Minghao 323
 Liu, Philip 177
 Liu, Ran 149
 Liu, Shing-Hwa 253, 310
 Liu, Tongjun 93
 Liu, Weimin 255
 Liu, Weiqing 87
 Liu, Wen-Chih 63
 Liu, X. Sherry 16, 35
 Liu, Xiaohua 70, 243
 Liu, Xiaonan 366
 Liu, Xiaowei 405
 Liu, Yao 223
 Liu, Yi 129, 173, 248
 Liu, Yi-Jui 384
 Liu, Ying 18
 Liu, Yu-Chuan 415
 Liu, Yuting 43
 Liu, Zhaoyang 144
 Liu, Zhenqing 190
 Liu, Ziyue 56, 334
 Livingston, Eric W 65
 Livingston, Eric W. 326
 Lix, Lisa 8, 38, 47, 103, 269

- Lix, Lisa M. 7, 12
 Lix, Lisa M. 100
 Lizarraga, Antonia 401
 Lo, Joan 166, 287, 289, 408
 Lobos, Stacey 405
 Lockhart, John 155
 Lockhart, John C 379
 Lockhart, Thurmon 125
 Loftus, Alexander 218
 Logan, John 105
 Logan, John G. 64
 Logan, Susan Jane Sinclair 186
 Logue, Jennifer 54
 Long, Caela 29, 352
 Long, Charles 426
 Long, Jin 209, 212
 Long, Sierra 426
 Looper, Amelia 327
 Loots, Gabriela 156, 337, 370, 375
 Looveren, Riet Van 244
 Lopes, Inês 102
 Lopez, Kelsie A. 201
 Lopez-Delgado, Laura 122
 Lopez-Olivo, Maria 411
 López-Romero, Pedro 113, 286
 López-Taylor, Juan 274, 308
 Lorentzon, Mattias 36, 46, 99, 104, 115, 271, 284, 392
 Lorenz, Madelyn 9
 Lorenz, Madelyn R 206
 Lorenzo, Joseph 35, 44
 Lorimer, Michelle 427
 Lorraine, Fitzpatrick 115
 Lotz, Jeffrey 161
 Lou, Yang 184
 Louis, Leeann 330
 Loundagin, Lindsay 330
 Louzada, Mário Jefferson Quirino 146, 328
 Low, Philip 32, 295
 Low, Stewart 32, 295
 Löwe, Axel Lennart 317
 Lowe, Catherine Minns 21
 Lowe, Walter 136, 370
 Lowe, Walter R. 292
 Lowery, Jonathan 314
 Lowry, Malcolm B. 351
 Lu, Aiping 10, 119
 Lu, Di 259
 Lu, Huifang 411
 Lu, Jean 415
 Lu, Jun 119
 Lu, Na 226
 Lu, Qinghua 221
 Lu, Sumei 79, 91, 254
 Lu, William 133, 208
 Lu, X. Lucas 89
 Lu, Yi-Chien 185, 262, 384
 Lubahn, Dennis 353
 Lubbe, Ryan 376
 Lubbe, Ryan J. 329
 Lubbers, Wouter 120
 Luca, Diana 50
 Lui, Julian 221
 Lui, Li-Yung 20, 24, 114
 Luna, Eduardo Dusty 162
 Luna, Jose Luis Ramirez-Garcia 64
 Lunde, Raine 362
 Lundh, Dan 46, 99
 Lundin, Hans Ranch 395
 Lundy, Mark W. 34, 407
 Luo, En 223
 Luo, Gangming 263
 Luo, Hongke 43
 Luo, Jack 350
 Luo, Yunhua 271
 Lupiáñez, Darío G. 144
 Luscher, Sergio 137
 Lutz, Laura 278, 352
 Luu, Simon 230
 Lyons, Karen 6
- M**
 Ma, Canchen 134
 Ma, Chi 70, 75, 243
 Ma, Liang 260
 Ma, Liting 31, 261
 Ma, Nina S. 422
 Ma, Shaocheng 410
 Ma, Xiaoli 85, 375
 Ma, Xinlong 292
 Ma, Yu-Heng 340
 Ma, Yu-Heng Vivian 260
 Ma, Yun 281
 Maalouf, Naim 298
 Macdonald, Heather 393
 Mace, Sarah 84
 Machida, Masafumi 264
 Machuca-Gayet, Irma 43
 Macica, Carolyn 304, 350
 Mack, Karen 181
 Macleod, Ryan 12
 Macneil, Adam J. 437
 Mac-Way, Fabrice 215, 234, 294, 324, 347, 348, 391
 Maeda, Takeyasu 257
 Maeda, Tomomi 147
 Maeda, Yukiko 78
 Maeda-Murohara, Eri 334
 Maehata, Yojiro 119
 Maekawa, Tomoki 257
 Maes, Frederik 244
 Magaziner, Jay 395
 Magee, Kristann 9
 Maggi, Daria 203
 Magnus, Jeanette H. 274
 Magnusson, Per 422
 Mahajan, Sahil 44
 Mahrous, Paul 193, 318, 318
 Mai, Ha 272
 Maier, Claudia S. 351
 Main, Russell 149, 383
 Maiz, Maria 296
 Majeed, Rukshana 61, 63, 129, 130, 203, 203
 Majeska, Robert 32, 161, 161
 Majeska, Robert J. 236
 Majeska, Robert J. 34, 407
 Majoor, Bas 51
 Majoor, Bas C.J. 297
 Majumdar, Sunipa 255
 Mak, Tak W. 369
 Makareeva, Elena 374
 Mäki-Jouppila, Jenni 188, 339
 Makin, Vinni 300
 Makino, Akito 295
 Mäkitie, Outi 417
 Malerba, Giovanni 312
 Malhan, Deeksha 346, 372
 Malhi, Pritpal 416
 Malhotra, Neil 185
 Malle, Oliver 101, 276
 Mallinson, Rebecca 402
 Malluche, Hartmut 176
 Malouf, Jorge 286
 Malouf-Sierra, Jorge 290
 Mamidi, Murali 19, 30
 Mampieri, Annie 307
 Mancini, Marianne 24
 Mandair, Gurjit 238
 Manduchi, Elisabetta 79, 91
 Manfrini, Silvia 203
 Mangano, Kelsey 229
 Mangiavini, Laura 5
 Manickam, Garthiga 343
 Manilay, Jennifer 337
 Mannan, Naila 105
 Mannfeld, Rachel 240
 Manning, Catherine 78
 Mannstadt, Michael 128, 357
 Manolagas, Stavros 23, 26, 53, 146, 239, 354
 Manolagas, Stavros C. 23, 345
 Manolson, Morris 426
 Manske, Sarah L 155
 Mansky, Kim 160, 195, 256
 Manson, Joann 8, 171, 284
 Mansur, Jose Luis 385
 Mantovani, Giovanna 40
 Manzano, Givenchy 369
 Mao, Meng 51, 55, 120
 Maquer, Ghislain 187
 Mara, Kristin 39
 Marahleh, Aseel 257, 258, 258, 378
 Marcadet, Laetitia 432
 Marchais-Oberwinkler, Sandrine 415
 Marchetto, Giulia 312
 Marcil, Valérie 143
 Marcocci, Claudio 321
 Marelli, Claudio 321
 Maren, Maud Van 291
 Margaritis, Ioannis 179
 Mariani, Eda 305
 Mariat, Christophe 173
 Marich, Alexandra 238
 Maridas, David 44, 232, 363, 373
 Marie, Louis Georges Ste 165
 Marin, Fernando 24, 113, 286
 Marini, Joan C. 16, 182
 Mark, Kronenberg 426
 Markwardt, Sheila 285
 Marom, Ronit 78
 Marques, Elisa A 11
 Marques-Vidal, Pedro-Manuel 428
 Marquis, Karine 215
 Marrie, Ruth Ann 284
 Marsh, Anthony 399
 Marshall, Randolph 323
 Marshall, Tanya 398
 Martelli, Yves 385
 Marth, Christian 55
 Martignène, Niels 105
 Martin, Aline 18, 260, 354
 Martin, Javier San 50, 51, 55, 56, 120, 122
 Martin, Natalia Bravo 298
 Martin, Regina M 299
 Martin, T John 1, 64, 293
 Martin, Tj 87
 Martinez, Jerahme 235, 404
 Martínez-Canarias, Susana 46
 Martínez-Gil, Núria 144, 144
 Martínez-Laguna, Daniel 54, 105
 Martin-Guerrero, Eduardo 149
 Martins, Csw 112
 Martins, Gisele 336
 Martins, Janaina 36
 Marty, Eric 13, 129, 200, 208
 Marzia, Marilena 187
 Masami, Iwasa 341
 Masamune, Hiroko 24
 Masedu, Francesco 45
 Maslin, Kate 109
 Masuda, Atsushi 213
 Masuzaki, Hideaki 68
 Matsuhisa, Munehide 234
 Matsui, Gen 369
 Matsumoto, Chiho 160
 Matsumoto, Hidehiro 411
 Matsumoto, Jane 420
 Matsumoto, Morio 308
 Matsumoto, Takumi 257
 Matsumoto, Tomoyuki 408
 Matsumoto, Toshio 132, 178, 234, 292, 341, 342
 Matsuo, Koichi 15
 Matsuo, Osamu 346
 Matsushita, Masaki 300
 Matsushita, Yuki 15
 Matteis, Antonella De 78
 Matthews, Brya 365
 Matthews, Brya G. 77, 87, 88
 Matthews, Robert 106
 Matthias, Julia 84, 434
 Matthys, Christophe 414
 Mattiuzzi, Andrea 209
 Mattson, Anna 96
 Matyas, John R 155
 Maulding, Nathan 424
 Maupin, Kevin 240, 361
 Maurano, Matthew 105
 Maurizi, Antonio 45, 123, 253
 Mawatari, Masaaki 258
 Mawatari, Taro 369
 Maxson, Julie 39
 May, Danielle 312
 Mayhew, Vera 73
 Mayman, David 248
 Maynard, Robert 227
 Maynard, Robert D. 205
 Mayo, Nancy E. 169
 Mayoral, Pedro Valencia 356
 Mayur, Jayenth 118
 Mazel, Martine 72
 Mazoni, Laura 321
 Mazur, Courtney M. 1
 Mazzetti, Tom 147
 Mbalaviele, Gabriel 137, 159, 364
 Mbimba, Thomas 253
 Mcalinden, Audrey 50
 Mcalister, William H 181
 Mcalister, William H. 57, 182, 420, 425
 Mcalpine, Michael D. 314, 437
 Mcandrews, Kevin 80, 82, 260, 296
 Mearthar, Caitlin 164, 277, 399, 400
 McCabe, George P. 296
 McCabe, George P. 323
 McCabe, Linda D 296
 Mccauley, Laurie 215, 216, 281
 McClain, Joyce 196
 Mcclloskey, Eugene 13, 39, 47, 108, 115, 115, 319, 392, 398
 Mcclung, James 278, 352
 Mcclung, Michael 115

- Mcclung, Mike 115
 Mccomb, Mark 382
 Mcconeghy, Kevin 54
 Mccool, Jillian 370
 Mccormack, Shana 28
 Mccready, Louise 145
 Mcculloch, Charles 20, 24
 Mcculloch, Kendal 155
 Mccutcheon, Sean 32
 Mcdermott, Scott 374
 Mcdonald, Matthew 133
 Mcdonald-Blumer, Heather 38, 438
 Mcdonough, Sean 134
 Mcgee-Lawrence, Meghan 93, 96, 153, 212, 242, 403, 414
 Mcgrath, Cody 237, 366
 Mcgrath, Sarah 379
 McGready, John 121
 Mcgregor, Narelle 1
 Mcilwain, David 369
 Mckee, Marc D 1
 Mckelvey, Kent 228
 Mckenna, Charles E. 22
 Mckenna, Malachi 301, 438
 Mckenzie, Jennifer 91, 229, 350
 Mclaughlin, Heather 417
 McLennan, Christine 154
 Mcmahon, Donald 113, 129, 323
 Mcmanus, Catherine 63, 324
 Mcmanus, Madison R. 206
 Mcwalter, Kirsty 417
 Md 140, 140, 419, 419, 419, 419
 Mead, Megan 215
 Meagher, Matthew 331
 Mealiffe, Matt 56, 122
 Medina-Gomez, Carolina 105, 125
 Meers, Grace 349
 Meghil, Mohamed 22
 Megret, Jerome 213
 Mehrotra, Meenal 124
 Mehrotra, Shikhar 124
 Mei, Kai 205, 327
 Mei, Xueting 260, 340
 Mei, Yixue 315
 Meier, Andreas 428
 Meier, Garnet 317
 Melbinger-Zeinitzer, Elisabeth . 55
 Melendez-Suchi, Christian . . 191
 Melk, Sameh 38
 Mellibovsky, Leonardo . . 144, 144
 Mellstrom, Dan 13, 36, 104, 271
 Mellström, Dan 310
 Melton, Mary 267
 Mendes, Jorge M 102
 Mendez, Melanie 156, 370
 Mendhe, Bharati 212
 Mendoza-Londono, Roberto . 426
 Menendez, Maria 432
 Meng, Fangang 250
 Mensch, Kenneth 272
 Menuki, Kunitaka 411
 Merabet, Ahmed 415
 Merametdijan, Laure 362
 Merceron, Christophe 5, 341
 Merkel, Alyssa 326
 Merle, Blandine 36
 Merle, Geraldine 64
 Merlijn, Thomas 8, 436
 Merling, Randall 338
 Mertens, Ann 414
 Mertz, Edward 374
 Merwin, Sara 360
 Merzoug, Valérie 418
 Mesfin, Addisu 238, 339
 Mesina, Kevin 118
 Messer, Larry 434
 Messer, Jonathan 33, 423
 Messina, Osvaldo D. 114
 Messner, Zora 116
 Metz, Juriaan R 403
 Metz-Estrella, Diana 43
 Metzger, Corinne 238, 327
 Metzger, Corinne E 382
 Meulemans, Ann 414
 Meulen, Marjolein Van Der . 208
 Mevel, Elsa 248
 Meyer, Haakon E. 274
 Meyer, Mark 19
 Meyer, Mark B 244
 Meyer, Ursina 109
 Meyers, Carina M G 160
 Meyers, Carolyn 367
 Meylan, Françoise 16
 Mhaske, Suhass 381
 Mi, Jie 270
 Miao, Dengshun 80, 81, 81, 226
 Miao, Zhiping 93
 Micha, Dimitra 304, 306
 Michalak, Geoff 387
 Michalski, Andrew 387
 Michalski, Megan 216
 Michelet, Franck 163, 263
 Michigami, Toshimi 301, 355
 Michou, Laetitia 351, 352
 Michou, Laëtitia 324
 Middleton, Kevin 340
 Migotsky, Nicole 91, 350
 Miguel, Gonzalo Allo 321
 Mihov, Borislav 54
 Mikhail, Mageda 202
 Mikki, Hirokazu 341, 342
 Mikolajewicz, Nicholas 313
 Mikolajewicz, Nicolas 189
 Mikuni-Takagaki, Yuko 119
 Milan, Anna 145
 Milano, Stephane 117, 118
 Milbrandt, Jeff. 206
 Millar, Adam 122
 Millard, Susan 72, 214
 Millecamps, Magali 214
 Miller, Freeman 432
 Miller, Michael 397
 Miller, Nicholas A. 201
 Miller, Paul D. 50
 Milovanovic, Petar 317, 348
 Mimura, Yusuke 176
 Mina, Mihaela 312
 Minami, Yasuhiro 49
 Minamizaki, Tomoko 293
 Minisola, Salvatore 61, 113, 147, 286
 Mintz, Douglas 208
 Miranda, Gustavo 6
 Miranda, Susan 6
 Miranda-Carboni, Gustavo . . 217
 Miranda, Anthony 86
 Mirisidis, Ioannis 179
 Mirzamohammadi, Fatemeh . . 14
 Misaghian-Xanthos, Negin . . 237
 Mishima, Kenichi 300
 Mishina, Yuji 30, 216, 258
 Misra, Madhusmita 29
 Missbichler, Albert 322
 Mitchell, Alexis 228, 362, 413, 426
 Mitchell, Claire H 93
 Mitchell, Deborah 29
 Mitchell, Jane 5, 252
 Mitchell, Jonathan 28, 188
 Mitlak, Bruce 20, 115
 Mitsuyasu, Hiroaki 369
 Mitteer, Richard 117
 Mittermayr, Rainer 116
 Mittman, Nicole 277
 Mittmann, Nicole 400
 Mitton, David 209
 Miura, Kiyonori 68
 Miura, Yasushi 408
 Miyagawa, Kazuaki 304, 380
 Miyagi, Masayuki 173, 175, 176
 Miyagi, Msayuki 408
 Miyajima, Tsuyoshi 290
 Miyakoshi, Naohisa 172, 175, 175, 179, 412
 Miyamoto, Chihiro 119
 Miyamoto, Takashi 262
 Miyamoto, Takeshi 257, 308
 Miyamura, Satoshi 387
 Miyaoka, Daichi 147, 355
 Miyata, Kei 211, 301
 Miyaura, Chisato 140, 160
 Mizoguchi, Toshihide 381
 Mizuhashi, Koji 344
 Mlineritsch, Brigitte 55
 Mo, Chenglin 213, 346
 Mobley, Tanner 242
 Mocanu, Veronica 286
 Modaff, Peggy 121
 Modan-Moses, Dalit 135
 Modlesky, Christopher 432
 Moe, Sharon 179, 297, 323
 Moericke, Ruediger 113
 Moffatt, Pierre 343, 350
 Moggia, Susana 184
 Mohamad, Safa 361
 Mohamed, Fatma 242
 Mohammad, Khalid 237
 Mohammad, Khalid S. 42
 Mohammadi, Moosa 352
 Mohan, Meera 219
 Mohan, Subburaman . 30, 42, 148, 231, 343, 344, 363
 Mohanty, Sarthak 150
 Mohanty, Sindhu 105
 Mohindroo, Neha 368
 Moini, Ariana 89
 Mok, Daniel Kam-Wah 297
 Mol, Merel O. 253
 Molina, Fidencio Cons 385
 Molinolo, Alfredo 424
 Molon, Rafael Scaf 294
 Molstad, David 96, 377
 Monache, Simona Delle 218
 Mondal, Nandan K 335
 Monegal, Ana 121, 172, 322
 Monette, Sébastien 369
 Monier, Daisy 92, 374
 Monistrol-Mula, Anna 144
 Monroe, David 17, 26, 111, 145, 371
 Montagna, Anna 352
 Montain, Scott 280
 Monteiro, Nelson 305
 Montenegro, Fabio M. 62
 Montoya, Juliana Marulanda 349
 Moody, Tania 51, 79
 Mooijaart, Simon P. 317
 Moon, Hyun Uk 276
 Moon, Rebecca 109, 356
 Moon, Seong 125
 Mooney, Robert 370
 Moore, Bethany 196
 Moore, Douglas 19, 88
 Moore, Harold 129
 Moore, Lynne 324
 Moore, Richard 432
 Mor, Vincent 54
 Morales, Blanca M 51
 Morales, Knashawn 188
 Morales-Torres, Jorge Alberto 274
 Moran, Meghan 363
 Moravits, Donald E. 206
 Morden, Nancy E. 319
 Moreau, Alain 143
 Moreira, Carolina 298
 Moreland, Jessica 215
 Moreno, Beatriz 46
 Moreno, Haritz 46
 Moreno, Julio Manuel Martinez . 353
 Moretón, Jordi 327
 Morfin, Cesar 375
 Morgan, Elise 141, 247, 356
 Morgan, Gareth 219, 342
 Mori, Antonio 312
 Mori, Giorgio 210
 Mori, Katsuhito 355
 Morin, Françoise 432
 Morin, Suzanne 8, 38, 47, 187, 269, 279, 279, 393
 Morin, Suzanne N. 7, 12, 107, 193, 351, 394, 438
 Morin, Suzanne N. 169, 268
 Morin, Trevor 377
 Moriscot, Anselmo 336
 Moriyo, Keiji 231
 Moriyko, Jukka 179, 295
 Morkos, Michael 193, 317, 318, 318
 Morozova, Ievgeniia 364
 Morrell, Andrea 382
 Morris, Carol 342
 Morris, John 39, 105
 Morris, John A. 70
 Morris, Michael D. 238
 Morse, Leslie 255
 Mortensen, Eva 201, 323
 Mortier, Geert 143
 Moseley, Kendall F. 201
 Mosialou, Ioanna 71, 71
 Mosti, Mats 297
 Mottes, Monica 312
 Motyl, Katherine 142, 232, 377
 Moui, Yvon 170
 Mourkioti, Foteini 87
 Moursi, Cleo 345
 Moussa, Fouad 253
 Moustafa, Mohamed Abdallah
 Mohamed 224
 Movérare-Skrtec, Sofia 14, 231
 Moyses, Rm 112
 Moyses, Rosa M. 62
 Mu, Fan 199
 Mudano, Amy 275, 276, 397
 Muderis, Munjed Al. 133, 208
 Mughal 356
 Mujica, Lady Serrano 345
 Mukaddam, Mona Al 282
 Mukaddam, Mona M. Al 420
 Mulawa, Emily 236
 Mullen, Zachary K. 98

- Müller, Sebastian T. 415
Mumm, Steven. .57, 181, 182, 306, 420, 422, 425
Mumtaz, Hammad 431
Mumtaz, Noreen. 435
Mun, Sehwan 95, 256
Munce, Sarah 399
Mundra, Jyoti Joshi. 220
Mundy, Christina 124
Muneoka, Ken 85, 372
Munivez, Elda 26
Munivez, Elda M 78
Mummun, Fahima 208
Munns, Craig55, 210, 333
Muñoz, Maximilian 118
Muñoz-Torres, Manuel 182
Munroe, Jenny. 147
Munshi, Lubna 415
Muraca, Maurizio 218
Murakami, Naoko. 68
Murase, Tsuyoshi 387
Murata, Kosuke . . . 173, 175, 176
Murata, Yuki. 160
Muratovic, Dzenita 247
Murphy, Aaron 369
Murphy, Andrew 320
Murphy, Andrew J. 196
Murphy, Joan 361, 393, 430
Mursic, Ines 224
Murthy, Sreemala 42
Muruges, Deepa . . . 156, 370, 375
Musarò, Antonio. 336
Muschitz, Christian 116
Museyko, Oleg. 164, 428
Musikarat, Suchawadee 265
Musson, David. 137, 295
Muthu, Muthu Lakshmi 435
Muthuri, Stella 280
Muxi, Africa 121
Muzzi, Bruno 162
Myers, Damian 153, 189
- N**
- Nabipour, Iraj 313, 439
Naciu, Anda Mihaela 203
Nadal-Desbarats, Lydie. 76
Nadeau, Geneviève 135
Nadesan, Puvindran 9
Nagahata, Itsuki. 172, 179
Nagai, Takashi. 408
Nagamani, Sandesh 26
Nagano, Kenichi. .29, 29, 232, 407
Nagao, Masashi 334
Nagasaki, Atsuhiko 423
Nagashima, Masato 290
Nagata, Yuki 147, 355
Nahrendorf, Matthias. 71
Naik, Vishal 362
Nair, Asha 154
Nair, Nandini 121, 199
Nakachi, Yutaka 42
Nakajo, Satoru. 412
Nakama, Gilberto 370
Nakamura, Akie. 122
Nakamura, Fumiya 133
Nakamura, Mary 51, 123
Nakamura, Masaya 308
Nakamura, Midori 381
Nakamura, Satoshi 308
Nakamura, Shingen 342
Nakamura, Singen. 341
Nakamura, Yukio 290, 422
Nakano, Satoshi 334
Nakano, Yukako. 211, 301
Nakaoka, Kanae. 178
Nakashima, Kazuhisa 136
Nakayama, Anna 278, 352
Nakayama, Hirofumi . . . 211, 301
Nakayama, Shogo 213, 241
Nakchbandi, Inaam . . . 138, 242
Nam, Hwa Kyung 92
Namba, Noriyuki 55
Nanclares, Guiomar Perez De . . . 40
Nango, Nobuhito 264
Nannuru, Kalyan 320
Nannuru, Kalyan C. 196
Naot, Dorit. 137, 295
Napierala, Dobrawa. 92, 374
Napoli, Nicola . . . 21, 25, 41, 106, 203
Narahara, Shun 158
Narayanan, S Anand 382
Narita, Eri 176
Narod, Steven 361, 430
Narod, Steven A. 393
Naruse, Koji 175, 176
Naseri, Take 311
Nasoori, Alireza 224
Navarro, Anderson Marliere 201
Nawata, Kiyoko 401
Nawrot-Wawrzyniak, Kamilla 184
Naylor, Kim 319
Nazhat, Showan N. 191
Negley, Brittany 26, 145
Nelson, Deborah J. 373
Nelson, Jessica H. 80, 260, 339
Nelson, Tracy 41
Nenninger, Angela. 57, 182
Neofiti-Papi, Bianca 336
Néo-Justino, Daniela Morilha 294
Nesterova, Galina 174
Netelenbos, Coen . . . 8, 120, 306, 436
Nethander, Maria . . . 14, 36, 273, 310
Neuburg, Samantha. 260
Neuburger, Jenny 269
Neugebauer, Romain . . . 287, 408
Neutel, Joel. 24
Neville, Kathryn. 278
Newby, Jordan. 314
Newman, Gregory. 304
Newman, Meredith 21
Ng, Bobby Kin-Wah. 27, 307
Ng, Pei Ying 94, 192
Nguyen, Hung T. 79
Nguyen, Huynh 64
Nguyen, Kevin. 434
Nguyen, Tuan 194, 272, 390
Nguyen, Tuan V. 79, 271
Nguyen-Yamamoto, Loan. 70
Ni, Amelia 208
Ni, Pu. 81, 353, 355
Nicklas, Barbara 399
Nickolas, Thomas 112, 323
Nicola, Angela Cristina . . . 146, 328
Nicolas, Gael. 64
Nieddu, Luciano. 61
Nielsen, Jeffery 32, 295
Nielsen, Tina Kamilla 216
Niemi, Eréne C 123
Nieten, Christopher 337
Nieves, Jeri. 113, 208
Nifuji, Akira 136
Nikel, Ondrej 332
Nilsson, Anna 104, 284
Nilsson, Karin 14, 296
Nilsson, Ola 55
Nimitphong, Hataikarn 265
Nisan, Bhattacharyya 424
Nishida, Takashi. 343
Nishida, Yosuke 177
Nishimori, Shigeki. 74, 425
Nishimoto, Hanako 408
Nishimura, Ichiro 22
Nishino, Yuichiro 262
Nishita, Michiru 49
Nishiyama, Kyle K 131, 325
Nissen, Urs 407
Nissenon, Robert . . . 189, 255, 437
Nistala, Harikiran 320
Nitta, Takaya 90
Niu, Fang. 287, 408
Noailly, Jérôme 327
Nocciolino, Laura Marcela . . . 137
Noda, Hiroshi 232, 425
Noda, Masaki 261
Noda, Seiko 178
Noel, Peter 205, 327
Noel, Sabrina 229
Noguchi, Takahiro. .257, 258, 258, 378
Nogueira, Addressa Vilas Boas 294
Nogueira-Barbosa, Marcello . . . 200
Nogues, Xavier. 249, 394
Nogués, Xavier. 144, 144
Noh, Sunggi 215, 338
Nolin-Lapalme, Alexis. 418
Nomura, Kazutaka 264
Nookaew, Intawat 146
Noonan, Megan 353, 362
Noonan, Megan L. 355
Norman, Brendan 145
Normand, Émilie 143
Normand, Myriam 173
Noss, Michael 318
Notomi, Takuya 261
Notsu, Masakazu 62
Noufaily, Angela 21
Novak, Sanja. 77, 87, 88, 365
Novince, Chad 31, 219
Nowson, Caryl. 20
Nozaka, Koji 175
Nozaki, Tadashige 261
Nozawa, Masahiko 334
Nozomi, Oki 368
Ntzani, Evangelia 105
Nuno, Natalia 187
Nyman, Jeffrey 326
- O**
- O'Brien, Charles 26, 237
O'Brien, Mara. 220
O'Brien, Mara H 156
O'Bryan, Linda 81
O'Connell, Thomas 313, 433
O'Donnell, Patricia 185
O'Donnell, Siobhan 7
O'Keefe, Regis. 50
O'Lear, Lauren 352
O'Malley, A. James 319
O'Neill, Terence 398
Oakes, Dana 303
Oberfield, Sharon 28
Oberger, Julia 298
Obermayer-Pietsch, Barbara. 224
Obrien, Charles 12
Ochi, Hiroki 97
Oda, Asuka 341, 342
Oda, Hiromi 42, 290
Odagaki, Naoya 149
Oden, Anders 13
Odén, Anders 115, 392
Odri, Guillaume 247
Oei, Edwin 279
Oei, Ling 279
Ogawa, Saika . . . 257, 258, 258, 378
Ogiso, Noboru 92
Oh, Han-Jin 384
Oh, Melissa 68
Ohara, Masaya 355
Ohata, Yasuhisa . . . 211, 301, 304, 380
Ohlsson, Claes . . . 13, 14, 24, 36, 69, 105, 226, 231, 273, 296, 310
Ohnishi, Yukiyo 132, 178
Oho, Fumitoshi.257, 258, 258, 378
Ohte, Satoshi. 123
Ohtori, Seiji 173, 214
Oida, Yasutaka 338
Oka, Kunihiko 387
Okabe, Iichiro 305
Okabe, Koji 257
Okada, Akiko 34
Okada, Hiroyuki. 257
Okada, Kiyotaka 346
Okamatsu-Ogura, Yuko. 224
Okamoto, Yasuyoshi. 409
Okawa, Atsushi 97
Okawa, Motomi 176
Okawa, Tokutaro 176
Okazaki, Jane Erika Frazao . . . 167
Okazaki, Jane Erika Frazão . . . 392
Okazaki, Narihiro . . . 68, 239, 262, 368, 403
Okazaki, Ryo 406
Okimoto, Nobukazu. 411
Okubo, Misato. 42
Okubo, Naoki 90
Okumoto, Katsumi 346
Olds, Timothy 68
Olender, Susan. 126
Oliva, Joan Carles. 383
Oliveira, Ivone B. 62
Oliver, Samuel 168
Oliveri, Beatriz 299, 421
Olivier, Patricia 135
Olmsted-Davis, Elizabeth. 366
Olson, Amber 396
Olson, Dawn A. 351
Olson, Mathew E. 80
Olsson, Lars-Eric 271
Olstad, Ole K. 228
Olszynski, Wojciech 193
Omeara, Maureen 357
Omeragic, Beatriz 61, 63, 129, 130, 203, 203
Omi, Maiko 258
Omma, Tulay 181
Omokehinde, Tolu 340
Omsland, Tone K. 274
Onal, Melda 19
Oneglia, Andrew. 402
Ong, Angel 279
Ongphiphadhanakul, Boonsong . . . 265
Onken, Jennifer 26
Ono, Mitsuaki 338
Ono, Noriaki 15, 344

- Ono, Yuichi 172, 179
 Ono, Yusuke 86
 Ooguro, Yukari 132
 Oohashi, Toshitaka 338
 Oosterwyck, Hans Van 244
 Or, Omer 200
 Orces, Carlos 429
 Orces, Daniella 429
 Ordovas, Jose 229
 Orme, Stephen 202
 Orr, Bradford 294
 Orschell, Christie 361
 Ortega, Alicia M. 326
 Ortendahl, Jesse D. 108
 Ortinau, Laura 6
 Ortíz, Maria Encarnacion
 Rodriguez 353
 Ortsater, Gustaf 267
 Orwig, Denise 24, 395
 Orwoll, Eric 13, 14, 40, 106, 147,
 285
 Orzabal, Marcus 362
 Orzuza, Ricardo 209
 Osaki, Makoto 68, 239, 262, 368,
 403
 Oshita, Yusuke 408
 Ostlund, Richard 148
 Ostovar, Afshin 313, 439
 Ostrowski, Michael C. 95
 Osuna, Maria Angeles Lillo 217
 Ota, Masahiro 34, 133
 Ota, Shusuke 409
 Othman, Ahmad 218
 Ott, Susan 287, 289, 408
 Ottenhoff, Tom Hm 51
 Oursler, Merry J 93
 Oursler, Merry Jo 96, 145, 293, 377
 Outman, Ryan 397
 Ouyang, Hongjiao 30, 218
 Owens, Brett 222
 Owens, Joshua A. 415
 Oya, Kaori 250
 Oyer, Mark 376
 Oz, Orhan 388
 Ozono, Keiichi 211, 300, 301, 322
- P**
- P, Hyoung Moo 409
 P, Olivier 43
 Pacak, Karel 430
 Paccou, Julien 105, 166
 Pacheco, Rafael 334
 Pacheco-Costa, Rafael 98
 Pacifici, Maurizio 124
 Pacifici, Roberto 35, 415
 Packer, Rebecca 236
 Paddidela, Raja 55, 120
 Padilla, Jaume 353
 Paes, Angela 186
 Paglia, David 118
 Pagnotti, Gabriel 237
 Pagnotti, Gabriel M. 42
 Pahapill, Richard 376
 Pählig, Sophie 415
 Paik, Julie M. 394
 Pajevic, Paola Divieti 162, 356, 382
 Pak, Kyoungjune 283
 Pal, Rimesh 166
 Palcu, Patricia 399
 Palermo, Andrea 203
 Palermo, Lisa 24
 Palmer, Abraham 363
 Palmer, Scott 134
 Palmieri, Michela 23, 23, 345
 Palomino, Pablo 13
 Palomo, Telma 422
 Pals, Gerard 304
 Pamperin, Jenny 73
 Pan, Feng 134, 167
 Pan, Kristen 424
 Pan, Kristen S 121, 183
 Panahifar, Arash 377
 Panellini, Tania 369
 Pang, Qian-Qian 143
 Pang, Ying 430
 Panitsas, Konstantinos 71
 Pannacciulli, Nico 114, 115, 290
 Pannacciulli, Nicola 21
 Pantano, Francesco 72
 Pantoja, Kimberly 281
 Panwar, Preety 370
 Paone, Riccardo 218
 Papadakis, Georgios 428
 Papadopoulos, Pericles 179
 Papageorghiou, Aris 109, 356
 Papaioannou, Alexandra 7, 107,
 164, 277, 394, 399, 400
 Papapoulos, Socrates E. 297
 Paparodis, Rodis D 199
 Papavasiliou, Kyriakos 179
 Papo, Niv 417
 Papp, Anne De 20, 24
 Paradise, Chris 254
 Paradise, Christopher 154, 251,
 364
 Paradise, Christopher R. 253
 Parajuli, Ashutosh 35, 235, 404
 Pardi, Elena 321
 Parent, Stefan 143
 Parés, Albert 172
 Paria, Nandina 244
 Parimi, Neeta 84, 106, 434
 Park, Cheol Woo 239, 335
 Park, Clara 329
 Park, Clara Yongjoo 435
 Park, Danbi 75
 Park, Dongsu 6
 Park, Eui Kyun 159
 Park, Han-Saem 435
 Park, Hyoung-Moo 380
 Park, Jai Hyung 278
 Park, Jihwan 313
 Park, Jin-Sung 176
 Park, Joo-Cheol 42, 151, 221
 Park, Jooyong 145
 Park, Na-Rae 329
 Park, Serk In 45, 340
 Park, Seung Shin 265
 Park, So Jeong 380, 429
 Park, Sungho 95
 Park, Sungjae 206
 Park, Ye Soo 176, 308
 Park, Yeoung Hyun 151
 Park, Yeoung-Hyun 221
 Park, Young Chang 116
 Park, Young Joo 45
 Park, Young-Eun 295
 Parkman, Virginia 29
 Parkmin, Kyung 256
 Park-Min, Kyung-Hyun 95
 Parnell, Laurence 229
 Parolini, Francesca 312
 Parsons, Camille 89, 109
 Parthasarathy, Sucharitha 235
 Partridge, Nicola 5, 118, 374
 Pascariu, Iulian 286
 Paschalis, Eleftherios 184, 311
 Paschalis, Eleftherios P. 111
 Pasco, Julie 99, 308, 392
 Pasco, Julie A 273
 Passeri, Giovanni 312
 Pastore, Anna 303
 Pastore, Raymond 173
 Pata, Monica 97
 Patel, Chirag 279
 Patel, Rajesh 46
 Patel, Rajvi 123
 Patel, Sapna 202
 Patel, Sharina 233, 240
 Paternoster (Cox), Lavinia 12
 Paternoster, Lavinia 369
 Patsch, Janina 310
 Patton, Daniella 209
 Patton, Daniella M. 238
 Patton, Olivia 413
 Pattyn, Ryan 42
 Paula, Francisco De 200
 Pauli, Richard 121
 Pauwels, Steven 147
 Pavlos, Nathan J. 192
 Peacock, Munro 50, 128, 296, 323
 Peal, Bridgette 134
 Pearson, Joseph 260
 Peault, Bruno 367
 Pecenkova, Kamila 333
 Peck, Sun 185
 Pedone, Claudio 203
 Peek, Christopher 194
 Peel, Nicola 129, 319
 Peissig, Peggy 47
 Pelle, Simone 305
 Pellegrini, Gretel G 209, 296
 Pellegrini, Miguel Angel 209
 Pelletier, Simon 170
 Pellicelli, Martin 332, 371
 Pelus, Louis 361
 Peña-Rodríguez, Pilar De La 274,
 308
 Peng, Matthew 101
 Peng, Yu 362
 Peng, Yuanzhen 337
 Peng, Zhiqi 179, 295
 Pennestri, Teresita 402
 Pennypacker, Brenda 294
 Pentyala, Srinivas 294
 Pepe, Jessica 61, 147, 223
 Poppel, Jeroen Van De 153
 Peppelenbosch, Maikel 153
 Pereira, Francisco De Assis 164
 Pereira, Patricia Monique Vila
 Nova 164
 Pereira, Renata 211
 Pereira, Renata C. 174
 Pereira, Rmr 112
 Peres, Sylvie Loiseau 166
 Perez-Campo, Flor M. 351
 Perez-Nuñez, Maria Isabel 351
 Peris, Pilar 121, 172, 322
 Periyasamy-Thandavan,
 Sudharsan 153, 403
 Perotti, Mc 417
 Perret, Christine 14
 Perrien, Daniel S 305
 Perrien, Daniel S. 59
 Perry, John 125
 Perry, Rachel 18
 Perwad, Farzana 56, 230
 Peters, Katherine 14
 Peters, Tim 398
 Petronglo, Jenna 315
 Petrovick, Martha 352
 Petryk, Anna 181, 322
 Petterson, Tanya 39
 Pettit, Allison 72, 214
 Pfeiler, Georg 55
 Pham, Hai 97
 Pham, Hai Thanh 338
 Pham, Thuy 272
 Phan, Peter 327
 Philippon, Marc J 370
 Phillips, Charlotte L. 349
 Phu, Steven 185, 189, 222
 Piacente, Laura 210
 Pialat, Jean-Baptiste 316
 Piao, Jinying 97
 Piazuolo, Blanca 194
 Piazzolla, Valentina 61
 Picard, Sylvain 294
 Picazo, Mirella López 163
 Piche, Nicolas 364
 Pichelin, Matthieu 17
 Pichurin, Oksana 254
 Picke, Ann-Kristin 231
 Picot, Tiphanie 3
 Picotto, Gabriela 255
 Pieber, Thomas R 224
 Picet, Isabelle 168, 182
 Pienkowski, David 176
 Pieper, Carl 272
 Pierce, Jessica 93
 Piet, Judith 190
 Pignatti, Emanuele 6
 Pignolo, Robert 26, 79, 111
 Pignolo, Robert J 22
 Pignolo, Robert J. 420
 Pihl, Susanne 201, 323
 Pike, J. Wesley 19
 Pikner, Richard 333
 Pilbeam, Carol 35
 Pilkey, A. Keith 327
 Pillai, Chanthu 334
 Pilot, Nicolas 137
 Pin, Fabrizio 188, 337
 Pinamont, William 249, 344
 Pinatti, Amanda 328
 Pineau, Joelle 39
 Pineda-Moncusí, Marta 394
 Pinel, Rosa Arboiro 298
 Pinali, Robert 150
 Pippin, James A. 79, 91
 Piquereau, Jérôme 76
 Pires, Geovanna O. 62
 Pissani, Leonardo 137
 Pitta, Michael 248
 Pitukcheewanont, Pisit 56, 134
 Plagge, Antonius 434
 Plankaert, Catherine 266
 Plasenzotti, Pia 184
 Plett, Artur 361
 Plotkin, Lilian 188, 334, 335
 Plotkin, Lilian I 296, 355
 Plotkin, Lilian I. 83, 95, 98
 Plovier, Hubert 296
 Plotkin, Lilian I. 260
 Poeze, M. 66
 Pohl, Sandra 4
 Poindexter, John 298

- Polk, John 207
 Pollard, Andrea 105
 Polly, David 181
 Pomer, Alysa 311
 Pomp, Daniel 434
 Ponte, Filipa 53
 Poole, Kenneth 90, 361
 Poon, Christina Chui Wa 297
 Popp, Kristin 170, 263, 265
 Portale, Anthony A. 55, 56, 120, 122
 Portela, MI Pita Martin De 417
 Portero-Muzy, Nathalie 206
 Portillo, Mariano Rodriguez 353
 Porzio, Ottavia 303
 Pöschl, Ernst 136
 Posey, Karen 304
 Potter, Lincoln 195
 Pouletaut, Philippe 76
 Poulides, Nicole 31
 Pourteymoor, Sheila 42, 343, 344
 Poveda, Jose 54
 Powell, Katherine 237, 331
 Pozzilli, Paolo 41, 203
 Prasad, Sadhana 277, 400
 Pratap, Jitesh 218
 Pregizer, Steven 433
 Preisig, Martin 428
 Premaor, Melissa 345
 Prenni, Jessica 236
 Prentice, Ann 109, 356
 Price, Iona 398
 Prideaux, Matt 261, 313, 433
 Prideaux, Matthew 355
 Prieto-Alhambra, Daniel 54, 105, 394, 398
 Prince, Richard 110, 264, 393
 Prior, Jerilynn 194, 390, 393, 395
 Prior, Jerilynn C 107, 193, 387, 394
 Prisby, Rhonda 58, 215, 338
 Probyn, Linda 387
 Procknow, Jesse D. 9
 Protheroe, Hayley J. 64
 Pruss, Cynthia 278, 355, 414
 Pryor, Jane 426
 Pucci, Sabina 336
 Pulliam, Alexis 331
 Pulumulla, Sree H 138
 Püschel, Christoph 116
 Pundole, Xerxes 411
 Punthakee, Zubin 122
 Puppali, Nagraj 30
 Purdue, Ed 416
 Püschel, Klaus 317, 348
 Putnam, Nicole 194, 314, 315
 Puzas, J Edward 43
- Q**
 Qi, Jiawei 257, 258, 258, 378
 Qi, Lixing 18, 260
 Qian, Airong 85, 93, 373, 375
 Qiao, Wanxin 81
 Qin, Ling 4, 117, 143, 313, 405
 Qin, Weiping 337
 Qin, Yi-Xian 245
 Qiu, Shijing 66, 99
 Qiu, Wei 41, 224
 Qiu, Wuxia 85
 Qiu, Yong 307
 Qu, Ruize 96
 Quaggin, Susan 354
- Que, Xuchu 23
 Quenneville, Eric 332
 Quillen, Ellen E. 206
 Quinn, Julian 105
 Quiroga, Felisa 299
 Quittner, Matthew 235
 Qureshi, Osama 372
 Qureshi, Shahar 413
- R**
 Rabadán, Raúl 71
 Rachner, Tilman 72
 Radcliff, Abigail 240
 Radmer, Sebastian 407
 Raganathan, Kavitha 5
 Raggio, Cathleen 180, 418
 Rahel, Braim 391
 Rahman, Munsur 207
 Rahme, Elham 279, 394
 Rahn, Elizabeth 275, 397
 Rai, Jyoti 424
 Raijmakers, Pieter 120
 Raine, Lauren 66
 Raj, Nirmal G 180
 Rajamani, Saathyaki 320
 Rajapakse, Chamith 4, 101, 202, 207
 Ramadoss, Jayanth 362
 Ramalho, Janaina 112
 Ramautar, Ashna 180
 Ramirez, Josue 362
 Ramos, Mercedes Aramendi 321
 Ramos-Platt, Leigh 134
 Rana, Ippolita 305
 Rana, Kavita 281
 Randall, Megan 317
 Ranganath, L R 245
 Ranganath, Lakshminarayan 145
 Rangel-Moreno, Javier 370
 Rannou, François 360
 Rantalainen, Timo 20, 235
 Rao, Sudhaker 66
 Rao, Sudhaker D 99, 180, 183
 Rao, Sudhaker D. 207, 386
 Rapp, Anna E. 231
 Rapp, Stephen 307
 Rasche, Leo 219
 Rascoe, Alexander 369
 Rashid, Harunur 140
 Raslan, Adnan 374
 Rasooly, Marjohn 298
 Rathbun, Alan 395
 Rathore, Roshita 388
 Rauch, Frank 50, 122, 123, 350, 421, 422
 Rauner, Martina 72
 Ravuri, Sudheer 370
 Raymond, Duncan A 21
 Raymond, Warren 256
 Raza, Azra 71
 Razaghi, Maryam 233, 240
 Read, Grant 426
 Reagan, Michaela 77
 Real, Alvaro Del 351
 Recker, Robert 121, 204, 213, 311
 Recker, Robert R. 199
 Rector, R. Scott 349
 Redae, Yonas 347
 Reddy, Sakamuri 31, 219
 Redline, Susan 285
 Redmond, Niamh 398
- Reesink, Heidi 134
 Reeve, Jonathan 105
 Rega, Laura Rita 303
 Rehan, Mohammad 30, 94
 Reichenberger, Ernst 183, 305
 Reid 356
 Reid, Ian 54
 Reifman, Jaques 170, 263, 265
 Reilly, Catherine 202
 Reimeringer, Michael 187
 Reinhardt, Dieter 435
 Reinhardt, Dieter P. 417
 Reinhold, Stefan 385
 Reis, Lm 112
 Reis, Luciene M. Dos 62
 Reis, Rui 431
 Reitsma, Shannon 156, 371
 Rejeski, Jack 399
 Rejnmark, Lars 47, 125, 277, 405, 422
 Relaix, Frédéric 213
 Remec, Katarina 173
 Ren, Rongguo 439
 Ren, Yinshi 4
 Ren, Yongxin 82
 Rendina-Ruedy, Elizabeth 225, 232, 346
 Rendu, Elisabeth Sornay-. 36
 Reppe, Sjur 228
 Resch, Heinrich 116
 Reseland, Janne 312
 Retrouvey, Jean-Marc 421
 Reutrakul, Sirimon 265
 Revel, Martin 209
 Revollo, Leila 363
 Revu, Shankar 30
 Reyes, Carlen 54
 Reyes, Monica 52, 181
 Reyes-Fernandez, Perla 84
 Reznikov, Natalie 364, 421
 Rhe, Frits Van 219
 Rhee, Yumie 127, 300, 429
 Rhodes, Sylvia 101
 Riancho, Jose A. 122, 351
 Riancho-Zarrabeitia, Leyre 122
 Ribom, Eva 13, 310
 Ricarte, Florante 5, 118, 374
 Ricci, Biancamaria 44, 159
 Richard, Céline 299
 Richard, Eastell 400
 Richards, Brent 105
 Richards, J Brent 39, 70
 Richette, Pascal 220
 Ricke, Darrell 352
 Rickel, Kirby 219
 Riddle, Ryan 10, 94
 Riddle, Ryan C. 77
 Ridgers, Nicola 235
 Ridout, Rowena 38, 438
 Riedel, Christoph 288
 Riemersma, Omar 299, 421
 Riesebo, Elise 304
 Rietbergen, B. Van 66
 Rietbergen, Bert Van 36, 102
 Rifai, Omar Al 80, 349
 Rinaldi, Gianmarco 221
 Río, Luis Del 163, 327
 Río, Luis Del 401
 Río, Luis Del 383
 Rios, Jonathan 244, 364
 Riquelme, Manuel 73, 341
 Ristic, Branko 24
- Ritchie, Robert 13
 Ritchie, Robert O. 317
 Rittweger, Joern 137
 Rivadeneira, Fernando 14, 105, 125, 279, 403
 Rizzì, Rita 217
 Rizzoli, Rene 275
 Rizzoli, René 36, 126, 223, 309
 Robbiani, Damian 302
 Robbins, Amy 345
 Roberts, Mary Scott 174, 332
 Roberts, Norman 145
 Robertson, Thomas 205
 Roberts-Pilgrim, Anna 374
 Robey, Pamela 338
 Robey, Pamela G 424
 Robinson) 356
 Robinson, Cemre 419
 Robinson, Dale 386
 Robinson, Jeremy 374
 Robinson, Jerid 195
 Robinson, Samantha 350
 Robinson, Samuel 358, 382
 Robinson-Cohen, Cassianne 230
 Robison, Lisa S 227
 Robles, Hero 9
 Robling, Alexander 136, 362
 Robling, Alexander G 82, 235
 Robling, Alexander G. 260
 Roblot, Pascal 130
 Roca, Hernan 215, 216, 281
 Roca-Ayats, Neus 144, 144
 Rocco, Maja Di 420
 Rocha-Braz, Manuela Gm 299
 Roche, Bernard 3
 Rochelle, Rachele 410
 Rockman-Greenberg, Cheryl 322
 Rockx, Barry 435
 Rødbro, Lene Langagergaard 125
 Rodeheffer, Matthew 41
 Rodeo, Scott 369
 Rodkey, William 370
 Rodondi, Nicolas 317
 Rodrigues, Ana Catarina 102
 Rodrigues, Ana Maria 102
 Rodrigues, Isabel Braganca 438
 Rodriguez, Alexander 110
 Rodriguez, Elena Gonzalez 317, 396, 428
 Rodriguez-Buritica, David 121
 Roedbro, Lene Langagergaard 277
 Roeder, Emilie 87
 Roetzer, Katharina 184
 Rohatgi, Nidhi 48
 Roizen, Jeffrey 29, 352
 Rojas, Maria 25
 Rokidi, Stamatia 111, 184, 311
 Roldán, Emilio 184
 Rolighed, Lars 47, 125, 277
 Rolvien, Tim 4, 5, 317
 Romano, Robert 348
 Romão, Elen Almeida 201
 Romero-Ibarra, Jaime 278
 Romme, Elisabeth 389, 391
 Rondinoni, Carlo 200
 Roodman, G 218
 Roodman, G. David 80, 304, 324, 339, 380
 Roper, Randall 350
 Rosario, Raysa 225
 Roschger, Paul 16, 184
 Rose, Marianne S 21, 108

- Rosen, Barry 361, 393, 430
 Rosen, Cliff J. 390
 Rosen, Clifford I, 17, 41, 71, 76, 77, 81, 87, 94, 168, 172, 223, 225, 232, 346, 434
 Rosen, Clifford J 90, 117, 118, 226, 345, 347
 Rosen, Clifford J. 319
 Rosen, Harold N. 394
 Rosen, Vicki 44, 232, 363, 373, 433
 Rosenfeld, Jill A. 78
 Rosenfeld, Lior 417
 Rosengren, Bjorn 13, 27
 Rosengren, Björn 310
 Rosete, Fernando R. 131, 325
 Rosner, Bernard A. 394
 Rosol, Thomas J. 95
 Ross, Gordon 145
 Ross, Ryan 331
 Rossi, Michela 303, 305
 Rossing, Maria. 419
 Rostom, Krista. 277
 Roszko, Kelly 430
 Roth, Theresa 255
 Rothenbuhler, Anya 418
 Rothman, Jeffrey 128
 Rothner, Ariel 437
 Rotman, Marlous 51, 417
 Roux, Christian 166, 418
 Roux, Jean-Paul 209, 316, 332
 Roux, Kyle 312
 Rowe, David 228, 426
 Roy, Savannah. 118
 Roychoudhury, Arindam 126
 Rozenfeld, Paula. 299, 421
 Rozental, Tamara D. 292
 Ruan, Ming 145, 293
 Rubin, Clinton 237
 Rubin, Clinton T. 42
 Rubin, Janet 154, 244, 321, 366
 Rubin, Katrine Hass 105
 Rubin, Mishaela 61, 63, 129, 130, 199, 203, 203
 Rucci, Nadia 45, 123, 218, 253
 Rudolph, Sara 265
 Rudolph, Sara E. 273
 Rue, Megan 142
 Rufus, Pamela 273, 308, 392
 Ruiz, Carlos 327
 Ruiz-Gaspa, Silvia. 322
 Ruiz-Gaspà, Silvia. 172
 Rupert, Joseph. 334
 Rupp, Markus 346, 372
 Ruppert, Kristine 142, 166
 Rush, Eric 301, 409
 Russell, Graham. 178
 Russo, Luis. 286
 Ryaby, James T. 251
 Ryan, Alice 395
 Ryan, Brittany A. 354
 Ryan, Denison S. 2, 2, 103
 Ryan, Patrick 272
 Rydzik, Renata 117
 Ryoo, Hyunmo 158
 Ryoo, Hyun-Mo 42, 79, 240, 241
 Ryu, Brian Y. 72
 Ryu, Euijung. 203
- S**
- Saad, Lina 97
 Saade, Marie-Béatrice 135
 Saag, Ken 290
 Saag, Kenneth 2, 106, 275, 276, 388, 397
 Sabik, Olivia 230
 Sabirova, Zarina. 189
 Sachdeva, Naresh 166, 180
 Sadrerafi, Keivan 22
 Sadvakassova, Gulzhakhan. 189
 Saedi, Ahmed Al. 153, 189, 222
 Saeki, Noritaka 86, 381
 Saetung, Sunee. 265
 Safadi, Fayez. 253, 368, 374
 Sagar, Rebecca. 202
 Sagebein, Carlos A. 412
 Saigopalakrishna, Yerneni S. 138
 Saika, Takashi 86
 Saita, Makiko 119
 Saito, Hiroaki 25, 29, 31, 49, 73
 Saito, Hiroki 176
 Saiyed, Rehan 13, 200
 Sajja, Puspaltha 233
 Sajjad, Muhammad 392
 Sakai, Akinori 411, 412
 Sakai, Yoshitada 408
 Sakakibara, Iori 86
 Sakamoto, Kei 74, 357
 Sakamoto, Yuko 334
 Sakashita, Naomi 375
 Sakhaee, Khashayar. 298
 Sakurai, Atsushi 167
 Salazar, Valerie 373
 Salcion, Axelle 418
 Saleh, Maleck 374
 Salga, Marjorie 214
 Salimi, Shabnam 395
 Salinas, Andrea 177
 Salinero, Abigail E. 227
 Salisbury, Elizabeth 366
 Salminen, Helena 395
 Salmon, Carlos 200
 Salmon, Jane. 369
 Salusky, Isidro 211
 Salusky, Isidro B. 174
 Sambandam, Yuvaraj 219
 Samelson, Elizabeth 36, 247
 Sami, Naveen 264
 Samsa, William 19, 30
 Samsonraj, Rebekah 111, 154
 Samuel, Andre 129
 Samuels, Blossom 248
 Samuvel, Devadoss J. 95
 Sande, Michiel Van De 51
 Sanders, Kerrie 20, 115, 392
 Sandhaus, Robert 418
 Sanesi, Lorenzo 210, 217, 312
 Sanjay, Archana 44, 153, 312
 Sankar, Uma 237, 248, 362
 Sankaran, Jeyantt 237
 Sankaran, Jeyantt S. 244
 Sankaran, Jeyantt S. 366
 Sanna, Joanna 220
 Santana, Josue 248
 Santana, Rodrigo Carvalho De 201
 Santesso, Nancy 438
 Santonati, Assunta. 203
 Santos, Fábio De Souza 164
 Santos, Fania Cristina 167, 392
 Sañudo, Carolina 351
 Saponaro, Federica 321
 Saramago, Ana 418
 Saripalli, K. Reddy 436
 Sarris, Ioannis 179
 Sato, Amy Y 82, 296, 355
 Sato, Chiaki 172, 179
 Sato, Dai 34
 Sato, Shingo 97
 Sato, Sunao 250
 Sato, Takenori 119
 Sattari, Maryam. 8
 Saule, Emilie. 275
 Savard, Louis Dore 191, 218
 Savitt, Anne 294
 Sawada, Yuichiro 86, 381
 Sawamura, Satoru. 167
 Sawatsubashi, Shun 234
 Sawyer, Rebecca. 205
 Sayani, Farzana 282
 Sayed, Riham El. 22
 Sayegh, Fares 179
 Sbrana, Francesca. 365
 Scadden, David 6, 71, 244
 Scadden, Elizabeth 71
 Scandling, Benjamin 354
 Scerpella, Tamara A. 135
 Schafer, Anne 189
 Schaffler, Mitchell 32, 161, 161, 236
 Schaffler, Mitchell B. 34, 236, 407
 Schaible, Eric 65
 Schanda, Jakob E. 116
 Scheffler, Julia 296
 Schei, Berit. 274
 Scheller, Erica L. 9, 206
 Scher, Judite 38
 Scherer, Samuel C. 277, 400
 Schilling, Lauren 31, 259
 Schima, Wolfgang 116
 Schindeler, Aaron 333
 Schini, Marian 129
 Schinke, Carolina 219
 Schinke, Thorsten 4, 5, 143
 Schipani, Ernestina 5, 312, 341, 425
 Schlecht, Stephen 209, 306
 Schlecht, Stephen H. 238
 Schlesinger, Paul H 373
 Schlezinger, Jennifer 356
 Schlussel, Yvette 110
 Schmidtsfeld, Jochen. 116
 Schmidt, Albrecht 224
 Schmidt, Felix N. 317, 348
 Schneider, Carrie 318
 Schneider, Peter 413
 Schneider, Prism S 389
 Schneider, Stephen 110
 Schneider, Vanessa Karine 294
 Schnitzer, Thomas 405
 Schober, Hans-Christof 407
 Schoenherr, Chris 196
 Schoenmaker, Ton 306
 Schoenmakers, Inez 109, 356
 Schoors, Sandra 244
 Schott, Eric 370
 Schousboe, John 8, 8, 38, 40, 269, 316, 391
 Schreuders-Koedam, Marijke 435
 Schreurs, Ann-Sofie 416
 Schröder, Fabian 310
 Schröder, Saskia 73
 Schroeder, William 214
 Schroijsen, Marielle 180
 Schueren, Bart Van Der 414
 Schulz, P.Christian 126
 Schulze, Kerry. 121
 Schurman, Charles 65
 Schwab, Frank. 129
 Schwarte, Lothar 120
 Schwartz, Ann 106, 168, 189, 310
 Schwartz, Ann V. 226
 Schwartz, Phillip 437
 Schweighofer, Natascha. 224
 Schweitzer, Dave. 169
 Scott, Daryl A 78
 Scott, David 110, 185, 307, 427
 Scott, Joanna 431
 Scott, Jonathan 278
 Scott, Laura 423
 Sebastian, Aimy 375
 Sedghizadeh, Parish. 178
 Seefried, Lothar 196, 320, 320, 322
 Seeman, Ego 38, 68, 362
 Séguin, Cheryle 57
 Segura, Noemi Vergara 353
 Seibel, Markus J. 9
 Seidah, Nabil G. 80
 Seijo, M 417
 Seiler, Michael 188
 Sekiguchi-Ueda, Sahoko 213, 241
 Sekine, Noriko 42
 Seldeen, Kenneth 347
 Selim, Abdulhafez 287
 Sellars, K. Berit 354
 Sellin, Karine 191
 Semionov, Alexandre 193
 Sen, Buer. 154, 237, 244, 366
 Senbanjo, Linda T. 219
 Sens-Albert, Carla. 138, 242
 Senwar, Bhavya 204
 Seo, Bo Yeon 340
 Seong, Sook Jin 257
 Seref-Ferlenguez, Zeynep 236, 236
 Serena, Michela 312
 Sergio, Marcelo 105
 Serna, Elena 121
 Serota, Alana. 248
 Serrat, Maria A 433
 Servitja, Sonia 394
 Sestak, Ivana. 46, 102
 Seuffert, Patricia. 412
 Seung-Hyun, Hong 228
 Sevelde, Paul. 55
 Sever, Mojca Jensterle 173
 Severe, Nicolas. 71
 Seymour, John. 412
 Sfeir, Jad 123, 127
 Shadman, Zhaleh 439
 Shafiee, Gita 313, 439
 Shah, Avni 334
 Shah, Jayesh 178
 Shah, Manasvi 6
 Shah, Ramille 329
 Shah, Roshan Pradip 89
 Shah, Viral 406
 Shainer, Reut 344
 Shane, Elizabeth. 121, 126, 131, 199, 266, 285, 325
 Shang, Peng 254, 337
 Shankar, Kartik 10
 Shapiro, Jay R. 182
 Shapses, Sue 110, 142, 399
 Shardell, Michelle 395
 Shares, Brianna 43, 154
 Sharifi, Farshad 313, 439
 Sharma, Anjali. 126
 Sharma, Anuj 93
 Sharma, Deepti 205
 Sharma, Karan 362, 435
 Sharma, Manisha 295

- Sharma, Shobhit 219
 Sharma, Sudarshana M. 95
 Shaul, Jonathan 280
 She, Yun 42
 Shea, M. Kyla 328
 Shea, Steven 285
 Sheets, Michael 26
 Shefelbine, Sandra 66, 190
 Shefferd, Kirsty 218
 Sheikh, Zeeshan 118
 Shen, Guofang 36
 Shen, Hui 80
 Shen, Jian 84, 147, 361
 Shen, Jie 50
 Shen, Leyao 86
 Shen, Lilia 348
 Shen, Wei-Ren . 257, 258, 258, 378
 Sheng, Rui 48
 Shepherd, John 28
 Shepstone, Lee 398
 Shergill, Arvind 387
 Shero, Nora 233, 240
 Sherry, Nicole 128, 199
 Sherwood, Richard 405
 Sheshbaradaran, Hooshmand 315
 Shetye, Sneha 207
 Sheu, Tzong-Jen 43
 Shevroja, Enisa 100, 163, 396
 Shi, Ce 258
 Shi, Chao 162
 Shi, Xingming 153, 242, 403
 Shi, Xing-Ming 93, 225, 414
 Shi, Zhenqu 379
 Shiau, Stephanie 121, 199, 285
 Shibata, Megumi 213, 241
 Shido, Rena 158
 Shieh, Albert 40, 177
 Shiekh, Adnan 235
 Shiftlett, Lora 336
 Shikh, Mohey Eldin El- 22
 Shillingford-Cole, Ventrice . . 272
 Shim, Jaehyuck 227
 Shim, Jae-Hyuck 3
 Shima, Kazuhiro 257, 258, 258, 378
 Shimada, Yoichi 172, 175, 175, 179
 Shimano, Antonio Carlos 431
 Shimizu, Tomohiro 34, 133
 Shimizu, Toshiaki 334
 Shimoido, Takeshi 346
 Shimosuru, Michito 224
 Shin, Bongjin 92, 380
 Shin, Chan Soo 145, 184, 265, 300, 311
 Shin, Dong Min 376
 Shin, Hong-In 159
 Shin, Hye-Rim 79, 240, 241
 Shin, Ikjae 342
 Shin, Woongchul 224
 Shin, Young Ho 388
 Shiraki, Makoto 258, 378
 Shirasawa, Eiki 176
 Shivappa, Nitin 190
 Shkhyan, Ruzanna 88
 Shoback, Dolores 189
 Shoback, Dolores M. 128
 Shon, Hyun Chul 278
 Shore, Eileen 79, 185, 302
 Shore, Eileen M 22, 305
 Shore, Eileen M. 87
 Shrestha, Rojesh 313
 Shropshire, Daniel 260, 341
 Shu, Aimee 201
 Shuhaibar, Leia C 196
 Shulman, Gerald 18
 Shum, Laura 154, 339
 Shumaker, Sally 307
 Shumate, Lauren 84, 434
 Shumate, Lauren Toyomi 181
 Shuwaikan, Raghad 382
 Shyu, Jia-Fwu 63
 Siao, Chia-Jen 320
 Sibai, Mohammad El 282
 Sidibe, Aboubacar 391
 Sidibé, Aboubacar 324
 Sidibé, Aboubacar James 215
 Siegel, Peter M. 189
 Siegel, Richard M. 16
 Siggeirsdottir, Kristin 392
 Siggeirsdottir, Kristin 11, 37
 Siggelkow, Heide 321
 Signorovitch, James 199
 Sigurdsson, Gunnar 11, 37, 226, 392
 Sigurdsson, Sigurdur 11, 37, 90, 168, 226
 Sihota, Praveer 207
 Sikaris, Ken 345
 Sikjær, Tanja 47
 Sikjaer, Tanja 125, 277, 422
 Silva, Barbara 162
 Silva, Caroline 162
 Silva, Cláudia Lobato Da 138
 Silva, Claudio 299
 Silva, Flavio Henrique Da 294
 Silva, Hugo Gomes Da 322
 Silva, Luis Fernando Negro 416
 Silva, Matthew. 53, 83, 83, 91, 229, 350
 Silva, Raquel A 67
 Silva, Raquel Assed 431
 Silva, Tiago 418
 Silva, William 336
 Silveira, Fernando 302
 Silverberg, Shonni 323
 Silverstein, Arlene 399
 Silvestre, Joao 336
 Silvina, Levis 291
 Sim, Ie-Wen 412
 Sim, Marc 110
 Sim, Sotheadt 332
 Simecek, Petr 434
 Siminoski, Kerry 7
 Simm, Peter 68
 Simmons, Jill H. 55
 Simoes, Vivian Rf 299
 Simonian, Narina 405
 Simonyan, David 234, 347
 Simpson, Christine 97, 402
 Sims, Natalie 214
 Sims, Natalie A 1, 64, 293
 Sinaki, Mehrsheed 401
 Sinder, Benjamin 216, 281
 Sinder, Benjamin P 77
 Sing, Chor-Wing 113
 Singer, Andrea J 108
 Singer, Christian F 55
 Singer, Frederick 194
 Singh, Harminder 103
 Singh, Harshvardhan 196, 388
 Singh, Priyanka 166
 Sipll, Rachel 406
 Sirbu, Paul Dan 24
 Sire, Alessandro De 223
 Siris, Ethel 21
 Sitara, Despina 352
 Siwarasanond, Nantaporn 265
 Sjögren, Klara 24, 69, 231, 296
 Skalicky, Susanna 310
 Skenandore, Cassandra 426
 Skinner, Jonathan 319
 Skjødtt, Michael K 7
 Skrinar, Alison 51, 55, 120
 Slane, Kevin 323
 Slayden, Alexandria 6
 Sliepka, Joseph 26
 Sliepka, Joseph M 78
 Slim, May 279
 Sloane, Richard 272
 Slørdahl, Tobias 341
 Smaldone, Silvia 320
 Smeenk, Frank 389, 391
 Smethurst, Victoria 92, 374
 Smid, Cory 121
 Smith, Alison 398
 Smith, Ashley 165
 Smith, David 21
 Smith, Jeremy 319
 Smith, Lachlan 185
 Smith, Michael 131
 Smith, Pamela S 422, 425
 Smith, Rosamund 81
 Smith, Tracey 280
 Smyth, Gordon K 64
 Snel, Marieke 180
 Snell-Bergeon, Janet 406
 Snyder, Michael 279
 Soares, Maria Marta 162
 Socorro, Mairobys 92, 374
 Soen, Satoshi 90
 Søgaard, Anne Johanne 274
 Sohn, Eric 256
 Solbakken, Siri Marie 274
 Solé, Thomas 296
 Solomon, Lauren 245
 Solomon, Lucian 205
 Somerman, Martha 423
 Son, Chul 151, 221
 Sonntag, Gregory 253
 Song, Hui 259
 Song, Hyunggi 151
 Song, I-Wen 78
 Song, Jun 364
 Song, Kee-Ho 283, 429
 Song, Min-Kyoung 259
 Song, Xiangqian 369
 Song, Yushan 315
 Sonnleitner, Linda 322
 Sood, Anil K 18
 Sornay-Rendu, Elisabeth 17, 38, 61, 173
 Sotunde, Olusola 152
 Sourice, Sophie 64, 362
 Southmayd, Emily 142, 402
 Souverein, Patrick C 269
 Souza, Mary Jane De 142, 402
 Souza, Pedro Paulo Chaves 294
 Sowder, Miranda 73, 340
 Sowe, Bintu 226
 Spagnoli, Anna 49, 53, 141, 246, 292, 343
 Spangeus, Anna 267
 Sparkes, Penny 105
 Spechbach, Herve 275
 Spencer, Taylor 345
 Spiegelman, Bruce 1
 Spiller, Kassandra 4
 Spray, David 32
 Spreicher, Sara 272
 Sprogøe, Kennett 323
 Squibb, Kathryn 134
 Srighanthan, Jeevitha 361, 430
 Srinivasan, Padma 235
 Srinivasan, Sundar 117, 359
 Srinivasan, Venkat 80
 Srinivasan, Venkatesan 45
 Srisukh, Sasima 265
 Sritara, Chanika 265
 Sritara, Piyamitr 265
 Srivastava, Alok 369
 Srivastava, Tarak 334
 Srividhya, Iyer 53
 Sroga, Grazyna 332
 Staa, Tjeerd P Van 269
 Staab, Jeffery 280
 Stabley, John 215
 Stadelmann, Marc 139, 187
 Stains, Joseph 359
 Stallard, Nigel 21
 Stamenkov, Roumen 205
 Standal, Therese 341
 Stankiewicz, Ann 148
 Stanley, Alexandra 87
 Stapledon, Catherine 205
 St-Arnaud, René 332, 354, 371
 Starr, Jessica 63
 Stechschulte, Lance 98, 315
 Steenackers, Ellen 143
 Stefanick, Marcia L. 434
 Stegen, Steve 221, 244
 Steger, Guenther G 55
 Stein, Daniel 135
 Stein, Emily 129, 248, 266
 Stein, Gary 49, 86
 Stein, Gary S 243
 Stein, Janet 86
 Stein, Janet L 243
 Stepan, Jan 113
 Stephan, Chris 124
 Stephen, Samuel 236
 Stephens, David 398
 Stephenson, Sonya 398
 Stephenson, Yvonne Coretha 68
 Sterenstein, Andrea 317
 Sternfeld, Barbara 142
 Stevens, Jan F 351
 Stewart, Rachel 26
 Stickland, Amy 206
 Stiers, Pieter-Jan 244
 Stirnemann, Jerome 275
 Stock, Stuart 376
 Stock, Stuart R 329
 Stodieck, Louis S 98, 326
 Stoetzel, Sabine 346
 Stoll, Delphine 3, 396
 Stolz, Donna 30
 Stolz, Donna Beer 373
 Stone, Katie 285, 361, 391
 Stone, Laura S 214
 Stone, Michael 398
 Storlino, Giuseppina 217, 413
 Stott, David J 317
 Stremke, Elizabeth R. 323
 Strickland, Ariana 209
 Strigini, Maura 296
 Strollo, Rocky 41
 Stroncek, John 410
 Strotmeyer, Elsa 106, 427
 Stubby, Julie 121, 199

- Stunes, Astrid Kamilla 297
 Sturgell, Emily 238
 Styner, Martin A. 237
 Styner, Maya. 237, 244, 366
 Su, Weiping 366
 Su, Yun 225
 Suadicani, Sylvia 236
 Suarez, Juan Miguel Villa . . . 182
 Suarez-Almazor, Maria 411
 Subburaj, Karupppasamy . . . 205
 Subburaman, Mohan 368
 Subler, Mark A. 324
 Subramaniam, Malayannan . . . 76
 Sudah, Suleiman 118
 Sueda, Reima 369
 Sugihara, Takaki 375
 Sugimoto, Toshitsugu 62, 70, 401
 Sugimura, Yoshihisa 241
 Suh, Joonho 42
 Suh, Sunghwan 283, 429
 Sui, Sophia 308
 Sultan, Hussein 22
 Sumita, Yoshinori 158, 375
 Summerford, David 140
 Summers, Megan 255
 Sumner, D. Rick 363
 Sumner, Rick 331
 Sun, Ben-Hua 53, 97
 Sun, Chunxiang 315
 Sun, Herb 236
 Sun, Hyun Jin 45
 Sun, Li 415
 Sun, Monica 354
 Sun, Ningyuan 162, 382
 Sun, Quanhong 138, 324
 Sun, Shuting 22, 178
 Sun, Weiwei 81
 Sun, Wenli 202
 Sun, Xuying 136, 292
 Sun, Yao 293
 Sun, Yuanyuan 439
 Sundan, Anders 341
 Sundh, Daniel 36, 104, 271, 284
 Sundquist, Kevin 104
 Sung, Hsiao Hsin 124
 Suominen, Mari I 188, 339
 Suri, Pradeep 247
 Surowiec, Rachel 124, 306
 Surridge, Rachel 212
 Susztak, Katalin 313
 Sutton, Vernon R 78
 Suva, Larry 219, 228, 238, 362, 413, 426
 Suvannasankha, Attaya 219
 Suzuki, Atsushi 213, 241
 Suzuki, Mitsuyoshi 334
 Suzuki, Miyako 214
 Suzuki, Takako 290, 422
 Svedbom, Axel 115
 Svensson, Hilda 271
 Svirskis, Darren 295
 Swallow, Elyse 199
 Swanson, Christine 285
 Swarnkar, Gaurav 137, 364
 Swart, Karin 8, 436
 Swekla, Kurtis 377
 Swinnen, Johan 244
 Syed, Shumayi 77
 Syversen, Unni 297
 Szabo, Eva 156, 371
 Szabo-Rogers, Heather 190
 Sztanyi, Istvan 24
 Sulz, Pawel 17, 36, 173, 266, 316
 Szymonifka, Jackie 369
T
 Taaffe, Dennis 20
 Tabacco, Gaia 61, 63, 63, 129, 130, 203, 203, 203, 324
 Tabaries, Sebastien 189
 Tabatabaie, Vafa 360
 Taguchi, Akira 274
 Taheri, Ehsaneh 439
 Tai, Nobuyuki 406
 Taipaleenmäki, Hanna 25, 31, 49, 73
 Tait, Jamie 20
 Tajima, Shuichiro 173, 176
 Takahashi, Naoyuki 381
 Takahashi, Nobunori 288
 Takahashi, Shun-Suke 119
 Takahashi, Takashi 181
 Takahashi, Yutaka 300
 Takahata, Masahiko 34, 133
 Takaishi, Kiyosumi 123
 Takano, Hajime 124
 Takashi, Yuichi 234
 Takaso, Masashi 173, 175, 176
 Takata, Shinjiro 375
 Takayama, Koji 408
 Takayanagi, Takeshi 213, 241
 Takeshita, Sunao 92
 Takeuchi, Ryohei 119
 Takeuchi, Tsutomu 90
 Takeuchi, Yasuhiro 177, 300
 Takeyari, Shinji 211, 301
 Takigawa, Masaharu 343
 Takyar, Farzin 18
 Talmo, Carl 154
 Tamimi, Faleh 364, 421
 Tamimi, Iskandar 364
 Tamura, Hikaru 257
 Tamura, Yukinori 346
 Tan, Nicholas 398
 Tan, Vivien 398
 Tanaka, Azusa 188
 Tanaka, Eiji 159, 341
 Tanaka, Hiroyuki 56, 387
 Tanaka, Ken-Ichiro 62, 70
 Tanaka, Sakae 90, 257
 Tanaka, Shinya 42, 290
 Tanaka, Yoshiya 90
 Tandon, Manish 218
 Tang, Hai 292
 Tang, Jonathan 168
 Tang, Jonathan C.Y. 437
 Tang, Yi 242
 Taniguchi, Keita 140, 160
 Tani-Ishii, Nobuyuki 119
 Tanimoto, Kotaro 341
 Tannous, Paul 210
 Tao, Jianguo 45
 Tao, Jianning 219, 312
 Tara, Zahra 29, 352
 Taranta, Anna 303
 Tarantino, Umberto 312, 336
 Tariq, Farhan 122, 409
 Taskaldiran, Isilay 181
 Tata, Zachary 5, 341
 Tatiparthi, Arun 81
 Tatsumi, Kohei 346
 Tauberg, Brandon 360
 Tauer, Josephine T. 225
 Tauqir, Madiha 409
 Tavares, Daniela Regina Brandao 167
 Tavares, Daniela Regina Brandão 392
 Tawfic, Monica 193
 Taxel, Pamela 140
 Tay, Donovan 130, 203
 Tay, Tabitha 410
 Tay, Yu-Kwang Donovan 61, 63
 Taylor, Brent 316, 391
 Taylor, Earnest 152
 Taylor, Erik 65
 Taylor, Erik A. 328
 Taylor, Kathryn 170
 Taylor, Kim 79
 Tchkonina, Tamar 26
 Tchkonina, Tamara 10
 Teare, Adrian 28
 Tebben, Peter 333
 Teguh, Dian 256
 Teitelbaum, Steven 48
 Teixeira, Andre L. 62
 Teixeira, Erica 161
 Tell, Grethe S. 274
 Tella, Sri Harsha 174
 Tembo, Monica 308
 Temple, Joseph 53, 141, 246, 343
 Tencerova, Michaela 216
 Tenn, Neil 57
 Tenorio, Jair 122
 Tenshin, Hirofumi 132, 341, 342
 Teramachi, Jumpei 132, 341, 342
 Terao, Yutaka 257
 Terhune, Elizabeth 214
 Terrill, Nick 410
 Tersey, Sarah 136
 Teti, Anna 45, 123, 253
 Teti, Anna Maria 218
 Teunissen, Bernd 120
 Thabane, Lehana 107, 277, 400
 Thacher, Tom 39
 Thai, Christine 318
 Thai, Lee 9
 Thakkar, Samarthkumar 317
 Thaler, Roman 251, 253, 254, 364
 Thanendrarajan, Sharmilan . . . 219
 Thapa, Prabin 203
 Theilen, Nicholas 229
 Theiler, Robert 109
 Theodore-Oklota, Christina 50, 56
 Thi, Ha Nguyen 338
 Thi, Mia 236
 Thicke, Brienne 17, 26, 145
 Thiele, Susanne 40
 Thies, Katie A. 95
 Thiagarajan, Ramkumar 347
 Thomas, Dominic 433
 Thomas, Jared 350
 Thomas, Mireille 3
 Thomas, N P. 245
 Thomas, Robert 147
 Thomas, Thierry 166, 173, 296
 Thompkins, Beatrice 182
 Thompson, William 237, 248, 362
 Thompson, William R. 42, 260, 355, 435
 Thomson, Seamus 133, 208
 Threadgill, David 413
 Threet, Dewayne 117, 359
 Thu, Ha Nguyen Thi 338
 Thu, Win Pa Pa 186
 Thumbigere-Math, Vivek 423
 Tian, Faming 82, 221
 Tian, Jing 167
 Tian, Li 143
 Tian, Ye 93, 375
 Tice, Matthew 297
 Tichy, Elisa 87
 Tickner, Jennifer 256
 Tiede-Lewis, Leann 383
 Tiedemann, Kerstin 189, 435
 Tien, Phyllis 193
 Tigyí, Gabor 43
 Tile, Lianne 38
 Timm, Wolfram 385, 436
 Tirado, Irene 149
 Tiso, Natascia 312
 Tobias, Jon H 271, 369
 Tobias, Jonathan 12, 105
 Tobin, Mark J 64
 Tocados, Juan Miguel Diaz 353
 Tokita, Akifumi 334
 Tom, Christina 345
 Tom, Kaitlyn 383
 Tomatsu, Eisuke 213, 241
 Tomazos, Ioannis 423
 Tominari, Tsukasa 140, 160
 Tomkinson, Ian 205
 Tomlinson, Ryan 82
 Tommasini, Steve 434
 Tommasini, Steven 41, 53, 350
 Tompkins, Douglas 219
 Ton, Amy 51
 Toner, Mehmet 71
 Tong, Wei 4
 Torgerson, David 398
 Toribio, Ramiro E. 95
 Toro-Ibacahe, Viviana 335
 Torossian, Frédéric 214
 Torrens, Sophie 221, 244
 Torres, Ferran 322
 Torres, Haydee 312
 Torres, Jorge LA Morales 278
 Torres, Vitor 336
 Torres-Naranjo, Francisco 274, 278, 308
 Torres-Quintana, María Angélica 335
 Toscani, Denise 218
 Toshihige, Masaaki 293
 Tosi, Laura L. 332
 Toth, Emese 105, 267
 Totten, Madeline 314
 Toumi, Hechmi 247
 Tourkova, Irina L 373
 Tower, Robert 4, 313, 405
 Towheed, Tanveer 387
 Towler, Dwight 215
 Toyone, Tomoaki 408
 Toyosawa, Satoru 250
 Trajanoska, Katerina 105
 Trajanoska, Katerina 125
 Tran, Christopher 277
 Tran, Doris 163
 Tran, Thach 194, 272, 390
 Tran, Thach S. 271
 Trani, Beatriz P 67
 Travnison, Thomas 247, 309
 Treece, Graham 90
 Trejo, Pamela 422
 Tremblay, Bradford 227
 Tremp, Brenna 78
 Treyball, Annika 232

- Tricarico, Domenico 136
 Trinh, Sophia 368
 Trippel, Stephen 248
 Tripto-Shkolnik, Liana 135
 Trivedi, Trupti 42
 Troen, Bruce 347
 Troka, Ildi 191
 Trollip, Jacques 387
 Trombetti, Andrea . . . 17, 126, 309
 Troy, Jordan 208
 Trudel, Guy 235
 Trudel, Yannick 416
 Truong, Kim 1
 Tsai, Jeffrey 424
 Tsai, Joy 20
 Tsai, Timothy 309
 Tsai, Yi-Wen 103
 Tsatsalis, Dimitrios 179
 Tseng, Hsu-Wen 214
 Tseng, Ing-Jy 185
 Tseng, Wei-Ju 16, 35
 Tsimikas, Sotirios 23
 Tsitouras, Dimosthenis 179
 Tsubota, Toshio 224
 Tsuchie, Hiroyuki 175
 Tsuchiya, Maho 176
 Tsuda, Eisuke 34, 381
 Tsuji, Kunikazu 97
 Tsuji, Shinnosuke 123
 Tsukamoto, Sho 123
 Tsukamoto, Sho 42
 Tsurukami, Hiroshi 412
 Tsurumoto, Toshiyuki 239
 Tu, Maxwell 41
 Tu, Qisheng 36, 111, 158, 191, 216, 223, 224, 281, 315, 372
 Tuari, Donna 295
 Tucker, Katherine 229
 Tuckermann, Jan 14, 231
 Turajane, Kathleen 416
 Turcotte, Anne-Frederique . . . 234, 347
 Turmezei, Thomas 90
 Turner, Joseph 311
 Turner, Mandy 278, 355, 414
 Turner, Mandy E. 147
 Turner, Russell T. 351
 Turner, Thomas 280
 Tusquets, Ignasi 394
 Tutino, Rebecca 345
 Tuukkanen, Juha 14, 69
 Twomey, Patrick 301
 Tyagi, Abdul Malik 35, 415
 Tyagi, Neetu 229, 335
 Tyagi, Suresh C 229, 335
 Tybulewicz, Victor 350
 Tye, Coralee 86
 Tye, Coralee E. 243
- U**
- Ucci, Argia 218
 Uchida, Kentaro 173, 176
 Uchiyama, Shigeharu 274
 Uda, Yuhei 162, 382
 Udagawa, Nobuyuki 381
 Uddin, Sardar Mz 294
 Uehara, Norihisa 252
 Uehara, Satomi 292
 Uehara, Shunsuke 381
 Uekusa, Yui 173, 176
 Ueno, Melise Jacou Peres 146, 328
 Ueno, Shuhei 176
 Ugur, Antonia 319
 Uitterlinden, Andre 279
 Uitterlinden, Andre G. 403
 Uitterlinden, Andre G. 125
 Uitto, Jouni 78
 Ulla, Maria Rosa 137
 Ullrich, Thomas 58
 Unasa-Apelu, Folla 311
 Underbjerg, Line 422
 Ung, Roth-Visal 215, 234, 294, 347, 348
 Unger, Sheila 299
 Unnikrishnan, Ginu 263, 265
 Unnikrishnan, Ginu 170
 Upala, Sikarin 396
 Uppuganti, Sasidhar 326
 Ural, Ani 65
 Urban, Robert 280
 Urban-Maldonado, Marcia . . . 236
 Usami, Yu 250
 Usardi, Alessia 40, 418
 Utheim, Tor P. 228
 Utsunomiya, Hajime 370
 Uyanik, Goekhan 184
 Uzer, Gunes 237, 244
- V**
- Vaaranemi, Jukka 179, 295
 Vaccaro, Chiara 35, 415
 Vacher, Jean 97, 293
 Vacher, Sophie 72
 Vaidyanathan, Sriram 294
 Vail, Thomas 161
 Valbret, Zoe 45
 Valderrabano, Rodrigo 434
 Valderrábano, Rodrigo J. 103
 Valdez, Sinai 83, 95
 Valenti, Maria Teresa 312
 Valero, Carmen 122, 351
 Valkema, Pieter 180
 Valland, Haldor 228
 Vallée, Maxime 351, 352
 Vallejo, Julian 431
 Vallejo, Julian A. 311
 Valta, Helena 417
 Vance, Eric A. 326
 Vancleave, Ashley 219
 Vandenberg, Andrew 71
 Vanden-Bossche, Arnaud 359
 Vandenput, Liesbeth 273, 310
 Vanderpuye-Orgle, Jacqueline 108
 Vanderschueren, Dirk 23, 402
 Vansickle, Judith 334
 Vanstone, Catherine. 152, 240, 279
 Vanstone, Catherine A. 233
 Vanwijnen, Andre 251
 Vargas, Geoffrey 72
 Vary, Calvin 77
 Vashishth, Deepak . . 138, 139, 297, 332
 Vasilakis, Naomi 398
 Vasilev, Krasimir 96
 Vassiliadis, John 26
 Vazquez, Maribel 32
 Vega, Gabriel Lopez. 360
 Veglahn, Tricia 199
 Veis, Deborah J 432
 Veis, Deborah J. 182, 192
 Veksler, Vladimir 76
 Velasquez-Forero, Francisco . 356
 Velde, Robert Y Van Der 397, 430
 Veldhuis-Vlug, Annegreet G. . 226, 347
 Venderschueren, Dirk 147
 Venditti, Rossella 78
 Vénica, C. 417
 Vennin, Severin 311
 Veras, Matthew 57
 Verbalis, Joseph G. 112
 Verdellis, Konstantinos 30
 Verdellis, Konstas 218
 Verdellis, Kostas 324
 Vered, Iris 135
 Verkerk, Annemieke Jmh. 403
 Verlinden, Lieve 414
 Verstappen, Johanna F.M. . . . 358
 Verstuyf, Annemieke 414
 Vesela, Iva 92
 Vesteragaard, Peter 7
 Vestergaard, Peter. 274
 Vico, Laurence. 3, 296, 359
 Vida, José María Gómez 182
 Vidmar, Gaj 173
 Vieira, Itamar O. 62
 Vieira, Margarida 418
 Vieira-Potter, Victoria. 353
 Vierlinger, Klemens 310
 Vigone, Giulia 196
 Villavicencio, Martha 112
 Violet, Lagari 291
 Visser, Jonathan V. 291
 Vito, Rita De 305
 Vitone, Gregory 18
 Vittinghoff, Eric . . . 20, 24, 106, 168, 226
 Vix, Justine 130
 Vlot, Mariska 274, 325
 Vo, Tammy 423
 Vo, Tien 316
 Vogrin, Sara 185
 Voight, Benjamin 28
 Vokes, Tamara 171, 396, 408
 Vokes, Tamara J. 128
 Volkman, Brian 153
 Volkman, Tammie 17
 Vollenweider, Peter 428
 Vollersen, Nele 5
 Vollmer, Günter 415
 Volpon, José B. 67
 Volpon, José Batista 431
 Vorland, Colby 179, 297
 Voronov, Irina 426
 Vos, Willem M De 296
 Voumard, Benjamin. 187
 Vracovska, Martina 333
 Vranken, Lisanne 397, 430
 Vries, Frank De 269, 270, 291
 Vries, Teun De 306
 Vrignaud, Arthur 170
 Vuilleumier, Patrik 126
 Vulpescu, Nicholas 105
- W**
- Waage, Anders 341
 Wacker, Michael. 383, 431
 Wacker, Michael J. 311
 Wactawski-Wende, Jean 8
 Wada, Satoshi 136
 Wadajkar, Aniket 255
 Wada-Takahashi, Satoko 119
 Waeber, Gerard 428
 Wagley, Yadav . . . 79, 91, 254, 376
 Wagman, Rachel B. 114
 Wagner, Diane 248
 Wagner, Philippe P 316
 Waguespack, Steven. 334
 Wake, Melissa 68
 Wakolbinger, Robert 116
 Waldorff, Erik I. 251
 Walji, Noosheen 340
 Walker, Emma 1
 Walker, Joanne 97
 Walker, Leila. 278
 Walker, Marcella 323
 Walkup, Michael 399
 Wall, Michelle 169
 Wallace, Joseph 212, 237, 331, 350
 Wallander, Marit 46
 Walls, Johnathon 320
 Wallwitz, Jacqueline . . . 280, 385
 Walsh, Jennifer 129, 319, 400
 Walsh, Neil. 168
 Wan, Mei. 245, 366
 Wan, Yong 190
 Wandel, Jasmin 187
 Wang, Andrew 426
 Wang, Bing 136
 Wang, Christine 115
 Wang, Chun 159
 Wang, Cuicui 50
 Wang, Cun-Yu. 190
 Wang, Dong 31, 439
 Wang, Elizabeth 5
 Wang, Haitao 111
 Wang, Haixing 379
 Wang, Hamilton 6
 Wang, Howard. 424
 Wang, Jefferey 177
 Wang, Jessie 199
 Wang, Ji 68
 Wang, Jia-Li 143
 Wang, Jingyi. 382
 Wang, Jinxi 221
 Wang, Jun 75
 Wang, Ke. 70
 Wang, Kun. 336
 Wang, Lai . . . 49, 53, 141, 246, 292, 343
 Wang, Lei 366
 Wang, Lijun 88
 Wang, Lili 196
 Wang, Ling. . . . 164, 264, 266, 390
 Wang, Liping 255, 437
 Wang, Liyun 35, 235, 404
 Wang, Luqiang 117, 313, 405
 Wang, Meng 252
 Wang, Mengyuan 48
 Wang, Rong 81
 Wang, Ruduan. 26
 Wang, Shenghang 254
 Wang, Tianlu 82, 249
 Wang, Ting. 50
 Wang, Wei 259
 Wang, Weiguang. 6
 Wang, Weihan 96
 Wang, Xi 77, 88, 153
 Wang, Xiao. 245
 Wang, Xiaodu 132
 Wang, Xiao-Fang 68
 Wang, Xiaoxuan 191, 281
 Wang, Xin-Luan. 143
 Wang, Xue 375
 Wang, Xuewei 139

- Wang, Xueyan 18, 260
 Wang, Yamei 104, 115, 292
 Wang, Yangang 178
 Wang, Yilin 31
 Wang, Yishu 31, 261
 Wang, Yi-Ting 103
 Wang, Yiyun 367
 Wang, Yongmei 82, 249
 Wang, Yongqiang 315
 Wang, Yu Jia 307
 Wang, Yuan 43
 Wang, Yuanyuan 367
 Wang, Yue Pei 215, 348
 Wang, Yue-Pei 391
 Wang, Yujia 27
 Wang, Zexi 89
 Wang, Zhaohua 9, 206
 Wang, Zhiying 213, 346
 Wang, Ziyi 149
 Wang, Zuqiang 84
 Wani, Mohan 381
 Waning, David 226
 Ward, Christopher 359
 Ward, Ferrous S. 238
 Ward, Kate 107, 280
 Ward, Leanne 55
 Ward, Linda 275
 Ward, Wendy E 438
 Ward, Wendy E. 314, 437
 Ware, Carl 413
 Wargny, Matthieu 17
 Wark, John 386
 Wark, John D. 277, 400
 Warman, Matthew 88
 Warner, Elizabeth 66, 99
 Warren, Aaron 26, 53, 191, 239, 354
 Warren, Gordon 195
 Warren, Mark L. 128
 Warshaw, Johanna 5, 118
 Warzecha, Maja 263
 Washbourne, Christopher 168
 Wastney, Meryl E. 323
 Watabe, Hirotaka 119
 Watamaniuk, Lelia 165
 Watanabe, Atsushi 92
 Watanabe, Kenta 140, 160
 Watanabe, Kounosuke 368
 Watanabe, Reiko 406
 Watkins, Marcus 91
 Watkns, Marcus 227
 Watson, Maureen 137, 295
 Watson, P 311
 Watson, Steven 402
 Watt, Heather 148
 Watt, James 356
 Watt, Torquil 405
 Watts, Nelson B. 128, 292
 Wayne, Jennifer 357
 Weaver, Connie 296
 Weber, Thomas 56
 Weber, Thomas J. 50
 Wee, Natalie K. 206
 Wee, Natalie Ky 77
 Weeks, Benjamin 402
 Weening, Bradley 409
 Wegrzyn, Julien 332
 Wehrli, Felix 202
 Wei, Bo 379
 Wei, Qiushi 245
 Wei, Shugin 240
 Wei, Shuqin 233
 Wei, Xin 439
 Weigley, Lindsay 332
 Weiler, Hope 152, 240, 279, 279
 Weiler, Hope A. 233
 Wein, Marc 74, 357
 Wein, Marc N. 14
 Weinhold, Niels 219
 Weins, Ashton M. 98
 Weinstein, Robert 23
 Weis, Lisa 400, 402
 Weis, Maryann 78, 424
 Weiss, Richard J. 104
 Weiss, Stephan 242
 Weisz-Hubshman, Monika 73
 Weivoda, Megan 145, 293
 Wek, Ronald 136
 Wells, Andrew 254
 Wells, Andrew D. 79, 91
 Welti, Laura 307
 Wen, Xialing 196
 Wenkert, Deborah 181, 182
 Wentworth, Kelly 51, 79
 Werfalli, Rafik El 122, 409
 Wergedal, Jon 363
 Wermers, Robert 199, 203
 Werner, Mathias 288
 Westbury, Leo 107
 Westendorf, Jennifer 96, 139, 152, 293, 377
 Westendorp, Rudi Gj 317
 Westerfield, Monte 78
 Westhrin, Marita 341
 Westhusin, Mark 426
 Westwater, Caroline 31
 Wette, Viktor 55
 Wetzel, Abigail I. 311
 Whalen, Jessica 209
 Whitaker, Adom 174
 Whitaker, Michael 125
 White, Fletcher 83
 White, James 9
 White, Kenneth 81, 353
 White, Kenneth E. 355
 White, Noelle 154
 White, Phillip 9
 White, Samantha 18
 Whitman, Malcom 363
 Whittier, Danielle E. 389
 Whyte, Michael P. 181, 432
 Whyte, Michael P. 51, 55, 57, 120, 130, 182, 306, 420, 422, 425
 Wientroub, Shlomo 333
 Wierpjes, Chantal 274, 325, 396
 Wierenga, Klaas J. 417
 Wijdeven, Katrien Van De 291
 Wijnen, Andre J Van 244, 254
 Wijnen, Andre J. Van 253, 366
 Wijnen, Andre Van 86, 154, 364
 Wilde, Aimee 314
 Wildman, Benjamin 30, 94
 Wiles, Crispin 410
 Willaert, Rebecca 417
 Willems, P.C. 66
 Willemsen, Rob 403
 Williams, Bart 259, 293
 Williams, Brett 26
 Williams, Diarra 228, 413, 426
 Williams, Graham 105
 Williams, Graham R. 64
 Williams, Greg 292
 Williams, John 61, 121, 126, 129, 130, 203, 323
 Williams, Katrina 359
 Williams, Nancy 142, 402
 Williams, Setareh A. 104
 Williams, Susan 300
 Willie, Bettina 313
 Wills, Karen 307
 Wilson, Brittany 363
 Wilson, David 154
 Wilson, Jonathan 81
 Wilson, Keith 194
 Wilson, Marques 280
 Wilsonsanthoshkumar, Aruni 344
 Wiluzanski, Diana 385, 410
 Windahl, Sara 273, 358
 Windle, Jolene 83
 Windle, Jolene J. 304, 324, 380
 Wing, Simon S. 70
 Winn, Nathan 353
 Winter, Liesbeth 180
 Winzenberg, Tania 109, 134, 185, 307
 Winzenrieth, Renaud 112, 264, 267, 401
 Wise, Carol 244, 364
 Witt-Enderby, Paula 208
 Witztum, Joseph L 23
 Wixted, John A. 184
 Wojda, Samantha 236
 Wolf, I 417
 Wolf, Jennifer 222
 Wolf, Myles 18, 260
 Wolf, Myles S. 230
 Wolfe, Lisa 236
 Wölfel, Eva Maria 288, 348
 Wolfgang, Michael J. 77
 Wollberg, Valerie 425
 Wollman, Caroline 134
 Wollny, Mathias 407
 Won, Ye-Yeon 276
 Wong, Andy 36
 Wong, Andy Kin On. 156, 371
 Wong, Andy Ko 387, 394
 Wong, Angel 113
 Wong, Carmen P. 351
 Wong, Ian 113
 Wong, Ka Ying 297
 Wong, Man-Sau 297
 Wong, Queenie 430
 Wong, Ronald Man Yeung 381
 Wong, Victoria Ho-Yee 177
 Woo, Jonathon 161
 Woo, Kyung-Mi 42, 79, 241
 Wood, Constance 176
 Wood, Nicholas 210
 Woods, Gina 106, 168
 Woods, Gina N. 226
 Woon, Song Dah 91
 Worton, Leah 117
 Wouters, Emiel 270, 389, 391
 Wouters, Fenne 306
 Wrann, Christianne 1
 Wright, Christian 362
 Wright, Christian S. 435
 Wright, Laura 237
 Wright, Laura E. 42
 Wright, Nicole 2, 54, 106, 267, 276
 Wright, Timothy 248
 Wu, Andy 72
 Wu, Chuanyue 31, 261
 Wu, Colleen 4
 Wu, Feitong 109
 Wu, Gang 358
 Wu, Gerald 80
 Wu, Joy 94, 279
 Wu, Joy Y. 434
 Wu, Jun 80
 Wu, Mengrui 29
 Wu, Po Hung 193
 Wu, Qing 168
 Wu, Shun-Cheng 413
 Wu, Xiaobo 48
 Wu, Xiaohao 119
 Wu, Xingwen 41, 191, 224, 281
 Wu, Yong 410
 Wu, Yunshu 43, 48
 Wu, Zixiang 373, 375
 Wuhler, Manfred 341
 Wulff, Birgit 348
 Wyers, Caroline E. 269, 291, 397, 430
 Wysolmerski, John 18

X

- Xi, Gang 81, 255
 Xia, Weibo 292
 Xian, Lingling 245
 Xiao, Guozhi 31, 261
 Xiao, Hui-Hui 297
 Xiao, Jianqiu 159
 Xiao, Lifeng 80
 Xiao, Liping 124, 281
 Xie, Han 357
 Xie, Hui 245
 Xie, Jing 43
 Xie, Liang 43, 48, 245
 Xie, Meng 367
 Xie, Yangli 84
 Xie, Yixia 383
 Xie, Zhihui 237, 244, 366
 Xie, Ziang 259
 Ximemez, João Paulo B. 67
 Ximenez, João Paulo 431
 Xin, Xiaonan 426
 Xing, Lianping 45, 178
 Xing, Mengdi 417
 Xing, Weirong 42, 343
 Xing, Yi 367
 Xiong, Guoming 218
 Xiong, Jinhui 12, 237
 Xiong, Qiuchan 48
 Xu, Chun 170, 263, 265
 Xu, Guoshuang 218
 Xu, Hanfei 36
 Xu, Huiyun 337
 Xu, Jiajia 367
 Xu, Jiake 256
 Xu, Jianrui 93, 414
 Xu, Kaipin 168, 189, 226
 Xu, Lan 26
 Xu, Li 266, 390
 Xu, Liangchen 260
 Xu, Liangcheng 340, 360
 Xu, Mingxin 368
 Xu, Qin 112
 Xu, Ren 3, 18
 Xu, Ruoshi 302, 338
 Xu, Xianghe 378
 Xu, Xiaoyu 383
 Xu, Yang 302
 Xu, Zech 147
 Xue, Yingben 70
 Xuereb-Anastasi, Angela 403

- Y**
- Yacoubian, Vahe 177
 Yadav, Ram Naresh 207
 Yadav, Sumit 156, 220
 Yalla, Naga 148
 Yallowitz, Alisha 3
 Yamada, Asako 178
 Yamada, Shuta 239
 Yamagata, Masayo 355
 Yamagiwa, Chiemi 177
 Yamamoto, Guilherme 417
 Yamamoto, Katsusuke 301
 Yamamoto, Keiko 301
 Yamamoto, Kenichi 211, 301
 Yamamoto, Masahiro 401
 Yamamoto, Takehisa 301
 Yamana, Kei 29
 Yamanaka, Hisashi 90
 Yamashita, Teruhito 136, 381
 Yamauchi, Mika 401
 Yan, Lin 12, 103
 Yan, Mingquan 85
 Yan, Qinnan 31, 261
 Yan, Shiguo 252
 Yan, Yinkun 270
 Yanagihara, Yuta 86, 381
 Yang, Chaofei 375
 Yang, Ethan 417
 Yang, Evan 124
 Yang, Fan 94
 Yang, Haisheng 149, 383
 Yang, Hou-Ting 384
 Yang, Jiancheng 254
 Yang, Jingyan 208
 Yang, Kyu Hyun 116
 Yang, Laiji 36
 Yang, Phillip 294
 Yang, Rong-Sen 253, 310
 Yang, Shuying 74, 93, 192
 Yang, Tao 259
 Yang, Wenjing 25
 Yang, Wentian 19, 88
 Yang, Xu 416
 Yang, Yajun 223
 Yang, Yang 140, 252
 Yang, Yi 109
 Yang, Yingzi 302
 Yang, Yu-Mi 376
 Yao, Gang Qing 235
 Yao, Gang-Qing 97
 Yao, Yeqi 426
 Yao, Zhenqiang 12, 45
 Yaoita, Eishin 213
 Yap, Patrick 417
 Yaqub, Maqsood 120
 Yarrow, Josh 33
 Yarrow, Joshua 423
 Yates, Christopher 386
 Yates, Nathan 218
 Yates, Sydney 314
 Yau, Diana 430
 Yau, Michelle 247
 Yazdani, Mazyar 228
 Ye, Ling 48
 Ye, Young-Min 283
 Ye, Zhou 195
 Yee, Cristal 161
 Yee, Cristal S. 1, 262
 Yeh, Randy 63, 324
 Yerges-Armstrong, Laura 395
 Yi, Haeyoung 348
- Yi, Jianxun 346
 Yi, Xin 237, 362, 435
 Yi, Young-Su 220
 Yin, Chong 373, 375
 Yin, Michael 126
 Yin, Michael T. 178
 Yin, Mt. 112
 Yin, Xiang 114, 290
 Yin, Yong 93
 Ying, Anita 334
 Yokogawa, Noriaki 238
 Yokota, Hiroki 34, 435
 Yokota, Kazuaki 403
 Yokozeiki, Yuji 173
 Yoneda, Masahiro 176
 Yoneda, Susumu 91
 Yoneda, Toshiyuki 90
 Yonezu, Daiki 409
 Yong, E.L. 186
 Yoo, Taekyeong 184
 Yoon, Donghoon 219, 342
 Yoon, Heein 79, 241
 Yoon, Hee-In 240
 Yoon, Hye-Jin 257
 Yoon, Sung-Hee Seanna 5
 Yoon, Won-Jun 240
 Yoon, Young-Ran 257
 Yorgan, Timur 5, 143
 Yorgan, Timur A. 4
 Yoshiko, Yuji 293
 Yoshimi, Akihide 71
 Yoshino, Yasumasa 213, 241
 Yoshinouchi, Shosei 140
 Yoshioka, Toru 411
 You, Lidan 260, 340, 360
 Youlten, Scott 105
 Youm, Yoosik 429
 Young, Edmond 340
 Young, Gregory 249
 Young, J.E.M. 122
 Young, Marian 97
 Young, Marian F. 344
 Young, Mariel 228
 Young, Robert 118
 Yu, Cindy 163
 Yu, Elaine 48
 Yu, Eric Y. 89
 Yu, Fangtang 80
 Yu, Fiona Wp 68
 Yu, Guangchuang 227
 Yu, Jungeun 31, 153, 259, 312
 Yu, Kanglun 93, 212
 Yu, Ling 85
 Yu, Mingcan 35, 415
 Yu, S. Michael 342
 Yu, Wei 292
 Yu, Wenxuan 297
 Yu, Y Eric 131
 Yu, Yilin 86
 Yu, Youcheng 41
 Yuan, Amy 20, 29, 263, 265
 Yuan, Quan 43, 48
 Yuasa, Yusuke 172, 179
 Yue, Hua 427
 Yue, Li 222
 Yue, Shanna 221
 Yue, Susan 115
 Yuen, Tony 415
 Yu-Kwang, Donovan Tay 129, 324
 Yun, Chawon 329, 376
 Yun, Huifeng 106, 276
- Z**
- Zaidi, Mone 415
 Zalzal, Paul 409
 Zamarioli, Ariane 67, 431
 Zambuzzi, Willian 153
 Zan, Pengfei 253
 Zanchetta, Jose Ruben 302
 Zanchetta, Maria Belen 302
 Zandieh-Doulabi, Behrouz 358
 Zandueta, Carolina 46
 Zangari, Maurizio 219, 342
 Zannettino, Andrew 424
 Zannit, Heather 83
 Zanotti, Stefano 31, 222, 259
 Zarecki, Patryk 267
 Zarecneva, Diana 73
 Zaritsky, Joshua 57
 Zarka, Mylène 360
 Zavala, Kathryn 177
 Zaweija, David C 382
 Zeana, Cosmina 126
 Zebaze, Roger 38, 68, 134, 362
 Zeitlin, Leonid 333
 Zemel, Babette 28, 112, 188, 212
 Zemelman, Boris 77
 Zeng, Erliang 219
 Zeng, Xuemei 218
 Zeni, Sn 417
 Zeni, Susana N. 209
 Zerbini, Cristiano 113
 Zeytinoglu, Meltem 171
 Zhang, Ben 227
 Zhang, Caibin 228
 Zhang, Chang-Qing 230
 Zhang, Chi 361
 Zhang, Chuan 432
 Zhang, Chunbin 44
 Zhang, Deyu 22
 Zhang, Fan 306, 425
 Zhang, Fenghe 259
 Zhang, Ge 119
 Zhang, Hao 303
 Zhang, Jane 402
 Zhang, Jia Jun 27, 307
 Zhang, Jian 254
 Zhang, Jiasheng 437
 Zhang, Lan 337
 Zhang, Lei 243
 Zhang, Leititia 367
 Zhang, Lin 56, 122
 Zhang, Liu 221
 Zhang, Mingcai 221
 Zhang, Nianli 251
 Zhang, Peng 300, 324
 Zhang, Ping 34, 379, 435
 Zhang, Qian 81, 94
 Zhang, Shu 168
 Zhang, Tingting 54
 Zhang, Xiao 80
 Zhang, Xin 23
 Zhang, Yan 93
 Zhang, Yang 351
 Zhang, Yejia 405
 Zhang, Yong 390
 Zhang, Yue 357
 Zhang, Yueqi 305
 Zhang, Zeijan 341
 Zhang, Zhendong 68
 Zhang, Zhenlin 292, 303, 427
 Zhang, Zhen-Lin 302
 Zhao, Baohong 3, 18
- Zhao, Binsheng 199
 Zhao, Fan 85
 Zhao, Gang 439
 Zhao, Haijun 10
 Zhao, Hong 383
 Zhao, Hongbo 16, 35
 Zhao, Hu 243
 Zhao, Jing 199, 219
 Zhao, Jinmin 139, 243
 Zhao, Junfei 71
 Zhao, Liang 18
 Zhao, Wei 337
 Zhao, Yiran 261
 Zhao, Yunpeng 96
 Zhao, Zhifeng 439
 Zheng, Li 139, 243
 Zheng, Liwei 338
 Zheng, Li-Zhen 143
 Zheng, Minghao 70
 Zheng, Rixin 43, 48
 Zheng, Xiaofei 43
 Zhong, Leilei 313
 Zhong, Qing 414
 Zhou, Baoyi 367
 Zhou, Bin 131
 Zhou, Daohong 23, 26, 239
 Zhou, Guang 19, 30
 Zhou, Hong 9
 Zhou, Hua 121, 199, 323, 324
 Zhou, Jingman 352
 Zhou, Jingsong 346
 Zhou, Liping 297
 Zhou, Michael 190
 Zhou, Shuanhu 230, 250
 Zhou, Weina 158, 216
 Zhou, Xichao 45
 Zhou, Xin 338
 Zhou, Xuedong 48, 224, 302, 338
 Zhou, Yongsheng 403
 Zhou, Yuqiao 30
 Zhu, Hui 94
 Zhu, Julia 26
 Zhu, Kun 110, 393
 Zhu, Mark 295
 Zhu, Meiling 97
 Zhu, Tracy Y. 68
 Zhu, Zoe (Xiaofang) 36
 Zhu, Zoe(Xiaofang) 223
 Zieba, Jennifer 26
 Zierau, Oliver 415
 Zillikens, M Carola 403, 438
 Zimmer, Katherine 372
 Zimmerman, Kristin 424
 Zimmermann, Elizabeth 313
 Zimmers, Teresa 334
 Zingman, Barry 126
 Zipeto, Donato 312
 Zirngibl, Ralph 426
 Zong, Xiaohua 9
 Zong, Xiaopeng 237
 Zou, Wei 48
 Zou, Weiguo 32
 Zullo, Andrew 54
 Zuloaga, Kristen L 227
 Zuo, Chunlin 88
 Zur, Yuval 417
 Zurynski, Yvonne 210
 Zuscik, Michael 117, 370
 Zweifler, Laura 216
 Zwettler, Elisabeth 184
 Zysset, Philippe 139, 187

